

Posterior Fossa Tumors in Children

M. Memet Özek
Giuseppe Cinalli
Virginia Maixner
Christian Sainte-Rose
Editors

Posterior Fossa Tumors in Children

M. Memet Özek • Giuseppe Cinalli
Virginia Maixner • Christian Sainte-Rose
Editors

Posterior Fossa Tumors in Children

 Springer

Editors

M. Memet Özek
Neurosurgery
Acibadem University
Istanbul
Turkey

Giuseppe Cinalli
Pediatric Neurosurgery
Santobono Children's Hospital
Naples, Napoli
Italy

Wirginia Maixner
Department of Neurosurgery
Royal Childrens Hospital
Melbourne, Victoria
Australia

Christian Sainte-Rose
Pediatric Neurosurgery
Hopital Necker-Enfants Malades
Paris
France

ISBN 978-3-319-11273-2 ISBN 978-3-319-11274-9 (eBook)
DOI 10.1007/978-3-319-11274-9

Library of Congress Control Number: 2015937189

Springer Cham Heidelberg New York Dordrecht London
© Springer International Publishing Switzerland 2015

This work is subject to copyright. All rights are reserved by the Publisher, whether the whole or part of the material is concerned, specifically the rights of translation, reprinting, reuse of illustrations, recitation, broadcasting, reproduction on microfilms or in any other physical way, and transmission or information storage and retrieval, electronic adaptation, computer software, or by similar or dissimilar methodology now known or hereafter developed.

The use of general descriptive names, registered names, trademarks, service marks, etc. in this publication does not imply, even in the absence of a specific statement, that such names are exempt from the relevant protective laws and regulations and therefore free for general use.

The publisher, the authors and the editors are safe to assume that the advice and information in this book are believed to be true and accurate at the date of publication. Neither the publisher nor the authors or the editors give a warranty, express or implied, with respect to the material contained herein or for any errors or omissions that may have been made.

Printed on acid-free paper

Springer International Publishing AG Switzerland is part of Springer Science+Business Media
(www.springer.com)

To my wife for 32 years, Eren, for her support and patience throughout my life.

M. Memet Özek

To my mother.

To Fabrizia, Francesco, and Maria Allegra because the time spent with them is the only real happiness.

and

To Roberta Migliorati who devoted her whole life to the care of children affected by Brain Neoplasms.

Giuseppe Cinalli

To my mentors and students and the children for whom we care.

Virginia Maixner

To all the young colleagues whom I have helped to progress in pediatric neurosurgery.

Christian Sainte-Rose

Preface

Tumors of the posterior fossa are one of the most challenging pathologies a neurosurgeon is called upon to deal with. The anatomical complexity of the region and the amazing variety of possible histologies of neoplastic lesions in this area in children make the therapeutic challenges even more difficult for the pediatric neurosurgeon. The frequent association with hydrocephalus and the options for its management before, during, or after the surgical procedure on the posterior fossa have given rise to significant controversies during recent years, and a consensus is still far from being obtained. During the last few years, we have witnessed impressive progress in the genetic and genomic profiling of some tumor lesions, allowing the identification of specific and very different prognostic subgroups previously labeled with the same name and often treated with the same protocols. With this new approach, we are entering an era in which we shall be able to tailor treatment protocols very precisely in order to avoid unnecessary procedures or therapeutic regimens, thus limiting the possible collateral effects that have always burdened the long-term prognosis and quality of life of survivors.

We have tried to group into different sections the main pathologies encountered in this age range. For each pathology, recognized experts thoroughly analyze all aspects of genetics, radiology, surgery, pathology, oncology, and radiotherapy. Although all of the editors are surgeons, only Section II is dedicated solely to surgical approaches and techniques, and a strong effort was made when profiling the book plan to offer a real multidisciplinary view of these pathologies. We hope that the final results will reflect this effort. Treatment of posterior fossa tumors in children is never a single person's work. Classification is complex, deeper expertise is demanded of actors in many different fields, and very strong and reliable teamwork is not simply an option but a real obligation.

An entire section has been dedicated to rare pathologies where early recognition may modify the therapeutic approach from the earliest stages, and the final section is devoted to an analysis of different standards of immediate postoperative care and the long-term general implications of follow-up and treatment.

The final result explains why gestation was long and complex, and we are very grateful to all contributors for their patience and to the Springer editorial staff, who believed in this project.

The final acknowledgment always goes to our patients and to their families, who are called upon to face something bigger than themselves and from whose terrible endurance and tribulations the cold scientific aspects of these pages are derived.

Istanbul, Turkey
Naples, Italy
Parkville, VIC, Australia
Paris, France

M. Memet Özek
Giuseppe Cinalli
Wirginia June Maixner
Christian Sainte-Rose

Contents

Part I General Principles of Treatment in Pediatric Posterior Fossa Tumors

- 1 History of Posterior Fossa Tumor Surgery 3**
James Tait Goodrich
- 2 Development of the Posterior Fossa Structures 61**
Martin Catala
- 3 The Anatomy of the Posterior Cranial Fossa 75**
Aşkın Şeker and Albert L. Rhoton Jr.
- 4 Anatomical Connection of the Cerebellum 101**
Akin Akakin and Albert L. Rhoton Jr.
- 5 Clinical Presentation and Neurologic Evaluation
in Posterior Fossa Tumors in Children 119**
Ugur Işık and M. Memet Özek
- 6 Principles of Molecular Biology in Posterior
Fossa Tumors 129**
Yuzo Terakawa, Jong Hee Chang, Christian Smith,
and James T. Rutka
- 7 Radiation Therapy in Posterior Fossa Tumors 147**
Thomas E. Merchant

Part II Surgical Approaches to Pediatric Posterior Fossa Tumors

- 8 Median Suboccipital Approach 177**
Benoit Jenny and Wirginia June Maixner
- 9 Paramedian Approaches to the Posterior Fossa 189**
Giuseppe Mirone, Pietro Spennato,
and Giuseppe Cinalli
- 10 Skull Base Approaches in Children 209**
Bernard George and Damien Bresson
- 11 Anterior Skull Base Approaches to the Posterior Fossa 219**
Dominic N.P. Thompson

12 Hydrocephalus in Pediatric Patients with Posterior Fossa Tumors	229
Mustafa Gdk and M. Memet zek	
13 Intraoperative Neurophysiological Monitoring in Posterior Fossa Surgery	239
Francesco Sala, Pasquale Gallo, Vincenzo Tramontano, and Massimo Gerosa	
Part III Pathologies in Pediatric Posterior Fossa Tumors: Medulloblastoma	
14 Molecular Biology and Genetics of Medulloblastoma	265
Pasquale De Antonellis, Livia Garzia, Antonio Verrico, Michael D. Taylor, and Massimo Zollo	
15 Imaging of Medulloblastoma	287
Anna Nastro, Maria Consiglio Buonocore, Domenico Cicala, Emilio Cianciulli, Daniele Cascone, and Maria Rita Panico	
16 Medulloblastoma: Surgery	313
Pietro Spennato, Claudio Ruggiero, and Giuseppe Cinalli	
17 Medulloblastoma: Pathology	333
Giuliana Di Martino, Elia Guadagno, and Maria Laura Del Basso De Caro	
18 Treatment of Medulloblastoma: Chemotherapy	349
Lucia Quaglietta, Virginia Vitale, Antonio Verrico, and Roberta Migliorati	
19 Radiotherapy in Medulloblastoma	363
Maurizio Mascarin, Francesca Maria Giugliano, and Elisa Coassin	
Part IV Pathologies in Pediatric Posterior Fossa Tumors: Ependymoma	
20 Ependymomas: Genetics	383
Stephanie Puget and Guillaume Bergthold	
21 Neuroimaging of Posterior Fossa Ependymoma in Children	393
Andrea Rossi	
22 Ependymomas: Surgery	407
Stephanie Puget and Christian Sainte-Rose	
23 Ependymoma	415
Pascale Varlet and Felipe Andreiuolo	
24 Oncological Management of Ependymomas	423
Jacques Grill and Maria-Jesus Lobon Iglesias	

**Part V Pathologies in Pediatric Posterior Fossa Tumors:
Cerebellar Astrocytoma**

- 25 Genetics of Cerebellar Low-Grade Astrocytomas** 431
Adam J. Fleming and Mark W. Kieran
- 26 Neuroimaging of Posterior Fossa Astrocytoma in Children** . . . 447
Daniele Cascone, Maria Rita Panico, Maria Consiglio Buonocore,
Domenico Cicala, Anna Nastro, and Emilio Cianciulli
- 27 Approaches to Cerebellar Astrocytoma in Pediatric Patients** . 457
Erica Jacobson, Grace K. Lai, and Wirginia June Maixner
- 28 Cerebellar Astrocytomas: Pathology** 467
Christian H. Rickert
- 29 Cerebellar Astrocytoma: Oncological Care** 487
Pratiti Bandopadhyay, Peter A. Downie, and David M. Ashley
- 30 Radiotherapy for Cerebellar Astrocytomas** 495
Greg C. Wheeler

**Part VI Pathologies in Pediatric Posterior Fossa Tumors:
Brain Stem Tumors**

- 31 Imaging of the Brainstem Tumors** 511
Charles Raybaud and Abeer Almehdar
- 32 Surgical Approach to Mesencephalic Tumors** 545
Bahattin Tanrikulu, Gurmit Singh, and M. Memet Özek
- 33 Surgery of the Pons** 557
Pablo F. Recinos, Violette Renard Recinos, and George I. Jallo
- 34 Surgery of Medulla Oblongata Tumors** 571
M. Memet Özek and Ulaş Yener
- 35 4D: Brain Stem Tumors – Pathology** 585
Aydin Sav and Pınar Karabağlı
- 36 Radiotherapy Options of Brainstem Tumors** 595
Hale Başak Çağlar
- 37 Oncologic Treatment of Pediatric Brainstem Tumors** 609
Cengiz Canpolat

Part VII Pathologies in Pediatric Posterior Fossa Tumors: AT/RT

- 38 Genetics** 629
Su Gulsun Berrak
- 39 Imaging Findings of CNS Atypical
Teratoid/Rhabdoid Tumors** 633
Alp Dinçer

40	Atypical Teratoid/Rhabdoid Tumor: Surgery	643
	Concezio Di Rocco and Luca Massimi	
41	Atypical Teratoid/Rhabdoid Tumor	651
	Pınar Karabağlı	
42	Atypical Teratoid/Rhabdoid Tumors: Current Chemotherapy and Future Directions	657
	Cengiz Canpolat	
43	Radiation Therapy in Atypical Teratoid/Rhabdoid Tumors ..	667
	Hale Basak Caglar	
 Part VIII Pathologies in Pediatric Posterior Fossa Tumors: Chordoma		
44	Molecular Biology and Genetics of Chordomas	675
	Mustafa Güdük and M. Memet Özek	
45	Imaging Findings of the Pediatric Clivus Chordomas	683
	Alp Dincer	
46	Chordomas: Pathology	693
	Aydin Sav and Pınar Karabağlı	
47	Chordomas and Their Management	703
	Kevin Beccaria, Stephanie Puget, Bernard George, and Christian Sainte-Rose	
 Part IX Pathologies in Pediatric Posterior Fossa Tumors: Rare Tumors		
48	Posterior Fossa Choroid Plexus Tumor	723
	Nobuhito Morota, Toshihiro Kumabe, and Akiyoshi Kakita	
49	Medical Management of Choroid Plexus Tumors	745
	Johannes E. Wolff, Mical Bahar, Anita Mahajan, and Su G. Berrak	
50	Vestibular Schwannoma	761
	Martin U. Schuhmann and Marcos S. Tatagiba	
51	Posterior Fossa Gangliogliomas	771
	Federico Di Rocco, Pascale Varlet, Nathalie Boddaert, Jacques Grill, Thomas Roujeau, Stephanie Puget, Bertrand Baussard, Michel Zerah, and Christian Sainte-Rose	
52	Dermoid Tumors	783
	M. Memet Özek and Saeed Kohan	
53	Epidermoid Tumors	795
	Saeed Kohan, Joachim Oertel, and M. Memet Özek	

54 Lhermitte–Duclos (Section Rare Tumors)	805
Pietro Spennato, Vincenzo Trischitta, Ferdinando Aliberti, and Giuseppe Cinalli	
55 Meningioma	813
Saeed Kohan and M. Memet Özek	
 Part X Pre- and Postoperative Care of Pediatric Posterior Fossa Tumors	
56 Immediate Postoperative Care	825
Martina Messing-Jünger, Michael Ehlen, and Ehrenfried Schindler	
57 Postoperative Care Following Surgery for Posterior Fossa Tumors	841
Vasilios Tsitouras and Spyros Sgouros	
58 Immediate Postoperative Care	847
Stephanie Puget, Antonio Vecchione, and Philippe Meyer	
59 Immediate Postoperative Care: Istanbul Experience	849
Nigar Baykan and M. Memet Özek	
60 Posterior Fossa Tumors: Immediate Postoperative Care	853
Il-Woo Lee	
61 Immediate Postoperative Care	857
Pietro Spennato, Anna Dolcini, Alessandra Alifuoco, and Giuseppe Cinalli	
62 Surgical Complications	861
Ram Kumar and Conor Mallucci	
63 Postoperative Vertebral Column Complications	885
Bahattin Tanrikulu, M. Memet Özek, and Deniz Konya	
64 Endocrinologic Complications and Late Sequela of Childhood Posterior Fossa Tumors	897
Abdullah Bereket	
65 Rehabilitation for Children with Posterior Fossa Tumors	907
Adam M. Scheinberg	
66 Psychosocial Coping with Neurosurgery: Children and Their Families	917
Banu Çankaya and M. Kemal Kuşcu	
Index	931

Contributors

Akin Akakin Department of Neurosurgery, Bahcesehir University, Beşiktaş, Istanbul, Turkey

Ferdinando Aliberti, M.D. Division of Pediatric Neurosurgery, Department of Neuroscience, Santobono-Pausilipon Children's Hospital, Naples, Italy

Alessandra Alifuoco Department of Pediatric Anesthesiology, Santobono-Pausilipon Children's Hospital, Naples, Italy

Abeer Almehdar, M.D. Department of Medical Imaging, King Abdulaziz Medical City, Jeddah, Saudi Arabia

Felipe Andreiuolo, M.D. Department of Neuropathology, Sainte-Anne Hospital, University Paris Descartes, Paris, France

David M. Ashley, M.D. Andrew Love Cancer Centre and Children's Cancer Centre, Barwon Health and Royal Children's Hospital, Melbourne, VIC, Australia

Pratiti Bandopadhyay, M.B.B.S., Ph.D. Pediatric Neuro-Oncology Program, Dana-Farber Cancer Institute, Boston Children's Hospital and Harvard Medical School, Melbourne, VIC, Australia

Bertrand Baussard, M.D. Department of Paediatric Neurosurgery, Necker Enfants Malades Hospital, Paris, France

Nigar Baykan, M.D. Department of Anesthesiology, Acibadem University, School of Medicine, Istanbul, Turkey

Kevin Beccaria, M.D. Division of Pediatric Neurosurgery, Department of Neurosurgery, Hopital Necker Enfants Malades, Université Paris Decartes, Paris, France

Abdullah Bereket, M.D. Division of Pediatric Endocrinology, Marmara University Hospital, Istanbul, Turkey

Guillaume Bergthold, M.D. Department of Vectorology and Anticancer Therapeutics, CNRS UMR 8203, University Paris sud XI, Institut Gustave Roussy, Villejuif, France

Su Gulsun Berrak, M.D. Division of General Pediatrics, LINCS, Children's Hospital at Montefiore, Albert Einstein College of Medicine, Bronx, NY, USA

Department of Pediatric Hematology Oncology, Marmara University Medical Center, Istanbul, Turkey

Nathalie Boddaert, M.D. Department of Radiology, Hopital Necker-Enfants Malades, Université Paris Decartes, Paris, France

Damien Bresson Department of Neurosurgery, Hôpital Lariboisière, Paris, France

Maria Consiglio Buonocore, M.D. Division of Pediatric Neuroradiology, Department of Neurosciences, Santobono-Pausilipon Children's Hospital, Naples, Italy

Hale Basak Caglar, M.D. Department of Radiation Oncology, Medipol University, Istanbul, Turkey

Banu Çankaya, Ph.D. Department of Psychology, Koç University, Istanbul, Turkey

Cengiz Canpolat, M.D. Division of Pediatric Oncology, Department of Pediatrics, Acibadem University, School of Medicine, Istanbul, Turkey

Daniele Cascone, M.D. Division of Pediatric Neuroradiology, Department of Neurosciences, Santobono Pausilipon Children's Hospital, Naples, Italy

Martin Catala, M.D., Ph.D. Faculté de Médecine Pitié-Salpêtrière (Université Paris 6), UMR CNRS and Paris VI 7622, Paris Cedex 05, France

Fédération de Neurologie, Hôpital Pitié-Salpêtrière, Paris Cedex 13, France

Jong Hee Chang, M.D. Division of Neurosurgery, Department of Surgery, The Hospital for Sick Children, The University of Toronto, Toronto, ON, Canada

Emilio Cianciulli, M.D. Division of Pediatric Neuroradiology, Department of Neurosciences, Santobono-Pausilipon Children's Hospital, Naples, Italy

Domenico Cicala, M.D. Division of Pediatric Neuroradiology, Department of Neurosciences, Santobono-Pausilipon Children's Hospital, Naples, Italy

Giuseppe Cinalli, M.D. Division of Pediatric Neurosurgery, Department of Neuroscience, Santobono-Pausilipon Children's Hospital, Naples, Italy
Department of Neurosurgery, University of L'Aquila, L'Aquila, Italy

Elisa Coassin, M.D. Pediatric Radiotherapy Unit, Department of Radiation Oncology, IRCCS – CRO Aviano Cancer Center (Italy), Aviano, Italy

Pasquale De Antonellis, M.D. Department of Molecular Medicine and Medical Biotechnologies, "Federico II" University of Naples, Naples, Italy

Maria Laura Del Basso De Caro, M.D. Department of Advanced Biomedical Sciences, University Federico II Naples, Naples, Italy

Giuliana Di Martino, M.D. Division of Pediatric Neurosurgery, Department of Neuroscience, Santobono-Pausilipon Children's Hospital, Naples, Italy

Concezio Di Rocco, M.D. Division of Pediatric Neurosurgery, Catholic University, Medical School-Rome, Rome, Italy

Federico Di Rocco, M.D. Department of Paediatric Neurosurgery, Hopital Necker-Enfants Malades, Université Paris Decartes, Paris, France

Alp Dinçer, M.D. Department of Radiology, Acibadem University, School of Medicine, Istanbul, Turkey

Anna Dolcini Department of Anesthesiology, Santobono-Pausilipon Children's Hospital, Naples, Italy

Peter A. Downie, M.D. Children's Cancer Centre, Royal Children's Hospital and Southernhealth, Melbourne, VIC, Australia

Michael Ehlen, M.D. Department of Pediatric Intensive Care and Neonatology, Asklepios Klinik Sankt Augustin, University-Hospital of Bonn, Bonn, Germany

Adam J. Fleming, M.A.Sc., M.D. Pediatric Hematology/Oncology, McMaster Children's Hospital, McMaster University, Hamilton, ON, Canada

Paquale Gallo, M.D. Pediatric Neurosurgery Unit, Institute of Neurosurgery, University Hospital, Verona, Italy

Livia Garzia, M.D. Arthur and Sonia Labatt Brain Tumor Research Centre, The Hospital for Sick Children, Toronto, ON, Canada

Bernard George Department of Neurosurgery, Hôpital Lariboisière, Paris, France

Massimo Gerosa Intraoperative Neurophysiology Unit, Institute of Neurosurgery, University Hospital, Verona, Italy

Francesca Maria Giugliano, M.D. Department of Radiation Oncology, II University of Naples (Italy), Aviano, Pordenone, Italy
Pediatric Radiotherapy Unit, Department of Radiation Oncology, IRCCS – CRO Aviano Cancer Center (Italy), Aviano, Italy

James Tait Goodrich, M.D., Ph.D., D.Sci. (Honoris Causa) Leo Davidoff Department of Neurological Surgery, Albert Einstein College of Medicine, Children's Hospital at Montefiore, Bronx, NY, USA

Jacques Grill, M.D., Ph.D. Pediatric and Adolescent Oncology, Institut Gustave Roussy, Villejuif, Ile de France, France

Elia Guadagno, M.D. Department of Advanced Biomedical Sciences, University Federico II Naples, Naples, Italy

Mustafa Güdük, M.D. Department of Neurosurgery, Acibadem University, School of Medicine, Istanbul, Turkey

Maria-Jesus Lobon Iglesias, M.D. Pediatric and Adolescent Oncology, Institut Gustave Roussy, Villejuif, Ile de France, France

Ugur Işık, M.D. Division of Pediatric Neurology, Department of Pediatrics, Acibadem University, Istanbul, Turkey

Erica Jacobson, M.D. Department of Neurosurgery, Prince of Wales Hospital, Randwick, NSW, Australia

George I. Jallo, M.D. Division of Pediatric Neurosurgery, Johns Hopkins University School of Medicine, Baltimore, M.D., USA

Benoît Jenny Department of Neurosurgery, Royal Children's Hospital Melbourne, Parkville, VIC, Australia

Akiyoshi Kakita, M.D., Ph.D. Department of Pathology and Resource Branch for Brain Disease Research CBBR, Brain Research Institute, University of Niigata, Chuo-ku, Niigata, Japan

Pınar Karabağlı, M.D. Department of Pathology, Selçuk University, Selçuklu School of Medicine, Konya, Turkey

Mark W. Kieran, M.D., Ph.D. Pediatric Neuro-Oncology, Dana-Farber Children's Hospital Cancer Center, Harvard Medical School, Boston, MA, USA

Saeed Kohan, MBBS, FRACS Department of Neurosurgery, Sydney Children's Hospital, Sydney, Australia

Deniz Konya, M.D. Department of Neurosurgery, Marmara University, School of Medicine, Istanbul, Turkey

Toshihiro Kumabe, M.D. Department of Neurosurgery, Tohoku University Graduate School of Medicine, Sagamihara, Kanagawa, Japan

Ram Kumar, M.D. Department of Neurology, Alder Hey Children's NHS Foundation Trust, Liverpool, UK

M. Kemal Kuşcu, M.D. Department of Psychiatry, Marmara University, School of Medicine, Istanbul, Turkey

Grace K. Lai, M.D. Department of Neurosurgery, Prince of Wales Hospital, Randwick, NSW, Australia

Il-Woo Lee, M.D., Ph.D. Department of Neurosurgery, Catholic University of Korea, Seoul, South Korea

Anita Mahajan, M.D. Department of Radiation Oncology, MD Anderson Cancer Center, Houston, TX, USA

Wirginia June Maixner, M.D. Department of Neurosurgery, Royal Children's Hospital Melbourne, Parkville, VIC, Australia

Conor Mallucci, M.D. Department of Neurosurgery, Alder Hey Children's NHS Foundation Trust, Liverpool, UK

Maurizio Mascarin, M.D. Pediatric Radiotherapy Unit, Department of Radiation Oncology, IRCCS – CRO Aviano Cancer Center (Italy), Aviano, Italy

Luca Massimi, M.D. Division of Pediatric Neurosurgery, Catholic University, Medical School-Rome/INI-Hannover, Rome, Italy

Thomas E. Merchant, D.O., Ph.D. Department of Radiation Oncology, St. Jude Children’s Research Hospital, Memphis, TN, USA

Martina Messing-Jünger, M.D., Ph.D. Department of Pediatric Neurosurgery, Asklepios Klinik Sankt Augustin, University-Hospital of Bonn, Bonn, Germany

Philippe Meyer, M.D. Department of Anesthesiology, Necker Hospital, Université Paris Descartes, Sorbonne Paris Cité, Paris, France

Roberta Migliorati, M.D. Department of Oncology, Division of Pediatric Oncology, A.O.R.N. Santobono-Pausilipon Children’s Hospital, Naples, Italy

Giuseppe Mirone Division of Neurosurgery, Department of Neurosciences, Santobono-Pausilipon Children’s Hospital, Naples, Italy

Nobuhito Morota, M.D. Division of Neurosurgery, National Medical Center for Children and Mothers, National Center for Child Health and Development, Setagaya, Tokyo, Japan

Anna Nastro, M.D. Service of Pediatric Neuroradiology, Department of Neurosciences, Santobono-Pausilipon Children’s Hospital, Naples, Italy

Joachim Oertel, M.D. Department of Neurosurgery, Universitätsklinikum des Saarlandes, Homburg-Saar, Germany

M. Memet Özek, M.D. Division of Pediatric Neurosurgery, Department of Neurosurgery, Acibadem University, School of Medicine, Istanbul, Turkey
Department of Neurosurgery, Acibadem University, Istanbul, Turkey

Maria Rita Panico, M.D. Division of Radiology, Department of Neurosciences, Federico II University, Naples, Italy

Ove Peters, M.D. Department of Pediatric Oncology, University of Regensburg, Regensburg, Germany

Stephanie Puget, M.D., Ph.D. Department of Pediatric Neurosurgery, Necker Hospital, Université Paris Descartes, Sorbonne Paris Cité, Paris, France

Lucia Quaglietta, M.D. Department of Oncology, Division of Pediatric Oncology, Santobono-Pausilipon Children’s Hospital, Naples, Italy

Charles Raybaud, M.D. Division Head of Neuroradiology, Hospital for Sick Children and University of Toronto, Toronto, ON, Canada

Pablo F. Recinos, M.D. Division of Pediatric Neurosurgery, Johns Hopkins University School of Medicine, Baltimore, M.D., USA

Violette Renard Recinos, M.D. Department of Neurosurgery, Cleveland Clinic, Cleveland, OH, USA

Albert L. Rhoton Jr., M.D. Department of Neurosurgery, Florida University, Gainesville, FL, USA

Christian H. Rickert, M.D., Ph.D., FRCPath, FFSc(RCPA) Department of Neuropathology and Paediatric Pathology, Vivantes Clinics Berlin, Berlin, Germany

Andrea Rossi, M.D. Department of Pediatric Neuroradiology, G. Gaslini Children's Hospital, Genoa, Italy

Thomas Roujeau, M.D. Department of Paediatric Neurosurgery, Necker Enfants Malades Hospital, Paris, France

Claudio Ruggiero, M.D. Division of Pediatric Neurosurgery, Department of Neuroscience, Santobono-Pausilipon Children's Hospital, Naples, Italy

James T. Rutka, M.D., Ph.D. Division of Neurosurgery, Department of Surgery, The Hospital for Sick Children, The University of Toronto, Toronto, ON, Canada

Christian Sainte-Rose, M.D. Department of Paediatric Neurosurgery, Necker Hospital, Université Paris Descartes, Sorbonne Paris Cité, Paris, France

Francesco Sala, M.D. Pediatric Neurosurgery Unit, Institute of Neurosurgery, University Hospital, Verona, Italy

Aydin Sav, M.D. Department of Pathology, Acıbadem University, School of Medicine, Istanbul, Turkey

Adam M. Scheinberg, M.D. Victorian Paediatric Rehabilitation Service, Royal Children's Hospital, Murdoch Children's Research Institute, Faculty of Medicine, Monash University, Parkville, VIC, Australia

Ehrenfried Schindler, M.D. Department of Anesthesiology and Critical Care Medicine, Asklepios Klinik Sankt Augustin, University-Hospital of Bonn, Bonn, Germany

Martin U. Schuhmann, M.D. Section of Pediatric Neurosurgery, Department of Neurosurgery, Eberhart Karls University Hospital of Tübingen, Tübingen, Germany

Aşkın Şeker, M.D. Department of Neurosurgery, Marmara University, Istanbul, Turkey

Mariasavina Severino, M.D. Department of Pediatric Neuroradiology, G. Gaslini Children's Hospital, Genoa, Italy

Spyros Sgouros, M.D., F.R.C.S. (S.N.) Department of Paediatric Neurosurgery, "Mitera" Children's Hospital, Athens, Greece
Department of Neurosurgery, University of Athens Medical School, Athens, Greece

Gurmit Singh, M.D. Department of Neurosurgery, Penang General Hospital, Penang, Malaysia

Christian Smith, Ph.D. Division of Neurosurgery, Department of Surgery, The Hospital for Sick Children, The University of Toronto, Toronto, ON, Canada

Pietro Spennato, M.D. Division of Pediatric Neurosurgery, Department of Neuroscience, Santobono-Pausilipon Children's Hospital, Naples, Italy

Bahattin Tanrikulu, M.D. Department of Neurosurgery, Marmara University, School of Medicine, Istanbul, Turkey

Marcos S. Tatagiba, M.D. Department of Neurosurgery, Eberhart Karls University Hospital of Tübingen, Tübingen, Germany

Michael D. Taylor, M.D. Arthur and Sonia Labatt Brain Tumor Research Centre, The Hospital for Sick Children, Toronto, ON, Canada

Yuzo Terakawa, M.D. Division of Neurosurgery, Department of Surgery, The Hospital for Sick Children, The University of Toronto, Toronto, ON, Canada

Department of Neurosurgery, Osaka City University Graduate School of Medicine, Osaka, Japan

Dominic N.P. Thompson, M.D., MBBS, BSc, FRCS (SN) Department of Pediatric Neurosurgery, Great Ormond Street Hospital for Children NHS Trust, London, UK

Vincenzo Tramontano Intraoperative Neurophysiology Unit, Institute of Neurosurgery, University Hospital, Verona, Italy

Vincenzo Trischitta, M.D. Division of Pediatric Neurosurgery, Department of Neuroscience, Santobono-Pausilipon Children's Hospital, Naples, Italy

Vasilios Tsitouras, M.D. Department of Pediatric Neurosurgery, "Mitera" Children's Hospital, Athens, Greece

Pascale Varlet, M.D. Department of Neuropathology, Sainte-Anne Hospital, University Paris Descartes, Paris, France

Department of Pathology, Sainte-Anne Hospital, Paris, France

Antonio Vecchione, M.D. Department of Anesthesiology, Necker Hospital, Université Paris Descartes, Sorbonne Paris Cité, Paris, France

Antonio Verrico, M.D. Department of Molecular Medicine and Medical Biotechnologies, "Federico II" University of Naples, Naples, Italy

Department of Oncology, Division of Pediatric Oncology, A.O.R.N. Santobono-Pausilipon Children's Hospital, Naples, Italy

Virginia Vitale, M.D. Department of Oncology, Division of Pediatric Oncology, Santobono-Pausilipon Children's Hospital, Naples, Italy

Greg C. Wheeler, M.D. Radiation Oncology and Cancer Imaging, Peter MacCallum Cancer Centre, East Melbourne, VIC, Australia

Johannes E. Wolff, M.D. Tufts Medical Center, Floating Hospital for Children, Boston, MA, USA

Department of Pediatrics, MD Anderson Cancer Center, Houston, TX, USA

Department of Pediatric Oncology, University of Regensburg, Regensburg, Germany

Department of Pediatric Hematology Oncology and Blood and Marrow Transplantation, Cleveland Clinic Children's, Cleveland, OH, USA

Brigitte Wrede, M.D. Department of Pediatric Oncology, University of Regensburg, Regensburg, Germany

Ulaş Yener, M.D. Department of Neurosurgery, Acibadem University, School of Medicine, Istanbul, Turkey

Michel Zerah, M.D. Department of Paediatric Neurosurgery, Necker Enfants Malades Hospital, Paris, France

Massimo Zollo, M.D. Department of Biochemistry and Medical Biotechnologies, "Federico II" University of Naples, Naples, Italy

Department of Molecular Medicine and Medical Biotechnologies, "Federico II" University of Naples, Naples, Italy

General Principles of Treatment in Pediatric Posterior Fossa Tumors

History of Posterior Fossa Tumor Surgery

1

James Tait Goodrich

1.1 Introduction

Development of surgical techniques for the treatment of posterior fossa disorders is, in the terms of historical events, very recent. In the sense of “modern” surgical techniques, we are only looking at a period that developed in the late quarter of the nineteenth century. In looking back at the historical literature, surgeons since the time of antiquity avoided any kind of surgical intervention within the posterior fossa. Early surgeons quickly realized that this region of the brain is extremely sensitive to any type of manipulation. Loss of respiration, sudden death, and distortion of the brain stem, all could lead to a rapid demise of the patient. As we shall see, surgery of the posterior fossa really only came in being with the origins of the twentieth century. A review of surgical textbooks in the latter half of the nineteenth century reveals only a minimal discussion of surgery in the posterior fossa. In the last 25 years, there has been a virtual explosion of techniques and equipment related to what is now called frameless surgical technology. To provide a historical perspective on this subject, the author will review the development of posterior fossa surgery with only

a brief look at antiquity and then quickly move to the Renaissance and the pioneering work of the anatomists of the sixteenth century. This chapter will review how the anatomy of the posterior fossa was first understood. The evolution of surgical technique and the individuals who provided us with these new ideas will be discussed.

In the twenty-first century, neurosurgeons now enter an operating room with an environment much more advanced and technically more complex than what was available to their colleagues just 30 years ago. In the 1970s, the surgical microscope revolutionized operative approaches with much improved visualization assisted by better illumination, and as a result, surgeons could now operate more safely on areas of the brain previously considered unapproachable. Looking to the future, likely within the next decade, with the advance in computer-assisted devices, the “hands-on surgeon” will become a relic of the past. The next generation of neurosurgeons will be “data suppliers,” i.e., a technician who makes entries into a database and then sits back and watches the robotics, e.g., the “da Vinci” perform the surgical operation.

Having said that, we have made enormous progress in surgical technique and the operative management of patients with complex posterior fossa disorders. To provide a comparison, I would like to present a scenario of a 1930s era operating room, what was then considered a “modern” operating theater. Paul Bucy, a pioneer in American neurosurgery, described the following

J.T. Goodrich, M.D., Ph.D., D.Sci. (Honoris Causa)
Leo Davidoff Department of Neurological Surgery,
Albert Einstein College of Medicine,
Children’s Hospital at Montefiore,
111 East 210th Street, Bronx, NY 10467, USA
e-mail: James.Goodrich@Einstein.yu.edu

scene at the Queens Square Hospital in London, where he was working as a visiting surgeon:

...[A]t the National Hospital were Sir Percy Sargent and Mr. Donald Armour. They were both poor surgeons, unbelievably crude in their surgical procedures. On one occasion (Gordon) Holmes told me to go with a patient to the operating theatre and tell Sargent that because the lesion was probably an arteriovenous malformation, he should use great care in exposing it. I did tell Sargent, but he paid no attention and proceeded to open the dura mater with a pair of sharp pointed scissors. In doing so he ripped the malformation wide open, resulting in a severe hemorrhage and the patient's death. On another occasion Armour performed an occipital craniectomy with hammer and chisel. This patient also did not survive the operation. There was a story current at the National Hospital that Denny-Brown, then a house officer, when assisting Armour in an operation would often remark that the blood had reached the drain in the floor on the far side of the room and that perhaps it would be wise to terminate the operation. [1]

This historical vignette clearly shows how far we have come in a fairly short period of time. A more complete anatomical foundation with a better understanding of the disease processes combined with computer technology has clearly led to better surgical outcomes and results in treating disorders of the posterior fossa. Understanding how we have managed to get to this point over time makes for an interesting historical review of our field.

This review will trace the origins of posterior fossa surgery from its antecedents in the Renaissance to the 1940s. Unfortunately, only a sampling of themes and personalities can be provided due to page constraints. Other authors in this monograph will deal with the developments in posterior fossa surgery from the 1940s forward.

1.2 Antiquity

Surgical operations on the posterior fossa have been dated back to antiquity [2]. From skulls excavated from around the world are examples of trephinations of the posterior fossa, most of which were done for trauma or other unknown reasons. In my own collection is a skull obtained from Peru in the 1950s that originates from a graveyard that dates back to 600 A.D. In the

mid-portion of the suboccipital bone is a large trephination with healed margins indicating the individual survived the surgical procedure. The reason for the trephination is not clear and it does not appear that it was done for trauma. In reviewing a number of trephined skulls over the years, the vast majority was performed over the convexity, and trephinations of the posterior fossa are actually quite rare Fig. 1.1.

The only accounts of posterior fossa surgery from the Greco-Roman era appear in the writings of Galen of Pergamon (130–200 A.D.), from an area of what is now Turkey [3–6]. In Galen's writings on anatomical procedures, he describes a series of animal dissections in which he exposed the cerebellum and the fourth ventricle, investigations which were done in the second century A.D. Using primarily the rat, he made a linear incision from the inion down to the foramen magnum. Galen studies were done in living animals with bleeding being controlled by finger pressure and scalp retractors. The craniectomy was done with a series of chisels, especially designed for this operation. After the skull bone was removed, Galen described the pulsating brain, especially seeing it rise up out of the craniectomy when the animal was agitated. Galen's technique of opening the dura was no different than what we do today. Galen used a small hook to elevate the dura away from the cerebellum and then incised it with a sharp knife carefully avoiding any of the venous sinuses, overlying cortical vessels, and the cerebellum. Galen pointed out in his discussion of the surgery that problems like cessation of breathing could occur along with motor or sensory loss. The voice could become hoarse and even death could occur. From experimentation, Galen noted that compression of the fourth ventricle could lead to severe impairments and even death. It is well known that Galen was a surgeon to the gladiators, so it is possible that he was involved in the treatment of traumatic injuries to the posterior fossa; whether he ever operated on these types of injuries is open to conjecture. Interestingly, Galen describes in his anatomical dissections splitting the vermis to expose the fourth ventricle in living animals. Galen carefully adds his comment that severe neurological impairments can happen with this technique; nevertheless, it was a useful way to

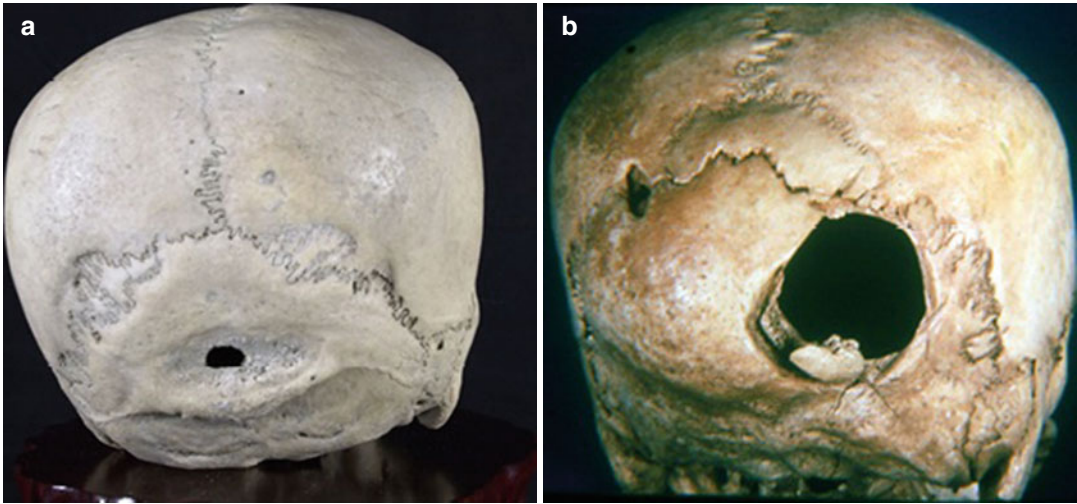


Fig. 1.1 (a) A human skull from Peru dating to about 600 A.D. In the occipital bone is a trephination done for unknown reasons. The well-healed bony margins indicate the “patient” survived the operation. From the author’s collection. (b) A skull with a large right occipital

trephination done for unknown reasons. Along the lower edge of the trephination are signs that show healing, so it is likely the patient survived this procedure. Courtesy of the Museum of Man collection, San Diego, California

expose the floor of the fourth ventricle. Galen was the first to describe the calamus scriptorius, which is seen on the floor of the fourth ventricle using this surgical exposure. Galen, throughout his writings, noted that knowledge of the surgical anatomy was absolutely key for the surgeon; without this knowledge, the surgeon would be prone to serious errors and bad outcomes. Unfortunately, much of Galen’s animal anatomy was incorrectly transliterated into human anatomy and then carried forward by various translations (e.g., Latin, Greek, and Arabic) to the time of the Renaissance. As we shall see, it was the Renaissance artist that led the drive to first understand and describe human anatomy from hands-on dissections of humans Fig. 1.2.

1.3 The Sixteenth Century: The Origins of Modern Anatomy and Surgical Investigation

At the end of the fifteenth century, the intellectual currents in Europe were undergoing profound changes. With the introduction of the printing press and moveable type, books could be more easily and cheaply produced. As the intellectual shackles of the Middle Ages were

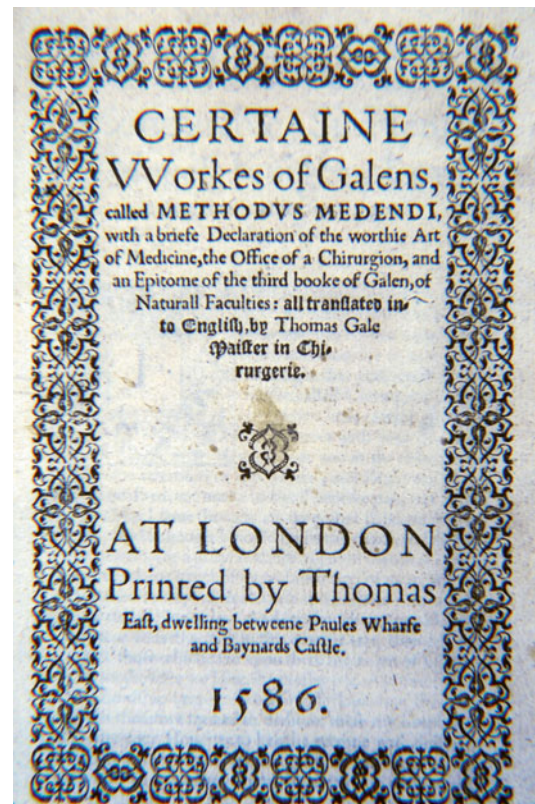


Fig. 1.2 An early English translation of Galen’s writing including his “office of a chirurgion” in which he details his surgical techniques along with general works on medicine [5]

being removed, physicians were beginning to rely more on what their eyes taught them at the bedside. The previously held concepts of the early anatomists like Galen of Pergamon and others would be challenged in their accuracy. One of the most important intellectual currents in surgery and medicine at this time were the schools of anatomical studies like Michelangelo, Titian, and Leonardo da Vinci among others [7, 8]. In an attempt to provide more realistic surface anatomy of the human, these individuals were doing hands-on dissection unencumbered with the earlier medieval anatomical texts and doctrines that were rife with errors. The “typical” surgeon at the beginning of the sixteenth century was nothing more than an unskilled and poorly educated barber surgeon. This surgeon could cut your hair, remove a tooth, and repair a hernia. There were a very few surgeons with either prominent personalities or formal education. The “educated” surgeon having learned medieval dogma remained buried in conjecture and training from centuries of beliefs based on earlier Greco-Roman and later Byzantine teachers and translators who continued to translate and repeated the errors of the past surgical history. In learning and then following these antiquated surgical writings, medieval surgeons often found themselves in conflict with their own bedside observations. As a result of these common conflicts of written text versus what was actually being seen in the anatomical amphitheater, a number of innovative personalities dually learned their surgical material not only as surgeons but also as anatomists. Within the origins of the intellectual climate of the Renaissance, we begin to see profound changes in learning, particularly in the anatomical investigations of the human body.

With the early origins of the Renaissance, we see a renewed interest in human anatomical dissection, anatomical dissections and drawings which at this point had been almost frozen in time for some 1400 years dating to the time of the Alexandrians. From the Byzantine era and through the Middle Ages, anatomy was based on the previous writings of the giants such as Galen of Pergamon who performed their anatomical dissections on non-human subjects and then morphing this informa-

tion to “human” anatomy. Ironically, it was the Renaissance artist followed by sixteenth-century anatomists and surgeons that led the movement in anatomy away from subservience to the medievalists. With great figures like Leonardo da Vinci (1452–1519), Berengario da Carpi (1470–1550), Johannes Dryander (1500–1560), Andreas Vesalius (1514–1564), and others that was to lead to a new movement based on a hands-on anatomical dissection of the human body. As a result, previous codified anatomical errors, many ensconced since the Greco-Roman era, were to be slowly corrected over the next several centuries. These changes in studies from codified manuscripts to a new and more accurate human anatomy also led to a surge of interest in surgery. The Renaissance surgeon, like the artist, became interested in trying to unravel the intricacies of the human body – without this foundation of knowledge, it would be impossible to correctly treat a disease much less perform a surgical resection. In the area of posterior fossa anatomy and surgery, a number of important Renaissance figures played pivotal roles in bringing forward posterior fossa surgery as both an art and a science.

While neither a surgeon nor a physician, *Leonardo da Vinci (1452–1519)* made enormous contributions to both medicine and surgery. Leonardo was the quintessential Renaissance man. Recognized as an artist, an anatomist, and a scientist, Leonardo learned human anatomy, both surface and deep to better provide more realistic artistic creations. Leonardo’s anatomical studies were extremely important in providing an early emancipation from the previous medieval teachings. Leonardo’s output in anatomical studies led to some 750 separate anatomical drawings. To modern scholars, Leonardo is now considered the founder of iconographic and physiologic anatomy [9–11].

Some of the earliest anatomical drawings on posterior fossa anatomy appear in Leonardo’s anatomical studies [9]. To Leonardo we owe the earliest surviving illustrations of the cranial nerves. Figures 1.3 and 1.4, Leonardo did not describe all 12 of the cranial nerves though he was the first to provide some reasonably accurate diagrams. To Leonardo we owe the first illustrations



Fig. 1.3 (a) An early copper engraving of Leonardo da Vinci (from the collection of author). (b) Leonardo's sketches of the “wax casting” of the ventricles of the brain. In these drawings, the third and fourth ventricles are anatomically outlined for the first time. In the bottom image is an early and rudimentary drawing of the cerebellum and brain stem [9]. (c) Da Vinci anatomical illustrations of the ventricular system – enlarged from b.

There are the earliest known anatomical drawings of the cerebral ventricles – for the first time demonstrating the third ventricle, aqueduct of Sylvius and the fourth ventricle [9]. (d) Leonardo's “layered” anatomical studies on the skull, brain, and cranial nerves, what would appear to be the earliest “realistic” anatomical demonstrations of the cranial nerves [9]

of the ventricular system. Using a uniquely designed “wax casting” of the ventricular system, Leonardo was able to detail the anatomical landmarks of these cavities including the fourth ventricle (see Fig. 1.3c). Leonardo's “wax casting” technique was quite innovative and involved

removing the brain from the skull and injecting melted wax through the fourth ventricle. Mental tubes were placed in each of the lateral ventricles to allow air to be released. Once the injected wax hardened, the brain was removed leaving behind a wax casting of ventricles.



Fig. 1.4 Leonardo's view of the ventricular system with the cranial nerves detailed at the skull base and exiting to supply the face, mouth, tongue, etc. [9]

In Leonardo's anatomical studies are several investigations that deal with the posterior fossa and its anatomy. His interest in these studies is not clear, as the findings would not have impacted theoretically on his artwork. Leonardo was also not a surgeon so there would not have been any surgical benefit from these studies. Yet his inquisitive mind provides for us some of the earliest and, at the time, the most accurate views of the posterior fossa. Unfortunately, Leonardo's great opus on anatomy, to be published in some 20 volumes, did not appear in print until the twentieth century [9, 10]. Leonardo's anatomical manuscripts did circulate in Italy throughout the sixteenth century among the artistic community; thanks to a close friend and companion, Francesco da Melzi [8]. Leonardo's manuscripts appear to have disappeared from general circulation in the latter half of the sixteenth century,

only to be rediscovered in the eighteenth century by William Hunter (1728–1793), a collection that is now part of the Windsor Castle collection, owned by the Queen of England, Elizabeth II. William Hunter was clearly awed by what he saw in Leonardo's drawing and he wrote of his views in a now rare series of eighteenth-century lectures on anatomy – Hunter comments that Leonardo "...was the best anatomist, at that time in the world" [12]. I have included the title and the comment by Hunter on this collection and the anatomy – the first sighting and investigations of these important anatomical illustrations since the sixteenth century. The real mystery is how these important drawings ended up in Scotland in the Windsor Castle collection (Fig. 1.5).

An interesting historical vignette was William Hunter's comment made upon seeing Leonardo's anatomical drawings: (In speaking of Leonardo) "Those very drawings and the writing, are happily found to be preserved in his Majesty's great collection of original drawings. Mr. Dalton, the King's librarian, informed me of this, and at my request procured me the honor of leave to examine them. I expected to see little more than such designs in Anatomy, as might be useful to a painter in his own professions. But I saw, and indeed with astonishment, that Leonardo had been a general and a deep student. When I consider what pains he has taken upon every part of the body, the superiority of his universal genius, his particular excellence in mechanics and hydraulics, and the attention with which such a man would examine and see objects which he was to draw, I am fully persuaded that Leonardo was the best Anatomist, at that time, in the world. We must give the fifteenth century the credit of Leonardo's anatomical studies, as he was 55 years of age at the close of that century" ([12], p 39).

The earliest printed work to appear on neurosurgery, in this case a monograph on head injury, was published in 1518 by *Berengario da Carpi* (1470–1550) [13, 14] (see Figs. 1.6 and 1.7). This book was published as a result of Berengario's success in treating a prominent Italian nobleman – Lorenzo de' Medici, Duke of

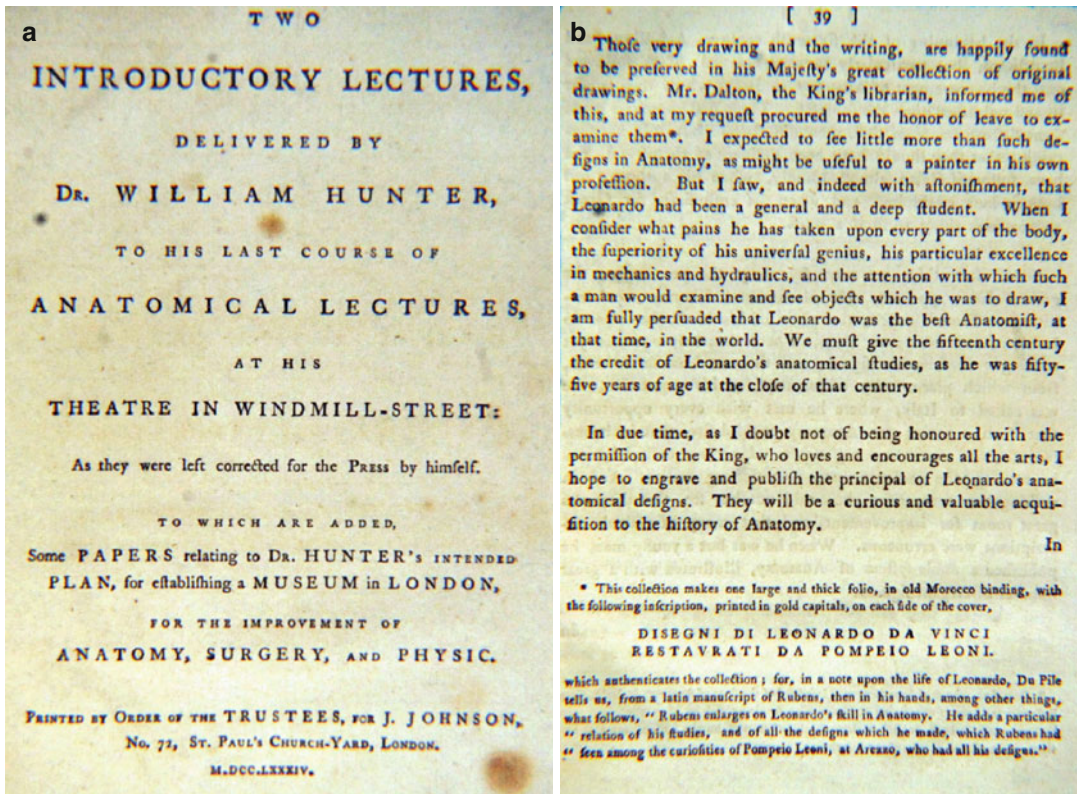


Fig. 1.5 (a) Title page from William Hunter's lecture on anatomy in which he announced the discovery of Leonardo's long-lost anatomical drawings which, for reasons that are not well known, ended up in the Windsor

Castle collection in Scotland [12]. (b) Hunter's description of the manuscripts and his initial thought of getting them published, an event that was not to happen until the turn of the twentieth century [12]

Urbino. Lorenzo was involved in a joust and sustained a serious cranial injury to his occipital bone and posterior fossa from which he survived. Shortly after this episode, Berengario was visited in a dream by a man wearing a cap adorned with a rooster feather and golden-winged sandals (i.e., Hermes Trismegistus, or the Third Mercury). Hermes encouraged Berengario to write a treatise on head injuries. Within this monograph are the earliest published surgical details dealing with head injuries and their treatment. Berengario designed his own surgical instruments for operating on the skull and brain. Illustrated in this monograph are trephine braces with interchangeable drill bits of different designs (Figs. 1.6 and 1.7). Berengario has an interesting writing style, a style that is verbose, pompous, and would be considered rather audacious by today's standards.

Yet within this treatise are descriptions of his early surgeries which are provided with descriptions of the patients, methods of treatment, and clinical outcomes. As a result, this work remains the best account of sixteenth-century brain surgery and the earliest to deal with any form of posterior fossa surgery.

Berengario besides being an innovative surgeon was also an excellent anatomist. Like Leonardo, Berengario provided one of the earliest and most complete discussions of the ventricular system. In his anatomical work *Isagoge Breves* published in 1522 [15], Berengario provided the earliest accurate descriptions of the sphenoid sinuses, pineal gland, choroid plexus, auditory ossicles, and lateral ventricles. Recent historians consider the anatomical illustrations in this volume to be the first anatomical



Fig. 1.6 (a) Portrait of Berengario da Carpi, author of the earliest printed work on injuries to the brain. (b) Title page from Berengario’s *Tractatus* [13]. (c) From Berengario’s *Tractatus* showing his design of what we now call a “Hudson Brace” – designed to perform

trephinations and with an interchangeable burr design [13]. (d) An illustration from Berengario’s *Tractatus* showing his various bur designs for performing trephinations, many designed to prevent “plunging” into the brain during the trephination [13]

illustrations published based on actual hands-on anatomical dissections.

In researching the early anatomical illustrations of the posterior fossa, a work that stands out was authored by *Johannes Dryander (Johann Eichmann)* (1500–1560), professor of surgery from Marburg, Germany. This richly illustrated

the work which first appeared in 1536 as a small monograph with limited illustrations. Dryander expanded this book further in 1537 and added additional illustrations [16, 17]. Within the 1537 edition are 16 plates showing successive layers of the traditional dissection of the brain as described by Galen in the second century. Of importance to



Fig. 1.7 Skull from Lorenzo da Medici showing the injury sustained to the posterior fossa during a jousting event – Berengario attended his surgery and care and from

which the patient survived what should have been a lethal injury (Courtesy of the University of Bologna Library Museum)



Fig. 1.8 (a) Portrait of Dryander, an early anatomist who provided some of the earliest anatomical descriptions of the posterior fossa and the cerebellum. From the author’s

personal collection. (b) Title page from Dr Dryander’s 1537 work on the anatomy of the skull and brain [16]

this chapter are the earliest realistic illustrations of the anatomy of the posterior fossa along with a primitive numbering of the cranial nerves. Illustrated by Dryander were nine cranial nerves

as originally described by Galen in the second century A.D. (see Figs. 1.8 and 1.9). Dryander details the earliest known description of tentorium, the structure separating the cerebellum

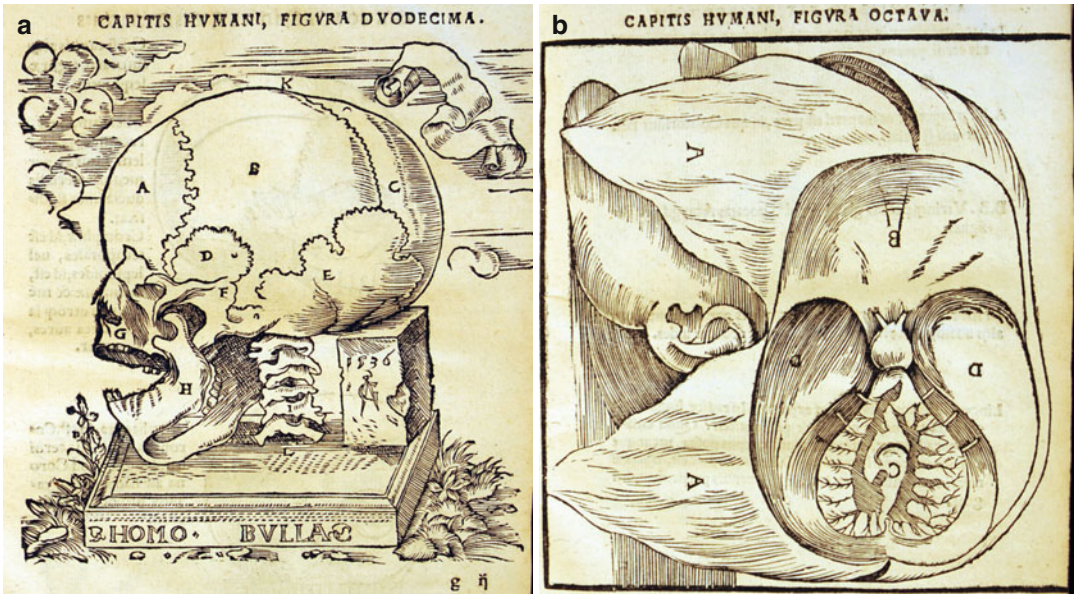


Fig. 1.9 (a) From Dryander's work on human anatomy detailing the human skull and accurately reflecting the sutures outlining the posterior fossa along with suboccipital cervical junction [17]. (b) Dryander provides in this

drawing the earliest detailed illustration of the posterior fossa including the details of the cerebellum and brain stem along with the middle and anterior fossae [17]

from the cerebrum. This book was heavily influenced by the writings of Galen and earlier medieval scholasticism, but despite these criticisms, this work can be considered the first textbook of neuroanatomy and the first to show somewhat realistic illustrations of the posterior fossa. Following a recently established Renaissance tradition, Dryander performed his own public dissections of the skull, dura, and brain without the use of dissector though referring at times to Galen's printed observations [17].

A landmark figure of the sixteenth century, both in anatomy and surgery, was the Italian physician and anatomist *Andreas Vesalius* (1514–1564). Vesalius argued strongly that the physician/anatomist must perform his own animal and human dissections. In 1543, at the young age of 28, Vesalius published his *magnum opus De Humani Corporis Fabrica* in Basel, Switzerland [18]. This folio volume is full of original and insightful anatomical observations and descriptions. Vesalius was a virulent critic of the early anatomists and their errors, in particular the writings of Galen. The *Fabrica* was done in collaboration with John Stephen of Calcar and the school of Titian. Vesalius adopted the viewpoint of earlier giants like Berengario da Carpi that the surgeon

must do his own dissections and then detail his own observations. In the elegant engraved title page of the *Fabrica*, Vesalius shows himself in an elaborate anatomical theater standing alongside a cadaver that he is in the process of dissecting sans dissector (Figs. 1.10, 1.11, and 1.12).

Book VII (Libri VII) of this *magnum opus* provides for us a detailed anatomical discussion of the brain and posterior fossa, each illustrated with excellent anatomical renderings. Ironically, the description of the cranial nerves remained heavily influenced by the anatomical numbering originally provided by Galen of Pergamon with nine cranial nerves described instead of 12. We have included two anatomical figures that show the posterior fossa exposed by elevating the cerebellar hemispheres up and exposing the brain stem and cervicomedullary junction. Figure 1.13b details the brain stem and cranial nerves in a rather primitive design. Vesalius notes that to get the best anatomical material, one should be friends with the judges so that the best and freshest of beheaded cadavers can be obtained immediately upon the execution of the criminal. Two eponyms employing Vesalius's name are still in use, and both involve the posterior fossa and skull base: the foramen of Vesalius, a small opening

Fig. 1.10 From the title page of 1543 *De Humani Corporis Fabrica* in which we see Vesalius (the bearded figure) standing alongside a human cadaver that is undergoing a public dissection [19] (courtesy of the Cambridge University Library – Cambridge, England)

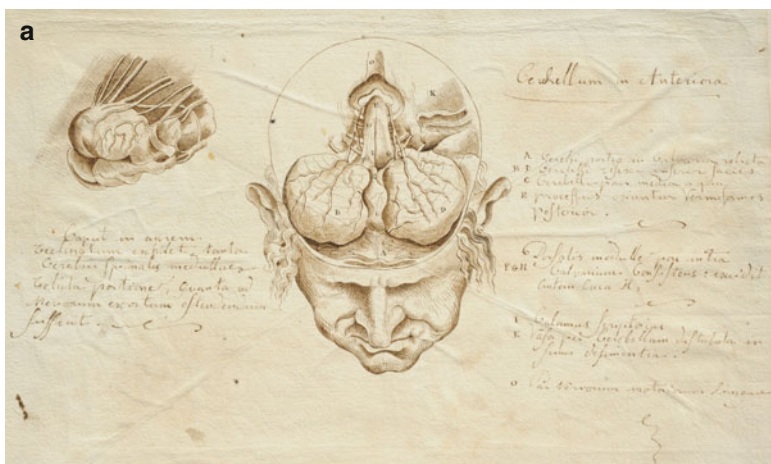


Fig. 1.11 (a) Early hand-drawn sketch illustrating the anatomy of the posterior fossa showing the cerebellum and brain stem being rotated forward, up, and out of the skull base. A primitive rendering of the cranial nerves is seen in the upper left figure. From the personal collection

of the author. (b) Early hand-drawn sketch illustrating the anatomy of the posterior fossa seen from an inferior view. The cranial nerves have been outlined along with the optic chiasm and the cerebellum. From the personal collection of the author

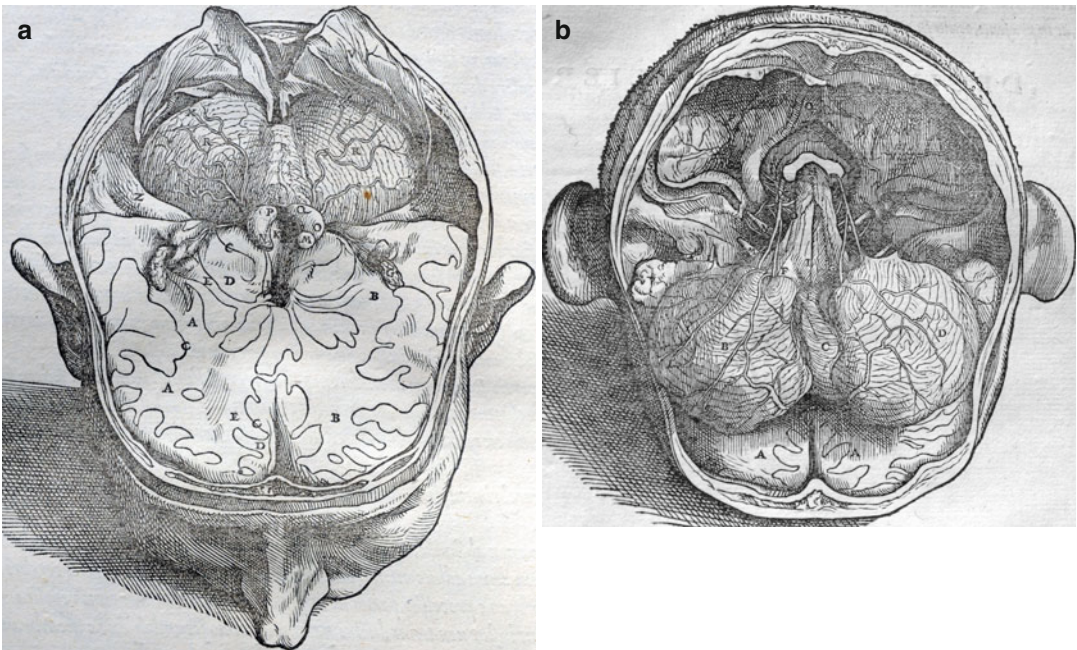
Fig. 1.11 (continued)

Fig. 1.12 (a) Drawing of the posterior fossa at the level of the tentorium likely drawn by Vesalius for his 1,543 book [18]. (b) Drawing of the posterior fossa with the cerebellum lifted up and out of the fossa with the brain stem exposed [18]

between the foramen ovale and the foramen rotundum. A small emissary vein which runs within the foramen of Vesalius is called the vein of Vesalius. These anatomical structures are actually anatomical variants in that they are seen in only about 10 % of anatomical dissections.

Another remarkable work on human anatomy and especially neuroanatomy was printed in

Paris, France, in 1546 by *Charles Estienne* (1504–1564) [20]. In reviewing this work, we see interesting and, in some cases, quite striking illustrations of the brain and in particular the posterior fossa. For the reader, the illustrations are quite imaginative with anatomical figures posed against elaborate Renaissance backgrounds that include noble living rooms and villa grounds.

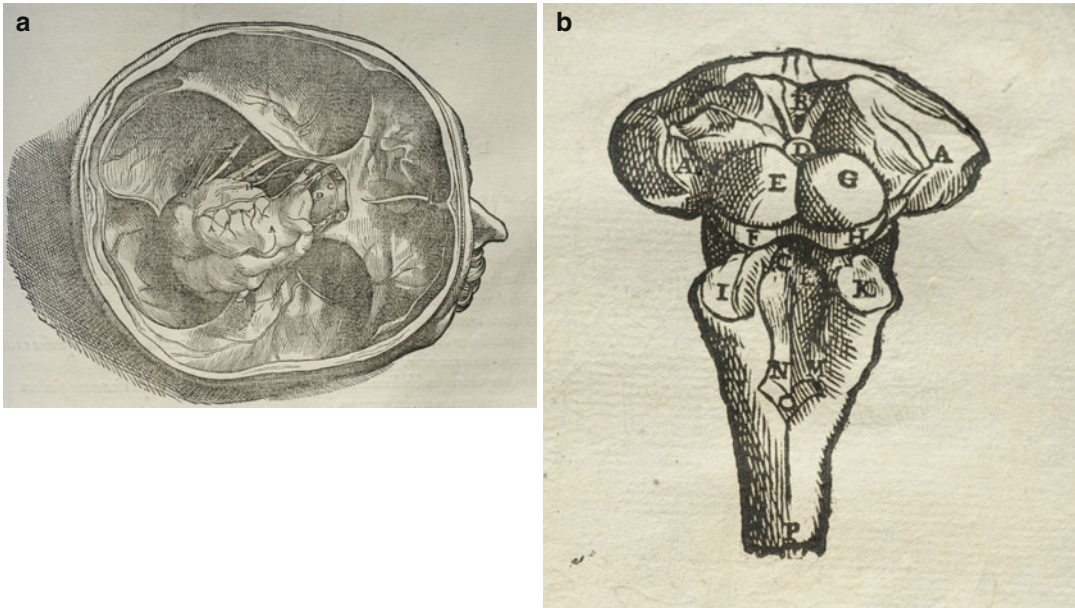


Fig. 1.13 (a) Drawing of the skull base with the brain and cerebellum removed exposing the brain stem and cranial nerves – a drawing felt to have been done by Vesalius [18].

(b) Drawing of the brain stem outlining the floor of the fourth ventricle, the colliculi, and inferior portion of the thalamus, surprising anatomical detail for this period [18]

In reviewing Estienne's writing, he is clearly strongly under the influence of Galen's writing on anatomy. In addition, the anatomical descriptions do not come to the level of writings of Vesalius (Figs. 1.14 and 1.15).

In reviewing the contributions of this period, an important surgical personality was *Ambroise Paré* (1510–1590) whom most historians considered the father of modern surgery [21–23]. Paré began his studies as a barber surgeon, starting at the age of 19 as a surgical dresser in a Paris hospital (Fig. 1.16). A common theme for surgeons was to train as a military surgeon; battlefield experience provided the ultimate surgical education. Paré was never formally trained in Latin and published his works in French, some of which were translated into English. As a result of Paré not publishing in Latin, rather in the vernacular, it led to a wider dissemination of his surgical works among barber surgeons and further enhanced his influence in the sixteenth century. From his successes as a military surgeon, Paré went on to become a much sought-after surgical figure among the European royalty. One of his most well-publicized surgical cases dealt with a

head injury sustained by Henri II of France. Paré attended the King and was also present at the autopsy. Paré discovered that Henri II had developed a subdural hematoma. Paré then recorded his clinical observations from the head injury and the resultant posterior fossa compression which included headache, blurred vision, vomiting, lethargy (i.e., weakness), and decreased respiration. Paré postulated that the injury was due to a tear in one of the bridging cortical veins, and this he confirmed at autopsy [23].

In Book X, of the *Collected Works* [21], Paré provides commentary on dealing with injuries to the brain and surgical techniques in treating these injuries. To assist the surgeon, Paré provides detailed discussions on the use of trepans, shavers, and scrapers (see Fig. 1.17c). Infections of the skull were common, and he describes techniques on how to remove an osteomyelitic bone and how to incise the dura and evacuate blood clots and pus. Paré's military experience led him to advocate wound debridement, emphasizing that all foreign bodies must be removed from the wound site. Paré's most humanitarian advance in surgery was the serendipitous discovery that

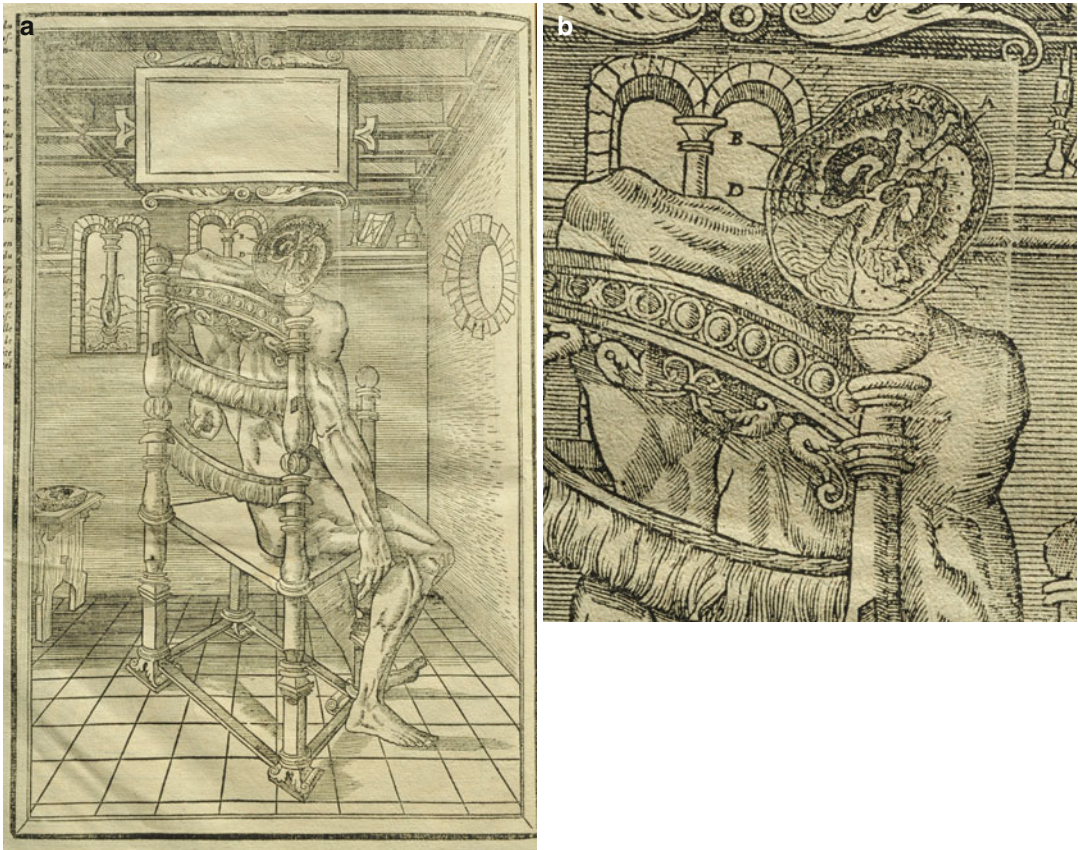


Fig. 1.14 (a–b) An anatomical scene from Estienne richly detailed anatomy book showing the anatomy of the brain in cross section including the cerebellum; image “b” is the figure enlarged showing better detail of the posterior fossa [20]

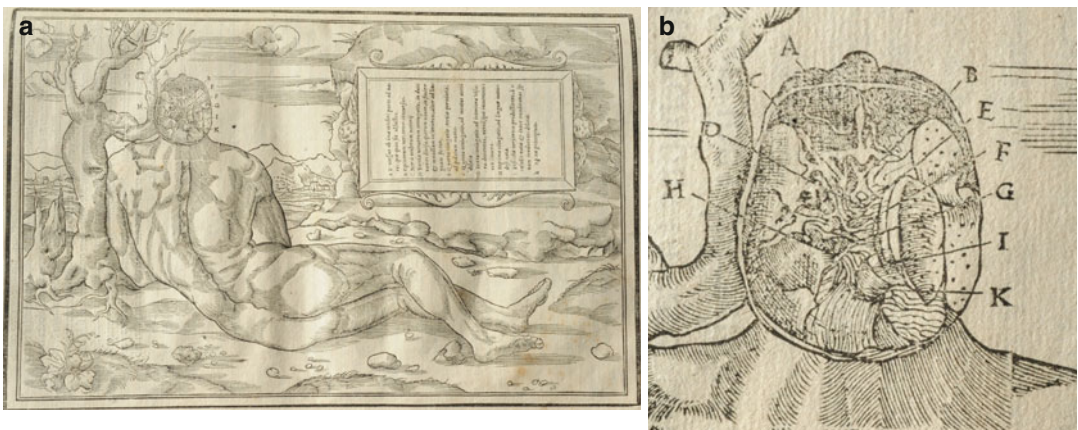


Fig. 1.15 (a–b) A “posed” anatomical dissection revealing an axial view of the skull and brain and detailing the brain and a cross section of the cerebellum. In Fig. 1.17b is an enlargement of the image [20]

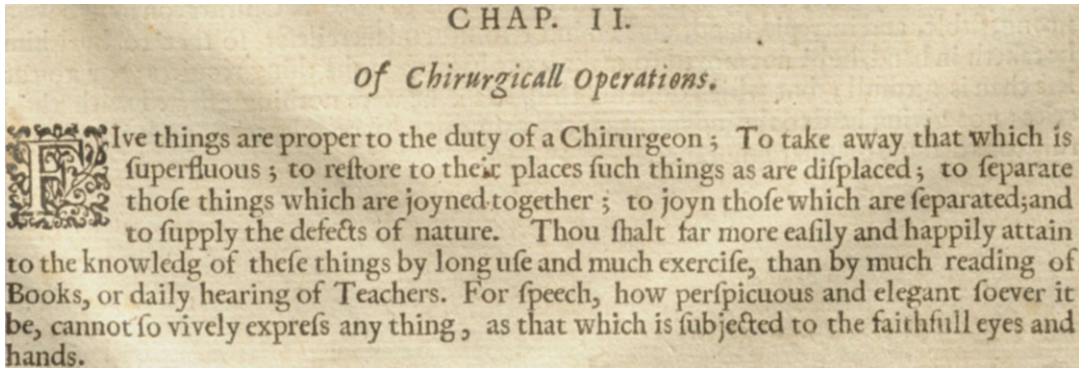


Fig. 1.16 In this introduction, Paré clearly outlines the “proper duties” of the surgeon, comments that still remain true today [21]



Fig. 1.17 (a) Title page from Paré first English edition of his collected surgical writings. [21]. (b) Vignette from the upper left corner of title page with a portrait of Paré and a trephination scene [21]. (c) Paré illustrates his surgical

instruments that he used for trephining the skull. A rotating hand brace along with various different drill designs allowed for more accurate hole placement and less risk of plunging [21]

boiling oil (previously poured into open surgical wounds) should not be used in gunshot wounds. Instead, he made a dressing made of egg yolk, rose oil, and turpentine, which he found led to

much improved wound healing. A long common method of controlling surgical wound bleeding was the application of the red-hot iron cautery to bleeding vessels. Paré replaced this barbaric

treatment of cautery with the use of ligatures placed around the bleeding vessels which led to not only better bleeding control but also substantially better wound healing.

1.4 **Seventeenth Century: An Age of Advancing Individual Scientific Endeavors in Anatomy and Physiology of the Brain**

The seventeenth century was an important period in the historical development of surgery; a period where both anatomy and physiology of the brain was being conceptualized for the first time. As the growth of both medicine and science took off exponentially with the contributions of Isaac Newton (1642–1727), Francis Bacon (1561–1625), William Harvey (1578–1657), and Robert Boyle (1627–1691), physics, experimental design, the discovery of the circulation of the blood, and physiological chemistry were introduced. We also see for the first time the development of the scientific societies (e.g., the Royal Society of London, the Académie des Sciences in Paris, and the Gesellschaft Deutscher Naturforscher und Aerzte in Germany). These societies and the inherent intellectual interchange would lead to dramatic advances in both medical and scientific education.

Reflecting back upon the seventeenth century, this was clearly the century that provided the first investigational studies leading to a modern understanding of the anatomy of the human brain. There turns out to be several individuals that contributed significant roles in understanding the structural anatomy of the human brain. One of the premier investigators was Englishman *Thomas Willis* (1621–1675), of the “circle of Willis” who published in his classic in 1664 a work he entitled *Cerebri Anatomie* [24]. In reviewing the text of the *Cerebri Anatomie*, the reader can clearly glean his methodical attention to anatomical detail. The book is provided with skillfully designed anatomical illustrations that provided then the most accurate detailed anatomy of the brain. Willis details a series of physiological demonstrations that clearly showed that when

parts of the “circle of Willis” were tied off, the anastomotic network would still provide blood to the brain via collaterals. For the first time, we are seeing anatomical structures of the brain clearly detailed and often forgotten, much of this was due to collaborative skills of Sir Christopher Wren (1632–1723) who drew the illustrations for the *Cerebri Anatomie* (Fig. 1.18).

For the surgeon, *Cerebri Anatomie* was among the first richly illustrated anatomical works to provide an accurate outline of the surface anatomy of the brain and the cranial nerves. The detail provided in the illustrations of the cerebellum and brain stem is considerably better detailed when compared to earlier anatomical works. In addition to his anatomical investigations, Willis introduced the concept of “neurology,” or the doctrine of neurons, though he used the term in a purely anatomical sense. The word “neurology,” in its modern usage, did not enter general nomenclature until Samuel Johnson defined it in his dictionary of 1755 [25]. Neurology would later come to encompass the entire field of neurological anatomy, function, and physiology.

While there were a number of important neuroanatomical works that came out in this period, one important book that is of posterior fossa historical interest was written by *Humphrey Ridley* (1653–1708) [26]. Ridley was educated at Merton College, Oxford, and at the University of Leyden, where he received his doctorate in medicine in 1679. At the time Ridley’s work on the brain appeared, many of the ancient Greek views of the brain still prevailed. Anatomy of the brain was now shifting away from the “cell-doctrine theory,” a concept that held that the functions of the brain were within the ventricles, not in the brain matter itself, concepts dating back to the Greco-Roman era. Ridley’s anatomical studies were conducted on freshly executed criminals which helped significantly in the anatomical investigations due to the vascular engorgement of the brain that occurred secondary to hangings. From his studies came the first descriptions of the cavernous sinuses, described by him after injection with mercury and wax. Ridley provided an even more complete description of the circle of Willis with better anatomical descriptions of the posterior cerebral and

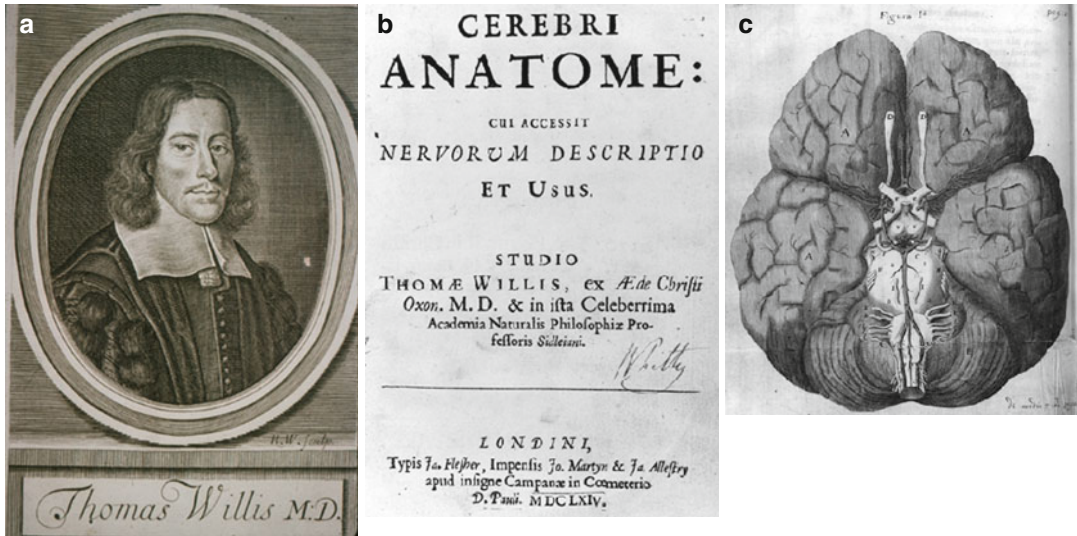


Fig. 1.18 (a) Portrait of Thomas Willis drawn during the time of writing of the *Cerebri Anatomie*. From the author's personal collection. (b) Title page from the first quarto edition of *Cerebri Anatomie* printed in London in 1664 [24]. (c) Willis illustration of the “circle” which

accurately details the posterior fossa, in particular the pons, brain stem, and the folia of the cerebellum. The cranial nerves also have better detail when compared to previous anatomical works [24]

superior cerebellar arteries. Ridley nicely detailed the transverse and lateral venous sinuses with the dura removed. The third cranial nerve is shown correctly as traversing in between the superior cerebellar artery and posterior cerebral artery, the first time this cranial nerve anatomy is correctly illustrated. It should be noted though that Ridley's cranial nerve descriptions followed the earlier Galenic tradition, describing only nine cranial nerves. In reviewing Ridley's cross sections of the cerebellum and brain stem, we find anatomical drawings clearly superior to Willis, and in these drawings, he outlined the deep nuclei in the cerebellum. Not well known it is to Ridley that we owe the first description of a pineal region tumor in a patient that developed an obstructive hydrocephalus. Ridley's description is interesting to review:

In an hydropical Brain of a strumous (sic) Boy, [here describing a child with hydrocephalus – author's note] I have see it (speaking of the pineal gland) swelled to a size of three times its ordinary magnitude, and by reason of the abundance of stagnate gelatinous Lympha contain'd in it, perfectly transparent. (Text and capitals as done by Ridley). ([26], pp 83–84)

Ridley is describing a gelatinous tumor of the pineal gland with a secondary obstructive hydrocephalus though he does not appear to recognize the association. Ridley goes on to note that the pineal gland is the region where Descartes has located the seat of the soul, a concept which he notes he agrees with (Figs. 1.19 and 1.20).

By the end of the seventeenth century, several key advances had occurred which laid a foundation that would eventually lead to an understanding of brain tumors and disorders of the posterior fossa. Neuroanatomy had developed to the point where identifiable structures were now consistently recognized in the brain. Brain function was now residing within the brain and not within the ventricles. Scientific societies were now providing public forums for disseminating scientific and medical information. For the surgeon, there still remain serious restrictions in surgical technique which would be the lack of antisepsis, anesthesia, and cerebral localization. The concept of a pathological basis to disease still had not yet been developed.

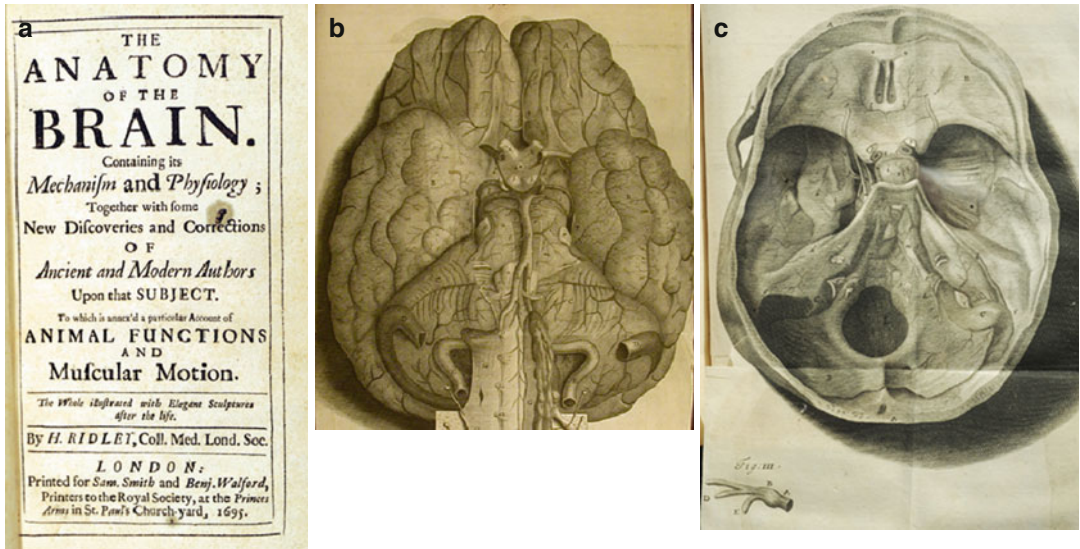


Fig. 1.19 (a) Title page from Ridley’s work on the brain [26]. (b) Ridley’s richly detailed anatomical illustration of the circle of Willis and the base of the

brain [26]. (c) Ridley’s detailed anatomical drawing of the skull base outlining the posterior fossa with the trigeminal nerve illustrated at the lower left [26]

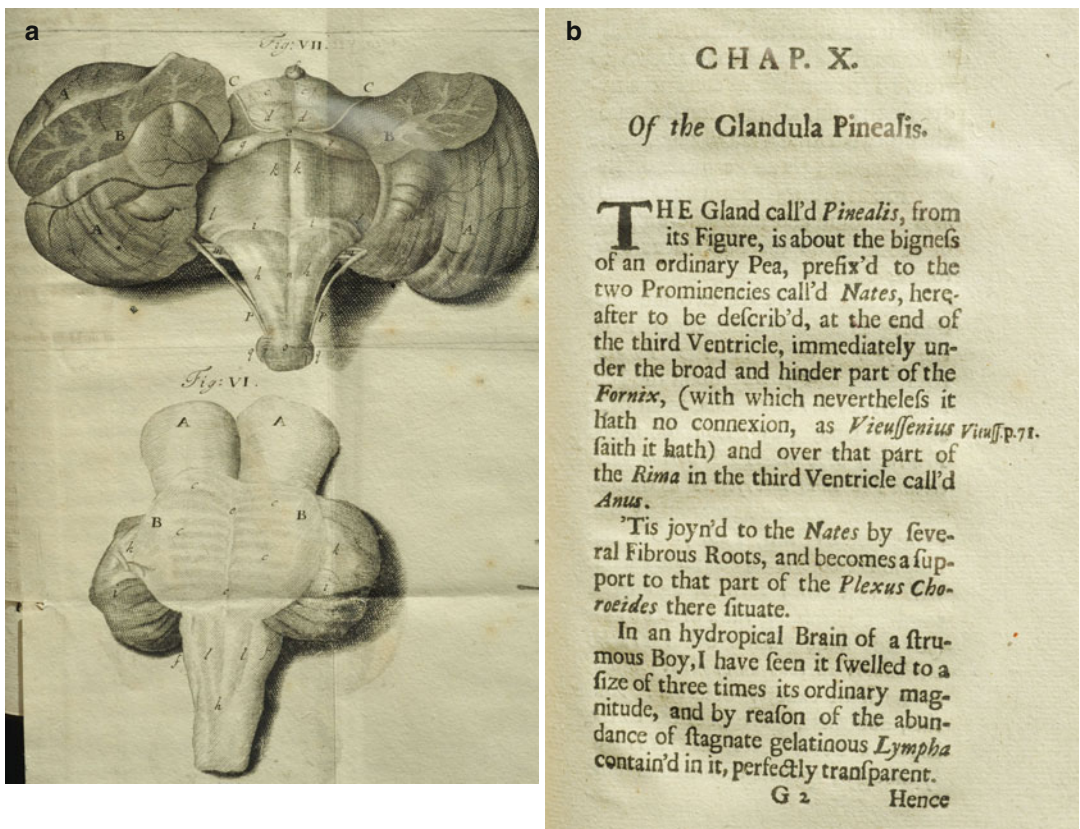


Fig. 1.20 (a) Ridley’s detailed anatomy of the cerebellum and brain stem is demonstrated here. The origins of the cranial nerves and each of the structures has been

labeled in the text [26]. (b) Ridley provides here the earliest description of a pineal gland tumor which caused secondary obstructive hydrocephalus [26]

1.5 Eighteenth Century: Development of Brain Surgery Beyond Just Trauma

Judgment in distinguishing, and ability in treating diseases, are not to be attained by a transient cursory view of them; merely running round an Hospital for a few months, or reading a general system of surgery, will not form a compleat (sic) practitioner: the man, who aims at that character, must take notice of many little things, which the inattentive pass over, and which cannot be remarked by writers; he must accustom himself to see, and to think for himself; and must regard the rules laid down by authors, as the outlines only of a piece, which he is to fill up and finish: books may give general ideas, but practice, and medication, must make him adroit and discerning; without these, his reading may possibly keep him clear of very gross blunders, but he will still remain injudicious, and inexpert – Percival Pott – 1760. [27]

The foundations of investigative science and medicine were beginning to be established in the eighteenth century. Chemistry was now recognized as a science from the works of Priestley, Lavoisier, Volta, Watt, and others. The practice of “bedside medicine,” which had not been practiced since the Byzantine era, was now being brought back into medical practice in the teachings and writings of Thomas Sydenham, William Cullen, and Herman Boerhaave. A bedside examination of the patient continued to be advanced with Auenbrugger’s introduction of percussion of the chest. William Withering introduced the use of digitalis for cardiac failure. William Jenner helped eliminate a worldwide scourge with the introduction of cowpox inoculation for small pox. At the same time, surgeons were becoming better skilled at surgical technique and even more importantly were entering the ranks of the educated as many were now obtaining university educations. While the surgical apprenticeship system was still very much in existence, the more learned surgeon was advancing the art of surgery with a better understanding of anatomy and physiology of the human body. An individual who clearly demonstrated this new orientation in training and surgical skills was *Percival Pott (1714–1788)*, a fashionable London surgeon who provided an early textbook devoted to the treatment of head injuries [27]. The treatment

of “tumors” was very primitive with almost no understanding of tumor genesis or even the pathological basis of a neoplasm. The most common concept of a brain tumor was a “fungus” or unexplained growth of the brain or skull. The cellular origin of a tumor was not developed until the late nineteenth century.

Rather unique for an eighteenth-century surgeon, Pott was a strong proponent of surgical intervention whether for trauma or tumor. With improved surgical instrumentation, a better understanding of human anatomy, and improved necropsy techniques, Pott and others were achieving better surgical outcomes. In dealing with surgery of the head, Pott challenged the earlier Hippocratic doctrines on whether *to trephine or not to trephine*. Because of the high morbidity associated with opening the dura and skull, few surgeons of this period were willing to accept the morbidity of trephination. Clearly, a more aggressive Pott strongly favored the use of the trephine in brain injury and treatment of brain pathology [27, 28] (Fig. 1.21a, b).

In 1718, *Lorenz Heister (1683–1758)* published a surgical textbook [30–32] that rapidly became one of the most popular surgical textbooks of this century. Heister broke away from the prevalent model of the traveling itinerant barber surgeon and instead advanced a more scientific-based approach to surgery. Heister firmly believed that to be a skilled surgeon, one began with strong education in both anatomy and surgical technique. Heister’s 1718 textbook described a number of cases in which “tumors” were surgically treated though none involved the brain [29]. Heister refined his techniques for trephining the skull and provided illustrations showing the tools and techniques. With a broad and well-developed surgical practice, it is quite likely that Heister performed surgeries for tumors such as meningiomas, particularly those that eroded through the skull. In reviewing his surgical technique, Heister offered some interesting tips for the young surgeon. For control of scalp bleeding and hemorrhage, Heister developed a “crooked needle and thread” and then zigzagged the suture on each side of the skin flap. When this suture was drawn tightly, it sharply reduced bleeding from the wound edges. To further assist

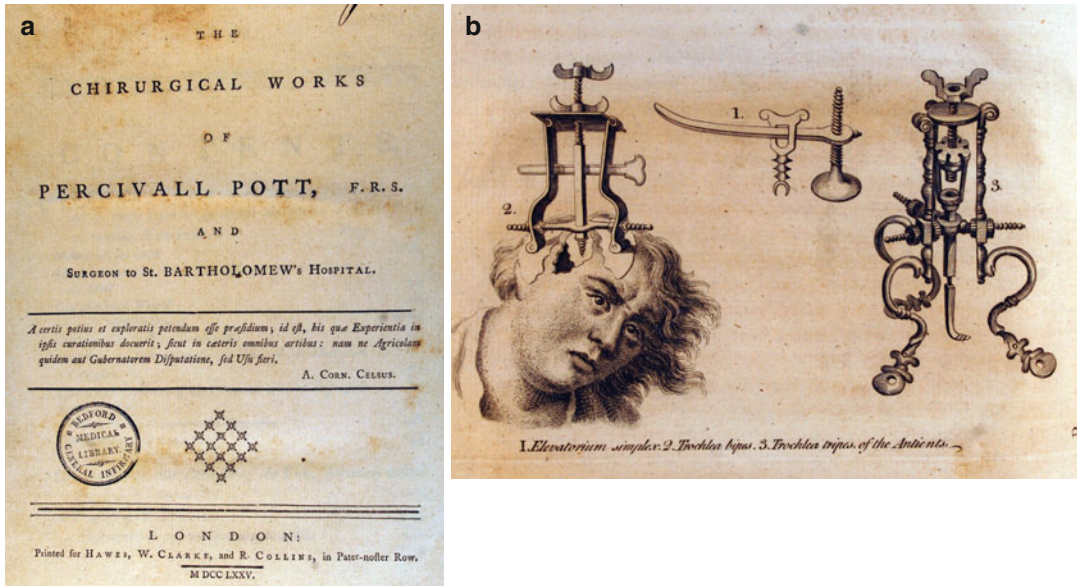


Fig. 1.21 (a) Title page from Pott's collected works on surgery [28]. (b) Pott's surgical devices for operating on the skull and brain were mainly of his own design. Illustrated here are two elaborate devices for dealing with

head trauma and depressed skull fractures. (The middle instrument was adapted from a device used to remove corks from a wine bottle [28])



Fig. 1.22 (a) Title page from a later edition (1750) of Heister's surgical textbook with his engraved portrait to the left [31]. (b) Heister's surgical textbook illustrating some of his instruments for operating on the brain and

skull along with an interesting technique for elevating a depressed skull fracture in a child –“Derby Hat fracture” elevation [30, 32]

control of scalp bleeding, Heister had his surgical assistant apply pressure to the skin edges. Harvey Cushing (1869–1939) adopted a similar technique when opening a scalp flap in the early 1900s (Fig. 1.22a, b).

In reviewing the eighteenth-century surgical literature on brain surgery, other than for trauma, surgery on the brain was quite rare. In 1743, a

French surgeon by the name of *Francois Quesnay* (1694–1774) argued that brain surgery could be done safely based on his experience with brain abscesses and removal of foreign bodies [107]. In his surgical treatise, Quesnay was adventurous enough to argue that incisions in the brain cortex could also be safely made. If tumors (which he called “fungous growths,” i.e., meningiomas)

were diagnosed, he argued they could be removed with minimal problems for the patient. Despite having made these statements, there is no evidence Quesnay actually ever removed a brain tumor.

In the year 1774, a treatise published by *Antoine Louis (1723–1792)* provides one of the earliest accounts of a successful brain tumor operation [33]. Antoine Louis was a French surgeon of considerable reputation having refined his surgical skills first as a military surgeon. Louis had an interesting personality and is remembered for a quarrelsome personality eager to come to physical blows with anyone who dare disagreed with him. In Louis's book is described an early surgical attempt at removing a brain tumor. Louis described a case involving a large petrus ridge meningioma (?) that deformed the left temporal and mastoid region causing a downward deviation of the ear [94]. Louis operated and describes debulking the tumor and felt successful in reducing its mass effect on the brain. To deal with tumors, Louis developed a number of ingenious surgical techniques, including one that involved tying a silk ligature around the base of a tumor and then cinching it down slowly over the next several days, in effect amputating the tumor and its blood supply at its base.

One of the first “successful” attempts to deal with a surgical problem in the posterior temporal region and mastoid was published by *Sauveur-Francois Morand (1697–1773)* in 1768. In his surgical monograph [34], Morand describes a case of a monk, who had an otitis media and subsequently mastoiditis with temporal bone and posterior fossa abscess. Morand describes his technique of trephining over the carious bone removing the infected bone and pus. Morand placed a catgut wick within the cavity to allow the surgical wound to continue to drain. The monk's clinical course continue to worsen so Morand reexplored the abscess site, but this time did something very aggressive in that he opened the dura through a cruciate incision. With this surgical maneuver, Morand was able to explore intracranially and describes how he drained a large brain abscess. Morand describes using his index finger as a probe and digitally explored the

abscess removing as much as he could. Morand further treated the abscess by filling the cavity with balsam and turpentine – an early example of antiseptic treatment. A silver tube was placed into the abscess cavity to allow continuous drainage (Table 1.1). As the wound healed, the silver tube was slowly withdrawn. The abscess healed; the patient survived leading Morand to report one of the earliest successful surgically treated lesion of the skull base and posterior fossa (Fig. 1.23).

A French surgeon that provided some interesting insights on surgery of the brain and the posterior fossa was *Louis Sebastian Saucerotte (1741–1814)* (also listed as Nicolas). As a French military surgeon, he obtained extensive experience in dealing with injuries and pathology of the brain [35]. Saucerotte was the first to describe gait ataxia with opisthotonos and rolling of the eyes in a patient with a cerebellum lesion. Saucerotte came up with the concept that different areas of the brain tolerated trauma better. Saucerotte recognized that the region of the brain most susceptible to trauma with poorer outcomes where those occurred was at the base of the brain, i.e., the region of the brain stem and cerebellum. Trauma and injuries of the forebrain were, in his experience, the best tolerated.

Surgical treatment of tumors, in all parts of the body, developed quite late in surgical history. Key to the treatment of any tumor was to separate its pathology from other commonly confused lesions like inflammation, syphilis, tuberculosis, and other “swellings” or “fungus-like” lesions. The first monograph to begin the differentiation of these concepts and introducing the field

Table 1.1 The numbering of the cranial nerves from Galen (second century A.D.) up to Soemmering (1778)

I = olfaction
II = optic
III = oculomotor
IV = trochlear
V = trigeminal
VI = abducens
VII = facial and auditory
VIII = vagus, glossopharyngeal, and cranial portion of the accessory
IX = hypoglossal plus spinal roots of accessory

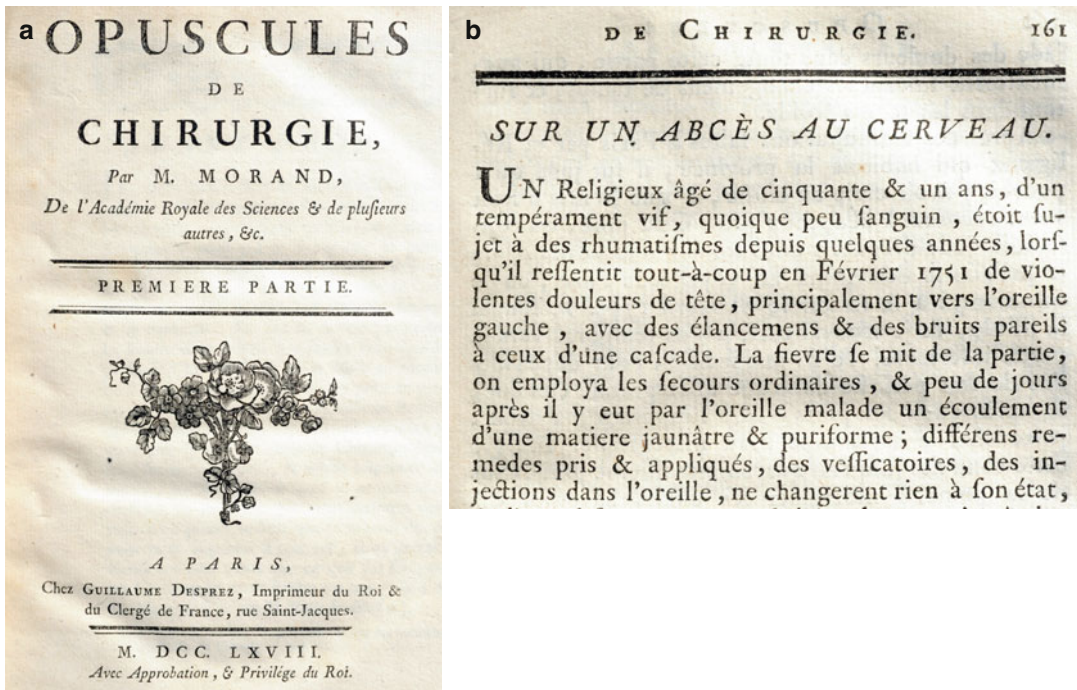


Fig. 1.23 (a) Title page from Morand's work in which he describes the successful treatment of a posterior temporal/mastoid region abscess – a rare adventurous procedure

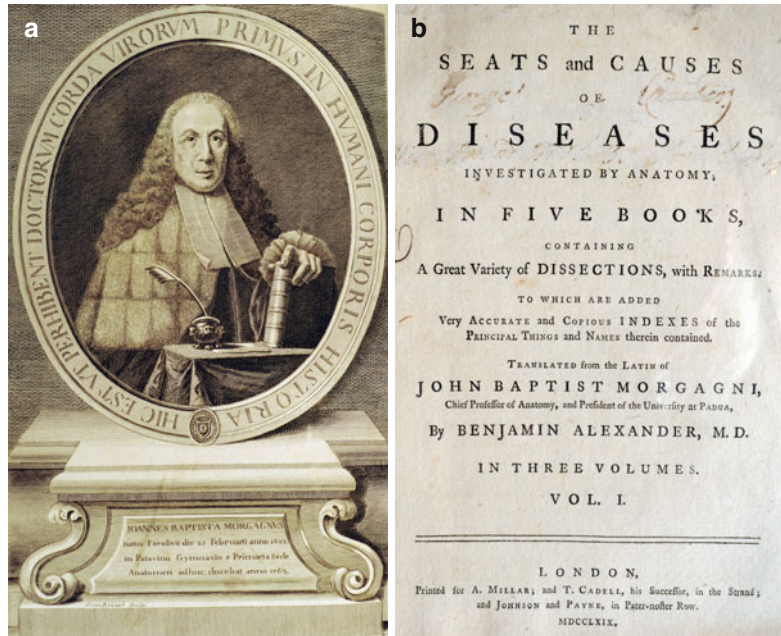
[34]. (b) Morand's description of his excision and treatment of a brain abscess [34]

of pathology was written by *Giovanni Battista Morgagni* (1682–1771), *De sedibus, et causis morborum per anatomen...* [36]. Morgagni's work was to revolutionize the treatment of diseases by laying, for the first time, a pathological foundation to various medical disorders. Morgagni's landmark work of 1761 was the first in a series of writings that categorized diseases into specific entities based on what he called “the seats and causes of disease” [37]. Morgagni studied under Valsalva and then at the unbelievably young age of 16, assumed the chair of anatomy at Padua in 1715. After a long and brilliant career, with a number of important publications already completed, he decided at the age of 79 to author his comprehensive work on the seat and causes of diseases which was based on over 700 autopsies that he had performed. From these pathological investigations, Morgagni offered a diagnosis, prognosis, and a specific treatment based on the pathological origin of a disease. In Morgagni's work are presented a series of cases that deal with

the pathological bases of diseases of the head and brain. Morgagni details some very interesting autopsy studies dealing with the brain and spine and at one point even comments on trephining on the brain. Morgagni's investigations clearly set the standards for a landmark work in pathology, but this work is also not often recognized as also a landmark work in the history of neurology and neurosurgery (Fig. 1.24).

Within the posterior fossa are the 12 cranial nerves of which each has their own particular tumor pathology. Cranial nerves have been described in some form, though often inaccurately since the time of Galen of Pergamon. It took over 2,000 years of anatomical history before the first complete description of all 12 cranial nerves would occur, and this was in the writings of *Samuel Thomas von Soemmering* (1755–1830). Soemmering was from Prussia and trained in Leyden having studied under H. A. Wrisberg (1739–1808) and Bernhard Albinus (1677–1770), all brilliant anatomists. From their

Fig. 1.24 (a) Contemporary portrait of Morgagni. From the author's personal collection. (b) Title page from the first English translation of Morgagni's work on the seats and causes of disease [37]



teachings and others, Soemmering learned to pay incredible attention to fine detail in anatomy. From this background, he went on to publish a series of important monographs dealing with the various senses. Germane to this chapter were his studies detailing the cranial nerves published in 1778, a book entitled *De basi encephali et originibus nervorum cranio egredientium* [38] (Fig. 1.25). This monograph originally appeared as a doctoral thesis and then was further expanded into a monograph within which he provided the first complete anatomical description of each of the 12 cranial nerves. Earlier anatomists, following Galen's original classification, had only previously described nine in total. The first description of the seventh and eighth nerves being two separate cranial nerves appears in this work. Soemmering also provided a clear anatomical description of the optic chiasm and pineal gland and in addition, detailed the topography of the cerebral hemispheres. Soemmering studies include the first detailed description of the substantia nigra. The anatomical details of the cranial nerves are further enhanced in the anatomical engravings that were provided by Soemmering's

artistic collaborator, Carl Christian Glassbach Jr. (fl. 1770).

Johann Friedrich Meckel, the Elder (1724–1774), was professor of anatomy, botany, and obstetrics in Berlin, Germany, at the time when the anatomy of the nervous system was undergoing detailed examination. Following the influence of Giovanni Morgagni and Alexander Monro II, Meckel undertook a number of investigations in regard to the anatomy of the brain. One of his most important works was his detailed anatomical investigation of the trigeminal nerve and the anatomical space in which the trigeminal ganglion laid – what is now called Meckel's cave. Meckel's cave (*cavum Meckeli*) or the *cavum trigeminale* is a space formed by two layers of dura mater that encases the trigeminal ganglion close to the apex of the petrous portion of the temporal bone (Fig. 1.26). In a brilliant doctoral dissertation, Meckel clearly detailed the anatomy of the nerve and region and then engraves the final result in a limited production book that appeared in 1748 – *Dissertatio inauguralis medica anatomica physiologica de Quinto*



Fig. 1.25 (a) Title page of Soemmerring’s anatomical work on the cranial nerves [38]. (b) Soemmerring’s illustration of a sagittal section of the brain with the cerebellum and brain stem elegantly illustrated along with cranial

nerves [38]. (c) Soemmerring’s detailed overview of what is now described as “12” cranial nerves [38]. (d) Soemmerring’s view of the base of the base with elegant details of the pontine cranial nerves [38]

Pare Nervorum Cerebri [39]. The illustrated details and the engraving show quite clearly the anatomy and the territory that the nerve innervates – in Fig. 1.26b, we see the elegant results that Meckel was able to achieve from his dissections.

The eighteenth century saw the first productions of elaborate and beautifully detailed ana-

tomical atlases of the brain. One individual who provided the first detailed colored anatomical views of the posterior fossa including surprisingly accurate diagrams of the cerebellum and brain stem was *Félix Vicq D’Azyr* (1748–1794) [40]. Vicq D’Azyr trained as an anatomist and further refined his studies with a keen interest in neuroanatomy. In his *Traité d’anatomie et de*

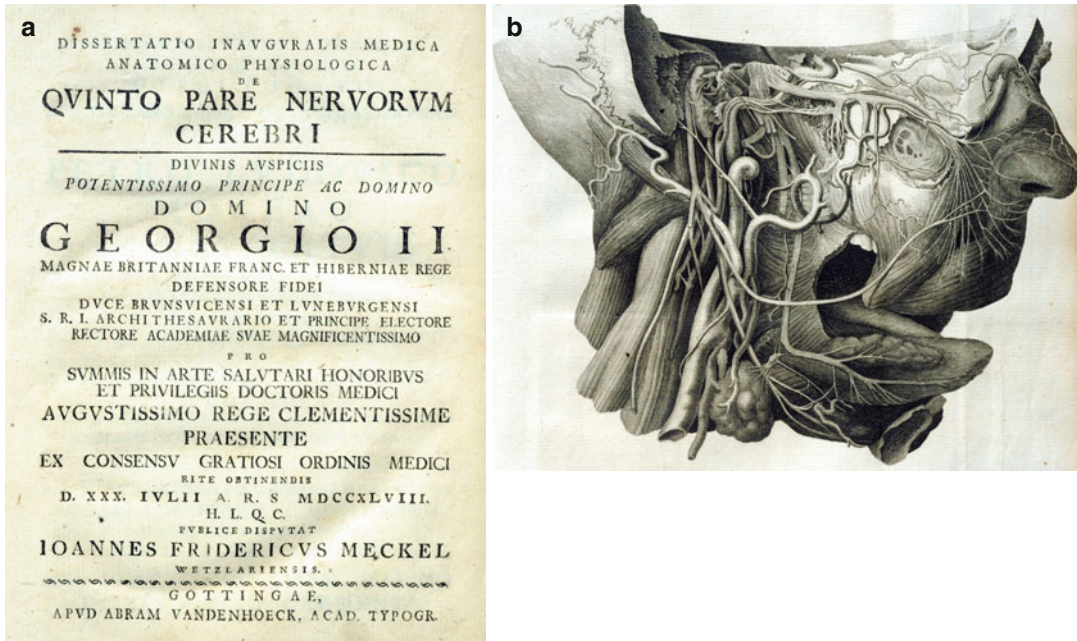


Fig. 1.26 (a) Title page from Meckel's dissertation on the anatomy of the trigeminal nerve and what is now called "Meckel's cave" [39]. (b) Illustration from

Meckel's monograph detailing the anatomical description of Meckel's cave and the anatomical distribution of the trigeminal nerve [39]

physiologie appeared 69 plates, of which 34 are hand-colored aquatints prepared by Alexandre Briceau [41], a noted Paris engraver. Vicq D'Azyr actually thanks his engraver in the preface for his skills, his stamina, and his endurance of "foul odors." Vicq D'Azyr prepared the drawings from fresh anatomical dissections that were fixed in alcohol allowing a better dissection. As a result, he was better able to outline the details of the gray and white matter and the cerebral convolutions using horizontal sections. Vicq D'Azyr was a firm proponent of integrating anatomy and physiology, and the concept of form had to be studied with function. Vicq D'Azyr is still remembered for the first description of the mammillothalamic tract that is now referred to as the tract of Vicq D'Azyr. Vicq D'Azyr also provided even more anatomical details of the substantia nigra. Within Vicq D'Azyr atlas are the first illustrations, done in aquatint color, of the structures of the posterior fossa, the vascular sinuses, and the brain stem along with the cranial nerves. The details and color make this work still one of the most beau-

tifully produced anatomical atlases of the brain ever produced (Fig. 1.27).

Another great eighteenth-century atlas that deals with brain and posterior fossa anatomy was prepared by Jacques Fabian Gautier D'Agoty (1717–1785) [41]. Gautier was a French print maker and pioneer in color printing. Gautier D'Agoty published a series of anatomical works that contained elegantly detailed anatomical plates illustrated in color, many of which were made in life-size formats (see Figs. 1.28 and 1.29). Joseph Guichard Du Verney (1648–1730) was responsible for the dissections and preparations on which this text was based. Germane to this chapter are the drawings of the internal anatomy of the brain and the posterior fossa that are both striking in color and meticulously executed.

By the end of the eighteenth century, surgeons were beginning to have a better understanding of brain disorders. Surgeons were becoming aggressive in the surgical treatment of disorders of the brain aggressively moving away from the earlier Hippocratic doctrine that feared operating on the

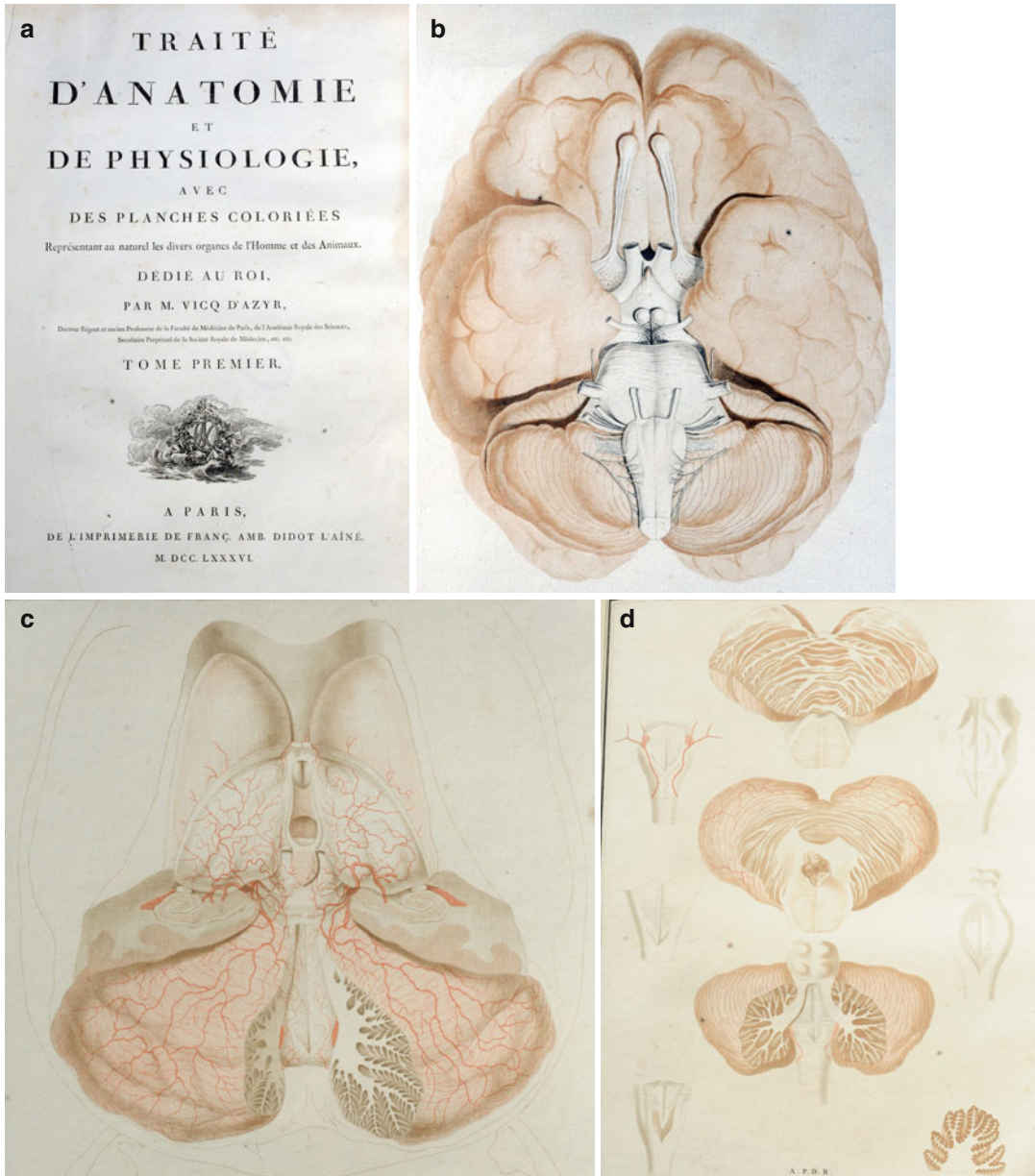


Fig. 1.27 (a) Title page from Vicq D'Azyr [40]. (b) Illustration from Vicq D'Azyr providing quite detailed anatomy of the pons and brain stem [40]. (c) Cross section of the cerebellum showing the folia patterns and details of the brain stem [40]. (d) Anatomy of the cerebellum shows the tracts and deep nuclei along with “shadow” views of

the brain stem [40]. (e) Among the earliest accurate dissections of the cerebellum, mesencephalon, colliculi, and pineal gland [40]. (f) In this image, Vicq D'Azyr has detailed the venous sinus drainage patterns of the posterior fossa [40]

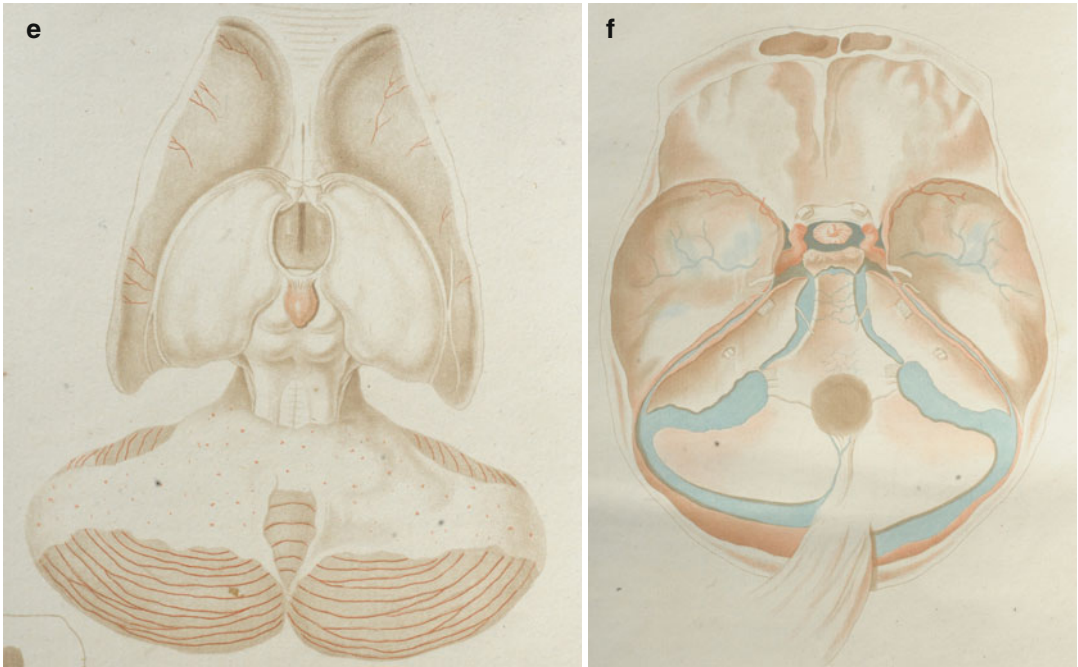


Fig. 1.27 (continued)

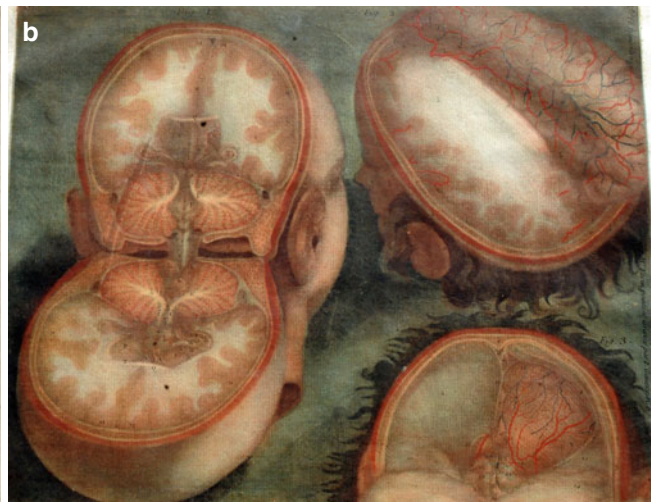
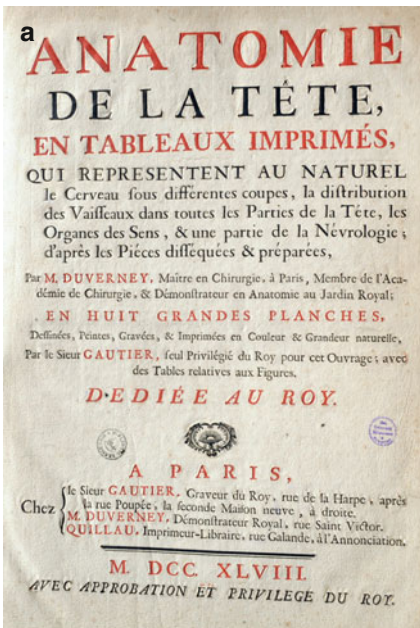


Fig. 1.28 (a) Title page from Gautier D’Agoty’s seminal work on brain anatomy [41]. (b) Gautier D’Agoty’s coronal section and posterior fossa exposure detailing the cerebellum and brain stem [41]. (c) Fig. 1.29b enlarged showing the unique detail of a coronal section of the brain

with cerebellum nicely outlined in color with brain stem well detailed [41]. (d) A striking anatomic view in which the brain and brain stem has been “lifted off” the skull base – colored details are quite striking for this period of brain anatomy illustration [41]

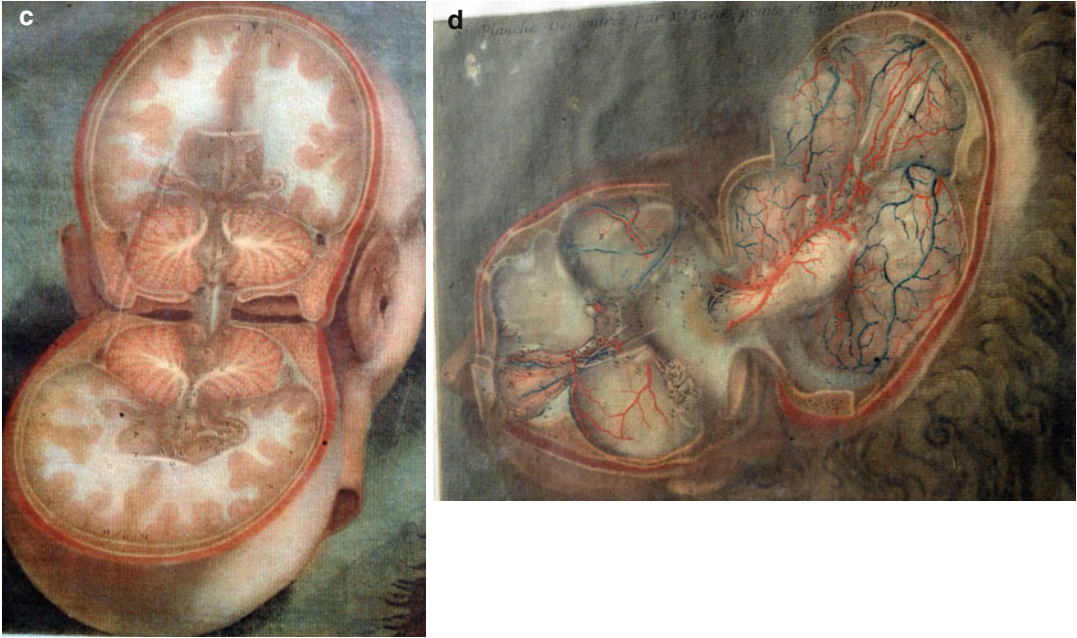


Fig. 1.28 (continued)

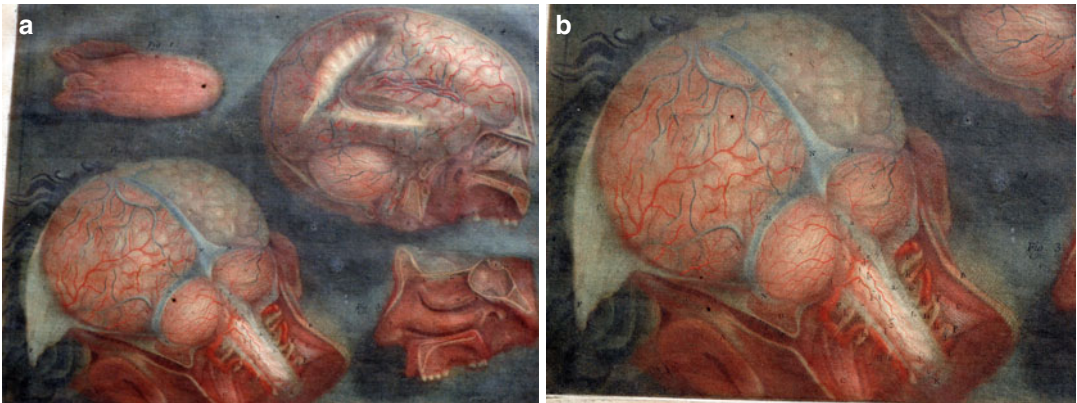


Fig. 1.29 (a) Several images of the brain and skull with the posterior fossa detailed in the lower left and enlarged in Fig. 1.29a [41]. (b) With the skull and dura “peeled

away,” Gautier D’Agoty details the venous sinuses and cerebellar hemispheres along with the cervical spine and nerve roots [41]

brain. The concept of different “pathologies” within the brain was becoming more defined and accepted. However, the concept of cerebral localization, the idea that each part of the brain had an individualized function, had not yet been clarified. In addition, there was no understanding of what caused infection and even more important

how to prevent infection in brain surgery. And not to be forgotten was the inability of the surgeon to provide “painless surgery”; pain alleviation existed in only the most crude forms. These important issues of infection, anesthesia, and cerebral location were only to be addressed in the coming nineteenth century.

1.6 Nineteenth Century: Introduction of Anesthesia, Antisepsis, and Cerebral Localization, The Origins of Modern Neurological Surgery as Practice

Surgery of the brain is the outgrowth of three discoveries of the nineteenth century, namely, anesthesia, asepsis and cerebral localization. Without asepsis or antisepsis, surgery of the brain would never be possible. With asepsis and without cerebral localization, it could be of but little value. With both asepsis and cerebral localization and without anesthesia, it would be possible but greatly limited. Although anesthesia had been in use nearly a quarter of a century before Lister's great discovery, surgery of the brain made no advance. And 17 additional years were required before the three combined discoveries were sufficiently secure and adequately correlated to permit this field of surgery to be fairly launched. [42]

Walter Dandy has clearly summarized the issues at this time in a most remarkable and poignant quote on the origins of neurosurgery. A modern reflection on this statement reveals Dandy clearly points out the important issues facing a nineteenth-century surgeon interested in operating on the brain. With the beginnings of the nineteenth century, surgeons were becoming more comfortable with some surgeries of the cerebral hemispheres, surgeries mostly related to trauma. Operating on or within the posterior fossa was still considered far too dangerous and not even in the surgical perspective for this era of surgeons. Several important and significant events had to occur before routine surgery of the brain, and in particular, surgery of the posterior fossa would become a reality.

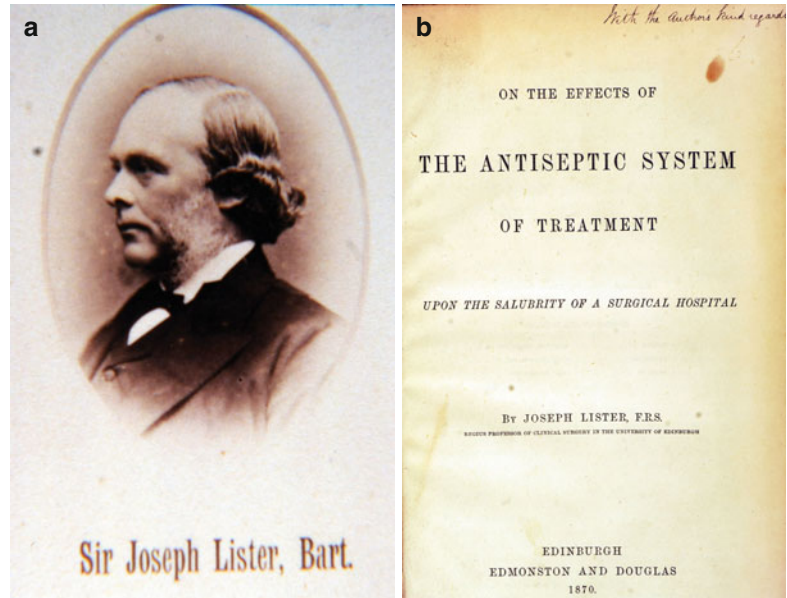
In 1844, a dentist from Hartford, Connecticut, by the name of Horace Wells (1815–1848) first used nitrous oxide as an anesthetic in a dental procedure. Unfortunately, a later overdose of the nitrous oxide led to the death of one of Wells' patients, and as a result, Wells stopped the use of nitrous oxide in his dental practice. Two years later, in Boston, MA, a man by the name of W.T.O. Morton (1819–1868) persuaded a Harvard surgeon, Dr. J. C. Warren (1778–

1856), to use ether to induce anesthesia [43]. On October 16, 1846, Warren did so, producing a state of insensibility in a patient during which a vascular tumor of the submaxillary region was removed. In the United Kingdom, efforts to induce painless surgery were furthered advocated by James Y. Simpson (1811–1870). Simpson's drug of choice was chloroform, which had just been introduced in 1847, and Simpson became a strong advocate of its use [44]. In reviewing the history of anesthesia, the introduction of "painless" surgery cannot be underestimated in the history of surgery. For the neurosurgeon, the ability to operate without disabling the patient in binding restraints, a no longer needed breakneck surgical speed, and all done with the patient comfortably asleep laid an important foundation for any surgery on the brain.

Throughout history the scourge of all surgeons has been the risk of infection within a surgical wound. In brain surgery, the risk of infection in the pre-antiseptic era approached 95 % meaning that even with good surgical technique, the patient still had a very high probability of dying of sepsis and meningitis. Surgical beliefs dating back to Hippocrates had led surgeons to avoid opening the dura, except in very extreme cases as the risk of infection inevitably led to death – a historically strong impedance to any form of brain surgery.

Several events took place in the nineteenth century that allowed surgeons, for the first time, to more safely perform a surgery on the brain along with a marked reduction in surgical infection. Two seminal events were the demonstrations by Oliver Wendell Holmes (1808–1894) [45] and Ignác Fülöp Semmelweis (1818–1865) [46] that puerperal fever, the scourge of the delivery room, was spread by the contaminated unwashed hands of the obstetrician. A mid-nineteenth-century obstetrician (and surgeon) entered the operating room wearing an unwashed black cloth coat soaked in blood, pus, and grime from many previous deliveries and surgeries. In contrast, midwives typically entered the delivery area with clean hands and clean clothes.

Fig. 1.30 (a) Nineteenth-century albumin portrait of Lister at the height of his career. From the collection of the author. (b) One of Lister's monographs detailing the "principles" of antiseptic surgery, an effort to reduce infection in patients undergoing surgical procedures [49]



Both Holmes and Semmelweis pointed out that hand washing before and after cases, particularly after postmortem examination, markedly reduced the frequency of infection. When this information on the transmission of infection was presented to the surgical profession, both Holmes and Semmelweis suffered severe ridicule from their colleagues. Holmes went on to comment: "Whatever indulgence may be granted to those who have heretofore been the ignorant cause of so much misery, the time has come when the existence of a private pestilence in the sphere of a single physician should be looked upon not as a misfortune but a crime" [45].

It took further studies on bacterial contamination, which were undertaken by Louis Pasteur (1822–1895) and Robert Koch (1843–1910), to convince surgeons and the world of the etiology of wound infection. The revolutionary work of Lord Lister (1827–1912) finally proved to surgeons that infection was due to contamination and that with antiseptic techniques, its incidence could be dramatically reduced (Fig. 1.30) [47–49]. As a result of the studies by Lister and others, a surgeon using antiseptic technique could operate on the brain with a much-reduced incidence of infection and subsequently an increased survival rate. Surgical infection would continue to be reduced with steam sterilization, use of ster-

ile gloves and gowns, and surgical instruments made of metal rather than wood.

Another key development of the nineteenth century was the development of a better understanding of what each region of the brain was responsible for, i.e., cerebral localization. As a result of a number of talented individuals, anatomical functions of various parts of the brain were becoming more clearly understood. One individual that stands out in these early neurological investigations was *Sir Charles Bell* (1774–1842). A Scottish surgeon and anatomist, Bell is remembered for his many contributions to the neurosciences, including the differentiation of the motor and the sensory components of the cranial nerves. Bell wrote a number of works on surgery, many of which were beautifully illustrated with his own drawings (Fig. 1.31). An early drawing of the brain stem was published by Bell which described very clearly the anatomy and the nerves of this structure. In the figure legend to this plate, Bell notes: "He who makes himself master of this plate can have no difficulty in comprehending the whole nervous system; – he holds the key to it in his hand". One of the first illustrations of a tumor of the posterior fossa appears in his 1830 monograph on the nerves [50]. This cerebellopontine angle tumor, which came from the fifth cranial nerve, was likely a

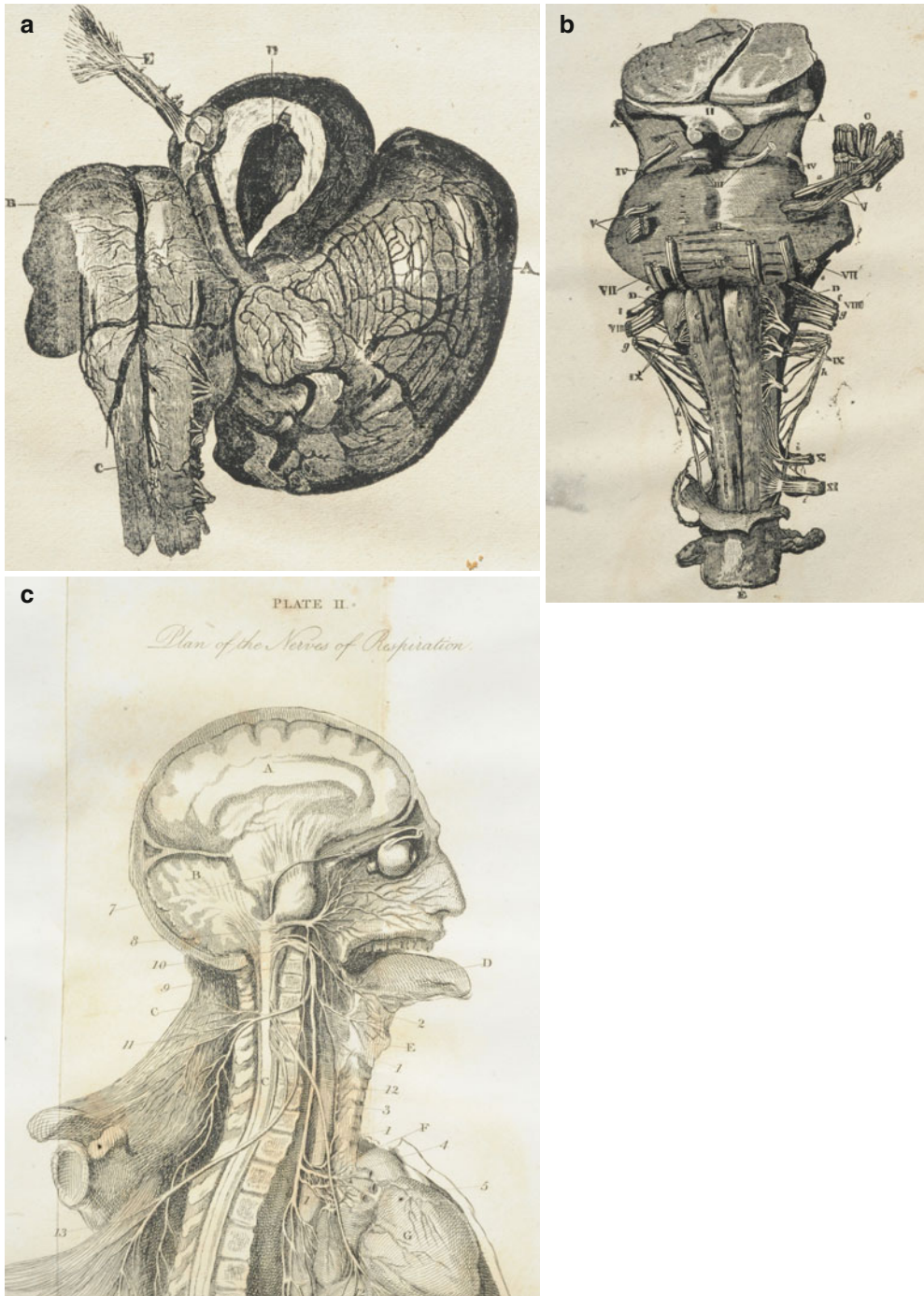


Fig. 1.31 (a) This illustration was drawn by Charles Bell and details a cerebellopontine angle tumor, a tumor arising from the fifth nerve. In the figure legend Bell describes a "...morbid sac which pressed upon and destroyed the fifth nerve on the left side." Bell notes the fifth nerve was wasted and almost "...reduced to cerebellar texture" [50]. (b) In Bell's writing on the nervous system are presented some of the earliest and best detailed descriptions of the

brain stem with very clearly outlined and labeled cranial nerves. As Bell noted in the text: "He who makes himself master of this plate can have no difficulty in comprehending the whole nervous system; he holds the key to it in his hand" [51]. (c) Both Bell's considerable artistic skills and anatomical dissections are clearly evident in this very finely detailed anatomy of the nerves of respiration, as they arise from the brain and brain stem [50]

Meckel's cave neuroma, which was not actually operated on but was illustrated in Bell's anatomical drawing.

Bell describes his technique of performing a trephination of the brain in 1821. It is interesting to read his surgical details from nearly 200 years ago and appreciate how far neurosurgical technique has come.

Let the bed or couch on which the patient is lying be turned to the light – have the head shaved – put a wax-cloth on the pillow – let the pillow be firm, to support the patient's head. Put tow [sic] or sponge by the side of the head – let there be a stout assistant to hold the patient's head firmly, and let others put their hands on his arms and knees.

The surgeon will expect the instruments to be handed to him in this succession – the scalpel; the rasparatory; the trephine; the brush, the quill, and probe, from time to time; the elevator, the forceps, the lenticular. [52]

In this era of computer-guided surgical technology, it is hard to appreciate how little was known of brain function and cerebral localization prior to the 1860s. The latter half of the nineteenth century led to many important developments in the understanding of brain anatomy and localization of function. Until we were able to develop this knowledge, operations on the brain and localization of brain lesions could not be possible.

If one was to describe the original “decade of the brain,” it would be the 1860s. Work by several investigators, including G. T. Fritsch (1838–1927) and E. Hitzig (1838–1907) [53] as well as Paul Broca (1824–1880) [54, 55], developed the important anatomical finding that each part of the brain had a particular function. From these foundation studies that were based on brain pathology, brain ablations, and stimulation, investigators gradually became able to localize speech, motor control, and vision, among other functions. Among these studies was the pioneering work by the English neurologist David Ferrier (1843–1928), investigations done in dogs, in which Ferrier removed various parts of the brain and then described the neurological deficit [56].

A rather unusual, if not controversial, series of cerebral localization studies were undertaken in the 1870s by an Ohio (USA) physician by the name of Roberts Bartholow (1831–1904).

Bartholow published a series involving three cases of tumors in the human brain in which he correlated clinical observations with the pathological findings [57, 58]. In 1874, Bartholow took under his care his house servant, a 30-year-old lady by the name of Mary Rafferty who had developed a large cranial defect from an “epithelioma” leaving exposed portions of each cerebral hemisphere [58]. Through these defects, he electrically stimulated the brain, carefully recording his observations. From these faradic studies, Bartholow was able to localize functional areas in the living human brain. Bartholow describes that during the series of stimulations, the patient developed focal and then generalized seizures with a hemiparesis of the right side. The patient died shortly after the studies and at autopsy was found to have a thrombosis and occlusion of the sagittal sinus. In commenting on this case, Bartholow felt the death was due to the autopsy examination and not his experimental studies! With present-day IRB standards, studies of this type would not be possible. Localization studies on the posterior fossa and cerebellum were the last to be done, being introduced with the stereotactic work of Victor Horsley and Clarke in the 1890s – a subject to be discussed further on in this chapter.

Pathological illustrations of diseases of the posterior fossa first appeared in the first half of the nineteenth century. At this point in surgical history, the cellular basis of brain pathology was not at all understood. Pathology illustrations being illustrated were literally what the eye would see. The atlas that stands out the most for posterior fossa pathology was illustrated and published by Jean Cruveilhier (1791–1874) [59, 60]. Cruveilhier became the first chairman of pathology at the University of Paris. Cruveilhier had at his disposal an enormous collection of pathological material provided by the dead house at the Salpêtrière and the Musée Dupuytren. Using this extensive autopsy material, he provided a number of original pathological descriptions of the nervous system including several lesions of the posterior fossa. Among the specimens illustrated was a cerebellopontine angle tumor along with a classic epidermoid tumor of the posterior fossa and brain stem (Fig. 1.32). Over a period

of 13 years, Cruveilhier issued a series of large fascicles with hand-colored illustrations. Harvey Cushing was the first to call attention to Cruveilhier's accuracy in correlating pathology

and the clinical history. Cushing used illustrations from Cruveilhier's works in both his treatise on acoustic neuromas [61] and his classic work on meningioma [62].

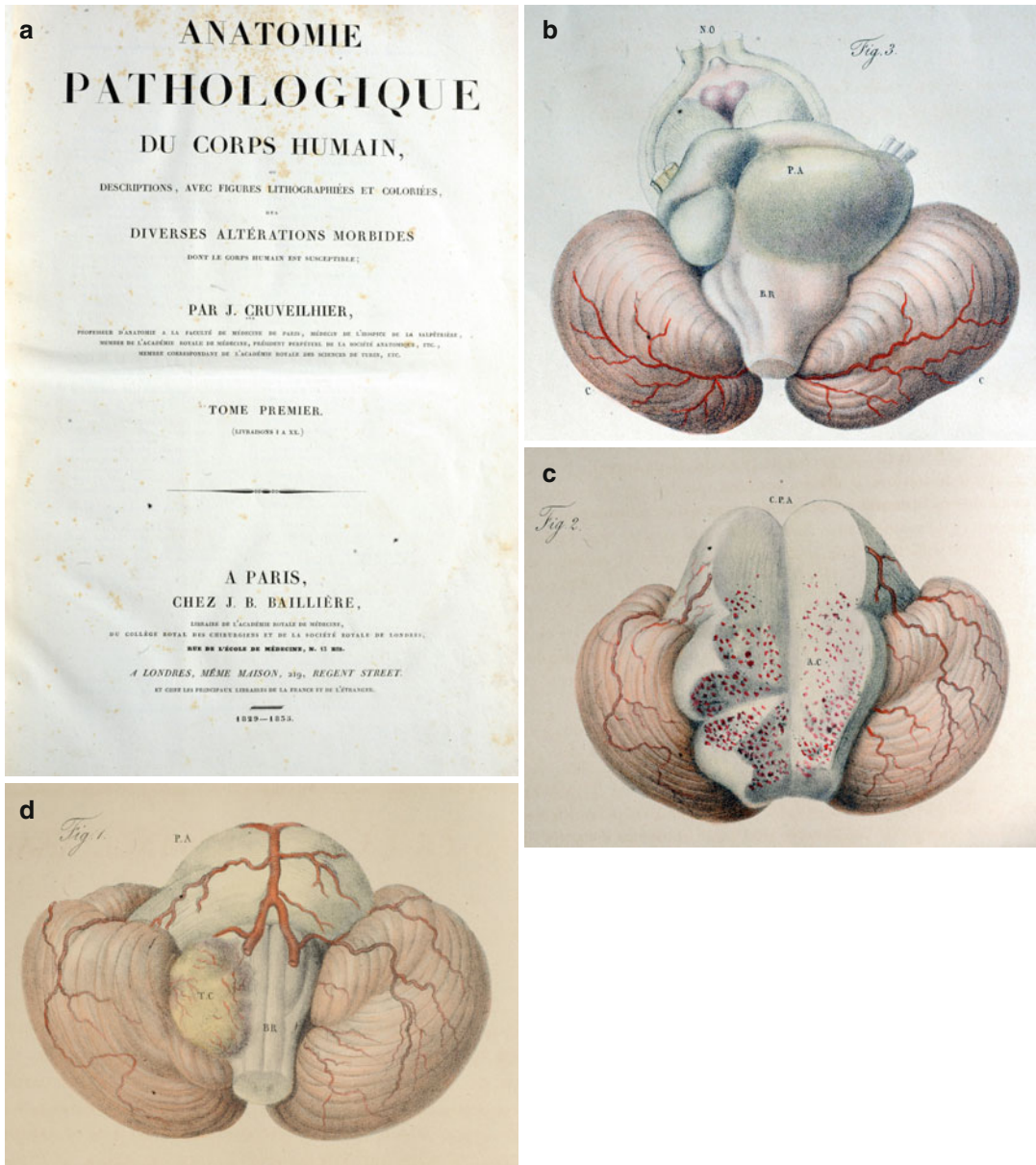


Fig. 1.32 (a) Title page from Cruveilhier's great pathological atlas including the brain pathology, following images are from this atlas [59]. (b) Infiltrating tumor of the pons, likely a pontine glioma [59]. (c) Infiltrating tumor of the brain stem seen in midsection with punctate hemorrhages [59]. (d) Exophytic tumor of medulla arising

from the pontine medullary junction [59]. (e) Midsagittal section of the brain stem with a large epidermoid of the superior brain stem. Cruveilhier described these lesions as "tumeurs d'apparence perlée fromées" [59]. (f) Large and extensive epidermoid tumor of the skull base encasing the cranial nerves and basilar artery [59]

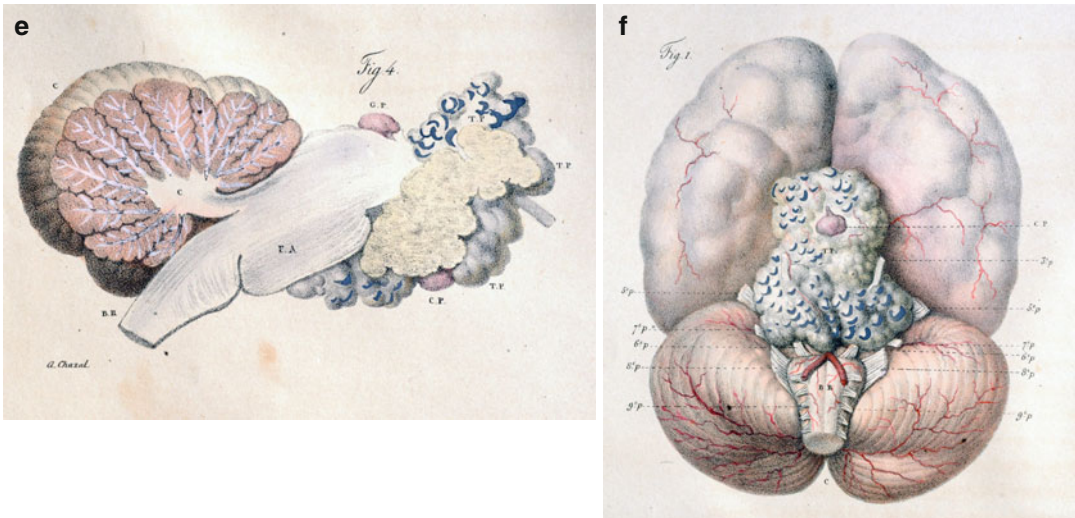


Fig. 1.32 (continued)

Another of the great nineteenth-century neuropathological atlases was produced by Richard Bright (1789–1858) who is best remembered as the eponymous discoverer of “Bright’s disease,” i.e., renal nephritis [63]. Bright’s interest to this chapter was his clinical observations of disease of the posterior fossa that were meticulously documented and then followed up by correlation with the postmortem findings. Not often appreciated by modern scholars was Bright’s contribution to neuropathology and in particular neuropathologies of the posterior fossa. In Bright’s two-volume atlas are several posterior fossa cases with detailed descriptions and clinical histories. Along with each clinical description, Bright provided a series of meticulously hand-colored plates detailing the pathological findings. The first illustrated case of a child with a pontine glioma and obstructive hydrocephalus was detailed by Bright – described as “tumor of the pons varolii.” In his description, Bright describes a 6.5-year-old girl that presented to Guy’s Hospital as a “delicate-looking” girl with a 3-month history of speech difficulty, a left facial paralysis (“when she slept, she never closed her left eye”), and progressive difficulty in ambulating. At the autopsy, Bright described the findings as: “Cutting into... this tumor...it

was found to consist of a peculiar gelatinous, somewhat translucent substance, with bands or fibres of whiter matter running through it, for the most part longitudinally, as if the natural texture had been separated by an infiltration between the fibres” (from volume II page 51). While microscopic pathology was not available at this time, this case clearly appears to be a pontine glioma. In this atlas, Bright also included cases involving abscesses and hemorrhage of the cerebellum hemispheres (Fig. 1.33).

In entering the fourth quarter of the nineteenth century, we now have developed a fundamental knowledge of brain pathology, cerebral localization, anesthesia, and antisepsis. For the first time, we find general surgeons, working in collaboration with neurologists, undertaking the first planned neurosurgical procedures. The earliest surgeries on the central nervous system were done on the cerebral hemispheres and the spine. By the 1890s, there develop some interesting and rather aggressive personalities advocating surgical treatments of disorders of the posterior fossa, and we will review a few of these pioneers and their efforts. One still has to keep in mind that all of these surgical personalities were general surgeons by training; neurosurgery as a subspecialty was not to occur until some 30 or so years later.

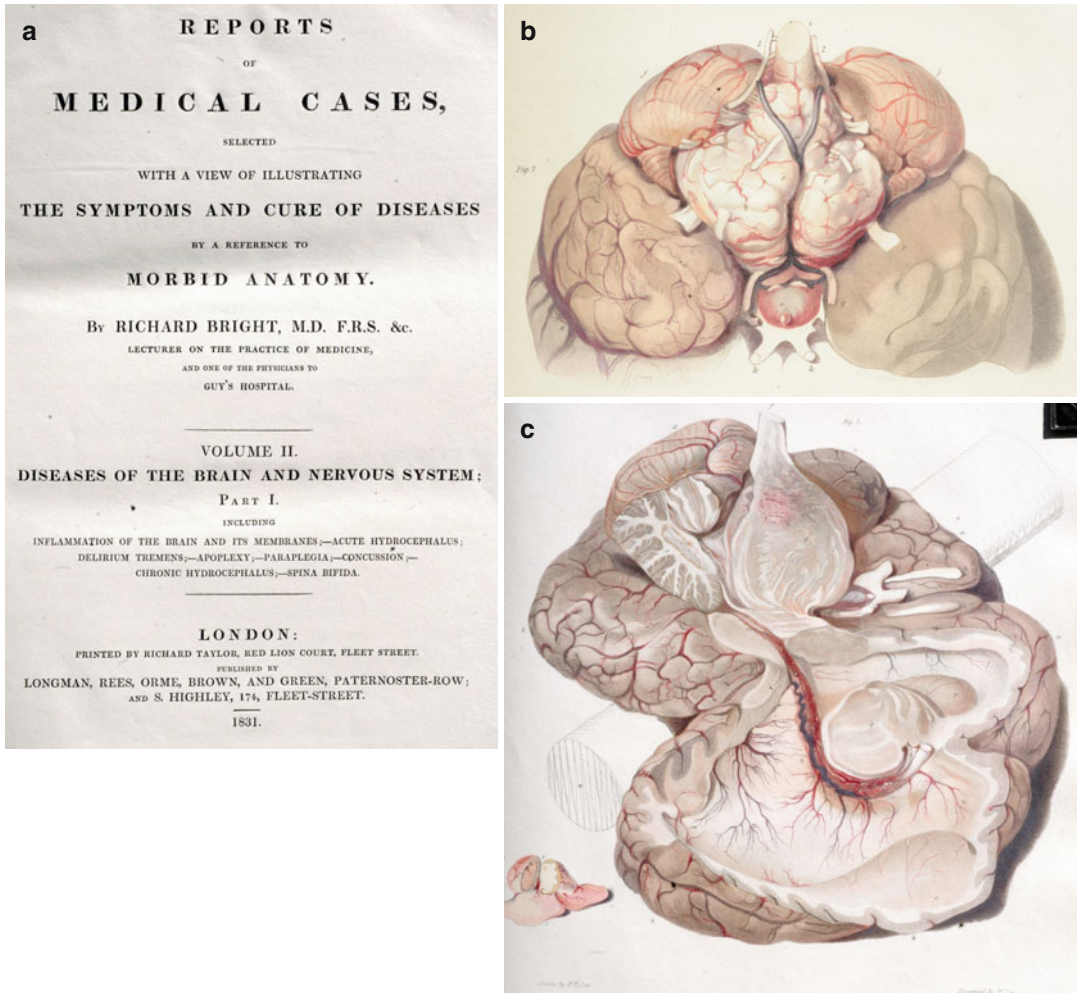


Fig. 1.33 (a) Title page from volume II of Bright's *Medical Reports* in which he details several cases of brain tumors and in particular a pontine glioma as illustrated in the next two figures [63]. (b) Bright's description of a diffusing infiltrating tumor of the pons likely a low-grade glioma. Bright's description: "Morbid enlargement of the Pons Varolii, involving the third, fourth, fifth, sixth, seventh, and eighth pair of nerves, all of which were soft, and

somewhat indistinctly seen" (from legend of plate 11) [63]. (c) In this illustration, Bright notes that he has made the cut just off the midline. Here again the diffusing infiltrating tumor can be seen and most likely consistent with a pontine. The diffuse infiltrating pattern in which the "whiter matter" has been disrupted; also note the small hemorrhages that have been nicely detailed [63]

In reviewing surgical operating room conditions, there are several interesting descriptions in the late nineteenth century; illustrated here is one example provided by an American general surgeon – John Wyeth (1845–1922):

The assistants should be as follows: A trained etherizer, and a first assistant to sponge and immediately help the operator, who stands usually just opposite him. A second assistant, to stand

conveniently to the instruments and the operator, whose duty it is to hand each instrument or article as called for with promptness, and as promptly to remove those which have been laid aside. A third assistant attends to the irrigation, regulating the supply at the indication of the chief. One supernumerary, for holding retractors, or performing any duty which may be required. A nurse to rinse the sponges and hand them to the first assistant. A second nurse to assist the etherizer. A supernumerary nurse for general usefulness. [64]

An early advocate of the Listerian antiseptic technique was an American surgeon – *William W. Keen (1837–1932)*, professor of surgery at Jefferson Medical College in Philadelphia [65]. In reviewing Keen’s textbook on surgery, coauthored with James White (1850–1916), Keen clearly details what he felt needed to be done to prevent infection in any surgical procedure. Keen’s surgical setup and his innovative approach to antisepsis and clean surgical technique are described here:

The operation was performed at the St. Mary’s Hospital, which had previously been a private home. All carpets and unnecessary furniture were removed from the patient’s room. The walls and ceiling were carefully cleaned the day before operation, and the woodwork, floors, and remaining furniture were scrubbed with carbolic solution. This solution was also sprayed in the room on the morning preceding but not during the operation. On the day before operation, the patient’s head was shaved, scrubbed with soap, water, and ether, and covered with wet corrosive sublimate dressing until operation, then ether and mercuric chloride washings were repeated. The surgical instruments were boiled in water for 2 hours, and new deep-sea sponges (elephant ears) were treated with carbolic and sublimate solutions before usage. The surgeon’s hand were cleaned and disinfected by soap and water, alcohol, and sublimate solution. ([65], p 502)

Keen made a number of advances in neurosurgical technique, one of which was his tapping the lateral ventricles to remove cerebrospinal fluid, done both for diagnosis and to reduce intracranial pressure – key concepts for any obstructive posterior fossa lesion. To help provide better visualization of brain structures, he bent kitchen spoons in various directions to provide an ingenious set of brain retractors. Keen was among the first surgeons to perform craniotomies rather than craniectomies using the recently designed Gigli saw, first described in Italy by an obstetrician in 1897 [66]. The craniotomy was accomplished with a series of bur holes and then connecting them with the Gigli saw. This technique quickly replaced the more gruesome “hammer and chisel” type of craniectomy. Before blood transfusions came available, Keen would stage the operations into two or more procedures, done to reduce the morbidity and mortality associated with excessive

blood loss. This staging technique was adopted by Keen after a visit to Victor Horsley in London.

Leonardo Gigli (1863–1908), of Florence, Italy, had designed the “Gigli saw” as a cutting wire to split the symphysis pubis during a childbirth [67] (Fig. 1.34). In describing his new saw, Gigli recommended it could also be used on skull bone. Not often appreciated was the fact that Gigli also introduced a curved metal guide to properly place the saw between the dura and skull. Alfred Obalinski [68] of Krakow, Poland, ignored or at least was not aware of Gigli’s recommendations and rapidly adopted this technique for craniotomies and recognized that it was much safer in a craniotomy to be able to cut bone from the inside out rather than the reverse. Gigli quickly appreciated this modification and published his technique in 1898 [67]. The general surgeons of this era very quickly adopted this technique for posterior fossa surgery.

In a further refinement of the craniotomy technique, *Wilhelm Wagner (1848–1900)* introduced the osteoplastic flap whereby the bone flap was elevated, leaving it attached to overlying soft tissue and muscle. Wagner first perfected this technique on a series of cadaver dissections and published his results in 1889 [69]. The series of surgical innovations led surgeons away from the earlier mutilating craniectomy technique of the hammer and chisel. By replacing the vascularized bone flap, the surgeon provided better post-operative brain protection and better esthetics for the patient.

An early successful pediatric neurosurgical case was reported by a Scotsman by the name of *William Macewen (1848–1924)*. In 1879, Macewen successfully removed a brain tumor from a 14-year-old child, a periosteal tumor over the right eye [70]. Using a new technique that he called “antiseptic trephining,” the tumor was resected and the child lived a further 8 years only to die of Bright’s disease. At the young age of 40, Macewen gave a classic address on his success in brain surgery to British Medical Association [71]. Macewen reported his results in 21 brain operations in which he had only three deaths and 18 successful recoveries, proving that brain surgery was now viable with the recently

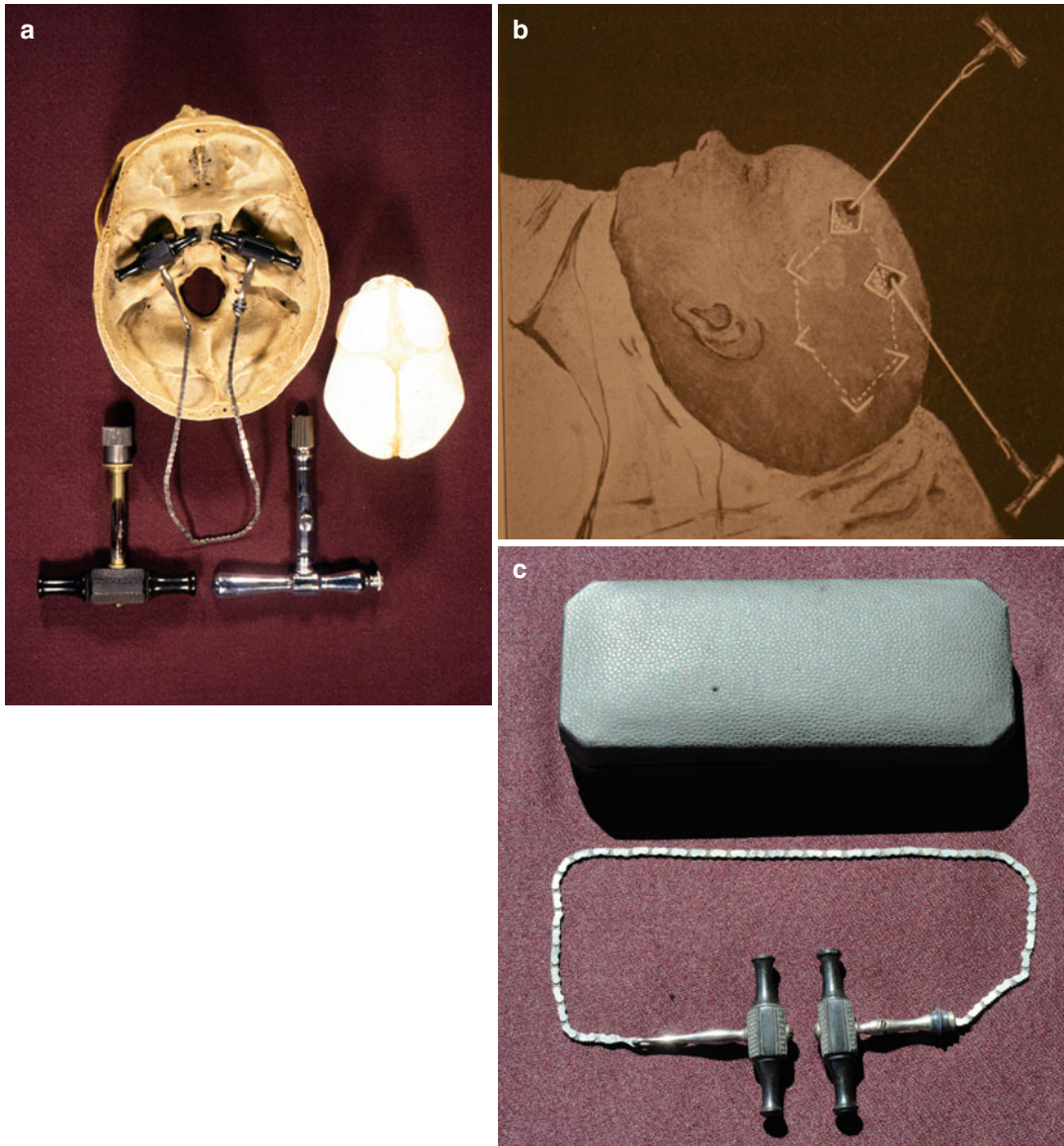


Fig. 1.34 (a) Gigli saw an early pre-Listerian (i.e., pre-antisepsis period) hand-driven ebony handle trephine on the lower left and with a steel trephine on the right, better able to be sterilized. From the author's collection. (b) The technique of connecting the bur holes with a Gigli saw;

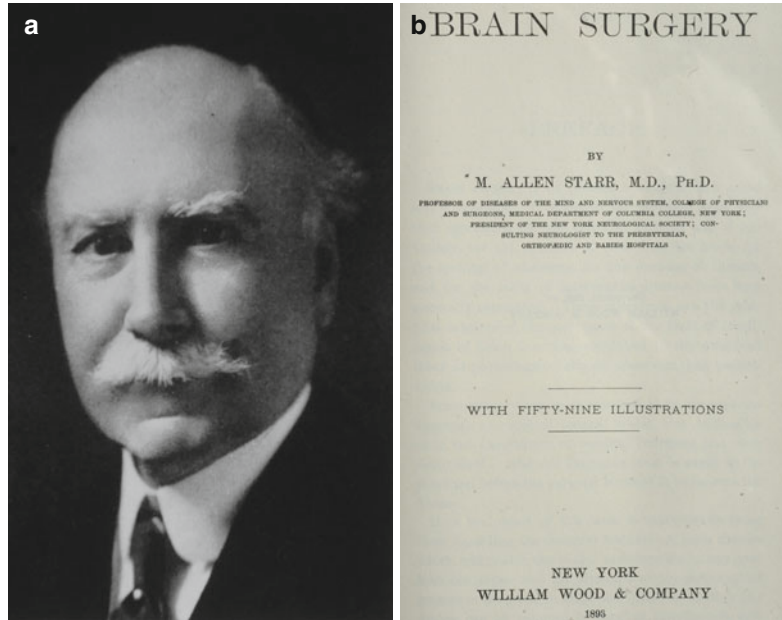
this technique replaced the “hammer and chisel” craniectomy [68]. (c) An early example of a Gigli saw with ebony handles and a traveling case; this would be a pre-Listerian example unable to be sterilized. From the author's collection

developed innovations of cerebral localization and Listerian antiseptic techniques. Macewen surgical results were summarized in a landmark neurosurgical textbook published in 1893 [72]. Of the 24 patients that he operated on, four had surgery within the posterior fossa, all within the cerebellum, and of this group, only one died,

clearly a remarkable advance in reducing mortality. In reflecting back on these results, Macewen made the following comment: “In uncomplicated abscess of the brain operated on at a fairly early period, recovery ought to be the rule [72].”

Macewen was a surgical innovator developing an anesthetic technique in which he used

Fig. 1.35 (a) M. Allen Starr, M.D. – a New York neurologist who authored the first American textbook on “Brain Surgery.” Photograph from author’s personal collection. (b) Title page from Starr’s remarkable early work detailing brain surgery at the turn of the twentieth century [73]



endotracheal intubation in place of the more commonly used tracheostomy in 1880. Macewen developed his own suture material made of catgut. He modified Lister’s antisepsis technique by using a carbolic spray rather than painting the surgical wound. Macewen was among the first to use a sterilized operating room gown, rather than entering the room in street clothes.

As we entered the 1890s, M. Allen Starr, M.D., a New York neurologist, offered the following contemporary view of neurosurgery – a surgical specialty only in existence for a decade at this point (Fig. 1.35):

Brain surgery is at present a subject both novel and interesting. It is within the past five years only that operations for the relief of epilepsy and of imbecility, for the removal of clots from the brain, for the opening of abscesses, for the excision of tumors, and for the relief of intracranial pressure have been generally attempted. These operations are the practical outcome of the acceptance of the facts of localization of brain function established by the combined labor of physiologist, clinical observers, and pathologists. ([73] – from the preface introduction)

Starr also notes an interesting observation on the differences of where tumors of the brain are likely to occur in adults and children; a view now well accepted – Starr comments:

It is evident...that all parts of the brain may be invaded by tumor, but that certain parts are invaded with special frequency both in childhood and in adult life. These parts are the cerebral axis and the cerebellum in children and the cortex in adults. ([73], p 209)

Starr went on to note that tumors of the cerebellum, in his series of 141 cases, were in pediatric patients more than twice as common as in adults. Starr then comments, “It is, therefore evident that children are especially liable to develop cerebellar tumors...but it may be stated here that they are most difficult to reach or to remove” ([73], p 212). Working with M. Allen Starr was a New York general surgeon named Charles McBurney, better remembered for “McBurney’s point” (appendicitis). McBurney performed a number of surgeries for brain tumors that were diagnosed and localized by Starr including cerebellar tumors. In Starr’s monograph on brain surgery, he describes a case of a child where he localized a lesion in the cerebellum. Starr asked McBurney to surgically remove the lesion on March 15, 1893. At surgery, McBurney found a “cystic tumor” within the hemisphere that he was able to remove and the patient survived ([73], pp 248–249). Starr also describes a case of a 7-year-old girl with a year of severe headaches,

vomiting, and staggering. The operative description is interesting to read as Starr notes that McBurney turned an osteoplastic flap with soft tissue left attached: “With chisel and mallet a considerable plate of bone was removed from over the centre of the cerebellar fossa, and the opening was then enlarged with rongeur forceps as much as was safe, having due regard for the venous sinuses.” While the operation went well, the patient expired 6 days later despite rectal stimulation due to weakness and convulsions. The autopsy revealed a large “gliosarcoma” which occupied the veriform lobe of the cerebellum and extended into both hemispheres ([73], pp 246–247).

A respected pioneer in neurosurgery and, in particular, posterior fossa surgery was a London surgeon – *Sir Victor Alexander Haden Horsley (1857–1916)*. Horsley was not only a general surgeon but also a talented investigator who did some of the very early faradic stimulation of the brain. Horsley’s original investigations were done in primates, studies done to analyze and localize brain function. Working with Gotch [74] and using a string galvanometer, they proved that electrical currents originated from within the brain. Horsley offered a number of innovative contributions to brain surgery including popularizing the use of bees wax to reduce bone bleeding. Horsley was an early advocate for performing a decompressive craniectomy for patients with inoperable tumors, particularly those of the posterior fossa. The Horsley-Clarke (Robert Henry Clarke 1850–1926) stereotactic frame was originally designed for stereotactic studies of the cerebellum in the primate [75]. This frame was then later adapted for work on the cerebrum though Horsley never used his instrument on humans, only in animal experimentation. The medical world had to wait some 50 years for the development of stereotactic frame in human neurosurgery, work published in 1947 by Spiegel and Wycis [76]. Horsley did a number of posterior fossa surgeries, the techniques of which he described in 1906 [77]. Horsley placed the patient in a lateral position preferring a craniectomy rather than a craniotomy using the hammer and chisel technique. Horsley’s skin incision started at the mastoid tip and then carried medially to the inion and then vertically

downward following the midline. When encountering a tumor within the cerebellum, Horsley argued to do only an internal decompression and not to attempt to remove it all, by doing this, the surgeon can significantly reduce morbidity and mortality (Fig. 1.36).

In the history of posterior fossa surgery, an individual often overlooked for his contributions was Sir Charles Ballance (1856–1936). A university college-educated surgeon, he went on to make a number of contributions to medicine and surgery. Germane to this chapter was his technique of a radical mastoidectomy with ligation of the jugular vein. He was among the first surgeons to develop a grafting technique for the facial nerve injury [78]. In his 1907 monograph on brain surgery, Ballance described a successful operation performed years earlier for an acoustic neuroma [79]. This was an adult patient that presented with headaches, vertigo, and tinnitus. Based on the clinical findings, Ballance operated on the patient via a posterior fossa craniectomy. This surgery was likely one of the first successful posterior fossa surgeries based on both localization and good surgical techniques. Ballance was also a strong early advocate of Listerian techniques.

Ballance gave the Lister Memorial Lecture in 1933 in which he reflected back over his long career. Ballance made the following comment which clearly shows the changes in surgery that had occurred over his lifetime:

Those who have recently joined the profession cannot in any way realise the paralysis of surgery sixty years ago in the presence of suppuration, cellulitis, erysipelas, septicaemia, pyaemia, acute traumatic gangrene, and tetanus, for which diseases there was as yet no means of prevention and no remedy....The operating theatre [of 1875] was of wood. The auditorium would seat several hundred persons. Each of the four surgeons had some two hours allotted to him for the performance of the ordinary operations of the week. The surgeon operated in a frock coat which had for a long time been kept in the theatre. It was stained with the blood and pus of previous operations. The instruments were placed in a tray lined with green baize. When a ligature was required the theatre attendant would put it on the stretch between his teeth and the fingers of the left hand. It was then waxed and handed to the surgeon.” [80]



b THE STRUCTURE AND FUNCTIONS OF THE CEREBELLUM
EXAMINED BY A NEW METHOD.

By SIR VICTOR HORSLEY, F.R.S., F.R.C.S.,

AND

R. H. CLARKE, M.A., M.B.

(From the Laboratory of Pathological Chemistry, University College, London.)

PART I.—METHODS.

- I.—INTRODUCTION.
- II.—RECTILINEAR TOPOGRAPHY.
- III.—STEREOTACTIC INSTRUMENT.
- IV.—ELECTROLYSIS.
- V.—EXCITATION.

I.—INTRODUCTION.

THE methods and experiments described in the following pages are the direct outcome of an investigation into the anatomical relations of the cortex of the cerebellum to its nuclei and peduncles, and to the rest of the brain and spinal cord. An account of that research was published in *Brain* in the spring of 1905.

When we began that work (1903) the view had been gaining ground that there was no direct path from the cortex of the cerebellum to the peduncles or to the spinal cord, and had been advanced by distinguished observers, especially Ferrier and Turner, Risien Russell and Thomas, who expressed themselves more or less definitely in favour of this opinion, and supported it with observations furnished by their own experiments. But although the evidence adduced established a strong probability we did not consider that it amounted to proof, as the conclusions were founded on lesions involving both cortex and nuclei, or complicated with injuries to other parts. Nor were all the conclusions of the authors absolutely definite. Marchi originally described a direct descending path in the spinal cord derived from the cerebellum. Ramon y Cajal spoke of this tract in a rather ambiguous way, leaving the reader in some doubt whether he recognized the tract himself or was merely quoting Marchi by calling it the *via descendente*. Ramon y Cajal also described some fibres passing from the cerebellar cortex to the superior peduncle.

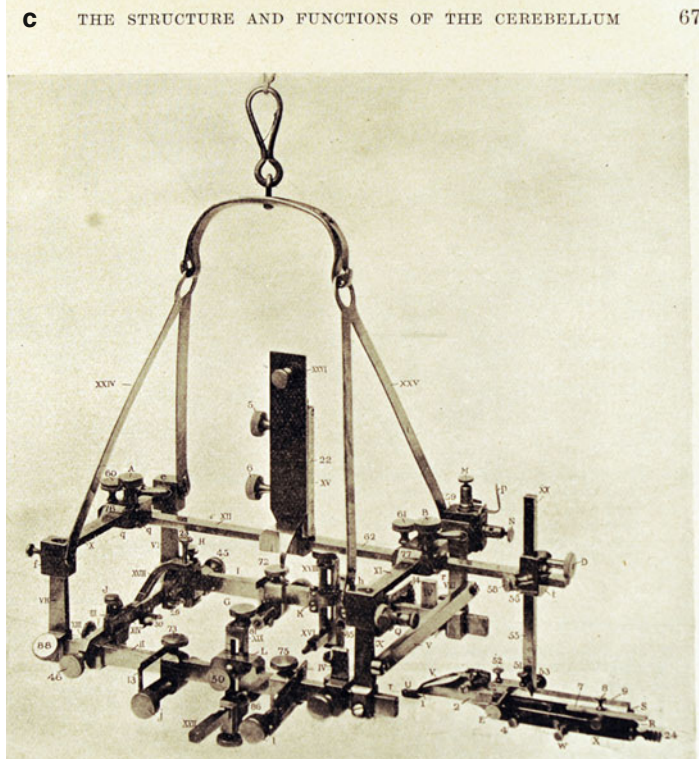


Fig. 1.36 (a) Portrait of Victor Horsley circa 1915. (b) Title page from Horsley and Clarke's monograph on a new stereotactic frame for animal brain experimentation [75]. (c) Horsley and Clark stereotactic frame [75]

In the early development of posterior fossa surgical techniques, we owe a great deal to the father of German neurological surgery, *Fedor Krause (1857–1937)*. Krause published a three-volume atlas on neurosurgery in 1909–1912, a revolutionary work detailing his surgical techniques. Krause’s illustrations and techniques for posterior fossa surgery were both innovative and aggressive [81]. Krause also recognized the advantages of aseptic technique in neurosurgery. A surgical approach still commonly used today for pineal region surgeries was the supracerebellar-infratentorial approach designed by Krause in 1926 [82]. Krause also provided some of the first detailed descriptions of surgical approaches to the cerebellopontine angle. The unilateral and bilateral osteoplastic craniotomy in posterior fossa surgery was elegantly detailed and illustrated in Krause surgical monograph. The bone flap was left attached to occipital muscles and hinged out of the field. This technique was not easy to do so it did not become popular with neurosurgeons. Krause’s outcome in the angle tumors was not so good as he reported 26 deaths in 31 cases [81]. Krause was also an early advocate for the craniectomy

for decompression in brain tumors (he called it “decompression trephining”) particularly in those cases where the tumor could not be removed or decompressed. Krause was also an early advocate for preoperative cannulation of the ventricles in posterior fossa tumor surgery to reduce increased intracranial pressure from hydrocephalus (Fig. 1.37).

Antony Maxine Nicholas Chipault (1866–1920) was the first French surgeon to devote his practice solely to neurosurgery (*Chirurgien-Neurologiste*) and in turn published several important papers and monographs dealing with neurosurgery at the turn of the twentieth century. Chipault started the first journal devoted to neurosurgery, but it had a short-lived run from 1896 to 1901 – *Travaux de Neurologie Chirurgicale* [83]. Chipault was the head of the surgical clinic at the La Salpêtrière but only for a short time. The tragedy of this individual was his rapid acceleration in neurosurgery and the equally rapid departure from medicine early in his life; he quit his practice at the age of 39 in 1905. Some writers have noted that he developed early signs of quadriplegia of unknown etiology. Unfortunately, Chipault’s life history still remains an obscure

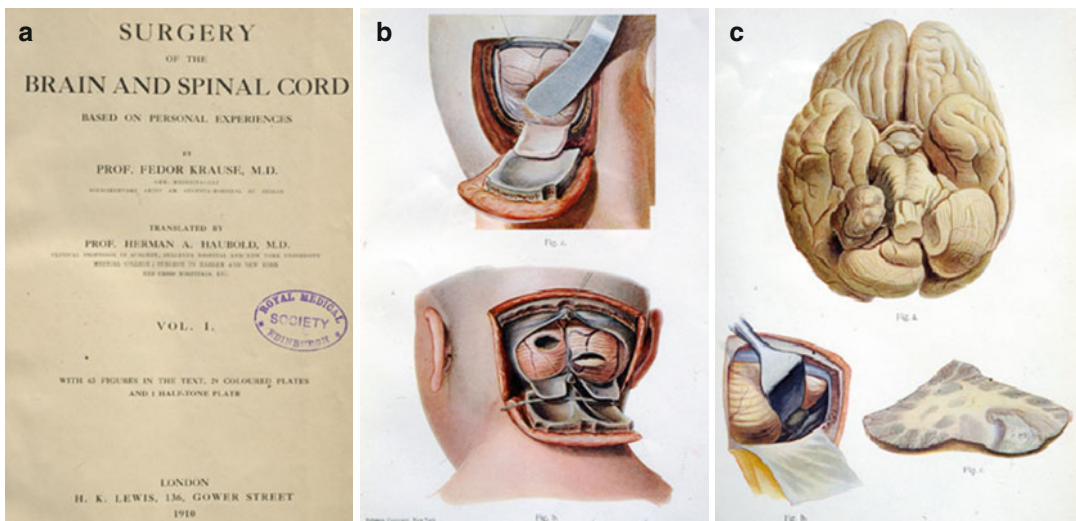


Fig. 1.37 (a) Title page from Krause’s neurosurgical monograph, the following images represent some of his surgical techniques [81]. (b) Krause’s technique for unilateral and bilateral osteoplastic craniotomies [81]. (c) In the upper image Krause is illustrating a right cerebellopontine angle tumor likely an acoustic neuroma. In

the lower left image is Krause’s cerebellopontine approach for an angle tumor. The image to the lower right is a cross-section of a cerebellar hemisphere tumor, likely an infiltrating glioma. (d) Krause’s “digital” technique of removing a tumor [81]. (e) Fungating lesion arising out of the lateral posterior fossa [81]

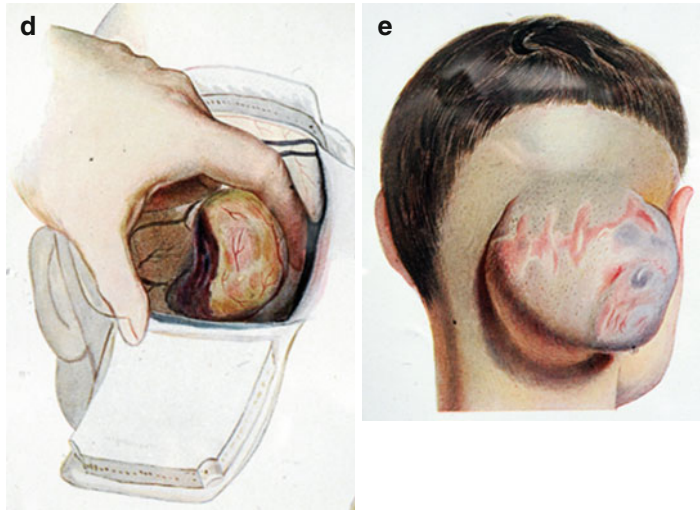


Fig. 1.37 (continued)

subject of which little is known. In 1894–1895, he published a two-volume work on surgery of the nervous system in which were introduced a number of new instruments and operative procedures [84]. An extraordinary contribution by Chipault was a lengthy table in his 1894–1895 text in which he reviewed the worldwide literature on brain tumors including age, pathology, surgery, and outcome. Within this series are several pediatric cerebellar tumors. In the outcome column, he used the word “mort” (i.e., death) quite often. By the end of the nineteenth century, surgery of the posterior fossa for tumors was clearly a business fraught with high risk and poor outcomes and undertaken by the very rare surgeon.

Chipault was an early advocate of the osteoplastic craniotomy. Chipault also published one of the earliest monographs dealing specifically with diseases and disorders of the spine and nerves. The first chapter of his work on the brain includes a then contemporary historical overview of neurosurgery as perceived by Chipault including a historical study on the development of trepanation back to ancient times [85].

Chipault appears to have been a gifted surgeon and clearly comfortable with operating on the brain and spine. Of his 22 brain tumor surgeries done between 1892 and 1905, two were of the posterior fossa. In personality, he was described as a very retiring, shy, very discreet man. In a

reply to a neurological colleague E. Brissaud who had made a comment on the sad state of brain tumor surgery at that time led Chipault to respond by saying:

The clinic is still sadder, which gives false, vague or too long delayed diagnoses. *We surgeons are ready from the technical point of view* (Italics mine), on the day when the clinicians are able to deliver to us cerebral tumors well localized, not too large or too diffuse. On that day their therapeutic convictions will be established as are ours already. Only surgical intervention can save the patient. It has sometimes done so already and one day will do so much more often. [86]

As a result of this lament, one of Chipault’s strong early interests was in a better understanding of cranio-encephalic topography devising some rather ingenious topographs of the head for cerebral localization. What is extraordinary to acknowledge is that Chipault did his first brain tumor in 1892 then retired in 1905, leaving behind a prodigious output of neurosurgical material – one could only imagine what his contributions would have been if he had been able to continue his surgical career longer.

An interesting aside at this point was a review by Robert H. Wilkins of neurosurgery at the end of the nineteenth century. Dr. Wilkins undertook a review of the Surgeon-General Index Catalogue for the years 1886–1896, a 10-year period following Horsley’s successful

removal of a brain tumor, and found that more than 500 general surgeons had reported cases of brain tumor surgery. However, that was to change dramatically as a subsequent review of the period 1896–1906 now showed only 80 cases. From 1906 to 1916, merely a handful of surgeons were reporting cases of brain tumor surgery – clearly a rude awakening of the dangers of brain tumor surgery settled in very quickly [87] (Fig. 1.38).

Further innovations in posterior fossa surgery were developed by a French surgical pioneer – *Thierry de Martel* (1875–1940). De Martel had a particularly strong interest in tumors of the posterior fossa and the cerebellopontine angle [88, 89] (see Fig. 1.39). De Martel was trained first as an engineer and took advantage of this training to design a number of surgical tools that included one of the first mechanically driven trephines. De Martel also designed the first electric

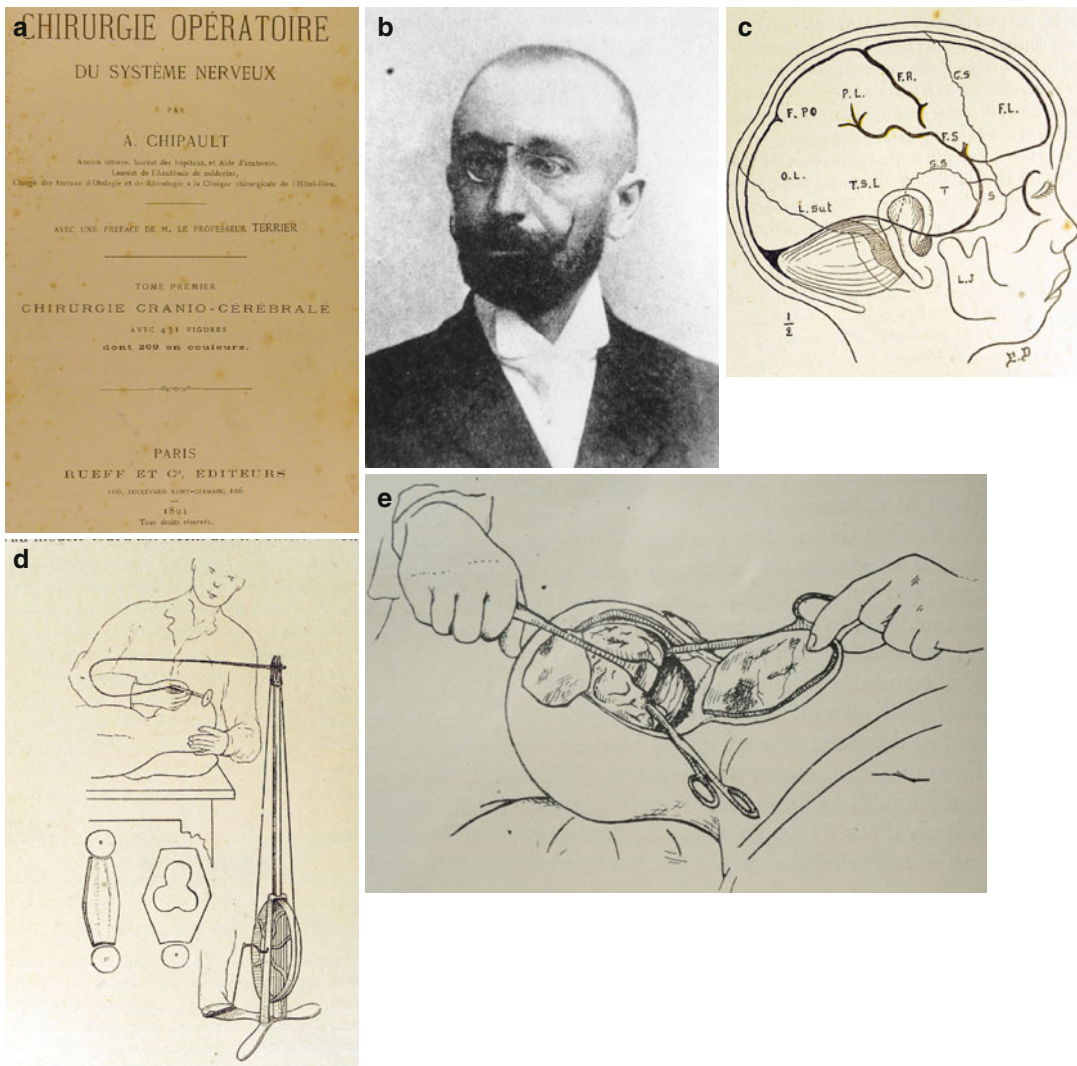


Fig. 1.38 (a) Title page from Chipault’s landmark publication on the surgery of the nervous system [84]. (b) Photograph of Chipault in mid-career and one of the few images of him that still exist. (c) Chipault’s anatomical landmarks used for localization of lesions in a child [84].

(d) Chipault’s design for a “surgical engine” which was foot-pedaled driven and used to perform a craniotomy [84]. (e) Chipault’s cerebellar “osteoplastic” flap for exposing the cerebellum [84]

motor-driven trephine that would disengage when reaching the inner table and dura. He further modified the Gigli saw with a metal guide to help pass the saw between bur holes. In posterior fossa surgery, de Martel was an early pioneer in the use of the sitting position for posterior fossa surgery. He designed his own surgical chair with various positioning devices to correctly position the patient [88]. De Martel also pioneered the technique of intraoperative cinematographic recordings and was among the first to use Kodachrome film to record operative techniques and findings. Sadly, de Martel ended his life by a self-injected lethal dose of potassium cyanide on the day the Germans invaded Paris at the advent of World War II.

A modification to the posterior fossa sitting position was introduced by Dawbarn [90]. Dawbarn developed a set of tourniquets that were placed around the legs. The tourniquets were tightened enough to allow arterial flow but restricted venous flow. During times of dropping blood pressure, the tourniquets could be opened allowing rapid infusion of blood into the body. The technique not only increased blood volume but also provided a form of autotransfusion.

An alternative surgical approach to cerebellopontine angle tumors was developed and published by R. Panse in 1904 – a translabyrinthine approach [91]. The limitation to this approach was the often-large size of the tumors upon presentation. The larger size of these tumors led to an

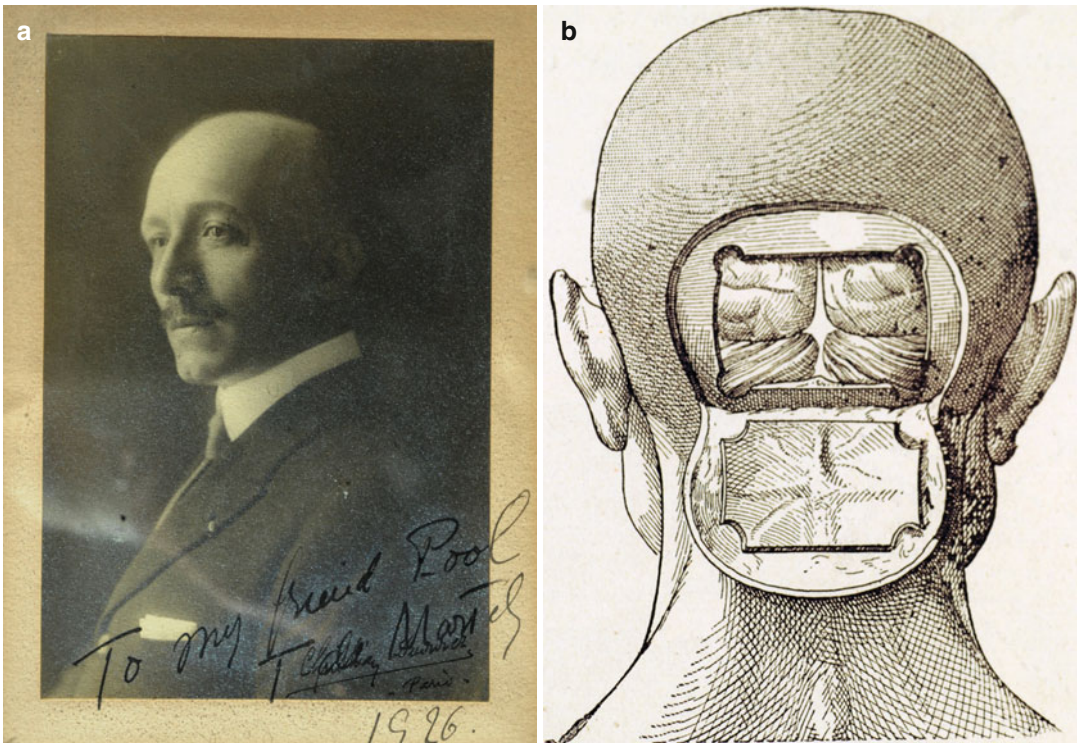


Fig. 1.39 (a) A photograph of de Martel inscribed to Larry Pool, M.D., at the height of his surgical career. From the author's collection. (b) De Martel's osteoplastic flap done bilaterally in which the transverse sinus, occipital lobes, and cerebellum are exposed – an aggressive surgical approach for this period [88]. (c) De Martel was an

early advocate for the sitting position in posterior fossa surgery and in this illustration he demonstrates his “sitting chair” with the head stabilization device [88]. (d) De Martel's uniquely designed chair with a tilting head piece that allowed him to place the head at various angles [88]

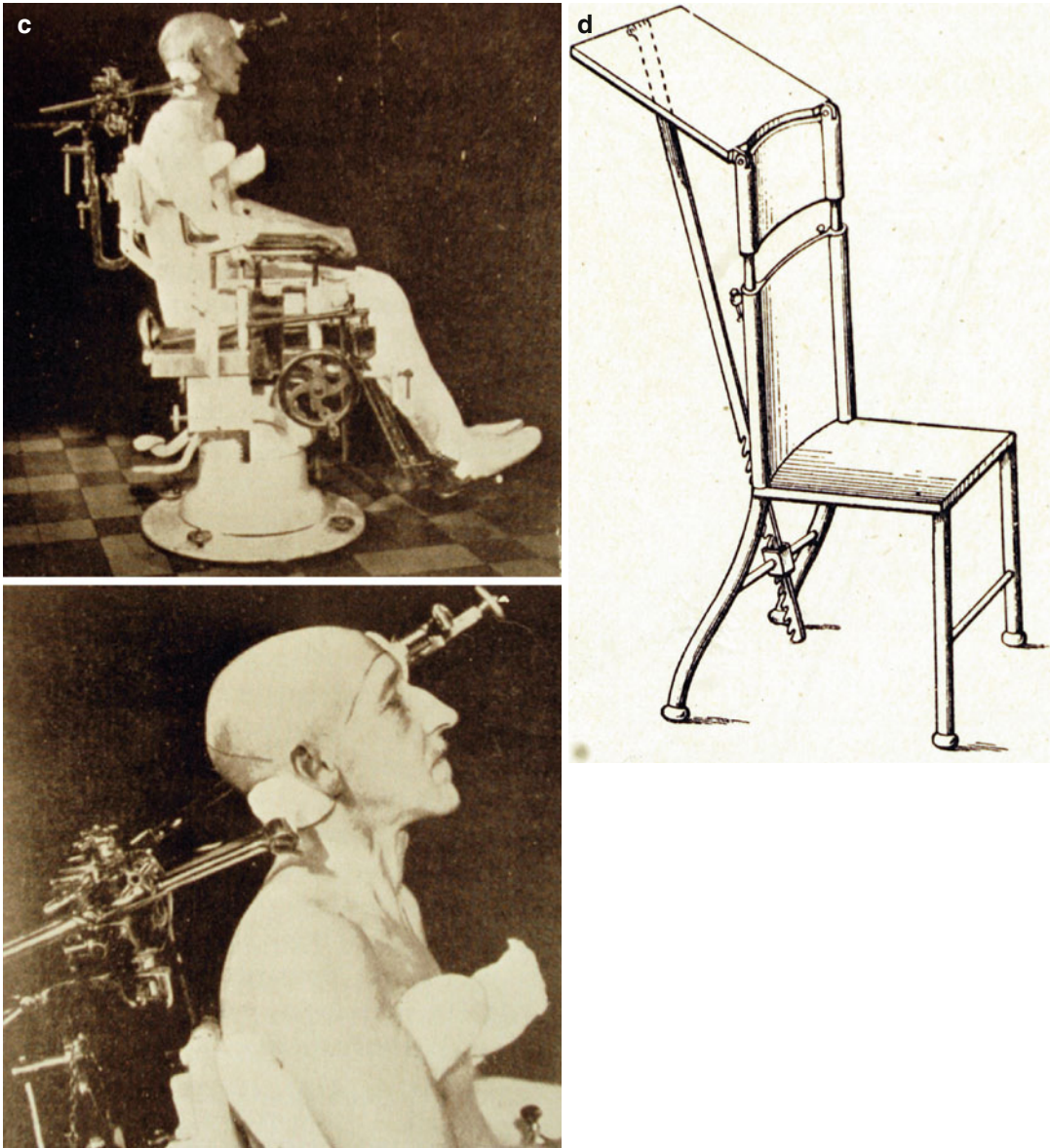


Fig. 1.39 (continued)

inevitable injury to the seventh nerve with facial palsy. A second and equally significant problem was the development of CSF leaks – these issues led to this technique not being popularly adopted. In recent years, there has been a renewed interest in the translabyrinthine technique due to better control of CSF leaks and the earlier detection of smaller tumors with better imaging techniques.

The difficulties that attend any attempt on the part of the surgeon to expose, much less remove tumors from the cerebellum, differ very materially from those encountered in tumors of the cerebrum. Speaking upon this subject on another occasion, I said it seemed as though, in encompassing the cerebellum with such large cranial sinuses, nature has intimated that this organ was never to be subjected to exposure at the hands of the surgeon. [92]

An influential American surgeon and an early pioneer in posterior fossa surgeries was Charles Frazier (1870–1936) of Philadelphia, PA. Frazier trained at Pennsylvania hospital and then went abroad and studied under Ernest von Bergmann and Rudolf Virchow among other prominent European personalities. Frazier was an early advocate of the aseptic technique and a sterile field for surgery, all in an effort to avoid the dreaded postoperative infection. To help speed up turnover time in the operating room, Frazier would grab a broom and a mop to help clean up at the end of a surgical case. Frazier became professor of surgery at the University of Pennsylvania and worked closely with two important early American neurologists, William G. Spiller, M.D., and Charles Mills, M.D. In collaboration with Spiller, Frazier made several important surgical contributions in the treatment of trigeminal neuralgia (Fig. 1.40). In reviewing Frazier's writings, he was clearly not an advocate of the craniotomy in the posterior fossa, rather preferred the craniectomy with hammer and chisel as he felt this was safer for the patient [93]. For posterior fossa surgery, Frazier preferred the prone position leading him to design an operating table with a headrest for the patient. Frazier introduced in 1926 the midline "bloodless" incision, which extended from theinion vertically to the cervical region [94]. The incision was "T" at the superior end, just above theinion and then carried down the midline of the neck. Frazier designed this incision to avoid the laterally perfusing occipital blood vessels that could bleed profusely when surgically disrupted. On occasion, Frazier would extend the superior end of the incision laterally to allow the surgeon a better exposure. In addition, this surgical maneuver also allowed placement of a bur hole for CSF removal to decompress the brain; most of these patients had obstructive hydrocephalus. Howard C. Naffziger, M.D. (1884–1961) later modified this midline incision by making it longer and thereby avoiding the lateral incisions [95]. Frazier was also an early advocate of removing the lateral third of the cerebellum, when necessary to provide exposure of the CP angle. Horsley, on the other hand, felt that you could easily retract the cerebellum

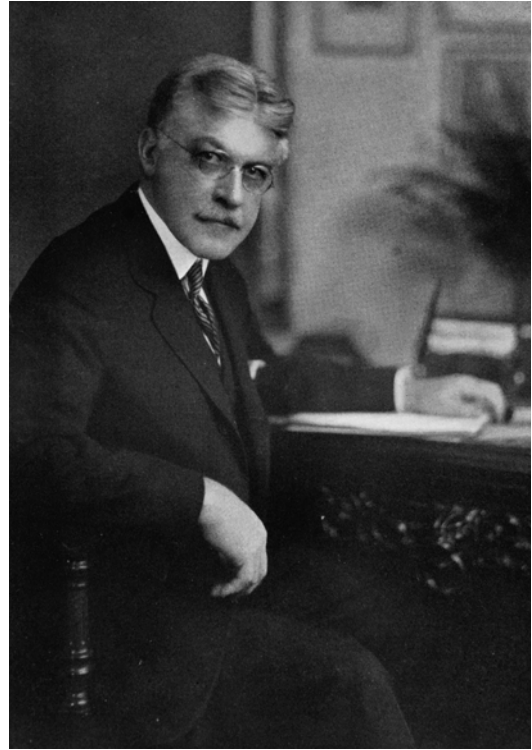


Fig. 1.40 Portrait of Charles Frazier, a pioneer in posterior fossa surgery and one who clearly recognized the complex nature of operating on this area due to the very high mortality and not insignificant morbidity. Frazier's contributions in surgery of the posterior fossa were clearly very much ahead of the time. From the author's collection

and provide the same exposure. When Frazier reported his series of posterior fossa surgeries in 1905, he had a surgical mortality of 42 %, a horrific number by today's standards yet considerably improved over his previous surgical colleagues [93] (Fig. 1.41).

If there is one figure in neurosurgery that stands out as a modern pioneer in posterior fossa surgery, it is Harvey W. Cushing (1869–1939). Cushing was educated at Johns Hopkins University under the tutelage of William H. Halsted (1852–1922) from whom he learned his meticulous surgical technique. Cushing developed his interest and insight into posterior fossa surgery early in his career while traveling abroad working with giants like Theodor Kocher (1841–1917). Cushing also spent time observing in the operating rooms of William Macewen and Victor Horsley among

other prominent European surgeons. Surgery within the posterior fossa was considered among the ultimate challenges at the turn of the last century. In this era of pre-steroids, lack of blood transfusion, and primitive imaging studies along with often very sick patients with acute hydrocephalus, these patients typically presented to the neurosurgeon gravely ill [97]. The associated high morbidity and mortality discouraged many surgeons from dealing with these complex posterior fossa surgical tumors. Following a different path and in typical Cushing fashion, he meticulously worked out surgical techniques to deal with lesions of the posterior fossa and as a result, published some of the early and best surgical outcomes in regard

to tumors of the cerebellum and brain stem [98]. Cushing's work on childhood medulloblastoma remains one of the classic studies [99]. In this particular tumor, Cushing argued that total resection was often not possible and a dangerous path to take if one wants to do so. Rather, Cushing argued it was best to do a posterior fossa decompression to relieve herniation, get a tissue diagnosis, and treat the hydrocephalus if present. Cushing was among the first to use radiation therapy in medulloblastomas and reported reasonable outcomes. For cerebellar astrocytomas, Cushing took a more aggressive approach in attempting to remove as much of the tumor as possible. When he published his numbers on astrocytomas in 1932, the

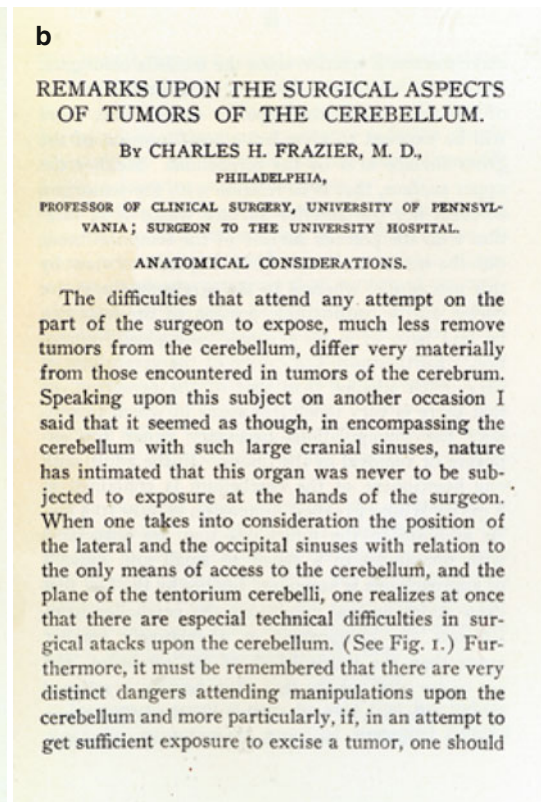
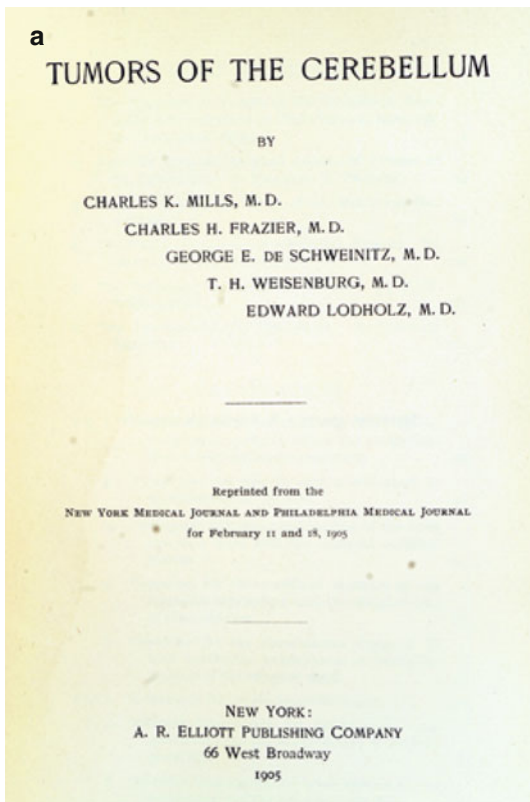


Fig. 1.41 (a) In the treatment of tumors of the cerebellum, this appears to be the first surgical monograph to deal with the disorder from both the clinical perspective and the surgical treatment [92]. (b) In this surgical monograph, Frazier offers a very poignant view of the dangers and difficulties of operating on lesions of the posterior fossa. A quite poignant view of surgery for this period [92]. (c) Frazier's technique for an osteoplastic flap for

exposure of the posterior fossa; Frazier clearly recognized the surgical dangers of exposing the transverse and lateral sinuses and potential injury to each [96]. (d) Frazier was not an advocate of the sitting position for posterior fossa surgery and so designed a table for a patient in the prone position with the head resting on a horseshoe-like device – a common positioning technique now used by many surgeons [96]

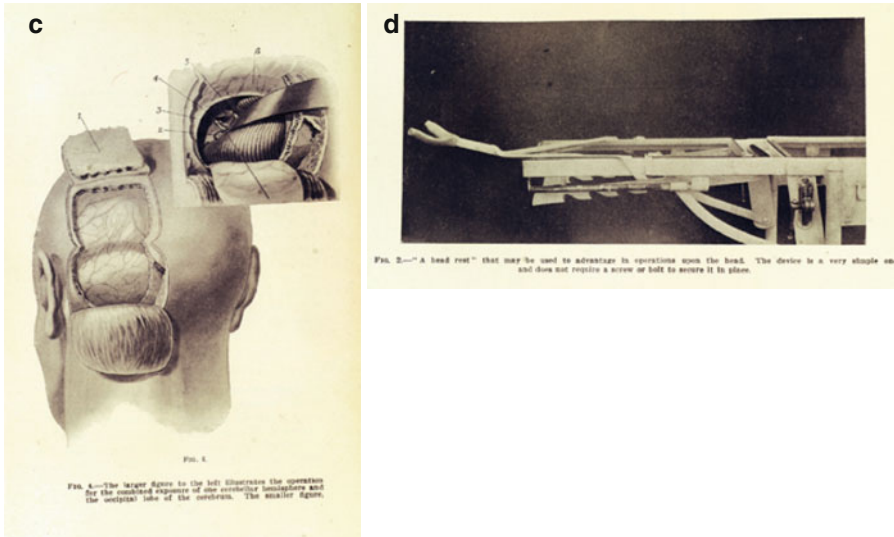


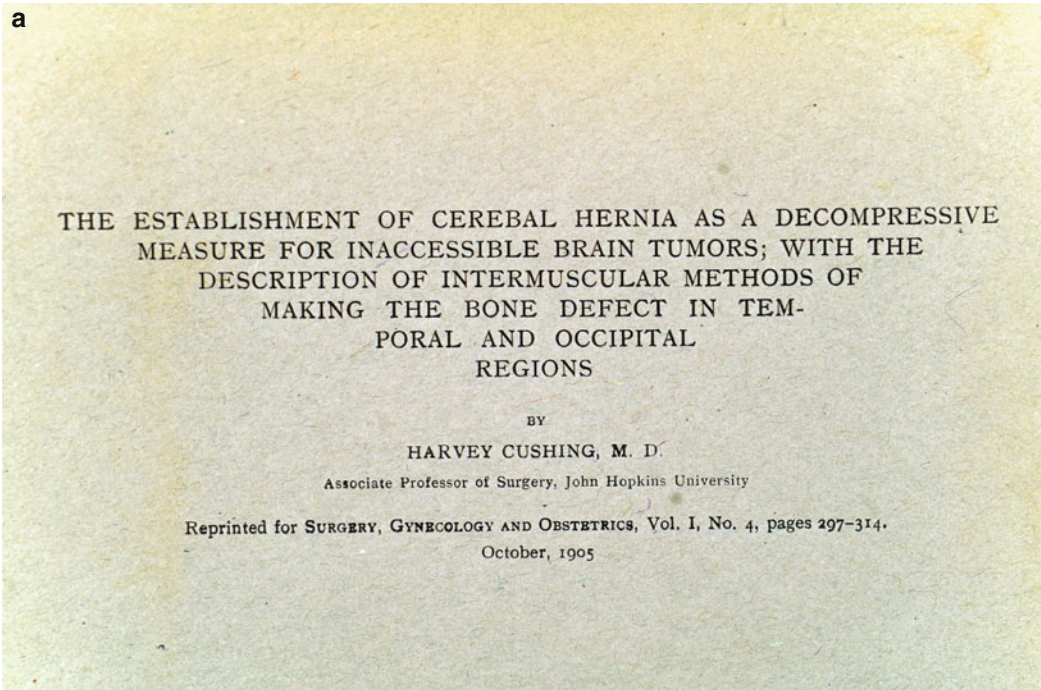
Fig. 1.41 (continued)

results were quite impressive – in 91 cases he had an operative mortality of 15 %, a dramatic improvement over earlier series [100]. Cushing operated mostly in the prone position and did not like the sitting position. He believed these surgeries should be attempted in a single stage, if possible, as the strain from additional surgeries was significant. For exposure, Cushing designed the “crossbow” incision that was a horizontal incision just above theinion and then carried down midline to the cervical region – an incision that never became popular. In Cushing’s hands, this incision allowed an adequate cerebellum exposure and also provided for an occipital bur hole for CSF decompression and relief from hydrocephalus. This incision also could be used to provide a posterior fossa decompression for the brain to herniate and decompress and thereby reduce increased intracranial pressure. Craniectomies for decompression of the brain were becoming a common form of treatment in this era of neurosurgery [101] (Fig. 1.42).

The first classification of brain tumors was developed by Cushing in collaboration with Percival Bailey (1892–1973), an American neuropathologist, and together published in 1926 a monograph entitled *A Classification of the Tumors of the Glioma Group on a Histogenetic basis with a correlated study of prognosis* [102]. Bailey began working with Cushing in 1919 at the Peter Bent Brigham Hospital where he developed an extensive pathological and histological series of studies from which ten different types of tumors or categories were developed and published. Bailey and Cushing were the first to describe in 1925 a tumor of the cerebellum usually associated with children that they coined “medulloblastoma cerebelli” [99]. These two physicians also described and introduced the term “hemangioblastoma” and also noted the association with Lindau’s disease [103]. The collaboration of these two individuals led to the first classification of brain tumors based on histology and cellular configuration (Fig. 1.43).

Fig. 1.42 (a) A very important paper by Cushing who offered a technique where by doing a “decompressive craniectomy,” a surgeon could treat and reduce increased ICP. These large craniectomies were done both supratentorially and infratentorially – at the time the only way to

reduce ICP when a tumor could not be found or removed – this in the pre-steroid era [101]. (b) Cushing innovated the “crossbow” incision to expose the posterior fossa which he has outlined here the incision and the exposure. Used for both tumor resection and reduction of increased ICP [101]



b Cushing: *Establishment of Cerebral Hernia.* 31

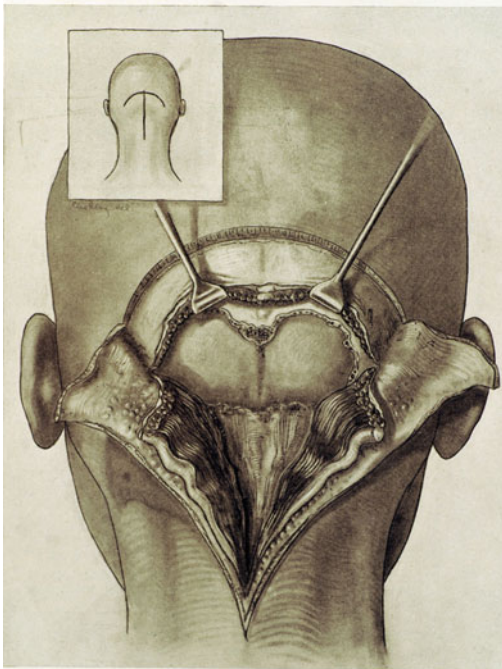
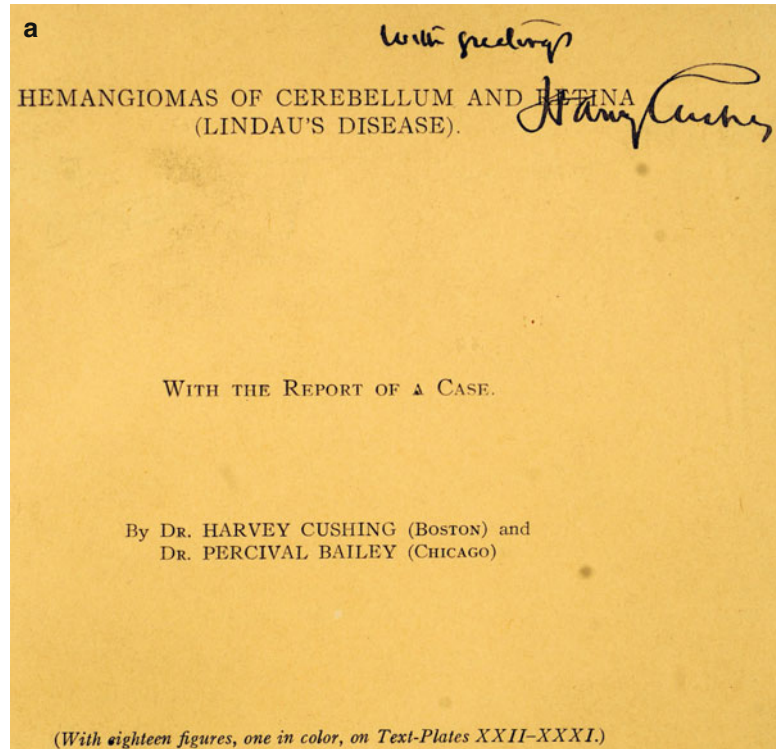


FIGURE 16.—Sketch of the field of operation, before opening the dura, in the suboccipital procedure. Note the high transverse cut of the "crossbow" incision.

Fig. 1.43 (a) Reprint of Cushing and Bailey's landmark paper on the hemangiomas of the cerebellum and the association with Lindau's disease – a signed presentation copy by Harvey Cushing [103]. (b) Cushing's postoperative sketch in which he outlines the hemangioma nodule and surrounding cyst; the position of the nodule is shown in a sagittal view [103]



b Arch. of Ophthal., Vol. LVII., No. 5.

Text-Plate XXII.

ILLUSTRATING ARTICLE OF DRs. HARVEY CUSHING AND PERCIVAL BAILEY,
"HEMANGIOMAS OF CEREBELLUM AND RETINA (LINDAU'S DISEASE)."

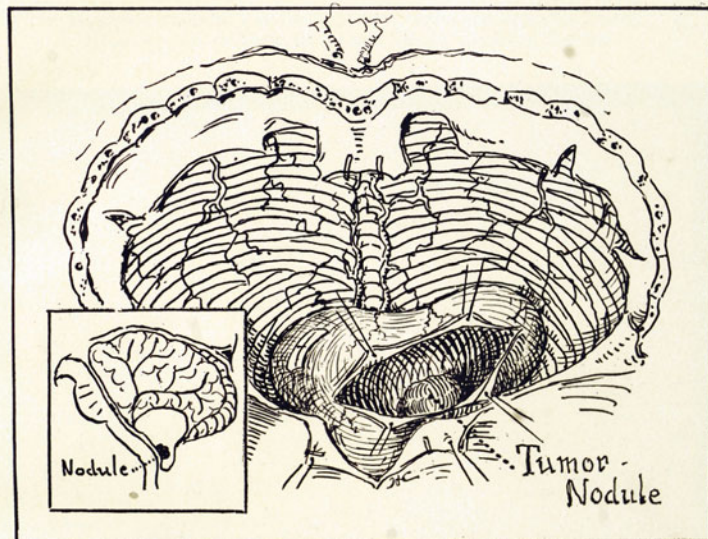


FIG. 1. Immediate postoperative sketch giving general appearance of operative field with cyst and position of nodule.

In tumors of the posterior fossa, Cushing developed a strong and early interest in the treatment of acoustic neuromas culminating in his clas-

sic monograph published in 1917 [104]. In his monograph on acoustic neuromas, which he called the "syndrome of cerebellopontine angle,"

Cushing described 30 cases. For the first time, surgery was being advanced as a reasonable treatment for lesions that had been considered unresectable because of their complex interrelationship with the cranial nerves and brain stem. Previous surgical monographs had described high morbidity and mortality that in reflection are clearly due to poor surgical technique. An example was the technique of Fedor Krause in which he removed the acoustic neuroma by taking his index finger and digitally removing it – the consequences were not only removal of the tumor but also the adjacent cranial nerves and anything adherent to the brain stem. To reduce morbidity, Cushing introduced the concept of the subcapsular resection of the tumor and thereby decompressing the brain stem and also reducing injury to the cranial nerves. Prior to Cushing's efforts in reviewing some of the other surgical studies, we find a very high surgical morbidity and mortality. For example, in reviewing a paper published in 1906 by Borchardt [104], he described 18 cases of angle tumors; in the outcomes of these 18 cases, there were 13 deaths. Fedor Krause reported his series of 31 cases with 26 deaths [105]. Cushing, in reviewing his earlier surgical literature, felt the high mortality was due to excessive surgical speed and the finger enucleating technique [61]. Cushing devised a more meticulous technique along with a subcapsular resection, and with this technique, Cushing was able to reduce his operative mortality to 15 % when he published his tumors of the nervous acoustic monograph in 1917 [61].

In 1932, Cushing retired from Harvard University as the Moseley Professor of Surgery. He had now completed his 2,000 brain tumor surgery, a career history that he summarized in his classic monograph of 1932 on intracranial tumors [100]. A combination of surgical technique, physiological research, and a career long attempt at understanding brain function – both physiology and pathology – all combined to allow Cushing to significantly reduce his overall mortality and morbidity in posterior fossa surgery to levels never before achieved.

Following up on the work of Harvey Cushing was his former student at Hopkins, Walter E. Dandy (1886–1946). Dandy was an equally brilliant surgical innovator but with an operating style more aggressive than Cushing. Their

differences in surgical techniques led to a number of rather acrimonious discussions over the years. Dandy's contributions to neurosurgery were also enormous in scope. Dandy's introduction of the technique of ventriculography allows neurosurgeons to localize mass lesions in an around the ventricle [106–108]. From his studies on ventriculography, Dandy and his pediatric colleague Kenneth Blackfan developed and clarified the earliest anatomic and physiological basis of hydrocephalus [109, 110].

Dandy's surgical style was completely the opposite of that of Cushing's. Dandy was more aggressive and typically performed more radical and complete surgical resections. These techniques were clearly disliked by Cushing who publicly commented on them to Dandy's dismay. Dandy was also a prodigious worker with packed work schedules. It was not at all unusual for him to do five to six surgeries in a day and typically working 6 days a week. Dandy offered a number of then unique innovations for increased nursing care in the postoperative period. These new innovations included the development of postoperative recovery room, an innovation that clearly led to better outcomes especially in posterior fossa surgery. During the postoperative period, Dandy developed protocols for aggressively monitoring and managing electrolytes. Dandy felt that aggressive management of airway issues was a new priority in the postoperative patient. When compared to Cushing, Dandy was clearly much more aggressive in his surgical management of cerebellopontine angle tumors such as acoustic neuromas. Dandy vocally and surgically differed from Cushing in surgical technique believing a total removal, rather than subcapsular, of the lesion should be done [111, 112]. Dandy's technique was to expose the tumor in the angle and incise the capsule. He would internally compress the tumor piecemeal. Once decompressed, the capsule would then be carefully dissected off the cranial nerves and brain stem [111, 112]. Cushing differed from Dandy as he preferred to leave the capsule attached to the brain stem and cranial nerves; aggressive removal here he felt led to unacceptable morbidity if not mortality. The letters exchanged between Cushing and Dandy over this subject provide for some interesting reading (Fig. 1.44).



a

b

**AN OPERATION FOR THE TOTAL EXTIRPATION
OF TUMORS IN THE CEREBELLO-PONTINE
ANGLE. A PRELIMINARY REPORT.**

By DR. WALTER E. DANDY

[From THE JOHNS HOPKINS HOSPITAL BULLETIN, September,
1922, XXXIII, Page 344.]

Fig. 1.44 (a) Portrait of Walter Dandy, courtesy of Mary Ellen Dandy Marmaduke. (b) Dandy's short paper published in 1922 in which he advocated for a gross total resection of acoustic tumors; this paper led to a bitter pub-

lic dialogue with Harvey Cushing [111]. (c) Dandy describes his total removal of acoustic tumors and here shows the technique of removing the outer lip of the acoustic foramen to follow the tumor into the petrous bone [111]

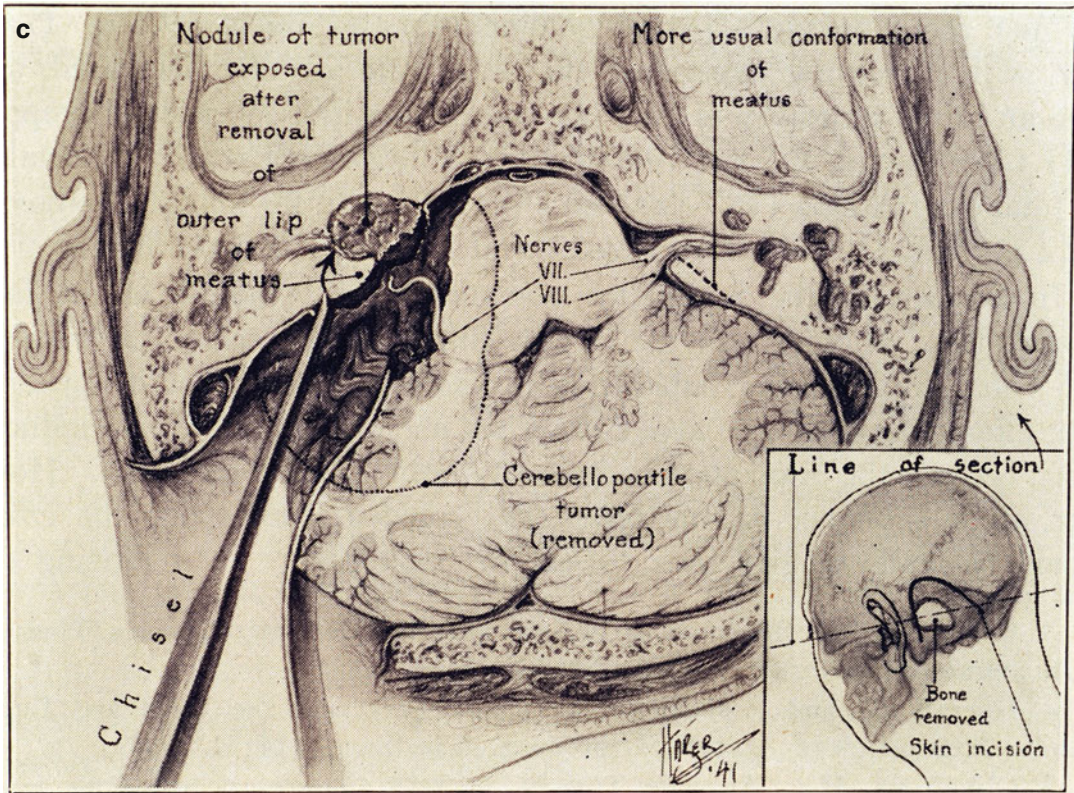


Fig. 1.44 (continued)

Dandy's surgical techniques involving posterior fossa surgery included treatment of trigeminal neuralgia via a suboccipital approach and sectioning of the fifth sensory root. His technique preserved both corneal function and motor function of the fifth nerve [113]. Dandy developed similar techniques for treatment of glossopharyngeal neuralgia [114, 115]. To expose the fourth ventricle, Dandy would split the vermis, which he noted could be safely done as long as the surgeon did not injure the dentate nucleus [116]. In posterior fossa surgery, Dandy also strongly felt a bur hole should be placed to decompress the brain secondary to hydrocephalus (Fig. 1.45).

Dandy had an early interest in surgery of the pineal region and the tumors located here. Dandy was not a proponent of the Krause's

supracerebellar-infratentorial approach, so he devised what is now called the "Dandy" approach, a large parieto-occipital flap and coming in over the tentorium by retracting the occipital lobe. The posterior two-thirds of the corpus callosum was transected thereby exposing the pineal region. Dandy, early on in his career, describes removing three tumors from this region in 1921, clearly aggressive surgery but with good outcomes [117].

When Dandy died on April 19, 1946, he had performed over 2,000 posterior fossa operations. When comparing operating numbers to Cushing, Dandy had done as many surgeries on the posterior fossa as Cushing had done on the brain in toto. Also interesting to note, Dandy's literary output now included 169 papers and five books, a more prodigious production than that of his teacher Harvey Cushing.

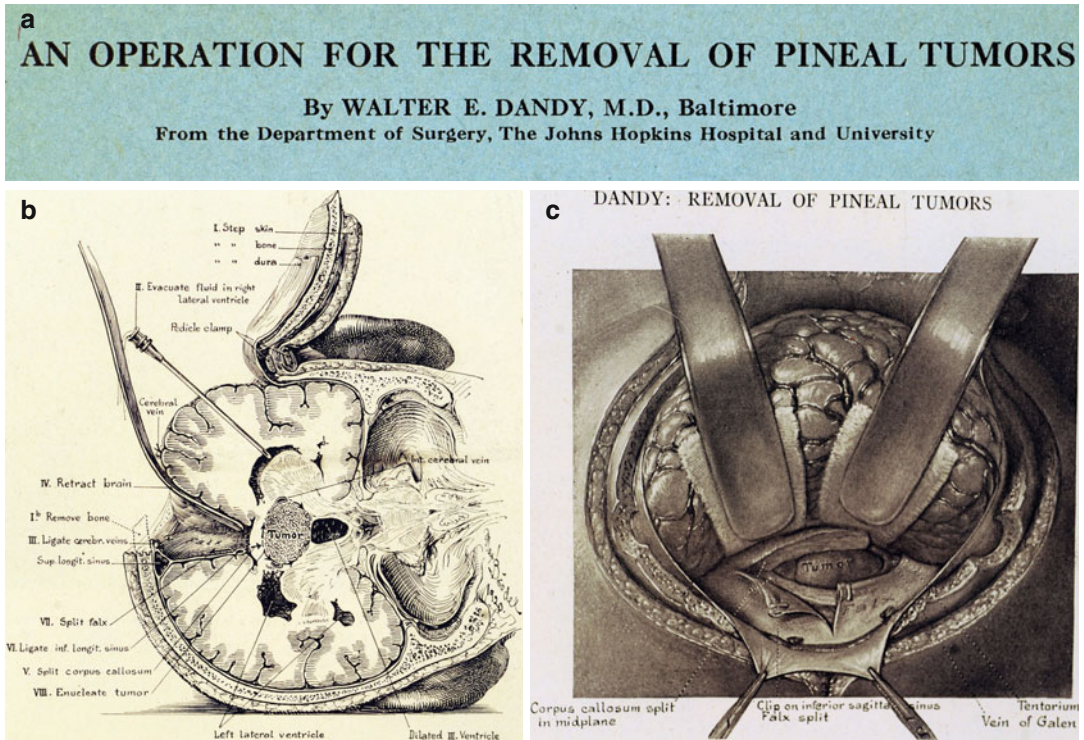


Fig. 1.45 (a) Reprint from an important paper by Dandy on a surgical technique for approaching the pineal region and its tumors [117]. (b) Dandy typically illustrated his surgical writings with elegant drawings, and here is a classic illustration of the approach to the pineal region as diagrammed by Max Brodel – note the lateral ventricle cannula

for decompression CSF prior to operative exposure. Dandy performed an osteoplastic flap for the craniotomy [117]. (c) Much like his teacher, Dandy liked to provide intraoperative views, and here he clearly delineates his approach to the pineal region with the pineal tumor exposed after longitudinally dividing the corpus callosum [117]

In the first half of the twentieth century, other innovative approaches to the posterior fossa were advocated. A novel approach to the brain stem was published in 1947 by *Gerard Guiot (1912)*. Guiot devised a subtemporal approach to the brain stem. Guiot did not use this approach for brain tumors, rather it was designed for pain treatment via mesencephalic tractotomy and also for the relief of Parkinsonian tremor with a peduncular tractotomy [118]. Guiot's approach has since been adopted by a number of surgical centers for dealing with tumors of the upper brain stem, in particular lesions of the tectal area and pons.

Conclusion

With the Renaissance, we had the introduction of anatomy, as it exist in life, not as written in outdated and inaccurate Greco-Roman texts.

The seventieth century brought us the basis of science and physiology in medicine and surgery. The eightieth century brought us surgeons that were both aggressive and innovative. The ninetieth century brought the development of anesthesia, antisepsis, and cerebral localization and the first understanding of the pathological basis of disease. The twentieth century brought imaging, better surgical equipment, the stereotactic device, the CT/MRI, and “frameless” computer-guided surgery. The twentieth century also brought us personalities like Cushing, Dandy, Krause, and de Martel among others who further developed an understanding of the physiology and pathology of the brain and in particular the posterior fossa. Brilliant minds lead to brilliant techniques and that continues still today. The next generation of neurosurgeons needs to be digitally gifted and

be able to wander the maze of the Internet and computers. It is quite likely that within the next generation, surgeons will no longer be “hands-on.” Rather, this generation will be data enterers – like a pilot flying an Airbus plane – their job will be to enter GPS coordinates and the computer will guide the robot to do the surgery via CT/MRI data points. Just as the plane takes off and lands based on a series of GPS grids, so will the surgery in which the operator with the computer and the robot.

References

- Bucy P (ed) (1985) *Neurosurgical giants: feet of clay and iron*. Elsevier, New York, p 5
- Rifkinson-Mann S (1988) Cranial surgery in ancient Peru. *Neurosurgery* 23:411–416
- Brock AJ (ed) (1916) *Galen on the natural faculties*. Cambridge University Press, Cambridge, UK
- Viale G (2007) The surgical approach to the posterior cranial fossa according to Galen. *Neurosurgery* 61:ON5399–ON5404
- Gale T (1586) *Certaines workes of Galens, called Methodus Medendi, with a brief declaration of the worthe art of medicine, the office of a chirurgion, and an epitome of the third books of Galen*. . . all translated into English by Thomas Gale, Maister in Chirurgie. Thomas East, London
- Galen of Pergamon (1576–1577) *Omnia quae extant opera in Latinum sermonem conversa*. (Quinta ed) Apud Juntas, Venice
- Garrison FG, Streeter EC (1920) *Sculpture and painting as modes of anatomical illustrations*. In: Choulant’s history and bibliography of anatomical illustrations, translated by Mortimer Frank. University of Chicago Press, Chicago
- Goodrich JT (1985) Sixteenth century renaissance art and anatomy: Andreas Vesalius and his great book – a new view. *Med Herit* 1:280–288
- Leonardo da Vinci (1911–1916) *Quaderni d’anatomia*. Jacob Dybwad, Christiania. In six volumes. See also Hopstock, H. Leonardo as an anatomist. In: Singer C (ed) (1921) *Studies in the history of medicine*. Clarendon Press, Oxford, pp 153–191
- Leonardo da Vinci (1979) *Corpus of the anatomical studies in the collection of Her Majesty the Queen at Windsor Castle*. Keele KD, Pedretti C (eds). Harcourt Brace Jovanovich, New York
- Todd EM (1991) *The neuroanatomy of Leonardo da Vinci*. American Association of Neurological Surgeons, Park Ridge
- Hunter W (1784) Two introductory lectures, delivered by Dr. William Hunter, to his last course of anatomical lectures, at his theatre in Windmill Street. London, printed by the order of the trustees for J. Johnson, 1784. See page 39 for Leonardo quote
- da Carpi JB (1518) *Tractatus de fractura calvae sive cranei*. Impressum per Hieronymum de Benedictus, Bologna
- Lind LR (1990) Berengario da Carpi on fracture of the skull or cranium. *Trans American Phil Soc* 80(4)
- da Carpi JB (1522) *Isagoge breves, perlucide ac uberime, in anatomia humani corporis*. Impressum per Benedictum Hectoris, Bologna
- Dryander J (1537) *Anatomiae*. Apud Eucharium Ceruicornum, Marburg
- Hanigan WC, Ragen W, Foster R (1990) Dryander of Marburg and the first textbook of neuroanatomy. *Neurosurgery* 26:489–498
- Vesalius A (1543) *De humani corporis fabrica libri septem*. Ex officina Joannis Oporini, Basel
- Pozeg ZI, Flamm ES (2009) Vesalius and the 1543 *Epitome* of his *De humani corporis Fabrica librorum*. A uniquely illuminated copy. *Proc Bibliogr Soc Am* 103:199–200
- Estienne C (1546) *De dissectione partium corporis humani libri tres*. Apud Simonen Colinaeum, Paris
- Paré A (1649) *The workes of that famous chirurgion ambroise parey translated out of Latine and compared with the French by Tho. Johnson*. Richard Coates, London
- Paré A (1582) *Opera*. A docto viro plerisque locis recognita: et Latinitate donata, Jacobi Guillemeau. Apud Jacobum Du-Puys, Paris, see Book X
- Paré A (1561) *Le Methode Curative des Playes et Fractures de la Teste Humaine*. A Paris, De l’imprimerie de Jehan Le Royer, Paris
- Willis T (1664) *Cerebri anatome: cui accessit nervorum descriptio et usus*. J. Flesher, London
- Johnson S (1755) *A dictionary of the english language*. W. Strahan for J. & P. Knapton, London
- Ridley H (1695) *The anatomy of the brain containing its mechanisms and physiology: together with some new discoveries and corrections of ancient and modern authors upon that subject*. Sam. Smith, London
- Pott P (1760) *Observations on the nature and consequences of wounds and contusions of the head, fractures of the skull, concussions of the brain*. C. Hitch and L. Hawes, London. See preface x–xi
- Pott P (1775) *The chirurgical works of percivall pott*. Hawke, W. Clarke, R. Collinsl, London
- Heister L (1718) *Chirurgie in welcher alles was zur Wund-Artzney gehöret, nach der neuesten und besten Art*. J. Hoffmann, Nürnberg
- Heister L (1743) *A general system of surgery in three parts*. W. Innys, London
- Heister L (1750) *Institutiones Chirurgicae, in qibus*. Apud Franciscum Pitteri, Venice
- Walker AE (1950) *A history of neurological surgery*. Williams & Wilkins, Baltimore. See p 333
- Quesnay F (1743) *Remarques sur les Playes de Cerveau, etc*. *Mém Acad Roy Chirurg* 1:310–316
- Morand FS (1768–1772) *Opuscules de Chirurgie*. Guillaume Desprez, Paris, pp 161–168

35. Saucerotte LS (1801) *Mélanges de chirurgie Neapoli*. Gay, Italy
36. Morgagni GB (1761) *De sedibus, et causis morborum per anatomem indagatis libri quinque*. Typog Remondiniana, Venetiis
37. Morgagni GB (1769) *The seats and cause of diseases investigated by anatomy*. Millar, London. Translated from the Latin by Benjamin Alexander
38. Soemmering ST (1778) *Dissertatio inauguralis anatomica de basi encephali et originibus nervorum cranio egredientium libri quinque*. apud A. Vanderboeck vid, Gottingae
39. Meckel JF (the Elder) (1748) *Tractatus anatomico-physiologicus de quinto pare nervorum cerebri*. A Vandenhoeck, Gottingae
40. Vicq d'Azyr F (1786) *Traité d'anatomie et de physiologie avec des planches coloriées représentant la nature les divers organes de l'homme et des animaux*. A. Didot l'aîné, Paris
41. Gautier D'Agoty JF (1748) *Anatomie de la tête*. Chez le sieur Gautier, M. Duverney, Quillau, Paris
42. Dandy WE (1945) *Surgery of the brain*. In: *Lewis practice of surgery*. W.F. Prior Co., Hagerstown, pp 6–7
43. Morton WTG (1847) *Remarks on the proper mode of administering sulphuric ether by inhalation*. MA. Dutton & Wentworth, Boston
44. Simpson JY (1847) *Discovery of a new anaesthetic agent, more efficient than sulphuric ether*. *Lond Med Gaz* 5n.s.:934–937
45. Holmes OW (1843) *The contagiousness of puerperal fever*. *N Engl Q J* 1:503–530
46. Semmelweis IF (1861) *Die Aetiologie, der Begriff und die Prophylaxis des Kindbettfiebers*. C.A. Hartleben's Verlags-Expedition, Pest, Vienna. See p 530 for quote
47. Lister J (1909) *Collected papers*. Clarendon Press, Oxford
48. Lister J (1891) *On the principles of antiseptic surgery*. *Int Beitr Wiss Med* 3:1–12, A paper in which Lister summarizes his work on antiseptics, presented in a festschrift to Rudolf Virchow on his 70th birthday
49. Lister J (1870) *On the effects of the antiseptic system of treatment upon the salubrity of a surgical hospital*. Edmonston & Douglas, Edinburgh
50. Bell C (1830) *The nervous system of the human body embracing the papers delivered to the Royal Society on the subject of nerves*. Longman, Rees, Orme, Brown, and Green, London. See clxxi plate V for the Meckel's cave neuroma
51. Bell C (1830) *The nervous system of the human body embracing the papers delivered to the Royal Society on the subject of nerves*. Longman, Rees, Orme, Brown, and Green, London. See pp clxix, plate IV for brain stem illustration
52. Bell C (1821) *Illustrations of the great operations of surgery, Trepan, Hernia, Amputation, Aneurism, and Lithotomy*. Longman, Hurst, Rees, Orme, and Brown, London
53. Fritsch GT, Hitzig E (1870) *Über die elektrische Erregbarkeit des Grosshirns*. *Arch Anat Physiol Wiss Med* 37:300–332
54. Broca P (1861) *Remarques sur le Siège de la faculté du langage articulé suivie d'une observation d'aphémie (perte de la parole)*. *Bull Soc Anthropol Paris* 36:330–336
55. Broca P (1861) *Perte de la parole; ramollissement chronique et destruction partielle du lobe antérieur gauche du cerveau*. *Bull Soc Anthropol Paris* 2:235–241
56. Ferrier D (1876) *The functions of the brain*. Smith, Elder and Co, London
57. Bartholow R (1868) *Tumours of the brain; clinical history and comments*. *Am J Med Sci* 110ns:339–359
58. Bartholow R (1874) *Experimental investigations into the functions of the human brain*. *Am J Med Sci* 67:305–313
59. Cruveilhier J (1829–1842) *Anatomie pathologique du corps humain*. J.-B. Baillière, Paris
60. Flamm ES (1973) *The neurology of Jean Cruveilhier*. *Med Hist* 17:343–353
61. Cushing H (1917) *Tumors of the nervus acusticus and the syndrome of the cerebellopontile angle*. WB Saunders, Philadelphia
62. Cushing H, Meningiomas EL (1938) *Their classification, regional behaviour, life history, and surgical end results*. Charles Thomas, Springfield
63. Bright R (1827–1831) *Reports of medical cases, selected with a view of illustrating the symptoms and cure of diseases by a reference to Morbid anatomy*. Richard Taylor for Longman et al., London
64. Wyeth JA (1889) *A textbook on surgery. General, operative, and mechanical*. Appleton & Co, New York
65. Keen WW, White JW (1899) *An American textbook of surgery of surgery from practitioners and students*, 3rd edn. Wm Saunders, Philadelphia
66. Keen WW (1898) *On the use of the Gigli wire saw to obtain access to the brain*. *Phila Med J* 1:32–33
67. Gigli L (1898) *Zur technik der temporären Schädelresektion mit meiner Drahtsäge*. *Centrabl für Chir* 25:425–428, For an English translation of this article see Wilkins RH (1965) *Neurosurgical classics*. Johnson Reprint Company, New York, pp 380–82
68. Obalinski A (1897) *Zur technik der Schädel-trepanation*. *Zentralbl FChir* 24:852–859
69. Wagner W (1889) *Die temporäre resektion der schädeldächer an stelle der trepanation*. *Centralbl Chir* 16:833–838
70. Macewen W (1881) *Localization of cerebral lesions and antiseptic trephining*. *Lancet* 2:581–582
71. Macewen W (1888) *An address on the surgery of the brain and spinal cord*. *BMJ* 2:302–309
72. Macewen W (1893) *Pyogenic infective diseases of the brain and spinal cord*. J. Maclehose & Sons, Glasgow
73. Starr A (1893) *Brain surgery*. William Wood & Company, New York
74. Gotch F, Horsley VAH (1891) *On the mammalian nervous system, its functions, and their localisation*

- determined by an electrical method. *Phil Trans R Soc B* 182:267–526
75. Horsley VAH, Clarke RH (1908) The structure and functions of the cerebellum examined by a new method. *Brain* 31:45–124
 76. Spiegel EA, Wycis HT, Marks M, Lee AJ (1947) Stereotaxic apparatus for operations on the human brain. *Science* 106:349–350
 77. Horsley V (1906) On the techniques of surgeries of the central nervous system. *BMJ* 2:411–423
 78. Ballance CA, Purves-Stewart J (1901) The healing of nerves. Macmillan and Co., London
 79. Ballance CA (1907) Some points in the surgery of the brain and its membrane. Macmillan and Co., London
 80. Ballance CA (1933) The Lister memorial lecture delivered in the theatre of the Royal College of surgeons in England on April 5, 1933. D.C. Thomson, Dundee. See pp 67–68
 81. Krause F (1909–1912) Surgery of the brain and spinal cord based on personal experiences. (trans: Haubold H, Thorek M). Rebman Co., New York. Issued in three volumes
 82. Krause F (1926) Operative freilegung der Vierhügel nebst beobachtungen über hirndruck und decompression. *Zentrabl Chir* 53:2812–2819
 83. Chipault A (ed) (1896–1901) *Travaux de Neurologie Chirurgicale*. Rueff et. e. Editeurs, Paris
 84. Chipault A (1894–1895) *Chirurgie Opératoire du Système Nerveus*. Rueff Et. C. Editeurs, Paris. For the pediatric cerebellar tumor cases listed by Chipault see case 23 and 24 on pp 333–34; case 79 on p 354; case 88 on p 357; case 118 on p 369
 85. Chipault A (1894) *Etudes de Chirurgie Médullaire (Historique, chirurgie opératoire, traitement)*. Felix Alcan, Paris
 86. Bucy P (ed) (1985) *Neurosurgical giants: feet of clay and iron*. Elsevier, New York, p 195
 87. Wilkins RW (1997) Treatment of craniocerebral infection and other common neurosurgical operations at the time of Lister and Macewen. In: Greenblatt SH (ed) *A history of neurosurgery in its scientific and professional contexts*. American Association of Neurological Surgeons, Chicago, pp 83–96
 88. Chatelin CH, de Martel T (1918) *Wounds of the skull and brain*. University of London Press, London
 89. De Martel T (1908) Un point de technique opératoire dans la craniectomie. *Presse Med* 16:641–643
 90. Dawbarn R (1907) Sequestration, anemia in brain and skull surgery. *Ann Surg* 45:161–187
 91. Panse R (1904) Ein Gliom des Akustikus. *Arch F Ohrenh* 61:251–255
 92. Frazier CH (1905) Remarks on the surgical aspects of tumors of the cerebellum. In: Mills CK, Frazier CH, de Schweinitz G, Weissenburg TH, Edward L (eds) *Tumors of the cerebellum*. A.R. Elliot, New York. See p 41 for quote
 93. Frazier CH (1905) Remarks on the surgical aspects of tumors of the cerebellum. *N Y S J Med* 18: 272–280; 332–337
 94. Frazier CH (1926) The midline bloodless approach to the posterior fossa. *Trans Am SA* 44:229–247
 95. Naffinger HC (1928) Brain surgery with special reference to exposure of the brain stem and posterior fossa, the principle of intracranial decompression, and the relief of impactions in the posterior fossa. *Surg Gynecol Obstet* 46:240–248
 96. Frazier CH (1905) In: Mills CK, Frazier CH, de Schweinitz G, Weissenburg TH, Lodholtz E (eds) *Tumors of the cerebellum*. A.R. Elliot, New York
 97. Cushing H (1927) The intracranial tumors of preadolescence. Report of a clinic for a combined meeting for the pediatric section of the New York Academy of Medicine, Philadelphia Pediatric Society, The New England Pediatric Society, held at the Peter Bent Brigham Hospital, Boston, October 16, 19. *Am J Dis Child* 33:551–584
 98. Cushing H (1931) Experiences with cerebellar astrocytomas. *Surg Gynecol Obstet* 52:129–204
 99. Cushing H (1930) Experiences with cerebellar medulloblastomas. *Acta Path Et Microb Scand* 7:1–86
 100. Cushing H (1932) Intracranial tumors. Notes on a series of two thousand verified cases with surgical mortality percentages pertaining thereto. Charles C. Thomas, Springfield
 101. Cushing H (1905) The establishment of the cerebral hernia as a decompressive measure for inaccessible brain tumors, with the description of the intermuscular making of the bone defects in the temporal and occipital regions. *Surg Gynecol Obstet* 1:297–314
 102. Bailey P, Cushing H (1926) A classification of the tumors of the Glioma group on a histogenic basis with a correlated study of prognosis. JB Lippincott Company, Philadelphia
 103. Cushing H, Bailey P (1928) Hemangiomas of cerebellum and Lindau's disease. *Arch Ophthalmol* 57:447–463
 104. Borchardt M (1913) Zur Technik der Blutstillung aus den Hirnblutleitern. *Zentralbl F Chir* 40: 1003
 105. Krause F (1913) Discussion of von Eiselsberg's paper. *Tr Int Cong Med Lond VII*:214
 106. Dandy WE (1918) Ventriculography following the injection of air into the cerebral ventricles. *Ann Surg* 68:5–11
 107. Dandy WE (1919) Röntgenography of the brain after the injection of air into the spinal canal. *Ann Surg* 70:397–403
 108. Dandy WE (1920) Localization or elimination of cerebral tumors by ventriculography. *Surg Gynecol Obstet* 30:329–342
 109. Dandy WE, Blackfan DD (1913) An experimental and clinical study of internal hydrocephalus. *JAMA* 61:2216–2217

110. Dandy WE, Blackfan DD (1914) Internal hydrocephalus: an experimental, clinical and pathologic study. *Am J Dis Child* 8:406–482
111. Dandy WE (1922) An operation for the total extirpation of tumors in the cerebellopontine angle. A preliminary report. *Bull Johns Hopkins Hosp* 33:344–345
112. Dandy WE (1925) An operation for the total removal of cerebellopontine (acoustic) tumors. *Surg Gynecol Obstet* 41:129–148
113. Dandy WE (1925) Section of the sensory root of the trigeminal nerve at the pons: preliminary report of the operative procedure. *Johns Hopkins Hosp Bull* 36:106
114. Dandy WE (1927) Glossopharyngeal neuralgia (tic douloureux): its diagnosis and treatment. *Arch Surg* 15:198–214
115. Dandy WE (1929) Operative relief from pain in lesions of the mouth, tongue and throat. *Arch Surg* 19(143–148):1929
116. Dandy WE (1932) The brain. In: *Lewis practice of surgery*, vol 12. WF Prior, Hagerstown
117. Dandy WE (1921) An operation for the removal of pineal tumors. *Surg Gynecol Obstet* 33:113–119
118. Guiot G, Forjaz S (1947) La tractotomie nesencéphalique par voie soustemporale. *Rev Neurol* 79:733–739

Development of the Posterior Fossa Structures

2

Martin Catala

The posterior fossa is a favorite subject for our colleagues involved in pediatric neurosurgery. Indeed, most of the serious illnesses affecting children lie at this level. It is therefore important to present here an aspect (albeit simplified) illustrating the development of these structures.

The development of a structure (or structures) reflecting the formation of the posterior fossa is very complex. Many current data came tearing down the Dogmas that are passed by reference books. Our project is not to destroy all these concepts but to try to enlighten our readers to understand that “Dogma reference works perpetuate themselves” in the words of Stephen Jay Gould. The posterior fossa is composed of three distinct elements: bones with essentially the occipital bone, the meninges, and the central nervous system. The bony elements of the posterior fossa represent a part of the skull base or chondrocranium that is characterized by the formation of a cartilage scaffolding prefiguring subsequent bone formation. This chondrocranium is one of the three parts of the cranium that is divided into the chondrocranium, the viscerocranium (i.e., the bones of the face), and the neurocranium (consisting of the bones of the vault).

M. Catala, M.D., Ph.D.
Faculté de Médecine Pitié-Salpêtrière
(Université Paris 6), UMR CNRS and Paris VI 7622,
9, quai Saint Bernard, 75252 Paris Cedex 05, France

Fédération de Neurologie, Hôpital Pitié-Salpêtrière,
47-83, Bd de l'Hôpital, 75651 Paris Cedex 13, France
e-mail: mcatala@snv.jussieu.fr

2.1 Development of the Occipital Bone

The bones that constitute the vault of the skull are dermal bones produced by membranous ossification, i.e., formation of bone cells from mesenchymal cells that are condensed during development. In humans, ossification begins around the 8th to 9th week of gestation. The first bones to ossify are the frontal and the supraoccipital bones. The parietal bone ossifies secondarily. These bones remain separated by a very active connective tissue, the suture. The latter allows the formation of new bone that is added to the already formed bone. This mode of growth is called accretion. The presence of an active suture is thus mandatory for the skull growth. Impairment of the sutures will lead to bone defect or to premature closure or craniosynostosis.

The occipital bone is included with the first cervical vertebrae into a very mobile region called the cranio-spinal hinge. This hinge is a region that has undergone profound changes over the phylogeny of vertebrates. In fish, the vertebrae, all along the axis of the body, do not exhibit major regional morphological differences, so it is not possible to describe various spinal regions. One of the first constraints that had to suffer the first terrestrial tetrapods was the opportunity to raise their head to better understand their visual environment. This evolutionary advantage is a major acquisition for the predators who can then locate their prey much better than if their eyes

remained near the ground plane. Such an adaptive advantage is also necessary for prey, which can then better understand the presence of predators. To acquire such a function, it was necessary that the spine undergoes a regionalization with mobile cervical vertebrae allowing extreme mobility of the skull and therefore the animal to acquire a better visual field. Furthermore, the mobility of the cephalic region has increased considerably during evolution. Thus, reptiles and birds have a cranio-spinal joint with a single degree of freedom. In contrast, mammals have a very mobile joint in three planes.

2.1.1 The Actors During Development of the Cranio-spinal Hinge: Somites, Sclerotome, and Cephalic Mesoderm

The somites, sclerotome, and cephalic mesoderm derive from paraxial mesoderm (Fig. 2.1). Their emergence takes place during the third week of development in humans during a stage called gastrulation (see [1] for a review). This phase of development is so important that embryo cannot survive without ensuring its successful gastrulation. This idea was put forward by the famous developmental biologist Lewis Wolpert who claimed “It is not birth, marriage, or death, but gastrulation which is truly the most important time in your life.” The mesoderm derive from cells initially located in the primitive streak in amniotes. Paraxial mesoderm originates from the rostral region of the primitive streak. The first contingent of the population forms the cephalic mesoderm that never segments. Slightly more caudally, the paraxial mesoderm becomes segmented some time after its formation. Each of these segments forms a cubic structure also known as a somite. The somites are produced according to a rostrocaudal gradient so that the first somites are formed before the more caudal somites. The total number of somites has been variously assessed by different authors in the textbooks of classic human embryology (from 40 to 44) [2–9]. However, the work of O’Rahilly and Müller [10] gives a number of 38–39. Yet this work is based on observation of human embryos of Carnegie collec-

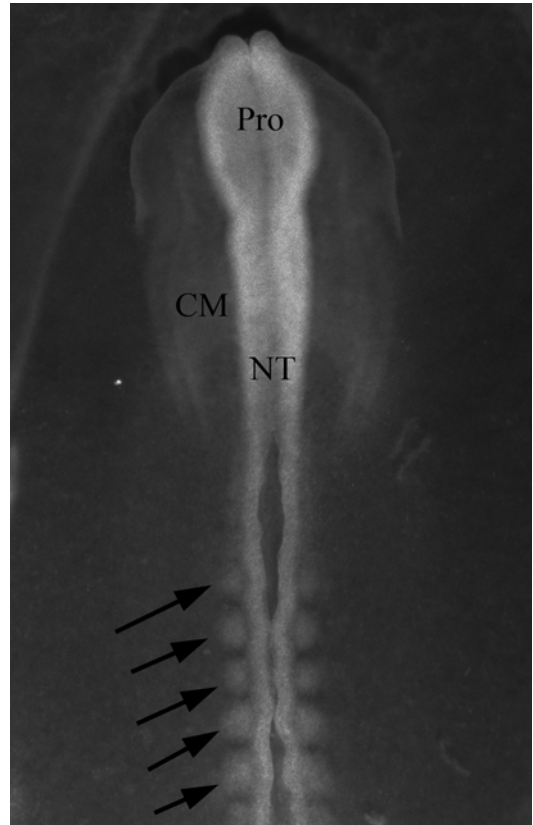


Fig. 2.1 Dorsal view of a chick embryo (8 somite stage) showing the neural tube (NT) that occupies the medial region and the paraxial mesoderm with the cephalic mesoderm (CM) and the somites (arrows)

tion contrarily to the statements of the other authors. This fact has only more valuable to us.

2.1.2 An Anatomical Lecture of the Development of the Occipital Bone

The classic description of medical anatomists, widespread in all their works, claims that the occipital bone of vertebrates is formed by four independent subunits. These are called: the basioccipital, the exoccipital, the supraoccipital, and the interparietal. A modern reader may reasonably wander about the relevance of this description for which the components of the occipital bone are in fact different morphogenetic elements. To unravel this mystery, we need to

appeal to the onset of ossification. Thus, the occipital bone that is one of the chondrocranium arises from a unique cartilaginous scaffold. Within the latter, ossification centers appear. Medical anatomists have therefore proposed that each of these points is actually a primitive bone that merges to create the definitive bones. This argument seems more obsolete now. Indeed, the endochondral ossification process develops late in development and does not prejudice the embryological data. Thus, the basioccipital, the exoccipital, and the supraoccipital cartilage matrix derived from a single primordium while the interparietal is a membranous bone. Sagacious readers, if they observe the primordial cartilage matrix, cannot recognize the different elements that have been described by the anatomists. Thus, it seems much more rigorous and much closer to the true reality of opposing a chondro-occipital (composed by the basioccipital, the exoccipital, and the supraoccipital) which is closely linked to the chondrocranium and an interparietal which is actually a bone of the skull vault the cells of which derived from neural crest.

2.1.3 Towards an Embryological Reading of the Occipital Bone

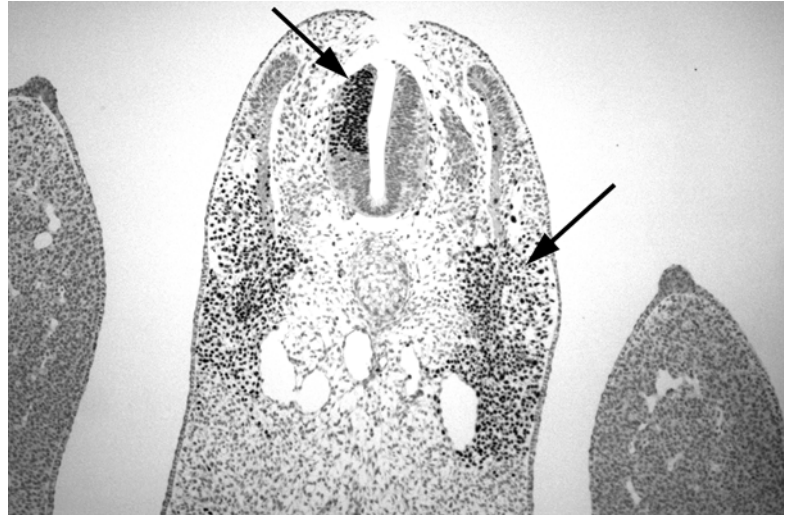
An avian fate map is available for the skull vault using the quail-chick chimera technique described by Nicole Le Douarin in 1969 [11]. This technique is based on the possibility of recognizing a nucleus of quail from that of chicken. Early studies were based on histochemical staining, the so-called Feulgen-Rossenbeck reaction, allowing to highlight DNA. In the quail, the heterochromatin is condensed and associated with the nucleolus when it is more diffuse in the chicken (Fig. 2.2). However, even if this technique has been very helpful, it generally does not allow immunostaining or in situ hybridization on the same sections. Only some very resistant antigens can produce an immunohistochemical reaction after Feulgen-Rossenbeck staining [12]. Thus, to differentiate the nuclei of quail and chicken, a monoclonal antibody (QCPN) that specifically recognizes quail nuclei but not the chicken is currently used (Fig. 2.3). This technique allows to constructing fate maps of embryonic territories. Consequently,



Fig. 2.2 A quail-chick chimera observed after Feulgen-Rossenbeck reaction. Neural crest cells from a quail embryo have been grafted into a chick host. Neurons of

the autonomous ganglion present a concentrated heterochromatin and are thus derived from the quail (*arrows*). The environment is derived from the chick (*arrowheads*)

Fig. 2.3 A quail-chick chimera observed after QCPN immunostaining. Tail bud cells from a quail embryo have been grafted into a chick host. The cells of the donor participate into the formation of the neural tube and the mesoderm (*arrows*)



Couly et al. [13] show that the skull has three distinct embryonic origins: the cephalic mesoderm (corresponding to the paraxial mesoderm located rostrally to the first somite) yields the supraoccipital, the postorbital, the orbitosphenoid, and the pleurospenoid bones. The first somites yield the exo- and the basioccipital. All the rest of the skull derives from the mesencephalic neural crest. In this study, the origin of the interparietal bone (a very tiny structure in birds located between the parietal and the supraoccipital bones) has not been reported. Furthermore, the cells of the mesencephalic neural crest differentiate into meninges, smooth muscle fibers of the media of the brain and cephalic vessels, and dermal cells. This work has been challenged more recently by a second group of embryologists [14]. Although the experimental approach is similar in both groups, the results are discordant. In particular, the exooccipital only derives from the first somite according to Couly et al. while Huang et al. recognize the participation of the first five somites. Similarly, the basioccipital comes from somites 2, 3, and 4 for Couly et al. and from the first five somites for Huang et al. The supraoccipital origin would be the cephalic mesoderm for Couly et al. whereas it is considered to derive from somites 1 and 2 for Huang et al. These conflicting results show the difficulty of interpreting experimental manipulations performed in the embryo. They must invite us to be very cautious in the use of these works for the understanding of human malformations.

Indeed, one cannot prefer the results of a group compared to the other. Furthermore, the shape of the occipital bone has changed considerably during evolution of vertebrates, and it is impossible to affirm the total homology between the different parts of this bone in birds and humans.

An alternative way to study the fate of neural crest cells in mouse embryos has been proposed recently [15]. The bacterial gene *Cre* (coding for the recombinase enzyme) is driven by the promoter sequence of the *Wnt1* gene. This gene is expressed by some cells of the neural tube and by neural crest cells. By crossing this transgenic line with the R26R line, it is possible to generate mice in which the *lacZ* gene (coding for beta galactosidase) is activated only in cells that express *Wnt1*. Revealing galactosidase activity allows to follow the fate of neural crest cells. In mouse, neural crest cells give rise to the nasal, the alisphenoid, the squamosal, the frontal, and the center of the interparietal bones. In contrast to the results published for birds, parietal bones do not arise from neural crest cells in the mouse.

Some of the discrepancies between the results gained by these studies can be easily explained. The orbitosphenoid participates in the formation of the vault in birds whereas it only gives rise to the lesser wing of the sphenoid in mammals. The postorbital bone does not exist in mammals. The pleurospenoid is not homologous to the alisphenoid that is the mammalian component of the vault. The alisphenoid derives from the palato-quadrate (the reptilian epipterygoid bone). This structure develops from

neural crest cells of the first branchial arch. The main discrepancies between the two studies correspond to the interparietal and the parietal bones. The interparietal bone gives rise to the part of the occipital bone located above the cerebellar tentorium. We can conclude that in mammals the occipital bone derives from both the mesoderm and the neural crest. The parietal bone is thought to arise from neural crest in birds and from mesoderm in mammals. This could represent a difference between these two species. Furthermore, Jiang et al. [15] doubt about the validity of Couly's results since the histological section Couly showed to prove the neural crest origin of the avian parietal bone does not pass through that bone.

2.1.4 The Genetic Lecture of the Development

The discovery of genes encoding the identity of a region has been gained from embryonic studies on *Drosophila melanogaster*. From the late nineteenth century, William Bateson observed transformations of a segment of invertebrate in another segment. He proposed the term "homeotic transformation" to account for this phenomenon. These transformations are particularly well known in *Drosophila*, a model organism in genetics used as early as the early twentieth century. Thus, a *Drosophila* wearing legs instead of antennae is called *Antennapedia*. Many other types of such transformations have been described (e.g., a *Drosophila* having eight legs instead of six, a *Drosophila* bearing four wings instead of two). The genetic study obtained by crossing these animals showed that only one gene is mutated. Homeotic transformation is actually a homeotic mutation and the causative gene is responsible for segmental identity. With the advent of molecular biology, genes responsible for homeotic mutations have been cloned. These genes encode transcription factors having a binding domain comprising three DNA helices. This domain was naturally called homeodomain by reference to the term homeotic. The region of DNA that encodes the homeodomain is called the homeobox. These genes are grouped into clusters in the DNA. Homologous genes to the drosophilian ones were found in all vertebrates. In these species, there are four clusters (A, B, C, and

D) carried by different chromosomes. Each cluster contains up to 13 genes (rated from 1 for the gene which is located on the more 5' extremity of the cluster to 13 for the most 3'). Each gene is defined by the term *Hox* (for Homeobox) a letter and a number. Genes whose location is the 5' extremity of the cluster are expressed more rostrally whereas those that lie in the 3' extremity are expressed more caudally. This property was described by Ed Lewis as the law of spatial colinearity.

This chapter has gained more and more importance nowadays. This could be explained by both the development of molecular biology and the development of human genetics. In terms of genetic regulations of morphogenesis, the vault of the skull can be divided into two parts: the supraoccipital bone and the rest of the vault.

2.1.4.1 *Hox d4*, a Key Gene for Vertebral Identity

The paraxial mesoderm of vertebrates is organized according to the rostrocaudal axis. The most rostral part of this domain represents the cephalic mesoderm (Fig. 2.1). All the rest of the paraxial mesoderm is segmented into somites that represent metameric units extending to the tip of the embryonic tail. The four first somites are called occipital somites since they contribute to the formation of the occipital bone [13, 14]. The fifth somite is the first cervical somite that participates into the formation of the first cervical vertebra.

Hox d4 is normally expressed from the first cervical vertebra caudalwards. If one forces the expression of *Hox d4* in more rostral mesoderm, both the supraoccipital and the exoccipital bones are transformed into occipital vertebrae [16]. This experiment indicates that the sole expression of *Hox d4* in the paraxial mesoderm is sufficient to induce the identity of a vertebra and to prevent the formation of the supraoccipital bone. It is important to note that the rest of the vault is normal in this experiment.

2.1.4.2 *Mhox (Prx-1)* Gene, a Key Regulator for the Formation of the Supraoccipital Bone

The *Mhox* gene codes for a transcription factor. The knockout of this gene leads to a total absence of the supraoccipital bone while the rest of the vault

is normally formed [17]. It is interesting to note that the interparietal bone is not affected by this mutation. This result shows that these two bones, which eventually fuse to form the contribution of the occipital bone to the vault, are not regulated by the same genes. Furthermore, other facial bones are involved by this knockout showing that the *Mhox* gene is not specific for the supraoccipital bone but participates into other patterning programs affecting the development of different bones.

2.2 The Meninges Are Responsible for the Proper Development of the Posterior Fossa Structures

2.2.1 Histological Description of the Meninges in Humans

The meninges form a wrap that surrounds the central nervous system (see [18] for a review). They consist of the dura mater (or pachymeninge) and a complex called arachnoid-pia mater (or leptomeninges). The dura is formed by collagen fibers grouped into dense bundles and fibroblasts. However, one can notice a heterogeneity within this pachymeninge: indeed, the innermost layers are composed of flattened and jointed cells (neurothelium or subdural mesothelium). Neurothelium is limited to the inner side by a basement membrane that separates it from the arachnoid. Neurothelium cells were also called dural border cells.

The arachnoid may be subdivided into two distinct layers. The outermost layer is composed by the arachnoid border cells (flat cells). These cells are joined by both gap junctions and desmosomes. These junctional devices reflect the role of barrier played by the external arachnoid. The innermost layer of the arachnoid consists in trabeculae that unit this layer to the pia mater. Intertrabecular domains form the subarachnoid space in which the CSF.

The pia mater is composed of a single cell layer in rodents and one to three layers in humans. Junctions that bind cells of the pia mater are the same as those that unite the arachnoid cells.

There are no histological criteria for distinguishing arachnoid trabecular cells from pial cells. Thus, modern histologists speak of leptomeningeal cells to define them.

Several authors have described a discontinuous pia mater in human. These postmortem studies are not correct and this discontinuity is actually an artifact. Finally, between the pia mater and the brain surface, lies a space (called subpial space) that contains a few collagen fibers.

2.2.2 Embryonic Origin of the Meninges

The embryological origin of the meninges is a topic that is widely established and demonstrated by developmental biologists. Thus, the old theory, now obsolete, which means that leptomeninges have a different origin as the pachymeninges and going back to the late 1920s is outdated. However, this theory remains in certain articles [19]. It is now well established that this information is obsolete particularly in higher vertebrates.

The origin of the meninges has been reestablished first in birds using the technique described by Nicole Le Douarin. The application of this technique showed that all cells of the spinal meninges are derived from somites [20, 21] and not the neural tube [22]. The cephalic mesoderm that is the rostral extension of the paraxial mesoderm (Fig. 2.1) gives rise to the meninges of the brain stem and cerebellum. In contrast, meningeal forebrain cells derive from neural crest and are generated by the cephalic mesectoderm (that is to say the mesoderm that is formed from the ectoderm) [23]. This origin in mammals has been confirmed by the work of Jiang et al. [15].

In conclusion, cells of the meninges (both pachymeninges and leptomeninges) sitting in the posterior fossa are derived from the cephalic mesoderm, a region of the paraxial mesoderm.

2.2.3 Developmental Interactions Assumed by the Meninges

The meninges are often seen as supporting tissues whose developmental role is relatively low.

Even if this assertion is widespread in the medical literature, it is false. First, the meninges induce the formation of the superficial glia limitans. Indeed, at the interface between neural tissue and meningeal region, develops a highly elaborate structure consisting of a variety of elements. The outermost region of the nervous system is composed of astrocytic feet that are joined together by gap junctions and form the glia limitans. This structure is covered with a basal lamina that is composed of laminin and collagen IV [24].

To highlight and demonstrate the role played by the cells of the meninges on the formation of the interface between the central nervous system and the outside, it is possible to selectively destroy the meningeal cells by injecting 6 OH dopamine in the subarachnoid space in the rodent newborn (see [25] for a review). In this case, the destruction of meningeal cells leads to a disappearance of the basement membrane and glia limitans [25].

The situation became even more complex now. These latest features are only the more fascinating because they introduce the problem of regionalization of cells according to the anteroposterior axis. Most medical authors consider that the meninges form a homogeneous tissue along this body axis. However, a new study shatters such insurance. Stephen Goff's group in La Jolla [26] generated a mouse that has both a conditional deletion of the *Abl* gene expressed only in neuronal and glial cells on a genetic background deficient in *Arg*. *Abl* and *Arg* are genes that code for two non-receptor tyrosine kinases that are involved in the transduction of the signal from the cell surface to the cytoskeleton. They observed that in this case, there is a severe cerebellar dysplasia with loss of basement membrane, an aspect which is reminiscent of that observed after local destruction of the meninges. Cautious analysis of this mutant shows that the defect is not related to impairment of cerebellar granule cells but to an intrinsic defect of the radial glia and Bergmann cells of the cerebellum. Besides the cognitive interest of such an outcome, it seems important to indicate that this defect only affects the cerebellum and that such topographic specificity could explain the existence of malformative lesions involving only parts of neuraxis in humans or pro-

liferative lesions specifically related to a particular anatomic location.

2.3 The Rhombomeres Are Segmented Structures That Generate the Brain Stem

In vertebrates, including humans, compartments (repetitive units) can be detected in the body of the adult. These are the case of both ribs and vertebrae. Regarding the central nervous system, such a research approach of the compartments is very old, since von Baer was the first to make reference to them from 1828 (Fig. 2.4). Now

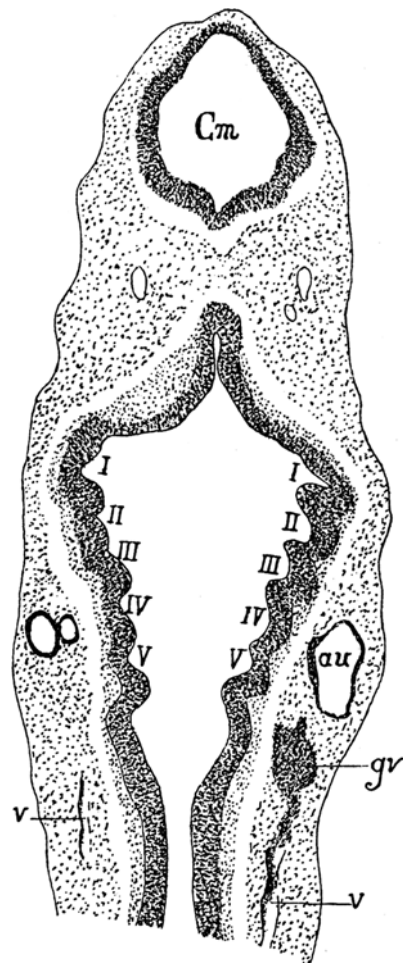


Fig. 2.4 The rhombomeres (I, II, III, IV, V) in a section from a pig embryo as illustrated in [43]. *au* otic vesicle, *Cm* midbrain, *gv* ganglion of the X cranial nerve, *v* X cranial nerve

these hindbrain compartments are baptized under the term of rhombomeres. In higher vertebrates, seven rhombomeres are individualized while the eighth have blurred boundaries (see [27] for a review).

The rhombomeres have histological individualization. Indeed, if we make histological sections in the embryonic hindbrain, we see that the inter-rhombomere boundaries are marked by a decrease in cell density. This purely morphological feature brings an element that is very tenuous sustaining the hypothesis that rhombomeres are in fact real compartments at the embryological meaning of the term. The second argument which argues for such a role played by rhombomeres is that neurons in even rhombomeres develop earlier than those of odd rhombomeres. Thus, this fact suggests that the genetic system controlling rhombomeric development differs if they are even or odd.

A third argument for thinking that the rhombomeres are embryological compartments was obtained by intracellular iontophoresis by Fraser et al. [28]. These authors injected a fluorescent dye of high molecular weight, lysinated rhodamine dextran (or LRD). This product has the distinction of remaining in the cytoplasm of the injected cell and does not pass through gap junctions. The authors use the chick embryo because it is more accessible during the embryonic period. Before the stage of 13 somites, there is no defined compartments. However, if the injection takes place immediately after this stage, the progeny of the injected cells remains within the inter-rhombomere limit (Fig. 2.5). This fact therefore shows that the inter-rhombomere boundary is established very gradually during development. Moreover, once this limit is established, the rhombomeres are true compartments within the meaning of embryological term. Yet this very net results worth to be modulated. Indeed, if we observe the embryos injected later than has been done, about 5 % of the clones do not meet the famous inter-rhombomere boundary [29]. In conclusion, the inter-rhombomere boundaries are not inviolable borders but they are limits that all the cells cannot cross freely.

How can we explain the absence of cell mixing between rhombomeres? If an even-numbered rhombomere is grafted adjacent to an odd-numbered

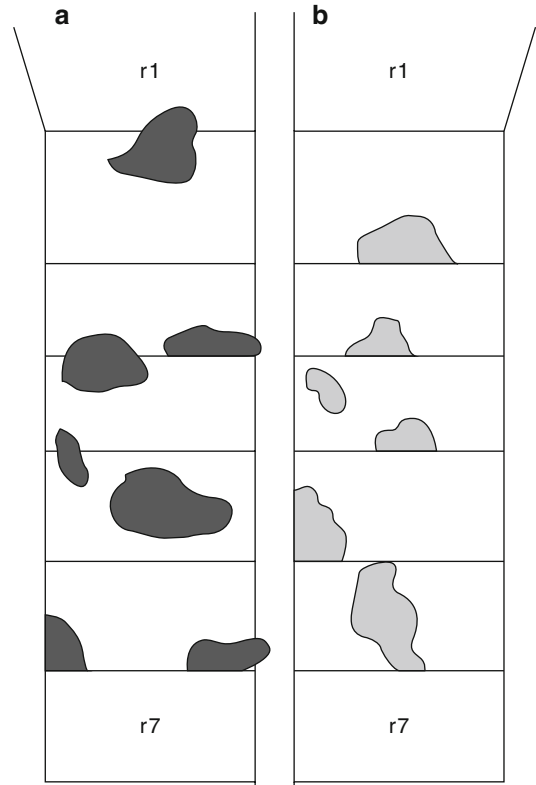


Fig. 2.5 Appearance of the rhombencephalic clones after a single cell injection of LRD. **(a)** If the injection is performed before boundary formation, some clones spread across the inter-rhombomeric limits. **(b)** If the injection is performed after the formation of the boundaries, the majority of clones does not cross the limits (Reproduced with permission from [27])

rhombomere, the cells of the grafted rhombomere will not mix with the cells of the host. In contrast, if an odd-numbered rhombomere is grafted adjacent to another odd-numbered rhombomere, the cells of the two rhombomeres intensively mix [30].

This result suggests that there are surface molecules that cause the repulsion of cells coming from an even rhombomere and placed into an odd environment. The molecular system in question is that of ephrin-Eph. These molecules are associated to the cell membrane. There are two classes of Eph-like molecules based on the presence or absence of a transmembrane domain. The members of Eph class A (A1–A8) have no transmembrane domain and are connected to the membrane by a glycosylphosphatidylinositol residue. Those of Eph class B (B1–B6) contain a transmembrane

domain. The EphAs bind to ephrins A (with the exception of EphA4). The EphBs bind to ephrins B. Recognition of ephrin by Eph generally causes a repellent effect. There are some cases where the effect is attractive. Rhombomeres 3 and 5 express EphA4, whereas rhombomeres 2, 4, and 6 express ephrin B2 [31]. The forced expression of EphA4 induces a cell with an odd identity while that of ephrin B2 induces an even identity. In conclusion, the ephrin-Eph system plays a role in controlling the inter-rhombomere boundaries.

Finally, some genes have an expression that is supportive of the role of rhombomeres in the hind-brain segmentation. Thus, *Hox b1* is expressed by the rhombomere 4 [32] and *Krox 20* by the rhombomeres 3 and 5 [32], as it is the case for *lunatic fringe* [33], *Kreisler* in rhombomeres 5 and 6 [34].

However, to be certain that these genes play a role in determining these segments or compartments, it is necessary to study the consequence of their inactivation in mice.

The *Kreisler* mutation was obtained by irradiation in the mouse and careful analysis of these showed that they lost rhombomeres 5 and 6. These rhombomeres are then replaced by a greatly enlarged rhombomere 4 [23]. The mutant mouse obtained by knock out gene *Krox-20* leads to a disappearance of rhombomeres 3 and 5 [24], that is to say rhombomeres within the grounds of which the gene is expressed.

2.4 Development of the Cerebellum

The phylotypic appearance of the cerebellum shows us that some very primitive species are devoid of granule cells. Such is the case for the amphioxus and hagfish. In the lamprey, shark and sturgeon, granule cells form two separate loci that are separated by the midline. From teleosts such as salmon, the cerebellum is an organ that fuses over the midline. These data show that the emergence of the cerebellum is a very old process on the phylogenetical background, suggesting that the molecular mechanisms involved in such an induction are largely conserved in all the vertebrate species.

2.4.1 The Isthmic Organizer

The cerebellum arises from the alar region of the metencephalon at the exact level of rhombomere 1. It is possible to induce diencephalon into cerebellum by placing it at the level of rhombomere 1. This result suggests that there are one or more molecules capable of inducing the differentiation of the grafted neural tube. The most serious candidate that was studied is FGF8 (which is a secreted protein that acts on a membrane receptor family belonging to the family of receptors with tyrosine kinase domain). *Fgf8* is expressed by a region located at the exact interface between the mesencephalon and the metencephalon called the isthmus (Fig. 2.6). It is possible to induce an ectopic cerebellum by increasing the amount of FGF8 pro-

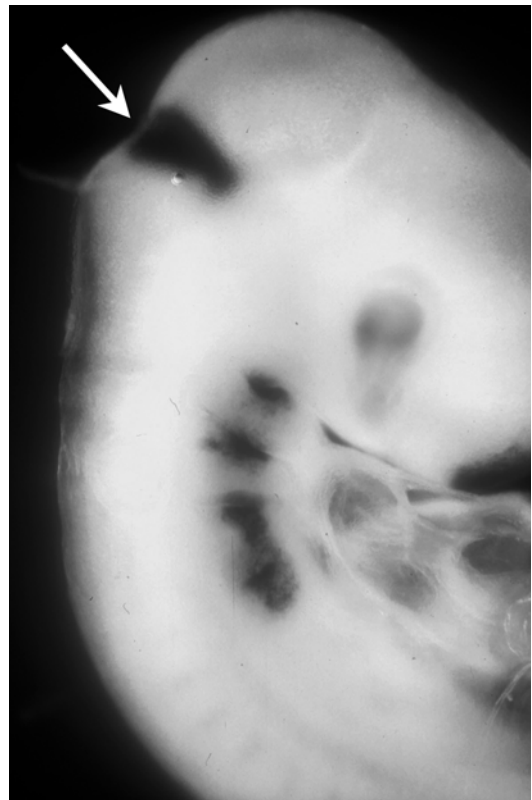


Fig. 2.6 In situ hybridization performed in toto on a 25-somite stage of a chick embryo. The probe is directed to detect mRNA specific for *Fgf8* gene. Note that the gene is strongly expressed at the isthmus region (namely, the border between mesencephalon and metencephalon) (arrow)

duced [35, 36]. Similarly, the conditional knock-out of *Fgf8* gene in mice can induce the absence of cerebellar differentiation [37]. These two experiments demonstrate that FGF8 is necessary and sufficient for differentiation of this region of the brain. Other FGFs are produced by this region but their expression is much wider and occurs later than *Fgf8*. In conclusion, the gene coding for FGF8 plays a crucial role in the induction of the cerebellar features by the metencephalon.

2.4.2 How to Control the Embryonic Position of the Isthmus

Very early, the anterior neural plate is regionalized, that is to say that certain regions express specific genes while others express a different set of genes. This set of genes expressed by the region and giving it a positional identity along the anteroposterior axis corresponds to a real molecular address. The anterior neural plate expresses the gene that encodes OTX2, a transcription factor. The caudal limit of expression of this gene corresponds to the level of the future isthmus. From this level and caudalwards, the neural plate expresses another gene, *Gbx2*. The expression of these two genes is mutually exclusive. The isthmus is formed at the exact border where the two areas of expression are meeting.

The activation of the receptor by FGF leads to an activation of a molecular cascade implying Ras, Raf, Mek, and eventually Erk that is translocated into the nucleus to induce the genes involved in cerebellar differentiation (reviewed in [38]).

2.4.3 The Formation of the Rhombic Lip

The primordium of the fourth ventricle develops very early during development and forms a diamond-shape structure. These anatomical features of this primordium can be explained by an expansion of the roof plate of the first rhombomeres. The region that marks the border between the roof plate and the rest of the neural tube is called the rhombic lip. R1 is composed by two parts: an anterior domain

lying rostrally to the fourth ventricle and a posterior part corresponding to the rostral rhombic lip (Fig. 2.7). The roof plate of this region is characterized by the expression of two genes, *Lmx1a* and *Gdf7* [39]. The roof plate will eventually give rise to choroid plexus but not to the cerebellum [39]. Using different genetic markers, Chizhilov et al. [39] decipher the rhombic lip into four subregions: c1 that expresses *Math1*, c2, c3, and c4 (Fig. 2.8). C1 cells will migrate rostrally and laterally to form the rostral rhombic lip stream which is fated to give rise to a secondary proliferative zone, the external granular layer. The roof plate secretes BMPs that are mandatory to induce the c1 phenotype [39]. In contrast,

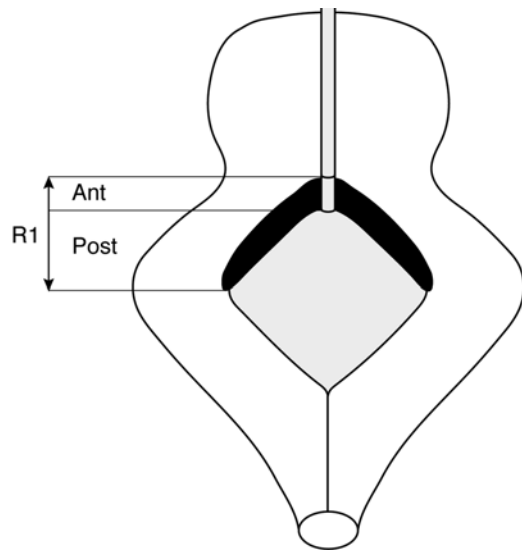


Fig. 2.7 Dorsal view showing the primordium of the fourth ventricle. The roof plate is indicated in gray. R1 territory could be divided into two parts: anterior and posterior. The primordium of the cerebellum (namely, the rhombic lip) is highlighted in black

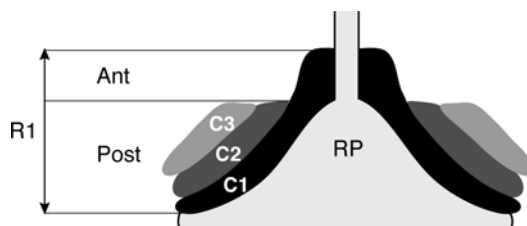


Fig. 2.8 The rhombic lip can be divided into bands oriented according to the mediolateral axis (c1, c2, c3)

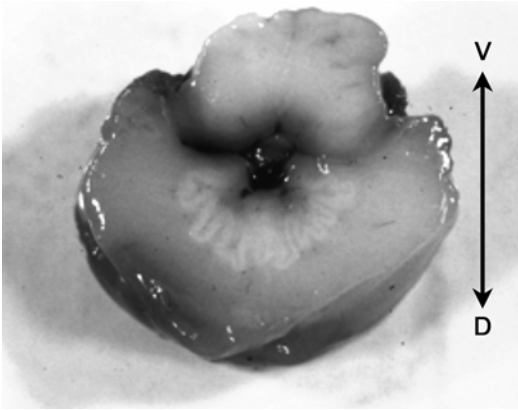


Fig. 2.9 Transverse section of the brain stem of a human fetus presenting the so-called rhombencephalosynapsis. Note that the medial part of the cerebellum is missing and that the lateral parts are fused together as can be evidenced by the fusion of the dentate nuclei

BMPs do not induce c2–4 cell-types but play a permissive role on these cells allowing their mitosis. Furthermore, at the early stages of development, the cerebellar primordium is separated into two parts by the midline. This isthmus midline plays an essential role for allowing cerebellar fusion [40]. So, in case of absence of midline fusion, the cerebellum will develop as two separate entities with a midline defect. The rostral part of c1 is fated to give rise to medial cerebellum whereas the caudal part of c1 will generate the lateral cerebellum [40]. So if the anterior c1 does not form, the lateral primordia will fuse on the midline forming the so-called rhombencephalosynapsis (Fig. 2.9).

2.4.4 Establishment of the Cells in the Cerebellum During Development

Neural tube cells usually divide at the ventricular zone. This general law does not apply to the cerebellum. The embryonic origin of the cerebellar cells has been extensively reviewed by Constantino Sotelo [41]. The ventricular zone of the primordium, corresponding to c2 subregion, gives rise to cerebellar neurons in the deep cerebellar ganglia and, with a slight temporal lag, to Purkinje cells and interneurons like basket cells, stellate cells,

and Golgi cells of the cerebellar cortex. The cells of the external granular layer give rise to cells of the internal granular layer (granule cells).

2.4.5 Molecular Control of Cell Proliferation in the External Granular Layer

The importance of this issue is not purely theoretical. Indeed, many authors agree that the origin of medulloblastomas seat in the external granular layer (reviewed in [42]). The molecular system implicated in the normal proliferation of the external granular layer is the sonic hedgehog (SHH) pathway [41, 42]. SHH is an analog of hedgehog, a morphogen molecule present in *Drosophila*. In mammals, this protein is synthesized and undergoes a cytoplasmic cleavage and two posttranslational modifications (a graft of a palmitoyl residue and a cholesterol radical). It is then secreted and acts on a 12-transmembrane receptor, the molecule patched. Patched is a part of a complex containing the smoothed receptor, a protein with seven transmembrane domains. In the absence of SHH, smoothed is inhibited and is not present at the plasma membrane. It is then sequestered in cytoplasmic vesicles. When SHH binds to patched, smoothed is exposed to the cytoplasmic membrane where it may act by phosphorylating the proteins GLI. These phosphorylated proteins are translocated to the nucleus where they act as transcription factors. It is interesting to note that the name of GLI comes from their isolation in tumor tissue (gliomas) in which they are hyper-expressed.

The role of the SHH pathway in humans has been demonstrated by the study of Gorlin syndrome. This rare genetic syndrome associates craniofacial dysmorphism, the emergence of basal cell skin cancers, and fewer cases of medulloblastoma. This syndrome has been localized to 9p22.3 in humans and corresponds to a mutation of the *PTCH* gene (encoding the receptor patched). However, only 10 % of the sporadic medulloblastomas can be explained by a somatic mutation affecting the gene *PTCH*.

The second human genetic syndrome that could account for the emergence of medulloblastomas

is Turcot syndrome (do not pronounce the final t). In this case, there is an association between colonic polyposis and medulloblastoma. The gene involved is the *APC* gene that plays a role in controlling the level of cytoplasmic beta-catenin (that is to say in the control of the canonical Wnt pathway). In case of mutation of the *APC* gene, the concentration of beta-catenin increases. The latter binds to TCF family members, allowing their nuclear translocation and consequently an increased rate of cell division. However, mutations in the *APC* gene play a negligible role in the occurrence of sporadic medulloblastomas even if, in these cases, an increase in the concentration of nuclear beta-catenin can be evidenced. This last observation calls us to search for other mutations in genes encoding molecules involved in the Wnt canonical pathway.

The development of structures of the posterior fossa is a largely studied problem in embryology. The processes that are involved are complex, especially since we know many genes that regulate the different stages of development. Knowledge of the broad outlines of these processes and their regulation is of interest to the pediatric neurosurgeons. Indeed, these mechanisms can help to understand some malformations (bone or nerve) and the emergence of tumors that affect this area particularly in children.

References

- Catala M (2003) Embryologie, développement précoce chez l'humain. Masson, Paris
- Encha-Razavi F, Escudier E (2003) Embryologie humaine; de la molécule à la clinique, 3rd edn. Masson, Paris
- Larsen WJ (2001) Human embryology, 3rd edn. Churchill-Livingstone, New York
- Moore KL, Persaud TVN (2003) The developing human, clinically oriented embryology, 7th edn. Saunders, Philadelphia
- Patten BM (1953) Human embryology, 2nd edn. Mc Graw Hill, New York
- Rabineau D (1989) Précis d'embryologie humaine. Ellipses, Paris
- Rouvière H (1978) Anatomie humaine. Descriptive, topographique et fonctionnelle, 11th edn. Masson, Paris
- Sadler TW (2004) Langman's medical embryology, 9th edn. Lippincott Williams and Wilkins, Philadelphia
- Tuchmann-Duplessis H (1965) Embryologie, travaux pratiques et enseignement dirigé. Fascicule premier. Masson, Paris
- O'Rahilly R, Müller F (1996) Human embryology and teratology, 2nd edn. Wiley Liss, New York
- Le Douarin N (1969) Details of the interphase nucleus in Japanese quail (*Coturnix coturnix japonica*). Bull Biol Fr Belg 103:435–452
- Catala M, Ziller C, Lapointe F, Le Douarin NM (2000) The developmental potentials of the caudal-most part of the neural crest are restricted to melonocytes and glia. Mech Dev 95:77–87
- Couly GF, Coltey PM, Le Douarin NM (1993) The triple origin of skull in higher vertebrates: a study in quail-chick chimeras. Development 117:409–429
- Huang R, Zhi Q, Patel K, Wilting J, Christ B (2000) Contribution of single somites to the skeleton and muscles of the occipital and cervical regions in avian embryos. Anat Embryol 202:375–383
- Jiang X, Iseki S, Maxson RE, Sucox HM, Morriss-Kay GM (2002) Tissue origins and interactions in the mammalian skull vault. Dev Biol 241:110–116
- Lufkin T, Mark M, Hart CP, Dollé P, Le Meur M, Chambon P (1992) Homeotic transformation of the occipital bones of the skull by ectopic expression of a homeobox gene. Nature 359:835–841
- Martin JF, Bradley A, Olson EN (1995) The paired-like homeo box gene *Mhox* is required for early events of skeletogenesis in multiple lineages. Genes Dev 9:1237–1249
- Weller RO (2005) Microscopic morphology and histology of the human meninges. Morphologie 89:22–34
- Sakka L, Chazal J (2005) The meninges, an anatomical point of view. Morphologie 89:35–42
- Bagnall KM, Higgins SJ, Sanders EJ (1988) The contribution made by a single somite to the vertebral column: experimental evidence of resegmentation using the quail-chick chimaera model. Development 103:69–85
- Bagnall KM, Higgins SJ, Sanders EJ (1989) The contribution made by cells from a single somite to tissues within a body segment and assessment of their integration with similar cells from adjacent segments. Development 107:931–943
- Halata Z, Grim M, Christ B (1990) Origin of the spinal cord meninges, sheaths of peripheral nerves, and cutaneous receptors including Merkel cells. An experimental and ultrastructural study with avian chimeras. Anat Embryol 37:529–537
- Couly GF, Coltey PM, Le Douarin NM (1992) The developmental fate of the cephalic mesoderm in quail-chick chimeras. Development 114:1–15
- Sievers J, Pehlemann FW, Gude S et al (1994) Meningeal cells organize the superficial glia limitans of the cerebellum and produce components of both the interstitial matrix and the basement membrane. J Neurocytol 23:135–149
- Catala M (2004) Development of the cerebrospinal fluid pathways during embryonic and fetal life in humans. In: Pediatric hydrocephalus. Springer, Milano
- Qiu Z, Cang Y, Goff SP (2010) Abl family tyrosine kinases are essential for basement membrane integrity

- and cortical lamination in the cerebellum. *J Neurosci* 30:14430–14439
27. Catala M (2005) Embryology of the brain. In: *Pediatric neuropathology, brain*. Springer, Milano
 28. Fraser S, Keynes R, Lumsden A (1990) Segmentation in the chick embryo hindbrain is defined by cell lineage restrictions. *Nature* 344:431–435
 29. Birgbauer E, Fraser SE (1994) Violation of cell lineage restriction compartments in the chick hindbrain. *Development* 120:1347–1356
 30. Guthrie S, Prince V, Lumsden A (1993) Selective dispersal of avian rhombomere cells in orthotopic and heterotopic grafts. *Development* 118:527–538
 31. Cooke J, Moens CB (2002) Boundary formation in the hindbrain: *Eph* only it were simple. *Trends Neurosci* 25:260–267
 32. Wilkinson D, Bhatt S, Chavrier P, Bravo R, Charnay P (1989) Segment-specific expression of a zinc-finger gene in the developing nervous system of the mouse. *Nature* 337:461–467
 33. Johnston SH, Ruaskolb C, Wilson R, Prabhakaran B, Irvine KD, Vogt TF (1997) A family of mammalian *Fringe* genes implicated in boundary determination and the *Notch* pathway. *Development* 124:2245–2254
 34. Mc Kay IJ, Muchamore I, Krumlauf R, Maden M, Lumsden A, Lexis J (1994) The Kreisler mouse: a hindbrain segmentation mutant that lacks two rhombomeres. *Development* 120:2199–2221
 35. Crossley PH, Martinez S, Martin GR (1996) Midbrain development induced by FGF8 in the chick embryo. *Nature* 380:66–68
 36. Liu A, Losos K, Joyner AL (1999) FGF8 can activate Gbx2 and transform regions of rostral mouse brain into a hindbrain fate. *Development* 126:4827–4838
 37. Meyers EN, Lewandoski M, Martin GR (1998) An *Fgf8* mutant allelic series generated by Cre- and Flp-mediated recombination. *Nat Genet* 18:136–141
 38. Nakamura H, Sato T, Suzuki-Hirano A (2008) Isthmus organizer for mesencephalon and metencephalon. *Dev Growth Differ* 50:S113–S118
 39. Chizhilov VV, Lindgren AG, Currie DS, Rose MF, Monuki ES, Mille KJ (2006) The roof plate regulates cerebellar cell-type specification and proliferation. *Development* 133:2793–2804
 40. Louvi A, Alexandre P, Métin C, Wurst W (2003) The isthmic neuroepithelium is essential for cerebellar midline fusion. *Development* 130:5319–5330
 41. Sotelo C (2004) Cellular and genetic regulation of the development of the cerebellar system. *Prog Neurobiol* 72:295–339
 42. Raffel C (2004) Medulloblastoma: molecular genetics and animal models. *Neoplasia* 6:310–322
 43. Prenant A. *Eléments d'Embryologie de l'homme et des vertébrés*. G. Steinheil, Paris. 1896.

The Anatomy of the Posterior Cranial Fossa

3

Aşkın Şeker and Albert L. Rhoton Jr.

The posterior cranial fossa, the largest and deepest of the three cranial fossae, contains the most complex intracranial anatomy. Here, in approximately one-eighth the intracranial space, are found the pathways regulating consciousness, vital autonomic functions, and motor activities and sensory reception for the head, body, and extremities, in addition to the centers for controlling balance and gait. Only 2 of the 12 pairs of cranial nerves are located entirely outside the posterior fossa; the ten other pairs have a segment within the posterior fossa [10, 12] (Fig. 3.1). The posterior fossa is strategically situated at the outlet of the cerebrospinal fluid flow from the ventricular system. The arterial relationships are especially complex, with the vertebral and basilar arteries having relatively inaccessible segments deep in front of the brainstem and the major cerebellar arteries coursing in relation to multiple sets of cranial nerves before reaching the cerebellum [3, 4, 7, 8].

The posterior fossa posteriorly is surrounded by the muscles attached to the occipital bone and upper cervical vertebrae (Fig. 3.1). The trapezius

covers the back of the head and neck. It extends from the medial half of the superior nuchal line, the external occipital protuberance, and the spinous processes of the cervical and thoracic vertebrae and converges on the shoulder to attach to the scapula and the lateral third of the clavicle. The sternocleidomastoid passes obliquely downward across the side of the neck from the lateral half of the superior nuchal line and mastoid process to the upper part of the sternum and the adjacent part of the clavicle. This muscle divides the side of the neck into an anterior triangle and a posterior triangle. The anterior triangle is bounded posteriorly by the anterior border of the sternocleidomastoid, above by the mandible, and anteriorly by the median line of the neck; the posterior triangle is bounded in front by the posterior border of the sternocleidomastoid, below by the middle third of the clavicle, and behind by the anterior margin of the trapezius. The splenius capitis, situated deep to and partially covered by the trapezius and sternocleidomastoid, extends from the bone below the lateral third of the superior nuchal line to the spinous processes of the lower cervical and upper thoracic vertebrae. Two muscles, both of which are situated deep to the splenius capitis and sternocleidomastoid and attach below to the upper thoracic and lower cervical vertebrae, are the semispinalis capitis, which attaches above in the area between the superior and inferior nuchal lines beginning medially at the external occipital crest and extending laterally to the occipitomastoid

A. Şeker, M.D. (✉)
Department Of Neurosurgery, Marmara University,
Istanbul, Turkey
e-mail: askinseker@hotmail.com

A.L. Rhoton Jr., M.D.
Department of Neurosurgery, Florida University,
100625, Gainesville, FL 32610, USA
e-mail: rhoton@neurosurgery.ufl.edu

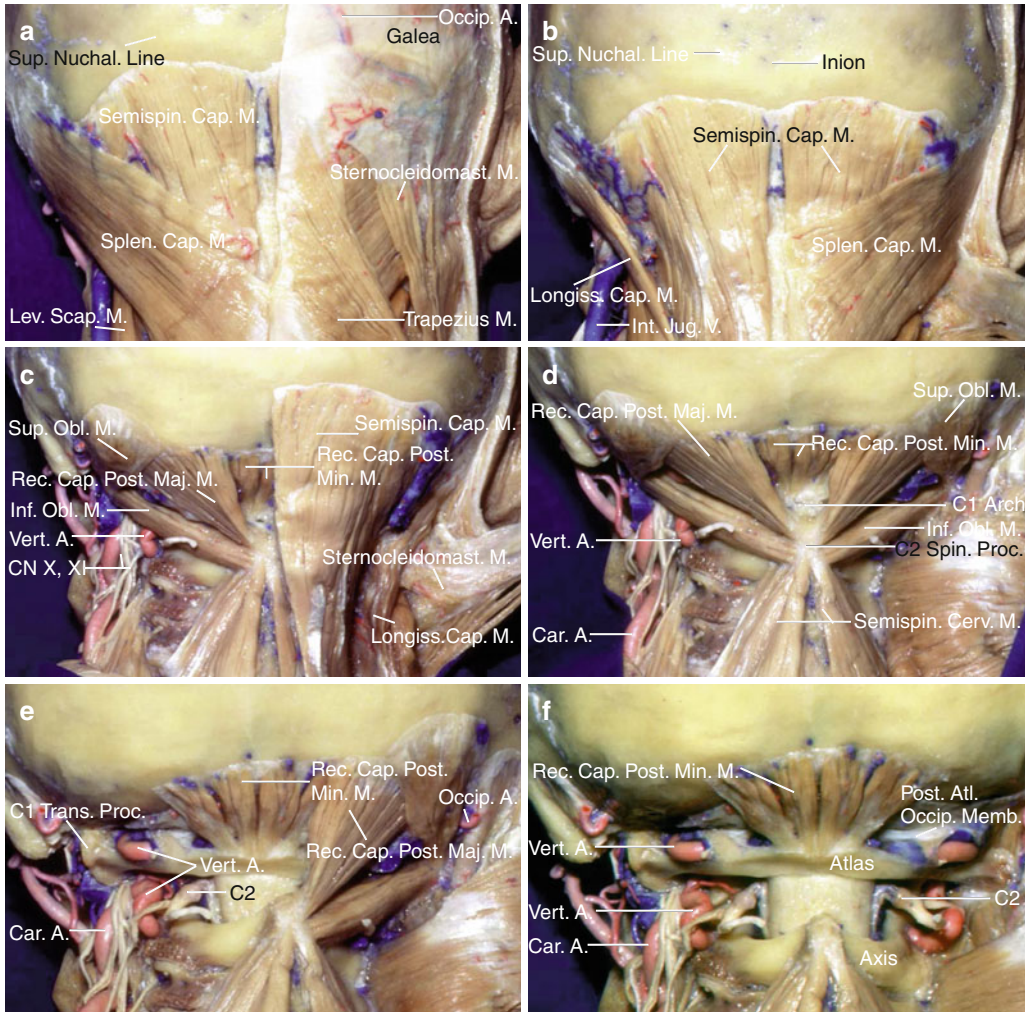


Fig. 3.1 Suboccipital muscles. Stepwise dissection. (a) The right trapezius and sternocleidomastoid have been preserved. The left trapezius and sternocleidomastoid have been reflected along with the galea aponeurotica to expose the underlying semispinalis capitis, splenius capitis, and levator scapulae. (b) The right sternocleidomastoid and trapezius have been reflected to expose the splenius capitis. The left splenius capitis has been removed to expose the underlying semispinalis and longissimus capitis. (c) The right splenius capitis has been removed to expose the semispinalis and longissimus capitis. The left semispinalis and longissimus capitis have been removed to expose the suboccipital triangle formed by the superior oblique, which passes from the C1 transverse process to the occipital bone; the inferior oblique, which extends from the transverse process of C1 to the spinous process of C2; and the rectus capitis posterior major, which extends from the occipital bone below the inferior nuchal line to the spinous process of C2. The vertebral artery courses in the depths of the suboccipital triangle as it passes behind the superior facet of C1 and across the upper edge of the posterior atlantal arch. (d) Both semispinalis capitis muscles have been reflected laterally to expose the suboccipital triangles

bilaterally. (e) The muscles forming the left suboccipital triangle have been removed. The vertebral artery ascends slightly lateral from the transverse process of C2 to reach the transverse process of C1 and turns medially behind the superior facet of C1 to reach the upper surface of the posterior arch of C1. The C2 ganglion is located between the posterior arch of C1 and the lamina of C2. The dorsal ramus of C2 produces a medial branch that forms the majority of the greater occipital nerve. (f) The muscles forming both suboccipital triangles have been removed. The rectus capitis posterior minor, which extends from the posterior arch of C1 to the occipital bone below the inferior nuchal line, has been preserved. The vertebral arteries cross the posterior arch of the atlas and penetrate the posterior atlanto-occipital membrane to reach the dura. A artery, *Atl* atlanto-, *Cap* capitis, *Car* carotid, *CN* cranial nerve, *Inf* inferior, *Int* internal, *Jug* jugular, *Lev* levator, *Longiss* longissimus, *M* muscle, *Maj* major, *Memb* membrane, *Min* minor, *Obl* oblique, *Occip* occipital, *Post* posterior, *Proc* process, *Rec* rectus, *Scap* scapulae, *Semispin* semispinalis, *Spin* spinalis, *Splen* splenius, *Sternocleidomast* sternocleidomastoid, *Sup* superior, *Trans* transverse, *V* vein, *Vert* vertebral

junction, and the longissimus capitis muscle, which attaches above to the posterior margin of the mastoid process.

The suboccipital muscles, located in the next layer, are a group of muscles situated deep to the splenius, semispinalis, and longissimus capitis in the suboccipital area. This group includes the superior oblique, which extends from the area lateral to the semispinalis capitis between the superior and inferior nuchal lines to the transverse process of the atlas; the inferior oblique, which extends from the spinous process and lamina of the axis to the transverse process of the atlas; the rectus capitis posterior major, which extends from and below the lateral part of the inferior nuchal line to the spine of the axis; and the rectus capitis posterior minor, which is situated medial to and is partially covered by the rectus capitis posterior major, extends from the medial part and below the inferior nuchal line to the tubercle on the posterior arch of the atlas. The suboccipital triangle is a region bounded above and medially by the rectus capitis posterior major, above and laterally by the superior oblique, and below and laterally by the inferior oblique (Fig. 3.1). It is covered by the semispinalis capitis medially and by the splenius capitis laterally. The floor of the triangle is formed by the posterior atlanto-occipital membrane and the posterior arch of the atlas. The structures in the triangle are the terminal extradural segment of the vertebral artery and the first cervical nerve.

The platysma is a broad sheet extending downward from the lower part of the face and across the clavicle to the fascia covering the pectoralis major and deltoid. The anterior vertebral muscles insert on the clival part of the occipital bone anterior to the foramen magnum. This group includes the longus colli, which attach to the anterior surface of the vertebral column between the atlas and the third thoracic vertebra; the longus capitis, which extends from the clivus in front of the foramen magnum to the transverse processes of the third through the sixth cervical vertebrae; the rectus capitis anterior, which is situated behind the upper part of the longus capitis and extends from the occipital bone in front of the occipital condyle to the anterior surface of the lateral mass and transverse process of the atlas; and the rectus capitis lateralis, which extends

from the jugular process of the occipital bone to the transverse process of the atlas (Fig. 3.1).

The posterior fossa extends from the tentorial incisura, through which it communicates with the supratentorial space, to the foramen magnum, through which it communicates with the spinal canal. It is surrounded by the occipital, temporal, parietal, and sphenoid bones (Figs. 3.2 and 3.3). It is bounded in front by the dorsum sellae, the posterior part of the sphenoid body, and the clival part of the occipital bone; behind by the lower portion of the squamosal part of the occipital bone; and on each side by the petrous and mastoid parts of the temporal bone, the lateral part of the occipital bone, and above and behind by a small part of the mastoid angle of the parietal bone. Its intracranial surface is penetrated by the jugular foramen, internal acoustic meatus, hypoglossal canal, the vestibular and cochlear aqueducts, and several venous emissary foramina (Fig. 3.4).

The cortical surfaces are divided on the basis of the structures they face, or along which they may be exposed, to make this description more readily applicable to the operative setting. The first surface, the tentorial surface, faces the tentorium and is retracted in a supracerebellar approach; the second surface, the suboccipital surface, is located below and between the lateral and sigmoid sinuses and is exposed in a suboccipital craniectomy; and the third surface, the petrosal surface, faces forward toward the posterior surface of the petrous bone and is retracted to expose the cerebellopontine angle. Each of the surfaces has the vermis in the midline and the hemispheres laterally and is divided by a major fissure named on the basis of the surface that it divides. The hemispheric lobules forming each of the three surfaces commonly overlap onto and form a part of the adjacent surfaces [10]. The fissures dividing the three cortical surfaces are to be distinguished from the fissures between the cerebellum and the brainstem (Fig. 3.5).

3.1 Tentorial Surface

The tentorial surface faces and conforms to the lower surface of the tentorium (Fig. 3.5). The anteromedial part of this surface, the apex, formed by the anterior vermis, is the highest

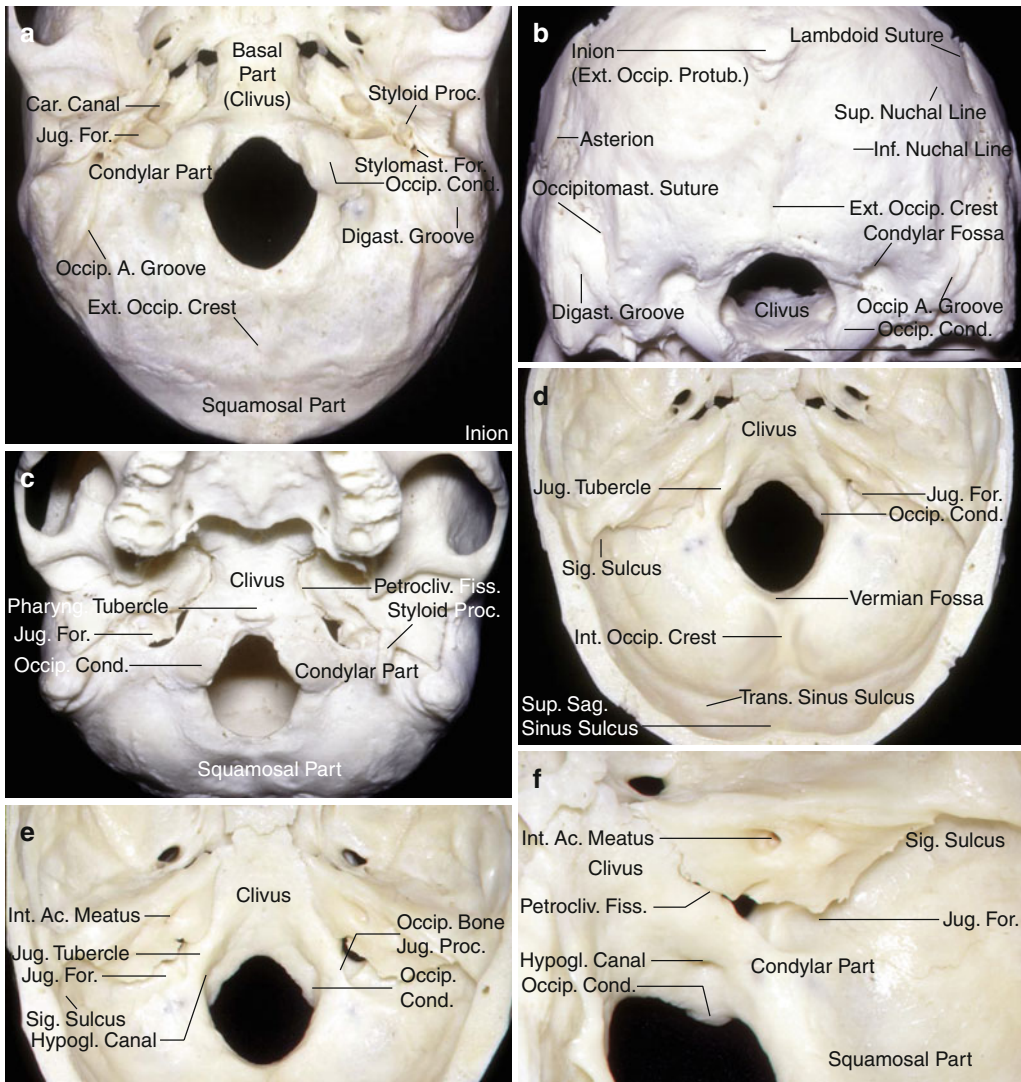


Fig. 3.2 Occipital bone and foramen magnum. (a) Inferior view. (b) Posteroinferior view. (c) Anterior-inferior view. (d) Superior view. (e) Posterosuperior view. (f) Oblique posterosuperior view. The occipital bone surrounds the oval-shaped foramen magnum, which is wider posteriorly than anteriorly. The occipital bone is divided into a squamosal part located above and behind the foramen magnum, a basal (clival) part situated in front of the foramen magnum, and paired condylar parts located lateral to the foramen magnum. The convex external surface of the squamosal part has several prominences. The largest prominence, the external occipital protuberance (inion), is situated at the central part of the external surface. The superior nuchal line radiates laterally from the protuberance. A vertical ridge, the external occipital crest, descends from the external occipital protuberance to the midpoint of the posterior margin of the foramen magnum. The inferior nuchal lines run laterally on both sides from the midpoint of the crest. The internal surface is divided into four unequal fossae by the sulcus of the superior sagittal sinus, the internal occipital crest, and the sulci for the

transverse sinuses. The basilar part of the occipital bone, which is also referred to as the clivus, is a thick quadrangular plate of bone that extends forward and upward to join the sphenoid bone just below the dorsum sellae. The clivus is separated on each side from the petrous part of the temporal bone by the petroclivial fissure that ends posteriorly at the jugular foramen. The condylar parts of the occipital bone, on which the occipital condyles are located, are situated lateral to the foramen magnum on the external surface. The hypoglossal canal is situated above the condyle. The jugular foramen is bordered posteriorly by the jugular process of the occipital bone and anteriorly by the jugular fossa of the petrous temporal bone. The jugular tubercle lies on the internal surface above the hypoglossal canal. A artery, *Ac* acoustic, *Car* carotid, *Cond* condyle, *Digast* digastric, *Ext* external, *Fiss* fissure, *For* foramen, *Hypogl* hypoglossal, *Inf* inferior, *Jug* jugular, *Occipitomast* occipitomastoid, *Occip* occipital, *Petrocliv* petroclivial, *Pharyng* pharyngeal, *Proc* process, *Protrub* protuberance, *Sag* sagittal, *Sig* sigmoid, *Sup* superior, *Trans* transverse

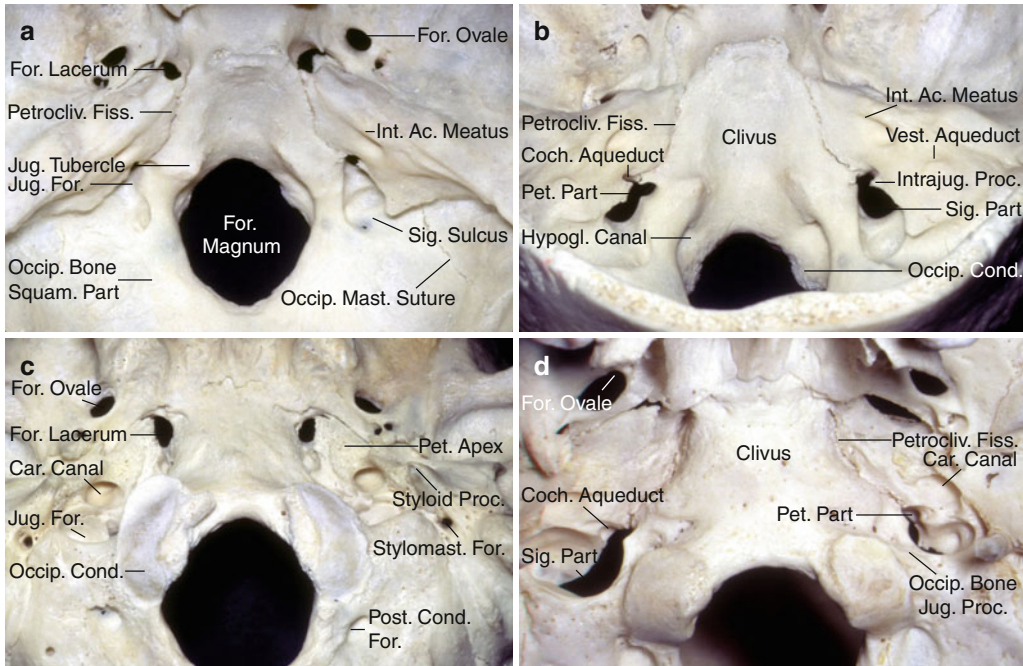


Fig. 3.3 Osseous relationships. (a) The jugular foramen is located between the temporal and occipital bones. (b) The view directed from posterior and superior shows the shape of the foramen, which is not seen on the direct superior view. The glossopharyngeal, vagus, and accessory nerves pass through the intrajugular portion of the foramen located between the sigmoid and petrosal parts. (c) Jugular foramen viewed from directly below. (d) The view directed from anterior and backward reveals the shape of the jugular foramen.

The posterior margin of the foramen is formed by the jugular process of the occipital bone, which connects the basal (clival) part of the occipital bone to the squamosal part. *Ac* acoustic, *Car* carotid, *Coch* cochlear, *Cond* condyle, *Fiss* fissure, *For* foramen, *Hypogl* hypoglossal, *Int* internal, *Intrajug* intrajugular, *Jug* jugular, *Mast* mastoid, *Occip* occipital, *Pet* petrous, *Petrocliv* petroclival, *Post* posterior, *Proc* process, *Sig* sigmoid, *Squam* squamosal, *Stylomast* stylomastoid, *Temp* temporal, *Vest* vestibular

point on the cerebellum. This surface slopes downward from its anteromedial to its posterolateral edge. On the tentorial surface, the transition from the vermis to the hemispheres is smooth and not marked by the deep fissures on the suboccipital surface between the vermis and hemispheres. Deep notches, the anterior and posterior cerebellar incisurae, groove the anterior and posterior edges of the tentorial surface in the midline. The brainstem fits into the anterior cerebellar incisura and the falx cerebelli fits into the posterior incisura (Fig. 3.6). The tentorial surface faces and conforms to the lower surface of the tentorium (Fig. 3.7). The anteromedial part of this surface, the apex, formed by the anterior vermis, is the highest point on the cerebellum. This surface slopes downward from its anteromedial to its posterolateral edge. On the tentorial surface, the transition from the vermis to the hemispheres is

smooth and not marked by the deep fissures on the suboccipital surface between the vermis and hemispheres. Deep notches, the anterior and posterior cerebellar incisurae, groove the anterior and posterior edges of the tentorial surface in the midline. The brainstem fits into the anterior cerebellar incisura and the falx cerebelli fits into the posterior incisura (Figs. 3.6 and 3.7).

The anterior border, separating the tentorial and petrosal surfaces, has a lateral part (the anterolateral margin) that is parallel to the superior petrosal sinus and separates the hemispheric part of the tentorial and petrosal surfaces, and a medial part (the anteromedial margin) that faces the midbrain and forms the posterior border of the fissure between the midbrain and cerebellum. The anterior angle formed by the junction of the anterolateral and anteromedial margins is directed anteriorly above the origin of the

Fig. 3.4 (a) Superior view of the posterior cranial fossa. The osseous walls of the posterior fossa are formed by the occipital, temporal, and sphenoid bones. (b) Nerves and arteries of the posterior fossa. Only 2 of the 12 pairs of cranial nerves course entirely outside the posterior fossa. The tentorium, which is attached along the petrous ridges, roofs the posterior fossa. A artery, *Ac* acoustic, *A.I.C.A* anteroinferior cerebellar artery, *Bas* basilar, *CN* cranial nerve, *For* foramen, *Int* internal, *Jug* jugular, *Occip* occipital, *P.C.A* posterior cerebral artery, *P.I.C.A* posteroinferior cerebellar artery, *S.C.A* superior cerebellar artery, *Temp* temporal, *Tent* tentorial, *Vert* vertebral

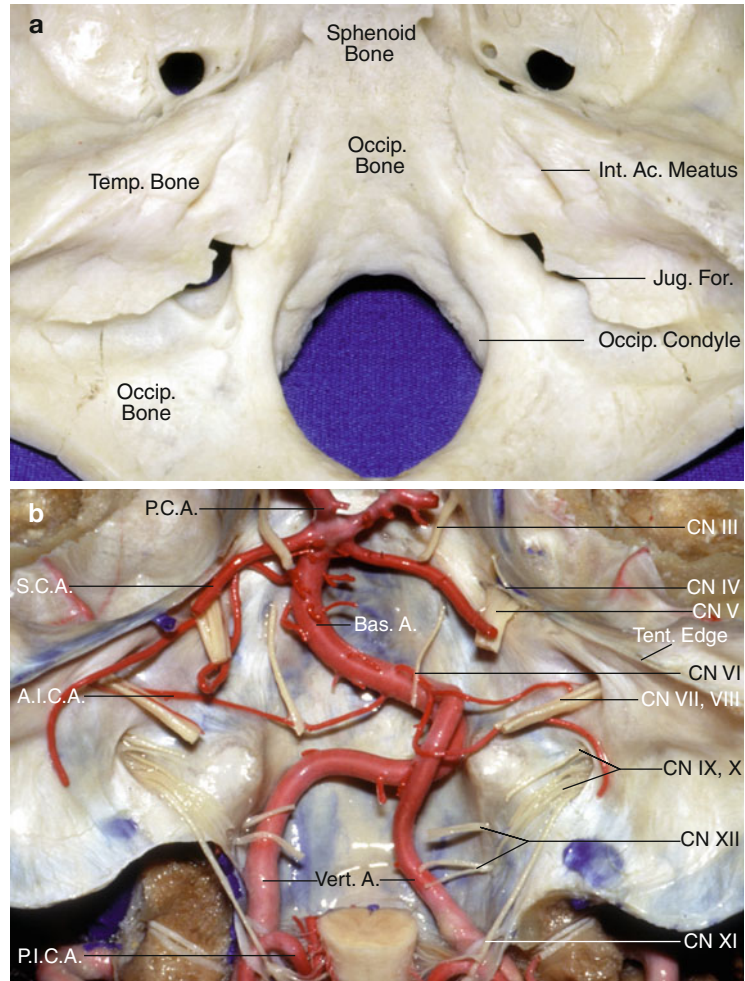
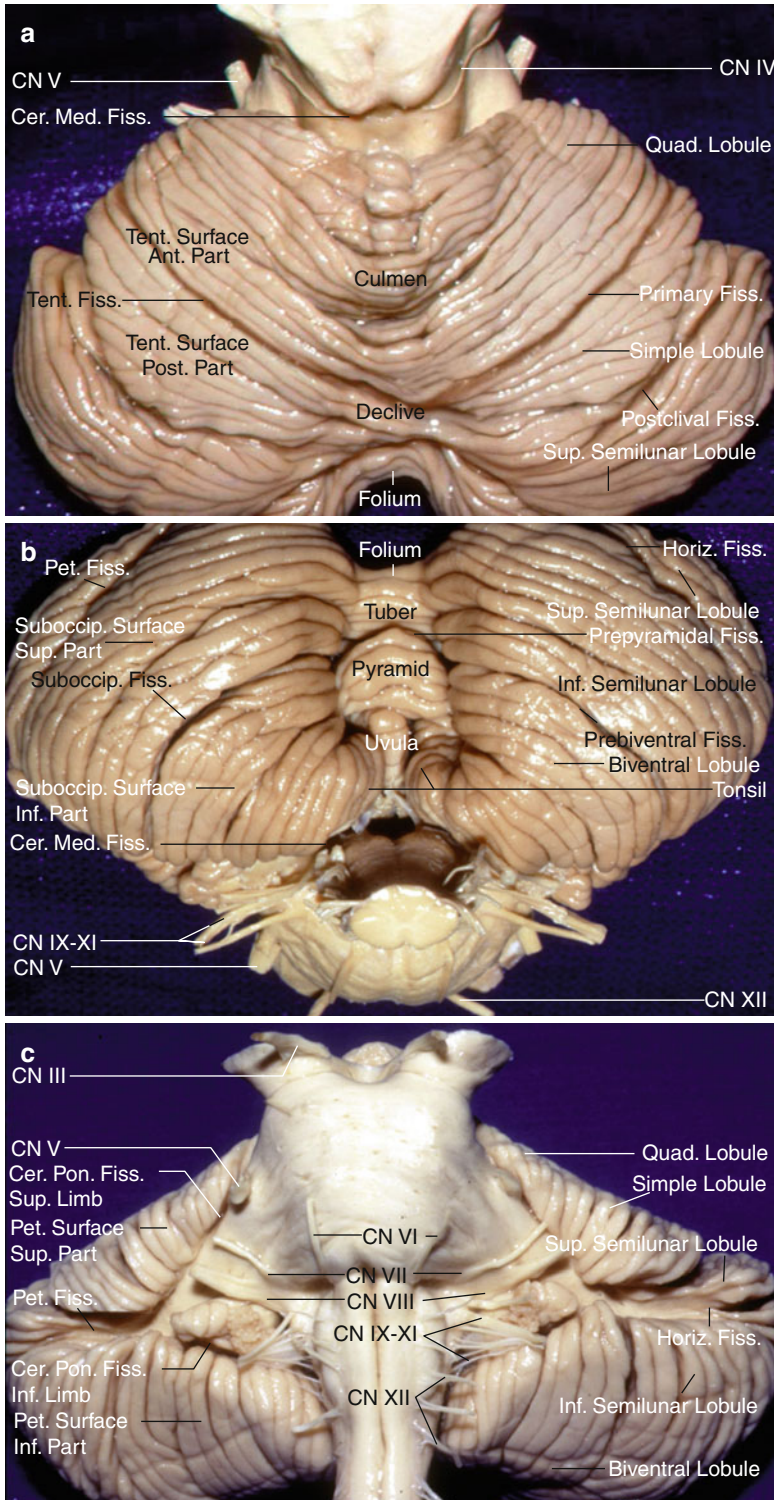


Fig. 3.5 Tentorial, suboccipital, and petrosal cerebellar surfaces. (a) The tentorial surface faces the lower surface of the tentorium. The anterior vermis is the most superior part of the tentorial surface. This surface slopes downward to its posterior and lateral margins. The fissure separates the hemispheric surface between the quadrangular and simple lobules and the vermis between the declive and culmen. (b) Suboccipital surface. The parts of the hemispheric surface from above to below are the superior and inferior semilunar and biventral lobules and the tonsils. These lobules extend beyond the suboccipital surface to the other surfaces of the cerebellum. The prebiventral fissures between the inferior semilunar and the biventral lobules separate the hemispheres into superior and inferior parts, and the prepyramidal fissure between the pyramid and tuber separates the vermis into superior and inferior parts. The petrosal (*horizontal*) fissure, the most prominent fissure on the petrosal surface, extends onto the

suboccipital surface and divides the superior half of the suboccipital surface between the superior and inferior semilunar lobules. The cerebellomedullary fissure extends superiorly between the cerebellum and medulla. (c) Petrosal surface. The petrosal surface faces forward toward the petrous temporal bone and is the surface that is retracted to surgically expose the cerebellopontine angle. The petrosal fissure divides the petrosal surface into superior and inferior parts. The cerebellopontine fissures are V-shaped fissures formed where the cerebellum wraps around the pons and the middle cerebellar peduncles. These fissures have a superior and an inferior limb, which meet at a lateral apex. The petrosal fissure extends laterally from the apex of the cerebellopontine fissures. *Ant* anterior, *Cer. Med* cerebellomedullary, *Cer. Pon* cerebellopontine, *CN* cranial nerve, *Fiss* fissure, *Horiz* horizontal, *Inf* inferior, *Pet* petrosal, *Post* posterior, *Quad* quadrangular, *Suboccip* suboccipital, *Sup* superior, *Tent* tentorial



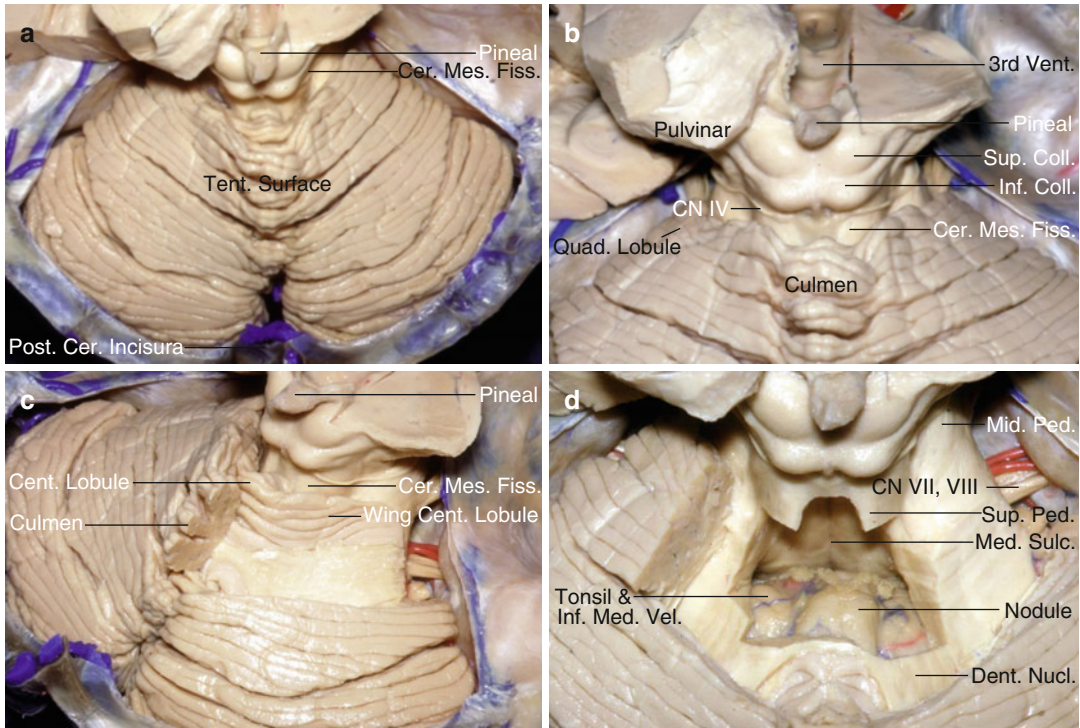


Fig. 3.6 Tentorial surface and cerebellomesencephalic fissure. **(a)** The surface slopes downward from the apex to the posterior and lateral margins. The anterior cerebellar incisura, the notch where the brainstem fits into the anterior part of the tentorial surface, is located anteriorly, and the posterior cerebellar incisura, the notch where the falx cerebelli fits into the cerebellum, is located posteriorly. **(b)** Enlarged view of the cerebellomesencephalic fissure, which extends downward between the midbrain and the cerebellum. The superficial part of the posterior lip is formed by the culmen in the midline and the quadrangular lobule laterally. The quadrigeminal cistern extends caudally from the pineal into the cerebellomesencephalic fissure. **(c)** The culmen has been removed to expose the central lobule and its wings, which form part of the

posterior lip of the cerebellomesencephalic fissure. **(d)** The central lobule and its wings, the lingula, the superior medullary velum, and medial part of the superior cerebellar peduncles have been removed to expose the fourth ventricle. The lower half of the roof is formed in the midline by the nodule and laterally by the inferior medullary velum, which passes laterally above, but is separated from the rostral pole of the tonsils by the cerebellomedullary fissure. *A.I.C.A* anteroinferior cerebellar artery, *Cent* central, *Cer* cerebellar, *Cer. Mes* cerebellomesencephalic, *Chor* choroid, *CN* cranial nerve, *Coll* colliculus, *Dent* dentate, *Fiss* fissure, *Flocc* flocculus, *Inf* inferior, *Lat* lateral, *Mid* middle, *Med* median, medullary, *Nucl* nucleus, *Ped* peduncle, *Plex Med. Vel.* posterior, *Quad* quadrangular, *Sulc* sulcus, *Sup* superior, *Tent* tentorial, *Vel* velum, *Vent* ventricle

posterior root of the trigeminal nerve. The posterior border between the tentorial and the suboccipital surfaces also has a lateral and a medial part. The lateral part (the posterolateral margin) is parallel and adjacent to the lateral sinus and separates the hemispheric part of the suboccipital and tentorial surfaces, and the short medial part (the posteromedial margin) faces the posterior cerebellar incisura and separates the vermic part of the two surfaces. The lateral angle, formed by the junction of the anterolateral and posterolateral margins, is located at the junction of sigmoid, lateral, and superior petrosal sinuses.

Veins often converge on the anterior and lateral angles. The hemispheric part of the tentorial surface includes the quadrangular, simple, and superior semilunar lobules, and the vermic part includes the culmen, declive, and folium. The vermic and the related hemispheric parts from above to below in sequence are the culmen and the quadrangular lobule, the declive and the simple lobule, and the folium and the superior semilunar lobule. The tentorial surface is divided at the site of its major fissure, the tentorial fissure, into anterior and posterior parts. This fissure, located between the quadrangular and the simple

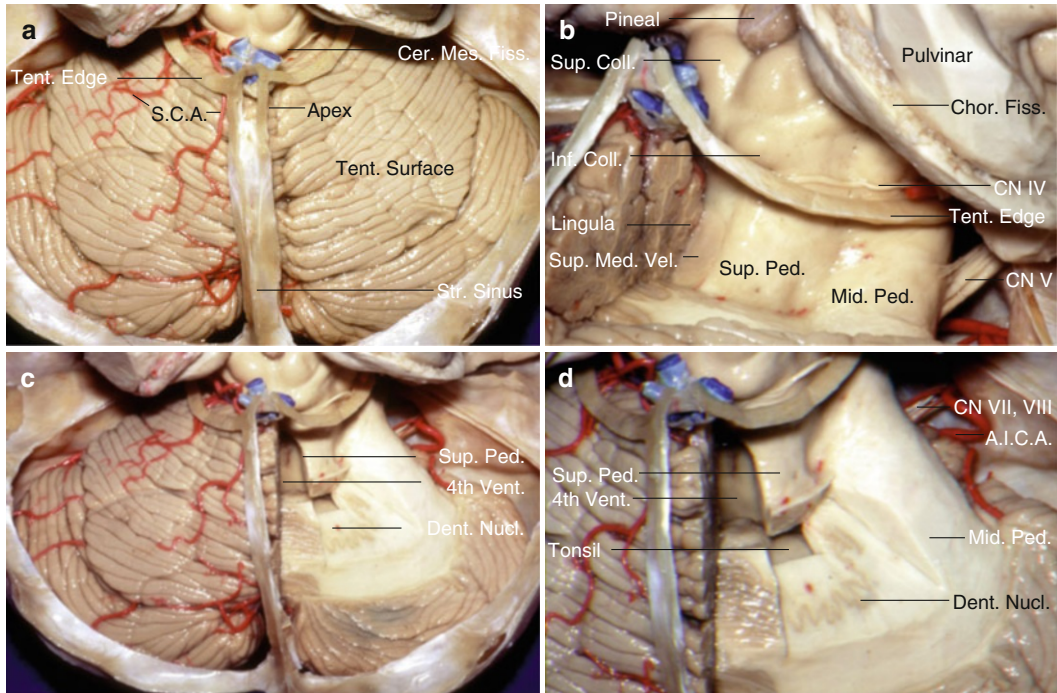


Fig. 3.7 Tentorial surface and cerebellomesencephalic fissure. (a) The tentorial cerebellar surface faces the tentorium and slopes downward from its apex located below the tentorial apex. The cerebellomesencephalic fissure extends forward between the cerebellum and midbrain. The SCA exits the cerebellomesencephalic fissure and supplies the tentorial surface. (b) The right half of the posterior lip of the cerebellomesencephalic fissure has been removed. The anterior wall of the fissure is formed in the midline by the collicular plate and lingula and laterally by the superior cerebellar peduncles. (c) The right half of the lingula and superior medullary velum has been

removed to expose the fourth ventricle. Additional white matter has been removed below the right superior peduncle to expose the dentate nucleus in which the superior peduncular fibers arise. (d) Enlarged view. The dentate nucleus appears to wrap around the rostral pole of the tonsil. *A.I.C.A.* anteroinferior cerebellar artery, *Cer. Mes* cerebellomesencephalic, *Chor* choroidal, *CN* cranial nerve, *Coll* colliculus, *Dent* dentate, *Fiss* fissure, *Inf* inferior, *Lat* lateral, *Med* medullary, *Mid* middle, *Nucl* nucleus, *Ped* peduncle, *S.C.A.* superior cerebellar artery, *Str* straight, *Sup* superior, *Tent* tentorial, *Vel* velum, *Vent* ventricle

lobules on the hemisphere and the culmen and the declive on the vermis, has also been called the primary fissure. The postclival fissure separates the simple and the superior semilunar lobules. The interfolial fissures on this surface pass anterolaterally from the midline and are continuous with the fissures on the superior half of the petrosal surface.

3.2 Suboccipital Surface

The suboccipital surface, located below and between the lateral and sigmoid sinuses, is the most complex of the three surfaces (Fig. 3.8). Operative approaches to the fourth ventricle and

most cerebellar tumors are commonly directed around or through this surface. It has a deep vertical depression, the posterior cerebellar incisura, which contains a fold of dura, the falx cerebelli. The vermis is folded into and forms the cortical surface within this incisura. The lateral walls of the incisura are formed by the medial aspects of the cerebellar hemispheres. Deep clefts, the vermohemispheric fissures, separate the vermis from the hemispheres. The vermian surface within the incisura has a diamond shape. The upper half of the diamond-shaped formation has a pyramidal shape and is called the pyramid. The folium and the tuber, superior to the pyramid, form the apex of the suboccipital part of the vermis. The lower half of the

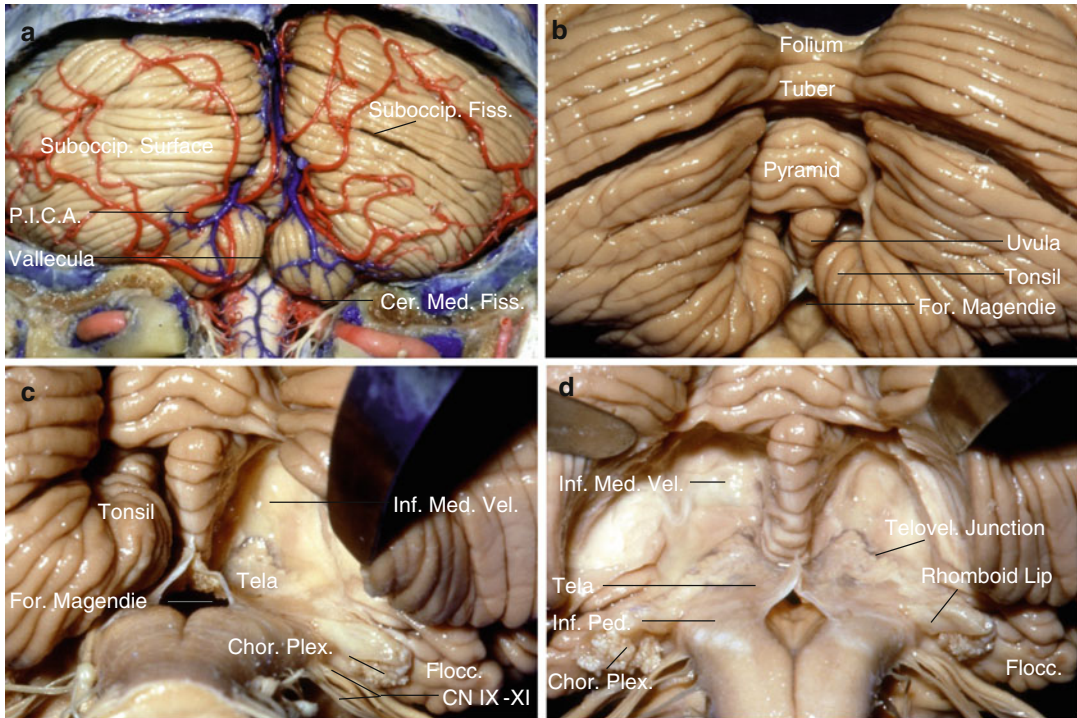


Fig. 3.8 Suboccipital surface of the cerebellum and the cerebellomedullary fissure. (a) The suboccipital surface is located below and between the sigmoid and lateral sinuses and is the surface that is exposed in a wide suboccipital craniectomy. The vermis sits in a depression, the posterior cerebellar incisura, between the hemispheres. The vallecule extends upward between the tonsils and communicates through the foramen of Magendie with the fourth ventricle. (b) Enlarged view. The lower parts of the vermis behind the ventricle are the pyramid and uvula. (c) The right tonsil has been removed to expose the lower part of the roof formed by the inferior medullary velum and tela choroidea. The uvula hangs downward between the tonsils, thus mimicking the situation in the oropharynx. The

choroid plexus arises on the inner surface of the tela and extends through the foramen of Luschka behind the glossopharyngeal and vagus nerve. The inferior medullary velum arises on the surface of the nodule, drapes across the superior pole of the tonsil, and blends into the flocculus laterally. (d) Both tonsils have been removed to expose the inferior medullary velum and tela choroidea bilaterally. The telovelar junction is the junction between the velum and tela. *Cer. Med* cerebellomedullary, *Chor* choroid, *CN* cranial nerve, *Fiss* fissure, *Floc* flocculus, *For* foramen, *Inf* inferior, *Lat* lateral, *Med* medullary, *Ped* peduncle, *P.I.C.A.* posteroinferior cerebellar artery, *Plex* plexus, *Suboccip* suboccipital, *Sup* superior, *Telovel* telovelar, *Vel* velum

diamond-shaped formation, the uvula, projects downward between the tonsils, thus mimicking the situation in the oropharynx. The rostromedial margin of the tonsils borders the tapering edges of the uvula. The nodule, the lowermost subdivision of the vermis, is hidden deep to the uvula. The strip of vermis within the incisura is broadest at the junction of the pyramid and uvula. Inferiorly, the posterior cerebellar incisura is continuous with the vallecule cerebelli, a cleft between the tonsils that leads through the foramen of Magendie into the fourth ventricle. The hemispheric portion of the suboccipital

surface is formed by the superior and inferior semilunar and biventral lobules and the tonsils, and the vermian portion is formed by the folium, tuber, pyramid, and uvula. The vermian and the related hemispheric parts from above to below are the folium and the superior semilunar lobules, the tuber and the inferior semilunar lobules, the pyramid and the biventral lobules, and the uvula and the tonsils. The suboccipital surface is divided at its major fissure, the suboccipital fissure, into superior and inferior parts. The suboccipital fissure has a vermian and a hemispheric part. The vermian part of this fissure, the

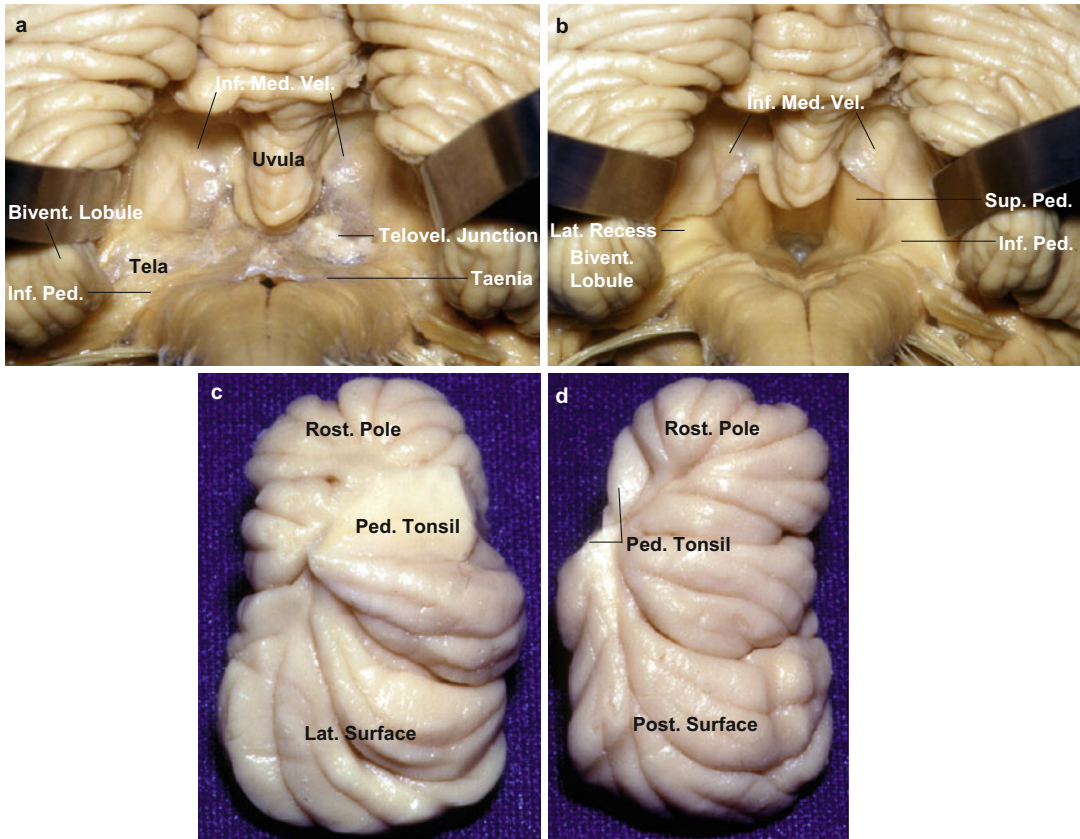


Fig. 3.9 Suboccipital surface and cerebellomedullary fissure. (a) Both tonsils have been removed by dividing the peduncle of the tonsil. Removing the tonsil exposes the inferior medullary velum and tela choroidea forming the lower part of the ventricular roof. (b) The tela, in which the choroid plexus arises, has been removed to expose both lateral recesses. The superior cerebellar peduncle forms the lateral wall of the upper half of the ventricle. The inferior cerebellar peduncle forms the anterior and upper margin of the lateral recess. (c) Lateral surface of the left tonsil. All of the tonsillar surfaces, except at the superolateral margin, are free surfaces. The peduncle of the tonsil, located along the superolateral margin of the

tonsil, attaches the tonsil to the remainder of the cerebellum. The posterior surface of the tonsil faces the cisterna magna. The medial surface faces the other tonsil. The anterior surface faces the posterior medulla. The rostral pole faces the inferior medullary velum and tela choroidea. The lateral surface below the peduncle of the tonsil faces the biventral lobule. (d) Posterior view of the left tonsil. The peduncle of the tonsil is located along the superolateral margin. Dividing the narrow peduncle allows the tonsil to be separated from the remaining cerebellum. *Bivent* biventral, *Inf* inferior, *Lat* lateral, *Med* medullary, *Ped* peduncle, *Post* posterior, *Rost* rostral, *Sup* superior, *Telovel* telovelar, *Vel* velum

prepyramidal fissure, separates the tuber and the pyramid, and the hemispheric part, the prebiventral fissure, separates the biventral and the inferior semilunar lobules. The prebiventral and prepyramidal fissures are continuous at the vermohemispheric junction, and together they form the suboccipital fissure. The petrosal fissure, the major fissure on the petrosal surface, extends from the petrosal surface onto the suboccipital surface and separates the superior and

inferior semilunar lobules laterally and the folium and the tuber medially. The tonsillobiventral fissure separates the tonsil and the biventral lobule.

The tonsils, the most prominent structure blocking access to the caudal part of the fourth ventricle, are a hemispheric component (Fig. 3.9). Each tonsil is an ovoid structure in the inferomedial part of the suboccipital surface that is attached to the remainder of the cerebellum along

its superolateral border by a white matter bundle called the tonsillar peduncle. The remaining tonsillar surfaces are free surfaces. The inferior pole and posterior surface face the cistern magna and are visible inferomedial to the remainder of the suboccipital surface. The lateral surface of each tonsil is covered by, but is separated from, the biventral lobule by a narrow cleft, except superiorly at the level of the tonsillar peduncle. The medial, anterior, and superior surfaces all face other neural structures but are separated from them by narrow fissures. The anterior surface of each tonsil faces and is separated from the posterior surface of the medulla by the cerebellomedullary fissure. The medial surfaces of the tonsils face each other across a narrow cleft, the vallecula, which leads into the fourth ventricle. The ventral aspect of the superior pole of each tonsil faces the three structures (tela choroidea, inferior medullary velum, and nodule) forming the lower half of the roof of the fourth ventricle. The superior pole is separated from the surrounding structures by a posterior extension of the cerebellomedullary fissure, called either the telovelotonsillar or supratonsillar cleft. The posterior aspect of the superior pole faces the uvula medially and the biventral lobule laterally (Fig. 3.9).

3.3 Petrosal Surface

The petrosal or anterior surface faces the posterior surface of the petrous bones, the brainstem, and the fourth ventricle (Figs. 3.3, 3.4, and 3.10). The lateral or hemispheric part of the petrosal surface rests against the petrous bone and is retracted to expose the cerebellopontine angle. The median or vermian part of the petrosal surface has a deep longitudinal furrow, the anterior cerebellar incisura, that wraps around the posterior surface of the brainstem and fourth ventricle. The right and left halves of the petrosal surfaces are not connected from side to side by a continuous strip of vermis, as are the suboccipital and tentorial surfaces, because of the interposition of the fourth ventricle between the superior and inferior part of the vermis. The vermal components rostral to the fourth

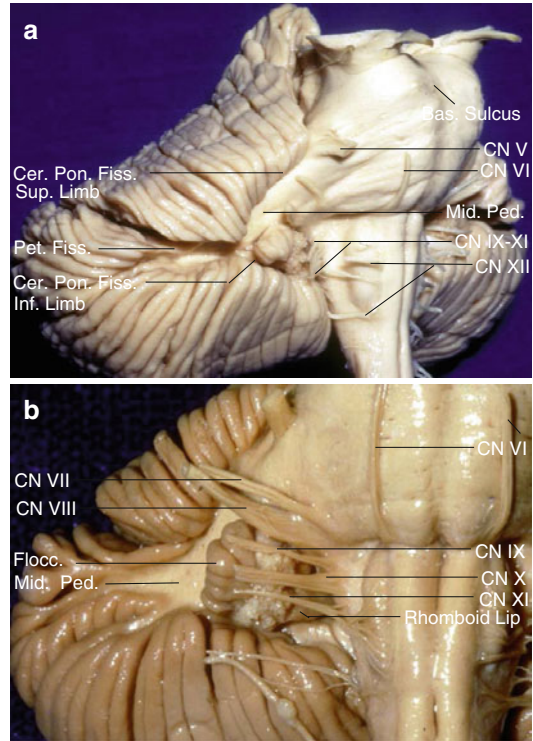


Fig. 3.10 Brainstem, petrosal surface, and cerebellopontine fissure. **(a)** Oblique view. The petrosal surfaces of the cerebellum face forward toward the petrous bone and are the surface that is retracted to expose the cerebellopontine angle. The cerebellopontine fissure, which might also be referred to as the cerebellopontine angle, is a V-shaped fissure formed where the cerebellum wraps around the pons and middle cerebellar peduncle cranial nerves V through XI arise within the margins of the cerebellopontine fissure. **(b)** Enlarged view of another brainstem. The facial and vestibulocochlear nerves join the brainstem 2 or 3 mm rostral to the glossopharyngeal nerve on a line drawn dorsal to the olive along the origin of the rootlets of the glossopharyngeal, vagus, and accessory rootlets. The rhomboid lip, a thin neural membrane in the ventral margin of the lateral recess, extends laterally behind the glossopharyngeal, vagus, and accessory nerves with the choroid plexus. *Bas* basilar, *Cer: Pon* cerebellopontine, *Chor* choroid, *CN* cranial nerve, *Fiss* fissure, *Floc* flocculus, *For* foramen, *Inf* inferior, *Mid* middle, *Ped* peduncle, *Pet* petrosal, *Plex* plexus, *Sup* superior

ventricle are the lingula, the central lobule, and the culmen, and those caudal to the fourth ventricle are the nodule and the uvula. The hemispheric surfaces are formed by the wings of the central lobule and the anterior surfaces of the quadrangular, simple, biventral, and superior and inferior semilunar lobules, the tonsils, and the flocculi. The vermian

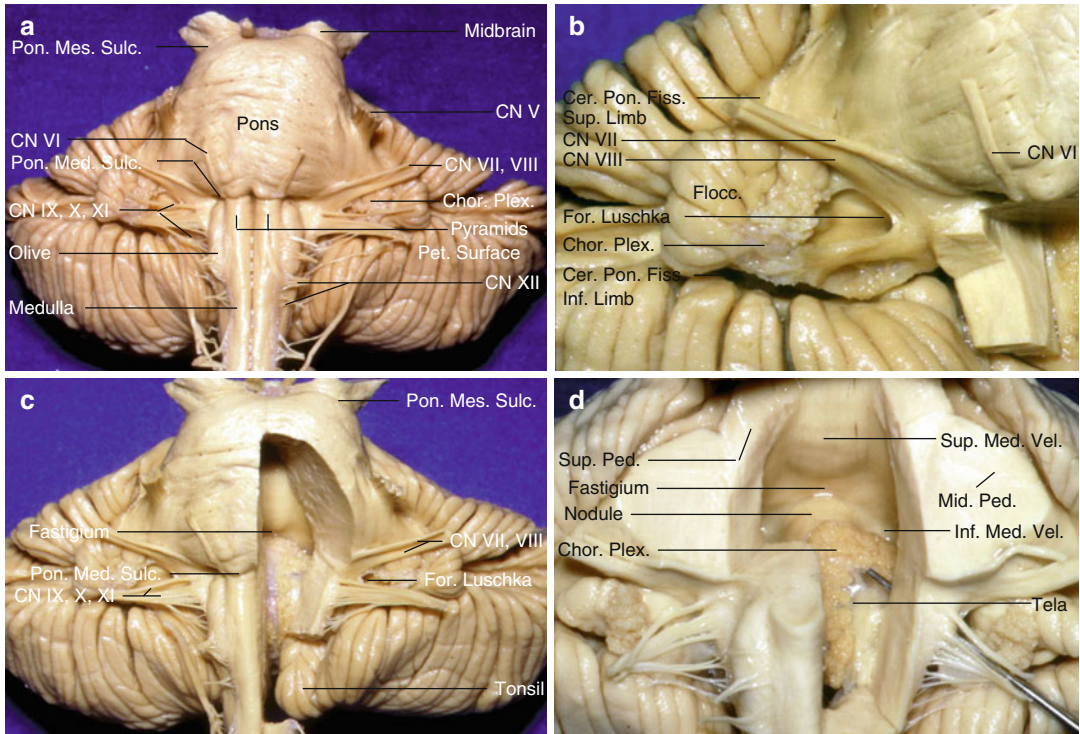


Fig. 3.11 Brainstem, fourth ventricle, and petrosal cerebellar surface. Stepwise anterior exposure. **(a)** The fourth ventricle is located behind the pons and medulla. The midbrain and pons are separated by the pontomesencephalic sulcus and the pons and medulla by the pontomedullary sulcus. The trigeminal nerves arise from the midpons. The abducens nerve arises in the medial part of the pontomedullary sulcus, rostral to the medullary pyramids. The facial and vestibulocochlear nerves arise at the lateral end of the pontomedullary sulcus immediately rostral to the foramen of Luschka. The hypoglossal nerves arise anterior to the olives and the glossopharyngeal, vagus, and accessory nerves arise posterior to the olives. Choroid plexus protrudes from the foramen of Luschka behind to the glossopharyngeal and vagus nerves. **(b)** The foramen of Luschka opens into the cerebellopontine angle below the junction of the facial and vestibulocochlear nerves with the lateral end of the pontomedullary sulcus.

Choroid plexus protrudes from the lateral recess and foramen of Luschka behind the glossopharyngeal, vagus, and accessory nerves. **(c)** The part of the pons and medulla forming the left half of the floor of the ventricle has been removed to expose the fastigium, which divides the ventricular roof into superior and inferior parts. **(d)** The right half of the pons has been removed to expose the upper half of the roof. The superior part of the roof is formed by the superior medullary velum. The rostral part of the lower half of the roof is formed by the nodule and inferior medullary velum and the caudal part is formed by the tela choroidea, a thin arachnoid-like membrane, in which the choroid plexus arises. *Cer Pon* cerebellopontine, *Chor* choroid, *CN* cranial nerve, *Fiss* fissure, *Flocc* flocculus, *For* foramen, *Inf* inferior, *Lat* lateral, *Med.* medial medullary, *Mid* middle, *Ped* peduncle, *Pet* petrosal, *Plex* plexus, *Pon. Med.* pontomedullary, *Pon. Mes.* pontomesencephalic, *Seg* segment, *Sulc.* sulcus, *Sup* superior, *Vel* velum

and related hemispheric parts are the central lobule and the wings of the central lobule, the culmen and the quadrangular lobules, the nodule and the flocculi, and the uvula and the tonsils. The major fissure on this surface, the petrosal fissure, also called the horizontal fissure, splits the petrosal surface into superior and inferior parts and extends onto the suboccipital surface between the superior and inferior semilunar lobules (Fig. 3.11).

3.4 The Fourth Ventricle and the Cerebellar-Brainstem Fissures

3.4.1 Fourth Ventricle

The fourth ventricle is a broad, tent-shaped midline cavity located between the cerebellum and the brainstem. It is connected rostrally

through the aqueduct with the third ventricle, caudally through the foramen of Magendie with the cisterna magna, and laterally through the foramina of Luschka with the cerebellopontine angles. Most of the cranial nerves arise near its floor. It has a roof, a floor, and two lateral recesses. It is ventral to the cerebellum, dorsal to the pons and medulla, and medial to the cerebellar peduncles.

The ventricular roof is tent shaped (Fig. 3.12). The roof expands laterally and posteriorly from its narrow rostral end just below the aqueduct to the level of the fastigium and lateral recess, the site of its greatest height and width, and from there it tapers to a narrow caudal apex at the level of the foramen of Magendie. The apex of the roof, the fastigium, divides it into superior and inferior parts. The superior part is distinctly different from the inferior part, in that the inferior part is formed largely by thin membranous layers and the superior part is formed by thicker neural structures.

The external or cisternal surfaces of the structures forming the roof are intimately related to the fissures between the cerebellum and brainstem. The three fissures formed by the embryological folding of the cerebellum around the brainstem are the cerebellomesencephalic fissure, which extends inferiorly between the cerebellum and mesencephalon and is intimately related to the superior half of the roof (Figs. 3.11, 3.12, and 3.13); the cerebellopontine fissures, which are formed by the folding of the cerebellum around the lateral sides of the pons and are intimately related to the lateral recesses (Figs. 3.11, 3.12, and 3.13); and the cerebellomedullary fissure, which extends superiorly between the cerebellum and the medulla and is intimately related to the inferior half of the roof (Figs. 3.11, 3.12, and 3.13).

A major cerebellar artery and vein course in each fissure. The superior cerebellar artery (SCA) and the vein of the cerebellomesencephalic fissure course within the cerebellomesencephalic fissure, the anteroinferior cerebellar artery (AICA) and the vein of the cerebellopontine fissure are related to the cerebellopontine fissure, and the posteroinferior cerebellar artery (PICA) and the vein of the cerebellomedullary fissure are intimately related to the cerebellomedullary

fissure. These arteries and veins will be reviewed in the next two chapters on the cerebellar arteries and posterior fossa veins [4, 7, 8].

Each fissure communicates with the adjacent fissure. The cerebellopontine fissures are continuous around the rostral surface of the middle cerebellar peduncles with the caudal edges of the cerebellomesencephalic fissure and around the caudal margin of the middle cerebellar peduncles with the rostral limits of the cerebellomedullary fissure. These fissures will be reviewed in greater detail in the discussion of the roof and lateral recesses of the fourth ventricle.

3.4.2 Upper Ventricular Roof and the Cerebellomesencephalic Fissure

The ventricular surface of the superior part of the roof of the fourth ventricle is divided into a single median and two lateral parts (Figs. 3.11 and 3.13). The median part is formed by the superior medullary velum, and the lateral parts (also referred to as the lateral walls) are formed by the inner surface of the cerebellar peduncles. The superior medullary velum is a thin lamina of white matter that spans the interval between the superior cerebellar peduncles and has the lingula, the uppermost division of the vermis, on its outer surface. It is continuous at the fastigium with the inferior medullary velum. The rostral portion of the ventricular surface of each lateral wall is formed by the medial surface of the superior cerebellar peduncle, and the caudal part is formed by the inferior cerebellar peduncle.

The middle cerebellar peduncle, although it is the largest component of the fiber bundle formed by the union of the three cerebellar peduncles, is separated from the ventricular surface by the fibers of the inferior and superior peduncles on its medial surface (Fig. 3.13). The fibers of the inferior cerebellar peduncle ascend in the posterolateral medulla and turn posteriorly in the inferomedial part of the fiber bundle formed by the union of the three peduncles to line the ventricular surface of the superior margin of the lateral recess and the inferior part of the lateral wall.

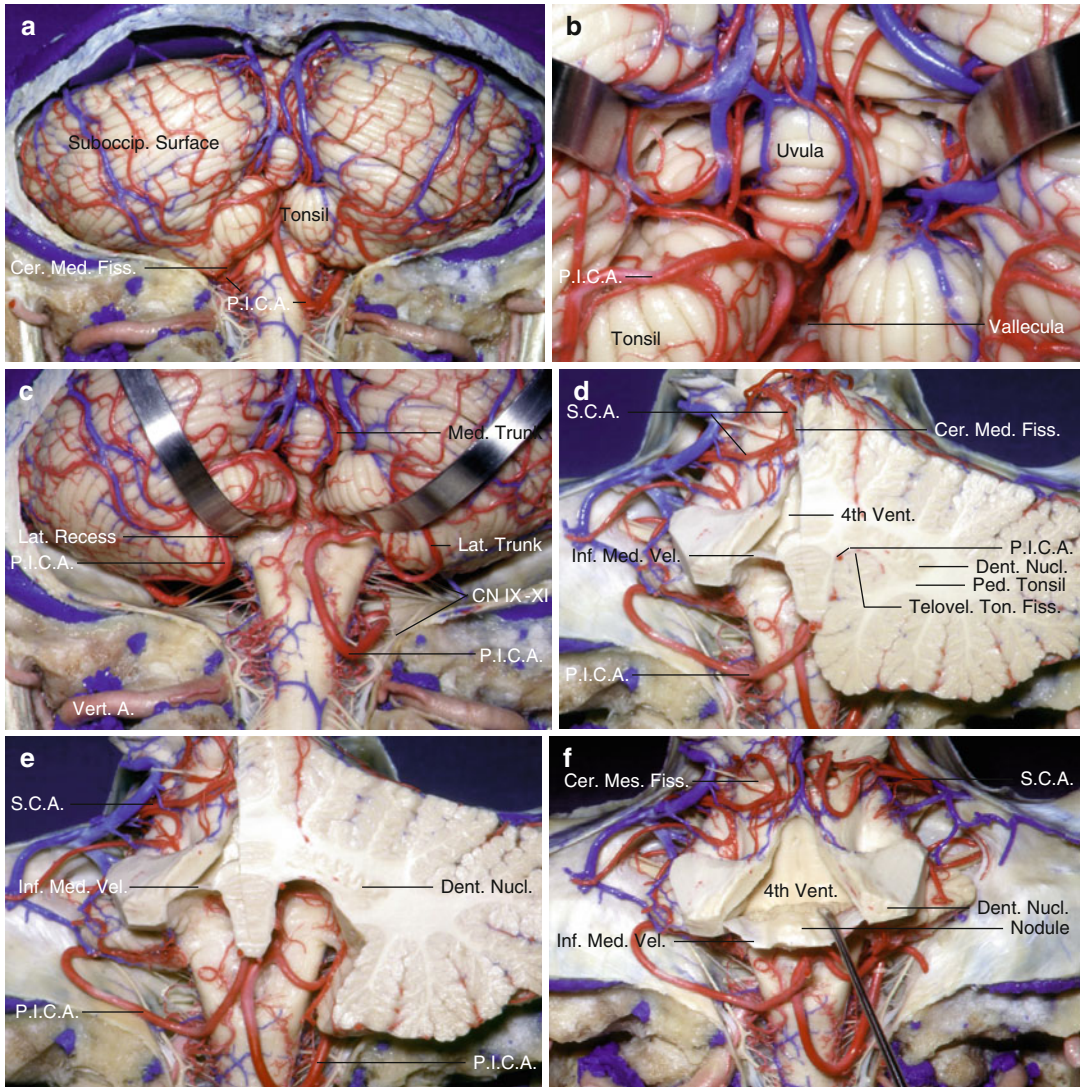


Fig. 3.12 Posterior views. Stepwise dissection examining the relationships of the inferior medullary velum, dentate nucleus, tonsil, and the cerebellomedullary and cerebellomesencephalic fissures. (a) The PICAs pass around the posterior medulla to reach the lower margin of the cerebellomedullary fissure. The left PICA courses around the lower pole of the tonsil. The right PICA descends well below the tonsil to the level of the foramen magnum before ascending along the medial tonsillar surface. (b) The PICAs ascend between the tonsils and medulla to reach the interval between the tonsil and uvula and to supply the suboccipital surface. (c) The posterior medullary segment of the right PICA divides into a medial trunk supplying the vermis and paravermian area and a lateral trunk supplying the hemisphere. (d) The cerebellum has been sectioned in an oblique coronal plane to show the relationship of the rostral pole of the tonsil to the inferior medullary velum and dentate nucleus. The den-

tate nucleus is located above the posterolateral part of the ventricular roof, near the fastigium, where it wraps around, and is separated from, the rostral pole of the tonsil by the inferior medullary velum. The left tonsil has been removed while preserving the left half of the inferior medullary velum. The SCAs course in the cerebellomesencephalic fissure. The PICA passes between the walls of the cerebellomedullary fissure formed above by the inferior medullary velum and below by the upper pole of the tonsil. (e) Both tonsils have been removed. The PICAs ascend through the cleft between the inferior medullary velum and rostral pole of the tonsil. (f) The superior part of the ventricular roof has been removed and the nodule and the inferior medullary velum has been folded downward to expose the floor. *Chor* choroid, *Dent* dentate, *Inf* inferior, *Lat* lateral, *Med.*, median medullary, *Mid* middle, *Nucl* nucleus, *P.I.C.A.* posteroinferior cerebellar artery, *Ped* peduncle, *Plex* plexus, *Sup* superior, *Vel* velum

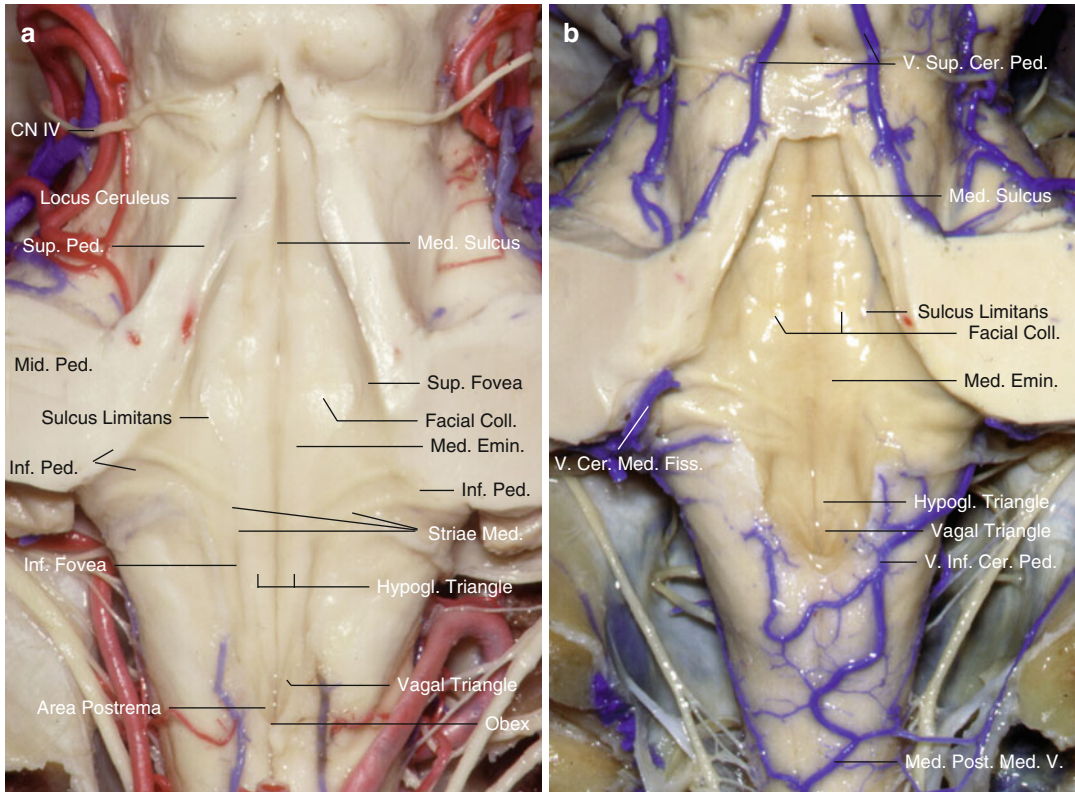


Fig. 3.13 Posterior views. (a) Enlarged view of the floor of the fourth ventricle. The median sulcus divides the floor longitudinally in the midline. Each half of the floor is divided longitudinally by an irregular sulcus, the sulcus limitans, which deepens lateral to the facial colliculus and hypoglossal triangles to form the superior and inferior foveae. A darkened area of cells, the locus ceruleus, is located at the rostral end of the sulcus limitans. The stria medullaris crosses the floor at the level of the lateral recess. The hypoglossal and vagal nuclei and the area postrema are stacked one above the other in the lower part of the floor to give the configuration of a pen nib and, thus, the area is referred to as the calamus scriptorius. (b) Another fourth ventricular floor. The paired veins of the

superior cerebellar peduncle course on the outer surface of the superior peduncles and join superiorly to form the vein of the cerebellomesencephalic fissure. The median posterior medullary vein ascends on the medulla and splits into the paired veins of the inferior cerebellar peduncle at the caudal margin of the floor. That left vein is hypoplastic. The left vein of the cerebellomedullary fissure passes along the lateral recess and ascends to join the petrosal group of veins in the cerebellopontine angle. *Cer Med* cerebellomedullary, *Cer* cerebellar, *CN* cranial nerve, *Coll* colliculus, *Emin* eminence, *Fiss* fissure, *Hypogl* hypoglossal, *Inf* inferior, *Med* median medullary, *Mid* middle, *Ped* peduncle, *Post* posterior, *Striae Med* stria medullaris, *Sup* superior, *V* vein

The fibers of the superior cerebellar peduncle arise in the dentate nucleus and ascend on the medial side of the middle cerebellar peduncle to form the ventricular surface of the superior part of the lateral wall.

The cisternal (external) surface of the structures forming the superior part of the roof also forms the anterior wall of the cerebellomesencephalic fissure. This fissure, which extends inferiorly between the cerebellum and midbrain, is V-shaped when viewed from superiorly (Figs. 3.14 and 3.15). This fissure

has also been referred to as the precentral cerebellar fissure. The dorsal half of the midbrain sits within the limbs of the V-shaped notch, and the cerebellum forms the outer margin, with the apex being posterior. The inner wall of the fissure, which forms the outer surface of the superior part of the roof, is composed of the lingula, the dorsal surface of the superior cerebellar peduncles, and the rostral surface of the middle cerebellar peduncles. The lingula, a thin, narrow tongue of vermis, sits on the outer surface of the superior medullary velum. The

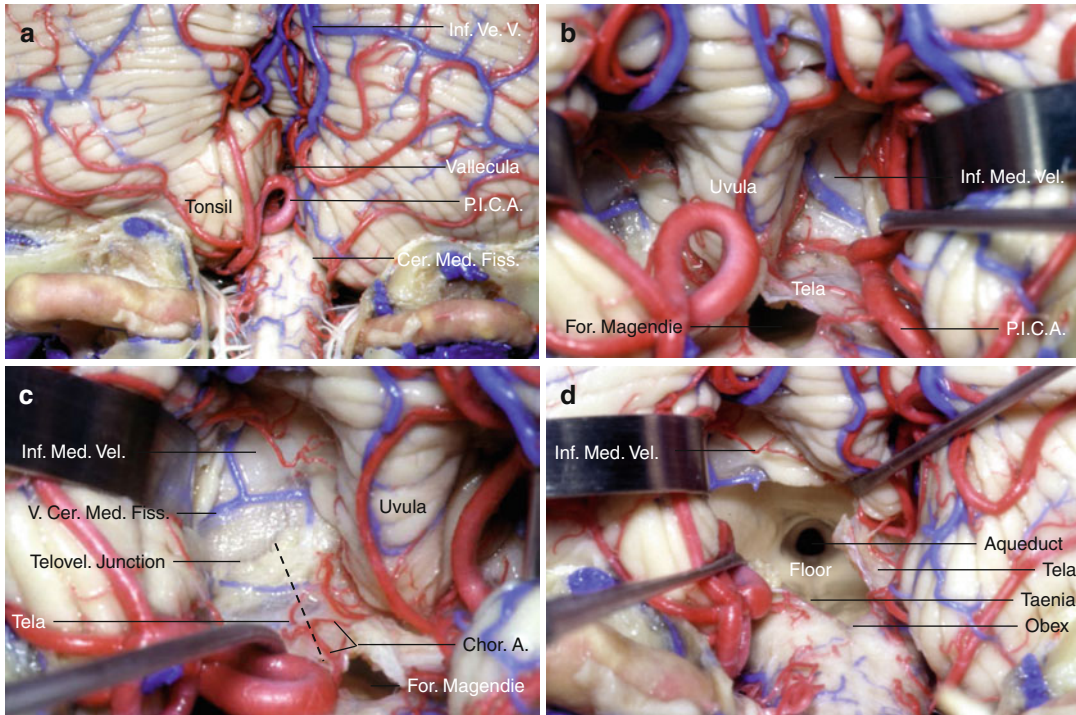


Fig. 3.14 Telovelar approach to the fourth ventricle. (a) The cerebellomedullary fissure extends upward between the tonsils posteriorly and the medulla anteriorly. The vallecule opens between the tonsils into the fourth ventricle. (b) Both tonsils have been retracted laterally to expose the inferior medullary velum and tela choroidea that form the lower part of the ventricular roof. The nodule of the vermis, on which the inferior medullary arises, is hidden deep to the uvula. (c) Enlarged view of the left half of the cerebellomedullary fissure. The choroidal arteries course along the tela choroidea from which the choroid plexus projects into the roof of the fourth ventricle. The vein of the cerebellomedullary fissure, which crosses the inferior

medullary velum, is the largest vein in the cerebellomedullary fissure. The interrupted line shows the site of the incision in the tela to provide the exposure seen in the next step. The telovelar junction is the line of attachment of the tela to the velum. (d) The tela choroidea has been opened extending from the foramen of Magendie to the junction with the inferior medullary velum. The uvula has been displaced to the right side to provide this view extending from the aqueduct to the obex. A artery, *Cer Med* cerebellomedullary, *Chor* choroidal, *Fiss* fissure, *For* foramen, *Inf* inferior, *Med* medullary, *P.I.C.A.* posteroinferior cerebellar artery, *Telovel* telovelar, *V* vein, *Ve* vermian, *Vel* velum

superior cerebellar peduncles form smooth longitudinal prominences on each side of the lingula before disappearing into the midbrain beneath the colliculi. The rostral surface of the middle cerebellar peduncles appears to wrap around the caudal margin of the superior cerebellar peduncles. A shallow groove, the interpeduncular sulcus, marks the junction of the superior and the middle cerebellar peduncles. The interpeduncular sulcus is continuous anteriorly with the pontomesencephalic sulcus, a transverse groove between the pons and midbrain, and superiorly with the lateral mesencephalic sulcus, a longitudinal fissure dorsal to the cerebral peduncle. The trochlear nerves arise in the

cerebellomesencephalic fissure below the inferior colliculi and pass anterolateral to exit the anterior part of the fissure. The outer wall of the cerebellomesencephalic fissure is formed by the culmen and the central lobule and its wings.

The neural structures separating the ventricular and cisternal surfaces of the superior part of the roof are thinnest in the area of the superior medullary velum and lingula and thickest in the area of the cerebellar peduncles. The rostral portion of each lateral wall, formed by only the superior cerebellar peduncle, is thinner than the caudal portion, which is formed by the three cerebellar peduncles after they have united.

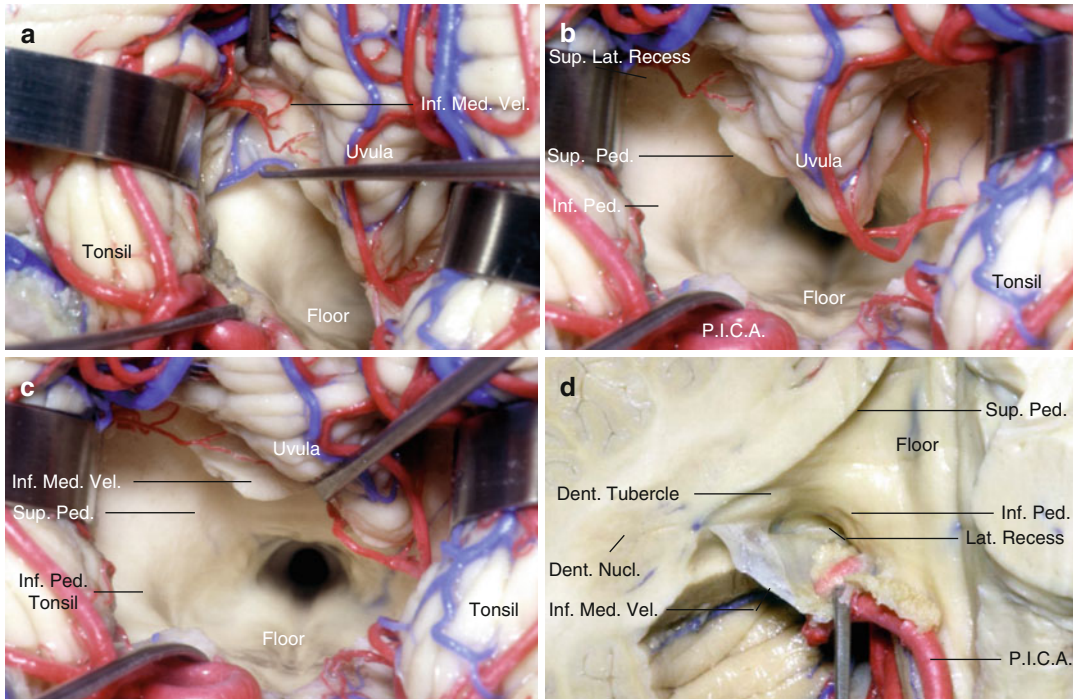


Fig. 3.15 Telovelar approach to the fourth ventricle. (a) The tip of a nerve hook placed inside the fourth ventricle is seen through the paper-thin inferior medullary velum. (b) The left half of the inferior medullary velum has been divided to expose the superolateral recess and the ventricular surface formed by the superior and inferior peduncles. (c) The uvula has been retracted to the right to expose all of the floor and much of the roof of the ventricle. (d) The right half of the cerebellum was removed by dividing the vermis sagittally and the cerebellar peduncles

transversely. The tonsil has been removed and the inferior medullary velum and the cranial loop of the PICA have been displaced downward to expose the opening into the lateral recess. The dentate nucleus forms a prominence, the dentate tubercle, in the superolateral recess of the roof of the fourth ventricle near the site of attachment of the inferior medullary velum. *Dent* dentate, *Inf* inferior, *Lat* lateral, *Med* medullary, *Nucl* nucleus, *P.I.C.A.* posteroinferior cerebellar artery, *Ped* peduncle, *Sup* superior, *Vel* velum

3.4.3 Lower Roof and Cerebellomedullary Fissure

The inferior portion of the roof slopes sharply ventral and slightly caudal from the fastigium to its attachment to the inferolateral borders of the floor (Figs. 3.14 and 3.15). The ventricular and cisternal surfaces are formed by the same structures, the tela choroidea and the inferior medullary velum, except in the rostral midline, where the ventricular surface is formed by the nodule and the cisternal surface is formed by the uvula. The choroid plexus is attached to the ventricular surface of the tela choroidea.

The ventricular surface is divided into a cranial part formed by the nodule and the inferior

medullary velum and a caudal part formed by the tela choroidea. The inferior medullary velum is a membranous layer and is all that remains of the connection between the nodule and the flocculi that form the flocculonodular lobe of the primitive cerebellum [5] (Figs. 3.14 and 3.15). It is a thin bilateral semitranslucent butterfly-shaped sheet of neural tissue that blends into the ventricular surface of the nodule medially and stretches laterally across, but is separated from, the superior pole of the tonsil by a narrow, rostral extension of the cerebellomedullary fissure. It blends into the dorsal margin of each lateral recess and forms the peduncle of each flocculus. The inferior medullary velum is continuous at the level of the fastigium with the superior medullary velum. Caudally it is attached to the tela choroidea.

The tela choroidea forms the caudal part of the inferior portion of the roof and the inferior wall of each lateral recess (Figs. 3.14 and 3.15). It consists of two thin, semitransparent membranes, each having a thickness comparable to arachnoid, between which is sandwiched a vascular layer composed of the choroidal arteries and veins. The choroid plexus projects from the ventricular surface of the tela choroidea into the fourth ventricle. The line of attachment of the inferior medullary velum to the tela choroidea, the telovelar junction, extends from the nodule into each lateral recess. The tela choroidea sweeps inferiorly from the telovelar junction around the superior pole of each tonsil to its attachment to the inferolateral edges of the floor along narrow white ridges, the taeniae, which meet at the obex. Cranially, the taeniae turn laterally over the inferior cerebellar peduncles and pass horizontally along the inferior borders of the lateral recesses. The tela choroidea does not completely enclose the inferior half of the fourth ventricle but has three openings into the subarachnoid space: the paired foramina of Luschka located at the outer margin of the lateral recesses and the foramen of Magendie located at the caudal tip of the fourth ventricle.

The cisternal (external) surface of the caudal half of the roof faces and is intimately related to the cerebellomedullary fissure (Figs. 3.14 and 3.15). This fissure is one of the most complex fissures in the brain. The ventral wall of the fissure is formed by the posterior surface of the medulla, the inferior medullary velum, and the tela choroidea. The dorsal wall of the fissure is formed by the uvula in the midline and the tonsils and biventral lobules laterally. It extends superiorly to the level of the lateral recesses and communicates around the superior poles of the tonsils with the cisterna magna, through the foramen of Magendie with the fourth ventricle, and around the foramina of Luschka with the cerebellopontine fissures. The rostral pole of the tonsils faces the inferior medullary velum, the tela choroidea, and the peritonsillar part of the uvula and the biventral lobule in the superior part of the fissure (Figs. 3.14 and 3.15). The portion of the fissure between the tonsil, the tela choroidea, and the inferior medul-

lary velum is called the telovelotonsillar cleft, and the superior extension of this cleft over the superior pole of the tonsil has been called the supratonsillar cleft.

3.5 Lateral Recess and Cerebellopontine Fissure

The lateral recesses are narrow, curved pouches formed by the union of the roof and the floor. They extend laterally below the cerebellar peduncles and open through the foramina of Luschka into the cerebellopontine angles (Figs. 3.11, 3.12, and 3.13). The ventral wall of each lateral recess is formed by the junctional part of the floor and the rhomboid lip, a sheetlike layer of neural tissue that extends laterally from the floor and unites with the tela choroidea to form a pouch at the outer extremity of the lateral recess. The rostral wall of each lateral recess is formed by the caudal margin of the cerebellar peduncles. The inferior cerebellar peduncle courses upward in the floor ventral to the lateral recess and turns posteriorly at the lower part of the pons to form the ventricular surface of the rostral wall. The peduncle of the flocculus interconnecting the inferior medullary velum and the flocculus crosses in the dorsal margin of the lateral recess. The caudal wall is formed by the tela choroidea that stretches from the lateral part of the taenia to the peduncle of the flocculus. The biventral lobule is dorsal to the lateral recess. The flocculus is superior to the outer extremity of the lateral recess. The rootlets of the glossopharyngeal and vagus nerves arise ventral to and the facial nerve arises rostral to the lateral recess. The fibers of the vestibulocochlear nerve cross the floor of the recess.

Each lateral recess opens into the cerebellopontine angle along the cerebellopontine fissure (Fig. 3.13). This V-shaped fissure is formed by the folding of the cerebellar hemisphere around the lateral side of the pons and the middle cerebellar peduncle. It has a superior limb between the rostral half of the middle cerebellar peduncle and the superior part of the petrosal surface and an inferior limb between the caudal half

of the middle cerebellar peduncle and the inferior part of the petrosal surface. The middle cerebellar peduncle fills the interval between the two limbs. The apex of the fissure is located laterally where the superior and inferior limbs meet. The petrosal fissure extends laterally from the apex. The lateral recess and the foramen of Luschka open into the medial part of the inferior limb. Other structures located along the inferior limb are the flocculus, the rhomboid lip, the choroid plexus protruding from the foramen of Luschka, and the facial, vestibulocochlear, glossopharyngeal, and vagus nerves. The trigeminal nerve arises from the pons along the superior limb of the fissure.

The superior limb of the cerebellopontine fissure communicates above the trigeminal nerve with the lateral part of the cerebellomesencephalic fissure, and the inferior limb communicates with the lateral part of the cerebellomedullary fissure at the level of the lateral recess. The flocculus projects into the cerebellopontine angle at the confluence of the cerebellopontine and cerebellomedullary fissures. The vestibulocochlear and facial nerves enter the brainstem anterosuperior to the flocculus, and the fila of the glossopharyngeal and the vagal nerves cross anteroinferiorly to it.

3.6 Choroid Plexus

The choroid plexus of the posterior fossa is composed of two inverted L-shaped fringes that arise on the ventricular surface of the tela choroidea and are located on each side of the midline [2] (Figs. 3.8 and 3.11). The paired longitudinal limbs bordering the median plane are the medial segments. The transverse limbs that originate from the rostral ends of the medial segments are the lateral segments. The entire structure presents the form of a letter T, the vertical limb of which, however, is double.

The medial segments are located in the roof near the midline, and the lateral segments extend through the lateral recesses and the foramina of Luschka into the cerebellopontine angles. The medial segments stretch from the level of the nodule anterior to the tonsils to the level of the for-

men of Magendie. Each medial segment is subdivided into a rostral or nodular part and a caudal or tonsillar part. The nodular parts are widest at their junction with the lateral segments.

The tonsillar parts are anterior to the tonsils and extend inferiorly through the foramen of Magendie. The rostral and caudal ends of the medial segments are often fused.

The lateral segments form a transversely oriented fringe that attach to the rostral part of the medial segments and extend parallel to the telovelar junction through the lateral recesses into the cerebellopontine angles. Each lateral segment is subdivided into a medial or peduncular part and a lateral or floccular part. The peduncular part forms a narrow fringe that is continuous with the rostral part of the medial segment and is attached to the tela choroidea covering the lateral recess inferior to the cerebellar peduncles. The floccular part is continuous with the peduncular part at the lateral margin of the cerebellar peduncles and protrudes through the foramen of Luschka into the cerebellopontine angle below the flocculus (Figs. 3.8, 3.11, 3.14, and 3.15).

3.7 Brainstem and Floor

3.7.1 Brainstem

The brainstem and ventricle floor are considered together because the brainstem forms the fourth ventricular floor. The brainstem in the posterior fossa is composed of the mesencephalon, pons, and medulla (Figs. 3.10 and 3.11). The mesencephalon consists of the cerebral peduncles, the tegmentum, and the tectum. It is demarcated superiorly from the diencephalon by the sulcus between the optic tracts and the cerebral peduncles and inferiorly from the pons by the pontomesencephalic sulcus. The interpeduncular fossa, a wedge-shaped depression between the cerebral peduncles, has the posterior perforated substance in its floor. The rootlets of the oculomotor nerves arise in the depths of the interpeduncular fossa and form the fossa's walls lateral to the posterior perforated substance. A small depression, the

superior foramen cecum, is located in the caudal part of the interpeduncular fossa. The pontomesencephalic sulcus runs from the superior foramen cecum around the cerebral peduncles to join the lateral mesencephalic sulcus, a vertical sulcus between the tegmentum and the cerebral peduncle.

The belly of the pons is convex from side to side, as well as from top to bottom, and is continuous on each side with the middle cerebellar peduncles. It has a shallow midline groove, the basilar sulcus, which extends from its superior to its inferior border. The posterior root of the trigeminal nerve emerges from the upper portion of the middle cerebellar peduncle just below the anterior angle of the cerebellum. The pons is demarcated inferiorly from the medulla by the pontomedullary sulcus, which extends laterally from the inferior foramen cecum (a midline dimple) to the supraolivary fossette (a depression located rostral to the olive). The rootlets of the facial and the vestibulocochlear nerves arise superior to this fossette and the rootlets of the glossopharyngeal and the vagal nerves originate dorsal to it.

The anterior surface of the medulla is formed by the medullary pyramids, which face the clivus, the anterior edge of the foramen magnum, and the rostral part of the odontoid process (Figs. 3.4 and 3.10). The anteromedian sulcus divides the upper medulla in the anterior midline between the pyramids and disappears on the lower medulla at the level of the decussation of the pyramids, but it reappears below the decussation and is continuous caudally with the anteromedian fissure of the spinal cord. The lateral surface of the medulla is formed predominantly by the inferior olives, which are situated lateral to and separated from the pyramids by the anterolateral (preolivary) sulcus. The rootlets of the hypoglossal nerves arise in the anterolateral sulcus. The lateral surface is demarcated posteriorly by the exits of the rootlets of the glossopharyngeal, vagus, and accessory nerves just dorsal to the posterolateral (postolivary) sulcus, which courses along the dorsal margin of the olive and is continuous below with the posterolateral sulcus of the spinal cord. The abducens nerves emerge from the pontomedullary sulcus rostral to the

pyramids. The posterior surface of the medulla is divided into superior and inferior parts. The superior part is composed in the midline of the inferior half of the floor of the fourth ventricle and laterally by the inferior cerebellar peduncles. The inferior part of the posterior surface is divided into two halves in the midline by the posteromedian sulcus, and each half is composed of the gracile fasciculus and tubercle medially and the cuneate fasciculus and tubercle laterally. The posteromedian sulcus of the medulla, which separates the paired gracile fasciculi in the midline, ends superiorly at the obex of the fourth ventricle and is continuous inferiorly with the posteromedian sulcus of the spinal cord. The posterior intermediate sulcus, which separates the gracile and cuneate fasciculi, is continuous inferiorly with the posterior intermediate sulcus of the spinal cord. The lower medulla blends indistinguishably into the upper spinal cord at the level of the C1 nerve roots (Figs. 3.4, 3.10, and 3.11).

3.7.2 Floor

The floor has a rhomboid shape (Fig. 3.13). The rostral two thirds of the floor is posterior to the pons and the caudal one-third is posterior to the medulla. Its cranial apex is at the level of the cerebral aqueduct; its caudal tip, the obex, is located at the rostral end of the remnant of the spinal canal, anterior to the foramen of Magendie; and its lateral angles open through the lateral recesses and foramina of Luschka into the cerebellopontine angles. A line connecting the orifices of the lateral recesses is located at the level of the junction of the caudal and the middle third of the length of the floor and also at the level of the junction of the pons and the medulla.

The floor is divided into three parts: a superior or pontine part, an intermediate or junctional part, and an inferior or medullary part. The superior part has a triangular shape: its apex is at the cerebral aqueduct, its base is represented by an imaginary line connecting the lower margin of the cerebellar peduncles, and its lateral limbs are formed by the medial surfaces of the cerebellar peduncles. The intermediate part is the strip between the lower margin of the cerebellar

peduncles and the site of attachment of the tela choroidea to the taeniae just below the lateral recesses. The intermediate part extends into the lateral recesses. The inferior part has a triangular shape and is limited laterally by the taeniae marking the inferolateral margins of the floor. Its caudal tip, the obex, is anterior to the foramen of Magendie.

The floor is divided longitudinally from the rostral apex to the caudal tip into symmetrical halves by the median sulcus. The sulcus limitans, another longitudinal sulcus, divides each half of the floor into a raised median strip, called the median eminence, that borders the midline and a lateral region called the vestibular area.

Each median eminence, the strip between the sulcus limitans and the median sulcus, from above to below contains the facial colliculus, a rounded prominence related to the facial nerve, and three triangular areas overlying the hypoglossal and vagus nuclei and the area postrema. The three triangular areas are paired and are stacked along the median sulcus to give the caudal part of the floor a feather or pen nib configuration; thus, the area is called the calamus scriptorius. At the pontine level the median eminence has a width equal to that of the full half of the floor and thus the sulcus limitans corresponds with the lateral limit of this part of the floor.

The sulcus limitans is discontinuous and is most prominent in the pontine and medullary portions of the floor, where it deepens at two points to form dimples called foveae, and is least distinct in the junctional part of the floor. One of the two dimples, the superior fovea, is located in the pontine portion of the floor and the other, the inferior fovea, is located in the medullary part of the floor. At the level of the superior fovea, the median eminence forms an elongated swelling, the facial colliculus, which overlies the nucleus of the abducens nerve and the ascending section of the root of the facial nerve. At the rostral tip of each sulcus limitans in the lateral margin of the floor is a bluish gray area, the locus ceruleus, which owes its color to a group of pigmented nerve cells. The hypoglossal triangle is medial to the inferior fovea and overlies the nucleus of the hypoglossal nerve. Caudal to the inferior fovea

and between the hypoglossal triangle and the lower part of the vestibular area is a triangular dark field, the vagal triangle, that overlies the dorsal nucleus of the vagus nerve. A translucent ridge, the funiculus separans, crosses the lower part of the vagal triangle. The area postrema forms a small tongue-shaped area between the funiculus separans and the gracile tubercle in the lower limit of the median eminence immediately rostral to the obex.

The vestibular area, the portion of the floor lateral to the median eminence and sulcus limitans, is widest in the intermediate part of the floor, where it forms a rounded elevation that extends into the lateral recess. White strands, the striae medullaris, course transversely from the region of the lateral recess across the inferior cerebellar peduncles above the hypoglossal triangles toward the midline and disappear in the median sulcus. The vestibular nuclei lie beneath the vestibular area. The auditory tubercle produced by the underlying dorsal cochlear nucleus and the cochlear part of the vestibulocochlear nerve forms a prominence in the lateral part of the vestibular area.

3.8 Vascular Relationships

Optimizing operative approaches to the posterior fossa requires an understanding of the relationship of the cerebellar arteries to the cranial nerves, brainstem, cerebellar peduncles, fissures between the cerebellum and brainstem, and the cerebellar surfaces [12]. When examining these relationships, three neurovascular complexes are defined: an upper complex related to the superior cerebellar artery (SCA), a middle complex related to the anteroinferior cerebellar artery (AICA), and a lower complex related to the posteroinferior cerebellar artery (PICA) (Figs. 3.4, 3.12, 3.14, and 3.15) [10].

The upper complex includes the SCA, midbrain, cerebellomesencephalic fissure, superior cerebellar peduncle, tentorial surface of the cerebellum, and the oculomotor, trochlear, and trigeminal nerves. The SCA arises in front of the midbrain and passes below the oculomotor and

trochlear nerves and above the trigeminal nerve to reach the cerebellomesencephalic fissure, where it runs on the superior cerebellar peduncle and terminates by supplying the tentorial surface of the cerebellum.

The middle complex includes the AICA, pons, middle cerebellar peduncle, cerebellopontine fissure, petrosal surface of the cerebellum, and the abducens, facial, and vestibulocochlear nerves. The AICA arises at the pontine level and courses in relationship to the abducens, facial, and vestibulocochlear nerves to reach the surface of the middle cerebellar peduncle, where it courses along the cerebellopontine fissure and terminates by supplying the petrosal surface of the cerebellum.

The lower complex includes the PICA, medulla, inferior cerebellar peduncle, cerebellomedullary fissure, suboccipital surface of the cerebellum, and the glossopharyngeal, vagus, spinal accessory, and hypoglossal nerves. The PICA arises at the medullary level and encircles the medulla, passing in relationship to the glossopharyngeal, vagus, accessory, and hypoglossal nerves to reach the surface of the inferior cerebellar peduncle, where it dips into the cerebellomedullary fissure and terminates by supplying the suboccipital surface of the cerebellum (Fig. 3.12).

3.8.1 The Cerebellar Arteries

Each wall of the fourth ventricle has surgically important arterial relationships: the SCA is intimately related to the superior half of the roof; the PICA is intimately related to the inferior half of the roof; the AICA is intimately related to the lateral recess and the foramen of Luschka; and the basilar and vertebral arteries give rise to many perforating branches that reach the floor of the fourth ventricle [1–4, 7, 8] (Figs. 3.12 and 3.14). The choroidal branches of the AICA supply the portion of the choroid plexus in the cerebellopontine angle and the adjacent part of the lateral recess, and the PICA supplies the choroid plexus in the roof and the medial part of the lateral recess [2]. There are no major veins within the cavity of the fourth ventricle.

3.8.2 The Superior Cerebellar Artery

The superior cerebellar artery (SCA) is intimately related to the cerebellomesencephalic fissure, the superior half of the fourth ventricular roof, the superior cerebellar peduncle, and the tentorial surface (Figs. 3.12 and 3.14). The SCA arises in front of the midbrain, usually from the basilar artery near the apex, and passes below the oculomotor nerve but may infrequently arise from the proximal PCA and pass above the oculomotor nerve. It dips caudally and encircles the brainstem near the pontomesencephalic junction, passing below the trochlear nerve and above the trigeminal nerve. Its proximal portion courses medial to the free edge of the tentorium cerebelli, and its distal part passes below the tentorium, making it the most rostral of the infratentorial arteries. After passing above the trigeminal nerve, it enters the cerebellomesencephalic fissure, where its branches make several sharp turns and give rise to the precerebellar arteries, which pass to the deep cerebellar white matter and the dentate nucleus. On leaving the cerebellomesencephalic fissure where its branches are again medial to the tentorial edge, its branches pass posteriorly under the tentorial edge and are distributed to the tentorial surface. It usually arises as a single trunk but may also arise as a double (or duplicate) trunk. The SCAs arising as a single trunk bifurcate into a rostral and a caudal trunk. The SCA gives off perforating branches to the brainstem and cerebellar peduncles. Precerebellar branches arise within the cerebellomesencephalic fissure. The rostral trunk supplies the vermis and paravermian area and the caudal trunk supplies the hemisphere on the suboccipital surface. The SCA frequently has points of contact with the oculomotor, trochlear, and trigeminal nerves [3, 4, 9, 11, 13].

3.8.3 Anteroinferior Cerebellar Artery

The anteroinferior cerebellar artery (AICA) courses through the central part of the cerebellopontine angle near the facial and vestibulocochlear

nerve (Fig. 3.4). It or its branches may be exposed in surgical approaches to cerebellopontine angle, basilar or vertebral arteries, clivus, and the fourth ventricle and cerebellum and during approaches directed through the temporal and occipital bones.

The AICA is intimately related to the pons, lateral recess, foramen of Luschka, cerebellopontine fissure, middle cerebellar peduncle, and petrosal cerebellar surface (Figs. 3.4, 3.14, and 3.15). The AICA originates from the basilar artery, usually as a single trunk, and encircles the pons near the abducens, facial, and vestibulocochlear nerves. After coursing near and sending branches to the nerves entering the acoustic meatus and to the choroid plexus protruding from the foramen of Luschka, it passes around the flocculus on the middle cerebellar peduncle to supply the lips of the cerebellopontine fissure and the petrosal surface. It commonly bifurcates near the facial-vestibulocochlear nerve complex to form a rostral and a caudal trunk. The rostral trunk sends its branches laterally along the middle cerebellar peduncle to the superior lip of the cerebellopontine fissure and the adjoining part of the petrosal surface, and the caudal trunk supplies the inferior part of the petrosal surface, including a part of the flocculus and the choroid plexus. The AICA gives rise to perforating arteries to the brainstem, choroidal branches to the tela and choroid plexus, and the nerve-related arteries, including the labyrinthine, recurrent perforating, and subarcuate arteries [8].

3.8.4 Posteroinferior Cerebellar Artery

The PICA has the most complex, tortuous, and variable course and area of supply of the cerebellar arteries. It may be exposed in surgical approaches to the foramen magnum, fourth ventricle, cerebellar hemisphere, brainstem, jugular foramen, cerebellopontine angle, petrous apex, and clivus [7].

The PICA is intimately related to the cerebellomedullary fissure, the inferior half of the ventricular roof, the inferior cerebellar peduncle, and the suboccipital surface (Figs. 3.4, 3.12, 3.14, and 3.15). The PICA, by definition, arises from the vertebral artery

near the inferior olive and passes posteriorly around the medulla. At the anterolateral margin of the medulla, it passes rostral or caudal to or between the rootlets of the hypoglossal nerve, and at the posterolateral margin of the medulla, it courses rostral to or between the fila of the glossopharyngeal, vagus, and accessory nerves. After passing the latter nerves, it courses around the cerebellar tonsil and enters the cerebellomedullary fissure and passes posterior to the lower half of the roof of the fourth ventricle. On exiting the cerebellomedullary fissure, its branches are distributed to the vermis and hemisphere of the suboccipital surface. Its area of supply is the most variable of the cerebellar arteries [6]. Most PICAs bifurcate into a medial and a lateral trunk. The medial trunk supplies the vermis and adjacent part of the hemisphere, and the lateral trunk supplies the cortical surface of the tonsil and the hemisphere. The PICA gives off perforating, choroidal, and cortical arteries. The cortical arteries are divided into vermian, tonsillar, and hemispheric groups.

The veins most intimately related to the fourth ventricle are those in the fissures between the cerebellum and the brainstem and on the cerebellar peduncle [9, 10]. The veins of the cerebellomesencephalic fissure and the superior cerebellar peduncle course on the superior part of the roof, the veins of the cerebellomedullary fissure and the inferior cerebellar peduncle drain the inferior half of the roof, and the veins of the cerebellopontine fissure and the middle cerebellar peduncle drain the lateral wall and the cerebellopontine angle around the lateral recess.

References

1. Duvernoy H (1978) Human brainstem vessels. Springer, Berlin
2. Fujii KLC, Rhoton AL Jr (1980) Microsurgical anatomy of the choroidal arteries: fourth ventricle and cerebellopontine angles. *J Neurosurg* 52:504–524
3. Hardy DG, Rhoton A Jr (1978) Microsurgical relationship of the superior cerebellar artery and the trigeminal nerve. *J Neurosurg* 49:669–678
4. Hardy DG, Rhoton A Jr (1980) Microsurgical anatomy of the superior cerebellar artery. *Neurosurgery* 6:10–28
5. Johnston T (1934) A note on the peduncle of the flocculus and the posterior medullary velum. *J Anat* 68:471–479

6. Kaplan HAFD (1966) Arteria cerebelli inferior posterior. In: *The brain vascular system*. Elsevier, Amsterdam, pp 93–95
7. Lister JR, Rhoton A Jr, Matsushima T, Peace DA (1982) Microsurgical anatomy of the posterior inferior cerebellar artery. *Neurosurgery* 10:170–199
8. Martin RG, Grant J, Peace D, Theiss C, Rhoton AL Jr (1980) Microsurgical nerve complex. *Neurosurgery* 6:483–507
9. Matsuno H, Rhoton AL Jr, Peace D (1988) Microsurgical anatomy of the posterior fossa cisterns. *Neurosurgery* 23:58–80
10. Matsushima TRAJ, Lenkey C (1982) Microsurgery of the fourth ventricle: part I—microsurgical anatomy. *Neurosurgery* 11:631–667
11. Ono M, Ono M, Rhoton AL Jr, Barry M (1984) Microsurgical anatomy of the region of the tentorial incisura. *J Neurosurg* 60:365–399
12. Rhoton AJ (1993) Microsurgical anatomy of posterior fossa cranial nerves. In: *Neurosurgical topics*. AANS, Chicago, pp 1–103
13. Rhoton AL Jr (2000) The cerebellar arteries. *Neurosurgery* 47:S29–S68

Akin Akakin and Albert L. Rhoton Jr.

The posterior cranial fossa contains the most complex intracranial anatomy. The posterior fossa is strategically important situated at the outlet of the cerebrospinal fluid flow from the ventricular system. The posterior fossa extends from the tentorial incisura, through which it communicates with the supratentorial space, to the foramen magnum, through which it communicates with the spinal canal. It is bounded in front by the dorsum sellae, the posterior part of sphenoid body, and clival part of the occipital bone; behind by the lower portion of the squamosal part of the occipital bone; and on each side by the petrous and mastoid parts of the temporal bone, the lateral part of occipital bone, and above and behind by a small part of mastoid angle of the parietal bone.

The cerebellum consists of three anatomical parts: a median vermis and two lateral hemispheres. The central vermis is elevated above the level of the hemispheres on the upper surface of the cerebellum, contrary to its deep depression on the suboccipital surface (Fig. 4.1).

The cerebellum has fissures that divide the organ into series of layers or leaves. The largest and deepest fissure is the horizontal sulcus. The horizontal sulcus divides the semilunar lobule into inferior and superior semilunar lobules.

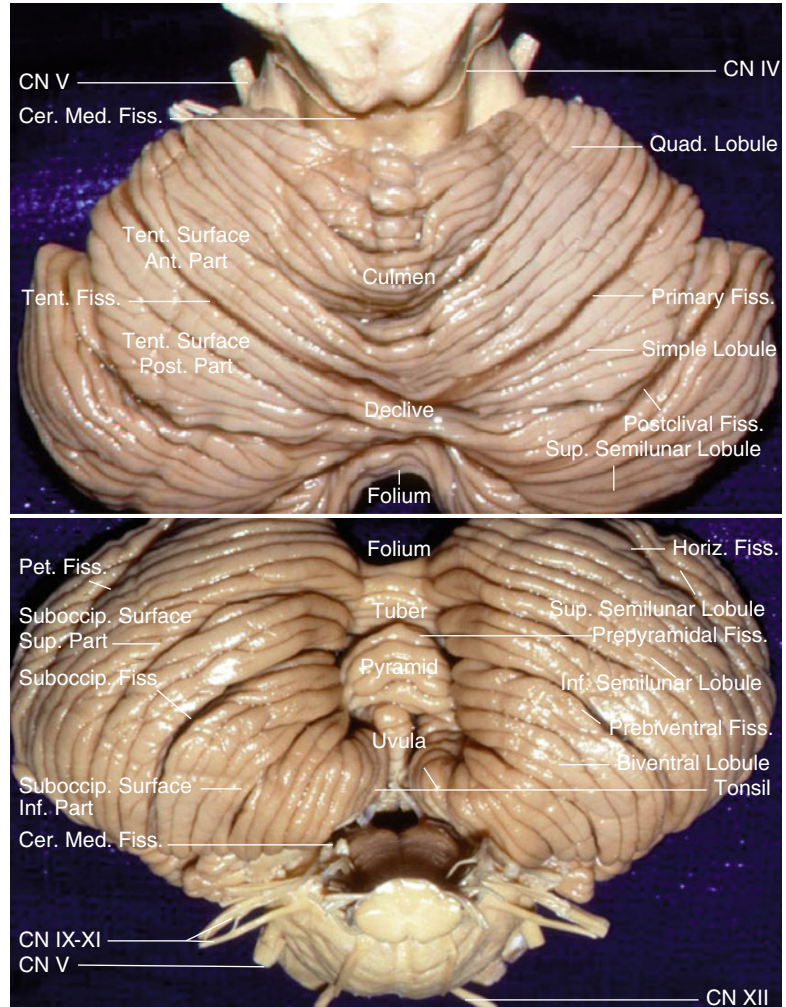
The vermis is positioned between the two hemispheres and is an important structure in the transvermian approach as it connects both hemispheres. Culmen represents the most apical part of the vermis at the tentorial surface. From posterior to anterior, the subdivisions of the superior vermis are represented by lingula, central lobule, monticulus, and folium vermis. Vermal parts of the posterior lobe are, in the following order, the declive, folium, tuber, pyramid, and uvula. This attachment area of the pyramid is a landmark for the dentate nucleus in cadaveric dissections. The lobus centralis is a small square lobule situated in the anterior cerebellar notch (Fig. 4.2).

The folium vermis is a short, narrow, and concealed band-like structure at the posterior extremity of the vermis. Laterally, it expands in either hemisphere into a sizeable lobule, the superior semilunar lobule which occupies the posterior third of the upper surface of the hemisphere and connected below by the horizontal sulcus. The superior semilunar lobule receives fibers mainly from middle cerebellar peduncles. These are known as pontocerebellar and corticocerebellar fibers.

A. Akakin (✉)
Department of Neurosurgery, Bahcesehir University,
Çırağan Caddesi Osmanpaşa Mektebi Sokak No: 4 – 6,
Beşiktaş, Istanbul 34353, Turkey
e-mail: drakinakakin@yahoo.com

A.L. Rhoton Jr., M.D.
Department of Neurosurgery, Florida University,
100625, Gainesville, FL 32610, USA
e-mail: rhoton@neurosurgery.ufl.edu

Fig. 4.1 Tentorial and suboccipital surface view of cerebellum



4.1 Lobes of the Cerebellum

The cerebellum consists of three parts, a median and two lateral, which are continuous with each other, and are substantially the same in structure. The median portion is constricted and is called the vermis. The hemispheres are separated below and behind by a deep notch, the posterior cerebellar notch, and in front by a broader shallower notch, the anterior cerebellar notch. The anterior notch lies close to the pons and upper part of the medullas, and its superior edge encircles the inferior colliculi and superior cerebellar peduncle. The posterior notch con-

tains the upper part of the falx cerebelli, fold of dura mater. The cerebellum is characterized by a laminated or foliated appearance; it is marked by deep, somewhat curved fissures and divides into a series of layers or leaves. The largest and deepest fissure is named horizontal sulcus. Several secondary but deep fissures separate the cerebellum into lobes, and these are further subdivided by shallower sulci, which separate the individual folia, though differing in appearance from the convolutions of the cerebrum, are analogous to them, in as much as they consist of central white substance covered by gray substance (Figs. 4.2 and 4.3).

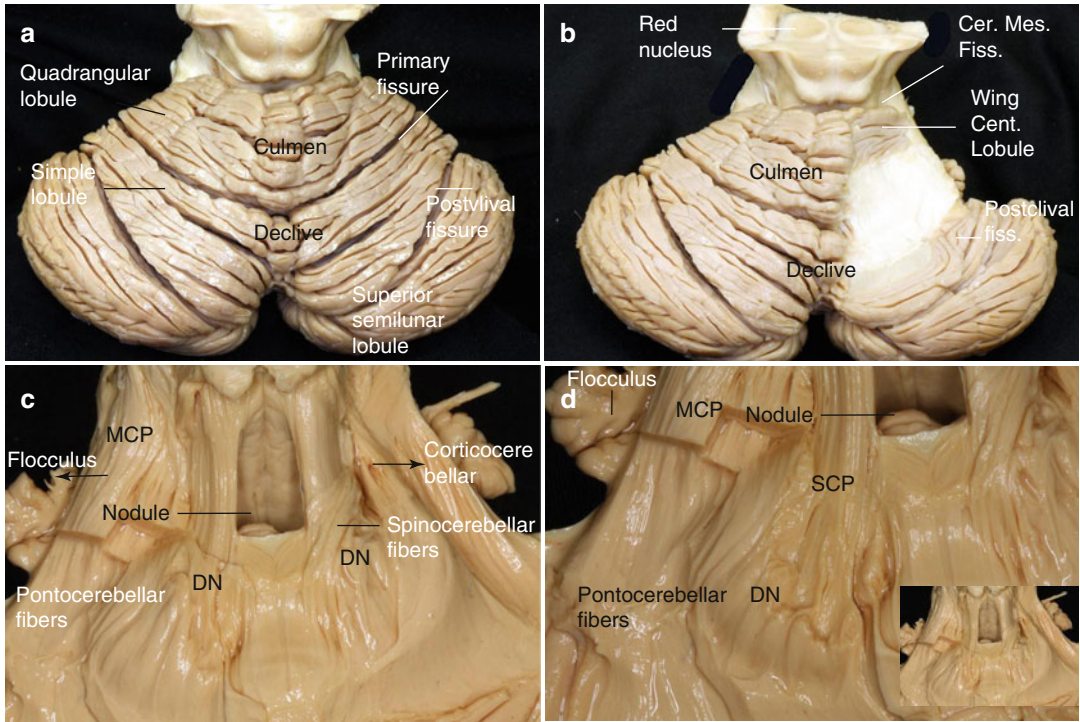


Fig.4.2 (a) On the tentorium surface the primary fissure is located in the DN area. The simple and quadrangular lobules have been retracted to expose the lateral part of the central lobule. Culmen is medial and above the DN from the tentorium surface. Its posteroinferior attachment area is approximately the beginning of the DN from the tentorium surface. If dissection begins from the primary fissure, after retraction of the simple and quadrangular lobules laterally, inferior cerebellar peduncle fibers can be followed from lateral to medial. (b) Inferior cerebellar peduncle has fibers crossing to the contralateral side of the cerebellum that pass anterior and inferior to the nodule. The hilus of the DN is approximately at this

level. (c) Superiorolateral side of the cerebellum, after removing quadrangular lobule on both sides. Superior medullary velum is dissected. After retraction of the superior cerebellar triangle laterally, the superiorolateral side of the choroid plexus and the fourth ventricle floor is observed with the facial colliculus and median eminence. (d) Closure view of image C with the retraction of the superior cerebellar peduncle. Some middle cerebellar peduncle fibers have been removed to expose the border of the DN. *CC* corticocerebellar, *DN* dentate nucleus, *MCP* middle cerebellar peduncle, *SCP* superior cerebellar peduncle

The upper surface of the cerebellum is elevated in the middle and sloped toward the circumference of the hemisphere being connected together by the superior vermis. The superior vermis is mainly subdivided into four parts: lingula, the lobus centralis, the monticulus, and folium vermis. These are continuous with corresponding parts of cerebellar hemisphere, except lingula (Fig. 4.3).

The lingula is a small tongue-shaped process consisting of four or five folia. Anteriorly it rests on the dorsal surface of the anterior medullary

velum and its white substance is continuous with that of the velum. Anteriorly it overlaps the lobulus centralis from which it is separated by the postcentral fissure. Laterally it is continuous with the quadrangular lobule in the hemispheres.

4.1.1 Superior Cerebellar Peduncle

On sagittal dissections, the superior cerebellar peduncle located approximately 5 mm from the midline can be identified lateral to superior med-

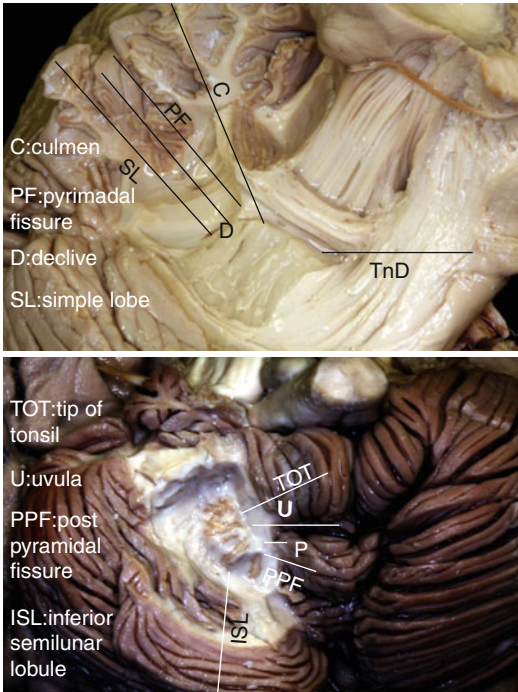


Fig. 4.3 Larger view of lateral appearance of cerebellum

ullary velum, tracking obliquely from the cerebellum to the midbrain. The superior cerebellar peduncle is the largest cerebellar efferent bundle. The superior cerebellar peduncles emerge from the upper and medial part of the white substance of the hemispheres, and they project in parallel and are placed undercover of the superior and inferior colliculi. They are joined by the superior medullary velum, can be followed up to the inferior colliculi, and disappear in the red nucleus.

The superior cerebellar peduncle is the largest efferent group of fibers of the DN. They form the upper lateral boundaries of the fourth ventricle, but as they ascend, they converge on the dorsal aspect of the ventricle and thus assist in the formation of its roof. The dentate-rubro-thalamic tract (dentatothalamic tract) is the major tract of the superior cerebellar peduncle. It ascends to the red nucleus, decussates, and projects to the ventrolateral side of the thalamus.

After exposure of the superior medullary velum, the nuclei of the abducens, the vestibular, and cochlear nerves can be readily seen in the fourth ventricle floor in anatomical specimens (Fig. 4.4).

4.1.2 Middle Cerebellar Peduncle

There are two groups of middle cerebellar peduncle fibers passing to the cerebellum. The first group of fibers is parallel to the midline and is essentially called the corticocerebellar fibers. The other group projects parallel to the DN, toward the posterior cerebellum to reach the superior and inferior semilunar lobules. This group is known as pontocerebellar fibers. Middle cerebellar peduncles radiate to entire cerebellar locations. Superior fibers of the middle cerebellar peduncle make a curve around the DN. These fibers cover the DN from medial to lateral direction. Middle cerebellar peduncle fibers wrap the DN superiorly and inferiorly. Fibers on the inferior side are named as the middle cerebellar inferior fibers and they project to the posterior cerebellum passing superiorly over the tonsils. These fibers constitute the pontocerebellar fibers. Fibers located superiorly are referred to as the middle cerebellar superior fibers and some of those fibers project mainly ipsilaterally while others project contralaterally. Middle cerebellar peduncle fibers curve over the DN and project to the contralateral side from the posterior of the nodule (Fig. 4.5).

4.1.3 Inferior Cerebellar Peduncle

The inferior cerebellar peduncle ascends from the medulla to the cerebellum conveying a number of fiber systems to the cerebellum. Inferior cerebellar peduncle fibers ascend to the cerebellum from the lateral pons and pass dorsally from the roof of the fourth ventricle. The inferior cerebellar peduncle fibers cross to the contralateral side of cerebellum over the nodule; however, some fibers follow an ipsilateral course from the lateral border of the nodule. They mainly carry the spinocerebellar, cuneocerebellar, olivocerebellar, and vestibulocerebellar pathways.

The nodule or the anterior part of the inferior vermis is located between the two DN's. It has a semilunar shape and its convex border is continuous with the white substance of the cerebellum,

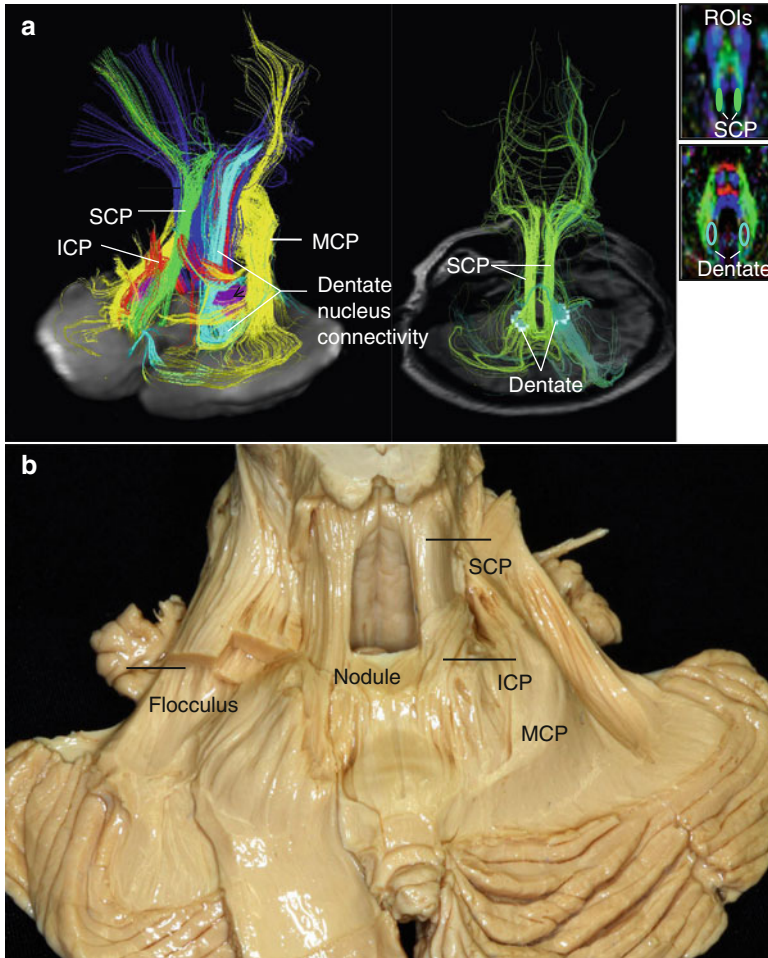


Fig. 4.4 Tractographic reconstruction (a) showing an oblique posterior view of cerebellum and cerebellar peduncles with dentate nucleus (arrow) and dentate nucleus connectivity on the right side (light blue). SCP is only shown on the left side. SCP (superior cerebellar peduncle, green), ICP (inferior cerebellar peduncle, red, bilateral), MCP (middle cerebellar peduncle, yellow, bilat-

eral), LM (lemniscus medialis, blue). (b) Enlarged view of the cerebellum with dissection of the tentorial surface. Middle cerebellar peduncle fibers are making a curve around the dentate nucleus. Inferior cerebellar peduncle fibers are passing anterior to the DN and crossing to other side anterior to the nodule. Dentate nucleus has projection fibers to posterior part of the inferior semilunar lobule

extending on either side up to the flocculus. On either side of the nodule, a thin layer of a white substance exists which it is referred to as the inferior medullary velum. It also has a semilunar form and its convex border is continuous with the white substance of the cerebellum. Inferior cerebellar peduncle fibers cross to the contralateral side superior to the nodule and some ipsilateral fibers project posteriorly through the superolateral side of the nodule.

While some of these fibers pass from the anterior surface of the DN projecting from lateral direction to the medial, some others follow a parallel course to the nodule and dorsally to the fourth ventricle roof. Dorsal spinocerebellar fibers ascend ipsilaterally in a tract that is located at the edge of the spinal cord and terminate ipsilaterally. The inferior cerebellar peduncle also carries the olivocerebellar pathway. This pathway is distributed to all parts of the cerebellum at

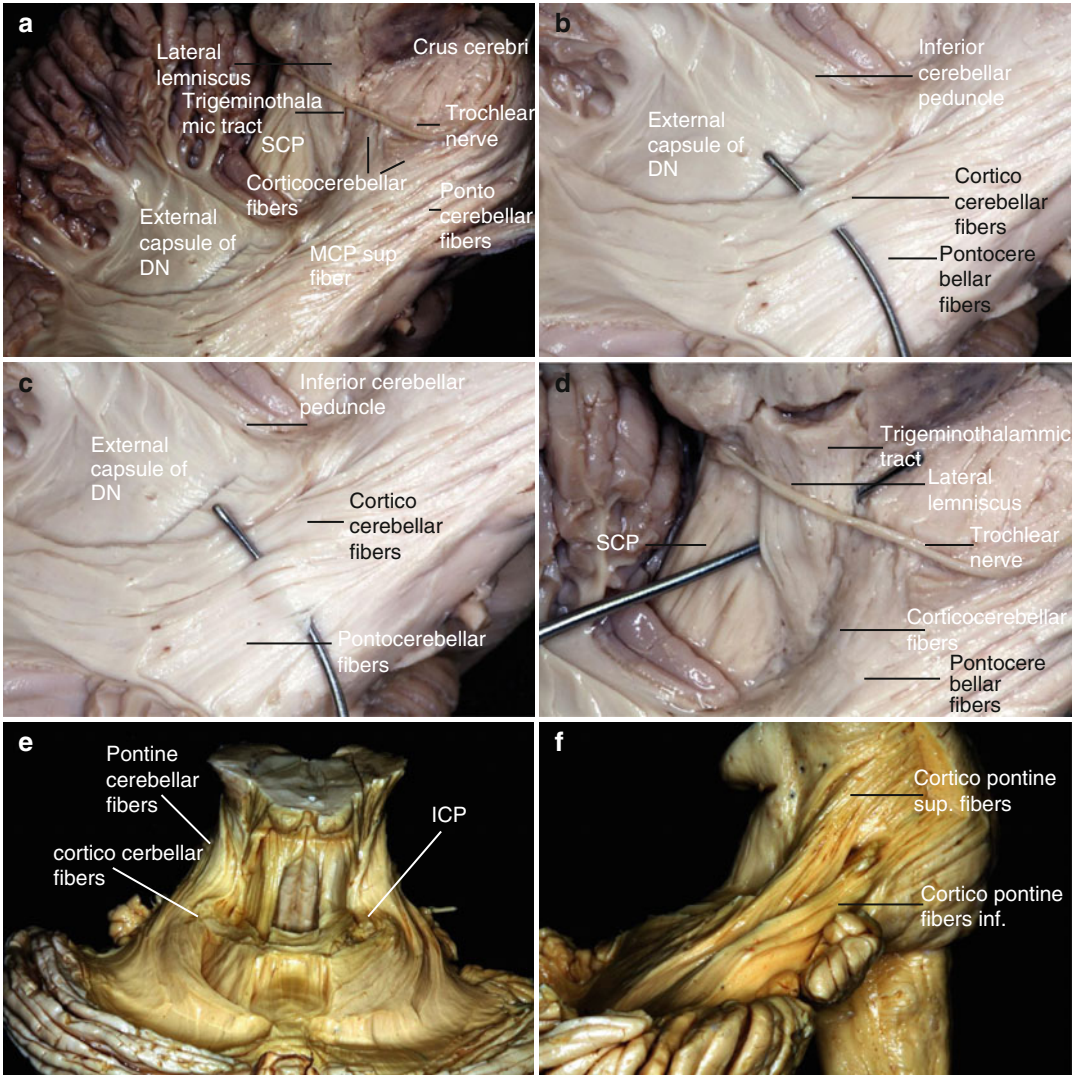
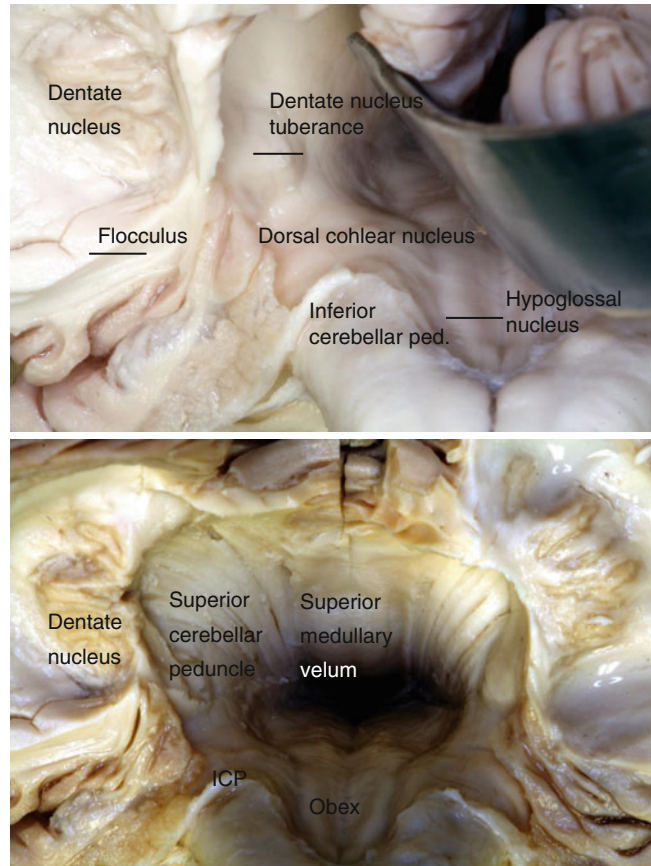


Fig. 4.5 On selective tracking, the images show very clearly the projection of the SCP. The importance of images showing the SCP suggests that these tracts correspond mainly to efferent cerebellar pathways. Nevertheless, there are images showing also fibers corresponding to the middle cerebellar peduncle (a). This is not surprising due to the fact that these nuclei are enveloped by the terminal fibers of this peduncle. The section corresponding to the anatomic specimen (b) shows very clearly the SCP with fibers from the dentate which cross the midline below the level of the red nucleus. The dentate nucleus is very outlined and could be traced with surrounding fibers. At the midbrain level, the ascending lateral lemniscus, the more oblique SCP, and the transverse crossing fibers will be easily distinguished by their different colors when they are analyzed on DTI. (c) The commissural vermian system was apparent in red on the

midline. The other anteroposterior or posteroanterior tracts appeared in green, and these correspond to the projections of the cerebellar hemispheres to the dentate. However, their more anterior components were intermixed with the afferent white matter projections following the MCP. (d) The same specimen with closure view; lateral lemniscus and trigeminothalamic tract dissected over the dissector. Trochlear nerve is passing over the lateral lemniscus. Superior cerebellar peduncle is passing medially and inferiorly to lateral lemniscus. (e) Inferior cerebellar peduncle passes other side of nodule. Middle cerebellar peduncle fibers are covering the dentate nucleus. (f) Lateral view of the same specimen trigeminal nucleus arising from the middle cerebellar peduncle. Flocculus is just lateral to the middle cerebellar peduncle fibers. Corticopontine cerebellar fibers are passing over the trigeminal nerve

Fig. 4.6 Inferior view of the fourth ventricle

the ipsilateral and contralateral sides. The cuneocerebellar tract conveys fibers from the ipsilateral accessory cuneate nucleus to the cerebellum (Fig. 4.6).

4.2 Cerebellar Surfaces

4.2.1 Tentorial Surface

The tentorial surface faces the tentorium and is retracted in the supracerebellar approach. The anteromedial part of the tentorial surface, the apex, formed by the anterior vermis, is the highest point on the cerebellum. Its surface slopes downward from its anteromedial to its posterolateral edge. The tentorial surface carries the inferior and middle cerebellar peduncle fibers from superioanterior to posteroinferior direction. The hemispheric part of the tentorial surface includes

the quadrangular, simple, and superior semilunar lobules and the vermian division includes the culmen, declive, and folium.

This lobe receives corticocerebellar and pontocerebellar fibers from the middle cerebellar peduncle. Anterior and medial to these fibers lie the inferior cerebellar peduncle fibers.

The tentorial surface is divided into anterior and posterior sections by its major fissure, the tentorial fissure. This fissure, located between the quadrangular and the simple lobules on the hemisphere and the culmen and the declive on the vermis, has also been called the primary fissure. The postclival fissure separates the simple and the superior semilunar lobules.

The dissection of the tentorial surface from the simple lobe to the superior semilunar lobule is shown. The superior cerebellar peduncle and lateral lemniscus can be seen after dissection of the simple and quadrangular lobules. The inferior cerebellar

peduncle fibers and superior cerebellar peduncle fibers can be observed after removing the simple and quadrangular lobules. After dissection of middle cerebellar peduncle fibers, a very thin external capsule is observed superior to the DN (Fig. 4.1).

4.2.2 Lateral Surface

The lateral recesses are narrow, curved pouches formed by the union of the roof and the floor. The rostral wall of each lateral recess is formed by the caudal margin of the cerebellar peduncles. The inferior cerebellar peduncle courses upward in the floor ventral to the lateral recess and turns posteriorly at the lower part of the pons to form the ventricular surface of the rostral wall. The inferior cerebellar peduncle ascends superomedial to the DN and courses between the superior and middle cerebellar peduncles. The biventral lobule that is inferomedial to the DN is dorsal to the lateral recess. The lateral lemniscus courses lateral and superior to the DN and just lateral to the inferior cerebellar peduncle, and it crosses the superior cerebellar peduncle. The trigeminothalamic tract passes lateral to the lateral lemniscus and reaches the ventral posteromedial nucleus of the thalamus ipsilaterally. It arises from the sensory trigeminal nucleus that is located lateral to the locus caeruleus and vestibular fibers that join the medial longitudinal fasciculus (Fig. 4.5).

4.2.3 Suboccipital Surface

Operative approaches to the fourth ventricle and to most cerebellar tumors commonly involve this surface and its close proximity. The lateral walls of the incisura are formed by the medial part of the cerebellar hemispheres. Deep clefts, known as the vermohemispheric fissures, separate the vermis from the hemispheres. The vermian surface within the incisura has a diamond shape. The upper half of the diamond-shaped formation has a pyramidal shape, thus called the pyramid. The folium and the tuber, superior to the pyramid, form the apex of the suboccipital part of the ver-

mis. These structures are posteromedial to the DN. The nodule, the lowermost subdivision of the vermis, is hidden deep to the uvula.

The hemispheric portion of the suboccipital surface is formed by the superior and inferior semilunar and biventral lobules and the tonsils. This portion is important for the supratonsillar and subtonsillar approaches.

The tonsils and biventral lobule have been separated and the white matter in between is known as the tonsillobiventral fissure. This is an important landmark for the supratonsillar approach. This white matter is formed mainly by the middle cerebellar peduncle fibers. On the suboccipital surface, the pyramid and uvula form the area where the DN is closest to the surface. The uvula and tonsil comprise the lobus uvula. The pyramid and biventral lobules constitute the lobus pyramidalis. The pyramid is a conical projection forming the largest prominence of the inferior vermis. The lateral border is separated from the inferior semilunar lobule by the postpyramidal fissure.

In the sagittal section through the center of the vermis, superior cerebellar peduncle fibers and superior medullary velum can be observed along with an arbor vitae appearance. After sharp dissection of the cerebellum from posterior to anterior, the fourth ventricle can be observed with the facial colliculus. Facial nucleus and its fibers have been dissected in the specimen as to demonstrate the relation of nucleus. When the cerebellum is sharply dissected step-by-step from posterior to anterior, no gray matter can be encountered in the first 2 cm of dissection. In the second 2 cm of dissection, symmetrical appearance of the DN can be observed. In the third 2 cm dissection, the DN disappears (Fig. 4.7).

4.2.4 Cerebellar Fissures

The first of the fissures is the cerebellomesencephalic fissure, which extends from the pineal region downward between the cerebellum and the superior half of the fourth ventricle. Superior cerebellar peduncles are located in the anterior wall of this fissure. The second fissure is the cerebel-

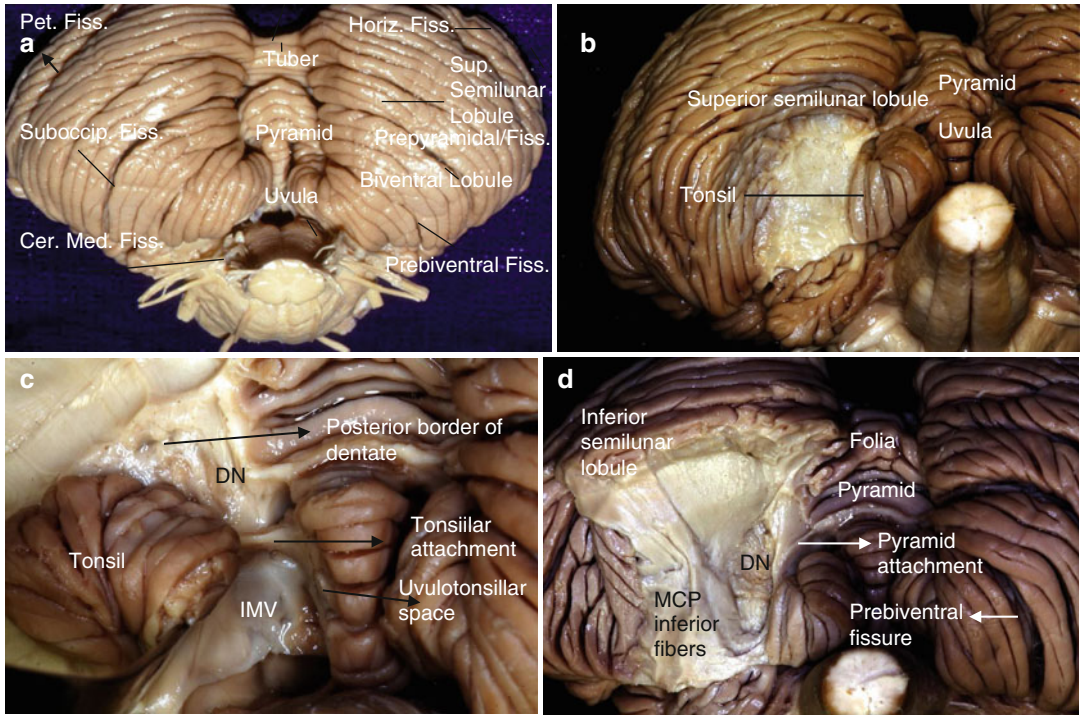


Fig. 4.7 (a) The suboccipital surface. The vermis sits in a large median depression, the posterior cerebellar incisura, between the cerebellar hemispheres. The portions of the vermis within the incisura from above to below are the folium, tuber, pyramid, and uvula. The parts of the hemispheric surface from above to below are the superior and inferior semilunar and biventral lobules and the tonsils. These lobules extend beyond the suboccipital surface to the other surfaces of the cerebellum. The prebiventral fissures between the inferior semilunar and the biventral lobules separate the hemispheres into superior and inferior parts, and the prepyramidal fissure between the pyramid and tuber separates the vermis into superior and inferior parts. From below to above, the corresponding vermian and hemispheric parts are the uvula and the tonsils, the pyramid and the biventral lobules, the tuber and inferior semilunar lobules, and the folium and the superior semilunar lobules. The petrosal (horizontal) fissure, the most prominent fissure on the petrosal surface, extends onto the suboccipital surface and divides the superior half of the suboccipital surface between the superior and inferior semilunar lobules. Between the biventral and tonsillar lobules there is prebiventral fissure which is important for approaching the fourth ventricle via the supratonsillar approach. (b) Biventral lobule has been dissected. The pyramid and biventral lobules constitute the lobuspyramidis. The pyramid is a conical projection, forming the largest prominence of the inferior vermis. The lateral border is separated from the inferior semilunar lobule by the postpyramidal fissure. The pyramid

has attachment to the DN laterally. The uvula has attachment at the base of the tonsils and the uvula and pyramid make an important landmark for the location of the DN. The base is directed forward, and is on a line with the anterior border of the tonsil, and is separated from the flocculus by the postnodular fissure. White matter in this area is formed with middle cerebellar peduncle fibers. (c) The pyramid attachment side to cerebellum is demonstrated. The folium and the tuber, superior to the pyramid, form the apex of the suboccipital part of the vermis. These structures are posteromedial to the DN. The uvula is the medial part of DN. The tonsil is located anterior, inferior and medial to the DN. (d) The lower half of the diamond-shaped formation, the uvula, projects downward between the tonsils. The uvula and pyramid are very close to the DN rather than the other midline structures. (e) There are some fibers projecting posteriorly called the middle cerebellar peduncle inferior fibers. Middle cerebellar peduncle fibers can be distinguished laterally and medially. Note the DN at this level, which is medial to the trajectory of the supratonsillar approach. (f) Closure view of (e). The DN border is inferior to the tonsil attachment area, medially pyramidal attachment is 1.8 mm away from the medial border of the DN. CC corticocerebellar, DN dentate nucleus, ICP inferior cerebellar peduncle, ISL inferior semilunar lobule, LL lateral lemniscus, MCP middle cerebellar peduncle, N nodule, PC pontocerebellar, SL simple lobule, SCP superior cerebellar peduncle, SMV superior medullary velum, SSL superior semilunar lobule

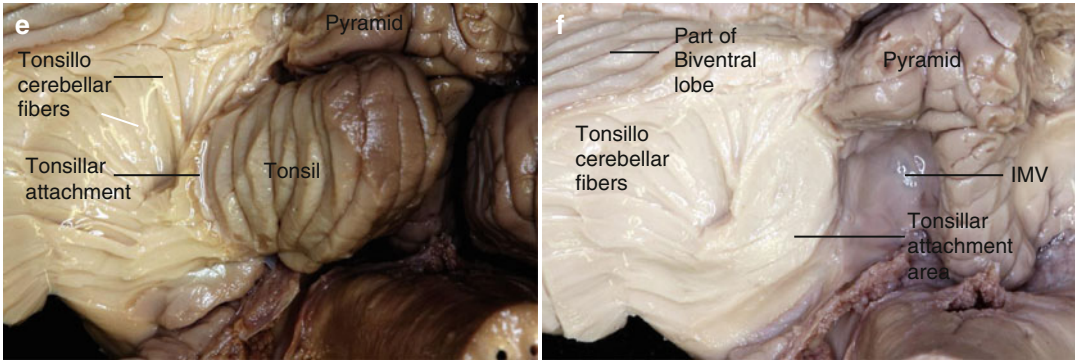


Fig. 4.7 (continued)

lopontine fissure that is formed by the folding of the cerebellum around the lateral sides of the pons and is intimately related to the lateral recesses. The middle cerebellar peduncle is located in this fissure and carries the corticocerebellar and pontocerebellar tracts. The third fissure is the cerebello-medullary fissure that extends superiorly between the cerebellum and the medulla and is intimately related to the inferior half of the roof. This fissure mainly carries the ICP fibers and extends upward around the cerebellar tonsils and the lower half of the roof of the fourth ventricle, which is formed by the tela choroidea and the inferior medullary velum. This fissure is highly important for the telovelar, subtonsillar, and transcerebellomedullary approaches (Figs. 4.2 and 4.3).

4.3 Dorsal Aspect of Brain Stem Nucleus Anatomy

Lesions of the fourth ventricle have posed a special challenge to neurosurgeons because of severe deficits that may occur after injury to cranial nerve nuclei and pathways in the floor. Approaching to the fourth ventricle could be obtained by splitting the cerebellar vermis, retraction of tonsils, or by removing part of a cerebellar hemisphere.

The medulla oblongata extends from the lower margin of the pons to a plane passing transversely below the pyramidal decussation and above the first pair of cervical nerves; this plane corresponds with the upper border of the atlas behind. Its posterior surface is received into the fossa

between the hemispheres of the cerebellum, and the upper portion of it forms the lower part of the floor of the fourth ventricle.

The medulla oblongata is pyramidal in shape, its broad extremity being directed upward toward the pons, while its narrow, lower end is continuous with the medulla spinalis. The central canal of the medulla spinalis is prolonged into its lower half and then opens into the cavity of the fourth ventricle; the medulla oblongata may therefore be divided into a lower closed part containing the central canal and an upper open part corresponding with the lower portion of the fourth ventricle.

It is a narrow groove and exists only in the closed part of the medulla oblongata; it becomes gradually shallower from below upward and finally ends about the middle of the medulla oblongata, where the central canal expands into the cavity of the fourth ventricle.

These two fissures divide the closed part of the medulla oblongata into symmetrical halves, each presenting elongated eminences which, on surface view, are continuous with the funiculi of the medulla spinalis. In the open part the halves are separated by the anterior median fissure and by a median raphe which extends from the bottom of the fissure to the floor of the fourth ventricle. This fissure extends into vestibular nucleus area. Similarly, the accessory, vagus, and glossopharyngeal nerves correspond with the posterior nerve roots and are attached to the bottom of a sulcus named the posterolateral sulcus. In this area, we can observe the vestibular nucleus laterally and hypoglossal nucleus more medially and inferior vestibular nucleus.

The lateral district is limited in front by the anterolateral sulcus and the roots of the hypoglossal nerve and behind by the posterolateral sulcus and the roots of the accessory, vagus, and glossopharyngeal nerves. Its upper part consists of a prominent oval mass which is named the olive, while its lower part is of the same width as the lateral funiculus of the medulla spinalis and appears on the surface to be a direct continuation of it. As a matter of fact, only a portion of the lateral funiculus is continued upward into this district, for the lateral cerebrospinal fasciculus passes into the pyramid of the opposite side, and the dorsal spinocerebellar fasciculus is carried into the inferior peduncle in the posterior district. The ventral spinocerebellar fasciculus is continued upward on the lateral surface of the medulla oblongata in the same relative position it occupies in the spinal cord until it passes under cover of the external arcuate fibers. It passes beneath these fibers just dorsal to the olive and ventral to the roots of the vagus and glossopharyngeal nerves; it continues upward through the pons along the dorsolateral edge of the lateral lemniscus. The remainder of the lateral funiculus consists chiefly of the lateral proper fasciculus. Most of these fibers dip beneath the olive and disappear from the surface, but a small strand remains superficial to the olive. In a depression at the upper end of this strand is the acoustic nerve (Figs. 4.6 and 4.7).

4.3.1 The Posterior District

It lies behind the posterolateral sulcus and the roots of the accessory, vagus, and the glossopharyngeal nerves and, like the lateral district, is divisible into a lower and an upper portion. The lower part is limited behind by the posterior median fissure and consists of the fasciculus gracilis and the fasciculus cuneatus. The fasciculus gracilis is placed parallel to and along the side of the posterior median fissure and separated from the fasciculus cuneatus by the postero-intermediate sulcus and septum. The gracile and cuneate fasciculi are at first vertical in direction, but at the lower part of the rhomboid fossa, they

diverge from the middle line in a V-shaped manner, and each presents an elongated swelling. That on the fasciculus gracilis is named the clava and is produced by a subjacent nucleus of gray matter, the nucleus gracilis; that on the fasciculus cuneatus is termed the cuneate tubercle and is likewise caused by a gray nucleus, named the nucleus cuneatus. The fibers of these fasciculi terminate by arborizing around the cells in their respective nuclei.

The upper part of the posterior district of the medulla oblongata is occupied by the inferior peduncle, a thick rope-like strand situated between the lower part of the fourth ventricle and the roots of the glossopharyngeal and vagus nerves. The inferior peduncles connect the medulla spinalis and medulla oblongata with the cerebellum and are sometimes named the restiform bodies. As they pass upward, they diverge from each other and assist in forming the lower part of the lateral boundaries of the fourth ventricle; higher up, they are directed backward, each passing to the corresponding cerebellar hemisphere. Near their entrance, into the cerebellum, they are crossed by several strands of fibers, which run to the median sulcus of the rhomboid fossa, and are named the striae medullares. The inferior peduncle appears to be the upward continuation of the fasciculus gracilis and fasciculus cuneatus. Stria medullaris is continuation of eight nerve fibers and pons over the inferior cerebellar peduncle.

Caudal to the striae medullares, the inferior peduncle is partly covered by the corpus pontobulbar, a thin mass of cells and fibers extending from the pons between the origin of the VII and VIII cranial nerves (Fig. 4.6).

Although the external form of the medulla oblongata bears a certain resemblance to that of the upper part of the medulla spinalis, its internal structure differs widely from that of the latter and this for the following principal reasons; certain fasciculi which extend from the medulla spinalis to the brain, and vice versa, undergo a rearrangement in their passage through the medulla oblongata; others which exist in the medulla spinalis end in the medulla oblongata; new fasciculi originate in the gray substance of the medulla oblongata and

pass to different parts of the brain; the gray substance, which in the medulla spinalis forms a continuous H-shaped column, becomes greatly modified and subdivided in the medulla oblongata, where also new masses of gray substance are added; on account of the opening out of the central canal of the medulla spinalis, certain parts of the gray substance, which in the medulla spinalis were more or less centrally situated, are displayed in the rhomboid fossa; the medulla oblongata is intimately associated with many of the cranial nerves, some arising from, and others ending in, nuclei within its substance.

4.4 Pons

The pons is situated in front of the cerebellum. Its dorsal or posterior surface is triangular in shape, is hidden by the cerebellum, and is bounded laterally by the superior peduncle; it forms the upper part of the rhomboid fossa.

From its superior surface the cerebral peduncles emerge, one on either side of the middle line. Curving around each peduncle, close to the upper surface of the pons, a thin white band, the taenia pontis, is frequently seen; it enters the cerebellum between the middle and superior peduncles. Behind and below, the pons is continuous with the medulla oblongata but is separated from it in front by a furrow in which the abducent, facial, and acoustic nerves appear.

Dorsal portion of the pons known as the pontine tegmentum is the rostral continuation of the medullary reticular formation. It contains cranial nerve nuclei, ascending and descending tracts, and reticular nuclei. Cranial nerve nuclei found in the pons are those cranial nerves facial, abducent, trigeminal, and vestibulocochlear.

Medial longitudinal fasciculus is situated dorsally on each side of the median raphe as in the medulla. The spinal trigeminal tract and nucleus lie medial to the inferior cerebellar peduncle. Vestibular nuclei are present in the floor of the fourth ventricle throughout the caudal pons. In pons area, there are the chief or pontine nucleus of trigeminal nerve, motor and sensory nucleus

of trigeminal nerve, facial nucleus and abducent nucleus.

The auditory division of the vestibulocochlear enters at the pons-medulla junction. Its fibers synapse in the cochlear nuclei and the central auditory pathway continues via the lateral lemnisci to the inferior colliculus. The vestibular division of vestibulocochlear nerve also enters at the pons-medulla junction and terminates in the vestibular nucleus which is an extensive area from high pons through the open medulla. Its connections are to the cerebellum, oculomotor, trochlear, and abducens nerve and form the vestibulospinal tracts. The medial lemniscus alters its position from that in the medulla. It moves laterally toward the spinothalamic tracts and lateral lemniscus in the ventral tegmentum.

The dorsal or tegmental part of the pons consist of transverse and longitudinal fibers and also contains important gray nuclei and is subdivided by a median raphe, however, does not extend into the basilar part, being obliterated by the transverse fibers. The transverse fibers in the lower part of the pons are collected into a distinct strand, named the trapezoid body. The longitudinal fibers, which are continuous with those of the medulla oblongata, are mostly collected into two fasciculi on either side. One of these lies between the trapezoid body and the reticular formation and forms the upward prolongation of the lemniscus; the second is situated near the floor of the fourth ventricle and is the medial longitudinal fasciculus (Figs. 4.8 and 4.9).

4.5 Midbrain

It is the short, constricted portion which connects the pons and cerebellum with the thalamencephalon and cerebral hemispheres. The cerebral peduncles are two cylindrical masses situated at the base of the brain and largely hidden by the temporal lobes of the cerebrum. The depressed area between the crura is termed the interpeduncular fossa and consists of a layer of grayish substance, the posterior perforated sub-

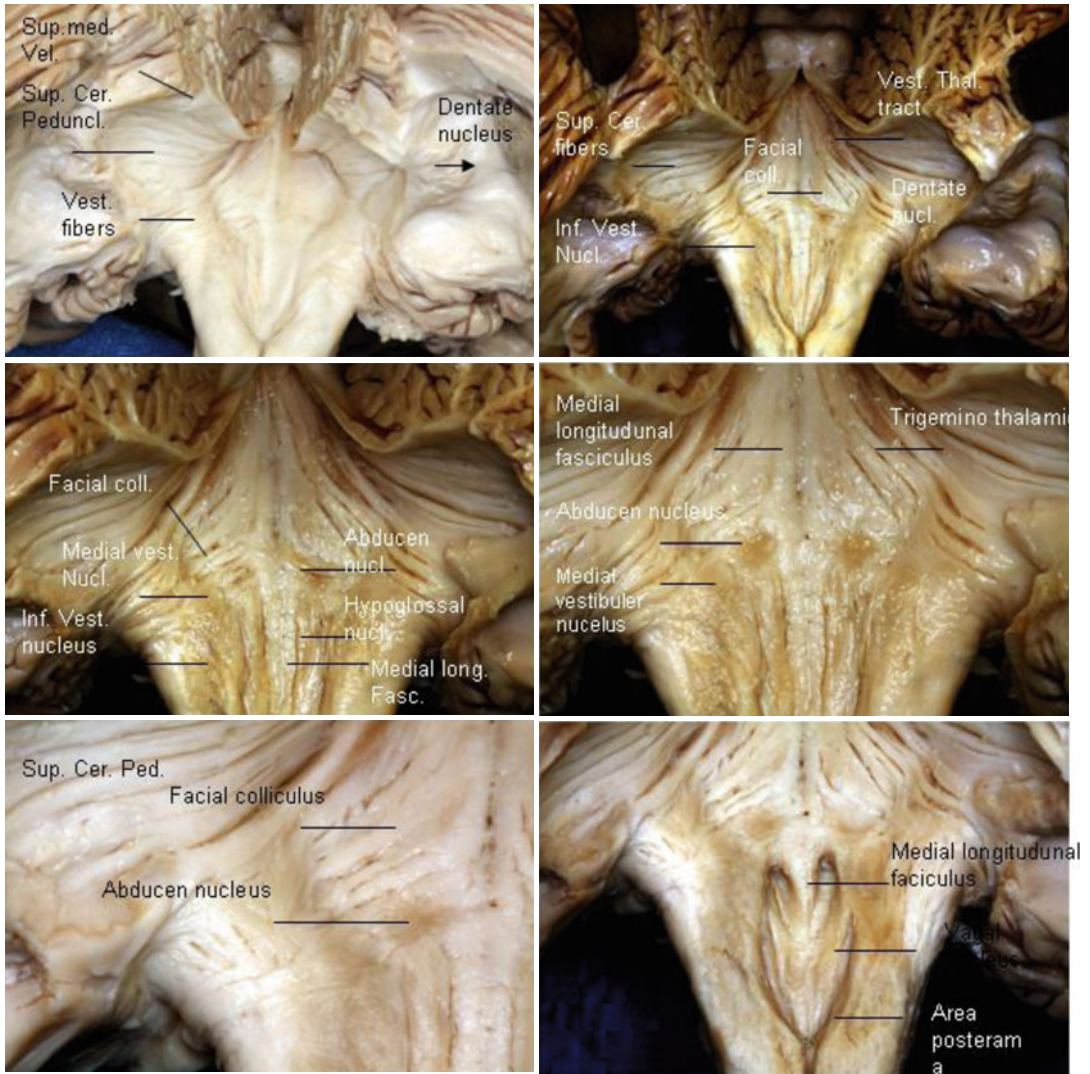


Fig. 4.8 Floor of the fourth ventricle

stance, and its upper part assists in forming the floor of the third ventricle. The medial surface of the peduncle forms the lateral boundary of the interpeduncular fossa and is marked by a longitudinal furrow, the oculomotor sulcus, from which the roots of the oculomotor nerve emerge. On the lateral surface of each peduncle, there is a second longitudinal furrow, termed the lateral sulcus; the fibers of the lateral lemniscus come to the surface in this sulcus, and

mass backward and upward, to disappear under the inferior colliculus.

4.6 Fourth Ventricle

The upper portion of the roof is formed by the superior peduncle and the anterior medullary velum; the lower portion, by the posterior medullary velum, the epithelial lining of the ventricle

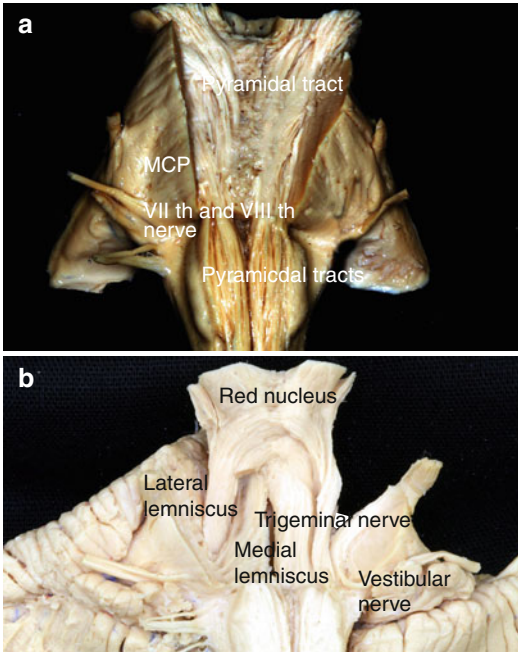


Fig. 4.9 (a) Anterior view of pons. Pyramidal tract with the middle cerebellar peduncle fibers (*MCP*). (b) After dissection of pyramidal tract: lateral lemniscus can be observed and inferior medial to lateral lemniscus, medial lemniscus is followed up. Lateral to lateral lemniscuses trigeminal nerve and vestibular nerve with middle cerebellar peduncle fibers can be observed

covered by the tela chorioidea inferior, the taeniae of the fourth ventricle, and the obex.

The superior peduncle pass upward and forward, forming at first the lateral boundaries of the upper part of the cavity; on approaching the inferior colliculi, they converge and their medial portions overlap the cavity and form part of its roof (Figs. 4.3 and 4.4).

The anterior medullary velum fills in the angular interval between the superior peduncle and is continuous behind with the central white substance of the cerebellum; it is covered on its dorsal surface by the lingula of the superior vermis.

The posterior medullary velum is continued downward and forward from the central white substance of the cerebellum in front of the nodule and tonsils and ends inferiorly in a thin concave. Below this margin the roof is devoid of nervous matter except in the immediate vicinity of the

lower lateral boundaries of the ventricle, where two narrow white bands, the taeniae of the fourth ventricle, appear; these bands meet over the inferior angle of the ventricle in a thin triangular lamina, the obex. The nonnervous part of the roof is formed by the epithelial lining of the ventricle from the deep surface of the posterior medullary velum to the corresponding surface of the obex and taeniae, and it is covered by the tela chorioidea of the fourth ventricle.

The taeniae of the fourth ventricle are two narrow bands of white matter which complete the lower part of the roof of the cavity. Each consists of a vertical and a horizontal part. The vertical part is continuous below the obex with the clava, to which it is adherent by its lateral border. The horizontal portion extends transversely across the inferior peduncle, below the striae medullares, and roofs in the lower and posterior part of the lateral recess; it is attached by its lower margin to the inferior peduncle and partly encloses the choroid plexus and hence this part of the taenia has been termed the cornucopia. The obex is a thin, triangular, gray lamina, which roofs in the lower angle of the ventricle and is attached by its lateral margins to the clavae. The posterior layer covers the anteroinferior surface of the cerebellum, while the anterior is applied to the structures which form the lower part of the roof of the ventricle, and is continuous inferiorly with the pia mater on the inferior peduncles and closed part of the medulla (Figs. 4.7 and 4.8).

4.6.1 Floor of Fourth Ventricle

The brainstem and ventricle floor are considered together because the brainstem forms the fourth ventricular floor. The interpeduncular fossa, a wedge-shaped depression between the cerebral peduncles, has the posterior perforated substance in its floor. The rootlets of the facial and the vestibulocochlear nerves arise superior to this fosse and the rootlets of the glossopharyngeal and the vagal nerves originate dorsal to it. The rootlets of the hypoglossal nerves arise in the anterolateral sulcus. The lateral surface is demarcated posteriorly by the exits of the rootlets

of the glossopharyngeal, vagus, and accessory nerves dorsal to the posterolateral sulcus.

The floor is divided into three parts: a superior or pontine part, an intermediate or junctional part, and an inferior or medullary part. The superior part has a triangular shape: its apex is at the cerebral aqueduct, its base is represented by an imaginary line connecting the lower margin of the cerebellar peduncles, and its lateral limbs are formed by the medial surfaces of the cerebral peduncles.

The intermediate part is the strip between the lower margin of the cerebellar peduncles and the site of attachment of the tela choroidea to the taeniae just below the lateral recesses. The intermediate part extends into the lateral recesses.

The inferior part has a triangular shape and is limited laterally by the taeniae marking the inferolateral margins of the floor. Its caudal tip, the obex, is anterior to the foramen of Magendie.

The floor is divided longitudinally from the rostral apex to the caudal tip into symmetrical halves by the median sulcus. The sulcus limitans, another longitudinal sulcus, divides each half of the floor into a raised median strip called the median eminence that borders the midline and a lateral region called the vestibular area.

Each median eminence, the strip between the sulcus limitans and the median sulcus, from above to below contains the facial colliculus, a rounded prominence related to the facial nerve, and three triangular areas overlying the hypoglossal and vagus nuclei and the area postrema. At the pontine level the median eminence has a width equal to that of the full half of the floor and thus the sulcus limitans corresponds with the lateral limit of this part of the floor. The sulcus limitans is discontinuous and is most prominent in the pontine and medullary portions of the floor, where it deepens at two points to form dimples called foveae, and is least distinct in the junctional part of the floor. One of the two dimples, the superior fovea, is located in the pontine portion of the floor and the other, the inferior fovea, is located in the medullary part of the floor. At the level of the superior fovea, the median eminence forms an elongated swelling, the facial colliculus, which overlies the nucleus of the abducens nerve and the ascending section of the root of the

facial nerve. At the rostral tip of each sulcus limitans in the lateral margin of the floor is a bluish-gray area, the locus ceruleus, which owes its color to a group of pigmented nerve cells. The hypoglossal triangle is medial to the inferior fovea and overlies the nucleus of the hypoglossal nerve. Caudal to the inferior fovea and between the hypoglossal triangle and the lower part of the vestibular area is a triangular dark field, the vagal triangle, that overlies the dorsal nucleus of the vagus nerve. A translucent ridge, the funiculus separans, crosses the lower part of the vagal triangle. The area postrema forms a small tongue-shaped area between the funiculus separans and the gracile tubercle in the lower limit of the median eminence immediately rostral to the obex.

The vestibular area, the portion of the floor lateral to the median eminence and sulcus limitans, is widest in the intermediate part of the floor, where it forms a rounded elevation that extends into the lateral recess. White strands, the striae medullaris, course transversely from the region of the lateral recess across the inferior cerebellar peduncles above the hypoglossal triangles toward the midline and disappear in the median sulcus. The vestibular nuclei lie beneath the vestibular area. The auditory tubercle produced by the underlying dorsal cochlear nucleus and the cochlear part of the vestibulocochlear nerve forms a prominence in the lateral part of the vestibular area.

In the superior part of the fossa, the medial eminence has a width equal to that of the corresponding half of the fossa, but opposite the superior fovea it forms an elongated swelling, the colliculus facialis, which overlies the nucleus of the abducent nerve and is, in part at least, produced by the ascending portion of the root of the facial nerve. In the inferior part of the fossa, the medial eminence assumes the form of a triangular area, the trigonum hypoglossi.

The sulcus limitans forms the lateral boundary of the medial eminence. In the superior part of the rhomboid fossa, it corresponds with the lateral limit of the fossa and presents a bluish-gray area, the locus caeruleus, which owes its color to an underlying patch of deeply pigmented nerve cells, termed the substantia ferruginea. At the level of the colliculus facialis, the sulcus limitans widens

into a flattened depression, the superior fovea, and in the inferior part of the fossa appears as a distinct dimple, the inferior fovea. Lateral to the foveae is a rounded elevation named the area acustica, which extends into the lateral recess and there forms a feebly marked swelling, the tuberculum acusticum. Winding around the inferior peduncle and crossing the area acustica and the medial eminence are a number of white strands, the striae medullares, which form a portion of the cochlear division of the acoustic nerve and disappear into the median sulcus. Below the inferior fovea and between the trigonum hypoglossi and the lower part of the area acustica is a triangular dark field, the ala cinerea, which corresponds to the sensory nucleus of the vagus and glossopharyngeal nerves. The lower end of the ala cinerea is crossed by a narrow translucent ridge, the funiculus separans, and between this funiculus and the clava is a small tongue-shaped area, the area postrema. On section it is seen that the funiculus separans is formed by a strip of thickened ependyma and the area postrema by loose, highly vascular, neuroglial tissue containing nerve cells of moderate size (Fig. 4.8).

4.6.2 Medial Lemniscus

In the pons, the medial lemniscus becomes flattened in a more mediolateral direction and ascends dorsal to the pontine nuclei. These continue upward in the pontine tegmentum ventral to medial to the spinal lemniscus. At the mesencephalic level, the medial lemniscus lies laterally to the mesencephalic decussation. It ascends within the mesencephalic tegmentum lateral and anteromedial to the spinal lemniscus. In the mesencephalodiencephalic level, it further ascends dorsal to the substantia nigra and lateral to the red nucleus (Figs. 4.5 and 4.9).

4.6.3 Lateral Lemniscus

The spinal lemniscus course ascends within the posterolateral part of the medulla oblongata dorsal to the principal nucleus of the inferior olivary nucleus and lateral to the medial lemniscus. The

lateral lemniscus lies within the anterolateral pontine tegmentum laterally to the medial lemniscus and dorsally to the pontine nuclei. It shifts slightly dorsolaterally at the level of the upper pons. At the mesencephalic level, the lateral lemniscus and medial lemniscus become more discernable, and the lateral lemniscus ascends more dorsolaterally to the medial lemniscus and terminates within the ventral posterolateral nucleus of the thalamus at the level of the diencephalon (Fig. 4.9).

4.7 Discussion

Surgical importance of cerebellum has been emphasized in many studies [1, 2, 18], which are very helpful in understanding the cerebellar anatomy. The major pathway from the superior cerebellar peduncle is the dentate-rubro-thalamic tract and major pathways from the middle cerebellar peduncle are the corticocerebellar and pontocerebellar tracts. Superior cerebellar peduncle fibers ascend anteriorly and superiorly to the DN. The middle cerebellar peduncle fibers wrap the DN superiorly and inferiorly.

In the supratonsillar approach, the DN is located under the biventral fissure and is thus more susceptible to injury when this approach is used for accessing the fourth ventricle. In subtonsillar and telovelar approaches, the DN remains in a safe area [3, 4, 18].

In the lateral mesencephalic approach, the superior cerebellar peduncle fibers lie very close to the lateral mesencephalic sulcus. In this approach, the trigeminothalamic tract, the lateral and medial lemniscuses, and the crus cerebri may be damaged.

The microsurgical anatomy of the cerebellomedullary fissure and the surgical entrance into the fourth ventricle and lateral recess through the tela choroidea and inferior medullary velum were first described in a series of papers from the University of Florida in the early 1980s [5]. The incision through the inferior portion of the vermis during the transvermian approach exposes the underlying nodule, which must be incised to gain access to the fourth ventricle. This incision through the vermis is limited by the position of

the superior medullary velum, which is closely related to the anterior portion of the nodule. The superior medullary velum forms the medial part of the superior half of the roof. The splitting of the inferior cerebellar vermis may cause caudal vermis syndrome [5, 6] resulting in an equilibrium disturbance with truncal ataxia, gait disturbance, oscillation of the head and trunk, and nystagmus.

When the DN is damaged, the resulting equilibrium disturbances are more severe than those observed with vermian lesions and are often accompanied by intentional tremor during voluntary movement of the extremities [7]. Splitting the inferior portion of the vermis may also play a role in cerebellar mutism [6], a transient complication following the removal of a cerebellar and fourth ventricle tumor [8, 9]. Although the exact anatomical substrate for cerebellar mutism remains unknown, the inferior portion of the vermis, including the pyramid, uvula, and nodule, has been implicated. The nodule area seems to be more important in mutism syndrome [10–13].

The vestibular area, the portion of the floor that is lateral to the median eminence and the sulcus limitans, is located at the lateral limit of the floor of the fourth ventricle. The DN is located lateral and superior to the vestibular area. The inferior fovea is a depression in the sulcus limitans located lateral to the hypoglossal triangle [11]. The median eminence contains the facial colliculi in its upper part and the hypoglossal and vagal triangles and the area postrema in its lower portion. DN tubercle is an important landmark while approaching the fourth ventricle floor and this may help explain the pathophysiology of oropharyngeal apraxia [12]. The median eminence is crossed by the funiculus separans. While approaching the brain stem lesions, median eminence can be used as a landmark microsurgically and endoscopically. Lateral to the median eminence there is another tubercle in lateral recess, which is known as the DN tubercle [13–15].

The fourth ventricle is continuous with the cerebellopontine angle through the foramen of Luschka at the lateral recess [11, 16, 17]. The superior half of the roof is formed medially by the superior medullary velum and laterally by the

inner surfaces of the superior cerebellar peduncles that carry the afferent fibers of the DN. The inferior medullary velum blends into the peduncles of the flocculus laterally and the surface of the nodule medially. Transvermian and superior medullary velum approaches require attention to the nucleus, which is located just lateral to the nodule.

References

1. Rhoton AL Jr (2000) Cerebellum and fourth ventricle. *Neurosurgery* 47:7–27
2. Matsushima T, Abe H, Kawashima M, Inoue T (2012) Exposure of the wide interior of the fourth ventricle without splitting the vermis: importance of cutting procedures for the tela choroidea. *Neurosurg Rev* 35:563–571
3. Tanriover N, Ulm AJ, Rhoton AL Jr, Yasuda A (2004) Comparison of transversmian and telovelar approach to the fourth ventricle. *J Neurosurg* 101:484–498
4. El-Bahy K (2005) Telovelar approach to the fourth ventricle: operative findings and results in 16 cases. *Acta Neurochir (Wien)* 147:137–142
5. Matsushima T, Rhoton AL Jr, Lenkey C (1982) Microsurgery of the fourth ventricle: part 1. Microsurgical anatomy. *Neurosurgery* 11:631–667
6. Salvati M, Missori P, Lunardi P, Orlando ER (1991) Transient cerebellar mutism after posterior cranial fossa surgery in an adult. *Clin Neurol Neurosurg* 93:313–316
7. Mussi AC, Rhoton AL Jr (2000) Telovelar approach to the fourth ventricle: microsurgical anatomy. *J Neurosurg* 92:812–823
8. Ravizza SM, McCormick CA, Schlerf JE, Justus T, Ivry RB, Fiez JA (2006) Cerebellar damage produces selective deficits in verbal working memory. *Brain* 129:306–320
9. Rhoton AL Jr (1993) Microsurgical anatomy of posterior fossa cranial nerves. In: Barrow DL (ed) *Surgery of the cranial nerves of the posterior fossa: neurosurgical topics*. AANS, Chicago, pp 1–103
10. Lechtenberg R, Gilman S (1978) Speech disorders in cerebellar disease. *Ann Neurol* 3:285–290
11. Cohen AR (ed) (1996) *Surgical disorders of the fourth ventricle*. Blackwell Science, Cambridge, pp 147–160
12. Dietze DD Jr, Mickle JP (1990) Cerebellar mutism after posterior fossa surgery. *Pediatr Neurosurg* 16:25–31
13. Jean WC, Abdel Aziz KM, Keller JT et al (2003) Subtonsillar approach to the foramen of Luschka: an anatomic and clinical study. *Neurosurgery* 52:860–866
14. Duvernoy HM (1995) *The human brainstem*. Springer, New York

15. Frazier CH (1918) Remarks upon the surgical aspects of tumors of the cerebellum. *N Y State J Med* 18(272–280):332–337
16. Ikezaki K, Matsushima T, Inoue T, Yokoyama N, Kaneko Y, Fukui M (1993) Correlation of microanatomical localization with postoperative survival in posterior fossa ependymomas. *Neurosurgery* 32: 38–44
17. Kellogg JX, Piatt JH Jr (1997) Resection of fourth ventricle tumors without splitting the vermis: the cerebellomedullary fissure approach. *Pediatr Neurosurg* 27:28–33
18. Akakin A, Peris-Celda M, Kılıç T, Seker A, Gutierrez-Martin A, Rhoton A Jr (2014) The dentate nucleus and its projection system in the human cerebellum: the dentate nucleus microsurgical anatomical study. *Neurosurgery* 74(4):401–424

Clinical Presentation and Neurologic Evaluation in Posterior Fossa Tumors in Children

5

Ugur Işık and M. Memet Özek

5.1 Signs of Posterior Fossa Tumors

The major neural structures of the posterior fossa are the brainstem, cranial nerves, and the cerebellum. Their anatomical features were written in great detail in the previous chapters.

5.1.1 Ataxia and Hypotonia

Ataxia refers to a disturbance in the smooth performance of voluntary motor acts [1]. In the absence of cerebellar inhibitory and modulating influences, skilled movements originating in the cerebral motor cortex become inaccurate and poorly controlled. Ataxia may affect the limbs, the trunk, or gait and may be of acute onset, episodic, or progressive. The term ataxia includes other abnormalities of voluntary movement control, such as asynergia (lack of

synergy of the various muscle components in performing more complex movements so that the movements are broken up into isolated successive parts – decomposition of movement), dysmetria (abnormal excursions in movement), dysdiadochokinesia (impaired performance of rapidly alternating movements), and past pointing. Also associated are an impaired checking response and an excessive rebound phenomenon when an opposed motion is suddenly released [2]. Typically patients with cerebellar disease have a wide-based stance and a gait characterized by staggering and impaired tandem walking [3]. Truncal instability may be manifested by falls in any direction. Truncal ataxia and titubations suggest midline cerebellar tumors such as medulloblastomas, ependymomas, and vermian astrocytomas. It is manifested by a tendency to fall frequently and a widely based gait. Hemicerebellar syndrome involves limb ataxia, nystagmus, and dysmetria [4].

The childhood cerebellar tumor most often presents a truncal ataxia, even when the bulk of the tumor is hemispherical rather than vermian. This apparent paradox is the result of the influence of the hydrocephalus which itself can produce a truncal form of ataxia. A wide-based gait with impairment of tandem walking is characteristic. Circle walking and hopping may bring out ataxic deficits which are not obvious. In hemispherical tumors with ipsilateral hypotonia, there is a marked tendency to fall to the side of the tumor. In vermian tumors or hemispherical tumors with

U. Işık, M.D. (✉)
Division of Pediatric Neurology,
Department of Pediatrics, Acibadem University,
Kozyatağı Acibadem Hastanesi İnönü Cad.
Okur sok. No:20, İstanbul, Turkey
e-mail: ugur.isik@acibadem.com.tr; uisik@asg.com.tr

M.M. Özek, M.D.
Division of Pediatric Neurosurgery,
Department of Neurosurgery,
Acibadem University, School of Medicine,
Kozyatağı Acibadem Hastanesi İnönü Cad.
Okur sok. No:20, İstanbul, Turkey
e-mail: mozek@turk.net

marked hydrocephalus, hypotonia may be most marked in both legs with a tendency to fall in place rather than to either side. Increased tone in the extremities indicates brainstem compression or actual invasion of the brainstem by the cerebellar tumor. Truncal ataxia combined with spasticity, in the absence of intracranial hypertension, should suggest intrinsic glioma of the brainstem rather than cerebellar tumor [4].

5.1.2 Rapid Alternating Movements

The ability of the patient to touch their index fingertips together in front of them with their eyes closed should be tested. The abnormality of both range and direction is referred to as dysmetria. The patients' ability to touch the tip of their nose and then the examiner's index finger is tested. This is known as the finger/nose test [5]. The value of the test is greatly enhanced if the examiner moves the target finger, varying both the direction and distance from the patient's nose. In this finger/nose/finger test quite mild incoordination, terminal intention tremor, and dysmetria can be more readily detected. The equivalent test in the legs is the heel/knee/shin test. The patient is asked to place the tip of the heel on the tibial tubercle of the leg and run the heel down the front of the shin. The heel is then lifted off and replaced on the tibial tubercle. Some mild incoordination is within normal limits for this test, the test must be performed properly, and overinterpretation of minor abnormalities should be avoided [5].

Rapid alternating movements, like a patient tapping himself on the back of one hand as fast as he can or tapping his foot on the floor or against the examiner's hand, detect fragmentation of movement or inaccuracy of movement, which is accentuated by the speed at which the movement is attempted. This is known as dysdiadochokinesia [4, 5].

5.1.3 Tremor

A major feature of cerebellar disease is the non-rhythmic tremor that appears on action, which is also known as action or intention tremor. At rest

the limbs are still, but in action tremulousness appears, which is maximal at the beginning and end of the range of movement and is sometimes referred to as terminal intention tremor. Truncal tremor can also occur. When sitting or standing these muscles are already in action, and a tremor of the trunk will appear and may become so violent that constant jerking movements of the head and body may occur, which may be backward and forward or even include lateral flexion or rotational movements [4, 5].

5.1.4 The Reflex Signs

The usual cerebellar tumor results in hypoactive deep tendon reflexes, especially in the lower extremities [4]. Plantar reflexes are normal. Hyperactive reflexes, a Babinski sign, or evidence of spasticity points to brainstem compression by the cerebellar tumor. The same effect can be produced by invasion of the brainstem by the cerebellar tumor. However, brainstem compression by a large cerebellar mass is more common than actual brainstem invasion by tumor [4].

5.1.5 Torticollis and Neck Stiffness

Torticollis is a hyperkinesia characterized by tonic or clonic contraction of the neck musculature, especially the sternocleidomastoid and trapezius muscles. Torticollis may occur as a sign of a posterior fossa tumor. Stiff neck may be due to herniation of a cerebellar tonsil or extension of tumor through the foramen magnum into the upper cervical canal. Neck stiffness tends to increase as intracranial pressure becomes marked [4] (Fig. 5.1).

5.1.6 Cerebellar Mutism

This sign is mostly seen after neurosurgical operations; however, it is also rarely seen in patients with posterior fossa tumors preoperatively. A tumor-related mutism in an adult subject has been described [6]. A 7-year-old boy was reported to have cerebellar mutism due to a hemorrhage of a neoplastic lesion (pilocytic astrocytoma) [7].



Fig. 5.1 Head tilt (torticollis) in a boy with posterior fossa tumor (chordoma)

5.1.7 Eye Abnormalities

5.1.7.1 Abducens Nerve Palsy

The paired abducens nucleus is located in the dorsal lower portion of the pons, separated from the floor of the fourth ventricle by the genu of the facial nerve (facial colliculus). The abducens motoneurons are intermixed with interneuronal neurons that send their axons across the midline to the opposite medial longitudinal fasciculus (MLF), where they ascend through the pons and midbrain to end in the third nerve nucleus. Thus, the abducens nuclear complex coordinates the action of both eyes to produce a horizontal gaze [2].

Localization of Lesions

Lesions of abducens nucleus early in life can cause Möbius syndrome or Duane's retraction syndrome. In addition to horizontal gaze disturbances, patients with Möbius syndrome have facial diplegia and may have other cranial nerve abnormalities. Duane's retraction syndrome is characterized by a narrowing of the palpebral fissure and occasionally globe retraction on adduction. Although Duane's retraction syndrome is predominantly congenital, and is thought to be due to anomalous innervation of the lateral rectus muscle by the inferior division of the oculomo-



Fig. 5.2 A boy with right lateral abducens palsy secondary to a posterior fossa tumor (ependymoma)

tor nerve, acquired Duane's syndrome has been described in patients with pontine glioma, with rheumatoid arthritis, following trigeminal rhizotomy, and after removal of an orbital cavernous hemangioma by lateral orbitotomy [8, 9].

Paralysis of the abducens nerve: Lesions of the abducens nerve cause impaired ipsilateral lateral gaze (Fig. 5.2). Therefore, patients with unilateral abducens palsy complain of horizontal diplopia, worst in the direction of the paretic lateral rectus muscle. Unlike a peripheral CN VI lesion, a nuclear CN VI lesion impairs ipsilateral gaze of both eyes. This is due to the fact that the abducens nuclear complex contains interneurons projecting via the medial longitudinal fasciculus (MLF) to the contralateral oculomotor nucleus (innervating the contralateral medial rectus muscle). Brainstem lesions (abducens nuclear lesions) produce a conjugate (both eyes involved) horizontal gaze palsy toward the side of the lesion, often associated with other neurologic signs of injury to the pons (usually ipsilateral peripheral CN VII palsy) [10]. In cerebellar tumors, abducens palsy with resultant diplopia is usually the result of increased intracranial pressure rather than direct brainstem compression by the cerebellar tumor. Compression of the dorsolateral pons can produce a facial asymmetry. Actual extension of cerebellar tumor into the brainstem can produce other cranial palsies [4].

B-nystagmus is an instability of gaze characterized by continuous movement of the eyes in any plane. When both arcs of the movement are of equal amplitude and the frequency is slow, this instability of gaze is referred to as *pendular nystagmus*. In most circumstances, pendular nystagmus is indicative of diminished visual acuity. If the amplitude of the movements is unequal

and the frequency is rapid, the abnormality is referred to as *jerk nystagmus*. Abnormalities involving the vestibular system result in jerk nystagmus. Gaze-evoked jerk nystagmus indicates vestibular abnormalities, whereas *vertical nystagmus* is indicative of *brainstem dysfunction*. If gaze-evoked nystagmus is unilateral, it may indicate ipsilateral *cerebellar or brainstem* pathology; if bilateral it is of limited localizing value [11].

In *downbeat nystagmus*, the most common cause is type I Chiari malformation and other surgically treatable pathology involving craniocervical junction must be excluded. It can also be seen vascular, demyelinating or neoplastic lesions in the same area [12]. *Upbeat nystagmus* is much less common and is usually due to a focal gray matter lesion either at the pontomesencephalic or pontomedullary junction [13]. *Up-beating vertical nystagmus* shows a high correlation with lesions of the cerebellar vermis and is often seen in children with medulloblastomas [12].

Torsional nystagmus is usually due to a lesion of the lateral medulla involving the vestibular nucleus although other brainstem sites of pathology may also be responsible. It beats away from the side of the lesion, increases on lateral gaze, and can be associated with skew deviation. *Seesaw nystagmus* consists of elevation of one eye with intorsion, accompanied by contralateral depression and extorsion, followed by reversal of the cycle. It may be asymmetric and is usually associated with midline mesodiencephalic or hypothalamic tumor or other pathology in this region. Chiasmal glioma in childhood may present this way, and there may be an associated bitemporal hemianopia [14].

Periodic alternating nystagmus is a primary position, horizontal nystagmus that changes direction, usually every 90 s in a crescendo-decrescendo fashion, often with a short-lived null period. It can occur in a large variety of clinical contexts, usually involving diffuse bilateral brainstem pathology such as MS [11].

How to Examine the Patient with Nystagmus

When nystagmus occurs in posterior fossa tumors, it is usually most marked on lateral gaze and is coarser to the side of a hemispheric.

When nystagmus is absent, the patient is rapidly brought to a full sitting position from the supine. Nystagmus induced by this maneuver can occur in vermian tumors of the cerebellum and in intrinsic brainstem tumors. Spontaneous vertical nystagmus can occur in anterior vermian tumors and in intrinsic brainstem tumors [4].

The higher the brainstem disorder, the greater the incidence of neurosurgical mass lesions because brainstem infarction most commonly involves the medulla oblongata, somewhat less often involves the pons, and occasionally is mesencephalic [4].

5.1.8 Midbrain Syndromes Associated with Tumors

Midbrain compression is usually due to a supratentorial-transtentorial process (e.g., uncal herniation), rather than due to a posterior fossa mass.

1. Internuclear ophthalmoplegia – paralysis of the adducting eye on attempted lateral gaze but preservation of convergence; horizontal nystagmus most marked in the abducting eye usually with multiple ocular deficits including skew deviation, paralysis of vertical gaze, and ptosis. Usually bilateral and often associated vertical nystagmus (MLF syndrome) – indicates an intra-brainstem lesion [4].
2. Intracranial hypertension with vertical gaze palsy, frequent convergence palsy, and occasional pupillary palsy (Parinaud's or sylvian aqueduct syndrome) – indicates a pineal tumor with aqueductal obstruction and dorsal midbrain compression [4]. The syndrome consists of a paralysis of conjugate upward movement of the eyes in the absence of paralysis of convergence. As the tumor grows into the tegmentum of the midbrain, there will be additional nuclear paresis of III with reflex pupilloplegia and paresis of IV. Compression of the aqueduct causes hypertensive hydrocephalus of lateral and third ventricles. Damage to the inferior colliculi produces hearing loss. There is a tendency to fall backward and to the opposite side [15].

5.1.9 Pontine Syndromes Associated with Tumors

The pons is critically important as a nuclear center and as a bridge between the forebrain and the hindbrain. In addition to a careful neuro-ophthalmologic evaluation, evidence for dysfunction of the pontine cranial nerve nuclei, long tracts, and cerebellar pathways is sought. Lesions in the basis pontis cause a paralysis which eventually shows hypertonus due to interruption of the corticospinal tracts, ataxia due to damage of the pontocerebellar tracts, and frequently paralysis of facial and lateral rectus muscles due to interruption of the facial and abducens tracts. In the tegmentum, the nuclei of the facial and abducens nerves may be damaged. Additionally the pontine gaze centers and medial longitudinal fasciculus (MLF) can be affected [16].

When tumors infiltrate the tegmentum, they damage both nuclei and tracts – an abducens and an ipsilateral gaze palsy will usually occur together. Findings which implicate only the ventral pons strongly suggest a mass, e.g., an infiltrating tumor, abscess, vascular malformation, large basilar aneurysm, or a clivus tumor [17].

Several classical pontine syndromes have been described. In dorsolateral pontine syndrome (Foville's syndrome), there is an ipsilateral gaze palsy and a contralateral hemiplegia; this results from involvement of both the basis and the tegmentum of the pons on one side [16]. The syndrome of Millard-Gubler or the ventral pontine syndrome is manifested by an ipsilateral facial and abducens palsy and a contralateral hemiplegia [16].

5.2 Symptoms Associated with Posterior Fossa Tumors

5.2.1 Headache

This is the most common symptom in patients with posterior fossa tumors. Headache is insidious and intermittent. It is most severe in the morning or after a nap because of increased intracranial pressure from recumbency and hypoventilation during sleep. Associated neck pain, stiffness, or head tilt suggest tonsillar herniation into the foramen magnum. Headache manifests in children as



Fig. 5.3 Left oculomotor nerve palsy (pupillary dilatation, left eye down and out) in a 5-year-old girl with metastatic brainstem tumor

irritability and difficulty to be handled. In a study of children with posterior fossa tumors, headache was present in 63.6 % of patients [18].

5.2.2 Nausea and Vomiting

They may be due to generalized intracranial hypertension or irritation of the vagal nuclei in the medulla oblongata or area postrema of the fourth ventricle. Vomiting (including projectile vomiting) may occur, usually in the morning. Vomiting sometimes relieves headache. In the same study as above, nausea and vomiting were present in 75.8 % if children with posterior fossa tumors [18].

5.2.3 Strabismus

It is secondary to sixth nerve palsies from intracranial hypertension. Third nerve palsies may also occur (Figs. 5.3 and 5.4).

5.2.4 Lethargy

Lethargy is a common symptom and it was present in 28.8 % of children in a study [18]. Young children may not complain of headache or diplopia; loss of normal childhood energy and vomiting may be the only symptoms due to pressure.

5.2.5 Hydrocephalus and Macrocephaly

In a study of children with posterior fossa tumors, 80.3 % demonstrated radiological evidence of

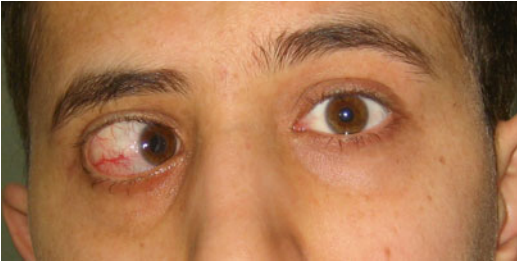


Fig.5.4 Strabismus secondary to the right abducens nerve palsy, this patient also has right facial nerve palsy and corneal changes on that side due to poor eye closure

hydrocephalus on their initial scan [18]. Children with posterior fossa tumors tend to present with a shorter duration of symptoms than supratentorial tumors secondary to early obstruction of cerebrospinal fluid (CSF) pathways [19]. In the first 6 months of life, the most common presenting signs are the signs of increased intracranial pressure and hydrocephalus [20, 21]. These infants are more likely to present with macrocephaly because their immature cranial vaults have the ability to accommodate the increased volume caused by the tumor, hydrocephalus, or a combination of both [20]. The intracranial hypertension and hydrocephalus may also contribute to the development of nystagmus, sundowning, and misalignment of the eyes. In addition, less specific complaints of emesis, lethargy, irritability, and poor feeding were more common than focal findings and seizures. The decreased incidence of focal neurologic deficits can be attributed to the relative immaturity of the neonatal brain [22]. Increased head circumference, hyperreflexia, hypotonia, stridor, pooling of secretions, abnormal gag reflex, nystagmus, dysconjugate eye movements, and facial palsy were reported in newborns with congenital diffuse intrinsic brainstem tumor [15].

5.2.6 Seizures

Posterior fossa tumors rarely can present with epilepsy. Pilocytic astrocytoma and ganglioglioma of the cerebellum can cause seizures [23, 24]. Hemifacial spasm in an infant due to fourth ventricular ganglioglioma has been described. Removal resulted in complete resolution of spasms [25]. Severe brainstem compression,

sometimes occurring during a hydrocephalic attack with an acute rise in intracranial pressure, can produce sudden and episodic extensor rigidity. The patient assumes the decerebrate posture, with autonomic instability, pupillary dilatation, and deep coma. Apnea and cyanosis may occur during such an attack [4].

5.2.7 Cerebellopontine Angle Syndrome

This is unusual in childhood although an acoustic neuroma can present early in neurofibromatosis type 2. Gradual unilateral deafness over months or years, with tinnitus, imbalance, and facial asymmetry are commonly noted. Intracranial hypertension is late, in contrast to the cerebellar tumors [4].

5.3 Signs and Symptoms in Different Types of Posterior Fossa Tumors

5.3.1 Medulloblastomas

Medulloblastomas are most frequently found in the fourth ventricle. Most patients with medulloblastoma have relatively short intervals between the onset of symptoms and diagnosis. Seventy to eighty percent of patients have it for less than 3 months [25–28].

The child with a medulloblastoma may present with obstructive hydrocephalus secondary to the posterior fossa mass followed by cerebellar dysfunction. Older children usually complain of morning headaches. Vomiting is frequent because of increased intracranial pressure. Later, patients develop ataxia caused by cerebellar compression and coexisting hydrocephalus. Development of a stiff neck or head tilt usually suggests tonsillar involvement by the tumor or signs of impending herniation [29–31]. When cerebellar symptoms are present, gait or truncal ataxia tend to predominate over any appendicular ataxia because of the midline location of these tumors [32]. Spinal drop metastases caused by the tumor spread into the subarachnoid space in the spinal canal may present with back pain, cranial neuropathies, seizures,

radiculopathies, and signs of meningeal irritation [33]. Less common at presentation are diplopia, facial paresis, lower cranial nerve palsies, head tilt, and seizures. Diplopia due to bilateral sixth nerve palsy is most often due to high ICP, but if the sixth nerve palsy is unilateral and accompanied by an ipsilateral lower motor neuron-type facial paresis, then brainstem invasion by the tumor must be suspected. Head tilt may be seen with impaction of the cerebellar tonsils at the foramen magnum against the C1 and C2 nerve roots, causing reflex nuchal muscle spasm. However, it is more often a sign of local extension of the tumor down into the upper spinal canal. Seizures, particularly focal ones, are almost certainly caused by cerebrospinal fluid metastasis of tumor cells to the cerebral cortex [25].

5.3.1.1 Pilocytic Astrocytomas

Pilocytic astrocytomas in children usually arise from the cerebellar hemispheres causing a predominant appendicular ataxia in contrast to medulloblastomas. Presentation is generally that of a posterior fossa mass with hydrocephalus. Headache is common. Usually it is present in the morning and may be associated with vomiting. The most common neuro-ophthalmologic finding is papilledema (about 50 %), diplopia (about 15 %), and nystagmus (about 5 %) [34]. Specifically complaints of limb clumsiness typically precede symptoms of raised intracranial pressure [33]. Interestingly some children are found to have macrocephaly at the time of diagnosis, and history of macrocephaly sometimes dates back to infancy. Some children still undergo extensive gastrointestinal or neuropsychological investigations because of chronic vomiting, altered behavior, or clumsiness [35]. In one review of 42 patients, the most common symptoms were headaches and vomiting (84 and 74 %, respectively). Altered gait was present in 70 %, an increased head size in 14 %, and blindness in 2.5 %. Two children presented in coma from large posterior fossa tumors and obstructive hydrocephalus [36]. Of the common signs, papilledema was seen in 84 %, ataxia in 75 %, and appendicular dysmetria in 39 %. Interestingly, some children are neurologically normal with

few cerebellar findings despite huge tumors. Still, a small number of children present as stuporous or comatose with projectile vomiting and oculomotor and facial palsies. Children with severe neck pain, opisthotonos, bradycardia, hypertension, and altered neurological function require immediate attention [35].

5.3.1.2 Ependymomas

The clinical resemblance of ependymomas is to medulloblastoma rather than to astrocytoma. The duration of symptoms is intermediate between medulloblastoma and astrocytoma, and average duration of symptoms before diagnosis is 2–3 months [25]. Children usually present with headache, vomiting, and lethargy subsequent to obstructive hydrocephalus. Later in the course of the disease, truncal ataxia, nystagmus, and sixth nerve palsy may develop. However, on occasion there is no hydrocephalus, indicating that the vomiting is secondary to the irritating effect of the tumor at the level of the obex and area postrema [25]. Ependymomas often extend through the foramen of Luschka into the cerebellopontine angle and cranial nerve dysfunction may be noted [37–39]. Some series report more than 50 % of patients having disturbances of the visual system at presentation. Although most findings are related to papilledema or nystagmus, a significant portion of patients have internuclear ophthalmoplegia, diplopia due to isolated cranial nerve palsy, or corneal problems due to a diminution of the protective blink reflex [34]. Torticollis is more frequently observed in ependymomas if compared to other posterior fossa tumor, due to the elective tendency of this kind of tumor to grow into the subarachnoid spaces in the region of the foramen magnum and in the upper cervical spine.

5.3.1.3 Diffuse Intrinsic Pontine Gliomas

Children with diffuse intrinsic pontine gliomas present with typical signs and symptoms secondary to the tumor's location and infiltrative nature. These patients often present with classic brainstem symptoms such as cranial nerve deficits, long-tract signs, ataxia, or a combination of the



Fig. 5.5 Hypoglossal nerve involvement (tongue deviation toward ipsilateral side) in a patient with a medulla oblongata tumor

three [40, 41]. Symptoms are usually of an acute onset and short duration often present for only 1–2 months prior to diagnosis [42]. Headache and motor complaints were the most common symptoms at onset in a retrospective analysis of 86 patients with brainstem gliomas, with the majority of patients being children [43]. The cranial nerve dysfunction can include diplopia from direct involvement of the oculomotor, trochlear, and abducens nerves or more complicated oculomotor disturbance [34]. Many of these tumors start in the region of the sixth nerve nucleus and any combination of a sixth and seventh nerve palsy should be regarded with suspicion. Minimal motor signs, brisk reflexes, and extensor plantar responses are often present but hemiplegia is not an early symptom. The sensory pathways also seem to be extremely resistant to infiltration by these tumors [44] (Fig. 5.5).

5.3.1.4 Cerebellar Hemangioblastoma (Von Hippel-Lindau Disease)

This usually nodular tumor consists of capillaries, is benign in its growth, and is usually seen in young and middle-aged adults. It is of diagnostic interest that this tumor is often associated with angiomatosis of the retina and capillary nevi in the skin, multiple cysts in kidneys and pancreas, and occasionally a renal cell carcinoma. This complex defines Von Hippel-Lindau disease. However, it is notable that only 10–20 % of the hemangioblastomas are associated with von Hippel-Lindau disease [26]. In most cases the tumor is small and is attached as

a hemorrhagic nodule to the wall of a large, well-defined cyst. Symptoms are usually mild and may consist of pain in the neck and occipital region, as a result of an increase in intracranial pressure [45]. Raised intracranial pressure and ataxia are the cardinal manifestations of the tumor [26]. It is of diagnostic interest that capillary hemangioblastomas are known to be associated with polycythemia. After resection of the neoplasm, the number of erythrocytes returns to normal [45].

References

1. Gilman S (1994) Cerebellar control of movement. *Ann Neurol* 35:3
2. Localization of lesions affecting the ocular motor system (1996) In: Brazis PW, Masdeu JC, Biller J (eds) *Localization in clinical neurology*, 3rd edn. Little, Brown and Company (Inc), Boston, pp 155–250
3. Gilman S (1992) Cerebellum and motor dysfunction. In: Asbury AK, McKhann GM, McDonald WI (eds) *Diseases of the nervous system. Clinical neurobiology*, 2nd edn. Saunders, Philadelphia, pp 319–341
4. Posterior fossa syndromes (1973) In: Needham CW (ed) *Neurosurgical syndromes of the brain*. Charles C Thomas, Springfield, pp 276–346
5. The extrapyramidal system and the cerebellum (1995) In: Patten J (ed) *Neurological differential diagnosis*, 2nd edn. Springer, London/New York, pp 178–212
6. Akil H, Statham PFX, Gotz M, Bramley P, Whittle IR (2006) Adult cerebellar mutism and cognitive-affective syndrome caused by cystic hemangioblastoma. *Acta Neurochir (Wien)* 148:597–598
7. Cerebellar mutism after spontaneous intratumoral bleeding involving the upper cerebellar vermis: a contribution to the pathophysiologic interpretation (2009) *Childs Nerv Syst* 25:7–11
8. De-Respinis PA et al (1993) Duane's retraction syndrome. *Surv Ophthalmol* 38:257
9. Miller NR (1985) *Walsh and Hoyt's neuro-ophthalmology*. Williams and Wilkins, Baltimore, p 698
10. Abducens nerve (2010) In: Binder DK, Sonne DC, Fischbein NJ (eds) *Cranial nerves, anatomy, pathology, imaging*. Thieme Medical Publishers, Inc., New York, pp 69–81
11. Elston JS (1992) Organization and control of eye movements. In: Crockard A, Hayward R, Hoff JT (eds) *Neurosurgery, the scientific basis of clinical practice*. Blackwell Scientific Publications, Boston, pp 224–235
12. Conjugate eye movements and nystagmus (1996) In: Patten J (ed) *Neurological differential diagnosis*, 2nd edn. Springer, London, pp 91–103

13. Gilman N, Baloh RW, Tomiyasu O (1977) Primary position upbeat nystagmus. *Neurology* 27:294–297
14. Bender MB (1980) Brain control of conjugate horizontal and vertical eye movements: a survey of the structural correlates. *Brain* 103:23–69
15. Brainstem and cranial nerves (1998) In: Duus P (ed) *Topical diagnosis in neurology-anatomy, physiology, signs and symptoms*. Thieme Medical Publishers, Inc., New York, pp 70–163
16. Ash PR, Keltner JL (1979) Neuro-ophthalmologic signs in pontine lesions. *Medicine* 58(4):304–320
17. Barnett HJ, Hyland HH (1952) Tumors involving the brainstem. *Q J Med* 21:265
18. Kameda-Smith MM, White MAJ, St. George EJ, Brown JIM (2013) Time to diagnosis of paediatric posterior fossa tumors: an 11-year West of Scotland experience 200–2011. *Br J Neurosurg* 27(3):364–369
19. Dörner I, Fritsch MI, Stark AM, Mehdorn HM (2007) Posterior fossa tumors in children: how long does it take to establish the diagnosis. *Childs Nerv Syst* 23:887–890
20. Isaacs H Jr (2002) I. Perinatal brain tumors: a review of 250 cases. *Pediatr Neurol* 27:249–261
21. Di Rocco C, Ceddia Alannelli A (1993) Intracranial tumors in the first year of life: a report of 51 cases. *Acta Neurochir (Wien)* 123:14–24
22. Mazewski CM, Hudgins RJ, Reisner A et al (1999) Neonatal brain tumors: a review. *Semin Perinatol* 23:286–298
23. Boop S, Wheless J, Van Poppel K, McGregor A, Boop FA (2013) Cerebellar seizures. *J Neurosurg Pediatr* 12(3):288–292
24. Chae JH, Kim SK, Wang KC, Kim KJ, Hwang YS, Cho BK (2001) Hemifacial seizure of cerebellar ganglioglioma origin: seizure control by tumor resection. *Epilepsia* 42(9):1204–1207
25. Chutorian AM, Masters RE, Heier LA. Neurology of the fourth ventricle (1996) In: Cohen AR (ed) *Surgical disorders of the fourth ventricle*. Blackwell Science, Inc, Cambridge, MA, pp 52–93
26. Whelan HT, Krower HG, Schmidt MH et al (1998) Current therapy and perspectives in the treatment of medulloblastoma. *Pediatr Neurol* 18:103–115
27. Modha A, Vassilyadi M, George A et al (2000) Medulloblastoma in children—the Ottawa experience. *Childs Nerv Syst* 16:341–350
28. Crawford JR, MacDonald TJ, Packer RJ (2007) Medulloblastoma in childhood: new biological advances. *Lancet Neurol* 6:1073–1085
29. Jenkin O (1996) The radiation treatment of medulloblastoma. *J Neurooncol* 29:45–54
30. Raimondi AJ, Tomita T (1982) Hydrocephalus and infratentorial tumors: incidence, clinical picture and treatment. *J Neurosurg* 55:174–182
31. Packer RJ, Cogen P, Vezina G, Rorke LB (1999) Medulloblastoma: clinical and biologic aspects. *Neuro Oncol* 1:232–250
32. Duffner PK (2008) Diagnosis of brain tumors in children. *Expert Rev Neurother* 23:179–183
33. Maher CO, Raffel C (2004) Neurosurgical treatment of brain tumors in children. *Pediatr Clin North Am* 51:327–357
34. Mapstone TB (1995) Brain tumors in children. In: Tomsak RL (ed) *Pediatric neuroophthalmology*. Butterworth-Heinemann, Boston, pp 77–114
35. Rutka JT, Hoffman HJ, Duncan JA (1996) Astrocytoma of the posterior fossa. In: Cohen AR (ed) *Surgical disorders of the fourth ventricle*. Blackwell Science, Inc, Boston, pp 189–208
36. Hoffman HJ, Berger MS, Becker LE (1990) Cerebellar astrocytomas. In: Deutsch M (ed) *Management of childhood brain tumors*. Kluwer Academic Publishers, Boston, pp 441–456
37. Sanford RA, Gajjar A (1997) Ependymomas. *Clin Neurosurg* 44:559–570
38. Lyons MK, Kelly PJ (1991) Posterior fossa ependymomas: report of 30 cases and review of the literature. *Neurosurgery* 28:659–665
39. Sutton LN, Goldwein J (2004) Intracranial ependymomas. In: Winn HR (ed) *Youmans neurological surgery*, 5th edn. WB Saunders, New York, pp 3623–3637
40. Hargrave D, Bartels U, Bouffet E (2006) Diffuse brainstem glioma in children: critical review of clinical trials. *Lancet Oncol* 7(3):241–248
41. Sandri A, Sardi N, Genitori L et al (2006) Diffuse and focal brainstem tumors in childhood: prognostic factors and surgical outcome. Experience in a single institution. *Childs Nerv Syst* 22(9):1127–1135
42. Finlay JL, Zacharoulis S (2005) The treatment of high grade gliomas and diffuse intrinsic pontine tumors of childhood and adolescence: a historical and futuristic perspective. *J Neurooncol* 75(3):253–266
43. Ueoka DI, Nogueira J, Campos JC, Filho PM, Ferman S, Lima MA (2009) Brainstem gliomas-retrospective analysis of 86 patients. *J Neurol Sci* 281:20–23
44. The brain stem (1996) In: Patten J (ed) *Neurological differential diagnosis*, 2nd edn. Springer, London, pp 162–177
45. Cerebellum (1998) In: Duus P (ed) *Topical diagnosis in neurology-anatomy, physiology, signs and symptoms*. Thieme Medical Publishers, Inc., New York, pp 164–179

Yuzo Terakawa, Jong Hee Chang, Christian Smith,
and James T. Rutka

6.1 Introduction

Brain tumors are the most common pediatric solid tumors, comprising 20–25 % of all childhood cancers. Although recent advances in the multidisciplinary care of the child with a brain tumor have taken place, brain tumors remain the leading cause of cancer-related death in the pediatric population. About 60–70 % of all the pediatric brain tumors occur in the posterior fossa. These tumors are clinically, pathologically, and genetically diverse and heterogeneous. While our understanding of the molecular mechanisms of these tumors is far from complete, the application of next generation lab-based strategies to pediatric brain tumors is closing our knowledge gap in a tangible way.

Y. Terakawa, M.D.

Division of Neurosurgery, Department of Surgery,
The Hospital for Sick Children,
The University of Toronto,
Suite 1503, 555 University Avenue,
Toronto, ON M5G 1X8, Canada

Department of Neurosurgery, Osaka City University
Graduate School of Medicine, Osaka, Japan

J.H. Chang, M.D. • C. Smith, Ph.D.

J.T. Rutka, M.D., Ph.D. (✉)

Division of Neurosurgery, Department of Surgery,
The Hospital for Sick Children,
The University of Toronto,
Suite 1503, 555 University Avenue,
Toronto, ON M5G 1X8, Canada
e-mail: james.rutka@sickkids.ca

In this chapter, we will summarize the current state of our knowledge of the molecular genetics of pediatric posterior fossa tumors such as medulloblastoma, ependymoma, pilocytic astrocytoma (PA), atypical teratoid/rhabdoid tumor (AT/RT), and choroid plexus (CP) tumor and emphasize the importance of future research effort in this field.

6.2 Hereditary Syndromes Predisposing to the Development of a Brain Tumor in the Posterior Fossa

A familial tumor syndrome is a rare hereditary disease in which patients are at an increased risk of various neoplasms. However, the investigation of such rare hereditary syndromes is invaluable since it has revealed specific gene defects responsible for various sporadic tumors and has contributed to the better understanding of the underlying mechanisms of some of the more common diseases. This is best illustrated in studies of retinoblastomas which have allowed researchers to establish current concepts of cancer biology [1–3].

While most brain tumors in the posterior fossa occur sporadically, some may arise within patients with hereditary syndromes. For example, Turcot, Gorlin, and Li-Fraumeni syndromes are syndromes which predispose kindreds in a family to the development of medulloblastomas [4–7]. In addition, several cases of CP papilloma have been observed in conjunction with

Aicardi syndrome, although they are located in the supratentorial compartment [8–10]. In this section, some of the hereditary syndromes associated with brain tumors in the posterior fossa are described.

6.2.1 Gorlin Syndrome

Gorlin syndrome, or nevoid basal cell carcinoma syndrome, is a rare autosomal dominant disorder characterized by multiple basal cell carcinomas of the skin, a variety of other tumors, including, but not limited to, ovarian fibromas and medulloblastomas, and developmental abnormalities. Developmental manifestations include macrocephaly, characteristic coarse facies, strabismus, dental malformations, jaw keratocysts, dermal pits of the palms and soles, rib abnormalities, dysgenesis of the corpus callosum, spina bifida occulta and other spine abnormalities, and ectopic calcification [11–13]. Gorlin syndrome is caused by mutation of the long arm of chromosome 9 (9q22.3–q31), and patients in this syndrome frequently have a germline mutation in the human homologue of the *Drosophila melanogaster patched* gene (*PTCH1*) [14–18]. The *PTCH1* gene encodes a transmembrane receptor protein for the secreted ligand, Sonic Hedgehog (Shh), and serves as a negative regulator of the Shh signaling pathway. Mutations in the *PTCH1* gene produce a truncated protein that is non-functional [19], thereby resulting in aberrant Shh signaling leading to the development of a transformed phenotype [20]. Consequently, patients with Gorlin syndrome are predisposed to a variety of tumors as well as multiple cutaneous basal cell carcinomas. The incidence of medulloblastomas in this syndrome ranges from 5 to 20 % [13, 21, 22].

6.2.2 Turcot Syndrome

Turcot syndrome is a rare hereditary disorder in which patients often present with colorectal cancer and a primary brain tumor [23–25]. This syndrome is known to be heterogeneous

but recently has been divided largely into two subtypes [25, 26]. One subtype of this syndrome involves a germline mutation in DNA mismatch-repair genes, such as *hMLH1* (*human mutL homolog 1*), *hMSH2* (*human mutS homolog 2*), and *hPMS1* and *hPMS2* (*human postmeiotic segregation 1 and 2*) [24]. These patients typically present with hereditary nonpolyposis colon cancer and glial tumors such as glioblastoma multiforme, but do not appear to have an increased risk of developing medulloblastomas. In contrast, the other subtype is characterized by medulloblastoma in the context of familial adenomatous polyposis where patients develop multiple colonic polyps that are predisposed toward malignant progression [27]. The molecular basis of this subtype involves a germline mutation in the tumor suppressor gene, *adenomatous polyposis coli* (*APC*), on chromosome 5q21 [24]. The *APC* protein is part of a polymeric protein complex that regulates the level of β -catenin, a downstream transcriptional activator of the Wntless (Wnt) signaling pathway, and thus altered regulation of the pathway can predispose to tumor formation.

6.2.3 Li-Fraumeni Syndrome

This familial cancer syndrome was first described by Li and Fraumeni in 1969, in which they described patients with rhabdomyosarcoma having an increased incidence of cancer in family members [28]. Criteria for the diagnosis of Li-Fraumeni syndrome are suggested by a proband with any childhood tumor or sarcoma, brain tumor, or adenocortical tumor under 45 years of age and an additional first- or second-degree relative with a typical Li-Fraumeni syndrome tumor at any age and another first- or second-degree relative with any cancer under the age 60 years [29, 30]. Patients with Li-Fraumeni syndrome have a predisposition to several malignant tumors including sarcomas, premenopausal breast cancer, acute leukemia, adenocortical carcinoma, and brain tumors such as medulloblastomas [29, 31]. Most cases of Li-Fraumeni syndrome are now secondary to germline mutations in *TP53* [32–35],

a tumor suppression gene responsible for several cell functions related to DNA repair, induction of apoptosis, and cell cycle arrest [36–38].

6.2.4 Aicardi Syndrome

Aicardi syndrome is a rare, X-linked dominant disorder secondary to mutation/deletion of a gene on the X chromosome that is seen almost exclusively in females as affected males are usually miscarried. Affected females have characteristic lacunar chorioretinopathy, flexor spasms, and agenesis of the corpus callosum [39]. These children have visual impairment, developmental delay, and intractable seizures. Several brain tumors have been reported associated with this syndrome. These brain tumors include CP papillomas and medulloblastoma [40]. Genetic analysis suggests that the mutations are localized in the Xp22 [41], but the molecular mechanisms predisposing to these brain tumors are not well known.

6.2.5 Rubinstein-Taybi Syndrome

Rubinstein-Taybi syndrome is a rare congenital anomaly syndrome characterized by microcephaly, facial abnormalities, broad thumbs and toes, and mental retardation [42]. The molecular basis of this syndrome involves mutation or deletion of the human CREB-binding protein (*CBP*) gene at chromosome 16p13.3 [43]. The functions of *CBP* include regulation of transcription factors, regulation of transcription by modifying DNA structure (chromatin), DNA repair, cell growth, and embryonic development. *CBP* is involved in integrating signals from multiple signaling pathways [44]. Pathways modulated by *CBP* include Hedgehog signaling, *TP53*, Wnt signaling, all of which have been implicated in the pathogenesis of medulloblastomas, as is discussed in the latter part of this chapter. Patients with Rubinstein-Taybi syndrome are predisposed to developing malignancies, especially of the central nervous system (CNS), including oligodendrogliomas, meningiomas, and medulloblastoma [45–48].

6.3 Developmental Signaling Pathways Involved in Medulloblastoma

Medulloblastoma, an embryonal tumor of the cerebellum, is the most common malignant solid neoplasm in children, classified as a brain tumor of grade IV according to the World Health Organization classification. Histologically, medulloblastoma is classified into five distinct subtypes; classic, desmoplastic/nodular, anaplastic, large cell, and medulloblastoma with extreme nodularity [49]. Desmoplastic/nodular medulloblastoma is typically associated with a more favorable prognosis as opposed to anaplastic and large cell medulloblastomas which have a poorer prognosis when compared to classic medulloblastoma [50].

Molecular genetic analysis of the aforementioned different familial hereditary syndromes has provided valuable insights into embryonic aberrations in key signaling pathways which are believed to contribute to the pathogenesis of brain tumors, especially medulloblastomas. The Shh, Wnt, and Notch signaling pathways are such key developmental pathways that control embryonic patterning and cell fate determination. These signaling pathways also regulate the development of the cerebellum including the proliferation of the granule cells in the external granular layer, the site of origin of at least a subset of medulloblastomas [20, 51–55]. Aberrancies in these signaling pathways can promote tumorigenesis [20, 53, 56]. Here, developmental signaling pathways involved in the molecular pathogenesis of medulloblastomas are described.

6.3.1 The Shh Pathway

The Hedgehog signaling pathway is composed of a number of secreted proteins expressed at different time points and locations in the course of development. The Hedgehog plays a vital role in regulating the behavior of neural stem and progenitor cells [20, 52–54]. Interestingly, mutations in certain Hedgehog genes may lead to severe defects in the CNS such as holoprosencephaly [52].

In vertebrates, the Hedgehog family consists of at least three genes, *Sonic*, *Indian*, and *Desert Hedgehog* [54].

Shh signaling pathway is known to be associated with midline facial development and the induction of neural tissue by mesodermal notochord [53]. Furthermore, Shh signaling pathway plays an active role in the formation of many vertebrate organ systems, especially the CNS including the cerebellum [57, 58].

During normal cerebellar development, the external granule layer (EGL) is formed when granule cell precursors (GCPs) migrate from the rhombic lip over the outer layer of the cerebellar surface where they initially undergo cell expansion. Subsequently, GCPs enter into a postmitotic phase and move into the inner EGL to generate the internal granule layer (IGL), where they undergo terminal differentiation. Shh, the most potent mitogen for GCPs, is secreted by Purkinje cells and is involved in the initial EGL cell expansion. Blocking this Shh function in vivo dramatically decreases the proliferation of cells in the EGL [59]. Furthermore, dysregulation of the molecular events regulating cerebellar GCPs may be responsible for uncontrolled cell growth leading to medulloblastoma formation [20, 52, 53, 56].

Shh proteins are synthesized as 45-kDa precursors, consisting of an N-terminal signaling domain and a C-terminal catalytic domain. Shh is secreted by Purkinje cells and is cleaved into two fragments. The amino-terminal fragment is covalently bound to cholesterol, so that it becomes hydrophobic. Consequently, Shh diffuses across the molecular layer of the cerebellum to the cells of the EGL, where it binds to PTCH and releases PTCH-mediated repression of smoothened (SMO), thus activating Shh signaling pathway [60].

The transduction of the Shh signal in cells is mediated by interactions between the Shh proteins and the multipass transmembrane protein PTCH. This interaction functions to activate the transmembrane protein SMO [52]. In the absence of the Shh ligand, PTCH constitutively represses SMO activity [61]. The derepression of SMO allows the activation of downstream transcription factors belonging to the Gli family, and these include Gli1, 2, and 3 in vertebrates. These transcription factors

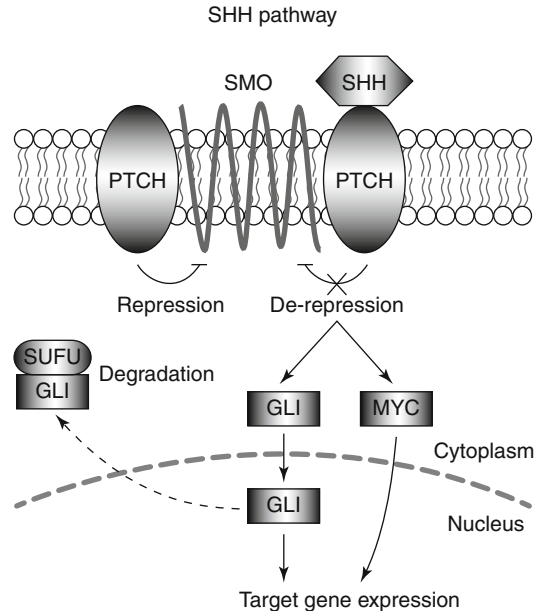


Fig. 6.1 A simplified scheme of the Sonic Hedgehog signaling pathway. *PTCH* patched, *SHH* Sonic Hedgehog protein, *SMO* smoothed, *SUFU* suppressor of fused

translocate into the nucleus and contribute to the expression of target genes related to the Hedgehog signaling pathway [52, 53, 62, 63]. Ultimately, these genes promote cell proliferation and differentiation and include: insulin-like growth factor 2, platelet-derived growth factor receptor α , N-myc, Myc, Bmi1, cyclins D1 and D2, Wnt, Hes1, or apoptosis (Bcl2) [64, 65]. Suppressor of fused (SUFU) is the Hedgehog protein known as a powerful antagonist of the Gli proteins, which acts to promote nuclear export, cytoplasm sequestration, and transcriptional inhibition of Gli proteins [53, 66, 67] (Fig. 6.1).

Aberrant activity of the Shh signaling pathway has been implicated in the pathogenesis of at least a subset of medulloblastomas [52]. Approximately 25 % of medulloblastomas carry mutations in genes of the Hedgehog pathway, and inappropriate activation of Hedgehog signaling occurs in approximately 60 % of tumors. Overactivity of Hedgehog signaling during GCP development may be a primary event in medulloblastoma pathogenesis [52]. The association between the Hedgehog signaling pathway and medulloblastomas is also supported by animal

models in which mice with *PTCH* gene mutations exhibit features of Gorlin syndrome and 14 % of them develop medulloblastoma [68, 69].

Medulloblastomas, especially of the desmoplastic subtype, are known to have loss of heterozygosity (LOH) on chromosome 9q, a region where the gene *PTCH1* is located [70]. On the other hand, subsequent studies of sporadic medulloblastomas have shown that mutations of *PTCH1* are not common among the sporadic tumors [71–73]. Sporadic medulloblastomas carrying LOH on chromosome 9q do not have readily detectable mutations of the other *PTCH1* allele. Moreover, medulloblastomas from *PTCH*^{+/-} mice retain the wild-type allele. These findings indicate that the loss of one allele of *PTCH1* may be sufficient to promote medulloblastoma formation [72, 74].

Activating mutations of *SMO* have been detected in approximately 5 % of sporadic medulloblastomas [75]. Germline and somatic mutations in the gene, *SUFU*, were found in approximately 9 % of children with medulloblastoma [76] and within the desmoplastic subtype in particular.

6.3.2 The Wnt Signaling Pathway

The Wnt signaling pathway is composed of a highly conserved group of more than 20 secreted proteins that play a role during embryonic development, stem cell regulation, and cell differentiation [51]. The Wnt signaling pathway can be divided into four subtypes: the canonical or Wnt/ β -catenin pathway and three noncanonical pathways, Wnt/Ca⁺⁺, planar cell polarity, and Wnt/protein kinase A pathways [77].

The Wnt/ β -catenin pathway has been well studied among these pathways, as sporadic colon cancer has shown to be frequently associated with mutations in this pathway [78]. Wnt protein is a secreted ligand that binds to its receptor, the seven-transmembrane protein Frizzled (FRZ) [79]. FRZ signaling is mediated by Dishevelled to a multiprotein complex composed of APC protein, axin protein, glycogen synthase kinase (GSK)-3 β , and β -catenin. In the absence of

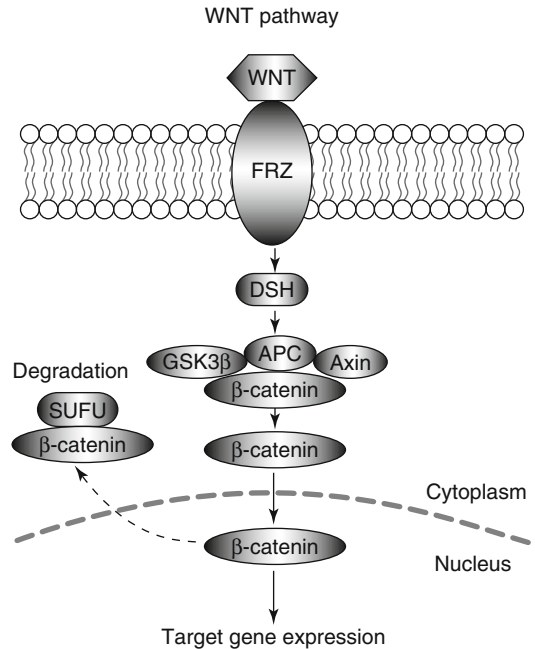


Fig. 6.2 A simplified scheme of the Wingless (*Wnt*) signaling pathway. *APC* adenomatous polyposis coli, *DSH* Dishevelled, *FRZ* frizzled, *GSK3 β* glycogen synthase kinase-3 β , *SUFU* suppressor of fused

Wnt signaling, the APC/axin/GSK-3 β complex phosphorylates the amino-terminal residues of β -catenin, thereby leading to degradation of β -catenin by the ubiquitin-proteasome pathway. As a consequence, the level of cytoplasmic β -catenin is downregulated. The binding of Wnt protein to the receptor complex inhibits the kinase activity of this protein complex, leading to β -catenin accumulation in the cytoplasm. When β -catenin accumulates in the cytoplasm, it can translocate to the nucleus where it binds to transcription factors thereby inducing the expression of known oncogenes, such as *c-myc* and *cyclin D* [80–82] (Fig. 6.2). Accumulation of β -catenin in cells with *APC* mutations has been shown to result in strong overexpression of the *c-myc* gene [80]. The protein *SUFU*, already described as responsible for nuclear exportation of Glis in Hedgehog signaling, is also responsible for nuclear exportation of β -catenin in the Wnt signaling pathway. Thus, it plays a significant role in two important pathways of medulloblastoma formation [51, 66, 83] (Fig. 6.2).

The identification of mutations of the tumor suppressor gene *APC* in the context of Turcot syndrome led to the recognition of the Wnt signaling pathway associated with medulloblastoma formation. Since then, several proteins related to this pathway have been studied to evaluate their participation in sporadic medulloblastomas [20, 55].

Immunohistochemical study showed that nuclear β -catenin was positive in 18 % of medulloblastomas, suggesting that Wnt signaling is overactive in about one-fifth of sporadic medulloblastomas [84]. β -Catenin was found to be overexpressed in the nucleus of medulloblastoma cells in 18–22 % of cases [85]. Activating mutations of β -catenin were also found in 3 of 67 sporadic medulloblastomas [86]. These data suggest that overactivity of the Wnt signaling pathway may contribute to the pathogenesis of sporadic medulloblastoma.

Although *APC* germline mutations are associated with medulloblastoma in Turcot syndrome, previous studies have failed to show LOH at the locus of *APC* and any somatic mutations in sporadic medulloblastomas [73, 87]. These results contrast with those found in sporadic colon cancer, where mutations of *APC* occur in almost 80 % of the cases. However, more recent study has shown missense mutations of *APC* gene in 2 of 46 sporadic medulloblastomas [88].

Mutational analysis of the *axin* gene has shown mutations in seven of 97 medulloblastomas including 86 sporadic cases. These mutations were primarily located at the *APC*-binding domain, possibly decreasing the ability of axin to bind *APC*, an interaction which is required to downregulate β -catenin [89]. Although GSK-3 β also acts as a downregulator of the Wnt signaling pathway, mutational analysis has failed to show any mutations of this gene in a series of medulloblastomas [86].

6.3.3 The Notch Signaling Pathway

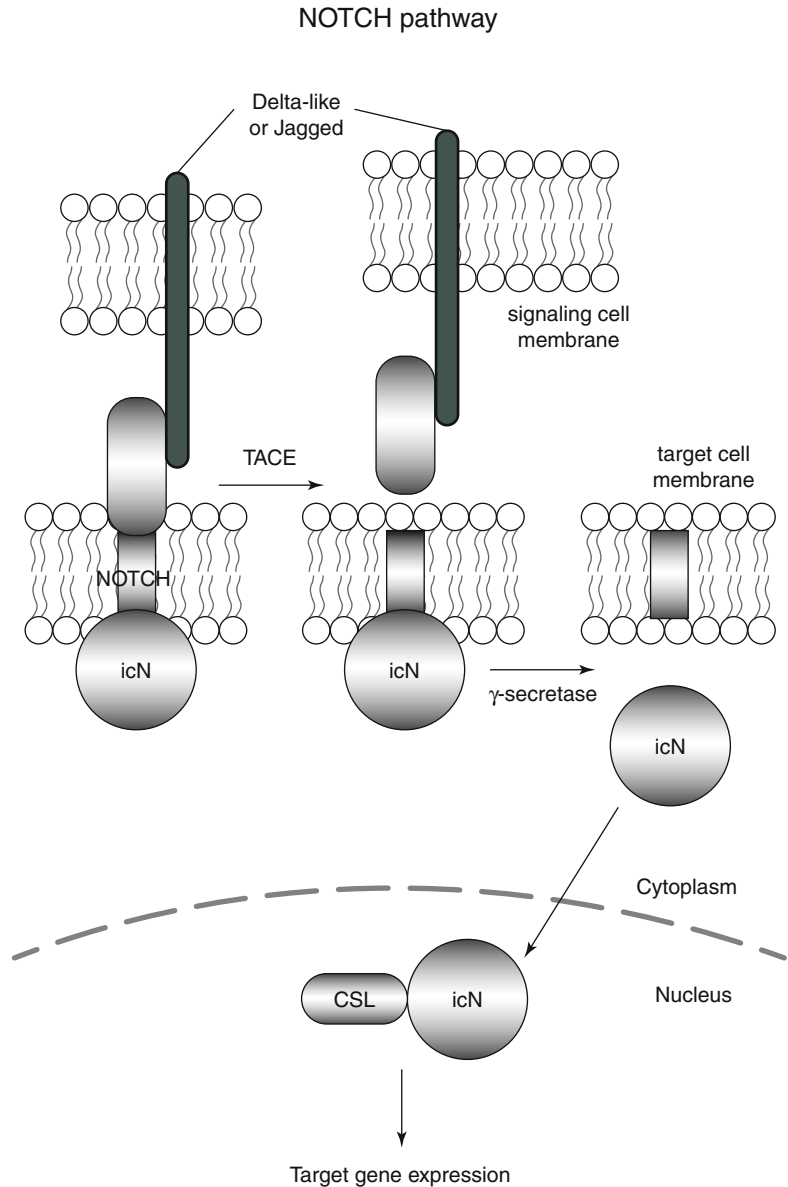
The Notch signaling pathway plays a general role in regulating cell fate choices and differentiation in several cells and tissues during development.

In mammals, five ligands (Delta-like-1, Delta-like-3, and Delta-like-4 and Jagged-1 and Jagged-2) and four transmembrane receptors (Notch1 to 4) have been identified in this signaling pathway [20, 56, 90].

The Notch receptor is a large single-pass transmembrane protein consisting of an extracellular domain responsible for ligand binding and a cytoplasmic domain. When activated by the binding of the ligand which is displayed on an adjacent cell, the Notch receptor undergoes two proteolytic cleavage processes to function. The first cleavage occurs at the extracellular portion mediated by an extracellular protease. The second cleavage is mediated by a γ -secretase complex at the transmembrane site, releasing the cytoplasmic domain of the receptor from the membrane, that is, the intracellular form of Notch (icN). The icN translocates to the nucleus where it forms a complex with the ubiquitously expressed transcription factor CSL (CBF/Suppressor of Hairless/LAG-1) and activates the transcription of target genes (such as *p21*, *cyclin D1* and *Hes*) and regulators of apoptosis [90] (Fig. 6.3).

Unlike the Shh and Wnt signaling pathways, no hereditary syndromes have been described associated with the Notch signaling pathway. Thus, its participation in medulloblastoma pathogenesis has not been well defined. However, recent analysis of embryonal brain tumor cell lines including medulloblastomas has shown that *Notch2* was amplified in 15 % of cases [91]. In contrast, another study of medulloblastomas showed *Notch1* was overexpressed in a majority of tumors, whereas *Notch2* expression was elevated only in a small number of cases [92]. The expression of the Notch target genes *Hes1* and *Hes5* has also been shown to be elevated in medulloblastomas [92]. Furthermore, Notch signaling inhibition with γ -secretase inhibitors induced a marked reduction of tumor cell growth [92]. Further studies are needed to elucidate the exact role of the Notch signaling pathway in medulloblastoma formation, but these studies indicate that dysregulation of the Notch signaling pathway may contribute to the pathogenesis of medulloblastoma.

Fig. 6.3 A simplified scheme of the Notch signaling pathway. *CSL* CBF/Suppressor of Hairless/ LAG-1 transcription factor, *icN* intracellular Notch, *TACE* TNF α converting enzyme-like protease



6.3.4 The EGFR Signaling Pathway

The epidermal growth factor receptor (EGFR) signaling pathway, comprising the EGFR family of receptor tyrosine kinases and their cognate ligands, is an evolutionarily conserved pathway that plays a crucial role in cell proliferation, survival, migration, and differentiation. Aberrant activation of this signaling pathway, in turn, leads to increased cell proliferation and altered cell

migration through the activation of transcription factor target proteins.

The EGFR family are composed of four distinct transmembrane receptors; ErbB1, ErbB2, ErbB3, and ErbB4 (also known as EGFR, HER2, HER3, and HER4, respectively). These receptors consist of an extracellular domain responsible for ligand binding and an intracellular domain which possesses enzymatic activity [93]. The binding of ligands to the

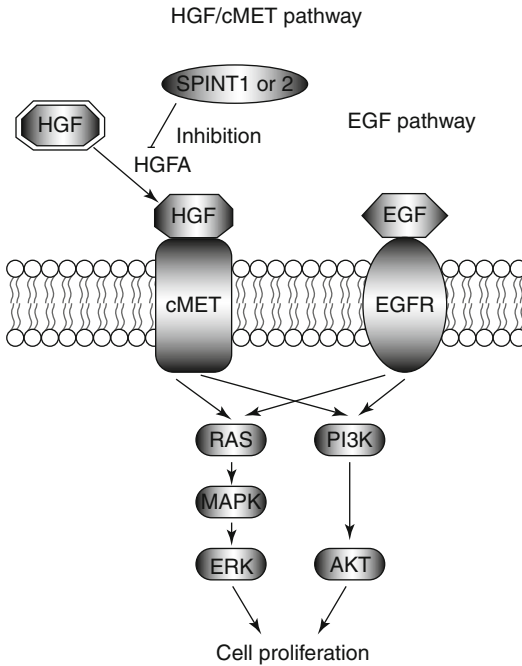


Fig. 6.4 A simplified scheme of the hepatocyte growth factor (*HGF*)/cMET and the epidermal growth factor (*EGF*) signaling pathways. *AKT* protein kinase B, *ERK* extracellular signal-regulated kinase, *HGFA* HGF activator, *PI3K* phosphoinositide 3-kinase

receptor induces receptor dimerization and cross-phosphorylation leading to activation of downstream signaling cascades such as phosphoinositide 3-kinase (PI3K), mitogen-activated protein kinase (MAPK), and protein kinase B (Akt) [94] (Fig. 6.4).

This EGFR signaling pathway has recently been implicated in the development and growth of several types of tumors including medulloblastoma. According to an immunohistochemical study, overexpression of the ErbB2 receptor was seen in 28 % of medulloblastomas [95], and coexpression of ErbB2 and ErbB4 was linked to unfavorable prognosis in the pediatric population [96]. Expression of ErbB2 and ErbB4 in association with a ligand of neureglin 1- β has been implicated in the metastatic behavior of medulloblastoma [97]. In addition, mutations of ErbB4 and upregulation of Akt and MAPK have also been described in association with medulloblastomas [98–100].

6.3.5 The HGF/cMET Signaling Pathway

The hepatocyte growth factor (HGF)/cMET signaling pathway plays a crucial role in diverse processes including development and tissue hemostasis. It promotes mitogenesis, morphogenesis, and cell motility in a variety of cell types including neurons [101]. HGF is a widely expressed multifunctional growth factor and serves as a ligand in this signaling pathway. HGF is produced in an inactive proform and then cleaved into its active heterodimer by the serine protease HGF activator (HGFA) [102, 103]. cMET is a transmembrane protein and the only receptor for HGF. The cytoplasmic domain of cMET has tyrosine kinase activity and is responsible for downstream signaling. The cMET receptor is normally activated by the binding of HGF. Upon binding of HGF, cMET undergoes autophosphorylation and recruits intracellular adapters which leads to the activation of downstream signaling such as Ras/MAPK, PI3K/Akt, and STAT pathways [101, 104–108] (Fig. 6.4).

Precise regulation of the HGF/cMET signaling is crucial for normal development. Several different mechanisms are involved in appropriate spatiotemporal expression of the cMET receptor along with HGF. In addition, the activity of HGFA which mediates HGF to activate is also tightly regulated. To date, two inhibitors of HGFA have been identified: SPINT1 and SPINT2 [109, 110]. These inhibitors prevent the HGF ligand from being activated, consequently leading to repression of the HGF/cMET signaling. Consequently, loss of inhibition due to reduced *SPINT1* or *SPINT2* expression may result in aberrant activation of the HGF/cMET signaling [111]. Aberrant overexpression of ligand or receptor may, in turn, upregulate HGF/cMET signaling [101]. Receptor amplification, activating mutations, or gene rearrangements may also increase HGF/cMET signaling [101, 111, 112].

Aberrant activation of HGF/cMET signaling has been implicated in promoting tumorigenesis and the metastatic phenotype, and several *cMET* activating mutations have been identified in a variety of cancers [111]. A recent study which

examined primary medulloblastomas by comparative genomic hybridization (CGH) has detected *cMET* gene copy number gains in 38.5 % of their cases [113]. High expression of *cMET* has been correlated with reduced overall survival [114]. Treatment of medulloblastoma cell lines with HGF increased cell proliferation and anchorage-independent growth and reduced apoptosis [114]. Following HGF treatment, the medulloblastoma cell lines exhibited a more malignant phenotype than the parental cell line [114]. Given these results, it is reasonable to hypothesize that the HGF/cMET signaling pathway may be involved in the pathogenesis of medulloblastoma.

6.4 Molecular Genetics of the Posterior Fossa Tumors in Children Other Than Medulloblastomas

6.4.1 Ependymomas

Ependymomas are the third most common pediatric brain tumor and account for 6.4 % of primary brain tumors in children aged 0–14 years and for 30 % of the tumors in children younger than 3 years [115]. Ependymomas can arise in three distinct locations: the spinal cord, supratentorial compartment, and the posterior fossa. Over 90 % of pediatric ependymomas arise intracranially with approximately 70 % of cases occurring in the posterior fossa. Interestingly, ependymomas located in these different anatomic sites are histologically indistinguishable. However, it is now known that different molecular genetic alterations occur in ependymomas depending on their site of origin.

Early cytogenetic and CGH studies which identified specific chromosomal aberrations exclusively in specific anatomical locations gave some indication that this might not be the case [116–118]. These reports were limited by the low resolution of techniques employed and small number of tumors analyzed from different locations and age of tumor onset. More recent studies on a larger number of tumor samples

at higher resolution have demonstrated that ependymomas arising in different anatomical compartments are characterized by distinct copy-number alterations and genetic signatures [119]. Chromosome 22 loss has been reported to be the most common copy-number alteration in both sporadic intracranial and spinal ependymomas. LOH and gene mutation point to *NF2* as a likely candidate in spinal ependymomas, but a chromosome 22 tumor suppressor gene, important in the case of pediatric intracranial ependymomas, remains unclear. The other frequent chromosomal abnormalities include losses on chromosomes 6q, 17p, and 22q and gains on 1q and 9q. Less frequent genetic alterations involve losses on chromosomes 7p, 9p, 10q, 13q, and 16q and gains on 4q, 5, 7, 8, 12q, 15q, 18, and 20. Mutational analysis used to find pathogenetically significant genes within regions of genetic alteration has yet to uncover causal targets, as somatic mutations in *NF2* (22q), *TP53* (17p), and *PTEN* (10q) are rare in childhood intracranial ependymoma [120, 121].

Recently, several publications have identified previously unknown focal amplifications of *MYCN*, *EGFR*, *NOTCH1*, *NOTCH4*, *VAV1*, and *YAP1* and deletion of *CDKN2A* and *SULT4A1* [119, 122–124]. Importantly, most pediatric ependymomas occur in the posterior fossa, and half of these cases demonstrated a balanced genomic profile with few detectable chromosomal abnormalities [121]. Modena et al. identified frequent deletion of chromosome 22q13.3 harboring a downregulated *SULT4A1* and amplification and overexpression of *YAP1* on chromosome 11q22 [122]. More recently, chromosome 9q33–34 was shown to be gained frequently in 30 % of ependymomas. Within this gene-rich locus, *NOTCH1* was shown to be a candidate gene and found to be overexpressed and mutated in a subset of ependymomas. These mutations occur in approximately 8.3 % of cases exclusively in ependymomas of the posterior fossa. Taylor et al. demonstrated that approximately 12 % of the genes amplified in ependymoma were overexpressed, compounding the difficulty in identifying potential oncogenes [119].

Despite the above limitations, our understanding of the genetic basis of pediatric ependymomas has advanced remarkably through gene expression profiling. By analyzing a cohort of ependymomas of different anatomic origin, Taylor et al. found that histologically identical, but genetically distinct, ependymomas exhibit patterns of gene expression that recapitulate those of radial glia cells in the corresponding region of the central nervous system [119]. Cancer stem cells isolated from ependymomas displayed a radial glia phenotype and formed tumors when transplanted into the intracranial compartment in mice. These findings suggest that ependymomas might arise within the radial glial cell lineage, and identify restricted populations of radial glia cells as candidate stem cells of the different subgroups of ependymoma. They also support a hypothesis that subgroups of the same histological tumor type are generated by different populations of progenitor cells in the tissues of origin.

6.4.2 Pilocytic Astrocytomas

PA is the most common cerebellar neoplasm in childhood. Most of these tumors arise in the cerebellum and generally are associated with a favorable outcome except tumors close to brainstem [125]. Patients with autosomal dominantly inherited neurofibromatosis type 1 (NF1) are at higher risk of developing low-grade astrocytomas than the general population, often along the optic pathways [126]. Neurofibromin, the gene product of the *NF1* gene, physiologically contributes to growth arrest of astrocytic cells and neuronal differentiation by downregulation of the MAPK signaling pathway via its GTPase-activating domain. Loss of neurofibromin expression conversely leads to increased Ras activity and astrocyte proliferation [127]. Similar activation of the MAPK pathway has been confirmed by gene expression profiles of both NF1-associated and sporadic PAs, suggesting activated MAPK signaling in most astrocytomas [128]. Even though activating

mutations in *KRAS* was previously identified and those mutations results in activation of MAPK signaling, in some sporadic PAs, alternative mechanisms of oncogenic MAPK activation in PA have not been clear yet [129].

Most PAs have a normal karyotype, and cytogenetic abnormalities may be more common in adult comparing to pediatric PAs. The presence of cytogenetic mutations may indicate tumor progression. Among the few recurrent aberrations, trisomy of chromosomes 5 and 7 and gain of 7q were the most consistent findings [130, 131]. Other chromosome aberrations are extremely rare, and cytogenetic abnormalities of chromosomes 6, 8, 11, 12, 17, 19, and 22 were described in only a few cases [130, 132–134]. With increased resolution of array-based DNA copy-number analysis in recent years, it has become possible to identify more discrete aberrations in PA, such as duplication at chromosome band 7q34.

Recently, Pfister et al. identified *BRAF* as a centrally important oncogene in the pathogenesis of pediatric PAs [134]. More than 50 % of PAs displayed a tandem duplication of the *BRAF* locus (7q34), and approximately 6 % of the remaining nonduplicated tumors showed an activating mutation of *BRAF* at codon 600 in exon 15, indicating that different mechanisms of oncogenic *BRAF* activation exist in these tumors. Several successive studies found a similar or even higher frequency of *BRAF* duplications in PA [133, 135–137].

Breakpoints in the *BRAF* gene and a previously uncharacterized gene, *KIAA1549*, led to the formation of an oncogenic fusion transcript incorporating the BRAF kinase domain and lacking the autoinhibitory domain of wild-type BRAF, thus rendering it constitutively active [136, 137].

More recently, another mechanism of MAPK activation in PA was described, namely, tandem duplications at 3p25 in a small percentage (2 %) of these tumors, leading to an in-frame oncogenic fusion between *SRGAP3* and *RAF1*, which shares high sequence homology with *BRAF* [132, 138]. In addition, one of the groups

described a novel insertion at codon 598 in *BRAF* that mirrors the hotspot V600E mutation, resulting in a transforming, constitutively active BRAF kinase [138]. Using combined molecular analysis of the BRAF-KIAA1549 fusion and mutational analysis of *IDH1*, PA can be sensitively and very specifically differentiated from diffuse astrocytoma. BRAF fusion is identified in at least 70 % of PAS, but neither *IDH1* nor *IDH2* mutations are present in PAs, whereas BRAF fusion occurs rarely in pediatric diffuse astrocytoma [134] and has never been found in adult diffuse astrocytoma [139].

6.4.3 AT/RTs

AT/RTs are aggressive embryonic tumors that usually are diagnosed in children under the age of 2 years. Approximately 30 % of AT/RTs occur infratentorially, and these tumors are also seen in the kidney and less commonly in a variety of locations in the soft tissue. The prognosis is significantly poor.

Rhabdoid tumors have a similar molecular origin regardless of their anatomical locations. Mutation or deletion of both copies of the *hSNF5/INI1* gene that maps to chromosome 22q11.2 is observed in approximately 70 % of primary tumors. Another 25 % of tumors have reduced expression at the RNA or protein level, indicative of a loss-of-function event. Deletions on chromosome 11 have also been found in rhabdoid tumors [140–145].

Versteeg et al. identified the rhabdoid tumor suppressor gene on chromosome 22q11 as the *hSNF5/INI1* (*human sucrose non-fermenting 5*) gene. This gene was biallelically inactivated by deletions and/or truncating mutations in a series of renal rhabdoid tumors [146]. This gene is highly conserved from humans to yeast, where it affects the yeast cell's ability to metabolize sucrose when mutated. Biegel and colleagues showed somatic deletions and/or truncating mutations of *hSNF5/INI1* in CNS AT/RTs. Subsequently, *hSNF5/INI1* mutations were also found in choroid plexus carcinomas (CPCs)

and possibly some primitive neuroectodermal tumors and medulloblastomas [147, 148]. Most mutations were found in tumors from very young children (age <2 years).

Some children with rhabdoid tumors have de novo germline mutations of *hSNF5/INI1*, suggesting that single mutation in the *hSNF5/INI1* gene was predisposed to develop rhabdoid tumors. In some families with an elevated incidence of rhabdoid tumors and/or CPCs, there may be an inherited germline mutation of the *hSNF5/INI1* gene that predisposes affected family members to cancer [149]. Subsequent generation of *SNF5/INI1* knockout mice by homologous recombination has shown that *SNF5/INI1* is important for development as *hSNF5/INI1*^{-/-} embryos die at embryonic day 7 [150, 151]. Furthermore, heterozygous *SNF5/INI1*^{+/-} mice develop tumors reminiscent of rhabdoid tumors, highly suggesting that it is also a tumor suppressor gene in mice, as well as providing an excellent model of the disease.

hSNF5/INI1 is almost ubiquitously expressed in both time and space in most tissues. It functions to regulate the structure of DNA to either allow or deny access of transcription factors to their respective promoters. *hSNF5/INI1* can promote expression of some genes while repressing others [152]. *hSNF5/INI1* interacts with the well-known proto-oncogene *c-myc* and may be involved in the *c-myc* mediated activation of apoptotic genes [153]. *hSNF5/INI1* may also be involved with regulation of the highly important tumor suppressor gene *RB1* (retinoblastoma susceptibility gene).

The *INI1* protein is a component of the SWI/SNF chromatin-remodeling complex. The complex is recruited to promoters of a large variety of genes involved in cell signaling, growth, and differentiation [145, 154, 155]. It is uncertain why loss of function of this highly conserved, ubiquitously expressed protein would induce the specific phenotypes in both humans and mice. Understanding the role of *INI1* as a member of the SWI/SNF complex in tumorigenesis will be important for identifying downstream target genes [145].

6.4.4 Choroid Plexus Papillomas

Primary CP tumors are the most common brain tumors in the first year of life. According to the 2007 WHO classification of tumors of the nervous system, these tumors are classified as CP papilloma (CPP, WHO grade I), atypical CPP (grade II), and CP carcinoma (CPC, grade III). While the patients with a CPP can be usually cured by surgical resection only, the prognosis of patients with a CPC is very poor.

CP tumors have been reported in families with germline mutations of *TP53* or *hSNF5/IN11*, while *TP53* mutations in sporadic CPCs are rare [149, 156–159]. Constitutional duplication of chromosome 9p is a rare anomaly with some of the patients reported having proliferative disorders of the CP [160]. Investigation of sporadic CP tumors showed extra copies of 9p further implicating genes on this chromosome arm in the pathogenesis of CP tumors. Overexpression of the SV40 Large T antigen oncogene in transgenic mice results in the formation of intracranial CP tumors [161, 162]. Carlotti et al. have shown overexpression of cell cycle gene products, such as pRB, cyclins, and E2F-1, in CPCs vs. CPPs. Furthermore, the MIB-1 labeling index of CPCs was significantly higher than that of the CPPs [163]. CP tumors were induced by the introduction of constitutively active Notch3 into periventricular cells of embryonic day 9.5 mice. These findings suggest that Notch signaling is important in this experimental model [164], while the significance of Notch signaling in human CP tumors remains unclear.

Conclusions

Recent technological advances and increased knowledge of molecular biology have brought us a better understanding of the molecular genetics of brain tumors in children as well as those in adults. As some examples, molecular genetic analyses of hereditary syndromes have revealed several specific gene mutations and signaling pathways involved in the pathogenesis of certain pediatric brain tumors, especially medulloblastoma. Many sporadic tumors exhibit frequent, nonrandom

cytogenetic alterations which are coming into greater focus given the widespread availability of advanced genetic sequencing techniques. These molecular genetic approaches have provided new insights into the major genes and pathways that appear to initiate a wide variety of pediatric brain tumors.

Although the translation of our understanding of the molecular genetics of brain tumors into a tangible benefit to the individual child is still some distance away, in some cases, our knowledge of the genetics of pediatric brain tumors is beginning to assist us in categorizing stages of disease, prognosticating outcome after therapy, and suggesting new targets for future therapy all the time. We anticipate that personalized therapies based of the molecular diversity of each patient's tumor will be feasible in the near future, which may have the potential to improve the outcome of a child with a malignant brain tumor.

Acknowledgements This work was supported by b.r.a.i.n.child, the Wiley Fund, and the Pediatric Brain Tumor Foundation of the United States.

References

1. Knudson AG Jr (1971) Mutation and cancer: statistical study of retinoblastoma. *Proc Natl Acad Sci U S A* 68:820–823
2. Cavenee WK, Hansen MF, Nordenskjold M, Kock E, Maumenee I, Squire JA, Phillips RA, Gallie BL (1985) Genetic origin of mutations predisposing to retinoblastoma. *Science* 228:501–503
3. Dunn JM, Phillips RA, Becker AJ, Gallie BL (1988) Identification of germline and somatic mutations affecting the retinoblastoma gene. *Science* 241:1797–1800
4. Raffel C (2004) Medulloblastoma: molecular genetics and animal models. *Neoplasia* 6:310–322
5. Taylor MD, Mainprize TG, Rutka JT (2000) Molecular insight into medulloblastoma and central nervous system primitive neuroectodermal tumor biology from hereditary syndromes: a review. *Neurosurgery* 47:888–901
6. Strahm B, Malkin D (2006) Hereditary cancer predisposition in children: genetic basis and clinical implications. *Int J Cancer* 119:2001–2006
7. Ng D, Stavrou T, Liu L, Taylor MD, Gold B, Dean M, Kelley MJ, Dubovsky EC, Vezina G, Nicholson HS, Byrne J, Rutka JT, Hogg D, Reaman GH, Goldstein

- AM (2005) Retrospective family study of childhood medulloblastoma. *Am J Med Genet A* 134:399–403
8. Taggard DA, Menezes AH (2000) Three choroid plexus papillomas in a patient with Aicardi syndrome. A case report. *Pediatr Neurosurg* 33:219–223
 9. Hamano K, Matsubara T, Shibata S, Hirano C, Ito Z, Ase Y, Kusakari J, Takita H (1991) Aicardi syndrome accompanied by auditory disturbance and multiple brain tumors. *Brain Dev* 13:438–441
 10. Uchiyama CM, Carey CM, Cherny WB, Brockmeyer DL, Falkner LD, Walker ML, Boyer RS (1997) Choroid plexus papilloma and cysts in the Aicardi syndrome: case reports. *Pediatr Neurosurg* 27:100–104
 11. Gorlin RJ (1995) Nevoid basal cell carcinoma syndrome. *Dermatol Clin* 13:113–125
 12. Gorlin RJ (1987) Nevoid basal-cell carcinoma syndrome. *Medicine (Baltimore)* 66:98–113
 13. Kimonis VE, Goldstein AM, Pastakia B, Yang ML, Kase R, DiGiovanna JJ, Bale AE, Bale SJ (1997) Clinical manifestations in 105 persons with nevoid basal cell carcinoma syndrome. *Am J Med Genet* 69:299–308
 14. Goldstein AM, Stewart C, Bale AE, Bale SJ, Dean M (1994) Localization of the gene for the nevoid basal cell carcinoma syndrome. *Am J Hum Genet* 54:765–773
 15. Chenevix-Trench G, Wicking C, Berkman J, Sharpe H, Hockey A, Haan E, Oley C, Ravine D, Turner A, Goldgar D et al (1993) Further localization of the gene for nevoid basal cell carcinoma syndrome (NBCCS) in 15 Australasian families: linkage and loss of heterozygosity. *Am J Hum Genet* 53:760–767
 16. Hahn H, Wicking C, Zaphiropoulos PG, Gailani MR, Shanley S, Chidambaram A, Vorechovsky I, Holmberg E, Uden AB, Gillies S, Negus K, Smyth I, Pressman C, Leffell DJ, Gerrard B, Goldstein AM, Dean M, Toftgard R, Chenevix-Trench G, Wainwright B, Bale AE (1996) Mutations of the human homolog of *Drosophila* patched in the nevoid basal cell carcinoma syndrome. *Cell* 85:841–851
 17. Farndon PA, Del Mastro RG, Evans DG, Kilpatrick MW (1992) Location of gene for Gorlin syndrome. *Lancet* 339:581–582
 18. Gailani MR, Bale SJ, Leffell DJ, DiGiovanna JJ, Peck GL, Poliak S, Drum MA, Pastakia B, McBride OW, Kase R et al (1992) Developmental defects in Gorlin syndrome related to a putative tumor suppressor gene on chromosome 9. *Cell* 69:111–117
 19. Wicking C, Shanley S, Smyth I, Gillies S, Negus K, Graham S, Suthers G, Haites N, Edwards M, Wainwright B, Chenevix-Trench G (1997) Most germ-line mutations in the nevoid basal cell carcinoma syndrome lead to a premature termination of the *PATCHED* protein, and no genotype-phenotype correlations are evident. *Am J Hum Genet* 60:21–26
 20. Marino S (2005) Medulloblastoma: developmental mechanisms out of control. *Trends Mol Med* 11:17–22
 21. Evans DG, Farndon PA, Burnell LD, Gattamaneni HR, Birch JM (1991) The incidence of Gorlin syndrome in 173 consecutive cases of medulloblastoma. *Br J Cancer* 64:959–961
 22. Friedrich RE (2007) Diagnosis and treatment of patients with nevoid basal cell carcinoma syndrome [Gorlin-Goltz syndrome (GGS)]. *Anticancer Res* 27:1783–1787
 23. Groden J (1995) Colon-cancer genes and brain tumors. *N Engl J Med* 332:884–885
 24. Hamilton SR, Liu B, Parsons RE, Papadopoulos N, Jen J, Powell SM, Krush AJ, Berk T, Cohen Z, Tetu B et al (1995) The molecular basis of Turcot's syndrome. *N Engl J Med* 332:839–847
 25. Paraf F, Jothy S, Van Meir EG (1997) Brain tumor-polyposis syndrome: two genetic diseases? *J Clin Oncol* 15:2744–2758
 26. Van Meir EG (1998) "Turcot's syndrome": phenotype of brain tumors, survival and mode of inheritance. *Int J Cancer* 75:162–164
 27. Hamada H, Kurimoto M, Endo S, Ogiuchi T, Akai T, Takaku A (1998) Turcot's syndrome presenting with medulloblastoma and familial adenomatous polyposis: a case report and review of the literature. *Acta Neurochir (Wien)* 140:631–632
 28. Li FP, Fraumeni JF Jr (1969) Rhabdomyosarcoma in children: epidemiologic study and identification of a familial cancer syndrome. *J Natl Cancer Inst* 43:1365–1373
 29. Varley JM, Evans DG, Birch JM (1997) Li-Fraumeni syndrome—a molecular and clinical review. *Br J Cancer* 76:1–14
 30. Birch JM, Hartley AL, Tricker KJ, Prosser J, Condie A, Kelsey AM, Harris M, Jones PH, Binchy A, Crowther D et al (1994) Prevalence and diversity of constitutional mutations in the p53 gene among 21 Li-Fraumeni families. *Cancer Res* 54:1298–1304
 31. Barel D, Avigad S, Mor C, Fogel M, Cohen IJ, Zaizov R (1998) A novel germ-line mutation in the noncoding region of the p53 gene in a Li-Fraumeni family. *Cancer Genet Cytogenet* 103:1–6
 32. Varley JM, McGown G, Thorncroft M, Santibanez-Koref MF, Kelsey AM, Tricker KJ, Evans DG, Birch JM (1997) Germ-line mutations of TP53 in Li-Fraumeni families: an extended study of 39 families. *Cancer Res* 57:3245–3252
 33. Frebourg T, Barbier N, Yan YX, Garber JE, Dreyfus M, Fraumeni J Jr, Li FP, Friend SH (1995) Germ-line p53 mutations in 15 families with Li-Fraumeni syndrome. *Am J Hum Genet* 56:608–615
 34. Malkin D, Li FP, Strong LC, Fraumeni JF Jr, Nelson CE, Kim DH, Kassel J, Gryka MA, Bischoff FZ, Tainsky MA et al (1990) Germ line p53 mutations in a familial syndrome of breast cancer, sarcomas, and other neoplasms. *Science* 250:1233–1238
 35. Srivastava S, Zou ZQ, Pirolo K, Blattner W, Chang EH (1990) Germ-line transmission of a mutated p53 gene in a cancer-prone family with Li-Fraumeni syndrome. *Nature* 348:747–749
 36. Almog N, Rotter V (1998) An insight into the life of p53: a protein coping with many functions! Review of the 9th p53 Workshop, Crete, May 9–13, 1998. *Biochim Biophys Acta* 1378:R43–R54

37. Bogler O, Huang HJ, Kleihues P, Cavenee WK (1995) The p53 gene and its role in human brain tumors. *Glia* 15:308–327
38. Giaccia AJ, Kastan MB (1998) The complexity of p53 modulation: emerging patterns from divergent signals. *Genes Dev* 12:2973–2983
39. Aicardi J, Chevrie JJ, Rousselle F (1969) Spasmodic flexion syndrome, callosal agenesis, chorioretinal abnormalities. *Arch Fr Pediatr* 26:1103–1120
40. Palmer L, Nordborg C, Steneryd K, Aman P, Kyllerman M (2004) Large-cell medulloblastoma in Aicardi syndrome. Case report and literature review. *Neuropediatrics* 35:307–311
41. Ballabio A, Andria G (1992) Deletions and translocations involving the distal short arm of the human X chromosome: review and hypotheses. *Hum Mol Genet* 1:221–227
42. Allanson JE, Hennekam RC (1997) Rubinstein-Taybi syndrome: objective evaluation of craniofacial structure. *Am J Med Genet* 71:414–419
43. Petrij F, Giles RH, Dauwerse HG, Saris JJ, Hennekam RC, Masuno M, Tommerup N, van Ommen GJ, Goodman RH, Peters DJ et al (1995) Rubinstein-Taybi syndrome caused by mutations in the transcriptional co-activator CBP. *Nature* 376:348–351
44. Giles RH, Peters DJ, Breuning MH (1998) Conjunction dysfunction: CBP/p300 in human disease. *Trends Genet* 14:178–183
45. Skousen GJ, Wardinsky T, Chenaille P (1996) Medulloblastoma in patient with Rubinstein-Taybi syndrome. *Am J Med Genet* 66:367
46. Taylor MD, Mainprize TG, Rutka JT, Becker L, Bayani J, Drake JM (2001) Medulloblastoma in a child with Rubenstein-Taybi Syndrome: case report and review of the literature. *Pediatr Neurosurg* 35:235–238
47. Miller RW, Rubinstein JH (1995) Tumors in Rubinstein-Taybi syndrome. *Am J Med Genet* 56:112–115
48. Evans G, Burnell L, Campbell R, Gattamaneni HR, Birch J (1993) Congenital anomalies and genetic syndromes in 173 cases of medulloblastoma. *Med Pediatr Oncol* 21:433–434
49. Louis DN, Ohgaki H, Wiestler OD, Cavenee WK, Burger PC, Jouvet A, Scheithauer BW, Kleihues P (2007) The 2007 WHO classification of tumours of the central nervous system. *Acta Neuropathol* 114:97–109
50. Gilbertson RJ, Ellison DW (2008) The origins of medulloblastoma subtypes. *Annu Rev Pathol* 3:341–365
51. Johnson ML, Rajamannan N (2006) Diseases of Wnt signaling. *Rev Endocr Metab Disord* 7:41–49
52. Dellovade T, Romer JT, Curran T, Rubin LL (2006) The hedgehog pathway and neurological disorders. *Annu Rev Neurosci* 29:539–563
53. Ingham PW, Placzek M (2006) Orchestrating ontogenesis: variations on a theme by sonic hedgehog. *Nat Rev Genet* 7:841–850
54. Fuccillo M, Joyner AL, Fishell G (2006) Morphogen to mitogen: the multiple roles of hedgehog signaling in vertebrate neural development. *Nat Rev Neurosci* 7:772–783
55. Reya T, Clevers H (2005) Wnt signalling in stem cells and cancer. *Nature* 434:843–850
56. Kelleher FC, Fennelly D, Rafferty M (2006) Common critical pathways in embryogenesis and cancer. *Acta Oncol* 45:375–388
57. Ingham PW (1998) The patched gene in development and cancer. *Curr Opin Genet Dev* 8:88–94
58. Ingham PW (1998) Transducing Hedgehog: the story so far. *Embo J* 17:3505–3511
59. Wechsler-Reya RJ, Scott MP (1999) Control of neuronal precursor proliferation in the cerebellum by Sonic Hedgehog. *Neuron* 22:103–114
60. Corcoran RB, Scott MP (2006) Oxysterols stimulate Sonic hedgehog signal transduction and proliferation of medulloblastoma cells. *Proc Natl Acad Sci U S A* 103:8408–8413
61. Stone DM, Hynes M, Armanini M, Swanson TA, Gu Q, Johnson RL, Scott MP, Pennica D, Goddard A, Phillips H, Noll M, Hooper JE, de Sauvage F, Rosenthal A (1996) The tumour-suppressor gene patched encodes a candidate receptor for Sonic hedgehog. *Nature* 384:129–134
62. Kiselyov AS (2006) Targeting the hedgehog signaling pathway with small molecules. *Anticancer Agents Med Chem* 6:445–449
63. Lauth M, Bergstrom A, Shimokawa T, Toftgard R (2007) Inhibition of GLI-mediated transcription and tumor cell growth by small-molecule antagonists. *Proc Natl Acad Sci U S A* 104:8455–8460
64. Browd SR, Kenney AM, Gottfried ON, Yoon JW, Walterhouse D, Pedone CA, Fuhs DW (2006) N-myc can substitute for insulin-like growth factor signaling in a mouse model of sonic hedgehog-induced medulloblastoma. *Cancer Res* 66:2666–2672
65. Hatton BA, Knoepfler PS, Kenney AM, Rowitch DH, de Alboran IM, Olson JM, Eisenman RN (2006) N-myc is an essential downstream effector of Shh signaling during both normal and neoplastic cerebellar growth. *Cancer Res* 66:8655–8661
66. Taylor MD, Zhang X, Liu L, Hui CC, Mainprize TG, Scherer SW, Wainwright B, Hogg D, Rutka JT (2004) Failure of a medulloblastoma-derived mutant of SUFU to suppress WNT signaling. *Oncogene* 23:4577–4583
67. Barnfield PC, Zhang X, Thanabalasingham V, Yoshida M, Hui CC (2005) Negative regulation of Gli1 and Gli2 activator function by Suppressor of fused through multiple mechanisms. *Differentiation* 73:397–405
68. Corcoran RB, Scott MP (2001) A mouse model for medulloblastoma and basal cell nevus syndrome. *J Neurooncol* 53:307–318
69. Kim JY, Nelson AL, Algon SA, Graves O, Sturla LM, Goumnerova LC, Rowitch DH, Segal RA, Pomeroy SL (2003) Medulloblastoma tumorigenesis diverges from cerebellar granule cell differentiation in patched heterozygous mice. *Dev Biol* 263:50–66

70. Schofield D, West DC, Anthony DC, Marshal R, Sklar J (1995) Correlation of loss of heterozygosity at chromosome 9q with histological subtype in medulloblastomas. *Am J Pathol* 146:472–480
71. Pietsch T, Waha A, Koch A, Kraus J, Albrecht S, Tonn J, Sorensen N, Berthold F, Henk B, Schmandt N, Wolf HK, von Deimling A, Wainwright B, Chenevix-Trench G, Wiestler OD, Wicking C (1997) Medulloblastomas of the desmoplastic variant carry mutations of the human homologue of *Drosophila* patched. *Cancer Res* 57:2085–2088
72. Raffel C, Jenkins RB, Frederick L, Hebrink D, Alderete B, Fults DW, James CD (1997) Sporadic medulloblastomas contain PTCH mutations. *Cancer Res* 57:842–845
73. Vortmeyer AO, Stavrou T, Selby D, Li G, Weil RJ, Park WS, Moon YW, Chandra R, Goldstein AM, Zhuang Z (1999) Deletion analysis of the adenomatous polyposis coli and PTCH gene loci in patients with sporadic and nevoid basal cell carcinoma syndrome-associated medulloblastoma. *Cancer* 85:2662–2667
74. Zurawel RH, Allen C, Chiappa S, Cato W, Biegel J, Cogen P, de Sauvage F, Raffel C (2000) Analysis of PTCH/SMO/SHH pathway genes in medulloblastoma. *Genes Chromosomes Cancer* 27:44–51
75. Reifenberger J, Wolter M, Weber RG, Megahed M, Ruzicka T, Lichter P, Reifenberger G (1998) Missense mutations in SMOH in sporadic basal cell carcinomas of the skin and primitive neuroectodermal tumors of the central nervous system. *Cancer Res* 58:1798–1803
76. Taylor MD, Liu L, Raffel C, Hui CC, Mainprize TG, Zhang X, Agatep R, Chiappa S, Gao L, Lowrance A, Hao A, Goldstein AM, Stavrou T, Scherer SW, Dura WT, Wainwright B, Squire JA, Rutka JT, Hogg D (2002) Mutations in *SUFU* predispose to medulloblastoma. *Nat Genet* 31:306–310
77. Liu H, Mohamed O, Dufort D, Wallace VA (2003) Characterization of Wnt signaling components and activation of the Wnt canonical pathway in the murine retina. *Dev Dyn* 227:323–334
78. Segditsas S, Tomlinson I (2006) Colorectal cancer and genetic alterations in the Wnt pathway. *Oncogene* 25:7531–7537
79. Yang-Snyder J, Miller JR, Brown JD, Lai CJ, Moon RT (1996) A frizzled homolog functions in a vertebrate Wnt signaling pathway. *Curr Biol* 6:1302–1306
80. He TC, Sparks AB, Rago C, Hermeking H, Zawel L, da Costa LT, Morin PJ, Vogelstein B, Kinzler KW (1998) Identification of c-MYC as a target of the APC pathway. *Science* 281:1509–1512
81. Korinek V, Barker N, Morin PJ, van Wichen D, de Weger R, Kinzler KW, Vogelstein B, Clevers H (1997) Constitutive transcriptional activation by a beta-catenin-Tcf complex in APC^{-/-} colon carcinoma. *Science* 275:1784–1787
82. Shtutman M, Zhurinsky J, Simcha I, Albanese C, D'Amico M, Pestell R, Ben-Ze'ev A (1999) The cyclin D1 gene is a target of the beta-catenin/LEF-1 pathway. *Proc Natl Acad Sci U S A* 96:5522–5527
83. Lee Y, Kawagoe R, Sasai K, Li Y, Russell HR, Curran T, McKinnon PJ (2007) Loss of suppressor-of-fused function promotes tumorigenesis. *Oncogene* 26:6442–6447
84. Eberhart CG, Tihan T, Burger PC (2000) Nuclear localization and mutation of beta-catenin in medulloblastomas. *J Neuropathol Exp Neurol* 59:333–337
85. Yokota N, Nishizawa S, Ohta S, Date H, Sugimura H, Namba H, Maekawa M (2002) Role of Wnt pathway in medulloblastoma oncogenesis. *Int J Cancer* 101:198–201
86. Zurawel RH, Chiappa SA, Allen C, Raffel C (1998) Sporadic medulloblastomas contain oncogenic beta-catenin mutations. *Cancer Res* 58:896–899
87. Mori T, Nagase H, Horii A, Miyoshi Y, Shimano T, Nakatsuru S, Aoki T, Arakawa H, Yanagisawa A, Ushio Y et al (1994) Germ-line and somatic mutations of the APC gene in patients with Turcot syndrome and analysis of APC mutations in brain tumors. *Genes Chromosomes Cancer* 9:168–172
88. Huang H, Mahler-Araujo BM, Sankila A, Chimelli L, Yonekawa Y, Kleihues P, Ohgaki H (2000) APC mutations in sporadic medulloblastomas. *Am J Pathol* 156:433–437
89. Dahmen RP, Koch A, Denkhaus D, Tonn JC, Sorensen N, Berthold F, Behrens J, Birchmeier W, Wiestler OD, Pietsch T (2001) Deletions of *AXIN1*, a component of the WNT/wingless pathway, in sporadic medulloblastomas. *Cancer Res* 61:7039–7043
90. Sjolund J, Manetopoulos C, Stockhausen MT, Axelson H (2005) The Notch pathway in cancer: differentiation gone awry. *Eur J Cancer* 41:2620–2629
91. Fan X, Mikolaenko I, Elhassan I, Ni X, Wang Y, Ball D, Brat DJ, Perry A, Eberhart CG (2004) Notch1 and notch2 have opposite effects on embryonal brain tumor growth. *Cancer Res* 64:7787–7793
92. Hallahan AR, Pritchard JI, Hansen S, Benson M, Stoeck J, Hatton BA, Russell TL, Ellenbogen RG, Bernstein ID, Beachy PA, Olson JM (2004) The SmoA1 mouse model reveals that notch signaling is critical for the growth and survival of sonic hedgehog-induced medulloblastomas. *Cancer Res* 64:7794–7800
93. Ullrich A, Schlessinger J (1990) Signal transduction by receptors with tyrosine kinase activity. *Cell* 61:203–212
94. Olayioye MA, Neve RM, Lane HA, Hynes NE (2000) The ErbB signaling network: receptor heterodimerization in development and cancer. *Embo J* 19:3159–3167
95. Gilbertson R, Wickramasinghe C, Hernan R, Balaji V, Hunt D, Jones-Wallace D, Crolla J, Perry R, Lunec J, Pearson A, Ellison D (2001) Clinical and molecular stratification of disease risk in medulloblastoma. *Br J Cancer* 85:705–712
96. Gilbertson RJ, Perry RH, Kelly PJ, Pearson AD, Lunec J (1997) Prognostic significance of HER2 and HER4 coexpression in childhood medulloblastoma. *Cancer Res* 57:3272–3280

97. Gilbertson RJ, Clifford SC, MacMeekin W, Meekin W, Wright C, Perry RH, Kelly P, Pearson AD, Lunec J (1998) Expression of the ErbB-neuregulin signaling network during human cerebellar development: implications for the biology of medulloblastoma. *Cancer Res* 58:3932–3941
98. Hartmann W, Digon-Sontgerath B, Koch A, Waha A, Endl E, Dani I, Denkhau D, Goodyer CG, Sorensen N, Wiestler OD, Pietsch T (2006) Phosphatidylinositol 3'-kinase/AKT signaling is activated in medulloblastoma cell proliferation and is associated with reduced expression of PTEN. *Clin Cancer Res* 12:3019–3027
99. Wlodarski P, Grajkowska W, Lojek M, Rainko K, Jozwiak J (2006) Activation of Akt and Erk pathways in medulloblastoma. *Folia Neuropathol* 44:214–220
100. Gilbertson R, Hernan R, Pietsch T, Pinto L, Scotting P, Allibone R, Ellison D, Perry R, Pearson A, Lunec J (2001) Novel ERBB4 juxtamembrane splice variants are frequently expressed in childhood medulloblastoma. *Genes Chromosomes Cancer* 31:288–294
101. Peruzzi B, Bottaro DP (2006) Targeting the c-Met signaling pathway in cancer. *Clin Cancer Res* 12:3657–3660
102. Abounader R, Lateral J (2005) Scatter factor/hepatocyte growth factor in brain tumor growth and angiogenesis. *Neuro Oncol* 7:436–451
103. Miyazawa K, Shimomura T, Kitamura A, Kondo J, Morimoto Y, Kitamura N (1993) Molecular cloning and sequence analysis of the cDNA for a human serine protease responsible for activation of hepatocyte growth factor. Structural similarity of the protease precursor to blood coagulation factor XII. *J Biol Chem* 268:10024–10028
104. Boccaccio C, Ando M, Tamagnone L, Bardelli A, Michieli P, Battistini C, Comoglio PM (1998) Induction of epithelial tubules by growth factor HGF depends on the STAT pathway. *Nature* 391:285–288
105. Machide M, Kamitori K, Kohsaka S (2000) Hepatocyte growth factor-induced differential activation of phospholipase C γ 1 and phosphatidylinositol 3-kinase is regulated by tyrosine phosphatase SHP-1 in astrocytes. *J Biol Chem* 275:31392–31398
106. Machide M, Kamitori K, Nakamura Y, Kohsaka S (1998) Selective activation of phospholipase C γ 1 and distinct protein kinase C subspecies in intracellular signaling by hepatocyte growth factor/scatter factor in primary cultured rat neocortical cells. *J Neurochem* 71:592–602
107. Rodrigues GA, Park M, Schlessinger J (1997) Activation of the JNK pathway is essential for transformation by the Met oncogene. *Embo J* 16:2634–2645
108. Khwaja A, Lehmann K, Marte BM, Downward J (1998) Phosphoinositide 3-kinase induces scattering and tubulogenesis in epithelial cells through a novel pathway. *J Biol Chem* 273:18793–18801
109. Kawaguchi T, Qin L, Shimomura T, Kondo J, Matsumoto K, Denda K, Kitamura N (1997) Purification and cloning of hepatocyte growth factor activator inhibitor type 2, a Kunitz-type serine protease inhibitor. *J Biol Chem* 272:27558–27564
110. Shimomura T, Denda K, Kitamura A, Kawaguchi T, Kito M, Kondo J, Kagaya S, Qin L, Takata H, Miyazawa K, Kitamura N (1997) Hepatocyte growth factor activator inhibitor, a novel Kunitz-type serine protease inhibitor. *J Biol Chem* 272:6370–6376
111. Danilkovitch-Miagkova A, Zbar B (2002) Dysregulation of Met receptor tyrosine kinase activity in invasive tumors. *J Clin Invest* 109:863–867
112. Jeffers MF (1999) Activating mutations in the Met receptor overcome the requirement for autophosphorylation of tyrosines crucial for wild type signaling. *Oncogene* 18:5120–5125
113. Tong CY, Hui AB, Yin XL, Pang JC, Zhu XL, Poon WS, Ng HK (2004) Detection of oncogene amplifications in medulloblastomas by comparative genomic hybridization and array-based comparative genomic hybridization. *J Neurosurg* 100:187–193
114. Li Y, Lal B, Kwon S, Fan X, Saldanha U, Reznik TE, Kuchner EB, Eberhart C, Lateral J, Abounader R (2005) The scatter factor/hepatocyte growth factor: c-met pathway in human embryonal central nervous system tumor malignancy. *Cancer Res* 65:9355–9362
115. Godfraind C (2009) Classification and controversies in pathology of ependymomas. *Childs Nerv Syst* 25:1185–1193
116. Carter M, Nicholson J, Ross F, Crolla J, Allibone R, Balaji V, Perry R, Walker D, Gilbertson R, Ellison DW (2002) Genetic abnormalities detected in ependymomas by comparative genomic hybridisation. *Br J Cancer* 86:929–939
117. Jeuken JW, Sprenger SH, Gilhuis J, Teepe HL, Grotenhuis AJ, Wesseling P (2002) Correlation between localization, age, and chromosomal imbalances in ependymal tumours as detected by CGH. *J Pathol* 197:238–244
118. Hirose Y, Aldape K, Bollen A, James CD, Brat D, Lamborn K, Berger M, Feuerstein BG (2001) Chromosomal abnormalities subdivide ependymal tumors into clinically relevant groups. *Am J Pathol* 158:1137–1143
119. Taylor MD, Poppleton H, Fuller C, Su X, Liu Y, Jensen P, Magdalen S, Dalton J, Calabrese C, Board J, Macdonald T, Rutka J, Guha A, Gajjar A, Curran T, Gilbertson RJ (2005) Radial glia cells are candidate stem cells of ependymoma. *Cancer Cell* 8:323–335
120. Dubuc AM, Northcott PA, Mack S, Witt H, Pfister S, Taylor MD (2010) The genetics of pediatric brain tumors. *Curr Neurol Neurosci Rep* 10:215–223
121. Mack SC, Taylor MD (2009) The genetic and epigenetic basis of ependymoma. *Childs Nerv Syst* 25:1195–1201
122. Modena P, Lualdi E, Facchinetti F, Veltman J, Reid JF, Minardi S, Janssen I, Giangaspero F,

- Forni M, Finocchiaro G, Genitori L, Giordano F, Riccardi R, Schoenmakers EF, Massimino M, Sozzi G (2006) Identification of tumor-specific molecular signatures in intracranial ependymoma and association with clinical characteristics. *J Clin Oncol* 24:5223–5233
123. Mendrzyk F, Korshunov A, Benner A, Toedt G, Pfister S, Radlwimmer B, Lichter P (2006) Identification of gains on 1q and epidermal growth factor receptor overexpression as independent prognostic markers in intracranial ependymoma. *Clin Cancer Res* 12:2070–2079
 124. Puget S, Grill J, Valent A, Bieche I, Dantas-Barbosa C, Kauffmann A, Dessen P, Lacroix L, Georger B, Job B, Dirven C, Varlet P, Peyre M, Dirks PB, Sainte-Rose C, Vassal G (2009) Candidate genes on chromosome 9q33-34 involved in the progression of childhood ependymomas. *J Clin Oncol* 27:1884–1892
 125. Ohgaki H, Kleihues P (2005) Population-based studies on incidence, survival rates, and genetic alterations in astrocytic and oligodendroglial gliomas. *J Neuropathol Exp Neurol* 64:479–489
 126. Listernick R, Ferner RE, Liu GT, Gutmann DH (2007) Optic pathway gliomas in neurofibromatosis-1: controversies and recommendations. *Ann Neurol* 61:189–198
 127. Yunoue S, Tokuo H, Fukunaga K, Feng L, Ozawa T, Nishi T, Kikuchi A, Hattori S, Kuratsu J, Saya H, Araki N (2003) Neurofibromatosis type I tumor suppressor neurofibromin regulates neuronal differentiation via its GTPase-activating protein function toward Ras. *J Biol Chem* 278:26958–26969
 128. Sharma MK, Mansur DB, Reifenberger G, Perry A, Leonard JR, Aldape KD, Albin MG, Emmett RJ, Loeser S, Watson MA, Nagarajan R, Gutmann DH (2007) Distinct genetic signatures among pilocytic astrocytomas relate to their brain region origin. *Cancer Res* 67:890–900
 129. Janzarik WG, Kratz CP, Loges NT, Olbrich H, Klein C, Schafer T, Scheurlen W, Roggendorf W, Weiller C, Niemeyer C, Korinthenberg R, Pfister S, Omran H (2007) Further evidence for a somatic KRAS mutation in a pilocytic astrocytoma. *Neuropediatrics* 38:61–63
 130. Jones DT, Ichimura K, Liu L, Pearson DM, Plant K, Collins VP (2006) Genomic analysis of pilocytic astrocytomas at 0.97 Mb resolution shows an increasing tendency toward chromosomal copy number change with age. *J Neuropathol Exp Neurol* 65:1049–1058
 131. Sanoudou D, Tingby O, Ferguson-Smith MA, Collins VP, Coleman N (2000) Analysis of pilocytic astrocytoma by comparative genomic hybridization. *Br J Cancer* 82:1218–1222
 132. Forshew T, Tatevossian RG, Lawson AR, Ma J, Neale G, Ogunkolade BW, Jones TA, Aarum J, Dalton J, Bailey S, Chaplin T, Carter RL, Gajjar A, Broniscer A, Young BD, Ellison DW, Sheer D (2009) Activation of the ERK/MAPK pathway: a signature genetic defect in posterior fossa pilocytic astrocytomas. *J Pathol* 218:172–181
 133. Jacob K, Albrecht S, Sollier C, Faury D, Sader E, Montpetit A, Serre D, Hauser P, Garami M, Bogner L, Hanzely Z, Montes JL, Atkinson J, Farmer JP, Bouffet E, Hawkins C, Tabori U, Jabado N (2009) Duplication of 7q34 is specific to juvenile pilocytic astrocytomas and a hallmark of cerebellar and optic pathway tumours. *Br J Cancer* 101:722–733
 134. Pfister S, Janzarik WG, Remke M, Ernst A, Werft W, Becker N, Toedt G, Wittmann A, Kratz C, Olbrich H, Ahmadi R, Thieme B, Joos S, Radlwimmer B, Kulozik A, Pietsch T, Herold-Mende C, Gnekow A, Reifenberger G, Korshunov A, Scheurlen W, Omran H, Lichter P (2008) BRAF gene duplication constitutes a mechanism of MAPK pathway activation in low-grade astrocytomas. *J Clin Invest* 118:1739–1749
 135. Bar EE, Lin A, Tihan T, Burger PC, Eberhart CG (2008) Frequent gains at chromosome 7q34 involving BRAF in pilocytic astrocytoma. *J Neuropathol Exp Neurol* 67:878–887
 136. Jones DT, Kocialkowski S, Liu L, Pearson DM, Backlund LM, Ichimura K, Collins VP (2008) Tandem duplication producing a novel oncogenic BRAF fusion gene defines the majority of pilocytic astrocytomas. *Cancer Res* 68:8673–8677
 137. Sievert AJ, Jackson EM, Gai X, Hakonarson H, Judkins AR, Resnick AC, Sutton LN, Storm PB, Shaikh TH, Biegel JA (2009) Duplication of 7q34 in pediatric low-grade astrocytomas detected by high-density single-nucleotide polymorphism-based genotype arrays results in a novel BRAF fusion gene. *Brain Pathol* 19:449–458
 138. Jones DT, Kocialkowski S, Liu L, Pearson DM, Ichimura K, Collins VP (2009) Oncogenic RAF1 rearrangement and a novel BRAF mutation as alternatives to KIAA1549:BRAF fusion in activating the MAPK pathway in pilocytic astrocytoma. *Oncogene* 28:2119–2123
 139. Korshunov A, Meyer J, Capper D, Christians A, Remke M, Witt H, Pfister S, von Deimling A, Hartmann C (2009) Combined molecular analysis of BRAF and IDH1 distinguishes pilocytic astrocytoma from diffuse astrocytoma. *Acta Neuropathol* 118:401–405
 140. Biegel JA, Allen CS, Kawasaki K, Shimizu N, Budarf ML, Bell CJ (1996) Narrowing the critical region for a rhabdoid tumor locus in 22q11. *Genes Chromosomes Cancer* 16:94–105
 141. Biegel JA, Burk CD, Parmiter AH, Emanuel BS (1992) Molecular analysis of a partial deletion of 22q in a central nervous system rhabdoid tumor. *Genes Chromosomes Cancer* 5:104–108
 142. Biegel JA, Rorke LB, Emanuel BS (1989) Monosomy 22 in rhabdoid or atypical teratoid tumors of the brain. *N Engl J Med* 321:906

143. Biegel JA, Rorke LB, Packer RJ, Emanuel BS (1990) Monosomy 22 in rhabdoid or atypical tumors of the brain. *J Neurosurg* 73:710–714
144. Hirose M, Yamada T, Toyosaka A, Hirose T, Kagami S, Abe T, Kuroda Y (1996) Rhabdoid tumor of the kidney: a report of two cases with respective tumor markers and a specific chromosomal abnormality, del(11p13). *Med Pediatr Oncol* 27:174–178
145. Biegel JA (2006) Molecular genetics of atypical teratoid/rhabdoid tumor. *Neurosurg Focus* 20:E11
146. Versteeg I, Sevenet N, Lange J, Rousseau-Merck MF, Ambros P, Handgretinger R, Aurias A, Delattre O (1998) Truncating mutations of hSNF5/INI1 in aggressive paediatric cancer. *Nature* 394:203–206
147. Sevenet N, Lellouch-Tubiana A, Schofield D, Hoang-Xuan K, Gessler M, Birnbaum D, Jeanpierre C, Jouvret A, Delattre O (1999) Spectrum of hSNF5/INI1 somatic mutations in human cancer and genotype-phenotype correlations. *Hum Mol Genet* 8:2359–2368
148. Gessi M, Giangaspero F, Pietsch T (2003) Atypical teratoid/rhabdoid tumors and choroid plexus tumors: when genetics “surprise” pathology. *Brain Pathol* 13:409–414
149. Taylor MD, Gokgoz N, Andrulis IL, Mainprize TG, Drake JM, Rutka JT (2000) Familial posterior fossa brain tumors of infancy secondary to germline mutation of the hSNF5 gene. *Am J Hum Genet* 66:1403–1406
150. Roberts CW, Galusha SA, McMenamin ME, Fletcher CD, Orkin SH (2000) Haploinsufficiency of Snf5 (integrase interactor 1) predisposes to malignant rhabdoid tumors in mice. *Proc Natl Acad Sci U S A* 97:13796–13800
151. Guidi CJ, Sands AT, Zambrowicz BP, Turner TK, Demers DA, Webster W, Smith TW, Imbalzano AN, Jones SN (2001) Disruption of *Ini1* leads to peri-implantation lethality and tumorigenesis in mice. *Mol Cell Biol* 21:3598–3603
152. Muchardt C, Yaniv M (2001) When the SWI/SNF complex remodels...the cell cycle. *Oncogene* 20:3067–3075
153. Cheng SW, Davies KP, Yung E, Beltran RJ, Yu J, Kalpana GV (1999) c-MYC interacts with INI1/hSNF5 and requires the SWI/SNF complex for transactivation function. *Nat Genet* 22:102–105
154. Phelan ML, Sif S, Narlikar GJ, Kingston RE (1999) Reconstitution of a core chromatin remodeling complex from SWI/SNF subunits. *Mol Cell* 3:247–253
155. Wang W, Xue Y, Zhou S, Kuo A, Cairns BR, Crabtree GR (1996) Diversity and specialization of mammalian SWI/SNF complexes. *Genes Dev* 10:2117–2130
156. Zwetsloot CP, Kros JM, Paz y Gueze HD (1991) Familial occurrence of tumours of the choroid plexus. *J Med Genet* 28:492–494
157. Sevenet N, Sheridan E, Amram D, Schneider P, Handgretinger R, Delattre O (1999) Constitutional mutations of the hSNF5/INI1 gene predispose to a variety of cancers. *Am J Hum Genet* 65:1342–1348
158. Vital A, Bringuier PP, Huang H, San Galli F, Rivel J, Ansoborlo S, Cazauban JM, Taillandier L, Kleihues P, Ohgaki H (1998) Astrocytomas and choroid plexus tumors in two families with identical p53 germline mutations. *J Neuropathol Exp Neurol* 57:1061–1069
159. Wolburg H, Paulus W (2010) Choroid plexus: biology and pathology. *Acta Neuropathol* 119:75–88
160. Norman MG, Harrison KJ, Poskitt KJ, Kalousek DK (1995) Duplication of 9P and hyperplasia of the choroid plexus: a pathologic, radiologic, and molecular cytogenetics study. *Pediatr Pathol Lab Med* 15:109–120
161. Symonds H, Krall L, Remington L, Saenz-Robles M, Lowe S, Jacks T, Van Dyke T (1994) p53-dependent apoptosis suppresses tumor growth and progression in vivo. *Cell* 78:703–711
162. Saenz Robles MT, Symonds H, Chen J, Van Dyke T (1994) Induction versus progression of brain tumor development: differential functions for the pRB- and p53-targeting domains of simian virus 40 T antigen. *Mol Cell Biol* 14:2686–2698
163. Carlotti CG Jr, Salhia B, Weitzman S, Greenberg M, Dirks PB, Mason W, Becker LE, Rutka JT (2002) Evaluation of proliferative index and cell cycle protein expression in choroid plexus tumors in children. *Acta Neuropathol* 103:1–10
164. Dang L, Fan X, Chaudhry A, Wang M, Gaiano N, Eberhart CG (2006) Notch3 signaling initiates choroid plexus tumor formation. *Oncogene* 25:487–491

Thomas E. Merchant

7.1 Introduction

The posterior fossa is the most commonly irradiated intracranial compartment in the treatment of childhood brain tumors and possibly the most commonly irradiated body site in children with cancer. An understanding of the pathophysiology of tumors in the posterior fossa is necessary in identifying the indications and contraindications for radiation therapy, the appropriate radiotherapy methods, potential for acute and long-term side effects, and developing trends relevant to the treatment of tumors at this intracranial site. An improved understanding of the goals of radiation therapy serves nonradiation oncology members of the treatment team by improving patient selection and treatment sequencing and provides insight into the differences in disease control and functional outcomes based on irradiation dose and volume. These differences underscore the role and the relative benefits and risks of irradiating children with posterior fossa tumors. Improved knowledge will lead to improved rates of cure and a reduction in the risk of treatment complications.

Based on the data from the United States, brain tumors comprise 20 % of all pediatric

malignancies. The 2000 US Standard Population Census indicate a standard population of 274,633,642, and 78,782,657 were aged 19 years and younger [1] (accessed December 11, 2010). According to the Central Brain Tumor Registry of the United States [2], the incidence of childhood primary brain and central nervous system tumors in individuals aged 0–19 years is 4.71 cases per 100,000 person-years and higher in males and children under the age of 4 years. There are approximately 4,000 cases of brain tumors diagnosed annually among those ages 0–19 years. The 2010 US population is expected to surpass 300,000,000 resulting in more than 4,200 cases annually.

Posterior fossa CNS embryonal tumors (medulloblastoma and atypical teratoid rhabdoid tumors), pilocytic astrocytoma, and ependymoma predominate in this age group. The distribution of tumor sites has been estimated by a number of organizations. The CBTRUS reports posterior fossa subsites including the cerebellum (15.6 %), brainstem (11.2 %), and cranial nerves (6.5 %) among the most common intracranial sites.

7.2 Characteristic Diagnoses and Tumor Locations

The posterior fossa is the site of some of the most and least curable brain tumors in children. Juvenile pilocytic astrocytoma can be irradiated with a high rate of success if not surgically

T.E. Merchant, D.O., Ph.D.
Department of Radiation Oncology,
St. Jude Children's Research Hospital,
262 Danny Thomas Place, Mail Stop 220,
Memphis, TN 38105-3678, USA
e-mail: thomas.merchant@stjude.org

resectable. Diffuse intrinsic pontine glioma is uniformly fatal despite irradiation. The most commonly irradiated tumors by age include medulloblastoma and atypical teratoid rhabdoid tumor (ATRT), juvenile pilocytic astrocytoma and other low-grade gliomas, ependymoma, brainstem glioma, and less commonly high-grade gliomas of the cerebellum, craniopharyngioma, and CNS germ cell tumors.

Tumor location is often characteristic of the diagnosis and has implications for radiation therapy planning. Medulloblastoma and ATRT may arise as a midline (vermian) or lateralized lesion of the cerebellum. Ependymoma characteristically fills the fourth ventricle and extends through the foramen magnum or Luschka. It may arise in the cerebellopontine angle. A low-grade glioma may arise in any part of the brainstem – midbrain, pons, or medulla – with an intrinsic, exophytic, or infiltrative pattern. A low-grade glioma may appear at the junction of other regions of the CNS (cervicomedullary or diencephalon). Cerebellar subsites are most common both superficial and deep and may involve the cerebellar peduncles.

Tumor extension to the posterior from other regions is exemplified by the craniopharyngioma with a posterior fossa component and other rare but relevant tumors including nerve sheath tumors (acoustic neuroma), base of skull tumors (chordoma), and meningioma. These tumors are considered within the purview of the radiation oncologist in the primary or adjuvant setting.

7.3 Surgical Optimization

Lack of surgical optimization is one of the leading causes of treatment failure when definitive irradiation is administered to potentially curable tumors of the posterior fossa. This comment applies mainly to ependymoma but is true for medulloblastoma and ATRT. Local failure as a component of failure is high in historical series for these tumors and attributed to the low rate of gross-total resection. In the current era where highly selective institutional series report gross-total resection rates in excess of 80 % for

ependymoma, cure rates have improved substantially. There are emerging data that suggest similar high rates of gross-total resection can be achieved in cooperative group trials as guidelines now urge more extensive resections and second surgery when feasible. These comments are not applicable to low-grade glioma, however, since the extent of resection has not been identified as a prognostic factor in irradiated children.

Lack of surgical optimization may lead to increased morbidity and mortality for children with posterior fossa tumors. This point is relevant when children with extensive posterior fossa ependymoma undergo minimal resection. Not only is the tumor undertreated but the symptoms usually persist and remain unimproved despite adjuvant therapy. Another example where surgery may optimize radiation therapy is target volume reduction. No longer do radiation oncologists treat the original tumor with a margin of security. The basis for current targeting guidelines is the postoperative tumor bed which includes the collapsed tumor bed. In modern radiation treatment planning, repositioning of normal tissues including the brainstem is accounted for.

Children with cervicomedullary tumors serve as an important example to demonstrate the role of surgery to optimize radiation therapy. Children with tumors in this location may have unresectable disease, infiltration and impingement of neural structures, and intense symptoms. These symptoms range from the expected headache, vomiting, and fatigue to swallowing difficulty, dysphagia, slurred speech, ataxia, singultus, and dysfunction of central homeostasis including abnormalities in heart rate and breathing. Relief of pressure by decompressing the occiput, laminotomy of the upper cervical elements, and partial resection may improve a child's ability to tolerate radiation therapy both during and after treatment and the phase of pseudoprogression and inflammation that may acutely or insidiously accompany irradiation. Acute symptoms of irradiation with this type of compartmentalization effect may present with abnormal patterns of breathing, especially during sleep, that may progress to seizure and death.

7.4 Modern Radiation Therapy Methods

In 1993 the International Commission on Radiation Units and Measurements (ICRU) issued a report [3] to provide guidance on the use of three-dimensional radiation therapy planning and delivery, defining target volumes and reporting dose. The methods and nomenclature outlined in the report were adopted for clinical trials involving children with brain tumors. The fundamental target volumes for pediatric neuroradiotherapy are applicable to posterior fossa tumors and outlined below.

7.4.1 Gross Tumor Volume

The gross tumor volume (GTV) is based on the postoperative MR examination and includes gross residual tumor and the tumor bed at the primary site. Including the tumor bed is not clearly in the definition of the GTV of the ICRU but does represent the location of greatest tumor burden which is included in the definition of the GTV. In defin-

ing the GTV one should consider the initial preoperative imaging examination that defined the extent of the tumor and the tissues involved anatomically. The GTV in most cases will be a contracted or collapsed tumor bed (Fig. 7.1). Tissue defects resulting from surgical approaches are not included as part of the GTV when not previously involved by a tumor. Registering the preoperative MR imaging sequence that best demonstrates the original tumor and contouring the volume are helpful when later delineating the GTV.

The GTV should take into account changes in the brain anatomy resulting from resection or shunt:

- The GTV is the volume of tissue containing the highest concentration of tumor cells.
- The GTV includes the postoperative tumor bed which is the edge of the resection cavity.
- The GTV includes residual disease defined by postoperative neuroimaging.
- The GTV does not include the surgical corridor unless suspected to contain a tumor.
- The GTV is the larger volume when there is discrepancy in imaging or operative findings.

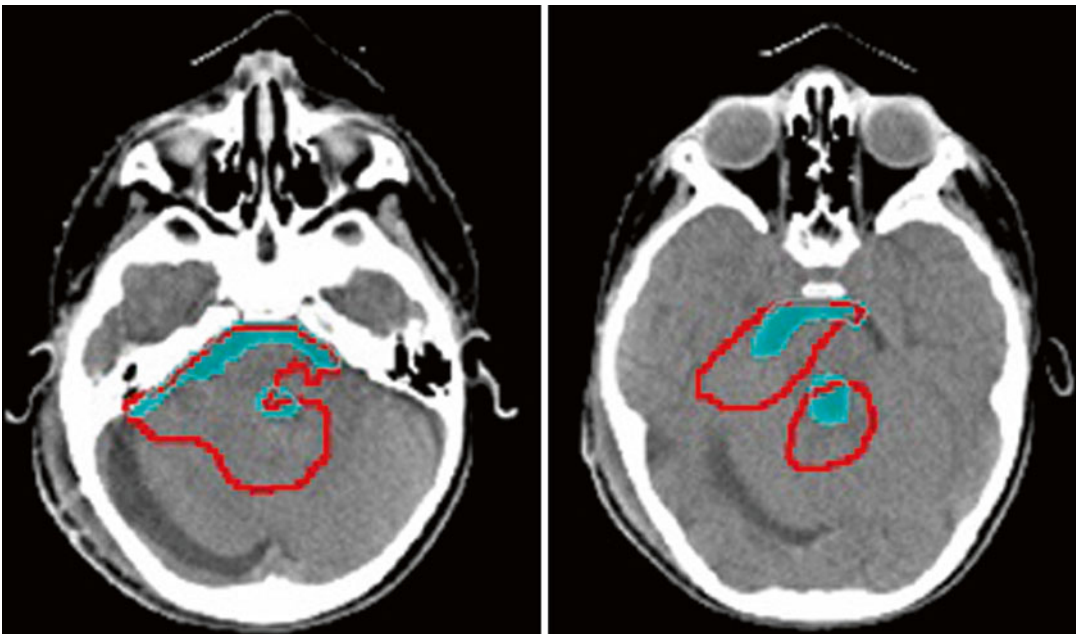


Fig. 7.1 A case of posterior fossa ependymoma where the initial tumor volume (*red*) and postoperative gross tumor (*light blue shaded*) have been delineated on axial MR imaging and presented on the treatment planning CT

7.4.2 Clinical Target Volume

The clinical target volume (CTV) includes the GTV with an added margin that is meant to treat subclinical microscopic disease and is usually “anatomically confined.” The term anatomically confined means that it does not extend beyond the bony calvarium, base of the skull, falx, or tentorium. The CTV extends to but not beyond neuroanatomic structures through which tumor extension or invasion is unlikely. When the GTV approaches the boundary of an anatomic compartment, the CTV extends to and includes the boundary (Fig. 7.2).

- The CTV is defined as the volume of tissue containing subclinical microscopic disease.
- The CTV should be tailored at tissue interfaces where invasion/infiltration is not likely.

7.4.3 Planning Target Volume

Planning target volume (PTV) includes a margin which is added to the CTV in three dimensions to create the PTV. It is geometric and not anatomically

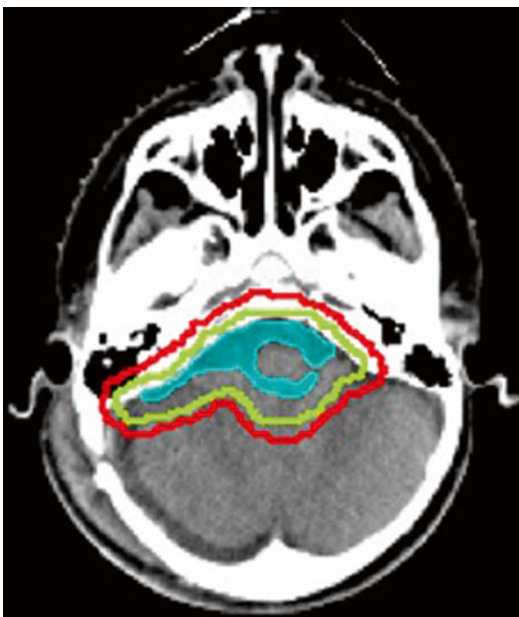


Fig. 7.2 A case of posterior fossa ependymoma where the postoperative gross tumor (light blue shaded), clinical target (yellow), and planning target (red) volume have been delineated on axial MR imaging and presented on the treatment planning CT

confined. The PTV has two components: the internal margin (IM) and the setup margin (SM). The IM is meant to compensate for all movements and variations in size and shape of the tissues contained within the CTV. The SM is meant to account for setup and mechanical and dosimetry uncertainties related to daily patient positioning and treatment equipment and software. For most brain tumor studies in children, the PTV margin is 3 or 5 mm (Fig. 7.2). The use of a PTV margin of 3 mm requires high precision immobilization and treatment verification methods known as image-guided radiation therapy. Given that the CTV is generally confined to the intracranial space, the PTV may extend into or beyond cranium but is unlikely to extend beyond the surface of the patient. Considering the CTV and PTV margins used for most brain tumor protocols in children, the imaging studies used to define the target volume should have a resolution less than the specified margins. Recent studies have shown that for children with brain tumors, a PTV margin of 3 mm is adequate provided that daily imaging is performed using cone beam CT [4]. Patients treated in the supine position have a smaller setup error than those treated in the prone position. The latter is often used for children with posterior fossa tumors. Similarly, those treated under anesthesia have the least amount of intra-fractional motion compared to children who are not anesthetized (Table 7.1). Children with posterior fossa tumors tend to be younger than those with supratentorial tumors.

Table 7.1 Data used to derive intra- and interfractional setup uncertainty including setup margins for pediatric patients with brain tumors

Cohort	CBCT	SE	RE	Uncertainty	Margin
Prone (25)	Pre	1.2	1.2	3.8	4.6
	Post	0.7	1.1	2.5	
Supine (75)	Pre	1.0	1.3	3.5	3.9
	Post	0.4	1.0	1.6	
GA (46)	Pre	1.1	1.2	3.7	4.0
	Post	0.4	0.8	1.5	
No-GA (54)	Pre	1.0	1.3	3.5	4.2
	Post	0.6	1.1	2.3	
All (100)	Pre	1.1	1.3	3.6	4.1
	Post	0.5	1.0	1.9	

GA general anesthesia, CBCT cone beam CT, pre before treatment, post after treatment, SE setup error, RE residual uncertainty, margin appropriate margin

7.5 Embryonal Posterior Fossa Tumors (Medulloblastoma, Atypical Teratoid Rhabdoid Tumor)

Medulloblastoma is the most common malignant tumor in children and is named for its posterior fossa location. It is the signature tumor when demonstrating the importance of pediatric neuroradiation therapy because of the curative potential of irradiation, the complexities of requisite craniospinal irradiation, and the systematic studies that have been performed to test craniospinal dose reduction and to prove the role of chemotherapy. It is the only pediatric brain tumor system to use a staging system to guide the use of radiation therapy – a staging system that has served investigators for nearly four decades with few modifications. Irradiation of medulloblastoma is notable for the evolution in target volumes, for the treatment of the primary site, and soon for future changes that will be driven by tumor biology. The specter of side effects observed after the irradiation of this disease is legendary in the field of pediatric oncology.

In the United States, the recent negative (no difference between treatment arms) A9961 trial [5] for standard risk (nonmetastatic) medulloblastoma in children ages 3–21 years, which compared two chemotherapy regimens, vincristine (VCR)/cisplatin (CDDP)/cyclophosphamide (CYC) versus VCR/CDDP/lomustine (CCNU),

was paused after nearly two decades of progress where standard dose craniospinal irradiation (36 Gy) and the posterior fossa boost (≥ 54 Gy) for all patients was replaced by reduced dose craniospinal irradiation (23.4 Gy) and the posterior fossa boost (55.8 Gy) followed by postirradiation chemotherapy to achieve an equivalent outcome in average-risk patients. Current and future progress includes further reducing the role of radiation therapy or at the very least the craniospinal dose for biologically favorable tumors, reducing the volume for the primary site boost (omitting the posterior fossa boost after craniospinal irradiation in favor of focal treatment of the primary site), increasing treatment intensity for biologically unfavorable or high-risk patients, and understanding better the effects of radiation dose and volume, clinical and treatment factors and host factors, and their effect on side effects after radiation therapy (Table 7.2).

Most clinical trials for medulloblastoma accrue a large number of patients and involve many institutions. Large trials are required to have the statistical power to detect small improvements in treatment. Large trials may lead to poor quality control in radiation therapy and diagnostic imaging [5, 6]. This is most evident in trials where craniospinal dose reductions have been the primary question and stems from inadequate staging or poor radiotherapy technique. This tragedy could be avoided if procedures were

Table 7.2 Recent clinical trials for medulloblastoma: sequencing of radiation and chemotherapy and radiotherapy parameters

Study/stages	Dates	CSI (Gy)	Primary site (Gy)	EFS	Chemotherapy
Average or standard risk (nonmetastatic medulloblastoma)					
A9961 [5]	1996–2000	23.4 CF	55.8 CF	5 years – 83 %	Post-RT
SJMB96 [9]	1996–2003	23.4 CF	55.8 CF	5 years – 83 %	Post-RT
AIEOP ^a [59]	1998–2003	36.0 HF (1.0)	66.0 HF (1.0)	5 years – 71 %	Pre- and post-RT
HIT-SIOP PNET4 [60]	2001–2006	36.0 HF	60.0 (68-R1) HF (1.0)	5 years – 79 %	Post-RT
High risk (metastatic medulloblastoma)					
CCG9931 ^b [61]	1994–1997	36.0 HF	72.0 HF	5 years – 43 %	Pre-RT
SJMB96 [9]	1996–2003	36.0–39.6 CF	55.8 CF	5 years – 70 %	Post-RT
GHOP-HIT 2000	2001–2007	40.0 HF	60.0 HF (68-R1)	4 years – 65 %	Pre- and post-RT
Milan [62]	1998–2007	39.0 HF (1.3)	60.0 HF (1.5)	5 years – 70 %	Pre- and post-RT
CCLG [63]	2002–2007	39.68 HF (1.24)	72.0 HF (1.24)		

CF conventional fractionation, HF hyperfractionation

^aTrial included M₁ patients

^bTrial included non-medulloblastoma patients

implemented to review all imaging and treatment plans prior to the initiation of treatment – a lofty goal which will not be achieved soon.

7.6 Medulloblastoma

As noted earlier, during the past two decades there has been considerable evolution in radiotherapy target volumes for CNS embryonal tumors including medulloblastoma (Table 7.3). When there was a preliminary indication that full posterior fossa irradiation was not required for children with medulloblastoma [7], investigators focused on testing the feasibility and safety of reducing the target volume for the treatment of the primary site which customarily follows the craniospinal component of therapy. The first prospective report was from the SJMB96 study which was a multi-institution collaborative study that included all types of CNS embryonal tumors [8]. The SJMB96 study [9] was carried out from 1996 to 2003 and included prospective treatment with postoperative, risk-adapted, craniospinal irradiation (CSI) and postirradiation chemotherapy that included dose-intense cyclophosphamide, vincristine, and cisplatin. Average-risk (nonmetastatic) cases ($n=148$) were treated using 23.4 Gy CSI, 36 Gy posterior fossa irradiation, and 55.8 Gy primary site irradiation using a 2 cm

CTV margin and daily fractionation of 1.8 Gy. High-risk cases were treated using 36–39.6 Gy CSI and 55.8 Gy primary site irradiation using a 2 cm (pre-2003). There was no difference in craniospinal dose, target volume margins, or cumulative total dose based on tumor type. The results of this study showed that the 5-year cumulative incidence of posterior fossa failure was only 4.9 ± 2.4 % for patients with average-risk tumors [8] with a median follow-up of more than 5 years. The targeting guidelines used in this study resulted in a mean reduction of 13 % in the volume of the posterior fossa receiving doses in excess of 55 Gy compared with conventionally planned posterior fossa boost. The prospective trial has demonstrated that irradiation of less than the entire posterior fossa after 23.4 Gy craniospinal irradiation for average-risk medulloblastoma results in disease control comparable to that after treatment of the entire posterior fossa. These guidelines were the first prospective series that showed the ability to reduce the targeted volume safely in children with CNS embryonal tumors. With the exception of the A9934 study, the other studies are works in progress. The A9934 study [10] was a trial of systemic chemotherapy, second-look surgery, and conformal radiation therapy limited to the posterior fossa and primary site for children between 8 months and 3 years with nonmetastatic medulloblastoma. Following

Table 7.3 Current target volume margins used for the treatment of posterior fossa embryonal tumors

Study	Dates	CSI	Clinical target volume margin (cm)			Dose (Gy)	Chemotherapy
			Medulloblastoma	ATRT	SPNET		
SJMB96 Age >3 years [9]	1996–2003	Yes	2.0	2.0	2.0	55.8	Post
A9934 Age 1–3 years [10]	2000–2006	Yes	1.5	n/a	n/a	54.0×	Pre and post
SJMB03 Age >3 years [64]	2003–present	Yes	1.0	1.0	1.0	55.8	Post
ACNS0331 Ages 1–22 years [65]	2004–present	Yes	1.5	n/a	n/a	54.0	Concurrent and post
ACNS0332 Ages 1–22 years [66]	2007–present	Yes	PF	n/a	1.0	55.8	Concurrent and post
SJYC07 Age 1–3 years [67]	2007–present	No	0.5	0.5	0.5	54.0	Pre and post
ACNS0333 Ages 1–22 years [68]	2008–present	No	n/a	1.0	n/a	54.0×	Pre and post

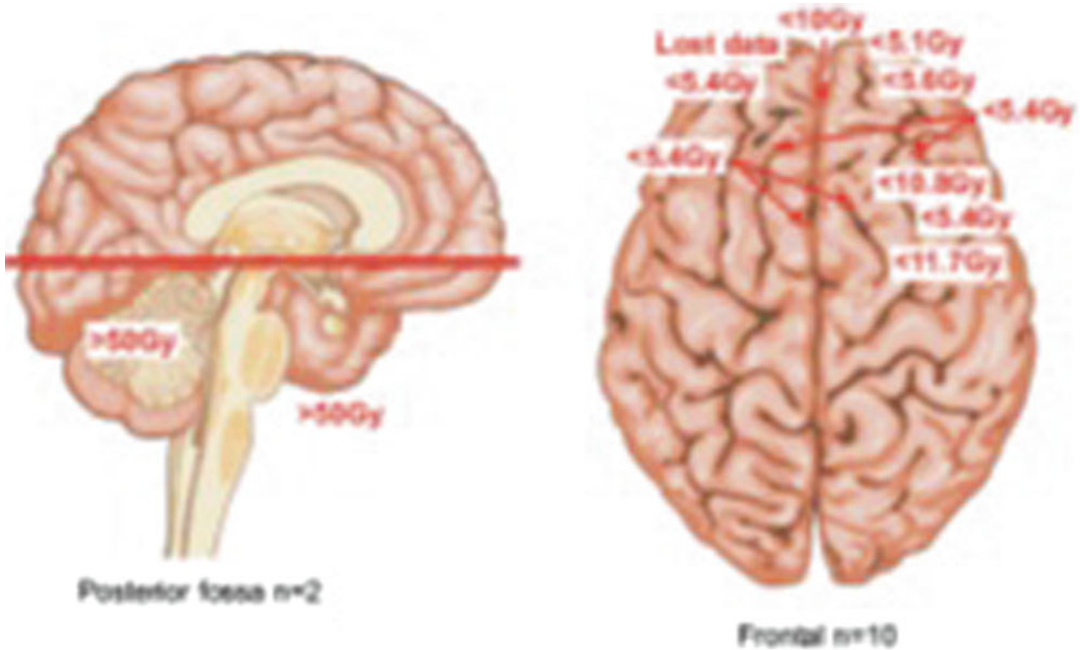


Fig. 7.3 Patterns of failure from the A9934 COG trial for non-metastatic medulloblastoma age <3 years

resection, these very young children received four 4-week courses of induction chemotherapy (cyclophosphamide, vincristine, cisplatin, and etoposide) followed by a second surgery when necessary and age- and response-adjusted irradiation of the tumor bed and posterior fossa. Patients then received maintenance chemotherapy consisting of four alternating cycles of cyclophosphamide and vincristine followed by oral VP-16. For the 78 eligible patients, the 3-year event-free survival (EFS) was approximately 50 % and by extent of resection 58 % (gross-total resection) and 36 % (<gross-total resection). There was a striking pattern of recurrence related to the timing of radiation therapy. Among the eight patients that progressed prior to irradiation, seven progressed with a component of failure in the posterior fossa or primary site. Among the 18 patients who progressed after irradiation, the initial sites of recurrence in 15 were either in the frontal lobes or the spinal compartment below C2/3. There was only one recurrence in the posterior fossa and there were no recurrences in the volume that received a dose in excess of 12–15 Gy (cumulative) during the 6 week course of the treatment.

It has been concluded that, despite the neuraxis failures, the addition of postoperative conformal radiation therapy limited to the posterior fossa and primary site appeared to be a promising treatment for nonmetastatic medulloblastoma in very young children (Fig. 7.3).

Critical to the success of this approach were the follow-up psychology data that suggested no significant or consistent decline in either cognitive or motor functioning as measured by either the phone-based interview technique or formal neuropsychologic assessments that could be performed after the delivery of chemotherapy and local conformal RT [11]. The approach of irradiating only the tumor bed in very young children has been carried forward by a number of groups and will likely be continued in the next series of cooperative group studies for intermediate- or higher-risk patients (unfavorable biology or residual or metastatic disease). Future studies will limit irradiation to the primary site and not include the posterior fossa as the initial volume (Fig. 7.4).

For patients with high-risk medulloblastoma, the use of high-dose craniospinal irradiation

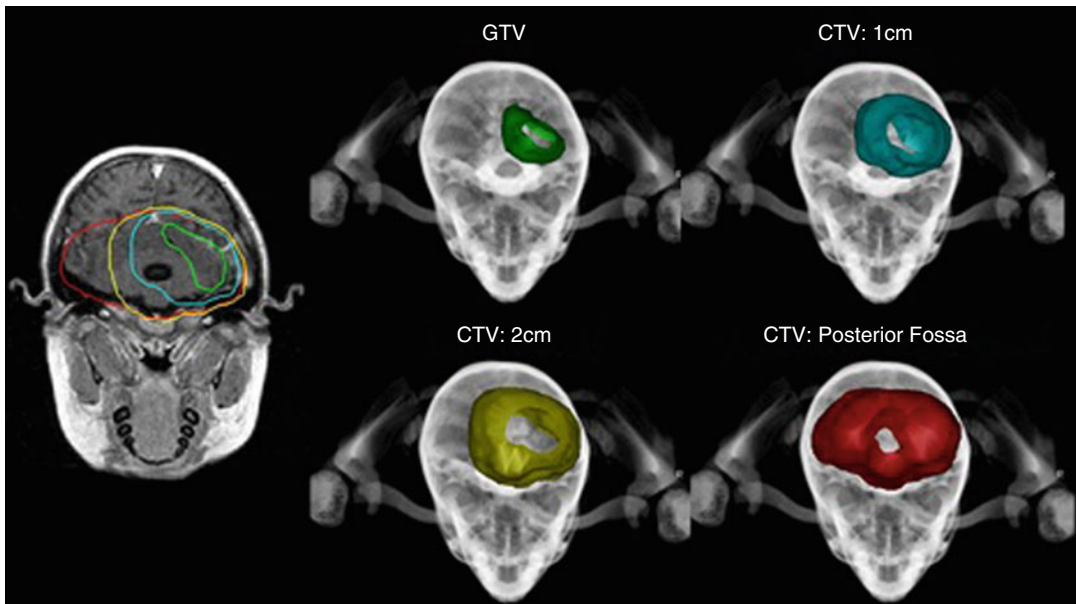


Fig. 7.4 Relative in situ differences in fundamental target volume guidelines for medulloblastoma

continues in combination with concurrent or postirradiation chemotherapy. The current approach of the Children's Oncology Group is an aggressive regimen of concurrent carboplatin and craniospinal irradiation. Other institutions favor postirradiation dose-intensive chemotherapy. In the St. Jude Children's Research Hospital series, high-risk medulloblastoma cases (metastatic disease or >1.5 cm residual disease) ($n=88$) were treated using 36–39.6 Gy CSI and 55.8 Gy primary site irradiation using a 2 cm (pre-2003) or (post-2003) 1 cm CTV margin. There are always risks associated with high-dose irradiation, most notably necrosis. With competing risk of death by any cause, the cumulative incidence (CI) of CNS necrosis at 5 years was 3.7% in a series that included 236 patients with embryonal tumors. The incidence was higher for the 196 patients with infratentorial tumor location 4.4 ± 1.5 %.

7.7 Ependymoma

The past results for the treatment of ependymoma have been dismal with very little changed until 20 years ago with the advent of conformal radiation therapy (Table 7.4). Conformal radiation

therapy was first introduced for very young children with this disease in the St. Jude RT1 protocol [12]. For the first time, children under the age of 3 years were offered immediate postoperative radiation therapy. The disease control rates increased significantly, especially for children who underwent gross-total resection prior to irradiation.

Radiation therapy for ependymoma can be very complex because of the configuration of the original tumor, postoperative changes, and the intimate association with vital structures. For example, these tumors can extend through the foramen magnum onto the surface of the upper cervical cord; through the foramen of Luschka to involve cranial nerves, the brainstem, and the basilar and vertebral arteries; or through the foramen of Magendie posteriorly into the subarachnoid space of the cisterna magna.

The standard treatment for localized ependymoma includes maximum safe resection followed by conformal or intensity-modulated radiotherapy. The extent of surgical resection is consistently the most important prognostic factor for these tumors. A 5-year survival for patients who have undergone a GTR is reported at 75–93% compared to 22–52.4% for those who received

Table 7.4 Recent clinical trials for ependymoma and radiotherapy parameters

Study	Dates	Total dose (Gy)	CTV (cm)	Chemotherapy	EFS ^a
					GTR ^b vs. <GTR
POG9132 [69]	1991–1994	69.6 ^c	Unknown	None	4 years EFS 70 % vs. 50 %
CCG9942 [70]	1995–1999	59.4	Original tumor ^d + 1.5 cm	STR only ^e	3 years 62 % vs. 55 %
RT1 [13]	1996–2009	59.4	1.0	None ^f	5 years 82 % vs. 41 %
ACNS0121 [22]	2003–2007	59.4	1.0	None	n/a
ACNS0831 [23]	2010–present	59.4	0.5	Post-RT ^g	n/a

^aEFS event-free survival^bGTR gross-total resection^cHyperfractionated irradiation 1.2 Gy BID^dConventional radiation therapy^eSTR subtotal resection^f35 of 153 patients received chemotherapy prior to irradiation^gRT radiation therapy

less than a GTR [13–15]. Radiation therapy has also demonstrated a survival advantage for these patients, with adjuvant radiotherapy resulting in a 5-year survival of 63 % compared to 23 % without radiotherapy in one series [15, 16]. Very often, disease control reports for ependymoma include patients with supratentorial tumors; however, in the recent publication by Merchant et al. [13], patients with infratentorial ependymoma appeared to have a poorer outcome than those with supratentorial ependymoma. This difference was not statistically significant.

The impact of histologic grade has been reported as controversial in the past; however, a report of 50 patients with localized ependymoma from St. Jude demonstrates a dramatic difference in a group of patients who received adjuvant radiotherapy [17]. The estimated 3-year progression-free survival rate was 28 % for patients with anaplastic ependymoma compared to 84 % for patients with differentiated ependymoma. Merchant et al. [17] provided further evidence from a prospective trial of conformal radiotherapy for resected ependymoma in which tumor grade had a significant impact on both EFS and overall survival (OS). A literature review of 1,444 pediatric patients with posterior fossa ependymoma suggests grade (WHO grade II vs. III) is an independent prognostic indicator for EFS but may not impact OS [18].

Craniospinal irradiation was once used prophylactically for ependymoma because of possible CNS dissemination; however, reviews demonstrated no benefit, even for anaplastic tumors. In fact, the most common site of recurrence is local. The best results in the literature come from the St. Jude prospective trial of conformal radiotherapy using a 10 mm margin which included patients 12 months of age or greater. The 7-year local control, EFS, and OS were 87.3, 69, and 81 %, respectively. The rate of gross-total resection in the study was 82 %, and the majority of patients had 59.4 Gy prescribed to their operative bed (children less than 18 months of age received 54 Gy).

The conformity of irradiation is key to decreasing long-term neurocognitive side effects and making radiation a safe option for young children. The percent volume of the supratentorial brain receiving radiation doses between 0 and 20 Gy, 20 and 40 Gy, and 40 and 65 Gy had a significant relationship with postirradiation IQ [19]. A prospective trial from St. Jude demonstrated that neurocognitive outcomes remained stable and within normal limits post radiotherapy for children receiving conformal adjuvant radiotherapy [12]. It is important to note that children less than 3 years of age at the time of conformal radiotherapy had significantly lower neurocognitive scores at baseline but demonstrated improvement

after radiotherapy. The ongoing COG trial now utilizes a 5 mm margin for the CTV, thus reducing normal tissue exposure to radiotherapy.

The role of adjuvant chemotherapy for ependymoma is an ongoing study question. Two cooperative group trials have utilized chemotherapy after craniospinal irradiation and found no clear benefit from the chemotherapy [20, 21]. A prospective cooperative group study randomized patients after postoperative CSI to receive lomustine, vincristine, and prednisone versus observation and found no benefit from the addition of chemotherapy for failure-free or OS [20]. A second prospective trial randomized patients to two adjuvant chemotherapy regimens: lomustine, vincristine, and prednisone versus the eight drugs in a 1-day chemotherapy regimen and found no difference between the regimens [21]. There was no difference between the two chemotherapy regimens and no benefit from radiotherapy alone when compared to other series. Seventy-one percent of the relapses on this trial were isolated local relapses, and only 47 % of patients received a gross-total resection. The impact of chemotherapy after more aggressive surgery and radiotherapy is not fully known.

Omitting radiotherapy from the treatment regimen of children with ependymoma has been an objective of two recent trials based on clinical factors that predict the low risk of failure even in the absence of radiation therapy. The recently completed COG ACNS0121 trial [22] and the current COG ACNS0831 trial [23] both include observation of children with supratentorial differentiated (WHO grade II) ependymoma after microscopically complete resection. These trials require central review of the neuropathology and written confirmation from the operating neurosurgeon that a microscope was used and that no visible tumor cells were present at the completion of surgery. That patients with supratentorial anaplastic ependymoma were not eligible for observation was based on data suggesting a higher rate of failure after radiation therapy of children with supratentorial anaplastic ependymoma regardless of the extent of resection [17]. Studies purely evaluating observations about the absence of chemotherapy have not been performed in children. Koshy et al. [24] reported using the SEER registry that

among 804 patients diagnosed with intracranial ependymoma between 1988 and 2005, postoperative radiation was administered only to 35 % of patients younger than 3 years and that among children younger than 3 years, the 3-year OS was significantly greater among those who received postoperative radiation compared to those who did not (81 % vs. 56 %, respectively, $p=0.005$). Indeed, RT is required for adult patients according to the work by Rogers et al. [25].

7.8 Brainstem Glioma

Brainstem glioma is a diffuse intrinsic tumor involving the pons. It has a characteristic appearance on MRI and does not require pathological confirmation. It is uniformly fatal despite excellent initial responses to irradiation; therefore, radiotherapy is considered palliative. Radiation dose escalation increases toxicity but does not improve outcome. Radiosensitizers have not improved the therapeutic ratio, and now biologics are combined with radiotherapy in clinical trials. Brainstem glioma (BSG) or diffuse infiltrating pontine glioma (DIPG) as it is also known is a tumor that extends along neural tracts to involve adjacent regions of the brain. The full extent of the tumor at diagnosis may not be fully appreciated but is readily apparent when it progresses after irradiation. When radiation therapy planning is performed, CT is used for dose calculation and verification. T2-weighted MRI is registered to the CT dataset for the purpose of targeting. A margin of security surrounding the obvious tumor is necessary to account for subclinical microscopic disease or extension along neural tracts, and an additional margin is subsequently added to account for variability in patient setup for daily (fractionated) radiation therapy. The MRI-visible tumor is called the gross tumor volume (GTV), the margin surrounding the gross tumor volume to account for subclinical microscopic disease and unappreciated tumor extension is called the clinical target volume (CTV), and the margin added to the CTV is called the planning target volume (PTV). The CTV margin used in clinical trials has been arbitrarily chosen

Table 7.5 Total doses and clinical target volume margins for pediatric brainstem glioma trials in the Pediatric Oncology Group (POG) and Children’s Oncology Group (COG)

Study	Dates	Total dose (Gy)	CTV margin (cm)	Chemotherapy
POG9836 [71]	1999–2001	54	1.5	Concurrent and post-RT VCR/ETO
ACNS0126 [72]	2002–2005	59.4	1.0	Concurrent and post-RT TMZ
ACNS0224 [73]	2005–2007	55.8	1.0	Concurrent topotecan
ACNS0222 [74]	2007–2008	54.0	1.5	Concurrent Motexafin-Gd
ACNS0927 [75]	2010–present	54.0	1.0	Concurrent and post-RT SAHA

VCR vincristine, ETO etoposide, TMZ temozolomide, TOPO topotecan, Gd gadolinium, SAHA suberoylanilide hydroxamic acid. Radiotherapy normal tissue dose limits: POG9836, no dose limits; ACNS0126, 50.4 Gy spinal cord, optic chiasm, and cochlea; ACNS0224, 50.4 Gy spinal cord, optic chiasm, and cochlea; ACNS0222, 54 Gy spinal cord, 50.4 Gy optic chiasm, and 45 Gy pituitary gland; ACNS0927, standard 3 days organ at risk guidelines

because pattern-of-failure data are not available to support a specific margin (Table 7.5).

To make progress and compare results among treatment regimens require uniform and consistent guidelines for irradiation. Because there is no agreement on target volume definitions for conformal treatment planning and some suggest that the first site of progression is at or beyond the targeted margin, the patterns of failure with respect to the targeted volume are currently under evaluation. T2-weighted MR imaging can be used to demonstrate treatment in almost all cases. Brainstem glioma extends along neuronal tracts in all dimensions including superiorly into the cerebral peduncles and thalamus, axially with posterior extension into the cerebellar peduncles, and in a limited manner into the cervical spinal cord. In one study [26], the average distances from the contoured GTV were superior, 1.1 cm with a range of 0.3–2.75 cm; inferior, 0.4 cm with a range of 0.1–0.6 cm; and lateral, 1.1 cm with a range of 0.3–2.0 cm. It was then recommended that the GTV should include identifiable tumor on post-contrast T1- and T2-weighted MRI. The CTV should include a 2 cm anatomical expansion in the transverse and inferior dimensions and a 3 cm anatomical expansion in the superior dimension. Tumors confined to the pons should have the CTV expanded superiorly to cover the midbrain. PTV margins should be individualized (0.3–0.5 cm) but not less than the MR image section thickness used for treatment planning. Treatment planning MRI should include the upper cervical spinal cord. In summary, the “required” CTV margin

used in the treatment of BSG will vary according to the location and volume of the GTV and access to specific neural pathways. Properly encompassing the tumor and subclinical microscopic disease will help patients to benefit most from radiation therapy while considering normal tissue effects which are often dose related.

7.9 Organs at Risk in the Treatment of Posterior Fossa Tumors

In some cases, photon IMRT may be the preferred treatment method to reduce dose to normal tissues despite some concern by treating physicians about the increased volume that receives the lowest doses.

The current normal tissue dose constraints for tumors of the posterior fossa are as follows:

Cochleae

- D50% < 3,500 cGy – goal (each cochlea).
- D50% < 2,000 cGy – preferred (each cochlea).
- Comment – there is no dose limit for the cochleae.
- Structure definition – using CT each cochlea should be contoured as a circular structure within the petrous portion of the temporal bone, and the contour should appear on at least two successive CT images.

Optic Nerves and Chiasm

- D90% < 1,000 cGy, D50% < 5,400 cGy, and D10% < 5,600 cGy – goal.

- $D90\% < 5,400$ cGy, $D50\% < 5,600$ cGy, and $D10\% < 5,800$ cGy – maximum.
- Comment – effort should be made to avoid direct treatment of the optic nerves and chiasm without compromising target volume coverage.
- Structure definition – the optic nerve may be contoured on CT or MR. The contour should appear on at least two successive CT or MR images.

Spinal Cord

- $D90\% < 300$ cGy, $D50\% < 2,600$ cGy, and $D10\% < 5,700$ cGy – goal.
- $D90\% < 900$ cGy, $D50\% < 5,000$ cGy, and $D10\% < 5,900$ cGy – maximum.
- Comment – effort should be made to minimize dose to the spinal cord without compromising target volume coverage.
- Structure definition – the spinal cord begins at the caudal aspect of the foramen magnum.

7.10 Late Effects

7.10.1 Hearing Loss

Hearing loss is considered a late complication of radiation therapy. Investigators have included audiometry in front-line studies to research the effect of therapy on hearing loss with various goals including those stated above. Absent direct auditory nerve damage from surgery, the risk of hearing loss increases with time and dose. The onset and severity of hearing loss is accelerated by ototoxic chemotherapy. There are additional factors such as sudden changes in intracranial pressure, hydrocephalus, CSF shunting, and perioperative complications including infections and ototoxic antibiotics. In planning for irradiation of posterior fossa tumors, consideration must be given to the target volume and its relationship to the cochleae. Except for tumors that require craniospinal irradiation, cochlear sparing is possible in most cases. Using the target volume margins now applied for pediatric CNS tumors, tumors centered in the fourth ventricle cochleae are unlikely to receive meaningful collateral

irradiation. For unilateral CP angle tumors, sparing the cochlea may be more difficult and considering the margins that are required to ensure that the PTV receives the prescription dose, sparing is unlikely. This is an important point regardless of the method of irradiation, appropriate target coverage should be the primary goal and pulling back to reduce the dose should not be considered. In cases of bilateral tumors, ensuring target coverage might mean that both cochleae receive the prescription dose. At this time, intensity-modulated radiation therapy (IMRT) might have a better chance of sculpting the dose away from the cochlea (Fig. 7.5).

Data published from the RT1 protocol at St. Jude (Table 7.6) that included patients treated with radiation therapy alone included 5 year estimates of hearing loss [31] and suggested that hearing loss at the highest (and most sensitive) frequencies is rare in patients treated with doses less than 35 Gy. In a separate publication from the same protocol, preliminary data were reported that included the effect of potentially ototoxic chemotherapy [32]. These data suggested the same as the Hua study [31]; however, for patients who received ototoxic chemotherapy, the incidence of hearing loss would be reduced in patients treated with levels at or below 20 Gy.

The goal of radiotherapy planning should be to reduce the dose to the cochlea to less than 35 Gy when RT alone is given, and when chemotherapy is given the dose should be 20 Gy or less. The key is to determine the true effect of chemotherapy. For children with medulloblastoma, proton therapy appears to reduce the rate and magnitude of hearing loss after craniospinal irradiation and postirradiation chemotherapy using cisplatin with mean cumulative doses of 300 mg/m². In this series, mean hearing threshold levels were lower at all frequencies, and the incidence of grades 3 and 4 ototoxicity at 1 year was reduced by 50 % when using proton therapy [27]. Others have found when using IMRT that a mean cochlear dose of >42 Gy, in combination with cisplatin chemotherapy (~375 mg/m²), results in a low rate of serious hearing loss and that there is a relationship between the incidence of hearing loss and cisplatin dose [28].

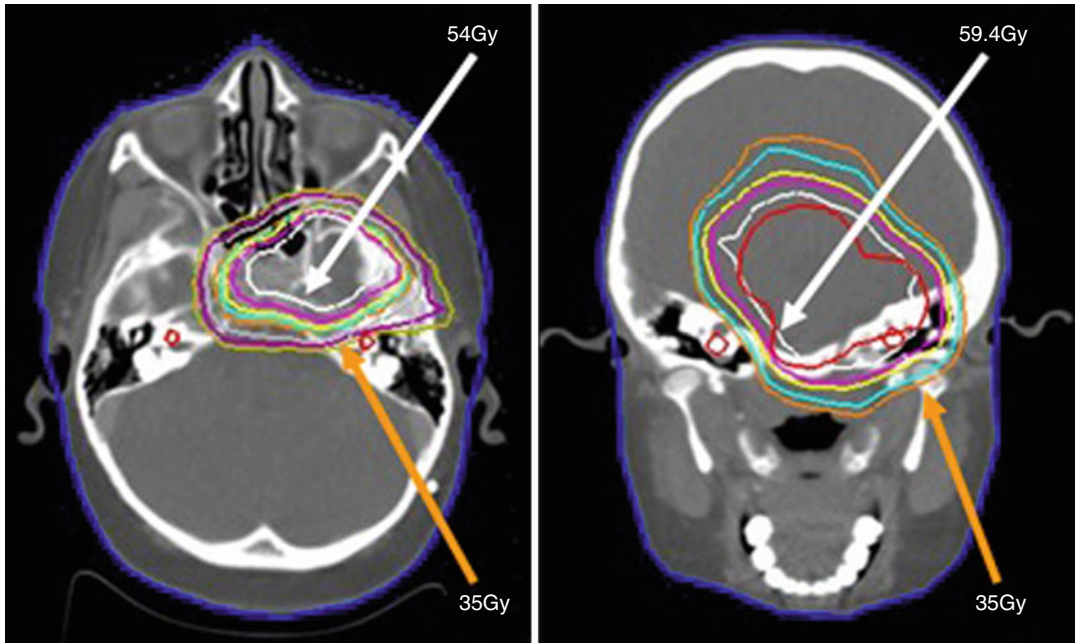


Fig. 7.5 Variability of dose to the cochleae and relative sparing in two example cases

Table 7.6 Probability of hearing loss at 6 and 8 kHz after radiation therapy alone

Hearing loss by dose	30 Gy	35 Gy	40 Gy	45 Gy	50 Gy	55 Gy	60 Gy
High-frequency 6 and 8 kHz	0 %	2 %	4 %	5 %	11 %	24 %	37 %

A recent report from the SJMB96/03 trials [33] showed the ability of amifostine to reduce the incidence of hearing loss (end point – hearing aid requirement) in patients treated with sequential irradiation and ototoxic chemotherapy – amifostine was administered with postoperative chemotherapy.

7.10.2 Endocrine

Hormone replacement therapy reduces the impact of radiation-induced endocrinopathy in children with brain tumors. The potential for endocrinopathy is not a contraindication to irradiation but should be understood because of its impact on general health and quality of life and its relationship to long-term cognitive effects for which data are emerging. One might question why a child with a posterior fossa tumor would be at risk for endocrinopathy. Tumors arising from the brainstem or

any posterior fossa subsite, with their applied margins, might encompass the hypothalamic-pituitary unit. One obvious example is a tumor that arises in the fourth ventricle or CP angle and tracks along the brainstem toward the anterior incisural space. Certainly tumors that require craniospinal irradiation will encompass the hypothalamic-pituitary unit at least to the dose level of the selected craniospinal dose. One should be cognizant that children treated with craniospinal irradiation are at risk for primary hypothyroidism secondary to the spinal field exit dose to the thyroid. Ovarian failure from the same mechanism may occur when the lower border of the spinal field includes the ovaries in the primary beam.

7.10.3 Cognitive

Due to the increasing long-term survival of patients treated for pediatric brain tumors,

especially those with tumors located in the posterior fossa, more focus has turned to the late effects of treatment. Intellectual ability, academic achievement, learning, and memory are usually negatively affected. Most studies have correlated lower achievement with the effects of radiation, chemotherapy, and surgery, and few have tried to find a relationship between neurocognitive deficits and the tumor, most notably hydrocephalus. The most commonly stated risk factor for neurocognitive sequelae is young age at the time of treatment. Mulhern et al. [29] have shown that this increased risk is associated with white matter loss, which is more marked in younger children. The volume of normal white matter in the brain is associated with IQ and attentional abilities: decreased volumes of normal white matter are related to reduced attentional abilities, which in turn have a negative effect on academic achievement. The development of white matter continues into adulthood, with the frontal and prefrontal lobes being the last areas to complete development. These areas are known to be involved in the "allocation of attentional resources." It makes sense, then, that treatment of tumor-related factors that cause injury to the developing white matter in these areas would negatively affect attentional abilities and from there produce the cascade of effects that lead to decreased achievement for long-term survivors of pediatric brain tumors.

Other areas of the brain are also believed to contribute to higher-order functions. Levisohn et al. [30] showed that resection itself may contribute to neuropsychological deficits in children with tumors of the cerebellum. The most common difficulties encountered were problems with visual-spatial tasks, language, sequencing memory, and regulation of affect. All of these can contribute to lower academic achievement and intelligence. This shows that connections between the cerebral hemispheres and the cerebellum are integral for higher-order functioning. Thus, when considering neuropsychological deficits, it is important to remember that radiation and the tumor may not be the only factors. However, it is usually hard to quantize the effect of surgery because radiation and chemotherapy effects often overlap and confound those of

surgery. It has also been shown that deficits in academic achievement among patients treated for medulloblastoma are due to a diminished capacity to learn new information, not the loss of previously learned information. It is likely that this is true for survivors of other brain tumors of the posterior fossa, such as ependymoma. Thus, standardized tests of learning, memory, and the ability to learn are of particular importance. Many studies have shown that higher radiation doses are correlated with neurocognitive impairments. Few have reported on the hypothesis that mal-effects of the tumor itself may have a significant impact on these impairments. Hydrocephalus is a commonly seen side effect of pediatric brain tumors, as most of the tumors affecting children occur in the posterior fossa and obstruct the ventricular pathway of cerebrospinal fluid. Hydrocephalus can be a major cause of white matter loss and thus may have an impact on academic achievement and other neuropsychologic outcomes.

7.10.4 Middle Ear Damage

Cerebellopontine angle tumors, especially those invading the internal auditory canal, are such that the tumor and the target volume for radiation therapy are within millimeters of the tympanic membrane and structures of the middle ear. Because of conformal treatment methods, middle ear damage is a rare but expected complication of posterior fossa tumor irradiation and may require microsurgical repair including tympanoplasty. Tympanoplasty can be used to repair damage to the tympanic membrane or middle ear and relies on autologous bone, temporalis fascia, or synthetic materials such as hydroxyapatite for the repair. The tympanoplasty procedure may be performed via either transcanal or the external auditory canal. In both instances irradiated bone may be further damaged leading to osteonecrosis and other complications. Care must be taken under these circumstances. The primary goal is to restore hearing when possible or to prevent infections of the middle ear. There is limited information on this for brain tumor patients as it

is relatively more common in irradiated patients with head and neck tumors [34].

7.10.5 Somatic

Children with posterior fossa tumors who require irradiation are at great risk for somatic effects especially when craniospinal irradiation is administered. Treatment of the entire brain and spine to comprehensively treat the subarachnoid volume encompasses a significant proportion of the osseous growth plates of the cranial vault, base of the skull, and axial skeleton. Small head size, short stature, and orthopedic deformities characterize this patient population and appear to be magnified in younger patients. Despite the extent of the problem and the large number of patients affected, there are limited data available to predict the incidence and severity of the problem in children who undergo craniospinal irradiation. In one series, significant growth effects were observed in the vertebral bodies of children treated with craniospinal irradiation, and region differences in the effect of radiation dose were noted and further modified by age and gender [35]. Orthopedic deformity and cervical subluxation have also been noted in very young children who are treated with focal irradiation. There are a number of factors that contribute to subluxation including multiple surgery procedures, chemotherapy, meningitis, and multilevel laminectomy. Subluxation is generally observed unless symptomatic or there is imaging evidence of cord impingement [36].

7.10.6 Hair Loss

Craniospinal irradiation may result in significant hair loss [37] including thinning of the vertex scalp that is most pronounced in high-risk patients. Damage to the skin and hair is a common effect of irradiation and is dose- and patient related [38]. Hair loss in patients treated with CNS irradiation may be more pronounced with chemotherapy [39]. Finally, hair loss at the point of beam entrance may be more pronounced in

patients treated with proton beam therapy because the skin dose is high and the number of beams is fewer.

7.10.7 Necrosis

Using fractionated irradiation, cumulative doses in the range of 54–59.4 Gy are commonly prescribed at 1.8 Gy per day. Based on available data, largely from adults, the risk of necrosis should be less than 5 % unless specific risk factors are present, most notably a history of diabetes mellitus, hypertension, and morbidity attributed to surgery [40–42]. While diabetes mellitus and nonsurgery-related hypertension are uncommon in the pediatric population, morbidity attributed to surgery is commonly seen in children with medulloblastoma, ependymoma, and low-grade glioma when the tumor is located within or adjacent to the brainstem. In some cases, the morbidity attributed to surgery can manifest in signs and symptoms that precede radiation necrosis. Hypertension resulting from surgery, postoperative seizure, postoperative cranial nerve deficits, evidence of ischemia on postoperative imaging, and the so-called posterior fossa or cerebellar mutism syndrome [43] appear to be risk factors for necrosis. The question is whether these findings, in any combination, should be considered as contraindications to radiation therapy. Cranial nerve deficits alone are probably not sufficient evidence to consider delaying or avoiding radiation therapy. This is a relatively common complication resulting from aggressive surgical resection [44], and it does not appear that high-dose postoperative irradiation impedes the recovery of cranial nerve function even when doses much higher than those reported in the adult literature are given to the brainstem of children with ependymoma [45]. Evidence of ischemia on MRI is relatively common after surgery for posterior fossa tumors, and because early postoperative treatment is a general requirement, there are no data to follow imaging findings to determine who will recover and who will not. We consider postoperative seizure and hypertension that requires medication, in addition to alterations in heart

rate, to be important signs of severe brainstem injury. When combined with the finding of extensive ischemia on MRI or extensive and severe cranial nerve deficits, these signs and symptoms might indicate damage to the brainstem and serve as contraindications for radiation therapy [13].

There are two additional scenarios in which severe brainstem injury leading to necrosis may occur: the first is shunt failure with prolonged increased intracranial pressure and the second is mass effect on the brainstem. Mass effect, largely from tumors such as craniopharyngioma or low-grade glioma that are prone to cyst expansion during and after treatment, may impinge on the brainstem and result in poor blood flow and regional hypoxia. Indeed, long-standing mass effect and possibly changing intracranial pressure may provide the environment for necrosis or similar complications. Patients who have received high-dose irradiation and who have shunts should be carefully followed including those who undergo surgery after radiation therapy who do not have a shunt. We know that these patients will be at increased risk for needing CSF diversion after more than one surgical procedure. Hiccups are an important sign in addition to swallowing dysfunction and long-tract signs. Any child who has received high-dose irradiation and who requires anesthesia or sedation for procedures should have their oxygen saturation and hemodynamic parameters monitored to avoid hypoxia of the brainstem and ischemic conditions. Acute onset of signs and symptoms considered to be harbingers of necrosis should be treated aggressively with corticosteroids, hyperbaric oxygen, or bevacizumab which has recently been shown to have therapeutic benefit in this setting [46]. In severe cases surgery should be considered when feasible [47]. There are special circumstances in which the risks of necrosis are higher: re-irradiation, radiosurgery [48], brainstem implants, and possible single-beam proton therapy [49, 50]. In cooperative group guidelines that include proton therapy, single-beam proton treatments are not permitted. Necrosis requires a variety of imaging studies including perfusion- and diffusion-weighted MRI, MRS, and PET for evaluation. The cumulative incidence of brainstem necrosis

at 7 years was 2.5 % (95 % CI 0.0–5.2) in a recent series of children with ependymoma treated with high-dose irradiation [13].

7.10.8 Secondary Tumors

Long-term survivorship after radiation therapy for posterior fossa brain tumors carries a lifetime risk of benign and malignant secondary tumor induction involving the brain and extra-axial and extra-CNS tissues subtended by the irradiated volume. The risks are greater at higher doses, and the probability is increased by the irradiated volume. Those treated with craniospinal irradiation are at greatest risk for this lethal complication because of the required doses and volumes. Although the use of conformal methods of irradiation purportedly irradiated a smaller volume of normal tissues to higher doses, it is unclear whether the reduction in the high-dose volume, which is most often the site of a secondary malignant brain tumor, is sufficiently meaningful to reduce this risk. Decreasing the high-dose volume often comes at the expense of an increase in the volume of normal tissue that receives the lowest doses – this includes tissues which may not have been irradiated in the era of nonconformal treatment planning. The potential difference is the risk of secondary tumors of the benign type (meningioma) or low-malignant potential (papillary thyroid cancer). Very low doses will induce some secondary tumors, mainly benign, while the highly malignant tumors are most often within the volume that receives the highest dose. The incidence of secondary tumors is largely related to time after irradiation – sufficient time must pass to attribute radiation therapy as the causative agent. In the era where combined modality therapy, including chemotherapy and radiation therapy, is more common, there is a concern that tumor induction will be increased by the use of chemotherapy. A recent report from the COG regarding the A9961 trial revealed that secondary tumors were more common than late relapses of medulloblastoma and a major cause of morbidity and mortality [51]. The cumulative incidence of malignant tumors in one series of

children with ependymoma treated with high-dose postoperative radiation therapy was 4.1 % (95 % CI 0.0–8.7) and of a malignant glioma 2.3 % (0.9–5.6) [13] at 7 years.

7.11 Future Trends of Radiotherapy in PFT

7.11.1 Low-Risk Medulloblastoma

Future trials for children with medulloblastoma will incorporate clinic-pathologic and biological risk stratification. At the present time there appear to be at least four groups based on biology; those with WNT, SHH, and two others. Concerning those with the lowest risk for failure, WNT, there are a number of possibilities to reduce therapy in this group. With an emphasis of reducing the risk of side effects due to radiotherapy, the following might be possible.

7.12 Measures to Reduce the Side Effects of Craniospinal Irradiation in Low-Risk Medulloblastoma

Despite the older age of the WNT cohort, there remains a risk for below-average cognitive function 5 years after 23.4 Gy CSI. We would estimate that the risk is greater than 5 % and probably

less than 40 % at 5 years based on recent data [52] Interpretation of the limited data available for children with WNT medulloblastoma is that they have some evidence of decline in cognition after treatment using 23.4 Gy CSI; therefore, further reductions in dose and volume are warranted based on risk of relapse and side effects. There are a variety of ways to reduce the dose to improve cognitive function and other anticipated side effects of irradiation considering the age of the patient and the potential for long-term survivorship. Very late and rare side effects, not just cognitive effects, should be considered in this group because of their potential for long-term survival. Proposals to reduce cognitive and other side effects in CNS embryonal tumors include reducing craniospinal dose and fractionation and considering different dose and fractionation schemes ($BED = nd(1 + d/\alpha\beta)$, where n = fractions, d = fractional dose, and $\alpha\beta = 2$ for normal tissues and 10, 20, or 50 for medulloblastoma (Table 7.7)).

The possible future regimens for patients with CNS embryonal tumors will (1) reduce cumulative dose to the primary site either limiting the dose to 54 Gy or using lower doses ranging from 45 to 50.4 Gy which appear to be therapeutic in recent studies, (2) use smaller CTV margins since a systematic study has shown the ability to safely reduce the CTV margins from 2 cm→1 cm→0.5 cm, and (3) use proton therapy which has a more precise and superior dose distribution and for which

Table 7.7 Different possible dose and fractionation regimens for medulloblastoma

Tissue	CSI dose (Gy)	Fractions	Dose/fraction (Gy)	α/β	BED	Diff (%)
Normal brain	23.4	13	1.8	2	44.5	0
Normal brain	24.0	16	1.5	2	42.0	-6
Normal brain	18.0	10	1.8	2	34.2	-23
Normal brain	18.0	12	1.5	2	31.5	-29
Normal brain	14.4	8	1.8	2	27.4	-38
Normal brain	15.0	10	1.5	2	26.3	-41
Tumor	23.4	13	1.8	50	24.2	0
Tumor	24.0	16	1.5	50	24.7	2
Tumor	18.0	10	1.8	50	18.6	-23
Tumor	18.0	12	1.5	50	18.5	-24
Tumor	14.4	8	1.8	50	14.9	-38
Tumor	15.0	10	1.5	50	15.5	-36
Tumor (A9934)	15.0	30	0.5	50	15.2	-38

models showed a benefit and will also reduce dose to extra-CNS tissues including the thyroid, heart, lungs, kidneys, ovaries, and vertebral growth plates.

7.13 Dorsally Exophytic Brainstem and Cervicomedullary Tumors

Exophytic tumors of the brainstem are most often low grade in nature, are of the pilocytic variety [53], and amenable to surgical resection [54]. These rare tumors respond well to irradiation, the patients experience limited radiation-related side effects because the treatment volume may be limited to the point of attachment when the operating neurosurgeon is able to document the same, and the likelihood of residual disease at adjacent subsites is low.

Cervicomedullary tumors represent a particularly morbid and dangerous entity after surgery and during or after irradiation [55, 56]. These low-lying lesions of the posterior fossa may present with life-threatening symptoms affecting autonomic processes based on invasion or extrinsic compression. Ganglioglioma has been commonly reported in this location, although other low-grade histologies are often present. It is important to consider surgical decompression to alleviate symptoms and improve the ability of the patient to tolerate radiation therapy and potential subsequent edema and inflammation (Fig. 7.6).

7.14 Re-irradiation

Children with recurrent ependymoma after prior irradiation have few treatment options and the majority will die within 2 years of initial disease progression. The pattern of failure after irradiation may include local progression, neuraxis dissemination, or a combination of the two with wide-ranging involvement of the central nervous system. There are various levels of disease burden when an ependymoma progresses after initial treatment; in most instances progressive disease is identified on surveillance imaging in asymptomatic patients. The experience with administering a second course of irradiation (re-irradiation) suggests that it is an effective treatment option for children with recurrent ependymoma when combined with resection of locally recurrent or metastatic disease [48]. Because most children initially treated for ependymoma receive radiation doses that approach the accepted tolerance levels of the brain and spinal cord, considering a second course of irradiation requires that the patient or their parents accept the risk for potentially devastating side effects that might compromise neurological function or even lead to death. To improve our understanding of the potential risks and benefits of re-irradiation requires systematic study of the clinical and biological factors critical to long-term disease control and tolerance to high-dose irradiation.

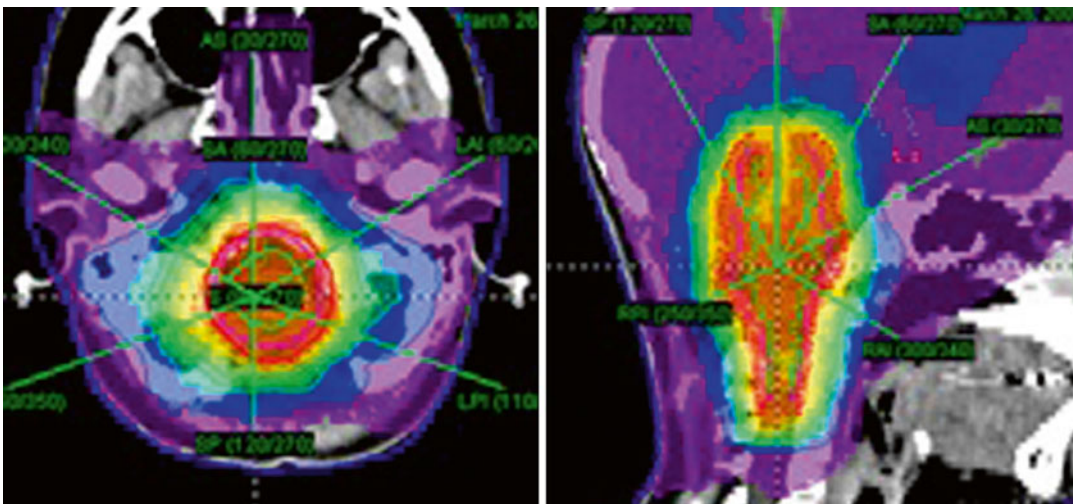


Fig. 7.6 Intensity-modulated radiation therapy dose distribution for cervicomedullary tumor

It is also important to understand the effects of re-treatment on function and quality of life. The treatment and follow-up of re-irradiated patients will provide an important opportunity to study the biology of recurrent ependymoma and factors predictive of disease control and normal tissue effects. So far no clinical protocols have been developed to systematically study this option that would identify patients who will benefit from re-irradiation and should provide a foundation for a combined modality approach to treatment failure with novel agents that enhance the effects of radiation or protect normal tissues. Fractionated re-irradiation has not been systematically explored for ependymoma mainly because it affects the very young and pediatric oncologists are not familiar with re-irradiation as a treatment option. In this study, we propose to irradiate children with an ependymoma that is recurrent after prior fractionated focal irradiation and to study the clinical and biologic features of these patients to predict disease control and toxicity. The indications for re-irradiation require exploration, and dose and volume guidelines need to be established. Three clinical risk groups have been identified that might help select patients for a particular treatment. Patients who progress at the primary site with no evidence of metastatic disease should be eligible for resection and re-irradiation using focal fractionated or craniospinal methods. Craniospinal irradiation might be considered for older patients based on the risk for metastatic progression. Focal fractionated irradiation should be the only option for younger patients to minimize the side effects of treatment. Patients with local failure should be offered both treatment options with recommendations dependent on patient age, prior treatment and morbidity, and other factors balancing the potential for cure with the risk of long-term effects. The low negative predictive value of CSF cytology and neuraxis imaging affects the selection of treatment for this group of patients. Improving the negative predictive value of these tests may be considered in this study. Patients who progress with metastatic disease but who remain controlled at the primary site should be considered for metastasectomy and craniospinal irradiation. This group of patients may have disease burdens ranging

from the resectable oligometastasis to extensive and unresectable neuraxis disease. Controlling metastatic disease requires a combination of craniospinal irradiation to neuraxis tolerance and supplemental irradiation to areas at highest risk for disease progression. Definitive treatment of these patients often requires exceeding generally acceptable normal tissue tolerance limits of the brain and spinal cord. Patients who progress with combined local and metastatic failure or diffuse neuraxis metastatic disease after prior radiation therapy appear to fare poorly with a second course of radiation therapy, although the number of patients with these clinical features appears to be small. Nevertheless, they should be considered for this treatment protocol that will set the stage for future experimental therapy including a combined modality approach that would involve craniospinal irradiation.

7.15 Technical Features of the Hardware Used for Irradiation of Posterior Fossa Tumors

Worldwide, radiotherapy is primarily administered using high-energy (≥ 6 MV) linear accelerators capable of isocentric treatment of the patient. During the past two decades, modifications to the linear accelerator have included increased precision of the treatment gantry and couch, multi-leaf collimation of the radiation beam, and onboard imaging devices or aftermarket hardware and software to improve localization and verification for daily (fractionated) treatments. A lesser equipment has no place in the treatment of children with brain tumors. This may be self-selecting by virtue of the fact that a center that is incapable of performing neurosurgery on a child is unlikely to have modern radiotherapy equipment (Fig. 7.7).

7.16 Gamma Knife

Gamma Knife is a form of radiosurgery that relies on concentrically placed cobalt sources that are individually collimated and directed to a precise location within the head of the device.

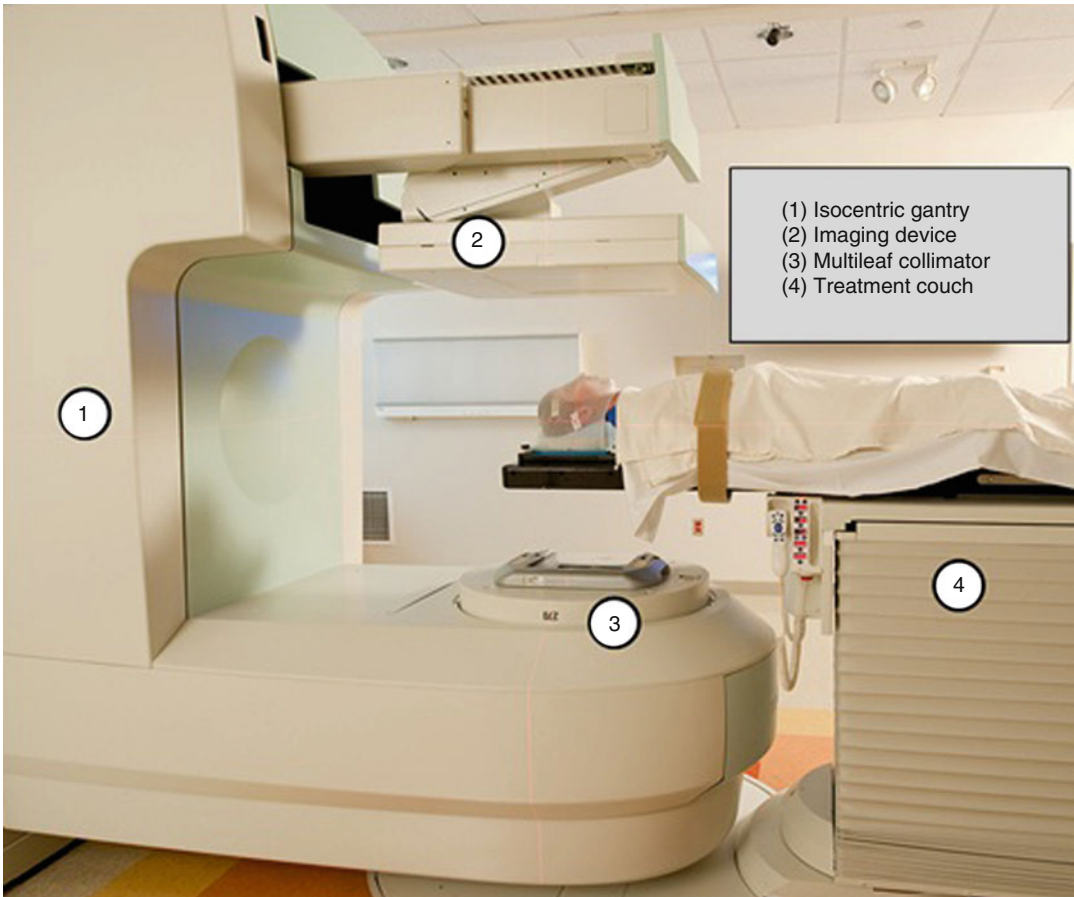


Fig. 7.7 Modern linear accelerator

The sharp falloff in dose and the extensive experience using this device for high-dose single-fraction treatment sets a standard to which other radiosurgery methods are compared. Dose is generally prescribed to an isodose that encompasses the treated lesion. Given the steep gradient of dose, the center of the lesion typically receives twice as much as the periphery. For metastatic lesions without normal tissue in the high-dose volume, the end point of necrosis is tolerable. When normal tissue is found within the volume, necrosis of the parenchyma may be problematic. Strict dose tolerances of the brainstem and other critical structures must be observed to minimize risks which are proportional to the irradiated volume [42]. There are data to suggest a potential benefit in the treatment of recurrent tumors of the posterior fossa, typically low-grade glioma and ependymoma, using this method. Less data are

available to support its use in the frontline management as an adjunct to surgery. Treatment of residual disease is a general requirement which seems to be fading in the treatment of adults with metastatic intracranial tumors following surgical resection (Fig. 7.8).

7.17 CyberKnife

CyberKnife (Accuray, Sunnyvale, CA) is a 6-MV linear accelerator mounted on a robotic arm that operates under computer control to deliver radiation beams at nearly unlimited angles to achieve a highly conformal treatment. Experience treating children using this form of radiosurgery is limited. There are few reports in the literature to document its effectiveness and safety and indications in pediatric posterior fossa tumors. Because

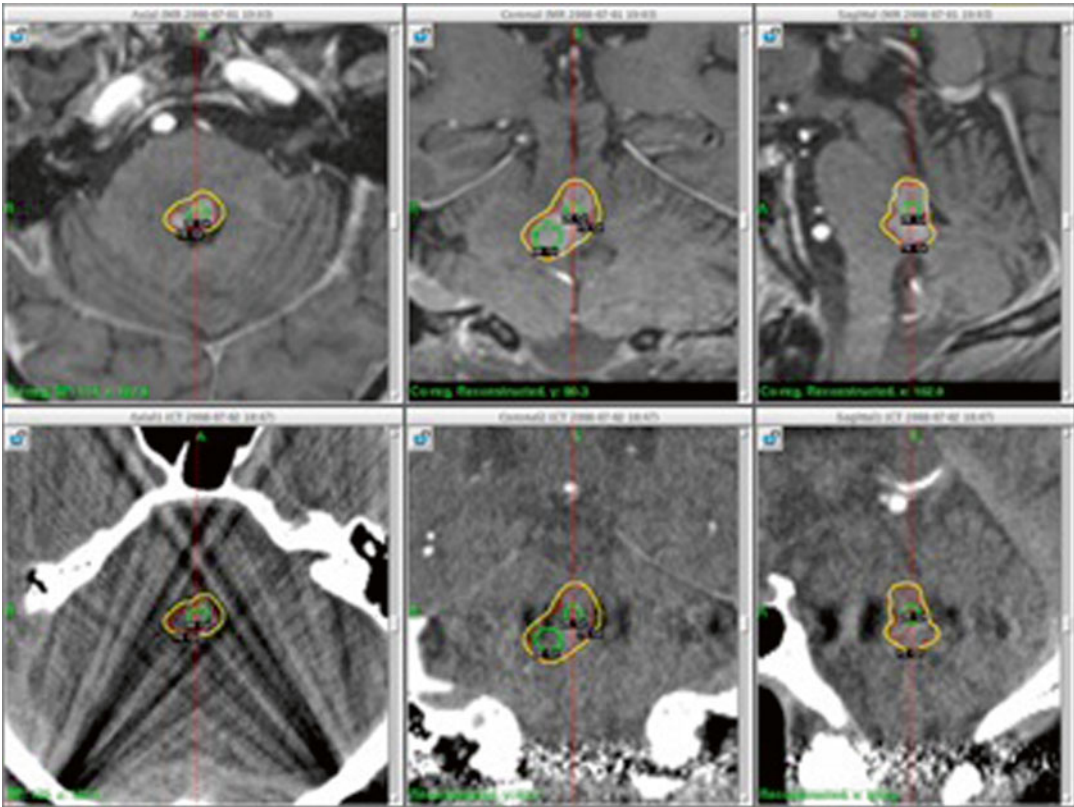


Fig. 7.8 Gamma Knife radiosurgery plan for the treatment of recurrent ependymoma on the dorsum of the brainstem

of the precision of this method, the dose per fraction may be increased and the total number of treatments reduced. It is uncertain whether this form of hypofractionated irradiation results in equivalent disease control or fewer side effects. Similar to other forms of radiosurgery and hypofractionated treatment, these methods are most often called upon to treat patients who have progressed after prior fractionated irradiation. This places the investigator and the method in a difficult situation. The method has to prove its usefulness in a setting that may be largely palliative. Of additional concern is the increased risk of side effects and necrosis due to the large size of the administered dose [57].

7.18 Proton Therapy

Protons appear to be comparable to high-energy photons in prescribed dose and the potential for side effects based on similar dose and volume;

however, the relative biologic effectiveness is on average of 1.1 and must be taken into account when prescribing a dose. The end of range for the proton beam has a slightly higher radiobiological effectiveness and should not be placed in a critical normal tissue volume. Single proton beams are not allowed in clinical trials for children with brain tumors in the Children's Oncology Group. It is important to note that using similar prescribed doses, protons do not have increased curative potential when compared to photons. Certainly the increased precision may be used to escalate the dose which is under consideration in clinical trial designs for ependymoma and other posterior fossa tumors. If there is a slight increase in the biological effectiveness of proton therapy despite the adjustments in physical dose when prescribing proton therapy to achieve the same effect, caution must be applied in the use of this modality in young patients and when the brainstem is partially or fully irradiated. Additional caution needs to be applied in the current area because

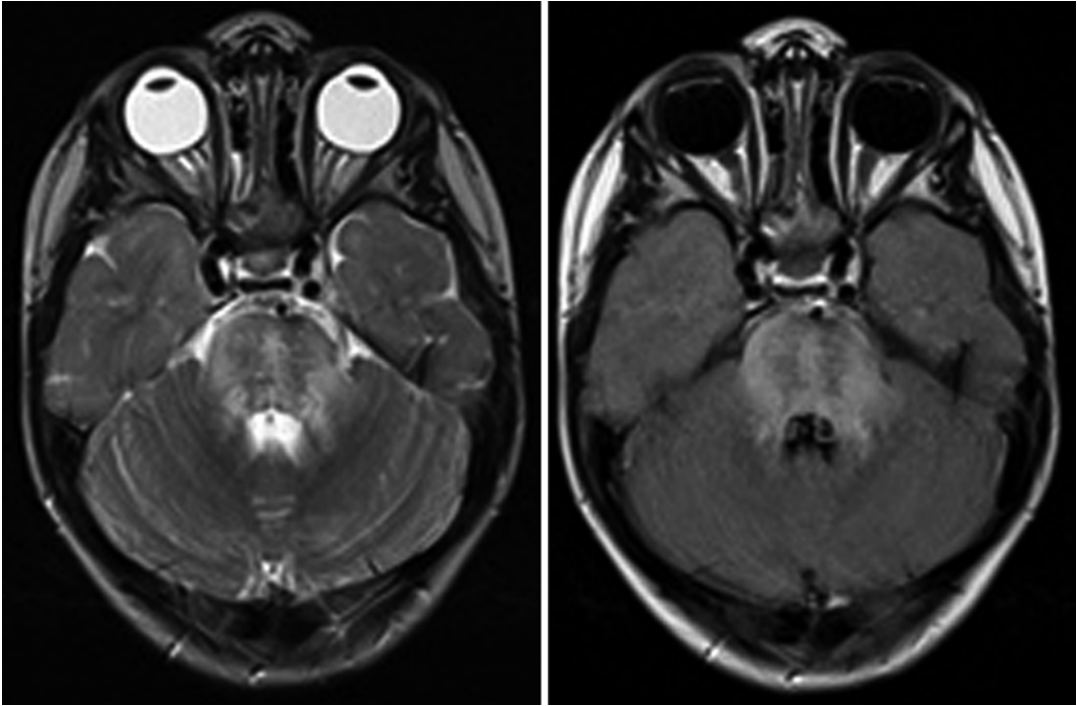


Fig. 7.9 Axial T2-weighted and FLAIR MRI demonstrating transient imaging changes in the brainstem of a child with ependymoma 6 months after completing

4 months of methotrexate-based chemotherapy and initiating proton therapy (5400CGE)

concurrent radiochemotherapy is becoming more widespread, and radiomimetic agents are often used before and after radiation therapy. The slight difference in radiobiological effectiveness may be exaggerated in such cases (Fig. 7.9).

Proton therapy is very expensive and requires industrial-size equipment (cyclotron, beam line, and gantry) for proper delivery in children with posterior fossa tumors. This type of treatment has been available for nearly 50 years but was only recently promoted for widespread clinical use by the industry with downscaled components and commercialization of hardware and software interfaces for clinical use. With the increasing number of proton facilities, more patients are being treated, and studies are underway to determine the potential benefits and risks. Considering that late effects may be a significant source of morbidity and mortality, the costs associated with proton therapy in selected cases may be justified. A review of the potential benefits of proton therapy in children with brain tumors that includes

dose-volume modeling was reported by groups from Memphis and Heidelberg [58].

Proton therapy is currently administered in the United States using the double-scattering method. Only a few centers worldwide are capable of performing the more sophisticated modulated pencil beam scanning method. Because proton therapy is in its early phase of development, there is little difference in the volume that receives the highest doses, and the real advantages are often limited to the volume that receives the lowest doses. This is illustrated in the comparative case of a relatively simple fourth ventricle differentiated ependymoma in a 6 year old child (Fig. 7.10). The original tumor was centered in the fourth ventricle and there was minimal bilateral extension into the foramen of Luschka. Comparing protons with photons, the volume of the brain receiving more than 50 % of the prescribed dose was nearly equivalent, but proton therapy resulted in exposure of a smaller volume receiving lower doses. Relevant to neuropsychological outcomes and

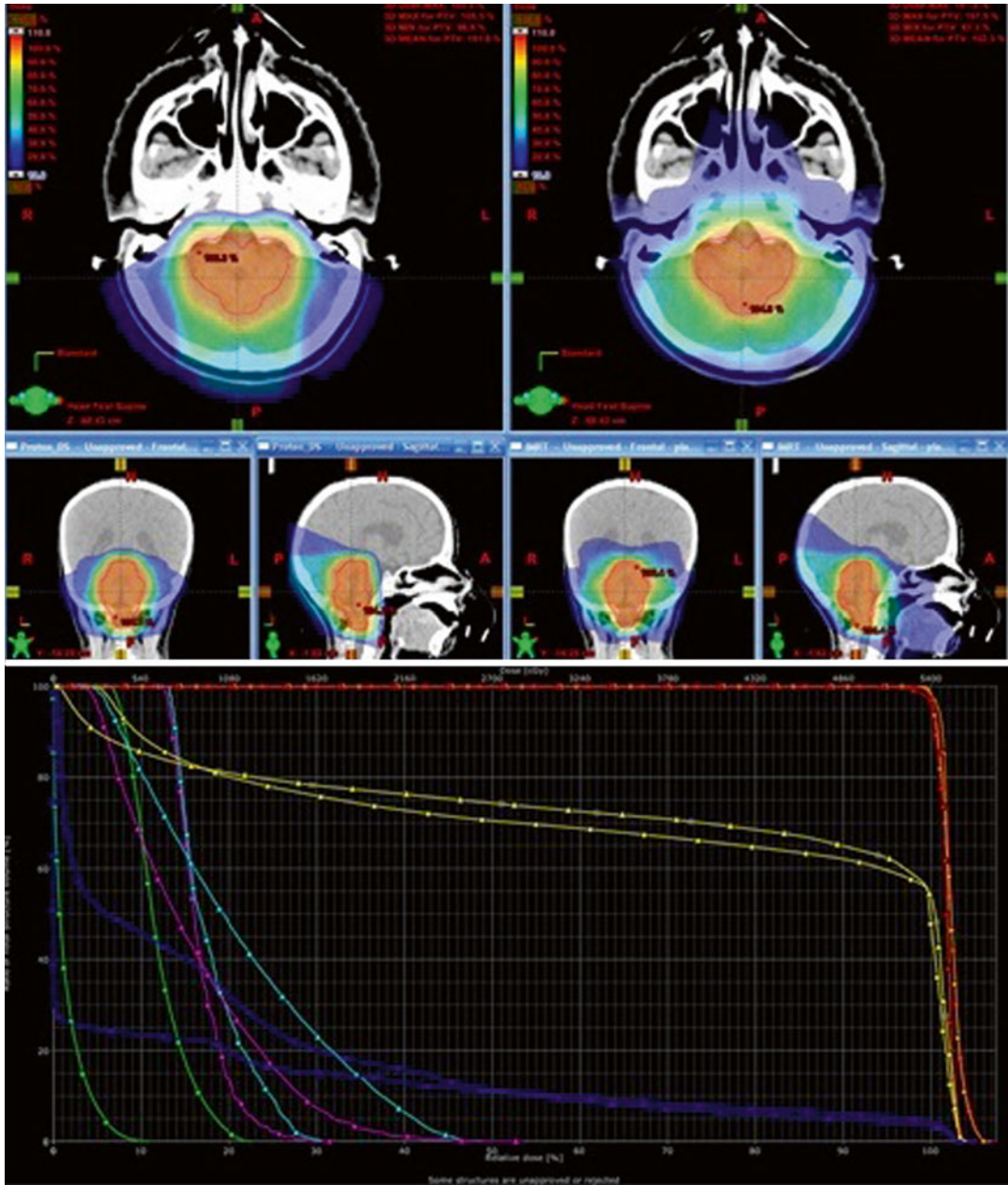


Fig. 7.10 Intensity-modulated photon therapy (left) compared to double-scattered proton therapy (right). Differences in the brain, cochleae, and hypothalamic dosimetry are shown in lower figure. Legend: proton – triangle, photon – square, red – target volume, yellow – brainstem, dark blue – brain, light blue – left cochlea, lavender – right cochlea, green – hypothalamus

available dose-effect models, this difference would not appear to be beneficial. The mean dose to the cochlea appears to be similar in both cases which would mean a low incidence of hearing

loss regardless of method. Finally, the proton therapy plan showed almost no dose to the hypothalamus whereas the photon plan, despite using intensity-modulated planning, resulted in dose

levels >10 Gy which would increase the risk of growth hormone deficiency and likely other endocrine effects during the first 5 years after treatment (Fig. 7.10).

References

1. SEER. Standard Populations (Millions) for Age-Adjustment. National Cancer Institute (NCI). 2011. 12-11-2010.

Ref Type: Online Source

2. CBTRUS (2010) Primary brain and central nervous system tumors diagnosed in the United States in 2004-2006. Hinsdale, Central Brain Tumor Registry of the United States. CBTRUS Statistical Report.

Ref Type: Report

3. International Commission on Radiation Units and Measurement (ICRU) (1993) Prescribing, recording and reporting photon beam therapy. ICRU. 50. Washington, DC.

Ref Type: Report

4. Beltran C, Krasin MJ, Merchant TE (2011) Inter- and intrafractional positional uncertainties in pediatric radiotherapy patients with brain and head and neck tumors. *Int J Radiat Oncol Biol Phys* 79(4):1266–74
5. Packer RJ, Gajjar A, Vezina G, Rorke-Adams L, Burger PC, Robertson PL, Bayer L, LaFond D, Donahue BR, Marymont MH, Muraszko K, Langston J, Spoto R (2006) Phase III study of craniospinal radiation therapy followed by adjuvant chemotherapy for newly diagnosed average-risk medulloblastoma. *J Clin Oncol* 24:4202–4208
6. Miralbell R, Fitzgerald TJ, Laurie F, Kessel S, Glicksman A, Friedman HS, Urie M, Kepner JL, Zhou T, Chen Z, Barnes P, Kun L, Tarbell NJ (2006) Radiotherapy in pediatric medulloblastoma: quality assessment of Pediatric Oncology Group Trial 9031. *Int J Radiat Oncol Biol Phys* 64:1325–1330
7. Merchant TE, Happersett L, Finlay JL, Leibel SA (1999) Preliminary results of conformal radiation therapy for medulloblastoma. *Neuro Oncol* 1:177–187
8. Merchant TE, Kun LE, Krasin MJ, Wallace D, Chintagumpala MM, Woo SY, Ashley DM, Sexton M,

- Kellie SJ, Ahern V, Gajjar A (2008) Multi-institution prospective trial of reduced-dose craniospinal irradiation (23.4 Gy) followed by conformal posterior fossa (36 Gy) and primary site irradiation (55.8 Gy) and dose-intensive chemotherapy for average-risk medulloblastoma. *Int J Radiat Oncol Biol Phys* 70:782–787
9. Gajjar A, Chintagumpala M, Ashley D, Kellie S, Kun LE, Merchant TE, Woo S, Wheeler G, Ahern V, Krasin MJ, Fouladi M, Broniscer A, Krance R, Hale GA, Stewart CF, Dauser R, Sanford RA, Fuller C, Lau C, Boyett JM, Wallace D, Gilbertson RJ (2006) Risk-adapted craniospinal radiotherapy followed by high-dose chemotherapy and stem-cell rescue in children with newly diagnosed medulloblastoma (St Jude Medulloblastoma-96): long-term results from a prospective, multicentre trial. *Lancet Oncol* 7:813–820
10. Ashley DM, Merchant TE, Zhou T, Coleman L, Pollack I, Duffner P, Burger P, Miller D, Buxton A, Douglas S (2008) Systemic chemotherapy, second look surgery and conformal radiation therapy limited to the posterior fossa and primary site for children >8 months and <3 years with nonmetastatic medulloblastoma: a Children's Oncology Group phase III Study (INF 12). Thirteenth International Symposium on Pediatric Neuro-Oncology (ISPNO). P9934.

Ref Type: Generic

11. Ashley DM, Lyon N, Bonner M, Michael M, Zhou T, Strother D, Merchant TE, Geyer R, Pollack I, Duffner P (2008) Developmental and functional outcome following postoperative chemotherapy and local conformal radiation in infants with medulloblastoma using a centrally administered phone-based interview technique (INF 5). Thirteenth International Symposium on Pediatric Neuro-Oncology (ISPNO).

Ref Type: Generic

12. Merchant TE, Zhu Y, Thompson SJ, Sontag MR, Heideman RL, Kun LE (2002) Preliminary results from a Phase II trial of conformal radiation therapy for pediatric patients with localised low-grade astrocytoma and ependymoma. *Int J Radiat Oncol Biol Phys* 52:325–332
13. Merchant TE, Li C, Xiong X, Kun LE, Boop FA, Sanford RA (2009) Conformal radiotherapy after surgery for paediatric ependymoma: a prospective study. *Lancet Oncol* 10:258–266
14. Pollack IF, Gerszten PC, Martinez AJ, Lo KH, Shultz B, Albright AL, Janosky J, Deutsch M (1995) Intracranial ependymomas of childhood: long-term outcome and prognostic factors. *Neurosurgery* 37:655–666

15. Rousseau P, Habrand JL, Sarrazin D, Kalifa C, Terrier-Lacombe MJ, Rekacewicz C, Rey A (1994) Treatment of intracranial ependymomas of children: review of a 15-year experience. *Int J Radiat Oncol Biol Phys* 28:381–386
16. van Veelen-Vincent ML, Pierre-Kahn A, Kalifa C, Sainte-Rose C, Zerah M, Thorne J, Renier D (2002) Ependymoma in childhood: prognostic factors, extent of surgery, and adjuvant therapy. *J Neurosurg* 97:827–835
17. Merchant TE, Jenkins JJ, Burger PC, Sanford RA, Sherwood SH, Jones-Wallace D, Heideman RL, Thompson SJ, Helton KJ, Kun LE (2002) Influence of tumor grade on time to progression after irradiation for localized ependymoma in children. *Int J Radiat Oncol Biol Phys* 53:52–57
18. Tihan T, Zhou T, Holmes E, Burger PC, Ozuysal S, Rushing EJ (2008) The prognostic value of histological grading of posterior fossa ependymomas in children: a Children's Oncology Group study and a review of prognostic factors. *Mod Pathol* 21:165–177
19. Merchant TE, Mulhern RK, Krasin MJ, Kun LE, Williams T, Li C, Xiong X, Khan RB, Lustig RH, Boop FA, Sanford RA (2004) Preliminary results from a phase II trial of conformal radiation therapy and evaluation of radiation-related CNS effects for pediatric patients with localized ependymoma. *J Clin Oncol* 22:3156–3162
20. Evans AE, Anderson JR, Lefkowitz-Boudreaux IB, Finlay JL (1996) Adjuvant chemotherapy of childhood posterior fossa ependymoma: cranio-spinal irradiation with or without adjuvant CCNU, vincristine, and prednisone: a Children's Cancer Group study. *Med Pediatr Oncol* 27:8–14
21. Robertson PL, Zeltzer PM, Boyett JM, Rorke LB, Allen JC, Geyer JR, Stanley P, Li H, Albright AL, McGuire-Cullen P, Finlay JL, Stevens KR Jr, Milstein JM, Packer RJ, Wisoff J (1998) Survival and prognostic factors following radiation therapy and chemotherapy for ependymomas in children: a report of the Children's Cancer Group. *J Neurosurg* 88:695–703
22. Clinical Trials. Phase II study of conformal radiotherapy for pediatric patients with localized ependymoma, chemotherapy prior to second surgery in pediatric patients with incompletely resected ependymoma, and observation only in pediatric patients with completely resected differentiated, supratentorial ependymoma. The Web Site of the National Cancer Institute (NCI)
23. Clinical Trials. Phase III randomized study of maintenance chemotherapy comprising vincristine sulfate, cisplatin, etoposide, and cyclophosphamide versus observation in pediatric patients with newly diagnosed ependymoma following induction chemotherapy and post-operative conformal radiotherapy. The Web Site of the National Cancer Institute (NCI)
24. Koshy M, Rich S, Merchant TE, Regine WF, Kwok Y (2009) Post-operative radiation improves overall survival in children age <3 years with intracranial ependymoma. *ASTRO*.
25. Rogers L, Pueschel J, Spetzler R, Shapiro W, Coons S, Thomas T, Speiser B (2005) Is gross-total resection sufficient treatment for posterior fossa ependymomas? *J Neurosurg* 102:629–636
26. Chang A, Merchant TE (2008) Patterns of failure for diffuse infiltrating brainstem glioma: New guidelines for radiotherapy planning. Thirteenth International Symposium on Pediatric Neuro-Oncology (ISPNO).

Ref Type: Generic

27. Moeller BJ, Chintagumpala M, Philip JJ, Woo SY, Wolff JE (2010) Proton radiotherapy for pediatric medulloblastoma: improved early ototoxicity. *Int J Radiat Oncol Biol Phys* 78:S18. [Abstract]
28. Vieira WA, Weltman E, Chen MJ, Silva NS, Cappellano AM, Pereira LD, Goncalves MR, Ferrigno R, Hanriot RM, Nadalin W (2010) Ototoxicity evaluation in medulloblastoma patients submitted to boost radiotherapy with intensity modulated radiation therapy (IMRT). *Int J Radiat Oncol Biol Phys* 78:S18–S19
29. Mulhern RK, Merchant TE, Gajjar A, Reddick WE, Kun LE (2004) Late neurocognitive sequelae in survivors of brain tumours in childhood. *Lancet Oncol* 5:399–408
30. Levisohn L, Cronin-Golomb A, Schmahmann JD (2000) Neuropsychological consequences of cerebellar tumour resection in children: cerebellar cognitive affective syndrome in a paediatric population. *Brain* 123(Pt 5):1041–1050
31. Hua C, Bass JK, Khan R, Kun LE, Merchant TE (2008) Hearing loss after radiotherapy for pediatric brain tumors: effect of cochlear dose. *Int J Radiat Oncol Biol Phys* 72:892–899
32. Merchant TE, Gould CJ, Xiong X, Robbins N, Zhu J, Pritchard DL, Khan R, Heideman RL, Krasin MJ, Kun LE (2004) Early neuro-otologic effects of three-dimensional irradiation in children with primary brain tumors. *Int J Radiat Oncol Biol Phys* 58:1194–1207
33. Fouladi M, Chintagumpala M, Ashley D, Kellie S, Gururangan S, Hassall T, Gronewold L, Stewart CF, Wallace D, Broniscer A, Hale GA, Kasow KA, Merchant TE, Morris B, Krasin M, Kun LE, Boyett JM, Gajjar A (2008) Amifostine protects against cisplatin-induced ototoxicity in children with average-risk medulloblastoma. *J Clin Oncol* 26:3749–3755
34. Hsu YC, Su CY (2006) Tympanoplasty for chronic otitis media in post-irradiated nasopharyngeal carcinoma patients. *Ann Otol Rhinol Laryngol* 115:330–333
35. Hartley KA, Li C, Laningham FH, Krasin MJ, Xiong X, Merchant TE (2008) Vertebral body growth after craniospinal irradiation. *Int J Radiat Oncol Biol Phys* 70:1343–1349
36. Fletcher DT, Warner WC, Muhlbauer MS, Merchant TE (2002) Cervical subluxation after surgery and irradiation of childhood ependymoma. *Pediatr Neurosurg* 36:189–196

37. Al-Mohanna H, Al-Khenaizan S (2010) Permanent alopecia following cranial irradiation in a child. *J Cutan Med Surg* 14:141–143
38. Ginot A, Doyen J, Hannoun-Levi JM (2010) Courdi A [Normal tissue tolerance to external beam radiation therapy: skin]. *Cancer Radiother* 14:379–385
39. Chua D, Krzakowski M, Chouaid C, Pallotta MG, Martinez JJ, Gottfried M, Curran W, Throuvalas N (2010) Whole-brain radiation therapy plus concomitant temozolomide for the treatment of brain metastases from non-small-cell lung cancer: a randomized, open-label phase II study. *Clin Lung Cancer* 11:176–181
40. Debus J, Hug EB, Liebsch NJ, O'Farrel D, Finkelstein D, Efrid J, Munzenrider JE (1997) Brainstem tolerance to conformal radiotherapy of skull base tumors. *Int J Radiat Oncol Biol Phys* 39:967–975
41. Lawrence YR, Li XA, El N I, Hahn CA, Marks LB, Merchant TE, Dicker AP (2010) Radiation dose-volume effects in the brain. *Int J Radiat Oncol Biol Phys* 76:S20–S27
42. Mayo C, Yorke E, Merchant TE (2010) Radiation associated brainstem injury. *Int J Radiat Oncol Biol Phys* 76:S36–S41
43. Robertson PL, Muraszko KM, Holmes EJ, Spoto R, Packer RJ, Gajjar A, Dias MS, Allen JC (2006) Incidence and severity of postoperative cerebellar mutism syndrome in children with medulloblastoma: a prospective study by the Children's Oncology Group. *J Neurosurg* 105:444–451
44. Morris EB, Li C, Khan RB, Sanford RA, Boop F, Pinlac R, Xiong X, Merchant TE (2009) Evolution of neurological impairment in pediatric infratentorial ependymoma patients. *J Neurooncol* 94:391–398
45. Merchant TE, Chitti RM, Li C, Xiong X, Sanford RA, Khan RB (2010) Factors associated with neurological recovery of brainstem function following postoperative conformal radiation therapy for infratentorial ependymoma. *Int J Radiat Oncol Biol Phys* 76:496–503
46. Wong ET, Huberman M, Lu XQ, Mahadevan A (2008) Bevacizumab reverses cerebral radiation necrosis. *J Clin Oncol* 26:5649–5650
47. Massengale JL, Levy RP, Marcellus M, Moes G, Marks MP, Steinberg GK (2006) Outcomes of surgery for resection of regions of symptomatic radiation injury after stereotactic radiosurgery for arteriovenous malformations. *Neurosurgery* 59:553–560
48. Merchant TE, Boop FA, Kun LE, Sanford RA (2008) A retrospective study of surgery and reirradiation for recurrent ependymoma. *Int J Radiat Oncol Biol Phys* 71:87–97
49. Boskos C, Feuvret L, Noel G, Habrand JL, Pommier P, Alapetite C, Mammar H, Ferrand R, Boisserie G, Mazon JJ (2009) Combined proton and photon conformal radiotherapy for intracranial atypical and malignant meningioma. *Int J Radiat Oncol Biol Phys* 75:399–406
50. Mullins ME, Barest GD, Schaefer PW, Hochberg FH, Gonzalez RG, Lev MH (2005) Radiation necrosis versus glioma recurrence: conventional MR imaging clues to diagnosis. *AJNR Am J Neuroradiol* 26:1967–1972
51. Packer RJ, Holmes E, Zhou T, Gajjar A, Vezina G (2010) Secondary malignant neoplasms (SMNS) following "successful" treatment of non-disseminated medulloblastoma (MB): a 10-year follow-up of patients treated on a COG study (SMNS). *ISPNO*. (ABSTRACT 29).

Ref Type: Generic

52. Merchant TE, Palmer SL, Lukose R, Wu S, Xiong X, Gajjar A (2010) Critical combinations of radiation dose and volume predict IQ and academic achievement after craniospinal irradiation in children. *ASTRO*.

Ref Type: Generic

53. Khatib ZA, Heideman RL, Kovnar EH, Langston JA, Sanford RA, Douglas EC, Ochs J, Jenkins JJ, Fairclough DL, Greenwald C (1994) Predominance of pilocytic histology in dorsally exophytic brain stem tumors. *Pediatr Neurosurg* 20:2–10
54. Pollack IF, Hoffman HJ, Humphreys RP, Becker L (1993) The long-term outcome after surgical treatment of dorsally exophytic brain-stem gliomas. *J Neurosurg* 78:859–863
55. Fujisawa H, Yoshida Y, Niida Y, Hasegawa M, Yamashita J (2005) Cyanotic breath-holding spell: a life-threatening complication after radical resection of a cervicomedullary ganglioglioma. *Pediatr Neurosurg* 41:93–97
56. Martin LD, Kaplan AM, Hernried LS, Fisher BJ (1986) Brainstem gangliogliomas. *Pediatr Neurol* 2:178–182
57. Sato K, Baba Y, Inoue M, Omori R (2003) Radiation necrosis and brain edema association with CyberKnife treatment. *Acta Neurochir Suppl* 86:513–517
58. Merchant TE, Hua CH, Shukla H, Ying X, Nill S, Oelfke U (2008) Proton versus photon radiotherapy for common pediatric brain tumors: comparison of models of dose characteristics and their relationship to cognitive function. *Pediatr Blood Cancer* 51:110–117
59. Bertin D, Vallero S, et al (2010) AIEOP (Associazione Italiana di Ematologia-Oncologia Pediatrica) SNC99 treatment protocol for standard risk childhood medulloblastoma: results of an Italian multicenter cooperative study.

Ref Type: Personal Communication

60. Lannering B et al (2011) HIT-SIOP PNET4 – A randomised multicentre study of hyperfractionated (HFRT) versus standard radiotherapy (StRT) in children with standard risk medulloblastoma.

Ref Type: Personal Communication

61. Allen J, Donahue B, Mehta M, Miller D, Rorke L, Jakacki R, Robertson P, Sposto R, Holmes E, Vezina G, Muraszko K, Puccetti D, Prados M (2008) Final report of CCG protocol 9931 for high-risk medulloblastoma/PNET: Neoadjuvant chemotherapy followed by hyperfractionated craniospinal radiotherapy. *Neuro Oncol* 3:479
62. Gandola L, Massimino M, Pecori E, Spreafico F, Berretta S, Pignoli E, Cefalo G, Luksch R, Poggi G, Ferrari A, Casanova M, Terenziani M, Bellani FF (2008) Hyperfractionated accelerated radiotherapy (Hart) and intensive postoperative chemotherapy for the treatment of metastatic medulloblastoma: Long term results of the milan strategy (PNET/MED16). Thirteenth International Symposium on Pediatric Neuro-Oncology (ISPNO).

Ref Type: Generic

63. Taylor R, Boota N, Bujkiewicz S, Lucas J, Robinson K, Robson K, Saran F, Michalski A, Pizer B (2008) Preliminary report of the children's cancer and leukemia group (CCLG) study of hyperfractionated accelerated radiotherapy (Hart) with chemotherapy for M1-3 Medulloblastoma (PNET/MED 37). Thirteenth International Symposium on Pediatric Neuro-Oncology (ISPNO).

Ref Type: Generic

64. St. Jude Children's Research Hospital. Treatment of patients with newly diagnosed medulloblastoma, supratentorial primitive neuroectodermal tumor, or atypical teratoid rhabdoid tumor (SJMB03). The Web Site of the National Institutes of Health
65. Clinical Trials. Phase III randomized adjuvant study of standard-dose versus reduced-dose craniospinal radiotherapy and posterior fossa boost versus tumor bed boost radiotherapy in combination with chemotherapy comprising vincristine, cisplatin, lomustine, and cyclophosphamide in pediatric patients with newly diagnosed standard-risk medulloblastoma. The Web Site of the National Cancer Institute (NCI)
66. Clinical Trials. Chemotherapy and radiation therapy in treating young patients with newly diagnosed, previously untreated, high-risk medulloblastoma or supratentorial primitive neuroectodermal tumor. The Web Site of the National Cancer Institute (NCI)

67. St. Jude Children's Research Hospital. Risk-adapted therapy for young children with embryonal brain tumors, choroid plexus carcinoma or ependymoma (SJYC07). The Web Site of the National Institutes of Health
68. Clinical Trials. Phase III study of induction therapy comprising vincristine, high-dose methotrexate, leucovorin calcium, etoposide, cisplatin, and cyclophosphamide followed by 3-dimensional conformal radiotherapy and high-dose consolidation therapy comprising carboplatin, thiotepa, and autologous peripheral blood stem cell rescue in pediatric patients with atypical teratoid/rhabdoid tumors of the central nervous system. The Web Site of the National Cancer Institute (NCI)
69. Kovnar EH, Curran W, Tomita T (1998) Hyperfractionated irradiation for childhood ependymoma: improved local control in subtotally resected tumors. *Childs Nerv Syst* 14:489. [Abstract]
70. Garvin J, Sposto R, Stanley P, Rorke L, Packer R (2004) Childhood ependymoma: Improved survival for patients with incompletely resected tumors with the use of pre-irradiation chemotherapy. International Symposium on Pediatric Neuro-Oncology (ISPNO).

Ref Type: Generic

71. Clinical Trials. Phase I pilot study of vincristine plus etoposide with concurrent radiotherapy in children with newly diagnosed diffuse intrinsic brain stem glioma. The Web Site of the National Cancer Institute (NCI)
72. Clinical Trials. Phase II pilot study of adjuvant temozolomide concurrently with postoperative radiotherapy and then alone as maintenance therapy in children with newly diagnosed anaplastic astrocytoma, glioblastoma multiforme, gliosarcoma, or diffuse intrinsic pontine glioma. The Web Site of the National Cancer Institute (NCI)
73. Clinical Trials. Phase I/II study of topotecan, filgrastim (G-CSF), and radiotherapy in young patients with newly diagnosed malignant intrinsic pontine brain stem glioma. The Web Site of the National Cancer Institute (NCI)
74. Clinical Trials. Phase II study of motexafin gadolinium and involved-field radiotherapy in pediatric patients with intrinsic pontine glioma. The Web Site of the National Cancer Institute (NCI)
75. Clinical Trials. Phase I/II study of vorinostat and local radiotherapy followed by maintenance vorinostat in pediatric patients with newly diagnosed intrinsic pontine gliomas. The Web Site of the National Cancer Institute (NCI)

Surgical Approaches to Pediatric Posterior Fossa Tumors

Benoit Jenny and Wirginia June Maixner

8.1 Introduction

The median suboccipital approach is the most commonly used approach to the posterior fossa in pediatric neurosurgery. In contrast to the retrosigmoid and far lateral approaches, it provides access to midline tumors in the cerebellum, particularly those arising from the fourth ventricle and the cerebellar vermis. Hemispheric cerebellar tumors may also be removed through this route, with a slight modification of the approach towards the side of the lesion. The most common pediatric posterior fossa tumors specifically pilocytic astrocytomas, medulloblastomas, or ependymomas can be removed with this approach. It provides access to the pineal region and permits the removal of those brain stem tumors with an exophytic component in the fourth ventricle.

Historically, surgery to the posterior fossa has not been without significant morbidity. Allen Starr, in 1893, published a series of 16 patients with cerebellar tumors, who had undergone attempted surgical resection. The tumor was not found in 11 patients, and of the 5 who had had tumor resection, 3 died [1]. In 1903, with improvement of

surgical technique, the same author described 58 surgical cases of cerebellar tumors with 16 being successfully removed and 8 deaths [2]. In 1909, the successful excision of a posterior fossa tumor in one patient was described. Interestingly it was noted that the major problem following tumor removal was control of bleeding, with the condition of the patient becoming “grave. The blood pressure fell... and a rapid closure was made with catgut.” After a stormy immediate postoperative course, this patient survived [3]. Over the last century, neurosurgical techniques improved substantially thus removing a posterior fossa tumor via a median suboccipital approach became standard practice. In 1996, Yasargil [4] modified the technique by dividing the median suboccipital approach into superior and inferior corridors. In the present day, the superior median approach provides good exposure of the inferior tentorial incisura, the dorsal mesencephalon, and the superior cerebellar hemisphere, while the inferior median approach provides access to the fourth ventricle and the posterior aspect of the pontobulbar region.

This chapter will highlight the general surgical principles necessary to enter the posterior fossa in the pediatric population. The relevant anatomy of the posterior fossa will be described with respect to the median suboccipital approach, with the different parts of the cerebellum accessed through this approach highlighted. Aspects of patient preparation relevant to this approach will be emphasized. The surgical

B. Jenny • W.J. Maixner, M.D. (✉)
Department of Neurosurgery,
Royal Children’s Hospital Melbourne,
Parkville, VIC, Australia
e-mail: wirgy@wirgy.com

techniques used in our department will be described incorporating the considerations of postoperative management.

8.2 Brief Overview of the Anatomy of the Posterior Fossa

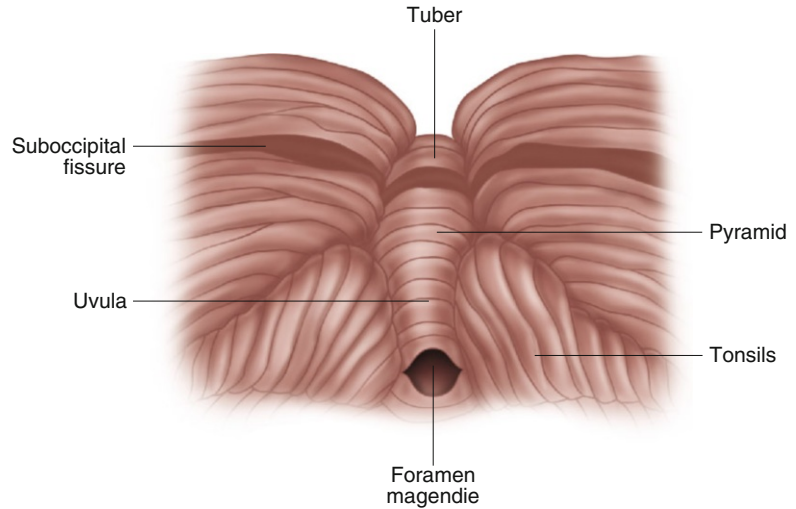
The surgical anatomy of the posterior fossa has been extensively illustrated by many authors. This section aims to provide a relevant overview only and readers are referred to the works of Yasargil and Rhoton for more detail [4, 5]. Briefly, the bony posterior fossa is surrounded anteriorly by the dorsum sellae and clivus and posteriorly and laterally by the occipital bone and the petrous and mastoid parts of the temporalis bone. On either side of the posterior fossa, the superior part of the petrous portion of the temporal bone provides attachment to the tentorium and contains the superior petrosal sinus. Posteriorly, both transverse sinuses delimit the superior aspect of the posterior fossa. They represent an important landmark to delineate the upper limit of the suboccipital craniotomy. The foramen magnum is positioned in the center of the floor of the posterior fossa and is delimited laterally by the occipital condyles, above which is situated the hypoglossal canal for the hypoglossal nerve. The jugular foramen is located between the lateral part of the occipital bone and the petrous portion of the temporal bone. Superior to the jugular foramen lies the internal acoustic meatus for the facial and acoustic nerves and internal auditory artery [6]. Posterior and superior to the foramen magnum are located the bilateral inferior occipital fossae which support the hemispheres of the cerebellum and are useful landmarks for burr hole placement. They are separated from each other by the internal occipital crest, which provides attachment to the falx cerebelli. It houses the occipital sinus, which can be a source of significant blood loss if not carefully closed during dural opening. The circular sinus, which traverses the posterior aspect of the foramen magnum, can also be a site of significant bleeding if not recognized during surgery [7].

The median suboccipital approach provides direct exposure of the cerebellum. The cerebellum presents three distinct surfaces: (1) the tentorial surface which faces the tentorium cerebelli and may be exposed in a superior median suboccipital approach, (2) the petrosal surface, retracted to access the cerebellopontine angle (usually via a retrosigmoid and far lateral approach), and (3) the suboccipital surface exposed in a median suboccipital craniotomy and through which access for most cerebellar tumors including access to the fourth ventricle is provided. This surface presents the cerebellar vermis and the two cerebellar hemispheres. The vermis is subdivided into the tuber superiorly and the pyramid and uvula inferiorly, separated by the horizontal suboccipital fissure which also divides the cerebellar hemispheres into superior and inferior parts. The suboccipital fissure delimits a superior and inferior surgical triangle providing access to either the superior part of the vermis including the culmen (superior triangle) or to the fourth ventricle, the inferior vermis, cerebellar hemispheres, and the foramen magnum (inferior triangle) (Fig. 8.1). The cerebellomedullary fissure is a natural cleft between the cerebellum and the medulla oblongata. It extends between the cerebellum and the medulla and forms part of the roof of the fourth ventricle [5]. It provides access to the fourth ventricle via the well-described telovelar approach through the tela choroidea [8].

The fourth ventricle, tentlike in appearance, is located between the cerebellum and brain stem. Dorsally, the roof is divided into superior and inferior parts. The ventricular surface of the superior part of the roof of the fourth ventricle is further divided into a median part formed by the superior medullary velum and two lateral parts formed by the inner parts of the cerebellar peduncles. Access to the fourth ventricle is therefore either by the cerebellomedullary fissure described above or through the vermis.

Understanding posterior fossa vasculature, in particular the supply to the cerebellum and the brain stem, is crucial to the safety of median suboccipital approaches. Three neurovascular complexes in the posterior fossa have been described by Rhoton [9]: an upper complex related to the

Fig. 8.1 Suboccipital surface of the cerebellum



superior cerebellar artery (SCA) which contains the midbrain; cranial nerves III, IV, and V; the cerebellomesencephalic fissure; the superior cerebellar peduncle; and the tentorial surface of the cerebellum. The middle complex, supplied by the anteroinferior cerebellar artery (AICA), contains the pons; the cranial nerves VI, VII, and VIII; the middle cerebellar peduncle; the cerebellopontine fissure; and the petrosal surface of the cerebellum. The lower complex, related to the posterior inferior cerebellar artery (PICA), contains the medulla and lower cranial nerves IX, X, XI, and XII. The PICA has the most tortuous course of the posterior circulation arteries and is exposed through a median suboccipital craniotomy. It is closely related to the cerebellomedullary fissure; coursing around the cerebellar tonsils, it enters the cerebellomedullary fissure and traverses the lower half of the roof of the fourth ventricle to finally exit the cerebellomedullary fissure. It provides branches that are distributed to the vermis and hemispheres of the suboccipital surface.

Veins of the posterior fossa may become an issue when enlarged due to tumor growth. They are divided into four groups: superficial, deep, brain stem, and bridging veins [7]. Of relevance to the median suboccipital approach are the large inferior vermian veins, which give rise to inferior hemispheric veins. These need to be carefully divided in midline approaches through the vermis.

This drawing represents an enlarged view of the suboccipital surface of the cerebellum. The suboccipital fissure divides the cerebellum into a superior and inferior part. Three different parts of the vermis are represented here: the tuber lies above the suboccipital fissure, the pyramid and the uvula below. The foramen of Magendie is located below the uvula, in the midline. The cerebellar tonsils lie lateral to the foramen of Magendie.

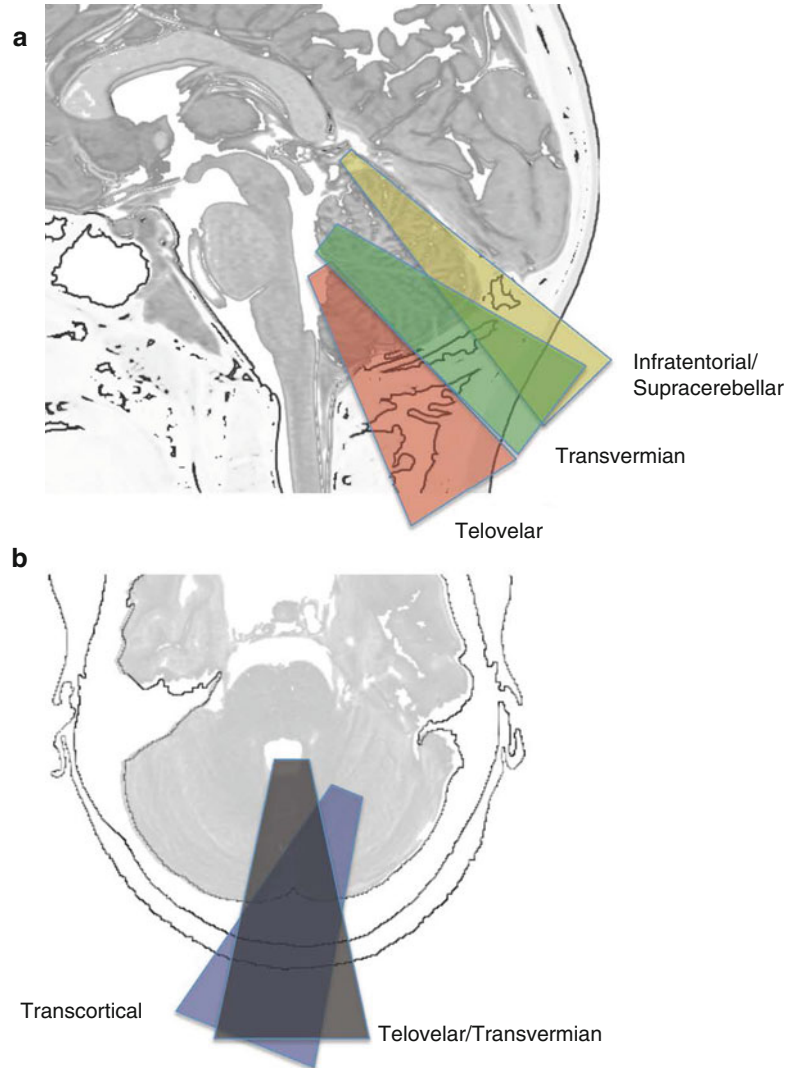
8.3 Goals of the Surgery

The aims of surgery for posterior fossa tumors, associated with brain stem compression and hydrocephalus, are (1) to decompress the brain stem and cerebellum, (2) to restore normal cerebrospinal fluid pathways through the fourth ventricle and the foramina of Luschka or Magendie, and (3) to attempt complete resection, without new neurological deficit, in order to improve postoperative survival.

8.4 Surgical Planning and Types of Approaches

The median suboccipital approach provides access to most pediatric tumors in the posterior fossa. Careful assessment of preoperative imaging

Fig. 8.2 Median suboccipital approaches to the posterior fossa. The main classical approaches to the posterior fossa via a median suboccipital approach are represented. **(a)** Sagittal view of the posterior fossa. Three surgical corridors are represented. In *yellow*, the infratentorial supracerebellar approach which gives access to pineal region tumors or to the superior part of voluminous posterior fossa tumors; in *green*, the transvermian approach, a classical route to access tumors from the vermis or within the fourth ventricle; in *red* the telovelar approach, which gives access to the fourth ventricle via the cerebellomedullary fissure after retraction of the cerebellar tonsils and dissection of the tela choroidea. **(b)** Axial view of the posterior fossa and the brain stem. Two surgical corridors are represented: in *gray* is the combination of the three approaches described above which are seen as one on this view. In *blue* is the corridor to access hemispheric tumors which have a median component



to determine tumor location within the fourth ventricle, the vermis, or cerebellar hemisphere is essential to determine the most appropriate surgical route and strategy. Depending on the tumor localization, approaches through a median suboccipital craniotomy can be classified into five major categories: (1) transcortical, (2) transvermian, (3) telovelar, (4) infratentorial supracerebellar, and (5) combined, involving a telovelar approach and a small inferior vermian incision or involving a telovelar approach and a supracerebellar approach as described recently [10]. Brain stem tumors can be resected either by a transvermian or telovelar approach (Figs. 8.2 and 8.3).

Initially, standard neurosurgical practice involved splitting the vermis to access “midline” posterior fossa tumors [11]. This approach was often associated with the known “cerebellar mutism syndrome” due to surgical incision of the vermis and lateral retraction to the dentate gyrus and its outflow tract [12–14].

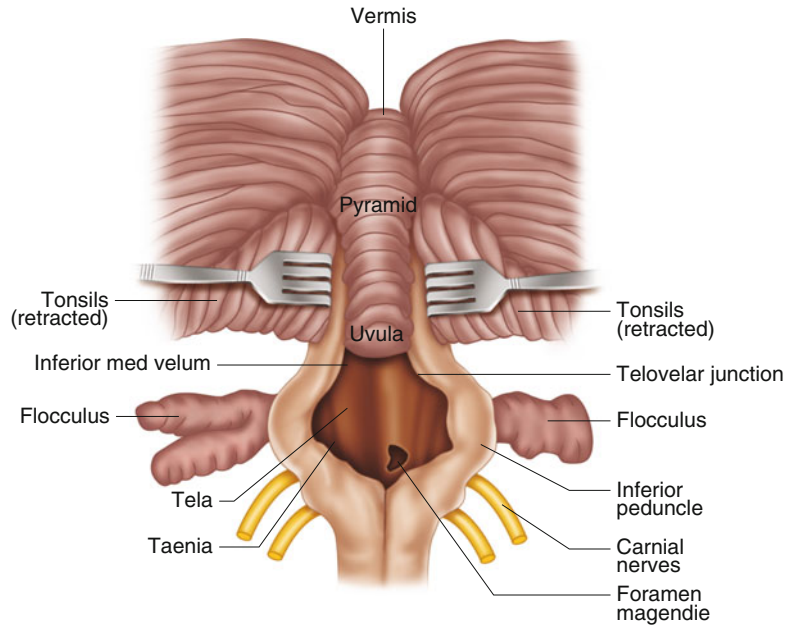
The telovelar approach is now a well-accepted surgical route and should be performed alone or in combination with incision of the inferior vermis dependent on the tumor size and its superior extension [15]. The microsurgical anatomy of this approach has been well described [8]. It involves gentle retraction of the tonsils laterally, which



Fig. 8.3 (a, b) Tumors of the fourth ventricle with compression of the vermis but no extensive vermian infiltration. These cases are good candidates to telovelar approach. (c) Tumor of the fourth ventricle with limited dimensions (<3 cm) but with extensive infiltration of the vermis. In this case telovelar approach with limited incision of the lower vermis was sufficient to achieve complete removal. (d) Tumor of the fourth ventricle with largest diameter >4 cm and extensive compression/

infiltration of the lower vermis. In similar cases incision of the lower vermis for traditional transvermian approach is usually necessary. (e) Large medulloblastoma of the upper vermis without involvement of the fourth ventricle. Transvermian approach with incision of the upper vermis is here the only option. (f, g) Medulloblastoma of the upper vermis with extensive lateral adhesion to tentorium. The tumor was completely removed through a supracerebellar approach

Fig. 8.4 Anatomy of the cerebellomedullary fissure



exposes both the tela choroidea and the inferior medullary velum. The tela choroidea is a thin arachnoid membrane and forms the lower portion of the inferior half of the roof of the caudal wall of each lateral recess. The foramen of Magendie delimits the lowest part of the membrane. In its superior parts and laterally to the uvula, it prolongs into the telovelar junction followed by the inferior medullary velum (Fig. 8.4). Opening of the tela gives access to the floor of the fourth ventricle, from the obex to the aqueduct. Further rostral opening of the velum gives additional access to the superior half of the roof of the fourth ventricle, the fastigium and the superolateral recess, a technique well described by Mussi [8].

Although this surgical corridor appears restricted, it has been shown to be sufficient to remove large fourth ventricle tumors without splitting the inferior vermis [15]. In cadaveric dissection it has been quantified, using triangles from defined anatomical points, that the telovelar approach with the removal of C1 posterior arch provided a larger working area than the transvermian approach except for a limited angle to the rostrum of the fourth ventricle [16]. These findings have been confirmed by other studies [17]. For ependymomas with lateral extension near the brain stem or cranial nerves, this surgical

corridor offers attractive possibilities, preventing potentially devastating complications associated with the transvermian approach [18]. For giant posterior fossa midline tumors, some surgeons have proposed a combined transventricular and infratentorial supracerebellar approach, highlighting that this was a safe technique, avoiding the incision of the vermis [10]. In contrast however, others have raised concerns regarding utilizing the telovelar approach for large fourth ventricular tumors, suggesting that a staged dissection of the tela and the uvulotonsillar cleft to be superior [19].

It is therefore imperative to consider on the basis of preoperative imaging the different approaches that are available and to define surgical strategy accordingly.

This drawing represents the surgical anatomy of the cerebellomedullary fissure. The tonsils have been retracted on both sides, and exposure of the tela choroidea on the left side of the drawing is seen. The inferior limit of the tela corresponds to the taenia and the superior part to the inferior medullary vellum. On the right side of the drawing, the tela has been removed, showing exposure of the fourth ventricle with the foramen of Magendie on its lowest aspect and the lateral limits represented by the inferior cerebellar peduncle.

8.5 Preoperative Consideration

8.5.1 Surgical Consent

Often, the diagnosis of a posterior fossa tumor in children is unexpected. Special care therefore needs to be taken in relaying the diagnosis and potential surgical risks to the parents [20]. Although surgical morbidity is low in most cases, significant neurological deficits are possible [21]. While the radiological appearances of the tumor may point to distinct pathologies, explicit management strategy discussions, particularly with respect to adjuvant chemotherapy and radiotherapy, should be delayed until the formal pathology is known. Signed consent is obtained from the parents. Age-appropriate information should be provided to the child regarding the proposed surgical procedure.

8.5.2 Anesthetic Considerations

Ideally, a specialized pediatric neuroanesthetic team should be involved with children, undergoing posterior fossa craniotomy for tumor excision. A full description of neuroanesthetic principles is however beyond the scope of this chapter. Of critical importance during surgery is monitoring for air embolism and hemodynamic fluctuations due to brain stem irritation or blood loss. The latter is of particular relevance in young children where rapid hypotensive shock can ensue. Routine anesthetic practice in our institution would include central venous and invasive arterial pressure monitoring and an indwelling urinary catheter. Mannitol is not given routinely. Perioperative antibiotic prophylaxis (cephazolin) and dexamethasone is used routinely.

8.5.3 Management of Hydrocephalus

The presence of hydrocephalus is assessed on preoperative imaging, and the necessity for its rapid treatment is dependent on the clinical state of the patient. If hydrocephalus does not need to be treated urgently, surgery to remove posterior

fossa tumors should be performed within 48 h of presentation and potentially on the day of admission if the child is critically unwell.

Different strategies are available to manage hydrocephalus in patients with posterior fossa tumors, including the insertion of an external ventricular drain (EVD), a ventriculoperitoneal shunt (VP) shunt, or performing a third ventriculostomy or the anticipated restoration of normal CSF flow secondary to tumor removal. There is no consensus yet as to which is the best option, often being dependent on surgical expertise and preference. The reader is referred to [Chap. 7](#) for a full discussion regarding hydrocephalus management in posterior fossa tumors. Recognition should be given, however, that unless critical the author's preference is to not treat the hydrocephalus separately to tumor removal.

Where significant hydrocephalus is present on preoperative imaging, the author's preference is to place an occipital EVD, prior to commencing the posterior fossa craniotomy. Reducing intracranial pressure in this way allows for a safer dural opening by reducing venous hypertension and reducing venous congestion of the cerebellum during the early phase of tumor removal. Where hydrocephalus is not severe, similar drainage of CSF may be enabled by entering into the cisterna magna initially prior to fully opening the dura. We would not recommend inserting a permanent VP shunt prior to surgery.

8.6 Operative Techniques

Different surgical techniques are available to remove posterior fossa tumors. General surgical principles, however, differ little between centers and thus we describe the surgical techniques used in our department.

8.6.1 Patient Positioning

Patient positioning depends on the surgeon's preference, and removing a pediatric posterior fossa tumor can be done in a prone "concorde,"

sitting or lateral position. The sitting position has the advantage that hemorrhage and CSF drain easily providing a clear operative field. It also provides superior exposure of the superior vermis and pineal region. It has the disadvantage of increased risk of air embolism, systemic hypotension, and intracranial air accumulation in the subdural and/or subarachnoid spaces. The surgeon's position during this approach with extended arms can be difficult to maintain.

In our neurosurgical unit all patients are operated upon in the prone position. The head is fixed in Mayfield pins if tolerated by the age of the patient; otherwise a soft horseshoe headrest is used. For small children extra padding is added to the horseshoe and to the dependent side of the head of the child to prevent pressure sores. Special attention is made to avoid pressure on the eyes. The eyes are filled with lubricant and covered to avoid inadvertent contamination by preparation solutions and blood. The patient is placed on a gel mat supported by gel rolls placed under the upper chest and pelvic regions. This allows the abdomen to be noncompressed improving venous return and aiding ventilation. A soft pad is placed under the patella tendon to allow the patella to have no contact with the mat, and the feet are elevated on a soft pillow. The rest of the patient is checked to avoid pressure areas.

The head is moderately flexed on an extended neck which opens the space between the foramen magnum and the posterior arch of C1. It is important not to compromise venous return thereby increasing cerebellar swelling. The bed is slightly tilted to place the occiput and the neck uppermost. View to the infratentorial space may be limited, due to the restricted head flexion during positioning, particularly in patients with a low-lying torcular.

A navigation system is utilized for all cases with posterior fossa tumors, even if positioning in pins is not possible. However, its utility once CSF and tumor cysts are drained is questionable.

After the patient's positioning has been checked, shaving is performed with the clipper which has been associated with a lower postoperative infection rate compared to the use of the razor [22]. At this stage of the preparation, it is important to have a visual concept of the anatomy

of the posterior fossa and its landmarks including the torcular, the transverse and sigmoid sinuses, and foramen magnum. It can be useful to draw the projection on the skin. An incision line is marked from the occipital protuberance to the level of C2 and the site of the potential insertion of the EVD.

8.7 Surgical Steps

8.7.1 Soft Tissue Preparation

The skin is prepped in three steps with chlorhexidine soap, alcoholic chlorhexidine solution, and alcohol. Care is taken not to allow the preparation solution to run down loosening taping of tracheal tubes and penetrating into the eyes. After draping, long-lasting local anesthetic is injected into the wound to improve the management of postoperative pain. A midline incision is carried out from the external occipital protuberance to the level of C2. In our experience, a midline incision is sufficient for most midline and hemispheric cerebellar tumors. Using monopolar cauterization, division of the fascia is performed in the avascular midline plane of the ligamentum nuchae. Either a linear midline incision can be made down to the bone with lateral exposure or a T-shaped incision of the fascia is made leaving a horizontal rim of tissue along the superior nuchal line (Fig. 8.5) used for later closure. The occipital bone is exposed to the foramen magnum. The posterior arch of C1 is exposed using a subperiosteal dissection technique with a combination of the monopolar cautery on low settings and sharp periosteal elevation. Bleeding from emissary veins is controlled with bone wax. In small children the posterior arch of C1 may be incompletely fused, and special attention is made not to cauterize the arch in the midline. The posterior arch of C1 is removed laterally up to the beginning of the groove of the vertebral artery. The atlantooccipital membrane is exposed. Careful dissection needs to be performed laterally to avoid injury to the vertebral arteries. A large circular sinus may cause significant bleeding but can often be controlled with the use of Surgicel® and pressure or bipolar electrocoagulation. Strong curved retractors are used to maintain adequate retraction of the muscles.

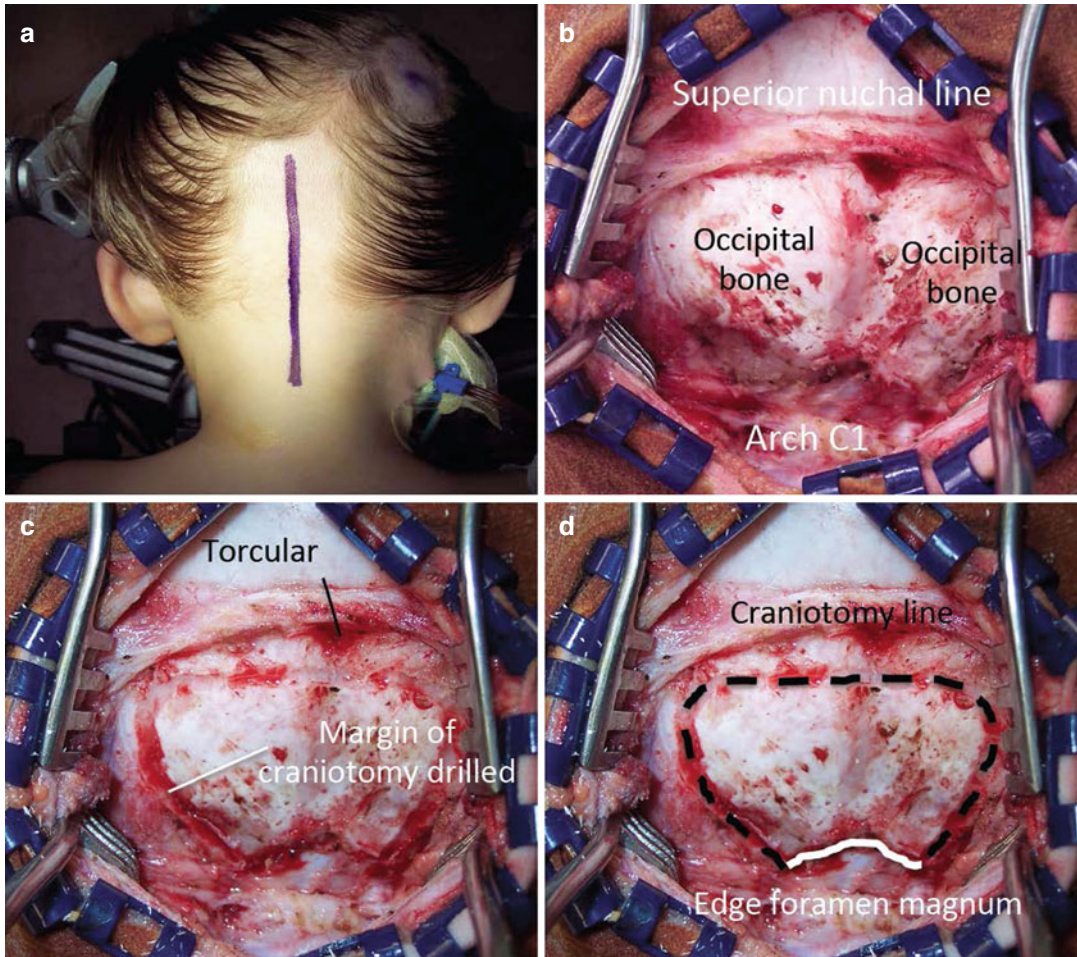


Fig. 8.5 Surgical steps to perform the suboccipital craniotomy flap. Representation of some of the different steps used to achieve a suboccipital craniotomy. (a) The incision line is drawn on the skin of the patient from the posterior occipital protuberance down to a level of C2. (b) Image representing the exposure of the occipital bone with the posterior arch of C1 and the atlantooccipital

membrane. The T-shaped incision of the muscle fascia along the superior nuchal line can be appreciated. (c) The edge of the craniotomy flap has been drilled with the M8 Midas Rex drill®. (d) Picture representing the line of the craniotomy edge which has been drilled (*curved dashed line*). The posterior aspect of the foramen magnum is exposed (*white line*)

8.7.2 Suboccipital Craniotomy

It is now well recognized that a suboccipital craniotomy with replacement of the bone flap is to be preferred to a craniectomy. It limits postoperative pseudomeningocele formation and headache [23]. The limits of the craniotomy can be drawn on the occipital bone. To elevate the bone flap, two options are possible: one is the placement of two burr holes on each side of the occipital plate just below the transverse sinus. The opening is then completed with the high-speed craniotome cutting a curved

line down to the foramen magnum. The cut joining the two burr holes just below the torcular can be initiated with the craniotome and completed with the drill or rongeurs to remove the triangular occipital crest. The second option is to elevate the entire bone flap with the high – speed M8 Midas Rex drill® (Fig. 8.5), which is our preferred option especially in small children. It allows preservation of the maximum size of the bone flap and provides also a safe option for bone removal in the midline below the torcular, and note should be made that posterior fossa tumors, particularly pilocytic astrocytomas,

may cause remodelling and marked thinning of the occipital bone. On elevation of the bone flap, the dura around the foramen magnum may be quite adherent. This can be separated by detaching the membranes with a scalpel or sharp periosteal elevator, always maintaining contact with the bone to avoid cerebellar/brain stem injury, and occasionally a fine point diathermy on low settings.

8.7.3 Opening of the Dura

Usually, the dura is opened in a Y-shaped or extended U-shaped fashion, starting above the cerebellar hemispheres and working down towards the midline at the level of the circular sulcus. Opening the dura in a tight posterior fossa, however, may be a difficult task due to the significant bleeding which may occur during division of the midline occipital sinus and due to tumor/cerebellar herniation. In this instance an EVD inserted to drain associated hydrocephalus or the tumor cyst may be drained. Alternatively the dura may be opened over the cisterna magna first allowing CSF egress. There are different ways of approaching the occipital sinus, we tend to use metal clips (Weck clips™) to progressively occlude and cut the sinus from each side and avoid major sudden bleeding. Alternatively the sinus may be oversewn. Once the dura is opened, a suture is inserted to the apex of the dura flap, which is reflected upward to limit bleeding from epidural spaces. Sutures are used around the Y-shaped dura opening to increase surgical exposure to the cerebellum and cisterna magna and limit extradural bleeding.

8.7.4 Tumor Excision

Midline cerebellar and fourth ventricular tumors can be often seen by gentle retraction of the cerebellar tonsils, division of the tela choroidea, and occasionally inferior vermian incision. Bilateral retractors are placed laterally to maintain exposure. Particular attention needs to be made to the inferior vermian and retromedullary portion of the PICA in this approach. Hemispheric tumors can be appreciated due to discoloration and swelling of the cerebellar surface. Cystic hemispheric

tumors may require cyst drainage with a Cushing needle prior to tumor dissection if swelling is significant otherwise initial preservation of the cyst is advantageous for the gradual dissection of the tumor wall from the cerebellar parenchyma.

As a general concept for tumor excision, the use of the Cavitron ultrasonic aspirator (CUSA) enables definition of the plane between the tumor and the adjacent cerebellar parenchyma. Dissection in this plane is performed, in general, prior to tumor debulking particularly in vascular tumors. This limits blood loss and improves the chance of complete excision particularly in low-grade astrocytomas.

Intraventricular tumors may be detached from the floor of the fourth ventricle via the CUSA except when direct tumor infiltration has occurred. In this case, resection should be stopped to avoid permanent neurological damage. The upper limit of the dissection of intraventricular tumors requires visualization of the aqueduct of Sylvius in general in order to confirm CSF flow reconstitution.

Once the tumor has been removed, the margins must be carefully inspected for residua.

8.7.5 Hemostasis

A critical part of the surgery is to achieve perfect hemostasis, which is done by coagulation of focal bleeding within the cavity of resection and local tamponade with cotton balls. If hemostasis cannot be achieved this way due to diffuse bleeding, hemostatic material such as fibrillary Surgicel® may be used. Hemorrhage into the ventricular system is to be avoided to minimize postoperative hydrocephalus, thus may be achieved by temporarily plugging the aqueduct of Sylvius with a small cottonoid. This should be removed when closing. Similarly the spinal subarachnoid space should be protected with temporary cotton pledgets.

8.7.6 Closure

A critical part of the surgery is dural closure. Opinions on whether the dura can be left open or not vary. As a principle we advise for watertight

closure to prevent the formation of pseudomeningocele, to reconstitute normal CSF pathways, and to restore normal anatomy should reoperation be necessary. In our practice we use a 5.0 Prolen® continuous suture and a pericranial duroplasty when necessary. Once the dura is closed, we place a square of Surgicel® over the suture line.

The bone flap is repositioned and attached to the edge of the craniotomy with 3.0 vicryl sutures or plates, but in children we recommend the use of sutures to secure the bone flap.

Muscle layers are closed with 3.0 vicryl sutures in the deeper layers. It is important that the “dead space” left between the dura and the inferior part of the craniotomy near the foramen magnum is minimized during this closure. The fascia layer is closed with 3.0 vicryl sutures in interrupted sutures. Perfect closure of this layer is critical to prevent CSF leak through the wound. The subcutaneous layers are closed with 3.0 vicryl sutures and the skin with running 5.0 vicryl rapide. The wound is then cleaned; the hair of the patient washed and a trimmed primapore dressing placed over the wound. A crepe bandage is applied.

8.8 Postoperative Management

In our practice patients are awoken and extubated directly after surgery. During this transition period it is important to minimize patient coughing to minimize the risk of venous bleeding. Once extubated patients are observed in recovery for 1–2 h. Neurological observations and vital parameters are obtained frequently and regularly. Once patients have regained an adequate conscious state, they are transferred to the neurosurgical ward in the high dependency unit, for continuous monitoring and neurological observation. Hemoglobin, blood cell count, electrolytes, and the C-reactive protein are monitored in the immediate postoperative period and for the following days until normalization. In our experience monitoring in an intensive care unit is not routinely necessary. Antibiotics are maintained for 24 h. Pain is relieved if a morphine infusion via a pump or patient controlled anesthesia (PCA) is administered. The wound is checked regularly for signs of CSF leakage or infection. Patients are

kept in the hospital until they have regained independent safe mobility and normal fluid and dietary intake, typically a period of 5–7 days.

8.9 Morbidities

Although safe in experienced hands, removal of a posterior fossa tumor in a child may still be associated with a range of minor to serious complications which can occur during the operative and perioperative periods.

Intraoperative morbidity can be due to a number of events including (1) significant bleeding in a highly vascularized tumor making it difficult to differentiate tumor, from adjacent important structures; (2) neurological impairment due to direct surgical trauma to the floor of the fourth ventricle, the medulla, or the lower cranial nerves particularly in tumors invading the fourth ventricular floor or extending into the cerebellomedullary and cerebellopontine cisterns, to the dentate nucleus leading to cerebellar mutism, or to the superior vermis leading to cerebellar ataxia; and (3) vascular injury to arterial brain stem perforators and PICA with resultant brain stem or cerebellar infarction.

Mild new postoperative neurological deficits, as temporary ataxia, mild diplopia, or mild facial hemiparesis, occur in about a third of the patient population and are reversible [21].

Postoperative complications may occur including the formation of a pseudomeningocele, CSF leakage through the wound, infection, meningitis, and persistent hydrocephalus.

Conclusions

The median suboccipital approach provided access to most posterior fossa tumors in the pediatric population. Different techniques can be used to perform the craniotomy and to remove the tumor. We have highlighted our goals and methods for this surgery. We feel that modern tools such as the high-speed drill, the ultrasonic aspirator, and a neuronavigation system should be used routinely to operate on these children in order to achieve maximum tumor removal and avoid neurological deficits to the patient.

References

1. Starr A (1893) Brain surgery. William Wood & Company, New York
2. Starr MA (1903) Organic nervous disease. Lea Brothers & Co, New York
3. Diller T (1909) The writings of Benjamin Franklin pertaining to medicine and the medical profession. *Aesculapian* 1(2):65–84
4. Yasargil (1996) Surgical approaches. In: Yasargil (ed) *Microneurosurgery of CNS tumours*. Thieme, Stuttgart, New York
5. Rhoton AL Jr (2000) Cerebellum and fourth ventricle. *Neurosurgery* 47(3 Suppl):S7–S27
6. Rhoton AL Jr (2000) The foramen magnum. *Neurosurgery* 47(3 Suppl):S155–S193
7. Rhoton AL Jr (2000) The posterior fossa veins. *Neurosurgery* 47(3 Suppl):S69–S92
8. Mussi AC, Rhoton AL Jr (2000) Telovelar approach to the fourth ventricle: microsurgical anatomy. *J Neurosurg* 92(5):812–823
9. Rhoton AL Jr (2000) The cerebellar arteries. *Neurosurgery* 47(3 Suppl):S29–S68
10. Hermann EJ, Rittierodt M, Krauss JK (2008) Combined transventricular and supracerebellar infratentorial approach preserving the vermis in giant pediatric posterior fossa midline tumors. *Neurosurgery* 63(1 Suppl 1):ONS30–ONS35; discussion ONS35–ONS37
11. Epstein FJ, Goh KC (2000) Ependymomas of the posterior fossa. In: Kaye AH, Black P (eds) *Operative neurosurgery*. Churchill Livingstone, London, pp 429–436
12. Kotil K et al (2008) Cerebellar mutism following posterior fossa tumor resection in children. *Turk Neurosurg* 18(1):89–94
13. Dailey AT, McKhann GM 2nd, Berger MS (1995) The pathophysiology of oral pharyngeal apraxia and mutism following posterior fossa tumor resection in children. *J Neurosurg* 83(3):467–475
14. Kellogg JX, Piatt JH Jr (1997) Resection of fourth ventricle tumors without splitting the vermis: the cerebellomedullary fissure approach. *Pediatr Neurosurg* 27(1):28–33
15. El-Bahy K (2005) Telovelar approach to the fourth ventricle: operative findings and results in 16 cases. *Acta Neurochir* 147(2):137–142; discussion 142
16. Deshmukh VR et al (2006) Quantification and comparison of telovelar and transvermian approaches to the fourth ventricle. *Neurosurgery* 58(4 Suppl 2):ONS-202–ONS-206; discussion ONS-206–ONS-207
17. Tanriover N et al (2004) Comparison of the transvermian and telovelar approaches to the fourth ventricle. *J Neurosurg* 101(3):484–498
18. Shimoji K et al (2009) Surgical considerations in fourth ventricular ependymoma with the transcerebellomedullary fissure approach in focus. *Child Nerv Syst* 25(10):1221–1228
19. Rajesh BJ et al (2007) Telovelar approach: technical issues for large fourth ventricle tumors. *Child Nerv Syst* 23(5):555–558
20. Greenberg ML, Hargrave D, Bond J (2004) Information needs for children and families. In: Walker DA (ed) *Brain and spinal tumors of childhood*. Arnold, London
21. Di Rocco C (1999) Cerebellar astrocytomas. In: Choux M (ed) *Pediatric neurosurgery*. Churchill Livingstone, London
22. Alexander JW et al (1983) The influence of hair-removal methods on wound infections. *Arch Surg* 118(3):347–352
23. Kurpad SN, Cohen AR (1999) Posterior fossa craniotomy: an alternative to craniectomy. *Pediatr Neurosurg* 31(1):54–57

Giuseppe Mirone, Pietro Spennato, and Giuseppe Cinalli

9.1 Introduction

Midline suboccipital craniotomies expose the fourth ventricle, upper brainstem, and pineal region, and it is widely used for lesions such as tumors of the culmen, pineal tumors, medulloblastoma, cerebellar hemisphere astrocytoma, ependymoma of the fourth ventricle, and foramen magnum tumors.

Otherwise, lateral suboccipital approaches (Fig. 9.1) give access to the cranial nerves, lateral brainstem, vertebrobasilar artery, extra axial lesions, and some lateral brainstem lesions. Upper lateral suboccipital and combined suboccipital approaches provide access to the tentorial area, incisura, upper clivus, upper cranial nerves, and petrous bone. Neurinomas, meningiomas, epidermoids, dermoids, chordomas, chondromas, metastases, and cysts constitute the majority of tumors in these regions.

In July 1897, Fedor Krause performed a unilateral suboccipital craniotomy in a patient

with a tumor involving the CPA [1]. Different neurosurgeons modified and refined the surgical technique [2–7], so that the Dandy's approach with an ipsilateral suboccipital flap [5, 6] evolved to what we call nowadays the retrosigmoid approach.

As indicated by Bassiouni et al., an extended suboccipital craniotomy including C1–C3 laminectomy was first performed in 1927 for successful removal of a foramen magnum meningioma [7]. These were among the first descriptions of posterolateral approaches to the posterior fossa and the craniocervical junction. It was not until more recently, however, that the far-lateral approach gained popularity. A combination of these approaches may be used for complex lesions of this region.

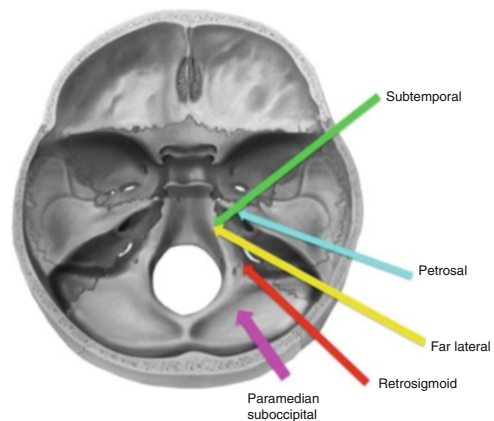


Fig. 9.1 Lateral approaches to posterior cranial fossa and its contents

G. Mirone (✉) • G. Cinalli, M.D.
Division of Pediatric Neurosurgery, Department of Neuroscience, Santobono-Pausilipon Children's Hospital, Naples, Italy

Department of Neurosurgery,
University of L'Aquila, L'Aquila, Italy
e-mail: peppemirone@fastwebnet.it;
giuseppe.cinalli@gmail.com

P. Spennato, M.D.
Division of Pediatric Neurosurgery,
Department of Neuroscience, Santobono-Pausilipon Children's Hospital, Naples, Italy

9.2 Surgical Anatomy of the Posterior Fossa and Craniovertebral Junction

9.2.1 Muscles

Several layers of musculature must be traversed during the exposure of the occiput and cervical vertebrae. The occipitofrontalis muscle is found superior to the line of attachment at the superior nuchal line than the trapezius, and sternocleidomastoid muscles are disconnected from the superior nuchal line. The sternocleidomastoid muscle is attached also to the posterolateral mastoid process. The deeper muscular layer includes the semispinalis capitis, splenius capitis, and longissimus capitis muscles. The first two muscles attach either on or below the superior nuchal line, while the longissimus capitis muscle, located most laterally of the three muscles, attaches to the mastoid process. The obliquus capitis superior, obliquus capitis inferior, rectus capitis posterior minor, and rectus capitis posterior major muscles form the deepest layer of musculature closest to the cervical vertebrae. To gain access to the occipitocervical junction and vertebral artery, their attachments to the occipital bone, to the spinous processes of C1 and C2, and to the transverse process of C1 must be resected.

The suboccipital triangle is a region bounded superiorly and medially by the rectus capitis posterior major muscle, superiorly and laterally by the superior oblique muscle, and inferiorly and laterally by the inferior oblique muscle. The floor of this space is occupied by the posterior atlanto-occipital membrane and the posterior arch of the atlas and within the triangle run both the extradural terminal segment of the vertebral artery and the first cervical nerve [8–10].

9.2.2 Occipital Artery

On the posterior side of the external carotid artery, at the level of the posterior belly of the digastric muscle, the occipital artery originates. It runs along the muscle to the mastoid where it passes under the longissimus and splenius

capitis muscles forming two terminal branches. The lateral branch carries on vertically upwards in the subcutaneous layer. The medial branch continues horizontally as far as the union before turning through a right angle to carry on vertically across the trapezius muscle, ending in the subcutaneous tissue. A paramedian skin flap hinged at the bottom to expose the posterior fossa can become necrotic if the stalk is too narrow.

9.2.3 The Vertebral Artery: The V3 and V4 Segments

The anatomy of the vertebral artery, especially the V3 and V4 segments, must be kept in mind when approaching lateral posterior fossa and the craniovertebral junction.

The V3 segment, also known as the “suboccipital segment,” extends from the C2 transverse process to the dura mater of the foramen magnum. Its course can be subdivided in three parts: a vertical segment, between the transverse processes of C2 and C1; a horizontal segment in the groove of the posterior arch of the atlas; and an oblique segment up to the dura mater [11]. The V3 segment is enclosed by a periosteal sheath that invaginates into the lateral dura at the level of the foramen magnum, thus forming a double furrow for 3–4 mm: indeed, the periosteal sheath is in continuity with the outer layer of the dura. The VA adventitia, adherent to the double furrow, forms sort of distal fibrous ring, so that, despite being the most mobile part, the V3 segment is fixed at its ends. Anatomical relations of the VA are modified by head movements of rotation, as well as during surgical positioning.

The V4 segment runs from the dura up to the anterior side of the pontomedullary sulcus where it joins the contralateral one to form the basilar artery. Initially, the V4 segment faces posteriorly and medially the occipital condyle, the hypoglossal canal, and the jugular tubercle. Later, the V4 segment lies on the clivus and runs in front of the hypoglossal and the lower cranial nerves rootlets. From the V4 segment originate several important branches: the PICA, the anterior spinal artery,

and the anterior and posterior meningeal arteries. The PICA origin can be variable: at, above, or below the FM level [12].

9.2.4 Venous Sinuses Relationships to Bony Landmarks

Despite the wide use of modern imaging guidance technology, the knowledge of superficial landmarks and their relationship to deeper intracranial structures are crucial in surgical planning of a lateral approach, and it is one of the keys to access the posterior fossa. The transverse sinus, the transverse-sigmoid junction, and the sigmoid sinus are deeply placed within a large bony groove which makes the first burr hole quite risky if wrongly planned. The precise placement of burr holes has several advantages allowing an accurate and small craniectomy laterally enough to decrease the risk of significant cerebellar retraction during approaches to the cerebellopontine angle. The asterion, a horizontal line from the superior aspect of the zygomatic arch (“zygomatic line”) and a vertical line from the mastoid notch (“mastoid line”), was thought to be the most important surface landmarks to localize the transverse and sigmoid junction [13].

9.2.5 Lower Cranial Nerves

The glossopharyngeal (CN IX), vagus (CN X), and spinal accessory (CN XI) nerves start as rootlets from the postolivary sulcus and go into the jugular foramen, passing ventral to the choroid plexus protruding from the foramen of Luschka and dorsal to the vertebral artery.

The accessory nerve is composed of rootlets originating from both the spinal cord and the medulla. Spinal rootlets join together to form the main trunk, which ascends through the foramen magnum running behind the dentate ligament and unites with the upper medullary rootlets.

The hypoglossal nerve (CN XII) arises from rootlets of the preolivary sulcus. It runs antero-lateral through the subarachnoid space and

pass behind the vertebral artery to reach the hypoglossal canal. Rarely, the VA separates the CN XII rootlets [14, 15].

9.2.6 The Greater Occipital Nerve

The greater occipital nerve is formed by the medial branch of the dorsal ramus of C2 that runs between the posterior arch of the atlas and lamina of the axis. The greater occipital nerve ascends between the inferior oblique and the semispinalis capitis muscles. It pierces the semispinalis capitis and the trapezius between the superior and inferior nuchal lines (2 cm below and lateral to the external occipital protuberance [16]). This nerve supplies the skin of the back of the scalp as far forward as the vertex of the skull. Obviously, transverse incision in this region could damage the nerve.

9.3 Surgical Approaches

9.3.1 General Principles

Preoperative clinical evaluation of the patient with lesions in the lateral part of the posterior fossa or close to the craniocervical junction is crucial. The clinical examination, as well as the radiologic information, will often help to decide from which direction to approach the ventral midline lesion in these lateral approaches (usually on the side with the pre-existing neurologic deficits). A careful preservation of the contralateral lower cranial nerves during tumor removal prevents devastating functional deficits with the airway speech, and oromotor functioning, often related to bilateral lower cranial nerve damage.

Valuable information can be gained from neuroimaging. CT allows assessment of the bony components of the craniocervical junction, mostly the occipital condylar-atlas-axis joint interfaces, and a view through the bony aperture of the foramen magnum. MRI indicates the extent of the lesion in relation to the brainstem and the upper spinal cord within the

posterior fossa. MRI angiography (MRA) helps to study vertebral artery anatomy and patency. If the surgeon is forced or plans to sacrifice one of the vertebral arteries, conventional angiography can provide more detailed anatomic information, as well as the functional status of the contralateral vertebral artery by a balloon occlusion test.

Neurophysiological monitoring is recommended during lateral suboccipital exposures. It includes somatosensory-evoked potentials, auditory-evoked responses, the monitoring of the facial nerve, and often cranial nerves IX through XII. Motor-evoked potentials are monitored when intraparenchymal tumors are resected.

The lateral suboccipital approaches have been usually performed with the patients in a lateral, park-bench, or sitting position. Even if the sitting position is ideal, most anesthetists reject its routine use for the lateral suboccipital approach because of a higher risk of air embolism. In the lateral or park-bench position, the shoulder of the pediatric patient, especially children whose neck is short, sometimes restricts both the surgeon's operative maneuvers and the direction of view of the microscope. Care must be taken to minimize tension on the cervical spine and brachial plexus with use of shoulder or axillary rolls where applicable.

9.3.2 Paramedian Unilateral Suboccipital

Possible indications for unilateral paramedian approach include hemispheric tumors of the cerebellum, angiomas, hemorrhages, space-occupying infarcted areas of the cerebellar hemisphere, malformations, and inflammatory processes.

The patient can be positioned both in the sitting and in the prone position. Use of the sitting position for surgery requires use of precordial ultrasonography and a central venous access at the level of the superior vena cava/right atrium for detection and treatment of air embolism. In both cases, the head is fixed in a three-pin head holder and carefully rotated about 30° toward the side of the lesion. Either an S-shaped or a straight skin incision may be used.

The greater occipital nerve and the accompanying artery and vein sometimes cannot be spared. As far as possible, the musculature is entered along the natural borders of adjoining muscles while the deeper muscles are divided by monopolar coagulation.

The first burr hole is planned in the occipital squama and the bone defect is extended to the desired size osteoclastically by forceps or by the craniotome forming a paramedian flap. The dura over the cerebellar hemisphere can be carefully opened in a cruciate fashion. At this point in case of intracerebellar lesions, neuronavigation or ultrasound can be very helpful in localizing the lesion. Sometimes it can be useful to insert a ventricular catheter under ultrasound guidance until the lesion (e.g., an hemorrhage) and then to follow the catheter into the cerebellar parenchyma until the lesion.

The dura is closed with interrupted sutures. Elevation sutures of the dura are placed prior to closure of the dura and are tied after the closure. Covering of the bone gap created by the osteoclastic craniotomy is not necessary. The wound is closed in layers.

Common errors during this approach can be overlooked: blood loss during the operation from skin, muscle, and/or bone especially in small children; lesions of the dura or cerebellar cortex; lost of orientation inside the cerebellar hemisphere; and postoperative bleeding from the cerebellar surface, from bridging veins, or due to inadequate dural elevation sutures.

9.3.3 Retrosigmoid Approach (Lateral Suboccipital Approach) (Figs. 9.7 and 9.8)

The retrosigmoid approach to the cerebellopontine angle is still an evolution of the lateral suboccipital craniectomy described by Dandy in 1929 and in 1934 [5, 6], which was later made through a straight lateral incision as proposed by Adson in 1941 [3] and then extended laterally and inferiorly as was already emphasized by Bucy in 1951 [4].

The retrosigmoid approach allows access to posterolateral pons, lateral middle cerebellar

peduncle, superior lateral medulla, and cerebellopontine angle.

Typical indications for retrosigmoid approach include space-occupying processes in the cerebellopontine angle, arteriovenous malformations, aneurysms, compression syndromes of cranial nerves, inflammatory processes, and tumors [17].

Cerebellopontine angle can be described as a pyramid-shaped space but inclined anteromedially with its apex extending to the posterior clinoid process and the base facing the inner surface of the squamosal part of the temporal and occipital bones. The superior side corresponds to the retrosellar area including the III cranial nerve and the inferior surface of the tentorium. The inferomedial side is close to the foramen magnum, including the vertebral artery and XII cranial nerve. The anterior side is represented by the posterior surface of the petrous bone, while the posterior side is limited by the petrosal surface of the brainstem and cerebellum. The medial third of the pyramid has the highest density of vital structures as the SCA, AICA, and PICA and the third to twelfth of cranial nerves.

Different variations of the shape, placement, and size of the retrosigmoid craniotomy can be planned to reach different target structures in the area of cerebellopontine angle.

The intradural compartments of the cerebellopontine angle are divided into (1) an inferior petroclival space with the medulla and the foramen magnum, (2) a middle space, and (3) a superior petroclival space.

These three compartments contain different neurovascular complexes: the upper around the trigeminal nerve, the middle around the vestibulocochlear-facial complex, and the lower around the lower cranial nerves [18, 19].

For a retrosigmoid approach the patient is placed in the horizontal position, either in the so-called park-bench (three quarters prone) position or in the supine position with the head turned away by about 30–40° from the surgeon. Each position offers different advantages and drawbacks.

We perform this approach with the patient fixed in the prone position with the neck rotated

25–30° to the side of the lesion and with the operating table rotated approximately 20° in the same direction. The surgeon is in a sitting position beside the contralateral shoulder of the patient so he can easily access the operative field, because the patient's shoulder contralateral to the lesion is shifted downward. In this way, the height of the patient's shoulder ipsilateral to the lesion is much lower than that in the lateral position, and it is also advantageous for a far-lateral approach.

The auricle is retracted with adhesive tape (or a suture). A slightly S-shaped skin incision is preferred. After soft tissue dissection, the key anatomical landmarks of the lateral temporo-occipital bones are precisely defined: the zygomatic arch, external auditory meatus, suprameatal crest, mastoid process and incisura, asterion, and external occipital protuberance. The asterion, defined as the junction of the lamboid, the occipitomastoid, and the parietomastoid sutures, has been proven a reliable marker in order to localize the junction between the transverse and sigmoid sinuses. The superior nuchal line is also identified by drawing a line from the root of the zygoma to theinion and the transverse-sigmoid junction is avoided by planning the burr holes below this line (1 or 2 cm below the asterion).

A craniotomy measuring approximately 3–5 cm in diameter is completed, bordering anteriorly the sigmoid sinus and superiorly the transverse sinus. Venous hemorrhages into the bone are controlled with bone wax, and emissaries are likewise sealed. If retrosigmoid mastoid air cells are entered, they must be exenterated of mucosa and then packed with muscle and iodinated bone wax.

The dura is subsequently widely opened in a curved fashion following the borders of the craniotomy, and the cerebellopontine angle is brought into view. Bridging veins can be coagulated and divided, to avoid they are not torn during placement of retractors and dissection. The cerebellum normally tends to fall away from the tumor once the subarachnoid space is opened and so it needs only to be very lightly retracted (Fig. 9.8). At this point, all the neurovascular structures in

the cerebellopontine angle are identified, and if available, neuromonitoring is used to look for cranial nerves. The facial nerve can be identified at or near the brainstem, and it is important to limit electrocautery as much as possible, depending on gentle blunt dissection to dissect blood vessels away from the lesion and the eighth cranial nerve, while using Gelfoam to stop light venous oozing. If the tumor is bulky, it may be decompressed with the use of an ultrasonic aspirator at this point.

At the end of the procedure, the intradural space is filled with Ringer solution at body temperature. The dura is closed with interrupted or continuous sutures in a watertight fashion, if necessary with the aid of a dural patch graft. The craniotomy and overlying soft tissues are then closed in standard fashion.

Common pitfalls can be wrong patient positioning (compression of the main cervical vessels or severe venous congestion in the posterior fossa), inaccurate placement of the burr holes (injury to venous sinuses), inadequate removal of CSF (severe cerebellar contusion due to spatula pressure), injury to sensitive vessels, and nerves in the cerebellopontine angle due to microsurgical dissection.

9.3.4 Far-Lateral Approach (Posterolateral Approach) (Figs. 9.2–9.7, 9.10, and 9.11)

The far-lateral approach, first developed by Seeger [20], has been an effective means of addressing intradural anterior and anterolateral craniovertebral junction lesions. The basic description of the far-lateral approach does not include resection of the occipital condyle, but the surgical corridor can be expanded by removing more bone from the cranial base (Fig. 9.9), which may be necessary depending on the nature, location, and extent of the lesion. Several variations of the far-lateral approach, including the transcondylar, supracondylar, and paracondylar approaches, have been proposed [21–27, 28–31]. These may be combined with other exposures as needed to optimally address each specific situation [32–37].

The anterior and lateral cervicomedullary junction, the foramen magnum, the lower clivus, medulla, lower pons, and lateral aspect of the inferior cerebellum are optimally accessed by the far-lateral approach (or posterolateral approach).

Accessible lesions include both intradural and extradural tumors as meningio-

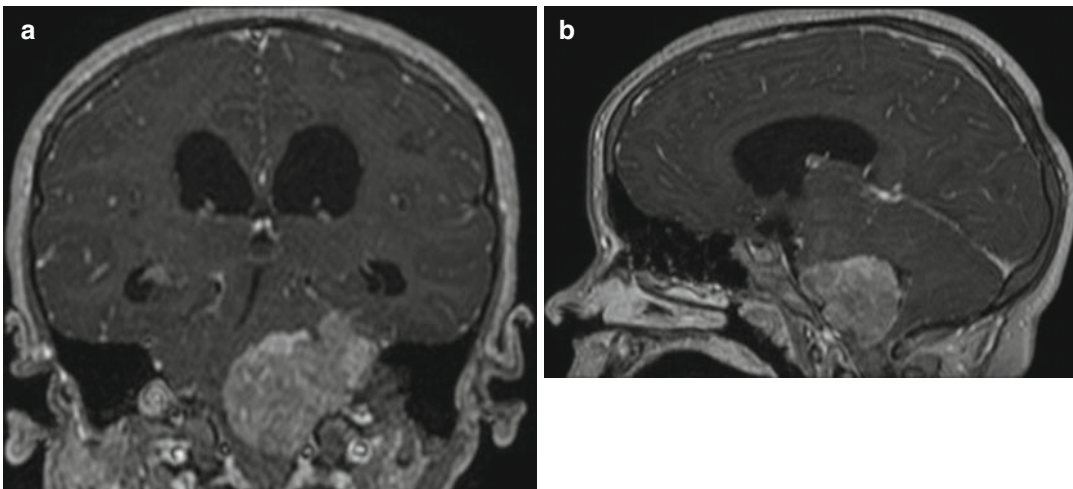


Fig. 9.2 Foramen magnum meningeoma in a 7-year-old girl with NF1. (a–c) Contrast-enhanced T1-weighted MRI scans that demonstrate a ventral, left-sided meningeoma at the foramen magnum. The mass reveals homogeneous enhancement on post-contrast injection with dural tail.

(d) There is significant mass effect and compression of the medullo-cervical region posteriorly. This tumor was completely resected using a far-lateral approach and suboccipital craniotomy with C1 laminectomy

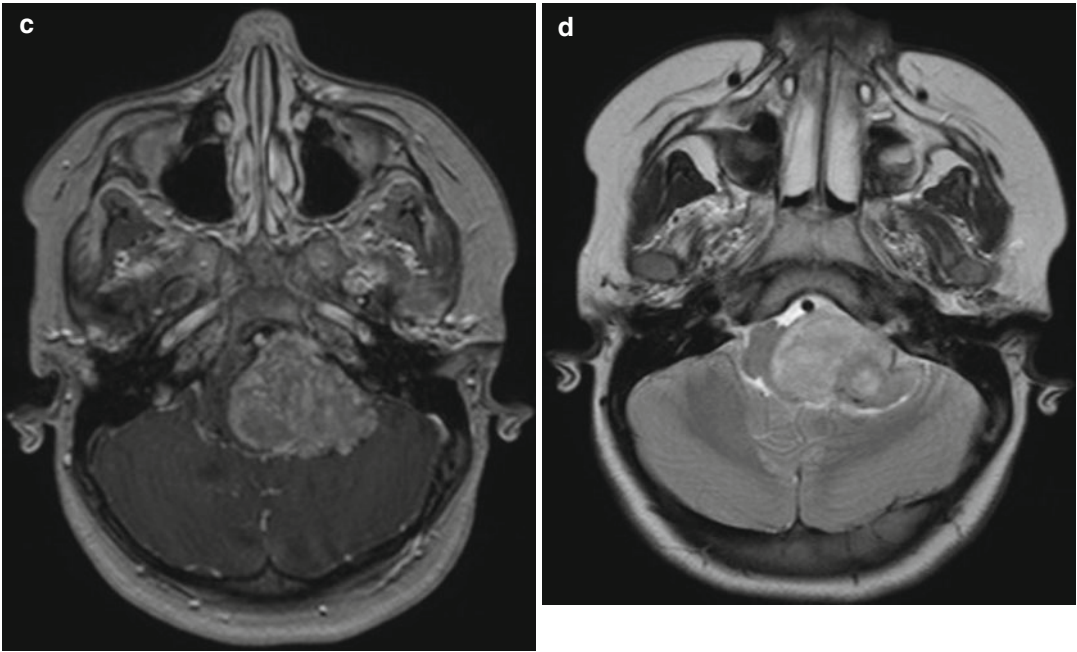


Fig. 9.2 (continued)

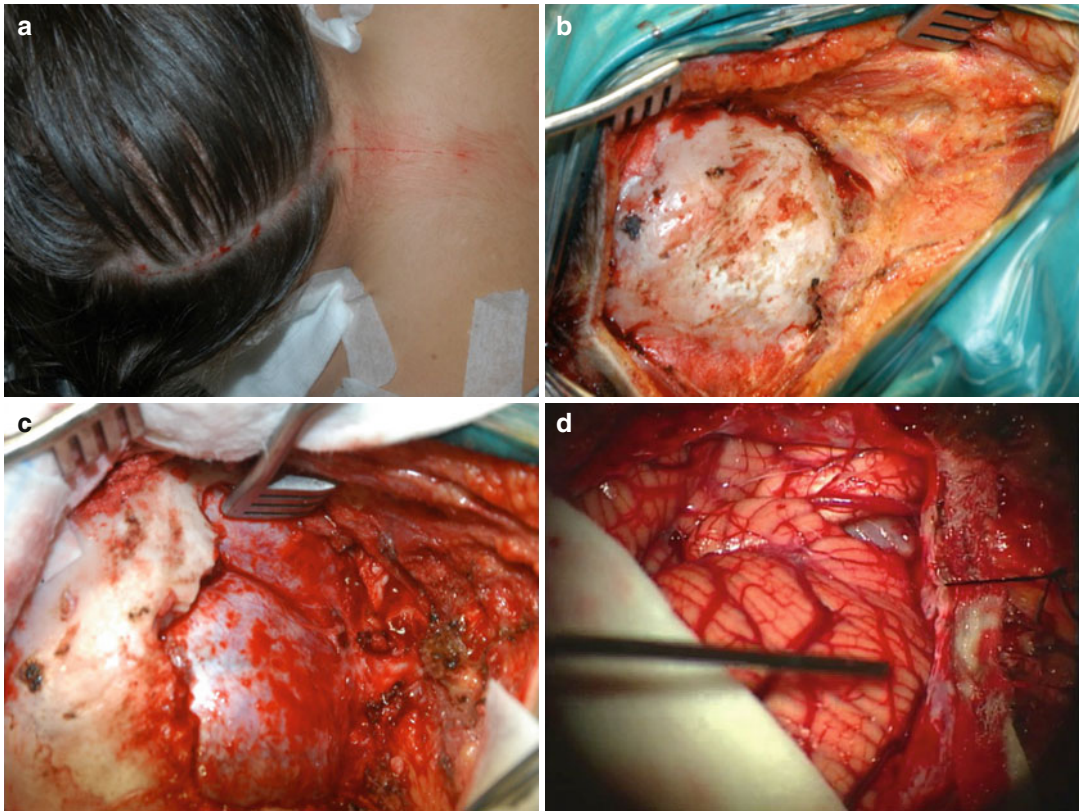


Fig. 9.3 Foramen magnum meningioma in a 7-year-old girl with NF1 (same as Fig. 9.2). (a) S-shaped skin incision. (b) Lateral suboccipital craniotomy with C1 lami-

nectomy. (c) After dural opening, the tumor appears under the left cerebellar tonsil that was partially resected (d) to enlarge the operative corridor

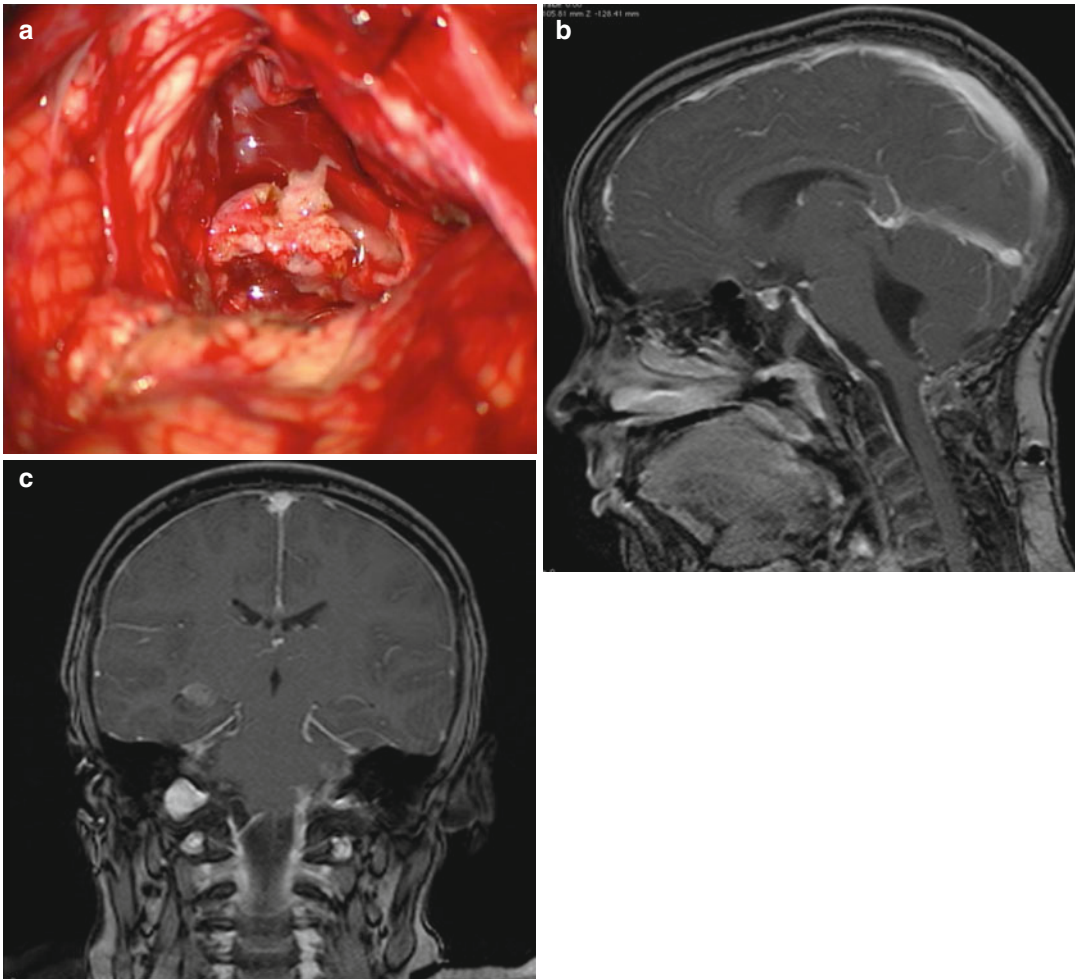


Fig. 9.4 Foramen magnum meningioma in a 7-year-old girl with NF1 (same as Figs. 9.2 and 9.3). (a) At the end of resection, a small piece of the tumor remains on the

vertebral artery. (b, c) Contrast-enhanced T1-weighted MRI scans at 3-year follow-up showing no recurrence

mas (Figs. 9.2–9.6), large glomus tumors, ependymoma (Figs. 9.7–9.9), vascular lesions of the brainstem and aneurysms of proximal basilar artery and PICA, and chondro-osseous lesions (Figs. 9.10 and 9.11) in the proximity of the craniocervical junction as chondromas [25, 28, 30, 33].

The key concept of the far-lateral approach is to access lesions of the craniocervical junction, with the benefits of proximal control and mobilization of the vertebral artery, minimal rotation and retraction of the neural axis, and the opportunity to combine other approaches, such

as the subtemporal and suboccipital approaches, to expand the field of exposure.

Key steps involve the identification and eventually the mobilization of the vertebral artery from the C2 transverse foramen to its intradural entry, bony removal of the lateral occipital bone and occipital condyle, partial or total laminectomy of the atlas and axis, tumor removal, and stabilization of the craniocervical junction, if necessary.

We use a modified park-bench position. The patient's neck is flexed in the anteroposterior plane, rotated 45° to the contralateral shoulder,

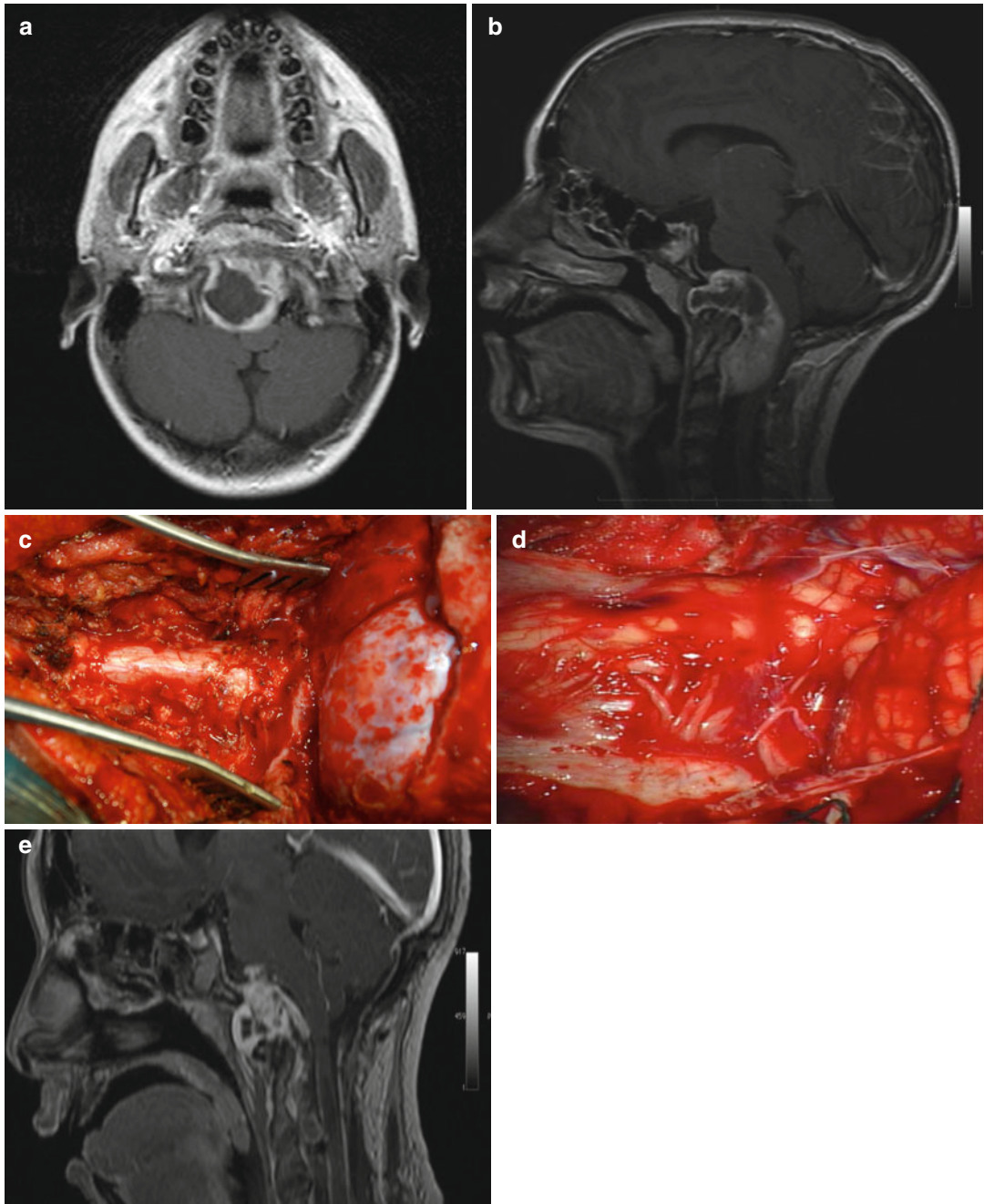


Fig. 9.5 Malignant peripheral nerve sheath tumor of the foramen magnum in a 12-year-old girl with NF1. (a, b) Preoperative contrast-enhanced T1-weighted MRI: the cystic regions did not enhance compared to the rest of the mass background that enhanced intensely.

(c) Far-lateral suboccipital approach combined with cervical laminotomy until C4. (d) After dural opening the tumor is removed working through the first cervical roots. (e) Postoperative MRI showing subtotal tumor removal with good decompression of the craniovertebral junction

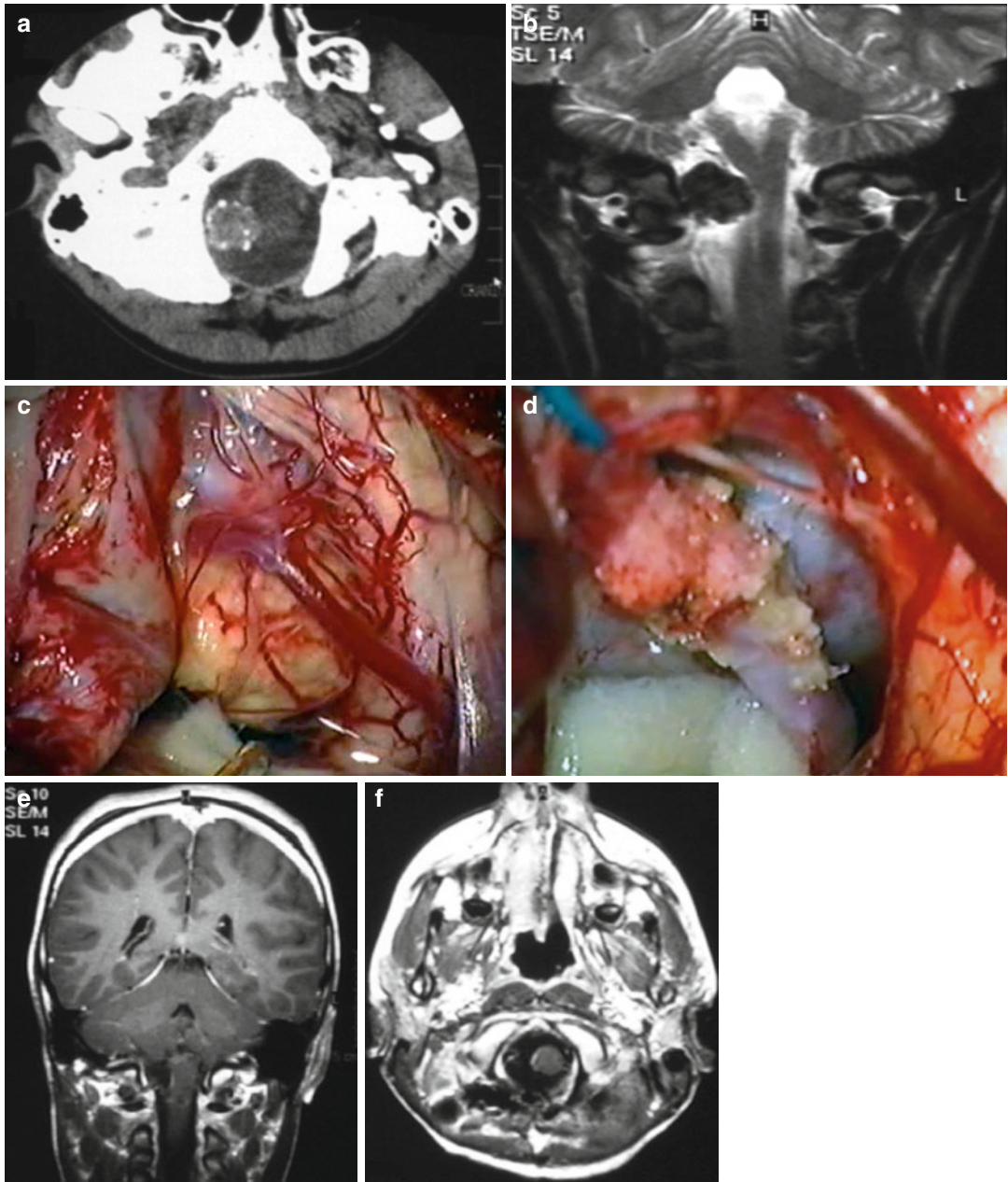


Fig. 9.6 Meningioma of the foramen magnum in a 10-year-old boy. **(a)** Preoperative CT showing calcification inside the tumor. **(b)** Preoperative MRI showing compression of the medullo-cervical region. **(c)** Meningioma exposed by a right far-lateral approach. **(d)** After gross tumor removal, a small piece of meningioma encasing the right vertebral artery is not resected. **(e, f)** Postoperative MRI showing no recurrence after 5 years

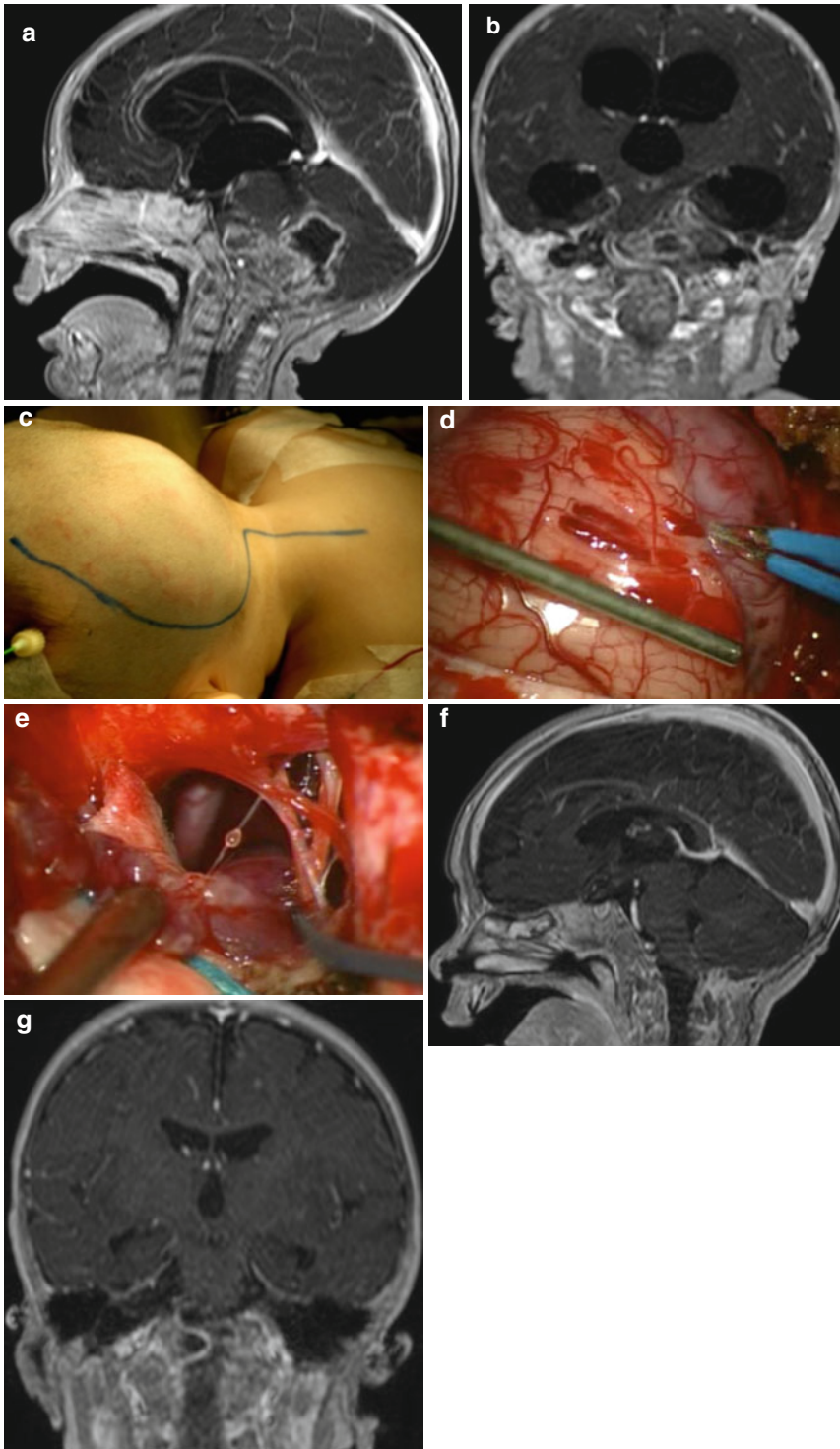


Fig. 9.7 Anaplastic ependymoma of the left cerebellopontine angle extending in the cervical region in a 3-year-old boy. (a, b) Preoperative contrast-enhanced T1W MRI showing the extension of the tumor. (c) Skin incision for a combined far-lateral and retrosigmoid approach.

(d) Tumor removal laterally to the left cerebellar hemisphere and the cerebellopontine angle. (e) Tumor removal at the craniovertebral junction between C1 roots and the displaced left vertebral artery. (f, g) Postoperative MRI showing complete removal

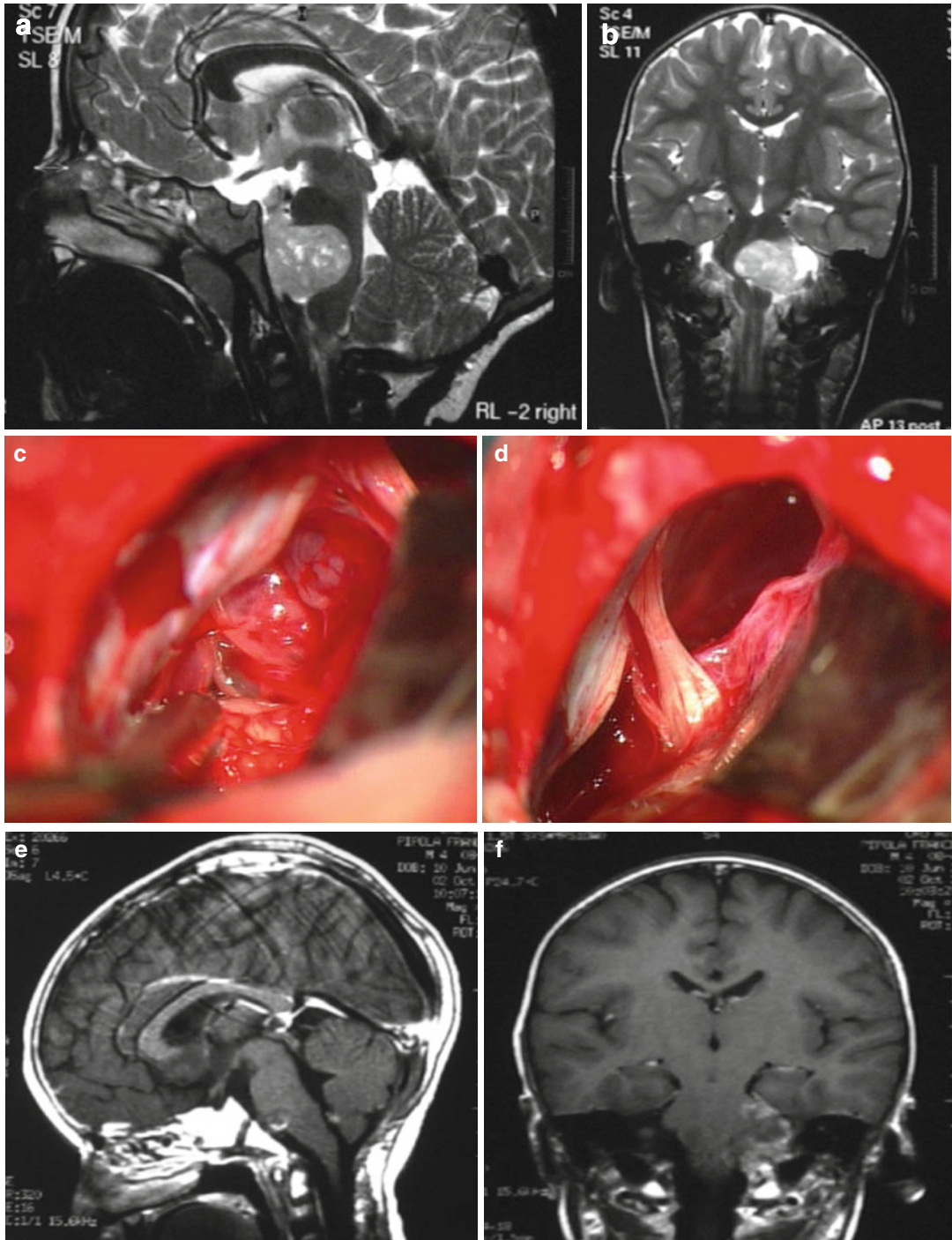


Fig. 9.8 PNET of the left cerebellopontine angle in a 4-year-old boy. (a, b) Preoperative MRI showing the extension of the tumor. (c, d) Tumor removal in the left cerebellopontine angle by a retrosigmoid approach. (e, f) Postoperative MRI at 2-year follow-up

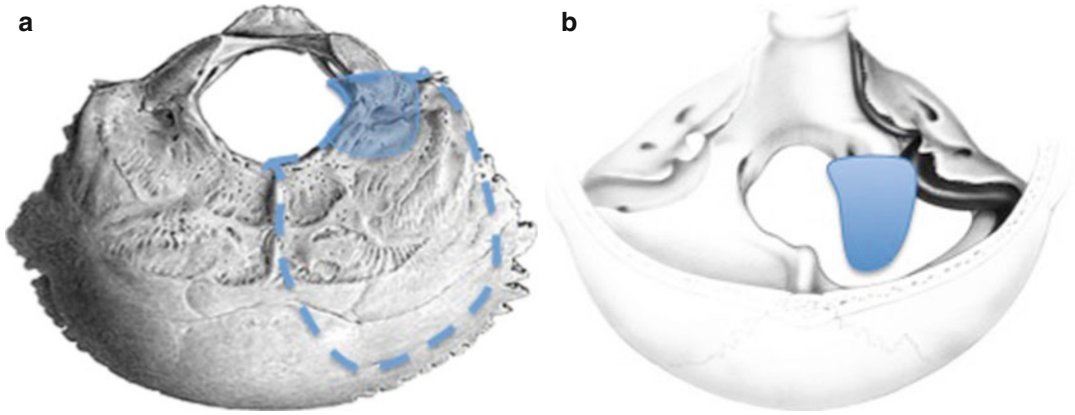


Fig. 9.9 Posterolateral approach (far-lateral approach). (a) Extent of the posterolateral approach (dotted line) and (b) foramen magnum opening with removal of the lateral two thirds of the condyle

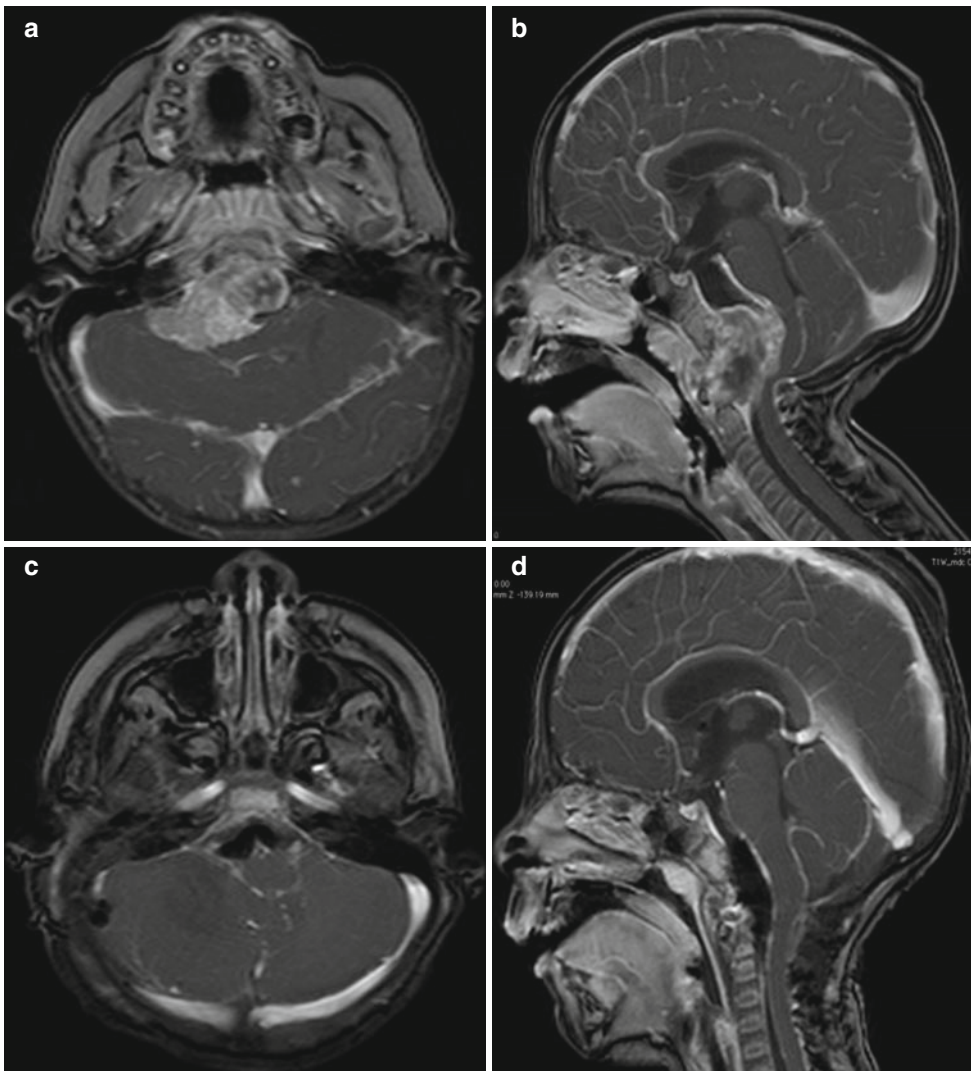


Fig. 9.10 Clival chordoma in a 3-year-old girl. (a, b) Preoperative MRI showing the extension of the tumor at the right craniovertebral junction. (c, d) Postoperative MRI showing subtotal removal of the lesion by right posterolateral (far-lateral) approach

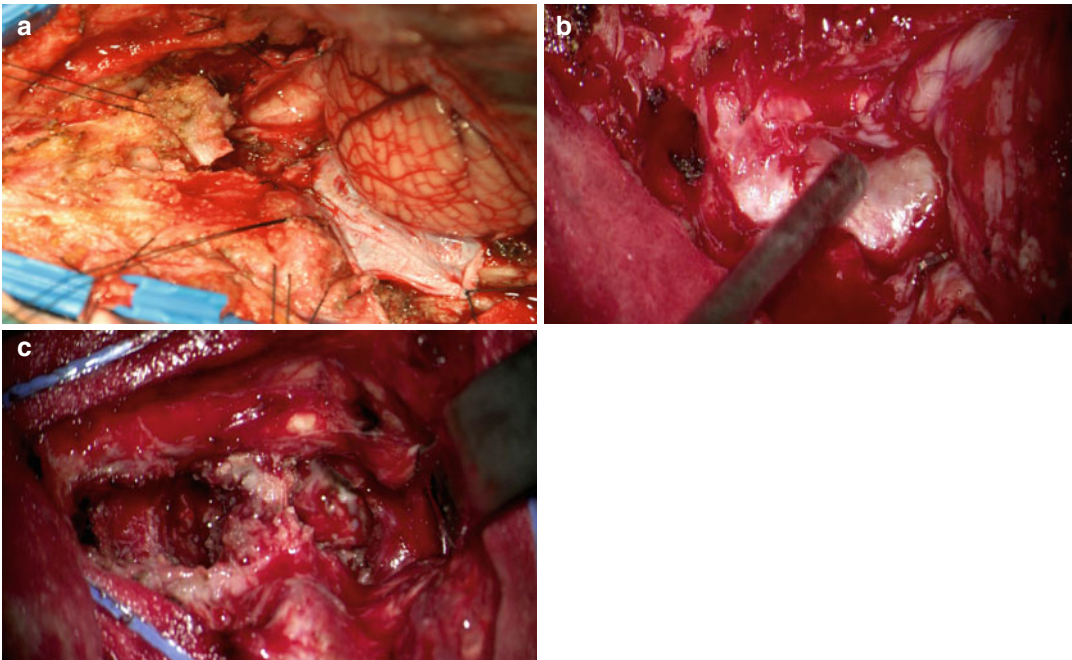


Fig. 9.11 Clival chordoma in a 3-year-old girl (same case of Fig. 9.10). (a) Right posterolateral approach. (b) Tumor extending at the right craniovertebral junction dis-

placing cord (exposure after sectioning the posterior root of C1). (c) Resection of the tumor sparing the right vertebral artery

and laterally flexed 30° to the floor. The sitting position has also been proposed, but the rich net of veins around the cervical muscles, vertebral artery, and bone in the region increases the risk of air embolism [38].

An inverted hockey stick incision is made from the midline at the level of the C4 spinous process and curved anterolaterally to the mastoid tip. The musculature is detached from the occipital bone laterally leaving a myofascial cuff on the bone for reattachment during closure. The soft tissues and underlying muscle flap are then retracted inferolaterally, exposing the craniocervical junction and the ipsilateral lamina of C1 and C2.

Alternatively, an S-shaped incision extending from the junction of the transverse and sigmoid sinuses superiorly and laterally to the midline C1 to C2 level inferiorly and medially can be used, followed by a muscle splitting approach (Figs. 9.3a and 9.7c). The muscle layers are incised with monopolar coagulation. Fishhooks are then used to retract the soft tissue from the field of view.

Subperiosteal dissection proceeds until the foramen magnum and C1 and C2 lamina are exposed. One of the main steps during the operation is the dissection of the vertebral artery (Figs. 9.4a and 9.6d). The vertebral artery is responsible for the blood supply to the upper spinal cord, brainstem, cerebellum, and the postero-inferior portion of the cerebral cortex. It is crucial to palpate and identify the vertebral artery between the occiput and C1 laterally. At this point, the vertebral artery should not be fully exposed, as it occasionally loops far medially and injury must be avoided. The best location to look for the vertebral artery in the far-lateral approach is between the atlas and axis: as the vertebral artery exits the transverse foramen of the atlas, it courses posteromedially in the arterial sulcus of the atlas (posterior atlas arch), prior to piercing the posterior atlantooccipital membrane. A small intraoperative Doppler ultrasound probe can be used to identify the course of the vertebral artery as it penetrates the dura.

There is an extensive venous plexus around the vertebral artery, and sometimes its mobilization may be time-consuming if excessive bleeding is encountered. Note that the vertebral artery may be very adherent to the periosteum, and vascular injury is possible if the bony removal of C1 and C2 is not carefully performed. With use of a subperiosteal dissection, the entire hemilamina of C1 is exposed and removed, avoiding to injure the vertebral artery along its course in the sulcus arteriosus. The vertebral artery seldom needs to be dissected free. Rather, its location should be respected and care taken to avoid injury.

Bony exposure is the most critical step in obtaining adequate exposure. The occipital bone is removed with a high-speed drill and can be completed as a craniotomy: it extends from the asterion and exposes the boundaries of the sigmoid and transverse sinuses. The craniotomy continues to the foramen magnum and rongeurs or a high-speed drill is then used to increase the lateral exposure.

Part of the occipital condyle can be removed, giving access to the midline and beyond at the level of the foramen magnum. The lateral two-thirds of the occipital condyle can be safely resected because the hypoglossal foramen resides in the anterior third of the condyle (Fig. 9.9). This removal is unnecessary in dealing with an intradural foramen magnum tumor while it can be useful for bony tumors of the craniocervical junction. Extradural masses that are directly in the midline are best approached by an anterior transoral route. Bony exposure should be as complete as needed to provide a trajectory that requires minimal, if any, retraction. If it is necessary to remove the condyle unilaterally and a posterior cervical fusion is planned, the original exposure is modified by leaving intact the transverse processes and lamina and also more occipital bone, so that rigid fixation plates may be secured to these areas. The fusion may be unilateral or bilateral, but, if there is an intact condylar articulation on the opposite side, unilateral fusion is enough. Craniocervical junction instability must be considered if extensive bony removal of the occipital condyle (greater than two-thirds),

atlas lateral mass, or axis facet joint is performed and no stabilization is attempted.

The dura is opened in a curvilinear fashion and reflected laterally. The underlying anterolateral medulla and cervicomedullary junction are visualized after retraction of the cerebellar hemisphere and tonsil. Sometimes it is possible to coagulate and remove partially the tonsil to increase the operative space and unmask the tumor.

Some anatomical considerations are extremely important because several structures may be involved in or obscured by the tumor. First, locate lower cranial nerves IX, X, and XI. Then visualize the location of the twelfth nerve: a unilateral twelfth nerve palsy is not a serious problem, but a bilateral paralysis is a catastrophe. Extubation and institution of an oral diet can only take place after thorough assurance of normal lower cranial nerve function postoperatively. Preparations for tracheostomy or enteral feedings must be initiated if there is lower cranial nerve dysfunction. One serious complication to the lower cranial nerves is related to the exposure. Particularly, the eleventh cranial nerve may be injured in its extracranial portion if the skin incision is carried too far anteriorly.

Identify the vertebral artery, the PICA, and their relationships to the tumor. Tumors often surround the vertebral artery and the vessel must be dissected throughout most of its intracranial course. If the upper cervical roots can be spared, they should be, but dividing them for exposure and good tumor removal is acceptable (Fig. 9.11b). If possible, work between the roots; otherwise, the rootlets can be clamped and cut, with bleeding vessels coagulated by fine bipolar coagulation. All manipulations should be performed under neurophysiological monitoring, and the retractors should be released and moved on a timed schedule. Use no more retraction than is necessary for the area where the surgeon is working. Sharp section of the arachnoid layer and superior dentate ligament allows gentle retraction of the upper spinal cord and lower brainstem.

Use of the far-lateral approach minimizes retraction during resection of lesions in this area. It also affords proximal and distal control of the

vertebral artery if needed for complex vascular lesions. Removal of a lesion depends on various factors including its size, vascularity, and firmness. Microsurgical techniques are combined with ultrasonic aspiration to resect most tumors, and when possible, tumor capsules and arachnoid planes are preserved to prevent injury to surrounding structures.

After the lesion has been resected, attention must be directed to ensure a watertight dural closure and closure of exposed mastoid air cells with muscle or fat, bone wax, and fibrin glue to avoid postoperative cerebrospinal fluid (CSF) leak and infection.

9.3.5 Subtemporal Approach (Figs. 9.12 and 9.13)

The posterior subtemporal approach allows to reach the region of the tentorial incisura and a safe dissection within the posterolateral prepontine, ambient, and quadrigeminal cisterns. An additional splitting of the tentorium provides access to the posterior cranial fossa and visualization of the tentorial surface of the cerebellum and structures of the cerebellopontine angle [39–41].

The patient is placed supine, with the head turned in a near horizontal position such that the zygomatic process is parallel to the floor, or in a true lateral position. A shoulder roll is always required to minimize the risk of injury to the brachial plexus and cervical spine. An inverted U-shaped incision is centered over the ear and the skin and underlying temporalis muscle reflected inferiorly.

A more posterior craniotomy placement allows a significantly reduced retraction of the temporal lobe compared to the anterior subtemporal approach. A temporal bone flap was fashioned with one burr hole on the superior temporal line, and craniotomy was performed extending from the asterion to a point placed about 1 cm above the zygoma until reaching the floor of the middle fossa. The bone flap is removed carefully to avoid injury to the transverse sinus often exposed at the posteroinferior aspect of the craniotomy. Usually, further bone must be drilled

or removed with rongeurs to ensure complete exposure of the middle cranial fossa floor and to minimize temporal lobe retraction. Mastoid air cells are often exposed during the craniotomy and must be packed with bone wax or fat to avoid postoperative CSF leakage.

Using the anatomical data acquired during the preoperative planning, attention was drawn to avoid injury to the junction of the sigmoid and transverse sinuses and the end of the vein of Labbé. Intraoperative accuracy of navigation was confirmed by placing the sterile navigation pointer at the inner edge of the craniotomy. The dura was then opened in an inverted U-shaped flap and reflected inferiorly. After identification of the vein of Labbé, the surgical route, anterior to the vein, was chosen by means of neuronavigation. The temporal lobe is gently retracted with care taken not to injure the vein of Labbé and inferior bridging veins. Thus, position and pressure of the brain spatula play a central role. It is advisable to place a lumbar drain preoperatively and use intraoperative osmotic diuretics and mild hyperventilation to ensure adequate brain relaxation. Opening the Sylvian fissure as well as the parasellar cisterns to drain the CSF facilitated brain retraction and prevented temporal lobe contusions without any significantly increase in the brain shift or limitation of the neuronavigational accuracy.

The tentorial edge is then identified with the closely associated trochlear nerve as well as the midbrain, oculomotor nerve, distal basilar artery, and its terminal branches. The tentorial edge often requires division posterior to the entry of the trochlear nerve into the tentorium and suturing of the respective flaps to the floor of the middle cranial fossa to visualize the pontomesencephalic junction and upper pons. Care must be taken during this process to avoid injury to the trochlear nerve. After a safe dissection and isolation from the underlying arachnoid bands and trochlear nerve using a Rhoton dissector, a small tentorial incision was made starting medially at the edge behind the entry point of CN IV into the dura, extended laterally to the superior petrosal sinus, and then divided

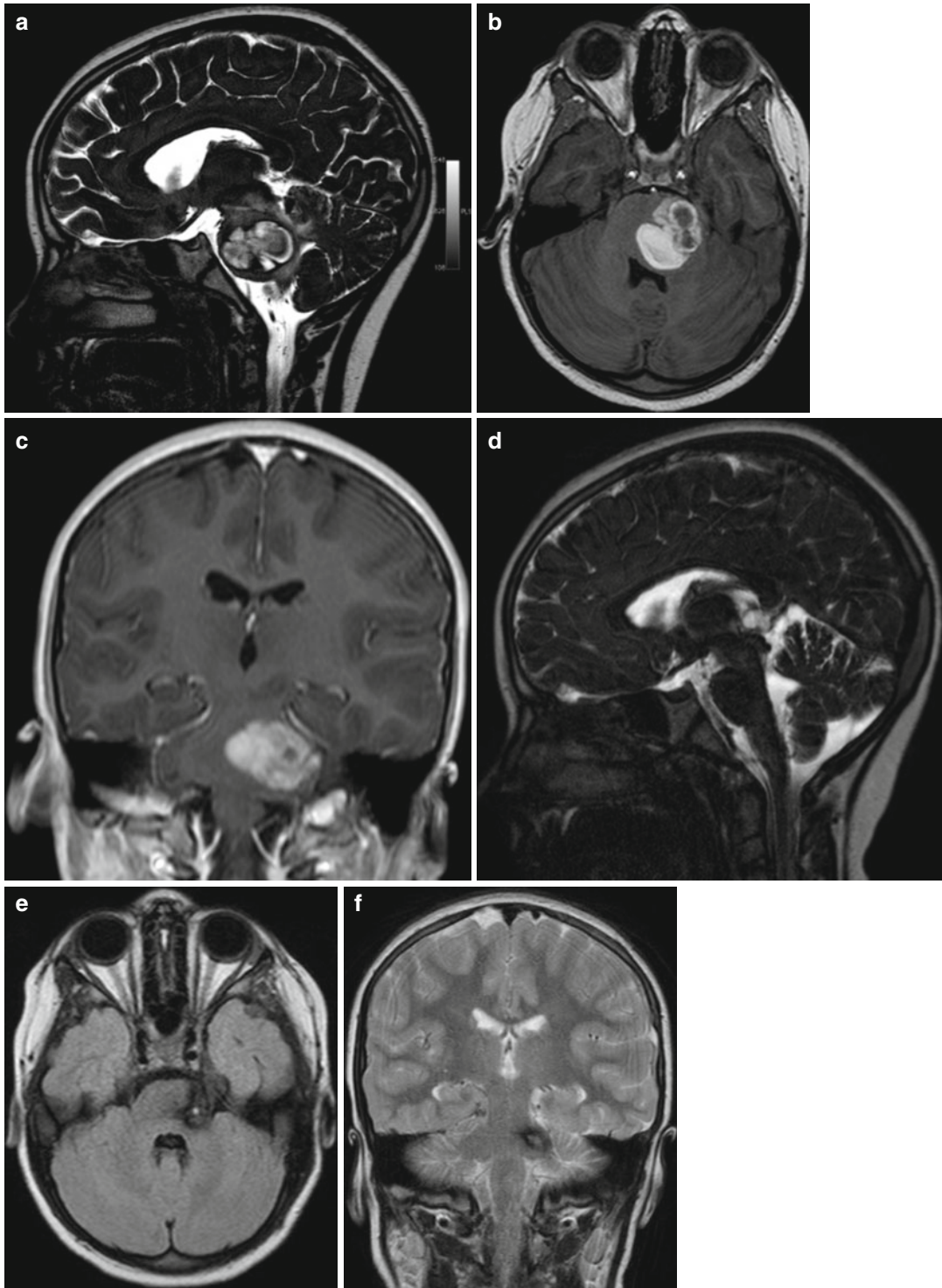


Fig. 9.12 Subtemporal approach for a large pontine cavernoma in a 10-year-old girl. (a–c) Preoperative MRI showing a large cavernoma in the left pons and cerebellar peduncle with signs of acute hemorrhage and surrounding

hemosiderin ring. The fourth ventricle is compressed. (d–f) Follow-up MRI at 24 months showing complete removal of the lesion

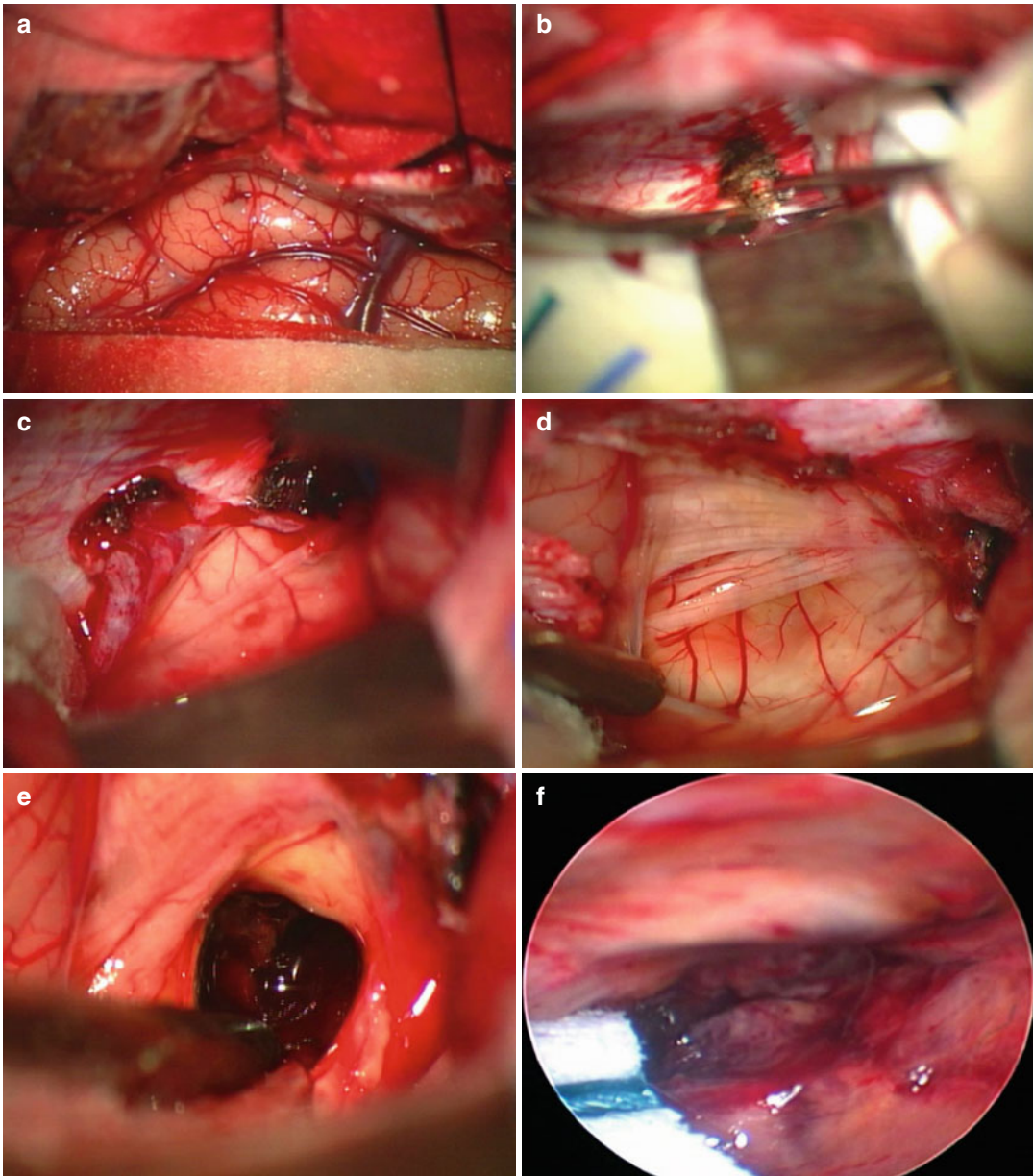


Fig. 9.13 Subtemporal approach for a large pontine cavernoma in a 10-year-old girl (same case as Fig. 9.12). (a) Temporal lobe after dural opening with the vein of Labbè. (b) Tentorial incision by laser after gentle retraction of the temporal lobe. (c) The fourth cranial

nerve appears in the free edge of the tentorium. (d) The area of bleeding is clearly visible on the surface of the pons. (e) Removal of the cavernoma. (f) Endoscopic exploration of the surgical cavity after removal of the cavernoma

between dural clips. The trochlear (IV) cranial nerve (CN), superior cerebellar artery, and vena petrosa were then extensively exposed in the cisterna ambiens.

9.3.6 Combined Approaches (Fig. 9.7)

Occasionally, it may be advantageous to perform two approaches in a combined fashion. This is

particularly true for lesions located in the superior and anterolateral aspect of the posterior fossa where exposure from above and below the tentorium greatly facilitates removal. The most commonly used exposure involves the use of the subtemporal and retrosigmoid approaches with splitting up the intervening tentorium. In this approach, the patient is positioned supine with the head turned contralateral to the lesion, using a shoulder roll for protection of the cervical spine and brachial plexus. A lumbar drain is positioned preoperatively to guarantee adequate brain relaxation. A standard retrosigmoid incision is carried superiorly and anteriorly, curving 1–2 cm above the ear before ending inferiorly at the roof the zygoma. After reflection of the skin flap and underlying temporal muscle, burr holes are drilled on either aspect of the transverse-sigmoid sinus junction before removal of the bone flap. The craniotomy can be performed using two separate bone flaps for each exposure with subsequent removal of the intervening bony bridge using a drill or rongeur. The dural openings are fashioned according to the anatomy of the bordering sinuses and floor of the middle cranial fossa with consideration given to the insertion of the neighboring anastomotic vein of Labbé. Occasionally, it may be necessary to ligate the transverse-sigmoid sinus for additional exposure if it is determined to be nondominant on the preoperative angiogram.

References

- Rosegay H (1992) The Krause operations. *J Neurosurg* 76(6):1032–1036
- Yasargil MG, Fox JL (1974) The microsurgical approach to acoustic neurinomas. *Surg Neurol* 2:393–398
- Adson AW (1941) A straight lateral incision for unilateral suboccipital craniotomy. *Surg Gynecol Obstet* 72:99–100
- Bucy PC (1951) Surgical treatment of acoustic tumors. *J Neurosurg* 8:547–555
- Dandy WE (1929) An operation for the cure of tic douloureux. Partial section of the sensory root at the pons. *Arch Surg* 18:687–734
- Dandy WE (1934) Removal of cerebellopontine (acoustic) tumors through a unilateral approach. *Arch Surg* 29:337–344
- Bassiouni H, Ntoukas V, Asgari S, Sandalcioğlu EI, Stolke D, Seifert V (2006) Foramen magnum meningiomas: clinical outcome after microsurgical resection via a posterolateral suboccipital retrocondylar approach. *Neurosurgery* 59(6):1177–1187
- Rhoton AL Jr (1984) Microsurgical anatomy of acoustic neuromas. *Neurol Res* 6:3–21
- Rhoton AL Jr (1986) Microsurgical anatomy of the brainstem surface facing an acoustic neuroma. *Surg Neurol* 25:326–339
- Rhoton AL Jr (1976) Microsurgical removal of acoustic neuromas. *Surg Neurol* 6:211–219
- Bruneau M, Cornelius JF, George B (2006) Anterolateral approach to the V3 segment of the vertebral artery. *Neurosurgery* 58(Suppl 1):ONS29–ONS35
- Sartor K, Flidner E, Pfingst E (1977) Angiographic demonstration of cervical extradural meningioma. *Neuroradiology* 14:147–149
- Tubbs RS, Loukas M, Shoja MM, Bellew MP, Cohen-Gadol AA (2009) Surface landmarks for the junction between the transverse and sigmoid sinuses: application of the “strategic” burr hole for suboccipital craniotomy. *Neurosurgery* 65(6 Suppl):37–41; discussion 41
- Rhoton AL Jr (2000) The cerebellopontine angle and posterior fossa cranial nerves by the retrosigmoid approach. *Neurosurgery* 47:S93–S129
- Rhoton AL Jr (1979) Microsurgical anatomy of the posterior fossa cranial nerves. *Clin Neurosurg* 26:398–462
- Berry M, Bannister LH, Standring SM (1999) Nervous system. In: Williams PL (ed) *Gray’s anatomy*, 38th edn. Churchill Livingstone, Edinburgh, pp 1262–1264
- Sinclair J, Kelly ME, Steinberg GK (2006) Surgical management of posterior fossa arteriovenous malformations. *Neurosurgery* 58(4 Suppl 2):ONS-189–ONS-201; discussion ONS-201
- Tedeschi H, Rhoton AL Jr (1994) Lateral approaches to the petroclival region. *Surg Neurol* 41(3):180–216
- Rhoton AL Jr (1994) The three neurovascular complexes in the posterior fossa and vascular compression syndromes (honored guest lecture). *Clin Neurosurg* 41:112–149
- Seeger W (1978) Atlas of topographical anatomy of the brain and surrounding structures for neuro surgeons, neuroradiologists, and neuropathologists. Springer, Vienna, pp 486–489
- George B, Laurian C (1979) Surgical possibilities in the third portion of the vertebral artery (above C2). Anatomical study and report of a case of anastomosis between subclavian artery and vertebral artery at C1–C2 level. *Acta Neurochir (Wien)* 28(1):263–269
- George B, Dematons C, Cophignon J (1988) Lateral approach to the anterior portion of the foramen magnum. Application to surgical removal of 14 benign tumors: technical note. *Surg Neurol* 29(6):484–490
- George B, Lot G, Boissonnet H (1997) Meningioma of the foramen magnum: a series of 40 cases. *Surg Neurol* 47(4):371–379

24. Heros RC (1986) Lateral suboccipital approach for vertebral and vertebrobasilar artery lesions. *J Neurosurg* 64(4):559–562
25. Samii M, Klekamp J, Carvalho G (1996) Surgical results for meningiomas of the cranio-cervical junction. *Neurosurgery* 39(6):1086–1095
26. Spetzler RF, Grahm TW (1990) The far-lateral approach to the inferior clivus and the upper cervical region. Technical note. *BNI Q* 6:35–38
27. Rhoton AL Jr (2000) The far-lateral approach and its transcondylar, supracondylar, and paracondylar extensions. *Neurosurgery* 47(suppl 3):S195–S209
28. Al-Mefty O, Borba LA, Aoki N, Angtuaco E, Pait TG (1996) The transcondylar approach to extradural non-neoplastic lesions of the craniovertebral junction. *J Neurosurg* 84(1):1–6
29. Arnold H, Sepehrnia A (1995) Extreme lateral transcondylar approach. *J Neurosurg* 82(2):313–314
30. Sen CN, Sekhar LN (1990) An extreme lateral approach to intradural lesions of the cervical spine and foramen magnum. *Neurosurgery* 27(2):197–204
31. Babu RP, Sekhar LN, Wright DC (1994) Extreme lateral transcondylar approach: technical improvements and lessons learned. *J Neurosurg* 81(1):49–59
32. Bertalanffy H, Seeger W (1991) The dorsolateral, suboccipital, transcondylar approach to the lower clivus and anterior portion of the craniocervical junction. *Neurosurgery* 29(6):815–821
33. Menezes AH (2008) Craniovertebral junction neoplasms in the pediatric population. *Childs Nerv Syst* 24(10):1173–1186
34. Sen CN, Sekhar LN (1993) Extreme lateral transcondylar and transjugular approaches. In: Sekhar LN, Janecka IP (eds) *Surgery of cranial base tumors*. Raven Press, New York, pp 389–411
35. Menezes AH (2008) Surgical approaches: postoperative care and complications “posterolateral-far lateral transcondylar approach to the ventral foramen magnum and upper cervical spinal canal”. *Childs Nerv Syst* 24(10):1203–1207
36. Karam YR, Menezes AH, Traynelis VC (2010) Posterolateral approaches to the craniovertebral approach. *Neurosurgery* 66(3 Suppl):135–140
37. Velat GJ, Spetzler RF (2012) The far-lateral approach and its variations. *World Neurosurg* 77(5–6):619–620
38. Kikuta KI, Miyamoto S, Kataoka H, Satow T, Yamada K, Hashimoto N (2004) Use of the prone oblique position in surgery for posterior fossa lesions. *Acta Neurochir (Wien)* 146(10):1119–1124; discussion 1124
39. Hernesniemi J, Ishii K, Karatas A et al (2005) Surgical technique to retract the tentorial edge during subtemporal approach: technical note. *Neurosurgery* 574(Suppl):E408; discussion E408
40. Hernesniemi J, Ishii K, Niemela M et al (2005) Subtemporal approach to basilar bifurcation aneurysms: advanced technique and clinical experience. *Acta Neurochir Suppl* 94:31–38
41. Drake C, Peerless S, Hernesniemi J (1996) *Surgery of vertebrobasilar aneurysms*. London, Ontario experience on 1767 patients, 1st edn. Springer, Vienna, pp 21–27

Bernard George and Damien Bresson

10.1 Introduction

Skull base surgery has incredibly developed over the last 25 years because of the improvement of pre- and intraoperative imaging, of instrumentation, of vision, of surgical instrumentation, and of new surgical approaches, the last ones being the consequence of the previously mentioned ones. In fact pediatric skull base surgery developed one step after the adult one was mastered for technical reasons, mainly the still more limited field, and for anesthetic reasons as it is often long with bleeding tendencies. Another limiting factor is the low incidence of skull base pathologies in the pediatric population.

As a matter of fact, the same surgical approaches are used in both the adult and pediatric populations. They can be divided into *anterior*, *lateral*, and *posterior* approaches, but for practical use, it is better to describe them following the skull base structures (or areas) that are intended to be reached (or where the pathology is located). Considering the posterior fossa, the skull base structures can be separated into the *petrous bone*, *jugular foramen*, *clivus*, and *cranio-cervical junction*.

B. George • D. Bresson (✉)
Department of Neurosurgery, Hôpital Lariboisière,
2, rue Ambroise Paré, Paris 75010, France
e-mail: bernard.george@lrp.aphp.fr;
damien.bresson@lrp.aphp.fr

10.2 Petrous Bone

Many approaches can lead to the petrous bone from different directions:

- A. Anteriorly, endoscopic endonasal approaches can be extended through the pterygoid process to the petrous apex and even reach the anterior edge of the internal auditory canal (IAC) [14]. Anterior approaches are presented in another chapter.
- B. Laterally, differentiated into the anterolateral, the lateral, and the posterolateral approaches.

10.2.1 Anterolateral Approaches

Anterolateral approaches include all the subtemporal approaches (Fig. 10.1 right) including the pterygoidal one [8]. They are performed on a patient in the supine position with the head slightly extended and rotated toward the opposite side. The skin incision is generally semi-circular, frontotemporal following the hair line. The temporal bone flap must always be as low as possible, sometimes including the zygomatic arch [11, 23]; it can be extended to the frontal bone with resection of the lesser wing (pterygoidal approach) and more or less anteriorly or posteriorly on the temporal bone depending on the area to be reached (petrous bone and tentorium). The temporalis muscle can be reflected in several directions but always in a different one from the anticipated axis of work which then must be

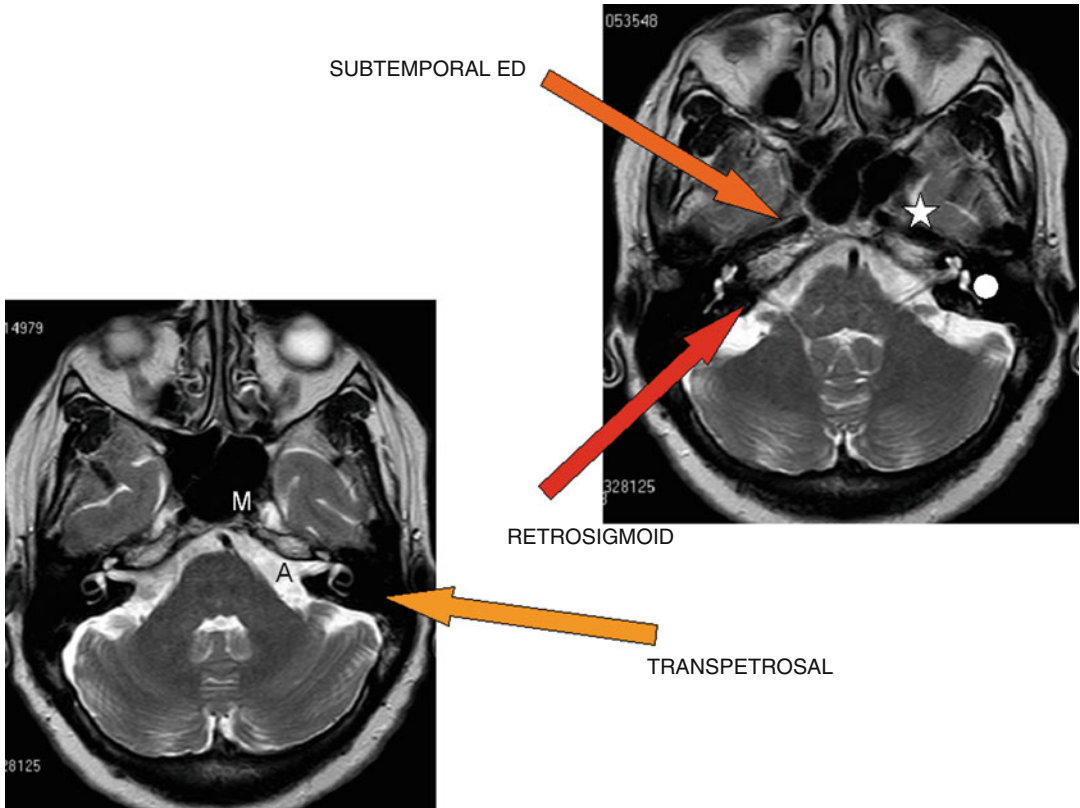


Fig. 10.1 Schematic presentation of (right) the extradural (ED) subtemporal and retrosigmoid approaches with the internal carotid artery (*star*) and internal auditory

canal and cochlea (*circle*) and of (left) the transpetrosal approach with *M* Meckel cave and *A* cerebellopontine angle

differentiated from the space of exposure which may be intradural, extradural, or both.

10.2.1.1 Extradural Exposure
(Fig. 10.2a)

The dura mater of the temporal lobe has to be elevated from the bone of the temporal fossa and then split from the dura propria of the cavernous sinus; this permits to expose the elements of the sphenoidal fissure, the V2 and V3 branches of the trigeminal nerve (CN V), and the horizontal part of the internal carotid artery (ICA) [15]. Venous bleeding from the cavernous sinus can be controlled by fibrin glue injection inside the cavernous sinus. With such an exposure, a view is given on the superior aspect of the petrous bone up to its ridge (superior petrosal sinus). Therefore it provides access to the IAC, to the cochlea and semi-circular canal (eminentia arcuata) from above

(Fig. 10.3) [3], and to the petrous apex (Kawase approach). Drilling the petrous apex medial to the ICA, anterior to the cochlea and IAC and posterior to V3 (CN V), permits to reach some bone tumors such as chordomas or chondrosarcomas and some cysts like cholesterol cysts or granulomas and to expose partially or totally neuromeningeal tumors like CN V schwannomas or petroclival meningiomas.

10.2.1.2 Intradural Exposure

The most frequent tumors for which intradural exposure is needed are meningiomas and neurinomas. So most of the time, it is achieved through a pterygoidal approach in which the temporal opening is more or less wide. Then a semi-circular dural incision gives a dural flap reflected anteriorly, and a contraincision gives another flap reflected inferiorly. The temporal lobe is retracted

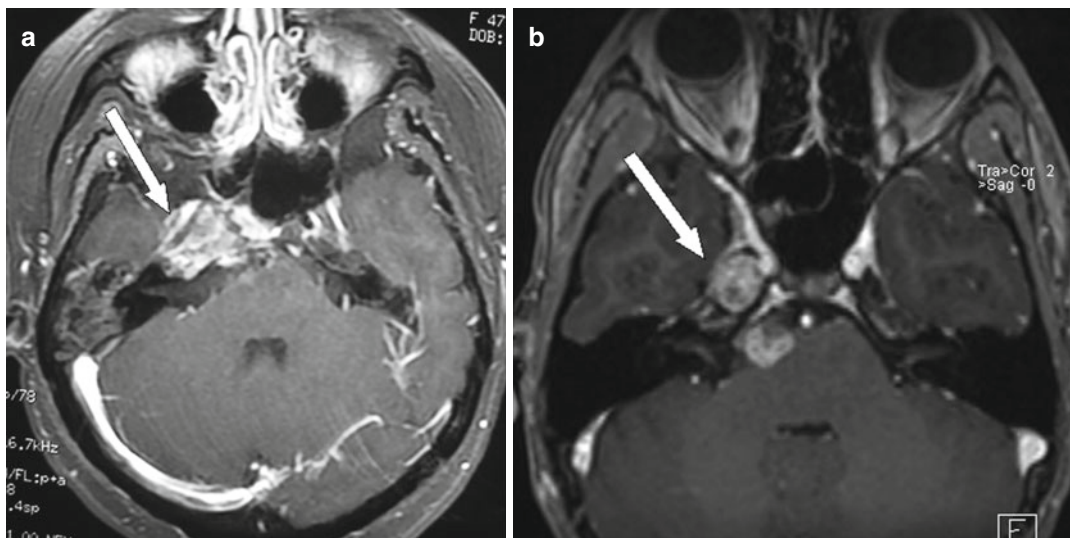


Fig. 10.2 (a) Chordoma of the petrous apex removed by an extradural subtemporal approach. (b) Fifth nerve neurofibroma removed by an extra-intradural subtemporal approach



Fig. 10.3 Facial nerve neurofibroma removed by a subtemporal approach

with the help of gravity provided by an adequate head positioning. For an approach toward the anterolateral aspect of the brain stem, the sylvian fissure is widely opened. Drilling of the posterior clinoid process (the so-called transcavernous approach) may help in case of superior tumoral extension. For posterior approach, the tentorium has to be divided after coagulation and/or clipping of the superior petrosal sinus. This is done behind the oculomotor nerve (CN III) more or

less close to it and after identification of the CN IV which should be separated from the tentorium.

In some cases the intradural exposure is combined with an extradural one (Fig. 10.2b); the dural incision on the temporal lobe is done horizontally, parallel to the superior petrosal sinus in order to protect the temporal lobe during its retraction; a blade is placed along the tentorium which is then cut. This allows to follow an intradural extension of a bone tumor (chordomas) or an infratentorial extension of a CN V neurofibroma or of a meningioma [12, 15, 21].

10.2.2 Lateral Approaches

Lateral approaches include all the routes going through the petrous bone [1, 2, 20]. They are usually named according to the petrous bone structures which are drilled out or preserved: the presigmoid retrolabyrinthine, translabyrinthine [7], transcochlear [13], and any combination up to total petrosectomy (Fig. 10.4). Obviously they require a perfect knowledge of the petrous bone anatomy or the assistance of an ENT surgeon. Most of them suppose the hearing function is lost or its sacrifice is accepted. The main problem in these approaches is the facial nerve (CN VII) which has generally to

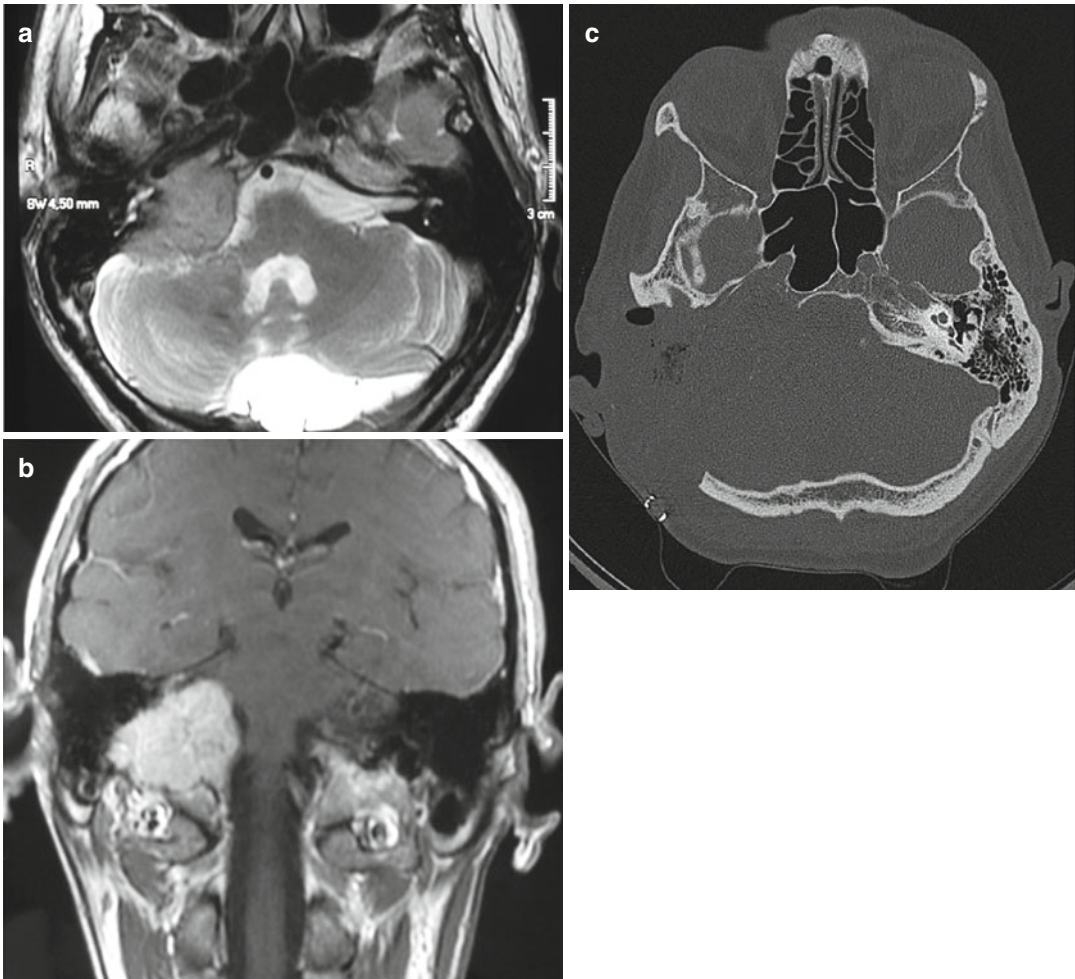


Fig. 10.4 Petrous bone tumor (paraganglioma). Preoperative axial (a) and coronal (b) MRI view and postoperative CT scanner (c) after total petrosectomy

be preserved either by keeping it inside its bony canal (the fallopian canal) whenever possible or mobilized or even transposed.

Generally the patient is in the supine position with the head rotated toward the opposite side; a cushion under the shoulder is often useful to help the rotation and reduce the jugular vein compression and intracranial hypertension. An alternative is the lateral position. The skin incision is generally a C-shape one running around the auricle. For wide approaches, the external auditory canal may need to be cut at its bony-cartilaginous junction and closed in a blind sac fashion. The middle ear is then excluded with occlusion of the eustachian tube by a piece of muscle; it leads to the external

semicircular canal. The drilling is then extended according to the selected approach. The dura mater of the posterior fossa and of the inferior aspect of the temporal lobe is usually exposed in between the superior petrosal sinus and its posterior limit the sigmoid sinus (SS).

Petrosal approaches are obviously used in bone tumors of the petrous bone. On the neurosurgical point of view, they are mostly utilized in acoustic neurinomas and in petrous bone meningiomas. In acoustic neurinomas (translabyrinthine approach), it gives a primary control onto the facial nerve and avoids cerebellar retraction; however the hearing function, if still present, is destroyed. In petrous bone meningiomas, the

petrosal approaches lead directly to their zone of insertion [2, 12, 21, 23] with a similar strategy as the one applied in convexity meningiomas; the tumor is first devascularized before being debulked. The extent of drilling has therefore to be adjusted to this zone of insertion. For this, it is useful to classify petrous bone meningiomas in A, anterior to the IAC; B, at the level of the IAC; and C, posterior to the IAC; accordingly class A meningiomas need at least a transcochlear approach, class B a translabyrinthine one, and class C may be limited to a retrolabyrinthine one.

Besides the problem of the facial nerve preservation, the dural closure is the main concern since many air cells and often the eustachian tubes are opened. Dural closure generally needs to pack a fat pad which must be prepared.

10.2.3 The Posterolateral Approaches

These are the approaches passing behind the petrous bone essentially represented by the retro sigmoid approach (Fig. 10.1 left). This approach can be realized in the semi-sitting, lateral, or supine position. The semi-sitting position has the advantage of less amount of bleeding and a cleaner field as the blood is flowing down away from the area of work; however for long surgeries, it needs an arm rest to avoid fatigue and pain in the surgeon's shoulders. Moreover air embolism is a possible complication. The lateral and supine positions are similar, the latter having the advantage to be more rapidly and simply achieved. In the supine positioning, the head is rotated toward the opposite side and tilted down a little (to see the tentorium). Rotation of the operating table must be possible during the surgery to better bring into view either the brain stem or the petrous bone. A cushion under the shoulder helps for the rotation as mentioned above. The lateral position is sometimes a better option when the tumor is on the right side (for a right-handed surgeon) since in the supine position, the shoulder of a short-neck patient is on the way of the hand holding the instruments. The skin incision is generally a C-shape one running around the auricle. The bone opening is on the

occipital bone and the mastoid process so as to expose the lateral aspect of the posterior fossa up to the sigmoid sinus (SS) and the beginning of the transverse sinus. There is no benefit of skelotonizing the SS. The dura is opened in a semicircular fashion (concavity toward the SS) for an easy and watertight closure. This approach leads to the cerebellopontine angle (CPA) up to the tentorium and down to the jugular foramen area, the bone and dura opening being extended as required. Its main indications are CPA tumors (acoustic neurinomas, meningiomas, epidermoid cysts, etc.).

The drilling of part of the petrous bone may be required to access the inside of the IAC (drilling of the posterior wall of the IAC) or the Meckel cave and posterior part of the cavernous sinus (drilling of the petrous apex).

In some cases, it may be useful to combine the retrosigmoid approach to a retrolabyrinthine and/or a subtemporal approach. The SS can be either mobilized or even transected [17] when there is a contralateral SS of good size; the superior petrosal sinus can be divided along with the tentorium enlarging the field superiorly.

10.3 Jugular Foramen

The jugular foramen (JF) area is a challenging area in which three different types of tumors can be observed essentially: glomus tumors (paragangliomas), neurinomas, and meningiomas. These tumors can be classified according to their development related to the JF: type A, intradural tumors; type B, foraminal tumors; and type C, extracranial (cervical) tumors. In fact many tumors exhibit a combination of types with a type A-B-C at the maximum. Approaches to the JF must be decided following this classification; intradural tumors are exposed by a retrosigmoid approach extended inferiorly or sometimes combined with a foramen magnum opening; extracranial tumors need a lateral cervical opening which should permit a control of all the vasculo-nervous elements running in or close to the JF (ICA, internal jugular vein (IJV), CN IX to XII). Foraminal tumors have always a more or less important extension, the intradural or extracranial; the

decision has to be made of the best choice between a retrosigmoid approach but without control of the distal part and an extracranial approach extended intracranially. There are mainly two extracranial approaches which can be used: the infratemporal and the juxtacondylar approaches.

10.3.1 Infratemporal Approach

It combines a cervical exposure to a transpetrosal approach, generally with a facial nerve transposition [10, 11]. Some variations have been proposed following the tumoral development and especially the tumoral relation to the petrosal ICA (tumor class C) and to the dura (tumor class D). It gives a lateral and superior route to the JF. The patient is in the supine position with the head slightly extended and rotated toward the opposite side. The skin incision is usually an interrogation mark following the superior part of the sternomastoid muscle (SM) up to the tip of the mastoid process, then curved along the mastoid process and turned around the auricle. The first step is the cervical dissection of all the vasculo-nervous elements. The EAC is transected and closed. Then the petrous bone is drilled extensively with exposure of the temporal and posterior fossa dura with skeletonization of the SS. The facial nerve is transposed anteriorly and the petrosal ICA controlled on the required length (vertical portion, genu, horizontal portion). The SS is ligated as well as the IJV on both sides of the tumor. The tumor is then resected up to the dura which is opened next, in case of intradural extension. The closure needs particular attention like in any transpetrosal approach in which the dura has been opened. In intradural tumors, the placement of an external lumbar drainage as the first step of the surgery is generally useful. It is kept for 3–4 days on average.

10.3.2 Juxtacondylar Approach

This approach is derived from the anterolateral (extreme lateral) approach with the same

position and skin incision as the infratemporal approach [4]. Therefore the first step is the cervical exposure of the vasculo-nervous elements including the VA with resection of the transverse process of C1. Generally the VA is kept in place, but a still wider access can be obtained by the posteroinferior transposition of the VA out of the C1 transverse process. This permits to control the IJV high up in the neck. The next step is the occipital bone resection and mastoid process drilling to expose the retrosigmoid dura and the whole length of the SS. Then the jugular foramen is opened on its posteroinferior aspect with resection of the bone (jugular tubercle) covering the junction between the SS and the IJV. This is quite sufficient to approach and resect a tumor (schwannomas) developed inside the JF. Of course tumors extending outside the JF toward the petrous bone (glomus tumors) need to enlarge the opening. However the petrous bone drilling can be very limited so that in many instances the facial nerve can be kept protected inside the fallopian canal. A better control and also preservation of the lower cranial nerves can also be expected. In case of strictly extradural tumor, the dura can be kept intact; even the occlusion of the SS can be realized without opening the dura. For this the distal SS wall is opened, and SURGICEL® is pushed inside, while a proximal occlusion is performed by compression.

10.4 Clivus

The lower clivus is in fact part of the craniocervical junction (CCJ) area, and its approach will be described in the next chapter. For the upper and middle clivus, the best approaches are anterior; formerly the subfrontal transbasal approach and different transfacial approaches (transsphenoidal, transmaxillary, extended transoral) were used [6]. Nowadays these approaches have been replaced by the endoscopic endonasal approaches [14]. The petrous bone approaches are still preferred only for petroclival tumors in which the clival part is not predominant.

10.5 Craniocervical Junction (CCJ) Area

This area includes the lower clivus, the atlas, and the C0–C1 and C1–C2 interspaces. This area can be approached from every aspect: anteriorly, most often by endoscopic endonasal approach and less by the transoral approach (see next chapter); posteriorly by the midline posterior approach; laterally by either the posterolateral (far lateral) or the anterolateral (extreme lateral) approach (Fig. 10.5) [4, 5].

Lateral approaches: basically the posterolateral approach is a lateral extension of the standard midline approach and mostly designed for intradural tumors (Fig. 10.6) and for extradural tumors located behind the occipital condyle and lateral mass of the atlas. The anterolateral approach is a route lateral to the IJV designed for extradural and bone lesions involving the lateral wall (occipital condyle, lateral mass of atlas) and anterior wall (tip of the clivus, anterior arch of the atlas, odontoid process) of the CCJ (Fig. 10.7).

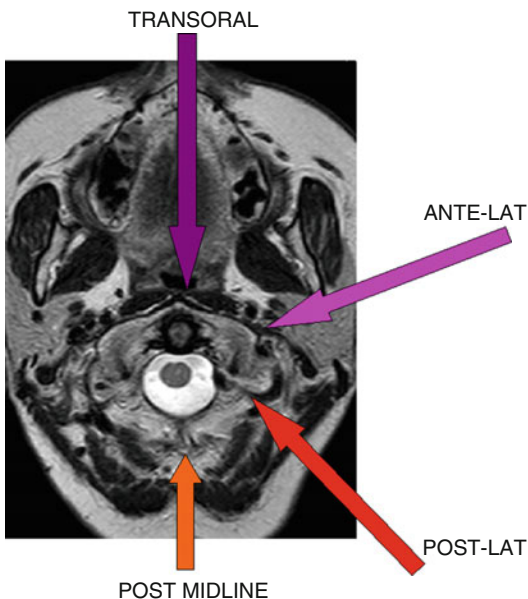


Fig. 10.5 Schematic presentation of the four available surgical approaches to the craniocervical junction

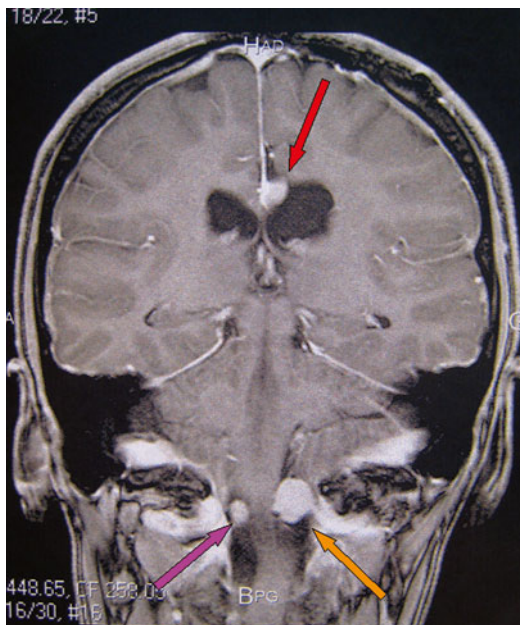


Fig. 10.6 Neurofibromatosis type II with three meningiomas, one on the falx and two at the foramen magnum level. Resection by a bilateral posterolateral approach

10.5.1 Posterolateral Approach

The patient may be in the sitting, lateral, or prone position with the head flexed but straight. The skin incision is on the midline up to the occipital protuberance then curved along the superior occipital line toward the mastoid. The inferolateral part of the posterior fossa is exposed as well as the posterior arch of the C1 and the laminae of C2; then the C1 posterior arch is subperiosteally exposed so that the VA can be controlled in its groove. The occipital bone and C1 posterior arch are resected including the bone above and below the VA. For intradural tumors (meningiomas and neurinomas), it is never useful to drill the occipital condyle or the lateral mass of the atlas. The dura is incised in a semicircular fashion and reflected laterally. It is often useful to cut the first arch of the denticulate ligament (encircling the intradural VA) and the first cervical nerve root so as to release the tension on the neuraxis and enlarge the access anterior to it.

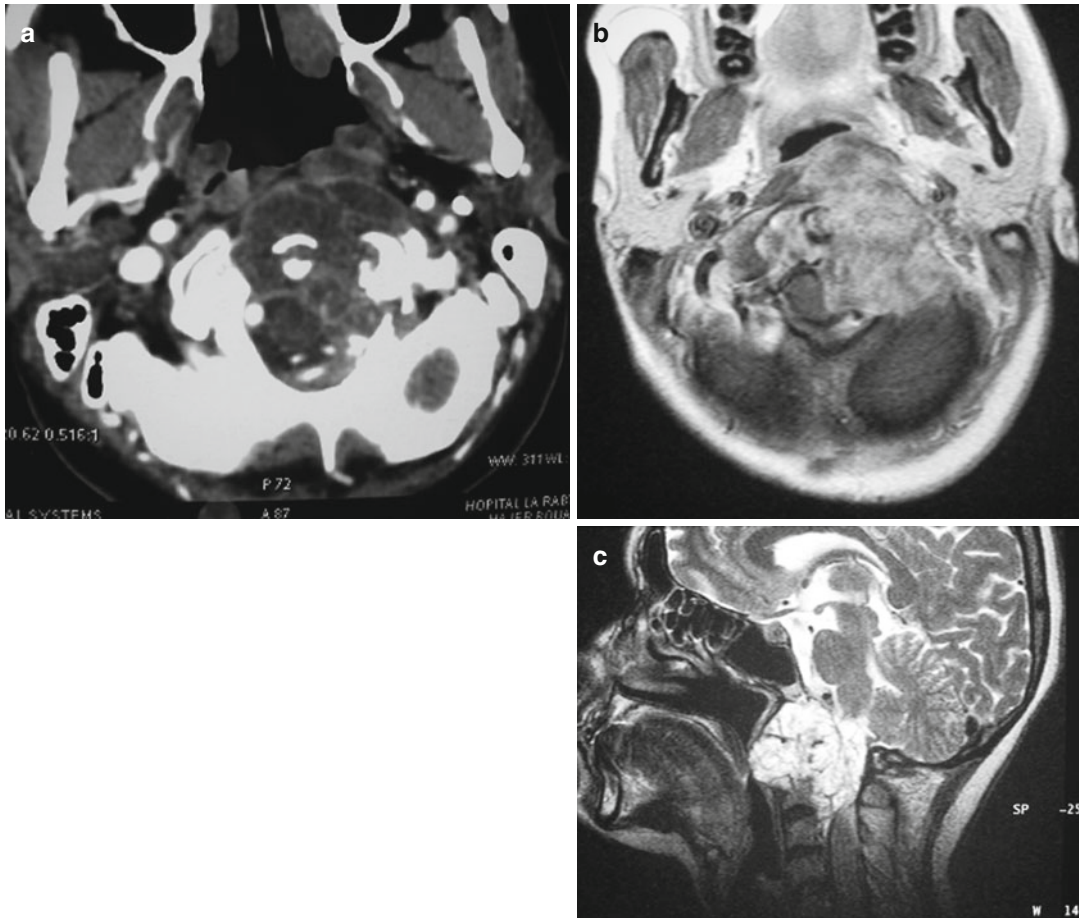


Fig. 10.7 Chordoma at the craniocervical junction level. (a) CT scanner (b) and (c) axial and sagittal MRI views. Resection by an anterolateral approach

10.5.2 Anterolateral Approach

The patient is in the supine position with the head slightly extended and rotated to the opposite side. The skin incision follows the medial edge of the SM muscle up to the mastoid tip, then along the mastoid process and more or less along the superior occipital line. The SM muscle is detached from the occipital bone and mastoid process; then the field between the IJV and medial aspect of the SM muscle is opened. In the depth of this field, the accessory nerve (CN XI) has to be identified and dissected free. Because of the head rotation, the transverse process of the atlas is projected anteriorly and is easily identified below the mastoid tip. The deep cervical muscles attached on the transverse process are divided

flush to it so that the two VA segments (above C1 and C1–C2) are exposed. These segments run parallel on both sides of the posterior arch of the atlas. This C1 arch is subperiosteally controlled up to the transverse process in order to find the entrance and exit of the VA into and from the C1 transverse foramen. This foramen can then be unroofed, and, if necessary, the VA can be mobilized outside the foramen. With the anterolateral approach, an access is gained to the lateral wall of the CCJ area including the jugular tubercle, occipital condyle, and lateral mass of the atlas. Access can be extended posteriorly toward the posterior arch of the atlas and occipital bone and anteriorly toward the anterior arch of the atlas and tip of clivus. It can also be extended superiorly to the JF area as described above.

10.6 General Principles

10.6.1 Choice of the Surgical Approach

The choice of the surgical approach depends on the tumoral location as precisely defined as possible by a complete preoperative imaging work-up including an MRI and a CT scanner with bone windows. A CT scanner is still useful for studying the bone variations and anomalies. It should be performed in any bone tumors and in any tumor extending into the bone (IAC, e.g., insertion osteoma of meningiomas, Fig. 10.3); it is also useful to look for air cells which may be opened by the bone opening (temporal bone, mastoid, etc.). MRI with various sequences provides identification of any tumoral extension and relation with the brain parenchyma (compression, edema) and also with most vasculo-nervous elements. Most cranial nerves can now be demonstrated on MRI; among vessels, the main arteries and branches can be visualized as well as the venous sinus and major veins. Analysis of these tumoral relations allows to imagine the tumoral origin and development. In fact it is generally a good principle to go first on the zone of tumoral origin and then to progress in the tumoral resection using the “tumor corridor” with minimal need of retraction.

Another principle in skull base surgery is to avoid “crossing the nerves.” The recognition of which direction nerves are displaced and which ones will be in the way is important to respect this rule. Similarly vascular problems with arteries but also veins should be anticipated. Angiography is only necessary when embolization or balloon occlusion test (BOT) is contemplated.

10.6.2 Brain Retraction

Brain retraction is one of the most deleterious effects of skull base surgery and much more if it is associated to vein compression which may lead to hemorrhagic infarction [22]. This may influence the choice of surgical approach; for instance, for a large petroclival meningioma on the left

side, a retrosigmoid approach may be preferred to a subtemporal one since cerebellar retraction is better tolerated.

Brain retraction can also be reduced by a lumbar drainage placed just prior to surgery; important also is the head positioning using gravity to make the brain fall by itself.

Enlargement of the bone opening down to the skull base and occasionally associated with zygomatic deposition or some bone drilling clearly reduces the need for brain retraction. Still better is the choice of an approach requiring no brain retraction such as transpetrosal or of course endoscopic endonasal approaches.

10.6.3 Sacrifice of Nerve or Vessel

Sometimes may be discussed the loss of a nerve function (hearing in translabyrinthine approach for CPA tumors or CN XII in CCJ tumor). Sacrifice of vessels is also possible but preferentially after a BOT; BOT can be realized on major vessels like ICA or VA but also on the veins and sinus. Definitive occlusion may be decided preoperatively or kept as a possibility intraoperatively in case of problem. In general, sacrifice or as a whole aggressive surgery has to be balanced with the aggressiveness of pathologies and with the quality of life. Therefore it is important to get preoperatively as much as possible an idea of the tumoral biological behavior. Markers of this behavior are still lacking in many pathologies. In the same spirit, radical tumoral resection must not be achieved at any price. With the modern techniques of radiotherapy, it is sometimes wise to leave a tumoral remnant preserving a function which will be treated by radiosurgery [9, 16, 18, 19].

Conclusion

The armamentarium of surgical approaches that can be used in skull base surgery has become important allowing efficient tumoral resection. A skull base surgeon must master all of them so as to be able to make the right choice for the right case. Many factors and not only the tumor location should be taken into account. Surgical technique is only part of the

problem, others being preoperative evaluation and intraoperative strategy. In the pediatric population because of their rarity, skull base tumors should be concentrated in reference centers where surgeons have accumulated sufficient experience.

References

1. Al-Mefty O, Ayoubi S, Smith RR (1991) The petrosal approach: indications, technique and results. *Acta Neurochir (Wien)* 53:166–170
2. Al-Mefty O, Fox JL, Smith RR (1988) Petrosal approach for petro-clival meningiomas. *Neurosurgery* 22:510–517
3. Bochenek Z, Kukwa A (1975) An extended approach through the middle cranial fossa to the internal auditory meatus and the cerebello-pontine angle. *Acta Otolaryngol* 80:410–414
4. Bruneau M, Cornelius JF, George B (2006) Anterolateral approach to the V3 segment of the vertebral artery. *Neurosurgery* 58(Suppl 1):29–35
5. Bruneau M, George B (2008) Foramen magnum meningiomas: detailed surgical approaches and technical aspects at Lariboisière Hospital and review of the literature. *Neurosurg Rev* 31:19–33
6. Crockard A, Steel T, Plowman N, Singh A, Crossman J, Revesz T, Holton JL, Cheeseman A (2001) A multidisciplinary team approach to skull base chordomas. *J Neurosurg* 95:175–193
7. Day JD, Chen DA, Arriaga M (2004) Translabyrinthine approach for acoustic neuroma. *Neurosurgery* 54:391–395
8. De Oliveira E (2001) Pterional approaches and perspectives. *Oper Tech Neurosurg* 4(2):59–107, Ed RF: Spetzler Saunders Philadelphia
9. Dufour H, Muracciole X, Metellus P, Regis J, Chinot O, Grisoli F (2001) Long term tumor control and functional outcome in patients with cavernous sinus meningiomas treated by radiotherapy with or without previous surgery: is there an alternative to aggressive tumor removal. *Neurosurgery* 48:285–294
10. Fisch U, Fagan P, Valavanis A (1984) The infratemporal fossa approach for the lateral skull base. *Otolaryngol Clin North Am* 17:513
11. Hakuba A, Liu S, Nishimura S (1986) The orbitozygomatic infratemporal approach: a new surgical technique. *Surg Neurol* 26:271–276
12. Hakuba A, Nishimura S, Jang BJ (1988) A combined retroauricular and preauricular transpetrosal-transtentorial approach to clivus meningiomas. *Surg Neurol* 30:108–116
13. House WF, Jitselberger WE (1976) The transcochlear approach to the skull base. *Arch Otolaryngol* 102:334–342
14. Kassam A, Snyderman CH, Mintz A, Gardner P, Carrau RL (2005) The expanded endonasal approach the rostrocaudal axis. Part II. Posterior clinoids to the Foramen Magnum. *Neurosurg Focus* 19(1):E4
15. Kawase T, Shiobara R, Toya S (1991) Anterior transpetrosal-transtentorial approach for sphenopetroclival meningiomas: surgical method and results in 10 patients. *Neurosurgery* 62:53–58
16. Konziolka D, Mathieu D, Lundsford LD, Martin JJ, Madhok R, Niranjana A, Flickinger JC (2008) Radiosurgery as definitive management of intracranial meningiomas. *Neurosurgery* 62:53–58
17. Mazzoni A, Sanna M (1995) A posterolateral approach to the skull base: the petro-occipital transsigmoid approach. *Skull Base Surg* 5:157–167
18. Regis J, Delsanti C, Roche PH, Thomassin JM, Pellet W (2004) Functional outcome of radiosurgical treatment of vestibular schwannomas: 1000 successive cases and review of the literature. *Neurochirurgie* 50:301–311
19. Regis J, Pellet W, Delsanti C, Dufour H, Roche PH, Thomassin JM, Zanaret M, Peragut JC (2002) Functional outcome after gamma knife surgery or microsurgery for vestibular schwannomas. *J Neurosurg* 97:1091–1100
20. Rhoton AL (2000) The temporal bone and transtemporal approaches. *Neurosurgery* 47:S211–S265
21. Sen CN, Sekhar LN (1990) The subtemporal and preauricular infratemporal approach to the intradural structures ventral to the brain stem. *Neurosurgery* 73:345–352
22. Sugita K, Kobayashi S, Yokoo A (1982) Preservation of large bridging veins during brain retraction. Technical note. *J Neurosurg* 57:856
23. Yoshida K, Kawase T (2002) Zygomatic transpetrosal approach for dumbbell shaped parasellar and posterior fossa Chordoma. *Oper Tech Neurosurg* 5(2):104–107, Ed:RF Spetzler Saunders Philadelphia

Dominic N.P. Thompson

11.1 Introduction

In rare instances a surgical approach to anterior boundary of the posterior fossa via the transoral route may be indicated. The transoral route has been well documented as a means of dealing with compressive pathologies at the clivus and craniovertebral junction in adults; however, the use of this approach in children has been less widely studied [1, 2]. Lesions that may have to be dealt with via this technique include congenital abnormalities, infectious and inflammatory lesions, as well as tumors.

11.2 History of Transoral Surgery

The evolution of the anterior approaches to the skull base can largely be traced back to the attempts by pioneers such as Kanaval and Cushing to access the pituitary and parasellar lesions in the early part of the twentieth century. It was not until the 1960s with the emergence of the operating microscope and microsurgical techniques that the transphenoidal approach to the pituitary became an established and indeed the preferred technique to access this region [3]. It was these advances combined with

improved imaging modalities that paved the way for the development of anterior approaches to the more posterior regions of the skull base including the clivus and anterior craniovertebral junction. While the transpharyngeal route had been used for many years by ENT surgeons to drain abscesses of the retropharynx, it was not until Fang and Ong described this route to access the upper cervical spine that the transoral era of transoral neurosurgery was born [4]. Unfortunately progress in developing this technique was cautious given the morbidity associated with complications such as infection, CSF leakage, and vertebral artery injury. There were however pioneers of skull base surgery who continued to develop and refine the technique with demonstrable improvement in morbidity [5, 6] and ensured that the transoral approach became an established operation in the neurosurgical repertoire. Modifications such as Le Fort I maxillotomy [7] and mandibular splitting [8] were introduced to increase the rostrocaudal exposure afforded by this approach.

The initial indications for these transoral approaches were predominantly compressive bony anomalies; however, the procedure was soon extended to the treatment of neoplastic lesions of the clivus and craniovertebral junction and even intradural pathologies [9]. Recent advances in endoscopic skull base surgery have heralded a new era in ventral approaches to the anterior boundaries of the posterior fossa. These techniques permit better access and obviate the need for some of the more extensive surgical exposures.

D.N.P. Thompson, M.D, MBBS, BSc, FRCS (SN)
Department of Paediatric Neurosurgery,
Great Ormond Street Hospital for Children NHS
Trust, Great Ormond Street, London WC1N 3JH, UK
e-mail: dominic.thompson@gosh.nhs.uk

11.3 Indications and Limitations of the Transoral Approach

The proximity of the posterior naso- and oropharyngeal wall to the clivus and anterior craniovertebral junction makes this an attractive route to access these otherwise restricted anatomical sites. A midline trajectory avoids the need to negotiate major neurovascular structures, which is a limitation of the more conventional routes from above via the middle cranial fossa or via the variety of lateral approaches through the posterior fossa.

Lesions ideally suited to the ventral approach are therefore those that are extradural and centered on the midline. For lesions related to the anterior foramen magnum, anterior arch of the atlas, and the odontoid, a direct transoral approach will usually suffice. More rostral lesions can also be accessed anteriorly though only with modifications to the approach. Lateral access is limited to 11–14 mm either side of the midline during the transoral approaches. This limitation is imposed by the vertebral artery and contents of the jugular foramen at the level of the foramen magnum and by the cavernous sinus and carotid arteries more rostrally [10]. This may not be a significant disadvantage where the primary surgical objective is decompression of the neuraxis as, for example, in the context of congenital bony malformations; however, it becomes a serious constraint in oncological surgery for laterally projecting tumors. In such instances one may have to consider an alternative surgical route or combining surgical approaches. The most commonly considered alternatives are the far lateral and extreme lateral approaches [11, 12]. Transdural or intradural lesions are not a contraindication to the transoral route; however, the risk of CSF leakage and infective complications is clearly greater, and in these circumstances lumbar drainage and formal dural repair need to be planned [9].

11.4 Pathology of Posterior Skull Base Tumors

Skull base tumors are rare in children compared with adults; moreover the spectrum of tumors affecting the skull base in children differs from that

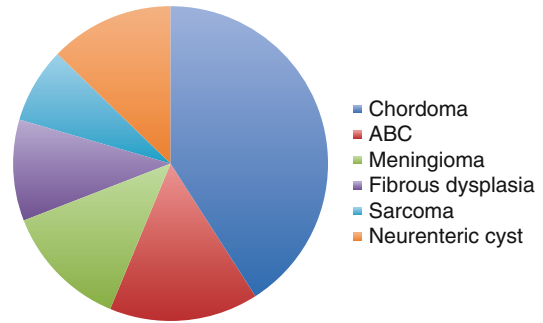


Fig. 11.1 Tumor types affecting the ventral craniocervical junction in 46 children (Composite data derived from the experience of Great Ormond Street Hospital, London, and Iowa Hospital, USA [2, 15])

in adults [13]. There is a greater variety of tumors affecting the anterior compared with the posterior skull base in children; furthermore the incidence of anterior skull base tumors is also much greater.

Overall there is a greater proportion of benign tumors in children, and tissue planes may be better preserved thus improving the prospects for useful tumor resection, and therefore prognosis has been reported to be more favorable in children compared with adults [14].

Tuite reported a series of 27 pediatric cases from Great Ormond Street Hospital who had required transoral surgery though in only 6 was this for tumor [2]. The rest were for ventral compression associated with congenital anomalies of segmentation or bone dysplasias. In cases operated on for tumor, the most common diagnosis was chordoma. In a subsequent cohort of patients, we have operated on a further 21 cases patients by this approach including 7 for tumor. The pathological diagnosis of the tumors operated on via the transoral approach comprises chordoma 8, aneurysmal bone cyst 2, sarcoma 1, and Langerhans cell histiocytosis 1. This distribution is replicated in other large series [15] Fig. 11.1.

11.4.1 T2 Chordoma

These are tumors of notochordal origin and are characteristically centered on the sphenoccipital synchondrosis. Local destruction of the clivus with extradural compression of the neuraxis is a characteristic feature (Fig. 11.2). Extension to the

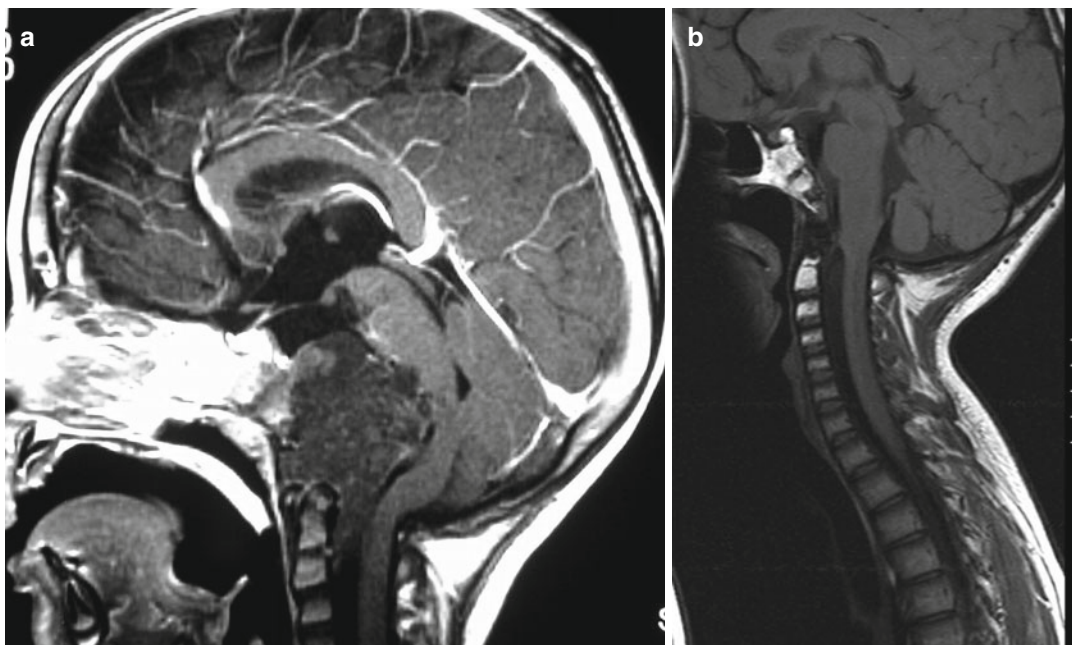


Fig. 11.2 Clival chordoma (a) sagittal MRI showing a clival chordoma in a 6-year-old girl causing severe brain stem compression. The tumor was debulked via a retrosigmoid approach in the first instance. A transoral approach was then

used to remove remaining tumor at the base of clivus and C1. The child was then treated with proton beam irradiation. The child is neurologically intact with no evidence of residual or recurrent tumor at 6 years posttreatment (b)

nasopharynx or upper cervical spine is well recognized though intradural extension is unusual. CT scanning is useful to delineate the extent of bony involvement. On MRI the lesion is hypointense on T1, hyperintense on T2, and commonly shows only modest enhancement.

In a review of the literature, Borba et al. found that only 57 % of children with chordoma were alive at a mean follow-up of 39 months [16]. Poor prognostic factors include young age at presentation (less than 5 years), atypical pathology [17], and the presence of metastases. At the time of presentation, these tumors are large and locally infiltrative compromising the prospects for complete resection. Surgery does however play an important role in the multidisciplinary management of these tumors in establishing accurate histological diagnosis and combining maximal resection with decompression of the neuraxis. Whilst surgery alone is ineffective in providing long-term tumor control the combination of surgery and radiotherapy confers a significant benefit. Given the proximity of the brain stem, proton beam irradiation is now the preferred irradiation

modality for this tumor resulting in better local control and survival [18]. Using combined proton and photon irradiation, almost 60–70 % 5-year local control has been reported [19, 20]. While many of the publications are predominantly adult series, there is increasing evidence that the benefit of proton therapy can be extended to chordoma and other aggressive tumors of the skull base in the pediatric population as well [21].

11.4.2 T2 Aneurysmal Bone Cyst (ABC)

These are benign cystic lesions of the bone that may occur either in isolation or in the context of an underlying bone neoplasm such as giant cell tumor, osteoblastoma or osteosarcoma. They more commonly present with pain than neuraxial compression. Pathologically ABCs consist of large cystic spaces separated by connective tissue trabeculae. In the craniovertebral region they most commonly arise within the axis or atlas vertebrae; involvement of the skull base is rare. They are expansile lesions best demonstrated on

CT. The observation of fluid levels, indicative of hemorrhage into the cysts, is a useful aid to diagnosis. These lesions can be exceedingly vascular, and preoperative embolization should be considered particularly in the larger lesions [22]. Embolization has been advocated as the definitive treatment modality [23]; however, at the craniovertebral junction the potential for extension of the embolic material compromising brain or spinal cord perfusion must be recognized [24]. The surgical goal is complete extirpation; subtotal removal is associated with high rate of local recurrence. If the tumor (or its removal) threatens the integrity of the anterior vertebral column, then concomitant spinal reconstruction or stabilization will be required as there is significant risk of postsurgical deformity and instability.

11.4.3 T2 Sarcoma

Chondrosarcoma, Ewings sarcoma, and epithelioid sarcoma are among the sarcomas that may

occur in the posterior skull base in children. Surgery for skull base sarcoma is rarely the sole treatment modality; precise histological diagnosis is essential in guiding therapy. These can be highly vascular, infiltrative tumors, and this strategy may optimize the prospects of safe complete resection. It may be necessary to use more than one surgical approach to achieve decompression of the neuraxis and maximal tumor debulking prior to adjuvant therapy (Fig. 11.3). In some instances, for example, in Ewings sarcoma once the tissue diagnosis is established, neoadjuvant treatment with chemotherapy followed by surgical resection of the involved field of any residual tumor is the preferred strategy.

11.4.4 T2 Other Lesions of the Posterior Skull Base in Children

A variety of other rare lesions of the posterior skull base may be encountered in the pediatric population; these include Langerhans cell

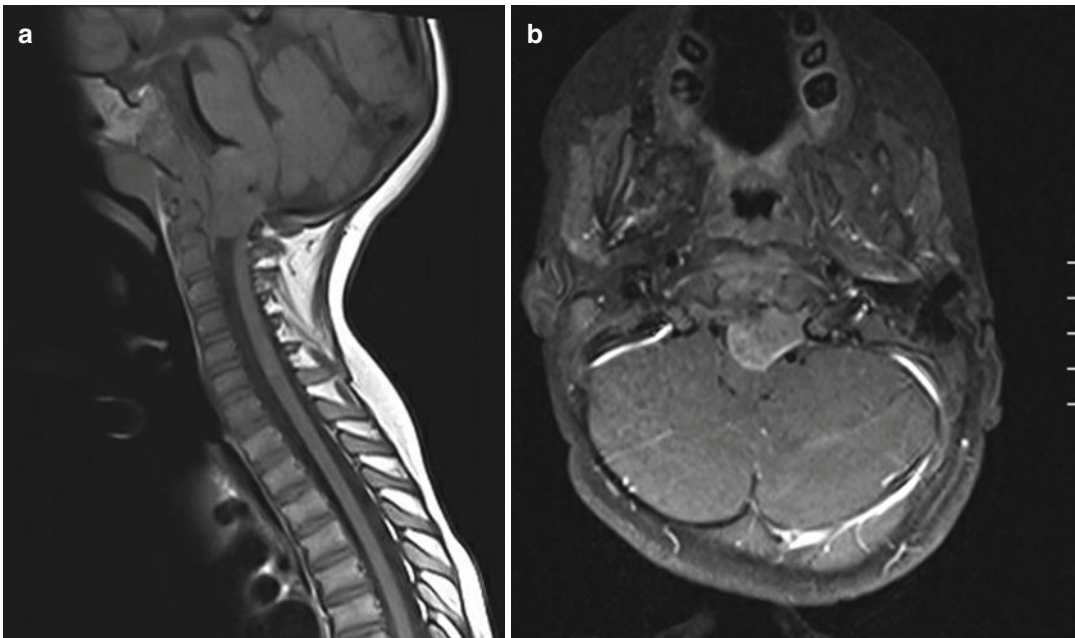


Fig. 11.3 Skull base sarcoma (a, b) pretreatment MRI scan of 2-year-old child with gait deterioration and bulbar dysfunction. A two-stage surgical approach (transoral resection followed by far lateral approach)

was used to debulk the tumor. The lesion was then treated with chemotherapy and involved field radiotherapy. The end of treatment scan shows no evidence of residual tumor (c, d)

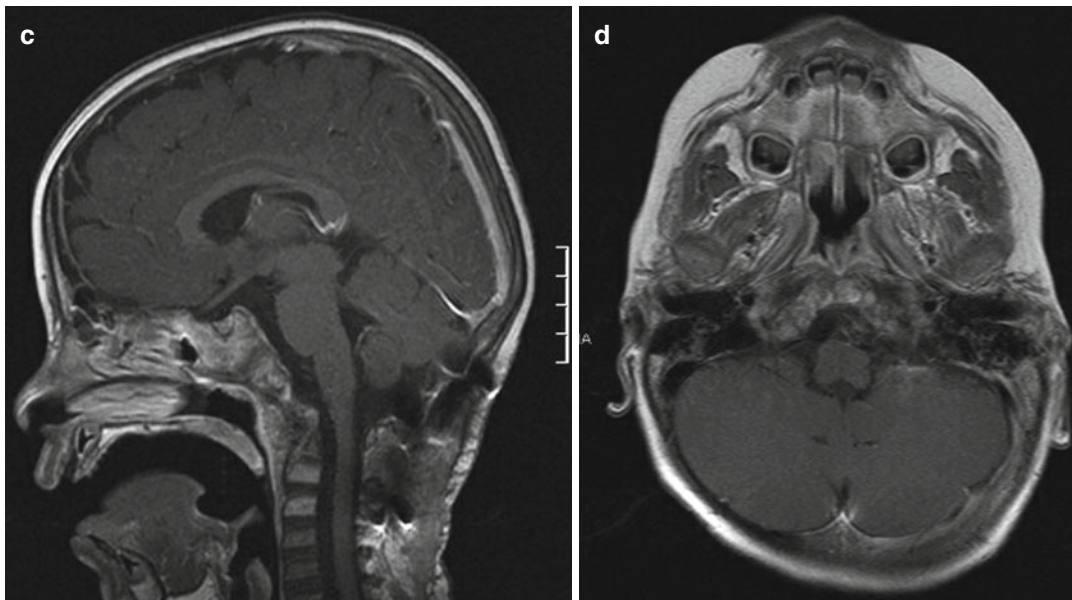


Fig. 11.3 (continued)

disorders, meningiomas, and nerve sheath tumors. These benign lesions can be treated successfully with surgery alone.

11.5 Transoral Approach in the Pediatric Age Group

While the principles of the surgical technique are broadly the same as in adults, there are additional considerations that need to be taken into account when performing transoral surgery in children. The most obvious of these is the smaller size and thus potential for more limited access. In reality however we have used the standard transoral instrumentation in children without particular difficulty; in our recent experience there have been six children under the age of 5 years (the youngest 2 years). Many children are operated on because of congenital deformity at the craniovertebral junction; in these circumstances the usual anatomical landmarks may be absent or misleading. Image guidance can be of help in negotiating distorted anatomy and may help in achieving a more predictable resection in the case of tumors accessed through this route [25].

The distance along the craniocaudal axis that can be accessed by the transoral approach is illustrated in Fig. 11.4. In most circumstances the standard transoral approach will permit access from the upper border of C1 to the base of C2. More cranial access has traditionally required complex craniofacial approaches such as the open-door maxillotomy [7]. Using this technique the clivus can be accessed as far as its upper third. There is significant morbidity associated with these extended approaches. There are now increasing reports of the use of skull base endoscopic techniques to access the upper clivus, and these have already virtually replaced the need for these extended approaches [26].

11.6 Preoperative Evaluation

MRI is the most sensitive modality by which to evaluate tumors in the region of the craniovertebral junction and posterior skull base. The effect on the brain stem and upper cervical spinal cord can be demonstrated, and the MR characteristics will aid in refining the differential diagnosis. Many of the tumors of this region will be of mesenchymal origin, arising in the bone or soft

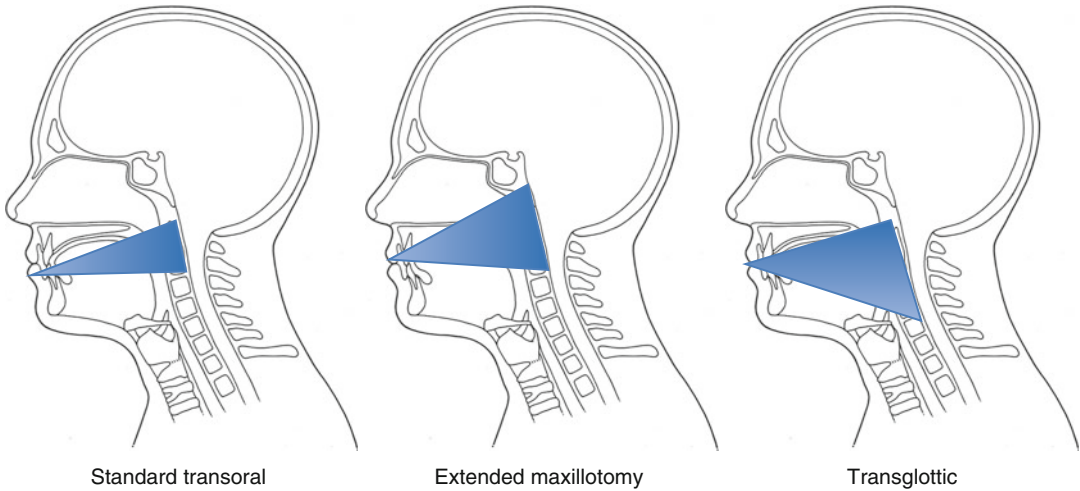


Fig. 11.4 Craniocervical access afforded by the transoral approach and its modifications

tissues and secondarily compromising the neuraxis. The extent of bone involvement by a tumor is better evaluated on CT scan; additionally CT will demonstrate the extent to which the craniocervical joints are involved and provide a means of assessing the suitability of the upper cervical vertebrae for instrumented stabilization should this be required.

Tumors at the craniocervical junction may be the cause of craniocervical instability; more commonly however instability occurs as a consequence of violating the apical, alar, and transverse ligaments in the course of the transoral approach. Preoperative flexion/extension cervical spine X-rays will reveal significant instability and will provide a baseline evaluation for comparison postoperatively.

In those situations where instability can be demonstrated prior to surgery or where it is felt to be inevitable as a consequence of the intervention (e.g., large tumors replacing bone or involving the craniocervical joints), prior immobilization in a halo body orthosis will provide temporary pre- and postoperative stability. This not only protects against inadvertent intra- and postoperative neurological damage due to hypermobility but also obviates the need to proceed to a posterior stabilization procedure in the same sitting. The immobilization also affords the opportunity

to use intraoperative image guidance using the halo frame as a reference [25].

The vertebral and the vertebrobasilar vessels may be involved or distorted by tumor and so may be vulnerable during the transoral procedure. In some cases CT angiography, combining bone and vascular imaging may assist in the planning of a safe resection [27].

11.7 Surgical Technique

An endonasal intubation is preferred to oral intubation as the latter risks further compromising the surgical access by crowding the oral cavity. Aqueous chlorhexidine is used to prepare the oral cavity, and metronidazole or co-amoxiclav is added to the usual neurosurgical antibiotic prophylaxis.

An integrated transoral retractor system (Codman/Crockard) is used (Fig. 11.5). The smaller tongue blades are usually more suitable for pediatric use. Care is needed to ensure that the tongue is not trapped between the blades and the occlusal surface of the teeth. The retractor system incorporates smaller blades for retraction of the soft palate and uvula. Once the retractors are in place, it is useful to assess the extent of rostrocaudal exposure using image intensifier or



Fig. 11.5 Codman-Crockard transoral instrumentation. The tongue blade and palatal retractors are shown

image guidance. The posterior pharyngeal wall is infiltrated with local anesthetic and adrenaline solution.

11.7.1 T2 Standard Approach

The posterior pharyngeal wall is incised along the midline. Cutting diathermy, on an extended handle, is used to dissect the submucosal tissues off the underlying bony structures. The anterior arch of the atlas is the first important bony landmark, assuming this is not involved or replaced by tumor. A subperiosteal dissection is continued laterally exposing as much of the anterior arch as possible. The dissection is continued inferiorly to the body of the axis and below if required. Caution is needed in dissecting above the atlantal arch as only the ligaments of the dens and tectorial membrane separate the submucosal layer from the dura. The atlantal arch is next drilled away revealing the odontoid process behind. The dens

is now removed, initially with a small cutting burr. It is important to remove the cancellous bone initially leaving a thin shell of posterior cortical bone intact. If the dura is exposed too early, it will tend to prolapse forward, obscuring the bone margin and increasing the risk of dural tear. The ligaments at the apex of the dens have to be sectioned to complete the bony decompression.

Prior to closure it is important to confirm that there has been no dural breach. A persisting CSF leak will significantly increase the risk of the procedure. If CSF leakage has been observed at any stage, then primary closure of the dura should be considered but is likely to be difficult particularly if the dura has been involved by tumor. A patch of surgical with application of a tissue sealant such as tisseal will usually suffice, and in the author's experience placement of lumbar drain to allow controlled CSF drainage during the early postoperative period is effective.

11.7.2 T2 Extended Approaches

The standard approach will provide good midline access from the tip of the dens to the C2/3 disc in the majority of cases. The approach can be modified to increase exposure.

11.7.3 T3 Palatal Split

The soft palate can be divided back to the hard palate providing useful extension to the anterior rim of the foramen magnum. At the end of the procedure, it is important to carefully close both the anterior and posterior mucosal surfaces as this extension increases the risk of velopharyngeal insufficiency and nasal regurgitation [2].

11.7.4 T3 Open Door Maxillotomy

This extension was designed to improve access in the treatment of basilar invagination, but it has been utilized in the approach to tumors involving the lower third of the clivus [7]. The maxillary

bone is exposed by a subperiosteal reflection above the gingival margin. A Le Fort 1 maxillectomy is carried and the vomer divided allowing the alveolar margin and the hard palate to be down fractured. Finally the hard palate is split from the incisors backwards. The two halves of the maxilla are retracted laterally exposing the mucosa over the lower clivus. While this extension improves the rostrocaudal access, the surgical corridor remains narrow compromising access to those lesions with significant lateral extension.

The open-door maxillectomy carries significant morbidity including sepsis, hemorrhage, and wound healing problems. In the pediatric population risk to the secondary dentition will usually preclude the use of this technique, and alternatives have to be sought. Modifications to the soft palate split, extending the incision into the hard palate without recourse to maxillectomy, have been recently described in children [28] but will still not achieve the rostral exposure afforded by the maxillectomy.

11.7.5 T3 Mandibular Glossotomy

Inferior extension of the transoral approach can be achieved by midline splitting of the lower lip, mandible, and tongue. This approach can be considered where the pathology extends into the midcervical spine or where mouth opening is limited as is more likely to be the case in the pediatric population [8]. The procedure results in a facial scar and problems such as damage to the dentition, dental malocclusion, and tongue mobility problems, as well as eating difficulties are reported. The procedure will also require a temporary tracheostomy in the majority of cases. In the author's experience an initial standard transoral procedure followed if required by a high anterior cervical approach will avoid the need for mandibular glossotomy in the majority of cases.

11.7.6 T4 Endoscopic Approaches

The recent evolution of endoscopic skull base techniques has profound implications for ventrally placed lesions at the craniovertebral

junction. Cadaveric studies have demonstrated both the feasibility and the improved access that can be achieved using endoscopic endonasal techniques [29, 30]. These procedures are now being increasingly described in clinical practice and it is to be hoped that these will obviate the need for the more invasive open midfacial approaches in the future [31]. It should not be assumed that these minimally invasive techniques necessarily equate with minimally morbidity. These are frequently lengthy operations, and there is a steep learning curve, major complications are well recognized, and however experienced practitioners are now developing sophisticated techniques to deal with problems such as major hemorrhage and CSF leakage.

11.7.7 Posterior Stabilization

Craniovertebral instability is a likely though not inevitable consequence of performing a transoral procedure. Where there is extensive bone destruction in particular where the occipital condyles and lateral masses of the atlas or axis are involved, the need for stabilization should be anticipated. In the author's experience 15 of 20 children who had undergone transoral procedures were deemed unstable and required a posterior stabilization procedure. This is comparable to the experience of Menezes who reported the need for posterior stabilization in 65 % of adults and 83 % of children who had undergone transoral transpharyngeal approaches [32]. The posterior fixation can be performed at the same time as the transoral procedure though more commonly a second operation is required. It is essential that the craniovertebral junction be adequately immobilized after the transoral procedure for fear of sudden cervicomedullary compression. Violation of the apical ligamentous complex as well as the transverse ligaments increases means that the occipitoatlantal as well as atlantoaxial articulation will be affected and so the arthrodesis will usually have to incorporate the occiput; occiput to C2 fixation will be the most usual. In the older child with more mature skeletal development, an instrumented fixation should be used; however,

in young children (less than 5 years) or in the context of bone dysplasia, this might not be possible, and in such cases an autologous bone graft technique is employed. The author's preference is full thickness calvarial graft secured with surgical cables [33].

Conclusions

Tumors of the posterior skull base in children are rare, and in the majority of such cases, the role of neurosurgery needs to be carefully defined in the context of the wider multidisciplinary oncological management. The anterior, transoral approaches to tumors of the posterior fossa may only occasionally be indicated; however, they remain a potentially useful component of the neurosurgical armamentarium either alone or in combination with other approaches. Transoral surgery can be carried out effectively and with low morbidity in the pediatric population; however, there are implications for craniovertebral stability and this needs to be accounted for in surgical planning.

Endoscopic skull base techniques are becoming increasingly important in accessing the anterior craniovertebral junction in adults and these are now also being reported in children. These minimally invasive approaches are likely to obviate the need for the extended transoral approaches.

References

- Menezes AH (1992) The anterior midline approach to the craniocervical region in children. *Pediatr Neurosurg* 18(5–6):272–281
- Tuite GF, Veres R, Crockard HA, Sell D (1996) Pediatric transoral surgery: indications, complications, and long-term outcome. *J Neurosurg* 84(4):573–583
- Hardy J (1969) Transphenoidal microsurgery of the normal and pathological pituitary. *Clin Neurosurg* 16:185–217
- Fang H, Ong G (1962) Direct approach to the upper cervical spine. *J Bone Joint Surg Am* 14:1588–1604
- Crockard HA (1995) Transoral surgery: some lessons learned. *Br J Neurosurg* 9(3):283–293
- Menezes AH (2008) Surgical approaches: postoperative care and complications “transoral–transpalatopharyngeal approach to the craniocervical junction”. *Childs Nerv Syst* 10:1187–1193
- James D, Crockard HA (1991) Surgical access to the base of skull and upper cervical spine by extended maxillotomy. *Neurosurgery* 3:411–416
- Brookes JT, Smith RJH, Menezes AH, Smith MC (2008) Median labiomandibular glossectomy approach to the craniocervical region. *Childs Nerv Syst* 24(10):1195–1201
- Crockard HA, Sen CN (1991) The transoral approach for the management of intradural lesions at the craniovertebral junction: review of 7 cases. *Neurosurgery* 1:88–97
- Bhangoo R, Crockard H (2000) Surgical approaches to the craniovertebral junction (C1–C2). In: Robertson J, Coakham H, Robertson J (eds) *Cranial base surgery*. Churchill Livingstone, London, pp 283–294
- Kawashima M, Tanriover N, Rhoton AL, Ulm AJ, Matsushima T (2003) Comparison of the far lateral and extreme lateral variants of the atlanto-occipital transarticular approach to anterior extradural lesions of the craniovertebral junction. *Neurosurgery* 53(3):662–674; discussion 674–5
- Heros RC (1986) Lateral suboccipital approach for vertebral and vertebralbasilar artery lesions. *J Neurosurg* 64(4):559–562
- Tsai EC, Santoreneos S, Rutka JT (2002) Tumors of the skull base in children: review of tumor types and management strategies. *Neurosurg Focus* 12(5):e1
- Teo C, Dornhoffer J, Hanna E, Bower C (1999) Application of skull base techniques to pediatric neurosurgery. *Childs Nerv Syst* 15(2–3):103–109
- Menezes AH (2008) Craniovertebral junction neoplasms in the pediatric population. *Childs Nerv Syst* 24(10):1173–1186
- Borba LA, Al-Mefty O, Mrak RE, Suen J (1996) Cranial chordomas in children and adolescents. *J Neurosurg* 84(4):584–591
- Coffin CM, Swanson PE, Wick MR, Dehner LP (1993) Chordoma in childhood and adolescence. A clinicopathologic analysis of 12 cases. *Arch Pathol Lab Med* 117(9):927–933
- Hug EB, Slater JD (2000) Proton radiation therapy for chordomas and chondrosarcomas of the skull base. *Neurosurg Clin N Am* 11(4):627–638
- Tai PT, Craighead P, Liem SK, Jo BH, Stitt L, Tonita J (2000) Management issues in chordoma: a case series. *Clin Oncol (R Coll Radiol)* 12(2):80–86
- Benk V, Liebsch NJ, Munzenrider JE, Efirid J, McManus P, Suit H (1995) Base of skull and cervical spine chordomas in children treated by high-dose irradiation. *Int J Radiat Oncol Biol Phys* 31(3):577–581
- Hug EB, Sweeney RA, Nurre PM, Holloway KC, Slater JD, Munzenrider JE (2002) Proton radiotherapy in management of pediatric base of skull tumors. *Int J Radiat Oncol Biol Phys* 52(4):1017–1024
- Saccomanni B (2008) Aneurysmal bone cyst of spine: a review of literature. *Arch Orthop Trauma Surg* 128(10):1145–1147
- Mohit AA, Eskridge J, Ellenbogen R, Shaffrey CI (2004) Aneurysmal bone cyst of the atlas: successful treatment through selective arterial embolization: case report. *Neurosurgery* 55(4):982

24. Turowski B, Schellhammer F, Herdmann J, Rommel F (2005) Fatal Ethibloc embolization of vertebrobasilar system following percutaneous injection into aneurysmal bone cyst of the second cervical vertebra. *AJNR Am J Neuroradiol* 26(7):1883–1884
25. Ternier J, Joshi SM, Thompson DNP (2009) Image-guided transoral surgery in childhood. *Childs Nerv Syst* 25(5):563–568
26. Hansen MA, da Cruz MJ, Owler BK (2008) Endoscopic transnasal decompression for management of basilar invagination in osteogenesis imperfecta. *J Neurosurg Spine* 9(4):354–357
27. Barker R, Fareedi S, Thompson D, Saunders D (2009) The use of CT angiography in the preoperative planning of cervical spine surgery in children. *Childs Nerv Syst* 25(8):955–959
28. Doorenbosch X, Santoreneos S, Molloy CJ, David DJ, Anderson PJ (2009) Modified transoral approach for resection of skull base chordomas in children. *Childs Nerv Syst* 25(11):1481–1483
29. Alfieri A, Jho H-D, Tschabitscher M (2002) Endoscopic endonasal approach to the ventral cranio-cervical junction: anatomical study. *Acta Neurochir (Wien)* 144(3):219–225; discussion 225
30. de Notaris M, Cavallo LM, Prats-Galino A, Esposito I, Benet A, Pobleto J et al (2009) Endoscopic endonasal transclival approach and retrosigmoid approach to the clival and petroclival regions. *Neurosurgery* 65(6 Suppl):42–50; discussion 50–2
31. El-Sayed IH, Wu J-C, Ames CP, Balamurali G, Mummaneni PV (2010) Combined transnasal and transoral endoscopic approaches to the cranio-vertebral junction. *J Craniovertebr Junction Spine* 1(1):44–48
32. Menezes AH, VanGilder JC (1988) Transoral-transpharyngeal approach to the anterior craniocervical junction. Ten-year experience with 72 patients. *J Neurosurg* 69(6):895–903
33. Casey AT, Hayward RD, Harkness WF, Crockard HA (1995) The use of autologous skull bone grafts for posterior fusion of the upper cervical spine in children. *Spine* 20(20):2217–2220

Mustafa Güdük and M. Memet Özek

12.1 Introduction

Hydrocephalus associated with posterior fossa tumors in children is a typical problem and can be lethal. It is usually of the obstructive type and its management has always been problematic both preoperatively and postoperatively. While the majority of patients will not require permanent treatment like endoscopic third ventriculostomy (ETV) or shunting procedures for hydrocephalus postoperatively, those patients who do so appear to suffer a stormier postoperative course [1] and are subject to the problems associated with these procedures and devices. Although in the past it was often appropriate to shunt all these patients preoperatively [2], technological advances and changes in the availability of neuroimaging have allowed earlier diagnosis of these tumors. Early surgery of the tumor is the mainstream of the treatment. However when early surgery is not possible, even though medical interventions like the use of corticosteroids, mannitol, and diuretics and fluid restriction can decrease the early

risks, the mortality and morbidity associated with hydrocephalus can make a surgical intervention like ETV, shunting, or temporary external ventricular drainage (EVD) for hydrocephalus inevitable. Also protocols of high-dose chemotherapy for medulloblastomas preoperatively make the concomitant management of hydrocephalus even more problematic and complex as any of those interventions bring its own risks with an unnecessary intervention.

In the literature, approximately one-third of all the patients will eventually require a shunt [1]. The factors associated with shunt placement have been retrospectively analyzed [1, 3] and include young age (<10 years), midline tumors, incomplete tumor resection, CSF infection, and persistent pseudomeningocele. Even though most of these patients do not require a permanent treatment for hydrocephalus after tumor resection, the associated mortality and morbidity of hydrocephalus need close follow-up. Contemporarily ETV has been shown to be an effective and safe method of treatment but shunt procedures are still required and widely used.

M. Güdük, M.D.
Department of Neurosurgery,
Acibadem University, School of Medicine,
Istanbul, Turkey

M.M. Özek, M.D. (✉)
Division of Pediatric Neurosurgery,
Department of Neurosurgery,
Acibadem University, School of Medicine,
Istanbul, Turkey
e-mail: memetozek@gmail.com

12.2 History and Contemporary Approach

Advances in molecular biological research, developments in neuroradiology allowing early diagnosis and close follow-up, microsurgical techniques, and medical pharmaceuticals have

increased survival and have improved the quality of life of pediatric posterior fossa tumor patients. Hydrocephalus either preoperatively or postoperatively is an important issue in these tumors. Even hydrocephalus should be considered and treated as a different entity from the neoplasia [4].

The management of hydrocephalus associated with posterior fossa tumors in children has always been problematic, and 60–90 % of children with posterior fossa tumors have hydrocephalus preoperatively [5, 6] and 18–40 % (mean 30 %) postoperatively [3, 7–10].

In the 1960s, when children presented in a poor clinical state as a result of a delayed diagnosis, the routine placement of a preoperative shunt significantly reduced the overall morbidity and mortality rates [11, 12], and postoperative permanent shunting was required in 40 % of patients within 4 weeks after the operation. Younger age, larger ventricles, and more extensive tumors (Chang’s stage T3 and T4) were all independently increasing the shunt dependency significantly [1, 13]. In addition to shunt dependency, shunt dysfunction, shunt infections, intraperitoneal tumor seeding, and shunt revisions to keep pace with growing children were problems associated with ventriculoperitoneal shunting, and even different approaches like placing a shunt between the third ventricle and cisterna magna (Torkildsen shunt) have been used [14].

The improvements in the availability and in the types of neuroimaging made markedly earlier diagnosis possible, and with the popularization of the shunt placement, frequent complications of shunts like infection and shunt malfunction, perioperative complications, and rarer complications like upward herniation, tumor hemorrhage, and peritoneal seeding began to be seen more commonly [15, 16], and treatment practice shifted to a more expectant policy of medical treatment with corticosteroids, diuretics, early surgery, and external ventricular drainage when needed [17–19]. In a study, perioperative and intraoperative factors which can influence the need for postoperative shunts like age at diagnosis, duration of symptoms, extent of hydrocephalus, tumor location, extent of tumor resection, presence and duration of an external ventricular

drain, flow of cerebrospinal fluid (CSF) through the fourth ventricle after tumor resection, presence of hemostatic cavity linings, method of dural closure, tumor type, CSF infection, CSF leak, and pseudomeningocele formation were reviewed [3]. Of these variables, young age at diagnosis, tumors affecting midline structures, subtotal tumor resection as determined by immediate postoperative scans, prolonged requirement of an external ventricular drain, use of cadaveric dural grafts, pseudomeningocele formation, and CSF infections were statistically significant factors associated with the need for postoperative shunt placement, which was required in 36 % of all patients [3]. However with the expectant treatment strategy, patients who were in need for shunt placement were facing increased risks of intracranial hypertension, increased rate of CSF leakage, pseudomeningocele formation, pseudobulbar palsy, CSF infections [20], intracranial hematomas with EVD, and prolonged hospitalization.

Due to these risk factors, complications, and shunt dependency of VPS, EVD prior to posterior fossa tumor surgery got popular. Dias et al. have reviewed retrospectively the records of 58 children with posterior fossa tumors and associated hydrocephalus, and they have found that 27 % of the “no treatment for hydrocephalus” group of children who had neither ventriculoperitoneal shunt (VPS) nor external ventricular drainage (EVD) needed a postoperative VPS. The “no treatment” group was stratified on the severity of preoperative hydrocephalus. They found that two factors were the main determinants: as the extent of resection decreased, the need for VPS increased, and those children whose dura were left open were more prone for the need of VPS. They have seen very few complications related with EVD, and they concluded that two-thirds to three-fourths of patients with childhood posterior fossa tumors and associated hydrocephalus may be managed with perioperative EVD and will not require shunts [5].

With the popularization of endoscopic surgery and its use in hydrocephalus treatment, ETV prior to resection of a posterior fossa tumor began to get popular [21, 22]. Jones et al. reported the

successful use of ETV in five patients with acquired aqueductal stenoses with no significant morbidity, and they mentioned even if ETV fails, the patients will be less shunt dependent [23]. Hopf et al. reviewed 100 cases who had ETV procedure performed, and the procedure had a 76 % overall success rate with the highest success rates in benign space-occupying lesions and non-tumorous aqueductal stenosis. There was no morbidity and mortality of the procedure [24].

Sainte-Rose et al. reported the role of ETV in a series of 96 pediatric patients with posterior fossa tumors. All the patients were stratified into three groups (Groups A, B, and C) based on the presence and extent of hydrocephalus. Group A had 67 patients with a more severe hydrocephalus ($p < 0.01$) present on admission in whom ETV was performed prior to tumor removal. Group B had 82 patients with hydrocephalus who did not undergo preliminary ETV but instead received conventional treatment, and Group C had 47 patients in whom no ventricular dilation was present on admission. In the follow-up, there were only four patients (6 %) in Group A compared with 22 patients (26.8 %) in Group B ($p = 0.001$) in whom progressive hydrocephalus required treatment following the removal of the posterior fossa tumor. Sixteen patients (20 %) in Group B underwent insertion of a ventriculoperitoneal shunt, significantly different from that demonstrated in Group A ($p < 0.016$). The other six patients (7.3 %) were treated by endoscopic third ventriculostomy after tumor resection. In Group C, two patients (4.3 %) with postoperative hydrocephalus underwent endoscopic third ventriculostomy. In three patients who required placement of CSF shunts, several episodes of shunt malfunction occurred that were ultimately managed by ETV and definitive removal of the shunt. There were no deaths; however, there were four cases of transient morbidity associated with ETV. They found that ETV at the time of initial tumor resection reduces the risk of postresection hydrocephalus from 26.8 to 6 %. Furthermore, in patients in whom CSF has caused spread of the tumor at presentation, ETV allows chemotherapy to be undertaken prior to tumor excision by controlling hydrocephalus.

Although the authors acknowledge that the routine application of ETV in selected patients results in a proportion of patients undergoing an “unnecessary” procedure, they believe that because patients’ postoperative courses are less complicated and because the incidence of morbidity is low and the success rate is high in those patients with severe hydrocephalus that further investigation of this protocol is warranted and in patients whom CSF has caused spread of the tumor at presentation, ETV allows chemotherapy to be undertaken prior to tumor excision by controlling hydrocephalus [21, 22].

Tamburrini et al. reviewed 104 children with posterior fossa tumors and associated hydrocephalus. They placed EVD if the child had hydrocephalus perioperatively, and 28.8 % of these children had persistent ventricular dilatation and abnormal intracranial pressure values and soon underwent ETV. The success rate of ETV was 90 % and neither operative mortality nor complications related to ETV were recorded, while two bacterial detections in CSF related with EVD were reported. They found that the only predictive factor for persistent postoperative hydrocephalus was the severity of the ventricular dilation at diagnosis. They concluded that ETV was a safe and effective procedure for postoperative persistent hydrocephalus in children with posterior fossa tumors [25]. In a series comparing VP shunt with ETV, it was seen that ETV was superior with no mortality, shorter duration of surgery, lower incidence of morbidity, no mortality, lower incidence of procedure failure, and the advantage of being shunt independent [26].

The use of ETV is criticized by the observation that the operation is performed in all patients before the excision of the tumor, whereas only a minority of children operated on for a posterior fossa tumor require a permanent postoperative CSF shunting procedure [27]. The importance of treating hydrocephalus in posterior fossa tumors is stressed in various studies. Kulkarni et al. found the need for permanent hydrocephalus treatment was the only variable associated with lower quality of life index in the long term, while a smaller posttreatment ventricle size was one of the significant factors associated with a high

quality of life index [28]. Also in another study, the quality of life was compared between patients with ETV and shunting procedures, and no substantial difference was noted [29]. In a retrospective study, patients who undergo CSF drainage procedures (either EVD or shunt placement) within 30 days of medulloblastoma resection had a significantly shorter survival time than those who do not [30]. However, treating all children with posterior fossa tumors this way potentially exposes nearly 70 % of patients to an unnecessary procedure that can have risks [8]. It will be beneficial for the patient with preoperative hydrocephalus secondary to a posterior fossa tumor if the neurosurgeon can predict the possibility of postoperative hydrocephalus requiring a CSF diversion procedure. In these cases, ETV can be considered prior to tumor resection, and postoperative EVD or shunt insertion can be avoided [31–33].

In their study, Kombogiorgis et al. showed that preoperative ventricular volume has a predictive value for the need of postresection hydrocephalus treatment, while no correlation was found between age at operation, presence of metastases, and amount of residual tumor [34]. However, in another study the patient’s age at surgery, ventricular index, and midline location of the tumor were predictive for postresection hydrocephalus treatment [35]. Surely, another variable which needs to be mentioned is the extent of tumor resection.

The “Canadian Preoperative Prediction Rule for Hydrocephalus” in children with posterior fossa neoplasms which is proposed by Riva-Cambrin is a working system for predicting and decision making. The system depends on seven different criteria which are assigned scores with a total possible value of 10 and predicts the probability of the need for postoperative hydrocephalus treatment [36]. A modification of this system was offered, and the “presence of papilledema” was replaced with the presence of “transependymal edema” which can be assessed with computerized tomography (CT) or magnetic resonance imaging (MRI) [37] (Tables 12.1 and 12.2).

The efficacy and safety of ETV as a preoperative treatment of posterior fossa tumor-associated

Table 12.1 The Canadian Preoperative Prediction Rule for Hydrocephalus (CPPRH) in children with posterior fossa neoplasms

Predictor	Score
Age <2 years	3
Presence of papilledema (later replaced with transependymal edema)	1
Moderate/severe hydrocephalus	2
Cerebral metastases	3
Preop estimated tumor diagnosis	
Medulloblastoma	1
Ependymoma	1
Dorsally exophytic brainstem glioma	1
Total possible	10

Table 12.2 The CPPRH’s predicted probabilities of postresection hydrocephalus at 6 months

CPPRH score	Probability of hydrocephalus at 6 months after resection
0	0.071
1	0.118
2	0.191
3	0.293
4	0.422
5	0.562
6	0.693
7	0.799
8	0.875
9	0.925
10	0.956

hydrocephalus is supported by literature and clinical practice; its use as a postresection treatment for persistent hydrocephalus is also mentioned in the literature. Even the combined use of perioperative ETV with ICP monitoring and postresection EVD in cases with persistent ventricular dilatation and persistently abnormal high ICP values and even VP shunt implementation in failed ETV cases are studied. The only factor associated with a higher rate of persistence of postoperative hydrocephalus was found to be the severity of the ventricular dilatation at diagnosis, and 93.3 % of children with persisting hydrocephalus had severe preoperative ventricular dilatation (Figs. 12.1, 12.2, 12.3, and 12.4). In 90 % of those cases ETV was successful [25]. In selected cases it makes biopsy possible too (Table 12.3).

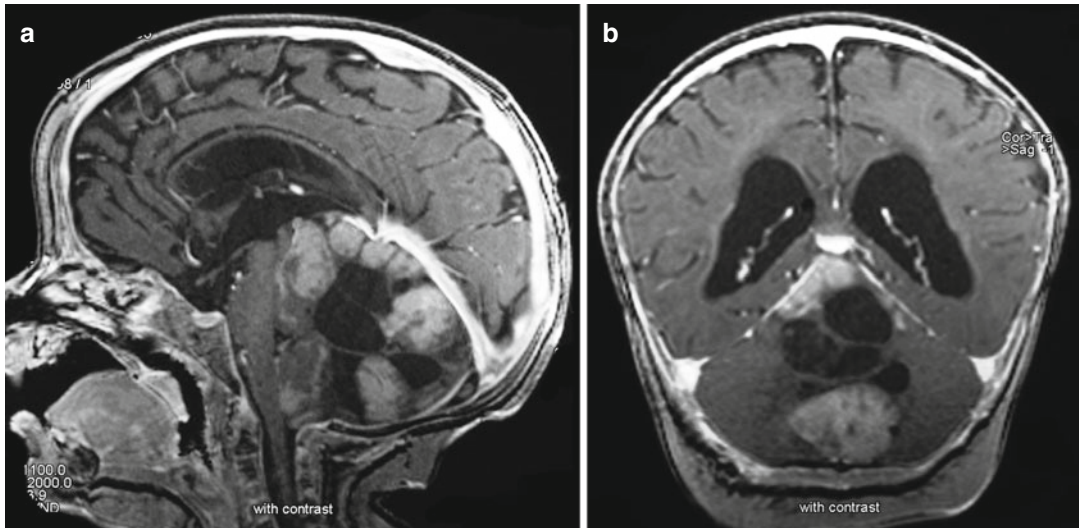


Fig. 12.1 The brainstem is pushed anteriorly toward the clivus (a) and also upward by a nodular-type medulloblastoma (b). The posterior part of the third ventricle is elevated. A preoperative ETV was performed

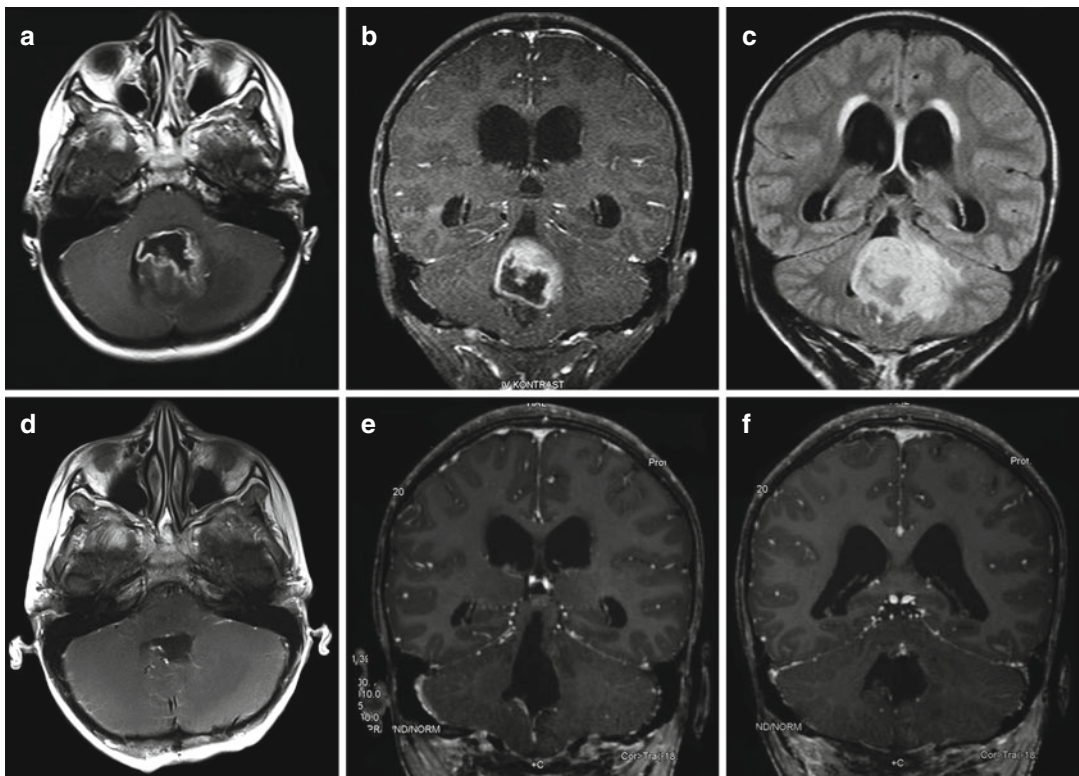


Fig. 12.2 A vermian tumor (pilocytic astrocytoma) (a) is presented with ventricular dilatation (b) and periventricular edema (c). Early postoperative study (d–f) demonstrates opening of the IV ventricle and resolving periventricular edema

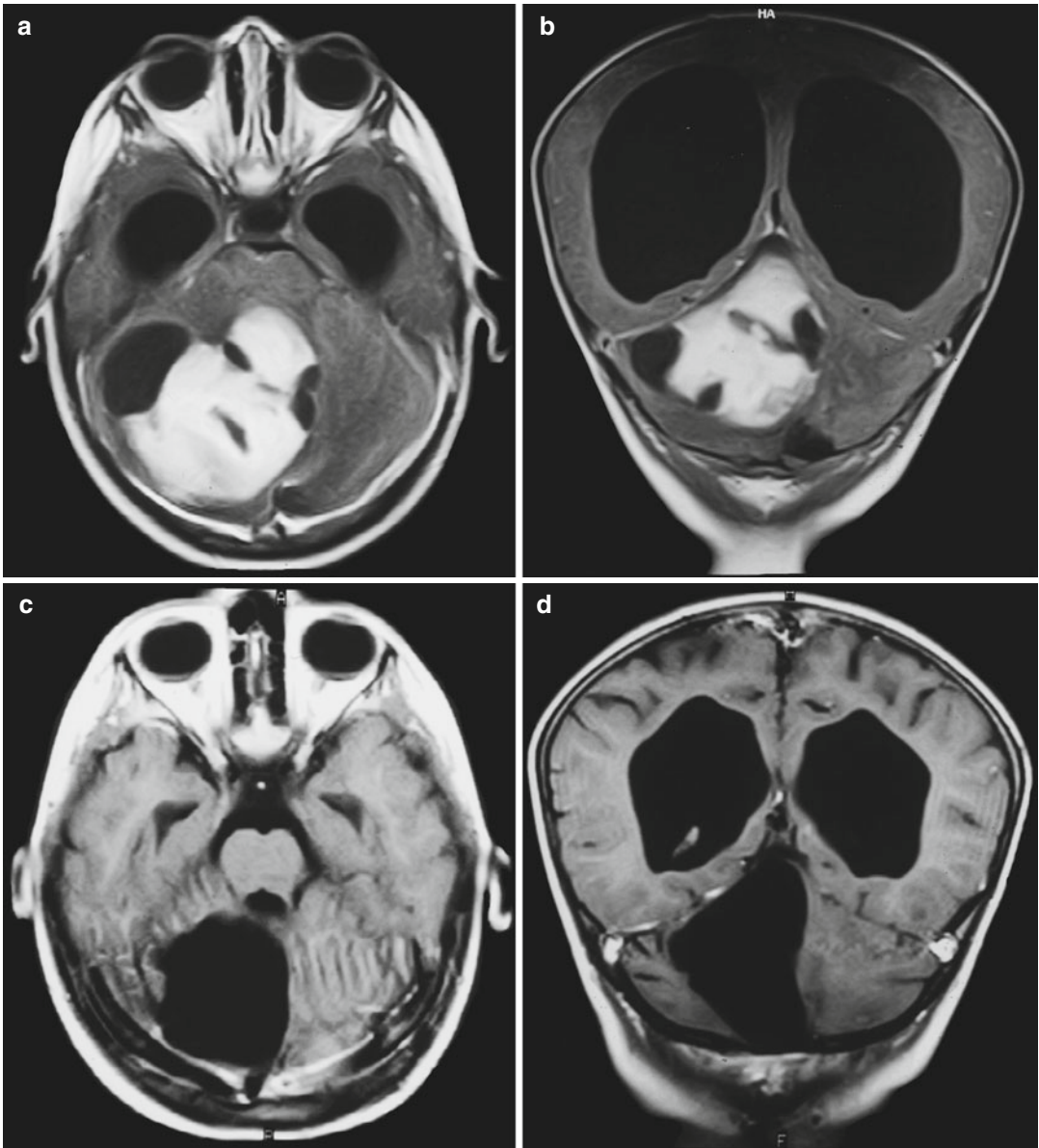


Fig. 12.3 A huge pilocytic astrocytoma case was admitted to the hospital in a precomatous condition at night (a, b). An EVD was inserted immediately and the patient was

operated the next morning. Three months after the surgery, the ventricles are still dilated without high pressure (c, d). There is no need for CSF diversion surgery

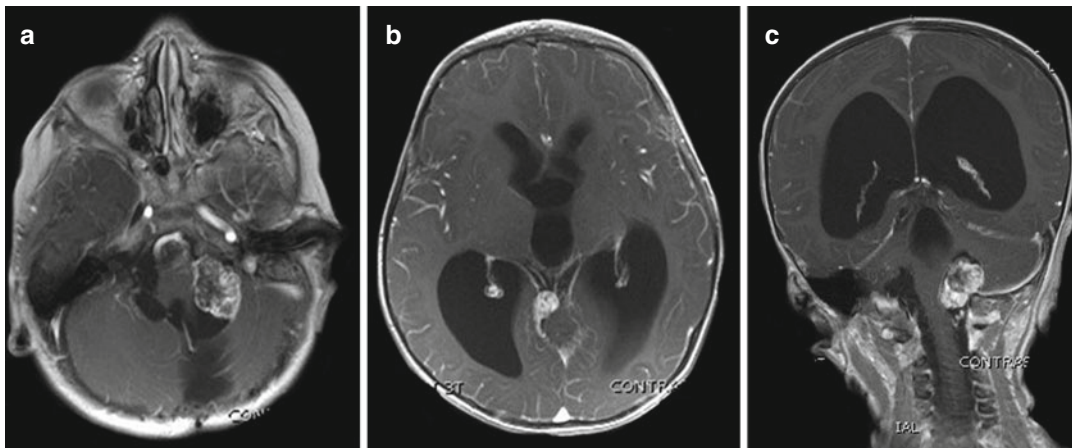


Fig. 12.4 An endependymoma case of posterior fossa with three different lesions (left PCA angle (a–b), prepontine cistern and tenorial incisor (c)). The IV ventricle is open (a). All three lesions were removed in the same session,

but hydrocephalus did not resolve. Because of multiple septations and adhesions at the interpeduncular and prepontine cistern, a VP shunt was inserted

Table 12.3 ETV procedures performed after removal of a posterior fossa tumor: review of the literature

Series reported in literature	Period of study (years)	Total no. of patients operated on for a posterior cranial fossa tumor with associated hydrocephalus	Total no. of patients with persisting hydrocephalus	No. of patients treated by postoperative ETV	Success rate of postoperative ETV (%)
Sainte-Rose et al. [22]	4	159	26	9	100
Ruggiero et al. [21]	3	46	6	4	50
Fritsch et al. [27]	4	52	6	2	100
Morelli et al. [8]	15	114	17	8	100
Due-Tonnessen and Helseth [38]	13	69	34	2	100
Tamburrini et al. [25]	6	104	30	30	90

Conclusion

Previously, before the standardization and advancement of endoscopic interventions, hydrocephalus was a big challenge; but contemporarily endoscopic interventions can be performed safely, efficiently, and in many medical centers. Due to the short-term and long-term effects of hydrocephalus on morbidity and mortality in this patient group, hydrocephalus needs to be handled usually primarily and prior to the tumor itself. Usually the drawbacks for ETV are doing an unnecessary surgery and possible failure, but when compared to the risks of hydrocephalus, doing an ETV is much more safer and should be considered whenever early surgery for the tumor cannot be done. ETV should be consid-

ered in persistent postoperative hydrocephalus cases too and, even if preoperative ETV fails, can be tried again. In the group that ETV is not possible or working efficiently, a shunting procedure can be done.

References

1. Lee M, Wisoff JH, Abbott R et al (1994) Management of hydrocephalus in children with medulloblastoma: prognostic factors for shunting. *Pediatr Neurosurg* 20:240–247
2. Albright L, Reigel DH (1977) Management of hydrocephalus secondary to posterior fossa tumors. *J Neurosurg* 46:52–55
3. Culley DJ, Berger MS, Shaw D, Geyer R (1994) An analysis of factors determining the need for ventriculoperitoneal shunts after posterior fossa tumor surgery

- in children. *Neurosurgery* 34:402–407; discussion 407–408
4. Raimondi AJ, Tomita T (1981) Hydrocephalus and infratentorial tumors. Incidence, clinical picture, and treatment. *J Neurosurg* 55:174–182
 5. Dias MS, Albright AL (1989) Management of hydrocephalus complicating childhood posterior fossa tumors. *Pediatr Neurosci* 15:283–289; discussion 290
 6. Gnanalingham KK, Lafuente J, Thompson D et al (2003) The natural history of ventriculomegaly and tonsillar herniation in children with posterior fossa tumours—an MRI study. *Pediatr Neurosurg* 39:246–253
 7. Kumar V, Phipps K, Harkness W, Hayward RD (1996) Ventriculo-peritoneal shunt requirement in children with posterior fossa tumours: an 11-year audit. *Br J Neurosurg* 10:467–470
 8. Morelli D, Pirotte B, Lubansu A et al (2005) Persistent hydrocephalus after early surgical management of posterior fossa tumors in children: is routine preoperative endoscopic third ventriculostomy justified? *J Neurosurg* 103:247–252
 9. Simon TD, Riva-Cambirin J, Srivastava R et al (2008) Hospital care for children with hydrocephalus in the United States: utilization, charges, comorbidities, and deaths. *J Neurosurg Pediatr* 1:131–137
 10. Kulkarni AV, Riva-Cambirin J, Butler J et al (2013) Outcomes of CSF shunting in children: comparison of Hydrocephalus Clinical Research Network cohort with historical controls: clinical article. *J Neurosurg Pediatr* 12:334–338
 11. Abraham J, Chandy J (1963) Ventriculo-atrial shunt in the management of posterior fossa tumours: preliminary report. *J Neurosurg* 20:252–253
 12. Hekmatpanah J, Mullan S (1967) Ventriculo-caval shunt in the management of posterior fossa tumors. *J Neurosurg* 26:609–613
 13. Chang CH, Housepian EM, Herbert C (1969) An operative staging system and a megavoltage radiotherapeutic technic for cerebellar medulloblastomas. *Radiology* 93(6):1351–1359
 14. Hoffman HJ, Hendrick EB, Humphreys RP (1976) Metastasis via ventriculoperitoneal shunt in patients with medulloblastoma. *J Neurosurg* 44:562–566
 15. Epstein F, Murali R (1978) Pediatric posterior fossa tumors: hazards of the “preoperative” shunt. *Neurosurgery* 3:348–350
 16. McLaurin RL (1983) Disadvantages of the preoperative shunt in posterior fossa tumors. *Clin Neurosurg* 30:286–292
 17. Shalit MN, Ben Ari Y, Eynan N (1979) The management of obstructive hydrocephalus by the use of external continuous ventricular drainage. *Acta Neurochir (Wien)* 47:161–172
 18. Rappaport ZH, Shalit MN (1989) Perioperative external ventricular drainage in obstructive hydrocephalus secondary to infratentorial brain tumours. *Acta Neurochir (Wien)* 96:118–121
 19. Muszynski CA, Laurent JP, Cheek WR (1994) Effects of ventricular drainage and dural closure on cerebrospinal fluid leaks after posterior fossa tumor surgery. *Pediatr Neurosurg* 21:227–231
 20. Schmid UD, Seiler RW (1986) Management of obstructive hydrocephalus secondary to posterior fossa tumors by steroids and subcutaneous ventricular catheter reservoir. *J Neurosurg* 65:649–653
 21. Ruggiero C, Cinalli G, Spennato P et al (2004) Endoscopic third ventriculostomy in the treatment of hydrocephalus in posterior fossa tumors in children. *Childs Nerv Syst* 20:828–833
 22. Sainte-Rose C, Cinalli G, Roux FE et al (2001) Management of hydrocephalus in pediatric patients with posterior fossa tumors: the role of endoscopic third ventriculostomy. *J Neurosurg* 95:791–797
 23. Jones RF, Stening WA, Brydon M (1990) Endoscopic third ventriculostomy. *Neurosurgery* 26:86–91; discussion 91–92
 24. Hopf NJ, Grunert P, Fries G et al (1999) Endoscopic third ventriculostomy: outcome analysis of 100 consecutive procedures. *Neurosurgery* 44:795–804; discussion 804–806
 25. Tamburrini G, Pettorini BL, Massimi L et al (2008) Endoscopic third ventriculostomy: the best option in the treatment of persistent hydrocephalus after posterior cranial fossa tumour removal? *Childs Nerv Syst* 24:1405–1412
 26. El-Ghandour NMF (2011) Endoscopic third ventriculostomy versus ventriculoperitoneal shunt in the treatment of obstructive hydrocephalus due to posterior fossa tumors in children. *Childs Nerv Syst* 27:117–126
 27. Fritsch MJ, Doerner L, Kienke S, Mehdorn HM (2005) Hydrocephalus in children with posterior fossa tumors: role of endoscopic third ventriculostomy. *J Neurosurg* 103:40–42
 28. Kulkarni AV, Piscione J, Shams I, Bouffet E (2013) Long-term quality of life in children treated for posterior fossa brain tumors. *J Neurosurg Pediatr* 12:235–240
 29. Kulkarni AV, Shams I, Cochrane DD, McNeely PD (2010) Quality of life after endoscopic third ventriculostomy and cerebrospinal fluid shunting: an adjusted multivariable analysis in a large cohort. *J Neurosurg Pediatr* 6:11–16
 30. David KM, Casey AT, Hayward RD et al (1997) Medulloblastoma: is the 5-year survival rate improving? A review of 80 cases from a single institution. *J Neurosurg* 86:13–21
 31. Cinalli G, Spennato P, Ruggiero C et al (2007) Complications following endoscopic intracranial procedures in children. *Childs Nerv Syst* 23:633–644
 32. Hader WJ, Drake J, Cochrane D et al (2002) Death after late failure of third ventriculostomy in children. Report of three cases. *J Neurosurg* 97:211–215

33. Drake JM (2007) Endoscopic third ventriculostomy in pediatric patients: the Canadian experience. *Neurosurgery* 60:881–886; discussion 881–886
34. Kombogiorgas D, Natarajan K, Sgouros S (2008) Predictive value of preoperative ventricular volume on the need for permanent hydrocephalus treatment immediately after resection of posterior fossa medulloblastomas in children. *J Neurosurg Pediatr* 1:451–455
35. Santos de Oliveira R, Barros Jucá CE, Valera ET, Machado HR (2008) Hydrocephalus in posterior fossa tumors in children. Are there factors that determine a need for permanent cerebrospinal fluid diversion? *Childs Nerv Syst* 24:1397–1403
36. Riva-Cambrin J, Detsky AS, Lamberti-Pasculli M et al (2009) Predicting postresection hydrocephalus in pediatric patients with posterior fossa tumors. *J Neurosurg Pediatr* 3:378–385
37. Foreman P, McClugage S, Naftel R et al (2013) Validation and modification of a predictive model of postresection hydrocephalus in pediatric patients with posterior fossa tumors. *J Neurosurg Pediatr* 12:220–226
38. Due-Tønnessen BJ, Helseth E (2007) Management of hydrocephalus in children with posterior fossa tumors: role of tumor surgery. *Pediatr Neurosurg* 43(2):92–96

Intraoperative Neurophysiological Monitoring in Posterior Fossa Surgery

13

Francesco Sala, Pasquale Gallo,
Vincenzo Tramontano, and Massimo Gerosa

13.1 Introduction

The surgical treatment of pediatric posterior fossa tumors has undergone many changes in the past century. The advent of operative magnification and ultrasonic surgical aspirator coupled with the introduction and refinement of MRI technology and with the advances in neuroanesthesia and neurointensive care has facilitated the resection of these tumors [8, 10, 11, 24, 53].

Even though operative mortality has decreased and survival rates of these patients continue to improve, a large number of survivors experience significant impairments following surgery, sometimes severely disabling. Furthermore, tumor recurrence remains a challenging management problem [16, 45, 51, 56, 75].

Despite it was thought that children were well suited to cope with brain damage, with respect to the cerebellum, the findings of recent studies suggest that cerebellar damage inflicted at a young age is not necessarily better compensated. In general, neurological impairment in pediatric brain tumor patients is poorly described. The literature

lacks prospective series that track the evolution of neurological deficits over time. Yet there are reports suggesting, for example, that children surgically treated for cerebellar pilocytic astrocytoma develop long-term disabilities [1, 16, 75].

Apraxia, motor neglect, dysarthric features, as well as language, attention, visual-spatial, executive, memory, and behavioral problems were observed in various combinations and to different degree [1]. Motor sequelae such as limb ataxia, truncal ataxia, dysarthria, and ocular movement disorders were also reported [75].

Similarly, surgery for fourth ventricle tumors carries significant morbidity. Ribi et al. [56] reported the outcomes in long-term survivors of pediatric medulloblastoma treated between 1980 and 2000 in a single institution (mean follow-up time 12.2 years). Neurological complications occurred in 72 % of patients. These complications included facial nerve palsy, strabismus, hearing impairment, visual impairment, hemi- and tetraparesis, and truncal ataxia.

Morris et al. [43] have characterized the incidence, evolution, and persistence of neurological impairment in 96 children with non-metastatic infratentorial ependymoma following maximal safe surgery and conformal or intensity-modulated radiation therapy. The most common deficits detected at baseline were limb dysmetria (55 %), cranial nerve VI palsy (51 %), VII palsy (50 %), limb paresis (40 %), dysphagia (39 %), and truncal ataxia and/or hypotonia (24 %). Overall, the number of neurological deficits per patient decreased

F. Sala, M.D. (✉) • P. Gallo, M.D.
Pediatric Neurosurgery Unit,
Institute of Neurosurgery, University Hospital,
Piazzale Stefani 1, Verona 37124, Italy
e-mail: francesco.sala@univr.it

V. Tramontano • M. Gerosa
Intraoperative Neurophysiology Unit,
Institute of Neurosurgery, University Hospital,
Verona, Italy

over time. Severe dysphagia was the function more resistant to improvement over time, no improvement was evident in 33 % of these patients, and 28 % had a gastrostomy tube placed. Baseline limb paresis and limb dysmetria were generally mild but did not improve at the follow-up. Facial paresis, dysphagia, and gait impairment improved within 36 months and then remained stable. Oculomotor dysfunction continued to improve at 60 months. In most patients neurological deficits were maximal in the postoperative period and either remained stable or improved during the posttreatment evaluation period.

Undoubtedly, the brainstem remains the most challenging location of posterior fossa tumors, due to the high concentration of neural structures so that even a small injury can result in severe and life-threatening morbidity.

During the past 20 years, there has been a resurgence of interest in operating on tumors within the brainstem. Due to the lack of redundancy, the brainstem surgical morbidity is significantly higher than in other areas of the central nervous system. Aggressive surgical treatment of mass lesions in the medulla oblongata incurs the risk of compromise the neural control of respiratory function and airway protection. Radical resection of cervicomedullary and medullary focal brainstem tumors threatens the patient's ability to swallow or protect the airway, resulting in the need for feeding gastrostomy and tracheostomy. Focal intrinsic tumors in the medulla have been associated with long progression-free survival; however, an overall risk of 15 % of permanent lower cranial nerve injury in children who underwent surgery for this subgroup of brainstem tumors has been reported [27].

Surgery in the pons and midbrain can result in diplopia due to internuclear ophthalmoplegia, with sixth and seventh nerve deficits [2, 8, 26].

In the mid-1990s, neurosurgeons have hardly worked to determine anatomical landmarks in the floor of the fourth ventricle to help localizing relatively safe entry routes to intrinsic brainstem tumors [32, 34, 67]. However, these landmarks seldom suffice to obtain this goal, as anatomy is often distorted by the tumor mass effect and is difficult to be recognized even under microscopic observation [41]. Moreover, during the surgical removal of brainstem and other posterior fossa

tumors, a number of maneuvers can expose to the risk of neurological injury: excessive coagulation or traction in the proximity of neural structures, improper or sustained use of retractors, drilling, inadvertent coagulation, or injury to perforating vessels to the brainstem.

Intraoperative neurophysiology (ION) fits in this effort to reduce postoperative complications and neurological morbidity providing real-time information on the functional integrity of neural structures contained in the posterior fossa and has become – over the last 10 years – one of the most valuable tools of neurosurgeons to protect patients from neurological injury during surgery [3, 60, 62].

ION is principally aimed to provide to the surgeon a real-time feedback on an impending injury to neural structures and pathways, in time for corrective measures to be taken and, possibly, avoid irreversible injury. On the other hand, ION may reassure that there is no impending injury to neural pathways, and therefore more radical surgery may be encouraged, when needed. Although predicting neurological outcome is one of the goal, to reduce neuromonitoring to a merely prognostic tool is unfair. Nowadays, most of the changes in intraoperative-evoked potentials are progressive or stepwise, and, if promptly recognized, there is time for taking action. In a study by McGill University [20], aimed to investigate the potential health benefit and budget impact of spinal cord monitoring, a review of the literature suggested that the rate of patients with intraoperative neurophysiological changes who benefited from corrective measures and avoided complications ranged from 63 to 100 %. They also observed that up to 20 % of all postoperative deficits that would occur in the absence of monitoring would be severe and persistent. Clearly, ION cannot prevent all neurological deficits, but some deficits that are not prevented are likely to be less severe as a consequence of the surgical adjustment resulting from monitoring. Other times, ION can only document but not prevent neural injury. For example, the inadvertent occlusion of a lenticulostriate perforating artery during aneurysm or insular tumor surgery results in a capsular infarct and will likely be not reverted by any surgical maneuver. Accordingly, motor-evoked potentials will permanently disappear. Similarly, in cerebellopontine angle surgery, a

vascular injury to the internal auditory artery will likely result in a permanent disappearance of the first peak of brainstem auditory-evoked responses. These situations fortunately represent the exception rather than the rule in ION.

In this chapter we will review and critically discuss the main ION techniques used during posterior fossa surgery in children.

13.2 Classification of ION Techniques in Posterior Fossa Surgery

Overall, neurophysiological techniques can be divided into two main categories (Fig. 13.1).

Mapping techniques: these techniques allow the functional identification of neural structures that are ambiguous from a merely anatomical standpoint. The following mapping techniques are relevant to posterior fossa surgery:

1. Identification of oculomotor nerves (III–(IV)–VI) through direct stimulation of the peripheral nerve
2. Identification of cranial motor nerves (VII–IX/X, XI, XII) through direct stimulation of the peripheral nerve
3. Identification of the oculomotor nerve nuclei at the level of the tectal plate
4. Identification of the corticospinal tract (CT) at the level of the cerebral peduncle through direct stimulation

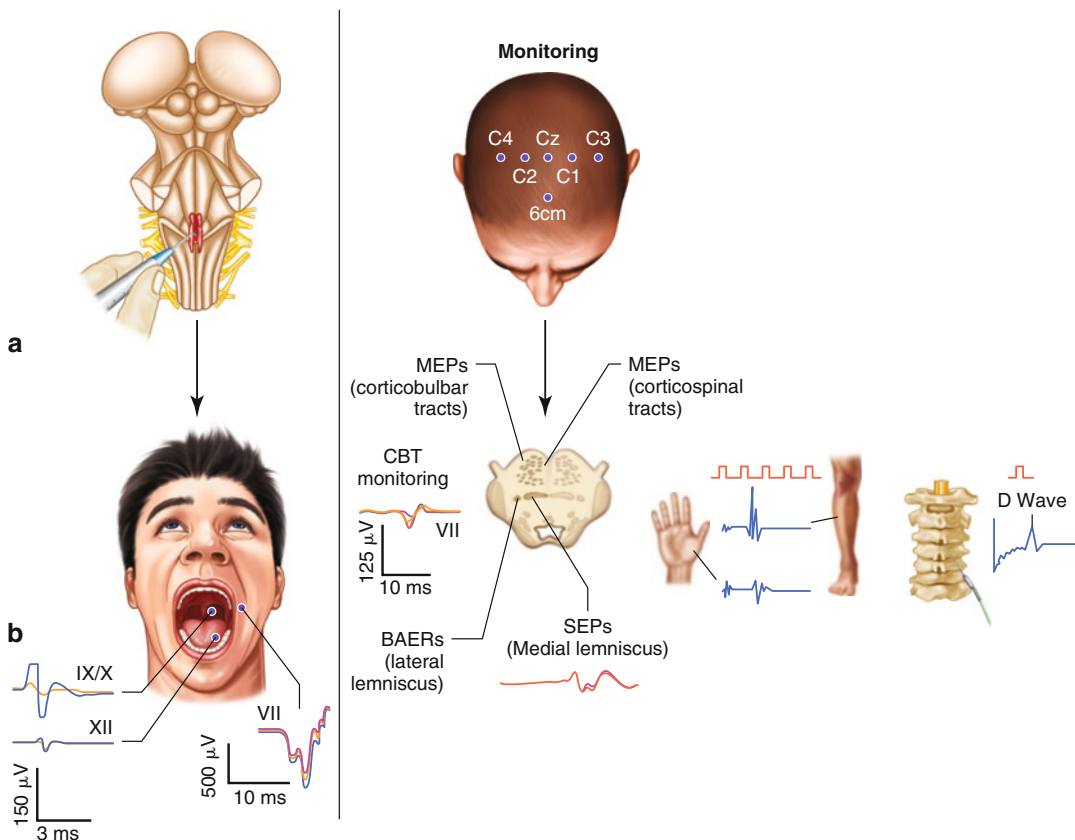


Fig. 13.1 Schematic classification of intraoperative neurophysiological techniques in the posterior fossa surgery. *Left panel:* neurophysiological mapping allows to identify the functional landmarks such as the nuclei of motor cranial nerves on the floor of the fourth ventricle. **(a)** A handheld monopolar probe is used to electrically stimulate the rhomboid fossa. **(b)** Compound muscle action potentials are recorded from the muscles innervated by motor cranial nerves. *VII* recording from the orbicularis oris for the facial

nerve, *IX/X* recording from the posterior wall of the pharynx for the glossopharyngeal/vagus complex, *XII* recording from the tongue muscles for the hypoglossal nerve. *Right panel:* neurophysiological monitoring allows to keep under control the functional integrity of neural pathways (motor, sensory, auditory,...) throughout the surgery. See the text for further details on each monitoring technique. *MEPs* motor-evoked potentials, *SEPs* somatosensory-evoked potentials, *BAERs* brainstem auditory-evoked responses, *CBT* corticobulbar tract

5. Identification of safe entry zones to the brainstem through direct mapping of the floor of the fourth ventricle to localize cranial motor nerve nuclei.

Mapping techniques allow identifying neural structures at a specific point in time but do not provide any information on what happens to these structures between one mapping and the following one. So, for example, we can identify the facial nerve nuclei on the floor of the fourth ventricle while approaching an intra-axial pontine lesion. Once the nuclei have been localized, the ependyma is open and dissection starts to detach the tumor from the surrounding parenchyma. If hazardous coagulation, traction, or any other surgical maneuver at this time compromises the brainstem through either mechanical and/or vascular injury, mapping techniques cannot assist to recognize these events. To do so, monitoring techniques should be used.

Monitoring techniques: these are true evoked potentials and provide continuous feedback on the functional integrity of neural pathways. Unlikely from mapping techniques, monitoring techniques do not localize function but are the best way to provide “online” information on the well-being of different pathways. The following are used in posterior fossa surgery.

1. Motor-evoked potential monitoring (MEP)
2. Corticobulbar motor-evoked potential monitoring (CBT MEP)
3. Free-running electromyography (EMG)
4. Somatosensory-evoked potentials (SEPs)
5. Brainstem auditory-evoked responses (BAERs)

13.2.1 Mapping Techniques

13.2.1.1 Identification of Oculomotor Nerves (III–(IV)–VI) Through Direct Stimulation of the Peripheral Nerve

Peripheral cranial motor nerves can be identified through direct stimulation. Either a handheld monopolar probe or a bipolar concentric probe can be used to deliver low-intensity stimuli directly to the nerve. The advantage of bipolar stimulation is a limited spreading of the current (rectangular

pulses of 0.2 ms duration at 1–3 Hz and intensity up to 0.5–3 mA). This could be advantageous when the goal is to identify a peripheral nerve encased in or dislocated by a tumor, to reduce the risk of activation of nearby fibers.

Recordings for mapping techniques are obtained by placing needle electrodes in the muscles innervated by their respective cranial nerves. However, these needles may be a bit traumatic in children, especially for hypoglossal, laryngeal, and, even more, oculomotor muscles, given their small sizes. Wire Teflon-coated electrodes may be used instead. The placement of recording electrodes in extrinsic oculomotor muscles may require the assistance of an ophthalmologist to avoid misplacement of the electrodes and injury to the ocular bulb, and one pair of electrodes is inserted in the superior rectus and the lateral rectus muscles to monitor the III and VI cranial nerve, bilaterally, and in the superior oblique for the trochlear nerve. When tissue of ambiguous origin is encountered during surgery, the tip of the stimulator is placed on the tissue, and the oscilloscope displays the recording muscles to determine whether this is a neural tissue or not. Similarly, mapping can also be used to confirm electrophysiologically the visual identification of a nerve. Especially when working in narrow spaces where the concentration of neural structures is high (e.g., the cavernous sinus), it is of utmost importance to adjust the stimulus intensity so that a response is obtained from only one muscle at a time. If the intensity is too high, the current may spread and the localizing value of the mapping decreases. Compound muscle action potentials (CMAPs) from extraocular muscles are usually of low amplitude as their muscle units have a considerably smaller number of fibers innervated by one axon, as compared to peripheral skeletal muscle units. Latency of the response obviously depends on the point of stimulation along the peripheral nerve, but in general it ranges between 2 and 5 ms [64, 65].

Other authors [21] have proposed less invasive recording using electrooculographic monitoring, but this was a rather small series, and the specificity and sensitivity of this method are not well established yet.

Overall, the application of intraoperative mapping of peripheral oculomotor nerves remains anecdotal and likely of little relevance in pediatric neurosurgery. Nevertheless it could be indicated during surgery for lesions involving the cisternal, cavernous, or intraorbital segment of these nerves.

13.2.1.2 Identification of Cranial Motor Nerves (VII–IX/X, XI, XII) Through Direct Stimulation of the Peripheral Nerve

Motor cranial nerves V–XII can be mapped during surgery for skull base and cerebellopontine angle tumors. Stimulation parameters similar to those used for mapping the oculomotor nerves can be used, considering that when stimulating directly the nerve, 0.1–0.3 mA usually suffices to elicit a CMAP; higher intensities could be required to elicit a response from nerve fibers encased in tumoral tissue. For recording, needle or wire electrodes are inserted in the following muscles: the masseter (V), orbicularis oculi and oris (VII), posterior wall of the pharynx (IX/X complex), vocal cords (X), trapezius (XI), and tongue (XII) (Fig. 13.2).

A typical example is the identification of the facial nerve in the cerebellopontine angle during

surgery for vestibular schwannomas in children with NF2. Besides the identification of the nerve or its fascicles during the removal of the tumor, some authors suggest to repeat a proximal stimulation (close to the brainstem) at the end of surgery, before closure, to assess the functional integrity of the nerve. A low stimulating threshold should warrant a good clinical outcome of the facial nerve [33]. Yet, a recent publication by Sugruhe et al. [68] suggests that elevated stimulation threshold exceeding >0.05 mA is a highly specific (90 %), but little sensitive (29 %) finding.

The possibility to locate other cranial nerves and record the so-called CMAP peripherally has become a standard technique in skull base surgery. In the pediatric population, it could be valuable, for example, when dealing with ependymomas invading the cerebellopontine angle through the lateral recess, in order to identify and preserve the lower cranial nerve peripherally.

13.2.1.3 Identification of the Oculomotor Nerve Nuclei at the Level of the Tectal Plate

Besides the identification of peripheral motor cranial nerves in the posterior fossa through direct stimulation, the same technique can be used to identify relatively safe entry zones into the

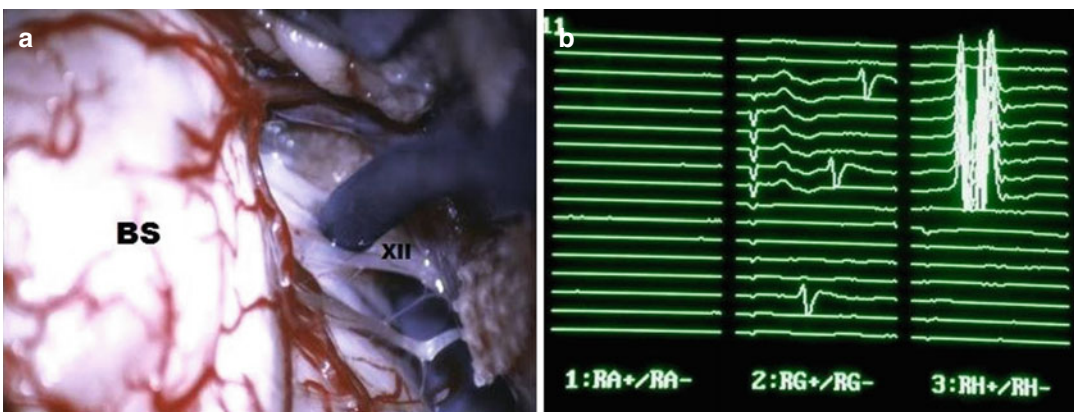


Fig. 13.2 Identification of cranial motor nerves through direct stimulation of the peripheral nerve. (a) Direct stimulation of the right hypoglossal nerve (XII) at its exit zone from the brainstem (BS). (b) Screenshot of online mapping results. A large compound action muscle potential (CMAP) is consistently recorded from the right hypoglossal muscles

(RH). A small CMAP is recorded also from the posterior wall of the pharynx muscles (RG), most likely due to some current spreading while using a monopolar stimulating probe. No responses are recorded from the right abductor pollicis brevis muscle (RA). Stimulation intensity was 0.2 mA and stimulus duration 0.5 ms

brainstem. Crowded by the cranial nerve nuclei and ascending, descending, and interconnecting fascicles, bundles, pathways, and reticular formation, the brainstem presents a highly complex structure both anatomically and functionally. This makes the brainstem a sort of neurological “minefield” such that surgical resection of brainstem tumors demands meticulous microsurgical technique due to the narrow routes leading to the lesion. If the tumor is exophytic outside the brainstem surface, its removal clearly begins at such outgrowth. In such cases, the tumor itself creates its own entry into the brainstem where it may be penetrated and eventually removed. However, tumors truly intrinsic with no surface component will require greater care and a full understanding of the local functional anatomy. This latter can be unpredictably abnormal due to tumoral mass effect and distortion of anatomical landmarks, to the point that ION may be invaluable to a reliable selection of safe entry zones.

The midbrain, which occupies the notch of the tentorium, consists of a dorsal part (the tectal plate), a large ventral portion (the tegmentum), and the cerebral peduncles. During dorsal approaches to treat intrinsic midbrain lesions, it is crucial to minimize injury to the oculomotor nerve nuclei and intramedullary tracts in order not to compromise the quality of life of these patients. This problem is not uncommon in the pediatric population that typically harbors a number of neoplastic lesions in this region. The great majority of midbrain gliomas are focal, benign astrocytomas. These tumors usually arise from either the tectal plate or tegmentum and may extend upward to the thalamus or downward to the pons, displacing but not infiltrating these structures [23, 39, 72]. Germinomas, teratomas, and primitive neuroectodermal tumors can also be found in this location.

Direct neurophysiological mapping of the tectal plate can therefore be used to identify safe entry zones to approach intrinsic midbrain lesions. Stimulation and recording techniques are the same used for mapping the peripheral oculomotor nerves, except for the stimulation intensity that at the level of the brainstem is usually kept

very low starting at 0.05 mA and usually not exceeding 1–1.5 mA. Reports are anecdotal [18, 25, 65], but it appears that direct mapping is of little help to select the entry zone as it is almost impossible to obtain a positive response when stimulating directly the superior collicula (Fig. 13.3c). This is because the superficial layers of the colliculus connect to the visual system by projection to the thalamus and the lateral geniculate nuclei, while the nuclei of the oculomotor nerves are embedded deeper in the periaqueductal gray matter, too far to be activated by superficial stimulation. This is in agreement also with our experience. Once in the brainstem, however, from the cavity wall it is possible to use neurophysiological mapping to localize the oculomotor nuclei (Fig. 13.3d).

Overall it could be concluded that the reliability of mapping the oculomotor nuclei and their tracts in the tegmentum is likely not as good as that achieved in direct mapping of other cranial nerves and of the floor of the fourth ventricle.

13.2.1.4 Identification of the Corticospinal Tract at the Level of the Cerebral Peduncle Through Direct Stimulation (Fig. 13.4)

With lesions involving the anterolateral aspect of the midbrain, it is crucial to avoid injuring the CT. The lateral mesencephalic vein [55], which courses into the lateral mesencephalic sulcus, is a useful anatomical landmark because it usually delimits posteriorly the corticospinal tract. Therefore, the entry zone to the brainstem is posterior to this sulcus in order to avoid injury to the pyramidal tract in the peduncle. However, local anatomy can be distorted by the tumor so that only a functional identification of the motor tracts can allow a safe entry to the lateral midbrain.

To identify the CT we use a handheld monopolar stimulator (tip diameter 0.75 mm) as cathode, with a needle electrode inserted in nearby muscles as anode. The response is recorded as a CMAP from one or more muscles of contralateral limbs, after a train of four to five stimuli of 0.5 ms duration, at 1–2 Hz. We usually increase

stimulation intensity up to 2 mA, starting from 0.5 mA. Other authors have successfully used higher intensities [70]. When a motor response is recorded, the probe is then moved in small increments of 1 mm in order to find the lowest threshold to elicit that response. In the case of cystic midbrain lesion (i.e., a pilocytic astrocytoma, common in this location), sometimes mapping of the CT is negative at the beginning of the procedure, but a positive response could be recorded when mapping from within the cystic cavity towards the anterolateral cystic wall.

13.2.1.5 Identification of Safe Entry Zones to the Brainstem Through Direct Mapping of the Floor of the Fourth Ventricle to Localize Cranial Motor Nerve Nuclei

For the great majority of surgical approaches to the intrinsic tumors of the pons and the medulla – especially for tumors located in the dorsal part of the pons and the open portion of the medulla – the access is by a *suboccipital craniotomy and trans-fourth-ventricle route*.

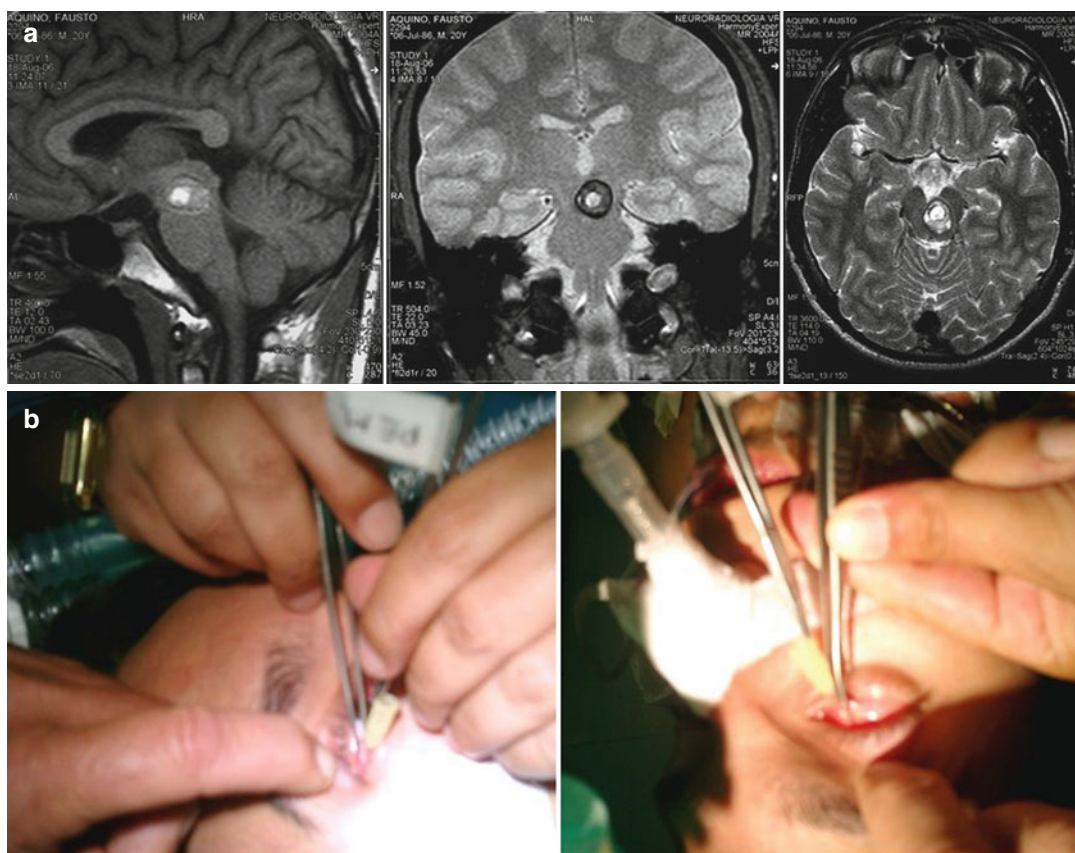


Fig. 13.3 Identification of the oculomotor nerve nuclei at the level of the tectal plate. **(a)** Sagittal (*left*), coronal (*middle*), and axial (*right*) magnetic resonance images of a midbrain cavernoma. **(b)** One pair of wire electrodes is inserted in the upper rectus and lateral rectus muscles, bilaterally, to record compound action muscle potentials (CMAPs) after stimulation of the III and VI cranial nerve nuclei, respectively. **(c)** Initially (time 12.33), direct stimulation of the superior colliculus (*left panel*) does not

elicit any response from the oculomotor muscles innervated by the III and VI cranial nerves (*right panel*). **(d)** Later on (time 13.41), stimulation from inside the surgical cavity, during removal of the cavernoma, elicits a consistent response (*arrow*) from the left upper rectus muscles (L III), indicating stimulation of the nearby nuclei. *R III* right upper rectus muscle, *L III* left upper rectus muscle, *R VI* right lateral rectus muscle, *L VI* left lateral rectus muscle

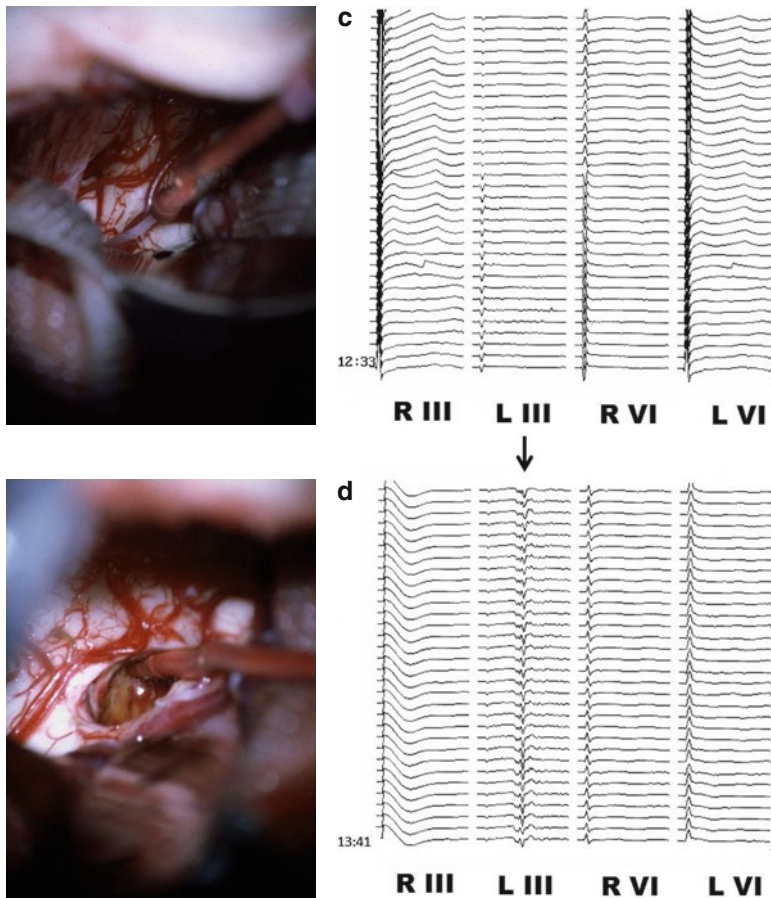


Fig. 13.3 (continued)

Entering the floor of the fourth ventricle requires a great understanding of the underlying structures.

At the level of the pons, the more prominent part of the median eminence, the facial colliculus, represents a highly dangerous brainstem “entry zone” through the rhomboid fossa [34]. Damage to this area invariably causes facial (VII) and abducens (VI) nerve paralysis as well as lateral gaze disturbances due to parabrachial reticular formation dysfunction. Injury to the medial longitudinal fascicles, which border the median sulcus and lie between the abducens and oculomotor nuclei (the so-called VI–III pathway), may result in internuclear ophthalmoplegia.

More caudally, at the level of the medulla, within the small concavity of the calamus scrip-

torius situated above the obex and usually below the striae medullaris lie two triangles of great functional importance: the hypoglossal triangle and the ala cinerea or vagal triangle. Immediately below the two medial triangles lie the hypoglossal nuclei, which control the muscles of the tongue. Due to the close proximity of the two nuclei, surgical injury to this area almost always results in severe tongue paralysis and atrophy. Since hypoglossal paralysis represents one of the most devastating cranial nerve deficits, even a minor injury in this area must be avoided.

Lateral to the hypoglossal are the vagal triangles and under these lie the dorsal nuclei of the vagus from where motor fibers to the bronchi, heart, and stomach originate. Slightly deeper and lateral lies the nucleus ambiguus, which gives

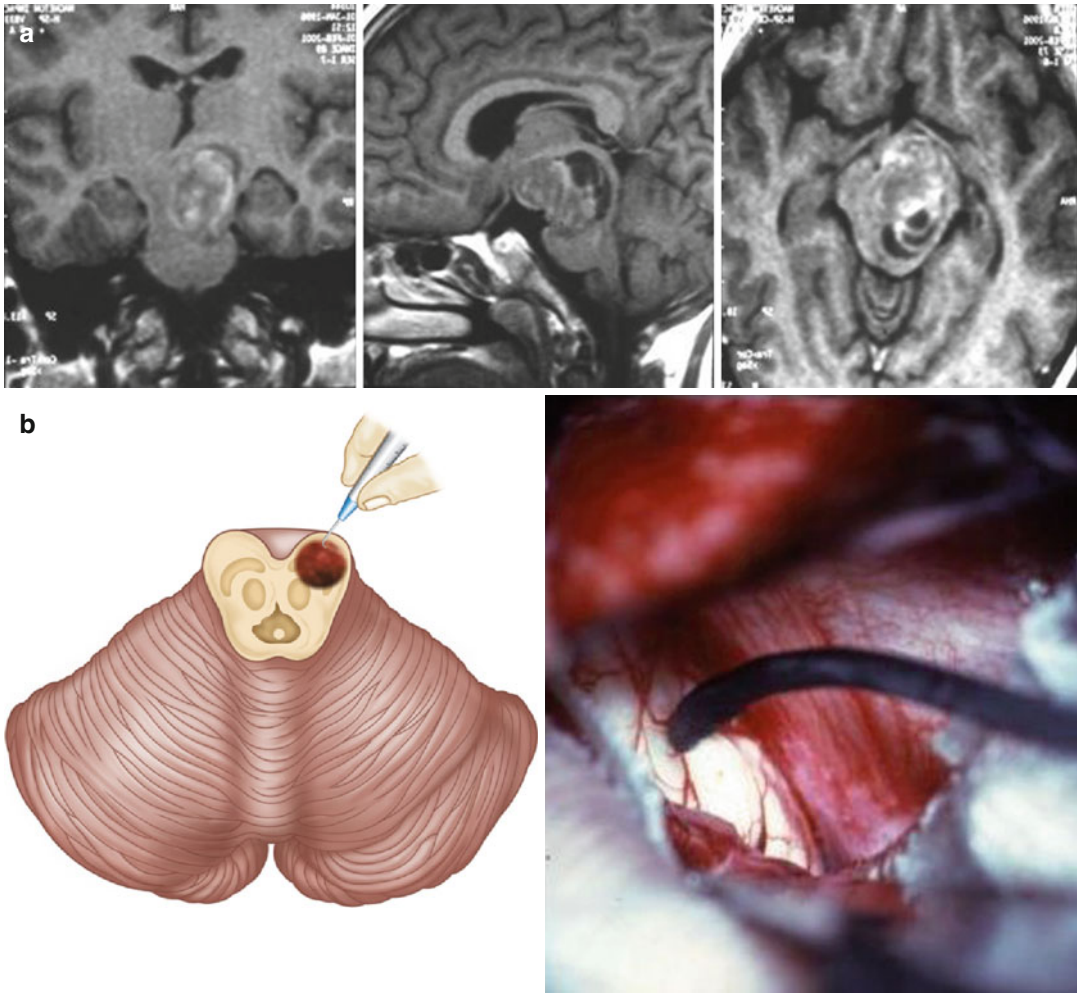


Fig. 13.4 Identification of the corticospinal tract at the level of the cerebral peduncle. **(a)** Preoperative gadolinium-enhanced T1-weighted images of a pilocytic astrocytoma of the left cerebral peduncle. Coronal (*left*), sagittal (*middle*), and axial (*right*) view. **(b)** Schematic illustration of direct stimulation of the corticospinal tract at the level of the cerebral peduncle by using a monopolar handheld probe with a short train of stimuli (each stimulus 0.5 ms duration) at 1 Hz and current up to 2 mA (*left panel*). Intraoperative view of stimulation of the left cerebral peduncle in the patient depicted in **(a)**. The tumor was approached through a left lateral supracerebellar infratentorial route (*right panel*). **(c)** Schematic illustration of the motor-evoked potential recorded from the abductor polli-

cis brevis (APB) muscle following direct stimulation of the cerebral peduncle (*left panel*). Mapping results in the same patients depicted in **(a, b)**. A consistent response from the left APB (LA) was recorded, while no responses were recorded in the left tibialis anterior muscle (LT) and in the right side muscles (RA and RT) (*right panel*). **(d)** The tumor was then removed entering the lateral midbrain posteriorly to the zone where the left APB response was elicited. Continuous transcranial MEP monitoring was performed during the surgery with no significant changes. The postoperative gadolinium-enhanced T1-weighted images documented a complete removal of the tumor, and the patient presented no additional motor deficits (Modified from Sala and Lanteri [61])

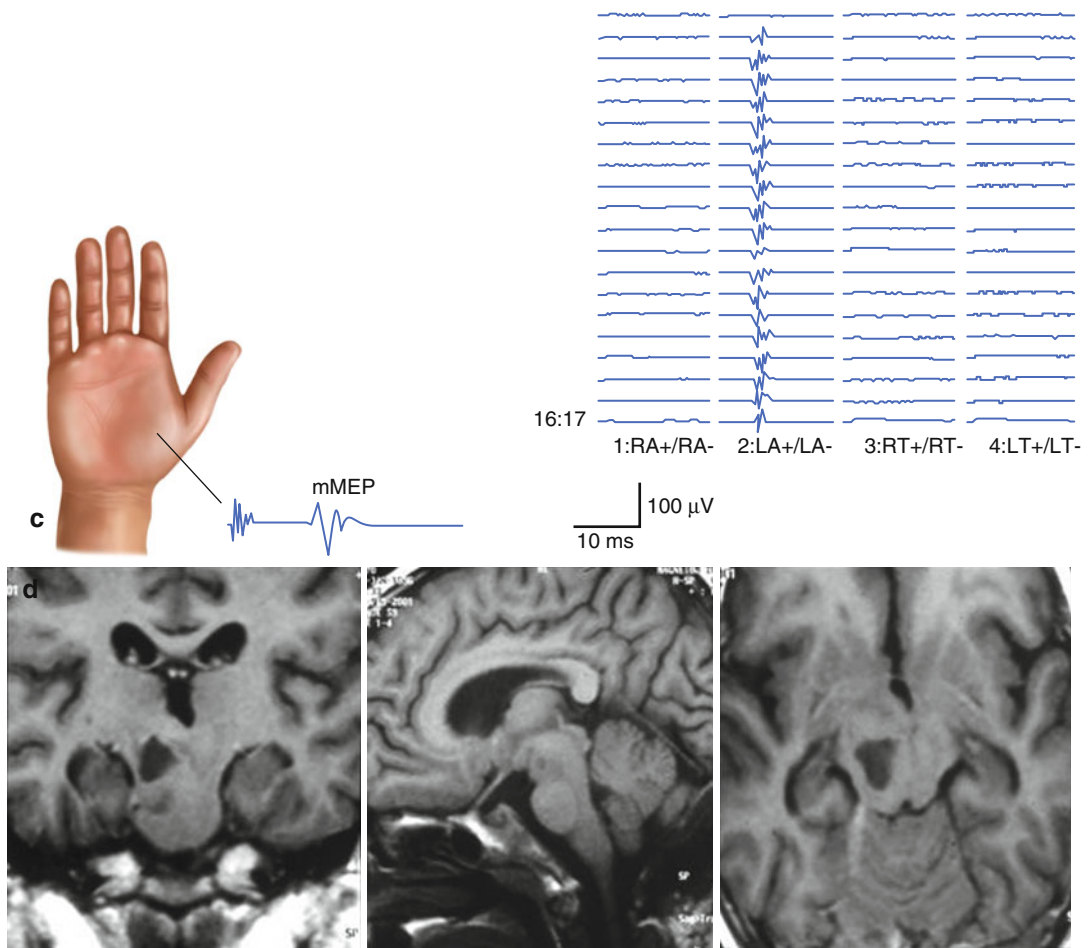


Fig. 13.4 (continued)

rise to fibers of the glossopharyngeal (IX), vagus (X), and accessory (XI) nerves, supplying musculature to the palate, pharynx, and larynx. Therefore, injury to this small area may result in deficits such as impaired swallowing, dysphonia, nose regurgitation, and coughing reflex loss, thus exposing the patient to the risk of aspiration pneumonia and incapacity to eat or drink [7].

Although anatomical landmarks have been described to safely enter the floor of the fourth ventricle [32, 34, 67], these may not be reliable due to distortion induced by the tumor (see Fig. 13.5). Displacement of a classical anatomical landmark such as the facial colliculus is commonly faced during brainstem surgery. Similarly, even when anatomy is not significantly distorted by the tumor, the identification of areas overlapping the lower cranial nerve motor nuclei can be

challenging. Mapping techniques are now available to intraoperatively identify the VII, X–IX, and XII motor nuclei or their intramedullary tracts on the floor of the fourth ventricle.

Similarly to what described for mapping the oculomotor nuclei in the midbrain, a hand-held monopolar stimulating probe can be used. CMAPs are then elicited in the muscles innervated by the cranial motor nerves. To record the responses from cranial motor nerves VII, IX/X, and XII, wire electrodes are inserted in their innervated muscles, as described above for direct mapping of the peripheral cranial nerves. A single stimulus of 0.2-msec duration is delivered at a repetitive rate of 1–2 Hz. There are two different mapping strategies that can be used. One can look, for each site, at the threshold intensity which allows recording a CMAP. Moving the

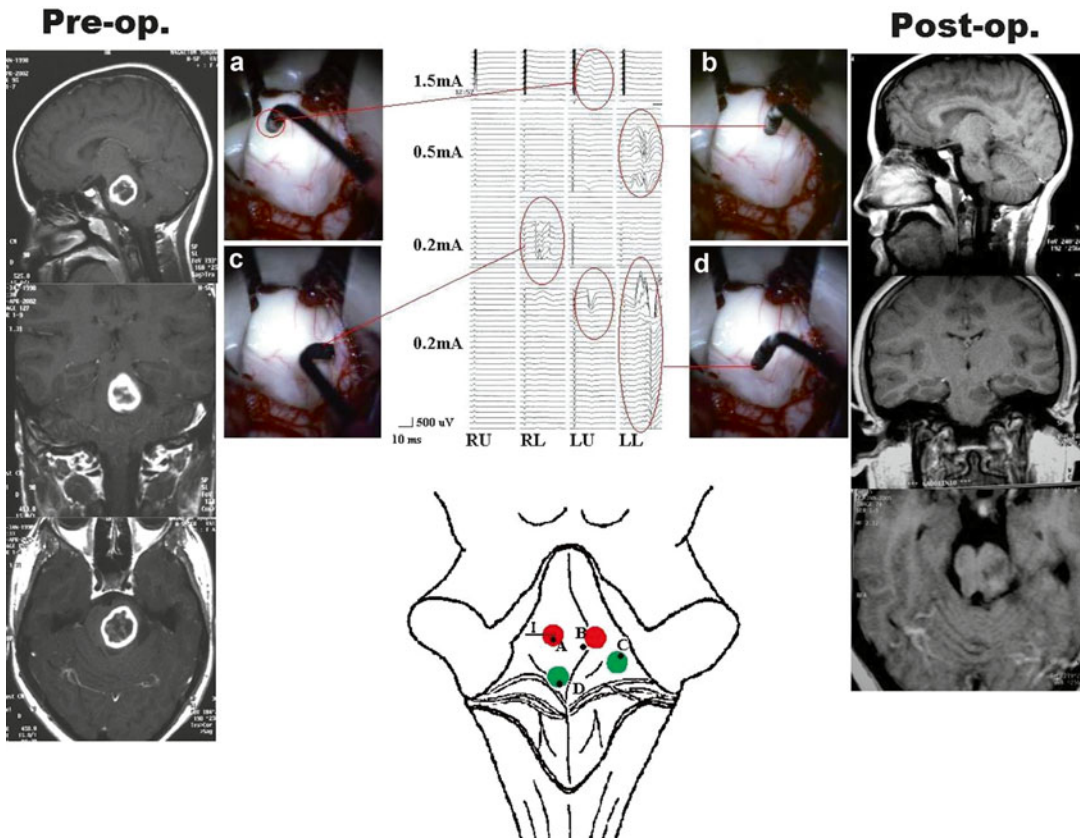


Fig. 13.5 Identification of the facial colliculus through direct mapping of the floor of the fourth ventricle. *Left panel:* preoperative contrast-enhanced T1-weighted MR images of a left pontine astrocytoma in a 12-year-old girl, sagittal (*top*), coronal (*middle*), and axial (*bottom*) view. The tumor was approached through a median suboccipital craniectomy. At surgery, the median sulcus on the floor of the ventricle was dislocated to the right, and the left median eminence was expanded. *Middle upper panel:* mapping of the facial nerve motor nuclei on the floor of the fourth ventricle. (a) On the left side, about 1.5 cm rostral to the striae medullares, a response was obtained from the left orbicularis oculi (LU) at 1.5 mA. (b) A response from the left orbicularis oris (LL) was recorded at a lower stimulation (0.5 mA) when the handheld probe was moved caudally and to the right. (c) When the probe was moved further down and to the right, the stimulation elic-

ited a consistent response from the right orbicularis oculi (RL) at an even lower intensity (0.2 mA). (d) Finally, by moving the probe paramedially to the left side, a clear response was recorded from both the left orbicularis oculi (LU) and oris (LL) at a similar intensity (0.2 mA). *Middle lower panel:* schematic summary of the mapping results (a–d) corresponding to the stimulating points illustrated in the upper panel. The conclusion was made that the actual location of the nuclei (green color) was more caudal than expected according to the normal anatomy (red color), especially on the left side, due to the tumor mass effect. Accordingly, the incision (I) was carried on transversally in correspondence of the stimulating point A. *Right panel:* postoperative contrast-enhanced T1-weighted MR images, sagittal (*top*), coronal (*middle*), and axial (*bottom*) view, showing complete removal of the tumor (Modified from Sala and Lanteri [61])

tip of the stimulator 1 mm apart, it is then possible to explore the floor of the fourth ventricle and identify the area with the lowest threshold (which is the one closer to either the nucleus or the intramedullary root of the nerve) and with the highest threshold or no response at all. These latter are likely the safer entry zones as the nuclei or tracts are far from the tip of the stimulator. The

other possibility is to work with an intensity of approximately 0.5–1 mA and determine for each point the amplitude of the muscle response. The point corresponding to the highest amplitude indicates the vicinity of the mapped nucleus, while small amplitudes or, better, no response at all suggests a safe distance from the nucleus or tracts (Fig. 13.5). In any case, no stimula-

tion intensity higher than 2 mA should be used to avoid cardiovascular derangements. Based on mapping studies, characteristic patterns of motor cranial nerve displacement, secondary to tumor growth, have been described (Fig. 13.6) [42].

These studies, although based on a small number of patients, suggest that motor nuclei dislocation is no random but rather corresponds to reproducible patterns so that the surgeon may to some extent predict where to look for the nuclei based

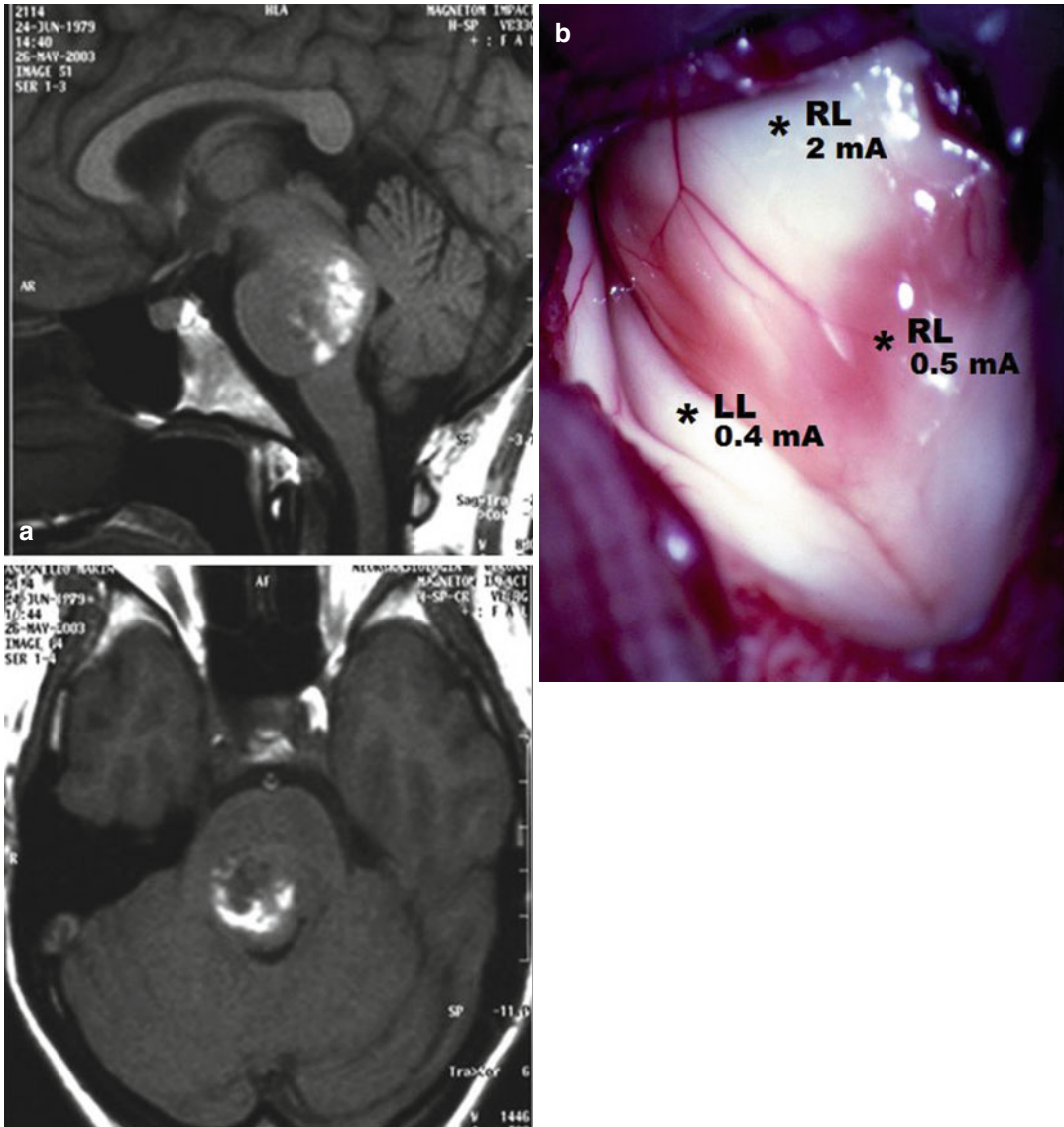


Fig. 13.6 Displacement of facial nerve nuclei. (a) Sagittal and axial T1-weighted MR images of a bleeding upper pontine cavernoma. (b) Intraoperative view of the distorted floor of the fourth ventricle with no anatomical landmarks to identify the facial colliculi. Results of neurophysiological mapping are displaced. Responses from the right lower facial muscle, orbicularis oris, (RL) are recorded following monopolar stimulation with 2 mA (0.5 ms duration) at the *upper asterisk*. Responses from the right lower facial muscle, orbicularis oris, (RL) are

recorded at lower intensity (0.5 mA) from the *lower right asterisk*, indicating a closer relationship with the right facial nerve nucleus or intramedullary root. Finally, responses from the left lower facial muscle, orbicularis oris, (LL) are recorded at low intensity (0.4 mA) from the *lower left asterisk*, indicating a close relationship with the left facial nerve nucleus or intramedullary root. (c) These results suggest a downward and lateral displacement of the facial nerve nuclei, consistent with the report of Morota et al. (see ref. [42])

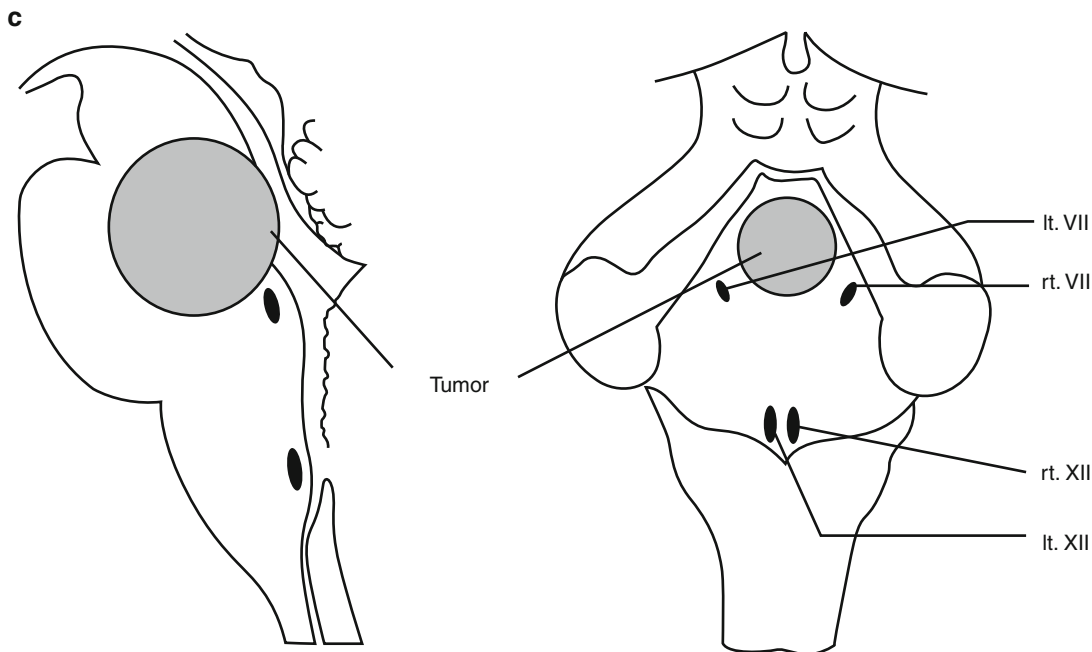


Fig. 13.6 (continued)

on the preoperative MRI. Obviously, intraoperative confirmation with direct mapping is absolutely crucial.

Despite the relative straightforwardness of the fourth ventricle mapping technique and its indisputable usefulness in planning the most appropriate surgical strategy to enter the brainstem, postoperative functional outcome is not always predicted by postresection responses. In the case of mapping of the motor nuclei of the seventh cranial nerve, brainstem mapping cannot detect injury to the supranuclear tracts originating in the motor cortex and ending on the cranial nerve motor nuclei. Consequently, a supranuclear paralysis would not be detected, although lower motoneuron integrity has been preserved. Similarly, the possibility of stimulating the intramedullary root more than the nuclei itself exists. This could result in a false-negative peripheral response still being recorded despite an injury to the motor nuclei [41].

Mapping of the glossopharyngeal nuclei has also some limitations. Recording activity from the muscles of the posterior pharyngeal wall after stimulation of the ninth cranial nerve motor nuclei on the floor of the fourth ventricle assesses only the functional integrity of the efferent arc of the

swallowing reflex. No information on the integrity of afferent pathways and afferent/efferent connections within the brainstem is provided, despite the fact that these pathways are indeed necessary to provide functions involving reflexive swallowing, coughing, and the complex act of articulation.

13.2.1.6 Brainstem Mapping for Fourth Ventricle Tumors

The same mapping techniques used to localize motor nuclei or cranial nerve intramedullary tracts during surgery for intrinsic brainstem tumors can also be used when dealing with tumors that either grow exophytically from the brainstem or grow primarily in the fourth ventricle and secondarily infiltrate the floor, entering the brainstem. In these cases brainstem mapping is used to decide when to stop removal rather than to select the entry zone to approach the tumor. Both in the case of a dorsally exophytic medullary glioma or of a fourth ventricle tumor, through a dorsal approach, the surgeon is faced first with the tumor, while the brainstem is displaced ventrally. In this situation, there is no point in mapping the nuclei at the beginning of the tumor removal, as these are ventral to the tumor, and CMAPs are likely not obtainable. Yet, when most of the exophytic

component of the glioma or the intraventricular part of the tumor has been removed, it is important to avoid entering the brainstem as the lower cranial nerve nuclei are just a few millimeters underneath the infiltrated ependyma. At this point it is useful to alternate a piecemeal removal of tumoral tissue with periodical mapping of the tumor to see if a CMAP is elicited. Using a monopolar probe, current spreads in a way that if we use intensity around 1–1.5 mA, it is possible to have some response even when there is still margin for more tumor removal. However, from now on, great care should be taken to avoid irreversible damage to the nuclei and is recommendable to stop removing the tumor when the threshold drops to less than 0.7–0.5 mA. In this setting, it is extremely valuable to combine direct mapping with the continuous monitoring of the corticobulbar tracts (Fig. 13.7).

From a neuro-oncological standpoint, it should be observed that brainstem tumors at the level of the medulla in children are often benign, low-grade astrocytomas [4]. So, even when a little sole of tumor is left behind on the floor of the fourth ventricle, this may remain indolent for many years and, occasionally, disappear, with no need for adjuvant treatments. Therefore, there is no justification to pursue a “total” tumor removal at all costs in this area because this will likely charge the child with life-threatening deficits such as dysphagia and absence of coughing reflex.

13.2.2 Monitoring Techniques

13.2.2.1 Brainstem Auditory-Evoked Potentials

Brainstem auditory-evoked potentials can provide useful information on the general well-being of the brainstem, especially during those procedures in which a significant surgical manipulation of the brainstem and/or of the cerebellum is expected. When interpreting brainstem auditory-evoked potential recordings, a thoughtful analysis of the waveforms and of their correlation with neural generators provides useful information about the localization of the changes. In summary, dysfunction of the eighth nerve proximal

to its cochlear end will cause a prolongation of the I–III interpeak interval, attenuation of waves III and V, or both. The latencies of waves III and V increase in parallel, while the III–V interpeak interval remains almost unchanged as long as the auditory pathways within the brainstem are not affected.

A disappearance of wave I only may also be indicative of cochlear ischemia secondary to the compromise of the internal auditory artery. Vice versa, if the cochlea is not injured and the damage to the eighth nerve occurs in the cerebellopontine angle, wave I may persist even if the eighth nerve is completely transected.

Damage to the lower pons, around the area of the cochlear nucleus or the superior olivary complex, will also affect waves III and V with delay in latency and drop in amplitude. Damage to the brainstem at the level of the midbrain will affect waves IV–V, but not waves I or III [36].

We have found BAERs to be more relevant during surgery of the cerebellopontine angle rather than in brainstem surgery where their value to localize the level of the injury needs experience in BAERs’ interpretation, and the area of the brainstem that can be evaluated with BAERs is circumscribed.

13.2.2.2 Somatosensory-Evoked Potentials

Like BAERs, SEPs have been extensively used to assess the functional integrity of the brainstem, although these two modalities, together, can evaluate only approximately 20 % of the brainstem pathways. As a result, their use is of limited value when the major concern is related to the corticospinal and cranial nerve motor function.

Yet, SEPs are valuable especially when approaching tumors at the level of the cervicomedullary junction where the dorsal column pathways end up in the Gall and Burdach nuclei. Here, however, similar limitations as those regarding SEP monitoring in intramedullary spinal cord tumors apply. The incision of the medial longitudinal rafe and the gentle lateral displacement of the dorsal column nuclei sometimes suffice to transiently compromised further monitoring with SEPs as they may drop significantly in amplitude

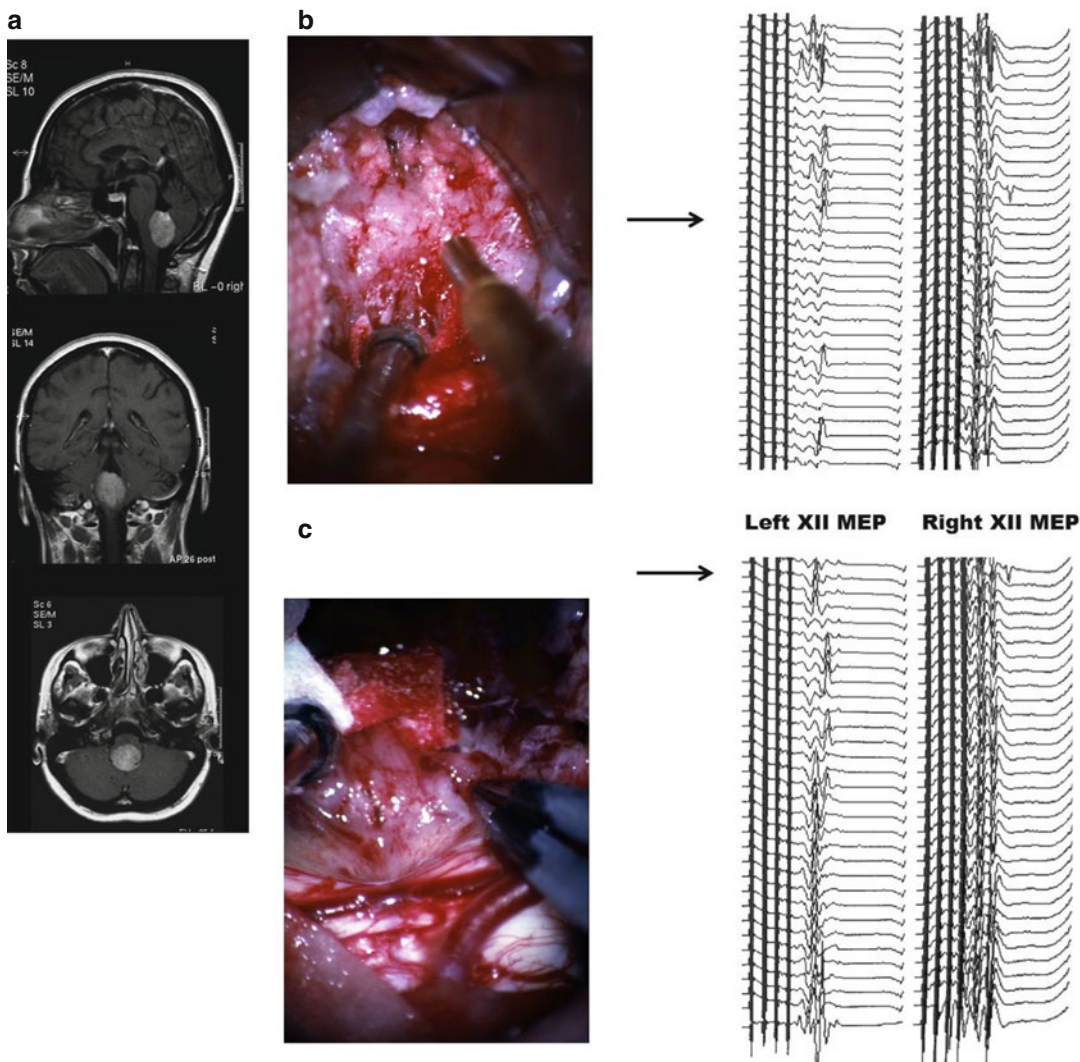


Fig. 13.7 Monitoring and mapping during surgery for fourth ventricle tumors. **(a)** (top to bottom): sagittal, coronal, and axial gadolinium-enhanced T1-weighted MR images of a fourth ventricle ependymoma infiltrating the floor at the level of the calamus scriptorius. During surgery, corticobulbar motor-evoked potentials (MEPs) were continuously monitored from the hypoglossal muscles after transcranial electrical stimulation at C3/Cz and C4/Cz with a train of four stimuli at 60 mA. **(b)** While using the CUSA (*left panel*) a significant drop in the amplitude of the left hypoglossal MEP was observed (*upper arrow*) and persisted for several minutes. At this point, surgery was transiently stopped to facilitate recovery of the corticobulbar MEPs. **(c)** When the amplitude recovered and a more consistent left hypoglossal MEP was recorded (*lower arrow*), surgery was resumed. Yet, the microscopic

view (*let panel*) suggested that the ependyma was infiltrated. **(d)** From now on, removal of little amount of tumor from the floor of the fourth ventricle was alternated with direct stimulation of the floor to localize the subependymal lower motor cranial nerve nuclei (*left panel*, surgical view). As soon as a clear compound muscle action potential (CMAP) was obtained from the left posterior wall of the pharynx muscles (glossopharyngeal/vagus complex) and the tongue muscles (hypoglossal nerve) (*right panel*), the decision was made to abandon surgery to avoid injuring the nearby nuclei. **(e)** (top to bottom): sagittal and coronal gadolinium-enhanced T1-weighted postoperative MR images showing gross total removal of the tumor and only a pinpoint enhancement at the bottom of the calamus scriptorius

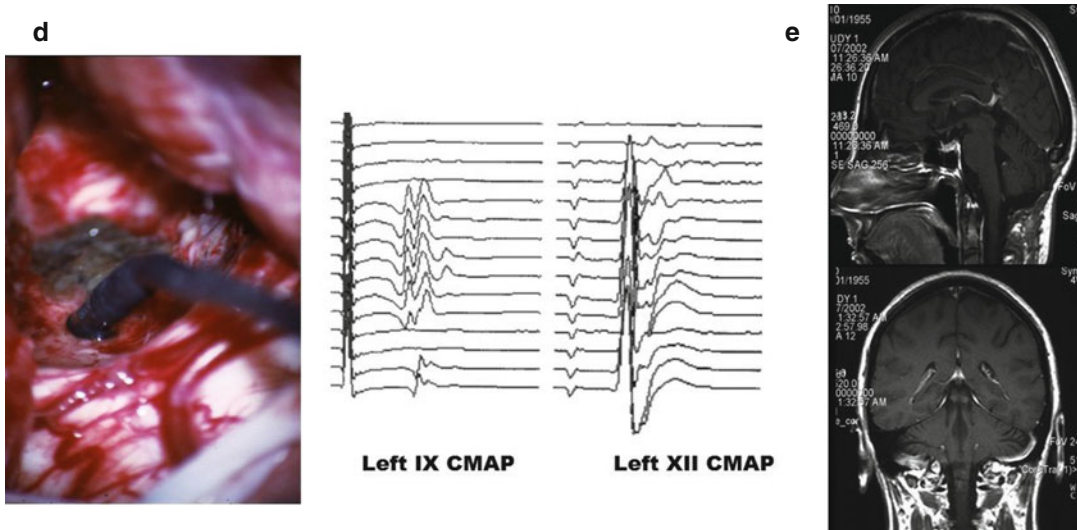


Fig. 13.7 (continued)

[13]. The SEP disappearance may be transient, and they may recover later during surgery or in the postoperative period. Accordingly, an intraoperative drop of the potentials may not necessarily correlate with a postoperative sensory deficit. This, in combination with the high sensitivity of SEP to surgical manipulation, explains why SEP changes only are not used as criteria to abandon surgery, although surgical manipulation may be transiently halted to favor the recovery of the potentials. For pontine and midbrain tumors, SEPs have little localizing value but can still be used to provide nonspecific information about the general functional integrity of the brainstem because it is expected that a major impending brainstem failure will be detected by changes in SEP parameters.

13.2.2.3 Motor-Evoked Potentials

With the advent of MEPs in the mid-1990s, ION has dramatically changed thanks to the possibility to specifically monitor motor pathways. MEPs have significantly impacted on brain surgery, spinal cord surgery, and brainstem surgery as well. Current techniques to intraoperatively monitor MEPs after TES have their origin in the work of Merton and Morton [40]. Since then, two methodologies for intraoperatively monitoring the motor pathways have been developed.

Transcranial Electrical Stimulation of the Motor Cortex and Muscle Recordings (Multipulse Technique) (Fig. 13.8)

The primary motor cortex is activated through transcranial electrical stimulation (TES). The main advantage of the multipulse TES is the ability to overcome the effects of anesthetics on a multisynaptic pathway and record mMEPs under general anesthesia [28, 50, 71]. TES is performed using corkscrew-like electrodes inserted in the scalp, since they are secure and provide low impedance. In children where the fontanel is still open, or in those with subcutaneous ventriculo-peritoneal shunts, great care should be taken to avoid penetrating the fontanel or the valve/shunt with the electrodes; in these patients cup electrodes should be preferred.

Short trains of five to seven square-wave stimuli of 0.5 ms duration and interstimulus interval of 4 ms are applied at a repetition rate of 1–2 Hz through electrodes placed at C1 and C2 scalp sites, according to the International 10/20 EEG system. A C1/C2 montage preferentially elicits mMEPs in the right limb muscles, while C2/C1 favors recordings from the left limb muscles. For the monitoring of lower extremity muscles, a Cz-C6 cm montage is usually preferred, where Cz is placed 1 cm behind the typical Cz point.

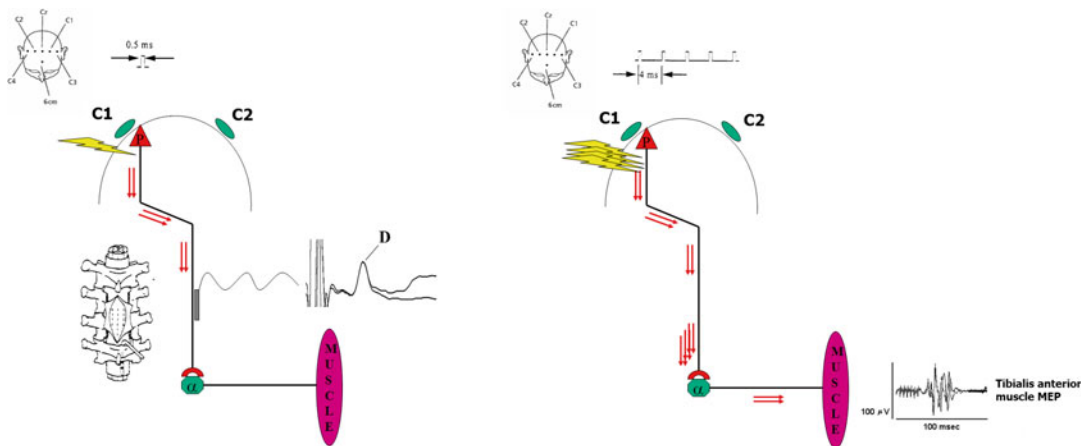


Fig. 13.8 Monitoring of motor-evoked potentials. Schematic illustration of motor-evoked potential monitoring. *Left panel:* transcranial electrical stimulation (TES) of the motor cortex and spinal epidural recordings. A single stimulus is delivered through TES. This activates directly the axon of the first motoneuron and travels along the fast conducting fibers of the corticospinal tract. Such potential is recorded by an epidural electrode at the spinal level and originates the so-called D(direct)-wave but cannot originate muscle motor-evoked potentials as anes-

thetic agents inhibit its synaptic transmission at the level of the α -motoneuron. *Right panel:* transcranial electrical stimulation (TES) of the motor cortex and muscle recordings. A short train of stimuli is delivered through TES. These stimuli sequentially activate descending volleys traveling along the axon of the first motoneuron. At the level of the α -motoneuron, the temporal and spatial summation of these volleys permits to reach the firing threshold, which then results in a muscle response

Using different montages of stimulating electrodes provides flexibility to optimize elicitation of muscle MEPs (mMEPs) without vigorous muscle twitching, which can interfere with surgery.

More lateral stimulating montages (C3/C4, C3/Cz, or C4/Cz) can induce more vigorous muscle twitching and, especially at high current intensities, may activate the CT tract deep within the brain or even at the brainstem level [58]. Therefore, the point of activation of descending motor pathways may be caudal to the level of surgery, even at the level of the peripheral nerve, exposing to the risk of false-negative results.

Other than that, TES is considered a safe method, and the report of serious complications is anecdotal [38]. It is always important to insert a tongue bite at the end of the anesthesiological preparation and electrode placement to avoid tongue injury during jaw muscle twitches that may occur during TES.

In young children, two opposite factors may affect the threshold to elicit mMEP after TES. The immaturity of the motor cortex and sub-cortical motor pathways may increase stimulat-

ing thresholds. However, this variable is to some extent counterbalanced by the thinner thickness of the skull which should facilitate motor cortex activation at lower intensities because of lower impedance.

The stimulation intensity usually should not exceed 150 mA, and in neurologically intact children upper limb mMEPs are sometimes recordable after stimulation intensities as low as 40–50 mA. Muscle responses are recorded via pairs of needle electrodes inserted into the upper and lower extremity muscles. We usually monitor the abductor pollicis brevis (APB) and the extensor digitorum communis for the arm and the tibialis anterior (TA) and the abductor hallucis for the leg. For supratentorial surgery, especially at the cortical level, it is important to monitor muscles from both the upper and lower extremities and the face in order to cover the entire representation of the homunculus and avoid falsely negative result. This is not needed at the level of the brainstem; here, the CT fibers are concentrated ventrally, in a very small area, so that selectively injuring CT fibers for only

one group of muscles is unlikely. Accordingly, most of the times it suffices to monitor the APB for the upper extremity and the TA for the lower extremity.

Before the advent of intraoperative mMEP monitoring, data from transcranial magnetic stimulation already showed that younger children had higher threshold to elicit mMEPs [44]. This is due to the immature myelination of the motor pathways. According to Nezu, electrophysiological maturation of the CT innervating hand muscles is complete by the age of 13 [47], and the CT appears to be the only spinal cord pathway with incomplete myelination at birth [31]. Actually, there is some evidence that full CT myelination may be reached as late as 16 years of age [6, 48].

Though the number of studies that have specifically looked at MEP monitoring in children is quite small [14, 35, 37, 69, 73], there is a similar evidence also in the intraoperative setting, under general anesthesia. This should be taken into account when performing MEP monitoring in younger children, as the stimulation intensity required may be significantly higher than in adults. One possibility to avoid strong intensities is to increase the number of stimuli to seven or nine or to slightly increase the pulse width, rather than the amperage.

Furthermore, the presence of mMEPs indicates that the functional integrity of not only the motor cortex and the CT but also the α -motor neuron, the peripheral nerve, and the neuromuscular junction has been maintained. One direct consequence of this technique is the ability to assess which extremity is going to be affected.

Unlike SEPs, mMEPs need no averaging, and, at a stimulation rate of 1–2 Hz, they provide rapid “online” feedback. Being generated through a polysynaptic pathway, however, mMEPs are very sensitive to the effect of anesthesia so that a wide variation in mMEP amplitude and latency can be observed [28, 74]. This variability explains the lack of a linear correlation between intraoperative changes in mMEP amplitude and/or latency and the motor outcome.

In terms of the warning criteria for mMEP interpretation indicative of an impending injury to the CTs, there are little data published with

regard to brainstem surgery. Our experience suggests that semiquantitative criteria should be applied. While in spinal cord tumor surgery, yes/no criteria have proved to correctly predict the outcome, in brainstem surgery – analogously to brain surgery – a significant drop in the mMEP amplitude, in the range of 50–80 %, should be taken into account as they are indicative of injury to the CT. Although only the mMEP disappearance strongly correlates with postoperative permanent paresis, persistent amplitude decrement may correlate with either a transient moderate deficit or, more rarely, a mild permanent deficit [46].

Transcranial Electrical Stimulation of the Motor Cortex and Epidural Recordings (Single Pulse Technique) (Fig. 13.8)

A single electrical stimulus applied transcranially or directly to the exposed motor cortex elicits a so-called direct (D) wave that can be recorded by a catheter electrode placed epi- or subdurally adjacent to the spinal cord. This wave form is a highly reliable parameter for monitoring the functional integrity of the CTs intraoperatively because it represents the direct activation of a population of synchronized fast conducting fibers of the CT [9, 29, 49]. The single stimulus technique is advantageous because it produces no muscle twitches, and the D-wave is very robust under general anesthesia [66] because no synapses are involved in its generation.

The D-wave is usually recorded in a “single-stimulus-single-response” fashion. The stimulation rate of 0.5–2 Hz, however, provides a fast feedback even when a few averages are needed. Signals are amplified 10,000 times, and the filter bandpass is set from 1.5 to 1,700 Hz. As the D-wave provides a semiquantitative assessment of the amount of preserved CT fibers, a decrease in the peak-to-peak amplitude mirrors a reduction in the number of preserved fibers. Fortunately, from a clinical perspective, the D-wave amplitude deteriorates in a stepwise incremental pattern. Thus, warning signs can be observed, and corrective measures can be taken before irreversible damage to the spinal cord occurs [12, 30].

D-wave monitoring is routinely performed at our institution during surgery for ISCTs, where a 50 % drop of the baseline amplitude is used as a warning sign to transiently stop or abandon surgery if the signals do not recover. This criterion is based on clinical experience more than on a strong neurophysiological background, as there is still no information available on the percentage of CT fibers necessary to support locomotion.

The combined use of the single (D-wave) and multipulse (mMEPs) techniques utilizes beneficial features of both while compensating for their disadvantages and allows predictions on short- and long-term neurological outcome. However, during brainstem surgery the risk of injury to the CT is relatively remote when the approach is from the fourth ventricle, as the tracts are ventrally located. The risk is higher for tumors located within the cerebral peduncle; in this case, yet, only a suboccipital supratentorial approach will allow to insert – after opening the dura in the posterior fossa – an epidural or subdural electrode at the level of C1–C2 to record the D-wave. Either the subtemporal lateral approach or the occipital transtentorial will not give access to the craniocervical junction. So, the D-wave electrode would have to be placed percutaneously, using a Tuohy needle, in the upper cervical spine, but this is, in our opinion, a risky maneuver, maybe not fully justified for the purpose of monitoring, especially in children.

Moreover, in a study by Szelenyi et al., in 19 children operated on for intramedullary spinal cord tumors (ISCTs) [69], the D-wave was present in 7 of 14 patients (50 %) aged 21 months or older but was never recorded in children younger than 21 months. This is likely due to the immaturity of the CT in younger children where incompletely myelinated fibers have variable conduction velocities resulting in desynchronization of the D-wave. So, although the CT fibers still conduct the descending volleys elicited by TES, these volleys are not synchronous and cannot be simultaneously picked up by a recording epidural spinal electrode to allow the recording of a potential with measurable amplitude.

For all these reasons, during brainstem surgery in children, we mostly rely on mMEP moni-

toring, limiting D-wave monitoring to selected cases such as, for example, cervicomedullary neoplasms that essentially behave like true spinal cord tumors.

13.2.2.4 Free-Running Electromyography (EMG)

Neurophysiological mapping of motor cranial nerve nuclei, intra-axial tracts, and peripheral nerves allows the functional identification of these anatomical neural structures without a continuous “online” assessment of their functional integrity. In addition, brainstem mapping cannot detect injury to the supranuclear tracts originating in the motor cortex and ending on the cranial nerve motor nuclei. Consequently, a supranuclear paralysis would not be detected when the motor neuron integrity has been preserved.

The standard technique for motor cranial nerve monitoring is the evaluation of the spontaneous electromyography (EMG) activity in the muscles innervated by motor cranial nerves [19, 22, 64]. This means that there is no stimulation of evoked potentials but simply the observation of the “spontaneous activity” of the peripheral muscles, recorded by the same needle or wire electrodes that can be used to record CMAPs after neurophysiological mapping.

Although several criteria have been proposed to identify EMG activity patterns suspicious for nerve injury, the terminology remains somewhat confusing, and convincing data regarding a clinical correlation between EMG activity and clinical outcome are still lacking [22, 64]. Paradoxically, the same electrical silence (no EMG activity) suggesting that no significant changes are occurring in the functional integrity of the nerve could be observed after a complete section of the peripheral nerve. On the other hand, some irritative EMG activity that persists behind the surgical manipulation of the nerve – and that is often considered indicative of a potential injury to the nerve – can be elicited by simply irrigating the surgical field with cold saline. Free-running EMG is therefore still lacking sensitivity and, to a larger extent, specificity, to the point

that strongly tailoring the surgical strategy on the basis of the different patterns of EMG activity may be hazardous. Recently some authors have shown the good predictive value of sustained neurotonic discharges, called A-train, to predict a postoperative facial palsy after surgery for vestibular schwannomas [52, 57]. Conversely, the reliability of free-running EMG in monitoring oculomotor and lower cranial nerves remains undetermined, if not poor.

An alternative technique is nowadays available, and it is based on the idea to extend the principles of mMEP monitoring to the muscle innervated by motor cranial nerves.

13.2.2.5 Monitoring of Corticobulbar Motor-Evoked Potentials (Fig. 13.9)

So-called corticobulbar mMEPs are recorded after TES. The main advantage is that these truly evoked potentials assess the integrity of the entire corticobulbar pathway from the motor cortex to the muscle.

TES is performed with a train of four stimuli at a rate of 1–2 Hz and intensity ranging between 60 and 120 mA. The electrode montage is usually C3/Cz for right side muscles and C4/Cz for left side muscles. For recording, electrodes are the same used to record CMAPs during map-

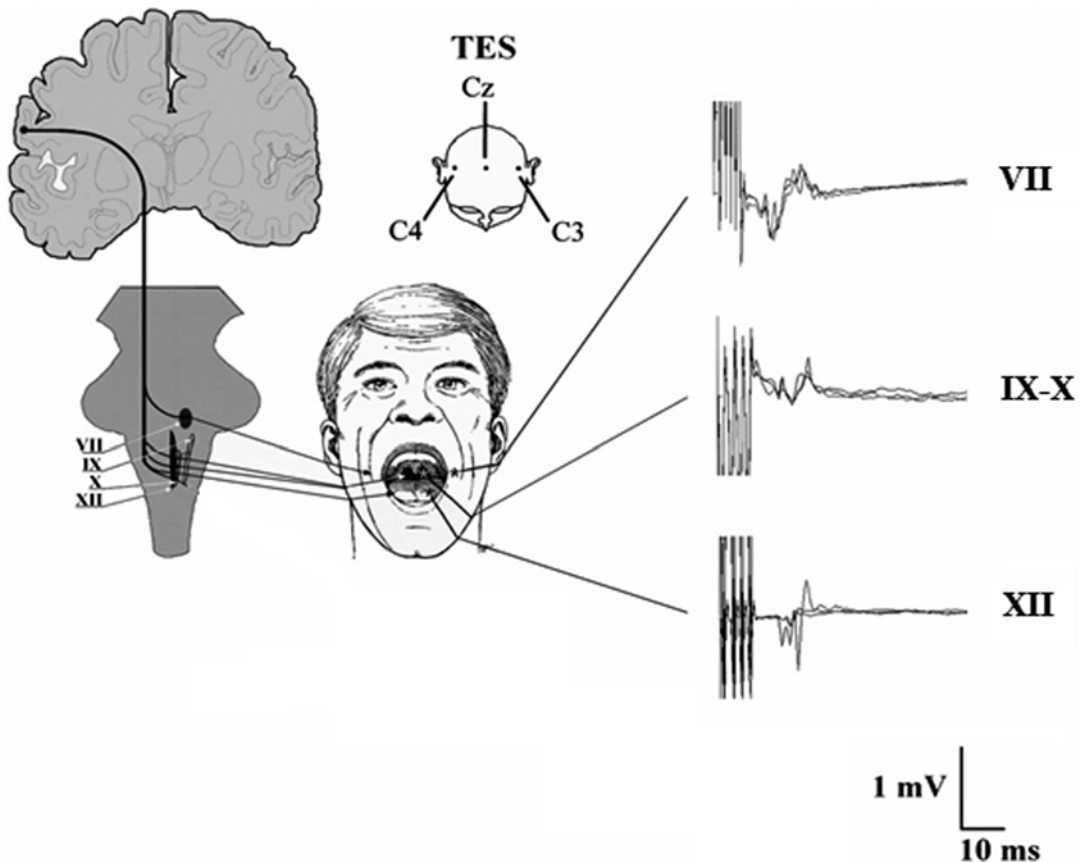


Fig. 13.9 Continuous monitoring of corticobulbar motor-evoked potentials. Schematic illustration of corticobulbar motor-evoked potentials elicited after transcranial electrical stimulation at C4/Cz (*left side* muscles) and C3/Cz (*right side* muscles). Responses are recorded

directly from the muscles innervated by motor cranial nerves VII, IX/X, and XII. The entire corticobulbar pathway, from the motor cortex to the muscles, is monitored with this technique (see text for details)

ping (Fig. 13.9). A reproducible mMEP can be continuously recorded from the facial, pharyngeal, and tongue muscles while the brainstem is surgically manipulated (Fig. 13.7).

There are, nevertheless, some theoretical and practical drawbacks that have so far limited the widespread use of this technique. First, from a neurophysiological perspective, using a lateral montage with C3 or C4 as an anodal stimulating electrode increases the risk that a strong TES may activate the corticobulbar pathways deep in the brain or even at the level of the brainstem/foramen magnum [58]. The possibility of a direct activation of the peripheral cranial nerve, especially the facial, can also not be excluded. Accordingly, an injury to the corticobulbar pathways rostral to the point of activation may be masked by a misleading preservation of the mMEP. Although we have not experienced false-negative results using this technique, this possibility should be taken into account, and the stimulation intensity should be kept as low as possible. Since a single pulse TES does not allow recording of mMEPs under general anesthesia, anytime a corticobulbar mMEP is recorded using multipulse TES, and TES should be repeated with the stimulation reduced to a single stimulus and all other stimulation parameters remaining the same. If a muscle response is still present (taking into account the shortening of the latency due to the smaller number of stimuli), this response is interpreted as a direct activation of the cranial nerve, hence not reliable for monitoring. Vice versa, if no mMEP responses are recorded after a single TES but only with the train, this is indicative of a proximal activation of the corticobulbar pathway at the level of the motor cortex. Given the continuous fluctuations in the threshold to elicit mMEPs intraoperatively – because of room temperature, anesthesiological regimen, physiological variability in mMEP threshold, etc. – it is recommended that the appropriate threshold for monitoring corticobulbar pathways be rechecked throughout the surgical procedure.

A second limitation of this technique is that spontaneous EMG activity, which is rather common during the manipulation of the brainstem and motor cranial nerves, can hinder the record-

ing of reliable mMEPs from the same muscles. In our experience, this spontaneous activity appears to be more common in the pharyngeal muscles as compared to the facial and tongue muscles. Finally, due to the limited experience with this technique, robust data about the prognostic role of these mMEPs with regard to the postoperative facial nerve paresis, dysphagia, and tongue paralysis are still lacking and warrant further investigation, but preliminary reports in the literature are encouraging [5, 15, 61].

Conclusions

Although the vast majority of current ION practice is not supported by evidence-based medicine standards, Class I studies have not been published and likely never will. In fact, it is accepted that the likelihood of deficit prevention using ION is so high that a controlled study comparing patients operated on with and without the assistance of neurophysiological monitoring would not be acceptable to most patients and surgeons who would need to participate. Similarly, even in the absence of class I evidence, many pediatric neurosurgical interventions are well established as the standard of care for their respective conditions, to the point that comparing an accepted surgical treatment with no treatment would rise ethical and medicolegal concerns. So, although Class I studies have not been published, the number of reports documenting the benefit of ION has constantly grown in the neurosurgical literature [17, 54, 63]. This, together with the evidence gained by Class II e Class III, suggests that ION is here to stay [59].

References

1. Aarsen FK, Van Dongen H, Paquier PF, Van Mourik M, Catsman-Berrevoets CE (2004) Long-term sequelae in children after cerebellar astrocytoma surgery. *Neurology* 62:1311–1316
2. Abbott R (1996) Brain stem glioma. In: McLone DG (ed) *Pediatric neurosurgery: surgery of the developing nervous system*. WB Saunders, Philadelphia, pp 859–867
3. Abbott R (2009) The use of physiological mapping and monitoring during surgery for ependymomas. *Childs Nerv Syst* 25:1241–1247

4. Abbott R, Shiminski-Maher T, Epstein FJ (1996) Intrinsic tumor of the medulla: predicting outcome after surgery. *Pediatr Neurosurg* 25:41–44
5. Akagami R, Dong CC, Westerberg BD (2005) Localized transcranial electrical motor evoked potentials for monitoring cranial nerves in cranial base surgery. *Neurosurgery* 57:78–85
6. Armand J, Olivier E, Edgley SA, Lemon RN (1996) The structure and function of the developing corticospinal tract: some key issues. In: Wing AM, Aggard P, Lanagan JR (eds) *Hand and brain*. Academic Press, San Diego, pp 125–145
7. Blessing W (1997) *The lower brainstem and bodily homeostasis*. Oxford University Press, New York
8. Bricolo A (2000) Surgical management of intrinsic brain stem gliomas. *Oper Tech Neurosurg* 3:137–154
9. Burke D, Hicks RG, Stephen JPH (1990) Corticospinal volleys evoked by anodal and cathodal stimulation of the human motor cortex. *J Physiol* 425:283–299
10. Cochrane DD, Gustavsson B, Poskitt KP, Steinbok P, Kestle JRW (1994) The surgical and natural morbidity of aggressive resection for posterior fossa tumors in childhood. *Pediatr Neurosurg* 20:19–29
11. Cushing H (1931) Experience with cerebellar astrocytomas. A critical review of seventy-six cases. *Surg Gynecol Obstet* 52:129–204
12. Deletis V, Kothbauer K (1998) Intraoperative neurophysiology of the corticospinal tract. In: Stålberg E, Sharma HS, Olsson Y (eds) *Spinal cord monitoring*. Springer, Vienna, pp 421–444
13. Deletis V, Sala F, Morota N (2000) Intraoperative neurophysiological monitoring and mapping during brain stem surgery: a modern approach. *Oper Tech Neurosurg* 3:109–113
14. DiCindio S, Theroux M, Shah S, Miller F, Dabney K, Brislin RP, Schwartz D (2003) Multimodality monitoring of transcranial electric motor and somatosensory-evoked potentials during surgical correction of spinal deformity in patients with cerebral palsy and other neuromuscular disorders. *Spine (Phila Pa 1976)* 28:1851–1855; discussion 1855–1856
15. Dong CC, MacDonald DB, Akagami R, Westerberg B, Alkhani A, Kanaan I, Hassounah M (2005) Intraoperative facial motor evoked potential monitoring with transcranial electrical stimulation during skull base surgery. *Clin Neurophysiol* 116:588–596
16. Due-Tonnesen B, Helseth E, Scheibe D, Skullerud K, Aamondt G, Lundar T (2002) Long term outcome after resection of benign cerebellar astrocytoma in children and young adults (0–19): report of 110 consecutive cases. *Pediatr Neurosurg* 37:71–80
17. Duffau H, Lopes M, Arthuis F, Bitar A, Sichez JP, Van Effenterre R, Capelle L (2005) Contribution of intraoperative electrical stimulations in surgery of low grade gliomas: a comparative study between two series without (1985–96) and with (1996–2003) functional mapping in the same institution. *J Neurol Neurosurg Psychiatry* 76:845–851
18. Duffau H, Sichez JP (1998) Intraoperative direct electrical stimulation of the lamina quadrigemina in a case of a deep tectal cavernoma. *Acta Neurochir (Wien)* 140:1309–1312
19. Eisner W, Schmid UD, Reulen HJ, Oeckler R, Olteanu-Nerbe V, Gall C, Kothbauer K (1995) The mapping and continuous monitoring of the intrinsic motor nuclei during brain stem surgery. *Neurosurgery* 37:255–265
20. Erickson L, Costa V, McGregor M (2005) *Use of intraoperative neurophysiological monitoring during spinal surgery*. McGill University Health Centre; Springer: Wien
21. Fukaya C, Katayama Y, Kasai M, Kurihara J, Yamamoto T (1999) Intraoperative electrooculographic monitoring of oculomotor nerve function during skull base surgery. Technical note. *J Neurosurg* 91:157–159
22. Grabb PA, Albright L, Sclabassi RJ, Pollack IF (1997) Continuous intraoperative electromyographic monitoring of cranial nerves during resection of fourth ventricular tumors in children. *J Neurosurg* 86:1–4
23. Hoffman HJ, Becker L, Craven MA (1980) A clinically and pathologically distinct group of benign brain stem gliomas. *Neurosurgery* 7:243–248
24. Humphreys RP (1982) Posterior cranial fossa brain tumors in children. In: Youmans JR (ed) *Neurological surgery*. Saunders, Philadelphia, pp 2733–2752
25. Ishihara H, Bjeljac M, Straumann D, Kaku Y, Roth P, Yonekawa Y (2006) The role of intraoperative monitoring of oculomotor and trochlear nuclei -safe entry zone to tegmental lesions. *Minim Invasive Neurosurg* 49:168–172
26. Jallo GI, Biser-Rohrbaugh A, Freed D (2004) Brainstem gliomas. *Childs Nerv Syst* 20:143–153
27. Jallo GI, Shiminski-Maher T, Velazquez L, Abbott R, Wisoff J, Epstein F (2005) Recovery of lower cranial nerve function after surgery for medullary brainstem tumors. *Neurosurgery* 56:74–78
28. Jones SJ, Harrison R, Koh KF, Mendoza N, Crockard HA (1996) Motor evoked potential monitoring during spinal surgery: responses of distal limb muscles to transcranial cortical stimulation with pulse trains. *Electroencephalogr Clin Neurophysiol* 100:375–383
29. Katayama Y, Tsubokawa T, Maemjima S, Hirayama T, Yamamoto T (1988) Corticospinal direct response in humans: identification of the motor cortex during intracranial surgery under general anesthesia. *J Neurol Neurosurg Psychiatry* 51:50–59
30. Kothbauer KF, Deletis V, Epstein FJ (1998) Motor-evoked potential monitoring for intramedullary spinal cord tumor surgery: correlation of clinical and neurophysiological data in a series of 100 consecutive procedures. *Neurosurg Focus* 4:e1, Article 1
31. Kubis N, Catala M (2003) Development and maturation of the pyramidal tract. *Neurochirurgie* 49:145–153
32. Kyoshima K, Kobayashi S, Gibo H, Kuroyanagi T (1993) A study of safe entry zones via the floor of the fourth ventricle for brain-stem lesions. Report of three cases. *J Neurosurg* 78:987–993
33. Lalwani AK, Butt FY, Jackler RK, Pitts LH, Yingling CD (1994) Facial nerve outcome after acoustic neuroma

- surgery: a study from the era of cranial nerve monitoring. *Otolaryngol Head Neck Surg* 111:561–570
34. Lang J Jr, Ohmachi N, Lang J Sr (1991) Anatomical landmarks of the rhomboid fossa (floor of the 4th ventricle), its length and its width. *Acta Neurochir (Wien)* 113:84–90
 35. Langeloo DD, Journee HL, Polak B, de Kleuver M (2001) A new application of TCE-MEP: spinal cord monitoring in patients with severe neuromuscular weakness undergoing corrective spine surgery. *J Spinal Disord* 14:445–448
 36. Legatt AD (2008) BAEPs in surgery. In: Nuwer MR (ed) *Intraoperative monitoring of neural function. Handbook of clinical neurophysiology.* Elsevier, Amsterdam, pp 334–349
 37. Lieberman JA, Lyon R, Feiner J, Diab M, Gregory GA (2006) The effect of age on motor evoked potentials in children under propofol/isoflurane anesthesia. *Anesth Analg* 103:316–321, table of contents
 38. MacDonald DB (2002) Safety of intraoperative transcranial electrical stimulation motor evoked potential monitoring. *J Clin Neurophysiol* 19:416–429
 39. May PL, Blaser SI, Hoffman HJ, Humphreys RP, Harwood-Nash DC (1991) Benign intrinsic tectal “tumors” in children. *J Neurosurg* 74:867–871
 40. Merton PA, Morton HB (1980) Stimulation of the cerebral cortex in the intact human subject. *Nature* 285:227
 41. Morota N, Deletis V, Epstein FJ, Kofler M, Abbott R, Lee M, Ruskin K (1995) Brain stem mapping: neurophysiological localization of motor nuclei on the floor of the fourth ventricle. *Neurosurgery* 37:922–930
 42. Morota N, Deletis V, Lee M, Epstein FJ (1996) Functional anatomic relationship between brain-stem tumors and cranial motor nuclei. *Neurosurgery* 39:787–793; discussion 793–784
 43. Morris EB, Li C, Khan RB, Sanford RA, Boop F, Pinlac R, Xiong X, Merchant TE (2009) Evolution of neurological impairment in pediatric infratentorial ependymoma patients. *J Neurooncol* 94:391–398
 44. Muller K, Homberg V, Lenard HG (1991) Magnetic stimulation of motor cortex and nerve roots in children. Maturation of cortico-motoneuronal projections. *Electroencephalogr Clin Neurophysiol* 81:63–70
 45. Neervoort FW, Van Ouwekerck W, Folkersma H, Kaspers GJL, Vandertop WP (2010) Surgical morbidity and mortality of pediatric brain tumors: a single center audit. *Childs Nerv Syst* 26:1583–1592
 46. Neuloh G, Pechstein U, Cedzich C, Schramm J (2004) Motor evoked potential monitoring with supratentorial surgery. *Neurosurgery* 54:1061–1070
 47. Nezu A, Kimura S, Takeshita S (1999) Topographical differences in the developmental profile of central motor conduction time. *Clin Neurophysiol* 110:1646–1649
 48. Olivier E, Edgley SA, Armand J, Lemon RN (1997) An electrophysiological study of the postnatal development of the corticospinal system in the macaque monkey. *J Neurosci* 17:267–276
 49. Patton HD, Amassian VE (1954) Single- and multiple unit analysis of cortical stage of pyramidal tract activation. *J Neurophysiol* 17:345–363
 50. Pechstein U, Cedzich C, Nadstawek J, Schramm J (1996) Transcranial high-frequency repetitive electrical stimulation for recording myogenic motor evoked potentials with the patient under general anesthesia. *Neurosurgery* 39:335–344
 51. Pompili A, Caperle M, Pace A, Ramazzotti V, Raus L, Jandolo B, Occhipinti E (2002) Quality-of-life assessment in patients who had been surgically treated for cerebellar pilocytic astrocytoma in childhood. *J Neurosurg* 96:229–234
 52. Prell J, Rampp S, Romstock J, Fahlbusch R, Strauss C (2007) Train time as a quantitative electromyographic parameter for facial nerve function in patients undergoing surgery for vestibular schwannoma. *J Neurosurg* 106:826–832
 53. Recinos PF, Sciubba DM, Jallo GI (2007) Brainstem tumors: where are we today? *Pediatr Neurosurg* 43:192–201
 54. Reithmeier T, Krammer M, Gumprecht H, Gerstner W, Lumenta CB (2003) Neuronavigation combined with electrophysiological monitoring for surgery of lesions in eloquent brain areas in 42 cases: a retrospective comparison of the neurological outcome and the quality of resection with a control group with similar lesions. *Minim Invasive Neurosurg* 46:65–71
 55. Rhoton AL (2000) The posterior fossa veins. *Neurosurgery* 47:S69–S92
 56. Ribic K, Rely C, Landolt MA, Alber FD, Boltshauser E, Grotzer MA (2005) Outcome of medulloblastoma in children: long term complications and quality of life. *Neuropediatrics* 36:357–365
 57. Romstock J, Strauss C, Fahlbusch R (2000) Continuous electromyography monitoring of motor cranial nerves during cerebellopontine angle surgery. *J Neurosurg* 93:586–593
 58. Rothwell J, Burke D, Hicks R, Stephen J, Woodforth I, Crawford M (1994) Transcranial electrical stimulation of the motor cortex in man: further evidence for the site of activation. *J Physiol* 481(Pt 1):243–250
 59. Sala F (2010) Intraoperative neurophysiology is here to stay. *Childs Nerv Syst* 26:413–417
 60. Sala F, Krzan MJ, Deletis V (2002) Intraoperative neurophysiological monitoring in pediatric neurosurgery: why, when, how? *Childs Nerv Syst* 18:264–287
 61. Sala P, Lanteri A, Bricolo (2004) Motor evoked potential monitoring for spinal cord and brainstem surgery. In: Dolenc VV, Lobo J, Antunes HJ, Reulen M, Sindou AJ, Strong N, de Tribolet CA, Tulleken F, Vapalahti M (eds). *Advanced and technical standards in neurosurgery. Vol.29.* Pickard JD (Editor in Chief), pp 133–169
 62. Sala F, Manganotti P, Grossauer S, Tramontano V, Mazza C, Gerosa M (2010) Intraoperative neurophysiology of the motor system in children: a tailored approach. *Childs Nerv Syst* 26:473–490
 63. Sala F, Palandri G, Basso E, Lanteri P, Deletis V, Faccioli F, Bricolo A (2006) Motor evoked potential monitoring improves outcome after surgery for intramedullary spinal cord tumors: a historical control study. *Neurosurgery* 58:1129–1143; discussion 1129–1143

64. Schlake HP, Goldbrunner R, Siebert M, Behr R, Roosen K (2001) Intra-Operative electromyographic monitoring of extra-ocular motor nerves (Nn. III, VI) in skull base surgery. *Acta Neurochir* 143:251–261
65. Sekiya T, Hatayama T, Shimamura N, Suzuki S (2000) Intraoperative electrophysiological monitoring of oculomotor nuclei and their intramedullary tracts during midbrain tumor surgery. *Neurosurgery* 47:1170–1176; discussion 1176–1177
66. Sloan TB (2002) Intraoperative neurophysiology and anesthesia management. In: Deletis V, Shils J (eds) *Neurophysiology in neurosurgery: a modern intraoperative approach*. Academic, San Diego, pp 451–474
67. Strauss C, Lutjen-Drecoll E, Fahlbusch R (1997) Pericolicular surgical approaches to the rhomboid fossa. Part I. Anatomical basis. *J Neurosurg* 87:893–899
68. Sughrue ME, Kaur R, Kane AJ, Rutkowski MJ, Kaur G, Yang I, Pitts LH, Parsa AT (2010) The value of intraoperative facial nerve electromyography in predicting facial nerve function after vestibular schwannoma surgery. *J Clin Neurosci* 17:849–852
69. Szelenyi A, Bueno de Camargo A, Deletis V (2003) Neurophysiological evaluation of the corticospinal tract by D-wave recordings in young children. *Childs Nerv Syst* 19:30–34
70. Tanaka S, Takashi J, Fujii K, Ujii H, Hori T (2007) Motor evoked potential mapping and monitoring by direct brainstem stimulation. Technical note. *J Neurosurg* 107:1053–1057
71. Taniguchi M, Cedzich C, Schramm J (1993) Modification of cortical stimulation for motor evoked potentials under general anesthesia; technical description. *Neurosurgery* 32:219–226
72. Vandertop WP, Hoffman HJ, Drake JM, Humphreys RP, Rutka JT, Armstrong DC, Becker LE (1992) Focal midbrain tumors in children. *Neurosurgery* 31:186–194
73. Wilson-Holden TJ, Padberg AM, Lenke LG, Larson BJ, Bridwell KH, Bassett GS (1999) Efficacy of intraoperative monitoring for pediatric patients with spinal cord pathology undergoing spinal deformity surgery. *Spine (Phila Pa 1976)* 24:1685–1692
74. Woodforth IJ, Hicks RG, Crawford MR, Stephen JP, Burke DJ (1996) Variability of motor-evoked potentials recorded during nitrous oxide anesthesia from the tibialis anterior muscle after transcranial electrical stimulation. *Anesth Analg* 82:744–749
75. Zuzak TJ, Poretti A, Drexel B, Zehnder D, Boltshauser E, Grotzer MA (2008) Outcome of children with low grade cerebellar astrocytoma: long term complications and quality of life. *Childs Nerv Syst* 24:1447–1455

Pathologies in Pediatric Posterior Fossa Tumors: Medulloblastoma

Giuseppe Cinalli

G. Cinalli, MD
Division of Pediatric Neurosurgery, Department of Neuroscience,
Santobono-Pausilipon Children's Hospital, Naples, Italy
Department of Neurosurgery, University of L'Aquila, L'Aquila, Italy

Pasquale De Antonellis, Livia Garzia,
Antonio Verrico, Michael D. Taylor,
and Massimo Zollo

Recent advances in molecular biology have led to the development of powerful tools for the study of medulloblastoma (MB) tumorigenesis, which have revealed new insights into the molecular and genetics basis of this disease. Throughout the life of an individual, the ~3 billion base pairs of DNA that constitute the human genome are exposed to mutagens and suffer errors in DNA replication; this assault leads to the acquisition of stable mutations through rounds of clonal selection and clonal expansion. The cancer genome, as a result of this process, is profoundly different from the genome that composes the constitutional DNA. The goal of cancer genomics is the study of the human cancer genome and the collection and description of all the alterations that make up for

its divergence from the constitutional DNA. The mutations, inherited or acquired, contribute in different degrees to the development of cancer and its progression from a localized cancer to one that grows uncontrolled and then metastasizes. Recent studies based on high-throughput mutation detection techniques have shown that cancer genomes harbor from 10 to over 100 mutations [1–5]. However, these studies are likely to underestimate the alterations caused by genomic rearrangements and copy number alterations (CNA); this suggests that the number of genes hit by somatic mutations is higher. Cell homeostasis can also be disrupted by mechanisms beyond the changes in DNA sequence; changes in DNA methylation status or histone acetylation can alter physiological cell processes like cell division [2, 6, 7, 8, 9]. For this reason a comprehensive description of cancer genetics has to include studies at the level of the genome, epigenome, and transcriptome, as schematized in Fig. 14.1.

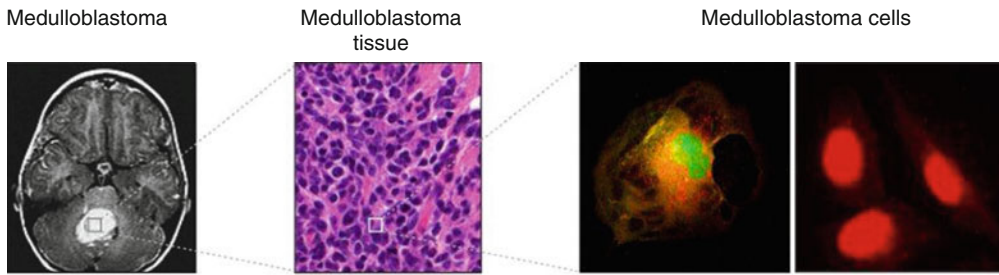
Medulloblastoma (MB) can occur in the setting of rare genetic syndromes characterized by increased incidence of malignancies, often at young age. Studies aimed to understand the genetic basis of such rare syndromes showed that the genes so far associated with predisposition to tumors appear to act as tumor suppressors; constitutional alterations associated with somatic loss or epigenetic silencing of the wild-type (wt) allele are observed in hereditary tumors, and often, biallelic somatic loss-of-function

P. De Antonellis, M.D. • A. Verrico, M.D.
Department of Molecular Medicine and Medical
Biotechnology, Federico II, University of Naples,
Naples, Italy

L. Garzia, M.D. • M.D. Taylor, M.D.
Arthur and Sonia Labatt Brain Tumor
Research Centre, The Hospital for Sick Children,
Toronto, ON, Canada
e-mail: michael_d.taylor@sickkids.ca

M. Zollo, M.D. (✉)
Department of Molecular Medicine and Medical
Biotechnology, Federico II, University of Naples,
Naples, Italy

Department of Biochemistry and Medical
Biotechnologies, Federico II, University of Naples,
Naples, Italy
e-mail: massimo.zollo@unina.it



Medulloblastoma Genetic Alterations

- Genetic alterations
 - somatic mutations
 - gene amplifications
 - gene deletions
- Epigenetic alterations
 - DNA methylation on cytosine residues in the CpG dinucleotides
 - modification of histone proteins, such as methylation, acetylation and phosphorylation
- Gene expression alterations
 - gene overexpression or downregulation
- Non-coding RNA alterations
 - miRNA overexpression or downregulation

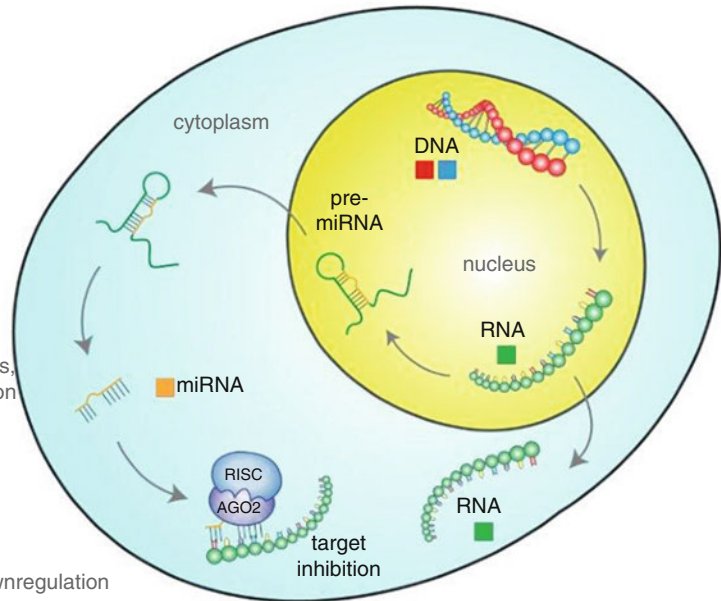


Fig. 14.1 Medulloblastoma tumor pathology: (*Top left panel*) representative axial midline vermian Medulloblastoma and photomicrographs of classic medulloblastoma; (*Top right panel*) representative immunofluorescence staining on

medulloblastoma cells; (*Bottom*); cartoon that comprehensively illustrates the known findings directing to medulloblastoma and reconstitute the different molecular alteration (Genetic, Epigenetic, of gene and miRNA expression)

(LOF) mutations and epigenetic silencing can be found in the corresponding sporadic tumors. Li-Fraumeni cancer family syndrome, Gorlin syndrome, and Turcot syndrome are commonly described conditions associated with an increased risk to develop MB.

14.1 Li-Fraumeni Cancer Family Syndrome and *TP53* Mutations in MB

In the early 1990s two groups reported germ line mutations in the *TP53* gene as the possible cause for the increased susceptibility to cancer observed in families affected by the Li-Fraumeni syndrome

(LFS). LFS is an autosomal dominant condition characterized by the occurrence of diverse cancers of mesenchymal and epithelial origin in multiple sites; affected families show particularly high rates of malignancy and a young age at onset of malignancies such as breast cancer, brain tumors, acute leukemia, soft tissue sarcomas, bone sarcomas, and adrenal cortical carcinoma [10, 11]. In terms of relative incidence, breast carcinomas are most frequent (24.0 %) followed by bone sarcomas (12.6 %), brain tumors (12.0 %), and soft tissue sarcomas (11.6 %) [12]. Among the brain tumors histologically analyzed ($N=29$), 69 % were of glial origin followed by a rate of 17 % for MBs and related primitive neuroectodermal tumors of childhood [12].

TP53 is a tumor suppressor gene that codifies for a 53 KDa protein which plays a key role in regulating crucial cellular processes deregulated during malignant transformation of the cells. P53 participates in DNA damage repair by holding the cell cycle at the G1/S regulation point on DNA damage recognition, allowing DNA repair processes to take place or signaling to sensor molecules in order to start an apoptotic program. During the G1/S checkpoint activated p53 binds DNA and activates expression of several genes, including *WAF1/CIP1* encoding for p21. p21 forms complexes with other proteins important for the G1/S transition in the cell cycle, inhibiting cell cycle progression when internal or external conditions are unfavorable to cell division. A decreased or aberrant activity of p53 will no longer prevent cells bearing damaged DNA from dividing, leading to uncontrolled division, genomic instability, and tumor formation.

TP53 mutations are also observed in sporadic MBs: early studies reported an incidence of mutation in 10 % of MBs [13, 14]; however, a higher frequency has been described in anaplastic MBs that show an occurrence of 27 % [15, 16]. *TP53* immunoreactivity accounts for one of the most reproducible molecular markers of poor outcome in MB, together with overexpression of survivin or *erbB2* and amplification of the *MYC* oncogene. In a recent study Tabori and colleagues correlated the incidence of *TP53* mutations and common biologic prognostic markers of MB outcome. The 5-year survival rate was negatively affected by *TP53* mutation; also *TP53*-mutated tumors recurred earlier, and 75 % of the recurrent tumors classified as average risk on the basis of WHO criteria showed to be mutated in *TP53* [16]. From a histological perspective in the cohort of 108 patients analyzed in the study, 50 % of the severely anaplastic MBs were *TP53* mutated. However, in the same study severe anaplasia was not predictive of disease outcome. In contrast with the findings reported for other molecular markers associated with negative outcome, such as *PDGFRA*, *TP53*-mutated tumors recurred locally, in a short time frame, with no dissemination, suggesting a possible role of *TP53* mutation in therapy resistance.

14.2 Gorlin Syndrome and Mutations in the *PTCH* (*Patched*) Gene

In 1960 Robert J. Gorlin and Robert W. Goltz described a genetic syndrome inherited in an autosomal dominant manner that greatly predispose to a skin cancer known as basal cell carcinoma. Patients affected by the Gorlin syndrome also present several abnormalities of the skin, skeleton, and nervous system, but more importantly they develop multiple cancers at an early age. About 90 % of the patients are affected by multiple basal cell carcinomas, while MB occurs less frequently in 3–5 % of affected patients [17, 18]. The peak incidence of MB in Gorlin syndrome-affected individuals is at approximately 2 years of age, while it is 7 years of age in the sporadic form of MB [19, 20]. The desmoplastic subtype is the only histopathologic subtype of MB reported in the current Gorlin syndrome population, while it accounts for no more than 20 % of sporadic MB [19]. The locus containing the causative gene was mapped to chromosome 9q22.3 by a combination of genetic linkage in five families affected by Gorlin syndrome supported by a loss-of-heterozygosity (LOH) study on sporadic basal cell carcinomas [21–23]. Fine mutational analysis of the locus 9q22.3 revealed alterations in the human homolog of the *Drosophila patched* (*ptc*) gene, whose reduced or absent expression was linked, respectively, to developmental abnormalities and tumorigenesis [24, 25]. The function of the *Drosophila* patched protein is well-studied: it acts as an inhibitor of the Hedgehog (HH) signaling pathway in the context of development. The HH signaling pathway is named after the family of extracellular HH ligands, of which there are three in mammals: Sonic Hedgehog (SHH), Indian Hedgehog (IHH), and Desert Hedgehog (DHH); *ptc* encodes for the receptor of such ligands and, in absence of ligand, it associates and represses the function of the seven-pass membrane protein Smoothened (SMOH) [26]. When *PTCH1* is ligand-bound, repression of SMOH is relieved and one or more of the GLI transcription factors are activated leading to the modulation of the transcription of downstream target genes. Given

the well-known role of the *Drosophila* homolog, human *PTCH1* was predicted and demonstrated to produce constitutive activation of *SHH* signaling after its biallelic inactivation; *PTCH1* fulfills the conditions to be defined as a classic tumor suppressor gene [27]. In sporadic MBs where no evidence of a familial predisposition can be asserted, there is a fraction of cases where mutations of the genes *PTCH1* and *SMOH* occur [28–32]; *GLI* gene family members, downstream effectors of the pathway, are instead amplified in glioblastoma [33]. These observations from human dataset, fortified with data from loss-of-function studies in mice (*Ptc*^{+/-} mice carrying one inactivated allele developed MB with a 30 % penetrance), helped to establish a role for aberrant SHH signaling in MB; more recently a whole transcriptome analysis on larger cohorts set around ~25–35 % the fraction of human MBs characterized by SHH pathway activation [34, 35].

14.3 Turcot Syndrome and Wnt Pathway

The Canadian surgeon Jacques Turcot in 1959 described a recessive hereditary condition defined by the association between familial polyposis of the colon and brain tumors. Nowadays this rare genetic condition is counted under the category of constitutional mismatch repair-deficiency (CMMR-D) as it is caused by homozygous mutations or compound heterozygosity of the mismatch repair (MMR) genes *MLH1*, *MSH2*, *MSH6*, or *PMS2*. Similarly families affected by the autosomal dominant disorder, familial adenomatous polyposis (FAP), also develop brain tumors associated with other neoplasms [36, 37]. These two conditions show enough similarities to support the proposed re-denomination of brain tumor-polyposis syndrome type 1 and brain tumor-polyposis syndrome type 2 (BTP-1 and BTP-2) to indicate, respectively, the Turcot and the FAP syndrome [38]. Early studies indicated that FAP is linked to Chr:5q15-q22 [39, 40]; in parallel LOF analysis on tumor tissues indicated how 20 % of sporadic colorectal adenocarcinomas lose one of the alleles on chromosome 5q

[41], and extracolonic neoplasms also confirmed the role of hemizygous or homozygously mutated *APC* gene in tumorigenesis [42–44]. *APC* gene mutations were also identified in 10 of 12 families with FAP in which at least one patient developed a central nervous system tumor, mainly MB (79 %), as an extracolonic manifestation of FAP [45]. In a recent study on 28 BTP subjects, MB was the most common brain tumor, with young females under the age of 20 most frequently affected [46]. *APC* exerts its tumor suppression function by inhibiting the activation of the Wnt signaling pathway preventing the uncontrolled growth of cells and, in turn, the tumorigenic process. The Wnt signaling pathway was at first described in *Drosophila*, where its components regulate embryonic development, cell differentiation, and cell polarity generation. Core elements of the signaling pathway include the “β-catenin destruction complex” composed of scaffold proteins like APC and AXIN, whose role is to cage β-catenin in the cytoplasm and direct it to proteasomal degradation; the interaction between β-catenin and the complex is regulated by a protein kinase like GSK3-β and CKI. In the presence of Wnt ligands, the destruction complex is destabilized, releasing β-catenin to enter the nucleus where it binds TCF/LEF family transcription factors to promote specific gene expression regulating cell cycle progression, apoptosis, and differentiation [47, 48]. A hint about the role of Wnt and its signaling pathway in cancer came from the discovery of the first Wnt gene: mice infected with mouse mammary tumor virus (MMTV) developed tumors; the provirus insertion sites were clustered around a locus on Chr:15 containing a putative oncogene, *Int1* (integration 1), that was activated as consequence of viral integration [49]. The putative oncogene *Int1* was then named *Wnt1* after its sequence homology with the *Drosophila* *Wg* gene. The high incidence of MB in BTP-2 patients has pointed toward the presence of abnormalities in the Wnt pathway; also in sporadic MB, about 15 % harbor mutations of pathway components *APC* and *CTNNB1* (encoding for β-catenin) [50–53]. A study conducted on 109 MB patients in 2005 showed that about 25 % of the tumors displayed β-catenin

nuclear staining, indicative of Wnt pathway activation. Nucleo-positive tumors were associated with a better overall survival and event-free survival (OS and EFS) than negative tumors; interestingly β -catenin nucleo-positivity was evident among classic and anaplastic MBs. Mutations in the GSK-3 β phosphorylation domain of CTNNB1 were associated with aberrant nuclear accumulation of β -catenin; notably these missense mutations frequently occurred in residues altered also in other cancers. In the majority of non-MB cancers, *APC* is inactivated by the effect of truncating mutations or deletions, but only missense mutations have been found in MB; if these mutations are sufficient to induce nuclear localization of β -catenin, with activation of the pathway, is debatable [52, 53].

The study of MB associated with cancer-predisposing genetic syndromes has shed light on the genetic pathways involved in MB development, confirming the early assumption, derived from histological observation of the tumor tissue, that MB is a disease of development. As other signaling pathways crucial for cerebellar development were screened for their role in MB, in a gene-candidate approach, it became evident that unbiased whole genome strategies would complement and broaden the pool of MB cancer genes, dramatically increasing the understanding of MB pathogenesis.

Our comprehension of the genetic base of MB has indeed progressed hand in hand with the refinement of high-throughput technologies, which have reached unprecedented resolution and sensitivity in the past 10 years.

14.4 MB Genome: A Low-Resolution Picture

The first report of G-banded karyotypes of MBs covered seven tumors and sought to determine if specific chromosomal abnormalities characterized the tumors; the predominant findings in the karyotyped samples were structural abnormalities consisting of both deletions and unbalanced translocations in what appeared a near-diploid karyotype [54]. Thus, even at a low-resolution analysis, human MB karyotypes were found to be profoundly different from malignant gliomas,

as MB contain mainly structural alterations of chromosomes 1, 3, 17, and 20, usually resulting in partial trisomy, whereas the most frequent abnormalities in malignant gliomas are gains of whole copies of chromosome #7 and losses of 10 [55, 56]. The most common abnormality found consistently in MB by several groups was isochromosome 17q [i(17q)]; this rearrangement resulted in trisomy for 17q and monosomy for 17p [54, 57, 58]. An i(17q) is also commonly found in chronic myeloid leukemia; a translocation of genetic material between chromosomes 15 and 17, t(15;17), is instead typical of acute promyelocytic leukemia; this alteration fuses part of the *PML* gene from chr15 with part of the *RARA* gene from chr 17. The complex structure of chromosome 17 predisposes it to a form of homologous recombination that occurs between two segments of DNA that display high sequence homology but are not on two different alleles; this results in DNA rearrangements that cause several disorders. Chromosome 17 contains between 2.5 % and 3 % of the total DNA in cells and about 1,200 protein-coding genes, among them are genes involved in early onset breast cancer (*BRCA1*), neurofibromatosis (*NFI*), and the DNA damage response (*TP53* encoding the p53 protein) [59, 60]. Even though i(17q) is the most common MB abnormality, unique in certain tumor samples, the gene or gene combination driving tumorigenesis has remained elusive. Cytogenetic studies can also detect gene amplification; frequently these events appear as small fragments of extrachromosomal DNA called double minutes (DM), and often these DNA lengths harbor oncogenes or gene related to drug resistance [61]. Human MB-derived cell lines analyzed at early passages as well as xenografts harbored amplification of the *MYC* oncogene [62–64]. The *MYC* gene is part of a gene family (*MYC*, *MYCN*, and *MYCL1*) that accounts for the most prevalent target of gene amplification in MB; the *MYC* gene maps to chr8q24 and encodes for a transcription factor that regulates genes involved in cell division, cell growth, and apoptosis [65–67]. The advent of comparative genomic hybridization (CGH), a molecular-cytogenetic method for the evaluation of copy number changes (gains/losses) in the DNA content of tumor cells, has

Table 14.1 Most prominent CNA in MB genome

Gains	Losses
Chromosome	
17q	10q
17p	11p
i(17q)	8p
7	16q
2p	9q
1q	17p
	6

revealed previously uncharacterized alterations in MB genome. Consistent gains on chromosomes 7 and 17q as well as losses on 10q, 11, 16q, 17p, and 8p were reported, together with the well-known i(17q) and gross losses of chromosome 1, 3, and 20 (see Table 14.1). When stringent methods of statistical analysis were applied, CGH data suggested a much higher degree of genomic imbalance in MB than has been possible to observe with lower-resolution techniques [68, 69]. However, an intrinsic limitation of CGH is that it will detect only chromosomal changes that alter the copy number; aberrations such as balanced reciprocal translocations or inversions cannot be detected, as they do not change the copy number. Although a technique that fuses fluorescence in situ hybridization (FISH) and CGH, known as spectral karyotyping, allows the detection of subtle genomic rearrangements like balanced translocation, it was not until the advent of high-resolution techniques that the full extent of MB genome aberrations was shown in detail [70].

14.5 MB Genome: Lessons from High-Resolution Studies

The most advanced tools available to omics scientists to detect genome abnormalities in the submegabase range are digital karyotyping, array comparative genomic hybridization (aCGH), single nucleotide polymorphism (SNP) arrays, and next-generation sequencing (NGS). Three independent groups have applied digital karyotyping to MB genomics; two cell lines D487Med and D425Med were analyzed, and both showed

amplification of the *OTX2* gene. The analysis of human tumors confirmed that *OTX2* was overexpressed in anaplastic MB [71, 72]. More recently, *OTX2* was found to be focally amplified in a large cohort of MB samples analyzed by high-density SNP array. *OTX2* protein acts as a transcription factor and plays a role in fore-brain development; in the cerebellum *OTX2* is expressed in proliferating granule cell precursors [73]. Nakahara and colleagues instead applied digital karyotyping and high-density SNP arrays to identify a rare, recurrent homozygous deletion of Kruppel-like factor 4 (*KLF4*); *KLF* is a well-characterized tumor suppressor gene in colonic, gastric, and pancreatic carcinoma [74–77]. Several groups have pursued a genome-wide survey of the oncogenes aberrantly expressed in MB through aCGH; gains of several candidate oncogenes as *MET* and *CDK6* have been found to be amplified in 38.5 % and 30 % of the analyzed cases [78, 79]. Although, in light of the recent advances in MB molecular classification, the traditional picture based on five distinct histological subgroups (classic, desmoplastic, anaplastic, large-cell, and MB with extensive nodularity) has lost a prime role in patient stratification, it is still worth of notice that genomics approaches have shed some light on the basis of the different histological presentations of MB. In a 2006 study, Ehrbrecht and colleagues investigated the genomics of desmoplastic MBs by CGH on a cohort of 22 sporadic cases followed by aCGH on a subset of samples that showed 9p and 17q22–q24 amplification. Among others, *JMJD2C* amplified on 9p24 was subsequently confirmed in an independent cohort [80, 81]; this gene encodes for a histone lysine demethylase that plays a key role in the posttranslational modification of histones and thus regulating the functional chromatin organization, a critical step in epigenetic regulation. As highlighted in the first part of this chapter, many developmental pathways are potentially involved in the MB pathogenesis; however, the genetic determinants of the deregulation still remain poorly characterized. The Wnt pathway is one of the signaling cascades that regulate cerebellar development; in the effort to understand the genetic base of the Wnt pathway alteration in

MB, two independent studies have used genomics approaches to identify potential mechanisms [35, 82]. Monosomy of chr6 stood out as the hallmark of MBs harboring nuclear β -catenin, *CTNNB1*, or *APC* mutations; the alteration has been consistently observed in following studies making monosomy of chr6/*CTNNB1* a genomic marker of Wnt pathway tumors that are consistently associated with a highly favorable prognosis [83, 84]. When the power of molecular techniques is applied to cohorts of an adequate number of samples with robust clinical follow-up, genomic data can be used to stratify patients in risk class based on their molecular profile, beyond the classic histological classification. The study by Pfister and colleagues pursued this goal with a cohort of 80 primary MBs and a validation set of 296 independent tumor samples; gain of chr6q, amplification of *MYC* and *MYCN*, and an isolated gain of 17q and i(17q) were all associated with a poor clinical outcome; the work also confirmed loss of 6q as indicator of good prognosis. The proposed molecular strategy was based on four markers: *MYC/MYCN* amplification and 6q loss as indicators of worse and of best outcome, respectively, and 6q gain, 17q gain, and 6q/17q balanced to further stratify the patients from poor to good prognosis [67]. As the study of the MB genome progressed, in the last decade it became clear how the bottleneck for a comprehensive picture of MB aberrations depended on the cohort size and the resolution of the platform utilized in the study. In their 2009 study, Northcott and colleagues collected an unprecedented number of tumor samples, 201 primary MB and 11 MB cell lines, and analyzed their genomes using high-resolution SNPs genotyping arrays [85]. The innovative technology allowed a resolution of at least an order of magnitude higher than any previous array-based study of the MB genome. This led to the identification of hundreds of high-level amplifications and homozygous deletions, but unexpectedly only a few amplifications and homozygous deletions were found in more than one sample. Narrowing down the analysis on one of the most interesting deletions, chr 9q34 which is among the more common alterations in MB, a single gene mapped to the minimal

deleted region: *EHMT1*. The gene encodes for a euchromatic histone (H3K9) methyltransferase which is part of a protein complex that mediates epigenetic silencing by demethylation of H3K9; further functional data in the study confirmed the key role of *EHMT1* as a tumor suppressor gene in MB [86]. In early 2011 a seminal study focusing on the genome-wide analysis of MB was published; the authors used a combination of next-generation sequencing on protein-coding exons and high-density SNP array on a discovery cohort of 22 MBs, 17 primary tumors, 4 tumors propagated as xenograft in nude mice, and one cell line. When analyzed at this unprecedented depth, the MB genome revealed an average of 11 alterations. *PTCH1*, *CTNNB1*, *MYC*, *PTEN*, *TP53*, and *OTX* were commonly mutated across different samples confirming the role of the SHH and Wnt pathway in MB pathogenesis; other genes as *MLL2*, *SMARCA4*, and *MLL3* indicated that mechanisms controlling chromatin remodeling and transcriptional regulation are frequently deregulated in MB [4].

14.6 MB Transcriptome

The collection of all mRNA transcripts in the cell, which are products of genes that are being actively expressed at any given time, constitutes the transcriptome. Several strategies have been employed to analyze comprehensively the MB transcriptome, from early serial analysis of gene expression (SAGE) approaches to more recent expression profile platforms. The first study which focused on the comparison of the MB transcriptome versus its normal counterpart, fetal brain at 24.5 weeks, was accomplished in 1999 by Michiels and colleagues. The authors compared mRNA from the two sources and found 138 genes with significant differential expression, two of these differentially expressed genes, *ZIC1* and *OTX2*, are usually expressed in the external granular layer of the cerebellum as well as in the subventricular zone, thus confirming the early assumptions that MB arises in pluripotent proliferating cells in the germinal areas of the cerebellum [87]. About 30 % of MB cases

are metastatic right at the moment of diagnosis, and metastases has been a well-characterized negative prognostic factor, indicative of a high-risk patient. In 2001 an expression profile study offered the scientific community with some molecular actors distinctive of metastatic MB. The study comprised 23 primary MBs (M+ or M0) whose analysis made possible to identify 85 genes as differentially expressed between the two classes. MacDonald and colleagues also translated this genes list in a gene signature able to predict the M status of a tumor with 72 % accuracy. This approach paved the way to following studies, which proved how molecular data can be predictive of some of MB clinical features. Notably, PDGFR and members of the Ras/MAPK pathway were among the genes upregulated in metastatic MB, a finding that was also confirmed by the work of an independent group [88, 89]. A substantial change in perspective on MB molecular profiling has to be credited to Pomeroy and colleagues; in 2002 they studied the expression profiles of 42 tumor samples: MBs (ten patients), atypical teratoid rhabdoid tumors (five patients), renal and extrarenal rhabdoid tumors (five patients), PNETs (eight patients), nonembryonal brain tumors (malignant glioma; ten patients), and the normal human cerebellum (four cases) [90]. By the way of an unsupervised approach, the authors showed a well-resolved molecular distinction between the different tumor types; in clinical settings MBs were accounted among the PNETs, and the therapeutic protocols were basically the same. Establishing the deep molecular distinction between histologically similar tumors such as MBs and sPNETs has been a seminal finding in MB research; nowadays, these two tumors are two recognized entities, and PNETs are characterized by a poorer outcome [91]. Several other studies recently offered also a comparison of the genome aberrations that discriminate MBs from PNETs [92, 93]. Following the McDonald study in using molecular profiling to understand the differences across MBs with distinctive clinical features, Pomeroy et al. also compared the profiles of desmoplastic MBs versus classic MBs, confirming that the SHH signaling pathway plays a crucial role in desmoplastic

MBs. The study was also pivotal in supporting the use of molecular profiling of human tumors to obtain indications about disease prognosis; the authors extrapolated a gene signature based on eight genes that successfully predicted the survival status for 47 of the 60 patients profiled. Many studies followed along the lines indicated by Pomeroy and McDonald studies; among them is worth to mention, the informative expression profile of 35 MBs that were generated by Neben and colleagues, to identify transcripts associated with patient outcome. Of note, the authors performed an mRNA expression analysis followed by validation on tissue macroarray (TMA), defining a *STK1554* as a negative prognostic marker of overall survival [94].

14.7 MB Molecular Subgroups: More Than One Disease

MB is the most common pediatric brain tumor, but it is still a rare disease compared to other childhood cancers. The necessity to collect large cohorts of samples has hindered the understanding of subtle molecular differences among different MB tumor samples for a long time; these molecular differences are now offering new and exciting perspectives on MB pathogenesis and progress. In their study from 2006 Thompson and colleagues were the first to apply unsupervised hierarchical clustering to a dataset of 46 MBs. They analyzed the tumor's expression profile and used the most differentially expressed genes to define five molecular subgroups of MB. Notably, the authors also showed that tumors harboring a *CTNNB1* mutation or monosomy of Chr 6 were also showing altered expression of *Wnt* pathway genes; the same can be said for mutations in *PTCH1*, which always correlate with alterations in SHH pathway genes [35]. Along the same line as the Thompson work, Kool and colleagues further explored the potential of molecular classification of MB in a dataset of 52 cases. The authors confirmed the five molecular subgroups previously identified but also made some unprecedented correlations between molecular subgroups and clinical features. The non-SHH/-Wnt subgroups were

found to be correlated with the presence of metastatic disease, supporting the potential of patient stratification based on molecular signatures [84]. Ultimately the understanding of MB genomics increases proportionally with the size of the tumor cohorts analyzed; a glimpse of the future potential of such studies come from two recent works from two different groups. Northcott and colleagues recently contributed to the definition of MB subgroups performing gene expression profiles and DNA copy number aberrations for 103 primary MBs. Through a combination of different bioinformatics approaches based on the most informative genes in the dataset, the authors defined four different molecular subgroups, Wnt, SHH, C, and D. These findings were confirmed by the way of immunohistochemistry in a large dataset of 294 MBs. The molecular subgroups showed specific demographics, histology, metastatic status, and DNA copy number aberrations. To translate the results in a flexible tool that could be applied routinely in pathology laboratories, the authors also characterized and refined a protocol based on four antibodies: DKK1 (WNT), SFRP1 (SHH), NPR3 (group C), and KCNA1 (group D) [34]. The vast majority of the tested samples stained uniquely for one of the four antibodies, allowing the reliable classification of formalin-fixed MBs. One of the most important finding of the study was the revision of clinical features and their relation with patients' prognosis. The metastatic status at the moment of diagnosis, which has been a well-established hallmark of poor outcome, was found to be not reliable in group C patients (NPR3-positive tumors) who exhibited a significantly diminished progression-free and overall survival irrespective of their metastatic status. Cho and colleagues, analyzing a dataset of 194 MBs by high-density SNPs array and by expression profile, further honed the molecular classification proposed by Northcott et al. They showed how the less-resolved molecular subgroups (C and D) could be further subtyped; the especially bad prognosis of the newly defined molecular group characterized by MYC amplification and transcriptionally by enrichment of photoreceptor pathways clearly indicates that MB molecular classification is necessary to develop new therapeutic strategies [65].

In 2012 a genetic molecular profiling on 1,000 MBs samples identified four prominent subgroups [95]. These pioneer studies driven by a clonal genetic selection describe each group origin. Group 1 tumors show mutations in *SHH* and its receptors; group 2 tumors are driven by changes in Wnt signaling, generally through its main effector gene, β -catenin; group 3 tumors are driven by changes in TGF β -OTX2 signaling; and group 4 tumors are driven by mutations in *MYC* and *MYCN* [96]. An additional study from Shih and colleagues has underscored, for the first time, the possibility to perform "subgroup-specific" risk stratification within these MB tumors, integrating both clinical and molecular variables. As aptly pointed out in their study, they were able to define for MB arising from different molecular subgroup, a small panel of cytogenetic biomarkers that reliably identified very high-risk and very low-risk groups of patients, making it an excellent and useful tool for selecting an appropriate therapy for patients [97].

14.8 Profiling MB Transcriptome: Noncoding RNA Alterations

A new class of genes producing small noncoding RNAs, the microRNAs (miRNAs), has been discovered over the last recent years. These short RNAs (18–24 nucleotides) bind to cis-regulatory elements mainly present in the 3' UTR of mRNAs, resulting in translational inhibition or mRNA degradation [98, 99]. In mammals, miRNAs are predicted to control the activity of ~50 % of all protein-coding genes. Functional studies indicate that miRNAs participate in the regulation of almost every cellular process investigated so far and that changes in their expression are associated with many human pathologies [100, 101]. MicroRNAs could be useful tools to control cancers; in fact, they might be able to fulfill this task through their simultaneous control of multiple target genes. MiRNAs have been linked to the initiation, progression, and metastasis of human malignancies, with some species displaying oncogenic and others tumor suppressive potential [102, 103]. They are often expressed

Table 14.2 Noncoding RNA alterations in MB

Noncoding RNAs	Noncoding RNA alterations and their functions in MB	References
miR-124	Targets CKD6 and regulation of cell cycle, its expression is inhibited in MB	[118]
miR-324-5p, miR-326, miR-19a, miR-20, miR-92	Hedgehog-dependent proliferation, downregulated in MB	[112]
miR-199b-5p	Targets Hes1, impairment of cancer stem cells CD133+, silenced in MB	[109]
miR-let7g, miR-9, miR-106b, miR-125a-b, miR-191	Regulation of proliferation and apoptosis of MB cells, found upregulated in MB	[117]
miR-17-92	Overexpressed in the Shh subgroup of MBs and elevated levels of MYC/MYCN expression	[66, 107]
miR30b, miR30d	Targets of a novel recurrent MB amplification at 8q24.22-q24.23	[120]
miR128	Targets Bmi-1 and inhibition of MB cell growth	[121]
miR34a	Targets Notch ligand Delta-like 1(Dll1), impairment of cancer stem cell compartments	[111]

aberrantly in tumors as compared to normal tissues and are likely to contribute to tumorigenesis by deregulating critical target genes [104–106]. Several miRNAs have been studied in MB, as listed in Table 14.2; the entries on this list are continuously growing with the number of studies published.

The miR-17/92 polycistron has been found recurrently amplified in 6 % of pediatric MBs by the way of profiling the expression of 427 mature miRNAs in a series of 90 primary human MBs [107, 108]. The components of this cluster (miR-92, miR-19a, and miR-20) are the most highly upregulated miRNAs in MB; of note their expression was highest in the subgroup of MBs associated with the activation of the SHH signaling pathway. In the subset of MBs with miR-17/92 upregulation, the authors also noted elevated levels of MYC/MYCN. Consistently with Shh regulation, the Shh treatment of primary murine cerebellar granule neuron precursors (CGNP), cells of origin of the SHH-associated MBs, resulted in increased miR-17/92 expression. In CGNPs, the Shh effector N-myc, but not Gli1, induced miR-17/92 expression. Furthermore, ectopic miR-17/92 expression in CGNPs synergized with exogenous Shh to increase proliferation and also enabled proliferation in the absence of Shh. MiR-17/92 is a positive effector of Shh-mediated proliferation, and aberrant expression/amplification of this miRNA confers a growth advantage to MBs [107]. Northcott and colleagues identified

a focal amplification on chromosome 13q31.3, which mapped to the same miRNA cluster. The expression of miR-17/92 was confirmed to be most elevated in MBs of the Shh subgroup and was also associated with elevated MYC/MYCN levels. These studies suggest that aberrant expression of miRNAs, encoded by the miR-17/92, enhances the growth potential of MB and that miRNA-mediated modulation of Hedgehog signaling may be an important contributing factor to MB pathogenesis [108].

Our group discovered for the first time a miRNA deregulated in MB that targets the Notch pathway and depletes the tumor stem cells quota [109]. We identified miR199b-5p as targeting HES1, the principal Notch effector, demonstrating a new mechanism of regulation of the Notch pathway. The miRNA 199b-5p inhibits HES1 expression by binding to its 3'UTR. It is known that HES1 plays a crucial role in MB biology because high levels of HES1 protein expression correlate with negative outcome in MB patients [110]. Furthermore, the miRNA 199b-5p affects MB cancer stem cells by decreasing the side population (SP) quota as well as the CD133+ cells compartment. In MB, the expression of the neural stem cell marker CD133 has been associated with both tumor initiation capacity and radioresistance. MiRNA 199b-5p was found downregulated in MB patients' tissues compared to healthy control cerebellum tissues. The analysis of 61 patients with MB showed that the expression of miR-199b-5p in the nonmetastatic cases was

significantly higher than in the metastatic cases. The correlation with survival for the patients with high levels of miR-199b expression showed a positive trend to better overall survival than for the low-expressing patients. We further showed that in a xenograft mouse model, MB tumor burden is reduced by miRNA 199b-5p, indicating the use of this miRNA as an adjuvant therapy after surgery, in combination with radiation and chemotherapy, for the improvement of anticancer MB therapies and patient quality of life. To date, this was the first report indicating that the expression of miRNA could deplete tumor stem cells, an interesting therapeutic approach for the targeting of these cells in brain tumors. In a recent finding by our group, miR34a was also found to play a role in the non-autonomous signaling of Notch; by controlling Notch ligand Delta-like 1(Dll1), miR34a induces neurogenesis of tumor spheres derived from a genetic animal model of MB (Patch1+/-p53-/-) [111].

The interest in miRNAs role in MB pathogenesis has been increasing over the last few years; the availability of high-throughput approaches to comprehensively profile miRNA expressions has allowed to investigate miRNAs involvement in MB carcinogenesis and their prognostic relevance. Specific miRNA expression patterns were correlated to MB histotypes (anaplastic, classic, and desmoplastic), to specific sets of molecular alterations (ErbB2- or MYC-overexpressing tumors), and to disease-risk stratification [112]. The group headed by Gulino studied miRNAs in the context of SHH signaling; miR-125b, miR-326, and miR-324-5p expression were found decreased in MB; the altered expression of these miRNAs led to tumor cell proliferation through an SHH-dependent mechanism. They identified 78 miRNAs with altered expression in MB compared with normal adult and fetal cerebellar cells. Several of the identified miRNAs have been implicated in other cancer types including glioblastoma [113]. The majority of these miRNAs were found downregulated in MB, supporting a role for miRNAs as tumor suppressors. Additionally, they found increased expression of miR-9 and miR-125a whose increased expression was capable of decreasing proliferation, augmenting apoptosis,

and ultimately promoting arrest of tumor growth. The pro-apoptotic effect was mediated by miR-9 and miR-125a targeting of the TrkC receptor, which was found in this study to be upregulated in MB cells. They also found that miR-let7g, miR-19a, miR-106b, and miR-191 were significantly upregulated in anaplastic compared with desmoplastic MBs tumors; miR-let7g and miR-106b were differentially expressed in desmoplastic compared with classic MBs. Changes in the expression of Her2 (ErbB2) and MYC have been demonstrated to impact biological activity and clinical features of MB [114–116]. The Gulino team additionally examined miRNAs expression from MBs overexpressing either Her2 or MYC and identified an miRNA signature in the two groups of MBs. The expression of miR-10b, miR-135a, miR-135b, miR-125b, and miR-153 was altered in Her2-overexpressing tumors, whereas MYC-overexpressing MBs had expression changes in miR-181b, miR-128a, and miR-128b. Additionally, the amount of expression change of two miRNAs correlated with disease risk. miR-31 and miR-153 were found downregulated in all MBs; the degree of change was directly proportional to disease severity [117]. Although these data are of interest, the identified signature would be of further importance as validation experiments in an independent cohort will be performed.

An additional study was related to miR-124, which is preferentially expressed in differentiating neurons and in CGNPs which are thought to be the cells of origin of MBs [118]. MiR-124 deregulation is common in MBs, and the restoration of its function inhibits cell proliferation, suggesting that it may act as a growth suppressor. Two targets of miR-124 have been identified: cyclin-dependent kinase 6 (CDK6) that was identified as an adverse prognostic marker in MB and SLC16A1 that may represent a novel therapeutic target for the treatment of malignant MBs [118]. SLC16A1, solute carrier family 16, functions to efflux lactic acid during aerobic glycolysis, and its inhibition resulted in a decrease of intracellular pH to a lethal level. This study demonstrates that miR-124 deregulation is common in MB, and the restoration of its function inhibits

cell proliferation, suggesting that miR-124 may act as a growth suppressor, raising the possibility that the miR-124/SLC16A1 pathway may represent a novel therapeutic target for the treatment of malignant MBs [119].

Further recent work demonstrated that miR-30b and miR-30d are amplified in MB and are putative oncogenic targets of a novel recurrent MB amplicon at 8q24.22-q24.23 [120]. miR-128a inhibits the growth of MB cells by targeting the Bmi-1 oncogene. This miRNA alters the intracellular redox state of the tumor cells and promotes cellular senescence. MiR-128a has growth suppression activity in MB cell lines, and this activity is partially mediated by targeting Bmi-1. This finding has implications for the modulation of redox states in cancer stem cells, which are thought to be resistant to therapy due to their low ROS states [121].

At this time, we can conclude that despite the amount of investigation related to miRNAs involvement in cancer, knowledge of their role in MB genetics is still at the beginning stage.

14.9 Profiling MB Transcriptome: Epigenetic Alterations

Epigenetic changes have been shown to be key players in tumorigenesis; they are defined as heritable changes in gene expression that are not accompanied by modifications in primary DNA sequence. Epigenetic modifications include DNA methylation on cytosine residues, most often in the context of CpG dinucleotides, as well as post-translational modification of histone proteins, such as methylation, acetylation, and phosphorylation [122–124]. Hypermethylation of CpG islands located at the 5' end of genes has been reported in most cancers, either alone or in combination with genetic alterations (as gene deletions or mutations); hypermethylation of CpG islands overall can contribute to tumor suppressor gene silencing [123]. The study of epigenetic changes in MB offers significant potential for an improved understanding of its genetics [125, 126]. Several studies have suggested that multiple loci undergo changes in their methylation sta-

tus during MB pathogenesis [85, 125, 126]. Among the earliest studies to implicate aberrant promoter methylation in MB on a global scale is the study by Frühwald and colleagues who used restriction landmark genomic scanning to analyze DNA methylation patterns in 17 primary MBs and 5 MB cell lines. Using this method, the authors identified methylation in up to 1 % of all CpG islands in primary tumors and up to 6 % in MB cell lines [125]. In addition, an association between hypermethylated sequences in MB and a poor prognosis were implied. Collectively, these findings provided early evidence that epigenetic events are likely to play a role in MB.

In another study, using microarray-based differential methylation hybridization, Waha and colleagues identified hypermethylation of the *SCG5* (secretory granule, neuroendocrine protein 1 gene) in 16 (~70 %) of 23 primary MBs and 7 (~87 %) of 8 MB cell lines [127]. The expression of *SCG5* was found to be down-regulated in the majority of primary samples and cell lines as compared with normal cerebellar controls, and *SCG5* transcription was restored in cell lines treated with the demethylating agent, 5-aza (5-aza-2'-deoxycytidine). Furthermore, the reexpression of *SCG5* in the D283Med cell line resulted in growth suppression and reduced colony formation, suggesting that *SCG5* may be a putative tumor suppressor gene in MB. A link between histone methylation genes and MB has also previously been hypothesized based on the observation that copy number alterations affecting chromosomal regions containing histone methyltransferases or demethylases occur in a subset of MBs [85, 128]. It is known that deregulation of Wnt signaling occurs in up to 20 % of MB. Kongkham et al., using a genome-wide approach, identified the secreted frizzled-related protein 1, 2, and 3 (*SFRP1*, *SFRP2*, and *SFRP3*) family of Wnt inhibitors as putative tumor suppressor genes silenced by promoter region methylation in MB. *SFRP1*, *SFRP2*, and *SFRP3* expression increased after 5-aza-2'-deoxycytidine treatment. *SFRP1*, *SFRP2*, and *SFRP3* methylation was identified in 23.5 %, 3.9 %, and 15.7 % of primary MB specimens, respectively,

by methylation-specific PCR; SFRP1 was expressed at levels twofold lower than that in the normal cerebellum. In MB, the loss of Wnt pathway inhibition due to SFRP gene silencing demonstrates an additional mechanism that may contribute to the deregulation of Wnt signaling [129]. *RASSF1A* (RAS association domain gene) regulates cyclin D1 expression, which is important in controlling the cell cycle. In contrast to other malignancies, hypermethylation of *RASSF1A* in MB is not accompanied by allelic loss of 3p21.3 or mutation, indicating that biallelic loss is the primary mechanism of inactivation of *RASSF1A* [130].

CASP8 is a cysteine protease involved in death-receptor-mediated apoptosis [131]. Promoter hypermethylation of *CASP8* leading to loss of *CASP8* mRNA expression induces resistance to apoptosis induced by tumor necrosis factor-inducing ligand (TRAIL). In primary tumors, aberrant promoter methylation of *CASP8* was seen most frequently in classic and anaplastic MBs and is an independent prognostic factor of poor outcome.

Transcriptional silencing of *SGNE1/7B2*, a gene located on 15q13.3, occurs predominantly in classic MB. *SGNE1* is a calcium-dependent serine protease that inhibits tumor cell proliferation. Another gene, *ZIC2*, a zinc-finger transcription factor essential for the development of the central nervous system was found downregulated in MBs [132]. Pfister and colleagues developed and applied a technique known as array-based profiling of reference-independent methylation status (aPRIMES) to globally survey DNA methylation patterns in the MB genome. They showed a striking association between samples classified as either “low methylators” or “high methylators” and patient outcome, with the high-methylator group exhibiting reduced overall survival. In addition, the C2H2-type zinc-finger protein *ZIC2* was identified as a hypermethylated candidate using aPRIMES and was subsequently confirmed to be epigenetically silenced in a panel of primary MB by using a combination of pyrosequencing and quantitative RT-PCR analysis. In total three other members of the S100 gene family were found to be aberrantly methylated

in 10–20 % of MBs [133]. Hypermethylation and silencing of *S100A6* are associated with the large-cell anaplastic subtype of MB. The pro-metastatic gene *S100A4* is a direct target of ErbB2 signaling and is associated with a poor prognosis in MB. MCG, a member of the DNAAJ protein family that influences chemotherapy resistance, was found inactivated by biallelic hypermethylation, but hypermethylation of one allele also occurs in combination with genetic loss of the second allele.

The 17p13.3 locus, the most common genetic defect in MB, contains the gene hypermethylated in cancer 1 (*HIC1*), a transcriptional repressor that is a frequent target of epigenetic gene silencing in MB [134]. The *Ptch1* gene is a well-characterized tumor suppressor in MB; when compared with *Ptch1*^{+/-} mouse mutants, compound *Ptch1/Hic1* heterozygotes display a fourfold increased incidence of MB. *Hic1* is a direct transcriptional repressor of Atonal Homolog 1 (*Atoh1*), a pro-neural transcription factor essential for cerebellar development [134].

An epigenome-wide screen in MB cell lines, using 5-aza-2 deoxycytidine to find genes aberrantly silenced by promoter hypermethylation, identified an inhibitor of HGF/MET signaling, serine protease inhibitor Kunitz-type 2 (*SPINT2/HAI-2*), as a putative tumor suppressor silenced by promoter methylation in MB [129]. *SPINT2* gene expression was downregulated, and *MET* expression was upregulated in 73.2 % and 45.5 % of tumors, respectively. *SPINT2* promoter methylation was detected in 34.3 % of primary MBs examined by methylation-specific PCR. *SPINT2* reexpression in MB cell lines reduced proliferative capacity, anchorage-independent growth, cell motility in vitro, and increased overall survival times in vivo in a xenograft model. These data support the role of *SPINT2* as another putative tumor suppressor gene methylated in MB [129]. The crucial role of epigenetic changes in MB was further underlined by Ecke and colleagues who showed reduced tumor incidence in heterozygous *Ptch1*^{+/-} mice after reduction of endogenous DNA methyltransferase 1 (*Dnmt1*) activity. This reduction was achieved by a combined treatment with the *Dnmt* inhibitor

5-aza-2 deoxycytidine (5-aza-dC) and the histone deacetylase (HDAC) inhibitor valproic acid (VPA). The combination of the two drugs efficiently prevented MB formation, whereas monotherapies with either drug were less effective. Wild-type *Ptch1* expression was efficiently reactivated in tumors by 5-aza-dC/VPA combination therapy. This was associated with reduced methylation of the *Ptch* promoter and induction of histone hyperacetylation suggesting the inhibition of HDACs in vivo. However, the treatment was not effective in advanced-stage tumors. This was the first in vivo demonstration that showed that targeting of *Dnmt* and HDAC activities is highly effective in preventing the formation of *Ptch*-associated tumors [135].

Although loss of 17p13 has been often associated with *p53* genetic alteration or *HIC1* gene hypermethylation, other tumor suppressor genes located in this region such as *KCTD11* (*KCTD11*) are potentially lost in human MB, in part by LOH and in part by uncharacterized epigenetic events [136]. Using a panel of 177 human tumor samples and their normal matching samples representing 18 different types of cancer, it was showed that the downregulation of *KCTD11* protein level is a specific and a diffusely common event in tumorigenesis. Additionally, it was identified that a CpG island and several Sp1 binding sites on *KCTD11* promoter, Sp1 transcription factor, and DNA methylation contribute, at least in part, in the regulation of *KCTD11* expression [136]. *KLF4* expression is also lost in more than 40 % of primary MBs both at the RNA and protein levels. MB cell lines drastically increase the expression of *KLF4* in response to the demethylating agent 5-azacytidine and demonstrate demethylation of the promoter CpG islands by bisulfite sequencing. Methylation-specific PCR, targeting the *KLF4* promoter, demonstrates CpG methylation in approximately 16 % of primary MBs. *KLF4* is inactivated by either genetic or epigenetic mechanisms in a large subset of MBs, and it likely functions as a tumor suppressor gene in the pathogenesis of MB [75].

A genome-wide method for detecting regions of CpG methylation on the basis of the increased melting temperature of methylated DNA, termed

denaturation analysis of methylation differences (DAMD), was developed by Diede S. J. and colleagues. They found common regions of cancer-specific methylation changes in primary MBs in critical developmental regulatory pathways, including *Shh*, *Wnt*, retinoic acid receptor (RAR), and bone morphogenetic protein (BMP). One of the commonly methylated loci is the *PTCH1-1C* promoter that is methylated in both primary patient samples and human MB cell lines. Treatment with the DNA methyltransferase inhibitor 5-aza-2'-deoxycytidine (5-aza-dC) increases the expression of *PTCH1* and other methylated loci. This data demonstrate that epigenetic silencing by DNA methylation of *PTCH1* contributes to the formation of this childhood cancer and suggests the use of DNA demethylating agents as a potential strategy for therapy [137].

Of particular interest are the findings of Northcott and colleagues that, using high-resolution SNP genotyping of 212 MBs, identified previously unknown amplifications and homozygous deletions, including recurrent, mutually exclusive, highly focal genetic events in genes targeting histone lysine methylation, particularly that of histone 3 lysine 9 (H3K9). Restoration of the expression of genes controlling H3K9 methylation greatly decreased the proliferation of MB in vitro. Copy number aberrations of genes with critical roles in writing, reading, removing, and blocking the state of histone lysine methylation, particularly at H3K9, suggest that defective control of the histone code contributes to the pathogenesis of MB [85]. A detailed summary of genes and literature describing their involvement in epigenetic changes of expression are shown in Table 14.3.

The recent epigenome studies of MB have demonstrated the implication of epigenetic gene silencing in this pediatric tumor as a crucial mechanism of tumor suppressor gene inactivation. The integration of epigenetic profiles and genome aberrations in the context of MB molecular subgrouping will be of invaluable significance to address important questions in MB pathogenesis and recurrence, paving the way for new therapeutic strategies.

Table 14.3 Genes epigenetically silenced in MB

Gene	Function	Reference
SCG5	Hypermethylation in 70 % of 23 primary MBs and 87 % of 8 MB cell lines	[138]
SFRP1, SFRP2, SFRP3	Wnt inhibitors, silenced by promoter region methylation in MB. Methylation was identified in 23.5 %, 3.9 %, and 15.7 % of primary MB	[139]
RASSF1A	Regulates cyclin D1 expression; hypermethylation in MB	[130]
CASP8	Cysteine protease involved in death-receptor-mediated apoptosis. In primary tumors, aberrant promoter methylation of CASP8 was seen most frequently in classic and anaplastic MB	[140]
SGNE1/7B2 and ZIC2	Calcium-dependent serine protease and zinc-finger transcription factor essential for the development of the central nervous system; silenced in MB	[132]
S100 gene family	S100A6 is hypermethylated and associated with large-cell anaplastic MB subtype while S100A4, a pro-metastatic gene, target of erbB2 signaling is hypomethylated	[93]
HIC1	Transcriptional repressor, direct inhibitor of Atonal Homolog 1 (Atoh1), a pro-neural transcription factor essential for cerebellar development. Epigenetic silencing in MB	[141]
SPINT2	Downregulated by promoter methylation in 34.3 % of primary MBs	[129]

Conclusions

The genomic landscape of MB has been shown, in all its complexity, by several intensive studies including genome-, transcriptome-, and epigenome-wide profiling of tumor cohorts. Genomics projects of unprecedented dimension have revealed new insight into molecular aberrations of the disease and have implicated new mechanisms leading to deregulation of the MB transcriptome. The molecular classification of MBs outperforms the classical histological stratification and is likely to revolutionize MB patient management and MB therapy. Although the understanding of the molecular genetics underlying MB pathogenesis has improved greatly, much has to be done to correlate the different aspects of MB genomics to clinical features of the disease: to achieve this goal large sample cohorts are necessary, and given the relative rarity of the disease, only integrative approaches based on the collaboration of several groups across the globe are likely to provide the comprehensive knowledge of MB that we crave for. Next-

generation sequencing technologies recently revolutionized the approach to cancer genomics: The Cancer Genome Atlas project is performing intensive studies to chart the genomic alterations involved in more than 20 types of cancer. As genomic studies proceed and produce a large amount of data, discriminating between so-called driver and passenger mutations will be the next challenge. Not all the alterations found in cancer genomes are thought to critically contribute to the progression of the disease, some are merely a bystander effect of generalized genome instability; to distinguishing mutations that confer a clonal advantage (drivers) in tumorigenesis from those that do not, a robust bioinformatics strategy will have to be implemented and candidates validated in relevant models. The future suggests to be an exciting time for MB researchers with a comprehensive catalogue of the key genomic changes to mine and explore in their relation to MB; cancer genomics will support advances in developing more effective ways to diagnose, treat, and prevent cancer.

References

- Link DC, Schuettelpelz LG, Shen D, Wang J, Walter MJ, Kulkarni S, Payton JE, Ivanovich J, Goodfellow PJ, Le Beau M, Koboldt DC, Dooling DJ, Fulton RS, Bender RH, Fulton LL, Delehaunty KD, Fronick CC, Appelbaum EL, Schmidt H, Abbott R, O'Laughlin M, Chen K, McLellan MD, Varghese N, Nagarajan R, Heath S, Graubert TA, Ding L, Ley TJ, Zambetti GP, Wilson RK, Mardis ER (2011) Identification of a novel TP53 cancer susceptibility mutation through whole-genome sequencing of a patient with therapy-related AML. *JAMA* 305(15):1568–1576. doi:[10.1001/jama.2011.473](https://doi.org/10.1001/jama.2011.473)
- Jones S, Zhang X, Parsons DW, Lin JC, Leary RJ, Angenendt P, Mankoo P, Carter H, Kamiyama H, Jimeno A, Hong SM, Fu B, Lin MT, Calhoun ES, Kamiyama M, Walter K, Nikolskaya T, Nikolsky Y, Hartigan J, Smith DR, Hidalgo M, Leach SD, Klein AP, Jaffee EM, Goggins M, Maitra A, Iacobuzio-Donahue C, Eshleman JR, Kern SE, Hruban RH, Karchin R, Papadopoulos N, Parmigiani G, Vogelstein B, Velculescu VE, Kinzler KW (2008) Core signaling pathways in human pancreatic cancers revealed by global genomic analyses. *Science* 321(5897):1801–1806. doi:[10.1126/science.1164368](https://doi.org/10.1126/science.1164368)
- Parsons DW, Jones S, Zhang X, Lin JC, Leary RJ, Angenendt P, Mankoo P, Carter H, Siu IM, Gallia GL, Olivi A, McLendon R, Rasheed BA, Keir S, Nikolskaya T, Nikolsky Y, Busam DA, Tekleab H, Diaz LA Jr, Hartigan J, Smith DR, Strausberg RL, Marie SK, Shinjo SM, Yan H, Riggins GJ, Bigner DD, Karchin R, Papadopoulos N, Parmigiani G, Vogelstein B, Velculescu VE, Kinzler KW (2008) An integrated genomic analysis of human glioblastoma multiforme. *Science* 321(5897):1807–1812. doi:[10.1126/science.1164382](https://doi.org/10.1126/science.1164382)
- Parsons DW, Li M, Zhang X, Jones S, Leary RJ, Lin JC, Boca SM, Carter H, Samayoa J, Bettegowda C, Gallia GL, Jallo GI, Binder ZA, Nikolsky Y, Hartigan J, Smith DR, Gerhard DS, Fults DW, VandenBerg S, Berger MS, Marie SK, Shinjo SM, Clara C, Phillips PC, Minturn JE, Biegel JA, Judkins AR, Resnick AC, Storm PB, Curran T, He Y, Rasheed BA, Friedman HS, Keir ST, McLendon R, Northcott PA, Taylor MD, Burger PC, Riggins GJ, Karchin R, Parmigiani G, Bigner DD, Yan H, Papadopoulos N, Vogelstein B, Kinzler KW, Velculescu VE (2011) The genetic landscape of the childhood cancer medulloblastoma. *Science* 331(6016):435–439. doi:[10.1126/science.1198056](https://doi.org/10.1126/science.1198056)
- Totoki Y, Tatsuno K, Yamamoto S, Arai Y, Hosoda F, Ishikawa S, Tsutsumi S, Sonoda K, Totsuka H, Shirakihara T, Sakamoto H, Wang L, Ojima H, Shimada K, Kosuge T, Okusaka T, Kato K, Kusuda J, Yoshida T, Aburatani H, Shibata T (2011) High-resolution characterization of a hepatocellular carcinoma genome. *Nat Genet* 43(5):464–469. doi:[10.1038/ng.804](https://doi.org/10.1038/ng.804)
- Brena RM, Costello JF (2007) Genome-epigenome interactions in cancer. *Hum Mol Genet* 16(Spec No 1):R96–R105. doi:[10.1093/hmg/ddm073](https://doi.org/10.1093/hmg/ddm073)
- Jones PA, Baylin SB (2002) The fundamental role of epigenetic events in cancer. *Nat Rev Genet* 3(6):415–428. doi:[10.1038/nrg816](https://doi.org/10.1038/nrg816)
- Noushmehr H, Weisenberger DJ, Diefes K, Phillips HS, Pujara K, Berman BP, Pan F, Pelloski CE, Sulman EP, Bhat KP, Verhaak RG, Hoadley KA, Hayes DN, Perou CM, Schmidt HK, Ding L, Wilson RK, Van Den Berg D, Shen H, Bengtsson H, Neuvial P, Cope LM, Buckley J, Herman JG, Baylin SB, Laird PW, Aldape K (2010) Identification of a CpG island methylator phenotype that defines a distinct subgroup of glioma. *Cancer Cell* 17(5):510–522. doi:[10.1016/j.ccr.2010.03.017](https://doi.org/10.1016/j.ccr.2010.03.017)
- Ting AH, Jair KW, Schuebel KE, Baylin SB (2006) Differential requirement for DNA methyltransferase 1 in maintaining human cancer cell gene promoter hypermethylation. *Cancer Res* 66(2):729–735. doi:[10.1158/0008-5472.CAN-05-1537](https://doi.org/10.1158/0008-5472.CAN-05-1537)
- Malkin D, Li FP, Strong LC, Fraumeni JF Jr, Nelson CE, Kim DH, Kassel J, Gryka MA, Bischoff FZ, Tainsky MA et al (1990) Germ line p53 mutations in a familial syndrome of breast cancer, sarcomas, and other neoplasms. *Science* 250(4985):1233–1238
- Srivastava S, Zou ZQ, Pirollo K, Blattner W, Chang EH (1990) Germ-line transmission of a mutated p53 gene in a cancer-prone family with Li-Fraumeni syndrome. *Nature* 348(6303):747–749. doi:[10.1038/348747a0](https://doi.org/10.1038/348747a0)
- Kleihues P, Schauble B, zur Hausen A, Esteve J, Ohgaki H (1997) Tumors associated with p53 germ-line mutations: a synopsis of 91 families. *Am J Pathol* 150(1):1–13
- Adesina AM, Nalbantoglu J, Cavenee WK (1994) p53 gene mutation and mdm2 gene amplification are uncommon in medulloblastoma. *Cancer Res* 54(21):5649–5651
- Saylor RL 3rd, Sidransky D, Friedman HS, Bigner SH, Bigner DD, Vogelstein B, Brodeur GM (1991) Infrequent p53 gene mutations in medulloblastomas. *Cancer Res* 51(17):4721–4723
- Frank AJ, Hernan R, Hollander A, Lindsey JC, Lusher ME, Fuller CE, Clifford SC, Gilbertson RJ (2004) The TP53-ARF tumor suppressor pathway is frequently disrupted in large/cell anaplastic medulloblastoma. *Brain Res Mol Brain Res* 121(1–2):137–140. doi:[10.1016/j.molbrainres.2003.11.016](https://doi.org/10.1016/j.molbrainres.2003.11.016)
- Tabori U, Baskin B, Shago M, Alon N, Taylor MD, Ray PN, Bouffet E, Malkin D, Hawkins C (2010) Universal poor survival in children with medulloblastoma harboring somatic TP53 mutations. *J Clin Oncol* 28(8):1345–1350. doi:[10.1200/JCO.2009.23.5952](https://doi.org/10.1200/JCO.2009.23.5952)
- Evans DG, Farndon PA, Burnell LD, Gattamaneni HR, Birch JM (1991) The incidence of Gorlin syndrome in 173 consecutive cases of medulloblastoma. *Br J Cancer* 64(5):959–961
- Kimonis VE, Goldstein AM, Pastakia B, Yang ML, Kase R, DiGiovanna JJ, Bale AE, Bale SJ (1997) Clinical manifestations in 105 persons with nevoid

- basal cell carcinoma syndrome. *Am J Med Genet* 69(3):299–308
19. Amlashi SF, Riffaud L, Brassier G, Morandi X (2003) Nevoid basal cell carcinoma syndrome: relation with desmoplastic medulloblastoma in infancy. A population-based study and review of the literature. *Cancer* 98(3):618–624. doi:[10.1002/cncr.11537](https://doi.org/10.1002/cncr.11537)
 20. Cowan R, Hoban P, Kelsey A, Birch JM, Gattamaneni R, Evans DG (1997) The gene for the naevoid basal cell carcinoma syndrome acts as a tumour-suppressor gene in medulloblastoma. *Br J Cancer* 76(2):141–145
 21. Farndon PA, Del Mastro RG, Evans DG, Kilpatrick MW (1992) Location of gene for Gorlin syndrome. *Lancet* 339(8793):581–582
 22. Gailani MR, Bale SJ, Leffell DJ, DiGiovanna JJ, Peck GL, Poliak S, Drum MA, Pastakia B, McBride OW, Kase R et al (1992) Developmental defects in Gorlin syndrome related to a putative tumor suppressor gene on chromosome 9. *Cell* 69(1):111–117
 23. Reis A, Kuster W, Linss G, Gebel E, Hamm H, Fuhrmann W, Wolff G, Groth W, Gustafson G, Kuklik M et al (1992) Localisation of gene for the naevoid basal-cell carcinoma syndrome. *Lancet* 339(8793):617
 24. Johnson RL, Rothman AL, Xie J, Goodrich LV, Bare JW, Bonifas JM, Quinn AG, Myers RM, Cox DR, Epstein EH Jr, Scott MP (1996) Human homolog of patched, a candidate gene for the basal cell nevus syndrome. *Science* 272(5268):1668–1671
 25. Uden AB, Holmberg E, Lundh-Rozell B, Stahle-Backdahl M, Zaphiropoulos PG, Toftgard R, Vorechovsky I (1996) Mutations in the human homologue of *Drosophila patched* (PTCH) in basal cell carcinomas and the Gorlin syndrome: different in vivo mechanisms of PTCH inactivation. *Cancer Res* 56(20):4562–4565
 26. Stone DM, Hynes M, Armanini M, Swanson TA, Gu Q, Johnson RL, Scott MP, Pennica D, Goddard A, Phillips H, Noll M, Hooper JE, de Sauvage F, Rosenthal A (1996) The tumour-suppressor gene patched encodes a candidate receptor for Sonic hedgehog. *Nature* 384(6605):129–134. doi:[10.1038/384129a0](https://doi.org/10.1038/384129a0)
 27. Gailani MR, Stahle-Backdahl M, Leffell DJ, Glynn M, Zaphiropoulos PG, Pressman C, Uden AB, Dean M, Brash DE, Bale AE, Toftgard R (1996) The role of the human homologue of *Drosophila patched* in sporadic basal cell carcinomas. *Nat Genet* 14(1):78–81. doi:[10.1038/ng0996-78](https://doi.org/10.1038/ng0996-78)
 28. Raffel C, Jenkins RB, Frederick L, Hebrink D, Alderete B, Fults DW, James CD (1997) Sporadic medulloblastomas contain PTCH mutations. *Cancer Res* 57(5):842–845
 29. Reifenberger J, Wolter M, Weber RG, Megahed M, Ruzicka T, Lichter P, Reifenberger G (1998) Missense mutations in SMOH in sporadic basal cell carcinomas of the skin and primitive neuroectodermal tumors of the central nervous system. *Cancer Res* 58(9):1798–1803
 30. Wolter M, Reifenberger J, Sommer C, Ruzicka T, Reifenberger G (1997) Mutations in the human homologue of the *Drosophila* segment polarity gene patched (PTCH) in sporadic basal cell carcinomas of the skin and primitive neuroectodermal tumors of the central nervous system. *Cancer Res* 57(13):2581–2585
 31. Xie J, Murone M, Luoh SM, Ryan A, Gu Q, Zhang C, Bonifas JM, Lam CW, Hynes M, Goddard A, Rosenthal A, Epstein EH Jr, de Sauvage FJ (1998) Activating Smoothed mutations in sporadic basal-cell carcinoma. *Nature* 391(6662):90–92. doi:[10.1038/34201](https://doi.org/10.1038/34201)
 32. Zurawel RH, Allen C, Chiappa S, Cato W, Biegel J, Cogen P, de Sauvage F, Raffel C (2000) Analysis of PTCH/SMO/SHH pathway genes in medulloblastoma. *Genes Chromosomes Cancer* 27(1):44–51
 33. Kinzler KW, Bigner SH, Bigner DD, Trent JM, Law ML, O'Brien SJ, Wong AJ, Vogelstein B (1987) Identification of an amplified, highly expressed gene in a human glioma. *Science* 236(4797):70–73
 34. Northcott PA, Korshunov A, Witt H, Hielscher T, Eberhart CG, Mack S, Bouffet E, Clifford SC, Hawkins CE, French P, Rutka JT, Pfister S, Taylor MD (2011) Medulloblastoma comprises four distinct molecular variants. *J Clin Oncol* 29(11):1408–1414. doi:[10.1200/JCO.2009.27.4324](https://doi.org/10.1200/JCO.2009.27.4324)
 35. Thompson MC, Fuller C, Hogg TL, Dalton J, Finkelstein D, Lau CC, Chintagumpala M, Adesina A, Ashley DM, Kellie SJ, Taylor MD, Curran T, Gajjar A, Gilbertson RJ (2006) Genomics identifies medulloblastoma subgroups that are enriched for specific genetic alterations. *J Clin Oncol* 24(12):1924–1931. doi:[10.1200/JCO.2005.04.4974](https://doi.org/10.1200/JCO.2005.04.4974)
 36. Gardner EJ (1951) A genetic and clinical study of intestinal polyposis, a predisposing factor for carcinoma of the colon and rectum. *Am J Hum Genet* 3(2):167–176
 37. Gardner EJ, Woolf CM (1952) Intestinal polyposis and carcinoma originating from a mutation in a family group. *Cancer* 5(4):695–699
 38. Paraf F, Jothy S, Van Meir EG (1997) Brain tumor-polyposis syndrome: two genetic diseases? *J Clin Oncol* 15(7):2744–2758
 39. Herrera L, Kakati S, Gibas L, Pietrzak E, Sandberg AA (1986) Gardner syndrome in a man with an interstitial deletion of 5q. *Am J Med Genet* 25(3):473–476. doi:[10.1002/ajmg.1320250309](https://doi.org/10.1002/ajmg.1320250309)
 40. Kobayashi T, Narahara K, Yokoyama Y, Ueyama S, Mohri O, Fujii T, Fujimoto M, Ohtsuki S, Tsuji K, Seino Y (1991) Gardner syndrome in a boy with interstitial deletion of the long arm of chromosome 5. *Am J Med Genet* 41(4):460–463. doi:[10.1002/ajmg.1320410416](https://doi.org/10.1002/ajmg.1320410416)
 41. Ashton-Rickardt PG, Dunlop MG, Nakamura Y, Morris RG, Purdie CA, Steel CM, Evans HJ, Bird CC, Wyllie AH (1989) High frequency of APC loss in sporadic colorectal carcinoma due to breaks clustered in 5q21-22. *Oncogene* 4(10):1169–1174
 42. Groden J, Thliveris A, Samowitz W, Carlson M, Gelbert L, Albertsen H, Joslyn G, Stevens J, Spirio L, Robertson M et al (1991) Identification and characterization of the familial adenomatous polyposis coli gene. *Cell* 66(3):589–600

43. Okamoto M, Sato C, Kohno Y, Mori T, Iwama T, Tonomura A, Miki Y, Utsunomiya J, Nakamura Y, White R et al (1990) Molecular nature of chromosome 5q loss in colorectal tumors and desmoids from patients with familial adenomatous polyposis. *Hum Genet* 85(6):595–599
44. van der Luijt RB, Tops CM, Khan PM, van der Klift HM, Breukel C, van Leeuwen-Cornelisse IS, Dauwerse HG, Beverstock GC, van Noort E, Snel P et al (1995) Molecular, cytogenetic, and phenotypic studies of a constitutional reciprocal translocation t(5;10)(q22;q25) responsible for familial adenomatous polyposis in a Dutch pedigree. *Genes Chromosomes Cancer* 13(3):192–202
45. Hamilton SR, Liu B, Parsons RE, Papadopoulos N, Jen J, Powell SM, Krush AJ, Berk T, Cohen Z, Tetu B et al (1995) The molecular basis of Turcot's syndrome. *N Engl J Med* 332(13):839–847. doi:[10.1056/NEJM199503303321302](https://doi.org/10.1056/NEJM199503303321302)
46. Attard TM, Giglio P, Koppula S, Snyder C, Lynch HT (2007) Brain tumors in individuals with familial adenomatous polyposis: a cancer registry experience and pooled case report analysis. *Cancer* 109(4):761–766. doi:[10.1002/cncr.22475](https://doi.org/10.1002/cncr.22475)
47. Klaus A, Birchmeier W (2008) Wnt signalling and its impact on development and cancer. *Nat Rev Cancer* 8(5):387–398. doi:[10.1038/nrc2389](https://doi.org/10.1038/nrc2389)
48. MacDonald BT, Tamai K, He X (2009) Wnt/beta-catenin signaling: components, mechanisms, and diseases. *Dev Cell* 17(1):9–26. doi:[10.1016/j.devcel.2009.06.016](https://doi.org/10.1016/j.devcel.2009.06.016)
49. Nusse R, van Ooyen A, Cox D, Fung YK, Varmus H (1984) Mode of proviral activation of a putative mammary oncogene (int-1) on mouse chromosome 15. *Nature* 307(5947):131–136
50. Baeza N, Masuoka J, Kleihues P, Ohgaki H (2003) AXIN1 mutations but not deletions in cerebellar medulloblastomas. *Oncogene* 22(4):632–636. doi:[10.1038/sj.onc.1206156](https://doi.org/10.1038/sj.onc.1206156)
51. Eberhart CG, Tihan T, Burger PC (2000) Nuclear localization and mutation of beta-catenin in medulloblastomas. *J Neuropathol Exp Neurol* 59(4):333–337
52. Huang H, Mahler-Araujo BM, Sankila A, Chimelli L, Yonekawa Y, Kleihues P, Ohgaki H (2000) APC mutations in sporadic medulloblastomas. *Am J Pathol* 156(2):433–437. doi:[10.1016/S0002-9440\(10\)64747-5](https://doi.org/10.1016/S0002-9440(10)64747-5)
53. Koch A, Waha A, Tonn JC, Sorensen N, Berthold F, Wolter M, Reifenberger J, Hartmann W, Friedl W, Reifenberger G, Wiestler OD, Pietsch T (2001) Somatic mutations of WNT/wingless signaling pathway components in primitive neuroectodermal tumors. *Int J Cancer* 93(3):445–449
54. Bigner SH, Mark J, Friedman HS, Biegel JA, Bigner DD (1988) Structural chromosomal abnormalities in human medulloblastoma. *Cancer Genet Cytogenet* 30(1):91–101
55. Bigner SH, Mark J, Bullard DE, Mahaley MS Jr, Bigner DD (1986) Chromosomal evolution in malignant human gliomas starts with specific and usually numerical deviations. *Cancer Genet Cytogenet* 22(2):121–135
56. Bigner SH, Mark J, Mahaley MS, Bigner DD (1984) Patterns of the early, gross chromosomal changes in malignant human gliomas. *Hereditas* 101(1):103–113
57. Biegel JA, Rorke LB, Packer RJ, Sutton LN, Schut L, Bonner K, Emanuel BS (1989) Isochromosome 17q in primitive neuroectodermal tumors of the central nervous system. *Genes Chromosomes Cancer* 1(2):139–147
58. Griffin CA, Hawkins AL, Packer RJ, Rorke LB, Emanuel BS (1988) Chromosome abnormalities in pediatric brain tumors. *Cancer Res* 48(1):175–180
59. Hubbard TJ, Aken BL, Beal K, Ballester B, Caccamo M, Chen Y, Clarke L, Coates G, Cunningham F, Cutts T, Down T, Dyer SC, Fitzgerald S, Fernandez-Banet J, Graf S, Haider S, Hammond M, Herrero J, Holland R, Howe K, Johnson N, Kahari A, Keefe D, Kokocinski F, Kulesha E, Lawson D, Longden I, Melsopp C, Megy K, Meidl P, Ouverdin B, Parker A, Prlic A, Rice S, Rios D, Schuster M, Sealy I, Severin J, Slater G, Smedley D, Spudich G, Trevanion S, Vilella A, Vogel J, White S, Wood M, Cox T, Curwen V, Durbin R, Fernandez-Suarez XM, Flicek P, Kasprzyk A, Proctor G, Searle S, Smith J, Ureta-Vidal A, Birney E (2007) Ensembl 2007. *Nucleic Acids Res* 35(Database issue):D610–D617. doi:[10.1093/nar/gk1996](https://doi.org/10.1093/nar/gk1996)
60. Zody MC, Garber M, Adams DJ, Sharpe T, Harrow J, Lupski JR, Nicholson C, Searle SM, Wilming L, Young SK, Abouelleil A, Allen NR, Bi W, Bloom T, Borowsky ML, Bugalter BE, Butler J, Chang JL, Chen CK, Cook A, Corum B, Cuomo CA, de Jong PJ, DeCaprio D, Dewar K, FitzGerald M, Gilbert J, Gibson R, Gnerre S, Goldstein S, Graffham DV, Grocock R, Hafez N, Hagopian DS, Hart E, Norman CH, Humphray S, Jaffe DB, Jones M, Kamal M, Khodiyar VK, LaButti K, Laird G, Lehoczky J, Liu X, Lokyitsang T, Loveland J, Lui A, Macdonald P, Major JE, Matthews L, Mauceli E, McCarroll SA, Mihalev AH, Mudge J, Nguyen C, Nicol R, O'Leary SB, Osogawa K, Schwartz DC, Shaw-Smith C, Stankiewicz P, Steward C, Swarbreck D, Venkataraman V, Whittaker CA, Yang X, Zimmer AR, Bradley A, Hubbard T, Birren BW, Rogers J, Lander ES, Nusbaum C (2006) DNA sequence of human chromosome 17 and analysis of rearrangement in the human lineage. *Nature* 440(7087):1045–1049. doi:[10.1038/nature04689](https://doi.org/10.1038/nature04689)
61. Barker PE (1982) Double minutes in human tumor cells. *Cancer Genet Cytogenet* 5(1):81–94
62. Bigner SH, Friedman HS, Vogelstein B, Oakes WJ, Bigner DD (1990) Amplification of the c-myc gene in human medulloblastoma cell lines and xenografts. *Cancer Res* 50(8):2347–2350
63. Friedman HS, Burger PC, Bigner SH, Trojanowski JQ, Brodeur GM, He XM, Wikstrand CJ, Kurtzberg J, Berens ME, Halperin EC et al (1988) Phenotypic and genotypic analysis of a human medulloblastoma cell line and transplantable xenograft (D341 Med) demonstrating amplification of c-myc. *Am J Pathol* 130(3):472–484
64. Raffel C, Gilles FE, Weinberg KI (1990) Reduction to homozygosity and gene amplification in central

- nervous system primitive neuroectodermal tumors of childhood. *Cancer Res* 50(3):587–591
65. Cho YJ, Tsherniak A, Tamayo P, Santagata S, Ligon A, Greulich H, Berhoulk M, Amani V, Goumnerova L, Eberhart CG, Lau CC, Olson JM, Gilbertson RJ, Gajjar A, Delattre O, Kool M, Ligon K, Meyerson M, Mesirov JP, Pomeroy SL (2011) Integrative genomic analysis of medulloblastoma identifies a molecular subgroup that drives poor clinical outcome. *J Clin Oncol* 29(11):1424–1430. doi:[10.1200/JCO.2010.28.5148](https://doi.org/10.1200/JCO.2010.28.5148)
 66. Northcott PA, Fernandez LA, Hagan JP, Ellison DW, Grajkowska W, Gillespie Y, Grundy R, Van Meter T, Rutka JT, Croce CM, Kenney AM, Taylor MD (2009) The miR-17/92 polycistron is up-regulated in sonic hedgehog-driven medulloblastomas and induced by N-myc in sonic hedgehog-treated cerebellar neural precursors. *Cancer Res* 69(8):3249–3255. doi:[10.1158/0008-5472.CAN-08-4710](https://doi.org/10.1158/0008-5472.CAN-08-4710)
 67. Pfister S, Remke M, Benner A, Mendrzyk F, Toedt G, Felsberg J, Wittmann A, Devens F, Gerber NU, Joos S, Kulozik A, Reifenberger G, Rutkowski S, Wiestler OD, Radlwimmer B, Scheurlen W, Lichter P, Korshunov A (2009) Outcome prediction in pediatric medulloblastoma based on DNA copy-number aberrations of chromosomes 6q and 17q and the MYC and MYCN loci. *J Clin Oncol* 27(10):1627–1636. doi:[10.1200/JCO.2008.17.9432](https://doi.org/10.1200/JCO.2008.17.9432)
 68. Reardon DA, Michalkiewicz E, Boyett JM, Sublett JE, Entrekin RE, Ragsdale ST, Valentine MB, Behm FG, Li H, Heideman RL, Kun LE, Shapiro DN, Look AT (1997) Extensive genomic abnormalities in childhood medulloblastoma by comparative genomic hybridization. *Cancer Res* 57(18):4042–4047
 69. Schutz BR, Scheurlen W, Krauss J, du Manoir S, Joos S, Bentz M, Lichter P (1996) Mapping of chromosomal gains and losses in primitive neuroectodermal tumors by comparative genomic hybridization. *Genes Chromosomes Cancer* 16(3):196–203. doi:[10.1002/\(SICI\)1098-2264\(199607\)16:3<196::AID-GCC7>3.0.CO;2-U](https://doi.org/10.1002/(SICI)1098-2264(199607)16:3<196::AID-GCC7>3.0.CO;2-U)
 70. Speicher MR, Carter NP (2005) The new cytogenetics: blurring the boundaries with molecular biology. *Nat Rev Genet* 6(10):782–792. doi:[10.1038/nrg1692](https://doi.org/10.1038/nrg1692)
 71. Boon K, Eberhart CG, Riggins GJ (2005) Genomic amplification of orthodenticle homologue 2 in medulloblastomas. *Cancer Res* 65(3):703–707
 72. Di C, Liao S, Adamson DC, Parrett TJ, Broderick DK, Shi Q, Lengauer C, Cummins JM, Velculescu VE, Fults DW, McLendon RE, Bigner DD, Yan H (2005) Identification of OTX2 as a medulloblastoma oncogene whose product can be targeted by all-trans retinoic acid. *Cancer Res* 65(3):919–924
 73. Adamson DC, Shi Q, Wortham M, Northcott PA, Di C, Duncan CG, Li J, McLendon RE, Bigner DD, Taylor MD, Yan H (2010) OTX2 is critical for the maintenance and progression of Shh-independent medulloblastomas. *Cancer Res* 70(1):181–191. doi:[10.1158/0008-5472.CAN-09-2331](https://doi.org/10.1158/0008-5472.CAN-09-2331)
 74. Ghaleb AM, Nandan MO, Chanchevalap S, Dalton WB, Hisamuddin IM, Yang VW (2005) Kruppel-like factors 4 and 5: the yin and yang regulators of cellular proliferation. *Cell Res* 15(2):92–96. doi:[10.1038/sj.cr.7290271](https://doi.org/10.1038/sj.cr.7290271)
 75. Nakahara Y, Northcott PA, Li M, Kongkham PN, Smith C, Yan H, Croul S, Ra YS, Eberhart C, Huang A, Bigner D, Grajkowska W, Van Meter T, Rutka JT, Taylor MD (2010) Genetic and epigenetic inactivation of Kruppel-like factor 4 in medulloblastoma. *Neoplasia* 12(1):20–27
 76. Wei D, Kanai M, Jia Z, Le X, Xie K (2008) Kruppel-like factor 4 induces p27Kip1 expression in and suppresses the growth and metastasis of human pancreatic cancer cells. *Cancer Res* 68(12):4631–4639. doi:[10.1158/0008-5472.CAN-07-5953](https://doi.org/10.1158/0008-5472.CAN-07-5953)
 77. Zhao W, Hisamuddin IM, Nandan MO, Babbitt BA, Lamb NE, Yang VW (2004) Identification of Kruppel-like factor 4 as a potential tumor suppressor gene in colorectal cancer. *Oncogene* 23(2):395–402. doi:[10.1038/sj.onc.1207067](https://doi.org/10.1038/sj.onc.1207067)
 78. Mendrzyk F, Radlwimmer B, Joos S, Kokocinski F, Benner A, Stange DE, Neben K, Fiegler H, Carter NP, Reifenberger G, Korshunov A, Lichter P (2005) Genomic and protein expression profiling identifies CDK6 as novel independent prognostic marker in medulloblastoma. *J Clin Oncol* 23(34):8853–8862. doi:[10.1200/JCO.2005.02.8589](https://doi.org/10.1200/JCO.2005.02.8589)
 79. Tong CY, Hui AB, Yin XL, Pang JC, Zhu XL, Poon WS, Ng HK (2004) Detection of oncogene amplifications in medulloblastomas by comparative genomic hybridization and array-based comparative genomic hybridization. *J Neurosurg* 100(2 Suppl Pediatrics):187–193. doi:[10.3171/ped.2004.100.2.0187](https://doi.org/10.3171/ped.2004.100.2.0187)
 80. Ehrbrecht A, Muller U, Wolter M, Hoischen A, Koch A, Radlwimmer B, Actor B, Mincheva A, Pietsch T, Lichter P, Reifenberger G, Weber RG (2006) Comprehensive genomic analysis of desmoplastic medulloblastomas: identification of novel amplified genes and separate evaluation of the different histological components. *J Pathol* 208(4):554–563. doi:[10.1002/path.1925](https://doi.org/10.1002/path.1925)
 81. Northcott PA, Nakahara Y, Wu X, Feuk L, Ellison DW, Croul S, Mack S, Kongkham PN, Peacock J, Dubuc A, Ra YS, Zilberberg K, McLeod J, Scherer SW, Sunil Rao J, Eberhart CG, Grajkowska W, Gillespie Y, Lach B, Grundy R, Pollack IF, Hamilton RL, Van Meter T, Carlotti CG, Boop F, Bigner D, Gilbertson RJ, Rutka JT, Taylor MD (2009) Multiple recurrent genetic events converge on control of histone lysine methylation in medulloblastoma. *Nat Genet* 41(4):465–472. doi:[10.1038/ng.336](https://doi.org/10.1038/ng.336)
 82. Clifford SC, Lusher ME, Lindsey JC, Langdon JA, Gilbertson RJ, Straughton D, Ellison DW (2006) Wnt/Wingless pathway activation and chromosome 6 loss characterize a distinct molecular sub-group of medulloblastomas associated with a favorable prognosis. *Cell Cycle* 5(22):2666–2670
 83. Fattet S, Haberler C, Legoux P, Varlet P, Lellouch-Tubiana A, Lair S, Manie E, Raquin MA, Bours D,

- Carpentier S, Barillot E, Grill J, Doz F, Puget S, Janoueix-Lerosey I, Delattre O (2009) Beta-catenin status in paediatric medulloblastomas: correlation of immunohistochemical expression with mutational status, genetic profiles, and clinical characteristics. *J Pathol* 218(1):86–94. doi:10.1002/path.2514
84. Kool M, Koster J, Bunt J, Hasselt NE, Lakeman A, van Sluis P, Troost D, Meeteren NS, Caron HN, Cloos J, Mrcic A, Ylstra B, Grajkowska W, Hartmann W, Pietsch T, Ellison D, Clifford SC, Versteeg R (2008) Integrated genomics identifies five medulloblastoma subtypes with distinct genetic profiles, pathway signatures and clinicopathological features. *PLoS One* 3(8):e3088. doi:10.1371/journal.pone.0003088
85. Northcott PA, Nakahara Y, Wu X, Feuk L, Ellison DW, Croul S, Mack S, Kongkham PN, Peacock J, Dubuc A, Ra YS, Zilberberg K, McLeod J, Scherer SW, Sunil Rao J, Eberhart CG, Grajkowska W, Gillespie Y, Lach B, Grundy R, Pollack IF, Hamilton RL, Van Meter T, Carlotti CG, Boop F, Bigner D, Gilbertson RJ, Rutka JT, Taylor MD (2009) Multiple recurrent genetic events converge on control of histone lysine methylation in medulloblastoma. *Nat Genet* 41(4):465–472
86. Tachibana M, Ueda J, Fukuda M, Takeda N, Ohta T, Iwanari H, Sakihama T, Kodama T, Hamakubo T, Shinkai Y (2005) Histone methyltransferases G9a and GLP form heteromeric complexes and are both crucial for methylation of euchromatin at H3-K9. *Genes Dev* 19(7):815–826. doi:10.1101/gad.1284005
87. Michiels EM, Oussoren E, Van Groenigen M, Pauws E, Bossuyt PM, Voute PA, Baas F (1999) Genes differentially expressed in medulloblastoma and fetal brain. *Physiol Genomics* 1(2):83–91
88. Gilbertson RJ, Clifford SC (2003) PDGFRB is over-expressed in metastatic medulloblastoma. *Nat Genet* 35(3):197–198. doi:10.1038/ng1103-197
89. MacDonald TJ, Brown KM, LaFleur B, Peterson K, Lawlor C, Chen Y, Packer RJ, Cogen P, Stephan DA (2001) Expression profiling of medulloblastoma: PDGFRA and the RAS/MAPK pathway as therapeutic targets for metastatic disease. *Nat Genet* 29(2):143–152. doi:10.1038/ng731
90. Pomeroy SL, Tamayo P, Gaasenbeek M, Sturla LM, Angelo M, McLaughlin ME, Kim JY, Goumnerova LC, Black PM, Lau C, Allen JC, Zagzag D, Olson JM, Curran T, Wetmore C, Biegel JA, Poggio T, Mukherjee S, Rifkin R, Califano A, Stolovitzky G, Louis DN, Mesirov JP, Lander ES, Golub TR (2002) Prediction of central nervous system embryonal tumour outcome based on gene expression. *Nature* 415(6870):436–442. doi:10.1038/415436a
91. Reddy AT, Janss AJ, Phillips PC, Weiss HL, Packer RJ (2000) Outcome for children with supratentorial primitive neuroectodermal tumors treated with surgery, radiation, and chemotherapy. *Cancer* 88(9):2189–2193
92. McCabe MG, Ichimura K, Liu L, Plant K, Backlund LM, Pearson DM, Collins VP (2006) High-resolution array-based comparative genomic hybridization of medulloblastomas and supratentorial primitive neuroectodermal tumors. *J Neuropathol Exp Neurol* 65(6):549–561
93. Pfister S, Remke M, Toedt G, Werft W, Benner A, Mendorzyk F, Wittmann A, Devens F, von Hoff K, Rutkowski S, Kulozik A, Radlwimmer B, Scheurlen W, Lichter P, Korshunov A (2007) Supratentorial primitive neuroectodermal tumors of the central nervous system frequently harbor deletions of the CDKN2A locus and other genomic aberrations distinct from medulloblastomas. *Genes Chromosomes Cancer* 46(9):839–851. doi:10.1002/gcc.20471
94. Neben K, Korshunov A, Benner A, Wrobel G, Hahn M, Kokocinski F, Golanov A, Joos S, Lichter P (2004) Microarray-based screening for molecular markers in medulloblastoma revealed STK15 as independent predictor for survival. *Cancer Res* 64(9):3103–3111
95. Northcott PA, Shih DJ, Peacock J, Garzia L, Morrissy AS, Zichner T, Stutz AM, Korshunov A, Reimand J, Schumacher SE, Beroukhir R, Ellison DW, Marshall CR, Lionel AC, Mack S, Dubuc A, Yao Y, Ramaswamy V, Luu B, Rolider A, Cavalli FM, Wang X, Remke M, Wu X, Chiu RY, Chu A, Chuah E, Corbett RD, Hoad GR, Jackman SD, Li Y, Lo A, Mungall KL, Nip KM, Qian JQ, Raymond AG, Thiessen NT, Varhol RJ, Birol I, Moore RA, Mungall AJ, Holt R, Kawauchi D, Roussel MF, Kool M, Jones DT, Witt H, Fernandez LA, Kenney AM, Wechsler-Reya RJ, Dirks P, Aviv T, Grajkowska WA, Perek-Polnik M, Haberler CC, Delattre O, Reynaud SS, Doz FF, Pernet-Fattet SS, Cho BK, Kim SK, Wang KC, Scheurlen W, Eberhart CG, Fevre-Montange M, Jouvett A, Pollack IF, Fan X, Muraszko KM, Gillespie GY, Di Rocco C, Massimi L, Michiels EM, Kloosterhof NK, French PJ, Kros JM, Olson JM, Ellenbogen RG, Zitterbart K, Kren L, Thompson RC, Cooper MK, Lach B, McLendon RE, Bigner DD, Fontebasso A, Albrecht S, Jabado N, Lindsey JC, Bailey S, Gupta N, Weiss WA, Bogner L, Klekner A, Van Meter TE, Kumabe T, Tominaga T, Elbabaa SK, Leonard JR, Rubin JB, Liao LM, Van Meir EG, Fouladi M, Nakamura H, Cinalli G, Garami M, Hauser P, Saad AG, Iolascon A, Jung S, Carlotti CG, Vibhakar R, Ra YS, Robinson S, Zollo M, Faria CC, Chan JA, Levy ML, Sorensen PH, Meyerson M, Pomeroy SL, Cho YJ, Bader GD, Tabori U, Hawkins CE, Bouffet E, Scherer SW, Rutka JT, Malkin D, Clifford SC, Jones SJ, Korbel JO, Pfister SM, Marra MA, Taylor MD (2012) Subgroup-specific structural variation across 1,000 medulloblastoma genomes. *Nature* 488(7409):49–56. doi:10.1038/nature11327, doi:nature11327 [pii]
96. Zollo M (2013) Genetics of recurrent medulloblastoma. *Lancet Oncol* 14(12):1147–1148. doi:10.1016/S1470-2045(13)70482-0, doi:S1470-2045(13)70482-0 [pii]
97. Shih DJ, Northcott PA, Remke M, Korshunov A, Ramaswamy V, Kool M, Luu B, Yao Y, Wang X, Dubuc AM, Garzia L, Peacock J, Mack SC, Wu X, Rolider A, Morrissy AS, Cavalli FM, Jones DT, Zitterbart K, Faria CC, Schuller U, Kren L, Kumabe T, Tominaga T, Shin Ra Y, Garami M, Hauser P, Chan JA, Robinson S, Bogner L, Klekner A, Saad AG, Liao LM, Albrecht S, Fontebasso A, Cinalli G,

- De Antonellis P, Zollo M, Cooper MK, Thompson RC, Bailey S, Lindsey JC, Di Rocco C, Massimi L, Michiels EM, Scherer SW, Phillips JJ, Gupta N, Fan X, Muraszko KM, Vibhakhar R, Eberhart CG, Fouladi M, Lach B, Jung S, Wechsler-Reya RJ, Fevre-Montange M, Jouveta A, Jabado N, Pollack IF, Weiss WA, Lee JY, Cho BK, Kim SK, Wang KC, Leonard JR, Rubin JB, de Torres C, Lavarino C, Mora J, Cho YJ, Tabori U, Olson JM, Gajjar A, Packer RJ, Rutkowski S, Pomeroy SL, French PJ, Kloosterhof NK, Kros JM, Van Meir EG, Clifford SC, Bourdeaut F, Delattre O, Doz FF, Hawkins CE, Malkin D, Grajkowska WA, Perek-Polnik M, Bouffet E, Rutka JT, Pfister SM, Taylor MD (2014) Cytogenetic prognostication within medulloblastoma subgroups. *J Clin Oncol* 32(9):886–896. doi:10.1200/JCO.2013.50.9539, doi:JCO.2013.50.9539 [pii]
98. Bartel DP (2004) MicroRNAs: genomics, biogenesis, mechanism, and function. *Cell* 116(2):281–297
99. Hammond SM (2006) MicroRNAs as oncogenes. *Curr Opin Genet Dev* 16(1):4–9
100. Krol J, Loedige I, Filipowicz W (2010) The widespread regulation of microRNA biogenesis, function and decay. *Nat Rev Genet* 11(9):597–610
101. DeSano JT, Xu L (2009) MicroRNA regulation of cancer stem cells and therapeutic implications. *AAPS J* 11(4):682–692
102. Calin GA, Croce CM (2006) MicroRNA signatures in human cancers. *Nat Rev Cancer* 6(11):857–866
103. Chen CZ (2005) MicroRNAs as oncogenes and tumor suppressors. *N Engl J Med* 353(17):1768–1771
104. Esquela-Kerscher A, Slack FJ (2006) Oncomirs – microRNAs with a role in cancer. *Nat Rev Cancer* 6(4):259–269
105. Kent OA, Mendell JT (2006) A small piece in the cancer puzzle: microRNAs as tumor suppressors and oncogenes. *Oncogene* 25(46):6188–6196
106. Croce CM (2009) Causes and consequences of microRNA dysregulation in cancer. *Nat Rev Genet* 10(10):704–714
107. Uziel T, Karginov FV, Xie S, Parker JS, Wang YD, Gajjar A, He L, Ellison D, Gilbertson RJ, Hannon G, Roussel MF (2009) The miR-17~92 cluster collaborates with the Sonic Hedgehog pathway in medulloblastoma. *Proc Natl Acad Sci U S A* 106(8):2812–2817
108. Northcott PA, Fernandez LA, Hagan JP, Ellison DW, Grajkowska W, Gillespie Y, Grundy R, Van Meter T, Rutka JT, Croce CM, Kenney AM, Taylor MD (2009) The miR-17/92 polycistron is up-regulated in sonic hedgehog-driven medulloblastomas and induced by N-myc in sonic hedgehog-treated cerebellar neural precursors. *Cancer Res* 69(8):3249–3255
109. Garzia L, Andolfo I, Cusanelli E, Marino N, Petrosino G, De Martino D, Esposito V, Galeone A, Navas L, Esposito S, Gargiulo S, Fattet S, Donofrio V, Cinalli G, Brunetti A, Vecchio LD, Northcott PA, Delattre O, Taylor MD, Iolascon A, Zollo M (2009) MicroRNA-199b-5p impairs cancer stem cells through negative regulation of HES1 in medulloblastoma. *PLoS One* 4(3):e4998
110. Fan X, Matsui W, Khaki L, Stearns D, Chun J, Li YM, Eberhart CG (2006) Notch pathway inhibition depletes stem-like cells and blocks engraftment in embryonal brain tumors. *Cancer Res* 66(15):7445–7452
111. de Antonellis P, Medaglia C, Cusanelli E, Andolfo I, Liguori L, De Vita G, Carotenuto M, Bello A, Formiggini F, Galeone A, De Rosa G, Virgilio A, Scognamiglio I, Sciro M, Basso G, Schulte JH, Cinalli G, Iolascon A, Zollo M (2011) MiR-34a targeting of Notch ligand delta-like 1 impairs CD15+/CD133+ tumor-propagating cells and supports neural differentiation in medulloblastoma. *PLoS One* 6(9):e24584. doi:10.1371/journal.pone.0024584, PONE-D-11-07916 [pii]
112. Ferretti E, De Smaele E, Miele E, Laneve P, Po A, Pelloni M, Paganelli A, Di Marcotullio L, Caffarelli E, Screpanti I, Bozzoni I, Gulino A (2008) Concerted microRNA control of Hedgehog signalling in cerebellar neuronal progenitor and tumour cells. *EMBO J* 27(19):2616–2627
113. Ciafre SA, Galardi S, Mangiola A, Ferracin M, Liu CG, Sabatino G, Negrini M, Maira G, Croce CM, Farace MG (2005) Extensive modulation of a set of microRNAs in primary glioblastoma. *Biochem Biophys Res Commun* 334(4):1351–1358
114. Herms J, Neidt I, Luscher B, Sommer A, Schurmann P, Schroder T, Bergmann M, Wilken B, Probst-Cousin S, Hernaiz-Driever P, Behnke J, Hanefeld F, Pietsch T, Kretzschmar HA (2000) C-MYC expression in medulloblastoma and its prognostic value. *Int J Cancer* 89(5):395–402
115. Gilbertson RJ, Perry RH, Kelly PJ, Pearson AD, Lunec J (1997) Prognostic significance of HER2 and HER4 coexpression in childhood medulloblastoma. *Cancer Res* 57(15):3272–3280
116. Grotzer MA, Hogarty MD, Janss AJ, Liu X, Zhao H, Eggert A, Sutton LN, Rorke LB, Brodeur GM, Phillips PC (2001) MYC messenger RNA expression predicts survival outcome in childhood primitive neuroectodermal tumor/medulloblastoma. *Clin Cancer Res* 7(8):2425–2433
117. Ferretti E, De Smaele E, Po A, Di Marcotullio L, Tosi E, Espinola MS, Di Rocco C, Riccardi R, Giangaspero F, Farcomeni A, Nofroni I, Laneve P, Gioia U, Caffarelli E, Bozzoni I, Screpanti I, Gulino A (2009) MicroRNA profiling in human medulloblastoma. *Int J Cancer* 124(3):568–577
118. Pierson J, Hostager B, Fan R, Vibhakhar R (2008) Regulation of cyclin dependent kinase 6 by microRNA 124 in medulloblastoma. *J Neurooncol* 90(1):1–7
119. Li KK, Pang JC, Ching AK, Wong CK, Kong X, Wang Y, Zhou L, Chen Z, Ng HK (2009) miR-124 is frequently down-regulated in medulloblastoma and is a negative regulator of SLC16A1. *Hum Pathol* 40(9):1234–1243
120. Lu Y, Ryan SL, Elliott DJ, Bignell GR, Futreal PA, Ellison DW, Bailey S, Clifford SC (2009) Amplification and overexpression of Hsa-miR-30b, Hsa-miR-30d and KHDRBS3 at 8q24.22-q24.23 in medulloblastoma. *PLoS One* 4(7):e6159

121. Venkataraman S, Alimova I, Fan R, Harris P, Foreman N, Vibhakar R (2010) MicroRNA 128a increases intracellular ROS level by targeting Bmi-1 and inhibits medulloblastoma cancer cell growth by promoting senescence. *PLoS One* 5(6):e10748
122. Kouzarides T (2007) Chromatin modifications and their function. *Cell* 128(4):693–705
123. Jones PA, Baylin SB (2002) The fundamental role of epigenetic events in cancer. *Nat Rev Genet* 3(6):415–428
124. Bernstein BE, Meissner A, Lander ES (2007) The mammalian epigenome. *Cell* 128(4):669–681
125. Fruhwald MC, O'Dorisio MS, Dai Z, Tanner SM, Balster DA, Gao X, Wright FA, Plass C (2001) Aberrant promoter methylation of previously unidentified target genes is a common abnormality in medulloblastomas—implications for tumor biology and potential clinical utility. *Oncogene* 20(36):5033–5042
126. Lindsey JC, Anderton JA, Lusher ME, Clifford SC (2005) Epigenetic events in medulloblastoma development. *Neurosurg Focus* 19(5):E10
127. Waha A, Koch A, Hartmann W, Milde U, Felsberg J, Hübner A, Mikeska T, Goodyer CG, Sorensen N, Lindberg I, Wiestler OD, Pietsch T, Waha A (2007) SGNE1/7B2 is epigenetically altered and transcriptionally downregulated in human medulloblastomas. *Oncogene* 26(38):5662–5668
128. Parsons DW, Li M, Zhang X, Jones S, Leary RJ, Lin JC, Boca SM, Carter H, Samayoa J, Bettegowda C, Gallia GL, Jallo GI, Binder ZA, Nikolsky Y, Hartigan J, Smith DR, Gerhard DS, Fuhs DW, VandenBerg S, Berger MS, Marie SK, Shinjo SM, Clara C, Phillips PC, Minturn JE, Biegel JA, Judkins AR, Resnick AC, Storm PB, Curran T, He Y, Rasheed BA, Friedman HS, Keir ST, McLendon R, Northcott PA, Taylor MD, Burger PC, Riggins GJ, Karchin R, Parmigiani G, Bigner DD, Yan H, Papadopoulos N, Vogelstein B, Kinzler KW, Velculescu VE (2011) The genetic landscape of the childhood cancer medulloblastoma. *Science* 331(6016):435–439
129. Kongkham PN, Northcott PA, Ra YS, Nakahara Y, Mainprize TG, Croul SE, Smith CA, Taylor MD, Rutka JT (2008) An epigenetic genome-wide screen identifies SPINT2 as a novel tumor suppressor gene in pediatric medulloblastoma. *Cancer Res* 68(23):9945–9953
130. Lusher ME, Lindsey JC, Latif F, Pearson AD, Ellison DW, Clifford SC (2002) Biallelic epigenetic inactivation of the RASSF1A tumor suppressor gene in medulloblastoma development. *Cancer Res* 62(20):5906–5911
131. Debatin KM, Krammer PH (2004) Death receptors in chemotherapy and cancer. *Oncogene* 23(16):2950–2966
132. Grotzer MA, Eggert A, Zuzak TJ, Janss AJ, Marwaha S, Wiewrodt BR, Ikegaki N, Brodeur GM, Phillips PC (2000) Resistance to TRAIL-induced apoptosis in primitive neuroectodermal brain tumor cells correlates with a loss of caspase-8 expression. *Oncogene* 19(40):4604–4610
133. Pfister S, Schlaefer C, Mendrzyk F, Wittmann A, Benner A, Kulozik A, Scheurlen W, Radlwimmer B, Lichter P (2007) Array-based profiling of reference-independent methylation status (aPRIMES) identifies frequent promoter methylation and consecutive downregulation of ZIC2 in pediatric medulloblastoma. *Nucleic Acids Res* 35(7):e51
134. Briggs KJ, Corcoran-Schwartz IM, Zhang W, Harcke T, Devereux WL, Baylin SB, Eberhart CG, Watkins DN (2008) Cooperation between the Hic1 and Pch1 tumor suppressors in medulloblastoma. *Genes Dev* 22(6):770–785
135. Ecker I, Petry F, Rosenberger A, Tauber S, Monkemeyer S, Hess I, Dullin C, Kimmina S, Pirngruber J, Johnsen SA, Uhmman A, Nitzki F, Wojnowski L, Schulz-Schaeffer W, Witt O, Hahn H (2009) Antitumor effects of a combined 5-aza-2'-deoxycytidine and valproic acid treatment on rhabdomyosarcoma and medulloblastoma in Pch mutant mice. *Cancer Res* 69(3):887–895
136. Mancarelli MM, Zazzeroni F, Ciccocioppo L, Capece D, Po A, Murgio S, Di Camillo R, Rinaldi C, Ferretti E, Gulino A, Alesse E (2010) The tumor suppressor gene KCTD11REN is regulated by Sp1 and methylation and its expression is reduced in tumors. *Mol Cancer* 9:172
137. Diede SJ, Guenther J, Geng LN, Mahoney SE, Marotta M, Olson JM, Tanaka H, Tapscott SJ (2010) DNA methylation of developmental genes in pediatric medulloblastomas identified by denaturation analysis of methylation differences. *Proc Natl Acad Sci U S A* 107(1):234–239
138. Waha A, Koch A, Hartmann W, Milde U, Felsberg J, Hübner A, Mikeska T, Goodyer CG, Sorensen N, Lindberg I, Wiestler OD, Pietsch T and Waha A (2007) SGNE1/7B2 is epigenetically altered and transcriptionally downregulated in human medulloblastomas. *Oncogene* 26:5662–5668. doi:10.1038/sj.onc.1210338; published online 5 March 2007
139. Kongkham PN, Northcott PA, Croul SE, Smith CA, Taylor MD, Rutka JT (2010) The SFRP family of WNT inhibitors function as novel tumor suppressor genes epigenetically silenced in medulloblastoma. *Oncogene* 29(20):3017–3024. doi: 10.1038/onc.2010.32. Epub 2010 Mar 8
140. Klaus-Michael Debatin and Peter H Krammer (2004) Death receptors in chemotherapy and cancer. *Oncogene* 23:2950–2966. doi:10.1038/sj.onc.1207558
141. Kimberly J Briggs, Eberhart CG, Watkins DN (2008) Just say no to ATOH: how HIC1 methylation might predispose medulloblastoma to lineage addiction. *Cancer Res* 68(21):8654–8856. doi: 10.1158/0008-5472.CAN-08-1904; Nov 1

Anna Nastro, Maria Consiglio Buonocore,
Domenico Cicala, Emilio Cianciulli,
Daniele Cascone, and Maria Rita Panico

15.1 Imaging Features

Neuroimaging of brain tumors has evolved from a strictly morphology-based discipline to one that encompasses function, physiology, and anatomy.

Medulloblastoma presents many faces on imaging.

The cerebellum is by far the most common location (94.4 %), with most medulloblastomas (75 %) arising in the midline, mainly in the middle and lower vermis. Dissemination to the cerebrospinal fluid is relatively common at presentation; spinal drop metastases and leptomeningeal tumor dissemination at the time of diagnosis were reported in up to 19.4 % of pediatric medulloblastomas.

Characteristic features, such as increased attenuation on unenhanced CT, midline location, and well-defined margins, are commonly present in childhood cases; however, atypical imaging

features are being noted more frequently with the increased use of MR as the diagnostic modality of choice.

Carefully performed CT and MR provide suitable topography and characteristics, but MR is superior in the detection of pre- or postoperative neoplastic spread elsewhere in the subarachnoid space. Careful assessment of disease extent is essential in planning both surgical resection and adjuvant therapy, and preoperative imaging of the entire neuraxis is critical given the high propensity of drop metastases.

15.2 Computed Tomography

Computed tomographic (CT) features of posterior fossa medulloblastoma in children have been well describe [1–6].

The CT typical appearance of a medulloblastoma is a well-defined, hyperattenuating, and homogeneous midline vermian mass surrounded by vasogenic edema, associated with hydrocephalus, and marked and homogeneous enhancement on contrast material-enhanced images (Fig. 15.1).

Medulloblastoma has characteristic hyperattenuation compared with normal gray matter on unenhanced CT that reflects the high nuclear-cytoplasmatic ratio seen at histologic analysis; the degree of hyperattenuation is variable.

Variable amounts of surrounding low density consistent with asymmetric vasogenic edema are reported in 95 % of the cases, and hydrocephalus

A. Nastro, M.D. (✉)
Service of Pediatric Neuroradiology, Department
of Neurosciences, Santobono-Pausilipon Children's
Hospital, Naples, Italy
e-mail: anna_nastro@libero.it

M.C. Buonocore, M.D. • D. Cicala, M.D.
E. Cianciulli, M.D. • D. Cascone
Division of Pediatric Neuroradiology, Department
of Neurosciences, Santobono-Pausilipon Children's
Hospital, Naples, Italy

M.R. Panico, M.D.
Division of Radiology, Department of Neurosciences,
Federico II University, Via Pansini n. 5, Naples., Italy

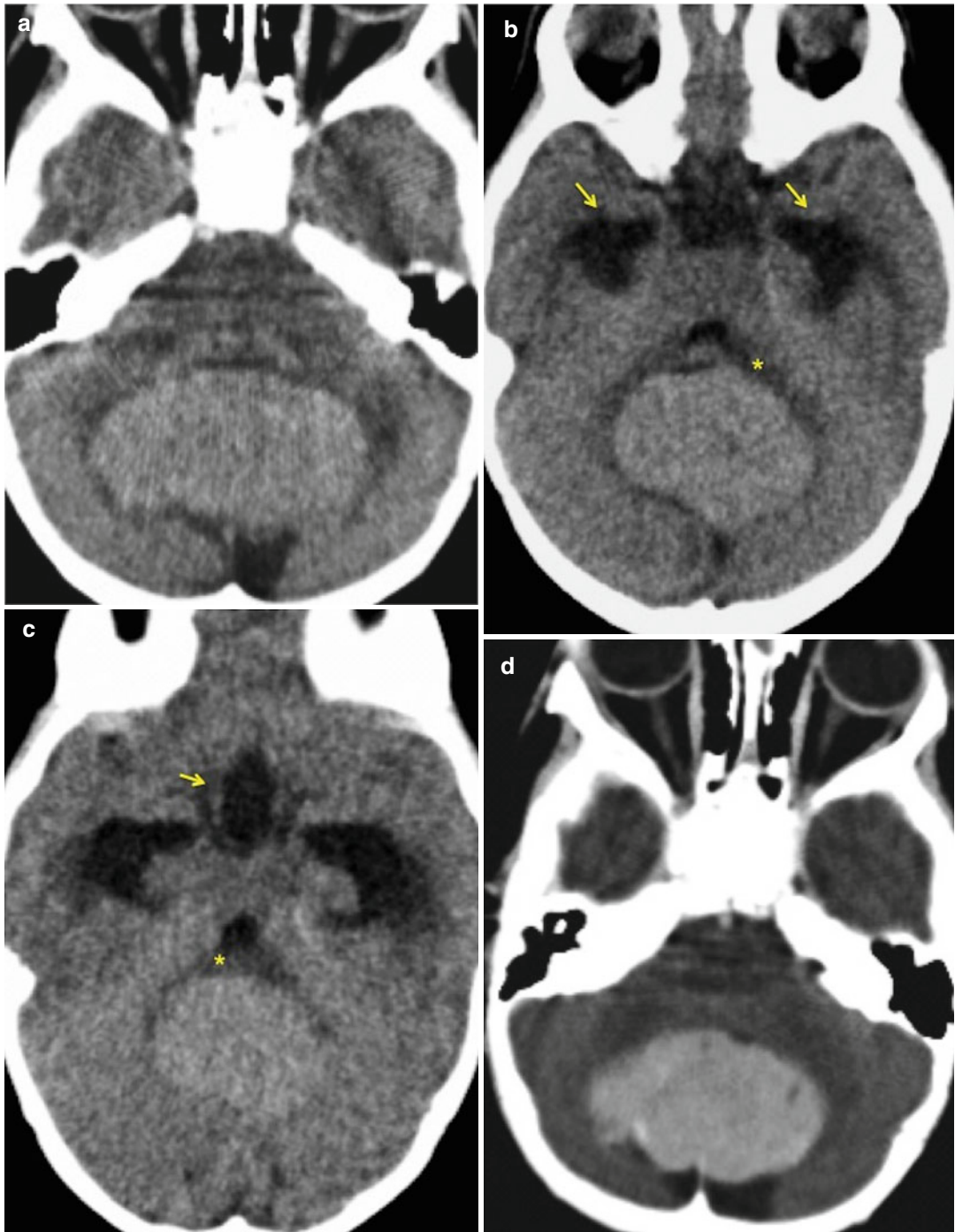


Fig. 15.1 Typical features CT: (a–c) unenhanced CT shows a well-defined, homogeneous hyperattenuated mass in the posterior fossa midline surrounded by vasogenic

edema (*asterisk*), associated with hydrocephalus (*yellow arrows*). (d–f) Contrast-enhanced CT image shows intense, nearly homogeneous enhancement of the mass

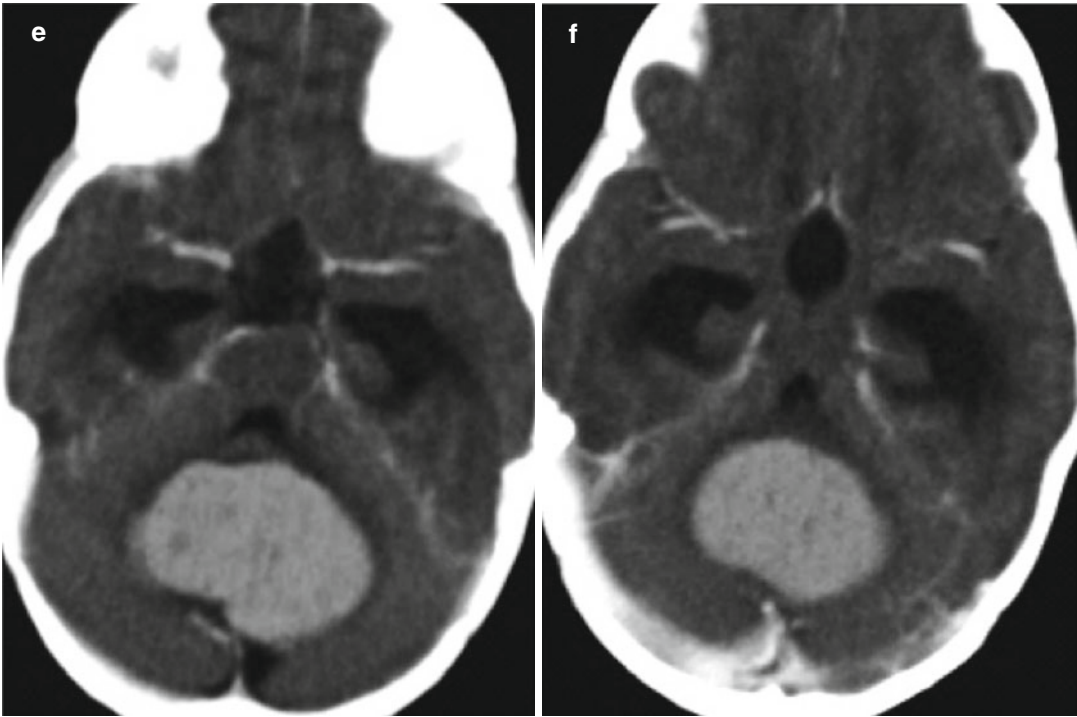


Fig. 15.1 (continued)

of various degrees of severity is evident in up to 95 % of the cases at presentation.

On enhanced CT scans, a marked enhancement of the mass, relatively homogeneous, occasionally patchy, is seen.

Nevertheless, variance from this characteristic features is common [3, 7, 8]. Several series have revealed atypical features, which include cystic or necrotic regions, calcification, ill-defined margins, and lack of enhancement. Intralesional areas of low density (usually <1 cm), consistent with intratumoral cystic and necrotic degeneration, can be depicted (Fig. 15.2).

The prevalence of cysts ranges from 30 to 60 %; some tumor has multiple small cysts, others have single large cavity and also calcifications can be seen (20–30 %).

Other less common atypical features include ill-defined margins, absence of vasogenic edema or hydrocephalus, hypoattenuation, hemorrhage, absence of enhancement on contrast-enhanced images, and the appearance of “primary” leptomeningeal dissemination.

Metastatic nodular seeding may be seen in the supratentorial subarachnoid space on contrast-enhanced CT scans and in the spinal canal on CT myelography. In the ventricle, typical area of metastases at diagnosis is the infundibular recess in the third ventricle.

Falcine calcification in children with medulloblastoma can suggest a nevoid basal cell carcinoma. For the reason that children with this tumor have a propensity to develop various basal cell carcinomas in irradiated fields, examination with CT in such patients is crucial, since it may influence therapeutic decision in the favor of chemotherapy or reduced-dose radiation therapy [9].

15.3 MR Imaging

The standard MRI protocol for pediatric intracranial tumors includes fluid-attenuated inversion recovery (FLAIR), T1-, T2-, axial diffusion-, and postcontrast T1-weighted sequences for brain and spine. Furthermore, MR angiography is regularly

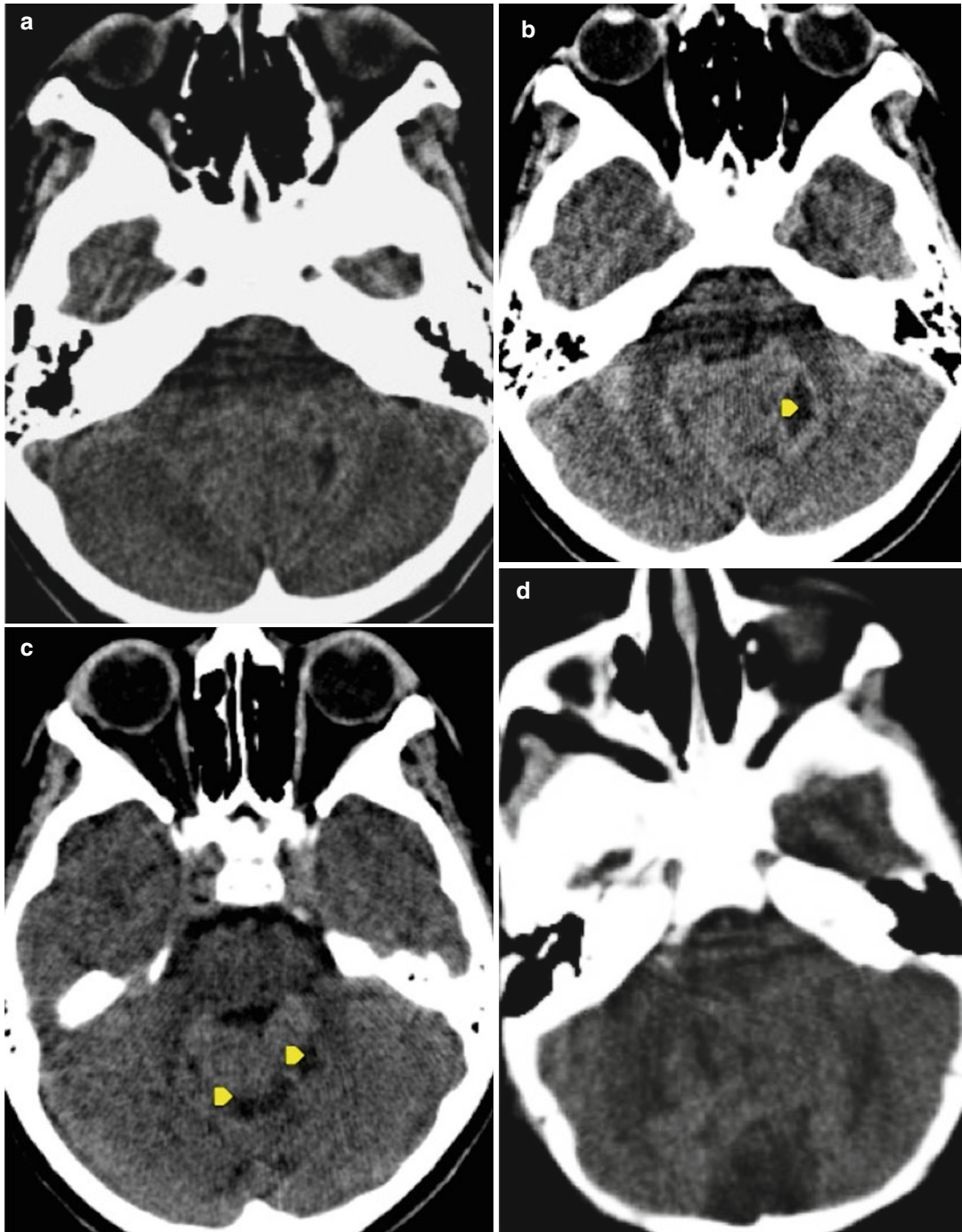


Fig. 15.2 Variability of medulloblastoma on CT images: (a–c) unenhanced CT image shows heterogeneous hyperdense mass with cystic/necrotic areas (*arrowheads*) in the posterior fossa midline. (d–f) On the unenhanced CT

image, the mass is hypo-hysodense compared with the surrounding normal cerebellum, and tumor has small cysts and a large cavity (*arrowheads*)

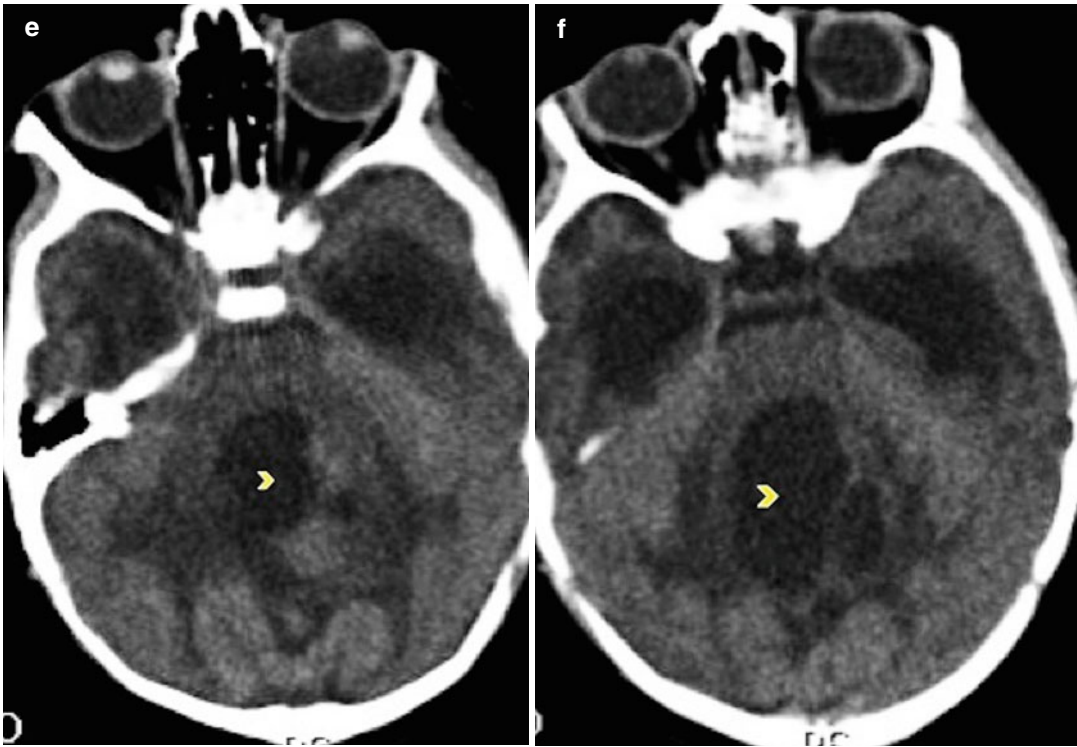


Fig. 15.2 (continued)

performed to better clarify the characteristics of the intratumoral circulation and to plan best way for the intervention. Susceptibility-weighted perfusion MRI and proton magnetic resonance (MR) spectroscopy are performed usually to distinguish post-treatment changes from recurrent tumor in the posttherapeutic setting, or occasionally when the neoplastic nature of a primary lesion is in question.

Preoperative evaluation of entire neuraxis and postoperative evaluation of surgical bed are key to prognosis (Fig. 15.3).

Bailey and Cushing in 1925 established the medulloblastoma principally as a tumor of the posterior vermis in children.

The medulloblastomas are most commonly situated in the region of the fourth ventricle as midline lesions involving the anterior portion of the vermis and can sometimes be seen originating from the inferior medullary velum; often the medulloblastomas are located in the middle and lower segments of the vermis. Less frequently can be seen originating from the superior zone of the vermis (Fig. 15.4) [10].

Medulloblastomas can be also off-midline tumors, located in cerebellar hemispheres (Fig. 15.5).

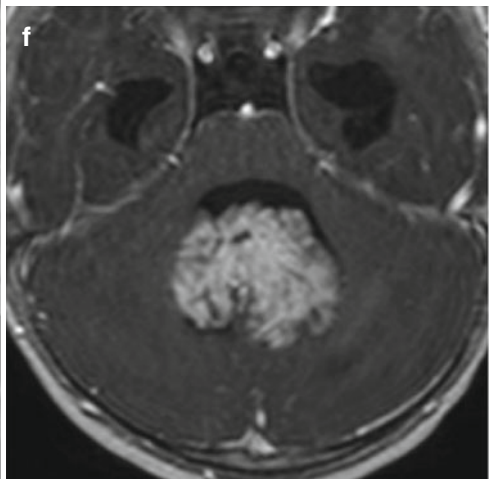
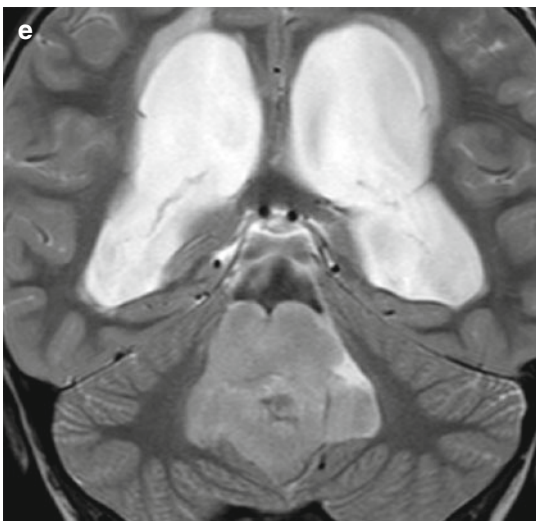
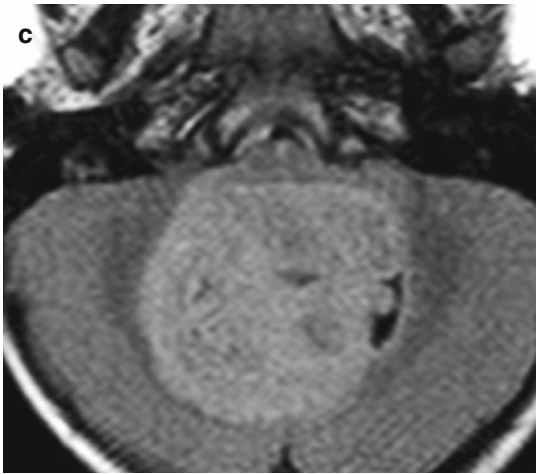
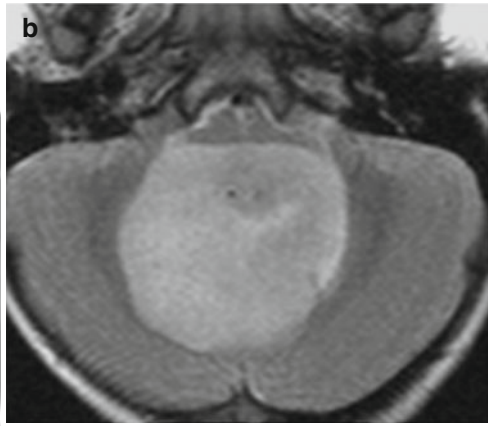
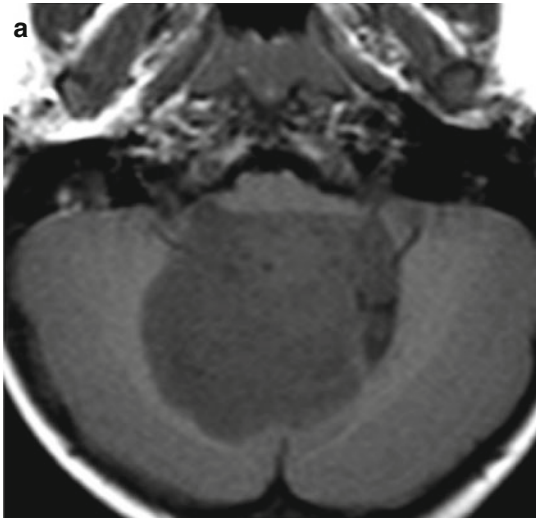
In 1930, Cushing included in an exhaustive survey of 61 cerebellar medulloblastomas, nine that were laterally situated, subsequently designated desmoplastic medulloblastoma (DMB).

Although much less common, medulloblastoma may also occur in adults, usually in the third and fourth decades of life, and the cerebellar hemispheres represent the most frequent location.

An off-midline location is common in desmoplastic medulloblastomas (DMB) and slightly more common in medulloblastomas with extensive nodularity variants (MB-EN).

Tumor margins are mostly convex and well defined on unenhanced spin-echo images. Lesions involving the vermis can occur as poorly defined zones of signal alteration on the long TR images only.

Foraminal extension from the fourth ventricle to involve the cerebellopontine angle, cisterna



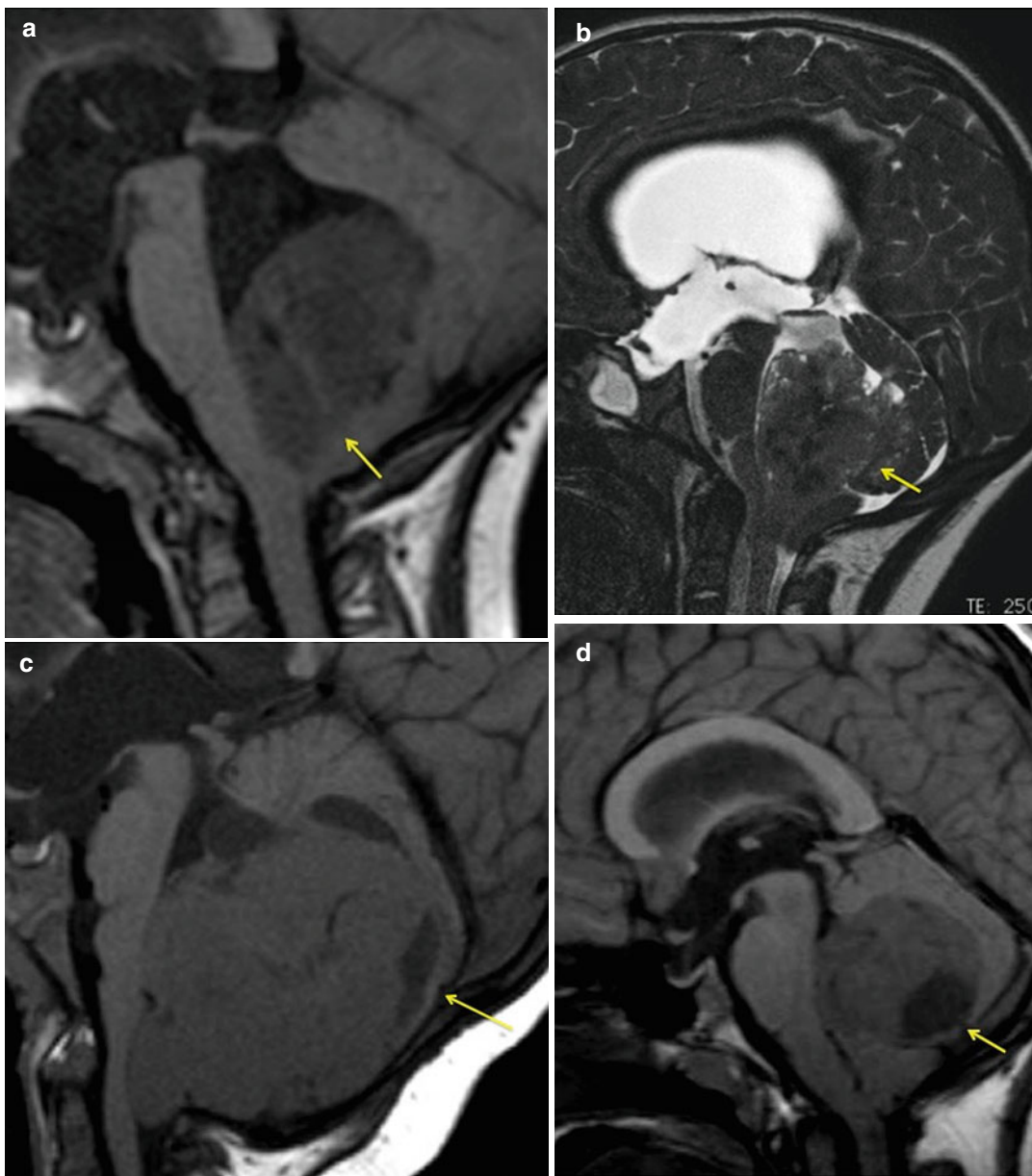


Fig. 15.4 Medulloblastomas in the region of the fourth ventricle originating from the inferior medullary velum (a–c) and mild vermis (d); medulloblastomas originating

from the posterior portion of the vermis (e, f), involving the inferior zone of the vermis (e) and the superior zone of the vermis (yellow arrows) (f)

Fig. 15.3 Medulloblastoma. MR typical features: (a) On an axial T1-weighted MR image, the mass is hypointense compared with the surrounding normal cerebellum with well-defined margins. (b) On an axial T2-weighted MR image, the mass shows mild hyperintensity compared with surrounding normal brain tissue. (c) On an axial FLAIR MR image, the tumor shows hyperintensity compared with surrounding normal brain tissue with well-defined margins. (d) Sagittal T1-weighted MR image shows ill-defined mass

originating from the inferior medullary velum compressing the fourth V and brainstem (arrows), causing obstructive hydrocephalus and projecting through the foramen magnum (arrowheads). Notice the hyposignal at C2–C3 level due to compression effect (asterisk). (e) On a coronal T2-weighted image, the mass shows hyperintensity and hydrocephalic dilatation of the lateral ventricles. (f) Contrast-enhanced axial T1-weighted MR image shows intense, nearly homogeneous enhancement of the mass

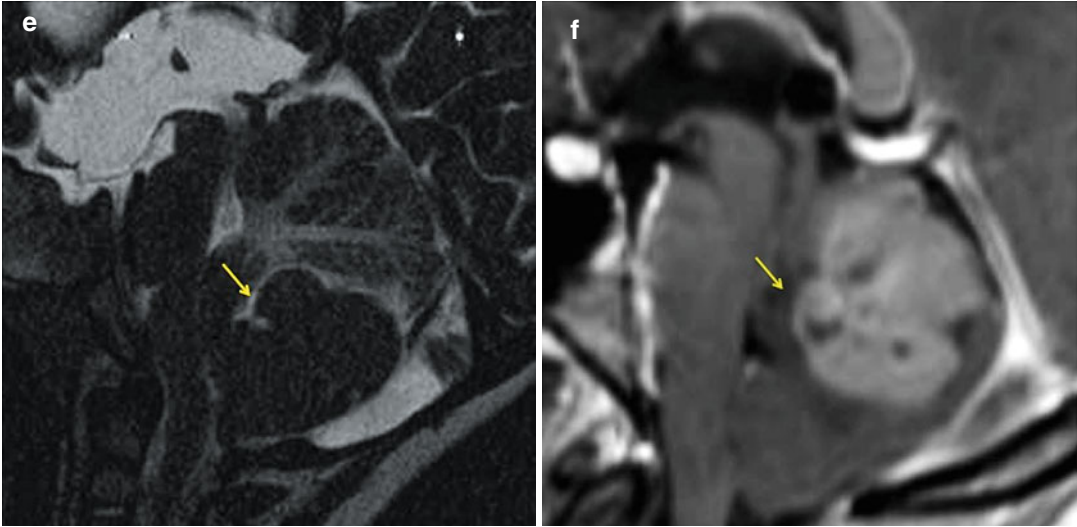


Fig. 15.4 (continued)

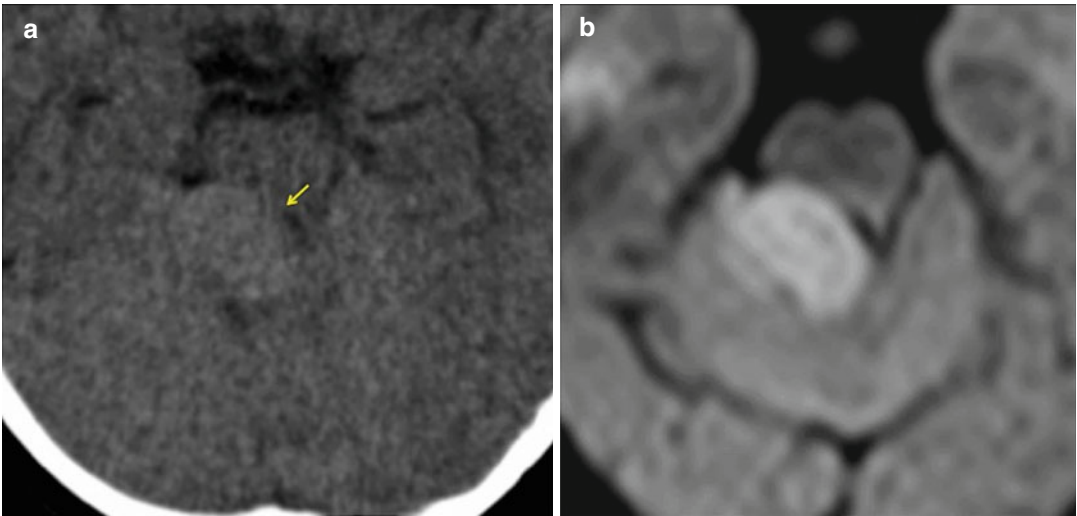


Fig. 15.5 Medulloblastoma in cerebellar hemisphere: desmoplastic MB in a 1-year-old girl (a) unenhanced CT shows a well-defined, homogeneous hyperattenuated right cerebellar hemispheric mass (*arrows*). (b) Axial DWI MR shows the tumor diffusivity to be increased to that in white matter. (c) On axial T1-weighted MR image, the lesion is hypointense com-

pared with normal cerebellum with well-defined margins. (d) Axial FLAIR MR image shows hyperintensity compared with surrounding normal brain tissue. (e) Coronal T2-weighted MR image shows hyperintensity compared with surrounding normal brain tissue. (f) Axial T1 C+ MR and (g) coronal T1 C+ MR show intense, homogeneous enhancement of the mass

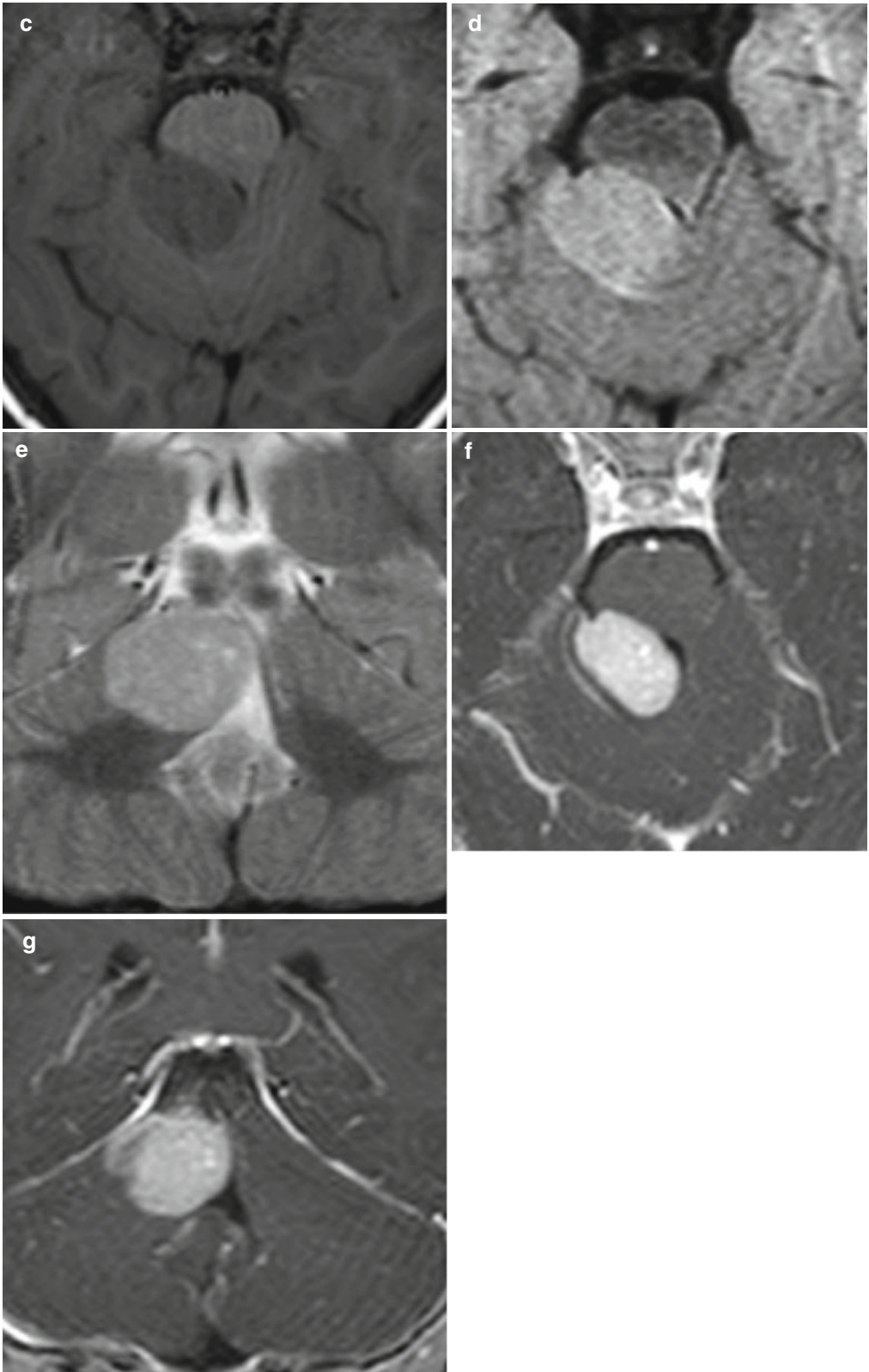


Fig. 15.5 (continued)

magna, and other cisternal compartments may occur but is not common [11].

Some reported cases of medulloblastoma involved the porus acusticus and simulated the

imaging features of a vestibular schwannoma [12] (Figs. 15.6 and 15.7).

At conventional MR imaging, the classic appearance of a medulloblastoma is iso-

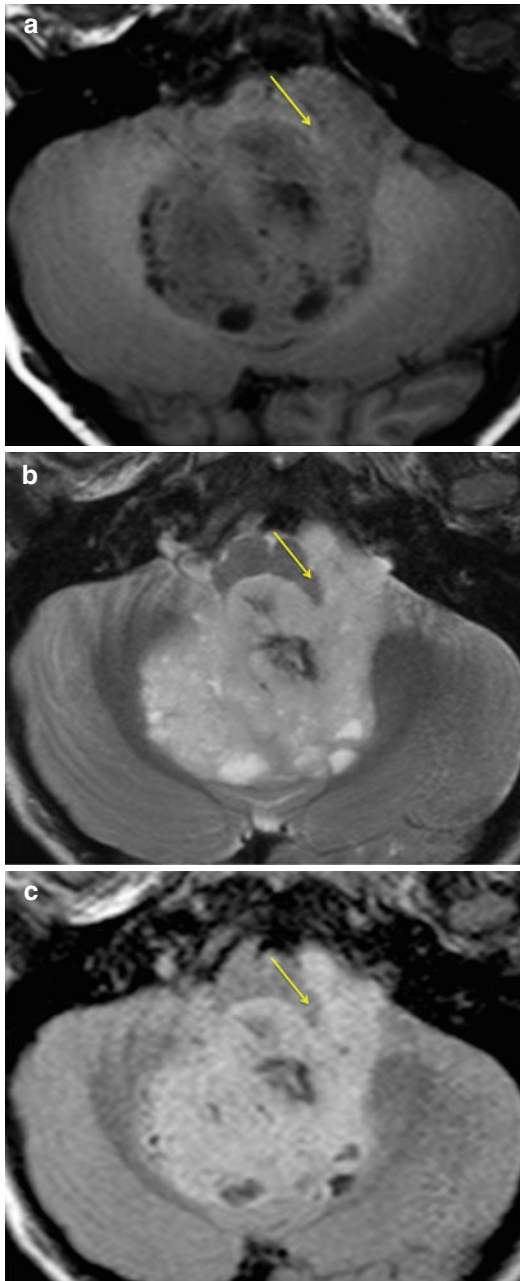


Fig. 15.6 Medulloblastomas with foraminal extension (arrows): (a) Axial T1- and (b) T2-weighted and (c) FLAIR images show foraminal extension from the fourth ventricle to the left foramen of Luschka

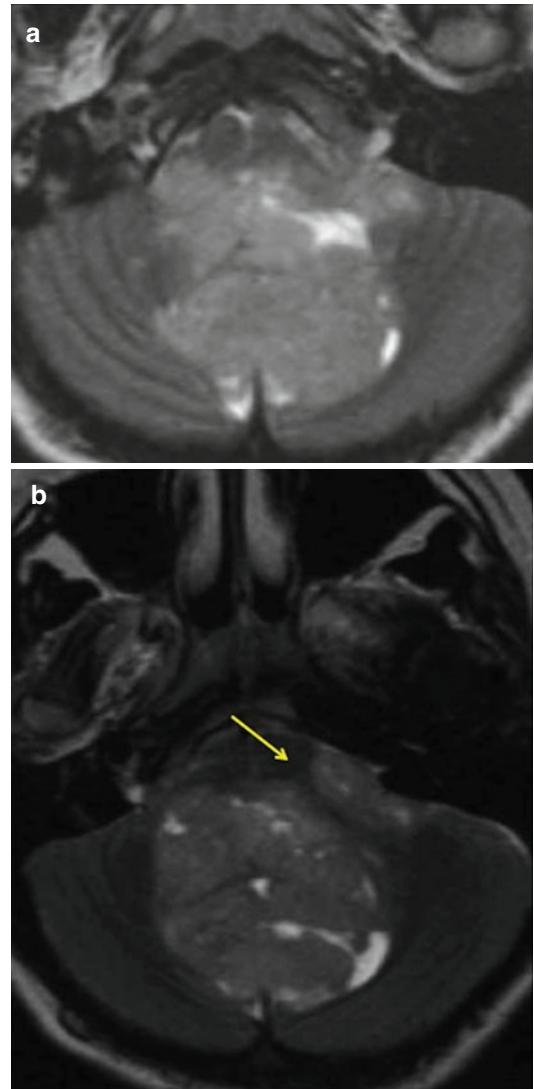


Fig. 15.7 Medulloblastomas with cerebellopontine angle cistern extension (arrows): (a, b) Axial T2-weighted images show foraminal extension from the fourth ventricle to the foramen of Luschka and to the cistern of left cerebellopontine angle. (d, c) Axial T2-weighted images shows metastatic MB (arrowsheads) with a lesion of the cistern of the left cerebellopontine angle



Fig. 15.7 (continued)

hypointense relative to gray matter with T1W sequences and variable signal intensity relative to grey matter with long repetition time pulse sequences [13]; the classic (CMB) and anaplastic medulloblastomas show commonly hyperintense signal on T2W images; DMB and MB-EN show commonly iso- to hyperintense signal on T2W images (Fig. 15.8) [14].

On postcontrast images, majority of CMB and medulloblastoma variants have a marked enhancement; in CMB, subtle, marginal, or only linear enhancement is also possible.

Large cell (LC) and anaplastic variants show often inhomogeneous but marked enhancement, with or without necrosis and cystic parts; DMB will show a wide spectrum of enhancement

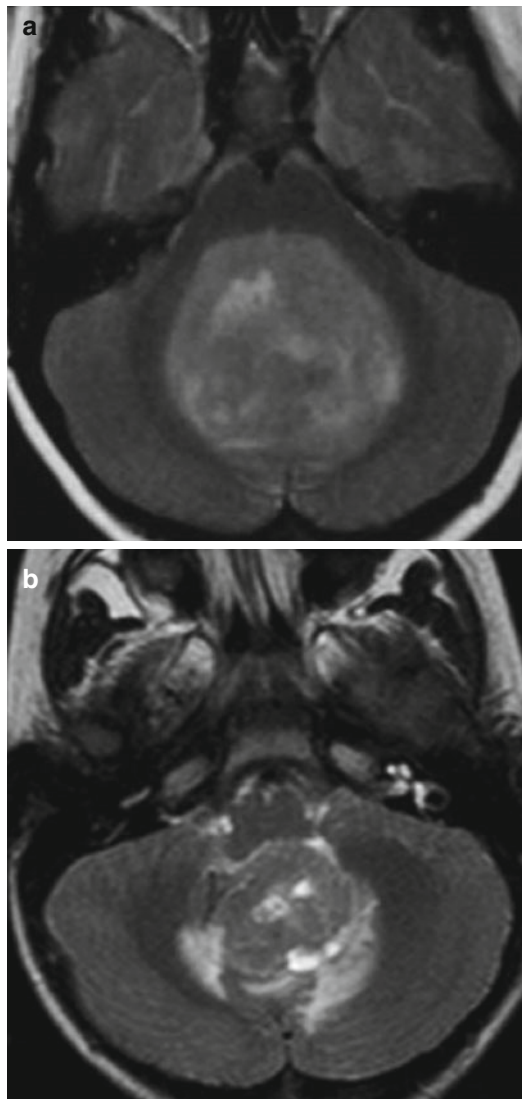


Fig. 15.8 Variability of signal intensity on T2-weighted images: (a) axial T2-weighted image shows a nearly heterogeneous hyperintense mass in the posterior fossa midline. (b) On an axial T2-weighted MR image, the mass is hypo-hysointense compared with the surrounding normal cerebellum with perilesional edema and well-defined margins. (c) Desmoplastic medulloblastoma: on an axial T2-weighted image, the mass, situated off-midline shows solid and fluid components, with iso-hyperintense signal of solid portion compared with surrounding normal brain tissue. (d) Medulloblastoma with extensive nodularity: on an axial T2-weighted image, the mass is heterogeneous hysointense with nodular aspect surrounding of vasogenic edema

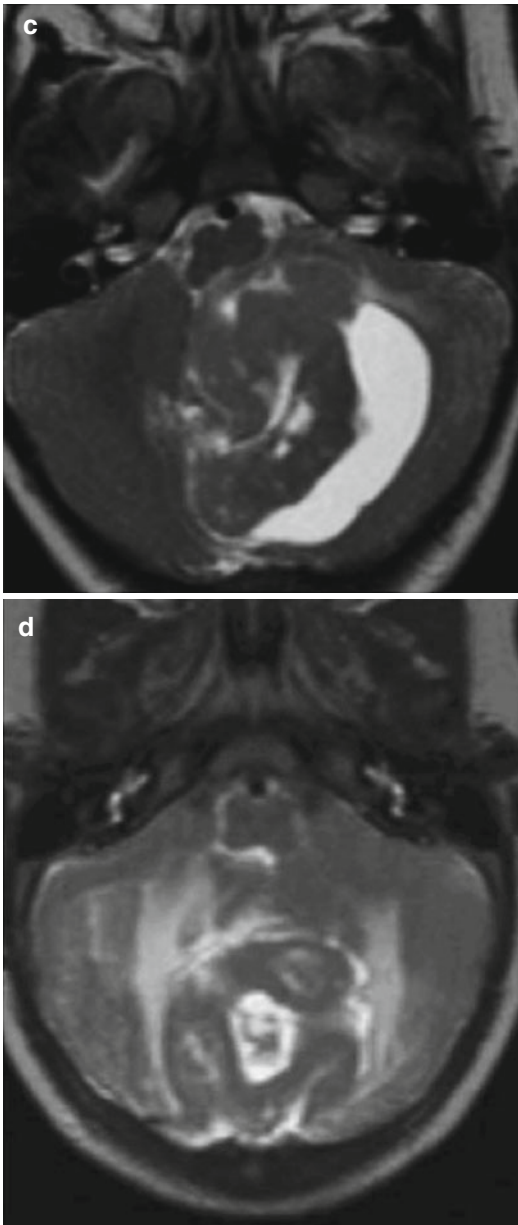


Fig. 15.8 (continued)

patterns, inhomogeneous, marked homogeneous, nodular appearance [14].

The typical appearance of the MB-EN variant is strongly, multifocal, homogeneously enhancing, grape-like tumor nodules, and it is possible depict a central “scar-like” enhancement; the degree of uptake better than that seen in CM may

indicate the neuronal differentiation known to be present within this variant [15] (Fig. 15.9).

At the time of the diagnosis, MBs are commonly associated with hydrocephalus.

Sometimes, herniation of cerebellar tonsils resulting from the tumors is observed.

In majority of the cases, findings consistent with peritumoral white matter edema are seen; typically, the patients with MBs had mild to moderate perifocal edema; DMB can show marked edema.

Intratumoural cystic areas are sometimes depicted in CMB and MB variants; calcifications and hemorrhagic component are not common features in MB variants but can be occasionally seen in CMB (Fig. 15.10).

However, conventional MRI has low sensibility and specificity in identifying specific medulloblastoma types and often cannot reliably differentiate between high-grade and low-grade tumors. Histopathologic evaluation of brain biopsies still remains the gold standard for definitive diagnosis.

Diffusion-weighted imaging (DWI) and apparent diffusion coefficient (ADC) maps, proton magnetic resonance spectroscopy (MRS), and perfusion imaging offer additional informations that can be helpful to determining tumor type and grade.

1H-MRS and DWI provide bio- and physico-chemical information that cannot be obtained with conventional imaging techniques alone. Thus, an approach combining both spectroscopic and diffusion imaging techniques has become obvious in the field brain tumors.

Several reports have shown that ADC values could be used to differentiate some tumors or evaluate their cellularity.

The use of short echo time MRS, still a more demanding technique in terms of analysis than long echo time spectroscopy, allows the detection of metabolites which have been suggested useful in the diagnosis of specific tumor histology. Short TE single-voxel 1H-MRS combined with DWI fully discriminates the most frequent posterior fossa tumors in children.

DWI is a technique in which dedicated phase-defocusing and phase-refocusing gradients

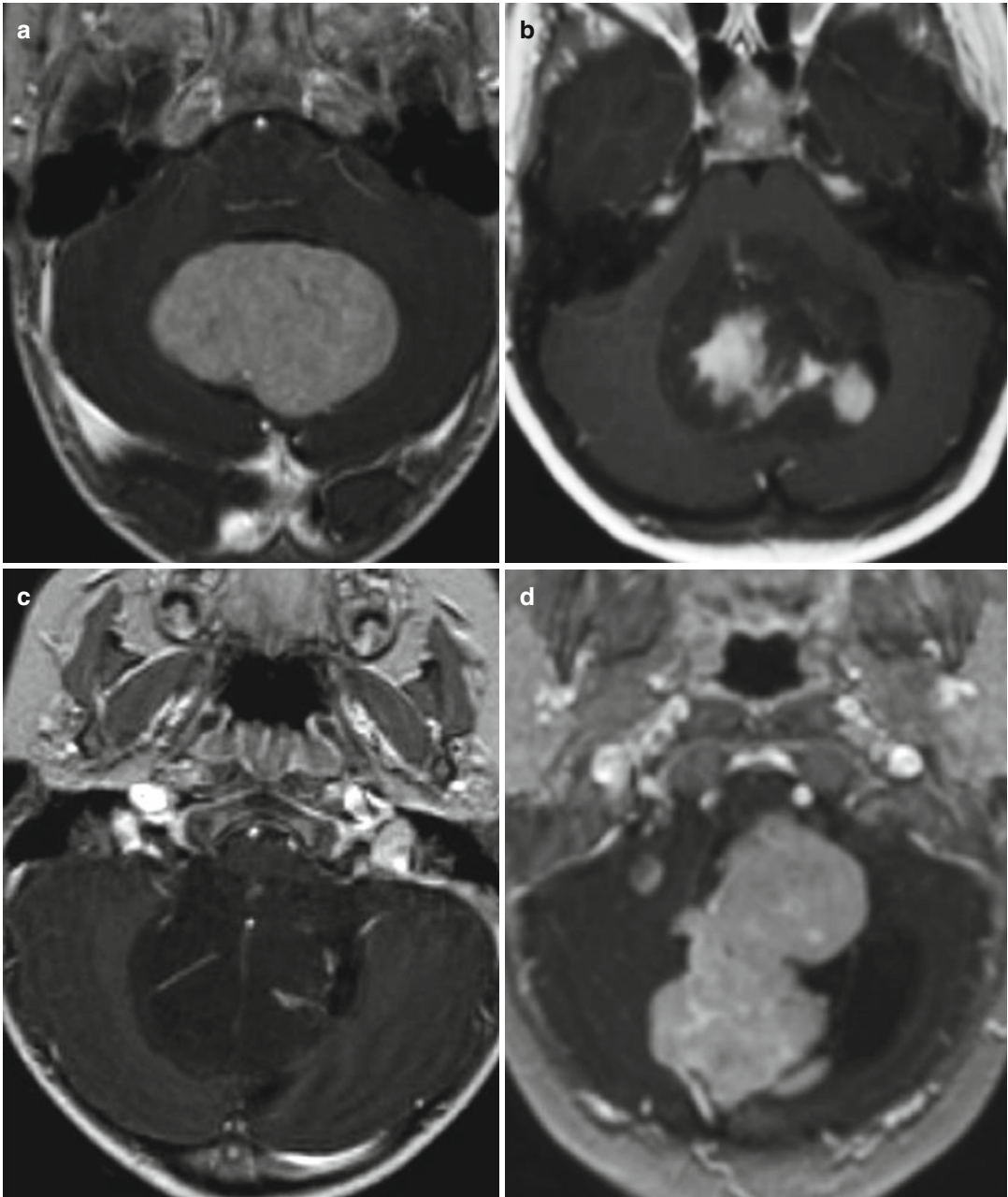


Fig. 15.9 Variability of contrast enhancement: (a) On an axial T1-weighted postcontrast image, medulloblastoma infant shows nearly homogeneous enhancement of the mass. (b, c) On an axial T1-weighted postcontrast image, classic medulloblastoma shows patchy (b) and linear (c) enhancement. (d) Desmoplastic medulloblastoma: on an axial T1-weighted postcontrast image, the mass shows

marked homogeneous enhancement with nodular aspect; notice nodular enhancement at the level of the right tonsilla cerebellar. (e, f) Medulloblastoma with extensive nodularity: on axial T1-weighted postcontrast images, the mass shows multifocal, heterogeneous enhancing, grape-like tumor nodules, and it is possible to depict a central “scar-like” enhancement

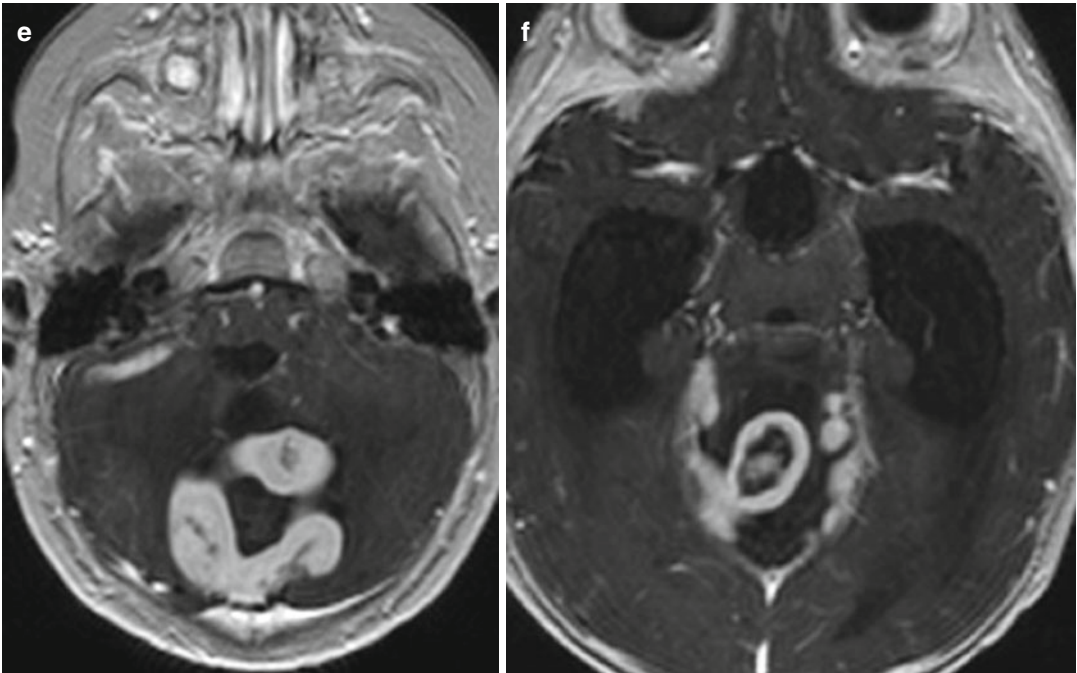


Fig. 15.9 (continued)

allows evaluation of the rate of microscopic water diffusion within tissues, where calculated ADC maps represent an absolute measure of average diffusion for each voxel [16].

It is used to distinguish necrosis from cyst formation or edema and has shown some efficiency in identifying different tumor types and delimiting their boundaries against normal cerebral tissue. DWI is helpful in distinguishing common pediatric cerebellar tumors on the basis of these tumors' different ADC values. Low tumor ADC values compared with normal brain parenchyma have been linked to hypercellularity of the tumors. The high cellularity of medulloblastoma is a well-known histologic feature of these tumors [17, 18]. Medulloblastoma characteristically shows patternless sheets of small cells with small areas of necrosis.

There is relative restriction to the random movement of the water molecules in the small cells of medulloblastoma. The densely cellular nature of medulloblastoma and the high nuclear-to-cytoplasm ratio lead to restriction of the water diffusion, resulting in high signal on trace DWI

and low ADC values (Fig. 15.11) [19]. Based on limited results, MB-EN and DMB may have a lower ADC compared to classic or LC/A variants. Studies with DWI measurements in larger numbers of patients with different MB variants are necessary to verify this and analyze further the value of DWI in distinguishing the variants of MB.

MRS analyzes the metabolic activity and chemical composition of the tissue studied through several major components such as choline-containing compounds (Cho), creatine plus phosphocreatine (Cr), N-acetylaspartate (NAA), and lactate (Lac).

Previous reports have demonstrated the ability of MRS to improve differentiation among tumors or even to identify specific histological tumor types.

These results have mainly been acquired at long echo time (TE 130 ms or longer), and only recently, MRS data obtained at short echo time (with a TE of 35 ms or less) have been published.

Most studies published have used long echo times (TE) and have focused on evaluating abnormalities of *N*-acetylaspartate (NAA), total choline (tCho), and lactate (Lac) by

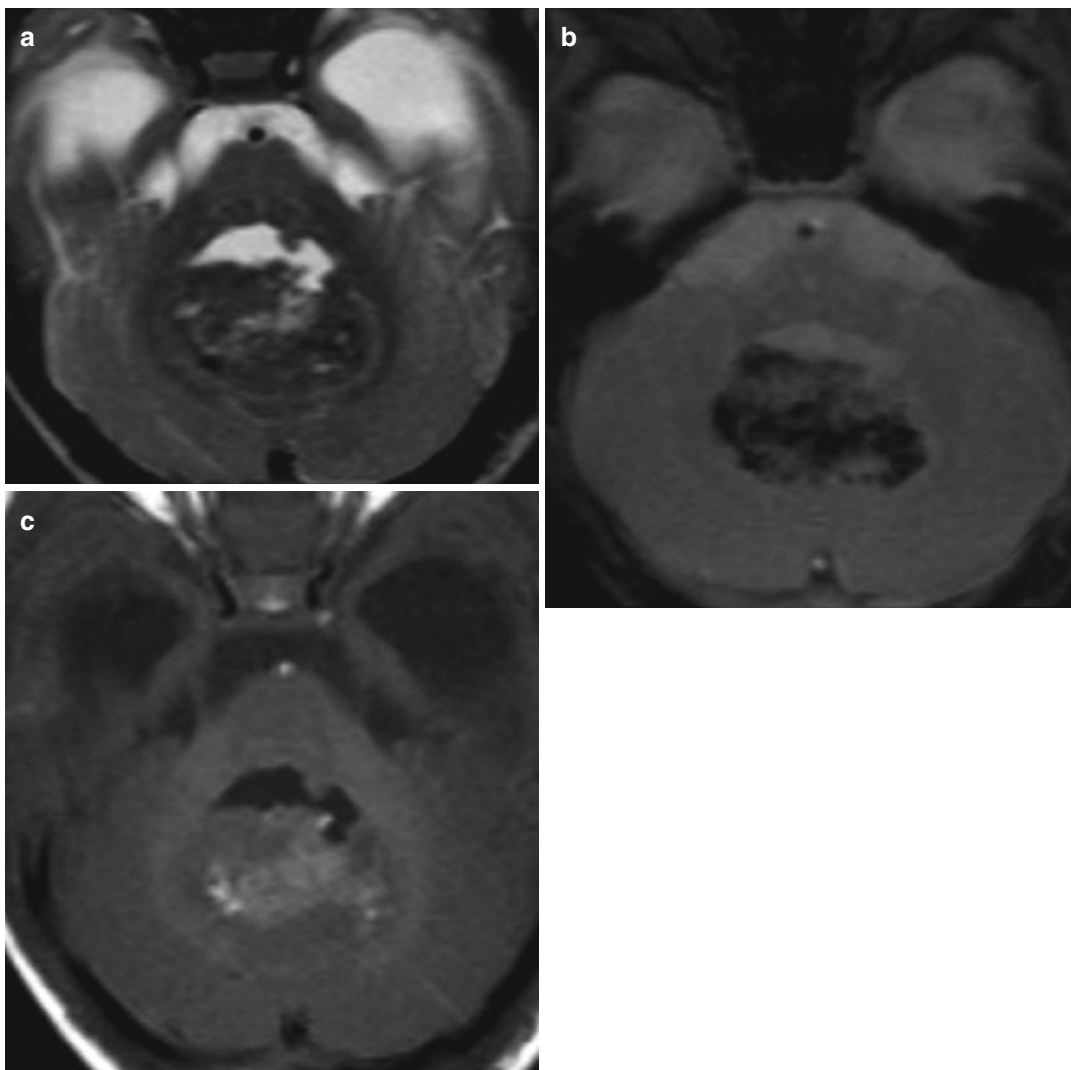


Fig. 15.10 Hemorrhagic medulloblastoma: (a) axial T2-weighted image. (b) Axial T2-GRE* image. (c) Axial T1-weighted image

analysis of ratios relative to creatine (Cr). These studies have shown that brain tumors in general have elevated choline peaks, reduced N-acetyl aspartate and creatine peaks, and occasionally elevated lipid and lactic acid peaks, a characteristic spectrographic signature for a neuroectodermal tumor but not necessarily specific for medulloblastoma.

Tumors also exhibited elevated Lac, which is believed to accumulate in necrotic areas of tumors or as a by-product of anaerobic glycolysis.

Compared to long TE, short TE spectroscopy permits the observation of additional metabolites which are characterized by a short T2 relaxation time at better signal-to-noise ratio (SNR), among others taurine (Tau), glutamine plus glutamate (Glx), myoinositol plus glycine (mI), or alanine (Ala). MRS and metabolite ratios and absolute quantification are increasingly used to better characterize tumor physiology in an attempt to distinguish normal from pathologic tissue or even identify specific tumor types.

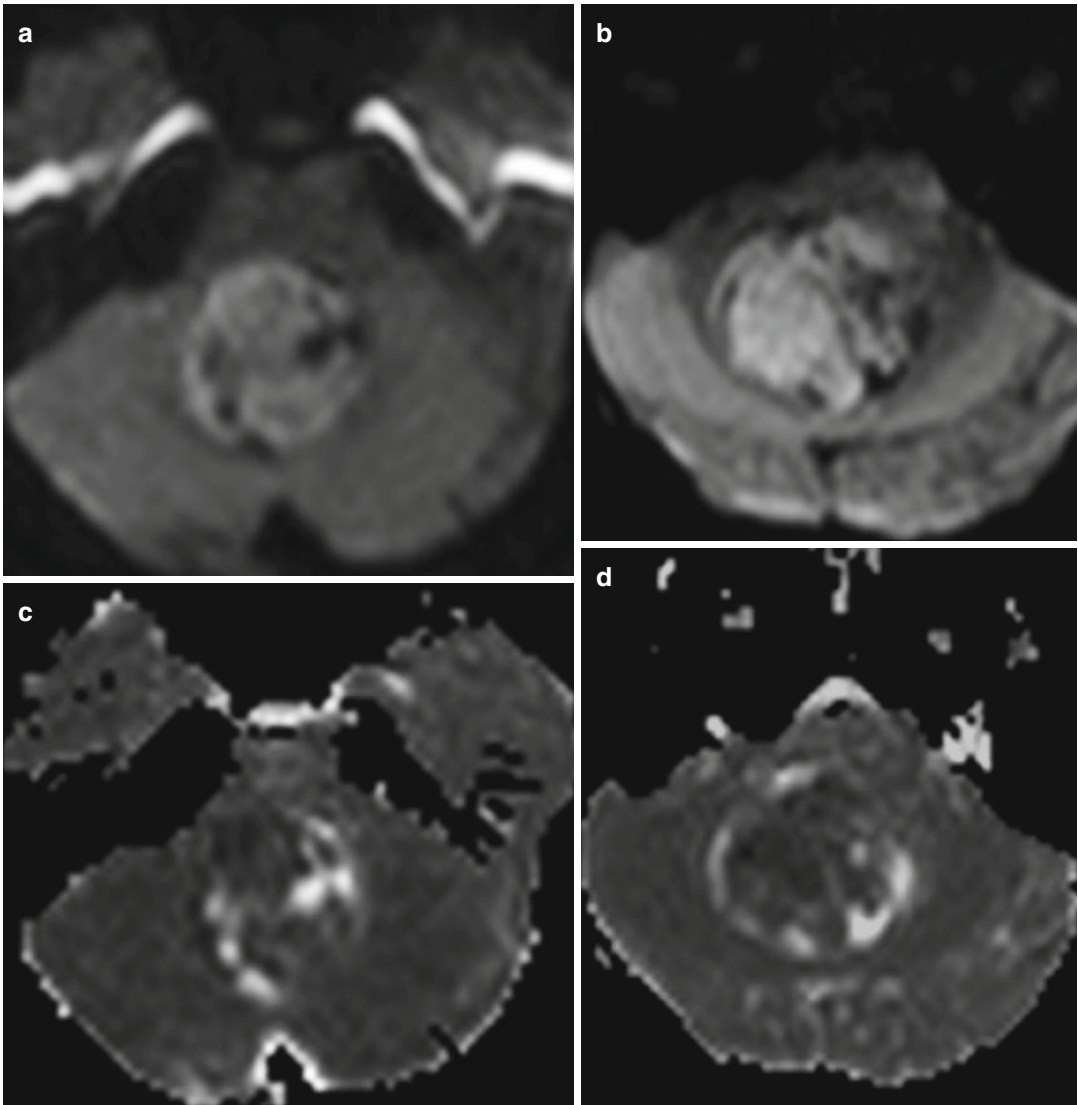


Fig. 15.11 (a, b) Diffusion-weighted MR images show extremely high intensity in the tumor. (c, d) On the axial ADC map, the tumors are well demarcated and isointense

to normal-appearing cerebellum. This finding is associated with high cellularity and small extracellular space at histologic examination

All MB show a consistent and significant elevation of Tau at 3.3 ppm and a significant increase in Cho (Fig. 15.12).

Tau is an aminosulfonic acid which localizes to the cerebellar molecular layer, Purkinje cells, basket cell axon terminals, and glial processes and is abundant in the developing cerebellum and isocortex. Tau seems associated with an increased cellular proliferation and tumoral aggressiveness.

Elevated taurine (Tau), an amino acid that has not been detected with long TE MR spectroscopy, has recently been observed independently in medulloblastoma by several groups using short TE MR spectroscopy and was found to be an important differentiator of this tumor type from other common pediatric brain tumors. High-grade tumors which are highly cellularized and have a high proliferative rate show increased Cho

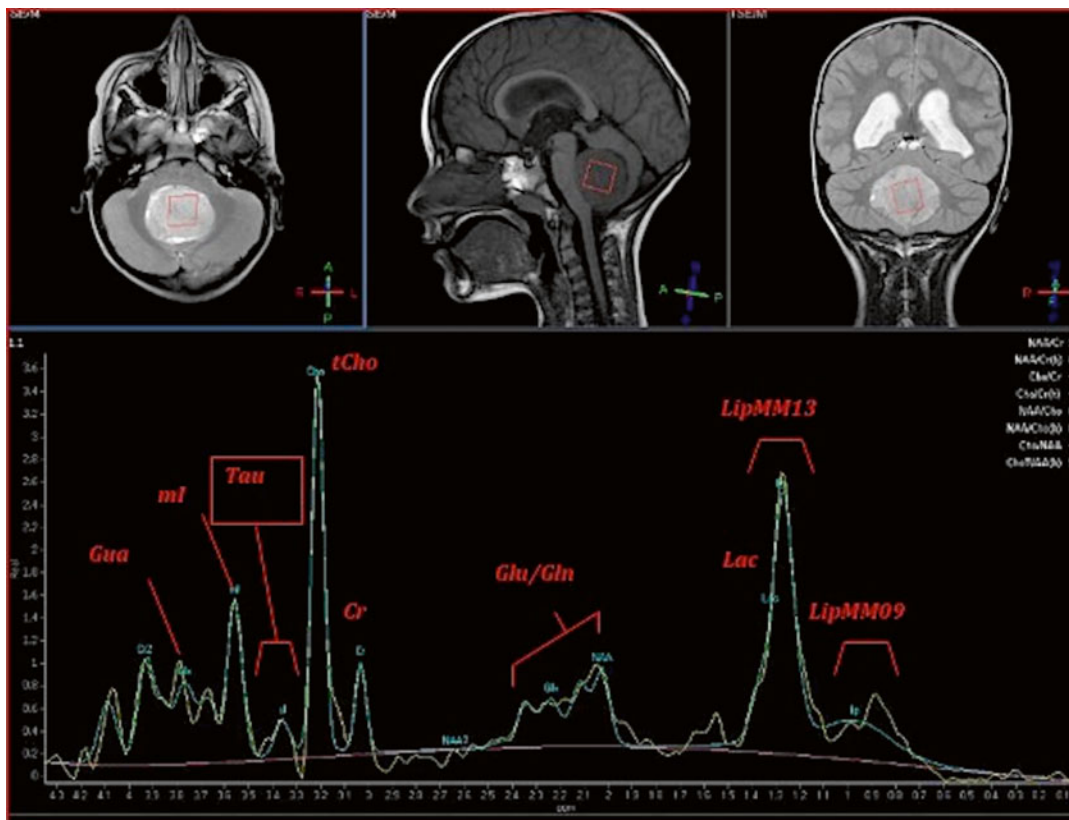


Fig. 15.12 Short TE (31 ms) 1H-MR spectroscopy of medulloblastoma: 1H spectrum of a solid-appearing medulloblastoma and corresponding T2-weighted transverse and coronal fast spin-echo MR images, T1-weighted sagittal spin-echo MR image, indicating the region of interest. Absolute quantitation included a correction for the fraction of cystic tissue (about 6 %). A singlet at 3.78 ppm consistent with guanidinoacetate

(Gua) is observed, and taurine (Tau) is detected as a complex signal intensity at \sim 3.4 ppm. Spectrum also exhibit broad lipid and macromolecule resonances at 0.9 and 1.3 ppm. One peak of the lactate (Lac) doublet at 1.33 ppm is detected as a shoulder of the broad LipMM13 resonance. *N*-acetylaspartate (NAA) is depleted, and total choline (tCho) is prominent in all spectra of medulloblastoma

levels in comparison to normal brain tissue. In a pediatric population, high levels seemed to correlate with tumor progression and a faster growth.

15.4 Differential Diagnosis

Intra-axial posterior fossa tumors in children are heterogeneous. Differential diagnosis includes above all ependymomas and pilocytic astrocytomas.

Ependymoma usually also presents as hyperattenuated midline cerebellar mass in a child.

In contrast to a medulloblastoma, an ependymoma is usually calcified and frequently extends from its ordinary fourth ventricular origin through

the foramen of Luschka into the adjacent cerebellopontine cistern [20].

For childhood masses that are within the cerebellar hemisphere, a pilocytic astrocytoma is the most likely tumor.

Hyperattenuation on nonenhanced CT scans is the signature imaging feature of the vast majority of cerebellar medulloblastomas and reflects the compact nature of the tumor seen at histologic study [21].

In agreement to Barkovich [22], this CT finding also accounts for the single most reliable imaging feature with which to distinguish a medulloblastoma from a pilocytic astrocytoma. Since cells of a pilocytic astrocytoma contain

abundant cytoplasm and form a less compact matrix, they tend to be hypoattenuated on nonenhanced CT scans unless calcification or hemorrhage is also present.

Posterior fossa tumors could be differentiated on the basis of ADC values and ADC ratios.

In a study by Rumboldt et al. [23], the mean ADC of medulloblastoma was $0.66 \times 10^{-3} \text{ mm}^2/\text{s}$. The assessment of ADC values of enhancing tumor parts in posterior fossa tumors in children revealed a cutoff value of $>1.4 \times 10^{-3} \text{ mm}^2/\text{s}$ for pilocytic astrocytoma and $<0.9 \times 10^{-3} \text{ mm}^2/\text{s}$ for medulloblastoma.

Very high ADC values and ratios are characteristic of pilocytic astrocytoma; the ADC values of pilocytic astrocytomas are also higher from ependymomas.

Medulloblastomas are uniformly hyperintense on DWI, with lower ADC values than those of ependymomas and juvenile pilocytic astrocytomas.

Medulloblastoma and atypical teratoid–rhabdoid tumor (AT–RT) constitute the majority of hypercellular primary CNS neoplasms of childhood. Differentiation of AT–RT from medulloblastoma has important clinical and prognostic implications because AT–RT has a more malignant biologic behavior and is less sensitive to therapy. The imaging characteristics and pathologic appearances of AT–RT and medulloblastoma are similar to each other.

AT–RT is a rare tumor that usually occurs in the cerebellum and is typically heterogeneous in appearance on MR imaging.

General imaging characteristics of AT–RT and medulloblastoma reflect the histopathologic similarities of these two tumors.

Typically, AT–RT presents at a younger age than medulloblastoma. Cerebellopontine angle involvement is significantly more common in AT–RT than in medulloblastoma. Intratumoral hemorrhage, described as T1 shortening, is more common in AT–RT than medulloblastoma.

Medulloblastoma was more commonly a solid or predominantly solid tumor compared with AT–RT; however, there is no statistically significant difference in the solid–cystic appearance of infratentorial AT–RT and medulloblasto-

mas. No statistically significant difference is seen in the enhancement characteristics, T2 signal intensity of the solid components, presence of extremely T2 hypointense foci, and presence of leptomeningeal spread–spinal drop metastasis between medulloblastoma and AT–RT. AT–RT is hyperintense on DWI and their ADC values are not significantly different from those of the medulloblastomas. Both tumors are hyperintense on DWI, and ADC values do not help distinguish these tumors from each other.

Therefore, for a pediatric posterior fossa neoplasm that is hyperintense on DWI, AT–RT has to be a consideration in addition to medulloblastoma.

In the posterior fossa tumors of children, lower ADC values are found in medulloblastoma and AT–RT compared with the ADC values of juvenile pilocytic astrocytomas and ependymomas. If a posterior fossa tumor showing restricted diffusion is not in the midline and if there is involvement of the CPA, it is more likely to be AT–RT than medulloblastoma.

Distinction between medulloblastoma and AT–RT is made by the presence of nests or sheets of rhabdoid cells in the latter, which are similar to those cells seen in the rapidly fatal rhabdoid tumor of the kidney. If the rhabdoid cells are few, immunohistochemical and molecular techniques are required to distinguish AT–RT from medulloblastoma.

In a study by Panighray et al. [24] single-voxel proton MR spectroscopy with a TE of 35 ms of 60 patients with untreated brain tumors (medulloblastomas, anaplastic astrocytomas, low-grade astrocytomas, pilocytic astrocytomas, anaplastic ependymomas, ependymomas, choroid plexus papillomas, choroid plexus carcinomas, and pineal germinomas) was performed, and absolute metabolite concentrations were determined by using fully automated quantitation.

Medulloblastomas show lower levels of ml compared to ependymoma and infiltrating glioma.

A prominent signal intensity from Tau was observed in all medulloblastoma spectra. Levels of Tau in medulloblastoma was higher than in all other and was the most significant differentiator of medulloblastoma from all other.

Of all tumor types studied, levels of tCho were highest in medulloblastoma.

Other considerations in the differential diagnosis include metastasis, hemangioblastoma, astrocytoma, lymphoma, and dysplastic cerebellar gangliocytoma (Lhermitte–Duclos disease).

Metastasis is the most common cerebellar mass in the adult population and has a variety of appearances.

Hemangioblastoma is the most common primary neoplasm of the cerebellum in adults.

The majority of these tumors have the classic imaging appearance of “a cystic mass with an enhancing mural nodule” and should be readily distinguishable from a medulloblastoma.

However, when the hemangioblastoma is in a solid or mixed form, its imaging appearance is nonspecific and it will be more difficult to differentiate from a medulloblastoma. Both lesions tend to be peripherally located. The presence of flow voids and intense enhancement on contrast-enhanced images may help correctly identify a hemangioblastoma [25].

About 10 % of all central nervous system lymphomas occur in the cerebellum. Hypointensity on T2-weighted images is characteristic of these lesions, which also tend to be periventricular in location.

The “striated cerebellum” is the classic imaging appearance of dysplastic cerebellar gangliocytoma, which carries the eponym of Lhermitte–Duclos disease. In support of the belief that this lesion is a hamartoma, it usually does not have surrounding vasogenic edema or enhancement and is not hyperattenuated on non-enhanced CT scans. The striped appearance is classic, but not all lesions will have this imaging manifestation. There is one case report of a medulloblastoma that had an imaging appearance mimicking a nonclassic appearance of a dysplastic cerebellar gangliocytoma (Lhermitte–Duclos disease) [26–28].

Several analyses demonstrate that the main variables which were able to isolate medulloblastoma from all other tumors consist of combination of elevation of Tau and Cho levels and reduction in ADC values.

15.5 Metastasis

Subarachnoid seeding is common in medulloblastomas, occurring in up to 33 % of all patients at the time of initial diagnosis [29].

Evidence of spread of medulloblastoma cells into the CSF is crucial to optimal patient management; its detection is a key factor in staging, prognosis, and treatment. Subarachnoid spread of disease can be detected by MRI or by CSF cytologic studies.

MRI is more sensitive than, and has replaced, CT myelography in the detection of leptomeningeal spread and is also likely more sensitive than CSF cytology for the detection of subarachnoid spread of primary brain tumors.

MR imaging and CSF cytologic analysis should be used in combination to establish the diagnosis.

Because the normal flow of CSF from the cisterna magna travels first along the posterior margin of the spinal cord before returning to the cistern along the ventral surface of the spinal cord, most metastases are found along the posterior margin of the spinal cord as the greatest concentration of malignant cells would be expected to be found there [30, 31].

Imaging manifestations of leptomeningeal spread of disease in the spine are variable and include smooth enhancement along the surface of the spinal cord, nodular enhancement in the extramedullary intradural or, occasionally, intramedullary space [32]; nerve root thickening, nodularity, or clumping; and thecal sac irregularity. The lumbosacral region, particularly the most caudal aspect of the thecal sac, is the most common location for “drop” metastases (Fig. 15.13).

MR sensitivity for leptomeningeal metastases increases with higher doses of contrast and the use of volumetric gradient-echo imaging to obtain thin section axial imaging of the spine. Small metastases on nerve roots can be detected if thin sections (3 mm or less) are used.

Postoperative MR for assessment of subarachnoid tumor spread should be performed no less than 2 weeks following surgery; in fact false-positive results can occur, either from the presence of methemoglobin or from

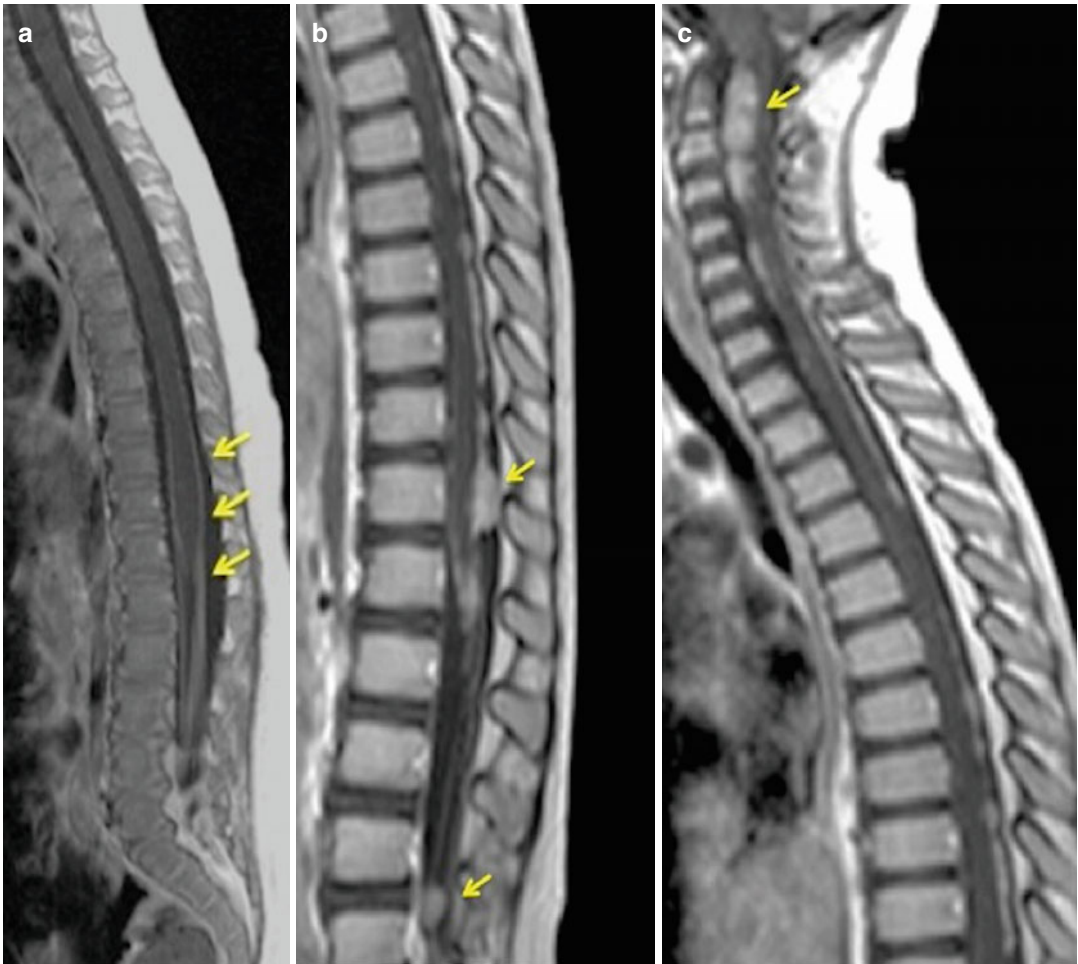


Fig. 15.13 Leptomeningeal spread: (a) Postcontrast sagittal T1-weighted image show smooth enhancement along the surface of spinal cord in the lumbosacral region

(arrows). Postcontrast sagittal (b) T1-weighted images of nodular enhancement in the extramedullary intradural space (arrows). (c) Intramedullary nodular enhancement

leptomeningeal irritation following posterior fossa craniectomy and can mimic leptomeningeal spread of disease.

For this reason, assessment of the spinal axis should be performed preoperatively during the initial MR imaging examination.

The most common locations for intracranial metastases are the vermian cisterns, the floor of the third ventricle, subependymal region of the lateral ventricles, and subfrontal region (Fig. 15.14).

While it is unusual for any central nervous system tumor to spread to remote sites, medullo-

blastoma has the third highest rate of extraneural metastasis, following glioblastoma multiforme and meningioma [33].

The prevalence of remote spread in children is increased in patients of a younger age, of male gender, and with diffuse subarachnoid disease. The presence of ventriculoperitoneal shunt may lead to metastatic spread in the abdominal cavity [34].

The addition of chemotherapy to the routine treatment protocol of patients with medulloblastoma is associated with a significantly decreased prevalence of extraneural metastasis. Still,

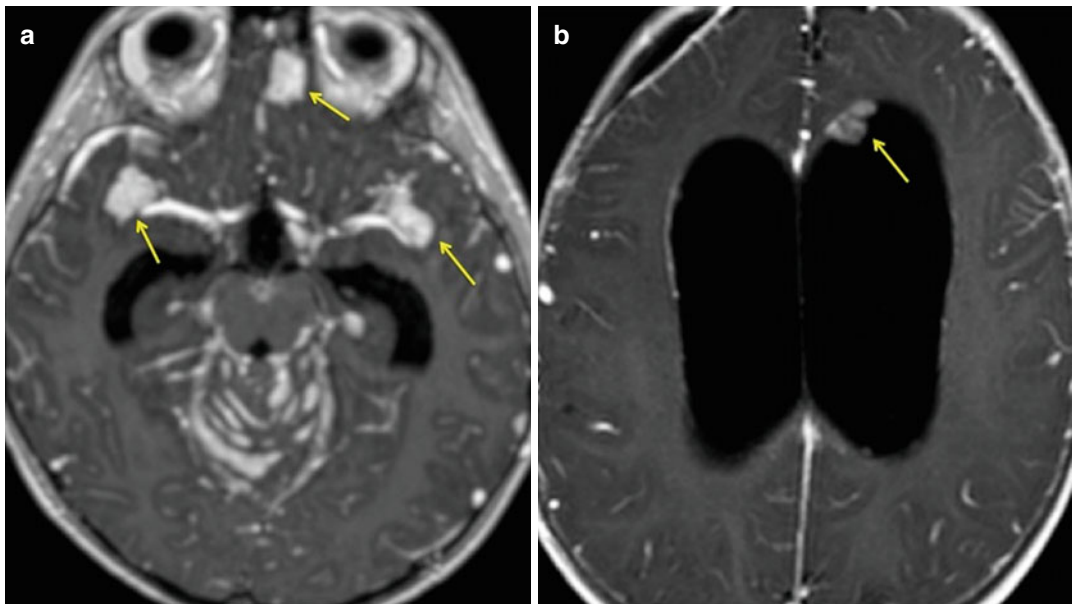


Fig. 15.14 (a) Axial T1-weighted postcontrast images in metastatic medulloblastoma with cerebellar leptomeningeal enhancement and nodular intracranial metastases in subfrontal and temporal region (*arrows*); (b) Axial

T1-weighted postcontrast images in metastatic medulloblastoma with a lesion in the subependymal region of the lateral ventricles (*arrow*)

extraneural metastasis may manifest up to several years after initial treatment, with a median time of 12–32 months [35].

By compiling data on 119 cases reported in the literature, Rochkind et al. [36] determined the overall prevalence of extraneural metastasis at 7.1 % of patients with a medulloblastoma. Bone is the most common (77 % of cases) extraneural site in both children and adults, followed by the lymph nodes (33 %). In children, liver (15 % of cases), lung (11 %), and muscle (2 %) are the next most common sites, whereas lung (17 %), muscle (13 %), and liver (10 %) are the next most common sites in adults (86). Less frequently, the pancreas (4 %), kidneys (2 %), testes (2 %), ureters (1 %), ovaries (1 %), and breast (1 %) may be involved.

15.6 Surveillance Imaging

MR is obtained immediately after surgery to evaluate the extent of resection and periodically thereafter for long-term surveillance for disease

recurrence. Following surgery, a thin rim of enhancement (likely representing granulation tissue) can be seen along the cavity margins beginning as soon as 24 h, which becomes progressively thicker and more nodular over the next several days. Therefore, imaging to assess extent of resection should be performed less than 48 h after surgery. Pregadolinium T1-weighted sequences are always included to distinguish perioperative hemorrhage from residual enhancing tumor. For pediatric patients, a head CT in the immediate postoperative period after craniotomy is reserved for delayed recovery from anesthesia or unexpected acute neurologic deficits or to assess changes in hydrocephalus after treatment. It should not be used as a surrogate for MR imaging to assess extent of resection.

Following the period after surgery, enhancement along the resection cavity margins progressively decreases beginning at approximately 5 weeks and usually resolves completely within 12 months. Therefore, any new or increasing enhancement after approximately 5 weeks after surgery should raise suspicion for tumor

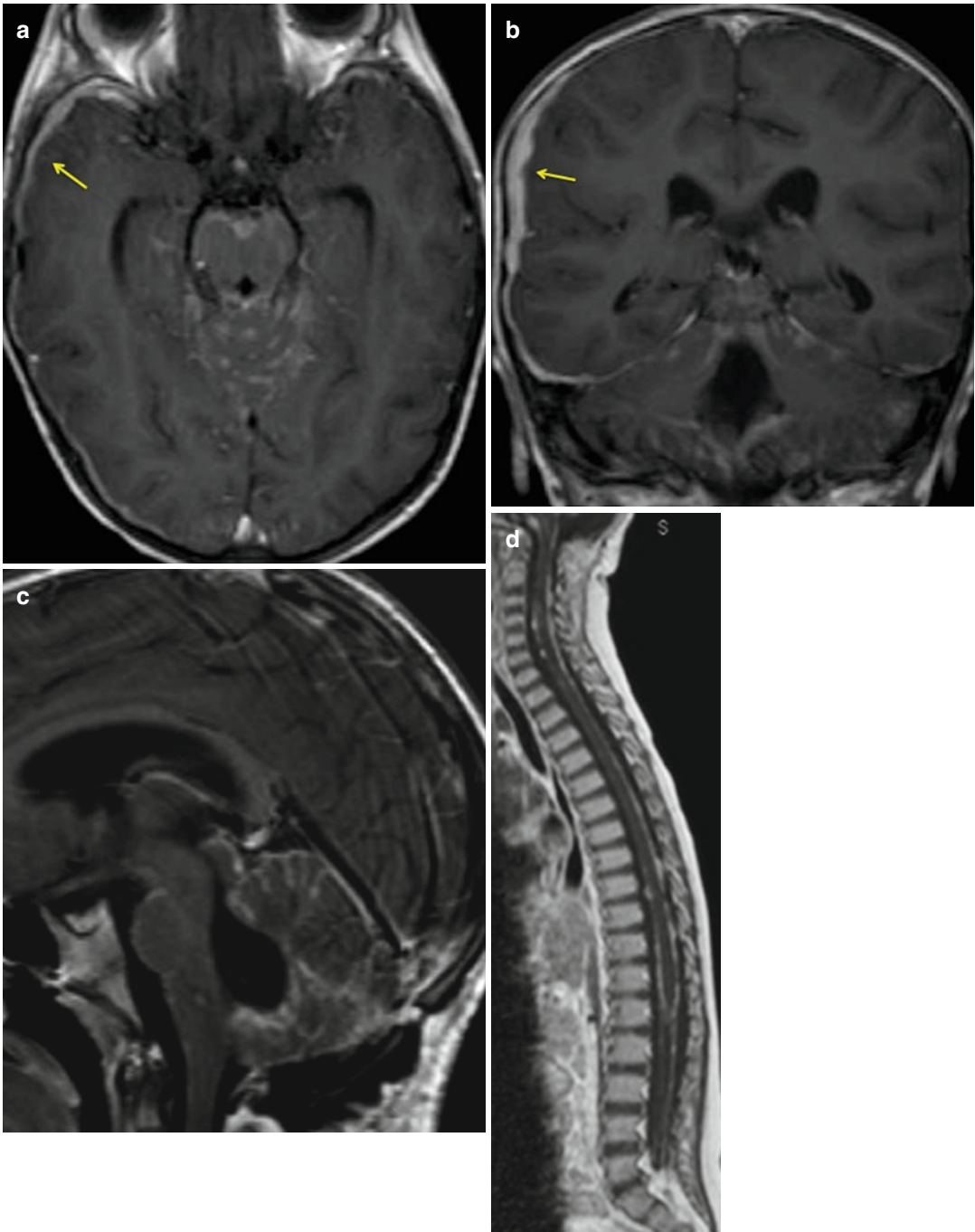


Fig. 15.15 Recurrence of medulloblastoma as leptomeningeal enhancement: (a) Axial (b) Coronal and (c) Sagittal T1 C+ MR show cerebellar leptomeningeal enhancement; notice

the metastatic thickening of the supratentorial dura (*arrows*); (d) Sagittal T1 C+ MR of the spine shows leptomeningeal enhancement and nodular surface metastatic lesions

recurrence. New contrast enhancement can also be seen several months to years (typically 4–6 months) after radiation therapy and has been attributed to late delayed injury resulting from permanent damage to blood vessels. Since recrudescence enhancement is sometimes attributable to these posttreatment effects rather than recurrent tumor, proton MR spectroscopy and perfusion MR can be helpful adjunct techniques in this setting to aid in the differentiation of tumor recurrence from posttreatment changes. In particular, necrosis, including that due to radiation injury, generally demonstrates concomitant reduction of NAA, choline, and creatine peaks, while a new or persistently elevated choline/NAA ratio raises concern for recurrent tumor.

Postoperative surveillance imaging of the brain and spine in patients with medulloblastoma should be employed with 3–6 month intervals during the first 5 years following initial diagnosis in the hope of detecting recurrent disease earlier. Although recommendations regarding the duration of surveillance imaging vary, periods of up to 10 years have been suggested for posterior fossa medulloblastoma.

Recurrence of medulloblastoma is unfortunately very common in both children and adults with the disease. Most recurrent disease in children develops in the first 2 years after initial treatment.

Recurrence of medulloblastoma most commonly manifests as leptomeningeal enhancement or focal parenchymal nodular enhancement within the CNS (Fig. 15.15).

Recurrent disease develops most frequently in the posterior fossa, with the subfrontal region being the second most common location, possibly reflecting the prone position commonly used during surgery and the use of lead blocks to spare the ocular system during radiation therapy.

Following therapy, patients with medulloblastoma have an increased risk for the development of secondary malignancies, a tendency that is partially attributable to the longer survival times for some patients and the use of radiation therapy and chemotherapy. Cases of meningioma, basal cell carcinoma, glioblastoma multiforme, thyroid cancer, cervical cancer, uterine cancer, and acute leukemias have all been noted in these patients (Fig. 15.16). As treatments extend survival times

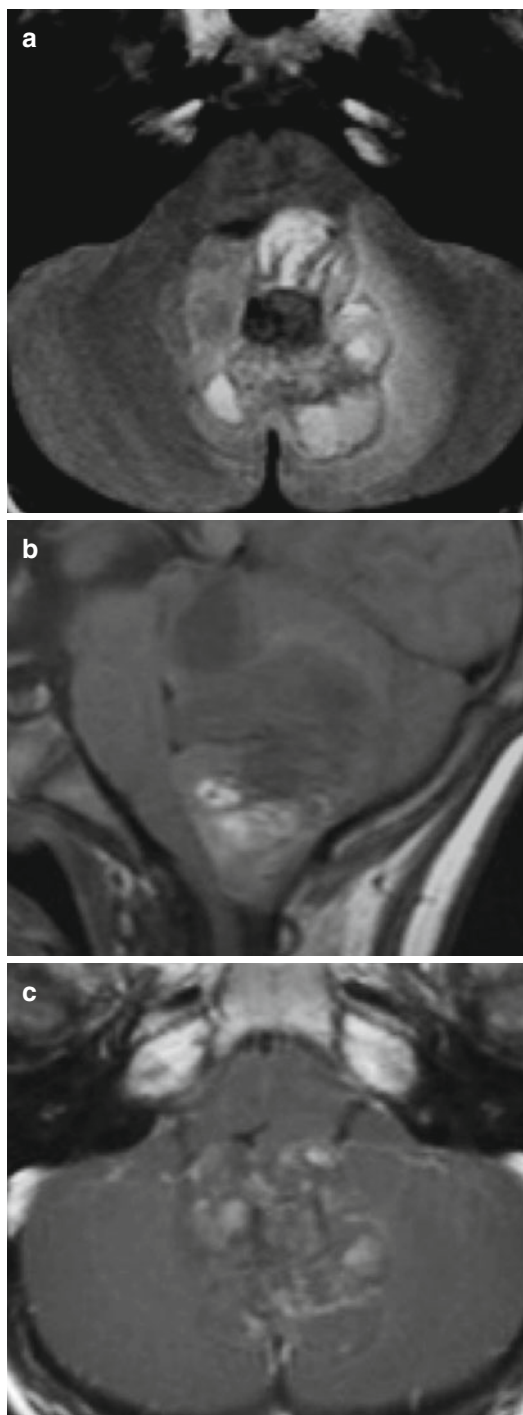


Fig. 15.16 Patient with medulloblastoma developed secondary malignancy: (a) Axial T2-, (b) sagittal T1-, (c) postcontrast axial T1-weighted images of medulloblastoma with hemorrhagic component in midline. (d) axial T2-, (e) sagittal T1-and, (f) postcontrast axial T1-weighted images, after 5 years the patient develop brainstem glioblastoma (arrows) secondary to therapy



Fig. 15.16 (continued)

for medulloblastoma patients, it is likely that secondary malignancies will be encountered.

Treatment-induced neurotoxicity—mainly that resulting from the deleterious effects of whole-brain irradiation on the white matter—is prevalent and manifests as diverse forms of cognitive dysfunction. However, because cognitive assessment of neurobehavioral morbidity is considered to be a late-outcome measurement, the identification of earlier and more sensitive markers of neurologic development and neurotoxicity can be the potential to limit or more effectively time (at developmentally advantageous points) neurotoxic treatments. By using diffusion-tensor magnetic resonance imaging, fractional anisotropy (FA) is reduced in the white matter of childhood medulloblastoma survivors after craniospinal irradiation and chemotherapy. Although it is not clear how these observations of reduced white matter anisotropy reflect the cognitive outcomes of patients who have been treated for medulloblastoma, determining the mean white matter FA value is potentially a useful outcome measure for evaluating treatment-induced neurotoxicity and may also be used for assessing the timing and application of neurotoxic treatments [37–41].

References

1. Zimmerman RA, Bilanuik LT, Phalajani H (1978) Spectrum of medulloblastomas demonstrated by computed tomography. *Radiology* 126:137–141
2. Gado M, Huete I, Mikhael M (1977) Computerized tomography of infratentorial tumors. *Semin Roentgenol* 12:109–120
3. Zee CS, Segall HD, Miller C et al (1982) Less common CT features of medulloblastoma. *Radiology* 144:97–102
4. Weisberg LA (1982) Computerized tomographic findings in medulloblastomas. *Comput Med Imaging Graph* 6:83–91
5. Naidich TP, Un JP, Leeds NE, Pudlowksi RM, Nordich JB (1977) Primary tumors and other masses of the cerebellum and fourth ventricle: differential diagnosis by computed tomography. *Neuroradiology* 14:153–174
6. Al-Mefty O, Jinkins JR, El-Senousse M, El-Shake M, Fox JL (1985) Medulloblastomas: a review of modern management with a report on 75 cases. *Surg Neurol* 24:606–624

7. Sandhu A, Kendall B (1987) Computed tomography in management of medulloblastomas. *Neuroradiology* 29:444–452
8. Nelson M, Diebler C, Forbes WSC (1991) Paediatric medulloblastoma: atypical CT features at presentation in the SIOP II trial. *Neuroradiology* 33:140–142
9. Stavrou T, Dubovsky EC, Reaman GH, Goldstein AM, Vezina G (2000) Intracranial calcifications in childhood medulloblastoma: relation to nevoid basal cell carcinoma syndrome. *AJNR Am J Neuroradiol* 21:790–794
10. Fruehwald-Pallamar J, Puchner SB, Rossi A, Garre ML, Cama A, Koelblinger C, Osborn AG, Thurnher MM (2011) Magnetic resonance imaging spectrum of medulloblastoma. *Neuroradiology* 53(6):387–396
11. Mueller DP, Moore SA, Sato Y, Yuh WTC (1992) MRI spectrum of medulloblastoma. *Clin Imaging* 16:250–255
12. House JL, Burt MR (1985) Primary CNS tumors presenting as cerebellopontine angle tumors. *Am J Otol Suppl*:147–153
13. Meyers SP, Kemp SS, Tarr RW (1992) MR imaging features of medulloblastomas. *AJR Am J Roentgenol* 158:859–865
14. Liu HQ, Yin X, Li Y, Zhang J, Wang Y, Tchoyoson Lim CC, Feng X (2012) MRI features in children with desmoplastic medulloblastoma. *J Clin Neurosci* 19(2):281–285
15. Naitoh Y, Sasajima T, Kinouchi H, Mikawa S, Mizoki K (2002) Medulloblastoma with extensive nodularity: single photon emission CT study with iodine-123 metaiodobenzylguanidine. *AJNR Am J Neuroradiol* 23:1564–1567
16. Rowley HA, Grant PE, Roberts TPL (1999) Diffusion MR imaging. *Neuroimaging Clin N Am* 9:343–361
17. Ellison D (2002) Classifying the medulloblastoma: insights from morphology and molecular genetics. *Neuropathol Appl Neurobiol* 28:257–282
18. Kleihues P, Louis DN, Scheithauer BW et al (2002) The WHO classification of tumors of the nervous system. *J Neuropathol Exp Neurol* 61:215–225
19. Pierce TT, Provenzale JM (2014) Evaluation of apparent diffusion coefficient thresholds for diagnosis of medulloblastoma using diffusion-weighted imaging. *Neuroradiol J* 27(1):63–74
20. Koeller KK, Sandberg GD (2002) Cerebral intraventricular neoplasms: radiologic-pathologic correlation. *RadioGraphics* 22:1473–1505
21. Bourgouin PM, Tampieri D, Grahovac SZ, Leger C, Del Carpio R, Melancon D (1992) CT and MR imaging findings in adults with cerebellar medulloblastoma: comparison with findings in children. *AJR Am J Roentgenol* 159:609–612
22. Barkovich AJ (2000) *Pediatric neuroimaging*, 3rd edn. Lippincott Williams & Wilkins, Philadelphia
23. Rumbolt Z, Camacho DLA, Lake D, Welsh CT, Castillo M (2006) Apparent diffusion coefficients for differentiation of cerebellar tumors in children. *Am J Neuroradiol* 27:1362–1369
24. Panigrahy A, Krieger MD, Gonzalez-Gomez I, Liu X, McComb JG, Finlay JL, Nelson MD Jr, Gilles FH, Blüml S (2006) Quantitative short echo time 1H-MR spectroscopy of untreated pediatric brain tumors: preoperative diagnosis and characterization. *AJNR Am J Neuroradiol* 27(3):560–572
25. Koci TM, Chiang F, Mehringer CM et al (1993) Adult cerebellar medulloblastoma: imaging features with emphasis on MR findings. *AJNR Am J Neuroradiol* 14:929–939
26. Koeller KK, Henry JM (2001) Superficial gliomas: radiologic-pathologic correlation. *RadioGraphics* 21:1533–1556
27. Chen KS, Hung PC, Wang HS, Jung SM, Ng SH (2002) Medulloblastoma or cerebellar dysplastic gangliocytoma (Lhermitte-Duclos disease)? *Pediatr Neurol* 27:404–406
28. Cidis-Meltzer C, Smirniotopoulos JG, Jones RV (1995) The “striated cerebellum”: an MR imaging sign in Lhermitte-Duclos disease (dysplastic gangliocytoma). *Radiology* 194:699–703
29. David KF, Casey ATH, Hayward RD, Harkness WFJ, Phipps K, Wade AM (1997) Medulloblastoma: is the 5-year survival rate improving?—a review of 80 cases from a single institution. *J Neurosurg* 86:13–21
30. George RE, Laurent JP, McCluggage CW, Cheek WR (1985) Spinal metastasis in primitive neuroectodermal tumors (medulloblastoma) of the posterior fossa: evaluation with CT myelography and correlation with patient age and tumor differentiation. *Pediatr Neurosci* 12:157–160
31. Stanley P, Senac MO Jr, Segall HD (1985) Intraspinal seeding from intracranial tumors in children. *AJR Am J Roentgenol* 144:157–161
32. Madhugiri VS, Pandey P, Indira Devi B, Santosh V, Yasha TC (2012) Intramedullary metastasis in a case of vermian medulloblastoma. *Br J Neurosurg* 26(2):278–280
33. Algra PR, Postma T, Van Groeningen CJ, Van Der Valk P, Bloem JL, Valk J (1992) MR imaging of skeletal metastases from medulloblastoma. *Skelet Radiol* 21:425–430
34. Roberts RO, Lynch CF, Jones MP, Hart MN (1991) Medulloblastoma: a population-based study of 532 cases. *J Neuropathol Exp Neurol* 50:134–144
35. Eberhart CG, Cohen KJ, Tihan T, Goldthwaite PT, Burger PC (2003) Medulloblastoma with systemic metastases: evaluation of tumor histopathology and clinical behavior in 23 patients. *J Pediatr Hematol Oncol* 25:198–203
36. Rochkind S, Blatt I, Sadeh M, Goldhammer Y (1991) Extracranial metastases of medulloblastoma in adults: literature review. *J Neurol Neurosurg Psychiatry* 54:70–86
37. Packer RJ, Spoto R, Atkins TE et al (1987) Quality of life in children with primitive neuroectodermal tumors (medulloblastoma) of the posterior fossa. *Pediatr Neurosci* 13:169–175

38. Johnson DL, McCabe MA, Nicholson HS et al (1994) Quality of long-term survival in young children with medulloblastoma. *J Neurosurg* 80:1004–1010
39. Silverman CL, Palkes H, Talent B, Kovnar E, Clouse JW, Thomas PRM (1984) Late effects of radiotherapy on patients with cerebellar medulloblastoma. *Cancer* 54:825–829
40. Walter AW, Mulhern RK, Gajjar A et al (1999) Survival and neurodevelopmental outcome of young children with medulloblastoma at St Jude Children's Research Hospital. *J Clin Oncol* 17:3720–3728
41. Poretti A, Meoded A, Huisman TA (2012) Neuroimaging of pediatric posterior fossa tumors including review of the literature. *J Magn Reson Imaging* 35(1):32–47

Pietro Spennato, Claudio Ruggiero,
and Giuseppe Cinalli

Prognosis of medulloblastoma has improved over the last two decades, for several reasons, such as early diagnosis, aggressive chemotherapeutic protocols, and craniospinal irradiation. However, surgery still retains a key role in the management of these tumors, so much that extent of surgical resection is one of the main factors affecting the prognosis and contributing in categorizing patients in standard risk or in high risk. Residual tumor after resection greater than 1.5 mm³ may lead to a worse prognosis [1].

The goals of medulloblastoma surgery are to treat associated hydrocephalus, obtain tissue sample for diagnosis and molecular investigations, decompress the brain stem, remove as much tumor as possible (with the aim of complete or near complete removal). Medulloblastoma is not always completely resectable: in cases with extensive and deep

infiltration of the fourth ventricle floor, it is preferable to leave residual tumor, rather than cause neurological deficit.

16.1 Surgical Considerations

Approximately 85 % of medulloblastomas are located in the cerebellar midline, typically arising from the inferior medullary velum. Microsurgical anatomy of this region has been reviewed in detail by Mussi and Rhoton [2]. Anatomy and neurosurgical relevance of the inferior medullary velum have been recently reviewed by Tubbs et al. [3]. The inferior medullary velum, together with the tela choroidea, forms the inferior half of the roof of the fourth ventricle (Fig. 16.1). The inferior medullary velum is a thin semitranslucent butterfly shaped sheet of neural tissue connecting the inferior vermis (uvula and nodule) with the two cerebellar hemispheres at the level of the flocculi (Fig. 16.2). Laterally it blends into the dorsal margin of the lateral recesses. Caudally it is attached to the tela choroidea, which forms the lower portion of the inferior half of the roof of the fourth ventricle. The junction between the inferior medullary velum and the tela choroidea (telovelar junction) is at the level of the lateral recess. The tela choroidea (two thin arachnoid like membranes sandwiching a vascular layer of choroidal vessels to which choroid plexus is attached) opens in three points in the subarachnoid spaces: bilaterally at the level of the lateral

P. Spennato, M.D. • C. Ruggiero, M.D.
Division of Pediatric Neurosurgery,
Department of Neuroscience,
Santobono-Pausilipon Children's Hospital,
Naples, Italy

G. Cinalli, M.D. (✉)
Division of Pediatric Neurosurgery,
Department of Neuroscience,
Santobono-Pausilipon Children's Hospital,
Naples, Italy

Department of Neurosurgery,
University of L'Aquila, L'Aquila, Italy
e-mail: giuseppe.cinalli@gmail.com

recesses forming the two foramina of Luschka and in the midline forming the foramen of Magendie. The external surface of the caudal half of the roof lies in the deep of the cerebellomedullary fissure. This is a complex cleft that extends

between the cerebellum and the medulla and communicates around the tonsils (paired ovoid structures attached to the cerebellar hemispheres along their superolateral borders) with the cisterna magna. Thereafter, usually medulloblastomas expand in the fourth ventricle (sometimes appearing to be entirely intraventricular) and/or in the cisterna magna, splitting the tonsils and elevating the vermis. Unusually the tumor may extend out of the foramen of Luschka: in fact this is more typical for ependymomas.

The remaining 15 % present as a lateral mass, located in the cerebellar hemisphere or in the cerebellopontine angle. They may also involve the cerebellar surface, resembling meningiomas (Fig. 16.3). Non-midline tumors present predominantly in older children and adults [4].

Any patients presenting with a cerebellar tumor are candidate to surgery. If the patient is stable, surgery can be scheduled for the next available operating time. Usually surgery can wait for appropriate imaging studies, particularly brain and spinal MRI. Sagittal MRI can help delineate relationship of the tumor to the

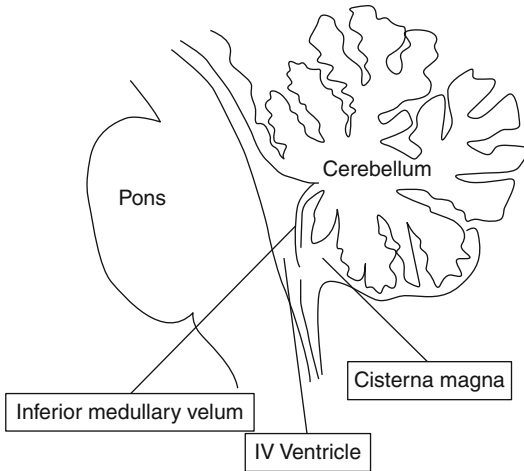


Fig. 16.1 Schematic drawing of the inferior medullary velum and its relationship with the fourth ventricle and cisterna magna

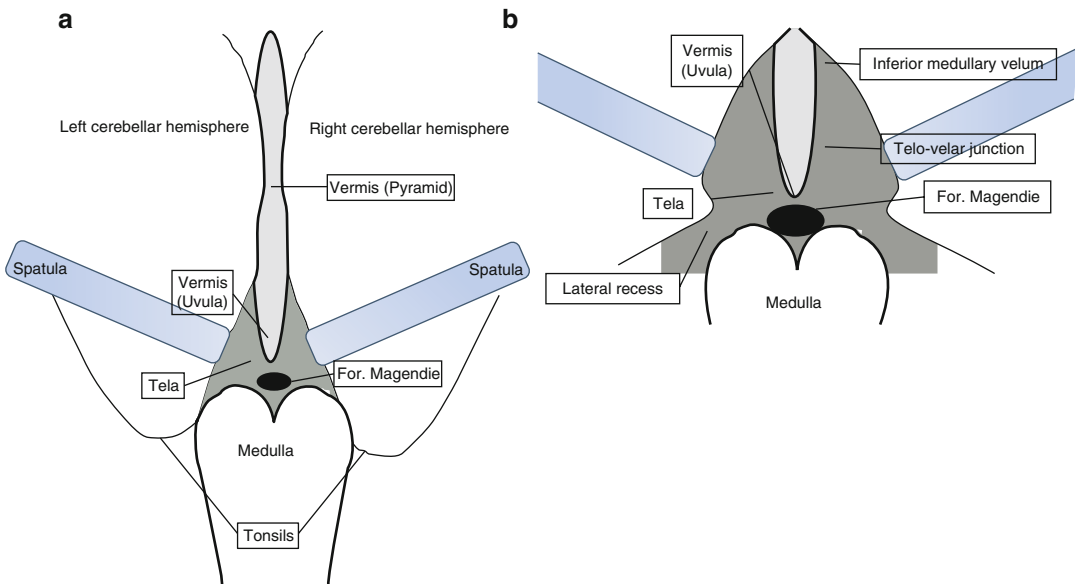


Fig. 16.2 Schematic drawing of the tela choroidea (a) and inferior medullary velum (b), following spatulation of the cerebellar tonsils

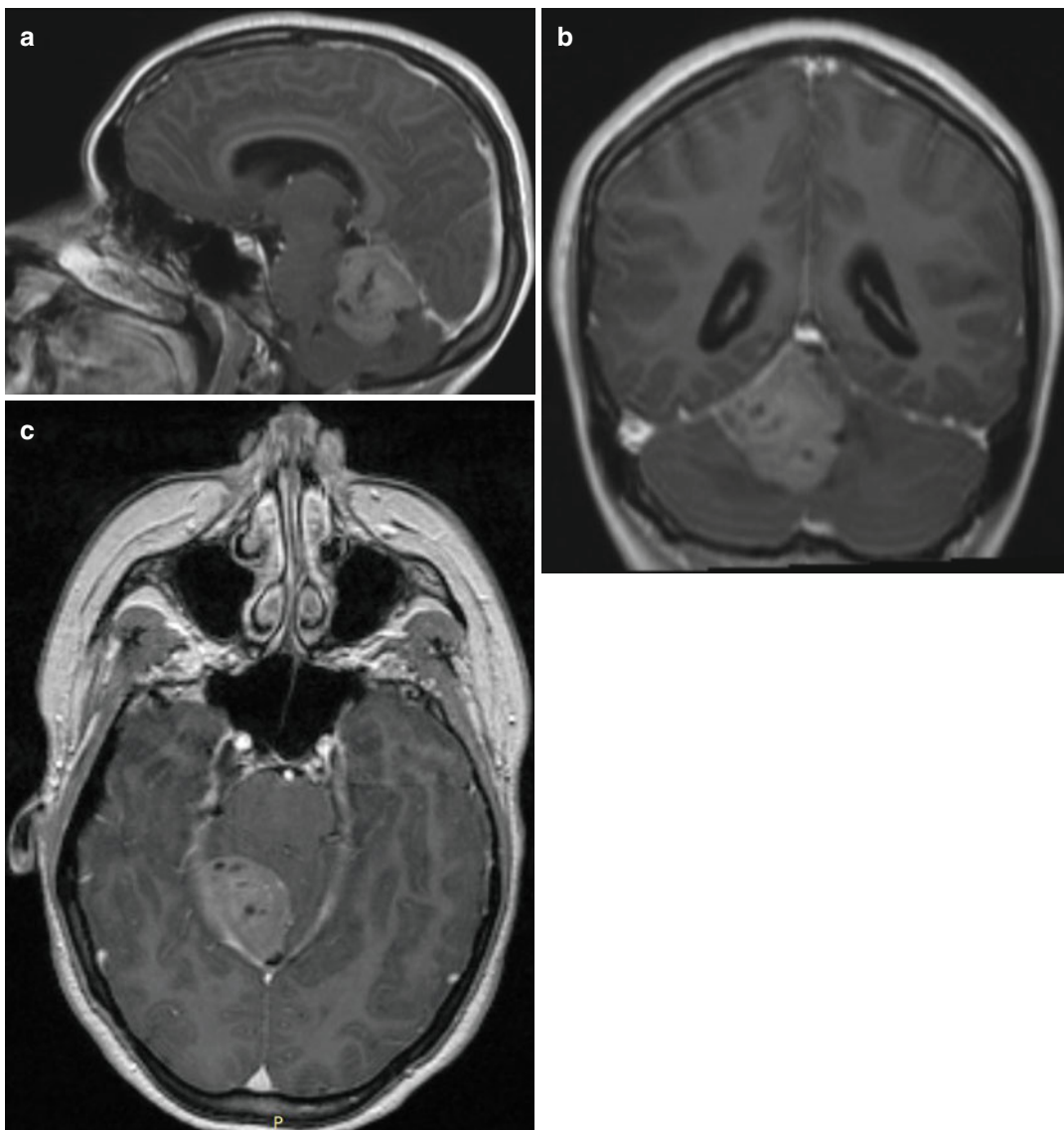


Fig. 16.3 Sagittal (a), coronal (b), and axial (c) T1 contrast-enhanced MRI showing a medulloblastoma of the tentorial notch

vermis, midbrain tectum, vein of Galen, and cervicomedullary junction and distinguish between true intraventricular tumor such as medulloblastomas that dislocate postero-superiorly the superior medullary velum and the quadrigeminal plate and widen the aqueduct [5] from vermian tumors such as astrocytomas, in which the quadrigeminal plate is dislocated anterior-inferiorly

(Fig. 16.4). Because of high frequency of craniospinal metastasis, even at presentation, all the neuraxis should be mandatorily scanned before surgery.

However, if the patient develops acute hydrocephalus and mental status or vital sign changes, it may be necessary to treat hydrocephalus on urgent basis [6].

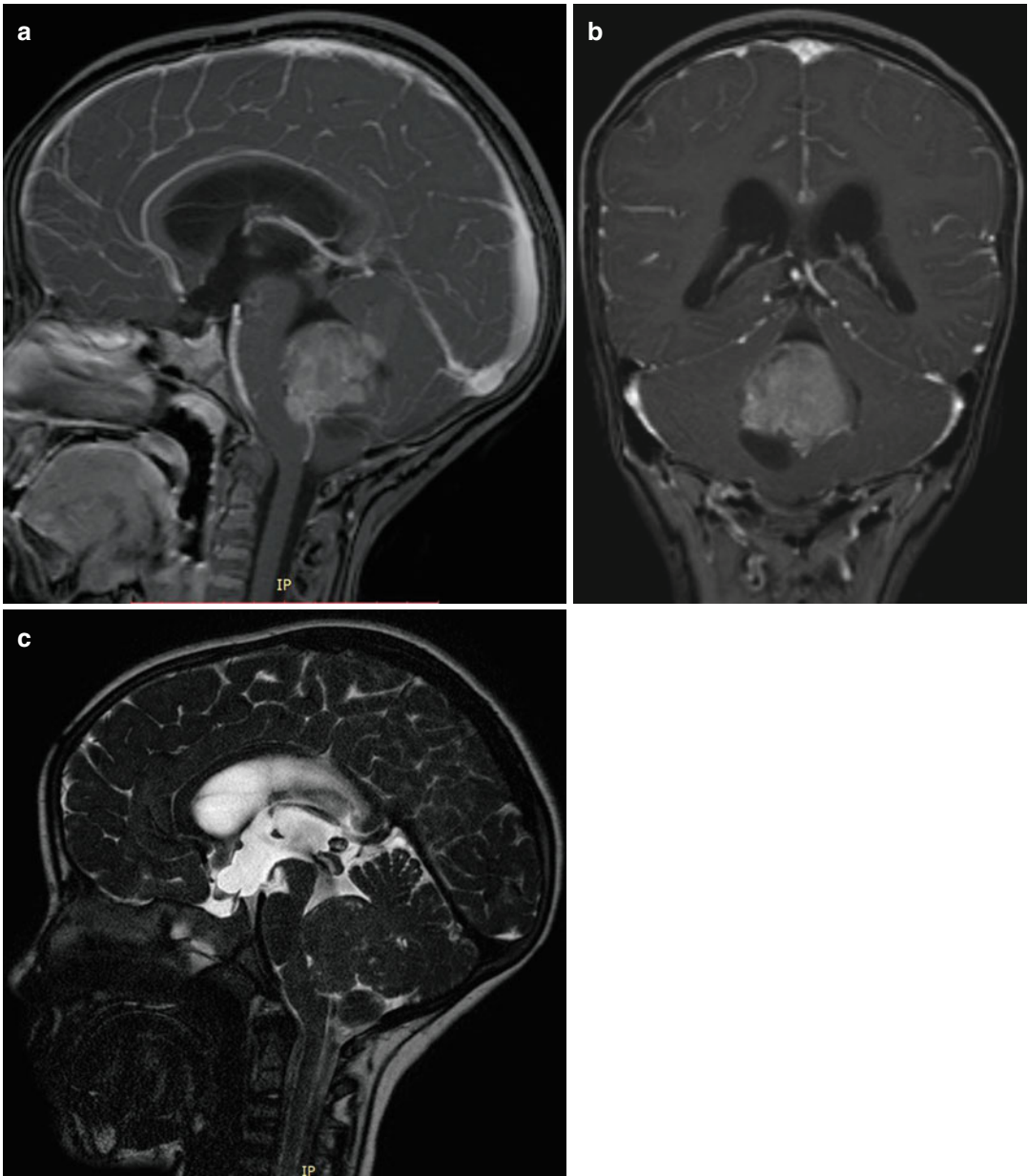


Fig. 16.4 MR images of typical medulloblastoma arising from the inferior medullary velum, filling the fourth ventricle. Sagittal and coronal contrast-enhanced T1 WI images (a, b); Midsagittal DRIVE sequence (c)

16.2 Management of Hydrocephalus

Hydrocephalus is a common presenting feature of medulloblastoma (about 80 % of cases), because of obstruction of egress foramina of the fourth

ventricle. In about one third of patients, hydrocephalus persists following tumor removal [7].

Management of hydrocephalus in posterior fossa tumors is controversial. The choice between the available options (steroids and early surgery; external ventricular drainage (EVD); placement

of ventriculoperitoneal (VP) shunt; endoscopic third ventriculostomy (ETV)) is usually left to the surgeon's preference.

ETV has been often utilized in the management of hydrocephalus associated with posterior fossa tumors, since the publication of the study of Sainte-Rose et al. in 2001 [8]. These authors observed definitive treatment of hydrocephalus, improvement of the patient's general condition, and improvement of postoperative course in most of their patients (94 %). Subsequent studies failed to confirm these very good results, questioning, above all, the possibility of ETV to provide long-term control of hydrocephalus [9–11]. Moreover due to the low incidence of persistent hydrocephalus following early tumor removal in some more recent series [9,10], many authors believe that the routine use of preoperative ETV is not entirely justified.

Medulloblastomas usually fall in the high-risk category for development of postoperative hydrocephalus: malignant histology, midline location, more severe ventricular enlargement at diagnosis, and younger age [12,13]. Patients with severe symptoms at presentation are also particularly at risk of a worse postoperative course [10].

In our centre, patients with midline tumors with severe hydrocephalus are considered candidate for preoperative ETV, rather than urgent posterior fossa surgery or external ventricular drainage. Tumor surgery is scheduled in the first available surgical session, following conclusion of the diagnostic workup and improvement of signs and symptoms of increased intracranial hypertension.

ETV eliminates the risks of CSF infection related to EVD and, providing more physiological CSF drainage than the other procedures, minimizes the risk of overdrainage. Placement of an EVD in these patients, in fact, must be exercised with caution because there is potential for upward herniation from posterior fossa mass effect.

El-Ghandour [14] reported the first study specifically addressed to midline posterior fossa tumors (medulloblastomas and ependymomas) in pediatric patients with advanced hydrocephalus. He compared pre-resectional ETV versus ventriculoperitoneal (VP) shunt. He concluded that the lower incidence of morbidity, the absence of

mortality, the lower incidence of procedure failure of ETV as compared to VP shunt, and the significant advantage of not becoming shunt dependent makes endoscopic third ventriculostomy to be recommended as the first choice in the treatment of pediatric patients with marked obstructive hydrocephalus due to midline posterior fossa tumors.

In our experience, in very young babies (under 6 months of age) harboring tumors with radiological features of medulloblastoma, the results of ETV were disappointing. In fact almost all children required ventriculoperitoneal (VP) shunt in the postoperative period in spite of complete tumor resection. Our current policy in case of very young children (under 6 months of age) with acute hydrocephalus and midline posterior fossa tumor with radiological features of malignancy is to offer VP shunt urgently. In metastatic medulloblastoma at presentation, the patient should be referred to chemotherapy and radiotherapy as soon as possible. In this situation, endoscopic approach may be very useful to treat hydrocephalus, if associated, and to biopsy intraventricular lesion. The patient can be referred to oncologists before posterior fossa surgery [15] (Fig. 16.5).

In rare cases during endoscopic surgery, unrecognized metastases can be detected, especially at the level of the infundibulum (Fig. 16.6). Biopsy-confirmed metastases may change the staging of the tumor, switching from standard risk to high risk.

In the management of postoperative hydrocephalus, ETV should be considered a valid alternative to shunt as a first option. In fact, there is agreement in the neurosurgical community in considering postoperative hydrocephalus obstructive in nature and to offer ETV to such patients [8–10].

Tamburrini et al. [16] have proposed a different strategy for management of hydrocephalus in posterior fossa tumors: perioperative external ventricular drainage positioned at time of tumor removal; postoperative ICP monitoring through the external ventricular drainage, ETV in case of persistent ventricular dilation and abnormally high ICP values, and VP shunt implantation in case of ETV failure.

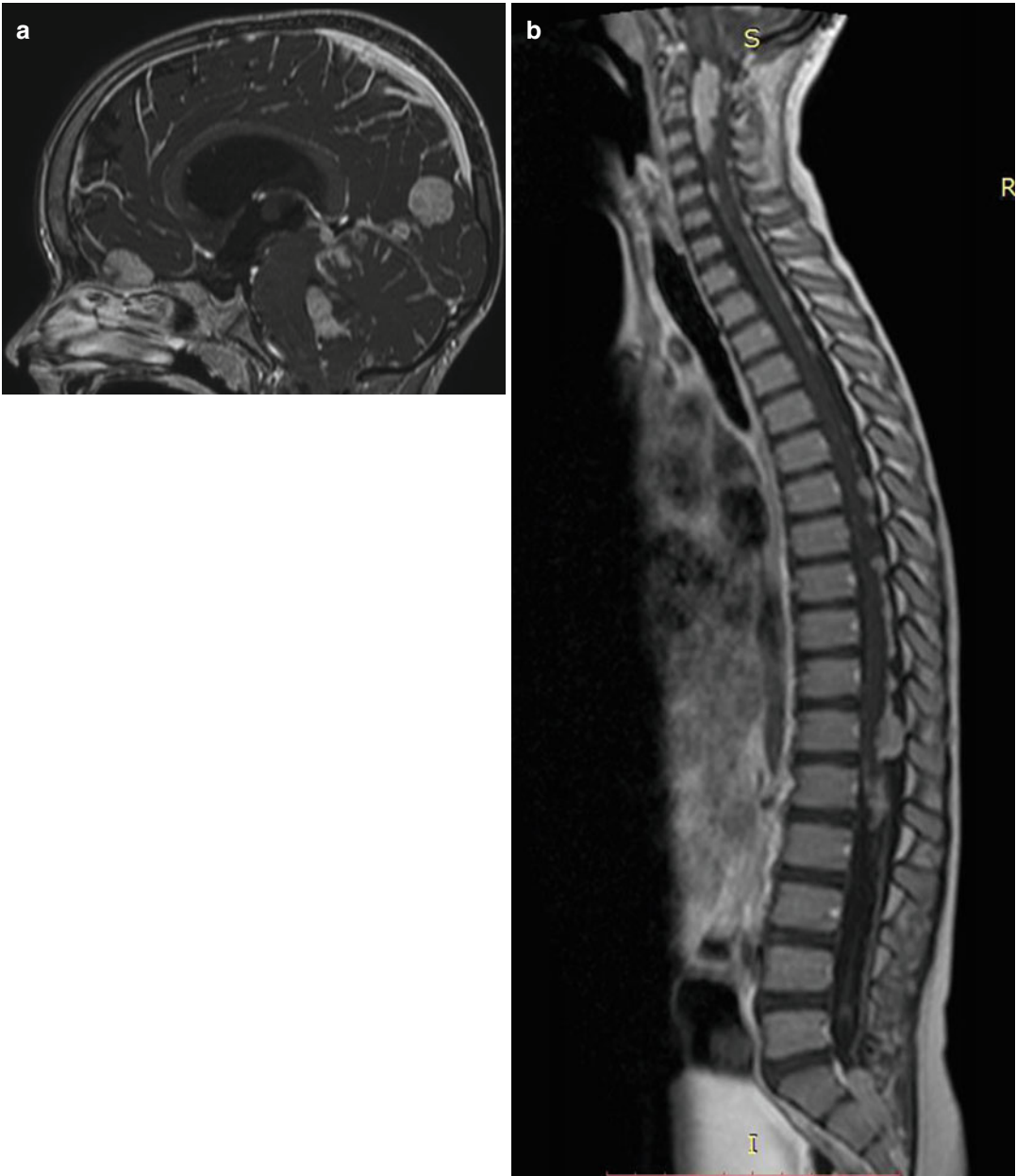


Fig. 16.5 Brain (a) and spinal (b) MRI of metastatic medulloblastoma at presentation. The patient presented with acute hydrocephalus and was managed with insertion of ventriculoperitoneal shunt and endoscopic inspection of the ventricles, through a standard right precoronal burr

hole. A small ependymal lesion was found at the level of the floor of the third ventricle that was biopsied. Histological diagnosis was medulloblastoma. The patient was referred to oncologists for chemotherapy and radiotherapy

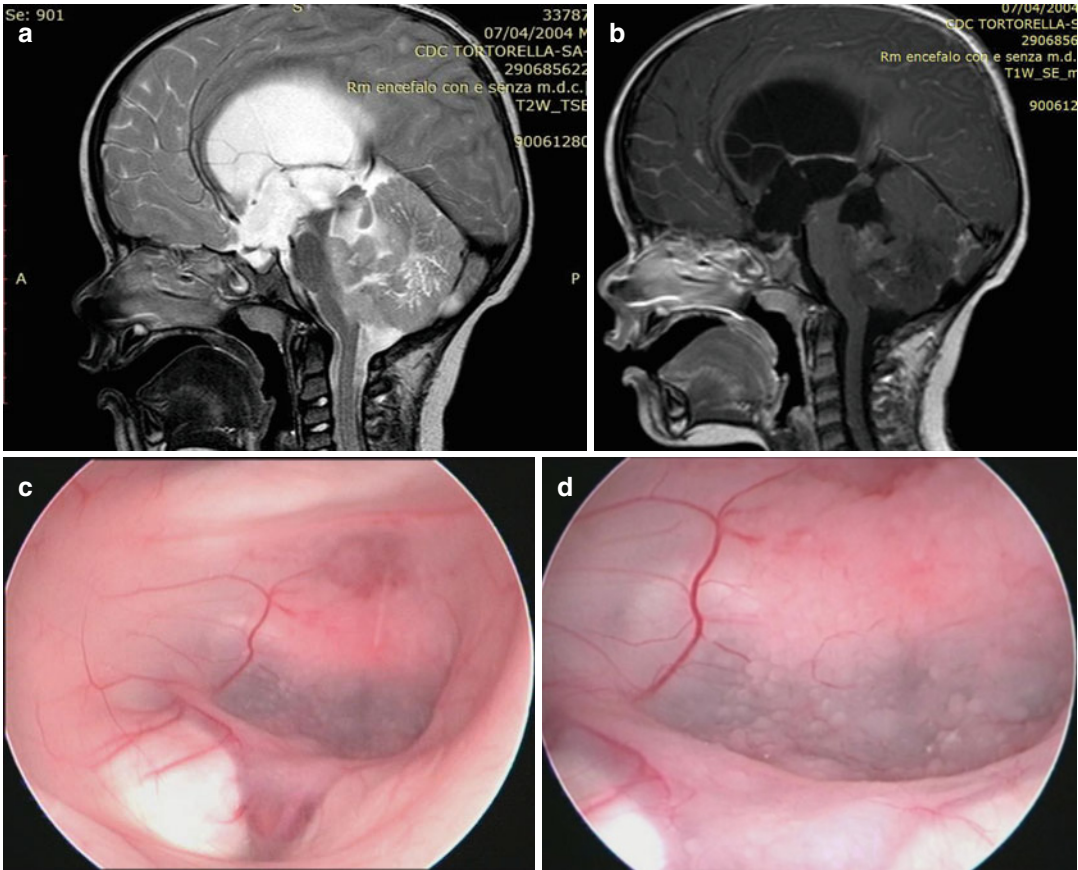


Fig. 16.6 Contrast-enhanced T1 WI MR images (a) and T2 MR images (b) of patient with a medulloblastoma, with no evidence of intraventricular metastases. (c, d):

endoscopic view of the third ventricular floor covered by several small nodules. Histology confirmed the presence of malignant cells

16.3 Anesthetic Considerations

Care must be taken to avoid respiratory depression in all phases of the diagnostic and therapeutic workup, especially during sedation to obtain imaging and at the induction of anesthesia: even mild respiratory depression can cause dangerous increase in intracranial hypertension. Before surgery, administration of corticosteroids for 24–48 h may help to control peritumoral edema. Electrolyte imbalance, secondary to vomiting, should be carefully corrected. Medulloblastomas are usually richly vascularized tumors; thereafter adequate venous

access (two to three peripheral venous catheters and a central venous line) is required. An arterial line for blood pressure monitoring is also mandatory.

The bladder is catheterized, and pulse oximetry, end-expiratory carbon dioxide, electrocardiography, blood pressure, body temperature are monitored.

For tumors that involve the brain stem, the use of motor, somatosensory, brain stem auditory evoked response, electromyographic monitoring of the lateral rectus and facial muscles, and direct electromyographic stimulation of relevant cranial nerves may be beneficial [17].

In our department, at the end of the procedure, it is customary to transfer the patient in ICU and keep him under controlled ventilation and sedoanalgesia until the next morning. We adopt this policy to avoid sudden modifications in arterial or venous pressure due to crying/coughing in the immediate postoperative hours and to allow a safer and easier postoperative MRI evaluation the following day. Mandatory prerequisite for this postoperative management is to achieve, by any means the surgeon prefers (ETV, EVD, VP shunt), preoperative control of hydrocephalus for tumors involving the fourth ventricle and the CSF pathways. In fact, the real major risk in posterior fossa surgery in children is acute postoperative hydrocephalus due to cerebellar swelling that typically occurs within the first 18–24 h after tumor removal. Postoperative swelling is less frequent in hemispheric lesions not involving the fourth ventricle. These lesions are usually approached through corticotomy and do not require vermian incision or significant cerebellar retraction. Postoperative swelling instead is very frequent in case that vermian incision, even partial, is required for approach or in cases with extensive parenchymal infiltration on the midline vermis that usually require more significant parenchymal retraction/manipulation even following telovelar approach. If swelling occurs, rapid obstruction to CSF pathways at the level of the outlets of the fourth ventricle may result, with consequent acute hydrocephalus with intracranial hypertension. If not resolved immediately with CSF drainage, this situation will result in downward and upward cerebellar herniation that may be rapidly fatal.

16.4 Operative Technique

16.4.1 Positioning

Despite some advantages of the sitting position, above all improved blood and CSF drainage from the operative field, in our institution, the prone position is preferred for all midline posterior fossa approaches. In fact there is a decreased risk

(if not nil) of air embolism and the absence of postoperative pneumocephalus that is instead a constant significant finding following posterior fossa surgery in the sitting position. Moreover the surgeon works more comfortably, and there is less risk of tearing bridging veins between the cerebellum and tentorium than in the seated position [18]. In rare cases in which an EVD is required (as discussed above, we prefer to perform ETV in case of urgent treatment of hydrocephalus), we prefer to place it frontally prior to positioning rather than occipitally when positioning is completed.

In older children the head can be fixed in a rigid pin-type head holder, such as Mayfield® or Doro® systems. In Doro® system, up to four pins can be used to widely distribute the total force. In very young babies, the pins can be replaced by silicone pillows. A horizontal pillow placed on the horizontal arm of the Mayfield® or Doro® frame offers additional support to the forehead, increasing the safety of the system. In alternative, a well-padded horseshoe headrest can be used. In this case, great care must be paid to avoid compression of the ocular globes due to the horseshoe arms. If an intraoperative image system, such as intraoperative CT scan, is used, the positioning and fixation of the head need to be adapted with dedicated material. For the last 3 years, we have routinely used intraoperative CT scan: we prefer to fix the head in a CT compatible horseshoe headrest (Fig. 16.7).

Flexion of the neck with reverse Trendelenburg positioning of the torso is very important because it allows for visualization of the rostral part of the posterior fossa, i.e., tentorium, pineal region, and cerebral aqueduct. Venous drainage is improved; as like dissection of the occipitocervical musculature [6]. However, care should be taken to avoid over flexion: it may be dangerous in case of tonsillar herniation through the foramen magnum, and may prevent adequate venous drainage through neck veins.

The iliac crests are supported with bolster; the abdomen is left free to avoid venous engorgement; the shoulders should be supported with adequate padded pillows to slightly project

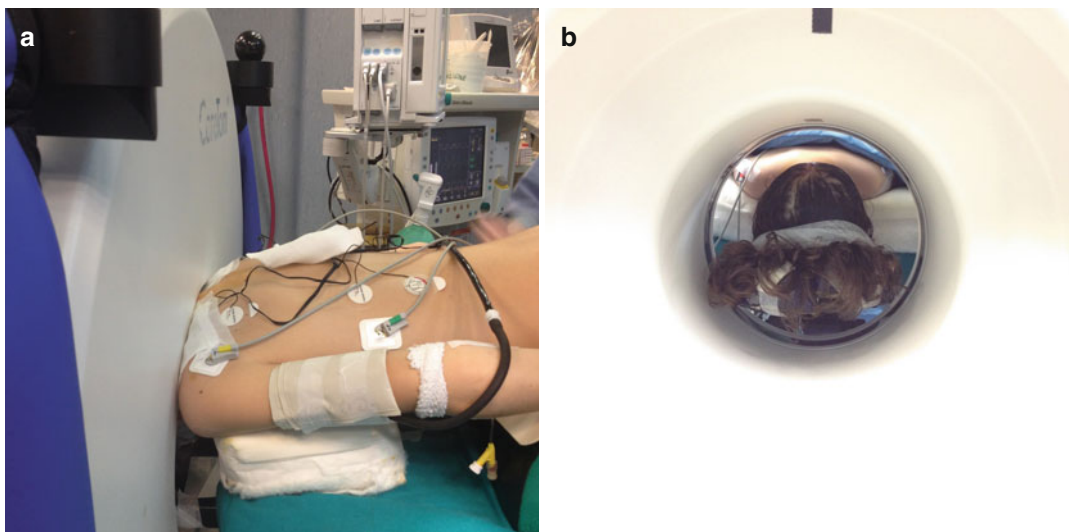


Fig. 16.7 Prone position with the head fixed in a CT compatible horseshoe headrest for intraoperative CT scanning. (a: lateral view, b: frontal view, through the scanner)

beyond the operating table, so that flexion of the neck will not place the endotracheal tube close to the table. In obese children silk tape should be used to pull the shoulders caudally and place the occipitocervical musculature under tension. All pressure points should be padded.

16.4.2 Surgical Approach

For most medulloblastomas, a standard midline posterior fossa approach, described in more details in another chapter of the present book, can be used.

A midline incision from theinion to C5 is traced. The dissection is taken through the avascular midline. Unless imaging studies suggest tumor extending caudally beyond C1, one should avoid taking the paraspinous muscles off the laminae of C2: this contributes to postoperative pain and may increase the risk of postoperative cervical instability.

At our institution, a craniotomy, rather than craniectomy, is used for all posterior fossa approaches. Two paramedian burr holes are drilled just below the lateral sinuses, on either side of the midline. Following the first burr

hole, if the lateral sinus is not visualized, further bone is removed cranially until visualization of the sinus, in order to exactly locate it and the torcula. The position of the second burr hole is modified accordingly. Another two more caudal and more lateral burr holes, on the cerebellar hemispheres, are drilled, in order to help dissecting the foramen magnum before craniotomy. The craniotome can then be used to turn as large a craniotomy as possible, joining the four burr holes and the foramen magnum. Usually it is necessary to further increase the bone exposure, with the help of rongeurs, especially at the level of the foramen magnum. If imaging studies reveal tumor below the level of the obex or tonsils caudally displaced, the posterior arch of C1 should also be removed, with the help of rongeurs.

Dura mater is opened in a Y shape, with the base along the lateral sinuses and midline durotomy extended caudally. Bleedings from the dura and occipital sinus should be controlled with dural clip or circumferential sutures with the technique. Every effort should be done to avoid mono or bipolar cautery on the dura. The dural flap should be retracted upward with sutures to expose as much cerebellum

as possible. The retracted dura should be left retracted upward and laterally under tension provided by retracting sutures, protected with a wet patty between the dura and the bone and a second wet patty above the dura. If a “Y” incision is done, two additional retracting sutures should be placed in the two points joining the cervical dura incision with the cerebellar dura incision, retracting the dura laterally towards the paraspinal muscles and keeping the dura under tension. Two additional long wet patties should be placed vertically under the cervical dura and under the retracting sutures, allowing to keep the cervical dura wet and avoiding blood to enter the surgical field from the extradural space at the level of the occipital foramen. Frequent moistening of these patties should be ensured by the scrub nurse. Absolute, perfect hemostasis of the extradural space and a perfectly clean operative field should be obtained before starting microsurgical dissection.

16.4.3 Microsurgical Dissection

If the medulloblastoma (like in the vast majority) is located into the fourth ventricle, microsurgical dissection begins with opening of the cistern magna (Fig. 16.8). This may help in relaxing the brain, releasing CSF. Many surgeons sample the CSF from cistern magna to determine if there are malignant cells on cytology (Fig. 16.9) [19]. Usually the tumor grows underneath the vermis, progressively filling the fourth ventricle and underneath between the cerebellar tonsils: initial exposure may be facilitated by splitting the tonsils if the tumor has not already done so (Fig. 16.10). The initial goal of dissection is to find and protect the floor of the fourth ventricle. If the tumor is not adherent at the level of the obex, microsurgical dissection of the arachnoid about the vermian peg will allow for elevation of the inferior pole of the tumor and visualization of the distal floor (Fig. 16.11).

The two most common surgical routes to expose medulloblastoma in the fourth ventricle are the transversian and telovelar approaches.

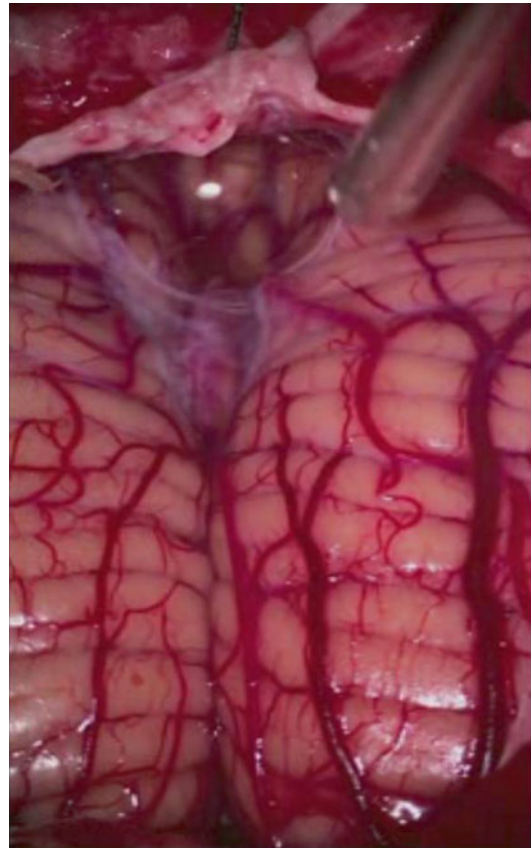


Fig. 16.8 Microsurgical dissection of the cisterna magna

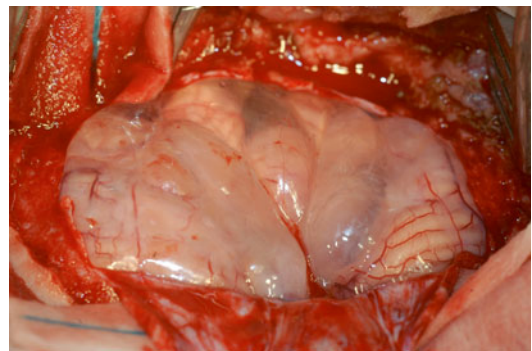


Fig. 16.9 Cisterna magna filled by several small tumoral nodules (same case of Fig. 16.6)

The first involves dividing the inferior vermis of the cerebellum and retracting the two halves of the vermis in opposite lateral directions (Fig. 16.12).

In the second approach, the tela choroidea and inferior medullary velum are opened, and the lower vermis is retracted superiorly [20].

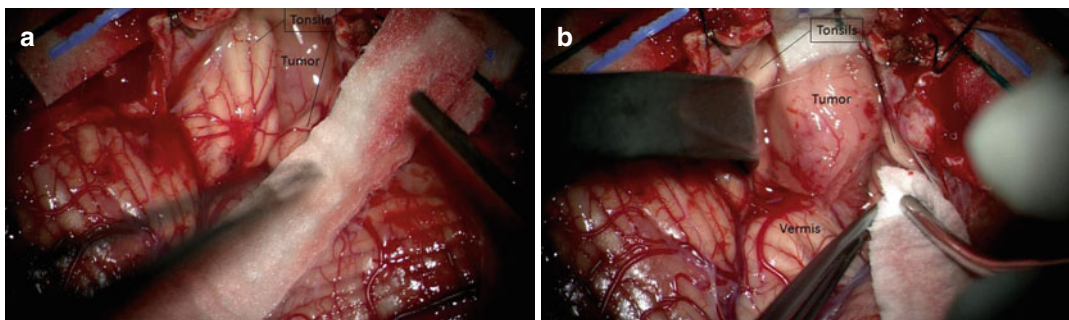


Fig. 16.10 The tumor is visible in the cisterna magna. The tonsils are gently divided following incision at the arachnoid (a). Further dissection of the tumor from

the cerebellar tonsils and inferior vermian allows better exposure of the tumor (b)

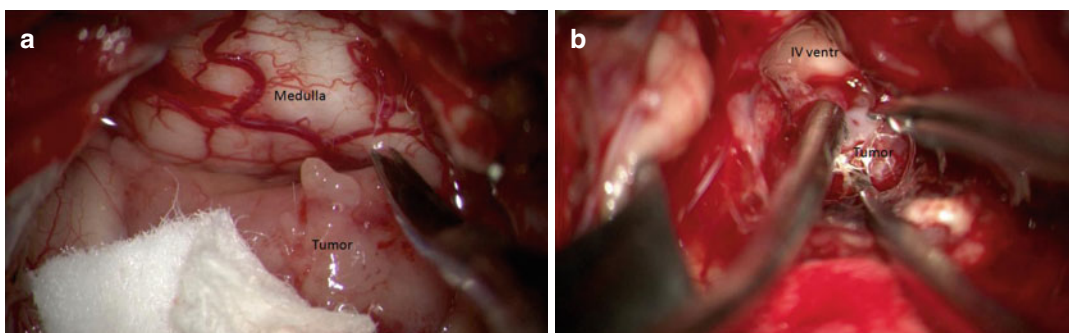


Fig. 16.11 The inferior pole of the tumor is dissected from the medulla at the level of the obex (a). Following dissection the inferior pole of the tumor is removed to expose the distal floor of the fourth ventricle (b)

Sometimes the two techniques can be fused: the initial dissection of the cerebellomedullary fissure allows exposition and removal of the lower pole of the tumor, identification of the fourth ventricle floor, and of possible tumor infiltration; if at this stage the surgeon realizes that the upper-posterior part of the lesion cannot be reached through this approach, then a 1 cm incision of the lower vermian (smaller than in traditional transvermian approach) can be used to complete the removal.

16.4.4 Telovelar Approach

The initial dissection for telovelar approach involves opening of the cisterna magna and lifting of the tonsils off the brain stem. These maneuvers will expose the intertonsillar space so that the tonsillomedullary part of the cerebellomedullary cleft is exposed. Following this, the foramen of Magendie is exposed and is enlarged by

cutting the tenia along the inferior cerebellar peduncles till the lateral recess (Fig. 16.13). Dissection is extended between the medial side of the tonsils and the adjacent edges of the uvula (uvulotonsillar cleft). Special attention is directed to the location and bifurcation of the PICA into medial and lateral trunks. Care should be taken to protect it. Complete dissection of this cleft will expose the inferior medullary velum, the incision of which will expose the superior and superolateral part of the fourth ventricle.

In more detail, according with Tanriover et al. [20], the telovelar incision can be divided in three parts. The first part of the incision, which opens the tela choroidea, begins inferiorly near the foramen of Magendie in the lower portion of the ventricle roof and extends upward to the level of the junction of the tela with the inferior medullary velum. In most cases, this is sufficient to expose the full length of the floor of the fourth ventricle. Less dissection of these structures is required in

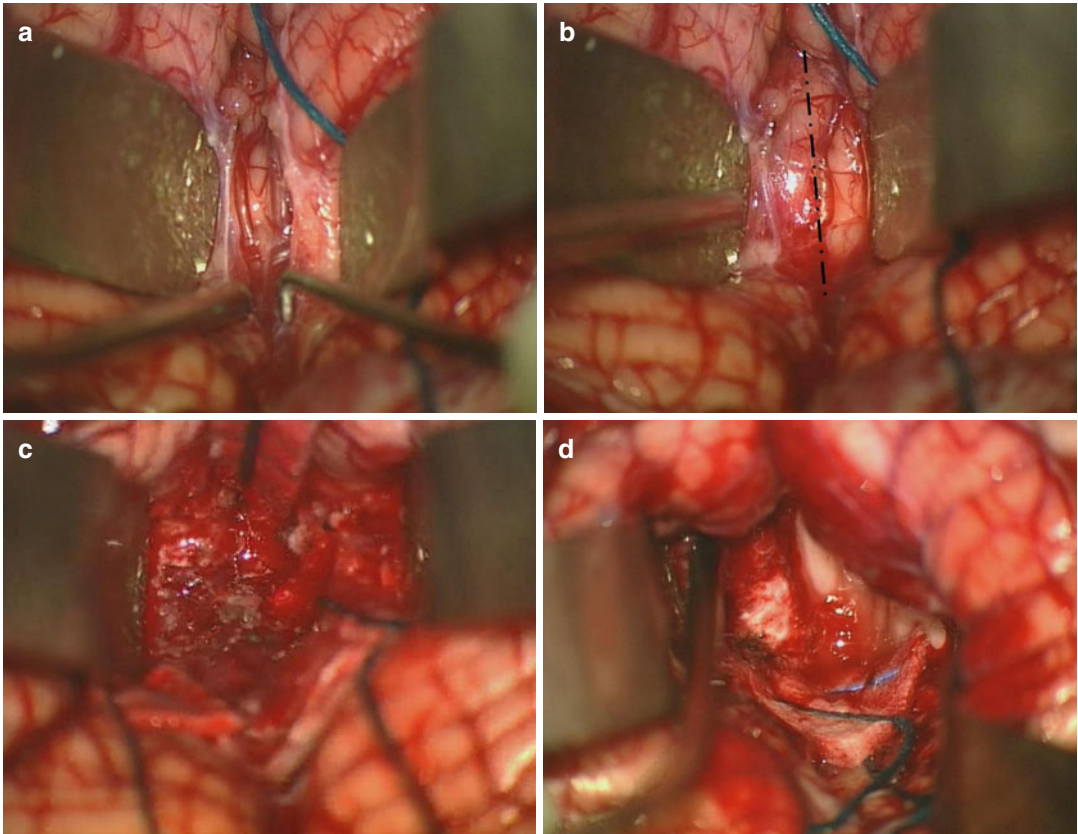


Fig. 16.12 Transvermian approach: arachnoid between the two cerebellar hemispheres is incised. (a) the two hemispheres are dissected away from the midline, and the inferior vermis

is exposed (b: dotted line: line of incision) The tumor is found few millimeters below the incision of the vermis and is debulked (c) Finally the fourth ventricle floor is exposed (d)



Fig. 16.13 The foramen of Magendie is exposed and enlarged

cases of large tumors, due to the distension at the foramen of Magendie produced by the tumor. The second part involves extending the incision superiorly through the inferior medullary velum, which is exposed in the depths of the uvulotonsillar space. The vein of the cerebellomedullary fissure, which crosses the inferior medullary velum, can be transected in some cases.

Incising the inferior medullary velum on one uvulotonsillar space exposes the ipsilateral superolateral recess and provides access to the entire floor of the fourth ventricle. Shifting the exposure to the opposite uvulotonsillar space and opening the tela and velum provide an identical exposure on the other side [20]. The third incision can be directed between the tonsil and medulla oblongata through the tela forming the lower posterior wall of the lateral recess: it provides additional access to the full length of the lateral recess and the foramen of Luschka.

16.4.5 Transvermian Approach

The transversmian approach is the oldest and most widely used. It consists of splitting the inferior vermis on the suboccipital surface, with variable extension depending on the location and size of the tumor. Most authors advocate limiting the vermian incision to the smallest possible length necessary to gain access to avoid complications. The midline incision of the inferior vermis is extended to the tela choroidea and inferior medullary velum: the full length of the floor (mean length 4 cm) from the aqueduct to obex can be exposed through this approach [20]. Adequate lateral exposure including the lateral recesses and both foramen of Luschka can be obtained, but it is of outmost importance combining the cerebellar retraction that should imperatively be as delicate and limited as possible, with the use of the full range of lateral bending of the operative microscope. This allows to put the whole volume of the fourth ventricle cavity in a line of sight adequate for less invasive surgery. Further help both for the upper part and for the lateral recesses of the fourth ventricle can be offered by the intraoperative use of the endoscope. Allowing excellent magnification and lightning with angled optics, endoscopes allow to see and remove under endoscopic control the most peripheral part of the tumor that would be difficult to see through traditional approaches described above. Nevertheless it should be stressed the use of endoscope for endoscope-controlled microsurgery requires additional and specific training.

As discussed in the study of Tanriover et al. [20], who confronted the two approaches on anatomical specimens, both the transversmian and telovelar approaches provide excellent exposure of the entire fourth ventricle. The telovelar approach provides additional access to the lateral recesses and foramen of Luschka. The transversmian approach provides a slightly better exposure of the midline superior half of the roof of the fourth ventricle and fastigium. However the article by Deshmukh et al. [21] emphasizes that this unique advantage of the transversmian approach is nullified by C1 laminotomy when added to the telovelar approach.

The transversmian approach requires an incision into the cortical and functional areas of the cerebellum. The splitting of the inferior cerebellar vermis may cause caudal vermis syndrome, resulting in an equilibratory disturbance with truncal ataxia, gait disturbance, oscillation of the head and trunk, and nystagmus. Also dentate nucleus, being located along the posterolateral margin of the roof of the fourth ventricle, is at risk. Lesions of the caudate nucleus may be responsible of more severe equilibratory disturbances often accompanied by intentional tremor during voluntary movement of the extremities [22]. Splitting the inferior portion of the vermis may also play a role in cerebellar mutism [23].

The telovelar approach is the preferred approach for all fourth ventricular tumors: medulloblastoma, protruding through the foramen of Magendie and stretching the tela choroidea and inferior medullary velum over its surface, is usually the ideal candidate for this approach [24].

Recently has been underlined that using the telovelar approach in very large and giant tumors may be hazardous [25]. In fact, in these cases, the anatomy is severely distorted and dissection in the uvulotonsillar cleft before decompression can result in breaching the pial plane and entering either vermis or tonsil leading to neurological deficit. Moreover, placing the retractor on the superomedial part of the tonsil can injure the dentate nucleus; inadvertent damage to veins and arteries can occur leading to ischemic injury to the vermis and deep cerebellar nuclei [25].

Such problems can be overcome by doing dissection and decompression simultaneously (Fig. 16.14). Initial decompression followed by dissection of the planes of the telovelar approach will help in minimizing retraction and reducing retraction-induced injuries [25].

The tumor is then dissected from surrounding cerebellar and brainstem structures using microsurgical techniques. Usually circumferential dissection of medulloblastomas is precluded by their size; thereafter debulking should proceed simultaneously with dissection also at this stage. Medulloblastomas have usually soft consistency; thereafter debulking may be done with either suction or ultrasonic aspirator. Small arterial feeders from the vermis, usually distal branches of the

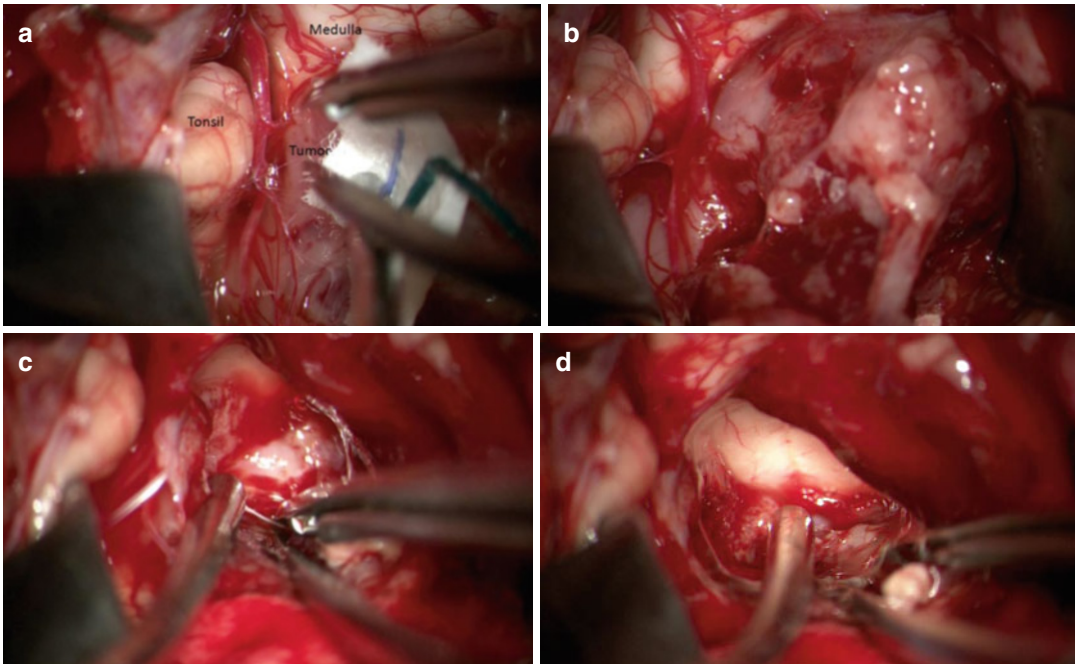


Fig. 16.14 The tumor is dissected laterally from the tonsil to expose the telovelar junction (a). The dissection is alternated with debulking (b, c), until the floor is exposed (d)

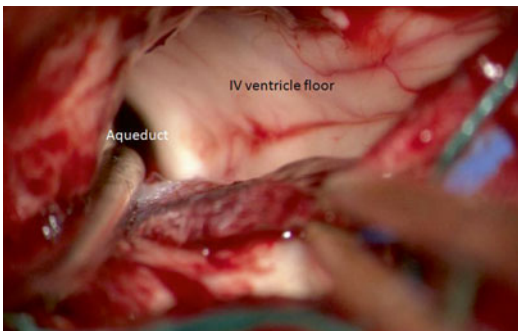


Fig. 16.15 Following debulking and dissection, the entire floor and the aqueduct are exposed

posterior inferior cerebellar artery, are cauterized. Resection of the central, more friable areas of the tumor, usually lead to a drier operative field. The surgeon should allow the tumor to deliver itself into the aspirator. Portions of the tumor not adherent to the floor of the fourth ventricle will deliver themselves, exposing the white floor, and rostrally the aqueduct (Fig. 16.15). A small cotton patty should be placed over the aqueduct to prevent blood from entering the ventricular system.

No forceful dissection should be attempted for medulloblastomas invading the floor of the fourth ventricle or the aqueduct. Once exposed the entire floor, dissection should proceed laterally to define a plane between the tumor and cerebellar hemispheres. Distinction between tumor and cerebellar white matter is usually clarified with high magnification. Great attention should be done to remove the tumor from the lateral recesses. The microscope should be rotated 90° on both sides to better visualize the recesses (Fig. 16.16).

Before closing, the walls of the resection cavity are checked carefully for residual pathological tissue. Some authors recommend to inspect the roof of the ventricle with a 30-degree rigid endoscope.

Adequate hemostasis is verified with a Valsalva maneuver and the surgical bed copiously irrigated with warm saline to remove debris and blood products. Attempts should be made to obtain hemostasis avoiding leaving behind hemostatic agents, such as oxycellulose, that may migrate and obstruct CSF pathways and will cause artifact on postoperative imaging.

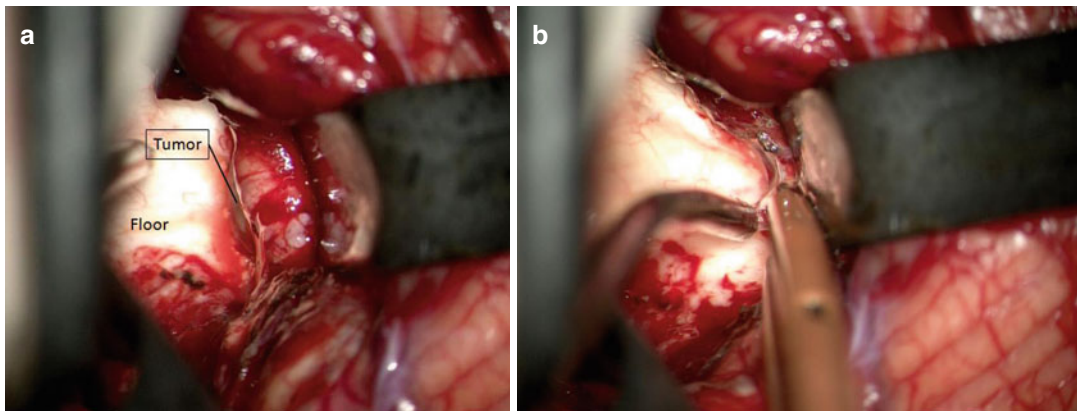


Fig. 16.16 Further exposure of the lateral recess revealed residual tumor (a), that was removed (b)

16.4.6 Non-midline Tumors

In case of large medulloblastomas, we prefer to perform a midline suboccipital approach, with bilateral dura opening, even if the tumor is entirely in a single hemisphere. Obviously bone and dura openings are more extended towards the side of tumor. Bilateral exposure and dural opening in fact dramatically reduces the risk of cerebellar swelling during opening. If the tumor is not visualized on the cortical surface, it can be located and the direction of dissection planned with intraoperative ultrasound. Hemispheric tumors are approached in the most direct manner through the thinnest portion of the cerebellar cortex via a horizontal incision.

Medulloblastomas may also present as cerebellopontine angle tumors. They may arise from the remnants of the external granular layer in the cerebellar hemisphere at the level of the flocculus or from proliferating residue of the lateral medullary velum where it projects into the cerebellopontine angle. These tumors can be operated via a standard suboccipital retromastoid approach [26]. Usually the approach should be extended to expose the transverse and sigmoid sinuses on the affected side. At advance stages, lateral dissection may reach cranial nerves. Because of the severe potential deficits and efficacy of chemotherapeutic protocols, dissemination among the cranial nerves should be removed with extreme caution, even leaving residual tumors.

In the largest series of cerebellopontine angle medulloblastomas [27], including 14 patients (nine adults and five children), seven patients underwent total excision of the tumor, while the remaining seven had a subtotal tumor resection.

Other localizations of medulloblastoma are exceptional. We observed a case of superior peduncle medulloblastoma in a 2-year-old baby girl. The tumor was removed through a supratentorial, subtemporal approach (Fig. 16.17).

16.4.7 Residual Tumor

Considering the efficacy of the adjuvant treatment, microsurgically complete resection should only be intended in case of tolerable risk. However, in case of significant residual tumor, particularly in nonmetastatic disease, second-look surgery should be discussed either directly after the primary operation or in the course of further treatment [28].

16.4.8 Surgery at Relapse

Treatment of relapsing medulloblastoma depends on several factors [29]. The role of surgery is usually limited and should be considered on a case-by-case basis. In older children who have already received craniospinal radiation as part of their initial therapy, surgery may be an option for solitary recurrences. However, prognosis following

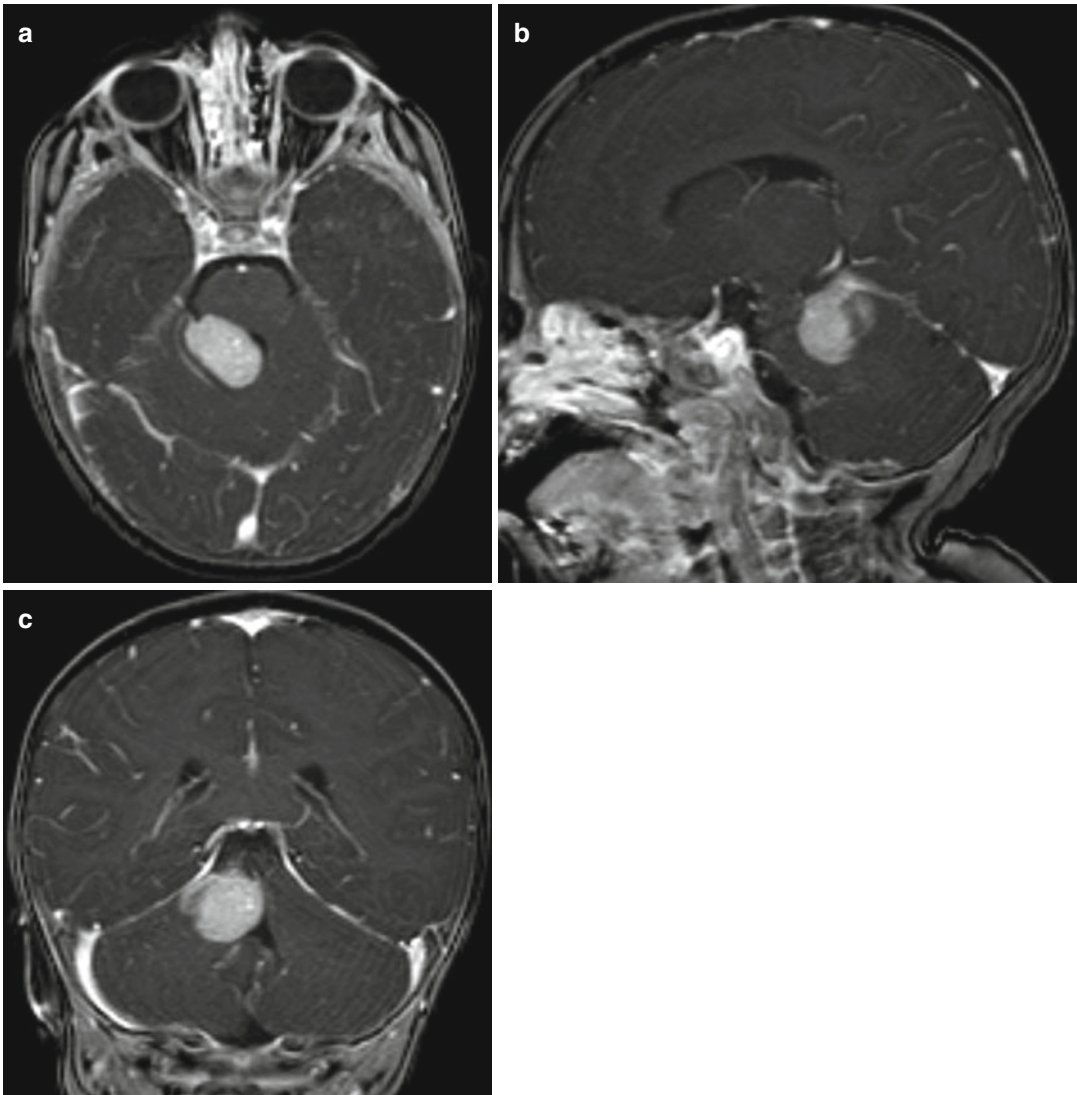


Fig. 16.17 Axial (a), sagittal (b), and coronal (c) T1 contrast-enhanced MRI of medulloblastoma originating in the right superior cerebellar peduncle

relapsing is poor with less than 5 % long-term survivors. Some patients with non-disseminated relapse may be salvaged with a multimodal therapy including surgery and focal re-irradiation [28].

16.5 Results

A near-total resection (greater than 90 % resection) consists of leaving less than 1.5 cc of tumor tissue on postoperative magnetic resonance

imaging (MRI). A gross total resection (minimal tumor visible on MRI), however, has the same overall prognosis as a near-total resection. A partial resection (less than 90 % resection or more than 1.5 cc of residual on MRI) is associated with a poor prognosis and should be avoided. This was clearly demonstrated by the Children's Cancer Group (CCG) on 203 patients [30].

If there is a large residual tumor on postoperative MRI, and surgeon did not stop due to excessive vascularity, or involvement of critical

anatomic structures, early repeat resection is advisable. Intraoperative MRI appears very useful for this issue. In alternative, postoperative MRI should be obtained immediately following closure or within the first 24 h.

Surgical mortality is low (less than 3 %) and morbidity is acceptable (5–10 %). Near total resection is attainable in more than 85 % of patients [31].

16.6 Complications

Intraoperative hemorrhage is a rare complication of medulloblastoma surgery [32]. It presents as massive cerebellar swelling, usually occurring following dural opening. It is probably related with ligation of the occipital sinus that in some cases may function as a drain from the tumor. Ligation of the occipital sinus may disturb the venous drainage and elevate the venous pressure. The specific vascular architecture of some tumors (presence of thin-walled vessels) may predispose to hemorrhage. Massive hemorrhages in the posterior cranial fossa can be fatal. To avoid this catastrophic complication, preoperative MRI venography should be obtained in order to detect venous hypertension and posterior fossa dura should be preferably opened without interruption of the sinus drainage. Intraoperative management is based on enlarging as much as possible suboccipital craniotomy and dural opening, followed by quick debulking of the tumor and hematoma.

Postoperative complications include hydrocephalus (discussed above), hematoma, aseptic meningitis, gastrointestinal hemorrhage, cervical instability, and neurological deficits secondary to damage of the cerebellum, brain stem and cranial nerves, such as truncal ataxia and hypotonia (lesions of the anterior lobe of the cerebellum); appendicular ataxia, hypotonia, and tremor (lesions of the posterior lobe); and hemiparesis and lower cranial nerve dysfunction (brainstem injury).

Cerebellum is also involved in higher cognitive processes: damage to the dentate nuclei, the vermis, and the right cerebellar hemisphere

result in significant reductions of intelligence quotient (IQ), with adverse neuropsychological outcomes.

The most characteristic complication following posterior fossa surgery in children is cerebellar mutism. This term refers to muteness that follows lesions of the cerebellum. Its unique features are delayed onset (1–6 days) and limited duration (1 day–4 months). Its incidence after posterior fossa surgery in children is 11–29 %. Recovery is spontaneous but not always complete, with a discrete number of patients presenting long-term speech and language dysfunction such as ataxic dysarthria, dysfluency, and slowed speech rate [33]. Several risk factors for the development of cerebellar mutism are identified, and the most significant are brainstem involvement by the tumor and midline location (vermis and fourth ventricle). These factors render medulloblastoma the most likely posterior fossa tumor to cause cerebellar mutism following surgery [33].

The anatomical substrate of cerebellar mutism is not completely understood. As recently underlined in an extensive review [33], bilateral interruption of the dentato–thalamo–cortical pathway (DTC) is considered the principal cause of cerebellar mutism. This complex system, together with monoaminergic areas in the mesencephalon (the periaqueductal gray matter and the substantia nigra), is implicated in genesis of “cerebellar” mutism that can result from injuries anywhere along the path. In a recent study, Soelva and co-workers, using diffusion-weighted MRI tractography, observed lower fronto-cerebellar association fibers tract volumes and diminished fiber signal intensities at the level of the superior cerebellar peduncles and in midline cerebellar structures in patients with postoperative cerebellar mutism. These data suggested an involvement of fronto-cerebellar association fibers in children with posterior fossa syndrome [34].

The nature of the injury is unknown; probably pathogenesis is related to dynamic perfusional disturbances, edema, transient disturbances in neurotransmitter release, and/or axonal injury.

The delayed onset of cerebellar mutism is so typical that if mutism is present immediately

after surgery, bulbar dysfunction caused by damage of cranial nerve nuclei in the brainstem should be suspected.

Cerebellar mutism may be part of a more complex syndrome, including other neurological problems such as ataxia, hypotonia, cranial nerve palsies, hemiparesis, and emotional lability (posterior fossa syndrome).

A recent study investigated incidence, risks, and sequelae of posterior fossa syndrome (PFS) in pediatric medulloblastoma [35]. PFS developed in 29 % of the patients of the study. Only 22 % of patients had complete recovery; the most common residual sequelae were dysarthric speech and ataxia. Brainstem invasion, midline tumor location, younger age, and the absence of radiographic residual tumor were found to be predictors of PFS. The authors concluded that incidence of PFS is increasing and parallels the current impetus to perform more aggressive surgery. They recommend to carefully evaluate the benefit-to-risk ratio of complete tumor removal in each case.

References

- Norris DG, Bruce DA, Byrd RL, Schut L, Littman P, Bilaniuk LT, Zimmerman RA, Capp R (1981) Improved relapse-free survival in medulloblastoma utilizing modern techniques. *Neurosurgery* 9:661–664
- Mussi AC, Rhoton AL Jr (2000) Telovelar approach to the fourth ventricle: microsurgical anatomy. *J Neurosurg* 92:812–823
- Tubbs RS, Bosmia AN, Loukas M, Hattab EM, Cohen-Gadol AA (2013) The inferior medullary velum: anatomical study and neurosurgical relevance. *J Neurosurg* 118:315–318
- Maleci A, Cervoni L, Delfini R (1992) Medulloblastoma in children and in adults: a comparative study. *Acta Neurochir (Wien)* 119:62–67
- Trasimeni G, Lenzi J, Di Biasi C, Anichini G, Salvati M, Raco A (2008) Midline medulloblastoma versus astrocytoma: the position of the superior medullary velum as a sign for diagnosis. *Childs Nerv Syst* 24:1037–1041
- Hoffmann HJ, Myseros JS (2000) Medulloblastoma. In: Kaye AH, Black PMcL (eds) *Operative neurosurgery*. Harcourt Publishers Limited, London, pp 417–427
- Lee M, Wisoff JH, Abbott R, Freed D, Epstein FJ (1994) Management of hydrocephalus in children with medulloblastoma: prognostic factors for shunting. *Pediatr Neurosurg* 20:240–247
- Sainte-Rose C, Cinalli G, Roux FE, Maixner R, Chumas PD, Mansour M, Carpentier A, Bourgeois M, Zerah M, Pierre-Kahn A, Renier D (2001) Management of hydrocephalus in pediatric patients with posterior fossa tumors: the role of endoscopic third ventriculostomy. *J Neurosurg* 95:791–797
- Fritsch MJ, Doerner L, Kienke S, Mehdorn HM (2005) Hydrocephalus in children with posterior fossa tumors: role of endoscopic third ventriculostomy. *J Neurosurg* 103(1 Suppl):40–42
- Morelli D, Pirotte B, Lubansu A, Detemmerman D, Aeby A, Fricx C, Berre J, David P, Brotchi J (2005) Persistent hydrocephalus after early surgical management of posterior fossa tumors in children: is routine preoperative endoscopic third ventriculostomy justified? *J Neurosurg* 103(3 Suppl):247–252
- Ruggiero C, Cinalli G, Spennato P, Aliberti F, Cianciulli E, Trischitta V, Maggi G (2004) Endoscopic third ventriculostomy in the treatment of hydrocephalus in posterior fossa tumors in children. *Childs Nerv Syst* 20:828–833
- Culley DJ, Berger MS, Shaw D et al (1994) An analysis of factors determining the need for ventriculoperitoneal shunts after posterior fossa tumor surgery in children. *Clinical study. Neurosurgery* 34:402–408
- Gopalakrishnan CV, Dhakoji A, Menon G, Nair S (2012) Factors predicting the need for cerebrospinal fluid diversion following posterior fossa tumorsurgery in children. *Pediatr Neurosurg* 48:93–101
- El-Ghandour NM (2011) Endoscopic third ventriculostomy versus ventriculoperitoneal shunt in the treatment of obstructive hydrocephalus due to posterior fossa tumors in children. *Childs Nerv Syst* 27:117–126
- Grill J, Lellouch-Tubiana A, Elouahdani S, Pierre-Kahn A, Zerah M, Renier D, Valteau-Couanet D, Hartmann O, Kalifa C, Sainte-Rose CJ (2005) Preoperative chemotherapy in children with high-risk medulloblastomas: a feasibility study. *Neurosurgery* 103(4 Suppl):312–318
- Tamburrini G, Pettorini BL, Massimi L, Caldarelli M, Di Rocco C (2008) Endoscopic third ventriculostomy: the best option in the treatment of persistent hydrocephalus after posterior cranial fossa tumor removal? *Childs Nerv Syst* 24:1405–1412
- Murazko KM, Braham B, Orringer D (2008) Medulloblastomas. In: Albright AL, Pollack IF, Adelson PD (eds) *Principles and practice of pediatric neurosurgery*, 2nd edn. Thieme, New York, pp 606–620
- Rajpa S, Iskandar BJ (2007) Surgical approaches to pediatric midline posterior fossa tumors. In: Badie B (ed) *Neurosurgical operative atlas. Neuro-oncology*, 2nd edn. Thieme, New York, pp 214–221
- Souweidane MM, Morgenstern PF, Christos PJ, Edgar MA, Khakoo Y, Rutka JT, Dunkel IJ (2009) Intraoperative arachnoid and cerebrospinal fluid sampling in children with posterior fossa brain tumors. *Neurosurgery* 65:72–78
- Tanriover N, Ulm AJ, Rhoton AL Jr, Yasuda A (2004) Comparison of the transvermian and telovelar approaches to the fourth ventricle. *J Neurosurg* 101:484–498

21. Deshmukh VR, Figueiredo EG, Deshmukh P, Crawford NR, Preul MC, Spetzler RF (2006) Quantification and comparison of telovelar and transvermian approaches to the fourth ventricle. *Neurosurgery* 58(ONS suppl 2):ONS 202–ONS 207
22. Ziyal IM, Sekhar LN, Salas E (1999) Subtonsillar-transcerebellomedullary approach to lesions involving the fourth ventricle, the cerebellomedullary fissure and the lateral brainstem. *Br J Neurosurg* 13:276–284
23. Dailey AT, McKhann GM II, Berger MS (1995) The pathophysiology of oral pharyngeal apraxia and mutism following posterior fossa tumor resection in children. *J Neurosurg* 83:467–475
24. Zaheer SN, Wood M (2010) experiences with the telovelar approach to fourth ventricular tumors in children. *Pediatr Neurosurg* 46:340–343
25. Rajesh BJ, Rao BRM, Menon G, Abraham M, Easwer HV, Nair S (2007) Telovelar approach: technical issues for large fourth ventricle tumors. *Childs Nerv Syst* 23:555–558
26. Spina A, Boari N, Gagliardi F, Franzin A, Terreni MR, Mortini P (2013) Review of cerebellopontine angle medulloblastoma. *Br J Neurosurg* 27:316–320
27. Jaiswal AK, Mahapatra AK, Sharma MC (2004) Cerebellopontine angle medulloblastoma. *J Clin Neurosci* 11:42–45
28. Gerber NU, Mynarek M, von Hoff K, Friedrich C, Resch A, Rutkowski S (2014) Recent developments and current concepts in medulloblastoma. *Cancer Treat Rev* 40:356–365
29. Massimino M, Giangaspero F, Garrè ML, Gandola L, Poggi G, Biassoni V, Gatta G, Rutkowski S (2011) Childhood medulloblastoma. *Crit Rev Oncol Hematol* 79:65–83
30. Albright AL, Wisoff JH, Zeltzer PM et al (1996) Effects of medulloblastoma resections on outcome in children: a report from the Children's cancer group. *Neurosurgery* 38:265–271
31. Taylor MD (2006) Medulloblastoma. In: Tonn J-C, Westphal M, Rutka JT, Grossman SA (eds) *Neuro-oncology of CNS tumors*. Springer, Berlin, pp 461–469
32. Fukai J, Uematsu Y, Shintani A, Nakai K, Itakura T (2002) Intraoperative hemorrhage in medulloblastoma: a case report and review of the literature. *Childs Nerv Syst* 18:356–360
33. Gudrunardottir T, Sehested A, Juhler M, Schmiegelow K (2011) Cerebellar mutism. Review of the literature. *Childs Nerv Syst* 27:355–363
34. Soelva V, Hernáiz Driever P, Abbushi A, Rueckriegel S, Bruhn H, Eisner W, Thomale UW (2013) Frontocerebellar fiber tractography in pediatric patients following posterior fossa tumor surgery. *Childs Nerv Syst* 29:597–607
35. Korah MP, Esiashvili N, Mazewski CM, Hudgins RJ, Tighiouart M, Janss AJ, Schwaibold FP, Crocker IR, Curran WJ Jr, Marcus RB Jr (2010) Incidence, risks, and sequelae of posterior fossa syndrome in pediatric medulloblastoma. *Int J Radiat Oncol Biol Phys* 1(77):106–112

Giuliana Di Martino, Elia Guadagno,
and Maria Laura Del Basso De Caro

17.1 Introduction

Medulloblastoma generally affects patients in the first two decades of life, accounting for about a fifth of all intracranial neoplasms of childhood [1]. According to the 2007 WHO classification [2] of tumors of the central nervous system, it belongs to primitive embryonal grade IV tumors (Table 17.1).

It mostly appears undifferentiated, but differentiation along different cell lineages (neuronal, glial, mesenchymal, melanotic) can sometimes be observed. This tumor shows wide heterogeneity from the histological and molecular point of view, reflecting distinct biological behavior and prognosis.

Its relationship with primitive neuroectodermal tumors (PNET) has changed over time. Since 1983, in fact, with the classification proposed by Rorke [3], they were considered a unique entity, being all pediatric cerebral high-grade undifferentiated neuroepithelial tumors and sharing an alleged common ontogenic origin. Despite many similarities, for the first time

in 2000, the WHO [4] issued a classification where medulloblastoma was distinguished from other embryonal tumors, and more recently, a molecular distinction of these tumors from PNETs has been demonstrated on the basis of microarray techniques [5].

Also the histological framework has changed with the last classification: two variants (medulloblastoma and melanotic medulloblastoma) have been excluded as distinct entities and one (medulloblastoma with extensive nodularity) has been added; moreover, anaplastic medulloblastoma and the large-cell variant have been separated into two different categories.

The actual classification, therefore, includes five variants: classic, desmoplastic/nodular, with extensive nodularity, anaplastic, and large cell.

Table 17.1 Embryonal tumors (From: the 2007 WHO classification of tumors of the central nervous system)

Embryonal Tumors
Medulloblastoma
Classic
Desmoplastic/nodular medulloblastoma
Medulloblastoma with extensive nodularity
Anaplastic medulloblastoma
Large-cell medulloblastoma
CNS primitive neuroectodermal tumors (PNET)
CNS neuroblastoma
CNS ganglioneuroblastoma
Medulloepithelioma
Ependymoblastoma
Atypical teratoid/rhabdoid tumor

G. Di Martino, M.D. (✉)
Department of Neurosciences,
Service of Pediatric Neurosurgery,
Santobono-Pausilipon Children's Hospital, Naples, Italy
e-mail: gdimart@hotmail.it

E. Guadagno, M.D. • M.L. Del Basso De Caro, M.D.
Department of Advanced Biomedical Sciences,
University Federico II Naples,
Via Pansini 5, 80131 Naples, Italy

Although currently risk and therapy stratification of patients is essentially based on clinical criteria (age, metastatic spread, and extent of surgical resection) [6], there is already an established consensus on histology and molecular genetic to play a relevant role for prognosis and rationalization of treatment protocols [7–10]. For example, desmoplastic variant is generally considered less malignant than classic one [7, 11], and medulloblastomas with extensive nodularity and anaplastic variant are poles apart, having the best and worst prognosis respectively. In the first case, thus, a lightening of adjuvant therapies may be justified to reduce long-term side effects without changing the outcome. However, between these two extreme entities, histology alone is inadequate for correct diagnostic and prognostic assessment, and at the same time, several transcriptional profiling studies have suggested the existence of multiple distinct molecular subgroups (*wingless/WNT*, *sonic hedge-hog/SHH*, groups 3 and group 4) that differ in their demographic distribution, genetic features, and clinical outcomes; their corresponding histological phenotypes can be variable [12]. Only in some cases a closer correspondence between histology and molecular subgroup can be found. Classic medulloblastoma, for example, is variably related to all four subgroups, and it also poses problems of differential diagnosis with teratoid/rhabdoid tumor on the bases of morphology alone [12]. For this reason, immunohistochemistry and sequencing technologies, although more expensive, should always be performed.

17.2 Origins and Historical Findings

The first description of this tumor, with the name of spongioblastoma multiforme, is to be referred to Globus and Strauss at the beginning of the last century [13]. The current nomenclature “medulloblastoma” was coined in 1925 by Bailey and Cushing [14, 15] for its similarity with embryonal medullary velum. They speculated that the progenitor cell was the “medulloblast” [16], a supposed multipotent cell, distinct from spongioblast and neuroblast but able to differentiate along both lineages. To date, the precursor cell remains

unknown and a matter of debate among neuropathologists. Microarray studies, however, demonstrated the existence of a strong link between medulloblastoma and normal cerebellum embryogenesis [17, 18]. In particular, mutations affecting the different cells and signal pathways (mainly SHH and WNT) that generate the different cellular layer of the cerebellum may produce different medulloblastoma variants. In fact, the tumor expresses immunohistochemical markers belonging either to the primary germinal zone (i.e., subventricular zone of the cerebellar anlage: calbindin-D28K, parvalbumin, nestin, vimentin, and GFAP) or to the secondary germinal zone (i.e., the granule neuron precursor cells that invade rostrally across the cerebellum anlage to produce the external germinal layer: p75^{NTR}, TrkC, Zic1, and Math1) [21]. These two immunohistochemical profiles are mutually exclusive [19–22]: the former is usually associated with the classic variant and the latter with the desmoplastic variant.

17.3 Macroscopic Aspects

The tumor generally appears as a soft, fleshy, and pink or gray mass but firm and well circumscribed in the desmoplastic variant; sometimes necrosis is observed, especially in the large-cell variant. Cysts can be found in 2–20 % of cases [23] and multiple microcysts are more often observable compared to single large cyst. Calcifications are detected in 10–20 % of cases [24] and a spontaneous tumor hemorrhage is found only in 3–5 % of medulloblastomas [23].

In most cases, the lesion is localized on the midline of the cerebellum, generally originating from the inferior medullary velum or from the roof of the fourth ventricle.

Lateral cerebellar location is observed more often in older children, in adults [25], and in the desmoplastic variant, while brainstem and cerebellopontine angle locations are exceptional [26].

In case of aggressive growth (Fig. 17.1), the mass can reach the surface of the cerebellar hemispheres, the floor of the fourth ventricle, often causing obstructive hydrocephalus, and infiltrate the leptomeninges. Medulloblastoma thus tends to spread via cerebrospinal fluid pathway (Fig. 17.2)

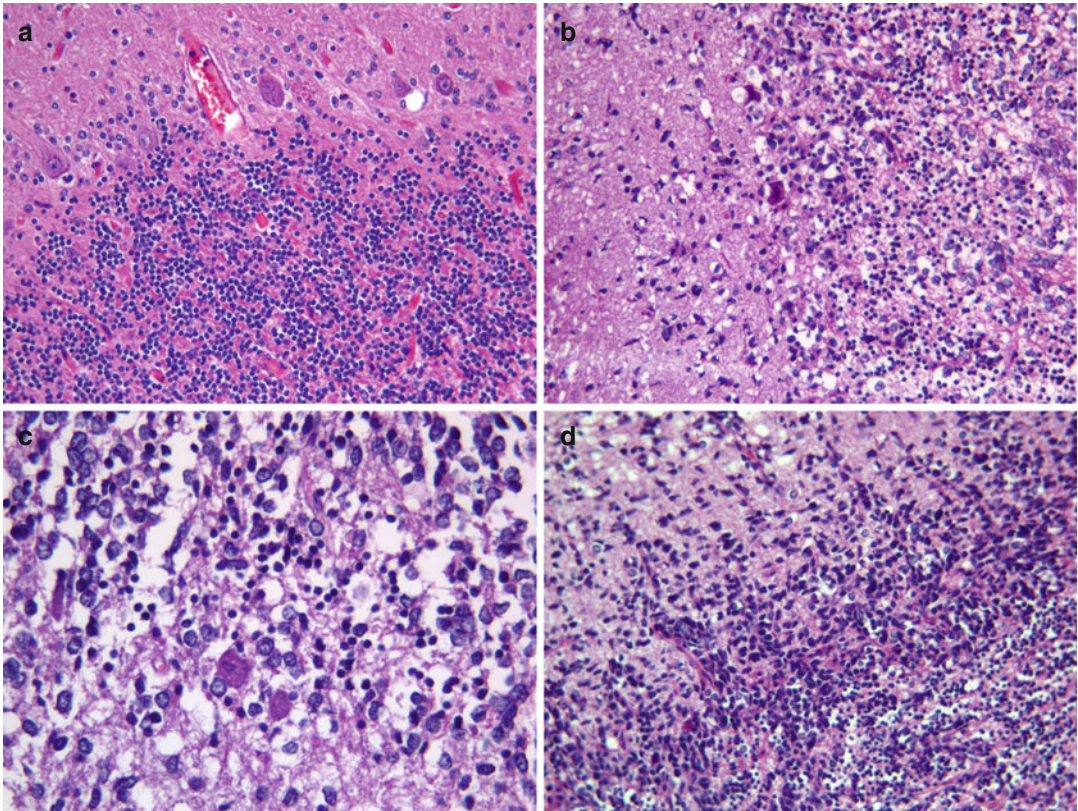


Fig. 17.1 (a) Normal cerebellum. (b) Infiltrative pattern: tumor cells (*right*) invade cerebellar cortex. (c) The cells of medulloblastoma with a larger and irregular nucleus intermingle with the regular, lymphocyte-like cells of the

internal granular layer of the normal cerebellum. (d) Neoplastic cells arranged in columns, at the level of the molecular layer. Hematoxylin and eosin stain: **a**, **b**, and **d** (20 \times), and **c** (40 \times)

along neuraxis generating distinct tumor nodules (e.g., the “drop metastases” among lumbar nerve roots) or, less frequently, a thickening of the pial or ventricular surface (“icing” of leptomeninges) [27]. Metastatic spread outside central nervous system is possible even if very rare [28–30], and the most common sites are bone, bone marrow, and lymph nodes; peritoneal dissemination through ventriculoperitoneal shunt is also reported [31].

17.4 Microscopic Aspects

17.4.1 Classic Medulloblastoma

Classic histology represents about 70 % of all medulloblastomas, mainly belonging to the molecular WNT subgroup (97 %), but even, to a

lesser extent, to group 3 and group 4 [32], affecting the prognosis.

It is a highly cellular neoplasm (Figs. 17.3, 17.4, and 17.5), composed of small round or oval-shaped cells, with hyperchromatic nuclei and little apparent cytoplasm [27]. Molding of the nuclei can be observed because of the high cellular density, even if it is a peculiarity of the anaplastic variant. Mitotic activity is usually conspicuous.

Necrosis and angiogenesis are variably present, but they are generally modest and lower than those seen in high-grade gliomas. Cells may be organized into rows, lobules, and twisted bundles or form neuroblastic (Homer-Wright) rosettes (Fig. 17.6). The latter are observed in not more than 40 % of cases and consist of tumor cell nuclei arranged in a radial fashion around a central tangle of fibrillar processes [27]. Like in neuroblastoma, pinealoblastoma, and primitive

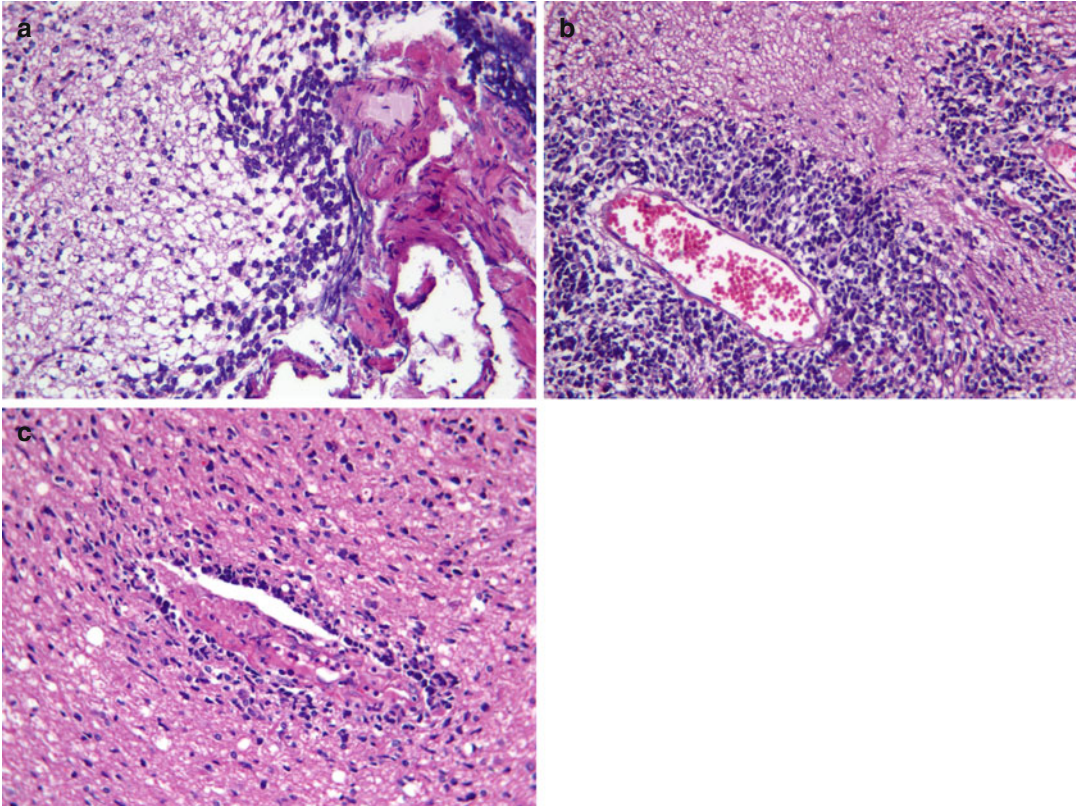


Fig. 17.2 Tumor cells fill the subarachnoid space (a) and reenter the brain along perivascular spaces (b, c). Hematoxylin and eosin stain (20×)

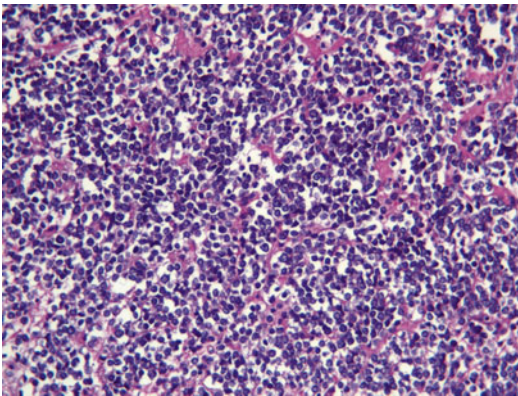


Fig. 17.3 Classic medulloblastoma. Densely cellular tumor, with non-nodular growth pattern. Hematoxylin and eosin stain (40×)

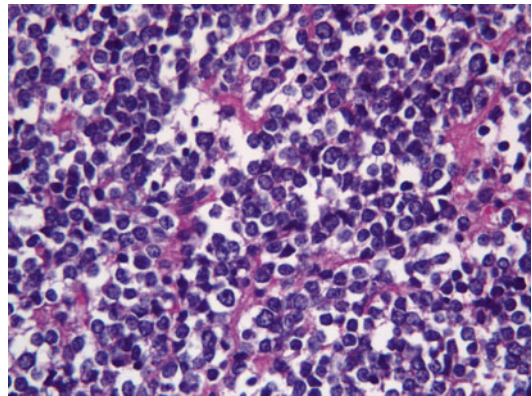


Fig. 17.4 Classic medulloblastoma. Sheets of cells with bland cytology and uniform distribution. Hematoxylin and eosin stain (63×)

neuroectodermal tumors of bone, they represent a phenotype of neuronal differentiation. Another possible structure is the “pseudorosette,” where fibrillar processes are projecting toward a central

blood vessel, resembling “spokes around the hub of wheel.”

Neuronal differentiation is the most common aspect, but morphological evaluation based on

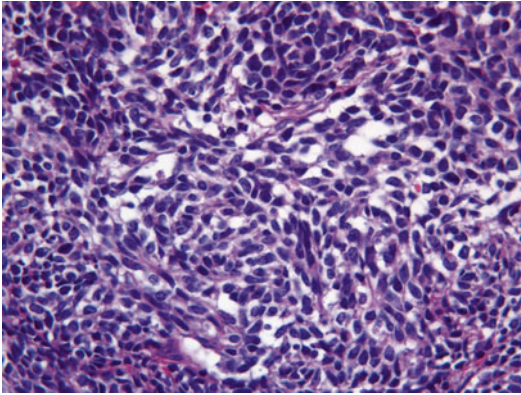


Fig. 17.5 Classic medulloblastoma with mild cytological atypia and minimal nuclear pleomorphism. Hematoxylin and eosin stain (40×)

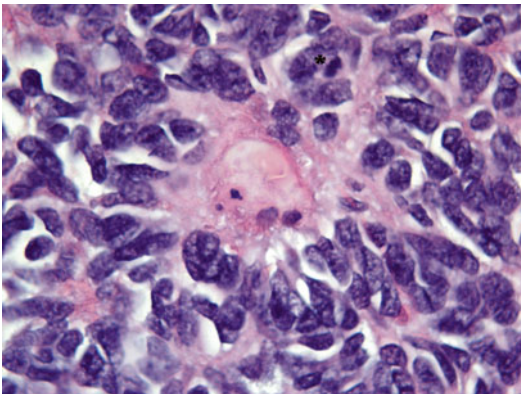


Fig. 17.6 Classic medulloblastoma. Detail of a Homer-Wright rosette: cells disposed in a radial fashion around a central core of fibrillar material. Note the mitotic figure (*). Hematoxylin and eosin stain (63×)

routine hematoxylin and eosin staining alone is not sufficient to reveal it. Immunohistochemistry becomes essential. In about 7 % of tumors, neurocytic or ganglion cells are found [18]. Glial differentiation is less frequent, and it is represented by mature glial cells with astrocytic phenotype, with eosinophilic cytoplasm and cell processes. Ependymal differentiation, on the contrary, is exceptional.

Rarely differentiation along mesenchymal line can occur. Medulloblastoma (classic, desmoplastic, and anaplastic) with foci of myogenic phenotype, with long cytoplasmic processes and striated muscle fibers, may be observed. This

entity, in the previous WHO classifications, was named medullomyoblastoma [33–35] and considered as a distinct variant; according to the current WHO classification (2007), the pathology report in these cases should refer to “medulloblastoma with myogenic differentiation” [2].

Another rare phenotype, previously described as a distinct variant, is melanotic medulloblastoma [18, 36, 37], now simply termed “medulloblastoma with melanotic differentiation” [2]. It is characterized by epithelioid pattern and the presence of cytoplasmic melanin pigments that have been proved to be both neuromelanin and oculocutaneous types. However, melanotic and medullomyoblastoma phenotypes can even coexist [38].

Cell proliferation in most classic medulloblastomas is generally high although variable [9, 39].

17.4.2 Desmoplastic Medulloblastoma

Desmoplastic/nodular variant accounts for about 16 % of cases, with a significantly higher prevalence in adults and infants (42 %) than in children (9 %) [32]. SHH molecular subgroup expresses this phenotype in the great majority with a good prognosis in infants and intermediate in others [12].

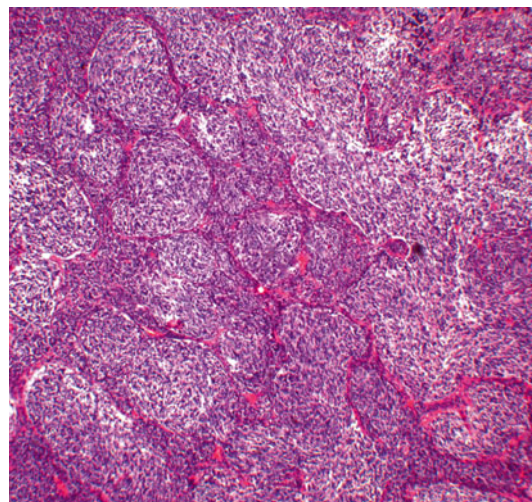


Fig. 17.7 Nodular/desmoplastic medulloblastoma, characterized by the alternating of pale and dark areas (hematoxylin and eosin stain; 10×)

It is characterized by coexisting of both nodular reticulin-free areas (“pale islands”) and desmoplasia (Figs. 17.7 and 17.8). Only one of these architectural elements, detectable separately in all variants of medulloblastomas, does not allow to classify it as desmoplastic [18]. They should be considered as distinct biological microenvironments [45] with different degrees of mitosis, apoptosis, and differentiation. Nodular areas appear as round or elongated zones of tumor cells, placed on a neuropil-like background, with neurocytic neuronal differentiation (Figs. 17.9 and 17.10), poor pro-

liferation, and scattered apoptotic cells. In some cases, nodule formation can be very focal with uninterrupted sheets of tumor cells, so there may be diagnostic problems because it is difficult to establish how many nodules or desmoplasias (Fig. 17.11) are required to make a correct diagnosis [45].

Desmoplasia is a pericellular reticulin-rich network that may represent also a reactive phenomenon like in leptomeningeal invasion [40]. Tumor cells in internodular regions tend to be more undifferentiated, sometimes with focal anaplasia, to be pleomorphic and mitotically

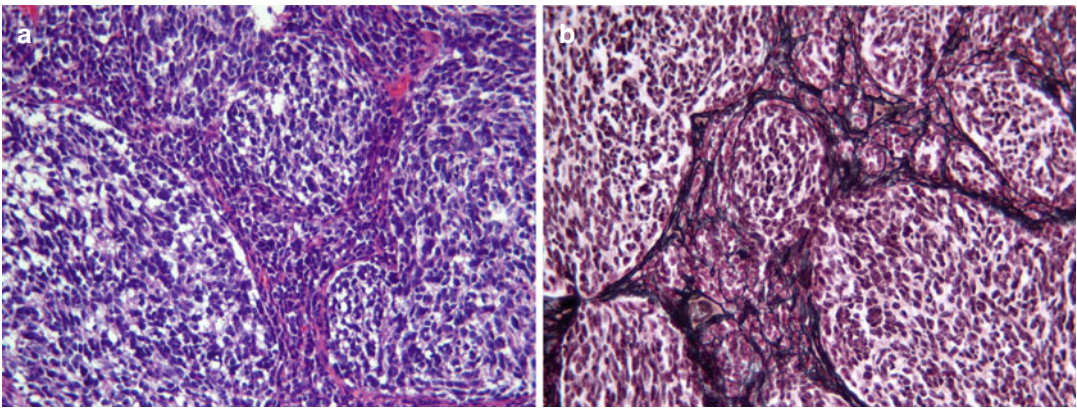


Fig. 17.8 Nodular/desmoplastic medulloblastoma. (a) Nodular areas appear as round or elongated zones of tumor cells, in contrast with the internodular regions

where cells appear more undifferentiated. Hematoxylin and eosin stain (40 \times). (b) Alternation of “pale islands,” reticulin-free, and dark zones, rich in reticulin (40 \times)

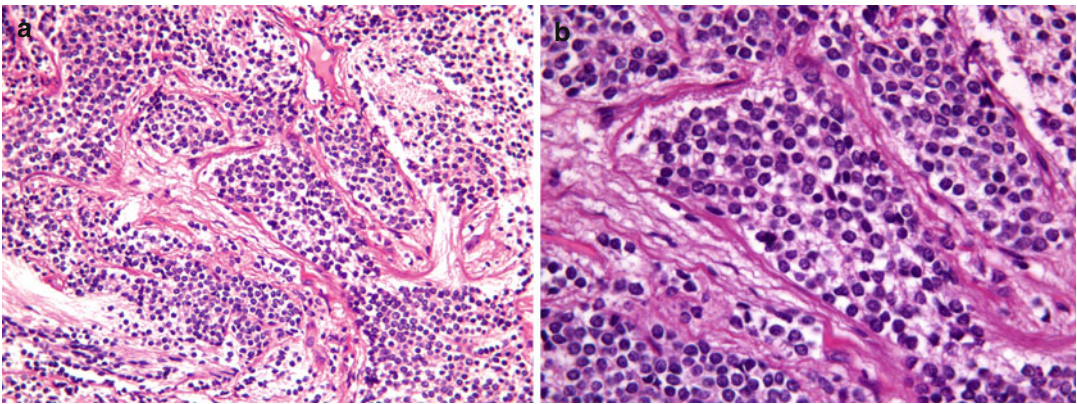


Fig. 17.9 Nodular/desmoplastic medulloblastoma. (a, b) Intranodular neurocytic differentiation. Hematoxylin and eosin stain (20 \times and 40 \times)

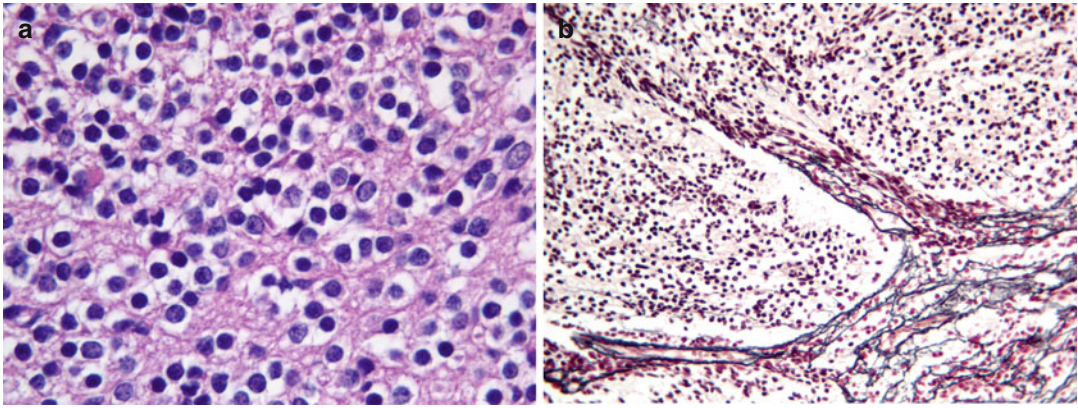


Fig. 17.10 Nodular/desmoplastic medulloblastoma. (a) Round bland cells with perinuclear halo. Hematoxylin and eosin stain (63×); (b) Nodular pattern highlighted by reticulin stain (20×)

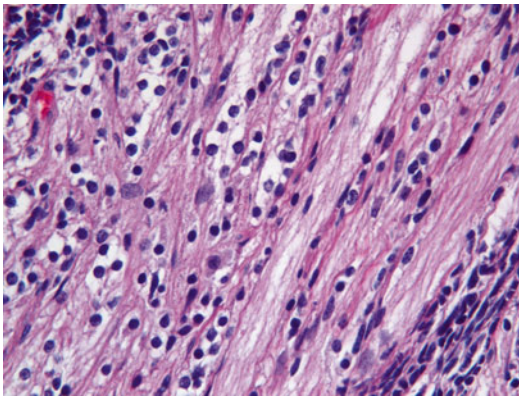


Fig. 17.11 Desmoplastic component. Streaming pattern of neoplastic cells (hematoxylin and eosin stain; 63×)

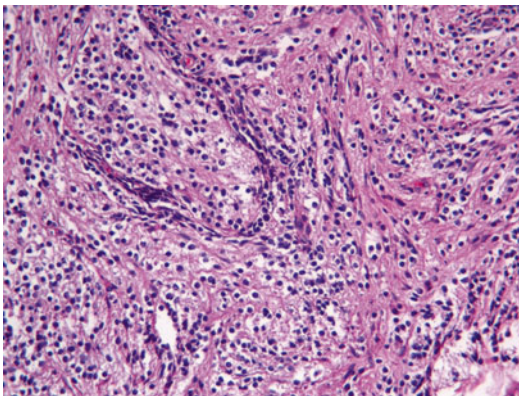


Fig. 17.12 Medulloblastoma with extensive nodularity. Large nodules of neoplastic cells with neurocytic differentiation interrupted by poor extranodular tissue. Hematoxylin and eosin stain (20×)

active, with greater nuclear/cytoplasmic ratio than nodular zones and a higher Ki67 (MIB1) Labeling Index [41].

17.4.3 Medulloblastoma with Extensive Nodularity (MBEN)

It is an uncommon variant, closely related to desmoplastic one [2] that was previously termed “cerebellar neuroblastoma” [42] and accounts for about 3 % of cases [43]. It occurs mainly below the age of 3 years, and it is associated to a good prognosis [44].

It may be considered as the most differentiated form of desmoplastic medulloblastoma (MB) [45] in which reticulin-free nodules are particularly large and numerous, while desmoplasia is markedly reduced or absent (Fig. 17.12). Intranodular cells show neurocytic differentiation and nuclear uniformity with features that resemble those of central neurocytoma. Occasionally, after radiotherapy and/or chemotherapy, medulloblastomas with extensive nodularity may evolve into a ganglioglioma [46].

17.4.4 Large Cell and Anaplastic (LCA)

These two histologies represent a morphophenotypic and biological continuum; for this reason

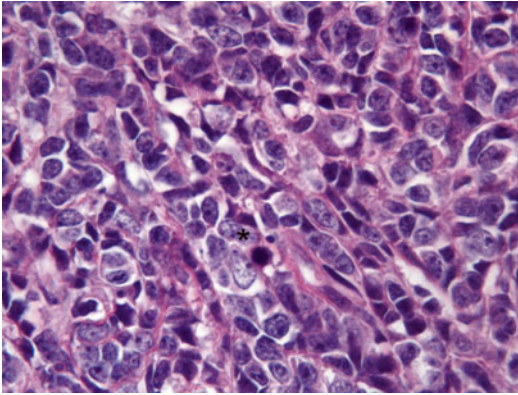


Fig. 17.13 Large-cell medulloblastoma. Large round cells with a vesicular nucleus and generally a prominent single nucleolus. Note the mitotic figure (*). Hematoxylin and eosin stain (63×)

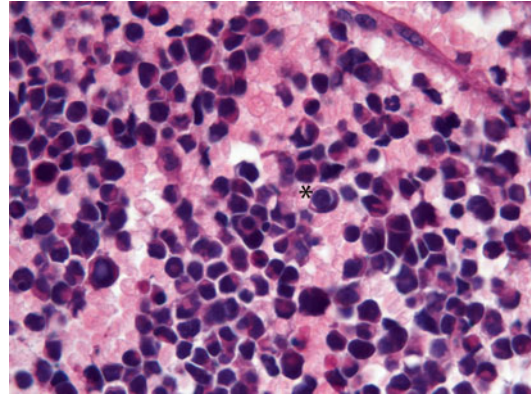


Fig. 17.15 Large-cell/anaplastic medulloblastoma. Nuclear pleomorphism and molding. Note the cell-cell wrapping (*). Hematoxylin and eosin stain (63×)

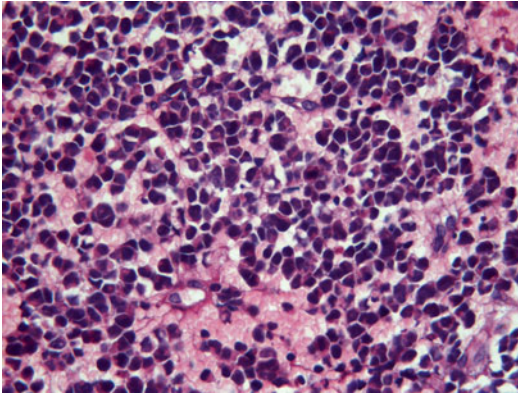


Fig. 17.14 Large-cell/anaplastic medulloblastoma. Large polyhedral cells which are densely packed with a paving-like pattern. Hematoxylin and eosin stain (40×)

in literature, they are usually considered as a single macrogroup (LCA tumors) [7].

Their prevalence accounts for 10 % of MBs, and it is lower in adults (3 %) [32]. They are equally associated to all the molecular subgroups except for WNT tumors in which a link is rarer, or among infants where the tumor always correspond to group 3, with poorer prognosis [32].

Large-cell medulloblastoma is composed of lobules or sheets of large round cells (two to three times greater than conventional small cells), with a vesicular nucleus and generally a prominent single nucleolus (Fig. 17.13). In some regions,

large cells can be polyhedral and densely packed with a paving-like pattern.

Anaplastic medulloblastoma (Figs. 17.14 and 17.15) is characterized by nuclear molding, cell-to-cell “wrapping,” nuclear pleomorphism [18, 47], and a peculiar apoptotic activity that can be so extensive to form small “lakes” [47].

Large-cell medulloblastoma always contains areas with anaplastic phenotype. When histology is dominated by this phenotype, anaplastic medulloblastoma variant is configured [18]. This entity was introduced in the 2007 WHO classification [2], and histological progression from non-anaplastic to anaplastic medulloblastoma is documented even within the same tumor [2, 8, 33, 48].

17.5 Immunohistochemistry

Medulloblastoma is mainly an undifferentiated neoplasm, referring solely on the light microscopic appearance, but at the immunohistochemical and ultrastructural level, it must be considered a neoplasm with neuronal or neuroblastic phenotype. Sometimes a differentiation toward glial lineage is detectable, almost exclusively after immunohistochemical investigation.

Clear positivity to synaptophysin (Fig. 17.16), class III β -tubulin, microtubule-associated protein 2 (MAP2), cromogranin, NSE, and NeuN may variably be observed [49, 50], especially in the fibrillar cores of

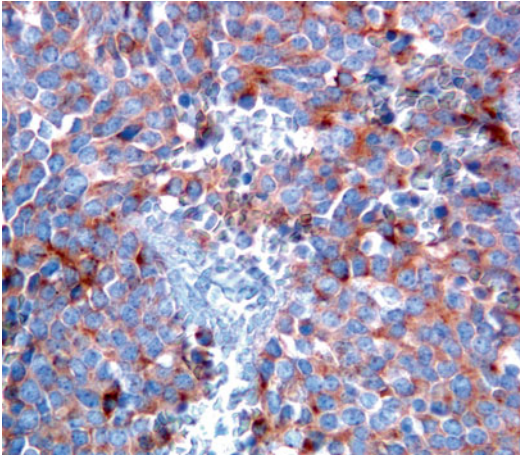


Fig. 17.16 Synaptophysin. Granular cytoplasmic immunoreactivity

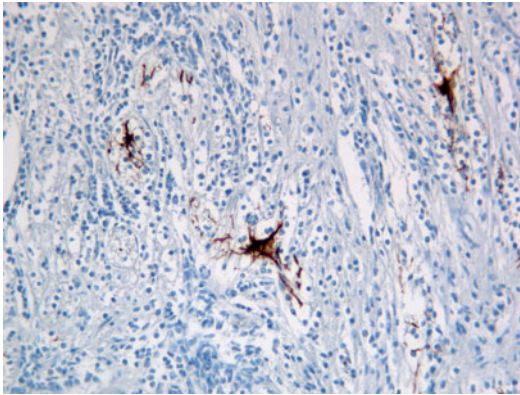


Fig. 17.17 GFAP. Rare entrapped glial cells reactive for GFAP

Homer-Wright rosettes and perivascular pseudorosettes and in the “pale islands” of the nodular variant; the expression of neurofilament protein is strictly tissue fixation-dependent.

GFAP (glial fibrillary acidic protein) positivity is of difficult interpretation, firstly because most of medulloblastomas contain reactive stellar-shaped astrocytes (Fig. 17.17), usually positioned around a vessel and whose long cytoplasmic processes can juxtapose to a neoplastic nucleus giving the false impression of a positive signal. Also “pale islands” of desmoplastic variant show GFAP positivity within evident network of fibrillar cells, denoting that intranodular areas represent a center of mixed neural and glial differentiation [51].

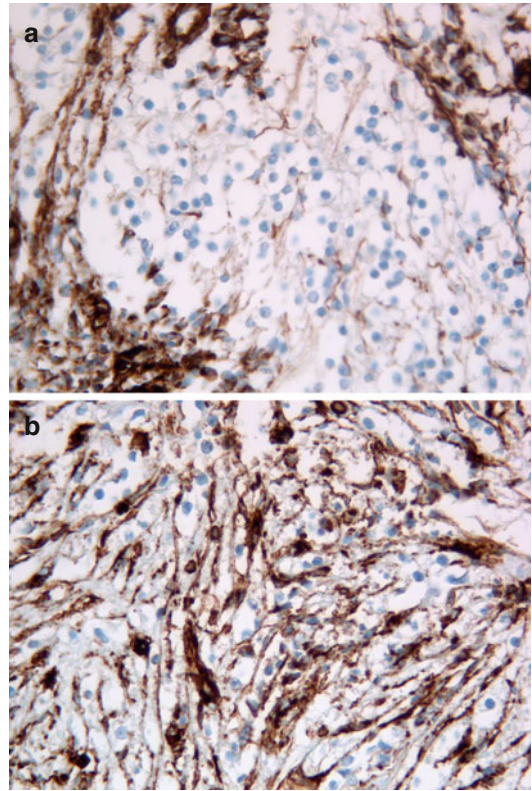


Fig. 17.18 Vimentin. Immunophenotype in the (a) nodular variant and in the desmoplastic area (b)

Large-cell variant never shows glial differentiation, while a strong positivity to synaptophysin, neurofilament protein, and chromogranin is often detected.

Occasionally, a photoreceptor differentiation is observed and therefore immunoreactivity to retinal-S-antigen and rhodopsin is detected.

Finally, immunophenotype of medulloblastoma may also include positivity (Fig. 17.18) to vimentin (mainly in classic form), nestin, neuronal cell adhesion molecule (NCAM), and nerve growth factor (NGF).

The Ki-67 (MIB1) antibody Labeling Index (Fig. 17.19) is among the highest detected in CNS tumors, owing to the high proliferative activity. It usually is not less than 30 % and even up to 80 %, revealing the large tumor aggressiveness. This wide range of expression, even inside the same tumor, is essentially function of the degree of differentiation. In fact, in the nodular

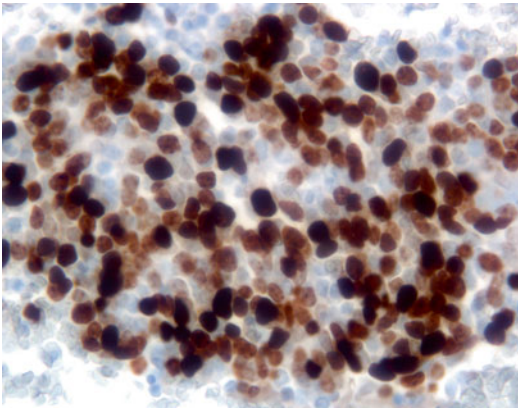


Fig. 17.19 Ki67. High Ki67 Labeling Index

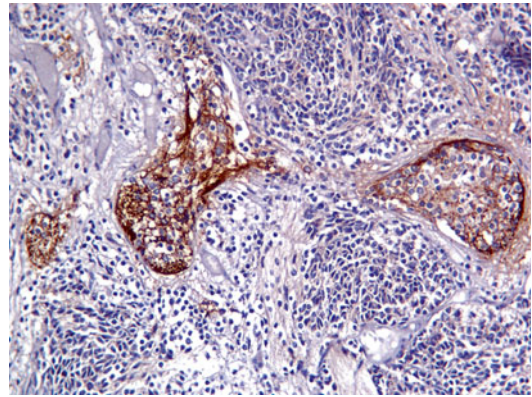


Fig. 17.21 CD133. Immunoreactivity for the stem cell marker CD133, detected inside the blades of islands in nodular medulloblastoma

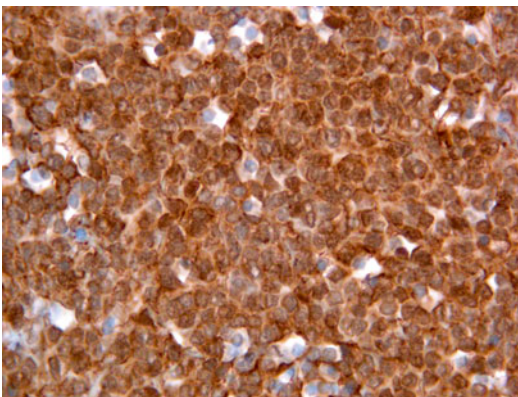


Fig. 17.20 β -catenin. Nuclear and cytoplasmic reactivity in medulloblastomas with a mutation in the β -catenin gene

variant, nodular foci, with neuronal or glial differentiation, usually show only scattered or peripheral positive nuclei, while the internodular zones explicit a much stronger signal. Higher rates are noted in the large-cell areas too.

Beyond the undoubted diagnostic utility, immunohistochemistry may play a relevant role for prognosis, patient stratification, and target therapy, although in a debated and not yet codified manner, being able to identify molecular subgroups of medulloblastoma, alternative to analysis of transcriptional profiling.

WNT subgroup medulloblastomas are characterized by nuclear immunoreactivity for both β -catenin [12, 52–57] and Dickkopf-related protein

1 (DKK1) [12, 56]. The former that also stains the cytoplasm (Fig. 17.20) generally shows a strong and diffused signal which, however, can also be moderate and patchy; DKK1 usually stains the cytoplasm.

SHH subgroup tumors are identified by cytoplasmic positivity to secreted frizzled-related protein 1 (SFRP1) [56, 60, 61], GRB2-associated-binding protein 1 (GAB1) [53], and GLI1 [56].

Both WNT and SHH subgroups are immunoreactive to cytoplasmic filamin A and YAP1 [61, 62], mainly within internodular regions of desmoplastic tumors: this panel allows to exclude a non-SHH/WNT molecular profile [53].

In fact, medulloblastomas belonging to groups 3 and 4 are usually immunonegative to all the abovementioned markers. However, group 3 and 4 tumors are identified respectively by positivity to natriuretic peptide receptor C/guanylate cyclase C (NPR3), and potassium channel Kv1.1 (KCNA1).

The association of more antibodies essentially strengthens the ascription of a medulloblastoma to a specific molecular subgroup, but there is a specific immunohistochemical panel that has been shown to have high diagnostic specificity.

Northcott et al. demonstrated that immunohistochemistry for DKK1 (WNT), SFRP1 (SHH), NPR3 (group C), and KCNA1 (group D) could univocally and reliably classify medulloblastomas,

Table 17.2 Chang's staging system for medulloblastoma

T1	Tumor less than 3 cm in diameter and limited to the midline position in the vermis, the roof of the fourth ventricle, and less frequently to the cerebellar hemispheres
T2	Tumor more than 3 cm in diameter, further invading 1 adjacent structure or partially filling the fourth ventricle
T3a	Tumor further invading 2 adjacent structures or completely filling the fourth ventricle with extension into the aqueduct of Sylvius, foramen of Magendie, or foramen of Luschka, thus producing marked hydrocephalus
T3b	Tumor arising from the floor of the fourth ventricle or brainstem and filling the fourth ventricle
T4	Tumor further spreading through the aqueduct of Sylvius to involve the third ventricle or midbrain or tumor extending to the upper cervical spinal cord
M0	No evidence of gross subarachnoid or hematogenous metastases
M1	Microscopic tumor cells in cerebrospinal fluid
M2	Gross nodular seeding demonstrated in cerebellar, cerebral, and subarachnoid space or in the third or lateral ventricles
M3	Gross nodular seeding in spinal subarachnoid space
M4	Extraneural metastasis

in approximately 98 % of patients, into four non-overlapping molecular variants [56].

A statistically significant negative correlation of stem cell markers (CD15 eCD133) positivity (Fig. 17.21) with EFS (event-free survival) was observed [66].

17.6 Staging

The most widespread staging system is Chang's one [62]. Born in premodern neuroimaging era and later adapted to it, it was determined on surgical and autopsy findings considering the size, invasiveness, and spread outside the posterior fossa (Table 17.2). In particular, the brainstem invasion was considered an important prognostic factor also for subtotal resection.

A more recent modification is that proposed by Langston [63] that includes radiological staging and does not account for hydrocephalus and number of structures invaded (Table 17.3).

Table 17.3 Langston modification of the Chang's T

T1	Tumor <3 cm in diameter
T2	Tumor ≥3 cm in diameter
T3a	Tumor ≥3 cm in diameter with extension
T3b	Tumor ≥3 cm in diameter with unequivocal extension into the brainstem
T4	Tumor ≥3 cm in diameter with extension up past the aqueduct of Sylvius and/or down past the foramen magnum (i.e., beyond the posterior fossa)

17.7 Cytology

The leptomeningeal disease is reported in about 30 % of medulloblastomas [64], and it is one of the major prognostic factors [6]. Therefore, the research of dissemination, by CSF cytology (lumbar and/or intracranial) together with magnetic resonance with gadolinium, plays a key role in the clinical management of these lesions.

The CSF examination generally shows small tumor cells, with a hyperchromatic nucleus; pleomorphism and apoptosis vary with the tumor grade. The little cytoplasm is often strongly basophilic especially at the level of the cell membrane [65]. Cell wrapping, or cannibalism, is also more common. In addition to the tumor cells, reactive CSF pleocytosis with prevalence of eosinophils may be evident. The differential diagnosis arises sometimes with lymphoblasts, with immature lymphocytes, and rarely with retinoblastoma. In these cases, immunocytochemical markers may be useful.

During intraoperative consultation, performing a cytologic "squash" (Fig. 17.22) can even be more useful than frozen sections.

17.8 Molecular and Cytogenetic Findings

The heterogeneity of this tumor is reflected also in the extreme heterogeneity of cytogenetic abnormalities. The most common one is the loss of all or part of chromosome 17p, often associated with duplication and translocation of chromosome 17q (isochromosome 17q). This

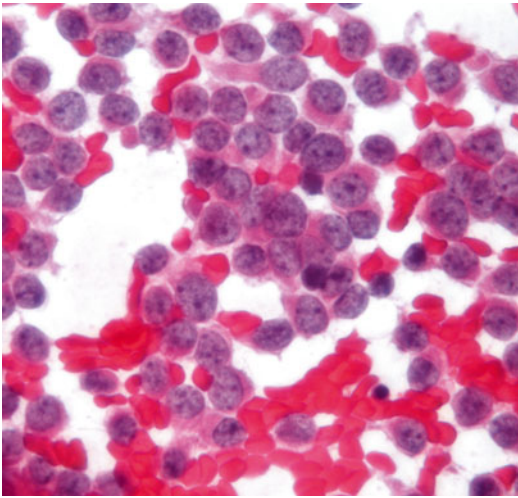


Fig. 17.22 Cytologic “squash” for intraoperative consultation. Small- and medium-sized cells with vesicular nuclei and multiple nucleoli and scant cytoplasm. Hematoxylin and eosin stain (63×)

alteration seems to be more expressed in non-nodular medulloblastomas, especially in higher-grade tumors.

High-level gains of chromosome 8q (*N-myc*) and 2p (*c-myc*) are frequently observed in anaplastic and large-cell medulloblastomas; the latter can be even characterized by amplification and overexpression of the oncogenes *c-myc* and *N-myc*. Overexpression of *c-myc* can also occur in non-anaplastic tumors, with negative, or unfavorable, prognostic significance.

Another molecular alteration is β -catenin nuclear positivity which characterizes the molecular subgroup of medulloblastomas associated with the activation of the WNT pathway. Immunohistochemical studies for β -catenin proved a statistical significant positive correlation with a better prognosis.

References

1. Packer RJ, Cogen P, Vezina G, Rorke LB (1999) Medulloblastoma: clinical and biologic aspects. *Neuro Oncol* 1(3):232–250
2. Louis DN, Ohgaki H, Wiestler OD, Cavenee WK, Burger PC, Jouvet A, Scheithauer BW, Kleihues P (2007) The 2007 WHO classification of tumours of

the central nervous system. *Acta Neuropathol* 114(2):97

3. Rorke LB (1983) The cerebellar medulloblastoma and its relationship to primitive neuroectodermal tumors. *J Neuropathol Exp Neurol* 42(1):1–15
4. Pomeroy SL, Tamayo P, Gaasenbeek M, Sturla LM, Angelo M, McLaughlin ME, Kim JY, Goumnerova LC, Black PM, Lau C, Allen JC, Zagzag D, Olson JM, Curran T, Wetmore C, Biegel JA, Poggio T, Mukherjee S, Rifkin R, Califano A, Stolovitzky G, Louis DN, Mesirov JP, Lander ES, Golub TR (2002) Prediction of central nervous system embryonal tumour outcome based on gene expression. *Nature* 415(6870):436–442
5. Kleihues P, Cavenee W (2000) Tumours of the nervous system. World Health Organization Classification of Tumours. IARC, Lyon
6. Zeltzer PM, Boyett JM, Finlay JL, Albright AL, Rorke LB, Milstein JM, Allen JC, Stevens KR, Stanley P, Li H, Wisoff JH, Geyer JR, McGuire-Cullen P, Stehbens JA, Shurin SB, Packer RJ (1999) Metastasis stage, adjuvant treatment, and residual tumor are prognostic factors for medulloblastoma in children: conclusions from the Children’s Cancer Group 921 Randomized Phase III Study. *J Clin Oncol* 17:832–845
7. Giangaspero F, Wellek S, Masuoka J, Gessi M, Kleihues P, Ohgaki H (2006) Stratification of medulloblastoma on the basis of histopathological grading. *Acta Neuropathol* 112(1):5–12
8. Eberhart CG, Kepner JL, Goldthwaite PT, Kun LE, Duffner PK, Friedman HS, Strother DR, Burger PC (2002) Histopathologic grading of medulloblastomas: a Pediatric Oncology Group study. *Cancer* 94(2):552–560
9. McManamy CS, Lamont JM, Taylor RE, Cole M, Pearson AD, Clifford SC, Ellison DW, United Kingdom Children’s Cancer Study Group (2003) Morphophenotypic variation predicts clinical behavior in childhood nondesmoplastic medulloblastomas. *J Neuropathol Exp Neurol* 62(6):627–632
10. Urberuaga A, Navajas A, Burgos J, Pijoán JI (2006) A review of clinical and histological features of Spanish paediatric medulloblastomas during the last 21 years. *Childs Nerv Syst* 22(5):466–474
11. Rutkowski S, Bode U, Deinlein F, Ottensmeier H, Warmuth-Metz M, Soerensen N, Graf N, Emser A, Pietsch T, Wolff JE, Kortmann RD, Kuehl J (2005) Treatment of early childhood medulloblastoma by postoperative chemotherapy alone. *N Engl J Med* 352(10):978–986
12. Taylor MD, Northcott PA, Korshunov A, Remke M, Cho YJ, Clifford SC, Eberhart CG, Parsons DW, Rutkowski S, Gajjar A, Ellison DW, Lichter P, Gilbertson RJ, Pomeroy SL, Kool M, Pfister SM (2012) Molecular subgroups of medulloblastoma: the current consensus. *Acta Neuropathol* 123(4):465–472
13. Globus JH, Strauss I (1925) Spongioblastoma multiforme. A primary malignant form of brain neoplasm:

- its clinical and anatomic features. *Arch Neurol Psychiatry* 14(2):139–191
14. Bailey P, Cushing H (1925) Medulloblastoma cerebelli: a common type of midcerebellar glioma of childhood. *Arch Neurol Psychiatry* 14:192–224
 15. Bailey OT (1985–1986) Genesis of the Percival Bailey-Cushing classification of gliomas. *Pediatr Neurosci* 12(4–5):261–265
 16. Cushing H (1930) Experiences in cerebellar medulloblastoma. *Acta Pathol Microbiol Scand* 1:1–86
 17. Sümer-Turanlıgil NC, Cetin EO, Uyanıkgil Y (2013) A contemporary review of molecular candidates for the development and treatment of childhood medulloblastoma. *Childs Nerv Syst* 29(3):381–388
 18. Gilbertson RJ, Ellison DW (2008) The origins of medulloblastoma subtypes. *Annu Rev Pathol* 3:341–365
 19. Bühren J, Christoph AH, Buslei R, Albrecht S, Wiestler OD, Pietsch T (2000) Expression of the neurotrophin receptor p75NTR in medulloblastomas is correlated with distinct histological and clinical features: evidence for a medulloblastoma subtype derived from the external granule cell layer. *J Neuropathol Exp Neurol* 59(3):229–240
 20. Pomeroy SL, Sutton ME, Goumnerova LC, Segal RA (1997) Neurotrophins in cerebellar granule cell development and medulloblastoma. *J Neurooncol* 35(3):347–352
 21. Salsano E, Pollo B, Eoli M, Giordana MT, Finocchiaro G (2004) Expression of MATH1, a marker of cerebellar granule cell progenitors, identifies different medulloblastoma sub-types. *Neurosci Lett* 370(2–3):180–185
 22. Yokota N, Aruga J, Takai S, Yamada K, Hamazaki M, Iwase T, Sugimura H, Mikoshiba K (1996) Predominant expression of human zic in cerebellar granule cell lineage and medulloblastoma. *Cancer Res* 56(2):377–383
 23. Choux M, Lena G, Gentet JC, Paz Paredes A (2001) Medulloblastoma. In: MacLone DG (ed) *Pediatric neurosurgery: surgery of the developing nervous system*. Elsevier Health Sciences, Philadelphia, pp 804–821
 24. Sandhou A, Kendall B (1987) Computed tomography in management of medulloblastomas. *Neuroradiology* 29:444–452
 25. Kleihues P, Cavenee W (eds) (2000) *Pathology and genetics of tumours of the central nervous system*. International Agency for Research on Cancer, Lyon, pp 129–137
 26. Choux M, Lena G (1982) Medulloblastoma. *Neurochirurgie* 28(Suppl):1–229
 27. Ellison DW, Clifford SC, Giangaspero F (2006) Medulloblastoma. In: McLendon RE, Rosenblum MK, Bigner DD (eds) *Russell and Rubinstein's pathology of tumors of the nervous system*. CRC Press, Boca Raton, FL, USA, pp 247–264
 28. Eberhart CG, Cohen KJ, Tihan T, Goldthwaite PT, Burger PC (2003) Medulloblastoma with systemic metastases: evaluation of tumor histopathology and clinical behaviour in 23 patients. *J Pediatr Hematol Oncol* 25:198–203
 29. Campbell AN, Chan HS, Becker LE, Daneman A, Park TS, Hoffman HJ (1984) Extracranial metastases in childhood primary intracranial tumors. A report of 21 cases and review of the literature. *Cancer* 53:974–981
 30. Sure U, Bertalanffy H, Isenmann S, Brandner S, Berghorn WJ, Seeger W, Aguzzi A (1995) Secondary manifestation of medulloblastoma: metastases and local recurrences in 66 patients. *Acta Neurochir* 136:117–126
 31. Kessler LA, Dugan P, Concannon JP (1975) Systemic metastases of medulloblastoma promoted by shunting. *Surg Neurol* 3:147–152
 32. Kool M, Korshunov A, Remke M, Jones DT, Schlanstein M, Northcott PA, Cho YJ, Koster J, Schouten-van Meeteren A, van Vuurden D, Clifford SC, Pietsch T, von Bueren AO, Rutkowski S, McCabe M, Collins VP, Bäcklund ML, Haberler C, Bourdeaut F, Delattre O, Doz F, Ellison DW, Gilbertson RJ, Pomeroy SL, Taylor MD, Lichter P, Pfister SM (2012) Molecular subgroups of medulloblastoma: an international meta-analysis of transcriptome, genetic aberrations, and clinical data of WNT, SHH, group 3, and group 4 medulloblastomas. *Acta Neuropathol* 123(4):473–484
 33. Leonard JR, Cai DX, Rivet DJ, Kaufman BA, Park TS, Levy BK, Perry A (2001) Large cell/anaplastic medulloblastomas and medulloblastomas: clinicopathological and genetic features. *J Neurosurg* 95(1):82–88
 34. Helton KJ, Fouladi M, Boop FA, Perry A, Dalton J, Kun L, Fuller C (2004) Medulloblastoma: a radiographic and clinicopathologic analysis of six cases and review of the literature. *Cancer* 101(6):1445–1454
 35. Smith TW, Davidson RI (1984) Medulloblastoma. A histologic, immunohistochemical, and ultrastructural study. *Cancer* 54(2):323–332
 36. Dolman CL (1988) Melanotic medulloblastoma. A case report with immunohistochemical and ultrastructural examination. *Acta Neuropathol* 76(5):528–531
 37. Jimenez CL, Carpenter BF, Robb IA (1987) Melanotic cerebellar tumor. *Ultrastruct Pathol* 11(5–6):751–759
 38. Kalimo H, Paljärvi L, Ekfors T, Pelliniemi LJ (1987) Pigmented primitive neuroectodermal tumor with multipotential differentiation in cerebellum (pigmented medulloblastoma). A case with light- and electron-microscopic, and immunohistochemical analysis. *Pediatr Neurosci* 13(4):188–195
 39. Gilbertson RJ, Jaros E, Perry RH, Kelly PJ, Lunec J, Pearson AD (1997) Mitotic percentage index: a new prognostic factor for childhood medulloblastoma. *Eur J Cancer* 33(4):609–615
 40. Rubinstein LJ, Northfield DW (1964) The medulloblastoma and the so-called “arachnoidal cerebellar sarcoma”. *Brain* 87:379–412
 41. McManamy CS, Pears J, Weston CL, Hanzely Z, Ironside JW, Taylor RE, Grundy RG, Clifford SC,

- Ellison DW, Clinical Brain Tumour Group (2007) Nodule formation and desmoplasia in medulloblastomas—defining the nodular/desmoplastic variant and its biological behavior. *Brain Pathol* 17(2):151–164
42. Pearl GS, Takei Y (1981) Cerebellar “neuroblastoma”: nosology as it relates to medulloblastoma. *Cancer* 47(4):772–779
 43. Massimino M, Giangaspero F, Garrè ML, Gandola L, Poggi G, Biassoni V, Gatta G, Rutkowski S (2011) Childhood medulloblastoma. *Crit Rev Oncol Hematol* 79(1):65–83
 44. Giangaspero F, Perilongo G, Fondelli MP, Brisigotti M, Carollo C, Burnelli R, Burger PC, Garrè ML (1999) Medulloblastoma with extensive nodularity: a variant with favorable prognosis. *J Neurosurg* 91(6):971–977
 45. Ellison D (2002) Classifying the medulloblastoma: insights from morphology and molecular genetics. *Neuropathol Appl Neurobiol* 28(4):257–282
 46. Geyer JR, Schofield D, Berger M, Milstein J (1992) Differentiation of a primitive neuroectodermal tumor into a benign ganglioglioma. *J Neurooncol* 14(3):237–241
 47. Brown HG, Kepner JL, Perlman EJ, Friedman HS, Strother DR, Duffner PK, Kun LE, Goldthwaite PT, Burger PC (2000) “Large cell/anaplastic” medulloblastomas: a pediatric oncology group study. *J Neuropathol Exp Neurol* 59(10):857–865
 48. Eberhart CG, Burger PC (2003) Anaplasia and grading in medulloblastomas. *Brain Pathol* 13(3):376–385
 49. Maraziotis T, Perentes E, Karamitopoulou E, Nakagawa Y, Gessaga EC, Probst A, Frankfurter A (1992) Neuron-associated class III beta-tubulin isotype, retinal S-antigen, synaptophysin, and glial fibrillary acidic protein in human medulloblastomas: a clinicopathological analysis of 36 cases. *Acta Neuropathol* 84(4):355–363
 50. Katsetos CD, Del Valle L, Legido A, de Chadarevian JP, Perentes E, Mörk SJ (2003) On the neuronal/neuroblastic nature of medulloblastomas: a tribute to Pio del Rio Hortega and Moises Polak. *Acta Neuropathol* 105(1):1–13
 51. Katsetos CD, Herman MM, Frankfurter A, Gass P, Collins VP, Walker CC, Rosemberg S, Barnard RO, Rubinstein LJ (1989) Cerebellar desmoplastic medulloblastomas. A further immunohistochemical characterization of the reticulin-free pale islands. *Arch Pathol Lab Med* 113(9):1019–1029
 52. Clifford SC, Lusher ME, Lindsey JC, Langdon JA, Gilbertson RJ, Straughton D, Ellison DW (2006) Wnt/Wingless pathway activation and chromosome 6 loss characterize a distinct molecular sub-group of medulloblastomas associated with a favorable prognosis. *Cell Cycle* 5(22):2666–2670
 53. Ellison DW, Dalton J, Kocak M, Nicholson SL, Fraga C, Neale G, Kenney AM, Brat DJ, Perry A, Yong WH, Taylor RE, Bailey S, Clifford SC, Gilbertson RJ (2011) Medulloblastoma: clinicopathological correlates of SHH, WNT, and non-SHH/WNT molecular subgroups. *Acta Neuropathol* 121(3):381–396
 54. Ellison DW, Kocak M, Dalton J, Megahed H, Lusher ME, Ryan SL, Zhao W, Nicholson SL, Taylor RE, Bailey S, Clifford SC (2011) Definition of disease-risk stratification groups in childhood medulloblastoma using combined clinical, pathologic, and molecular variables. *J Clin Oncol* 29(11):1400–1407
 55. Ellison DW, Onilude OE, Lindsey JC, Lusher ME, Weston CL, Taylor RE, Pearson AD, Clifford SC, United Kingdom Children’s Cancer Study Group Brain Tumour Committee (2005) beta-Catenin status predicts a favorable outcome in childhood medulloblastoma: the United Kingdom Children’s Cancer Study Group Brain Tumour Committee. *J Clin Oncol* 23(31):7951–7957
 56. Northcott PA, Korshunov A, Witt H, Hielscher T, Eberhart CG, Mack S, Bouffet E, Clifford SC, Hawkins CE, French P, Rutka JT, Pfister S, Taylor MD (2011) Medulloblastoma comprises four distinct molecular variants. *J Clin Oncol* 29(11):1408–1414
 57. Remke M, Hielscher T, Korshunov A, Northcott PA, Bender S, Kool M, Westermann F, Benner A, Cin H, Ryzhova M, Sturm D, Witt H, Haag D, Toedt G, Wittmann A, Schöttler A, von Bueren AO, von Deimling A, Rutkowski S, Scheurlen W, Kulozik AE, Taylor MD, Lichter P, Pfister SM (2011) FSTL5 is a marker of poor prognosis in non-WNT/non-SHH medulloblastoma. *J Clin Oncol* 29(29):3852–3861
 58. Fernandez-L A, Northcott PA, Dalton J, Fraga C, Ellison D, Angers S, Taylor MD, Kenney AM (2009) YAP1 is amplified and up-regulated in hedgehog-associated medulloblastomas and mediates Sonic hedgehog-driven neural precursor proliferation. *Genes Dev* 23(23):2729–2741
 59. Zhao B, Wei X, Li W, Udan RS, Yang Q, Kim J, Xie J, Ikenoue T, Yu J, Li L, Zheng P, Ye K, Chinnaiyan A, Halder G, Lai ZC, Guan KL (2007) Inactivation of YAP oncoprotein by the Hippo pathway is involved in cell contact inhibition and tissue growth control. *Genes Dev* 21(21):2747–2761
 60. Al-Halabi H, Nantel A, Klekner A, Guiot MC, Albrecht S, Hauser P, Garami M, Bogner L, Kavan P, Gerges N, Shirinian M, Roberge D, Muanza T, Jabado N (2011) Preponderance of sonic hedgehog pathway activation characterizes adult medulloblastoma. *Acta Neuropathol* 121(2):229–239
 61. Remke M, Hielscher T, Northcott PA, Witt H, Ryzhova M, Wittmann A, Benner A, von Deimling A, Scheurlen W, Perry A, Croul S, Kulozik AE, Lichter P, Taylor MD, Pfister SM, Korshunov A, Thompson MC, Fuller C, Hogg TL, Dalton J, Finkelstein D, Lau CC, Chintagumpala M, Adesina A, Ashley DM, Kellie SJ, Taylor MD, Curran T, Gajjar A, Gilbertson RJ (2006) Genomics identifies medulloblastoma subgroups that are enriched for specific genetic alterations. *J Clin Oncol* 24(12):1924–1931
 62. Chang CH, Housepain EM, Herbert C Jr (1969) An operative staging system and a megavoltage radio-

- therapeutic technic for cerebellar medulloblastomas. *Radiology* 93(6):1351–1359
63. Halperin EC, Constine LS, Tarbell NJ et al (1999) Tumors of the posterior fossa and the spinal cana. In: *Pediatric radiation oncology*, 3rd edn. Lippincott-Williams & Wilkins, Philadelphia, pp 80–125
64. Terterov S, Krieger MD, Bowen I, McComb JG (2010) Evaluation of intracranial cerebrospinal fluid cytology in staging pediatric medulloblastomas, supratentorial primitive neuroectodermal tumors, and ependymomas. *J Neurosurg Pediatr* 6(2):131–136
65. Wiczorek V, Kluge H, Linke E, Zimmermann K, Kuehn HJ, Witte OW, Isenmann S (2007) Pathological CSF cell findings in primary and metastatic CNS tumors, malignant lymphoma and leukemia. In: Kluge H (ed) *Atlas of CSF cytology*. Thieme, Stuttgart, Germany, pp 84–87
66. Gowda KK, Gupta K, Kapoor R, Vasishta RK (2012) Nuclear expression of β -catenin and stem cell markers as potential prognostic indicators in medulloblastoma. *Neurol India* 60(5):487–494

Lucia Quaglietta, Virginia Vitale, Antonio Verrico,
and Roberta Migliorati

18.1 Introduction

18.1.1 Epidemiology

Tumors of the central nervous system (CNS) represent in children the second most frequent type of cancer after leukemia, with an incidence of about 2.8 cases per 100,000 children per year. Medulloblastoma (MB) accounts for approximately 20 % of all CNS tumors, thereby representing one of the most common malignant brain tumors in childhood [1]. Most cases of MB occur in children younger than 10 years of age. Incidence is significantly higher in boys than in girls (about 60 % boys). The annual incidence rate is higher in children between 1 and 9 years of age (eight per million) and slightly reduced in infants (six per million), and it is lowest in 10–14-aged children (four

per million) [2]. Between 2000 and 2002, 5-year overall survival (OS) in European children with diagnosis of MB was 66 %, and infants had the worst prognosis. There was a significant improvement of survival for children diagnosed in 2000–2002 compared to those diagnosed in 1995–1999 and the risk of dying was reduced by 30 % [3].

18.1.2 Clinical, Histopathological, and Molecular Markers of Prognosis

Usually, MB patients are stratified into standard and high-risk groups for therapy, according to the clinical presentation, depending on the presence of metastases (M1–M4) or residual disease >1.5 cm² evaluated by early postoperative magnetic resonance imaging (MRI), according to North American stratification [4]. The type of risk group is determined according to Chang's classification for metastases (Table 18.1). Risk-stratified

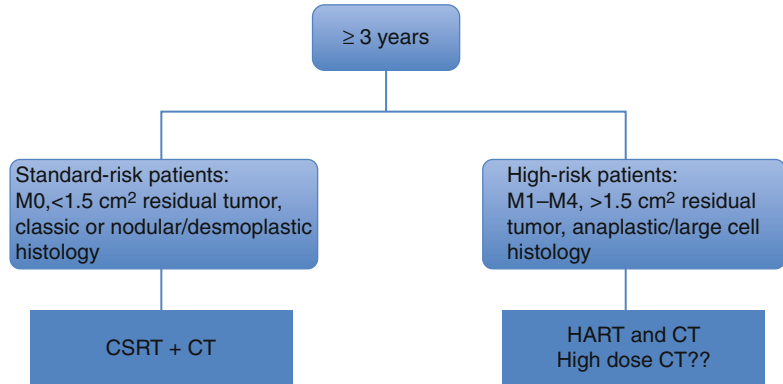
L. Quaglietta, M.D. (✉) • V. Vitale, M.D.
R. Migliorati, M.D.
Department of Oncology, Division of Pediatric
Oncology, A.O.R.N. Santobono-Pausilipon
Children's Hospital,
Via Posillipo n°226, 80123 Naples, Italy
e-mail: oncologia pediatricanapoli@gmail.com;
virginia.viT80@gmail.com;
roberta.migliorati@gmail.com

A. Verrico, M.D.
Department of Oncology, Division of Pediatric
Oncology, A.O.R.N. Santobono-Pausilipon
Children's Hospital,
Via Posillipo n°226, 80123 Naples, Italy
e-mail: antonioverrico@gmail.com

Table 18.1 Chang classification for metastases

M0	No gross nodular or laminar subarachnoid or hematogenous metastasis
M1	Microscopic tumor cells in the cerebrospinal fluid
M2	Gross nodular or laminar seeding in the cerebellum, cerebral subarachnoid space, or in the third or fourth ventricles
M3	Gross nodular or laminar seeding in the spinal subarachnoid space
M4	Extra-neuraxial metastases

Fig. 18.1 Stratification of patients according to clinical risk factors. *M* metastases, *CSRT* craniospinal radiotherapy, *CT* chemotherapy, *HART* hyperfractionated accelerated radiotherapy



schemes of the patients older than 3 years of age, on the basis of the extent of residual disease and dissemination, are reported in Fig. 18.1. Standard-risk (SR) patients are those diagnosed when they are older than the age of 3 years with nonmetastatic and totally or near-totally resected (<1.5 cm² on postoperative MRI) disease; patients not fulfilling these criteria are regarded as high risk (HR). This clinical stratification has only proven useful as a rough guide for predicting prognosis; in particular, it does not identify the 20–30 % of SR patients with resistant disease or rather those patients who might be overtreated with current protocols [5]. More recently, the histological subtype and molecular characteristics of the tumor are going to be added to the list of possible prognostic factors for survival: the presence of widespread anaplasia or large cell morphology was added to risk-stratification criteria after these cytologic phenotypes showed to be associated with decreased progression-free survival. In infants, nodular/desmoplastic tumors seem to carry a better prognosis [6–8]. The prospective multicenter trial HIT 2000 confirmed the prognostic impact of histology: in patients aged <4 years desmoplastic/nodular histology was an independent prognostic factor for EFS. In these subgroup of children, the tumor control was obtained by chemotherapy alone [9].

Over the last decade, studies of mRNA expression profiles identified medulloblastomas are not a single disease entity. Extensive efforts using integrative genomics to allow for genetic and

molecular stratification of the disease brought to the current consensus on four molecular subgroups of medulloblastoma each with distinct genetic profiles, pathway signatures, and clinicopathological features: WNT, SHH, Group 3, and Group 4 [10]. This work not only established the complexity of this most common embryonal CNS tumor but also provided insight into biological subgroups and their prognostic relevance [11] along with clinical and histopathological stratification that have not been supplanted. WNT activation in medulloblastoma is associated with good outcome and immunohistochemistry analysis for nuclear accumulation of β -catenin is a marker of immediate clinical impact for upcoming trials aiming to test the feasibility of reducing therapy intensity in WNT-driven medulloblastoma. SHH and Group 4 are generally associated with an intermediate prognosis, whereas Group 3 with a poor one.

18.1.3 Chemosensitivity

Chemotherapy is presently an integral component of treatment for all infants and children with medulloblastoma. Because of its chemosensitivity, MB was one the first pediatric brain tumors to have chemotherapy extensively evaluated in different contexts: to increase disease control and patient survival, to decrease adverse effects of radiation therapy, and to postpone or avoid the need for radiation therapy in very young children. Objective

response rates have been documented with cisplatin, etoposide, and a variety of different alkylators, with the best responses being seen with multidrug regimens [12] (Figs. 18.2, 18.3, and 18.4).

Historically, neither the first trial of the International Society of Paediatric Oncology

(SIOP) nor the trial of the Children's Cancer Study Group (CCSG) could demonstrate a significant long-term survival difference in favor of chemotherapy, although children with more extensive tumors benefited from the addition of chemotherapy in the latter study. The second

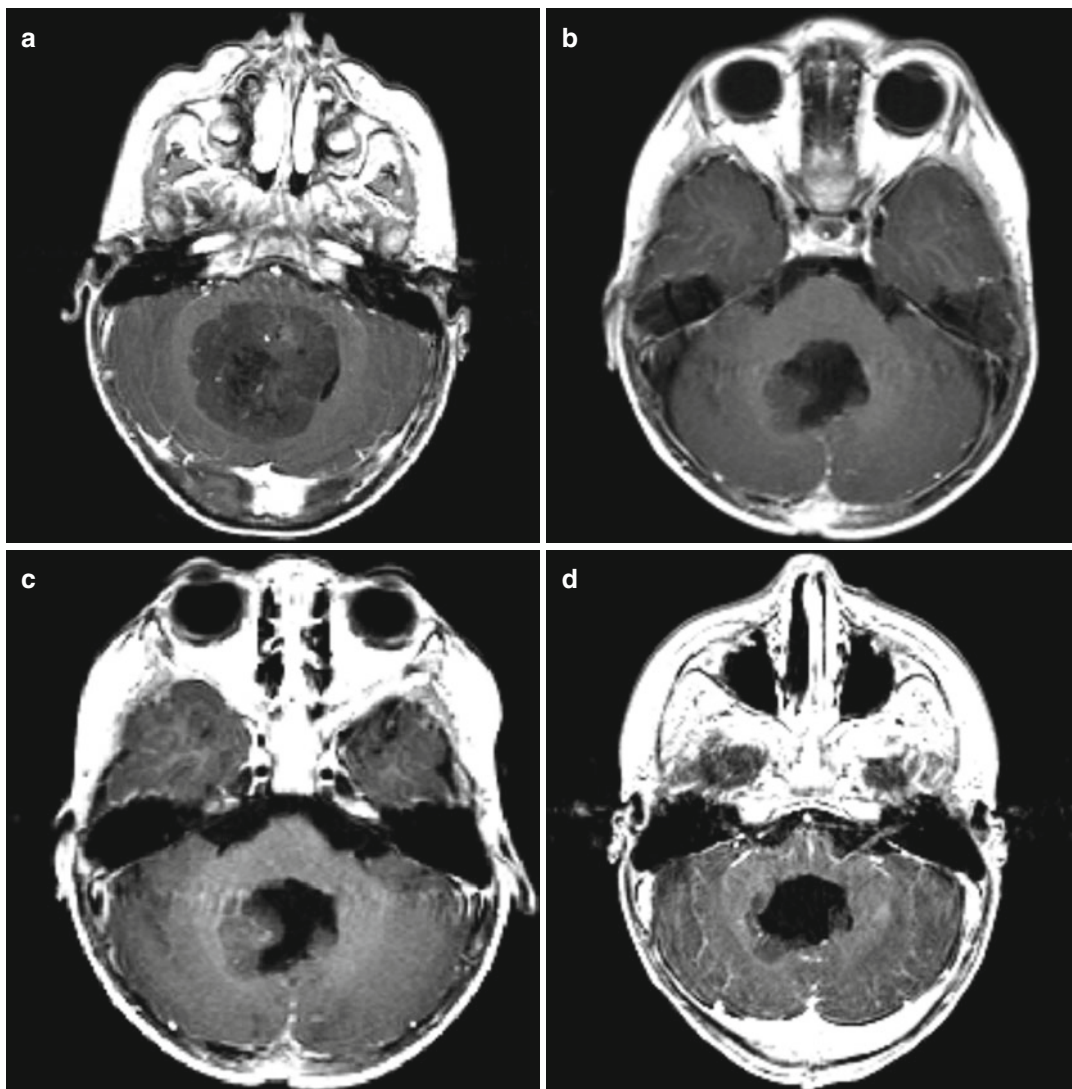


Fig. 18.2 (a) Example of chemoresistance: 2-year-old baby girl presenting with vomiting and ataxic gait. Post-contrast axial T1-weighted MRI shows a non-enhancing lesion of cerebellar origin extending into the fourth ventricle. (b) Post-contrast MRI performed 12 h after partial removal. Residual tumor >1.5 cm² is visible within the fourth ventricle, adherent to the right cerebellar hemisphere. A diagnosis of MB was made. (c) Post-contrast

MRI performed 4 months after surgery and 4 cycles of HD chemotherapy (vincristine, MTX, VP16, cyclophosphamide, carboplatin). Residual tumor is still visible within the fourth ventricle. No variations if compared with (b). (d) Post-contrast MRI performed 12 h after second-look surgery. No residual tumor is visible in the fourth ventricle cavity. (e) Post-contrast MRI performed 6 months after the end of chemo and radiotherapy

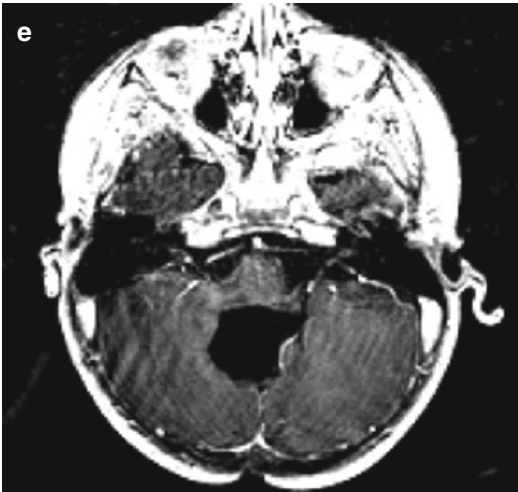


Fig. 18.2 (continued)

SIOP study (SIOP II) aimed to improve survival of children and, where possible, to reduce the dose of craniospinal radiotherapy (CSRT) to 25 Gray (Gy), but no benefit of neoadjuvant chemotherapy could be demonstrated for any group of children. Furthermore, children who received reduced-dose radiotherapy had the worst prognosis [13]. Similarly, Jakacki et al. reduced the craniospinal radiation dose to 18 Gy after chemotherapy in seven young children with localized MB, but they concluded that this dose could not be adequate to prevent recurrences [14]. The third SIOP study (PNET 3) randomized nonmetastatic patients to receive radiotherapy with or without chemotherapy. This prospective randomized multicenter study demonstrated an improved event-free survival (EFS) in the chemotherapy group, but the difference in overall survival (OS) was not statistically significant [15]. A past nonrandomized study by the Children's Cancer Group (CCG) demonstrated a 5-year progression-free survival (PFS) of 79 % for children with not disseminated MB treated with a combination of adjuvant chemotherapy and a reduced dose of CSRT [16]. Later, the CCG conducted a study where children affected by not disseminated standard-risk MB received reduced-dose

CSRT and then were randomized to receive two different chemotherapy schedules; they demonstrated a 5-year EFS and OS of 81 % and 86 %, respectively [17].

In order to improve survival of high-risk patients (very young children or children with disseminated disease) with a dismal prognosis, a wide number of studies demonstrated a good result with chemotherapy alone in young children, as in the study of Rutkowski et al. [18]. For young children with localized MB, they found 5-year PFS and OS rates of 68 % and 77 %, respectively; in contrast for those with metastases, the 5-year PFS and OS rates did not exceed 33 % and 38 %, respectively. Similarly, the treatment with “eight drugs in one day” for infants without and with metastases demonstrated a 3-year PFS rate of 29 % and 11 %. A study by Perez-Martinez et al. reported a 2-year EFS of 71 % in very young children treated with high-dose chemotherapy followed by stem cell rescue (SCR) [19]. The French Society of Pediatric Oncology (SFOP) showed that conventional chemotherapy alone could cure young children with localized MB who had gross total resection in 41 % of cases. In addition, they demonstrated a 3-year OS of 61 % in locally relapsed nonmetastatic patients younger than 3 years old of age rescued by high-dose chemotherapy plus SCR followed by posterior fossa radiotherapy. Five of 15 patients with metastatic relapse are alive after salvage therapy which included high-dose chemotherapy; however, the prognosis in metastatic patients was dismal with a 5-year PFS of 13 % and none of the children with disease progression responded to salvage therapy. Conventional chemotherapy alone can be used to cure young children with nonmetastatic medulloblastoma who have gross total resection confirmed by early radiological assessment, but is not sufficient for treatment of those with metastatic or incompletely resected medulloblastoma. Salvage treatment followed by posterior fossa radiotherapy can effectively treat local relapses or progression [20].

18.2 Treatment

18.2.1 Standard Risk

Traditionally, the milestone for treatment of standard-risk patients has consisted of complete or near complete surgical resection followed by postoperative CSRT. Using conventional

doses of radiotherapy (36 Gy to the craniospinal axis together with a boost of 18–20 Gy to the posterior fossa, with a total dose of 54–56 Gy), different studies reported that after 5 years from diagnosis, between 55 % and 70 % of children are alive and free of progressive disease [21]. It is noteworthy that an elevated percentage of survivors have significant long-term sequelae, mostly

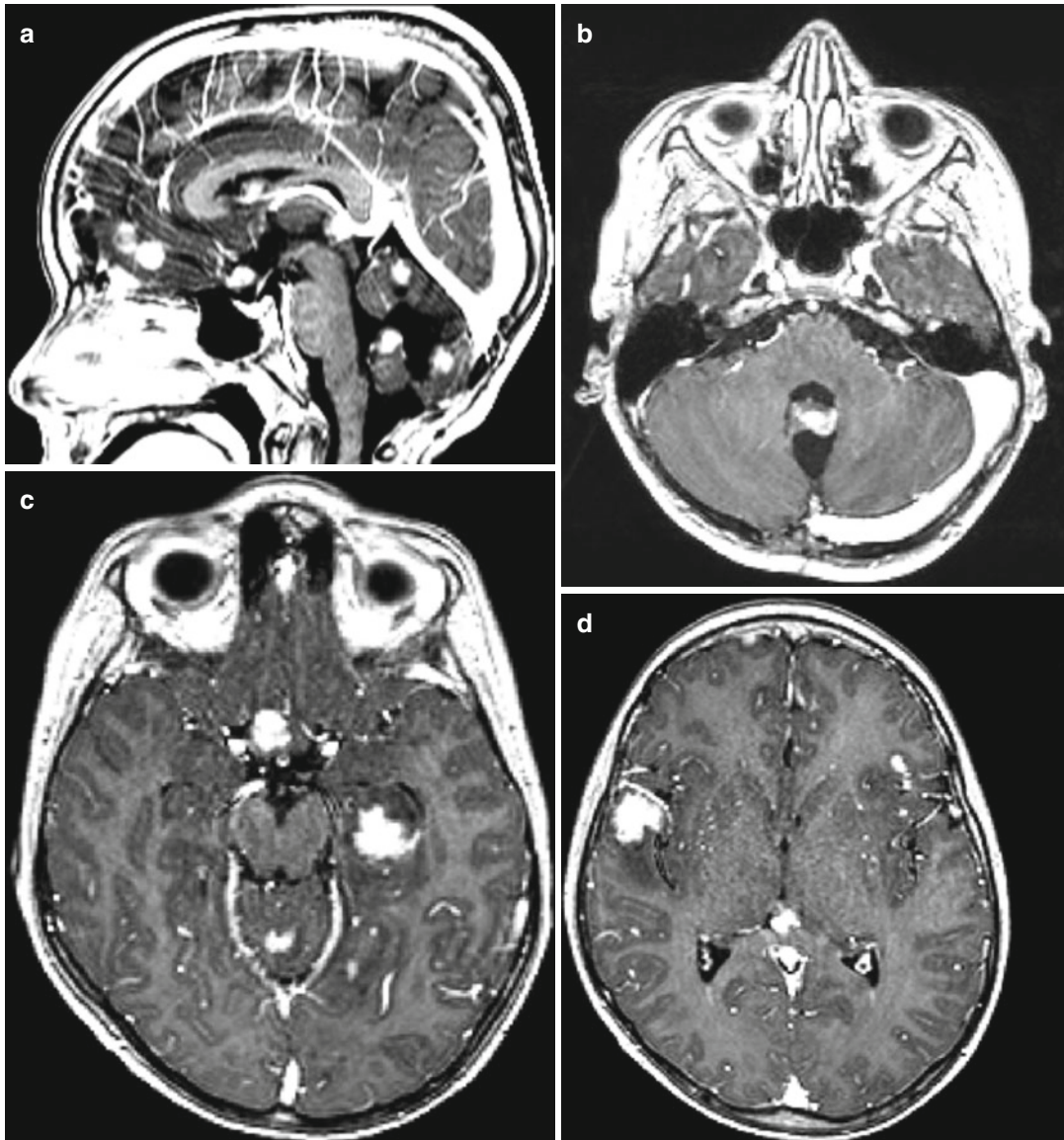


Fig. 18.3 (a–e) Example of chemosensitivity: 11-year-old patient referred by another country where 3 years before, he had been treated for complete removal of vermian MB followed by radiotherapy (25.5 Gy on neuraxis,

15.3 Gy on spinal cord, 30.4 Gy on the posterior fossa). MRI performed for vomiting showed recurrent tumor in both infra- and supratentorial space (a–d), in the lateral ventricle (e)



Fig. 18.3 (continued)

neuropsychological deficits, linear growth deficit, and endocrine dysfunction due to irradiation of the pituitary gland and hypothalamic regions together with the effects of whole spine radiotherapy. In order to decrease the long-term neurocognitive effects of radiation and to control tumor growth, especially in young children, the dose administered to the brain and spine has been reduced.

At present, there is general agreement that after surgical resection, the gold standard treatment for patients older than 3 years at diagnosis is “reduced-dose” CSRT: a total dose of 23.4 Gy to the craniospinal axis within 40 days from surgery plus a localized boost to the posterior fossa (total dose of 54–55.8 Gy). The treatment is usually combined with weekly concurrent single administration of vincristine and followed by a multidrug regimen (cisplatin, vincristine, and lomustine or cisplatin, vincristine, and cyclophosphamide) [17] that provided a 5-year event-free survival of 80 %. The reduced-dose CSRT (23.4 Gy vs. 36 Gy) without the adjuvant chemotherapy has shown a higher number of early failures. The Children Oncology Group (COG) is evaluating in a randomized study further reduction of CSRT and posterior fossa boost dose, but at present, this treatment is not recommended.

The HIT-SIOP PNET 4 trial, recently closed in Europe, compared the use of conventionally fractionated radiotherapy at a dose of 23.4 Gy plus boost versus hyperfractionated radiotherapy (HFRT) (1 Gy/fraction, 2 fractions/day) at a dose of 36 Gy plus boost, both followed by chemotherapy schedule with eight courses of vincristine (1.5 mg/m² for three doses), cisplatin (70 mg/m²), and lomustine (CCNU, 75 mg/m²). EFS and OS for HFRT were not better than the conventional one, which therefore remains standard of care in this disease [22]. However, a French study on standard-risk MB patients treated by hyperfractionated radiotherapy without adjuvant chemotherapy showed a 3-year PFS of 83 % with a good neuropsychological outcome at follow-up [23]. Future trials are needed to further evaluate the efficacy and safety of these treatment modalities.

Molecular biology has changed our knowledge of MB and has implications for diagnostic stratification and treatment. As newer biological agents are translated from the lab to the bedside, clinicians need to understand the fundamental signalling pathways that are targeted during therapy. More knowledge of the molecular biology of MB is needed so that more children will be cured or have an improved quality of life. Future protocols will stratify treatments on the basis of biological factors, such as beta-catenin, so a subgroup of “low-risk” patients will be identified to be addressed to only surgery and radiotherapy or chemotherapy without risk of relapse.

18.2.2 High Risk

Prospective randomized studies performed as early as the late 1970s by the CCG and the SIOP, which compared PFS and OS in children treated with radiotherapy alone to those receiving radiotherapy plus chemotherapy given during and after radiation, demonstrated a statistically significant 15–20 % survival advantage for patients with poorer risk disease (defined as those with disseminated disease or larger and more infiltrative tumors and/or significant amounts of tumor left after surgery, as determined by postoperative

MRI). These results were the basis of a series of trials performed over the ensuing two decades evaluating the efficacy of chemotherapy given at higher dose, coupled with other agents, or given in various sequences with radiotherapy [15, 17, 24]. Once again, studies using chemotherapy prior to radiotherapy have not shown benefit and possibly may have demonstrated inferior overall disease control rate [15]; on the other hand, chemotherapy treatment during and after radiotherapy has conducted to an improvement of survival rate [12]. Chemotherapy is therefore part of adjuvant treatment in this group of patients but optimal timing and schedule are not yet established.

A mono-institutional trial considering the use of CSRT followed by vincristine, cisplatin, and CCNU in high-risk patients reported a survival rate of around 85 % [25]. In an SIOP trial published with a 76-month follow-up, 27 metastatic patients treated with standard-dose RT followed by CCNU and vincristine obtained a 5-year PFS of 43 % [13]. Similar results have been reported by the SFOP study, which treated high-risk patients with the “eight-drugs-in-one-day” chemotherapy regimen, followed by two cycles of high-dose MTX, radiotherapy, and then further “eight-in-one” chemotherapy. The French national study confirmed the low rate of response to the “sandwich” chemotherapy

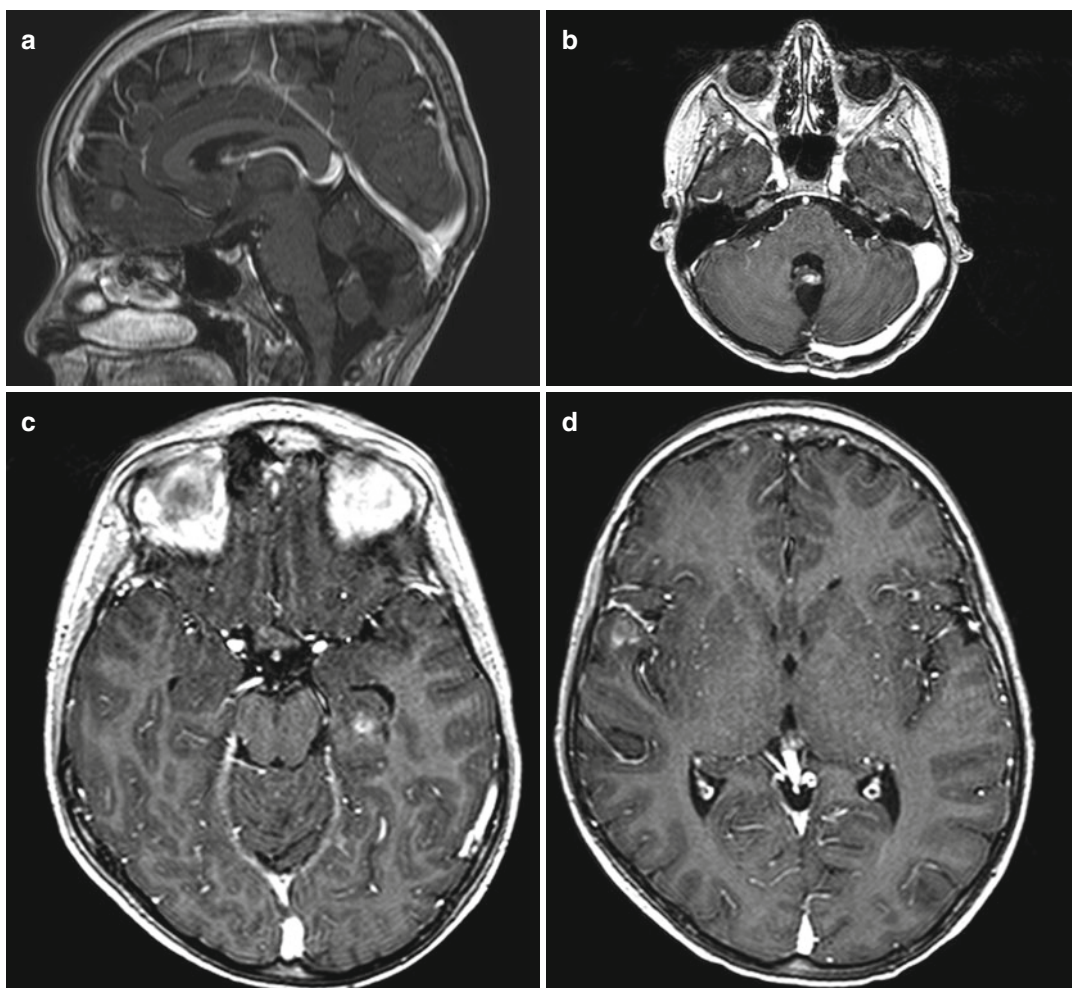


Fig. 18.4 (a–e) MRI performed after two cycles of HD chemotherapy (vincristine, Endoxan, VP16). Significant reduction of the lesions is evident. The patient was addressed to autologous bone marrow transplantation

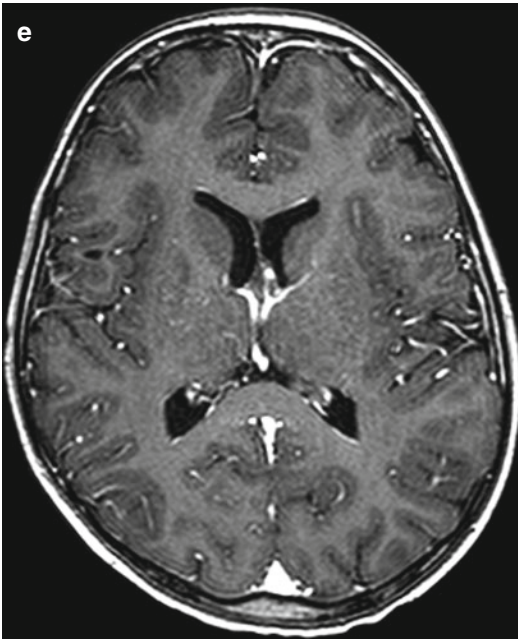


Fig. 18.4 (continued)

without significant improvement in either M1 or M2/M3 patients, showing a 5-year EFS of 58.8 % and 43.1 %, respectively [26]. The “eight-in-one” chemotherapy regimen before and after RT has been also proposed by the CCG 921 randomized phase III trial, which reported a significantly lower PFS for metastatic patients [57 % M1; 40 % M2; 78 % M0, ($p=0.0006$)] [27]. The randomized prospective multicenter trial HIT’91 compared two treatments: the postoperative neoadjuvant chemotherapy (ifosfamide, etoposide, high-dose methotrexate, cisplatin, and cytarabine given in two cycles) followed by CSRT and maintenance chemotherapy after immediate postoperative RT. For all randomized patients, the PFS resulted 65 % for M1 patients and 30 % for M2–M3 patients after 3 years of follow-up confirming that metastases stage plays a prognostic role [28]. Recently, high-dose chemotherapy and autologous stem cell transplantation provided encouraging results. Strother et al. reported that after 2 years, the PFS was 73.7 % \pm 10.5 % in 19 enrolled patients with metastases treated by surgical resection and topotecan in a 6-week face window followed by CSRT and four cycles of high-dose cyclophosphamide (4,000 mg/m²

per cycle), with cisplatin (75 mg/m² per cycle) and vincristine (two 1.5 mg/m² doses per cycle). Support with SCR or bone marrow rescue was administered after each cycle of high-dose CT [29]. Results of a study conducted on nine patients affected by supratentorial primitive neuroectodermal tumors and metastatic MB treated with high-dose chemotherapy (cyclophosphamide, cisplatin, vincristine, etoposide, and high-dose MTX) for two to three cycles before radiotherapy showed, after a median follow-up of 27 months, that seven patients remained in continuous complete remission [30]. More recently, 21 young patients with high-risk or disseminated MB were enrolled in order to evaluate the response rate to an intensified induction chemotherapy regimen and single myeloablative chemotherapy cycle with autologous SCR. This was followed by RT for patients more than 6 years of age or with evidence of residual disease on completion of the induction chemotherapy if under 6 years old. The 3-year EFS and OS were 49 and 60 %, respectively [31]. The European phase III clinical trial SIOP/UKCCSG PNET 3 demonstrated an unsatisfactory outcome in metastatic patients treated with neoadjuvant CT (vincristine, cisplatin, etoposide, and cyclophosphamide) followed by a standard CSRT dose with a posterior fossa boost and/or a boost to metastases, obtaining a 5-year PFS of less than 40 % [15]. Recently, Gandola et al. [32] reported 33 consecutive patients receiving postoperative high-dose chemotherapy (HDCT) with methotrexate plus vincristine, etoposide, cyclophosphamide, and carboplatin in a 2-month schedule. Hyperfractionated accelerated radiotherapy (HART) was delivered at a total dose to the neuraxis of 39 Gy (1.3 Gy/fraction, 2 fractions/day) with a posterior fossa boost up to 60 Gy (1.5 Gy/fraction, 2 fractions/day). In addition, patients with persistent disseminated disease before HART underwent two courses of myeloablative chemotherapy and circulating progenitor cell rescue. Otherwise, patients in complete remission received maintenance chemotherapy with vincristine and CCNU for 1 year. Of 32 evaluable patients (one patient dead by sepsis before radiotherapy), 22 responded to chemotherapy. 12/22 patients achieved complete

remission (CR) before the radiation phase and 10/22 had radiological partial response (PR). In the remaining patients, disease was stable in five and progressed in five. All patients underwent radiotherapy. Fourteen of the 32 patients received consolidation therapy after HART. Eight patients relapsed after a median of 12 months after beginning chemotherapy. With a median follow-up of 82 months, the 5-year EFS, PFS, and OS were 70, 72, and 73 %, respectively. No severe clinical complications of HART have been reported. HART with intensive postoperative chemotherapy and myeloablative chemotherapy seems to be feasible without limiting major toxicity in children with metastatic MB.

None of these studies has so far provided results concerning the role of chemotherapy, administered before or after radiotherapy, the efficacy of high-dose chemotherapy followed by the SCR, and the contribution of high doses of CSRT, possibly delivered through a hyperfractionated/accelerated modality, to achieve better disease control. Wider phase III trials are desirable to obtain stronger evidence.

18.2.3 Infant

In the past, the survival of infants with MB was lower compared to older children. Then, in 1980s, a cut-off age level of 3 years for radiotherapy had been introduced in order to reduce unacceptable sequelae caused by irradiation. Thus, in the USA in the 1980s and then in Europe after 1985, trials were performed using up-front CT so as to delay or avoid radiotherapy.

The first Pediatric Oncology baby protocol (POG1) that aimed to delay irradiation by using conventional CT was followed by several North American and European Cooperative studies [33–36].

In the POG1 study, the CT for 1 or 2 years, respectively, for children who were 2–3 and <2 years of age was provided. At the end of CT, both groups were eligible for radiotherapy when they were 3-year-old. The 5-year EFS and OS were 30 % and 69 %, respectively. Radical surgical intervention was a favorable prognostic fac-

tor, as 69 % of M0/T0 cases became long-term survivors (13 cases) [37]. The CCG study tested the “eight-in-one” protocol. After a median follow-up of 6 years, the 3-year EFS was 22 % while the long-term survival was below 30 % in M0/T0 cases [38]. These early results lead to following European and North American studies which intensified systemic CT (POG2) or added intraventricular CT (HIT-SKK’92) or high-dose systemic methotrexate (AIEOPSN9501). Standard CT in France (Baby SFOP Protocol) included courses of carboplatin/procarbazine, etoposide/cisplatin, and vincristine/cyclophosphamide for 18 months. The OS was 76 %, but 33/47 M0/T0 patients progressed during/after CT. The results in metastatic cases were poor and unsatisfactory (PFS 16 %); nevertheless, localized failures in M0/T0 were successfully rescued by high-dose CT, with or without reoperation, followed by focal irradiation [33]. The German study investigated about intraventricular CT in 43 patients showing the best known OS and EFS in 17 M0/T0 patients without irradiation. Results are especially promising for patients without initial metastases, in whom radiotherapy should be reserved for salvage strategies at relapse [18]. These results need to be reproduced in a larger international cooperative study.

The Italian AIEOP infant pilot study, which uses HDCT followed either by conformal RT on the residual tumor or by CSRT in patients with metastases, shows that 5-year EFS in 20 enrolled patients increased (70 %) [35].

It is still unclear whether the subset of infants that were cured in each study had peculiar biological features that favored survival.

The HIT-SKK’92s reported a high frequency of desmoplastic medulloblastoma (40 %), with a significantly better prognosis compared with classic MB [18]. A recent single institution retrospective study reports a similar observation, confirming the high frequency of desmoplastic variants and particularly of extensive nodularity medulloblastomas (MBEN) in young age and the high frequency of association between Gorlin syndrome and MBEN, which was observed in 40 % of cases [39]. Further prospective cooperative studies will clarify the prognostic role of

desmoplasia, biological markers, and postoperative residual tumor in order to improve stratification criteria by risk-adapted treatment recommendations.

On account of the higher frequency (28 %) of cancer predisposition syndromes (mainly Gorlin syndrome) in young patients with MB [39], future trials should include guidelines for the identification of such conditions and for genetic counseling to families. In infants with Gorlin syndrome, every attempt should be made to avoid radiotherapy because of the increased risk of secondary tumors and the frequency of nevoid basal cell carcinomas in irradiated fields.

18.2.4 Relapse

The treatment strategies for relapsed patients or patients with refractory disease include repeat surgical resection, re-irradiation when feasible, high-dose chemotherapy followed by autologous hematopoietic cell transplantation, and early phase clinical trials. Actually, there is no current standard of care in the treatment of recurrent-refractory MB as no one strategy has proven superior. Recent reports have clearly distinguished two groups of patients with relapsing MB: children not undergoing irradiation at diagnosis because of their young age (<3–5-year-old at the time) and older children who commonly underwent CSRT as part of their first-line treatment. In the first group, radiotherapy can be used at relapse, combined with various chemotherapy schedules mostly with myeloablative dosages [40]. This option can obtain a progression-free survival rate of approximately 50 %. For the second group, the cure is exceptional: approximately 20 % of patients who experience relapse after irradiation cannot be cured by salvage therapy, with very rare exceptions (<5 % of those who experience relapse) [41, 42]. In older children who received CSRT as part of their initial therapy, reoperation followed by focal radiation with conformal techniques or proton beam might be an option for solitary recurrences and should be considered on a case-by-case basis [43]. Trials of

idarubicin, taxol, topotecan, temozolomide plus oral etoposide, and irinotecan recorded few and not lasting responses with development of further tumor progression. Recently, the combination of bevacizumab and irinotecan, with or without temozolomide, produces objective responses with minimal toxicity in children with recurrent medulloblastoma [44]. Under investigation is the use of a low-dose chemotherapy regimen called “metronomic” therapy, such as oral etoposide or temozolomide, with the intent to stabilize the disease minimizing symptoms and with preservation of quality of life as long as possible. Several groups have reported the feasibility of this approach for treating pediatric brain tumors in case series, although no formalized clinical trials have been published to date. The main concerns about this approach are the hematological toxicity and the long-term risk of secondary tumors. More clinical trials are needed to validate this line of therapy. Several drugs act on tumor clonal cells, but not on tumor stem cells, which seem to show a multidrug resistance.

18.2.5 New Frontiers

The goal of molecular therapy could be to eliminate tumor stem cells of the tumor bulk. The identification of activated signalling pathway components of stem cells may help to develop new treatment strategies in aggressive tumors such as resistant/relapsed MB. A phase II trial with smoothed inhibitors for SHH-driven relapsed medulloblastoma (SHH-MBs, clinicaltrials.gov, ID: NCT01708174) showed how infant (36 %) and childhood (45 %) SHH-MBs frequently have mutations downstream of SMO, which makes these tumors intrinsically resistant to drugs targeting SMO [45] and highlighting genetic heterogeneity within the disease subgroups need to be elucidated before starting treatment. In line with this finding, it has recently been proposed “6 packs” of fluorescence in situ hybridization tests (GLI2, MYC, 14q, 17p, 17q, and 11q) to evaluate heterogeneity within subgroups; indeed, C-MYC/N-MYC amplification is

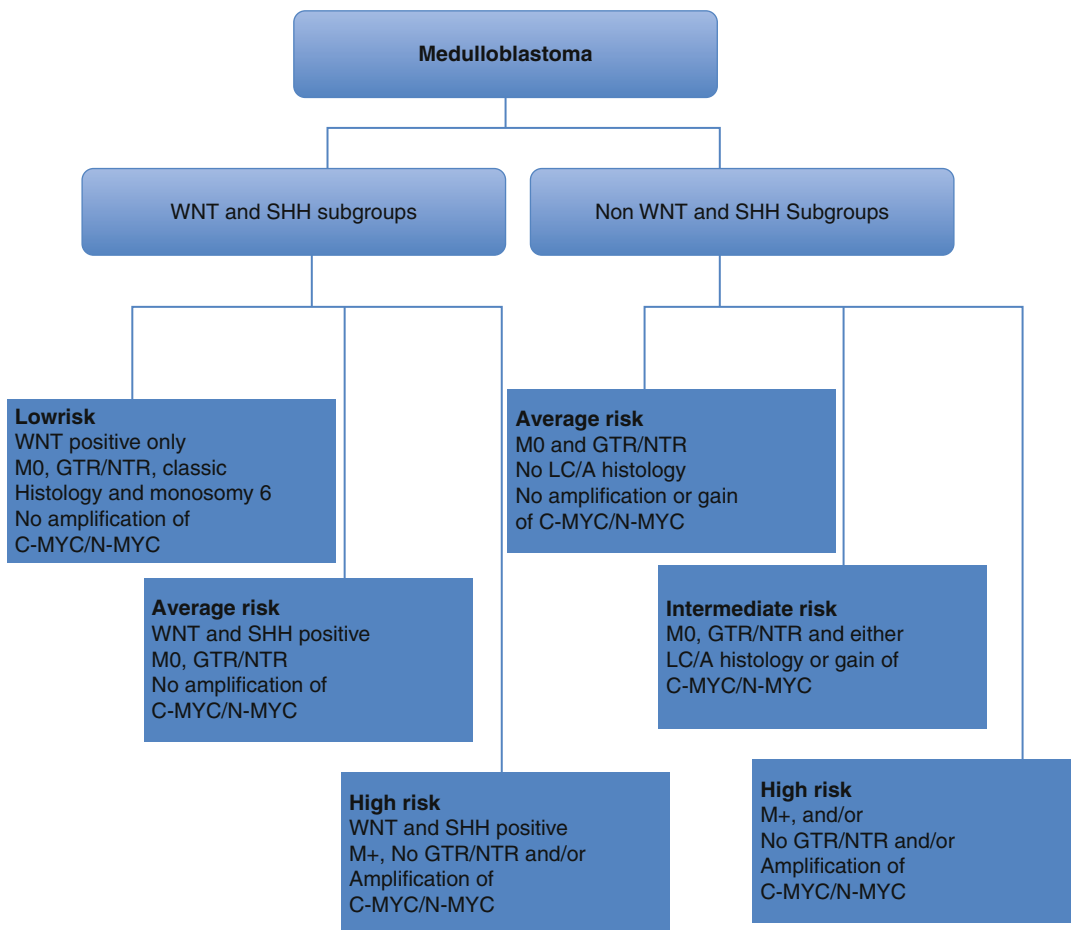


Fig. 18.5 New stratification of patients according to clinical and molecular risk factors in opened St. Jude frontline medulloblastoma protocol (SIMB 12)

already considered an exclusion criterion from low average-risk protocols [46].

Prospective clinical trials being planned for medulloblastoma will assess the stratification of patients using the above-mentioned molecular and histological biomarkers, alongside clinical indices, to select favorable-, standard-, and high-risk treatment groups (Fig. 18.5). This selection will underpin SIOP PNET 5 MB (clinicaltrials.gov, ID: NCT02066220), which will test whether treatment can be reduced for a favorable-risk disease subgroup, with the aim of maintaining survival rates while reducing late effects.

References

1. Michiels EMC, Schouten-Van Meeteren AYN, Doz F et al (2010) Chemotherapy for children with medulloblastoma (Protocol). *Cochrane Lib* 1:1–8
2. Peris-Bonet R, Martinez-Garcia C, Lacour B et al (2006) Childhood central nervous system tumours—incidence and survival in Europe (1978–1997): report from Automated Childhood Cancer Information System project. *Eur J Cancer* 42:2064–2080
3. Gatta G, Zigon G, Capocaccia R et al (2009) Survival of European children and young adults with cancer diagnosed 1995–2002. *Eur J Cancer* 45:992–1005
4. Packer RJ, Rood BR, MacDonald TJ (2003) Medulloblastoma: present concepts of stratification into risk groups. *Pediatr Neurosurg* 39:60–67

5. Gajjar A, Hernan R, Kocak M et al (2004) Clinical, histopathologic and molecular markers of prognosis: toward a new disease risk stratification system for medulloblastoma. *J Clin Oncol* 22(6):984–993
6. Eberhart CG, Kepner JL, Goldthwaite PT et al (2000) Histopathologic grading of medulloblastomas: a Pediatric Oncology Group study. *Cancer* 94(2):552–560
7. Massimino M, Antonelli M, Gandola L et al (2013) Histological variants of medulloblastoma are the most powerful clinical prognostic indicators. *Pediatr Blood Cancer* 60(2):210–216
8. McManamy CS, Lamont JM, Taylor RE et al (2003) Morphophenotypic variation predicts clinical behavior in childhood non-desmoplastic medulloblastomas. *J Neuropathol Exp Neurol* 62(6):627–632
9. Von Bueren AO, Von Hoff K, Pietsch T et al (2011) Treatment of young children with localized medulloblastoma by chemotherapy alone: Results of the prospective, multicenter trial HIT 2000 confirming the prognostic impact of histology. *Neuro Oncol* 13(6):669–679
10. Taylor MD, Northcott P, Korshunov A et al (2012) Molecular subgroups of medulloblastoma: the current consensus. *Acta Neuropathol* 123(4):465–472
11. Pietsch T, Schmidt R, Remke M et al (2014) Prognostic significance of clinical, histopathological, and molecular characteristics of medulloblastomas in the prospective HIT2000 multicenter clinical trial cohort. *Acta Neuropathol* 128(1):137–149
12. Pizzo PA, Poplack DG (2011) Principles and practice of pediatric oncology. Lippincott Williams & Wilkins/Wolters Kluwer Business, Philadelphia
13. Bailey CC, Gnekow A, Welke S et al (1995) Prospective randomised trial of chemotherapy given before radiotherapy in childhood medulloblastoma. International Society of Paediatric Oncology (SIOP) and the (German) Society of Paediatric Oncology (GPO): SIOP II. *Med Pediatr Oncol* 25:166–178
14. Jakacki RI, Feldman H, Jamison C et al (2004) A pilot study of preirradiation chemotherapy and 1800 cGy craniospinal irradiation in young children with medulloblastoma. *Int J Radiat Oncol Biol Phys* 60(2):531–536
15. Taylor RE, Bailey CC, Robinson KJ et al (2005) Outcome for patients with metastatic (M2-3) medulloblastoma treated with SIOP/UKCCSG PNET-3 chemotherapy. *Eur J Cancer* 41:727–734
16. Packer RJ, Goldwein J, Nicholson HS et al (1999) Treatment of children with medulloblastoma with reduced-dose craniospinal radiation therapy and adjuvant chemotherapy: a Children's Cancer Group study. *J Clin Oncol* 17(7):2127–2136
17. Packer RJ, Gajjar A, Vezina G et al (2006) Phase III study of craniospinal radiation therapy followed by adjuvant chemotherapy for newly diagnosed average-risk medulloblastoma. *J Clin Oncol* 24(25):4202–4208
18. Rutkowski S, Bode U, Deinlein F et al (2005) Treatment of early childhood medulloblastoma by postoperative chemotherapy alone. *N Engl J Med* 352:978–986
19. Pérez-Martínez A, Quintero V, Vicent MG et al (2004) High-dose chemotherapy with autologous stem cell rescue as first line of treatment in young children with medulloblastoma and supratentorial primitive neuroectodermal tumors. *J Neurooncol* 67:101–106
20. Grill J, Sainte-Rose C, Jouvét A et al (2005) Treatment of medulloblastoma with postoperative chemotherapy alone: an SFOP prospective trial in young children. *Lancet Oncol* 6:573–580
21. Massimino M, Giangaspero F, Garrè ML et al (2011) Childhood medulloblastoma. *Crit Rev Oncol Hematol* 79(1):65–83, Epub 2010 Dec 3
22. Lannering B, Rutkowski S, Doz F et al (2012) Hyperfractionated versus conventional radiotherapy followed by chemotherapy in standard-risk medulloblastoma: results from the randomised multicenter HIT-SIOP PNET 4 trial. *J Clin Oncol* 30(26):3187–3193
23. Carrie C, Muracciole X, Gomez F et al (2005) Conformal radiotherapy, reduced boost volume, hyperfractionated radiotherapy, and online quality control in standard-risk medulloblastoma without chemotherapy: results of the French M-SFOP 98 protocol. *Int J Radiat Oncol Biol Phys* 63:711–716
24. Gajjar A, Chintagumpala M, Ashley D et al (2006) Risk-adapted craniospinal radiotherapy followed by high-dose chemotherapy and stem-cell rescue in children with newly diagnosed medulloblastoma (St. Jude Medulloblastoma-96): long-term results from a prospective, multicentre trial. *Lancet Oncol* 7(10):813–820
25. Packer RJ, Siegel KR, Sutton LN et al (1988) Efficacy of adjuvant chemotherapy for patients with poor-risk medulloblastoma: a preliminary report. *Ann Neurol* 24:503–508
26. Verlooy J, Mosseri V, Bracard S et al (2006) Treatment of high risk medulloblastomas in children above the age of 3 years: a SFOP study. *Eur J Cancer* 42:3004–3014
27. Zeltzer PM, Boyett JM, Finlay JL et al (1999) Metastasis stage, adjuvant treatment, and residual tumor are prognostic factors for medulloblastoma in children: conclusions from the Children's Cancer Group 921 randomized phase III study. *J Clin Oncol* 17:832–845
28. Kortmann RD, Kuhl J, Timmermann B et al (2000) Postoperative neoadjuvant chemotherapy before radiotherapy as compared to immediate radiotherapy followed by maintenance chemotherapy in the treatment of medulloblastoma in childhood: results of the German prospective randomized trial HIT '91. *Int J Radiat Oncol Biol Phys* 46:269–279
29. Strother D, Ashley D, Kellie SJ et al (2001) Feasibility of four consecutive high-dose chemotherapy cycles with stem-cell rescue for patients with newly diagnosed medulloblastoma or supratentorial primitive neuroectodermal tumor after craniospinal radiotherapy: results of a collaborative study. *J Clin Oncol* 19:2696–2704
30. Dhodapkar K, Dunkel IJ, Gardner S et al (2002) Preliminary results of dose intensive pre-irradiation

- chemotherapy in patients older than 10 years of age with high risk medulloblastoma and supratentorial primitive neuroectodermal tumors. *Med Pediatr Oncol* 38:47–48
31. Chi SN, Gardner SL, Levy AS et al (2004) Feasibility and response to induction chemotherapy intensified with high-dose methotrexate for young children with newly diagnosed high-risk disseminated medulloblastoma. *J Clin Oncol* 22:4881–4887
 32. Gandola L, Massimino M, Cefalo G et al (2009) Hyperfractionated accelerated radiotherapy in the Milan strategy for metastatic medulloblastoma. *J Clin Oncol* 27:566–571
 33. Duffner PK, Horowitz ME, Krischer JP et al (1993) Postoperative chemotherapy and delayed radiation in children less than three years of age with malignant brain tumors. *N Engl J Med* 328:1725–1731
 34. Ater JL, van Eys J, Woo SY et al (1997) MOPP chemotherapy without irradiation as primary postsurgical therapy for brain tumors in infants and young children. *J Neurooncol* 32:243–252
 35. Garrè ML, Massimino M, Cefalo G et al (2003) High-risk malignant CNS tumours in infants: standard vs myeloablative chemotherapy: the experience of the Italian cooperative study for children <3 years of age. *Neuro Oncol* 1:40
 36. Rutkowski S, Gerber NU, von Hoff K et al (2009) Treatment of early childhood medulloblastoma by postoperative chemotherapy and deferred radiotherapy. *Neuro Oncol* 11:201–210
 37. Duffner PK, Horowitz ME, Krischer JP et al (1999) The treatment of malignant brain tumors in infants and very young children: an update of the Pediatric Oncology Group experience. *Neuro Oncol* 1:152–161
 38. Geyer JR, Sposto R, Jennings M et al (2005) Multiagent chemotherapy and deferred radiotherapy in infants with malignant brain tumors: a report from the Children's Cancer Group. *J Clin Oncol* 23:7621–7631
 39. Garrè ML, Cama A, Bagnasco F et al (2009) Medulloblastoma variants: age-dependent occurrence and relation to Gorlin syndrome—a new clinical perspective. *Clin Cancer Res* 15:2463–2471
 40. Ridola V, Grill J, Doz F et al (2007) High-dose chemotherapy with autologous stem cell rescue followed by posterior fossa irradiation for local medulloblastoma recurrence or progression after conventional chemotherapy. *Cancer* 110:156–163
 41. Bouffet E, Doz F, Demaille MC et al (1998) Improving survival in recurrent medulloblastoma: earlier detection, better treatment or still an impasse? *Br J Cancer* 77:1321–1326
 42. Massimino M, Gandola L, Spreafico F et al (2009) No salvage using high-dose chemotherapy plus/minus reirradiation for relapsing previously irradiated medulloblastoma. *Int J Radiat Oncol Biol Phys* 73:1358–1363
 43. Saran F, Baumert BG, Creak AL et al (2008) Hypofractionated stereotactic radiotherapy in the management of recurrent or residual medulloblastoma/PNET. *Pediatr Blood Cancer* 50:554–560
 44. Aguilera D, Mazewski C, Fangusaro J et al (2013) Response to bevacizumab, irinotecan, and temozolomide in children with relapsed medulloblastoma: a multi-institutional experience. *Childs Nerv Syst* 29(4):589–596
 45. Kool M, Jones DTW, Jager N et al (2014) Genome sequencing of SHH medulloblastoma predicts genotype-related response to smoothed inhibition. *Cancer Cell* 25(3):393–405
 46. Gottardo NG, Hansford JR, McGlade JP et al (2014) Medulloblastoma down under 2013: a report from the third annual meeting of the International Medulloblastoma Working Group. *Acta Neuropathol* 127:189–201

Maurizio Mascarin, Francesca Maria Giugliano,
and Elisa Coassin

19.1 Introduction

Medulloblastoma (MB) is a relatively radiosensitive tumor. Radiotherapy (RT) together with surgery and chemotherapy provide a better outcome, and it is an integral component of the initial management of MB. The tumor generally arises in the posterior fossa (PF) and has a predisposition to spread to the subarachnoid space of the central nervous system (CNS). For this reason, from the late 1960s craniospinal irradiation (CSI) plus a PF boost has become the standard of care [1]. The rationale for additional radiation to the tumor bed is based on the observation that 50–70 % of tumor recurrences occur in the PF [2, 3]. Results obtained in the following two decades suggested that 5-year survival rates of 50–55 % would be realistically obtained in an overall sur-

vival (OS) for children under 16 years of age treated with radical surgery and a full course of megavoltage RT compared with about 40 % rates, as assessed in previous reviews [4]. Since late effects (hormonal deficits, decreased bone growth, and especially intellectual outcome) with these approaches remain suboptimal, investigators have considered new ways to further reduce the side effects of radiotherapy, combining treatment with chemotherapy, reducing the neuraxis dose, and using more conformal techniques. Until now, with the exception of children younger than 3 years, CSI is standard. It is well established that the primary site needs to receive >50 Gy for better PF control [5].

The RT of children with MB can be divided into three main categories: standard-risk MB, high-risk MB in patients older than 3 years of age, and MB in infants and young children.

Established risk factors for an adverse prognosis in terms of progression-free and overall survival are metastatic disease at diagnosis (M1-M3), residual tumor of >1.5 cm (largest extent in an axial plane) on postoperative imaging, young age, and anaplastic or large-cell histological subtype. Future trials would include also biological and molecular features (e.g., beta-catenin and neurotrophin receptor TrkC associated with a favorable outcome, in opposition to myc amplification and chromosome 17 imbalance associated with poor prognosis) into the clinical stratification, to find more efficient treatment strategies and to minimize long-term sequelae of tumor treatment [6].

M. Mascarin (✉) • E. Coassin
Pediatric Radiotherapy Unit, Department of
Radiation Oncology, IRCCS CRO Centro di
Riferimento Oncologico,
Via Gallini, 2, Aviano, (Pordenone), Italy
e-mail: mascarin@cro.it; elisa.coassin@gmail.com

F.M. Giugliano
Pediatric Radiotherapy Unit, Department of
Radiation Oncology, IRCCS CRO Centro di
Riferimento Oncologico,
Via Gallini, 2, Aviano, (Pordenone), Italy

Department of Radiation Oncology,
IRCCS Fondazione Pascale,
Via Mariano Semmola, Naples 80131, Italy
e-mail: francesca_giugliano@hotmail.com

The CSI dose is modulated on the base of risk factors and combined or not with chemotherapy. CSI dose for high-risk patients is actually 36–40 Gy; for standard risk it is 23.4 Gy when RT is given with chemotherapy, with a PF boost to a total dose of 54–55.8 Gy. CSI is complex and should be applied in centers with adequate experience both in technique and the scheduling of clinical follow-up to monitor later side effects, because the quality of treatment, including radiation dose and volume, has a significant impact on the outcome, and it is the cornerstone of curative management [7–9].

19.2 Radiotherapy Planning and Delivery

19.2.1 Timing and Duration of Radiotherapy

Following definitive surgery, patients in standard-risk categories should if possible begin RT within 42 days and preferably within 28 days [10]. Moreover, the overtime-dose relationships were proven important in many cancer sites. A study conducted by the University of Florida in about 53 MB patients showed that duration of the treatment course (≤ 45 days vs. > 45 days) was the only RT-related variable with a significant impact on freedom from relapse and PF control [11].

The International Society of Paediatric Oncology (SIOP) primitive neuroectodermal tumors (PNET) 3 trial showed that pre-RT chemotherapy did not improve 5-year OS [12] and suggested a negative effect of RT treatment time prolongation. Event-free survival (EFS) was significantly worse for patients whose RT course took more than 50 days to be delivered (EFS 78.5 % vs. 53.7 %) [13].

The German Society of Pediatric Hematology and Oncology, recruiting patients with M2-M3 disease and postsurgical residual disease, also conducted a randomized trial (HIT '91) using postoperative neoadjuvant chemotherapy before RT as opposed to maintenance chemotherapy after immediate postoperative RT. Neoadjuvant chemotherapy was accompanied by increased

myelotoxicity causing an interruption in RT in 35 % of patients in the first arm as compared to 19.3 % in the second. Delayed and/or protracted RT may therefore have a negative impact on outcome [14].

19.2.2 Equipment

The simulation is done by a simulation computer tomography (CT) and with the patient in the treatment position. The slice thickness is no greater than 5 mm. Three-dimensional treatment planning optimization is strongly recommended for any phase of the treatment.

Photon linear accelerators should be used for the cranial (whole brain) and for the spinal fields, as a standard treatment. In the past, treatment of spinal fields with electrons was approved due to the better sparing of deep-seated normal structures [15]. However, the need of a sufficient energy, tissue heterogeneity, and junction difficulties needs to be precisely calculated.

19.2.3 Energy

The cranial fields should be treated with megavoltage photons in the energy range of 4–6 MV. Energies greater than 6 MV should be avoided for the brain, because of underdosage to the lateral meninges due to dose buildup effects. For PF and tumor bed boost and spinal fields, higher energy could be necessary. In order to reduce the anterior exit dose from the spinal radiation field, some institutions treat the spine with electrons [16]. However, treating with electrons poses the persistent difficulty of matching the spinal field with the cranial field and the challenge of inhomogeneities based on the differing electron absorption in compact bone especially in robust children. The radiobiological efficacy of electrons is poorly understood and may add yet another confounding factor to the determination of adequate dose to the spinal cord [17, 18]. Finally, proton radiation therapy (PRT) offers several advantages for the treatment of children with CNS tumors. Protons are particles with

charge and mass. They deliver maximum dose at a finite range determined by energy, in contrast to photons that have infinite range with dose decreasing exponentially to depth.

19.2.4 Position for Treatment and Simulation

Patients should be immobilized using an immobilization system according to local practice to maintain the same position during the treatment and assure its reproducibility. Careful positioning of the patients and optimal placement of the junction are important to avoid inclusion of the mandible in the exit of the spinal field. For this reason, the head is slightly extended. Prone positioning is generally used because it allows a direct visualization of the junction between the cranial lateral fields and the posterior cervical field and between the last field and the lumbar field (Fig. 19.1a). The patient facing downward, an undesirable position from the anesthesiologist's viewpoint complicates the problem of access, just as repositioning of the patient during daily treatment. Given that many patients who require CSI are very young children and need sedation or anesthesia (with intubation), some cancer centers

have recently also adopted the supine position with linear accelerator, even if this technique does not allow a direct visualization of the junction [19–21]. Helical tomotherapy (HT), a recent technique able to deliver the dose in a helical mode, allows supine positioning without the inconvenience of multiple field junction [22]. Devices such as personalized body “cradles” or vacuum bags and thermoplastic masks could be used for immobilization. The patient is positioned as comfortable as possible, and the bags need to be long enough to cover the cervical, thoracic, and lumbar-sacral region (Fig. 19.1b).

19.2.5 Target Volumes, Organs at Risk, and Techniques

The following organs at risk (OARs) will be routinely outlined: eyes, lenses, optic nerves, pituitary gland, optic chiasm, cochlea, brain, supratentorial brain, brainstem, thyroid gland, heart, lungs, breast, liver, kidneys, bowel, bladder, and gonads (if visible). For any of these organs, a dose-volume histogram (DVH) should be constructed for plan analysis. Dose constraints for various OAR are as follows: optic chiasm and optic nerves, 55 Gy [23]; brainstem, 54 Gy [24];



Fig. 19.1 Prone (a) and supine (b) positioning for craniospinal irradiation with personalized thermoplastic mask and vacuum bag immobilizer

spinal cord, 50.4 Gy [25]; lenses, 8 Gy; and cochlea for sensor neural hearing loss, as low as possible (conservatively ≤ 35 Gy) [26].

The following target volumes should be observed: craniospinal axis, PF, and tumor bed. Fusion magnetic resonance imaging (MRI) with simulation CT is ideal for planning to determine the extent of presurgical–postsurgical disease. T1 gadolinium-enhanced MRI may be ideal. According to the International Commission on Radiological Units and Measurements (ICRU), specification of volumes and doses is necessary for prescribing, documenting, and reporting therapy [27]. The gross tumor volume (GTV) includes all gross residual tumor and/or tumor bed at the primary site as determined by the preoperative MRI initially defining the tissues involved with disease and the postoperative MRIs identifying residual disease and/or tumor bed. GTV in most cases is a contracted or collapsed tumor bed. Tissue defects resulting from surgical approaches are generally not included as part of GTV.

In the whole brain, the clinical target volume (CTV) should extend frontally to include the entire frontal lobe, the cribriform plate region, and the temporal lobes.

If present, the metastatic deposits should be determined on a planning CT. The field arrangement for boost delivery in these areas must be chosen accurately to provide a high conformity index, avoiding OARs where possible.

The complexity and volume irregularity typical of CSI have led to the development of several new techniques. Relative to the conventional technique, the geometric edge of the cranial shield on the film should extend at least 5 mm below the cribriform plate and 10 mm below the lowest part of the temporal fossa [28]. Often the margin of anterior shielding needs to include the posterior part of the orbit so as to encompass the cranial meninges [17]. The cribriform region should be evaluated with modern techniques like CT or MRI, because conventional treatment planning of the brain area, using lateral radiographs, provides ambiguous information on its localization [29]. If the brain is treated by a pair of paral-

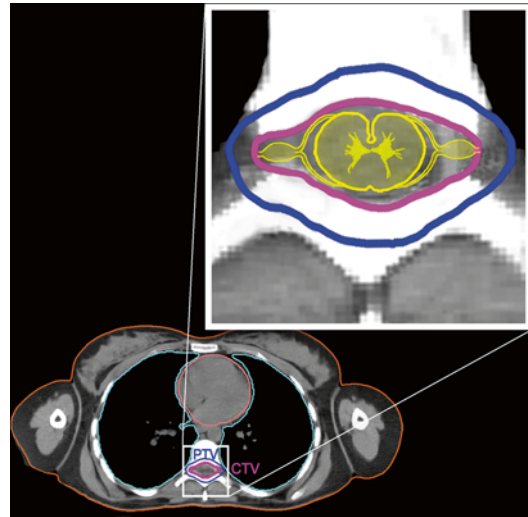


Fig. 19.2 The lateral extension of CTV (*fuchsia*) in the spinal target volume should include the entire subarachnoid space along the posterior spinal ganglia (*yellow*), located in the intervertebral foramina. Because of a less accurate immobilization of the spinal target compared to the brain target, fixed with mask, a 5–10-mm margin is added for spinal PTV (*blue*), according to center’s setup policy

lel opposed fields, the dose should be defined at the midpoint of the central axis.

It is our policy to extend, as much as possible, the lower lip of the cervical spinal volume in the lateral cranial fields avoiding the shoulders. This is advised for three reasons: avoiding most thyroid tissue by shielding this within the cranial volume, minimizing the risk of the junction being close to the primary tumor, and avoiding the exit of the posterior spinal field through the mandible.

The aim of the spinal CTV is to include the entire subarachnoid space with extension along the nerve roots as far as the intervertebral foramina (Fig. 19.2). The width between the intervertebral and the sacral foramina increases no more than 20 mm, as one moves from cranial to caudal regions. The use of a “spade”-shaped field to treat the lumbar-sacral spine is no longer recommended [17]. The lower limit of CTV is the terminal part of the thecal sac, evaluable on a spinal MRI and usually extending inferiorly to at least the lower border of the S2–S3 sacral vertebra. A study on MRI showed that the caudal sac end is at the

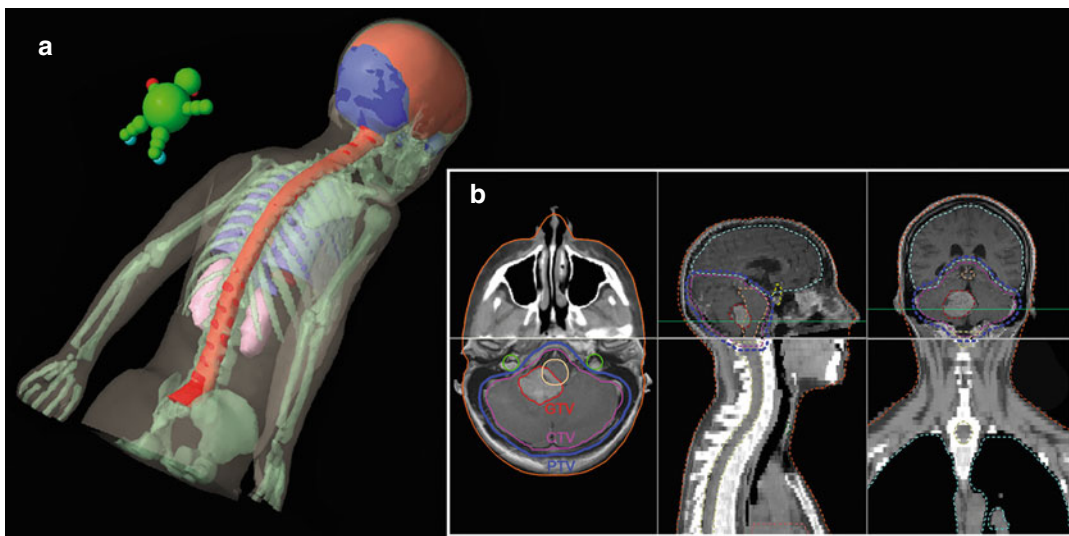


Fig. 19.3 Volumetric reconstruction of the craniospinal target (*red*). The posterior fossa volume is highlighted in *blue* (**a**). Axial, sagittal, and coronal MRI reconstruction fuse with simulation CT of pre-operative GTV (*red*) and CTV (*fuchsia*) including the entire posterior fossa and fur-

ther 5-mm expansion to PTV (*blue*). Cochlea (*green*), pituitary gland (*yellow*), and brainstem (*orange*) outlined (**b**) (CT-MRI fusion obtained with Oncentra MasterPlan, Nucletron®, The Netherlands)

bottom of S1 in about 17 %, at the bottom of S2 in about 50 %, and at S3 in about 33 % of children [30] (Fig. 19.3a). An additional margin, generally 5–10 mm on CTV, should be added for the planning target volume (PTV), depending on the center's setup techniques.

The PF is the typical anatomic region in which MB develops. It is delimited superiorly by the tentorium (superior field edge will also be estimated as 10 mm above the midpoint of a line drawn between the foramen magnum and the vertex), posteriorly by the outer table of the skull, frontally by the posterior clinoid (the pituitary should be shielded unless tumor extends to that region), and inferiorly by the outer table of the skull at the foramen magnum with a safety margin of 10 mm, typically at the lower border of C1 (Fig. 19.3b). The brainstem was part of the volume in the entire PF boost irradiation. The reduction of boost volume to the tumor bed instead of the entire PF is under investigation in the current COG-ACNS0331 study for standard-risk patients [31]. The optimal CTV for a reduced-volume posterior fossa boost remains to be defined, although an anatomically confined expansion of

1.5–2 cm around the GTV (preoperative extension based upon the T1 signal changes with and without gadolinium contrast and anatomic shifts or changes after surgery) seems to be reasonable. In standard-risk patients the CTV does not extend to the bony confines of the PF. The brainstem is included in the entire CTV PF boost, but only the portion of brainstem close to the tumor bed is carefully included in the tumor bed boost. Indeed, invasion of the brainstem or cerebellum-pontine peduncle is often the limiting factor for radical resection. The PTV is defined as the CTV with a 3–5-mm margin for both PF boost or tumor bed boost, to account for a day-to-day setup variation and center's setup techniques. The entire PTV should be covered by at least 95 % of the prescription dose; however, no part of PTV should receive less of 90 % of prescribed dose or more than 110 % of the prescribed dose.

With conventional treatment, the head and the upper cervical spine are treated with parallel-opposed fields. Lateral fields need to be carefully matched over the cervical spinal cord with the spinal field which extends superiorly to form an accurate match with the lower border of the cranial

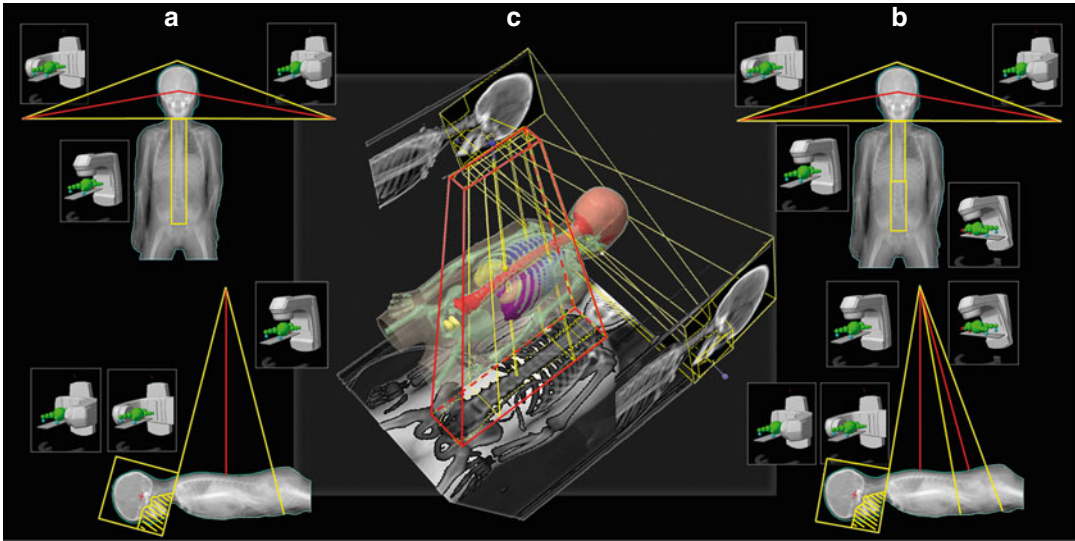


Fig. 19.4 Schematic representation of craniospinal irradiation setup for a young child (a) and for a taller patient requiring two posterior fields to cover the entire spinal

volume (b). Digitally reconstructed radiographs (DRR) and field geometry reconstruction are shown (c) (Courtesy of Sartor G, Med Physics, CRO Aviano, Italy)

fields. Some centers apply a 5-mm gap between adjacent fields, but this results frequently in a “cold spot.” To avoid over- or underdosage in this region, most centers recommend moving (“feather”) the junction during treatment with a gap of 5–10 mm which does not generate hot-cold spots [17].

We obtain abutting fields, rotating the collimator for the lateral fields to match the divergence of the posterior field and simultaneously the foot of the couch toward the entering lateral fields, with an angle that is a function of the divergent fields (Fig. 19.4a). A second posterior field will be required if the length of the spinal field is excessive and the geometry at this junction differs from that over the cervical spinal cord. To avoid hot spots in the same area, the anatomic junction site needs to be shifted at least 5–10 mm every 9 Gy, once a week. Rather than a classical geometric junction, we prefer a couch rotation with abutting fields in the dorsolumbar region (Fig. 19.4b). This technique avoids delivering a double dose in front of the spinal canal at the level of the junction area, although giving an existing dose to the lower anterior part of the abdomen, a risk for females. When necessary, to reduce the dose inhomogeneity inside the spinal target volume, we use the “field in field” technique (Fig. 19.4c).

In recent years, it is customary in standard-risk patients to switch from traditional opposite lateral field boost of the entire PF volume to highly conformal techniques like three-dimensional conformal radiation therapy (3DCRT) and intensity-modulated radiation therapy (IMRT).

High conformal techniques in MB have not been confined to the boost but also to addressing CSI volumes. IMRT planning and delivery techniques are increasingly employed. They represent one of the most promising methods of treatment, especially for large and non-regular tumors located close to critical areas. In particular, IMRT may be used as an option for reducing the radiation dose to the cochlea and has also been used to improve homogeneity of spinal RT. Modern techniques to deliver IMRT are HT and volumetric modulated arc therapy (ArcT) (Fig. 19.5).

HT is a high conformal technique, allowing RT guided by the images through a system in which a linear accelerator emits a narrow fan beam traveling in a spiral mode [32]. HT is mainly of interest for CSI because of the ability to deliver an IMRT plan, advancing the patient slowly through the gantry, allowing the dose to be sculpted around a complex target, and avoid-

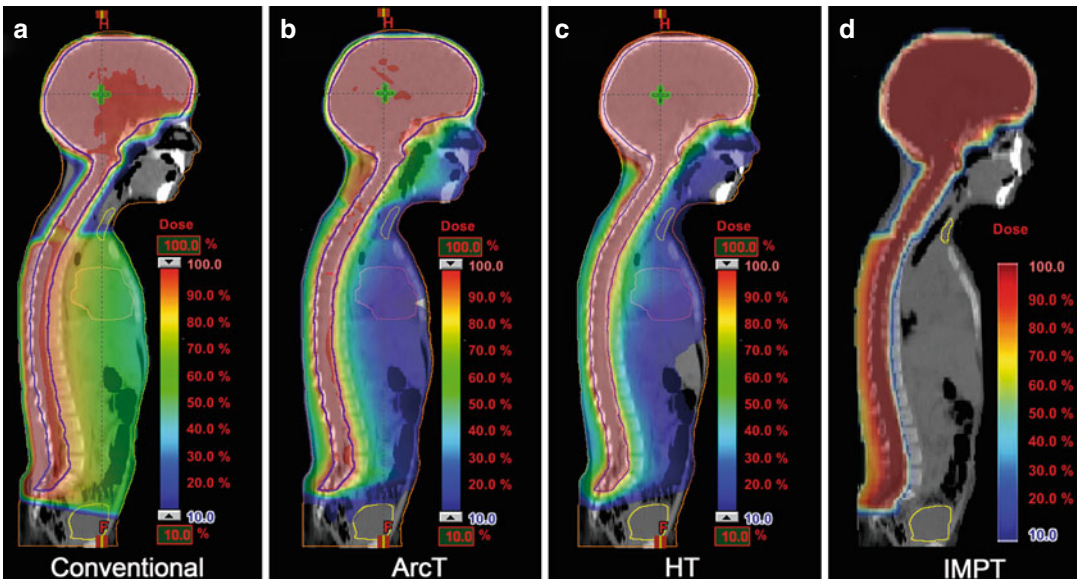


Fig. 19.5 Midsagittal dose distribution in 4-year-old child affected by standard-risk medulloblastoma. Comparison between conventional craniospinal irradiation (cCSI) (a), arc therapy (*ArcT*) (b), helical tomotherapy (*HT*) (c), and intensity modulated proton therapy (*IMPT*) (d). Conformation to the target increases from cCSI, through *ArcT*, and *HT*, up to *IMPT*. Exit dose of the prescribed dose to the anterior part of the abdomen is

50–60 % for cCSI, 18 % for *ArcT*, 10 % for *HT*, and 0 % for *IMPT* (cCSI and *ArcT* plans calculated by Eclipse Varian®, Palo Alto, USA; *HT* plan calculated by Hi-Art TomoTherapy Inc.®, Madison, USA) (*ArcT* plan is a courtesy of Chiovati P, Med Physics, CRO Aviano, Italy) (*IMPT* plan is a courtesy of Widesott L and Amichetti M, ATreP Trento, Italy)

ing issues of beam matching, junctions, multiple isocenter, and beam gaps that are common in conventional CSI techniques [33]. Moreover, with *HT* technique the children can be placed in supine position, which assures comfort and improves the security during the anesthesia procedures. In our experience in 15 CSI patients younger than 8 years treated with *HT*, an inspection of DVH reveals excellent conformal quality both for CTV brain and spinal cord with better sparing of OARs close to the target. In comparison with 3DCRT, CSI delivered with *HT* is able to give a more homogeneous dose and better conformation of the dose to the target, delivering a low-dose bath to the organs around the PTV and slightly increasing the whole body integral dose, which is inherent to the technique [34].

ArcT is instead a dynamic rotational RT using a linear accelerator, in which the gantry speed, multileaf collimator leaf position, and dose rates vary continuously during delivery [33, 35, 36]. To

deliver *ArcT* CSI multiple isocenter is necessary. Generally the first isocenter is located in the brain region; the second isocenter is located in the lumbar region; and in some cases (highest in children or adolescents) the third isocenter is used in the upper thoracic region. For each isocenter a different number of arcs (ranging from 1 to 2) are applied [37]. We generally apply two full arcs (clockwise and counterclockwise) for the brain area and one partial arc for each spinal cord region, with an overlap length of about 3–10 cm for each center. For spinal cord region partial arcs are generated with an avoidance sector in the angle of shoulders and harms for supine positioned patients (e.g., from 50° to 115° and from 245° to 310° arc) (Chiovati P, Med Physics, CRO Aviano, Italy, personal communication) (Fig. 19.6). *ArcT* has the ability to reduce field junction difficulties that are encountered in conventional treatment by accounting for the overlapping area between arcs during the process of optimization [33, 37]. With this strategy no field matching (potentially leading

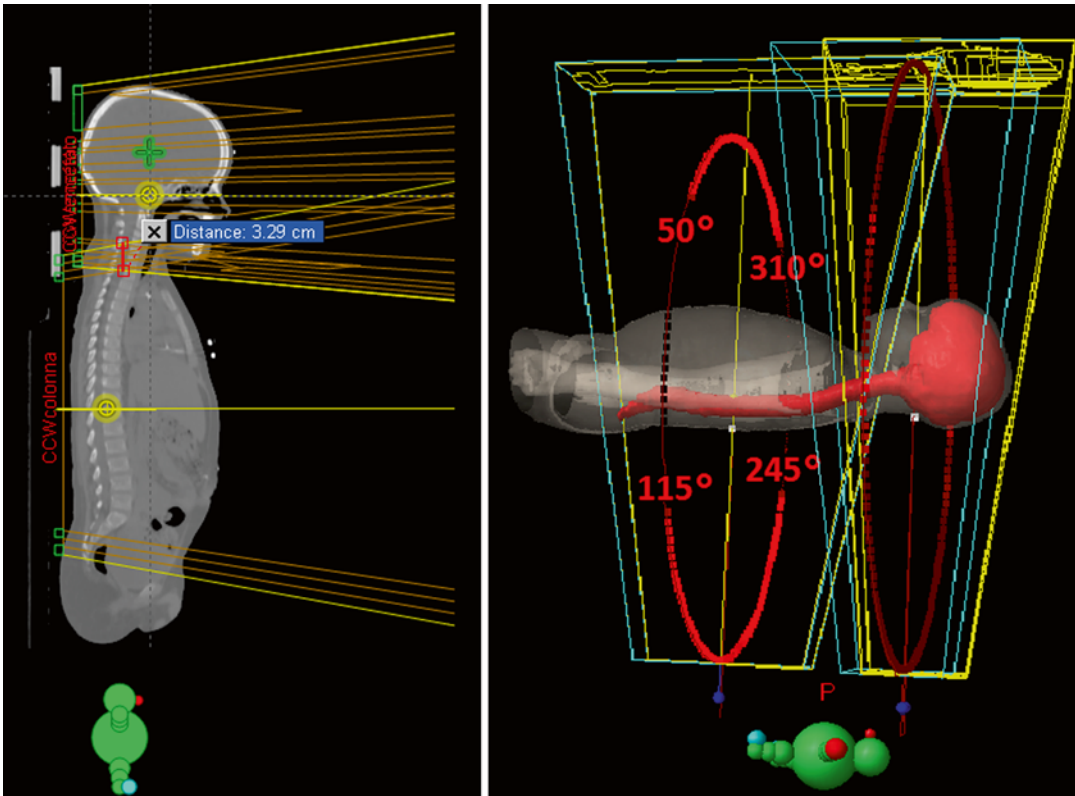


Fig. 19.6 Craniospinal irradiation delivered with Arc Therapy (ArcT). Multiple isocenter are necessary. Generally the first isocenter is located in the brain region (two full arcs clockwise and counterclockwise); the second isocenter is located in the dorsolumbar region (one partial arc). For spinal cord region a partial arc is generated with an avoidance sector in the angle of shoulders and

to hot and/or cold spots) is necessary, and the uniform dose transition task is demanded to the optimizer [37]. This technique has been recently applied in CSI patients and for PF tumors, obtaining similar results than HT both on target and OAR [32, 33, 35, 37] (Fig. 19.5).

19.3 The Rationale of Dose and Volume Reduction in Standard-Risk Patients

Historically the postsurgical treatment for standard-risk patients has been 36 Gy CSI together with a boost of 18–20 Gy to the PF (total dose 54–56 Gy). Under these conditions, the 5-year recurrence-free survival rate was approximately 60 % [38].

harms for supine positioned patients (e.g., from 50° to 115° and from 245° to 310° arc). In this case the length of overlapping region for each field/center is 3.29 cm and the uniform dose transition task is demanded to the optimization process (ArcT plan calculated by Eclipse Varian®, Palo Alto, USA)

Although using such doses has demonstrated a long, recurrence-free survival rate 5 years from diagnosis, there is a spectrum of radiation-related treatment effects. These include hearing loss, endocrine deficiencies, somatic effects, cognitive decline (especially in children younger than 7–8 years), and cerebrovascular damage. Furthermore, the estimated cumulative 10-year rate of secondary neoplasms is 4.2 %, in a population base of 379 standard-risk MB patients treated according to COG trial A9961 with standard RT and adjuvant chemotherapy [39]. Many studies indicate that 2 factors influence the effects of RT: the dose and the age younger than 4 at the time of diagnosis, especially when the 2 are combined. Children who received a lower dose (25 Gy vs. 35 Gy) exhibited less impairment in

Table 19.1 Radiotherapy recommendations

Risk-adapted craniospinal irradiation in medulloblastoma patients	
<i>Standard risk</i>	CSI 23.4 Gy
	PF boost up to 55.8 Gy (reduction of the boost volume to the tumor bed is currently being investigated)
<i>High risk residual >1.5 cm</i>	Post-RT chemotherapy
	CSI 36–39.6 Gy
	PF boost up to 55.8 Gy
	Combined with chemotherapy
<i>High risk M+</i>	Second look surgery
	CSI 36–39.6 Gy
	PF boost up to 55.8 Gy
	Nodular leptomeningeal disease up to 45–50 Gy
	Combined with intensified chemotherapy (pre- and/or post RT)
<i>Infant (<3 years old) standard risk</i>	HART could be considered
	Chemotherapy alone for selected patients
	In desmoplastic/nodular variant, elimination of RT could be an appropriate strategy
	RT is delayed as much as possible using chemotherapy
<i>Infant (<3 years old) high risk</i>	RT possibly restricted to the posterior fossa (54 Gy)
	Intensified chemotherapy
	Second look surgery
	RT is delayed as much as possible using chemotherapy
	Local RT (54 Gy) and/or age-adapted CSI (18–23.4 Gy) is required in these subgroups
	Nodular leptomeningeal disease 45 Gy

CSI craniospinal irradiation, PF posterior fossa, RT radiotherapy, HART hyperfractionated accelerated radiotherapy

measures of verbal and visual-spatial intelligence [40], verbal fluency, immediate word list recall, block design, and fine motricity of the dominant hand [41].

Recently, reduced-dose CSI with 23.4 Gy and a boost to the PF (total dose 55.8 Gy) have been used for standard-risk MB (Table 19.1).

The minimal dose of RT needed for disease control is still unknown, but since the 1990s, several authors reported their experience of

reduced-dose CSI. In a combined Children's Cancer Group (CCG, 923) and Pediatric Oncology Group (8631) study, patients 3–21 years of age with standard-risk MB were randomized to receive either standard-dose (36 Gy) or reduced-dose (23.4 Gy) CSI, followed by a PF boost. The protocol was terminated prematurely because of early relapses in the reduced-dose arm. Long-term follow-up confirmed this data, with a 67 % EFS at 5 years for patients treated with standard-dose CSI and 52 % for the reduced dose ($p=0.08$) [42].

If, on one hand, this trial failed to formally demonstrate equivalent survival after reduced-dose CSI, on the other hand, adding combination chemotherapy allowed goal achievement. Packer et al. investigated the use of reduced-dose CSI of 23.4 Gy with a PF boost to 55.8 Gy, followed by chemotherapy in carefully selected standard-risk patients. Chemotherapy consisted of 8 cycles of vincristine, lomustine, and cisplatin. Results showed 5-year progression-free survival (PFS) of 79 %. This outcome supported the use of reduced-dose CSI along with adjuvant chemotherapy for patients with standard-risk MB [43].

The evolved standard for MB standard risk now includes postoperative CSI to 23.4 Gy, irradiation of the anatomic PF to 55.8 Gy, and about 11 months of combination chemotherapy [44, 45].

Unfortunately, studies on intellectual outcome of children treated for MB showed significant neurocognitive complications even after 23.4 Gy of CSI, especially in younger children. Mulhern et al. reported on the neuropsychological outcome for 22 children. At a median time of 8 years from diagnosis, patients had a median Full-Scale IQ of 82.9. Children who were younger than 8 years of age at diagnosis and received 23.4 Gy CSI (median Full-Scale IQ=85 for 5 children) had a median 15 IQ point advantage when compared to children receiving full-dose CSI to 36 Gy (median Full-Scale IQ=70 for 6 children) [46]. Ris et al. describe the significant decline over time in both intellectual and academic domains in a population of 110 patients (COG A9961) treated with 23.4 Gy CSI plus adjuvant chemotherapy. The decline was greater in children who were younger at diagnosis and had higher initial intelligence test score [47].

Since intellectual outcome with these protocols remains suboptimal, investigators are now considering new ways to further reduce the side effects of RT. The first approach is an attempt to reduce the neuraxis dose to 18 Gy. There are only limited data on the efficacy of this strategy [48], and other studies are ongoing [31]. An effective method is targeting less than the entire PF for the boost phase of therapy. Among others, the St Jude Group explored the role of conformal RT boost in 86 newly diagnosed standard-risk MB subjects. RT began within 28 days of definitive surgery and consisted of CSI (23.4 Gy), conformal to PF (36 Gy), and primary site RT (55.8 Gy). Five-year EFS was 83 %, comparable to historical CSI and PF. The targeting guidelines used in this study resulted in a mean reduction of 13 % in the volume of PF receiving doses >55 Gy compared with conventionally planned RT. The dose reductions to the temporal lobes, cochleae, and hypothalamus were statistically significant. The 5-year cumulative incidence of 4.9 % local failure was comparable to results reported for similar patients treated with 23.4 Gy CSI and adjuvant chemotherapy in which the entire PF was irradiated to 55.8 Gy [49]. These data have been confirmed in a recent study by Paulino et al. in which the PF and tumor boost were delivered with IMRT technique [50]. These studies have been built to reduce the side effect of RT and are based on consideration that local failure in the PF outside the tumor bed is rare as the solitary site of failure [2, 3].

Based on this data, the Children's Oncology Group is currently undertaking a 4-arm clinical trial for patients between 3 and 21 years of age with standard-risk MB. Children aged 3–7 years are randomized twice: one randomization will determine whether the child receives standard (23.4 Gy) or reduced radiation to the brain and spine (18 Gy) and the second randomization will determine whether they receive a standard RT boost to the entire PF or reduced boost to the tumor bed only (total dose 55.8 Gy). Children of 8 years or older will all receive the standard radiation dose to the brain and spinal cord, but will be randomized to either a standard or reduced-volume “boost” dose. In this study, children receive weekly vincristine during RT and lomus-

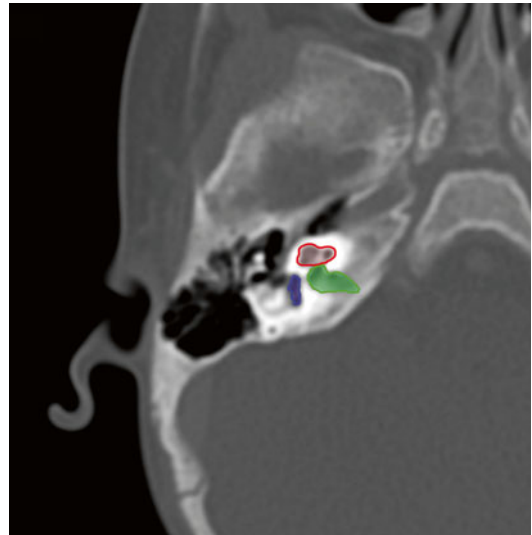


Fig. 19.7 Axial CT image of 18-month-old girl through the skull base. Cochlea (*red*), vestibule (*blue*), and internal auditory canal (*green*) outlined

tine, vincristine, cisplatin, etoposide, and cyclophosphamide after RT. The final data collection date for primary outcome measure is scheduled in July 2016 [31].

An additional side effect is hearing loss that usually develops within 6–12 months after cochlea irradiation (Fig. 19.7). Although the mechanism remains unproven, it is generally thought to be caused by RT-induced changes in the cochlea or vasculature [51]. Platinum agents play an important role in chemotherapy regimens for MB, but also in inducing ototoxicity. It has been shown to be even more significant when RT and cisplatin chemotherapy are used in combination. Schell et al. predicted that the probability of developing substantial hearing loss with cranial radiation was 40–60 % at cisplatin doses of 270 mg/m². With doses of 450 mg/m², the risk increased to 80–100 % [52]. Conventional treatment of the entire PF with 2 opposite fields will irradiate the cochlea fully. Instead, the application of conformal techniques like 3DCRT, IMRT, or PRT to PF [51] or of a reduced-volume PF boost [36, 49] is an attempt to limit the cochlear dose. 3DCRT and IMRT reduce cochlear doses to less than 70 % of the mean target dose [53]. In our experience, HT-IMRT used for PF boost is

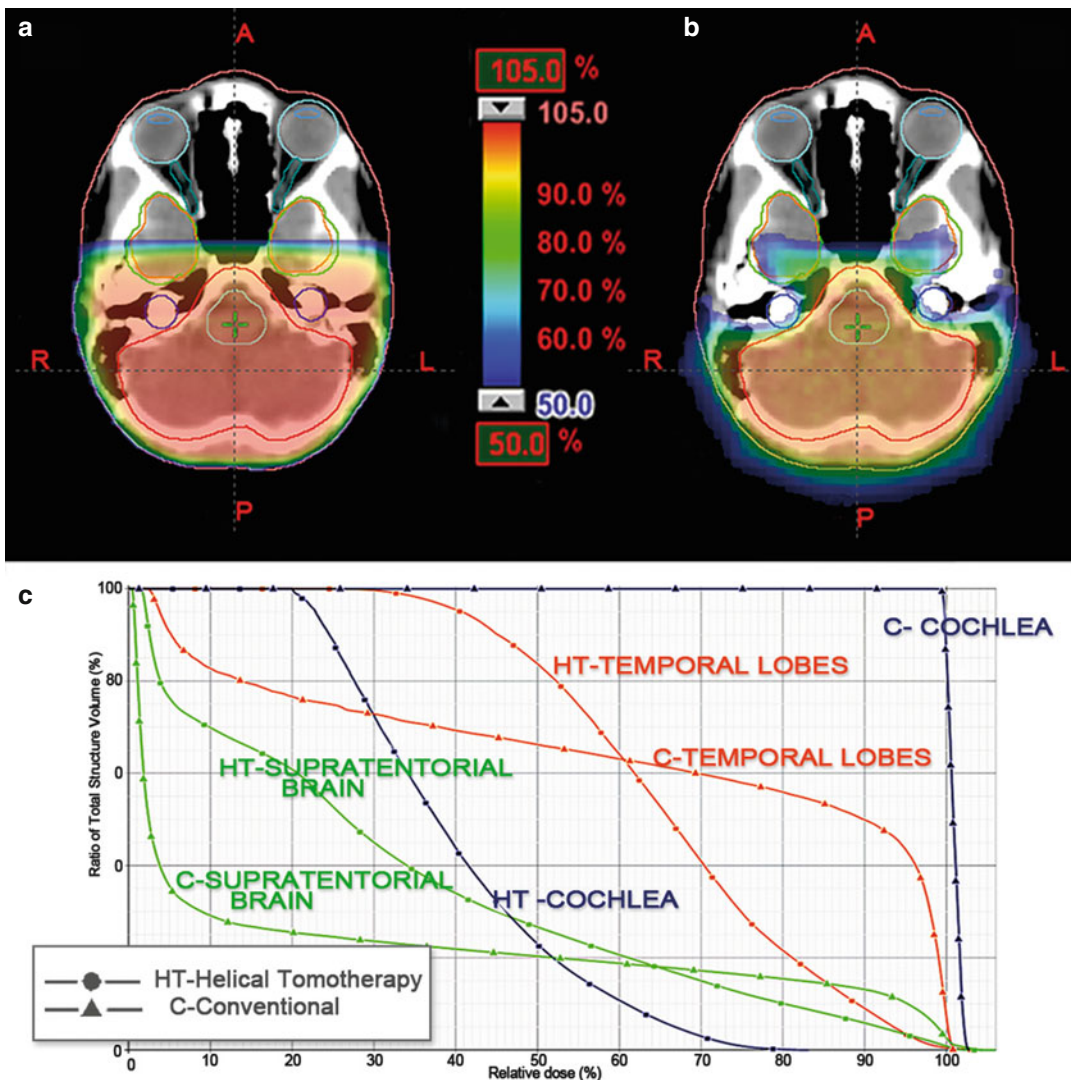


Fig. 19.8 Posterior fossa boost and skull base axial dose distribution in 18-year-old female affected by standard-risk medulloblastoma. A dose-volume analysis for the cochlea is not easy reproducible due to its small volume and the limitations with its delineation: so the cochlea volume (blue) has been deliberately enlarged to obtain a better optimization in this area. DVH comparison between conventional RT, using two parallel-opposed lateral fields

(a), and helical tomotherapy (HT) (b): reduced cochlea region irradiation to less than 50 % of prescribed dose. Simultaneously HT treatment reduces the higher doses to temporal lobes (red) and supratentorial brain (green), but increases low-intermediate doses (c) (Conventional posterior fossa boost plan calculated by Eclipse Varian®, Palo Alto, USA; HT plan calculated by Hi-Art Tomotherapy Inc.®, Madison, USA)

able to reduce the cochlear area dose to less than 50 %, simultaneously decreasing the higher dose to the temporal lobes and supratentorial brain, although there is a greater spread of medium dose toward the pituitary region (Fig. 19.8).

Finally, investigators worldwide have tested different strategies to reduce treatment-related

toxicity using hyperfractionated radiation therapy (HFRT) for both the CSI and boost phases. HFRT is a technique that separates radiation into 2 doses per day, giving a higher overall dose, theoretically increasing the chance of irradiating actively dividing cells without killing normal cells. In HIT-SIOP PNET 4 trial, 340 standard-risk patients

were randomly assigned to receive HFRT (36 Gy, 1 Gy/fraction b.i.d. to the craniospinal axis followed by a hyperfractionated boost to the whole PF at a dose of 60 Gy with a further boost to the tumor bed at a dose of 68 Gy) or standard conventional fractionated RT (23.4 Gy to the craniospinal axis and 54 Gy to whole PF, given in 30 daily fractions of 1.8 Gy each). Thus, the HFRT technique aims to improve the therapeutic ratio, either by enhancing the antitumor effect without an increase in later side effects or by maintaining the same level of antitumor effects and reducing later morbidity. In both arms adjuvant chemotherapy started 6 weeks after the end of RT, consisting of 8 cycles of cisplatin, lomustine, and vincristine. The OS and EFS in the HFRT arm were not superior to standard fractionated RT group [54].

In addition, Full-Scale IQ drops and thyroid function seem to be less pronounced than previously reported with standard irradiation regimens [55–57].

19.4 Proton Beam Radiation Therapy

PRT currently represents the most conformal approach for CSI. Protons provide a dose distribution that cannot yet be achieved by the most sophisticated photon beam treatment planning. The major disadvantages of PRT are the restricted access and high cost.

When protons come to the end of their penetration range and stop, they deposit all their radiation dose (Bragg peak). Beyond the peak, no further dose deposition occurs with a clear reduction of unintended irradiation of OARs [58], despite active debate on secondary neutron contamination. Bragg peak can be employed to achieve a high conformation around the target. Indeed charge particles (like protons) have a unique advantage over photons because of the ability to confine the high-dose region to the tumor volume and minimize the dose to the surrounding tissue [59, 60], thus reducing the potential for treatment-related complications.

Neurocognitive damage is generally considered the most devastating sequelae; however, protons cannot reduce this by themselves. PRT increases

dose conformation to the PF and subsequently reduces the higher doses to supratentorial brain [61].

Long-term toxicity with emphasis on hearing, endocrine, cardiac, gonadic function, and secondary tumors should be substantially improved secondary to nontarget tissue sparing achieved with protons [62]. Sparing of these OARs may be an additional advantage in assuring long-term, post-treatment morbidity-free survival [63]. With conventional photons, the PF boost delivers a substantial dose to the cochlea, spared with PRT, limiting radiation-induced ototoxicity [61]. The dose to 90 % of the cochlea was reduced from 101.2 % of the prescribed PF boost dose from conventional X-rays to 33.4 and 2.4 % from IMRT and PRT, respectively. Dose to 50 % of the heart volume was reduced from 72.2 % for conventional X-rays to 29.5 % for IMRT and 0.5 % for PRT [64]. With the future development of intensity-modulated proton therapy (IMPT), both the exit and entrance dose could be further reduced with less normal tissue unnecessarily irradiated (Fig. 19.5) and integral dose sparing [58], and also the neutron component is decreased compared to passive scattering technique. As more hospital-based proton treatment centers become operational, prospective trials that assess the late toxicity of different radiation techniques are needed to substantiate the expected reduction in long-term side effects with PRT.

19.5 Radiotherapy in Young Children with Medulloblastoma

Given the reluctance to use extensive RT (especially CSI) and increased susceptibility of the immature brain to therapy-induced cognitive deficits incremental years after RT, age limitation becomes an issue in the use of RT in this set of patients [65]. Strategies for CSI dose reduction and delay or avoidance of RT by postoperative chemotherapy have been investigated, especially in children younger than 3–5 years of age [66].

More recent strategies to delay or avoid CSI have provided evidence for improved survival rates by intensive systemic and intraventricular chemotherapy alone or by intensified systemic chemotherapy and high-dose, marrow-ablative

chemotherapy with or without RT. Thus, RT when delivered is applied according to age, response, and M risk status.

The COG P9934 study recruited 74 infants with nonmetastatic MB. They were treated, after initial surgery, with induction chemotherapy, secondary surgery, 3DCRT limited to PF (18–23.4 Gy) and tumor bed boost (cumulative 50.4–54 Gy), and maintenance chemotherapy. The 4-year EFS and OS were 50 and 69 %, respectively. The addition of 3DCRT increases the EFS compared with the use of postoperative chemotherapy alone, without interfering in cognitive or motor function [67].

Postoperative residual tumor and metastatic disease have been identified as negative clinical prognostic factors, leading to the concept of stratifying young children into three different risk groups: localized disease and gross total tumor resection (M0/R0); localized disease and postoperative residual tumor (M0/R+); and metastatic MB (M+) [68]. In their meta-analysis, Rutkowski et al. indicate that controlled de-escalation of treatment strategies without RT may be appropriate for young children with desmoplastic/nodular variant of MB, as a possible favorable prognostic factor in early childhood MB [68], in which elimination of RT could be an appropriate strategy [8, 69]. In contrast, given the relatively low survival rates in children with classical MB and large-cell/anaplastic MB, treatment intensifications with or without reintroduction of local or age-adapted CSI may be required in these subgroups [68] (Table 19.1).

19.6 Radiotherapy in High-Risk Patients

The high-risk disease category is heterogeneous including patients with postoperative residual disease >1.5 cm² without leptomeningeal spread, and even those with M1 disease, for whom it may be appropriate to consider a different treatment approach from M2-M3 disease patients. The prognosis for metastatic MB is still unsatisfactory. Most clinical trials have been directed at intensification of therapy. Studies adopting a “sandwich” schedule, such as the French Society of Pediatric Oncology Study [70], or a sandwich

plus a maintenance phase, such as the CCG 921, failed to improve much on the 40–50 % PFS for patients with M1-M3 disease. Other studies have been oriented to investigate high-dose chemotherapy and autologous stem cell transplantation rescue [71]. Other than chemotherapy regimens, research has focused on the timing of RT delivery, changes in fractionation scheduling, and dose.

An important question was addressed by Taylor et al. to determine whether chemotherapy given after surgery and before RT would improve high-risk outcome. Results of a randomized study of pre-RT chemotherapy versus RT alone, for MB high risk, were presented by SIOP/United Kingdom Children’s Cancer Study Group (UKCCSG) PNET 3. M2-M3 MB patients were treated with surgery and chemotherapy (vincristine, etoposide, carboplatin, and cyclophosphamide), followed by CSI (35 Gy/21 fractions with a PF boost, 20 Gy/12 fractions) or RT alone at the same dose, no significant impact on OS or EFS between the two groups [72]. Pediatric Oncology Group Trial 9031 aimed to study the relative benefit of cisplatin and etoposide in high-risk MB patients to pre-RT vs. post-RT treatments. The use of a higher CSI dose (40 Gy craniospinal plus 5 Gy boost to macroscopic disease) produced excellent early results: 2-year EFS for M1-M4 patients was 61 % in the first arm chemotherapy vs. 74 % in the first arm RT [73]. Gajjar et al. investigate the effectiveness of risk-adapted RT followed by a shortened period of dose-intense chemotherapy in children with high-risk MB. CSI dose was 36–39.6 Gy. The 5-year EFS was 70 % [74]. Between 1998 and 2007, Gandola et al. studied a modified accelerated fractionation radiotherapy (HART) in 33 consecutive patients (M1-M4). They received postoperative high-dose chemotherapy (methotrexate, etoposide, cyclophosphamide, and carboplatin) and then HART with a maximal dose to the neuraxis of 39 Gy (1.3 Gy/fraction, b.i.d.) and a PF boost up to 60 Gy (1.5 Gy/fraction, b.i.d.). Patients with persistent disseminated disease before HART were consolidated with 2 myeloablative courses and circulating progenitor cell rescue. Seven patients younger than 10 years with complete response after chemotherapy received a lower dose to the neuraxis (31.2 Gy). The 5-year EFS, PFS, and OS rates were

70, 72, and 73 %, respectively. No severe clinical complications of HART have emerged so far [75], but longer follow-up is needed. The results have generally been accepted as very encouraging even if they need confirmation in larger series. The Children's Cancer and Leukaemia Group (CCLG) conducted a phase II study of HART (1.24 Gy/fraction b.i.d.; CSI dose 39.68 Gy in 32 fractions, followed by entire PF boost 22.32 Gy in 18 fractions) in 34 M1-M3 MB patients. Preliminary results showed 2-year EFS at 68.1 % [76]. A recently published study on high-risk MB showed the effects of reduced-dose CSI (23.4 Gy CSI and local RT at 30.6 Gy) followed by tandem high-dose chemotherapy with autologous stem cell rescue. Even if only 9 patients with M+MB were enrolled, the results showed limited toxicity and favorable EFS rate (77.8 % at 3 years) [77]. Finally, in the POG 9031 protocol for high-risk medulloblastoma, the investigators explored the role of chemotherapy (3 cycles of cisplatin and etoposide) delivered before ("chemotherapy first CT1") or after RT ("radiation therapy first RT1"). The study enrolled 112 patients: 5-year EFS was 66 % in the CT1 arm and 70 % in the RT1 arm ($p=0.54$) [78].

In conclusion, the optimal treatment for children with metastatic or unresectable tumors is unknown. In high-risk MB no reduction of doses or volumes in radiation fields are allowed (recommended doses are CSI 36–39.6 Gy, PF boost up to 55.8 Gy, and spinal metastasis site boost up to 45–50 Gy) to maintain survival with standard chemotherapy regimens (Table 19.1). The optimal treatment for these children is still under investigation, and these patients should be included on a clinical protocol whenever possible.

19.7 The Role of Radiation Therapy in Recurrent Medulloblastoma

Recurrence is not uncommon and may develop many years after initial treatment [79]. Disease may recur at the primary tumor site or by cerebrospinal fluid dissemination. Patients with recurrent MB may be candidates for salvage chemotherapy and/or stereotactic irradiation, although long-

term disease control is rare. Entry into trials of novel therapeutic approaches including new agents, high-dose chemotherapy, and autologous stem cell rescue should be considered at the time of relapse after RT alone or RT-chemotherapy.

It is known that in previously nonirradiated children aged <3 years, the success of salvage therapy results most likely when RT is added as part of the salvage regimen. Older children, usually already treated with radiation dose at the limit of radiation tolerance to the brainstem or the CNS at the time of their first diagnosis, also show a better outcome if their recurrence treatment includes reirradiation [80, 81].

The CCLG initiated an observational study to test a strategy including high-dose chemotherapy with autologous stem cell rescue for recurrent CNS PNET in children and adolescents. An important component of this protocol was that patients should, if possible, receive further RT following relapse. In recent years, it has become clear that after initial course of RT (at least 1–2 years), there is a degree of CNS tolerance recovery to further RT. This will enable giving low to moderate doses of RT, even after prior CSI, that may contribute to tumor response in combination with chemotherapy. The results showed that patients who suffer a localized relapse, where second surgery and possibly second RT can be undertaken, may have a better chance of long-term survival than those with a more diffuse pattern of relapsed disease [82].

Recently the Memorial Sloan Kettering Cancer Center published its experience in use of thiotepa-based high-dose chemotherapy for previously irradiated recurrent MB. Notably, a trend toward better EFS was reported in the 5 patients who received additional RT as part of their retrieval therapy ($p=0.07$) [83]. The Milan group reported their data in treating relapsed MB in 17 patients; 16 received prior CSI. Ten patients were treated with cisplatin-etoposide chemotherapy, 3 underwent complete resection of recurrence, and 10 underwent reirradiation. There was only one survivor who had had a single spinal metastasis that was excised and irradiated [84].

Saran et al. described the use of hypofractionated stereotactic radiotherapy (SCRT) in the

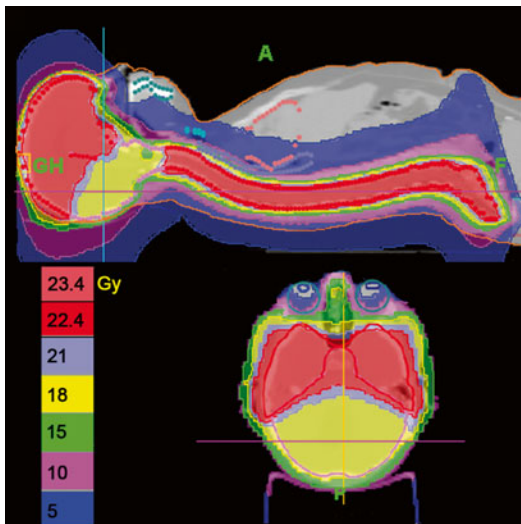


Fig. 19.9 A case of palliative craniospinal reirradiation in an 11-year-old male with recurrent metastatic medulloblastoma. The helical tomotherapy (HT) plan we prescribed 23.4 Gy to the entire neuraxis and simultaneously a lower dose was delivered to the posterior fossa (18 Gy) where the patient had been previously irradiated to the full dose (55.8 Gy)

management of recurrent or residual MB/PNET. This therapy offers possible accurate delivery of high-dose radiation to an area of recurrent disease, while significantly sparing surrounding normal tissue. Such an approach is mandatory if re-treatment is considered due to the potential risk of radiation necrosis, particularly to the brainstem. In this study, 14 patients with nonmetastatic, locally recurrent, or residual MB/PNETs were treated with hypofractionated SCRT. Nine patients underwent surgical resection prior to RT and 13 received chemotherapy prior to RT. Thirteen patients with recurrent disease were treated with chemotherapy prior to RT. Four patients received high-dose chemotherapy and peripheral blood stem cell rescue. The local control rate was 80 % at 1 year. Only one patient experienced radiation necrosis due to an extremely high cumulative dose of radiation. No other late sequelae were noted during follow-up [85].

Both in Parker [86] and our experience, HT has been used to re-treat patients with previously irradiated recurrent MB to deliver a simultaneous dose reduction to the PF at the time of relapse.

HT allows dose modulations to areas previously irradiated with higher dosage like PF (Fig. 19.9).

A recent German experience of stereotactic interstitial brachytherapy using (¹²⁵)iodine seeds has been proposed as salvage therapy for patients with recurrent MB [87].

However, caution must be taken in the application of reirradiation: time course from previous RT, target volume, tissue tolerance, and patient age need to be carefully considered.

Acknowledgment We thank Ms. Sarah Wilson for editorial assistance and Ms. Elisa Cipolat Gotet for illustration assistance.

References

1. Bloom HJ, Wallace EN, Henk JM (1969) The treatment and prognosis of medulloblastoma in children. A study of 82 verified cases. *Am J Roentgenol Radium Ther Nucl Med* 105:43–62
2. Fukunaga-Johnson N, Lee JH, Sandler HM, Robertson P, McNeil E, Goldwein JW (1998) Patterns of failure following treatment for medulloblastoma: is it necessary to treat the entire posterior fossa? *Int J Radiat Oncol Biol Phys* 42:143–146
3. Wolden SL, Dunkel IJ, Souweidane MM et al (2003) Patterns of failure using a conformal radiation therapy tumor bed boost for medulloblastoma. *J Clin Oncol* 21:3079–3083
4. Bloom HJ (1982) Medulloblastoma in children: increasing survival rates and further prospects. *Int J Radiat Oncol Biol Phys* 8:2023–2027
5. Silverman CL, Simpson JR (1982) Cerebellar medulloblastoma: the importance of posterior fossa dose to survival and patterns of failure. *Int J Radiat Oncol Biol Phys* 8:1869–1876
6. Gerber NU, Mynarek M, von Hoff K et al (2014) Recent developments and current concepts in medulloblastoma. *Cancer Treat Rev* 40:356–365
7. Taylor RE, Bailey CC, Robinson KJ et al (2004) Impact of radiotherapy parameters on outcome in the International Society of Paediatric Oncology/United Kingdom Children's Cancer Study Group PNET-3 study of preradiotherapy chemotherapy for M0-M1 medulloblastoma. *Int J Radiat Oncol Biol Phys* 58:1184–1193
8. von Hoff K, Rutkowski S (2012) Medulloblastoma. *Curr Treat Options Neurol* 14:416–426
9. Bartlett F, Kortmann R, Saran F (2013) Medulloblastoma. *Clin Oncol (R Coll Radiol)* 25:36–45
10. Rieken S, Mohr A, Habermehl D et al (2011) Outcome and prognostic factors of radiation therapy for medulloblastoma. *Int J Radiat Oncol Biol Phys* 81:e7–e13

11. del Charco JO, Bolek TW, McCollough WM et al (1998) Medulloblastoma: time-dose relationship based on a 30-year review. *Int J Radiat Oncol Biol Phys* 42:147–154
12. Pizer BL, Weston CL, Robinson KJ et al (2006) Analysis of patients with supratentorial primitive neuro-ectodermal tumours entered into the SIOP/UKCCSG PNET 3 study. *Eur J Cancer* 42:1120–1128
13. Taylor RE, Bailey CC, Robinson K et al (2003) Results of a randomized study of preradiation chemotherapy versus radiotherapy alone for nonmetastatic medulloblastoma: The International Society of Paediatric Oncology/United Kingdom Children's Cancer Study Group PNET-3 Study. *J Clin Oncol* 21:1581–1591
14. Kortmann RD, Kühl J, Timmermann B et al (2000) Postoperative neoadjuvant chemotherapy before radiotherapy as compared to immediate radiotherapy followed by maintenance chemotherapy in the treatment of medulloblastoma in childhood: results of the German prospective randomized trial HIT '91. *Int J Radiat Oncol Biol Phys* 46:269–279
15. Li C, Muller-Runkel R, Vijayakumar S et al (1994) Craniospinal axis irradiation: an improved electron technique for irradiation of the spinal axis. *Br J Radiol* 67:186–193
16. Gaspar LE, Dawson DJ, Tilley-Gulliford SA, Banerjee P (1991) Medulloblastoma: long-term follow-up of patients treated with electron irradiation of the spinal field. *Radiology* 180:867–870
17. Halperin EC (1996) Impact of radiation technique upon the outcome of treatment for medulloblastoma. *Int J Radiat Oncol Biol Phys* 36:233–239
18. Bernier V (2004) Technical aspects in cerebrospinal irradiation. *Pediatr Blood Cancer* 42:447–451
19. Thomadsen B, Mehta M, Howard S, Das R (2003) Craniospinal treatment with the patient supine. *Med Dosim* 28:35–38
20. Parker WA, Freeman CR (2006) A simple technique for craniospinal radiotherapy in the supine position. *Radiother Oncol* 78:217–222
21. Zaghoul MS, Eldebawy E, Attalah E et al (2012) Craniospinal irradiation in children: patient position modification, dose uniformity and early adverse effects. *Gulf J Oncolog* 1:7–15
22. Mascarin M, Giugliano FM, Coassin E (2011) Helical tomotherapy in children and adolescents: dosimetric comparisons, opportunities and issue. *Cancers* 3:3972–3990
23. Mayo C, Martel MK, Marks LB et al (2010) Radiation dose-volume effects of optic nerves and chiasm. *Int J Radiat Oncol Biol Phys* 76(3 Suppl):S28–S35
24. Mayo C, Yorke E, Merchant TE (2010) Radiation associated brainstem injury. *Int J Radiat Oncol Biol Phys* 76(3 Suppl):S36–S41
25. Kirkpatrick JP, van der Kogel AJ, Schultheiss TE (2010) Radiation dose-volume effects in the spinal cord. *Int J Radiat Oncol Biol Phys* 76(3 Suppl):S42–S49
26. Bhandare N, Jackson A, Eisbruch A et al (2010) Radiation therapy and hearing loss. *Int J Radiat Oncol Biol Phys* 76(3 Suppl):S50–S57
27. ICRU Report 50 (1994) Prescribing, recording and reporting photon beam therapy. *Med Phys* 21:833–844
28. Carrie C, Hoffstetter S, Gomez F et al (1999) Impact of targeting deviations on outcome in medulloblastoma: study of the French Society of Pediatric Oncology (SFOP). *Int J Radiat Oncol Biol Phys* 45:435–439
29. Gripp S, Kambergers J, Wittkamp M et al (2004) Coverage of anterior fossa in whole-brain irradiation. *Int J Radiat Oncol Biol Phys* 59:515–520
30. Dunbar SF, Barnes PD, Tarbell NJ (1993) Radiologic determination of the caudal border of the spinal field in cranial spinal irradiation. *Int J Radiat Oncol Biol Phys* 26:669–673
31. Michalski JM, Children's Oncology Group. A Study Evaluating Limited Target Volume Boost Irradiation and Reduced Dose Craniospinal Radiotherapy (18.00 Gy) and Chemotherapy in Children With Newly Diagnosed Standard Risk Medulloblastoma: A Phase III Double Randomized Trial. (Last updated: August 12, 2014) Accessible at: <http://clinicaltrials.gov/ct2/show/study/NCT00085735>
32. Sharma DS, Gupta T, Jalali R et al (2009) High-precision radiotherapy for craniospinal irradiation: evaluation of three-dimensional conformal radiotherapy, intensity-modulated radiation therapy and helical TomoTherapy. *Br J Radiol* 82:1000–1009
33. Myers P, Stathakis S, Gutiérrez AN et al (2013) Dosimetric Comparison of Craniospinal Axis Irradiation (CSI) treatments using helical tomotherapy, Smartarc™, and 3D conventional radiation therapy. *Int J Med Phys Clin Eng Radiat Oncol* 2:30–38
34. Mascarin M, Chiovati P, Drigo A (2010) New technologies and therapeutic index in pediatric radiotherapy. *Tumori* 10:R63–R65
35. Lee YK, Brooks CJ, Bedford JL et al (2012) Development and evaluation of multiple isocentric volumetric modulated arc technique for craniospinal axis radiotherapy planning. *Int J Radiat Oncol Biol Phys* 82:1006–1012
36. Beltran C, Gray J, Merchant TE (2012) Intensity-modulated arc therapy for pediatric posterior fossa tumors. *Int J Radiat Oncol Biol Phys* 82:e299–e304
37. Fogliata A, Bergström S, Cafaro I et al (2011) Craniospinal irradiation with volumetric modulated arc therapy: a multi-institutional treatment experience. *Radiother Oncol* 99:79–85
38. Jenkin D, Goddard K, Armstrong D et al (1990) Posterior fossa medulloblastoma in childhood: treatment results and a proposal for a new staging system. *Int J Radiat Oncol Biol Phys* 19:265–274
39. Packer RJ, Zhou T, Holmes E et al (2013) Survival and secondary tumors in children with medulloblastoma receiving radiotherapy and adjuvant chemotherapy: results of Children's Oncology Group trial A9961. *Neuro Oncol* 15:97–103
40. Grill J, Renaux VK, Bulteau C et al (1999) Long-term intellectual outcome in children with posterior fossa tumors according to radiation doses and volumes. *Int J Radiat Oncol Biol Phys* 45:137–145

41. Kieffer-Renaux V, Bulteau C, Grill J et al (2000) Patterns of neuropsychological deficits in children with medulloblastoma according to craniospinal irradiation doses. *Dev Med Child Neurol* 42:741–745
42. Thomas PR, Deutsch M, Kepner JL et al (2000) Low-stage medulloblastoma: final analysis of trial comparing standard-dose with reduced-dose neuraxis irradiation. *J Clin Oncol* 18:3004–3011
43. Packer RJ, Goldwein J, Nicholson HS et al (1999) Treatment of children with medulloblastomas with reduced-dose craniospinal radiation therapy and adjuvant chemotherapy: a Children's Cancer Group Study. *J Clin Oncol* 17:2127–2136
44. Packer RJ, Gajjar A, Vezina G et al (2006) Phase III study of craniospinal radiation therapy followed by adjuvant chemotherapy for newly diagnosed average-risk medulloblastoma. *J Clin Oncol* 24:4202–4208
45. Sirachainan N, Nuchprayoon I, Thanarattanakorn P et al (2011) Outcome of medulloblastoma in children treated with reduced-dose radiation therapy plus adjuvant chemotherapy. *J Clin Neurosci* 18:515–519
46. Mulhern RK, Kepner JL, Thomas PR et al (1998) Neuropsychologic functioning of survivors of childhood medulloblastoma randomized to receive conventional or reduced-dose craniospinal irradiation: a Pediatric Oncology Group study. *J Clin Oncol* 16:1723–1728
47. Ris MD, Walsh K, Wallace D et al (2013) Intellectual and academic outcome following two chemotherapy regimens and radiotherapy for average-risk medulloblastoma: COG A9961. *Pediatr Blood Cancer* 60:1350–1357
48. Goldwein JW, Radcliffe J, Johnson J et al (1996) Updated results of a pilot study of low dose craniospinal irradiation plus chemotherapy for children under five with cerebellar primitive neuroectodermal tumors (medulloblastoma). *Int J Radiat Oncol Biol Phys* 34:899–904
49. Merchant TE, Kun LE, Krasin MJ et al (2008) Multi-institutional prospective trial of reduced-dose craniospinal irradiation (23.4 Gy) followed by conformal posterior fossa (36 Gy) and primary site irradiation (55.8 Gy) and dose-intensive chemotherapy for average-risk medulloblastoma. *Int J Radiat Oncol Biol Phys* 70:782–787
50. Paulino AC, Mazloom A, Teh BS et al (2011) Local control after craniospinal irradiation, intensity-modulated radiotherapy boost, and chemotherapy in childhood medulloblastoma. *Cancer* 117:635–641
51. Huang E, Teh BS, Strother DR et al (2002) Intensity-modulated radiation therapy for pediatric medulloblastoma: early report on the reduction of ototoxicity. *Int J Radiat Oncol Biol Phys* 52:599–605
52. Schell MJ, McHaney VA, Green AA et al (1989) Hearing loss in children and young adults receiving cisplatin with and without prior cranial irradiation. *J Clin Oncol* 7:754–760
53. Breen SL, Kehagioglou P, Usher C, Plowman PN (2004) A comparison of conventional, conformal and intensity-modulated coplanar radiotherapy plans for posterior fossa treatment. *Br J Radiol* 77:768–774
54. Lannering B, Rutkowski S, Doz F et al (2012) Hyperfractionated versus conventional radiotherapy followed by chemotherapy in standard-risk medulloblastoma: results from the randomized multicenter HIT-SIOP PNET 4 trial. *J Clin Oncol* 30:3187–3193
55. Carrie C, Grill J, Figarella-Branger D et al (2009) Online quality control, hyperfractionated radiotherapy alone and reduced boost volume for standard risk medulloblastoma: long-term results of MSFOP 98. *J Clin Oncol* 27:1879–1883
56. Ricardi U, Corrias A, Einaudi S et al (2001) Thyroid dysfunction as a late effect in childhood medulloblastoma: a comparison of hyperfractionated versus conventionally fractionated craniospinal radiotherapy. *Int J Radiat Oncol Biol Phys* 50:1287–1294
57. Gupta T, Jalali R, Goswami S et al (2012) Early clinical outcomes demonstrate preserved cognitive function in children with average-risk medulloblastoma when treated with hyperfractionated radiation therapy. *Int J Radiat Oncol Biol Phys* 83:1534–1540
58. Hoffman KE, Yock TI (2009) Radiation therapy for pediatric central nervous system tumors. *J Child Neurol* 24:1387–1396
59. Fossati P, Ricardi U, Orecchia R (2009) Pediatric medulloblastoma: toxicity of current treatment and potential role of protontherapy. *Cancer Treat Rev* 35:79–96
60. Howell RM, Giebler A, Koontz-Raisig W et al (2012) Comparison of therapeutic dosimetric data from passively scattered proton and photon craniospinal irradiations for medulloblastoma. *Radiat Oncol* 7:116
61. Miralbell R, Lomax A, Russo M (1997) Potential role of proton therapy in the treatment of pediatric medulloblastoma/primitive neuro-ectodermal tumors: spinal theca irradiation. *Int J Radiat Oncol Biol Phys* 38:805–811
62. Brodin NP, Munck Af Rosenschöld P, Aznar MC et al (2011) Radiobiological risk estimates of adverse events and secondary cancer for proton and photon radiation therapy of pediatric medulloblastoma. *Acta Oncol* 50:806–816
63. Merchant TE, Hua CH, Shukla H et al (2008) Proton versus photon radiotherapy for common pediatric brain tumors: comparison of models of dose characteristics and their relationship to cognitive function. *Pediatr Blood Cancer* 51:110–117
64. St Clair WH, Adams JA, Bues M et al (2004) Advantage of protons compared to conventional X-ray or IMRT in the treatment of a pediatric patient with medulloblastoma. *Int J Radiat Oncol Biol Phys* 58:727–734
65. Kiltie AE, Lashford LS, Gattamaneni HR (1997) Survival and late effects in medulloblastoma patients treated with craniospinal irradiation under three years old. *Med Pediatr Oncol* 28:348–354
66. Duffner PK, Horowitz ME, Krischer JP et al (1993) Postoperative chemotherapy and delayed radiation in children less than three years of age with malignant brain tumors. *N Engl J Med* 328:1725–1731

67. Ashley DM, Merchant TE, Strother D et al (2012) Induction chemotherapy and conformal radiation therapy for very young children with nonmetastatic medulloblastoma: Children's Oncology Group study P9934. *J Clin Oncol* 30:3181–3186
68. Rutkowski S, von Hoff K, Emser A et al (2010) Survival and prognostic factors of early childhood medulloblastoma: an international meta-analysis. *J Clin Oncol* 28:4961–4968
69. Leary SE, Zhou T, Holmes E et al (2011) Histology predicts a favorable outcome in young children with desmoplastic medulloblastoma: a report from the children's oncology group. *Cancer* 117:3262–3267
70. Verlooy J, Mosseri V, Bracard S et al (2006) Treatment of high risk medulloblastomas in children above the age of 3 years: a SFOP study. *Eur J Cancer* 42:3004–3014
71. Strother D, Ashley D, Kellie SJ et al (2001) Feasibility of four consecutive high-dose chemotherapy cycles with stem-cell rescue for patients with newly diagnosed medulloblastoma or supratentorial primitive neuroectodermal tumor after craniospinal radiotherapy: results of a collaborative study. *J Clin Oncol* 19:2696–2704
72. Taylor RE, Donachie PHJ, Weston CL et al (2009) Impact of radiotherapy parameters on outcome for patients with supratentorial primitive neuroectodermal tumours entered into the SIOP/UKCCSG PNET 3 study. *Radiother Oncol* 92:83–88
73. Tarbell NJ, Friedman H, Kepner J et al (2000) Outcome for children with high stage medulloblastoma: results of the pediatric oncology group 9031. *Int J Radiat Oncol Biol Phys* 48:179 (abstr)
74. Gajjar A, Chintagumpala M, Ashley D et al (2006) Risk-adapted craniospinal radiotherapy followed by high-dose chemotherapy and stem-cell rescue in children with newly diagnosed medulloblastoma (St Jude Medulloblastoma-96): long-term results from a prospective, multicentre trial. *Lancet Oncol* 7:813–820
75. Gandola L, Massimino M, Cefalo G et al (2009) Hyperfractionated accelerated radiotherapy in the Milan strategy for metastatic medulloblastoma. *J Clin Oncol* 27:566–571
76. Taylor RE, Boota N, Bujkiewicz S et al (2009) Children's Cancer and Leukemia Group (CCLG) Study of Hyperfractionated Accelerated Radiotherapy (HART) with Chemotherapy for M1–3 Medulloblastoma (MB). *Int J Radiat Oncol Biol Phys* 75:S38 (abstr)
77. Kim SY, Sung KW, Hah JO et al (2010) Reduced-dose craniospinal radiotherapy followed by high-dose chemotherapy and autologous stem cell rescue for children with newly diagnosed high-risk medulloblastoma or supratentorial primitive neuroectodermal tumor. *Korean J Hematol* 45:120–126
78. Tarbell NJ, Friedman H, Polkinghorne WR et al (2013) High-risk medulloblastoma: a pediatric oncology group randomized trial of chemotherapy before or after radiation therapy (POG 9031). *J Clin Oncol* 31:2936–2941
79. Jenkin D, Greenberg M, Hoffman H et al (1995) Brain tumors in children: long-term survival after radiation treatment. *Int J Radiat Oncol Biol Phys* 31: 445–451
80. Bakst RL, Dunkel IJ, Gilheaney S et al (2011) Reirradiation for recurrent medulloblastoma. *Cancer* 117:4977–4982
81. Shih CS, Hale GA, Gronewold L et al (2008) High-dose chemotherapy with autologous stem cell rescue for children with recurrent malignant brain tumors. *Cancer* 112:1345–1353
82. Pizer B, Donachie PHJ, Robinson K et al (2011) Treatment of recurrent central nervous system primitive neuroectodermal tumours in children and adolescents: results of a Children's Cancer and Leukaemia Group study. *Eur J Cancer* 47:1389–1397
83. Dunkel IJ, Gardner SL, Garvin JH Jr et al (2010) High-dose carboplatin, thiotepa, and etoposide with autologous stem cell rescue for patients with previously irradiated recurrent medulloblastoma. *Neuro Oncol* 12:297–303
84. Massimino M, Gandola L, Spreafico F et al (2009) No salvage using high-dose chemotherapy plus/minus reirradiation for relapsing previously irradiated medulloblastoma. *Int J Radiat Oncol Biol Phys* 73:1358–1363
85. Saran F, Baumert BG, Creak AL et al (2008) Hypofractionated stereotactic radiotherapy in the management of recurrent or residual medulloblastoma/PNET. *Pediatr Blood Cancer* 50:554–560
86. Parker W, Brodeur M, Roberge D, Freeman C (2010) Standard and nonstandard craniospinal radiotherapy using helical Tomo Therapy. *Int J Radiat Oncol Biol Phys* 77:926–931
87. El Majdoub F, Simon T, Hoevens M et al (2011) Interstitial brachytherapy using stereotactic implanted (125)iodine seeds for recurrent medulloblastoma. *Clin Oncol (R Coll Radiol)* 23:532–537

Pathologies in Pediatric Posterior Fossa Tumors: Ependymoma

Stephanie Puget

Stephanie Puget, M.D., Ph.D
Department of Pediatric Neurosurgery, Necker Hospital, Université Paris Descartes,
Sorbonne, Paris, France

Stephanie Puget and Guillaume Bergthold

20.1 Introduction

Ependymoma represents the third pediatric most frequent brain tumor behind astrocytoma and medulloblastoma [1]. It is a glial tumor expressing GFAP, but not Olig2, that is supposed to be derived from radial glial cells [2]. The prognosis of these tumors remains rather dark with an average survival rate at 5 years of 50 % and a 5-year progression-free survival between 30 % and 60 % according to the studies published in the literature [3, 4]. Long-term survival is still unsatisfactory despite increased use of radiotherapy even in young children [3]. The histological grading according to the WHO classification based on morphological criteria has shown limits to predict the outcome, especially in young children [5]. Using four European trials cohorts, the authors found a better reproducibility using a more prescribed scheme derived from the WHO classification but without improving the prognostication.

S. Puget, M.D., Ph.D. (✉)
Department of Pediatric Neurosurgery,
Necker Hospital, Université Paris Descartes,
Sorbonne, Paris, France
e-mail: stephanie.puget@gmail.com

G. Bergthold, M.D.
Department of Vectorology and Anticancer Therapeutics,
CNRS UMR 8203, University Paris sud XI,
Institut Gustave Roussy,
Rue Edouard Vaillant, Villejuif 94805, France

The low prevalence of this tumor in children also represents a handicap in research, due to the low number of available tumor samples. However, the cooperative work helped to refine the knowledge of the origin and progression of ependymoma. Despite histological similarities, ependymomas have different prognoses and molecular abnormalities according to age and location, showing they are different diseases. The objective of this review is to expose the recent advances that identified biological subgroups and pointed out new prognostic markers and potential therapeutic targets.

20.2 Pediatric and Adults Ependymomas Are Different Diseases

Although histologically similar, ependymomas in children and adults differ in terms of outcome with a worse prognosis for children [6, 7]. With regard to location, posterior fossa tumors occur more commonly in children, whereas supratentorial and spinal cord tumors dominate in adults. If we consider the influence of location on the biology of these tumors, it is not surprising that children and adult ependymomas have distinct chromosomal abnormalities (Table 20.1). In a meta-analysis of 13 CGH studies, the two most characteristic differences between adult and pediatric ependymomas were the gain of 1q (20 % and 8 % of pediatric and adults ependymomas, respectively) and the absence of

Table 20.1 Chromosomal imbalances of pediatric and adult ependymomas [8–12]

Array CGH	Children		Adults
	<4 years	>4 years	
Balanced profile	Few imbalances	Few imbalances	Extensive imbalances
Gains		1q, 7, 9q	7, 9, 12, 5, 18, X, 2
Losses		22, 3, 9p, 13q, 6q, 1p, 17, 6	22/22q, 10, 13q, 6, 14q

chromosomal imbalances which was very common in children, especially younger [8]. The number and complexity of chromosomal rearrangements is also different according to age subgroups with mean genomic imbalances of 7.5 and 3.8 per adult and pediatric tumors, respectively [8]. In a large series of 122 adult and pediatric ependymomas analyzed by CGHarray, Korshunov et al. [9] confirmed previous results from Dyer et al. [10] and Puget et al. [11] that children less than 4 years have frequently a balance profile, with an average of 0.5 chromosome aberration, while patients older than 4 years have tumors with a statistically higher chromosomal rearrangements rate with an average of 6.4 chromosomal aberration.

Witt et al. focused on posterior fossa ependymoma in 177 adults and children and identified two distinct molecular subtypes [12]. The subtype A occurred in younger patients (median of 2.5 years old) with relatively less genomic instability. The most frequent DNA copy number variants included gain of chromosome 1 and loss of chromosome 22. On the other hand, subtype B occurred in older patients (median of 20 years old) with extensive chromosomal aberrations. More recently, Mack et al. [13] and Parker et al. [14] found that supratentorial ependymomas carry an intrachromosomal translocation that creates a new tumor-driving gene, posterior fossa type A lack tumor-driving mutations, but has aberrant epigenetic modifications, and type B shows neither gene mutations nor epigenetic aberrations.

20.3 The Location of Ependymoma Influences Its Genetic Landscapes

The meta-analysis made by Kilday et al. revealed location-specific abnormalities as shown by CGHa [8]. Recent genome-wide expression analyses have revealed that despite histological similarities, ependymomas arising from different locations of the CNS are biologically distinct in terms of genetic aberrations and transcriptional profiles [2, 9, 11–20]. Table 20.2 recapitulates the main biological characteristics associated with tumor location reported in literature.

20.3.1 Identification of Key Players in the Tumorigenesis and Progression of Pediatric Ependymomas

It is now clear that ependymomas from distinct locations will be initiated and will progress through different biological pathways. In 2005, Taylor et al. showed that supratentorial posterior fossa and spinal ependymomas have distinguishable gene expression signatures and proposed radial glia cells as the cell of origin for supratentorial and spinal cord ependymomas [2]. They showed also an upregulation of EphB–ephrin in the supratentorial group compared to the others. Neuronal differentiation has been recently shown to be characteristic of supratentorial ependymomas (68 % IHC positivity in supratentorial tumors and only 12.5 % for infratentorial ependymoma) with the positivity of NEFL70 (neurofilament light polypeptide) associated with a better prognosis [19]. On the opposite, RELN (reelin) and TN-C (tenascin C, an extracellular matrix protein of the stem cell niche), both belonging to the Notch1 gene signaling pathway, have been found significantly upregulated in infratentorial ependymoma [11, 12, 15–19].

To better understand the biological abnormalities underlying ependymoma progres-

Table 20.2 Biological characteristics of pediatric ependymomas according to location

Location	Biological characteristics	Role	References
Supratentorial	Ch 9 deletion	Uncertain	[8, 9, 15, 17]
	ECM and cytoskeleton genes	Mesenchymal transition	[18]
	EphB–ephrin and Notch signaling	Tumor stem cell expansion	[2, 11, 16, 20]
	CyclinD1	Increased proliferation rate	[2]
	NEFL70, LHX2, FOXP1, TLX1	Neuronal differentiation, better prognosis	[19]
	Ch11 translocation (C11orf95–RELA fusion)	Involve in NF-κB signaling. Induces ependymoma-like tumors in mouse brain	[14]
Posterior fossa	Ch 1q gain	Worse prognosis	[8]
	Ch 9q33 – 34 gain at relapse		[11, 17]
	PAX3, OGN, FMO1	None identified	[15]
	ZIC1,2,3,4 and LFNG	Unknown	[16]
	ID1,2,4	Glial stem cell marker	[2]
	AQP1,3,4	Angiogenesis and invasion	[2]
	TNC overexpression	Worse prognosis	[12, 19]
	CpG island methylator phenotype	Repression of differentiation genes	[13]
Spinal	Ch 7 and 9 gains		
	Overexpression of HOX genes	Alteration of anteroposterior differentiation	[2, 16]
	IGF1	Increased cell growth	[2, 16]

sion, Puget et al. [11] analyzed 59 pediatric ependymoma by CGHarray including 33 tumors at the time of diagnosis and 26 at relapse. By comparing genomic abnormalities of these two groups of tumors, they observed a significant increase of chromosomal imbalances in relapsed ependymoma compared to those analyzed at the diagnosis, such as gain of the 9qter and 1q and loss of 6q. The presence of the 9qter gain was a sign of tumor aggressiveness as it was associated with more pejorative prognostic and occurred preferentially at relapse in children over 3 years and located in the posterior fossa. Two important genes located in this region, NOTCH1 and tenascin C (TN-C) were overexpressed in ependymoma compared to normal and fetal brain. Quantitative PCR analyses of the tumor samples highlighted overexpression of the Notch1 pathway target genes, such as *DLL1* (ligand), and four effector genes (*HES1*, *HEY1*, *MYC*, and *TNC*) and the repression of *FBXW7*, a Notch1 repressor, involved in Notch1 ubiquitination (Fig. 20.1). Finally, mutations of *NOTCH1* gene were identified

both in TAD and in the HD domains. To date, this is one of the few candidate oncogenes identified in ependymoma [11, 12, 15–20].

To better understand the biological mechanisms involved in ependymoma relapse, Peyre et al. compared CGHarray and gene expression in 17 ependymoma tumors at the time of diagnosis and at subsequent relapses [18]. A tumor relapse signature based on the gene expression changes was established. They found a frequent overexpression of genes involved in the kinetochore (including ASMP, already described in the mechanisms of malignant glioma progression, and kinesin KIF11) and gene implied in neuronal development (CD133, Wnt and Notch signaling pathways). Conversely, metallothionein genes (including MT3, also known as neuronal growth inhibitory factor) were described as downregulated in more than 80% of the recurrent ependymoma compared with the diagnosis. These data were confirmed by immunohistochemistry of ASMP and MT3 proteins on paired tumors at diagnosis and relapse on independent series. Some of these proteins could represent potential therapeutic option in the future.

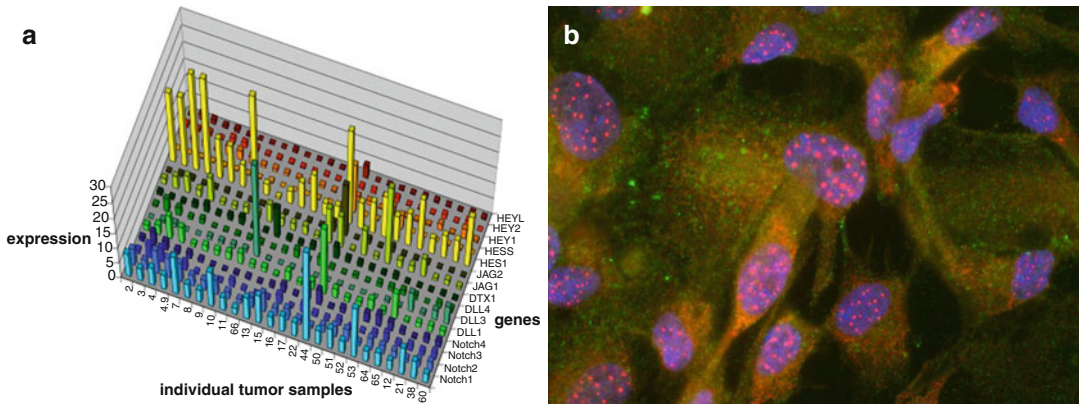


Fig. 20.1 (a) Notch pathway landscape in pediatric ependymoma. This figure shows the RT PCR expression of some of the Notch pathway genes, both ligands and

effectors. (b) Immunocytochemistry for HES1 (red dots) in pediatric ependymomas stem cells

20.3.2 Identification of Ependymoma Subgroups and Oncogenesis Pathways

Gilbertson's team crossed the database of genomic abnormalities of human ependymoma to those of tumor models developed in mice [20]. They first identified subgroups of similar genomic alteration from 83 ependymomas (adults and children). Comparing their genomic abnormalities, they identified nine different subgroups, divided according to age and location. The transcriptome of human tumors was then crossed with those derived from murine neural stem cells (NSCs), isolated from different parts of the CNS, at different stages of development and having either a locus *Ink4a/Arf*, encoding for *CDKN2A* and *CDKN2B*, wild type or deleted. They showed that only the transcriptome of human supratentorial ependymoma which specifically amplifies the oncogene *EPHB2* matched with NSCs isolated from *Ink4a/Arf* $-/-$ mouse brain. Based on these results, they generated the first mouse model for supratentorial ependymoma. Mice transplanted with mouse NSCs *Ink4a/Arf* $-/-$ and activating *EPHB2* signaling developed brain ependymomas. Further comparative analysis of matched mouse models and a supratentorial ependymoma subgroup showed deregulation of genes implied in synaptogenesis, pinpointing disruption of this pathway as a

critical event in the oncogenesis of this supratentorial subgroup. These data support strongly the hypothesis that ependymoma variants arise from specific combinations of susceptible NSCs and matched mutations. The driver mutations of the eight other subgroups they have described have yet to be identified.

Work from Witt et al. focused on posterior fossa ependymoma and identified two distinct molecular subtypes, each with unique gene expression signatures, different levels of genomic instability, and different prognosis [12]. These two subtypes were concordant with an independent patient cohort. The subtype A occurred in younger patients with lateral extension in the cerebellopontine angle with relatively less genomic instability. This subtype had enrichment of genes associated for signaling pathways for angiogenesis, PDGF, MAPK, EGFR, TGF- β , integrins, extracellular matrix (ECM) assembly, RAS/GTPase, and tyrosine kinase receptors. On the other hand, subtype B occurred in older patients and was more likely located in the spinal cord or the midline cerebellum with extensive chromosomal aberrations. This subtype had enrichment of genes associated with ciliogenesis, microtubule assembly, and mitochondria/oxidation metabolism. These findings were confirmed by immunohistochemistry of two markers of ECM signaling for subtype A, named TNC and LAMA2 (laminin alpha 2), and two markers of

ciliogenesis signaling and microtubule assembly for subtype B, named KIF27 (kinesin family number-27) and NELL2 (neural epidermal growth factor-like 2). Some of these proteins could probably help to stratify ependymomas patients, although the cohort analyzed included both adults and children.

Two recent papers using whole genome and whole exome sequencing [13, 14] found that supratentorial ependymomas carry an intrachromosomal translocation that creates a new tumor-driving gene (C11orf95–RELA fusion on chromosome 11), whereas posterior fossa ependymomas type A and B did not reveal any recurrently mutated gene or translocation. Mack et al. did find increased DNA methylation of specific genes, as well as silencing of their expression, in type A, but not type B posterior fossa ependymomas. Indeed, they found H3K27me3 marks on many of the genes with DNA methylation in posterior fossa type A tumors.

20.4 Prognostic Biomarkers

In recent years, efforts have been made to search for optimal molecular markers for ependymomas, but the degree to which they could accurately predict outcome is limited for several of them. Our knowledge has been hampered by results of cohorts including both adult and pediatric ependymomas, and most of the putative prognostic biomarkers identified so far still lack validation in prospective cohorts. For instance, members of the receptor tyrosine kinase 1 (RTK1) family have been proposed as potential prognostic markers for pediatric ependymomas [21, 22]. It concerned ERBB2/ERBB4 and EGFR, but the results on mixed cohorts were not confirmed in subsequent pure pediatric series [21].

20.4.1 Chromosomal Imbalances

Several studies have revealed chromosome 1q gain as a pejorative prognostic marker in ependymoma [9, 10, 23, 24]. Some genes located within 1q locus have been proposed as potential

candidate oncogene, such as DUSP12, members of the S100 family, and CHI3L1, but they have to be validated in large series of pediatric ependymomas. The recent results from Korshunov et al. on 122 ependymomas confirm and validate previous results [9]. They also pointed out a small group of poor prognosis associated with CDKN2A deletion and another group characterized by chromosomal imbalances associated with a better prognosis that have not been confirmed by another study yet. Considering that the cohort included both adult and pediatric ependymomas, all of the findings may not apply to children.

Loss expression of genes within 22q12 and 22q13 has also been frequently observed in pediatric ependymoma. A retrospective analysis of 47 pediatric ependymoma found frequent loss of C22ORF2 and RAC2, this latter being associated with poorer overall survival [25]. Finally, the loss of many loci of chromosome 6q has been described and seemed exclusive to posterior fossa ependymomas at relapse in a meta-analysis, but no putative gene identified in the deleted regions has been validated in further pediatric cohorts [8].

20.4.2 hTERT and Nucleolin

Human telomerase reverse transcriptase (hTERT) expression has been found to be a strong independent prognostic factor of pediatric ependymoma relapse and poor survival [26, 27]. Immunohistochemical analysis performed on 65 pediatric ependymoma revealed positive staining of hTERT in 58 % of tumors with a worse prognosis in multivariate analysis [26]. Importantly, another study based on the review of 80 pediatric intracranial ependymomas showed that the antibody used recognized in fact nucleolin, a chaperone protein of nuclear enzyme hTERT [28]. In this series, the EFS at 5 years was 31 % for the tumors with a strong nucleolin expression and 74 % for those with low expression. The role of this prognostic marker has been evaluated in a wide meta-analysis conducted by three European cooperative groups, but the results of the two previous teams could not be confirmed [29].

20.4.3 Neuronal Differentiation

Neuronal differentiation as shown by NEFL70 expression on immunohistochemical experiment has recently been associated with supratentorial location of pediatric ependymomas compared to posterior fossa ones [19]. Among the supratentorial tumors, strong staining for NEFL was significantly associated with better 5-year EFS (90 % for NEFL high staining versus 0 % for NEFL low staining). NEFL immunopositivity was associated with other neuronal markers such as chromogranin A and synaptophysin.

20.4.4 Tenascin C

The tenascin C (TN-C) gene situated on chromosome 9q has been found upregulated in pediatric ependymomas series [7, 11, 15]. Because of few number of tumor samples, multicentric studies containing many tumors represent a significant strength in the analysis of new ependymoma prognostic markers. This is the case of a European study regrouping 260 pediatric ependymoma, from France, UK, and Italy. Immunohistochemical analysis of the main potential prognostic markers was carried out on each tumor and correlated with the clinical patient data. In a multivariate analysis, the strong expression of TNC in the tumor was significantly correlated with a poorer median survival, independent on the quality of the surgical resection. The TNC may thus be considered as a bad prognostic marker in pediatric ependymomas that could be used for the stratification of treatments in pediatric ependymoma future trials [19].

20.4.5 Other Potential Markers

Recently, Koos et al. aimed to identify pathways operative in the development of infratentorial ependymomas and compared gene expression profiles of tumor cell laser microdissected from infratentorial ependymomas with that of nonneoplastic ependymal cell laser microdissected from autopsy tissue [30]. They

found an overexpression (up to 35-fold) of the transcription factor EVI1 (ecotropic viral integration site 1). They also identified MDS1/EVI1 fusion transcripts in 17 of 28 infratentorial ependymomas, and the transfection of primary posterior fossa ependymomas cells with EVI1-specific siRNAs resulted in significant growth inhibition. Using an independent cohort, they confirmed that high EVI1 expression was associated with shorter overall survival and progression-free survival. These data have to be confirmed in prospective pediatric cohort, as there were some adult samples in this series.

In a recent study performed on a small series of 19 pediatric ependymoma samples, Donson et al. described the importance of the innate and adaptative immunity in the prognosis of this tumor [31]. After classification according to their evolution in recurrent tumor or not, they analyzed the profile expression of 127 genes involved in immune functions. Ontology analyses revealed that genes associated with nonrecurrent ependymoma were predominantly immune function related. Additionally, increased expression of immune-related genes was correlated with longer time to progression in recurrent ependymoma. Histological analysis of the location of these genes that are upregulated in non-relapse tumors showed that their expression was essentially localized in a restricted cell population, the tumor-infiltrating lymphocytes (TIL), especially CD4+ T lymphocytes. Thus, the presence of these cells, mediators of adaptative inflammatory response against cancer cell, seems to play a protective role in the progression of the ependymoma. Other complementary larger cohort studies are needed to confirm these works, but these preliminary results suggest that immunotherapy could be envisaged in the treatment of these tumors.

20.5 Future Therapeutic Options

Recent advances in the identification of new therapeutic targets and pathways involved in pediatric ependymoma tumor allowed to propose new therapies complementing conventional treatment.

Proposing a therapy based on the biology of tumor fits into the emerging concept of personalized medicine therapy.

20.5.1 Gamma-Secretase Inhibitors

The Notch signaling pathway has been described as involved in the ependymoma oncogenesis and tumor progression mechanisms [2, 11, 19]. The pharmacological class of gamma-secretase inhibitors (GSI) prevents the cleavage of the Notch protein, a transmembrane receptor. This cleavage of the protein receptor represents the last step of the activation of the pathway signaling. Under the action of the GSI enzyme, the intracellular portion of the Notch protein cannot be released into the cytoplasm and nucleus to activate the transcriptional machinery. Through its action, the Notch signaling pathway (whose main effector genes are HES1 HEY1, MYC) is inhibited. As shown by Puget et al. [11], they may be interesting drug candidates against ependymomas stem cells.

20.5.2 Histone Deacetylase Inhibitors (HDACi)

As shown above, ependymomas have relatively few chromosomal abnormalities compared with other tumors, especially in young children and infants [8, 9]. Aberrant epigenetic regulation of gene expression may therefore be implicated in tumor initiation. Little is known about methylation in ependymomas, except the frequent methylation of RASSF1A and TRAIL pathway-related genes [32]. Numerous studies have suggested that HDACi may be potent anticancer drugs allowing the re-expression of tumor suppressor genes. A recent study in vitro evaluating the efficacy of a HDACi (trichostatin A) in pediatric high-grade brain tumor cell lines (PNET, medulloblastoma, and ependymoma) showed a reduction of cell proliferation associated with a phase G2/M arrest, DNA damage, and induction of apoptosis in the three types of cell lines [33]. In vitro analysis on pediatric ependymoma short-term cultures

has shown that HDACi class caused a significant increase in the level of expression of the MT3 which seems to be involved in mechanisms of tumor progression [18]. HDACi could restore the level of expression of MT3 and could represent a therapeutic option in the future to decrease risk of relapse.

20.5.3 Antiangiogenic Drugs

Angiogenesis may also be a relevant target in ependymomas. Preliminary clinical data have been reported in recurrent adult ependymoma showing that bevacizumab, an anti-VEGF (vascular epithelial growth factor) monoclonal antibody, could be efficient [34]. Although the study included only a small number of patients, bevacizumab associated with carboplatin, temozolomide, and irinotecan showed benefit effect to radiological response. Clinical studies are currently developed in adults. These agents should also be evaluated in pediatric cohorts.

20.5.4 Telomerase Inhibitors

Expression of hTERT telomerase has been described in some studies as a pejorative prognostic marker in pediatric ependymoma [26, 27]. According to this hypothesis, Hawkins et al. have recently published a study evaluating the effect of a telomerase inhibitor in ependymoma primary cultures (MST-312) [35]. Inhibition of telomerase on this cell population leads to a significant reduction in their viability with DNA damage (via YH2AX expression) as well as an increase of 50 % of death by apoptosis.

20.5.5 Antimetabolites

The polyamine metabolism may be critical for ependymoma as shown by Smith et al. who treated tumor xenograft model with a conformationally restricted analog of the natural polyamine spermine that competitively inhibits natural polyamine functions leading to cancer

cell growth inhibition [36]. The single case of tumor regression in their experiment occurred in an ependymoma xenograft. Other metabolites such as methotrexate and 5-FU may also deserve further testing in the clinic.

20.5.6 Targeting mTOR Pathway

In a brief report of a 6-year-old child with a multiple progressive ependymoma, Bowers et al. have shown a near complete response to sirolimus [37]. Immunohistochemistry for phosphorylated S6, which has been reported to be associated with tumor sensitivity to mTORC1 inhibitors, was positive in this patient's tumor. This result suggests that sirolimus may be a useful therapeutic agent in a subgroup of pediatric ependymomas with mTOR pathway activation.

20.5.7 Targeting Epigenetic Modifiers

Recently, Mark et al. performed whole genome and whole exome sequencing of 47 hindbrain ependymoma type A [13]. They showed that they exhibited a CpG island methylator phenotype. Transcriptional silencing driven by CpG methylation converged exclusively on targets of the polycomb repressive complex 2 which represses expression of differentiation genes through trimethylation of H3K27. Importantly, CpG island methylator phenotype-positive hindbrain ependymomas were responsive to epigenetic modifiers such as 5-aza-2'-deoxycytidine (a DNA demethylating agent) or 3-deazaneplanocin A (an inhibitor of H3K27me3) both in vitro and in vivo. These epigenetic modifiers are thus very promising therapeutic candidates for this disease.

Conclusion

Advances in the biological understanding of childhood ependymoma have been significant in the past decade. New biomarkers should be used for patient stratification and in a near future for treatment decisions. The diagnosis work-out should currently comprise a CGHarray analysis and immunohistochemistry for the

prognosis biomarkers such as TNC. New molecular findings as epigenetic changes specific to pediatric posterior fossa ependymomas brought new insight in the development of this disease. Given the rarity of this tumor, multicentric collaboration that designs prospective studies is necessary to validate known biomarkers and discover other target genes.

References

1. Mc Lendon RE, Wistler OD, Kros JM et al (2007) Ependymoma. In: Louis DN (ed) WHO classification of tumors of the central nervous system. IARC, Lyon, pp 74–78
2. Taylor MD, Poppleton H, Fuller C et al (2005) Radial glia cells are candidate stem cells of ependymoma. *Cancer Cell* 8:323–335
3. Merchant TE, Li C, Xiong X, Kun LE et al (2009) Conformal radiotherapy after surgery for paediatric ependymoma: a prospective study. *Lancet Oncol* 10(3):206–207
4. Massimino M, Buttarelli FR, Antonelli M et al (2009) Intracranial ependymoma: factors affecting outcome. *Future Oncol* 5(2):207–216
5. Ellison DW, Kocat M, Figarella-Branger D et al (2011) Histopathological grading of pediatric ependymoma: reproducibility and clinical relevance in European trial cohorts. *J Negat Results BioMed* 10:7
6. Hamilton RL, Pollack IF (1997) The molecular biology of ependymomas. *Brain Pathol* 7:807–822
7. Korshunov A, Golanov A, Timirgaz V (2002) Immunohistochemical markers for prognosis of ependymal neoplasms. *J Neurooncol* 58:255–270
8. Kilday JP, Rahman R, Dyer S et al (2009) Pediatric ependymoma: biological perspectives. *Mol Cancer Res* 7:765–786
9. Korshunov A, Witt H, Hielscher T et al (2010) Molecular staging of intracranial ependymoma in children and adults. *J Clin Oncol* 28(19):3182–3190
10. Dyer S, Prebble E, Davison V et al (2002) Genomic imbalances in pediatric intracranial ependymomas define clinically relevant groups. *Am J Pathol* 161:2133–2134
11. Puget S, Grill J, Valent A et al (2009) Candidate genes on chromosome 9q33-34 involved in the progression of childhood ependymomas. *J Clin Oncol* 27:1884–1892
12. Witt H, Mack SC, Ryzhova M et al (2011) Delineation of two clinically and molecularly distinct subgroups of posterior fossa ependymoma. *Cancer Cell* 20:143–157
13. Mack SC, Witt H, Piro RM et al (2014) Epigenomic alterations define lethal CIMP-positive ependymomas of infancy. *Nature* 506(7489):445–450

14. Parker M, Mohankumar KM, PUNCHIHEWA C et al (2014) C11orf95-RELA fusions drive oncogenic NF- κ B signalling in ependymoma. *Nature* 506(7489):451–455
15. Modena P, Lualdi E, Facchinetti F et al (2006) Identification of tumor-specific molecular signatures in intracranial ependymoma and association with clinical characteristics. *J Clin Oncol* 24:5223–5233
16. Palm T, Figarella-Branger D, Chapon F et al (2009) Expression profiling of ependymomas unravels localization and tumor grade-specific tumorigenesis. *Cancer* 115(17):3955–3968
17. Schneider D, Monoranu CM, Huang B et al (2009) Pediatric supratentorial ependymomas show more frequent deletions on chromosome 9 than infratentorial ependymomas: a microsatellite analysis. *Cancer Genet Cytogenet* 191(2):90–96
18. Peyre M, Commo F, Dantas-Barbosa B et al (2010) Portrait of ependymoma recurrence in children: biomarkers of tumor progression identified by dual color microarray-based gene expression analysis. *PLoS One* 5(9):e12932
19. Andreiulo F, Puget S, Peyre M et al (2010) Neuronal differentiation distinguishes supratentorial and infratentorial childhood ependymomas. *Neuro Oncol* 12(11):1126–1134
20. Johnson RA, Wright KD, Poppleton H et al (2010) Cross-species genomics matches driver mutations and cell compartments to model ependymoma. *Nature* 466(7306):632–636
21. Gilbertson RJ, Bentley LH, Hernan R et al (2002) ERBB receptor signaling promotes ependymoma cell proliferation and represents a potential novel therapeutic target for this disease. *Clin Cancer Res* 8:3054–3064
22. Poppleton H, Gilbertson RJ (2007) Stem cells of ependymoma. *Br J Cancer* 96:6–10
23. Carter M, Nicholson J, Ross F et al (2002) Genetic abnormalities detected in ependymomas by comparative genomic hybridization. *Br J Cancer* 86:929–939
24. Mendrzyk F, Korshunov A, Benner A et al (2006) Identification of gains on 1q and epidermal growth factor receptor overexpression as independent prognostic markers in intracranial ependymoma. *Clin Cancer Res* 12:2070–2079
25. Karakoula K, Suarez-Merino B, Ward S et al (2008) Real-time quantitative PCR analysis of pediatric ependymomas identifies novel candidate genes including TPR at 1q25 and CHIBBY at 22q12-q13. *Genes Chromosomes Cancer* 47:1005–1022
26. Tabori U, Ma J, Carter M et al (2006) Human telomere reverse transcriptase expression predicts progression and survival in pediatric intracranial ependymoma. *J Clin Oncol* 24:1522–1528
27. Tabori U, Ma WV, Tabori U, Wong V, Ma J et al (2008) Telomere maintenance and dysfunction predict recurrence in paediatric ependymoma. *Br J Cancer* 99(7):1129–1135
28. Ridley L, Rahman R, Brundler MA et al (2008) Multifactorial analysis of predictors of outcome in pediatric intracranial ependymoma. *Neuro Oncol* 10:675–689
29. Andreiulo F, Mauguen A, Kilday J et al (2010) Tenascin-C is an independent prognostic marker in pediatric ependymoma: an international collaborative study. *Neuro Oncol* 12:ii26, Abstract ISPNO, Vienna
30. Koos B, Bender S, Witt H et al (2011) The transcription factor Evi-1 is overexpressed, promotes proliferation, and is prognostically unfavorable in infratentorial ependymomas. *Clin Cancer Res* 17:3631–3637
31. Donson AM, Birks DK, Barton VN et al (2009) Immune gene and cell enrichment is associated with a good prognosis in ependymoma. *J Immunol* 183(11):7428–7440
32. Michalowski MB, de Fraipont F, Michelland S et al (2006) Methylation of RASSF1A and TRAIL pathway related genes is frequent in childhood intracranial ependymoma and benign choroid plexus papilloma. *Cancer Genet Cytogenet* 166:74–81
33. Rahman R, Osteso-Ibanez T, Hirst RA et al (2010) Histone deacetylase inhibition attenuates cell growth with associated telomerase inhibition in high-grade childhood brain tumor cells. *Mol Cancer Ther* 9:2568–2581
34. Green RM, Cloughesy TF, Stupp R et al (2009) Bevacizumab for recurrent ependymoma. *Neurology* 73(20):1677–1680
35. Wong VC, Morrison A, Tabori U et al (2010) Telomerase inhibition as a novel therapy for pediatric ependymoma. *Brain Pathol* 20(4):780–786
36. Smith MA, Maris JM, Lock R et al (2011) Initial testing (stage 1) of the polyamine analog PG11047 by the pediatric preclinical testing program. *Pediatr Blood Cancer* 57:268–274
37. Bowers DC, Kucejova B, Margraf L et al (2011) mTORC1 activation in childhood ependymoma and response to sirolimus. *J Neurooncol* 103:797–801

Andrea Rossi

21.1 Introduction

Neuroimaging studies are crucial for the identification and characterization of posterior fossa ependymomas as well as in the presurgical planning and evaluation of treatment results including the outcome of surgery, chemotherapy, and irradiation. Magnetic resonance imaging (MRI) and computerized tomography (CT) are the imaging methods in current use to evaluate these, as well as other, brain tumors. These methods detect tumors as lesions whose density and signal intensity are different from those of normal brain, with a variable degree of mass effect causing distortion of normal structures. MRI is superior to CT in the characterization of brain tumors and in the follow-up after treatment, thanks to its greater soft tissue contrast and multiplanar imaging capability without the burden of ionizing radiations, an especially relevant issue in infants and children who are more susceptible than adults to radiation-induced complications, including malignancy. Furthermore, advanced MRI modalities such as diffusion, perfusion, and spectroscopy provide additional information regarding functional features of brain tumors, including cellularity, hemodynamics, and metabolism, which may add

significant information regarding their biological behavior and prognosis [1].

Despite advances in imaging, microsurgical techniques, and adjuvant radiotherapy, morbidity and mortality in patients harboring posterior fossa ependymomas have remained significant [2]. Among prognostic factors influencing long-term survival rates, the extent of surgical resection remains the most relevant [3]. This is, in turn, influenced by tumor location and anatomical origin. Thus, the main goal of preoperative imaging is, other than the differential diagnosis from other posterior fossa tumors typical of the pediatric age group, a careful assessment of the anatomical features and extension of the lesion.

21.2 Technical Issues

MRI is the main neuroimaging method for patients affected by posterior fossa ependymomas, as well as other forms of brain tumor. State-of-the-art scanners working at 1.5 or 3 tesla field strength are to be preferred over low-field magnets because of their superior signal-to-noise and contrast-to-noise characteristics. In all instances, both at presentation and on follow-up, imaging studies should include the entire neuraxis, i.e., the brain and the whole spine, in order to detect possible leptomeningeal spread. Brain MRI should be performed using dedicated head coils. Parallel imaging coils have proved advantageous over conventional quadrature head coils in terms

A. Rossi, M.D.
Department of Pediatric Neuroradiology,
G. Gaslini Children's Hospital,
Via G. Gaslini 5, Genova 16147, Italy
e-mail: andrearossi@ospedale-gaslini.ge.it

of scan duration and should be preferred whenever available. The scanning protocol should include thin-slice (typically 3 mm) T2-weighted images in all three planes of space and axial FLAIR images at 3–4 mm slice thickness; T1-weighted images should be acquired both in the axial and the sagittal planes at 3–4 mm slice thickness. Gradient-echo imaging is also mandatory in order to detect calcification and/or hemorrhage, both frequent features of ependymomas; susceptibility-weighted imaging (SWI) has proven advantageous over conventional gradient-echo T2* imaging in this respect [4]. Following intravenous gadolinium-chelate administration, T1-weighted images should be acquired in the three planes of space. Finally, three-dimensional contrast-enhanced T1-weighted or T2-weighted sequences may be acquired and transferred online to a computerized system in the surgical room (neuronavigator) which guides the neurosurgeon's instrument to the selected target during surgery. Spinal MRI is typically obtained just after completion of the brain portion of the imaging study. The optimal technique involves the use of phased-array surface coils which allow for inclusion of the whole spine in a single sagittal acquisition using a large field of view. Typically, post-contrast sagittal T1-weighted images will suffice to ascertain the presence of leptomeningeal spread to the spine. However, sagittal T2-weighted or axial T1-weighted images can be added to the protocol at the expense of a few minutes scan time in order to clarify doubtful findings.

Regarding advanced brain MRI modalities, diffusion-weighted imaging (DWI) should be acquired in the axial plane and apparent diffusion coefficient maps should be calculated. This is usually done by internal machine software. The ADC values are obtained by placing manually drawn region of interests on solid (i.e., nonnecrotic, noncalcified, nonhemorrhagic) portions of the mass. In the field of brain tumor imaging, DWI is mainly used to estimate cellularity, which is a function of tumor grading. In general, ADC values are inversely correlated with tumor grade, i.e., high-grade tumors have lower ADCs than low-grade tumors, although some degree of overlap exists between certain tumor types [5]. There is no currently recognized indication for diffusion

tensor imaging studies or tractography for the presurgical evaluation of posterior fossa tumors, including ependymomas.

Proton MR spectroscopy (MRS) can be acquired with single-voxel and multi-voxel (i.e., chemical shift imaging (CSI)) methods. Single-voxel MRS is more widespread and used routinely; it produces spectra from manually selected volumes of interest. Acquisition is possible at short (20–30 ms), intermediate (135–144 ms), and long (270–280 ms) echo times, yielding different possibilities for metabolite identification and peak analysis. The metabolites normally detected in the brain, regardless of the adopted echo time, include N-acetylaspartate (NAA), a neuronal marker; choline (Cho), a membrane marker; and creatine (Cr), an energy metabolism marker. Short echo-time techniques allow for additional metabolite identification, including myoinositol (mI), a glial marker. Other metabolites, including lactate (a marker of anaerobic glycolysis in hypoxic regions), lipids, and glutamine-glutamate complexes, are undetectable in normal conditions. Thus, their identification indicates the presence of an abnormal process, although specificity is limited to a few disorders. Albeit technically possible, absolute quantification of normal or abnormal metabolites is not routinely performed. Relative changes of concentrations in the form of metabolite ratios are frequently used instead.

Perfusion-weighted imaging (PWI) can also be acquired with several methods. The most widely available is T2*-weighted dynamic susceptibility contrast (DSC) imaging. This requires the bolus intravenous administration of paramagnetic contrast material and the rapid acquisition of images over time during the first pass of contrast material through the capillary bed by means of echo-planar imaging techniques. Of all measurable perfusional parameters, the relative cerebral blood volume (rCBV), defined as the volume of blood in an area of brain tissue expressed in mm³/100 g, is the most commonly evaluated in the field of brain tumor imaging as it grossly correlates with tumor grade. Arterial spin labeling is an alternative perfusional technique that does not require an exogenous tracer. While promising, this technique suffers limitations at lower magnet

fields (i.e., 1.5 tesla) and is challenging in the posterior fossa due to susceptibility artifacts. Currently, PWI is performed in only a limited number of cases, usually to distinguish treatment-related changes from recurrent tumor.

The role of CT scanning is presently limited to the initial recognition of a posterior fossa tumor mass in patients who present with suggestive clinical findings. Most patients will initially undergo CT because it is generally more readily available than MRI, and rapid imaging acquisition greatly reduces the need for sedation also in uncooperative patients. Once a tumor mass is detected, however, the patient should immediately be referred for MRI. There is usually no indication, in our opinion, to proceed with

post-contrast CT scanning when the patient will regardless have to perform MRI as well. Post-contrast CT imaging is, however, mandatory when MRI is not available for further neuroimaging assessment. Helical acquisitions should be preferred since they allow for better reformatting and multiplanar morphological assessment.

21.3 Classification

Posterior fossa ependymomas originate from the ependymal layer of the fourth ventricle either on a midline or, less frequently, a lateral position. The classification of Ikezaki et al. [3] categorizes ependymomas into three variants (Fig. 21.1):

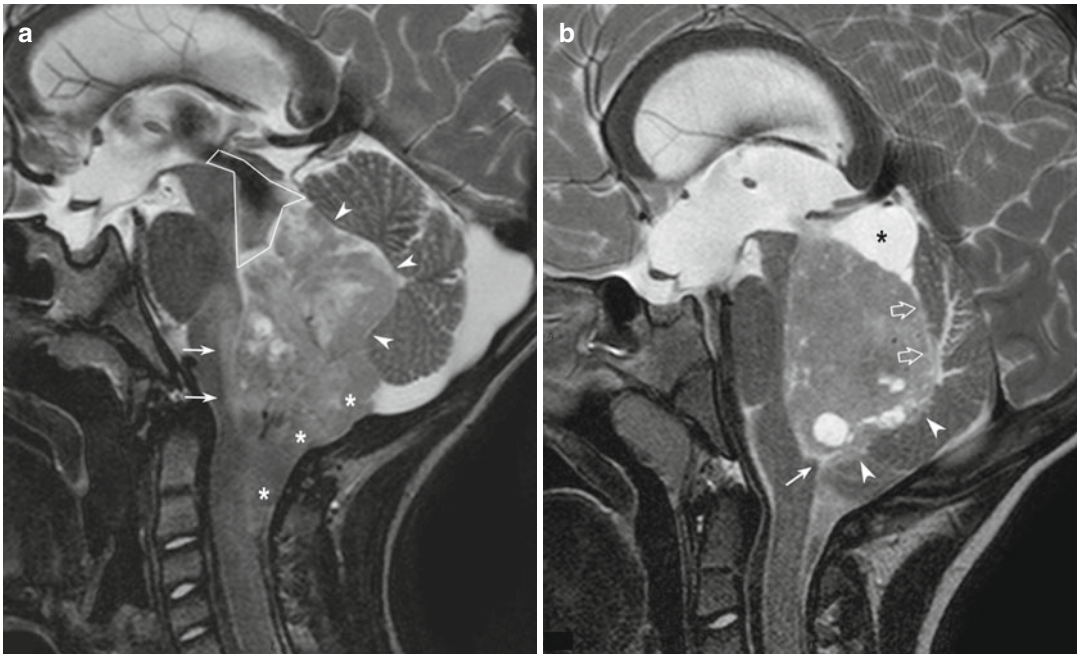


Fig. 21.1 Origin and classification of ependymomas. (a) Midfloor type. Sagittal T2-weighted image (a) shows tumor almost completely filling the fourth ventricle with a clear-cut cleavage with the vermis (arrowheads). The whole length of the brainstem is visualized. The obex is not visible at the site of origin of the tumor from the floor of the fourth ventricle (arrows). There is tumor extension into the cistern magna and foramen magnum (asterisks). Dilatation of the cerebral aqueduct and superior fourth ventricle (squared area) is due to CSF flow obstruction; notice signal loss due to turbulent flow at this level. (b) Roof type. Sagittal T2-weighted image shows intra-fourth-ventricular mass with lack of demarcation from the inferior portion of the roof (arrowheads) but preservation

of a cleavage plane above the fastigium (empty arrows). The entire length of the brainstem is visible, and the obex is preserved (arrow) although the brainstem is globally displaced anteriorly. There is a superiorly located large peripheral cystic component (asterisk). (c, d) Lateral type. Sagittal T2-weighted image (c) shows tumor extending anteriorly (arrows) and displacing the brainstem, which is consequently no longer visible in its entirety along the midline. Tumor also extends inferiorly in the cistern magna and foramen magnum (asterisks). Axial T2-weighted image (d) shows lateral displacement of the brainstem (arrows) and lateral extension into the right Luschka foramen and cerebellopontine cistern (asterisks), leading to encasement of the basilar trunk (b)



Fig. 21.1 (continued)

- (i) “Midfloor type”: It is a midline tumor arising from the inferior half of the fourth ventricular floor beneath the stria medullaris and representing the most common type; technically, it is a dorsally exophytic brainstem tumor, however usually lacking significant infiltration of the fourth ventricular floor and growing into the fourth ventricle.
- (ii) “Roof type”: It is a midline tumor arising from the inferior medullary velum forming the roof of the fourth ventricle.
- (iii) “Lateral type”: It is an off-midline tumor that originates into the vestibular area or lateral recess of the fourth ventricle.

An accurate localization of the site of origin of posterior fossa ependymomas on neuroimaging carries important prognostic implications. It is ascertained that midline (either midfloor or roof) tumors carry a more favorable prognosis than lateral types, mainly because a gross total resection is more difficult to achieve for lateral masses owing to their deep location and intimate relationships with arteries and lower cranial nerves into the cerebellopontine angle and lateral medullary cisterns [6]. On the other hand, midline lesions are usually less firmly adherent to vital structures, although infiltration of the fourth

ventricular floor may limit the extent of surgical removal, thus increasing the chance of recurrence and worsening the prognosis [7].

21.4 Macroscopic Features and Growth Pattern

Ependymomas are nodular, lobulated neoplasms with a macroscopically solid appearance on neuroimaging studies. Usually, nervous tissue infiltration only occurs at the site of origin; the latter may, however, not always be clearly recognizable on imaging and is often ascertained only on surgical observation. Owing to their soft consistency and slow growth rate [8], these masses tend to adapt their shape to that of surrounding structures and grow along existing anatomic structures without infiltrating the adjacent nervous tissues. This results in the typical “plastic development” [9] (Figs. 21.1 and 21.2), a term that describes the tendency of these tumors to spread as ribbonlike extensions throughout the outlet foramina of the fourth ventricle into the subarachnoid spaces of the posterior fossa and cervical spinal canal while maintaining a clear-cut edge toward the adjacent nervous tissue. On ground of their soft consistency,

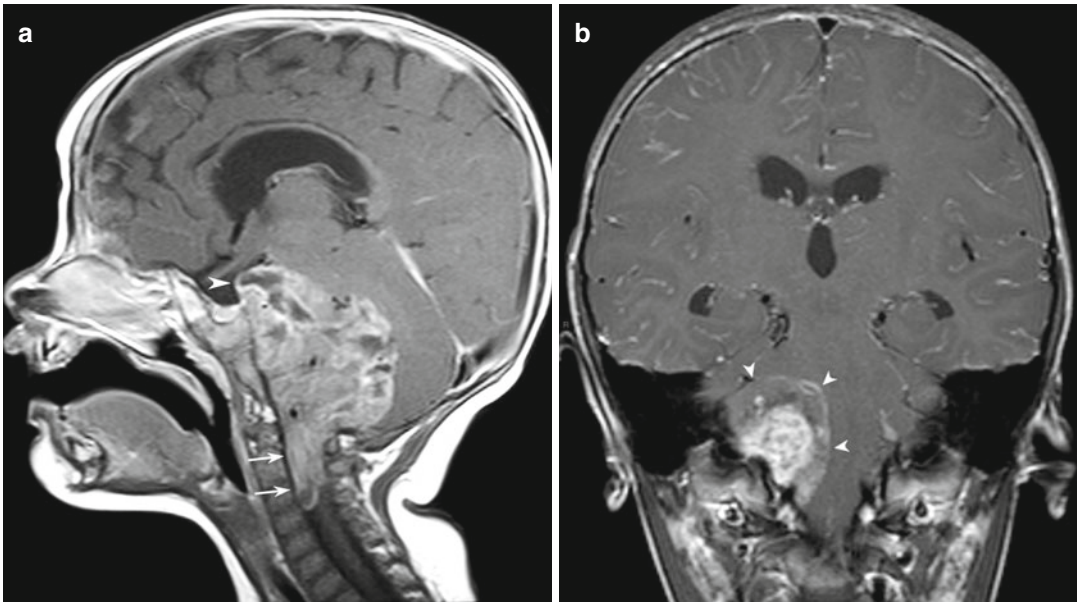


Fig. 21.2 Plastic development of ependymomas. (a) Contrast-enhanced sagittal T1-weighted image shows tumor extending caudally into the foramen magnum and cervical spinal canal (arrows). The tumor has also extended cranially through the prepontine cistern and

into the interpeduncular fossa, where it abuts the suprasellar cistern (arrowhead). (b) Contrast-enhanced coronal T1-weighted image shows inhomogeneously enhancing tumor (arrowheads) into the right cerebellopontine angle cistern

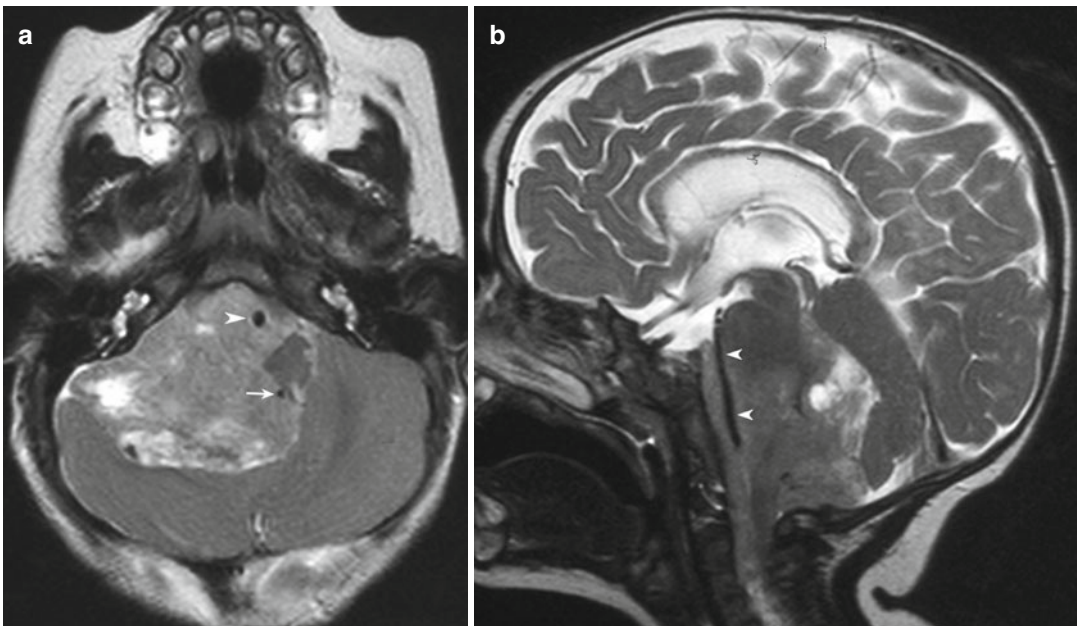


Fig. 21.3 Vessel encasement in ependymomas. (a) Axial T2-weighted image shows lateral ependymoma encasing the basilar trunk (arrowhead) and posterior inferior cerebellar artery (arrow). (b) Sagittal T2-weighted image shows the full length of the basilar trunk (arrowheads) is engulfed by the tumor. (c) Contrast-enhanced coronal

T1-weighted image shows encasement of the right vertebral artery (arrow). Notice the caliber of the artery is not reduced. (d) Sagittal T2-weighted image shows cluster of encased small-caliber vessels (arrows). The finding of small encased vessels is almost constant in posterior fossa ependymomas

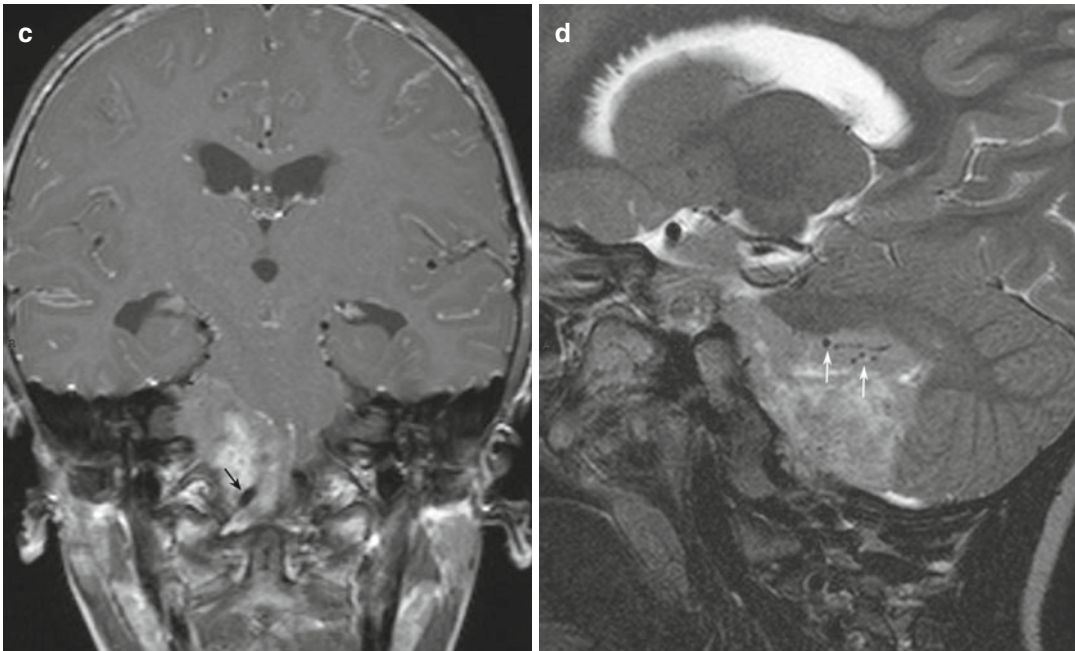


Fig. 21.3 (continued)

ependymomas also typically encase vessels (both arteries and veins) and nerves. Radiologically, encasement of vessels is defined as a tumor-vessel relationship in which the tumor is inseparable from the vessel wall for 180° or more of the vessel circumference [2] (Figs. 21.1 and 21.3).

On presentation, supratentorial hydrocephalus is common due to cerebrospinal fluid flow obstruction from the intraventricular mass. Capped hyperintensities on T2-weighted and FLAIR images around the horns of the lateral ventricles indicate periventricular edema in the setting of progressive uncompensated hydrocephalus. These represent a frequent indication to emergent surgery for shunt placement before the actual surgical operation for tumor excision.

21.4.1 Midline Ependymomas (Midfloor and Roof Types)

These masses are centered on the midline and fill the fourth ventricle to a variable degree. The differentiation of these two types from one another may not be feasible on imaging when the lesion is sufficiently large as to almost completely fill the

fourth ventricle. The superior portion of the fourth ventricle is typically free of tumor and forms, together with the overlying dilated cerebral aqueduct, a triangular or oval shape that has been called a “capped fourth ventricle” [8]. By virtue of their midline location, these tumors displace the brainstem anteriorly, but not laterally; thus, the entire length of the brainstem is visible on midsagittal MR images [2]. The obex (i.e., the point on the midline of the dorsal surface of the medulla at the most caudal aspect of the fourth ventricle floor) is seen to be infiltrated in the midfloor type but not in the roof type (Fig. 21.1). Conversely, there is a clear-cut cleavage plane between the posterior surface of the tumor and the vermis in the midfloor type. This morphological appearance on midsagittal images is extremely important in the differentiation from medulloblastomas, which originate from the vermis and project anteriorly in the fourth ventricle without any such separation. In the roof variant, the demarcation between tumor and vermis may not be as conspicuous owing to the tumor’s origin from the ependyma of the inferior medullary velum; however, the cleavage is usually visible at least in the superior portion of the fourth ventricle roof, above the fastigium (Fig. 21.1).

Plastic extension occurs either through the foramen of Magendie or the foramina of Luschka (Figs. 21.1 and 21.2). Extension through the Magendie causes the tumor to grow into the cisterna magna and, often, to herniate into the foramen magnum and cervical spinal canal, surrounding and compressing the medulla and spinal cord [8]. Extension into the lateral recess and Luschka foramen may occur either mono- or bilaterally and may involve the cerebellopontine angle; however, midline lesions typically do not extend further into the prepontine cistern [2].

21.4.2 Lateral Ependymomas

These masses are centered off the midline, as they typically arise in one lateral recess of the fourth ventricle and displace the brainstem laterally, but not anteriorly. This morphological arrangement is the opposite to that of midline (either midfloor or roof) variants. As a consequence of this displacement, the entire length of the brainstem cannot be seen in one single midsagittal plane (Fig. 21.1).

Lateral ependymomas often extend through the homolateral Luschka foramen into the cerebello-pontine angle and may reach the prepontine cistern, where the mass engulfs the basilar artery (Fig. 21.3), a feature not seen in midline lesions. However, they typically do not extend across the fourth ventricle floor into the contralateral recess and Luschka foramen, unlike the midfloor type. Lateral tumors may also extend inferiorly into the cisterna magna through the Magendie foramen. However, the obex is consistently not infiltrated and can therefore be recognized as a discrete structure [2]. Engulfment of nerves and vessels in the cisternal spaces makes radical excision difficult if not impossible and is the main reason for the worse prognosis as compared with midline tumors.

21.5 Structural Imaging Features

Calcification has been regarded as the most specific neuroimaging feature of ependymomas [10] (Fig. 21.4). However, it is present in only 25–50 % of cases [8]. Hemorrhage also is frequent

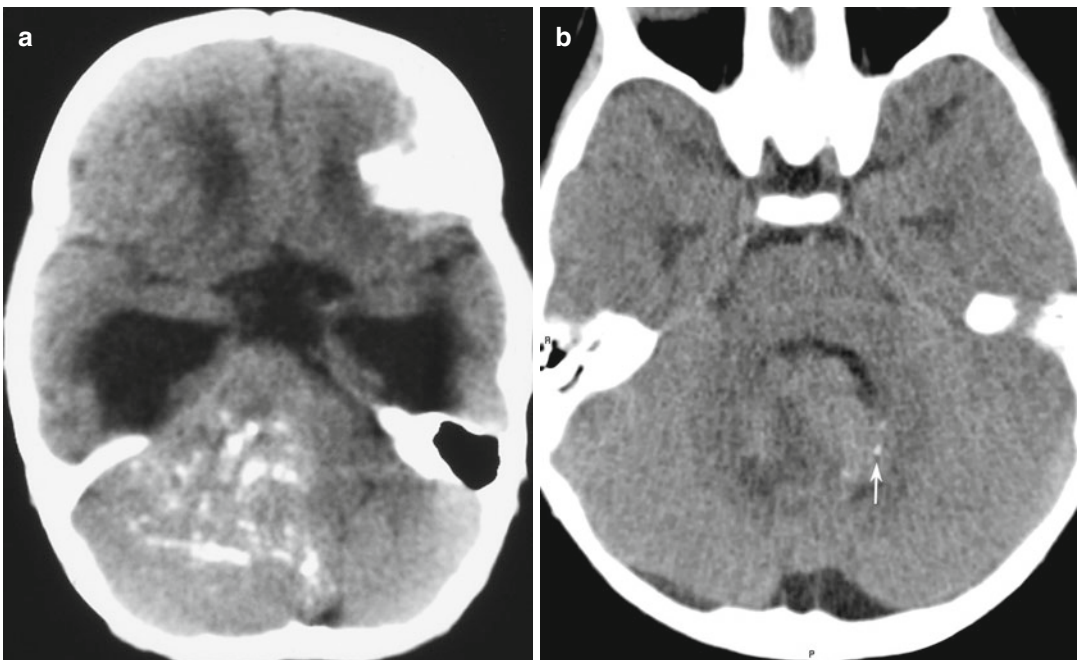


Fig. 21.4 Calcifications in ependymomas. (a) Axial CT in a case of diffusely calcified anaplastic ependymoma. (b, c) In a different case, axial CT scan shows isolated

calcified foci (*arrow*) in an otherwise isodense ependymoma. Axial susceptibility-weighted MR image reveals calcifications as a cluster of tiny hypointense spots (*arrow*)

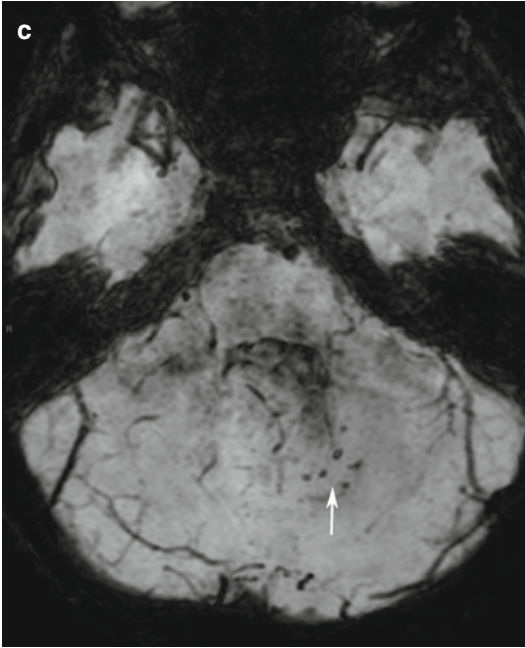


Fig. 21.4 (continued)

(Fig. 21.5). Structural heterogeneity is typical [10] with frequent occurrence of necrotic-cystic portions within the mass.

The solid components (Fig. 21.6) are isointense with gray matter on T1-weighted MRI images. Signal behavior is more variable in T2-weighted images due to pathological heterogeneity, variable cellularity, and hydration of the mass, with most tumors being iso- to hyperintense to gray matter. On FLAIR, signal intensity is intermediate to high. Contrast enhancement of the solid components is variable, ranging from marked to absent, and often is not homogeneous because of an admixture of markedly, poorly, or non-enhancing soft tissue areas [8]. On CT, the solid portion generally is isodense with normal gray matter (Fig. 21.6); hemorrhage and calcifications are easily detected as hyperdense areas. Conventional MRI characteristics cannot definitively distinguish between grade II ependymomas and anaplastic grade III

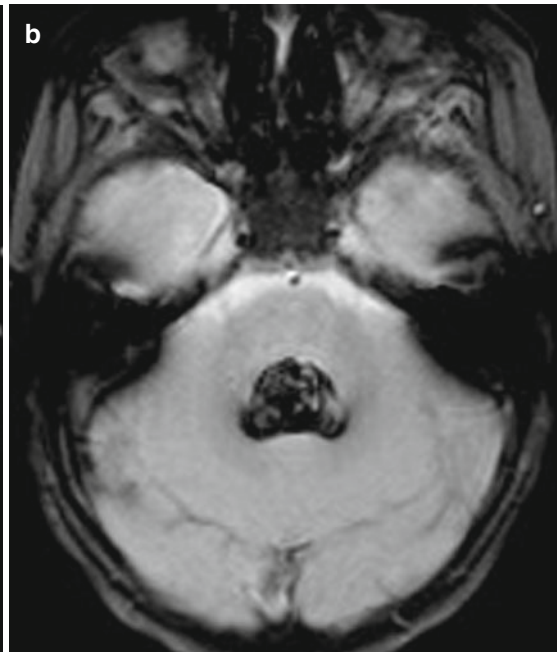


Fig. 21.5 Hemorrhage in ependymomas. (a–c) Hemorrhagic anaplastic ependymoma. Axial CT scan (a) shows hyperdense lesion filling the fourth ventricle. Axial gradient-echo T2*-weighted image (b) confirms the acute hemorrhage. (c) Sagittal T2-weighted image shows midline-type lesion with infiltration of the fourth ventri-

cle floor at the obex (*white arrowheads*). The tumor shows plastic development through the Magendie into the cisterna magna. Blood extends superiorly into the posterior third ventricle (*black arrowheads*). (d) In a different case, axial T2-weighted image shows focal hemorrhagic necrosis with dependent fluid-fluid level (*arrows*)

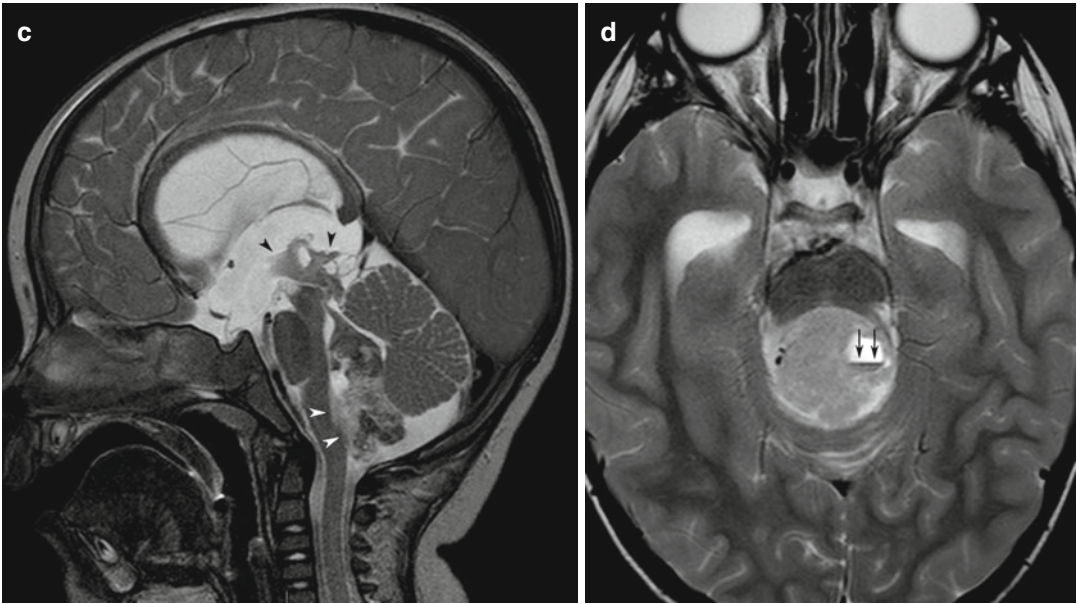


Fig. 21.5 (continued)

ependymomas [11]. On DWI, grade II ependymomas show normal to mildly increased diffusivity with respect to normal brain (Fig. 21.6), while there is a trend toward restricted diffusion for grade III anaplastic ependymomas due to higher cellularity and nuclear-to-cytoplasmic ratios; however, there is too much overlap to predict the grade of individual cases [12].

Cystic and necrotic portions typically are hypointense on T1-weighted images and hyperintense on T2-weighted images, due to their hydration and low protein content; consequently, they result in increased diffusivity with high ADC values. The mass is frequently associated with a mild or moderate degree of vasogenic edema in the adjacent cerebellum.

Metastatic spread is uncommon at presentation but becomes more frequent after surgical removal (Fig. 21.7) [8, 13]. The close relationship between the tumor and the fourth ventricle could be expected to favor CSF seeding, but CSF metastases are not frequent at presentation; in our experience, we never encountered metastases at the onset. Leptomeningeal spread due to CSF seeding is the most common form of metastatic involvement in ependymomas and may involve both the brain and spine, justifying post-contrast

MRI evaluation of the whole neuraxis. Post-contrast FLAIR imaging may be useful to confirm subtle subarachnoid spread.

MRS (Fig. 21.8) may help to increase diagnostic accuracy in ependymomas and to distinguish recurrent tumor from postoperative or treatment-related changes. Among the various metabolite ratios, Cho/NAA is a gross marker of tumor grade, as greater ratios indicate increasing myelin turnover associated with loss of neuroaxonal integrity. In ependymomas, the Cho/NAA ratio is intermediate between those of medulloblastomas and pilocytic astrocytomas, although significant overlap exists in individual cases. Additionally, the Cr/Cho ratio is the highest among posterior fossa tumors [14]. Lactate is not usually found.

21.6 Postsurgical and Surveillance Imaging

The extent of surgical resection is the main factor determining long-term survival. Therefore, the purpose of surveillance imaging for posterior fossa ependymomas is to recognize residual or recurrent tumor as early as possible in order to institute second-look surgery. The initial

Fig. 21.6 Typical density and signal behavior of posterior fossa ependymomas. (a) Axial CT scan shows noncalcified posterior fossa ependymoma. Isodensity of the tumor with the surrounding hindbrain makes it virtually indiscernible if not for absent visualization of the fourth ventricle, which is filled by the tumor. (b) Axial T1-weighted image shows the tumor to be isointense with cerebellar gray matter. The margins of the tumor are not clearly visualized. (c) Axial T2-weighted image shows the tumor is heterogeneously hyperintense to gray matter. Notice encased vessels (*arrowheads*) and extension into the right cerebellopontine angle cistern (*asterisk*). (d) Contrast-enhanced axial T1-weighted image shows the tumor enhances very heterogeneously, with large completely unenhancing portions. (e) Axial diffusion-weighted image and (f) corresponding ADC map show increased diffusivity with respect to normal cerebellum

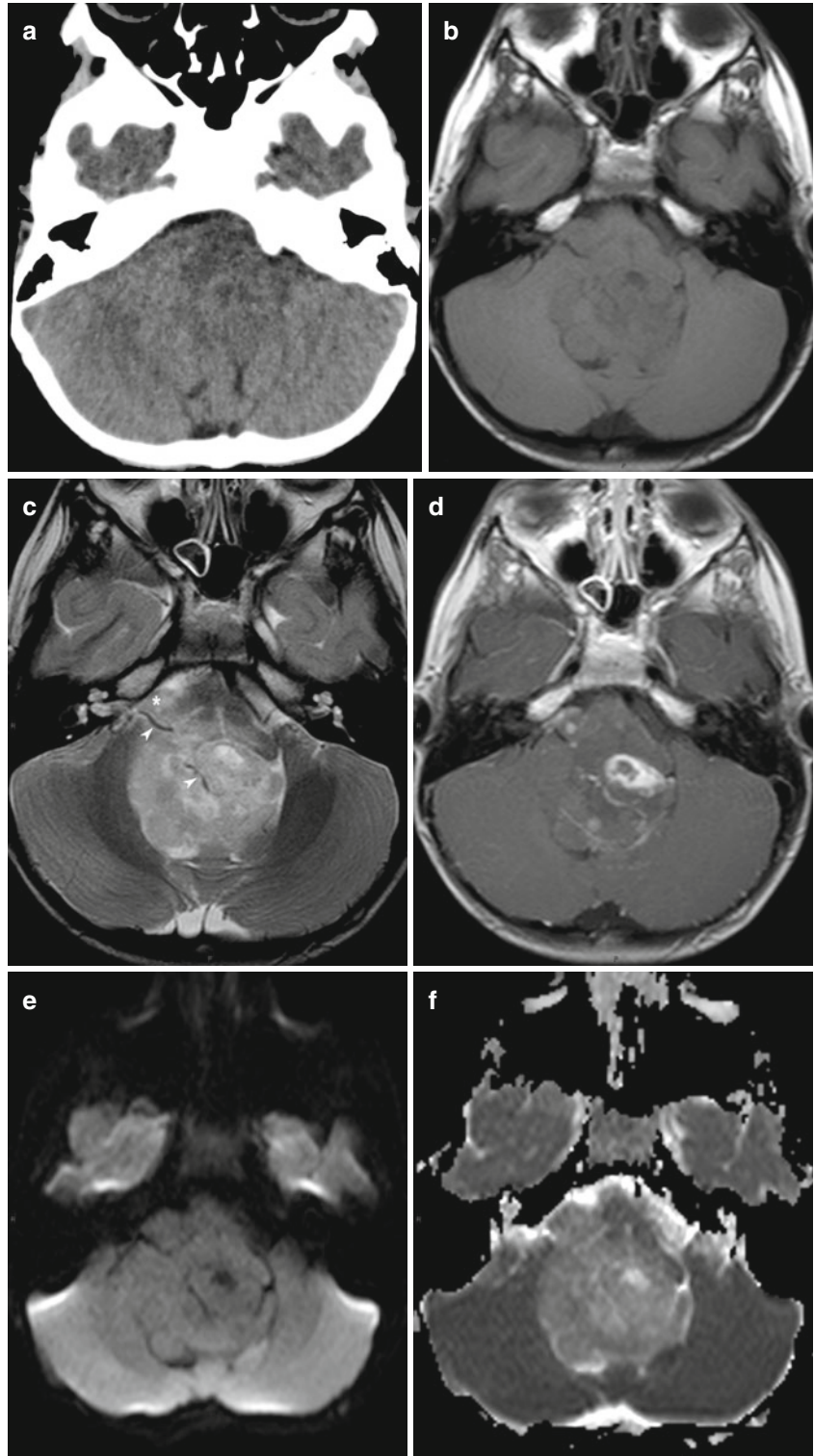




Fig. 21.7 Leptomeningeal metastases of ependymomas. (a) Contrast-enhanced axial T1-weighted image shows structurally heterogeneous ependymoma. (b) Contrast-enhanced axial T1-weighted image obtained 1.5 years after radical removal shows local relapse (arrow). (c) Contrast-enhanced sagittal T1-weighted image shows relapsing tumor (arrow) as well as a huge hypothalamic

metastasis (thick arrows). Notice the aqueduct is plugged by the lesion (arrowhead). (d) Contrast-enhanced sagittal T1-weighted image of the spine obtained at the same time shows the bottom of the thecal sac is filled with drop metastases (arrowheads). Also notice faintly enhancing leptomeningeal nodule at T12 (arrow)

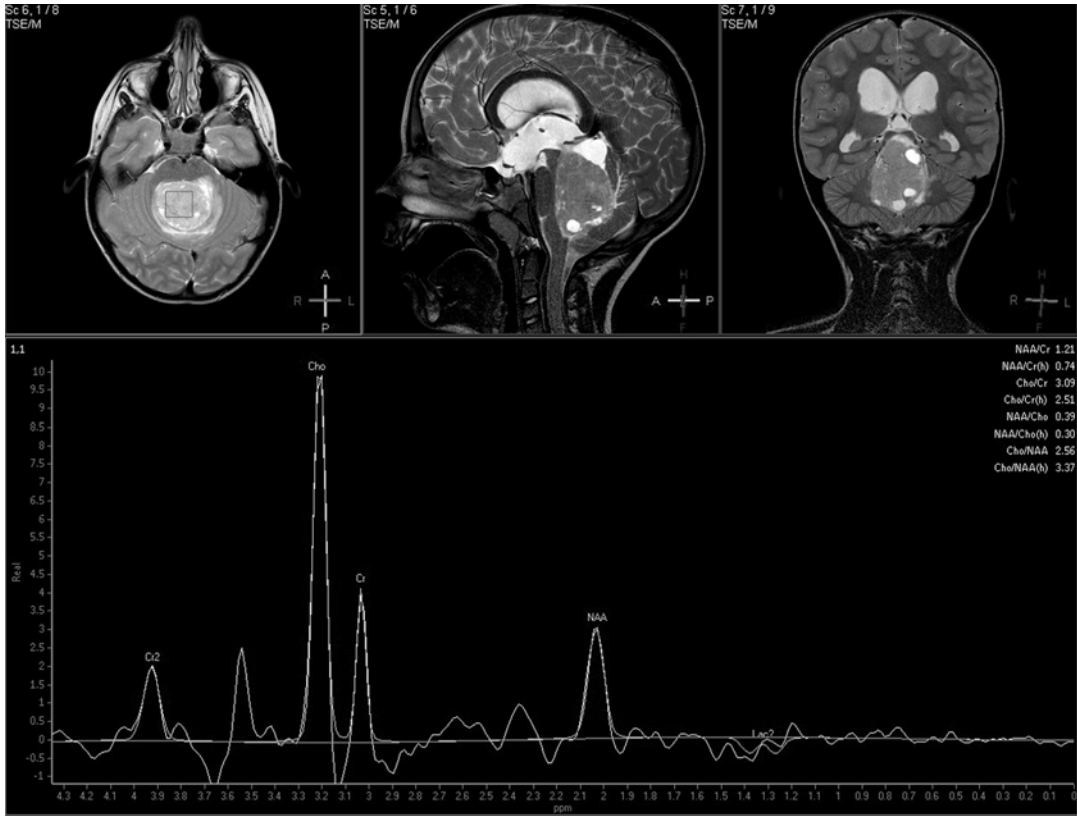


Fig. 21.8 MR spectroscopy findings in ependymomas. MR spectroscopy obtained with a single-voxel technique at TE 144 ms shows an aspecifically pathologic pattern

with increased choline (Cho)/creatinine (Cr), reduced N-acetylaspartate (NAA)/Cr, and absent lactate

postoperative MRI should be performed within 48 h of surgery. The frequency of subsequent surveillance imaging is variable, depending on the treatment protocol, the level of concern, and the risk of residual or recurrent tumor [2]. Typically, craniospinal MRI is performed at 3–6 months' intervals for the first year and 6 months thereafter for the next 5 years.

Signal changes due to surgical injury to the margins of the operative bed are invariably found on early postoperative neuroimaging studies. These changes correspond to localized ischemic-hemorrhagic areas and behave as such, with initial restricted diffusion and contrast enhancement at the operative site that progressively resolves on follow-up studies. On the other hand, residual tumor appears as nodular lesions located in areas that were involved by tumor on presurgical imaging and have signal characteristics compatible with those of the primitive tumor (Fig. 21.9).

Lateral-type tumors that extend into the cerebellopontine angle and prepontine cistern beyond the plane of the cranial nerves and encase arterial vessels are at higher risk for postsurgical residual. Neuroimaging studies must be of the highest technical profile in order to detect subtle tumor nodules that are often strictly adherent to and isointense with adjacent nervous tissue and may not enhance. As opposed to residual tumor, recurrence implies the detection of a new mass or nodular or mass-like enhancement either at the primary site (Fig. 21.7) or elsewhere. Metastatic spread typically occurs by CSF seeding into the subarachnoid spaces and appears as nodular or diffuse enhancement along the leptomeningeal surface of the brain and spine. Peculiar anatomic areas may favor dependent accumulation of metastatic cells and therefore represent frequent areas of recurrence. These areas, prominently including the inner acoustic canals, hypothalamic

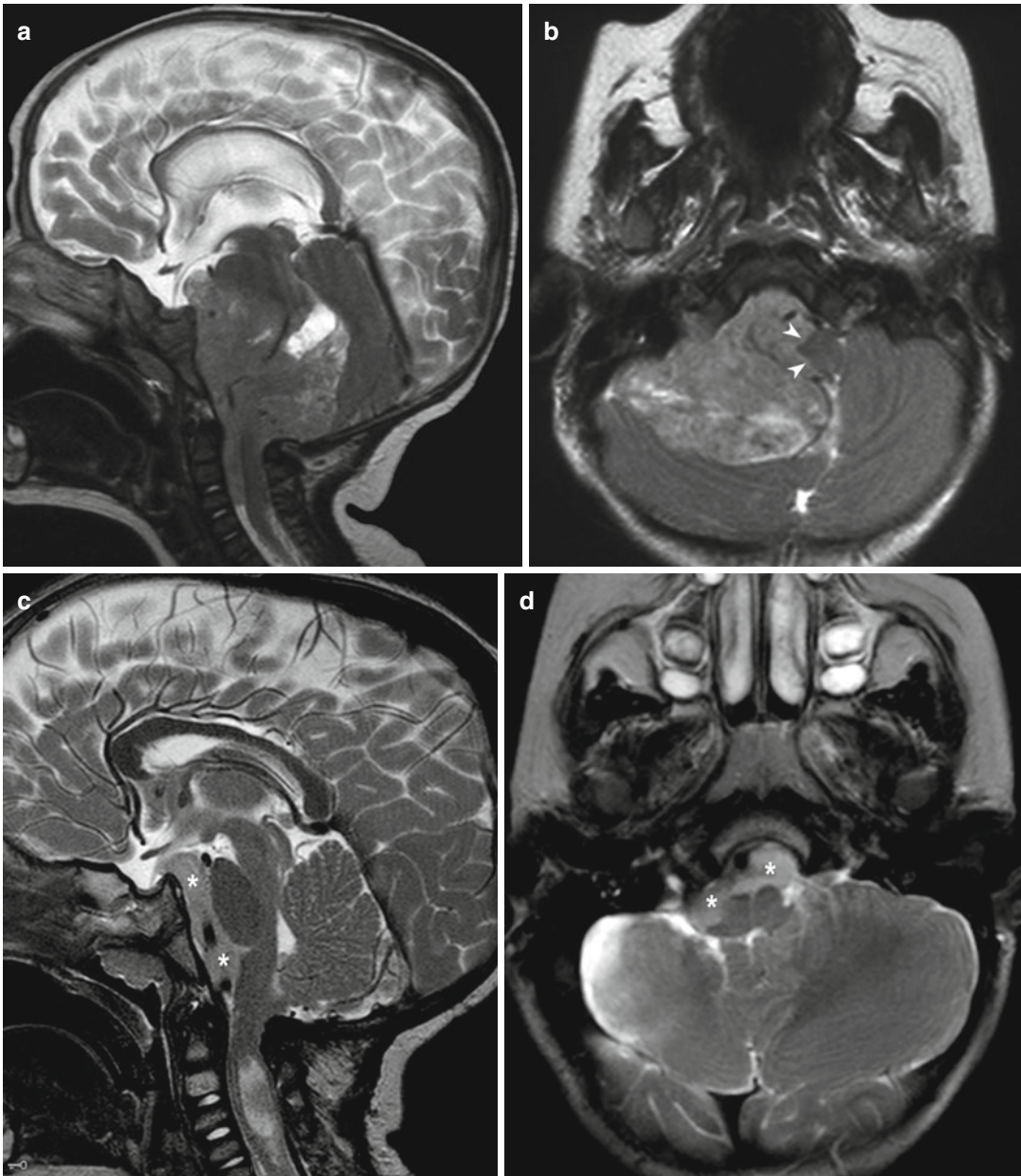


Fig. 21.9 Postsurgical residual tumor in a lateral anaplastic ependymoma. **(a)** Sagittal T2-weighted image shows huge tumor partially filling the fourth ventricle and extending both in the cervical canal and prepontine cistern. **(b)** Axial T2-weighted image shows lateral location with marked displacement of the brainstem (*arrowheads*).

(c) Sagittal T2-weighted image and **(d)** axial T2-weighted images obtained after surgery show residual tumor in front of the brainstem (*asterisks*). The fourth ventricle is re-expanded and free of tumor. The brainstem is no longer displaced. A syrinx has developed in the cervical cord

infundibulum, interpeduncular fossa, and the bottom of the spinal thecal sac (Fig. 21.7), must always be very carefully scrutinized.

Chemotherapy is used in attempts to avoid radiation therapy. In very young children with

brain tumors, primary chemotherapy, omitting radiation therapy, has been reported to improve neurodevelopmental outcome and survival. Treatment-related complications are manifold and their description falls off the purpose of

this paper. Patients undergoing chemotherapy regimens may experience adverse CNS complications ranging from leukoencephalopathy to the posterior reversible encephalopathy syndrome (PRES) which may usually be completely reversible. Patients treated with irradiation may be at risk for focal or diffuse radiation necrosis, cavernous malformations [15], and second tumors occurring in the radiation field. These complications may occur years after completion of the treatment regimen and require long follow-ups in order to be identified.

References

- Rossi A, Gandolfo C, Morana G, Severino M, Garrè ML, Cama A (2010) New MR sequences (diffusion, perfusion, spectroscopy) in brain tumours. *Pediatr Radiol* 40:999–1009
- U-King-Im JM, Taylor MD, Raybaud C (2010) Posterior fossa ependymomas: new radiological classification with surgical correlation. *Childs Nerv Syst* 26:1765–1772
- Ikezaki K, Matsushima T, Inoue T, Yokoyama N, Kaneko Y, Fukui M (1993) Correlation of microanatomical localization with postoperative survival in posterior fossa ependymomas. *Neurosurgery* 32:38–44
- Tong KA, Ashwal S, Obenaus A, Nickerson JP, Kido D, Haacke EM (2008) Susceptibility-weighted MR imaging: a review of clinical applications in children. *AJNR Am J Neuroradiol* 29:9–17
- Yamasaki F, Kurisu K, Satoh K, Arita K, Sugiyama K, Ohtaki M, Takaba J, Tominaga A, Hanaya R, Yoshioka H, Hama S, Ito Y, Kajiwara Y, Yahara K, Saito T, Thohar MA (2005) Apparent diffusion coefficient of human brain tumors at MR imaging. *Radiology* 235:985–991
- Figarella-Branger D, Civatte M, Bouvier-Labit C, Gouvernet J, Gambarelli D, Gentet JC, Lena G, Choux M, Pellissier JF (2000) Prognostic factors in intracranial ependymomas in children. *J Neurosurg* 93:605–613
- Nagib MG, O'Fallon MT (1996) Posterior fossa lateral ependymoma in childhood. *Pediatr Neurosurg* 24:299–305
- Tortori-Donati P, Fondelli MP, Cama A, Garrè ML, Rossi A, Andreussi L (1995) Ependymomas of the posterior cranial fossa: CT and MRI findings. *Neuroradiology* 37:238–243
- Courville CB, Broussalian SL (1961) Plastic ependymomas of the lateral recess. Report of eight verified cases. *J Neurosurg* 18:792–796
- Spoto GP, Press GA, Hesselink JR, Solomon M (1990) Intracranial ependymoma and subependymoma: MR manifestations. *AJNR Am J Neuroradiol* 11:83–91
- Martínez León MI, Vidal Denis M, Weil Lara B (2011) Magnetic resonance imaging of infratentorial anaplastic ependymoma in children. *Radiologia* 54:59–64
- Jaremko JL, Jans LB, Coleman LT, Ditchfield MR (2010) Value and limitations of diffusion-weighted imaging in grading and diagnosis of pediatric posterior fossa tumors. *AJNR Am J Neuroradiol* 31:1613–1616
- Nazar GB, Hoffman HJ, Becker LE, Jenkin D, Humphreys RP, Hendrick EB (1990) Infratentorial ependymomas in childhood: prognostic factors and treatment. *J Neurosurg* 72:408–417
- Wang Z, Sutton LN, Cnaan A, Haselgrove JC, Rorke LB, Zhao H, Bilaniuk LT, Zimmerman RA (1995) Proton MR spectroscopy of pediatric cerebellar tumors. *AJNR Am J Neuroradiol* 16:1821–1833
- Martínez León MI (2011) Early magnetic resonance imaging detection of a cavernous angioma after cranial radiotherapy for an anaplastic ependymoma in a boy. *Radiologia* 55:541–545

Stephanie Puget and Christian Sainte-Rose

22.1 Introduction

Surgical treatment plays an important role in the treatment of ependymoma as the quality of resection represents, with radiotherapy the main prognosis factor in this disease. Surgery plays a role in both the treatment of frequently associated hydrocephalus and the tumor itself. It will indeed help in the histological and genetic diagnosis by sampling the tumor tissue, relieving the brainstem compression from the tumor, and reducing the volume of local disease.

Surgical treatment for these tumors has improved dramatically over the past 30 years. This is primarily related to imaging improvement and fundamental innovations in surgery and medical technology including the use of diathermy and microscopes, new surgical instruments, and ultrasonic aspiration in conjunction with significant

improvements in general anesthesia and intensive and postoperative care.

Different operative approaches have been described through the years. Most of these tumors arise in the fourth ventricle and can be reached through a trans-vermian or a telovelar approach. In case of development in the cerebellopontine angle and/or the spine, the surgical approach is tailored to the location.

The single most important determinant of outcome in this disease is the extent of resection. This places a great deal of responsibility on the pediatric neurosurgeon to achieve a maximal safe resection. The 5-year survival in children who receive gross total resection (GTR) is 67–80 % and the 5-year progression free survival (PFS) rate is 51–75 % [1–4]. After subtotal resection, the 5-year survival ranges from 22 to 47 % and the 5-year PFS rate is 0–26 %.

22.2 Preoperative Evaluation and Treatment Strategies

The treatment strategies are based on the evaluation of clinical and radiological patient status. The use of steroids is often useful as they decrease the peri-tumoral edema and favors the CSF circulation thus decreasing the signs of raised ICP.

The presence of hydrocephalus and clinical signs of raised ICP will determine whether or not the CSF diversion procedure will take place in emergency before the tumor resection.

S. Puget, M.D., Ph.D. (✉)
Department of Pediatric Neurosurgery,
Necker Hospital, Université Paris Descartes, ,
Sorbonne, Paris, France
e-mail: stephanie.puget@gmail.com

C. Sainte-Rose, M.D.
Department of Pediatric Neurosurgery,
Necker Hospital, Université Paris Descartes,
Sorbonne Paris Cité, Rue de Sèvres, Paris 75015, France

Department of Paediatric Neurosurgery,
Necker Enfants Malades Hospital, Paris, France
e-mail: chsaintrose@gmail.com

The diagnosis of posterior fossa ependymoma is usually suspected from the preoperative imaging studies. An image of a tumor within the fourth ventricle with extensions through the Luschka and Monroe foramen is highly suspect of this tumor.

A complete craniospinal MRI examination should ideally be obtained before any surgery. Indeed, any procedure such as lumbar puncture, ventriculostomy, CSF drainage, and tumor resection may lead, in the following days, to spinal MRI images that could be misdiagnosed as metastasis. However, on the contrary to medulloblastoma, metastatic dissemination at diagnosis is rare [1].

In case of localized ependymoma, all the current protocols are advocated for gross total resection before adjuvant radiotherapy. Chemotherapy plays a less-defined role in a minority of patients [5].

Technological aids and advances in supportive care have made surgery safer. However, the presence of extended tumors in cerebellopontine cisterns, fourth ventricle, and sometimes the spine, especially in the youngest, should lead the surgeon to staged surgeries. It is particularly important to minimize the risk of neurological complications that may be due to removing the tumor from critical locations such as the low cranial nerves, to avoid tracheostomy and/or gastrostomy. Moreover, it has been recently recognized that injury to the dentate nuclei and vermis is linked to cognitive impairment in children with posterior fossa tumors [6, 7]. Therefore, damage to those anatomical structures is likely to have a strong impact as an unfavorable cognitive and functional outcome with those children.

Posterior fossa ependymomas typically fill the cavity of the fourth ventricle. They often infiltrate the dorsal brainstem and especially the obex and attach laterally to the cerebellar peduncles. The tumor extension in the Luschka and Monroe foramen is very frequent. They may also have prepontine extension with vertebral and basilar arteries encasement. Even with modern imaging, it is still difficult to preoperatively predict the attachment or invasion of functional anatomical structures by the tumor. U-King-Im proposed a radiological classification correlated with surgical findings

and risk of postoperative residual disease [8]. They described the “midfloor-type” tumor (infiltration of obex and anterior displacement of brainstem) and the “lateral type” more frequently associated with extension into prepontine and cerebellopontine cisterns. They have shown that risk of residual tumor was higher in case of lateral-type tumor compared to midfloor type and higher in case of vessel encasement or prepontine extension.

In both cases, our team recommends the use of endoscopy-assisted microscopic resection to improve the quality of resection of these tumors, therefore their prognosis.

22.3 Hydrocephalus Management

Children with ependymomas may have cranial nerve palsy at the time of presentation but more typically have signs of increased raised intracranial pressure (ICP). They may therefore complain of headaches, episodes of vomiting, or be lethargic. These symptoms are usually the result of acute obstructive hydrocephalus rather than due to direct compression of the brainstem from the tumor. There are a few different options in the management of hydrocephalus for those patients, which include administration of preoperative steroids, endoscopic third ventriculostomy, insertion of extraventricular drain, and placement of ventriculoperitoneal shunt before excision of the ependymoma. Although many studies and opinions have been reported in the literature regarding the management of obstructive hydrocephalus in children with posterior fossa tumors including ependymoma, there is no consensus about the optimum management of that group of patients [9–12].

The rate of permanent treatment of hydrocephalus with a shunt or endoscopic third ventriculostomy (ETV) after the primary ependymoma resection usually ranges between 22 and 63 % in different series [13, 14].

In our practice, when symptomatic obstructive hydrocephalus occurs in children with ependymomas, we first perform an ETV. We have shown that it statistically reduces the

incidence of postoperative hydrocephalus requiring permanent treatment from 27 to 6 % [9, 11]. Some authors argue that routine application of ETV results in a significant proportion of patients undergoing an unnecessary procedure with risk of potential complications [15, 16]. However, in our experience of more than 600 ETV procedures, we showed no mortality or serious complication from delaying the tumor treatment. These results must be balanced with potential complications as a result of other CSF diversion procedures such as infection, upward brain herniation due to CSF hyperdrainage, or tumor hemorrhage. Importantly, the effectiveness of ETV is similar for nonmetastatic or metastatic posterior fossa tumors [9].

22.4 Operative Positioning

There is still considerable controversy among neurosurgeons and anesthesiologists regarding the optimum intraoperative positioning of a patient with a posterior fossa tumor. We consider that the best one is the one you are more comfortable with. Each of them has advantages and drawbacks.

In prone position, the risk of air embolism, frontal pneumocephalus, and systemic hypotension associated with the sitting position is minimized, and the surgeon's arms become less fatigued. Children 3 years of age or older are flexed and held in position with three-point pin fixation. It is recommended that short "pediatric"

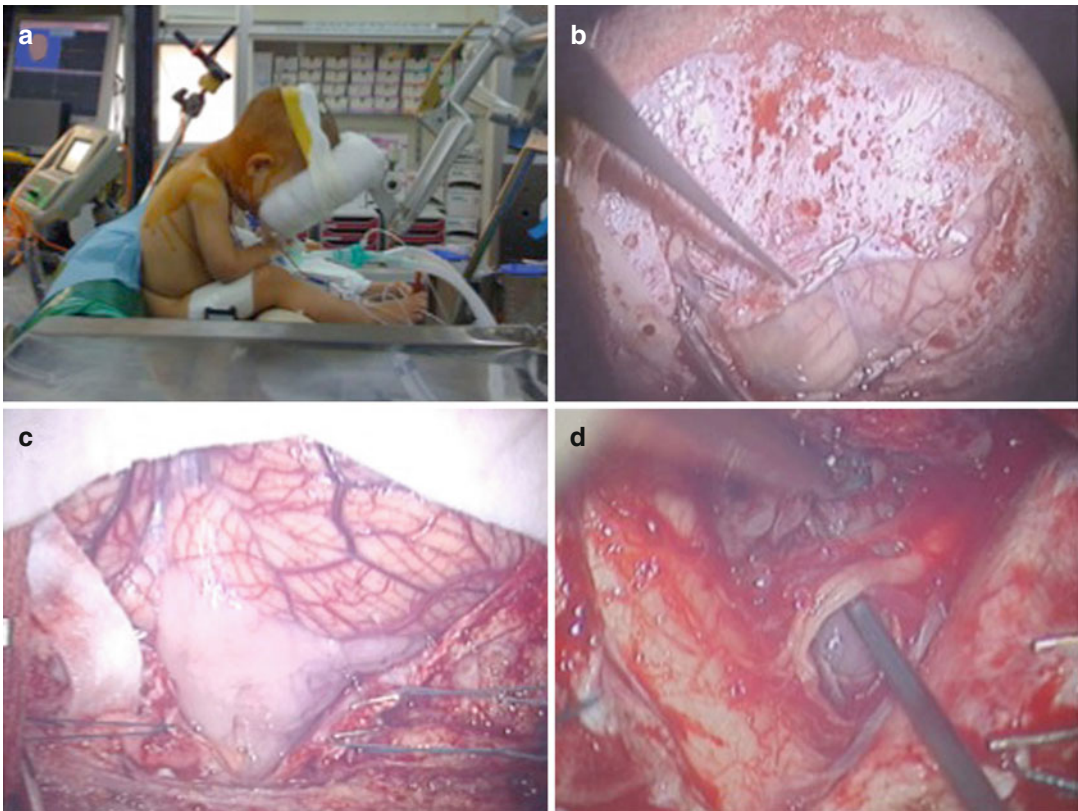


Fig. 22.1 (a) Sitting position for a young child. (b) The dura is opened in a U-shaped fashion down to the occipito-C1 ligament that will facilitate the dura closure. When little vessels bleed during this opening, dura coagulation should be avoided as it generates its retraction and complicates the closure. We use dura clips that are removed at closure time. (c) The dura is

opened in a Y-shaped fashion, showing the ependymoma bulging out from underneath the arachnoid splaying of the cerebellar tonsils. (d) Right lateral view of the upper cervical spinal canal. The caudal and superficial portion of the tumor has been removed in one piece. We can see ependymoma in the cerebellopontine right cistern, in front of the spinal roots

pins be used in prepubertal children. In children less than 3 years old, in whom pins might perforate the skull or result in a depressed skull fracture (“ping-pong type of fracture”), the head is supported with a padded horseshoe-shaped rest. By standing at the side of the patient facing the head, the operating surgeon obtains an excellent view, and exposure is correct far upward as the upper vermis and tentorial notch. Occasionally, flexion of the neck will occlude the endotracheal tube, which will result in high inflating airway pressures and venous bleeding in the operative field. This requires immediate readjustment of the head holder.

The sitting position provides several potential advantages to both surgeon and anesthesiologist and can be used at every age (Fig. 22.1a). Specific advantages include an improved surgical exposure and anatomical orientation with optimal instrumental access to structures of the rostral levels of the posterior fossa; decreased bleeding; improved CSF and blood drainage; less impairment of diaphragmatic motion and improved ventilation with lower airway pressures; improved access to the tracheal tube, thorax, and extremities; and the ability to observe the face for signs of surgical stimulation of cranial nerves [17–19]. On the other hand, there are significant drawbacks with the sitting position. These include an increased incidence of venous air embolism (very rare in our experience), undesirable hemodynamic changes, tension pneumocephalus, postoperative bleeding, lingual or laryngeal edema, brachial plexus, sciatic or peroneal nerves injuries, and quadriparesis [17–19].

However, the prone position is itself also associated with some disadvantages, including increased bleeding and decreased CSF and blood drainage, and it does not eliminate the risk of venous air embolism [17, 18]. In 2001, our team published a study in which the results are not in agreement with this consensus [18]. We studied 79 children in whom 60 children were operated on in the sitting position and 19 in the prone position. The patients in the prone position group received a significantly larger volume of blood transfusion during the surgical procedure than the patients in the sitting group ($P=0.04$).

Intraoperative (surgical difficulties, cardiac dysrhythmias, arterial hypo-/hypertension) complications were statistically significant and more frequent in the prone position group ($P=0.01$). There was no significant difference between the two groups regarding the overall number of postoperative complications or the percentage of patients with a postoperative complication, while there was a significantly more frequent need for early re-intervention in the prone position group, 47 % versus 17 % ($p: 0.02$). Also, the duration of tracheal intubation, the intensive care stay, and the hospital stay were statistically significantly longer in the prone position group compared with sitting position group. A significant difference was observed between the two groups, with severe complications, reversible only with intervention, being more frequent in the prone position group ($P=0.01$). There was no significant difference in the overall number of postoperative complications.

22.5 Surgical Technique

Before surgery, a careful examination of the MRI imaging is critical in reaching the goal of gross total resection. It helps to determine the surgical approach, to be prepared for surgical difficulties, and to anticipate a second staged surgery for large tumors.

The “crossbow incision” was first described by Cushing in 1905 and involved a midline sagittal skin incision in the suboccipital region, with a “T”-like horizontal incision at its superior extent. In 1928, Naffziger described the straight midline sagittal incision, which had been used by neurosurgeons up to date. At present, a midline incision is made from theinion down to the C3–C4 cervical lamina by splitting the nuchal ligament. In case of cerebellopontine involvement, an invert “L”-like incision is recommended.

The craniotomy should extend rostrally up to the level of the torcular, laterally (driven by size and tumor location, i.e., along the sigmoid sinus in case of cerebellopontine cisterns extension) and caudally down to the foramen magnum. A laminectomy of C1 at least may be necessary if

the tumor has a spinal extension. A pedicle of muscle and fascia can be left attached to the external occipital protuberance in order to facilitate muscular closure at the end of the operation.

The dura matter may be opened in a “U-” or “Y”-shaped fashion. The authors use a U-shaped opening down to the occipito-C1 ligament, which facilitates the dura closure (Fig. 22.1b). In case of bulbar, cerebellopontine cisterns, or spinal involvement, a “Y”-shaped opening is necessary to better expose the structures (Fig. 22.1c).

If the patient is in a sitting position, the surgeon has to ask for jugular compression at each step of the opening to limit the risk of air embolism.

Some patients have a midline occipital sinus that can be a source of bleeding when the dura mater is opened. This bleeding can be controlled by clips that should be removed at the time of dura closure. Dura coagulation should be avoided as it generates its retraction and complicates the primary closure of the dura. The dura leaves are tacked to the margins of the muscle with sutures. The dura is covered with cottonoids and maintained wet throughout the surgery to reduce the degree of its retraction.

Often the ependymoma can be seen bulging out from underneath the arachnoid splaying of the cerebellar tonsils (Fig. 22.1c). The arachnoid is incised and opened over the cisterna magna for drainage of cerebrospinal fluid, except if it is filled by the ependymoma. The caudal portion of the tumor may be separated first from the medulla by using an arachnoid dissector, with care not to injure the spinal roots. In some cases with upper cervical spinal canal extension, the lower part of the tumor can be gently pulled from the spinal subarachnoid space and removed in one piece, avoiding extended laminectomy (Fig. 22.1d). In some other cases, it may stick to the spinal pia thus leading to tailored laminectomy and dissection along the medulla. Once the cisterna magna is free, a cottonoid is placed at its level to decrease the risk of drop metastases entering the spinal canal and reducing the amount of blood that escapes to subarachnoid space.

In case of midfloor-type ependymoma, the surgical steps are very similar to those used for

medulloblastoma resection. A careful dissection of the telovelar fissure(s) is made depending on the tumor location. It can be done unilaterally or bilaterally avoiding the vermis incision. Involvement of one or both posterior inferior cerebellar artery(ies) (PICA) should be recognized on preoperative MRI and leads to a careful dissection of these arteries. The vascular supply to the tumor comes off of the PICA. Coagulation of large feeders to the tumor from the PICA will reduce the vascularity of the tumor and decrease preoperative bleeding. The tumor is then gradually removed using either the bipolar/suction technique or the ultrasonic aspirator, preferred by the authors. During excision of the tumor, cottonoids can be placed between the lateral capsule of the tumor and cerebellar tissue. In case of large tumors, internal debulking helps in reducing the need for cerebellar retraction during excision of the tumor. Moreover, when the interface between the normal tissue and the ependymoma is not so clear at the lower part, a superior and midline debulking to the aqueduct of Sylvius may help in the recognition of the normal fourth ventricle structures. The resection will then be made from back to front. Biopsy sampling for histology and genetic assessment is performed. If the ependymoma arises from the floor, a tiny portion of the tumor is left to avoid sequels. Also the tumor has been lifted off the floor of the fourth ventricle, and initially a cottonoid is placed between the tumor and the floor of the fourth ventricle for protection of the fourth ventricle floor structures. Ependymomas often stick to the obex, where their resection can be associated with cardio-rhythmic disorders. It is important to know that this complication may not be reproducible during a second step surgery for the same patient. The inferior pole is then dissected along its lateral margins, through the Luschka foramen, ideally controlled by endoscopy to avoid missing a small piece of tumor. After the tumor has been resected, careful inspection of the tumor bed can be assisted by the use of an endoscope, especially at the level of the roof of the fourth ventricle and the Luschka foramen.

In case of lateral-type ependymoma, the tumor often sticks to the lateral wall of the brainstem, at

the junction of the pons and the medulla. In such cases, ependymoma may raise the cerebellum, distort the brainstem, and envelop the cranial nerves. Once the spinal portion has been removed, the vertebral artery can be traced. The tumor is then debulked laterally, until the lower cranial nerves are identified. They may be separated from the tumor in arachnoid folds or may strongly stick to it. Even with modern imaging, it is still difficult to preoperatively predict the attachment or invasion of these structures by the tumor. The authors recommend identifying the cranial nerves at the level of their foramen, dissecting them to the brainstem. The Luschka foramen is explored and tumor removed. In case of prepontine extension with basilar artery encasement, care must be taken not to injure perforating arteries, as the tumor can be developing in between these arteries and the brainstem. For this anterior portion, the use of an endoscope can be helpful to improve the quality of resection.

After ependymoma removal, meticulous hemostasis is crucial. The dura is closed in a watertight fashion. In our experience, the need for a dural graft is exceptional in children if the dura is kept wet, stretched, and not coagulated during the procedure. The bone flap is put back and fixed in place according to the surgeon's preference (absorbable sutures are used by the authors). The surgical wound is closed in layers with absorbable sutures in the muscles and fascia. Use of absorbable or nonabsorbable sutures in the skin is the surgeon's preference.

In case of reoperation, we advocate a linear dura opening (vertical/horizontal) with a monopolar microneedle as it avoids elevation of the dura from the surface of the cerebellum, which may adhere to it.

22.6 Postoperative Surgical Complications

The most common postoperative complication of posterior fossa tumor surgery includes hematoma, infection/meningitis, aseptic meningitis, hydrocephalus, pseudomeningocele, CSF leak, cerebellar mutism, cranial nerve palsy, and hemiparesis. The specific risk after removal of

pediatric ependymoma is the low cranial nerve palsy or paralysis causing inability to swallow, vocal cord paralysis, or reduced or absent gag/cough reflex resulting in recurrent aspiration pneumonia. Vocal cord paralysis, when present, should be unilateral. A bilateral injury will mandate a tracheostomy and a gastrostomy. To avoid such complication, the authors recommend a two-step surgery in case of bilateral cerebello-pontine cistern involvement.

"Aseptic meningitis" is another well-recognized postoperative syndrome. Cushing described that syndrome in 1931, which consisted of fever, photophobia, nuchal rigidity, and CSF pleocytosis. It occurs in association with blood-stained CSF, and serial spinal taps to clear the CSF were recommended [20]. The syndrome typically appears 5–7 days after surgery, often as steroids are being weaned. Cerebrospinal fluid should be obtained by spinal tap or from the shunt or ventriculostomy to rule out bacterial infection. If CSF microscopy and culture results are negative for infection, Sutton et al. suggested an increase in corticosteroid dose for several days followed by a 2-week taper, which usually relieves the symptoms [20].

Postoperative pseudomeningocele may occur after posterior fossa tumor surgery in children if the closure of the dura and the soft tissue was not appropriate, leaving behind dead space. However, wound revision is rarely necessary. Occipital pseudomeningoceles may be treated initially with intermittent lumbar puncture and removal of 10–20 ml of CSF daily and wrapping the head with an elastic bandage. If children develop persistent hydrocephalus, if the wound is threatening to leak spinal fluid, CSF diversion is required by performing an ETV or inserting a ventriculoperitoneal shunt.

Although, spinal deformity is an unusual complication of posterior fossa tumor resection, it is well documented in the literature. It is typically seen within a year of surgery. Steinbock et al. reported a series of 72 children who had undergone resection of a posterior fossa tumor [21]. Four of them developed a cervical spinal instability and deformity. Factors that predisposed to this complication included laminectomy of C2 or lower, local wound complications, and possibly

postoperative neck weakness. It is important to be aware that cervical subluxation can occur after resection of posterior fossa tumors, when a laminectomy extends below the C1 level. Subsequently, those patients should be followed closely in order to prevent neurological deficits.

Conclusion

Ependymoma is a neurosurgical disease, with local control being the most important prognostic factor. Neurosurgeons, aided by modern technology (microscope, CUSA, surgical tools, neuronavigation), make considerable efforts to achieve complete or near complete resection of the ependymoma. Careful scrutiny of the preoperative imaging is necessary to estimate the extent of the tumor and anticipate the surgical challenges. In case of bilateral cerebellopontine cistern involvement, the surgery should be done in two steps to avoid irreversible lower cranial nerve palsy. Such surgery can bring an increased risk of neurological deficits of a temporary or even a permanent nature. Postoperative complications and neurological deficits resulting from surgery not only impact upon quality of survival but may also contribute to delay in commencing adjuvant therapy.

References

- Perilongo G, Massimino M, Sotti G, Belfontali T, Masiero L, Rigobello L et al (1997) Analyses of prognostic factors in a retrospective review of 92 children with ependymoma: Italian pediatric neuro-oncology group. *Med Pediatr Oncol* 29(2):79–85
- Horn B, Heideman R, Geyer R, Pollack I, Packer R, Goldwein J et al (1999) A multi-institutional retrospective study of intracranial ependymoma in children: identification of risk factors. *J Pediatr Hematol Oncol* 21(3):203–211
- Robertson PL, Zeltzer PM, Boyett JM, Rorke LB, Allen JC, Geyer JR et al (1998) Survival and prognostic factors following radiation therapy and chemotherapy for ependymomas in children: a report of the children's cancer group. *J Neurosurg* 88(4):695–703
- Pejavar S, Polley MY, Rosenberg-Wohl S, Chennupati S, Prados MD, Berger MS et al (2012) Pediatric intracranial ependymoma: the roles of surgery, radiation and chemotherapy. *J Neurooncol* 106(2):367–375
- Strother DR, Lafay-Cousin L, Boyett JM, Burger P, Aronin P, Constine L et al (2014) Benefit from prolonged dose-intensive chemotherapy for infants with malignant brain tumors is restricted to patients with ependymoma: a report of the pediatric oncology group randomized controlled trial 9233/34. *Neuro Oncol* 16(3):457–465
- Puget S, Boddaert N, Viguier D, Kieffer V, Bulteau C, Garnett M et al (2009) Injuries to inferior vermis and dentate nuclei predict poor neurological and neuropsychological outcome in children with malignant posterior fossa tumors. *Cancer* 115(6):1338–1347
- Ojemann JG, Partridge SC, Poliakov AV, Niazi TN, Shaw DW, Ishak GE et al (2013) Diffusion tensor imaging of the superior cerebellar peduncle identifies patients with posterior fossa syndrome. *Childs Nerv Syst* 29(11):2071–2077
- UK-I JM, Taylor MD, Raybaud C (2010) Posterior fossa ependymomas: new radiological classification with surgical correlation. *Childs Nerv Syst* 26(12):1765–1772
- Sainte-Rose C, Cinalli G, Roux FE, Maixner R, Chumas PD, Mansour M et al (2001) Management of hydrocephalus in pediatric patients with posterior fossa tumors: the role of endoscopic third ventriculostomy. *J Neurosurg* 95(5):791–797
- Schijman E, Peter JC, ReKate HL, Sgouros S, Wong TT (2004) Management of hydrocephalus in posterior fossa tumors: how, what, when? *Childs Nerv Syst* 20(3):192–194
- Schmid UD, Seiler RW (1986) Management of obstructive hydrocephalus secondary to posterior fossa tumors by steroids and subcutaneous ventricular catheter reservoir. *J Neurosurg* 65(5):649–653
- Morelli D, Pirotte B, Lubansu A, Detemmerman D, Aeby A, Fricx C et al (2005) Persistent hydrocephalus after early surgical management of posterior fossa tumors in children: is routine preoperative endoscopic third ventriculostomy justified? *J Neurosurg* 103(3 Suppl):247–252
- Due-Tonnessen BJ, Helseth E (2007) Management of hydrocephalus in children with posterior fossa tumors: role of tumor surgery. *Pediatr Neurosurg* 43(2):92–96
- Kumar V, Phipps K, Harkness W, Hayward RD (1996) Ventriculo-peritoneal shunt requirement in children with posterior fossa tumours: an 11-year audit. *Br J Neurosurg* 10(5):467–470
- Hopf NJ, Grunert P, Fries G, Resch KD, Perneczky A (1999) Endoscopic third ventriculostomy: outcome analysis of 100 consecutive procedures. *Neurosurgery* 44(4):795–804; discussion –806
- Feng H, Huang G, Liao X, Fu K, Tan H, Pu H et al (2004) Endoscopic third ventriculostomy in the management of obstructive hydrocephalus: an outcome analysis. *J Neurosurg* 100(4):626–633
- Black S, Ockert DB, Oliver WC Jr, Cucchiara RF (1988) Outcome following posterior fossa craniectomy in patients in the sitting or horizontal positions. *Anesthesiology* 69(1):49–56

18. Orliaguet GA, Hanafi M, Meyer PG, Blanot S, Jarreau MM, Bresson D et al (2001) Is the sitting or the prone position best for surgery for posterior fossa tumours in children? *Paediatr Anaesth* 11(5):541–547
19. Matjasko J, Petrozza P, Cohen M, Steinberg P (1985) Anesthesia and surgery in the seated position: analysis of 554 cases. *Neurosurgery* 17(5):695–702
20. Sutton LN, Phillips PC, Molloy PT (1996) Surgical management of medulloblastoma. *J Neurooncol* 29(1):9–21
21. Steinbok P, Boyd M, Cochrane D (1989) Cervical spinal deformity following craniotomy and upper cervical laminectomy for posterior fossa tumors in children. *Childs Nerv Syst* 5(1):25–28

23.1 Histopathological Definition

Ependymoma is a glial tumor presenting ependymal differentiation. Key histological features are perivascular pseudorosettes (tumor cell cytoplasmic processes converging to blood vessels) and more occasionally true ependymal rosettes (single layers of well-differentiated ependymal cells) (Figs. 23.1 and 23.2). As opposed to the other groups of malignant gliomas, ependymomas are well circumscribed and usually do not infiltrate diffusely peritumoral tissue.

23.2 WHO Subtypes and Grading

According to WHO 2007 classification, main histological variants include classic, cellular, clear cell, papillary, tancytic, and myxopapillary ependymomas [16]. As for meningioma, some histological subvariants are correlated with the WHO grade, for instance, myxopapillary and subependymoma are grade I. Of note, in the pediatric population, the tancytic and myxopapillary ependymoma variants are exceptional and classic and clear cell ependymoma (grade II or III) are the most frequent (Figs. 23.1, 23.2, and 23.3). Clear cell ependymoma is more often observed in supratentorial location.

The current WHO 2007 distinguishes grade II from grade III ependymomas (anaplastic ependymoma) (Fig. 23.4), but important uncertainties about the prognostic value of this grading still persist, especially among children. Tihan et al. have performed a meta-analysis on 24 pediatric intracranial ependymoma studies using the WHO grading system between 1990 and 2005 [24]. Twelve studies found no impact of grading criteria or grade on survival, whereas five found a statistical significant negative impact of high grade on OS. The remaining studies found a variable prognostic impact in terms of EFS or PFS. The ratio of grade II versus III is strikingly heterogeneous in the different cohorts (ranging from 7 % to 89 %), highlighting the numerous potential selection biases in age, location, tissue sampling, and interobserver discrepancies in the application of the WHO grading scheme [10]. The literature on the issue remains controversial due to multiple factors: retrospective monocentric studies extending over a long period of time, mixture of hybrid adult and pediatric cohorts, inclusion of ependymoma from different locations, and inclusion of grade I myxopapillary and subependymoma variants. Furthermore, all these confounding factors are not always appropriately considered in multivariate analyses, particularly in this disease in which clinical characteristics as age and extent of surgery have major impacts on survival. From a histopathological standpoint, major difficulties stem from the absence of precise WHO guidelines, a variable definition of grading criteria (particularly extensive or focal anaplastic

P. Varlet, M.D., Ph.D. (✉) • F. Andreiuolo, M.D., Ph.D.
Department of Neuropathology, Sainte-Anne
Hospital, University Paris Descartes, Paris, France
e-mail: P.VARLET@ch-sainte-anne.fr

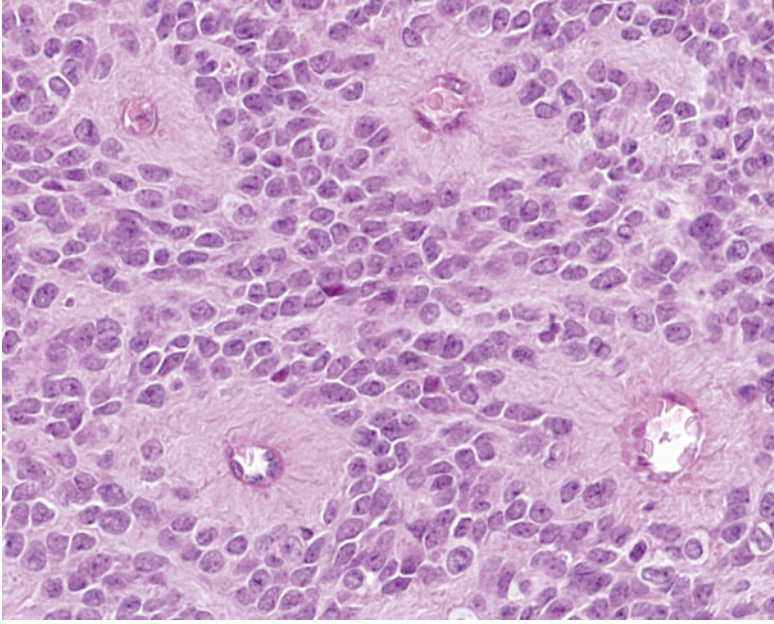


Fig. 23.1 Perivascular pseudorosettes

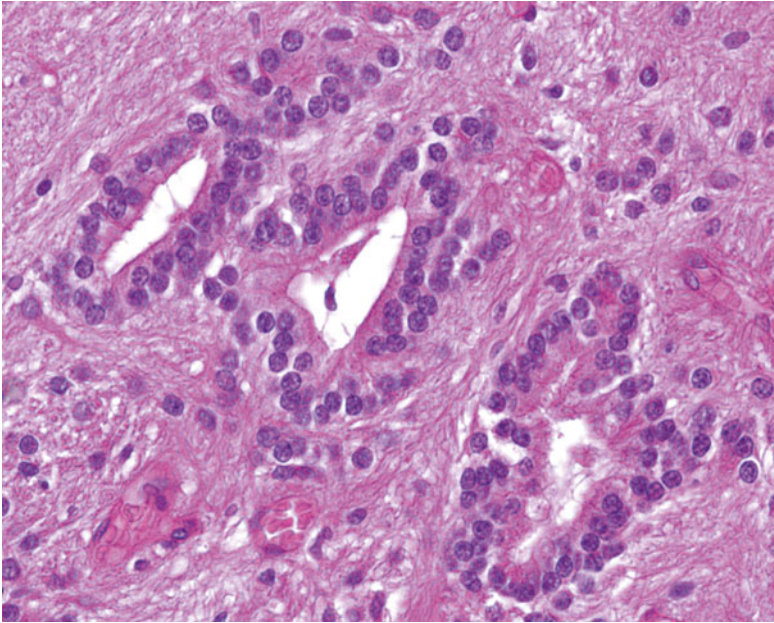


Fig. 23.2 Ependymal rosettes

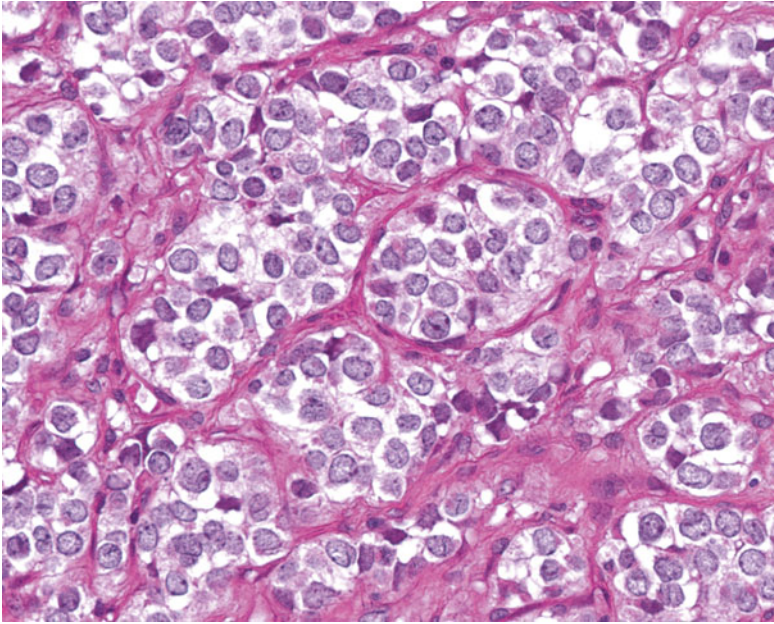


Fig. 23.3 Clear cell ependymoma

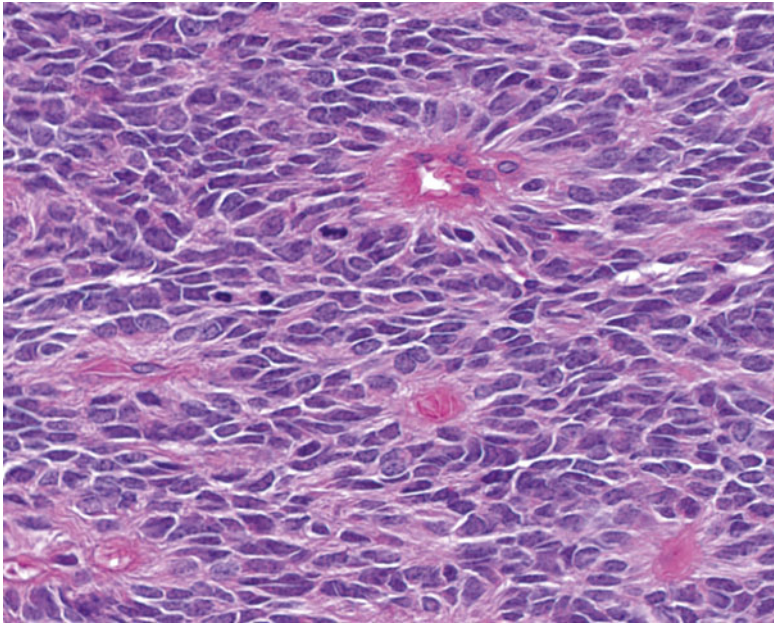


Fig. 23.4 Anaplastic ependymoma. Densely cellular and poorly differentiated tumor with high mitotic activity

areas, cellularity, necrosis) and different cutoff values for the mitotic rate.

Currently, WHO grading criteria used to define an anaplastic ependymoma are “high mitotic activity often accompanied by microvascular proliferation and pseudopalisading necrosis” [16]. The exact definitions and thresholds are not yet clearly established. In general, most studies have identified the parameters of cellular proliferation as significant for prognosis [8, 13, 17, 27]. Ellison et al. have proposed a cutoff value for mitoses of more than 5 mitoses per 10 HPF, associated or not with microvascular proliferation and taking into account the presence of hypercellular nodules [7]. Tihan et al. used a mitotic rate greater than 10 per HPF to identify grade III lesions but failed to find a prognostic correlation between grade III and OS [24].

The development of limited, well-defined, reproducible histological criteria associated with simultaneous biomarkers might be a useful approach to optimize the WHO grading scheme and to identify patients who could benefit from additional treatment.

23.3 Immunohistochemical Findings

Immunohistochemical stains in ependymoma generally show strong cytoplasmic positivity for glial fibrillary acidic protein (GFAP), vimentin, S-100, and CD56. Perivascular pseudorosettes are GFAP positive and typically express S-100 and vimentin, whereas true rosettes are largely GFAP negative. EMA immunostains are variable from case to case, usually highlighting dot-like punctuate perinuclear staining, ringlike intracytoplasmic microluminal positivity, or less frequently a linear staining along the luminal surface of ependymal rosettes. Dot-like EMA positivity is neither necessary nor specific to the diagnosis of ependymoma but remains a strong positive argument. Olig2 is not expressed by ependymal cells or is limited to scattered positive nuclei. Negativity for Olig2 represents a good criterion to eliminate the diagnostic hypothesis of other gliomas mimicking ependymoma such as an astrocytic tumor or oligodendroglioma [30].

23.4 Differential Diagnosis

Architectural features such as clear delineation from surrounding nonneoplastic tissue and perivascular pseudorosettes are robust diagnostic criteria, but the frequent heterogeneity of classic ependymoma (cellular and paucicellular areas) as well as the existence of clear cell and papillary variants sometimes lead to challenging diagnostic problems.

A common diagnostic issue in classic or cellular ependymoma is the distinction from another malignant glioma, glioblastoma (GBM), since this entity also presents a perivascular tropism. Features identifying GBM are extensive pseudopalisading necrosis, absence of dot-like EMA positivity, extended Olig2 positivity, and more importantly peritumoral diffuse infiltration. Ependymoma particularly in the spinal cord or in the fourth ventricle must be distinguished from pilocytic astrocytoma (PA) since this tumor also displays perivascular formations and a frequent clear cell component. Features identifying PA are intratumoral Rosenthal fibers, extensive Olig2 positivity, and the absence of dot-like punctuate EMA positivity.

Clear cell ependymoma can be confused with oligodendroglioma, central neurocytoma, and metastatic renal carcinoma since all these entities comprise neoplastic uniform round cells with encircling clear cytoplasm. Features identifying clear cell ependymoma are perivascular pseudorosettes even if these present only focally and GFAP and vimentin positivity associated with negativity for Olig2 (or with some rare positive nuclei), NeuN, and synaptophysin.

Papillary ependymoma could be confused with choroid plexus tumors and metastatic papillary carcinoma, as this ependymoma variant is characterized by epithelial-appearing cells supported by fibrovascular stalks. Ependymoma, as opposed to choroid plexus papilloma, lacks the PAS-positive basement membrane and is widely positive for GFAP. Ependymoma exhibits much weaker staining for keratins, such as CAM5.2, CK7, and CK18 [26].

It is also important to precise that the presence of foci of true ependymal differentiation in a CNS

tumor is not synonymous of an ependymoma. For example, ependymal features may be encountered in mixed neuronal-glial tumors such as dysembryoblastic neuroepithelial tumor, ganglioglioma, or angiocentric glioma [5, 14, 15, 21, 25] and also in embryonal tumors such as atypical teratoid/rhabdoid tumor, PNET, and embryonal tumor with abundant neuropil and true rosettes (ETANTR) [6]. Exceptional childhood neuroepithelial tumors can display ependymal differentiation such as chordoid glioma of the third ventricle or papillary tumor of the pineal region [14].

23.5 New Generation of Predictive Biomarkers

Cooperative studies – necessary to achieve an adequate cohort, sufficient for a robust statistical analysis in this relatively rare disease, and associated with the recent technical progress in genetics and transcriptional profiling – have permitted the identification of ependymoma molecular subtypes. Location stands out as a major driver for the biology of ependymoma [2, 23]. Studies on biomarkers have consistently confirmed the major differences between ependymomas in children and adults, well described also on a clinical basis, as besides different preferential location (supratentorial and spinal in adults, posterior fossa in children); ependymomas in children have been largely shown to have a worse prognosis [10].

In comparison to adult counterparts, pediatric ependymomas display a higher frequency of 1q gain (20 % vs. 8 %, $p=0.0040$) which has been linked to an adverse prognosis in several retrospective cohorts and more recently in two infant and young children trial cohorts [11].

A microarray study on a mixed adult and pediatric population has shown two different prognostic groups in posterior fossa ependymoma, according to their gene expression profiles [29]. Group A showed worse outcome, more frequent location in the cerebellopontine angle and cerebellar invasion, younger age, and overexpression of laminin a2 (LAMA2) or tenascin C (TN-C); group B was composed mainly of adolescent/adult

patients with intraventricular and intramedullary tumors overexpressing NELL2 and genes involved in ciliogenesis or microtubule assembly. The 5-year progression-free and overall survival was significantly worse for group A (44 vs. 75 %; $p=0.017$ and 65 vs. 95 %; $p=0.0048$). These data have been partially confirmed by an independent group [28] but need further validation.

Several potential prognostic immunomarkers have been studied in retrospective studies such as metallothionines, metalloproteinase, ezrin, P-glycoprotein, P53, bcl2, p14ARF, VEGF, hTERT, HIF, vitronectin, survivin, EGFR, and neuronal markers – for review see [3, 10]. Unfortunately, these results are generally based on small or large but mixed adult/pediatric series, have used non-standardized immunostaining scores and have not yet been verified prospectively on independent and homogeneously treated cohorts. Thus, it is critical to determine if those biomarkers have a definitive correlation with prognosis.

Numerous studies have focused on the assessment of the proliferation index in pediatric ependymomas by immunohistochemistry for Ki67 and its relation with prognosis. Although most authors have shown an inverse and significant correlation between proliferation and prognosis [4, 8, 9, 18, 31], other groups did not confirm these data [17, 20, 22]. All were retrospective studies, and for the great majority, the association was not confirmed in multivariate analysis. Moreover, the labeling index used as a cutoff in these various studies was extremely variable (from 1% to 25 %), which renders definite conclusions difficult as to its prognostic value in pediatric ependymoma.

A candidate gene strategy exploring the 9q33–34 gain discovered TN-C as significantly overexpressed both at the mRNA and protein levels [19]. Tenascin C (TN-C) is an extracellular matrix glycoprotein involved in the differentiation of gliogenic precursors from glial radial cells which has been described as one of the targets of the Notch1 signaling pathway. Two retrospective studies have described TN-C immunorexpression as a marker correlated with a worse prognosis in ependymoma [12, 31]. Moreover, TN-C is overexpressed in posterior fossa ependymoma in

a group of patients with worse outcome [29]. These findings have been confirmed by a large international study, including over 400 pediatric ependymomas from France, the UK, Italy, and Germany. TN-C overexpression shown by immunohistochemistry was associated with a 1.7-fold increase in relapse or death in multivariate analysis [1]. TNC is therefore proposed as a marker of poor prognosis in pediatric ependymoma and could be used in the future for the therapeutic stratification.

References

1. Andreiuolo F, Mauguen A, Kilday J, Modena P, Massimo M, Varlet P et al (2010) Tenascin-C is an independent prognostic marker in pediatric ependymoma: an international collaborative study. *Neuro Oncol* 12:ii26
2. Andreiuolo F, Puget S, Peyre M, Dantas-Barbosa C, Boddaert N, Philippe C, Mauguen A, Grill J, Varlet P (2010) Neuronal differentiation distinguishes supratentorial and infratentorial childhood ependymomas. *Neuro Oncol* 12:1126–1134
3. Andreiuolo F, Ferreira C, Puget S, Grill J (2013) Current and evolving knowledge of prognostic factors for pediatric ependymomas. *Future Oncol Lond Engl* 9:183–191
4. Bennetto L, Foreman N, Harding B, Hayward R, Ironside J, Love S, Ellison D (1998) Ki-67 immunolabelling index is a prognostic indicator in childhood posterior fossa ependymomas. *Neuropathol Appl Neurobiol* 24:434–440
5. Burel-Vandenbos F, Varlet P, Lonjon M, Chanalet S, Chatel M, Michiels JF (2007) Ependymal variant of dysembryoplastic neuro-epithelial tumor. *Ann Pathol* 27:320–323
6. Dunham C, Sugo E, Tobias V, Wills E, Perry A (2007) Embryonal tumor with abundant neuropil and true rosettes (ETANTR): report of a case with prominent neurocytic differentiation. *J Neurooncol* 84:91–98
7. Ellison DW, Kocak M, Figarella-Branger D, Felice G, Catherine G, Pietsch T, Frappaz D, Massimino M, Grill J, Boyett JM et al (2011) Histopathological grading of pediatric ependymoma: reproducibility and clinical relevance in European trial cohorts. *J Negat Results Biomed* 10:7
8. Figarella-Branger D, Civatte M, Bouvier-Labit C, Gouvernet J, Gambarelli D, Gentet JC, Lena G, Choux M, Pellissier JF (2000) Prognostic factors in intracranial ependymomas in children. *J Neurosurg* 93:605–613
9. Gilbertson RJ, Bentley L, Hernan R, Junttila TT, Frank AJ, Haapasalo H, Connelly M, Wetmore C, Curran T, Elenius K et al (2002) ERBB receptor signaling promotes ependymoma cell proliferation and represents a potential novel therapeutic target for this disease. *Clin Cancer Res Off J Am Assoc Cancer Res* 8:3054–3064
10. Kilday J-P, Rahman R, Dyer S, Ridley L, Lowe J, Coyle B, Grundy R (2009) Pediatric ependymoma: biological perspectives. *Mol Cancer Res MCR* 7:765–786
11. Kilday J-P, Mitra B, Domerg C, Ward J, Andreiuolo F, Osteso-Ibanez T, Mauguen A, Varlet P, Le Deley M-C, Lowe J et al (2012) Copy number gain of 1q25 predicts poor progression-free survival for pediatric intracranial ependymomas and enables patient risk stratification: a prospective European clinical trial cohort analysis on behalf of the Children's Cancer Leukaemia Group (CCLG), Societe Francaise d'Oncologie Pediatrique (SFOP), and International Society for Pediatric Oncology (SIOP). *Clin Cancer Res Off J Am Assoc Cancer Res* 18:2001–2011
12. Korshunov A, Golanov A, Timirgiz V (2002) Immunohistochemical markers for prognosis of ependymal neoplasms. *J Neurooncol* 58:255–270
13. Kurt E, Zheng P-P, Hop WCJ, van der Weiden M, Bol M, van den Bent MJ, Avezaat CJJ, Kros JM (2006) Identification of relevant prognostic histopathologic features in 69 intracranial ependymomas, excluding myxopapillary ependymomas and subependymomas. *Cancer* 106:388–395
14. Lehman NL (2008) Central nervous system tumors with ependymal features: a broadened spectrum of primarily ependymal differentiation? *J Neuropathol Exp Neurol* 67:177–188
15. Lellouch-Tubiana A, Boddaert N, Bourgeois M, Fohlen M, Jouveta A, Delalande O, Seidenwurm D, Brunelle F, Sainte-Rose C (2005) Angiocentric neuroepithelial tumor (ANET): a new epilepsy-related clinicopathological entity with distinctive MRI. *Brain Pathol Zurich Switz* 15:281–286
16. Mc Lendon RE, Wiestler OD, Kros JM, Korshunov A, Ng H-K (2007) Ependymoma. In: Louis DN, Deutsches Krebsforschungszentrum Heidelberg, International Agency for Research on Cancer, World Health Organization (eds) WHO classification of tumours of the central nervous system. WHO Press, World Health Organization, Geneva
17. Prayson RA (1999) Clinicopathologic study of 61 patients with ependymoma including MIB-1 immunohistochemistry. *Ann Diagn Pathol* 3:11–18
18. Preusser M, Heinzl H, Gelpi E, Höftberger R, Fischer I, Pipp I, Milenkovic I, Wöhrer A, Popovici F, Wolfsberger S et al (2008) Ki67 index in intracranial ependymoma: a promising histopathological candidate biomarker. *Histopathology* 53:39–47
19. Puget S, Grill J, Valent A, Bieche I, Dantas-Barbosa C, Kauffmann A, Dessen P, Lacroix L, Geoerger B, Job B et al (2009) Candidate genes on chromosome 9q33-34 involved in the progression of childhood ependymomas. *J Clin Oncol Off J Am Soc Clin Oncol* 27:1884–1892

20. Ridley L, Rahman R, Brundler M-A, Ellison D, Lowe J, Robson K, Prebble E, Luckett I, Gilbertson RJ, Parkes S et al (2008) Multifactorial analysis of predictors of outcome in pediatric intracranial ependymoma. *Neuro Oncol* 10:675–689
21. Rodriguez FJ, Scheithauer BW, Robbins PD, Burger PC, Hessler RB, Perry A, Abell-Aleff PC, Mierau GW (2007) Ependymomas with neuronal differentiation: a morphologic and immunohistochemical spectrum. *Acta Neuropathol (Berl)* 113:313–324
22. Shuangshoti S, Rushing EJ, Mena H, Olsen C, Sandberg GD (2005) Supratentorial extraventricular ependymal neoplasms: a clinicopathologic study of 32 patients. *Cancer* 103:2598–2605
23. Taylor MD, Poppleton H, Fuller C, Su X, Liu Y, Jensen P, Magdaleno S, Dalton J, Calabrese C, Board J et al (2005) Radial glia cells are candidate stem cells of ependymoma. *Cancer Cell* 8:323–335
24. Tihan T, Zhou T, Holmes E, Burger PC, Ozuysal S, Rushing EJ (2008) The prognostic value of histological grading of posterior fossa ependymomas in children: a children's oncology group study and a review of prognostic factors. *Mod Pathol Off J U S Can Acad Pathol Inc* 21:165–177
25. Varlet P, Peyre M, Boddaert N, Miquel C, Sainte-Rose C, Puget S (2009) Childhood gangliogliomas with ependymal differentiation. *Neuropathol Appl Neurobiol* 35:437–441
26. Vege KD, Giannini C, Scheithauer BW (2000) The immunophenotype of ependymomas. *Appl Immunohistochem Mol Morphol AIMM Off Publ Soc Appl Immunohistochem* 8:25–31
27. Versteegen MJT, Leenstra DTS, Ijlst-Keizers H, Bosch DA (2002) Proliferation- and apoptosis-related proteins in intracranial ependymomas: an immunohistochemical analysis. *J Neurooncol* 56:21–28
28. Wani K, Armstrong TS, Vera-Bolanos E, Raghunathan A, Ellison D, Gilbertson R, Vaillant B, Goldman S, Packer RJ, Fouladi M et al (2012) A prognostic gene expression signature in infratentorial ependymoma. *Acta Neuropathol (Berl)* 123:727–738
29. Witt H, Mack SC, Ryzhova M, Bender S, Sill M, Isserlin R, Benner A, Hielscher T, Milde T, Remke M et al (2011) Delineation of two clinically and molecularly distinct subgroups of posterior fossa ependymoma. *Cancer Cell* 20:143–157
30. Yokoo H, Nobusawa S, Takebayashi H, Ikenaka K, Isoda K, Kamiya M, Sasaki A, Hirato J, Nakazato Y (2004) Anti-human Olig2 antibody as a useful immunohistochemical marker of normal oligodendrocytes and gliomas. *Am J Pathol* 164:1717–1725
31. Zamecnik J, Snuderl M, Eckschlager T, Chanova M, Hladikova M, Tichy M, Kodet R (2003) Pediatric intracranial ependymomas: prognostic relevance of histological, immunohistochemical, and flow cytometric factors. *Mod Pathol Off J U S Can Acad Pathol Inc* 16:980–991

Jacques Grill and Maria-Jesus Lobon Iglesias

24.1 Introduction

Despite its frequency (third most common brain tumor in children), publications about ependymomas per year are three times less frequent than for medulloblastomas (120 vs. 330). The knowledge and the sophistication of the protocols are lagging behind those of medulloblastomas. Accordingly, this has limited the progress made for these tumors. The improvement of neurosurgery is probably the driving force improving the outcome of children affected with this disease in the last 20 years. The three main questions that remain for ependymomas are the following: (i) Which biomarkers are useful to understand the oncogenesis and prognosis? (ii) Is there a role for chemotherapy? (iii) What is the appropriate strategy at the time of relapse?

The management of ependymomas is currently mainly based on surgery and radiotherapy because of the relative inefficacy of chemotherapy. At each step of the management, these two treatments have to be considered for an optimal care. Presently oncological management for all intracranial ependymomas is homogenous despite the recent findings that ependymoma biology may largely differ by location.

J. Grill, M.D., Ph.D. (✉) • M.-J.L. Iglesias, M.D.
Pediatric and Adolescent Oncology,
Institut Gustave Roussy, Rue Edouard Vaillant,
Villejuif, Ile de France 94805, France
e-mail: jacques.grill@gustaveroussy.fr;
mj_lobon@hotmail.com

24.2 First-Line Treatment: Surgery

The initial surgical management is aiming at complete removal of the tumor, if necessary in more than one step because it remains the principal risk factor for survival. Indeed, in case of incomplete resection, one should not proceed to irradiation. Risk of relapse is five times higher in case of incomplete resection even after full-dose radiation therapy [1]. In the Saint-Jude series, presently the best results published so far, 5-year event-free survival is only 41 % (95 % CI=18–64 %) in case of near-total or subtotal resection versus 81.5 % (95 % CI=73–90 %) in case of gross-total resection, $p < 0.0001$. Any attempt should therefore be made to obtain a macroscopically complete resection. In between two surgeries, there is no definitive indication for chemotherapy since most of the regimens tested have not shown many responses [2]. Pre-irradiation chemotherapy may compensate for an incomplete resection as it has been shown with a recently published phase II using a standard chemotherapy regimen based on cisplatin in patients with incompletely resected; in this report, patients with incompletely resected ependymomas treated with pre-irradiation chemotherapy had similar although slightly lower EFS than those with completely resected ependymomas treated with irradiation only [3]. In addition, some anecdotal reports have shown that second surgery may be facilitated by a course or two of

chemotherapy by reducing vascularization and bleeding. Evaluating new agents could therefore be introduced as upfront window in between two surgeries; this strategy will be part of the next SIOP trial for ependymoma. Multiple steps are sometimes necessary to reach macroscopic resection before embarking into the adjuvant treatment.

24.3 Adjuvant Treatment: Radiation Therapy

In most of the cases, ependymomas cannot be cured by surgery only, and adjuvant treatment has to be associated. Surgery can however be enough to cure completely resected low-grade ependymomas in the spine or in the supratentorial brain. Small series of supratentorial low-grade ependymomas treated with surgery alone have shown that a small proportion of patients, around one third, may be cured without recourse to any adjuvant treatment [4, 5]. Actual guidelines for the management of myxopapillary and intramedullary ependymoma indicate that adjuvant treatment can be omitted after complete resection [6]. Although ependymomas occurring in the superior part of the spine tend to have a better prognosis, there is currently no consensus for a different management according to the location of the ependymoma in the spine [7].

In all the other situations, ependymomas should receive adjuvant treatment after surgery.

It has been the rule to avoid radiation therapy in young children in the past 20 years [8, 9]. Despite disappointing long-term results with only 30–50 % of relapse-free survivors at 5 years, this strategy allows to cure some patients without recourse to radiation therapy. It is, therefore, possible to choose this option either in children with very good prognostic factors, see below, or in children too young to receive irradiation. Presently and because of the progress of radiation techniques, irradiation can be considered in children down to 1 year for posterior fossa tumors where we know that the consequences of radiation therapy to the posterior fossa are limited [10, 11]. There is more debate

for supratentorial ependymomas, but some studies have shown that cognition may be preserved with more conformal techniques [12]. Decision to embark with adjuvant radiation therapy in infants with supratentorial ependymomas may be defined on an individual basis considering both prognostic biomarkers and the size of the field of irradiation. For children that do not receive radiation therapy, dose dense chemotherapy such as the combinations used in the UK [9] or the intensified baby-POG regimen is a valuable option [13].

In the other children requiring adjuvant treatment, radiotherapy is delivered routinely with local fields because craniospinal irradiation was unable to prevent distant/metastatic relapses [14]. Recent studies have shown that the radiation field can be limited to the tumor bed without the need to irradiate the whole posterior fossa [9, 15]. The best results are obtained with higher doses of irradiation up to 59.4 Gy culminating in 5-year overall survival above 75 % [1]. These doses may have to be mitigated depending on the organ at risk such as the upper spinal cord or optic tracts.

There is currently no proof that the addition of chemotherapy on top of irradiation could improve the outcome of the patients. Indeed, the only randomized study published was underpowered and could not show any advantage with a relatively mild chemotherapy [16]. It will however be the purpose of the new SIOP ependymoma trial, to test the addition of a more intensive chemotherapy alternating cisplatin and the VEC (vincristine-etoposide-cyclophosphamide combination) [17].

24.4 Relapse Strategy

Recurrences are mostly local despite the use of high dose of irradiation. After a chemotherapy-first approach, around 90 % of relapses are in the tumor bed [8, 9]. After a radiotherapy-first approach in older children however, the percentage of local relapses is slightly lower, i.e., around 60 % [1]. This calls for improvement in the local

control, i.e., with an additional boost. The feasibility and safety of this approach will be tested as a phase I trial in incompletely resected tumors in the next SIOPE protocol.

Whenever possible, reoperation is key for disease control after relapse as shown irrespective of the initial treatment [8, 18]. Even when the relapse can be treated with re-irradiation, most of the patients whose disease can be durably controlled are those who could undergo a complete surgery of the relapse. This is true for local as well as distant relapses.

The benefit of chemotherapy is limited at this stage. Numerous chemotherapy regimens have been tested at relapse. Response rate for single agents are usually below 20 % except for cisplatin and etoposide [2]. Best results reported with combinations were seen with ICE [19] and VEC [17]. High-dose chemotherapy is of no benefit [20]. Antiangiogenic agents such as bevacizumab have also failed to control recurrent ependymomas [21]. Metronomic therapy has shown some benefit in selected cases [22]. Recent drug screen in preclinical models have shown that 5-FU may be an option [23]. New agents are definitively needed to improve the prognosis of ependymomas.

Re-irradiation has been attempted with many techniques depending on the type of relapse and on the availability of new radiation modalities: stereotactic hypofractionated irradiation [24, 25], conformal conventionally fractionated full-dose irradiation [18, 26], and Gamma knife [27]. Local relapses have been treated usually with local re-irradiation and metastatic relapses with cranio-spinal irradiation. Time to progression after re-irradiation has been shown to be possibly longer than the time to progression after the first irradiation [18, 24, 26]. Tolerance has been shown to be good in most of the cases, although radionecrosis is not uncommon [24]. Some patients could eventually receive more than one course of stereotactic re-irradiation. There has been no formal comparison of these different modalities. There is however a clear indication that these re-irradiations are effective in terms of tumor control provided that the recurrence is not metastatic, the tumor is supratentorial, and the

interval since previous radiotherapy is superior to 18 months [25].

24.5 Treatment Stratification

Grading of ependymomas is not reproducible and is rarely associated with survival as shown by an international panel of pathologists reviewing four different trials cohorts [28]. Numerous biomarkers have therefore been tested, usually only in single-center cohorts.

A small but significant proportion of young children with ependymomas can be cured with chemotherapy. Combining two trial cohorts of children below the age of 5, Kilday et al. could show that the 1q gain was an adverse prognostic factor for recurrence but not for survival [29]. Similar data in children treated with irradiation will soon be published by the German HIT group (Pietsch, personal communication). The value of this strong adverse biomarker is limited by the proportion of patients with this gain that is below 20 % and cannot account for all children who experience a relapse.

Ependymomas cannot be considered as a single entity anymore. Indeed, posterior fossa tumors have been divided into two groups according to the methylation profile of the DNA; a hypermethylated profile is associated with the expression of mesenchymal markers such as LAMA2 or tenascin-C and a worse survival [30, 31]. Epigenetic modifiers such as 5-aza-2'-deoxycytidine (a DNA-demethylating agent) or 3-deazaneplanocin A (an inhibitor of the methylation of histones) have an antitumor effect *in vitro* [31]. Likewise, supratentorial ependymomas are divided into a poor prognosis group based on the presence of a specific translocation involving the RELA gene [32] and a good prognostic group that could be characterized by the overexpression of neuronal markers [33]. These categories may be considered for treatment stratification, provided that they could be validated in independent cohorts.

Others biomarkers deserve further investigations before becoming of clinical meaningful

use [34]. Recently, PIK3 pathway activation has been associated with poor outcome and could become a relevant target in the future [35].

References

- Merchant TE, Li C, Xiong X, Kun LE, Boop FA, Sanford RA (2009) Conformal radiotherapy after surgery for paediatric ependymoma: a prospective study. *Lancet Oncol* 10(3):258–266
- Grill J, Chastagner P, Kalifa C (2003) Childhood ependymoma: a systematic review of treatment options and strategies. *Paediatr Drugs* 5(8):533–543
- Garvin JH Jr, Selch MT, Holmes E, Berger MS, Finlay JL, Flannery A, Goldwein JW, Packer RJ, Rorke-Adams LB, Shiminski-Maher T, Spoto R, Stanley P, Tannous R, Pollack IF (2012) Children's Oncology Group. Phase II study of pre-irradiation chemotherapy for childhood intracranial ependymoma. Children's Cancer Group protocol 9942: a report from the Children's Oncology Group. *Pediatr Blood Cancer* 59(7):1183–1189
- Palma L, Celli P, Mariottini A, Zalaffi A, Schettini G (2000) The importance of surgery in supratentorial ependymomas. Long-term survival in a series of 23 cases. The importance of surgery in supratentorial ependymomas. Long-term survival in a series of 23 cases. *Childs Nerv Syst* 16(3):170–175
- Hukin J, Epstein F, Lefton D, Allen J (1998) Treatment of intracranial ependymoma by surgery alone. *Pediatr Neurosurg* 29(1):40–45
- Figueiredo N, Brooks N, Resnick DK (2013) Evidence-based review and guidelines for the management of myxopapillary and intramedullary ependymoma. *J Neurosurg Sci* 57(4):327–341
- Oh MC, Sayegh ET, Safaee M, Sun MZ, Kaur G, Kim JM, Aranda D, Molinaro AM, Gupta N, Parsa AT (2013) Prognosis by tumor location for pediatric spinal cord ependymomas. *J Neurosurg Pediatr* 11(3):282–288
- Grill J, Le Deley MC, Gambarelli D, Raquin MA, Couanet D, Pierre-Kahn A, Habrand JL, Doz F, Frappaz D, Gentet JC, Edan C, Chastagner P, Kalifa C (2001) French Society of Pediatric Oncology. Postoperative chemotherapy without irradiation for ependymoma in children under 5 years of age: a multicenter trial of the French Society of Pediatric Oncology. *J Clin Oncol* 19(5):1288–1296
- Grundy RG, Wilne SH, Robinson KJ, Ironside JW, Cox T, Chong WK, Michalski A, Campbell RH, Bailey CC, Thorp N, Pizer B, Punt J, Walker DA, Ellison DW, Machin D (2010) Children's Cancer and Leukaemia Group (formerly UKCCSG) Brain Tumour Committee. primary postoperative chemotherapy without radiotherapy for treatment of brain tumours other than ependymoma in children under 3 years: results of the first UKCCSG/SIOP CNS 9204 trial. *Eur J Cancer* 46(1):120–133
- von Hoff K, Kieffer V, Habrand JL, Kalifa C, Dellatolas G, Grill J (2008) Impairment of intellectual functions after surgery and posterior fossa irradiation in children with ependymoma is related to age and neurologic complications. *BMC Cancer* 8:15
- Conklin HM, Li C, Xiong X, Ogg RJ, Merchant TE (2008) Predicting change in academic abilities after conformal radiation therapy for localized ependymoma. *J Clin Oncol* 26(24):3965–3970
- Landau E, Boop FA, Conklin HM, Wu S, Xiong X, Merchant TE (2013) Supratentorial ependymoma: disease control, complications, and functional outcomes after irradiation. *Int J Radiat Oncol Biol Phys* 85(4):e193–e199
- Strother DR, Lafay-Cousin L, Boyett JM, Burger P, Aronin P, Constine L, Duffner P, Kocak M, Kun LE, Horowitz ME, Gajjar A (2014) Benefit from prolonged dose-intensive chemotherapy for infants with malignant brain tumors is restricted to patients with ependymoma: a report of the Pediatric Oncology Group randomized controlled trial 9233/34. *Neuro Oncol* 16(3):457–465
- Rousseau P, Habrand JL, Sarrazin D, Kalifa C, Terrier-Lacombe MJ, Rekaewicz C, Rey A (1994) Treatment of intracranial ependymomas of children: review of a 15-year experience. *Int J Radiat Oncol Biol Phys* 28(2):381–386
- Paulino AC (2001) The local field in infratentorial ependymoma: does the entire posterior fossa need to be treated? *Int J Radiat Oncol Biol Phys* 49(3):757–761
- Evans AE, Anderson JR, Lefkowitz-Boudreaux IB, Finlay JL (2014) Adjuvant chemotherapy of childhood posterior fossa ependymoma: cranio-spinal irradiation with or without adjuvant CCNU, vincristine, and prednisone: a Children's Cancer Group study. *Neuro Oncol* 16(3):457–465
- Massimino M, Gandola L, Giangaspero F, Sandri A, Valagussa P, Perilongo G, Garrè ML, Ricardi U, Forni M, Genitori L, Scarzello G, Spreafico F, Barra S, Mascarin M, Pollo B, Gardiman M, Cama A, Navarria P, Brisigotti M, Collini P, Balter R, Fidani P, Stefanelli M, Burnelli R, Potepan P, Podda M, Sotti G, Madon E (2004) AIEOP Pediatric Neuro-Oncology Group. Hyperfractionated radiotherapy and chemotherapy for childhood ependymoma: final results of the first prospective AIEOP (Associazione Italiana di Ematologia-Oncologia Pediatrica) study. *Int J Radiat Oncol Biol Phys* 58(5):1336–1345
- Merchant TE, Boop FA, Kun LE, Sanford RA (2008) A retrospective study of surgery and reirradiation for recurrent ependymoma. *Int J Radiat Oncol Biol Phys* 71(1):87–97
- Fouladi M, Baruchel S, Chan H, Grant R, Malkin D, Weitzman S, Greenberg ML (1998) Use of adjuvant ICE chemotherapy in the treatment of anaplastic ependymomas. *Childs Nerv Syst* 14(10):590–595

33. Andreiuolo F, Puget S, Peyre M, Dantas-Barbosa C, Boddaert N, Philippe C, Mauguén A, Grill J, Varlet P (2010) Neuronal differentiation distinguishes supratentorial and infratentorial childhood ependymomas. *Neuro Oncol* 12(11):1126–1134
34. Andreiuolo F, Ferreira C, Puget S, Grill J (2013) Current and evolving knowledge of prognostic factors for pediatric ependymomas. *Future Oncol* 9(2): 183–191
35. Rogers HA, Mayne C, Chapman RJ, Kilday JP, Coyle B, Grundy RG (2013) PI3K pathway activation provides a novel therapeutic target for pediatric ependymoma and is an independent marker of progression-free survival. *Clin Cancer Res* 19(23):6450–6460

Pathologies in Pediatric Posterior Fossa Tumors: Cerebellar Astrocytoma

Wirginia J. Maixner

W.J. Maixner, M.D
Department of Neurosurgery,
Royal Children's Hospital, Parkville, VIC, Australia

Adam J. Fleming and Mark W. Kieran

Low-grade gliomas are the most frequently encountered primary central nervous system (CNS) tumor in the pediatric population. They account for almost 40 % of CNS tumors, making them one of the most common solid tumors found in children [1, 2]. In contrast, adult low-grade gliomas appear to have a different biology and clinical behavior [3]. A number of histologic subtypes can be included in the general term “low-grade glioma” [4]. The World Health Organization (WHO) classification and nomenclature still stands as the gold standard for diagnosis, but the past decade has brought about an exponential increase in our understanding of these tumors at the molecular and genetic level. This chapter will aim to provide an overview of the current knowledge of the genetics of pediatric

astrocytomas [5] of the posterior fossa and will highlight many recent advances [1].

25.1 Incidence of Pediatric Low-Grade Gliomas

A number of national datasets on childhood brain tumors are published regularly and include the National Cancer Institute’s Surveillance Epidemiology End Results (SEER) Report [6] and the Central Brain Tumor Registry of the United States (CBTRUS) [7]. These detailed reports provide excellent resources for tracking trends on the incidence and survival by age, geography, race, and tumor type of different brain tumors in both adult and pediatric patients. According to the latest CBTRUS report (February 2011), the average annual incidence of brain tumors diagnosed in the 0–19 year old age group is 4.84 per 100,000 population [7]. This includes all primary CNS tumors, including both those classified as malignant and nonmalignant. Based on these data, approximately 4,150 people under the age of 20 are expected to develop a primary brain tumor in the United States in 2010. A similar incidence of pediatric low-grade gliomas has been reported in other national databases from around the world [8–11] and suggests that local environmental factors are not the primary cause of these tumors. The prevalence of primary CNS tumors in children 0–19 years old is estimated at 35.4 per 100,000 population, meaning that over

A.J. Fleming, M.A.Sc., M.D.
Pediatric Hematology/Oncology, McMaster
Children’s Hospital, McMaster University,
1280 Main Street West, Hamilton, ON, Canada

Division of Pediatric Oncology, Organization of
Montreal Children’s Hospital,
McGill University, 2300 Tupper, Montreal, QC,
Canada
e-mail: Adam.Fleming@MUHC.MCGILL.CA;
afleming@mcmaster.ca

M.W. Kieran, M.D., Ph.D. (✉)
Pediatric Neuro-Oncology,
Dana-Farber Children’s Hospital
Cancer Center, Harvard Medical School,
450 Brookline Avenue, Rm SW331,
Boston, MA, USA
e-mail: Mark_kieran@dfci.harvard.edu

28,000 children are living with this diagnosis in the United States.

25.2 Signs and Symptoms of Posterior Fossa Low-Grade Gliomas

The signs and symptoms that a patient will demonstrate when presenting with a low-grade glioma are varied and are predominately dictated by the tumor location. Typically, the rate of growth is slow and patients may experience several months or years of subtle symptoms before the final diagnosis becomes evident [12]. In some cases, neuroimaging is obtained for an unrelated reason, and a low-grade brain tumor is identified without having any associated symptoms. For cerebellar tumors, the slowly progressive neurologic symptoms that are often associated with these tumors suddenly become acute when blockage of the fourth ventricle results in obstructive hydrocephalus and acute signs of raised intracranial pressure ensue [13]. Differing molecular profiles of cerebellar tumors do not seem to be related to the presenting symptoms of posterior fossa low-grade gliomas except in patients with neurofibromatosis type I. In these patients, imaging in asymptomatic patients (either for screening in the NF1 population or to follow an optic pathway low-grade glioma) will frequently identify an asymptomatic lesion in the brainstem or cerebellum [14]. The role of NF1 and low-grade gliomas will be discussed in more detail below, but in patients with this genetic predisposition, it is critical to institute therapy only if the tumor is causing problems.

25.3 Treatment of Posterior Fossa Low-Grade Gliomas

25.3.1 Surgery

There are three main therapeutic approaches for the treatment of pediatric low-grade gliomas. The primary approach involves assessment for surgical resection and can be used to relieve obstructive

hydrocephalus when present (often by third ventriculostomy [15]) to obtain material for diagnostic and molecular profiling and/or to remove the tumor in its entirety. For posterior fossa low-grade gliomas, a complete resection can be “curative” in a significant percentage of cases; on the other hand, low-grade gliomas are typically slow growing and less invasive than high-grade tumors, with less chance for metastatic spread, and the long-term survival is very good even when residual tumor is left behind, suggesting that aggressive surgical resection is not always indicated [16, 17]. However, even in patients treated with conservative resection alone, long-term cognitive effects can still be identified [18]. Infants with low-grade gliomas do not do as well as older children, although the biologic reason for this remains unknown [19]. Transformation of pilocytic astrocytomas to malignant gliomas is extremely rare in pediatrics [20]. Low-grade glial tumors invasive into the brainstem are difficult to completely resect but still have an excellent long-term prognosis, and aggressive surgical resection is often detrimental to the patient. Low-grade gliomas of the tectum have an excellent outcome even without biopsy [21] and suggest a different biology from other low-grade gliomas in this region. Extra-axial posterior fossa juvenile pilocytic astrocytomas have been reported [22] but are extremely rare. These findings have supported the overall approach that maximal but safe surgery should be considered for all patients with tumors in this region. Patients with incompletely resected pilocytic astrocytomas of the brainstem have a greater recurrence rate and so careful surveillance is required and adjuvant therapy is often required [23]. While tumor-specific molecular factors have not been identified to differentiate the location of low-grade gliomas in the posterior fossa, increased rates of progression are observed in those at young age, WHO grade II (vs. grade I for pilocytic astrocytomas) pathology, and lower extent of surgical resection [24].

25.3.2 Chemotherapy

For some patients who are unable to undergo total resection and in those with progressive lesions,

chemotherapy has emerged over the past couple of decades as a viable treatment option [25]. Chemotherapy has become widely used in the past two decades to control tumor growth of pediatric low-grade gliomas. Several different options have emerged that seem to provide comparable results with respect to event-free survival and overall survival, and these chemotherapy options are relatively well tolerated and allow for a good quality of life. Standard regimens include vincristine and carboplatin [26] and TPCV (thioguanine, procarbazine, lomustine, vincristine) [27]. Progression of disease can still occur on these chemotherapy regimens, but changing treatment to an alternate chemotherapy will often result in cessation of growth [28]. For reasons that are poorly understood, the majority of pediatric low-grade gliomas will stop progressing as children enter adulthood, suggestive of changes in development cues that drive these lesions.

25.3.3 Radiation Therapy

Radiation is the third and usually least desirable treatment option for pediatric patients with low-grade gliomas. Although focal radiation is effective in most cases of pediatric low-grade gliomas, a substantial amount of radiation is required and the severity of side effects is inversely proportionate to the age of the patient [29]. Neurocognitive decline with memory loss and concentration difficulties top the list of side effects, while vasculopathy, secondary tumors, and endocrinopathies can be common [30]. Since most pediatric patients with low-grade gliomas of the posterior fossa and brainstem will be long-term survivors [31]; these patients will have to live with the long-term toxicities resulting from radiotherapy [32]. Stereotactic radiosurgery or Gamma Knife have been used in patients with recurrent pilocytic astrocytomas, and while there is good initial control of tumor progression, recurrences can occur, and the late effects are still of a concern [33]. Overall, the long term survival rates for pediatric low-grade gliomas (in particular juvenile pilocytic astrocytomas) remains excellent [34].

25.4 Imaging of Posterior Fossa Low-Grade Gliomas

The imaging characteristics of posterior fossa tumors can be very characteristic. Grade I astrocytomas are typically intensely homogeneous, well-circumscribed, contrast-enhancing lesion with minimal surrounding edema. Lesions are typically bright on both T1 and T2 images. Tumoral cysts are prevalent in the cerebellum and often possess a contrast-enhancing mural nodule. Grade II astrocytomas are usually less enhancing, although there can be considerable overlap between grade I and grade II tumors. While molecular imaging is just now being brought into practice, it is not sufficient to make the diagnosis in the absence of a biopsy. The imaging characteristics of other low-grade gliomas of the tectum and brainstem will not be discussed here [1].

Using diffusion tensor (DT) imaging and white matter tractography, the location of the white matter tracts in relation to the tumor can be identified and may be useful in planning the operative trajectory [35] with the goal of reducing postoperative morbidity. Assessment of apparent diffusion coefficient (ADC) values of enhancing solid tumor is a simple and reliable technique for preoperative differentiation of pilocytic astrocytomas and medulloblastoma tumors in pediatric patients [36] but is unable to differentiate different low-grade gliomas from each other [37]. The presence of a lactate peak can be present in a large percentage of low-grade gliomas and therefore does not exclude the diagnosis of a pilocytic astrocytoma [38]. Postoperative imaging to follow tumors after resection is important and should continue for some period afterwards due to the possibility of late recurrences [39].

25.5 Histology/ Immunohistochemistry of Posterior Fossa Low-Grade Gliomas

Surgery is performed in children in order to relieve symptoms and determine the diagnosis of the tumor. Therefore, most patients with

low-grade astrocytomas undergo surgical resection or biopsy and tumor tissue is obtained. Samples are sent either “fresh” (frozen) or fixed (in formalin) to the neuropathologist who prepares thin cut slides from larger pieces of tissue. These are stained for various markers, helping to differentiate between the types and grades of gliomas and other CNS tumors that can be found in the cerebellum, posterior fossa, and brainstem of children.

Typically, the most common type of low-grade glioma is the juvenile pilocytic astrocytoma (JPA). These will classically exhibit Rosenthal fibers, biphasic architecture, and eosinophilic granular bodies [4]. In small biopsies, some of the characteristic components of the tumor may be absent, making a definitive diagnosis by grade difficult. Tumors that cannot be graded are often referred to as low-grade astrocytomas, astrocytomas with piloid features, or low-grade glioma NOS (not otherwise specified). Pathologic expertise in pediatric low-grade gliomas is important in the evaluation of these tumors, although many series have found the overall outcome of “low-grade glioma” similar to that of grade I pilocytic astrocytoma [40]. Pilocytic astrocytomas can have both mitotic activity and vascular proliferation based on the WHO grading criteria [4], hallmarks of malignant gliomas even though they maintain their much more benign clinical behavior. Pilomyxoid astrocytomas have recently been separated from classic pilocytic astrocytomas [4] and appear to have a more aggressive clinical course, often associated with leptomeningeal dissemination [41, 42]. While now considered histologically distinct, the molecular classification of these tumors and their relation to pilocytic astrocytomas is lacking [43].

Eosinophilic granular bodies are a common feature of pilocytic astrocytomas and have been shown to be proximal to areas of the cystic changes that are common in pilocytic astrocytomas and may play a role in cyst development [44]. With regards to immunohistochemical staining, pilocytic astrocytoma will typically be diffusely positive for glial fibrillary acid protein

(GFAP) but may also express positivity for vimentin, S-100 protein, microtubule-associated protein 2 (MAP2), and others [45]. Neuronal markers are uncommon in pediatric low-grade glioma [46]. The stem cell marker Olig2 is commonly expressed in pediatric low-grade gliomas [47] and, in addition to providing an additional marker of the astrocytic lineage [47, 48], suggests that these tumors may be stuck in an early developmental program.

Histology has been a long-standing method of determining tumor type, and there are many ways in which histologic features have helped define the clinical risk stratification for a given tumor. To date, histology provides the diagnostic criteria for establishing the grade of glial tumors (WHO grades I–IV) [4], although it is not clear that histologic classification predicts outcome [49]. Variations in the microscopic appearance of pilocytic astrocytomas have been noted and may impact their outcome [50].

The microscope has long been the primary tool for the diagnosis and grading of tumors. The outward appearance of cell morphology fails to recognize the unique molecular differences between tumors of the same grade. Even with the robust use of immunohistochemistry and decades of experience, there is an increasing need to define tumor characteristics by multiple methods, going beyond their appearance under a microscope. Expert opinion and interobserver variability are factors that make robust genetics or molecular testing appealing, at least as a supplementation to the “art of histology.” This inherent weakness in classic histology must be balanced by the heterogeneity associated with sampling error in small biopsy material, which may underrepresent certain components of the tumor [51]. A small study of seven non-NF1 pilocytic astrocytoma samples used single nucleotide polymorphism techniques and direct PCR sequencing to determine “allele-specific expression” (ASE) across the X chromosome. They came to the conclusion that pilocytic astrocytoma tumor cells are most likely derived from a single clonal population of glial origin, rather than an overgrowth of heterogeneous cells [52].

25.5.1 MIB-1/Ki67

MIB-1 refers to an immunohistochemistry tool that provides an estimate of the percentage of tumor cells that have exited G0 (i.e., G1, S, M, or G2) and are at some stage of cellular proliferation (proliferative index). Since low-grade gliomas can take a long period of time to go through the cell cycle, the MIB-1 index must be differentiated from the mitotic index, which assesses the number of cells in the M phase of cellular replication. Although MIB-1 has been correlated with poor outcome in higher-grade glioma [53], expression does not correlate with outcome in pilocytic astrocytomas [50, 54–56], although it can differentiate high-grade glioma from pilocytic astrocytoma [57, 58]. However, in another study of 80 pilocytic astrocytoma samples from incompletely resected tumors, an MIB-1 labeling index of >2 was associated with tumor progression and a significantly shorter event-free survival [59, 60]. The inability of MIB-1 to consistently correlate with outcome in pilocytic astrocytoma may in part be related to the identification of mitotically active microglial and lymphocytic cells in these tumor rather than just the tumor cells themselves [61].

25.5.2 p53

Tumor protein 53 (p53) mutations are one of the most widely identified mutations in human cancers and have been shown to present in a significant majority of malignant gliomas [62]. Immunohistochemical staining for mutant TP53 has been correlated to poor outcomes in some pediatric tumors [63, 64], but in pilocytic astrocytomas, mutant TP53 immunohistochemistry has showed scattered positivity in up to 80 % of samples and mutation in 35 % of cases but has not correlated with poor outcome [50, 65–67]. Positive p53 staining was described in another study to be strongly focused in areas of anaplasia [68], areas which also had a mean MIB1 proliferative index of 24.7 %.

25.5.3 IDH1

A marker called IDH-1 has been shown to exist in adult gliomas, and its expression is inversely proportional to grade. This was found to be an independent marker of prognosis in higher-grade gliomas, with an overall survival of 150.9 months versus 60.1 months [69]. IDH1 is expressed in adult grade 2 astrocytomas and those of older adolescence [70] but not pilocytic astrocytomas [71, 72]. However, pediatric low-grade gliomas are a unique entity, and one study compared adult and pediatric samples; no mutations of IDH 1/2 or p53 were found compared to adults where these were found in a large proportion of low-grade gliomas [73].

25.5.4 MGMT

Epigenetic promoter methylation of O⁶-methylguanine-DNA methyltransferase (MGMT) has been an area of great interest in adult gliomas. In high-grade gliomas, it has been correlated to respond to chemotherapy and has therefore been implicated as a prognostic marker in these tumors [74] and in guiding therapy with temozolomide [75]. MGMT was analyzed by immunohistochemistry in one study, where 87 % of low-grade gliomas showed little to no MGMT staining while 13 % showed positivity in the nuclei. However, there was no correlation with prognosis or disease location in a relatively large sample of 118 pilocytic astrocytomas [50]. Another study looked at MGMT in pilocytic astrocytomas along with two other emerging immunohistochemical markers: mini-chromosomal maintenance protein 2 (MCM2) and phosphohistone H3 (PHH3). Neither of these showed a significant association with survival or tumor progression [60, 76].

25.5.5 miRNA

MicroRNAs (miRNA) are nonprotein-coding RNAs that act as a critical regulator of protein expression via posttranscriptional regulation of

mRNA [77]. Aberrant microRNA expression has been suggested to play a role in the biology of brain tumors. An assessment of several pediatric CNS tumors, including four patients with JPA, demonstrated overexpression of five different miRNAs (miR-432, 29a, 138, 299-5p, 34a) while five were underexpressed (miR-93, 135a, 129, 135b, 106b) in comparison to normal brain tissue. This preliminary work has the potential to expand their use as a biomarker, with diagnostic or prognostic significance [77].

25.5.6 Telomeres

Telomere length is an important component of the cellular senescence program [78] and was examined in a subset of 56 pediatric gliomas, under investigation as a potential prognostic marker. Telomere activity was found in 0 of 11 pilocytic astrocytomas, while telomere shortening was observed in eight of eight patients with additional lesions biopsied years later. The authors speculated that this may provide a biologic mechanism for the tendency for pediatric low-grade gliomas to exhibit growth arrest and even spontaneous regression after many years [79]. An analysis of telomere-associated promyelocytic leukemia bodies (TPBs) in pilocytic astrocytomas may indicate that telomere maintenance occurs by an alternate mechanism to telomerase activity [80].

25.5.7 Chromosomal Integrity

Information is constantly emerging about the genetics of low-grade gliomas in children, yet many studies suggest that normal karyotypes and chromosome copy numbers are the most common finding in these tumors [81]. The profiling of pilocytic astrocytomas has demonstrated two major groupings for these tumors in cell adhesion, regulation of cell growth, cell motility, nerve ensheathment, and angiogenesis [82]. In this series, the immunohistochemical analysis also found a higher incidence of recurrent pilocytic astrocytomas in tumors without myelin basic protein (MBP) expression [82].

Pilocytic astrocytomas are generally thought to have a relatively stable genome, but whole chromosome gains have been described. The most frequent changes in one study of pilocytic astrocytomas were gains of chromosome 5, 6, 7, and 11; these were identified in 9 out of 32 cases [83]. Another study analyzed a series of astrocytomas by CGH and found chromosomal number alterations in 5 out of 35 pilocytic astrocytoma samples (14 %). Chromosome gains were reported as 6q, 7q, and 12q, and losses in 1p and 16p were each seen in single cases [84]. The small number of alterations found precluded clinical correlation. An earlier study used CGH in a series of 48 pilocytic astrocytoma samples, 7 of which showed chromosomal abnormalities with single gains in chromosomes 5, 6, 7, and 9 [85]. However, another study described changes in two-thirds, with an average number of 2.5 gains or losses per sample; chromosomes involved included 2q, 4, 5q, 6q, 7q, 9, and 13q with losses in 1p, 9q, 7q, and 12q [86]. High-resolution array CGH in 14 low-grade glioma samples found alterations (gain of 1q) in only 2 (14.3 %); however, these were samples from the only two patients that required re-resection for recurrent disease. This suggests that complex genetic alterations may correlate with less favorable outcomes [87].

The genetics of pilocytic astrocytomas by tumor location has also been an area of research, with an aim to determine prognosis beyond surgical resectability. BRAF rearrangements are more common in cerebellar tumors than non-cerebellar tumors [88]; they also are found more commonly in the classic biphasic histology which is frequently identified in the cerebellum. The clinical outcome for these pilocytic astrocytomas was independent of BRAF status. Deletion of p16 has also been found to be location specific, occurring more commonly in pilocytic astrocytomas of the midbrain, brainstem, and spinal cord. Loss of heterozygosity (LOH) for 17p13 was correlated in this same study with increased risk of recurrence in cerebellar tumors [88]. Other studies suggest that common alterations such as p16 deletions, PTEN mutations, and 10q23 LOH are much less commonly found in pilocytic

astrocytomas, while occasional TP53 mutations have been described along with p53 overexpression and 17p LOH [89]. Overall, these results suggest that pilocytic astrocytomas have intact chromosomes in the majority of cases, a finding that is consistent with the low malignant potential.

25.5.8 NF1 and ras

Neurofibromatosis type 1 (NF1) is a relatively common autosomal dominant genetic disease that involves mutations within a large gene on chromosome 17. The NF1 gene product is neurofibromin, a protein that normally plays a role in astrocyte growth arrest and neuronal differentiation; it accomplishes this by downregulating ras-GTP via its GTPase-activating domain. Since activation of the ras-MAPK signaling pathway has been found in most astrocytomas, this is thought to be a mechanism of tumor development in NF1 patients. Patients with NF1 are particularly prone to developing brain tumors, and these are commonly low-grade glioma of the optic pathway, although tumors in other locations can occur [90, 91]. Optic pathway gliomas (OPGs) have a more indolent behavior in NF1 patients than in non-NF1 patients, although those that require therapy can recur requiring repeated therapy [92]. Those associated with fibrillary histology appear to behave more like grade II astrocytomas in non-NF1 patients [93].

While approximately 15 % of NF1 patients will develop a low-grade glioma, the vast majority of patients that present with low-grade gliomas arise sporadically in patients without NF1 or any other detectable hereditary genetic disorder [94]. Knowing that a significant proportion of NF1 patients will develop low-grade gliomas, there has been recent work to determine which patients are at higher risk. The NF1 gene is large and mutations can be challenging to identify, but one study looked at 29 patients with NF1 and found a strong tendency for the NF1 mutation to occur toward the 5' end of the gene. NF1 will likely be a critical gene to aid in our understanding of low-grade gliomas, given the high

incidence of tumor occurrence in these patients and the importance of the ras/raf/mek/erk pathway in the development of these tumors (see below).

In one study of 41 microarray-based gene expression pilocytic astrocytomas, NF1 “inactivation” was only found in NF1-PAs, which were also distinguished by their less aggressive clinical behavior. Compared to spontaneous pilocytic astrocytomas, they found a limited number of NF1-unique transcripts. Importantly, these were not expressed in the patient’s NF1 deficient cells but rather only in the associated pilocytic astrocytoma cells [95]. The immunohistochemical expression of p53, p16, retinoblastoma (RB), epidermal growth factor receptor (EGFR), cyclin-dependent kinase 4 (CDK4), platelet-derived growth factor A (PDGF-A), and PDGF receptor alpha (PDGF-Ralpha) protein expression profiles were also not altered in NF1-associated low-grade gliomas [96].

Gene expression has also been used to evaluate for differences in the location of NF1-associated low-grade gliomas. For the forebrain, LHX2, NR2E1, and SIX3 genes were implicated in suprasellar tumor location, while PAX3, IRX2, and IRX5, which are associated with hindbrain development, were increased in posterior fossa pilocytic astrocytomas [95, 97]. NF1-associated low-grade gliomas are not usually associated with the truncated duplication of BRAF at 7q34 [98], likely because they already have constitutive activation of the ras/raf pathway.

It is important to follow NF1 patients carefully because they have an increased risk of degeneration of low-grade tumors into malignant astrocytomas [99, 100].

25.5.9 Subependymal Giant Cell Astrocytoma (SEGA)

Tuberous sclerosis is a genetic disease characterized by mutations in the TSC genes, which are a critical component of the AKT/mTOR pathway. These patients are at risk for the development of tumors called SEGAs that may arise in the posterior fossa. These may be treated by

surgical resection [101], and more recently, with the use of mTOR inhibitors [102–104]. The majority of these tumors do not express the genetic rearrangements found with sporadic or NF1-associated low-grade gliomas [105].

25.5.10 BRAF Duplication

Over the past decade, the most illuminating research on pilocytic astrocytomas has been with regards to the alterations in BRAF, which is a part of the mitogen-activated protein kinase (MAPK) cascade (including ras/raf/mek/erk) [106, 107]. BRAF serves as a regulator in the MAPK pathway, and a truncated duplication at 7q34 called *KIAA1549-BRAF* creates a fused oncogene product that is constitutively active compared to wild-type BRAF [83, 88, 98, 108–112]. The fusion of *KIAA1549-BRAF* leads to loss of its inhibitory domain and therefore uncontrolled downstream (ERK) activation. Localization of this truncated mutation of BRAF is predominantly identified in pilocytic astrocytomas of the posterior fossa and brainstem and less frequently from the optic pathway or cortex. This duplication is rare in patients with NF1 [98]. This pathway has been an area of tremendous research, and BRAF alterations have been found in various studies at a rate of 50–100 % of all pilocytic astrocytomas. Immunohistochemistry staining of 43 pilocytic astrocytomas identified ERK phosphorylation in 81 %, supporting the premise that increase in the MAPK (BRAF-MEK-ERK) signaling pathway would result [109]. Others have found ERK/MAPK pathway activation in 100 % of cerebellar pilocytic astrocytomas [83]. BRAF duplication was identified as the most frequent genomic aberration in 63 % of cerebellar pilocytic astrocytoma but only 33 % of anaplastic pilocytic astrocytomas [108]. Gains of 7q34 point to the *KIAA1549-BRAF* fusion. However, some diffuse astrocytomas (WHO grade II) have been associated with ERK/MAPK pathway activation in the absence of 7q34 gain or RAS mutations [83]. Pilocytic astrocytomas that demonstrate the fusion may be associated with a less aggressive phenotype. In one study, 146 samples were

analyzed, and the *KIAA1549-BRAF* fusion gene alteration was found in 62 %. Multivariate analysis identified this as the strongest predictor of good clinical outcome, independent of patient age, tumor location, or specific pathology [113]. Another study investigated 125 pilocytic astrocytoma samples and found the *KIAA1549-BRAF* in 72 %. Also, rare mutations in BRAF, KRAS, NF1, and RAF1 gene fusions were mutually exclusive to the *KIAA1549-BRAF* fusion and found in 16 of the 125 samples [114]. A different but smaller study identified the *KIAA1549-BRAF* fusion in 100 % (10 out of 10) of the pilocytic astrocytomas and none of the higher-grade tumors. In the same study, none of the pilocytic astrocytomas had the BRAF^{v600e} missense mutation [115]. One study of 25 pilocytic astrocytomas compared 5 supratentorial tumors with 20 from the cerebellar area. Seventeen of the cerebellar tumors demonstrated copy number increases in the 7q34 region, covering exons known to encode the BRAF kinase domain. In this study, three out of the six pilocytic astrocytomas with 7q34 copy number gains also had high levels of ERK and MEK [109].

25.5.11 SRGAP3-RAF1

Although the BRAF fusion with *KIAA1549* has been a major area of research, *SRGAP3* is highly expressed in brain tissue. Fusion of *SRGAP3* (slit-robo GTPase-activating protein) to RAF1 (at chromosome 3p25) has been identified in pilocytic astrocytoma [83]. Low-grade astrocytoma samples from 50 pediatric patients were screened in one study for fusion genes activating the ERK/MAPK pathway. Five variants of the *KIAA1549-BRAF* fusion were found in 30 of 32 cerebellar cases [83]. In addition, two samples demonstrated a *SRGAP3-RAF1* fusion protein. In this same study, one cerebellar pilocytic astrocytoma was found to demonstrate an activating mutation in KRAS. BRAF^{v600e} mutations found were in a PXA and a WHO grade II diffuse astrocytoma [83]. Another study identified novel *SRGAP3-RAF1* gene fusions in 2 out of 125 samples [114]. *FAM131B-BRAF* gene fusion with chromosome

7q34 is a novel finding that was demonstrated in three cases and was thought to lead to a constitutively active BRAF kinase [114].

Recently, the BRAF duplication has been detected when using archival paraffin samples, which has a far greater practical implication in widespread use [116, 117]. In the first study, 27 out of 29 reviewed JPA samples were positive for the BRAF duplication by PCR, which is comparable to FISH and CGH techniques. The ability to process tumor tissue of varying age and preservation methods is a key component of translating targets of this therapy into practice as a useful diagnostic tool for clinicians.

25.5.12 BRAF Mutations

Many different activating mutations of signaling molecules have been described which mimic phosphorylation and thereby make a constitutively active protein product. The most common in low-grade gliomas is an activating mutation that substitutes valine for glutamate at amino acid position 600, referred to as BRAF^{v600e}. First described in melanoma, colon, and certain types of thyroid cancer, the BRAF^{v600e} mutation has been well described in pediatric low-grade gliomas [118]. In a large study of 1,320 brain tumor samples, BRAF^{v600e} mutations were most frequent in two-thirds of pleomorphic xanthoastrocytomas [119] and 20–40 % of gangliogliomas (WHO grade I) [107, 120]. The mutation was detected in only 9 % of the pilocytic astrocytoma samples, but the authors noted a strong association with JPAs located outside of the cerebellum (2 % of cerebellar pilocytic astrocytomas vs. 20 % of pilocytic astrocytomas outside the cerebellum). This mutation was not detected in non-glial CNS tumors [107].

CLIA-certified assays for the BRAFV600E mutation are now widely available by PCR [120] and immunohistochemistry [121].

The exciting therapeutic implications of finding a constitutively activated gene product are the potential for rapid translation to the clinic. For example, there are a number of BRAF^{V600E}-specific inhibitors in clinical development. MEK1/2

inhibition may target the immediate downstream phosphorylation target of BRAF [108] and are therefore ideal for the truncated-duplicated form of BRAF. From a therapeutic standpoint, medical treatment for low-grade gliomas can expand greatly using these discoveries. These findings are also of considerable interest in helping understand the underlying biology of low-grade gliomas, which have both a proliferative phase and an arrested growth and senescence phase [122, 123].

25.5.13 PI3K/AKT

Another oncogenic pathway associated with glial tumors is the PI3K/AKT cascade [124]. One study compared different subsets of pilocytic astrocytoma using “classic” versus “clinically aggressive” groupings. PTEN deletions and p16 deletions, both of which are regulators of the AKT pathway, were found in anaplastic pilocytic astrocytoma tumors suggesting that activation of the PI3K/AKT pathway was associated with a more aggressive form of pilocytic astrocytoma [124]. The clinical utility of such findings could be very helpful in determining which patients justify the use of more aggressive therapy to improve long-term survival outcomes.

25.5.14 WNT

The beta-catenin gene (chromosome 3p2.1) is part of the Wnt signaling cascade, a pathway of interest in pediatric brain tumors, especially based on its role in medulloblastoma [125]. In a series of pilocytic astrocytoma from patients over a wide age range, studies demonstrated that beta-catenin expression by immunohistochemistry was related to clinical prognosis; patients with a higher expression did better [126] in pediatrics but did worse in adult astrocytomas [127]. FRAT-1 (frequently rearranged in advanced T-cell lymphomas-1) is a positive regulator of the Wnt/beta-catenin pathway and is overexpressed in several human cancers and was recently shown to be expressed in a series of 76 astrocytomas and corresponded to grade, with the weakest

expression in low-grade astrocytomas [128]. Epigenetic modification has also been postulated via Wnt inhibitory factor-1 (WIF-1), which can bind and inhibit signaling. In astrocytomas, one study demonstrated promoter hypermethylation of WIF-1 in astrocytomas and postulated that this could lead to uncontrolled Wnt signaling [129].

25.5.15 Sonic Hedgehog (SHH)

Hedgehog signaling (Hh) plays a role in medulloblastoma and high-grade gliomas. The regulator of the Hh pathway transcription target *PTCH* has been studied in pilocytic astrocytomas [130]. Twenty samples of pediatric pilocytic astrocytoma underwent analysis by PCR, and overexpression was seen in 45 %. This was more pronounced in younger children (<10 years of age) [130] which may therefore be suggestive of a more aggressive clinical course.

25.5.16 KIT/PDGFR

“KIT” is a member of the platelet-derived growth factor receptor (PDGFR) family, a group of receptor tyrosine kinases. KIT has been investigated in adult gliomas and was overexpressed in the endothelium of 35 % of pilocytic astrocytomas [131]. PDGFR alpha has been shown by immunoreactivity to be positive in more than half (56 %) of pilocytic astrocytomas in one study [47], and a dramatic response in a case of disseminated pilocytic astrocytoma with imatinib has been reported. Interestingly, the tumor cells were negative for PDGFR and KIT and raised the possibility that the response was mediated by targeting of the endothelium [132].

25.5.17 EGFR

The EGFR inhibitor gefitinib has arrested the proliferation of pilocytic astrocytoma cells in vitro in spite of the absence of EGFR expression in these cells, suggesting an additional target

for this agent [133]. The role of EGFR therefore remains poorly defined in pediatric low-grade astrocytomas [134]. Since these receptor tyrosine kinases signal through the ras/raf/mek/erk pathway, the possibility that they are involved in the signaling of some of these tumors remains a possibility [135].

25.5.18 VEGF

Angiogenesis is an area of interest in many different tumor types, referring to the ability of a tumor to generate its own blood and nutrient supply via the formation of new blood vessels. Microvascular proliferation can frequently be seen in pilocytic astrocytomas [136], and VEGFR2 expression in pilocytic astrocytomas is found in the tumor endothelium [137]. With regimens in development that are able to target angiogenesis as a therapeutic approach [138, 139], there are efforts to identify which tumors express the appropriate potential receptor targets. The protein expression of vascular endothelial growth factors (VEGF) has been demonstrated in low-grade astrocytomas [140]. In one study, 17 snap frozen pediatric pilocytic astrocytomas were analyzed for VEGF receptors 1–3 by immunohistochemical staining and showed a high level of expression in the endothelial cells lining the tumor vasculature. Furthermore, in situ techniques were applied that showed that these receptors are in a phosphorylated state [137]. The expression of VEGF and endothelial proliferation were examined in low-grade gliomas. VEGF expression by immunohistochemistry was diffusely seen in one-third of the patients and at least focally in two-thirds. Endothelial proliferation was observed focally in all samples, but approximately 20 % had an extensive pattern. Despite these observations there was no correlation with clinical prognosis [141]. Cox-2 is thought to be a regulator of angiogenesis by modulating endothelial cell proliferation and VEGF production and in one study was shown by immunohistochemistry to be overexpressed in 60 % of low-grade astrocytomas, providing another potential

target [142] that has been used in metronomic regimens which included celecoxib, an inhibitor of Cox-2 [143]. Pilocytic astrocytomas have been shown to have a similar percentage of immature vessels in comparison to high-grade gliomas, both by morphology and by angiopoietin (ang 1&2). In 59 samples, VEGF expression and endothelial cell turnover supported exploration of the role of anti-angiogenic therapy [136].

25.5.19 Epigenetics

The ten-eleven translocation 2 (TET2) gene at chromosome 4q24 has been recently described in certain cancers and seems to play a role in epigenetic modification. This was recently assessed in a study of 29 low-grade astrocytoma samples, but evidence for either the mutation or the promoter methylation was not found [144]. The “ten-eleven translocation 2” TET2 is involved with DNA methylation and seems to be mutually exclusive of the IDH-1 mutations seen in a large proportion of adult low-grade gliomas. Whether this is clinically relevant in the pediatric population remains to be seen [144].

Conclusions

Our knowledge of the histology, biology, and genetic variants found in low-grade gliomas has been accelerating over the past decade. Low-grade gliomas, while the most common brain tumor in the pediatric population, are rare in the general population and are therefore difficult to study unless large sample databases are created. BRAF duplication is one of the best examples of a genetic change that has been identified in a significant portion of low-grade gliomas, specifically juvenile pilocytic astrocytoma. The role of biologic, genetic, and molecular markers in helping prognosticate for pilocytic astrocytomas is emerging, which will be particularly relevant for tumors that are not surgically resectable. Our expanding knowledge seems to offer a multitude of ways in which we will soon be able to “target” therapy and halt tumor cell

growth. With this increasing knowledge of pathway activation, physicians must remain cautious; not all receptors that are “overexpressed” will be causative of tumor growth. Such findings will allow us to postulate the driving forces behind tumorigenesis and will hopefully lead to new drug targets and a better understanding of how to treat this challenging group of diseases.

References

1. Orkin SH, Fisher DE, Look TA et al (eds) (2009) *Oncology of infancy and childhood*, 1st edn. Saunders, Elsevier, Philadelphia
2. Qaddoumi I, Sultan I, Broniscer A (2009) Pediatric low-grade gliomas and the need for new options for therapy: why and how? *Cancer Biol Ther* 8(1):4–10
3. Schiff D, Brown PD, Giannini C (2007) Outcome in adult low-grade glioma: the impact of prognostic factors and treatment. *Neurology* 69(13): 1366–1373
4. Louis DN, Ohgaki H, Wiestler OD et al (2007) WHO classification of tumours of the central nervous system, 4th edn, World Health Organization classification of tumours. International Agency for Research on Cancer, Lyon, p 309
5. Bernaerts A, Vanhoenacker F, Debois V et al (2003) Juvenile pilocytic astrocytoma. *JBR-BTR* 86(3): 142–143
6. Surveillance, Epidemiology, and End Results (SEER) Program Research Data (1973–2011), National Cancer Institute, Division of Cancer Control and Population Sciences (DCCPS). <http://www.seer.cancer.gov>. Accessed Feb 2012
7. Ostrom QT, Gittleman H, Liao P et al (2014) CBTRUS statistical report: primary brain and central nervous system tumors diagnosed in the United States in 2007–2011. *Neuro Oncol* 16(Suppl 4):iv1–iv63
8. Houben MP, Aben KK, Teepen JL et al (2006) Stable incidence of childhood and adult glioma in The Netherlands, 1989–2003. *Acta Oncol* 45(3): 272–279
9. Lanngren B, Sandstrom PE, Holm S et al (2009) Classification, incidence and survival analyses of children with CNS tumours diagnosed in Sweden 1984–2005. *Acta Paediatr* 98(10):1620–1627
10. Dobs M, Shadbolt B, Khurana VG et al (2011) A multicenter study of primary brain tumor incidence in Australia (2000–2008). *Neuro Oncol* 13(7): 783–790
11. Kohler BA, Ward E, McCarthy BJ et al (2011) Annual report to the nation on the status of cancer, 1975–2007, featuring tumors of the brain and other nervous system. *J Natl Cancer Inst* 103(9): 714–736

12. Bilginer B, Narin F, Oguz KK et al (2011) Benign cerebellar pilocytic astrocytomas in children. *Turk Neurosurg* 21(1):22–26
13. Sridhar K, Sridhar R, Venkatprasanna G (2011) Management of posterior fossa gliomas in children. *J Pediatr Neurosci* 6(Suppl 1):S72–S77
14. Williams VC, Lucas J, Babcock MA et al (2009) Neurofibromatosis type 1 revisited. *Pediatrics* 123(1):124–133
15. Sainte-Rose C, Cinalli G, Roux FE et al (2001) Management of hydrocephalus in pediatric patients with posterior fossa tumors: the role of endoscopic third ventriculostomy. *J Neurosurg* 95(5):791–797
16. Oh KS, Hung J, Robertson PL et al (2011) Outcomes of multidisciplinary management in pediatric low-grade gliomas. *Int J Radiat Oncol Biol Phys* 81(4):e481–e488
17. Wisoff JH, Sanford RA, Heier LA et al (2011) Primary neurosurgery for pediatric low-grade gliomas: a prospective multi-institutional study from the Children's Oncology Group. *Neurosurgery* 68(6):1548–1554; discussion 1554–1555
18. Turner CD, Chordas CA, Liptak CC et al (2009) Medical, psychological, cognitive and educational late-effects in pediatric low-grade glioma survivors treated with surgery only. *Pediatr Blood Cancer* 53(3):417–423
19. Rivera-Luna R, Zapata-Tarres M, Medina-Sanson A et al (2007) Long-term survival in children under 3 years of age with low-grade astrocytoma. *Childs Nerv Syst* 23(5):543–547
20. Parsa CF, Givrad S (2008) Juvenile pilocytic astrocytomas do not undergo spontaneous malignant transformation: grounds for designation as hamartomas. *Br J Ophthalmol* 92(1):40–46
21. Ternier J, Wray A, Puget S et al (2006) Tectal plate lesions in children. *J Neurosurg* 104(6 Suppl):369–376
22. Martin DS, Geller TJ, Falbo S et al (2000) Exophytic juvenile pilocytic astrocytomas of the posterior fossa. *J Child Neurol* 15(4):262–265
23. Kestle J, Townsend JJ, Brockmeyer DL et al (2004) Juvenile pilocytic astrocytoma of the brainstem in children. *J Neurosurg* 101(1 Suppl):1–6
24. Stokland T, Liu JF, Ironside JW et al (2010) A multivariate analysis of factors determining tumor progression in childhood low-grade glioma: a population-based cohort study (CCLG CNS9702). *Neuro Oncol* 12(12):1257–1268
25. Zacharoulis S, Kieran MW (2004) Treatment of low-grade gliomas in children: an update. *Expert Rev Neurother* 4(6):1005–1014
26. Packer RJ, Ater J, Allen J et al (1997) Carboplatin and vincristine chemotherapy for children with newly diagnosed progressive low-grade gliomas. *J Neurosurg* 86(5):747–754
27. Prados MD, Edwards MS, Rabbitt J et al (1997) Treatment of pediatric low-grade gliomas with a nitrosourea-based multiagent chemotherapy regimen. *J Neurooncol* 32(3):235–241
28. Scheinemann K, Bartels U, Tsangaris E et al (2011) Feasibility and efficacy of repeated chemotherapy for progressive pediatric low-grade gliomas. *Pediatr Blood Cancer* 57(1):84–88
29. Merchant TE, Conklin HM, Wu S et al (2009) Late effects of conformal radiation therapy for pediatric patients with low-grade glioma: prospective evaluation of cognitive, endocrine, and hearing deficits. *J Clin Oncol* 27(22):3691–3697
30. Packer RJ (2010) Radiation therapy for pediatric low-grade gliomas: survival and sequelae. *Curr Neurol Neurosci Rep* 10(1):10–13
31. Fisher PG, Tihan T, Goldthwaite PT et al (2008) Outcome analysis of childhood low-grade astrocytomas. *Pediatr Blood Cancer* 51(2):245–250
32. Benesch M, Lackner H, Sovinz P et al (2006) Late sequela after treatment of childhood low-grade gliomas: a retrospective analysis of 69 long-term survivors treated between 1983 and 2003. *J Neurooncol* 78(2):199–205
33. Kano H, Niranjana A, Kondziolka D et al (2009) Stereotactic radiosurgery for pilocytic astrocytomas part 2: outcomes in pediatric patients. *J Neurooncol* 95(2):219–229
34. Daszkiewicz P, Maryniak A, Roszkowski M et al (2009) Long-term functional outcome of surgical treatment of juvenile pilocytic astrocytoma of the cerebellum in children. *Childs Nerv Syst* 25(7):855–860
35. Moshel YA, Elliott RE, Monoky DJ et al (2009) Role of diffusion tensor imaging in resection of thalamic juvenile pilocytic astrocytoma. *J Neurosurg Pediatr* 4(6):495–505
36. Rumboldt Z, Camacho DL, Lake D et al (2006) Apparent diffusion coefficients for differentiation of cerebellar tumors in children. *AJNR Am J Neuroradiol* 27(6):1362–1369
37. Davies NP, Wilson M, Harris LM et al (2008) Identification and characterisation of childhood cerebellar tumours in vivo proton MRS. *NMR Biomed* 21(8):908–918
38. Hwang JH, Egnaczyk GF, Ballard E et al (1998) Proton MR spectroscopic characteristics of pediatric pilocytic astrocytomas. *AJNR Am J Neuroradiol* 19(3):535–540
39. Dorward IG, Luo J, Perry A et al (2010) Postoperative imaging surveillance in pediatric pilocytic astrocytomas. *J Neurosurg Pediatr* 6(4):346–352
40. Bristol RE (2009) Low-grade glial tumors: are they all the same? *Semin Pediatr Neurol* 16(1):23–26
41. Forbes JA, Mobley BC, O'Lynnger TM et al (2011) Pediatric cerebellar pilomyxoid-spectrum astrocytomas. *J Neurosurg Pediatr* 8(1):90–96
42. Mahore A, Kammar A, Dange N et al (2011) Diencephalic juvenile pilomyxoid astrocytoma with leptomeningeal dissemination. *Turk Neurosurg* 21(2):222–225
43. Amatya VJ, Akazawa R, Sumimoto Y et al (2009) Clinicopathological and immunohistochemical features of three pilomyxoid astrocytomas: comparative

- study with 11 pilocytic astrocytomas. *Pathol Int* 59(2):80–85
44. Tung JN, Tsao TY, Tai CJ et al (2010) Distribution of lysosome-associated membrane proteins-1 and -2, and cathepsin D in eosinophilic granular bodies: possible relationship to cyst development in pilocytic astrocytomas. *J Int Med Res* 38(4):1354–1364
 45. Pfister S, Witt O (2009) Pediatric gliomas. *Recent Results Cancer Res* 171:67–81
 46. Donek K, Scheithauer BW, Rodriguez FJ et al (2010) Expression of diagnostic neuronal markers and outcome in glioblastoma. *Neuropathol Appl Neurobiol* 36(5):411–421
 47. Takei H, Yogeswaren ST, Wong KK et al (2008) Expression of oligodendroglial differentiation markers in pilocytic astrocytomas identifies two clinical subsets and shows a significant correlation with proliferation index and progression free survival. *J Neurooncol* 86(2):183–190
 48. Otero JJ, Rowitch D, Vandenberg S (2011) OLIG2 is differentially expressed in pediatric astrocytic and in ependymal neoplasms. *J Neurooncol* 104(2):423–438
 49. Bernhardtsten T, Laursen H, Bojsen-Moller M et al (2003) Sub-classification of low-grade cerebellar astrocytoma: is it clinically meaningful? *Childs Nerv Syst* 19(10–11):729–735
 50. Horbinski C, Hamilton RL, Lovell C et al (2010) Impact of morphology, MIB-1, p53 and MGMT on outcome in pilocytic astrocytomas. *Brain Pathol* 20(3):581–588
 51. Wemmert S, Romeike BF, Ketter R et al (2006) Intratumoral genetic heterogeneity in pilocytic astrocytomas revealed by CGH-analysis of microdissected tumor cells and FISH on tumor tissue sections. *Int J Oncol* 28(2):353–360
 52. Payton JE, Schmidt J, Yu J et al (2011) Genome-wide polymorphism analysis demonstrates a monoclonal origin of pilocytic astrocytoma. *Neuropathol Appl Neurobiol* 37(3):321–325
 53. Kayaselcuk F, Zorludemir S, Gumurduhu D et al (2002) PCNA and Ki-67 in central nervous system tumors: correlation with the histological type and grade. *J Neurooncol* 57(2):115–121
 54. Roessler K, Bertalanffy A, Jeza H et al (2002) Proliferative activity as measured by MIB-1 labeling index and long-term outcome of cerebellar juvenile pilocytic astrocytomas. *J Neurooncol* 58(2):141–146
 55. Paixao Becker A, de Oliveira RS, Saggioro FP et al (2010) In pursuit of prognostic factors in children with pilocytic astrocytomas. *Childs Nerv Syst* 26(1):19–28
 56. Machen SK, Prayson RA (1998) Cyclin D1 and MIB-1 immunohistochemistry in pilocytic astrocytomas: a study of 48 cases. *Hum Pathol* 29(12):1511–1516
 57. Matsumoto T, Fujii T, Yabe M et al (1998) MIB-1 and p53 immunocytochemistry for differentiating pilocytic astrocytomas and astrocytomas from anaplastic astrocytomas and glioblastomas in children and young adults. *Histopathology* 33(5):446–452
 58. Nakamizo A, Inamura T, Ikezaki K et al (2002) Enhanced apoptosis in pilocytic astrocytoma: a comparative study of apoptosis and proliferation in astrocytic tumors. *J Neurooncol* 57(2):105–114
 59. Bowers DC, Gargan L, Kapur P et al (2003) Study of the MIB-1 labeling index as a predictor of tumor progression in pilocytic astrocytomas in children and adolescents. *J Clin Oncol* 21(15):2968–2973
 60. Margraf LR, Gargan L, Butt Y et al (2011) Proliferative and metabolic markers in incompletely excised pediatric pilocytic astrocytomas – an assessment of 3 new variables in predicting clinical outcome. *Neuro Oncol* 13(7):767–774
 61. Klein R, Roggendorf W (2001) Increased microglia proliferation separates pilocytic astrocytomas from diffuse astrocytomas: a double labeling study. *Acta Neuropathol* 101(3):245–248
 62. Levidou G, El-Habr E, Saetta AA et al (2010) P53 immunorexpression as a prognostic marker for human astrocytomas: a meta-analysis and review of the literature. *J Neurooncol* 100(3):363–371
 63. Tabori U, Baskin B, Shago M et al (2010) Universal poor survival in children with medulloblastoma harboring somatic TP53 mutations. *J Clin Oncol* 28(8):1345–1350
 64. Tabori U, Shlien A, Baskin B et al (2010) TP53 alterations determine clinical subgroups and survival of patients with choroid plexus tumors. *J Clin Oncol* 28(12):1995–2001
 65. Hayes VM, Dirven CM, Dam A et al (1999) High frequency of TP53 mutations in juvenile pilocytic astrocytomas indicates role of TP53 in the development of these tumors. *Brain Pathol* 9(3):463–467
 66. Cheng Y, Pang JC, Ng HK et al (2000) Pilocytic astrocytomas do not show most of the genetic changes commonly seen in diffuse astrocytomas. *Histopathology* 37(5):437–444
 67. Tibbetts KM, Emmett RJ, Gao F et al (2009) Histopathologic predictors of pilocytic astrocytoma event-free survival. *Acta Neuropathol* 117(6):657–665
 68. Rodriguez FJ, Scheithauer BW, Burger PC et al (2010) Anaplasia in pilocytic astrocytoma predicts aggressive behavior. *Am J Surg Pathol* 34(2):147–160
 69. Sanson M, Marie Y, Paris S et al (2009) Isocitrate dehydrogenase 1 codon 132 mutation is an important prognostic biomarker in gliomas. *J Clin Oncol* 27(25):4150–4154
 70. Pollack IF, Hamilton RL, Sobol RW et al (2010) IDH1 mutations are common in malignant gliomas arising in adolescents: a report from the Children's Oncology Group. *Childs Nerv Syst* 27(1):87–94
 71. Korshunov A, Meyer J, Capper D et al (2009) Combined molecular analysis of BRAF and IDH1 distinguishes pilocytic astrocytoma from diffuse astrocytoma. *Acta Neuropathol* 118(3):401–405

72. Mukasa A, Takayanagi S, Saito K et al (2012) Significance of IDH mutations varies with tumor histology, grade, and genetics in Japanese glioma patients. *Cancer Sci* 103(3):587–592
73. Jones DT, Mulholland SA, Pearson DM et al (2011) Adult grade II diffuse astrocytomas are genetically distinct from and more aggressive than their paediatric counterparts. *Acta Neuropathol* 121(6):753–761
74. Hegi ME, Diserens AC, Gorlia T et al (2005) MGMT gene silencing and benefit from temozolomide in glioblastoma. *N Engl J Med* 352(10):997–1003
75. Stupp R, Mason WP, van den Bent MJ et al (2005) Radiotherapy plus concomitant and adjuvant temozolomide for glioblastoma. *N Engl J Med* 352(10):987–996
76. Hongeng S, Brent TP, Sanford RA et al (1997) O6-Methylguanine-DNA methyltransferase protein levels in pediatric brain tumors. *Clin Cancer Res* 3(12 Pt 1):2459–2463
77. Birks DK, Barton VN, Donson AM et al (2011) Survey of MicroRNA expression in pediatric brain tumors. *Pediatr Blood Cancer* 56(2):211–216
78. Wai LK (2004) Telomeres, telomerase, and tumorigenesis – a review. *MedGenMed* 6(3):19
79. Tabori U, Vukovic B, Zielenska M et al (2006) The role of telomere maintenance in the spontaneous growth arrest of pediatric low-grade gliomas. *Neoplasia* 8(2):136–142
80. Slatter T, Gifford-Garner J, Wiles A et al (2010) Pilocytic astrocytomas have telomere-associated promyelocytic leukemia bodies without alternatively lengthened telomeres. *Am J Pathol* 177(6):2694–2700
81. Zattara-Cannoni H, Gambarelli D, Lena G et al (1998) Are juvenile pilocytic astrocytomas benign tumors? A cytogenetic study in 24 cases. *Cancer Genet Cytogenet* 104(2):157–160
82. Wong KK, Chang YM, Tsang YT et al (2005) Expression analysis of juvenile pilocytic astrocytomas by oligonucleotide microarray reveals two potential subgroups. *Cancer Res* 65(1):76–84
83. Forshew T, Tatevossian RG, Lawson AR et al (2009) Activation of the ERK/MAPK pathway: a signature genetic defect in posterior fossa pilocytic astrocytomas. *J Pathol* 218(2):172–181
84. Ward SJ, Karakoula K, Phipps KP et al (2010) Cytogenetic analysis of paediatric astrocytoma using comparative genomic hybridisation and fluorescence in-situ hybridisation. *J Neurooncol* 98(3):305–318
85. Sanoudou D, Tingby O, Ferguson-Smith MA et al (2000) Analysis of pilocytic astrocytoma by comparative genomic hybridization. *Br J Cancer* 82(6):1218–1222
86. Shlomit R, Ayala AG, Michal D et al (2000) Gains and losses of DNA sequences in childhood brain tumors analyzed by comparative genomic hybridization. *Cancer Genet Cytogenet* 121(1):67–72
87. Faria C, Miguens J, Antunes JL et al (2010) Pediatric brain tumors: genetics and clinical outcome. *J Neurosurg Pediatr* 5(3):263–270
88. Horbinski C, Hamilton RL, Nikiforov Y et al (2010) Association of molecular alterations, including BRAF, with biology and outcome in pilocytic astrocytomas. *Acta Neuropathol* 119(5):641–649
89. Hartmann C, Hentschel B, Tatagiba M et al (2011) Molecular markers in low-grade gliomas: predictive or prognostic? *Clin Cancer Res* 17(13):4588–4599
90. Ullrich NJ, Raja AI, Irons MB et al (2007) Brainstem lesions in neurofibromatosis type I. *Neurosurgery* 61(4):762–766; discussion 766–767
91. Pascual-Castroviejo I, Pascual-Pascual SI, Viano J et al (2010) Posterior fossa tumors in children with neurofibromatosis type 1 (NF1). *Childs Nerv Syst* 26(11):1599–1603
92. Hernaiz Driever P, von Hornstein S, Pietsch T et al (2010) Natural history and management of low-grade glioma in NF-1 children. *J Neurooncol* 100(2):199–207
93. Rodríguez FJ, Perry A, Gutmann DH et al (2008) Gliomas in neurofibromatosis type 1: a clinicopathologic study of 100 patients. *J Neuropathol Exp Neurol* 67(3):240–249
94. Avery RA, Fisher MJ, Liu GT (2011) Optic pathway gliomas. *J Neuroophthalmol* 31(3):269–278
95. Sharma MK, Mansur DB, Reifenberger G et al (2007) Distinct genetic signatures among pilocytic astrocytomas relate to their brain region origin. *Cancer Res* 67(3):890–900
96. Li J, Perry A, James CD et al (2001) Cancer-related gene expression profiles in NF1-associated pilocytic astrocytomas. *Neurology* 56(7):885–890
97. Sharma MK, Watson MA, Lyman M et al (2006) Matrillin-2 expression distinguishes clinically relevant subsets of pilocytic astrocytoma. *Neurology* 66(1):127–130
98. Jacob K, Albrecht S, Sollier C et al (2009) Duplication of 7q34 is specific to juvenile pilocytic astrocytomas and a hallmark of cerebellar and optic pathway tumours. *Br J Cancer* 101(4):722–733
99. Huttner AJ, Kieran MW, Yao X et al (2010) Clinicopathologic study of glioblastoma in children with neurofibromatosis type 1. *Pediatr Blood Cancer* 54(7):890–896
100. Peters KB, Cummings TJ, Gururangan S (2011) Transformation of juvenile pilocytic astrocytoma to anaplastic pilocytic astrocytoma in patients with neurofibromatosis type I. *J Pediatr Hematol Oncol* 33(5):e198–e201
101. de Ribaupierre S, Dorfmueller G, Bulteau C et al (2007) Subependymal giant-cell astrocytomas in pediatric tuberous sclerosis disease: when should we operate? *Neurosurgery* 60(1):83–89; discussion 89–90
102. Campen CJ, Porter BE (2011) Subependymal Giant Cell Astrocytoma (SEGA) Treatment update. *Curr Treat Options Neurol* 13(4):380–385
103. Moavero R, Pinci M, Bombardieri R et al (2011) The management of subependymal giant cell tumors in tuberous sclerosis: a clinician's perspective. *Childs Nerv Syst* 27(8):1203–1210
104. Krueger DA, Care MM, Holland K et al (2010) Everolimus for subependymal giant-cell astrocytomas

- in tuberous sclerosis. *N Engl J Med* 363(19):1801–1811
105. Rickert CH, Paulus W (2002) No chromosomal imbalances detected by comparative genomic hybridisation in subependymal giant cell astrocytomas. *Acta Neuropathol* 104(2):206–208
 106. Jeuken J, van den Broecke C, Gijsen S et al (2007) RAS/RAF pathway activation in gliomas: the result of copy number gains rather than activating mutations. *Acta Neuropathol* 114(2):121–133
 107. Schindler G, Capper D, Meyer J et al (2011) Analysis of BRAF V600E mutation in 1,320 nervous system tumors reveals high mutation frequencies in pleomorphic xanthoastrocytoma, ganglioglioma and extra-cerebellar pilocytic astrocytoma. *Acta Neuropathol* 121(3):397–405
 108. Pfister S, Janzarik WG, Renke M et al (2008) BRAF gene duplication constitutes a mechanism of MAPK pathway activation in low-grade astrocytomas. *J Clin Invest* 118(5):1739–1749
 109. Bar EE, Lin A, Tihan T et al (2008) Frequent gains at chromosome 7q34 involving BRAF in pilocytic astrocytoma. *J Neuropathol Exp Neurol* 67(9):878–887
 110. Jones DT, Kocialkowski S, Liu L et al (2008) Tandem duplication producing a novel oncogenic BRAF fusion gene defines the majority of pilocytic astrocytomas. *Cancer Res* 68(21):8673–8677
 111. Sievert AJ, Jackson EM, Gai X et al (2009) Duplication of 7q34 in pediatric low-grade astrocytomas detected by high-density single-nucleotide polymorphism-based genotype arrays results in a novel BRAF fusion gene. *Brain Pathol* 19(3):449–458
 112. Lawson AR, Tatevossian RG, Phipps KP et al (2010) RAF gene fusions are specific to pilocytic astrocytoma in a broad paediatric brain tumour cohort. *Acta Neuropathol* 120(2):271–273
 113. Hawkins C, Walker E, Mohamed N et al (2011) BRAF-KIAA1549 fusion predicts better clinical outcome in pediatric low-grade astrocytoma. *Clin Cancer Res* 17(14):4790–4798
 114. Cin H, Meyer C, Herr R et al (2011) Oncogenic FAM131B-BRAF fusion resulting from 7q34 deletion comprises an alternative mechanism of MAPK pathway activation in pilocytic astrocytoma. *Acta Neuropathol* 121(6):763–774
 115. Schiffman JD, Hodgson JG, VandenBerg SR et al (2010) Oncogenic BRAF mutation with CDKN2A inactivation is characteristic of a subset of pediatric malignant astrocytomas. *Cancer Res* 70(2):512–519
 116. Tian Y, Rich BE, Vena N et al (2011) Detection of KIAA1549-BRAF fusion transcripts in formalin-fixed paraffin-embedded pediatric low-grade gliomas. *J Mol Diagn* 13(6):669–677
 117. Setty P, Gessi M, Waha A et al (2011) Sensitive determination of BRAF copy number in clinical samples by pyrosequencing. *Diagn Mol Pathol* 20(3):148–157
 118. Dougherty MJ, Santi M, Brose MS et al (2010) Activating mutations in BRAF characterize a spectrum of pediatric low-grade gliomas. *Neuro Oncol* 12(7):621–630
 119. Dias-Santagata D, Lam Q, Vernovsky K et al (2011) BRAF V600E mutations are common in pleomorphic xanthoastrocytoma: diagnostic and therapeutic implications. *PLoS One* 6(3):e17948
 120. MacConaill LE, Campbell CD, Kehoe SM et al (2009) Profiling critical cancer gene mutations in clinical tumor samples. *PLoS One* 4(11):e7887
 121. Capper D, Preusser M, Habel A et al (2011) Assessment of BRAF V600E mutation status by immunohistochemistry with a mutation-specific monoclonal antibody. *Acta Neuropathol* 122(1):11–19
 122. Raabe EH, Lim KS, Kim JM et al (2011) BRAF activation induces transformation and then senescence in human neural stem cells: a pilocytic astrocytoma model. *Clin Cancer Res* 17(11):3590–3599
 123. Jacob K, Quang-Khuong DA, Jones DT et al (2011) Genetic aberrations leading to MAPK pathway activation mediate oncogene-induced senescence in sporadic pilocytic astrocytomas. *Clin Cancer Res* 17(14):4650–4660
 124. Rodriguez EF, Scheithauer BW, Giannini C et al (2011) PI3K/AKT pathway alterations are associated with clinically aggressive and histologically anaplastic subsets of pilocytic astrocytoma. *Acta Neuropathol* 121(3):407–420
 125. Ullrich NJ, Pomeroy SL (2006) Molecular genetics of pediatric central nervous system tumors. *Curr Oncol Rep* 8(6):423–429
 126. Sareddy GR, Geeviman K, Panigrahi M et al (2011) Increased beta-catenin/Tcf signaling in pilocytic astrocytomas: a comparative study to distinguish pilocytic astrocytomas from low-grade diffuse astrocytomas. *Neurochem Res* 37(1):96–104
 127. Zhang LY, Jiang LN, Li FF et al (2010) Reduced beta-catenin expression is associated with good prognosis in Astrocytoma. *Pathol Oncol Res* 16(2):253–257
 128. Guo G, Liu B, Zhong C et al (2011) FRAT1 expression and its correlation with pathologic grade, proliferation, and apoptosis in human astrocytomas. *Med Oncol* 28(1):1–6
 129. Yang Z, Wang Y, Fang J et al (2010) Expression and aberrant promoter methylation of Wnt inhibitory factor-1 in human astrocytomas. *J Exp Clin Cancer Res* 29:26
 130. Rush SZ, Abel TW, Valadez JG et al (2010) Activation of the Hedgehog pathway in pilocytic astrocytomas. *Neuro Oncol* 12(8):790–798
 131. Puputti M, Tynninen O, Pernila P et al (2010) Expression of KIT receptor tyrosine kinase in endothelial cells of juvenile brain tumors. *Brain Pathol* 20(4):763–770
 132. McLaughlin ME, Robson CD, Kieran MW et al (2003) Marked regression of metastatic pilocytic astrocytoma during treatment with imatinib mesylate (STI-571, Gleevec): a case report and laboratory investigation. *J Pediatr Hematol Oncol* 25(8):644–648

133. Foreman NK, Gore L, Wells D et al (2006) Gefitinib is effective against juvenile pilocytic astrocytoma in vitro. *Pediatr Blood Cancer* 47(3):293–298
134. Huang H, Hara A, Homma T et al (2005) Altered expression of immune defense genes in pilocytic astrocytomas. *J Neuropathol Exp Neurol* 64(10): 891–901
135. Anagnostopoulos AK, Dimas KS, Papathanassiou C et al (2011) Proteomics studies of childhood pilocytic astrocytoma. *J Proteome Res* 10(5):2555–2565
136. Sie M, de Bont ES, Scherpen FJ et al (2010) Tumour vasculature and angiogenic profile of paediatric pilocytic astrocytoma; is it much different from glioblastoma? *Neuropathol Appl Neurobiol* 36(7):636–647
137. Sikkema AH, de Bont ES, Molema G et al (2011) Vascular endothelial growth factor receptor 2 (VEGFR-2) signalling activity in paediatric pilocytic astrocytoma is restricted to tumour endothelial cells. *Neuropathol Appl Neurobiol* 37(5):538–548
138. Kieran MW, Billett A (2001) Antiangiogenesis therapy. Current and future agents. *Hematol Oncol Clin North Am* 15(5):835–851, viii
139. Packer RJ, Jakacki R, Horn M et al (2009) Objective response of multiply recurrent low-grade gliomas to bevacizumab and irinotecan. *Pediatr Blood Cancer* 52(7):791–795
140. Yao Y, Kubota T, Sato K et al (2001) Prognostic value of vascular endothelial growth factor and its receptors Flt-1 and Flk-1 in astrocytic tumours. *Acta Neurochir (Wien)* 143(2):159–166
141. Kurwale NS, Suri V, Suri A et al (2011) Predictive factors for early symptomatic recurrence in pilocytic astrocytoma: does angiogenesis have a role to play? *J Clin Neurosci* 18(4):472–477
142. El-Sayed M, Taha MM (2011) Immunohistochemical expression of cyclooxygenase-2 in astrocytoma: correlation with angiogenesis, tumor progression and survival. *Turk Neurosurg* 21(1):27–35
143. Kieran MW, Turner CD, Rubin JB et al (2005) A feasibility trial of antiangiogenic (metronomic) chemotherapy in pediatric patients with recurrent or progressive cancer. *J Pediatr Hematol Oncol* 27(11):573–581
144. Kim YH, Pierscianek D, Mittelbronn M et al (2011) TET2 promoter methylation in low-grade diffuse gliomas lacking IDH1/2 mutations. *J Clin Pathol* 64(10):850–852

Daniele Cascone, Maria Rita Panico,
Maria Consiglio Buonocore, Domenico Cicala,
Anna Nastro, and Emilio Cianciulli

26.1 Introduction

Pilocytic astrocytoma (PA) is the most common pediatric cerebellar neoplasm and the most common pediatric glioma, constituting 85 % of all cerebellar astrocytomas and 10 % of all cerebral astrocytomas in this age group [1]. PAs are usually clinically benign and are classified as grade I by the World Health Organization (WHO) [2].

The incidence is approximately 4.8 cases per million people per year, with 2.3–6 % of all brain tumors classified as PA [3]. They have a peak incidence between the age of 5 and 13 years and occur equally frequent in boys and girls [1].

Cerebellar astrocytomas are usually sporadic, but association with neurofibromatosis type 1, Turcot syndrome, PHACE(S) syndrome, and Ollier's disease has been reported [4]. The prognosis depends particularly on tumor characteristics (location, gross structure, and size) and the completeness of resection. Complete resection, hemispheric location, small size, and presence of cysts are favorable prognostic factors [5].

They are potentially curable by surgery and are associated with a longer survival, with the 25 years survival rate being close to 90 % [6].

Very rarely, a PA may undergo spontaneous malignant transformation and become an anaplastic astrocytoma. Accurate interpretation of imaging studies plays an essential role in directing treatment of these tumors. Patients with cerebellar PA typically present with a gradual onset of symptoms due to the slow growth of the tumor. Common presenting symptoms include headache, nausea and vomiting, and gait imbalance. Common clinical findings include truncal ataxia and papilledema (due to increased intracranial pressure) [7] (Fig. 26.1).

D. Cascone, M.D. (✉)

Division of Pediatric Neuroradiology, Department of Neurosciences, Santobono Pausilipon Children's Hospital, Naples, Italy

Department of Neurosciences, Service of Neuroradiology, Santobono Pausilipon Children's Hospital, Via Mario Fiore n.6, Naples 80129, Italy
e-mail: d.cascone@santobonopausilipon.it

M.R. Panico, M.D. (✉)

Division of Radiology, Department of Neurosciences, Federico II University, Via Pansini n. 5, Naples, Italy

M.C. Buonocore • D. Cicala • A. Nastro
E. Cianciulli, M.D.

Division of Pediatric Neuroradiology, Department of Neurosciences, Santobono Pausilipon Children's Hospital, Naples, Italy

26.2 Classifications

26.2.1 Regional

PAs were classified as being located in the cerebellar hemisphere or within the vermis. They

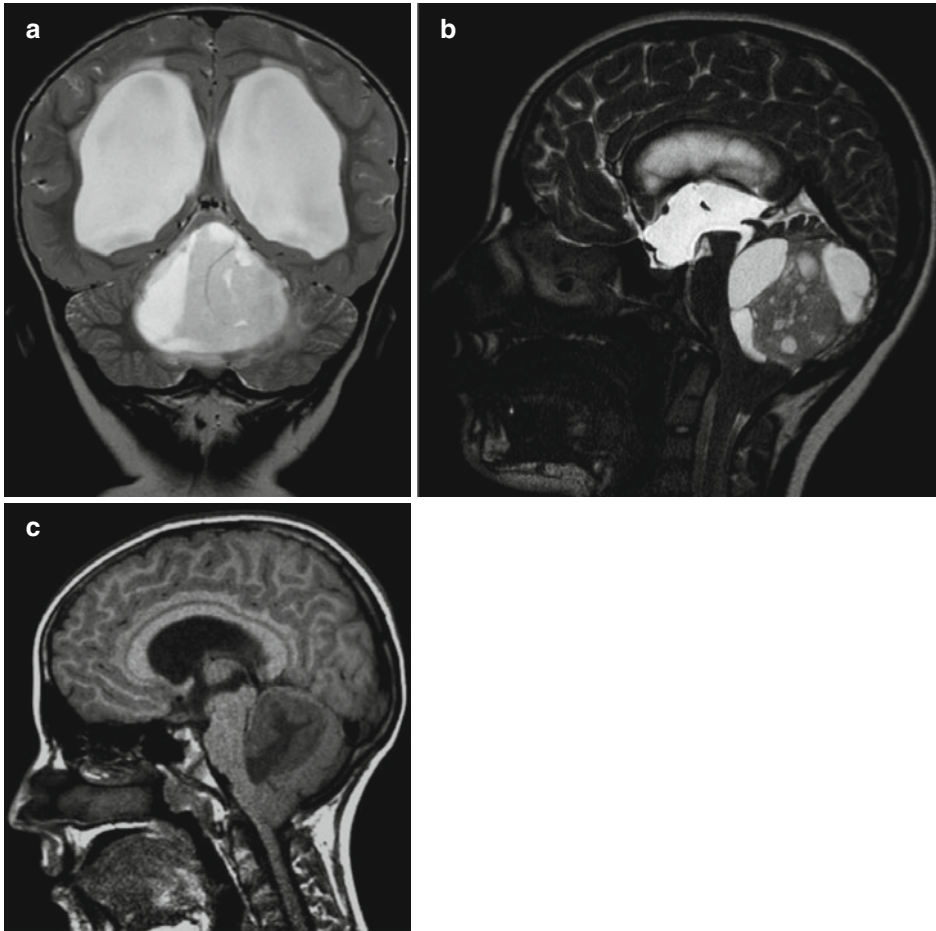


Fig. 26.1 Hydrocephalus (a) coronal TSE T2-image show evident hydrocephalic enlargement of lateral ventricles, area of hyperintensity in periventricular white matter to be attributed to ependymal transudation; (b) sagittal

DRIVE T2-image show triventricular hydrocephalus due to obstruction of fourth ventricle by the lesion; (c) sagittal TSE T1 – notice downward tonsillar displacement (*arrow*) below the McRae line (*white line*)

were further classified according to the presence of brainstem involvement. It can be difficult to differentiate between tumors that originate primarily within the brainstem and those that originate in the cerebellum when both involve intermediary structures (the middle cerebellar peduncle). The term “transitional astrocytoma” has been applied to PA that has a predominantly cerebellar origin but also involve the brainstem (Fig. 26.2). These tumors show a higher incidence of nonpilocytic histologies and are usually incompletely resectable.

This results in a higher proportion of tumor recurrence and, subsequently, a significantly poorer length of survival and long-term neurological outcome than purely cerebellar tumors [8].

26.2.2 Morphologic

The appearance of PA on MR is variable and depends on the tumor’s size and structure. Four predominant imaging patterns of PA have been described:

- I. Typical large cyst with a nonenhancing cyst wall and intensely enhancing mural nodule (sometimes en plaque) (Fig. 26.3)
- II. Cystic mass with an enhanced cyst wall and the mural nodule (Figs. 26.4 and 26.5)
- III. Tumor appearing largely necrotic with no identifiable mural nodule (falsely cystic) (Fig. 26.6)
- IV. Solid or mainly solid tumor, with irregular contrast enhancement [8] (Fig. 26.7)

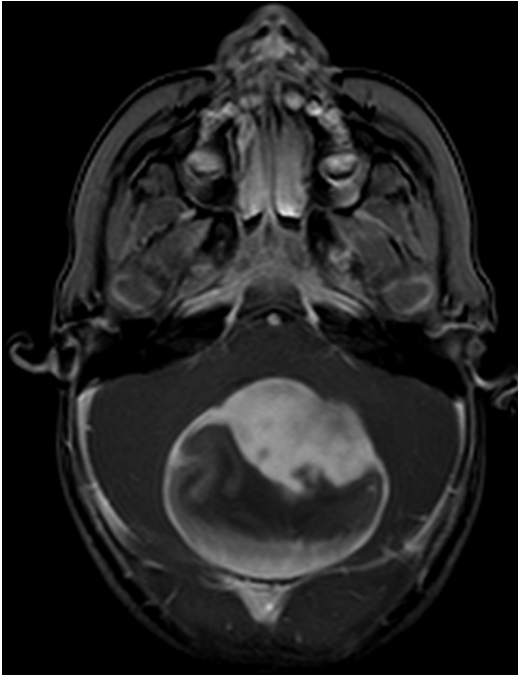


Fig. 26.2 Transitional astrocytoma. Gd-enhanced axial T1-weighted image. Transitional astrocytoma has a predominantly cerebellar origin but also involve the brainstem

Approximately 50 % of PAs are well circumscribed, round or ovoid, and have a large cystic component with a mural nodule. A less common appearance (approximately 10 %) is a solid component peripherally with central necrosis [4, 9].

26.3 Computed Tomography (CT)

On CT, the cystic component of PA is hypodense or slightly hyperdense than the CSF owing to its higher protein content; the solid nodular component is isodense compared to the surrounding brain parenchyma. With contrast administration, there is avid enhancement of the solid nodule and occasionally the walls of the cyst; enhancement of the cyst wall suggests but is not diagnostic of the presence of tumor cells within the cyst wall lining. However, enhancement may be scant in some cases. Larger masses result in compression and obstruction of the fourth ventricle with associated hydrocephalus. If uncompensated, transependymal flow of CSF may be seen along the margins of the lateral ventricles [10]. Tumor calcification is rare but tends to resemble flecks

when it does occur [4]. Adjacent parenchymal edema may occur but is less common, due to the indolent nature of PA.

26.4 Magnetic Resonance (MR)

On MR, the cystic components are hyperintense, not suppressed, in FLAIR; iso- to slightly hyperintense to CSF on T1; and iso-/hyperintense to CSF on T2 sequences.

The solid portions are iso-/hypointense to gray matter (GM) and hyperintense in T2, FLAIR to GM. Vasogenic edema, when present, is relatively mild compared to the size of the lesion and is T2 hyperintense. After contrast administration, there is avid enhancement of the solid nodular component, reflecting the typically rich vascularity with absent BBB. As discussed above, enhancement of the cyst wall may occasionally be seen and is suggestive but not diagnostic of tumor cells lining the cyst wall. MR also depicts associate features such as herniation of the tonsils and superior vermis. Surrounding edema is scant or even absent [10].

On diffusion-weighted imaging, cystic components of the mass exhibit the diffusion properties of CSF. The solid component displays high apparent diffusion coefficient (ADC) values, which indicate the low cellularity of PA [11] (Fig. 26.8).

Information on the metabolism of brain tissue may be obtained from proton MR spectroscopy (MRS). MRS performed on the solid portion of pilocytic astrocytomas shows slight elevation of choline compared to N-acetyl aspartate (NAA), with a ratio of approximately 1.6 to 2.3 to 1 [12]. This ratio is only from the solid portions of the tumor.

The cystic portions of the tumor often show only elevated lactate levels and lack of other metabolites. This pattern is paradoxical because it does not reflect the quiescent clinical behavior of the tumor. The elevated lactate levels in the cystic portion of PAs do not reflect necrosis, which is rare in pilocytic astrocytomas. The presence of lactate within pilocytic tumors might be explained by several mechanisms, such as an abnormal number or dysfunction of mitochondria (which would interfere with the processes of oxidative phosphorylation and electron transport); alterations in proportional oxygen delivery,

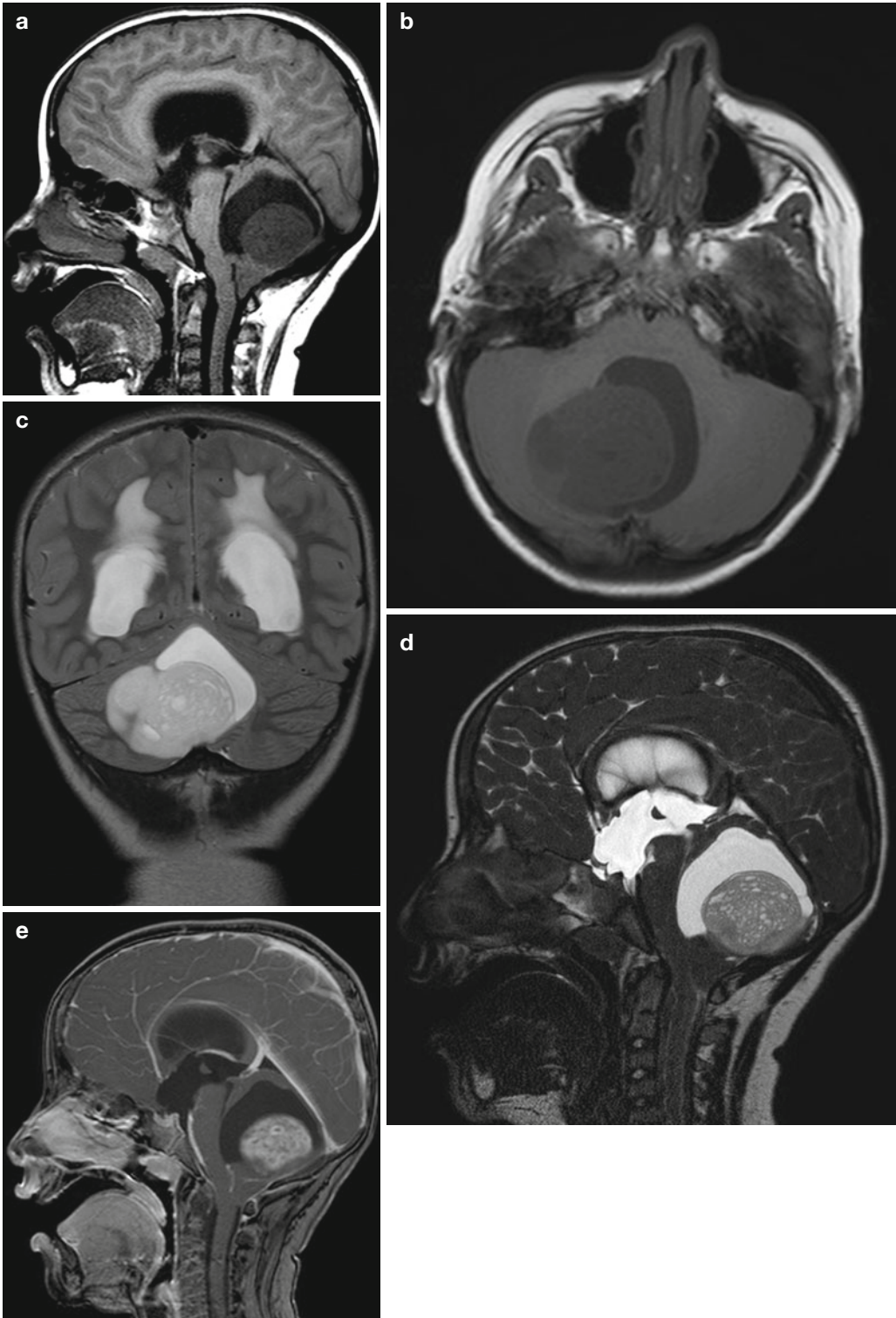


Fig. 26.3 Pilocytic astrocytoma, type I. (a) Sagittal T1 TSE; (b) Axial TSE T1; (c) Coronal T2 TSE; (d) DRIVE T2 Sag; (e) Gd-enhanced Sagittal T1-weighted image. There is a huge cystic lesion with mural nodule. The mural nodule is hypointense on (a, b) T1-weighted

images; hyperintense on T2-weighted image (c, d), and enhances markedly (e). The cyst is hypointense on T1-weighted images (a, b), hyperintense on T2-weighted images (c, d). Note nonenhancing cyst wall in (e)

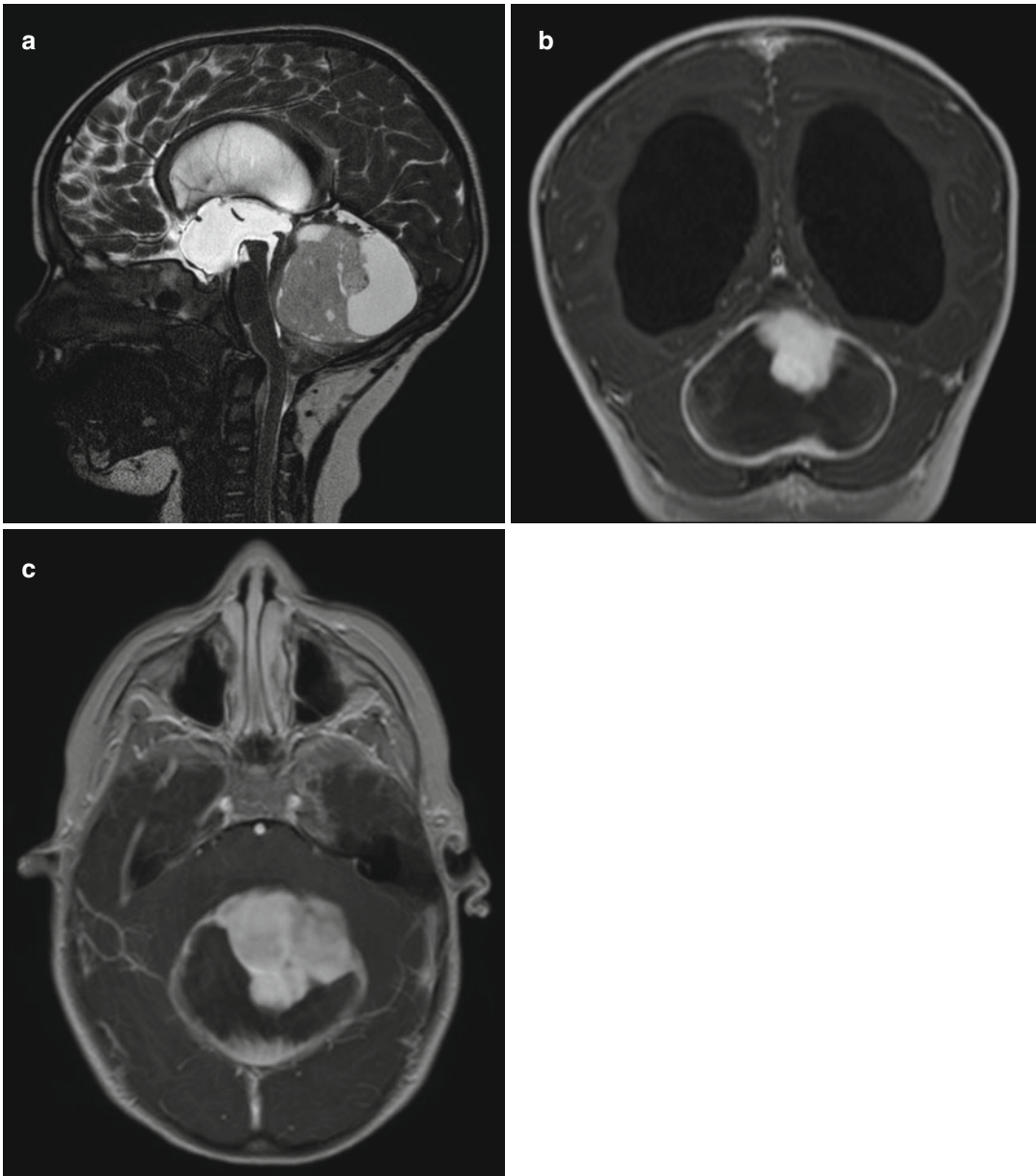


Fig. 26.4 Pilocytic astrocytoma, type II. (a), Sagittal DRIVE T2-weighted image; (b, c) Gd-enhanced coronal and axial T1-weighted image. Selected images from an MR of the posterior fossa demonstrates a large cystic

mass with peripheral nodular enhancement. It appears to be displaced and compressing the fourth ventricle. Given the patient's age, the ventricles appear enlarged in keeping with hydrocephalus

oxygen extraction, or oxygen usage by the tumor; or anaerobic glycolysis by tumor cells (Fig. 28.9).

Although investigators report that cerebellar PA with anaplastic features is more often solid than cystic from a neuroimaging standpoint, CT and MR findings are inadequate to predict these histologic features [13].

26.5 Differential Diagnosis

The differentiation from other posterior fossa tumors may not be immediate when the mass is solid and located in the vermis or fourth ventricle. However, knowledge of the density on CT and signal behavior on MR usually will allow one to



Fig. 26.5 Pilocytic astrocytoma, type II. Gd-enhanced axial T1 fat sat-weighted image. The cystic mass with an enhanced cyst wall and mural nodule

make the correct diagnosis. Therefore, when a typical solid-cystic tumor is found on MR in a patient younger than 20 years of age, the most probable diagnosis is PA, particularly when it is located in the posterior fossa.

PA may mimic hemangioblastomas on conventional MR by appearing as a cystic mass with an enhancing mural nodule; however, perfusion MR may confidently allow distinction between these tumors because relative cerebral blood volume (rCBV) has been shown to be significantly less in PAs than in hemangioblastomas [14].

Diffusion-tensor imaging (DTI) has been shown to be a useful adjunct in differentiating thalamopeduncular pilocytic astrocytomas from infiltrating tumors in the posterior fossa because pilocytic astrocytomas displace corticospinal tracts, whereas other tumors may encase them or disrupt them [15].

Differential diagnosis of CPA in children mainly includes ependymoma and medulloblastoma.

- Medulloblastomas are malignant and invasive embryonal tumors of the cerebellum which classically shows densely packed tumor cells. Typical imaging features reflecting this high cell density are hyperdensity on CT, gray matter signal on T2-weighted images, and ADC reduction (less than $80 \text{ \AA} \sim 10\text{--}5 \text{ mm}^2/\text{s}$) [16, 17].
- Ependymomas might have calcifications (50 %) and tend to extend laterally to the cerebellopontine angles, while medulloblastomas tend to disseminate through CSF spaces to the brain and spine [4] and ADC between 80 and $120 \text{ \AA} \sim 10\text{--}5 \text{ mm}^2/\text{s}$ [17].

26.6 Postsurgical and Surveillance Imaging

The goal of surgery, when feasible, remains gross-total resection, which in many cases results in “cure,” without the need for adjunctive therapy. This goal is achieved in 60–80 % of operative cases with a 10-year survival rate of more than 94 % [3]. The initial postoperative MR should be performed within 24 h of surgery.

Follow-up surveillance imaging of cerebellar pilocytic astrocytoma is recommended at every 3 months for 2 years, followed by every 6 months for an additional 2 years, and then annually after 4 years from the time of treatment [18].

The presence of nodular tumor enhancement on the initial postoperative MR had predictive value for recurrent disease, which improved with the incorporation of Ki 67 and CD68 as pathological variables for predicting progressive disease. However, cases of delayed recurrence of gross-totally resected tumors in purportedly low-risk patients emphasize that the absence of abnormalities on surveillance imaging does not eliminate the risk of developing recurrence [19].

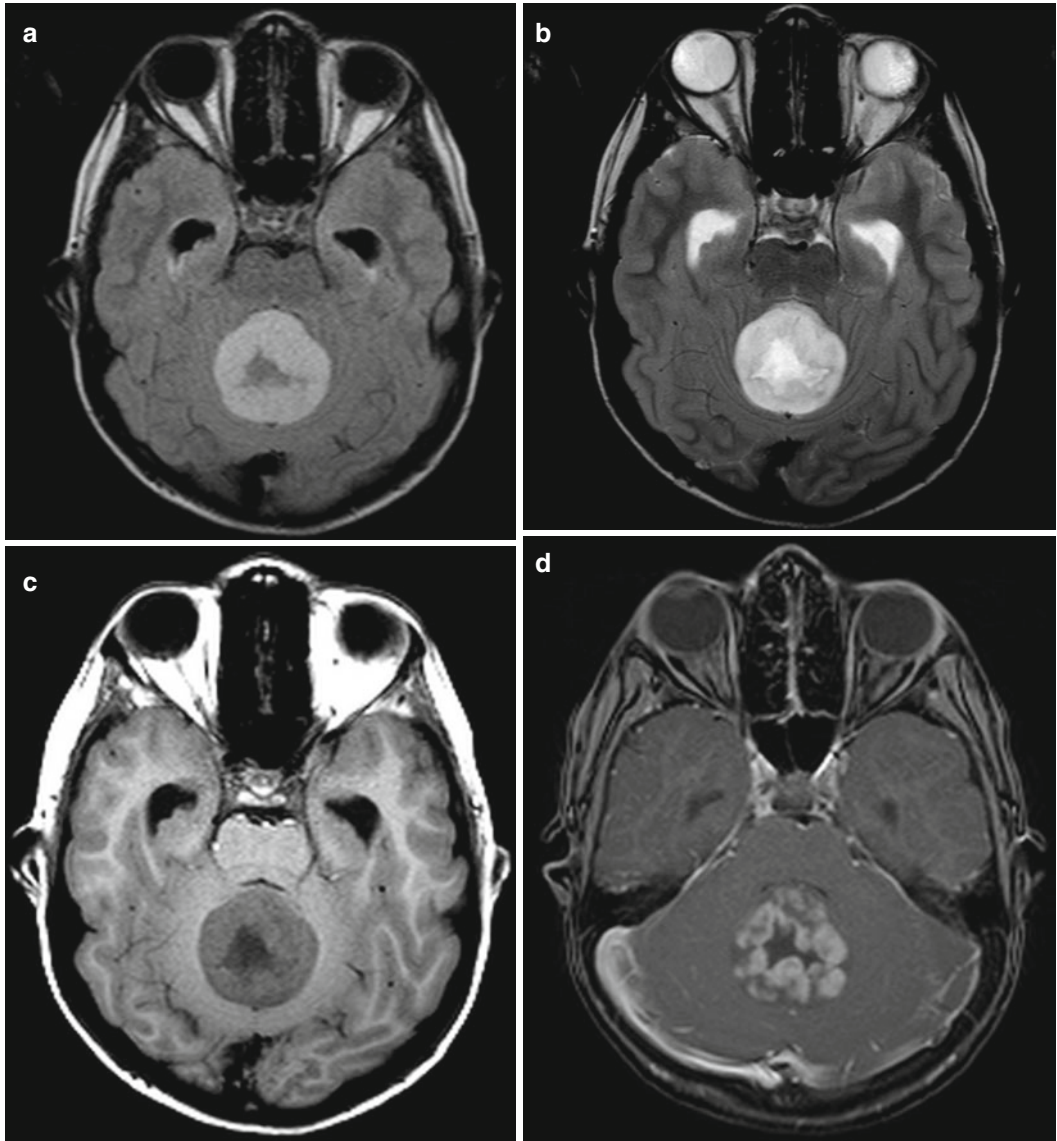


Fig. 26.6 Pilocytic astrocytoma type III. (a) Axial FLAIR-weighted image; (b) axial T2-weighted image; (c) Axial T1-weighted image; (d) Gd-enhanced axial

T1-weighted image. The tumor appearing largely necrotic with no identifiable mural nodule (falsely cystic)

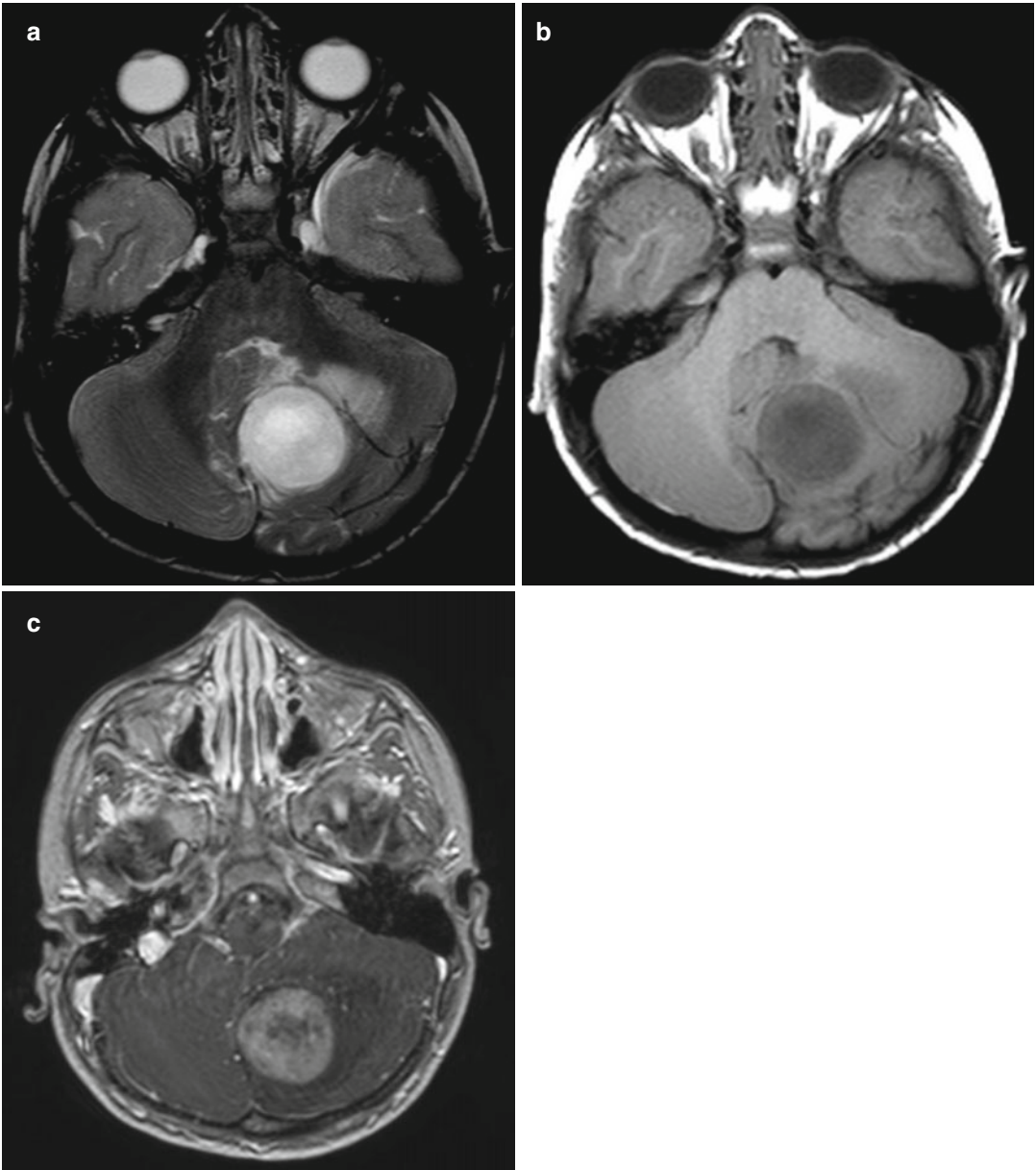


Fig. 26.7 Pilocytic astrocytoma, type IV. (a) Axial T2-weighted image; (b) axial T1-weighted image; (c) Gd-enhanced axial T1 fat sat-weighted image. The tumor appearing solid with irregular contrast enhancement

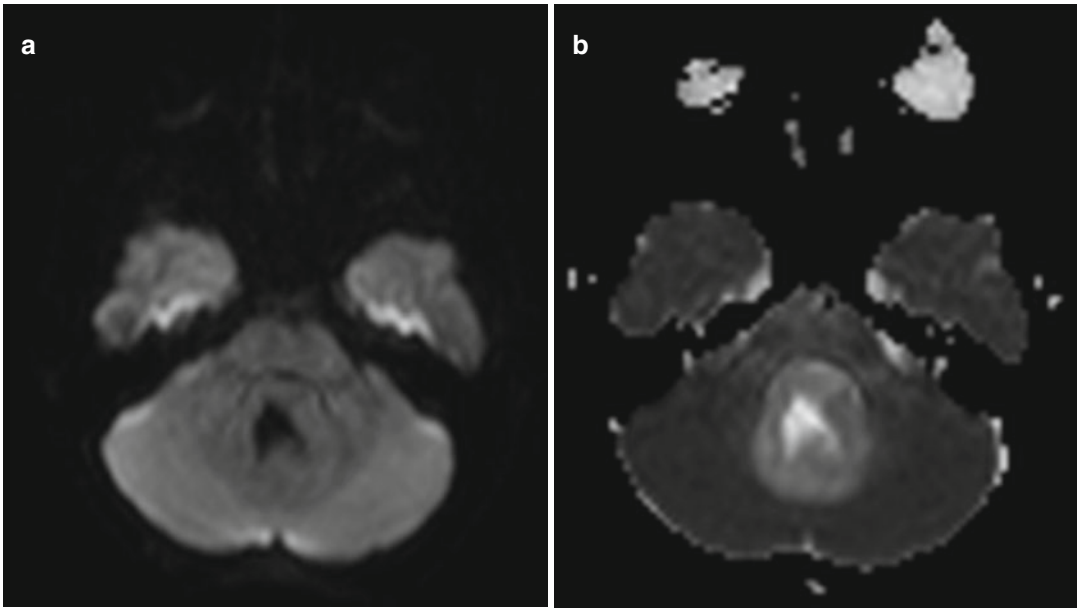


Fig. 26.8 Diffusion-weighted imaging (DWI) and apparent diffusion coefficient (ADC): (a) DWI and (b) ADC. On DWI, cystic components of the mass exhibit the diffusion properties of CSF. The solid component displays high ADC values, which indicate the low cellularity of PA

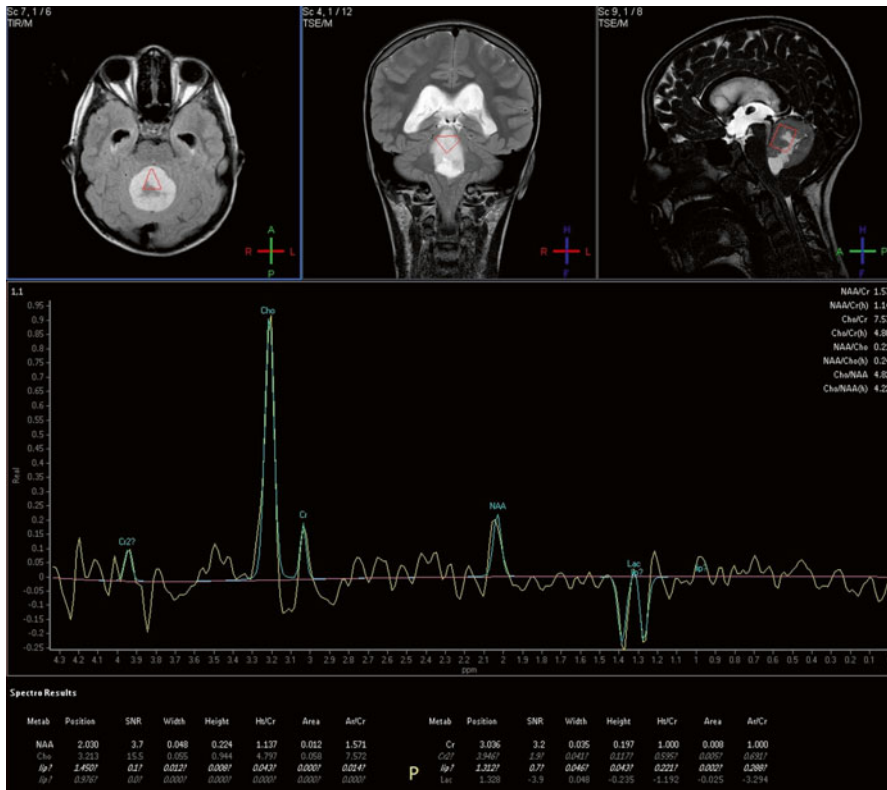


Fig. 26.9 MR spectroscopy (MRS). MRS performed on the solid portion of pilocytic astrocytomas shows slight elevation of choline compared to N-acetyl aspartate (NAA)

References

1. Burger PC, Scheithauer BW, Paulus W, Szymas J, Giannini C, Kleihues P (2000) Pilocytic astrocytoma. In: Kleihues P, Cavenee W (eds) *Pathology and genetics of tumours of the nervous system*. IARC, Lyon, pp 45–51
2. Scheithauer BW, Hawkins C, Tihan T et al (2007) Pilocytic astrocytoma. In: Louis DN, Ohgaki H, Wiestler OD et al (eds) *WHO classification of tumours of central nervous system*. IARC, Lyon, pp 14–21
3. Burkhard C, Di Patre PL, Schuler D et al (2003) A population-based study of the incidence and survival rates in patients with pilocytic astrocytoma. *J Neurosurg* 98:1170–1174
4. Poretti A, Meoded A, Huisman TA (2012) Neuroimaging of pediatric posterior fossa tumors including review of the literature. *J Magn Reson Imaging* 35(1):32–47
5. Villarejo F, de Diego JM, de la Riva AG (2008) Prognosis of cerebellar astrocytomas in children. *Childs Nerv Syst* 24:203–210
6. Kuroiwa T, Ohta T, Tsutsumi A (1999) Malignant pilocytic astrocytoma in the medulla oblongata: case report. *Brain Tumor Pathol* 16:81–85
7. Reinberg M, Hammad O (2014) Cerebellar astrocytoma presenting with headache and nystagmus in a 20-year-old male. *Emerg Med* 46(4):e121–e124
8. Pencolet P, Maixner W, Sainte-Rose C, Lellouch-Tubiana A, Cinalli G, Zerah M, Pierre-Kahn A, Hoppe-Hirsch E, Bourgeois M, Renier D (1999) Benign cerebellar astrocytomas in children. *J Neurosurg* 90:265–273
9. Chourmouzi D, Papadopoulou E, Konstantinidis M, Syrris V, Kouskouras K, Haritanti A, Karkavelas G, Drevelegas A (2014) Manifestations of pilocytic astrocytoma: a pictorial review. *Insights Imaging* 5(3):387–402
10. Lee YY, Van Tassel P, Bruner JM, Moser RP, Share JC (1989) Juvenile pilocytic astrocytomas: CT and MR characteristics. *AJR Am J Roentgenol* 152(6):1263–1270
11. Rumboldt Z, Camacho DLA, Lake D et al (2006) Apparent diffusion coefficients for differentiation of cerebellar tumors in children. *AJNR Am J Neuroradiol* 27:1362–1369
12. Sutton LN, Wang Z, Gusnard D, Lange B, Perilongo G, Bogdan AR, Detre JA, Rorke L, Zimmerman RA (1992) Proton magnetic resonance spectroscopy of pediatric brain tumors. *Neurosurgery* 31(2):195–202
13. Panigraphy A, Krieger MD, Gonzalez-Gomez I et al (2006) Quantitative short echo time 1H-MR Spectroscopy of untreated pediatric brain tumors: pre-operative diagnosis and characterization. *AJNR Am J Neuroradiol* 27:560–572
14. Bing F, Kremer S, Lamalle L et al (2009) Value of perfusion MRI in the study of pilocytic astrocytoma and hemangioblastoma: preliminary findings. *J Neuroradiol* 36:82–87
15. Broadway SJ, Ogg RJ, Scoggins MA, Sanford R, Patay Z, Boop FA (2011) Surgical management of tumors producing the thalamopeduncular syndrome of childhood. *J Neurosurg Pediatr* 7:589–595
16. Arai K, Sato N, Aoki J, Yagi A, Taketomi-Takahashi A, Morita H, Koyama Y, Oba H, Ishiuchi S, Saito N, Endo K (2006) MR signal of the solid portion of pilocytic astrocytoma on T2-weighted images: is it useful for differentiation from medulloblastoma? *Neuroradiology* 48:233–237
17. Pavlisa G, Pavlisa G, Rados M (2011) Diffusion differences between pilocytic astrocytomas and grade II ependymomas. *Radiol Oncol* 45(2):97–101
18. Schneider JH Jr, Raffel C, McComb JG (1992) Benign cerebellar astrocytomas of childhood. *Neurosurgery* 30:58–63
19. Dorward IG, Luo J, Perry A, Gutmann DH, Mansur DB, Rubin JB, Leonard JR (2010) Postoperative imaging surveillance in pediatric pilocytic astrocytomas. *J Neurosurg Pediatr* 6(4):346–352

Erica Jacobson, Grace K. Lai,
and Wirginia June Maixner

Key Points

- Benign astrocytomas are common pediatric tumors with an excellent survival rate of 80–100 %.
- Tumors can have significant neurological consequences, including invasion of the brainstem.
- Surgical excision is the first- and best line of treatment.
- Surgical technique for excision can be used to address other infratentorial tumors, e.g., medulloblastomas and ependymomas.

signs. They rarely metastasize. Because of their benign nature, surgical resection is the mainstay of treatment. The extent of surgical resection is the best predictor of the patient's outcome [1, 7, 10, 15]. Complete surgical resection is not always possible. In this group, there are often good long-term outcomes that are well documented even for subtotal excision of tumors [10]. Thus, subtotal resection remains a viable option in situations where complete surgical resection may significantly affect quality of life.

While JPAs are the most common astrocytic tumor of the cerebellum, other astrocytic tumors such as fibrillary astrocytomas (grade II), high-grade astrocytoma, and pilomyxoid astrocytomas also occur. These have implications for prognosis, but such information can only be determined by formal pathological assessment after surgery.

This chapter focuses on the construction and execution of a surgical plan to manage benign cerebellar astrocytomas in pediatric patients. The pathology and epidemiology of these tumors are discussed elsewhere in this book.

The nature of the tumor, by its location, features, and behavior, as well as the age of the patient, provides its own unique challenges. These challenges include surgical approach, perioperative care, and postoperative evaluation. We will also briefly consider the management of recurrent and malignant cerebellar astrocytomas. There still exists debate regarding the management of certain features, such as the cyst wall and

27.1 Introduction

The majority of posterior fossa astrocytomas (85 %) are juvenile pilocytic astrocytomas (JPA) and are grade I tumors. These are slow-growing, intra-axial tumors that usually present as large masses of the midline vermis or hemisphere, causing obstruction to CSF flow and cerebellar

E. Jacobson, M.D. (✉) • G.K. Lai, M.D.
Department of Neurosurgery, Prince of Wales
Hospital, Barker St, Randwick, NSW 2031, Australia
e-mail: dvetica@mac.com; Glai7159@gmail.com

W.J. Maixner, M.D.
Department of Neurosurgery,
Royal Children's Hospital, Flemington Road,
Parkville, VIC 3052, Australia
e-mail: wirgy@wirgy.com

tumors that are involved. The authors aim to provide an overview of the surgical management, for both surgeons and clinicians, and, for experienced surgeons, an advance on the debate on the optimal management of cerebellar astrocytomas.

27.2 Preoperative Assessment

CT is often the instrument of initial diagnosis, but it is rarely of use in surgical planning unless bony structures need to be assessed [5, 13, 14].

The mainstay of preoperative planning is MRI. It allows assessment of the location, size, and morphology of the tumor to plan the surgical approach. It can show involvement of surrounding structures (exophytic tumors) or invasion of the brainstem which have prognostic implications. It has the added benefit of being able to assess the viability of performing a third ventriculostomy if this is planned as the initial procedure.

MRI of the brain and spine, with and without contrast, should be performed. T1-weighted images demonstrate a mass that is hypo- or isointense to the surrounding brain; on T2-weighted images, the lesion is often hyperintense, particularly if there is a cystic component. Gadolinium may show a mural nodule in a cyst and enhancement of the cyst wall. MRI of the whole spine will exclude spinal drop metastases that may suggest an alternative pathology and assist in staging.

Preoperative blood test should include routine full blood count, electrolytes, coagulation studies, and a crossmatch. Crossmatch is preferable to a simple group and hold as torrential bleeding is a potential complication of surgery.

27.3 Anesthetic Considerations

A detailed discussion of neuroanesthesia is beyond the scope of this chapter. However, all patients require a full neuroanesthetic, nasotracheal intubation, arterial and central lines to monitor BP and venous filling, and an indwelling catheter to assist aggressive monitoring.

There are some specific considerations for these cases.

- Positioning of the patients can require extreme positions for the neck. A reinforced endotracheal tube may be needed to prevent kinking. Further, venous hypertension caused by such positions may add to the risk of bleed with venous sinus injuries.
- Venous sinus injuries can cause air embolism or torrential bleeding. A precordial Doppler ultrasound is useful in detecting the former. Transfusable blood ready and available is important for the latter.
- Choose an inhalational anesthetic agent when using neuromonitoring, as this may avoid depressing potentially useful recordings.
- Manipulation of the brainstem and surrounding structures may cause bradycardia or even asystole. Communication between the surgical and anesthetic team is important: the surgeon should let the anesthetist know when he is approaching the brainstem; the anesthetist in turn should notify the surgeon immediately of any variations in heart rate or blood pressure.

Preoperative medications include corticosteroids, which are given as a loading dose of 0.5–1 mg/kg to continue postoperatively at a maximum dose of 4 mg q6 hours (for adult-sized pediatric patients). This can be weaned over 2–4 weeks. Mannitol can be considered in extreme conditions. There is no indication for prophylactic anticonvulsants for posterior fossa pathology.

27.4 The Approach to Surgery

The aims of surgery are:

- To manage any associated hydrocephalus
- To obtain tissue diagnosis
- To treat the mass effect of the tumor
- To achieve maximal safe debulking of the tumor

All four may be achieved from a single surgical procedure. The location and size of the tumor determine the surgical approach. Involvement of surrounding structures, including invasion of the brainstem, have implications for the extent of surgical resection possible and hence the long-term prognosis.

In planning surgery, the complications specific to these procedures should be considered to minimize the risks to the patient. These include the risks of the different positions, the risks of air embolus and bleeding from injury to venous sinuses, and the risks of injury to important local structures.

27.5 Management of Hydrocephalus

Hydrocephalus is commonly occurring in up to 93 % of patients with a posterior fossa astrocytoma that have hydrocephalus at presentation [15]. It is often symptomatic (79 % of patients in Due-Tønnessen and Helseth's retrospective series of 87 pediatric patients).

The acuity of the hydrocephalus may establish the first step in treatment. A child with grossly symptomatic hydrocephalus – headaches, gross papilledema, vomiting, etc. – may require urgent treatment of the hydrocephalus prior to considering the tumor mass. Options include a third ventriculostomy, with or without a reservoir, or a ventriculoperitoneal shunt. The former is preferable in a setting where the histological diagnosis of the tumor has not yet been established. On rare occasions the patient may present in extremis directly due to tumor mass, in which case urgent surgery for diagnosis and to prevent death may be required.

More usually the hydrocephalus and the tumor are significant but not immediately life-threatening. This allows for preoperative planning. Minor symptoms may improve with steroids, to continue until after surgery has been performed. Hydrocephalus resolves without treatment in up to 60 % of patients after the posterior fossa tumor has been removed [9]. In these cases, a temporizing EVD placed prior to surgery via Kocher's point or at surgery via a Dandy/Frasier approach allows CSF decompression initially. Overdrainage should be avoided to prevent the risk of upward herniation before the posterior fossa is opened.

Hydrocephalus can be cured in up to 90 % of patients with primary tumor surgery or third ventriculostomy [9]. In resistant cases, a ventriculoperitoneal shunt may be required. Postoperatively,

persistent hydrocephalus may occur. Postoperative hydrocephalus can be prevented by avoiding entry into the normal CSF pathways such as the fourth ventricle or cisterna magna. This is easier in the case of JPA as the tumors are more often intra-axial and do not necessarily extend into the CSF pathways. In cases where there is likely to be a breach of the normal CSF pathways, Pencalet et al. [15] recommend conducting a third ventriculostomy prior to definitive tumor surgery.

Recurrent or new onset hydrocephalus more than 30 days after surgery may herald tumor recurrence and should be investigated as such [9].

27.6 Surgical Approaches

There are two main surgical approaches:

1. Midline suboccipital craniotomy which is suitable for most midline and large hemispheric lesions
2. Retromastoid approach for more laterally placed tumors

27.6.1 Midline Suboccipital Craniotomy

This is suitable for the vast majority of cerebellar astrocytomas but is particularly good for midline and large hemispheric lesions. A good lateral extent of resection can be obtained.

27.6.1.1 Positioning

The patient can be positioned in either a prone or a seated position for the retrosigmoid approach:

- (a) *The prone position* is adequate for nearly all midline approaches. It can be used to adequately expose midline or hemispheric lesions that do not extend deep to invade the peduncles and brainstem. For more lateral lesions a modified unilateral approach using a hockey stick incision can aid exposure.

In the prone position, the neck must be in a posturally neutral position with the head flexed at the craniocervical junction to flatten out the horizontal portion of the occipital bone. This also opens out the dura between

the foramen magnum and C1. Three-pin fixation is required to adequately achieve this position. Over-flexing the craniocervical junction can compress the endotracheal tube and can obstruct venous outflow, so the degree of flexion must be checked with the anesthetist. The head of the operating table can then be elevated to allow adequate venous drainage.

This position has the advantage of being ergonomic for the surgeon, with the microscope directly above the opening. As long as the neck is not too flexed, a balance between venous drainage and venous outflow can be achieved, minimizing the risk of air embolism and blood loss.

The main disadvantage of the prone position is the pooling of blood and CSF into the wound. Also, retraction of the cerebellar tissue is more likely to be required for adequate exposure.

- (b) *The sitting position* has gone somewhat out of vogue, but it is useful for midline and superiorly placed lesions. It allows natural drainage of blood and CSF away from the surgical site and allows natural retraction of the cerebellum from the tentorium. Care should be taken that the small superior cerebellar veins do not tear and cause bleeding.

This position needs careful anesthetic planning. The head is well above the heart and the ensuing negative pressure in the venous sinuses increases the risk of air embolism. Strict precordial monitoring is required. Some of the negative venous pressure can be obviated by the use of a mast suit, compressing distal veins and increasing venous return to the heart.

Another potential complication includes slumping of the brain causing traction on mid-brain structures (Goodrich p. 276). The elevation of the head may also decrease cerebral perfusion pressure adding risk in situations where blood loss occurs.

Ergonomically the surgeon must have the operating microscope horizontally and his arms elevated, a tiring position for long procedures, and one that requires longer arms.

27.6.1.2 Exposure

Incisions should be marked prior to opening so that adequate draping can be done after the skin prep. If an EVD is used, a linear incision over Frazier's point (6 cm above and 4 cm lateral to the inion) should be marked out along with the main midline incision which extends from the greater occipital protuberance (inion) to the level of the C2 spinous process. The fascia deep to the skin is opened in the same line, except at its superior extent just below the inion, where a Y-shaped incision allows a more airtight closure to prevent CSF leak.

A deeper dissection should follow the avascular midline. This can be done with sharp dissection or cautery. The final exposure should provide a wide view of the squamous occipital bone down to the arch of C1. As wide a periosteal dissection as possible should be performed for large lesions. This can be modified for smaller lesions or more lateral lesions.

The occipital bone can be exposed using cautery to prevent blood loss from the bone. Cautery should be used with care between the foramen magnum and the C1 arch. It is useful for clearing muscles from the occiput, but one should be cautious in infants in whom cautery can penetrate thin bone. The foramen magnum and C1 arch should be exposed using sharp and blunt dissection, with dissecting scissors preferred over cautery as the dura can easily be breached, and the C1 arch may be incomplete or cartilaginous in the young. It is also best to avoid dissection of muscles off the C2 spinous process, where there are significant muscular attachments of the axial cervical spine to the skull. This minimizes post-operative pain. Bleeding can occur laterally, at the edge of the foramen magnum, or on the C1 arch. This indicates that one is approaching the vertebral artery laterally and no further dissection is needed. Bleeding can be controlled with Surgicel or Gelfoam.

27.6.1.3 Occipital Craniotomy

The superior and lateral borders can be cut using a match-head bur and tracing the outline of the craniotomy or by placing two bur holes at the superolateral edges of the craniotomy and finishing with the cutting blade. If the latter is done, the

dura should be separated from the skull using a Penfield no. 3 or a Watson-Cheyne dissector. The authors prefer to use a matchstick bur to cut the whole bone flap, as there is less risk of entering the transverse sinus or torcula, but this has the disadvantage of more bone loss. At the inferolateral margins, if there is still bone, a small Kerrison rongeur can be used to remove the last connections.

The occiput can be hinged up a little on the inferior edge, stripping the dura from the bone using a round periosteal elevator. The inferior edge of the occiput at the foramen magnum is tightly adherent to the underlying periosteum but can be dissected off using a curette, a periosteal elevator, and/or sharp dissection with a 15-blade knife. The bone can be replaced and secured at the end of a case. In general, a craniotomy is preferable to a craniectomy [15], and its replacement assists in the prevention of CSF leaks.

There are some controversy as to whether removing the C1 arch is of benefit. The arch is not important for spinal stability, so it can be sacrificed. It is probably not required if the tumor does not extend beyond the foramen magnum.

27.6.1.4 Dural Opening

A Y-shaped incision starting laterally over the hemispheres allows safe approach to the dural sinuses. These are always encountered in the midline (cerebellar or occipital sinus).

Failure to control the opening can result in air embolism or significant blood loss. Opening bilaterally toward the midline allows judicious application of Ligaclips across the sinus, occluding the sinus and allowing the dura to be opened fully. Similar care should be taken as the durotomy crosses the foramen magnum as a circular sinus is present in a significant number of patients. Diathermy to control dural bleeding should be avoided as this causes shrinkage of the dura, which is then hard to close later.

27.6.1.5 Tumor Resection

At this point, the operating microscope is introduced. A stereotaxy can be used to help locate the

tumor, though this is rarely necessary with large tumors.

These are intra-axial tumors and may not present to the surface. The corticectomy should be planned accordingly. For vermian tumors, a vertical vermian split can be used, with care not to extend the corticectomy too superiorly. If hemispheric, a horizontal approach following the natural line of the folia is recommended to minimize neurological damage. If there is a large cystic component, fluid can be drained using a brain needle prior to conducting the corticectomy to provide some decompression.

Once the cortex is opened, the tumor is often readily identified, being a pinkish gray or brown that contrasts with the normal white matter of the cerebellum. Often a plane can be established between the tumor and brain. Tumor removal can be performed using bipolar cautery and suction or the ultrasonic aspirator or laser. Bipolar cautery should be used with care when near the brainstem. Sometimes a cyst wall can be gently teased off surrounding the brain [17]. Controversy exists as to whether the cyst wall should be removed [15, 17]. Resection should continue as far as is safely possible.

If a good plane is seen around the tumor, gross total resection can be achieved. Factors which limit this include loss of a good plane between normal and abnormal tissue, invasion into the brainstem, and leptomeningeal spread [3, 16].

Complete resection may be limited by invasion into the brainstem or gross leptomeningeal spread [3, 16]. Intraoperative MRI, where available, may be helpful in demonstrating additional resectable tissue to achieve maximal safe resection.

27.6.1.6 Closure

Hemostasis can be achieved using irrigation, Surgicel, Gelfoam, and cautery. Hemostatic agents such as Surgicel and Gelfoam can cause artifacts in the postoperative MRI and should be avoided if possible. Cautery should be used cautiously near the brainstem. Patience is sometimes a virtue using irrigation.

The rest of the closure should be done carefully and thoroughly to minimize the risk of CSF leak.

The dural should be closed in a watertight fashion using muscle or fascia if needed. The bone flap is best replaced and can be held in place with a rigid fixation system such as plates and screws or CranioFix. Muscle, fascial, and skin closure should be done carefully and meticulously.

27.6.2 Retrosigmoid craniotomy

This is useful for lateral hemispheric lesions with extension into the cerebellopontine angle and for tumors of the brainstem. It is not as commonly needed but can be useful in resecting exophytic brainstem tumors.

27.6.2.1 Positioning

Again there are two main positions: either a lateral position or a supine position.

- (a) *The lateral position* provides good access and view of the cerebellopontine angle. The patient is positioned with the side of access up. The head is rotated away to allow a more vertical projection of the petrous temporal bone. It is then laterally flexed away from the ipsilateral shoulder to allow for a degree of head elevation without loss of a direct line of vision. The shoulder should be retracted inferiorly away from the neck to allow better access, but with care not to pull too hard to avoid inadvertent brachial plexus injury.

The advantage of the lateral position is a good line of sight into the CP angle which can be adjusted with minimal bed rotation during the procedure if needed. There is little venous compression, minimizing raised ICP and bleeding.

The main disadvantage is the risk of pressure areas which must be cushioned, especially under the axilla and the hip.

- (b) *The supine position* is the most familiar with surgeons. Access to the retrosigmoid incision is much easier in children whose necks rotate with ease. A roll under the shoulder aids rotation and is useful to prevent extreme rotation of the neck. There are fewer risks of pressure areas, but more neck rotation is required which may affect venous drainage and

increase the ICP [1]. It may also have implications with endotracheal tube obstruction.

27.6.2.2 Opening

The incision is planned according to the location of the transverse and sigmoid sinuses. Surface anatomy can be used to trace both sinuses from the greater occipital protuberance to horizontally to a point directly above the mastoid for the transverse sinus and from the mastoid up to join this line at a right angle. A stereotaxy can provide these landmarks.

The incision can be linear, a lazy S shape, or C-shaped. The choice depends on the inferior extension and whether modification to a far-lateral approach is needed. It must allow enough exposure such that the dura over the transverse and sigmoid sinus is exposed.

Dissection with diathermy can proceed directly down to the skull and can be used to dissect the muscle and periosteum off as well. There is often an emissary vein at the transverse sigmoid junction which should be controlled with bone wax.

27.6.2.3 Craniotomy

The aim is to expose the transverse and sigmoid sinuses, thus allowing access to the lateral extent of the cerebellar hemisphere. The bone is quite thick as one approaches the mastoid. A disk of bone can be removed by tracing a thin bur line with a match-head drill, with care taken over the sinuses. The sinuses should be exposed by the craniotomy as important guiding landmarks.

27.6.2.4 Durotomy

Once open, the dura can be opened in a T or X shape with the long arm of the T extending up to the transverse sigmoid junction. One of the arms should then extend down toward the mastoid stopping just short of the sigmoid sinus.

27.6.2.5 Tumor Resection

Once the dura is opened, patient is drained of CSF to allow for some natural brain relaxation and the ventral aspect of the cerebellar hemisphere can be exposed and traced medially. Retraction should be kept to a minimum to avoid

traction on nerves which may be tethered by tumor and to prevent tearing of small veins entering into the superior petrosal sinus superiorly.

Exophytic tumors will envelope and obscure important anatomical structures. If the intention is to explore the brainstem, important structures should be identified: cranial nerves VII, V, and VI superiorly and cranial nerves IX, X, and XII; the vertebral artery with its branches (anterior spinal artery); and the posterior inferior cerebellar artery inferiorly. Damage to any of these structures can result in significant morbidity, particularly in the case of the lower cranial nerves.

Complete tumor resection may not be achievable if these are obscured or if there is significant invasion of the brainstem.

27.6.2.6 Closure

Again this involves careful hemostasis and then a tight dural closure. The latter can be difficult to achieve if the dura has dried out or if it has been cauterized at any time. If this is an issue, galea can be harvested as dural replacement and sewn in place. The disk of bone can be replaced and secured. This minimizes headaches caused by muscle traction on the dura. Careful, multilayered muscular and skin closure is also required to help prevent CSF leaks.

27.7 Complications

Common complications of surgery include the formation of a pseudomeningocele deep in the wound which may progress to a CSF wound leak; meningitis; aggravation of hydrocephalus; cerebellar mutism; cerebellar symptoms of truncal ataxia, or peripheral ataxia and nystagmus depending on the location of the tumor; and rarely disabling symptoms such as bulbar dysfunction from cranial nerve or brainstem injury. Dirven et al. [8] report an overall surgical morbidity rate of 15 %.

As noted above, it is easier to prevent problems than to treat them, so the surgical technique is important in minimizing complications. Table 27.1 delineates risk factors for and methods to minimize complications when operating on posterior fossa tumors.

Cerebellar mutism is a disturbing complication, more commonly seen in younger patients, and with larger midline tumors that extend into the fourth ventricle. Originally reported in 1985 by Rekat et al. and Yonemasu, cerebellar mutism may occur in as many as 30 % of patients after resection of a cerebellar tumor [4, 11, 18, 21]. It is thought to be less common in patients with cerebellar pilocytic astrocytomas. The symptoms may last for weeks to months with a gradual return of speech that is often dysarthric as it improves. Persistent cognitive and verbal deficits are common [11, 19].

Longer-term consequences including learning difficulties, motor planning, as well as ongoing cerebellar motor symptoms may be due to direct cerebellar injury. Patients with preoperative deficits are more likely to have postoperative deficits. These may affect a child's learning abilities, and early intervention should be organized to maximize learning.

Death is, thankfully, rare with modern techniques and is reported in <1–5 % of patients in most series (Dirven, Villarejo, DiRocco). In Villarejo's series, perioperative mortality was 17.5 % prior to 1974 and 3.2 % after 1974. DiRocco notes that in more modern series, mortality is approaching zero.

27.8 Surgical Outcomes

The most important prognostic factor in the management of cerebellar astrocytomas is the extent of surgical resection [2, 20]. Complete resection for juvenile pilocytic astrocytoma affords a nearly 100 % long-term survival rate compared with the overall 10 year survival rate of 65. Gross total resection, as judged by an immediate postoperative MRI, occurs in 60–70 % of cases [2, 8, 12]. Location is a good determinant of how easily a GTR may be achieved, with Akay's series describing a higher percentage in patients with single hemispheric lesions. The extent of resection is often overestimated by the operating surgeon [8]! This is reflected in Desai's series in which the surgeon reported an 80 % incidence of GTR, while this was seen in only 70 % of postoperative scans [6].

Table 27.1 Common complications and techniques to avoid them

Complication	Predisposing factors	Preventive techniques
CSF leak/pseudomeningocele	Hydrocephalus wound infection	Clean cuts to structurally important tissue (fascia, dura) Avoid diathermy to same Complete dural closure using galea graft or substitute if it cannot be achieved primarily Y- or T-shaped incision in fascia just below theinion to assist in a tight closure Careful reconstruction of the normal planes Replacement of the bone flap (craniotomy vs. craniectomy) Minimize dead space in muscular layers Treat hydrocephalus
Blood loss	Higher risk in infants with low blood volume	Appropriate positioning to prevent venous hypertension Use of a Colorado needle in infants and young children Control of hemostasis as bleeding occurs Active control of the venous sinuses (occipital and circular sinuses) at dural opening Judicious use of bipolar and other hemostatic techniques during tumor removal Minimization of cerebellar retraction, use of gravity or otherwise, especially superiorly and superolaterally to the cerebellum
Hydrocephalus	Preoperative hydrocephalus	Avoid opening into CSF spaces if possible (easier with JPAs as they are mostly intra-axial tumor that do not extend into the fourth ventricle) Minimize blood contamination of subarachnoid space/cisterna magna Careful monitoring of signs of hydrocephalus
Neurological deficit/cerebellar mutism	Large tumors Midline tumors	Gentle handling of normal neural tissue Avoid retraction of normal neural tissue Minimize use of diathermy especially near peduncles/brainstem Identify normal structures early

It is not surprising then that factors which limit the resection, such as the size and extent of the tumor, brainstem invasion, leptomeningeal spread or multifocal disease, are associated with

a worse prognosis. Thus, the recurrence rates in patients with a gross total resection are of the order of 2–5 %, while it is 42–45 % in patients with subtotal removal of tumor [8, 12]. In patients

with residual tumor, about half progress, and the rest remain static or regress with time [8]

The histology of the tumor affects prognosis. In Desai's series of cerebellar astrocytomas, 57 % had pilocytic astrocytomas, 35 % had low-grade fibrillary astrocytomas, and 8 % had high-grade astrocytomas. Pilocytic tumors had a much better long-term survival. This has not been confirmed in all series. There is great variability in the biological behavior of the pilocytic subtype in itself. Some authors believe that cystic tumors carry a better prognosis than solid tumors [15]. At present there is still little information explaining the variable behavior of pilocytic tumors, which, while generally benign can occasionally behave in a malignant fashion, may transform later in to malignant tumors [12] or which may regress.

There are few other proven prognostic factors. Age is said to be a factor with children under 5 years or younger having a shorter survival period compared to those aged older than 5 years [10]. This may reflect different tumor biology. It may also reflect the greater dangers for smaller children. In Desai's series, in which five mortalities were recorded, 3/5 children who died postoperatively were infants less than 1 year of age.

27.9 Postoperative Care

The patient should be managed in a pediatric intensive care unit for the first 24–48 h. Where the operation has been long, or if the patient's preoperative condition was serious, extubation can be delayed. Placement of an EVD intraoperatively allows for monitoring of the intracranial pressure during this period. Neurological and other physiological observations should be closely monitored (half hourly) for the first 6 h. Steroids can continue at a higher dose for 24–48 h, but weaning should start as soon as tolerated by the patient.

A postoperative MRI with contrast should be done within 72 h of the operation, preferably within 24 h, to assess the extent of surgical resection. Where there is residual tumor that is surgi-

cally accessible, further resection is a viable option.

The patient should have a careful neurological assessment, as their condition permits, to assess potential deficits.

The CSF circulation can be tested by gradual elevation of the external drain, then clamping, prior to removal. The wound should be checked for the formation of a pseudomeningocele or a frank CSF leak, which may indicate that CSF flow is obstructed. This may need to be addressed further.

Long-term follow-up for tumor recurrence or progression is imperative. In general, postoperative review of the patient is required every 3 months for at least 2 years with a lengthening between reviews over time. In patients with disease absent at 5 years, the period of review can be lengthened still. Close review is required in patients with residual tumor and those with more aggressive pathologies. Reoperation and adjuvant therapies should be considered in patients in whom the tumor recurs.

Conclusion

Cerebellar astrocytomas typically have an excellent prognosis with surgical excision as the first line of treatment. In the era of MRI and pediatric ICU, pediatric patients are typically presenting for elective resection, allowing time to plan surgical approaches that minimize complications. Potential complications, such as cerebellar mutism, can be rare but significant and are made more likely by the extension of the tumor into the brainstem or leptomeningeal spread. The authors suggest that as surgical resection is the key prognostic factor, these lesions should be pursued to the maximum of their margin of safety, irrespective of their pathological grade.

References

1. Akalan N (2009) Intracranial tumours in childhood. In: Practical handbook of neurosurgery, Springer, Berlin, Part 6, pp 1043–1059

2. Akay KM, Izci Y, Baysefer A, Atabey C, Kismet E, Timurkaynak E (2004) Surgical outcomes of cerebellar tumors in children. *Pediatr Neurosurg* 40(5): 220–225
3. Auer RN, Rice GP, Hinton GG, Amacher AL, Gilbert JJ (1981) Cerebellar astrocytoma with benign histology and malignant clinical course. Case report. *J Neurosurg* 54(1):128–132
4. Catsman-Berrevoets CE, van Dongen HR, Mulder PG, Geuze D, Paquier PF, Lequin MH (1999) Tumour type and size are high risk factors for the syndrome of “cerebellar” mutism and subsequent dysarthria. *J Neurol Neurosurg Psychiatry* 67:755–757
5. Chang T, Teng MM, Lirng JF (1993) Posterior cranial fossa tumours in childhood. *Neuroradiology* 35(4): 274–278
6. Desai KI, Nakdarni TD, Muzumdar DP, Goel A (2001) Prognostic factors for cerebellar astrocytoma in children: a study of 102 cases. *Pediatr Neurosurg* 35:311–317
7. DiRocco C Cerebellar (1999) astrocytomas. In: Choux M, DiRocco C, Hockley A, Walker M (eds) *Pediatric neurosurgery*. Churchill Livingstone, London, p 451
8. Dirven CM, Mooij JJ, Molenaar WM (1997) Cerebellar pilocytic astrocytoma: a treatment protocol based upon analysis of 73 cases and a review of the literature. *Childs Nerv Syst* 13(1):17–23
9. Due-Tønnessen BJ, Helseth E (2007) Management of hydrocephalus in children with posterior fossa tumors: role of tumor surgery. *Pediatr Neurosurg* 43:92–96
10. Garcia DM, Latifi HR, Simpson JR, Picker S (1989) Astrocytomas of the cerebellum in children. *J Neurosurg* 71:661–664
11. Gudrunardottir T, Sehested A, Juhler M, Schmiegelow K (2011) Cerebellar mutism: review of the literature. *Childs Nerv Syst* 27(3):355–363
12. Krieger MD, Gonzalez-Gomez I, Levy ML, McComb JG (1997) Recurrence patterns and anaplastic change in a long-term study of pilocytic astrocytomas. *Pediatr Neurosurg* 27(1):1–11
13. Lee YY, Van Tassel P, Bruner JM, Moser RP, Share JC (1989) Juvenile pilocytic astrocytomas: CT and MR characteristics. *AJR Am J Roentgenol* 152(6): 1263–1270
14. Morreale VM, Ebersold MJ, Quast LM, Parisi JE (1997) Cerebellar astrocytoma: experience with 54 cases surgically treated at the Mayo Clinic, Rochester, Minnesota, from 1978 to 1990. *J Neurosurg* 87(2):257–261
15. Pencalet P, Maixner W, Sainte-Rose C, Lellouch-Tubiana A, Cinalli G, Zerah M, Pierre-Kahn A, Hoppe-Hirsch E, Bourgeois M, Renier D (1999) Benign cerebellar astrocytomas in children. *J Neurosurg* 90(2):265–273
16. Pollack IF, Hurtt M, Pang D, Albright AL (1994) Dissemination of low grade intracranial astrocytomas in children. *Cancer* 73:2869–2878
17. Raimondi AJ (1998) *Pediatric neurosurgery. Theoretical principles art of surgical techniques*. Springer, Berlin
18. Rekate HL, Grubb RL, Aram DM, Hahn JF, Ratcheson RA (1985) Muteness of cerebellar origin. *Arch Neurol* 42(7):697–698
19. Riva D (1997) The neuropsychology of the cerebellum. In: Choux M, DiRocco C, Hockley A, Walker M (eds) *Pediatric neurosurgery*. Churchill Livingstone, London, pp 452–453
20. Villarejo F, de Diego JM, de la Riva AG (2008) Prognosis of cerebellar astrocytomas in children. *Childs Nerv Syst* 24(2):203–210
21. Yonemasu Y (1985) Cerebellar mutism and speech disturbance as a complication of posterior fossa surgery in children. 13th Annual Meeting of the Japanese Society for Pediatric Neurosurgery, Tsukuba

Christian H. Rickert

28.1 Pathology

Although gross and microscopic features of central nervous system (CNS) tumors are identical regardless of the age of the patient, the incidence of various specific histological tumor types varies widely in those 18 years or under in contrast to adults. Whereas the most common tumors in adults are high-grade astrocytic tumors, meningiomas, and metastases, in children astrocytic tumors are the most common CNS neoplasms, account for 47.3 % of lesions, and tend to be low grade [1]. At the same time particular entities can be almost exclusively found among children, e.g., pilocytic and pilomyxoid astrocytomas. Another fundamental difference between adult and childhood CNS tumors lies in the site of origin. Whereas the cerebrum is the favored site among adults, the infratentorial compartment including the cerebellum gives rise to between 21.7 and 60.2 % of all primary brain tumors in children aged 15–17 years and 3–5 years, respectively, with an overall rate throughout childhood of 46.7 % [1].

Cerebellar astrocytomas are common tumors in children, accounting for approx. 5–6 % of all gliomas, 20 % of all pediatric CNS tumors, and 30–40 % of the tumors developing within the

posterior cranial fossa [2]. They are predominantly tumors of early life with three-quarters of them occurring in children and adolescents with a main peak incidence between 6 and 9 years of age and a second lower peak in young adulthood, with nearly 90 % being low-grade tumors. Although some series have shown a slight female preponderance, in most larger series the gender ratio is approx. 1:1 [2]. The most common subtype of glioma in childhood is pilocytic astrocytomas, the majority of which are located in the cerebellum (69 %); they can usually be cured by surgery alone and tend not to recur when totally resected [3]. High-grade astrocytic tumors of childhood, on the other hand, are less frequently encountered in the posterior fossa with 13 % of pediatric anaplastic astrocytomas and glioblastomas occurring in the cerebellum [3].

28.1.1 Pilocytic Astrocytoma (WHO Grade I: ICD-O Code 9421/1)

28.1.1.1 Definition

A relatively circumscribed, slowly growing, often cystic astrocytoma occurring in children and young adults histologically characterized by a biphasic pattern with varying proportions of compacted bipolar cells associated with Rosenthal fibers and loose-textured multipolar cells associated with microcysts and eosinophilic granular bodies/hyaline droplets [4].

C.H. Rickert, M.D., Ph.D., FRCPath, FFSc(RCPA)
Department of Neuropathology and Paediatric
Pathology, Vivantes Clinics Berlin,
Landsberger Allee 49, Berlin 10249, Germany
e-mail: christian.rickert@vivantes.de

28.1.1.2 Incidence, Age, Localization, and Sex Distribution

Pilocytic astrocytomas comprise approx. 5–6 % of all gliomas with an incidence of 3.7 per million per year. They are the most common glioma in children in whom the majority (67 %) arises in the cerebellum. Pilocytic astrocytomas most commonly develop without gender predilection in the first two decades of life, comprising 23.5 % of pediatric brain tumors [1]. They are the principal CNS tumor associated with neurofibromatosis NF1 with approx. 15 % of NF1 patients developing a pilocytic astrocytoma [4].

28.1.1.3 Macroscopy

Most pilocytic astrocytomas are soft, gray, and discrete. Intra- or peritumoral cyst formation

is common. Chronic lesion may contain calcium or hemosiderin deposits. Primary diffuse leptomenigeal pilocytic astrocytoma is a rarity [4].

28.1.1.4 Histopathology

Pilocytic astrocytomas are tumors of low to moderate cellularity exhibiting an often biphasic pattern with varying proportions of compacted bipolar cells with Rosenthal fibers and loose-textured multipolar cells with microcysts and eosinophilic granular bodies/hyaline droplets (Fig. 28.1). This classical biphasic pattern is best seen in cerebellar tumors. Rare mitoses, hyperchromatic and pleomorphic nuclei, glomeruloid vascular proliferation, infarct-like necrosis, and infiltration of leptomeninges are compatible with a diagnosis of

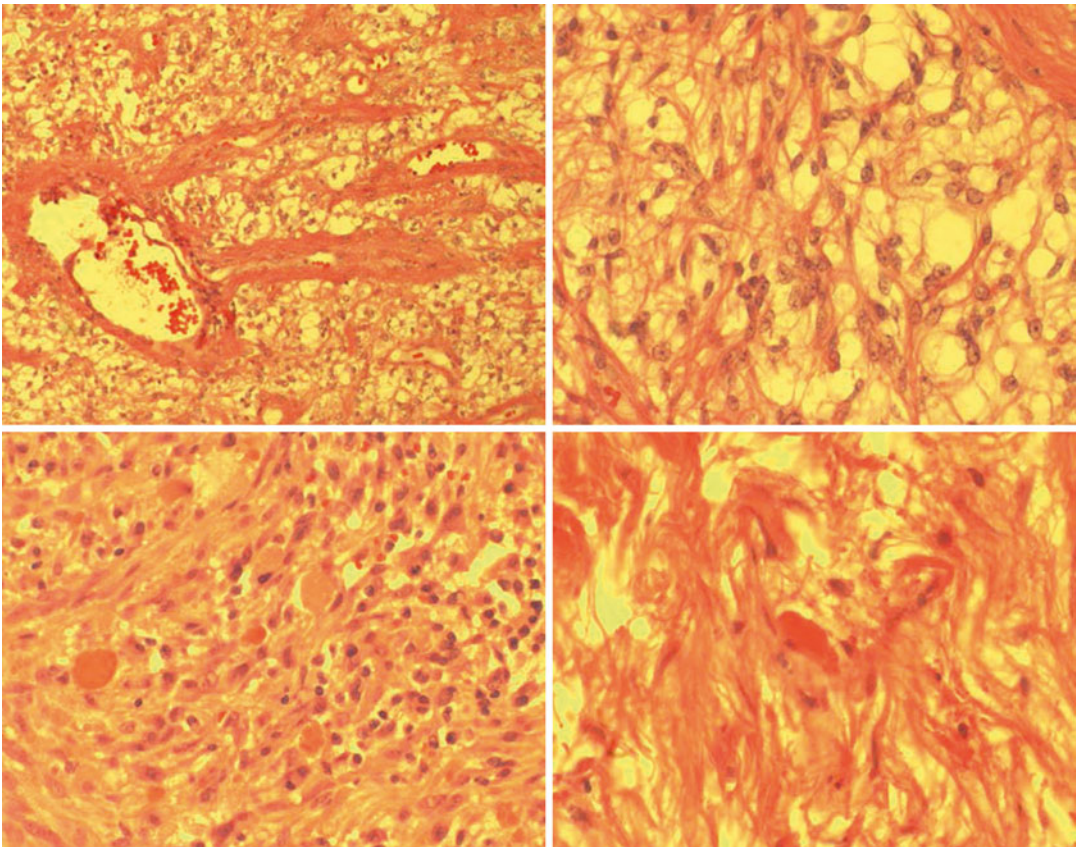


Fig. 28.1 Pilocytic astrocytomas are tumors of low to moderate cellularity exhibiting an often biphasic pattern with varying proportions of compacted bipolar cells (*top left and right*) with Rosenthal fibers (*bottom right*) and

loose-textured multipolar cells with microcysts and eosinophilic granular bodies/hyaline droplets (*bottom left*). Hyalinized vessels and perivascular lymphocytes are prominent features (*top left*)

pilocytic astrocytoma and are not signs of malignancy. Occasionally, oligodendroglioma-like cells may be seen, especially in cerebellar examples. A striking feature in some pilocytic astrocytomas is alignment of cells in prominent regimented palisades (in pattern that used to be called “primitive polar spongioblastoma”).

Compact portions of the tumor yield bipolar piloid cells, long hairlike processes that often extend across a full microscopic field and Rosenthal fibers. Their nuclei are typically elongate and cytologically bland. Due to their high fibril content, these cells are strongly positive for GFAP. Cells derived from microcystic areas possess round to oval cytologically bland nuclei, a small cell body, and relatively short cobweb-like processes which are fibril-poor and only weakly GFAP positive. This growth pattern is typically associated with eosinophilic granular bodies and/or hyaline droplets. Some pilocytic astrocytomas show considerable hyperchromasia and pleomorphism with mitoses encountered in up to 30 % of tumors. In particular cerebellar lesions show a sometimes more diffuse growth pattern reminiscent of diffuse astrocytoma. Hyalinized and glomeruloid vessels and perivascular lymphocytes are prominent features, and necrosis when seen is often infarct-like and non-palisading. The MIB-1/Ki-67 proliferation indices have been found to be in the range of 0–3.9 % with a mean of 1.1 % [5].

Rosenthal fibers are tapered corkscrew-shaped brightly eosinophilic hyaline intracytoplasmic masses and are most common in compact piloid tissue. Although helpful in diagnosis, their presence is not required nor are they exclusive to pilocytic astrocytoma or even indicative of neoplasia as they are also encountered in gangliogliomas and chronic reactive gliosis. They lie within astrocytic processes and are composed of α -B-crystallin but lack GFAP immunoreactivity.

Eosinophilic granular bodies form globular aggregates within astrocytic processes. They are brightly eosinophilic in H&E and PAS positive and show immunoreactivity for α -1-antichymotrypsin and α -1-antitrypsin. Their intracellular localization is usually not discernible in tissue sections. Eosinophilic granular bodies are an important diagnostic feature of several

neoplasms but are in themselves not indicative of neoplasia.

Pilocytic astrocytomas are highly vascular as evidenced by their contrast enhancement. Glomeruloid vasculature may be seen; however, endothelial proliferation (a feature of high-grade astrocytic tumors) is generally not encountered. Such neovascularity often lines cyst walls, thus explaining the narrow band of intense contrast enhancement seen at the circumference of some cysts. Involvement of the subarachnoid space is a common finding, particularly in the cerebellum, and is not indicative of aggressive or malignant behavior nor does it portend subarachnoid dissemination. Surprisingly, otherwise typical pilocytic astrocytomas very occasionally seed the neuraxis, rarely even before the primary tumor is detected; however, even this finding is not a predictor of future aggressive behavior [4].

As a group, pilocytic astrocytomas are remarkable in maintaining their WHO grade I over years and decades with changes being commonly of a regressive rather than anaplastic nature. However, there have been rare examples of pilocytic astrocytomas undergoing malignant transformation [6]. They often feature multiple mitoses per high-power field, endothelial proliferation, and palisading necrosis and warrant the designation of “anaplastic pilocytic astrocytoma” rather than “glioblastoma” as their prognosis is not uniformly grim.

28.1.2 Pilocytic Astrocytoma (WHO Grade II: Provisional ICD-O Code 9425/3)

28.1.2.1 Definition

A piloid neoplasm, closely related to pilocytic astrocytoma that has a prominent mucoid matrix and angiocentric arrangement of monomorphic, bipolar tumor cells typically without Rosenthal fibers or eosinophilic granular bodies/hyaline droplets [4].

Earlier reports refer to tumors with similar features as “infantile” pilocytic astrocytoma, and the occasional phenotypical conversion of a

pilomyxoid astrocytoma to a typical pilocytic astrocytoma supports a common origin for these two tumors [4].

28.1.2.2 Incidence, Age, Localization, and Sex Distribution

The incidence of pilomyxoid astrocytomas is not known. They present in the very young (median 10 months) but can occur in older children without gender predilection [4]. Although mostly located in the hypothalamic/chiasmatic region, they can occur in the cerebellum [7]. Two patients with pilomyxoid astrocytomas and neurofibromatosis 1 (NF1) have been reported [8].

28.1.2.3 Macroscopy

Pilomyxoid astrocytomas present as solid gelatinous masses partly infiltrating parenchyma; thus a clear surgical plane may not be identified [9].

28.1.2.4 Histopathology

Pilomyxoid astrocytomas show a markedly mucoid matrix, monomorphous bipolar cells, and a predominantly angiocentric cell arrangement (Fig. 28.2). The tumor typically has a compact, rather solid architecture while others are more infiltrative. The lesion is composed of relatively monomorphous, medium-sized bipolar cells, the processes of which may radiate from vessels in a pseudorosette fashion; cells may also be aligned along the long axis of vessels. When strictly defined,

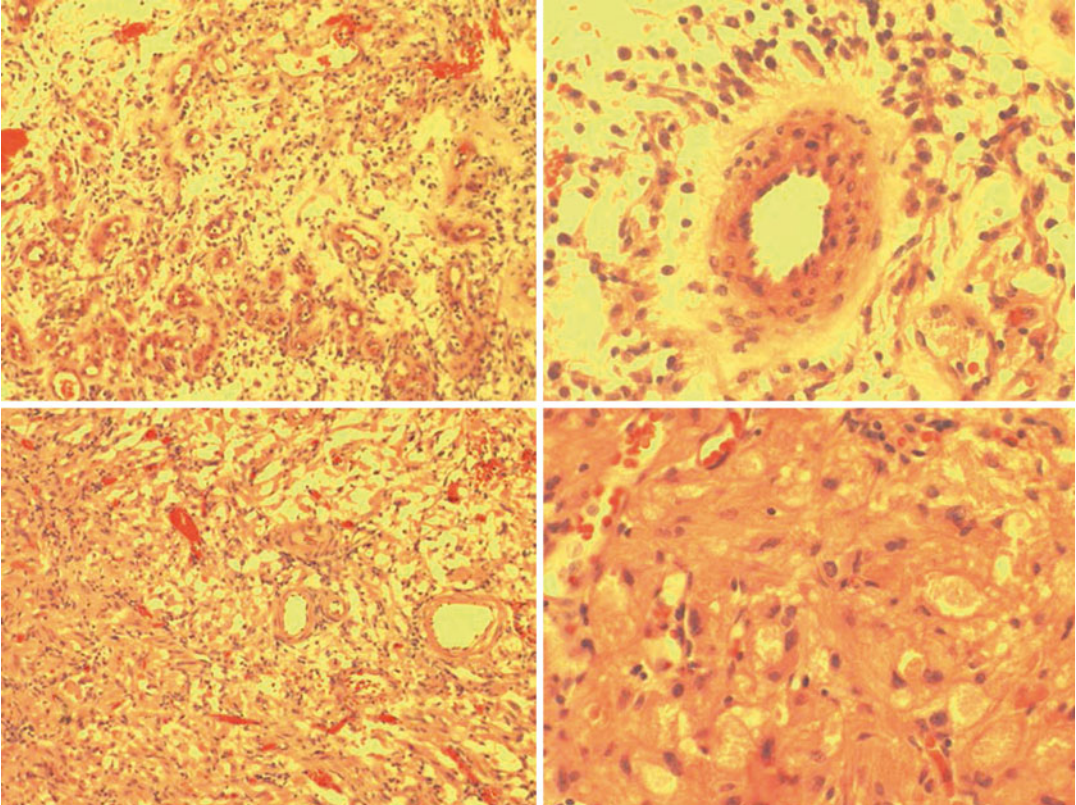


Fig. 28.2 Pilomyxoid astrocytomas show a markedly mucoid matrix (*top left*), monomorphous bipolar cells, and a predominantly angiocentric cell arrangement of cell processes which may radiate from vessels in a pseudorosette fashion (*top right*). Pleomorphic xanthoastrocytomas

are characterized by spindly elements intermingled with mono- or multinucleated giant astrocytes with hyperchromatic and pleomorphic nuclei (*bottom left*) as well as the presence of large xanthomatous cells showing intracellular accumulation of lipid droplets (*bottom right*)

the tumor does not contain Rosenthal fibers or eosinophilic granular bodies/hyaline droplets. Mitotic figures and vascular proliferation may be present, and rare examples may be focally necrotic.

Immunohistologically, tumors are positive for GFAP, S-100 protein, and vimentin and may show expression for synaptophysin but are negative for neurofilament protein and chromogranin. MIB-1/Ki-67 labelling indices were found to vary substantially between 2 and 20 % [4].

28.1.3 Pleomorphic Xanthoastrocytoma (WHO Grade II: ICD-O Code 9424/3)

28.1.3.1 Definition

An astrocytic neoplasm with a relatively favorable prognosis typically encountered in children and young adults; characteristic histological features include pleomorphic and lipidized cells expressing GFAP and often surrounded by a reticulin network as well as eosinophilic granular bodies. Lesions with significant mitotic activity (five or more mitoses per 10 HPF) and/or with areas of necrosis may be designated as “pleomorphic xanthoastrocytoma with anaplastic features” [10].

28.1.3.2 Incidence, Age, Localization, and Sex Distribution

Pleomorphic xanthoastrocytomas account for less than 1 % of all astrocytic neoplasms. They are mainly encountered in the second decade of life and account for 1.9 % of pediatric brain tumors [1], with two-thirds of patients being under 18 years of age without gender predilection [10]. A superficial location involving the meninges and cerebrum is typical for pleomorphic xanthoastrocytomas; however, they can also occur in the cerebellum [11].

28.1.3.3 Macroscopy

Pleomorphic xanthoastrocytomas are mainly superficial tumors attached to the meninges; they are frequently accompanied by a cyst, sometimes forming a mural nodule within the cyst wall [10].

28.1.3.4 Histopathology

The key histopathological features are contained in its designation: “pleomorphic” refers to the variable histological appearance of the tumor in which spindly elements are intermingled with mono- or multinucleated giant astrocytes with hyperchromatic and pleomorphic nuclei with frequent intranuclear inclusions (Fig. 28.2). “Xanthoastrocytoma” refers to the presence of large xanthomatous cells showing intracellular accumulation of lipid droplets. Granular bodies are an almost constant feature as well as focal collections of small lymphocytes and reticulin fibers visualized using silver impregnation surrounding the individual tumor cells.

Immunohistochemically, tumor cells express GFAP and S-100 protein but also show significant neuronal differentiation (synaptophysin, neurofilament protein, MAP2) as well as CD34 expression. The MIB-1/Ki-67 labelling index is usually <1 % [10].

28.1.4 Diffuse Astrocytoma (WHO Grade II: ICD-O Code 9400/3)

28.1.4.1 Definition

A diffusely infiltrating astrocytoma characterized by a high degree of cellular differentiation and slow growth. The tumor has an intrinsic tendency for malignant progression to anaplastic astrocytoma and, ultimately, glioblastoma [12].

28.1.4.2 Incidence, Age, Localization, and Sex Distribution

Diffuse astrocytomas represent 10–15 % of all astrocytic CNS tumors with an incidence rate of 1.4 per million per year. Fibrillary astrocytomas are fairly rare in childhood and make up 5.0 % of CNS tumors encountered in this period [1]. Epidemiological data suggest that the incidence in children has increased slightly over the past three decades. There is a slight predilection for males (1.18:1), and approximately 10 % occur below the age of 20 years. Localization in the cerebellum is distinctly uncommon [12].

28.1.4.3 Macroscopy

Because of their infiltrative nature, diffuse astrocytomas usually show blurring of the gross anatomical boundaries. There is enlargement and distortion but no destruction of the invaded structures. Smaller or larger cysts, granular areas, and zones of firmness or softness may be seen. Extensive microcyst formation may cause a gelatinous appearance. Focal calcification may be present [12].

28.1.4.4 Histopathology

Diffuse astrocytoma is composed of well-differentiated fibrillary or gemistocytic neoplastic astrocytes in a background of a loosely structured, often microcystic, tumor matrix (Fig. 28.3). The cellularity is moderately increased and occasional nuclear atypia is a typical feature. Mitotic activity is generally absent; however, a single mitosis does not yet allow the diagnosis of anaplastic astrocytoma. The presence of necrosis or microvascular proliferation is incompatible with the diagnosis of diffuse astrocytoma. Histological recognition of neoplastic astrocytes depends mainly on nuclear characteristics of atypia: whereas normal astrocyte nuclei are oval to elongate and vesicular, often with a distinct nucleolus, neoplastic astrocytes show enlarged, cigar-shaped, or irregular hyperchromatic nuclei. Reactive astrocytes, on the other hand, present with stainable cytoplasm while normal and tumor astrocytes show no discernible or scant cytoplasm (“naked nuclei”) [12].

28.1.5 Anaplastic Astrocytoma (WHO Grade III: ICD-O Code 9401/3)

28.1.5.1 Definition

A diffusely infiltrating malignant astrocytoma histologically characterized by nuclear atypia increased cellularity and significant proliferative activity. The tumor may arise from diffuse astrocytoma or de novo, i.e., without evidence of a less malignant precursor lesion, and has an inherent tendency to undergo progression to glioblastoma [13].

28.1.5.2 Incidence, Age, Localization, and Sex Distribution

Anaplastic astrocytomas are rare in children and within the cerebellum. They account for 7.2 % of childhood brain tumors [1] and show a male gender predilection with a ratio of between 1.1 and 1.6:1 [13].

28.1.5.3 Macroscopy

Anaplastic astrocytomas have a tendency to infiltrate the surrounding brain without frank tissue destruction which often leads to a marked enlargement of invaded structures such as gyri and basal ganglia. Cysts are uncommon but areas of granularity, opacity, and soft consistency are frequent. On cut surface the higher cellularity of anaplastic astrocytomas produces a discernable tumor mass with a clearer distinction from surrounding structures than in diffuse astrocytomas WHO grade II [13].

28.1.5.4 Histopathology

The principal histological features are those of a diffusely infiltrating astrocytoma with increased cellularity compared with a WHO grade II tumor, distinct nuclear atypia (variations in nuclear size, shape, coarsening and dispersion of chromatin, prominent and multiple nucleoli) and mitotic activity (Fig. 28.3), the latter depending on the size of the sample (one mitosis in stereotactic biopsy sample equals a significant proliferation but not in a large surgical tumor sample; immunohistochemistry for MIB-1/Ki-67 may be helpful which usually ranges between 5 and 10 %). Additional signs of anaplasia are multinucleated cells and abnormal mitoses. By definition, microvascular proliferation (multilayered vessels) and necrosis are absent [13].

28.1.6 Glioblastoma (WHO Grade IV: ICD-O Code 9400/3)

28.1.6.1 Definition

The most malignant neoplasm with predominant astrocytic differentiation; histopathological features include nuclear atypia, cellular pleomorphism, mitotic activity, vascular thrombosis,

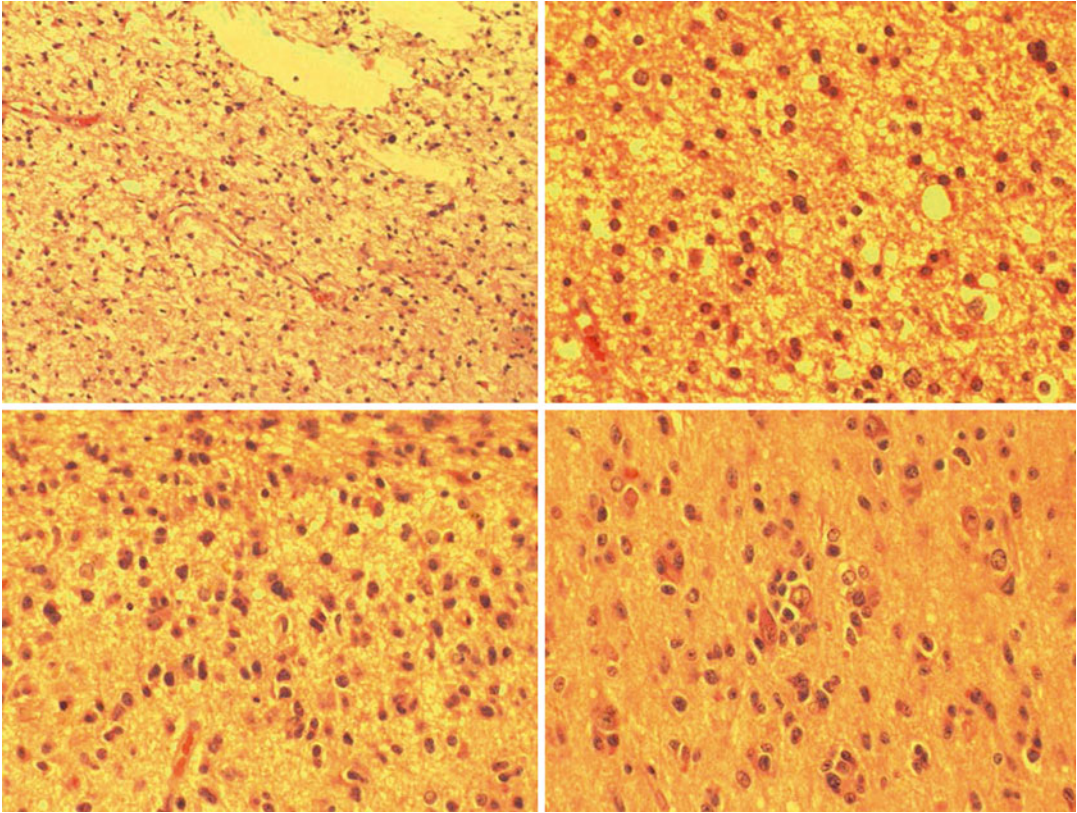


Fig. 28.3 Diffuse astrocytoma is composed of well-differentiated fibrillary or gemistocytic neoplastic astrocytes in a background of a loosely structured, often microcystic tumor matrix (*top left*). The cellularity is moderately increased and occasional nuclear atypia is a typical feature whereas mitotic activity is generally absent (*top right*). In contrast, anaplastic astrocytoma is a diffusely infiltrating lesion with increased cellularity

compared with a WHO grade II tumor, distinct nuclear atypia (variations in nuclear size, shape, coarsening and dispersion of chromatin, prominent and multiple nucleoli) and mitotic activity whereas microvascular proliferation and necrosis are absent (*bottom left*). In the cortex, perineuronal satellitosis (tumor cells surrounding cortical nerve cells) is a common feature (*bottom right*)

microvascular proliferation, and necrosis. Most glioblastomas manifest rapidly *de novo*, without recognizable precursor lesions (primary glioblastoma). Secondary glioblastomas develop slowly from diffuse astrocytoma or anaplastic astrocytoma. Due to their invasive nature, glioblastomas cannot be completely resected. The term “glioblastoma” is used synonymously with “glioblastoma multiforme” [14].

28.1.6.2 Incidence, Age, Localization, and Sex Distribution

Glioblastoma may manifest at any age but is the most frequent CNS tumor in adults, accounting for 12–15 % of all intracranial

neoplasms and 60–75 % of astrocytic tumors with an incidence of 30–40 new cases per million per year. The majority (>90 %) develops very rapidly with a short clinical history (usually <3 months): primary or *de novo* glioblastomas, whereas secondary glioblastomas develop through progression from diffuse (WHO grade II) or anaplastic (WHO grade III) astrocytomas. Glioblastomas are relatively rare in children with 1 % of glioblastomas encountered in patients under the age of 20 years. They account for 7.2 % of childhood brain tumors and are rarely encountered in the cerebellum [1]. The male to female ratio is about 1.26–1.28 [14].

28.1.6.3 Macroscopy

Despite the short duration of symptoms in many cases of glioblastoma, the tumors are often surprisingly large. The lesion is usually unilateral but bilateral symmetrical extension is seen supratentorially due to growth along myelinated structures like the corpus callosum (“butterfly glioma”). Glioblastomas are diffuse and poorly delineated with the cut surface showing a variable color with peripheral grayish tumor masses and central areas of yellowish and red from necrosis, myelin breakdown, and hemorrhage. The central necrosis may occupy as much as 80 % of the total tumor mass and is typically stippled with red and brown foci of recent and remote bleeding; extensive hemorrhages may occur and evoke stroke-like symptoms. Macroscopic cysts contain a turbid fluid

and represent liquefied necrotic tissue. Most glioblastomas have their epicenter in the white matter. Multifocal glioblastomas occur in approximately 2.4 % of cases; penetration of the subarachnoid space, dura, venous sinus, or bone is exceptional [14].

28.1.6.4 Histopathology

Glioblastoma is a malignant cellular glioma composed of poorly differentiated, often pleomorphic astrocytic tumor cells with marked nuclear atypia and brisk mitotic activity (Fig. 28.4). Prominent microvascular proliferation (multilayered vessels) and necrosis are essential diagnostic features. Necroses often take the shape of multiple band-like or serpiginous foci surrounded by radially oriented and densely packed tumor cells in a pseudopalisading pattern.

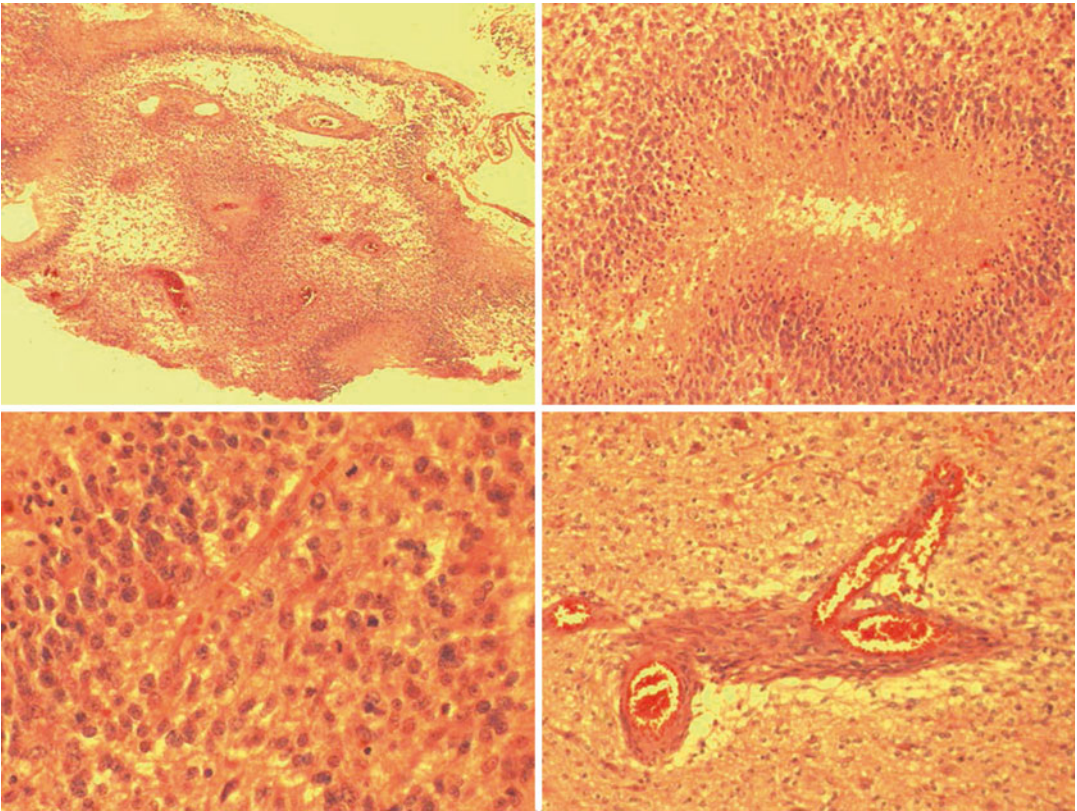


Fig. 28.4 Glioblastoma is composed of poorly differentiated, often pleomorphic astrocytic, tumor cells with marked nuclear atypia and brisk mitotic activity (*bottom left*). Prominent microvascular proliferations/multilayered vessels (*bottom*

right) and/or necrosis are essential diagnostic features. Necroses often take the shape of multiple band-like or serpiginous foci surrounded by radially oriented and densely packed tumor cells in a pseudopalisading pattern (*top left and right*)

As the term “glioblastoma multiforme” implies, the histopathology of this tumor is extremely variable. While some tumors show a high degree of cellular and nuclear pleomorphism with multinucleated giant cells, others are highly cellular but rather monotonous. The regional heterogeneity of glioblastoma is remarkable and poses challenges to the diagnosis of specimens obtained by stereotactic needle biopsies.

The diagnosis of glioblastoma is typically based on the tissue pattern rather than the identification of certain cell types. The distribution of the diagnostic key elements (highly anaplastic glial cells, mitotic activity, vascular proliferation and/or necrosis) is variable, but large necrotic areas usually occupy the tumor center, while viable tumor cells tend to accumulate in the periphery. The circumferential region of high cellularity and abnormal vessels corresponds to the contrast-enhancing ring seen radiologically. Occasionally, glioblastomas contain foci of glandular epithelial structures which usually can unequivocally be established as being astrocytic in nature. Cellular pleomorphism also includes formation of small undifferentiated as well as lipidized, granular, and large multinucleated giant cells. The latter are often considered a hallmark of glioblastoma; however, they are not an obligatory feature, are not associated with a more malignant clinical course, and are generally regarded as a type of regressive change. If they dominate, a designation of “giant cell glioblastoma” is justified. In addition to necrosis, the presence of microvascular proliferations is a histopathological hallmark of glioblastoma. They typically appear as “glomeruloid tufts” which are most commonly located in the vicinity of necrosis and appear directionally oriented to it. Microvascular proliferations consist of multilayered, mitotically active endothelial cells together with smooth muscle cells and pericytes. Proliferative activity is usually prominent with detectable and frequently atypical mitoses in nearly every high-power field. The growth fraction shows great regional variation with mean MIB-1/Ki-67 values of 15–20 % [14].

28.2 Prognostic Value of Histopathological, Immunohistochemical, Cytogenetic, and Molecular Genetic Features Among Astrocytic Tumors of Childhood

A number of studies have been performed into the predictive prognostic value of morphological features among tumors in general and pediatric CNS neoplasms in particular in order to be able to predict the clinical course, stratify the therapy regimen, or avoid potentially fruitless and deleterious interventions. Not surprisingly, these have yielded wildly diverse and sometimes contradictory results. A plethora of statistically significant histopathological, immunohistochemical, cytogenetic, and molecular genetic parameters has been put forward (Table 28.1), none of which are currently applied in a clinical setting. It comes as little surprise that extent of tumor resection, patient age, and WHO grade still feature most prominently in predicting the clinical course and prognosis of children affected by astrocytic CNS lesions. Significant results are listed in Table 28.1. For a more detailed review of this topic, the interested reader may find these reviews rewarding [15, 16].

28.2.1 General

A study of 30 pediatric astrocytic tumors of various histologies found ploidy to be a statistically significant predictor of survival independent of tumor grade, age, gender, and extent of resection [17]. DNA diploidy was demonstrated in 21 patients and aneuploidy in 9 patients, and of the patients with diploid tumors, 81 % survived compared to only 33 % among patients with aneuploid tumors [17]. Another investigation of 43 astrocytic lesions of different grades evaluated the correlation between outcome and proliferative potential as measured by the bromodeoxyuridine (BrdU) labelling index. A high BrdU labelling index regardless of tumor grade highly correlated with short survival, whereas the association between malignant histology and short

Table 28.1 Summary of statistically significant prognostic histopathological, immunohistochemical, cytogenetic, and molecular genetic factors with their clinical relevance in pediatric astrocytic tumors

Tumor entity				
Source	Feature	Prognostic relevance	<i>p</i>	<i>N</i>
<i>General</i>				
[18]	High BrdU labelling index	Worse OS	0.0001	43
[17]	Aneuploidy	Worse OS	<0.0011	30
<i>Low-grade astrocytomas</i>				
[18]	Tumor grade (low vs high grade)	Worse OS	0.019	43
[19]	Tumor grade (pilocytic vs fibrillary)	Better 5-year OS	<0.001	132
		Better 10-year OS	<0.001	132
		Better 20-year OS	<0.001	132
[23]	MIB-1 proliferation index >0 %	Worse 5-year CSS	0.005	35
		Worse 5-year PFS	0.006	35
[20]	Tumor grade (pilocytic vs fibrillary)	Better 5-year PFS	<0.001	29
		Better 5-year OS	<0.001	29
<i>Pilocytic astrocytomas</i>				
[25]	Mixed pattern/additional non-pilocytic glial component	Worse OS	0.008	78
[9]	Monomorphous pilomyxoid features	Worse 1-year PFS	0.04	31
		Worse 2-year OS	0.001	31
[28]	MIB-1 proliferation index >2 %	Worse 5-year PFS	0.035	118
[7]	Monomorphous pilomyxoid features	Worse 5-year PFS	ND	78
		Worse 5-year OS	ND	78
<i>Pleomorphic xanthoastrocytomas</i>				
No significant data				
<i>Fibrillary astrocytomas</i>				
[24]	MIB-1 proliferation index >11 %	Worse OS	<0.0001	34
<i>High-grade astrocytic tumors</i>				
[40]	High immunohistochemical expression of bFGF	Shorter median PFS	0.006	27
		Shorter median OS	0.03	27
[35]	Immunohistochemical p53 overexpression	Shorter median PFS	0.019	29
		Shorter median OS	0.013	29
	TP53 mutations	Worse median PFS	0.04	29
[39]	PTEN mutations	Decreased OS	0.006	39
		Worse OS	0.004	17
[36]	MIB-1 proliferation index >25 %	Worse OS	<0.001	33
[29]	Topoisomerase II alpha expression index >12 %	Worse 5-year PFS	0.011	17
		Worse OS	0.004	17
[38]	High immunohistochemical expression of p53	Worse 5-year PFS	<0.001	115
		Worse 5-year OS	<0.001	115
	Overexpression and mutation of p53	Worse 5-year PFS	<0.001	88
		Worse 5-year OS	<0.001	88
[37]	MIB-1 proliferation index >36 %	Worse 5-year PFS	0.003	98
<i>Anaplastic astrocytomas</i>				
[24]	MIB-1 proliferation index >11 %	Worse OS	<0.001	33
[36]	Gain of chromosome 1q	Worse OS	<0.05	10
[37]	MIB-1 proliferation index	Worse 5-year PFS	0.02	98
<i>Glioblastomas</i>				
[36]	Tumor grade (vs anaplastic astrocytoma)	Worse OS	<0.05	23
[37]	MIB-1 proliferation index	Worse 5-year PFS	0.046	98

ND no data available, OS overall survival, PFS progression-free survival

survival was weaker but still significant, indicating that BrdU labelling index may be a significant predictor of outcome in children with astrocytomas [18].

28.2.2 Low-Grade Astrocytic Tumors

A large cohort of cerebellar low-grade astrocytomas consisting of 105 pilocytic astrocytomas and 27 diffuse astrocytomas revealed that the separation into pilocytic and diffuse histological type was the most significant prognostic factor influencing survival: the 5-, 10-, and 20-year survival rates were 85, 81, and 79 %, respectively, for pilocytic and 7 % each for diffuse astrocytomas [19]. Whereas several additional studies also found better survival rates in children with pilocytic compared to diffuse astrocytomas, one of them highly significantly with children with WHO grade I tumors having a superior progression-free and overall survival than those with grade II tumors [20], histological subclassification of low-grade cerebellar astrocytomas in children was found by other authors to be insufficient for predicting prognosis and biological behavior as both WHO tumor grades I and II showed similar survival rates [21, 22]. Furthermore, among 35 pediatric low-grade astrocytomas, patients with MIB-1/Ki-67-negative tumors, i.e., showing no proliferation, had a 5-year cause-specific survival and progression-free survival of 100 % which declined significantly to 84 and 67 %, respectively, for patients with tumors demonstrating any degree of Ki-67 positivity [23]. Similar results were published from a survey of 34 children with diffuse fibrillary astrocytomas which showed that an MIB-1 proliferation index of <11 % was associated with significantly better overall survival compared with those with MIB-1 >11 % [24].

Cytogenetic analysis was performed on 29 pediatric low-grade astrocytomas and revealed one or more chromosomal abnormalities in eight tumors while normal karyotypes were observed in 21 cases [20]. There was a trend for

a better clinical course for tumors with chromosomal changes with 5-year progression-free survivals estimated at 87.5 % for children with abnormal vs 43 % with normal cytogenetics and with 5-year overall survival of 83 % for those with abnormal vs 78 % with normal cytogenetics [20].

28.2.3 Pilocytic and Pilomyxoid Astrocytomas

Several investigations on pilocytic astrocytomas have encountered pilomyxoid features or a mixed pattern with additional non-pilocytic glial components which were found to convey an unfavorable clinical course. One study of 31 cases concluded that pilocytic astrocytomas with monomorphous pilomyxoid features had a less favorable outcome with higher rates of recurrence and CSF dissemination than cases with classical histological features, resulting in 1-year progression-free survival of 38.7 % (vs 69.2 %) and 2-year overall survival of 38.7 % (vs 100 %), thus qualifying as a more aggressive variant and separate entity [9]; this fact was appreciated by including the pilomyxoid astrocytoma as a separate entity in the latest WHO classification of CNS tumors [4]. A study on 58 classic pilocytic astrocytomas and 20 pilomyxoid astrocytomas revealed the pilomyxoid variant to be associated with a worse prognosis in univariate but not in multivariate analysis [7]. A further survey on 78 cerebellar pilocytic astrocytomas revealed a classic pilocytic/microcystic pattern in 62 cases whereas 16 showed a mixed pattern with an additional non-pilocytic glial component which was associated with a significantly poorer survival [25]. The conjunction of mitoses, nuclear atypia, and increased cellularity, designated as “atypical pilocytic astrocytoma,” was found to be rare and less reliably correlated with prognosis than in patients with fibrillary astrocytomas [6].

Several investigations have examined the influence of proliferation upon juvenile pilocytic astrocytomas, using among others the

currently most widely employed proliferation marker Ki-67/MIB-1. No significant differences were encountered between subgroups of pilocytic astrocytomas showing an MIB-1 index $<5\%$ (PFS=87.4 %) vs MIB-1 $>5\%$ (PFS=76.3 %) [26], while there was also no association found between survival and MIB-1 labelling index or any histological parameter in 131 pilocytic astrocytomas [5]. Another investigation on 48 cases showed adverse outcome in patients with pilocytic astrocytoma to be related to the extent of surgical resection and not to correlate with histology, MIB-1 labelling indices, or cyclin D1 immunoreactivity [27]. Interestingly, one study on 118 pilocytic astrocytomas found an MIB-1 index of $>2.0\%$ to be associated with shortened progression-free survival; however, restricting evaluation to only incompletely resected tumors resulted in an insignificant trend of patients with tumors showing an MIB-1 index $>2.0\%$ having a shortened progression-free survival [28]. Another group investigated the immunohistochemical expression of topoisomerase II alpha, a marker of cell cycle turnover and determinant of tumor cell resistance to chemotherapy, whose labelling index was found to range from 0 to 11.6 and was closely correlated to the MIB-1 index; however, topoisomerase II alpha expression did not correlate with patient survival or recurrence [29].

28.2.4 Pleomorphic Xanthoastrocytoma (PXA)

PXA are mainly encountered in the second decade of life and have a generally good prognosis despite their pleomorphic appearance. Factors influencing clinical outcome include extent of resection and histological features such as mitotic index, necrosis, and lymphocytic infiltration, whereas necrosis has occasionally been put forward as a hallmark of unfavorable prognosis; additionally, findings of no or rare degeneration, atypical mitoses, as well as high mitotic activity and MIB-1 labelling index seem to correlate with

a worse biological behavior of PXA [30]. This is corroborated by two publications which find anaplastic transformation and increased mitotic activity of PXA to confer a much worse prognosis [31], while conversely, a low mitotic index of $<5/10$ HPF is postulated to be predictive of a more favorable recurrence-free and overall survival [30].

As to the significance of TP53 mutations regarding malignant progression or recurrence, no prognostic value has yet been established in two independent investigations [32, 33]. One PXA revealing multiple genetic alterations after investigation by comparative genomic hybridization (CGH) showed a poor prognosis [34]; however, no large series relating chromosomal aberrations to survival exists.

28.2.5 High-Grade Astrocytic Tumors

A study on 26 patients with high-grade astrocytic tumors found a striking difference in outcome between tumors with MIB-1 indices $<12\%$ and those with indices $>12\%$ [35], another on 33 cases found a prognostically significant cutoff MIB-1 proliferation index of 25% [36]. Median progression-free survival in the former study was >48 months in the low compared with only 6 months in the high MIB-1 group, whereas median overall survival was >48 months in the low compared with only 16 months in the high MIB-1 group. Although MIB-1 index was found to be associated with histopathological grade, it proved to be a much stronger predictor of outcome than histology [35]. A later study by the same group on 98 high-grade gliomas showed a strong association between MIB-1 labelling and patient outcome: the 5-year progression-free survival was 33% in 43 patients with MIB-1 indices of $<18\%$, 22% in 27 patients with MIB-1 between 18 and 36% , and 11% in 28 patients with MIB-1 $>36\%$ [37]. Not surprisingly, a strong association was also observed between tumor grade and MIB-1. Notwithstanding this correlation, a significant association was noted between MIB-1 and progression-free survival even after stratification by

histology. Thus, although histology had an independent association with outcome, the prognostic value of MIB-1 labelling transcended histological subgrouping and was apparent both in anaplastic astrocytomas and glioblastomas, with tumors showing MIB-1 labelling indices >36 % having an almost uniformly poor outcome regardless of histology [37].

The same group also analyzed immunohistochemical expression of p53 in 115 high-grade astrocytic tumors, among which a significant association between p53 overexpression and outcome was found independent of histological features, age, sex, the extent of resection, and tumor location [38]. The rate of 5-year progression-free survival was 44 % among the 74 patients with low p53 expression and 17 % among the 41 patients with p53 overexpression indicating that overexpression of p53 in malignant gliomas of childhood is strongly associated with an adverse outcome, possibly because P53-dependent pathways influence the cytotoxic effects of conventional chemo- and radiotherapy [38]. The study corroborated an earlier investigation by the same authors who had already encountered a significant association between p53 overexpression and a shorter progression-free and overall survival in a smaller cohort [35]. However, while a later study on a group of 39 high-grade astrocytomas found a significant association between PTEN mutations and decreased survival among children regardless of patient age or tumor grade, mutations in TP53 or amplifications of MDM2 and CDK4 were not significantly linked to outcome [39].

Immunoreactivity for basic fibroblast growth factor (bFGF), a mitogenic and angiogenic factor, among 27 malignant childhood gliomas found a significant difference in outcome between patients with high and those with low bFGF expression with median progression-free survival of >66 months in the low and 6 months in the high bFGF group as well as an overall survival of >66 months in the low and 18 months in the high bFGF group, pointing toward a strong association between tumor bFGF expression and outcome in children with high-grade gliomas [40]. The same authors later investigated nuclear DNA

topoisomerase II alpha (TII alpha), a marker of cell cycle turnover and determinant of tumor cell resistance to chemotherapy, in a series of 17 pediatric high-grade gliomas [29]. A cutoff labelling index of 12 % was found to define two prognostic subgroups with profoundly different 5-year progression-free (60 % vs 8 %) and overall survival (100 % vs 8 %) for cases with an index >12 % [29].

28.2.6 Anaplastic Astrocytoma

An investigation of the proliferative potential of 33 childhood anaplastic astrocytomas showed a significantly better survival for tumor carriers with an MIB-1 index <11 % compared to those with an index >11 % [24]. Furthermore, a CGH study on 10 anaplastic astrocytomas of childhood found a significantly shorter survival for children whose tumors showed gains of chromosome 1q [36].

28.2.7 Glioblastoma

Within the group of pediatric glioblastomas, the clinical outcome for the giant cell type of glioblastoma seems to be somewhat better than for classical glioblastomas with children surviving up to 11 years, possibly can be due to their less infiltrative nature [41]. Equally, in the setting of Turcot syndrome type 1 (autosomal dominant disorder characterized by colorectal polyps and malignant neuroepithelial tumors), glioblastomas tend to show a remarkably longer survival time (27 vs 12 months) compared with sporadic cases [42].

28.3 Comparative Genomic Hybridization (CGH) in Astrocytic Tumors of Childhood and Adolescence

CGH is a cytogenetic technique that is particularly useful in the study of solid tumors and which was first introduced in 1992. CGH offers

advantages over other cytogenetic and molecular genetic methods like loss of heterozygosity analysis (LOH) and classic karyotyping in that it does not involve in vitro culture of tumor tissue or necessitate healthy tissue or blood from a given patient, allows rapid detection and localization of gains and losses across the entire genome, and offers higher resolution than conventional cytogenetics. DNA from archival material can be used, and CGH can be successfully performed using very small amounts of DNA in the order of nanograms. The entire genome is screened for gains and losses of genetic material relative to the ploidy level in a single experiment, and the method is essentially a modified in situ hybridization. However, there is a limit to the resolution of this technique: losses are only detectable when the region affected exceeds 10 Mb, whereas gains are detected if there is a high-level amplification of approximately 2 Mb, and balanced structural rearrangements like balanced translocations, inversions, and ring chromosomes cannot be detected at all. Once regions of gain or loss have been established, they can be further

delineated by FISH or other molecular genetic techniques, e.g., LOH analysis and sequencing in order to identify proto-oncogenes and tumor suppressor genes [43]. A summary of the most common CGH findings in 154 pediatric astrocytic tumors is listed in Table 28.2.

28.3.1 Pilocytic Astrocytomas

Two CGH studies altogether with 50 cases showed very few chromosomal imbalances [44, 45]. The most common aberration affecting a mere 10 % of all tumors consisted of gains of 6q followed by gains of 7q in 8 % of cases whereas the most common loss affects 9q and is found in just 4 % of cases [44, 45]. The last two imbalances are noteworthy in that +7q is encountered in other gliomas like pleomorphic xanthoastrocytomas, ependymomas, and gangliogliomas but also in choroid plexus papillomas, classic medulloblastomas, and PNET, while -9q is the main aberration in pleomorphic xanthoastrocytomas and is also found in anaplastic astrocytomas and astroblastomas [43].

Table 28.2 Summary of the most common CGH findings in 154 pediatric astrocytic tumors

Tumor entity			
Source	N	Frequent gains (%)	Frequent losses (%)
<i>Pilocytic astrocytomas</i>			
[44]	9	6q(44),4q(33),5q,7q,11q,13q(22)	1p,9q(22)
[45]	41	7(5),5,6,9(3)	None
<i>Pleomorphic xanthoastrocytomas</i>			
[46]	50	X(14),7,9q,20(8)	9(48),17(10)
[34]	3	7(67),2p,4p,11q,12,15q,19(33)	8p(67),9p,10p,13q(33)
<i>Fibrillary astrocytomas</i>			
[47]	8	9,11,19(13)	2,22q(13)
<i>Anaplastic astrocytomas</i>			
[48]	2	None	None
[36]	10	5q(40),1q(30)	22q(50),6q,9q(40),12q(30)
[49]	3	2q,6q,7q,11q,12q,13q(33)	16p(67)
<i>Glioblastomas</i>			
[36]	13	1q(54),3q(38),2q,17q(23)	6q,8q,10q,13q,17p(31)
[50]	5 ^a	17,20q(40)	13q,Y(40)
[49]	10	2q,4q,5q,12q,13q(40),8q(30)	16p(50),17p,19p,22q(40),19q(30)

^aAfter radiochemotherapy

28.3.2 Pleomorphic Xanthoastrocytomas (PXA)

Two CGH investigations on 53 cases found loss of chromosome 9 to be by far the single most common aberration affecting 49 % of specimens whereas gains of chromosome X and losses of 7 were far rarer with 14 and 11 %, respectively [34, 46].

28.3.3 Fibrillary Astrocytomas

Only one CGH study of eight cases has been performed and showed no chromosomal aberrations in four tumors whereas the other tumors presented with no distinct pattern of gains and losses [47]. Loss of 22q – the most frequent aberration among anaplastic astrocytomas – was encountered in one tumor.

28.3.4 Anaplastic Astrocytomas

Three studies have investigated altogether 15 anaplastic astrocytomas by CGH [36, 48, 49]. The most common chromosomal aberrations among these tumors were gains of 5q (27 %) and 1q (20 %) as well as losses of 22q (40 %), 9q (33 %), and 12q (27 %) [36]. Interestingly, one study found a significantly shorter survival among patients with anaplastic astrocytomas showing +1q [36], an association that has also been reported for ependymomas which when shown to harbor +1q tended to occur in the posterior fossa of children and behave aggressively [15, 43].

28.3.5 Glioblastomas

Three studies have investigated altogether 28 pediatric glioblastomas by CGH [36, 49, 50], of which five were examined after radiochemotherapy [50]. Similar to anaplastic astrocytomas, the most common chromosomal aberrations were gains of 1q and 2q (25 %

each), 3q and 17q (18 % each), as well as losses of 17p (29 %) and 13q (21 %) [36]. Compared with adult cases, gains of 1p, 2q, and 21q as well as losses of 6q, 11q, and 16q were more frequently observed among pediatric malignant astrocytomas showing that chromosomal aberrations do not only differ between pediatric anaplastic astrocytomas and glioblastomas but also between pediatric and adult high-grade astrocytomas, supporting the notion of different genetic pathways [36].

28.4 Extraneural Metastases of Astrocytic Brain Tumors in Childhood

Extraneural metastases from brain tumors are an unusual event; their incidence, however, has increased over the years along with improved patient survival due to more aggressive and effective therapy. As to their pathogenesis, the relationship between surgery and metastasis is unclear: while it is possible that in some cases the appearance of extraneural tumor foci simply reflects prolonged survival time of these patients, the overwhelming majority of patients with extraneurally metastasising brain tumors have undergone some form of prior surgical manipulation of the primary neoplasm, be in the shape of a previous stereotactic or open biopsy, surgery, or a shunt procedure. The diagnosis of extraneural metastases in the pediatric population is of more than just academic interest as these lesions do not necessarily occur in conjunction with a local recurrence of the CNS tumor and the investigating pathologist has to be aware that a tumor at a particular site and in a specific age group could also represent metastatic spread of a cerebral neoplasm.

A survey of extraneural metastases occurring in children under the age of 18 years revealed 245 cases of which 28 (11.4 %) were patients suffering from astrocytic lesions (for references to specific cases see [51]): 14 with glioblastomas (6.9 % of all cases), 6 with pilocytic astrocytomas (2.9 %), t3 each with astrocytomas not

otherwise specified and gliosarcomas (1.5 % each), respectively, and 2 with anaplastic astrocytomas (1.0 %, Table 28.3). Glioblastomas predominantly metastasized to bone (57.1 % of astrocytic tumors), with vertebrae being particu-

larly common targets and 3 out of 14 cases presenting with multiple osseous sites of involvement (Table 28.3). Of all 28 astrocytic tumors, 57.1 % spread to mainly regional, i.e., cervical, lymph nodes, interestingly unrelated to WHO grade of

Table 28.3 Demographic data, tumor histology, metastatic sites, latency, and survival among 28 children with extraneural metastases of astrocytic tumors

Age/sex	Histology	Metastatic sites			Latency	Surv
		Bone (including bone marrow)	Lymph nodes	Visceral/others		
<i>(a) Metastases after surgical intervention (operation, biopsy, and/or shunt insertion)</i>						
4/M	PA	–	Cervical	Skin	48	>90
3/M	AA	–	–	Epidural	ND	ND
3/F	GBM	Skull	Pulmonary	Lung, pleura	ND	31
7/F	GBM	Jaw, ver, sca, hum, pel, fem, tib	Supraclavicular	–	12	7
9/M	GBM	Bone NOS	–	–	2	3
9/F	GBM	–	Cervical	–	ND	19
12/M	GBM	Pelvis	–	–	5	ND
12/F	GBM	Bone NOS	Cervical	Lung	ND	7
17/F	GBM	–	–	Lung	24	ND
6/M	GS	–	–	Lung	ND	17
6/M	GS	–	–	Lung	ND	7
11/F	GS	–	–	Lung	1	0
<i>(b) Spontaneous metastases without prior surgical intervention</i>						
4/M	PA	–	–	Lung, muscle	0	ND
3/M	AA	–	Cervical	–	0	2
11/F	GBM	Skull, jaw, ver, rib, hum, uln, fem, pel, tib, fib	–	–	–	6
<i>(c) Shunt-related metastases</i>						
6 m/M	PA	–	–	Peritoneum	2	>106
19 m/M	PA	–	–	Peritoneum	47	10
3/M	PA	–	–	Peritoneum	6	>12
6/F	PA	–	–	Peritoneum	122	5
4/F	A NOS	–	–	Peritoneum	5	1
12/F	A NOS	–	–	Lung, liver	ND	0
17/M	A NOS	Bone NOS	Nodes NOS	Pleura, soft tissue	ND	28
1/F	GBM	–	–	Peritoneum	ND	ND
7/F	GBM	Vertebrae	Pulmonary	Pleura, liver, adre	ND	ND
9/M	GBM	–	–	Peritoneum	9	ND
9/F	GBM	–	–	Peritoneum	2	4
13/M	GBM	–	–	Peritoneum	3	4
14/F	GBM	Vertebrae, rib, sternum	Aorta, mediast	Pleura, lung	ND	13

M male, *F* female, *PA* pilocytic astrocytoma, *A* astrocytoma, *AA* anaplastic astrocytoma, *GBM* glioblastoma, *GS* gliosarcoma; *adre* adrenal, *fem* femur, *fib* fibula, *hum* humerus, *mediast* mediastinum, *pel* pelvis, *sca* scapula, *tib* tibia, *uln* ulna, *ver* vertebrae

Latency interval between brain surgery and extraneural metastasis (in months), *Surv* survival after extraneural metastasis (in months), *NOS* not otherwise specified, *ND* no data available

malignancy. In regard to visceral metastases, there was a clear distinction between shunt-related metastases, of which all 13 cases showed tumor seeding in the compartments that the previously inserted shunt was draining to (pleura, peritoneum), whereas 7 out of the 15 remaining cases showed pulmonary metastases, all but one of them stemming from glioblastomas or gliosarcomas [51]. Not surprisingly, particularly grave outcomes were found among children with glioblastomas and gliosarcomas, of which all died within a time span of at most 31 months, while long-term survival of between 1 and 11 years was encountered among children suffering from pilocytic astrocytoma [51].

Acknowledgements Many thanks and heartfelt best wishes to my former clinical colleagues at the Royal Children's Hospital in Melbourne (Australia) – may the Hawthorn Hawks win many more flags! Thanks, too, to Werner Paulus for years of teaching, advice, and help.

References

- Rickert CH, Paulus W (2001) Epidemiology of central nervous system neoplasms in childhood and adolescence based on the new WHO classification. *Childs Nerv Syst* 17:503–511
- Di Rocco C (1999) Cerebellar astrocytomas. In: Choux M, Rocco D, Hockley AD, Walker ML (eds) *Pediatric neurosurgery*. Churchill Livingstone, London, pp 427–459
- Rorke LB (1999) Pathology of brain and spinal cord tumors. In: Choux M, Rocco D, Hockley AD, Walker ML (eds) *Pediatric neurosurgery*. Churchill Livingstone, London, pp 395–426
- Scheithauer BW, Hawkins C, Tihan T, VandenBerg SR, Burger PC (2007) Pilocytic astrocytoma. In: Louis DN, Ohgaki H, Wiestler OD, Cavenee WK (eds) *WHO classification of tumours of the central nervous system*. IARC, Lyon, pp 14–21
- Giannini C, Scheithauer BW, Burger PC, Christensen MR, Wollan PC, Sebo TJ, Forsyth PA, Hayostek CJ (1999) Cellular proliferation in pilocytic and diffuse astrocytomas. *J Neuropathol Exp Neurol* 58:46–53
- Tomlinson FH, Scheithauer BW, Hayostek CJ, Parisi JE, Meyer FB, Shaw EG, Weiland TL, Katzmann JA, Jack CR Jr (1994) The significance of atypia and histologic malignancy in pilocytic astrocytoma of the cerebellum: a clinicopathologic and flow cytometric study. *J Child Neurol* 9:301–310
- Fernandez C, Figarella-Branger D, Girard N, Bouvier-Labit C, Gouvernet J, Paz Paredes A, Lena G (2003) Pilocytic astrocytomas in children: prognostic factors – a retrospective study of 80 cases. *Neurosurgery* 53:544–553
- Khanani MF, Hawkins C, Shroff M, Dirks P, Capra M, Burger PC, Bouffet E (2006) Pilomyxoid astrocytoma in a patient with neurofibromatosis. *Pediatr Blood Cancer* 46:377–380
- Tihan T, Fisher PG, Kepner JL, Godfraind C, McComb RD, Goldthwaite PT, Burger PC (1999) Pediatric astrocytomas with monomorphous pilomyxoid features and a less favorable outcome. *J Neuropathol Exp Neurol* 58:1061–1068
- Giannini C, Paulus W, Louis DN, Liberski P (2007) Pleomorphic xanthoastrocytoma. In: Louis DN, Ohgaki H, Wiestler OD, Cavenee WK (eds) *WHO classification of tumours of the central nervous system*. IARC, Lyon, pp 22–24
- Gil-Gouveia R, Cristino N, Farias JP, Trindade A, Ruivo NS, Pimentel J (2004) Pleomorphic xanthoastrocytoma of the cerebellum: illustrated review. *Acta Neurochir* 146:1241–1244
- von Deimling A, Burger PC, Nakazato Y, Ohgaki H, Kleihues P (2007) Diffuse astrocytoma. In: Louis DN, Ohgaki H, Wiestler OD, Cavenee WK (eds) *WHO classification of tumours of the central nervous system*. IARC, Lyon, pp 25–29
- Kleihues P, Burger PC, Rosenblum MK, Paulus W, Scheithauer BW (2007) Anaplastic astrocytoma. In: Louis DN, Ohgaki H, Wiestler OD, Cavenee WK (eds) *WHO classification of tumours of the central nervous system*. IARC, Lyon, pp 30–32
- Kleihues P, Burger PC, Aldape KD, Brat DJ, Biernat W, Bigner DD, Nakazato Y, Plate KH, Giangaspero F, von Deimling A, Ohgaki H, Cavenee WK (2007) Glioblastoma. In: Louis DN, Ohgaki H, Wiestler OD, Cavenee WK (eds) *WHO classification of tumours of the central nervous system*. IARC, Lyon, pp 33–49
- Rickert CH (2004) Prognosis-related molecular markers in pediatric central nervous system tumors. *J Neuropathol Exp Neurol* 63:1211–1224
- Rickert CH, Paulus W (2005) Prognosis-related histomorphological and immunohistochemical markers in central nervous system tumors of childhood and adolescence. *Acta Neuropathol* 109:69–92
- Ben Arush MW, Linn S, Ben-Izhak O, Levy R, Nahum MP, Tsuk-Shina T, Guilbord JN, Elhasid R, Postovsky S (1999) Prognostic significance of DNA ploidy in childhood astrocytomas. *Pediatr Hematol Oncol* 16:387–396
- Prados MD, Krouwer HG, Edwards MS, Cogen PH, Davis RL, Hoshino T (1992) Proliferative potential and outcome in pediatric astrocytic tumors. *J Neuro Oncol* 13:277–282
- Hayostek CJ, Shaw EG, Scheithauer B, O'Fallon JR, Weiland TL, Schomberg PJ, Kelly PJ, Hu TC (1993) Astrocytomas of the cerebellum. A comparative clinicopathologic study of pilocytic and diffuse astrocytomas. *Cancer* 72:856–869
- Orr LC, Fleitz J, McGavran L, Wyatt-Ashmead J, Handler M, Foreman NK (2002) Cytogenetics in

- pediatric low-grade astrocytomas. *Med Pediatr Oncol* 38:173–177
21. Pencolet P, Maixner W, Sainte-Rose C, Lellouch-Tubiana A, Cinalli G, Zerah M, Pierre-Kahn A, Hoppe-Hirsch E, Bourgeois M, Renier D (1999) Benign cerebellar astrocytomas in children. *J Neurosurg* 90:265–273
 22. Bernhardt T, Laursen H, Bojsen-Møller M, Gjerris F (2003) Sub-classification of low-grade cerebellar astrocytoma: is it clinically meaningful? *Childs Nerv Syst* 19:729–735
 23. Fisher BJ, Naumova E, Leighton CC, Naumov GN, Kerkvliet N, Fortin D, Macdonald DR, Cairncross JG, Bauman GS, Stitt L (2002) Ki-67: a prognostic factor for low-grade glioma? *Int J Radiat Oncol Biol Phys* 52:996–1001
 24. Ho DM, Wong TT, Hsu CY, Ting LT, Chiang H (1998) MIB-1 labeling index in non-pilocytic astrocytoma of childhood. *Cancer* 82:2459–2466
 25. Haapasalo H, Sallinen S, Sallinen P, Helen P, Jääskeläinen J, Salmi TT, Paetau A, Paljärvi L, Visakorpi T, Kalimo H (1999) Clinicopathological correlation of cell proliferation, apoptosis and p53 in cerebellar pilocytic astrocytomas. *Neuropathol Appl Neurobiol* 25:134–142
 26. Roessler K, Bertalanffy A, Jeza H, Ba-Ssalamah A, Slavc I, Czech T, Budka H (2002) Proliferative activity as measured by MIB-1 labeling index and long-term outcome of cerebellar juvenile pilocytic astrocytomas. *J Neuro Oncol* 58:141–146
 27. Machen SK, Prayson RA (1998) Cyclin D1 and MIB-1 immunohistochemistry in pilocytic astrocytomas: a study of 48 cases. *Hum Pathol* 29:1511–1516
 28. Bowers DC, Gargan L, Kapur P, Reisch JS, Mulne AF, Shapiro KN, Elterman RD, Winick NJ, Margraf LR (2003) Study of the MIB-1 labeling index as a predictor of tumor progression in pilocytic astrocytomas in children and adolescents. *J Clin Oncol* 21:2968–2973
 29. Bredel M, Pollack IF, Hamilton RL, Birner P, Hainfellner JA, Zentner J (2002) DNA topoisomerase II α predicts progression-free and overall survival in pediatric malignant non-brainstem gliomas. *Int J Cancer* 99:817–820
 30. Giannini C, Scheithauer BW, Burger PC, Brat DJ, Wollan PC, Lach B, O'Neill BP (1999) Pleomorphic xanthoastrocytoma: what do we really know about it? *Cancer* 85:2033–2045
 31. Macaulay RJ, Jay V, Hoffman HJ, Becker LE (1993) Increased mitotic activity as a negative prognostic indicator in pleomorphic xanthoastrocytoma. *J Neurosurg* 79:761–768
 32. Munoz EL, Eberhard DA, Lopes MBS, Schneider BF, Gonzales F, VandenBerg SR (1996) Proliferative activity and p53 mutation as prognostic indicators in pleomorphic xanthoastrocytoma. *J Neuropathol Exp Neurol* 55:606
 33. Paulus W, Lisle DK, Tonn JC, Wolf HK, Roggendorf W, Reeves SA, Louis DN (1996) Molecular genetic alterations in pleomorphic xanthoastrocytoma. *Acta Neuropathol* 91:293–297
 34. Yin XL, Hui AB, Liang EC, Ding M, Chang AR, Ng HK (2002) Genetic imbalances in pleomorphic xanthoastrocytoma detected by comparative genomic hybridization and literature review. *Cancer Genet Cytogenet* 132:14–19
 35. Pollack IF, Campbell JW, Hamilton RL, Martinez AJ, Bozik ME (1997) Proliferation index as a predictor of prognosis in malignant gliomas of childhood. *Cancer* 79:849–856
 36. Rickert CH, Sträter R, Kaatsch P, Wassmann H, Jürgens H, Dockhorn-Dworniczak B, Paulus W (2001) Pediatric high-grade astrocytomas show chromosomal imbalances distinct from adult cases. *Am J Pathol* 158:1525–1532
 37. Pollack IF, Hamilton RL, Burnham J, Holmes EJ, Finkelstein SD, Spoto R, Yates AJ, Boyett JM, Finlay JL (2002) Impact of proliferation index on outcome in childhood malignant gliomas: results in a multi-institutional cohort. *Neurosurgery* 50:1238–1244
 38. Pollack IF, Finkelstein SD, Woods J, Burnham J, Holmes EJ, Hamilton RL, Yates AJ, Boyett JM, Finlay JL, Spoto R (2002) The Children's cancer group. Expression of p53 and prognosis in children with malignant gliomas. *N Engl J Med* 346:420–427
 39. Raffel C, Frederick L, O'Fallon JR, Atherton-Skaff P, Perry A, Jenkins RB, James CD (1999) Analysis of oncogene and tumor suppressor gene alterations in pediatric malignant astrocytomas reveals reduced survival for patients with PTEN mutations. *Clin Cancer Res* 5:4085–4090
 40. Bredel M, Pollack IF, Campbell JW, Hamilton RL (1997) Basic fibroblast growth factor expression as a predictor of prognosis in pediatric high-grade gliomas. *Clin Cancer Res* 3:2157–2164
 41. Klein R, Mölenkamp G, Sörensen N, Roggendorf W (1998) Favorable outcome of giant cell glioblastoma in a child. Report of an 11-year survival period. *Childs Nerv Syst* 14:288–291
 42. Van Meir EG (1998) "Turcot's syndrome": phenotype of brain tumors, survival and mode of inheritance. *Int J Cancer* 75:162–164
 43. Rickert CH, Paulus W (2004) Comparative genomic hybridization in central and peripheral nervous system tumors of childhood and adolescence. *J Neuropathol Exp Neurol* 63:399–417
 44. Rienstein S, Aviram-Goldring A, Daniely M, Amerigleo N, Simoni F, Goldman B, Barkai G, Rechavi G, Constantini S (2000) Gains and losses of DNA sequences in childhood brain tumors analyzed by comparative genomic hybridization. *Cancer Genet Cytogenet* 121:67–72
 45. Sanoudou D, Tingby O, Ferguson-Smith MA, Collins VP, Coleman N (2000) Analysis of pilocytic astrocytoma by comparative genomic hybridization. *Br J Cancer* 82:1218–1222
 46. Weber RG, Kaulich K, Ehrler M, Blaschke B, Jauch A, Weber S, von Deimling A, Wiestler OD, Reifenberger G (2002) Genomic and expression profiling of pleomorphic xanthoastrocytomas. *Acta Neuropathol* 104:575 (abstract)

47. Schröck E, Blume C, Meffert MC, du Manoir S, Bersch W, Kiessling M, Lozanowa T, Thiel G, Witkowski R, Ried T, Cremer T (1996) Recurrent gain of chromosome arm 7q in low-grade astrocytic tumors studied by comparative genomic hybridisation. *Gene Chromosome Cancer* 15:199–205
48. Kunwar S, Mohapatra G, Bollen A, Lamborn KR, Prados M, Feuerstein BG (2001) Genetic subgroups of anaplastic astrocytomas correlate with patient age and survival. *Cancer Res* 61:7683–7688
49. Warr T, Ward S, Burrows J, Harding B, Wilkins P, Harkness W, Hayward R, Darling J, Thomas D (2001) Identification of extensive genomic loss and gain by comparative genomic hybridisation in malignant astrocytoma in children and young adults. *Gene Chromosome Cancer* 31:15–22
50. Romeike BFM, Graf N, Jung V, Krenn T, Zang KD, Urbschat S, Feiden W (2002) Diffuse small cell glioblastomas (DSCG) after radio-chemotherapy of pediatric malignancies: histopathologic and molecular genetic characterization. *Acta Neuropathol* 104:566 (abstract)
51. Rickert CH (2003) Extraneural metastases in paediatric brain tumours. *Acta Neuropathol* 105:309–327

Pratiti Bandopadhyay, Peter A. Downie,
and David M. Ashley

29.1 Introduction

Astrocytomas are the most common pediatric brain tumor. These glial tumors encompass a heterogeneous group of tumors of which pilocytic astrocytomas (WHO grade 1) are the most frequent. Higher-grade tumors, including anaplastic astrocytoma (WHO grade III) and glioblastoma multiforme (WHO grade IV), also do occur in the cerebellum. Although much less frequent, they carry a poorer prognosis compared to their grade I counterpart. The management of astrocytomas is a balance between optimizing long-term survival and minimizing long-term morbidity in survivors.

P. Bandopadhyay, M.B.B.S., Ph.D (✉)
Pediatric Neuro-Oncology Program, Dana-Farber
Cancer Institute, Boston Children's Hospital and
Harvard Medical School, Melbourne, VIC, Australia
e-mail: pratiti_bandopadhyay@dfci.harvard.edu

P.A. Downie, M.D.
Children's Cancer Centre, Royal Children's Hospital
and Southernhealth, Melbourne, VIC, Australia
e-mail: Peter.Downie@rch.org.au

D.M. Ashley, M.D.
Andrew Love Cancer Centre and Children's Cancer
Centre, Barwon Health and Royal Children's
Hospital, Melbourne, VIC, Australia
e-mail: David.Ashley@barwonhealth.org.au

29.2 Clinical Presentation

Like all brain tumors, the clinical presentation of cerebellar astrocytoma reflects the anatomic position of the tumor.

The site of origin of brain tumors in childhood is a considerable factor in prognosis because of differences in biology and surgical accessibility. The symptoms and signs in a child with a brain tumor reflect the neurological dysfunction of the affected site but can also be due to obstruction of normal flow of CSF, localized edema, and associated raised intracranial pressure. These symptoms and signs are varied and are dependent on many factors such as premorbid developmental stage, age, and site of origin. The same symptoms and signs are therefore seen in children regardless of specific tumor histopathology. In infancy, there may be increased head circumference. Brain tumors, especially posterior fossa tumors, should be considered in the differential diagnosis of infantile hydrocephalus. Irritability, anorexia, developmental delay, and regression of intellectual and motor milestones are signs seen in infants and young children. Cranial sutures and fontanelles may remain open due to raised ICP, and fundal examination may therefore show optic pallor rather than papilledema. Separation of cranial sutures leads to resonance on skull percussion (the Macewen or "cracked pot" sign). The well-described "setting sun" sign is seen with downward eye deviation, which is often accompanied by a high-pitched cry. Clinical assessment

should always include head circumference, fundal examination, and developmental appraisal.

Symptoms and signs in older children with posterior fossa brain tumors may be more subtle and nonspecific. In school-aged and older children, morning headaches, vomiting, and lethargy make up the typical triad seen with raised intracranial pressure. The headache may have physical suboccipital localization and is rarely continuous. Vomiting is not accompanied by nausea. Raised intracranial pressure can affect other intracranial structures; sixth nerve palsy results in diplopia or blurred vision. This may be a false localizing sign and does not necessarily mean the presence of a posterior fossa lesion, as raised intracranial pressure can be due to other diseases. Deficits of cranial nerves V, VII, and XI should direct investigation to the brainstem. There may be long tract upper motor neuron signs of weakness, hyperreflexia, clonus, and hypertonia, cerebellar signs may result in nystagmus, as well as non-lateralizing gait or truncal ataxia. In any child who presents with visual problems, the optic nerve, chiasm, and visual fields should be carefully evaluated. An afferent pupil defect will be shown by comparing evaluation of both direct and consensual pupillary response to a bright light (Marcus Gunn pupil). It is worth emphasizing that nonlocalizing symptoms of raised intracranial pressure will be the predominant symptoms early in the course of disease.

29.3 Cerebellar Pilocytic Astrocytoma

Pilocytic astrocytomas are slow-growing tumors with a low frequency of malignant transformation and characteristically on imaging have mixed solid and cystic characteristics. These tumors occur most commonly in the cerebellum, optic nerves, or chiasm, with the cerebellum representing the most frequent site [1]. The reported incidence of cerebellar astrocytoma approaches 25 % of all primary pediatric CNS tumors [2]. Cerebellar astrocytoma is most commonly seen in early childhood, with age of peak diagnosis being in the first 14 years of life and a median age of diagnosis at 6 years [3, 4]. This is most likely

a reflection of brain maturation and development processes being linked with pathogenesis. The notion that pathways involved in early brain development are involved in the pathogenesis of pediatric cerebellar astrocytomas is supported by distinct differences between pediatric cerebellar astrocytomas and their adult counterparts. While the histology of these tumors, as described in Section 35 is similar between pediatric and adult pilocytic astrocytomas, the genetic profiles are distinct [3, 5], highlighting the need to consider pediatric cerebellar astrocytomas as a separate disease entity to adult tumors when considering therapeutic options. The genetics of pediatric cerebellar astrocytomas are described in Section 32. While these tumors can arise *de novo*, an increased risk is associated with particular genetic constitutions. In particular, children with neurofibromatosis are at a significantly higher risk of pilocytic astrocytomas, not only in the optic nerves which are the most frequent site of presentation, but also for cerebellar pilocytic astrocytomas [6, 7].

29.4 Management of Cerebellar Pilocytic Astrocytomas

The overall prognosis of children with cerebellar astrocytomas is excellent, with some studies reporting overall 5- and 10-year survival figures of between 80 and 100 % [8–10]. Survival of adult survivors of Pediatric Low-Grade Gliomas is excellent and these tumors do not frequently transform to higher grade tumors [40]. Furthermore, as noted above, the peak incidence of cerebellar astrocytomas is in the preschool and early school years, at a time when postnatal maturation of the brain is occurring. In this group, childhood milestones are developing exponentially, and therapy for cerebellar tumors therefore has potential for significant neurocognitive deficits. The principle of treatment of cerebellar astrocytomas is to attempt maximal tumor control with minimal long-term deficits. It is also clear that the clinical behavior of these tumors is variable, with periods of growth and periods of stability [11]. The therapy modalities available include observation, surgery, chemotherapy, and radiation therapy.

29.5 Principles of Therapy

The initial modality of therapy in a child with a cerebellar astrocytoma is surgical, and this has been described in Section 34. Briefly, surgical therapy is directed at controlling complications of the tumor, in particular hydrocephalus, and maximal safe resection of the primary tumor while attempting to minimize long-term surgical morbidity. Gross total resection confers the most favorable prognosis and is considered to be curative in the majority of children [9, 12] with 10-year progression-free survival of up to 95 %. Gross total resection is achievable in 60–80 % of children with cerebellar astrocytoma [12].

Historically, children with subtotal resections were treated with radiation therapy. However, given the morbidity of radiation therapy and the understanding that these tumors have a variable course, are unlikely to undergo malignant transformation, and have periods of extended stability, current therapy strategies aim to defer radiation therapy. Instead they are observed closely and upon clear documentation of disease progression, other therapy is utilized including second-look surgery or chemotherapy [10–13]. Using this approach, children undergo surveillance imaging at three to six monthly intervals. Prospective surveillance studies have reported 5-year progression-free survival rates of between 45 and 65 % in children with residual tumor postprimary resection [14, 15].

In children who have progression after either initial gross total resection or subtotal resection, a multidisciplinary approach to the management is vital. Single institute studies have demonstrated the feasibility of second-look surgery on tumor progression prior to initiation of chemotherapy or radiation therapy. If second-look surgery is able to be performed safely, there is demonstrated reduction in long-term morbidity [11].

Multiple chemotherapy regimen has been utilized to defer radiation. This approach to use chemotherapy was originally for newly diagnosed children but is now also utilized for documented progression. Pilocytic astrocytomas were first shown to be sensitive to carboplatin and vincristine in the 1990s [16]. There is ongoing

debate about the utility of vincristine to be effective in crossing the blood-brain barrier, and current treatment incorporates carboplatin, with or without vincristine to stabilize tumors, limit progression or make them potentially amendable to second-look surgery [11]. Other chemotherapy regimens include procarbazine, 6-thioguanine, CCNU, dibromodulcitol with vincristine, and the combination of CCNU with vincristine [17]. Cyclophosphamide in combination with carboplatin and vincristine has not been shown to have any added benefit [18]. However, cyclophosphamide and vincristine has reported to improve progression-free survival [19]. Carboplatin in combination with etoposide has also been reported to result in objective responses in progressive astrocytomas [13]. These studies all show that pilocytic astrocytomas are chemoresponsive.

These agents all have their unique side-effect profiles, and the challenge is to use the least morbid regimen without compromising tumor control. The COG study A9952 evaluated event-free survival in children treated with either the carboplatin and vincristine or the TPCV (thioguanine, procarbazine, CCNU, and vincristine) protocol. In this randomized study, there was no statistical difference in outcome; however, there was a trend to improved survival using the TPCV protocol [20]. Carboplatin is very well tolerated, with adverse effects including development of hypersensitivity, thrombocytopenia, myelosuppression, and low incidence of sensorineural hearing. In contrast, alkylating agents such as CCNU carry with them risks of secondary malignancy including myeloid leukemia. Many centers around the world therefore use carboplatin, either with or without vincristine as first-line therapy on documented progression, with the more morbid regimens being reserved for subsequent progression. Children with NF1 carry a higher risk of secondary malignancies, and in these children, alkylating agents, if possible, should be avoided.

While once standard of care postsurgical resection, radiation therapy in children with cerebellar pilocytic astrocytomas is now reserved for those with recurrent episodes of progression that are not stabilized by chemotherapy and in whom further surgery is no longer an

option. Section 37 focuses on the role of radiation therapy in cerebellar astrocytomas. Almost all children with PLGGs can be treated without radiation therapy. Given these children are likely to be long-term survivors, attempts are made to spare them the long-term morbidities associated with radiation therapy including second malignancies, vasculopathy and neuro-cognitive deficits. With regard to radiation, caution also needs to be exercised with regard to children with neurofibromatosis type-1 (NF-1) as there is an increased risk of radiation-induced vasculitis (including Moyamoya disease), as well as the aforementioned risk of second malignancy. In what is therefore generally considered a benign tumor, the role of radiation should be reserved for tumors where standard first-line therapy of surgery and/or chemotherapy has failed. With the increasing understanding of the somatic alterations that contribute to tumor formation, targeted therapies are now possible. These include BRAF inhibitors for tumors that harbor the BRAFV600E mutations, MEK inhibitors for those that harbor BRAF duplications, mTOR inhibitors and other targeted therapeutics.

29.6 Long-Term Outlook of with Cerebellar Pilocytic Astrocytomas

As mentioned above, the long-term prognosis of children with pilocytic astrocytomas is excellent. The majority of children with completely resected tumors are cured and require no further therapy for tumor control. In these children, the focus of therapy is directed toward recognizing potential long-term neurocognitive effects that occur as a result of the tumor, the concurrent hydrocephalus, and subsequent surgical management. Of the children who undergo a subtotal resection, approximately half enjoy 5-year progression-free survival. In these children, the focus is on surveillance for progression, rehabilitation of functional deficits, and surveillance for long-term neurocognitive deficits.

For the children who do have tumor progression postsurgical resection, vincristine and carbopla-

tin are able to either stabilize the tumor or induce partial responses and achieve 3-year progression-free survival of 68 % [16]. These children may subsequently experience further tumor progression and require further therapy with alternate chemotherapy regimens and/or ultimately with radiation therapy once older. In these children, surveillance for tumor and therapy-related morbidity is of paramount importance as the overall survival outcomes of these children remains very good with subsequent therapy. In a recent analysis of greater than 4000 patients treated for a pediatric low-grade glioma, the majority of patients had excellent very long-term survival, well into their adult years. Importantly these tumors are unlikely to transform to higher grade tumors [40].

29.7 Future Directions for Targeted Therapy in Pilocytic Astrocytomas

Genetic alterations in pediatric astrocytomas are distinct from their adult counterparts. Genome-wide analysis of DNA copy number aberrations in pediatric low-grade astrocytomas have identified both duplication of the BRAF proto-oncogene and activating BRAF mutations. In addition, fusions between KIAA1549 and BRAF are seen in up to 100 % frequency in tumors [21–24]. In vitro analysis of tumor cell lines suggests that activation of the mitogen-activated protein kinase (MAPK) pathway may be involved in the pathogenesis of these tumors [21]. In vitro experiments have demonstrated that when BRAF is silenced, tumor cells undergo cell cycle arrest. These promising results have led to the development of new and more specific agents targeting the MAPK pathway which are currently entering early phase studies in children with low-grade gliomas.

29.8 Grade II Tumors

While WHO grade I tumors are noninfiltrating, grade II tumors are diffuse astrocytomas which have different genetic characteristics to grade I tumors. They include diffuse fibrillary

astrocytoma and pleomorphic xanthoastrocytoma. The initial therapeutic considerations in this group of tumors are similar to grade I tumors. Outcomes for children with Grade II PLGGs is also excellent (and distinct from adult patients) with the majority of patients expected to be long-term survivors [25, 40].

29.9 Grade III or IV Cerebellar Astrocytomas

Malignant astrocytomas can occur anywhere in the central nervous system, including the posterior fossa. They include anaplastic astrocytoma (WHO grade III) and glioblastoma multiforme (WHO grade IV). Pediatric malignant gliomas differ in their molecular and genetic characteristics when compared to adult gliomas. In particular the incidence of mutations of the epidermal growth factor receptor and the presence of Pten deletions and p53 mutations is less frequent in the pediatric population than adult tumors [26, 27]. In children, these tumors are most commonly supratentorial and account for <5 % of cerebellar astrocytomas [28, 29]. High-grade gliomas are rare in infants compared to older children [2]. Like low-grade gliomas, constitutional chromosomal disorders such as NF-1 increase the risk of developing high-grade gliomas. Prior exposure to radiation therapy also increases the risk of developing high-grade gliomas and can be seen following therapy for other malignancies such as medulloblastoma or leukemia. Overall prognosis remains poor. There is high recurrence without adjuvant therapy with overall 2-year survival of between 32 and 45 % following adjuvant therapy [30]. Anatomical location confers prognostic significance; posterior fossa tumors have a poorer prognosis than supratentorial high-grade gliomas [31].

29.10 Management of High-Grade Astrocytomas

The initial management of children with high-grade gliomas is maximal surgical resection, with studies demonstrating that the most favorable

prognostic factor is gross total resection, with no evidence of residual tumor on postoperative MRI [29]. This is followed by involved field irradiation therapy, concurrent administration of the alkylating agent temozolomide, followed by maintenance therapy also with temozolomide.

This adjuvant chemotherapy regimen is based on studies with an adult patient population that showed improved survival in patients receiving radiotherapy and concomitant and adjuvant temozolomide for glioblastoma [32]. In this study, the addition of temozolomide, given concomitant to radiation and as maintenance adjuvant therapy, increased 2-year overall survival of adult patients with high-grade glioma to 26.5 % compared to 10.4 % in those patients who had received postoperative radiation therapy alone. Studies in the pediatric population have failed to reproduce convincing survival benefits from the addition of temozolomide. The COG study ACNS 0126 compared the outcomes of children newly diagnosed with high-grade gliomas treated with radiation therapy and concurrent temozolomide therapy with historical controls and was not able to document any improvement in survival with temozolomide, with a 3-year event-free survival of 11 % [33]. However, given the results in the adult population, this approach is currently the standard of care in children with high-grade tumors [31].

In a phase 2 study conducted by the Children's Oncology Group investigating the responses to temozolomide in children with a variety of CNS malignancies, only one response (partial response) was observed in 23 children with malignant astrocytomas. It is important to note, however, that these children were treated on progression, not "up-front" up as is the current practice [34].

As described above, the molecular characteristics of pediatric malignant astrocytomas are considerably different to their adult counterparts, and they are considered separate disease entities in the two age groups. Extrapolating results from adult studies to pediatric patients, especially without current phase III studies, may therefore not be valid and may account for the difficulty in demonstrating improved survival with temozolomide

in the pediatric population. Despite this, however, concurrent temozolomide with radiation remains the current standard of care, while other targeted therapies are being investigated for pediatric malignant astrocytomas.

High-grade tumors are usually very vascular tumors and molecular analysis of adult tumors have shown that proangiogenic factors including vascular endothelial growth factor (VEGF) are upregulated, leading to the hypothesis that antiangiogenic agents may have therapeutic benefits [35]. The agent that has undergone most clinical testing is bevacizumab, a monoclonal anti-VEGF-A antibody. Bevacizumab in combination with other chemotherapeutic agents such as irinotecan has been shown to increase progression-free survival in adults with refractory high-grade glioma [36, 37]. However, increased tumor invasion has been described [38]. The role of bevacizumab in recurrent or refractory pediatric tumors remains unclear, with a phase II pediatric brain tumor consortium study failing to detect objective responses in children with recurrent malignant glioma or diffuse brainstem glioma [39]. Further studies investigating the role of antiangiogenics in children with high-grade gliomas are continuing.

29.11 Long-Term Follow-Up

It is clear that although there has been an increase in the 5-year survival of children with cerebellar astrocytomas, the consequences of therapy can result in potential intellectual, neurological, and endocrine deficits. The magnitude of these problems often depends on the anatomical site and mode of therapy. For example, intellectual impairment is one of the most frequent problems seen in young children who have been treated with radiation therapy. Likewise, damage to normal brain development from raised intracranial pressure and surgical trauma can result in neurological sequelae. Chemotherapy can have acute effects such as hair loss and myelosuppression, but longer-term side effects such as hearing loss and renal impairment from platinum compounds can have longer-lasting consequences. Early

intervention to correct deficits is being trialed, and MRI may be a useful means of locating and tracking potential white and gray matter changes. Further investigation of functional MRI may provide better means of early intervention which is specifically targeted.

References

1. Sievert AJ, Fisher MJ (2009) Pediatric low-grade gliomas. *J Child Neurol* 24(11):1397
2. Rickert CH, Paulus W (2001) Epidemiology of central nervous system tumors in childhood and adolescence based on the new WHO classification. *Childs Nerv Syst* 17:503
3. Kieran MW, Walker D, Frappaz D, Prados M (2010) Brain tumors: from childhood through adolescence into adulthood. *J Clin Oncol* 28(32):4783
4. Steinbok SC, Mutat A (1999) Chapter 35: Cerebellar astrocytoma. In: Albright AL, Pollack IF, Adelson PD (eds) *Principles and practice of pediatric neurosurgery*. New York: Thieme, p 1300
5. Lawso ARJ, Tatevossian RG, Philipps KP et al (2010) RAF gene fusions are specific to pilocytic astrocytoma in a broad paediatric brain tumour cohort. *Acta Neuropathol* 120:271
6. Kluwe L, Hagel C, Tatagiba M et al (2001) Loss of NF1 alleles distinguish sporadic from NF-1 associated pilocytic astrocytomas. *J Neuropathol Exp Neurol* 60(9):917
7. Listernick R, Charrow J, Gutmann DH (1999) Intracranial gliomas in neurofibromatosis type 1. *Am J Med Genet* 89(1):38
8. Garcia DM, Latifi HR, Simpson JR et al (1989) Astrocytomas of the cerebellum in children. *J Neurosurg* 71(5):661
9. Burzynski SR (2006) Treatments for astrocytic tumors in children. *Pediatr Drugs* 8(3):167
10. Packer RJ, Ater J, Allen J, Phillips P et al (1986) Carboplatin and vincristine chemotherapy for children with newly diagnosed progressive low grade gliomas. *J Neurosurg* 86:747
11. Bowers DC, Krause TP, Aronson LJ et al (2001) Second surgery for recurrent pilocytic astrocytoma in children. *Pediatr Neurosurg* 34:229
12. Gajjar A, Sanford RA, Heideman R et al (1997) Low grade astrocytoma: a decade of experience at St. Jude Children's Research Hospital. *J Clin Oncol* 15(8):2792
13. Castello MA, Schiavetti A, Varrasso G et al (1998) Chemotherapy in low grade astrocytoma management. *Childs Nerv Syst* 4:6
14. Fisher BJ, Leighton CC, Vujovic O et al (2001) Results of a policy of surveillance alone after surgical management of pediatric low grade gliomas. *Int J Radiat Oncol Biol Phys* 51(3):704

15. Shaw EG, Wisoff JH (2003) Prospective clinical trials of intracranial low grade glioma in adults and children. *Neuro Oncol* 5(3):153
16. Packer RJ, Ater J, Allen J et al (1997) Carboplatin and vincristine chemotherapy for children with newly diagnosed progressive low grade gliomas. *J Neurosurg* 86:747
17. Lefkowitz IB, Packer RJ, Sutton LN et al (1988) Results of the treatment of children with recurrent gliomas with lomustine and vincristine. *Cancer* 61:896
18. Kadota RP, Kun LE, Langston JW et al (1999) Cyclophosphamide for the treatment of progressive low-grade astrocytoma: a Pediatric Oncology Group phase II study. *J Pediatr Hematol Oncol* 21(3):198
19. Longee DC, Friedman HS, Albright RE et al (1990) Treatment of patients with recurrent gliomas with cyclophosphamide and vincristine. *J Neurosurg* 72:583
20. Ater A, Holmes E, Zhou T et al (2008) Abstract LGG 18: results of COG protocol A9952: a randomised phase 3 study of two chemotherapy regimens for incompletely resected low grade glioma in young children. *Neuro-Oncology* 10:369
21. Pfister S, Janzarik W, Remke M et al (2008) BRAF gene duplication constitutes a mechanism of MAPK activation in low grade astrocytomas. *J Clin Invest* 118(5):1739
22. Sievert A, Jackson EM, Gai X et al (2009) Duplication of 7q34 in pediatric low grade astrocytomas detected by high density single nucleotide polymorphism-based genotype arrays results in a novel BRAF fusion gene. *Brain Pathol* 19:449
23. Bar E, Lin A, Tihan T et al (2008) Frequent gains at chromosome 7q34 involving BRAF in pilocytic astrocytoma. *J Neuropathol Exp Neurol* 67(9):878
24. Forsheo T, Tatevossian R, Lawson A et al (2009) Activation of the ERK/MAPK pathway: a signature genetic defect in posterior fossa pilocytic astrocytomas. *J Pathol* 218:172
25. Wu X, Bandopadhyay P, Ng J et al (2011) The evolution of the histology in pleomorphic xanthoastrocytomas in children: a study of 15 cases. *Pathology* 43(1):9
26. Kieran MW, Walker D, Frappaz DM et al (2010) Brain tumors: from childhood through adolescence into adulthood. *J Clin Oncol* 28(32):4783–4789
27. Pollack IF, Hamilton RL, James CD et al (2006) Rarity of PTEN deletions and EGFR amplification in malignant gliomas of childhood: results from the Children's Cancer Group 945 cohort. *J Neurosurg* 105(5 Suppl):418
28. Conway PD, Oechler HW, Kun LE et al (1991) Importance of histologic condition and treatment of pediatric cerebellar astrocytoma. *Cancer* 67:2772
29. Song KS, Phi JH, Cho BK et al (2010) Long-term outcomes in children with glioblastoma. *J Neurosurg Pediatr* 6:145–149
30. Perkins SM, Rubin JB, Leonard JR et al (2011) Glioblastoma in children: a single institution experience. *Int J Radiat Oncol Biol Phys* 80:1117–1121
31. Bartels U, Baruchel S, Carret AS et al (2011) The use and effectiveness of temozolamide in children with central nervous system tumours: a survey from the Canadian paediatric brain tumour consortium. *Curr Oncol* 18(1):e19
32. Stupp R, Mason WP, van den Bent MJ et al (2005) Radiotherapy plus concomitant and adjuvant temozolamide for glioblastoma. *N Engl J Med* 352:987–996
33. Cohen K, Pollack I, Zhou T et al (2011) Temozolamide in the treatment of high-grade gliomas in children: a report from the Children's Oncology Group. *Neuro-Oncology* 13(3):317
34. Nicholson HS, Kretschmar CS, Krailo M et al (2007) Phase 2 study of temozolamide in children and adolescents with recurrent central nervous system tumours. A report from the Children's Oncology Group. *Cancer* 110(7):1542–1550
35. Folkman J (2006) Angiogenesis. *Annu Rev Med* 57:1
36. Cloughesy T, Prados M, Wen P et al (2008) A phase II, randomised, non-comparative clinical trial of the effect of bevacizumab (BV) alone or in combination with irinotecan (CPT) on 6 month progression free survival (PFS6) in recurrent, treatment-refractory glioblastoma (GBM). *J Clin Oncol* 26
37. Norten A, Drappatz J, Wen P (2009) Antiangiogenic therapies for high-grade glioma. *Nat Rev Neurol* 5:610
38. Narayana A, Kelly P, Gofinos J et al (2009) Antiangiogenic therapy using bevacizumab in recurrent high grade glioma: impact on local control and patient survival. *J Neurosurg* 110:173
39. Gururangan S, Chi S, Young Poussaint T et al (2010) Lack of efficacy of bevacizumab plus irinotecan in children with recurrent malignant glioma and diffuse brainstem glioma: a pediatric brain tumor consortium study. *J Clin Oncol* 28(18):3069
40. Bandopadhyay P, Berghold G, London WB et al (2014) Long-term outcome of 4,040 children diagnosed with pediatric low-grade gliomas: an analysis of the Surveillance Epidemiology and End Results (SEER) database. *Pediatr Blood Cancer* 61(7):1173–1179. doi: [10.1002/pbc.24958](https://doi.org/10.1002/pbc.24958). Epub 2014 Jan 30

Greg C. Wheeler

30.1 Introduction

The classification, pathology, presentation, and genetics of cerebellar astrocytomas (CA) have been discussed in earlier sections of this text. Cerebellar astrocytomas make up 10–15 % of all childhood brain tumors and one quarter of posterior fossa tumors in children. Most are pilocytic astrocytomas (PAs); of these about 85 % are WHO grade 1 tumors, with the majority of the remainder WHO grade 2 tumors. Cerebellar PAs represent approximately 40 % of all pilocytic astrocytomas and two thirds of PAs in children [1]. The incidence of PAs in a Swiss series was 8.3 per million per year in children under 15 years old [1].

High-grade malignant tumors are rare. These may arise as a second malignant neoplasm resulting from prior posterior fossa irradiation for the treatment of medulloblastomas, ependymomas, or other tumors. In young children (<3 years old) high-grade astrocytomas are uncommon, and about one quarter are in the cerebellum [2]. In some series, the incidence of high-grade astrocytomas in the cerebellum is as high as 24 % [3].

The median age at presentation of CAs is 5–6 years [4] with 20 % under 3 at diagnosis.

G.C. Wheeler, M.D.
Radiation Oncology and Cancer Imaging,
Peter MacCallum Cancer Centre,
St. Andrews place, East Melbourne,
VIC 3002, Australia
e-mail: Greg.Wheeler@petermac.org

This is an important consideration in the management of these children, as the late effects of radiation treatment are more significant the younger the child is at treatment; indeed, age is a more important factor in neurocognitive decline than total dose [5]. Each year of increasing age decreases the monthly IQ loss by 0.0275 points per month [5].

Types of Cerebellar Astrocytomas

Juvenile pilocytic astrocytomas (JPA) (WHO grade 1)

Diffuse fibrillary astrocytomas (WHO grade 2)

Anaplastic astrocytomas (AA) (WHO grade 3)

Glioblastoma multiforme (GBM) (WHO grade 4)

30.2 Treatment

Surgery is the treatment of choice for most cerebellar astrocytomas. Ideally a complete resection is obtained. In the ANZCCSG Baby Brain study [6] where intensive chemotherapy was given to children under 4 years old for CNS tumors in an effort to delay radiotherapy, the 5-year event-free survival (EFS) was significantly improved if a complete resection was able to be undertaken (60 % vs 22 %). If complete resection is achieved, observation is appropriate for low-grade tumors.

Adjuvant chemotherapy (usually carboplatin based) is considered where there has been a progression of tumor, again with the intention of delaying the need for radiotherapy until the child is older.

Complete resection also improves the outcome in high-grade tumors [2]. In a St. Jude series, the 10-year overall survival (OS) was 70 % versus 30 % ($p=0.24$) where resection was incomplete. In the same series, all children under 1 year of age at diagnosis were alive at 5 years, compared to 37.5 % for those aged 1–3 years old [2]. This effect was independent of the extent of resection ($p=0.67$) and became significant when analyzed as a continuous variable using the Cox model ($p=0.047$).

Radiotherapy is rarely used in the juvenile PA group.

30.3 Radiotherapy

Table 30.1 shows a summary of the radiotherapeutic management of cerebellar astrocytomas.

30.3.1 Timing

In pilocytic and low-grade tumors, a complete resection does not require adjuvant radiation (RT) [7, 8].

In low-grade CAs after a complete resection, approximately 13 % of patients relapse, half of those occurring between 6 and 12 months of surgery [4]. In those not requiring surgery at recurrence, three of six in one series regressed, while the others had further treatment [4].

Table 30.1 Radiotherapy treatment summary of cerebellar astrocytomas

Timing of radiotherapy	Low-grade gliomas	High-grade gliomas
	At progression, usually after chemotherapy	Postoperatively
Dose	54 Gy in 1.8 Gy fractions	59.4 Gy in 1.8 Gy fractions
GTV	Tumor bed + solid and cystic tumor on T1 MTR	Tumor bed + solid and cystic tumor on T1 MTR
CTV	GTV + 1.0 cm	GTV + 2.0 cm
PTV	CTV + 3–5 mm	CTV + 3–5 mm
PFS 5 years	68–87 %	30 %
OS 5 years	80–100 %	60–66 %

In the Mishra series, 5-year progression-free survival (PFS) rates were 79 % ± 13 % for patients treated with complete resection (CR), 60 % ± 8 % for those with subtotal resection (STR), and 46 % ± 8 % for those with biopsies alone. Five-year OS rates were 100 % for those treated with CR, 88 % ± 5 % for those with STR, and 89 % ± 5 % for those with biopsies alone. Ten-year PFS rates were 45 % ± 8 % for patients with STR and 30 % ± 8 % for those with biopsies alone. Ten-year OS rates were 82 % ± 6 % for patients with STR and 76 % ± 8 % for those with biopsies. The hazard ratio (HR) for PFS with a complete resection was 0.14 when compared to biopsy alone. This did not translate to a significant hazard ratio for OS [7].

In the setting of an incomplete resection, adjuvant chemotherapy may be considered either at initial diagnosis or at progression.

Low-grade tumors have been reported to spontaneously regress with no further treatment or following incomplete surgical resection [4, 8]. In Saunders et al., 5 of 11 patients who were observed after an incomplete resection progressed at a mean of 12 months; 5 of 11 showed tumor regression at a mean of 32 months [4]. The remaining patient progressed as a high-grade tumor. In the Netherlands, a retrospective review of 25 children (mean age 10.8 years) with pilocytic CAs who had undergone a subtotal resection showed that 15 progressed, 8 were stable, 1 spontaneously regressed, and the last regressed after irradiation [8].

A review by Palma revealed that incompletely resected pilocytic tumors remain stable in about one third of cases and spontaneously regress in about 14 % [9].

In the event of progression, radiation can be utilized if further surgery is not feasible or if there is an incomplete resection at the salvage procedure.

Against this approach, the Kidd series demonstrated increase relapses after radiation in the group who were treated at recurrence, rather than at the initial diagnosis (see below) [10]. However, only 5 of the 20 patients in this series were infratentorial.

Grade 2 tumors similarly do not necessarily require radiation as part of their initial management [7]. A retrospective review of grade 2 astrocytomas in children at Memorial Sloan Kettering showed similar PFS and OS when comparing those receiving RT at initial diagnosis versus no initial RT. The respective 5- and 10-year PFS rates were $59\% \pm 13\%$ and $43\% \pm 14\%$ for those not receiving radiation at diagnosis, as compared with $60\% \pm 7\%$ and $44\% \pm 8\%$ for those who did. The respective 5- and 10-year OS rates were $93\% \pm 6\%$ and $82\% \pm 12\%$ for those receiving no radiation at diagnosis, as compared with $84\% \pm 5\%$ and $77\% \pm 7\%$ for those who did. Importantly, this analysis removed children under 3 and those who had undergone a gross total resection to remove selection bias for radiation [7]. Only 10% of the patients had infratentorial tumors in this study.

In the adult setting, a large randomized EORTC study showed no difference in overall survival in those who were observed (7.4 years, 5 years) compared to those offered early radiation (7.2 years). There was a significantly reduced progression-free survival in the observation group (55% 5 years PFS vs 35%), with the observation group having a longer time from relapse to death (in part due to the use of radiation as salvage therapy) [11].

In high-grade tumors, consideration may be given to intensive chemotherapy to delay the need for radiotherapy in children under 3–4 years of age [6]. However, if it is considered that the supratentorial volumes can be minimized and thus the neurocognitive effects reduced, then initial irradiation may be preferable [5, 12]. In very young patients (<3 years old) with high-grade tumors, an appropriate strategy is to achieve a maximal safe resection followed by adjuvant chemotherapy with radiation held in reserve until progression or relapse [2].

30.3.2 Radiation Dose

The results of the prospective EORTC study 22844 of dose response in low-grade gliomas in

adults demonstrated no significant difference in survival or PFS between administration of 45 and 59.4 Gy in 379 patients [13]. This was also seen when allowance was made for incomplete versus complete resection. Interestingly however twice the number of patients (26 vs 13) in the higher-dose arm had interruptions to their radiotherapy of a week or more, and nine of those had treatment discontinued.

In the prospective St Jude series [5, 14] of conformal radiotherapy for low-grade gliomas, a dose of 54 Gy was used in 1.8 Gy per fraction (#), over 6 weeks. There were 17 cerebellar tumors in this cohort of 78. Similar fractionation schedules have been reported by other groups [3, 10].

As a result, many centers use 54 Gy as their routine dose for low-grade gliomas.

In high-grade gliomas, there have been conflicting results regarding dose response. In the adult population there were equivalent results between 35 Gy in 10 #s and 60 Gy in 30 #s in Phillips' study, although it was closed due to poor accrual [15]. In a recent pilot study, Beauchesne et al. [16] examined thrice daily (TDS) radiation of 0.75 Gy up to 67.5 Gy total and found that, in comparison to the EORTC-NCIC 26981-22981 study, the OS and PFS (5.1 and 9.5 months, respectively) were superior to conventional radiotherapy alone, but not to RT and temozolomide.

An older study of hyperfractionation to adult gliomas (61.4, 71.2, and 80 Gy) showed no improvements in OS between the dose groups [17]. Another Japanese series [18] using 60–80 and 90 Gy in 2 Gy per fraction 5 days per week showed no improvement in the overall survival of patients with differing doses, but there were fewer local failures in the 90 Gy group (94/13 vs 16 of 19).

Most centers and studies use radiation of 54–60 Gy, with a recent St Jude series of high-grade gliomas (in children) with temozolomide mandating 59.4 Gy in 1.8 Gy fractions.

30.3.3 Radiation Volumes

The volume for irradiation in cerebellar astrocytomas is local conformal. A clinical and autopsy

series [19] (in adults) demonstrated that in 15 patients with infratentorial glioblastoma, there was no evidence of CSF spread, indicating no need for craniospinal irradiation (CSI). However a small study from Toronto [20] demonstrated that three of four pediatric patients with cerebellar glioblastoma ultimately relapsed in the spine; similarly a Japanese series had five consecutive patients with malignant cerebellar astrocytomas relapsing with leptomeningeal disease [21]. Other authors have suggested CSI in this group [22]. Some centers have given craniospinal irradiation for glioblastomas, but this is not a routine in the absence of CSF seeding [3].

It is essential that dedicated spinal MRIs and CSF cytology be performed prior to planning radiotherapy to determine whether craniospinal irradiation is required.

In adult series, the majority of failures of non-JPA astrocytomas occur in the previously treated field with only a few at the field edge [23].

In the St Jude series [5, 24], the gross tumor volume (GTV) was taken to be the solid and cystic tumor seen on multisequence MRI before radiotherapy. A 10 mm expansion was made to the clinical target volume (CTV), and the planning target volume (PTV) was a 3–5 mm expansion on the CTV depending on the degree of immobilization. In this group (overall) there was only one marginal failure, with four failing metastatically and eight being local failures. The marginal failure was in a patient with optic glioma.

Jalali has reported using a 5 mm GTV-CTV expansion with a 3 mm PTV expansion in low-grade and benign tumors with similar results [25].

Thus, the use of a 10 mm GTV-CTV expansion is considered safe for low-grade tumors.

In high-grade tumors such as glioblastoma, larger margins are needed. In a landmark paper, Halperin et al. performed autopsy studies on 15 adults who had died of GBM [26]. Neuropathological analysis was performed identifying malignant cells, and the distribution was traced onto diagrams of the whole-mount histological sections. Radiotherapy plans were carried out using the most recent CT scan, with reference

to the contrast-enhancing area and edema. In nine patients, a 1 cm margin on the contrast-enhancing area would have missed the identified tumor on histology. Expanding the volume to the tumor, the edema and 1 cm would have covered only six patients, whereas a 3 cm margin covered all the tumor in all patients. There was evidence of tumor tracking along neural pathways and crossing of the corpus callosum.

In a clinical study, Wallners group looked at patterns of failure in AAs and GBMs treated with irradiation. Using the CT contrast enhanced as the initial tumor volume, 56 % of patients recurred within 1 cm and 78 % within 2 cm. All patients received whole brain radiotherapy of the order of 40 Gy with the majority having a boost to 51–70 Gy. There was no mention as to the margins used for the boost therapy.

Kelly et al. from the Mayo Clinic took 195 samples from 40 patients and found that contrast enhancement most often corresponded to tumor tissue without intervening parenchyma; hypodensity corresponded to parenchyma infiltrated by isolated tumor cells or in some instances to tumor tissue in low-grade gliomas or to simple edema, and isolated tumor cell infiltration extended at least as far as T2 prolongation on magnetic resonance images in both high- and low-grade tumors.

Extrapolating these results to children, a margin of CTV expansion of 2 cm from the GTV, the contrast-enhanced mass (T1 post-gadolinium or tumor bed) plus the associated T2 or FLAIR abnormalities, is appropriate [27].

The use of functional imaging in brain tumors is also increasing. In a series of 36 patients, pre-treatment methionine PET scans were performed in patients with glioblastoma. Of 19 patients with uptake in the tumor, the five who had activity outside the high-dose radiotherapy area all had non-central failures; as compared to 2 of the remaining 14 who had activity inside the high-dose radiotherapy area [28]. MET PET has also been shown to be a strong predictor of disease involvement when used to guide stereotactic biopsies (61 of 61 in 32 patients) [29]. It has proved useful in modifying the surgical volumes in a large Belgian series in both high- and low-grade tumors [30].

It is quite likely that functional imaging will become integrated into radiotherapy planning as an adjunct to MRI and CT.

30.4 Technique

30.4.1 Modality

The increasing complexity of planning systems in addition to other technological advances means that treatment can be offered with less damage to the normal brain tissue than the previous [12, 14, 31].

Conformal 3D noncoplanar plans have become the standard of care in many institutions. The addition of noncoplanar beams allows relative sparing of the temporal lobes and the subventricular/hippocampal regions implicated in late neurocognitive complications [12, 31, 32]. Figures 30.1, 30.2, 30.3, and 30.4 demonstrate the benefits of a six-field noncoplanar plan versus a three-field coplanar plan.

Intensity modulated radiotherapy (IMRT) has been used in posterior fossa tumors. The main advantage is in reducing the inner ear/cochlear dose to less than 30–35 Gy which should result in less hearing loss, particularly high-frequency deafness [33–35]. IMRT therapy does increase the volumes of the normal brain receiving low doses which may theoretically increase the incidence of second malignancies and may also contribute to [36] some late neurocognitive effects [12].

Using *stereotactic radiosurgery* of 12–18 Gy to the 50–80 % isodose line, results have been reported equivalent to standard conformal therapy in grade 1 tumors [10]. In a series from Tapei which examined gamma knife treatment for low-grade gliomas, by covering the T1- and T2-weighted abnormalities with a median of 14 Gy, the 10-year PFS was 65 %. All local failures in this series were within the high-dose volume, including patients receiving SRS after progressing through initial therapy [23]. Similar results using a median of 15 Gy have been reported by Hadjipanayis et al. [37] and Kano et al. [38].

The number of centers offering proton therapy has increased in the last decade and in many countries has become a viable option for patients. Proton therapy has the benefit of reducing auditory apparatus dose and sparing the temporal lobes from both low- and high-dose exposure [36, 39]. There is no difference reported in PFS or OS in the low-grade glioma group [40].

30.4.2 Results

The survival of CAs is highly dependent on the histology [41, 42]. Glioblastomas that are EGFR immunonegative appear to be more radiosensitive and thus have better control rates [43]. In a large series of CNS tumors, Morris et al. [44] found that a 15-year overall survival for low-grade gliomas was approximately 90 %, whereas for high-grade gliomas it was around 60 %. In the Swiss series [1] of pilocytic astrocytomas, there was a 100 % 5-year OFS and 96.8 % 10-year OFS.

Functional imaging is proving to be important in the predictions of outcome. FET PET showing uptake with a diffuse pattern on MRI in low-grade gliomas has a poorer outcome than diffuse tumors with no uptake; the best outcomes occurred in circumscribed tumors with no uptake [45].

Saunders group treated 12 children with RT for low-grade tumors with regression or stabilization first occurring at a mean age of 6 months with complete changes at 14.9 months. Only one child progressed [4].

Kidd et al. similarly found 100 % OS at 5 years and 80 % at 10 years in pediatric patients receiving radiotherapy for grade 1 tumors. The 5-year progression-free survival was 68 %, with those having upfront therapy faring better than those after disease progression (77 % vs 50 %, $p=0.013$) [10]. The infratentorial group fared better than the supratentorial group (80 % PFS 5 years vs 59 %). Patient age had no impact on outcome.

In the Merchant series [5, 14], the overall survival was 98.5 % at 5 years and 95.9 % at



Figs. 30.1 and 30.2 A three-field coplanar field arrangement showing dose distribution (Fig. 30.1) and the dose volume histogram (DVH) for the plan in Fig. 30.1 (Fig. 30.2)

10 years, the event-free survival was 87.4 % (5 years) and 74.3 % (10 years). The 5- and 10-year local failure rate was 8.7 and 16.4 %, respectively.

For high-grade gliomas, overall the prognosis is better than in the adult setting with a 5-year OS of 66 % but a 5-year event-free survival of 28 % [2].The median survival of adults with



Figs. 30.3 and 30.4 The same tumor volumes now planned with a six-field noncoplanar arrangement. Note the reduction in temporal lobe dose (Fig. 30.3) and the DVH for the plan in Fig. 30.3. Note the improvement in temporal lobe doses (Fig. 30.4)

high-grade cerebellar astrocytomas is of the order of 14 months [14]. In some series, there is no difference in outcomes for AA versus GBM in children under 3.

30.4.3 Surveillance

In low-grade tumors, the need for routine surveillance is less marked than in high-grade

tumors, ependymomas, or medulloblastoma [4]. The Saunders group recommends routine surveillance imaging for low-grade CAs at 6 months, 1, 2, 3.5, and 5 years after either complete surgical resection or radiotherapy [4]. In the incompletely resected group, they recommend surveillance at six monthly intervals for 3 years, then yearly for 2 years, and two yearly thereafter [4].

Dirven's group recommends fewer scans again; surveillance scans at 1 and 4 years for complete resection and yearly for residual disease [8].

In the future, the response to treatment using functional imaging may become an important tool to guide the frequency of assessment.

30.4.4 Toxicity: Acute

Acute side effects of posterior fossa radiotherapy are generally mild and easily managed. The most common side effects are alopecia, otitis, and effects consistent with peritumoral swelling (headache, nausea, and vomiting) [11].

In the weeks and months after radiotherapy, changes in the capillary permeability and transient demyelination may cause headaches, somnolence, fatigability, and worsening of the initial presenting symptoms. This occurs in up to 60–70 % of children receiving cranial radiation and is proportional to the whole brain DVH [46, 47]. This effect is self-limiting and usually recovers after 2–3 weeks. It should not progress into further neurological compromise [46, 48, 49].

30.5 Intermediate Imaging Changes

In the weeks and months following radiotherapy for low-grade tumors, routine imaging may reveal an increase in asymptomatic edema and/or cyst development [14, 38]. The latter effect may even occur during the radiotherapy treatment itself. This should settle spontaneously but may necessitate surgical drainage of the cyst should symptoms develop [14]. It can be mistaken for a local recurrence and therefore may cause signifi-

cant distress to patients, their families, and the treating team. If there is doubt, then functional imaging or a biopsy may be required. Mostly repeat imaging is all that is needed approximately 6 weeks later.

30.6 Toxicity: Late

The impact of treatment on later health is significant in children who have had brain tumors. The incidence of death due to medical complications occurred 25 times more than expected in the matched population in Morris' review of the St Jude series [44]. This is in addition to the significant health and functional effects that the treatment of brain tumors entails.

30.6.1 Neurocognition

There is limited data on the long-term toxicity of cerebellar astrocytomas. Much of the appropriate data comes from series which examine gliomas at any site or radiation given for other posterior fossa tumors.

It is important to appreciate that radiotherapy alone is not the sole cause of neurocognitive impairment in children with brain tumors. More surgical complications are associated with a sharper decline in later IQ [50]. Increased inattentiveness has been observed in children undergoing two or more surgical procedures as compared to one [51]. Hydrocephalus requiring a shunt has been linked to impaired attention, slowed processing, and lower scores on the Child Behaviour Checklist [5, 51–54]. Results are also better before radiation in children who have a biopsy only in comparison to a subtotal resection [5].

Some chemotherapeutic agents have been implicated in reduced neurocognitive functioning, particularly intrathecal methotrexate [55] although this is not routinely used in the management of astrocytomas. The most common agents used in CAs (temozolomide and carboplatin) have not been shown to affect cognition. However, in Merchant's series [5] a trend was

seen to higher scores on visual auditory learning (10.7 points $p=0.0983$) in those not treated with chemotherapy.

The Aarsen series [56] examined 35 patients with infratentorial tumors of whom 15 required remedial teaching and seven needed special education. The majority had received radiotherapy postoperatively. Importantly, the mean preoperative bicaudate index of hydrocephalus was 0.22 in this group, compared to 0.13 in the supratentorial group. They also found that, compared to the normal population, these patients had significantly lower scores on verbal intelligence, sustained attention, speed (cancellation test speed), long-term visual-spatial memory, executive functioning, and naming. Further sub-analysis showed that children with a cerebellar PA had significantly lower scores on all these tests with exception of verbal intelligence in comparison to the norms [56].

The largest single institution study of localized pediatric brain tumors has been reported by the Merchant group from St Jude Children's Research Hospital [5, 12, 31, 51, 53, 57]. They have demonstrated less inattentiveness in children with posterior fossa syndromes as opposed to supratentorial ones, provided that tight conformal therapy and attention to supratentorial structures are performed [51]. In this series, the most severe decline in cognitive performance was in those children under 5 years old. Neurocognitive impairment appears to be worse in children with NF-1 compared to those without NF-1, and they had lower IQ scores before radiotherapy commenced. It appears that the volumes of brain receiving 30–60 Gy are more important than those receiving 0–30 Gy. The predicted IQ decline can be found using this derived equation for the volumes of supratentorial brain irradiated [5]:
$$IQ = 95.5545 + (Age \times 0.3291) + Time \text{ (months)} \times (Age \times 0.00273) - (V_{0-30 \text{ Gy}} \times 0.0027) - (V_{30-60 \text{ Gy}} \times 0.0047).$$

30.6.2 Hearing

The impact of radiation on hearing loss is well recognized, particularly in combination with

platinum-containing chemotherapeutic agents. In the radiotherapy alone group, hearing loss tends to occur 3–5 years after the completion of therapy. There does appear to be a dose threshold of approximately 30–35 Gy and is worse with pre (or concurrent) ototoxic chemotherapy, CSF shunting, and is more common on the right side [33–35]. Overall, hearing loss occurred in about 15 % of children treated [5, 58]. Deficits tend to be in higher frequencies more than lower frequencies [5, 58].

30.6.3 Vasculopathy

The incidence of vasculopathy in post-RT imaging is about 5 % of patients at 7 years; this was 12.5 % for patients less than 5 years of age compared to 3.8 % for those over 5 [14].

30.6.4 Neuroendocrine

There is evidence that up to 24 % of patients have reduced GH production on provocative testing after surgery and before radiation, and 12 % have precocious puberty [5]. In the same series, the 5-year, 10-year, and 10-year (hypothalamic dose >40 Gy) cumulative incidence, respectively, of growth hormone replacement were 46.0, 48.9, and 54.7 %; of thyroid hormone replacement, 61.4, 64.0, and 69.1 %; of glucocorticoid replacement, 19.2, 19.2, and 20.0 %; of DDAVP replacement, 2.1, 5.2, and 6.2 %; of sex hormone replacement, 8.0, 14.1, and 16.4 %; and of GnRH analog therapy, 31.8, 34.2, and 35.3 % [5].

In young children (<3 years old) with high-grade tumors, most have endocrinopathies [2].

30.6.5 Second Malignancies

In the Morris study reviewing 672 patients who had CNS tumors [44], 1.2 % of patients with posterior fossa tumors later succumbed to a second malignant neoplasm (SMN) compared to 3.9 % of those patients who had supratentorial tumors. Overall, 2.3 % of low-grade tumors and 3.9 % of

high-grade gliomas died of a second malignancy. The median time to development of an SMN was 9.8 years and from then to death was 10.5 months [44]. There have been reports of malignant astrocytomas resulting from prior radiation and also of malignant transformation of low-grade into high-grade tumors [44, 59, 60]. Radical re-treatment is feasible provided that sufficient time has passed from the initial radiation. In a rhesus monkey spinal cord model [61], substantial recovery of asymptomatic radiation damage can occur over a couple of years. Vascular injury is slower to recover than white matter changes.

30.7 Re-treatment

A local recurrence of a primary tumor or the development of a second malignancy is devastating for the patient, their families, and the treating team. Often treatment is limited due to concerns of breaching tolerance of critical structures which were in the initial radiotherapy field. In adults, re-treatment using fractionated stereotactic radiotherapy using 15–36 Gy [62] in 2 Gy #s has been reported; in 172 patients only one developed radiation necrosis. In this study, patients who had WHO grade 2, 3, and 4 astrocytomas were treated; histology and time to initial progression were prognostic factors. One adult series [63] re-treated 32 patients with a resulting median survival of 36 months, with a 6 % incidence of radionecrosis. 9 % suffered from severe neurological sequelae. In another series of 42 patients, reirradiation to 46 Gy after an initial 54 Gy demonstrated a good quality of life until relapse (8.6 months, less in astrocytomas.) The prognostic factors for survival were the WHO grade of the recurrence, the length of time between treatments, the initial histology, and the response to initial treatment [64].

A review of available reirradiation data found that brain radionecrosis occurs after an NTD (cumulative) of 100 Gy. Higher doses were tolerated with stereotactic techniques which limit the normal brain dose. Interestingly, there was no correlation seen with the time from the initial treatment. A Californian series of patients with a median age of 19 years demonstrated small

survival or palliative benefits with a 9 % incidence of radionecrosis. There are few reports of reirradiation in CA specifically; an Italian study of 31 cerebellar astrocytomas in children had two patients who each had three courses of radiotherapy. Both subsequently died, one from radionecrosis (histologically confirmed) [9].

The use of high-dose stereotactic radiation in recurrent high-grade gliomas after initial radiotherapy in adults has been shown to be feasible [65, 66]. Fogh et al. found that using 3.5 Gy per fraction of stereotactic radiosurgery, with the PTV = GTV = the contrast-enhanced tumor on T1 post-gadolinium MRI, the significant prognostic factors were younger age, smaller GTV, and shorter interval from initial RT with a trend ($p=0.07$) of dose greater than 35 Gy. There were no reports of necrosis in this group [65].

In the pediatric population, reirradiation has been reported in recurrent ependymoma [67]. In this series, the main toxicity was seen in a patient who had radiosurgery of a single 18 Gy fraction to the brainstem. Another series using SRS for both upfront and recurrent treatment in the pediatric group with low-grade tumors reported excellent outcomes of 70.8 % PFS at 5 years [38].

30.8 Long-Term Follow-Up

The upsurge of interest in the long-term effects of cancer treatment has led to the formation of many bodies to review these sequelae. The Children's Oncology Group has developed a series of evidence-based guidelines for follow-up of children and young adults who have had cancer treatment [68]. They are updated regularly in accordance with emerging evidence with specific recommendations depending on the type of treatment received. The next update is due towards the end of 2011. It is clear that surveillance for long-term effects needs to be lifelong [60], but carried out in a manner which allows the survivors to lead as normal a life as possible.

Acknowledgments The author thanks Dr. Josie Samers and Ms Maria Portillo for their help with the text and figures respectively.

References

- Burkhard C, Di Patre PL, Schuler D, Schuler G, Yasargil MG, Yonekawa Y et al (2003) A population-based study of the incidence and survival rates in patients with pilocytic astrocytoma. *J Neurosurg* 98(6):1170–1174
- Sanders RP, Kocak M, Burger PC, Merchant TE, Gajjar A, Broniscer A (2007) High-grade astrocytoma in very young children. *Pediatr Blood Cancer* 49(7):888–893
- Viano JC, Herrera EJ, Suarez JC (2001) Cerebellar astrocytomas: a 24-year experience. *Childs Nerv Syst* 17(10):607–610; discussion 11
- Saunders DE, Phipps KP, Wade AM, Hayward RD (2005) Surveillance imaging strategies following surgery and/or radiotherapy for childhood cerebellar low-grade astrocytoma. *J Neurosurg* 102(2 Suppl):172–178
- Merchant TE, Conklin HM, Wu S, Lustig RH, Xiong X (2009) Late effects of conformal radiation therapy for pediatric patients with low-grade glioma: prospective evaluation of cognitive, endocrine, and hearing deficits. *J Clin Oncol* 27(22):3691–3697
- Bandopadhyay P, Hassall TE, Rosenfeld JV, Wheeler GC, Downie PA, Kirby ML et al (2011) ANZCCSG BabyBrain99; intensified systemic chemotherapy, second look surgery and involved field radiation in young children with central nervous system malignancy. *Pediatr Blood Cancer* 56:1055–1061
- Mishra KK, Puri DR, Missett BT, Lamborn KR, Prados MD, Berger MS et al (2006) The role of up-front radiation therapy for incompletely resected pediatric WHO grade II low-grade gliomas. *Neuro Oncol* 8(2):166–174
- Dirven CM, Mooij JJ, Molenaar WM (1997) Cerebellar pilocytic astrocytoma: a treatment protocol based upon analysis of 73 cases and a review of the literature. *Childs Nerv Syst* 13(1):17–23
- Palma L, Celli P, Mariottini A (2004) Long-term follow-up of childhood cerebellar astrocytomas after incomplete resection with particular reference to arrested growth or spontaneous tumour regression. *Acta Neurochir (Wien)* 146(6):581–588; discussion 8
- Kidd EA, Mansur DB, Leonard JR, Michalski JM, Simpson JR, Perry A (2006) The efficacy of radiation therapy in the management of grade I astrocytomas. *J Neurooncol* 76(1):55–58
- van den Bent MJ, Afra D, de Witte O, Ben Hassel M, Schraub S, Hoang-Xuan K et al (2005) Long-term efficacy of early versus delayed radiotherapy for low-grade astrocytoma and oligodendroglioma in adults: the EORTC 22845 randomised trial. *Lancet* 366(9490):985–990
- Merchant TE, Kiehna EN, Li C, Xiong X, Mulhern RK (2005) Radiation dosimetry predicts IQ after conformal radiation therapy in pediatric patients with localized ependymoma. *Int J Radiat Oncol Biol Phys* 63(5):1546–1554
- Karim AB, Maat B, Hatlevoll R, Menten J, Rutten EH, Thomas DG et al (1996) A randomized trial on dose-response in radiation therapy of low-grade cerebral glioma: European Organization for Research and Treatment of Cancer (EORTC) study 22844. *Int J Radiat Oncol Biol Phys* 36(3):549–556
- Merchant TE, Kun LE, Wu S, Xiong X, Sanford RA, Boop FA (2009) Phase II trial of conformal radiation therapy for pediatric low-grade glioma. *J Clin Oncol* 27(22):3598–3604
- Phillips C, Guiney M, Smith J, Hughes P, Narayan K, Quong G (2003) A randomized trial comparing 35Gy in ten fractions with 60Gy in 30 fractions of cerebral irradiation for glioblastoma multiforme and older patients with anaplastic astrocytoma. *Radiation Oncol* 68(1):23–26
- Beauchesne P, Bernier V, Carnin C, Taillandier L, Djabri M, Martin L et al (2010) Prolonged survival for patients with newly diagnosed, inoperable glioblastoma with 3-times daily ultrafractionated radiation therapy. *Neuro Oncol* 12(6):595–602
- Fulton DS, Urtasun RC, Scott-Brown I, Johnson ES, Mielke B, Curry B et al (1992) Increasing radiation dose intensity using hyperfractionation in patients with malignant glioma. Final report of a prospective phase I-II dose response study. *J Neurooncol* 14(1):63–72
- Nakagawa K, Aoki Y, Fujimaki T, Tago M, Terahara A, Karasawa K et al (1998) High-dose conformal radiotherapy influenced the pattern of failure but did not improve survival in glioblastoma multiforme. *Int J Radiat Oncol Biol Phys* 40(5):1141–1149
- Kopelson G, Linggood R (1982) Infratentorial glioblastoma: the role of neuraxis irradiation. *Int J Radiat Oncol Biol Phys* 8(6):999–1003
- Kulkarni AV, Becker LE, Jay V, Armstrong DC, Drake JM (1999) Primary cerebellar glioblastomas multiforme in children. Report of four cases. *J Neurosurg* 90(3):546–550
- Endo H, Kumabe T, Jokura H, Shirane R, Ariga H, Takai Y et al (2003) Leptomeningeal dissemination of cerebellar malignant astrocytomas. *J Neurooncol* 63(2):191–199
- Salazar OM (1981) Primary malignant cerebellar astrocytomas in children: a signal for postoperative craniospinal irradiation. *Int J Radiat Oncol Biol Phys* 7(12):1661–1665
- Wang LW, Shiau CY, Chung WY, Wu HM, Guo WY, Liu KD et al (2006) Gamma Knife surgery for low-grade astrocytomas: evaluation of long-term outcome based on a 10-year experience. *J Neurosurg* 105(Suppl):127–132
- Merchant TE, Kiehna EN, Kun LE, Mulhern RK, Li C, Xiong X et al (2006) Phase II trial of conformal radiation therapy for pediatric patients with cranio-pharyngioma and correlation of surgical factors and radiation dosimetry with change in cognitive function. *J Neurosurg* 104(2 Suppl):94–102
- Jalali R, Budrukkar A, Sarin R, Sharma DS (2005) High precision conformal radiotherapy employing

- conservative margins in childhood benign and low-grade brain tumours. *Radiother Oncol* 74(1):37–44
26. Halperin EC, Bentel G, Heinz ER, Burger PC (1989) Radiation therapy treatment planning in supratentorial glioblastoma multiforme: an analysis based on post mortem topographic anatomy with CT correlations. *Int J Radiat Oncol Biol Phys* 17(6):1347–1350
 27. Halperin ECC, Tarbell NJ, Kun LE (2011) *Pediatric radiation oncology*, 5th edn. Williams & Wilkins, Lippincott
 28. Lee IH, Piert M, Gomez-Hassan D, Junck L, Rogers L, Hayman J et al (2009) Association of 11C-methionine PET uptake with site of failure after concurrent temozolomide and radiation for primary glioblastoma multiforme. *Int J Radiat Oncol Biol Phys* 73(2):479–485
 29. Pirotte B, Goldman S, Massager N, David P, Wikler D, Vandesteene A et al (2004) Comparison of 18F-FDG and 11C-methionine for PET-guided stereotactic brain biopsy of gliomas. *J Nucl Med* 45(8):1293–1298
 30. Pirotte B, Goldman S, Dewitte O, Massager N, Wikler D, Lefranc F et al (2006) Integrated positron emission tomography and magnetic resonance imaging-guided resection of brain tumors: a report of 103 consecutive procedures. *J Neurosurg* 104(2):238–253
 31. Merchant TE, Mulhern RK, Krasin MJ, Kun LE, Williams T, Li C et al (2004) Preliminary results from a phase II trial of conformal radiation therapy and evaluation of radiation-related CNS effects for pediatric patients with localized ependymoma. *J Clin Oncol* 22(15):3156–3162
 32. Fouladi M, Gilger E, Kocak M, Wallace D, Buchanan G, Reeves C et al (2005) Intellectual and functional outcome of children 3 years old or younger who have CNS malignancies. *J Clin Oncol* 23(28):7152–7160
 33. Merchant TE, Gould CJ, Xiong X, Robbins N, Zhu J, Pritchard DL et al (2004) Early neuro-otologic effects of three-dimensional irradiation in children with primary brain tumors. *Int J Radiat Oncol Biol Phys* 58(4):1194–1207
 34. Grewal S, Merchant T, Reymond R, McInerney M, Hodge C, Shearer P (2010) Auditory late effects of childhood cancer therapy: a report from the children's oncology group. *Pediatrics* 125(4):e938–e950
 35. Huang E, Teh BS, Strother DR, Davis QG, Chiu JK, Lu HH et al (2002) Intensity-modulated radiation therapy for pediatric medulloblastoma: early report on the reduction of ototoxicity. *Int J Radiat Oncol Biol Phys* 52(3):599–605
 36. Lin R, Hug EB, Schaefer RA, Miller DW, Slater JM, Slater JD (2000) Conformal proton radiation therapy of the posterior fossa: a study comparing protons with three-dimensional planned photons in limiting dose to auditory structures. *Int J Radiat Oncol Biol Phys* 48(4):1219–1226
 37. Hadjipanayis CG, Kondziolka D, Flickinger JC, Lunsford LD (2003) The role of stereotactic radiosurgery for low-grade astrocytomas. *Neurosurg Focus* 14(5):e15
 38. Kano H, Niranjan A, Kondziolka D, Flickinger JC, Pollack IF, Jakacki RI et al (2009) Stereotactic radiosurgery for pilocytic astrocytomas part 2: outcomes in pediatric patients. *J Neurooncol* 95(2): 219–229
 39. Merchant TE, Hua CH, Shukla H, Ying X, Nill S, Oelfke U (2008) Proton versus photon radiotherapy for common pediatric brain tumors: comparison of models of dose characteristics and their relationship to cognitive function. *Pediatr Blood Cancer* 51(1):110–117
 40. Hug EB, Muentner MW, Archambeau JO, DeVries A, Liwnicz B, Loredo LN et al (2002) Conformal proton radiation therapy for pediatric low-grade astrocytomas. *Strahlenther Onkol* 178(1):10–17
 41. Hayostek CJ, Shaw EG, Scheithauer B, O'Fallon JR, Weiland TL, Schomberg PJ et al (1993) Astrocytomas of the cerebellum. A comparative clinicopathologic study of pilocytic and diffuse astrocytomas. *Cancer* 72(3):856–869
 42. Conway PD, Oehler HW, Kun LE, Murray KJ (1991) Importance of histologic condition and treatment of pediatric cerebellar astrocytoma. *Cancer* 67(11):2772–2775
 43. Saito T, Hama S, Kajiwara Y, Sugiyama K, Yamasaki F, Arifin MT et al (2006) Prognosis of cerebellar glioblastomas: correlation between prognosis and immunoreactivity for epidermal growth factor receptor compared with supratentorial glioblastomas. *Anticancer Res* 26(2B):1351–1357
 44. Morris EB, Gajjar A, Okuma JO, Yasui Y, Wallace D, Kun LE et al (2007) Survival and late mortality in long-term survivors of pediatric CNS tumors. *J Clin Oncol* 25(12):1532–1538
 45. Floeth FW, Pauleit D, Sabel M, Stoffels G, Reifenberger G, Riemenschneider MJ et al (2007) Prognostic value of O-(2-18F-fluoroethyl)-L-tyrosine PET and MRI in low-grade glioma. *J Nucl Med* 48(4):519–527
 46. Ch'ien LT, Aur RJ, Stagner S, Cavallo K, Wood A, Goff J et al (1980) Long-term neurological implications of somnolence syndrome in children with acute lymphocytic leukemia. *Ann Neurol* 8(3):273–277
 47. Vern TZ, Salvi S (2009) Somnolence syndrome and fever in pediatric patients with cranial irradiation. *J Pediatr Hematol Oncol* 31(2):118–120
 48. Faithfull S, Brada M (1998) Somnolence syndrome in adults following cranial irradiation for primary brain tumours. *Clin Oncol (R Coll Radiol)* 10(4):250–254
 49. Kelsey CR, Marks LB (2006) Somnolence syndrome after focal radiation therapy to the pineal region: case report and review of the literature. *J Neurooncol* 78(2):153–156
 50. Kao GD, Goldwein JW, Schultz DJ, Radcliffe J, Sutton L, Lange B (1994) The impact of perioperative factors on subsequent intelligence quotient deficits in children treated for medulloblastoma/posterior fossa primitive neuroectodermal tumors. *Cancer* 74(3):965–971
 51. Kiehna EN, Mulhern RK, Li C, Xiong X, Merchant TE (2006) Changes in attentional performance of children and young adults with localized primary

- brain tumors after conformal radiation therapy. *J Clin Oncol* 24(33):5283–5290
52. Reimers TS, Mortensen EL, Schmiegelow K (2007) Memory deficits in long-term survivors of childhood brain tumors may primarily reflect general cognitive dysfunctions. *Pediatr Blood Cancer* 48(2):205–212
 53. Merchant TE, Lee H, Zhu J, Xiong X, Wheeler G, Phipps S et al (2004) The effects of hydrocephalus on intelligence quotient in children with localized infratentorial ependymoma before and after focal radiation therapy. *J Neurosurg* 101(2 Suppl):159–168
 54. Merchant TE, Kiehna EN, Miles MA, Zhu J, Xiong X, Mulhern RK (2002) Acute effects of irradiation on cognition: changes in attention on a computerized continuous performance test during radiotherapy in pediatric patients with localized primary brain tumors. *Int J Radiat Oncol Biol Phys* 53(5):1271–1278
 55. Moleski M (2000) Neuropsychological, neuroanatomical, and neurophysiological consequences of CNS chemotherapy for acute lymphoblastic leukemia. *Arch Clin Neuropsychol* 15(7):603–630
 56. Aarsen FK, Paquier PF, Arts WF, Van Veelen ML, Michiels E, Lequin M et al (2009) Cognitive deficits and predictors 3 years after diagnosis of a pilocytic astrocytoma in childhood. *J Clin Oncol* 27(21):3526–3532
 57. Merchant TE (2009) Three-dimensional conformal radiation therapy for ependymoma. *Childs Nerv Syst* 25(10):1261–1268
 58. Hua C, Bass JK, Khan R, Kun LE, Merchant TE (2008) Hearing loss after radiotherapy for pediatric brain tumors: effect of cochlear dose. *Int J Radiat Oncol Biol Phys* 72(3):892–899
 59. Furuta T, Sugiu K, Tamiya T, Matsumoto K, Ohmoto T (1998) Malignant cerebellar astrocytoma developing 15 years after radiation therapy for a medulloblastoma. *Clin Neurol Neurosurg* 100(1):56–59
 60. Wisoff HS, Llana JF (1989) Glioblastoma multiforme of the cerebellum five decades after irradiation of a cerebellar tumor. *J Neurooncol* 7(4):339–344
 61. Ang KK, Price RE, Stephens LC, Jiang GL, Feng Y, Schultheiss TE et al (1993) The tolerance of primate spinal cord to re-irradiation. *Int J Radiat Oncol Biol Phys* 25(3):459–464
 62. Combs SE, Thilmann C, Edler L, Debus J, Schulz-Ertner D (2005) Efficacy of fractionated stereotactic reirradiation in recurrent gliomas: long-term results in 172 patients treated in a single institution. *J Clin Oncol* 23(34):8863–8869
 63. Dritschilo A, Bruckman JE, Cassady JR, Belli JA (1981) Tolerance of brain to multiple courses of radiation therapy. I. Clinical experiences. *Br J Radiol* 54(645):782–786
 64. Veninga T, Langendijk HA, Slotman BJ, Rutten EH, van der Kogel AJ, Prick MJ et al (2001) Reirradiation of primary brain tumours: survival, clinical response and prognostic factors. *Radiother Oncol* 59(2):127–137
 65. Fogh SE, Andrews DW, Glass J, Curran W, Glass C, Champ C et al (2010) Hypofractionated stereotactic radiation therapy: an effective therapy for recurrent high-grade gliomas. *J Clin Oncol* 28(18):3048–3053
 66. Patel M, Siddiqui F, Jin JY, Mikkelsen T, Rosenblum M, Movsas B et al (2009) Salvage reirradiation for recurrent glioblastoma with radiosurgery: radiographic response and improved survival. *J Neurooncol* 92(2):185–191
 67. Merchant TE, Boop FA, Kun LE, Sanford RA (2008) A retrospective study of surgery and reirradiation for recurrent ependymoma. *Int J Radiat Oncol Biol Phys* 71(1):87–97
 68. Children's Oncology Group. <http://www-survivorshipguidelines.org/pdf/LTFUGuidelines.pdf>. Long-term follow-up guidelines for survivors of childhood, adolescent, and young adult cancers 2008 [cited 9 Apr 2011]; Available from <http://www-survivorshipguidelines.org>

Pathologies in Pediatric Posterior Fossa Tumors: Brain Stem Tumors

M. Memet Özek

M.M. Özek, M.D.
Division of Pediatric Neurosurgery,
Acibadem University, School of Medicine, Istanbul, Turkey

Charles Raybaud and Abeer Almehdar

Brainstem tumors are common in children: 10–15 % of the CNS tumors [1–4], 7–16 % of intracranial tumors [5–9], 13–30 % of posterior fossa tumors [5, 7, 8], and 25 % of gliomas [1] in that age range. They affect males and females equally, typically about 7–9 years of age [10], although they can be seen in neonates like in young adults [11]. Their prognosis is typically dismal: most are malignant gliomas and even when they are of low grade, the anatomical and functional complexity of the brainstem is such that complete surgical exeresis is impossible. MR imaging is important to provide a diagnosis of lesion obviously, to locate it, to recognize it as a tumor, and to identify an appropriate surgical approach if partial exeresis or biopsy is felt to be potentially useful. However, biopsy itself is often felt hazardous in the brainstem, and MR imaging may actually represent a good approach to the histological diagnosis [8]. As it is usual with brain tumors, the nature and histological grade of

the tumor may be inferred from both its location and its appearance.

Brainstem tumors are usually astrocytic gliomas. They may be pilocytic astrocytomas (PA, WHO grade 1) or more rarely gangliogliomas or pilomyxoid astrocytomas (PMA, WHO grade II). Within the pons, they are typically fibrillary astrocytomas, which may be of various grades (FA, WHO grades II, III, IV). All grow within the brainstem, but they often develop exophytic components into the surrounding ventricular and/or cisternal spaces.

31.1 Anatomical Features of the Brainstem Pertinent to Imaging

The brainstem is the portion of the neuraxis that is interposed between the cord caudally and the diencephalon rostrally. It is classically subdivided longitudinally into three segments, the *medulla*, the *pons*, and the *midbrain* separated by the pontomesencephalic and the pontomedullary sulci. The midbrain corresponds to the cerebral peduncles and tectal plate; it contains the aqueduct of Sylvius; the pons corresponds to the cerebellar peduncles and relates to the upper half of the fourth ventricle; the medulla relates to the lower half of the fourth ventricle but extends further caudally just below the medullary pyramids.

The simplest structure in the neural tube is represented by the spinal cord. It is made of a ventro-

C. Raybaud, M.D. (✉)
Division Head of Neuroradiology,
Hospital for Sick Children and University of Toronto,
555 University Avenue, Toronto, ON
M5G1X8, Canada
e-mail: charles.raybaud@sickkids.ca

A. Almehdar, M.D.
Department of Medical Imaging,
King Abdulaziz Medical City,
9515, Jeddah 28273, Saudi Arabia
e-mail: dr_amehdar@hotmail.com

lateral basal plate (motor) and a dorsolateral alar plate (sensory); the ventral midline forms the floor and the dorsal midline forms the roof, both devoid of cellular bodies. The peripheral marginal zone contains the white matter tracts. The brainstem pattern is similar but it has become more complex with the development of the ventricles and, dorsal to them, of highly cellular roof plates (cerebellum, tectal plate). Each segment can be divided from ventral to dorsal into a ventral base, an intermediate tegmentum (ventral to the ventricular cavities, aqueduct, or fourth ventricle), and (for the midbrain and pons at least) a dorsal roof of gray matter forming the quadrigeminal or tectal plate and the cerebellum, respectively. The motor basal plate is ventromedial, while the sensory alar plate is ventrolateral, and the dorsal tectum/cerebellum has become prominent. The medulla however has no roof: in its rostral part the ventricle remains open dorsally into the cisterna magna (“open” medullary portion); in its caudal part at and below the obex and the pyramidal decussation, it lacks a cellular roof and is closed like the cord (“closed” portion). The corticospinal tracts course in the ventral base, the ascending sensory tracts in the tegmentum. The inferior olivary nuclei (medulla), the pontine nuclei, the substantia nigra (midbrain), and the red nuclei are ventral. The cranial nerve nuclei and the reticular formation are tegmental. The dorsal roof (tectum and cerebellum) has complex integrative functions. Beside the descending and ascending white matter tracts, transverse, decussating fibers are important as they are assumed to create “barriers” which would limit the expansion of the benign tumors of the brainstem [12]. Such barriers would be: the pyramidal decussation, internal arcuate fibers, and olivocerebellar tracts between the caudal and rostral medulla; the pontocerebellar fibers and the trapezoid body between the rostral medulla and the pons; and the pontocerebellar fibers and the decussation of the superior cerebellar peduncle between the midbrain and the pons. On the contrary the caudal medulla is freely continuous with the upper cervical cord and the rostral midbrain is freely continuous with the posterior diencephalon and infralenticular hemispheric white matter.

Beside the classical anatomy and its organization, the modern concepts of neuromeric

compartmentation of the neuraxis may also explain the existence of biological barriers along the brainstem, and actually the two visions may be linked. The initial organization of the neural tube in the fifth embryonal week comprises a rostral prosencephalon (forebrain), an intermediate mesencephalon (midbrain), and a caudal rhombencephalon (hindbrain) in addition to the cord. The further neuromeric compartmentation that develops is genetically defined by specific segmentation genes. Within each neuromere the aggregation and organization of specific neurons is facilitated, while the inter-neuromeric boundaries prevent the migrating cells to proceed longitudinally along the neural tube, at least in the early stages. The midbrain has two *mesomeres* (mesencephalic neuromeres), rostral and caudal, and a specialized zone identified as the *isthmical organizer* (or midbrain-hindbrain boundary organizer) just caudal to the caudal mesomere [13]. The hindbrain comprises eight *rhombomeres*: the first one forms the pons and dorsally, together with part of the caudal mesomere, the cerebellum. Two by two, the following rhombomeres correspond to the branchial organization with their specific nerves [13, 14]; r8 includes the caudalmost medulla and the whole cord. In the same way the forebrain is segmented into six *prosomeres*, the three caudal ones forming the posterior diencephalon and the three rostral ones forming the anterior diencephalon together with the overlying telencephalon [15, 16]. The neuromeric segmentation of the brainstem results in a segmentation of the columns of gray matter that prolongs the anterior and posterior horns of the cord, which results in the individualization of the cranial nerves nuclei. Like the gray matter in the cord, these cranial nerves nuclei originate from the correspondingly segmented subependymal proliferative neuroepithelium.

By contrast, the later-developing dorsal gray matter (cerebellum, tectal plate) and the precerebellar nuclei are made of neuroblasts which migrate regardless of the inter-neuromeric boundaries: neuroblasts from the isthmical organizer migrate longitudinally to the tectal plate and the upper median cerebellum; neuroblasts from the caudal rhombic lips travel to the inferior olive,

pontine nuclei, and the corresponding reticular area. Given the new understanding of the biology of brain tumors, which implies an interaction between a stem cell – normal or tumoral – and the regional environment where it migrates [17–19], these developmental processes are important to keep in mind when the diagnosis of a brainstem tumor is approached morphologically.

From a practical imaging point of view, a few anatomical landmarks are important to recognize when assessing the brainstem anatomically for a mass lesion. The midline sagittal cut (Fig. 31.1a, b) across the midbrain demonstrates the posterior commissure, the quadrigeminal plate, and the anterior medullary velum; the tegmental cap of the midbrain forming the third ventricular floor posterior to the mamillary bodies and the smooth sweep of the sylvian aqueduct; the deep indentation of the interpeduncular fossa; and the inferiorly oblique boundary between the midbrain and the pons. More caudally, the wedge-shaped pons is prominent, with a generally rounded/oblong section, well demarcated posteriorly from the tegmentum pontis; dorsal to this the ventricular floor is flat. Just caudal to the pons, the deep indentation of the pontomedullary sulcus is found where it crosses the median medullary sulcus, as well as the superiorly oblique pontomedullary boundary. The medulla tapers toward the upper cervical cord; its open cranial portion corresponds to the inferior part of the fourth ventricle, with the opening of the central canal of the cord covered dorsally with the obex; the caudal closed medulla is more like the cord. In addition to the midline sagittal cut, the superior, inferior, and middle cerebellar peduncles show well on the parasagittal cuts.

Coronal cuts (Fig. 31.1c) are useful to show the whole extent of the brainstem from the thalami to the cord, and especially to demonstrate the three cerebellar peduncles. However, the most useful plane beside the sagittal one is the axial plane, with cuts spanning the whole neuraxis from the upper cord (C2 or C3) to the thalami (Fig. 31.1d–i). The upper cord presents a transverse oblong appearance. The caudal medulla presents with the anterior bilateral protrusion of the pyramidal decussation (giving it kind of a triangular shape) and a tiny ependymal canal. The cut through the mid-portion

of the rostral medulla shows the anterolateral prominence of the inferior olivary nuclei with the posterior widening of the lower third ventricle. One step above, the cut includes the pontomedullary sulcus with the lateral recesses, the inferior cerebellar peduncles, and the emergences of the facial and acoustic nerves. A cut through the caudal pons beautifully demonstrates the pons itself (transverse “bridge”) with the middle cerebellar peduncles, the tegmentum pontis posteriorly, as well as the ventricular floor with its median sulcus and medial eminences (colliculi faciales); a more rostral cut crosses the rostral pons anteriorly but the tegmentum mesencephali posteriorly (due to the obliquity of the midbrain-pons interface) as well as the superior cerebellar peduncles. Finally the last two axial cuts demonstrate the aqueduct and periaqueductal gray matter, the inferior and superior colliculi, the red nuclei and substantia nigra, and the diverging cerebral peduncles forming the junction with the base of the cerebral hemispheres.

31.2 Radiological Features of Brainstem Tumors

Old imaging modalities such as pneumoencephalography could not assess the parenchyma itself. Angiography could demonstrate a global swelling of the brainstem, sometimes some abnormal vascularity, and the frequent encasement of the basilar artery by the anterior exophytic portions of the tumor. Because no surgery was performed, and no biopsy, all brainstem tumors were categorized as a single group with a uniformly poor prognosis. CT for the first time allowed a parenchymal evaluation which, beside morphology, provided information on the structure of the mass (solid/cystic/edematous/hemorrhagic) and on its vascularity and blood-brain-barrier status. It was only after clinical experience with CT had accumulated that it became apparent that brainstem tumors could be subdivided in very different specific entities [1, 5]. This obviously could only be amplified by the generalized use of MR imaging after 1985, which resulted in a complete metamorphosis of the way brainstem tumors are seen, from both the anatomical and the structural points of view.

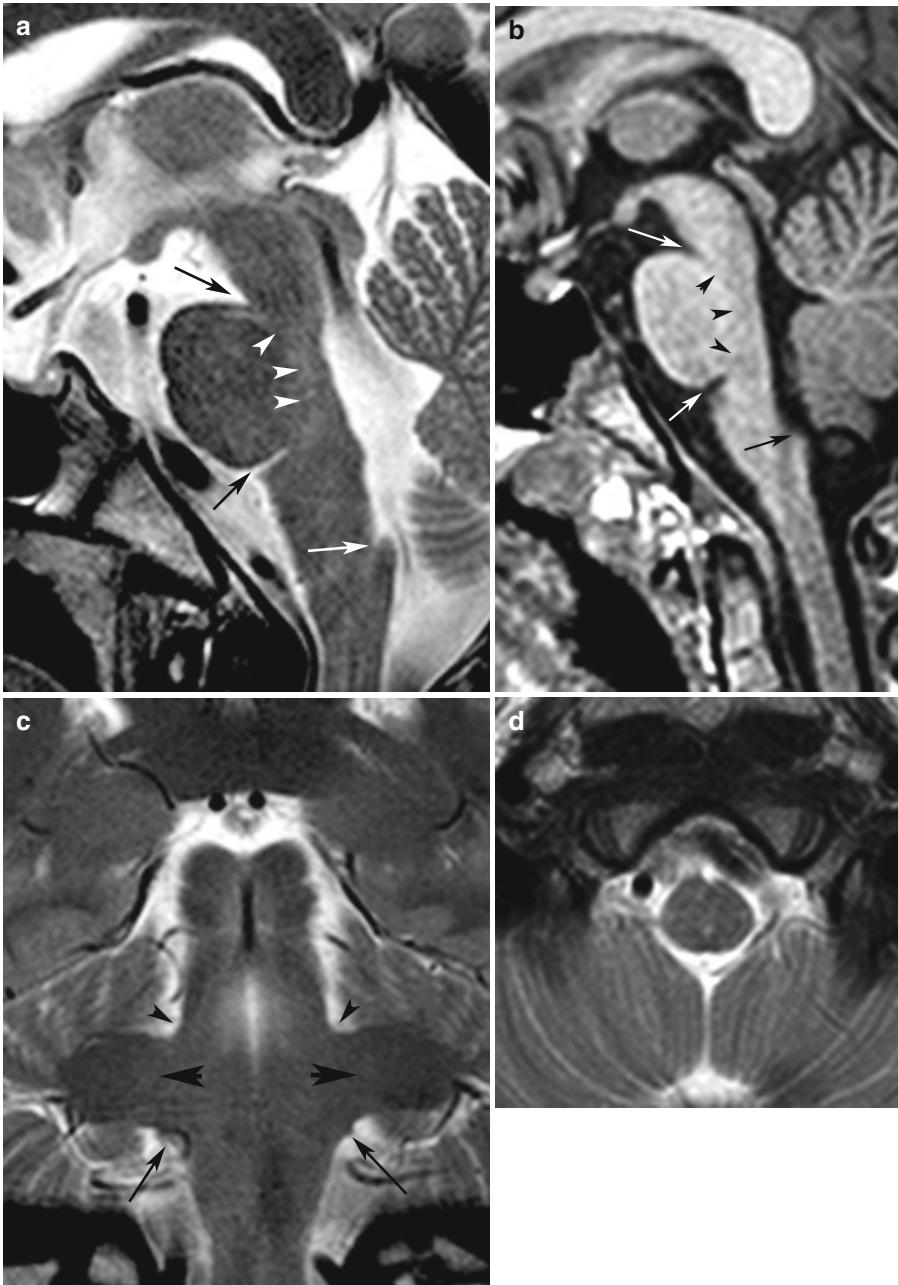


Fig. 31.1 MR anatomy of the brainstem. (a) Midline sagittal T2. Pontomesencephalic and pontomedullary sulci (*black arrows*). Limits of the basis pontis (*white arrowheads*), with the tegmentum pontis behind. Caudalmost limit of the fourth ventricle marking the lower limit of the “open” medulla (*white arrow*). The “closed” medulla extends from there to the plane of the foramen magnum. (b) Midline sagittal T1. Same landmarks. (c) Coronal T2. It shows the three cerebellar peduncles: superior (*small arrowheads*), middle (*large arrowheads*), and inferior (*arrows*). (d) Axial T2 through the “closed” medulla with the pyramids ventrally. (e) Axial T2 through the “open”

medulla with the inferior olivary nuclei anterolaterally, the inferior cerebellar peduncles posterolaterally, and the lower fourth ventricle dorsally. (f) Axial T2 through the pontomedullary sulcus, showing the lateral medullary fossa (*white arrow*). (g) Axial T2 through the pons showing the basis pontis anteriorly, the tegmentum pontis posteriorly (*white arrowheads*) with the median sulcus (*black arrow*), and the facial colliculi on either side. (h) Axial T2 through the cerebral peduncles with the superior cerebellar peduncles. (i) Axial T2 through the superior midbrain with the cerebral peduncles, the tegmentum mesencephali, the aqueduct (*flow void*), and the tectal plate dorsally

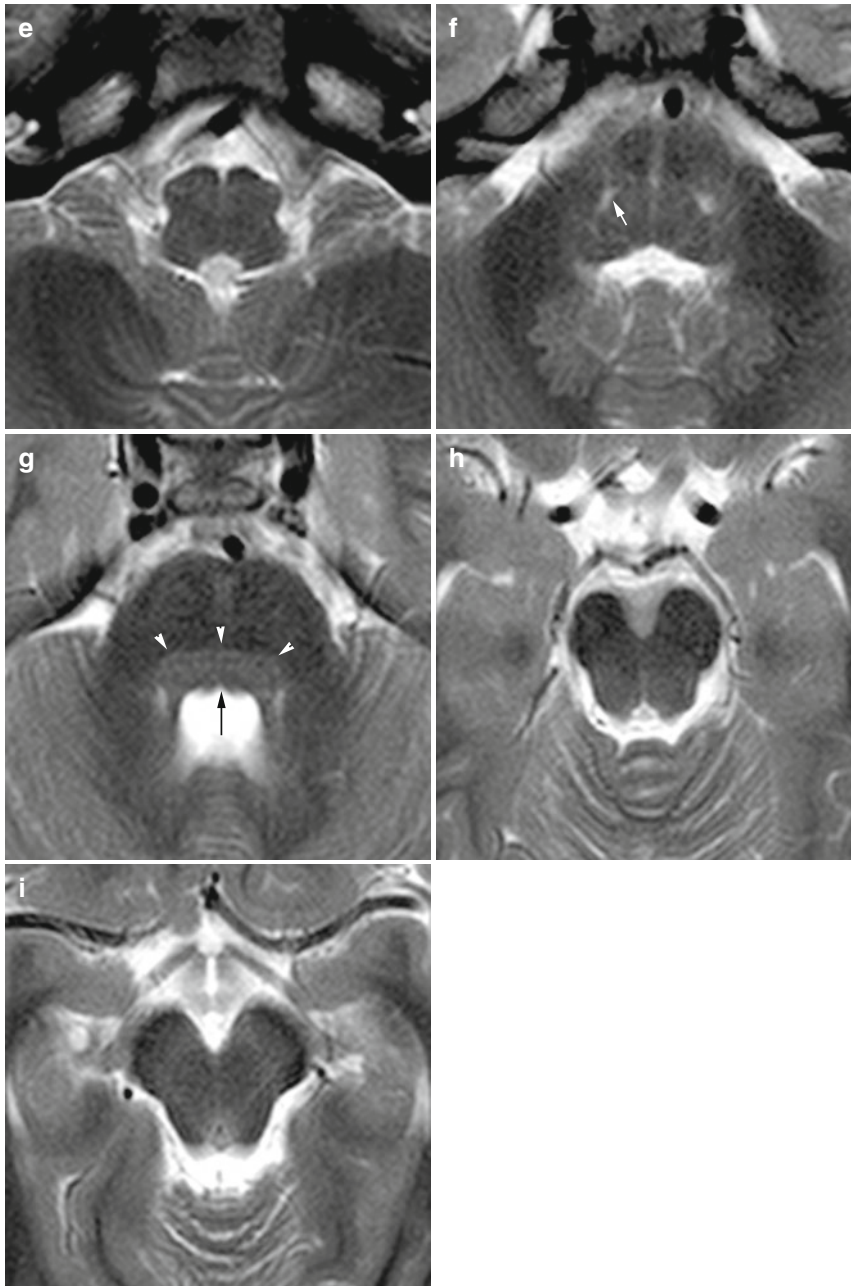


Fig. 31.1 (continued)

31.2.1 The Imaging Tools

MR imaging is an extremely versatile modality. The information it provides can be described as depending on *relaxation imaging* (classical T1- and

T2-weighted imaging with its specific variants), *proton diffusion imaging* (diffusion-weighted and diffusion tensor imaging), *proton metabolic imaging* (MR spectroscopy, chemical shift imaging), and *vascular* and *blood-brain-barrier imaging*.

In clinical settings, MR technology investigates protons only, whose behavior when excited by appropriate radio waves depends on their particular immediate physicochemical environment intrinsic (e.g., proteins) or extrinsic (e.g., gadolinium compound).

Relaxation imaging comprises the classical T1, T2, FLAIR, and T2*/susceptibility imaging.

T1 imaging, whatever the specific sequence design used, demonstrates the anatomy nicely, with a good gray-white contrast. The CSF is black. The gray matter depending on its organization is of intermediate signal and the white matter is bright. This is primarily due to myelin, or rather to the components of myelin which shorten the T1 relaxation time of the protons (magnetization transfer effect). This occurs quite early in the development because of the accumulation of myelin precursors, the more so in the brainstem as myelination proceeds from the cord to the forebrain. The “mature” T1 pattern is present early in the brainstem, about the end of the first semester. Whatever process changes the myelin content (edema, necrosis, gliosis) decreases the signal as well (it becomes dark). On the contrary gadolinium exerts a strong magnetization effect and induces a very bright signal.

T2 imaging also is good for anatomy, especially the anatomy of the brainstem nuclei. The CSF is white. The gray matter is of variable degrees of intermediate density, depending on the cellularity, the amount of myelinated fibers, and the amount of iron deposition. The white matter is dark (short T2 relaxation time), not as much as a direct effect of myelin but rather because the accumulation of compacted myelin, which has a weak T2 signal, correlates with a decrease of water content. The “mature” pattern on T2 imaging is present in the brainstem about the end of the first year (even though myelination is not completed until the end of adolescence). Whatever increases the relative amount of water in the tissue (edema, or lack, loss or replacement of myelin) appears as a bright signal. T2 imaging is insensitive to gadolinium. T2 spin-echo (or fast spin-echo) sequences are devised to neutralize local magnetic susceptibility artifacts induced, for example, by iron (notably blood or blood residue), air-bone interfaces, etc.

In *susceptibility-weighted sequences* (SWI, T2*GE, etc.) on the contrary, artifacts related to local magnetic field heterogeneities are maintained and even enhanced, in order to better demonstrate tiny foci of hemorrhage often associated with malignancy, blood residues (e.g., hemosiderin in macrophages) [9, 20, 21], calcium, metallic fragments, etc. Specific sequence design may also demonstrate the intraparenchymal blood-containing venous channels nicely [22].

T2-FLAIR sequences are true T2 sequences in which the signal of the free water (normally bright) is specifically cancelled (appears black) by an appropriate radiofrequency pulse. This allows differentiating the bound water associated with cellular membranes, proteins, or even gadolinium (remains bright) from the CSF or CSF-like (e.g., interstitial fluid) collections (blackened). The interstitial water is suppressed in the neonatal brain (white matter is dark) because there is not enough myelin to bind it. Yet after a few weeks, the accumulation of myelin precursors increases the amount of bound water and reduces that of free water, and the white matter becomes bright. Thereafter, the signal proceeds as with conventional T2 sequences, except that the mature pattern is not reached until later than on classical T2 sequences. T2-FLAIR sequences are optimal to appreciate structural changes and to recognize faintly bloody or hyperproteinic CSF, cystic or interstitial fluids. On 3 T magnets, the iron-related hyposignal in the globi pallidi and the red nuclei often is especially prominent.

T2 steady-state sequences (CISS/FIESTA) produce 3D-T2 submillimetric images with an outstanding morphological definition but poor demonstration of the intrinsic parenchymal structures. They are therefore of limited use in this type of pathology except for the demonstration of an aqueductal obstruction and, in the follow-up of brainstem tumor patients with hydrocephalus, demonstration of the patency of a third ventriculostomy.

Diffusion imaging uses the Brownian motion of the protons at the body temperature. It comprises the classical diffusion-weighted imaging (DWI/ADC) and the more quantitative diffusion tensor imaging (DTI). Totally independent from the

relaxation parameters T1 and T2, it is based on the fact that with optimized sequences (defined by the factor b, typically b1000), the range of diffusion of the protons in a living tissue at 37 °C is of the same order as the size of the extracellular space.

DWI/ADC mapping is intended to reveal restriction of the proton motion mostly in the extracellular spaces. The freer the protons are to move (e.g., in the ventricles), the more de-phased they become and the weaker the returned signal is (CSF is black). The more restricted their motion is by the surrounding cells, the more coherent and stronger their returned signal remains (the lesion is bright). DWI therefore has the ability to detect a restricted diffusion, due to a decrease of the extracellular spaces, but it cannot appreciate an increased diffusion. The calculated correlate of the restricted diffusion imaging is the ADC mapping (apparent diffusion coefficient) where areas of free motion appear bright, while areas of restricted motion appear dark. In tumor pathology, restricted diffusion may be demonstrated when a dense cellularity restricts the extracellular spaces.

DTI goes one step further as it has the capability to quantify the diffusivity: therefore, it can evaluate both decreased and increased diffusions, that is, both restricted and expanded extracellular space. In a fascicular structure such as the white matter, diffusivity parameters can be appreciated three-dimensionally according to the direction of the fibers: axial diffusivity is parallel to the fibers and radial diffusivities are perpendicular to the fibers; they are measured in mm²/s. The directionality of the structure can be expressed by a fractional anisotropy index (FA) which may vary from zero (the motion of the proton is the same in every directions, like in the ventricles) to one (motion is in one direction only). In normal fascicular white matter, intermediate FA values are obtained as the diffusivity is more along the fibers than perpendicular to them. With appropriate post-processing it is possible to use FA mapping to represent the anatomical organization of the white matter fascicles (fiber tracking). Decreased FA may reflect a decrease of axial diffusivity (altered fascicular organization, hypercellularity) or an increase of radial diffusivity (loss of fibers and/or myelin, extracellular edema) or both. In brainstem glioma, fiber tracking is used

to help differentiate infiltrative tumors from compact tumors and from necrosis and tumors from inflammation [7, 23–25].

Metabolic imaging includes MR spectroscopy (typically monovoxel) and metabolic cartography with chemical shift imaging (CSI).

Proton MR spectroscopy (¹H MRS) has been included in many routine MR protocols for about two decades. The measurement is usually done in a single voxel of approximately 2 by 2 by 2 cm selected in the region of interest. Given its overwhelming abundance, the signal of the free water has to be cancelled by specific radiofrequencies. MRS is based on the fact that the resonant frequency of the excited proton depends on its molecular environment: this phenomenon is called the chemical shift. Different proton-containing molecules may be differentiated, thanks to their specific molecular arrangements, resulting in separate peaks on the spectrum (the shift is measured in parts per million or ppm), and their relative amount is reflected by the relative size/area of the peaks. For tumors, MR spectra obtained with a long echo time provide most of the information needed in a reasonably short time: lactate (energy failure, necrosis) at 1.33 ppm, NAA (neuroaxonal activity mostly) at 2.01 ppm, creatine (energetic metabolism) at 3.02 (more or less invariant in the neural tissue), and choline (cellular turnover) at 3.22 ppm. By using a short echo time, more metabolites can be identified such as the macromolecules (necrosis) at 0.9–1.3 ppm, myoinositol (a marker of the glia) at 3.56 ppm, or taurine (a marker of embryonal tumors) at 3.35 ppm. Absolute metabolite concentrations may be extrapolated also [6, 26–28].

Instead of investigating a single voxel, *CSI* investigates a plane or even a volume, assessing the core of the tumor as well as its margins and the surrounding normal tissue [28]. Given the small size of the brainstem, however, and the proximity of the bony structures with the related distortion of the magnetic field, it is usually not the procedure of choice in brainstem tumors.

Perfusion imaging provides information on focal relative cerebral blood volume (CBV), transit time (TT), and relative cerebral blood flow (CBF). Therefore, it has the potential of being

useful to differentiate benign from malignant tumors as well as radiation necrosis from tumors. It may also be helpful to appreciate the effects of therapy when antiangiogenic drugs are used. Perfusion data are obtained by analyzing the curve of a single-pass bolus of gadolinium contrast (dynamic susceptibility-weighted contrast-enhanced perfusion imaging DSC). It may also be done by labeling the incoming arterial blood with a specific inversion pulse (arterial spin labeling ASL) [29]. When performed by using a bolus of gadolinium compound, it may also be used to evaluate the vascular permeability and to document the degree of impairment of the blood-brain barrier: after the first pass the curve remains above base level because of the accumulation of contrast into the tissue due to the leaking abnormal or impaired BBB [30]. However, perfusion studies are difficult to perform in a small structure like the brainstem that is surrounded by so many artifact-producing structures; they are not routinely used [31].

31.2.2 Imaging Protocols

High-field clinical magnets (3.0 T) and multiple array coils in general yield images with good definition. The location in the posterior fossa however is typically associated with more artifacts than the supratentorial space due to the proximity of bone (susceptibility artifacts), the pulsatility of blood in the basilar artery and transverse sinuses, and the CSF-flow artifacts in the cisterns and fourth ventricle.

Imaging protocols are many, depending on local traditions and technical availabilities. Obviously MR imaging is the modality of choice and, as always, it must be multi-planar and multi-sequential. Because the brainstem is so small (diameters of the medulla are 11–13 mm, those of the midbrain, 20–27 mm; those of the pons are the largest, at 20–40 mm), thin slices (2–3 mm) are needed, without any significant gap. 3D-T1GE millimetric images (either MPRAGE or TFE or SPGR depending on the vendor) are useful, given their excellent gray-white contrast and the possi-

bility of secondary reformation of the images in any plane. Thin sagittal T2 sections are useful too: both T1 and T2 sagittal sections show the craniocaudal extent of the lesion well. T2-FLAIR is often considered the best sequence to appreciate the full extent of glioma [3], and axial cuts are especially useful to show the transverse extent of the lesion. The three T1, T2, and FLAIR sequences contribute to the analysis of the structural changes (solid, cystic, necrotic, edematous components); because of their high degree of hydration, gliomas typically are dark on T1 and bright on T2 and T2-FLAIR. However, isolated hypercellular malignant foci may appear as T2-dark nodules surrounded by a bright edematous tissue.

In all varieties of gliomas, conventional *DWI/ADC* typically shows no restriction, but *quantitative DTI* is more sensitive and it provides a quantification of the diffusivity and may therefore demonstrate foci of high cellularity [4]. *Susceptibility imaging* may demonstrate the presence of intratumoral hemorrhages: this feature, although not absolutely specific, is strongly suggestive of a high-grade tumor [9]. Also, *DTI tractography* (although not done routinely) may assess the involvement of the main fiber tracts, assist in the differential diagnosis, and help to direct a surgical biopsy or even an open surgical approach, especially when integrated in the neuronavigation program [7, 23–25]. From a strictly anatomical point of view, the corticospinal tract; the superior, medial, and inferior cerebellar peduncles; and the medial lemnisci can be identified [7].

To evaluate the vascular bed and the vascular permeability (BBB), contrast administration is always mandatory, with axial (usually done according to the requisites of the surgical neuronavigation), sagittal, and coronal imaging planes. For medullary tumors, the cervical spine must be imaged as well, as the tumor often extends caudally, and a subjacent hydrosyringomyelia should then be ruled out. Pilomyxoid astrocytomas may originate in the brainstem [32] and often disseminate in the leptomeninges [33], which justifies whole spinal imaging, typically not at the first

study however as the precise diagnosis may be attained later in the course of the disease.

CT has a limited role to play in the diagnosis of brainstem tumors. Its main contributions in a context of tumors are the demonstration of calcification, which are more common in gangliogliomas than in typical gliomas, and a high attenuation suggestive of a densely packed cellular tumor, which is typically not observed into the brainstem.

31.2.3 Imaging Findings

Location is, in tumors of the brainstem like elsewhere in the CNS, an important point to consider when assessing a tumor. Several classifications of the brainstem tumors have been suggested [34], and in all the most important point is to differentiate infiltrative tumors of the pons from tumors elsewhere [35–37], as pontine tumors are essentially all of poor prognosis (FA grade II, III, IV) [11]. This topographic specificity is expressed by giving it the specific name of *diffuse intrinsic pontine glioma*.

Diffuse intrinsic pontine gliomas (DIPG) (Figs. 31.2, 31.3, 31.4, and 31.5) are centered within the ventral pons (or basis pontis, where the numerous transverse pontocerebellar fibers are located), and typically they expand the pons in every direction. On a sagittal plane the upper and lower boundaries or the pons (pontomesencephalic and pontomedullary) tend to be displaced as the tumor appears initially to squeeze more than to invade the midbrain and medulla. Yet, invasion does occur, and the fact that the tumor crosses the anatomic boundaries of the pons is felt to reflect its malignant nature [12] (Fig. 31.2a, b). In an axial plane the tumor is essentially bilateral, more or less symmetrical (Fig. 31.2c–h). The DIPG often are exophytic anteriorly, filling the cisterns and engulfing the basilar artery (Fig. 31.2c–g), but not so much posteriorly into the fourth ventricle: on the contrary the ventricular floor is stretched transversely and craniocaudally so that the ventricular lumen is expanded rather than effaced, and hydrocephalus

is typically absent, at least in the early stages of the disease.

Uncommonly, *dorsal exophytic gliomas* may originate in the tegmentum pontis, and they typically are of low grade (PA grade I). They protrude into the fourth ventricle and are associated with hydrocephalus. Also, *lateral tumors* (Figs. 31.6 and 31.7) may develop into the brachium pontis (middle cerebellar peduncles) and seem to be more commonly of low grade (PA grade I) as well.

Cervicomedullary gliomas are another typical presentation of brainstem tumors [38] (Figs. 31.8, 31.9, and 31.10). They are centered at the junction of and occupy the upper cord and caudal medulla, which are both circumferentially expanded (Fig. 31.8c), typically with an exophytic component into the caudal part of the fourth ventricle resulting in its obstruction (Fig. 31.8a, b, d); hydrocephalus may or may not be present [39]. The histology of these tumors is characteristically benign (PA grade I). It has been suggested that their particular pattern of extension sparing the rostral medulla (Fig. 31.8a, b, d) was related to the decussation plane (pyramidal decussation, internal arcuate fibers, olivocerebellar tracts) (it might perhaps reflect the brainstem compartmentation in rhombomeres as well.) and that this behavior would reflect their nonmalignant nature [12]. This may not be absolutely true however as some truly benign cervicomedullary tumors may secondarily invade the upper medulla (Fig. 31.9b) and may extend to the pons (Fig. 31.10). Extension often is more lateral toward the inferior cerebellar peduncle as well. Strictly *focal intrinsic medullary* tumors are uncommon, typically (but not always) benign, and may be exophytic (Fig. 31.11) or infiltrative, in a surgically difficult location [40, 41].

From a developmental point of view, *tectal plate* tumors should be differentiated from the rest of the midbrain tumors, in the same way as the cerebellar tumors should be differentiated from the pontine tumors; the differentiation however is not always easy to make as tectal tumor may extend ventrally while periaqueductal tumors may involve the tectal plate. Pineal regions tumors

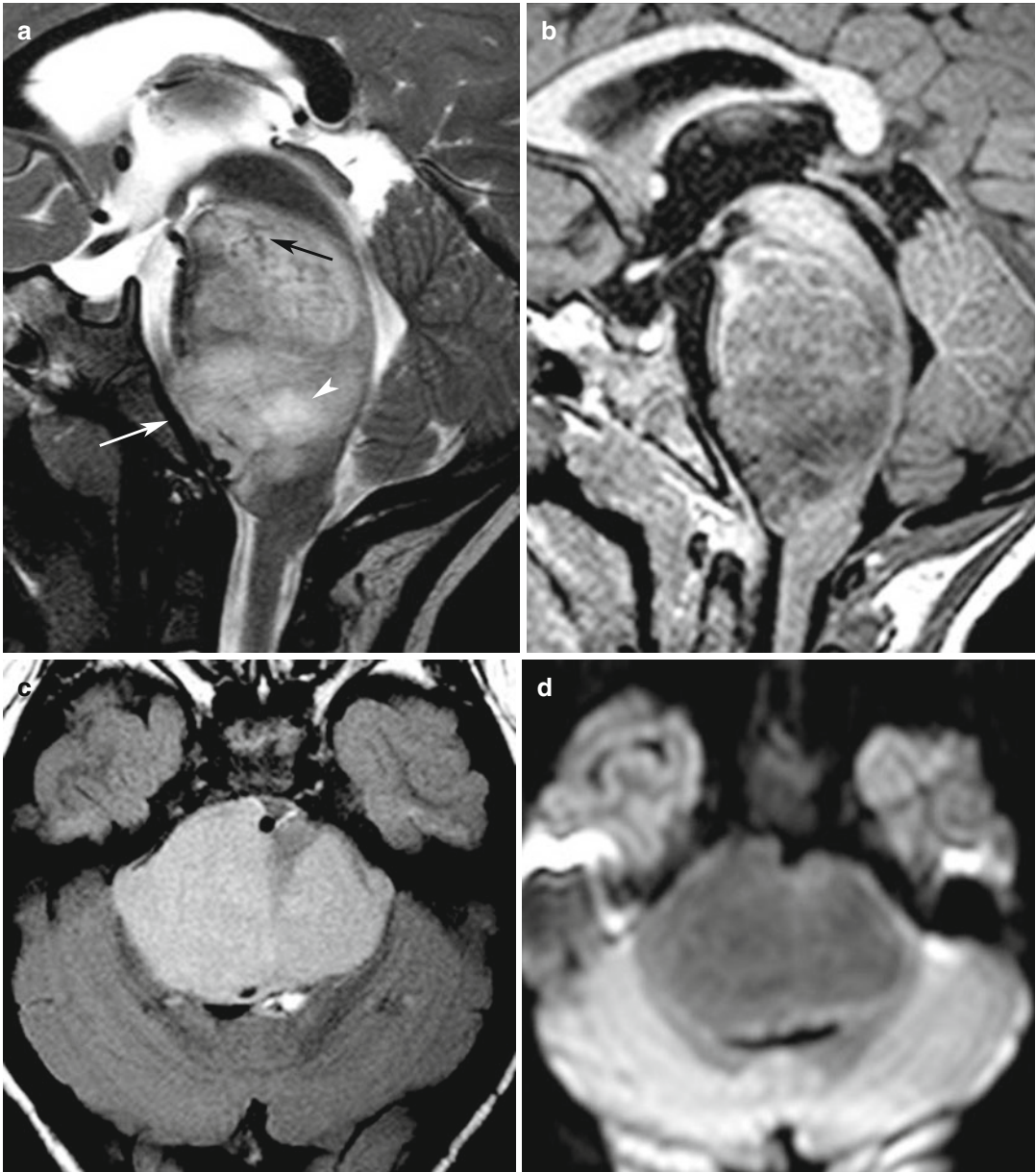


Fig. 31.2 Diffuse intrinsic pontine glioma. (a) Midline sagittal T2. Diffuse expansion of the pons with smooth posterior displacement of the fourth ventricle and patent aqueduct. Filling of the prepontine cisterns by exophytic components (*white arrow*). Upward compression of the midbrain and downward compression of the medulla. The mass is heterogeneous with areas of necrosis (*white arrowhead*) and petechial hemorrhages (*black arrow*). (b)

Midline sagittal T1 shows the anatomy, not so much the structure. (c) Axial FLAIR, assumedly the best to appreciate the limits of the tumor. (d) DWI. Uniformly high diffusion with no evidence of restriction. (e–h) Axial T2. Sequential cuts demonstrating the heterogeneity of the lesion with irregular preservation of some tracts and nuclei, areas of necrosis, petechial hemorrhages, etc.

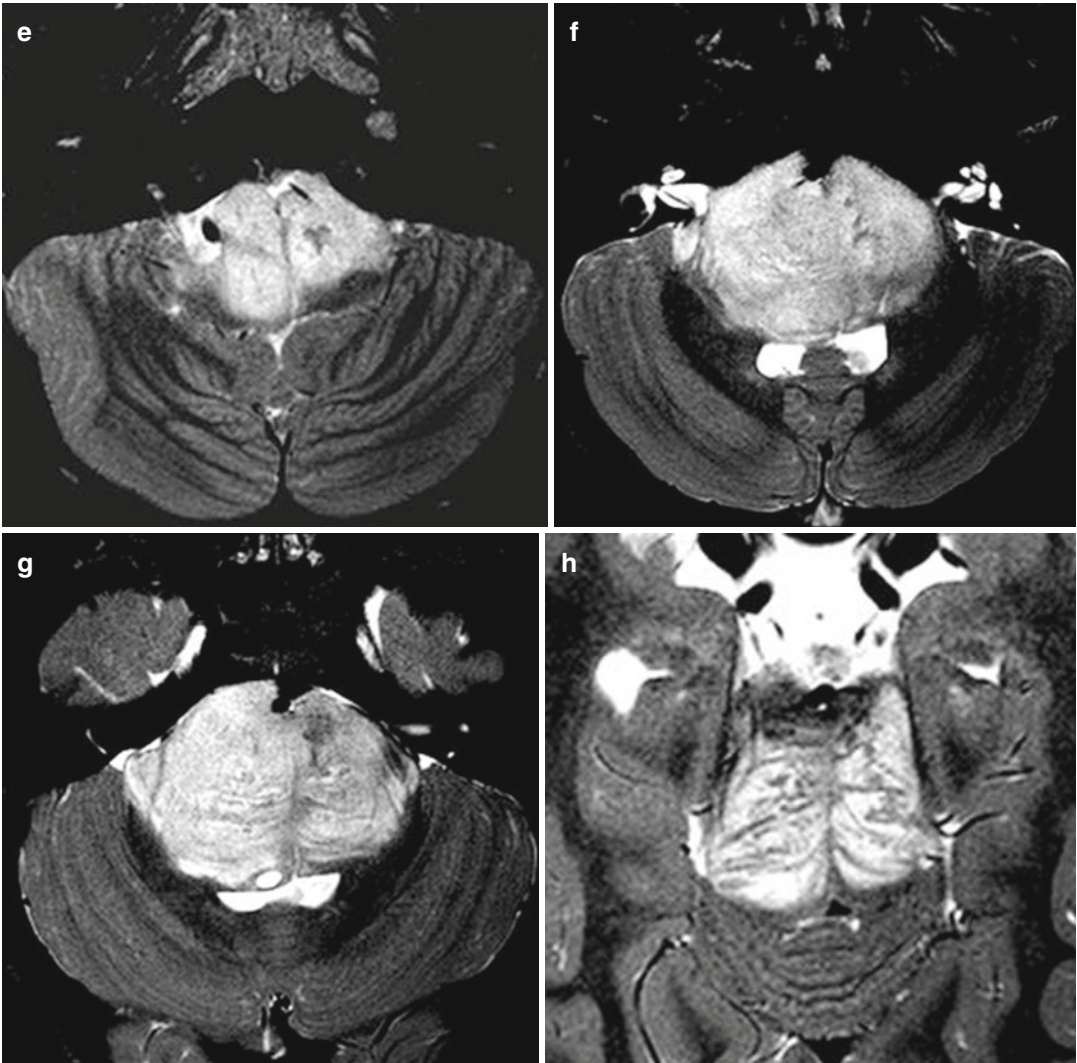


Fig. 31.2 (continued)

invading the tectal plate should be excluded as they are typically of different nature (germ cell tumors or pineoblastomas) and centered more on the posterior aspect of the third ventricle. Tectal plate tumors almost always result in hydrocephalus [42] (Figs. 31.12 and 31.13). They may develop symmetrically or asymmetrically. Some of them are extremely indolent, presenting as a stable swelling of the tectal plate with a loss of the quadrigeminal sulcus and aqueductal stenosis

(Fig. 31.12); they have occasionally been described as “hamartomas” [42, 43]. However, some tectal tumors may be more aggressive and expand progressively [42, 44, 45] (Fig. 31.13). It is suggested that the size at discovery is the best indicator of evolutivity: lesions of less than 2 cm [45] or 4 cm³ [42] seem to be less likely to expand. It has been suggested that the expanding tumors could originate from the region of the posterior commissure with secondary invasion of the tectal plate and/or

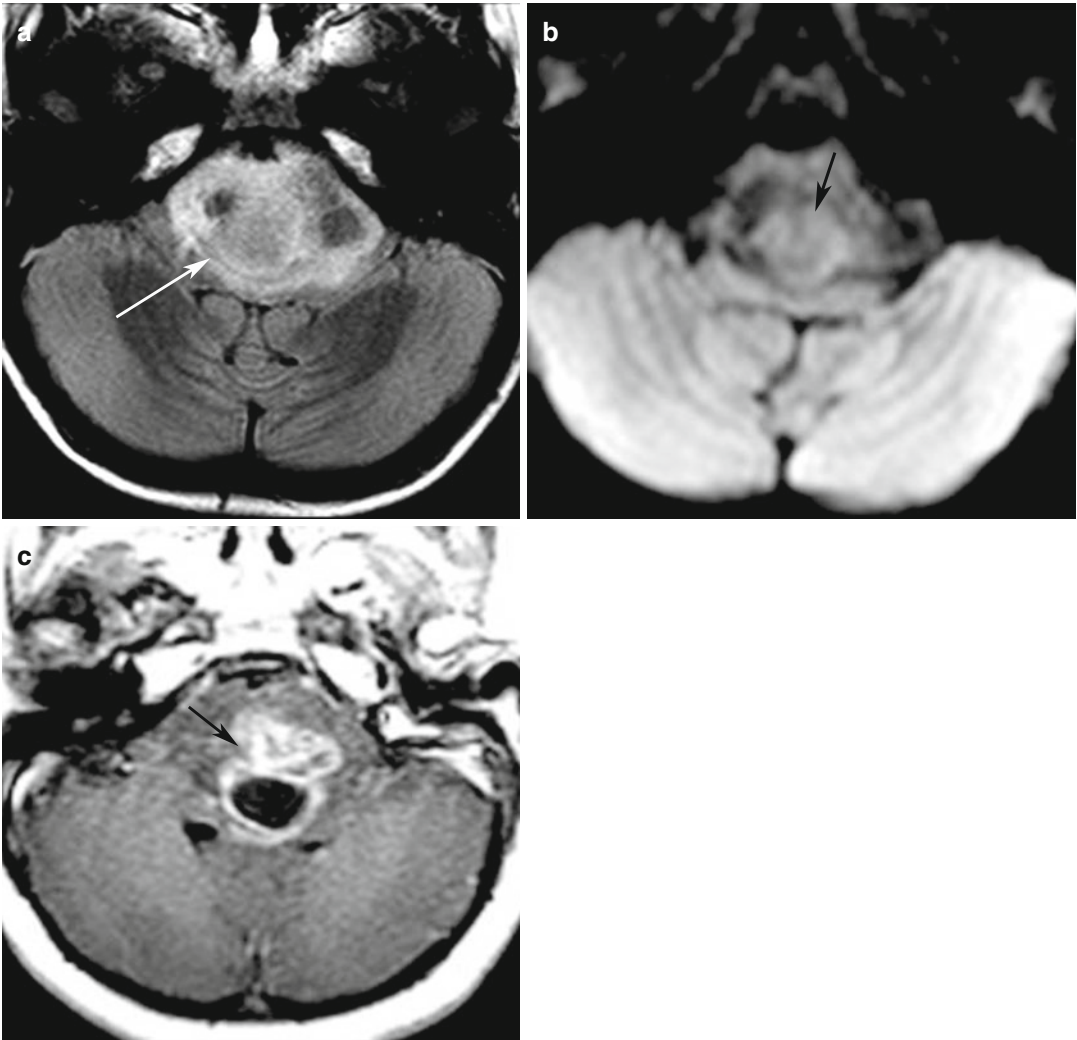


Fig. 31.3 Diffuse intrinsic pontine glioma. Cellular density. (a) Axial FLAIR. In the heterogeneous bright signal of the infiltrative tumor, there is an ill-defined area of lower signal (*white arrow*). (b) Axial DWI, same level.

This area shows some restriction of the water diffusion (*black arrow*), suggesting high cellularity. (c) Axial gadolinium-enhanced T1. Follow-up study after 3 months demonstrates high vascularity (*black arrow*) and necrosis

thalamus, so that it was proposed to give them the specific name of *peritectal tumor* [44].

Tegmental midbrain tumors are typically lateral (Fig. 31.14), well circumscribed, and often associated with hydrocephalus [46]; although there is some confusion with the terms, it seems that some of them may be located within the *cerebral peduncle* more than in the *tegmentum stricto sensu* [46, 47] (Fig. 31.14): this may have some bearing on the invasiveness pattern, as well as from a developmental point of view. Tegmental tumors may remain within the brainstem, or they

may extend rostrally into the thalamus and caudally into the tegmentum pontis or the brachium pontis (Fig. 31.15). Most are gliomas, but within that group examples of all PA-FA grades I–IV have been reported [34, 36, 37, 44–48]. A particular variant of midbrain tumor is the uncommon “pencil” *periaqueductal glioma* of the midbrain [48–50], forming a dormant infiltrative mass that surrounds the aqueduct and is characterized by a long-standing hydrocephalus; various histological types have been reported, including *hamartomas* in fetuses [51].

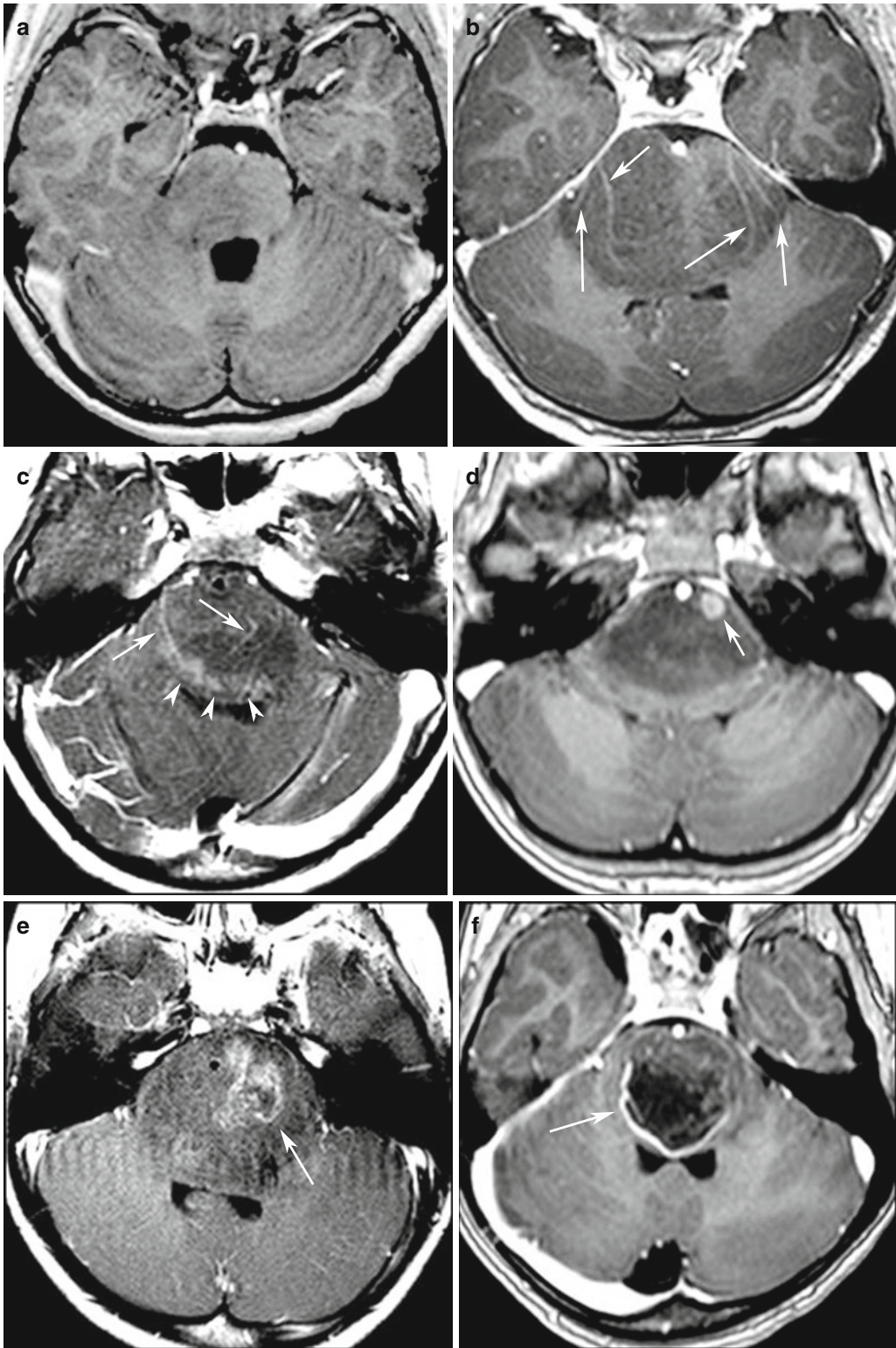


Fig. 31.4 Diffuse intrinsic pontine glioma. Enhancement patterns (axial T1 post-gadolinium administration). (a) No enhancement. (b) Dilated vessels, likely veins (arrows), reflecting the increased blood flow. (c) Dilated

vessels (arrows) with ill-defined area of faint enhancement (arrowheads). (d) Nodular enhancement (arrow). (e) Irregular patchy enhancement (arrow). (f) Ringlike enhancement with central necrosis (arrow)

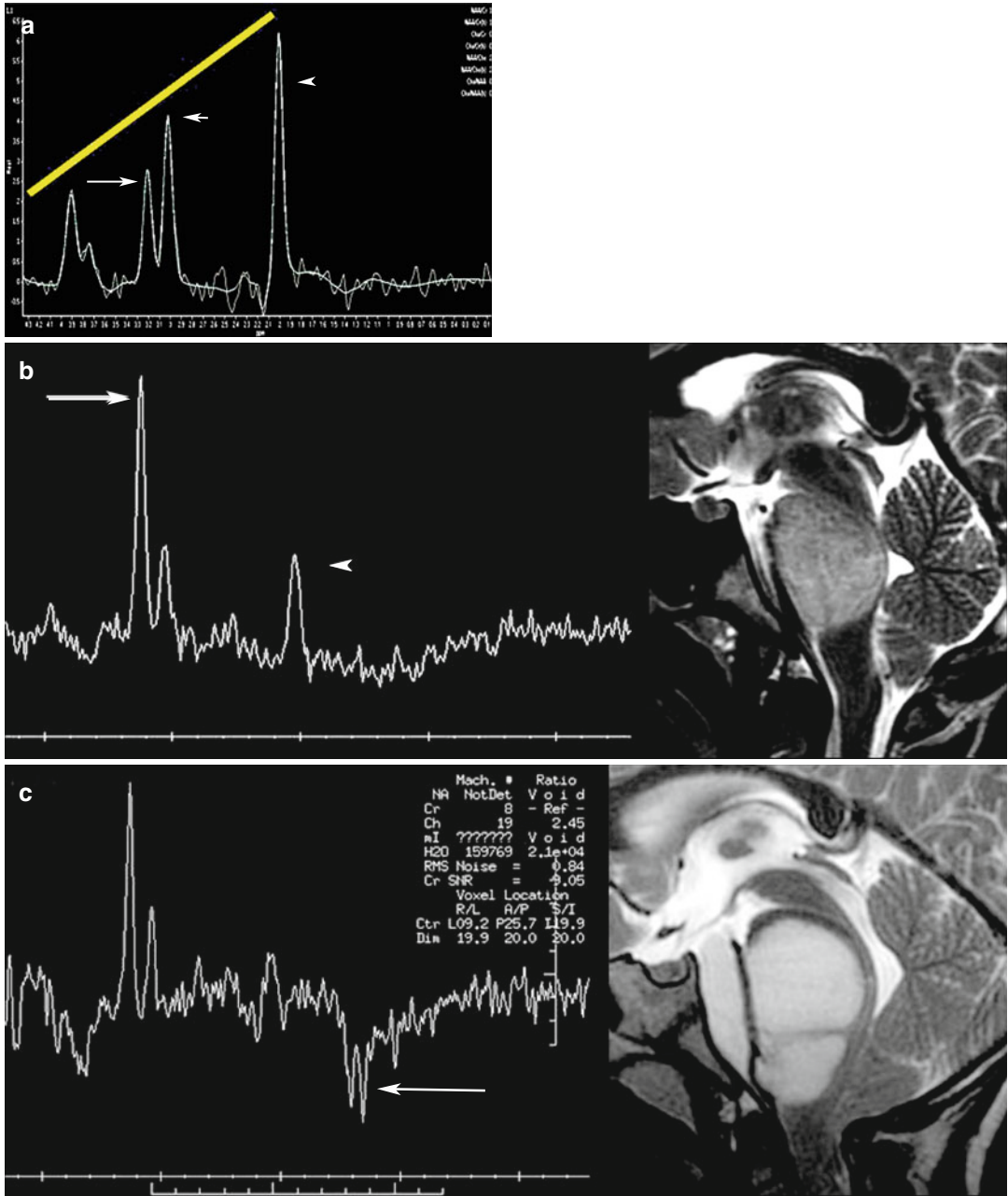


Fig. 31.5 MR spectroscopy of pontine tumors. (a) Normal pattern. NAA (arrowhead) is higher than Cr (short arrow) and Cho (long arrow). The three are aligned, the peaks decreasing from right to left (yellow line). (b) DIPG. Assuming that Cr remains invariant, NAA (neuronal activity) is low (arrowhead), and Cho (cellular turnover) is extremely high (long arrow). (c) DIPG. Same pattern but in addition there is a lactate doublet (arrow) that reflects cellular necrosis

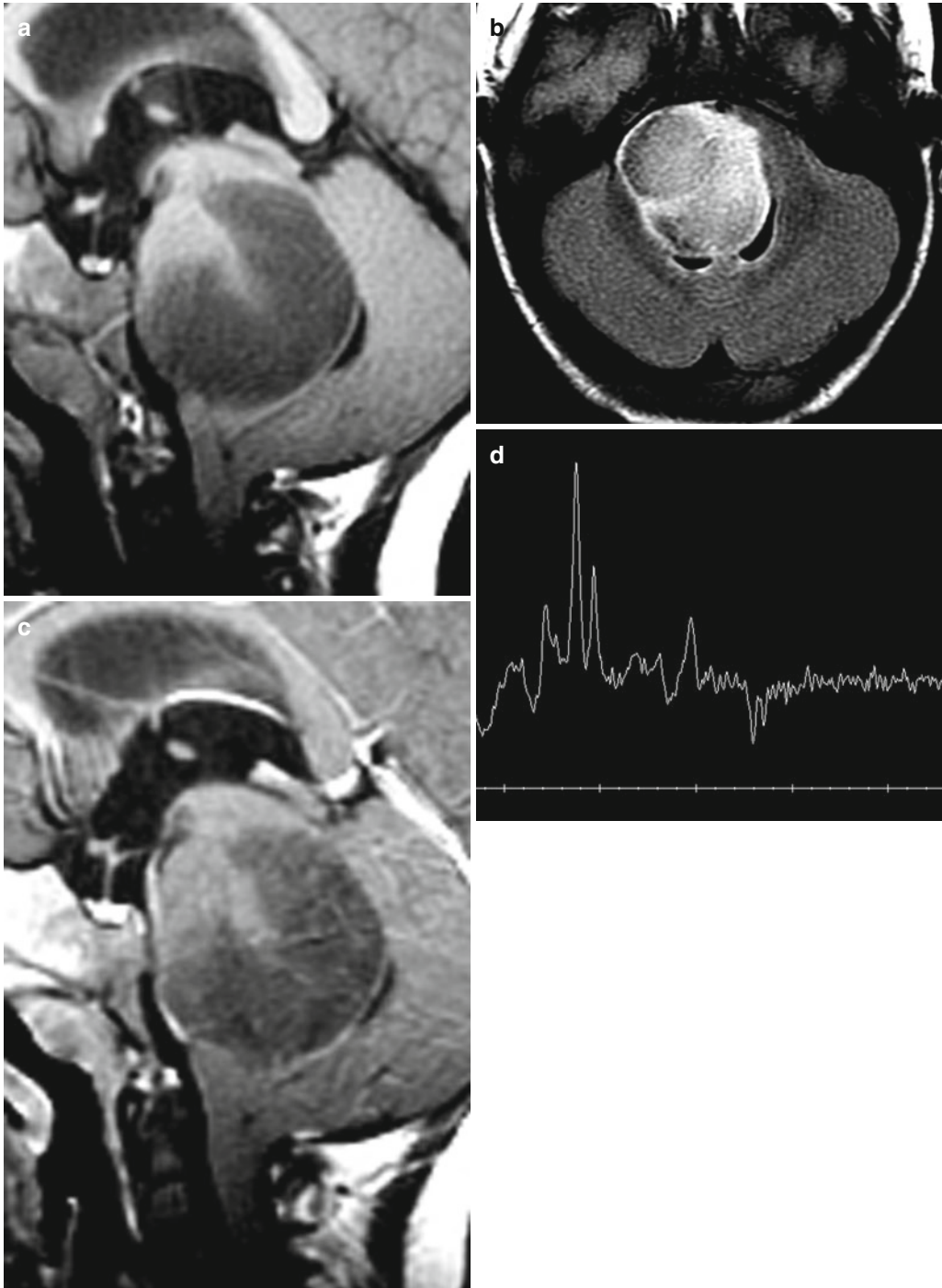


Fig. 31.6 Lateral pontine glioma (pilocytic astrocytoma). (a) Sagittal T1. Huge pontine mass, heterogeneous, with significant posterior expansion and hydrocephalus (dilated third ventricle). (b) Axial FLAIR. The mass is centered on the right middle cerebellar peduncle. (c) Axial T1 with contrast administration. No significant enhancement. (d) “Malignant” pattern of the MR spectrum with increased Cho (high cellular turnover), low NAA (neuronal activity)

and Lac doublet. A surgical partial exeresis of the posterior exophytic component disclosed a pilocytic astrocytoma (WHO grade I). (This case illustrates the fact that when dealing with gliomas, location is more contributive to the diagnosis than MRS.) Perfusion would have shown a low CBF and high contrast leakage in this case of PA, in contrast with a high-grade glioma which would have shown a high CBF

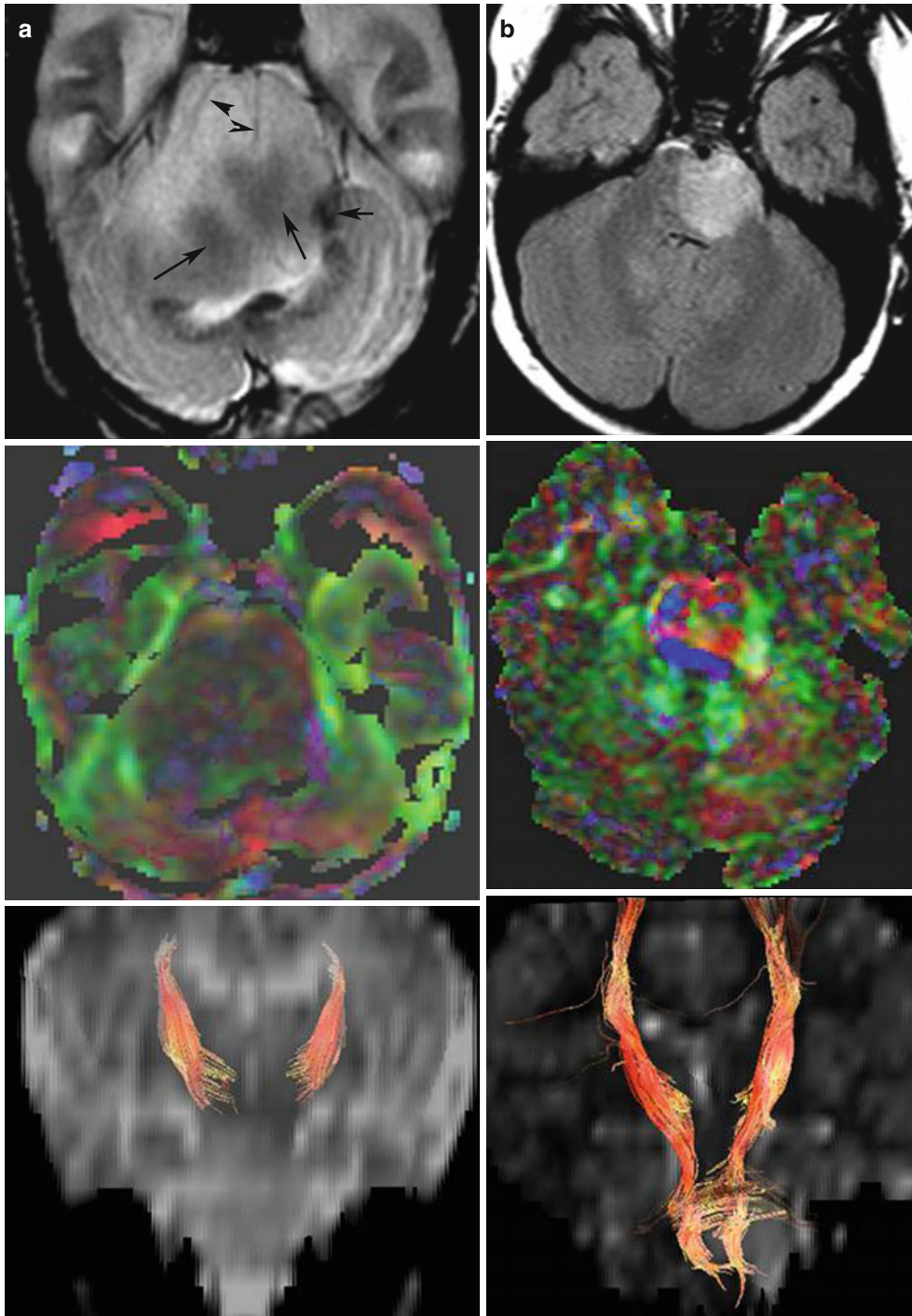


Fig. 31.7 DTI tractography. (a) Highly malignant pontine tumor. (Upper) Axial T2 demonstrates areas of high cellularity (long arrows), hemorrhage (short arrow), and dilated vessels (arrowheads). (Middle) FA map demonstrates complete loss of the organization of the fiber tracts in the pons. (Lower) Craniocaudal fiber-tracking of the corticospinal tract reveals that they are interrupted at the level of the tumor. This may reflect a destruction of the

fibers, or a massive extracellular edema with loss of anisotropy. (b) Low-grade lateral pontine glioma. (Upper) On the axial FLAIR image the tumor is centered on the left cerebellar peduncle. (Middle) The FA map shows a partial distortion but a general preservation of the organization of the fiber tracts (compare with a). (Lower) The corticospinal tract on the left is displaced medially but otherwise preserved

31.2.3.1 Structural Changes: Conventional Imaging

Assessing the structure is the second step of the radiological approach to the diagnosis of brainstem tumor. As mentioned above, essentially all ventral pontine tumors are malignant, and most tumors in other locations are not.

Essentially all are low signal on T1WI and bright signal on T2WI and FLAIR and present without evidence of restriction on diffusion imaging.

However, *malignant tumors* may be characterized by a few particular features: foci of T2 low density reflecting local anaplasia and high cellular density [4] (Figs. 31.3a and 31.7a), poorly

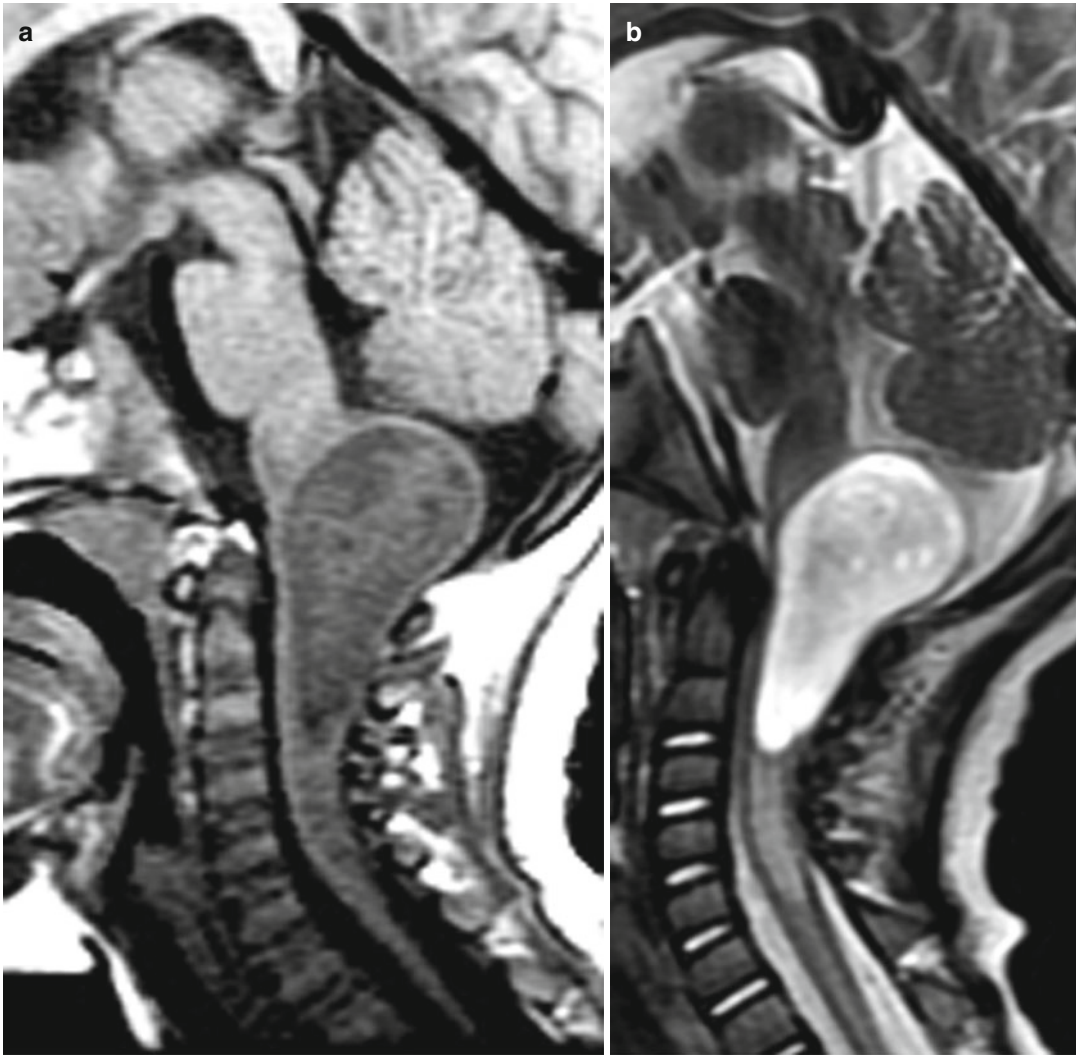


Fig. 31.8 Cervicomedullary pilocytic astrocytoma. **(a)** Midline sagittal T1. The tumor seems to originate from the upper cord, to extend into the lower medulla and to emerge from the dorsal surface of the lower medulla into the cisterna magna: this fits the model according to which the tumor wouldn't cross the decussation plane (or the inter-rhombomeric plane). The mass appears homogeneous, solid, and on its dorsal exophytic component lined

with a normal-looking layer of brain tissue. **(b)** Midline sagittal T2. Similar findings, with the core of the tumor being bright; the cord below the tumor seems to be edematous. **(c)** Axial FLAIR. Diffuse enlargement with concentric bulging into the cisterna magna. **(d)** Midline sagittal T1 post-gadolinium. Diffuse enhancement of the mass with a few necrotic patches, consistent with the diagnosis of low-grade PA

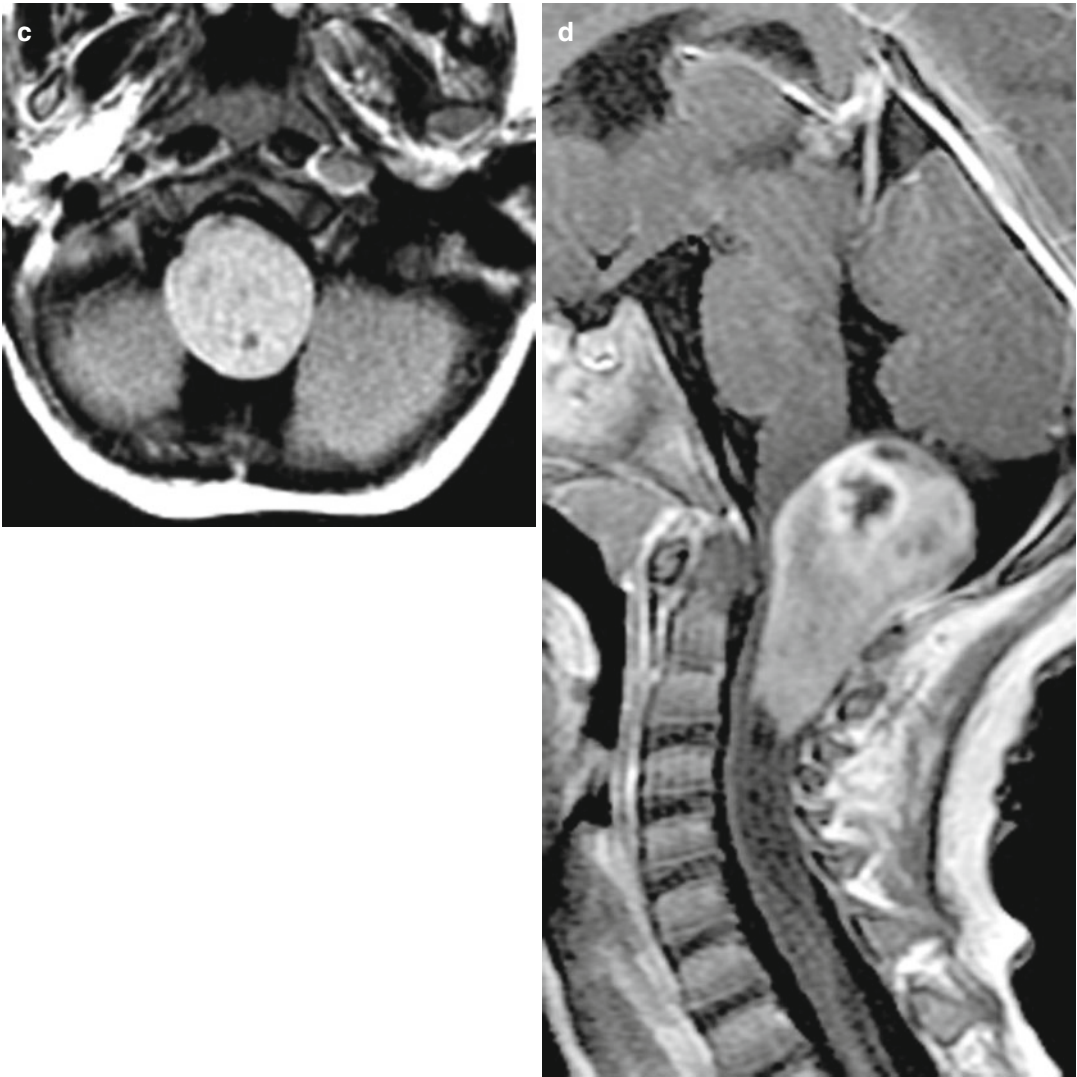


Fig. 31.8 (continued)

defined limits, surrounding edema (difficult however to differentiate from the core of the tumor), extensions across anatomical boundaries (Fig. 31.2a), hemorrhages (especially multiple tiny diffusely distributed petechial hemorrhages) [9, 52] (Fig. 31.2a, e–h), and necrosis (Figs. 31.2a, g, 31.3c and 31.4f). Enhancement is extremely variable from nonexistent to faint, patchy, or to ringlike surrounding a necrotic areas (Figs. 31.3c and 31.4a–f). In the basis pontis one of the main features of the high-grade gliomas is the exophytic outgrowth of the tumor into the prepontine cistern;

it surrounds the basilar artery without really invading it (Figs. 31.2a, c–h, 31.3a, 31.4b–e and 31.5c). In every location, another feature of malignancy is the progressive expansion of the tumor on follow-up studies performed *at short intervals* (3 months or less), and this often correlates with a short duration of the symptoms. Obviously, leptomeningeal dissemination is suspicious for high grade (Fig. 31.13e).

Benign brainstem tumors typically are pilocytic astrocytomas. Although they may extend diffusely across the brainstem, they usually



Fig. 31.9 Cervicomedullary pilocytic astrocytoma. Long-term progression. (a) Midline sagittal T2, age 6 years. Tumor of the upper cord with exophytic growth into the cisterna magna, sparing the upper medulla. (b)

Midline sagittal T1, age 12 years. The tumor has expanded into the medulla and is now reaching the pontomedullary boundary (therefore has crossed the decussation plane)

appear well demarcated from the surrounding parenchyma (Fig. 31.6); they do not cross anatomic boundaries (Figs. 31.8 and 31.9); they form relatively compact masses (Fig. 31.8), without or with cystic components (Fig. 31.9b); and they tend to enhance more diffusely and homogeneously (Figs. 31.8d and 31.15d). They are commonly exophytic, often dorsally into the fourth ventricle but also anteriorly or laterally in the perimedullary or the cerebellopontine angle cisterns, and anywhere around the midbrain. On repeated study, the growth of the mass is slow, hardly apparent on short follow-ups, reflecting a usually long clinical history. However, the uncommon, infiltrative, usually non-enhancing fibrillary astrocytoma grade II may evolve toward anaplasia so that its structural pattern is secondarily modified.

From a blinded multicentric study of a group, 142 cases of pediatric brainstem lesions including 78 cases of tumors, by using 14 imaging criteria in conjunction with clinical and laboratory data (the latter mostly to exclude infection and inflammation) compared with histopathological data, it appeared that biopsy was only rarely needed to reach the exact diagnosis and that appropriate care could be provided to most patients with brainstem tumors on the basis of radiological imaging alone [8]. (The imaging criteria taken into account in this study are listed in Table 31.1.) This however is controversial, and in some specialized centers, a surgical biopsy is recommended for precise identification of the histological and cytogenetic subtype.

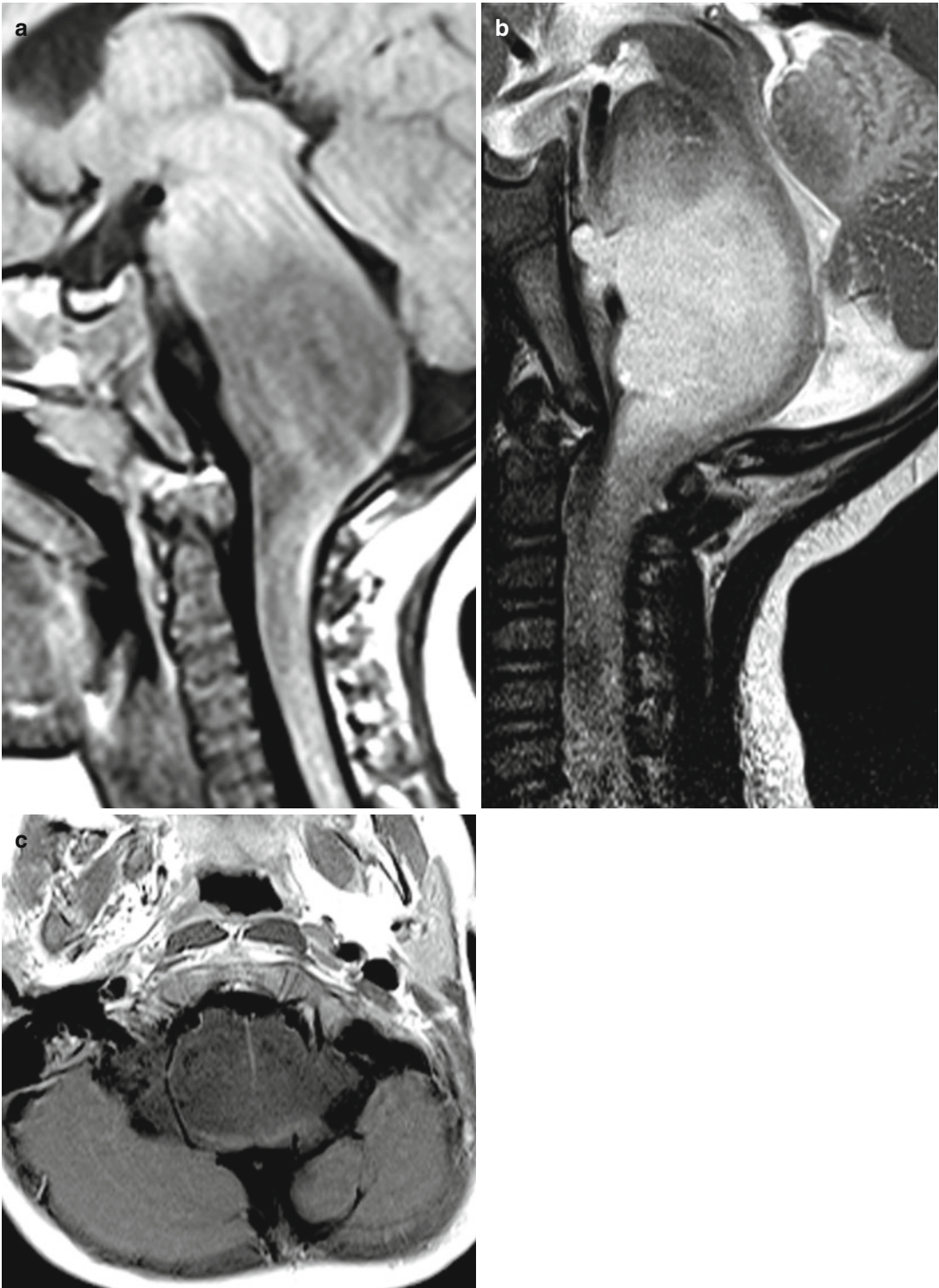


Fig. 31.10 Cervico-medullo-pontine diffuse glioma, identified as low-grade (13-month-old boy). **(a)** Sagittal T1. The tumor is centered on the medulla and extends toward both the upper cord and the pons. **(b)** Midline sagittal T2. The tumor appears ventrally located with exo-

phytic nodules in the prepontine and premedullary cisterns while the dorsal aspect of the medulla appears better preserved. **(c)** Axial T1 post-contrast. Dilated vessels, concentric enlargement of the medulla with apparent preservation of its dorsalmost aspect

31.2.3.2 Structural Changes: Advanced Imaging

In addition to conventional imaging, a few noninvasive MR techniques may provide useful data. In patients with apparently classical imaging of DIPG, *MR spectroscopy* was able to demonstrate different spectral profiles in patient with long survival as compared with those with short survival [26]; however, the MR spectrum of pilocytic grade I astrocytomas may be puzzling (Figs. 31.5 and 31.6d). MR spectroscopy also detects a malignant evolution in initially low-grade pontine gliomas, when the initially low total choline increases while NAA, creatine, and myoinositol decrease [27]. Using *DTI*, a quanti-

tative evaluation of the diffusivity of the proton may appreciate a decreased diffusivity, meaning high cellularity, in cases where conventional diffusion imaging does not show any apparent restriction. Tractography demonstrates dispersion of the white matter fibers in cases of infiltrative tumors, while they are rather pushed aside in focal benign lesions. It was demonstrated in cases of DIPG that not only a Wallerian antero-grade degeneration occurred in the sensory tracts but also a retrograde degeneration along the corticospinal tracts, more pronounced in the vicinity of the tumor but still apparent close to the cortex [24]. Finally *perfusion imaging* is an efficient tool to appreciate the grading of a tumor by measur-

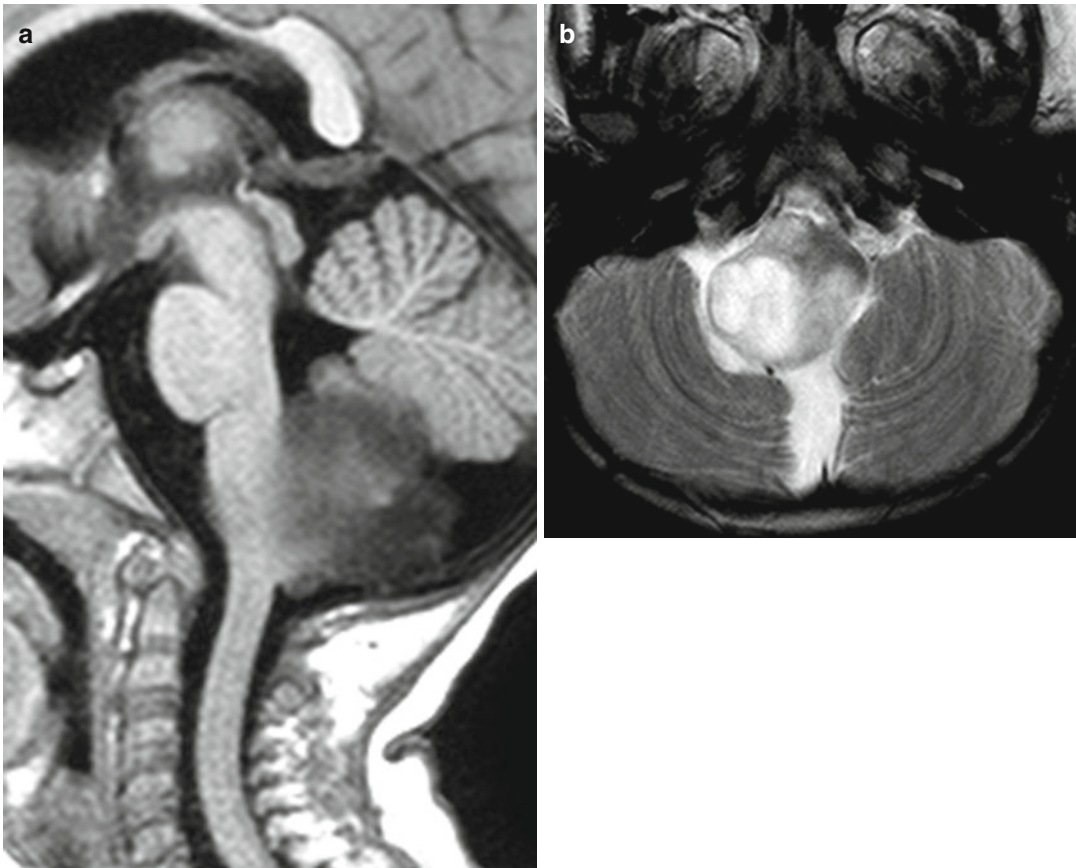


Fig. 31.11 Medullary glioma, focal. (a) Midline sagittal T1. The tumor is located in the medulla and is exophytic dorsally into the cisterna magna. (b) Axial T2. The tumor is mostly dorsal, somewhat lateralized to the right. (c) Axial FLAIR. The tumor appears essentially solid. (d) Lateral sagit-

tal T1 post-gadolinium. The tumor is irregularly enhanced, which still is consistent with the diagnosis of low-grade glioma. It extends superiorly into the inferior cerebellar peduncle

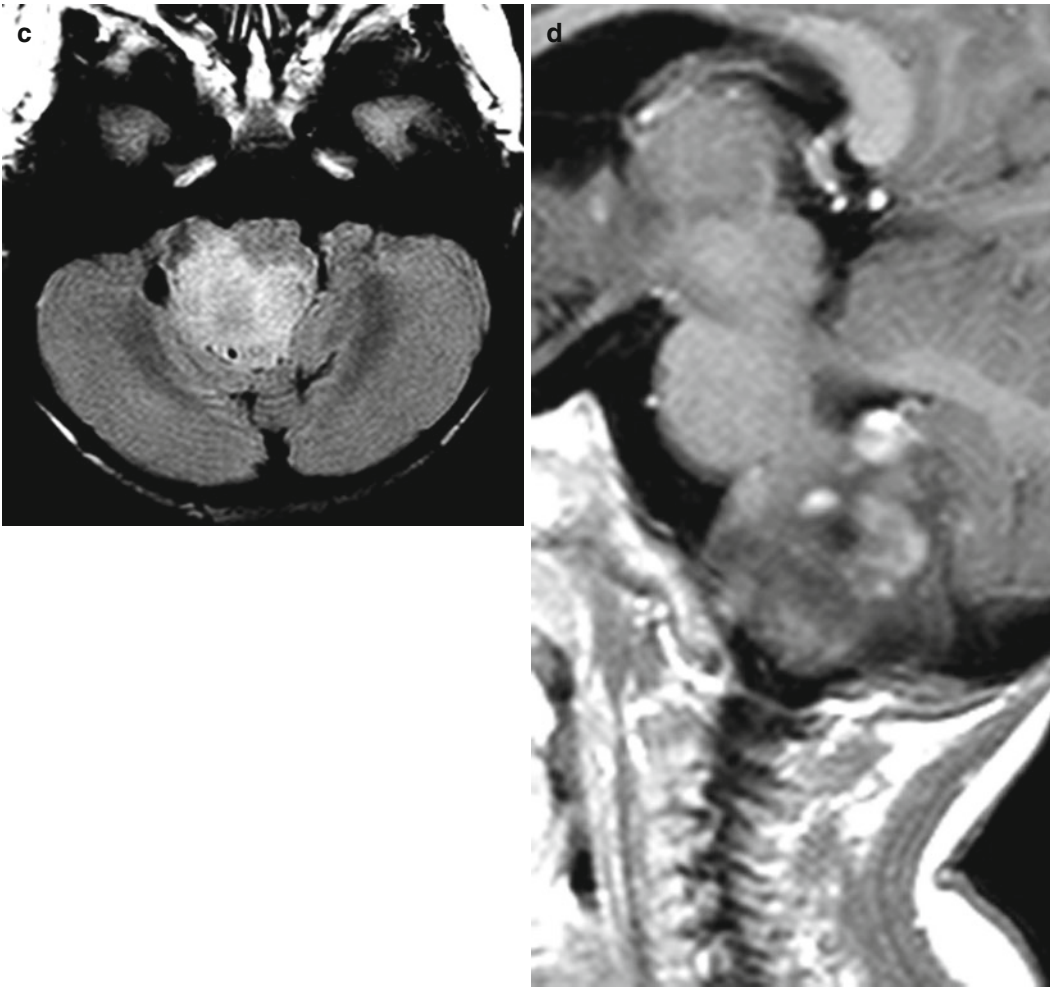


Fig. 31.11 (continued)

ing the regional CBF and CBV. Increased perfusion is often reflected on imaging by a prominent dilation of the vessels, mostly the veins, in the brainstem (Fig. 31.4b, c). In cases of malignant glioma (grades II–IV), CBV is significantly increased and the time-curve remains above the baseline after the first pass because of leakage of contrast accumulating in the interstitial fluid [30]. In fibrillary astrocytoma grade II the CBV is similar to normal brain with no leakage of contrast after the first pass [30]. In pilocytic astrocytoma grade I CBV is low (poor vascular bed) but the time-curve remains above the baseline after the first pass because of massive leakage

of contrast into the interstitial fluid [30, 53, 54]; this presumably is due to the fact that PA present a hyaline degeneration of the vessels while the endothelial cells have no tight junctions and open fenestrae allowing for the extravasation of the contrast media [53].

As mentioned before DTI is more sensitive than DWI/ADC mapping in detecting an hypercellularity. Tractography may be helpful in showing that the fibers tracts are spread apart or even destroyed by the highly malignant DIPG (Fig. 31.7a), while they are simply displaced by the more compact pilocytic astrocytomas (Fig. 31.7b).

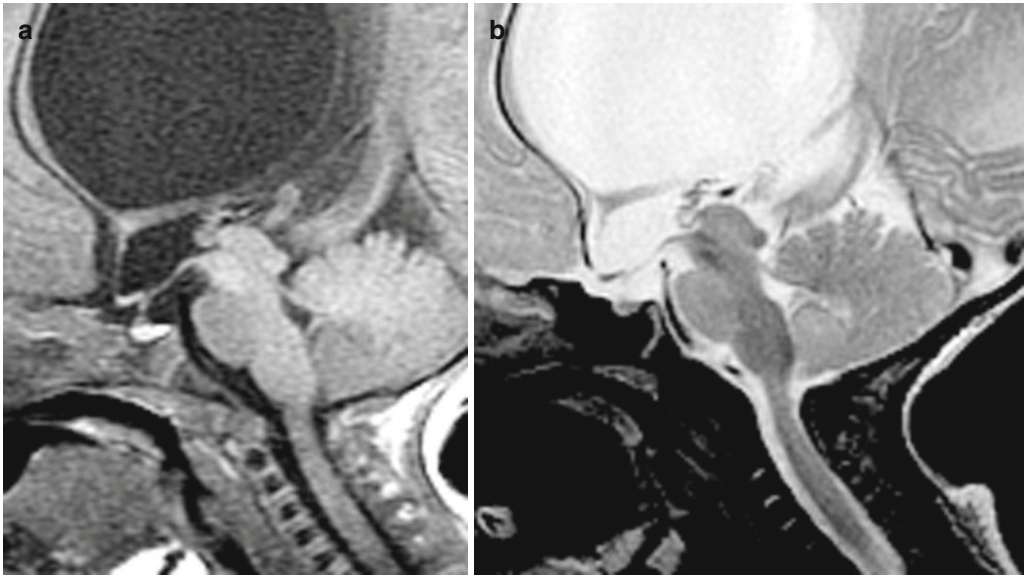


Fig. 31.12 “Dormant” tectal tumor, presumably glioma (or hamartoma) in a 5-week-old girl. (a) Midline sagittal T1. Presumably congenital hydrocephalus with aqueductal stenosis; this is explained by a bulky tectal plate with loss of the quadrigeminal sulcus. (b) Midline sag-

ittal T2. The normal tectal plate is myelinated early: in this case its rostral portion is too bright (high T2 signal). Hydrocephalus was treated and follow-up studies over 5 years showed no change in the appearance of the tectal plate lesion

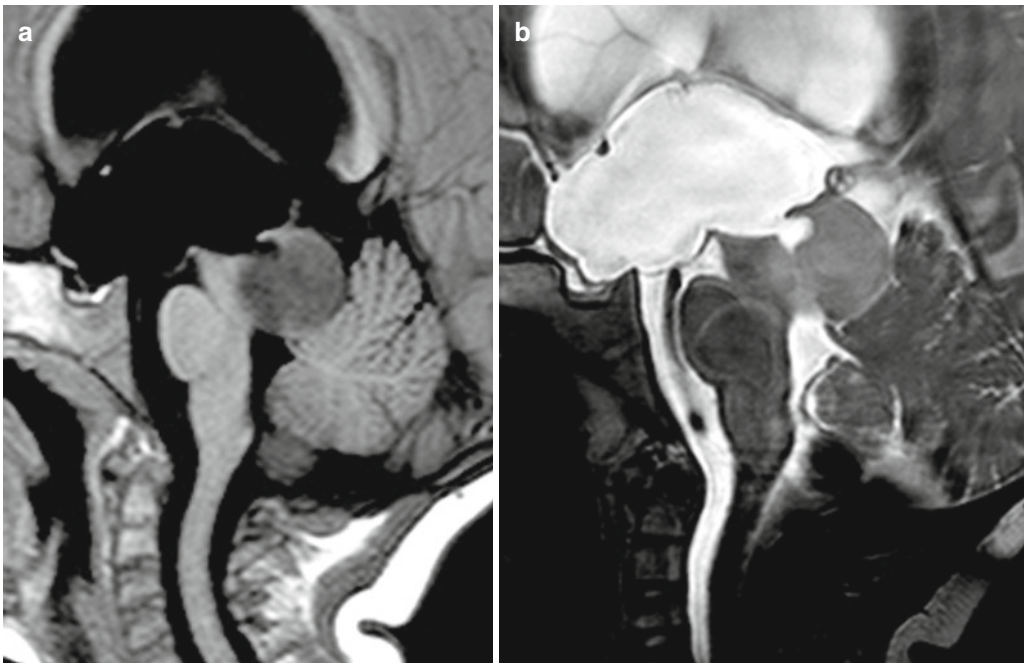


Fig. 31.13 Evolute tectal glioma (25 mm diameter). (a) Midline sagittal T1. Rounded mass developed on the posterior part of the tectal plate, invading the adjacent tegmentum and aqueduct, and the rostral part of the anterior medullary velum. Severe hydrocephalus. The mass is homogeneously hypointense. (b) Midline sagittal T2/FIESTA (high definition T2). The tectal mass encroaches upon the distal portion of the aqueduct. Massive dilation of the third ventricle. (c) Axial

FLAIR. Well circumscribed, homogeneously hyperintense mass surrounding the aqueduct and slightly lateralized to the right. Note a massive high-pressure hydrocephalus with periventricular interstitial edema. (d) Sagittal T1 post-gadolinium. Homogeneous enhancement of the mass, suggestive of a low-grade glioma. (e) Spinal sagittal T1 post-gadolinium. Drop metastase on the right posterolateral aspect of the conus, suggesting some invasiveness (pilomyxoid astrocytoma?)

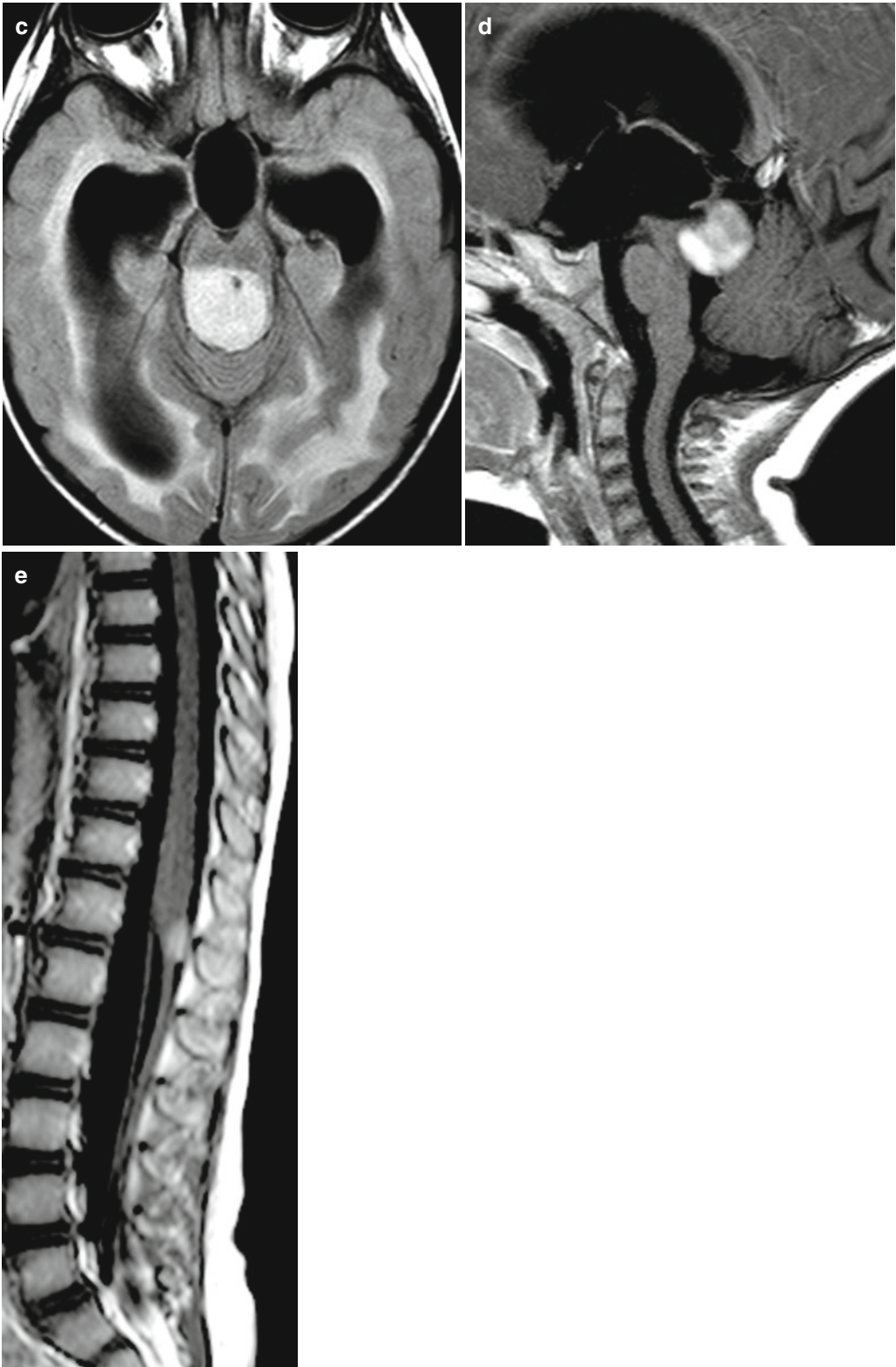


Fig. 31.13 (continued)

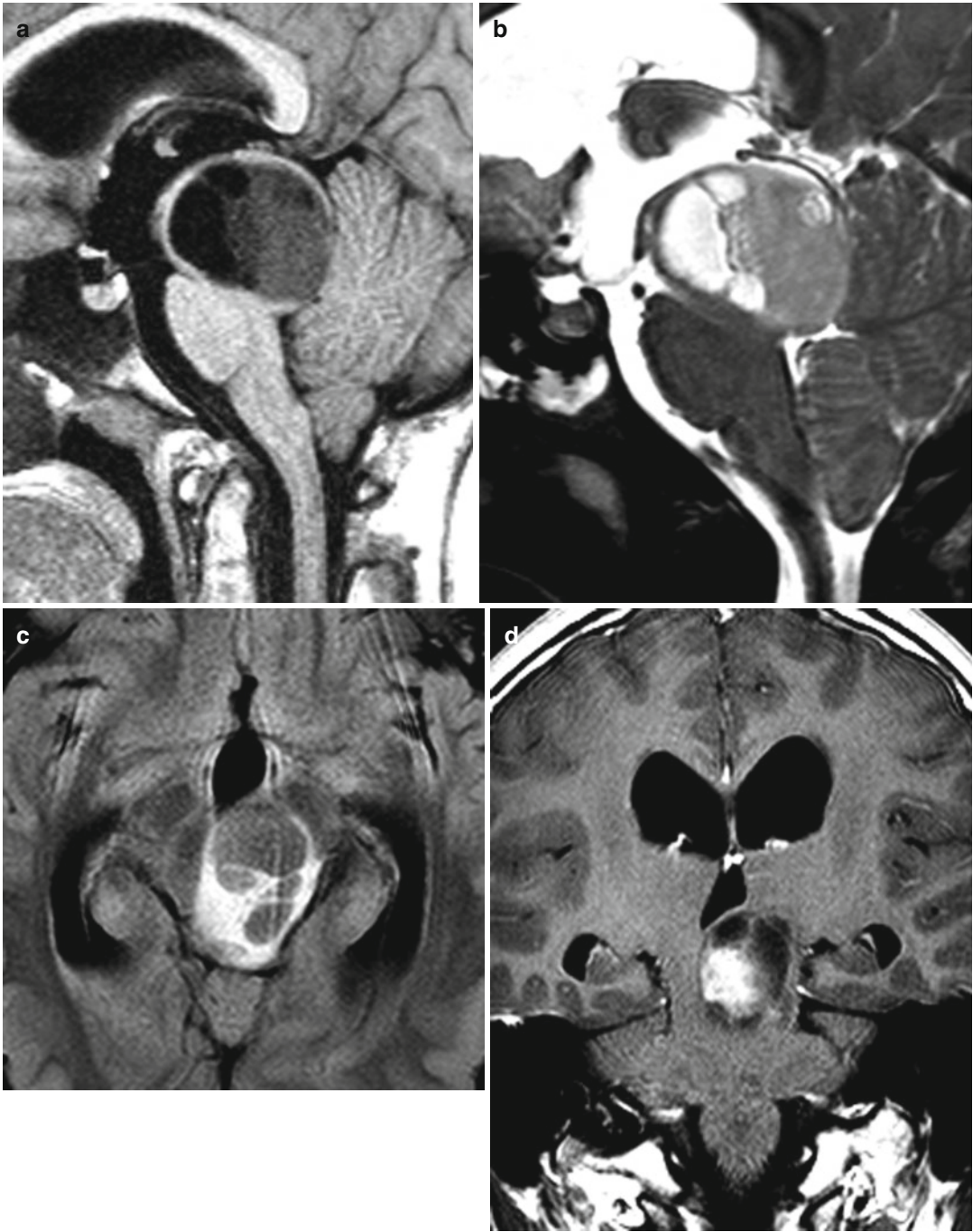


Fig. 31.14 Midbrain tumor. (a) Midline sagittal T1. Large, possibly cystic mass in the tegmentum and peduncle. (b) Midline sagittal T2/FLAIR. Multiloculated anterior cysts. The tectal plate is stretched and partly separated from the tumor by the aqueduct. (c) Axial

FLAIR. Well-circumscribed solid/cystic tumor lateralized to the left tegmentum and cerebral peduncle. (d) Homogeneous enhancement of the solid portion of the tumor. Superior expansion toward the subthalamic region



Fig. 31.15 Mesencephalo-thalamic glioma. **(a)** Sagittal lateral T1. Huge, relatively homogeneous mass extending from the suprasellar region to the upper portion of the pons, with a significant exophytic component. **(b)** Coronal FLAIR. It shows the full extent of the mass, partly cystic in its more lateral component. Associated changes in the stria-

tum, of uncertain nature. **(c)** Axial T2. It shows the mesencephalic component of the mass (tegmentum and right peduncle). **(d)** Sagittal lateral T1 with gadolinium. It reveals the diffuse, strong enhancement consistent with a low-grade glioma

Table 31.1 MR imaging characteristics important for the diagnosis of brainstem gliomas (Ref. [8])

1. Intrinsic structures	Homogeneous/heterogeneous
2. Margin of the lesion	Delineated/blurred Regular/irregular
3. Enhancement	Diffuse, focal, ringlike
4. Reaching the brain surface	Dorsal Lateral Ventral
5. Necrosis	0–20 % 21–40 % 41–60 % 61–80 % 81–100 %
6. Edema	<1 cm 1–2 cm >2 cm
7. Cysts	<0.5 cm 0.5–1 cm >1 cm
8. Brainstem expansion	Mild Moderate Severe
9. Hydrocephalus	Mild Moderate Severe
10. Bleeding	
11. Calcification	
12. Extension into fourth ventricle	
13. Contact to cranial nerves and dura	
14. Aqueductal stenosis	

31.3 Other Histological Types of Intrinsic Brainstem Tumors

The vast majority of brainstem tumors consists of *astrocytic gliomas* (fibrillary astrocytomas grade II–III, pilocytic astrocytomas grade I, and glioblastomas grade IV) and corresponds to the descriptions above. *Gangliogliomas* may be found as well,

although not common, presenting typically like pilocytic astrocytomas; as they may be calcified, they appear spontaneously diffusely dense on CT, sometimes with coarse calcifications, and relatively dark T2 on MR; they have a very slow evolution (Fig. 31.16). A *desmoplastic infantile ganglioglioma* was reported in a 22-month-old boy, with diffuse meningeal involvement [55]. *Pilomyxoid astrocytomas* may develop in the brainstem as well [32]; they may not be differentiated radiologically from classical pilocytic astrocytomas except for possible leptomeningeal dissemination. Other than that, *oligoastrocytoma* or *oligodendroglioma* have been observed, but only secondarily diagnosed from the biopsy [42, 48]. An angiocentric glioma-like tumor has been reported as well [56].

In the context of a *neurofibromatosis type 1 (NF1)*, brainstem gliomas seem to be the most commonly observed type of tumor after the anterior optic pathway/hypothalamic tumors [57–59]. Their real incidence is uncertain as the lesion often is detected incidentally while following up an optic/hypothalamic mass. In children with NF1, brainstem tumors develop at a later age than the optic/hypothalamic tumors but still may be apparent before the age of 10 years. Like the optic/hypothalamic tumors, they seem to be much more indolent than similar tumors encountered without the NF1 context, and like for optic/hypothalamic glioma, spontaneous regression does occur. They are most often located in the medulla, then in the midbrain, and much less in the pons. Histologically they seem to consist mostly of fibrillary astrocytomas [57], typically low grade with only one grade III (anaplastic) reported [57]. The main diagnostic problem is to differentiate such potentially developing tumors from the classical UBOs (“unidentified bright objects”) which are extremely common in the brainstem, cerebellar peduncles, and cerebellar white matter. UBOs tend to be slightly bulky, and may occasionally enhance faintly, but are considered *never to be associated with symptoms*. In a child with NF1, the diagnosis of tumor will be suspected if symptoms and signs referable to the brainstem are noted; if a significant mass effect (especially if this mass effect progresses between two MR studies) is observed; if there is clear hypointensity on

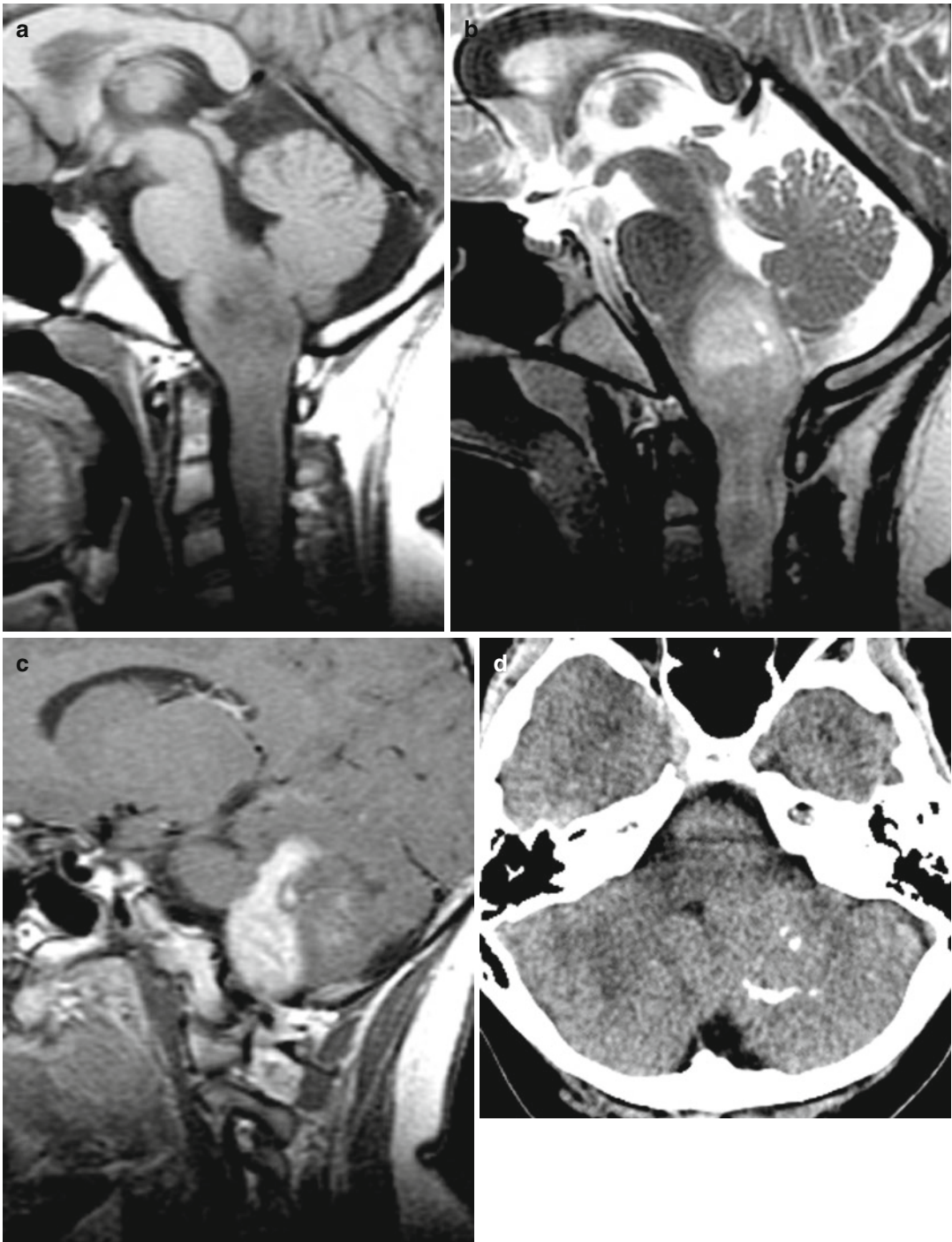


Fig. 31.16 Cervicomedullary ganglioglioma. **(a)** Midline sagittal T1. Mildly heterogeneous tumor of the upper cord and medulla, with a signal close to that of the normal brain. **(b)** Midline sagittal T2. Similarly, the signal is mildly heterogeneous, mostly close to that of the normal neural tissue. **(c)** Sagittal lateral T1 with gadolinium. Diffuse enhance-

ment of the portion of the mass that extends into the inferior cerebellar peduncle and cerebellar white matter. **(d)** Unenhanced CT. The mass on the left side of the fourth ventricle is isodense to the cerebellar cortex, which is unexpected for an astrocytoma; this is associated with coarse calcifications and is highly suggestive of a ganglioglioma

T1 imaging and clear hypersignal on T2/FLAIR; if a hemorrhage, a necrosis, or a cyst is present; if the tumor is exophytic; and if the tumor is avidly enhancing. In the majority of the cases, clinical and radiological regression will occur, both in treated and in untreated patients [59].

As can be expected, *ependymomas* have been reported in the region of the aqueduct, have no specific features, and are diagnosed on the basis of the biopsy only [34, 48, 60]. Another report of an ependymoma within the basis pontis [61] is more surprising, however, as ependymomas typically develop in the laterodorsal aspect of the neuraxis. When they develop from the medulla (i.e., from the inferior rhombic lips), ependymomas do not invade the brainstem but rather behave as purely exophytic tumors extending into the cisterns (cisterna magna or cerebellopontine angle cistern) and usually (but not always) the fourth ventricle, with no more than their insertion being attached on the dorsal (obex) or dorsolateral (lateral recess) brainstem [62].

In young children, *PNETs* also may be found in the brainstem [34, 63], mostly in the pons and brachium pontis [63]. They are focal masses which present with low T1 and high T2/FLAIR signals [63] and tend to become exophytic and to disseminate [63]. The diagnosis of PNET is suggested preoperatively by the usually clear restriction of diffusion demonstrated on DWI and ADC mapping. They seem not to enhance [63]. The possible occurrence of another embryonal tumor, the *atypical teratoid rhabdoid tumor (ATRT)*, is mentioned also, with features grossly similar to those of the PNET, notably on DWI/ADC.

Rarely in children hemangioblastoma may develop in the dorsal medulla (Fig. 31.17) and may be both solid and cystic. Their appearance however is different from that of the PA because they are vascular, high blood flow tumors and contain numerous prominent vascular flow voids on T2 (Fig. 31.17a); MRA may demonstrate a hypervascularization (Fig. 31.17b) and enhancement by contrast is intense. Of course, intraaxial tumors of extraneural origin such as a lymphoma or a Langerhans cell histiocytosis (LCH) [64] may occur, although exceptionally, and be mistaken for an intrinsic tumor.

31.4 Differential Diagnosis

A comprehensive coverage of the differential of both focal and diffuse brainstem lesions would cover nearly the whole spectrum of neurological diseases [65, 66]. The diagnosis of tumor may be difficult on conventional imaging alone in case of a large, single edematous lesion of *ADEM* and other demyelinating diseases; DTI fiber tracking would show extreme paucity and even truncation of the pyramidal fibers with very low FA in case of ADEM and displacement and distortion of the fibers with normal to mildly low FA in case of tumor [25]. These data however may need to be confirmed in larger series. *Behçet's disease* also may present as a nonspecific inflammatory mass of the brainstem with diffuse enhancement and may therefore suggest a tumor both clinically and radiologically. The so-called infectious *rhombencephalitis* is uncommon and affects the cerebellum mostly.

Centro-pontine myelinolysis is rare in children and develops in specific contexts.

Abscesses may look like tumors, especially when surrounded by massive edema, even though the brainstem is an uncommon location in children. Beside the clinical context is usually different, and DWI/ADC mapping would demonstrate restricted diffusion within the pus-filled cavities.

Dysembryoplastic inclusion cysts may rarely be found in the brainstem, either neuroenteric cysts or dermoid cysts. They form very slow-growing mass lesions, typically on the midline, and their MR signal on T1, T2, or FLAIR wouldn't be consistent with either a tumoral cyst or a necrosis: fat and skin products for the dermoid and mucus for the neuroenteric cyst. Dermal tracts and cysts are always dorsal to the fourth ventricle or central canal.

Cavernomas are the second cause of intracerebral bleed in children, after arteriovenous malformations, and in this age range, the brainstem appears to be a common location [67]. However, the multiloculated, blood-filled appearance of the lesion; its hemorrhagic pattern when it bleeds, quite different from the common petechial hemorrhages in brainstem malignant glioma; and the surrounding blooming artifacts on susceptibility

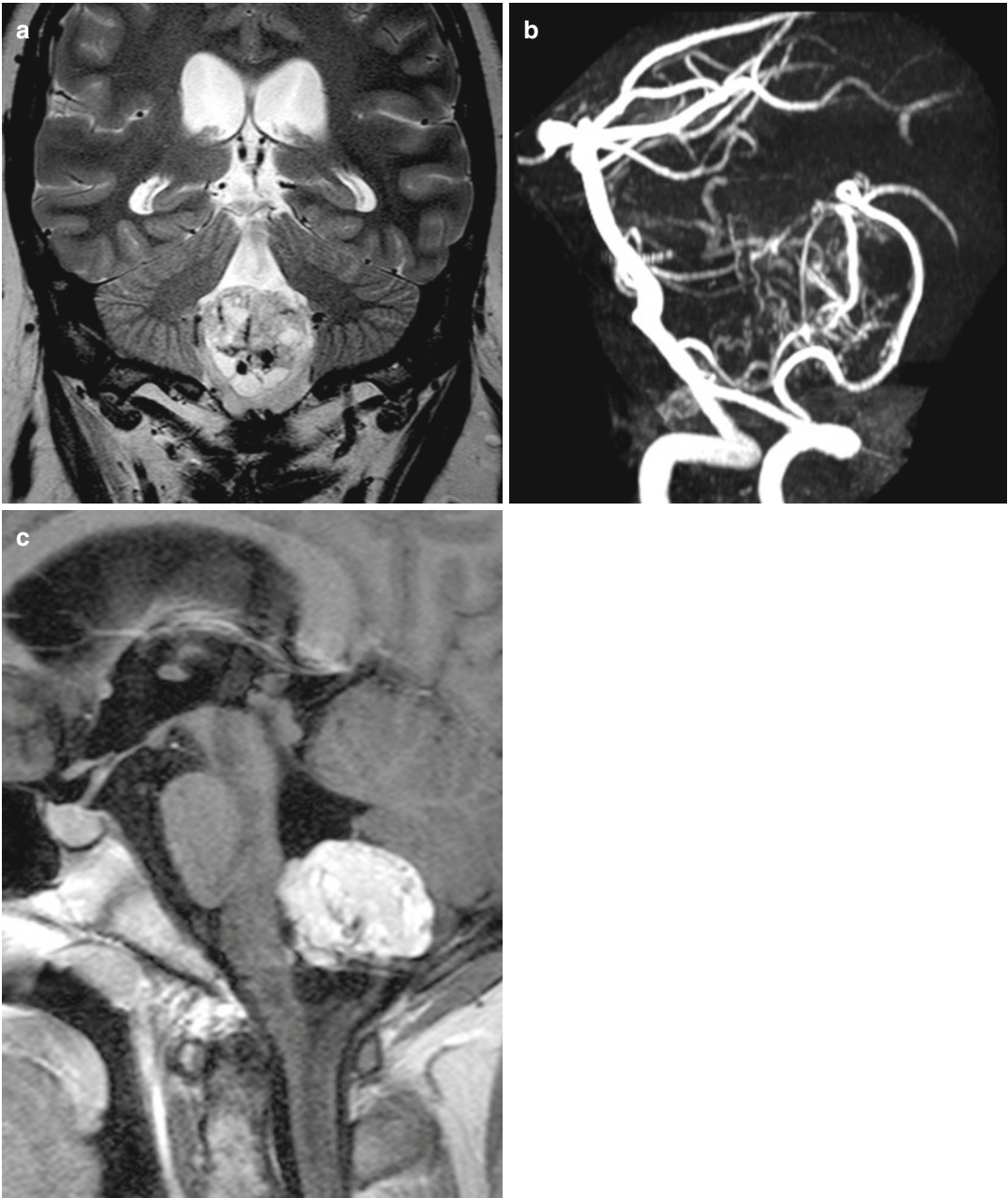


Fig. 31.17 Hemangioblastoma of the medulla. (a) Coronal T2. Hyperintense tumor protruding in the cisterna magna, with numerous flow voids. (b) MR-angiography. Rich vascularity originating from the

cisternal segments of both PICA. (c) Midline sagittal T1 post-gadolinium. Significant widening of the lower medulla with small cystic formation and an avidly enhancing solid exophytic portion bulging in the cisterna magna

imaging concur in making the diagnosis of a cavernoma quite straightforward.

Finally some *metabolic diseases* may produce lesions that resemble brainstem tumors; such cases have been reported for mitochondrial diseases [68] and in one instance of Alexander disease [69].

31.5 Follow-Up Studies

Follow-up studies of brainstem tumors are usually defined, for sequences and timing, by multicentric therapeutic protocols. In essence, the imaging protocols are not different for the surveillance and for the initial diagnosis, being essentially based on the same sequences of conventional imaging, sometimes associated with more advanced imaging such as MR spectroscopy, DTI, and perfusion for specific purposes. Measurements of the tumors usually consist of the longest diameter, usually craniocaudal in brainstem tumors, and of its largest perpendicular diameters in the transverse and the anterior-posterior (dorsoventral) planes. Because of the commonly associated edema, the measurement are somewhat observer dependent; it is generally felt that in the case of gliomas, FLAIR sequences are the most reliable in this respect [3]. It appears clear now that DIPG often disseminates secondarily into the leptomeninges [70–72] and that as a consequence the whole spinal axis must be investigated after administration of gadolinium compound.

There is some evidence that under treatment, malignant DIPG tend to decrease in size, mostly in transverse and dorsoventral diameters but that in the same time they tend to grow along the neural axis into the adjacent midbrain and medulla [73]. The morphological decrease of the mass effect often goes along with an improvement of the clinical symptoms and signs [73], a reduction of the DTI alterations [74], and a trend toward normalization of the MR spectroscopic parameters [28]. However, these findings do not help in prognosticating the duration of the progression-free or overall survival. A secondary deterioration of the spectroscopic parameters (increase of choline, decrease of NAA, increase of lactates and lipids) develops months before a

clinical deterioration and announces the eventual relapse [27]. The development of new areas of high cellularity on T2, DWI, or DTI, of micro-hemorrhages on SWI, of enhancement and/or of necrosis also tells that the tumor is becoming more aggressive.

During evolution, it may be important to differentiate between *radiation necrosis* and recurrent malignant glioma. Perfusion imaging may help by demonstrating a significant increase of rCBV in the latter, against a significant decrease in the former [75]. Quantitative DTI may show a decreased diffusivity in case of recurrence (reflecting the high cellularity) against a high diffusivity in the radiation necrosis (reflecting the interstitial edema) [4, 75]. MR spectroscopy as well would demonstrate a higher peak of choline in case of relapse than in case of necrosis [75].

In the cases of the more benign fibrillary or pilocytic astrocytomas which have been operated upon, follow-up imaging appreciates the extent of the resection and the eventual growth of new foci, and in cases of cervicomedullary tumors, it can appreciate the spinal postsurgical stability [34].

References

1. Epstein F (1985) A staging system for brain stem gliomas. *Cancer* 56:1804–1806
2. CBTRUS (2007–2008) Primary brain tumors in the United States. Statistical report 2000–2004
3. Hayward RM, Patronas M, Baker EH et al (2008) Inter-observer variability in the measurement of diffuse intrinsic pontine gliomas. *J Neurooncol* 90:57–61
4. Löbel U, Sedlacik J, Reddick WE et al (2011) Quantitative diffusion-weighted and dynamic susceptibility-weighted contrast-enhanced perfusion MR imaging analysis of T2 hypointense lesion components in pediatric diffuse intrinsic pontine glioma. *AJNR Am J Neuroradiol* 32(2):315–322
5. Berger MS, Edwards MSB, LaMasters D et al (1983) Pediatric brain stem tumors: radiographic, pathological and clinical correlations. *Neurosurgery* 12:298–302
6. Curless RC, Bowen BC, Pattany PM et al (2002) Magnetic resonance spectroscopy in childhood brainstem tumors. *Pediatr Neurol* 26:374–378
7. Helton KJ, Phillips NS, Khan RB et al (2006) Diffusion tensor imaging of tract involvement in children with pontine tumors. *AJNR Am J Neuroradiol* 27:786–793
8. Schumacher M, Schulte-Mönting J, Stoeter P et al (2007) Magnetic resonance imaging compared with

- biopsy in the diagnosis of brainstem diseases of childhood: a multicenter review. *J Neurosurg* 106(2 Suppl Pediatrics):111–119
9. Löbel U, Sedlacik J, Sabin ND et al (2010) Three-dimensional susceptibility-weighted imaging and two-dimensional T2*-weighted gradient-echo imaging of intratumoral hemorrhages in pediatric diffuse intrinsic pontine glioma. *Neuroradiology* 52:1167–1177
 10. Recinos PF (2007) Brainstem tumors: where are we today? *Pediatr Neurosurg* 43:192–201
 11. Fischbein NJ (1996) Radiological classification of brain stem tumors: correlation of magnetic resonance imaging appearance with clinical outcome. *Pediatr Neurosurg* 24:9–23
 12. Epstein FJ, Farmer JP (1993) Brain-stem glioma growth patterns. *J Neurosurg* 78:408–412
 13. ten Donkelaar HJ, Lammens M, Cruysberg JRM, Cremers CWJR (2006) Development and developmental disorders of the brain stem. In: ten Donkelaar HL, Lammens M, Hori A (eds) *Clinical neuroembryology*. Springer, Berlin Heidelberg pp 269–308
 14. Keynes R, Lumsden A (1990) Segmentation and the origin of regional diversity in the vertebrate central nervous system. *Neuron* 2:1–9
 15. ten Donkelaar HJ, Lammens M, Cruysberg JRM et al (2006) Development and developmental disorders of the forebrain. In: ten Donkelaar HL, Lammens M, Hori A (eds) *Clinical neuroembryology*. Springer, Berlin Heidelberg pp 345–428
 16. Puelles L, Rubenstein LR (2003) Forebrain gene expression domains and the evolving prosomeric model. *Trends Neurosci* 26:469–476
 17. Vescovi AL, Galli R, Reynolds BA (2006) Brain tumour stem cells. *Nat Rev Cancer* 6:425–436
 18. Gilbertson RJ, Gutmann DH (2007) Tumorigenesis in the brain: location, location, location. *Cancer Res* 67:5579–5582
 19. Dirks PB (2008) Brain tumour stem cells: the undercurrents of human brain cancer and their relationship to neural stem cells. *Phil Trans R Soc B* 363:139–152
 20. Sehgal V, Delproposito Z, Haacke EM et al (2005) Clinical applications of neuroimaging with susceptibility-weighted imaging. *J Magn Reson Imaging* 22:439–450
 21. Sehgal V, Delproposito Z, Haddad D et al (2006) Susceptibility-weighted imaging to visualize blood products and improve tumor contrast in the study of brain masses. *J Magn Reson Imaging* 24:41–51
 22. Rauscher A, Sedlacik J, Barth M et al (2005) Noninvasive assessment of vascular architecture and function during modulated blood oxygenation using susceptibility-weighted magnetic resonance imaging. *Magn Reson Med* 54:87–95
 23. Chen X, Weigel D, Ganslandt O et al (2007) Diffusion tensor imaging and white matter tractography in patients with brainstem lesions. *Acta Neurochir (Wien)* 149:1117–1131
 24. Helton KJ, Weeks JK, Phillips NS et al (2008) Diffusion tensor imaging of brainstem tumors: axonal degeneration of motor and sensory tracts. *J Neurosurg Pediatrics* 1:270–276
 25. Giussani C, Poliakov A, Ferri RT et al (2010) DTI fiber tracking to differentiate demyelinating diseases from diffuse brain stem glioma. *NeuroImage* 52:217–223
 26. Krieger MD, Blüml S, McComb JG (2003) Magnetic resonance spectroscopy of atypical diffuse pontine masses. *Neurosurg Focus* 15(1):E5
 27. Panigrahy A, Nerson MD Jr, Finlay JL et al (2008) Metabolism of diffuse intrinsic brainstem gliomas in children. *Neuro-Oncology* 10:32–44
 28. Laprie A, Pirzkall A, Haas-Kogan DA et al (2005) Longitudinal multivoxel MR spectroscopy study of pediatric diffuse brainstem glioma treated with radiotherapy. *Int J Radiat Oncol Biol Phys* 62:20–31
 29. Warmuth C, Günther M, Zimmer C (2003) Quantification of blood flow in brain tumors: comparison of arterial spin labeling and dynamic susceptibility-weighted contrast-enhanced MR imaging. *Radiology* 228:523–532
 30. Grand S, Lefournier V, Krainik A et al (2007) Imagerie de perfusion: principes et applications cliniques. *J Radiol* 88:444–471
 31. Alvarez-Linera J (2010) Magnetic resonance techniques for the brainstem. *Semin Ultrasound CT MRI* 31:230–245
 32. Komotar RJ, Zacharia BE, Sughrue ME et al (2008) Magnetic resonance imaging characteristics of pilomyxoid astrocytomas. *Neurol Res* 30:945–951
 33. Lee IH, Kim JH, Suh YL et al (2010) Imaging characteristics of pilomyxoid astrocytoma in comparison with pilocytic astrocytomas. *Eur J Radiol* 79:311–316
 34. Jallo GI, Biser-Rohrbaugh A, Freed D (2004) Brainstem gliomas. *Childs Nerv Syst* 20:143–153
 35. Hoffman HJ, Becker L, Craven MA (1980) A clinically and pathologically distinct group of benign brainstem gliomas. *Neurosurgery* 7:243–248
 36. Farmer JP, Montes JL, Freeman CR et al (2001) Brainstem gliomas. *Pediatr Neurosurg* 34:206–214
 37. Kestle J, Townsend JJ, Brockmeyer DL, Walker ML (2004) Juvenile pilocytic astrocytoma of the brainstem in children. *J Neurosurg (Pediatrics)* 2 101:1–6
 38. Epstein F, Wisoff J (1987) Intraaxial tumors of the cervicomedullary junction. *J Neurosurg* 67:483–487
 39. Poussaint TY, Yousuf N, Barnes PD et al (1999) Cervicomedullary astrocytomas of childhood: clinical and imaging follow-up. *Pediatr Radiol* 29:662–668
 40. Abbott R, Shiminski-Maher T, Wisoff JH, Epstein FJ (1991) Intrinsic tumors of the medulla: surgical complications. *Pediatr Neurosurg* 17:239–244
 41. Sandri A, Sardi N, Genitori L et al (2006) Diffuse and focal brain stem tumors in childhood: prognostic factors and surgical outcome. *Childs Nerv Syst* 22: 1127–1135
 42. Ternier J, Wray A, Puget S et al (2006) Tectal plate lesions in children. *J Neurosurg* 104(6 Suppl Pediatrics):369–373
 43. Konno H, Yamamoto T, Iwasaki Y et al (1985) A case of quadrigeminal hamartoma. *Acat Neuropathol (Berl)* 68:155–159
 44. Robertson PL, Murazko KM, Brunberg JA et al (1995) Pediatric midbrain tumors: a benign subgroup of brainstem gliomas. *Pediatr Neurosurg* 22:65–73

45. Dağlıoğlu E, Çataltepe O, Akalan N (2003) Tectal gliomas in children: the implications for natural history and management strategy. *Pediatr Neurosurg* 38:223–231
46. Vandertop WP, Hoffman HJ, Drake JM et al (1992) Focal midbrain tumors in children. *Neurosurgery* 31:186–194
47. Tomita T, Cortes RF (2002) Astrocytomas of the cerebral peduncle in children: surgical experience in seven patients. *Childs Nerv Syst* 18:225–230
48. Sun B, Wang CC, Wang G (1999) MRI characteristics of midbrain tumors. *Neuroradiology* 41:158–162
49. Sanford RA, Bebin J, Smith WR (1982) Pencil glioma of the aqueduct of Sylvius. *J Neurosurg* 57:690–696
50. Boydston WR, Sanford RA, Muhlbauer MS et al (1991–1992) Glioma of the tectum and periaqueductal region of the mesencephalon. *Pediatr Neurosurg* 17:234–238
51. Marcorelles P, Fallet-Bianco C, Oury JF et al (2005) Fetal aqueductal glioneuronal hamartoma : a clinicopathological and physiopathological study of three cases. *Clin Neuropathol* 24:155–162
52. Broniscer A, Laningham FH, Kocak M et al (2006) Intratumoral hemorrhage among children with newly diagnosed, diffuse brainstem glioma. *Cancer* 106:1364–1371
53. Grand SD, Kremer S, Tropres IM et al (2007) Perfusion-sensitive MRI of pilocytic astrocytomas: initial results. *Neuroradiology* 49:545–550
54. Kumar VA, Knopp EA, Zagzag D (2010) Magnetic resonance dynamic susceptibility-weighted contrast-enhanced perfusion imaging in the diagnosis of posterior fossa hemangioblastomas and pilocytic astrocytomas: initial results. *J Comput Assist Tomogr* 34:825–829
55. Milanaccio C, Nozza P, Ravegnani M et al (2005) Cervico-medullary desmoplastic infantile ganglioglioma: an unusual case with diffuse leptomeningeal dissemination at diagnosis. *Pediatr Blood Cancer* 45:986–990
56. Covington DB, Rosenblum MK, Brathwaite CD, Sandberg DI (2009) Angiocentric glioma-like tumor of the midbrain. *Pediatr Neurosurg* 45:429–433
57. Bilaniuk LT, Molloy PT, Zimmerman RA et al (1997) Neurofibromatosis type 1: brain stem tumors. *Neuroradiology* 39:642–653
58. Rosser T, Packer RJ (2002) Intracranial neoplasms in patients with neurofibromatosis 1. *J Child Neurol* 17:630–637
59. Ulrich NJ, Raja AI, Irons MB et al (2007) Brainstem lesions in neurofibromatosis type 1. *Neurosurgery* 61:762–767
60. Terazaki M, Uchikado H, Takeuchi Y, Shigemori M (2005) Minimally invasive management of ependymoma of the aqueduct of Sylvius: therapeutic considerations and management. *Minim Invasive Neurosurg* 48:322–324
61. Keene DL, Hsu E, Ventureyra E et al (1998) An unusual behavior of brainstem ependymoma. *J Child Neurol* 13:86–88
62. U-King-Im JM, Taylor MD, Raybaud C (2010) Posterior fossa ependymomas: new radiological classification with surgical correlation. *Childs Nerv Syst* 26:1765–1772
63. Zagzag D, Miller DC, Knopp E et al (2000) Primitive neuroectodermal tumors in the brainstem: investigation of seven cases. *Pediatrics* 106:1045–1053
64. Gavriel H, Shuper A, Kornreich L et al (2000) Diffuse intrinsic brainstem disease with neurologic deterioration : not what it seemed. *Med Ped Oncol* 34:213–214
65. Guzmán-de-Villoria JA, Fernández-García P, Ferreiro-Argüelles C (2010) Differential diagnosis of T2 hyperintense brainstem lesions. Part 1. Focal lesions. *Semin Ultrasound CT MRI* 31:246–259
66. Guzmán-de-Villoria JA, Fernández-García P, Ferreiro-Argüelles C (2010) Differential diagnosis of T2 hyperintense brainstem lesions. Part 2. Diffuse lesions. *Semin Ultrasound CT MRI* 31:260–274
67. Giliberto G, Lanzino DJ, Diehn FE et al (2010) Brainstem cavernous malformations : anatomical, clinical and surgical considerations. *Neurosurg Focus* 29:E9
68. Lebre RM, de Lonlay P, Valayannopoulos V et al (2010) Mitochondrial ND5 mutations mimicking brainstem tectal glioma. *Neurology* 75:93
69. van Poppel K, Broniscer A, Patay Z, Morris EB (2009) Alexander disease: an important mimicker of focal brainstem glioma. *Pediatr Blood Cancer* 53:1355–1356
70. Wagner S, Benesh M, Berthold F et al (2006) Secondary dissemination in children with high-grade malignant gliomas and diffuse pontine gliomas. *Brit J Cancer* 95:991–997
71. Singh S, Bhutani R, Jalali R (2007) Leptomeninges as a site of relapse of locally controlled, diffuse pontine glioma with review of the literature. *Childs Nerv Syst* 23:117–121
72. Sethi R, Allen J, Donahue B et al (2010) Prospective neuraxis MRI surveillance reveals a high risk of leptomeningeal dissemination in diffuse intrinsic pontine glioma. *J Neurooncol* 102:121–127
73. Kornreich L, Schwarz M, Kamarzyn B et al (2005) Role of MRI in the management of children with diffuse pontine tumors: a study of 15 patients and review of the literature. *Pediatr Radiol* 35:872–879
74. Prabhu S, Ng S, Vajapeyam S et al (2011) DTI assessment of the brainstem white matter tracts in pediatric BSG before and after therapy. *Childs Nerv Syst* 27:11–18
75. Bobek-Billiewicz B, Stasil-Pres G, Majchrzak H, Zarudzki L (2010) Differentiation between brain tumor recurrence and radiation necrosis using perfusion, diffusion-weighted imaging and MR spectroscopy. *Folia Neuropathol* 48:81–92

Bhattin Tanrikulu, Gurmit Singh,
and M. Memet Özek

Primary brain stem tumors are a group of diseases that may be located in the mesencephalon, pons, and medulla oblongata. They are generally considered as diseases with a poor prognosis, because surgery nearby such eloquent structures within the brain stem is a great challenge for many neurosurgeons and complete resection can be achieved in only a small number of selected patients.

Most of them are gliomas [1, 2], frequently occur in children and account for 10–20 % of all brain tumors of childhood with no gender, race, or geographic predilection. Most of them are low-grade (WHO I or II) gliomas [3, 4]. These tumors are most frequently seen in the first decade of life [5–7]. High-grade or diffuse brain stem gliomas have poor prognosis when compared with low-grade, focal, or exophytic ones [8].

Mesencephalic gliomas are typically noninvasive even though they may reach large sizes and are associated with deterioration of neurological function due to involvement of corticospinal

tracts, mesencephalic nuclei, and brain stem centers [9].

Mesencephalic gliomas can be classified as tectal gliomas and tegmental gliomas according to their anatomical location.

32.1 Tectal Tumors

Tectal gliomas are rare group of intrinsic mesencephalic tumors encompassing different histological subtypes, astrocytomas being most frequent [10, 11]. They make up less than 5 % of brain stem tumors in children [12, 13]. Age at diagnosis ranges from 3.3 to 16.6 years [14, 15].

Within this usually indolent group of tumors however, a proportion may show progressive tumor growth with the anatomic, physiologic, and neurologic deficits associated with the space-occupying lesion [9].

Tectal plate gliomas are a subgroup of tectal gliomas. They are slow growing low-grade tumors, which rarely produce focal neurologic deficit. They generally become symptomatic as late-onset hydrocephalus [11, 16, 17].

32.1.1 Basic Anatomy

The tectum is the most posterior part of the mesencephalon. It is located just posterior to ventricular system (cerebral aqueduct). Tectum consists of a pair each of superior and inferior colliculi.

B. Tanrikulu, M.D.
Department of Neurosurgery,
Marmara University, School of Medicine,
Istanbul, Turkey

G. Singh, M.D.
Department of Neurosurgery,
Penang General Hospital, Penang, Malaysia

M.M. Özek, M.D. (✉)
Division of Pediatric Neurosurgery,
Acibadem University, School of Medicine,
Istanbul, Turkey
e-mail: memetozek@gmail.com

The combination of four colliculi is commonly called the corpora quadrigemina [14]. The four colliculi sit on tectal plate. The superior colliculus receives retinal inputs directly via brachium of superior colliculus and also receives inputs from ipsilateral visual cortex. It mediates oculomotor responses such as horizontal conjugate gaze [9, 18]. The inferior colliculus receives auditory inputs from the pons and medulla via the lateral lemniscus. Its axonal fibers travel from the brachium to the medial geniculate nucleus.

The posterior margin of the quadrigeminal plate is covered by pia mater and thick arachnoid membrane. Combination of these structures forms the quadrigeminal cistern. These structures may act as a barrier to prevent the dorsal extension of tectal tumors [19]. Detailed anatomy of this region is described in chapters “Development of the posterior fossa structures” and “The anatomy of the posterior cranial fossa”.

32.1.2 Clinical Presentation

Tectal tumors because of their close relationship with the cerebral aqueduct mostly become

symptomatic as a result of raised intracranial pressure caused by progressive obstruction of the aqueduct (Figs. 32.3a, b and 32.4a, b). The signs and symptoms include papilledema, headache, nausea, vomiting, visual changes, oculomotor deficits, Parinaud’s syndrome, decreased school performance, and very rarely patients present with pyramidal tract dysfunction, ataxia, and other cranial nerve palsies [10, 11, 20].

32.1.3 Radiology

Tectal tumors are generally small and appear isodense with normal brain parenchyma on computerized tomography (CT) images. They show minimal or no contrast enhancement (Fig. 32.1a–c) [19]. The CT scan fails to detect 50 % of cases with tectal glioma [21]. Many cases that were only scanned with CT in pre-magnetic resonance imaging (MRI) era are misdiagnosed as congenital aqueductal stenosis [21, 22].

MRI is more reliable than CT for the visualization of tectal tumors and it should be ordered in every child and adolescent with hydrocephalus [9, 23]. MRI reliably detects a tectal mass and

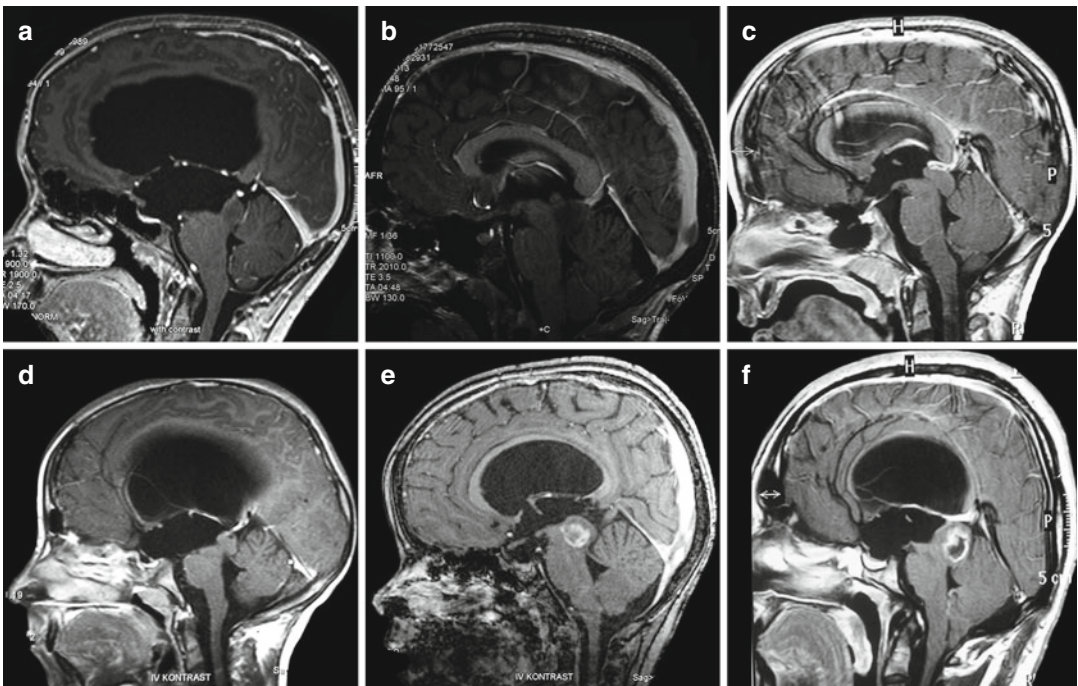


Fig. 32.1 Tectal plate glioma cases with i.v. contrast MR study. (a–c) does not have contrast enhancement and (d) minimal, whereas (e, f) demonstrates significant contrast enhancement

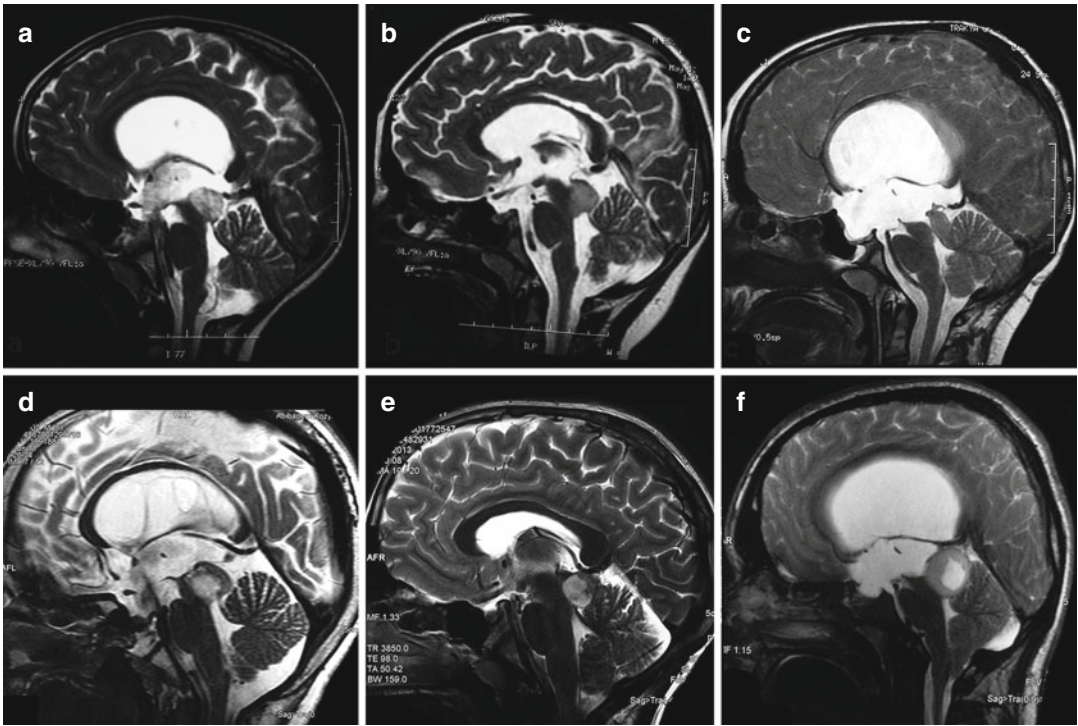


Fig. 32.2 The T-2 weighted images give more detailed anatomical information. In the six cases shown above (a–f) the boundaries of the tectal lesions are very clear in T2 sequences

it is a reliable imaging modality for follow-up [15, 24]. There has been no consensus on significance of contrast enhancement in the tectal region yet [10]. Contrast enhancement at presentation is seen in up to 18 % of cases [24, 25]. It is speculated that there is no correlation between contrast enhancement in the first imaging and tumor progression during follow-up. On the other hand, there is contrast enhancement in all cases with tumor enlargement during follow-up (Fig. 32.1d–f) [19, 24]. The T2-weighted images give more detailed anatomical information about these lesions particularly growth direction and relationship of the tumor with cerebellum and tegmentum (Fig. 32.2a–f).

32.1.4 Surgical Treatment

The goal of treatment in tectal plate gliomas is to reverse the signs and symptoms of hydrocephalus and improve neurologic deficits and to prevent further neurologic damage [10]. One of the earliest treatment options is shunting of cerebrospi-

nal fluid to peritoneum via a ventriculoperitoneal (VP) shunt [26].

Pollack al. [18] describe hydrocephalus for this group of patients to be more challenging than the usual hydrocephalic patient.

18.75 % of the patients (3 out of 16) in this report developed subdural hematomas.

Chapman [27] encountered similar problems in his shunted cases with 28.57 % (2 out of 7) cases resulting in subdural hematomas. Subsequent management is open-ended follow-up with neuroimaging. The second option is endoscopic third ventriculostomy (ETV). It is the gold standard for the management of hydrocephalus induced by tectal plate gliomas (Fig. 32.3a–d) and additionally allows the surgeon to take a biopsy from the lesion [28–30]. The third but less frequently used option is endoscopic aqueductoplasty with or without stenting [10].

There are well-described safe and unsafe entry zones for open midbrain surgery [31]. It is advocated to use supracollicular incision, infracollicular incision, and lateral mesencephalic sulcus to enter the mesencephalon, whereas it is

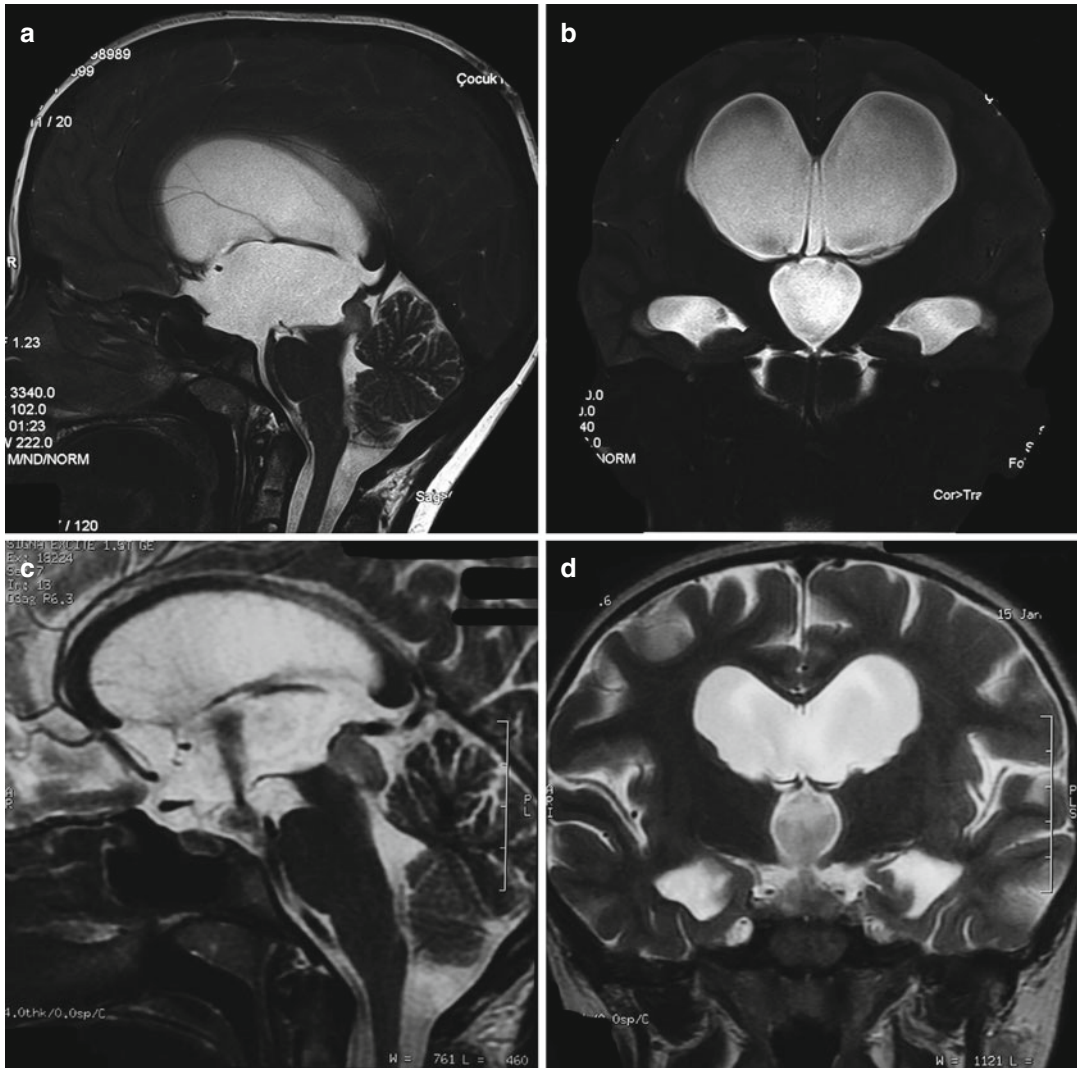


Fig. 32.3 Tectal plate glioma case presenting with hydrocephalus (a, b). After endoscopic third ventriculostomy (c, d)

not advised to use incisions through superior and inferior colliculi [31].

The lesions in the tectal plate can be reached easily by occipital transtentorial and infratentorial supracerebellar approaches.

Occipital transtentorial approach has been adopted by many neurosurgeons for tumors located in this region, to avoid possible damage to colliculi (Fig. 32.4a–d). In this approach a right occipital craniotomy is performed and tentorium is incised just adjacent to the straight sinus. The direct visualization of the fissure between the superior vermis, quadrigeminal

plate, and superior medullary velum is the advantage, whereas a probable visual defect resulting from occipital lobe retraction is the disadvantage of this approach [32, 33]. The same area can be also easily reached through standard infratentorial supracerebellar approach which is first described for pineal region tumors [33, 34]. Infratentorial supracerebellar approach can be used for more caudally located median tumors with infracollicular entry to avoid ocular and auditory disturbances [32]. Ternier et al. [35] centered their decision based on tumor volume. Tumors less than 4 cm³ are less likely to progress

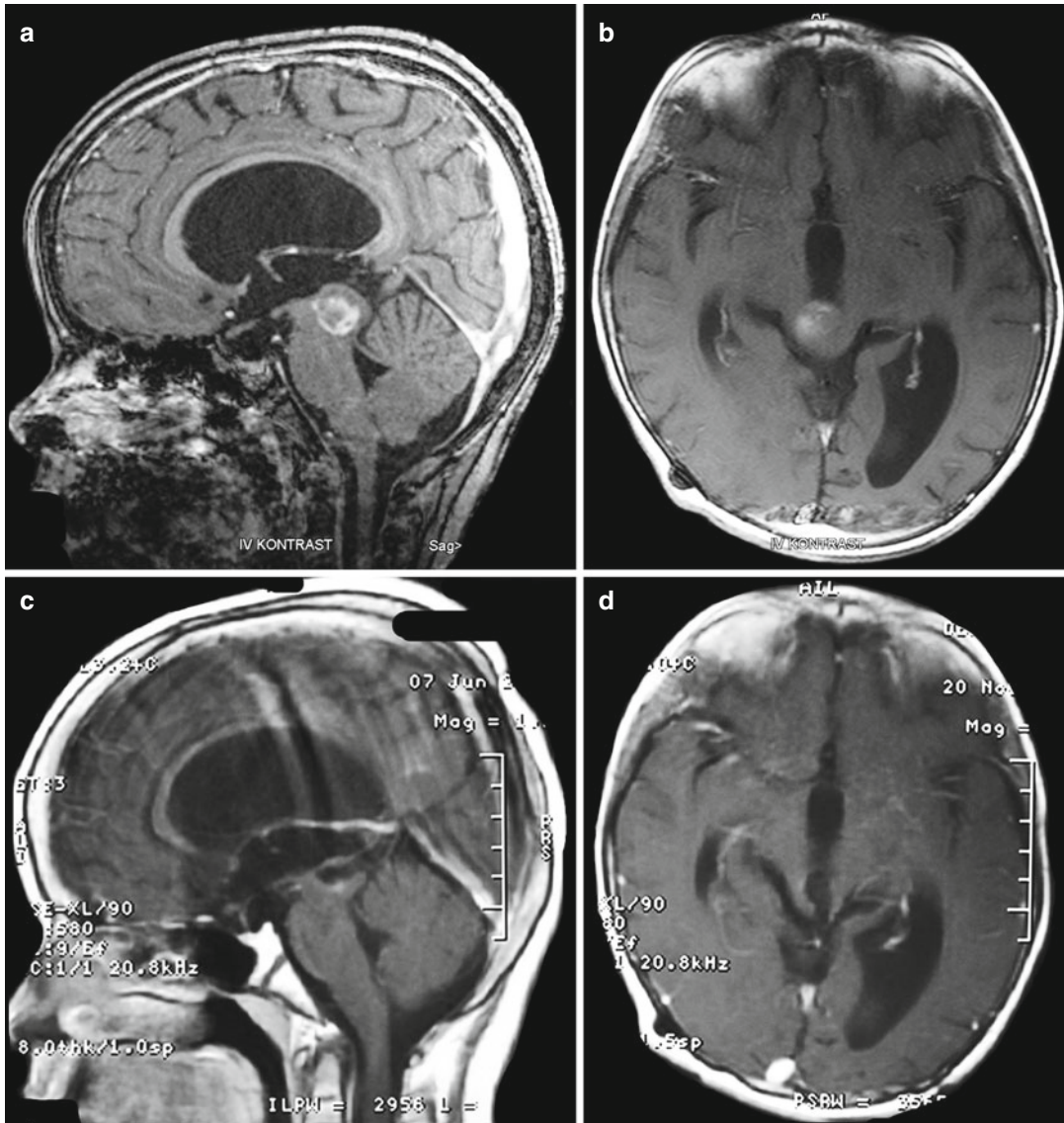


Fig. 32.4 Tectal plate glioma case with documented tumor growth (a, b) treated via occipital transtentorial approach (c, d)

(hamartomas); lesions with volumes greater than 10 cm³ warrant consideration for an early intervention. Those in between, 4–10 cm (hamartomas or tumors), will benefit from frequent initial imaging.

Possibility exists that the majority of these tumors increase and cause new deficits; thus, diligent long-term follow-up becomes a part of the armamentarium of the surgeon. Pollack et al. [14] recommend MR imaging and clinical examinations every 6 months for the 1st year after the

diagnosis and then yearly for 4 years in patients who are asymptomatic. From the 6th year onwards, yearly clinical evaluation is sufficient and imaging studies are obtained every 2–3 years or in the interim if new symptoms develop. It is vital that the patients are warned there is a possibility of tumor progression (6.9 years from shunt insertion and 11.5 years from the onset of initial symptoms) in a certain percentage of patients, despite the so-called indolent nature of their tumors, and hence not to neglect follow-up [14].

32.2 Tegmental Tumors

Tumors arising from the tectum may extend upward to the thalamus or downward to the pons. They displace but do not infiltrate intrinsic mesencephalic nuclei and tracts although they may reach enormous size so that they may be candidates for surgical resection (Figs. 32.6a–c, 32.7a–c, and 32.10a–c) [32].

They are almost always focal low-grade astrocytomas. Therefore, total excision should be the aim for surgery of these tumors.

32.2.1 Basic Anatomy

Tectum consists of two cerebral peduncles, substantia nigra, red nuclei, oculomotor nerve nuclei, and medial and lateral longitudinal fasciculus. A tumor originating from tectum may show many different clinical presentations upon involvement of these structures [32]. On the other hand posterior cerebral and superior

cerebellar arteries encircle the midbrain and are in close relationship with the oculomotor and trochlear nerve through their course. It is important to decide the most appropriate surgical approach that allows sufficient exposure of the chosen entry area while minimizing the damage to normal neurovascular structures [32, 36].

32.2.2 Clinical Presentation

The patient may present with hemiparesis, hemihypoesthesia, headache, bilateral papilledema, vertical gaze deficiency, oculomotor paresis, or paralysis upon involvement of midbrain structures [37].

32.2.3 Radiology

Tegmental gliomas are more frequently focal, round-shaped hypo- or isointense on T1-weighted MRI series, whereas they appear hyperintense on T2-weighted MRI series (Fig. 32.5a–c). They

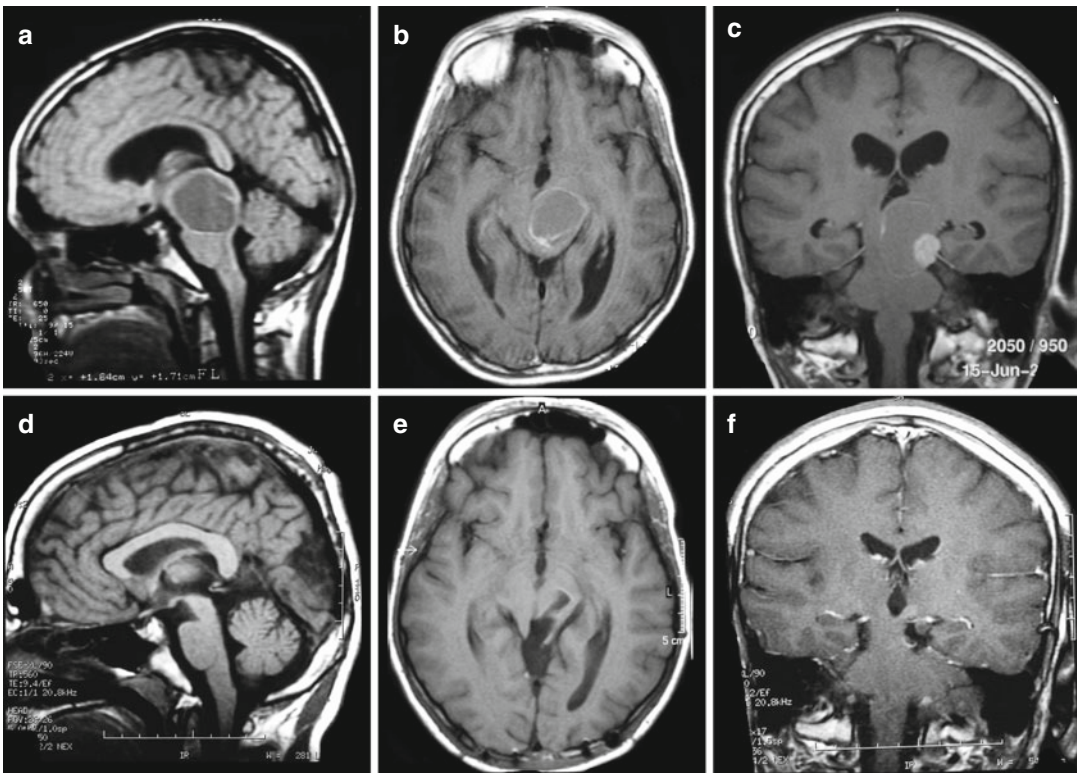


Fig. 32.5 Left sided tegmental cystic tumor with mural nodule (a–c). After tumor resection (d–f)

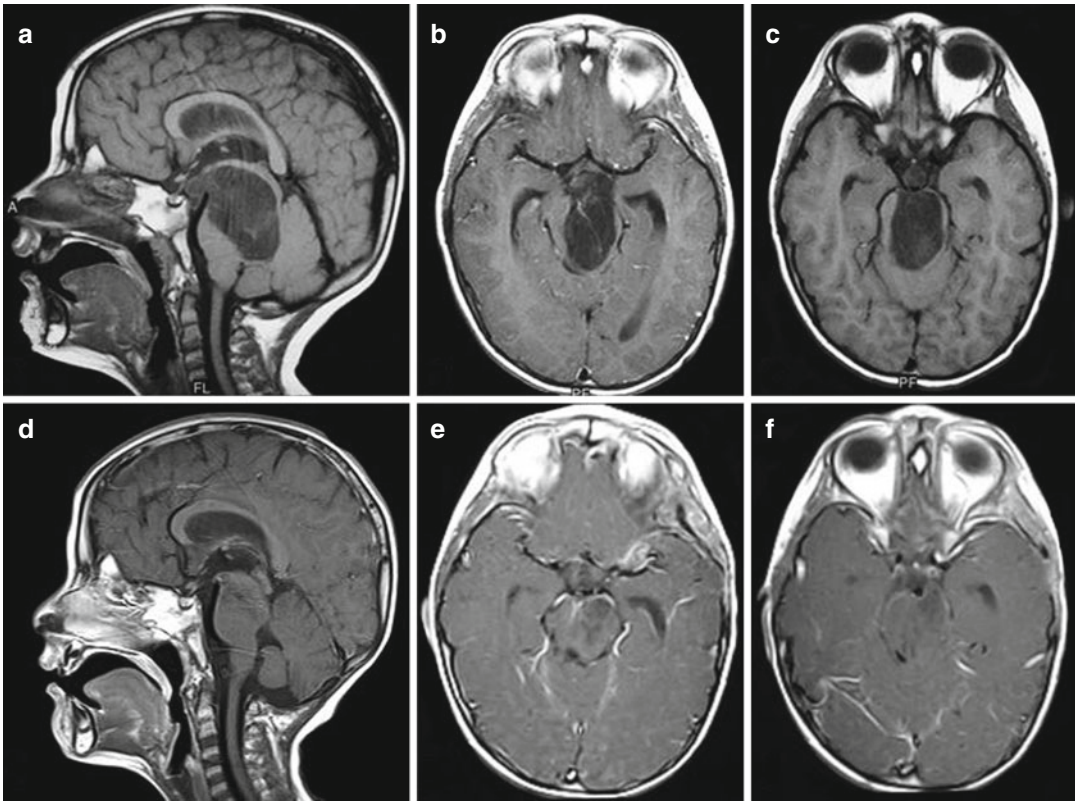


Fig. 32.6 Tegmentum tumor without contrast uptake (a–c). Staged surgery via pterional transsylvian and median suboccipital craniotomies (d–f)

generally show no or little contrast enhancement on contrasted MRI scans (Fig. 32.6a–c) [19]. But some rare cases can present with strong enhancement (Figs. 32.8a–c and 32.10a–c). Cystic tumors should be evaluated in detail about their cyst configuration and location, since entering through a right area in the cyst will give a nice exposure for the removal of the solid part (Figs. 32.5a–c and 32.10a–c).

32.2.4 Surgery

Surgical exposure to the mesencephalon is a challenge. With such a complex anatomy and a variety of sites where tumors may arise, there is no single approach that can provide optimal pathway.

The mesencephalic tegmental tumors can be divided into three groups:

- (a) Dorsal
- (b) Dorsolateral
- (c) Lateral

Success depends on detailed study of imaging and selection of appropriate route according to the location of the pathology that will facilitate maximal safe resection with minimal morbidity [38, 39].

Porter et al. [40] uses a two-point method to select the best approach. A line is drawn between the point where the tumor is closest to the surface and another at the center of the lesion. This will give an indication of which approach to utilize to excise the lesion. Ultimately, route to be selected should allow for excellent exposure and contribute to minimal retraction of brain tissue, vasculature, and cranial nerves ensuring complete excision of tumor with no or minimal complications.

Dorsal tumors of tegmentum can be reached by occipital transtentorial, infratentorial supracerebellar, or midline telovelar approach.

Occipital transtentorial approach is used for lesions superior to pontomesencephalic junction. In dorsal lesions there is a very thin amount of

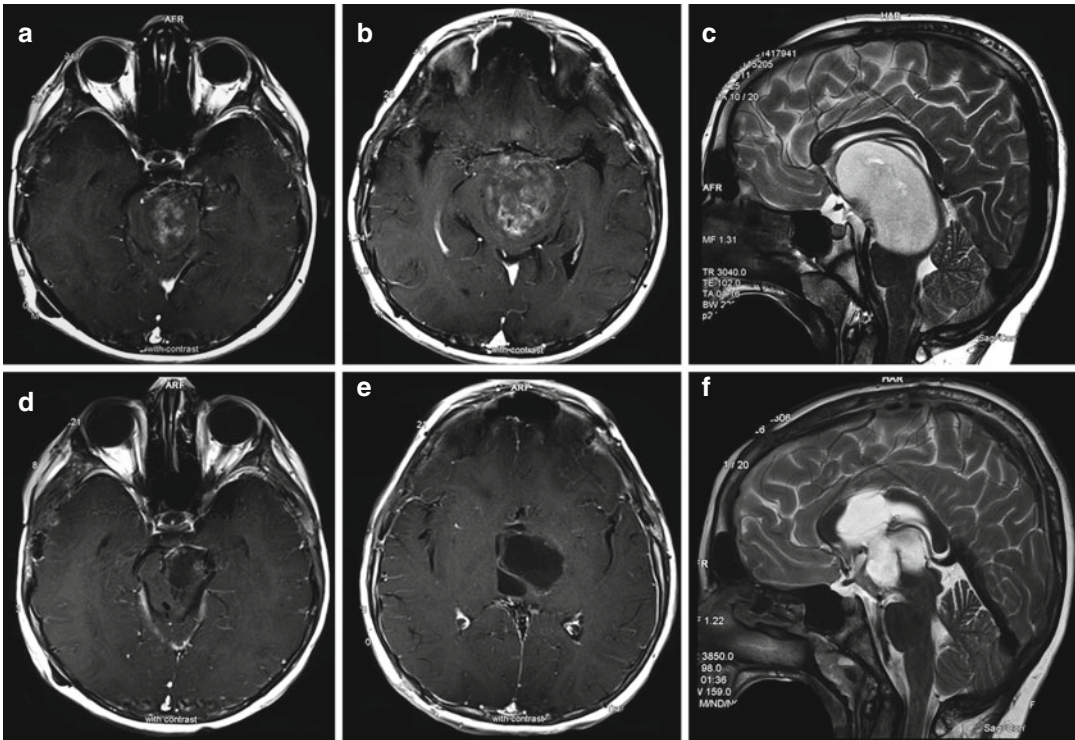


Fig. 32.7 Mesencephalic tumor growing into the third ventricle with little contrast uptake (a–c). After transcallosal resection (d–f)

tissue under the pia. The supracollicular area is the entry point into mesencephalon, avoiding causing visual and oculomotor disturbances. In case of a cystic mass, the entry point should give a good vision to the solid part (Fig. 32.5d–f). Since use of a retractor will be not possible in such a deep area, a long plated bayonet can be used for retraction [41, 42]. During the resection of the tumor, pulling the tissue is not recommended; instead an ultrasonic aspirator should be used.

Infratentorial supracerebellar approach can also be used in removal of tegmental lesions. To reach tegmental lesions with this approach, the dural opening should be extended more laterally close to sigmoid sinus. Careful dissection of arachnoid allows wide opening of cerebello-mesencephalic fissure. It is important to identify the lateral mesencephalic vein, which lies in the lateral mesencephalic sulcus. To avoid pyramidal tract injury, the entry zone should be posterior to lateral mesencephalic sulcus [32].

In case tumor is extending downward to the pons and the IV ventricle, a midline telovelar

approach can be used (Fig. 32.6d–f). The disadvantage of this approach is the long distance to the lesion and working through the IV ventricle. The floor of the IV ventricle should be covered with cotton patties to avoid possible damage during the tumor removal. For big lesions which expand to the suprasellar area, the treatment can be staged and for the second step, a pterional approach can be utilized (Fig. 32.6).

Tumors which extend upward to the thalamus and the ventricle can be excised through an inter-hemispheric transcallosal approach (Fig. 32.7d–f). If tumors with this location have associated big size cysts growing into the supratentorial area, a transcystic approach through inferior temporal sulcus may be feasible (Fig. 32.10d–f).

Tumors located on the anterolateral aspect of the midbrain can be accessed via subtemporal transtentorial approach (Fig. 32.8c, d) [43]. It provides access to the cisternal and crural segments of the anterior choroidal and medial posterior choroidal arteries and exposes the interpeduncular and crural cisterns as well as the lower half of

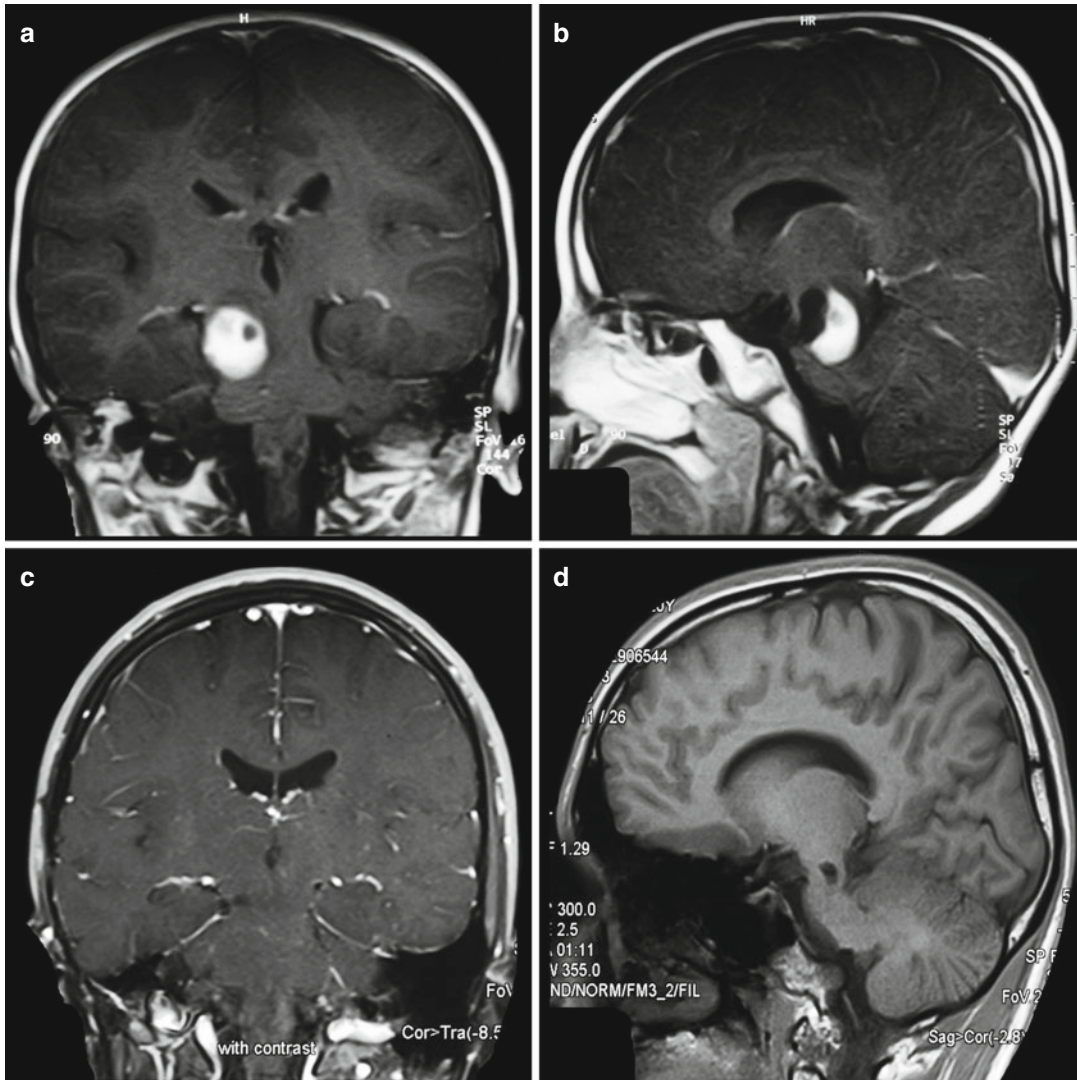


Fig. 32.8 Solid tegmentum tumor with lateral localization (a, b). After subtemporal approach (c, d)

the ambient cistern. The tentorial incision is made posterior to the entry of trochlear nerve, which allows exposure to anterolateral mesencephalon and upper pons. However, this route carries the potential risk of injuring vein of Labbe due to excessive temporal lobe retraction and may result in temporal lobe swelling and infarct [32, 44].

Posterolateral lesions in the contrary can be reached by a retrosigmoid approach (Figs. 32.9 and 32.10) [44].

Lateral approaches provide shorter working distances to the mesencephalon.

However, standard lateral approaches still have tentorium or petrous bone obstructing, preventing clear access. Hence, anterior and posterior petrosectomy, which involves drilling the petrous away, were developed [44].

Mesencephalic tumors located near median ventral surface can be accessed through a pterional transsylvian route after a frontotemporal craniotomy, described by Yasargil et al. [45]. After opening of the Sylvian fissure, the tentorial edge, third cranial nerve, and interpeduncular cisterns are exposed. Anatomical landmark

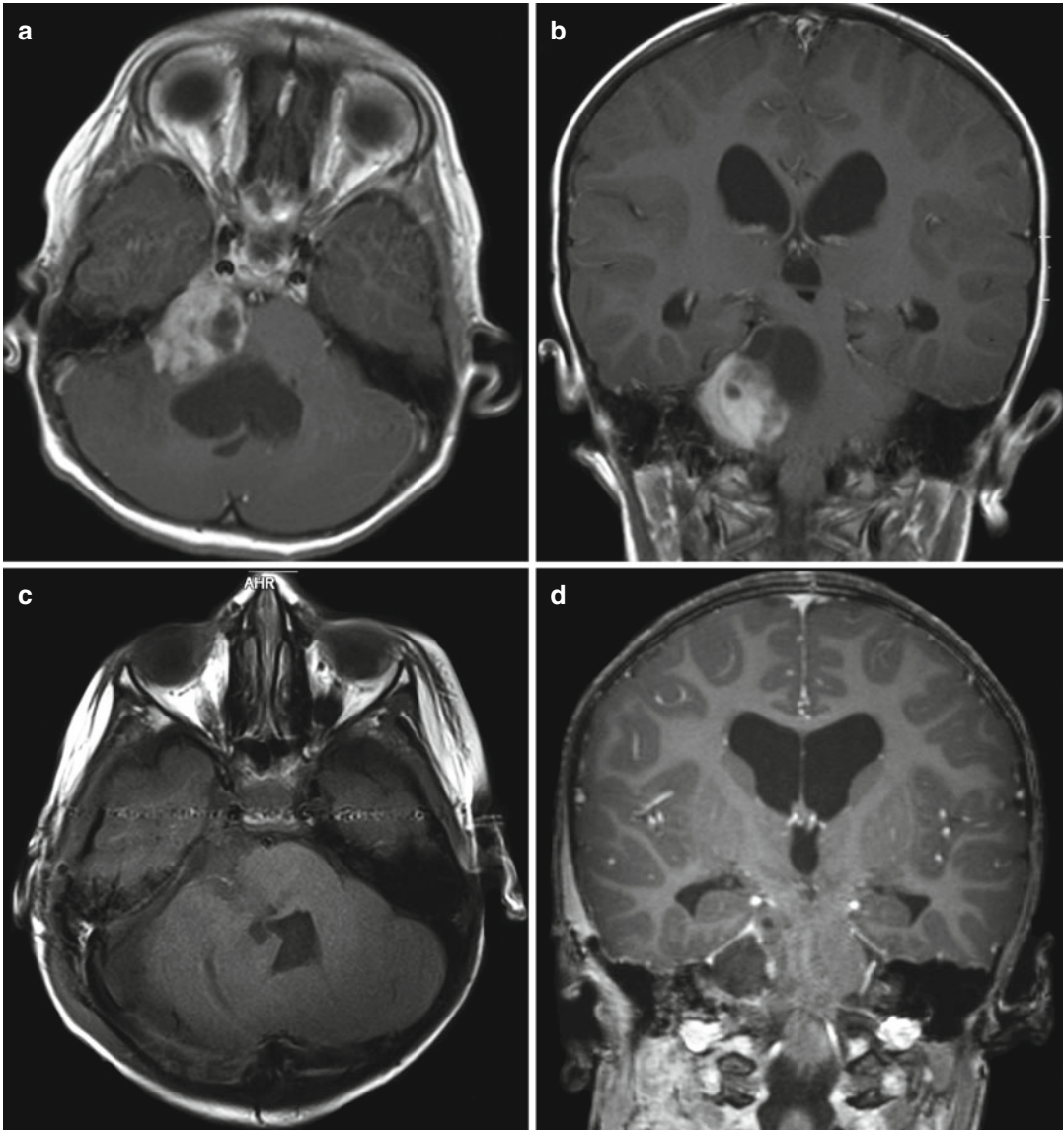


Fig. 32.9 Pontomesencephalic junction tumor with cystic component (a, b). A right sided retrosigmoid approach was used for resection (c, d)

of the target area is exit of the oculomotor nerve from midbrain with posterior cerebral artery above. The safe entry zone into the midbrain in this approach is a small rectangular area bounded medially by the exit of oculomotor nerve and basilar artery, inferiorly by the superior cerebellar artery, superiorly by the posterior cerebral artery, and laterally by the tentorial edge [46]. This relatively safe area allows surgical entrance to midbrain through more medial to

cerebral peduncle and enables sparing the motor tract [32, 45].

Using the orbitozygomatic approach, the interpeduncular fossa view is greatly enhanced by the downward retraction of the globe giving an upward and oblique view of the anterior aspect of mesencephalon. In comparison with standard frontotemporal craniotomy, this approach shortens the working distance to interpeduncular fossa by 3 cm [47].

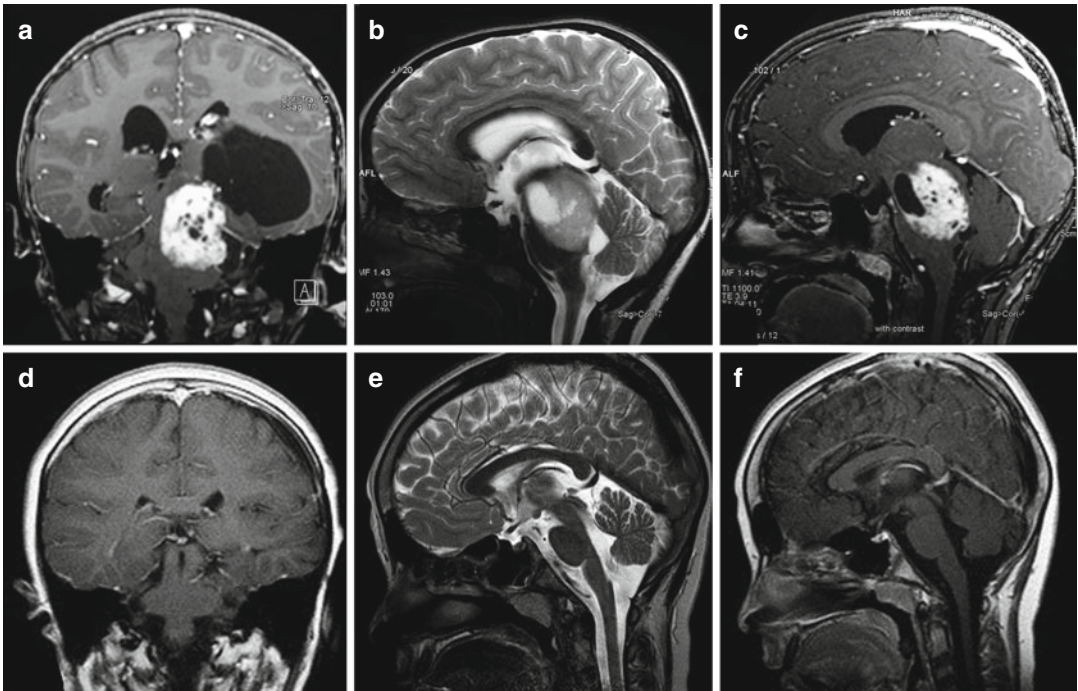


Fig. 32.10 Tegmental tumor with huge cyst (a–c). A transcystic approach was used for radical tumor resection (d–f)

References

- Garzon M et al (2013) Brain stem tumors in children and adolescents: single institutional experience. *Childs Nerv Syst* 29(8):1321–1331
- Recinos PF, Sciubba DM, Jallo GI (2007) Brainstem tumors: where are we today? *Pediatr Neurosurg* 43(3):192–201
- Alaqeel AM, Sabbagh AJ (2014) Pediatric brainstem tumors. Classifications, investigations, and growth patterns. *Neurosciences (Riyadh)* 19(2):93–99
- Walker DA, Punt JA, Sokal M (1999) Clinical management of brain stem glioma. *Arch Dis Child* 80(6):558–564
- Tokuriki Y et al (1986) Brainstem glioma: an analysis of 85 cases. *Acta Neurochir (Wien)* 79(2–4):67–73
- Littman P et al (1980) Pediatric brain stem gliomas. *Cancer* 45(11):2787–2792
- Babu R et al (2014) Malignant brainstem gliomas in adults: clinicopathological characteristics and prognostic factors. *J Neurooncol* 119:177–185
- Farmer JP et al (2001) Brainstem gliomas. A 10-year institutional review. *Pediatr Neurosurg* 34(4):206–214
- Igboechi C et al (2013) Tectal plate gliomas: a review. *Childs Nerv Syst* 29(10):1827–1833
- Stark AM et al (2005) Management of tectal glioma in childhood. *Pediatr Neurol* 33(1):33–38
- Lapras C et al (1994) Tectal plate gliomas. Part I: microsurgery of the tectal plate gliomas. *Acta Neurochir (Wien)* 126(2–4):76–83
- Burger PC (1996) Pathology of brain stem astrocytomas. *Pediatr Neurosurg* 24(1):35–40
- Fisher PG et al (2000) A clinicopathologic reappraisal of brain stem tumor classification – identification of pilocytic astrocytoma and fibrillary astrocytoma as distinct entities. *Cancer* 89(7):1569–1576
- Poussaint TY et al (1998) Tectal tumors of childhood: clinical and imaging follow-up. *AJNR Am J Neuroradiol* 19(5):977–983
- Boydston WR et al (1991) Gliomas of the tectum and periaqueductal region of the mesencephalon. *Pediatr Neurosurg* 17(5):234–238
- Javadpour M, Mallucci C (2004) The role of neuroendoscopy in the management of tectal gliomas. *Childs Nerv Syst* 20(11–12):852–857
- Yeh DD, Warnick RE, Ernst RJ (2002) Management strategy for adult patients with dorsal midbrain gliomas. *Neurosurgery* 50(4):735–738; discussion 738–740
- Pollack IF, Pang D, Albright AL (1994) The long-term outcome in children with late-onset aqueductal stenosis resulting from benign intrinsic tectal tumors. *J Neurosurg* 80(4):681–688
- Pollack IF, Shultz B, Mulvihill JJ (1996) The management of brainstem gliomas in patients with neurofibromatosis 1. *Neurology* 46(6):1652–1660

20. Grant GA et al (1999) Management of intrinsic gliomas of the tectal plate in children. A ten-year review. *Pediatr Neurosurg* 31(4):170–176
21. Bognar L et al (1994) Tectal plate gliomas. Part II: CT scans and MR imaging of tectal gliomas. *Acta Neurochir (Wien)* 127(1–2):48–54
22. May PL et al (1991) Benign intrinsic tectal “tumors” in children. *J Neurosurg* 74(6):867–871
23. Holland BA et al (1985) Magnetic resonance imaging of primary intracranial tumors: a review. *Int J Radiat Oncol Biol Phys* 11(2):315–321
24. Squires LA et al (1994) Focal tectal tumors: management and prognosis. *Neurology* 44(5):953–956
25. Bowers DC et al (2000) Tectal gliomas: natural history of an indolent lesion in pediatric patients. *Pediatr Neurosurg* 32(1):24–29
26. Daszkiewicz P et al (1999) Benign tectal tumors: clinical and neuroradiological correlations. *Neurol Neurochir Pol* 33(4):847–855
27. Chapman PH (1990) Indolent gliomas of the midbrain tectum. In: *Concepts in pediatric neurosurgery*. Basel, Karger, p 97–107
28. Wellons JC 3rd et al (2002) Long-term control of hydrocephalus via endoscopic third ventriculostomy in children with tectal plate gliomas. *Neurosurgery* 51(1):63–67; discussion 67–68
29. Oka K et al (1999) Neuroendoscopic approach to tectal tumors: a consecutive series. *Neurosurg Focus* 6(4):e14
30. Mizoguchi M et al (2000) Neuroendoscopic biopsy of tectal glioma: a case report. *Minim Invasive Neurosurg* 43(1):53–55
31. Bricolo A, Turazzi S (1995) Surgery for gliomas and other mass lesions of the brainstem. *Adv Tech Stand Neurosurg* 22:261–341
32. Bricolo A (2000) Surgical management of intrinsic brainstem gliomas. *Oper Tech Neurosurg* 3:137–154
33. Mottolese C et al (2014) Supracerebellar infratentorial approach for pineal region tumors: Our surgical and technical considerations. *Neurochirurgie pii: S0028-3770(14)00039-3*
34. Luo SQ (1982) Infratentorial supracerebellar approach for removing tumors of the pineal region in children (author’s transl). *Zhonghua Wai Ke Za Zhi* 20(3):184–185
35. Ternier J et al (2006) Tectal plate lesions in children. *J Neurosurg* 104(6 Suppl):369–376
36. Ono M et al (1984) Microsurgical anatomy of the region of the tentorial incisura. *J Neurosurg* 60(2):365–399
37. Wang C et al (2000) Surgical treatment of primary midbrain gliomas. *Surg Neurol* 53(1):41–51
38. Ulm AJ et al (2004) Microsurgical approaches to the perimesencephalic cisterns and related segments of the posterior cerebral artery: comparison using a novel application of image guidance. *Neurosurgery* 54(6):1313–1327; discussion 1327–1328
39. Martinez JAG, De Oliveira E, Tedeschi H, Wen HT, Rhoton AL (2000) Microsurgical anatomy of the brain stem. *Oper Tech Neurosurg* 3:80–86
40. Porter RW, Detwiler P, Spetzler RE (2000) Surgical approaches to the brain stem. *Oper Tech Neurosurg* 3:114–123
41. Epstein FJ, Ozek M (1993) The plated bayonet: a new instrument to facilitate surgery for intra-axial neoplasms of the spinal cord and brain stem. Technical note. *J Neurosurg* 78(3):505–507
42. Teo C, Siu TL (2008) Radical resection of focal brainstem gliomas: is it worth doing? *Childs Nerv Syst* 24(11):1307–1314
43. Lobato RD et al (2004) Meningiomas of the basal posterior fossa. Surgical experience in 80 cases. *Neurocirugia (Astur)* 15(6):525–542
44. Jittapiromsak P et al (2010) The challenge of access to the pontomesencephalic junction: an anatomical study of lateral approach and exposure. *Skull Base* 20(5):311–320
45. Yasargil MG, Teddy PJ, Roth P (1985) Selective amygdalo-hippocampectomy. Operative anatomy and surgical technique. *Adv Tech Stand Neurosurg* 12:93–123
46. Recalde RJ, Figueiredo EG, de Oliveira E (2008) Microsurgical anatomy of the safe entry zones on the anterolateral brainstem related to surgical approaches to cavernous malformations. *Neurosurgery* 62(3 Suppl 1):9–15; discussion 15–17
47. Hakuba A, Liu S, Nishimura S (1986) The orbitozygomatic infratemporal approach: a new surgical technique. *Surg Neurol* 26(3):271–276

Pablo F. Recinos, Violette Renard Recinos,
and George I. Jallo

33.1 Introduction

Tumors of the brainstem make up 10–20 % of all tumors of the central nervous system in the pediatric population. In the United States, there are 150–300 annual cases each year. The average age of diagnosis is 7–9 years old and both males and females are equally affected [1, 2]. The term “brainstem tumor” in the pediatric population refers to a heterogeneous group of tumors that arise in the midbrain, pons, and medulla. Diffuse gliomas make up to 75 % of all brainstem tumors [3]. In the pons, diffuse gliomas are the most common tumor type, although focal tumors are also seen. Diffuse brainstem gliomas have a poor prognosis and their natural history is similar to that of glioblastoma multiforme [4]. Focal tumors, on the other hand, comprise approximately 25 % of brainstem tumors and have a much better prognosis (Fig. 33.1) [3].

Although pediatric brainstem tumors were historically lumped together into a single group, it

is now understood that their behavior depends on their location and histopathology. The location and imaging characteristics now guide the treatment of pediatric brainstem tumors. In the same vein, tumors of the pons behave differently depending on their focality, histopathology, and location within the pons. Current surgical treatments include biopsy and open resection, while future surgical treatment likely will incorporate local drug-delivery techniques. In order to appropriately treat pediatric pontine tumors, an understanding of the tumor classification schemes, pathophysiology, and surgical options is necessary.

33.2 Classification Schemes

Several classification systems have been proposed to categorize brainstem tumors (Table 33.1). The earliest classification systems were based on the natural history without intervention combined with the tumor characteristics on computed tomography (CT) [5–7]. More recent systems have been primarily based on MRI appearance [8–11]. The simplest schemes classify tumors based on growth pattern, either focal or diffuse. The more detailed systems subdivide tumors based on location (midbrain, pons, medulla, cervicomedullary), whether an exophytic component is present, presence of hydrocephalus or hemorrhage, and contrast enhancement pattern.

The most recent radiographic classification, as proposed by Choux et al., is based on

P.F. Recinos, M.D. (✉) • G.I. Jallo, M.D.
Division of Pediatric Neurosurgery,
Johns Hopkins University School of Medicine,
600 North Wolfe Street, Harvey 811,
Baltimore, MD 21287, USA
e-mail: pablo@jhmi.edu; gjallo1@jhmi.edu

V.R. Recinos, M.D.
Department of Neurosurgery, Cleveland Clinic,
171 Burwick Road Highland Heights,
Cleveland, OH 44143, USA
e-mail: recinov@ccf.org

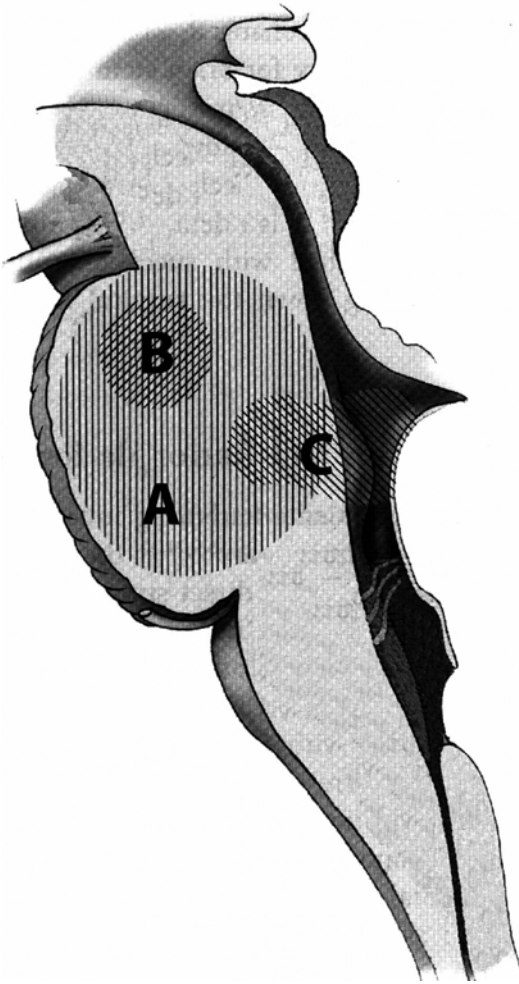


Fig. 33.1 Illustration representing the different types of pontine tumors. Diffuse pontine gliomas (A) are invasive tumors that involve the pontine parenchyma and are the most common type. Focal intrinsic tumors (B) are well-circumscribed, intra-axial tumors. Dorsal exophytic tumors (C) arise from the dorsal pontine surface and expand into the fourth ventricle

both CT and MRI data and classifies brainstem tumors into four types [12]. Type I tumors are diffuse and account for approximately 75 % of all brainstem tumors [8, 13]. Radiographically, they have poorly demarcated edges on CT and are usually hypointense on T1 MRI sequences (Fig. 33.2). They usually do not enhance with contrast. Histopathologically, they are most commonly malignant gliomas (WHO grade III or IV); however, diffuse tumors can be low-grade

gliomas as well [12, 14, 15]. Type II tumors are focal, intrinsic masses that can be solid or cystic in appearance. The main distinguishing radiographic feature is their well-demarcated appearance relative to surrounding tissue (Fig. 33.3) [12]. Histopathologically, they are most commonly low-grade gliomas (WHO grade I or II); however, high-grade lesions have been reported to present in this way as well [4, 15]. Type III tumors are dorsal exophytic masses that originate from the subependymal glial tissue of the floor of the fourth ventricle [12, 16]. Radiographically, they have well-demarcated borders and demonstrate a dorsal and lateral growth pattern (Fig. 33.4). Histopathologically, they are commonly low-grade gliomas. It has been observed that the higher-grade exophytic brainstem tumors tend to have a lateral and ventral growth pattern compared to lower-grade exophytic lesions, which tend to extend dorsally [4, 17, 18]. Type IV tumors are cervicomedullary masses that present and behave very similar to intrinsic cervical spinal cord tumors [6, 12]. Histopathologically, most of these lesions are non-infiltrative, low-grade lesions whose growth pattern is limited rostrally by the white matter of the medial lemniscus and corticospinal tract [18].

33.2.1 Presentation

Pontine tumors are distinguished by three characteristics: (1) signs and symptoms related to intra-axial location, (2) signs and symptoms related to hydrocephalus, and (3) timing of symptom onset. Whether a tumor is diffuse or focal affects each of these characteristics.

The most common signs and symptoms of diffuse pontine tumors are due to cerebellar dysfunction and cranial nerve palsies [19]. Cerebellar dysfunction can manifest as both appendicular and axial ataxia, although ataxia is not specific to diffuse tumors as it can commonly be seen in focal tumors [3]. Cranial nerve palsies are also common in both diffuse and focal tumors. Diffuse tumors tend to present with sixth and seventh nerve palsies, while focal tumors tend to present more commonly with diplopia

Table 33.1 Classification systems for brainstem tumors

Author	Classification system
Epstein et al. [5]	Intrinsic <ol style="list-style-type: none"> 1. Diffuse 2. Focal 3. Cervicomedullary Exophytic <ol style="list-style-type: none"> 1. Anterolateral into cerebellopontine angle 2. Posterolateral and into brachium pontine Disseminated <ol style="list-style-type: none"> 1. Positive cytology 2. Positive myelography
Epstein et al. [6]	Diffuse Focal Cervicomedullary
Stroink et al. [7]	Group I – dorsal exophytic glioma Group IIa – intrinsic brainstem tumors Hypodense, no enhancement Group IIb – intrinsic brainstem tumors Hyperdense, contrast enhancing, exophytic Group III – focal cystic tumor with contrast enhancement Group IV – focal intrinsic isodense, contrast enhancing
Barkovich et al. [9]	Location (midbrain, pons, medulla) Focality (diffuse or focal) Direction and extent of tumor growth Degree of brainstem enlargement Exophytic growth Hemorrhage or necrosis Evidence of hydrocephalus
Albright [8]	Diffuse Focal (midbrain, pons-intrinsic, dorsally exophytic, medulla)
Fischbein et al. [10]	Midbrain <ol style="list-style-type: none"> 1. Diffuse 2. Focal 3. Tectal Pons <ol style="list-style-type: none"> 1. Diffuse 2. Focal Medulla <ol style="list-style-type: none"> 1. Diffuse 2. Focal 3. Dorsal exophytic
Rubin et al. [11]	Cervicomedullary Exophytic Cystic Focal Diffuse
Choux et al. [12]	Type I – diffuse Type II – intrinsic, focal Type III – exophytic, focal Type IV – cervicomedullary

CT computerized tomography, *MRI* magnetic resonance imaging

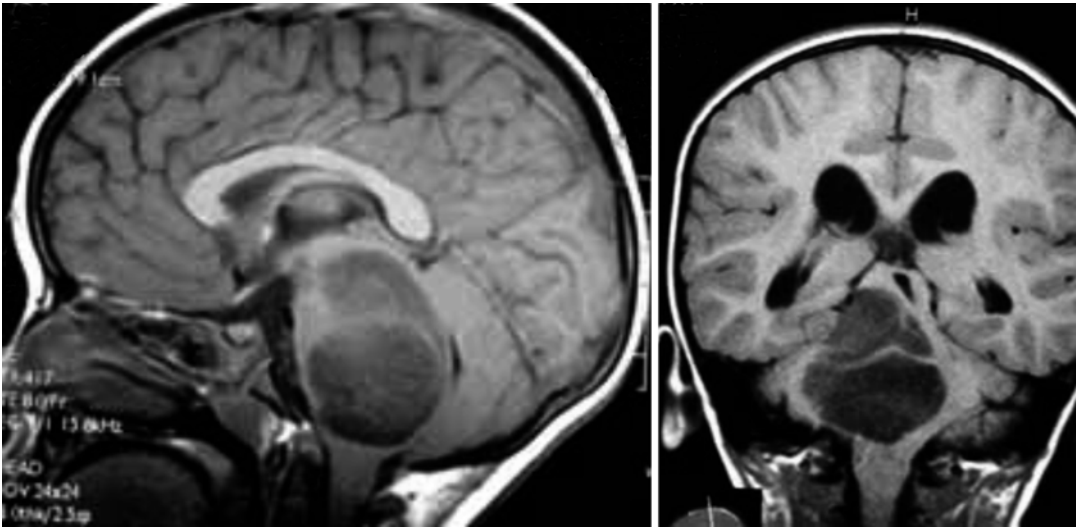


Fig. 33.2 Diffuse pontine glioma as seen on sagittal (left) and coronal (right) T1 gadolinium-enhanced MRI sequences. The typical imaging characteristics are seen

including heterogeneous tumor mass, poorly demarcated borders, and global expansion of the pons

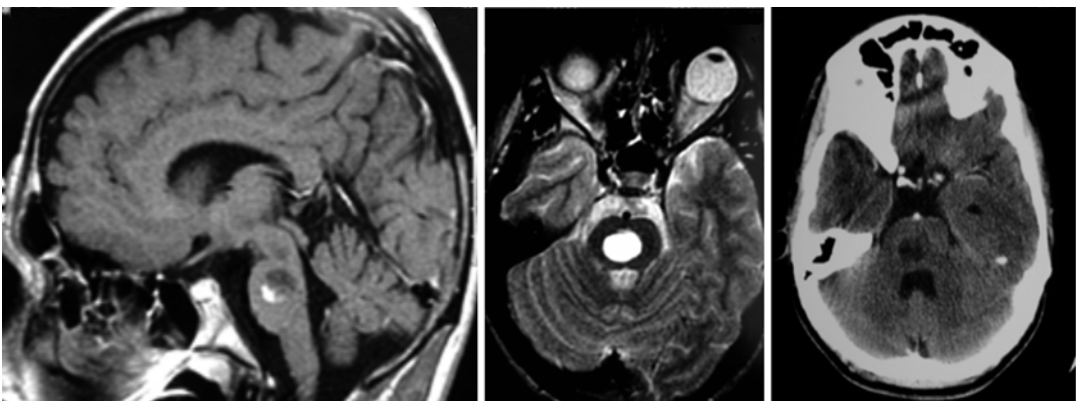


Fig. 33.3 Focal intrinsic pontine tumor as seen on T1 gadolinium-enhanced sagittal MRI (left), T2 axial MRI (middle), and axial CT (right). It is notable that the tumor is fully within the pons and has well-demarcated borders in contrast to the global expansion of brainstem classically

seen in diffuse pontine gliomas. In this case, the tumor has a cystic component, but focal intrinsic pontine tumors can appear solid as well. Pathological diagnosis was juvenile pilocytic astrocytoma

and facial weakness [3, 14]. Interruption of the fibers of the corticospinal tracts resulting in the upper motor neuron syndrome is characteristic of pontine tumors [19]. These signs and symptoms include loss of fine motor skills, spasticity, initial hyporeflexia followed by hyperreflexia, and upgoing extensor plantar reflex.

Development of hydrocephalus is highly dependent on tumor location. Dorsal, exophytic

tumors are found on the floor of the fourth ventricle and commonly produce obstruction of CSF flow as they grow. Although diffuse intrinsic tumors can produce enlargement of the brainstem, they rarely produce obstructive hydrocephalus [18, 20, 21].

The timing of symptom onset is dependent on aggressiveness of the tumor and whether hydrocephalus is present. Behnke et al. reported a series

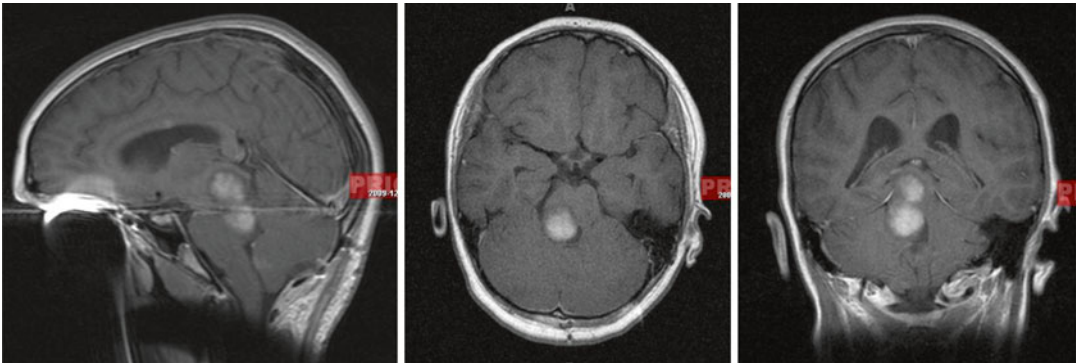


Fig. 33.4 Dorsal exophytic tumor as seen on sagittal (*left*), axial (*middle*), and coronal (*right*) T1 gadolinium-enhanced MRI sequences. The tumor is arising from the dorsal pontine surface along the floor of the fourth ventricle. It is notable that the tumor has well-demarcated

borders and has grown dorsally and cranially. The mass effect exerted on the brainstem without parenchymal invasion is typical for these tumors. Pathological diagnosis was juvenile pilocytic astrocytoma

of 30 children with intra-axial, endophytic tumors of the pons and cervicomedullary junction. They noted that symptoms >6 months in duration were indicative of a benign brain tumor. With one exception, those patients did not have a PNET or malignant astrocytoma [14]. In patients with a history <6 months of duration, a malignant astrocytoma or PNET was much more likely. However, as has previously been demonstrated, patients with grade I and II astrocytomas can present with clinical symptoms of <6 months duration [14, 22]. In their study, 27 % of patients had hydrocephalus on presentation. Other studies report similar percentages of patients presenting with moderate to severe hydrocephalus [9, 14, 23, 24]. In contrast, only 26 % of patients in a series by Villani and co-workers presented with a history >6 months. However, the incidence of hydrocephalus was much higher (85 %) and possibly explained the differences in the two series [14, 25].

33.2.2 The Role of Biopsy

The use of biopsy in the management of tumors of the brainstem has come in and out of favor with technological advances and has changed with increased understanding of tumor behavior. Surgery as a whole was initially considered to play no role in the treatment of all brainstem gliomas. In 1939, Bailey postulated that “until

some effective treatment other than surgery is devised, gliomas of the brainstem will be hopeless problems for treatment” [26]. Surgical techniques to approach eloquent brain structures were introduced prior to modern imaging techniques. In 1949, Spiegel and colleagues first reported the use of frame-based stereotaxy to perform a medial thalamotomy to reduce emotional reactivity [27]. This was the first description of the safe use of stereotaxis to approach deep-seated structures. The use of frame-based stereotaxy was then applied to approach the brainstem in a monkey model as reported by Ward in 1958 [28].

Despite early technical advances in approaches to the brainstem, surgical interventions, whether through biopsy or more open procedure, were not universally accepted. In 1967, Lassman and Arjona concluded that the diagnosis of pontine glioma could be made by ventriculography alone and that surgical management should be limited to control of hydrocephalus [23]. In 1969, Madson echoed Bailey’s early opinion when he stated that “regardless of specific histology, brainstem gliomas must be classified as malignant tumors since their location in itself renders them inoperable” [29]. Surgery would continue to not play a significant role in the management of brainstem tumors until after the advent of CT. The advent of CT allowed the brainstem anatomy and location of brainstem tumors to be studied with improved definition. The combination of CT

and frame-based stereotactic techniques greatly facilitated biopsy of deep structures of the brain.

In 1978, image-directed biopsy of deep brain structures was first reported by Gleason and co-workers [30]. In the 1980s, multiple brainstem biopsy series reported a high diagnostic yield with low complication rate in both adult and pediatric patients [31–38]. The proponents of brainstem biopsy argued that a histopathological diagnosis provided important prognostic information and guided therapeutic decisions [39, 40]. Additionally, it was clear that brainstem tumors did not all exhibit the same behavior as once thought [5, 6, 13, 16, 41]. Epstein was the first to classify brainstem tumors based on location and focality, distinguishing more favorable focal lesions from less favorable diffuse lesions [5]. It appeared that with the combination of radiographic location and histopathology, empiric radiotherapy for a presumed brainstem glioma would no longer be necessary [42].

As MRI became increasingly available in the 1980s, it was noted that the resolution of normal anatomy and pathology of the brainstem was superior to CT. On MRI, the imaging characteristics finally reflected the heterogeneous nature of these lesions. As the experience with MR imaging of brainstem tumors increased, Barkovich et al. proposed the first classification scheme based on MRI criteria in 1990 [9]. Not only had MRI replaced CT as the primary imaging modality for brainstem tumors, certain groups were suggesting that it could replace stereotactic biopsy as the diagnostic tool of choice [43, 44]. Perhaps the most notable report favoring abandonment of biopsy in the workup of brainstem tumors came from Albright and co-workers [45]. Their report summarized the recommendations from the Children's Cancer Group studying the effects of radiotherapy on brainstem tumors. Out of 120 patients, 45 (38 %) had either a stereotactic or open biopsy. All of these patients had either low-grade or high-grade gliomas on histopathology. Postoperative neurological complications occurred in five (11 %) of the operative cases. Due to the fact that MRI diagnosis correlated highly with diagnosis of glioma, it was recommended that MRI alone should be the diag-

nostic modality of choice for diffuse brainstem gliomas [45].

The shift in diagnostic criteria of brainstem tumors, from a combination of histological and radiological characteristics to purely radiological criteria, was reflected in several proposed brainstem tumor classification systems [5, 6, 8, 9, 12]. All of these classification systems made a distinction between focal and diffuse lesions. In 1986, Epstein and McCleary defined a diffuse lesion as any lesion greater than 2 cm. Their classification scheme was one of the earliest and perhaps the most influential. In their series of 34 patients, which served as the basis for their classification, 22 patients had lesions greater than 2 cm and were classified as diffuse. All of those patients had malignant gliomas (grade III–IV) [6]. Although CT was the primary imaging modality used to diagnose patients in this study, their definition of “diffuse” was more clearly defined than more recent studies.

In contrast, the study by Fishbein and colleagues defined diffuse tumors as being “poorly marginated, involving more than one half of the involved brain stem segment, or infiltrating both the segment of brain superior to and the segment inferior to the segment of origin” [10]. The two most important prognostic factors in their study were focality and location. In concordance with previous studies, patients with focal tumors had higher long-term survival than patients with diffuse tumors [6, 12, 16]. Likewise, patients with pontine tumors did worse than patients with tumors of the midbrain or cervicomedullary junction [11, 41]. However, 6 out of 29 patients with diffuse, pontine tumors were alive with a mean follow-up time of 2.6 years [10]. This is in stark contrast to the series reported by Epstein and McCleary, in which all 22 patients with diffuse brainstem tumors died within 6–12 months [6]. One possible explanation for the differences in these studies is that the classification criteria defining “diffuse tumors” was significantly different so that “diffuse” tumors in each study were not directly comparable. Another explanation is that the sample size of each study was not large enough to give an accurate representation of tumor behavior.

Despite the fact that it was not clear how to select the few patients with diffuse pontine tumors that had longer survival, it was clear that patients with diffuse pontine tumors generally did not benefit from aggressive surgery and that most patients had a dismal prognosis [13, 46]. Given the reported experience at the time, Albright concluded that “there is probably no other intrinsic brainstem tumor with the same MRI appearance as diffuse brainstem glioma, with the possible exception of hamartoma, which is exceedingly rare and generally presents when the patient is younger than 2 months old” [3]. This led to a paradigm shift in the early 1990s in the management of children with brainstem tumors. For those patients who presented with signs and symptoms consistent with a brainstem glioma and who had a diffuse brainstem mass, biopsy was no longer considered necessary and stopped being standard of care [3, 45, 47].

However, others have shown that the appearance of a diffuse brainstem mass does not always yield a histopathological diagnosis of malignant glioma. Roujeau et al. presented a series of 24 children with diffuse pontine tumors not amenable to surgical resection. Of the 24 patients who underwent stereotactic, frame-based biopsy, 22 children had malignant gliomas while 1 had a grade II astrocytoma and 1 had a grade I astrocytoma. Given these results, the two patients with low-grade tumors did not receive up-front radiation therapy. Upon progression, the patient with the grade I tumor underwent surgery to attempt resection, while the patient with the grade II tumor was treated with radiation therapy [48]. Behnke and co-workers reported a series of 30 patients with intra-axial, endophytic tumors of the pons and medulla who underwent open surgery for excision. Although most malignant astrocytomas did demonstrate a diffuse pattern of growth on MRI, there were five cases that had a focal appearance. Likewise, three out of ten grade I and all six grade II astrocytomas had a diffuse growth pattern on MRI [14]. Unlike the early experience with brainstem tumors, histopathologically benign tumors clearly can mimic malignant tumors radiographically [14, 15]. In 2010, Kumar and colleagues presented a series of 100

patients harboring grade I astrocytomas with features mimicking high-grade gliomas on MRI. Of these patients, 76 were pediatric patients and 24 patients had brainstem tumors [15].

Currently, the role of biopsy in the management of brainstem tumors is being revisited [47]. For the past 20 years, it has been argued that sampling tissue was unnecessary and harmful to patients harboring diffuse brainstem tumors given that a diagnosis could be made on clinical presentation and imaging alone [12, 45]. At present, it is clear that the appearance of a diffuse brainstem mass on MRI correlates to a high-grade glioma in the majority but not all cases [14, 15, 48]. Additionally, advances in molecular genetics and drug-delivery mechanisms raise the possibility of improved therapies and outcomes for patients who would otherwise have a dismal prognosis [46, 47, 49]. Obtaining tissue is of central importance to study the molecular and genetic foundation and to better understand the biology of these tumors to develop therapies. The dilemma of whether to biopsy brainstem tumors lies in whether it is preferable to perform a biopsy on a large number of patients in order to find the few patients with low-grade tumors versus empirically treating patients with diffuse pontine tumors with radiation, knowing that the management would likely be different if there was a known diagnosis of low-grade glioma. Ideally, tissue diagnosis should be obtained in combination with testing a novel therapy in a clinical trial [49]. In routine practice, however, performing a biopsy on patients with diffuse, pontine tumors remains controversial.

33.2.3 Surgical Indications and Approaches

One of the first neurosurgeons to advocate surgery for select brainstem tumors was J.L. Pool, who reported a survival of 10–25 years after operating on three children [50]. By the early 1980s, several pioneering neurosurgeons also reported favorable surgical outcomes for certain types of brainstem gliomas [6, 7, 13, 16, 51] and introduced classification systems in an attempt to identify those tumors that could be successfully

treated with surgery. Although the role of surgery in patients presenting with a diffuse pontine tumor continues to be controversial, surgery is the first-line treatment for patients with focal intrinsic and dorsal exophytic brainstem tumors. Focal intrinsic brainstem tumors are characterized as solid or cystic lesions that have well-defined borders on MRI and that do not show local tissue invasion. Dorsal exophytic brainstem gliomas arise from the subependymal glial tissue, with the majority of the tumor lying in the fourth ventricle [20, 21]. In the pons, focal and dorsal exophytic tumors are rare as they tend much more common in the midbrain, medulla, and cervicomedullary junction. In a series reported by Jallo et al., only 7 out of 85 patients (8.2 %) with focal or dorsally exophytic brainstem tumors were localized in the pons. Given that most focal and dorsal exophytic brainstem tumors tend to be histologically benign, surgical excision can significantly change the natural history of the disease [14, 21].

33.2.4 Focal Intrinsic Tumors

Although surgical excision of focal intrinsic tumors of the pons is the treatment of choice, it carries a high morbidity. Preoperatively, the risk of surgery is judged based on the specific location of the tumor, preoperative functional status, preoperative neurological deficits, and comorbidities. Although most new postoperative deficits are temporary, the possibility of permanent, devastating complications must not be underestimated. An open discussion with the family outlining possible complications, including need for tracheostomy and feeding gastrostomy, is imperative [20].

The surgical approach for focal pontine tumors is determined by the location of the tumor. For tumors located in the dorsal pons, a midline suboccipital craniotomy is preferred. For tumors in the ventral pons that extend into the cerebellopontine angle, a lateral retrosigmoid approach is utilized. Neurophysiologic mapping is indispensable to obtain feedback regarding the integrity of the motor and sensory pathways.

Cerebellar mutism and pseudobulbar symptoms can result from excessive traction of the cerebellar hemispheres, so excessive retraction should be avoided [52–54]. Replacement of the bone flap improves postoperative healing and protects the area of surgical dissection. It is also helpful to find surgical planes should a future resection be necessary [17].

33.2.5 Dorsal Exophytic Tumors

Gross total resection is the primary goal for dorsal exophytic tumors in the hopes of achieving cure and to treat secondary hydrocephalus. A midline suboccipital craniotomy with or without C1 laminectomy is the standard approach for dorsal exophytic tumors located in the pons. A telovelar approach is used to expose the fourth ventricle. This avoids injury to the vermis and cerebellar tonsils. It is important to remember that dorsal exophytic tumors arise from the ependymal cells of the fourth ventricular floor [21] (Fig. 33.5). Therefore, great care must be taken when resecting the intrinsic brainstem portion. Neurophysiological monitoring and mapping are critical to avoid cranial nerve and motor track damage if a significant portion of the tumor lies within the brainstem. Subtotal resection should be

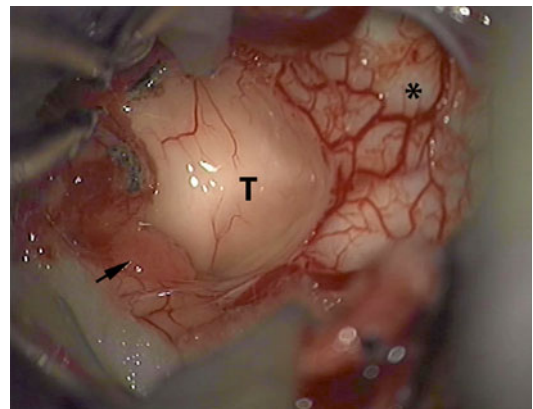


Fig. 33.5 Intraoperative view of a dorsal exophytic tumor. The choroid plexus (*arrow*) is seen on the caudal end of the operative. The tumor [T] has been exposed with a clear plane visible at the interface between the tumor and the floor of the fourth ventricle [*]

performed if gross resection can only be achieved with resultant brainstem injury. If hydrocephalus subsequently develops or persists, it can easily be treated with CSF diversion [13, 17, 55].

33.2.6 Role of Neuromonitoring

Intraoperative neurophysiologic monitoring (IONM) has played an important role in guiding surgery of the supratentorial space as well as the spinal cord. In surgery of the brainstem, IONM has not been as extensively utilized compared with supratentorial and spinal cord surgery. Nonetheless, it is becoming increasingly clear that IONM can provide useful feedback to guide the surgical approach and extent of resection in brainstem tumor surgery. In order to utilize IONM appropriately, it is important for the surgeon to be familiarized with the technical setup, type of information that can be obtained, and limitation of each IONM modality.

Brainstem mapping (BSM) is a technique used to localize the cranial nerve nuclei found on the floor of the fourth ventricle (Fig. 33.6). It is indicated when surgery will proceed through a midline approach into the pons or when a tumor extends out into the fourth ventricle. It is not useful for tumors located on the ventral or lateral pons [56, 57]. A monopolar or bipolar probe is set to a current of 2.0 mA and moved at 1 mm intervals to create a functional map of the fourth ventricular floor. It is applied for no greater than 5 s to avoid tissue damage [57]. In the pons, the

most important cranial nerve nuclei are the paired facial nerve nuclei. Once the facial nerve nuclei respond at the initial current setting, the current is lowered in a stepwise manner in order to precisely map their location. When a pontine tumor is present, the position of the facial nerve nuclei can be distorted, making them vulnerable to iatrogenic damage [58]. Tumors located in the rostral pons typically shift the facial nuclei caudally. Likewise, tumors located in the caudal end of the pons typically shift the facial nuclei rostrally. In these situations, the critical resection zone is the edge of the tumor which abuts the facial nerve nuclei [57]. Therefore, the myelotomy should be started in the region most distant to the facial nerve nuclei. Likewise, retraction in the direction of the facial nerve nuclei should be avoided. Once the resection is underway, the resection bed can be intermittently mapped in order to know when the facial nerve nuclei are being approached. There are disadvantages of BSM; it disrupts the flow of the procedure each time mapping is done and it only maps out the efferent segment of the cranial nerve pathway. In cranial nerves with complex pathways, the afferent pathway may be damaged without any change in BSM [56, 57]. This is not an issue for mapping of the facial nerve nuclei since the pathway of the facial nerve is primarily efferent. However, it is applicable to the lower cranial nerves and can be an issue when operating on pontine tumors with extensive caudal extension.

The use of motor evoked potentials (MEPs) can be used to monitor the corticospinal tract



Fig. 33.6 Intraoperative view of brainstem mapping technique for a focal pontine tumor. The myelotomy location is planned by mapping out the paired facial nuclei with a monopolar or bipolar probe. (*Left*) The myelotomy incision is then made in the region most distal to the facial

nuclei. (*Middle*) Parenchymal resection then proceeds to approach the tumor. (*Right*) The resection bed is then periodically remapped to reconfirm the location of the facial nuclei because tissue shifts can occur while working within the pons

(CST) and the corticobulbar tract (CBT). In supratentorial surgery, a decrease of 50 % in the MEPs is a warning of impending damage to the CST. In spinal cord surgery, damage to the CST is predicted in a binary manner (i.e., if the MEPs are present or absent). In contrast, MEPs in surgery of the brainstem are neither predictive based on a set threshold nor in a binary manner. Neuloh and colleagues examined the role of MEPs in 70 patients with either intraparenchymal or extraparenchymal brainstem lesions. They found that reversible MEP loss and irreversible deterioration wave amplitude were predictive of a temporary postoperative motor paresis. In contrast, complete, irreversible MEP loss resulted in permanent paresis [59].

CBT-MEP is performed in the same way as standard MEP except that it uses the muscles innervated by the motor branches of cranial nerves VII, IX, X, and XII. These muscles are the same ones that are used for BSM. CBT-MEP can be more difficult to interpret than standard MEP because the muscles can be stimulated either through a multisynaptic pathway or through direct cranial nerve stimulation. As in standard MEP, the goal is to monitor through multisynaptic pathway. Direct stimulation of a cranial nerve can lead to false-positive monitoring feedback [56]. In contrast to BSM, CBT-MEP is advantageous because it provides real-time feedback without having to interrupt the procedure and can be used for tumors in any location of the brainstem. However, the use of CBT-MEP in brainstem surgery is not as well defined and studied compared to the use of MEP in supratentorial and spinal cord surgery [56].

Monitoring of sensory pathways can be done via somatosensory evoked potentials (SSEPs) and brainstem auditory evoked potentials (BAEPs). However, SSEPs and BAEPs combined only monitor about 20 % of the brainstem and therefore have a limited role in surgery for intrinsic brainstem lesions [60, 61]. Unlike MEPs, they do not provide real-time information as the data can be delayed by 1 min [60]. Given that they monitor the sensory pathways, they are, at best, an indirect indicator of motor damage. SSEPs are commonly normal throughout an entire procedure in which brainstem injury occurs that results

in a postoperative deficit [59]. However, despite their disadvantages, SSEPs and BAEPs are easy to obtain and provide the surgeon additional data points reflective of the brainstem function.

Proper communication with the anesthesia team is critical to obtain useful feedback from IONM. In general, using a continuous infusion of intravenous anesthetics, such as propofol and fentanyl, works well. Intermittent bolus of intravenous anesthetics, use of halogenated anesthetics, and hypothermia can all dampen sensory and motor signals and should be avoided. Usage of paralytics during intubation is acceptable, but should not be used during the operation to maintain MEPs [57, 60].

33.3 Future Directions

Surgical resection of focal intrinsic and dorsal exophytic pontine tumors will continue to be the first-line therapy. However, as previously discussed, treatment of diffuse pontine tumors is more complicated. Diffuse malignant tumors of the pons are rapidly progressive and almost uniformly fatal. Although radiation can provide symptomatic relief and increase progression-free survival, it does not improve overall survival [46]. Malignant gliomas are challenging to treat because pathophysiologically they induce angiogenesis, inhibit apoptosis, and proliferate uncontrollably. Future therapies will likely have complementary and/or synergistic antitumoral effects [46]. Additionally, chemotherapy has not been shown to improve overall survival likely because the blood-brain barrier (BBB) does not allow good access of systemically administered therapies to the brainstem [4]. Therefore, local delivery of therapeutics has been proposed as one possible method to circumvent the BBB [46].

Local delivery of therapeutics using surgical techniques is challenging due to the highly eloquent nature of the brainstem. For example, placing biodegradable polymers loaded with a chemotherapeutic has been an effective method to bypass the BBB for supratentorial tumors [62]. However, placement of bulky polymers is not feasible in the brainstem. Convection-enhanced delivery (CED) is another method to locally

deliver therapeutics by infusing tissue using a continuous pressure gradient [63]. CED has been shown to achieve local drug concentrations 10,000 times greater than that achieved by intravenous administration, while not producing significant systemic exposure [64, 65]. CED of carboplatin has been shown to increase survival in a rat brainstem tumor model [66]. CED has also been safely utilized for drug delivery in two human patients with Gaucher's disease [67]. It remains to be seen whether CED of chemotherapy will be successful in changing the outcome treat brainstem tumors.

33.4 Summary/Conclusion

Pediatric brainstem tumors are a heterogeneous group of tumors whose behavior is predicted by their location, focality, and histopathology. In the pons, the majority of these tumors are diffuse and a minority are focal intrinsic and dorsal exophytic. For patients harboring focal intrinsic and dorsal exophytic pontine tumors, surgical resection is the treatment of preference. While diffuse pontine tumors are generally malignant gliomas that carry a very poor prognosis, a minority of tumors have a diffuse appearance but are histologically benign. In lesions with a questionable appearance, a biopsy can be useful in predicting the tumor behavior and determining the most appropriate treatment. Historically, diffuse pontine gliomas have not responded favorably to medical, surgical, and radiation treatment. Convection-enhanced delivery of therapeutics and other novel delivery methods are the future hope for making meaningful change in the otherwise dismal prognosis that these patients have.

References

1. Littman P, Jarrett P, Bilaniuk LT, Rorke LB, Zimmerman RA, Bruce DA, Carabell SC, Schut L (1980) Pediatric brain stem gliomas. *Cancer* 45:2787–2792
2. Berger MS, Edwards MS, LaMasters D, Davis RL, Wilson CB (1983) Pediatric brain stem tumors: radiographic, pathological, and clinical correlations. *Neurosurgery* 12:298–302

3. Albright AL, Pollack IF (2003) Brainstem gliomas. In: Winn HR (ed) *Youmans neurological surgery*. Saunders, Philadelphia, pp 3663–3670
4. Recinos PF, Sciubba DM, Jallo GI (2007) Brainstem tumors: where are we today? *Pediatr Neurosurg* 43:192–201
5. Epstein F (1985) A staging system for brain stem gliomas. *Cancer* 56:1804–1806
6. Epstein F, McCleary EL (1986) Intrinsic brain-stem tumors of childhood: surgical indications. *J Neurosurg* 64:11–15
7. Stroink AR, Hoffman HJ, Hendrick EB, Humphreys RP, Davidson G (1987) Transependymal benign dorsally exophytic brain stem gliomas in childhood: diagnosis and treatment recommendations. *Neurosurgery* 20:439–444
8. Albright AL (1996) Brain stem gliomas. In: Winn HR (ed) *Youmans neurological surgery*. Saunders, Philadelphia, pp 2603–2611
9. Barkovich AJ, Krischer J, Kun LE, Packer R, Zimmerman RA, Freeman CR, Wara WM, Albright L, Allen JC, Hoffman HJ (1990) Brain stem gliomas: a classification system based on magnetic resonance imaging. *Pediatr Neurosurg* 16:73–83
10. Fischbein NJ, Prados MD, Wara W, Russo C, Edwards MS, Barkovich AJ (1996) Radiologic classification of brain stem tumors: correlation of magnetic resonance imaging appearance with clinical outcome. *Pediatr Neurosurg* 24:9–23
11. Rubin G, Michowitz S, Horev G, Herscovici Z, Cohen IJ, Shuper A, Rappaport ZH (1998) Pediatric brain stem gliomas: an update. *Childs Nerv Syst* 14:167–173
12. Choux M, Lena G, Do L (2000) Brainstem tumors. In: Choux M, Di Rocco C, Hockley A (eds) *Pediatric neurosurgery*. Churchill Livingstone, New York, pp 471–491
13. Epstein F, Wisoff JH (1988) Intrinsic brainstem tumors in childhood: surgical indications. *J Neurooncol* 6:309–317
14. Behnke J, Christen HJ, Brück W, Markakis E (1997) Intra-axial endophytic tumors in the pons and/or medulla oblongata. I. Symptoms, neuroradiological findings, and histopathology in 30 children. *Childs Nerv Syst* 13:122–134
15. Kumar AJ, Leeds NE, Kumar VA, Fuller GN, Lang FF, Milas Z, Weinberg JS, Ater JL, Sawaya R (2010) Magnetic resonance imaging features of pilocytic astrocytoma of the brain mimicking high-grade gliomas. *J Comput Assist Tomogr* 34:601–611
16. Hoffman HJ, Becker L, Craven MA (1980) A clinically and pathologically distinct group of benign brain stem gliomas. *Neurosurgery* 7:243–248
17. Jallo GI, Biser-Rohrbaugh A, Freed D (2004) Brainstem gliomas. *Childs Nerv Syst* 20:143–153
18. Epstein F, Farmer JP (1993) Brain-stem glioma growth patterns. *J Neurosurg* 78:408–412
19. Kaplan AM, Albright AL, Zimmerman RA, Rorke LB, Li H, Boyett JM, Finlay JL, Wara WM, Packer RJ (1996) Brainstem gliomas in children. A Children's Cancer Group review of 119 cases. *Pediatr Neurosurg* 24:185–192

20. Klein O, Chastagner P, Joud A, Marchal JC, Léna G (2008) Pontine tumors. *J Neurosurg Pediatr* 1:423–424
21. Jallo GI, Freed D, Roonprapunt C, Epstein F (2003) Current management of brainstem gliomas. *Ann Neurosurg* 3:1–17
22. Cohen ME, Duffner PK, Heffner RR, Lacey DJ, Brecher M (1986) Prognostic factors in brainstem gliomas. *Neurology* 36:602–605
23. Lassman LP, Arjona VE (1967) Pontine gliomas of childhood. *Lancet* 1:913–915
24. Gjerris F (1978) Clinical aspects and long-term prognosis of infratentorial intracranial tumours in infancy and childhood. *Acta Neurol Scand* 57:31–52
25. Villani R, Gaini SM, Tomei G (1975) Follow-up study of brain stem tumors in children. *Childs Brain* 1:126–135
26. Bailey P, Buchanan DN, Bucy PC (1939) Gliomas of the brainstem. In: Bailey P (ed) *Intracranial tumors of infancy and childhood*. University of Chicago Press, Chicago, pp 188–241
27. Spiegel EA, Wycis HT, Marks M, Lee AJ (1947) Stereotaxic apparatus for operations on the human brain. *Science* 106:349–350
28. Ward AA Jr (1958) Trends in the application of stereotaxy to the brain stem. *Clin Neurosurg* 6:223–239
29. Matson D (1969) Tumors of the posterior fossa. In: Thomas C (ed) *Neurosurgery of infancy and childhood*. Thomas, Springfield, pp 469–477
30. Gleason CA, Wise BL, Feinstein B (1978) Stereotactic localization (with computerized tomographic scanning), biopsy, and radiofrequency treatment of deep brain lesions. *Neurosurgery* 2:217–222
31. Artigas J, Ferszt R, Brock M, Kazner E, Cervos-Navarro J (1988) The relevance of pathological diagnosis for therapy and outcome of brain stem gliomas. *Acta Neurochir Suppl (Wien)* 42:166–169
32. Broggi G, Franzini A, Migliavacca F, Allegranza A (1983) Stereotactic biopsy of deep brain tumors in infancy and childhood. *Childs Brain* 10:92–98
33. Coffey RJ, Lunsford LD (1985) Diagnosis and treatment of brainstem mass lesions by CT-guided stereotactic surgery. *Appl Neurophysiol* 48:467–471
34. Coffey RJ, Lunsford LD (1985) Stereotactic surgery for mass lesions of the midbrain and pons. *Neurosurgery* 17:12–18
35. Frank F, Fabrizi AP, Frank-Ricci R, Gaist G, Sedan R, Peragut JC (1988) Stereotactic biopsy and treatment of brain stem lesions: combined study of 33 cases (Bologna-Marseille). *Acta Neurochir Suppl (Wien)* 42:177–181
36. Franzini A, Allegranza A, Melcarne A, Giorgi C, Ferraresi S, Broggi G (1988) Serial stereotactic biopsy of brain stem expanding lesions. Considerations on 45 consecutive cases. *Acta Neurochir Suppl (Wien)* 42:170–176
37. Kratimenos GP, Nouby RM, Bradford R, Pell MF, Thomas DG (1992) Image directed stereotactic surgery for brain stem lesions. *Acta Neurochir (Wien)* 116:164–170
38. Thomas DG, Bradford R, Gill S, Davis CH (1988) Computer-directed stereotactic biopsy of intrinsic brain stem lesions. *Br J Neurosurg* 2:235–240
39. Albright AL, Price RA, Guthkelch AN (1983) Brain stem gliomas of children. A clinicopathological study. *Cancer* 52:2313–2319
40. Reigel DH, Scarff TB, Woodford JE (1979) Biopsy of pediatric brain stem tumors. *Childs Brain* 5:329–340
41. Epstein F, Wisoff J (1987) Intra-axial tumors of the cervicomedullary junction. *J Neurosurg* 67:483–487
42. Pincus DW, Richter EO, Yachnis AT, Bennett J, Bhatti MT, Smith A (2006) Brainstem stereotactic biopsy sampling in children. *J Neurosurg* 104:108–114
43. Lee BC, Kneeland JB, Walker RW, Posner JB, Cahill PT, Deck MD (1985) MR imaging of brainstem tumors. *AJNR Am J Neuroradiol* 6:159–163
44. Sanford RA, Freeman CR, Burger P, Cohen ME (1988) Prognostic criteria for experimental protocols in pediatric brainstem gliomas. *Surg Neurol* 30:276–280
45. Albright AL, Packer RJ, Zimmerman R, Rorke LB, Boyett J, Hammond GD (1993) Magnetic resonance scans should replace biopsies for the diagnosis of diffuse brain stem gliomas: a report from the Children's Cancer Group. *Neurosurgery* 33:1026–1029; discussion 1029–1030
46. Frazier JL, Lee J, Thomale UW, Noggle JC, Cohen KJ, Jallo GI (2009) Treatment of diffuse intrinsic brainstem gliomas: failed approaches and future strategies. *J Neurosurg Pediatr* 3:259–269
47. Handler MH, Foreman NK (2010) Pontine gliomas. *J Neurosurg Pediatr* 5:140–141; author reply 141–142
48. Roujeau T, Machado G, Garnett MR, Miquel C, Puget S, Geoerger B, Grill J, Boddaert N, Di Rocco F, Zerah M, Sainte-Rose C (2007) Stereotactic biopsy of diffuse pontine lesions in children. *J Neurosurg* 107:1–4
49. Dunkel IJ, Souweidane MM (2009) Pontine glioma. *J Neurosurg Pediatr* 3:257; author reply 257–258
50. Pool JL (1968) Gliomas in the region of the brain stem. *J Neurosurg* 29:164–167
51. Alvisi C, Cerisoli M, Maccheroni ME (1985) Long-term results of surgically treated brainstem gliomas. *Acta Neurochir (Wien)* 76:12–17
52. Pollack IF, Polinko P, Albright AL, Towbin R, Fitz C (1995) Mutism and pseudobulbar symptoms after resection of posterior fossa tumors in children: incidence and pathophysiology. *Neurosurgery* 37:885–893
53. Steinbok P, Cochrane DD, Perrin R, Price A (2003) Mutism after posterior fossa tumour resection in children: incomplete recovery on long-term follow-up. *Pediatr Neurosurg* 39:179–183
54. Wisoff JH, Epstein FJ (1984) Pseudobulbar palsy after posterior fossa operation in children. *Neurosurgery* 15:707–709
55. Pollack IF, Hoffman HJ, Humphreys RP, Becker L (1993) The long-term outcome after surgical

- treatment of dorsally exophytic brain-stem gliomas. *J Neurosurg* 78:859–863
56. Morota N, Ihara S, Deletis V (2010) Intraoperative neurophysiology for surgery in and around the brainstem: role of brainstem mapping and corticobulbar tract motor-evoked potential monitoring. *Childs Nerv Syst* 26:513–521
 57. Morota N, Deletis V (2006) The importance of brainstem mapping in brainstem surgical anatomy before the fourth ventricle and implication for intraoperative neurophysiological mapping. *Acta Neurochir (Wien)* 148:499–509; discussion 509
 58. Morota N, Deletis V, Lee M, Epstein FJ (1996) Functional anatomic relationship between brainstem tumors and cranial motor nuclei. *Neurosurgery* 39:787–793; discussion 793–794
 59. Neuloh G, Bogucki J, Schramm J (2009) Intraoperative preservation of corticospinal function in the brainstem. *J Neurol Neurosurg Psychiatry* 80:417–422
 60. Sala F, Krzan MJ, Deletis V (2002) Intraoperative neurophysiological monitoring in pediatric neurosurgery: why, when, how? *Childs Nerv Syst* 18:264–287
 61. Fahlbusch R, Strauss C (1991) Surgical significance of cavernous hemangioma of the brain stem. *Zentralbl Neurochir* 52:25–32
 62. Legnani FG, Pradilla G, Wang PP, Brem H, Olivi A, Dimeco F (2003) Local delivery of antineoplastic agents using biodegradable polymers for the treatment of malignant brain tumors. *Expert Rev Neurother* 3:533–546
 63. Bobo RH, Laske DW, Akbasak A, Morrison PF, Dedrick RL, Oldfield EH (1994) Convection-enhanced delivery of macromolecules in the brain. *Proc Natl Acad Sci U S A* 91:2076–2080
 64. Groothuis DR, Ward S, Itskovich AC, Dobrescu C, Allen CV, Dills C, Levy RM (1999) Comparison of ¹⁴C-sucrose delivery to the brain by intravenous, intraventricular, and convection-enhanced intracerebral infusion. *J Neurosurg* 90:321–331
 65. Occhiogrosso G, Edgar MA, Sandberg DI, Souweidane MM (2003) Prolonged convection-enhanced delivery into the rat brainstem. *Neurosurgery* 52:388–393; discussion 393–394
 66. Wu Q, Guarnieri M, Tyler B, Clatterbuck RE, Liu Y, Carson BS (2004) Section on tumors: Young Investigator Award: local release of carboplatin via an Alzet mini-osmotic pump prolongs survival in a rat brainstem tumor model. *Clin Neurosurg* 51:332–339
 67. Lonser RR, Warren KE, Butman JA, Quezado Z, Robison RA, Walbridge S, Schiffman R, Merrill M, Walker ML, Park DM, Croteau D, Brady RO, Oldfield EH (2007) Real-time image-guided direct convective perfusion of intrinsic brainstem lesions. Technical note. *J Neurosurg* 107:190–197

M. Memet Özek and Ulaş Yener

Tumors of medulla oblongata are considered as a unique entity and due to their anatomical relationship their surgical resection is challenging. They can be classified as focal (solid or cystic), exophytic (dorsally or laterally), or diffuse (which may also involve pons or rarely the upper cervical cord). In addition to these main classical groups, there are two subgroups of medulla tumors, namely, the pontomedullary junction and cervicomedullary junction tumors which have unique clinical and radiological presentation.

34.1 Clinical Presentation

Each type can present with distinct symptoms.

Focal tumors (Figs. 34.1a, b and 34.2a, b) present with insidious history. Patient may complain from nausea, vomiting, poor appetite, and speech disorders. As the tumor progresses and exhibits mass effect, brain stem findings like unilateral cranial nerve dysfunction, long tract findings, and cerebellar dysfunction may be

seen. A long history usually indicates a benign tumor and can be mentioned as a favorable diagnostic factor [1–4].

Dorsally exophytic tumors (Fig. 34.3a, b) present with posterior fossa symptoms like vomiting, headache, and ataxia. Due to tumor growth pattern into the fourth ventricle, it can cause cerebrospinal obstruction. Long tract sign is rare. Torticollis may be seen in dorsolateral exophytic lesions (Fig. 34.4a, b).

Lateral exophytic tumors (Figs. 34.5a, b and 34.6a, b) present mainly with ataxia especially those at the gracilis and cuneate tubercles. They may also present cranial nerve dysfunction due to compression or stretching of the lower cranial nerves (Fig. 34.5b).

Cervicomedullary tumors (Fig. 34.7a) originate either from upper cervical spinal cord or medulla of the brain stem. Most are low-grade lesions. Presenting complaints are due to medullary dysfunction. Usually neck pain, hoarseness, and lately weakness in the extremities with hyperreflexia can be seen. Recurrent respiratory tract infections are common. Sometimes torticollis may present. Signs and symptoms of raised intracranial pressure are uncommon in cervicomedullary junction tumors.

Diffuse tumors (Fig. 34.8a, b, d–f) are infiltrative and grow by using the fiber tracts to reach pons rostrally and upper cervical cord caudally. They typically present with a short duration of symptoms. Due to wide settlement of the tumor, they may affect the vital functions

M.M. Özek, M.D. (✉)
Division of Pediatric Neurosurgery,
Acibadem University, School of Medicine,
Istanbul, Turkey

Department of Neurosurgery,
Acibadem University, Istanbul, Turkey
e-mail: memetozek@gmail.com

U. Yener, M.D.
Department of Neurosurgery,
Acibadem University, Istanbul, Turkey

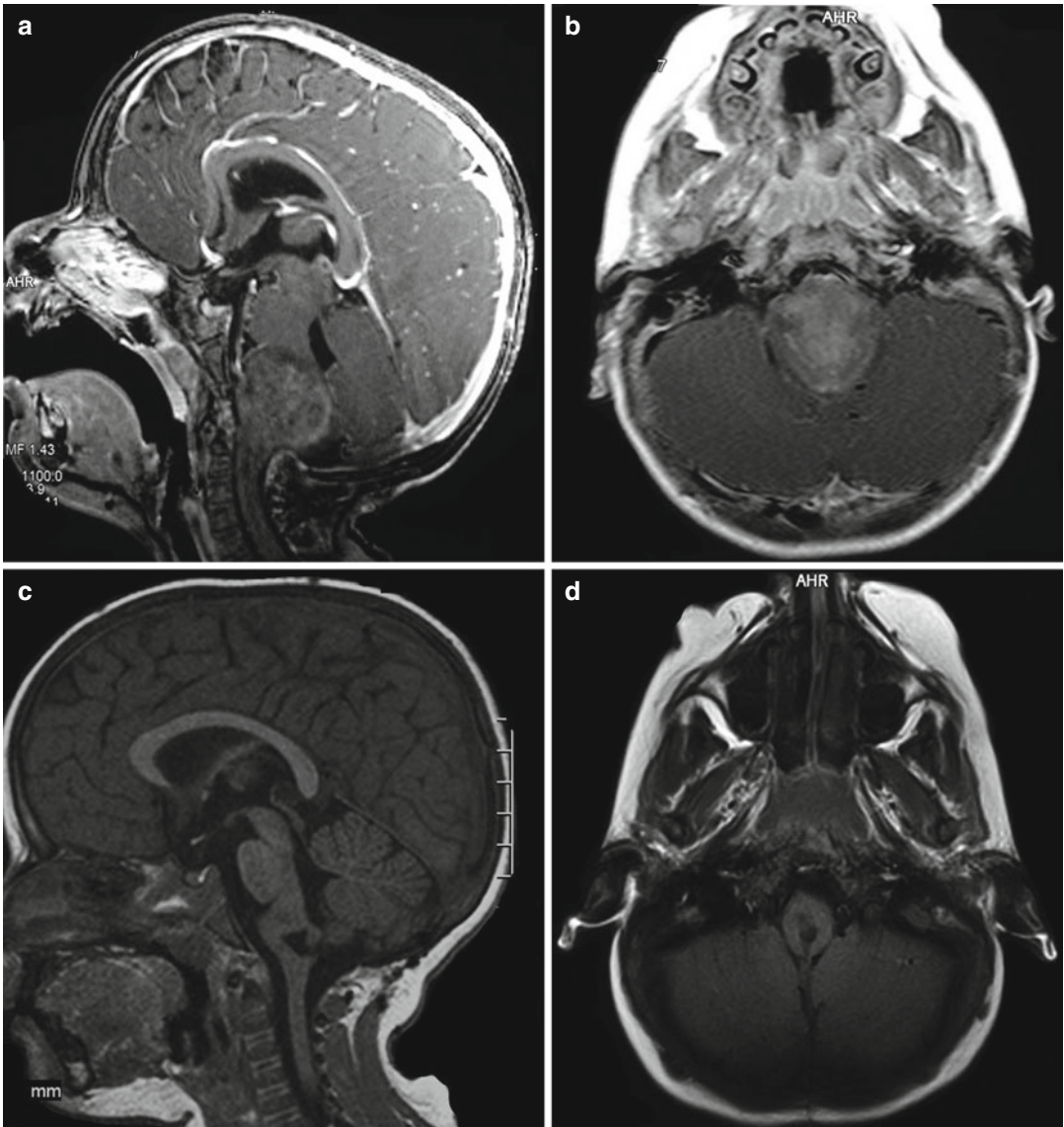


Fig. 34.1 (a) Focal medulla oblongata tumor with contrast enhancement, sagittal view. (b) Axial cut demonstrates a very thin layer of medulla. (c) Postoperative sagittal view. (d) Postoperative axial cut after midline approach

of the brain stem and they can present with a history of bilateral cranial nerve dysfunction, long tract findings, and cerebellar dysfunction. Multiple cranial nerve palsies are reported as a predictor of bad outcome [5]. Detailed physical examination can reveal altered facial

expression, diplopia, diminished gag reflex, change in vocal quality, diffuse weakness with hyperreflexia, and ataxia. Small portion of patients have hydrocephalus at the time of diagnosis [2]. Majority of these children die within the 2 years after the diagnosis [6].

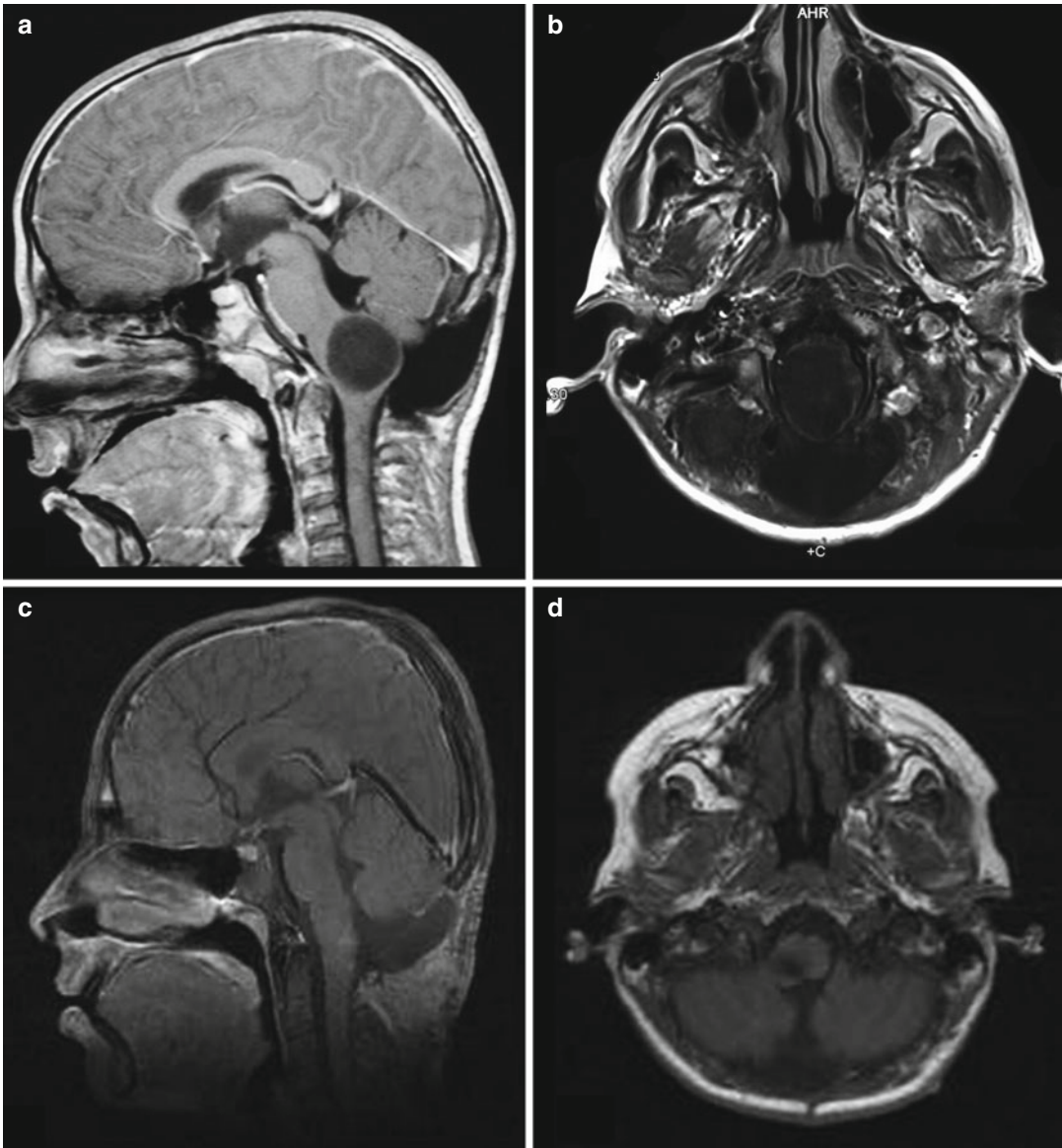


Fig. 34.2 (a) Focal tumor without contrast enhancement. Tumor is covered by a thin layer of normal tissue. (b) Axial cut demonstrates a well demarcated lesion.

(c) Postoperative sagittal view. (d) Axial cut shows the recovery of the medulla after resection

34.2 Diagnosis

MRI is the first radiologic diagnostic tool. The radiological evaluation of brain stem lesions is discussed in the chapter “Genetics”. The authors

just want to underline basic points which are very important during decision-making on these lesions. The study has to demonstrate in detail the normal anatomical structures and the extent of the pathology. We should compare

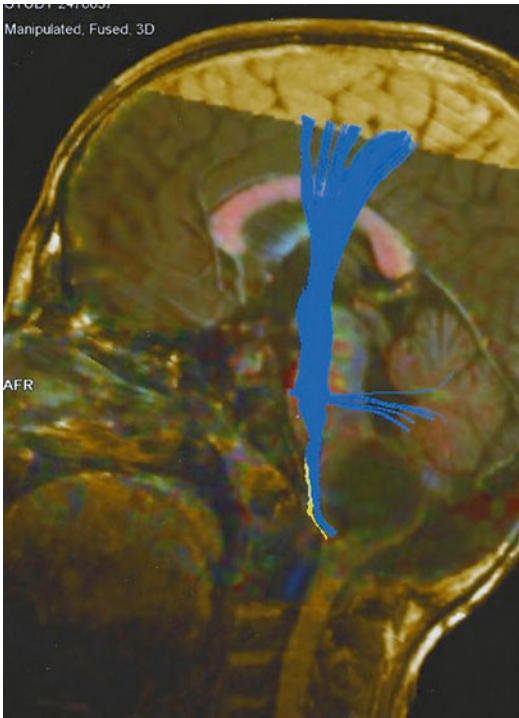


Fig. 34.3 DTI demonstrates the anterior displacement of the fibers

the volume of the lesion on T1- and T2-weighted images which can be informative for differentiating between the diffuse and the focal tumor. In diffuse tumors there isn't any distinct boundary and the tumor can be demonstrated as a hypointense on T1-weighted and hyperintense on T2-weighted MR images expanding the entire medulla throughout to pons. In a large radiological study (without histopathological verification), Barkovich et al. [7] showed that the "brain stem hypertrophy" is a predictor for a bad outcome of brain stem gliomas (Fig. 34.8a, b). Also Albright et al. proposed MRI instead of biopsy or operation to confirm the diagnosis for the diffuse tumors [8]. Contrary to this, Behnke stated that MRI has little predictive value for histopathological diagnosis in intra-axial brain stem tumors [2].

Focal tumors are well circumscribed with a limited size (<2.5 cm). Tumor may be cystic or solid that may or may not enhance. Pilocytic tumors usually enhance homogeneously due to characteristic vascular proliferation of the tumor [9]. Abbott et al. reported that cysts that are enhancing are pathognomonic for a malignant glioma. As the tumor grows, it can reach to

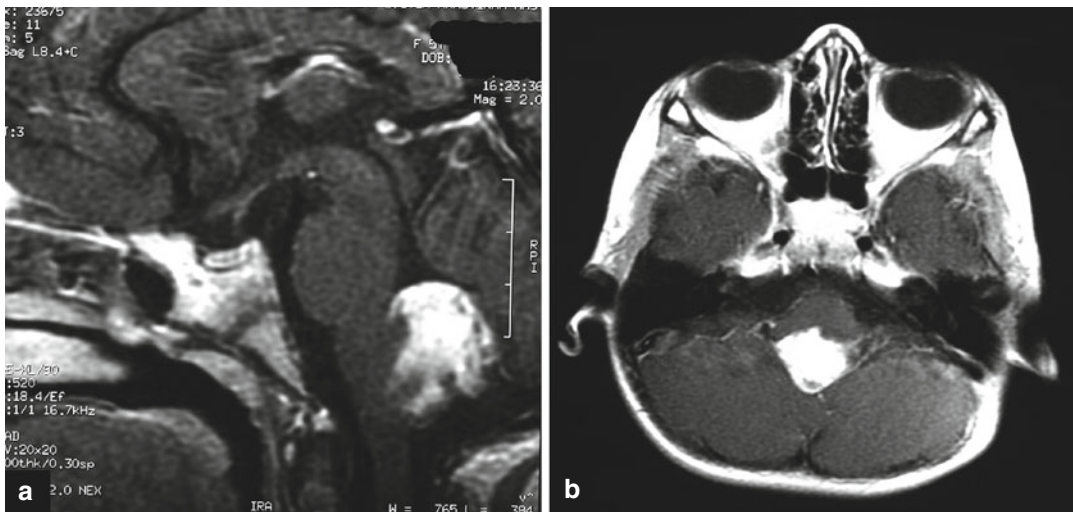


Fig. 34.4 (a) Dorsal exophytic medulla lesion with contrast enhancement. (b) Tumor growth into the fourth ventricle. (c) Sagittal contrast study shows the radical excision of the lesion. (d) Postoperative axial view

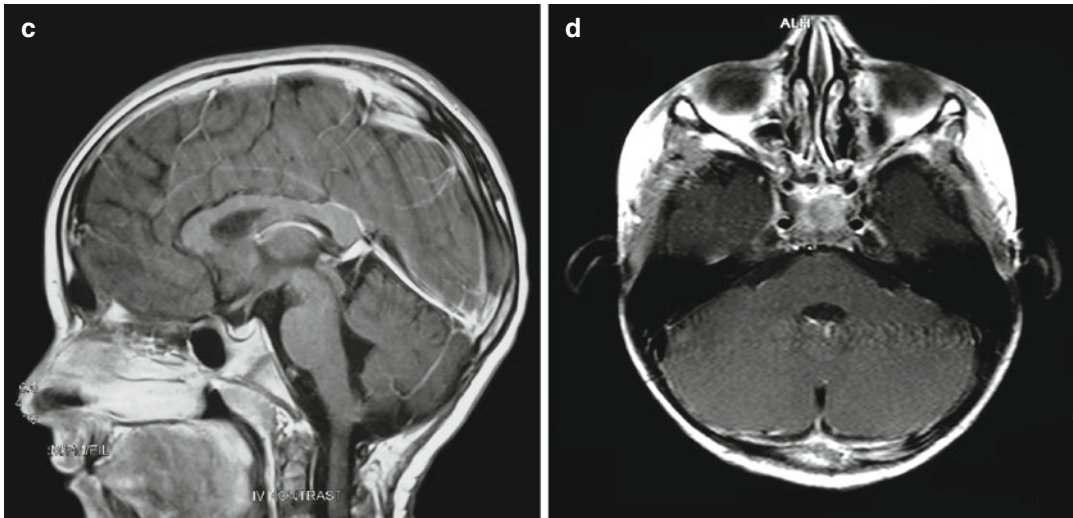


Fig. 34.4 (continued)

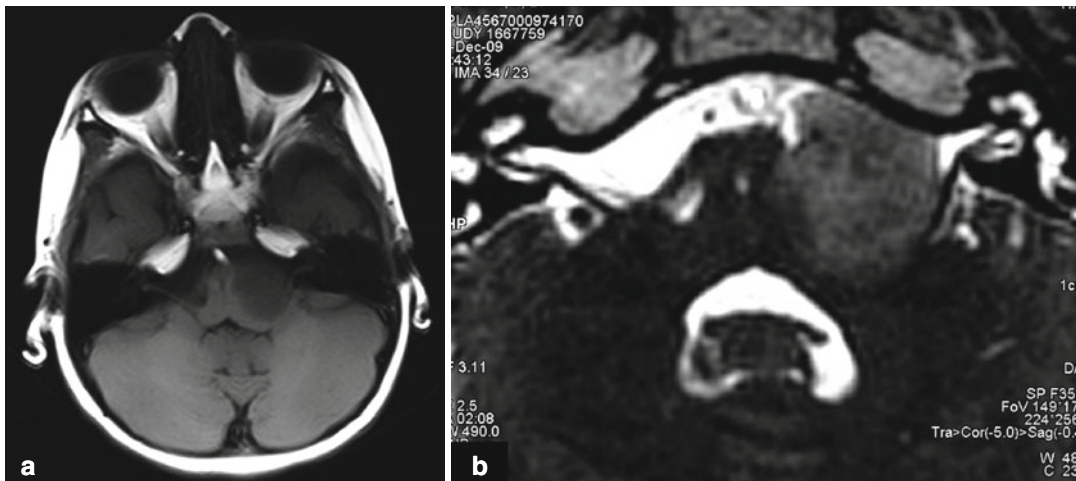


Fig. 34.5 (a) Lateral exophytic medulla tumor on the left side. (b) The tumor has stretched the VII and VIII nerves and fills the cisternal cavity on the left side

surface and can make the exophytic component [10]. Dorsal exophytic neoplasms are also not biologically similar to anterior and lateral exophytic tumor.

Cervicomedullary tumors respect the boundaries. Their axial growth is limited by the pyramidal decussation at cervicomedullary junction, at which point the tumor growth turns posteriorly

towards the fourth ventricle. Small proportion of tumors have invasive potential in this location; therefore, they grow through the decussation and do not show posterior exophytic component. MR scan shows distortion of the medulla with enlarged upper cervical cord (Fig. 34.8c). Tumors can enhance gadolinium either homogeneously or nonhomogeneously.

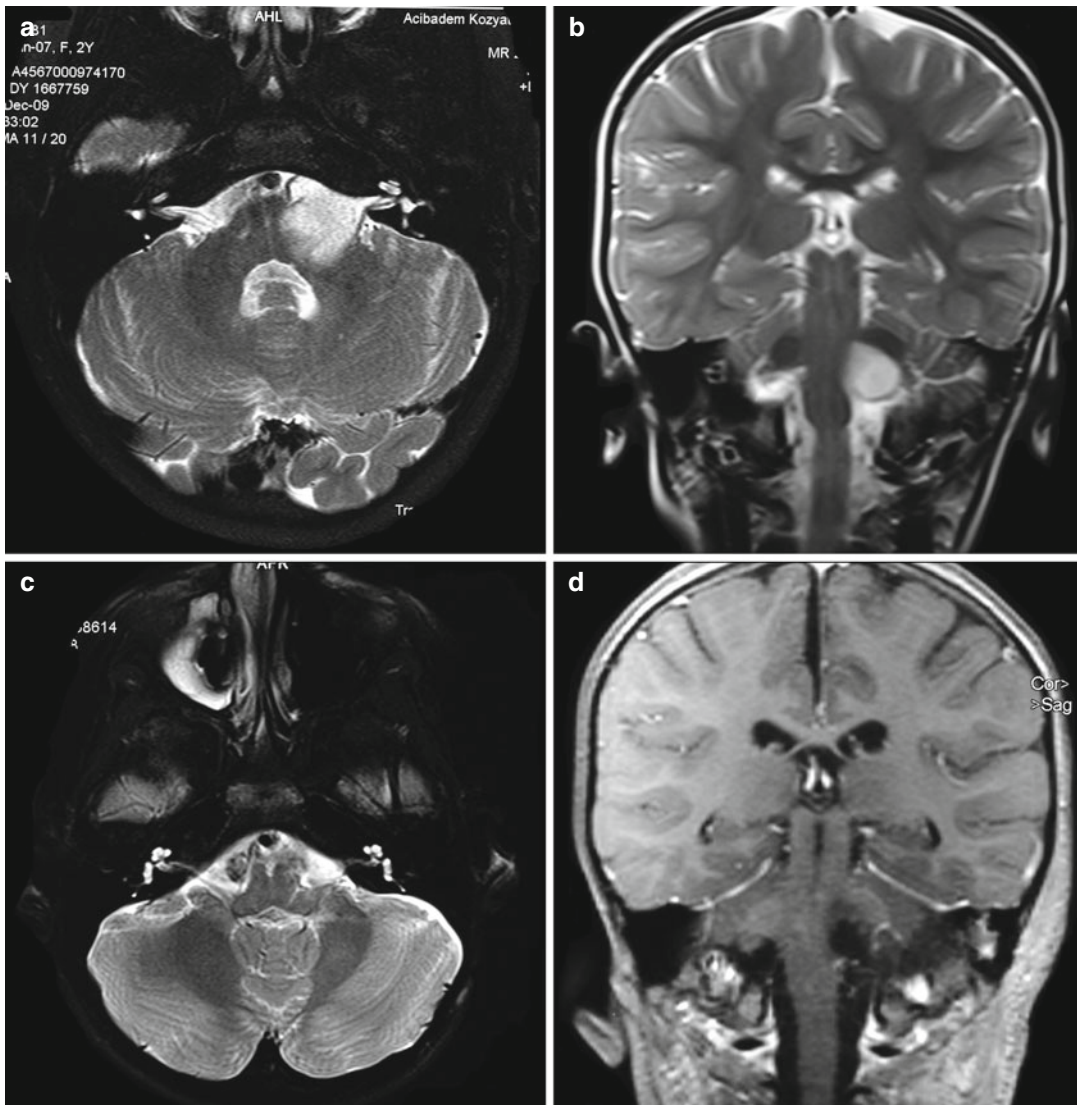


Fig. 34.6 (a, b) Lateral exophytic tumor on T2-weighted images. (c, d) The lesion is removed via retrosigmoid approach

A preoperative DTI study is also essential to have an idea of the location of corticospinal tracts (Fig. 34.9). We also agree that the histopathology of the medulla tumors cannot be reliably predicted by means of MRI alone [11].

34.3 Treatment

The main objectives for surgery of the medulla tumors are to obtain tissue samples for pathological examination and to decrease the tumor volume. The extent of tumor resection should

be as large as possible in exophytic tumors to relieve from preoperative clinical signs and symptoms. Radical tumor removal is important for the patient's survival; unfortunately the surgical removal of the medullary tumors carries a high risk of surgically related complications since the tumor infiltration may preclude the functional preservation of the surrounding brain stem parenchyma. In experienced hands the risk of morbidity is acceptable and results for complete or subtotal resection are good. In the management of diffuse tumors, surgery has no role.

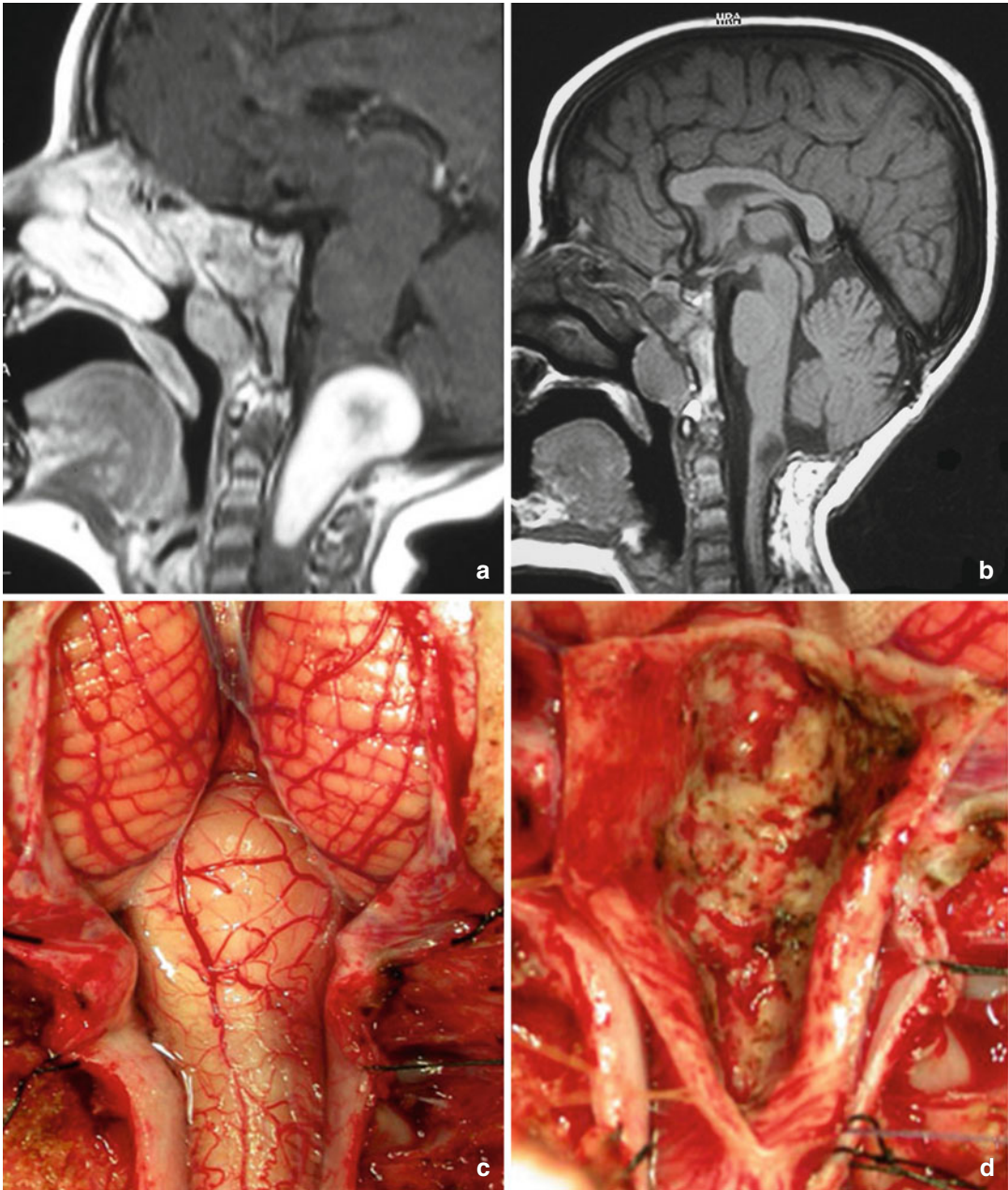


Fig. 34.7 (a) Cervicomedullary junction lesion with homogeneous contrast enhancement. (b) Radical resection of the lesion. (c) View after opening the dura. The

lesion is covered with a very thin normal tissue. (d) A midline approach and radical resection of the low-grade glioma

34.4 Preoperative Considerations

Analysis of the clinical history and physical and neurological evaluation must be done precisely. Short duration of symptoms and presence of multiple cranial nerve deficits are suggestive of a

diffuse tumor which in most cases is a high-grade pathology with a bad outcome [2, 7, 12]. In such a condition, a radical excision is not indicated [4].

Detailed MRI workup in three planes is necessary to have an idea about the anatomical relationship of the lesion with normal structures.

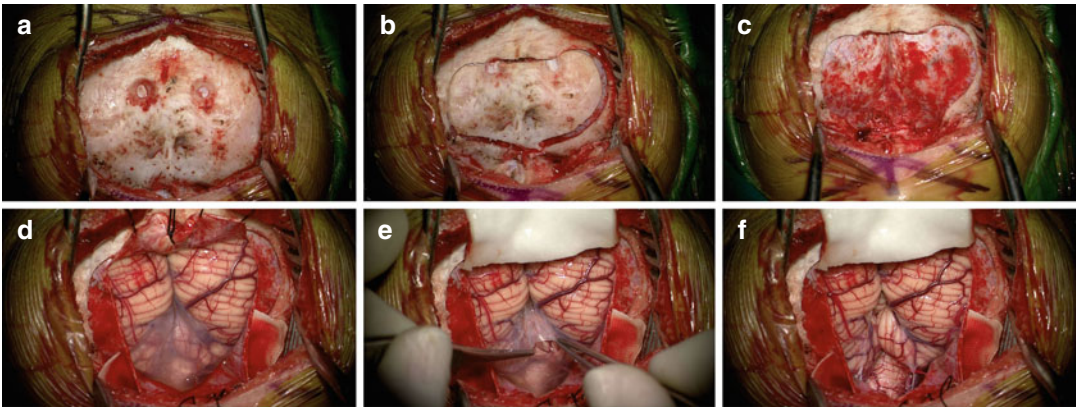


Fig. 34.8 (a) Two burr holes close to the midline. (b) Craniotomy is performed. (c) Bone flap is removed. (d) Dura is opened in a “Y” shape. (e) Arachnoidal opening. Dura is kept wet. (f) Exposure of the posterior fossa

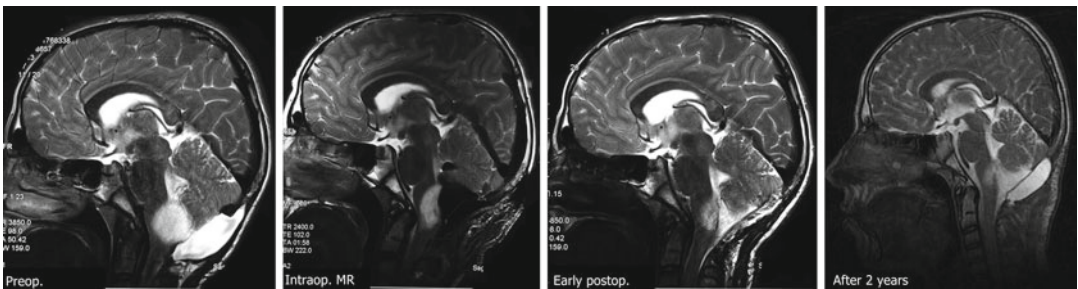


Fig. 34.9 A dorsal exophytic tumor without contrast enhancement. The ioMR demonstrates a big residual part of the tumor. Early postoperative scan shows minimal

residual lesion in the medulla. Two years after the surgery, there is no tumor regrowth

All of the probable complications must be told with precise detail to the patient relatives before the operation. They should be informed about the serious complications of loss of swallowing and airway protection, resulting to the need for gastrostomy and tracheostomy.

A good preoperative evaluation of the patient by the anesthesiology team will help to avoid intraoperative and early postoperative complications.

Operations inside the medulla are delicate because of many important structures that are located within a very small volume of brain tissue. Morbidity can be decreased by using intraoperative neurophysiological methods which are described in detail in chapter “[Treatment of medulloblastoma: chemotherapy.](#)” Motor structures can be identified by electrically stimulating the lower part of the surface of the floor of the fourth ventricle and recording the EMG

responses from muscles that are innervated by the respective motor systems. The hypoglossal nerve can be identified and recordings are made from genioglossal muscle. IX, X, and XI cranial nerves can be identified using similar methods [13]. SEP and MEP usage allows surgeons to be more aggressive on the tumor [13, 14].

Intraoperative magnetic resonance imaging (ioMR) has been shown to be a useful tool for maximizing the extent and safety of resection in glioma surgery [15]. The image quality provided by current high- and ultrahigh-field ioMR imaging systems is not more inferior to postoperative MR imaging studies. Therefore, an optimal evaluation of the surgical outcome can be obtained during the procedure, and further improvements can be performed before the procedure ends without increasing morbidity. Whether this further resection of LGGs without increasing surgical

morbidity will translate into prolonged survival is not currently known.

Three-tesla ioMR imaging protocol takes less than 10 min including the transfer and the authors obtain very high-resolution T2-weighted MR images without the use of intravenous contrast [16]. Functional imaging sequences, such as DTI sequences, were effectively used pre- and postoperatively but were not successful intraoperatively because of magnetic inhomogeneity [15].

34.5 Operation

There are three major steps during the surgical intervention of medulla lesions:

- The surgical approach
- The point of entry into the medulla
- Removal of the lesion

34.6 Positioning

The prone and the lateral positions are used to approach to the medulla tumors. Prone position is widely used for the midline lesions. To avoid compression on eyes, chest, knees and hip in this position, special care must be given.

The lateral or park bench position is the way to approach the lateral exophytic tumors. Usually the surgeon's preference and experience along with the localization of the tumor determines the way of approach.

34.7 Surgical Approach and Surgery

Midline tumors either focal or dorsally exophytic can be reached with a midline approach. It provides a wide visualization of the cerebellar hemispheres, the fourth ventricle, obex, and the cervicomedullary junction. A midline skin incision extended from the inion to C1 level is done. To reach to the occipital squamous bone, midline avascular ligamentum nuchae is followed. This provides clean dissection of the muscular layer in infants where minimal blood loss is especially

important for maintenance of cardiovascular stability. Dissection and retraction of the muscular layer provides wide access to the occipital and the posterior cervical region. C1 posterior laminectomy is required for tumor extending to the cervicomedullary junction.

Following the muscle retraction, a midline standard suboccipital craniotomy is performed (Fig. 34.10a–c). After bone removal, dura can be opened in Y-shaped fashion incision and retracted (Fig. 34.10d). In infants, intradural sinuses are well developed in the midportion of the dura, so caution must be paid to them. Closure of these sinuses after cutting must be performed as quick as possible by using hemoclips. Dura should be retracted and covered with cotton to keep it wet (Fig. 34.10e). Opening of the arachnoid membrane gives a good view to the posterior fossa (Fig. 34.10f).

The authors' preference is the telovelar approach to avoid injury to the vermis [17, 18]. Telovelotonsillar segment must be dissected and caution must be paid to telovelotonsillar segment of the PICA. Only one-sided retraction is enough to have a wide exposure to the medulla.

In *focal tumors of the medulla*, the point of entry into the brain stem may be marked by a small area of discoloration or elevation seen through the ependyma or pia-arachnoid. This area is checked with the brain stem mapping techniques. The experience of the surgeon with distorted anatomy of the medulla is important. The forbidden entry point is the gracilis and cuneate tubercles; on the contrary posterior median fissure below obex, posterior lateral sulcus, and posterior intermediate sulcus are relatively safe zones to enter the medulla (Fig. 34.1c, d) [14, 19]. The DTI of the patient will give us an additional information about the possible no entry zones (Fig. 34.9). The ependyma should be incised at these relatively safe areas sharply by using an arachnoid blade gently 4–5 mm and dissection should be carried out with blunt tip bayonets [20]. At that point a biopsy for frozen section is taken. If the frozen section reports high-grade tumor, then aggressive resection is not indicated. In case of a low-grade lesion, the surgery is continued with the help of ultrasonic aspirator. The authors use the plated bayonet as a dissection and retraction tool to

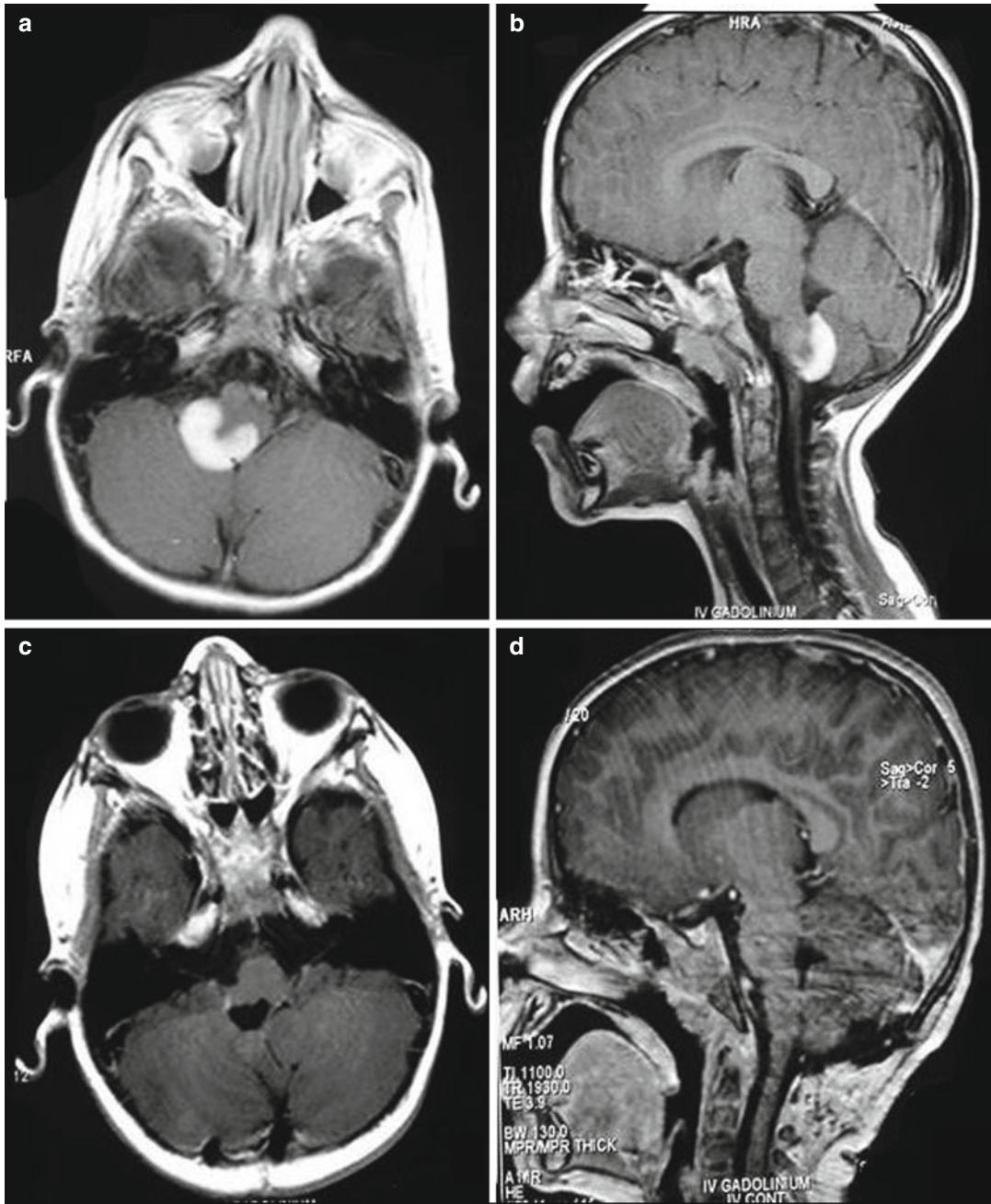


Fig. 34.10 (a, b) A dorsolateral exophytic tumor of medulla with homogeneous contrast enhancement. The 5-year-old boy presented with torticollis. (c, d) Postoperative MR scan. The torticollis improved dramatically

spread the fibers of the white matter. When the discolored tumor tissue is reached between the two tips of the bayonet, ultrasonic aspirator is used with low power settings. The first attempt is always an internal debulking, and then further

dissection around the lesion is carried out. It is the authors experience for the last 8 years to use ioMR for brain stem lesions. At the point when we are not sure about the margins of the tumor, we ask for an ioMR evaluation (Fig. 34.11).

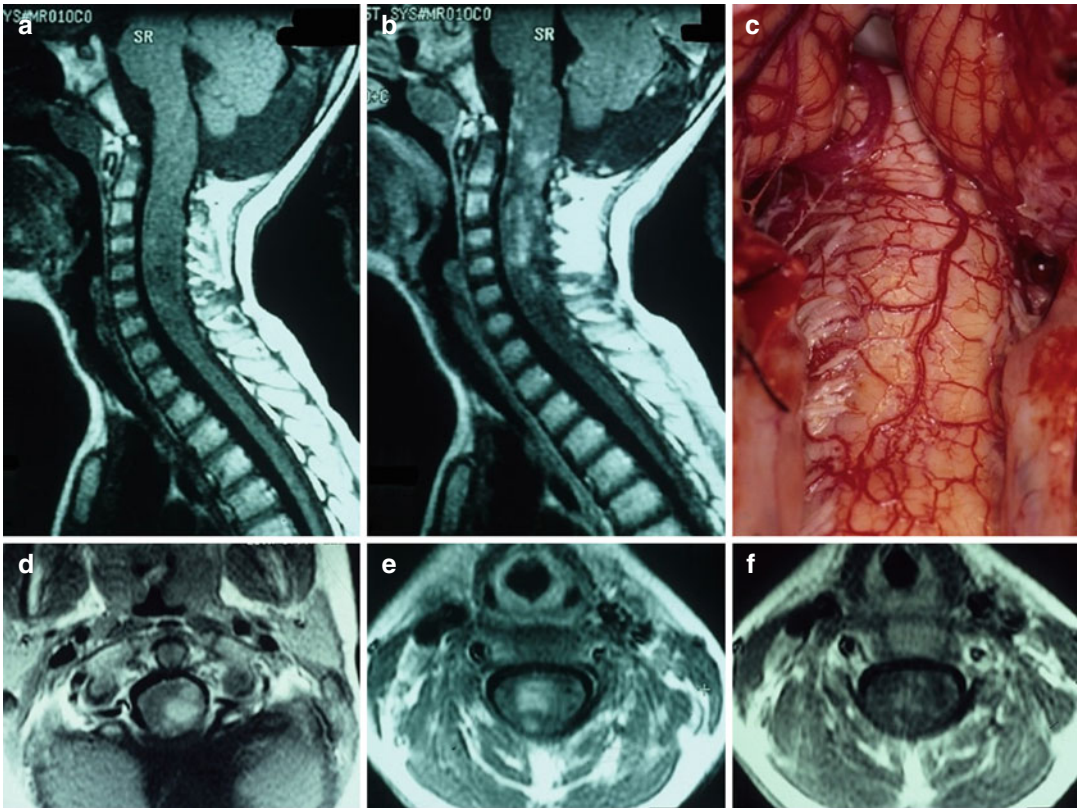


Fig. 34.11 (a) A diffuse medulla oblongata tumor on T1-weighted image. The patient has a very long history of neck pain and torticollis. (b) Heterogeneous contrast

enhancement. (c) Torsion of the medulla and upper cervical cord. (d–f) Axial cut studies demonstrate irregular enhancement in the medulla and upper cervical cord

In case of residual lesion, the surgery is continued. Intraoperative ultrasonography would be another option to have an idea about the amount of resection. Rarely the focal medullary lesions are cystic. The cystic component may be quite large to the size of the solid portion and this cystic portion makes natural pathway to reach to the nodular tumor. It is the author's experience that tumors with no enhancement on the MR are softer and easy to aspirate. There is always a clear-cut border between the lesion and the medulla on this group of tumors (Fig. 34.2c, d).

In *dorsally exophytic* lesions the tumor can be seen immediately after cerebellar retraction. Again a lower fourth ventricle mapping is performed before starting with the tumor removal. Ultrasonic aspirator with medium level suction power is used. When we get closer to the surface of the fourth ventricle, suction power should

be reduced. Bipolar coagulation of the minor bleedings should be avoided; with continuous irrigation these bleedings will stop. Abnormal hemodynamics during extirpation of medulla tumors is common and may be associated with direct vagal stimulation of the medullary circuit [21]. Abnormal hemodynamics was defined as a >20 % change from the means of the intraoperative mean arterial pressure and heart rate. Also short asystolic crises, especially during manipulations in the superficial layers of pontomedullary junction, can be observed [11]. In case of an increase of bleeding, the anesthesiology team should be informed about a possible hemodynamic change. After meticulous dissection and use of ultrasonic aspirator, we can realize that we have reached the lower boundary of the lesion (Fig. 34.3c, d). For dorsolateral lesions in a semi-lunar location, the retractor should be on the

side of lateral extension. The power of retraction should be stronger to the end of resection in order to have a wider view on the lateral aspect of the tumor. A stimulation of the lower cranial nerves may be necessary at that point (Fig. 34.4a–d).

In *cervicomedullary tumors* a cervical osteoplastic laminectomy in addition to the occipital craniotomy has to be performed. It is essential that laminectomy must involve the caudal pole of the tumor for adequate exposure [4]. After opening the dura to avoid injury to posterior columns, myelotomy is done in the midline [22, 23]. In some cases torsion of the cord and medulla complicates to find the midline. Then the midpoint between the nerve roots will be the entry into the spinal cord (Fig. 34.7c). Pial sutures are applied and the cord is retracted to the lateral side. Again with the help of the plated bayonet, the dissection is continued and with the ultrasonic aspirator a piece meal resection is performed (Fig. 34.7b, d).

At the end of the procedure, surgical field walls are visualized and checked carefully for sources of bleeding and possible tumor remnants. One should never coagulate those feeding vessels which are entering the cord through the midline. With the help of pial sutures, the cord surface is closed. Dura is closed in watertight fashion. Laminas and the craniotomy flab are fixed with absorbable sutures. Cervical and nuchal muscles are reconstructed separately in order to reduce the risk of CSF leakage.

34.8 Lateral Approach

In case of a tumor settled laterally, especially confined to the CPA, a retrosigmoid skin incision must be carried out in order to make a retromastoid craniotomy. Paramedian incision is followed by muscular dissection. Special care must be paid to avoid excessive blood loss while cutting the muscular layers by cautery. Bone removal can be done either by craniotomy or by craniectomy. After gentle retraction of the cerebellum and CSF release, the exophytic tumor can be seen. Because of the distorted anatomy due to the tumor, it is better to separate the tumor from the

cranial nerve proceeding laterally and then medially. Additionally, marker points can be used as a landmark (e.g., internal acoustic foramen to preserve VII and VIII cranial nerves, jugular foramen to preserve IX and X cranial nerves). Use of a nerve stimulator can again be helpful. After having a biopsy for the frozen section, the tumor is removed with ultrasonic aspirator. We always start from the medial part of the lesion and proceed to the lateral aspect. There should be no pressure on the tumor tissue while removing it since in most of the cases the lower cranial nerves are stretched and an additional pressure on them may cause a postoperative nerve dysfunction (Fig. 34.5b). To achieve maximal degree of tumor resection, intraoperative MRI or ultrasound guidance can be used (Fig. 34.6c, d).

34.9 Postoperative

Most serious and immediate postoperative complication is respiratory insufficiency. Care must be taken for the risk of postoperative respiratory collapse due to CO₂ retention [23]. In our department we keep the patients intubated for 24 h postoperatively until they demonstrate adequate respiratory drive. We do not have the tendency to start early with feeding in infants with the medulla tumors. We always start to feed the patient after 24 h with an NG tube. Oral feeding starts only on the third day when we are sure there is no problem with swallowing. In case of swallowing difficulties and absence of gag reflex, a gastrostomy is performed.

34.10 Outcome

Patients with low-grade focal tumors of the medulla have a long overall survival and stable progression after surgery [18, 24]. However, significant lower cranial nerve dysfunction has been reported and is associated with preoperative clinical presentation. In a series of 41 patients reported by Jallo et al. [24], 19 patients (46 %) had significant lower cranial nerve deficits that required a tracheostomy, postoperative

ventilation, and a feeding gastrostomy. However, a majority of these patients (79 %) experienced complete cranial nerve recovery or demonstrated significant resolution of their deficits after surgery. Patients that present with a history of voice changes, pneumonia, and upper respiratory infections have a higher risk of requiring postoperative ventilation [10].

Dorsal exophytic tumors have a much better prognosis. Khatib et al. [25] reported a 92 % long-term survival in a series of 12 patients, with one death in a nonsurgically treated patient. Likewise, Pollack et al. [26] reported a long-term survival of 94 % in their series of 18 patients, with one death related to a shunt malfunction. They also reported complete disappearance or stable residual disease in 11 patients. Tumor regrowth was seen in four patients, all of whom were treated with reoperation or irradiation.

Postoperative morbidity after resection of cervicomedullary junction tumors directly correlates with preoperative function [18]. In a series of 17 patients reported by Robertson et al. [22], five patients had a history of moderate–severe symptoms preoperatively and all of them had significant postoperative neurological complications. The 12 patients who presented with mild preoperative symptoms remained stable or improved postoperatively. Postoperative outcome is directly related to the duration of the prodrome. Weiner et al. [27] reported progression-free, 5-year survival in 72 % of patients with preoperative symptoms that lasted greater than 15 weeks and only in 46 % of those who presented with symptoms lasting less than 15 weeks.

References

- Cohen ME, Duffner PK, Heffner RR, Lacey DJ, Brecher M (1986) Prognostic factors in brainstem gliomas. *Neurology* 36:602–605
- Behnke J, Christen HJ, Bruck W, Markakis E (1997) Intra-axial endophytic tumors in the pons and/or medulla oblongata. I. Symptoms, neuroradiological findings, and histopathology in 30 children. *Childs Nerv Syst* 13:122–134
- Teo C, Siu TL (2008) Radical resection of focal brainstem gliomas: is it worth doing? *Childs Nerv Syst* 24:1307–1314
- Abbott R (1993) Tumors of the medulla. *Neurosurg Clin N Am* 4:519–527
- Albright AL (1993) Pediatric brain tumors. *Cancer* 43:272–288
- Villani R, Gaini SM, Tomei G (1975) Follow-up study of brain stem tumors in children. *Childs Brain* 1:126–135
- Barkovich AJ, Krischer J, Kun LE, Packer R, Zimmerman RA, Freeman CR, Wara WM, Albright L, Allen JC, Hoffman HJ (1990) Brain stem gliomas: a classification system based on magnetic resonance imaging. *Pediatr Neurosurg* 16:73–83
- Albright AL, Packer RJ, Zimmerman R, Rorke LB, Boyett J, Hammond GD (1993) Magnetic resonance scans should replace biopsies for the diagnosis of diffuse brain stem gliomas: a report from the Children's Cancer Group. *Neurosurgery* 33:1026–1029, discussion 1029–1030
- Russell DS (1989) Pathology of tumors of the nervous system, 5th edn. Williams&Wilkins, Baltimore
- Abbott R, Shiminski-Maher T, Epstein FJ (1996) Intrinsic tumors of the medulla: predicting outcome after surgery. *Pediatr Neurosurg* 25:41–44
- Behnke J, Christen HJ, Mursch K, Markakis E (1997) Intra-axial endophytic tumors in the pons and/or medulla oblongata. II. Intraoperative findings, postoperative results, and 2-year follow up in 25 children. *Childs Nerv Syst* 13:135–146
- Albright AL, Guthkelch AN, Packer RJ, Price RA, Rourke LB (1986) Prognostic factors in pediatric brain-stem gliomas. *J Neurosurg* 65:751–755
- Moller AR (2006) Identification of specific neural tissue. In: Møller AR (ed) Intraoperative neurophysiological monitoring. Humana Press, Totowa
- Bricolo A, Sala F (2002) Surgery of brainstem lesions. In: S J, Deletis V (eds) Neurophysiology in neurosurgery. Academic, Amsterdam
- Pamir MN, Ozduman K, Dincer A, Yildiz E, Peker S, Ozek MM (2010) First intraoperative, shared-resource, ultrahigh-field 3-tesla magnetic resonance imaging system and its application in low-grade glioma resection. *J Neurosurg* 112:57–69
- Pamir MN, Peker S, Ozek MM, Dincer A (2006) Intraoperative MR imaging: preliminary results with 3 tesla MR system. *Acta Neurochir Suppl* 98:97–100
- Tanriover N, Ulm AJ, Rhoton AL Jr, Yasuda A (2004) Comparison of the transvermian and telovelar approaches to the fourth ventricle. *J Neurosurg* 101:484–498
- Recinos PF, Sciubba DM, Jallo GI (2007) Brainstem tumors: where are we today? *Pediatr Neurosurg* 43:192–201
- Recalde RJ, Figueiredo EG, de Oliveira E (2008) Microsurgical anatomy of the safe entry zones on the anterolateral brainstem related to surgical approaches to cavernous malformations. *Neurosurgery* 62:9–15, discussion 15–17
- Epstein FJ, Ozek M (1993) The plated bayonet: a new instrument to facilitate surgery for intra-axial neoplasms of the spinal cord and brain stem. Technical note. *J Neurosurg* 78:505–507

21. Ideguchi M, Kajiwara K, Yoshikawa K, Sadahiro H, Nomura S, Fujii M, Suzuki M (2013) Characteristics of intraoperative abnormal hemodynamics during resection of an intra-fourth ventricular tumor located on the dorsal medulla oblongata. *Neurol Med Chir* 53:655–662
22. Robertson PL, Allen JC, Abbott IR, Miller DC, Fidel J, Epstein FJ (1994) Cervicomedullary tumors in children: a distinct subset of brainstem gliomas. *Neurology* 44:1798–1803
23. Abbott R, Shiminski-Maher T, Wisoff JH, Epstein FJ (1991) Intrinsic tumors of the medulla: surgical complications. *Pediatr Neurosurg* 17:239–244
24. Jallo GI, Shiminski-Maher T, Velazquez L, Abbott R, Wisoff J, Epstein F (2005) Recovery of lower cranial nerve function after surgery for medullary brainstem tumors. *Neurosurgery* 56:74–77, discussion 78
25. Khatib ZA, Heideman RL, Kovnar EH, Langston JA, Sanford RA, Douglas EC, Ochs J, Jenkins JJ, Fairclough DL, Greenwald C et al (1994) Predominance of pilocytic histology in dorsally exophytic brain stem tumors. *Pediatr Neurosurg* 20:2–10
26. Pollack IF, Hoffman HJ, Humphreys RP, Becker L (1993) The long-term outcome after surgical treatment of dorsally exophytic brain-stem gliomas. *J Neurosurg* 78:859–863
27. Weiner HL, Freed D, Woo HH, Rezai AR, Kim R, Epstein FJ (1997) Intra-axial tumors of the cervicomedullary junction: surgical results and long-term outcome. *Pediatr Neurosurg* 27:12–18

Aydin Sav and Pinar Karabağlı

35.1 Introduction

The most common intrinsic tumor of the brain stem is the astrocytoma. The majority of brain stem gliomas are diffuse with an epicenter in the pons [1–3]. Histologically, these brain stem astrocytomas are fibrillary (80 %) or pilocytic (20 %). On rare tumors within the brain stem include subependymomas, lymphomas, gangliogliomas, and oligodendrogliomas [4–6]. Brain tumors, primarily gliomas, are more common in those with neurofibromatosis type 1 (NF1) than in the general population [7].

Brain stem tumors are a heterogeneous group of tumors, which may be diffuse, focal, dorsally exophytic, or cervicomedullary [4, 8, 9]. Pathologic type was significantly associated with location [10].

A. Sav, M.D. (✉)
Department of Pathology,
Acıbadem University, School of Medicine,
Gülsuyu Mah., Fevzi Çakmak Cd, Divanyolu Sk,
1, Maltepe, İstanbul 34848, Turkey
e-mail: murataydinsav@gmail.com

P. Karabağlı, M.D.
Department of Pathology,
Selçuk University, Selçuklu School of Medicine,
Alaaddin Keykubat Campus, Konya 42075, Turkey
e-mail: hakankarabagli@yahoo.com

35.2 Gliomas

Diffuse brain stem gliomas are the most encountered tumor of the brain stem, comprising between 58 and 75 % of all gliomas in this area [11–14]. About two thirds of cases of diffuse type brain stem glioma were classified as high-grade (WHO grade III to IV) glioma in postmortem studies [1–4]. They infiltrate along the fiber tracts into the midbrain and medulla oblongata. Almost 16 % of patients in one series observed leptomenigeal metastases [3]. Grossly, the brain stem appears diffusely swollen [9]. Unlike most pediatric tumors, these tumors have genetic mutations similar to those of adult gliomas [1, 4, 9]. Proliferative potential of diffuse type brain stem gliomas is as high as that of an adult supratentorial glioblastoma. The mean MIB-1 proliferating cell index of glioblastoma is 20.4 % [2]. Louis reported that half of the patients exhibited TP53 mutations [15]. A recent study, analyzing 28 brain stem gliomas, demonstrated a correlation, between the tumor grade and EGFR (epidermal growth factor receptor) protein expression. EGFR gene amplification was observed in only a minority of these neoplasm, particularly in grade III and IV tumors [16]. Approximately 50 % of all cases in one series demonstrated allelic loss in the long arm of chromosome 10 [15]. Diffuse pontine gliomas carry a poorer prognosis than other brain stem tumors [1, 5]. Less than 10 % of children with diffuse brain stem gliomas survive 2 years [5].

Focal tumors are defined as demarcated lesions. These tumors can arise anywhere within the brain stem [1]. They may be solid or cystic. They are mostly histologically benign (WHO grade I or II) lesions. Focal tumors of the brain stem number no more than 25 % of newly diagnosed brain stem gliomas. These tumors include not only low-grade fibrillary astrocytomas, pilocytic astrocytomas, gangliocytomas, and gangliogliomas but also gangliogliomas and primitive neuroectodermal tumors (PNETs) [1, 4, 9].

Dorsally exophytic brain stem gliomas most often have a low-grade glial histology. These tumors grow from subependymal glial tissue out into the fourth ventricle [1]. They are typically grade I or grade II astrocytomas. The histology of these lesions is usually pilocytic astrocytoma, and outcome is generally good, although higher-grade astrocytomas and gangliogliomas have been reported [4, 7, 10].

Cervicomedullary brain stem gliomas are predominantly benign low-grade gliomas [4]. Reported histology is predominately fibrillary or pilocytic astrocytomas, but ependymomas, gangliogliomas, and rarely high-grade astrocytomas are reported [7, 10].

35.3 Diffuse Astrocytic Neoplasms/ Brain Stem Gliomas

Diffuse astrocytoma (WHO grade II), anaplastic astrocytoma (WHO grade III), and glioblastoma (WHO grade IV) constitute a range of diffusely infiltrating astrocytic neoplasms, which occur throughout the CNS. The diffuse astrocytic neoplasms are commonest in the brain stem in children [17].

Diffuse infiltrating astrocytoma (WHO grade II) is characterized by a high degree of cellular differentiation and slow growth [18] (Fig. 35.1). Fibrillary astrocytomas are the most frequent histological subtype of diffuse astrocytoma WHO grade II, involving the brain stem of children and adolescents [17–20].

Grossly, astrocytoma of the brain stem expands normal tissues in a fusiform fashion. Brain stem

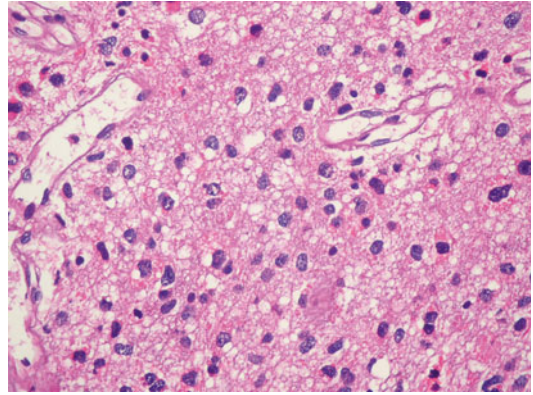


Fig. 35.1 Diffuse astrocytoma, grade WHO grade II is characterized by a high degree of cellular differentiation

astrocytomas are frequently centered in the pons and an exophytic component may encircle the basilar artery [17, 21]. Because of their infiltrative nature, these tumors usually show blurring of the gross anatomical boundaries [18].

If there is only a limited material for histopathologic examination, e.g., from a stereotactically obtained biopsy, diagnosis of astrocytoma may be difficult to make, especially if the biopsy is sampled from infiltrating edge of tumor [17]. A firm intraoperative diagnosis of infiltrative astrocytoma requires an unequivocal increase in cellularity, irregular distribution of glial cells, nuclear atypia, and, in some instances, presence of microcysts [21] (Fig. 35.2). Intraoperative smears readily demonstrate the fibrillary matrix, which is usually more ill defined than the background accompanying reactive astrocytosis. The nuclei of the tumor cells are slightly larger and more irregular and hyperchromatic with coarser chromatin than those of reactive astrocytes. Cytoplasmic morphology ranges from a scant perinuclear rim with ill-defined borders to more stellate shape [20].

Histologically fibrillary astrocytoma is predominantly composed of fibrillary neoplastic astrocytes. Cellularity is moderately increased, and nuclear atypia is a typical feature but mitotic activity, necrosis, and microvascular proliferation absent [18]. The cells of fibrillary astrocytomas may appear as bare nuclei, their tenuous fibrillary processes blending with the brain's parenchyma.

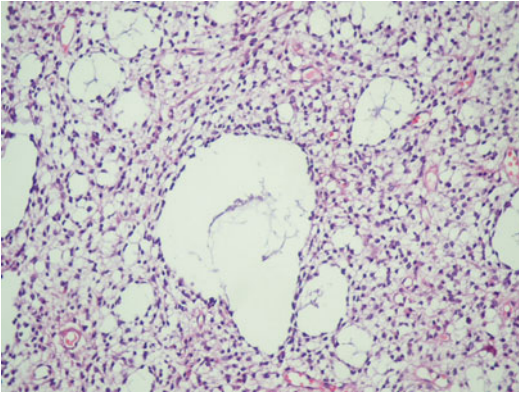


Fig. 35.2 Diffuse astrocytoma, WHO grade II showing increase in cellularity, irregular distribution of glial cells, minimal nuclear atypia associated with microcysts

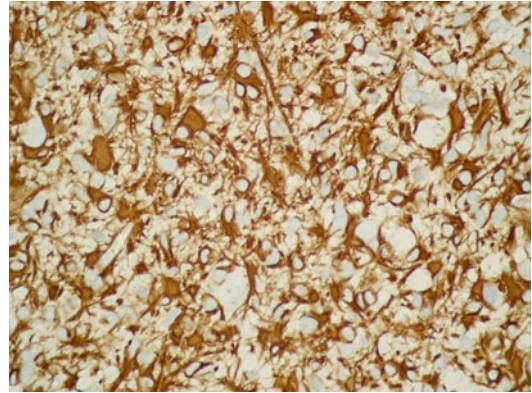


Fig. 35.4 Intense reactivity for glial fibrillary acidic protein (GFAP) is characteristic

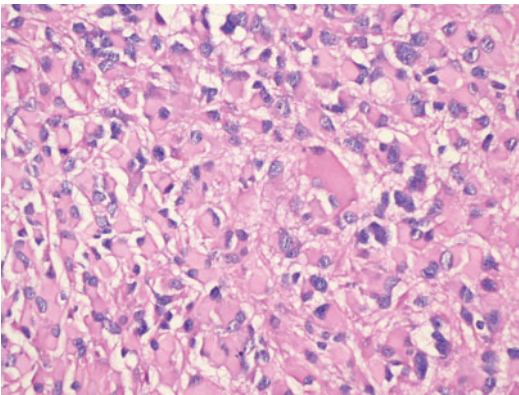


Fig. 35.3 Gemistocytic phenotype is associated in a fibrillary astrocytoma

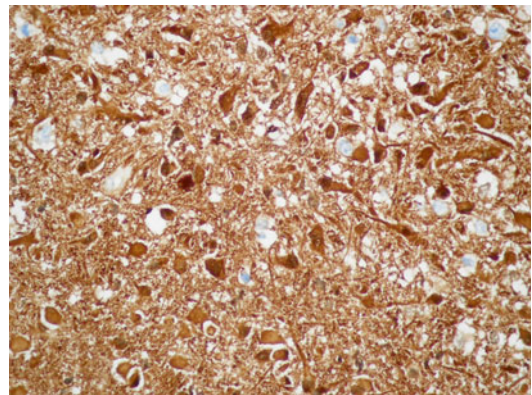


Fig. 35.5 Diffuse nuclear and cytoplasmic immunoreactivity for S-100 protein

Alternatively they show varying degrees of astrocytic differentiation, exhibiting prominent fibrillary strands of eosinophilic cytoplasm, or a plump cell body in which the nucleus is displaced by homogeneously eosinophilic cytoplasm, the gemistocytic phenotype [17, 18] (Fig. 35.3).

The presence of microcystic spaces is a distinctive and diagnostically helpful feature of gliomas. Microcysts containing mucinous fluid are a characteristic feature. Cartilage formation is very rare [18, 21].

Immunohistochemical Findings. The cytoplasm often is immunopositive for glial fibrillary acidic protein (GFAP), although to a variable degree and not by all cells of tumor

(Fig. 35.4). The fibrillary matrix forms diffuse GFAP positive background. Vimentin is usually expressed in astrocytic tumors, with similar distribution to GFAP but with less prominence. Tumor cells are also immunoreactive for S-100 protein, in both nuclei and cytoplasmic processes, but this feature has no diagnostic relevance [18, 20, 21] (Fig. 35.5).

The growth fraction, as determined by the Ki67/MIB-1 labeling indices of astrocytoma grade II, has generally been less than 4 %, with a mean of 2.5 % (Fig. 35.6). Staining for p53 protein is variable in diffuse astrocytomas (Fig. 35.7). A higher percentage is present in gemistocyte-rich lesions [18, 21].

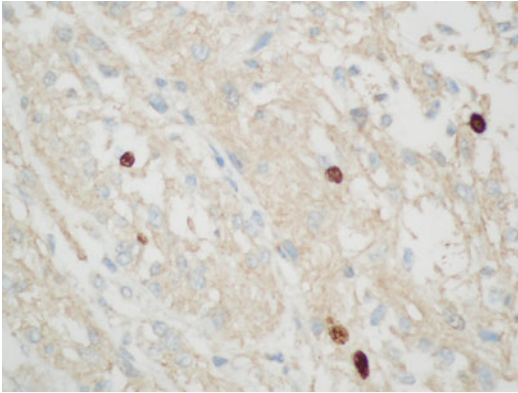


Fig. 35.6 Ki67/MIB-1 is relatively low in WHO grade II astrocytoma

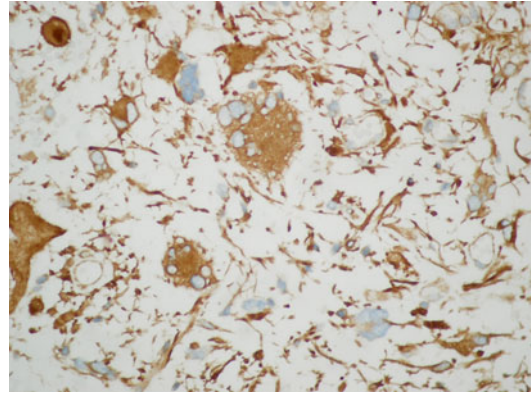


Fig. 35.8 A number of WHO grade II astrocytomas shows EGFR reactivity

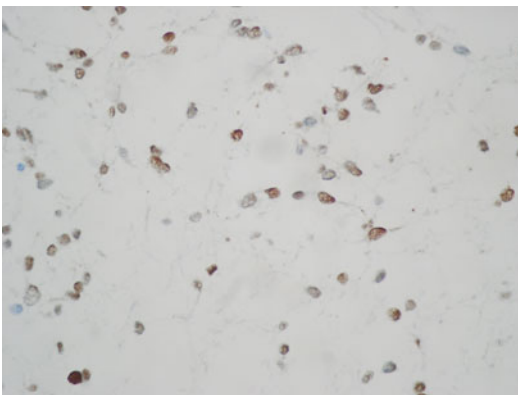


Fig. 35.7 Staining for p53 protein is inconsistent

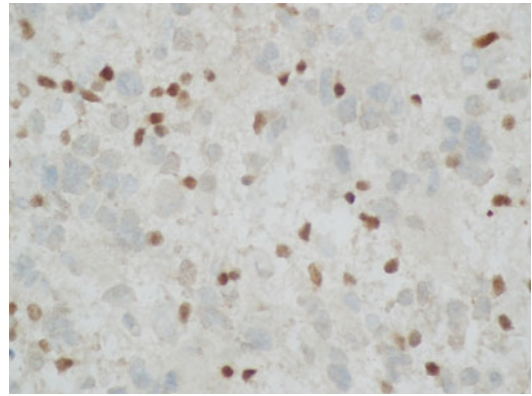


Fig. 35.9 MGMT promoter methylation is detected in this grade II astrocytoma

Genetic abnormalities have been described in less than 100 pediatric patients with diffuse brain stem gliomas in the literature. Half of the patients exhibited TP53 mutations, and in one study, half of the patients with this mutation also exhibited loss of the other p53 allele [5, 15].

Similarly, both p53 gene mutations and increased expression of platelet-derived growth (PDGF) and insulin-like growth factor I (IGF-1) appear to occur early in the tumorigenesis of the diffuse type astrocytomas. Altered growth factor activity occurs in the astrocytic tumors either by changes in ligand or receptor expression, including PDGF, bFGF, TGF α , TGF β , and IGF-1 [17, 20].

Comparative genomic hybridization (CGH) analyses showed a gain of chromosome 7q and

amplification of 8q as the most frequent genomic imbalance. Loss of heterozygosity (LOH) on 22q was found at one or more loci in 27–33 % grade II diffuse astrocytomas. Approximately 50 % of all pediatric patients with diffuse brain stem gliomas in one series demonstrated allelic loss in the long arm of chromosome 10 [18].

In a study EGFR gene amplification was observed in only a minority of low grade II diffuse astrocytomas neoplasms [16] (Fig. 35.8). Approximately one third of low-grade astrocytomas show p14ARF promoter methylation. MGMT promoter methylation was detected in approximately 50 % of low-grade diffuse astrocytomas, and this was significantly associated with TP53 mutations [18–20] (Fig. 35.9).

35.4 Anaplastic Astrocytomas

Anaplastic astrocytomas may occur in neonatal and pediatric groups in brain stem [2, 3, 5]. It is often difficult grossly distinguish between anaplastic and diffuse astrocytoma [17, 21].

Anaplastic astrocytoma is a WHO grade III tumor with which is characterized by its diffusely infiltrating features furnished by distinct nuclear atypia, hypercellularity, and mitotic activity (Fig. 35.10). MIB-1 labeling index is usually in the range of 5–10 % (Fig. 35.11). Multilayered microvascular proliferation and necrosis are absent. Microcysts may be seen in mitotically

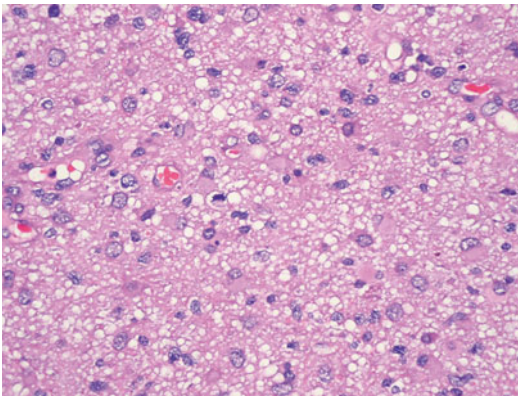


Fig. 35.10 Anaplastic astrocytoma, (WHO grade III), is characterized by distinct nuclear atypia, hypercellularity, and mitotic activity

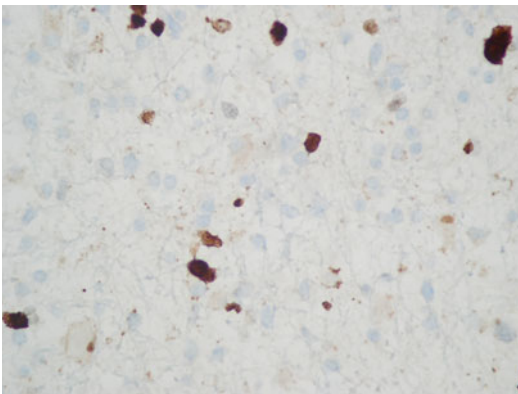


Fig. 35.11 Anaplastic astrocytoma reflects Ki67/MIB-1 index of 10 %

active anaplastic astrocytomas, although they are more common in grade II diffuse astrocytoma. Its immunohistochemical features are similar as those of glioblastoma and grade II diffuse astrocytoma.

Anaplastic progression of astrocytomas WHO grade II to anaplastic astrocytoma WHO grade III is usually accompanied by genetic losses on chromosome 19q, CDK4 overexpression/amplification, Rb gene pathway alterations, LOH on chromosome 13q, and 11p is lost. It has a high frequency of TP53 mutations and LOH 17p (50–60 %), similar to that of diffuse astrocytoma WHO grade II [22]. Approximately 10–17 % of anaplastic astrocytomas have EGFR gene amplification (Fig. 35.12). Approximately 18 % of anaplastic astrocytomas have PTEN point mutations, and these tumors also have a significantly worse prognosis [23].

35.5 Glioblastoma

Glioblastoma is the most malignant neoplasm with predominant astrocytic differentiation that appears to originate either de novo (primary glioblastoma) or in transition from diffuse astrocytoma and anaplastic astrocytoma (secondary glioblastoma). Glioblastoma of the brain stem is often affects neonatal and pediatric groups [1, 2, 5, 19–21]. Secondary type glioblastomas usually present

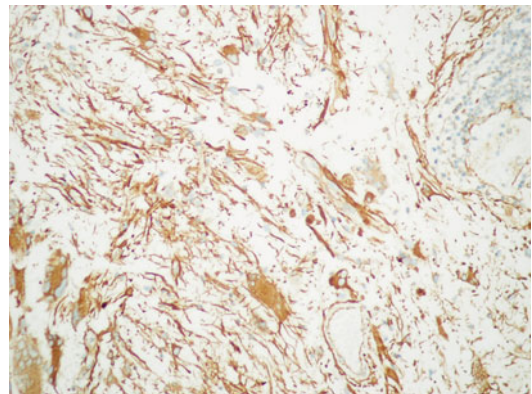


Fig. 35.12 Diffuse and intense reactivity for EGFR is spotted in an anaplastic astrocytoma

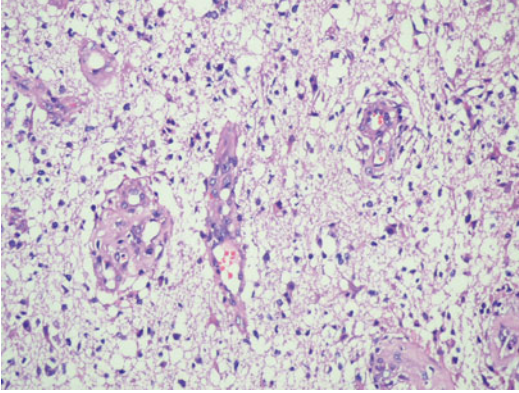


Fig. 35.13 Both necrosis and/or prominent microvascular proliferation are characteristic features of glioblastoma

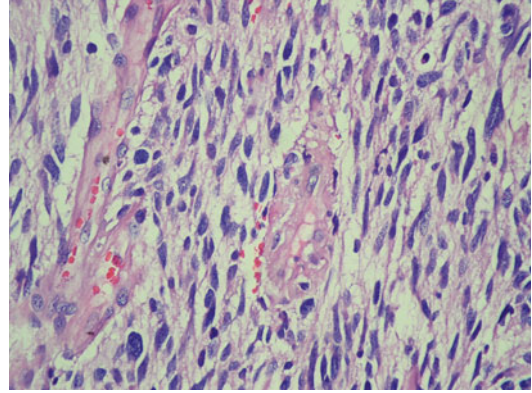


Fig. 35.14 Thrombosed vessels are not uncommon in glioblastoma

in younger patients. Diffuse astrocytomas of the brain stem in children may be of this type [21].

These lesions can be bilaterally symmetrical located in the brain stem. The cut surface of the tumor shows variable color with peripheral grayish tumor masses and central areas of yellowish necrosis. Foci of cyst formation, necrosis, and hemorrhage can be frequently seen in glioblastomas [21].

Microscopically, although some regions of glioblastoma may appear like an astrocytoma or anaplastic astrocytoma, necrosis and/or prominent microvascular proliferation are the key features separating glioblastoma from the other two diffuse astrocytic neoplasms [17] (Fig. 35.13). Thrombi are often found in the aberrant vessels and are responsible for the foci of necrosis (Fig. 35.14). Large, multinucleated tumor cells are often considered a hallmark of about 5 % of glioblastomas. TP53 mutations occur in giant cell variant at a much higher frequency [17, 19] (Fig. 35.15).

Mitotic figures, including atypical forms, are frequent and the MIB-1 proliferative index is usually high. Mean values of 15–20 % have been reported [2, 19].

Most of high-grade astrocytomas (WHO grades II–III) are focally immunoreactive for S-100 protein. GFAP immunoreactivity is variable but is generally positive. Cytokeratin expression is not uncommon in glioblastomas. Immunopositivity is especially likely with antibodies AE1/AE3; CAM5.2 is more likely to be negative [20, 21].

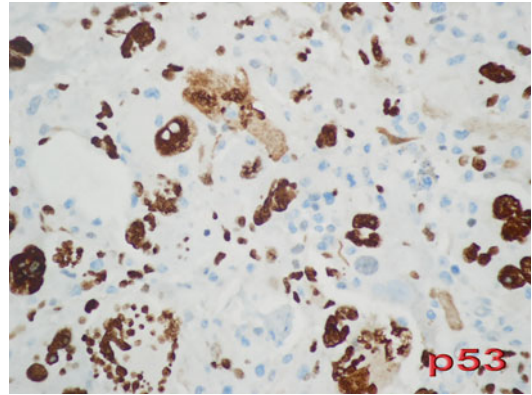


Fig. 35.15 An infrequent feature is high p53 reactivity in giant cell glioblastoma

Most important, p53 point mutations were statistically significantly more common in the anaplastic astrocytomas than in the glioblastomas [23]. In both primary and secondary GBM have the LOH at 10q is the most frequent genetic lesion [17, 19].

Deletions of the p16 (CDKN2a) gene appear in primary glioblastomas (31 %), often in association with EGFR gene amplification which occurs in approximately 40–60 % of tumors [23]. In contrast to adult primary glioblastomas, EGFR amplification is very uncommon in pediatric tumors [17]. However, in another series analyzing 28 brain stem gliomas demonstrated a correlation between WHO tumor grade and EGFR protein expression and all grade IV tumors had EGFR protein [16]. PTEN mutations statistically are significantly more common among younger patients

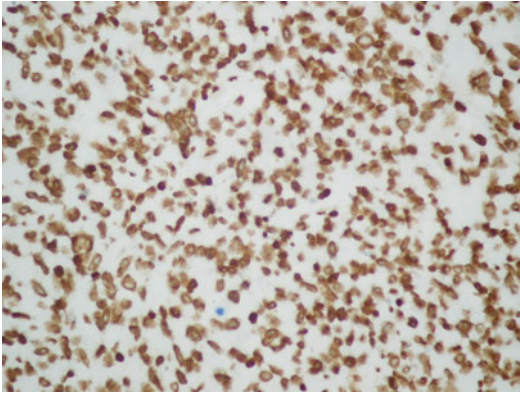


Fig. 35.16 Intense reactivity for PTEN is a common feature of primary glioblastoma

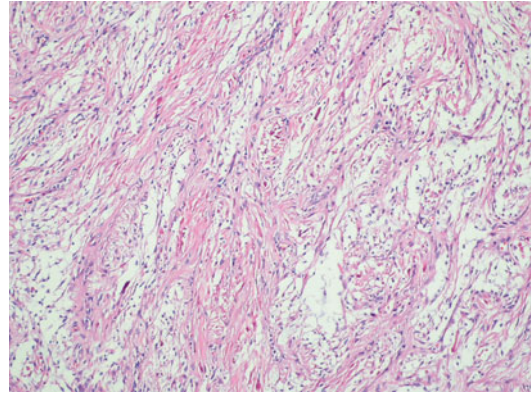


Fig. 35.17 Pilocytic astrocytomas are biphasic tumors composed of a compact and loosely knit microcysts bearing components

with primary glioblastomas [23] (Fig. 35.16). In secondary glioblastomas, deletions of the p16 gene, EGFR amplifications, and PTEN mutations occur with lower frequencies [17].

Increased mRNA expression of the platelet-derived growth factor α (PDGFR α) has been observed in astrocytic tumors of all stages, but gene amplification was only detected in a small subset of glioblastomas [18].

35.6 Pilocytic Astrocytoma

Pilocytic astrocytomas of brain stem are considerably less common than the classic brain stem glioma of the diffuse type. Pilocytic tumors of the brain stem are usually dorsal and exophytic or just into the cerebellopontine angle. Microscopically, pilocytic astrocytomas are usually biphasic tumors. The two components are present to varying degrees. Pilocytic astrocytoma is formed of compact tissue, consisting of elongated and highly fibrillated cells, that alternates with loosely knit spongy tissue in which microcysts are prominent (Fig. 35.17). The compact tissue contains abundant Rosenthal fibers, granular hyaline droplets, and eosinophilic intracytoplasmic bodies. Mitotic rates are usually very low, with MIB-1 labeling indices ranging from 0 to 4%. While many pilocytic are benign, some show considerable hyperchromasia and pleomorphism. Glomeruloid capillary and endothelial

proliferations are common. In small specimens, as those from the brain stem, distinctive architectural feature may not be present.

Immunohistochemical staining for neurofilament protein determines the numbers of axons within the mass, which is generally higher in diffuse astrocytoma. The highly fibrillary, piloid cells are GFAP immunoreactive, while stellate cells of the microcystic areas are only weakly GFAP positive. Vimentin is conspicuously immunopositive in cellular processes [17, 20, 21, 24].

Unlike diffuse astrocytomas, pilocytic astrocytomas have a very low frequency of TP53 mutation. About 15–30% of pilocytic astrocytomas occur in patients with neurofibromatosis 1 (NF1). Approximately 20% of sporadic pilocytic astrocytomas show loss of chromosome 17q but no mutation of the NF1 gene [17, 21].

35.7 Ganglion Cell Tumors

Gangliocytoma and ganglioglioma are well-differentiated neuroepithelial tumors. Ganglion cell tumors are generally circumscribed. They are usually firm and gray and frequently contain calcification and small cysts [17, 25].

Ganglion cell tumors composed of large, mature but dysmorphic, neurons. These tumors are grade I in the WHO classification system, whereas gangliogliomas with anaplastic glial

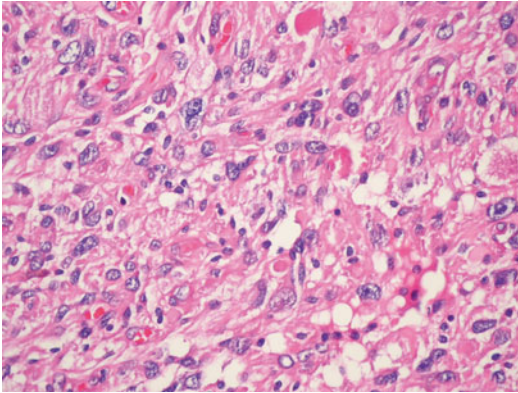


Fig. 35.18 Gangliogliomas are mainly consisted of an admixture of neuronal and glial components and decorated focal collections of hyaline protein droplets, or eosinophilic granular bodies

component are grade III. The glial component in gangliogliomas may include cell types resembling fibrillary astrocytoma, oligodendroglioma, or pilocytic astrocytoma. Diagnostically important features of ganglion cell tumors, both are focal collections of hyaline protein droplets or eosinophilic granular bodies (Fig. 35.18). Ganglion cell tumors may contain aggregates of lymphoid cells along perivascular spaces or within tumor/brain parenchyma. Mitotic figures are rare. MIB-1 labeling involves only the glial component, mean values ranging from 1.1 to 2.7 % [21, 25].

Immunohistochemically, neurofilaments, synaptophysin, NeuN, and MAP2 are useful to demonstrate the neural component in gangliogliomas. There is no specific marker available to differentiate dysplastic neurons from normal counterparts. Strong surface staining for synaptophysin is normal in certain large neurons, as in brain stem. Immunoreactivity of ganglion cells for CD34 is common. CD34 is not present in neural cells of the adult brain. Astrocytes in ganglion cell tumors are reactive for both S-100 protein and GFAP [21, 25].

Chromosomal abnormalities were recorded in one third. Gain of chromosome 7 has been the most recurrent alteration. However, TP53 mutation, PTEN mutation, and CDK4 and EGFR amplification have not been not detected [25].

References

1. Abbott R, Goh KYC (1999) Brainstem gliomas. In: Albright AL, Pollack IF, Adelson PD (eds) Principles and practice of pediatric neurosurgery. Thieme, New York, pp 629–633
2. Yoshimura J, Onda K, Tanaka R et al (2003) Clinicopathological study of diffuse type brainstem gliomas: analysis of 40 autopsy cases. *Neurol Med Chir (Tokyo)* 43:375–382
3. Hong S, Kim H II, Wang KC (2005) Outcome and prognostic factors of childhood diffuse brain-stem glioma. *Cancer Res Treat* 37:109–113
4. Roonprapunt C, Abbott (2002) Surgical treatment of brainstem gliomas in children. *Neurosurg Q* 12:160–170
5. Broniscer A, Gajjar A (2004) Supratentorial high-grade astrocytoma and diffuse brainstem glioma: two challenges for the pediatric oncologist. *Oncologist* 9:197–206
6. Koral K, Kedzierski GB, Gomez A, Rollins NK (2008) Subependymoma of the cerebellopontine angle and prepontine cistern in a 15-year-old adolescent boy. *AJNR Am J Neuroradiol* 29:190–191
7. Cohen BH, Nicholson CL (2005) Brainstem gliomas. In: Schiff D, O'Neill BP (eds) Principles of neuro-oncology. McGraw-Hill, New York, pp 333–341
8. Ebstein F, McCleary EL (1986) Intrinsic brain-stem tumors in childhood: surgical indications. *J Neurosurg* 64:11–15
9. Abbott R (2001) Brain stem gliomas. In: McLone DG (ed) Pediatric neurosurgery, surgery of the developing nervous system. W.B. Saunders, Philadelphia, pp 859–867
10. Fisher PG, Breiter SN, Carson BS et al (2000) A clinicopathologic reappraisal of brain stem tumor classification. Identification of pilocytic astrocytoma and fibrillary astrocytoma a distinct entities. *Cancer* 89:1569–1576
11. Ebstein F, Wisoff J (1988) Intrinsic brainstem tumors in childhood: surgical indications. *J Neurooncol* 6: 309–317
12. Nishio S, Fukui M, Tateishi J (1988) Brain stem gliomas: a clinicopathological analysis of 23 histologically proven cases. *J Neurooncol* 6:245–250
13. Albright A (1996) Brain stem gliomas. In: Youmans J (ed) Neurological surgery, vol 4. WB Saunders, Philadelphia, pp 2603–2611
14. Fischbein N, Prados M, Wara W et al (1996) Radiologic classification of brain stem tumors: correlation of magnetic resonance imaging appearance with clinical outcome. *Pediatr Neurosurg* 24:9–23
15. Louis DN, Rubio MP, Correa KM et al (1993) Molecular genetics of pediatric brain stem gliomas. Application of PCR techniques to small and archival brain tumor specimens. *J Neuropathol Exp Neurol* 52:507–515

16. Gilbertson RJ, Hill DA, Hernan R et al (2003) ERBB1 is amplified and over expressed in high –grade diffusely infiltrative pediatric brain stem glioma. *Clin Cancer Res* 9:362–3624
17. Ellison D, Love S, Chimelli L, Harding BN, Lowe J, Vinters HV (eds) (2004) *Neuropathology a reference text of CNS pathology*. Mosby, Edinburg
18. von Deimling A, Burger PC, Nakazato Y et al (2007) Diffuse astrocytoma. In: Louis DN, Ohgaki H, Wiestler OD, Cavenee WK (eds) *WHO classification of tumours of the central nervous system*. IARC Press, Lyon, pp 25–29
19. Kleihues P, Burger PC, Aldape KD et al (2007) Glioblastoma. In: Louis DN, Ohgaki H, Wiestler OD, Cavenee WK (eds) *WHO classification of tumours of the central nervous system*. IARC Press, Lyon, pp 33–49
20. Lopes MBS, VanderBerg SR (2007) Tumors of the central nervous system. In: Fletcher CDM (ed) *Diagnostic histopathology of tumors, vol 2*. Elsevier, China, pp 1653–1670
21. Burger PC, Scheithauer BW (eds) (2007) *Tumors of the central nervous system*. American Registry of Pathology, Washington, DC
22. Kitange GJ, Templeton KL, Jenkins RB (2003) Recent advances in the molecular genetics of primary gliomas. *Curr Opin Oncol* 15:197–203
23. Smith JS, Tachibana I, Passe SM et al (2001) PTEN mutation, EGFR amplification, and outcome in patients with anaplastic astrocytoma and glioblastoma multiforme. *J Natl Cancer Inst* 93:1246–1256
24. Scheithauer BW, Hawkins C, Tihan T et al (2007) Pilocytic astrocytoma. In: Louis DN, Ohgaki H, Wiestler OD, Cavenee WK (eds) *WHO classification of tumours of the central nervous system*. IARC Press, Lyon, pp 14–20
25. Becker AJ, Wiestler OD, Figarella-Branger D et al (2007) Ganglioglioma and gangliocytoma. In: Louis DN, Ohgaki H, Wiestler OD, Cavenee WK (eds) *WHO classification of tumours of the central nervous system*. IARC Press, Lyon, pp 103–105

Hale Başak Caglar

The brainstem is the connecting structure that joins the long tract from the cerebral hemispheres and midline diencephalic nuclei with the cerebellar tracts, forming the spinal cord as the tracts exit through the foramen magnum. Within the brainstem are the nuclei of the cranial nerves, the reticular activating system, and vital function centers (e.g., respiratory). The brainstem includes three anatomic segments: the midbrain, the pons, and the medulla.

Brainstem gliomas account for approximately 20 % of all central nervous system tumors among children younger than age 15. The peak incidence occurs between ages of 5 and 9 years.

They are a heterogeneous group of tumors that share common astrocytic histologies but evidence divergent clinical behavior related to the anatomic region of involvement and the pattern of growth. Historically tumors arising in this location were regarded as single entity and treated without histologic confirmation of diagnosis. As a result of the advances in neuroimaging and particularly with the advent of MRI, it has become clear that tumors in the brainstem are of several distinct types that can be identified by their apparent anatomic segment of origin and the macroscopic appearance as diffuse or focal lesions. The ones so-called the more favorable group are low-grade focal, dorsal

exophytic, and cervicomedullary tumors and the more aggressive group are diffuse intrinsic tumors. Focal lesions are tumors that are limited in size (typically defined as involving less than 50 % of the anatomic structure of origin or less than 2 cm in maximal diameter), well circumscribed on imaging (with no evidence of infiltration or edema beyond the primary lesion), and often showing juvenile pilocytic histology if biopsied and have a good prognosis. They may be cystic, and as with cystic tumors at other sites, they may be large relative to the solid and biologically active component. Focal tumors may occur at any level in the brainstem but are most frequently seen in midbrain and medulla (Fig. 36.1). This tumor type represents 15–20 % of brainstem lesions. They usually present with a long history of localizing findings such as an isolated cranial nerve deficit and a contralateral hemiparesis. Signs and symptoms of raised intracranial pressure are uncommon except in patients with tumors arising in the tectal region that may cause aqueduct stenosis while still small. In most of the cases, the tumor enhances with gadolinium on MRI.

Over the same period improvements in neurosurgical techniques and perioperative care have made surgery feasible for all except diffuse intrinsic tumors [1].

The classically quoted incidence of brainstem tumors in children identifies 70–80 % as diffusely infiltrating lesions (primarily arising in the pons) with the remainder identified as one

H.B. Caglar, M.D.
Medipol University, Istanbul, Turkey
e-mail: halebasakcaglar@gmail.com



Fig. 36.1 Focal brainstem glioma, sagittal T1 image

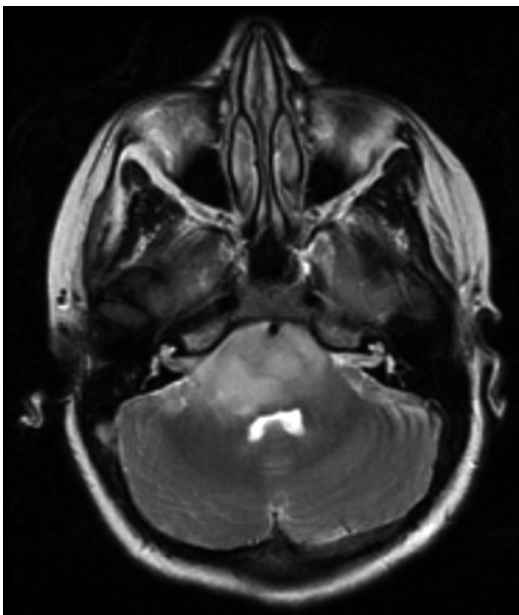


Fig. 36.2 Diffuse pontine glioma, axial T2 image

of the focal or benign tumor types. They arise in the pons and cause diffuse enlargement of the brainstem (Fig. 36.2). Extension to the midbrain and medulla and/or exophytic growth is seen in at least two thirds of cases. The histologies are usually fibrillary astrocytomas with a potential for malignant change and have a very poor prognosis. The most common presenting symptoms for the diffusely infiltrating pontine gliomas include diplopia, motor weakness, and difficulty with

speech, swallowing, and walking. Neurologic signs include ataxia, cranial nerve palsies (most commonly pontine nerves followed by the medullary nerves), and long tract signs. Only 10 % of the lesions have hydrocephalus at diagnosis. Tumors of the midbrain and medulla may be diffuse or focal, even diffuse tumors show much less infiltration and expansion of the brainstem than seen with the pontine gliomas.

The duration of symptoms correlates with the type of brainstem glioma. Children with diffusely infiltrating pontine gliomas have a brief history of neurologic symptoms almost appears in weeks and usually less than 6 months. The more focal, less aggressive brainstem tumors are often associated with prolonged symptoms, typically confined to deficits in one or two cranial nerves alone unlike diffusely infiltrating tumors.

MRI is the definitive test for diagnosis and delineation of tumor extent and type. The typical diffusely infiltrating pontine glioma is homogeneous or hypodense on T1 imaging. The tumor expands the pons and infiltrates into other brainstem segments. They are best seen on T2 weighted or FLAIR MRI which should be the imaging modality of choice. There is often little or no enhancement, but inhomogeneous areas of enhancement can be noted [2]. The presence of a ring enhancement is suggestive of high-grade histology. Biopsy of the classic, diffusely infiltrating pontine glioma is generally unnecessary, and there is no clear benefit derived from biopsy when the imaging and clinical picture show a typical diffusely infiltrating tumor. Histological series show equal proportions of low and high grade [3]. There is no consistent correlation between histology and outcome; generally all diffusely infiltrating pontine tumors show poor duration of response to irradiation, and median survival is less than 1 year [4–9]. It is of interest that most such tumors show malignant astrocytoma at autopsy even the ones showing low-grade histology at initial diagnosis.

Brainstem tumors have recently been shown to express ERBB1 with the degree of overexpression is proportional with increasing g grade [10]. These findings suggest that EGFR inhibitors can be worth studying in these kinds of tumors in

conjunction with radiation. One of the studies ongoing among the Pediatric Tumor Consortium examines gefitinib and radiation in pediatric patients newly diagnosed with brainstem tumors in a phase I/II manner.

The management of pediatric brainstem gliomas basically depends on the location of the tumor and the specific imaging characteristics of the tumor. Patients with nonenhancing focal tumors in the tectal region who present with only hydrocephalus may do well without any treatment other than CSF diversion. Active intervention including biopsy is reserved for clinical and radiologic progression. Surgery is the treatment of choice for focal tumors at other locations that are surgically accessible (either they extend toward the surface of the brainstem laterally or at the floor of the fourth ventricle) and have imaging characteristics of low-grade histology (uniform bright enhancement with contrast material which correlated with pilocytic histology, the absence of peritumoral hypodensity) as mentioned above. Similar to completely or subtotally resected low-grade gliomas at other sites results can be excellent in a high percentage [3, 11]. Results are less satisfactory for patients with bulky tumors and for patients in the medulla with lower cranial nerve deficits because of high risk of postoperative complication in these cases. For surgically inaccessible focal lesions, conventional radiotherapy should be the standard of care. Looking at the treatment results of the series using conventional radiotherapy in the brainstem tumors, it is reasonable to assume that 50–70 % of focal lesions may be permanently controlled with such treatment [2–4, 9, 12]. Dorsal exophytic lesions are treated with surgery, and ultrasound guidance is used to achieve maximal tumor resection during the procedure. However, as there is no definite interface between tumor and brainstem in most of the cases, there are usually a thin layer of residual tumor cells after the surgery on the floor of the fourth ventricle. Nonetheless there is no standard postoperative radiation therapy for these kinds of tumors as the majority of the children do well following surgery. Radiotherapy should be considered for patients that found to have high-grade lesions

or for patients that have low-grade tumors who are found to have progressive disease in the first 1–9 months after the surgery. For patients that recur after this period re-surgery, further surgery should be considered and radiation should be reserved for those who have inoperable disease. According to the literature, the salvage is possible with excellent overall prognosis, especially for dorsal exophytic lesions [11, 13, 14].

Cervicomedullary lesions arise in the upper cervical cord and grow rostrally beyond the foramen magnum, and they are usually low-grade lesions whose axial growth is limited by the pyramidal decussations located at the junction of cervical cord and medulla. The tumor grows posteriorly causing a bulge in the dorsal of medulla toward the fourth ventricle. Surgery is the treatment of choice in these tumors with a gross total resection achieved in 75 % of the cases and subtotal resection in the remaining 25 %. For the typical low-grade lesions, outcomes after surgery are excellent. There is no routine indication for postoperative radiotherapy for these kinds of lesions. Radiation is reserved for surgically inaccessible lesions and high-grade tumors.

Surgery has no role in the management of diffuse intrinsic lesions. Even biopsy is no longer considered as necessary in the context of a typical clinical presentation with the characteristic MRI findings; histology does not affect the outcome of these patients and does not influence the treatment [15, 16]. In conventional radiation, the majority of the patients (75 % and over) with diffuse intrinsic tumors improve clinically. The improvements in signs and symptoms begin after several weeks during and after irradiation. Improvement in MRI has been reported in 30–70 % of children. However, the progression-free interval is short with a median of less than 6 months, and survival is poor with median survival less than 1 year and survival rates at 2 years is less than 20 % [3–5, 7, 12, 17]. Intrinsic focal pontine lesions often must be irradiated at diagnosis because of the neurological signs. With the availability of the precision volume techniques, the risk benefit ratio may favor early intervention in these lesions.

36.1 Technology of Radiotherapeutic Management

36.1.1 3D Conformal Radiotherapy

Powerful x-ray CT simulation and three-dimensional treatment planning systems (3DTPS) have been commercially available since the early 1990s, and three-dimensional conformal radiation therapy (3DCRT) is now firmly in place as the standard of practice. In addition, advances in radiation treatment-delivery technology continue, and medical linear accelerators now come equipped with sophisticated computer-controlled multileaf collimator systems (MLCs) and integrated volumetric imaging systems that provide beam aperture and/or beam-intensity modulation capabilities that allow precise shaping and positioning of the patient's dose distributions. Conformal treatment plans generally use an increased number of radiation beams that are shaped to conform to the target volume (Figs. 36.3, 36.4, and 36.5). Forward-based 3D planning for conformal therapy typically involves a series of procedures summarized below:

- Step 1: Patient positioning and immobilization
- Step 2: Image acquisition and input (CT, MRI, or other imaging data)
- Step 3: Anatomy definition (contours for organs at risk, target volumes)
- Step 4: Dose prescription (for planning target volume and organs at risk)
- Step 5: Beam technique (beam arrangements, field shape, beam modifiers, beam weighting)
- Step 6: Dose calculations
- Step 7: Plan evaluation/improvement (two- and three-dimensional displays, dose volume histograms, and isodose curves)
- Step 8: Plan review and documentation
- Step 9: Plan implementation and verification

36.1.2 Intensity-Modulated Radiation Therapy

Since its introduction into clinical use, intensity-modulated radiation therapy has generated widespread interest. IMRT optimally assigns nonuniform intensities to tiny subdivisions of beams, which have been called rays

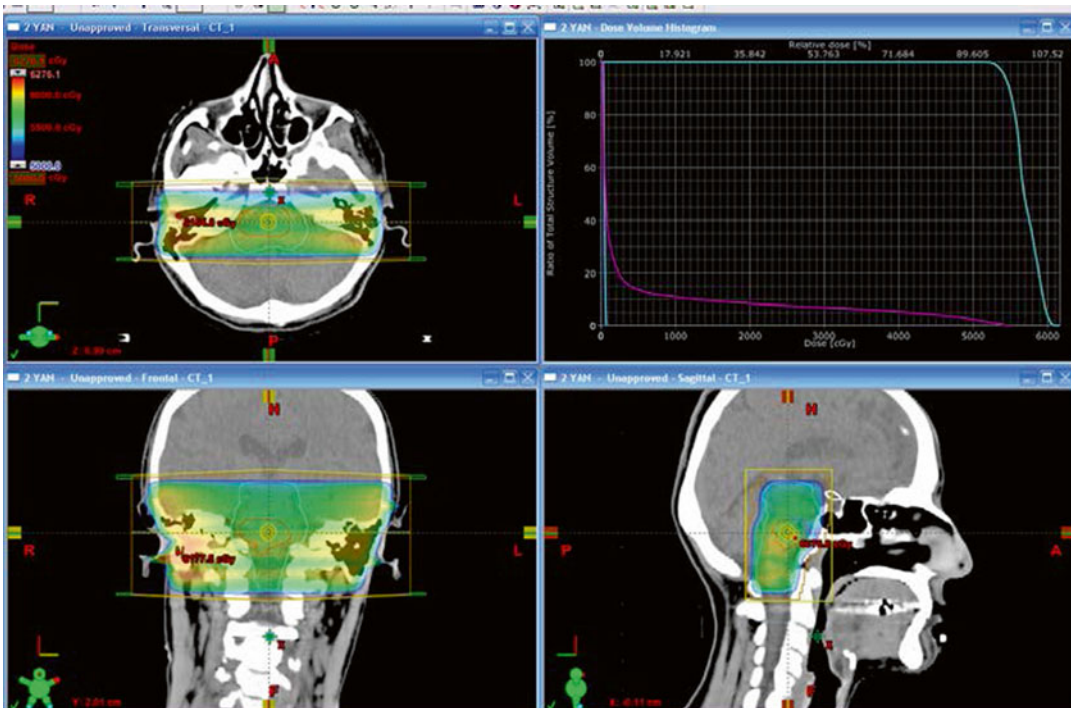


Fig. 36.3 3D conformal radiotherapy with two-field technique

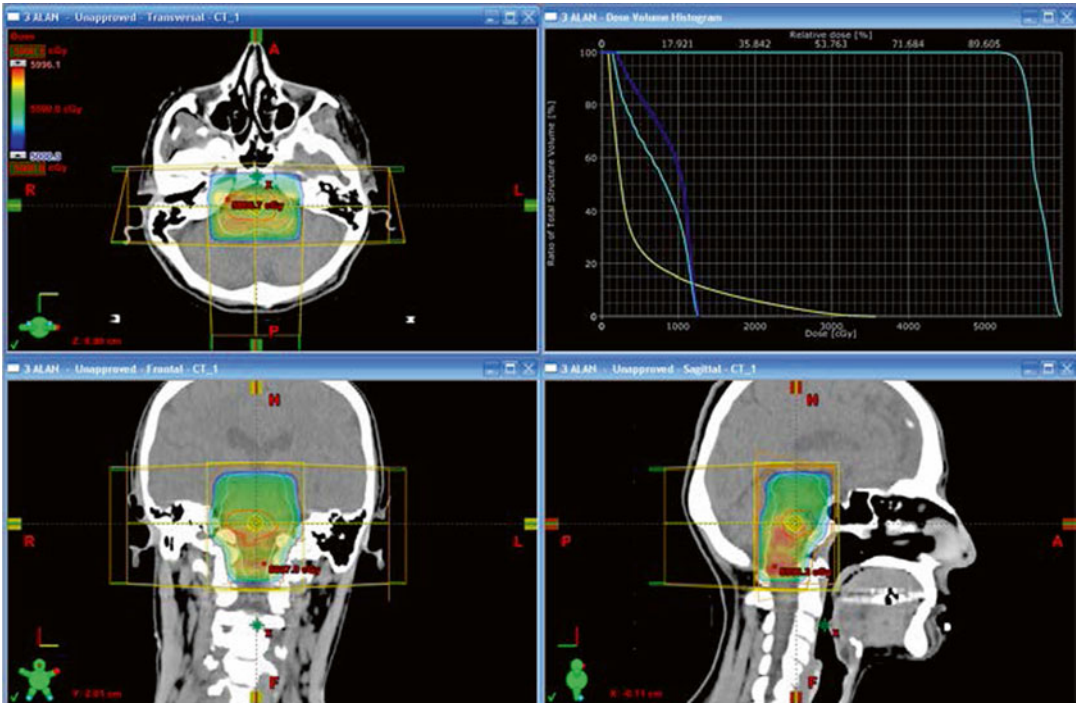


Fig. 36.4 3D conformal radiotherapy with three-field technique

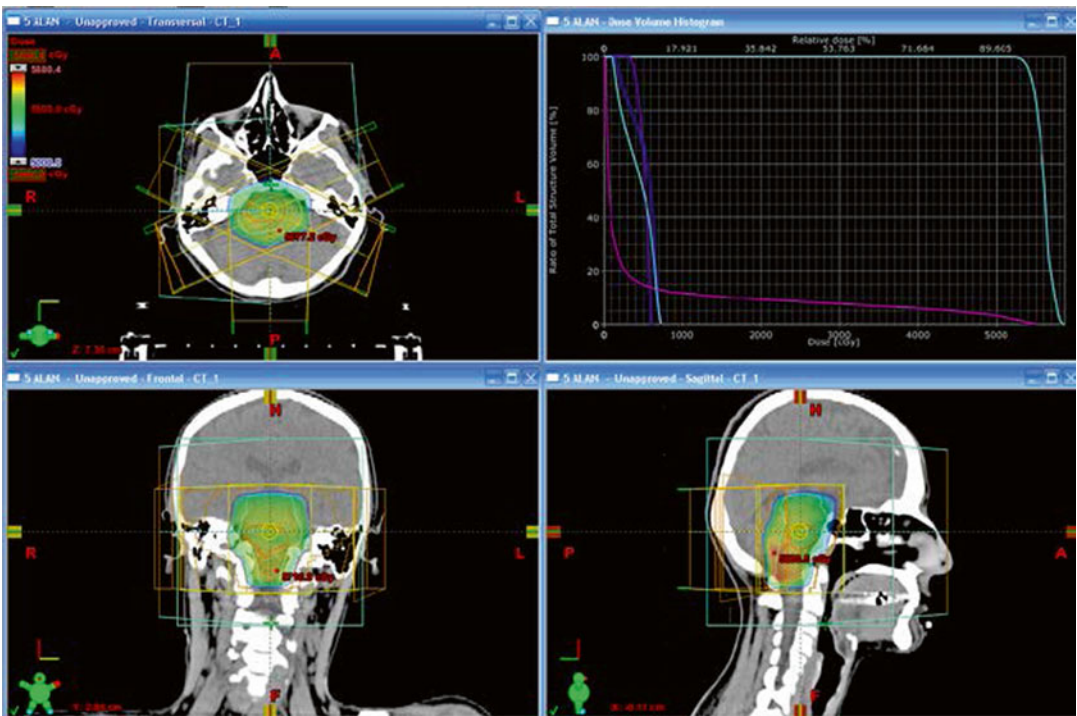


Fig. 36.5 3D conformal radiotherapy with five-field technique

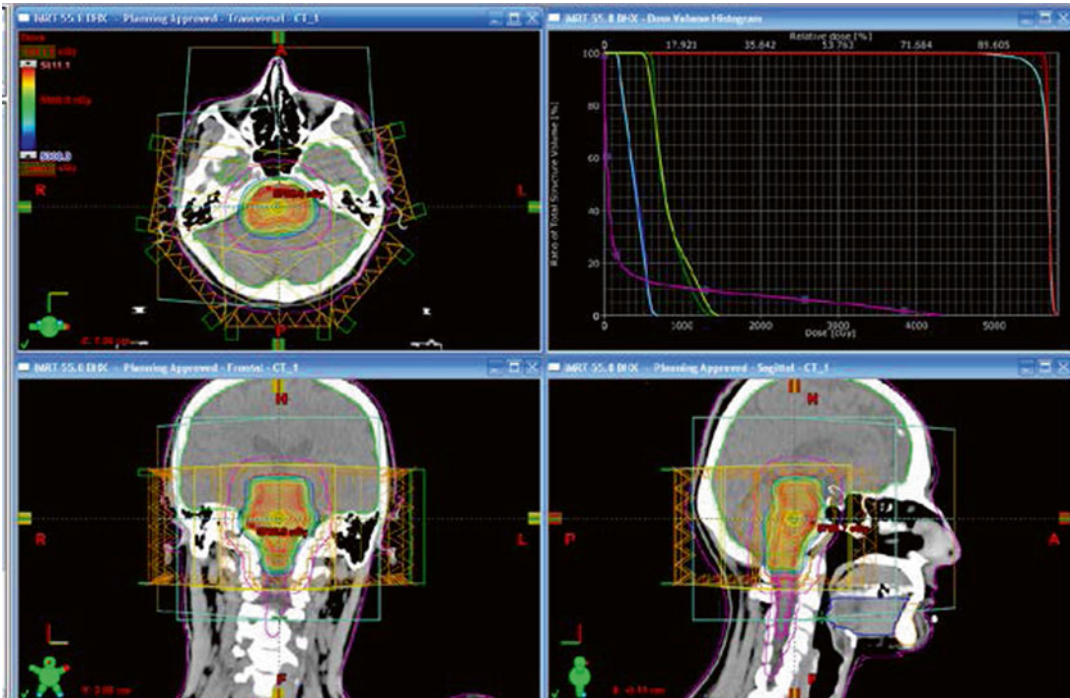


Fig. 36.6 Intensity-modulated radiation therapy technique

or beamlets. The improved dose distributions potentially may lead to improved tumor control and reduced normal tissue toxicity (Fig. 36.6). IMRT requires the settings of the relative intensities of tens of thousands of rays comprising an intensity-modulated treatment plan. This task cannot be accomplished manually and requires the use of specialized computer-aided optimization methods. IMRT dose distributions can be created to conform much more closely to the target volume, particularly for those volumes having complex/concave shapes, and shaped to avoid critical normal tissues in the irradiated volume. This increased conformality results in IMRT treatments being much more sensitive to geometric uncertainties than the two-dimensional or 3DCRT approaches and has spurred the development of treatment machines integrated with advanced volumetric imaging capabilities, which is again pushing the edge of our frontiers in conformal therapy practice from IMRT to what is now referred to as image-guided IMRT or simply image-guided radiation therapy (IGRT). It should be

understood that most of concepts and tasks discussed apply equally well as in 3DCRT to IMRT and IGRT, particularly with regard to target volume definition.

36.1.3 Stereotactic Radiosurgery and Radiotherapy

Stereotactic radiosurgery and radiotherapy are techniques to administer precisely directed, high-dose irradiation that tightly conforms to an intracranial target to create a desired radiobiologic response while minimizing radiation dose to surrounding normal tissue. These techniques exploit the fact that the radiation tolerance of normal tissue is volume-dependent. With these techniques, the complication risks for any radiation dose delivered are reduced by minimizing or eliminating the margin of normal tissue otherwise included in the radiation treatment volume with conventional radiotherapy techniques. In the case of radiosurgery, all of the irradiation is done in a single session or fraction, while in stereotactic

radiotherapy (SRT), more than one fraction of irradiation is administered. The key requirements for stereotactic treatments should be:

1. Small target/treatment volume: Reduction of the volume of normal and target tissue irradiated to high doses improves tolerance.
2. Sharply defined target: Can be treated with little or no extra margin of surrounding normal tissue and/or without unintentional under dosage of the target (marginal miss).
3. Accurate radiation delivery: No margin of normal tissue is needed for setup error and/or reduced chance of underdosing target.
4. High conformality: Reduces the treatment volume to match the target volume.
5. Sensitive structures excluded from target: Dose-limiting structures (optic chiasm, spinal cord) should be able to be defined and excluded from the target volume to limit the risk of radiation injury.

Advances in imaging, computers, and treatment planning in the last two decades have led to the development of a variety of different stereotactic radiosurgery/radiotherapy techniques and their wider applications. Successful clinical experience with intracranial radiosurgery for a variety of applications has led to a reexamination of radiobiology and exploration of both fractionated approaches and extracranial applications. Margin reduction with radiosurgery and fractionated stereotactic irradiation techniques makes target definition accuracy more critical.

36.1.4 Volumetric Arc Therapy

Improvements in patient care achieved through image-guided positioning and plan adaptation have resulted in an increase in overall treatment times. IMRT has also increased treatment time by requiring a larger number of beam directions, increased monitor units (MU), and, in the case of tomotherapy, a slice-by-slice delivery. The solution in volumetric arc therapy is a novel aperture-based algorithm for treatment plan optimization where dose is delivered during a single gantry arc of up to 360°. The technique is similar to tomotherapy in that a full 360° of beam directions is

available for optimization but is fundamentally different in that the entire dose volume is delivered in a single source rotation. The new technique is referred to as volumetric-modulated arc therapy (VMAT). Multileaf collimator (MLC) leaf motion and number of MU per degree of gantry rotation is restricted during the optimization so that gantry rotation speed, leaf translation speed, and dose rate maxima do not excessively limit the delivery efficiency. During planning, investigators model continuous gantry motion by a coarse sampling of static gantry positions and fluence maps or MLC aperture shapes. The technique is unique in that gantry and MLC position sampling is progressively increased throughout the optimization. Using the full gantry range will theoretically provide increased flexibility in generating highly conformal treatment plans (Fig. 36.7). In practice, the additional flexibility is somewhat negated by the additional constraints placed on the amount of MLC leaf motion between gantry samples. A series of studies are performed that characterize the relationship between gantry and MLC sampling, dose modeling accuracy, and optimization time. The competing benefits of having small and large sample spacing are mutually realized using the progressive sampling technique described here. Preliminary results show that plans generated with VMAT optimization exhibit dose distributions equivalent or superior to static gantry IMRT. Timing studies have shown that the VMAT technique is well suited for online verification and adaptation with delivery times that are reduced to approximately 1.5–3 min for a 200 cGy fraction.

36.2 Treatment Volume

36.2.1 Definitions of Tumor and Target Volumes

The International Commission on Radiation Units and Measurements (ICRU) first addressed the issue of consistent volume and dose specification in radiation therapy with the publication of ICRU Report 29 in 1978 [18]. In retrospect, ICRU Report 29 recommendations were well

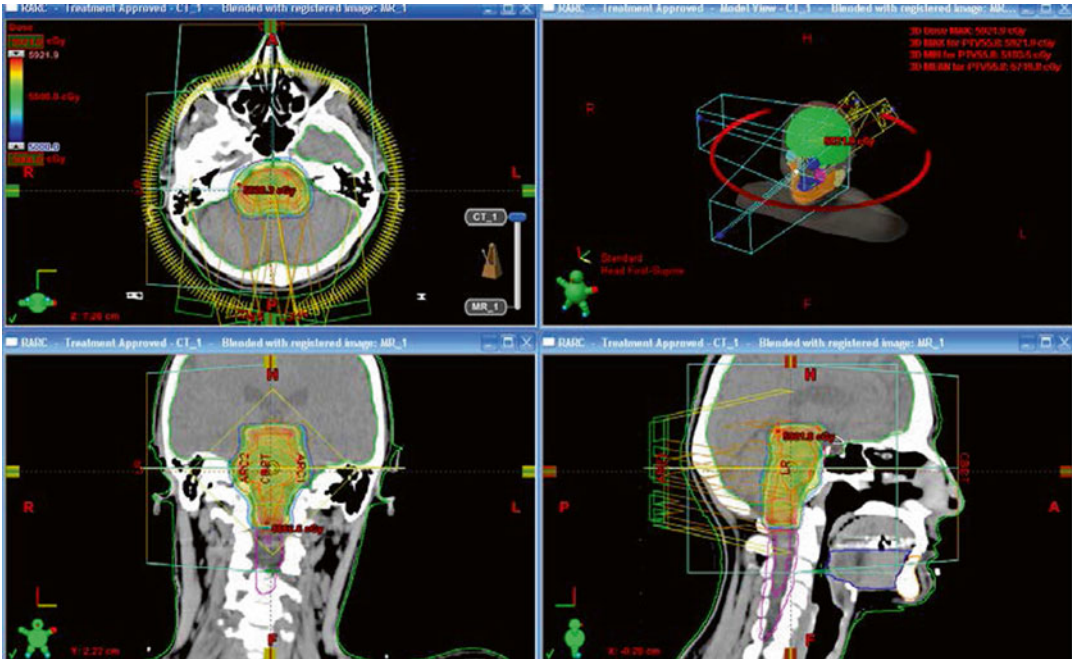


Fig. 36.7 Volumetric arc radiation therapy technique

suites for the technology of the 1970s and 1980s, that is, using a conventional simulator to generate a planning radiograph for designing beam portals based on bony and soft tissue landmarks for standardized beam arrangement techniques applied to whole classes of comparable patients.

In 1993, the ICRU updated its recommendations for specifying dose/volume in Report 50 and were well suited for conformal therapy [19]. The target volume definition was separated into three distinct volumes: (a) visible tumor, that is, gross tumor volume (GTV); (b) a volume to account for uncertainties in microscopic tumor spread, that is, clinical target volume (CTV); and [3] a volume to account for geometric and other uncertainties, that is, planning target volume (PTV) as illustrated in Fig. 36.8.

The GTV and CTV are anatomic-clinical concepts that should be defined before a choice of treatment modality and technique is made. Labels or subscripts with the GTV nomenclature can be used to distinguish between primary disease and other areas of macroscopic tumor involvement. Note that even if the GTV has been removed by radical surgery, the volume can be designated

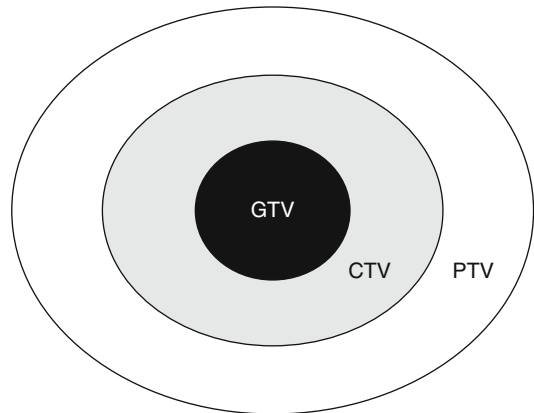


Fig. 36.8 ICRU definitions for target volumes

as CTV. In specifying the CTV, the physician must not only consider microextensions of the disease near the GTV but also the natural avenues of spread for the particular disease and site. The PTV is defined by specifying the margins that must be added around the CTV to manage the effects of organ, tumor and patient movements, inaccuracies in beam and patient setup, and any other uncertainties. The PTV is a static,

geometrical concept used for treatment planning and for specification of dose. Its size and shape depend primarily on that of the GTV/CTV, and the effects caused by internal motions of organs and the tumor, technical aspects of treatment technique (e.g., patient fixation). The PTV can be considered a 3D envelope in which the tumor and any microscopic extensions reside and move within this envelope. Once the PTV is defined, appropriate beam sizes to account for penumbra and beam arrangements must be selected to ensure the desired dose coverage of the PTV.

Report 50 refined the definition of organs at risk as normal tissues whose radiation sensitivity may significantly influence treatment planning and/or prescribed dose. The report did state that any possible movement of the organ at risk during treatment, as well as uncertainties in the setup during the whole treatment course, must be considered, but did not provide a method to do so. The hot spot definition was modified to be a volume outside the PTV that received a dose larger than 100 % of the specified PTV dose. This was considered clinically meaningful only if the minimum diameter exceeded 15 mm.

Report 50 was well suited to conformal therapy; however, its use raised new questions and prompted numerous publications [20, 21]. Also, as previously pointed out, irradiation techniques continued to evolve (e.g., IMRT), and advances in imaging procedures (e.g., PET, MRI) provided even more information on functionality; the location, shape, and limits of tumor/target volumes; and organs at risk. In response to these developments, the ICRU in 1999 published Report 62 [22], which expanded on some of the definitions and concepts of Report 50 and took into account the consequences of the technical and clinical progress, referred to previously. ICRU Report 62 refined the definition of PTV by introducing the concept of an internal margin to take into account variations in size, shape, and position of the CTV in reference to the patient's coordinate system using anatomic reference points and also the concept of a setup margin to take into account all uncertainties in patient-beam positioning in reference to the treatment machine coordinate system. Setup margin uncertainties are related

largely to technical factors that can be dealt with by more accurate setup and immobilization of the patient and improved mechanical stability of the machine. ICRU Report 62 refined the definition of the two dose volumes defined ICRU Report 50 as follows: The treated volume is the tissue volume that (according to the approved treatment plan) is planned to receive at least a dose selected and specified by radiation oncology team as being appropriate to achieve the purpose of the treatment, e.g., tumor eradication or palliation, within the bounds of acceptable complications. The irradiated volume is the tissue volume that receives a dose that is considered significant in relation to normal tissue tolerance.

Report 62 refined the definition of organs at risk as normal tissues (e.g., spinal cord) whose radiation sensitivity may significantly influence treatment planning and/or prescribed dose. Report 62 also addressed what was perhaps the most criticized limitation of Report 50, which was that it did not provide a method to account for organ at risk movements and changes in shape and/or size, as well as setup uncertainties. To account for such spatial uncertainties, Report 62 introduced the concept of the planning organ at risk volume (PRV), in which a margin is added around the organ at risk to compensate for that organ's geometric uncertainties. The PRV margin around the organ at risk is analogous to the PTV margin around the CTV. The introduction of the PRV concept is timely as its use is even more important for those conformal therapy cases involving IMRT because of the increased sensitivity of this type treatment to geometric uncertainties.

36.2.2 Treatment Volume for Brainstem Gliomas

MRI and autopsy studies document contiguous extension of pontine gliomas linearly through the adjacent medulla or midbrain and axially into the brachium pontis, the cerebellopontine angle, and adjacent structures of the cerebellar hemispheres [2, 23]. Leptomeningeal involvement has been noted in up to 15 % of children with diffusely

infiltrating pontine lesions mostly involving the subarachnoid space at the level of the brainstem, the basal cistern, or the upper cervical cord. Spinal canal involvement has also been documented [4, 24, 25]. Only a small proportion of focal, low-grade lesions are associated with neuroaxis dissemination mostly noted at diagnosis [26]. The most common pattern of failure is locally. Local irradiation is indicated with target volumes subtending both the pons and the adjacent regions both linearly (the adjacent midbrain and medulla) and axially (the adjacent anterior cerebellum).

Volume definition for the treatment should rely on the MRI of the patient performed before or during the treatment planning. Although the calculations are performed with CT images, for the effective volume determination, image fusion with MRI is usually the preferred method for planning.

Diffusely infiltrating pontine gliomas often are incompletely or nonenhancing lesion, so the greatest tumor extent on T1 or T2 images should define the GTV. For infiltrating tumors of the midbrain and medulla, margins of 1–2 cm beyond the lesion are appropriate.

Focal lesions of the tectum can be treated with limited target volumes; treatment of discrete lesions generally entails treating only the identifiable tumor with a 1 cm or less CTV for the enhancing lesions on T1-weighted images and/or hyperintense area on the T2-weighted images [4]. Fractionated stereotactic radiosurgery has been used for these tumor types [27], and more recent experience favors 3DCRT or IMRT in this setting.

For dorsally exophytic tumors, the volume can conform to the disease process based on MRI; the anterior margin at the brainstem should encompass at least 5 mm of apparently normal brainstem ventral to the tumor as documented on MRI. 3DCRT or IMRT can spare radiation dosage to temporal lobes especially for the young age population where long life expectancy takes place.

36.3 Dosage

Currently, the standard radiation treatment for brainstem tumors consists of 54 Gy given in 30 daily fractions over 6 weeks to the GTV

as demonstrated by enhancing tumor on T1-weighted images or hyperintense volume on T2-weighted or FLAIR MRI with a margin for the CTV of 1–1.5 cm.

A lot of trials evaluated the impact of high dose, hyperfractionated irradiation for brainstem gliomas. Despite dose escalation from 66 to 70–72 to 75.6–78 Gy using twice-daily fractions of 100–126 cGy, no durable improvement was documented in disease control or survival. Outcome after conventionally fractionated irradiation to 54 Gy or hyperfractionated irradiation to 70–78 Gy has been consistently documented at median times to progression of 8 months and 2-year survival rates of 10 % [4–8, 12, 17, 28–31]. The use of conventionally fractionated irradiation (typically 180 cGy once daily) has been shown to be equivalent to the best of the hyperfractionated regimens (70.2 Gy in 60 fractions using 117 cGy twice daily with a 6 h interfraction interval) in a prospective randomized trial in Pediatric Oncology Group. Similarly a trial of accelerated fractionation conducted in the United Kingdom using 180 cGy twice daily with interfraction intervals of 8 h to 48.8 and 50.4 Gy showed no superior results with 1 and 2-year survival rates of 32 % and 11 % respectively.

Despite all of these efforts to improve the outcomes, the number of long-term survivors with diffusely infiltrating pontine gliomas remains small; an update of the Pediatric Oncology Group Study, including 3 serially escalating dose arms between showed only 9 survivors out of 130 patients enrolled [6]. So, the standard management of diffusely infiltrating brainstem gliomas should be to use conventional fractionation (typically 180 cGy once daily) to 54–55.8 Gy. This type of radiation can be combined with chemotherapy for radiosensitization or biologically targeted therapy within a protocol addressing the effectiveness. For focal or dorsally exophytic lesions, similar dosage and fractionation are incorporated with a higher likelihood of longer-term survival, avoiding the potential risks of higher radiation doses, accelerated fractionation regimens, or concurrent chemotherapy or biologically targeted therapy.

Attempts to identify radiosensitization by concurrent chemotherapy using cisplatin or etoposide in the previous years or more recently

with temozolomide, biologic response modifiers with interferon or tamoxifen and hypoxic cell sensitizers have been disappointing [32–36]; studies with anti-EGFR drugs combined with radiation is under way [37].

36.4 Radiotherapy Technique

Diffusely infiltrating pontine gliomas typically were irradiated with parallel opposed lateral fields to encompass the tumor volume with a safety margin of 2–3 cm as in the former studies [17], but current approaches more often include 3DCRT, IMRT, or VMAT that enable to spare the temporal lobes as discussed in detail above.

For focal brainstem gliomas (including tectal plate lesions, dorsally exophytic pontomedullary tumors, focal intrinsic lesions of the midbrain, pons, or medulla), tumor size, margination, and location define the volume to minimize the dose beyond the primary target volume and long-term toxicity.

Children with large diffusely infiltrating tumors usually need corticosteroids at diagnosis to control neurologic symptoms especially at the initiation of radiation therapy with low-dose regimen (dexamethasone at 2–4 mg) as additional or progressive neurologic signs may appear. Children with rapidly deteriorating signs may need higher doses of corticosteroids to control mass effect prior to irradiation.

Irradiation is generally well tolerated although acute reactions including radioepidermitis especially in the external auditory canal and the retroauricular region can be seen. These reactions are more pronounced with hyperfractionated radiotherapy and less with the implementation of new technologies discussed above.

The majority of the patients with brainstem tumors demonstrate clinical and imaging evidence of apparent progressive tumor within 1–4 months after the completion of radiation therapy [3, 7, 17, 38], but these patients should not be considered as therapeutic failures immediately as majority of children stabilize or improve after 3–12 weeks. Imaging changes during this interval include focal enhancement often in a previously nonenhancing lesion, cyst formation or cystic degeneration, intralesional hemorrhage,

and necrosis [31, 38]. Differentiating such subacute phenomena from tumor progression may be extremely difficult, and conventional MRI at presentation does not predict clinical response [39]. Positron emission tomography using fluorodeoxyglucose and magnetic resonance spectroscopy has been of some value in differentiating tumor progression from postirradiation changes in this interval [40, 41]. Similar changes can occur for focal lesions, and medical support during this period including corticosteroids may be necessary until the lesion regresses over several months.

36.5 Results of the Treatment

Approximately 60–70 % of patients with pontine gliomas have a stabilization or improvement of their functional status after irradiation. Although time to progression may be difficult to document in this tumor system, cooperative group studies report median time to progression as 6–8 months. Median survival is 8–12 months for the high-risk diffuse gliomas, and the rate of surviving patients beyond 2 years is less than 20 % [4–8, 12, 17, 28, 32]. A recently published review of clinical trials about diffuse brainstem gliomas in children evaluated the outcomes of 973 children treated between 1984 and 2005. Looking at the results of the review overall radiotherapy induces neurological improvement, allows reduction or discontinuation of steroids, and is associated with clinical response (85 % clinical, 50 % radiological response). The response is similar between the patients who received hyperfractionation or hypofractionation techniques and those who received conventional fractionation. No treatment has shown any benefit over conventional fractionation. The use of chemotherapy either before or after radiation has not shown any survival advantage. Similarly concomitant radiotherapy and radiotherapy do not show any survival benefit [42, 43]. Treatment results to different radiotherapy and chemotherapy schedules are presented in Table 36.1.

Children with focal, intrinsic tumors of the midbrain or medulla show long-term survival after irradiation of 50–70 % [2–4, 9, 12]. Survival at 10 years after surgery with or without

Table 36.1 Treatment results to different radiotherapy and chemotherapy schedules

Schedule	Complete response	Partial response	Minor response	Stable disease	Progressive disease	<i>n</i>	Reference
Hyperfractionation at 68.4	1	2	9	2	1	15/16	[44]
Hyperfractionation at 66	0	5	0	20	8	33/34	[45]
Hyperfractionation 70.2	1	3	0	40	8	33/34	[46]
Hyperfractionation 75.6	1	5	0	20	3	29/39	[17]
Hyperfractionation 78	1	7	12	24	0	44/66	[7]
Hypofractionation 48–50	0	14	0	6	6	26/28	[31]
Chemotherapy before hyperfractionation 66	0	4	0	12	4	20/32	[47]
Chemotherapy during hyperfractionation 70.2	0	2	2	5	0	9/9	[33]
Chemotherapy during hyperfractionation 72	1	14	0	8	6	29/34	[48]
Chemotherapy during hyperfractionation 70.2	1	15	0	23	12	51/64	[30]
Chemotherapy + 54 Gy	1	18	0	25	13	57/66	[30]
Chemotherapy during and after 50–56 Gy	0	3	0	8	3	22/27	[49]
Chemotherapy + 59.4 Gy	0	2	2	7	1	12/13	[50]
Chemotherapy before and after 55.8 Gy	0	7	0	25	0	32/33	[51]

necessary irradiation for dorsally exophytic brainstem gliomas approaches 75 % survival rates, and similar rates are quoted for the focal pontine lesions of limited size after localized irradiation.

36.6 Future Prospects

Several studies on new chemotherapeutic agents, small molecules, or radiation sensitizers are ongoing. The precise pattern of genetic abnormalities within the group of diffuse pontine glioma is still poorly documented. A study has suggested that the genetics of these tumors is complex and includes grade-dependent amplification and overexpression of epidermal growth factor receptor (EGFR) and grade-independent expression and mutation of P53 [52]. With the development of targeted therapies, the issue of stereotactic or open biopsies for diffuse brainstem glioma is being readdressed by some cooperative groups to correlate biological findings with drug activity.

References

- Epstein F, Constantini S (1996) Practical decisions in the treatment of pediatric brain stem tumors. *Pediatr Neurosurg* 24:24–34
- Barkovich AJ, Krischer J, Kun LE et al (1990) Brain stem gliomas: a classification system based on magnetic resonance imaging. *Pediatr Neurosurg* 16(2):73–83
- Farmer JP, Montes JL, Freeman CR et al (2001) Brainstem gliomas. A 10 year institutional review. *Pediatr Neurosurg* 34(4):206–214
- FrFreemaneeman CR, Farmer JP (1998) Pediatric brain stem gliomas: a review. *Int J Radiat Oncol Biol Phys* 40(2):265–271
- Shrieve DC, Wara WM, Edwards MS et al (1992) Hyperfractionated radiation therapy for gliomas of the brainstem in children and in adults. *Int J Radiat Oncol Biol Phys* 24(4):599–610
- Freeman CR, Bourgouin PM, Sanford RA et al (1996) Long term survivors of childhood brain stem gliomas treated with hyperfractionated radiotherapy. Clinical characteristics and treatment related toxicities. *Cancer* 77(3):555–562
- Packer RJ, Boyett JM, Zimmerman RA et al (1993) Hyperfractionated radiation therapy (72 Gy) for children with brain stem gliomas. A Children's Cancer Group phase I/II trial. *Cancer* 72(4):1414–1421
- Packer RJ, Boyett JM, Zimmerman RA et al (1994) Outcome of children with brain stem gliomas after treatment with 7800 cGy of hyperfractionated radiotherapy. A Children's Cancer Group phase I/II trial. *Cancer* 74(6):1827–1834
- Albright AL, Guthkelch AN, Packer RJ et al (1986) Prognostic factors in pediatric brain-stem gliomas. *J Neurosurg* 65(6):751–755
- Gilbertson RJ, Hill DA, Hernan R et al (2003) ERBB1 is amplified and overexpressed in high-grade diffusely infiltrative pediatric brain stem glioma. *Clin Cancer Res* 9(10 Pt 1):3620–3624
- Pollack IF, Hoffman HJ, Humphreys RP et al (1993) The long-term outcome after surgical treatment of dorsally exophytic brain-stem gliomas. *J Neurosurg* 78:859–863

12. Prados MD, Wara WM, Edwards MS et al (1995) The treatment of brain stem and thalamic gliomas with 78 Gy of hyperfractionated radiation therapy. *Int J Radiat Oncol Biol Phys* 32(1):85–91
13. Hoffman HJ (1996) Dorsally exophytic brain stem tumors and midbrain tumors. *Pediatr Neurosurg* 24:256–262
14. Khatib ZA, Heideman RL, Kovnar EH et al (1994) Predominance of pilocytic histology in dorsally exophytic brain stem tumors. *Pediatr Neurosurg* 20:2–10
15. Albright AL, Packer RJ, Zimmerman R et al (1993) Magnetic resonance scans should replace biopsies for the diagnosis of diffuse brain stem gliomas: a report from the Children's Cancer Group. *Neurosurgery* 33:1026–1029
16. Albright AL (1996) Diffuse brainstem tumors: when is a biopsy necessary? *Pediatr Neurosurg* 24:252–255
17. Freeman CR, Krischer JP, Sanford RA et al (1993) Final results of a study of escalating doses of hyperfractionated radiotherapy in brain stem tumors in children: a Pediatric Oncology Group study. *Int J Radiat Oncol Biol Phys* 27(2):197–206
18. ICRU Report 29 (1978) Dose specification for reporting external beam therapy with photons and electrons. International Commission on Radiation Units and Measurements, Washington, DC
19. ICRU Report 50 (1993) Prescribing, recording, and reporting photon beam therapy. International Commission on Radiation Units and Measurements, Bethesda
20. Antolak JA, Rosen II (1999) Planning target volumes for radiotherapy: how much margin is needed. *Int J Radiat Oncol Biol Phys* 44:1165–1170
21. Remeijer P, Rasch C, Lebesque JV et al (1999) A general methodology for three-dimensional analysis of variation in target volume delineation. *Med Phys* 26:931–940
22. ICRU Report 62 (1999) Prescribing, recording, and reporting photon beam therapy (Supplement to ICRU Report 50). International Commission on Radiation Units and Measurements, Bethesda
23. Halperin EC (1985) Pediatric brain stem tumors: patterns of treatment failure and their implications for radiotherapy. *Int J Radiat Oncol Biol Phys* 11(7):1293–1298
24. Yoshimura J, Onda K, Tanaka R et al (2003) Clinicopathological study of diffuse type brainstem gliomas: analysis of 40 autopsy cases. *Neurol Med Chir (Tokyo)* 43(8):375–382
25. Donahue B, Allen J, Siffert J et al (1998) Patterns of recurrence in brain stem gliomas: evidence for craniospinal dissemination. *Int J Radiat Oncol Biol Phys* 40(3):677–680
26. Gajjar A, Sanford RA, Heideman R et al (1997) Low-grade astrocytoma: a decade of experience at St. Jude Children's Research Hospital. *J Clin Oncol* 15(8):2792–2799
27. Dunbar SF, Tarbell NJ, Kooy HM et al (1994) Stereotactic radiotherapy for pediatric and adult brain tumors: preliminary report. *Int J Radiat Oncol Biol Phys* 30(3):531–539
28. Freeman CR, Kepner J, Kun LE et al (2000) A detrimental effect of a combined chemotherapy-radiotherapy approach in children with diffuse intrinsic brain stem gliomas. *Int J Radiat Oncol Biol Phys* 47(3):561–564
29. Mandell L, Kadota R, Douglass EC et al (1997) It is time to rethink the role of hyperfractionated radiotherapy in the management of children with newly diagnosed brainstem? Results of a Pediatric Oncology Group Phase III trial comparing conventional versus hyperfractionated radiotherapy. *Int J Radiat Oncol Biol Phys* 39:143
30. Mandell LR, Kadota R, Freeman C et al (1999) There is no role for hyperfractionated radiotherapy in the management of children with newly diagnosed diffuse intrinsic brainstem tumors: results of a Pediatric Oncology Group phase III trial comparing conventional vs hyperfractionated radiotherapy. *Int J Radiat Oncol Biol Phys* 43:959
31. Lewis J, Lucraft H, Gholkar A (1997) UKCCSG study of accelerated radiotherapy for pediatric brain stem gliomas. *Int J Radiat Oncol Biol Phys* 38(5):925–929
32. Packer RJ, Prados M, Phillips P et al (1996) Treatment of children with newly diagnosed brain stem gliomas with intravenous recombinant beta-interferon and hyperfractionated radiation therapy: a Children's Cancer Group phase I/II study. *Cancer* 77(10):2150–2156
33. Walter AW, Gajjar A, Ochs JS et al (1998) Carboplatin and etoposide with hyperfractionated radiotherapy in children with newly diagnosed diffuse pontine gliomas: a phase I/II study. *Med Pediatr Oncol* 30(1):28–33
34. Jalali R, Raut N, Arora B et al (2010) Prospective evaluation of radiotherapy with concurrent and adjuvant temozolomide in children with newly diagnosed diffuse intrinsic pontine glioma. *Int J Radiat Oncol Biol Phys* 77(1):113–118
35. Chiang KL, Chang KP, Lee YY et al (2010) Role of temozolomide in the treatment of newly diagnosed diffuse brainstem glioma in children: experience at a single institution. *Childs Nerv Syst* 26(8):1035–1041
36. Sharp JR, Bouffet E, Stempak D et al (2010) A multi-centre Canadian pilot study of metronomic temozolomide combined with radiotherapy for newly diagnosed paediatric brainstem glioma. *Eur J Cancer* 46(18):3271–3279
37. Geyer JR, Stewart CF, Kocak M et al (2010) A phase I and biology study of gefitinib and radiation in children with newly diagnosed brain stem gliomas or supratentorial malignant gliomas. *Eur J Cancer* 46(18):3287–3293, Epub 2010 Aug 12
38. Packer RJ, Zimmerman RA, Kaplan A et al (1993) Early cystic/necrotic changes after hyperfractionated radiation therapy in children with brain stem gliomas. *Cancer* 71(8):2666–2674
39. Liu AK, Brandon J, Foreman NK et al (2009) Conventional MRI at presentation does not predict clinical response to radiation therapy in children with diffuse pontine glioma. *Pediatr Radiol* 39(12):1317–1320

40. Griebel M, Friedman HS, Halperin EC et al (1991) Reversible neurotoxicity following hyperfractionated radiation therapy of brain stem glioma. *Med Pediatr Oncol* 19(3):182–186
41. Taylor JS, Langston JW, Reddick WE et al (1996) Clinical value of proton magnetic resonance spectroscopy for differentiating recurrent or residual brain tumor from delayed cerebral necrosis. *Int J Radiat Oncol Biol Phys* 36(5):1251–1261
42. Hargrave D, Bartels U, Bouffet E (2006) Diffuse brainstem glioma in children: critical review of clinical trials. *Lancet Oncol* 7(3):241–248
43. Freeman CR, Perilongo G (1999) Chemotherapy for brain stem gliomas. *Childs Nerv Syst* 15:545–553
44. Packer RJ, Littman PA, Sposto RM et al (1987) Results of a pilot study of hyperfractionated radiation therapy for children with brain stem gliomas. *Int J Radiat Oncol Biol Phys* 13:1647–1651
45. Freeman CR, Krischer J, Sanford RA et al (1988) Hyperfractionated radiotherapy in brain stem tumors: results of a Pediatric Oncology Group study. *Int J Radiat Oncol Biol Phys* 15:311–318
46. Freeman CR, Krischer J, Sanford RA et al (1991) Hyperfractionated radiation therapy in brain stem tumors: results of treatment at the 7020 cGy dose level of Pediatric Oncology Group study #8495. *Cancer* 68:474–481
47. Kretschmar CS, Tarbell NJ, Barnes PD et al (1993) Preirradiation chemotherapy and hyperfractionated radiation therapy 66 Gy for children with brain stem tumors: a phase II study of the Pediatric Oncology Group, Protocol 8833. *Cancer* 72:1404–1413
48. Allen J, Siffert J, Donahue B et al (1999) A phase I/II study of carboplatin combined with hyperfractionated radiotherapy for brainstem gliomas. *Cancer* 86:1064–1069
49. Wolff JE, Westphal S, Molenkamp G et al (2002) Treatment of paediatric pontine glioma with oral trophosphamide and etoposide. *Br J Cancer* 87:945–949
50. Packer RJ, Krailo M, Mehta M et al (2005) A phase I study of concurrent RMP-7 and carboplatin with radiotherapy for children with newly diagnosed brainstem gliomas. *Cancer* 104:1968–1974
51. Broniscer A, Iacono L, Chintagumpala M et al (2005) Role of temozolomide after radiotherapy for newly diagnosed diffuse brainstem glioma in children: results of a multiinstitutional study (SJHG-98). *Cancer* 103:133–139

Cengiz Canpolat

Tumors of the brainstem comprise 10–20 % of all central nervous system tumors in the pediatric population. Fifteen to 20 % of these are low-grade astrocytomas that have characteristic clinical features and growth patterns and follow an indolent course. The importance of recognition of these relatively favorable brainstem tumors cannot be overemphasized, since the management will be quite different from that of the more common diffuse intrinsic lesion [1, 2]. Some may not require any treatment. Others may be amenable to surgical resection and not require adjuvant therapy. When surgery is not feasible or at the time of development of progressive disease that is not resectable, treatment options for these patients include radiotherapy and/or chemotherapy depending on the specific clinical situation, especially the age of the child. Most are low-grade astrocytomas and may be expected to respond to chemotherapy similarly to low-grade astrocytomas at other sites. Approximately 75 % of tumors arising in the brainstem are diffuse intrinsic lesions [3, 4]. There is an equal predilection for males and females, and these tumors are typically diagnosed between ages 7 and 9 [5, 6]. This generic term comprises a heterogeneous set of neoplasms that arise in the midbrain, pons, medulla, and upper

cervical spine. These lesions are typically one of the most difficult pediatric cancers to treat and are recognized histologically as a heterogenic group of tumors. Children with these infiltrating fibrillary astrocytomas often present with progressive symptoms such as ataxia and multiple deficits of the cranial nerves, long tracts, and cerebellum. Their natural history and poor prognosis are similar to glioblastoma multiforme, which is the most common primary supratentorial tumor in adults. Focal lesions represent the minority of brainstem tumors and have a good prognosis.

The most recent classification system of the brainstem tumors by Choux et al. [7] utilizes both CT and MRI images to group brainstem tumors into four types. *Type I* tumors are *diffuse brainstem gliomas*, accounting for up to 75 % of all tumors [4, 5]. These lesions appear hypointense on CT with nondelineated borders, and do not significantly enhance on T1-weighted MRI sequences. They are characterized by diffuse infiltration and swelling of the brainstem and are generally >2 cm at time of presentation. Typically, these lesions are malignant fibrillary astrocytomas (WHO grade III or IV). *Type II* tumors are *focal*, intrinsic tumors that can be cystic or solid. Unlike type I lesions, these tumors are sharply demarcated from surrounding tissue on MRI sequences and are associated with less brainstem edema. The majority of these lesions are low-grade gliomas (WHO I or II). *Type III* tumors are *exophytic* tumors that arise from the subependymal glial tissue of the fourth

C. Canpolat, M.D.
Division of Pediatric Oncology,
Department of Pediatrics,
Acibadem University, School of Medicine,
Istanbul, Turkey
e-mail: cccانpolat@yahoo.com

ventricle and mostly grow dorsally or laterally. Radiographically, they possess MRI characteristics similar to type II lesions, and histologically, these lesions are usually low-grade lesions (WHO I or II) like type II lesions. Interestingly, some authors have noted that exophytic tumors that grow laterally and ventrally into the brainstem are higher-grade lesions compared to those that project dorsally [8]. *Type IV* lesions are *cervicomedullary* brainstem gliomas similar in imaging, histology, and behavior to intramedullary spinal cord gliomas. The majority of type IV lesions are low-grade, non-infiltrative tumors, and thus their growth is usually confined rostrally by the white matter of the corticospinal tract and medial lemniscus.

Radiation and chemotherapy are the current mainstay of therapy for diffuse brainstem gliomas [9]. Radiotherapy is the only definitely indicated treatment for diffusely infiltrating pontine gliomas and remains the best option with local field radiotherapy amounting to a total dose of 54–60 Gy in 6 weeks. Without radiation, the median survival rate is approximately 20 weeks [10]. However, this treatment modality produces transient improvements in neurological function and a progression-free survival benefit in nearly 70 % of patients, but does not improve overall survival [11]. The median onset of disease progression following irradiation is often <6 months, with a median survival of ~10 months and prolonged survival (i.e., 24 months) in <10 % of all patients. Furthermore, delayed toxicity associated with such radiation includes potential radiation necrosis of the brainstem and radiation-induced injury to the occipital lobes and the hypothalamic axis. Evidence of transient response to radiotherapy has influenced numerous groups to attempt trials of increased radiotherapeutic dosage by using a hyperfractionated treatment regimen [12–16]. These studies have shown that increased amounts of radiation and hyperfractionation as well as brachytherapy have been unable to afford any additional survival benefit, however, while inducing more severe side effects because of intratumoral necrosis, steroid dependency, and other chronic factors [17–19].

Various treatment modalities in addition to standard-dose and high-dose hyperfractionated radiotherapy have been studied, such as preradiation chemotherapy followed by conventional radiotherapy [20], preradiation chemotherapy followed by hyperfractionated radiotherapy [12, 21], concurrent chemotherapy with radiotherapy [22–24], conventional radiotherapy followed by chemotherapy [25–27], and conventional high-dose chemotherapy with stem cell rescue [28]; however, survival remains poor.

37.1 Pre-irradiation Chemotherapy

The efficacy of chemotherapy in addition to surgery and irradiation has been studied in several clinical trials during the last two decades. Several groups of investigators have tested the utility of the administration of chemotherapy prior to radiotherapy. In a French Society of Pediatric Oncology study, Doz et al. investigated the efficacy of carboplatin prior to and during conventional radiotherapy and achieved minor response in 2, stable disease in 6, and progressive disease in 19 patients with a median survival of 11 months [20]. On behalf of Children's Oncology Group (CCG), Dunkel et al. published the results of a multicenter study in which investigators evaluated the use of high-dose thiotepa and etoposide-based chemotherapy regimens with autologous bone marrow rescue prior to hyperfractionated radiotherapy in 16 patients and concluded that high-dose chemotherapy regimens did not prolong survival when compared with standard therapy [21]. In a phase II study conducted by CCG (9941), investigators evaluated the efficacy of two different chemotherapy arms on a combined 63 patients. First treatment group received carboplatin, etoposide, and vincristine, while the second group was treated with cisplatin, etoposide, and cyclophosphamide. In both groups, patients received hyperfractionated radiotherapy following chemotherapy. The authors did not observe any improvement in the response rate, event-free survival, or overall survival when compared with the previous studies

dealing with patients who were treated with radiation with or without chemotherapy. Median survival of the patients in this study was less than 1 year [29]. Kretschmar et al. reported in a POG phase II study (8833) on the utilization of cisplatin and cyclophosphamide in children with brainstem tumors prior to hyperfractionated radiotherapy. This treatment scheme produced 3 partial responses, 23 stable disease, and 6 progressive disease with a median survival of 9 months. There were only three long-term survivors of more than 2 years [30]. Despite these discouraging results, Frappaz et al. decided to test the feasibility of preradiation chemotherapy in 23 pediatric patients with diffuse intrinsic brainstem glioma [31]. The chemotherapy protocol consisted of alternating hematotoxic and nonhematotoxic schedules. Each cycle included three courses delivered monthly. The first course was BCNU and cisplatin, and the second and third were high-dose methotrexate. Three patients could only receive one cycle, five patients three cycles, and ten patients four cycles. Twenty of the 23 patients eventually received local radiation therapy. Fourteen patients who previously received only radiotherapy served as controls. There were chemotherapy-related infections in 4 patients, and 11 patients required platelet transfusions. Median survival increased significantly from 9 to 17 months in patients included in this protocol though hospitalization was prolonged (Table 37.1).

37.2 Concomitant Chemotherapy and Radiotherapy

Based on the efficacy of radiotherapy for achieving at least temporary disease regression in children with brainstem gliomas, investigators designed an alternative strategy involving administration of radiosensitizing agents concurrently with irradiation, with the goal of potentiating the efficacy of this treatment modality. Radiosensitization is thought to synergistically potentiate the efficacy of irradiation within rapidly dividing tumor cells. Multiple studies have been conducted to evaluate the response of patients with brainstem gliomas to treatment with chemotherapy during radiotherapy [22, 32–35]. One of the earliest studies was conducted by Jakacki et al. which investigated the concurrent radiotherapy and dose-intensive chemotherapy with procarbazine, lomustine and vincristine. Six patients with diffuse brainstem glioma treated according to this regimen. Patients underwent PBSC harvesting after mobilization with G-CSF. Chemotherapy consisted of CCNU 130 mg/m² on day 0, vincristine 1.5 mg/m² on days 0 and 7, and procarbazine 150 mg/m² on days 1–7. PBSCs were reinfused on day 9 of each course. Four courses of chemotherapy were administered 28 days apart or when counts recovered. Involved field radiation was administered to newly diagnosed high-grade glioma patients following recovery from chemotherapy. The

Table 37.1 Literature review of clinical trials of pre-irradiation chemotherapy

Authors and year (reference)	No. of patients	Treatment	Outcome
Doz et al. (2002) [20]	19	CCNU, VCR; PCB2 + PBSC infusion × 4 courses/XRT	Median survival 11 months
Dunkel et al. (1998) [21]	16	HD thiotepa and VP-16 with ABMT	Median survival 11.4 months
Jennings et al. (2002) [29]			
Group A	32	Carboplatin, VP-16, VCR	7PR, 5SD, 11PD
Group B	31	Cisplatin, CTX, VP-16, VCR	5PR, 4 SO, 9P0
Kretschmar et al. (1993) [30]	32	Cisplatin, CTX	3PR, 23SD, 6 PD median survival 9 months
Frappaz et al. (2008) [31]	23	BCNU, cisplatin, HDMTX ×2	Median survival 17 months

ABMT Autologous bone marrow transplantation, MR Minor response, SD Stable disease, PD progressive disease, PR partial response, HD High dose, VP-16 Etoposide, VCR Vincristine, CTX Cyclophosphamide, HDMTX High-dose methotrexate

reported median overall survival time was 11 months [28]. Packer et al. assessed the concurrent administration of radiotherapy and chemotherapy consisting of carboplatin as a radiosensitizer and a bradykinin analog RMP-7 as a selective-blood-brain-barrier permeability increasing agent [33]. Carboplatin dose was 35 mg/m², and RMP-7 was given at a dose of 0.3 mg/kg of ideal body weight as a 10-min intravenous infusion beginning 5 min before the end of the carboplatin infusion. These two drugs were given for 5 successive days during radiotherapy. Thirteen patients were treated whose median age was 7 years. The estimated median survival was reported as 328 days with only one patient remaining disease progression-free more than 400 days from the initiation of treatment. Nine patients were treated with hyperfractionated radiotherapy and chemotherapy with carboplatin and etoposide [35] in a phase I/II study setting. Carboplatin, given in combination with fixed-dose etoposide, was escalated in successive cohorts to determine its maximum tolerated systemic exposure. Eight of the nine children on this study died of their disease at a median of 44 weeks, essentially the same survival as those treated on a previous Pediatric Oncology Group study using hyperfractionated radiation therapy alone. Allen and his colleagues [22] evaluated the usefulness of administration of carboplatin as a single agent for the purpose of radiosensitization along with radiotherapy. Carboplatin was infused twice-weekly in a dose-escalating manner with a maximum tolerated dose of 110 mg/m² or a total cumulative dose of 1,540 mg/m² over 7 weeks. A total of 38 patients were enrolled with a median age of 7.8 years. Median progression-free survival was 8 months, and the overall survival was 12 months. Five long-term survivors remained in continuous remission after a mean follow-up period of 79 months. In a Brazilian cooperative study, Broniscer et al. used tamoxifen concurrent with radiation treatment [36]. Tamoxifen was administered orally with a dose of 200 mg/m² per day along with conventional radiotherapy and for 52 additional weeks. Of 29 patients treated, 27 completed radiotherapy. Eleven of the 22 assessable patients had an objective radiologic response. Only three patients completed the entire course

of treatment without tumoral progression or significant toxicity. Median survival was 10.3 months, and the 1-year survival rate was 37±9.5%. As a result, the authors recommended alternative treatments be tested in patients with diffuse brainstem glioma. Bernier-Chastagner et al. [23] conducted a phase II study to evaluate the survival and toxicity in children with diffuse brainstem glioma treated with daily radiotherapy with topotecan as a radiosensitizer. Topotecan was administered intravenously at a dose of 0.4 mg/m² per day within 1 h before irradiation. All 32 patients who were included in the study completed the treatment. Only partial responses were observed occurring in 40% of the patients. The 9-month and the 12-month survival rates were 34.4 and 25.5%, respectively. The median duration of survival was 8.3 months. The results were not encouraging, and this treatment at this schedule and doses was not recommended for the treatment of patients with brainstem glioma. A recent study by Turner et al. [37] aimed at assessing the efficacy of administering daily thalidomide concomitantly with radiation and continuing for up to 1 year following radiation. Thirteen children, 12 with brainstem glioma, were enrolled. All patients received focal radiotherapy to a total dose of 5,580 cGy. Thalidomide was administered once daily beginning on the first day of radiation and continued for 12 months or until the patient came off study. The starting dose was 12 mg/kg (rounded down to the nearest 50 mg) and was increased by 20% weekly, if tolerated, to 24 mg/kg or 1,000 mg. No patients completed the planned 12 months of thalidomide therapy, and all have since died of disease progression. The median duration of therapy was 5 months (range 2–11 months). The median time to progression was 5 months (range 2–11 months), and the median time to death was 9 months. With these results, adding thalidomide to radiation was not considered to improve survival comparing to historical controls; however, toxicity appeared to be increased. In another phase I study done by Greenberg et al. [24], investigators enrolled seven brainstem glioma patients in order to be treated as an induction therapy with oral etoposide, continuous infusion cyclosporine A given with escalating doses of vincristine, and concomitant

standard-dose irradiation. Maintenance therapy was to be administered after induction comprising six 28-day cycles with the same drugs as in induction. All seven patients completed radiotherapy, while only three completed more than 1 month of chemotherapy because of disease recurrence. The study was closed before completion because of dose-limiting neurotoxicity. One patient had tumor necrosis at 6 weeks suggesting some antitumor effect. Median survival for the whole group was 11 months. Cyclosporine A was utilized in this study with the intension of modifying the P-gp, competitively binding to and inhibiting the efflux function of the protein, but actually no clear benefit was achieved from it but it rather increased the drug levels of neurotoxic chemotherapeutic agents in the central nervous system. Considering the fact that the use of concurrent radiotherapy with temozolomide has become the standard care for adult patients with malignant gliomas, Sirachainan et al. [38] decided to investigate the usefulness of the same agent in pediatric patients with diffuse intrinsic brainstem glioma. Twelve children were treated with concurrent radiotherapy with temozolomide followed by adjuvant temozolomide and *cis-retinoic acid*. Radiotherapy was administered at a conventional dose at the tumor site with temozolomide (75 mg/m²/day) for 6 weeks

followed by temozolomide 200 mg/m²/day for 5 days with *cis-retinoic acid* (100 mg/m²/day) for 21 days with a 28-day cycle after concurrent radiotherapy. Ten of the 12 patients experienced clinical response after radiotherapy. Seven patients had partial response, four had stable disease, and one had progressive disease. At the time of the publication, 9 of the 12 patients had died of tumor progression, 1 was alive with progression, and 2 patients were alive with clinical improvement. One-year progression-free survival was 41.7 %, and the median survival was 13.5 months. One-year overall survival was 58 %. In a Children's Oncology Group phase II study, Korones et al. [39] evaluated the efficacy of vincristine and oral etoposide with radiotherapy in children with diffuse brainstem glioma. Patients received local radiotherapy of 54 Gy. Chemotherapy consisted of two 28-day cycles of vincristine 1.5 mg/m² on days 1 and 8 and oral etoposide 50 mg/m² days 1–21 administered concurrent with radiation and continuing for ten cycles following radiation. Of the 30 children enrolled, 7 had a partial response, 18 had stable disease, and 2 had progressive disease. Response in three patients could not be evaluated. All 30 children died. Overall survival at 1 and 2 years were 27 and 3 %, respectively. Median survival was 9 months (Table 37.2).

Table 37.2 Literature review of clinical trials of concomitant chemotherapy and radiotherapy

Authors and year (reference)	No. of patients	Treatment	Outcome
Jakacki et al. (1998) [28]	6	CCNU, VCR, PCB2 + PBSC infusion × 4 courses/XRT	Median survival 11 months
Packer et al. (2005) [33]	13	XRT/carboplatin, RMP 7	Median survival 328 days
Walter et al. (1998) [35]	9	XRT/carboplatin, VP-16	Median survival 44 weeks
Allen et al. (1999) [22]	38	XRT/carboplatin	PFS 8 months, OS 12 months
Broniscer et al. (2000) [36]	29	XRT/tamoxifen	Median survival 10.3 months
Bernier-Chastagner et al. (2005) [23]	32	XRT/topotecan	Median survival 8.3 months
Turner et al. (2007) [37]	13	XRT/thalidomide	Median survival 9 months
Greenberg et al. (2005) [24]	7	XRT/VP + 6, cyclosporine A, VCR	Median survival 11 months
Sirachainan et al. (2008) [38]	12	XRT/TM2 and TM2 and <i>cis-retinoic acid</i>	Median survival 13.5 months
Korones et al. (2008) [39]	30	XRT/VCR, VP-16	Median survival 9 months

VCR Vincristine, PCB2 Procarbazine, PBSC Peripheral blood stem cell, VP + 16 etoposide, PFS Progression-free survival, OS Overall survival, XRT: Radiotherapy, TM2 Temozolomide

37.3 Chemotherapy Following Radiotherapy

The role of chemotherapy administration after radiotherapy has been investigated in several studies [25–27]. In one of them, Bouffet et al. [40] assessed the benefit of high-dose chemotherapy (HDC) after radiotherapy in 35 children with newly diagnosed diffuse pontine gliomas. Two to three months after radiotherapy, all patients received busulfan (150 mg/m² on days 8, 7, 6, and 5) and thiotepa (300 mg/m² on days 4, 3, and 2) followed by autologous bone marrow transplantation. Eleven patients could not receive HDC because of early progression [9] or parental refusal [2]. Three patients died of HDC-related complications. All 21 patients who survived HDC eventually died of disease progression. The median survival time was 10 months. Statistical analysis did not suggest any evidence of survival benefit. A prospective randomized Children's Cancer Study Group trial [25] included 74 children who received either a combination of carmustine, vincristine, and prednisone or no treatment after conventional radiotherapy. The overall 5-year survival rate was 20 %, and was not prolonged with the adjuvant chemotherapy regimen compared to radiotherapy alone. Wolff et al. [27] assessed the efficacy of a combination of trofosfamide and etoposide during and after conventional radiation treatment in 20 patients with diffuse pontine gliomas. None of the 12 evaluable patients showed complete response to therapy. In three patients partial response was achieved; stable disease and progressive disease were observed in four and five patients, respectively. All tumors progressed locally, and all patients died. The overall median survival was 8 months. The authors concluded that oral trofosfamide in combination with etoposide did not prolong survival of pontine glioma patients. On the other hand, a study done by Benesch et al. [41] included 11 children with brainstem glioma who were treated with external beam radiation simultaneous with an intensive chemotherapy consisting of two cycles of ifosfamide, etoposide, methotrexate, cisplatin, and cytarabine separated by a 3-week interval. Maintenance

chemotherapy with carmustine, carboplatin, and vincristine (eight cycles over a 1-year period) was given to those patients who showed clinical or radiographic response to induction chemotherapy. Six of 11 patients showed an objective reduction in tumor size on magnetic resonance imaging, and 4 of 11 were reported to be alive at the time of report >22, >22, >90, and >92 months, respectively, after diagnosis without radiographic evidence of tumor progression (one complete remission, two partial remissions, one stable disease) but had suffered from moderate to severe long-term side effects. Three patients died due to disease progression, and the tumors in four patients showed short-term stabilization, and these patients died within 1 year after diagnosis. This intensive combined modality treatment yielded objective responses in more than 50 % and long-term survival in one third of the patients that was considered encouraging when compared with the historical cases. Wagner et al. [42] reviewed the data of 153 patients with pontine gliomas treated in different prospective multicenter studies that were registered in HIT-GBM (Hirntumor glioblastoma multiforme) database. Ninety children received chemotherapy according to the HIT-GBM protocols. Conventional fractionated radiotherapy with a total dose of 54–60 Gy was a part of each induction regimen. Radiotherapy was combined with oral trofosfamide and etoposide in the HIT-GBM A protocol, with simultaneously given intensive chemotherapy comprising carboplatin, etoposide, and ifosfamide in the HIT-GBM B protocol and with further intensified chemotherapy (addition of vincristine) in HIT-GBM C protocol. The 1-year overall survival rate of all patients was 39.9 %. Favorable prognostic factors were found to be age less than 4 years, low-grade histology, and smaller tumor. As a result of the statistical analysis, chemotherapy was found beneficial in achieving a better overall survival. A group of investigators from Mexico has initiated several chemotherapy trials for the treatment of brainstem gliomas in children. Their first experience was with a combination chemotherapy consisting of BCNU (120 mgm² on day 1 every 6 weeks), procarbazine (100 mg/m² for 14 days

Table 37.3 Literature review of clinical trials of chemotherapy following radiotherapy

Authors and year (reference)	No. of patients	Treatment	Outcome
Bouffet et al. (2000) [40]	35	Busulfan and thiotepa followed by ABMT	Median survival 10 months
Jenkin et al. (1987) [25]	74	Either carmustine, VCR and PRO or no treatment	5-year OS rate 20 % in either arm
Wolff et al. (2002) [27]	20	Trofosfamide and VP-16 during and after XRT	Median survival 8 months
Benesch et al. (2001) [41]	11	XRT with IFX, VP-16, MTX, cisplatin and Ara-C and carmustine, carboplatin, and VCR as maintenance	Objective response in >50 % and long-term survival in 1/3 of the patients
Wagner et al. (2006) [42], HIT-GBM studies	90	XRT with trofosfamide and VP-16 in HIT-GBMA XRT with carboplatin, VP-16 and IFX in HIT-GBMB XRT with carboplatin, VP-16, IFX, and VCR in HIT-GBMC	1-year OS 39.9 %

ABMT Autologous bone marrow transplantation, *VCR* Vincristine, *PRD* Prednisone, *VP-16* Etoposide, *XRT* Radiotherapy, *IFX* Ifosfamide, *MTX* Methotrexate, *Ara-C* Cytosine arabinoside, *HIT-GBM* Hirn tumor glioblastoma multiforme, *OS* Overall survival

every month for 12 months), and vincristine (2 mg/m² every 6 weeks for 12 months) given subsequent to surgery and conventional dose radiotherapy. Patients had a 5-year survival of 29 % (unpublished data). It was then followed by a new protocol in 1994 including four courses of neoadjuvant ifosfamide, carboplatin, and etoposide (ICE) followed by hyperfractionated radiotherapy and four more courses of ICE. Initial tumor reduction was observed after two courses of chemotherapy, but progressive disease was found after the fourth course. Survival was only 20 % at 18 months [43]. More recently the same group tried four courses of ICE associated with temozolomide (200 mg/m² for 5 days) every 4 weeks followed by 54 Gy hyperfractionated radiotherapy. Four high-grade brainstem tumors were treated with 30 % survival at 18 months (unpublished data) (Table 37.3).

37.4 Antiangiogenic Therapy

Recently investigators in the field of cancer have introduced new therapeutic approaches such as the administration of antiangiogenic drug. Angiogenesis is a fundamental process of blood vessel growth that is a hallmark of cancer. Survival of the tumor depends on the generation

of new blood vessels which assure the distribution of oxygen and the nutrients as well as the excretion of toxins. Angiogenesis is tightly regulated by proangiogenic and antiangiogenic factors. Among proangiogenic ones vascular endothelial growth factor (VEGF) is the most studied and serve as a key regulator of endothelial cell proliferation and migration. Angiopoietin, FGFs, PDGFs, and hepatocyte growth factor/scatter factor (HGF/SF) are other known proangiogenic factors. Angiostatin, endostatin, thrombospondin, and interleukin-12 are antiangiogenic factors [44]. Pathologic angiogenesis is caused by the imbalance between proangiogenic and antiangiogenic forces, a process called “angiogenic switch.” Hypoxia, acidosis, low blood glucose, mechanical stress from proliferating tumor cells, inflammatory responses, and genetic alterations of angiogenic regulators can trigger this switch [45]. Malignant glioma is one of the most vascularized tumors with expression of VEGF and high microvessel density. Increased microvessel density has been associated with poor prognosis in patients with malignant gliomas [46]. Inhibition of angiogenesis may contribute to the prevention of angiogenic switch intervening in the rapid expansion of small tumors as well as inducing the regression of large cancers [47]. More than 75 antiangiogenic compounds have

entered clinical trials. Preliminary results of these trials suggest that these drugs as single agents are poorly active in advanced tumors, and responses can only be created if they are used in association with chemotherapy. Bevacizumab (Avastin) is a recombinant human neutralizing monoclonal antibody of VEGF and is the first FDA-approved antiangiogenic agent in cancer treatment [48]. It has been shown to decrease tumor vascularity, enhance tumor apoptosis, and prolong survival in a rat intracranial C6 glioma model [49]. The antitumor mechanism of bevacizumab includes decreasing vessel diameter, density, and permeability; reducing the pressure of the interstitial fluid; and in some studies increasing the intratumoral uptake of chemotherapy [50, 51]. Bevacizumab has demonstrated a promising anti-tumor activity when used with a topoisomerase I inhibitor, irinotecan in an anecdotal series [52]. Vredenburg et al. has treated 32 adult patients with GBM and WHO grade III gliomas with bevacizumab 10 mg/kg every 2 weeks along with irinotecan 125 mg/m² for patients not on enzyme-inducing anticonvulsants (EIACs) or 340 mg/m² for patients on EIACs. This drug combination induced a radiographic response rate of 61 % for recurrent anaplastic gliomas. The median progression-free survival was 23 weeks for all patients. The 6-month progression-free survival probability was 38 %, and the 6-month overall survival probability was 72 %. Few patients developed venous thromboembolism, and one patient had an arterial ischemic stroke [53]. A case report on an adult patient with progressive diffuse brainstem glioma treated with bevacizumab and irinotecan demonstrated remarkable improvement in the clinical condition of the patient as well as significant radiographic response [54]. Bevacizumab has been used in children with pontine gliomas as therapy for radiation necrosis. Four children treated with irradiation later developed radiation necrosis in the brainstem. They then received bevacizumab as a treatment for the radiation necrosis. After bevacizumab therapy, three children had significant clinical improvement and were able to discontinue steroid use. One child continued to decline and, in retrospect, had disease progression, not radiation necrosis.

In all cases, bevacizumab was well tolerated [55]. Another agent that inhibits VEGF by blocking ligand-receptor binding is VEGF-trap (regeneron). A clinical trial of VEGF-trap in recurrent malignant gliomas is ongoing. Recently there has been a shift in thinking towards the view that more fractionated schedules of drug administration using smaller doses than the maximum tolerated dose would be as or perhaps even more effective than the classic chemotherapy administration. Such schedules known as metronomic schedules increase the antiangiogenic activity of certain drugs [56]. Metronomic chemotherapy may delay the onset of acquired drug resistance as the target of the therapy is the endothelial cell rather than the cancer cells [56, 57]. In addition, antiangiogenic drugs do not need to cross the blood-brain barrier as they target endothelial cells. A number of agents such as etoposide, temozolomide, cyclophosphamide, and vinblastine are currently used in metronomic schedules against pediatric brain tumors [58–60]. Recently Aguilar et al. [61] described the results of their phase II study of metronomic chemotherapy with thalidomide, carboplatin, vincristine, and fluvastatin in the treatment of brainstem tumors in children. Their objective was to determine tumor response to chemotherapy combined with an antiangiogenic drug thalidomide and fluvastatin that decreases the cholesterol substrate necessary for cancer cell growth by inhibiting biosynthesis of cholesterol. Nine recently diagnosed pediatric brainstem glioma patients were included. Patients received four continuous courses of chemotherapy consisting of carboplatin on day 1, vincristine on day 1, fluvastatin orally every 24 h on days 1–14, carboplatin and vincristine same dosage on day 15, and thalidomide orally on days 15–28. One month after finishing the last course of chemotherapy, patients underwent hyperfractionated radiotherapy followed by the administration of four more courses of the same chemotherapy. There was a significant reduction in the tumor volume, and overall survival was 71.5 % after 24 months. In this trial the antitumor effect of fluvastatin could not be attributed only to ability to inhibit cholesterol biosynthesis but also its potential to inhibit *Ras* farnesylation.

Table 37.4 Literature review of clinical trials of antiangiogenic therapy

Authors and year (reference)	No. of patients	Treatment	Outcome
Vredenburg et al. (2007) [53]	32 adult patients with GBM and WHO grade III gliomas	Bevacizumab and irinotecan	Median PFS 23 weeks 6 months PFS 38 % 6 months OS 72 %
Aguilar et al. 2008 [61]	9	Carboplatin, VCR, and fluvastatin and thalidomide (metronomic therapy) followed by XRT and the same chemotherapy × 4 courses	2-year OS 71.5 %

GBM Glioblastoma multiforme, *XRT* Radiotherapy, *PFS* Progression-free survival, *OS* Overall survival

More recently fluvastatin has been reported to activate caspase-1 and induce a small secretion of IL-18 in human peripheral blood mononuclear cells. This interleukin is known to exhibit antitumor activities by activation of cytotoxic T lymphocytes and natural killer cells by production of IFN-gamma and by inhibiting angiogenesis [62]. Thalidomide was investigated as an antineoplastic drug because of its known anti-inflammatory and immunomodulatory activities through degradation of mRNA encoding tumor necrosis factor-alpha in monocytes [63]. Thalidomide has also been shown to be antiangiogenic in the rabbit cornea micropocket assay [64] involving the anti-hypoxia-inducible factor pathway [65]. Results show a poor response when used as monotherapy but potential benefit when used in combination with other drugs [65] (Table 37.4).

37.5 Immunostimulatory Therapy

Despite advances in surgical-, radiation-, and chemotherapy-based strategies, malignant gliomas continue to be associated with a poor prognosis. Immunostimulants offer a novel treatment approach. Early attempts at glioma therapy based on immunostimulants failed to demonstrate effectiveness. Current immunostimulant therapies have shifted to a more multifaceted approach combining two or more different immunotherapeutic strategies. Immunotherapy, and in particular immunostimulants (also known as biologic modifiers), is an example of an area of research into novel therapy for use in high- and low-grade gliomas. Immunotherapy, or treatment that uses the body's immune system to combat tumors, is

attractive for cancer therapy for several reasons, including the conviction that it would be less toxic than the traditional cytotoxic therapies and may lead to sustained responses through immunologic memory. A group of immunostimulants commonly used are interferons. IFNs are glycoproteins, which are cell-signaling molecules produced by the cells of the immune system in response to challenges such as viruses and tumor cells. IFNs assist the immune response by inhibiting viral replication within host cells, activating natural killer cells and macrophages, increasing antigen presentation to lymphocytes, and inducing the resistance of host cells to viral infection. A member of the group is interferon-beta (IFN-beta). IFN-beta exerts its antitumor effect by inhibiting glioma cells in the S phase, enhancing natural killer cell and cytotoxic T-cell activity, and perhaps synergizing with cytotoxic chemotherapies [66]. An earlier example of immunostimulatory therapy was carried out by Packer et al. who attempted to treat newly diagnosed children with brainstem glioma with recombinant beta-interferon combined with hyperfractionated radiation therapy [19]. Thirty-two children with diffuse intrinsic brainstem gliomas were included in the study who were treated with 72 Gy of hyperfractionated radiotherapy along with beta-interferon that was initially begun at 12.5×10^6 IU/m² and escalated up to 400×10^6 IU/m². The safe starting dose was determined to be 100×10^6 IU/m². Due to unacceptable toxicity, the maintenance dose was reduced to 200×10^6 IU/m². Interferon-beta was continued for 8 weeks following radiotherapy. Unfortunately 30 of the 32 patients have developed progressive disease. The median time to progression from study entry was 5 months,

Table 37.5 Literature review of clinical trials of immunostimulatory therapy

Authors and year (reference)	No. of patients	Treatment	Outcome
Packer et al. (1996) [19]	32	XRT and IFN- β	MTP 5 months, MTD 9 months
Ohno et al. (2009) [67]	15	IFN- β , MCNU, and XRT	Median survival 14.7 months
Wolff et al. (2006) [75]	24	Cycle A, cisplatin; VP-16 Cycle B, Cisplatin; VP-16 and IFX maintenance, IFN γ and CTX	Median survival ~10 months

XRT Radiotherapy, MTP Median time to progression, MTD Median time to death, IFN- β interferon-beta, VP-16 etoposide, IFX Ifosfamide, IFN- γ Interferon-gamma, CTX Cyclophosphamide

and the median time to death was 9 months. This therapy did not result in a higher rate of disease control. Ohno et al. [67] evaluated the effects of treatment with IFN-Beta, MCNU, and radiotherapy (IMR therapy). Another aim of the study was to determine patient response to IMR therapy by evaluating O6-methylguanine-DNA methyltransferase (MGMT) promoter methylation in serum DNA. Fifteen newly diagnosed children with brainstem tumors were administered IFN-beta (1–2 MIU/day, days 1–7, 0.5–1 MIU/day, days 8–14) and MCNU (80 mg/m² on day 2) concurrent with conventional radiotherapy. Of the 15 patients, partial response, stable disease, and progressive disease were noted in 5 patients each. The median overall survival and the median progression-free survival were 14.7 and 4.6 months, respectively. The MGMT promoter methylation status in the serum appeared to correlate with a positive response to IMR therapy. Another IFN that was used for the treatment of glioma is IFN-gamma. IFN-gamma causes increased major histocompatibility complex expression on brain cells, class 1 antigen on local endothelial and ependymal cells, and class 2 antigen on microglial, ependymal, and perivascular cells. It also recruits lymphocytes and other inflammatory cells. These effects were accompanied by significant upregulation of tumor MHC-1 and MHC-2 expression. In addition, therapy downregulated the expression of endothelial Fas ligand, a cell membrane protein implicated as a contributor to immune privilege in cancer. It also promotes Th1 development by enhancing IL-12 secretion from macrophages and maintaining the expression

of IL-12R on CD4+ cells making them more responsive to IL-12. IFN-gamma and IL-12 production appear to correlate with the induction of antitumor activity [68–71]. The proliferation, adhesion to hyaluronic acid, and the migratory capacity of the glioma cells that express IFN-gamma receptor are inhibited by IFN-gamma [72, 73]. Interferon-gamma also has significant anti-angiogenic effects [74]. Wolff et al. investigated the usefulness of interferon-gamma and low-dose cyclophosphamide as a maintenance treatment in pediatric high-grade glioma patients [75]. Mitsuoka et al. first showed the immunomodulatory effect of cyclophosphamide, when given in lower doses [76]. A specific sensitivity of immunosuppressive T cells to very low concentration of cyclophosphamide has been shown in vitro [77]. The protocol in Wolf's study [75] used two cycles of chemotherapy consisting cisplatin and etoposide in the first and cisplatin, etoposide, and ifosfamide in the second cycle. Following induction, the maintenance therapy started with IFN-gamma with a starting dose of 25 mcg/m²/day which increased by 25 mcg/m² per week up to a maximum of 175 mcg/m². When the maximum dose of IFN was reached, cyclophosphamide was initiated as a 1 h infusion of 300 mg/m² to be repeated every 21 days. Forty pediatric high-grade glioma patients were enrolled, 24 of whom had brainstem tumors. The median overall survival of 1 year was not statistically different from the historical controls. The pontine glioma patients fared even worse, and this treatment was found to have no sufficient benefit for the treatment of such patients (Table 37.5).

37.6 Molecularly Targeted Therapies

In the light of the disappointing results of radiotherapy alone, in combination with, or followed by single or multiple agent chemotherapy for the treatment of pediatric brainstem tumors, there is a strong need to identify new therapeutic approaches that target features of these tumors that account for their dysregulated growth. Studies have demonstrated that malignant gliomas are driven to proliferate by aberrant activation of growth factor receptor-mediated signal transduction pathways [78]. The traditional approach of administering cytotoxic agents at the maximum tolerated dose is being supplanted by the development of molecularly targeted agents aimed at critical cellular changes that are responsible for the growth and spread of cancer cells. These agents theoretically should be more specific for tumor cells and less toxic to normal cells. Two general approaches to targeting cancer cells include (a) targeting critical cellular changes that are responsible for the growth and spread of a cancer cell (i.e., molecular targets) and (b) targeting specific antigens not present on normal cells. Recent advances in molecular biology have identified critical cellular changes within pediatric brain tumors, suggesting that molecularly targeted therapy may have a role in the treatment of these patients. Protein receptor tyrosine kinases (RTK) are a family of enzyme-linked surface receptors that interact to form a complex signaling network, integrating external stimuli from the cell surface with internal cellular responses. These enzymes reversibly phosphorylate proteins after a ligand binds to its receptor, leading to activation of signaling pathways [79, 80]. One important receptor pathway involves platelet-derived growth factor (PDGF) which encompasses a family of ligands (AA, AB, BB, CC, and DD) that bind to a pair of receptors (a and b) [81]. Concurrent expression of one or more of these ligands and their receptors has been observed in a high percentage of malignant gliomas [82, 83], allowing autocrine and paracrine stimulation for tumor cell growth [84, 85]. Inhibition of PDGF receptor (PDGFR)

activation, as well as pharmacological blockade of PDGFR, has been shown to inhibit glioma growth both in vitro and in vivo [85–87]. It has been demonstrated that PDGF plays a role in supporting the angiogenesis in malignant gliomas [84]. Inhibition of PDGFR in this regard may simultaneously block tumor growth and tumor-induced angiogenesis. Like PDGFR, EGFR has been frequently found to be amplified, overexpressed, or rearranged in gliomas. It is a member of the ErbB family of membrane receptors which include four related transmembrane glycoproteins [88]. Signaling by way of the ErbB receptor tyrosine kinase family has been implicated in the development of both normal and malignant tissue within the nervous system [89].

Pediatric brain tumor consortium conducted two phase I studies using a tyrosine kinase inhibitors imatinib (PDGFR inhibitor) and gefitinib (EGFR inhibitor) for the treatment of newly diagnosed or recurrent brainstem glioma in children. Patients received the drugs concurrently with and after radiation therapy. Radiation was conventional with a total dose of 5,580 cGy. These agents were continued for approximately a year in the absence of progression or serious toxicity. Unfortunately an unusually high number of patients experienced intratumoral hemorrhage which raised the concern that this could be related to these new agents; the studies were then amended to exclude the patients with radiological evidence of intratumoral hemorrhage not related to previous surgery and to start these molecules 2 weeks after radiotherapy [90, 91]. Another phase I study on an EGFR tyrosine kinase inhibitor tipifarnib by Haas-Kogan et al. [92] investigators used the agent orally 100–150 mg/kg/dose twice daily in children with newly diagnosed brainstem glioma both concurrent and following radiation. Postradiation dose was 200 mg/m²/dose bid for 21 consecutive days in 28-day cycles for up to 24 months in the absence of disease progression or severe toxicity. The maximum tolerated dose (MTD) of tipifarnib was 125 mg/m²/dose bid. Dose-limiting toxicities (DLT) were rash, infection, and neutropenia. One-year survival and progression-free survival of the patients were

36.4 and 9.4 %, respectively. Overall, minimal efficacy has been demonstrated for these single agents tested in the pediatric brain tumor population to date.

Human malignant glioma cell lines and adult brain tumors overexpress high levels of interleukin-13 receptor alpha 2 chain (IL-13Ralpha2). Joshi et al. [93] investigated the presence of this receptor in specimens of diffusely infiltrative pediatric brainstem gliomas using immunohistochemical (IHC) and in situ hybridization (ISH) assays and detected high levels of IL-13Ralpha2 RNA in tumor samples by Q-dot ISH but only weak RNA expression in normal brain tissue. There was significant agreement between IHC and ISH. IL-13Ralpha2 protein and mRNA are expressed to significantly higher levels in brainstem glioma than in normal brain tissue. Investigators concluded that this receptor could be an important new drug target for treatment of this disease. Okada and colleagues [94] studied the expression of three glioma-associated antigens EphA2, IL-13Ralpha2, and survivin by immunochemistry on paraffin-embedded tissue of 15 brainstem glioma and 12 non-brainstem glioma cases and found that 13 of the 15 BSGs and 12 of NBSGs expressed at least 1 antigen and 7 BSGs and 9 NBSGs expressed 2 antigens at higher levels than normal brain. They stated that these antigens are suitable targets for developing vaccine strategies for pediatric brainstem gliomas.

Gilbertson and colleagues performed molecular analysis on 28 brainstem glioma samples and found out that a large percentage of tumors were expressing EGFR with an intensity that correlated with the tumor grade [95]. Following this, Bode et al. carried out a study examining the effect of nimotuzumab (an anti-EGFR monoclonal antibody) in 22 children with relapsing malignant gliomas and pontine tumors. Ten patients showed stable disease and partial remissions [96].

37.7 New Drug Delivery Methods

Tumor progression in children with malignant gliomas typically results from failure of disease control at the primary tumor site. This factor

suggests that improvements in outcome may be feasible if strategies can be devised for enhancing the delivery of therapeutically active agents into the brain tumor microenvironment. Since blood–brain barrier restricts the entrance into the brain tumor of many chemotherapeutic agents and large macromolecules [95], strategies have been developed in finding ways of circumventing this obstacle. Two applications of these approaches in neuro-oncology are interstitial chemotherapy and convection-enhanced drug delivery. Interstitial chemotherapy using carmustine-impregnated polymers has been the most widely applied local delivery strategy for adult patients with brain tumors. These polymers are directly implanted into the tumor resection cavity at the time of surgery. Carmustine produces an antineoplastic effect by alkylating DNA and RNA. With this method, high intratumoral concentrations of the active agent can be achieved without any significant systemic toxicity [96, 97], in comparison with adult malignant gliomas, implementation of this technique in pediatric neuro-oncology has been limited because of the growth pattern differences of many pediatric brain tumors.

Although interstitial delivery represents a useful strategy for administering low-molecular-weight chemotherapy agents, such as BCNU, into the tumor resection cavity and periresectional brain, different approaches are required to deliver higher-molecular-weight agents, such as immunotoxins, that target cell surface proteins selectively expressed on glioma cells relative to normal brain. Studies by Oldfield and collaborators demonstrated the feasibility of using positive-pressure microinfusion at flow rates in the range of 0.5–6 $\mu\text{l}/\text{min}$, via catheters implanted into the brain, as a way to enhance the distribution of macromolecules of this size by convection, rather than diffusion [98, 99]. With this technique, ligands or antibodies coupled to a mutated toxin, such as pseudomonas exotoxin (PE38) or diphtheria toxin (CRM107) [100, 101], can be targeted against receptors overexpressed on brain tumor cells relative to normal brain. To date, a variety of receptors have been targeted, including the epidermal growth factor receptor (EGFR), the interleukin 4 (IL4) and 13 (IL13) receptors, the transferrin

receptor (TfR), and the urokinase-type plasminogen activator receptor (uPAR). All convection-enhanced delivery studies to date have been performed on supratentorial hemispheric tumors in adult patients. Since many pediatric brainstem tumors share many receptor expression characteristics with non-brainstem malignant gliomas, interest has been directed at exploring the use of convection-enhanced delivery of immunotoxin conjugates for such tumors in children. It has been shown with animal model studies that convection-enhanced delivery to brainstem is possible and tolerable with adequate distribution of the infusate throughout the brainstem parenchyma [102, 103]. The results of these studies may eventually be translated into clinical practice.

Interstitial brachytherapy has long been used in the adult patients with good results, but its utilization in the pediatric patient remains limited predominantly to patients with cystic craniopharyngiomas and focal gliomas [104]. Pollack et al. [105] used intracavitary P-32 in a series of children with cystic craniopharyngioma and demonstrated radiological evidence of cyst regression. The application of interstitial radiation to cystic gliomas has also demonstrated efficacy [106] and may be considered an option for adjunct therapy in the young patient with brainstem cystic gliomas. With the aim of improving local control, investigators utilized I-125 implants in the brainstem and cerebral hemispheres of children with recurrent brainstem and supratentorial gliomas followed by conventional external beam radiation [107, 108]. Significant improvement has been observed in a number of patients with minimal morbidity.

37.8 Targeted Monoclonal Antibody

Gilbertson and colleagues performed molecular analysis on 28 brainstem glioma samples and found out that a large percentage of tumors were expressing EGFR with an intensity that correlated with the tumor grade [109]. Following this, Bode et al. carried out a study examining the effect of nimotuzumab (an anti-EGFR monoclonal

antibody) in 22 children with relapsing malignant gliomas and pontine tumors. Ten patients showed stable disease and partial remissions [110]. Another report published by Massimo et al. revealed the activity of nimotuzumab in a phase II trial on 47 relapsing pediatric patients with diffuse intrinsic pontine gliomas and high-grade gliomas. This was a multicenter study combining nimotuzumab and radiotherapy demonstrating disease control and overall patient survival similar to previous experiences with good quality of life and minimal side effects [111].

37.9 Chemotherapy for Nondiffuse Brainstem Gliomas

The majority of focal midbrain tumors, either tectal or tegmental, are grade I or grade II astrocytomas [8]. Tectal plate tumors are often small and produce hydrocephalus with or without midbrain eye signs. They can be followed by serial MRIs, but often these will remain unchanged for many years. For tumor progression, surgery is indicated with the aim of total resection if possible. Tegmental and other non-tectal midbrain tumors tend to be larger and more frequently show sign and symptoms of brainstem involvement [112]. Surgery is indicated for these tumors followed by radiotherapy for the incompletely resected ones. An increasing number of patients are being treated with systemic chemotherapy for symptomatic and recurrent low-grade tumors. The commonly used regimens contain carboplatin and vincristine and nitrosurea-containing multiagent chemotherapy drugs. Cervicomedullary tumors are essentially very rostral intrinsic spinal cord tumors approximately 90 % of which are low-grade astrocytomas. These tumors are also associated with a favorable prognosis. Both gangliogliomas and ependymomas have also been reported in this region [113, 114]. About 10 % of the tumors originating from the cervicomedullary region are anaplastic astrocytomas. Opinions differ about the role of chemotherapy in the treatment of cervicomedullary gliomas. Some argue that it should be used as the initial treatment for children under 10 years old or for older patients

whose tumors have progressed after irradiation. Others recommend it only in children when surgery has failed or as an adjuvant therapy [113, 115, 116]. Single- and multidrug regimens have been tested. Actinomycin-D and vincristine allow deferment of radiotherapy in children younger than 5 years old. Alternatively, carboplatin, currently the most effective drug, can be used alone or in combination with vincristine [117, 118]. Dorsally exophytic subtype of brainstem tumors make up approximately 14–24 % of the whole population [119–121]. These tumors occur at a younger age than other brainstem tumors, and over one quarter of patients present in the first year of life [119, 120]. Compared to diffuse brainstem gliomas, dorsally exophytic lesions tend to have a longer duration of symptoms, which is generally over 6 months [120, 121]. Of all the brainstem glioma subtypes, dorsally exophytic lesions are the most surgically accessible. The mainstay of treatment is surgical debulking followed by close observation. Radiotherapy and chemotherapy are reserved for the recurrent lesions. For low-grade gliomas, particularly those that cannot be surgically resected, chemotherapy has a role in disease stabilization [122]. This is particularly useful in younger children in order to delay radiotherapy. Although a variety of both single agents and combined therapies have been studied, the combination of vincristine with carboplatin is the most widely utilized [117, 118]. This regimen has produced approximately 50–60 % radiographic response rates in children with progressive disease.

References

- Walker DA, Punt JA, Sokal M (1999) Clinical management of brainstem glioma. *Arch Dis Child* 80:558–564
- Allen J (1983) Brain stem glioma. *Neurol Neuro Surg Updat Ser* 20:2–7
- Freeman CR, Farmier JP (1998) Pediatric brain stem gliomas: a review. *Int J Radiat Oncol Biol Phys* 40:265–271
- Albright AL, Pollack IF (2004) Brainstem gliomas. In: Winn HR (ed) *Youmans neurological surgery*, vol 3. Saunders, Philadelphia, pp 3663–3669
- Littman P, Jarrett P, Bilaniuk LT, Rorke LB et al (1980) Pediatric brain stem gliomas. *Cancer* 45:2787–2792
- Berger MS, Edwards MS, LaMasters D et al (1983) Pediatric brain stem tumors: radiographic, pathological, and clinical correlations. *Neurosurgery* 12:298–302
- Choux M, Lena G, Do L (2000) Brainstem tumors. In: Choux M, Di Rocco C, Hockley A (eds) *Pediatric neurosurgery*. Churchill Livingstone, New York, pp 471–491
- Jallo GI, Biser-Rohrbaugh A, Freed D (2004) Brainstem gliomas. *Childs Nerv Syst* 20:143–153
- Allen JC, Siffert J (1996) Contemporary chemotherapy issues for children with brainstem gliomas. *Pediatr Neurosurg* 24:98–102
- Langmoen IA, Lundar T, Storm-Mathisen I et al (1991) Management of pediatric pontine gliomas. *Childs Nerv Syst* 7:13–15
- Albright AL, Price RA, Buthkelch AN (1983) Brain stem glioma in children. *Cancer* 52:2313–2319
- Edwards MS, Wara WM, Urtasun RC et al (1989) Hyperfractionated radiation therapy for brainstem glioma: a phase I-II trial. *J Neurosurg* 70:691–700
- Freeman CR, Krischer J, Sanford RA et al (1988) Hyperfractionated radiotherapy in brainstem tumors: results of a Pediatric Oncology Group Study. *Int J Radiat Oncol Biol Phys* 15:311–318
- Freeman CR, Krischer J, Sanford RA et al (1991) Hyperfractionated radiotherapy in brainstem tumors. Results of treatment at the 7020 cGy dose level of Pediatric Oncology Group study #8495. *Cancer* 68:474–481
- Lewis J, Lucraft H, Gholkar A (1997) UKCCSG study of accelerated radiotherapy for pediatric brainstem gliomas. United Kingdom Childhood Cancer Study Group. *Int J Radiat Oncol Biol Phys* 38:925–929
- Packer RJ, Boyett JM, Zimmerman RA et al (1994) Outcome of children with brain stem gliomas after treatment after treatment with 7800 cGy of hyperfractionated radiotherapy. A Children's Cancer Group Phase I/II Trial. *Cancer* 74:1827–1834
- Packer RJ, Boyett JM, Zimmerman RA et al (1993) Hyperfractionated radiation therapy (72Gy) for children with brain stem gliomas. A Children's Cancer Group Phase I/II trial. *Cancer* 72:1414–1421
- Packer RJ, Littman PA, Sposto RM et al (1987) Results of a pilot study of hyperfractionated radiation therapy for children with brainstem gliomas. *Int J Radiat Oncol Biol Phys* 13:1647–1651
- Packer RJ, Prados M, Phillips P et al (1996) Treatment of children with newly diagnosed brainstem gliomas with intravenous recombinant beta-interferon and hyperfractionated radiation therapy. A Children's Cancer Group Phase I/II Study. *Cancer* 77:2150–2156
- Doz F, Neuenschwander S, Bouffet E et al (2002) Carboplatin before and radiation therapy for the treatment of malignant brain stem tumors: a study by Societe Francaise d'Oncologie Pediatric. *Eur J Cancer* 38:815–819

21. Dunkel IJ, Garvin HJ Jr, Goldman S et al (1998) High-dose chemotherapy with autologous bone marrow rescue for children with diffuse pontine brain stem tumors. *Children's Cancer Group. J Neurooncol* 37:67–73
22. Allen J, Siffert J, Donahue B et al (1999) A phase I/II study of carboplatin combined with hyperfractionated radiotherapy for brainstem gliomas. *Cancer* 86:1064–1069
23. Bernier-Chastagner V, Grill J, Doz F et al (2005) Topotecan as a radiosensitizer in the treatment of children with malignant diffuse brainstem gliomas; result of a French Society of Paediatric Oncology Phase II Study. *Cancer* 104:2792–2797
24. Greenberg ML, Fisher PG, Freeman C et al (2005) Etoposide, vincristine, and cyclosporine A with standard dose radiation therapy in newly diagnosed diffuse intrinsic brainstem gliomas: a pediatric oncology group phase I study. *Pediatr Blood Cancer* 45:644–648
25. Jenkin RD, Boesel C, Ertel I et al (1987) Brain-stem tumors in childhood: a prospective randomized trial of irradiation with and without adjuvant CCNU, VCR and prednisone. A report of the Children's Cancer Study Group. *J Neurosurg* 66:227–233
26. Wakabayashi T, Yoshida J, Mizuno M et al (1992) Effectiveness of interferon-beta, ACNU, and radiation therapy in pediatric patients with brainstem glioma. *Neurol Med Chir (Tokyo)* 32:942–946
27. Wolff JE, Westphal S, Molenkamp G et al (2002) Treatment of paediatric pontine glioma with trophosphamide and etoposide. *Br J Cancer* 87:945–949
28. Jakacki RI, Jamison C, Mathews VP et al (1998) Dose-intensification of procarbazine, CCNU (lomustine), vincristine (PCV) with peripheral blood stem cell support in young patients with gliomas. *Med Pediatr Oncol* 31:483–490
29. Jennings MT, Sposto R, Boyett JM et al (2002) Preradiation chemotherapy in primary high-risk brainstem tumors: phase II study CCG-9941 of the Children's Cancer Group. *J Clin Oncol* 20:227–233
30. Kretschmar CS, Tarbell NJ, Barnes PD et al (1993) Pre-irradiation chemotherapy and hyperfractionated radiation therapy 66 Gy for children with brain stem tumors. A phase II study of the Pediatric Oncology Group, Protocol 8833. *Cancer* 72:1404–1413
31. Frappaz D, Schell M, Thiesse P et al (2008) Preradiation chemotherapy may improve survival in pediatric diffuse intrinsic brainstem gliomas: final results of BSG 98 prospective trial. *Neuro Oncol* 10(4):599–607
32. Mandell LR, Kadota R, Freeman C et al (1999) There is no role for hyperfractionated radiotherapy in the management of children with newly diagnosed diffuse intrinsic brainstem tumors: results of a Pediatric Oncology Group phase III trial comparing conventional vs. hyperfractionated radiotherapy. *Int J Radiat Oncol Biol Phys* 43:959–964
33. Packer RJ, Krailo M, Mehta M et al (2005) Phase I study of concurrent RMP-7 and carboplatin with radiotherapy for children with newly diagnosed brainstem gliomas. *Cancer* 104:1281–1287
34. Sanghavi SN, Needle MN, Krailo MD et al (2003) A phase I study of topotecan as a radiosensitizer for brainstem glioma of childhood: first report of the Children's Cancer Group-0952. *Neuro Oncol* 5:8–13
35. Walter AW, Gajjar A, Ochs JS et al (1998) Carboplatin and etoposide with hyperfractionated radiotherapy in children with newly diagnosed diffuse pontine gliomas: a phase I/II study. *Med Pediatr Oncol* 30:28–33
36. Broniscer A, Leite CDC, Lanchote VL et al (2000) Radiation therapy and high-dose tamoxifen in the treatment of patients with diffuse brainstem gliomas: results of a Brazilian Cooperative Study. *J Clin Oncol* 18:1246–1253
37. Turner CD, Chi S, Marcus KJ et al (2007) Phase II study of thalidomide and radiation in children with newly diagnosed brain stem gliomas and glioblastoma multiforme. *J Neurooncol* 82:95–101
38. Sirachainan N, Pakakasama S, Visudithbhan A et al (2008) Concurrent radiotherapy with temozolomide followed by adjuvant temozolomide and cis-retinoic acid in children with diffuse intrinsic pontine glioma. *Neuro-Oncology* 10:577–582
39. Korones DN, Fisher PG, Kretschmar C et al (2008) Treatment of children with diffuse intrinsic pontine glioma with radiotherapy, vincristine, and oral VP-16: a Children's Oncology Group Phase II Study. *Pediatr Blood Cancer* 50:227–230
40. Bouffet E, Raquin M, Doz F et al (2000) Radiotherapy followed by high dose busulfan and thiotepa: a prospective assessment of high dose chemotherapy in children with diffuse pontine gliomas. *Cancer* 88:685–692
41. Benesch M, Lackner H, Moser A et al (2001) Outcome and long-term side effects after synchronous radiochemotherapy for childhood brain stem glioma. *Pediatr Neurosurg* 35:173–180
42. Wagner S, Warmuth-Metz M, Emser A et al (2006) Treatment options in childhood pontine gliomas. *J Neurooncol* 79(3):281–287
43. Lopez Aguilar E, Sepulveda-Vildosola AC, Riviera-Marquez H et al (2003) Preirradiation ifosfamide, carboplatin and etoposide (ICE) for the treatment of high-grade astrocytomas in children. *Child Nerv Syst* 19:818–823
44. Tuettenberg J, Friedel C, VAjkoczy P (2006) Angiogenesis in malignant glioma- a target for antitumor therapy. *Crit Rev Oncol Hematol* 59:181–193
45. Carmeliet P, Jain RK (2000) Angiogenesis in cancer and other diseases. *Nature* 407:249–257
46. Leon SP, Folkerth RD, Black PM (1996) Microvessel density is a prognostic indicator for patients with astroglial brain tumors. *Cancer* 77:362–372
47. Folkman J (1971) Tumor angiogenesis: therapeutic implications. *N Engl J Med* 285:1182–1186
48. Ferrera N, Hillan KJ, Gerber HP et al (2004) Discovery and development of bevacizumab, an anti-VEGF antibody for treating cancer. *Nt Rev Drug Discov* 3:391–400
49. Rubenstein JL, Kim J, Ozawa T et al (2000) Anti VEGF-antibody treatment of glioblastoma prolongs

- survival but results in increased vascular cooption. *Neoplasia* 2:306–314
50. Wildiers H, Guetens G, De Boeck G et al (2003) Effect of antivascular endothelial growth factor treatment on the intratumoral uptake of CPT-11. *Br J Cancer* 88:1979–1986
 51. Gerber HP, Ferrera N (2005) Pharmacology and pharmacodynamics of bevacizumab as monotherapy or in combination with cytotoxic therapy in preclinical studies. *Cancer Res* 65:671–680
 52. Stark VV (2005) Bevacizumab and CPT-11 in the treatment of relapsed malignant glioma. *Neuro Oncol* 7:369
 53. Vredenburgh JJ, Desjardins A, Herndon JE et al (2007) Phase II trial of bevacizumab and irinotecan in recurrent malignant glioma. *Clin Cancer Res* 13:1253–1259
 54. Torcuator R, Zuniga R, Loutfi R et al (2009) Bevacizumab and irinotecan treatment for progressive diffuse brainstem glioma: case report. *J Neurooncol* 93:409–412
 55. Liu AK, Macy ME, Foreman NK (2009) Bevacizumab as therapy for radiation necrosis in four children with pontine gliomas. *Int J Radiat Oncol Biol Phys* 75:1148–1154
 56. Laquente B, Vinals F, Germa JR (2007) Metronomic chemotherapy: an antiangiogenic scheduling. *Clin Transl Oncol* 9:93–98
 57. Benbrahim Z, Assard C, El Mesbahi O (2011) Metronomic chemotherapy in 2011: update and perspectives. *Bull Cancer* 98:1447–1454
 58. Sterba J, Pavelka Z, Stampa P (2002) Concomitant radiotherapy and metronomic temozolomide in pediatric high-risk brain tumors. *Neoplasia* 49:117–120
 59. Herrlinger U, Rieger J, Steinbach JP et al (2005) UKT-04 trial of continuous low dose metronomic therapy with methotrexate and cyclophosphamide for recurrent glioblastoma. *J Neurooncol* 71(3):295–9
 60. Peyrl A, Chocholous M, Kieran MW et al (2012) Antiangiogenic metronomic therapy for children with recurrent embryonal brain tumors. *Pediatr Blood Cancer* 59:511–517
 61. Lopez Aguilar E, Sepulveda-Vildosola AC, Cabrera YB et al (2008) Phase II study of metronomic chemotherapy with thalidomide, carboplatin, vincristine, fluvastatin in the treatment of brain stem tumors in children. *Arch Med Res* 39:655–662
 62. Kohka-Takashi H, Weitz-Schmidt G, Iwagaki H et al (2006) Hypothesis: the antitumor activity of statins may be mediated by IL-18. *J Leukocyte Biol* 80:215–216
 63. Teo S, Colburn W, Tracewell W et al (2004) Clinical pharmacokinetics of thalidomide. *Clin Pharmacokin* 43:311–327
 64. D' Amato RJ, Loughnan MS, Flynn E et al (1994) Thalidomide is an inhibitor of angiogenesis. *Proc Natl Acad Sci U S A* 91:4082–4085
 65. Jouanneau E (2008) Angiogenesis and gliomas: current issues and development of surrogate markers. *Neurosurgery* 98:353–364
 66. Denbo JW, Williams RF, Orr WS et al (2011) Continuous local delivery of interferon-beta stabilizes tumor vasculature in an orthotopic glioblastoma xenograft resection model. *Surgery* 150:497–504
 67. Ohno M, Natsume A, Fujii M et al (2009) Interferon-beta, and conventional radiotherapy for pediatric patients with brainstem glioma. *Pediatr Blood Cancer* 53:37–41
 68. Bach EA, Auget M, Schreiber RD (1997) The IFN gamma receptor: a paradigm for cytokine receptor signaling. *Annu Rev Immunol* 15:563–591
 69. Abbas AK, Murphy KM, Sher A (1996) Functional diversity of helper T lymphocytes. *Nature* 383:787–793
 70. Dredge K, Marriot JB, Todryk SM et al (2002) Adjuvants and the promotion of Th-1 type cytokines in tumour immunotherapy. *Cancer Immunol Immunother* 51:521–531
 71. Knüpfner MM, Poppenborg H, Van Gool SW et al (1997) Interferon-gamma inhibits proliferation and adhesion of T98G human malignant glioma cells in vitro. *Klin Pediatr* 209:271–274
 72. Knüpfner MM, Knüpfner A, Van Gool SW et al (2000) Interferon-gamma inhibits proliferation and hyaluronic acid adhesion of human malignant glioma cells in vitro. *Cytokine* 12:409–412
 73. Knüpfner MM, Knüpfner A, Jendrossek V et al (2001) Interferon-gamma inhibits growth and migration of A172 human glioblastoma cells. *Anticancer Res* 21:3989–3994
 74. Beatty G, Paterson Y (2001) IFN-g-dependent inhibition of tumor angiogenesis by tumor-infiltrating CD4+ T cells requires tumor responsiveness to IFN-g. *J Immunol* 166:2276–2282
 75. Wolff JE, Wagner S, Reinert C et al (2006) Maintenance treatment with interferon-gamma and low-dose cyclophosphamide for pediatric high-grade glioma. *J Neurooncol* 79:315–321
 76. Mitsuoka A, Baba M, Morikawa S (1976) Enhancement of delayed hypersensitivity by depletion of suppressor T cells with cyclophosphamide in mice. *Nature* 262:77–78
 77. Ozer H, Cowens JW, Colvin M et al (1982) In vitro effects of 4-hydroperoxy-cyclophosphamide in human immunoregulatory T subset function. I. Selective effects on lymphocyte function in T-B collaboration. *J Exp Med* 155:276–290
 78. Nathoo N, Goldlust S, Vogelbaum M (2004) Epidermal growth factor receptor antagonists: novel therapy for the treatment of high grade gliomas. *Neurosurg Online* 54:1480–1488
 79. Ulrich A, Schlessinger J (1990) Signal transduction by receptors with tyrosine kinase activity. *Cell* 61:203–212
 80. Sibley D, Benovic J, Caron M et al (1987) Regulation of transmembrane signalling by receptor phosphorylation. *Cell* 48:913–922
 81. Kapoor G, O'Rourke D (2003) Receptor tyrosine kinase signaling in gliomagenesis. *Cancer Biol Ther* 2:330–342

82. Maher E, Furnari F, Bachoo R et al (2001) Malignant glioma: genetics and biology of a grave matter. *Genes Dev* 15:1311–1333
83. Westermark B, Heldin C, Nister M (1995) Platelet-derived growth factor in human glioma. *Glia* 15:257–263
84. Lokker N, Sullivan C, Hollenbach S et al (2002) Platelet-derived growth factor (PDGF) autocrine signaling regulates survival and mitogenic pathways in glioblastoma cells: evidence that the novel PDGF-C and PDGF-D ligands may play a role in the development of brain tumors. *Cancer Res* 62:3729–3735
85. Kilic T, Alberta J, Zdunek P (2000) Intracranial inhibition of platelet-derived growth factor mediated glioblastoma cell growth by an orally active kinase inhibitor of 2-phenylaminopyridine class. *Cancer Res* 60:5143–5150
86. Traxler P, Bold G, Buchdunger E et al (2011) Tyrosine kinase inhibitors: from rational design to clinical trials. *Med Res Rev* 21:499–512
87. Mauroro A, Bulfone A, Turco E et al (1991) Coexpression of platelet-derived growth factor (PDGF) B chain and PDGF B-type receptor in human gliomas. *Childs Nerv Syst* 7:432–436
88. Baselga J (2002) Why the epidermal growth factor receptor? The rationale for cancer therapy. *Oncologist* 7:2–8
89. Gilbertson R, Herna R, Pietsch T et al (2001) Novel ERBB4 receptor spliced variants are frequently expressed in childhood medulloblastoma. *Genes Chromosomes Cancer* 31:288–294
90. Pollack IF, Jakacki RI, Blaney SM et al (2007) Phase I trial of imatinib in children with newly diagnosed brainstem and recurrent malignant gliomas: a Pediatric Brain Tumor Consortium report. *Neuro Oncol* 9:145–160
91. Geyer JR, Boyett J, Douglas J et al (2004) Phase I trial of ZD1839 (Iressa TM) and radiation in pediatric patients newly diagnosed with brainstem tumors or incompletely resected supratentorial malignant gliomas. In: *ASTRO 46th annual meeting, 2004 Atlanta: International Journal of radiation Oncology Biology and Physics*; pp S251
92. Haas Kogan DA, Banerjee A, Kocak M et al (2008) Phase I trial of tipifarnib in children with newly diagnosed intrinsic diffuse brainstem glioma. *Neuro Oncol* 10:341–347
93. Joshi BH, Puri RA, Leland P et al (2008) Identification of interleukin-13 receptor alpha2 chain overexpression in situ in high-grade diffusely infiltrative pediatric brainstem glioma. *Neuro Oncol* 10:265–274
94. Okada H, Low KL, Kohanbash G et al (2008) Expression of glioma-associated antigens in pediatric brain stem and non-brain stem gliomas. *J Neurooncol* 88(3):245–250
95. Groothuis DR (2000) The blood-brain and blood-tumor barriers: a review for strategies for increasing drug delivery. *Neuro-Oncology* 2:45–49
96. Sipes E, Tyler B, Piantadosi S et al (1997) Optimizing interstitial delivery of BCNU from controlled release polymers for the treatment of brain tumors. *Cancer Chemother Pharmacol* 39:383–389
97. Wang C, Li J, Teo CS, Lee T (1999) The delivery of BCNU to brain tumors. *J Control Release* 61:21–41
98. Bobo RH, Laske D, Akbasak A et al (1994) Convection-enhanced delivery of macromolecules in the brain. *Proc Natl Acad Sci* 91:2076–2080
99. Liebermann DM, Laske DW, Morrison PF et al (1995) Convection-enhanced distribution of large molecules in gray matter during interstitial drug infusion. *J Neurosurg* 82:1021–1029
100. Pastan I, Fitzgerald D (1991) Recombinant toxin for cancer treatment. *Science* 254:1173
101. Greenfield L, Johnson VG, Youle RJ (1987) Mutations in diphtheria toxin separate binding from entry and amplify immunotoxin selectivity. *Science* 238:536–539
102. Occhigrosso G, Edgar MA, Sandberg DI (2003) Prolonged convection-enhanced delivery into rat brainstem. *Neurosurgery* 52:388–393
103. Lonser RR, Walbridge S, Garmestani K et al (2002) Successful and safe perfusion of the primate brainstem: in vivo magnetic resonance imaging of macromolecular distribution during infusion. *J Neurosurg* 97:905–913
104. Bernstein M, Laperriere NJ (1990–1991) A critical appraisal of the role of brachytherapy for pediatric brain tumors. *Pediatr Neurosurg* 16:213–218
105. Pollack IF, Lundsford LD, Slamovitz TL et al (1998) Stereotactic intracavitary irradiation for cystic cranio-pharyngiomas. *J Neurosurg* 68:227–233
106. Hood TW, McKeever PE (1988) Stereotactic management of cystic gliomas of the brain stem. *Neurosurgery* 24:373–378
107. Fontanesi J, Heideman RL, Muhlbauer M et al (1995) High-activity 125-I interstitial irradiation in the treatment of pediatric central nervous system tumors: a pilot study. *Pediatr Neurosurg* 22:289–295
108. Chujba PJ, Zamarano L, Hamre M et al (1998) Permanent I-125 brainstem implants in children. *Childs Nerv Syst* 14:570–577
109. Gilbertson RJ, Hill DA, Hernan R (2003) ERBB 1 is amplified and overexpressed in high-grade diffusely infiltrative pediatric brainstem gliomas. *Clin Cancer Res* 9:3620–3624
110. Bode U, Buchen S, Warmuth-Metz M et al (2007) Final report of a phase II trial of nimotuzumab in the treatment of refractory and relapsed high-grade gliomas in children and adolescents. *J Clin Oncol*. 2007 ASCO Annual Meeting Proceedings; (abstract) 25, 18S (20 Jun Supplement)
111. Massimo M, Bode U, Biassoni V et al (2011) Nimotuzumab for pediatric diffuse intrinsic pontine gliomas. *Expert Opin Biol Ther* 11:247–256
112. Fischbein NJ, Prados MD, Wara W et al (1996) Radiologic classification of brainstem tumors: correlation of magnetic resonance imaging appearance with clinical outcome. *Pediatr Neurosurg* 24:9–23
113. Klimo P Jr, Pai Panandiker AS, Thompson CJ et al (2013) Management and outcome of focal low-grade brainstem tumors in pediatric patients: the St. Jude experience. *J Neurosurg Pediatr* 11:274–281

114. Alaqeel AM, Sabbagh AJ (2014) Pediatric brainstem tumors. Classifications, investigations, and growth patterns. *Neurosciences* 19:93–99
115. Rubin G, Miskowitz S, Horev G et al (1998) Pediatric brain stem gliomas: an update. *Childs Nerv Syst* 14:167–173
116. Di Maio S, Gul SM, Cochrane DD et al (2009) Clinical, radiologic and pathologic features and outcome following surgery for cervicomedullary gliomas in children. *Childs Nerv Syst* 25:1401–1410
117. Packer RJ, Lange B, Ater J et al (1993) Carboplatin and vincristine for recurrent and newly diagnosed low-grade gliomas of childhood. *J Clin Oncol* 11:850–856
118. Ronghe M, Hargrave D, Bartels U et al (2010) Vincristine and carboplatin chemotherapy for unresectable and/or recurrent low-grade astrocytoma of the brainstem. *Pediatr Blood Cancer* 55:471–477
119. Hoffman HJ (1996) Dorsally exofitric brain stem tumors and midbrain tumors. *Pediatr Neurosurg* 24:256–262
120. Polalck IF, Hoffman HJ, Humphreys RP et al (1993) The long-term outcome after surgical treatment of dorsally exophytic brain stem gliomas. *J Neurosurg* 78:859–863
121. Garzon M, Garcia-Fructuoso G, Guillen A et al (2013) Brain stem tumors in children and adolescents: single institutional experience. *Childs Nerv Syst* 29:1321–1331
122. Khatib ZA, Heideman RL, Kovnar EH et al (1994) Predominance of pilocytic histology in dorsally exophytic brain stem tumors. *Pediatr Neurosurg* 20:2–10

Pathologies in Pediatric Posterior Fossa Tumors: AT/RT

Concezio Di Rocco

C. Di Rocco, M.D.
Division of Pediatric Neurosurgery,
Catholic University, School of Medicine, Rome, Italy

Su Gulsun Berrak

Atypical teratoid/rhabdoid tumors (AT/RTs) of central nervous system (CNS) are rare and among the most malignant neoplasms in children younger than 3 years of age. AT/RT is composed of rhabdoid cells that were first reported in 1985 by Briner et al. [1]. However, its clinical and pathological features remained obscure until 1995 [2–4]. AT/RT is characterized by gene abnormalities within the long arm of chromosome 22. The mutations of the SMARCB1 gene [MIM *601607] that is located on the long arm of chromosome 22 – i.e. 22q11.2 region – have been identified in approximately in 75 % of ATRTs. The SMARCB1 gene that is also known by other names such as INI1 or hSNF5 is part of the SWI/SNF chromatin-remodeling complex. It functions as a DNA-binding protein, facilitating SWI/SNF mediated co-transactivation of genes involved in cell cycle regulation [2, 5, 6]. Mutations of the SMARCB1 gene leads to cell cycle arrest via the SWI/SNF pathway [6–9]. It is known that the SMARCB1 gene is inactivated either by gross chromosomal aberrations or loss of heterozygosity (LOH) of the chromosomal region 22q11.2 containing the SMARCB1 gene, as well as a

range of private point mutations [10]. In addition to mutations of the SMARCB1 gene within the tumor, there are reports of patients from the same family that were found to have germline mutations in one allele of the SMARCB1 gene, and the remaining allele has been found to be lost within their tumors [10–13]. This is called Rhabdoid Tumor Predisposition Syndrome (RTPS) [MIM #609322]. RTPS is an autosomal dominant cancer syndrome predisposing to renal or extrarenal malignant rhabdoid tumors [12]. RTPS is usually due to LOH of the SMARCB1 gene and rarely of the SMARCA4 gene located in 19p13 [14]. Several authors have confirmed that the presence of such germline mutations is almost always associated with a lower median age at diagnosis and worse overall survival rate [10, 15]. These three findings qualified the SMARCB1 gene as a tumor suppressor gene [5, 16–18]:

- Homozygous somatic loss of function mutations resulting in sporadic tumors
- Germline anomalies associated with somatic loss of the wild-type allele in tumors resulting in a dominantly inherited cancer predisposition syndromes
- Development of rhabdoid like tumors in all mice with heterozygous mutation of the SMARCB1 gene.

In one of the early studies, Berrak et al. [19] have demonstrated high expression of abnormal pRb and p16 and low expression of abnormal p53 and MMAC/PTEN within the AT/RTs that

S.G. Berrak, M.D.
Division of General Pediatrics, LINCOS,
Children's Hospital at Montefiore, Albert Einstein
College of Medicine, 3415 Bainbridge Avenue,
Bronx, NY 10467, USA
e-mail: sberrak@montefiore.org

indicates an alteration of the G1-to-S-phase step in the cell cycle within the tumor. At the same time Zhang et al. [20] suggested that one of the mechanisms by which the SMARCB1 gene exerts its tumor suppressor function is by mediating the cell cycle arrest due to the direct repression of the cyclin D1 gene thereby causing G0–G1 arrest. After a set of experiments, McKenna et al. [17] demonstrated that the tumor suppressor activity of the SMARCB1 gene that features as a gatekeeper in cell cycle S-phase entry arises from epigenetic reader activity rather than from its role in DNA repair and maintenance of genome stability. Epigenetic activity includes methylation of cytosine bases in DNA, posttranslational modifications of histone proteins, as well as the positioning of nucleosomes along the DNA. Since epigenetic changes are known to be potentially reversible – unlike the genetic mutations – this might present as a significant therapeutic option in AT/RTs. The epigenetic pathway inhibitors such as histone deacetylase inhibitors [21–23] and DNA methylation inhibitors have been trialed on in vitro and in vivo models with promising success [21, 24]. There are also studies that show fibroblast growth factor receptors, Cyclin D1 and Aurora Kinase A as novel possible therapeutic targets in AT/RTs [25, 26]. Further molecular analysis of AT/RTs with the aim of identifying potential therapeutic targets in order to improve survival rates in children is the ultimate goal.

Conclusion

AT/RT is a rare disease with poor prognosis and aggressive phenotype. There is a clear need for further molecular analysis of AT/RTs with the aim of identifying novel treatment strategies that target the genetic abnormalities.

References

1. Briner J, Bannwart F, Kleihaus P, Odermatt B, Janzer R, Willi U, Boltshauser E (1985) Malignant small cell tumour of the brain with intermediate filaments—a case of primary cerebral rhabdoid tumour. *Pediatr Pathol* 3:117–118 [Abstract]
2. Rorke LB, Packer R, Biegel J (1995) Central nervous system atypical teratoid/rhabdoid tumors of infancy and childhood. *J Neurooncol* 24:21–28
3. Rorke LB, Packer RJ, Biegel JA (1996) Central nervous system atypical teratoid/rhabdoid tumors of infancy and childhood: definition of an entity. *J Neurosurg* 85:56–65
4. Biegel JA, Rorke LB, Packer RJ, Emanuel BS (1990) Monosomy 22 in rhabdoid or atypical tumors of the brain. *J Neurosurg* 73:710–714
5. Roberts CW, Orkin SH (2004) The SWI/SNF complex—chromatin and cancer. *Nat Rev Cancer* 4:133–142
6. Rousseau-Merck MF, Versteeg I, Legrand I, Couturier J, Mairal A, Delattre O et al (1999) hSNF5/INI1 inactivation is mainly associated with homozygous deletions and mitotic recombinations in rhabdoid tumors. *Cancer Res* 59:3152–3156
7. Betz BL, Strobeck MW, Reisman DN, Knudsen ES, Weissman BE (2002) Re-expression of hSNF5/INI1/BAF47 in pediatric tumor cells leads to G1 arrest associated with induction of p16ink4a and activation of RB. *Oncogene* 21:5193–5203
8. Bruch LA, Hill DA, Cai DX, Levy BK, Dehner LP, Perry A (2001) A role for fluorescence in situ hybridization detection of chromosome 22q dosage in distinguishing atypical teratoid/rhabdoid tumors from medulloblastoma/central primitive neuroectodermal tumors. *Hum Pathol* 32:156–162
9. Fuller CE, Pfeifer J, Humphrey P, Bruch LA, Dehner LP, Perry A (2001) Chromosome 22q dosage in composite extrarenal rhabdoid tumors: clonal evolution or a phenotypic mimic? *Hum Pathol* 32:1102–1108
10. Kordes U, Gesk S, Fruhwald MC, Graf N, Leuschner I, Hasselblatt M et al (2010) Clinical and molecular features in patients with atypical teratoid rhabdoid tumor or malignant rhabdoid tumor. *Genes Chromosome Cancer* 49:176–181
11. Biegel JA, Fogelgren B, Wainwright LM, Zhou JY, Bevan H, Rorke LB (2000) Germline INI1 mutation in a patient with a central nervous system atypical teratoid tumor and renal rhabdoid tumor. *Genes Chromosome Cancer* 28:31–37
12. Sevenet N, Sheridan E, Amram D, Schneider P, Handgretinger R, Delattre O (1999) Constitutional mutations of the hSNF5/INI1 gene predispose to a variety of cancers. *Am J Hum Genet* 65:1342–1348
13. Taylor MD, Gokgoz N, Andrulis IL, Mainprize TG, Drake JM, Rutka JT (2000) Familial posterior fossa brain tumors of infancy secondary to germline mutation of the hSNF5 gene. *Am J Hum Genet* 66:1403–1406
14. Schneppenheim R, Fruhwald MC, Gesk S, Hasselblatt M, Jeibmann A, Kordes U et al (2010) Germline nonsense mutation and somatic inactivation of SMARCA4/BRG1 in a family with rhabdoid tumor predisposition syndrome. *Am J Hum Genet* 86:279–284
15. Bourdeaut F, Lequin D, Brugieres L, Reynaud S, Dufour C, Doz F et al (2011) Frequent hSNF5/INI1 germline mutations in patients with rhabdoid tumor. *Clin Cancer Res* 17:31–38

16. Lu P, Roberts CW (2013) The SWI/SNF tumor suppressor complex: regulation of promoter nucleosomes and beyond. *Nucleus* 4:374–378
17. McKenna ES, Sansam CG, Cho YJ, Greulich H, Evans JA, Thom CS et al (2008) Loss of the epigenetic tumor suppressor SNF5 leads to cancer without genomic instability. *Mol Cell Biol* 28: 6223–6233
18. Biegel JA (2006) Molecular genetics of atypical teratoid/rhabdoid tumor. *Neurosurg Focus* 20:E11
19. Berrak SG, Özek MM, Canpolat C, Dagginar A, Sav A, El-Naggar A et al (2002) Association between DNA content and tumor suppressor gene expression and aggressiveness of atypical teratoid/rhabdoid tumors. *Childs Nerv Syst* 18:485–491
20. Zhang F, Tan L, Wainwright LM, Bartolomei MS, Biegel JA (2002) No evidence for hypermethylation of the hSNF5/INI1 promoter in pediatric rhabdoid tumors. *Genes Chromosome Cancer* 34: 398–405
21. Knipstein JA, Birks DK, Donson AM, Alimova I, Foreman NK, Vibhakar R (2012) Histone deacetylase inhibition decreases proliferation and potentiates the effect of ionizing radiation in atypical teratoid/rhabdoid tumor cells. *Neuro Oncol* 14:175–183
22. Algar EM, Muscat A, Dagar V, Rickert C, Chow CW, Biegel JA et al (2009) Imprinted CDKN1C is a tumor suppressor in rhabdoid tumor and activated by restoration of SMARCB1 and histone deacetylase inhibitors. *PLoS One* 4:e4482
23. Thiemann M, Oertel S, Ehemann V, Weichert W, Stenzinger A, Bischof M et al (2012) In vivo efficacy of the histone deacetylase inhibitor suberoylanilide hydroxamic acid in combination with radiotherapy in a malignant rhabdoid tumor mouse model. *Radiat Oncol* 7:52
24. Alimova I, Birks DK, Harris PS, Knipstein JA, Venkataraman S, Marquez VE et al (2013) Inhibition of EZH2 suppresses self-renewal and induces radiation sensitivity in atypical rhabdoid teratoid tumor cells. *Neuro Oncol* 15:149–160
25. Venkataraman S, Alimova I, Tello T, Harris PS, Knipstein JA, Donson AM et al (2012) Targeting Aurora Kinase A enhances radiation sensitivity of atypical teratoid rhabdoid tumor cells. *J Neurooncol* 107:517–526
26. Wohrle S, Weiss A, Ito M, Kauffmann A, Murakami M, Jagani Z et al (2013) Fibroblast growth factor receptors as novel therapeutic targets in SNF5-deleted malignant rhabdoid tumors. *PLoS One* 8:e77652

Alp Dinçer

Atypical teratoid/rhabdoid tumor (AT/RT) is an uncommon malignant CNS tumor typically seen in infant and children less than 3 years of age [1–6]. Although these tumors can be seen at any location in the CNS, approximately half of all tumors are located at the posterior fossa. The striking heterogeneity of the AT/RT apparently reflects the radiologic complexity of these tumors. They are typically large, heterogeneous masses that commonly contain cysts, hemorrhage, calcifications, and solid parts with increased cellularity [1–6]. Approximately 20 % of AT/RT present with disseminated disease at the time of diagnosis.

The radiologic descriptions of AT/RT appeared in the literature in 1990s [7]. Since then, imaging characteristics of AT/RT including diffusion-weighted imaging (DWI) and magnetic resonance spectroscopy (MRS) were reported in numerous manuscripts [1–11]. But, most previous reports describe the imaging features of AT/RT as nonspecific, and there is significant overlap in the imaging appearance of AT/RT and the other common posterior fossa masses especially medulloblastoma which can have identical histopathology to AT/RT. However,

some distinguishing morphological, spectroscopic, and diffusion features of computed tomography (CT) and magnetic resonance imaging (MRI) may help differentiate AT/RT from others, and a combination of these single characteristics together is suggestive of an AT/RT.

39.1 Location

Although usually arise intra-axial from the cerebellum, infratentorial AT/RT tends to occur off-midline and grow into the adjacent space of the cerebellopontine angle (Figs. 39.1 and 39.2). However, extra-axial location is not rare and can be extend from posterior fossa to supratentorial (Figs. 39.3 and 39.4). The tumor may also be multifocal at presentation and can be found rarely both infra and supratentorial. Drop metastasis to spinal and supratentorial pial surface is not rare and should be investigated at the initial diagnosis (Fig. 39.5). Hematogenous metastasis from posterior fossa AT/RT to extracranial organs is not described yet. However, due to its aggressive nature, contrary to other high-grade tumors of the posterior fossa, the adjacent dural and bone invasion can be occurred [8]. Hydrocephalus due to compression and obstruction of the fourth ventricle and the cerebral aqueduct occurs in approximately 60–65 % of cases, which is less frequent than with medulloblastoma.

A. Dinçer, M.D.
Department of Radiology, Acibadem University,
School of Medicine, Istanbul, Turkey
e-mail: adincer@asg.com.tr

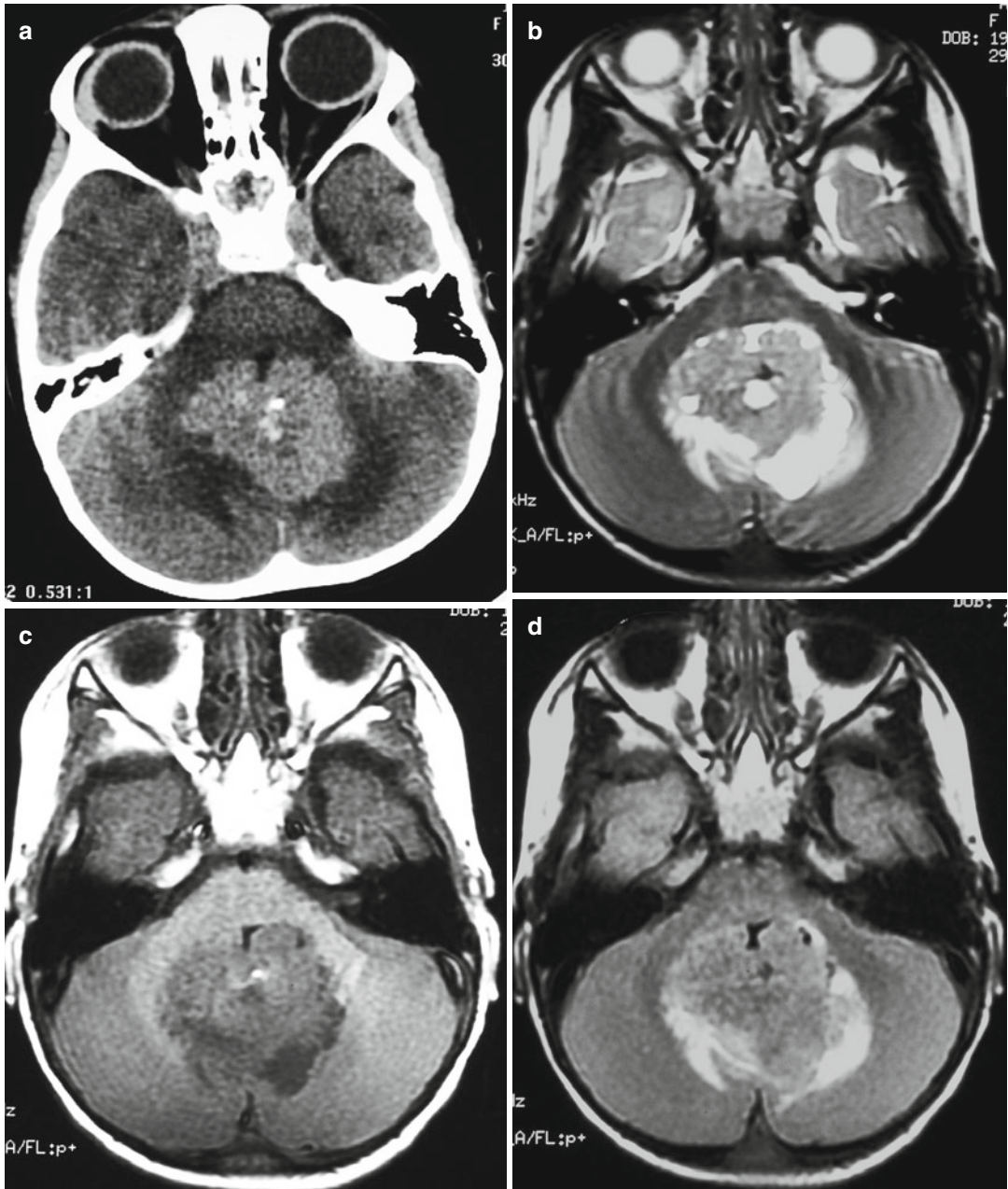


Fig. 39.1 Axial CT and MRI posterior fossa images of a 3 years old boy. CT section without contrast through the midpons level shows a hyperattenuated heterogeneous midline mass with foci of calcification (**a**). Corresponding T2 weighted image reveals a T2 hyperintense mass filling the fourth ventricle with eccentric multiple cysts (**b**). There is a slight heterogeneity within mass containing a minimal peripheral vasogenic edema. It is hard to depict calcifica-

tion with T2 weighted images alone. However, T1 weighted axial image at the same level demonstrate calcification as a small foci of hyperintensity, which is unusual (**c**). It is easy with FLAIR (fluid attenuated inversion recovery) to separate solid component, cysts and surrounding edema (**d**). There is avid heterogeneous enhancement after contrast administration including the eccentric cyst wall (**e**)

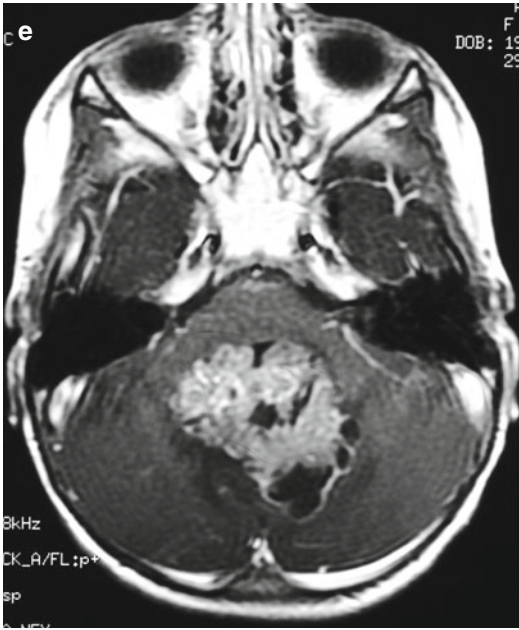


Fig. 39.1 (continued)

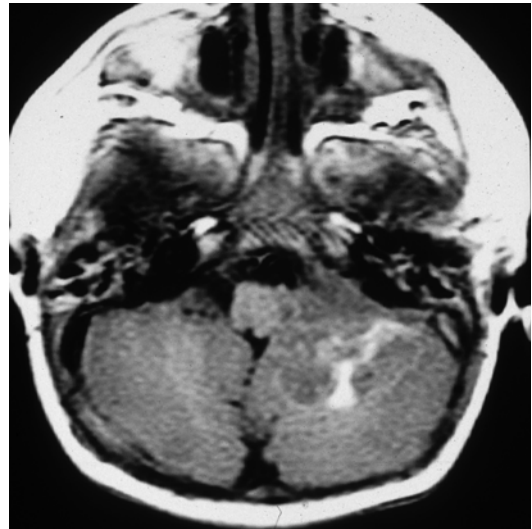


Fig. 39.3 A heterogeneous extra-axial mass located in cerebellopontine angle with avid but patchy enhancement is seen on axial post-contrast T1-weighted image of a year old boy with a posterior fossa AT/RT



Fig. 39.2 Coronal T1 weighted image after contrast administration of a 2 years old female. There is a strong wavy rim of peripheral contrast enhancement of a AT/RT in posterior fossa. Central necrotic or cystic zone is seen. Although rare, this sign could be specific to AT/RT

39.2 Calcification and Hemorrhage

CT is usually demonstrated foci of calcification (Figs. 39.1a and 39.4a). Although it can be seen hypointense foci on all sequences and may demonstrate blooming on gradient echo sequences, susceptibility-weighted imaging (SWI) is very sensitive to it and readily demonstrates both calcification and intratumoral hemorrhage as intratumoral susceptibility dots (Fig. 39.6). In addition to that, phase images of SWI may make a differentiation between them.

39.3 CT

The increased cellularity of the solid part of tumor may make the appearance on CT to have increased attenuation without contrast (Figs. 39.1a and 39.4a). But it can be iso- or hypodense comparing to adjacent brain

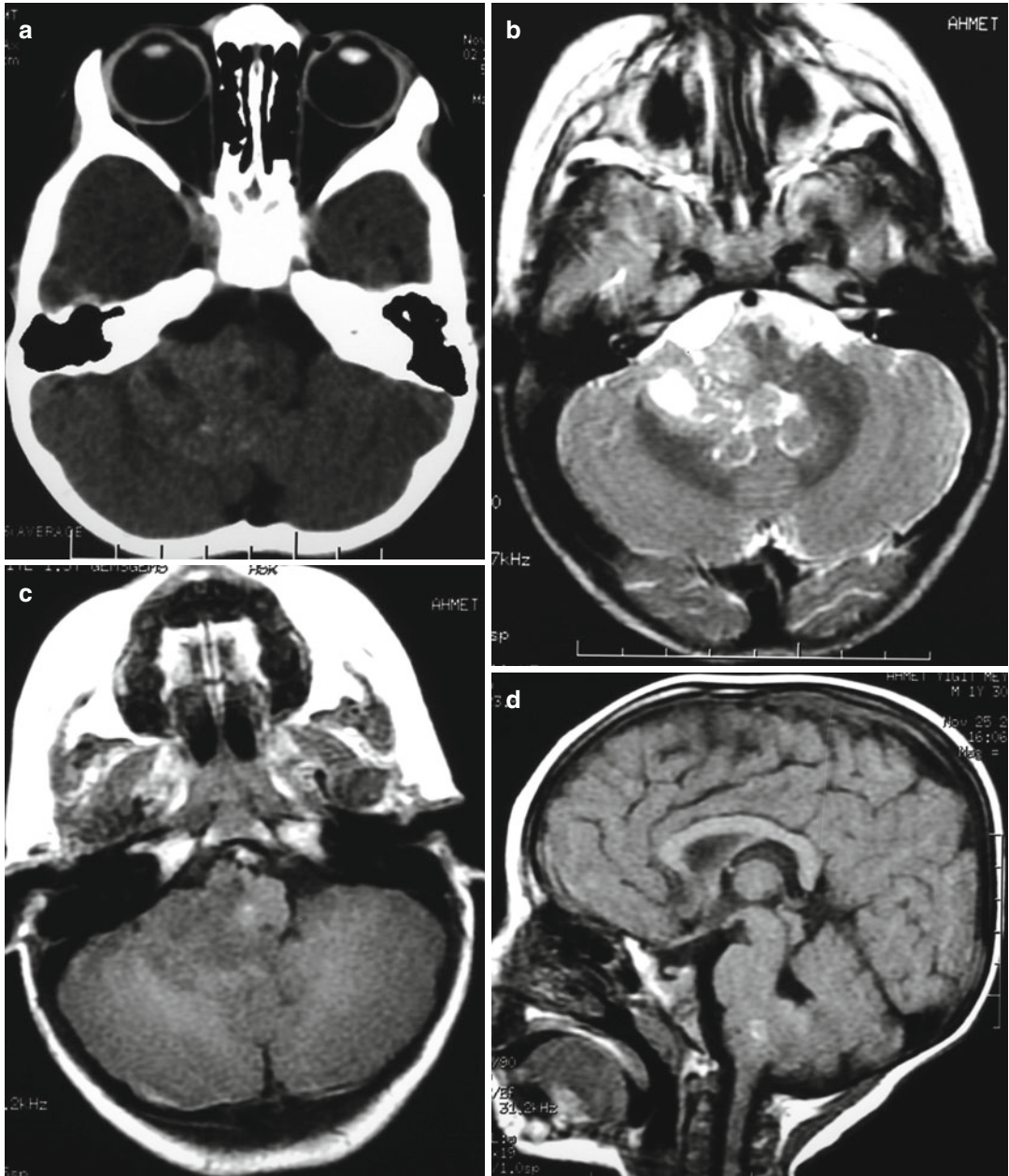


Fig. 39.4 Axial CT section through the posterior fossa without contrast (a), axial T2 (b), axial T1 (c), sagittal T1 without contrast (d) and axial T1 with contrast (e) demonstrate hyperattenuated intra-axial masses with tiny foci of

calcifications extending to the cerebellopontine angle in a 3 years old female. Eccentric cystic component, intratumoral hemorrhage as a T1 hyperintense foci, avid but heterogeneous enhancement are seen



Fig. 39.4 (continued)

parenchyma. Calcification, hemorrhage, and intratumoral cysts are giving an CT appearance to AT/RT rather heterogeneous.

39.4 MRI

Findings on T1- and T2-weighted images are variable (Figs. 39.1, 39.2, 39.4, and 39.6). AT/RT is typically iso- to hypointense compared to white matter on T1-weighted sequences; however, intratumoral hemorrhage will demonstrate regions of T1 hyperintensity, which are more characteristic of AT/RT compared to medulloblastoma (Fig. 39.1). T2 signal intensity is variable and usually heterogeneous; more cellular components are T2 hypointense, while less cellular components are iso- to mildly hyperintense compared to white matter (Figs. 39.1 and 39.6). Despite the aggressive features, there is often little or no vasogenic edema within the surrounding parenchyma (Fig. 39.1b). Peripherally located and relatively large eccentric cysts are frequently seen and are T2 hyperintense (Figs. 39.1, 39.4, and 39.7). T1 signal intensity of the cyst is usu-

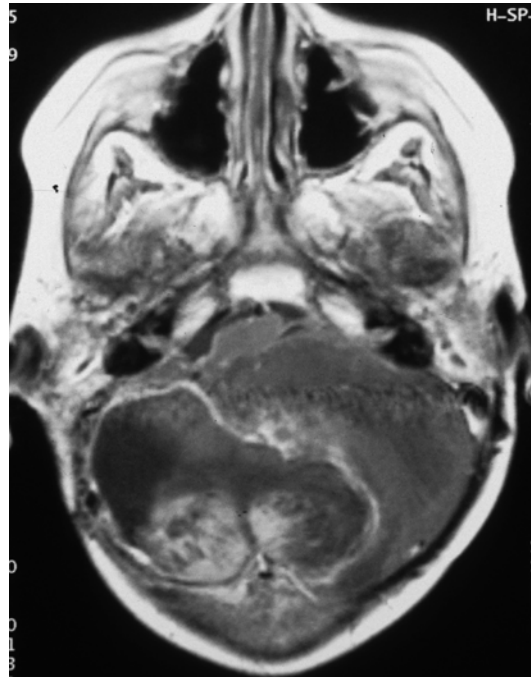


Fig. 39.5 A large cystic cerebellar mass and diffuse leptomeningeal spreading including the bilateral seventh cranial nerves are seen in an infant

ally hypointense but can be variable. T1 hyperintense cysts which have protein rich content can be seen (Fig. 39.4d).

39.5 Contrast Enhancement

AT/RT usually but not always demonstrates avid and heterogeneous enhancement of solid components, including the walls of the eccentric cysts (Figs. 39.1e, 39.3, 39.6c, and 39.7d). A thick band like wavy rim of strong and uniform enhancement completely or only partially surrounding a central cystic or necrotic area has been demonstrated in some AT/RT cases (Fig. 39.2) [2]. However, this pattern does not seem to be frequent and specific; if it is present, it could help in the differential diagnosis of posterior fossa tumors of early childhood. CSF dissemination may present as regions of leptomeningeal enhancement or multifocal masses with similar imaging characteristics to the primary tumor [9].

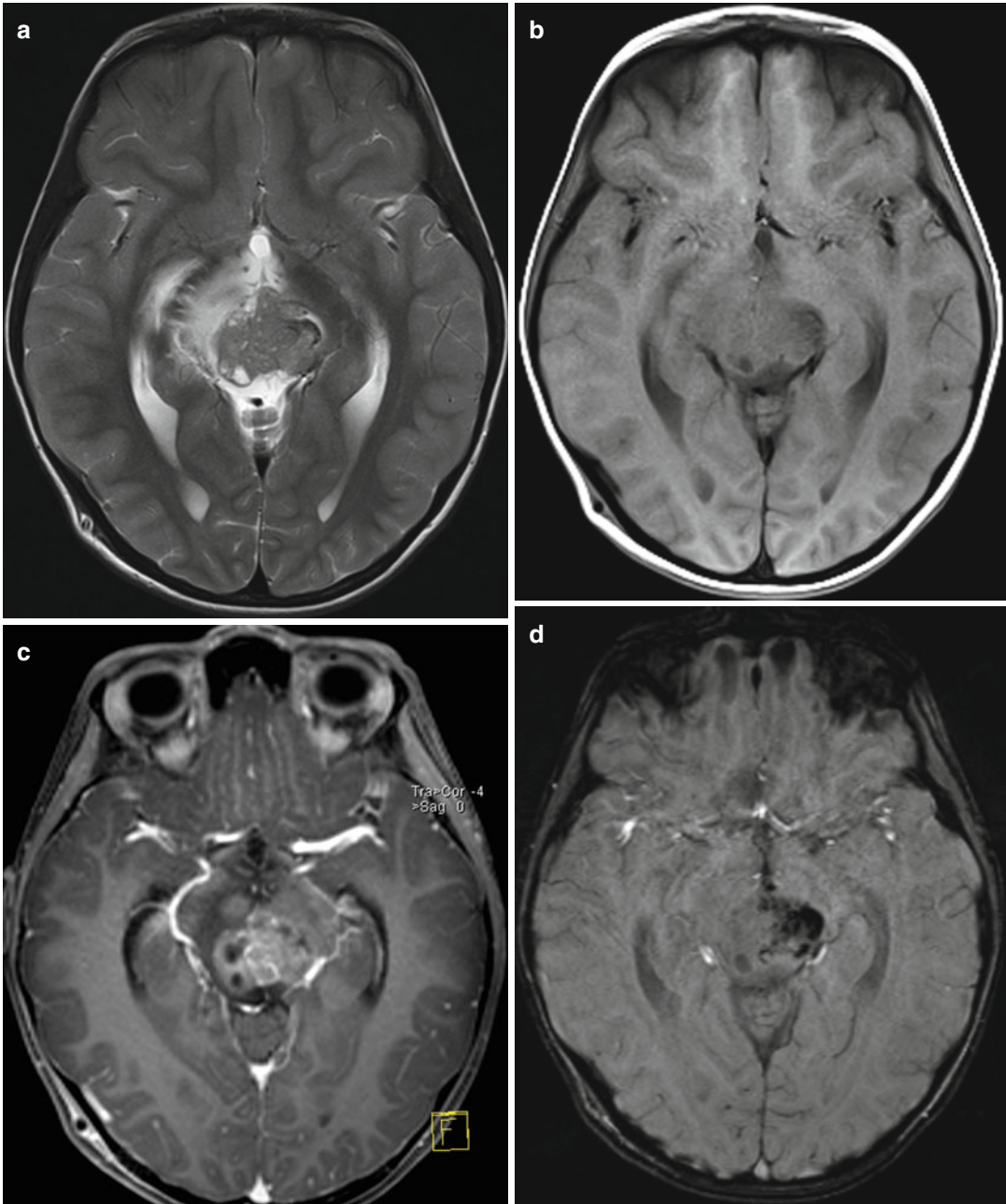


Fig. 39.6 A large midline posterior fossa mass including cerebellum, mesencephalon and pineal gland extending to supratentorial area in a 6 year old boy with AT/RT is seen on axial T2 (a), T1 (b), T1 with contrast (c), SWI (d), DWI (e), and ADC map (f). Heterogeneous midline mass includes eccentric cysts and surrounding marked vaso-

genic edema. There is an excessive hemorrhage within it. But it is hard to pick up these hemorrhages with conventional sequences including DWI. However, SWI clearly depicts them as intratumoral susceptibility dots. Strong diffusion restriction is seen as hyperintensity on DWI and hypointensity on ADC map

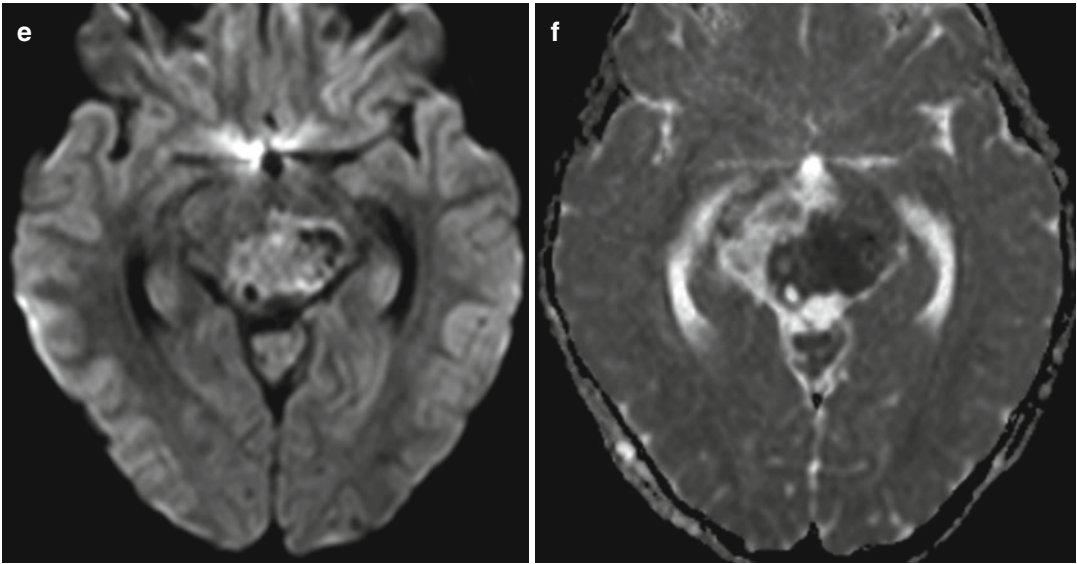


Fig. 39.6 (continued)

39.6 DWI

High cellularity of solid components of AT/RT leads to an inhomogeneous pattern of restricted diffusion which is seen as hyperintensity on DWI and hypointensity on ADC (apparent diffusion coefficient) maps, similar to medulloblastoma (Figs. 39.6 and 39.7) [5, 10]. Cystic components of AT/RT shows hyperintensity ADC map with hypointensity on corresponding DWI. However, if AT/RT contains excessive hemorrhage and/or calcification which cause increased susceptibility, DWI could not be diagnostic (Fig. 39.7).

39.7 MRS

Although proton MRS is validated to provide important diagnostic information about pediatric brain tumor, there is a little information in the literature regarding MRS utility for diagnosing AT/RT. However, a marked increase in choline and lipids peaks and a decrease in N-acetylaspartate and myoinositol peaks have been reported in children with AT/RT reflecting underlying histopathological features including necrosis and hemorrhage. These meta-

bolic profiles may provide potentially distinct metabolite information from other malignant pediatric brain tumors, including medulloblastoma [3, 11].

39.8 Differential Diagnosis

Differential diagnosis includes mostly medulloblastoma and anaplastic ependymoma. Although ependymoma usually demonstrates distinct imaging features with different diffusion properties on DWI, general imaging characteristics of AT/RT and medulloblastoma reflect the histopathologic similarities of these two tumors. Both tumors are hyperintense on DWI and hypointensity is seen on corresponding ADC map. Lower ADC values for both tumors do not help distinguish them from each other. However, AT/RT is more likely to appear heterogeneous compared to medulloblastoma with large eccentric cystic components, visible calcifications, intratumoral hemorrhage, and an inhomogeneous avid contrast-enhancing solid component. AT/RT tends to occur off-midline, whereas medulloblastoma more commonly arise near the midline. Peripherally located cysts are often present

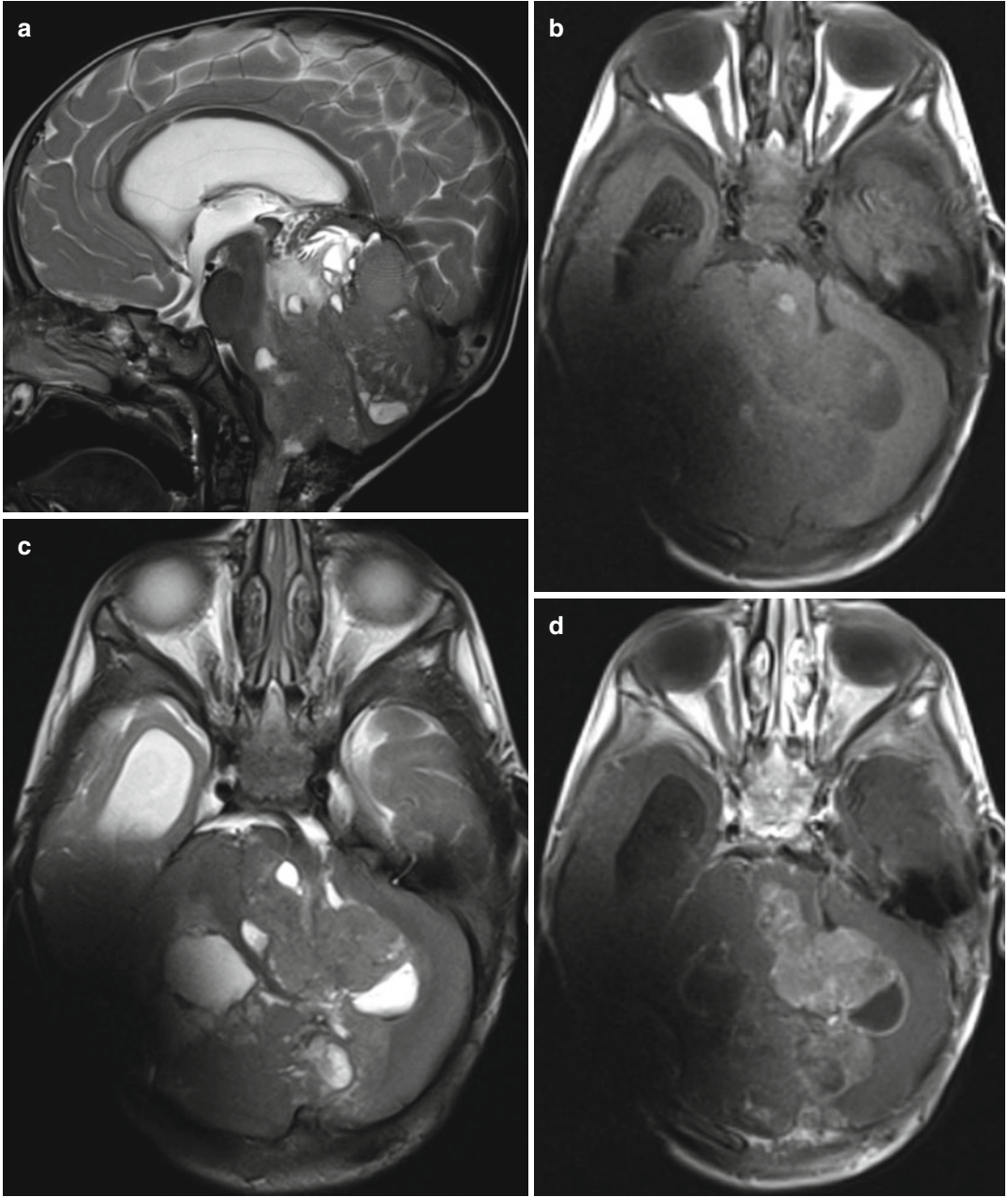


Fig. 39.7 A huge posterior fossa mass which causes nearly complete obliteration of it is seen on sagittal midline T2 (a), axial T1 (b), axial T2 (c), axial T1 with contrast (d), DWI (e) and ADC map (f) through the pons. Mass contains large eccentric cyst with strong cyst wall enhancement; some of them is seen as T1 hyperintense

due to protein rich content. There is an excessive susceptibility due to ventriculo-peritoneal shunt reservoir on the right occipital bone. Although there is an excessive artifact especially on DWI, Diffusion restriction can be interpreted with ADC map

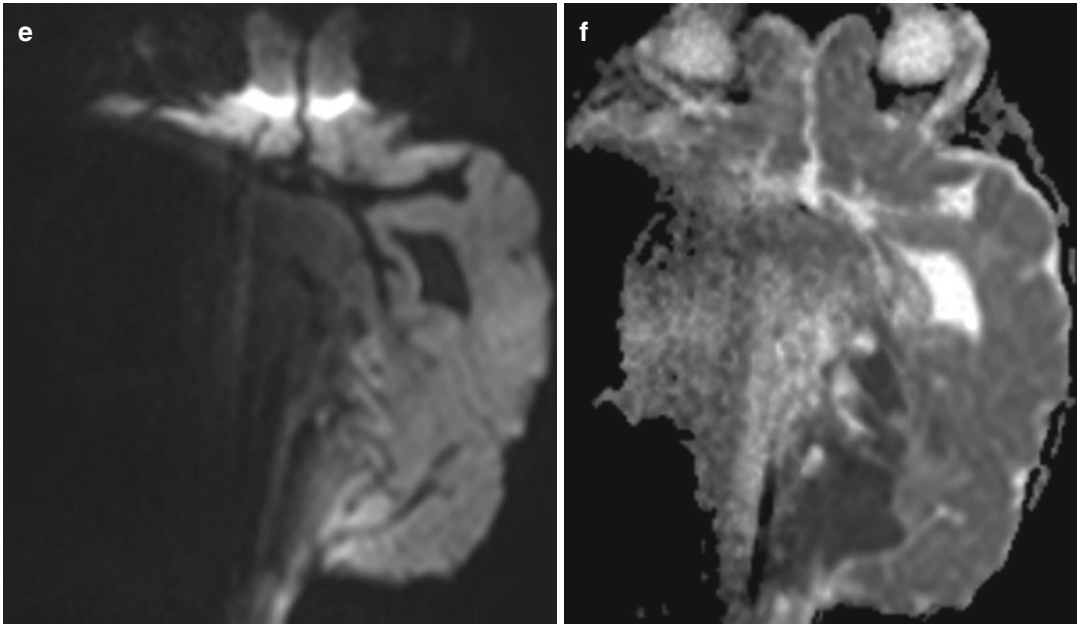


Fig. 39.7 (continued)

in AT/RT, whereas medulloblastoma tend to be a more homogeneous solid mass. If a pediatric posterior fossa mass displays restricted diffusion on DWI and elevated lipids in spectra is involving the cerebellopontine cistern, AT/RT is a more likely consideration than medulloblastoma especially in children less than 3 years of age.

References

1. Parmar H, Hawkins C, Bouffet E, Rutka J, Shroff M (2006) Imaging findings in primary intracranial atypical teratoid/rhabdoid tumors. *Pediatr Radiol* 36(2):126–132
2. Warmuth-Metz M, Bison B, Dannemann-Stern E, Kortmann R, Rutkowski S, Pietsch T (2008) CT and MR imaging in atypical teratoid/rhabdoid tumors of the central nervous system. *Neuroradiology* 50(5):447–452
3. Jin B, Feng XY (2013) MRI features of atypical teratoid/rhabdoid tumors in children. *Pediatr Radiol* 43(8):1001–1008. doi:10.1007/s00247-013-2646-9, Epub 2013 Mar 7. PubMed PMID: 23467756
4. Arslanoglu A, Aygun N, Tekhtani D, Aronson L, Cohen K, Burger PC, Yousem DM (2004) Imaging findings of CNS atypical teratoid/rhabdoid tumors. *AJNR Am J Neuroradiol* 25(3):476–480
5. Koral K, Gargan L, Bowers DC, Gimi B, Timmons CF, Weprin B, Rollins NK (2008) Imaging characteristics of atypical teratoid-rhabdoid tumor in children compared with medulloblastoma. *AJR Am J Roentgenol* 190(3):809–814
6. O'Brien W (2013) Imaging of primary posterior fossa brain tumors in children. *J Am Osteopath Coll Radiol* 2(3):2–12
7. Muñoz A, Carrasco A, Muñoz JM, Esparza J (1995) Cranial rhabdoid tumor with marginal tumor cystic component and extraaxial extension. *Am J Neuroradiol* 16:1727–1728
8. Warmuth-Metz M, Bison B, Gerber NU, Pietsch T, Hasselblatt M, Frühwald MC (2013) Bone involvement in atypical teratoid/rhabdoid tumors of the CNS. *AJNR Am J Neuroradiol* 34(10):2039–2042
9. Meyers SP, Khademian ZP, Biegel JA, Chuang SH, Korones DN, Zimmerman RA (2006) Primary intracranial atypical teratoid/rhabdoid tumors of infancy and childhood: MRI features and patient outcomes. *AJNR Am J Neuroradiol* 27(5):962–971
10. Koral K, Zhang S, Gargan L, Moore W, Garvey B, Fiesta M, Seymour M, Yang L, Scott D, Choudhury N (2013) Diffusion MRI improves the accuracy of pre-operative diagnosis of common pediatric cerebellar tumors among reviewers with different experience levels. *AJNR Am J Neuroradiol* 34(12):2360–2365. doi:10.3174/ajnr.A3596, Epub 2013 Jun 20
11. Bruggers CS, Moore K (2014) Magnetic resonance imaging spectroscopy in pediatric atypical teratoid rhabdoid tumors of the brain. *J Pediatr Hematol Oncol* 36(6):e341–5

Concezio Di Rocco and Luca Massimi

40.1 Targets

The main goals of surgery for atypical teratoid/rhabdoid tumor (AT/RT) are: (1) to obtain tumor samples for histological examination, (2) to achieve cytoreduction of the tumor mass to decompress the surrounding neural structures and to favor the adjuvant treatments, and (3) to treat the possibly associated hydrocephalus.

A biopsy should be performed as the first step of the tumor resection to assure the good quality of the specimen in order to favor a reliable pathological analysis. Frozen tumor samples should also be collected for possible further genetic investigations. CSF samples are taken for cytological examination.

The extent of tumor resection should be as large as possible to relief from preoperative clinical signs and symptoms. Moreover, the gross total tumor removal is considered important for the patient's survival, which is usually very short in this highly malignant tumor. Unfortunately, the common huge size of the tumor at diagnosis and the young age of the affected children may prevent a massive excision in several cases. In some instances, it could be advisable to resect the

tumor in two or more steps, in order to obtain a satisfactory mass reduction safely. Such a strategy bears also a minor risk of postoperative neurological deficits. Indeed, the surgical removal of AT/RT carries a high risk of surgically related complications since the tumor infiltration may preclude the functional preservation of the surrounding cerebellar parenchyma (e.g., the sparing of the dentate nucleus or the upper cerebellar vermis to reduce the risk of postoperative cerebellar mutism syndrome).

Endoscopic third ventriculostomy (ETV) is currently the best option for the management of hydrocephalus associated to posterior cranial fossa (PCF) tumors. We suggest to perform ETV after tumor resection instead that preoperatively to avoid an unnecessary procedure and to reduce the risk of early closure of the stoma [12]. In case of leptomeningeal spreading of the AT/RT, ventriculoperitoneal shunt has to be considered.

40.2 Timing and Preparation

The surgical operation is carried out in emergency in several cases due to the rapid tumor growth and the severe preoperative hydrocephalus which may cause an abrupt clinical deterioration. Therefore, the surgical treatment should be advocated as soon as the preoperative workup is completed. Both the tumor resection and the treatment of the hydrocephalus are addressed at the same time, whenever possible. Instead, should

C. Di Rocco, M.D. (✉) • L. Massimi, M.D.
Division of Pediatric Neurosurgery,
Catholic University, Medical School-Rome,
Largo A. Gemelli, 8, Rome 00168, Italy
e-mail: cdirocco@rm.unicatt.it;
profconceziodirocco@gmail.com;
lmassimi@email.it; lucamax30@hotmail.com

severe raised intracranial hypertension prevent the completion of the preoperative assessment or the transfer to a referral center, the treatment of hydrocephalus may be considered first.

In case of operation in emergency, a quick anamnesis and neurological evaluation should be associated to urgent blood examinations, stabilization of the child clinical condition with the help of the PICU team, and medical therapy with intravenous steroids (0.5 mg/kg each 6 h) and mannitol 18 % (0.5–1 g/kg bolus, then 0.25 mg/kg each 4–6 h) in order to obtain urgent brain MRI or, if unavailable, CT scan and then transfer the child immediately to the surgical ward.

In case of routine operation, the preparation includes the following: (1) analysis of the clinical history, physical, neurological, and neuropsychological evaluation, and routine blood examinations; (2) brain and spinal cord MRI (looking for possible tumor spreading); (3) medical therapy with intravenous or intramuscular or per os steroids (0.2–0.3 mg/kg each 8 h) and mannitol 18 % (0.25–0.5 g/kg bolus, then 0.25 g/kg each 6–8 h); (4) adequate abstinence from food; and (5) antibiotic prophylaxis (usually starting immediately before surgery).

40.3 Anesthesiological Considerations

The young age of children harboring AT/RT and the huge size and the critical location of the tumor make the anesthesiological preparation and monitoring particularly relevant for a good surgical outcome. Anesthesia is induced and maintained by inhalation gas or intravenous drugs or both. Sevoflurane is the inhalation anesthetic drug most commonly utilized in pediatric neuroanesthesia. Hypnotic drugs (propofol, etomidate), mio-relaxing drugs (atricure, rocuronium), and opioids (remifentanyl, alfentanil, sufentanyl) represent the pharmacological armamentarium to maintain the sedation during surgery.

Central venous line is mandatory for an adequate monitoring and for the rapid transfusion of blood derivatives, if needed. An accurate intraoperative monitoring should include heart rate,

invasive arterial blood pressure, central venous pressure, pulse oximetry, spirometry, end-tidal carbon dioxide, urine output, peripheral and core temperature, acid/base status (serial determinations), blood loss, and clotting function (serial determinations).

Precordial or esophageal Doppler is required to look for possible air embolism when the seated position is used. Ventilation with 100 % O₂, compression of the jugular veins, and refill of the operating field with saline solution are the key maneuvers to be quickly done when this complication occurs.

If the prone position is utilized, special care has to be taken to avoid excessive head flexion or extension during the patient's positioning, to fix the endotracheal tube, and to prevent compression on the eyes, chest, knees, and hips.

Due to the frequent invasion/compression of the brainstem by the tumor, the strict feedback between anesthesiologist and neurosurgeon is crucial to avoid severe cardiovascular complications. Similarly, the timing for extubation should be carefully evaluated because of the possible impairment of the brainstem respiratory centers.

40.4 The Operation

40.4.1 Positioning

Three main positions are used to approach AT/RT: the prone, the seated, and the lateral position. The first one provides a wide access to the cerebellar hemisphere, the IV ventricle, and the cervicomedullary junction. This is the most widely utilized and the most comfortable position for the surgeon; it is ideal for huge, hemispheric AT/RT. The seated position gives a more direct access to the inferior aspect of the tentorium and the upper cerebellar vermis, being the best option for AT/RT extending rostrally. This position also offers the advantage of a bloodless operating field though with an increased risk of air embolism and systemic blood hypotension. The lateral or park bench position is the best way to approach AT/RT mainly confined to the cerebellopontine angle. It

is worth reminding that the choice of the patient's position is based on the surgeon's preference and experience other than on the tumor location.

The patient's head is supported and fixed by a Mayfield 3-pin holder. In infants and young children, who represent the group age mostly affected by AT/RT, an alternative head holder is recommended (e.g., Mayfield-like holder with soft pillows or Olivecrona head holder).

40.4.2 Surgical Approach

Skin incision is extended from theinion to C3–C4 level to achieve an optimal exposure of the PCF. It is carried out along the midline for a standard suboccipital craniotomy/craniectomy. In case of AT/RT confined to the cerebellar hemisphere or the CP angle, the incision can be lateralized or performed in the retromastoid region, respectively.

Muscular incision and division follow the avascular midline area represented by the ligamentum nuchae. This avascular structure offers the possibility to spare blood and to avoid injury to the muscular layer that, especially in infants and young children, is thin and should be preserved for an appropriate reconstruction during closure. After division, dissection, and retraction of the muscles of the neck, the occipital squama and the posterior arch of C1 are exposed. C1 surface is reached by a subperiosteal dissection to reduce the risk of vertebral artery injury.

Suboccipital craniotomy is realized through two burr holes, placed in each side of the occipital squama just below the transverse sinus and conjoined by a linear craniectomy and through one curvilinear craniectomy extending from the burr hole of each side to the foramen magnum (with the concavity facing the midline). Both high-speed craniotome and bone rongeur may be used for this procedure. *Suboccipital craniectomy* is performed by some surgeons instead of craniotomy, especially when severe intracranial hypertension is expected. *C1 posterior laminectomy* is required for AT/RT extending to the cervicomedullary junction or to improve the exposure of the PCF content.

Opening of the dura is usually carried out with a Y-shaped incision, the vertical arm running

along the midline and extending up to the upper cervical region. Attention has to be paid to the intradural sinuses that are still well developed in infants since their delayed clipping or occlusion can result in profuse bleeding. In case of dural tension (large tumor and associated hydrocephalus), an *external ventricular drainage* (EVD) may be placed to reduce the intracranial hypertension through a controlled, slow intraoperative CSF withdrawal. Such a maneuver is done prior to open the dura to avoid the extrusion and the strangulation of the PCF content. EVD is realized with the patient in prone position through an occipital burr hole just before the dural opening (to prevent the upward cerebellar herniation possibly resulting from CSF escape) or through a frontal burr hole immediately before the operation (paying special care to avoid the aforementioned complication).

40.4.3 Tumor Excision

Lateral AT/RT involving the hemisphere is usually revealed by the distortion of the midline and the distension of the cerebellar folia (Fig. 40.1).

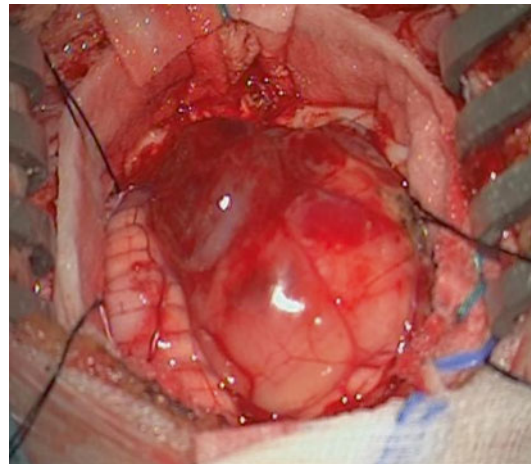


Fig. 40.1 Intraoperative view (prone position) of an AT/RT of the left cerebellar hemisphere. The huge tumor inflates the left cerebellar hemisphere (the normal architecture of its folia disappeared) and compresses the right one. The midline cannot be visualized. Note the dishomogeneous appearance of the mass, with the hemorrhagic area along its lower aspect

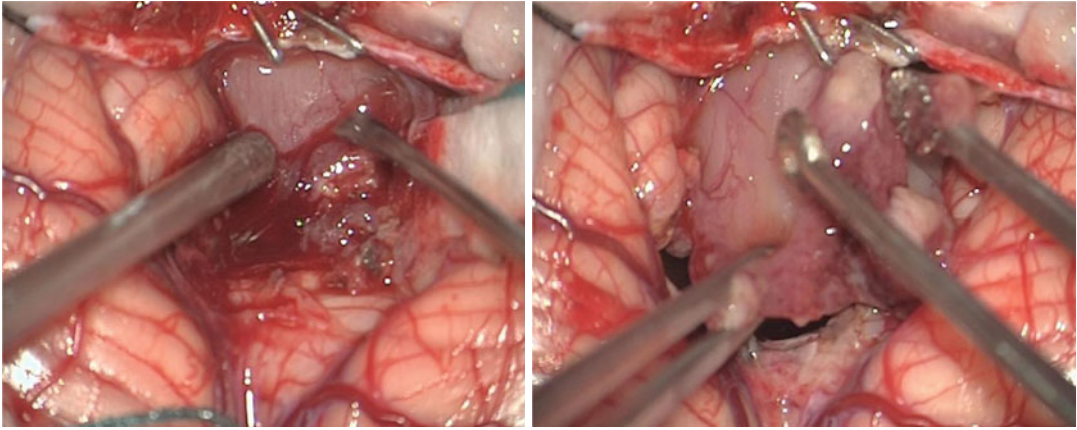


Fig. 40.2 Typical appearance of a midline AT/RT during a piecemeal excision (prone position). The tonsils are divaricated and the vermis upward displaced. The tumor

appears as a reddish, soft, and bleeding mass. These features make AT/RT similar to medulloblastoma

It is approached through a small corticotomy, with an incision placed parallel to the folia where the tumor is more superficial. Sometimes, lateral AT/RT is made recognizable by its protrusion through the pial surface; this transcortical protrusion, in turn, should not be confused with areas of leptomeningeal dissemination, which is quite common. *Midline AT/RT*, on the other hand, may present no revealing signs, the tumor being located within the fourth ventricle. In this instance, the tumor is reached by a transvermian approach to the fourth ventricle, with incision of the inferior aspect of the cerebellar vermis followed by distraction of the two hemispheres (Fig. 40.2). The telovelar approach is advocated by some authors to reduce the risk of cerebellar mutism by avoiding injuries to the vermis [3, 13]. However, in our experience as well as in that of other authors [5], such a surgical option does not result in a significant reduction of mutism. Not infrequently, midline AT/RT protrudes through the Magendie foramen into the cisterna magna so that it can be firstly approached from the cisternal spaces.

Tumor resection is usually carried out under magnification. The first step consists of a careful microdissection of the tumor away from the surrounding cerebellar tissue. Although AT/RT is easily distinguished from the normal tissue, appearing as a reddish pink (or gray), richly vascularized mass, an obvious interface with the surrounding neural structures may be lacking

because of its infiltrative growth. The peripheral supplying vessels are progressively coagulated to reduce the bleeding from the tumor. Since such a bleeding is often profuse, the visual intraoperative control of the major arteries providing the vascular supply (namely, PICA) is recommended. Therefore, both PICAs should be identified at the beginning of the procedure prior to attempt the tumor excision. When a demarcation plane from normal tissue is completely missing, the mass removal has to start from inside the neoplasm. The tumor excision is carried out in a piecemeal fashion as the tumor size and infiltration rarely allow the surgeon to perform an “en bloc” resection (Fig. 40.2). The piecemeal removal, however, favors the tumor bleeding, and, considering that this bleeding usually stops only when the resection is completed, the removal should be realized as quickly as possible using both microsurgical instruments and ultrasonic aspirator. At the end of the procedure, the walls of the surgical field are carefully checked looking for possible tumor remnants or sources of bleeding. During this step, self-retaining retractors can be used to improve the visualization of the residual surgical cavity. We actually utilize retractors only during the late phases of cytoreduction in order to avoid unnecessary retraction and stretching of the cerebellar structures which may result in further edema when applied on the normal tissues already compressed by the tumor itself at the beginning of the operation.

The *involvement of brainstem and cranial nerves* is one of the most critical steps of AT/RT excision. When dealing with AT/RT located within the fourth ventricle, it is recommended to dissect the tumor up to visualize the ventricular floor before starting the tumor reduction; such a maneuver allows the surgeon to use the ventricular floor as a marker to avoid injury to the brainstem. When the superficial portion of the mass has been removed, the tumor is progressively excised starting from the inferior portion (close to the cervical region) and proceeding cephalad until the Sylvius' aqueduct is visualized, opened (if needed), and protected with Gelfoam; finally, the tumor can be gently detached from the fourth ventricle floor trying to reduce its manipulation as well as bipolar cautery on the ventricular surface as much as possible. In case of infiltration of the floor (which is not infrequent), attempts to follow the tumor inside the brainstem should be avoided to decrease the risk of perioperative and postoperative damages (namely, cardiorespiratory impairment, VI and VII cranial nerve palsy, vomiting syndrome) (Fig. 40.3). Similarly, a cautious dissection of the tumor from the lower cranial nerves is recommended unless a clear infiltration of nerve sheath or a severe encasement of the structures of the CP angle is present (Fig. 40.4).

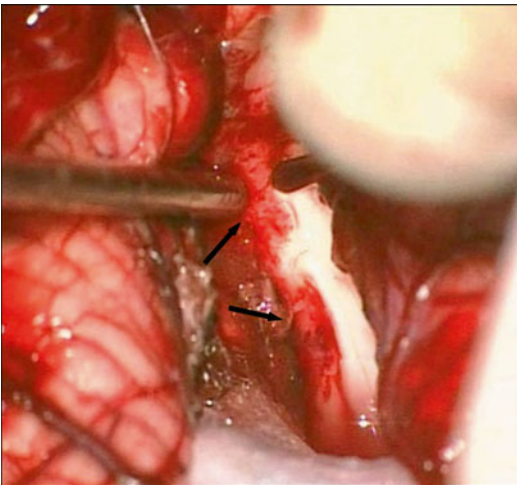


Fig. 40.3 Intraoperative view of a brainstem infiltration (prone position). After removal of the tumor, which involved the IV ventricle extending into the right CPA, an extensive infiltration of the right lateral surface of the brainstem is evident (*arrows*)

Such a dissection may result very hard as the anatomy is often completely distorted. For this reason, it is advisable to separate the tumor from the cranial nerve proceeding from laterally to medially, trying to individuate as many marker points as possible (e.g., internal acoustic foramen to preserve VII and VIII cranial nerves, jugular foramen to preserve IX and X cranial nerves). The dissection of the tumor from the cranial nerve carried out from the medial surface of the brainstem, indeed, is more likely to result in cranial nerve loss because of the usually severe encasement at this level.

40.4.4 Closure

After irrigation of the surgical field with saline solution to reduce the inflammatory reaction and to counterbalance the cerebellar collapse, the dura is watertight closed. Dural substitutes or muscular fascia is utilized for a duraplasty in case of shrinking of the autologous dura mater. Afterwards, the bone flap is replaced and secured with reabsorbable plates and screws or silk sutures. The bone replacement prevents postoperative cerebellar ptosis and ensures protection to the PCF content. Cervical and nuchal muscles are then reconstructed and carefully closed to reduce the risk of CSF leakage. Such a complication and the following risk of CSF infection, indeed, prolong the postoperative course delaying the adjuvant treatments that are mandatory for children with such a dismal prognosis like those with AT/RT. Finally, subcutaneous sheet and skin are sutured in separate layers.

40.4.5 Surgical Armamentarium

The operation is carried out by means of standard microsurgical instrumentarium, microscope, and ultrasonic aspirator. However, some adjunctive intraoperative tools can make surgery safer and more effective: (1) Ultrasounds may be utilized to evaluate the real tumor extension and to correctly plan the corticotomy for those embedded within the cerebellar hemisphere. They also allow the surgeon to receive real-time information on

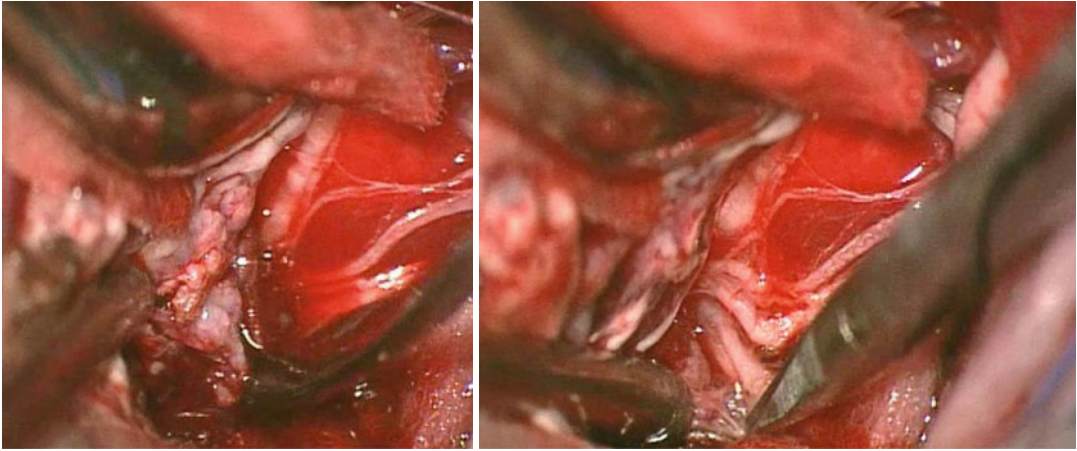


Fig. 40.4 AT/RT of the left CPA. Intraoperative view (prone position) of the tumor dissection and detachment from the lower cranial nerves. The medial portion of the tumor is still adherent to the brainstem

the extent of the tumor resection and to identify encased vascular structures (Doppler mode). (2) MRI-based neuronavigation plays a similar role in assessing the extension of resection and reducing the risk of damaging critical structures. The accuracy of this image guidance system is progressively decreased during the tumor excision because of the post-registration brain shift. The advent of electromagnetic image guidance system permits to employ the neuronavigation also in infants where the use of Mayfield holder is not appropriate. (3) Intraoperative neurophysiological monitoring should be utilized routinely when brainstem and cranial nerve are involved. This kind of monitoring modulates the surgical resection through a continuous electrophysiological feedback, often making it more radical and less risky. BAEPs and monitoring of cranial nerve or their nuclei are the most appropriate type of monitoring [4]. (4) Intraoperative MRI is the best way to assess the extent of surgical resection (and, in case, to improve it) and to find out possible early complications. Unfortunately, its diffusion is still limited.

40.5 Postoperative Period

The immediate postoperative course usually takes place within the PICU. The patient can be extubated just after the end of the operation

or mechanically ventilated for another 12–24 h or more if brainstem impairment is expected. During this time, EVD is particularly useful to monitor the ICP other than to manage persistent hydrocephalus and to permit CSF washing from surgical debris. Steroid therapy is continued to prevent postsurgical inflammation concerning the cerebellum, brainstem, and cranial nerves. Mannitol, instead, is administered only in case of suboptimal decompression of the PCF not to increase the collapse of the cerebellar hemisphere after a gross total tumor resection.

Once the stabilization of the clinical condition is verified, the child is referred to the surgical floor where steroids, analgesic therapy, and antibiotic prophylaxis are continued according to the patient's condition and to the adopted protocol. Adequate hydration and feeding are provided. Rehabilitation therapy should be started as soon as possible, if needed. EVD is removed after an appropriate monitoring period, while patients with persistent hydrocephalus undergo ETV or extrathecal CSF shunting.

Early neuroimaging investigation (brain MRI or CT scan with contrast medium administration within 48–72 h from surgery) is obtained to rule out possible surgical complications and to assess the extent of tumor resection. Following MRIs

are planned according to the clinical course and the adjuvant therapies.

40.6 Surgical Outcome

Surgery is attempted to obtain a gross total tumor resection; however, such a goal can be achieved in no more than 50–70 % of cases [8, 11, 14]. The infiltrative growth pattern, the frequent involvement of the multiple cranial nerves, vascular structures, and brainstem, and the large tumor extent are the main reasons limiting the surgical excision [1, 7].

Although there are not specific data, mortality and morbidity following resection of AT/RT seem to overlap those resulting from surgery for other pediatric malignant PCF tumors. Currently, such a mortality accounts for about 1–3 % of cases, and morbidity ranges from 5 to 10 % though the latter increases up to 30 % when dealing CP angle tumors [2, 10]. Cranial nerve palsy, motor-sensitive deficit, and cerebellar signs are the most common neurological sequelae. Cerebellar mutism can occur isolated or as part of PCF syndrome (hypokinesia, irritability, sphincter incontinence, cerebellar and pyramidal tracts impairment). This multifactorial syndrome is thought to result from the interaction between the tumor damages (infiltration, preoperative hemorrhage, associated disease like hydrocephalus) and the surgical injuries (mainly to the dentate nucleus, the dentatohalamocortical pathway, the cerebellar vermis). The tumor seems to play an important role in this syndrome as we recently demonstrated in our series where preoperative language impairment was found in most of the children developing postoperative mutism. This would explain the significantly higher incidence of this complication in children with malignant PCF tumors (namely, medulloblastoma) compared with those with benign histotypes [9].

Although there are not prospective data on the effects of surgery, initial gross total resection is thought to contribute to prolong the survival. In the Hilden and coworkers' registry series, chil-

dren who underwent a gross total tumor excision (47 %) had both median survival and event-free survival longer than those who received initial partial resection or biopsy (20 months vs. 15.25 months and 14 months vs. 9.25 months, respectively) [6].

References

1. Biswas A, Goyal S, Puri T, Das P, Sarkar C, Julka PK, Bakhshi S, Rath GK (2009) Atypical teratoid rhabdoid tumor of the brain: case series and review of the literature. *Childs Nerv Syst* 25: 1495–1500
2. Dubey A, Sung WS, Shaya M, Patwardhan R, Willis B, Smith D, Nanda A (2009) Complications of posterior cranial fossa surgery—an institutional experience of 500 patients. *Surg Neurol* 72:369–375
3. El-Bahy K (2005) Telovelar approach to the fourth ventricle: operative findings and results in 16 cases. *Acta Neurochir (Wien)* 147:137–142
4. Galloway GM, Zamel K (2011) Neurophysiologic intraoperative monitoring in pediatrics. *Pediatr Neurol* 44:161–170
5. Heuer GC, Jackson EM, Magge SN, Storm PB (2007) Surgical management of pediatric brain tumors. *Expert Rev Anticancer Ther* 7:S61–S68
6. Hilden JM, Meerbaum S, Burger P, Finlay J, Janss A, Scheitauer BW, Walter AW, Rorke LB, Biegel JA (2004) Central nervous system atypical teratoid/rhabdoid tumor: results of therapy in children enrolled in a registry. *J Clin Oncol* 22:2877–2884
7. Packer RJ, Biegel JA, Blaney S, Finlay J, Geyer JR, Heideman R, Hilden J, Janss AJ, Kun L, Vezina G, Rorke LB, Smith M (2002) Atypical teratoid/rhabdoid tumor of the central nervous system: report on workshop. *J Pediatr Hematol Oncol* 24: 337–342
8. Reddy AT (2005) Atypical teratoid/rhabdoid tumors of the central nervous system. *J Neurooncol* 75:309–313
9. Robertson PL, Muraszko KM, Homes E, Spoto R, Packer RJ, Gajjar A, Dias MS, Allen JC (2006) Incidence and severity of postoperative cerebellar mutism syndrome in children with medulloblastoma: a prospective study by the Children's Oncology Group. *J Neurosurg (Pediatr)* 105: 444–451
10. Sanford RA, Merchant TE, Zwienenberg-Lee M, Kun LE, Boop FA (2009) Advances in surgical techniques for resection of childhood cerebellopontine angle ependymomas are key to survival. *Childs Nerv Syst* 25:1229–1240
11. Strother D (2005) Atypical teratoid rhabdoid tumors of childhood: diagnosis, treatment and challenges. *Exp Rev Anticancer Ther* 5:907–915

12. Tamburrini G, Massimi L, Caldarelli M, Di Rocco C (2008) Antibiotic impregnated external ventricular drainage and third ventriculostomy in the management of hydrocephalus associated with posterior cranial fossa tumours. *Acta Neurochir (Wien)* 150:1049–1055
13. Tanriover N, Ulm AJ, Rhoton AL Jr, Yasuda A (2004) Comparison of the transvermian and telovelar approaches to the fourth ventricle. *J Neurosurg* 101:484–498
14. Tekautz TM, Fuller CE, Blaney S et al (2005) Atypical teratoid/rhabdoid tumors (atrt): improved survival in children 3 years of age and older with radiation therapy and high-dose alkylator-based chemotherapy. *J Clin Oncol* 23:1491–1499

Pınar Karabağlı

41.1 Introduction

Embryonal tumors of the central nervous system (CNS) include medulloblastoma (MB), atypical teratoid/rhabdoid tumor (AT/RT), and supratentorial primitive neuroectodermal tumor (PNET). Cytologic polymorphism in embryonal tumors of the central nervous system (CNS) often alerts the pathologist to the diagnostic possibility of an AT/RT [1, 2].

AT/RT is a distinct tumor of young children based on morphological, immunohistochemical, and cytogenetic characteristics [1, 3]. In 1993, it was included in the World Health Organization (WHO) classification as a grade IV embryonal neoplasm [4].

Malignant rhabdoid tumors were originally described as a renal neoplasm of infancy or childhood. These tumors may arise in the kidney or at a variety of other sites including the brain and are associated with an extremely poor prognosis [5, 6]. The tumor was defined in 1987 as a distinct malignant CNS tumor of infancy because of its pathologic and genetic characteristics [7].

Grossly, AT/RTs tend to be soft, pinkish-red, and bulky and often appear to be demarcated from adjacent parenchyma. They typically contain necrotic foci and may be hemorrhagic [1].

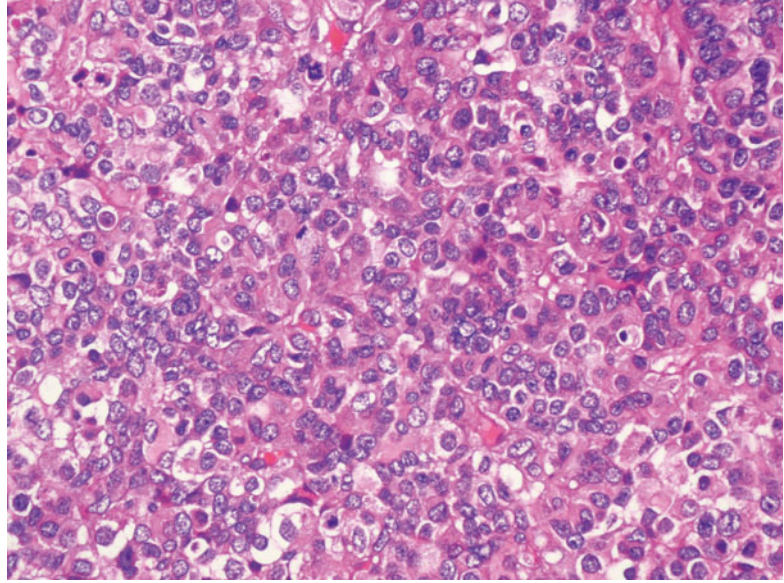
41.2 Microscopic Findings

Histologically, AT/RTs are morphologically heterogeneous lesions that are sometimes difficult to recognize using only histopathologic criteria [1, 7]. AT/RT is characterized by the presence of rhabdoid cells, that is, large cells with abundant cytoplasm containing juxtannuclear, eosinophilic inclusions, and nuclei that display a single, prominent eosinophilic nucleolus in vesicular chromatin [1, 3, 8, 9] (Fig. 41.1). This rhabdoid phenotype was not prevalent. Cell transitions between pale and the typical rhabdoid cells were occasionally seen. The cytoplasm of pale cells has a fine granular homogeneous character or may contain a poorly defined dense pink “body” [1, 3]. Most tumors contain variable components with primitive neuroectodermal, mesenchymal, and epithelial features [1, 9]. Undifferentiated primitive neuroectodermal component consisting of small cells with high nuclear/cytoplasmic ratio and oval hyperchromatic nuclei is encountered, in about two thirds of tumors. Mesenchymal differentiation is less common and appears as areas with spindle-shaped cells or fascicular growth pattern. Moreover, the tumor cells may be arranged in cords or trabeculae

P. Karabağlı, M.D.

Department of Pathology, Selcuk University, School of Medicine, Alaeddin Keykubad Campus- Selcuklu, Konya 42075, Turkey
e-mail: pinarkarabagli@yahoo.com

Fig. 41.1 Typical rhabdoid cells with granular chromatin, prominent nucleolus and eosinophilic cytoplasm, brisk mitoses, and apoptotic bodies (HE, $\times 100$)



that are embedded within a basophilic or mucopolysaccharide mucinous background [1, 9–11]. Epithelial structures characterized with poorly formed glands, papillae, or rosettes are seen in a minority of patients [1, 10]. Flexner-Wintersteiner or Homer Wright rosettes may be seen [10].

Reticulin may be abundant in some AT/RTs, especially in the perivascular regions [10]. The mitotic count is high, and necrosis is common. Microvascular proliferation in AT/RT very rarely shows the endothelial proliferation characteristic of some gliomas [1, 2].

Cytologic examination by scraping and smearing squash preparation or fine-needle aspiration offers a useful alternative to frozen section during intraoperative consultation. Cytomorphologic features are unique and lead to an accurate diagnosis in the right clinico-radiologic context [12]. Cytomorphologically, the smears are hypercellular with primitive-type small, round neoplastic cells admixed with large-sized rhabdoid cells in varying proportions. The rhabdoid cells have abundant eosinophilic cytoplasm, eccentrically located hyperchromatic nucleus with prominent nucleolus and irregular nuclear contour [12, 13]. Mitosis, necrosis, and dystrophic calcification may be present.

Ultrastructurally, the rhabdoid cells, which can be prominent but often not dominant, show intracytoplasmic, paranuclear whorls of intermediate

filaments [3, 12]. Rhabdoid cells contain multiple nuclei with invagination. In small cells, cytoplasmic organelles are poorly seen. Epithelial cells formed nests separated from the stromal elements by basement membrane material [3, 14].

41.3 Immunohistochemical Findings

Immunohistochemical staining shows diffuse expression of vimentin. Both rhabdoid and epithelial cells are immunoreactive for epithelial membrane antigen, and cytokeratins are positive in most cases [1, 3, 10, 14] (Figs. 41.2 and 41.3). In more than half AT/RT cases, the rhabdoid cells/pale cells and scattered spindle cells are positive for smooth muscle actin [3, 10] (Fig. 41.4). They may also express GFAP, neurofilament protein, and synaptophysin (Figs. 41.5 and 41.6). Germ cell markers such as human chorionic gonadotropin and placental alkaline phosphatase are generally negative [1, 3, 10]. However one series found limited alpha-fetoprotein staining in large cells [10]. Supplementing these immunohistochemical characteristics, the absence of nuclear expression of INI1 has emerged as a critical tool for accurate AT/RT diagnosis [1].

AT/RTs in children have marked MIB-1 labeling indices that are often more than 50 %,

Fig. 41.2 Most of tumor cells show strong expression of membranous and cytoplasmic EMA (streptavidin-biotinylated complement; $\times 400$)

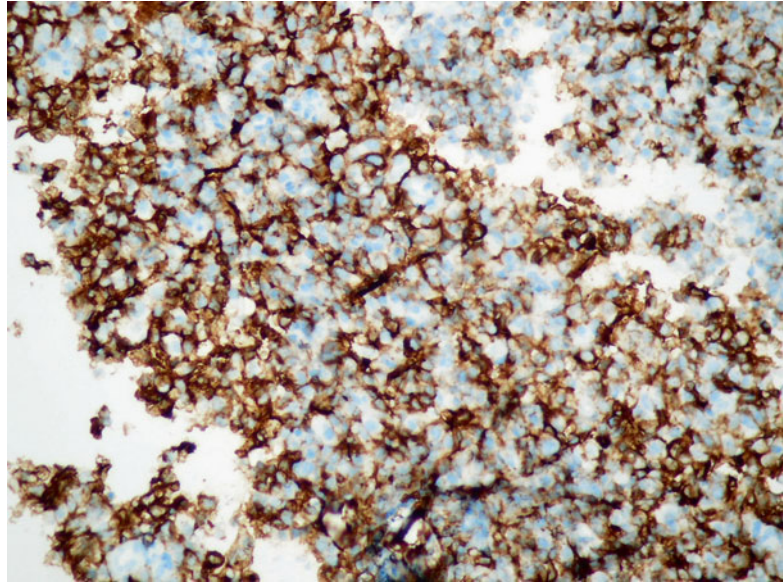
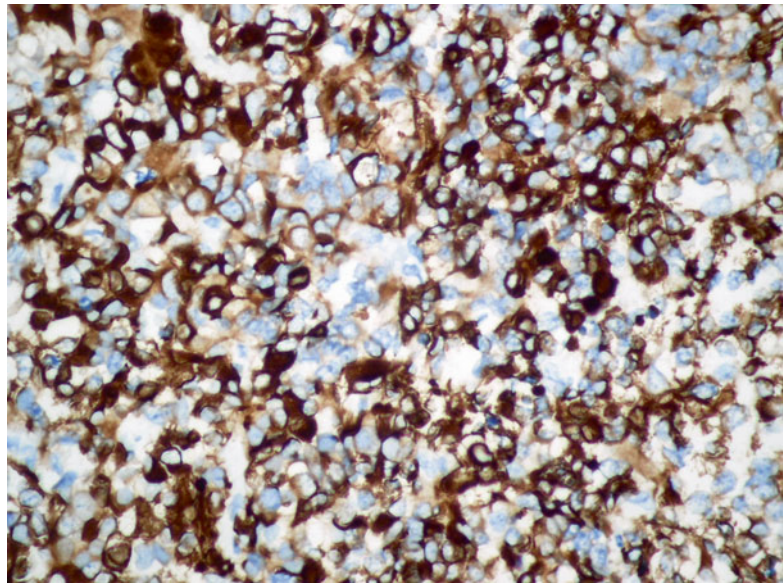


Fig. 41.3 Tumor cells show strong expression of cytoplasmic pan CK (streptavidin-biotinylated complement; $\times 400$)



but in some cases the labeling index may be significantly lower [1, 9, 14] (Fig. 41.7).

41.4 Differential Diagnosis

In most cases, when the neoplasm occurs in the cerebellum of an infant, the principal differential diagnostic issue is MB. This distinction

may be difficult to resolve if a small specimen contains only the small cell component. In contrast to MB, the AT/RT has a high incidence of necrosis with calcification, frequent broad fibrovascular septa, a population of large cells, and a lack of nodularity. Immunoreactivity for a broad range of antigens and the presence of chromosome 22 alterations are additional points of distinction [10].

Fig. 41.4 Some tumor cells show strong expression of cytoplasmic synaptophysin (streptavidin-biotinylated complement; $\times 400$)

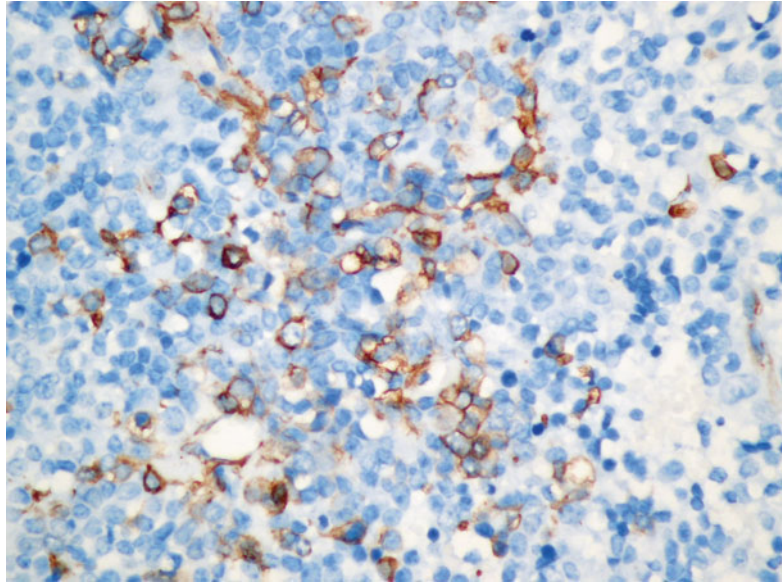
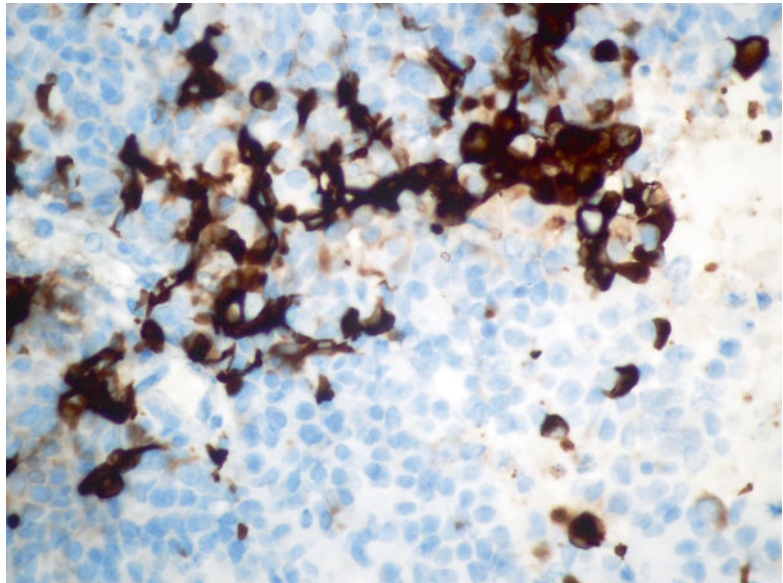


Fig. 41.5 Focal reactivity of cytoplasmic GFAP (streptavidin-biotinylated complement; $\times 400$)



The cytomorphic differential diagnosis includes MB, PNET, metastatic adenocarcinoma, gemistocytic astrocytoma, oligodendroglioma, non-Hodgkin lymphoma (NHL), malignant melanoma, and germinoma [12]. It is important to consider the diagnosis of AT/RT in patients aged <1 year who have specimens that demonstrate cytomorphic features of MB or PNET. AT/RT may show a cytomorphology of predominantly primitive-looking neuronal cells mimicking MB

or PNET. Finding larger cells with eccentric nuclei or rhabdoid cells suggests against a diagnosis of MB/PNET and should be considered as a characteristic feature of AT/RT. Gliomas show significant pleomorphism with a characteristic fibrillary background. Care must be taken, however, not to confuse gemistocytes in a glioma with the rhabdoid cells of an AT/RT. Gemistocytes are significantly larger cells with abundant, glassy-looking cytoplasm and often are binucle-

Fig. 41.6 Focal cytoplasmic smooth muscle actin alpha 8 [SMAA] (streptavidin-biotinylated complement; $\times 400$)

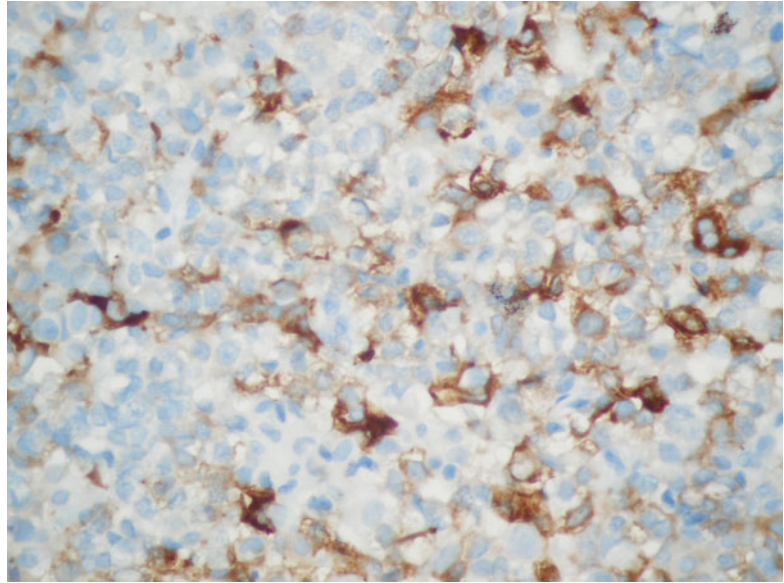
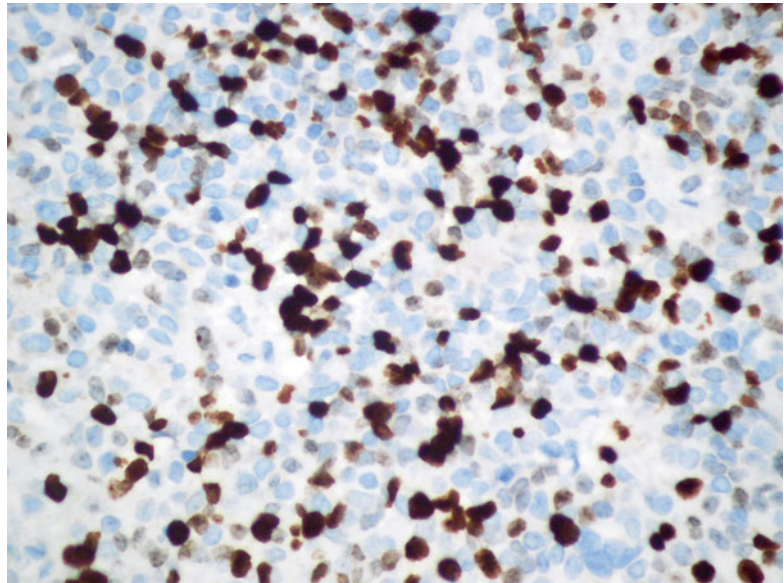


Fig. 41.7 Ki67 labeling index of 40 % (streptavidin-biotinylated complement; $\times 400$)



ated. Oligodendroglioma shows small, uniform cells, often with fragile cytoplasm, leading to a large population of naked, “lymphocyte-like” nuclei. Microgemistocytes may be seen in these neoplasms. NHL has cells with scant basophilic cytoplasm or naked nuclei, often with irregular-shaped nuclei and prominent nucleoli. Lymphoglandular bodies may also be helpful [12]. Metastatic adenocarcinoma sometimes shows eccentric nuclei, but carcinoma usually

occurs in older age. Cells of malignant melanoma are similar in that they have bizarre nuclei with prominent red nucleoli. They often show nested cell clusters, and the nucleus is usually centrally located. The cells of germinoma are characterized by a round, vesicular, and centrally positioned nuclei, prominent nucleoli, discrete cell membrane, and relatively abundant cytoplasm. In addition, the age of patients is slightly older than that of AT/RT [13].

Diagnosis of AT/RTs based on adequate biopsy material, on the other hand, is relatively straightforward and involves techniques and immunostains which are routinely used on histological tissues. Although loss of nuclear expression of INI1 is believed to be highly specific for AT/RT and retention of nuclear expression of INI1 strongly suggests an alternate diagnosis, loss of INI1 staining has been reported rarely in other tumors [15]. Some authors have reported inactivation of INI1 in choroid plexus carcinoma [16, 17].

References

- Judkins AR, Eberhart CG, Wesseling P (2007) Atypical teratoid/rhabdoid tumour. In: Louis DN, Ohgaki H, Wiestler OD, Cavenee WK (eds) WHO classification of tumors of the central nervous system. IARC, Lyon, pp 147–149
- Ellison D, Love S, Chimelli L et al (2004) Neuropathology: a reference text of CNS pathology, 2nd edn. Mosby, Philadelphia, pp 671–672
- Oka H, Scheithauer BW (1999) Clinicopathological characteristics of atypical teratoid/rhabdoid tumor. *Neurol Med Chir (Tokyo)* 39(7):510–517; discussion 517–518
- Kleihues P, Louis DN, Scheithauer BW, Rorke LB, Reifenberger G, Burger PC, Cavenee WK (2002) The WHO classification of tumors of the nervous system. *J Neuropathol Exp Neurol* 61(3):215–225, discussion 226–229
- Beckwith JB, Palmer NF (1978) Histopathology and prognosis of Wilms tumors: results from the first National Wilms' Tumor Study. *Cancer* 41(5):1937–1948
- Montgomery P, Kuhn JP, Berger PE (1985) Rhabdoid tumor of the kidney: a case report. *Urol Radiol* 7(1):42–44
- Rorke LB, Packer RJ, Biegel JA (1996) Central nervous system atypical teratoid/rhabdoid tumors of infancy and childhood: definition of an entity. *J Neurosurg* 85(1):56–65
- Dufour C, Beaugrand A, Le Deley MC, Bourdeaut F, André N, Leblond P, Bertozzi AI, Frappaz D, Rialland X, Fouyssac F, Edan C, Grill J, Quidot M, Varlet P (2012) Clinicopathologic prognostic factors in childhood atypical teratoid and rhabdoid tumor of the central nervous system: a multicenter study. *Cancer* 118(15):3812–3821. doi:10.1002/cncr.26684
- Mohapatra I, Santosh V, Chickabasaviah YT, Mahadevan A, Tandon A, Ghosh A, Chidambaram B, Sampath S, Bhagavatula ID, Chandramouli BA, Kolluri SV, Shankar SK (2010) Histological and immunohistochemical characterization of AT/RT: a report of 15 cases from India. *Neuropathology* 30(3):251–259. doi:10.1111/j.1440-1789.2009.01075
- Burger PC, Yu IT, Tihan T, Friedman HS, Strother DR, Kepner JL, Duffner PK, Kun LE, Perlman EJ (1998) Atypical teratoid/rhabdoid tumor of the central nervous system: a highly malignant tumor of infancy and childhood frequently mistaken for medulloblastoma: a Pediatric Oncology Group study. *Am J Surg Pathol* 22(9):1083–1092
- Yachnis AT, Perry A (2009) Embryonal (primitive) neoplasms of the central nervous system. In: Perry A, Brat DJ (eds) *Practical surgical neuropathology: a diagnostic approach*. Churchill Livingstone, Philadelphia, pp 163–176
- Parwani AV, Stelow EB, Pambuccian SE, Burger PC, Ali SZ (2005) Atypical teratoid/rhabdoid tumor of the brain: cytopathologic characteristics and differential diagnosis. *Cancer* 105(2):65–70
- Choi J, Kim H, Kim SH (2012) Atypical teratoid/rhabdoid tumor: analysis of cytomorphologic features in CSF, focused on the differential diagnosis from mimickers. *Diagn Cytopathol* 40(7):592–596. doi:10.1002/dc.21594
- Seno T, Kawaguchi T, Yamahara T, Sakurai Y, Oishi T, Inagaki T, Yamanouchi Y, Asai A, Kawamoto K (2008) An immunohistochemical and electron microscopic study of atypical teratoid/rhabdoid tumor. *Brain Tumor Pathol* 25(2):79–83. doi:10.1007/s10014-008-0236-6
- Livermore LJ, Dabbous B, Hofer M, Kueker W, Jayamohan J, Wimalaratna S (2013) Primary diffuse leptomeningeal atypical teratoid/rhabdoid tumour in an adolescent. *Clin Neurol Neurosurg* 115(10):2170–2173. doi:10.1016/j.clineuro.2013.05.036
- Gessi M, Giangaspero F, Pietsch T (2003) Atypical teratoid/rhabdoid tumors and choroid plexus tumors: when genetics “surprise” pathology. *Brain Pathol* 13(3):409–414
- Judkins AR, Burger PC, Hamilton RL, Kleinschmidt-DeMasters B, Perry A, Pomeroy SL, Rosenblum MK, Yachnis AT, Zhou H, Rorke LB, Biegel JA (2005) INI1 protein expression distinguishes atypical teratoid/rhabdoid tumor from choroid plexus carcinoma. *J Neuropathol Exp Neurol* 64(5):391–397

Atypical Teratoid/Rhabdoid Tumors: Current Chemotherapy and Future Directions

42

Cengiz Canpolat

Atypical teratoid/rhabdoid tumors (AT/RT) are relatively uncommon malignancies that can arise anywhere in the body, most frequently in the kidneys and the central nervous system (CNS) [1]. The central nervous system atypical teratoid/rhabdoid tumor (CNS AT/RT) is a highly malignant neoplasm that commonly affects infants and young children and has an extremely poor prognosis.

While AT/RT accounts for 1–2 % of childhood tumors in the brain, it may constitute more than 20 % of CNS tumors in infants [2–5]. AT/RT, first described in 1987 by Rorke and colleagues [6], was often classified as a medulloblastoma, primitive neuroectodermal tumor, or choroid plexus carcinoma prior to its recognition as a separate entity. AT/RTs were defined as an entity in 1996 and added to the World Health Organization (WHO) brain tumor classification in 2000 [7].

AT/RT is the first nervous system tumor for which the genetic etiology has been discovered. The tumor suppressor gene, *INI1*, has been identified by Biegel and colleagues as abnormal in the majority of AT/RT tumors [8]. There is an alteration of the SMARCB1 (*hSNF5/INI1*) gene at chromosomal locus 22q11.23, resulting in loss of nuclear protein expression. Consistent with the role

of a tumor suppressor gene, biallelic inactivation of SMARCB1 is present in rhabdoid tumors, and AT/RTs may occur sporadically or in the setting of a rhabdoid predisposition syndrome [9, 10].

Ten to twenty percent of AT/RTs are seen in patients less than 3 years old and also tend to originate in infratentorial regions [3, 6].

Occurrence of the majority of this tumor in children under 3 years of age necessitates avoidance of radiation therapy which further complicates treatment and effects of prognosis. This aggressive tumor remains a significant challenge in pediatric neuro-oncology, and new therapeutic approaches are desperately needed. AT/RT is a deadly disease, with initial retrospective studies reporting a survival of approximately 12 months from time of diagnosis following use of therapy standard for other malignant brain tumors in children [2, 6, 11].

Due to the rarity of the disease and the lack of large formal prospective trials, the patients were usually treated in a heterogeneous manner, and no definitive guidelines for optimal treatment have been established. Despite often impressive responses to chemotherapy (CT), the majority of patients in all published studies developed progressive disease early, within 24 weeks of diagnosis, suggesting a rapid development of resistance in AT/RTs [12–14]. More recently, long-term survivors including patients with recurrent and disseminated disease have been reported, and disease-specific protocols and registries combining maximal surgical resection, intensive

C. Canpolat, M.D.
Division of Pediatric Oncology,
Department of Pediatrics, Acibadem University,
School of Medicine, Istanbul, Turkey
e-mail: cccانpolat@yahoo.com

chemotherapy with or without stem cell support, and radiotherapy (RT) have been opened and show encouraging, albeit preliminary results [15, 16].

42.1 Chemotherapy

The Children's Hospital of Philadelphia (CHOP) first described a 5-year-old patient with CNS primary rhabdoid tumor in 1991. They chose to treat the patient with 3,600 cGy craniospinal radiation with an unspecified boost dose to the primary site along with CT consisting of cisplatin, cyclophosphamide, vincristine, and etoposide [17].

Following this, Weinblatt and Kochen from Cornell submitted a letter describing a patient they treated in 1985 with a primary CNS rhabdoid tumor. They removed the tumor with a gross total resection and then applied 4,140 cGy focal radiation followed by an intensive CT according to the IRS-III protocol including weekly vincristine during radiation, actinomycin-D, doxorubicin, and triple intrathecal chemotherapy with hydrocortisone, methotrexate, and cytosine arabinoside [18]. Olson et al. then reported an additional three cases successfully treated with IRS-III. These patients also received RT. Two of these patients (including a patient with disseminated disease at diagnosis) are alive and well without evidence of disease 12.5 and 8 years from diagnosis [19].

Since AT/RT was thought to be similar to parameningeal rhabdomyosarcomas choosing IRS-III as the CT protocol seemed to be justified as it was found easy to adapt the protocol to RT and intrathecal CT. Zimmerman and colleagues from Dana Farber Cancer Institute published a report on four children with CNS AT/RT two with newly diagnosed and two with progressive disease after multi-agent CT who were long-term survivors (median follow-up of 37 months) using a combination of surgery, RT, and intensive CT. The CT component was modified from the Intergroup Rhabdomyosarcoma Study Group (IRS-III) parameningeal protocol. The DFCI/IRS-III-based therapy was maintained close to the original, but a few potentially significant modifications to the therapy were made. For children less than three, craniospinal irradiation (CSI) was

omitted and substituted with focal stereotactic RT. Second, DTIC was substituted with temozolomide, both of which are converted to MTIC but for which dosing and administration are easier with temozolomide. Finally, the use of the cardioprotectant dexrazoxane in patients receiving doses of doxorubicin in excess of 360 mg/m² was included. The authors concluded that the toxicity associated with the delivery of this therapy was significant since all patients experienced significant episodes of neutropenia, occasionally with fever. Difficulties with maintaining weight were also common and required careful attention to nutritional supplementation. The aggressive utilization of intrathecal drug administration also created difficulties for patients, with the need for Ommaya insertion and frequent procedure-related sedation [15].

DFCI then continued with a phase II trial and treated 20 patients with AT/RT with a modified IRS-III protocol. Eight of the 20 patients had relapses by the time of publication, giving a 1-year progression-free survival (PFS) rate of 70 ± 10 % and overall survival (OS) of 75 ± 10 % and 2-year PFS of 53 ± 13 % and OS 70 % ± 10 %. Univariate analysis showed that PFS and OS were significantly influenced by the extent of resection. OS was also affected by tumor location, and patients with posterior fossa tumors had better survival. The reported PFS and OS were significantly better than those seen in other clinical trials, but due to small numbers, it was impossible to make comparisons to determine why there was such an improvement [14].

In order to increase the number of patients and apply a uniform treatment protocol, CCG enrolled 299 children less than 3 years old with multiple tumor types on protocol CCG9921 from April 1993 through June 1997. This regimen included two induction courses with ifosfamide or cyclophosphamide along with vincristine, cisplatin, and etoposide. Induction was followed by maintenance with vincristine, etoposide, carboplatin, and cyclophosphamide. There were 28 rhabdoid tumors (9.4 % of patients enrolled), 24 of those had treatment failures. The 1-year and 5-year event-free survival (EFS) rates were 32 ± 9 % and 14 ± 7 %, respectively, and the 5-year OS was 29 ± 9 % [20].

The Pediatric Oncology Group treated 36 patients with AT/RT using standard versus dose-intensified CT to delay radiation in POG 9233/34 (Baby POG 2). CT included cyclophosphamide, vincristine, cisplatin, and etoposide. Patients on the dose-intensified arm had better responses, but all patients with rhabdoid tumors ultimately died, with a median survival of 6.7 months (personal communication, Douglas Strother).

Tekautz et al. from St Jude Children's Research Hospital reviewed the treatment of 37 patients with AT/RT during the 19-year period. Six patients were excluded from this clinical review based on pathologic or clinical criteria. Of the remaining 31 patients, 22 were younger than 3 years. Posterior fossa primary lesions and metastatic disease at diagnosis were more common in younger patients. All patients underwent surgical resection; 30 received subsequent CT. Treatment included alkylator-based CT (cyclophosphamide/cisplatin/vincristine/etoposide, carboplatin/ifosfamide/etoposide (ICE), high-dose cyclophosphamide and topotecan followed by autologous hematopoietic stem cell reconstitution (AHSR), and oxaliplatin/topotecan). The majority of patients aged 3 years or older received postoperative CSI. Two-year EFS and OS of children aged 3 years or older (EFS, $78 \pm 14\%$; OS, $89 \pm 11\%$) were significantly better than those for younger patients (EFS, $11 \pm 6\%$; OS, $17 \pm 8\%$); no other clinical characteristics were predictive of survival. Three of four patients 3 years or older with progressive disease were successfully rescued with ifosfamide, carboplatin, and etoposide therapy [3].

Lafay-Cousin et al. from the Canadian Pediatric Brain Tumor Consortium published a retrospective review of 50 children (31 males; median age at diagnosis of 16.7 months) with a central nervous system AT/RT between 1995 and 2007. Twelve patients were older than 36 months and 52 % of the tumors were located infratentorially. Nineteen patients had metastatic disease. Fifteen underwent gross total resection. Ten patients underwent palliation. Twenty-two of the 40 remaining patients received conventional CT and 18 received high-dose chemotherapy (HDCT) regimens. Among the HDCT patients, nine received intrathecal CT and 15

received adjuvant RT. Thirty of the 40 treated patients relapsed/progressed at a median time of 5.5 months. The median survival time of the entire cohort was 13.5 months. Age, tumor location, and metastatic status were not found to be of prognostic significance. Patients with gross total resection had a better survival, and HDCT conferred better outcome. Upfront radiation did not provide survival benefit. Six of the 12 survivors did not receive radiation [12].

Since 2008, the Children's Oncology Group (COG) has been enrolling patients with AT/RT on a clinical trial that incorporates five cycles of CT: two cycles of induction therapy followed by three cycles of consolidation therapy. The two induction cycles each include cyclophosphamide, etoposide, vincristine, cisplatin, and high-dose methotrexate. Three cycles of consolidation consist of thiotepa and carboplatin with ASCR. Peripheral blood stem cells are harvested after each cycle of induction to provide support of the subsequent three consolidation cycles. For all patients with residual disease, second-look surgery is strongly recommended. After completion of induction, radiation therapy is administered to patients with localized disease who were greater than or equal to 6 months of age at end of induction for infratentorial tumors and greater than or equal to 12 months of age at the end of induction for supratentorial tumors. This is followed by three cycles of consolidation CT each consisting of carboplatin and thiotepa followed by ASCR. Patients, who are disseminated at diagnosis or who are younger than the ages specified above, receive induction and consolidation CT prior to RT. High-dose methotrexate (HDMTX) is included based on data from the Head Start (HS) protocols, and the three cycles of consolidation are based on CCG 99703 protocol. The study was closed for 1 year due to the toxic death of one patient but has been reopened with amendments concerning pulmonary toxicity monitoring and increased time between consolidation courses. Enrollment is ongoing, and the accrual rate is as expected for this rare tumor.

A report published by Campen et al. from Stanford University on ten patients with CNS high-risk embryonal tumors investigated feasibility

and efficacy of intravenous cyclophosphamide administered concurrently with CSI followed by alkylator-based CT. Cyclophosphamide was given 1 g/m^2 on day 1 and 2 of irradiation. Following a median of 36 cGy CSI plus tumor boost, adjuvant treatment consisted of 21 doses of oral etoposide and alkylator-based CT from five to eight cycles. Median survival was 3.3 years, with a 3-year PFS of 50 %. Median time to progression was 1.3 years. Although there was only one patient with CNS AT/RT, the study concluded that the regimen was well tolerated and a phase II trial was warranted [21].

Finally a very recently published study from Medical University of Vienna by Slavc et al. investigated the treatment outcome of 22 consecutive patients from 1992 to 2012. First nine patients with a median age of 24 months who were originally diagnosed correctly were treated according to an intensive multimodal regimen consisting of three 9-week courses of a dose-dense regimen including doxorubicin, cyclophosphamide, vincristine, ifosfamide, cisplatin, etoposide, and methotrexate augmented with intrathecal therapy, followed by high-dose chemotherapy (HDCT) and completed with local radiotherapy (MUV-AT/RT). Thirteen patients with a median age of 30 months were treated differently according to protocols in use for their respective diagnoses. Most patients in cohort B were treated according to the HIT brain tumor protocols proposed by the German Society for Paediatric Oncology and Haematology (GPOH) and in use for their respective diagnoses at the time, that is, HIT SKK 92 and HIT 91. As of July 2013, 5-year OS and EFS for all 22 consecutive patients was $56.3 \pm 11.3 \%$ and $52.9 \pm 11.0 \%$, respectively. For MUV-AT/RT regimen-treated patients, 5-year OS was 100 %, and EFS was $88.9 \pm 10.5 \%$. For patients treated differently, 5-year OS and EFS were $28.8 \pm 13.1 \%$. All nine MUV-AT/RT regimen-treated patients were alive for a median of 76 months (range: 16–197), eight in first complete remission. The authors concluded at the end that the drug combination and sequence used in the proposed MUV-AT/RT regimen appear to be efficacious in preventing early relapses also in young children with M1–M3 stage disease allowing postponement of radiotherapy until after HDCT [22].

42.2 High-Dose Chemotherapy

Investigators have used HDCT with ASCR not only as salvage therapy for patients with relapsed disease but also as a method of intensifying initial CT to delay irradiation in young patients. Researchers from Saint Jude Children's Research Hospital published a report on 27 children with recurrent CNS malignancies who received HDCT and ASCR between 1989 and 2004. The median age at diagnosis was 4.5 years and that at ASCR was 6.7 years. Diagnoses included medulloblastoma (13 patients), primitive neuroectodermal tumor (three patients), pineoblastoma (two patients), AT/RT (two patients), ependymoma (three patients), anaplastic astrocytoma (two patients), and glioblastoma multiforme (two patients). The 5-year OS and PFS rates were 28.2 and 18.5 %, respectively. The 5-year PFS rate for patients aged <3 years at diagnosis (57.1 %) was significantly better than older patients (5.0 %). This difference was likely because the patients younger than three were able to be salvaged with HDCT and radiation, whereas those older than three had previously received radiation so it was not an option for salvage. Among the six long-term survivors (five with M0 disease and one with M3 disease at diagnosis), five received both RT and HDCT as part of their salvage regimen; four were aged less than 3 years at diagnosis and had received CT only as part of frontline therapy. Two patients died of transplant-related toxicities; 44 % experienced grade 3 or 4 transplant-related toxicities. The authors concluded that HDCT with ASCR is not an effective salvage strategy for older children with recurrent CNS malignancies. The significantly better outcome in the younger cohort was most likely related to the use of RT as part of the salvage strategy [23].

Gardner et al. reported their experience of 13 children newly diagnosed with CNS ATRT enrolled on the Head Start I (HS I) or "Head Start II (HS II) regimens" therapy included resection followed by five cycles of cisplatin, vincristine, cyclophosphamide, and etoposide. HDMTX was added to each of the five induction courses in HS II. Consolidation for both regimens included carboplatin, thiopeta, and etoposide with ASCR. If

the patient had no evidence of disease at the end of induction, regardless of second-look surgery, then the patient proceeded to consolidation. If there was evidence of residual disease locally or with positive cerebrospinal cytology, consolidation was followed by RT. Six children were treated on HS I, and seven children were treated on HS II. One patient received CSI following ASCR but prior to recurrence. Three of seven children with CNS AT/RT treated on HS II have experienced long-term remissions. None received RT. The authors conclude that long-term survival could be achieved in a subset of young children with CNS AT/RT following resection with the use of multidrug CT including HDMÖTX and myeloablative CT without RT [24].

Fidani and colleagues from Italy reported eight patients with CNC AT/RT treated on a clinical trial starting from 1999. The patients were treated after primary surgery with four courses of conventional CT followed by HDCT and at the end of treatment RT. Conventional CT consisted of two courses of ICE, two courses of cyclophosphamide/etoposide/carboplatin/thiotepa (CECAT), or two other ICE courses. Eight patients underwent primary surgery achieving a complete removal in three. Progressive disease (PD) occurred in 2/8 patients during ICE courses and in 3/4 during CECAT courses. After four courses, five patients presented a PD. HDCT was performed in three patients followed by local RT. OS and EFS probability at 5 years were estimated to be 50 and 33 %, respectively. The investigators admit that the patient numbers were too small to make any real determination of survival compared with historic controls. Of the five patients who were reported as still alive at the time of publication, one did not proceed to HDCT, one had relapse before HDCT, one had relapse after HDCT but was alive with salvage therapy, one proceeded through planned therapy including HDCT and has no evidence of disease, and one was currently on therapy at the time of publication [25].

Researchers from Hospital for Sick Children in Toronto evaluated eight AT/RT patients who were identified during a period 2003–2008. Tumor location was supratentorial in three cases,

infratentorial in three cases, and multifocal in two patients. Two patients did not receive any therapy. Surgery was performed in six patients who were also given induction CT followed by sequential HDCT with ASCR. Two patients receive focal irradiation. At a median follow-up of 52 months, they reported that four of six patients were alive with no evidence of disease at a median follow-up of 52 months, and three of the four patients did not receive any radiation [26].

Nine children with AT/RT were treated at the University of California San Francisco between 1997 and 2007 with HDCT and ASCR. They received varied postsurgical therapy and conditioning regimens. As of the date of publication, there were two long-term survivors with no evidence of disease 78 and 98 months from diagnosis. One patient was reported alive with disease after 19 months. The authors suggested that at least a subset of patients could be cured with this approach [27].

More recently investigators from Korea used tandem HDCT and ASCR following six cycles of induction CT for the treatment of nine children with AT/RT. RT was administered if the tumor relapsed or progressed; otherwise, it was administered after 3 years of age. During therapy, five of the nine had progressive disease, and one patient died of disease. The remaining four patients were treated with transplantation using the same conditioning regimen. A total of five patients were alive with a median follow-up of 20 months from diagnosis. Four of five patients who received RT after relapse/progression are alive. The probability of overall survival at 3 years from diagnosis was 53.3 ± 17.3 %. The authors concluded that early administration of RT prior to tandem HDCT/ASCR improved survival [28].

42.3 Novel Therapies

Recently, a small subset of ion channels have been found to be overexpressed in a variety of malignant cells. Ion channels have been shown to regulate growth factor signaling, angiogenesis, and survival of tumor cells by their antiapoptotic properties. These properties of ion channels

appear not to be present in normal nondividing cells; thus, they may be an attractive target for drug development for difficult to treat tumors [29–31]. Volume-sensitive ion channels (VSCs) are responsible for counteracting cellular swelling. The activation of VSCs allows efflux of potassium (K⁺) and chloride (Cl⁻) ions and organic osmolytes via specific channels. The imbalance resulting from this osmolyte loss leads to an efflux of water that, in turn, reduces cell volume. Cell shrinking is a feature of apoptosis, and this depends primarily on ion efflux through K and Cl⁻ channels [32, 33]. The specific role of ion channels in apoptosis is cell type dependent and appears to involve their interplay with components of the apoptosis pathways.

Investigators from Canada examined the role of volume-sensitive ion channels in AT/RT cell lines and have found that chloride-selective VSCs are particularly active in AT/RT cell lines, compared to non-tumor cells. They evaluated specific inhibitors for activity against these ion channels and found out that inhibiting these channels reduce the growth and development of the tumor cells *in vitro*. They also showed that ion channel inhibition enhanced the activity of certain anti-neoplastic agents, suggesting its value in effective drug combination protocols. They suggested that the possibility of considering VSCs as the eventual targets in the therapy against AT/RT should be further investigated [34].

Since 1998, when the hSNF5/INI1 gene was identified as playing a role in malignant rhabdoid tumors (MRTs), much research has been done to understand the mechanism that derives AT/RT, resulting in findings that may be potential targets in the treatment of these highly malignant tumors. Morozov et al. used MON cell lines in which they introduced INI1 and then analyzed a cDNA microarray to determine expression changes and found 18 genes that were important in mitoses downregulated. These genes were topoisomerase II alpha (TOP2A), aurora A (STK6), polo-like kinase (PLK), kinesin family member 2C (KIF2C), centromere protein F (CENPF), and pituitary tumor-transforming gene 1 (PTTG1). They found that interferon-stimulated genes were significantly increased early after the reintroduc-

tion of INI1. Keeping this in mind, they treated MON and STA- WT1 rhabdoid cell lines with interferon-alpha or interferon-beta and found that cells reduced in number in 5–7 days after treatment also with their PLK1 genes downmodulated. The researchers concluded that drugs that induce interferons or target PLK1 or cyclin D1 may be effective [35].

Further investigation into the association of INI1 and cyclinD1 showed that loss of INI1 results in depression of the transcription of cyclinD1, which may drive the cell through G1 cell cycle restriction. A group at CHOP investigated 25 AT/RT and 11 non-CNS MRT samples with confirmed *SMARCB1* loss. They aimed to find the relationship between *SMARCB1*, p16INK4A, and cyclinD1. When they stained the samples for p16INK4A, they found that 17 of 25 of AT/RT and 4 of 11 of non-CNS MRT were negative. They demonstrated expression of cyclinD1 in 20 of 25 of ATRT and six of 11 of non-CNS MRT. The authors conclude that cyclin D1, which is expressed in majority of primary AT/RT tumor samples, may be a driving factor and an effective therapeutic target for rhabdoid tumors [36].

Histone deacetylase (HDAC) inhibitors such as MS-275 or trichostatin A have been shown to decrease the expression of cyclin D1 and cell proliferation in culture [37, 38]. Knipstein and colleagues from the University of Colorado at Denver investigated the effects of three HDAC inhibitors: trichostatin A, suberoylanilide hydroxamic acid, and SNDX-275 on AT/RT cell lines and a primary short-term culture of a tumor sample. They showed that all tested HDAC inhibitors decreased proliferation and that SNDX-275 increased the sensitivity of BT12 and BT16 cell lines to ionizing radiation [39].

Retinoids such as all-trans retinoic acid have also been shown in the laboratory to inhibit cyclins and cyclin-dependent kinases [40]. Other vitamin A analogs such as the rexinoid bexarotene have been shown to decrease the expression of cyclin D1, and this effect can be reversed by the HDAC inhibitor trichostatin A [41].

A group from Albert Einstein College of Medicine investigated the role of *Aurora A* in rhabdoid tumors. They used rhabdoid tumor cell lines and demonstrated that introduction of

INI1 resulted in down-modulation of Aurora A by repression of gene promoter activity. They used human and mouse tumor cells and showed that all had severalfold increase of Aurora A messenger RNA and all stained with Aurora A antibody. Then they used si-Aurora A to down-modulate Aurora A in the cells and saw a significant decrease in growth and enlarged cells with 12–15 % cell death [42].

Pediatric Preclinical Testing Program showed intermediate to high response rates in rhabdoid mouse xenograft models treated with the Aurora A inhibitor MLN8237 [43].

Many other aurora kinase inhibitors are being tested in clinical trials that may be candidates for the treatment of patients with AT/RT [44].

Positive immunohistochemical staining with IGF-IR and its ligand IGF-II has been shown first in two AT/RT samples. Then investigators from CHOP confirmed IGF-IR expression in eight formalin-fixed paraffin-embedded AT/RT samples suggesting the involvement of an autocrine/paracrine loop in AT/RT. Tumor cells treated with IGF-IR antisense oligonucleotides decreased proliferation, increased apoptosis, and increased chemotherapeutic sensitivity to doxorubicin and cisplatin [45, 46].

ATRT cell lines grown in serum-free media have been shown by other researchers to secrete insulin supporting the autocrine/paracrine theory and that use of the IGF-IR inhibitor NVP-AEW541 inhibited proliferation and increased caspase three activation, although only at a high concentration [47]. There are several preclinical studies and clinical trials related to the development of IGF inhibitors, whether through small molecule inhibitors such as nordihydroguaiaretic acid in prostate cancer or breast cancer or receptor-inhibiting antibodies in multiple solid tumors [48–50].

IGF inhibitors have been investigated for the treatment of other cancers such as prostate and breast tumors by several other investigators in preclinical and clinical trials.

A group in Germany investigated five AT/RT and 18 non-CNS MRT samples as well as two cell lines for expression of tyrosine kinases and found c-Abl staining in all of them. Imatinib as well as specific targeting of c-Abl with siRNA

significantly reduced proliferation of both cell lines [51]. Jayanthan et al. utilized sorafenib and sunitinib on BT12, BT16, and KCCF1 cell lines and showed dose-dependent inhibition of growth. Significant levels of platelet-derived growth factor and vascular endothelial growth factor have been shown in the supernatant of cell culture media. They also used irinotecan on the cell lines and achieved the same effect and concluded that tyrosine kinase inhibitors and irinotecan, when used in combination, had a synergistic effect. Others have reported that expression of epidermal growth factor receptor was absent in nine tumor samples of AT/RT tested by FISH and immunohistochemistry and suggested that this may not be an effective target in AT/RT [52, 53].

The prognosis for AT/RT is poor especially for those with metastatic disease and in children who are under 3 years of age. Radiotherapy seems to be the most important part of therapy although multiple chemotherapeutic approaches have been tried in an attempt to increase survival but without much success. Despite all these efforts, we still need more laboratory and clinical work to find out more effective and targeted therapies for the treatment of this tumor, and this should be accomplished rapidly for the future sake of our patients.

References

1. Beckwith JB, Palmer NF (1978) Histopathology and prognosis of Wilms' tumor: results from the first National Wilms' Tumor Study. *Cancer* 41:1937–1948
2. Packer RJ, Biegel JA, Blaney S et al (2002) Atypical teratoid/rhabdoid tumor of the central nervous system: report on workshop. *J Pediatr Hematol Oncol* 24:337–342
3. Tekautz TM, Fuller CE, Blaney S et al (2005) Atypical teratoid/rhabdoid tumors (ATRT): improved survival in children 3 years of age and older with radiation therapy and high-dose alkylator-based chemotherapy. *J Clin Oncol* 23:1491–1499
4. Von Hoff K, Hinkes B, Dannenmann-Stern E et al (2011) Frequency, risk factors and survival of children with atypical teratoid rhabdoid tumors (AT/RT) of the CNS diagnosed between 1988 and 2004, and registered to the German HIT database. *Pediatr Blood Cancer* 57:978–985
5. Lefkowitz IB, Rorke LB, Packer RJ et al (1987) Atypical teratoid tumor of infancy: definition of an entity. *Ann Neurol* 22:448–449

6. Rorke LB, Packer RJ, Biegel JA (1996) Central nervous system atypical teratoid/rhabdoid tumors of infancy and childhood: definition of an entity. *J Neurosurg* 85:56–65
7. Kleihues P, Cavaneer WK (2000) Pathology and genetics of tumours of the nervous system, 3rd edn. IARC Press, Lyon
8. Biegel JA, Zhou JY, Rorke LB et al (1999) Germ-line and acquired mutations of INI1 in atypical teratoid and rhabdoid tumors. *Cancer Res* 59:74–79
9. Bourdeaut F, Lequin D, Brugieres L, Reynaud S, Dufour C, Doz F et al (2011) Frequent hSNF5/INI1 germline mutations in patients with rhabdoid tumor. *Clin Cancer Res* 17:31–38
10. Eaton KW, Tooke LS, Wainwright LM, Judkins AR, Biegel JA (2011) Spectrum of SMARCB1/INI1 mutations in familial and sporadic rhabdoid tumors. *Pediatr Blood Cancer* 56:7–15
11. Burger PC, Yu IT, Tihan T et al (1998) Atypical teratoid/rhabdoid tumor of the central nervous system: a highly malignant tumor of infancy and childhood frequently mistaken for medulloblastoma. *Am J Surg Pathol* 22:1083–1092
12. Lafay-Cousin LC, Hawkins AS, Carret D et al (2012) Central nervous system atypical teratoid rhabdoid tumours: the Canadian Paediatric Brain Tumour Consortium experience. *Eur J Cancer* 48:353–359
13. Ginn KF, Gajjar A (2012) Atypical teratoid rhabdoid tumor: current therapy and future directions. *Front Oncol* 2:114
14. Chi SN, Zimmerman MA, Yao X et al (2009) Intensive multimodality treatment for children with newly diagnosed CNS atypical teratoid rhabdoid tumor. *J Clin Oncol* 27:385–389
15. Zimmerman MA, Goumnerova LC, Proctor M et al (2005) Continuous remission of newly diagnosed and relapsed central nervous system atypical teratoid/rhabdoid tumor. *J Neurooncol* 72:77–84
16. Athale UH, Duckworth J, Odame I et al (2009) Childhood atypical teratoid rhabdoid tumor of the central nervous system: a meta-analysis of observational studies. *J Pediatr Hematol Oncol* 31:651–663
17. Perilongo G, Sutton L, Czaykowski D et al (1991) Rhabdoid tumor of the central nervous system. *Med Pediatr Oncol* 19:310–317
18. Weinblatt M, Kochen J (1992) Rhabdoid tumor of the central nervous system. *Med Pediatr Oncol* 20:258
19. Olson T A, Bayar E, Kosnik E et al (1995) Successful treatment of disseminated central nervous system malignant rhabdoid tumor. *J Pediatr Hematol Oncol* 17:71–75
20. Geyer JR, Sposto R, Jennings M et al (2005) Multi agent chemotherapy and deferred radiotherapy in infants with malignant brain tumors: a report from the Children's Cancer Group. *J Clin Oncol* 23:7621–7631
21. Campen CJ, Dearlove J, Pertap S et al (2012) Concurrent cyclophosphamide and craniospinal radiotherapy for pediatric high-risk embryonal brain tumors. *J Neurooncol* 110:287–291
22. Slave I, Chocholous M, Leiss U et al (2014) Atypical teratoid rhabdoid tumor: improved long-term survival with an intensive multimodal therapy and delayed radiotherapy. The Medical University of Vienna Experience. *Cancer Med* 3(1):91–100
23. Shih CS, Hale GA, Gronewold L, Tong X, Laningham FH, Gilger EA, Srivastava DK, Kun LE, Gajjar A, Fouladi M (2008) High-dose chemotherapy with autologous stem cell rescue for children with recurrent malignant brain tumors. *Cancer* 112(6):1345–1353
24. Gardner SL, Asgharzadeh S, Green A (2008) Intensive induction chemotherapy followed by high dose chemotherapy with autologous hematopoietic progenitor cell rescue in young children newly diagnosed with central nervous system atypical teratoid rhabdoid tumors. *Pediatr Blood Cancer* 51(2):235–240
25. Fidani P, De Loris MA, Serra A et al (2009) A multimodal strategy based on surgery, radiotherapy, ICE regimen and high dose chemotherapy in atypical teratoid/rhabdoid tumours: a single institution experience. *J Neurooncol* 92:177–183
26. Finkelstein-Shechter T, Gassas A, Mabbott D et al (2010) Atypical teratoid or rhabdoid tumors: improved outcome with high-dose chemotherapy. *J Pediatr Hematol Oncol* 32:182–186
27. Nicolaidis T, Tihan T, Horn B et al (2010) High-dose chemotherapy and autologous stem cell rescue for atypical teratoid/rhabdoid tumor of the central nervous system. *J Neurooncol* 98:117–123
28. Park ES, Sung KW, Baek HJ et al (2012) Tandem high-dose chemotherapy and autologous stem cell transplantation in young children with atypical teratoid/rhabdoid tumor of the central nervous system. *J Korean Med Sci* 27:135–140
29. Prevarskaya N, Skryma R, Shuba Y (2010) Ion channels and the hallmarks of cancer. *Trends Mol Med* 16:107–121
30. Davies AR, Melsy MJ, Kozlowski RZ (2004) Volume sensitive organic osmolyte anion channels in cancer. *Ann N Y Acad Sci* 1028:38–55
31. Sontheimer H (2008) An unexpected role for ion channels in brain tumor metastasis. *Exp Biol Med* 233:779–791
32. Banderali U, Roy G (1992) Anion channels for amino acids in MDCK cells. *Am J Physiol* 263:C1200–C1207
33. Kirk K, Strange K (1998) Functional properties and physiological roles of organic solute channels. *Annu Rev Physiol* 60:719–739
34. Banderali U, Jayanthan A, Hoeksema KA et al (2012) Ion channels in pediatric CNS Atypical Teratoid/Rhabdoid Tumor (AT/RT) cells: potential targets for novel therapeutic agents. *J Neurooncol* 107:111–119
35. Morozov A, Lee SJ, Zhang ZK et al (2007) N11 induces interferon signaling and spindle checkpoint in rhabdoid tumors. *Clin Cancer Res* 13:4721–4730
36. Venneti S, Le P, Martinez D et al (2011) p16INK4A and p14ARF tumor suppressor pathways are deregulated in malignant rhabdoid tumors. *J Neuropathol Exp Neurol* 70:596–609

37. Rosato RR, Almenara JA, Grant S (2003) The histone deacetylase inhibitor MS-275 promotes differentiation or apoptosis in human leukemia cells through a process regulated by generation of reactive oxygen species and induction of p21CIP1/WAF11. *Cancer Res* 63:3637–3645
38. Alao JP, Stavropoulo AV, Lam EW et al (2006) Histone deacetylase inhibitor, trichostatin A induces ubiquitin-dependent cyclin D1 degradation in MCF-7 breast cancer cells. *Mol Cancer* 5:8
39. Knipstein JA, Birks DK, Donson AM et al (2012) Histone deacetylase inhibition decreases proliferation and potentiates the effect of ionizing radiation in atypical teratoid/rhabdoid tumor cells. *Neurooncology* 14:175–183
40. Kosaka C, Sasaguri T, Komiyama Y et al (2001) All-trans retinoic acid inhibits vascular smooth muscle cell proliferation targeting multiple genes for cyclins and cyclin dependent kinases. *Hypertens Res* 24:579–588
41. Li Y, Shen Q, Kim HT et al (2011) The rexinoid bexarotene represses cyclin D1 transcription by inducing the DEC2 transcriptional repressor. *Breast Cancer Res Treat* 128:667–677
42. Lee S, Cimica V, Ramachandra N et al (2011) Aurora A is a repressed effector target of the chromatin remodeling protein INI1/hSNF5 required for rhabdoid tumor cell survival. *Cancer Res* 71:3225–3235
43. Maris JM, Morton CL, Gorlick R et al (2010) Initial testing of the aurora kinase A inhibitor MLN 8237 by the Pediatric Preclinical Testing Program (PPTP). *Pediatr Blood Cancer* 55:26–34
44. Dar AA, Goff LW, Majid S et al (2010) Aurora kinase inhibitors rising stars in cancer therapeutics. *Mol Cancer Ther* 9:268–278
45. Ogino S, Kubo S, Abdul-Karim FW et al (2001) Comparative immunohistochemical study of insulin-like growth factor II and insulin-like growth factor receptor type I in pediatric brain tumors. *Pediatr Dev Pathol* 4:23–31
46. D’Cunja J, Shalaby T, Rivera P et al (2007) Antisense treatment of IGF-IR induces apoptosis and enhances chemosensitivity in central nervous system atypical teratoid/rhabdoid tumour cells. *Eur J Cancer* 43:1581–1589
47. Arcaro A, Doepfner KT, Boller D et al (2007) Novel role for insulin as an autocrine growth factor for malignant brain tumour cells. *Biochem J* 406:57–66
48. Ozkan EE (2011) Plasma and tissue insulin-like growth factor-I receptor (IGF-IR) as a prognostic marker for prostate cancer and anti-IGF-IR agents as novel therapeutic strategy for refractory cases: a review. *Mol Cell Endocrinol* 344:1–24
49. Rowe DL, Ozbay T, Bender LM et al (2008) Nor dihydroguaiaretic acid, a cytotoxic insulin-like growth factor-I receptor/HER2 inhibitor in trastuzumab-resistant breast cancer. *Mol Cancer Ther* 7:1900–1908
50. Adam PJ, Ostermann E, Lamche HR et al (2011) Pharmacodynamic properties and antitumor efficacy of BI 836845, a fully human IGF1 ligand neutralizing antibody. *Mol Cancer Ther* 10(Suppl 11):abstr. A208
51. Koos B, Jeibmann A, Lunenburger H et al (2010) The tyrosine kinase c- Abl promotes proliferation and is expressed in atypical teratoid and malignant rhabdoid tumors. *Cancer* 116:5075–5081
52. Jayanthan A, Bernoux D, Bose P et al (2011) Multi-tyrosine kinase inhibitors in preclinical studies for pediatric CNSAT/RT: evidence for synergy with Topoisomerase-I inhibition. *Cancer Cell Int* 11:44
53. Jeibmann A, Buerger H, Fruhwald M et al (2006) No evidence for epidermal growth factor receptor amplification and overexpression in a typical teratoid/rhabdoid tumors. *Acta Neuropathol* 112:513–514

Hale Basak Caglar

43.1 Introduction

The first description of primary malignant rhabdoid tumor was made by Beckwith and Palmer in 1978 as a highly malignant pediatric tumor of the kidney [1]. Since then, this neoplasm appeared in many other parts of the body, including the central nervous system (CNS). The CNS variant of this tumor was recognized as the atypical teratoid rhabdoid tumor (AT/RT) when added as a separate entity to the World Health Organization (WHO) in 1993 [2]. AT/RT is a malignant embryonal tumor of the CNS that is composed of rhabdoid cells, with or without fields resembling classical primitive neuroectodermal tumor [3]. Although the morphological pattern resembles other embryonal tumors of the CNS (medulloblastoma, PNET), it is shown to exhibit different serum marker expression and immunohistochemical (IHC) staining patterns from them and proved significantly more aggressive [4]. To date, approximately 300 cases of AT/RT have been described in the literature. It is likely that the incidence of AT/RT has been underestimated given the clinical and histological similarities to medulloblastoma and the previous unavailability of IHC for routine diagnosis. Prior to recognition of AT/RT as a unique entity, many

cases of AT/RT may have been misdiagnosed as medulloblastoma. Since the rise in accessibility of IHC testing in the late 1990s, the recognition of AT/RT has increased. Results from a pathological review of a Children's Cancer Group study of children with malignant brain tumors suggest that although AT/RT is a relatively rare disease, accounting for less than 5 % of all pediatric CNS tumors, up to 20 % of malignant CNS tumors diagnosed before the patient is 3 years old are AT/RTs [4–6].

In addition to the histological similarities, AT/RT has many common radiological and clinical characteristics with medulloblastoma. It commonly affects infants and young children. It can be located both infratentorial and supratentorial although posterior fossa is more common.

Looking at the clinical and pathological similarities between these two entities, it is important to realize that the clinical outcomes of these tumors are somehow different. Over the past 30 years, the overall survival of medulloblastoma has increased from 25 to 65 % [7], while the numbers are still the same for AT/RT with a median survival of almost a year especially when metastases were found at the time of diagnosis, an entity seen in 20 % of the patients [6]. The patients with AT/RT tend to be refractory to standardized therapies, especially chemotherapy for medulloblastoma. A significant portion dies of local recurrence.

Majority of the patients with AT/RT present at an age of less than 3 years, radiation therapy has usually been withheld as a standard treatment

H.B. Caglar, M.D.
Department of Radiation Oncology,
Medipol University, Istanbul, Turkey
e-mail: halebasakcaglar@gmail.com

option right away from surgery. However, the most recent evidence suggests that long-term survival can be obtained with the use of more intensive and aggressive chemotherapy with adjuvant radiation therapy still presents a particular dilemma as young patients with this disease may experience serious late effects of therapy if with longer follow-up.

The first and the most important step of treating this tumor is achieving the correct diagnosis for directing the patient to the most proper therapy. As approximately two-thirds of the patients with AT/RT have pathologic samples that contain cells resembling medulloblastoma [7]. IHC is the most objective and reliable way to make a differentiation.

The earliest publication for the association of AT/RT with chromosomal abnormalities especially chromosome 22 was from Rorke et al. in 1995 [8]. Through subsequent years, specific gene mutations were identified on a specific locus of the chromosome. The identification of hSNF5/INI1 gene mutation is now used for the definition of the disease.

43.2 Treatment Strategies

Much of the management of AT/RT has evolved from medulloblastoma because of the similarities. The central pathologic review of the data collected from protocols for medulloblastoma and PNET have shown that a number of these patients are actually AT/RT. By this, a retrospective analysis of these tumors was performed to evaluate response for standard treatment strategies.

A multi-institutional registry of patients with AT/RT with complete information on surgery, chemotherapy, and radiotherapy was published by Hilden et al. in 2006 [6]. Complete information was observed for 42 patients. Primary therapy included chemotherapy in all patients, radiotherapy in 13 patients (31 %), stem-cell rescue in 13 patients (31 %), and intrathecal chemotherapy in 16 patients (38 %).

Achieving a complete resection appears to be a significant prognostic factor for overall survival (OS) [6, 9]. Among the three strategies, chemotherapy has been the most studied one. As most of the children present at an early age of less than 3 years, chemotherapy is usually started after surgery as a

way of postponing radiation. The initial response to medulloblastoma/PNET protocols is very poor, so more aggressive chemotherapy combinations with intrathecal applications are recommended.

The role of radiation therapy is much less studied than chemotherapy in the management of AT/RT. The most recent evidences support the use of early and effective radiotherapy for making long-term survival possible in this group of patients. The rationale of radiation is to prevent local recurrences as in many other tumor sites. In the early report of the registry, the majority of the recurrences were in the primary tumor site. Another role for radiation could be the prevention of leptomeningeal disease especially when performed as a full axis irradiation. Although long-term detrimental effects of radiation in patients aged less than 3 years old has been clearly identified, the disadvantages of radiation should be weighed given the dismal prognosis of the disease especially in the presence of new technological advances of the treatment [10].

43.3 The Necessity of Adjuvant Radiation Therapy for AT/RT

Immediate initial radiation therapy for AT/RT is a controversial issue as most of the patients are under the age of 3 years. Postponing radiotherapy until after 3 years because of the highlighted side effects such as endocrine dysfunction, cognitive disturbances, and mental retardation has been the trend for various neoplasms in this age group. Duffner et al. reported the effects of delaying radiotherapy in children that have neoplasms under 3 years old with chemotherapy in a POG study in 1993 [11]. The progression-free survival (PFS) at 1 and 2 years were reported to be 41 and 39 %, respectively. Although the results of this study confirmed the safety of deferring radiation until 3 years as a standard management strategy for patients diagnosed as having a medulloblastoma and PNET under 3 years old, there still might be some high-risk patients leading to poorer outcomes with this delay [12]. Additionally it has to be emphasized that these are the evidence for medulloblastoma and PNET, which is known to have better outcomes with less aggressive thera-

pies from AT/RT. As the number of the patients with AT/RT is much less than other histologies, currently there is not any prospective data for the postponement of radiation. Looking at the retrospective evidence with small number of patients, AT/RT is less sensitive to traditional chemotherapy regimens used for medulloblastoma and has a high rate of relapse within the first year [13].

In the AT/RT registry report, a total of 42 patients were included where 28 of them experienced progression and recurrence. Eight of the 13 children who were clinically without evidence of disease at least 19 months after diagnosis had received radiation therapy as part of their initial treatment regimen [6].

The initial report of 37 cases of AT/RT diagnosed at St. Jude's Children's Research Hospital over a 19-year interval was published in 2005 by Tekautz et al. They reported 22 patients who were less than 3 years old at the time of diagnosis, and of these patients, there were only two long-term survivors. Both long-term survivors received initial radiation therapy as part of their treatment protocol. The majority of patients who were older than 3 years old at diagnosis received craniospinal irradiation as part of their primary treatment. The only significant prognostic factor for event-free survival (EFS) and OS was the age at diagnosis [5]. The same group updated their data in 2012 according to radiotherapy sequencing as a prognostic factor [14]. Thirty-one patients at a median age of 2.3 years at diagnosis were enrolled into protocols that included risk- and age-stratified radiotherapy. Radiation was delayed more than 1 month in 24; seven patients received immediate postoperative irradiation (majorly craniospinal irradiation) preceding high-dose alkylator-based chemotherapy. At a median follow-up of 48 months, children receiving delayed RT were more likely to experience local failure.

A retrospective review from Taiwan reported 17 patients with AT/RT. All patients were treated with primary surgery and then radiation therapy. All but one patient in this series were 3 years or older at the time of radiation therapy. There were five patients in the series that were disease-free for a period of 25 months or longer, of which three remain disease-free. Median overall survival

and failure-free survival were 17 and 11 months, respectively. The three longest surviving patients were older, underwent gross tumor removal, and completed both craniospinal and focal boost irradiation. Multivariate analysis revealed a significant relationship between performance status, total irradiation dose, time interval between surgery and radiotherapy initiation, and time interval between surgery and radiotherapy end point [15].

A Surveillance Epidemiology and End Results (SEER) database was used to identify 144 patients with ATRT from 1973 to 2008. The median age at diagnosis was 1 year, gross total resection of the primary tumor was achieved in 39 % of patients, and 33 % of patients received RT. From 1992 to 2008, RT use increased 2.4-fold in patients aged less than 3 years. The median OS for was 10 months. In multivariate analyses, metastatic disease and radiation treatment were identified as independent predictors of survival [16].

Another SEER study from 2012 confirmed similar results in infant brain tumors which included mixed histologies including ATRT [17]. For infants with medulloblastoma and ATRTs, improved survival was observed in patients treated with both surgery and early radiation compared with those treated with surgery alone.

The fact that long-term survivors of AT/RT were more likely to have had initial radiation provides an argument for the use of initial radiation therapy as part of a treatment regimen for AT/RT. The dismal salvage rate for AT/RT also suggests that the best opportunity to cure this disease is prior to relapse or disease progression. The only prospective data included radiation as a primary adjuvant treatment in all age groups [18]. Based on the current available evidence, the NCI AT/RT workshop in 2001 recommended that involved field radiation therapy be included in the developing COG protocol for CNS AT/RT [19].

43.4 Radiation Therapy Techniques

There is even less evidence for the dose and volume of radiation therapy delivered to patients with AT/RT. Major variations in the treatment techniques

were detected in small number retrospective reports including whole-brain radiation, craniospinal irradiation, and involved-field radiation. Weiss reviewed the 36 cases of CNS malignant rhabdoid tumor reported in the literature prior to 1998. Of these patients, 14 were reported to have received craniospinal irradiation as part of the treatment regimen. Of the patients in the AT/RT registry, only 4 of the 42 patients had craniospinal irradiation as part of their initial treatment [6].

The reason of administering craniospinal irradiation to patients with AT/RT is because of the high frequency of the disease to disseminate throughout the craniospinal axis. The frequency of relapses involving the spine was found to be 42 % in ATRT [21]. Out of a total of 52 cases reviewed by Burger, 24 relapsed at the primary site, 9 relapsed both at the primary site and with craniospinal metastases, and 16 developed craniospinal metastases without clinically evident local recurrence [13]. One-third of the patients were found to have leptomeningeal dissemination at the time of initial diagnosis [5, 14–16].

While there may be a theoretical benefit from craniospinal irradiation, this benefit is not without significant morbidity, particularly in very young patients. Irradiation of the neuraxis may increase the risk of growth retardation and damage to organs anterior to the spinal cord when compared with conformal focal radiation especially in younger children. Although the NCI recommended involved field radiation therapy as the treatment fields to be used in developing a COG protocol, radiation treatment fields for AT/RT remain controversial [19].

Similar to the treatment fields, the dose of the radiation has not been well established [20]. The dose is decided according to the age of the patient, size and the location of the tumor, dissemination to the neuraxis, and response to previous treatment. The doses usually are derived from the treatment of medulloblastoma. Craniospinal radiation consists of 25–36 Gy doses followed by a boost to the primary site to a dose of 45–63 Gy [5, 14–16]. The total radiotherapy dose (less than 50 Gy vs greater than 50 Gy) was found to be significantly associated with failure-free survival in the report from Taiwan [15]. No other studies evaluated the effect of radiation dose in this patient group.

The use of more conformal radiation techniques for patients with AT/RT allows for sparing of critical structures that might influence the long-term side effects of radiation therapy. Intensity-modulated radiation therapy (IMRT) has been used in the treatment of patients with childhood brain tumors in order to spare critical structures in the brain such as the cochlea and the optic apparatus. More recently the use of volumetric helical IMRT technologies for craniospinal irradiation yielded better dose heterogeneity especially at junctions compared with conventional techniques [22]. However with the use of IMRT, the integral dose delivered to the surrounding tissues increase at a significant rate, so it might be harmful to the developing brain. Sufficient follow-up for the late effects is not available, but they might include secondary cancers at most.

Proton therapy is another way of utilizing conformal radiotherapy with the physical properties of rapid dose falloff distal to the target volume. Protons produce little to no exit dose, thus minimizing the exposure of normal brain tissue to ionizing radiation. The integral dose of proton therapy is significantly less than that of photon-IMRT. Proton has been shown to spare critical structures compared with other techniques in craniospinal radiation [23, 24]. In a very recent report from Boston, ten patients with the diagnosis of ATRT were treated with upfront local 3D conformal proton therapy [25]. With a median follow-up of 27.3 months, only two patients relapsed, and at the last follow-up, nine patients were alive without the evidence of disease.

43.5 Radiation Therapy as a Salvage Treatment

Because of the dismal prognosis of AT/RT after relapse, there is no clear evidence for successful salvage therapy after initial therapy. Radiation should be considered as a salvage treatment if not yet been administered as an initial adjuvant treatment.

Reirradiation with stereotactic radiosurgery can be applied for small, non-infiltrative in-field recurrences. As the use of primary radiation increases with evidence, radiosurgery provides

potential as a salvage modality to patients previously irradiated by decreasing the risk of radionecrosis, which would occur after a second course of conventional radiation therapy [7].

There are reports of successful usage of stereotactic radiosurgery as a salvage procedure to achieve long-term control of AT/RT [9, 26–28].

43.6 Adverse Effects of Radiation Therapy

Although the age at initial presentation of STRT is majorly below 3 years, radiation therapy plays an important role in achieving local control. Aggressive treatment including initial radiation therapy has been shown as the most effective for long-term survival. The risk of radiation-induced damage is usually increased in younger children majorly due to the irradiation of immature CNS tissue. The evidence to support a relationship between younger age at time of radiation and severity of late effects has been shown before [10]. While there is emerging evidence for the potential benefit of initial radiation in patients with AT/RT, careful consideration of the side-effect profile is warranted because of the nature and severity of such effects [7].

43.7 Enhancing the Effect of Radiotherapy

As ATRT is a highly malignant neoplasm that has poor outcomes, new therapies are urgently needed. Knipstein et al. have evaluated the effect of histone deacetylase inhibitors (HDIs) as a radiosensitization strategy in ATRT cell lines in vitro [29]. They act as epigenetic modifiers and lead to re-expression of inappropriately repressed genes, proteins, and cellular functions.

They have showed that HDI pretreatment effectively potentiates the effect of ionizing radiation on ATRT cells as measured by clonogenic assay.

Another study examined inhibition of aurora kinase A which was found to be one of the multiple kinases that was found to be elevated in gene expression analysis of ATRT tissues [30].

The objective of the study was to evaluate the impact of aurora kinase A inhibition in ATRT cell lines. The analysis revealed that inhibition of aurora kinase A sensitizes these cells to radiation.

43.8 Summary

ATRT is a rare disease seen in the CNS in young ages with a dismal prognosis despite various treatment modalities. Although data is limited, there is evidence for the routine use of radiation initially after surgery in order to achieve long-term survival concurrently with intense and aggressive chemotherapy. The majority of the recurrences are local and the survival after recurrence is very poor.

Currently, radiation is included to ongoing multi-institutional prospective trials as an initial adjuvant treatment procedure for newly diagnosed ATRT regardless of patient age. The radiation fields usually consist of local primary tumor volume when there is no proven dissemination to the neuraxis.

References

1. Beckwith JB, Palmer NF (1978) Histopathology and prognosis of wilms tumors: results from the first national wilms' tumor study. *Cancer* 41(5): 1937–1948
2. Ginn KF, Gajjar A (2012) Atypical teratoid rhabdoid tumor: current therapy and future directions. *Front Oncol* 2(114):1–13
3. Kleihues P, Louis DN, Scheithauer BW et al (2002) The WHO classification of tumors of the nervous system. *J Neuropathol Exp Neurol* 61:215–225
4. Packer RJ, Biegel JA, Blaney S et al (2002) Atypical teratoid/ rhabdoid tumor of the central nervous system: report on workshop. *J Pediatr Hematol Oncol* 24(5):337–342
5. Tekautz TM, Fuller CE, Blaney S et al (2005) Atypical teratoid / rhabdoid tumors (ATRT): improved survival in children 3 years of age and older with radiation therapy and high-dose alkylator-based chemotherapy. *J Clin Oncol* 23(7):1491–1499
6. Hilden JM, Meerbaum S, Burger P et al (2004) Central nervous system atypical teratoid/rhabdoid tumor: results of therapy in children enrolled in a registry. *J Clin Oncol* 22:2877–2884
7. Squire SE, Chan MD, Marcus KJ (2007) Atypical teratoid/rhabdoid tumor: the controversy behind radiation therapy. *J Neurooncol* 81:97–111

8. Rorke LB, Packer R, Biegel J (1995) Central nervous system atypical teratoid/rhabdoid tumors of infancy and childhood. *J Neurooncol* 24:21–28
9. Zimmerman MA, Goumnerova LC, Proctor M et al (2005) Continuous remission of newly diagnosed and relapsed central nervous system atypical teratoid/rhabdoid tumor. *J Neurooncol* 72(1):77–84
10. Duffner PK, Cohen ME, Thomas PR et al (1985) The long term effects of cranial irradiation on the central nervous system. *Cancer* 56(7 Suppl):1841–1846
11. Duffner PK, Horowitz ME, Krischer JP et al (1993) Postoperative chemotherapy and delayed radiation in children less than three years of age with malignant brain tumors. *N Engl J Med* 328(24):1725–1731
12. Grill J, Sainte-Rose C, Jouvet A et al (2005) Treatment of medulloblastoma with postoperative chemotherapy alone: an SFOP prospective trial in young children. *Lancet Oncol* 6(8):573–580
13. Burger PC, Yu IT, Tihan T et al (1998) Atypical teratoid/rhabdoid tumor of the central nervous system: a highly malignant tumor of infancy and childhood frequently mistaken for medulloblastoma: a pediatric oncology group study. *Am J Surg Pathol* 22(9):1083–1092
14. Pai Panandiker AS, Merchant T, Beltran C et al (2012) Sequencing of local therapy affects the pattern of treatment failure and survival in children with atypical teratoid rhabdoid tumors of the central nervous system. *Int J Radiat Oncol Biol Phys* 85(2):1756–1763
15. Chen YW, Wong TT, Ho DM et al (2006) Impact of radiotherapy for pediatric CNS atypical teratoid/rhabdoid tumor (single institute experience). *Int J Radiat Oncol Biol Phys* 64(4):1038–1043
16. Buscariollo DL, Park HS, Roberts KB et al (2012) Survival outcomes in atypical teratoid rhabdoid tumor for patients undergoing radiotherapy in a Surveillance, Epidemiology, and End Results analysis. *Cancer* 118(17):4212–4219
17. Bishop AJ, McDonald MW, Chang AL et al (2012) Infant brain tumors: incidence, survival, and the role of radiation based on Surveillance, Epidemiology, and End Results (SEER) data. *Int J Radiat Oncol Biol Phys* 82(1):341–347
18. Chi SN, Zimmerman MA, Yao X et al (2009) Intensive multimodality treatment for children with newly diagnosed CNS atypical teratoid rhabdoid tumor. *J Clin Oncol* 27(3):385–389
19. Combination chemotherapy, radiation therapy, and an autologous peripheral blood stem cell transplant in treating young patients with atypical teratoid/rhabdoid tumor of the central nervous system. <http://www.cancer.gov/clinicaltrials/search/view?cdrid=592812&version=healthprofessional>
20. Weiss E, Behring B, Behnke J et al (1998) Treatment of primary malignant rhabdoid tumor of the brain: report of three cases and review of the literature. *Int J Radiat Oncol Biol Phys* 41(5):1013–1019
21. Perreault S, Lober RM, Carret AS et al (2013) Relapse patterns in pediatric embryonal central nervous system tumors. *J Neurooncol* 115(2):209–215
22. Studenski MT, Shen X, Yu Y et al (2013) Intensity-modulated radiation therapy and volumetric-modulated arc therapy for adult craniospinal irradiation—a comparison with traditional techniques. *Med Dosim* 38(1):48–54
23. St Clair WH, Adams JA, Bues M et al (2004) Advantage of protons compared to conventional x-ray or IMRT in the treatment of a pediatric patient with medulloblastoma. *Int J Radiat Oncol Biol Phys* 58(3):727–734
24. Song S, Park HJ, Yoon JH et al (2014) Proton beam therapy reduces the incidence of acute haematological and gastrointestinal toxicities associated with craniospinal irradiation in pediatric brain tumors. *Acta Oncol* 10:1–7
25. De Amorim BK, Sethi R, Trofimov A et al (2013) Early clinical outcomes using proton radiation for children with central nervous system atypical teratoid rhabdoid tumors. *Int J Radiat Oncol Biol Phys* 86(1):114–120
26. Hirth A, Pedersen PH, Wester K et al (2003) Cerebral atypical teratoid/rhabdoid tumor of infancy: long-term survival after multimodal treatment, also including triple intrathecal chemotherapy and gamma knife radiosurgery –case report. *Pediatr Hematol Oncol* 20(4):327–332
27. Giller CA, Berger BD, Pistenmaa DA et al (2005) Robotically guided radiosurgery for children. *Pediatr Blood Cancer* 45(3):304–310
28. Nanda R, Dhabbaan A, Janss A et al (2014) The feasibility of frameless stereotactic radiosurgery in the management of pediatric central nervous system tumors. *J Neurooncol* 117(2):329–335
29. Knipstein JA, Birks DK, Donson AM et al (2012) Histone deacetylase inhibition decreases proliferation and potentiates the effect of ionizing radiation in atypical teratoid/rhabdoid tumor cells. *Neuro Oncol* 14(2):175–183
30. Venkataraman S, Alimova I, Tello T et al (2012) Targeting Aurora Kinase A enhances radiation sensitivity of atypical teratoid rhabdoid tumor cells. *J Neurooncol* 107(3):517–526

Pathologies in Pediatric Posterior Fossa Tumors: Chordoma

Christian Sainte-Rose

C. Sainte-Rose, M.D.
Department of Paediatric Neurosurgery,
Necker Enfants Malades Hospital, Paris, France

Mustafa Gdk and M. Memet zek

44.1 Introduction

Chordomas are extra-axial, low-grade malignancies growing slowly, located anywhere from the clivus to the sacrum on the axial skeleton. Grossly they are unencapsulated, usually lobulated, pink-gray colored, invasive tumors with foci of hemorrhage and calcifications exhibiting epithelial phenotype. Histopathologically they are classified as classic chordomas, chondroid chordomas, and atypical chordomas [1, 2]. Classic chordomas are characterized by the presence of physaliferous cells which are large, vacuolated, mucus-containing cells with hyperchromatic, eccentric nuclei having prominent nucleoli rarely demonstrating atypia and reticulated cytoplasm due to intracellular accumulation of glycosaminoglycans, similar to the cells of notochord. The cytoplasm is eosinophilic and stains positive with the periodic acid Schiff stain. Other cell types are stellate cells and intermediate or transitional cells [3].

M. Gdk, M.D. (✉)
Department of Neurosurgery, Acibadem University,
School of Medicine, Istanbul, Turkey
e-mail: mustafa.guduk@acibadem.edu.tr

M.M. zek, M.D.
Division of Pediatric Neurosurgery, Department of
Neurosurgery, Acibadem University, School of
Medicine, Istanbul, Turkey
e-mail: mozek@turk.net

Annual incidence of chordomas is 0.08 per 100,000 population, more common in males (1.0) than females (0.6), and rare in patients under 40 years and blacks. Within the axial skeleton, 2 % are cranial, 32.8 % spinal, and 29.2 % sacral. Younger age and female sex are associated with a higher likelihood of cranial presentation. While the biological activity of chordomas varies considerably, more aggressive behavior is usually seen in the younger age group [4].

Chordomas are extremely rare tumors in children which are supposed to arise from the remnants of the embryonic notochord (from the Greek noton or notos, meaning back, +Latin chorda, meaning cord) originating from the ectoderm during the third week of embryogenesis, influencing the development of perinotochordial mesenchymal elements, and serving as the axial skeleton of the embryo until the formation of other vertebral elements. The notochord which expresses type X collagen is replaced by bone, but between the vertebrae, the notochord which does not express type X collagen expands and forms the nucleus pulposus. The notochord is most likely a primitive relative of cartilage and shares many characteristics with it like aggrecan, Sox9, calmodulin, and type II and IX collagen expressions [5].

Benign forms of chordal ectopias are called echordosis physaliphora and commonly encountered in the cranial base and axial skeleton of adults. In autopsy and radiologic studies, its incidence is 0.5–2 %. In a report of 100 autopsies, microscopic

notochordal intraosseous remnants are found in 11 % of the clivus and 19 % of spinal vertebrae [6]. The supposed origin of ecchordosis physaliphora from the notochord is supported by electron microscopy and immunohistochemical studies. Some authors have proposed a chordoma tumorigenesis from these benign remnants, while others hypothesize a *de novo* origin. The hypothesis of chordomas originating from ecchordosis physaliphora is supported by similar morphology, similar immunophenotype, and similar localization [7, 8].

There are both genetic and immunohistochemical studies which find brachyury, a T-box transcription factor gene product, expression in embryonal notochord, and chordomas. Brachyury expression is required for the specification of mesodermal identity, representing one of the key genes regulating notochord formation and the differentiation of the notochord to nucleus pulposus, while it is absent in the nucleus pulposus. The brachyury protein is a useful marker for chordomas in cases where diagnosis and differentiation is difficult, increasing the sensitivity and specificity of the diagnosis. Expression of this protein specifically in the notochord and the chordomas is considered to be an evidence of the notochordal origin of chordomas.

The studies on the molecular biology and genetics of chordomas are increasing although most of the series have limited numbers, and there is not a specific study regarding pediatric age group chordomas. The studies show polyclonal origin of chordomas [9], and the genome-wide studies using comprehensive array techniques are still of limited number.

44.2 Familial Chordomas

First data regarding the genetics of chordomas came from familial chordoma cases. Foote et al. reported sacrococcygeal chordomas in middle-aged siblings [10], followed by few other familial chordoma reports [11–20]. Although congenital chordomas have been reported [21, 22], the youngest patient with a chordoma family history was a 3-year-old child [23].

Although familial chordomas were reported, cytogenetic or detailed genetic studies came later.

Four affected patients in two generations were reported with a probable autosomal dominant inheritance pattern with complete penetrance but without cytogenetic abnormality [12], and the first cytogenetic study of familial chordomas (father and two daughters) found chromosomal hypo- or nearly diploidy and had a pronounced karyotypic heterogeneity with clonal and non-clonal rearrangements affecting several chromosomes, and a dic(1;9)(p36.1;p21) was found by fluorescence in situ hybridization (FISH) technique, and especially chromosome 1p appeared to be involved in unbalanced translocations with different chromosomes, leading to variable losses of 1p [13]. This family and six other sporadic tumors were studied later by combined use of loss of heterozygosity (LOH) and haplotype analyses, and they have found a susceptibility region on 1p36 related with a tumor suppressor gene [14]. In 2001, Kelley et al. have linked chordomas to chromosome 7q33 by performing linkage analysis using microsatellite markers in an extended pedigree of the family reported by Stepanek and other two unrelated families in a total of 16 chordoma patients [12, 15]. They have corroborated their results by using chromosome 7 and 1p36 single nucleotide polymorphisms (SNPs) in these families but could not detect the same changes in another fourth family in a study in 2005 which was studied previously by LOH and linkage analysis [16]. In another study, 7q LOH in one familial chordoma case was reported [18]. Yang et al. reviewed previously studied four chordoma families by using high-resolution array-comparative genomic hybridization (CGH) and identified a unique duplication of a region on 6q27 which contains only the T gene (brachyury) [20].

44.3 Genome-Wide Studies

Genome-wide studies in chordomas have shown many diverse chromosome aberrations, while most of them were hypodiploid or near diploid with both structural and numerical abnormalities. Karyotype analyses are comparable between chordoid and classic chordomas, and aneuploidy is rare in both types of chordomas. Those which have abnormal karyotype have higher recurrence rates.

In a study using CGH and FISH, the most common DNA copy number alterations in 16 chordomas were losses on chromosomal arms 3p (50 %) and 1p (44 %) suggesting tumor suppressor genes or mismatch repair genes (located at 1p31 and 3p14), and the most common gains involved 7q (69 %), 20 (50 %), 5q (38 %), and 12q (38 %) suggesting oncogenes (located in 7q36) might be involved in chordoma genesis [24].

Hallor et al. have published the first array-based genome study of chordomas in 30 tumor samples from 26 patients. All of those tumors were located in the spinal axis, and the median age of patients was 60 years. They have found multiple chromosome imbalances, and those which showed no karyotype anomaly had genomic imbalances upon aCGH analysis, especially CDKN2A, and CDKN2B deletions (9p21) have been found meaningful and expected larger deletions in that region with higher-resolution arrays [25]. In another study, chordomas highly expressed genes like type II collagen, aggrecan, SOX 9, and CD-RAP which are commonly found in the cartilage. They also found components of the activator protein 1 (AP-1) transcription factor to be highly expressed in chordomas in comparison to nucleus pulposus and articular cartilage tissue. The same pattern of expression was seen with FOSB, c-Fos, and c-Jun. Deregulation of AP-1 transcription factor is thought to be sufficient for tumorigenesis, and AP-1 is considered critical in the function of dominant oncogenes and plays a role in the invasiveness of the chordomas. Several genes are known to be regulated by AP-1 like EGFR, MMP3, and MMP9 [26]. Genes like T brachyury; CD24; keratins 8, 13, 15, 18, and 19; and discoidin domain receptor 1 were found to be highly expressed in concordance with the findings of Vujovic et al. They found that T brachyury was significantly expressed in chordomas but nucleus pulposus in concordance with other studies [27]. The fibroblastic growth factor receptor-RAS/RAF/MEK/ERK-ETS2/brachyury signalling pathway was later studied, but no mutation could be shown to be related with pathogenesis [28]. Diaz et al. have done high-resolution whole-genome analysis of skull base chordomas and have found a deletion at 9p involving

CDKN2A, CDKN2B, and MTAP but at a much lower rate (22 %) than previously reported for sacral chordomas. At a similar frequency (21 %), they found aneuploidy of chromosome 3. Tissue microarray immunohistochemistry demonstrated absent or reduced fragile histidine triad (FHIT) protein expression in 98 % of sacral chordomas and 67 % of skull base chordomas suggesting that chromosome 3 aneuploidy and epigenetic regulation of FHIT contribute to loss of the FHIT tumor suppressor in chordomas [29].

44.4 Telomere Maintenance

Butler et al. studied five lumbosacral chordomas and found increased telomere length in four of them and increased telomerase activity in one of two of those tumors studied for telomerase activity [30], and in a later study, they found telomere elongation in four chordomas and no consistent chromosomal alterations [31]. In another study, Pallini et al. found correlation between human telomerase reverse transcriptase (TERT)-mRNA expression and shorter recurrence-free survival in 26 skull base chordomas. Most of the hTERT-positive tumors were also positive for p53 mutations, suggesting that telomerase dysfunction is combined with abnormal p53 function to initiate the unrestrained clonal expansion of the tumor cells [32]. In another study, low telomerase activity was found, but the study had only one chordoma case [33], while in another study, none of the three chordomas had telomerase activity [34]. Ricci et al. have established a tumor cell line from three chordomas which were aggressive, recurrent tumors; all of them had overexpressed telomerase activity and expressed hTERT immunohistochemically [35].

44.5 The Rb Gene, P53, and Cell Cycle Control

The Rb gene is one of the well-characterized tumor suppressor genes, and its inactivation has been shown to be associated with a number of cancers. The Rb gene is located on chromosome 13q14. The Rb gene plays a pivotal role in regulating the

cell cycle, specifically control of the G1-S transition via its interaction with E2F transition complex and also can induce apoptosis through a pathway that involves p53 through a pathway involving P14 and MDM2 and p21.

LOH in the Rb gene has been demonstrated in two of seven chordomas at genetic level [36]. Alterations of pRb proteins have also been investigated in relation to MIB-1 labeling index, but no significant relation have been found [37].

Bergh, Kilgore, Naka, and Pallini found p53 overexpression in 0, 27 %, 30 %, and 40 % of the chordoma cases in their cohorts, respectively [32, 37–39]. In a comprehensive analysis, Naka et al. showed that high p53 levels in 30 % of their cases correlated well with increased mitotic index and decreased patient survival. In a significant proportion of human cancers, increased p53 levels result from mutations in the p53 gene. However, the authors found no mutations in the p53 gene in cases with increased p53 levels, possibly indicating an alternative mechanism for p53 protein accumulation. Mdm2 overexpression is a common mechanism of p53 inactivation in sarcomas, but not in chordomas [37]. Toguchida et al. could find no p53 mutations in three chordoma cases [40].

44.6 1p36 Locus

Genetic changes mapping to 1p36 have been found by Miozzo et al. in a family which was previously reported by Dalpra and six sporadic chordomas from five patients, and the additional LOH data performed on those sporadic tumors defined an SRO (the smallest region of overlapping loss) from 1p36.31 to 1p36.13 probably carrying a tumor suppressor gene [14]. Riva et al. performed a linkage analysis in 27 sporadic chordoma cases and mapped a defect to 1p36.13, common to 85 % of the cases. By performing RT-PCR analysis on candidate genes in this region, the authors suggested that caspase 9, ephrin 2A, and DVL1 genes may play a role in chordoma tumor suppression [41]. Yang et al. have studied a chordoma family which was studied before by using combined LOH and linkage analysis and reported to be linked to 1p36, by using SNP and microsatellite (STR) markers

for 1p36, but they could not corroborate the same result [13, 16]. In another study using interphase FISH technique which included 7 primary and 11 recurrent chordomas from seven patients, 1p36 deletion was observed in 28.5 % of primary chordomas and 30 % of recurrent tumors, while 1p36 amplification was present in 14.2 % of primary chordomas and 60 % of recurrent chordomas [42]. Defects in 1p may be an early change in chordoma oncogenesis. Longoni et al. studied 1p36 expression in 16 skull base chordomas from 15 patients. They performed LOH analysis using 33 microsatellite markers mapped at 1p36.33–1p36.12 region, five microsatellite markers mapped at 1p, and six microsatellites mapped at 1q; 75 % of chordomas had 1p36 LOH. They have also studied eight apoptotic genes located in 1p36; superfamily of four tumor necrosis factor receptors, TNFRSF1B, TNFRSF8, TNFRSF9, and TNFRSF14, involved in cell death or survival signaling; CASP9, involved in the activation cascade of caspases and responsible for apoptosis execution; DFFA and DFFB, effectors of DNA fragmentation after apoptotic stimuli; and TP73, encoding a member of the p53 family. They studied the presence/absence of the transcripts of the above genes in the 15 chordoma samples by RT-PCR and compared the expression profiles of those with that of adult nucleus pulposus. In order to define an expression profile specific for nucleus pulposus for this set of genes, they also investigated other normal tissues: lymphocytes, placenta, fetal brain, fetal heart, fetal aorta, fetal skeletal muscle, and fetal and adult liver. Most of the studied genes were expressed evenly in nucleus pulposus compared to the other tissues. A notable exception was TP73, which was peculiarly not expressed in nucleus pulposus, whereas TNFRSF9 was expressed only in nucleus pulposus and lymphocytes. A third gene that did not show a similar expression profile in normal tissues was TNFRSF8 which was not detected in nucleus pulposus. They found widespread deregulation of TNFRSF8, TNFRSF9, and TNFRSF14 in the chordoma samples [43].

Considering all the selected genes, tumor samples showed variable expression profiles, none of which matched that of nucleus pulposus. The TNFRSF14 gene was differently expressed

in six samples in comparison with nucleus pulposus; TP73 was differently expressed in two tumors, DFFB in four, TNFRSF9 in eight, DFFA in one, TNFRSF8 in seven, TNFRSF1B in three, and CASP9 in two chordomas. None of the analyzed samples showed the same expression profile observed in the reference tissue for all of the tested genes.

They then grouped the patients according to LOH status at 1p36 and observed that all events (recurrence/death) clustered in the group of 1p36 LOH-positive patients. They also grouped patients according to expression/non-expression for each of the mentioned genes. They observed that all events (recurrence or death) clustered in the group of TNFRSF8 expression-negative patients. They found no correlations between expression/non-expression of the other studied genes and clinical outcome [43].

44.7 Tuberos Sclerosis Complex, PTEN, and Akt/mTOR Pathway

There are case reports of chordomas in patients with the tuberous sclerosis complex. Two genes have been identified in tuberous sclerosis: TSC1 and TSC2. The TSC1 gene on chromosome 9q34 encodes a protein known as hamartin (from hamartoma); the TSC2 gene on chromosome 16p13.3 encodes for a protein called tuberin. TSC1/TSC2 complex inhibits the mammalian target of rapamycin (mTOR) signaling pathway, therefore suppressing cell growth. The mTOR pathway is a growth-promoting pathway and plays an essential role in a wide array of cellular processes including translation, transcription, trafficking, and autophagy. In two tuberous sclerosis complex patients, one with a germ-line TSC2 and the other with a germ-line TSC1 mutation having sacrococcygeal chordomas, Lee-Jones et al. showed somatic inactivation of the other wild-type allele by LOH and immunohistochemistry, but a causal relationship was not proven [44].

Another important negative regulator of the Akt/mTOR pathway is PTEN (phosphatase and tensin homologue deleted on chromosome 10). The TSC/

mTORC1 pathway is dysregulated in several hamartoma syndromes as well as in many cancers. It is shown by Western blot and immunohistochemistry analysis in ten sporadic chordoma cases and one TSC chordoma case and also U-CH1 chordoma cell line that Akt/mTOR pathway is hyperactivated with PTEN loss and rapamycin, a strong inhibitor of this pathway, strongly inhibits cell growth in U-CH1 cell culture [45]. In another immunohistochemical study including five chordomas, Akt/mTOR pathway activation was noted [46].

44.8 JAK/STAT Pathway

Signal transducers and activators of transcription 3 (Stat3) belongs to a family of cytoplasmic transcription factors which are activated by cytokines and growth factor receptors. The STAT transcription factors serve as direct links between both cytokine and growth factor receptors on the cell surface and regulation of gene expression in the nucleus.

pStat3 levels in 70 chordoma patients (51 males, 19 females) were studied by tissue microarray, and worse prognosis in patients expressing high levels of pStat3 was found. Rate of pStat3 in recurrent tumors was greater compared with primary tumors. Strikingly, pStat3 expression of chordomas with metastasis was increased in comparison to primary chordomas without metastasis [47]. This result of increased pStat3 expression was verified in another study too [48]. The expression of antiapoptotic proteins Bcl-xL and MCL-1 was also inhibited in three chordoma cell lines after treatment with those drugs, and poly (ADP-ribose) polymerase cleavage, an apoptosis-associated biochemical event, was detected in all three chordoma cell lines after treatment [47].

44.9 Oncogene Activation

Most studies on oncogene activation in chordomas are about receptor tyrosine kinases (RTKs) and comes from the use of inhibitors like imatinib in recurrent/refractory chordomas [49–51]. Burger et al. studied c-KIT and PDGFR alpha and PDGFR beta mutations in 17 chordomas. They

could find no mutations in those tumors [52]. Weinberger et al. studied other members of RTKs like EGFR, c-Met (the hepatocyte growth factor/scatter factor receptor) in their study including ten chordomas (30 % skull base, 50 % sacral, 20 % sacral) and found consistent immunoreactivity for EGFR and c-Met receptors, robust expression in 50 and 70 %, respectively. HER2/neu receptor expression was present in 70 % of the tumors [51]. Finding of increased c-Met expression in most chordomas is important. The chromosomal site of the c-met proto-oncogene has been located at 7q31. Scheil et al. found that gains of 7q were among the most common chromosomal alterations noted, and 69 % of chordomas studied demonstrated 7q gain. Thus, gain of c-Met expression via 7q amplification may represent an early event in chordoma progression [24, 51]. In another study, gain of chromosome 7 was correlated with EGFR gene status and EGFR and c-MET protein expression in 22 chordoma samples. Copy number analysis of chromosome 7 was done by chromogenic in situ hybridization (CISH) and protein expression of EGFR and c-MET by immunohistochemistry. Aneusomy of chromosome 7 was seen in 73 % of the samples, 62 % of primary tumors and in all recurrent chordomas. EGFR and c-MET were both expressed, but only c-MET protein expression was found to be significantly correlated with chromosome 7 aneusomy [53]. Naka et al. also studied and documented c-Met expression in both primary and recurrent tumors by immunohistochemistry [54–56].

44.10 Experimental Models

Explant cultures have been performed by Horten et al. from human sacral chordomas [57]. The first chordoma cell line, U-CH1, was generated from a recurrent sacral chordoma by Scheil et al., and they described its chromosomal abnormalities [24]. After that other cell lines like EACH-1, CH22 [58, 59], and a xenograft model have been established [60]. A zebrafish model of chordoma initiated by notochord-driven expression of HRASV12 is reported, and they have studied the effects of rapamycin which delays

HRASV12-dependent notochord tumor formation and seen that it extends survival [61].

References

1. Heffelfinger MJ, Dahlin DC, MacCarty CS, Beabout JW (1973) Chordomas and cartilaginous tumors at the skull base. *Cancer* 32:410–420
2. Mitchell A, Scheithauer BW, Unni KK et al (1993) Chordoma and chondroid neoplasms of the sphenocciput. An immunohistochemical study of 41 cases with prognostic and nosologic implications. *Cancer* 72:2943–2949
3. Richardson MS (2001) Pathology of skull base tumors. *Otolaryngol Clin North Am* 34:1025–1042, vii
4. McMaster ML, Goldstein AM, Bromley CM et al (2001) Chordoma: incidence and survival patterns in the United States, 1973–1995. *Cancer Causes Control* 12:1–11
5. Schwab JH, Boland PJ, Agaram NP et al (2009) Chordoma and chondrosarcoma gene profile: implications for immunotherapy. *Cancer Immunol Immunother* 58:339–349
6. Yamaguchi T, Suzuki S, Ishiwa H, Ueda Y (2004) Intraosseous benign notochordal cell tumours: overlooked precursors of classic chordomas? *Histopathology* 44:597–602
7. Nishiguchi T, Mochizuki K, Tsujio T et al (2010) Lumbar vertebral chordoma arising from an intraosseous benign notochordal cell tumour: radiological findings and histopathological description with a good clinical outcome. *Br J Radiol* 83:e49–e53
8. Yamaguchi T, Yamato M, Saotome K (2002) First histologically confirmed case of a classic chordoma arising in a precursor benign notochordal lesion: differential diagnosis of benign and malignant notochordal lesions. *Skelet Radiol* 31:413–418
9. Klingler L, Trammell R, Allan DG et al (2006) Clonality studies in sacral chordoma. *Cancer Genet Cytogenet* 171:68–71
10. Foote RF, Ablin G, Hall WW (1958) Chordoma in siblings. *Calif Med* 88:383–386
11. Kerr WA, Allen KL, Haynes DR, Sellars SL (1975) Letter: familial nasopharyngeal chordoma. *S Afr Med J* 49:1584
12. Stepanek J, Cataldo SA, Ebersold MJ et al (1998) Familial chordoma with probable autosomal dominant inheritance. *Am J Med Genet* 75:335–336
13. Dalprà L, Malgara R, Miozzo M et al (1999) First cytogenetic study of a recurrent familial chordoma of the clivus. *Int J Cancer* 81:24–30
14. Miozzo M, Dalprà L, Riva P et al (2000) A tumor suppressor locus in familial and sporadic chordoma maps to 1p36. *Int J Cancer* 87:68–72
15. Kelley MJ, Korczak JF, Sheridan E et al (2001) Familial chordoma, a tumor of notochordal remnants, is linked to chromosome 7q33. *Am J Hum Genet* 69:454–460

16. Yang XR', Beerman M, Bergen AW et al (2005) Corroboration of a familial chordoma locus on chromosome 7q and evidence of genetic heterogeneity using single nucleotide polymorphisms (SNPs). *Int J Cancer* 116:487–491
17. Weber W, Scott RJ (2005) Case report: familial gastric cancer and chordoma in the same family. *Hered Cancer Clin Pract* 3:81–84
18. Bhadra AK, Casey ATH (2006) Familial chordoma. A report of two cases. *J Bone Joint Surg (Br)* 88: 634–636
19. Coppens JR, Ric Harnsberger H, Finn MA et al (2009) Oronasopharyngeal chordomas. *Acta Neurochir (Wien)* 151:901–907
20. Yang XR, Ng D, Alcorta DA et al (2009) T (brachyury) gene duplication confers major susceptibility to familial chordoma. *Nat Genet* 41:1176–1178
21. Probst EN, Zanella FE, Vortmeyer AO (1993) Congenital clivus chordoma. *AJNR Am J Neuroradiol* 14:537–539
22. Goel A, Nadkarni TD, Kirtane MV (1996) Clival chordoma in an infant. *J Postgrad Med* 42:51–53
23. Chetty R, Levin CV, Kalan MR (1991) Chordoma: a 20-year clinicopathologic review of the experience at Groote Schuur Hospital, Cape Town. *J Surg Oncol* 46:261–264
24. Scheil S, Brüderlein S, Liehr T et al (2001) Genome-wide analysis of sixteen chordomas by comparative genomic hybridization and cytogenetics of the first human chordoma cell line, U-CH1. *Genes Chromosomes Cancer* 32:203–211
25. Hallor KH, Staaf J, Jönsson G et al (2008) Frequent deletion of the CDKN2A locus in chordoma: analysis of chromosomal imbalances using array comparative genomic hybridisation. *Br J Cancer* 98:434–442
26. Ozanne BW, Spence HJ, McGarry LC, Hennigan RF (2006) Transcription factors control invasion: AP-1 the first among equals. *Oncogene* 26:1–10
27. Vujovic S, Henderson S, Presneau N et al (2006) Brachyury, a crucial regulator of notochordal development, is a novel biomarker for chordomas. *J Pathol* 209:157–165
28. Shalaby AAE, Presneau N, Idowu BD et al (2009) Analysis of the fibroblastic growth factor receptor-RAS/RAF/MEK/ERK-ETS2/brachyury signalling pathway in chordomas. *Mod Pathol* 22:996–1005
29. Diaz RJ, Guduk M, Romagnuolo R et al (2012) High-resolution whole-genome analysis of skull base chordomas implicates FHIT loss in chordoma pathogenesis. *Neoplasia* 14:788–798
30. Butler MG, Dahir GA, Hedges LK et al (1995) Cytogenetic, telomere, and telomerase studies in five surgically managed lumbosacral chordomas. *Cancer Genet Cytogenet* 85:51–57
31. Butler MG, Sciadini M, Hedges LK, Schwartz HS (1996) Chromosome telomere integrity of human solid neoplasms. *Cancer Genet Cytogenet* 86:50–53
32. Pallini R, Maira G, Pierconti F et al (2003) Chordoma of the skull base: predictors of tumor recurrence. *J Neurosurg* 98:812–822
33. Aue G, Muralidhar B, Schwartz HS, Butler MG (1998) Telomerase activity in skeletal sarcomas. *Ann Surg Oncol* 5:627–634
34. Lauer NK, Maier SM, Oberringer M et al (2002) Absence of telomerase activity in malignant bone tumors and soft-tissue sarcomas. *Sarcoma* 6:43–46
35. Ricci-Vitiani L, Pierconti F, Falchetti ML et al (2006) Establishing tumor cell lines from aggressive telomerase-positive chordomas of the skull base. Technical note. *J Neurosurg* 105:482–484
36. Eisenberg MB, Woloschak M, Sen C, Wolfe D (1997) Loss of heterozygosity in the retinoblastoma tumor suppressor gene in skull base chordomas and chondrosarcomas. *Surg Neurol* 47:156–160, discussion 160–1
37. Naka T, Boltze C, Kuester D et al (2005) Alterations of G1-S checkpoint in chordoma: the prognostic impact of p53 overexpression. *Cancer* 104: 1255–1263
38. Bergh P, Kindblom LG, Gunterberg B et al (2000) Prognostic factors in chordoma of the sacrum and mobile spine: a study of 39 patients. *Cancer* 88: 2122–2134
39. Kilgore S, Prayson RA (2002) Apoptotic and proliferative markers in chordomas: a study of 26 tumors. *Ann Diagn Pathol* 6:222–228
40. Toguchida J, Yamaguchi T, Ritchie B et al (1992) Mutation spectrum of the p53 gene in bone and soft tissue sarcomas. *Cancer Res* 52:6194–6199
41. Riva P, Crosti F, Orzan F et al (2003) Mapping of candidate region for chordoma development to 1p36.13 by LOH analysis. *Int J Cancer* 107:493–497
42. Bayrakli F, Guney I, Kilic T et al (2007) New candidate chromosomal regions for chordoma development. *Surg Neurol* 68:425–430, discussion 430
43. Longoni M, Orzan F, Stroppi M et al (2008) Evaluation of 1p36 markers and clinical outcome in a skull base chordoma study. *Neuro Oncol* 10:52–60
44. Lee-Jones L, Aligianis I, Davies PA et al (2004) Sacrococcygeal chordomas in patients with tuberous sclerosis complex show somatic loss of TSC1 or TSC2. *Genes Chromosome Cancer* 41:80–85
45. Han S, Polizzano C, Nielsen GP et al (2009) Aberrant hyperactivation of akt and Mammalian target of rapamycin complex 1 signaling in sporadic chordomas. *Clin Cancer Res* 15:1940–1946
46. Dobashi Y, Suzuki S, Sato E et al (2009) EGFR-dependent and independent activation of Akt/mTOR cascade in bone and soft tissue tumors. *Mod Pathol* 22:1328–1340
47. Yang C, Schwab JH, Schoenfeld AJ et al (2009) A novel target for treatment of chordoma: signal transducers and activators of transcription 3. *Mol Cancer Ther* 8:2597–2605
48. Yang C, Hornicek FJ, Wood KB et al (2010) Blockage of Stat3 with CDDO-Me inhibits tumor cell growth in chordoma. *Spine (Phila Pa 1976)* 35:1668–1675
49. Casali PG, Messina A, Stacchiotti S et al (2004) Imatinib mesylate in chordoma. *Cancer* 101: 2086–2097

50. Stacchiotti S, Marrari A, Tamborini E et al (2009) Response to imatinib plus sirolimus in advanced chordoma. *Ann Oncol* 20:1886–1894
51. Weinberger PM, Yu Z, Kowalski D et al (2005) Differential expression of epidermal growth factor receptor, c-Met, and HER2/neu in chordoma compared with 17 other malignancies. *Arch Otolaryngol Head Neck Surg* 131:707–711
52. Burger H, den Bakker MA, Kros JM et al (2005) Activating mutations in c-KIT and PDGFRalpha are exclusively found in gastrointestinal stromal tumors and not in other tumors overexpressing these imatinib mesylate target genes. *Cancer Biol Ther* 4:1270–1274
53. Walter BA, Begnami M, Valera VA et al (2011) Gain of chromosome 7 by chromogenic in situ hybridization (CISH) in chordomas is correlated to c-MET expression. *J Neurooncol* 101:199–206
54. Naka T, Boltze C, Samii A et al (2009) Expression of c-MET, low-molecular-weight cytokeratin, matrix metalloproteinases-1 and -2 in spinal chordoma. *Histopathology* 54:607–613
55. Naka T, Iwamoto Y, Shinohara N et al (1997) Expression of c-met proto-oncogene product (c-MET) in benign and malignant bone tumors. *Mod Pathol* 10:832–838
56. Naka T, Kuester D, Boltze C et al (2008) Expression of hepatocyte growth factor and c-MET in skull base chordoma. *Cancer* 112:104–110
57. Horten BC, Montague SR (1976) In vitro characteristics of a sacrococcygeal chordoma maintained in tissue and organ culture systems. *Acta Neuropathol* 35:13–25
58. Liu X, Nielsen GP, Rosenberg AE et al (2012) Establishment and characterization of a novel chordoma cell line: CH22. *J Orthop Res* 30:1666–1673
59. DeComas AM, Penformis P, Harris MR et al (2010) Derivation and characterization of an extra-axial chordoma cell line (EACH-1) from a scapular tumor. *J Bone Joint Surg Am* 92:1231–1240
60. Trucco MM, Awad O, Wilky BA et al (2013) A novel chordoma xenograft allows in vivo drug testing and reveals the importance of NF-κB signaling in chordoma biology. *PLoS ONE* 8:e79950
61. Burger A, Vasilyev A, Tomar R et al (2014) A zebrafish model of chordoma initiated by notochord-driven expression of HRASV12. *Dis Model Mech* 7(7): 907–13

Alp Dincer

Both computed tomography (CT) and magnetic resonance imaging (MR) are required for evaluation of clivus chordomas due to anatomic complexity of the skull base, bone involvement, and the proximity of these tumors to many important neural and vascular structures [1]. They have complementary roles in the evaluation of chordoma. The excellent imaging capabilities of MRI and CT allow precise delineation of the clivus chordoma with respect to volume and relation to adjacent structures. The pretreatment goal of the imaging of clivus chordomas is to delineate the tumor margins, adjacent cranial nerves, and vascular structures. The posttreatment goal of the imaging is to define the extent of the surgery; to guide for the additional therapy, if needed; and to differentiate the recurrence from the post-therapy changes. The classical radiologic feature of the clivus chordoma is a destructive soft-tissue mass with calcification due to sequestra from bone destruction and/or dystrophic mineralization [1–8] (Fig. 45.1a–c). Intracranial chordomas most often originate from the sphenoid-occipital synchondrosis of the clivus and are located in the midline (Fig. 45.2). However, it presents with

more or less marked symmetric or asymmetric lateral extension (Fig. 45.3a–j). Furthermore, it may extend into the cavernous sinus, sphenoid sinus, and nasopharynx [9–11]. But the site of origin is usually along the caudal margin of the clivus and extension through the foramen magnum is common in younger children (Fig. 45.4a, b). But it may also be originated from the cranial margin of the clivus [1, 8] (Fig. 45.5a).

45.1 Computed Tomography

CT scanning is essential, highly sensitive, and accurate for evaluating bony integrity, bone destruction, and calcifications or bone fragments within the lesion [3, 6]. CT should be reviewed in both soft and bone algorithm with multiplanar reconstruction (Fig. 45.3h, i). The classic appearance of the clivus chordomas at CT is that of a centrally located, well-circumscribed expansile soft-tissue mass with extensive lytic bone destruction [12] (Fig. 45.2b). The margin between the tumor and adjacent bone is not sclerotic. CT easily defines the exact nature and extent of the bone destruction caused by the tumor. CT is valuable in evaluating the integrity of cranio-vertebral junction and reliably demonstrates the lysis of the skull base foramina. The bulk of the tumor is usually hyperattenuating relative to the neighboring neural axis. Intratumoral calcifications appear irregular (Figs. 45.1c and 45.3h). Moderate to marked enhancement following administration

A. Dincer, M.D.
Department of Radiology,
Acibadem University, School of Medicine,
Istanbul, Turkey
e-mail: adincer@asg.com.tr

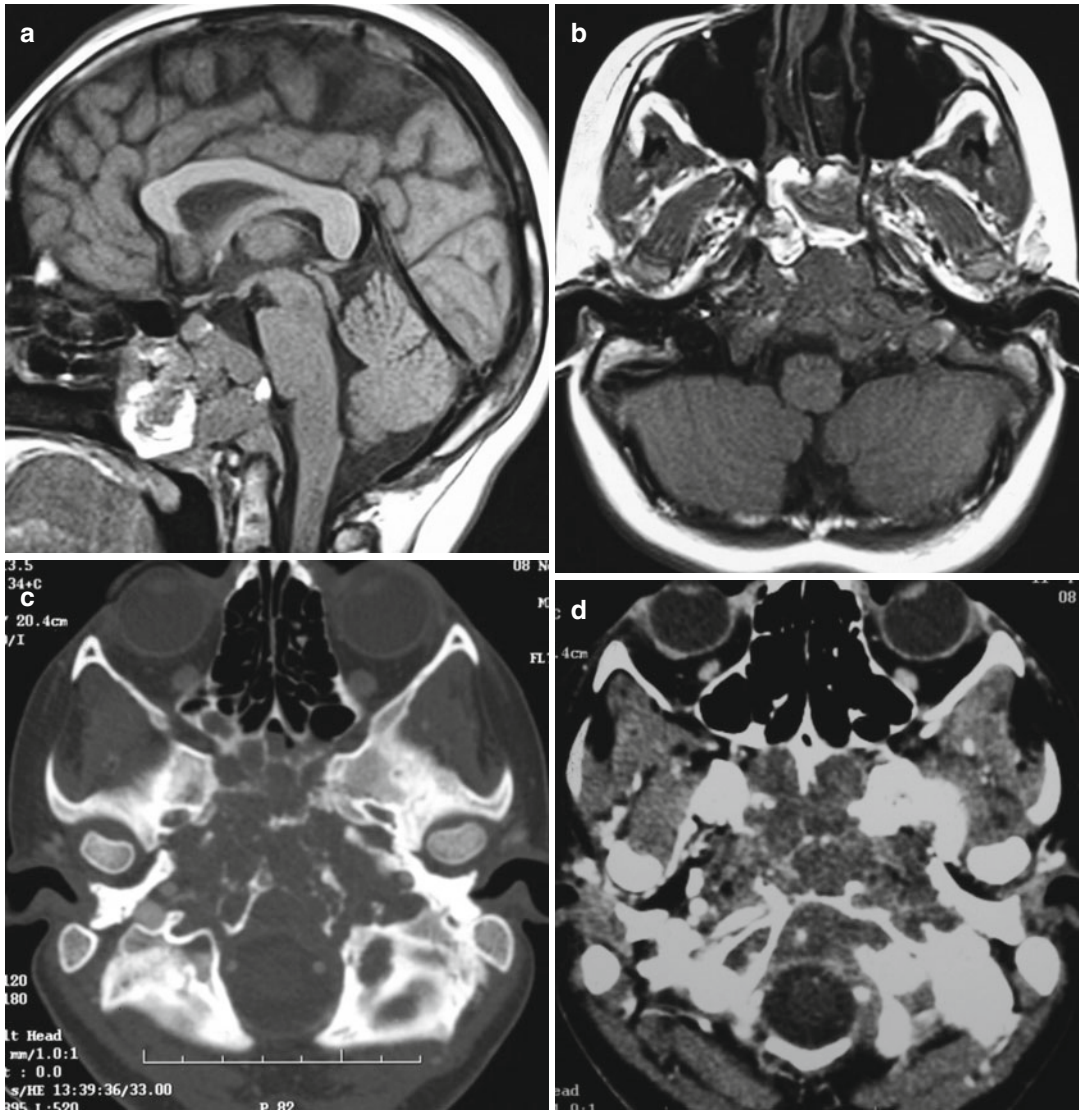


Fig. 45.1 MRI and CT findings in a 10-year-old-girl with a clival chordoma. Sagittal T1-weighted MR image shows a clival mass that has a hyperintense focus which represents highly proteinaceous material or blood products (a). Axial T1-weighted MR image shows an isointense clivus mass with hyperintense focus (b).

Axial CT scan demonstrates lytic bone destructions with intratumoral bone or calcifications (c). Contrast-enhanced axial CT scan shows irregular tiny enhancement (d)

of iodinated contrast material is seen in almost every case (Fig. 45.1d). Solitary or multiple low-attenuation areas are sometimes seen within the soft-tissue mass representing gelatinous material seen at gross examination (Fig. 45.2b). The bone changes and the extent of the resection after operation are precisely interpreted at CT [1].

45.2 MRI

Clivus chordomas have intermediate to low signal intensity and is easily recognized within the high signal intensity of the fat of the bone marrow of clivus on T1-weighted MR images (Figs. 45.1a, b, 45.3b and 45.4b). Small foci of hyperintensity

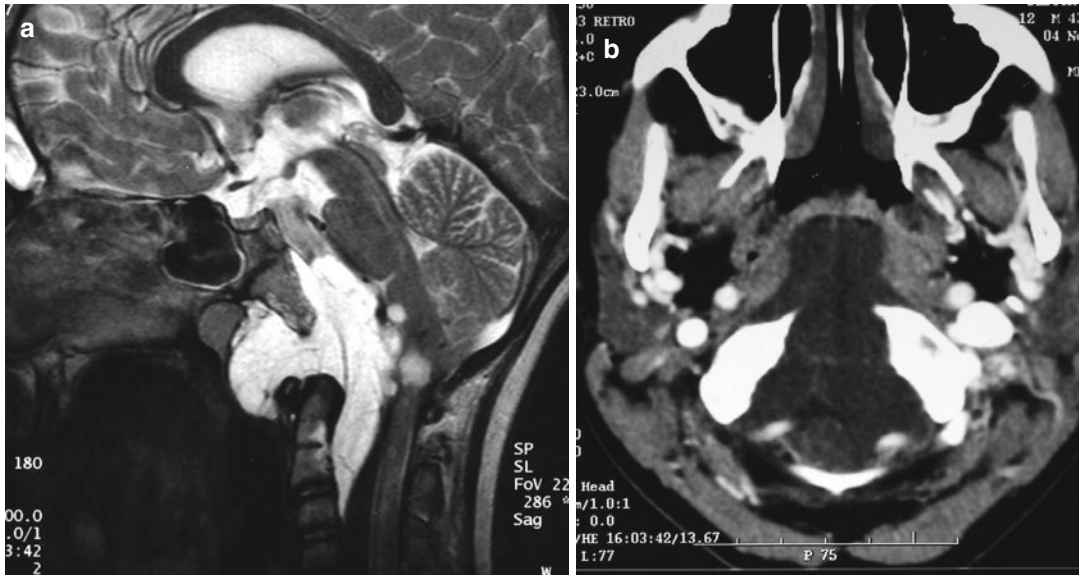


Fig. 45.2 MRI and CT findings in an 11-year-old boy with a clival chordoma. Sagittal T2-weighted image represents a clivus mass with irregular tiny septa, extending

to the upper cervical spine (a). There is extensive brainstem compression. Axial postcontrast CT scan demonstrates a clivus mass with a little enhancement (b)

can be visualized within the tumor on T1-weighted images which may represent a protein-rich content or intratumoral hemorrhage [1, 13] (Fig. 45.4b). Typically, intracranial chordoma has high signal intensity on T2-weighted images due to the high fluid content of cellular components (Figs. 45.2a and 45.4a). The intratumoral areas of calcification, hemorrhage, and a highly proteinaceous mucus pool usually demonstrate heterogeneous hypointensity at T2-weighted images (Fig. 45.3a, c). Low-signal-intensity irregular septations that separate high-signal-intensity lobules are commonly seen (Figs. 45.2a and 45.4a). MRI provides accurate evaluation of the involvement of the adjacent soft tissues, including vasculature, cranial nerve involvement, and changes in the brainstem related to tumor itself [1, 2, 6] (Figs. 45.3a and 45.4a). Fat saturation with T2-weighted images can be used to increase in delineation of the border of the tumor (Fig. 45.3a). Gradient echo T2* or susceptibility-weighted images (SWI) may show intratumoral calcification or hemorrhage better than conventional T1- and T2-weighted images (Fig. 45.3c).

Furthermore, SWI can make a differentiation between calcification and hemorrhage with phase reconstruction algorithm.

There is no data in the literature concerning the diffusion properties of the clivus chordomas. However, our cases demonstrate a slight hyperintensity in ADC maps, which may help in differentiation between very rare confusing clivus lesions with extensive diffusion restriction such as dermoid/epidermoid cysts and chordoma (Fig. 45.3e, f).

The pattern of contrast enhancement is related to the pathological features of these tumors which are organized in lobules with mucinous and gelatinous contents. The majority of intracranial chordomas demonstrate moderate to marked heterogeneous enhancement following contrast material injection (Fig. 45.3d). Clivus chordomas usually show lobulated areas after gadolinium with a “honeycomb” appearance corresponding to low-signal areas within the tumor [2] (Figs. 45.4c and 45.6). The application of fat saturation after contrast material may augment the enhancement and delineation of the tumor border from adjacent bright fat marrow (Fig. 45.3d).

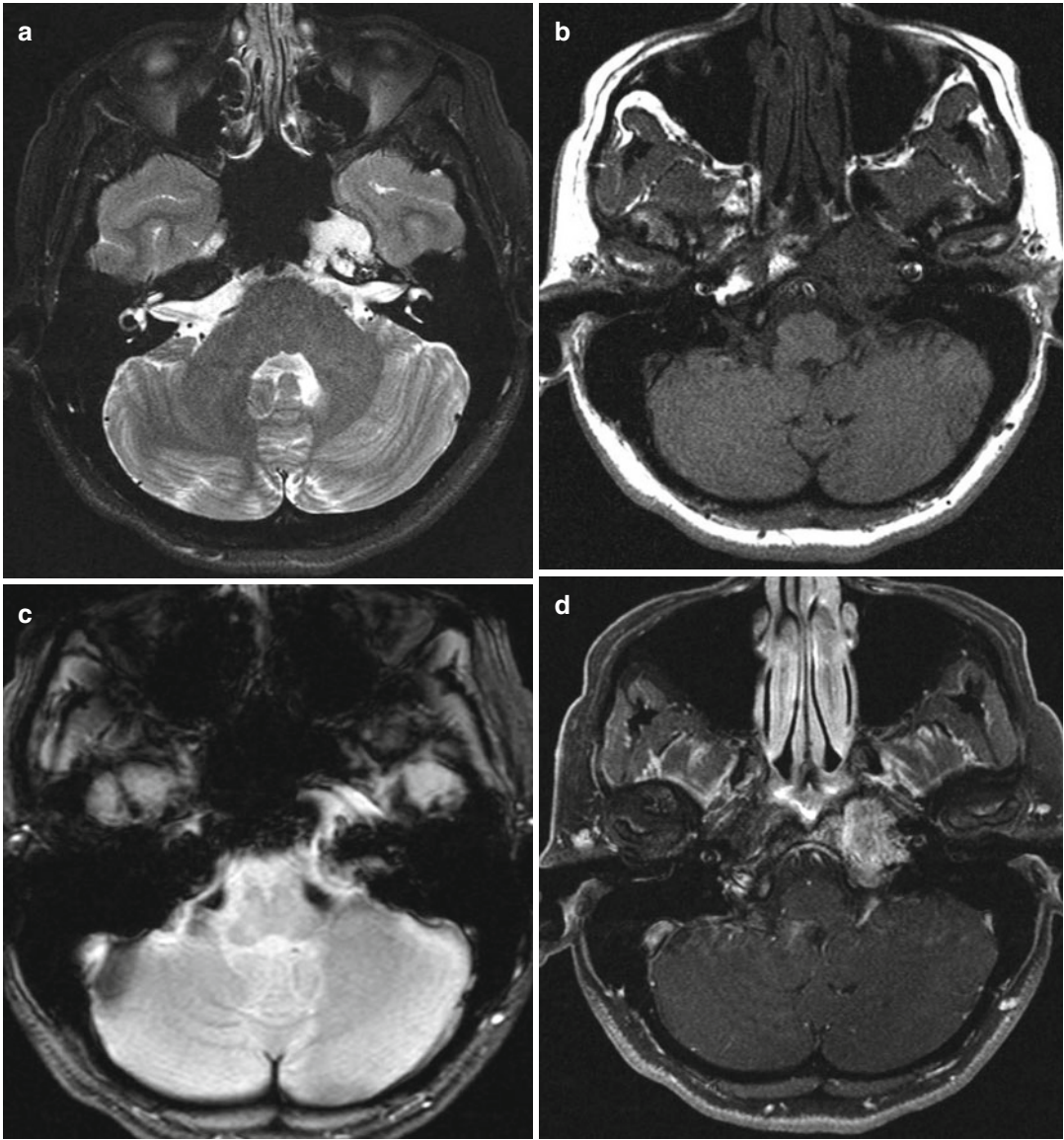


Fig. 45.3 CT, MRI, and angiographic findings in an 18-year-old woman with a skull base chordoma. Axial fat saturation T2-weighted image (**a**) shows a parasagittal mass extending to the sphenoid sinus. The mass is hyperintense and contains hypointense focus compatible with bone remnant or calcifications. The mass displaces and compresses the left internal carotid artery anteromedially (**a**, **k**). Axial unenhanced T1-weighted image demonstrates the border of the tumor (**b**). There is marked enhancement on contrast-enhanced fat-saturated T1-weighted image which also delin-

eates the border of the tumor (**d**). Axial GRE T2* image depicts the calcifications better than the other sequences (**c**). Axial diffusion-weighted image and corresponding ADC map reveal an increase in diffusion (**e**, **f**). The soft and bone tissue algorithm of axial CT scan demonstrate the border and contents of the tumor (**h**, **i**). Axial collapsed MIP image of 3D TOF MR angiography demonstrates the displacement in internal carotid artery (**g**). Left internal carotid arteriogram confirms the vascular displacement (**j**). There is no staining of the tumor in the arterial phase

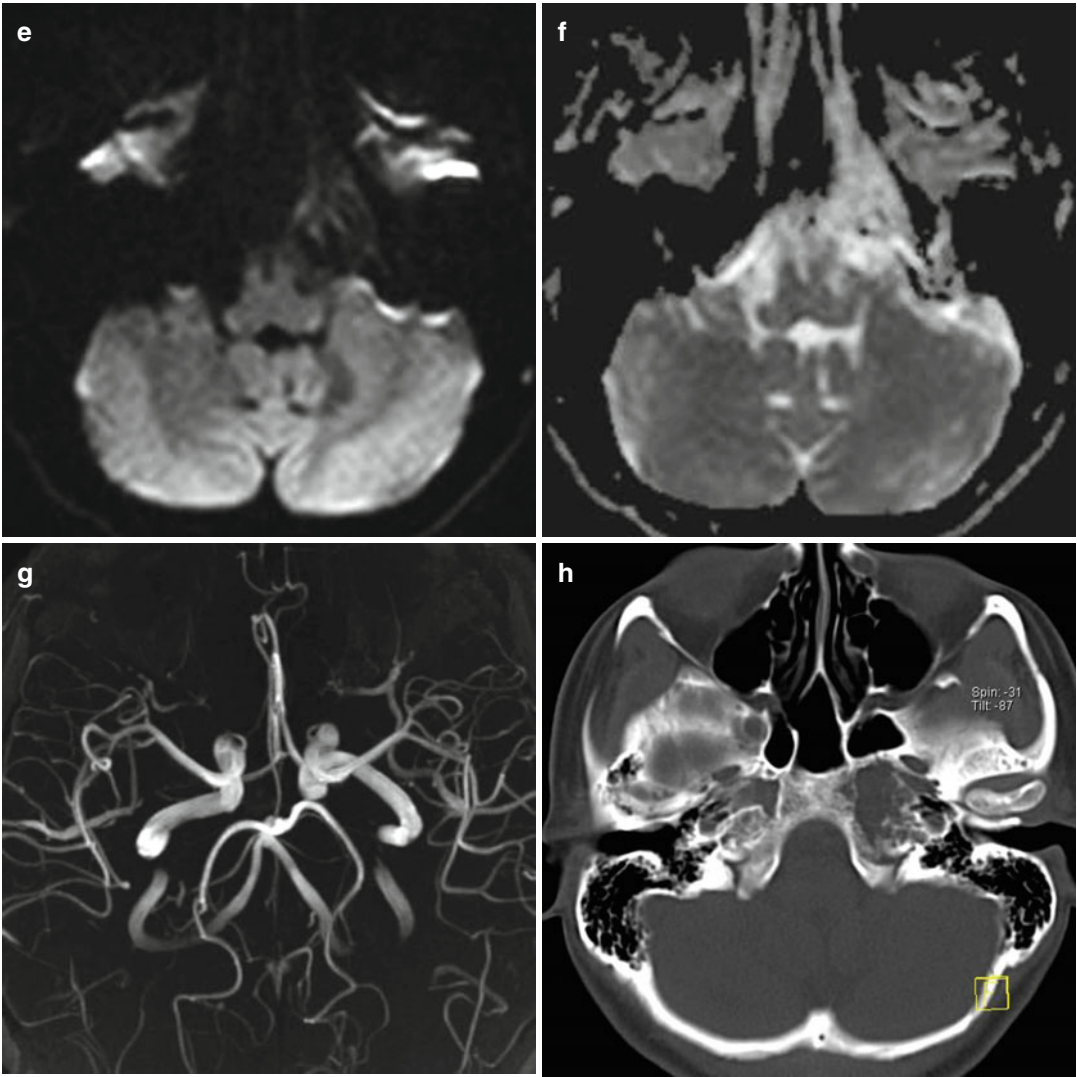


Fig. 45.3 (continued)

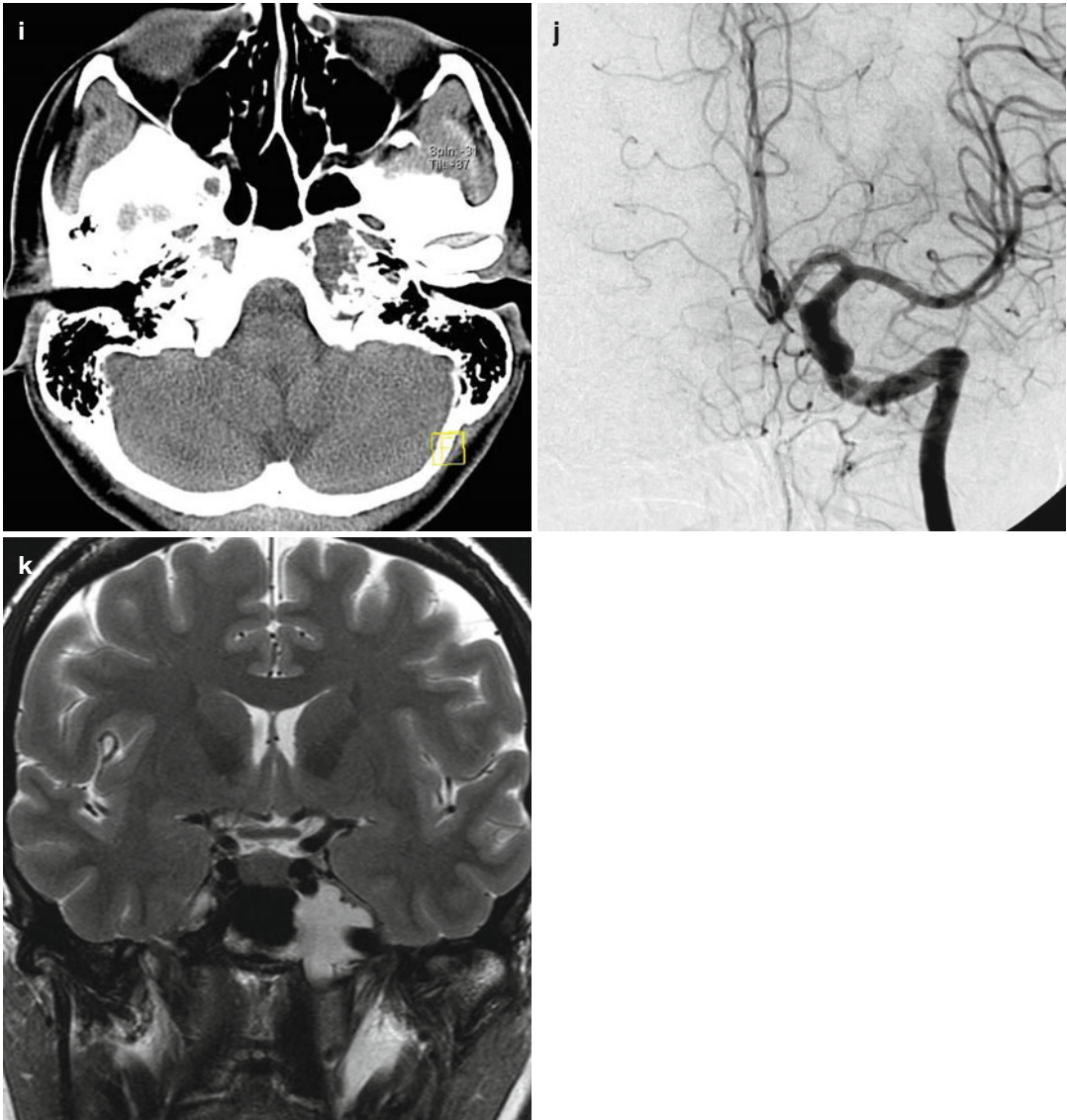


Fig. 45.3 (continued)

Vascular encasement can be appreciated with conventional T1- and T2-weighted images (Fig. 45.3a, k). In equivocal cases, MR angiography or CT angiography can give additional information to demonstrate displacement, encasement, or narrowing of the internal carotid or vertebral artery (Fig. 45.3g). Furthermore, MR venography precisely demonstrates venous involvement or occlusion. Conventional selective angiographic evaluation is reserved for cases with significant displacement, encasement, or narrowing of the

internal carotid or vertebral artery at MR angiography to demonstrate the collateral circulation and to be able to perform temporary balloon occlusion. Abnormal tumor vascularity or staining is very rare in cases with clivus chordomas [1, 14].

MR imaging is the modality of choice for postsurgical follow-up and detection of recurrence which is more common following subtotal or partial resection (Fig. 45.7a–c). Prominent hyperintensity at T2-weighted images is seen in tumor recurrence rather than postoperative

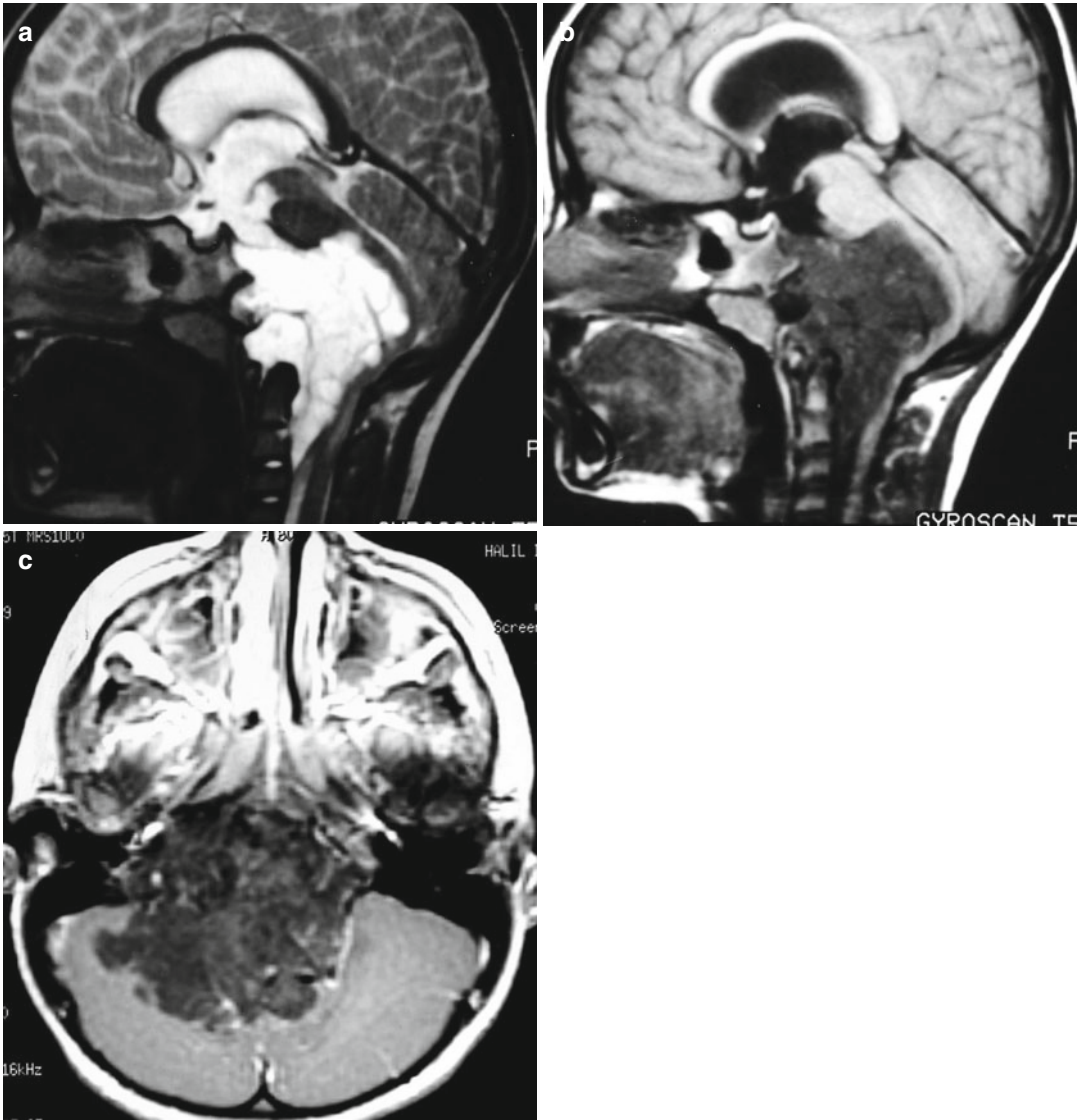


Fig. 45.4 MR findings of a 5-year-old-boy with clivus chordoma. Sagittal T2-weighted image demonstrates an intracranial chordoma with slight irregular hyperintensity due to tiny hypointense septa (a). The huge mass extends

to the upper cervical spine and compresses the brainstem posteriorly (a, b). Axial contrast-enhanced T1-weighted image shows a large clival mass with variable enhancement (honeycomb enhancement pattern) (c)

changes. Contrast-enhanced fat-saturated images are also valuable in making this distinction and in delineating recurrent tumor margins. Tumor recurrence can occur along the surgical pathway but is very uncommon [15]. Distant metastasis is rarely seen [16–18].

45.3 Differential Diagnosis

The differentiation between chondrosarcomas and clivus chordomas is difficult in terms of both imaging and pathology. Unlike midline clivus chordomas, the majority of chondrosarcomas

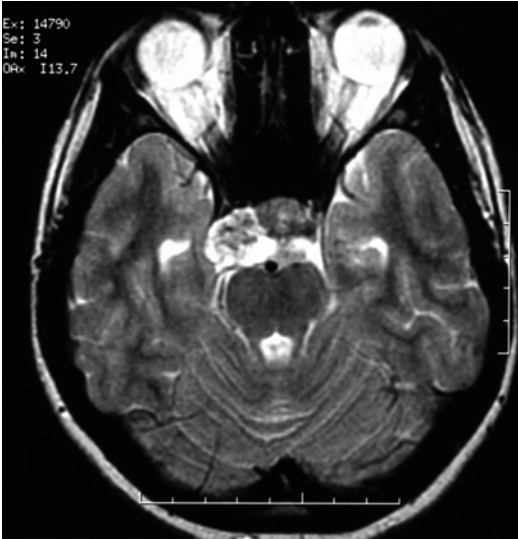


Fig. 45.5 Axial T2-weighted image of a 17-year-old girl with clivus chordoma shows a heterogeneous mass in the upper part of the clivus extending to the right cavernous sinus

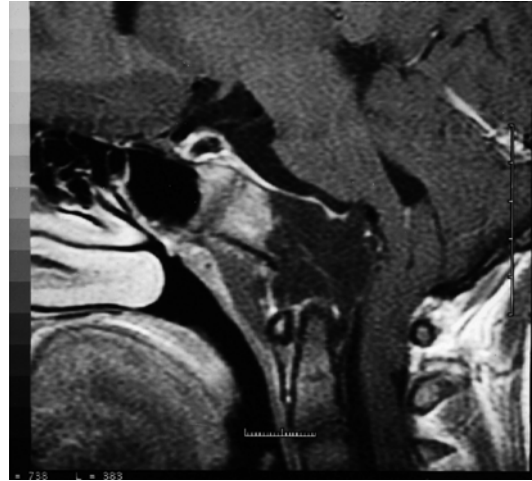


Fig. 45.6 Postcontrast sagittal T1-weighted image of a 13-year-old-boy with clivus chordoma shows “honeycomb” enhancement

arise along the petro-occipital fissure. However, chondrosarcomas can sometimes have a mid-line location. Furthermore, the two tumors have similar signal intensity on T1- and T2-weighted MR images. The linear or globular calcifications make the diagnosis of chondrosarcomas more likely. Clival meningiomas, nasopharyngeal

malignancies, plasmacytoma, lymphoma, craniopharyngiomas, rhabdomyosarcoma, aggressive pituitary adenoma, histiocytosis X, dermoid and epidermoid cysts, trigeminal neuroma, and fibrous dysplasia in pediatric population cause rarely diagnostic difficulties [1, 6].

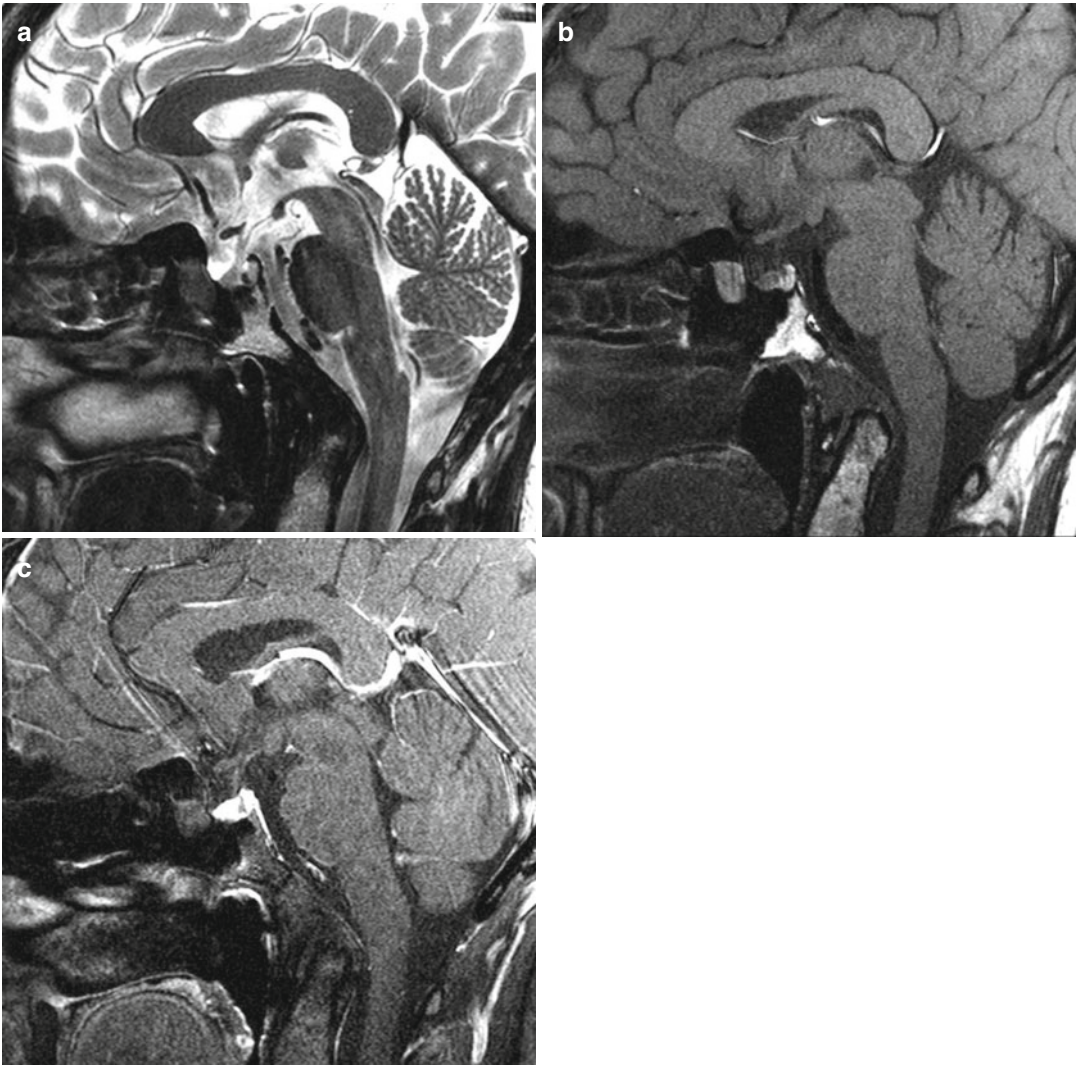


Fig. 45.7 Postoperative follow-up MRI findings of an 18-year-old-girl with clivus chordoma. Sagittal T2-weighted image (a), sagittal T1-weighted image (b),

and sagittal postcontrast fat-saturated T1-weighted image reveal a gross total resection of tumor without any finding compatible with recurrence

References

1. Erdem E et al (2003) Comprehensive review of intracranial chordoma. *Radiographics* 23(4):995–1009
2. Doucet V et al (1997) MRI of intracranial chordomas. Extent of tumour and contrast enhancement: criteria for differential diagnosis. *Neuroradiology* 39(8): 571–576
3. Gehanne C et al (2005) Skull base chordoma: CT and MRI features. *JBR-BTR* 88(6):325–327
4. Menezes AH (2008) Craniovertebral junction neoplasms in the pediatric population. *Childs Nerv Syst* 24(10):1173–1186
5. Niida H et al (1994) Clival chordoma in early childhood without bone involvement. *Childs Nerv Syst* 10(8):533–535
6. Oot RF et al (1988) The role of MR and CT in evaluating clival chordomas and chondrosarcomas. *AJR Am J Roentgenol* 151(3):567–575
7. Poskitt KJ et al (1995) Pediatric case of the day. Chordoma of the clivus. *Radiographics* 15(6):1507–1509

8. Weber AL et al (1994) Chordomas of the skull base. Radiologic and clinical evaluation. *Neuroimaging Clin N Am* 4(3):515–527
9. Yan ZY et al (2010) Primary chordoma in the nasal cavity and nasopharynx: CT and MR imaging findings. *AJNR Am J Neuroradiol* 31(2):246–250
10. Coppens JR et al (2009) Oronasopharyngeal chordomas. *Acta Neurochir* 151(8):901–907
11. Nguyen RP et al (2009) Extraosseous chordoma of the nasopharynx. *AJNR Am J Neuroradiol* 30(4):803–807
12. Meyer JE, Oot RF, Lindfors KK (1986) CT appearance of clival chordomas. *J Comput Assist Tomogr* 10(1):34–38
13. Machida T et al (1986) Magnetic resonance imaging of clival chordomas. *Acta Radiol Suppl* 369:167–169
14. Smink KW, Hekster RE, Bots GT (1977) Clivus chordoma with distinct vascularity demonstrated by angiography. *Neuroradiology* 13(5):273–277
15. Fischbein NJ et al (2000) Recurrence of clival chordoma along the surgical pathway. *AJNR Am J Neuroradiol* 21(3):578–583
16. Horton KM et al (1989) Metastasizing chordoma in early childhood: report of a case at 1.5 T. *Magn Reson Imaging* 7(6):689–691
17. Sibley RK et al (1987) Metastasizing chordoma in early childhood: a pathological and immunohistochemical study with review of the literature. *Pediatr Pathol* 7(3):287–301
18. Plese JP et al (1978) Unusual subarachnoid metastasis of an intracranial chordoma in infancy. *Childs Brain* 4(4):251–256

Aydin Sav and Pinar Karabağlı

46.1 Introduction

Chordoma is a rare, low- to intermediate-grade, primary malignant bone tumor originating from primitive notochord remnants, those of which form the primitive cell line around which the skull base and vertebral column develop [1–7]. Remnants of the notochord usually remain in or close to the midline. The anatomical distribution of these tumors mirrors the location of notochord remnants [8]. As a rule, sacrum represents the more common anatomical site of origin accounting for 50–60 % of all cases followed by skull base region (25–37 % of cases), cervical vertebrae (approximately 10 % of cases), and thoracolumbar vertebrae (approximately 5 % of cases) [2, 5, 6, 9].

For the most part, intracranial chordomas most frequently originate from the clivus. Among other sites of origin are the petrous apex, sellar area, and sphenoid sinus. On the other hand, although exceptional, the nasopharynx, maxilla, paranasal sinuses, and intradural region are also involved

[5]. Skull base chordoma affects younger patients compared with nonskull base chordoma [3, 9].

Grossly, chordomas tend to be soft, lobulated, mucoid, semitranslucent gray often hemorrhagic masses that permeate and destroy. Chondroid regions or calcifications are encountered primarily in clival examples. Seldom chordoma may show cystic changes. The majority of lesions are 2–5 cm in size [1, 6, 10].

46.2 Microscopic Findings

Chordomas have been divided into three histopathologic subtypes: typical or conventional chordomas, chondroid chordomas, and dedifferentiated chordomas [4, 5]. Typical chordomas are always lobulated lesions and lobules are separated by fibrous septa. Cells are arranged in sheets and cords or float singly within an abundant mucoid matrix. Therefore, their cytological appearance varies from cells with nonvacuolated eosinophilic cytoplasm, containing a single large vacuole and having signet ring cell appearance, to multivacuolated cells with bubbly cytoplasm so called “physaliphorous cells” (Fig. 46.1).

The cells contain relatively uniform, small, oval, eccentric nuclei with smooth nuclear contours and evenly distributed chromatin. Although rare, nuclear pleomorphism characterized by anisonucleosis and hyperchomasia might be associated with infrequent mitoses [1, 5, 6, 10–12]. In addition,

A. Sav, M.D. (✉)
Department of Pathology,
Acibadem University, School of Medicine,
Istanbul, Turkey
e-mail: murataydinsav@gmail.com

P. Karabağlı, M.D.
Department of Pathology,
Selçuk University, School of Medicine,
Konya, Turkey
e-mail: hakankarabagli@yahoo.com

Fig. 46.1 Physaliferous cells with multivacuolation swimming in mucin-rich matrix

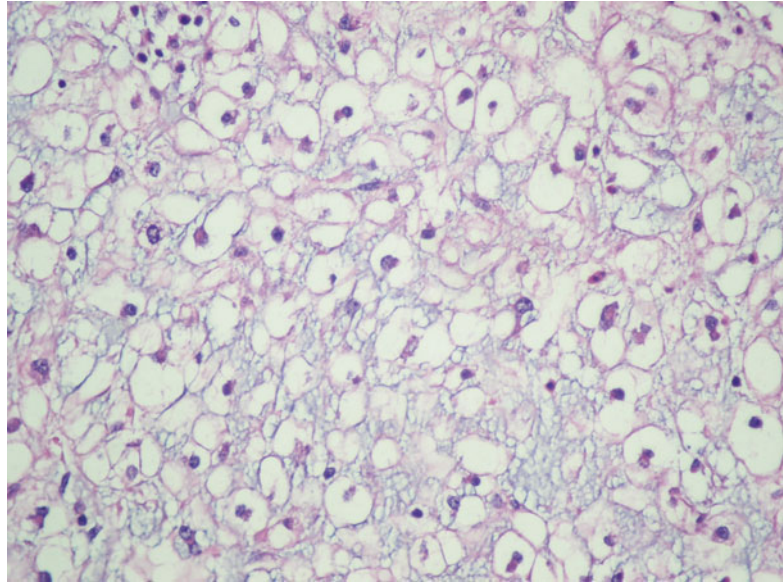
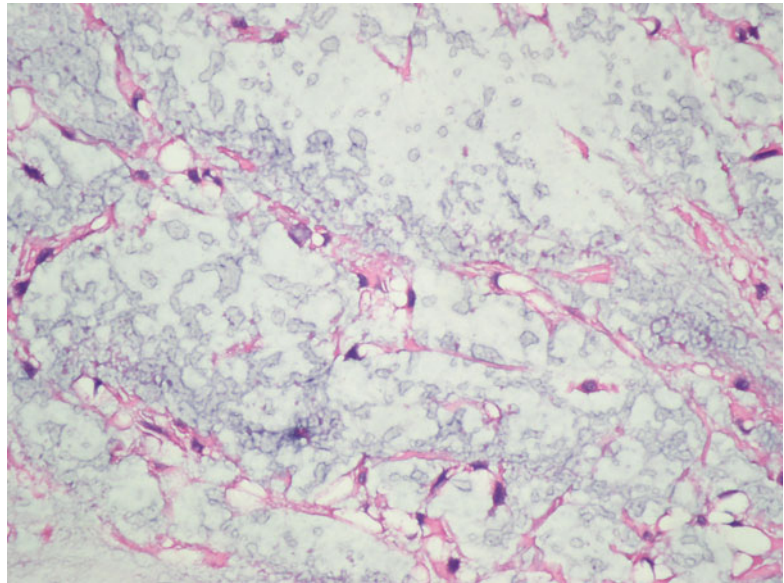


Fig. 46.2 Physaliferous cells floating in mucin-rich chondroid matrix



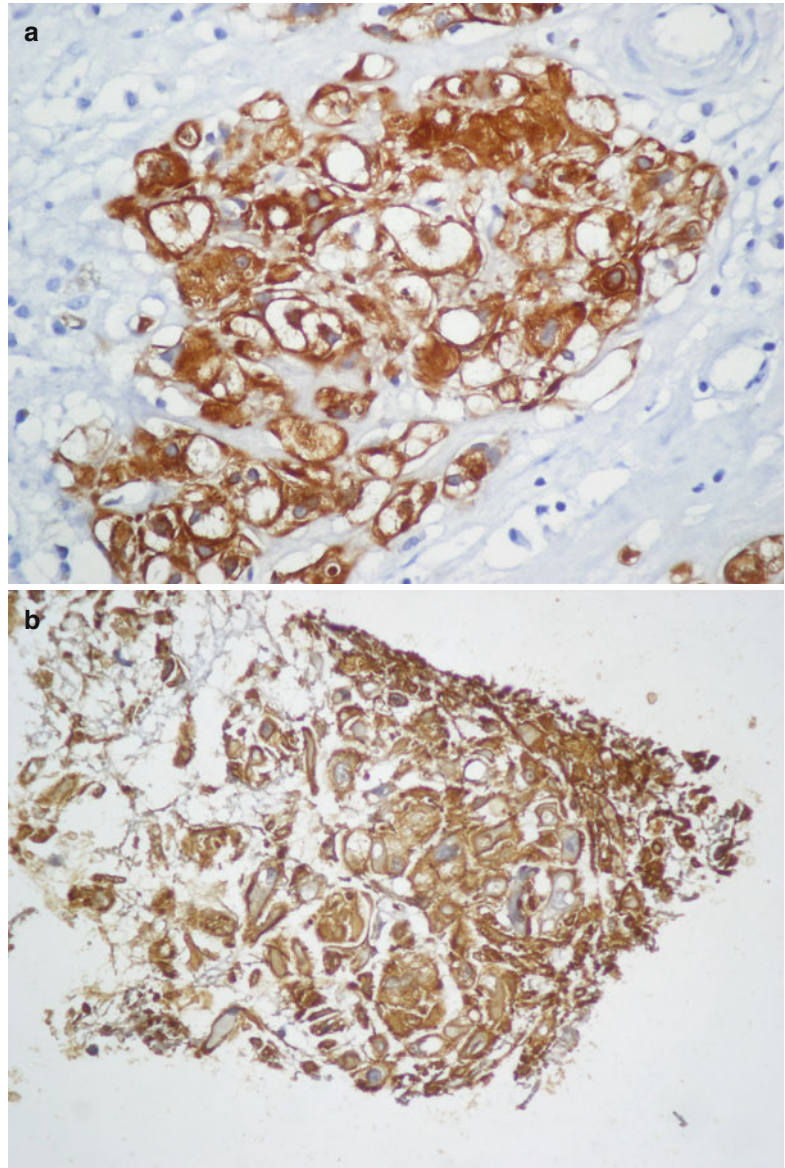
typical chordomas contain areas of coagulation necrosis, recent and old hemorrhage, and entrapped bone trabeculae [1, 12]. Likewise, vascular invasion is rare and tumor matrix varies in appearance [12].

Chondroid chordoma is a variant of chordoma first identified by Heffelfinger et al. that demonstrates better prognosis than the conventional chordomas [3, 5, 6, 10, 11]. This variant is more commonly seen in the skull base [1, 10, 11]. In chondroid chordomas, although varying in percentage,

hyaline or myxoid cartilage resembling stroma wraps neoplastic cells in lacunae unlike classic chordomas (Fig. 46.2). It is widely accepted that chondroid chordomas may be histologically indistinguishable from well-differentiated chondrosarcoma when a classic chordomatous component is not present [5, 7, 10, 11].

Chordoma associated with a high-grade sarcoma is called “dedifferentiated” chordoma or sarcomatoid chordoma [3, 5]. Therefore, they are

Fig. 46.3 (a) Multivacuolated “physaliferous” cells of chordoma with strong cytoplasmic reactivity for cytokeratin (cytokeratin). (b) “Physaliferous” cells with strong cytoplasmic reactivity for cytokeratin (cytokeratin)



biphasic tumors composed of both typical chordoma and a pleomorphic sarcomatous component [5, 10]. Dedifferentiated chordoma is a high-grade subtype of chordoma, often results in distant metastasis, and most patients have a poorer prognosis. They account for less than 5 % of all chordomas.

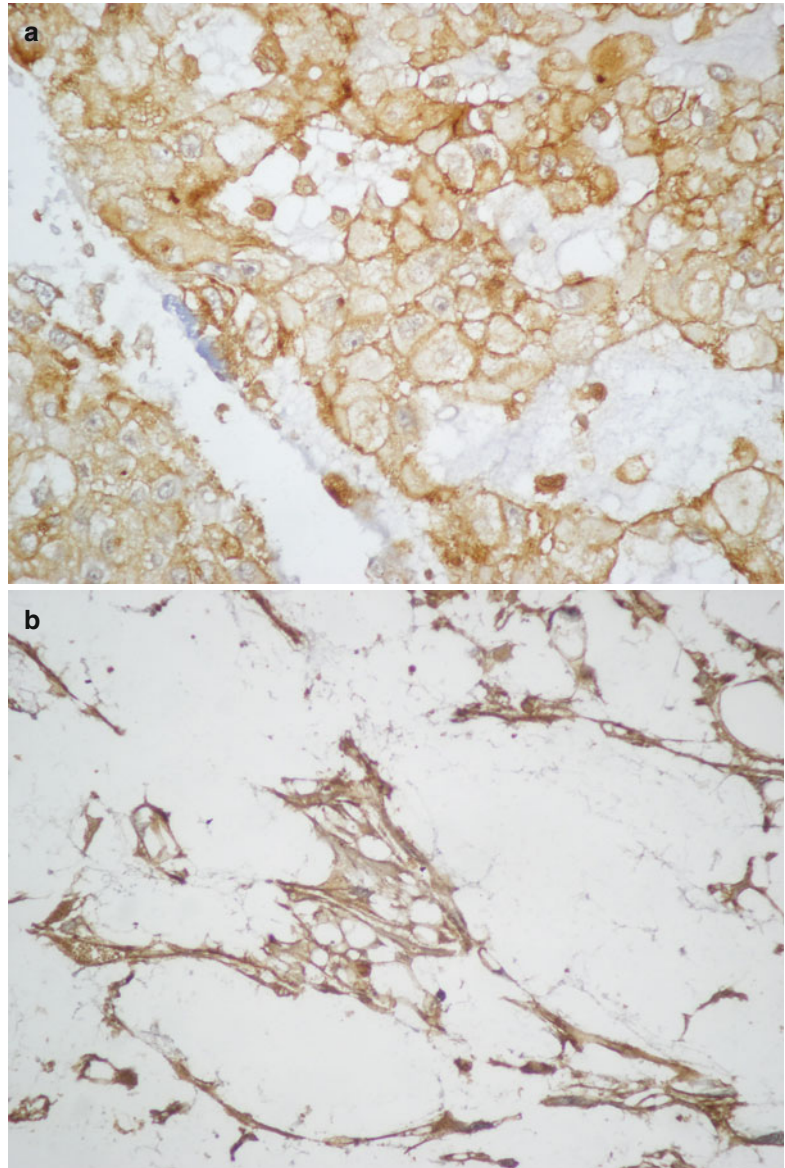
Histologically, the mucoid matrix in nonskull base chordomas was more abundant than in skull base chordomas. Conversely, skull base chordomas presented with phagocytosis (hemosiderin deposits) more frequently compared with nonskull base chordomas [3].

Increased patient age, clinical status, and nuclear pleomorphism are found to be closely related to the proliferative ability of conventional chordoma particularly those of originating from skull base [3, 12].

46.3 Immunohistochemical Findings

Chordoma (Fig. 46.3a) and chondroid chordoma (Fig. 46.3b) are immunopositive for epithelial markers including cytokeratin AE1/AE3 and

Fig. 46.4 (a) Chordoma cell membranes reacting with EMA (EMA). (b) Bubbles bearing tumor cell membranes reacting with EMA in chondroid chordoma (EMA)



epithelial membrane antigen (EMA) (Fig. 46.4a, b). The majority of conventional (Fig. 46.5a) and chondroid chordomas (Fig. 46.5b) are positive for S-100 protein [5, 7, 10, 11, 13]. On the contrary, dedifferentiated chordomas lack reactivity for epithelial markers [10].

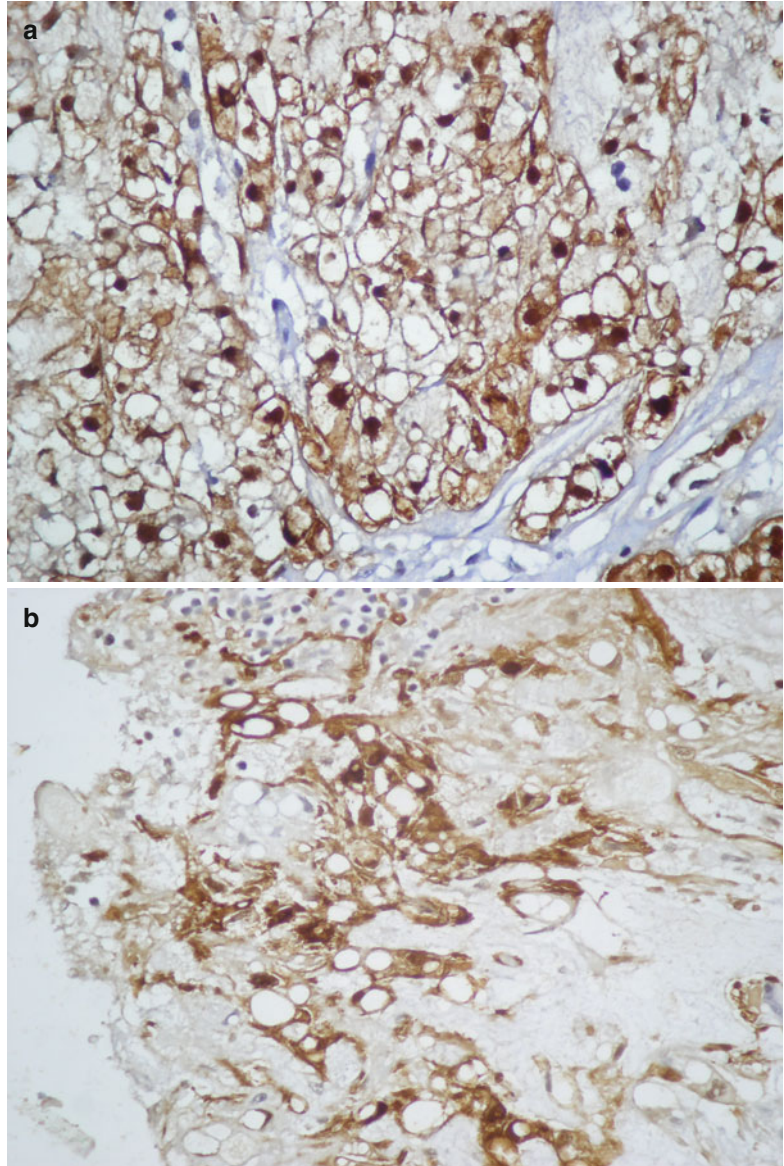
Genuine notochordal origin is supported by their expression of brachyury and CD 24, which may prove to be useful diagnostic markers [6, 13]. Brachyury is the transcription factor protein product of a T-box gene whose function is to reg-

ulate formation of the mesoderm and notochord in humans. Specifically, immunohistochemical expression of brachyury is highly sensitive and specific for chordomas. Interestingly, brachyury is apt to be lost in histologically and clinically more aggressive chordomas. As another example, less than 60 % chordomas are positive for CD24, polyclonal CEA, and GFAP [13].

MIB-1 labeling and E-cadherin were correlated with disease-free survival and recurrence in pediatric skull base chordomas [9, 14].

Fig. 46.5 (a)

Multivacuolated “physaliferous” cells of chordoma with strong nuclear and cytoplasmic reactivity for S-100 (S-100). **(b)** Multivacuolated “physaliferous” cells with strong nuclear and cytoplasmic reactivity for S-100 (S-100)

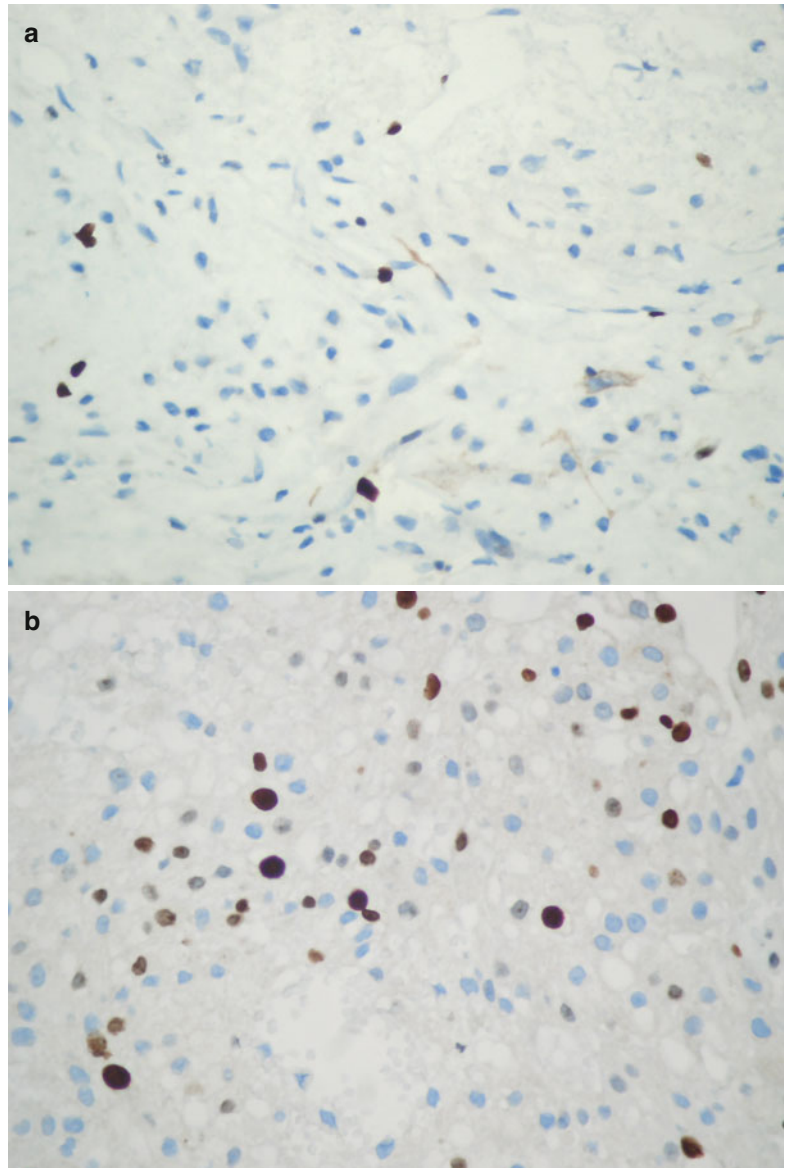


MIB-1 labeling index (LI) of nonskull base chordomas was higher than that of skull base chordomas (Fig. 46.6a, b). Being an independent factor, increased patient age is directly proportional with MIB-1 LI [3, 15]. In the same way, immunohistochemical staining of p53 protein is associated with a worse prognosis and decreased survival in patients with chordoma [9, 16] (Fig. 46.7).

Chordomas commonly express cyclooxygenase 2(COX-2), androgen receptor (AR), and estrogen receptor- β (ER- β), whereas estrogen

receptor- α (ER- α) and progesterone receptor (PR) are immunonegative. Bcl-2, actin, D2-40, and CD117 are not detectable in most chordomas [17, 18]. Likewise, in a study, descriptive data from immunohistochemical analyses of chordomas suggest that high levels of TGF- α and bFGF expression are linked to aggressive biological behavior. Similarly, strong fibronectin expression may be an additional confirmatory marker of aggressiveness, especially when accompanied by intense reactivity for TGF- α and bFGF [19].

Fig. 46.6 (a) Skull base chordoma showing a MIB-1 LI 3 % (Ki-67). (b) Nonskull base chordoma showing a high MIB-1 LI 15 % (Ki-67)



46.4 Cytological Findings

Vacuolated physaliphorous cells and more epithelioid appearing cells are positioned in a mucinous matrix [10].

46.5 Differential Diagnosis

The differential diagnosis includes mainly chondrosarcoma, many other chordoid tumors and metastatic carcinoma.

Chondroid chordoma and chondrosarcoma have a common presentation and similar anatomic locations and can be difficult to distinguish before histopathologic and immunohistochemical examination. It is unusual to observe a conventional chondrosarcoma involving base of the skull. Chordoma and chondroid chordoma are immunopositive for epithelial markers including cytokeratin and epithelial membrane antigen (EMA), whereas chondrosarcoma is negative for both but only S-100 positive [1–3, 11, 14].

Fig. 46.7 Diffuse and intense nuclear p53 reactivity (p53)

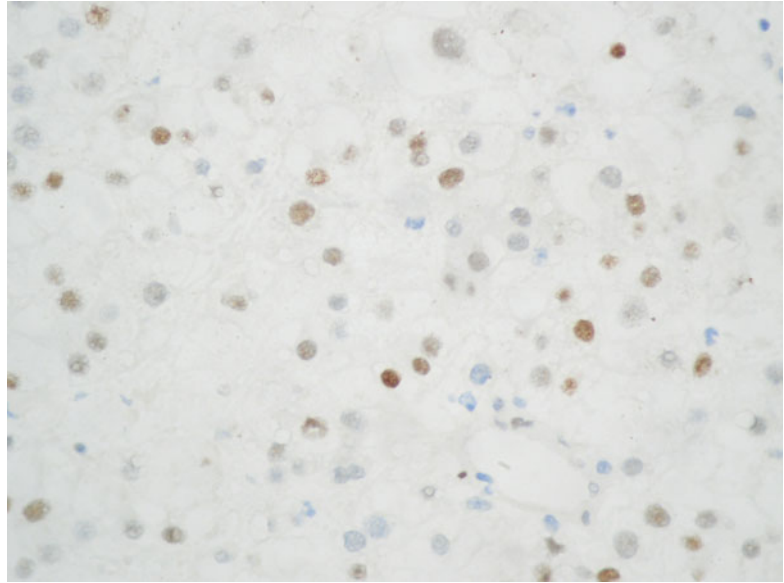
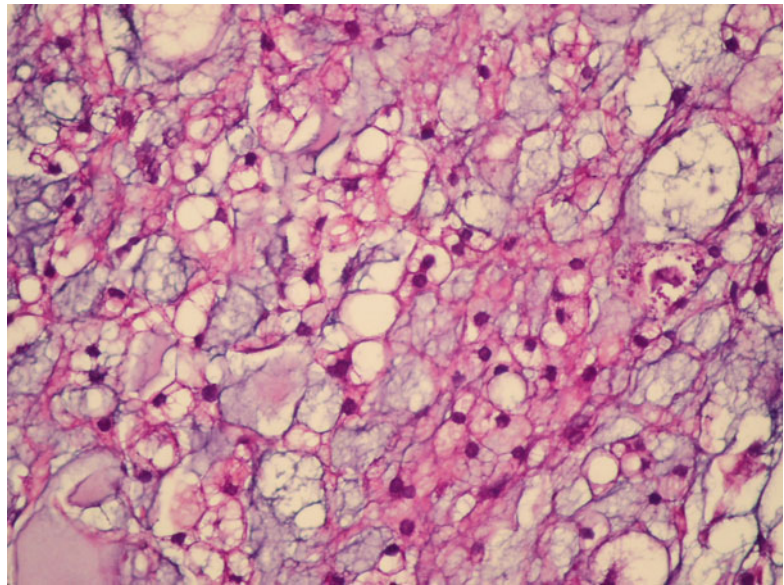


Fig. 46.8 Acidic mucinous material in chordoma (Alcian blue /PAS)

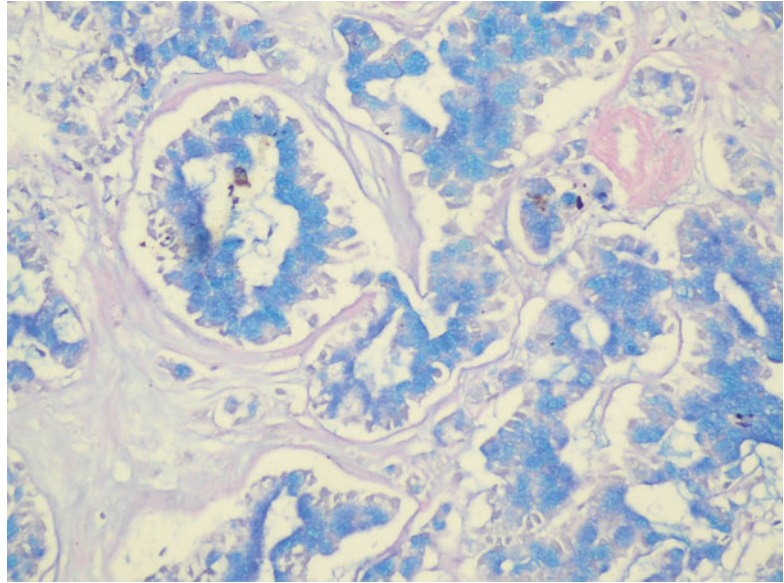


Tumors in the skull base or around the third ventricle can imitate chordoid meningioma, chordoid glioma of the third ventricle, and, rarely, metastatic carcinomas with myxoid or myxohyaline stroma. Likewise, chordoid meningiomas are typically large, supratentorial tumors. Similarly, in meningiomas, immunohistochemical studies reveal diffuse positive reaction for EMA whereas negativity for cytokeratin antibodies. Histologically, chordoid gliomas consisted of clusters, cords, and streams of eosinophilic, somewhat epithelioid cells

in a mucinous stroma, often comprising a lymphoplasmacytic infiltrate with speckled Russell bodies. For this reason, immunoreactivity for S-100 protein and often GFAP is widespread, and only focal EMA and/or keratin reactivity may be seen.

Chordoma must also be distinguished from metastatic mucinous adenocarcinoma. Histochemically, the mucin type in chordoma is acidic in nature (Fig. 46.8). However, mucin in carcinomas is neutral and epithelial type which reacts with periodic acid-Schiff (PAS) (Fig. 46.9) [10]. Above all, both

Fig. 46.9 Neutral mucin in a metastatic adenocarcinoma (Alcian blue/PAS)



metastatic carcinomas and chordomas stain positively for epithelial markers. However, chordomas are positive for S-100 protein. It is unusual to see a distinctive lobulated growth pattern with fibrous septa in metastatic carcinoma [6, 20].

References

1. Erdem E, Angtuaco EC, Hemert RV et al (2003) Comprehensive review of intracranial chordoma. *Radiographics* 23:995–1009
2. Ferraresi V, Nuzzo C, Zoccali C et al (2010) Chordoma: clinical characteristics, management and prognosis of a case series of 25 patients. *BMC Cancer* 10(22):1–10
3. Naka T, Boltze C, Samii A et al (2003) Skull base and nonskull base chordomas. *Am Cancer Soc* 98:1934–1941
4. Tamborini E, Miselli F, Negri et al (2006) Molecular and biochemical analyses of platelet-derived growth factor receptor (PDGFR) b, PDGFRA, and kit receptors in chordomas. *Clin Cancer Res* 12:6920–6928
5. Mirra JM, Rocca CD, Nelson SD, Mertens F (2002) Chordoma. In: Christopher DM, Fletcher CDM, Unni KK, Mertens F (eds) *Pathology and genetics of tumours of soft tissue and bone*. IARC Press, Lyon, pp 316–317
6. Unni KK, Inwards CY (2007) Tumors of the osteoarticular system. In: Fletcher CDM (ed) *Diagnostic histopathology of tumors*, vol 2. Elsevier, Philadelphia, PA 1632–1633
7. Tihan T, Kilpatrick R (2010) Mesenchymal tumors of the central nervous system. In: Perry A, Brat DJ (eds) *Practical surgical neuropathology a diagnostic approach*. Elsevier/Churchill Livingstone, Philadelphia, PA 219–234
8. Brüderlein S, Sommer JB, Meltzer PS et al (2010) Molecular characterization of putative chordoma cell lines. *Sarcoma* 2010:1–14, Article ID 630129
9. Longoni M, Orzan F, Stropi M, Boari N, Mortini P, Riva P (2007) Evaluation of 1p36 markers and clinical outcome in a skull base chordoma study. *Neuro Oncol* 10:52–60
10. Burger PC, Scheithauer BW (eds) (2007) *Tumors of the central nervous system*. American Registry of Pathology, Washington, DC
11. Almefty K, Pravdenkova S, Colli BO et al (2007) Chordoma and chondrosarcoma similar, but quite different, skull base tumors. *Cancer* 110:2457–2467
12. O'Connell JX, Renard LG, Liebsch NJ et al (1994) Base of skull chordoma. *Cancer* 74:2261–2267
13. Oakley GJ, Fuhrer K, Seethala RR (2008) Brachyury, SOX-9, and podoplanin new markers in the skull base chordoma vs chondrosarcoma differential: a tissue microarray-based comparative analysis. *Mod Pathol* 21:1461–1469
14. Naka T, Oda Y, Iwamoto Y et al (2001) Immunohistochemical analysis of e-cadherin, α -catenin, β -catenin, and neural cell adhesion molecule (NCAM) in chordoma. *J Clin Pathol* 54:945–950
15. Naka T, Boltze C, Kuester D et al (2005) Intralesional fibrous septum in chordoma. *Am J Clin Pathol* 124:288–294
16. Naka T, Boltze C, Kuester D et al (2005) Alterations of G1-S checkpoint in chordoma the prognostic impact of p53 overexpression. *Am Cancer Soc* 104:1255–1263

17. Daugaard S, Christensen LH, Hogdall E (2009) Markers aiding the diagnosis of chondroid tumors: an immunohistochemical study including osteonectin, bcl-2, cox-2, actin, calponin, D2-40 (podoplanin), mdm-2, CD117 (ckit), and YKL-40. *Authors J Compilation* 117:518–525
18. Fasig JH, Dupont WD, Olson SJ et al (2007) Steroid hormone receptor and cox-2 expression in chordoma. *Anat Pathol* 128:375–381
19. Deniz ML, Kilic T, Almaata I, Kurtkaya O, Sav A, Pamir MN (2002) Expression of growth factors and structural proteins in chordomas: basic fibroblast growth factor, transforming growth factor alpha, and fibronectin are correlated with recurrence. *Neurosurgery* 51(3):753–760
20. Ellison D, Love S, Chimelli L, Harding BN, Lowe J, Vinters HV (eds) (2004) *Neuropathology a reference text of CNS pathology*. Mosby, Edinburgh/London/New York

Kevin Beccaria, Stephanie Puget, Bernard George,
and Christian Sainte-Rose

Chordomas are tumours arising from primitive notochordal remnants. They are rare tumours, comprising 0.2 % of primary brain tumours [1, 2] and less than 5 % of primary bone tumours [1, 3, 4]. They occur in less than one/million population [3, 5], with a peak incidence occurring between the fourth and sixth decades [3, 6, 7]; less than 5 % of chordomas present in the first two decades [7–10], with a male to female ratio of close to 1 [9]. In contrast to chordomas in the adult population where the majority are located within the sacrum [6], chordomas in children are more commonly located within the cranium, particularly the clivus [9]. Case reports of extraskel-etal chordomas have been published [11–26].

Chordomas are characterised by their aggressive potential and their frequency of recurrence. This risk of recurrence is due in part to the difficulty in obtaining complete surgical resection of these tumours, situated in anatomical locations difficult to access and rich in neurovas-

cular structures. Metastatic dissemination may occur with an incidence varying between 8.6 and 58 % in paediatric series [27, 28]. A particularly aggressive form occurs in young children in whom progression is often rapid.

Management of these tumours is based on a complete primary resection as possible followed by local irradiation, ideally proton therapy.

The results from our series (36 cases) have been compared to those in the literature (120 papers reporting more than 250 cases of paediatric chordomas).

47.1 Background

47.1.1 History

Luschka [29] was the first to describe, in 1857, the existence of small soft transparent “jelly-like” tumours of the *clivus blumenbachii* (*dorsum sellae*).

Virchow [30] performed the first histological study the same year. He called them *ecchondrosis spheno-occipitalis physaliphora sive prolifera*, in reference to their microscopic appearance (from the Greek word *physallis*, meaning bubble; *-phore*, meaning to hold) and their presumed cartilaginous origin.

In 1858, Müller [31], whilst studying the anterior prolongation of the notochord, observed that it extended to the inferior part of the sella turcica. He put forward the theory that the lesions described by

K. Beccaria, M.D. • S. Puget, M.D., Ph.D.
Department of Pediatric Neurosurgery,
Necker Hospital, Université Paris Descartes,
Sorbonne, Paris, France

B. George
Département de Neurosurgery, Hôpital Lariboisière,
Paris, France

C. Sainte-Rose (✉)
Department of Paediatric Neurosurgery,
Necker Enfants Malades Hospital, Paris, France
e-mail: chsaintrose@gmail.com

Luschka and Virchow were not cartilaginous growths as previously thought but rather arose from chordal tissue. Müller's theory, however, was not unanimously accepted, and it would take until the work of Ribbert (an anatomopathologist of Bonn) in 1895 [32] that the notochordal origin of these tumours was firmly established. Ribbert and his pupil Steiner based their theory on both histological and experimental data. They punctured the lumbar intervertebral discs of rabbits thereby causing expulsion of fragments of *nucleus pulposus*. They observed that the expelled tissue demonstrated cellular proliferation and an increase in volume. The experimental cultures resorbed after a year, but their histological characteristics were those of the ecchondrosis as described by Virchow. Ribbert therefore renamed these lesions *ecchordosis physaliphora* and gave birth to the term "chordoma".

Stewart and Burrow [33] suggested in 1923 to distinguish terminologically these two clinical entities. They proposed the term "chordomas" to represent symptomatic malignant tumours and *ecchordosis physaliphora* for benign clival lesions with limited growth potential.

If one adheres to this definition, then one of the first cases of chordoma (*clinically symptomatic*) was described by Klebs in 1864 [34]. The same author described in 1889 the first case of a chordoma in the cervical spine [35]. Linck [36] described in 1909 a case of nasopharyngeal chordoma presenting with otitis and a pharyngeal mass. One year later, Feldmann [37] published the first case of sacrococcygeal chordoma in a 46-year-old woman presenting with a progressive soft swelling of the sacro-perineal region over a year.

Paediatric cases were also reported in the same period. André-Thomas [38] and Adson [39] reported the case of an 18-year-old girl and an 8-year-old boy with clival chordomas in 1923 and 1935, respectively. The first case of sacrococcygeal chordoma in an infant was reported by Argaud [40] in 1926; then in 1935 and 1940, Ellis [41] and Mixter [42] described cases of a young girl of 8 years and a boy of 14 presenting with lumbar (L2–L3) and cervical chordomas (C2–C4), respectively.

Since then, numerous cases of paediatric chordomas have been published. Currently, more than 250 cases of chordomas in children have been

reported, in all locations. However, the majority are case reports with paediatric series of greater than ten patients being rare [7, 27, 28, 43, 44].

47.1.2 Embryology

The term "notochorde" comes from the ancient Greek *noton* (back) and *chordê* (cord), literally "dorsal cord". It is a dorsal tubular structure occurring in embryos of all chordates [45]. In vertebrates, a phylum of *Chordata*, the notochord is replaced during development by the vertebral column and part of the cranial base.

The nucleus pulposus, considered by some to be the sole remnant of the notochord, has long been considered to be the point of origin of chordomas. However, clinical observation shows that chordomas almost always arise from the vertebral bodies and not the intervertebral discs, which are generally respected by the tumour. Similarly, chordomas arise, in the majority, at the extremities of the cranio-vertebral axis, at the level of the clivus and sacrococcygeal region and thus at a distance from the intervertebral discs [6, 9, 46]. Finally, certain authors have shown that brachyury, a growth factor implicated in the development of the notochord, was also a specific marker of chordomas even though it was not found in the nucleus pulposus of intervertebral discs [47]. These different pieces of evidence strongly place into doubt the link between chordomas and the nucleus pulposus.

The fact that chordomas arise from notochordal cells is supported by different arguments. Apart from their identical location, there exists morphological and immunophenotypical similarities between the cells of chordomas and those of the notochord [48]. In fact, chordomas arise from notochordal remnants from an incomplete involution of the notochord and different from "normal" remnants potentially found in the *nuclei pulposi*.

47.2 Necker-Lariboisière Series

A retrospective analysis of paediatric chordomas operated upon from 1980 to 2012 at the Hôpital Necker-Enfants Malades and the Hôpital

Lariboisière was performed. Of the 36 children operated upon for a chordoma during this period, 5 were lost to follow-up. Clinical history, pathological anatomy, management and outcome were thus available in 31 children in this series and were compared to those in the literature.

Chordomas in children are particularly rare representing less than 1 % of intracranial tumours in children [7] and less than 5 % of chordomas in all ages [1, 7, 49, 50]. Only 2 series report more than 15 cases. In 2006, Hoch [44] reported 73 cases of chordomas of the cranial base: essentially an anatomic-pathological study with little clinical information. In 2010, Ridenour [28] published 35 cases of whom 20 were children.

47.2.1 Age at Diagnosis

In the literature, the average age at diagnosis was around 10 years [9, 10, 27, 28, 43, 44]; the youngest case described was in a neonate with a tumour of the clivus [51]. The average age of patients in our series was 11.8 years (range 3.6–18 years).

In contrast to adults [1, 3, 52], sacrococcygeal chordomas in children occur at a younger age than those in the cranium. This tendency was noted in our review of the literature of 249 cases: the average age being 9 years in 193 children with clival chordomas, 10.5 years in 34 children with vertebral chordomas (cervical, thoracic or lumbar) and 5.6 years in 22 children with sacrococcygeal chordomas.

47.2.2 Sex Ratio

The sex ratio in our series was 2, with a male predominance (20M/11F). This does not correspond to those seen in the literature.

In adults there is a slight male predominance for all locations (60 % males); intracranial chordomas were more frequent in females compared with those in the sacrococcygeal region or in the spine being more common in males [49, 53, 54].

It is difficult to evaluate the male to female ratio in the paediatric population given the heterogeneity in the literature. For all locations, the

male to female ratio is reported as 0.7–1 [9, 28]. This figure varies little according to tumour location (0.72–1.17 [10, 44] intracranial chordomas, 1.11 sacrococcygeal chordomas and 1 for chordomas of the spinal column).

47.2.3 Histology

The classic forms are more frequent in children greater than 5 years of age. Atypical chordomas are generally seen in younger children (50–65 % in the series of Borba [10], in those less than 5 years of age).

Even if certain authors state that childhood chordomas are characterised by a greater pleomorphism than those of adults [27, 46], the “classic” form has been described in 57–89 % of paediatric series [7, 28, 43, 44]. We found in our series 80.6 % classic chordomas, 12.9 % chondroid chordomas and 6.5 % atypical/poorly differentiated chordomas (two patients aged 4.3 and 3.6 years).

47.2.4 Clinical History

47.2.4.1 Intracranial Chordomas

(Figs. 47.1 and 47.2)

Impairment of cranial nerve function is the principal presenting feature of chordomas of the cranial base, occurring in approximately 60 % of cases [43, 46]. The sixth nerve is most frequently involved (55–72 % of cases) [10]. Headaches occur in less than 40 % of cases [10, 46], occurring as part of an intracranial hypertensive syndrome (ICH) in 28 % of cases [46]. According to the same authors, long tract signs with a pyramidal syndrome occurs in 36 % of cases.

Children less than 5 years of age present more frequently with intracranial hypertension (72 %) or with long tract signs (43 %) than older children who present with diplopia or isolated headaches (55 and 42 %, respectively) [46, 51, 55].

Nolte was the first to describe four types of clival tumour extension (superior, inferior, anterior, posterior). The inferior extension, according to him, was more frequently found in children less than 5 years of age, perhaps explaining the

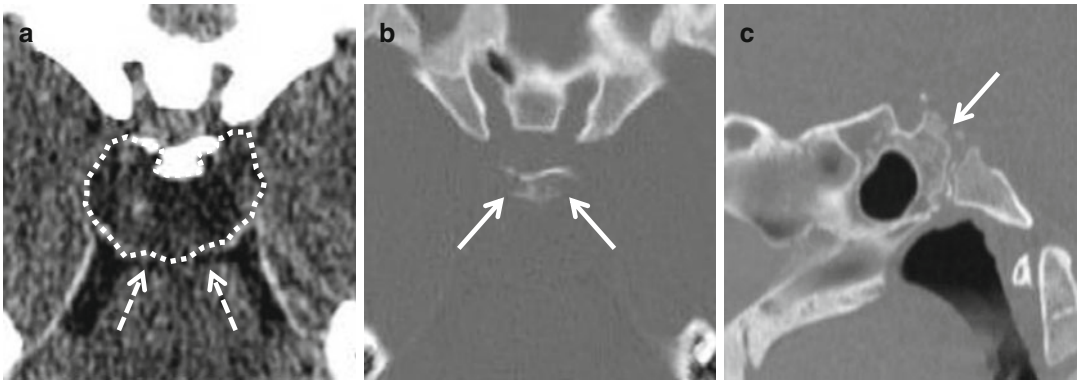


Fig. 47.1 CT scan of a clival chordoma (a) Axial slice showing a hypodense mass of the posterior aspect of the clivus (*dotted line*) contacting the brainstem (*arrows*) (b) Axial slice on bone windows demonstrating a lytic lesion

eroding the superior aspect of the clivus and posterior clinoid processes (*arrows*) (c) Sagittal slice on bone windows demonstrating a lytic lesion eroding the posterior cortex of the sphenoid bone (*arrows*)

frequent involvement of the long tracts and lower cranial nerves and the presence of torticollis [55].

47.2.4.2 Sacrococcygeal Chordomas

These present with the rapid appearance of an eventually ulcerated subcutaneous mass [56–58] occasionally massive within the presacral space. Perineal pain is often present and may be associated with radicular pain [58, 59] or cauda equina syndrome. Bladder and bowel dysfunction is common through compression and/or invasion of the nerves of the cauda equina or by direct compression of the urinary tract and colon by the presacral mass [56, 60].

47.2.4.3 Vertebral Column Chordomas

(Figs. 47.3 and 47.4)

The predominant symptoms depend on the orientation and development of the tumour. In the majority of cases, posterior enlargement of the tumour causes compression of the spinal cord or cauda equina [27, 41, 49, 61–63]. Anterior progression can present with respiratory dysfunction and/or dysphagia in those tumours of the cervical and thoracic regions [64]. In general, pain is common, often insidious in onset and becoming progressively more severe. The cause is mixed: displacement of soft tissues, bone destruction, nerve root compression, and vertebral instability [64]. Rigidity and/or spinal deformity have been similarly reported [27, 41, 65, 66].

47.2.5 Anatomical Localisation and Metastatic Dissemination

47.2.5.1 Anatomical Localisation

Skeletal Localisation (Fig. 47.5)

In the literature, childhood chordomas are clearly distinguished from their adult counterparts by their anatomical distribution. Adult chordomas are primarily found in the sacrococcygeal region [6, 9, 46, 55, 67], whereas in children, intracranial chordomas occur in the majority [7, 9, 27, 62, 68]. In our series, the majority of cases were situated at the level of the clivus and/or cervical spine.

Extraskelletal Localisation

Outside of these typical skeletal sites, ectopic extraskelletal chordomas have been described in children. We have not observed any in our series. They have been reported in the gluteal region [11], the paranasal sinuses [12], the ethmoid and maxillary sinuses [13], the temporal bone [14] and three cases of intradural lesions [15–17].

Finally, a certain number of cases have been published describing chordomas arising in the paravertebral or paraclival regions without associated bony invasion [18–26].

47.2.5.2 Metastatic Dissemination

The incidence of chordoma metastases is quite variable, from 10 to 48 % in adults [3, 6, 49, 53, 69]

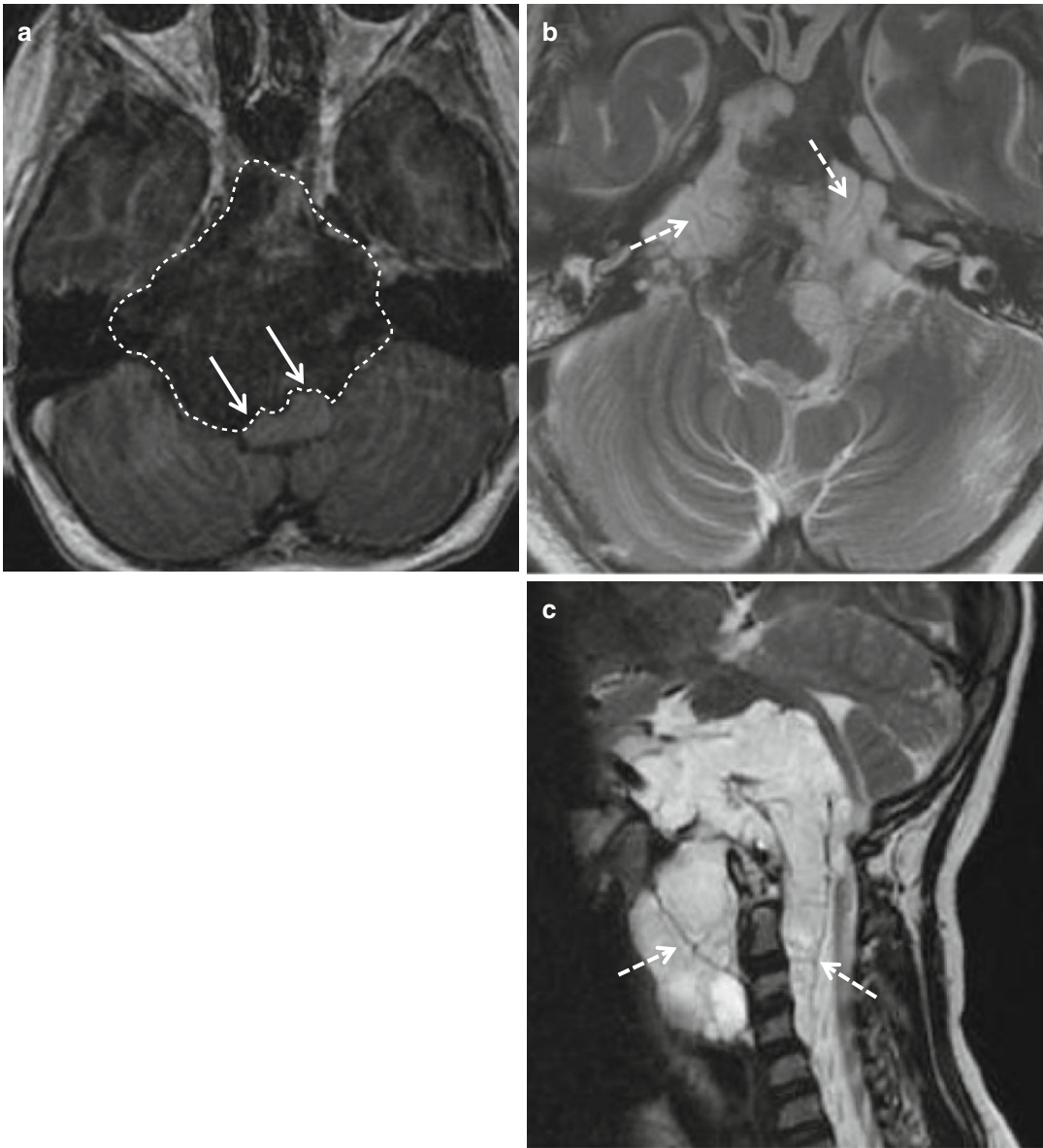


Fig. 47.2 MRI of a clival chordoma (a) Axial T1 post-contrast. Large hypointense, heterogenous mass (*dotted line*) of the posterior aspect of the clivus displacing the brainstem (*arrows*). Contrast enhancement is minimal and heterogenous. (b) T2 axial image showing a multilobular mass, hyperintense on T2 extending into the prepontine

region and invading the two posterior clinoid processes. Hypointense intratumoural septations are seen (*arrows*) (c) T2 sagittal image. The chordoma is visible as hyperintense on T2, extending from the sella turcica to C5. Hypointense intratumoural septations are well seen (*arrows*)

and from 8.6 to 58 % in children [9, 27, 28, 43]. It was 9.7 % in our series.

Metastatic spread seems to be the prerogative of the under 5-year-olds [10, 46, 70]. Tumours

located in the sacrococcygeal region or of the spinal column seem to have a greater tendency to metastasize. In our review, the incidence in children was 55 % in sacrococcygeal chordomas

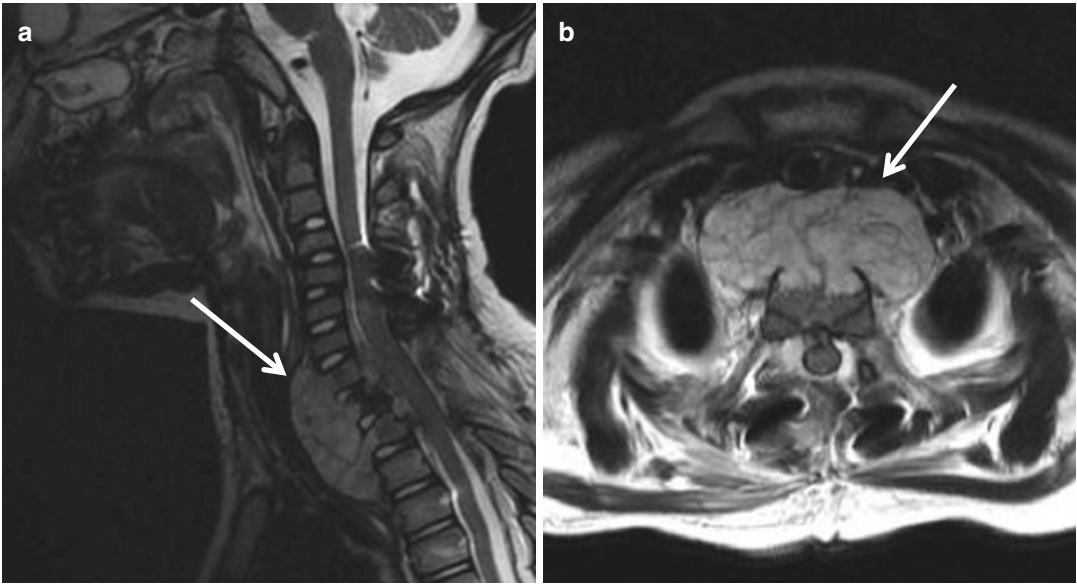


Fig. 47.3 Chordoma of the cervicothoracic junction with anterior extension (*arrows*) diagnosed due to respiratory difficulties (stridor)

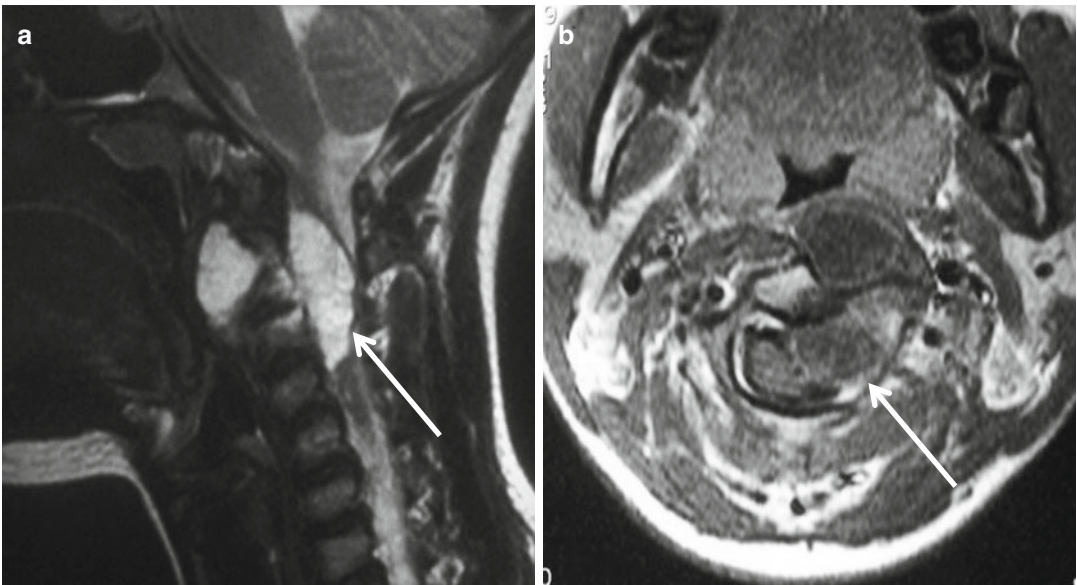


Fig. 47.4 Cervical chordoma with posterior extension into the spinal canal (*arrows*) presenting with neurological involvement (right upper limb paresis, C5–7 radiculopathy)

with an average delay of 1.4 months, compared to 13.2 % for intracranial chordomas with an average delay of 4.5 months (Table 47.1).

Metastatic dissemination primarily occurs via the blood circulation, particularly via the dural

venous sinuses for clival chordomas [71], and the presacral veins for sacrococcygeal chordomas. Dissemination via the cerebrospinal fluid has also been reported, either via the subarachnoid spaces [70, 72] or through ventricular shunting

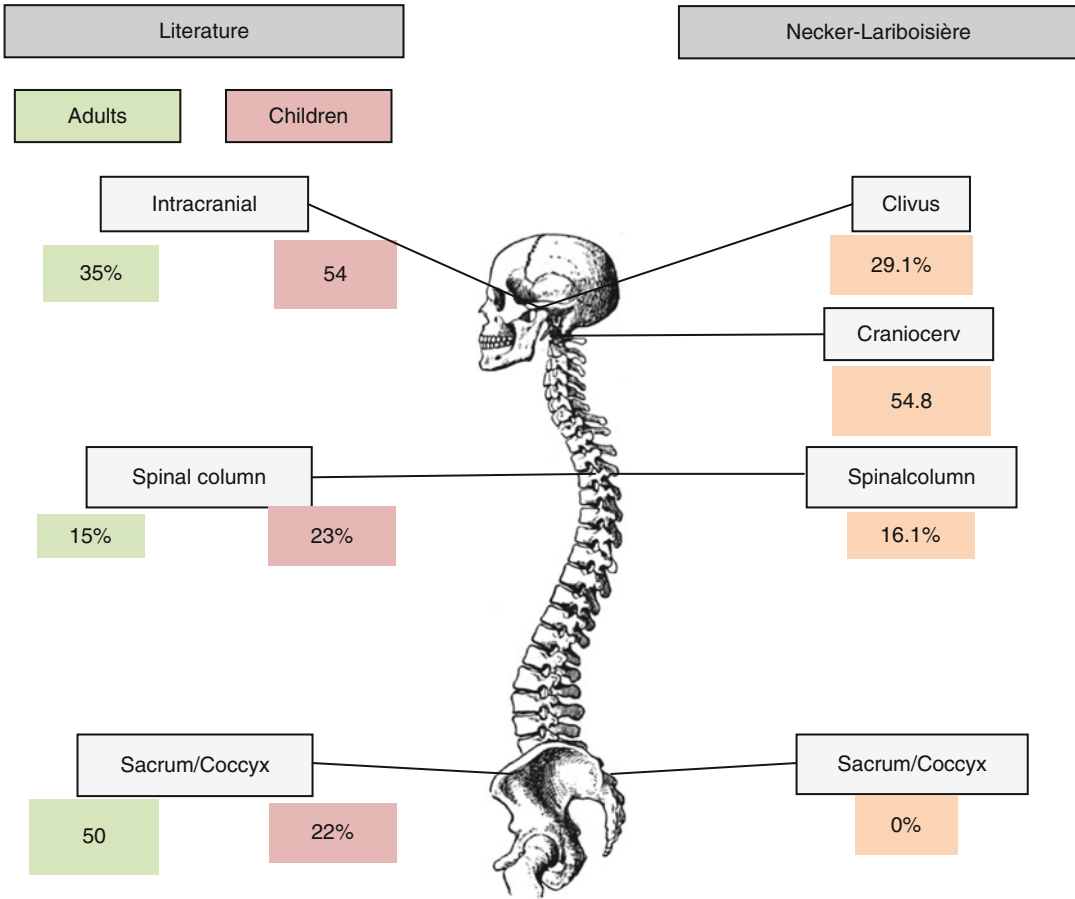


Fig. 47.5 Distribution of anatomical location of chordomas in the literature in adults and children from the literature and in our series

Table 47.1 Incidence and delay to metastases in chordomas of children in the literature

Site	M+	M-	UKN	M+ at diagnosis	M+ secondary	Avg. delay in months (med; min-max)
Intracranial (n=194)	22 (13.2 %)	145 (86.8 %)	27	5 (3 %)	6 (3.6 %)	4.5 (1; 0-18)
Sacrococcygeal (n=22)	11 (55 %)	9 (45 %)	2	5 (25 %)	3 (15 %)	1.4 (0; 0-6)
Spinal column (n=34)	10 (41.7 %)	14 (58.3 %)	10	1 (4.2 %)	3 (12.5 %)	3.3 (2; 0-9)

Max maximum, Med median, Min minimum, M+ metastases, M- no metastases, UKN unknown

[17]. There is also the risk of metastatic tumour deposition through the surgical route [73]. In our series, we reported one case of chordoma arising at the site of abdominal fat graft harvest, 10 months after the initial surgery.

The principal site of metastases is the lungs [9, 10, 17, 27, 40, 72, 74-76], followed by the bone [70, 76], lymph nodes (cervical, inguinal, subclavicular) [9, 27, 71, 76], skin [70, 77], liver [43, 70, 77] and anecdotally the brain and spinal

Table 47.2 Progression-free survival and overall survival related to the length of follow-up in the major paediatric series and those of Necker-Lariboisière

Series	Number of patients	Av. follow-up in months (min-max)	Progression-free survival (%)	Overall survival (%)
Benk et al. [43]	18	72 (19–120)	63 (5 years)	68 (5 years)
Borba et al. [10]	79 (review)	39 (1–300)	–	56,8
Hoch et al. [44]	73	90 (12–252)	–	81
Ridenour et al. [28]	35	129 (1–501)	–	63
Necker-Lariboisière	31	78 (0.3–239)	54,3 (15 years)	63

cord [77], meninges [70, 72], heart [77, 78], pleural cavity [9], kidneys [77] and suprarenal glands [27, 46]. It is not uncommon for metastases to be present at diagnosis in contrast to that observed in adults. In our review of the literature, 25 % of patients with sacrococcygeal chordomas had metastases at diagnosis compared with 3 % of those with intracranial chordomas and 4.2 % of those with chordomas of the spinal column (Table 47.2). There appears to be a link between the incidence of metastases and local recurrence [43, 53]. In our series, metastases often occurred late in the illness (from 24 to 67 months) and each time was in the context of local recurrence.

47.2.6 Management

Management of chordomas is multidisciplinary and relies on a collaboration between neurosurgeons, radiotherapists, radiologists, oncologists and sometimes ENT surgeons. Due to the poor outcome of the disease, management must be aggressive in order to limit the risk of local recurrence and metastatic dissemination. The advent of MRI, the advances in neurosurgery (endoscopy) and the contribution of proton therapy have allowed considerable prolongation of life for these patients. Today, treatment relies on as complete a surgical resection as possible followed by adjuvant radiotherapy by proton therapy. Standard chemotherapy has no role even if certain authors have utilised chemotherapy with occasionally encouraging results.

47.2.6.1 Surgery

Surgery is the essential step in the treatment of chordomas. The objectives are twofold: (1) maximal reduction in tumour volume with obtaining a

macroscopically complete excision and (2) removal of any possible tumour residual away from the brainstem to maximise radiotherapy dose.

As in adults, all authors agree that the largest surgical resection possible must be achieved at the initial surgery [6, 7, 43, 79–82]. This attitude is commonly accepted, even if the paediatric series in the literature are too little to allow a real statistical analysis.

Ridenour observed a better survival following a complete excision versus an incomplete excision in 35 children, without achieving statistical significance [28]. We observed a similar result in our series, with a greater overall survival in patients with a complete excision before radiotherapy compared to those whose excision was incomplete.

The location of these tumours and the complexity of their extension allow a complete resection in the minority of cases [2, 83] due to the proximity to neural structures (cranial nerves, brainstem, sacral nerves) or vascular structures. Modern imaging techniques, neuronavigation, microsurgery and endoscopy have allowed surgeons to be more aggressive and to obtain better surgical excisions than in the past. However, the rate of complete surgical excision remains low in the major paediatric series published and varies between 0 and 36.4 %; it was 19.4 % in our series. These rates of clearance are less than those seen in other tumours of the cranial base in children (posterior fossa ependymoma, craniopharyngioma) [84, 85]. This is due to the fact that chordomas (1) are multilobulated tumours, often insinuated between nerves and arteries to which they adhere, (2) have osseous invasion and are located within the spine and cranial base whereby macroscopic clearance would cause significant

mutilation and (3) often have an intradural component (50 % in our series) and sometimes insinuated within the dural layers.

Maximal tumour resection often requires many surgical attempts [86], in utilising different surgical routes in one or more procedures. In our series, 82 procedures were performed in 31 patients (on average 2.6 per patient). Complete excision was able to be achieved in only six patients (after one to three surgeries per patient).

The majority of routes to the cranial base currently used in adults may be applied to children with little modification and are well tolerated [87]: suboccipital [7, 61], retrosigmoid [16], infratentorial far-lateral and anterolateral [82], infra-temporal [55, 70, 88], transoral [43, 89–91] and transsphenoidal [7, 43, 92] routes. For spinal chordomas, the route can be posterior (laminectomy) [43], anterior (thoracotomy, retroperitoneal) or anterolateral [64], or a combination of these [63, 66].

In our series, the two routes used more frequently were the suboccipital retrosigmoid and anterolateral routes in 20.7 and 19.5 % of cases, respectively. When the tumors is originated from the clivus with an anterior extension into the sphenoid bone (body, sinus, sella turcica) and/or retropharyngeal, the classical routes employed have been transsphenoidal and transoral. This latter route was abandoned by numerous teams in favour of endonasal endoscopy [93, 94, 109], which is utilised to approach the craniocervical junction [110].

Orthopaedic management is rarely reported in the paediatric literature; in 34 cases of vertebral column chordomas, spinal fixation has only been reported in 3 cases [63, 64, 66, 68, 95]. In our series, the spine was involved in 22 children in whom 11 required fusion. Nine patients required temporary bracing.

Apart from tumoural reduction, the other objective of surgery is to remove as far as possible the tumour residual from functional anatomical tissues (spinal cord, brainstem, large vessels, internal auditory meatus, optic pathways and hypophysis) in order to deliver the maximal radiotherapy dose whilst minimising secondary effects.

47.2.6.2 Radiotherapy

Radiotherapy is an integral part of the treatment of chordomas, even if few paediatric series have truly evaluated the effectiveness of this treatment in this population.

Conventional Radiotherapy

Despite the fact that chordomas have been considered as relatively radioresistant tumours, the utilisation of high doses of conventional radiotherapy has provided a certain degree of tumoural control, and early on, the majority of authors have recommended adjuvant radiotherapy [1, 65, 96, 97].

Apart from isolated cases reported in the literature, only the series of Wold has provided long-term results of conventional adjuvant radiotherapy and surgical excision in an exclusively paediatric population [7]. In this series, Wold reported a group of 12 patients, with an average age of 13.6 years, presenting with intracranial chordomas (clival or of the sella region). All the patients had been treated by surgery primarily, radical ($n=4$) or partial ($n=2$) excision and unknown in 2; conventional adjuvant radiotherapy was given in 10 (5,115 rads on average, unknown in 4). The average follow-up was 67 months (1–252 months). During the follow-up period, two patients died from tumour progression after 26 and 44 months and two others due to unrelated causes (pneumonia in one and cause unknown in another). Survival rates in this series were thus close to 75 % at 5 years.

On another level, the interest in the association between surgery and radiotherapy in the paediatric population seems confirmed by Borba who in his review of the literature on intracranial chordomas confirmed that surgical excision, whether complete or incomplete, followed by radiotherapy (type not precise), offered a better outcome than surgical excision alone ($p=0.004$) [10].

Proton Therapy

Radiotherapy in growing children has, however, its limits and can give rise to numerous complications [98]. In this context, proton therapy has become little by little the radiotherapy modality of choice in this condition [99, 100] in reducing by a factor of 2–3 the dose

delivered to neighbouring structures (encephalon, hypophysis, cochlear...) [101]. In the series published by Hoch, 73 children had been treated for cranial base chordomas by surgical excision followed by proton therapy [44]. The average age at diagnosis was 9.7 years (1–18 years). The overall survival rate was 81 % with an average follow-up of 7.25 years (1–21 years). The authors considered the prognosis to be better than in adults where it ranged from 23 to 66 % in various series [102–104]. In the series of Benk, 18 cranial base and cervical chordomas were treated by incomplete surgery followed by fractionated radiotherapy as a mixture of photons and protons, to doses of between 55.8 and 75.6 CGE (median 69 CGE) [43]. The overall rate of survival progression-free survival at 5 years was 68 and 63 %. The authors considered the morbidity of the technique to be acceptable; two patients developed growth hormone deficiency requiring replacement, one patient developed an asymptomatic necrosis of the temporal lobe at last follow-up and three patients developed unilateral hearing loss.

In our series, all the patients were irradiated except two (one death in the immediate postoperative period, one tumour with rapid progression motivated chemotherapy at the outset). Routine access to proton therapy in our service commenced at the beginning of 2000: all the patients irradiated by photons alone were before 2001; thus, the majority irradiated by protons (alone or in combination with photons) were from 2000. Our series illustrates one of the interesting aspect of proton therapy, the ability to irradiate in higher doses without affecting surrounding healthy tissues in the majority: the average dose used was 55 Gy Eco in patients irradiated with photons alone, compared with 72 Gy Eco in patients irradiated with protons alone.

Of note in our series, 14 patients had tumoral progression. Six out of the seven children who died had been irradiated prior to progression, whilst six of seven survivors had been irradiated after progression. In cases of progression following radiotherapy, one can contemplate focal irradiation (Gamma knife, Cyberknife, Novalis).

47.2.6.3 Chemotherapy

Similar to adults, utilisation of chemotherapy in the management of paediatric chordomas is anecdotal with only 20 or so cases reported in the literature [7, 27, 43, 71, 77, 105–108]. In our series, only four patients had been treated by chemotherapy with disappointing results, all having died in the month following treatment.

Some authors consider that chemotherapy used for sarcomas can also be used in undifferentiated chordomas [77, 109]. The agent most commonly used is ifosfamide, frequently in association with étoposide [71, 105] or doxorubicin [105, 108]. In more recent years, Gleevec® (imatinib mesylate), a specific inhibitor of tyrosine kinase receptors (notably PDGFR α , PDGFR β and KIT), has been used in adults with encouraging results [109]. Whatever the agent used, the indication for chemotherapy differs among authors, but is commonly the last option when all standard treatments (surgery and radiotherapy) are not possible or have failed.

Some very young children have been treated primarily with chemotherapy if the tumour has been considered inoperable or has already metastasised. Unfortunately, all these children died over some weeks to months [27, 71, 106, 108]. Lountzis has reported the only case of disease control with chemotherapy. This was in a 20-month-old child who presented with a clival chordoma extending to C1 with multiple metastases (cutaneous, cerebral, spinal cord, pulmonary, cardiac, hepatic and renal), treated by chemotherapy with cisplatin, doxorubicin, VP-16, vincristine and ifosfamide over 9 months with stability of the tumour. Due to the toxicity of the cumulated effects of the drugs used, second-line treatment with oral VP-16 was used for 24 months resulting in complete remission at 30 months of follow-up [77].

In other reports, chemotherapy has been proposed in cases of progression or recurrence of tumours previously treated with a standard protocol [7, 27, 43, 107]. This treatment seemed to have a benefit in only a small number of cases.

In our series, chemotherapy was not successful in disease control in any of the four children.

None of our patients received ifosfamide-etoposide or ifosfamide-doxorubicin.

Based on recent studies in molecular biology, the tendency has become to use targeted therapies. Only adult series are available. Gleevec® (imatinib) has been utilised in a series of adult patients and infrequently in children (one child in our series). This tyrosine kinase inhibitor is specific for PDGFR α , PDGFR β and KIT which are overexpressed on the surface of chordoma cells [109]; symptomatic and radiological improvement has been observed in adults treated with Gleevec® [109]. Inhibitors of the mTOR pathway (sirolimus) have also been used in cases of resistant chordomas [111]. A partial clinical response has been shown in a patient with metastatic chordoma of the sacrum treated with cetuximab/gefitinib, inhibitors of EGFR [112]. These observations need to be confirmed through large cohort studies with sufficient follow-up. With the exception of Gleevec®, these different agents have not been the subject of paediatric studies.

47.2.6.4 Treatment-Related Morbidity Literature

Even though approximately 250 cases of paediatric chordoma have been reported in the literature, reporting of morbidity from therapy is remarkably lacking. To our knowledge, only three studies have documented treatment-related complications; elsewhere, infrequent descriptions have been published in case reports.

In the series of Wold [7], two patients developed complications following surgery and radiotherapy (hypopituitarism/obesity and epilepsy).

Benk [43] reported 14 % growth hormone deficiency. In others, three developed hearing loss, one patient developed temporal lobe necrosis and one developed temporalis muscle fibrosis following a transmandibular route.

Dhall [105] insists on the importance of an optimal surgical resection despite the morbidity that can ensue. In his series, two children had a subtotal excision with significant postsurgical sequelae (ventilator dependence and tracheostomy, cranial nerve dysfunction, quadriplegia and hemiparesis, swallowing difficulties and gastrostomies), and four children had a partial excision

without notable neurological complications. In our series, one patient had hearing loss, one maxillary hypoplasia and one acute myeloid leukaemia.

Borba [10] reported a perioperative mortality of 12.8 % in children between 5 and 20 years.

Necker-Lariboisière Series

In our series, 13 patients (41.9 %) had complications directly related to surgery. The major morbidity related to aggravation postoperatively of premonitory neurological symptoms: cranial nerve deficits (6.5 % IX and X, 19.4 % XII), cervical nerve roots or Horner's syndrome. One child had a pseudomeningocele from a suboccipital exposure and two had episodes of cerebrospinal fluid leakage from a retrosigmoid approach and an endoscopic transclival approach. Five patients developed postoperative infections – at the operative site ($n=2$) or meningitis ($n=3$) – giving an overall infection rate of 16.1 % in our series. Finally, one patient died from pulmonary complications 9 days following a complete surgical excision.

Cranial nerve dysfunction leading to a gastrostomy occurred in three children and to a tracheostomy in seven. In all patients, these were temporary for a period of several months (5 months for the tracheostomies and 10 months for the gastrostomies).

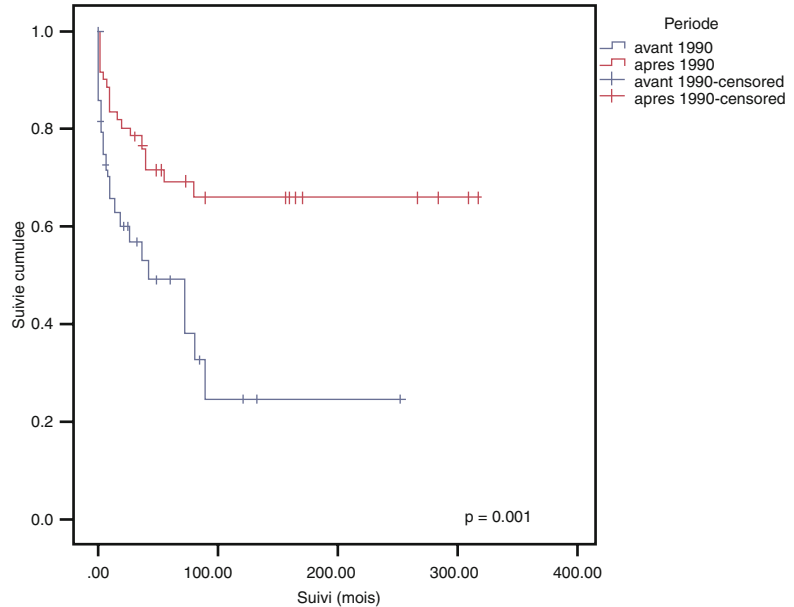
Morbidity from radiotherapy in our series was evidenced as endocrinological and auditory dysfunction. Six patients (19.6 %) developed endocrine insufficiency with panhypopituitarism ($n=2$), growth hormone deficiency ($n=3$) or mixed thyroid and growth hormone deficiency ($n=1$). Four patients developed hearing loss, these in children with large lesions requiring irradiation of the inner ear.

One death in the postoperative period occurred in our series giving an overall surgical mortality of 3.2 %. This was less than that reported in the literature which is approximately 12.8 % according to the paper of Borba [10].

47.2.7 Survival and Prognostic Factors

Globally survival is better in children than in adults except for the aggressive form of chordomas occurring in children under 5 years of age.

Fig. 47.6 Overall survival in the literature of children with chordomas according to period of treatment (before or after 1990)



47.2.7.1 Survival Rates in the Paediatric Population

With an average survival of 6.5 years, the overall survival and disease-free survival at 15 years are 63 and 54.3 %, respectively, in our series. This is similar to the major paediatric series in the literature where the overall survival varies between 56.8 and 81 % (Table 47.2).

In comparing the survival rates of children treated before and after 1990 in the literature, there is a statistically significant difference in overall survival with the more recent cases having a better outcome (Fig. 47.6).

These results observed in the paediatric population are generally better than those seen in adults where the survival varies from 23 to 66 % [102, 103].

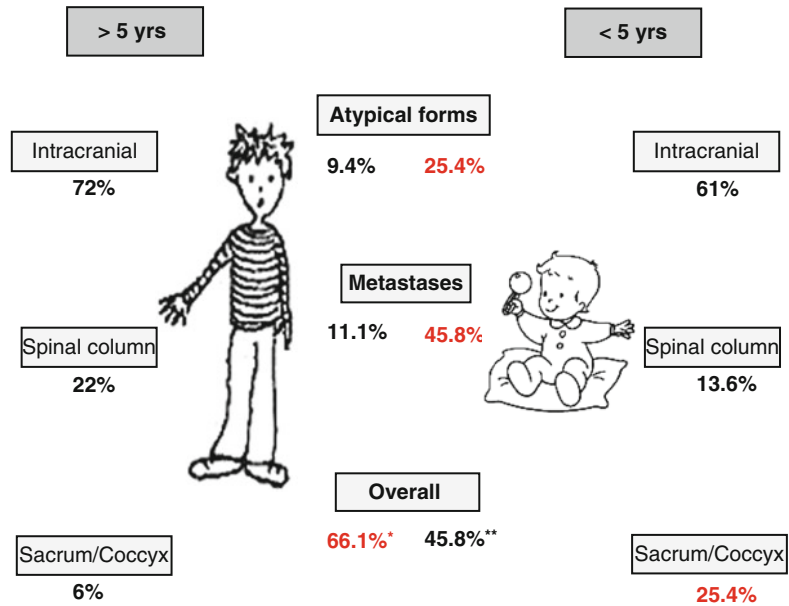
47.2.7.2 Aggressive Form in Young Children

The first prognostic factor identified in chordomas was age of onset, and it is notable in the literature that the worst progression occurs in very young children, particularly those under the age of 5 years [10, 27, 46, 70, 99, 113]; the review of intracranial chordomas by Borba is quite clear on this subject [10]. Age, where children under 5 years are more prone to develop more aggressive tumours, however, is not the only factor

associated with a poorer outcome. Tumour-related factors include:

- The majority of chordomas occur in the sacrococcygeal region. In our review of the literature, 6 % of children greater than 5 years presented with sacrococcygeal tumours; this figure rose to 25.4 % in children less than 5 years of age. Similarly, 68.2 % of children less than 5 years of age had sacrococcygeal chordomas with those intracranial and spinal column involvement in 29.5 % and 23.5 %, respectively.
- Atypical histologies occur predominantly in the younger child; this is probably the least important prognostic factor. In our review, atypical forms represented, respectively, 33.3 %, 6.7 % and 25 % of intracranial, sacrococcygeal and spinal column chordomas in children under 5 years, comparative figures for the over-5-year age group being 7.1, 42.9 and 8 %, respectively. The smaller proportion of atypical forms observed in the children under 5 years with sacrococcygeal chordomas is probably biased by the not insignificant number of unspecified histologies in these patients (46.7 %).
- Metastatic dissemination is more frequent. Borba estimated the rate of metastases to be 57.9 % in the under 5-year-olds, compared to only 8.5 % in patients 5–20 ans. In our review,

Fig. 47.7 Major anatomic, clinical and prognostic differences between children younger and older than 5 years of age according to our review of the literature. *: with an average follow-up of 55.4 months; **: with an average follow-up of 30.1 months



45.8 % of children less than 5 years had metastases compared with 11.1 % in those over 5.

- Finally, overall survival in these children is clearly less than those over 5 years of age. Apart from a few cases, the majority of children less than 5 years died within 18 months following diagnosis despite surgery, radiotherapy and/or chemotherapy [9, 27, 46, 55, 67, 70, 71, 73, 76, 78, 106, 108]. In our review of the literature, 54.2 % of children less than 5 years of age died with an average follow-up of 30.1 months compared with only 33.9 % of children older than 5 years with an average follow-up of 55.4 months.

The differences seen in children younger and older than 5 years from our review of the literature are summarised in Fig. 47.7.

The two children less than 5 years of age included in the Necker-Lariboisière series also presented with rapid progression of their tumour. One died day 9 after an incomplete excision of their lesion due to pulmonary complications. The second presented with a rapidly progressive clival tumour which extended into the spinal column; this patient died 4 months later. In contrast to the majority of children in this age group, these two children had tumours located in the clivus and had not developed metastases (within the limits investigations performed). Both had atypical chordomas histologically.

47.2.7.3 Histological Type

Histological subtype is probably the most important prognostic factor.

In the series of Ridenour [28], the rate of mortality in atypical and undifferentiated forms was 67 %, compared with 27 % on average for conventional and chondroid forms. In the series of Hoch [44], the rate of mortality for conventional, chondroid and poorly differentiated forms were 14, 18 and 83 %, respectively, over an average follow-up of 7.25 years. In the series of Coffin [27], the six patients with the atypical form of chordoma died during follow-up, between 3 weeks and 6 months after diagnosis (the delay was not reported in two patients). The results of our series were similar; we found a significant difference between the overall rates of survival and progression-free survival ($p \leq 0.016$ and $p \leq 0.035$, respectively) related to the histological subtype (classical form compared to the atypical forms).

47.2.7.4 Anatomic Localisation

The primary location of the chordoma in children would seem to be a prognostic factor. In our series, we demonstrated a tendency to a better prognosis in chordomas of the clivus compared to those of the spine. Analysis of the literature would divide this further with intracranial lesions having a better outcome than those in the spinal

column, which have a better outcome than those in the sacrococcygeal region [27, 28, 43].

Our review of the literature confirmed these findings: the rate of survival being 64.5, 45.5 and 50 % at an average follow-up of 54.8, 14.6 and 37.1 months for tumours in intracranial, sacrococcygeal and spinal column locations, respectively.

47.2.7.5 Tumour Volume

Tumour volume is not considered to be a prognostic factor for paediatric chordomas [43]. In fact, it is the degree of tumour extension and its relationship to adjacent structures that constitutes the true prognostic risk.

Conclusion

Chordomas are rare malignant tumours which involve the cranial base and spinal column in children. They are characterised by a high risk of local recurrence. Outcome is generally better than in adults even though there are more aggressive forms in the paediatric population often of atypical histology, freely metastatic, which occur in children under 5 years of age and which progress rapidly.

A major advancement in therapy of these tumours has occurred since 1990, with an analysis of paediatric literature showing a statistically significant improvement in survival before and after 1990 (32.6 versus 66 %, respectively, $p=0.001$).

With 31 cases studied, our series is the largest paediatric surgical series in the literature. The progression-free survival and overall survival rates are 54.3 and 63 %, respectively, at 15 years, and are in accordance with other paediatric series already published. These results have been obtained with a multidisciplinary therapeutic strategy. This strategy consists of as complete a surgical excision as possible followed by radiotherapy, ideally with protons.

Factors associated with an improved outcome as found in the literature include complete tumour excision, classic histology ($p=0.016$ in our series), irradiation and clival

location. In order to obtain a complete surgical excision, it is often necessary to utilise multiple surgical procedures via multiple routes adapted to the site of tumour extension. Progress in MRI, the development of endoscopy has helped improve operative procedures. Surgery, however, remains particularly difficult with low rates of complete excision (19.4 % in our series, 0–34 % in the literature). Utilisation of tracheostomy and/or a gastrostomy may be necessary, albeit temporarily, and are predictable complications associated with multiple surgeries which are often aggressive. Proton therapy has become the adjuvant treatment of choice in chordomas and allows improvement in local control by targeted high dose irradiation. The use of chemotherapy is anecdotal in the literature and in our series; some recent results, however, are encouraging.

Despite the inherent difficulty in treating these tumours, 25.8 and 37.8 % of patients in our series had, respectively, a complete remission or stability of disease at last follow-up. Long-term sequelae when they exist have generally been amenable to specific therapies (hormone replacement, surgery for oculomotor dysfunction, etc.), and the majority of those who survive can attend a normal school with longer-term social and professional lives with minimal.

Surgery and radiotherapy remain the pillars of treatment for chordomas, their ongoing challenges being to be as aggressive as possible without inducing iatrogenic complications. In order to improve the outcome in these patients, there are three promising avenues:

- The quality of surgical excision remains too often disappointing in this rare pathology where it is difficult to develop a real expertise.
- Recent developments in the molecular biology of brain tumours have opened up new developments in targeted therapies.
- Finally, the evaluation of the place of focal re-irradiation in recurrences.

References

- Dahlin DC, Maccarty CS (1952) Chordoma. *Cancer* 5(6):1170–1178
- Krayenbuhl H, Yasargil M (1975) Cranial chordomas. *Prog Neurol Surg* 6:380–434
- Eriksson B, Gunterberg B, Kindblom LG (1981) Chordoma. A clinicopathologic and prognostic study of a Swedish national series. *Acta Orthop Scand* 52(1):49–58
- Mirra JM, Picci P (1989) Bone tumors: clinical, radiologic, and pathologic correlations, vol 1. Lea & Febiger, Philadelphia
- McMaster ML, Goldstein AM, Bromley CM, Ishibe N, Parry DM (2001) Chordoma: incidence and survival patterns in the United States, 1973–1995. *Cancer Causes Control* 12(1):1–11
- Heffelfinger MJ, Dahlin DC, MacCarty CS, Beabout JW (1973) Chordomas and cartilaginous tumors at the skull base. *Cancer* 32(2):410–420
- Wold LE, Laws ER Jr (1983) Cranial chordomas in children and young adults. *J Neurosurg* 59(6):1043–1047
- Nix WL, Steuber CP, Hawkins EP, Stenback WA, Pokorny WJ, Fernbach DJ (1978) Sacrococcygeal chordoma in a neonate with multiple anomalies. *J Pediatr* 93(6):995–998
- Sibley RK, Day DL, Dehner LP, Trueworthy RC (1987) Metastasizing chordoma in early childhood: a pathological and immunohistochemical study with review of the literature. *Pediatr Pathol* 7(3):287–301
- Borba LA, Al-Mefty O, Mrak RE, Suen J (1996) Cranial chordomas in children and adolescents. *J Neurosurg* 84(4):584–591
- Jain SP, Agrawal PK, Jain S, Pandey UC, Samuel KC, Sinha N (1981) Chordoma presenting in the gluteal region in the child. Report of a rare case. *Indian J Cancer* 18(2):160–162
- Tao Z-Z, Chen S-M, Liu J-F, Huang X-L, Zhou L (2005) Paranasal sinuses chordoma in pediatric patient: a case report and literature review. *Int J Pediatr Otorhinolaryngol* 69(10):1415–1418
- Berdal P, Myhre E (1964) Cranial chordomas involving the paranasal sinuses. *J Laryngol Otol* 78:906–919
- Yoneoka Y, Tsumanuma I, Fukuda M et al (2008) Cranial base chordoma—long term outcome and review of the literature. *Acta Neurochir (Wien)* 150(8):773–778; discussion 778
- Dow GR, Robson DK, Jaspan T, Punt JAG (2003) Intradural cerebellar chordoma in a child: a case report and review of the literature. *Childs Nerv Syst* 19(3):188–191
- Chang SW, Gore PA, Nakaji P, Rekate HL (2008) Juvenile intradural chordoma: case report. *Neurosurgery* 62(2):E525–E526; discussion E527
- Figueiredo EG, Tavares WM, Welling L, Rosemberg S, Teixeira MJ (2011) Ectopic pineal chordoma. *Surg Neurol Int* 2:145
- Horton KM, Levey MS, Owl-Smith FA, Azizkhan RG, Schiebler ML (1989) Metastasizing chordoma in early childhood: report of a case at 1.5 T. *Magn Reson Imaging* 7(6):689–691
- Bianchi PM, Marsella P, Masi R et al (1989) Cervical chordoma in childhood: clinical statistical contribution. *Int J Pediatr Otorhinolaryngol* 18(1):39–45
- Jallo J, Nathan D, Bierbrauer K, Farber E (1997) Chordoma: a case report. *Surg Neurol* 48(1):46–48
- Zhou H, Liu Z, Liu C et al (2009) Cervical chordoma in childhood without typical vertebral bony destruction: case report and review of the literature. *Spine* 34(14):E493–497
- Sebag G, Dubois J, Beniaminovitz A, Lelouch-Tubiana A, Brunelle F (1993) Extraosseous spinal chordoma: radiographic appearance. *AJNR Am J Neuroradiol* 14(1):205–207
- Clemons RL, Blank RH, Hutcheson JB, Ruffolo EH (1972) Chordoma presenting as a posterior mediastinal mass. A choristoma. *J Thorac Cardiovasc Surg* 63(6):922–924
- Stratt B, Steiner RM (1980) The radiologic findings in posterior mediastinal chordoma. *Skeletal Radiol* 5(3):171–173
- Niida H, Tanaka R, Tamura T, Takeuchi S (1994) Clival chordoma in early childhood without bone involvement. *Childs Nerv Syst* 10(8):533–535
- Kombogiorgas D, St George EJ, Chapman S, English M, Solanki GA (2006) Infantile clivus chordoma without clivus involvement: case report and review of the literature. *Childs Nerv Syst* 22(10):1369–1374
- Coffin CM, Swanson PE, Wick MR, Dehner LP (1993) Chordoma in childhood and adolescence. A clinicopathologic analysis of 12 cases. *Arch Pathol Lab Med* 117(9):927–933
- Ridenour RV 3rd, Ahrens WA, Folpe AL, Miller DV (2010) Clinical and histopathologic features of chordomas in children and young adults. *Pediatr Dev Pathol* 13(1):9–17
- Luschka PH (1857) Ueber gallertartige Auswüchse am Clivus Blumenbachii. *Arch Für Pathol Anat Physiol Für Klin Med* 11(1):8–12
- Virchow R (1857) Untersuchungen über die Entwicklung des Schädelgrundes. Berlin: Reimer
- Müller (1858) *Z Ration Med* 2:262
- Ribbert H (1895) Ueber die experimentelle Erzeugung einer Ecchondrosis physalifora. *Verh Kong Inn Med* 13:455
- Burrow JLF, Stewart MJ (1923) Original papers: malignant sphenoccipital chordoma. *J Neurol Psychopathol* 4(15):205–217
- Klebs E (1864) Ein Fall von Ecchondrosis sphenoccipitalis amyloacea. *Virchows Arch* 31(3):396–399
- Klebs D (1889) *Handbuch der allgemeinen Pathologie* Jena
- Linck A (1909) Chordoma Malignum. Ein Beitrag zur Kenntnis des Geschwülste an der Schädelbasis. *Zieglers Beitr* 46:573
- Feldmann (1910) Chordoma ossis sacri. *Zieglers Beitr* 43:630

38. André-Thomas J (1923) Chordome de la région sphéno-basilaire. *Rev Neurol* 1:300–304
39. Adson A, Kernohan J, Woltman H (1935) Cranial and cervical chordomas. *Arch Neurol Psychiatry* 33:241–61
40. Argaud R, Lestrade A (1926) Sur la précocité de certains chordomes sacrococcygiens. *Bull Acad Med* 95:375–377
41. Ellis V (1935) Notochordal tumor of cauda equina in a child of 8 years. *Brit Jr Surg* 23:25–30
42. Mixter C, Mixter W (1940) Surgical management of sacrococcygeal and vertebral chordoma. *Arch Surg* 41:408–421
43. Benk V, Liebsch NJ, Munzenrider JE, Efirid J, McManus P, Suit H (1995) Base of skull and cervical spine chordomas in children treated by high-dose irradiation. *Int J Radiat Oncol Biol Phys* 31(3):577–581
44. Hoch BL, Nielsen GP, Liebsch NJ, Rosenberg AE (2006) Base of skull chordomas in children and adolescents: a clinicopathologic study of 73 cases. *Am J Surg Pathol* 30(7):811–818
45. Harvey W, Dawson E (1941) Chordoma. *Edinb Med J* 48(2):713–735
46. Matsumoto J, Towbin RB, Ball WS Jr (1989) Cranial chordomas in infancy and childhood. A report of two cases and review of the literature. *Pediatr Radiol* 20(1–2):28–32
47. Vujovic S, Henderson S, Presneau N et al (2006) Brachyury, a crucial regulator of notochordal development, is a novel biomarker for chordomas. *J Pathol* 209(2):157–165
48. Salisbury JR (1993) The pathology of the human notochord. *J Pathol* 171(4):253–255
49. Higinbotham NL, Phillips RF, Farr HW, Hustu HO (1967) Chordoma. Thirty-five-year study at memorial hospital. *Cancer* 20(11):1841–1850
50. Rich TA, Schiller A, Suit HD, Mankin HJ (1985) Clinical and pathologic review of 48 cases of chordoma. *Cancer* 56(1):182–187
51. Probst EN, Zanella FE, Vortmeyer AO (1993) Congenital clivus chordoma. *AJNR Am J Neuroradiol* 14(3):537–539
52. Mabrey R (1935) Chordoma: a study of 150 cases. *Am J Cancer* 25:501–17
53. Chambers PW, Schwinn CP (1979) Chordoma. A clinicopathologic study of metastasis. *Am J Clin Pathol* 72(5):765–776
54. Soo MY (2001) Chordoma: review of clinicoradiological features and factors affecting survival. *Australas Radiol* 45(4):427–434
55. Nolte K (1979) Malignant intracranial chordoma and sarcoma of the clivus in infancy. *Pediatr Radiol* 8(1):1–6
56. Richards AT, Stricke L, Spitz L (1973) Sacrococcygeal chordomas in children. *J Pediatr Surg* 8(6):911–914
57. Cable DG, Moir C (1997) Pediatric sacrococcygeal chordomas: a rare tumor to be differentiated from sacrococcygeal teratoma. *J Pediatr Surg* 32(5):759–761
58. Al-Adra D, Bennett A, Gill R, Lees G (2011) Pediatric metastatic sacrococcygeal chordoma treated with surgery. *Eur J Pediatr Surg* 21(3):196–198
59. Kozłowski K, Barylak A, Campbell J et al (1990) Primary sacral bone tumours in children (report of 16 cases with a short literature review). *Australas Radiol* 34(2):142–149
60. Shinmura Y, Miura K, Yajima S, Tsutsui Y (2003) Sacrococcygeal chordoma in infancy showing an aggressive clinical course: an autopsy case report. *Pathol Int* 53(7):473–477
61. Congdon CC (1952) Benign and malignant chordomas; a clinico-anatomical study of twenty-two cases. *Am J Pathol* 28(5):793–821
62. Occhipinti E, Mastrostefano R, Pompili A, Carapella CM, Caroli F, Riccio A (1981) Spinal chordomas in infancy. Report of a case and analysis of the literature. *Childs Brain* 8(3):198–206
63. Huang S-M, Chen C-C, Chiu P-C, Lai P-H, Ho J-T, Tseng H-H (2003) Unusual presentation of posterior mediastinal chordoma in a 2-year-old boy. *J Pediatr Hematol Oncol* 25(9):743–746
64. Choi GH, Yang M-S, Yoon DH et al (2010) Pediatric cervical chordoma: report of two cases and a review of the current literature. *Childs Nerv Syst* 26(6):835–840
65. Windeyer BW (1959) Chordoma. *Proc R Soc Med* 52:1088–1100
66. Killampalli VV, Power D, Stirling AJ (2006) Preadolescent presentation of a lumbar chordoma: results of vertebrectomy and fibula strut graft reconstruction at 8 years. *Eur Spine J* 15(Suppl 5):621–625. doi:10.1007/s00586-006-0138-4
67. Sassin JF, Chutorian AM (1967) Intracranial chordoma in children. *Arch Neurol* 17(1):89–93
68. Proyard G, Dony H (1965) Chordoma of the cervical spine. *Acta Chir Belg* 64:132–139
69. Kamrin RP, Potanos JN, Pool JL (1964) An evaluation of the diagnosis and treatment of chordoma. *J Neurol Neurosurg Psychiatry* 27:157–165
70. Kaneko Y, Sato Y, Iwaki T, Shin RW, Tateishi J, Fukui M (1991) Chordoma in early childhood: a clinicopathological study. *Neurosurgery* 29(3):442–446
71. Auger M, Raney B, Callender D, Eifel P, Ordóñez NG (1994) Metastatic intracranial chordoma in a child with massive pulmonary tumor emboli. *Pediatr Pathol* 14(5):763–770
72. Plese JP, Borges JM, Nudelman M, Lefèvre AB, Sallum J (1978) Unusual subarachnoid metastasis of an intracranial chordoma in infancy. *Childs Brain* 4(4):251–256
73. Sen CN, Sekhar LN, Schramm VL, Janecka IP (1989) Chordoma and chondrosarcoma of the cranial base: an 8-year experience. *Neurosurgery* 25(6):931–940; discussion 940–941
74. Garofalo E, Minerva A, Baltieri G (1976) Sacrococcygeal chordoma in a 19-month-old boy. *Minerva Pediatr* 28(31):1909–1914
75. Worthy T (1965) Sacrococcygeal chordoma – two cases with unusual features. *Clin Radiol* 16(4):412–413
76. Nakamura Y, Becker LE, Marks A (1983) S100 protein in human chordoma and human and rabbit notochord. *Arch Pathol Lab Med* 107(3):118–120

77. Lountzis NI, Hogarty MD, Kim HJ, Junkins-Hopkins JM (2006) Cutaneous metastatic chordoma with concomitant tuberous sclerosis. *J Am Acad Dermatol* 55(2 Suppl):S6–10
78. Schneegans E, Mandigas M (1938) Hydrocephalie non communicante due a un chordome malin. *Bull Soc pédiat* 36:535–38
79. Amendola BE, Amendola MA, Oliver E, McClatchey KD (1986) Chordoma: role of radiation therapy. *Radiology* 158(3):839–843
80. Berson AM, Castro JR, Petti P et al (1988) Charged particle irradiation of chordoma and chondrosarcoma of the base of skull and cervical spine: the Lawrence Berkeley Laboratory experience. *Int J Radiat Oncol Biol Phys* 15(3):559–565
81. Taylor R, Eldridge P, Errington R, Jones B, Punt J, Spooner D (2000) Proton therapy for base of skull chordoma: a report of the Royal College of Radiologists. *Clin Oncol* 12:75–79
82. Carpentier A, Polivka M, Blanquet A, Lot G, George B (2002) Suboccipital and cervical chordomas: the value of aggressive treatment at first presentation of the disease. *J Neurosurg* 97(5):1070–1077
83. Lanzino G, Dumont AS, Lopes MB, Laws ER Jr (2001) Skull base chordomas: overview of disease, management options, and outcome. *Neurosurg Focus* 10(3):E12
84. Cage TA, Clark AJ, Aranda D et al (2013) A systematic review of treatment outcomes in pediatric patients with intracranial ependymomas. *J Neurosurg Pediatr* 11(6):673–681
85. Puget S, Garnett M, Wray A et al (2007) Pediatric craniopharyngiomas: classification and treatment according to the degree of hypothalamic involvement. *J Neurosurg* 106(1 Suppl):3–12
86. Menezes AH (2008) Craniovertebral junction neoplasms in the pediatric population. *Childs Nerv Syst* 24(10):1173–1186
87. Kennedy JD, Haines SJ (1994) Review of skull base surgery approaches: with special reference to pediatric patients. *J Neurooncol* 20(3):291–312
88. Inagaki H, Anno Y, Hori T, Ohama E (1992) Clival chordoma in an infant; case report and review of the literature. *No Shinkei Geka* 20(7):809–813
89. Arana-Iñiguez R, Castillo LA, Benedek P, Folle JA (1968) Transoral approach in clivus and high cervical chordomas. *Acta Neurol Latinoam* 14(1):65–73
90. Handa J, Suzuki F, Nioka H, Koyama T (1987) Clivus chordoma in childhood. *Surg Neurol* 28(1):58–62
91. Nagib MG, Wisol ES, Simonton SC, Levinson RM (1990) Transoral labiomandibular approach to basiocciput chordomas in childhood. *Childs Nerv Syst* 6(3):126–130
92. Schamschula RG, Soo MY (1993) Clival chordomas. *Australas Radiol* 37(3):259–264
93. Chivukula S, Koutourousiou M, Snyderman CH, Fernandez-Miranda JC, Gardner PA, Tyler-Kabara EC (2013) Endoscopic endonasal skull base surgery in the pediatric population. *J Neurosurg Pediatr* 11(3):227–241
94. Hickman ZL, McDowell MM, Barton SM, Sussman ES, Grunstein E, Anderson RCE (2013) Transnasal endoscopic approach to the pediatric craniovertebral junction and rostral cervical spine: case series and literature review. *Neurosurg Focus* 35(2):E14
95. Tuite GF, Veres R, Crockard HA, Sell D (1996) Pediatric transoral surgery: indications, complications, and long-term outcome. *J Neurosurg* 84(4):573–583
96. Tewfik HH, McGinnis WL, Nordstrom DG, Latourette HB (1977) Chordoma: evaluation of clinical behavior and treatment modalities. *Int J Radiat Oncol Biol Phys* 2(9–10):959–962
97. Reddy EK, Mansfield CM, Hartman GV (1981) Chordoma. *Int J Radiat Oncol Biol Phys* 7(12):1709–1711
98. Habrand JL, Bondiau PY, Dupuis O, Lévy-Piedbois C, Marin JL, Oberlin O (1997) Late effects of radiotherapy in children. *Cancer Radiother* 1(6):810–816
99. Hug EB, Sweeney RA, Nurre PM, Holloway KC, Slater JD, Munzenrider JE (2002) Proton radiotherapy in management of pediatric base of skull tumors. *Int J Radiat Oncol Biol Phys* 52(4):1017–1024
100. Igaki H, Tokuyue K, Okumura T et al (2004) Clinical results of proton beam therapy for skull base chordoma. *Int J Radiat Oncol Biol Phys* 60(4):1120–1126
101. Habrand J-L, Bolle S, Datchary J et al (2009) Proton beam therapy in pediatric radiotherapy. *Cancer Radiother* 13(6–7):550–555
102. O'Connell JX, Renard LG, Liebsch NJ, Efirid JT, Munzenrider JE, Rosenberg AE (1994) Base of skull chordoma. A correlative study of histologic and clinical features of 62 cases. *Cancer* 74(8):2261–2267
103. Mitchell A, Scheithauer BW, Unni KK, Forsyth PJ, Wold LE, McGivney DJ (1993) Chordoma and chondroid neoplasms of the sphenoid-occiput. An immunohistochemical study of 41 cases with prognostic and nosologic implications. *Cancer* 72(10):2943–2949
104. Nielsen G, Rosenberg A, Liebsch N (1996) Chordomas of the base of skull in children and adolescents: a clinicopathologic study of 35 cases. *Mod Pathol* 9:11A
105. Dhall G, Traverso M, Finlay JL, Shane L, Gonzalez-Gomez I, Jubran R (2011) The role of chemotherapy in pediatric clival chordomas. *J Neurooncol* 103(3):657–662
106. Brooks M, Kleefeld J, O'Reilly GV, Haykal HA, MacLeod M (1987) Thoracic chordoma with unusual radiographic features. *Comput Radiol* 11(2):85–90
107. Chetty R, Levin CV, Kalan MR (1991) Chordoma: a 20-year clinicopathologic review of the experience at Groote Schuur Hospital Cape Town. *J Surg Oncol* 46(4):261–264
108. Scimeca PG, James-Herry AG, Black KS, Kahn E, Weinblatt ME (1996) Chemotherapeutic treatment of malignant chordoma in children. *J Pediatr Hematol Oncol* 18(2):237–240

109. Casali PG, Messina A, Stacchiotti S et al (2004) Imatinib mesylate in chordoma. *Cancer* 101(9): 2086–2097
110. Fleming GF, Heimann PS, Stephens JK et al (1993) Dedifferentiated chordoma. Response to aggressive chemotherapy in two cases. *Cancer* 72(3):714–718
111. Stacchiotti S, Marrari A, Tamborini E et al (2009) Response to imatinib plus sirolimus in advanced chordoma. *Ann Oncol* 20(11):1886–1894
112. Hof H, Welzel T, Debus J (2006) Effectiveness of cetuximab/gefitinib in the therapy of a sacral chordoma. *Onkologie* 29(12):572–574
113. Yadav YR, Kak VK, Khosla VK, Khandelwal N, Radotra BD (1992) Cranial chordoma in the first decade. *Clin Neurol Neurosurg* 94(3):241–246

Pathologies in Pediatric Posterior Fossa Tumors: Rare Tumors

M. Memet Özek

M.M. Özek, M.D.
Division of Pediatric Neurosurgery,
Acibadem University, School of Medicine, Istanbul, Turkey

Nobuhito Morota, Toshihiro Kumabe,
and Akiyoshi Kakita

48.1 Introduction

Posterior fossa choroid plexus tumors (CPTs) are quite unusual tumors for pediatric neurosurgeons to encounter. It is rare not only in terms of tumor prevalence in the ventricular system but also rare in terms of age-dependent tumor location in CPTs. However, it is important to remind and differentiate CPTs before surgery of more common posterior fossa tumors in and around the fourth ventricle since surgical tactics, tumor vascularity, and postoperative management of the tumor are quite different.

The term CPT consists of two pathologies, choroid plexus papilloma (CPP) and carcinoma

(CPC). In addition, a tumor which presents some malignancy in pathology but does not fulfill the criteria of CPC is called atypical CPP. A recently reported meta-analysis of CPTs collected 857 documented cases: among them, CPP accounted 495 cases (58 %), CPC 347 cases (40 %), and atypical CPP 15 cases (2 %) [101]. Other lesions such as choroid plexus cyst and diffuse villous hyperplasia can develop pathological condition in the posterior fossa, but only one choroid plexus cyst in the vermis has been published yet [41, 72].

In this chapter, we focus on CPTs in the posterior fossa and describe their clinical features with special emphasis on the surgical anatomy and tactics. It should be reminded that any series of CPTs in the posterior fossa are too small in number that makes general statement in clinical issues difficult.

N. Morota, M.D. (✉)

Division of Neurosurgery, National Medical Center for Children and Mothers, National Center for Child Health and Development,
2-10-1 Okura, Setagaya, Tokyo 157-8535, Japan
e-mail: morota-n@ncchd.go.jp

T. Kumabe, M.D.

Department of Neurosurgery,
University of Kitasato, School of Medicine,
1-15-1 Kitasato, Minami-ku, Sagami-hara,
Kanagawa 252-0374, Japan
e-mail: kuma@kitasato-u.ac.jp

A. Kakita, M.D., Ph.D.

Department of Pathology and Resource Branch for Brain Disease Research CBBR, Brain Research Institute, University of Niigata, School of Medicine,
1 Ashahi-machi, Chuo-ku, Niigata 951-8585, Japan
e-mail: kakita@bri.niigata-u.ac.jp

48.2 General Remarks

The incidence of CPT is about 0.5 % in all intracranial tumors [2, 91]. They account for about 2–4 % of the brain tumors that develop in pediatric population [32]. The incidence increases up to 10–20 % among the brain tumor in the first year of life [39, 50, 76, 99]. Although the data is old, Laurence collected the published data before 1974 and reported that 45 % of CPTs presented in the first year of life, which reaches 74 % among the first decades of life [52]. Not a small number of

reports have described congenital CPTs [1, 10, 18, 55, 73, 84, 93]. CPTs comprise 7.9 % of prenatally diagnosed fetal brain tumors [85]. In general, it is widely noted that more than 70 % of CPTs develop in childhood and more than 50 % are diagnosed under the age younger than 2 years [27].

The ratio of CPPs in the previous reports, probably some of them including atypical CPP, out-numbers CPCs with the rate of 3–5:1 [2, 48, 91, 99]. CPCs are more common among pediatric population predominantly under the age of 2 years. The lateral ventricle is the main location where the CPC in childhood develops [49, 50, 86, 99].

The main location of CPTs in the posterior fossa is in the fourth ventricle, followed by the cerebellopontine (CP) angle. CPTs in the fourth ventricle seem rare in children and occur commonly among adult patients. The majority of CPTs in pediatric population develop in the lateral ventricle (79 %) and are followed by the fourth (14 %) and third ventricle (7 %) [35, 95]. In other reports subjecting CPTs in pediatric population, one paper reported only one CPP in the fourth ventricle among 16 CPTs and the other 5 from the fourth ventricle and 3 from the CP angle among 38 CPTs [23, 76]. A latest paper described four posterior fossa CPTs among 37 CPTs [50]. Contrary to CPTs in the lateral ventricle, those in the fourth ventricle distribute in all age group [2, 76, 99]. It is reported that the median age of CPTs in the lateral and third ventricle is 1.5 years old while that in the fourth ventricle 22.5 years old. CPTs in the CP angle are even older as 35.5 years old [99]. The CP angle CPT is reported to associate with older age, benign histology, and female gender predominance [99]. CPTs in the CP angle can arise directly from the choroid plexus tuft through the foramen of Luschka or are formed by drop metastasis or seeding along the CSF pathway. The latter two compiles a subgroup of the CPT which are called as extraventricular CPTs [15]. A very unusual manifestation of bilateral CP angle CPPs has been reported [9, 21]. There have been reports of extraventricular CPTs arising from the cerebellar hemisphere as an intraparenchymal mass [37, 85].

Clinical presentation of CPTs in the posterior fossa is location dependent and similar to those

tumors observed more commonly in the posterior fossa. Hydrocephalus and associated signs and symptoms are present if the fourth ventricle CPT is large enough to obstruct the CSF flow [53]. Other findings associated with posterior fossa CPTs would be signs of brain stem compression, cranial nerve paresis, and cerebellar dysfunction [28].

48.3 Anatomy

The choroid plexus is derived from the ventricular epithelium. Embryologically, differentiation of the choroid plexus from the ventricular ependyma starts at around 6 weeks gestation from the fourth ventricle. The lateral ventricle is the next place where the choroid plexus appears and followed by the third ventricle [72]. Initially, the roof plate of the fourth ventricle consists of a single layer of ependymal cells. The ventricular surface of the ependymal layer is covered by a vascular-rich mesenchyme layer and both layers give rise to the tela choroidea. The vascular-rich mesenchyme shows high proliferation activity and invaginates to protrude into the fourth ventricle. The invaginated tissue from the tela choroidea forms the choroid plexus whose shape is compared to a cauliflower [52].

The role of the choroid plexus is highly specialized to produce cerebrospinal fluid (CSF) in the central nervous system (CNS). As is shown embryologically deprived from vascular mesenchyme, the choroid plexus is a vascular-rich tissue. Its capillaries have a unique structure known as fenestrated, noncontinuous capillary wall. Contrary to the adjacent choroid plexus epithelial cell which has tight junctions, the fenestrated endothelial cell of the choroid plexus capillaries allows free movement of small molecules through the fenestration [72]. Histologically, the cuboidal epithelium covered the surface of the choroid plexus. Surface area of the choroid plexus is further expanded by a well-developed brush border on the ventricular side of the cuboidal epithelium layer.

The choroid plexus attached the ventricular wall tightly and vascular loops enter the epithelium of the choroid plexus through the attachment. The attachment of the choroid plexus to the

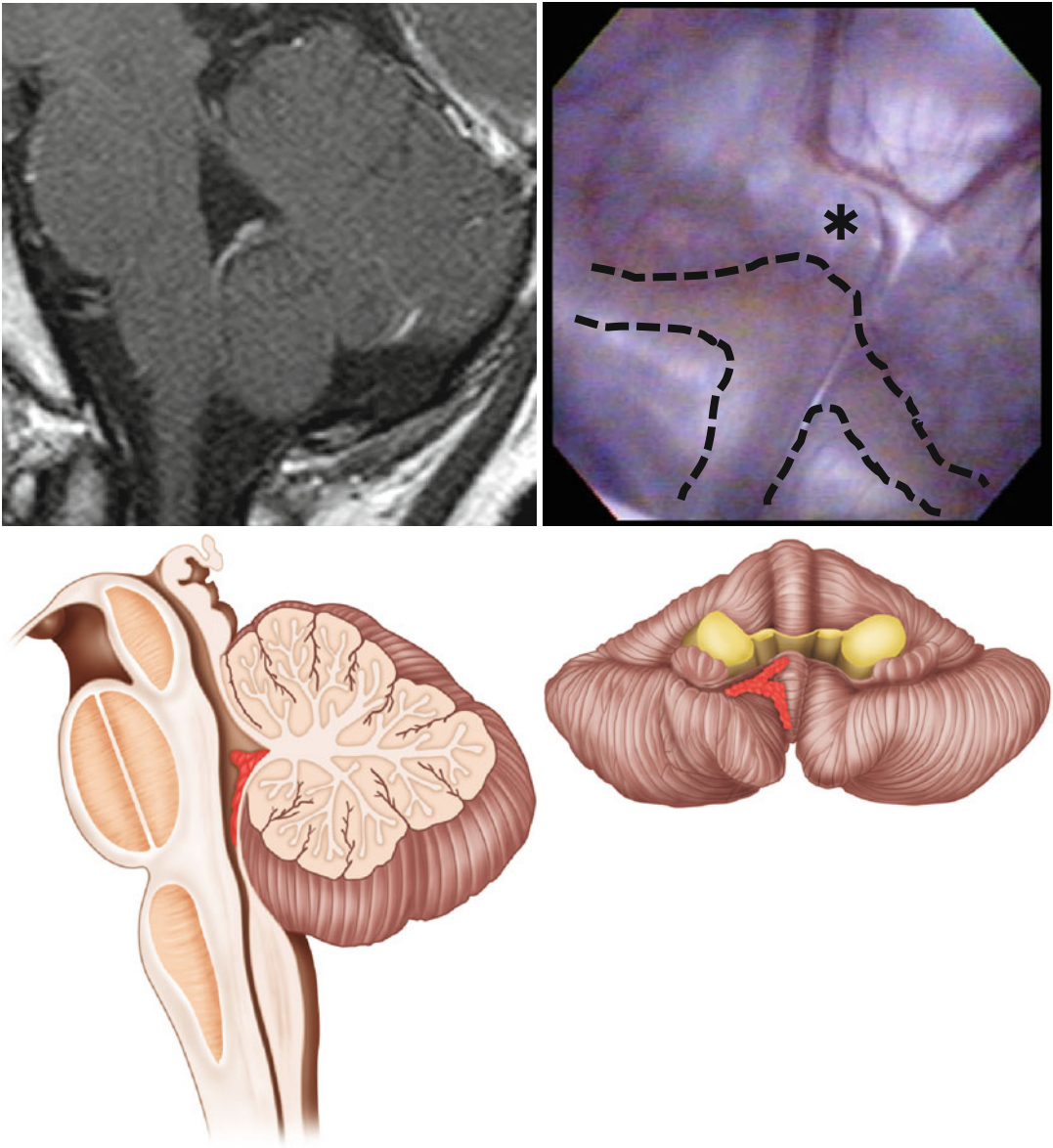


Fig. 48.1 Choroid plexus: normal shape and location. The rostral end of the choroid plexus locates at the fastigium and extends to caudal and lateral directions on the inferior velum. The choroidal plexus can be observed on MRI gadolinium-enhanced T1WI in the midsagittal image as a linear enhancement along the surface of the inferior velum (above *left* and lower *left*). The above *right* photograph shows the roof of the

fourth ventricle and choroid plexus taken during an endoscopic surgery for Dandy-Walker syndrome. The shape of the choroid plexus looks like two inverted L-shaped fringes that form a T shape (*dotted line*, choroid plexus; *, fastigium). The lower *right* scheme shows the right choroid plexus observed from the ventral side (*, fastigium)

ventricle wall forms a linear structure on the ventricular wall, which is called the taenia choroidea. Other parts of the choroid plexus move freely in the CSF as a willow that trembles in the breeze.

The choroid plexus in the posterior fossa attaches on the roof of the fourth ventricle (Fig. 48.1). There is variety in size and shape of the choroid plexus in the fourth ventricle. The

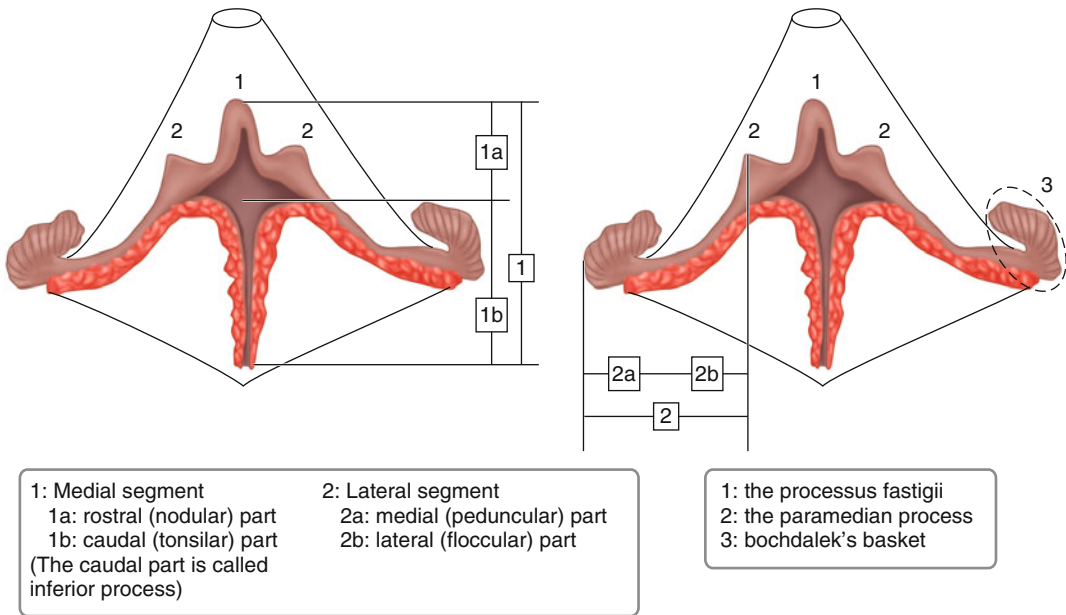


Fig. 48.2 Choroid plexus: normal shape and anatomy. *Left:* the choroid plexus is superimposed on the floor of the fourth ventricle. The choroid plexus is divided into two segments, medial and lateral one. *Left:* the medial segment is further divided into a rostral or nodular part and a caudal or tonsillar part. The paramedian process presents inferolateral side of the processus fastigii. The

caudal part is called inferior processes. There is a plexus-free central space between the medial segments of each choroid plexus. *Right:* the lateral segment of the choroid plexus is subdivided into a medial or peduncular part and a lateral or floccular part. The choroid plexus out of the foramen of Luschka is called Bochdalek's baskets due to its shape

shape of the choroid plexus in the fourth ventricle is not simple compared with that in the lateral and third ventricles. It looks like two inverted L-shaped fringes that form a T shape when it is observed dorsally (Fig. 48.2). However, its actual shape is more complicated like an opened umbrella or a bat opening its wings. The rostral end of the choroid plexus locates at the fastigium and extends to caudal and lateral directions on the inferior velum. No choroid plexus exists rostral to the fastigium, meaning no choroid plexus on the superior velum [51, 82].

The choroid plexus is divided into two segments, medial and lateral one (Fig. 48.2). The medial segment is further divided into a rostral or nodular part and a caudal or tonsillar part [82]. The rostral part consists of the processus fastigii at its rostral top forming a nodule which connects bilaterally the choroid plexus. The paramedian process presents the inferolateral side of the processus fastigii. The caudal part is called inferior processes. The caudal end of the inferior process often goes down out of the foramen of

Magendie. There is a plexus-free central space between the medial segments of each choroid plexus [51].

The choroid plexus extends laterally from the paramedian process. The lateral segment of the choroid plexus is subdivided into a medial or peduncular part and a lateral or floccular part [82]. The tip of the lateral segment of the choroid plexus projects through the foramen of Luschka to the cerebellopontine angle cistern. The choroid plexus out of the foramen of Luschka is called Bochdalek's baskets due to its shape. The choroid plexus at the foramen of Luschka turns sharply toward the rostromedial direction [51]

The shape of the choroid plexus can be compared to a human body, like the processus fastigii as a head, the paramedian process as a shoulder, the peduncular part of the lateral segment as an arm, the floccular part as a hand, and the inferior process as a leg.

Vascular supply to the choroid plexus mainly comes from the posterior inferior cerebellar artery

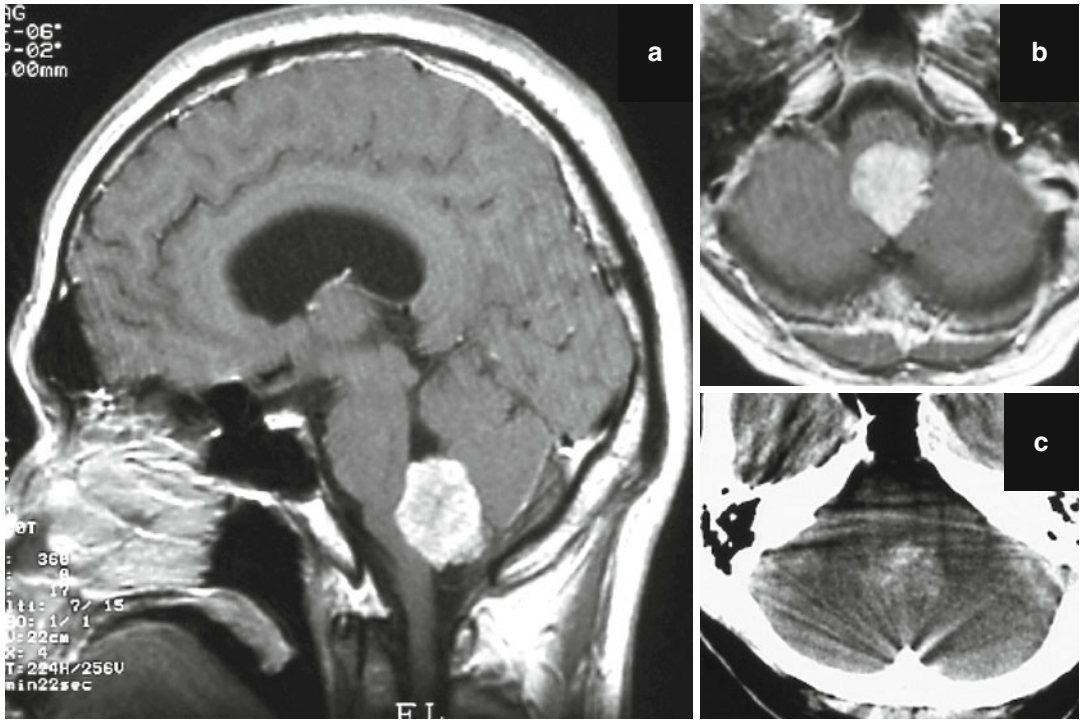


Fig. 48.3 Fourth ventricular choroid plexus papilloma. MRI gadolinium-enhanced T1WI sagittal (a) and axial (b) views and a plain CT axial view (c)

(PICA). Most of the medial segment and the paramedian part of the lateral segment of the choroid plexus are fed by arterial branches which originate from the telovelotonsillar segment of the PICA. It means that the midline structure of the choroid plexus as well as the tela choroidea in the fourth ventricle is supplied by the PICA, which runs paramedian the ventral surface of the tonsil. The lateral part of the lateral segment receives vascular supply from the anterior inferior cerebellar artery (AICA), especially from its caudal trunks. Vascular supply to the choroid plexus from the AICA is supplemental to the PICA. The AICA gives rise to branches where the PICA does not reach [83].

48.4 Radiology

Diagnostic tools for CPTs are either computed tomography (CT) or magnetic resonance images (MRI). MRI is preferred to CT in terms of no radiation exposure in children. However, CT still remains the initial diagnostic tool for screening

because of its clinical convenience. A normal choroid plexus is shown as iso-gray density on CT and iso-gray intensity on MRI. If the choroid plexus is calcified, the part of calcification is depicted as punctuated foci of high density on CT and hypointensity on MRI. Absence of the blood-brain barrier due to fenestrated epithelium of the choroid plexus capillaries results in homogeneous enhancement of the choroid plexus after intravenous injection of contrast materials on CT and MRI [28, 38].

The neuroradiological feature of the posterior fossa CPT is the same with other locations (Figs. 48.3 and 48.4). Most of the CPTs present as iso- or high-density mass in the ventricle, while some shows low or mixed density on CT. Associated calcification is observed in about 25 % of the CPTs. The tumor demonstrated iso- or hypointense mass on T1-weighted MRI and heterogeneous hyperintensity on T2-weighted one [28, 38, 96]. The tumor is generally large in size and spherical in shape. Some CPTs contain cystic component in the tumor. Detailed observation

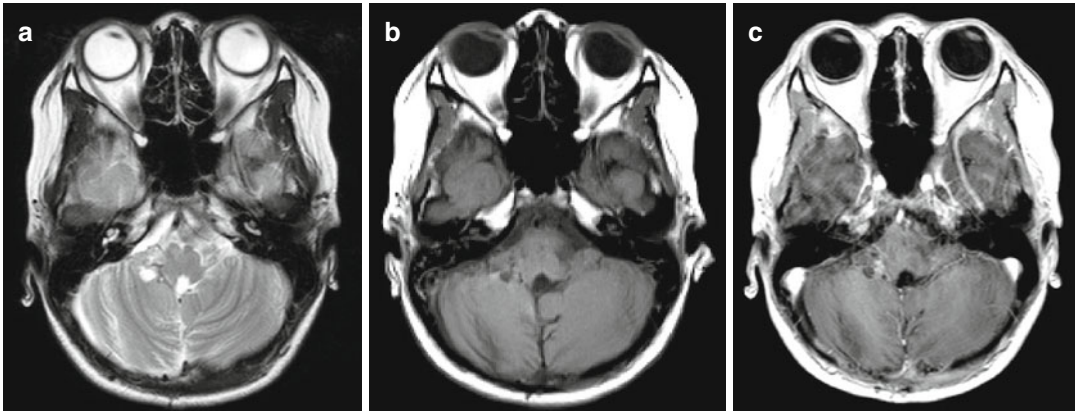


Fig. 48.4 Cerebellopontine angle atypical choroid plexus papilloma. Heterogeneously enhanced tumor is observed in the *right* cerebellopontine angle. (a) T2WI, (b) T1WI without contrast enhancement, (c) T1WI with

gadolinium enhancement (Courtesy of Takaaki Yanagisawa, Associate Professor, Department of Neuro-oncology, Saitama Medical University International Medical Center)

may reveal lobulated surface with heterogeneous proliferation in cauliflower shape in the ventricular side. The tumor attaching the ventricular wall may be well demarcated, but the border could be obscured due to parenchymal invasion and subsequent peritumoral edema. The CPT demonstrates marked contrast enhancement on CT and MRI. Enhancement pattern is usually homogeneous, but nodular or cystic enhancement could be involved [28].

Differentiation of CPTs from other tumors in the fourth ventricle depends on its shape as cauliflower surface, MRI imaging pattern, location in the fourth ventricle, and hypervascularity [79]. Since the choroid plexus locates in the lower half of the fourth ventricle below the fastigium, CPTs usually do not extend to the aqueduct unless they grow larger [96]. Instead, enlarged CSF space presents rostral to the tumor in the fourth ventricle due to the CSF obstruction and overproduction by the tumor (Fig. 48.5). On MRI, irregular-shaped signal voids indicating enlarged blood vessel are not unusually observed. The sign is a relatively specific finding compared with other more common posterior fossa tumors in childhood such as medulloblastoma and ependymoma, but could be observed as a more immature tumor like atypical teratoma/rhabdoid tumor (AT/RT) in the posterior fossa. Presence of signal voids in the CPT strongly alarms hypervascularity of the tumor, and surgeons should

be prepared to shut down the vascular supply before tumor resection. Apart from signal void in the tumor, enlarged vessels feeding the tumor can be described as signal void in the ventricle around the tumor capsule.

CPPs in the CP angle can arise bilaterally. There is a report of a middle-aged woman whose atypical CPP mimicked neurofibromatosis 2 with multiple lesions along the craniocervical region [9]. Another adolescent case showed bilateral CP angle CPPs associated with diffuse craniospinal extension [21].

There are no definitive characteristic or specific findings to differentiate CPPs from CPCs. Nevertheless, some findings such as extensive parenchymal invasion and presence of marked peritumoral vasogenic edema in the white matter tend to suggest that the tumor is more likely the CPC than CPP, but the finding is not a definitive one and could be associated with the CPP [7, 16, 75, 90]. Other findings favor the diagnosis of the CPC: irregular contour of the tumor surface, mixed density/intensity with variable enhancement pattern, and presence of cysts and hemorrhage within the tumor [7, 61, 90]. Presence of disseminated tumor would strongly support the preoperative diagnosis of CPC [61].

Currently, MRI is being established as the diagnostic imaging study of choice in pediatric brain tumors. In CPTs, MRI demonstrates detailed ana-

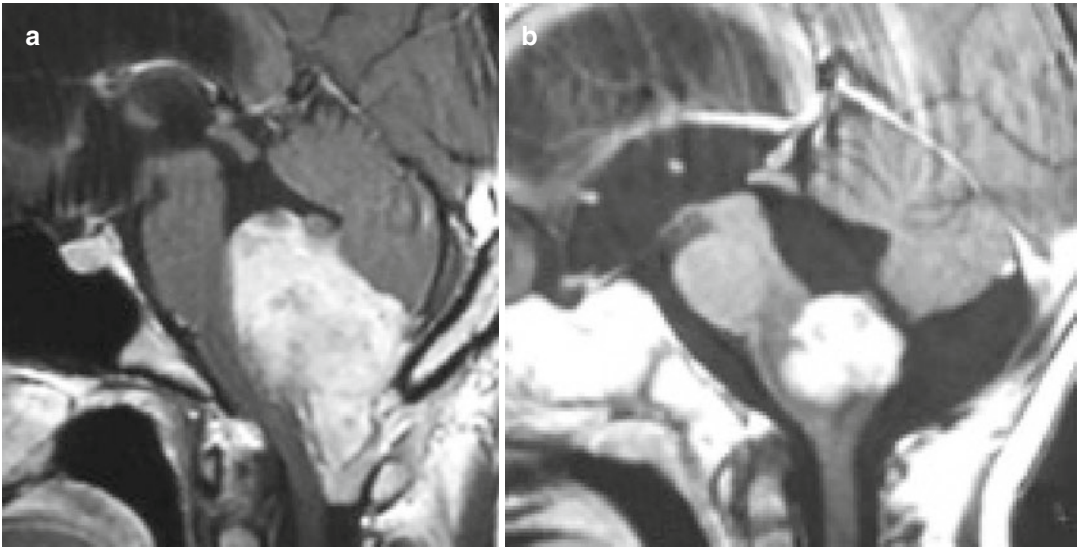


Fig. 48.5 Extension of choroid plexus tumor. The tumor locates caudal to the fastigium and the rostral half of the fourth ventricle is enlarged by associated hydrocephalus.

Note that the tumor tends to infiltrate into the floor of the fourth ventricle regardless of its size (*left*, adult choroid plexus carcinoma; *right*, pediatric choroid plexus carcinoma)

tomical relationship with the tumor and surrounding neural structures in multiplanar images. MR angiography enables to reveal 3D relationship between the tumor and main feeding arteries and is taking place for the conventional transfemoral angiography [28]. Detail of the vascular supply to the CPT in the fourth ventricle has been described in the anatomy section in this chapter.

48.5 Pathology

48.5.1 Histopathological Features

(Fig. 48.6)

According to the WHO classification of tumors of the nervous system, primary tumors of the choroid plexus are classified as CPP (WHO grade I), atypical CPP (grade II), and CPC (grade III) [76]. There are no remarkable histopathological differences between choroid plexus tumors in the fourth ventricle and those in other ventricular systems.

CPP resembles the native choroid plexus, showing an orderly layer of columnar epithelium on a basement membrane that overlies delicate fibrovascular stalks (Fig. 48.6a). The cells have sometimes higher cellular density and are more

columnar and more varied in nuclear size (Fig. 48.6b) than those of the normal choroid plexus epithelium. Transition of the neoplasm to normal choroid plexus is common. Almost all well-differentiated CPPs are overtly papillary; however, there are exceptional cases showing acinar or tubular features, in part [3, 5]. CPP commonly exhibits focal glial differentiation in the form of elongated glial fibrillary acidic protein (GFAP)-positive cells with tapering processes [11]. Other interesting features are pigmentation [97], oncocyctic change [11], calcification, xanthomatous change, and bone [23] and cartilage sclerosis (Fig. 48.6c) [11]. Large CPP may inexplicably have foci of necrosis, presumably infarction, without any other anaplastic features. Tumors of the fourth ventricle may be heavily calcified.

Atypical CPP constitutes a group that is intermediate between well-differentiated papilloma and obvious carcinoma. They exhibit significant cytologic atypia, increased nuclear to cytoplasmic ratios, and variable number of mitotic figures (Fig. 48.6d). A follow-up study of 124 choroid plexus tumors suggested that atypical CPP can be distinguished from CPP on the bases of mitotic activity—two or more mitotic figures in ten high-power fields [44]. Foci of necrosis are not uncommon.

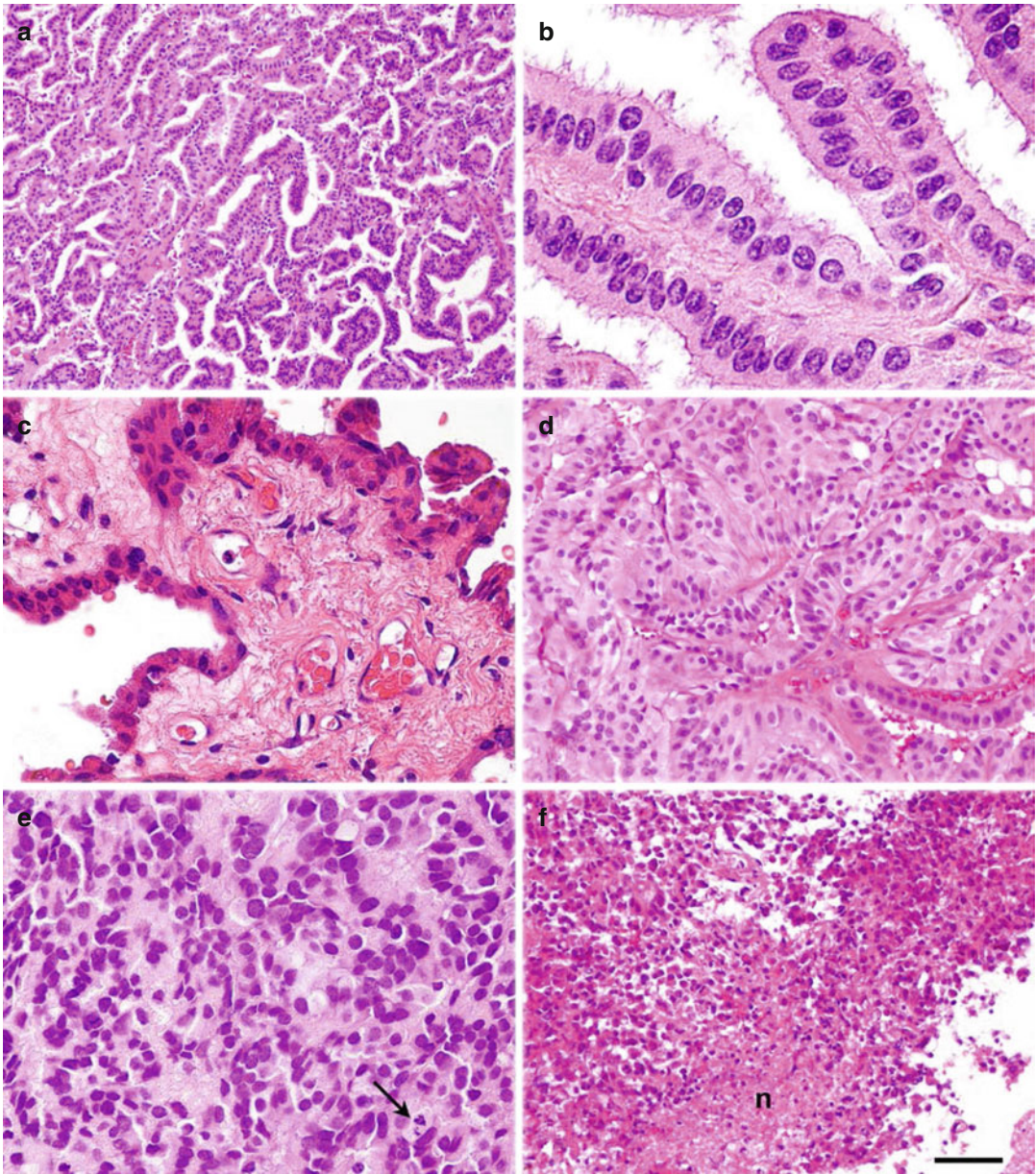


Fig. 48.6 Histopathological features of choroid plexus tumors. Choroid plexus papilloma (CPP) in the fourth ventricles (**a–c**) of a 31-year-old woman (**a, b**) and a 43-year-old woman (**c**), atypical CPP in the fourth ventricle of a 60-year-old woman (**d**), and choroid plexus carcinoma (**e, f**) in the lateral ventricle of a 14-year-old girl (**e**) and in the fourth ventricle of a 1-year-old boy (**f**). (**a**) A low-power view shows fibrovascular papillary structures lined by bland cuboidal to columnar epithelial cells. (**b**) A higher-magnification view demonstrates the cuboidal epithelial cells with flatter apical surfaces and

increased nuclear to cytoplasmic ratios. (**c**) The fibrovascular stroma shows sclerotic change with proliferation of connective tissue. (**d**) A tumor lesion with highly differentiated, clear epithelium, but with scattered mitoses, possessing difficulty to place into either papilloma or carcinoma category. (**e**) A lesion showing increased cellular density, nuclear atypia, a mitotic figure (*arrow*), and blurring of the papillary pattern. (**f**) An area of highly cellular proliferation of small, anaplastic cells with necrosis (**n**). (**a–f**) Hematoxylin and eosin stain. Bar = (**a**) 120 μ m, (**b**) 20 μ m, (**c**) and (**e**) 30 μ m, and (**d**) and (**f**) 60 μ m

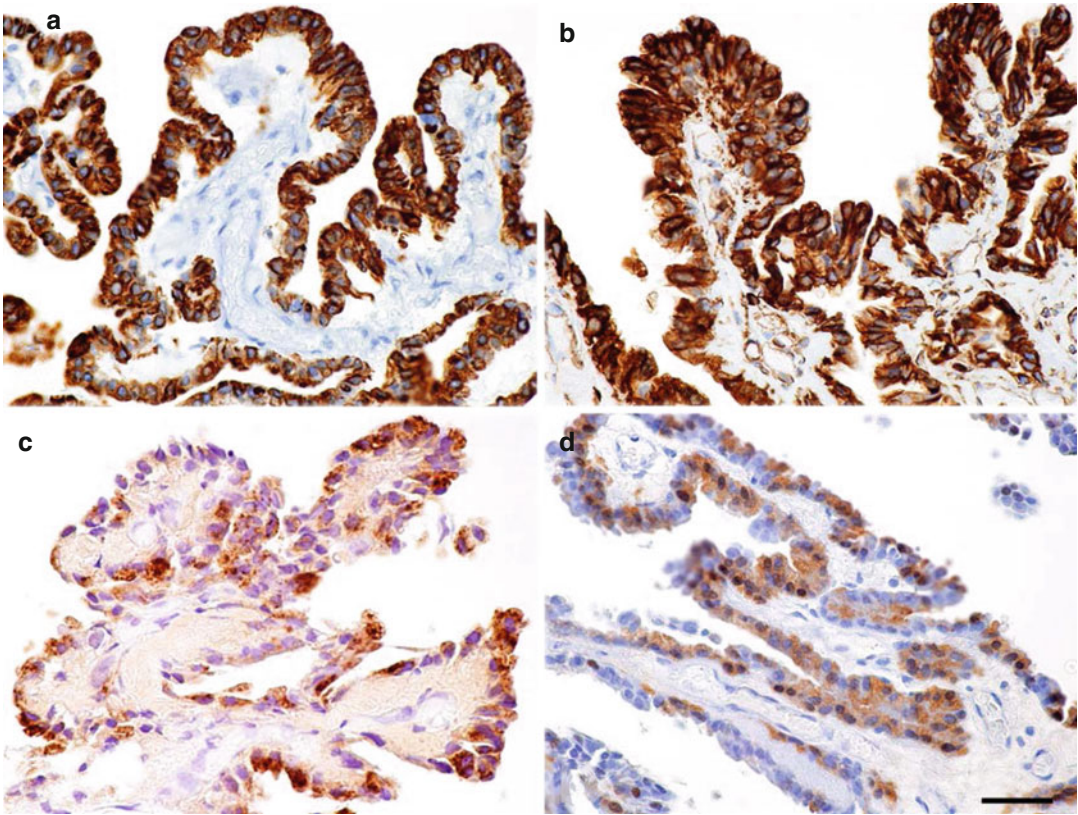


Fig. 48.7 Immunohistochemical profiles. A CPP in the fourth ventricle of a 43-year-old woman. Almost all of the epithelial cells are strongly labeled with antibodies against cytokeratin (a) and vimentin (b). The cytoplasm of a large

proportion of the cells is reactive for S-100 protein (c) and transthyretin (d) in granular and dot-like patterns. (a–d) Immunostaining with diaminobenzidine as the chromogen. Bar = (a–d) 40 μ m

One study suggests that atypical CPPs behave like CPPs rather than CPCs [65].

The CPC demonstrates apparently anaplastic features. The cells are no longer constrained to a simple columnar epithelium, but form solid masses in variable proportions to the papillary component (Fig. 48.6e). Nuclear atypia is obvious, mitoses are abundant, and necrosis is common (Fig. 48.6f). Hyaline protein droplets may be seen. Sometimes, there are anaplastic lesions composed of sheets of cells with perinuclear halos that lend a somewhat oligodendroglial appearance. Other anaplastic features with complex architectural arrangements of rhabdoid cells, creating confusion with AT/RT. CPCs may invade the brain through the ependymal lining.

48.5.2 Immunohistochemistry (Fig. 48.7)

CPTs express cytokeratins (Fig. 48.7a), vimentin (Fig. 48.7b), synaptophysin, and podoplanin and often GFAP, S-100 protein (Fig. 48.7c), and epithelial membrane antigen [40], presumably indicating hybrid, epithelial-neuroepithelial nature of the choroid plexus epithelium.

Several studies have indicated the diagnostic utility of immunoreactivity of the choroid plexus for prealbumin (synonymous: transthyretin) [42]. Both neoplastic and normal choroid plexus epithelia are reactive for prealbumin (Fig. 48.7d). Since occasional metastatic carcinomas are positive, staining for transthyretin cannot be considered entirely as choroid plexus specific [6].

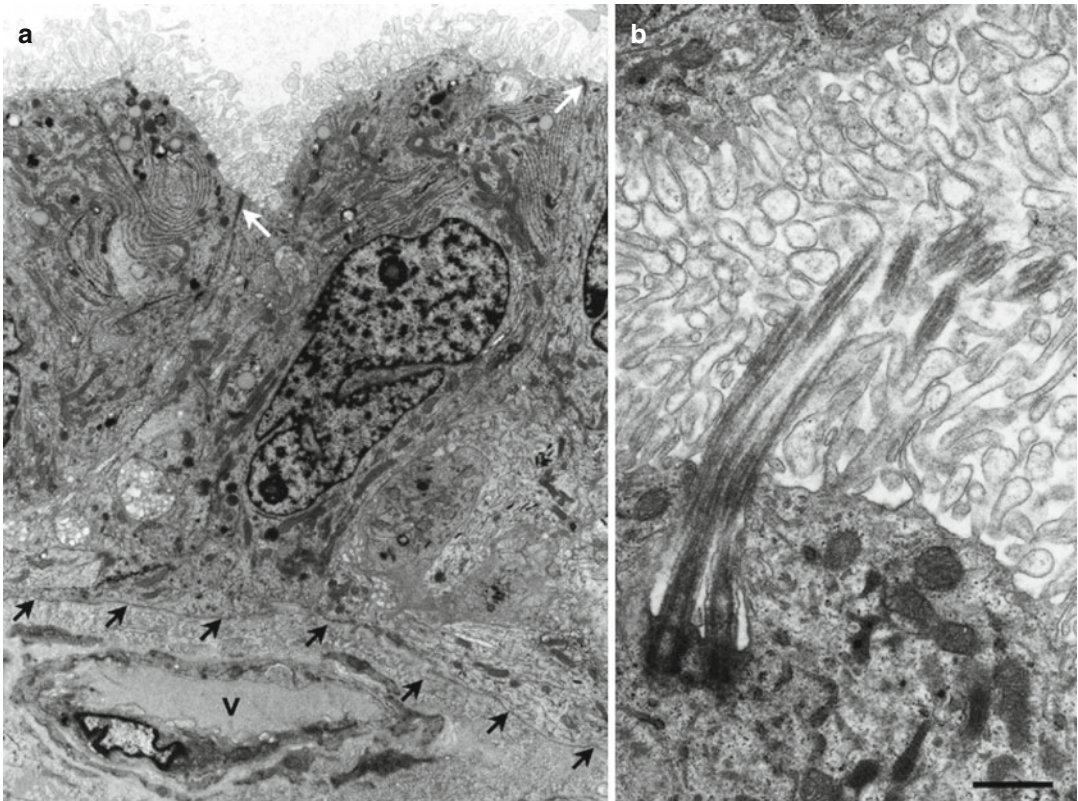


Fig. 48.8 Electron micrographs of CPP in the fourth ventricle of a 43-year-old woman. (a) The cells showing a distinct apical (*upper*)-basal (*lower*) orientation with abundant apical microvilli. The cytoplasm of the cells contains abundant mitochondria and parallel stacks of rough endoplasmic reticulum. The basal surface is covered by

basement membrane (*black arrows*). Abundant collagen and a capillary vessel (v) are seen underneath the basement membrane. The apical surfaces of adjacent cells are joined by junctional complexes (*white arrows*). (b) A higher-magnification view demonstrates cilia projecting from the apical surface of the cell. Bar = (a) 3 μm and (b) 0.6 μm

A clinicopathological study has demonstrated that CPCs in children are characterized by a higher MIB-1 labeling index and greater cell cycle dysregulation than CPPs [14]. In another study, the MIB-1 index was less than 10 % in 73 % of CPPs, but never above 25 %. No CPC had an index less than 10 %, and 69 % of malignant tumors had indices greater than 25 % [13].

48.5.3 Ultrastructure (Fig. 48.8)

The ultrastructural appearances of CPP are closely similar to those of the normal choroid plexus, suggesting that the neoplastic cells may have retained the ability to produce CSF. The cells rest upon basal laminae, interdigitate lateral

cell membranes, grasp adjacent cells by desmosomes and regular apical junctional complexes, produce occasional bundled intermediate filaments, and project both apical microvilli and scattered cilia [31, 57].

48.5.4 Differential Diagnosis on Histological Sections

Many CPCs arise in young children. In this clinical setting, a malignant papillary tumor in a ventricle is highly likely to be a CPC, since metastatic carcinomas from visceral organs are solely rare in children. On the other hand, intraventricular metastatic papillary carcinoma in adults becomes an important consideration. Metastasis to the choroid

plexus in situ is rare but well documented [80]. Immunoreactivity for cytokeratin does not distinguish metastatic carcinoma and CPC, but when combined with positivity for S-100 protein and synaptophysin, strongly favors a primary CPT, as does the rate occurrence of GFAP staining in better-differentiated examples. The majority of CPTs have a cytokeratin (CK) 7-positive/CK20-negative immunophenotypes; therefore, these profiles may be useful in differentiating these lesions from metastatic carcinomas [40]. Complicating this issue is that positivity for prealbumin has been noted in some metastatic carcinomas [4, 6]. Antibodies Ber-EP4 and HEA-25 may be useful because only a rare CPC is positive for either antibody [34]. Synaptophysin is diffusely positive in many choroid plexus tumors, but may be also present in metastases. In some instances, only the diagnosis of high-grade papillary carcinoma can be rendered, with resolution of the problem left to a search for a systemic primary.

Solid, nonpapillary variants of CPC can resemble AT/RT. The CPC affects mainly young children but is not as likely as AT/RT to present in infancy. At present, immunostain for INI-1 is thought to be useful for identifying AT/RT, as this antigen should be lost from the nuclei of tumor cells in that tumor but retained in most of all CPCs [46].

The distinction between the CPC and small-cell embryonal tumor is not always easy, particularly if the carcinoma is largely undifferentiated, but even then, the CPC may show pleomorphic cellular features. Embryonal carcinomas are characteristically positive for placental alkaline phosphatase and CD30. In medulloepithelioma, the primitive epithelioid-appearing cells are typically negative for cytokeratin.

Papillary ependymoma infrequently enters the differential diagnosis of CPTs because ependymoma showing epithelial-papillary pattern only throughout the resected specimen seems quite rare.

48.6 Treatment Strategy

Matson once mentioned in his textbook that “optimum treatment of papilloma of the choroid plexus consists of total excision with the least possible damage to normal brain tissue” [56].

The total removal of tumor still remains the major goal for curative treatment of CPTs. Because the extent of surgical resection of CPTs is the single most determinant factor for long-term survival, radical resection of the tumor must be attempted in all children with CPTs. The challenge in surgical resection of CPTs stems from the fact that the tumor is highly vascularized and hemorrhagic. Thus, obliteration of vascular supply before tumor resection is ideal but not always possible. Possible choices of treatment for controlling intraoperative hemorrhage are:

1. Preoperative embolization of the feeding artery
2. Neoadjuvant chemotherapy
3. Intraoperative coagulation of the feeding artery

Preoperative embolization of CPTs in the posterior fossa is not straightforward because of the tortuous nature of the choroidal branch from the PICA/AICA and its close proximity to the brain stem. Previous successful reports for preoperative embolization of CPTs in childhood mostly located in the lateral and the third ventricles [20, 71, 74, 77]. In addition, bilateral embolization is required for the CPT in the fourth ventricle. Despite recent advancement of endovascular treatment, preoperative embolization of CPTs in the posterior fossa seems difficult for practical use.

Neoadjuvant chemotherapy seems a more reliable, promising treatment for CPTs. Chemotherapy before radical resection of CPTs helps reduce intraoperative bleeding and tumor size and thus contributes to gross total resection of the tumor and subsequent prognosis [36, 49, 80, 89]. From a surgical viewpoint, marked reduction of the tumor vascularity is the main advantage for radical resection. Chemotherapy alone is not curative, but the use of chemotherapy after biopsy or failed radical resection would allow more complete tumor resection in the second stage surgery [49, 89].

Whatever the treatment is applied before surgery, surgeons should pay every effort to shut down the vascular supply to the CPTs intraoperatively by coagulation, if possible, before starting tumor resection. For this purpose, the cerebello-medullary fissure needs to be opened widely to access bilateral PICA vermian branches where

feeding choroidal arteries to the fourth ventricle CPTs originate [83]. If the CPT locates in the cerebellopontine angle, standard retromastoid lateral approach would be sufficient, but more basal approach can be required for large tumor to locate the AICA beforehand.

48.7 Surgery

48.7.1 Surgical Anatomy

The CPT in the fourth ventricle usually presents in the lower half of the fourth ventricle along the midline. Extension of the CPT toward the upper half of the fourth ventricle to the aqueduct seems unusual since the choroid plexus doesn't exist rostral to the fastigium. The CPT tends to extend caudally as the tumor grows larger through the foramen of Magendie. It is important to be reminded that the upper half of the floor of the fourth ventricle can be secured if the tumor is detached from the cerebellar vermis in the early stage of the surgery.

Despite the fact that the CPT grows from the choroid plexus tissue attached on the roof of the fourth ventricle, the tumor can infiltrate to the brain stem as it grows larger. Preoperative finding of high signal intensity in the brain stem by MRI T2WI is a warning sign which strongly suggests tumor invasion to the fourth ventricle floor.

Vascular supply to the CPT in the fourth ventricle comes from the bilateral PICAs which feed the tumor from the ventrolateral direction. Those feeders should be cut in the cerebellomedullary fissure after the arteries to the brain stem are branched.

In general, the CPT originates from the lower half of the fourth ventricle roof and hangs in the ventricular space in the early stage. As the CPT grows, it compresses or attaches the floor of the fourth ventricle and can invade into the brain stem if the tumor is likely to be malignant. The CPT tends to extend caudally through the foramen of Magendie. The upper half of the fourth ventricle to the aqueduct often remains tumor free. Instead, the space would be enlarged due to associated hydrocephalus.

48.7.2 Surgical Approach

Surgical approach to the CPT in the fourth ventricle is the same with that of more common pediatric brain tumors which locate in the fourth ventricle. The choice of intradural approach to the tumor is the transcerebellomedullary fissure approach instead of the traditional vermis splitting one [26, 33, 58, 59, 70]. Postoperative mutism that could happen after the vermis splitting approach would be avoided by the transcerebellomedullary fissure approach [78].

Detail of the surgical procedure regarding the transcerebellomedullary fissure (Telovelar) approach has been described elsewhere [58, 59, 70]. We describe the procedure when it is applied for the surgery of the CPT in the fourth ventricle.

A midline skin incision is made from theinion to C2. Cervical muscle layers are divided on the midline and dissected from the occipital bone. The C1 lamina is exposed. The C1 laminectomy is required whenever the CPT is large and a secured extensive surgical field is preferred. Two burr holes are opened on the occipital bone, one on each sides, and suboccipital craniotomy is performed. Lateral edge of the foramen magnum is resected. The dura is opened between the foramen magnum and C1 lamina. The subarachnoid space has sufficient space and the venous sinus doesn't exit this part of the dura. The dura can be safely opened without damaging the neural tissue even if the tumor is large and the cerebellum is compressed dorsally. After copious cerebrospinal fluid (CSF) is drained and the dura over the cerebellar hemisphere became slack, both rostrrolateral ends of the dura are opened easily. The dura is incised toward the center of the foramen magnum and three incisions are connected to form a Y-shaped incision after shutting down the venous sinuses. Care should be paid to preserve abnormally enlarged draining veins whenever they were observed.

An operative microscope is introduced for the intradural procedure hereafter (Fig. 48.9). The tonsil is elevated and retracted laterally so that the cerebellomedullary fissure is opened widely. A slightly pinky or brownish dark-colored tumor with granular surface is exposed. The tela choroidea is incised along the taenia choroidea. Any vascular supply to the tumor from the PICA needs to be

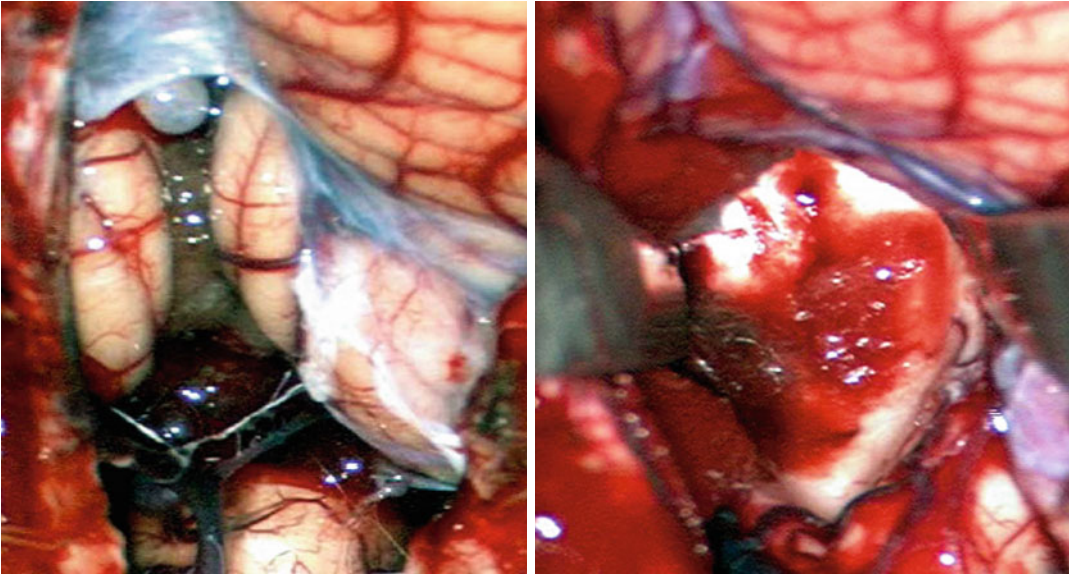


Fig. 48.9 Intraoperative photograph of choroid plexus papilloma in the fourth ventricle. *Left:* a brownish dark-colored tumor is observed between the cerebellar tonsils. Enlarged draining veins run on the cervical cord toward

the caudal direction. *Right:* the tumor attachment on the floor of the fourth ventricle is shown after gross total resection of the tumor (same patient with Fig. 48.3)

coagulated and cut while the branches to the brain stem be preserved. The tumor is detached from the inferior velum where it attaches. By this step, most of the vascular supply to the tumor is reduced markedly and debulking of the tumor becomes much easier [48]. Tumor debulking at this stage directs not to the ventral but to the rostral side so that the CSF space in the upper half of the fourth ventricle is opened. Once the rostral border of the tumor is confirmed, the rostral side of the floor of the fourth ventricle is secured. It is critical to avoid injury to the floor of the fourth ventricle (Figs. 48.9 and 48.10). The dissection plane connecting the rostral normal floor of the fourth ventricle and the obex is assumed, and the tumor resection using an ultrasonic surgical aspirator is resumed paying special attention not to cross the dissection plane. It should be reminded that the CPT tends to infiltrate on the surface of the fourth ventricle irrespective of the tumor size. Meticulous dissection technique enables gross total resection of the tumor when the tumor infiltration is limited on the surface of the fourth ventricular floor (Fig. 48.10).

Application of the intraoperative neurophysiological procedure such as brain stem mapping or

the monitoring of the corticobulbar tract motor evoked potential (MEP) would help accomplish sufficient tumor resection while preserving function of cranial motor nuclei [17, 22, 67–69]. Tumors attaching the floor of the fourth ventricle can be left untouched for functional preservation.

If the tumor is large enough to extend from the fourth ventricle to the CP angle, skull base approach such as transcondylar fossa approach would suffice for tumor resection [60]. Standard retromastoid suboccipital approach is chosen for surgical resection of the primary CP angle CPT [103].

The basic principle of the posterior fossa CPT surgery would be summarized as follows:

1. Early reduction of vascular supply
2. Tumor detachment from the cerebellum
3. Preservation of brain stem and/or cranial nerve function

48.7.3 Intraoperative Neurophysiology

Intraoperative neurophysiology can help avoid damage to the cranial motor nuclei and nerves during surgery in and around the brain stem [17,

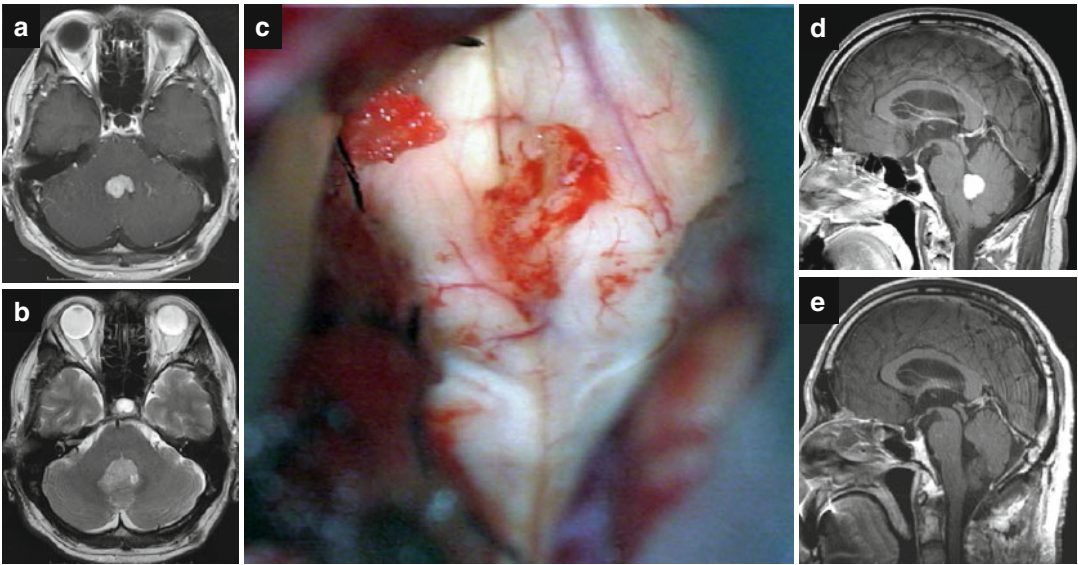


Fig. 48.10 Intraoperative photograph of choroid plexus papilloma in the fourth ventricle. (a) Preoperative MRI T1WI axial view with gadolinium enhancement, (b) preoperative MRI T2WI axial view, (c) intraoperative photograph after tumor resection, (d) preoperative MRI T1WI sagittal

view with gadolinium enhancement, (e) postoperative MRI T1WI sagittal view with gadolinium enhancement. Note that even this relatively small choroid plexus papilloma infiltrates on the surface of the fourth ventricle floor. Meticulous dissection technique enables gross total resection of the tumor

22, 67–69]. Surgery involving the floor of the fourth ventricle places the cranial motor nuclei at risk of direct damage. Brain stem mapping can locate the cranial motor nuclei on the floor of the fourth ventricle before tumor resection, thus can avoid direct damage during surgical manipulation. In addition, monitoring the corticobulbar tract MEP reflects the functional integrity of the cranial motor nerve. Combination of both procedures would give the neurosurgeon the best chance to preserve critical brain stem function with optimal tumor resection [69]. Whenever the CPT in the fourth ventricle involves its floor or the CPT locates in the CP angle, application of intraoperative neurophysiology should be considered.

48.7.4 Management of Hydrocephalus

Hydrocephalus can be associated with the CPT in the fourth ventricle and, some case, that in the CP angle [19, 48]. Pathogenesis of hydrocephalus in the CPT can be multifactorial [76, 80]. Hydrocephalus is caused by either or both overproduction of CSF [66], obstruction of the CSF pathway by tumor itself (in case of the fourth ventricle

CPT), or tumor compression (in case of the CP angle CPT) [87]. Complex interaction of CSF overproduction and partial restriction of the CSF flow is suggested for the pathogenesis of hydrocephalus in CPPs [81]. Impaired CSF absorption can be another pathogenesis of hydrocephalus in neonate and infant cases [63]. Functional obstruction at the level of the arachnoid granulations due to the high CSF protein and/or compressed subarachnoid space due to long-standing hydrocephalus can contribute to the disturbed CSF absorption [77]. Therefore, like the CPT in the supratentorial location, resection of the CPT does not always promise the resolution of hydrocephalus.

Hydrocephalus, typically triventricular enlargement, associates almost all cases of the posterior fossa CPT [39]. It is expected that the rate of shunt dependency might be lower than other locations because other clinical presentations such as brain stem and cerebellar dysfunction develop in the early stage due to narrow posterior fossa. However, in Kumabe's report of 5 CPTs in the fourth ventricle, two patients required treatment of hydrocephalus. Compared with more than 75 % association of hydrocephalus and high shunt dependency that ranged from

24 % to 78 % in all CPTs, the ratio of hydrocephalus and VP shunt requirement seems approximately the same in the posterior fossa CPTs [27, 43, 48, 54, 77]. It should be noted that only one pediatric case in Kumabe's series developed hydrocephalus and had endoscopic third ventriculostomy (ETV) [48]. Pediatric patients with posterior fossa CPTs may have higher risk of developing hydrocephalus than adults.

Management of pre- and postoperative hydrocephalus is the same with the one associated with other posterior fossa tumors. Special consideration would be necessary in case of CPCs since remote dissemination could happen to the abdomen after VP shunt [62]. ETV would be preferred to VP shunt if the situation allows its indication.

48.7.5 Surgical Outcome

Even in the era of modern neurosurgery, intraoperative death due to hemorrhage seems not necessarily unusual. Intraoperative death in some reports ranges from 5 % to 13 % [24, 49, 77]. Overall operative mortality rate reaches unignorable level of about 30 % [27, 54]. Further investigation reveals that most of those ominous cases are located in the lateral ventricle, the pathology is predominantly CPCs, and the tumor is large in size. The cause of bleeding is most likely from the tumor itself but in selected case injury of the midline deep draining veins at the last stage of surgery [77].

It seems that such fatal bleeding, though the tumor is highly vascularized, can be an unusual encounter in case of posterior fossa CPTs. Early obliteration of the feeding arteries would be possible if appropriate surgical approach is chosen and massive venous bleeding looks less likely to happen. Nevertheless, surgeons should be prepared for critical situation beforehand.

48.8 Postoperative Management of the CPT (Adjuvant Therapy)

There is wide agreement that if the CPP is completely resected, no further treatment is required. Adjuvant therapy is required for the incompletely resected CPCs. Controversy remains in case of

incompletely resected CPPs or completely resected CPCs.

Chemotherapy for CPCs is not curative but can contribute to improve overall prognosis. Survival following complete resection and adjuvant therapy of CPCs varies from about 60–90 %, and the survival rate is better than those with complete resection without adjuvant therapy [29]. Efficacy of chemotherapy comes from marked reduction of tumor vascularity and results in reduction of tumor volume [36, 80, 88, 89]. Fibrosis and collagenization within the tumor have been also evidenced in a recent report [49]. There are several choices of chemotherapy agents. Platinum agents seem to play a central role in recent regimens with the combination of other agents [30, 49]. Recently published data derived from meta-analysis reached a conclusion that chemotherapy was highly significantly linked to better prognosis [101].

Radiation remains a part of adjuvant therapy in older children with CPCs. Survival time of the CPC after recurrence was significantly better in those who had received irradiation than those without irradiation [99, 101]. Response to irradiation in recent study revealed its efficacy, and irradiation is strongly recommended even after gross total resection of CPCs [98, 101]. Impact of stereotactic radiosurgery for the CPT in the posterior fossa has not been established.

Postoperative adjuvant therapy may play a critical role for the posterior fossa CPT since aggressive surgical resection could be unachieved by brain stem involvement. All CPCs require adjuvant therapy regardless of the amount of tumor resection by surgery. Chemotherapy for young children and chemo- and radiotherapy for older children are the modality of adjuvant therapy for children with CPCs [8, 25, 99, 101]. Neoadjuvant therapy followed by a second look surgery would be another choice of treatment strategy [49].

A different approach would be appropriate for CPPs. Aggressive surgical resection promises the best prognosis in almost all CPPs [94]. No universal agreement exists on what the treatment of choice for incompletely resected CPPs, which could happen in the case of posterior fossa CPPs. Recurrence or metastasis of CPPs, although

unusual for pediatric patients, has been reported [12, 45, 64]. However, based on the fact that prognosis at the time of recurrence remains acceptable, “wait and see” policy is recommended [99]. Probably, this conservative attitude and reoperation with or without adjuvant therapy would be sufficient for CPPs left in the brain stem.

48.9 Prognosis

Prognosis of pediatric CPTs in the posterior fossa would depend on two factors as those in other locations. The one is the extent of surgical resection. Difference from CPTs in other locations comes from the fact that the brain stem invasion modifies surgical respectability irrelevant for the tumor pathology. Another factor is the pathology of CPTs.

CPPs are surgically curable tumors that have 1-, 5-, and 10-year projected survival rates which account for 90 %, 81 %, and 77 %. When the tumor is completely resected, the expected 10-year survival reaches 85 %, while those who had incomplete resection fall 56 % [99]. In another paper, 5-year local control, distant brain control, and overall survival of CPP are described as 84 %, 9 %, and 97 %. Complete surgical resection results in 100 % local control which is much better than incompletely resected group with 68 % local control at 5 years [47]. Metastasis of CPP in the posterior fossa is quite unusual, but there have been two case reports published [45, 64]. Both are adult cases: one originated in the fourth ventricle and another in the CP angle.

Prognosis of atypical CPP is favorable but stays slightly worse than that of CPP [102]. Age distribution of atypical CPP is significantly younger than those with CPP or CPC. Complete resection was achieved in more than 60 % and the 5-year event free survival was 83 %, again much better than CPC but slightly worse than CPP. Rapid growth of a cystic atypical CPP at the time of recurrence has been reported [92]. Wrede concluded that atypical CPP responded favorably to chemotherapy, and its intermediate position between CPP and CPC in terms of clinical feature and outcome was supported [102].

Prognosis of CPCs remains in an unsatisfactory level. One-, 5-, and 10-year projected survival rates are 71, 41, and 35 %, far behind those in CPPs. Still, radical surgical resection is desirable whenever possible since a 2-year survival rate reaches 72 % in completely resected group, while those with incomplete resection stay 34 % [99]. Other papers reported similar 5-year survival rate of 26–40 % [8, 77].

As is expected, prognosis of CPTs in the fourth ventricle could be poorer than those in other locations since the tumor infiltrating the brain stem is unresectable and most surgeries fall in the group of incomplete resection at best. However, there is only one reported series and its result is not disappointing. Kumabe’s report of five patients (2 CPPs and 3 CPCs, with four brain stem invasions on MRI) resulted in one total resection and four subtotal to partial resections. All three CPCs had adjuvant therapies and two CPPs with subtotal resection received no adjuvant therapy. During the follow-up that ranged from 23 to 130 months (average 64 months), none of them showed tumor progression [48]. In addition, there are two reports which treated predominantly adult patients and thus included more CPTs in the fourth ventricle [47, 103]. Adjuvant therapy was done only for CPCs or for subtotally resected recurrent CPPs. “Wait and see” policy for incompletely resected CPPs and adjuvant therapy for all CPCs would be a strategic approach for CPTs in the fourth ventricle.

Regarding CPTs in the CP angle, CPP is a more frequent pathology [99]. Thus, better prognosis is expected, but there has been no published data focused on the prognosis of CPTs in this specific location.

48.10 CPT-SIOP-2000

The latest prospectively collected data from the CPT-SIOP-2000 can bring critical change in terms of treatment protocol for the CPT in the future [100]. This international study included 163 patients (CPP 57, APP 49, CPC 57). The gross total resection was achieved in 79 % of CPPs, 92 % of atypical CPPs, and 61 % of CPCs.

A controversial result was revealed that the 2-year overall survival in the gross totally resected CPCs was 67 % while that in partial resection 83 %. It means that the extent of surgical resection does not necessarily reflect the prognosis of CPCs. Instead, the impact of chemotherapy could be a more influential factor for survival of CPCs [50, 100]. Further study is required, but it should be reminded that the role of surgery could be modified by the recent advancement of chemotherapy.

48.11 Summary

Rare occurrence of the tumor, rare occurrence of the location, and, furthermore, rare occurrence of age distribution make it difficult to reach any specific conclusions in terms of pediatric posterior fossa CPTs. However, general tendency of surgical outcome and prognosis seems the same with the CPT in other locations. Kumabe's series of five patients, though four of them were adults and three including one child were CPCs, is encouraging because all patients remained progression free even after subtotal or partial resection of the tumor [48]. Recent advancement of chemo- and radiotherapies would enable the tailored surgery for the posterior fossa CPT when it involves the brain stem.

From the surgical viewpoint, the surgeon should be prepared for the following for the surgery of fourth ventricle CPTs:

1. Preoperative diagnosis of tumor infiltration to the fourth ventricle. If the tumor infiltration is strongly suggested by MRI, application of intraoperative neurophysiology would help preserve the critical brain stem function.
2. Early reduction of vascular supply to the tumor during surgery. Preoperative embolization seems impractical for the posterior fossa CPT, but chemotherapy as a neoadjuvant therapy can contribute to reduce tumor vascularity.
3. Application of transcerebellomedullary approach for wide exposure of the tumor and vascular supply from the PICA. It will lessen the possible postoperative development of mutism.
4. Expose the rostral part of the floor of the fourth ventricle by detaching the tumor from the vermis. The procedure enables to assume the plane of the floor of the fourth ventricle before removing the ventral part of the tumor.
5. Tailor the surgical resection if the tumor invades or tightly attaches the floor of the fourth ventricle. Functional preservation of the brain stem has higher priority than tumor resection.
6. "Wait and see" policy for incompletely resected CPPs while aggressive adjuvant therapy for all CPCs. A second look surgery may be indicated in selected cases of CPCs.

The tumor involvement of the brain stem and cranial nerves hinders total resection of the CPT in the posterior fossa. Total resection of CPTs in the fourth ventricle is difficult [48]. Considering recent advancement of neuroendoscopic technology and chemotherapy, a model of treatment of fourth ventricle CPTs in the future could be endoscopic third ventriculostomy for hydrocephalus and concomitant endoscopic tumor biopsy, followed by several courses of neoadjuvant chemotherapy before radical resection of the tumor [49]. A combined multidisciplinary approach seems mandated for the CPT in the posterior fossa.

Acknowledgement The authors thank Takaaki Yanagisawa, M.D., for his kind assistance and critical remarks in editing the paper.

References

1. Adra AM, Mejides AA, Salmoan FA, Landy HJ, Helfgott AW (1994) Prenatal sonographic diagnosis of a third ventricle choroid plexus papilloma. *Prenat Diagn* 14:865–867
2. Aguzzi A, Brandner S, Paulus W (2000) Choroid plexus tumours. In: Kleihues P, Cavenee WK (eds) *Pathology and genetics. Tumours of the nervous system*. WHO, Lyon, pp 84–86
3. Ajir R, Chanbusarakum K, Bolles JC (1982) Acinar choroid plexus adenoma of the fourth ventricle. *Surg Neurol* 17:290–292
4. Albrecht S, Rouah E, Becker LE, Bruner J (1991) Transthyretin immunoreactivity in choroid plexus neoplasms and brain metastases. *Mod Pathol* 4:610–614
5. Andreini L, Doglioni C, Giangaspero F (1991) Tubular adenoma of choroid plexus: a case report. *Clin Neuropathol* 10:137–140
6. Ang LC, Taylor AR, Bergin D, Kaufmann JC (1990) An immunohistochemical study of papillary tumors in the central nervous system. *Cancer* 65: 2712–2719

7. Barkovich AJ (1996) Pediatric neuroimaging, 2nd edn. Lippincott-Raven, Philadelphia, pp 406–408
8. Berger C, Thiesse P, Lellouch-Tubiana A, Kalifa C, Pierre-Kahn A, Bouffet E (1998) Choroid plexus carcinomas in childhood: clinical features and prognostic factors. *Neurosurgery* 42:470–475
9. Borota OC, Jacobsen EA, Scheie D (2006) Bilateral atypical choroid plexus papillomas in cerebellopontine angles mimicking neurofibromatosis 2. *Acta Neuropathol* 111:500–502
10. Body G, Darnis E, Pourcelot D, Santini JJ, Gold F, Soutoul JH (1990) Choroid plexus tumors: antenatal diagnosis and follow-up. *J Clin Ultrasound* 18: 575–578
11. Bonnin JM, Colon LE, Morawetz RB (1987) Focal glial differentiation and oncocytic transformation in choroid plexus papilloma. *Acta Neuropathol* 72: 277–280
12. Buetow PC, Smirniotopoulos JG, Done S (1990) Congenital brain tumor: a review of 45 cases. *Am J Neuroradiol* 11:793–799
13. Burger PC, Scheithauer BW (2007) Tumors of the Neuroglia and Choroid Plexus. In: tumors of the central nervous system. AFIP Atlas of Tumor Pathology, Fourth Series, Fascicle 7. ARP Press, Washington, DC, pp 33–208
14. Carlotti CG Jr, Salhia B, Weitzman S, Greenberg M, Dirks PB, Mason W, Becker LE, Rutka JT (2002) Evaluation of proliferative index and cell cycle protein expression in choroid plexus tumors in children. *Acta Neuropathol* 103:1–10
15. Carter AB, Price DL Jr, Tucci KA, Lewis GK, Mewborne J, Singh HK (2001) Choroid plexus carcinoma presenting as an intraparenchymal mass. *J Neurosurg* 95:1040–1044, Case report
16. Coates TL, Hinshaw DB Jr, Peckman N, Thompson JR, Hasso AN, Holshouser BA (1989) Knierim DS: pediatric choroid plexus neoplasms: MR, CT, and pathologic correlation. *Radiology* 173:81–88
17. Deletis V, Sala F, Morota N (2000) Intraoperative neurophysiological monitoring and mapping during brainstem surgery. A modern approach. *Oper Tech Neurosurg* 3:109–113
18. Rocco D (1997) Ianelli a: poor outcome of bilateral congenital choroid plexus papilloma with extreme hydrocephalus. *Eur Neurol* 37:33–37
19. Dinda AK, Mahapatra AK, Sarkar C, Dhir R, Kharbanda K (1994) Primary cerebellopontine angle choroid plexus papilloma: a case report and review of literature. *Indian J Cancer* 31:48–51
20. Do HM, Marx WF, Khanam H, Jensen ME (2001) Choroid plexus papilloma of the third ventricle: chorography, preoperative embolization, and histology. *Neuroradiology* 43:503–506
21. Doglietto F, Lauretti L, Tartaglione T, Gessi M, Fernandez E, Maira G (2005) Diffuse craniospinal choroid plexus papilloma with involvement of both cerebellopontine angles. *Neurology* 65:842
22. Dong CCJ, MacDonald DB, Akagawa R, Westerberg B, AlKhani A, Kanaan I, Hassounah M (2005) Intraoperative facial motor evoked potential monitoring with transcranial electrical stimulation during skull base surgery. *Clin Neurophysiol* 116: 588–596
23. Doran SE, Blaivas M, Dauser RC (1995) Bone formation within a choroid plexus papilloma. *Pediatr Neurosurg* 23:216–218
24. Due-Tonnessen B, Helseth E, Skullerud K, Lundar T (2001) Choroid plexus tumors in children and young adults: report of 16 consecutive cases. *Childs Nerv Syst* 17:252–256
25. Duffner PK, Kun LE, Burger PC, Horowitz ME, Cohen ME, Sanford RA, Krischer JP, Mulhern RK, James HE, ReKate HL, Friedman HS (1995) Postoperative chemotherapy and delayed radiation in infants and very young children with choroid plexus carcinomas. *Pediatr Neurosurg* 22:189–196
26. El-Bahy K (2005) Telovelar approach to the fourth ventricle: operative findings and results in 16 cases. *Acta Neurochir (Wien)* 147:137–142
27. Ellenbogen RG, Winston KR, Kupsky WJ (1989) Tumors of the choroid plexus in children. *Neurosurgery* 25:327–335
28. Ellenbogen RG, Donovan DJ (2001) Choroid plexus tumors. In: Keating RF, Goodrich JT, Packer RJ (eds) Tumor of the pediatric central nervous system. Thieme, New York, pp 339–350
29. Fitzpatrick LK, Aronson LJ, Cohen KJ (2002) Is there a requirement for adjuvant therapy for choroid plexus carcinoma that has been completely resected? *J Neuro Oncol* 57:123–126
30. Fouladi M, Gururangan S, Moghrabi A, Phillips P, Gronewold L, Wallace D, Sanford RA, Gajjar A, Kun LE, Heideman R (2009) Carboplatin-based primary chemotherapy for infants and young children with CNS tumors. *Cancer* 115:3243–3253
31. Gaudio RM, Tacconi L, Rossi ML (1998) Pathology of choroid plexus papillomas: a review. *Clin Neurol Neurosurg* 100:165–186
32. Gjerris K, Agerlin N, Borgesen SE, Buhl L, Hasse J, Kliken L, Mortensen AC, Oslen JH, Ovesen N, Reske-Nielsen E, Schimdt K (1998) Epidemiology and prognosis in children treated for intracranial tumours in Denmark 1960–1984. *Childs Nerv Syst* 14:302–311
33. Gok A, Alptekin M, Erkuclu I (2004) Surgical approach to the fourth ventricle cavity through the cerebellomedullary fissure. *Neurosurg Rev* 27:50–54
34. Gottschalk J, Jautzke G, Paulus W, Goebel S, Cervos-Navarro J (1993) The use of immunomorphology to differentiate choroid plexus tumors from metastatic carcinomas. *Cancer* 72:1343–1349
35. Gradin WC, TAYLON C, Fruin AH (1983) Choroid plexus papilloma of the third ventricle: case report and review of the literature. *Neurosurgery* 12:217–220
36. Greenberg ML (1999) Chemotherapy of choroid plexus carcinoma. *Childs Nerv Syst* 15:571–577
37. Greene RC (1951) Extraventricular and intra-cerebellar papilloma of the choroid plexus. *J Neuropathol Exp Neurol* 10:204–207

38. Guermazi A, De Kerviler E, Zagdanski AM, Fria J (2000) Diagnostic imaging of choroid plexus disease. *Clin Radiol* 55:503–516
39. Gupta N (2004) Choroid plexus tumors. In: Gupta N, Banerjee A, Haas-Kogan D (eds) *Pediatric CNS tumors*. Springer, Berlin, pp 157–166
40. Gyure KA, Morrison AL (2000) Cytokeratin 7 and 20 expression in choroid plexus tumors: utility in differentiating these neoplasms from metastatic carcinomas. *Mod Pathol* 13:638–643
41. Handa H, Bucy PC (1956) Benign cysts of the brain simulating brain tumor. *J Neurosurg* 13:489–499
42. Herbert J, Cavallaro T, Dwork AJ (1990) A marker for primary choroid plexus neoplasms. *Am J Pathol* 136:1317–1325
43. Humphreys RP, Nemoto S, Hendrick EB, Hoffman HJ (1987) Childhood choroid plexus tumors. *Conc Pediatr Neurosurg* 7:1–18
44. Jeibmann A, Hasselblatt M, Gerss J, Wrede B, Egensperger R, Beschoner R, Hans VH, Rickert CH, Wolff JE, Paulus W (2006) Prognostic implications of atypical histologic features in choroid plexus papilloma. *J Neuropathol Exp Neurol* 65:1069–1073
45. Jinhu Y, Jianping D, Jun M, Hui S, Yepeng F (2007) Metastasis of a histologically benign choroid plexus papilloma. Case report and review of literature. *J Neuro Oncol* 83:47–52
46. Judkins AR, Burger PC, Hamilton RL, Kleinschmidt-DeMasters N, Perry A, Pomeroy SL, Rosenblum MK, Yachnis AT, Zhou H, Rorke LN, Biegel JA (2005) INI1 protein expression distinguishes atypical teratoid/rhabdoid tumor from choroid plexus carcinoma. *J Neuropathol Exp Neurol* 64:391–397
47. Krishnan S, Brown PD, Scheithauer BW, Ebersold MJ, Hammack JE, Bucher JC (2004) Choroid plexus papillomas: a single institutional experience. *J Neuro Oncol* 68:49–55
48. Kumabe T, Fujimura M, Jokura H, Tominaga T (2008) Surgical treatment for choroid plexus tumors in the fourth ventricle: brain stem infiltration hinders total extirpation. *Neurosurg Rev* 31:165–172
49. Lafay-Cousin L, Mabbott DJ, Halliday W, Taylor MD, Tabori U, Kamaly-Asl ID, Kulkarni AV, Bartels U, Greenberg M, Bouffet E (2010) Use of ifosfamide, carboplatin, and etoposide chemotherapy in choroid plexus carcinoma. *J Neurosurg Pediatr* 5:615–621
50. Lafay-cousin L, Kene D, Carret AS, Fryer C, Brossard J, Crooks B, Eisenstat D, Johnston D, Larouche V, Silva M, Wilson B, Zelcer S, Bartels U, Bouffet E (2011) Choroid plexus tumors in children less than 36 months: the Canadian Pediatric Brain Tumor Consortium (CPBTC) experience. *Child Nerve Syst* 27:259–264
51. Lang J (1983) *Clinical anatomy of the head. Neurocranium, orbit, craniocervical regions*. Springer, New York, pp 340–341
52. Langman J (1975) *Medical embryology*, 3 Asianth edn. Igaku Shoin Ltd, Tokyo, pp 340–351
53. Laurence KM (1974) The biology of choroid plexus papilloma and carcinoma of the lateral ventricle. In: Vinken PJ, Bruyn GW (eds) *Handbook of clinical neurology*. Elsevier, New York, pp 555–595
54. Lena G, Genitori L, Molina J, Legatte JR, Choux M (1990) Choroid plexus tumours in children. Review of 24 cases. *Acta Neurochir (Wien)* 106:68–72
55. Lippa C, Abroms IF, Davidson R, De Girolami U (1989) Congenital choroid plexus papilloma of the fourth ventricle. *J Child Neurol* 4:127–130
56. Matson DD (1969) *Neurosurgery of infancy and childhood*, 2nd edn. Charles C Thomas, Springfield, Illinois 581–595
57. Matsushima T (1983) Choroid plexus papillomas and human choroid plexus. A light and electron microscopic study. *J Neurosurg* 59:1054–1062
58. Matsushima T, Fukui M, Inoue T, Natori Y, Baba T, Fujii K (1992) Microsurgical and magnetic resonance imaging anatomy of the cerebellomedullary fissure and its application during fourth ventricle surgery. Experimental and clinical study. *Neurosurgery* 30:325–330
59. Matsushima T, Inoue T, Inamura T, Natori Y, Ikezaki K, Fukui M (2001) Transcerebellomedullary fissure approach with special reference to methods of dissecting the fissure. *J Neurosurg* 94:257–264
60. Matsushima T, Matsukado K, Natori Y, Inamura T, Hitotsumatsu T, Fukui M (2001) Surgery on a saccular vertebral artery – posterior inferior cerebellar artery aneurysm via the transcondylar fossa (supracondylar transjugular tubercle) approach or the transcondylar approach: surgical results and indications for using two different lateral skull base approaches. *J Neurosurg* 95:268–274
61. Mayer SP, Khademian ZP, Chuang SH, Pollack IF, Korones DN, Zimmerman RA (2004) Choroid plexus carcinomas in children: MRI features and patient outcome. *Neuroradiology* 46:770–780
62. McCallum S, Cooper K, Franks DN (1988) Choroid plexus carcinoma. Cytologic identification of malignant cells in ascitic fluid. *Acta Cytol* 32:263–266
63. McDonald JV (1969) Persistent hydrocephalus following the removal of papilloma of the choroid plexus of the lateral ventricle. Report of two cases. *J Neurosurg* 30:736–740
64. McEvoy AW, Galloway M, Revesz T, Kitchen ND (2002) Metastatic choroid plexus papilloma: a case report. *J Neuro Oncol* 56:241–246
65. McGirr SJ, Ebersold MJ, Scheithauer BW, Quast LM, Shaw EG (1988) Choroid plexus papillomas: long-term follow-up results in a surgically treated series. *J Neurosurg* 69:843–849
66. Milhorat TH, Hammock MK, Davis DA, Fenstermacher JD (1976) Choroid plexus papilloma. I. Proof of cerebrospinal fluid overproduction. *Childs Brain* 2:273–289
67. Morota N, Deletis V, Epstein FJ, Kofler M, Abbott R, Lee M, Ruskin K (1995) Brain stem mapping: neurophysiological localization of motor nuclei on the floor of the fourth ventricle. *Neurosurgery* 37:922–930

68. Morota N, Deletis V (2006) The importance of brainstem mapping in brainstem surgical anatomy before the fourth ventricle and implication for intraoperative neurophysiological mapping. *Acta Neurochir (Wien)* 148:499–509
69. Morota N, Ihara S, Deletis V (2010) Intraoperative neurophysiology for surgery in and around the brainstem: role of brainstem mapping and corticobulbar tract motor-evoked potential monitoring. *Childs Nerv Syst* 26:513–521
70. Mussi ALM, Rhoton AL Jr (2000) Telovelar approach to the fourth ventricle: microsurgical anatomy. *J Neurosurg* 92:812–823
71. Nagib MG, O'Fallon MT (2000) Lateral ventricle choroid plexus papilloma in childhood: management and complications. *Surg Neurol* 54:366–372
72. Naeini RM, Yoo JH, Hunter JV (2009) Spectrum of choroid plexus lesions in children. *AJR Am J Roentgenol* 192:32–40
73. Noguchi A, Shiokawa Y, Kobayashi K, Saito I, Tsuchiya K, McMenomey SO, Delashaw JB (2004) Choroid plexus papilloma of the third ventricle in the fetus. Case illustration. *J Neurosurg* 100:224, Pediatrics 2
74. Otten ML, Riina HA, Gobin YP, Souweidane MM (2006) Preoperative embolization in the treatment of choroid plexus papilloma in an infant. Case report. *J Neurosurg* 104(6 Suppl):419–421
75. Packer RJ, Perilongo G, Johanson D, Sutton LN, Vezina G, Zimmerman RA, Ryan J, Reaman G, Schut L (1992) Choroid plexus carcinoma of childhood. *Cancer* 69:580–585
76. Paulus W, Brandner S (2007) Choroid plexus tumours. In: Louis DN, Ohgaki H, Wiestler OD, Cavenee WK (eds) WHO classification of tumours of the central nervous system. IARC Press, Lyon, pp 82–85
77. Pencanalet P, Sainte-Rose C, Lellouch-Tubiana A, Kalifa C, Brunelle F, Sgouros S, Meyer P, Cinalli G, Zerah M, Pierre-Khan A, Renier D (1998) Papilloma and carcinomas of the choroid plexus in children. *J Neurosurg* 88:521–528
78. Pollack IF, Polinko P, Albright AL, Towbin R, Fitz C (1995) Mutism and pseudobulbar symptoms after resection of posterior fossa tumors in children: incidence and pathophysiology. *Neurosurgery* 37: 885–893
79. Ralia FA, Bottoms TW Jr, Fratkin JD (1998) Solitary choroid plexus metastasis from a renal cell carcinoma. *South Med J* 91:1159–1162
80. Razzaq AA, Cohen AR (1997) Neoadjuvant chemotherapy for hypervascular malignant brain tumors of childhood. *Pediatr Neurosurg* 27:296–303
81. ReKate HL, Erwood S, Brodkey JA, Chizeck HJ, Spear T, Ko W, Montague F (1985–1986). Etiology of ventriculomegaly in choroid plexus papilloma. *Pediatr Neurosci* 12:196–201
82. Rhoton AL (2003) Cerebellum and fourth ventricle. *Neurosurgery* 53:439–459
83. Rhoton AL (2003) The cerebellar arteries. *Neurosurgery* 53:461–500
84. Rickert CH, Paulus W (2001) Tumor of the choroid plexus. *Microsc Res Tech* 52:104–111
85. Robinson RG (1955) Two cerebellar tumors with unusual features. 1. Cystic astrocytoma. 2. Papilloma of the choroid plexus. *J Neurosurg* 12:183–186
86. Russel DS, Rubinstein LJ (1989) Choroid plexus tumours. In: Pathology of tumours of the nervous system, 5th edn. Williams & Wilkins, Baltimore, pp 394–404
87. Sahar A, Feinsod M, Beller AJ (1980) Choroid plexus papilloma: hydrocephalus and cerebrospinal fluid dynamics. *Surg Neurol* 13:476–478
88. Souweidane MM, Johnsen JH, Lis E (1999) Volumetric reduction of a choroid plexus carcinoma using preoperative chemotherapy. *J Neuro Oncol* 43: 167–171
89. St Clair SK, Humphreys RP, Pillay PK, Hoffman HJ, Blaser SI, Becker LE (1991–1992). Current management of choroid plexus carcinoma in children. *Pediatr Neurosurg* 17:225–233
90. Taylor MB, Jackson RW, Hughes DG, Wright NB (2001) Magnetic resonance imaging in the diagnosis and management of choroid plexus carcinoma in children. *Pediatr Radiol* 31:624–630
91. The Committee of Brain Tumor Registry of Japan (2003). Report of brain tumor registry of Japan (1969–1996). *Neurol Med Chir (Tokyo)* 43 (Suppl):36–43
92. Tanaka K, Sasayama T, Nishihara M, Sakagami Y, Kondoh T, Ohbayashi C, Kohmura E (2009) Rapid regrowth of an atypical choroid plexus papilloma located in the cerebellopontine angle. *J Clin Neurosci* 16:121–124
93. Tomita T, Naidich TP (1987) Successful resection of choroid plexus papillomas diagnosed at birth: report of two cases. *Neurosurgery* 20:774–779
94. Tomita T, McLone DG, Flannery AM (1988) Choroid plexus papilloma of neonate, infants and children. *Pediatr Neurosci* 14:23–30
95. Thompson JR, Harwood-Nash DC, Fitz CR (1973) The neuroradiology of childhood choroid plexus neoplasms. *Am J Roentgenol Radium Ther Nucl Med* 118:116–133
96. Vazquez E, Ball WS, Prenger EC, Castellote A, Crone KR (1991) Magnetic resonance imaging of fourth ventricular choroid plexus neoplasms in childhood. *Pediatr Neurosurg* 17:48–52
97. Watanabe K, Ando Y, Iwanaga H, Ochiai C, Nagai M, Okabe K, Watanabe N (1995) Choroid plexus papilloma containing melanin pigment. *Clin Neuropathol* 14:159–161
98. Wolff JEA, Sajedi M, Coppes MJ, Anderson RA, Egeler RM (1999) Radiation therapy and survival in choroid plexus carcinoma. *Lancet* 353:2126
99. Wolff JE, Sajedi M, Brant R, Coppes MJ, Egeler RM (2002) Choroid plexus tumors. *Br J Cancer* 87:1086–1091
100. Wolff JE, Wrede B, Weinberg J, Peters O, Hahajan A, Thall P, Witt O, Kutluk T, Diez B, Rutkowski S, Carret AS, Hauser P, Hasselblatt M (2010) Resection

- not so important after all? - analysis of the choroid plexus tumor SIOP study. *Neuro Oncol* 12:ii49
101. Wrede B, Liu P, Wolff JE (2007) Chemotherapy improves the survival of patients with choroid plexus carcinoma: a meta-analysis of individual cases with choroid plexus tumors. *J Neuro Oncol* 85:345–351
102. Wrede B, Hasselblatt M, Peters O, Thall PF, Kutluk T, Moghrabi A, Mahajan A, Rutkowski S, Diez B, Wang X, Pietsch T, Kortmann RD, Paulus W, Jeibmann A, Wolff JEA (2009) Atypical choroid plexus papilloma: clinical experience in the CPT-SIOP-2000 study. *J Neuro Oncol* 95:383–392
103. Yasargil MG (1996) Choroid plexus tumors. In: *Microneurosurgery of CNS tumors* 4B. Thieme, Stuttgart, pp 326–327

Johannes E. Wolff, Mical Bahar, Anita Mahajan,
and Su G. Berrak

49.1 Background

49.1.1 Pathology

Tumors of the choroid plexus epithelium are rare [1, 2]. The most frequently cited number for the total frequency is 0.5 % of all brain tumors in adults and children [3].

Choroid plexus tumors are intraventricular, papillary neoplasms. The WHO classification of central nervous system tumors classifies the relatively benign “choroid plexus papilloma” (CPP) as grade I, “atypical choroid plexus papilloma” (APP) as grade II, and “choroid plexus carcinoma” (CPC) as grade III. Choroid plexus tumors most frequently occur in the lateral ventricles, but are also encountered in the third and fourth ventricle. Rare cases of ectopic CPT are on record [4, 5].

Choroid plexus papillomas (CPPs) are composed of delicate fibrovascular connective tissue fronds, which are covered by a single layer of epithelial cells with round or oval monomorphic nuclei. Mitotic activity is extremely low. Brain invasion, high cellularity, necrosis, nuclear pleomorphism, and focal blurring of the papillary pattern are unusual, but may occur. Rarely, CPPs may acquire unusual histological features, including oncocyctic change, mucinous degeneration, melanization, as well as formation of bone, cartilage, adipose tissue, or neuropil islands. Malignant progression [6] or CSF-mediated metastases [7] may occur, but are exceedingly rare.

Atypical choroid plexus papilloma (APP) has been defined as CPP with increased mitotic activity in the latest revision of the WHO classification [8]. A mitotic index of two or more mitoses per 10 randomly selected HPF (one HPF corresponding to 0.23 mm²) can be used to establish the diagnosis [9].

Choroid plexus carcinoma is characterized by frank signs of malignancy, including at least four

J.E. Wolff, M.D. (✉)

Department of Pediatric Hematology Oncology and Blood and Marrow Transplantation, Cleveland Clinic Children’s, Cleveland, OH, USA

Department of Pediatrics, Anderson Cancer Center, Houston, TX, USA

Department of Pediatric Oncology, University of Regensburg, Regensburg, Germany
e-mail: wolffj@ccf.org

M. Bahar

Department of Pediatric Hematology Oncology and Blood and Marrow Transplantation, Cleveland Clinic Children’s, Cleveland, OH, USA

A. Mahajan, M.D.

Department of Radiation Oncology, Anderson Cancer Center, Houston, TX, USA

S.G. Berrak

Department of Pediatric Hematology Oncology, Marmara University Medical Center, Istanbul, Turkey

Division of General Pediatrics, Children’s Hospital at Montefiore, Albert Einstein College of Medicine, Bronx, NY, USA

of the following five features: frequent mitoses (usually greater than 5 per 10 HPF), increased cellular density, nuclear pleomorphism, blurring of the papillary pattern, and necrosis. Diffuse brain invasion is common. CSF-mediated metastases may occur.

49.1.2 Etiology

Choroid plexus tumors are the model for viral induction of brain tumors. The simian virus 40 (SV40), which naturally infects Asian macaques, has been shown in several lines of evidence to induce choroid plexus tumors. The virus is capable of transforming human choroid cells in vitro [10–12] and creates CPT in hamsters [13, 14] and mice [15–18]. Transgenic mice harboring the SV40 large T antigen gene developed papillomas of the choroid plexus by 80–90 days [19]. Tumors in these mice develop focally, but when the T antigen is controlled by another virus, the proliferation is uniform [20]. Within the SV40 virus, the T antigen is sufficient to induce the tumors, and the SV40 enhancer (72-base-pair repeat region) has a role in directing tumors to the choroid plexus [21]. The T antigen of the virus binds to tumor suppressor genes such as p53 [21] and pRB [20]. Interestingly, dogs develop spontaneous plexus tumors [22–25]. In human plexus choroid plexus tumors, SV40 is frequently found [26–29]. Involvement of the p53 tumor suppressor gene in patients is suggested by the occurrence of two cases of CPC [30, 31] and two cases of CPP in families with Li-Fraumeni syndrome [32] and one case with p53 inactivation demonstrated in tumor tissue [33]. This is a quite strong evidence for SV40-induced tumorigenesis. The only higher level of evidence would be a controlled experiment with humans. This cannot be done, but in the 1970s the vaccine for poliomyelitis was contaminated with the SV40. As an infection with SV40 is not pathogenic for humans, the contamination was not recognized clinically. If SV40 infection results in choroid plexus tumors, the frequency of those tumors should be higher in the population immunized during that time. The data, however, are inconclusive. It, therefore, still

remains questionable if SV40 induces choroid plexus tumors in humans, while the link to Li-Fraumeni syndrome is certain.

49.1.3 Symptoms and Signs

CPTs are associated with cerebrospinal fluid overproduction and blockage of the cerebrospinal fluid reabsorption pathways, which predominantly results in hydrocephalus in addition to the space-occupying effect of the lesion [34, 35]. Ataxia and nystagmus are common space-occupying effects in fourth ventricular CPTs.

49.1.4 Radiological Diagnosis

Among the relatively noninvasive neuroradiological imaging techniques, for supratentorial tumors at least a computer tomography (CT) without and with contrast and for infratentorial tumors or pineal tumors at least an MRI without and with contrast should be performed. And the practical hint here is for children with infratentorial tumors, who require anesthesia for MRI tomography, the whole spinal cord should be examined with the first MRI.

CPTs usually appear as lobulated, homogeneously enhancing lesions that are often associated with hydrocephalus. Sometimes there is calcification in CT scans. Presence of inhomogeneous signal intensity that is consistent with necrosis in the center of the tumor could be seen particularly in CPCs. In addition to that feature, CPCs may demonstrate areas of brain invasion in MRI.

49.1.5 Further Radiodiagnostic Options

Preoperatively in cases of uncertain diagnoses, the following diagnostic methods might be used in addition:

1. Fluorodeoxyglucose PET
2. Thallium scan
3. Alpha-methyltyrosine scan
4. Sestamibi (MIBI-SPECT) [36]

49.2 General Treatment Experience of Choroid Plexus Tumors

Due to the low incidence of this tumor, only one randomized trial has ever been done (CPT-SIOP-2000); the code of which is still closed [1, 2]. Therefore, only lower-level evidence is available. Most of these data come from individual case reports, small series [36–39], or systematic literature reviews, which created an ever growing patient database from published cases. In those data, choroid plexus papilloma patients did better than choroid plexus carcinoma patients. Surgery was a significant variable in both choroid plexus papilloma and choroid plexus carcinoma even if a second resection is necessary [40]. The data further support importance of radiation if the patient is old enough [41, 42] and the importance of chemotherapy at least when the tumor is less than completely resected [43]. The five most frequently used drugs are cisplatin, vincristine, cyclophosphamide, carboplatin, and etoposide. Of those, etoposide (VP16) was most frequently involved in protocols creating response and had the most convincing survival benefit in various multivariate analyses [4].

49.2.1 CPT-SIOP-2000 Study

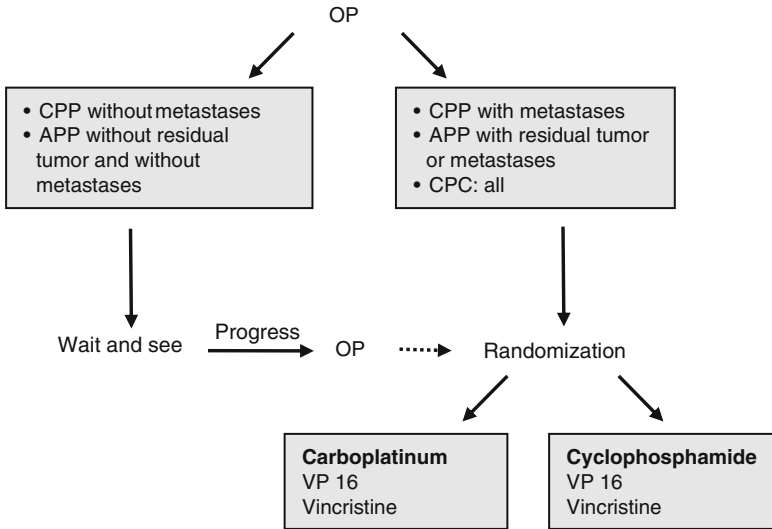
In 2000, a study was launched with the aim to gain information concerning the specific role of single treatment agents, upon which further studies could be build. The available evidence suggested benefit of surgery for all patients and irradiation for patients over 3 years of age. Among the chemotherapeutic agents the best evidence was found for VP16, followed by vincristine, cyclophosphamide, and the platinum drugs. Among many interesting treatment questions, only one variable could be compared in the small number of patients available. An international discussion around this study, which occurred from 1998 to 2000 in various national and international groups, showed that the comparison of cyclophosphamide with carboplatin was the best feasible question. Carboplatin was preferred over cisplatin because of the lower ototoxicity and the difficulties in testing hearing in

infants. Multiagent treatment was viewed as standard care in many centers. Therefore, the most frequently used drugs, VP16 and vincristine, were added to both arms of the protocol. This combination of DNA-binding drugs, with topoisomerase inhibitors and mitosis inhibitors, was well based on theoretical/preclinical thinking and was generally used in almost all pediatric brain tumor protocols. The majority of patients were young and most physicians agreed that they should not receive irradiation. Therefore, radiotherapy could not be a randomized study objective internationally. For patients over 3 years of age, the CPT-SIOP-2000 study includes irradiation, based upon the literature review conducted for this study [40–44]. The CPT-SIOP-2000 study was the first international study for children and adults with tumors of the choroid plexus and is formally closed. The results suggest, either Arm A or Arm C as the treatment of choice for patients with CPT. The study is currently substituted with a collaborative international chart review.

49.2.2 Treatment Protocol

After maximal possible resection, all patients with CPC, metastasized tumors, and incompletely resected atypical plexus papilloma were randomized to a treatment with either carboplatin or cyclophosphamide given together with etoposide and vincristine. After the first interim analysis at the committee meeting in Vancouver 2005, it was decided to stratify the randomization by age to keep an even number of radiated patients in each treatment group. A total of six courses of chemotherapy (VP16 100 mg/m² d1-5, vincristine 1.5 mg/m² d1, and either carboplatin 350 mg/m² d1+2 or cyclophosphamide 1,000 mg/m² d1+2), and additional irradiation after the second course for those who are older than 3 years of age, was given. Patients with metastasized APP and CPC and patients with non-metastasized CPC nonresponsive to chemotherapy (SD, PD) received craniospinal irradiation with 35 Gy and local boost up to a total of 54 Gy. Patients with choroid plexus papilloma and completely resected atypical papilloma were closely followed without further treatment.

49.2.3 CPT-SIOP-2000 Study Design



49.2.3.1 Treatment Algorithm

Based upon the available literature, the experience of the prospective trial CPT-SIOP-2000, and expert opinion, an international meeting decided guidelines how choroid plexus tumors should be treated.

49.2.3.2 Choroid Plexus Papilloma

The first step of treatment is maximal possible resection. This might take more than one surgery.

Tumor at diagnosis: histology and location	Postop: residual tumor	1st treatment (2 cycles) induction	Response to first two cycles (or other follow-ups)	2nd treatment(± XRT + 4 cycles ChT)
Localized CPP	Regardless	Watch	No progression	Watch and wait
	Regardless	Watch and wait	Local tumor progression	2nd OP if second resection is completed, then treat like first resection. If there is residual tumor or already at third resection, then move down in algorithm; treat as if localized APP with residual tumor (localized or metastatic)
	Regardless	Watch	Metastatic progression	Move down in algorithm; treat as if localized APP with residual tumor (localized or metastatic)
Metastatic CPP	No	Watch	CCR	Watch and wait
	No	Watch	Tumor progression	2nd OP if possible. Start 1st systemic chemotherapy with IT. Reevaluate. Continue 1st ChT if SD or better without XRT; change treatment if progression, single site resect + 2nd ChT, multiple sites <3 years, 2nd ChT, multiple sites >3years CSI followed by 2nd ChT
	Yes	1st ChT + ith	CR, PR, SD	Continue ChT +ith; complete protocol; start watch and wait without XRT
	Yes	1st ChT + ith	PD single site	If further resection successful, watch and wait. If resection impossible, 2nd ChT 2 cycles. Reevaluate. If PR or CR, continue 2nd ChT. If PD or SD, local XRT and 3rd ChT for >1.5 years and or only 3rd chemo if <1.5 years
	Yes	1st ChT + ith	PD multiple sites	>3 years, CSI + 2nd ChT >2.5–3 years, 2nd.ChT +ith, delay CSI, <2.5 years, 2nd ChT+ ith no XRT

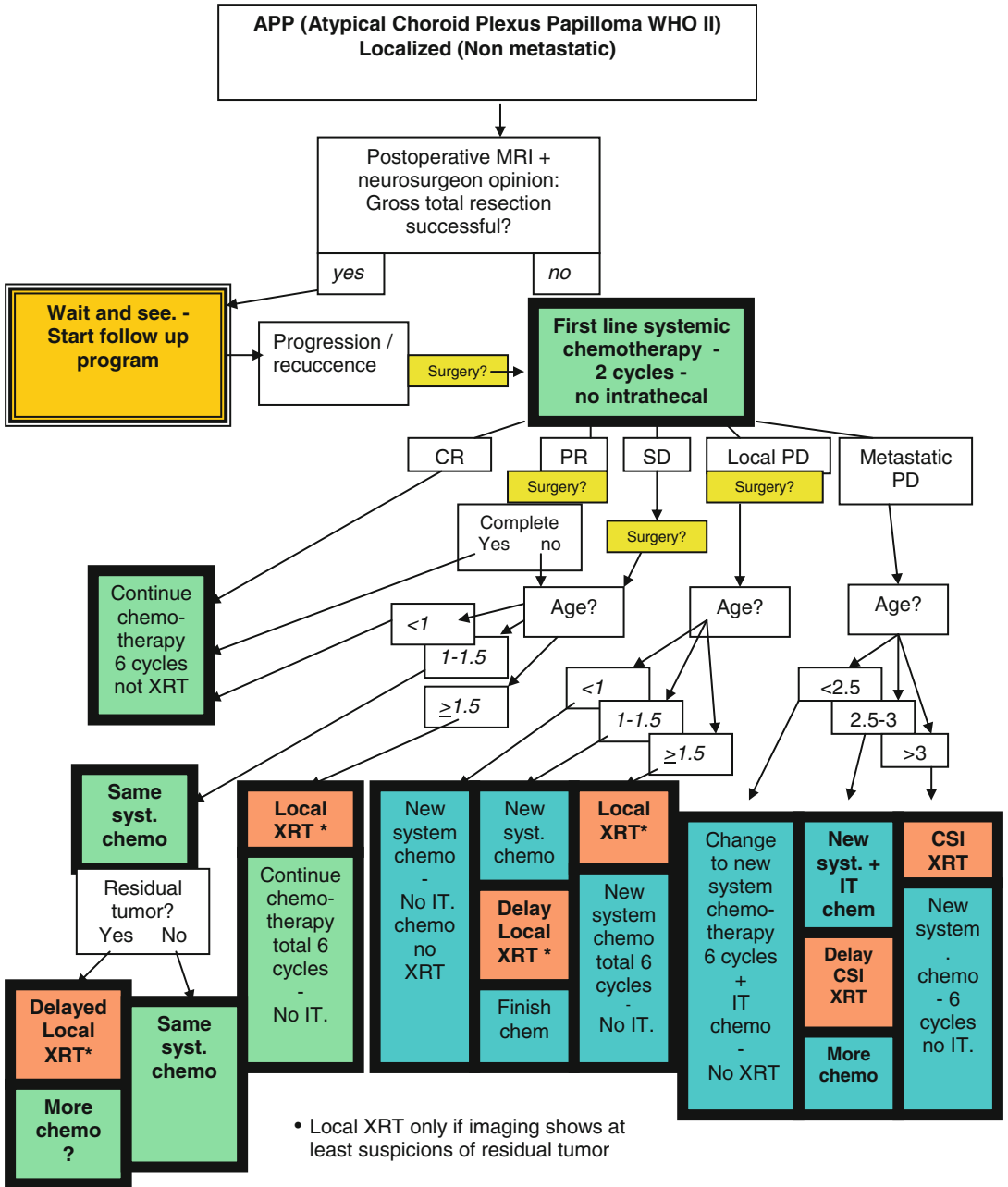
1st ChT first-line systemic chemotherapy, 2nd ChT second-line systemic chemotherapy, 3rd ChT third-line systemic chemotherapy, XRT radiation therapy, CSI craniospinal irradiation with boost, IT intrathecal chemotherapy, localXRT local radiation therapy

49.2.3.3 Localized Atypical Choroid Plexus Papilloma

The first step of treatment is maximal possible resection. This might take more than one surgery.

Postop: residual tumor	1st treatment (2 cycles) induction	Response to first two cycles (or other follow-ups)	2nd treatment (+/- XRT + 4 cycles ChT)
No	Watch and wait	CCR	Watch and wait as long as no recurrence
No	Watch and wait	Tumor progression	Consider resecting the tumor. But move on in treatment regardless of success. Start 1st chemotherapy without intrathecal chemotherapy. Follow guidelines as if newly diagnosed APP with residual tumor (one line lower)
Yes	1st ChT	CR	Complete chemotherapy protocol. No XRT. No IT chemo
Yes	1st ChT	PR	Attempt resection again. If resection complete, continue 1st ChT without radiation. If resection incomplete, treat age dependently: <1 year, continue ChT without radiation; 1–1.5 years, continue 1st ChT, give delayed local RT to residual tumor; >1.5 year, give local RT to residual tumor and continue 1st ChT. No IT ChT
Yes	1st ChT	SD	Attempt resection again. Independent of result of resection, treat age dependently: <1 year, continue ChT without radiation; 1–1.5 years, continue 1st ChT, give delayed local RT to residual tumor; >1.5 year, give local RT to residual tumor without delay and continue 1st ChT. No IT ChT
Yes	1st ChT	PD in single site	Attempt resection. <1 year, 2nd ChT no IT, no XRT; 1–1.5 years, 2nd ChT no IT delayed local XRT; >= 1.5 years, local XRT 2nd ChT no IT;
Yes	1st ChT	PD multiple sites	>3 years, CSI + 2nd ChT without IT; >2.5–3 years, 2nd ChT + IT, delayed CSI complete 2nd ChT without IT; <2.5 years, 2.ChT+IT (CSI for third recurrence)

1st ChT first-line systemic chemotherapy, *2nd ChT* second-line systemic chemotherapy, *XRT* radiation therapy, *CSI* craniospinal irradiation with boost, *IT* intrathecal chemotherapy, *localXRT* local radiation therapy



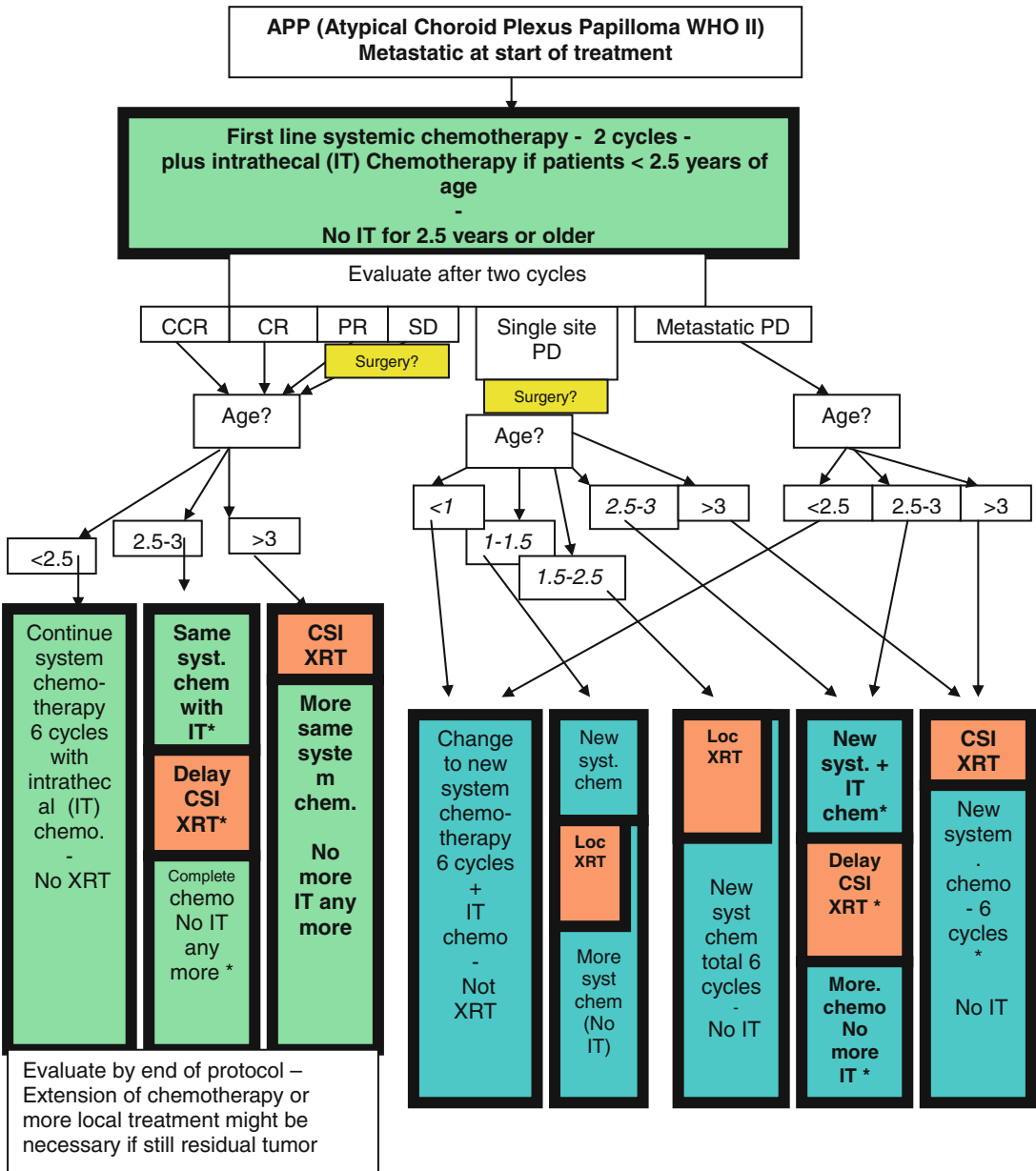
49.2.3.4 Metastatic Atypical Choroid Plexus Papilloma

After maximal possible resection, start treatment with two cycles of first-line systemic chemotherapy

(1st ChT) including intrathecal chemotherapy (IT). Evaluate response. Further treatment is stratified by treatment result and patient age.

Response to first two cycles	Age of patient	Treatment
CCR or CR	<2.5 years	Continue 1st CT with IT chemotherapy. Evaluate by the end of the protocol. If there is still no tumor, watch and wait protocol
	2.5–3 years	Continue 1st CT with IT. Delay CSI XRT until patient is 3 years old. Finish protocol without IT. Evaluate after 6 cycles. Continue if there is still detectable tumor with less intense treatment and reconsider surgery
	>3 years	CSI XRT until patient is 3 years old. Continue 1st ChT without IT. Evaluate after 6 cycles. Continue if there is still detectable tumor with less intense treatment and reconsider surgery
PR or SD	<2.5 years	Consider surgery. Continue 1st CT with IT chemotherapy. Evaluate by the end of the protocol. If there is still no tumor, watch and wait protocol
	2.5–3 years	Consider surgery. Continue 1st CT with IT. Delay CSI XRT until patient is 3 years old. Finish protocol without IT. Evaluate after 6 cycles. Continue if there is still detectable tumor with less intense treatment and reconsider surgery
	>3 years	Consider surgery CSI XRT until patient is 3 years old. Continue 1st ChT without IT. Evaluate after 6 cycles. Continue if there is still detectable tumor with less intense treatment and reconsider surgery
PD in single site	<1	Change treatment to 2nd ChT and 2nd IT. No XRT
	1–1.5	Change treatment to 2nd ChT and 2nd IT. Delay local XRT until 1.5 years. Finish 2nd ChT without IT after XRT
	1.5–2.5	Change treatment to 2nd ChT; start simultaneously with local XRT. Finish 2nd ChT without IT after XRT
	2.5–3	Change treatment to 2nd ChT with 2nd IT. Delay XRT until 3 years; then give CSI. Finish 2nd ChT without IT after XRT
	>3	CSI XRT followed by 2nd ChT without IT
PD in multiple sites	<2.5	Change treatment to 2nd ChT and 2nd IT. No XRT
	2.5–3	Change treatment to 2nd ChT with IT. Delay XRT until 3 years; then give CSI. Finish 2nd ChT without IT after XRT
	>3	CSI XRT followed by 2nd ChT without IT

1st ChT first-line systemic chemotherapy, *2nd ChT* second-line systemic chemotherapy, *XRT* radiation therapy, *CSI* craniospinal irradiation with boost, *IT* intrathecal chemotherapy, *localXRT* local radiation therapy



* Extending systemic chemotherapy followed by CSI XRT has increased risk of bone marrow failure. Interindividual differences are large. In general, not more than four cycles are recommended prior to CSI, and chemotherapy after CSI might need dose reduction.

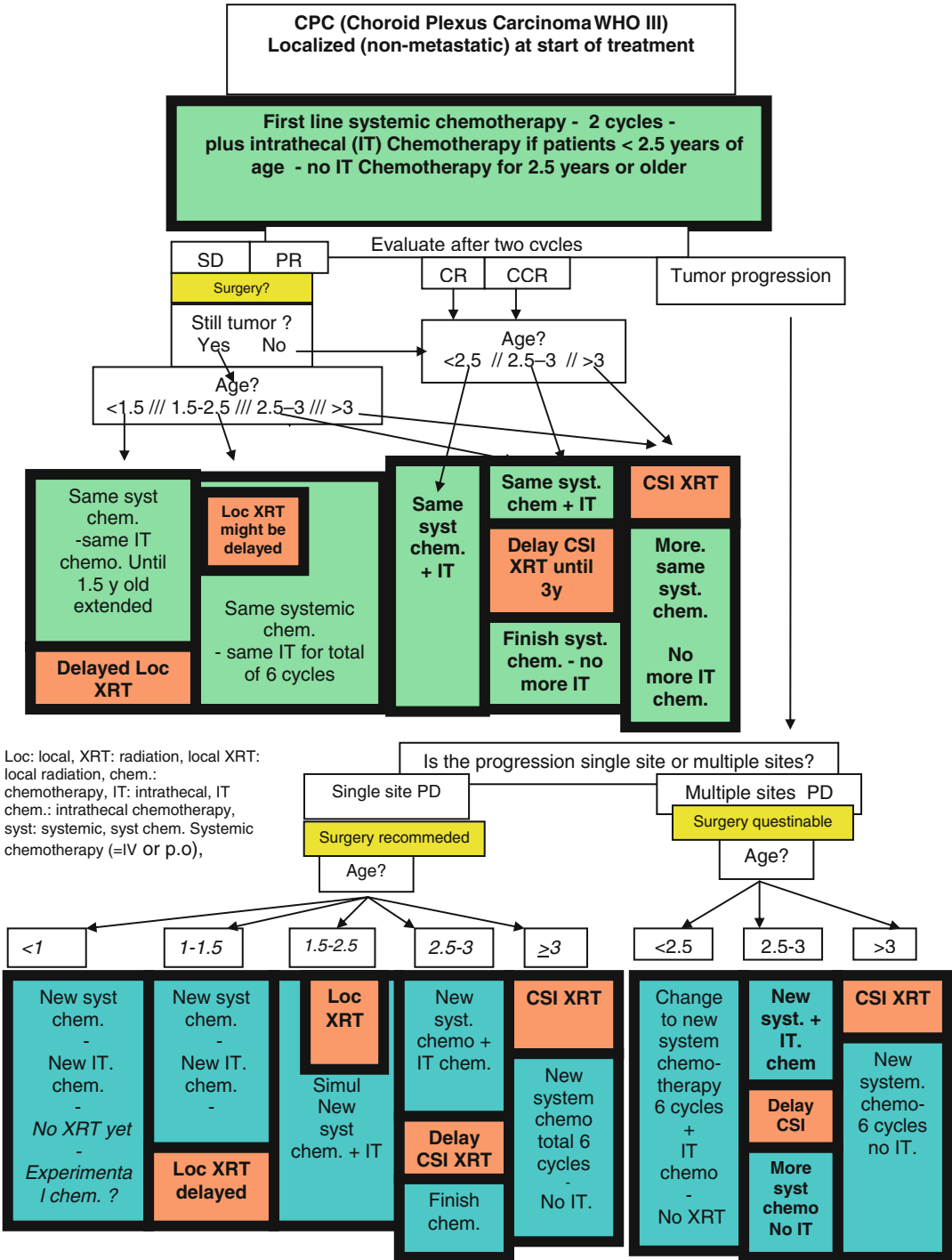
49.2.3.5 Localized Choroid Plexus Carcinoma

After maximal possible resection, start treatment with two cycles of first-line systemic chemotherapy

(1st ChT) including intrathecal chemotherapy (IT). Evaluate response. Further treatment is stratified by treatment result and patient age.

Result of 1st ChT	Patient age	Treatment
CCR or CR	<2.5 years	Continue same 1st ChT with IT. No XRT. Reevaluate. Start watch and wait
	<2.5–3 years	Continue same 1st ChT with IT. Delay XRT until 3 years old; then give CSI XRT. Finish 1st ChT without further IT. Reevaluate. Start watch and wait
	>3 years	CSI XRT followed by same 1st ChT without IT. Evaluate. Watch and wait
PR or SD	<1.5	Reoperate. Continue same 1st ChT with IT until 1.5 years old. Reevaluate. If there is still a residual, give local XRT. Otherwise, just watch and wait
	1.5–2.5 years	Reoperate. Continue same 1st ChT with IT for a total of 6 cycles. Local XRT might be delayed but should be given regardless of tumor status
	2.5–3 years	Continue same 1st ChT with IT. Delay XRT until 3 years old; then give CSI XRT. Finish 1st ChT without further IT. Reevaluate. Start watch and wait
	>3 years	CSI XRT followed by same 1st ChT without IT. Evaluate. Watch and wait
PD single site	<1 years	Consider resection. Change chemotherapy: 2nd ChT with 2nd IT, no XRT
	1–1.5 years	Consider resection. Change chemotherapy: 2nd ChT with 2nd IT; delay local XRT until 1.5 years
	1.5–2.5 years	Consider resection. Local XRT + changed chemotherapy: 2nd ChT with 2nd IT start simultaneously with XRT
	2.5–3	Consider resection. Change chemotherapy: 2nd ChT with 2nd IT; delay XRT until 3 years; then give CSI. Complete protocol after CSI without IT. Might need dose reduction for bone marrow toxicity
PD multiple sites	<2.5 years	Change chemotherapy: 2nd ChT with 2nd IT, no XRT. Reevaluate by the end of the protocol. If there is still tumor, reconsider local therapy or low-intense long-term chemo
	2.5–3 years	Change chemotherapy: 2nd ChT with 2nd IT; delay XRT until 3 years; then give CSI. Complete chemotherapy without IT. Might need dose reduction for bone marrow toxicity
	>3 years	CSI XRT, followed by changed chemotherapy: 2nd ChT without IT

1st ChT first-line systemic chemotherapy, *2nd ChT* second-line systemic chemotherapy, *XRT* radiation therapy, *CSI* craniospinal irradiation with boost, *IT* intrathecal chemotherapy, *localXRT* local radiation therapy



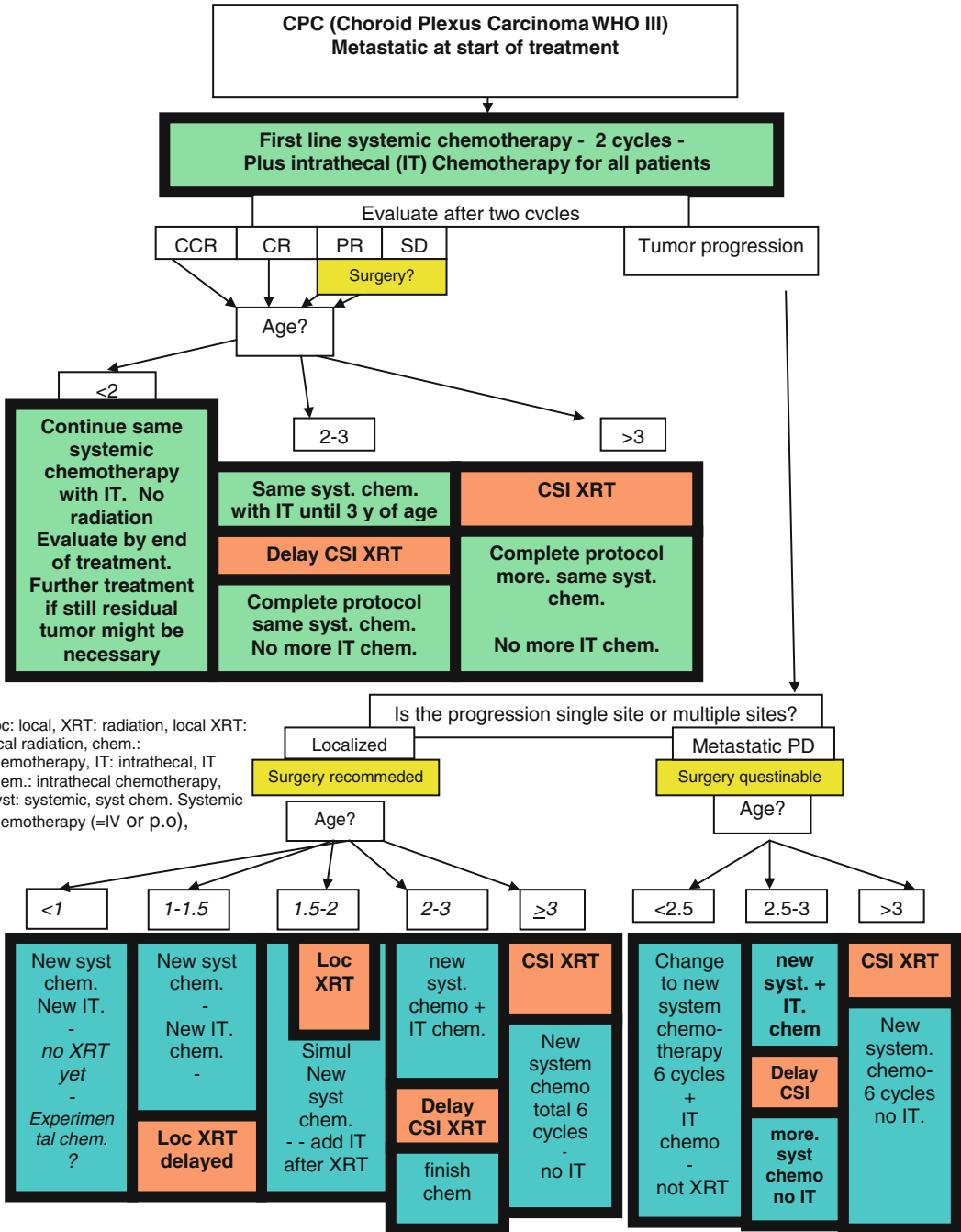
49.2.3.6 Metastatic Choroid Plexus Carcinoma

After maximal possible resection, start treatment with two cycles of first-line systemic

chemotherapy (1st ChT) including intrathecal chemotherapy (IT). Evaluate response. Further treatment is stratified by treatment result and patient age.

Result of 1st ChT	Patient age	Treatment
CCR or CR	<2 years	Continue same 1st ChT with IT. No XRT. Reevaluate. Start watch and wait
	<2–3 years	Continue same 1st ChT with IT. Delay XRT until 3 years old, might require reducing intensity after 6 cycles. Then give CSI XRT. Finish 1st ChT without further IT. Reevaluate. Start watch and wait program
	>3 years	CSI XRT followed by same 1st ChT without IT. Evaluate. Watch and wait
PR or SD	<2 years	Continue same 1st ChT with IT. No XRT. Reevaluate. Start watch and wait
	<2–3 years	Continue same 1st ChT with IT. Delay XRT until 3 years old, might require reducing intensity after 6 cycles. Then give CSI XRT. Finish 1st ChT without further IT. Reevaluate. Start watch and wait program
	>3 years	CSI XRT followed by same 1st ChT without IT. Evaluate. Watch and wait
PD single site	<1 year	Consider resection or at least biopsy. Change chemotherapy: 2nd ChT with 2nd IT, no XRT
	1–1.5 years	Consider resection or at least biopsy. Change chemotherapy: 2nd ChT with 2nd IT; delay local XRT until 1.5 years
	1.5–2 years	Consider resection or at least biopsy. local XRT + changed chemotherapy: 2nd ChT with 2nd IT start simultaneously with XRT
	2–3	Consider resection or at least biopsy. Change chemotherapy: 2nd ChT with 2nd IT, might need reduction of intensity later to be continued until patients are 3 years old. Then give CSI XRT. Complete chemo protocol after CSI without IT. Might need dose reduction for bone marrow toxicity
	>3	Consider resection or at least biopsy. CSI XRT, followed by changed chemotherapy: 2nd ChT without IT
PD multiple sites	<2 years	If multiple sites are growing, surgery is only of limited value, might be built in later. Change chemotherapy: 2nd ChT with 2nd IT, no XRT. Reevaluate by the end of the protocol. If there is still tumor, reconsider local therapy or low-intense long-term chemo
	2–3 years	If multiple sites are growing, surgery is only of limited value, might be built in later. Change chemotherapy: 2nd ChT with 2nd IT, might need reduction of intensity later to be continued until patients 3 years. Then give CSI XRT. Complete chemo protocol after CSI without IT. Might need dose reduction for bone marrow toxicity
	>3 years	If multiple sites are growing, surgery is only of limited value, might be built in later. CSI XRT, followed by changed chemotherapy: 2nd ChT without IT

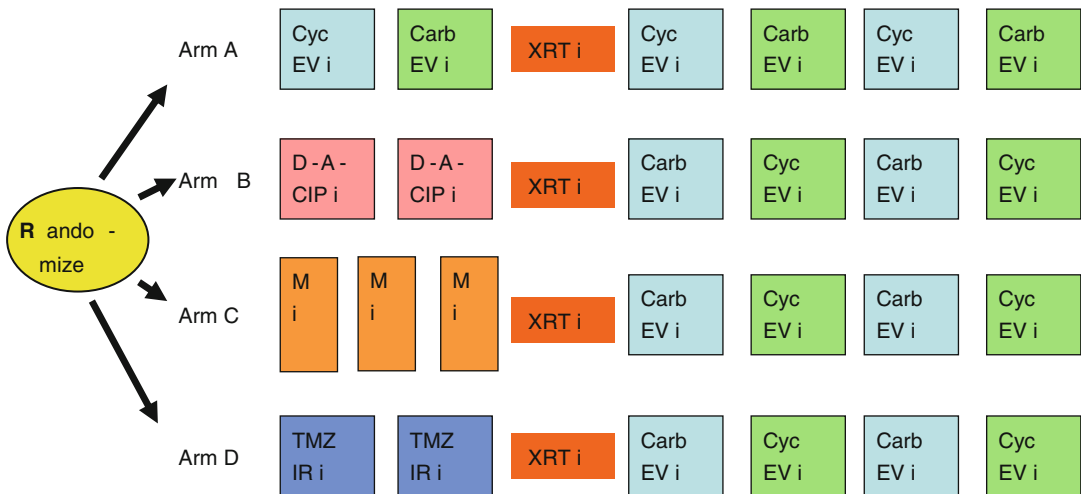
1st ChT first-line systemic chemotherapy, *2nd ChT* second-line systemic chemotherapy, *XRT* radiation therapy, *CSI* craniospinal irradiation with boost, *IT* intrathecal chemotherapy, *localXRT* local radiation therapy



For patients that are part of the wait and see program, i.e., the patients that are not receiving any additional treatment, they should have physical exam and neuroimaging every 3 months for

the first year and then every 6 months till fifth year and annually afterward.

49.3 CPT: SIOP-2009 Protocol Overview



Details of the treatment are:

- Standard arm:** Alternating chemotherapy cycles with VP16 100 mg/m² over 1 h on days 1–5, carboplatin 350 mg/m² over 2 h on days 2 and 3, and vincristine 1.5 mg/m² on day 5 alternating with VP16 100 mg/m² over 1 h on days 1–5, cyclophosphamide 1 g/m² over 1 h on days 2 and 3, and vincristine 1.5 mg/m² on day 5. Six blocks are given in 4-week intervals (day 1 to day 1). Radiation is given between the second and the third cycle only to a small subgroup of patients defined by age histology staging and response to the first two cycles of chemotherapy.
- Doxorubicin/cisplatin arm:** Doxorubicin 25 mg/m²/day over 12 h on days 1–3, dactinomycin 45 µg/kg/day (max. 2 mg) i.v. on day 1, cisplatin 70 mg/m²/d over 6 h on day 4, and vincristine 1.5 mg/m²/day (max. 2 mg) i.v. on days 8 and 15. An identical second cycle is started on day 28 if the side effects
- Methotrexate arm:** 5 g/m² over 24 h with leucovorin rescue at hour 42 given three times on days 1, 15, and 29. The further treatment is identical in all four treatment arms.
- Temozolomide irinotecan arm:** Temozolomide is given at 150 mg/m²/day × 5 days orally and combined with irinotecan 50 mg/m²/day × 5 days as 1 h infusions. Two of these cycles are followed by the common radiation – four-cycle chemotherapy protocol.

49.4 Radiation

Radiation therapy is accepted as part of the standard treatment for patients with choroid plexus

carcinoma [41, 42]; however, data is lacking regarding the radiation dose responsiveness and appropriate target volumes with respect to histological grade and extent of disease at diagnosis. A literature search suggested that the use of radiation therapy has a significant influence in the survival outcomes in patients with choroid plexus carcinoma [41, 42]. Craniospinal irradiation (CSI) should be performed with X-rays with a nominal energy of ≥ 4 MV or electron-proton beam radiation can be used if the institution has experience with these techniques. While planning radiation therapy, the gross tumor volume should include all gross residual tumors and/or the surgical cavity at the primary site after the initial imaging examination and on subsequent imaging done prior to the radiotherapy if there has been disease progression or anatomic changes because of resolution of postoperative changes.

Prescribed doses should be as follows:

Attained age	CSI	Partial brain	GTV/brain met boost	Boost to spinal metastases
<1.5 years	None	None	n/a	n/a
≥ 1.5 years to <2.5 years ^a	None	50.4 Gy	n/a	n/a
≥ 2.5 years to <3 years ^a	Delay to 3 years	54 Gy	n/a	n/a
≥ 3 years	If not needed	54 Gy (no CSI)	n/a	n/a
≥ 3 years	36 Gy	–	18 Gy	9 Gy at cord, 14.4 Gy below cord

^aPatients <3 years will not receive CSI but may receive partial brain RT

In summary, the treatment of choroid plexus tumors should include maximal possible surgery, and adjuvant treatment with chemotherapy and/or radiotherapy should be considered for all patients with various risk factors as mentioned in the text.

Acknowledgement The text is in part identical with the SIOP-CPT-2009 protocol; we thank the authors for permission. No conflicts of interest.

References

- Wolff J (2008) Choroid plexus tumoren. In: Korinthenberg R, Ritter J (eds) Pädiatrische Hämatologie und Onkologie. Springer Science and Business Media, Heidelberg, p 2
- Wolff JE, Finlay J (2009) Choroid plexus tumors. In: Carroll WL, Finlay JL (eds) Cancer in children. Jones & Bartlett Publishers, Sudbury
- Zulch KJ (1957) Brain tumors: their biology and pathology. Springer, New York
- Berrak SG, Liu DD, Wrede B et al (2011) Which therapy works better in choroid plexus carcinomas? J Neurooncol 103(1):155–162
- Ma YH, Ye K, Zhan RY et al (2008) Primary choroid plexus papilloma of the sellar region. J Neurooncol 88(1):51–55
- Jeibmann A, Wrede B, Peters O et al (2007) Malignant progression in choroid plexus papillomas. J Neurosurg 107(3 Suppl):199–202
- McEvoy AW, Galloway M, Revesz T et al (2002) Metastatic choroid plexus papilloma: a case report. J Neurooncol 56(3):241–246
- Louis DN, Ohgaki H, Wiestler OD et al (2007) The 2007 WHO classification of tumours of the central nervous system. Acta Neuropathol 114(2):97–109
- Jeibmann A, Hasselblatt M, Gerss J et al (2006) Prognostic implications of atypical histologic features in choroid plexus papilloma. J Neuropathol Exp Neurol 65(11):1069–1073
- Carruba G, Dallapiccola B, Brinchi V et al (1983) Ultrastructural and biological characterization of human choroid cell cultures transformed by Simian Virus 40. In Vitro 19(6):443–452
- Carruba G, Dallapiccola B, Mantegazza P et al (1984) Transformation of human choroid cells in vitro by SV40. Ultrastructural and cytogenetic analysis of cloned cell lines. J Submicrosc Cytol 16(3):459–470
- Shein HM, Enders JF, Levinthal JD (1962) Transformation induced by simian virus 40 in human renal cell cultures. II. Cell-virus relationships. Proc Natl Acad Sci U S A 48:1350–1357
- Davis LE, Nager GT, Johnson RT (1979) Experimental viral infections of the inner ear. II. Simian virus 40 induced tumors of the temporal bone. Ann Otol Rhinol Laryngol 88(2 Pt 1):198–204
- Kirschstein RL, Gerber P (1962) Ependymomas produced after intracerebral inoculation of SV40 into new-born hamsters. Nature 195:299–300

15. Brinster RL, Chen HY, Messing A et al (1984) Transgenic mice harboring SV40 T-antigen genes develop characteristic brain tumors. *Cell* 37(2):367–379
16. Enjoji M, Iwaki T, Hara H et al (1996) Establishment and characterization of choroid plexus carcinoma cell lines: connection between choroid plexus and immune systems. *Jpn J Cancer Res* 87(9):893–899
17. Reynolds RK, Hoekzema GS, Vogel J et al (1988) Multiple endocrine neoplasia induced by the promiscuous expression of a viral oncogene. *Proc Natl Acad Sci U S A* 85(9):3135–3139
18. Small JA, Blair DG, Showalter SD et al (1985) Analysis of a transgenic mouse containing simian virus 40 and v-myc sequences. *Mol Cell Biol* 5(4):642–648
19. Cho HJ, Seiberg M, Georgoff I et al (1989) Impact of the genetic background of transgenic mice upon the formation and timing of choroid plexus papillomas. *J Neurosci Res* 24(1):115–122
20. Chen J, Tobin GJ, Pipas JM et al (1992) T-antigen mutant activities in vivo: roles of p53 and pRB binding in tumorigenesis of the choroid plexus. *Oncogene* 7(6):1167–1175
21. Palmiter RD, Chen HY, Messing A et al (1985) SV40 enhancer and large-T antigen are instrumental in development of choroid plexus tumours in transgenic mice. *Nature* 316(6027):457–460
22. Kurtz HJ, Hanlon GF (1971) Choroid plexus papilloma in a dog. *Vet Pathol* 8(1):91–95
23. Ohashi F, Kotani T, Onishi T et al (1993) Magnetic resonance imaging in a dog with choroid plexus carcinoma. *J Vet Med Sci* 55(5):875–876
24. Ribas JL, Mena H, Braund KG et al (1989) A histologic and immunocytochemical study of choroid plexus tumors of the dog. *Vet Pathol* 26(1):55–64
25. Steiss JE, Cox NR, Knecht CD (1990) Electroencephalographic and histopathologic correlations in eight dogs with intracranial mass lesions. *Am J Vet Res* 51(8):1286–1291
26. Bergsagel DJ, Finegold MJ, Butel JS et al (1992) DNA sequences similar to those of simian virus 40 in ependymomas and choroid plexus tumors of childhood. *N Engl J Med* 326(15):988–993
27. Lednický JA, Garcea RL, Bergsagel DJ et al (1995) Natural simian virus 40 strains are present in human choroid plexus and ependymoma tumors. *Virology* 212(2):710–717
28. Martini F, Iaccheri L, Lazzarin L et al (1996) SV40 early region and large T antigen in human brain tumors, peripheral blood cells, and sperm fluids from healthy individuals. *Cancer Res* 56(20):4820–4825
29. Tabuchi K, Kirsch WM, Low M et al (1978) Screening of human brain tumors for SV40-related T antigen. *Int J Cancer* 21(1):12–17
30. Garber JE, Burke EM, Lavally BL et al (1990) Choroid plexus tumors in the breast cancer-sarcoma syndrome. *Cancer* 66(12):2658–2660
31. Yuasa H, Tokito S, Tokunaga M (1993) Primary carcinoma of the choroid plexus in Li-Fraumeni syndrome: case report. *Neurosurgery* 32(1):131–133; discussion 133–134
32. Kleihues P, Schauble B, zur Hausen A et al (1997) Tumors associated with p53 germline mutations: a synopsis of 91 families. *Am J Pathol* 150(1):1–13
33. Vajtai I, Varga Z, Bodosi M et al (1995) Melanotic papilloma of the choroid plexus: report of a case with implications for pathogenesis. *Noshuyo Byori* 12(2):151–154
34. Buxton N, Punt J (1997) Choroid plexus papilloma producing symptoms by secretion of cerebrospinal fluid. *Pediatr Neurosurg* 27(2):108–111
35. Fujimoto Y, Matsushita H, Plese JP et al (2004) Hydrocephalus due to diffuse villous hyperplasia of the choroid plexus. Case report and review of the literature. *Pediatr Neurosurg* 40(1):32–36
36. Wolff JE, Myles T, Pinto A et al (2001) Detection of choroid plexus carcinoma with Tc-99 m sestamibi: case report and review of the literature. *Med Pediatr Oncol* 36(2):323–325
37. Asai A, Hoffman HJ, Hendrick EB et al (1989) Primary intracranial neoplasms in the first year of life. *Childs Nerv Syst* 5(4):230–233
38. Berger C, Thiesse P, Lellouch-Tubiana A et al (1998) Choroid plexus carcinomas in childhood: clinical features and prognostic factors. *Neurosurgery* 42(3):470–475
39. Packer RJ, Perilongo G, Johnson D et al (1992) Choroid plexus carcinoma of childhood. *Cancer* 69(2):580–585
40. Wrede B, Liu P, Ater J et al (2005) Second surgery and the prognosis of choroid plexus carcinoma—results of a meta-analysis of individual cases. *Anticancer Res* 25(6C):4429–4433
41. Wolff JE, Sajedi M, Brant R et al (2002) Choroid plexus tumours. *Br J Cancer* 87(10):1086–1091
42. Wolff JE, Sajedi M, Coppes MJ et al (1999) Radiation therapy and survival in choroid plexus carcinoma. *Lancet* 353(9170):2126
43. Wrede B, Liu P, Wolff JE (2007) Chemotherapy improves the survival of patients with choroid plexus carcinoma: a meta-analysis of individual cases with choroid plexus tumors. *J Neurooncol* 85(3):345–351
44. Wrede B, Hasselblatt M, Peters O et al (2009) Atypical choroid plexus papilloma: clinical experience in the CPT-SIOP-2000 study. *J Neurooncol* 95(3):383–392

Martin U. Schuhmann and Marcos S. Tatagiba

50.1 Incidence and Association to NF2

Vestibular schwannomas (VS, also referred to as acoustic neuroma) are the most common infratentorial brain tumors in adults, accounting for about 8–10 % of the primary intracranial tumors and 80–90 % of those tumors located within the cerebellopontine angle (CPA) [1]. In children they constitute less than 1 % of all primary pediatric brain tumors, even less than 1 % of all posterior fossa tumors [2]. In most cases the presence of vestibular schwannomas in childhood and adolescence is connected to the coexistence of neurofibromatosis type 2 (NF2).

Vestibular schwannomas are benign tumors assigned to WHO Grade I. Derived from Schwann cells they are histologically dominated by spindle cells which form two characteristic patterns: Antoni A and Antoni B.

The overall incidence of VS is estimated to be 1 in 80,000 per year, cumulating to a lifetime risk of 1:1,000 in the general population [3, 4]. Most patients with unilateral sporadic VS present at an age beyond 40 years [3, 5]. Therefore, sporadic VS in childhood are extremely rare. In a large series of 1,000 surgically treated VS in a renowned skull base center specializing in VS treatment, only 3 of 880 patients with a sporadic unilateral VS (0.34 %) were treated at an age of 11–17 years (personal communication by [5]).

Around 5–7 % of all VS are due to NF2, an autosomal dominant inherited disease, which has an estimated incidence of 1:25,000 at birth [4]. Although NF2 is characterized by bilateral vestibular schwannomas at the time of presentation, up to 10–25 % of NF2-associated VS might initially be presenting unilaterally [6]. It could recently be shown that patients presenting with unilateral VS and other tumors typically related to NF2 (and thus fulfilling the NIH criteria for diagnosing NF2) had a high risk of 82 % of developing a contralateral VS, if initial diagnose was established at an age below 18 years [7]. The average age of clinical onset in NF2 patients, however, is 18–24 years, thus just beyond adolescence [8]. Of 1,000 surgically treated VS, 120 were operated in 82 NF2 patients at a mean age of 27.5 years [5, 9]. Most pediatric cases treated at an age below 18 years will be associated with NF2. In the above-named series, 14 of 17 patients (82 %) operated between 11 and 17 years of age

M.U. Schuhmann, M.D. (✉)
Section of Pediatric Neurosurgery, Department of
Neurosurgery, Eberhart Karls University Hospital of
Tübingen,
Hoppe-Seyler-Str. 3, Tübingen 72076, Germany
e-mail: martin.schuhmann@med.uni-tuebingen.de

M.S. Tatagiba, M.D.
Department of Neurosurgery, Eberhart Karls
University Hospital of Tübingen,
Hoppe-Seyler-Str. 3, Tübingen 72076, Germany
e-mail: marcos.tatagiba@med.uni-tuebingen.de

were associated with NF2 (personal communication by [5]). In our own series of 413 cases of surgically treated VS during the last 7 years, 3.4 % were children and 82 % of them were associated with NF2.

50.2 Symptomatology and Establishment of Diagnosis

Sporadic VS and VS in NF2 patients diagnosed in adulthood often present with impairment of VIII nerve function like hearing impairment, tinnitus, vertigo, and balance problems. Children with NF, especially those where the diagnosis is established at an age below 10 years of age, are different in our experience and according to others [10–12]. Here, other signs and symptoms like subtle skin tumors, posterior capsular cataracts, or retinal dysplasia, symptoms associated to other schwannomas or NF2-related peripheral neuropathy, prevail at the time of clinical diagnosis or have been present years before establishment. The clinical suspicion of NF2, especially in absence of a noticeable hearing impairment, has to be prompted by immediate high-resolution MRI with contrast application. MRI is the method of choice to establish the diagnosis of vestibular schwannomas and, if VS are bilaterally present, of NF2.

If NF2 is diagnosed early, children will still be asymptomatic regarding hearing. VS are therefore often an incidental finding. On the other hand, those children with early diagnosis of NF2 due to skin or eye involvement or other tumors than VS belong to the severe type (Wishart type) of NF2 [11]. In these children VS will most likely grow rather earlier than later (Fig. 50.1).

Therefore, in all NF2 children surveillance MRI scanning is mandatory at least every 12 months to detect VS growth in time. We perform in addition audiograms with speech discrimination tests and brain stem auditory evoked potential (BAEP) every 6 months, as also has been suggested by others [13].

All children with persistent unilateral hearing impairment, tinnitus, or balance problems without other signs of NF2 have to undergo MRI as well to rule out or diagnose VS as an underly-

ing cause. The presence of a facial nerve paresis at the time of diagnosis of a tumor involving the internal auditory canal arises the suspicion of a facial nerve schwannoma, in case of known NF2, or, in absence of NF2, of a rare differential diagnosis like teratoma.

Vestibular schwannomas in childhood usually involve the internal auditory canal and are rarely located in the cerebellopontine cistern alone. Tumors located solely within the cerebellopontine cistern, even if associated with unilateral hearing loss, are in our experience more likely to belong to more typical pediatric tumor entities of the posterior fossa like ependymoma or medulloblastoma. This is especially true if there is any suspicion of involvement of the cerebellum or the lateral recess of the fourth ventricle.

Typical MRI features of vestibular schwannomas are the presence of an isointense to mixed isointense-hypointense mass in T1-weighted images showing a rather homogeneous enhancement (two thirds homogeneous, one third inhomogeneous) after contrast application. Central slightly irregular hypointensities in post-contrast images of larger tumors extending into the cerebellopontine angle are common. This corresponds to circumscribed degenerative cystic and necrotic areas [14]. Lesions are slightly hyperintense in T2-weighted images. High-resolution CISS or true FISP images often allow to delineate, especially in smaller tumors, the course of the neighboring cochlear and facial nerve within the cistern or even within the internal auditory canal.

Tumor extension is best described according to the Hannover classification to provide a uniform anatomical basis for the process of decision making in the later course of the disease: T1 = purely intrameatal; T2 = intrameatal and limited extrameatal extension; T3A = filling the cerebellopontine cistern, not reaching the brain stem; T3B = filling the cerebellopontine cistern and reaching the brain stem; T4A = compressing the brain stem; and T4B = hydrocephalus secondary to compression of the fourth ventricle [5].

In all cases where surgery is planned, a thin-sliced (2 mm) bone window CT scan in reduced radiation dose has to be performed, since it provides the surgeon with critical information like position of emissary veins and of the jugular bulb

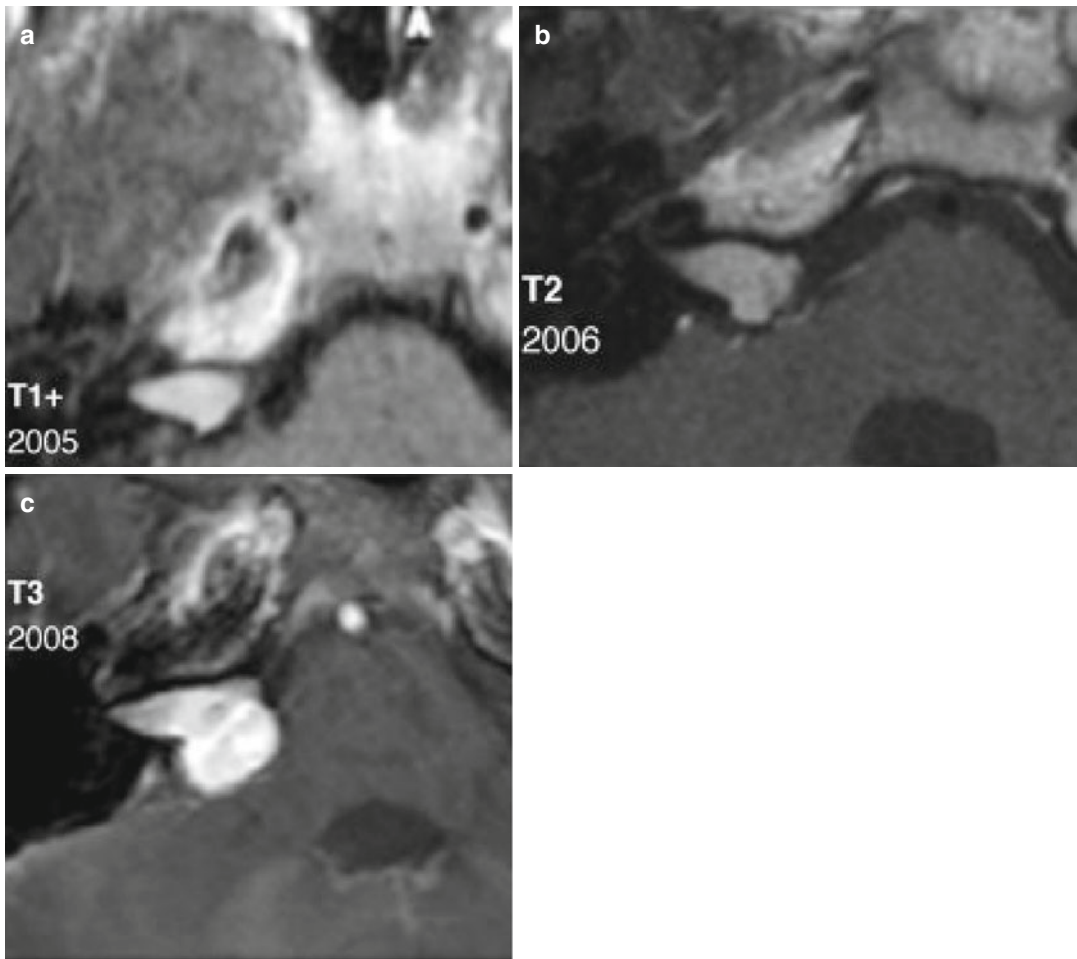


Fig. 50.1 MRI surveillance scans of a boy with Wishart type of NF2. After hearing-preserving partial resection of the VS on the left side at age 13, the tumor on the right side (T1+) was observed (a). At age 14, when tumor

growth to T2 was evident (b), the family was not ready for a second intervention. At age 16 the tumor size had grown to T3 (c) and the boy underwent partial resection

(high riding?) and the topographical orientation of the semicircular canals in relation to the planned opening of the internal auditory canal to avoid injury of the former.

50.3 Treatment Options

As in all tumors of the central nervous system, the basic three treatment options are neurosurgical resection, radiotherapy, and chemotherapy. Since VS are benign tumors, WHO I, standard chemotherapy and conformal radiotherapy are per se no primary treatment options. Purely from the point of tumor biology, gross total surgical

resection is the treatment of choice since it carries the strongest potential of cure. However, in VS surgery functionality of the involved cochlear nerve and facial nerve is the most important cofactor. The rate of functional preservation is on one hand strongly dependent on the experience of the surgeon and the employed microsurgical technique; on the other hand, it depends on tumor-associated factors like adherence/infiltration, tumor size, and level of preoperative hearing [15, 16]. In case of bilateral VS in NF2, a real long-term threat of bilateral deafness and facial nerve paralysis exists. Therefore, the avoidance of functional deficits has even higher priority, especially in children. Consequently, we have

shifted our surgical strategy in children away from GTR as outlined below.

In sporadic unilateral VS in adults, Gamma Knife radiosurgery is meanwhile a firmly established alternative treatment option for smaller- to medium-sized tumors with a large body of available literature, suggesting good tumor control rates in the 90 % range, preservation rate for serviceable hearing of 50–80 %, and long-term facial nerve injury rate of 1 % [17–20]. Long-term outcome analysis beyond 15 years however is still rare in the literature.

Only a few studies have targeted a larger number of NF2 patients with radiosurgery [21–25]. However, in none of those series, the few included pediatric patients have been analyzed separately. Concerns regarding Gamma Knife treatment in VS of NF2, as evident from the most recent series [21] like lower control rates in younger patients, rather rapidly decrease of hearing function over the first 5 years from 76 % after 1 year to 48 % after 5 years and the fact that there is a 18.8 relative risk for induction of new schwannomas and a real risk of malignant transformation after radiosurgery [26] do apply even more to the pediatric age group, where long-term stability is the most prominent treatment goal in smaller tumors with preserved hearing. In one series of NF2 patients treated with Gamma Knife, only 6 of 14 NF2 patients (43 %) maintained their preoperative useful hearing at 3 years [25]. Furthermore, our adult experience from surgical intervention in growing tumors after radiosurgery is that of very difficult tumor removals with a high risk of facial nerve injury. We therefore do not recommend radiosurgery in the management of pediatric VS, especially in the most common setting of NF2.

An experimental chemotherapeutic approach with bevacizumab has shown some promising results very recently in NF2 patients regarding tumor response and hearing improvement [27, 28]. However, it could be shown that this effect is only sustained under continued therapy and rebound occurs after therapy stops [29]. No experiences in adolescence have been published so far. Therefore, this option, which remains experimental since the drug is not approved for the use in NF2 and schwannomas, is not suitable for pediatric application.

50.4 Surgical Treatment Algorithm

Children without NF2 and sporadic vestibular schwannomas will most likely be diagnosed at a time of beginning hearing loss when the tumor has already grown to a considerable size of at least T3, mostly T4a and T4b. In a series of seven sporadic pediatric VS [30], the average tumor size was even considerably larger than in a meta-analysis of 1,345 adult patients [31]. In these children both the (beginning of) hearing impairment and brain stem compression are indications for surgical treatment.

Children with NF2 are different, especially if they are diagnosed early at a time of unimpaired hearing harboring still small tumors. The major threat coming from those early diagnosed bilateral VS to children is the development of complete deafness in the next 10–20 years, not brain stem compression. The latter is most of the time present in late discovered cases which are often unilaterally deaf. Therefore, a pediatric treatment algorithm has to aim primarily at hearing preservation and, consequently, only second at facial nerve integrity and then at brain stem compression and lastly at gross total resection. Multiple management strategies are at hand. Already the question of timing of interventions ranges theoretically from prophylactic treatment despite unimpaired hearing at the time of discovery to prophylactic treatment despite unimpaired hearing at the time of proven growth, to intervention at the time of beginning hearing loss, to treatment after loss of functional hearing, to, finally, treatment only at the time of brain stem compression.

Figure 50.2 presents the “Tübingen algorithm” for the treatment of pediatric VS in NF2 patients, which is derived from treatment principles put forward by Samii and coworkers already years ago [9]. According to this algorithm, a treatment indication exists in T1 and T2 tumors at the time of tumor growth; in T3a we discuss with the family to wait or not until tumor growth has been proven. In T3b and T4a and T4b, we recommend treatment at time of diagnosis.

In all cases of functional hearing and bilateral T1, T2, and T3a, the goal is to perform a decom-

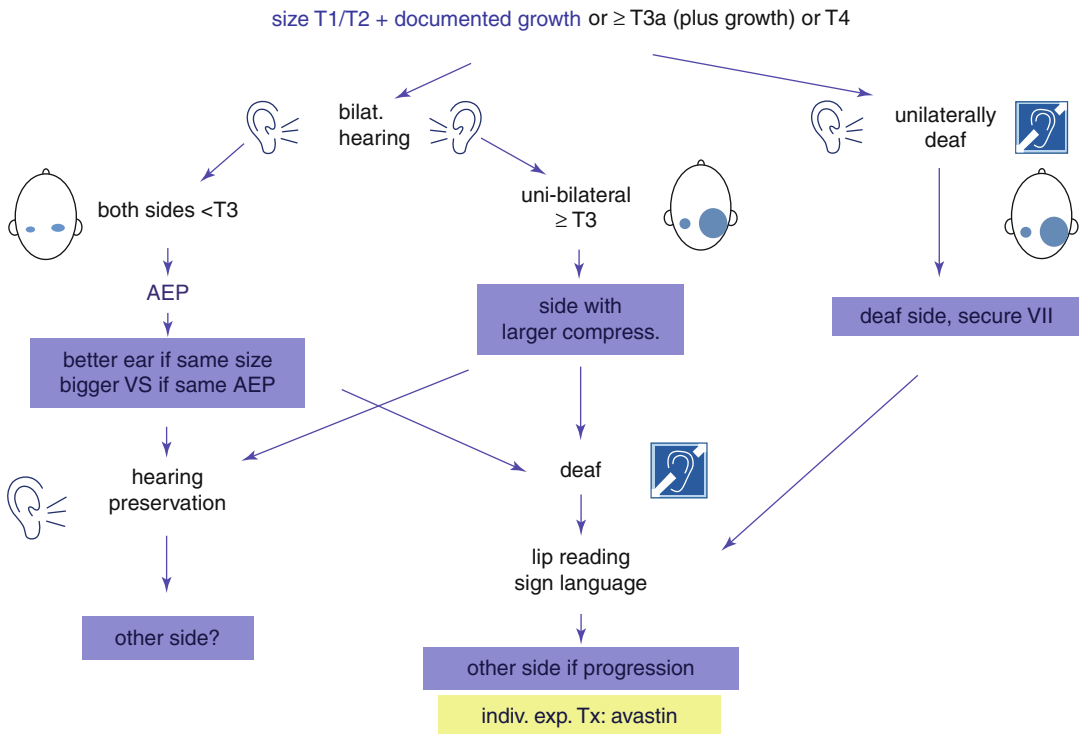


Fig. 50.2 The Tübingen algorithm for surgical treatment of VS in children with NF2

pression of the cochlear nerve by (a) opening the bony posterior circumference of the internal auditory canal and (b) partial resection of the tumor under strict control of the integrity of BAEP. The resection is stopped if BAEP starts to deteriorate and does not recover within a short time to the baseline levels.

The quality of preoperative bilateral BAEP is essential in the decision-making process. If the tumor size is similar, the side with the better BEAP is operated first since the better BEAP, the more sensitive and reliable is the intraoperative guidance according to neurophysiological monitoring and the higher are the chances of preservation of functional hearing. If BEAP is of similar good quality on both sides, we operate on the side of the larger VS first. If the presurgical goal of hearing preservation has been achieved, we operate on the other side, as soon as there is documented growth. If hearing has deteriorated to a nonfunctional level due to surgery, the patient has to undergo training for lip reading and sign language. Treatment of the other side is then delayed

and performed, according to the same principles, if tumor size is progressing significantly. Only in rare case BEAP is deteriorating without discernible tumor growth.

If tumors are uni- or bilaterally larger than T3a and the child has maintained bilateral functional hearing, we recommend surgery at the time of diagnosis and treat the side of more significant brain stem compression first, again aiming at hearing preservation and not at total removal. In case of preservation or loss of hearing, treatment of the other size is as in smaller tumors.

In patients with unilateral functional hearing loss or complete deafness at the time of diagnosis, tumors are almost always larger than T3a on the more severely affected side. The aim is now to resect the VS on this side as radical as possible, guided by the preservation of facial nerve function according to intraoperative facial motor evoked potentials and responses to direct stimulation of the facial nerve. The treatment of the other, still hearing, side follows the same principles as outlined above.

In patients with bilateral loss of functional hearing, the side with the larger brain stem compression is of course treated first, again aiming primarily at preservation of facial nerve function and not at total removal.

50.5 Surgical Technique

In T1, T2, and T3a tumors, we perform surgery in supine position with the head turned to the contralateral side, the same positioning as used for vascular decompression procedures in the cerebellopontine angle. A park bench position is not necessary in children who usually have no limitations in head rotation. In larger tumors we prefer a semi-lying position under permanent surveillance of the right atrium via transesophageal ultrasound for early and highly sensitive detection of air embolism. The semi-lying position combines an upright head position with higher intrathoracic and cervical venous pressure than in sitting position which reduces the risk of air embolism. The major surgical advantage of the vertical head position is the fact that irrigation replaces suction to keep the operating field clear of blood and that bimanual dissection by the surgeon, which in our experience is the key feature for preservation of function, is enabled.

We perform a retrosigmoid lateral suboccipital approach via craniotomy, which is placed just medial to the sigmoid sinus and below the transverse sinus according to landmarks and thorough study of the bone window CT scans. A craniectomy, which is our standard procedure in adults, is not warranted since the dura is not firmly attached to the bone and robust in children and adolescents. Dura opening is performed in parallel to the transverse and sigmoid sinus and the CPA cistern opened to drain CSF. Afterward the cerebellum is smoothly retracted and the tumor exposed. The dura covering the posterior petrous bone is cut in a semicircular fashion with its base at the meatus of the internal auditory canal (IAC) and the dura excised. The posterior wall of the IAC is then completely removed with a diamond drill exposing the IAC as far lateral as possible. The preoperative bone window CT scan provides the necessary information to define the limits of a

safe approach sparing functionally important structures like the labyrinth [32, 33]. Opening of labyrinthine structures results in irreversible hearing loss due to outflow of the endolymph from the inner ear.

In NF2, the tumor in the IAC is more likely to be firm and strongly adhesive than soft and unattached to the cochlear nerve. Thus, the tumor is reduced in size under strict control of the BEAP. Any mechanical force transmission to the attached cochlear nerve like traction has to be avoided, and the amount of mass reduction with micro grasping forceps and CUSA is therefore very limited in firm tumors. In these cases the use of a 2 μm laser fiber for touch-free reduction of the tumor without mechanical stress to the attached cochlear nerve has been very useful; however, thermal effects require great caution with this modality as well. The extent of resection within the IAC has to be strictly tailored by BEAP integrity and requires experience with cochlear nerve handling (see Fig. 50.3).

In case of a nonfunctional hearing preoperatively, which is often found in larger tumors greater than T3a, the limitation regarding total tumor removal is the preservation of the facial nerve function. Facial nerve MEP provides additional information about the nerve integrity before the facial nerve is identified and exposed for direct stimulation. However, the correct interpretation of facial nerve MEP and the distinction between centrally and peripherally evoked potentials are essential and difficult at the same time and require experience. The preservation of facial nerve function has priority over total resection. In case of severe facial nerve infiltration, which is most of the time associated with a preoperative facial nerve paralysis, the attempt is made to reconstruct the facial nerve with a sural nerve graft in those cases where a proximal stump at the brain stem level and a distal stump at the fundus of the IAC exist. If not, a hypoglossal facial nerve anastomosis can be used for reanimation of facial nerve function in the further course, provided that the hypoglossal nerve is still functioning and not bearing a schwannoma, as can be the case in severe manifestation of NF2 (Wishart type).

After tumor removal all bony openings in case of pneumatization of the petrous bone

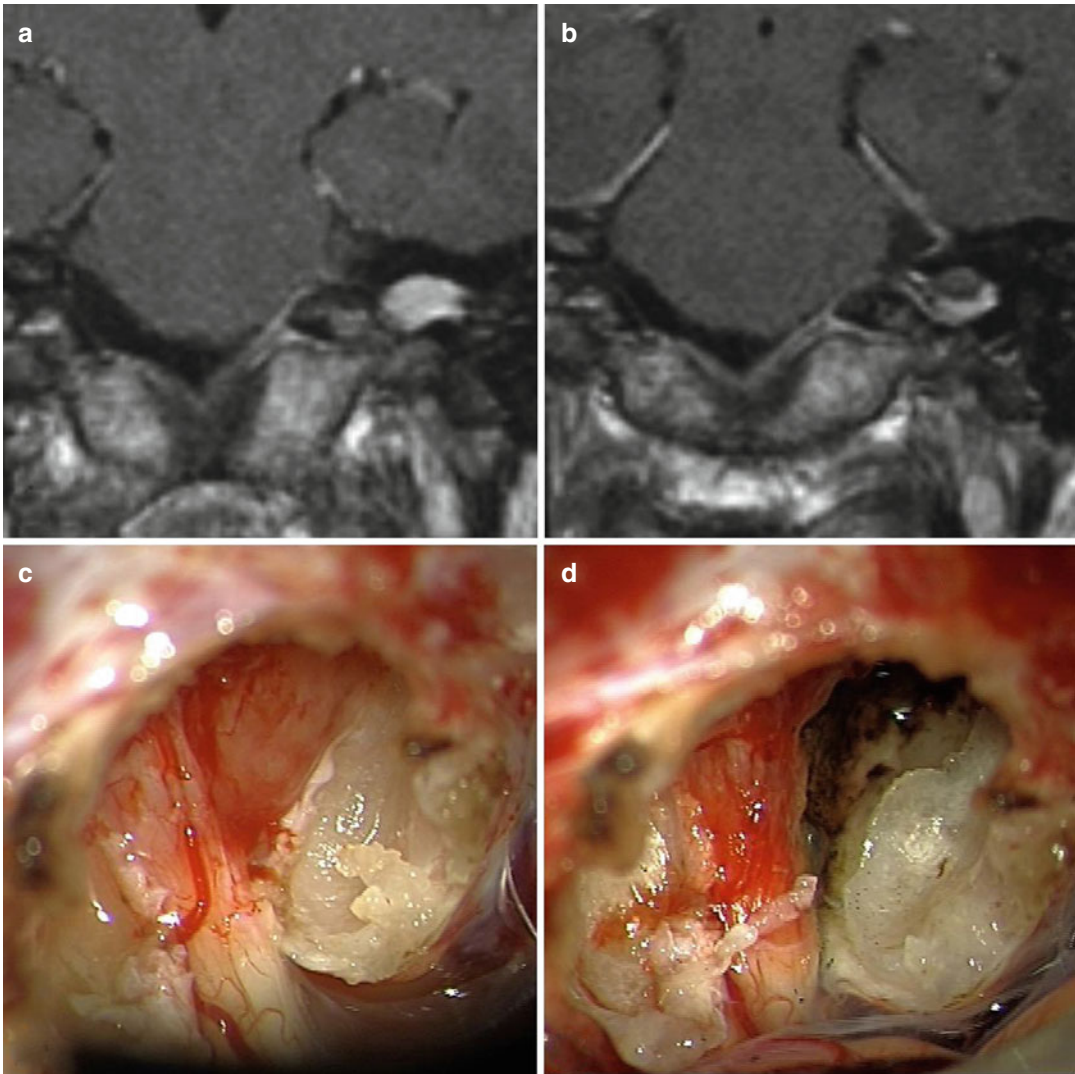


Fig. 50.3 An 11-year-old boy with Wishart type of NF2, who had already undergone removal of a tuberculum sellae meningioma. The left-sided VS showed growth and partial decompression after opening of the internal auditory canal was performed using forceps, CUSA and finally 2 μ m laser under strict guidance of BAEP integrity. (a) pre-operative MRI: coronal T1 weighted MRI after

contrast application. (b) post-operative scan in same orientation. (c) intra-operative view of the tumor after bony decompression of the internal audireotey canal. The yellowish tumor is next to the vestibulocochlear and facial nerve. (d) view of internal auditory canal after laser supported partial resection of the tumor masses cranial to the nerves.

in the area of drilling and at the lateral boarder of the craniotomy are covered/sealed with muscle and fibrin glue. The dura is closed watertight and covered with a resorbable sponge, and the bone flap is reinserted and fixed with sutures or microplates, depending on the patient's age. No drain is placed, the muscles are readapted, and the fascia is closed watertight with a running suture.

50.6 Postoperative Care and Surgical Outcome

Children usually recover well from surgical intervention and are kept on ICU for the first night. A control CT scan to rule out postoperative hemorrhage in the CPA and to assess the amount of intracranial air after semi-lying position is performed the next morning before transfer to

the regular ward. High-dose dexamethasone, which has been given as single shot at a dose of 0.3–0.4 mg/kg body weight intraoperatively, is initially continued at 0.05 mg/kg body weight three times a day and tapered to zero within 4 days postoperatively. Intravenous opioids are given for 2–3 days along with NSAIDs for pain control. Nausea and vomiting, sometimes vertigo, can be present in the first days. A firm head bandage is kept for 5 days to prevent subcutaneous serous or CSF collections. Patients usually feel fit enough for mobilization on the ward after discontinuation of opioids at days 3–5 and are discharged usually without any pain medication at postoperative days 7–8. Physiotherapy for restoration of full head movement is recommended for 4 weeks; thereafter, children return to school. We do not allow participation in school sports for 3 months to secure full wound healing and firm fixation of the bone flap.

Our rate of successful functional hearing preservation in T1 tumors has been in the range of 80 % if the above-described surgical strategies were employed. The larger the tumor (T2 and T3a) and the worse the quality of preoperative BEAP, the lower is the rate of hearing preservation (only 33 %). This highlights the importance of close follow-up surveillance in those patients for optimal timing of an intervention. If preoperative hearing is lost and tumor size is below T4, the rate of gross total removal with preserved facial nerve function can be as high as 80 %.

The long-term success of this strategy regarding the number of extra years of hearing preservation after decompression/partial resection in small T1 tumors as opposed to the natural course or an intervention later when hearing is already deteriorating is not known due to small numbers and the lack of a prospectively randomized trial.

However, we have not had a case of deafness during the second decade in those cases which were treated in our institution according to the proposed algorithm right from the beginning, nor did a patient die due to brain stem compression early on. This means, so far all children could finish school and continue education without becoming deaf. Patients with a severe manifestation of NF2, however, usually are deaf by the end

of the third decade, and multiple meningioma manifestations/meningiomatosis is evolving to be a life-threatening factor. It seems that the general severity of the NF2 manifestation is the key factor regarding long-term overall outcome beyond pediatric neurosurgery.

50.7 Follow-Up

Patients are followed postoperatively with an intensified schedule compared to preoperatively in case of NF2. This means audiograms and BEAP are performed every 3 months; imaging is done for the first time at 3 months postoperatively and then every 6 months. The reason for shorter surveillance intervals is the fact that most tumors showed growth before surgery and most children are in puberty at this time. The growth stimulus thus persists and changes in tumor size should be detected early.

Children with sporadic VS undergo as well a first postoperative MRI at 3 months; then surveillance scanning is continued every year for 5 years; then we switch to a 2-year cycle for further 6 years in case there was no tumor growth.

References

1. Urich H, Tien RD (1998) Tumors of the cranial, spinal and peripheral nerve sheaths. In: Bigner DD, McLendon RE, Bruner JM, Russell DS (eds) Russell and Rubinstein's pathology of tumors of the nervous system. Arnold, Oxford University Press, London
2. Pollack IF (1994) Brain tumors in children. *N Engl J Med* 331:1500–1507
3. Tos M, Charabi S, Thomsen J (1999) Incidence of vestibular schwannomas. *Laryngoscope* 109:736–740
4. Evans DG, Moran A, King A, Saeed S, Gurusinge N, Ramsden R (2005) Incidence of vestibular schwannoma and neurofibromatosis 2 in the North West of England over a 10-year period: higher incidence than previously thought. *Otol Neurotol* 26:93–97
5. Matthies C, Samii M (1997) Management of 1000 vestibular schwannomas (acoustic neuromas): clinical presentation. *Neurosurgery* 40:1–9
6. Evans DG, Lye R, Neary W, Black G, Strachan T, Wallace A, Ramsden RT (1999) Probability of bilateral disease in people presenting with a unilateral vestibular schwannoma. *J Neurol Neurosurg Psychiatry* 66:764–767

7. Evans DG, Ramsden RT, Shenton A, Gokhale C, Bowers N, Huson SM, Wallace AJ (2008) What are the implications in individuals with unilateral vestibular schwannoma and other neurogenic tumors? *J Neurosurg* 108:92–96
8. Evans DG, Huson SM, Donnai D, Neary W, Blair V, Newton V, Harris R (1992) A clinical study of type 2 neurofibromatosis. *Q J Med* 84:603–618
9. Samii M, Matthies C, Tatagiba M (1997) Management of vestibular schwannomas (acoustic neuromas): auditory and facial nerve function after resection of 120 vestibular schwannomas in patients with neurofibromatosis 2. *Neurosurgery* 40:696–705; discussion 705–696
10. Mautner VF, Tatagiba M, Guthoff R, Samii M, Pulst SM (1993) Neurofibromatosis 2 in the pediatric age group. *Neurosurgery* 33:92–96
11. Evans DG, Birch JM, Ramsden RT (1999) Paediatric presentation of type 2 neurofibromatosis. *Arch Dis Child* 81:496–499
12. MacCollin M, Mautner VF (1998) The diagnosis and management of neurofibromatosis 2 in childhood. *Semin Pediatr Neurol* 5:243–252
13. Evans DG, Newton V, Neary W, Baser ME, Wallace A, Macleod R, Jenkins JP, Gillespie J, Ramsden RT (2000) Use of MRI and audiological tests in presymptomatic diagnosis of type 2 neurofibromatosis (NF2). *J Med Genet* 37:944–947
14. Duvoisin B, Fernandes J, Doyon D, Denys A, Sterkers JM, Bobin S (1991) Magnetic resonance findings in 92 acoustic neuromas. *Eur J Radiol* 13:96–102
15. Samii M, Matthies C (1997) Management of 1000 vestibular schwannomas (acoustic neuromas): the facial nerve—preservation and restitution of function. *Neurosurgery* 40:684–694; discussion 694–685
16. Samii M, Matthies C (1997) Management of 1000 vestibular schwannomas (acoustic neuromas): hearing function in 1000 tumor resections. *Neurosurgery* 40:248–260; discussion 260–242
17. Hasegawa T, Fujitani S, Katsumata S, Kida Y, Yoshimoto M, Koike J (2005) Stereotactic radiosurgery for vestibular schwannomas: analysis of 317 patients followed more than 5 years. *Neurosurgery* 57:257–265; discussion 257–265
18. Lunsford LD, Niranjana A, Flickinger JC, Maitz A, Kondziolka D (2005) Radiosurgery of vestibular schwannomas: summary of experience in 829 cases. *J Neurosurg* 102(Suppl):195–199
19. Paek SH, Chung HT, Jeong SS, Park CK, Kim CY, Kim JE, Kim DG, Jung HW (2005) Hearing preservation after gamma knife stereotactic radiosurgery of vestibular schwannoma. *Cancer* 104:580–590
20. Kondziolka D, Lunsford LD, McLaughlin MR, Flickinger JC (1998) Long-term outcomes after radiosurgery for acoustic neuromas. *N Engl J Med* 339:1426–1433
21. Mathieu D, Kondziolka D, Flickinger JC, Niranjana A, Williamson R, Martin JJ, Lunsford LD (2007) Stereotactic radiosurgery for vestibular schwannomas in patients with neurofibromatosis type 2: an analysis of tumor control, complications, and hearing preservation rates. *Neurosurgery* 60:460–468
22. Rowe JG, Radatz MW, Walton L, Soanes T, Rodgers J, Kemeny AA (2003) Clinical experience with gamma knife stereotactic radiosurgery in the management of vestibular schwannomas secondary to type 2 neurofibromatosis. *J Neurol Neurosurg Psychiatry* 74:1288–1293
23. Roche PH, Regis J, Pellet W, Thomassin JM, Gregoire R, Dufour H, Peragut JC (2000) Neurofibromatosis type 2. Preliminary results of gamma knife radiosurgery of vestibular schwannomas. *Neurochirurgie* 46:339–353
24. Kida Y, Kobayashi T, Tanaka T, Mori Y (2000) Radiosurgery for bilateral neurinomas associated with neurofibromatosis type 2. *Surg Neurol* 53:383–389
25. Kondziolka D, Subach BR, Lunsford LD, Bissonette DJ, Flickinger JC (1998) Outcomes after gamma knife radiosurgery in solitary acoustic tumors and neurofibromatosis type 2. *Neurosurg Focus* 5:e2
26. Evans DG, Birch JM, Ramsden RT, Sharif S, Baser ME (2006) Malignant transformation and new primary tumours after therapeutic radiation for benign disease: substantial risks in certain tumour prone syndromes. *J Med Genet* 43:289–294
27. Mautner VF, Nguyen R, Kutta H, Fuensterer C, Bokemeyer C, Hagel C, Friedrich RE, Panse J (2010) Bevacizumab induces regression of vestibular schwannomas in patients with neurofibromatosis type 2. *Neuro Oncol* 12:14–18
28. Plotkin SR, Stemmer-Rachamimov AO, Barker FG 2nd, Halpin C, Padera TP, Tyrrell A, Sorensen AG, Jain RK, di Tomaso E (2009) Hearing improvement after bevacizumab in patients with neurofibromatosis type 2. *N Engl J Med* 361:358–367
29. Mautner VF, Nguyen R, Knecht R, Bokemeyer C (2010) Radiographic regression of vestibular schwannomas induced by bevacizumab treatment: sustain under continuous drug application and rebound after drug discontinuation. *Ann Oncol* 21:2294–2295
30. Walcott BP, Sivarajan G, Bashinskaya B, Anderson DE, Leonetti JP, Origitano TC (2009) Sporadic unilateral vestibular schwannoma in the pediatric population. Clinical article. *J Neurosurg Pediatr* 4:125–129
31. Smouha EE, Yoo M, Mohr K, Davis RP (2005) Conservative management of acoustic neuroma: a meta-analysis and proposed treatment algorithm. *Laryngoscope* 115:450–454
32. Samii A, Brinker T, Kaminsky J, Lanksch WR, Samii M (2000) Navigation-guided opening of the internal auditory canal via the retrosigmoid route for acoustic neuroma surgery: cadaveric, radiological, and preliminary clinical study. *Neurosurgery* 47:382–387
33. Matthies C, Samii M, Krebs S (1997) Management of vestibular schwannomas (acoustic neuromas): radiological features in 202 cases—their value for diagnosis and their predictive importance. *Neurosurgery* 40:469–481; discussion 481–462

Federico Di Rocco, Pascale Varlet,
Nathalie Boddaert, Jacques Grill, Thomas Roujeau,
Stephanie Puget, Bertrand Baussard, Michel Zerah,
and Christian Sainte-Rose

51.1 Introduction

Gangliogliomas (GGs) are an uncommon primary neoplasm of the central nervous system. They account for 0.4–1.3 % of all intracranial tumors [51]. GGs are typically identified in

F. Di Rocco, M.D. (✉) • T. Roujeau, M.D.
B. Baussard, M.D. • M. Zerah, M.D.
C. Sainte-Rose, M.D.
Department of Paediatric Neurosurgery,
Necker Enfants Malades Hospital, Paris, France
e-mail: fdirocco@iol.it;
christian.sainte-rose@nck.ap-hop-paris.fr

P. Varlet, M.D.
Department of Neuropathology, Sainte-Anne
Hospital, University Paris Descartes, Paris, France

Department of Pathology, Sainte-Anne Hospital,
Paris, France
e-mail: P.VARLET@ch-sainte-anne.fr

N. Boddaert, M.D.
Department of Paediatric Neurosurgery,
Necker Enfants Malades Hospital, Paris, France

Department of Radiology, Necker Enfants
Malades Hospital, Paris, France

J. Grill, M.D., Ph.D.
Pediatric and Adolescent Oncology,
Institut Gustave Roussy, Villejuif, France
e-mail: jacques.grill@igr.fr

S. Puget, M.D., Ph.D.
Department of Pediatric Neurosurgery,
Necker Hospital, Université Paris Descartes,
Sorbonne, Paris, France

adolescents and young adults. Eighty percent of the GGs occur, in fact, in patients younger than 30 years with a peak age of incidence between 10 and 20 years [13]. GGs are mostly a supratentorial with the majority of the tumors occurring in the temporal lobe. However, they may be found in any location of the central nervous system [31]. Infratentorial GGs are considered to be exceedingly rare. However, the development of modern pathological diagnostic techniques has suggested that these lesions might be more common than originally stated.

51.2 Background

The term *ganglioglioma* was originally used by Loretz in 1870 and was later popularized by Perkins in 1926 to refer to an intracranial tumor composed of a mixed population of neoplastic astrocytes and atypical ganglion cells [27]. GGs were described by Cushing in his monograph published in 1927. In 1930, Courville correctly acknowledged the mixed histological composition of mature ganglion cells and glial cells of varying proportions and degrees of differentiation [11]. The first descriptions of infratentorial GG go back to 1911 with Pick and Bielschowsky [17]. Later Foerster and Gagel in 1932 provided the first documented reports of medullary GG [17].

51.3 Epidemiology of Infratentorial GG

The actual incidence of GG is difficult to evaluate with data varying from 0.4 to 7.6 according to the type of series (pediatric series or series comprising patients of all ages) [[31, 51]; Idlar]. According to Zulch and Cushing, these tumors are extremely rare. Indeed, in their reports, GG accounted for 0.4 % and 0.3 % of all brain tumors, respectively [51].

GGs are prevalently located within the supratentorial compartment, the temporal lobe being most commonly affected, followed by the parietal and frontal lobes [13, 29, 31, 51]. The infratentorial location of GG, both within the cerebellum and the brainstem, is rare, with few anecdotal cases reported in the literature [43]. The brainstem location has been more frequently described than the cerebellar one (SSA, CDR). In 1984, by reviewing the literature, Garcia and coworkers [19] found only 14 cases, and more recently, in 2001, Lagares et al. [32] reported 31 cases of brainstem GG in patients of all ages. Lang and associates [33] in their series on GG found among 58 cases from 3 months to 66 years of age an infratentorial location in 9. To date, 41 cases of infratentorial GG have been described in children. Within posterior fossa lesions, the proportion of GG remains low. In the series by Chang and associates, among 133 posterior cranial fossa tumors, only 1 case of GG was described [9]. In 2001, Farmer et al. [16] found only three cases of GG in their 10-year review of brainstem gliomas. Similarly in 2003, Goncalves-Ferreira and coworkers [22] identified one case of GG in their series of 30 cases of focal brainstem expanding lesions. The age at presentation of infratentorial GG shows a wide range, beginning from 2 weeks to 59 years in brainstem GG and from 11 weeks to 60 years in cerebellar tumors. In general, the tumor affects mostly patients younger than 30 years with a peak age of incidence between 10 and 20 years [31, 32, 51].

No significant preference for sex or ethnicity has been reported.

51.4 Clinical Presentation

The clinical history of infratentorial GG before diagnosis is generally short compared to GG within the cerebral hemisphere (6 years and 1.25 years, respectively [33]). In children, however, the duration of symptoms before diagnosis can be as long as 7 years [3].

The clinical presentation of infratentorial GG depends on the structures involved. Pure cerebellar forms are rare. In most of the cases, the GGs are located within the brainstem or cerebellar peduncles (brainstem or transitional forms [38]).

Such brainstem location is the most common within the posterior cranial fossa. It is commonly revealed by focal motor and sensorial long pathway impairment and/or cranial nerve deficits, namely, hearing loss, intractable facial pain, hemifacial seizures, and hemiparesis. Cerebellar hemispheric signs and gait disturbance may also contribute to the picture. Headache is common [1, 3, 5, 14, 17, 24, 32].

More rarely, brainstem GGs may cause respiratory problems, syncope, and even sudden death [17, 32]. In fact, many of the brainstem GGs reported in the past were only detected by the postmortem.

Cerebellar GGs are more often hemispheric and present with slowly progressive cerebellar signs, eventually associated to gait disturbance. There are some reports describing epilepsy of cerebellar origin in patients with cerebellar GG [8, 24, 36]. Whether the cerebellar tumor initiates the seizure or simply lowers their epileptic threshold is still debated. Although the exact mechanism for the epilepsy arising in the cerebellum is not known, invasive electrophysiologic monitoring with depth electrodes has confirmed the cerebellum as the site of seizure origin [24]. It is thought that seizures arise in the cerebellum to subsequently generalize by involving the cortical surface secondarily [8, 24].

In spite of the location, hydrocephalus is rarely found in children with posterior fossa GG.

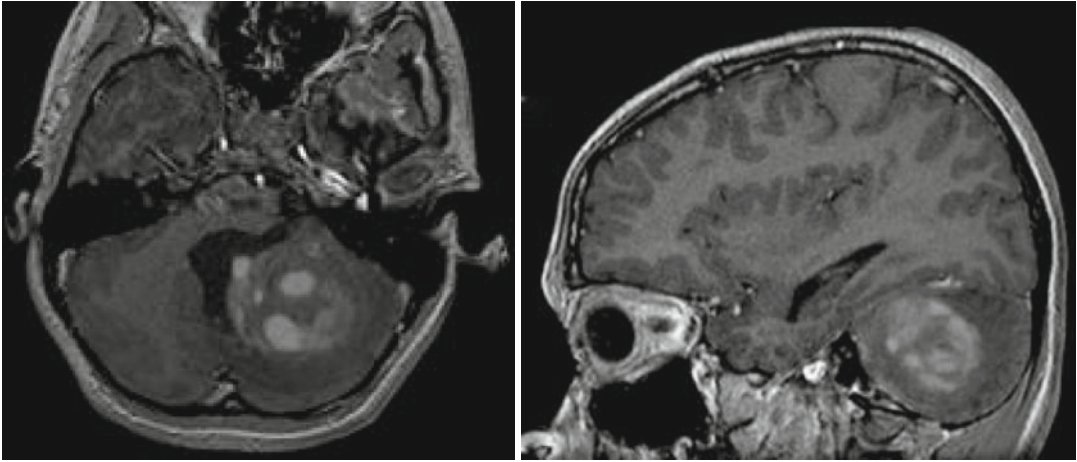


Fig. 51.1 Axial and sagittal post-gadolinium T1-weighted images show a typical aspect of ganglioglioma in the left cerebellar hemisphere with a mass effect. The enhanced-T1 image demonstrates patchy enhancement

51.5 Radiology Findings

On CT scans, most of GG present as masses with low density [5, 31, 51]]. Calcifications reported in the literature in 20–50 % of the cases [5, 31, 51]]. The degree of contrast uptake is variable, with 16–80 % of the patients showing an obvious enhancement [31]. Occasionally, GG can escape CT recognition consequently delaying the correct diagnosis (SSA). Even though MR imaging has proved to be more sensitive in identifying GG, the MR appearance is also variable and often nonspecific, with a spectrum of signal intensity ranging from hypointense to hyperintense on short MR images and hyperintense relative to the gray matter on long TR images [5, 31]. GG may appear cystic, solid, or mixed with nonspecific gadolinium enhancement [51]. The imaging features of infratentorial gangliogliomas seem to differ from those of a supratentorial location. The lesion is heterogeneous on imaging, appearing hypointense on T1-weighted images and hyperintense on FLAIR or T2-weighted sequences. In addition, the tumor seems often infiltrating with mass effect. In the majority of cases, the pattern of contrast enhancement on the T1-weighted images

consists of small, patchy areas of enhancement. Tumor enhancement is in fact very common in infratentorial GG [3], whereas in other location it varies greatly [13]. The pattern of enhancement observed in infratentorial GG is often relatively specific when showing areas of patchy enhancement within the tumor mass as opposed to supratentorial gangliogliomas that often appear as a delineated uniformly enhancing mass. The lesion appears thus as a dysplastic infiltrating lesion with some enhancing areas (Fig. 51.1). Cystic components have been reported in 30–57 % of the cases [3, 7, 23]. In posterior fossa, the cystic aspect might remind that of a pilocytic astrocytoma (Fig. 51.2). Although the tumor usually appears as an intra-axial avascular mass, extra-axial or vascular presentation may occur too [2]] (Fig. 51.3).

51.6 Histopathology

51.6.1 WHO Definition

Gangliogliomas belong to the group of glioneuronal tumors, morphologically characterized by a biphasic population of neuronal ganglion cell and

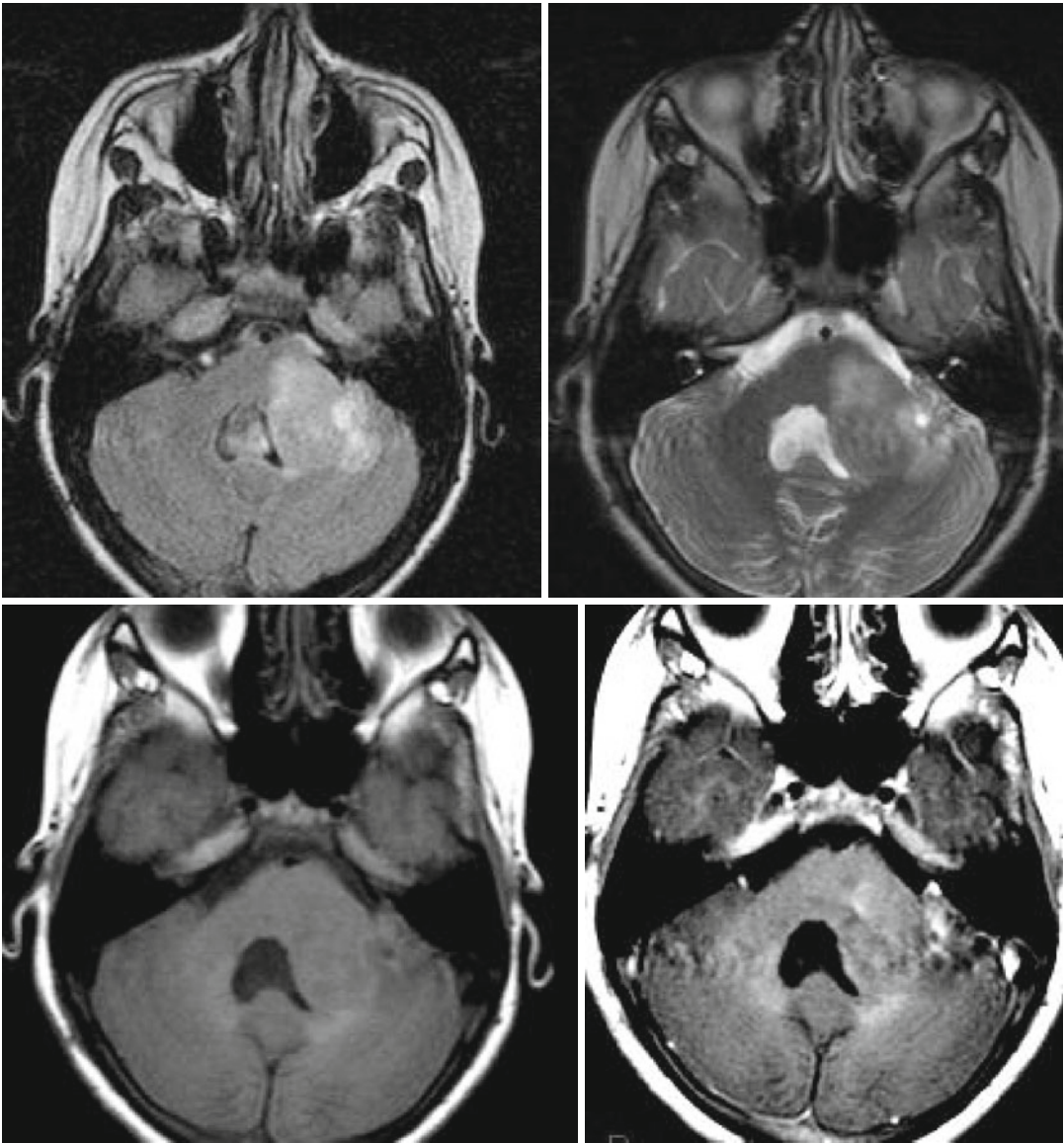


Fig. 51.2 FLAIR, T2, T1, and post-gadolinium T1 axial images show that the lesion is heterogeneous on imaging, appearing iso-intense on T1-weighted images and

hyperintense on FLAIR or T2-weighted sequences. The tumor is infiltrating and mass effect was noted

glial cell components. According to the WHO 2007 classification, GGs correspond to benign WHO grade I. Some rare GGs presenting the same anaplastic features found in aggressive gliomas are considered WHO grade III. Criteria for defining GG grade II have been not yet established (ref [4]).

51.6.2 Pathological Findings

GGs are characterized by a mixed glioneuronal phenotype usually composed of a major glial morphotype associated with a neuronal ganglion cell component (Fig. 51.4). The histopathological identification of GG is notoriously challenging

because both glial and neuronal populations may exhibit marked phenotypic heterogeneity and distribution. Consequently, GG morphological spectrum can range from a predominantly glial phenotype with exceptional ganglion cells to predominantly neuronal population. Glial elements are usually piloid astrocytic, but the glial cells

can also present with an oligodendroglial, clear cell, gemistocytic, or ependymal morphology [4, 6, 37, 49]. Ganglion cells are characterized by their abnormal noncortical localization and distribution as well as by cytomegaly, bizarre shape, vesicular nuclei, and abnormally aggregated Nissl substance. All these criteria are not always associated. Consequently, a broad neuronal spectrum may be observed, leading to potential discrepancies between true neoplastic ganglion cells and dystrophic residual neurons, particularly in anatomic areas containing pyramidal or large neurons as it occurs in temporal or brainstem structures. Binucleated or multinucleated neurons are pathognomonic but unfortunately rare and heterogeneously distributed. Additional histopathological features such as Rosenthal fibers, eosinophilic granular bodies, perivascular lymphoid infiltrates, and abundant capillary networks with many parallel capillaries are also encountered frequently. These nonspecific features may alert and motivate a careful analysis of all the samples to search for a ganglion cell component. Desmoplasia (connective tissue component intermingled with glial lobules) is a common associated feature and should not be interpreted as an aggressive metastatic leptomeningeal extension. Histologically, as compared to pilocytic astrocytoma, GGs are

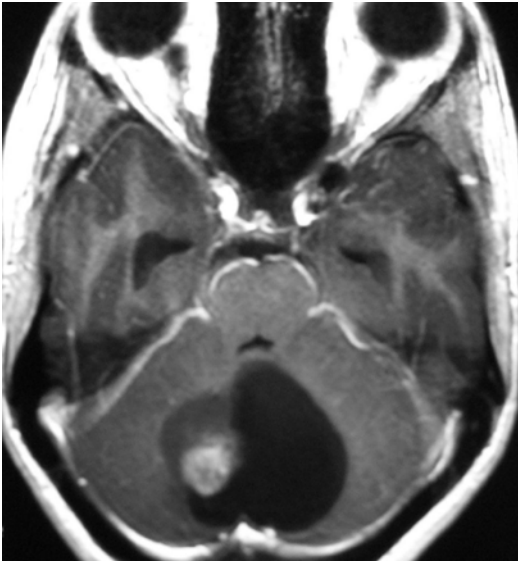


Fig. 51.3 Axial post-gadolinium T1-weighted images show a cystic tumor with an enhancing solid nodule

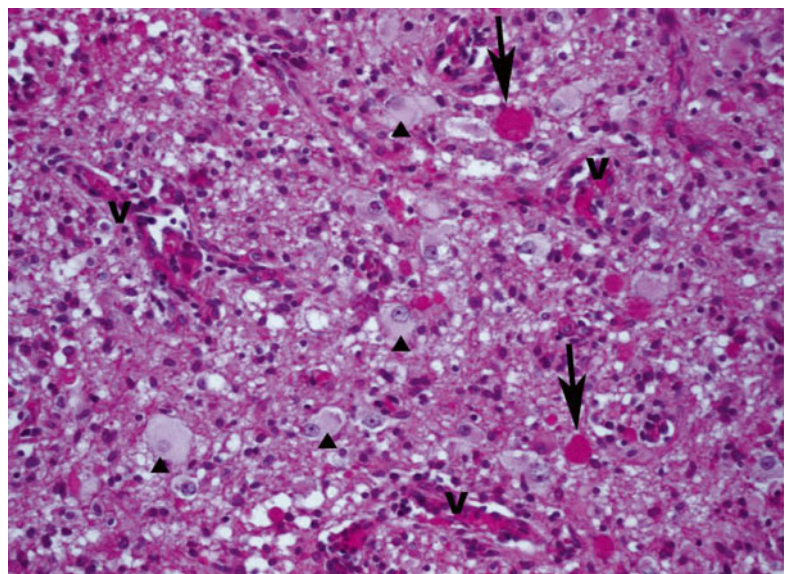


Fig. 51.4 Histological appearance of a typical ganglioglioma with double neuronal and glial component composed many ganglion neurons (*arrow-head*) and accompanied by granular body (*arrows*) characteristic but nonspecific. Vasculature is unique with many parallel capillaries (*V*) surrounded by perivascular lymphocytic infiltrate

not frequently well defined from the surrounding brain structures. They are associated with areas of marked dysplastic and/or atrophic parenchyma, leading in MRI to pseudo-infiltrating images.

The immunohistochemical profile of GG reflects the mixed glioneuronal nature, and many neuronal routine markers (such as chromogranin A, synaptophysin, NF70, and NeuN) are heterogeneously positive in ganglion cells. It is important to note that all these markers are not specific to neoplastic ganglion cells and are also positive in normal residual neurons. As a consequence, neuronal markers should be interpreted carefully and comparatively, preferentially in areas of tumoral tissue or in desmoplastic areas. Recently, studies suggested that the oncofetal CD34 transiently expressed during early neural development is frequently expressed in GG [6, 12]. These intratumoral and peritumoral highly ramified CD34 immunopositive cells are encountered in 66–74 % of gangliogliomas and are negative or only exceptional in DNET, pilocytic astrocytoma, or the infiltrative areas of low-grade oligodendroglioma or astrocytoma. Although the exact nature of the CD34-positive cells is not known, it has been suggested that they represent a glioneuronal progenitor cell as the majority of CD34-positive cells co-localized with S100 protein and more rarely with neuronal antigens [6, 12]. Thus, CD34 represents a valuable marker for the diagnostic evaluation of GG. MIB-1 index is generally low with a mean value ranging from 1 to 2.7 % [34].

51.6.3 Molecular Findings

Nonconsistent and recurrent allelic alterations have been identified, but gain of chromosomes 5, 7, 8, and 12 and loss of chromosomes 9, 10, and 22 have been described too [26]. No TP53 mutation, PTEN mutation, KRAS or IDH 1 mutation, or EGFR amplification [15, 50] has been documented. Mutational analysis in the coding region of the tuberous sclerosis 1 and 2 genes (TSC1, TSC2) did not discover any mutation on genes involved in the Reelin pathway [34]. However, in the two past years, the pathogenesis of GG is moving up by the involvement

of an aberrant mitogen-activated protein kinase (MAPK) pathway activation due to the identification of BRAF activating mutation [46]. The mechanism of MAPK activation seems to be different than in pilocytic astrocytoma (PA). Many recent studies have demonstrated gene fusions between KIAA1549 and BRAF in the majority of the PA, whereas BRAF activating mutation, particularly V600E, represents the genetic hallmark of GG [15, 34, 39, 45, 47]. These recent data, described in a small number of GG, need further translational studies particularly to establish the prognostic significance and more interestingly whether children with GG may benefit from inhibitors of the MAPK signaling pathway.

51.7 Differential Diagnosis

Two main groups of differential diagnoses should be considered:

1. Diffuse infiltrating gliomas containing residual trapped neurons. This possible “overdiagnosis” of GG is of importance as it can impact on the management and prognosis. Radiological and histopathological correlations may assist in distinguishing between these two entities. Diffuse gliomas present ill-defined margins on T2-weighted images without contrast enhancement, whereas GG is a more well-delineated, often cystic lesion. Furthermore, GG may present contrast-enhancing nodules. Unfortunately, reliable histopathological and immunophenotypical distinguishing criteria are scarce. Only binucleated neurons and CD34 extravascular positivity represent good arguments in favor of the neoplastic nature of the neuronal component.
2. CNS lesions containing ganglion cells: pilocytic astrocytoma, dysembryoplastic neuroepithelial tumor (DNET), pleomorphic xantho-astrocytoma (PXA), cortical dysplasia, Lhermitte-Duclos disease, and desmoplastic infantile ganglioglioma (DIG). The differential diagnosis with this type of tumors is particularly important. PA, DNET, and focal cortical dysplasia are stable lesions, while GG can undergo malignant transformation, even though rarely.

Pilocytic astrocytoma: The differential diagnosis with PA may be particularly difficult as the most frequent glial component of GG is morphologically piloid and frequently associated with Rosenthal fibers and eosinophilic granular bodies. Clinical and radiological considerations are of little help because these two entities are very similar with regard to the natural history and neuroradiological findings. The lack of CD34 immunoreactivity is a consistent finding in pilocytic astrocytoma and can help in the distinction between the two entities [6]. More recently, tandem duplication in chromosome band 7q34 with a KIAA1549-BRAF fusion has been described specifically in PA but not in GG [15, 39, 45, 47].

Dysembryoplastic neuroepithelial tumor (DNET): Complex form of DNET containing the specific glioneuronal element (GNE) but presenting frequently a neuronal component as intracortical lesion should be considered as DNET even if focally a dysmorphic neuronal component is observed. The recent findings of the absence of BRAF V600E mutation in DNETs and overlapping cases of DNET/GG support this idea [15]. The more challenging differential diagnosis is represented when the GNE is damaged, rare, or fragmented in biopsy or small specimens. In this situation, multiple histological sections and CD34 immunostainings can be useful as CD34 positivity is more frequent in GG than in DNET [12].

Pleomorphic xantho-astrocytoma (PXA): PXA corresponds to an astrocytic neoplasm grade II, characterized by pleomorphic and lipidized astrocyte, according to the WHO 2007 classification. However, this entity presents numerous clinical, radiological, and histological features overlapping those of GG. All the key histopathological features characterizing PXA could be encountered in GG, namely, granular bodies, perivascular lymphocytes, and dense reticulin fiber network. Moreover, PXA may express neuronal markers as well as CD34 with a variable frequency [20, 42]. The recent findings of BRAF 600E mutations in a subset of PXAs support the fact that GG, PXA, and DIG/DIA represent a same pathological spectrum, containing more or less ganglion cells or desmoplastic features [15, 18].

51.8 Malignant Transformation and Prognostic Factors

Histological grading of GG is still controversial. In particular, criteria for grade II have not been defined in the last WHO 2007 classification. It is important to note that the classical criteria used for purely astrocytic adult gliomas have been applied to GGs. A specific and dedicated GG grading system is thus challenging due to the rarity of grade II or grade III GG, estimated to, respectively, 10–2 % of the cases [35]. In a large series of 203 GGs, a 3-tiered grading system was found to be statistically significant. The authors found a 5-year OS in grade II estimated at 79 % versus 53 % for the grade III [35]. In the HIT-GBM database, the 5-year overall survival of GG grade III was comparable at 88 % [30].

A gemistocytic component, increased proliferative activity, increased cellularity, nuclear pleomorphism, and high MIB-1 labeling index may herald an adverse clinical course [40; Majores 2008]. However, these potential prognostic features should be better defined and further confirmed.

51.9 Management of Infratentorial GG

51.9.1 Surgical Management

The treatment of choice for gangliogliomas is total macroscopic excision whenever possible [3, 23, 27, 33]. Total removal is associated with the highest probability of a long-term disease-free survival.

Unfortunately, infratentorial gangliogliomas are amenable to total excision only when the tumor is confined to the cerebellum. The excision is often incomplete if the tumor extends to the cerebellar peduncle and partial in practically all cases of brainstem involvement. Despite the difficulties that might be encountered during the removal of such lesions in these particular locations, surgery should still be considered as first treatment. It is worth to note that the removal of the enhancing portion of the tumor can result in a long event free survival even in the absence of any further treatment. In patients with residual

nonenhancing tumors, no evidence of tumor progression or enhancement has been reported, with a follow-up of at least 2.5 years [3].

Because of the characteristics of the tumor, however, a postoperative neurological deterioration has been reported in about 30 % of the cases with infratentorial GGs [33]. This elevated morbidity reflects the difficulties related to the infiltrative nature of these tumors and the risks of a too aggressive surgery within the brainstem. This morbidity can, in fact, be lowered by limiting the surgery to the enhancing component of the tumor [3].

51.9.2 Medical Treatment

There are only limited reports about the use of adjuvant therapy in patients with infratentorial GG. Scarce information is available from the experience with supratentorial GG as adjuvant therapy is commonly not utilized in these tumors usually amenable to radical excision, except in case of malignant subtypes. In case of residual tumors, adjuvant therapy has utilized either in the early postoperative period or at the moment of disease progression [29, 33]. The efficacy of adjuvant therapy to control tumor progression is, however, not clear from the literature. Its use may be also weighted by potentially fatal complications such as severe hematological aplasia [3]. Responses to chemotherapy of non-pilocytic glioma have usually been reported less frequently [21]. Frequently, chemotherapy alone fails to control on the long run the progression of the tumor requiring therefore additional radiotherapy. The absent or modest benefit of chemotherapy explains why it is not utilized even in case of residual tumor [3, 28, 48].

Radiotherapy has been used for treatment of some brainstem GGs, but, similarly, its usefulness has yet to be proven [32, 41]. The deleterious side effects on the developing nervous system have been a strong argument against the use of this treatment modality in children [29]. Moreover, some reports suggest that postoperative radiation may favor the malignant degeneration [25, 44]. Due to bias in patient selection for radiotherapy (more aggressive tumors, incomplete resections, early postoperative progressions, etc.), it is dif-

ficult to assign the transformation to the effect of radiation therapy. However, secondary tumors have been extensively documented after brain irradiation.

51.9.3 Prognostic Factors

Infratentorial gangliogliomas are generally benign tumors, but their natural course is difficult to predict.

Although infratentorial GGs frequently are resected only partially, the overall survival time does not seem reduced as compared with supratentorial GG where a more radical resection can be achieved [32]. Among brainstem tumors, gangliogliomas have a better prognosis than other brainstem gliomas [16].

Further, invasiveness on radiographic studies or anaplasia within a GG seems not to correlate with clinical outcome. However, the risk of recurrence is higher for brainstem and spinal GGs than for supratentorial GGs [5, 33].

Brainstem gangliogliomas have a fivefold increased risk of recurrence compared with equivalent tumors in the cerebral hemisphere [33]. However, not all incomplete resections ultimately show an evolution toward a recurrence. Among nine patients with a posterior fossa gangliogliomas with at least 75 % reduction in their volume after surgery, the tumor recurred in only two cases [33].

The presence or absence of contrast enhancing within the residual tumor seems to correlate with the risk of recurrence. When no postoperative enhancement in the residual tumor is found, no disease progression might be observed for many years [3]. Conversely, in patients with an enhancing residual lesion, tumor progression is common [3]. This finding implies that children with posterior fossa gangliogliomas may benefit from the removal of the enhancing component of the tumor, which consequently should be attempted when possible.

Conclusions

Gangliogliomas are rare and generally benign tumors that might occur in the posterior fossa. The MR images of these tumors show patchy

enhancement after gadolinium administration, in contrast to gangliogliomas found in the supratentorial compartment. A total macroscopic excision of the tumor is often impossible because of its location within cerebellar peduncle and/or the brainstem. Nevertheless, in some cases, the mere excision of the enhancing portion of the tumor may suffice to obtain long progression-free survivals. In cases of progression of the residual tumor, further excision may be effective in controlling disease progression. Chemotherapy is of scarce usefulness. The use of radiotherapy is limited in many cases because of the location of the tumor, the age of the patient, and the risk of malignant degeneration.

References

- Athale S, Hallett KK, Jinkins JR (1999) Ganglioglioma of the trigeminal nerve: MRI. *Neuroradiology* 41:576–578
- Baltuch GH, Farmer JP, Meagher-Villemure K, O’Gorman AM, Montes JL (1993) Ganglioglioma presenting as a vascular lesion in a 10-year-old boy: case report. *J Neurosurg* 79:920–923
- Baussard B, Di Rocco F, Garnett MR, Boddaert N, Lellouch-Tubiana A, Grill J, Puget S, Roujeau T, Zerah M, Sainte-Rose C (2007) Pediatric infratentorial gangliogliomas: a retrospective series. *J Neurosurg* 107(4 Suppl):286–291
- Becker AJ, Wiestler OD, Figarella-Branger D, Blumcke I (2007) Ganglioglioma and gangliocytoma, 4th edn. IARC, Lyon, pp 103–105, WHO
- Blatt GL, Ahuja A, Miller LL, Ostrow PT, Soloniuk DS (1995) Cerebellomedullary ganglioglioma: CT and MR findings. *AJNR Am J Neuroradiol* 16:790–792
- Blümcke I, Wiestler OD (2002) Gangliogliomas: an intriguing tumor entity associated with focal epilepsies. *J Neuropathol Exp Neurol* 61(7):575–584
- Castillo M, Davis PC, Takei Y, Hoffman JC Jr (1990) Intracranial ganglioglioma: MR, CT and clinical findings in 18 patients. *AJR Am J Roentgenol* 154:607–612
- Chae JH, Kim SK, Wang KC, Kim KJ, Hwang YS, Cho BK (2001) Hemifacial seizure of cerebellar ganglioglioma origin: seizure control by tumor resection. *Epilepsia* 42:1204–1207
- Chang T, Teng MM, Lirng JF (1993) Posterior cranial fossa tumours in childhood. *Neuroradiology* 35:274–278
- Courville CB (1930) Gangliogliomas: tumor of the central nervous system—review of the literature and report of 2 cases. *Arch Neurol Psychiatry* 24:39–91
- Courville CB, Anderson FM (1941) Neuro-gliogenic tumor of the central nervous system: report of two additional cases of ganglioglioma of the brain. *Bull Los Angeles Neurol Soc* 6:154–176
- Deb P, Sharma MC, Tripathi M, Sarat Chandra P, Gupta A, Sarkar C (2006) Expression of CD34 as a novel marker for glioneuronal lesions associated with chronic intractable epilepsy. *Neuropathol Appl Neurobiol* 32(5):461–468
- Demierre B, Stichnoth FA, Hori A, Spoerri O (1986) Intracerebral ganglioglioma. *J Neurosurg* 65:177–182
- Dhillon RS (1987) Posterior fossa ganglioglioma: an unusual cause of hearing loss. *J Laryngol Otol* 101:714–717
- Dougherty MJ, Santi M, Brose MS, Ma C, Resnick AC, Sievert AJ, Storm PB, Biegel JA (2010) Activating mutations in BRAF characterize a spectrum of pediatric low-grade gliomas. *Neuro Oncol* 12:621–30
- Farmer JP, Montes JL, Freeman CR, Meagher-Villemure K, Bond MC, O’Gorman AM (2001) Brainstem gliomas: a 10-year institutional review. *Pediatr Neurosurg* 34:206–214
- Friedman WA, Vries JK, Quisling RG (1979) Ganglioglioma of the medulla oblongata. *Surg Neurol* 12:105–108
- Epstein N, Epstein F, Allen JC, Aleksic S (1982) Intractable facial pain associated with a ganglioglioma of the cervicomedullary junction: report of a case. *Neurosurgery* 10:612–616
- Forsheew T, Tatevossian RG, Lawson AR, Ma J, Neale G, Ogunkolade BW, Jones TA, Aarum J, Dalton J, Bailey S, Chaplin T, Carter RL, Gajjar A, Broniscer A, Young BD, Ellison DW, Sheer D (2009) Activation of the ERK/MAPK pathway: a signature genetic defect in posterior fossa pilocytic astrocytomas. *J Pathol* 218(2):172–181
- Garcia CA, McGarry PA, Collada M (1984) Ganglioglioma of the brain stem: case report. *J Neurosurg* 60:431–434
- Giannini C, Scheithauer BW, Lopes MB, Hirose T, Kros JM, VandenBerg SR (2002) Immunophenotype of pleomorphic xanthoastrocytoma. *Am J Surg Pathol* 26(4):479–485
- Gnekow AK, Kortmann RD, Pietsch T, Emser A (2004) Low grade chiasmatic-hypothalamic glioma—carboplatin and vincristine chemotherapy effectively defers radiotherapy within a comprehensive treatment strategy – report from the multicenter treatment study for children and adolescents with a low grade glioma – HIT-LGG 1996 – of the Society of Pediatric Oncology and Hematology (GPOH). *Klin Padiatr* 216(6):331–342
- Goncalves-Ferreira AJ, Herculano-Carvalho M, Pimentel J (2003) Stereotactic biopsies of focal brainstem lesions. *Surg Neurol* 60:311–320
- Haddad SF, Moore SA, Menezes AH, Van Gilder JC (1992) Ganglioglioma: 13 years of experience. *Neurosurgery* 31:171–178
- Harvey AS, Jayakar P, Duchowny M et al (1996) Hemifacial seizures and cerebellar ganglioglioma: an

- epilepsy syndrome of infancy with seizures of cerebellar origin. *Ann Neurol* 40:91–98
25. Hayashi Y, Iwato M, Hasegawa M, Tachibana O, von Deimling A, Yamashita J (2001) Malignant transformation of a gangliocytoma/ganglioglioma into a glioblastomamultiforme: amoleculargenetic analysis—case report. *J Neurosurg* 95:138–142
 26. Hoischen A, Ehrler M, Fassunke J, Simon M, Baudis M, Landwehr C, Radlwimmer B, Lichter P, Schramm J, Becker AJ, Weber RG (2008) Comprehensive characterization of genomic aberrations in gangliogliomas by CGH, array-based CGH and interphase FISH. *Brain Pathol* 18(3):326–337
 27. Ildan F, Tuna M, Gocer IA, Erman T, Cetinalp E (2001) Intracerebral ganglioglioma: clinical and radiological study of eleven surgically treated cases with follow-up. *Neurosurg Rev* 24:114–118
 28. Im SH, Chung CK, Cho BK, Wang KC, Yu IK, Song IC, Cheon GJ, Lee DS, Kim NR, Chi JG (2002) Intracranial ganglioglioma: preoperative characteristics and oncologic outcome after surgery. *J Neurooncol* 59(2):173–183
 29. Johnson JH Jr, Hariharan S, Berman J et al (1997) Clinical outcome of pediatric gangliogliomas: ninety-nine cases over 20 years. *Pediatr Neurosurg* 27:203–207
 30. Karremann M, Pietsch T, Janssen G, Kramm CM, Wolff JE (2009) Anaplastic ganglioglioma in children. *J Neurooncol* 92(2):157–163
 31. Koeller KK, Henry JM (2001) Superficial gliomas: radiologic-pathologic correlation. *Armed Forces Institute of Pathology, Radiographics* 21:1533–1556
 32. Lagares A, Gomez PA, Lobato RD, Ricoy JR, Ramos A, de la Lama A (2001) Ganglioglioma of the brainstem: report of three cases and review of the literature. *Surg Neurol* 56:315–324
 33. Lang FF, Epstein FJ, Ransohoff J et al (1993) Central nervous system gangliogliomas. Part 2: clinical outcome. *J Neurosurg* 79:867–873
 34. Luyken C, Blümcke I, Fimmers R, Urbach H, Wiestler OD, Schramm J (2004) Supratentorial gangliogliomas: histopathologic grading and tumor recurrence in 184 patients with a median follow-up of 8 years. *Cancer*. 1 Jul 101(1):146–55. MacConaill LE, Campbell CD, Kehoe SM, Bass AJ, Hatton C, Niu L, Davis M, Yao K, Hanna M, Mondal C, Luongo L, Emery CM, Baker AC, Philips J, Goff DJ, Fiorentino M, Rubin MA, Polyak K, Chan J, Wang Y, Fletcher JA, Santagata S, Corso G, Roviello F, Shivdasani R, Kieran MW, Ligon KL, Stiles CD, Hahn WC, Meyerson ML, Garraway LA (2009) Profiling critical cancer gene mutations in clinical tumor samples. *PLoS ONE*. 18 Nov 4(11):e7887. Majores M, Schick V, Engels G, Fassunke J, Elger CE, Schramm J, Blümcke I, Becker AJ (2005) Mutational and immunohistochemical analysis of ezrin-, radixin-, moesin (ERM) molecules in epilepsy-associated glioneuronal lesions. *Acta Neuropathol*. Dec. 110(6):537–46
 35. Majores M, von Lehe M, Fassunke J, Schramm J, Becker AJ, Simon M (2008) Tumor recurrence and malignant progression of gangliogliomas. *Cancer* 113(12):3355–3363
 36. McLone DG, Stieg PE, Scott RM, Barnett F, Barnes PD, Folkerth R (1998) Cerebellar epilepsy. *Neurosurgery* 42:1106–1111
 37. Miller DC, Lang FF, Epstein FJ (1993) Central nervous system gangliogliomas. Part 1: pathology. *J Neurosurg* 79(6):859–866
 38. Pencalet P, Maixner W, Sainte-Rose C, Lellouch-Tubiana A, Cinalli G, Zerah M, Pierre-Kahn A, Hoppe-Hirsch E, Bourgeois M, Renier D (1999) Benign cerebellar astrocytomas in children. *J Neurosurg* 90(2):265–273
 39. Pfister S, Janzarik WG, Remke M, Ernst A, Werft W, Becker N, Toedt G, Wittmann A, Kratz C, Olbrich H, Ahmadi R, Thieme B, Joos S, Radlwimmer B, Kulozik A, Pietsch T, Herold-Mende C, Gnekow A, Reifenberger G, Korshunov A, Scheurlen W, Omran H, Lichter P (2008) BRAF gene duplication constitutes a mechanism of MAPK pathway activation in low-grade astrocytomas. *J Clin Invest* 118(5):1739–1749
 40. Prayson RA, Khajavi K, Comair YG (1995) Cortical architectural abnormalities and MIB1 immunoreactivity in gangliogliomas: a study of 60 patients with intracranial tumors. *J Neuropathol Exp Neurol* 54(4):513–520
 41. Probst A, Ulrich J, Zdrojewski B, Hirt HR (1979) Cerebellar ganglioglioma in a child. *J Neuropathol Exp Neurol* 38:57–71
 42. Reifenberger G, Kaulich K, Wiestler OD, Blümcke I (2003) Expression of the CD34 antigen in pleomorphic xanthoastrocytomas. *Acta Neuropathol* 105(4):358–364
 43. Safavi-Abbasi S, Di Rocco F, Chantra K, Feigl GC, El-Shawarby A, Samii A, Samii M (2007) Posterior cranial fossa gangliogliomas. *Skull Base* 17(4):253–264
 44. Sasaki A, Hirato J, Nakazato Y, Tamura M, Kadowaki H (1996) Recurrent anaplastic ganglioglioma: pathological characterization of tumor cells—case report. *J Neurosurg* 84:1055–1059
 45. Schiffman JD, Hodgson JG, VandenBerg SR, Flaherty P, Polley MY, Yu M, Fisher PG, Rowitch DH, Ford JM, Berger MS, Ji H, Gutmann DH, James CD (2010) Oncogenic BRAF mutation with CDKN2A inactivation is characteristic of a subset of pediatric malignant astrocytomas. *Cancer Res* 70(2):512–519
 46. Sievert AJ, Jackson EM, Gai X, Hakonarson H, Judkins AR, Resnick AC, Sutton LN, Storm PB, Shaikh TH, Biegel JA (2009) Duplication of 7q34 in pediatric low-grade astrocytomas detected by high-density single-nucleotide polymorphism-based genotype arrays results in a novel BRAF fusion gene. *Brain Pathol* 19(3):449–458, Epub 2008 Oct 21
 47. Tatevossian RG, Lawson AR, Forshew T, Hindley GF, Ellison DW, Sheer D (2010) MAPK pathway

- activation and the origins of pediatric low-grade astrocytomas. *J Cell Physiol* 222(3):509–514
48. Tamburrini G, Colosimo C Jr, Giangaspero F, Riccardi R, Di Rocco C (2003) Desmoplastic infantile ganglioglioma. *Childs Nerv Syst* 19(5–6):292–297
49. Varlet P, Peyre M, Boddaert N, Miquel C, Sainte-Rose C, Puget S (2009) Childhood gangliogliomas with ependymal differentiation. *Neuropathol Appl Neurobiol* 35(4):437–441
50. Yin XL, Hui AB, Pang JC, Poon WS, Ng HK (2002) Genome-wide survey for chromosomal imbalances in ganglioglioma using comparative genomic hybridization. *Cancer Genet Cytogenet* 134(1):71–76
51. Zentner J, Wolf HK, Ostertun B et al (1994) Gangliogliomas: clinical, radiological, and histopathological findings in 51 patients. *J Neurol Neurosurg Psychiatry* 57:1497–1502

52.1 Introduction

Dermoid tumors are congenital, nonneoplastic, inclusion lesions which have epidermal capsule and contain dermal appendages such as hair and sebaceous glands. They can occur anywhere along the neuraxis. In the literature, they are often referred to as “cysts” which refers to their histological structure and the presence of secretions (sebum) within the tumor, as well as indicates a nonneoplastic nature of these lesions. Although benign biologically, they can have malignant behavior due to their location causing mass effect and compression of vital structures or having potentially fatal complications such as abscess, spontaneous rupture, and hydrocephalus [1–4]. Remak [5] was the first to suggest displacement of epithelial rests and defective closure of the neural tube as the cause for development of these lesions. The first description of an occipital dermal sinus connected to a dermoid tumor is attributed to Olge [6] in 1865. Later in 1897, Bostroem [1] suggested ectopic inclusion of dermis and

epidermis during embryonic development as the cause for formation of dermoids and epidermoids, respectively. This theory was further supported by Bailey in 1920 and later Citchley and Furguson in 1928 who further proposed that dermoids and epidermoids were the result of fetal inclusion of epidermal cells, depending on the depth of the layer or according to embryonic age [1].

Logue and Till [7] classified posterior fossa dermoids into four groups depending on extradural and interadural location with absent, partial, or complete dermal sinus connection. The significance of this classification was the risk of infection. This classification is not in common use.

52.2 Epidemiology

Dermoid cysts in pediatric age group are often reported in association with dermal sinuses and also in larger series are collectively reported with epidermoids. These tumors are generally rare accounting for 0.1–0.7 % of all intracranial tumors [8]. Epidermoids and dermoids together account for approximately 0.7–1.8 % of all intracranial masses, with epidermoid 4–10 times as common [1, 9–11]. Dermoids are usually reported in younger age, in the first decade of life, while epidermoids classically present later in adulthood [10, 12–14]. Dermoids are reported to affect both sexes equally or with slight male predominance [9, 13, 15]. Twelve out of 19 pediatric patients in

M.M. Özek, M.D. (✉)
Division of Pediatric Neurosurgery, Department
of Neurosurgery, Acibadem University, School
of Medicine, Kozyatağı Acibadem Hastanesi İnönü
Cad. Okur sok. No:20, Istanbul, Turkey
e-mail: memetozek@gmail.com; mozek@turk.net

S. Kohan, MBBS, FRACS
Department of Neurosurgery,
Sydney Children’s Hospital, High St.,
Randwick, Sydney 2031, Australia

Caldarelli et al. series were male [2]. This group reported the first large pediatric series of intracranial dermoids and epidermoids. Of the 19 patients they treated over 20-year period, 16 were dermoids and only 3 were epidermoids and the mean age of 5.5 years [2]. On the other hand, Fornari et al. [5] also reported on 36 cases of CNS dermoids and epidermoids in patients younger than 20 years of age and found only 3 dermoids out of 17 intracranial lesions of which one was infratentorial. The mean age was 16 years, with slight male predominance (20–16) [5]. Lunardi et al. [13] reported on dermoids and epidermoids of posterior fossa exclusively. In their series, they had 16 patients, 9 of whom had dermoids, with average age of 6.4 years, while the average for epidermoids was 40 years and no gender difference. These findings are summarized in Table 52.1.

The incidence of congenital dermal sinus is reported approximately 1 in 2,500–3,000 births. These are mostly in the lumbosacral region, and only a small percentage is found in the occipital region [16].

52.3 Embryology

Embryologically dermoid tumors are thought to result from inclusion of ectodermal elements at the time of the closure of the neural groove during the third to fifth embryonic life [1, 5, 10, 17, 18]. This is the same as epidermoid as opposed to teratomas where mesoderm also is involved.

In terms of time profile for development of dermoid tumors in relation to epidermoids, the current theory suggests that these lesions occur earlier in embryonic life than epidermoid tumors. Therefore, displaced cells lie near midsagittal plane and as sometimes noted are associated with defect in closure of overlying skin [5, 10]. This is in contrast to epidermoids which most often occupy a more lateral position, in particular in intracranial location. This

is postulated to result either from inclusions of ectoderm at a later stage of embryogenesis or displacement during formation of secondary cerebral vesicles, i.e., the otic and optic vesicles [1]. On the other hand, lateral displacement of the primitive ectodermal and mesenchymal cells caused by the developing cerebral vasculature along Virchow-Robin spaces gives rise to laterally positioned dermoids [2, 6, 12].

The congenital dermal sinus that often is found in association with dermoids suggested to represent abnormal adhesion between the skin and neural ectoderm during development [9, 15] (Fig. 52.1a). This tract, depending on its degree of incomplete separation, may end up in subcutaneous tissue, bone, dura, subdural space, or extend at any length into the parenchyma and ultimately within the fourth ventricle. The dermal sinuses can be blind or connect to dermoid [15] (Fig. 52.1c). Rarely there may be more than one dermal sinus present [15].

In recent years, concurrent finding of a rare phenomenon of vertebral anomalies, namely, Klippel-Feil syndrome, with posterior fossa dermoids, has led some authors to propose theories on common embryological process, which suggests dermoid tumors being a late embryonic developmental anomaly [19–21]. It is proposed that this may be related to under-expression of *pax* gene that leads to segmentation failure of cervical somites that alters tissue tension at craniocervical junction leading to entrapment of dermal elements and development of posterior fossa dermoids [20, 21]. On the other hand, some have suggested that segmentation failure affects cervical flexure formation which in turn reduces fetal movements at rhombencephalo-cervical junction ultimately trapping ectodermal elements and leading to formation of dermoid tumors [19]. These theories remain unproven.

Other rare concurrent anomalies such as Dandy-Walker syndrome, callosal agenesis, and diastematobulbia in association with posterior fossa dermoid cyst have also been reported, but the significance of these anomalies remains to be explained [2, 22].

Table 52.1 Major series of mixed posterior fossa lesions

Series	Number of patients (M:F)	Age range (mean)	Pathology	Location in PF	Outcome/complication	Recurrence/reoperation	f/u period (mean)
Schijman et al. [15]	7 2:5	2–6 years	2 dermoids 5 epidermoids (1 + DS)	PF	2 deaths (1 dermoid, 1 epidermoid), 1 severe am	–	–
Yasargil et al. [12]	35 21:14 8(6:2)	18–62 years (37) 19–53 years (36)	Epidermoid Dermoid	10 ST, 22 CPA, 3 IV vent 7 ST, 1 in IV ventricle	8 am, 2 bm, 7 transient deficits 2 deaths (epidermoids)	No symptomatic recurrences	1 month–20 years
Fomari et al. [5]	17 9:8 (of 36 total)	6 months–20 years (16 years)	3 dermoids 14 epidermoids	5 PF	1 death (CPA)	2 reoperation	6–29 years (13)
Lunardi et al. [13]	16	(6.4 years) (40 years)	9 dermoids (3 with DS) 7 epidermoids	2 in IV vent 6 in IV vent	3 deaths (all epidermoid), 1 am (epidermoid)	1 recurrence (epidermoid)	(17.3)
Martinez-Lage et al. [6]	3 (0:3)	6 months–2 years	Dermoid	Extradural	Severe sinus hemorrhage	nil	1–12 years
Caldarelli et al. [2]	19 12:7	3 months–16 years (5.5 years) 6 (<1 year)	16 dermoids (12 + DS) 3 epidermoids	5 CM, 2 IV vent. 1 PMJ	No deaths	2 recurrences (1 dermoid, 1 epidermoid)	8–237 months (92 months)
Zuccaro et al. [37]	30 12:18	1 month–18 years (13 years)	8 acoustics 6 meningiomas, 2 astrocytomas, 3 arach. cysts, 2 epidermoids, others	CPA	7 deaths (6 with recurrences), 3 VPS	6 recurrences	1–12 years

CPA cerebellopontine angle, am aseptic meningitis, PF posterior fossa, ST supratentorial, PMJ pontomedullary junction

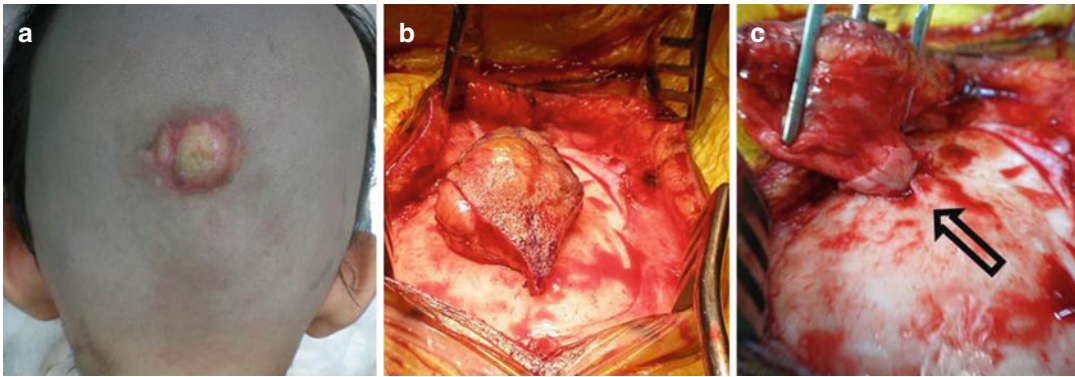


Fig. 52.1 (a) An infected occipital dermal sinus, (b) Intra-op image showing skin flap incision around the dilated dermal sinus dilatation, (c) Entrance of the dermal sinus into the cranium (*arrow*)

52.4 Pathology

Most pediatric intracranial dermoids arise in the posterior fossa, in midline position, i.e., cerebellar vermis and adjacent meninges being more common locations [1, 2, 18]. These tumors are also found in the cavity of the fourth ventricle [2, 13, 18], although this is not the most common location within the posterior fossa. Of the 16 pediatric dermoids in one study, 8 (50 %) were in the posterior fossa with the cisterna magna as the most common location [2] (see Table 52.1). Intra-axial location, cerebellum or brainstem, is exceptionally rare [2, 23, 24]. Intracranial extradural dermoids are also reported as rare [6]. The significance of this location becomes apparent in the review by Martinez-Lage et al. [6] where four out of nine reported cases were closely related to venous sinuses with three intraoperative hemorrhages. The other favored intracranial location is in the parasellar region [10]. Interestingly in contrast to teratomas, dermoids rarely are reported in the pineal region [10].

Grossly well-circumscribed, opaque, oval, or round multi-lobulated masses are generally well demarcated from surrounding tissues. The wall is formed by a fibrous material that varies in thickness and degree of adherence to the surrounding structures [1, 10]. Often there is a layer of reactive gliosis in the adjacent brain tissue. Calcification may be seen in the wall of the cyst [10]. The material within the cyst can vary between a dense (sometimes described as

“cheesy”) substance and a more brown, mucoid consistency fluid. The presence of hair is common within the tumor [5]. Pus-like fluid due to sebaceous secretions and desquamation, to a more yellowish-brown mucoid fluid, has also been described. Teeth are rarely seen. Some investigators have reported more than one cyst in the same location [10]. Dermoid tumors grow faster than epidermoids [9]. This is due to secretions as well as desquamation process. This may also explain their earlier presentation in life.

The presence of dermal sinus in the occipital region is an important clue to the underlying dermoid cyst and considered by some a diagnostic feature [10]. The importance of the dermal sinus lies in the fact that the open connection between the skin surface and the cyst is a direct route for bacterial infection and thus the source for recurrent meningitis or abscess formation. Most tumors are associated with a complete or incomplete dermal sinus; however, the IV ventricle tumors may not have an associated sinus [2, 18]. In McComb’s experience, the lesions involving the region of the IV ventricle have all been dermoids and all been associated with dermal sinus [9]. In another study, 89 % of dermal sinuses are associated with an inclusion tumor and were mostly dermoid tumors, with 18 % only found extradurally, and the rest were intradural [25]. The congenital dermal sinuses associated with dermoid tumor have both dermal and epidermal elements, and it can sometimes regress to a

Fig. 52.2 Dermoid cyst lined by stratified squamous epithelium (HE, $\times 40$)

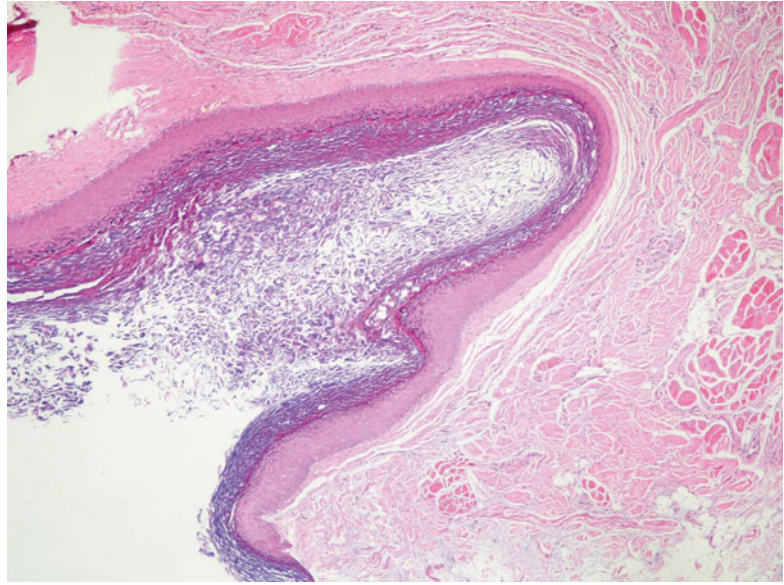
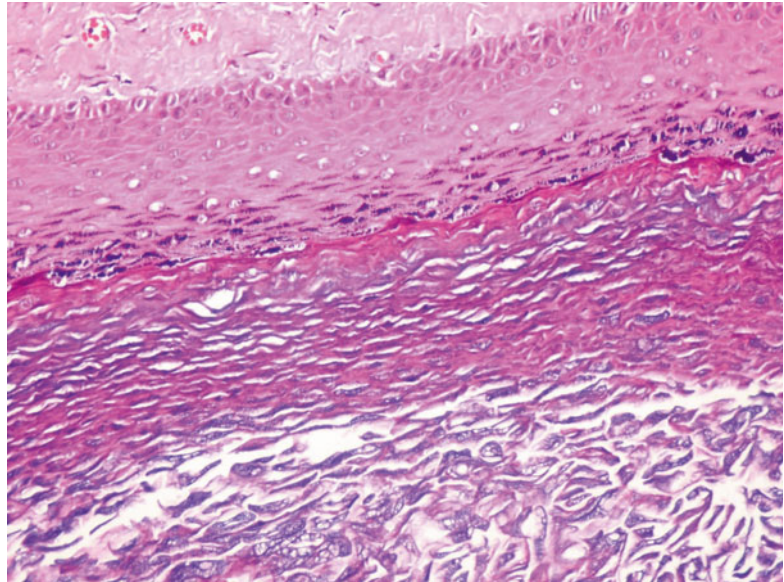


Fig. 52.3 Dermoid cyst lined by cornified epithelium has a distinct granular layer and contains anucleate squames (HE, $\times 200$)



connective tissue band or a nodule. There may be enlargements along the tract forming other dermoid cysts [9]. The opening of the tract is usually very small and difficult to see without shaving the hair on occipital region [18].

Microscopically, the wall of the dermoid cyst (or the capsule of the tumor) is formed by stratified squamous epithelium as seen in the skin and includes hair follicles and sebaceous and sweat

glands [1] (Figs. 52.2 and 52.3). Much of the lining of the cyst may be simple squamous epithelium supported by collagen, similar to epidermoid tumors, while in the thicker parts it is supported by dermis and its appendages [10, 17]. It is important to emphasize that dermoid cysts do not contain *fat cells* per se as this is of mesodermal origin, and the lipid metabolites seen are the result of breakdown products of hair and glandular secretions [26].

52.5 Clinical Manifestations

Symptoms from dermoid tumors generally result from mass effect, infection, inflammation, or occasionally hydrocephalus as presenting symptom [9, 15, 27–29]. Recurrent hyperpyrexia without meningism was the presenting symptom in 4 out of 8 pediatric posterior fossa dermoids, while only one presented with aseptic meningitis [2]. Another common finding in pediatric age is localized swelling secondary to inflammation and infection which may or may not be accompanied by discharge from the dermal sinus. These symptoms are often reported for one or more episodes before patient is brought to attention [2, 9].

Recurrent bacterial meningitis is thought to result from bacterial entry via the dermal tract as the port of entry into the subarachnoid space [9]. Recurrent septic meningitis should alert the physician to the possibility of dermal tract existence [10, 15, 18, 30]. The usual infecting organism is *Staphylococcus epidermidis*, but other organisms such as *Klebsiella*, *Proteus* species, pneumococcus, and even *E. coli* have been reported [15, 18, 30, 31].

Cerebellar abscess is a rare and serious sequela of posterior fossa dermoid cyst with dermal sinus which may or may not be associated with bacterial meningitis [9, 29] (Fig. 52.4a–c). This will result in significant inflammation and more rapid

rise in size of the lesion and consequently more significant mass effect, exacerbating the symptoms of posterior fossa mass. Akhddar et al. [29] in their review of literature between 1943 and 2001 identified 14 such cases.

Hydrocephalus may be obstructive due to mass effect within the IV ventricle or communicating secondary to arachnoiditis caused by repeated bouts of meningitis [9, 15, 18, 30]. Although hydrocephalus due to mass effect is a late-onset phenomenon, these lesions are slow growing and the surrounding brain tissue accommodates them until they reach a large size [9].

The rare intra-axial brainstem location is reported in association with intermittent cranial nerve palsy probably secondary to transient ischemic attacks, which is thought to be due to spillage of cyst contents within the CSF spaces [32].

Spontaneous or traumatic rupture of the cyst has been reported, which can present with mild to severe neck pain and headache, confusion, and decreased level of consciousness [1]. Histologically, rupture can cause severe granulomatous meningitis with formation of foreign body giant cell reaction to the contents of the cyst and hydrocephalus [3, 10, 33]. This is well demonstrated with the presence of fat droplets within the ventricles on MRI [3, 33]. The cause of spontaneous rupture is not clear. However, El-Bahy and his colleagues [4] reported two cases

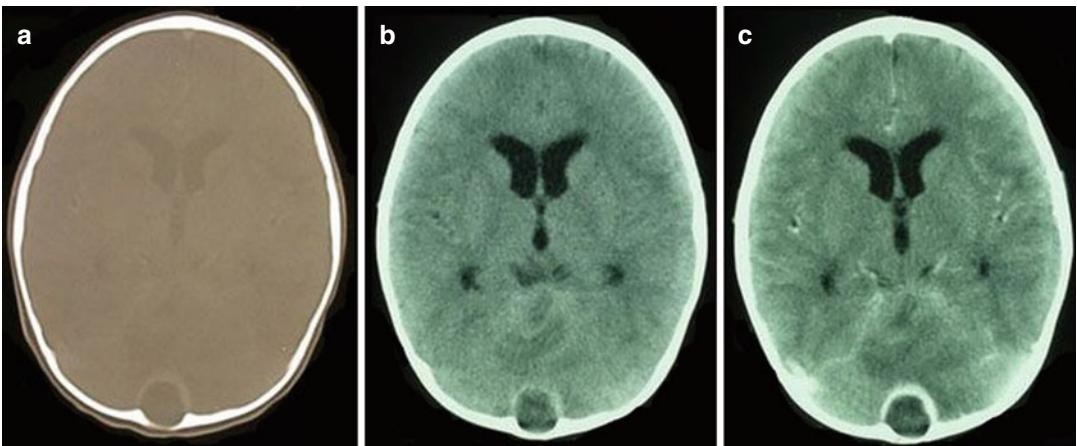


Fig. 52.4 CT images of an occipital dermoid. (a) Bone window study demonstrates scalloping of the occipital bone, (b) non-contrast CT, (c) contrast enhancement of the cyst wall due to inflammation

(16- and 18-year-olds) of spontaneous rupture and reviewed 49 reported cases of ruptured dermoid cyst in the literature. They supported Stendel's theory [34] that the spontaneous rupture can be explained by age-dependent hormonal changes which leads to increase secretion within the cyst and hence faster enlargement and subsequent leakage. The presence of fat within the ventricles and subarachnoid space causes hydrocephalus, meningitis, vasospasm, and cerebral ischemia [4].

52.6 Diagnosis

52.6.1 History and Examination

History of recurrent meningitis, in particular aseptic meningitis, or discharge from a pimple-like lesion on the head which is not healing should raise suspicion. Furthermore, the symptoms of intracranial hypertension, posterior fossa mass (e.g., nausea, vomiting, unsteady gait, nystagmus), as well as cranial nerve palsies should be sought [1, 6, 12]. The natural history of these tumors consists of slow growth which eventually will lead to hydrocephalus, seizures, dysarthria, and dementia [1].

Protracted history is reported in most series with the average length to presentation of 6.8 years in one series, with only one of eight patients presenting in less than 1 year [12].

The slow presentation of these lesions is because of a linear slow rate of growth as opposed to neoplastic lesions that have exponential growth [1]. The duration of symptoms before the era of modern imaging as reported often extended for several years. However, symptoms can also rarely present more acutely as a result of development of hydrocephalus or meningitis. Rupture of a cyst and release of cholesterol-rich contents can cause severe inflammatory reaction, leading to chemical meningitis, acute brain swelling, and vascular compromise.

On the other hand, in pediatric series the duration of symptoms was commonly short, with average of only 1.5 months in one series [13]. In this series, most common presenting symptoms were due to raised ICP followed by bacterial meningitis [13].

Inspection of scalp may reveal the opening of the dermal sinus that is often very small and may be associated with other cutaneous markers such as protruding hair from the opening, capillary telangiectasis, abnormal pigmentation, or increased subcutaneous fat tissue. The presence of abnormal hair pattern is more indicative of rudimentary encephalocele rather than a dermal sinus. There may also be evidence of infection such as skin inflammation or discharge [9]. Gentle pressure around the dermal sinus can help detection of discharging material; however, probing the sinus or injecting the tract (e.g., with contrast material) must be avoided as it can introduce bacteria [9].

52.6.2 Imaging

Plain skull films may reveal an occipital bony defect with densely sclerosing margins and a hypodense tract, although a small tract going obliquely in posterior fossa can be difficult to detect [9, 28]. The films are normal in the absence of dermal sinus. Furthermore, if any evidence of a lesion is seen, further examination with CT or preferably MRI is required. Therefore, the use of plain x-rays is no longer appropriate when other methods are available.

Dermoid tumors usually have low density on CT in keeping with their fatty content (Fig. 52.5b). The contents however more typically have density between that of fat and CSF [18, 35], although rarely isodense or hyperdense lesions have been reported [12, 15, 35, 36]. Enhancement of the wall is uncommon and is thought to be due to the presence of inflammation [15, 35] (Fig. 52.5c). Vasogenic edema is almost never seen in an uncomplicated cyst [36]. In some instances, the contents can have CSF density; hence, the cyst can look similar to normal CSF spaces or an arachnoid cyst if large enough [9]. The presence of calcification within the wall of the cyst is also commonly demonstrated on CT scans [35]. CT scans can also demonstrate scalloping of the cranial bone and the presence of hydrocephalus [9] (Fig. 52.5a), and in cases with ruptured cyst hypodense lipid droplets within the subarachnoid space or ventricles have been demonstrated [33].

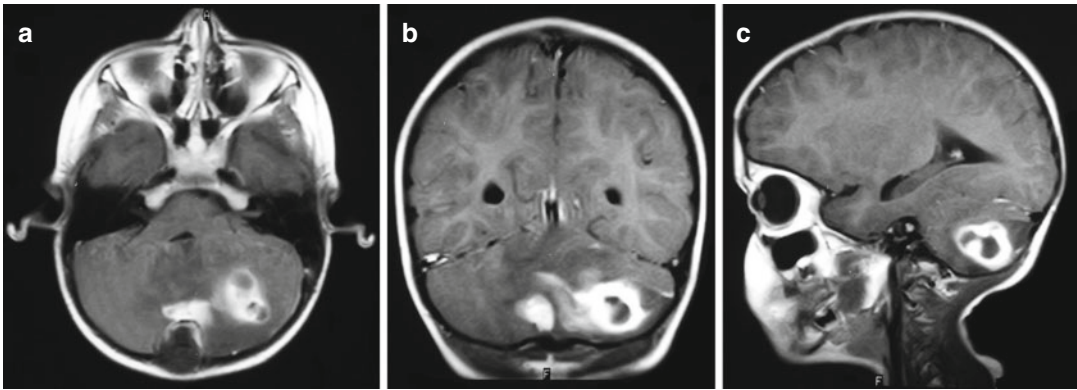


Fig. 52.5 MRI images showing a complicated occipital dermoid at the torcula with associated cerebellar abscess and significant amount of edema involving the cerebellar hemispheres

Although CT scans can demonstrate the lesion, it cannot help in distinguishing it from other lesions, and therefore the next step would be MR imaging. Thus, in cases where history and/or examination suggests this pathology, MRI scan with various sequences can assist in making the diagnosis and therefore is the investigation of choice as first step [2].

Uncomplicated dermoid tumors appear as well-circumscribed lesions with no vasogenic edema, hyperintense on T1W, and hypo- to hyperintense or heterogeneous on T2W images [2, 35, 36] (Fig. 52.6a–e). Fourth ventricular lesions have been reported with mixed hypointensity on T1W [28].

Fat suppression sequence is very useful for detection of lipid, after rupture or within the lesion for establishing a diagnosis [4, 35]. The fat droplets can be detected by hyperintense signal within the cyst [35]. Another useful MR sequence is the diffusion-weighted images (DWI). With this technique, epidermoid tumors show “restricted diffusion” (high signal), while dermoids do not.

Angiography is not proven useful in investigation of these lesions as they are avascular, and it will only confirm the presence of space-occupying lesion.

The differential diagnosis for dermoid cysts includes atretic cephalocele, arachnoid cyst, and

low-grade gliomas [2, 23, 28]. Atretic cephalocele lesions which may look similar to subgaleal dermoids enhance with contrast, while dermoids usually do not, and MRI sequences as described above should distinguish these lesions from a glioma or an arachnoid cyst.

52.7 Management

Once the diagnosis is established, the surgical intervention with complete removal is the definitive treatment. These tumors are not radiosensitive and have risk of recurrence if partially removed [2, 9, 12, 18]. Although it is not an urgent issue in an uncomplicated dermoid tumor (e.g., no hydrocephalus, severe compression, or abscess), no significant delay should intervene, in particular when associated dermal sinus is present, due to risk of infection [9].

Complicated lesions presenting with infection, abscess, or ruptured cyst require urgent surgery. Patients with meningitis must be treated with broad-spectrum antibiotics covering for gram-positive cocci with optimal CSF penetration, and if abscess is present, anaerobic cover must be added [16]. In cases of ruptured cyst, most authors suggest prompt surgery and wash-out of subarachnoid and ventricular spaces (some with hydrocortisone solution) and insertion of

ventricular drain [4]. In the presence of abscess and mass effect, urgent surgical intervention with appropriate antibiotic cover is recommended.

In relation to dermal sinuses, it is important to note that when a dermal sinus is detected, the presence of the tract or bony defect can still be missed on CT or MR imaging, and hence the sinus must be explored with preparation for posterior fossa exploration. In these cases, if no bony

defect is detected, this excludes intracranial extension [9].

Repeated infections can cause increased adhesions and make the removal even more difficult. Hence, prompt surgery is advisable upon discovery of the sinus to prevent further infection morbidity and adhesions from surgical point of view. One should plan for a major posterior fossa exploration once dermal sinus is discovered [18].

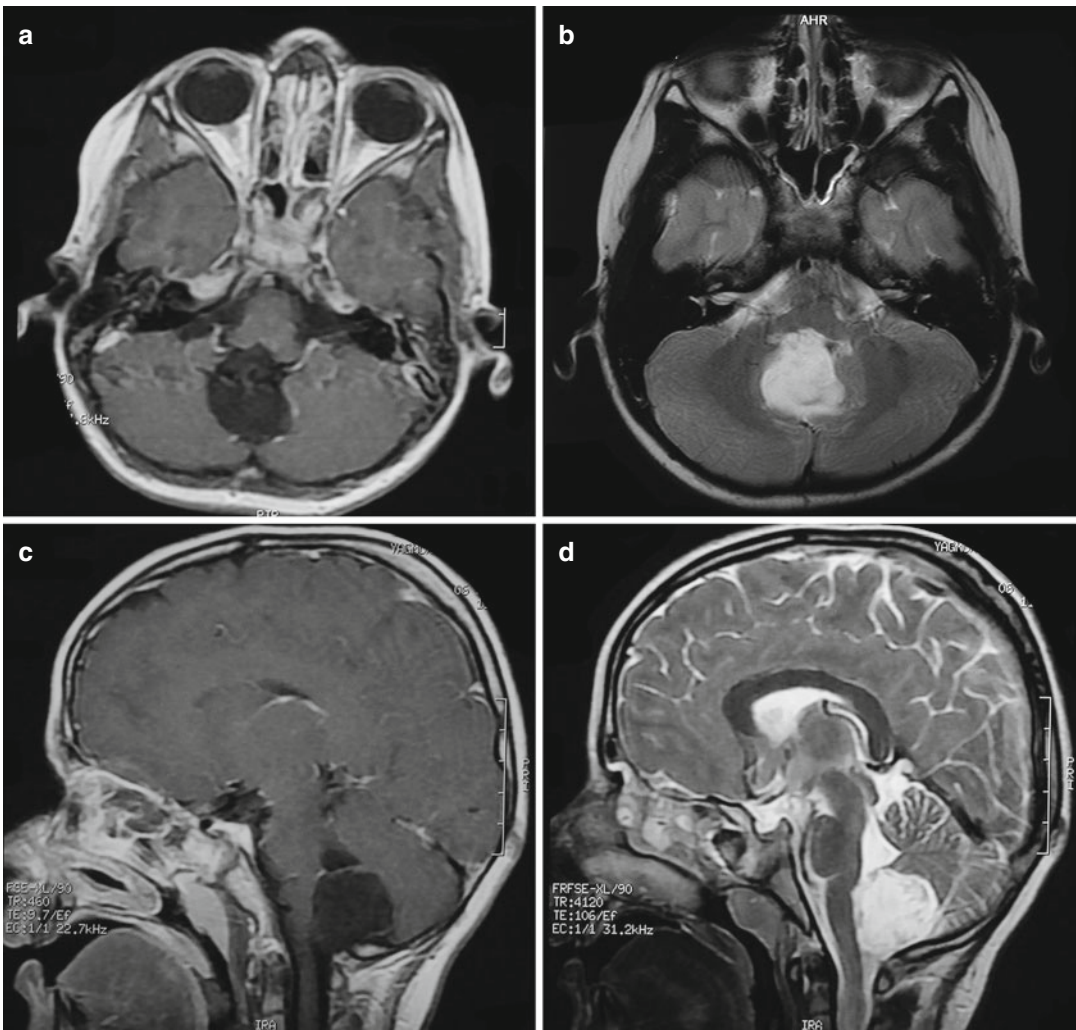


Fig. 52.6 (a–d) Axial and sagittal MRI images (T2 and T1) demonstrating a well-circumscribed posterior fossa lesion with CSF intensity and no surrounding edema but sig-

nificant mass effect at midline, (e) dermoid tumor with hair content in the cisterna magna

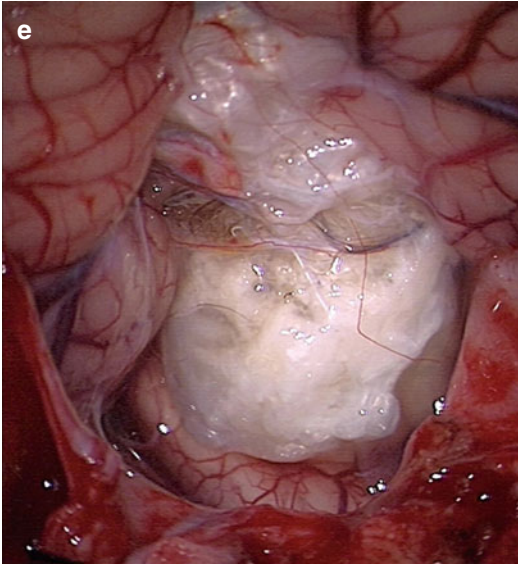


Fig. 52.6 (continued)

52.8 Preoperative Considerations

An important surgical anatomy to consider is the direction of occipital dermal sinuses which is typically directed inferiorly, and when extending intracranially, they enter below the torcula and can be adherent to dural sinus [6, 9, 15, 28]. Another well-described consideration is to avoid spillage of content within subarachnoid space. Leakage of contents may lead to meningitis as well as deposition epithelial cells within the surgical field and increase risk of recurrence [15]. To minimize the spillage of contents into the subarachnoid space, if the cyst is punctured, the contents must be aspirated promptly, and avoid irrigating the area until contents cleared. However, if spillage does occur, after aspirating the content, the operative site must be thoroughly irrigated, and corticosteroid wash has been recommended by some authors [12, 26]. On the other hand, if the cyst is large, deliberate drainage of the contents through a small opening may be necessary to allow working space and decrease manipulation of surrounding already compressed tissues [2, 12, 15].

If obstructive hydrocephalus is present, the removal of the tumor should obviate the need for the treatment of hydrocephalus as in none of the

posterior fossa lesions in Caldarelli's pediatric series [8] required shunt insertion.

52.9 Technical Consideration

With the use of microscope and microsurgical techniques, it is often possible to achieve complete removal. Starting with the removal of dermal sinus, an elliptical skin incision is made around the dermal sinus opening in order to remove the tract completely (Fig. 52.1b). The extent of the craniotomy can be limited superiorly as the tract travels obliquely and inferiorly [9]. To accommodate resection of the dermoid tumor within the fourth ventricle or cisterna magna, a standard suboccipital exposure and craniotomy are necessary. Care must be taken when lifting the bone flap as the tract can be attached to the dura and venous sinuses [15]. Where the sinus is entering the dura, a small elliptical dural incision should be made to make certain the entire tract is removed. Again one should be prepared to deal with venous sinus bleeding in particular when close to the torcula. Once the tract is separated from the dura, the durotomy is extended via a vertical linear incision to gain access to intradural structures and the dermoid cyst. Maximal care must be taken to keep the capsule intact, which can be adherent to the surrounding tissues, including the brain and vascular tissue. Adhesions can be more significant if an abscess is present, which also can make the wall more friable.

Extradural location of dermoid tumors is very rare as reported by Martinez-Lage [6], and as these lesions occur close to the torcula, the high risk of significant hemorrhage must be kept in mind when performing the craniotomy.

52.10 Postoperative Considerations

During early post-op period, the main concerns are with infection, aseptic meningitis, hydrocephalus or pseudomeningocele, and CSF leak [9]. Aseptic meningitis is reported in many series, which is transient and self-limiting, with routine

administration of corticosteroids for few days postoperatively [9, 12].

Follow-up imaging in the form of MRI should be obtained within first 24 h, to look for possible residual and give a baseline for comparison for future studies should the need arise. In our unit, we prefer CT scan immediately post-op to detect any significant post-op hematoma and perform an MRI on the following day as for all tumor surgery procedures. Provided hydrocephalus is not a concern, follow-up imaging can be performed after 3 months and then at 1 year. If no evidence of tumor or recurrence is found, no further imaging is necessary.

Long-term follow-up, up to 17 years, has been reported in the literature, and several studies have reported very rare incidence of recurrence after partial removal [1, 10, 13]. Caldarelli et al. reported residual in three patients out of eight posterior fossa dermoids and one recurrence during an 8-year follow-up which occurred 2 years after initial operation and required surgery 5 years later [2]. Although incomplete removal rather than risk of significant morbidity with aggressive surgery is warranted [1], some authors recommend consideration for re-exploration if a significant residual exists [9]. Malignant changes have been reported but are extremely rare [4, 10].

In summary, dermoid tumors are rare. Clinically, recurrent meningitis or presences of dermal sinus are important clues in diagnosis of intracranial dermoid tumors. Surgical key points include attention to possible involvement of dural sinuses by the dermal sinus and avoiding spillage of the contents. Dermoids generally have less complicated postoperative period compared with epidermoids, and complete removal is curative.

References

1. Cobbs CS, Pitts LH, Wilson CB (1997) Epidermoid and dermoid cysts of the posterior fossa. *Clin Neurosurg* 44:511–528
2. Caldarelli M, Massimi L, Kondageski C et al (2004) Intracranial midline dermoid and epidermoid cysts in children. *J Neurosurg (Pediatrics 5)* 100:437
3. Oursin C, Wetzel SG, Lyrer P, Bachli H, Stock KW (1999) Ruptured intracranial dermoid cyst. *J Neurosurg Sci* 43(3):217–221
4. El-Bahy K, Kotb A, Galal A, El-Hakim A (2006) Ruptured intracranial dermoid cysts. *Acta Neurochir* 148:457–462
5. Fornari M, Solero CL, Lodrini S et al (1990) Surgical treatment of infratentorial dermoid and epidermoid cysts in children. *Childs Nerv Syst* 6:66–70
6. Martinez-Lage J, Ramos J et al (1997) Extradural dermoid tumours of the posterior fossa. *Arch Dis Child* 77:427–430
7. Louge V, Till K (1952) Posterior fossa dermoid cysts with special reference to intracranial infection. *J Neurol Neurosurg Psych* 15:1–12
8. Lunardi P, Missori P, Innocenzi FM et al (1990) Long-term results of surgical treatment of cerebello-pontine angle epidermoids. *Acta Neurochir* 103:105–108
9. McComb JG (1996) Congenital dermal sinus and dermoid/epidermoid tumors. In: Cohen Allan R (ed) *Surgical disorders of the fourth ventricle*, Blackwell Science, Massachusetts, USA, pp 222–234
10. Russell DS, Rubinstein LJ (1989) Dermoid and Epidermoid cysts. In: Russell DS, Rubinstein LJ (ed) *Pathology of Tumours of the Nervous System*, Edward Arnold, London, pp 690–795
11. Baxter JW, NM (1985) Epidermoid and dermoid tumors: pathology. In: Wilkins RH (ed) *Neurosurgery*. R.S, McGraw-Hill, New York, USA, pp 655–661
12. Yasargil GM, Abernathy CD, Sarioglu A (1989) Microsurgical treatment of intracranial dermoid and epidermoid tumors. *Neurosurgery* 24(4):561–567
13. Lunardi P, Missori P, Gagliardi FM, Fortuna A (1992) Dermoid and epidermoid cysts of the midline in the posterior cranial fossa. *Neurosurg Rev* 15:171–175
14. Gelabert-Gonzalez M (1998) Intracranial epidermoid and dermoid cysts. *Rev Neurol* 27:777–782
15. Schijman E, Monges J, Craganz R (1986) Congenital dermal sinuses, dermoid and epidermoid cysts of the posterior fossa. *Childs Nerv Syst* 2:83–89
16. McIntosh R, Merrit KK, Richards MR et al (1954) The incidence of congenital malformations, a study of 5,964 pregnancies. *Pediatrics* 14:505–521
17. Parisi J, Nelson SJ, Schochet SS (1993) *Principles and practice of neuropathology*. Mosby, St. Louis, pp 226–227
18. McLaurin RL, ed. (1989) In: *Pediatric neurosurgery*. W.B. Saunders Company, Philadelphia, Pennsylvania, pp 365–372
19. Chandra P, Gupta A, Mishra NK et al (2005) Association of craniovertebral and upper cervical anomalies with dermoid and epidermoid cysts: report of four cases. *Neurosurgery* 56(5):E1155
20. Hinojosa M, Tatagiba M, Harada K, Samii M (2001) Dermoid cyst of the posterior fossa accompanied by Klippel-Feil syndrome. *Childs Nerv Syst* 17:97–100
21. Muzumdar D, Goel A (2001) posterior cranial fossa in association with craniovertebral and cervical spinal anomaly: report of two cases. *Pediatr Neurosurg* 35:159–161
22. Ciurea AV, Coman T, Tascu A, Ionescu V (2005) Intradural dermoid tumor of the posterior fossa in a child with diastematobulbia. *Surg Neurol* 63:571–575

23. Pant I, Joshi SC (2008) Cerebellar intra-axial dermoid cyst: a case of unusual location. *Childs Nerv Syst* 24:157–159
24. Caldarelli M, Colosimo C, Di Rocco C (2001) Intra-axial dermoid/epidermoid tumors of brainstem in children. *Pediatr Neurosurg* 56:97–105
25. French BN (1990) Midline fusion defects and defects of formation. In: Win R (ed) *Youman's neurological surgery*, Saunders, Philadelphia, Pennsylvania, pp 1164–1169
26. Kim KS, Weinberg PE (1981) Dermoid tumors. *Surg Neurol* 15:375–376
27. McLendon RE (1985) Epidermoid and dermoid tumors: pathology. In: Rengachary S, Wilkins RH (eds) *Neurosurgery*. McGraw-Hill, New York, pp 655–661
28. Higashi S, Takinami K, Yamashita J (1995) Occipital dermoid sinus associated with dermoid cyst in the fourth ventricle. *Am J Neuroradiol* 16:945–948
29. Akhaddar A, Mohamed J, Chakir N et al (2001) Cerebellar abscesses secondary to occipital dermoid cyst with dermal sinus. *Surg Neurol* 58:266–270
30. Cai C-Q, Zang Q,-J, Hu X-L et al (2008) Dermoid cyst of the posterior fossa associated with congenital dermal sinus in child. *World J Pediatr* 4(1):66–69
31. Layadi F, Louhab N et al (2006) Cerebellar dermoid cyst with occipital dermal sinus. *Pediatr Neurosurg* 42:387–390
32. Ford K, Drayer B, Osborne D, Dubois P (1981) Transient cerebral ischemia as a manifestation of ruptured intracranial dermoid cyst. *J Comput Assist Tomogr* 5:895–897
33. Kim I-Y, Jung S, Jung T-Y (2008) Traumatic rupture of an intracranial dermoid cyst. *J Clin Neurosci* 15:469–471, e.a
34. Stendel R, Pietilä T, Lehmann K et al (2002) Ruptured intracranial dermoid cyst. *Surg Neurol* 57:391–398
35. Osborn AG (1994) Nonneoplastic tumorlike lesions. In: Osborn A (ed) *Diagnostic neuroradiology*. Mosby, St. Louis, pp 631–636
36. Brown JY, Morokoff AP, Mitchell PJ et al (2001) Unusual imaging appearance of an intracranial dermoid cyst. *Am J Neuroradiol* 22:1970–1972
37. Zúccaro G, Sosa F (2007) Cerebellopontine angle lesions in children. *Childs Nerv Syst*. 23:177–183

53.1 Introduction

Epidermoid tumors are congenital, nonneoplastic, slow-growing lesions that can occur anywhere along the neuroaxis similar to dermoid tumors [1]. The historical background to these lesions has been described along with dermoid tumors previously.

53.2 Epidemiology

The incidence of these tumors is between 0.5 and 2 % of all intracranial tumors [2–7]. Epidermoid tumors are found in all age groups but more commonly become symptomatic in adults between the fourth and sixth decade of life [4–6, 8–11]. Epidermoids are found to be four to ten times more common than dermoids when considering adult and pediatric series [11–13]. However, when considering pediatric series alone, dermoids-to-epidermoids ratio is reported as high

as 6:1 [3, 12, 14]. Onset in pediatric age is very unusual; association with cutaneous stigmata, i.e., dermal sinus, is reported in about 1.5 % of cases [6]. The sex distribution for epidermoids is approximately equal [11, 15–17].

53.3 Location

Compared to dermoids which are found more commonly in the supratentorial compartment (up to seven times more frequent [13]), epidermoids are more frequently observed in the infratentorial space. The ratio of infratentorial to supratentorial occurrence is reported from 1:1 to 2:1 [16]. They generally occupy a paramedian location with the most common locations described in the literature being cerebellopontine angle, followed by fourth ventricle, parasellar, diploe of the skull, and intraspinal [3, 4, 11]. They can also occur in the petrous apex causing progressive facial palsy and very rarely within the cerebral hemisphere and pineal region [4].

In their review of literature of posterior fossa epidermoids, Talacchi et al. [17] found that the most common site is the cerebellopontine angle (60 % of all intracranial epidermoids), making them the third most common tumor in this location after vestibular schwannomas and meningiomas. The second most common location in the posterior fossa is the fourth ventricle (5–18 % of all intracranial epidermoids) [3, 18]. Intraventricular epidermoids are rare in pediatric age with only one

S. Kohan, MBBS, FRACS
Department of Neurosurgery,
Sydney Children's Hospital, Sydney, Australia

J. Oertel, M.D.
Department of Neurosurgery, Universitätsklinikum
des Saarlandes, Homburg-Saar, Germany

M.M. Özek, M.D. (✉)
Division of Pediatric Neurosurgery, Department
of Neurosurgery, Acibadem University,
School of Medicine, Istanbul, Turkey
e-mail: memetozek@gmail.com; mozek@turk.net

Table 53.1 Posterior fossa epidermoid classification according to Samii et al. [5]

Tumor location and extension	No. of cases (40)
CPA alone	15
CPA with transtentorial extension	3
CPA with middle fossa extension	5
CPA with foramen magnum extension	9
CPA with transtentorial and foramen magnum extension	8

reported case among 100 reported cases between 1974 and 2003 [6].

In pediatric population, epidermoids are reported forming less than 1 % of CP angle lesions being the fifth most common lesion after vestibular schwannoma, meningioma, low-grade astrocytoma, and arachnoid cysts [19]. In contrast, other series have reported epidermoids to account for 4.6–6.3 % of all CP angle tumors [11].

Brain stem location is also rare with only 19 cases reported between 1978 and 2004 [7]. Nine out of the 19 cases were in pediatric age, probably indicating early presentation due to involvement of highly eloquent area. The midline location in cases of ventricular or brain stem lesions is suggested to be due to midline contact between cutaneous and neuroectoderm where the cells are left on the inner or outer surface or within the neural tube ectoderm [20]. The tumor is believed to extend from cisternal spaces into the brain stem and usually appears as an exophytic lesion in the pons and medulla, where gradually the brain stem parenchyma may cover the cyst content and give rise to an intraparenchymal lesion [7].

Various classifications based on tumor locations have been suggested in order to help with surgical decision making and choice of treatment as well as prognosis [5, 13, 17]. Samii et al. [5] have published a classification of cerebellopontine angle epidermoids based on the extension of the tumor in order to better define the size and therefore the surgical implications (Table 53.1), while Talacchi et al. [17] described a classification for the posterior fossa epidermoids based on tumor location and extension (Table 53.2). Although these classifications are not in common use, their clinical significance is the possibility of radical removal which is associated with a decreased risk of recurrence.

Table 53.2 Posterior fossa epidermoid tumor anatomical classification according to Talachi et al. [17]

Location (no. of cases)	Tumor extension (no. of cases)
CPA (20)	Pure CPA (6)
	Suprasellar/chiasmatic (5)
	Parasellar/temporobasal (3)
	Mesencephalic/pineal (6)
Posterior fossa basal (3)	Parasellar/temporobasal (2)
	Mesencephalic/pineal (1)
Fourth ventricle (5)	

53.4 Pathology

Cruvellier in 1829 originally described these lesions as “pearly tumor” due to significant sheen and whitish appearance [1, 4]. Macroscopically, they consist of circumscribed, smooth, and irregular surface (described as “cauliflower shaped” by some authors) sometimes with foci of calcifications in the capsule, containing concentric lamellae of soft, white, and waxy flakes [1, 3, 4, 12]. The content is rich in cholesterol and results from progressive desquamation of epithelial lining of the cyst. Thick viscous and brown content secondary to breakdown products of keratin similar to that in dermoids has also been described [1, 4].

The main microscopic difference from dermoids is the lack of skin appendages (hair follicles, sebaceous and sweat glands). The cyst wall consists of simple stratified squamous epithelium, supported by an outer layer of collagenous tissue [4]. The wall of the epidermoids is thinner than that of dermoids and usually do not cause as much reactive fibrosis as the wall of dermoids do [1].

The growth rate of these lesions is said to be linear and similar to normal skin unlike the exponential growth of neoplastic tissues [4, 21], although malignant transformation has rarely been reported for epidermoid as well as for dermoid cyst [22, 23]. The germinal cell layer is spread out over the outer surface giving rise to vertically or radially orientated mitoses. Epidermoids grow slowly as dry keratin cells accumulate in the avascular center of the tumor [21]. Alvord suggests that due to increased

pressure from within the tumor, the outer basal cells divide in tangential direction giving rise to increase basal cell layer and consequently the surface area. The theoretical surgical implication of the germinal cell layer being on the surface is that the capsule needs to be completely removed to minimize the risk of recurrence, although this must be weighed against risk of neurovascular and cranial nerve injury. Epidermoids tend to have a soft malleable consistency which allows them to extend between cranial nerves and vessels engulfing these structures [13, 17, 24, 25]. The expanding tumor conforms to the shape of the cavity. It occupies and does not displace the neurovascular structures until all the available space is filled [13]. The delay in onset of symptoms has been attributed to this characteristic of these lesions.

53.5 Embryology

The embryogenesis of epidermoid lesions is generally agreed to be similar to that of dermoids, i.e., arising from inclusion of ectodermal elements at the time of neural tube formation between the third and fifth week of embryological life [1, 4, 26]. However, epidermoids, in particular intracranial ones, are thought to occur at a later stage of development, namely, during formation of secondary cerebral vesicles (optic and otic vesicles) at the fourth and fifth week, as they lay in a more lateral location and are differentially unipotent cells [1, 4].

Kaido et al. [27] reporting on intraparenchymal epidermoids put forward a hypothesis on development of these lesions explaining their locations. According to this theory, if sequestration of ectodermal elements occurs early during formation of primary central vesicles in the third week of gestation, the ectodermal cells are more likely to be “trapped” within the neural tube giving rise to intraparenchymal or intraventricular epidermoids, while sequestration later during the fifth week of gestation and the development of secondary cerebral vesicles (otic and optic) will lead to lesions located in CP angle, middle ear, and orbit.

53.6 Clinical Manifestation

The signs and symptoms caused by epidermoid tumors in general relate to their location, mass effect, or chemical meningitis. The tumor location is the key feature, and with slow growth recorded in adult patients, they are typically reported to cause symptoms for several years before detection [1, 11, 13, 16, 17]. With posterior fossa location in particular CP angle, clinical symptoms typically include cranial nerve abnormalities, such as facial palsy, hearing loss, vertigo, trigeminal neuralgia, as well as ataxia, hemiparesis, and hemianesthesia [1, 4, 13, 17, 28]. Particularly for cranial nerves VII, VIII, VI, and V, clinical signs have been reported [4, 5, 11]. Nystagmus and ataxia secondary to cerebellar compression have also been commonly observed [13, 29]. Chu et al. [28] have reported on cases of CPA epidermoids with audiovestibular deficits due to eighth nerve compression which returned to normal after surgery.

Raised intracranial pressure signs and symptoms including nausea, vomiting, headache, and transitory loss of consciousness have been reported with intraventricular or posteriorly located tumors within the infratentorial space [17, 24] causing CSF flow obstruction.

Rupture of epidermoids can result in granulomatous meningitis, which could lead to communicating hydrocephalus if repeat episodes do occur [1, 4], while the presence of dermal sinus can be a portal entry for bacterial meningitis [4].

Epidermoids usually are characterized by subtle and prolonged symptoms prior to diagnosis, and acute presentation (less than 1 week) is rare and associated with hydrocephalus and leakage of cyst contents into subarachnoid space causing chemical meningitis. Other acute presentations include bacterial meningitis, tension pneumocephalus, hemorrhage, and traumatic rupture [14, 30, 32]. Traumatic rupture of epidermoid cyst has also been reported with patient presenting few hours after cranial trauma with hemiparesis [30].

An interesting phenomenon reported in fourth ventricular lesions is the lack of correlation of ventricular enlargement and significant dimensions of the tumor [6]. Furthermore, patients have

also been reported to have spontaneous improvement of their symptoms leading to the wrong diagnosis in some cases [6, 24]. The mechanism involved has been suggested to be either due to small leakages and subsequent tumor decompression or slow growth of the tumor and extension along the subarachnoid spaces without significant compression [6, 24]. The overall incidence of hydrocephalus has been reported to be less than 50 % with intraventricular lesions [24].

Bartal et al. [24] analyzed the clinical presentation of patients with posterior fossa epidermoids during CT era and divided them to two clinically distinguishable groups: those posteriorly located, which presented predominantly with the symptoms and signs of raised intracranial pressure, and those with anterior lesions which presented with cranial nerve deficit without features of raised intracranial pressure.

Association with other congenital abnormalities including nasal dermal sinus and congenital defects in the vertebral column has been reported [4, 30].

53.7 Imaging

CT scan is the common starting point for diagnosis of intracranial lesions. However, the appearance and location of epidermoid tumors can be similar to several other lesions including arachnoid cyst, meningioma, dermoid tumor, and vestibular schwannoma. Epidermoids typically appear as low-density extra-axial lesion due to the fat content and therefore have similar attenuation to dermoids and CSF in arachnoid cysts. On occasions, the higher keratin content of the epidermoids can appear as hyperdensity on CT [1], in which case it may carry a differential diagnosis of meningioma or vestibular schwannoma. Li et al. [31] reported on 15 cases where hyperdense lesions were seen on CT. The incidence of such lesions was reported in 3 % of their cases over 20 years (15/596). It was hypothesized that recurrent leakage of the content with subsequent chemical inflammatory response may be responsible for this appearance [31]. Other causes of hyperdense appearance on CT imaging are

thought to be intracystic hemorrhage [19]. Enhancement with contrast on CT scans is rare and occurs at the margins [1, 6]. Bone absorption surrounding the epidermoid cyst can occasionally be a clue to the diagnosis [1].

Magnetic resonance imaging (MRI) is the investigation of choice for diagnosis of epidermoid cysts allowing the differential diagnosis with dermoids, arachnoid cysts, lipomas, and cholesterol granulomas [33, 34]. MRI is especially useful in assessing the extent of the lesion and relationship to the surrounding anatomy using the images in various planes [35]. Generally, they have low intensity on T1W images and high intensity on T2W images (Fig. 53.1). This appearance may be very similar to that of CSF, and therefore the diffusion-weighted imaging (DWI) technique is the ideal sequence for discriminating between these two entities, where the epidermoid cysts appear hyperintense [1]. DWI is also useful in distinguishing between epidermoids and encephalomalacia [1]. Signal intensity varies depending on the relative lipid, cholesterol, and keratin composition [35]. They generally do not show contrast enhancement [35]. In postoperative cases, cholesterol crystals are clues for capsule remnant [7]. Proton density (PD)-weighted images are also helpful in differential diagnosis, where structural heterogeneity of the lesion can be a distinguishing feature from brain tissue and CSF [17].

53.8 Management

The first line of treatment of epidermoid tumors is surgical resection. Ideally, complete excision should be the aim of the surgery, as they carry risk of recurrence and do not respond to adjuvant therapy such as chemotherapy or radiation [4, 5, 11, 13]. However, it should be emphasized that when a risk of neurological deficit due to surgery exists, a conservative approach is more appropriate, as these lesions are histologically benign and very slow growing [5, 6]. Furthermore, even a subtotal resection alleviates patient's symptoms, allowing normal life for many years.

Standard surgical approaches have been used for removal of these lesions. The principle

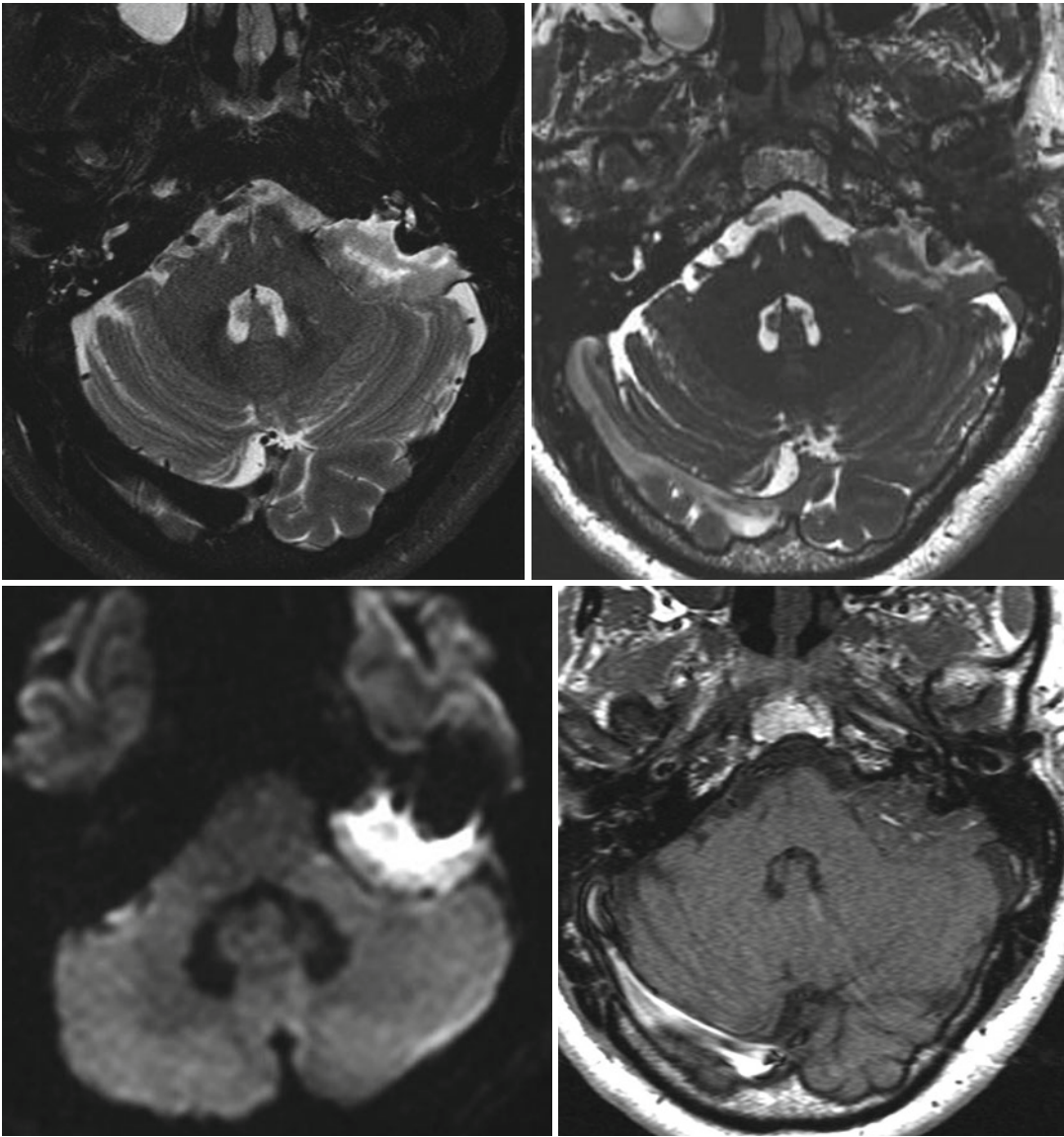


Fig. 53.1 Clockwise from *top left*: Axial TSE T2: A hyperintense mass with hypointense complete thin rim is seen. The cystic mass compresses the left middle cerebellar peduncle, eroding the temporal bone. Axial 3D CISS: A well-defined heterogeneous hypointense mass comparing to the CSF. Axial DWI: There is a restricted diffusion

in the mass, characteristic for epidermoid. Ax TSE T1: There is a slightly hyperintense and heterogeneous mass comparing to the CSF in the cerebellomedullary and cerebellopontine cisterns, eroding temporal bone in axial TSE image through the posterior fossa. Punctate apparent focal hyperintense points are also seen in the lesion

approach undertaken is to firstly access the cistern where the lesion arises. Depending on the size of the tumor and location, this is then followed by evacuation or removal of the contents carefully avoiding spillage, and then attempt to excise the cyst wall by tracing the wall along

various compartments. Epidermoid tumors are less likely to have dense reactive involvement of the arachnoid membranes compared to dermoids and have a thinner wall [13].

Yasargil et al. [13] in their series of 43 cases approached all parasellar lesions from a

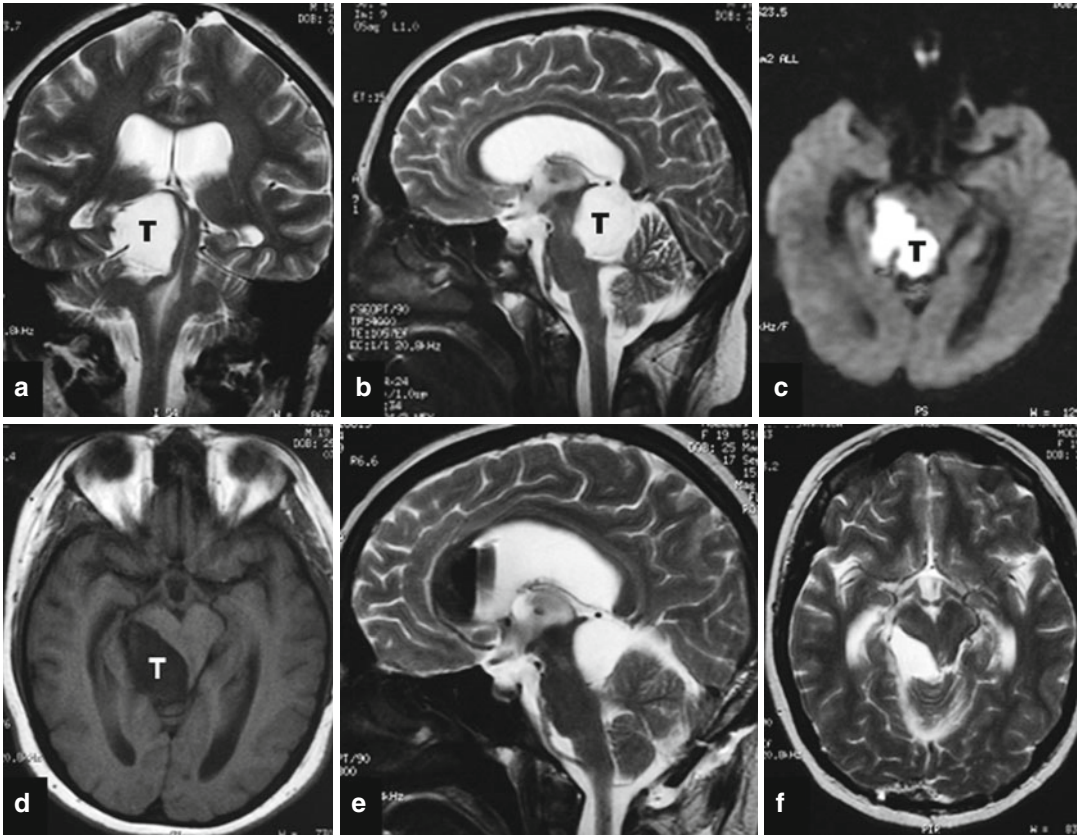


Fig. 53.2 Pre- and postoperative MRI of an epidermoid of the pineal region. (a) T2W coronal section with the hyperintense tumor (T) compressing the brain stem/midbrain. (b) T2W sagittal section with the tumor (T). (c) DWI with the hyperintense tumor clearly to differentiate from the CSF. (d) T1W non-enhanced axial section dem-

onstrating the brain stem compression of the tumor (T). (e) Early postoperative MRI (T2W sagittal section) showing the decompression of the brain stem/midbrain and cerebellum. (f) Axial T2W postoperative image demonstrating the midbrain decompression

pterional route, while the posterior fossa tumors were accessed via midline suboccipital route for fourth ventricle or centrally located tumors and through a retromastoid approach for masses in CP angle. Following the conduit created by the tumor and creating a plane between the capsule and the overlying arachnoid, Yasargil and colleagues [13] reported complete removal of the lesions in one-stage operations. Another important observation in this series was the fact that these lesions did not cross the midline to the contralateral subarachnoid spaces, although they may bulge across the midline [13]. This was thought to be due to possible fenestration existing between some cisterns, while others have no such communication.

In terms of surgical technique based on tumor location and extension, Samii et al. [5] divided the posterior fossa into four compartments. The first lies between undersurface of the tentorium and the fifth cranial nerve, the second from fifth to the lower border of seventh nerve, the third down to the lower cranial nerves, and the fourth compartment from lower cranial nerves to the foramen magnum. The authors suggested their technique of starting in lateromedial direction, from the bony surface and moving toward the brain stem, in each compartment sequentially. This will allow easier identification of the cranial nerves near or at their bony or dural entrance/exit where their anatomy is relatively well preserved [21]. Burger et al. [9] based on their series

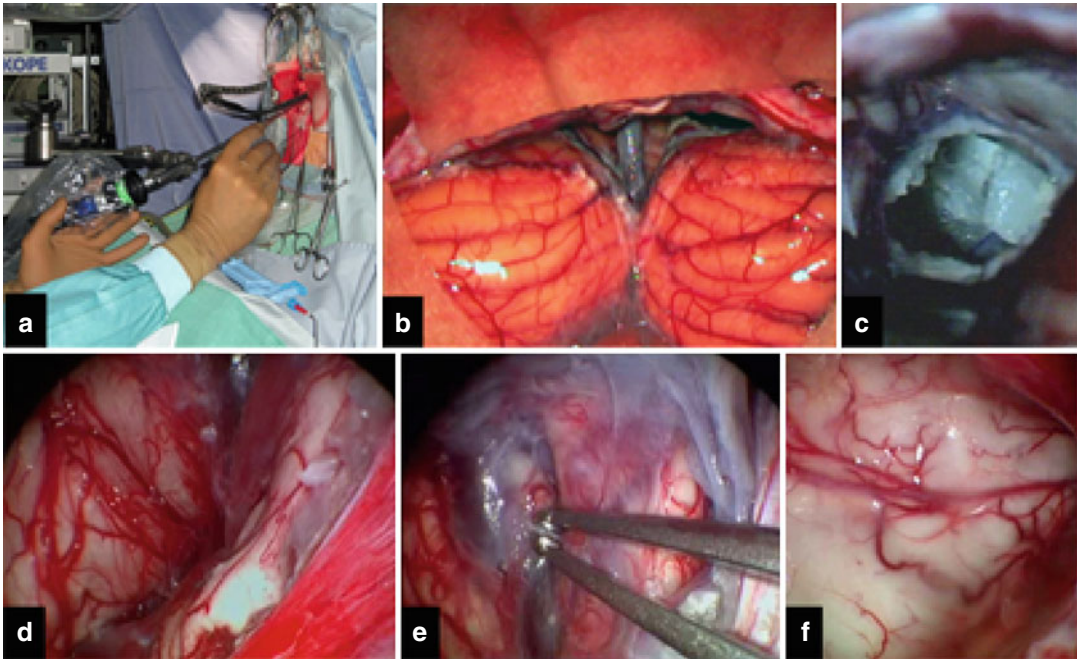


Fig. 53.3 Intraoperative setting of the case of Fig. 53.1 for endoscopic-assisted removal. (a) Tumor removal under endoscopic assistance in the semisitting position. (b) Microscopic view of the supracerebellar infratentorial approach. (c) Microscopic view of the typical whitish

epidermoid tumor. (d–f) Endoscopic-assisted removal of the capsule remnants under view of a 70° angle Hopkins rod-lens scope with achieved complete tumor resection at the end of the procedure (f)

believed radical resection of the capsule is not appropriate for epidermoids although mentioned the use of dental mirrors to assist with removal of the cyst content from areas without direct vision.

Currently, endoscopically assisted techniques are becoming more and more utilized in removing these tumors as they are well recognized to extend along the paths of least resistance to adjacent compartments where direct visualization is not possible. In the experience of the authors with more than 200 endoscopic-assisted intracranial skull base procedures in the last 10 years, only 15 procedures were undertaken for endoscopic-assisted epidermoid removal [36, 37]. The tumors were located in the CPA in 11 cases, purely temporobasal engulfing the brain stem/midbrain in 1 and in the pineal region in 3. Careful selection of the approach is of utmost importance. In general, the authors recommend to select the approach which allows gross subtotal microsurgical removal of the lesion mass. In the authors' series, a retromastoid suboccipital approach was selected

in eight cases, a pterional craniotomy in four cases including three tumors with extension to the upper compartment of the CPA. For the deep-seated posterior tumors, an infratentorial supracerebellar approach was performed in one and an interhemispheric supratentorial approach in two.

For surgery, the patient receives a bolus of dexamethasone just before the start of the procedure. Antibiotic agents are administered as single shot. After induction of general anesthesia, the patient is positioned either supine for the pterional approach or semisitting for the retromastoid and posterior midline approaches (Fig. 53.3a). The park bench position for the retromastoid approach and the prone position for the posterior midline approach are also an option although avoidance of manipulation of the cranial nerves is more challenging. A standard craniotomy is performed and the tumor microsurgically exposed. The capsule is incised, and as much tumor mass is evacuated and aspirated as possible under microscopic view. Always an attempt should be made to resect the

tumor capsule completely. However, if there is any risk of injury to neurovascular structures or to the cranial nerves because of capsule adherence to these structures, parts of the capsule should be left in place since the lesion is very slow growing. As soon as removal of the tumor under microscopic view is completed, the endoscope is introduced. For the endoscopic-assisted removal, the optical quality of the neuroendoscope is very important. Also, the endoscope should be bayonet shaped to allow easy maneuvering of the instruments next to the endoscope and camera. The authors recommend to use 30°, 45°, and 70° angles of view. For endoscopic inspection of the extent of tumor removal, the endoscope can be applied in a free-hand fashion. If tumor remnants are found and endoscopic-assisted resection is performed, the endoscope should be fixed with a self-retaining holding device. Irrigation to cool the endoscope has to be used frequently, and care must be taken to avoid any contact of the endoscope to cranial nerves since injury of cranial nerves by the heat of the endoscope is well known. If these necessities are considered, the endoscopic-assisted removal can be performed safely, and even lesions in almost 90° angle to the straight approach such as in Meckel's cave can be resected safely. With the endoscope-assisted microsurgical technique, epidermoid tumor extensions into adjacent cranial compartments can be removed with the same approach without retracting neurovascular structures or enlarging the craniotomy (Fig. 53.2).

With regard to the fourth ventricular epidermoids, Tancerdi et al. [6] recently reported on their largest series with comprehensive review of the literature with 100 reported cases between 1974 and 2003. In that series, only three tumors were confined to the fourth ventricle, while four had extension into the cisterna magna and two others with extension into cervical subarachnoid space or CP angle [37]. Complete resection was reported in only two of nine cases, emphasizing the close adherence of the tumor to the floor of the ventricle making the complete resection of the capsule hazardous.

In the literature, heterogeneous results have been reported on the extent of tumor removal. This appears to be related to the biological behavior of

the tumor, i.e., extension along paths of lowest resistance and firm adhesions to structures.

Avoiding or minimizing the spillage of tumor contents into the subarachnoid space is vital as there is theoretical risk of seeding as well as reported postoperative aseptic meningitis [9, 13, 17]. Aseptic meningitis is marked by high fever and intense local pain [38, 39], as well as confusion and decreased level of consciousness. Lumbar puncture must be performed which often demonstrates cloudy fluid with neutrophils and lymphocytes but negative cultures [1]. Routine postoperative dexamethasone is recommended by most authors [1, 17], and broad-spectrum antibiotics are recommended until the culture results are available, when appropriate treatment should be continued accordingly [39].

53.9 Complications

An important observation from several series was that postoperative period for epidermoid cases was generally more complicated with more incidence of aseptic meningitis and mortality [13, 15]. Incidence of postoperative aseptic meningitis reported in literature is between 2 and 50 % of cases, majority of which is associated with subtotal resection [7, 10, 11, 17]. The rate of chemical meningitis postoperatively is found to be less when the tumor was removed completely [11].

Prevention of this complication is important as it can further lead to communicating hydrocephalus and perineural and perivascular fibrosis [6]. Post-removal irrigation with hydrocortisone solution and administration of dexamethasone postoperatively have been reported to reduce the risk of aseptic meningitis [9, 11, 13].

53.10 Prognosis

Complete removal of an epidermoid cyst is curative; however, they can recur if removal is incomplete [4]. The rate of regrowth again follows the slow linear pattern of normal epidermis. If the growth rate is considered approximately one generation per month, the expected time to symptomatic

recurrence is estimated as patient's age at diagnosis plus 9 months [21]. The recurrences reported in the literature with incomplete removal of brain stem epidermoids occurred within 2 years [40]. This however also depends on how much of the contents were removed during initial operation. In another series, Fornari et al. [15] reported two recurrences, one after an apparent complete resection 11 years later and one 5 years later, after partial removal of supratentorial lesions.

Malignant changes with infiltration of the surrounding brain are very rare but have been reported in several case reports including pediatric cases, even many years after apparent complete removal [1, 4, 23, 30]. Prolonged inflammatory reaction from these lesions is thought to be the predisposing factor in development of squamous cell carcinoma, similar to changes seen in chronic ulcers and draining sinuses [41]. The prognosis when carcinomatous changes occur is poor as complete removal is difficult [41]. In their review of literature, Tamura et al. [23] identified 14 cases of malignant transformation of epidermoids reported between 1965 and 2006. Based on this review, newly identified areas of enhancement during follow-up imaging were found to be strongly suggestive of malignant transformation with postoperative interval before transformation ranging from 3 months to 33 years. Various adjuvant treatments have been employed following surgery for malignant cases where radiotherapy and Gamma Knife radiosurgery have been the main treatments [23]. Surgery alone has had the poorest outcome, while surgery with radiotherapy and/or radiosurgery has been associated with long survival up to 3.5 years. Although new enhancement is suggestive of possible malignant transformation, tissue diagnosis is necessary as foreign body giant cell reaction in the postoperative period can have the same appearance [42].

Symptomatic recurrence was seen in 42 % of intraventricular epidermoids after 10–17 years, all of which were incompletely removed initially [6], indicating the need for long-term follow-up in such cases. Recurrences may not be easily identified in this location as the neural tissue re-expands very slowly or does not at all [6].

Brain stem lesions are associated with highest mortality when comparing various locations with 6 out of 18 reported cases in the literature dying due to progressive deterioration [7].

Lunardi et al. [18], based on their experience with seven intraventricular epidermoids with recurrences after 13 and 17 years postoperatively, suggested that epidermoid tumors do not regrow at the same constant rate as in preoperative period after incomplete resection. This was thought to be due to amount of tumor left, decreased blood supply, and surgical trauma. Length of time to recurrence was about 9 years in the Yamakawa series [18], for the first recurrence in 7 out of 33 patients, and 12.5 years between second and third reoperation. They had three deaths in patients with CPA tumors and one with suprasellar tumor.

In summary, epidermoid tumors are rare lesions in pediatric age and are less common than dermoids in children. Cerebellopontine angle and fourth ventricle are most common locations for these lesions within posterior fossa. Epidermoid tumors generally engulf the neurovascular structures and by the time of their diagnosis often have extended to adjacent compartments. This “fluid” tendency makes the total removal of the lesion more difficult, and therefore epidermoids are associated with higher rate of postoperative complications and recurrence.

References

1. Cobbs CS, Pitts LH, Wilson CB (1997) Epidermoid and dermoid cysts of the posterior fossa. *Clin Neurosurg* 44:511–528
2. Akhavan-Sigari R, Bellinzona M, Becker H, Samii M (2007) Epidermoid cysts of the cerebellopontine angle with extension into the middle and anterior cranial fossae: surgical strategy and review of the literature. *Acta Neurochir* 149:429–432
3. Caldarelli M, Massimi L, Kondageski C et al (2004) Intracranial midline dermoid and epidermoid cysts in children. *J Neurosurg (Pediatr)* 5: 100:437–480
4. Russell DS, Rubinstein LJ (1989) Dermoid and epidermoid cysts. In: *Pathology of tumours of the nervous system*, 5th edn. Edward Arnold, London, pp 690–795
5. Samii M, Tatagiba M, Piquer J et al (1996) Surgical treatment of epidermoid cysts of the cerebellopontine angle. *J Neurosurg* 84:14–19

6. Tancredi A, Fiume D, Gazzeri G (2003) Epidermoid cysts of the fourth ventricle: very long follow up in 9 cases and review of the literature. *Acta Neurochir* 145:905–911
7. Ziyal IM, Bilginer B, Bozkurt G et al (2005) Epidermoid cyst of the brainstem symptomatic in children. *Child Nerv Syst* 21:1025–1029
8. Altschuler EM, Jungreis CA, Sekhar LN, Jenneta PJ, Sheptak PF (1990) Operative treatment of intracranial epidermoid cysts and cholesterol granulomas: report of 21 cases. *Neurosurgery* 26:606–614
9. Berger MS, Wilson CB (1985) Epidermoid cysts of the posterior fossa. *J Neurosurg* 62:214–219
10. Liang-Fu Z (1990) Intracranial epidermoid tumors: thirty-seven years of diagnosis and treatment. *Br J Neurosurg* 4(3):211–216
11. Yamakawa K, Shitara N, Genka S et al (1989) Clinical course and surgical prognosis of 33 cases of intracranial epidermoid tumors. *Neurosurgery* 24:568–573
12. Baxter JW, Netsky MG (1985) Epidermoids and dermoids tumors: pathology. In: Wilkins RH, Rengachary S (eds) *Neurosurgery*. McGraw-Hill, New York, pp 655–661
13. Yasargil G, Abernathy CD, Sarioglu A (1989) Microsurgical treatment of intracranial dermoid and epidermoid tumors. *Neurosurgery* 24:561567
14. Conley FK (1985) Epidermoids and dermoids: clinical features and surgical management. In: Wilkins RH, Rengachary S (eds) *Neurosurgery*. McGraw-Hill, New York, pp 668–673
15. Fornari M, Solero CL, Lodrini S et al (1990) Surgical treatment of infratentorial dermoid and epidermoid cysts in children. *Childs Nerv Syst* 6:66–70
16. Lunardi P, Missori P, Gagliardi FM et al (1992) Dermoid and epidermoid cysts of the midline in the posterior cranial fossa. *Neurosurg Rev* 15:171–175
17. Talacchi A, Sala F, Alessandrini F et al (1998) Assessment and surgical management of posterior fossa epidermoid tumors: report of 28 cases. *Neurosurgery* 42:242–251
18. Lunardi P, Missori P, Gagliardi FM et al (1990) Epidermoid tumors of the 4th ventricle: report of seven cases. *Neurosurgery* 27:532–534
19. Zuccaro G, Fidel S (2007) Cerebellopontine angle lesions in children. *Childs Nerv Syst* 23:177–183
20. Chandler W, Farhat S, Paufi FJ et al (1975) Intrathalamic epidermoid tumor. Case report. *J Neurosurg* 43:614–617
21. Alvord EC (1977) Growth rates of epidermoid tumors. *Ann Neurol* 2:367–370
22. Oertel J, Piek J, Müller J-U, Vogelgesang S, Warzok R, Gaab MR (2002) Posterior fossa squamous cell carcinoma due to dedifferentiation of a dermoid cyst in Klippel-Feil syndrome. *J Neurosurg* 97:1244
23. Tamura K, Aoyagi M, Wakimoto H et al (2006) Malignant transformation eight years after removal of a benign epidermoid cyst: a case report. *J Neurooncol* 79:67–72
24. Bartal A, Razon N, Avram J et al (1988) Infratentorial epidermoids. *Acta Neurochir* 42:142–146
25. Tytus JS, Pennybaker J (1956) Pearly tumours in relation to the central nervous system. *J Neurol Neurosurg Psychiatry* 19:241–259
26. Nelson J, Parisi JE, Schchet SS (1993) Epidermoid and dermoid cysts. In: *Principles and practice of neuropathology*. Mosby, St. Louis, pp 226–228, 262
27. Kaido T, Okazaki A, Kurokawa S et al (2003) Pathogenesis of intraparenchymal epidermoid cyst in the brain: a case report and review of the literature. *Surg Neurol* 59:211–216
28. Chu C, Tseng H, Young Y (2006) Clinical presentation of posterior fossa epidermoid cysts. *Eur Arch Otorhinolaryngol* 263:548–551
29. Sabin HI, Bordi LT, Symon L et al (1987) Epidermoid cysts and cholesterol granulomas centered on the posterior fossa: twenty years. *Neurosurgery* 21:798–805
30. Netsky MG (1988) Epidermoid tumors. *Surg Neurol* 29:477–483
31. Li F, Zhu Y, Liu G et al (2007) Hyperdense intracranial epidermoid cysts: a study of 15 cases. *Acta Neurochir* 149:31–39
32. Hsieh CH, Huang KM, Kao MC et al (1996) Hemorrhage in intracranial epidermoid cyst. *J Formos Med Assoc* 95:173–175
33. Doll A, Eid M, Kehrl P et al (2000) Aspect of FLAIR sequence, 3D CISS and diffusion-weighted MR imaging of intracranial epidermoid cysts. *J Neurosurg* 27:101–106
34. Karantanis AH (2001) MR imaging of intracranial epidermoid tumors: specific diagnosis with Turbo-FLAIR pulse sequence. *Comput Med Imaging Graph* 25:249–255
35. Eytan A, Chen D, Chen JM (2003) Posterior fossa epidermoid cyst. *Otol Neurotol* 24:699–700
36. Oertel J, Gaab MR (2008) Endoscopic assisted surgery in posterior fossa lesions: results with 132 cases. Abstract book, 59th annual meeting of the German Society of Neurosurgery, Würzburg, Germany, June 2008. <http://www.egms.de/en/meetings/dgnc2008/08dgnc240.shtml>
37. Schroeder HWS, Oertel J, Gaab MR (2004) Endoscope-assisted microsurgical resection of epidermoids in the cerebellopontine angle. *J Neurosurg* 101:227–232
38. Aramson RC, Morawetz R, Schlitt M (1989) Multiple complications from an intracranial epidermoid cyst: case report and literature review. *Neurosurgery* 24:574–578
39. Long DM (1993) Intracranial epidermoid tumors. In: Apuzzo MLJ (ed) *Brain surgery*. Churchill Livingstone, New York, pp 669–688
40. Caldarelli M, Colosimo C, Di Rocco C (2001) Intra-axial dermoid/epidermoid tumors of brainstem in children. *Pediatr Neurosurg* 56:97–105
41. Abramson RC, Morawetz RB, Schlitt M (1989) Multiple complications from an intracranial epidermoid cyst: case report and literature review. *Neurosurgery* 24:574–578
42. Moran CC, Vakili ST, Caldmeyer KS et al (1995) Foreign body giant cell reaction associated with epidermoid tumor: CT and MR findings. *J Comput Assist Tomogr* 19:628–630

Pietro Spennato, Vincenzo Trischitta,
Ferdinando Aliberti, and Giuseppe Cinalli

54.1 Introduction

Lhermitte-Duclos disease (LDD), also known as dysplastic cerebellar gangliocytoma, is a rare mass lesion of the cerebellum. It was first described in 1920 [1]. The lesion may be part of a syndrome and associated with congenital malformations, such as megalencephaly, hemihypertrophy, partial gigantism, and polydactyly. Its nature is controversial, and the debate whether it represents a tumor, malformation, or hamartoma is still open [2, 3].

The morphologic and cytologic aspects may indicate that LDD may be the consequence of a disorder of growth and migration of the granular cells of the cerebellar cortex. LDD is characterized by an overgrowth of hypertrophic ganglion cells that replace the granular-cell layer and Purkinje cells, resulting in global thickening of the cerebellar folia, and a gross reduction of the central white matter [4]. However, some authors

support the neoplastic nature of LDD, underlining the resemblance of the large granular cells to blastomas, as well as of the tendency to growth and recur after resection. On the other hand, the similar orientation of the enlarged cells to normal granule cells, lack of mitotic figures, and low proliferation index underscore the benign character of LDD. Recurrence may represent progressive growth of minimally affected regions that appeared normal on MRI at the time of initial resection.

Anyway, in the 2007 WHO classification of tumors of the central nervous system, LDD is classified as grade I tumor, among “neuronal and mixed neuronal-glia tumours” [5].

54.2 Genetic Aspects

The deviant migration and cellular growth in LDD have been linked to a germline mutations of a tumor suppressor gene, named PTEN (phosphatase and tensin homologue deleted). PTEN is located on chromosome 10q22–23 and regulates cell apoptosis, growth, migration, and differentiation. PTEN inactivation results in the loss of inhibition of pAKT and mTOR pathways, promoting hypertrophy and survival of the granule cells in LDD. Recent data suggest that PTEN pathway may contribute to an overgrowth of both neoplastic and nonneoplastic cells: dysregulation of PTEN pathway could determine, in nonneoplastic cells, cell survival and pro-inflammatory

P. Spennato, M.D. • V. Trischitta, M.D.
F. Aliberti, M.D.

Division of Pediatric Neurosurgery, Department
of Neurosciences, Santobono-Pausilipon Children’s
Hospital, Naples, Italy

G. Cinalli, M.D. (✉)
Division of Pediatric Neurosurgery, Department
of Neurosciences, Santobono-Pausilipon Children’s
Hospital, Naples, Italy

Department of Neurosurgery,
University of L’Aquila, L’Aquila, Italy
e-mail: giuseppe.cinalli@gmail.com



Fig. 54.1 Cutaneous lesions of Cowden syndrome

stimulation, mediated by the expression of molecules such as β -catenin, $\text{TNF}\alpha$, and $\text{TNF}\alpha$ receptors, which could predispose to the development of multiple cancers [6]. LDD has been associated with Cowden disease, an autosomal dominant syndrome, which also carries germline mutations of *PTEN* [7]. Association is so strong that LDD is a major diagnostic criterion for Cowden syndrome [8].

Cowden syndrome is an autosomal dominant multiple hamartomatous syndrome, characterized by trichilemmomas (hamartomas of the infundibulum of the hair follicle), mucocutaneous papillomatous papules, macrocephaly, and an increased risk of breast, thyroid, endometrial, and cerebellar tumors (Fig. 54.1). Over 80 % of patients with Cowden disease carry germline mutations in *PTEN*. It remains unclear whether all cases of LDD, even without features of CS, are caused by germline *PTEN* mutation and whether somatic *PTEN* mutation occurs in sporadic LDD. Recent

immunohistochemical studies of tissues from patients with adult-onset LDD have demonstrated activation of the *PTEN/Akt/mTOR* pathway also in patients without Cowden syndrome. However, pathogenesis may be different in the childhood variant of LDD, as the pathway was not constitutively active in these cases [9].

Nowadays, there is tendency to include LDD and Cowden syndrome in *PTEN* hamartomatous tumor syndromes (PHTS): a collection of syndromes characterized by germline mutations in *PTEN* that include also Bannayan–Riley–Ruvalcaba syndrome (association of macrocephaly, developmental delay, intestinal hamartomas, lipomatosis, hemangiomas, speckled penis in males) and *Proteus* and *Proteus*-like syndromes (congenital malformations, tissue overgrowth, epidermal nevi, hyperostosis). The nature of *PTEN* mutations may be specific for each syndrome [8, 10].

PTEN and β -catenin pathways are also implicated in the midbrain development. In conditional mutant mice, deletion of *PTEN* and/or β -catenin genes resulted in enlargement of mid-brain structures and hydrocephalus secondary to aqueductal stenosis [11]. These data may explain macrocephaly and hydrocephalus associated with Cowden syndrome.

Individuals with LDD, even without apparent CS features, should be thereafter counseled as in Cowden syndrome, in order to reduce the risk of developing malignancies [12]. The likelihood that a patient affected by Cowden syndrome will develop breast, thyroid, or endometrial cancer in his or her lifetime is 30–50 %. The screening includes: breast self-exam and education, starting at 18 years of age; medical breast exam for men and women since 25 years of age; annually mammography for women, starting at 30–35 years of age; physical exam with careful attention to the skin and neck region; and thyroid, endometrial, and renal ultrasound with follow-up for any anomalies.

54.3 Clinical Aspects

The distribution of males and females is equal; LDD may present at any age (from neonates to the elderly), but many are diagnosed in the third

to fourth decades of life, with very few pediatric cases reported in the literature.

It can occur both sporadically and in familial form. Cowden syndrome is associated with LDD in approximately 40 % of patients.

Patients present with symptoms of a slow-growing cerebellar mass: headaches, nausea, vomiting, ataxia, diplopia, gait disturbances, and cranial nerve dysfunctions. Usually presentation is not acute, with long-standing history of poor localized neurological symptoms. The duration of symptoms ranges from 1 to 3 years. Some patients, in which the cerebellar lesion was not recognized, have been misdiagnosed having chronic tonsillar herniation (Chiari malformation) and syringomyelia and treated with foramen magnum decompression [13]. Occasionally, the patients may even have sudden neurological deterioration due to acute or decompensated chronic hydrocephalus. In children, symptoms or signs such as developmental delay, hemiparesis, and complex ocular movement disturbance have been reported [14]. Orthostatic hypotension and acute subarachnoid hemorrhage have been described among atypical clinical appearances [15].

54.4 Histopathology

Macroscopically LDD is characterized by the presence of thickened and distorted folia. Microscopically, histological architecture of the cerebellar cortex is reproduced within the lesion in a disorganized fashion. The normal cerebellar cortex consists of three constant layers: the molecular layer (outermost), the Purkinje layer, and the granular layer (innermost). In dysplastic gangliocytoma, an abnormal population of large neurons is present in the granular layer, and aberrant myelination is seen in the molecular layer. This is associated with a generalized thickening of the cerebellar cortex and scarcity or absence of the central white matter. The granular layer is thickened because of hypertrophy of granule cells; the molecular layer is thickened by hyperplasia and hypertrophy of the myelinated fibers extending from abnormal cells in the granular layer. The Purkinje cells are scarce [15, 16]. The

lesion gradually blends into normal cerebellar tissue making the complete surgical removal difficult.

At immunohistochemistry, the dysplastic neurons are positive for neuronal markers (synaptophysin, neurofilaments) and usually show complete or partial loss of PTEN expression accompanied by elevated phosphorylated Akt. No evidence of proliferation is usually shown. This led to the hypothesis that growth of tumor should be produced by increasing size of the abnormal cells rather than multiplication of cells [17]. Malignant transformation of residual or recurrent lesions has never been observed.

Numerous associated abnormalities have been described in patients with LDD. These include megalencephaly, microgyria, spongioblastomas, peritheliomas, hydromyelia, partial gigantism, hemangiomas, polydactyly, macroglossia, and leontiasis ossea [4].

54.5 Imaging

Neuroimaging, showing the presence of enlarged and disorganized cerebellar folia, is so typical that is usually diagnostic for LLD [18]. Magnetic resonance imaging is the imaging modality of choice; however, the lesion can be recognized also on CT scan. It appears on CT scan as a cerebellar mass of mixed density with iso- and hypodense regions, occasionally with scattered or laminar calcification.

This striated or layered appearance (“tiger-striped pattern”) is better appreciable on MRI, especially on T2-weighted images (Fig. 54.2), in which the lesions present with a well-circumscribed high intensity and a striated pattern with isointense bands within these hyperintense areas [19]. Kulkanstrakorn et al. [20] reported that the high signal intensity band corresponded to the inner molecular layer and the granular cell layer. The outer portion of the folia consisting of the outer molecular layer and leptomeninges within effaced sulci created the band isointense to cerebellar grey matter. On T1-weighted images, the striations have been described as hypointense and isointense, respectively, to the cerebellar gray

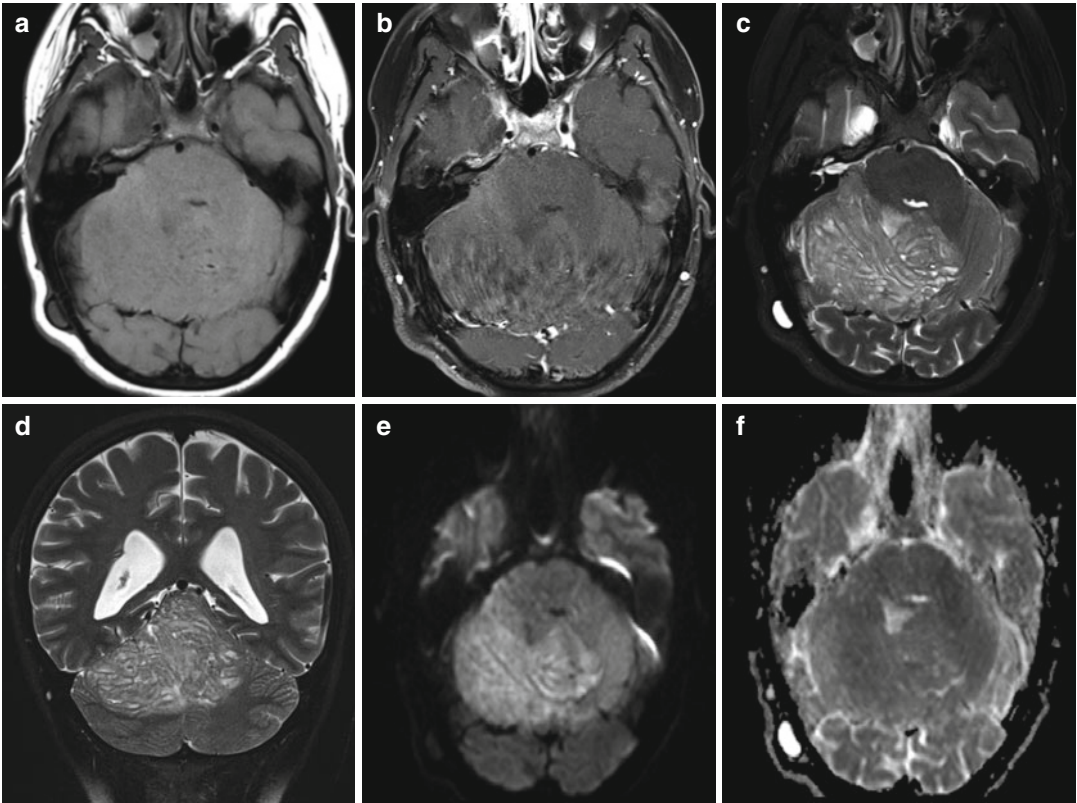


Fig. 54.2 Typical MRI findings of Lhermitte–Duclos disease. T1-weighted axial imaging shows a non-enhancing hypointense cerebellar mass on the right hemisphere (a), with no contrast enhancement (b). T2-weighted axial (c) and coronal (d) imaging reveals a well-circumscribed

hyperintense mass with lamellar areas of isointensity (tiger-striped pattern). The lesion demonstrates high signal intensity on axial diffusion-weighted image (DWI) (d), with patchy mixed diffusion pattern on corresponding ADC map fig. (e–f) (Courtesy of Prof. Dr. Memet Ozek)

matter. On the short TI inversion recovery (STIR) sequence and the turbo inversion recovery magnitude (TIRM) sequence, the morphologic features of the LDD may be clearly demonstrated [21]. The lesions may demonstrate mass effect on the adjacent cerebellar parenchyma and fourth ventricle with hydrocephalus and tonsillar herniation (Figs. 54.2, 54.3, and 54.4). Lesion usually does not enhance following gadolinium (Fig. 54.2), even if proliferating veins within the lesion, and the surrounding leptomeninges, can do. The disease involves one hemisphere, but it occasionally extends to the vermis or to the contralateral hemisphere (Fig. 54.4).

Perfusion-weighted imaging demonstrates elevated regional cerebral blood volume and regional cerebral blood flow rCBF. On diffusion-weighted

images, there may be variable restriction of diffusion depending on contributions from the inner layer and the thick outer molecular layer with large dysplastic neurons, the loss of Purkinje cells, and thinning of medullary white matter. Apparent diffusion coefficient (ADC) mapping may show no disturbance of water diffusion [21]. As compared with the other sequence, the ADC mapping may be helpful in postoperative control, because it delineates tumor from surgical resection margins (Fig. 54.2) [21–23].

Functional imaging (positron emission tomography and magnetic resonance spectroscopy) has also been recently used in diagnosis. F18-fluoro-D-glucose reveals hypermetabolism of the lesion. The reasons for this high uptake, which mimic a malignant tumor, may be increased in overall cell

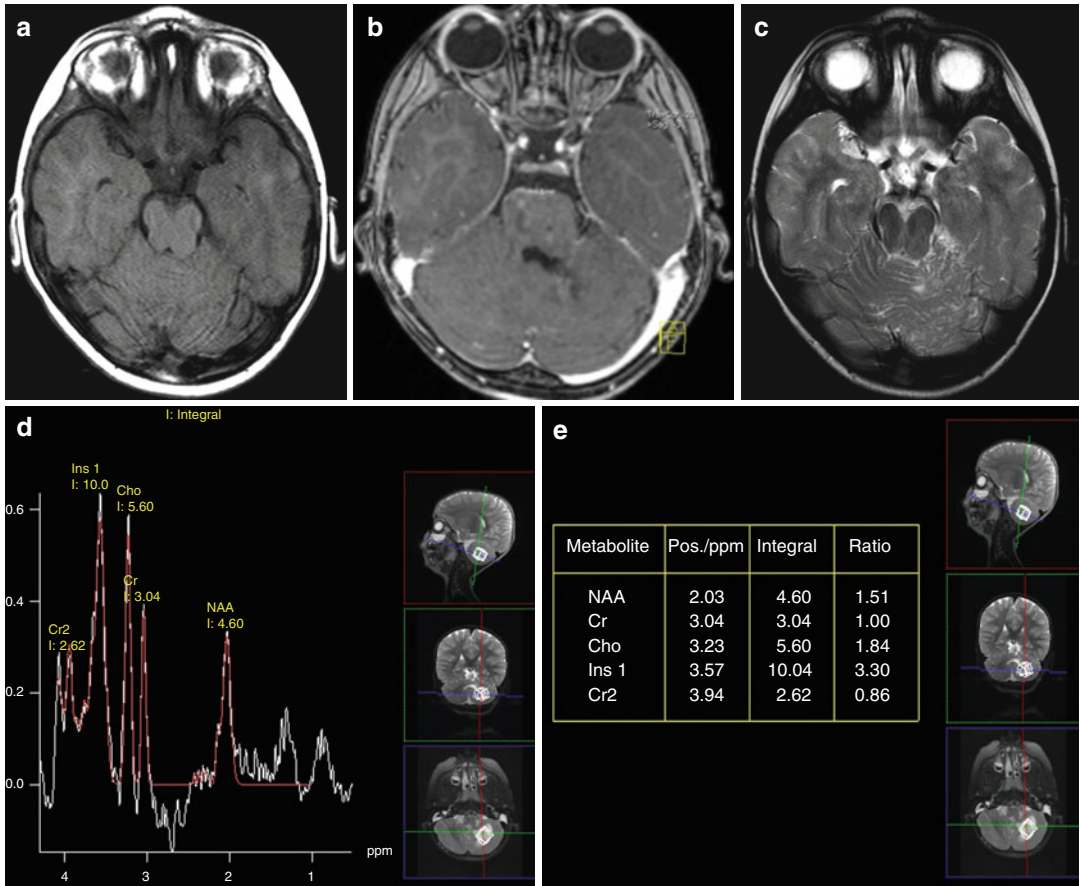


Fig. 54.3 T1- (a–b) and T2 (c)-weighted axial MRI showing LDD in the left cerebellar hemisphere. (d–e) Magnetic resonance spectroscopy, demonstrating elevated

Cho\Cr ratio and elevated Ins peak with reduced Naa\Cr and NAA/Choline (Cho) ratios, as well as an obvious lactate peak in this case (Courtesy of Prof. Dr. Memet Ozek)

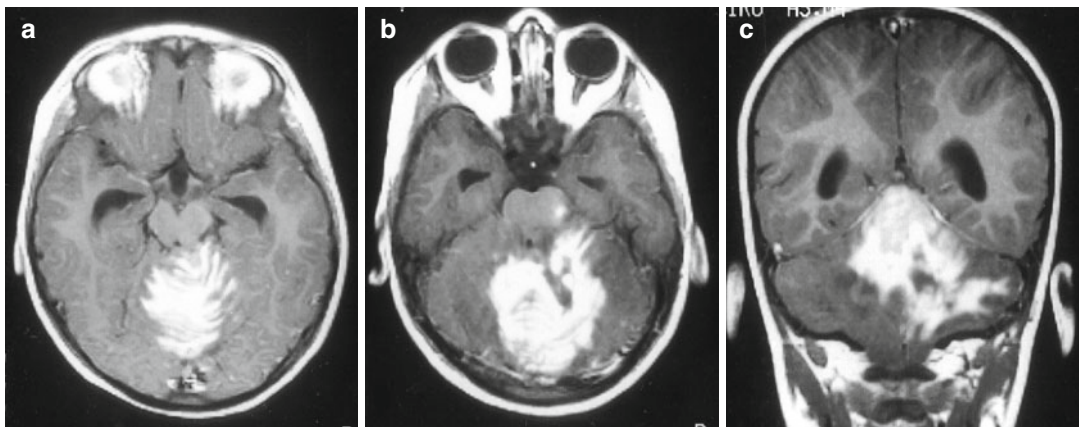


Fig. 54.4 Axial (a, b) and coronal (c) T1-weighted MR images with gadolinium, showing the typical “tiger-striped pattern” of the cerebellar folia. This case showed

an atypical enhancement following gadolinium, associated with involvement of the upper cerebellar peduncle and brain stem

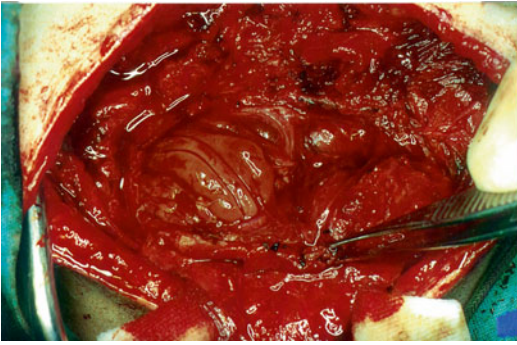


Fig. 54.5 Intraoperative aspect of the hypertrophic cerebellar folia

metabolism, increased in cell density, and isolated upregulation in enzyme activity of hexokinase within the lesion [13, 24].

The appearance of LDD on magnetic resonance spectroscopy is also variable. The most frequent findings are elevated level of lactate, near-normal values of Cho/Cr, and decreased ratios in N-acetylaspartate/creatine (NAA/Cr) and NAA/choline (Cho), secondary to a decrease in the concentration of NAA. These can be attributed to a lack of neuronal architecture (a hallmark of hamartoma) and/or the presence of embryonic neural tissue, which fails to express NAA (Fig. 54.3d–e) [25]. The near-normal values of Cho/Cr ratios in LDD indicate a lack of cell turnover or proliferation (increases in Cho levels are associated with enhanced membrane turnover). These results are in favor of “benign” hamartoma rather than a tumor. In other cerebral neoplasia, a decrease in NAA or NAA/Cr ratio is associated with an increase in Cho or Cho/Cr ratio. Lactate, normally undetectable in the brain, accumulates in cysts, necrotic tissue, or within active tumors because of the high rate of glycolysis. Combined with the histopathologic findings of no necrotic areas within the LDD lesion, the elevated lactate levels do not represent cell death, but an abnormal high glucose metabolism [25]. Therefore, LDD has some characteristics of tumors such as decreased NAA and increased lactate, but not increased levels of Cho [26].

In summary, the typical appearance of LDD is “tiger-striped” mass, with restricted or normal diffusion, high vascularity, preserved blood–brain

barrier permeability and peak of lactate, normal choline, and decrease in NAA.

Differential diagnosis is usually simple, even if cases of medulloblastomas mimicking LDD were reported: as well as LDD they presented typical band-like lamination along the cerebellar cortex, no contrast enhancement and normal diffusivity [27].

54.6 Treatment and Prognosis

Treatment of LDD is surgical resection, even in case of incidental discover lesion because its propensity to grow. Goto et al. [13], observing an initially asymptomatic patient for long time, calculated a tumor doubling time of about 42 months (the tumor doubling time of asymptomatic meningiomas is 93.6). They also observed a linear growth pattern, rather than exponential growth like other neuroglial tumors.

The surgical procedure, usually through a suboccipital approach, should be as radical as possible especially in young patients, [28]. At surgery, the cerebellum may exhibit minimal surface abnormalities (Fig. 54.5). Sometimes, during surgical exploration, no tumor mass can be found [29]. The absence of tumor limits in the depth of the cerebellar hemisphere constitutes the major technical problems during surgery. During removal of the deep portions of the hemispheric tumors, the surgeon should be careful to not damage the cerebellar nuclei and the upper cerebellar peduncle: an unusually high rate of complications were reported following LDD surgery, including cerebellar mutism and persistent cerebellar syndrome (truncal and limbs ataxia, gait disturbance, hypotonia, scanning speech, intention tremor, and nystagmus) [29, 30].

The lack of sharp border between the tumor and normal cerebellar tissue accounts for a recurrence rate that approaches 30 %. Intraoperative biopsies in the suspected border region of the tumor may also be helpful in achieving complete tumor removal, as well as the use of an intraoperative MRI unit [31].

The presence of residual or recurrent disease at follow-up MRI is indication for reoperation,

even if on histological examination at first operation no mitoses were seen [32]. The efficacy of radiation therapy is unknown and should be not considered even if the lesion has been incompletely resected [32].

Nowadays, the prognosis is good and the mortality low. In pre-MRI era, about one-third of the reported patients died [2], including one newborn [33]. Over the recent decades, MR imaging has proven to prompt early diagnosis and appropriate surgical treatment.

Long-term follow-up observation may identify recurrences and facilitate early detection of concomitant malignancies [34].

References

- Lhermitte J, Duclos P (1920) Sur un ganglioneurome diffus du cortex du Cervelet. *Bull Assoc Fr Center* 9:99–107
- Nowak DA, Trost HA, Porr A, Stölzle A, Lumenta CB (2001) Lhermitte-Duclos disease (Dysplastic gangliocytoma of the cerebellum). *Clin Neurol Neurosurg* 103:105–110
- Williams DW, Elster AD, Ginsberg LE, Stanton C (1992) Recurrent Lhermitte-Duclos disease: report of two cases and association with Cowden's disease. *Am J Neuroradiol* 13:287–290
- Amler M, Pogacar S, Sidman R (1969) Lhermitte-Duclos disease (granule cell hypertrophy of the cerebellum) pathological analysis of the first familial cases. *J Neuropathol Exp Neurol* 28:622–647
- Louis DN, Ohgaki H, Wiestler OD, Cavenee WK (eds) (2007) WHO classification of tumours of the central nervous system. IARC, Lyon
- Galatola M, Paparo L, Duraturo F, Turano M, Rossi GB, Izzo P, De Rosa M (2012) Beta catenin and cytokine pathway dysregulation in patients with manifestations of the “PTEN hamartoma tumor syndrome”. *BMC Med Genet* 13:28
- Liaw D, Marsh DJ, Li J, Dahia PL, Wang SI, Zheng Z, Bose S, Call KM, Tsou HC, Peacocke M, Eng C, Parsons R (1997) Germline mutations of the PTEN gene in Cowden disease, an inherited breast and thyroid cancer syndrome. *Nat Genet* 16:64–67
- Lopiccolo J, Ballas MS, Dennis PA (2007) PTEN hamartomatous tumor syndromes (PHTS): rare syndromes with great relevance to common cancers and targeted drug development. *Crit Rev Oncol Hematol* 63:203–214
- Abel TW, Baker SJ, Fraser MM et al (2005) Lhermitte–Duclos disease: a report of 31 cases with immunohistochemical analysis of the PTEN/AKT/mTOR pathway. *J Neuropathol Exp Neurol* 64:341–349
- Hollander MC, Blumenthal GM, Dennis PA (2011) PTEN loss in the continuum of common cancers, rare syndromes and mouse models. *Nat Rev Cancer* 11:289–301
- Ohtoshi A (2008) Hydrocephalus caused by conditional ablation of the Pten or beta-catenin gene. *Cerebrospinal Fluid Res* 5:16
- Govindan A, Premkumar S, Alapatt JP (2012) Lhermitte-Duclos disease (dysplastic gangliocytoma of the cerebellum) as a component of Cowden syndrome. *Indian J Pathol Microbiol* 55:107–108
- Goto Y, Hashimoto N, Okita Y, Goto T, Rabo C, Hirayama H, Horikawa Y, Kinoshita M, Kagawa N, Yoshimine T (2010) A surgically treated case of Lhermitte-Duclos disease with a precise natural history and high uptake of FDG on PET. *J Neurooncol* 97:445–450
- Capone Mori A, Hoeltzenbein M, Poetsch M, Schneider JF, Brandner S, Boltshauser E (2003) Lhermitte-Duclos disease in 3 children: a clinical long-term observation. *Neuropediatrics* 34:30–35
- Kumar R, Vaid VK, Kalra SK (2007) Lhermitte-Duclos disease. *Childs Nerv Syst* 23:729–732
- Roski RA, Roessmann U, Spetzler RF, Kaufman B, Nulsen F (1981) Clinical and pathological study of dysplastic gangliocytoma. *J Neurosurg* 55:318–321
- Hair LS, Symmans F, Powers JM, Carmel P (1992) Immunohistochemistry and proliferative activity in Lhermitte-Duclos disease. *Acta Neuropathol (Berl)* 84:570–573
- Asley DG, Chi-Shing Z, Chandrasoma PT, Segall HD (1990) Lhermitte–Duclos disease: CT and MRI findings. *J Comput Assist Tomogr* 14:984–987
- Meltzer CC, Smirniotopolous JG, Jones RV (1995) The striated cerebellum: an MR imaging sign in Lhermitte–Duclos disease (dysplastic gangliocytoma). *Radiology* 194:699–703
- Kulkantrakorn K, Awwad EE, Levy B, Selhorst JB, Cole HO, Leake D, Gussler JR, Epstein AD, Malik MM (1997) MRI in Lhermitte-Duclos disease. *Neurology* 48:725–731
- Sen KK, Gunasekaran K, Kanagaraj V (2013) Imaging in Lhermitte-Duclos disease. *South Asian J Cancer* 2:131
- Moonis G, Ibrahim M, Melhem ER (2004) Diffusion-weighted MRI in Lhermitte-Duclos disease: report of two cases. *Neuroradiology* 46:351–354
- Klisch J, Jeungling F, Spreer J, Koch D, Thiel T, Buchert M, Arnold S et al (2001) Lhermitte–Duclos disease: assessment with MR imaging, positron emission tomography, single-photon emission CT, and MR spectroscopy. *Am J Neuroradiol* 22:824–830
- Calabria F, Grillea G, Zinzi M, Barbarisi M, Siravo E, Bartolo M, Cantore G, Colonnese C, Grasso C, Schillaci O (2012) Lhermitte-Duclos disease presenting with positron emission tomography-magnetic resonance fusion imaging: a case report. *J Med Case Rep* 6:76
- Nagaraja S, Powell T, Griffiths PD, Wilkinson ID (2004) MR imaging and spectroscopy in Lhermitte–Duclos disease. *Neuroradiology* 46:355–358

26. Wu CH, Chai JW, Lee CH, Chen WH, Lee T, Chen CC (2006) Assessment with magnetic resonance imaging and spectroscopy in Lhermitte-Duclos disease. *J Chin Med Assoc* 69:338–342
27. Douglas-Akinwande A, Payner TD, Hattab EM (2009) Medulloblastoma mimicking Lhermitte-Duclos disease on MRI and CT. *Clin Neurol Neurosurg* 111:536–539
28. Tuli S, Provias JP, Bernstein M (1997) Lhermitte-Duclos disease: literature review and novel treatment strategy. *Can J Neurol Sci* 24:155–160
29. Prestor B (2006) Dysplastic gangliocytoma of the cerebellum (Lhermitte-Duclos disease). *J Clin Neurosci* 13:877–881
30. Afshar-Oromieh A, Linhart H, Podlesek D, Schrempf W, Schackert G, Krex D (2010) Postoperative cerebellar mutism in adult patients with Lhermitte-Duclos disease. *Neurosurg Rev* 33:401–408
31. Buhl R, Barth H, Hugo H-H, Straube T, Mehdorn HM (2003) Dysplastic gangliocytoma of the cerebellum: rare differential diagnosis in space occupying lesions of the posterior fossa. *Acta Neurochir* 145:509–512
32. Marano SR, Johnson PC, Spetzler RF (1998) Recurrent Lhermitte-Duclos disease in a child, case report. *J Neurosurg* 69:599–603
33. Roessmann U, Wongmongkolrit T (1984) Dysplastic gangliocytoma of cerebellum in a newborn, case report. *J Neurosurg* 60:845–847
34. Wei G, Zhang W, Li Q, Kang X, Zhao H, Liu X, Tang X, Wu Y, Han J, Yin H (2014) Magnetic resonance characteristics of adult-onset Lhermitte-Duclos disease: an indicator for active cancer surveillance? *Mol Clin Oncol* 2:415–420

55.1 Introduction

There are many similarities between pediatric meningiomas and adult counterparts. However, there are several characteristics that are unique to pediatric meningiomas, and these include male predominance, often larger size at presentation, lack of dura attachment, and unusual anatomical locations [1]. In contrast to adult intracranial meningiomas, pediatric meningiomas only account for 2–4.2 % of all pediatric tumors [2–4].

One of the controversies in relation to pediatric meningiomas is with regard to their recurrence and long-term outcomes. Few series have claimed poorer prognosis [2–5]. Some of this conclusion may be drawn based on studies that included significant number of patients with subtotal resection [5]. Whether the behavior of meningiomas in pediatric age group is more aggressive is another potential conclusion drawn by these studies. As some series report,

recurrence is seen more often even with totally resected tumors [6]. Nonetheless, all could imply need for lifelong surveillance and follow-up. Furthermore, there seem to be higher proportion of these tumors in pediatric age with WHO grades II and III [4, 5].

55.2 Epidemiology

The majority of pediatric meningiomas are seen in the second decade of life [5, 7, 8]. The incidence of childhood meningiomas is reported in most series between 2 and 4 % [4, 5, 9]. Rosenberg and Fujiwara reported the incidence of pediatric nervous system meningiomas [10]. They reported a 3 % incidence of intracranial meningiomas out of 1,058 cases. In terms of WHO grading, pediatric meningiomas show higher percentage of high-grade tumors. Thuijs et al. reported on 72 patients over a 35-year period where grades II and III combined formed 35 % of total number of tumors [5]. Similarly a more recent outcome analysis by Kotecha et al. reported 30 % WHO grade II and III meningiomas in total of 261 tumors [4].

Increasing incidence of meningiomas with age is demonstrated on several studies. Male predominance is consistently found in majority of studies with larger number of patients [1, 4, 8, 9, 11–13]. This may be related to lack of hormonal influences in the prepubertal age group as hormonal effects beginning in this group would not manifest

S. Kohan, MBBS, FRACS
Department of Neurosurgery,
Sydney Children's Hospital, High St.,
Randwick, Sydney 2031, Australia

Suite 17 Level 5, St. George Private Hospital,
1 South St Kogarah, NSW, Sydney 2217, Australia

M.M. Özek, M.D. (✉)
Division of Pediatric Neurosurgery,
Department of Neurosurgery, Acibadem University,
School of Medicine, Istanbul, Turkey
e-mail: memetozek@gmail.com

themselves for several years [14]. The mean age at presentation in most reported series are around 11–13 years of age which are generally later than typical pediatric CNS tumors [7, 8, 11, 13, 15].

Neurofibromatosis is found in 10–20 % of pediatric age group with meningiomas [4, 8, 14].

55.3 Predisposing Factors

Most frequently suggested factors predisposing to development of posterior fossa meningiomas are radiation and neurofibromatosis [3, 11, 16].

The first large series indicating association of meningiomas and radiation was reported with connection of children radiating for tinea capitis in Israel [17]. This study reviewed 10,834 children who had undergone low-dose radiation (850 cGY) compared with age and sex match-controlled population. Those irradiated were found to have four-fold increase in development of meningioma. This had direct relationship with increased dose of radiation. Pettoriani and colleagues [18] reviewed pediatric population with meningioma and found a median age at radiation for grade I tumors of 5.4 years and that for atypical tumors of 5.1 years of age with latency period of 13.7 years (range between 6 months and 28 years) and for grade II of 21.1 years (range 8–63 years).

The most consistent chromosomal abnormality associated with development of meningiomas is seen in patients with NF2. An abnormality of chromosome 22 has been reported for both sporadic and NF2-associated meningiomas [1].

Meningiomas are the first solid tumors to be associated with cytogenetic abnormalities, with most tumors showing monosomy of chromosome 22 and some with partial deletion or rearrangement of chromosome 22q [19, 20].

Bhattacharjee et al. reported 40–60 % of meningiomas showing allelic losses of chromosome 22q [19]. Other larger series also have shown between 23 and 58 % association with neurofibromatosis in patients with pediatric meningiomas [12, 21, 22]. An interesting feature of pediatric meningiomas associated with neurofibromatosis is in terms of location, where these children have higher incidence of extracranial, intraocular, and

multifocal meningiomas indicating the need for closer monitoring as well as investigating children with these unusual features particularly for presence of neurofibromatosis.

55.4 Clinical Features

55.4.1 Signs and Symptoms of Posterior Fossa Meningiomas

Symptoms of raised intracranial pressure including nausea, vomiting, and headache are the most common presenting symptoms with pediatric posterior fossa meningiomas [7, 8, 14]. Focal neurological signs are less frequent in some series, at around 20 % of cases reviewed [8, 14]. Raised ICP may also be due to presence of hydrocephalus. Increasing head circumference is one of the key features in particular at younger age where nonspecific symptoms and signs such as irritability and poor feeding due to raised ICP may also be present [2, 23].

55.5 Imaging

Imaging findings in pediatric meningiomas are mostly similar to adults. However, there are few particular imaging characteristics which are more commonly noted in pediatric age group [1]. With the current era of availability of MRI scans, many physicians proceed directly to MRI scan for investigations of suspected intracranial lesion in children. However, CT scanning is still a common screening tool.

On plain radiographs, many series have reported a higher percentage of calcification, as well as calvarial erosion and hyperostosis. Abnormal calcifications were seen in 21 % of cases reported [24]. Skull radiographic abnormalities showing hyperostosis, calvarial bulging, and focal erosion were seen in 7 out of 11 cases reported by Im and colleagues [25] and 7 out of 33 tumors in another series [26].

The typical computed tomography (CT) features include presence of an extra-axial lesion, with associated hyperostosis, irregularity of underlying cerebellar cortex, and calcification

within the tumor in up to 25 % of cases demonstrated as hyperdense areas. An extra-axial mass is identified by its broad base toward the dural surface, causing displacement of gray matter (“buckled”), and there may be a thin cerebrospinal fluid (CSF) rim between the tumor and the cortex. More than 90 % of these lesions enhance strongly with contrast [18]. Other described findings on CT scans include sharp and lobulated margins and homogeneous post-contrast enhancement, with limited peritumoral edema which were found in all 24 cases reported in one study [6], while in the series of Im and colleagues [25] examination by CT and magnetic resonance imaging (MRI) showed about 20 % of tumors with poor demarcation and less than 10 % poorly enhancing with contrast [25].

Cystic areas have been reported in up to 3 % of mixed series, although their presence in pediatric meningiomas is commonly reported to be higher [14]. In combined series Artico and colleagues [26] found 25 cystic meningiomas in 210 reported cases representing 12 % of these tumors. Also in other studies, cystic tumors have been reported in up to 8 % versus 3–5 % in adults [12, 14, 17] and in 155 patients reviewed by Liu and colleagues [27] where 21 % had cystic changes.

One of the commonly reported features of pediatric meningiomas is their large size regardless of their location at presentation. In their combined series of 166 patients, Liu and colleagues [27] reported the mean diameter of 5.2 cm with the range of 2–11 cm. The clinical significance of cystic changes is unclear from the literature, although Tufan and colleagues [15] reported 4 cystic tumors out of 11 reported cases, all of which were grade II or III. The cystic feature is best appreciated on MRI.

MRI is the investigation of choice for meningiomas in providing three-dimensional anatomic details and the relationship of the tumors to other structures, as well as avoiding radiation.

On standard sequences, these lesions typically appear isointense or occasionally hypointense to the cortex on T1-weighted images and hyperintense or mixed intensity on T2 imaging (Fig. 55.1a). The majority of these lesions (>90 %) enhance strongly with contrast (Figs. 55.1b,

55.2a, and 55.3a). The extent of edema (50–65 %) and the presence of a CSF rim around the tumor are also better seen on MRI (T2 weighted), which can confirm the extra-axial nature of these lesions.

One of the features that have commonly been reported in the literature is absence of a dural tail in a high percentage of pediatric meningiomas (Fig. 55.2a) [2, 24, 28]. Dural thickening or “tail” is the best diagnostic feature of meningiomas and is reported in 35–80 % of cases. However, it is not pathognomonic for meningiomas. Drake and colleagues [2] reported 23 % of the tumors in their series which did not have dural attachment. This feature is also mentioned in other studies with 11–15 % variability [21, 29].

In a recent series Sitthinamsuwan et al. reported on 243 consecutive cases where the MRI scans were viewed and found the signal intensity on T2WI and FLAIR images were useful in predicting the consistency of meningiomas [30]. These investigators found hypointense tumors on these sequences tended to be hard whereas tumors showing hyperintensity in T2WI and FLAIR to be associated with softer consistency.

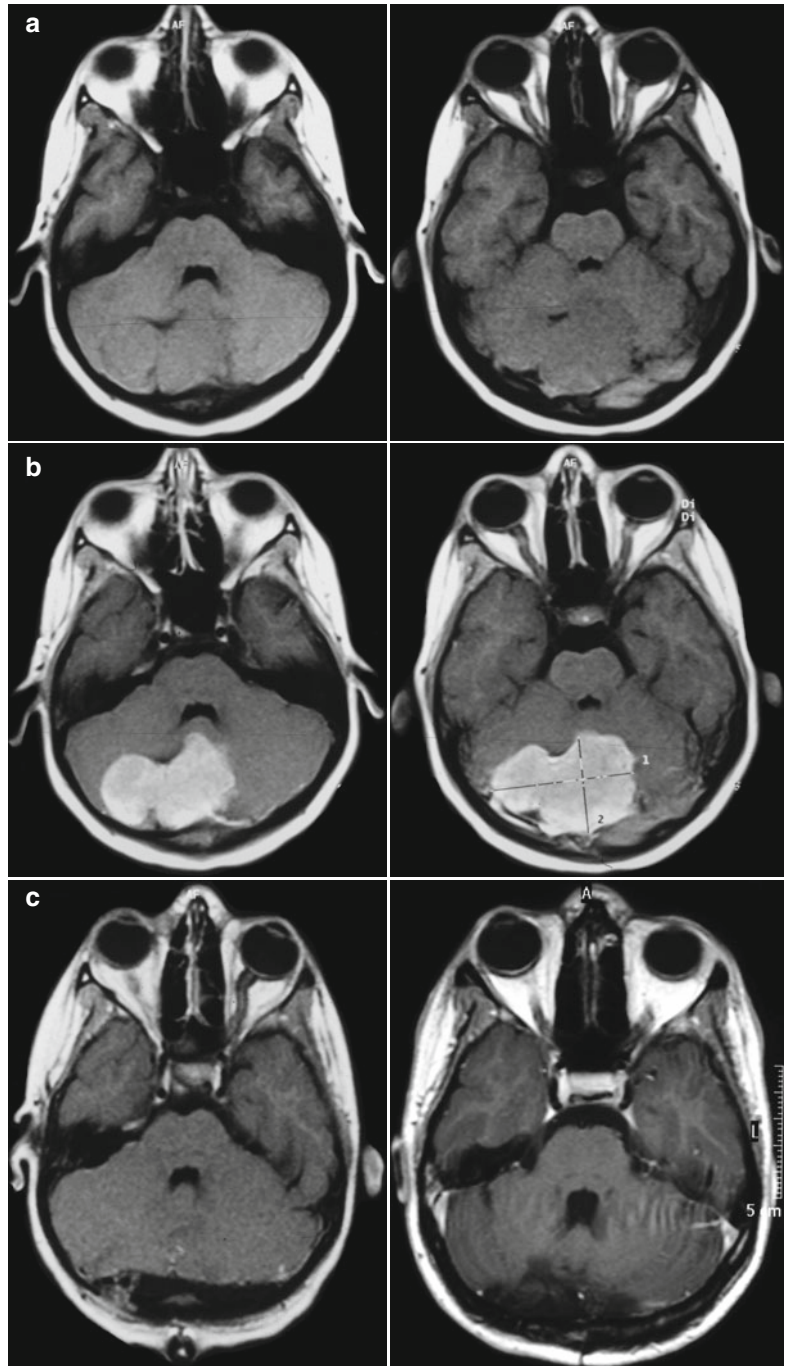
MR spectroscopy has been reported as a useful tool in differentiating meningiomas from other lesions in particular metastases and gliomas [16]. These are described as low N-acetylaspartate (NAA) and free lipids and high concentration of glutamate/glutamine compounds in meningiomas. High glutathione (GSH) peak on MR spectroscopy is described [31]. In the modern area of readily available MRI or at least CT scans, no specific indication or reason was found for performing angiography in more recent series. But the authors recommend having a MR venography to have an idea about the major venous sinuses for posterior fossa meningiomas (Fig. 55.2b).

The need for embolization for pediatric meningiomas is also limited due to the risk of morbidity and availability of modern surgical care [6].

55.6 Pathology

Cystic tumors and large size of pediatric meningiomas at presentations are significant macroscopic features reported [2, 15, 25, 27].

Fig. 55.1 (a) Isointense appearance of a posterior fossa meningioma in a 9-year-old girl. Despite the big size of the lesion, there is no obstruction of the four ventricle. (b) Strong homogeneous enhancement. (c) After tumor resection



Histopathologically there seems to be higher representation of atypical and malignant (WHO grades II and III) associate with these features.

Meningiomas are currently divided into 13 histological types, separated over 3 grades

according to the WHO grading system. Majority of these tumors are grade 1 and considered benign (meningotheial, psammomatous, transitional, fibrous, etc.). The atypical (grade 2) tumors are chordoid, clear cell, and atypical; and

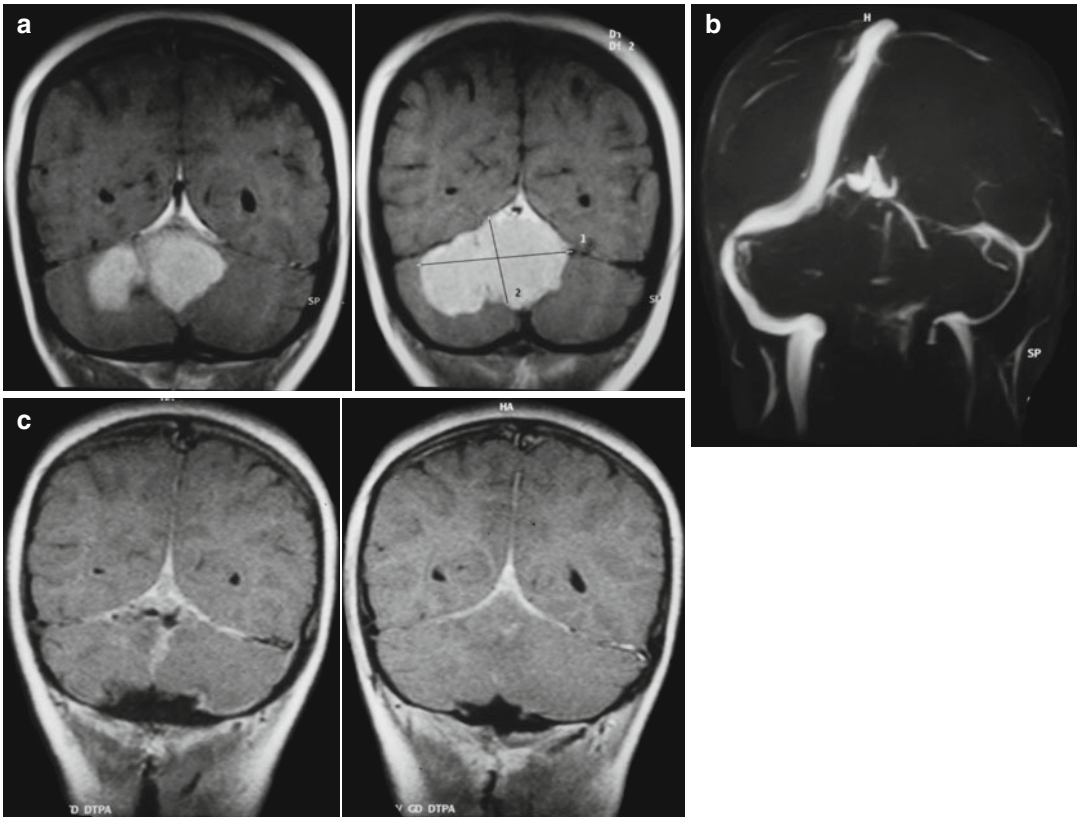


Fig. 55.2 (a) Post-contrast coronal view. There is no “tail” sign. (b) No blood flow through the right transverse sinus. (c) After tumor resection

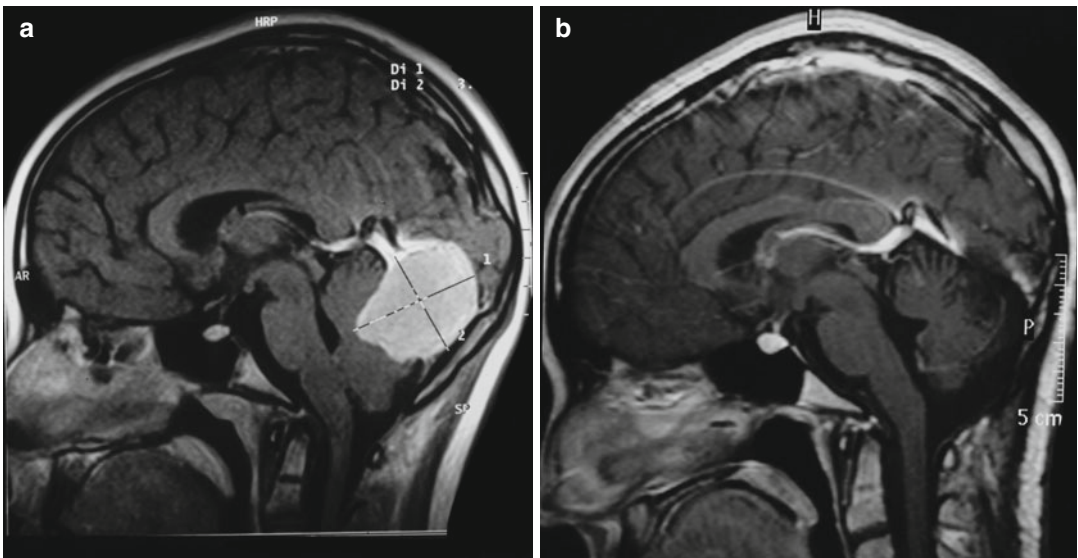


Fig. 55.3 (a) Preoperative sagittal view of the same case. (b) After tumor resection

grade 3 (anaplastic) tumors are rhabdoid, anaplastic, and papillary [32]. These have been associated with prognostic significance.

Immunohistochemistry in recent years has been of significant importance in diagnosing these tumors. MIB-1 is an anti-Ki67 monoclonal antibody which is immunoreactive for the nuclei of cells in non-G0 phases [13]. The ratio of MIB-1-positive cells (MIB-1 index) is reported to correlate well with histological grading. High immunohistochemical proliferation index is found to be associated with increased risk of recurrence [33]. Sandburg et al. [33] studied 14 pediatric tumors and found MIB-1 index of 12.3 % (range 7–31.6 %) in atypical and malignant and 7 % (range 1.2–12.6 %) for grade I meningiomas. When patients with NF2 or history of radiation were excluded, the difference between the MIB-1 index medians for benign and atypical/malignant tumors was even more significant (median of 8.4 % vs. 25.7 %). The authors concluded that the elevated MIB-1 index correlated well with atypia and more aggressive behavior of pediatric meningiomas. Im et al. [25] observed high MIB-1 (≥ 5 %) in 3 of 11 cases and noted recurrence after 2 years in one case with transitional meningioma and MIB-1 of 10 %. They also noted direct correlation of higher MIB-1 and size of the tumor (5–9 cm), while all were grade one tumors with different histological subtypes. Also Perry et al. [34] studied 19 sporadically occurring pediatric and 14 children and 7 adults NF 2 associated meningiomas in details. The percentages of high-grade (II and III) tumors were 57 %, 60 %, and 67 % in pediatric non-NF2, pediatric NF2, and adults with NF2, respectively. The rate of recurrences was highest in the pediatric non-NF2 patients of 50 % vs. 23 % in pediatric NF2 tumors and 40 % in adults with NF2.

The number of mitotic figures per high power field (1 HPF=0.16 mm²) is one of the WHO criteria for grading of meningiomas. According to these criteria, 4 or more mitosis/10 HPFs is consistent with atypical meningiomas, and 20 or more is consistent with anaplastic types. The identification of the morphological changes within cells and consequently accurate diagnosis can be difficult. Recently a mitosis-specific antibody against

phosphorylated histone H3 (PHH3) has been developed which makes identification of proliferating cells much more accurate [13].

Meningiomas in particular fibroblastic type may be difficult to differentiate from schwannomas with routine staining, especially when located in posterior fossa or spinal canal. Commonly, immunostaining for epithelial membrane antigen (EMA) is significantly higher in meningioma and S100 in schwannoma, but neither immunostain is 100 % specific. For this purpose, another immunohistochemical stain for claudin-1, a key structural protein of tight junctions, has been developed that reacts with meningioma cells but has been shown to have no reactivity with schwannomas [14].

In more recent studies, the incidence of atypical pediatric meningiomas is reported between 11 and 18 %, while grade III meningiomas were around 7 % [4, 5, 8].

55.7 Management Strategies

Before considering the approaches to the pediatric meningiomas, it is important to point out that the concept of outcome in pediatric neurosurgery patient is perhaps more complex and multifaceted. The factor that plays a significant role in this long-term outlook is the child's development both cognitively and socially, in order to allow the child to become at least independent or ideally a functional member of the society. The care for the pediatric patient becomes even more complex as one is faced with the child's carers (usually very anxious parents).

Observation in pediatric posterior fossa meningiomas may be justified for short term but suboptimal for long-term management of these tumors [1]. In the short term, observation may be appropriate to optimize the patient conditions or in cases of small tumors when there is little or no neurological deficit or significant mass effect. However, although these tumors are slow growing, the long-life expectancy of children and the presence of mass effect during their developmental period necessitate definitive management in the long term.

55.8 Surgery

Surgery has been the main stay of treatment of pediatric posterior fossa meningiomas and is found to be the main factor affecting the long-term outcome in this population [4, 5, 34]. Factors complicating surgery include unusual location in the posterior fossa, large size, compression of the lower cranial nerves, infiltration and obstruction of the sinuses, and tumor vascularity, as well as patient-related factors due to prolonged surgery and risks of hypothermia and massive blood transfusion [26].

Recurrence is reported in many series mostly in association with subtotal resection. Given that these lesions are mostly benign and been shown to have good prognosis with total resection, complete surgical resection should be attempted while avoiding further neurological deficit.

With the importance of complete resection being increasingly realized, it has been suggested the complete resection should be attempted even if this is done in two or three stages [35]. Some authors also suggest “second-look” surgery in order to avoid radiation and its long-term complication including secondary tumors [27, 36]. Staged surgery is also an option for the cases with high blood loss [27]. In our institution we take the approach of maximal resection even if this may require further surgery, in order to avoid radiation and its long-term complications [1].

Risk factors for perioperative mortality include tumor characteristics such as the size, location within the posterior fossa, and the vascularity of the tumor. In a series of 152 combined cases, 5 perioperative deaths were recorded [27]. Three died due to brainstem injury and intraoperative hemorrhage, respectively, and two died of intracranial infection. On their review of literature, Liu et al. reported perioperative mortality between 0 and 8.3 % with the mean mortality of 3.3 % [27].

Significant brain edema as cause of perioperative death has been reported in several series [26]. Arivazhagan et al. [26] suggested preoperative CSF diversion, anti-edema measures, and postoperative ventilation as some of strategies to avoid this complication.

55.9 Adjuvant Treatment: Role of Radiotherapy and/or Chemotherapy

The utility of radiation in the treatment of meningioma has been demonstrated in adult tumors. Local control and recurrence rates differ between studies, with rates between 46 % 5 years local control and 100 % 10 years recurrence-free probability being reported [20]. However, it is generally recognized that surgical resection continues to offer superior local control than radiation, for cases where it is suitable. The role of radiation therapy as an adjunct to surgery, in cases of incomplete resection, is more universally supported, particularly in cases of WHO grade 2 and 3 tumors [20].

Before considering radiation in children, however, potential adverse effect such as secondary tumors, hormonal deficiency, growth retardation, or cognitive impairment, particularly in younger patient, must be weighed against potential benefits [1].

Libel and colleagues used upfront radiation to delay recurrent tumor [32]. However, some others have suggested re-operation as an option for avoiding radiation for recurrent tumors [26]. The reason for postoperative radiotherapy has been mostly with recurrent tumor or presence of atypical or malignant tumors in most series [5, 8, 9, 20]. In series reviewed, radiotherapy was recommended for high-grade tumors in children older than 5 years of age and in particular where residual was present and further surgery was not feasible.

Rochat et al. [24] reported on 22 pediatric meningiomas in Denmark between 1935 and 1984. Eight children were irradiated of whom two had partial resection and survived for 18.5 and 39 years. In our series we did not perform radiotherapy for residual or recurrent tumors.

Chemotherapy has little to offer in the treatment of meningioma and is typically employed in salvage therapy of refractory, recurrent tumors, especially of high-grade type.

55.10 Outcomes

Factors found to be associated with recurrence are completeness of resection, tumor location, and the histopathological grading of the tumor

[15, 27, 35, 37]. Several series where NF patients were included, presence of neurofibromatosis was suggested as another factor associated with higher recurrences and deaths [21, 26, 35]. The 10-year recurrence rates reported by Erdiçler et al. [12] in their series of 29 patients were 82 and 33 % for total and subtotal resections, respectively. Mallucci et al. [3] despite the majority of patients predating the modern era, reported 92 % long-term (40 years) survival in the group with complete resection.

Recurrences after total resection have been reported. Amirjamshidi et al. [6] and Rochat et al. [24] reported 6 out of 21 and 6 out of 11 recurrences after reported total resection, respectively. Lack of optimal post-op imaging to accurately assess the degree of resection and accuracy of histopathological diagnosis at the time may have contributed to these findings.

Higher proliferation index (MIB-1) is also associated with higher recurrence [24]. Perry et al. [38] correlated the grading of the meningiomas with rates of recurrences and deaths. Despite higher recurrences, there was significantly lower death in pediatric non-NF2 patients due to tumor recurrence. Given that five of pediatric NF2 patients were diagnosed during the course of the study, the authors recommended that any child with meningioma to be carefully examined and followed up since this could be the initial presentation of NF2.

Interestingly in their series, Arivazhagan et al. [26] have reported three cases of progression to higher histological grade. These were found on examination of the specimen obtain during surgery of three recurrent tumors which were compared with original diagnosis.

In review of morbidity in survivors of childhood meningioma, Kotecha et al. reported on 261 patients [4]. Overall these investigations found 48 % of patients had completely normal life with no morbidity, while 25 % had moderate to severe morbidity associated with their original diagnosis. The factors that affected the increased risk of long-term morbidity included association with neurofibromatosis, location of the tumor at the skull base, and recurrence of tumor. These investigators again concluded aggressive surgical

management for children and adolescents with meningioma both at the primary operation and for the relapse is a determining factor for better outcome.

Lastly, in a recent study, Surov et al. reported on presence of distant metastases associated with meningioma which previously was thought to be extremely rare [39]. These investigators in review of literature estimated 6.1 % metastases with primary tumor and in 0.9 % metastases were identified before the primary tumor was found. The most frequent site for these included the lungs in 37.2 %, bones in 16.5 %, and intraspinal in 15.2 % with liver involved in 9.2 % of cases [39]. Given the long survival expected in pediatric meningiomas and higher percentage of grade II and III lesions, this may be a fact to keep in mind.

References

- Ozek MM, Kohan S (2010) Pediatric meningiomas. In: Pamir MN, Black PM, Fahlbusch R (eds) Meningiomas. Saunders Elsevier, Philadelphia, pp 581–591
- Drake JM, Hoffman HJ (1991) Meningiomas in children. In: AL-Mefty O (ed) Meningiomas. Raven Press, Ltd., New York, pp 145–152
- Mallucci CL, Parkes SE, Barber P, Powell J, Stevens MCG, Walsh AR, Hockley AD (1996) Paediatric meningeal tumours. *Childs Nerv Syst* 12:582–589
- Kotecha R, Jacoby P, Cole C, Gottardo N (2013) Morbidity in survivors of child and adolescent meningioma. *Cancer* 119:4350–4357
- Thuijs N, Uitdehagg B, Van Ouwkerk W et al (2012) Pediatric meningiomas in The Netherlands 1974–2010- a descriptive epidemiological case study. *Childs Nerv Syst* 28:1009–1015
- Amirjamshidi A, Mehrazin M, Abbassioun K (2000) Meningiomas of the central nervous system occurring below the age of 17: report of 24 cases not associated with neurofibromatosis and review of literature. *Childs Nerv Syst* 16:406–416
- Lakhdar F, El Ouahadi A, Rifi L, Darraz S, El Khamlichi A (2010) Intracranial meningioma in children- different from adult forms? A series of 21 cases. *Neurochirurgie* 56:309–314
- Gao X, Zhang R, Mao Y, Wang Y (2009) Childhood and juvenile meningiomas. *Childs Nerv Syst* 25:1571–1580
- Ravindranath K, Vasudevan M, Pande A, Symss N (2013) Management of pediatric intracranial meningiomas- an analysis of 31 cases and review of literature. *Childs Nerv Syst* 29:573–582

10. Rosemberg S, Fujiwara D (2005) Epidemiology of pediatric tumors of the nervous system according to the WHO 2000 classification: a report of 1,195 cases from a single institution. *Childs Nerv Syst* 21:940–944
11. Lund-Johansen M, Scheie D, Muller T, Lundar T, Helseth E (2001) Neurosurgical treatment of meningiomas in children and young adults. *Childs Nerv Syst* 17:719–723
12. Erdinçler P, Lena G, Sarioglu AC, Kaday C, Choux M (1998) Intracranial meningiomas in children: review of 29 cases. *Surg Neurol* 49:136–141
13. Herz DA, Shapiro K, Shulman K (1980) Intracranial meningiomas of infancy, childhood and adolescence. *Childs Brain* 7:43–56
14. Moores LE, Cogen PH (2001) Intracranial meningioma. Tumors of the pediatric central nervous system. Thiemes Medical, New York, pp 351–360
15. Tufan K, Dođulu F, Kurt G, Emmez H, Çeviker N, Baykaner MK (2005) Intracranial meningiomas of childhood and adolescence. *Pediatr Neurosurg* 41: 1–7
16. Rutten I, Raket D, Francotte N, Philippet P, Chao SL, Lemort M (2006) Contribution of NMR spectroscopy to the differential diagnosis of a recurrent cranial mass 7 years after irradiation for a pediatric ependymoma. *Childs Nerv Syst* 22:1475–1478
17. Modan B, Mart H, Baidatz D, Steiniz R, Levin SG (1974) Radiation –induced head and neck tumors. *Lancet* 1:227–279
18. Pettorini BL, Park YS, Caldarelli M, Massimi L, Tamburrini G, Rocco C (2008) Radiation-induced brain tumours after central nervous system irradiation in childhood: a review. *Childs Nerv Syst* 24:793–805
19. Bhattacherjee MB, Armstrong DD, Vogel H, Cooley LD (1997) Cytogenetic analysis of 120 primary pediatric brain tumors and literature review. *Cancer Genet Cytogenet* 97:39–53
20. Li Z, Zhang Y, Wang E, Wang Z et al (2012) Distant metastases in meningioma- an underestimated problem. *Childs Nerv Syst* 28:2143–2151
21. Merten DF, Gooding CA, Newton TH, Malamud N (1974) Meningiomas of childhood and adolescence. *J Pediatr* 84:696–700
22. Deen HG Jr, Scheithauer BW, Ebersold MJ (1982) Clinical and pathological study of meningiomas of the first two decade of life. *J Neurosurg* 56:317–322
23. Katayama Y, Tsubokawa T, Yoshida K (1986) Cystic meningiomas in infancy. *Surg Neurol* 25:43–48
24. Rochat P, Johannesen HH, Gjerris F (2004) Long-term follow up of children with meningiomas in Denmark: 1935 to 1984. *J Neurosurg (Pediatr)* 100: 179–182
25. Im SH, Wang KC, Kim DG, Hong SK, Kim NR, Chi JG, Cho BK (2001) Childhood meningioma: unusual location, atypical radiological findings, and favorable treatment outcome. *Childs Nerv Syst* 17:656–662
26. Arivazhagan A, Indira Devi B, Kolluri SVR, Abraham RG, Sampath S (2008) Pediatric intracranial meningiomas do they differ from their counterparts in adults? *Pediatr Neurosurg* 44:43–48
27. Liu Y, Li F, Zhu S, Liu M, Wu C (2008) Clinical feature and treatment of meningiomas in children: report of 12 cases and literature review. *Pediatr Neurosurg* 44:112–117
28. Sano K, Wakai S, Ochiai C, Takakura K (1981) Characteristics of intracranial meningiomas in childhood. *Childs Brain* 8:98–106
29. Doty JR, Schut L, Bruce DA, Sutton LN (1987) Intracranial meningiomas of childhood and adolescence. *Prog Exp Tumor Res* 30:247–254
30. Sitthinamsuwan B, Khampalikit I, Nunta-aree S et al (2012) Predictors of meningioma consistency- a study in 243 consecutive cases. *Acta Neurochir* 154:1383–1389
31. Optad KS, Provencher SW, Bell BA, Griffiths JR, Howe FA (2003) Detection of elevated glutathione in meningiomas by quantitative in vivo ¹H MRS. *Magn Reson Med* 49:632–637
32. Libel SA, Wara WM et al (1976) The treatment of meningiomas in childhood. *Cancer* 37:2709–2712
33. Sandberg D, Edgar MA, Resch L, Rutka JT, Becker LE, Souweidane MM (2001) MIB-1 staining index of pediatric meningiomas. *Neurosurgery* 48:590–597
34. Stafford SL et al (1998) Primarily resected meningiomas: outcome and prognostic factors in 581 Mayo Clinic patients, 1978–1988. *Mayo Clin Proc* 73:936–942
35. Baumgartner JE, Sorenson JM (1996) Meningioma in the pediatric population. *J Neurooncol* 29:223–228
36. Rickert CH, Paulus W (2001) Epidemiology of central nervous system tumors in childhood and adolescence based on the new WHO classification. *Childs Nerv Syst* 17:503–511
37. Darling CF, Byrd SE, Reyes-Mugica M, Tomita T, Osborn RE, Radkowski MA, Allen ED (1994) MR of pediatric intracranial meningiomas. *Am J Neuroradiol* 15:435–444
38. Perry A, Giannini C, Raghavan R, Schethauer BW, Benerjee R, Margraf L, Browsers DC, Lytle RA, Newsham IF, Gutmann DH (2001) Aggressive phenotypic and genotypic features in pediatric and NF2-associated meningiomas: a clinicopathologic study of 53 cases. *J Neuropathol Exp Neurol* 60(10):994–1003
39. Surov A, Gottschling S, Bolz J, Kornhuber M, Alfieri A, Holzhausen HJ, Abbas J, Kösling S (2013) Distant metastases in meningioma: an underestimated problem. *J Neuro Oncol* 112:323–327

Pre- and Postoperative Care of Pediatric Posterior Fossa Tumors

Martina Messing-Jünger, Michael Ehlen,
and Ehrenfried Schindler

This chapter will focus on the direct postoperative management after the removal of a posterior fossa tumor. There are general principles that can be applied to any kind of tumor surgery in the posterior fossa and its adjacent structures, but specific aspects depending on the different pathologies found in this region are addressed as well. General principles as well as personal statements reflecting the authors' experience in the treatment of such entities are presented. A special emphasis is put on early postoperative complications.

56.1 Operating Room and Postanesthesia Care Unit

Immediately after finishing the operative procedure, the surgeon communicates with the anesthesiology team. Limits of blood pressure and heart

rate, in which the patient is considered to be safe, are thus set by the surgeon. The final hemoglobin level is addressed in order to determine any necessity for transfusion and as a baseline for further controls. The question whether to extubate or not is to be discussed before the induction of the patient. There is no general rule in which pathology a prolongation of postoperative ventilation is mandatory or not. In some centers, all children remain intubated after posterior fossa procedures. To the authors' opinion early extubation should always be considered, mainly because complications related to ventilation are reduced and clinical and neurological functions can be monitored better. Transportation in remote wards could be an argument for keeping the patient intubated for safety issues during transfer. Extubation is performed after a period of intensive care surveillance as long as typical postsurgical complications become more unlikely or are excluded. Extended ventilation should not be necessary in cases of uncomplicated hemostasis and if there are no signs of brain tissue swelling during the procedure as long as brainstem and cranial nerve functions are unaffected. But before immediate postoperative extubation, the surgeon must be sure that there is no functional disorder of the brainstem or the cranial nerves with breathing dysfunction or impaired laryngeal or pharyngeal functions. Elevated intracranial pressure also prohibits extubation [1]. Patients with preexisting pathologies are potentially more prone to develop postsurgical complications, and thus, secondary extubation should be discussed.

M. Messing-Jünger, M.D., Ph.D. (✉)
Department of Pediatric Neurosurgery,
Asklepios Klinik Sankt Augustin,
Sommelweis University, Campus Hamburg,
Sankt Augustin, Germany
e-mail: m.messing@asklepios.com

M. Ehlen, M.D.
Department of Pediatric Intensive Care and
Neonatology, Asklepios Klinik Sankt Augustin,
Sommelweis University, Campus Hamburg,
Sankt Augustin, Germany

E. Schindler, M.D.
Department of Anesthesiology and Critical Care
Medicine, Asklepios Klinik Sankt Augustin,
Sommelweis University, Campus Hamburg,
Sankt Augustin, Germany

Total intravenous anesthesia (TIVA) with propofol and an ultrashort-acting opioid (remifentanyl) has become more popular in neurosurgery, also for pediatric patients [2–4]. Some clinical studies suggest that TIVA compared to a combination with volatile anesthetics leads to a decrease of intracranial pressure, while the cerebral perfusion pressure is increased [5]. Extubation times are shorter in some cases and a prompt cognitive recovering can be expected. Given these advantages early extubation is less dangerous, and testing of critical neurological functions like spontaneous breathing and cough and gag reflexes is possible before finally removing the tube. Balanced anesthesia with inhalational agents could be a possible alternative to TIVA-based anesthesia. Sevoflurane is the volatile agent of choice in pediatric patients [6, 7]. The choice of TIVA versus balanced anesthesia is secondary. In a large patient series, no differences could have been shown in regard to the incidence of postoperative nausea and vomiting (PONV) or pain medication [8, 9]. Compared to the choice of anesthetic agent, it is more important to keep the mean arterial pressure in high normal range and therefore to maintain adequate cerebral perfusion pressure [10].

In any case, postoperative nausea and vomiting (PONV) as well as pain must strictly be avoided because of being a potential source to increase intracranial pressure. In the early postoperative period, pain therapy should therefore be initiated during induction of anesthesia [11]. For this paracetamol (rectally 40 mg/kg BW) or ibuprofen (rectally 10 mg/kg BW) could be considered. For basic postoperative pain therapy in children younger than 3 months of age, ibuprofen 10 mg/kg orally up to three times per day and in children older than 3 months 15 mg/kg BW is recommended. Additionally, opioids can supplement the pain medication if needed [11]. For PONV prophylaxis ondansetron 0.1 mg/kg BW intravenously could be administered. Dexamethasone (dosage 0.15 mg/kg BW, maximum 25 mg) proved to be an effective prophylactic antiemetic alternative for PONV in children [12].

Vital parameters like blood pressure, heart rate, and possibly intracranial pressure are monitored. As long as the child is still sleepy, regular control of

pupillary reflexes and GCS is performed. In order to assure immediate emergency management, central and peripheral venous and intra-arterial lines as well as gastric and urinary catheters remain in place for the next 24–48 h.

In case of persistent external ventricular drainage, the catheter must be fixated sufficiently and handled with care. It should be disconnected or closed for transportation in order to avoid accidental disconnection or removal as well as unintended CSF drainage. This can lead to significant CSF loss with potential intracranial low pressure risks like bleeding and cardiac arrest, e.g., in young infants.

All wound sites have to be checked before leaving the operating room. The head is elevated. Intracranial air and negative intracranial pressure can cause headache and nausea or vomiting. In such cases, head elevation might not be tolerated [13, 14].

The surgeon and anesthesiologist define essential treatment issues in a protocol. Postoperative dexamethasone and antibiotic treatment are to be recommended in selected cases. Anticonvulsive medication is rarely indicated in posterior fossa surgery. Less than 2 % of patients develop seizures after posterior fossa surgery, one third of them within 24 h postoperatively. Medulloblastoma patients have the highest incidence. Whether supratentorial CSF tumor spread is the cause remains unclear. The most important predisposing factors are metabolic acidosis and hyponatremia, but also previous hydrocephalus treatment might be a factor [15, 16].

Pain management including antiemetic treatment is generally realized by the anesthesiology team. In the first postoperative phase, intravenous physiological electrolyte solutions and eventual electrolyte supplements are administered. In cases of blood pressure beyond the range recommended by the surgeon, vasoactive medication to lower the blood pressure might be indicated. Intravenous morphine typically started at 0.1 mg/kg BW will decrease elevated blood pressure in most of the cases sufficiently and will eliminate pain as a potential source of elevated blood pressure [17]. If the blood pressure has to be elevated in case of low cardiac output, an exact diagnosis is recommended at first. Central or mixed venous oxygenation

saturation in combination with standard laboratory parameters (base excess, pH, lactate) could serve to estimate circulation. Based on that information one must consider to add volume or inotropes to increase cardiac output. In case of elevated intracranial pressure, it is mandatory to restrict volume therapy; therefore, early inotropic support is needed. In pediatric patients, dopamine is still an interesting alternative to start with. An initial dose of 5 µg/kg/min should be considered.

After surgery in sitting position and the rare event of air embolism, persistent arterial hypotension is a possible complication [18].

A direct postoperative T scan or MRI scan is recommended only in suspected complication. A sudden increase of blood pressure or marked tachy- or bradycardia as well as mydriasis that cannot be explained by other factors can indicate postoperative bleeding, massive swelling, or new hydrocephalus as well as epileptic seizure. Shunt failure must also be ruled out in cases with preexisting CSF shunts.

Early routine imaging of the brain is not necessary and should be performed later. A chest x-ray is most often done to verify correct placement of the central intravenous line and exclude pneumothorax.

When the child is extubated in the operating room, it is monitored in the postanesthesia care unit. During this time, vital parameters and intracranial pressure via ventricular drainage, if in place, are recorded. As soon as adequate reactions and stable conditions are present, the transfer to the intensive care unit for further surveillance is organized. It is recommended that transportation is conducted by a team familiar with in-house emergencies. In any case of complications, the surgeon should be informed immediately.

An easily accessible CT or MRI unit is a basic prerequisite for immediate postoperative care.

56.2 Intensive Care Unit and Pediatric Ward

After arrival at the ICU, the child is connected to the monitoring unit, and all relevant information concerning surgery, medication, and postoperative

controls are personally communicated between the anesthesiologist, surgeon, and ICU staff.

Given the fact that parents are very much concerned about the course and findings during surgery, early communication with them is strongly advised. If the child's condition allows it, the authors would admit parents' visit as early as possible. In most cases, the child will respond positively and excitation can be reduced.

Depending on the treated pathology and the given postoperative neurological state, different management strategies are to be applied.

In a child with no obvious neurological dysfunction besides a typical mild cerebellar ataxia and without elevated ICP, basic postoperative ICU monitoring is sufficient. Control of hemostasis, vegetative parameters, and a protocol for pain medication and antiemesis are the key points of postoperative treatment.

In our department, single-shot antibiotic prophylaxis prior to skin incision is standard in all neurosurgical procedures. Extended prophylaxis is only given after very long surgical procedures and in cases of external ventricular drainage (EVD) or implanted shunt. A first- or second-generation cephalosporin is indicated in uncomplicated cases. The incidence of infection after elective neurosurgical procedures was less than 1 % in our institution. In general, indications for other prophylactic antibiotic regimens are rare. Modified or prolonged antibiotic treatment protocols should be discussed in patients with signs of postoperative infection unrelated to the surgery and in patients who require reoperation. Other associated risk factors for infection can be an obvious or suspected CSF leak or a concurrent systemic infection.

Postsurgical dexamethasone is indicated to decrease tumor- and surgery-related edema (cytotoxic and vasogenic). In order to minimize adverse effects, only short-time and careful administration is recommended [19–21]. Dexamethasone dosage is 0.5–1 mg/kg BW IV loading dose (maximum 10 mg) followed by 0.25–0.5 mg/kg BW/day IV or po divided in single doses each 6 h.

Short-time dexamethasone side effects in pediatric patients are mainly hyperglycemia and an increased risk of gastrointestinal complications.

Hyperglycemia is a well-known complication in patients receiving dexamethasone and should be strictly avoided in neurosurgical patients in order to decrease the risk of neurological complications. After perioperative dexamethasone administration, blood glucose concentrations increase with a peak after 12–24 h [22].

Blood glucose monitoring is therefore strongly recommended. Blood glucose levels are taken every 4 h 1 day after surgery. Blood glucose levels up to 150 mg/dl (8.3 mmol/l) are tolerated. In case of higher concentrations, glucose supply must be reduced to age-adapted minimal rates (4–10 g/kg BW/day). If blood glucose levels still remain above 150 mg/dl, IV insulin therapy must be considered. In cases with normal blood glucose levels, controls each 8 h after the first day are sufficient.

Gastrointestinal perforation and hemorrhage are rare side effects in short-time use of perioperative dexamethasone in children. Stress ulcers in newborns are associated with dexamethasone; the incidence in older children remains unclear.

Histamine-2 blockers or proton pump inhibitors are used to inhibit gastric acid production in children. Alkaline suspensions are used to directly neutralize gastric acid secretions.

A prophylactic medication with histamine-2 blockers or proton pump inhibitors is given to any patient with dexamethasone. Ranitidine for prophylaxis of stress-induced gastric ulcers is administered in the following dosage: neonates receive 5 mg/kg BW/day po or IV divided into three doses. Patients older than 1 month up to 16 years are treated with 1 mg/kg BW IV each 6–8 h or 2–4 mg/kg/BW/day po divided into two doses.

Alternatively, famotidine is given to patients between 1 and 16 years: 0.5 mg/kg BW/day po or 0.25 mg/kg IV each 12 h. Studies with omeprazole and pantoprazole in intravenous forms have been encouraging, but they are not yet approved for use in children.

Corticosteroids may exacerbate systemic fungal infections and, therefore, should not be used.

In patients with a previous history of corticosteroid therapy who are subjected to unusual stress, increased dosage of rapidly acting corticosteroids before, during, and after the stressful situation, e.g., repeated surgery, is indicated.

Drug-induced secondary adrenocortical insufficiency may result from rapid withdrawal of corticosteroids and may be minimized by gradual reduction of dosage. This type of relative insufficiency may persist for months after discontinuation of the therapy; therefore, in any situation of stress occurring during that period, hormone therapy should be reinstated. If a patient is already receiving steroids, dosage adaptation should be considered. Since mineralocorticoid secretion may be impaired, salt and/or a mineralocorticoid should be administered concurrently.

Corticosteroids may mask some signs of infection, and new infections, especially ventilator-associated pneumonia, may appear during steroid therapy.

Dexamethasone should be used cautiously in combination with vancomycin because dexamethasone may decrease the transport of vancomycin into the CSF.

Pain and nausea are common problems in children following craniotomy. Younger age is strictly associated with increased pain after intracranial surgery. All patients have to be scored with special pediatric pain scales and treated with standardized analgesic regimens.

Possible analgesic drugs are paracetamol, NSAID, and opioids (i.e., piritramide, morphine). Strong opioids (i.e., fentanyl, remifentanyl) in combination with midazolam can be used in ventilated children.

Possible methods of analgesic drug administration are continuous infusion, PCA (patient-controlled analgesia, possible in children older than 5–6 years of age), NCA (nurse-controlled analgesia), and intermittent IV boluses.

Paracetamol, ibuprofen, and metamizole are used as intermittent oral or rectal analgesic drugs and opioids as intermittent IV boluses or continuous IV infusions.

In our institution we use a continuous IV application of metamizole (1–2 mg/kg BW/h) in all patients older than 3 months after craniotomy and in addition NCA with IV boluses of piritramide (0.05 mg/kg BW) in children younger than 5–6 years and PCA with piritramide (loading dose 0.1 mg/kg, boluses 0.02–0.04 mg/kg, maximum 10 boluses in a 4 h period).

Postoperative nausea and vomiting (PONV) are frequent problems in children undergoing neurosurgical procedures. In children receiving dexamethasone, postoperative nausea is less common.

Oral or rectal application of dimenhydrinate and IV 5-HT(3) antagonists (ondansetron, granisetron, tropisetron) are possible therapeutic agents. Prophylactic intraoperative use of IV 5-HT(3) antagonists should be considered. Metoclopramide and droperidol should not be used in children as a first-line therapy because of possible extrapyramidal symptoms [23]. After uncomplicated neurosurgical procedures, early enteral feeding is recommended. Such a management protects the gut, therefore reduces gastrointestinal complications, enhances immunity, and shortens the length of ICU stay. Nevertheless, there are no clear guidelines about the best nutrition for critically ill children [24].

Early enteral feeding may start postoperatively as soon as the child is neurologically and hemodynamically stable. In most cases, enteral feeding can be initiated within 6–12 h after surgery. Starting with clear fluids, such as tea or water, one will follow as soon as possible with a light and simple diet for the first days. Nutrition according to the child's age can be continued after this period.

During enteral feeding gastrointestinal tolerance must closely be observed. High gastric residuals are the most frequent gastrointestinal complication. Persistent nausea and vomiting and the use of paralytic drugs, such as opioids, are also associated with feeding intolerance. In these cases, additional age- and weight-adapted IV fluids are necessary. A profound knowledge of fluid requirements in children is essential in such situations. The following calculation may be used to estimate the approximate maintenance requirement of children above 1 year of age: 4 ml/kg BW/h for the first 10 kg, 2 ml/kg BW/h for 11–20 kg, for each kilogram >20 kg BW 1 ml/kg BW/h.

Children younger than 12 months of age need larger amounts of fluid in order to achieve an adequate fluid balance (120–150 ml/kg BW/day).

Replacement of preexisting fluid losses, ongoing fluid losses such as postoperative vomiting,

or drain losses should also be calculated and replaced.

In most situations, 2.5–5 % dextrose containing solutions with 0.45 % up to 0.9 % sodium chloride is indicated. Potassium chloride (1–2 mmol/kg BW/day) should be added.

The use of solutions with lower levels than 0.45 % sodium chloride is not recommended because SIADH (syndrome of inappropriate antidiuretic hormone secretion) is common in the postoperative period in infants and children.

For this reason we restrict fluids initially to a 70–80 % maintenance in children with a higher risk of SIADH, i.e., after neurosurgery. All children must be closely monitored for serum electrolytes, glucose, and fluid balance.

Enteral nutrition may not be started in all PICU (pediatric intensive care unit) patients after neurosurgery. In case of prolonged neurological dysfunction with intolerance of normal feeding, nasogastric and orogastric tubes for short-term enteral nutrition should be considered. Transpyloric feedings may be better tolerated in case of prolonged necessity of tube feeding or for those children who are at a high risk for aspiration. Intermittent tube feeding seems to be more physiological and is indicated for children who are clinically stable; continuous tube feeding is better tolerated in critically ill children.

If enteral feeding cannot be started, additional parenteral nutrition should be started at day 3 depending on the preoperative nutritional status. Indications therefore are rare in elective neurosurgery.

Antithrombotic prophylaxis is indicated for children who have reached the age of puberty (Tanner stage greater than 1). It may also be discussed after insertion of a central venous catheter because of the risk of catheter-associated venous thrombosis in children. In our institution, we use low-molecular-weight heparin for girls older than 12 years and boys older than 14 years of age. The first dose is given some hours after surgery. We prefer enoxaparin based on the greater experience with this LMWH preparation in childhood. We use a single daily dose of 20 mg SC. Compression stockings are also indicated in this group. Children with inserted central venous

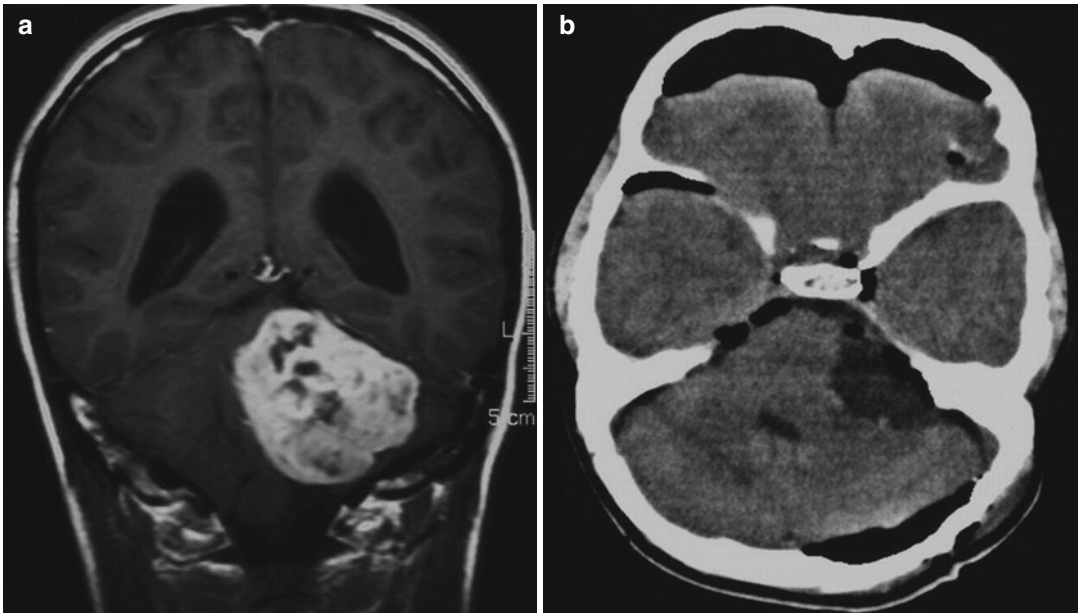


Fig. 56.1 Extensive acoustic schwannoma in a 14-year old girl with dysostosis cleidocranialis and complete left-sided hearing loss (a). Early postoperative CAT scan after

removal in sitting position. Extensive air in supratentorial subdural spaces as well as infratentorially. Severe headache in upright position and sleepiness for 48 hours (b)

catheters, especially via the femoral veins or the left subclavian vein, receive a prophylaxis against catheter-associated thrombosis (0.5 I.E./kg BW/h systemic heparin via central venous catheter). Higher doses of heparin must be discussed individually with the neurosurgeon. Postoperative mobilization is performed as soon as possible according to the individual status of the child.

Physiological monitoring, pain control, and frequent neurological evaluation are essential in the postoperative period. After admission to the PICU, the strategy for each child between the neurosurgical and the intensive care team must be planned.

In children with no obvious neurological dysfunction and without signs of elevated ICP, basic postoperative ICU monitoring is sufficient. All patients are monitored for vital parameters such as pulse, respiratory rate, invasive blood pressure, oxygen saturation, and temperature. Immediately after admission blood gas analysis with additional measurement of glucose, electrolytes, hematocrit, and lactate is conducted. Laboratory tests for CBC, platelets, electrolytes, glucose, and coagulation studies are additionally performed.

Chest x-ray is a routine procedure for all children with inserted central venous catheters.

Blood pressure levels are determined individually. Neurological examination by PICU nurses (modified Glasgow Coma Scale for children) is performed every 2 h in uncomplicated patients.

The PICU environment exposes a child to constant and frequent noise, as well as to excessive and permanent light. Additionally, pain and discomfort will lead to feelings of loneliness, anxiety, and isolation. Adequate analgesia, encouraging the family to visit and communicate, noise level reduction, and an age-appropriate, personalized communication are several essentials to reduce distress in PICU patients.

Compared to other neurosurgical approaches, a typical suboccipital access causes significant soft tissue pain. Additionally, negative intracranial pressure and pneumocephaly can lead to severe headache and nausea, e.g., when the head is elevated. Patients operated in a sitting position are more often affected (Fig. 56.1a, b).

Posterior fossa surgery has a higher incidence of postoperative complications compared to other neurosurgical operations, and a broad variety of typical but also rare adverse events may endanger the patient. Careful observation and the awareness of this fact are always mandatory.

Multiple causes for postoperative airway obstruction after posterior fossa approaches are known. Some of them are related to the patient's unusual position during surgery. Pharyngeal swelling after intraoperative endotracheal ultrasound [25] or macroglossia after prone position [26, 27] is reported. In soft tissue swelling, anti-phlogistics and steroids are indicated.

In uneventful courses, a routine postoperative MRI for assessment of the resection extent must be organized in between 72 h after surgery. Only during this early period no blood-brain barrier disruption other than tumor will allow contrast enhancement [28]. After 3 days, a false-positive contrast uptake will not allow to distinguish between tumor and surgical lesions. This period lasts until 6 weeks postoperatively. Most brain tumor protocols ask for T1 sequences in all three dimensions pre and post contrast. In primarily non-enhancing tumors, T2 and FLAIR sequences are more significant.

In the authors' experience perioperative EVD has become the exception in posterior fossa tumor surgery, since improved surgical techniques and the possibility of endoscopic third ventriculostomy (ETV) are available [29–35]. In most cases of mild to moderate hydrocephalus, tumor surgery is performed the day after admission without any particular treatment of the hydrocephalus itself, if intraoperative patency of CSF pathways is assured.

In severe symptomatic hydrocephalus without prospect of resolution after tumor surgery and occluded infratentorial CSF spaces, ETV does not seem to be promising and shunting would be performed. Only in emergency situations, the authors would primarily insert an EVD (herniation, bleeding, etc.). This can be done as regular OR procedure or immediately on the ICU with special needle systems [36]. In some centers, perioperative EVD is still a routine for having immediate access to the ventricles in case of sudden ICP rise. In general, a handling guideline for EVD management is recommended in order to avoid related complications.

Once an EVD is in place, weaning should be started as soon as the assumed cause for eventual hydrocephalus or elevated ICP is solved or

became unlikely. The first step is to gradually elevate the draining pressure above normal pressure ranges (depending on the patient's age up to 15 cm H₂O). If no symptoms are overt, closure of the drainage can be attempted with intermediate pressure measurements. Alternatively, continuous ICP monitoring can be performed instead of keeping the drainage open.

Should the intracranial pressure levels remain in normal ranges, removal of the EVD is carried out. In persistent intracranial hypertension, shunting is indicated after or MRI scan to exclude unexpected causes.

In modern series of experienced departments, postoperative complication rate is very low. Typical surgical complications are bleeding into the tumor bed and remote bleeding due to excessive brain slacking mostly after operating in sitting position, e.g., subdural (Fig. 56.2), epidural, or intra-axial hemorrhage [37–41]. But also swelling of cerebellar and brainstem tissue, vascular infarction, and severe pneumocephaly (Fig. 56.3) can be responsible for impairment of neurological functions and indicate further ventilation and special treatment aspiration/drainage [42]. In rare cases, secondary emergency opera-



Fig. 56.2 Bilateral subdural hygroma after surgery of a large medulloblastoma and previous shunting



Fig. 56.3 Early postoperative CT scan after removal of a medulloblastoma in the IVth ventricle. Free air is visible in the bifrontal subdural space and suprasellar cistern and a marked edema in the right paraventricular (paravermian) region

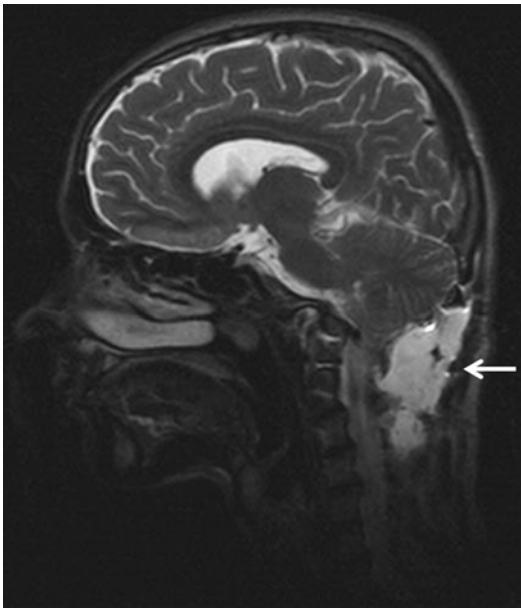


Fig. 56.4 Suboccipital pseudomeningocele (→) after posterior fossa surgery in a 16-year old boy. Symptoms: local pain, orthostatic dysfunction and signs of aseptic meningitis

tions are necessary, mainly to remove a clot or to perform posterior fossa decompression. In most cases, re-bleeding after brain tumor resection is caused by tumor remnants that should also be removed if localization allows it. A coagulation disorder must be ruled out as well [43].

Complications related to the CSF system are most frequently seen after posterior fossa surgery. The syndrome of aseptic meningitis is characterized by spiking fever and meningismus. CSF analysis reveals pleocytosis and elevated protein, while cultures remain negative. It counts for up to 25 % of all postoperative complications with the highest rate after tumor surgery [44–46]. Bacterial meningitis is rare, but the immunosuppressive effects of corticosteroids can lead to serious and lethal infections and this fact has to be taken into consideration [47].

Suboccipital pseudomeningoceles (Fig. 56.4) and CSF fistulas also belong to the most frequent complications and occur in 10–25 %. Depending on skin penetration, aseptic or septic meningitis can develop.

Aseptic meningitis is related to certain tumors (10 % in cerebellar astrocytomas) or to the implantation of an artificial dura substitute. The risk of septic meningitis following a CSF fistula is enhanced by steroid medication. Small pseudomeningoceles without progression can be watched and sometimes punctured. In many cases, they resolve spontaneously or remain uncomplicated. CSF fistulas require immediate closure before any deep or CSF infection. In most cases, single compression sutures will solve the problem. Lumbar puncture with the aim to lower the intrathecal pressure, shunting procedures in underlying CSF circulation disorders, and finally secondary revision have to be considered [48, 49].

Not all pseudomeningoceles become clinically apparent. One retrospective series reports about 16 % symptomatic pseudomeningoceles, although a total of 41 % showed CSF accumulations on postoperative MRI at days 1–5. These findings progressively resolved in nearly all patients spontaneously after 10–15 months. The risk to develop a CSF leak was higher in patients with pseudomeningoceles (39 % versus 13 %). Additionally, the hospital stay was markedly prolonged in this patient group. Suboccipital craniectomy compared

to craniotomy seemed to be a predisposing factor (69 % versus 38 %) [32, 50].

Unusual surgical complications can be seen as well. Especially, young children with thin calvarial bone can develop epidural hematoma in case of pin penetration in Mayfield fixation, but also air embolism caused by fixation pins in sitting position is described [51]. Surgery in sitting position, e.g., in large tumor masses in the posterior fossa and rapid tumor removal, may lead to tension pneumocephaly, which is always a life-threatening situation with potential for severe neurological damage [52–59]. Rarely compression of a venous sinus by hemostyptic material or bone wax can cause intracranial hypertension [60, 61]. Extradural pneumatocele due to open mastoid cells is also described [62], as well as rhabdomyolysis after operations in sitting position [63].

In another 10-year (1992–2002) retrospective study of all posterior fossa surgeries, data from 500 patients were obtained and the overall complication rate was 31.8 %. Cerebrospinal fluid leaks were the most frequent complication in 13 %, followed by meningitis in 9.2 % and wound infection in 7 %. After tumor surgery cerebellar edema occurred in 5 %, hydrocephalus in 4.6 %, cerebellar hematoma in 3 %, and cerebellar mutism in 1.2 % of patients of all ages.

The authors found that compared to other surgical sites, posterior fossa surgery involves greater morbidity and mortality and has a wider variety of complications [64, 65].

Spinal structures can also be involved in postoperative complications, mainly due to positioning and the given vicinity to the posterior fossa. Cervical instability [66], myelopathy [67], spinal subdural hematoma [68, 69], tetraparesis [70, 71], and spinal cord infarction [72] have been described.

Other rare complications are inverse herniations due to large tumor masses and bradycardia after the instillation of hydrogen peroxide for hemostasis [73, 74].

An orbital emphysema after posterior fossa surgery in sitting position for pilocytic astrocytoma and ETV in a 4-year-old girl is reported [75] as well as cerebral ischemia after venous air embolism [76].

The mortality rate during the early postoperative period is very low and tends toward zero.

Morbidity is mainly caused by neurological deficits and is most often transient. Additional new deficits occur in about one third of the patients. Significant persisting impairment is to be expected, when the cranial nerves and brainstem are involved.

Other non-neurological causes for postoperative morbidity are rare in childhood. Cerebellar ataxia is the most common and obvious neurological deficit found pre and post surgically. Depending on the site of the postoperative lesion, different symptoms are found, although in most cases a spatial and functional overlapping exists: Should the neocerebellum (cerebellar hemispheres) be affected, limb ataxia, dysmetria, dysdiadochokinesia, tremor, and muscular hypotension as well as ataxic dysarthria (scanning speech) will occur. Lesions in the paleocerebellum (cerebellar vermis and paravermal zone) lead to truncal ataxia, which is also the case in affections of the archicerebellum (nodulus and flocculus cerebella) that is connected to vestibular neurons. Vertigo and nausea are typical focal symptoms.

Nystagmus is a common finding after posterior fossa surgery as well and follows in irritations or lesions of cerebellar or brainstem structures.

Vomiting can be a side effect of anesthesia or a symptom of a gastric problem, but there are different specific reasons related to posterior fossa surgery: pneumocephaly, raised ICP, and irritation of the area postrema, the brain's vomiting center located at the obex. Additionally, irritation of the vestibular system also provokes vomiting. Careful indication of antiemetic medication is recommended and persistent vomiting should implicate further diagnostics. Refractory emesis can be life threatening, e.g., in small infants [77].

Brainstem lesions might result in severe cranial nerve deficits and impaired coordination of vital vegetative functions like blood pressure, heart rate, vessel reactivity, breathing, and somatic reflexes (swallowing reflex, gag reflex, cough reflex). Additional long tract affections will give rise to internuclear ophthalmoplegia (dysconjugate gaze) and sensomotoric deficits. A typical nasal and slurry speech is part of a bulbar palsy, too [1, 78, 79]. In these brainstem affections, rapid improvement is not common and permanent impairment is to be considered. In vocal cord paralysis and missing somatic reflexes, early

tracheostomy and feeding tube, followed by gastrostomy (percutaneous endoscopic gastrostomy, PEG), become necessary. Early radiographic swallowing assessment prior to oral feeding is recommended by some authors. Furthermore, fiber-optic vocal cord and pharyngeal function can be assessed. A team of neurosurgeon, otolaryngologist, pediatric intensivist, and speech therapist should be involved ensuring optimal management of these dysfunctions [80, 81].

Facial nerve malfunction causes lagophthalmos (Bell's palsy), and especially during night eye closure is incomplete and the cornea might dry out. Infection and corneal ulcers are typical complications. The affected eye must be protected with overnight monocular and eye ointment or artificial tears.

Double vision can be a sequel of direct nerve root malfunction or brainstem lesion. If there is no early recompensation of oculomotor function, covering of one eye is necessary. Otherwise, mobilization, e.g., in cerebellar ataxia and vertigo, is not possible, due to the lack of optic control [82]. Another rare complication after cerebellar tumor surgery is a transient cerebellar eye closure (TCES). The pathogenesis is unclear [83].

Tumors affecting the medulla oblongata potentially cause progressive CO₂ retention and sleep apnea; therefore, preoperative blood gas analysis is recommended as well as frequent postoperative breathing parameter checkup and close breath monitoring [84, 85].

Cerebellar mutism or posterior fossa syndrome is a complex of multiple symptoms that exclusively occurs after posterior fossa surgery in young individuals. So far, the pathophysiological background is not well understood, but a multifunctional organic genesis is assumed [86–98]. Several observations, regarding the patient's constellation, allow a risk estimation in advance. The syndrome occurs in up to 20 % of pediatric patients after tumor removal in the posterior fossa. Predisposing factors are medulloblastoma; large tumor mass; midline involvement, e.g., the fourth ventricle and brainstem; and preexisting hydrocephalus (Fig. 56.5a–d) [99–105].

Primary brainstem lesions may also cause mutism [106]. After a period of few hours up to 2 days

of normal speech production, the child becomes mute or utters only single words, sometime toneless. Additional dysfunction of oral and pharyngeal muscle coordination is obvious in some patients, and consecutively drinking and eating are no longer possible. Both phenomena have been discussed in the past as psychological reactions to the situation. The fact that the syndrome is only observed after posterior fossa surgery and not after involvement of cerebral hemispheres makes a single psychological cause unlikely. The affected child might react apathetically or be suffering and whining or crying and sometimes rejecting his/her own mother [107]. In most cases, significant truncal ataxia is evident [88–96, 108–112]. Visual impairment is also described [113].

The symptoms last for weeks up to months and are followed by a phase of dysarthric speech before spontaneous resolution. Deficient speech up to a certain extent remains in most children, though. In the course of investigations regarding the pathophysiological background of cerebellar mutism, possible neuropsychological functions of the cerebellum have been addressed as well. It is now well accepted that the cerebellum plays an important role in neuropsychological and cognitive processes, e.g., in complex speech functions, and is widely connected with higher cerebral structures [114–118].

Recently, it has been shown that patients with a history of cerebellar mutism bear an increased risk for neurocognitive impairment [119, 120].

So far, no specific treatment is known to influence the course of the syndrome. Therefore, cerebellar mutism should be part of the preoperative information, given to the parents, e.g., in cases of large midline tumors suspicious for medulloblastoma. Only a few reports exist describing a positive effect of bromocriptine on cerebellar mutism analogous to the effect on akinetic mutism in Parkinson syndromes, which is also observed in hydrocephalic patients developing an aqueductal syndrome [121–123].

Generally, brain tumors should be treated in an interdisciplinary team and each individual case must be evaluated according to available protocols [124]. In some countries, national boards coordinate treatment protocols and all

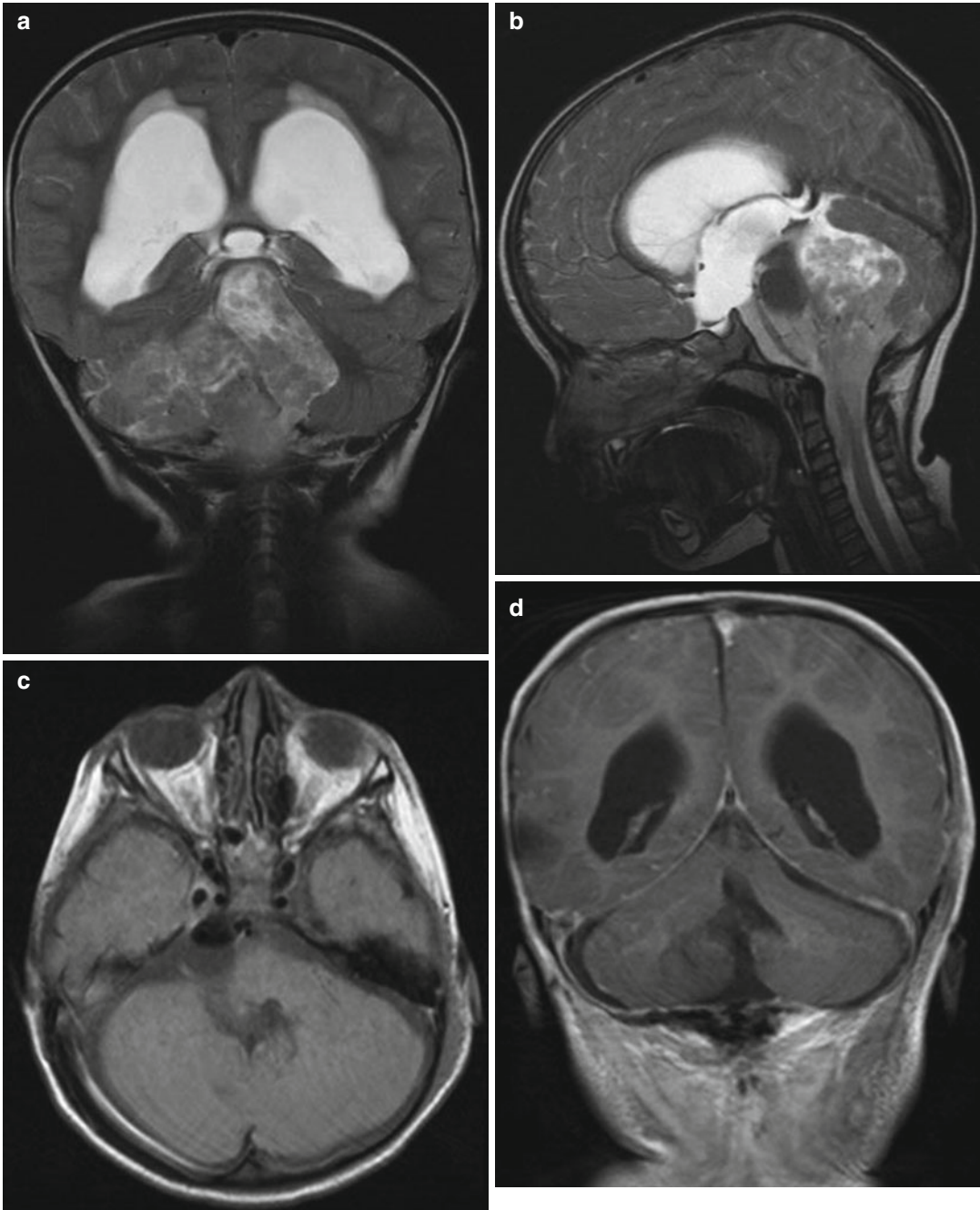


Fig. 56.5 Coronal (a) and sagittal (b) T2 weighted MRI of large ependymoma of the posterior fossa and upper cervical cord with marked occlusive hydrocephalus in a 3 year old boy. Primary symptoms: signs of lower cranial nerve impairment and gait ataxia with bilateral papilloedema. Predisposing factors for cerebellar mutism: large

tumor mass, marked hydrocephalus, brainstem involvement. Early postoperative contrast T1 weighted axial (c) and coronal (d) MRI after gross total resection and preoperative shunt placement. Symptoms: transient facial and vocal cord paresis and cerebellar mutism

relevant findings, together with reference pathologies that are obtained and shared with the expert team. Also international working groups and boards exist and will be contacted depending on the pathology. In rare histological tumor entities, individual regimens can be defined together with the pediatric neuro-oncology group.

The aim of this strategy is to assure the most promising treatment option in respect of outcome and quality of life for each individual pediatric tumor patient [125].

Postoperative tumor staging should be performed as soon as possible and starts with contrast MRI in the first 72 h after removal. If not performed prior to surgery, spinal MRI is also necessary in tumor types that tend to spread along the CSF pathways, e.g., medulloblastoma, ependymoma, and some astrocytomas [126]. In case of incomplete tumor resection in the posterior fossa, it must be discussed in the interdisciplinary tumor board, whether second look operation is recommended before starting adjuvant therapy or if a wait-and-watch strategy is feasible. In medulloblastoma, only significant tumor remnants of more than 1.5 cm [2] should be reoperated before further adjuvant therapy, due to better outcome statistics for total resection or near total resection [36, 127]. Ependymoma has a significantly better outcome after complete resection due to poor chemo- and radiosensitivity. Indication for second-look surgery should be generous if the tumor localization and the expected neurological deficits allow this [128–133].

In summary, tumor surgery of the posterior fossa is generally more prone for the development of surgical and neurological complications compared to operative procedures of other localizations. Therefore, the postoperative management should be in the hands of an experienced team, specially dedicated to the care of children with severe neuro-oncological diseases [134].

References

1. Yates AP, Sumner E, Lindahl SG (1986) Respiratory disturbance and posterior fossa surgery. A case report. *Anaesthesia* 41(12):1214–1218
2. Cole CD, Gottfried ON, Gupta DK, Couldwell WT (2007) Total intravenous anesthesia: advantages for

- intracranial surgery. *Neurosurgery* 61(5 Suppl 2):369–377
3. Davis PJ, Cladis FP (2005) The use of ultra-short-acting opioids in paediatric anaesthesia: the role of remifentanyl. *Clin Pharmacokinet* 44(8):787–796
4. Escarment J, Donne X, Palmier B et al (1992) Quality of sedation and neurologic evaluation following surgery of the posterior cranial fossa: the importance of propofol. *Cah Anesthesiol* 40(1):29–35
5. Kikuta K, Takagi Y, Nozaki K et al (2007) Effects of intravenous anesthesia with propofol on regional cortical blood flow and intracranial pressure in surgery for moyamoya disease. *Surg Neurol* 68(4):421–424
6. Duffy CM, Matta BF (2000) Sevoflurane and anesthesia for neurosurgery: a review. *J Neurosurg Anesthesiol* 12(2):128–140
7. Sponheim S, Skraastad O, Helseth E, Due-Tonnesen B, Aamodt G, Breivik H (2003) Effects of 0.5 and 1.0 MAC isoflurane, sevoflurane and desflurane on intracranial and cerebral perfusion pressures in children. *Acta Anaesthesiol Scand* 47(8):932–938
8. Schindler E, Benson M, Junger A, Muller M, Sticher J, Hempelmann G (2000) Recovery of balanced anesthesia with various inhalation anesthetics in comparison to intravenous anesthetics: a retrospective analysis of 20,060 patients. *Anesthesiol Intensivmed Notfallmed Schmerzther* 35(6):375–380
9. Neufeld SM, Newburn-Cook CV, Schopfloch D, Dundon B, Yu H, Drummond JE (2009) Children's vomiting following posterior fossa surgery: a retrospective study. *BMC Nurs* 8:7
10. Rupp SM, Wickersham JK, Rampil IJ, Wilson CB, Donegan JH (1989) The effect of halothane, isoflurane, or sufentanil on the hypertensive response to cerebellar retraction during posterior fossa surgery. *Anesthesiology* 71(5):660–663
11. Kraemer FW, Rose JB (2009) Pharmacologic management of acute pediatric pain. *Anesthesiol Clin* 27(2):241–268
12. Liechti M, Feurer R, Gross D et al (2007) Prevention of postoperative nausea and vomiting in children following adenotonsillectomy, using tropisetron with or without low-dose dexamethasone. *J Anesth* 21(3):311–316
13. Di LN, Caruso R, Floris R, Guerrisi V, Bozzao L, Fortuna A (1986) Pneumocephalus and tension pneumocephalus after posterior fossa surgery in the sitting position: a prospective study. *Acta Neurochir (Wien)* 83(3–4):112–115
14. Hernandez-Palazon J, Martinez-Lage JF, de la Rosa-Carrillo VN, Tortosa JA, Lopez F, Poza M (2003) Anesthetic technique and development of pneumocephalus after posterior fossa surgery in the sitting position. *Neurocirugia (Astur)* 14(3):216–221
15. Lee ST, Lui TN, Chang CN, Cheng WC (1990) Early postoperative seizures after posterior fossa surgery. *J Neurosurg* 73(4):541–544
16. Suri A, Mahapatra AK, Bithal P (1998) Seizures following posterior fossa surgery. *Br J Neurosurg* 12(1):41–44

17. Duedahl TH, Hansen EH (2007) A qualitative systematic review of morphine treatment in children with postoperative pain. *Paediatr Anaesth* 17(8):756–774
18. Bithal PK, Pandia MP, Dash HH, Chouhan RS, Mohanty B, Padhy N (2004) Comparative incidence of venous air embolism and associated hypotension in adults and children operated for neurosurgery in the sitting position. *Eur J Anaesthesiol* 21(7): 517–522
19. McClelland S III, Long DM (2008) Genesis of the use of corticosteroids in the treatment and prevention of brain edema. *Neurosurgery* 62(4):965–967
20. Kaal EC, Vecht CJ (2004) The management of brain edema in brain tumors. *Curr Opin Oncol* 16(6): 593–600
21. Sinha S, Bastin ME, Wardlaw JM, Armitage PA, Whittle IR (2004) Effects of dexamethasone on peritumoural oedematous brain: a DT-MRI study. *J Neurol Neurosurg Psychiatry* 75(11):1632–1635
22. Lukins MB, Manninen PH (2005) Hyperglycemia in patients administered dexamethasone for craniotomy. *Anesth Analg* 100(4):1129–1133
23. Kovac AL (2007) Management of postoperative nausea and vomiting in children. *Paediatr Drugs* 9(1):47–69
24. Joffe A, Anton N, Lequier L et al (2009) Nutritional support for critically ill children. *Cochrane Database Syst Rev* (2), CD005144
25. Pandia MP, Bithal PK, Bhagat H, Sharma M (2007) Airway obstruction after extubation following use of transesophageal echocardiography for posterior fossa surgery in the sitting position. *J Clin Neurosci* 14(11):1139–1141
26. Pivalizza EG, Katz J, Singh S, Liu W, McGraw-Wall BL (1998) Massive macroglossia after posterior fossa surgery in the prone position. *J Neurosurg Anesthesiol* 10(1):34–36
27. Tsung YC, Wu CT, Hsu CH, Yeh CC, Lin SL, Wong CS (2006) Macroglossia after posterior fossa surgery in the prone position—a case report. *Acta Anaesthesiol Taiwan* 44(1):43–46
28. Pollack IF (1999) Pediatric brain tumors. *Semin Surg Oncol* 16(2):73–90
29. El Beltagy MA, Kamal HM, Taha H, Awad M, El KN (2010) Endoscopic third ventriculostomy before tumor surgery in children with posterior fossa tumors, CCHE experience. *Childs Nerv Syst* 26:1699–1704
30. Morelli D, Piroette B, Lubansu A et al (2005) Persistent hydrocephalus after early surgical management of posterior fossa tumors in children: is routine preoperative endoscopic third ventriculostomy justified? *J Neurosurg* 103(3 Suppl):247–252
31. Ruggiero C, Cinalli G, Spennato P et al (2004) Endoscopic third ventriculostomy in the treatment of hydrocephalus in posterior fossa tumors in children. *Childs Nerv Syst* 20(11–12):828–833
32. Santamarta D, Blazquez JA, Maillo A, Munoz A, Caballero M, Morales F (2003) Analysis of cerebrospinal fluid related complications (hydrocephalus, fistula, pseudomeningocele and infection) following surgery for posterior fossa tumors. *Neurocirugia (Astur)* 14(2):117–126
33. Sainte-Rose C, Cinalli G, Roux FE et al (2001) Management of hydrocephalus in pediatric patients with posterior fossa tumors: the role of endoscopic third ventriculostomy. *J Neurosurg* 95(5):791–797
34. Lapras C, Patet JD, Derex MC, Nicolas A, Bret P, Hor F (1983) Astrocytoma of the cerebellum in children. Apropos of 57 cases. *Neurochirurgie* 29(4): 241–246
35. Parizek J, Mericka P, Nemecek S et al (1998) Posterior cranial fossa surgery in 454 children. Comparison of results obtained in pre-CT and CT era and after various types of management of dura mater. *Childs Nerv Syst* 14(9):426–438
36. Schaller C, Meyer B, Rohde V, Hassler W (1994) Emergency ventriculostomy-experience with a new screw device: technical note. *Neurosurgery* 35(5): 982–984
37. Bucciero A, Quaglietta P, Vizioli L (1991) Supratentorial intracerebral hemorrhage after posterior fossa surgery. Case report. *J Neurosurg Sci* 35(4):221–224
38. Haines SJ, Maroon JC, Jannetta PJ (1978) Supratentorial intracerebral hemorrhage following posterior fossa surgery. *J Neurosurg* 49(6):881–886
39. Pandey P, Madhugiri VS, Sattur MG, Devi BI (2008) Remote supratentorial extradural hematoma following posterior fossa surgery. *Childs Nerv Syst* 24(7): 851–854
40. Tondon A, Mahapatra AK (2004) Superatentorial intracerebral hemorrhage following infratentorial surgery. *J Clin Neurosci* 11(7):762–765
41. Wolfsberger S, Gruber A, Czech T (2004) Multiple supratentorial epidural haematomas after posterior fossa surgery. *Neurosurg Rev* 27(2):128–132
42. Ram Z, Knoller N, Findler G, Sahar A (1992) Delayed intraventricular tension pneumocephalus complicating posterior fossa surgery for cerebellar medulloblastoma. *Childs Nerv Syst* 8(6):351–353
43. Vrettou CS, Stavrinou LC, Halikias S et al (2010) Factor XIII deficiency as a potential cause of supratentorial haemorrhage after posterior fossa surgery. *Acta Neurochir (Wien)* 152(3):529–532
44. Carmel PW, Greif LK (1993) The aseptic meningitis syndrome: a complication of posterior fossa surgery. *Pediatr Neurosurg* 19(5):276–280
45. Kaufman HH, Carmel PW (1978) Aseptic meningitis and hydrocephalus after posterior fossa surgery. *Acta Neurochir (Wien)* 44(3–4):179–196
46. Ramos-Martinez A, de Las Heras-Carballo T, Fernandez-Mateos C et al (2009) Postsurgical meningitis. Differential characteristics of aseptic postsurgical meningitis. *Neurocirugia (Astur)* 20(2):103–109
47. Dickerman RD, Stevens QE, Schneider SJ (2004) Sudden death secondary to fulminant intracranial aspergillosis in a healthy teenager after posterior fossa surgery: the role of corticosteroids and prophylactic recommendations. *J Neurosurg Sci* 48(2):87–89
48. Black P (2000) Cerebrospinal fluid leaks following spinal or posterior fossa surgery: use of fat grafts for prevention and repair. *Neurosurg Focus* 9(1):e4

49. Hillier CE, Stevens AP, Thomas F, Vafidis J, Hatfield R (2000) Aseptic meningitis after posterior fossa surgery treated by pseudomeningocele closure. *J Neurol Neurosurg Psychiatry* 68(2):218–219
50. Gnanalingham KK, Lafuente J, Thompson D, Harkness W, Hayward R (2003) MRI study of the natural history and risk factors for pseudomeningocele formation following postfossa surgery in children. *Br J Neurosurg* 17(6):530–536
51. Cabezedo JM, Gilsanz F, Vaquero J, Areitio E, Martinez R (1981) Air embolism from wounds from a pin-type head-holder as a complication of posterior fossa surgery in the sitting position. Case report. *J Neurosurg* 55(1):147–148
52. Biyani N, Silbiger A, Ben-Ari J, Constantini S (2007) Postoperative brain stem tension pneumocephalus causing transient locked-in syndrome. *Pediatr Neurosurg* 43(5):414–417
53. Bilginer B, Ziyal IM, Celik O, Ayhan S, Akalan N (2007) Enlargement of postoperative aqueductal air due to elevated body temperature. Case report. *Turk Neurosurg* 17(1):37–39
54. Kishan A, Naidu MR, Muralidhar K (1990) Tension pneumocephalus following posterior fossa surgery in sitting position. A report of 2 cases. *Clin Neurol Neurosurg* 92(3):245–248
55. Lunsford LD, Maroon JC, Sheptak PE, Albin MS (1979) Subdural tension pneumocephalus. Report of two cases. *J Neurosurg* 50(4):525–527
56. Prabhakar H, Bithal PK, Garg A (2003) Tension pneumocephalus after craniotomy in supine position. *J Neurosurg Anesthesiol* 15(3):278–281
57. Satapathy GC, Dash HH (2000) Tension pneumocephalus after neurosurgery in the supine position. *Br J Anaesth* 84(1):115–117
58. Suri A, Mahapatra AK, Singh VP (2000) Posterior fossa tension pneumocephalus. *Childs Nerv Syst* 16(4):196–199
59. MacGillivray RG (1982) Pneumocephalus as a complication of posterior fossa surgery in the sitting position. *Anaesthesia* 37(7):722–725
60. Crocker M, Nesbitt A, Rich P, Bell B (2008) Symptomatic venous sinus thrombosis following bone wax application to emissary veins. *Br J Neurosurg* 22(6):798–800
61. Keiper GL Jr, Sherman JD, Tomsick TA, Tew JM Jr (1999) Dural sinus thrombosis and pseudotumor cerebri: unexpected complications of suboccipital craniotomy and translabyrinthine craniectomy. *J Neurosurg* 91(2):192–197
62. Hong KS, Park K (2010) Delayed progressive extradural pneumatocele due to incomplete sealing of opened mastoid air cell after micro-vascular decompression. *J Korean Neurosurg Soc* 47(6):477–479
63. Portilla HD, Fuentes R, Sanchez M, Morales J, Torres LM (2001) Rhabdomyolysis and the seated position during posterior fossa surgery. *Rev Esp Anesthesiol Reanim* 48(1):44
64. Dubey A, Sung WS, Shaya M et al (2009) Complications of posterior cranial fossa surgery—an institutional experience of 500 patients. *Surg Neurol* 72(4):369–375
65. Dubey PK, Singh AK (2000) Venous oxygen embolism due to hydrogen peroxide irrigation during posterior fossa surgery. *J Neurosurg Anesthesiol* 12(1):54–56
66. Gangemi M, Renier D, Daussange J, Hirsch JF, Rigault P (1982) Children's cervical spine instability after posterior fossa surgery. *Acta Neurol (Napoli)* 4(1):39–43
67. Haisa T, Kondo T (1996) Midcervical flexion myelopathy after posterior fossa surgery in the sitting position: case report. *Neurosurgery* 38(4):819–821
68. Hicdonmez T, Kilincer C, Hamamcioglu MK, Cobanoglu S (2006) Paraplegia due to spinal subdural hematoma as a complication of posterior fossa surgery: case report and review of the literature. *Clin Neurol Neurosurg* 108(6):590–594
69. Porto L, Kieslich M, Turowski B, Lanfermann H, Zanella FE (2002) Spinal subdural haematoma mimicking tethered cord after posterior fossa open surgery. *Neuroradiology* 44(5):415–417
70. Kurze T, Gross JD (1997) Tetraparesis after posterior fossa surgery. *J Neurol Neurosurg Psychiatry* 63(2):255
71. Rau CS, Liang CL, Lui CC, Lee TC, Lu K (2002) Quadriplegia in a patient who underwent posterior fossa surgery in the prone position. Case report. *J Neurosurg* 96(1 Suppl):101–103
72. Martinez-Lage JF, Almagro MJ, Izura V, Serrano C, Ruiz-Espejo AM, Sanchez-Del-Rincon I (2009) Cervical spinal cord infarction after posterior fossa surgery: a case-based update. *Childs Nerv Syst* 25(12):1541–1546
73. Prabhakar H, Umesh G, Chouhan RS, Bithal PK (2003) Reverse brain herniation during posterior fossa surgery. *J Neurosurg Anesthesiol* 15(3):267–269
74. Prabhakar H, Rath GP, Dash HH (2006) Bradycardia following hydrogen peroxide irrigation during posterior fossa surgery. *Anaesthesia* 61(9):914
75. Solivera J, Navarro R, Costa JM (2007) Orbital emphysema after endoscopic third ventriculostomy and posterior fossa surgery in the sitting position. *Childs Nerv Syst* 23(1):27–29
76. Tommasino C, Rizzardi R, Beretta L, Venturino M, Piccoli S (1996) Cerebral ischemia after venous air embolism in the absence of intracardiac defects. *J Neurosurg Anesthesiol* 8(1):30–34
77. Guttuso T Jr, Vitticore P, Holloway RG (2005) Responsiveness of life-threatening refractory emesis to gabapentin-scopolamine therapy following posterior fossa surgery. Case report. *J Neurosurg* 102(3):547–549
78. Ali Z, Prabhakar H, Rath GP (2010) Persistent postoperative hypertension following posterior fossa surgery—a case report. *Middle East J Anesthesiol* 20(4):571–572
79. Farmer J-P, McNeely PD, Freeman CR (2008) Brainstem gliomas. In: Albright AL, Pollack IF, Adelson PD (eds) *Principles and practice of pediatric neurosurgery*, 2nd edn. Thieme, New York, pp 640–654
80. Newman LA, Boop FA, Sanford RA, Thompson JW, Temple CK, Duntch CD (2006) Postoperative swallowing function after posterior fossa tumor resection

- in pediatric patients. *Childs Nerv Syst* 22(10):1296–1300
81. Thompson JW, Newman L, Boop FA, Sanford RA (2009) Management of postoperative swallowing dysfunction after ependymoma surgery. *Childs Nerv Syst* 25(10):1249–1252
 82. Chern JJ, Relyea K, Edmond JC et al (2009) Transient selective downward gaze paralysis complicating posterior fossa tumor resection in children. Report of 2 cases. *J Neurosurg Pediatr* 3(6):467–471
 83. Nasser MJ (2009) Transient cerebellar eye closure after posterior fossa surgery in a 5-year-old child. *Childs Nerv Syst* 25(5):635–637
 84. Greenough G, Sateia M, Fadul CE (1999) Obstructive sleep apnea syndrome in a patient with medulloblastoma. *Neuro Oncol* 1(4):289–291
 85. Howard R, Mahoney A, Thurlow AC (1990) Respiratory obstruction after posterior fossa surgery. *Anaesthesia* 45(3):222–224
 86. Buzunov E, Ojemann JG, Robinson FR (2010) Rhesus macaque as an animal model for posterior fossa syndrome following tumor resection. *Pediatr Neurosurg* 46(2):120–126
 87. Ersahin Y, Yararbas U, Duman Y, Mutluer S (2002) Single photon emission tomography following posterior fossa surgery in patients with and without mutism. *Childs Nerv Syst* 18(6–7):318–325
 88. Janssen G, Messing-Junger AM, Engelbrecht V, Gobel U, Bock WJ, Lenard HG (1998) Cerebellar mutism syndrome. *Klin Padiatr* 210(4):243–247
 89. Kingma A, Mooij JJ, Metzemaekers JD, Leeuw JA (1994) Transient mutism and speech disorders after posterior fossa surgery in children with brain tumours. *Acta Neurochir (Wien)* 131(1–2):74–79
 90. Kotil K, Eras M, Akcetin M, Bilge T (2008) Cerebellar mutism following posterior fossa tumor resection in children. *Turk Neurosurg* 18(1):89–94
 91. Kusano Y, Tanaka Y, Takasuna H et al (2006) Transient cerebellar mutism caused by bilateral damage to the dentate nuclei after the second posterior fossa surgery. Case report. *J Neurosurg* 104(2):329–331
 92. Mastronardi L (1996) Mutism and pseudobulbar symptoms after resection of posterior fossa tumors in children: incidence and pathophysiology and transient cerebellar mutism after posterior fossa surgery in children. *Neurosurgery* 38(5):1066
 93. Papavasiliou AS, Kotsalis C, Trakadas S (2004) Transient cerebellar mutism in the course of acute cerebellitis. *Pediatr Neurol* 30(1):71–74
 94. Paquier P, van Mourik M, van Dongen H, Catsman-Berrevoets C, Brison A (2003) Cerebellar mutism syndromes with subsequent dysarthria: a study of three children and a review of the literature. *Rev Neurol (Paris)* 159(11):1017–1027
 95. Salvati M, Cervoni L, Santoro A (1996) Cerebellar mutism after posterior cranial fossa surgery. *J Neurosurg Sci* 40(1):59–63
 96. Van CF, Van de Laar A, Plets C, Goffin J, Casaer P (1995) Transient cerebellar mutism after posterior fossa surgery in children. *Neurosurgery* 37(5):894–898
 97. Ildan F, Tuna M, Erman T, Gocer AI, Zeren M, Cetinalp E (2002) The evaluation and comparison of cerebellar mutism in children and adults after posterior fossa surgery: report of two adult cases and review of the literature. *Acta Neurochir (Wien)* 144(5):463–473
 98. Ozgur BM, Berberian J, Aryan HE, Meltzer HS, Levy ML (2006) The pathophysiologic mechanism of cerebellar mutism. *Surg Neurol* 66(1):18–25
 99. Akhaddar A, Belhachmi A, Elasri A et al (2008) Cerebellar mutism after removal of a vermian medulloblastoma in an adult. *Neurochirurgie* 54(4):548–550
 100. Al-Jarallah A, Cook JD, Gascon G, Kanaan I, Siqueira E (1994) Transient mutism following posterior fossa surgery in children. *J Surg Oncol* 55(2):126–131
 101. Asamoto M, Ito H, Suzuki N, Oiwa Y, Saito K, Haraoka J (1994) Transient mutism after posterior fossa surgery. *Childs Nerv Syst* 10(4):275–278
 102. Baillieux H, Weyns F, Paquier P, De Deyn PP, Marien P (2007) Posterior fossa syndrome after a vermian stroke: a new case and review of the literature. *Pediatr Neurosurg* 43(5):386–395
 103. Boratynski W, Wocjan J (1993) Mutism after surgeries with removal of posterior cranial fossa neoplasms. *Neurol Neurochir Pol* 27(2):261–265
 104. Catsman-Berrevoets CE, Van Dongen HR, Mulder PG, Geuze D, Paquier PF, Lequin MH (1999) Tumour type and size are high risk factors for the syndrome of “cerebellar” mutism and subsequent dysarthria. *J Neurol Neurosurg Psychiatry* 67(6):755–757
 105. Daniels SR, Moores LE, DiFazio MP (2005) Visual disturbance associated with postoperative cerebellar mutism. *Pediatr Neurol* 32(2):127–130
 106. Frim DM, Ogilvy CS (1995) Mutism and cerebellar dysarthria after brain stem surgery: case report. *Neurosurgery* 36(4):854–857
 107. Punzo A, De Marinis P, Ruggiero C, D’Arienzo G, Ambrosio G, Graziano DV (1992) Psychic disorders. An unknown complication of surgery of the posterior cranial fossa. *Minerva Anestesiol* 58(4 Suppl 1):161–163
 108. Ersahin Y, Mutluer S, Cagli S, Duman Y (1996) Cerebellar mutism: report of seven cases and review of the literature. *Neurosurgery* 38(1):60–65
 109. Ferrante L, Mastronardi L, Acqui M, Fortuna A (1990) Mutism after posterior fossa surgery in children. Report of three cases. *J Neurosurg* 72(6):959–963
 110. Frassanito P, Massimi L, Caldarelli M, Di RC (2009) Cerebellar mutism after spontaneous intratumoral bleeding involving the upper cerebellar vermis: a contribution to the physiopathogenic interpretation. *Childs Nerv Syst* 25(1):7–11
 111. Gelabert-Gonzalez M, Fernandez-Villa J (2001) Mutism after posterior fossa surgery. Review of the literature. *Clin Neurol Neurosurg* 103(2):111–114
 112. Germano A, Baldari S, Caruso G et al (1998) Reversible cerebral perfusion alterations in children with transient mutism after posterior fossa surgery. *Childs Nerv Syst* 14(3):114–119
 113. Liu GT, Phillips PC, Molloy PT et al (1998) Visual impairment associated with mutism after posterior fossa surgery in children. *Neurosurgery* 42(2):253–256

114. Yildiz O, Kabatas S, Yilmaz C, Altinors N, Agaoglu B (2010) Cerebellar mutism syndrome and its relation to cerebellar cognitive and affective function: review of the literature. *Ann Indian Acad Neurol* 13(1):23–27
115. Wells EM, Walsh KS, Khademian ZP, Keating RF, Packer RJ (2008) The cerebellar mutism syndrome and its relation to cerebellar cognitive function and the cerebellar cognitive affective disorder. *Dev Disabil Res Rev* 14(3):221–228
116. Di Rocco C (1999) Cerebellar astrocytomas. In: Choux M, Di Rocco C, Hockley A, Walker M (eds) *Pediatric neurosurgery*, 1st edn. Churchill Livingstone, London, pp 427–460
117. Ichimura S, Ohira T, Kobayashi M et al (2010) Assessment of cognitive function before and after surgery for posterior cranial fossa lesions using computerized and conventional tests. *Neurol Med Chir (Tokyo)* 50(6):441–448
118. Vandeinse D, Hornyak JE (1997) Linguistic and cognitive deficits associated with cerebellar mutism. *Pediatr Rehabil* 1(1):41–44
119. Palmer SL, Hassall T, Evankovich K et al (2010) Neurocognitive outcome 12 months following cerebellar mutism syndrome in pediatric patients with medulloblastoma. *Neuro Oncol* 12:1311–1317
120. Grill J, Viguier D, Kieffer V et al (2004) Critical risk factors for intellectual impairment in children with posterior fossa tumors: the role of cerebellar damage. *J Neurosurg* 101(2 Suppl):152–158
121. Mateo-Sierra O, Gutierrez FA, Fernandez-Carballal C et al (2005) Akinetic mutism related to hydrocephalus and cerebellar surgery treated with bromocriptine and ephedrine. A pathophysiological review. *Neurocirugia (Astur)* 16(2):134–141
122. Adachi J, Nishikawa R, Hirose T, Matsutani M (2005) Mixed neuronal-glioma of the fourth ventricle and successful treatment of postoperative mutism with bromocriptine: case report. *Surg Neurol* 63(4):375–379
123. Caner H, Altinors N, Benli S, Calisaneller T, Albayrak A (1999) Akinetic mutism after fourth ventricle choroid plexus papilloma: treatment with a dopamine agonist. *Surg Neurol* 51(2):181–184
124. Choux M, Lena G, Do L (1999) Brainstem tumors. In: Choux M, Di Rocco C, Hockley A, Walker M (eds) *Pediatric neurosurgery*, 1st edn. Churchill Livingstone, London, pp 471–492
125. Lena G, Gentet J-C (1999) Medulloblastoma. In: Choux M, Di Rocco C, Hockley A, Walker M (eds) *Pediatric neurosurgery*, 1st edn. Churchill Livingstone, London, pp 461–470
126. Muraszko KM, Brahma B, Orringer D (2008) Medulloblastomas. In: Albright AL, Pollack IF, Adelson PD (eds) *Principles and practice of pediatric neurosurgery*, 2nd edn. Thieme, New York, pp 606–620
127. Albright AL, Wisoff JH, Zeltzer PM, Boyett JM, Rorke LB, Stanley P (1996) Effects of medulloblastoma resections on outcome in children: a report from the Children's Cancer Group. *Neurosurgery* 38(2):265–271
128. Sanford RA, Merchant T (2008) *Ependymomas*, 2nd edn. Thieme, New York
129. Tomita T (1994) Miscellaneous posterior fossa tumors. In: Cheek WR (ed) *Pediatric neurosurgery: surgery of the developing nervous system*, 3rd edn. W B Saunders, Philadelphia, pp 383–391
130. Massimino M, Buttarelli FR, Antonelli M, Gandola L, Modena P, Giangaspero F (2009) Intracranial ependymoma: factors affecting outcome. *Future Oncol* 5(2):207–216
131. Figarella-Branger D, Civatte M, Bouvier-Labit C et al (2000) Prognostic factors in intracranial ependymomas in children. *J Neurosurg* 93(4):605–613
132. Pollack IF, Gerszten PC, Martinez AJ et al (1995) Intracranial ependymomas of childhood: long-term outcome and prognostic factors. *Neurosurgery* 37(4):655–666
133. Healey EA, Barnes PD, Kupsky WJ et al (1991) The prognostic significance of postoperative residual tumor in ependymoma. *Neurosurgery* 28(5):666–671
134. Stavrinou NG, Taylor R, Rowe A, Whittle IR (2008) Posterior fossa surgery complicated by a pseudomeningocele, bilateral subdural hygromata and cerebellar cognitive affective syndrome. *Br J Neurosurg* 22(1):107–109

Postoperative Care Following Surgery for Posterior Fossa Tumors

57

Vasilios Tsitouras and Spyros Sgouros

As immediate postoperative period is considered the time from recovery of anesthesia to discharge from the hospital, usually from 1 to 4 weeks, although in some countries (e.g., the United Kingdom), legally the postoperative period extends to the first 4 weeks from operation, and every complication in that period is considered a result of, or intimately related to, the operation, regardless of whether the patient has gone home. Posterior fossa surgery poses many dangers and the postoperative period requires particular vigilance [7].

An important determinant of postoperative course is the preoperative clinical condition. A fully alert patient with minor preoperative neurological deficit has better chance of good postoperative recovery than a patient with severe deficit or impaired state of consciousness. Two major factors that determine the postoperative management are uneventful surgery and the findings of the immediate postoperative MRI scanning.

Important surgical aspects are minimal blood loss, respect of normal neural (cerebellar and brainstem) tissue, and reduced (as much as possible) operative time [3].

In our department immediately after wound closure and before the patient is awake, a contrast-enhanced MR scan is performed. This requires coordination with the anesthetist at the beginning of the operation, to avoid placement of an armored endotracheal tube. Although currently we are lacking an intraoperative MR facility, the proximity of the radiology department to the operating theaters allows this transfer safely. The MR findings will determine further management. A postoperative hematoma needs immediate reoperation and evacuation. It should be stated that an immediate postoperative MR scan safeguards to a large extent from postoperative hematoma in the absence of a coagulation disorder, as in practice it takes a good half hour from skin closure to the acquisition of the MR images, time period enough for a postoperative hematoma to accumulate if there is active hemorrhage from unrecognized bleeding vessel in the operative field. Only in patients with coagulation disorder (e.g., low platelet count following chemotherapy) there is high risk of developing hematoma later postoperatively. The presence of an accessible tumor residual of significant size (nominally more than 15 % of its original size or more than 1.5 cm² in its largest slice) is an indication for reoperation at the same setting. A clear tumor bed, without notable edema or hematoma, and

V. Tsitouras, M.D.
Department of Paediatric Neurosurgery,
“Mitera” Children’s Hospital, Erythrou Stavrou 6,
Marousi, Athens 151 23, Greece

S. Sgouros, M.D., F.R.C.S. (S.N.) (✉)
Department of Paediatric Neurosurgery,
“Mitera” Children’s Hospital, Erythrou Stavrou 6,
Marousi, Athens 151 23, Greece

Department of Neurosurgery, University of Athens
Medical School, Athens, Greece
e-mail: sgouros@med.uoa.gr

ventricular system of acceptable size are strong indicators for patient's extubation, especially if there have been no untoward intraoperative events (e.g., repeat episodes of severe bradycardia or hypertension). The anesthesiologist will decide the time for extubation based on satisfactory respiratory drive, cardiopulmonary sufficiency, spontaneous ventilation, satisfactory gag reflex, and state of awakesness (good level of consciousness, appropriate responses to pain stimuli or even verbal commands). Usually, if the operation went well without untoward intraoperative events, the patients wake up immediately and are able to defend their airways well, while maintaining good respiratory drive. Failure to wake up needs transfer of the patient to the pediatric intensive care unit (PICU) for further management.

When the patient is extubated, a clinical examination is performed and recorded as a baseline. Important checkpoints are respiratory rate and pattern, vital signs, and neurological examination (eye opening, verbal and motor response, cranial nerves, sensory and motor examination of extremities).

An extubated child with satisfactory clinical state and negative MR findings is safe to be nursed at the ward. Transfer to the pediatric intensive care unit with child awake is also an option especially if the child is less than 2 years old or agitated and excessively vomiting. We prefer to keep the patient at the ward, on bed rest together with his/her parents under close follow-up. For the first 4 h vital signs and neurological assessments are performed every half hour and then every hour. Indwelling nasogastric and Foley catheters are avoided if possible at this early postoperative period. An attempt is made for light feeding the same evening if an adequate swallowing mechanism is preserved.

Postoperative medications are kept to minimal. Analgesia is achieved with acetaminophen (10–15 mg/kg IV every 6 h). If preoperative steroids (usually dexamethasone) were administered, then they are continued for the first few postoperative days on a tapered dosage. An H₂ antagonist (ranitidine) is given as prophylaxis. On excessive vomiting, which is not uncommon in posterior fossa surgery, ondansetron is an

option (0.1 mg/kg IV every 12 h) [5, 12]. Antibiotics are given only preoperatively (one dose of second-generation cephalosporin 30 min prior to incision) [14]. A second dose is administered if the operation lasts more than 6 h. Fluid replacement during the first 24 h is usually held with a dextrose saline solution (sodium chloride 0.18 % + dextrose 4.3 %) on a rate dependent on the child's weight and additional fluid losses (e.g., vomiting). In the next morning, a blood sample is withdrawn for standard lab tests (full blood count, electrolytes, renal profile). At the first postoperative day (the morning after the operation), the child is encouraged to mobilize out of bed, and a further clinical examination is made focusing on truncal or gait disturbances. The wound is inspected for CSF leakage.

Failure to progress or deterioration in the early postoperative period usually implies either postoperative hematoma at the resection site (acute presentation with rapid clinical deterioration within hours) or hydrocephalus (slow insidious presentation over the first 7–10 days)

Four issues which are encountered in the early postoperative period merit separate discussion: hydrocephalus, pseudomeningocele/CSF leak, mutism, and aseptic meningitis.

57.1 Hydrocephalus

Approximately 80 % of children with posterior fossa tumors present preoperatively with hydrocephalus. Almost exclusively this hydrocephalus is obstructive due to the proximity of these tumors to the fourth ventricle and the aqueduct. Brainstem tumors and midline cerebellar tumors, commonly medulloblastomas and ependymomas, have a higher incidence of need of postoperative shunting in comparison to tumors situated in the cerebellar hemispheres [8]. There is controversy surrounding the management of hydrocephalus in children with posterior fossa tumors [17]. Some surgeons prefer to treat hydrocephalus prior to tumor excision by means of external ventricular drainage (EVD), ventriculoperitoneal (VP) shunting, or endoscopic third ventriculostomy

(ETV) if the child's condition is critical due to elevated ICP and the tumor surgery is delayed for any reason (usually practicalities of operating theaters). An endoscopic ventriculostomy preoperatively has been advocated to reduce the incidence of postoperative need for shunt insertion [16]. Overall, persistent or progressive hydrocephalus needing operative treatment has been reported in 25–30 % of cases postoperative. This means that in approximately three out of four children, tumor excision will lead to avoidance of shunting. Hence, one should avoid preoperative shunting, especially if the patient is not acutely well or rapidly deteriorating, and aim instead for early tumor removal. In medulloblastomas the postoperative incidence of hydrocephalus is higher (22–63 %), and the need for shunt insertion has been found to correlate with the preoperative ventricular volume [10]. Other factors that could raise the need for shunting are age younger than 3 years at diagnosis, midline tumor location, subtotal tumor resection, prolonged requirement of an EVD, the use of cadaveric dural grafts, pseudomeningocele formation, and CSF infections [4]. We prefer to avoid shunting pre- or postoperatively. After an uncomplicated tumor removal, the child is observed for the next few days for potential symptoms and signs of hydrocephalus. If this occurs we perform a CT or MR scan in order to compare ventricular size with the immediate postoperative MR scan. Increase of the ventricular size associated with symptoms and signs or raised ICP, or pseudomeningocele/CSF leak, is treated with an endoscopic third ventriculostomy as the first choice [11]. Moderate ventricular size reduction after ETV should be sufficient for clinical improvement but very often is less than expected. In these circumstances the patient should be followed clinically for a few days or weeks until CSF dynamics convert from a shunt-dependent to a shunt-independent state [13]. If hydrocephalus remains symptomatic, we perform one or two lumbar punctures to provide a pressure gradient between the third ventricle and the subarachnoid space in order to accelerate CSF circulation and absorption. If these measures still do not work, then a VP shunt is placed. Manifestation of active

hydrocephalus with pseudomeningocele or CSF leak responds better to ventricular shunting rather than ETV.

57.2 Pseudomeningocele/CSF Leak

An early manifestation of postoperative hydrocephalus could be the formation of pseudomeningocele and/or CSF leak. After posterior fossa operations CSF leakage is a major concern and many efforts should focus on preventing it. A clean operation field with minimal blood loss and generous irrigation can protect from excessive arachnoiditis. Watertight dural closure is important to prevent pseudomeningocele and/or CSF leak. It should be remembered that commonly the operation of the removal of posterior fossa tumor takes several hours, during which the dura, under the heat of the microscope light, shrinks, making watertight closure difficult. Avoidance of dural substitutes, especially cadaveric, is an important technical tip. The use of pericranial graft is preferred in filling dural gaps during closure. Some surgeons in cases of insufficient dural edges would leave the dura wide open and rely on the musculature closure, provided that normal CSF dynamics are anticipated. Cranioplasty with replacement of the bone flap has been shown to be protective [9]. The upper part of the incision covering the occiput is considered as the most vulnerable site due to the limited subgaleal tissue. Some tips are the Y incision of the galea and the maintenance of a cuff of occipital musculature on the bone during opening, to allow a stronger watertight reattachment of the occipital muscles. These muscles should be reattached with meticulous anatomical technique using strong absorbable sutures. Subcutaneous and skin sutures – continuous or interrupted – should prevent gaps and avoid wound ischemia. Some surgeons use a pressure bandage or keep the head elevated postoperatively. The usefulness of these measures is limited and they are not recommended.

CSF leak should be treated immediately, in order to prevent infection. As a first step one or more sutures can reinforce wound closure.

A pseudomeningocele as only an imaging finding can be left and followed. If it increases or contributes to a persistent CSF leak, then it should be treated by means of CSF diversion. A few lumbar punctures, a lumbar drain, or an EVD left for 2–3 days could rectify the problem. As mentioned, a pseudomeningocele formation or a difficult to treat CSF leak could be the result of active hydrocephalus. In this case a permanent treatment option is considered with a VP shunt being more favorable than an ETV. Care should be taken not to place a shunt in the presence of CSF infection due to CSF leak. Small pseudomeningoceles are expected to resolve spontaneously after a few weeks in the absence of abnormal CSF flow. As a last option the wound can be reopened, explored, and reclosed provided that CSF dynamics are under control.

57.3 Cerebellar Mutism

After resection of vermian tumors, most commonly medulloblastomas, impaired speech or true cerebellar mutism can be seen in a child that is progressing initially well [6]. Typically, it appears after postoperative days 1–4 with a varying incidence in different studies among 2–40 % [2]. Additional signs such as ataxia, hypotonia, emotional lability, and behavioral abnormalities constitute the so-called posterior fossa syndrome [18]. The severity of this cerebellar mutism syndrome (CMS) has been classified as mild, moderate, and severe, with ataxia being the most prominent finding [15]. No specific demographic, clinical, or radiological features can predict preoperatively which patients with medulloblastoma will develop this syndrome. Disruption or malfunction of the dentatohalamocortical outflow tracts is a possible etiology of the syndrome and can result from extended vermian splitting, edema, or vasospasm. Tumor size and hydrocephalus haven't been found to associate with CMS. Focal postoperative edema in the middle and superior cerebellar peduncles and the brainstem has been reported as a prominent MR finding in children with CMS. Previously it was thought that most of the syndrome's features

were transient, but recent data have demonstrated more persistent impairments of speech and language as well as inattention, executive dysfunction, and behavioral dysregulation [19]. It is believed that a more aggressive surgical technique can increase the incidence of the syndrome and that usage of surgical retractors and of ultrasonic aspirator should be kept in minimal. A low-dose corticosteroid administration is recommended by many surgeons in cases of CMS, but the most effective therapy at the moment is prevention by smooth and gentle surgical manipulations.

57.4 Aseptic Meningitis

It is thought to result from the presence of blood degradation products in the subarachnoid space or into the ventricles and occurs at the third to fifth postoperative day with an incidence of 2 %. Mild fever, headache, meningismus with negative CSF cultures, and pleocytosis (with lymphocyte predominance) are the most common findings [1]. A brief period of steroid (dexamethasone) administration is attempted combined with one or two lumbar punctures. Occasionally, aseptic meningitis can take several weeks to settle.

In conclusion, removal of posterior fossa tumors is safe nowadays with the use of modern neurosurgical technical adjuncts (microscope, Cavitron Ultrasonic Surgical Aspirator, neuronavigation, nerve monitoring), and careful technique respecting normal neural tissue allows direct waking up and extubation of most patients immediately postoperatively and speedy mobilization and recovery, facilitating further oncological management.

References

1. Carmel PW, Greif LK (1993) The aseptic meningitis syndrome: a complication of posterior fossa surgery. *Pediatr Neurosurg* 19(5):276–280
2. Charalambides C, Dinopoulos A, Sgouros S (2009) Neuropsychological sequelae and quality of life following treatment of posterior fossa ependymomas in children. *Childs Nerv Syst* 25(10):1313–1320

3. Cochrane DD, Gustavsson B, Poskitt KP, Steinbok P, Kestle JR (1994) The surgical and natural morbidity of aggressive resection for posterior fossa tumors in childhood. *Pediatr Neurosurg* 20(1):19–29
4. Culley DJ, Berger MS, Shaw D, Geyer R (1994) An analysis of factors determining the need for ventriculoperitoneal shunts after posterior fossa tumor surgery in children. *Neurosurgery* 34(3):402–407; discussion 407–408
5. Culy CR, Bhana N, Plosker GL (2001) Ondansetron: a review of its use as an antiemetic in children. *Paediatr Drugs* 3(6):441–479
6. Dailey AT, McKhann GM 2nd, Berger MS (1995) The pathophysiology of oral pharyngeal apraxia and mutism following posterior fossa tumor resection in children. *J Neurosurg* 83(3):467–475
7. Dubey A, Sung WS, Shaya M, Patwardhan R, Willis B, Smith D, Nanda A (2009) Complications of posterior cranial fossa surgery—an institutional experience of 500 patients. *Surg Neurol* 72(4):369–375
8. Due-Tonnessen BJ, Helseth E (2007) Management of hydrocephalus in children with posterior fossa tumors: role of tumor surgery. *Pediatr Neurosurg* 43(2):92–96
9. Gnanalingham KK, Lafuente J, Thompson D, Harkness W, Hayward R (2002) Surgical procedures for posterior fossa tumors in children: does craniotomy lead to fewer complications than craniectomy? *J Neurosurg* 97(4):821–826
10. Kombogiorgas D, Natarajan K, Sgouros S (2008) Predictive value of preoperative ventricular volume on the need for permanent hydrocephalus treatment immediately after resection of posterior fossa medulloblastomas in children. *J Neurosurg Pediatr* 1(6):451–455
11. Kulkarni AV, Drake JM, Kestle JR, Mallucci CL, Sgouros S, Constantini S (2010) Predicting who will benefit from endoscopic third ventriculostomy compared with shunt insertion in childhood hydrocephalus using the ETV Success Score. *J Neurosurg Pediatr* 6(4):310–315
12. Neufeld S, Dundon B, Yu H, Newburn-Cook C, Drummond J (2009) Midline location of tumour is a risk factor for postoperative vomiting in children requiring posterior fossa tumour resection. *Can J Neurosci Nurs* 31(3):10–14
13. Nishiyama K, Mori H, Tanaka R (2003) Changes in cerebrospinal fluid hydrodynamics following endoscopic third ventriculostomy for shunt-dependent non-communicating hydrocephalus. *J Neurosurg* 98(5):1027–1031
14. Rangel SJ, Fung M, Graham DA, Ma L, Nelson CP, Sandora TJ (2011) Recent trends in the use of antibiotic prophylaxis in pediatric surgery. *J Pediatr Surg* 46(2):366–371
15. Robertson PL, Muraszko KM, Holmes EJ, Spoto R, Packer RJ, Gajjar A, Dias MS, Allen JC (2006) Incidence and severity of postoperative cerebellar mutism syndrome in children with medulloblastoma: a prospective study by the Children’s Oncology Group. *J Neurosurg* 105(6 Suppl):444–451
16. Sainte-Rose C, Cinalli G, Roux FE, Maixner R, Chumas PD, Mansour M, Carpentier A, Bourgeois M, Zerah M, Pierre-Kahn A, Renier D (2001) Management of hydrocephalus in pediatric patients with posterior fossa tumors: the role of endoscopic third ventriculostomy. *J Neurosurg* 95(5):791–797
17. Schijman E, Peter JC, ReKate HL, Sgouros S, Wong TT (2004) Management of hydrocephalus in posterior fossa tumors: how, what, when? *Childs Nerv Syst* 20(3):192–194
18. Steinbok P, Cochrane DD, Perrin R, Price A (2003) Mutism after posterior fossa tumour resection in children: incomplete recovery on long-term follow-up. *Pediatr Neurosurg* 39(4):179–183
19. Wells EM, Khademian ZP, Walsh KS, Vezina G, Spoto R, Keating RF, Packer RJ (2010) Postoperative cerebellar mutism syndrome following treatment of medulloblastoma: neuroradiographic features and origin. *J Neurosurg Pediatr* 5(4):329–334

Stephanie Puget, Antonio Vecchione,
and Philippe Meyer

58.1 The Neurosurgical Care

The complications associated with surgical procedures in the posterior fossa are linked to the anatomical structures involved and the risk of hydrocephalus if the tumor was developed in the ventricles or the cerebellopontine angle.

58.1.1 Avoidance of Cerebrospinal Fluid Leakage

A watertight closure may be obtained and require sometimes the use of pericranium patch, some sealant, or fibrin glue. Closing the different layers of muscles is also essential.

We also pay special attention to make a large and compressive dressing for at least 5 days, redone after 1 or 2 days. The compression has to be moderate to avoid eschar, especially in front of the occipital protuberance. According to us, it

can help also to maintain the head in straight line to decrease the pain and avoid torticollis. In case of leakage in the subgaleal space, we performed local and lumbar taps and apply again a compressive dressing.

58.2 The Intensivist Care

Although rare, occurring in less than 10 % of the cases, complications are life-threatening and require immediate recognition and prompt treatment that could be best achieved in a dedicated pediatric neurointensive care unit (NICU) with large caseload and optimized ICU resource management. Most children with posterior fossa brain tumor resection could be discharged to the surgical ward after an uneventful scheduled overnight ICU stay and satisfactory control of brain imaging. The main issues, for anesthesiologists in the immediate postoperative period, are to insure adequate timing for tracheal extubation, prompt effective neurological evaluation, and pain and postoperative nausea and vomiting (POVN) control.

In our department, complete anesthesia reversal is achieved in the eight-bed pediatric NICU. Patients are kept intubated at the end of the procedure and transferred directly from the operative room. Pain control is achieved with nurse-controlled analgesia (NCA) using IV morphine, with or without continuous infusion, in all patients. Low doses of clonazepam are frequently added in order to prevent neck pain

S. Puget, M.D., Ph.D. (✉)
Department of Pediatric Neurosurgery,
Necker Hospital, Université Paris Descartes,
Sorbonne, Paris, France
e-mail: stephanie.puget@gmail.com

A. Vecchione, M.D. • P. Meyer, M.D.
Department of Anesthesiology, Necker Hospital,
Université Paris Descartes, Sorbonne Paris Cité,
Rue de Sèvres, Paris 75015, France
e-mail: vecchione.antonio@gmail.com;
philippe.meyer@nck.aphp.fr

and contracture, especially in older children and adolescents operated in the sitting position. Ondansetron is used systematically to prevent POVN that are almost constant [1]. Within the first 24 h, a no-glucose infusion policy using normal saline is adopted in order to prevent hyperglycemia and hyponatremia [2].

Most patients could rapidly be weaned from ventilation, and the trachea is extubated in 90 % of them within the first 3 h. Progressive and complete anesthesia reversal, careful rewarming, and effective pain control are the key issues to prevent agitation, arterial hypertension, cough reflex, laryngotracheal spasm, and hypoxia upon tracheal tube removal that are major sources of postoperative ICH and bleeding. Children, especially those under 2 years of age, experiencing heavy blood losses, long-lasting procedures with perioperative brain stem structure stimulations, and those with tumors making them at particular risks of deglutition disorders, are kept intubated under light sedation with a titrated association of IV morphine and benzodiazepine infusion, until

autonomous upper airway control could be achieved. Only those children requiring long-term mechanical ventilation will need an NICU stay exceeding 24 h. Careful monitoring of bed availability is essential and could be best achieved provided that priority could be given to free NICU beds as soon as possible, to insure efficient control of pain and POVN allowing easy transfer to the general ward or to intermediate care unit when needed and preventing early emergency ICU readmission.

References

1. Kathirvel S, Dash HH, Bhatia A, Subramaniam B, Prakash A, Shenoy S (2001) Effect of prophylactic ondansetron on postoperative nausea and vomiting after elective craniotomy. *J Neurosurg Anesthesiol* 13(3):207–212
2. Pietrini D, Di Rocco C, Di Bartolomeo R, Conti G, Ranelletti FO, De Luca D et al (2009) No-glucose strategy influences posterior cranial fossa tumors' postoperative course: introducing the Glycemic Stress Index. *J Neurooncol* 93(3):361–368

Nigar Baykan and M. Memet Özek

Immediate postoperative period in pediatric posterior fossa surgery requires special measures regarding the perioperative and early complications related to surgical procedure and anesthesia. Immediate postoperative care starts in the operating room, including the recovery room and transportation to the intensive care unit (ICU). Close care continues at least 24 h until the vital stabilization and complication-free status are confirmed by final evaluation after MRI control.

59.1 Anesthetic Management and Emergency from Anesthesia

Anesthesia for posterior fossa surgery requires rapid control of anesthetic levels for neurological examination. Remifentanyl with either propofol or sevoflurane is used for the maintenance of anesthesia. Both anesthetic drugs have very short-term effect, provide rapid return of consciousness, and reduce respiratory complications, making them suitable for planned extubation at the end of

surgery [1, 2]. Remifentanyl infusion is used in our routine anesthesia practice for posterior fossa surgery combined with either sevoflurane infusion for patients under age 4 or propofol infusion for patients over age 4. At the time of dural closure, patients receive low-dose propofol (1–3 mg/kg/h) or sevoflurane (MAC 0.4–0.5) until the beginning of skin closure. After head dressing remifentanyl (0.1 µg/kg/h) is discontinued, and continuing full monitorization, patient is placed in supine position and neuromuscular blockers are fully reversed. While moving the patient to supine position, the head and neck must be fixed in the axis of the body. Then neuromonitorization is discontinued and nasogastric catheter is removed. Patients with medulla oblongata and pons disorders are left intubated for 24 h.

Fentanyl (0.1 µg/kg) is almost routinely administered for postoperative analgesia after immediate examination at the operating room.

Respiratory dysfunction is the leading complication after posterior fossa surgery. The most immediate postoperative complication is apnea. Careful consideration must be made regarding the timing of extubation [3]. In the case of apnea, it is very important to make distinct diagnosis for anesthetic-related apnea. Ischemia or edema of the respiratory centers in the brainstem interferes with the respiratory control and may lead to postoperative apnea. It is crucial to keep in mind that after endotracheal intubation the infant in prone position with a tight-fitting endotracheal tube is always at risk for subglottic obstruction secondary

N. Baykan, M.D. (✉)
Department of Anesthesiology, Acıbadem University,
School of Medicine, Istanbul, Turkey
e-mail: nigarbaykan@yahoo.com

M.M. Özek, M.D.
Division of Pediatric Neurosurgery, Acıbadem
University, School of Medicine, Istanbul, Turkey

to mucosal swelling. In the case of localized airway edema in the recovery room, racemic epinephrine inhalation is used.

59.2 Immediate Evaluation

All patients are examined for potential complications after extubation. Respiratory, hemodynamic, and neurological status (new motor deficit, unexpected delay of awakening) is evaluated and recorded. It must be taken into account that the specificity of early postoperative findings for long-term neurological and developmental abnormalities is limited, with surprising ability of the neonatal and infant brain to withstand and recover from perioperative injury.

59.3 Transport and Monitoring

All patients are monitored regarding respiratory (pulse oximetry, capnography) and hemodynamic parameters (heart rate, ECG, invasive arterial blood pressure, and body temperature) during transport and are accompanied by an anesthesiologist since arrival at the ICU. During transportation and in the ICU, all patients must be placed in semi-fowler position.

59.4 ICU

Children with posterior fossa craniectomy are subjected to cranial nerve injuries that have implications for the anesthesiologist. Close observation in an ICU with serial neurological examinations and invasive hemodynamic monitoring is helpful for the prevention and early detection of postoperative problems. Identifying perioperative neurological injury may be challenging. It is important to diagnose cranial nerve defect early by assessing the ability to handle secretions since the insidious aspiration is a frequent cause of postoperative morbidity. Whenever the lower cranial nerves are traumatized, the anesthesiologist should be notified. If cranial nerves IX, X, and XII are injured, the patient is at

increased risk of aspiration pneumonitis and hypoxia.

Nausea and vomiting can cause early postoperative complications in patients subjected to posterior fossa surgery and should be treated with nonsedating antiemetics. However, prophylactic administration of ondansetron during surgery is not effective in decreasing the incidence of vomiting following craniotomies in children [4].

A cranial CT scan control is performed at the first hour of admission to the ICU. Vital parameters are monitored and level of consciousness is assessed regularly.

59.5 Prophylaxis and Maintenance

Antibiotics, steroids, analgesics, antiemetics, and H₂ receptor blockers are used routinely for prophylaxis and maintenance.

Antibiotic prophylaxis is performed at 100 mg/kg/day (ampicillin 4 × 1).

Steroids are also used for prevention of intracranial edema. Dexamethasone is administered at 0.1 mg/kg/day.

Metoclopramide (at 0.5 mg/kg/day) is used for antiemesis.

Ranitidine (at 1 mg/kg/day) is also used routinely.

Postoperative pain relief is provided by paracetamol (at 40 mg/kg/day) four times a day and fentanyl (at 1 µg/kg) when needed.

On the first postoperative day, MRI control scanning and neurosurgical consultation are performed; oral feeding is started after the assessment of gag reflex and swallowing function. In patients with medulla oblongata and pons disorders, oral feeding is started after 48 h. In patients with swallowing dysfunction, percutaneous endoscopic gastrostomy (PEG) is carried out before discharging from the ICU.

References

1. Wong AY, O'Regan AM, Irwin MG (2006) Total intravenous anesthesia with propofol and remifentanyl for elective neurosurgical procedures: an audit of

- early postoperative complications. *Eur J Anaesth* 23: 586–590
2. Sneyd JR, Andrews CJ, Tsubokawa T (2005) Comparison of propofol/remifentanyl and sevoflurane/remifentanyl for maintenance of anesthesia for elective intracranial surgery. *Br J Anaesth* 94: 778–783
 3. Bhagat H, Dash HH, Bithal PK et al (2008) Planning for early emergence in neurosurgical patients: a randomized prospective trial of low-dose anesthetics. *Anesth Analg* 107:1348–1355
 4. Furst SR, Sullivan LJ, Soriano SG et al (1996) Effects of ondansetron on emesis in the first 24 hours after craniotomy in children. *Anesth Analg* 83:325–328

Il-Woo Lee

60.1 Immediate Postoperative Care

Immediate postoperative care is very important for preventing complications and reducing postoperative morbidity and mortality after posterior fossa tumor surgery in children. The posterior fossa has relatively small volume than the supratentorial space but contains many important neural structures. Minor complications after operation may result in severe neurological damages to the patients.

After surgery, the patient is placed in the intensive care unit for the first 1–3 days, and during that period, close observation and monitoring should be done. In the intensive care unit, arterial pressure, pulse, continuous electrocardiogram, water and electrolyte balance, blood gases, and urine output are closely monitored. The body temperature should be kept in normal range, while hyperthermia aggravates cerebral edema and hypothermia reduces the cerebral perfusion.

The patient's head should be placed slightly elevated to reduce intracranial pressure (ICP). Care should be taken on the surgical wound not to be compressed when large craniectomy is performed. Careful attention also must be given to reduce the risk of aspiration pneumonia due to vomiting.

Children who are in satisfactory postoperative neurologic condition are extubated immediately after surgery in the operating room or recovery room. But when the surgery takes a long time or adjacent structure is injured during the tumor removal, there would be potential problems of vocal cord function and swallowing. In that case, it is safer to leave the patient intubated overnight and that an experienced otolaryngologist extubates him and assesses vocal cord movement and gag reflex. If the vocal cord function is inadequate, the patient remains extubated and in continuous monitoring for 24 h in the intensive care unit [1, 2].

After posterior fossa tumor surgery, increased intracranial pressure is a common cause of neurological morbidity and may result in herniation and even death. Postoperative bleeding and brain edema due to excessive brain retraction and subtotal resection of tumor are major causes of increased intracranial pressure [3]. In the event of a neurological deterioration or if a patient does not awake in the immediate postoperative period, a CT scan should be performed to rule out a postoperative hematoma, brain edema, or persistent hydrocephalus [4]. ICP monitoring is very useful for early detection of such complications.

Subdural-type pressure transducer and ventriculostomy are the two most common types of ICP monitoring that the authors prefer to use. Normal ICP varies according to age, and physiological level is less than 2 mmHg in a neonate, 1.5–6 mmHg in infant, and 3–7 mmHg in young children [5]. In general, treatment is not needed

I.-W. Lee, M.D., Ph.D.
Department of Neurosurgery, Catholic University
of Korea, Seoul, South Korea
e-mail: leeilwoo@catholic.ac.kr

when the ICP is below 20 mmHg, but an ICP elevation over 20 mmHg requires treatment. When the patients have external ventricular drainage (EVD) after operation, EVD is adjusted to drain at 10–15 cm above head level for 1–3 days. If the patient has no headache or neurological deterioration, EVD is clamped and connected to the pressure transducer for 1 day for continuous intracranial pressure monitoring. When the ICP is within normal range, EVD is removed. When the ICP increases over 20 mmHg during monitoring, the EVD catheter is opened to allow more drainage and will be left open for a few more days, without exceeding 7 days in total. If the EVD is still needed 7 days after operation, it is our practice to replace another new EVD for 1 week. If the symptoms of hydrocephalus persist, permanent shunt is inserted [6].

Steroids are frequently used postoperatively for decreasing peritumoral edema. The recommended daily dose is 0.25–0.5 mg/kg for 2–3 days and then tapered over 3–5 days [7].

A hyperosmolar agent, such as mannitol or glycerol, can be used if the ICP is not controlled by extraventricular drainage. Monitoring of plasma osmolality is essential to prevent renal failure when the hyperosmolar agent is used.

The use of prophylactic antibiotics has some debates among surgeons, but the author believes that it lowered the rate of postoperative infection. Broad-spectrum antibiotics covering the skin flora are continued for 2–3 days or, if an EVD is in place, until the EVD is removed.

The use of prophylactic anticonvulsant is also controversial, but the author prefers to use it for a couple of weeks for reducing the risk of postoperative seizure [8].

Most surgeons recommended a postoperative MRI within 48 h before substantial tissue granulation or inflammation occurs to assess the extent of tumor resection of surgery. The postoperative MRI is predictive of tumor recurrence and patient survival. Postoperative enhancement is a common finding on imaging performed between 1 day and 1 year following surgery, and it is most pronounced between postoperative days 3 and 21. Nodular enhancement is characteristic of residual tumors [9–12].

The neurologic consequences of the tumor removal will be apparent postoperatively. The risk of a new postoperative neurological deficit depends on the location of tumor and aggressiveness of resection. The most frequent neurological sequela is deterioration of cerebellar function, with increased limb or truncal ataxia. Sixth cranial nerve dysfunctions may occur if dissection occurs along the floor of the fourth ventricle, and other cranial nerve complications may occur when tumor resection involves the cerebellomedullary or cerebellopontine angle. Cerebellar mutism may occur in less than 5 % of children. The pathogenesis is not clear and it can occur when the operative procedure seems to go well. The deficits improve within several weeks and most patients recover completely [13–15].

References

1. Thompson JW, Newman L, Boop FA, Sanford RA (2009) Management of postoperative swallowing dysfunction after ependymoma surgery. *Childs Nerv Syst* 25(10):1249–1252
2. Sanford RA, Merchant TE, Zwienerberg-Lee M, Kun LE, Boop FA (2009) Advances in surgical techniques for resection of childhood cerebellopontine angle ependymomas are key to survival. *Childs Nerv Syst* 25(10):1229–1240
3. Constantini S, Cotev S, Rappaport ZH, Pomeranz S, Shalit MN (1988) Intracranial pressure monitoring after elective intracranial surgery. A retrospective study of 514 consecutive patients. *J Neurosurg* 69(4): 540–544
4. O'Brien M, Krisht A Chapter: 26. Cerebellar astrocytomas. In: Cheek WR (ed) (1994) *Pediatric neurosurgery*, 3rd edn. Philadelphia: WB Saunders, pp 356–331
5. Lieberman DM, Russo CL, Berger MS (1994) Brain tumor during the first 2 years of life. In: Albright AL, Pollak IF, Adelson PD (eds) *Principles and practice of pediatric neurosurgery*. Albright AL, Pollack IF, Adelson PD (Eds.). New York, NY: Thieme, pp 476–481
6. Taylor WA, Todd NV, Leighton SE (1999) CSF drainage in patients with posterior fossa tumors. *Acta Neurochir (Wien)* 117(1–2):1–6
7. Badr A Ishak, Zehava L Noah Chapter 17: Neurologic intensive care. In: Batjer HH, Loftus CM (eds) (1999) *Textbook of neurological surgery: Principles and Practice* Philadelphia: Lippincott Williams and Wilkins, pp 509–517
8. Warnick RE Chapter 50: Surgical complications and their avoidance. In: Youmans (ed) (2004) *Neurological*

- surgery, 5th edn. Saunders (Elsevier), Philadelphia, pp 931–940
9. Maher C, Friedman JA, Raffel C (2004) Chapter 71: Posterior fossa tumors in children. In: Batjer HH, Loftus CM (eds) Textbook of neurological surgery. Principles and Practice. Philadelphia: Lippincott Williams and Wilkins, pp 989–993
 10. Abmed KM, Chiocca EA Chapter 60: Surgical management of cerebellar astrocytoma in adult. In: Shmideck HH, Roberts DW (eds) (2005) Operative neurosurgical techniques, 5th edn. Philadelphia: WB Saunders, pp 878–880
 11. Steinbok P, Hentschel S, Cochrane DD, Kestle JR (2005) Value of postoperative surveillance imaging in the management of children with some common brain tumors. *J Neurosurg* 84(5):726–732
 12. Saunders DE, Phipps KP, Wade AM, Hayward RD (2005) Surveillance imaging strategies following surgery and/or radiotherapy for childhood cerebellar low-grade astrocytoma. *J Neurosurg* 102(2 Suppl):172–178
 13. Campbell JW, Scott RM Chapter 235: Cerebellar astrocytoma in children. In: Youmans (ed) (2004) Neurological surgery, 5th edn. Saunders (Elsevier), Philadelphia, pp 3658–3661
 14. Leland Albright Posterior fossa tumors (2004). In: Berger MS (ed) (1992) Pediatric neurooncology. Neurosurgery Clinics of North America, WB Saunders, Philadelphia, pp 881–891
 15. Chapter 26: Cerebellar astrocytomas. In: Albright AL, Pollak IF, Adelson PD (eds) (1999) Principles and practice of pediatric neurosurgery. New York, NY: Thieme, pp 652–662

Pietro Spennato, Anna Dolcini, Alessandra Alifuoco,
and Giuseppe Cinalli

Children who underwent posterior fossa tumor surgery are complex patients, and, in almost all cases, they need postoperative monitoring in an intensive care unit. They are, in fact, at high risk of hypotension, hypoxia, and intracranial hypertension.

Following the surgical procedure, they remain intubated and ventilated and are transferred to an intensive care unit (ICU) for extubation at a later time. In our department, during prone position surgery, a wire-reinforced endotracheal tube is usually used. It is necessary to replace this tube with a conventional tracheal tube, in order to reduce pressure sores during prolonged intubation and artifacts on postoperative MRI.

Most patients will be successfully extubated within the first 24 h postoperatively. Before awakening, MR imaging of the brain is obtained, to assess extension of surgery and presence of complications and brainstem edema that may affect respiratory and cardiovascular systems. In these cases sedation will be prolonged, until resolution of brainstem edema, as assessed by MRI obtained 3–4 days later.

Benefits of continuing postoperative intensive care are [1]:

1. Airway protection
2. Metabolic, water, and electrolyte balance
3. Optimal balance of blood gases
4. Hemodynamic stability
5. A good level of analgesia and sedation

In neurosurgical patients, these benefits overcome the benefits of immediate extubation: it has been reported that in case of manipulation of critical brain areas, cardiovascular stability with tight ventilation control may increase the chances of an optimal recovery. Sedation is also advised in patients with raised intracranial pressure (ICP) or in whom ICP is expected to increase following operation [1].

The use of short-acting anesthetic agents (e.g., desflurane and remifentanyl) may allow rapid assessment of the level of consciousness and ability to protect the airway. Patients may be easily sedated again if extubation criteria are not met. In our center, analgo-sedation is maintained with midazolam and remifentanyl. Postoperative analgesia, following awakening,

P. Spennato, M.D.
Division of Pediatric Neurosurgery,
Department of Neuroscience, Santobono-Pausilipon
Children's Hospital, Naples, Italy
e-mail: pierospennato@gmail.com

A. Dolcini • A. Alifuoco
Division of Anesthesia and Intensive Care,
Santobono-Pausilipon Children's Hospital,
Naples, Italy

G. Cinalli, M.D. (✉)
Division of Pediatric Neurosurgery,
Department of Neuroscience, Santobono-Pausilipon
Children's Hospital, Naples, Italy

Department of Neurosurgery,
University of L'Aquila, L'Aquila, Italy
e-mail: giuseppe.cinalli@gmail.com

is obtained with intravenous infusion of ketorolac and tramadol, associated with ondansetron and proton pump inhibitors.

61.1 Monitoring

Hypoxia and hypotension are the two most important insults following brain damage. Therefore, oxygen saturation by pulse oximetry and blood pressure are continuously monitored. Although evidence is lacking, continuous intra-arterial blood pressure monitoring is preferable because even short periods of hypotension may compromise cerebral perfusion and oxygenation. The arterial partial pressure of CO₂ (PaCO₂) is an important determinant of cerebral blood flow (CBF) [2].

Three additional parameters must be monitored closely: temperature, glucose, and sodium. Both hyperthermia and hyperglycemia are associated with poor outcome in patients with cerebral insults.

Rapidly changing sodium levels may lead to fluid shifts across the blood-brain barrier, and severe hyponatremia may trigger seizures. In neurosurgical patients, hyponatremia can be attributed to syndrome of inappropriate antidiuretic hormone secretion (SIADH) or to salt-wasting brain syndrome. The former causes hyponatremia resulting from excessive water retention, whereas the latter is characterized by hyponatremia, polyuria, and dehydration. Hypothalamic-pituitary axis tumors may course with both complications, whereas other tumors, including posterior fossa tumors, most commonly course with SIADH. Hydrocephalus and its treatment (endoscopic third ventriculostomy) may also be responsible of a hypothalamic damage and electrolyte imbalance. Differential diagnosis between these two clinical conditions is fundamental, since treatment is completely different: in SIADH, due to an excess ADH secretion, the patient should be kept in fluid restriction (approximately 70 mL/100 kcal). Depending on volume status, loop diuretics (furosemide) and/or increased sodium supply may be prescribed. In the salt-losing syndrome,

volume replacement with an isotonic solution and increased sodium supply are necessary, given the severe dehydration risk [3]. Clinical and laboratory criteria for differential diagnosis reflect the dehydration state that characterizes the salt-wasting brain syndrome and the water intoxication that characterizes SIADH: fluid balance is zero or slightly positive in SIADH, negative in salt-wasting syndrome; hematocrit and serum albumin are normal in SIADH, increased in salt-wasting syndrome; and jugular venous distention is present in SIADH, absent in salt-wasting syndrome.

Usually ICP is not monitored after tumor resection, unless an external ventricular drainage is inserted perioperatively.

61.2 Drugs

Surgical handling of the central nervous system may cause perilesional edema. Postoperative systemic corticosteroid use is usual in pediatric neurosurgery aiming to reduce complications; however, there is no evidence warranting a benefit from the use of these drugs. Mannitol is often used in the postoperative period.

Risk of postoperative bacterial meningitis is low following brain surgery. Usually only intraoperative prophylaxis is administered during brain surgery.

Most cases presenting with postoperative fever have no etiological or topographical diagnosis of infection, and they are cause for warning and exhaustive clinical and laboratory investigation for better understanding of the subject.

Following posterior fossa surgery, seizure prophylaxis is not routinely utilized.

61.3 Intensive Care Unit Discharge Criteria

Before safe transfer to the general neurosurgical ward is considered, a number of criteria must be met as reviewed by Pritchard and Radcliff [4]. The patient must have a patent airway with protective reflexes present and oxygen saturations

maintained at an appropriate level (usually above 95 %), with oxygen as necessary. Breathing must be spontaneous and regular, pulse and blood pressure within normal levels, and invasive arterial monitoring and unnecessary venous cannulae removed. Neurologically, the patient must have an appropriate GCS assessment, with no acute reduction or asymmetry in limb power and no new or unexplained pupillary changes. The patient should have effective analgesia, antiemetics, and intravenous fluids prescribed and temperature lying within normal limits.

References

1. Lowes T, Wright J (2006) Anaesthesia and postoperative ventilation. *Curr Anaesth Crit Care* 17:43–53
2. Pfister D, Strelbel SP, Steiner LA (2007) Postoperative management of adult central neurosurgical patients: systemic and neuro-monitoring. *Best Pract Res Clin Anaesthesiol* 21(4):449–463
3. Mekitarian Filho E, Carvalho WB, Cavalheiro S (2012) Perioperative patient management in pediatric neurosurgery. *Rev Assoc Med Bras* 58(3): 388–396
4. Pritchard C, Radcliff J (2011) General principles of postoperative neurosurgical care. *Anaesth Intensive Care Med* 12(6):233–2011

62.1 Introduction

Complications after posterior fossa tumor surgery are common [1]. Estimates of 32–62 % of children are reported in case series to experience some form of complication after surgery [2–4]. Although frequently these complications are mild or transient, they can still lead to discomfort and delayed hospital discharge. More serious complications will cause prolonged discomfort and disability or even death.

Reducing the incidence and severity of surgical complications is thus integral to improving outcomes for children with posterior fossa tumors. One of the outcome goals of a comprehensive posterior fossa tumor treatment program, which includes surgery as one of the major treatment modalities, is to optimize the “quality of survival” of the children, rather than just the length of their survival. The concept of quality of survival takes account of the children’s level of disability and discomfort, as well as the more established and readily observable measure of length of survival, in judging whether surgery and the overall treatment program are a “success.” In order to reduce surgical complication rates, the predisposing risk

factors and etiological mechanisms for these complications need to be identified along with potential methods of mitigating these risks.

The goal of reducing surgical complications cannot be seen in isolation from other established goals of surgical management: relieving deficits and disability caused by the tumor itself, optimizing the use of adjunctive treatments such as chemotherapy and radiotherapy (each of which causes their own adverse effects and disability), and achieving long-term recurrence-free survival. There is often a trade-off between these surgical goals, that is, the need to balance the benefits and the harm of surgery in any one child. This is most clearly seen in diffuse intrinsic brainstem glioma, in which surgical treatment is limited due to the unacceptable risk of injury including life-supporting structures. On the other hand, the goal for surgery in a child with a malignant tumor in a more accessible area (e.g., ependymoma) may be gross total resection to improve the length of recurrence-free survival, at the cost of more post-operative neurological deficits (e.g., bulbar weakness causing dysphagia and apnea) due to the extent of surgery required. Therefore, what in isolation may be considered a risk factor for surgical complication (extent of resection) may well be a beneficial factor for overall tumor treatment effectiveness. The desire to maximize treatment effectiveness in terms of surgical resection while simultaneously avoiding surgical complications has been the motivation to develop preoperative surgical planning, perioperative anesthetic and nursing care, and intraoperative monitoring technology.

R. Kumar, M.D. (✉) • C. Mallucci, M.D.
Department of Neurology, Alder Hey Children’s
NHS Foundation Trust, Eaton Road,
Liverpool L12 2AP, UK
e-mail: ram.kumar@alderhey.nhs.uk;
Conor.mallucci@alderhey.nhs.uk; cons@msu.com

In this chapter, we summarize what is known regarding complications following posterior fossa tumor surgery in children. The focus is on those complications and related issues which are most specific to posterior fossa tumor surgery rather than generic complications of any cranial surgery. In line with the earlier discussion, for each complication we attempt to identify predisposing risk factors and methods for reducing these risks, accepting that much of the evidence is of low validity.

To complement the practical issues on individual complications, we first provide a brief theoretical overview of the study of complications of treatments drawing in analogies from the more established work on patient safety and adverse effects in pharmaceutical treatments. We finish this chapter with a discussion on practical ways forward in monitoring surgical complications as part of clinical quality improvement of posterior fossa tumor treatment in children.

62.2 Theoretical Considerations on Surgical Complications

In this section we provide some general theoretical considerations on definitions of surgical complications and related issues, with some illustrative examples relevant to posterior fossa tumor surgery in children. This will inform more detailed discussions in the following section on individual surgical complications and assessing the literature on predisposing risk factors and means of mitigation. At the outset, we emphasize that the purpose of this section is not to aid in the management of any individual child at the point of care. Rather, the goal of this section is to aid in case reviews (including medicolegal cases), tumor surgery program quality improvement, and future research.

62.2.1 What Is a Complication? Reliability and Validity Issues

It may seem self-evident what a surgical complication is. Indeed in published series on surgical outcomes of posterior fossa tumors, the inclusion and exclusion criteria for what constitutes a complication are rarely stated. The result is reduced reliability and validity of the conclusions

Table 62.1 List of potential complications of posterior fossa tumor surgery in children

<i>Neurological syndromes</i>
Prolonged coma
Posterior fossa syndrome/cerebellar mutism
Dysphagia including lower cranial nerve palsy
Dysarthria
Apnea and other neuro-respiratory disturbances
Vomiting
Ataxia
Limb weakness
Diplopia and other visual disturbances
Hearing loss
Facial weakness
Headache and pain
Cognitive-affective dysfunction
<i>Regional complications</i>
CSF leak
Pseudomeningocele
Hydrocephalus progression
Intracranial hemorrhage and infarction
Cerebellar edema
Meningoencephalitis
Superficial and deep wound infection
<i>Systemic complications</i>
Hemodynamic instability
Systemic infections including urinary and pulmonary infections
Deep vein thrombosis
<i>Salient events and "rescue treatments"</i>
Unplanned return to theater
Unplanned admission to intensive care unit
Prolonged intubation
Gastrostomy requirement
Large volume blood transfusion
Prolonged length of stay in hospital

to be drawn from the published literature on the incidence rate and risk factors for some important posterior fossa tumor surgical complications. We discuss below some further challenges to the reliability and validity of the data on surgical complications which are essential to take into account. This is particularly important if the aim is to compare the reported outcomes of individual neurosurgeons and institutions performing posterior fossa tumor surgery in children.

A simple definition of a surgical complication is an unwanted event, problem, or clinical syndrome (cluster of signs or symptoms) caused by surgery. Table 62.1 is a list of the commonly

Table 62.2 Potential pathophysiological mechanisms underlying neurological complications. Multiple mechanisms are likely to be present in any individual child

Pathophysiological mechanisms	Examples
Global cerebral ischemic injury	Raised intracranial pressure, systemic hemodynamic instability
Focal ischemic-contusion injury	Retraction, edema, vasospasm
Direct tumor-related focal injury	Invasion, hemorrhage
Direct local injury by surgery	Neurotmesis
Remote injury mechanisms	Diaschisis, transsynaptic degeneration

described events and syndromes that can be caused by posterior fossa tumor surgery, categorized according to whether they are neurological, regional, or systemic in nature.

The definition may include complications due to closely related interventions to surgery, for example, general anesthesia – this may be implied by using the more general term “postsurgical complications.” Clinical events and “rescue treatments” such as unexpected return to theater can also be considered a sentinel feature of a complication having occurred and can be useful in monitoring purposes (see section 62.3).

The complication may be reported as an externally observable clinical syndrome (e.g., prolonged coma, CSF leak, posterior fossa syndrome, and dysphagia) or the pathophysiological etiological mechanism that led to the clinical syndrome. The etiological mechanism may be observable only using investigations such as radiology or detailed examination (e.g., edema, hydrocephalus decompensation, hemorrhage, cranial nerve lesion). These distinct categories of complications – mechanisms and clinical syndromes – are often conflated but should be distinguished. Table 62.2 lists the most common etiological mechanisms along with syndromes they can cause.

As an example, a clinical syndrome such as dysarthria can arise from multiple causative mechanisms such as direct cranial nerve section (neurotmesis) or parenchymal edema causing transient dysfunction of the brainstem cranial nerve nuclei. These have different implications for avoidance,

early management, and prognosis for recovery. Clinical syndromes are also more readily observed than etiological mechanism and are thus more likely to be accurately recorded in some situations. For example, dysphagia as a clinical syndrome is more likely to be recorded as a complication in a questionnaire-based survey or retrospective case note-based review of complication rates than an underlying bulbar cranial nerve lesion which would require formal neurological or speech therapist examination in a prospective study design. A related issue is that clinical symptoms which are not accompanied by observable signs such as pain may be under ascertained, for example, surgical incision site pain, allodynia, and taste disturbance.

Some authors include in their definition that a complication should be an unexpected event [1]. Using this criterion, events are excluded as complications if they are held to be unavoidable and thus are accepted as part of the postoperative course. The “unexpectedness” of an event is however a somewhat subjective assessment and this is likely to lead to further systematic bias. Without a reliable definition of “unexpectedness,” events or problems that may be expected postoperatively but are nevertheless more severe than expected may not be noted as a surgical complication even if they are potentially avoidable. An example is ataxia, which is a typical presenting sign of the tumor, but often unquantified in its severity. The ataxia may be more severe or qualitatively different after surgery, for example, the child may be able to walk with ataxia pre surgery, but unable to even sit independently post surgery. It should also be noted that a postoperative problem simply being expected does not mean it is unavoidable with appropriate refinements in surgical technique, preoperative planning including use of alternative nonsurgical strategies, etc. Accepting the problem as unavoidable a priori runs the danger of becoming a self-fulfilling prophecy and lack of innovative solutions.

The final related issue that impacts on reliability is deciding that the postoperative problem was caused by the surgery, since this is part of the definition of a complication. Causality is usually assigned by “global introspection,” that is, informal and unstructured personal judgment based on the evidence at hand. The evidence for surgery being the cause of a problem noted in a child who is assessed some time later is not always clear. The distinction

between an unwanted event following but unrelated to surgery and thus not a complication (e.g., a symptom of the natural progression of the tumor) and one due to surgery itself is not always straightforward. Causation may be inferred by factors such as how specific the clinical syndrome or event is to the postoperative situation. A clinical syndrome or event that is not seen as a presenting sign of the untreated tumor and is not seen following other treatments (e.g., radiotherapy) independent of surgery is more likely to be considered a surgical complication. An example is posterior fossa syndrome which is a qualitatively specific syndrome seen after posterior fossa surgery. On the other hand, where a postoperative syndrome is similar to the presenting features of the untreated tumor or the complications of another treatment, that is, it has low specificity as a surgical complication, it may not be considered to be a complication. An example is persistent postsurgical vomiting; this, in our experience, can be a debilitating problem which is underreported as a surgical complication in the literature. This underrecognition as a complication is presumably because vomiting appears similar to the presenting features of a posterior fossa tumor and vomiting is also a complication of radiotherapy and chemotherapy that the children often receive following surgery.

62.2.2 Methods of Improving Reliability and Validity: Lessons from Medicines Regulation and Adverse Drug Reactions

There are useful lessons to be drawn on how to improve reliability and validity of identifying surgical complications from analogous work in medicines regulation on adverse drug reactions. By analogy, a surgical complication can be regarded as an “adverse surgical reaction.” In European

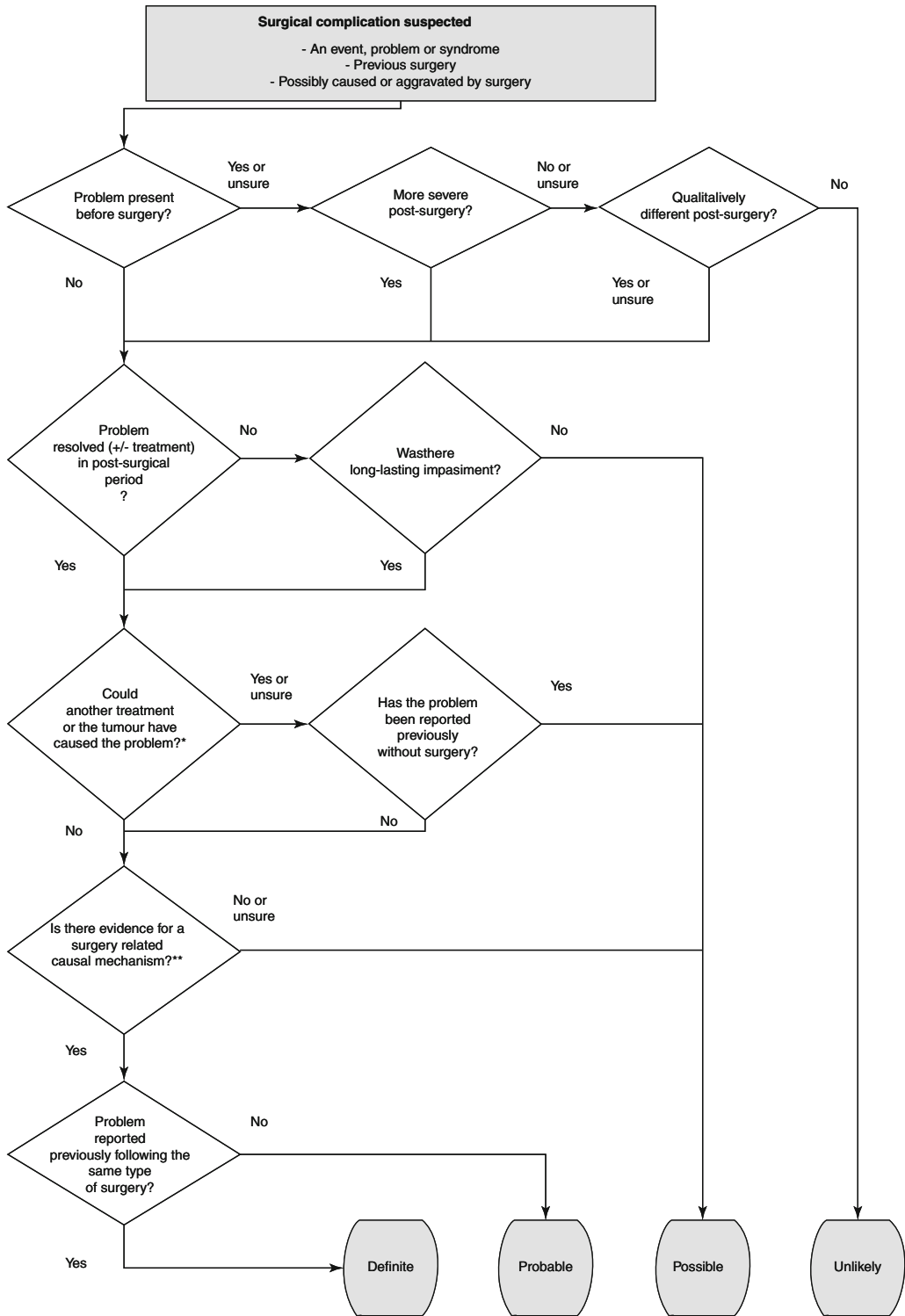
medicines regulation for human drug trials, there is a two-step process to identifying a suspected adverse drug reaction: first identify if an adverse event not necessarily caused by the drug has occurred, and then identify if the adverse event is caused by the drug, that is, an adverse drug reaction. Additional formal definitions are provided from medicines regulatory agencies to decide whether the adverse reaction is serious and unexpected.

Applying these ideas from the medicines regulation to the study of surgical complications, we propose that all adverse events following surgery should be recorded prior to deciding whether or not they are expected or a complication of surgery. A serious adverse event can be defined as one that is life threatening, results in prolongation of hospitalization, or results in significant disability without additional corrective treatment. We also propose that surgical complications should include expected and unexpected adverse events due to surgery. From a practical point of view, expected complications would be those which are listed as common or serious (based on current knowledge) in a patient/parent information sheet provided as part of consent prior to surgery. This corresponds to the definition of an unexpected adverse drug reaction as a reaction that is not described in the product information for the drug.

There are also lessons to be applied from medicines research to improve on the subjective nature of determining causality, that is, whether the adverse postoperative event is caused by surgery. An ongoing research in our institution on adverse drug reactions in children has led to the development of a decision analysis tool in the form of a flowchart with the aim of improving the reliability and validity of the judgment on whether a drug caused an adverse event. We have developed an analogous decision analysis tool for determining causality in adverse events following surgery, the Liverpool Neurosurgical Complication Causality Assessment Tool (Fig. 62.1).

Fig. 62.1 A proposed causality assessment tool to identify whether an event or syndrome identified in a child following brain tumor surgery may be a surgical complication (Reproduced by permission Copyright © 2011 Alder Hey Children’s NHS Foundation Trust). *Notes:* *Examples: intervening adjunctive treatments (e.g., radiotherapy and

chemotherapy) prior to the problem being noted; problem more characteristic of adjunctive treatment than surgery (e.g., hearing deficit in non-cerebellopontine angle tumors).**Examples of evidence: radiology (MRI T2 hyperintensities in areas consistent with neurological deficit), neurophysiology (EMG revealing acute denervation), re-exploration surgery findings



The tool is yet to be validated, and we emphasize that the purpose is not for point-of-care use in the individual child, but rather to improve concordance between individual reviewers of a case and research workers on whether an adverse event is a surgical complication.

The causality tool provides a structured decision process involving the following key questions:

1. Was the problem present prior to the surgery?
2. If so, did it worsen or change qualitatively after surgery?
3. Is the problem specific to the postsurgical situation or can it be caused by other treatments or the tumor itself?
4. Is there evidence of a basic causal mechanism by which surgery caused the problem in this child?

Depending on yes or no answers, and taking into account that it may not be possible to answer these questions with the patient information available, the case is categorized into one of the following causality groups: unlikely, possible, probable, and definite surgical complication.

Illustrative examples of problems where these questions arise following posterior fossa tumor surgery are hydrocephalus, ataxia, and vomiting. These are very common presenting features of posterior fossa tumors, for example, 71–90 % of posterior fossa tumors have hydrocephalus at presentation [5]; 90 % of children with infratentorial tumors had ataxia [6]. Vomiting can also be caused by adjunctive treatments such as analgesia, radiotherapy, and chemotherapy. Thus, hydrocephalus, ataxia, and vomiting noted after surgery have low specificity for being considered surgical complications, in contrast to problems such as posterior fossa syndrome and CSF leak which are very specific to being surgical complications. However, hydrocephalus, ataxia, and vomiting can worsen following surgery (e.g., ataxia but able to walk pre surgery, ataxia with inability to sit or stand post surgery) indicating that these may be surgical complications. There can also be qualitative changes in syndromes present before surgery, for example, vomiting may be positioning provoked after surgery limiting rehabilitation,

rather than the early morning non-positioning-related vomiting that was present prior to surgery. Often these quantitative and qualitative changes in syndromes are not recorded. At best these problems are marked only as being present or absent; thus, there is insufficient information to judge if problems worsened after surgery. In this situation, other supporting evidences must be used to decide if these problems were surgical complications. This could include postoperative CT or MRI scan demonstrating hemorrhage or signal abnormalities consistent with surgical injury to key anatomical structures, for example, deep cerebellar nuclei related to vestibular function and balance.

Some postoperative syndromes will still be difficult to allocate causality to surgery and thus may not be considered a surgical complication even using the causality tool. This is important if modifications to surgical technique could reduce the severity of problems that can cause persistent disability, that is, avoidable problems. This is often the case with syndromes that cause “invisible” or “silent” deficits, that is, problems that are not externally visible and require detailed assessment. An example is higher cognitive function deficit, for example, the cerebellar cognitive-affective syndrome. These silent deficits may not be evident in the early postoperative period and if they have not been assessed in detail prior to surgery. For example, preoperative detailed cognitive assessment is often not possible because of the child’s age or degree of obtundation [2]. There may be intervening treatments after surgery, such as radiotherapy, given before the problem comes to light which obscure judgment on what portion of the silent deficit is specifically due to modifiable surgical factors [3].

Using the systematic methods described above of defining and identifying complications will be essential to improve the current rather poor evidence base on risk factors, described in the following section. A benefit of reconciling the definitions of adverse reactions/complications in medicines research with that in surgery is that it will aid in future comparative

effectiveness research studies comparing surgery against pharmaceutical treatments for posterior fossa tumors.

62.3 Complications After Posterior Fossa Tumor Surgery: Risk Factors and Presenting Features

In this section, we discuss the surgical complications (Table 62.1) with a focus on those most specific to posterior fossa tumors in children, their predisposing risks and potential means of mitigation. In Table 62.1, we have used a widely recognized categorization of neurosurgical complications: neurological, regional, and systemic complications. The neurological and regional complications are those most specific to posterior fossa tumor surgery; thus, we do not provide a detailed description of the general risks of surgery and anesthesia although these are of course of major importance, for example, blood loss; obtundation; chest, skin, and urine tract infections in the postoperative period. Many of these systemic complications will account for the additional complication category of “salient events” and “rescue treatments” we have introduced in Table 62.1. “Salient events” include events such as unplanned admission to intensive care for resuscitation and unplanned return to theater within the initial postoperative period to deal with a regional complication such as CSF leak. The concept of a “rescue treatment” is that it is an additional postoperative procedure that was required to prevent an established complication from causing greater injury or death, for example, large volume blood transfusion from intraoperative blood loss in an infant. The rescue treatment may itself lead to iatrogenic harm.

Before discussing the individual complications in detail, we first provide an overview of the relevant predisposing and causative factors. Much of this has been covered in the earlier individual chapters on the different tumor histologies and the chapters on surgical approaches and intraoperative monitoring which have been moti-

vated by the need to reduce surgical complications. The aim is to draw comparisons and contrasts in the specific complications across these areas of work. For the majority of presumptive risk factors, we are not able to provide absolute and relative risk figures for the complications, given the lack of reliable study design. Only a minority of studies are prospective consecutive cohort with predefined operational definitions for the risks and complications and both presurgical and post-surgical assessment. Where the frequency of postoperative complications is stated, this presumably indicates systemic complications and other neurological and regional complications evident in the early postoperative period. Figures of 35–42 % appear to be common for postoperative complications after posterior fossa tumor surgery in children [3, 4].

62.3.1 Risk Factors for Complications

The main categories of risk factors and potential mitigating factors for surgical complications are shown in Fig. 62.2. These factors are not independent of each other, but rather are codependent, for example, surgical approach routes are dependent on the location of the tumor, which is related to the tumor histology.

As discussed in the preceding section, unless there has been a detailed preoperative assessment, it is not always clear from reviewing the literature whether a neurological finding after surgery was caused by the tumor itself or by the surgery. Given the interrelated nature of the risks, for example, large tumors distorting the regional anatomy and thus predisposing to further surgical injury, both tumor-related factors and surgical factors will need to be considered together.

The predisposing risk factors for complications are important to consider for a number of reasons:

1. At a practical level, it allows the neurosurgeon to counsel the child and parent appropriately regarding the nature and likelihood of complications as part of informed consent.

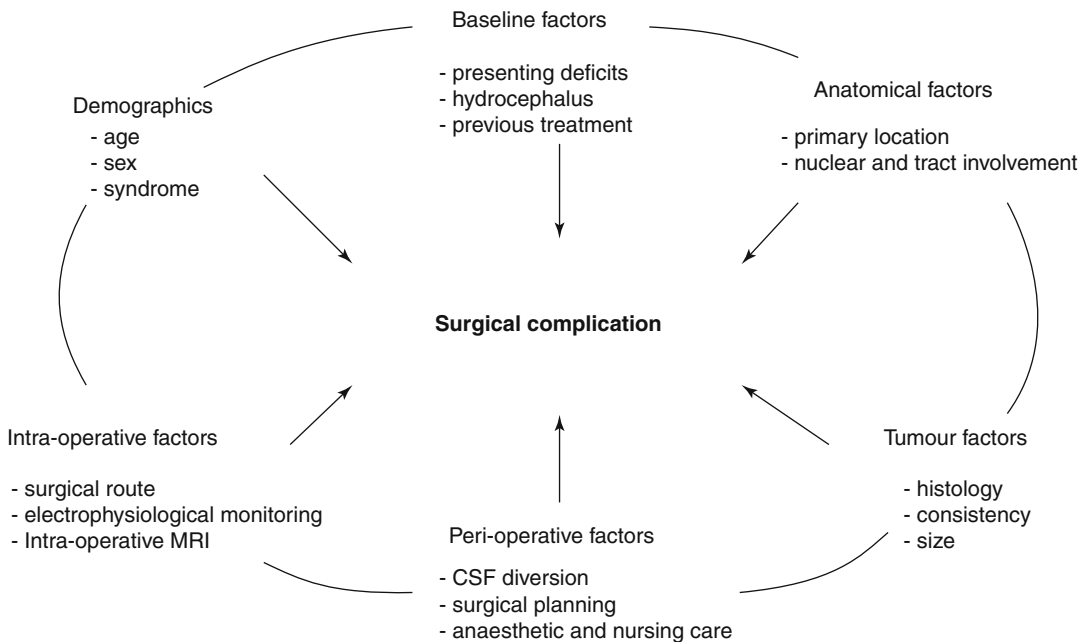


Fig. 62.2 The broad categories of predisposing risk factors and mitigating factors for surgical complications in posterior fossa tumor surgery

- More generally, it allows consideration of whether complications are modifiable, using, for example, mitigating techniques such as preoperative planning and intraoperative monitoring. In Table 62.3, we highlight examples of how risk factors for complications may be modified.
- Risk factor adjustment (“adjusting for case-mix”) is also necessary if surgical complication rates are to be validly monitored and compared across surgeons and provider institutions.

62.3.1.1 Tumor Type, Location, and Surgical Approaches as Risk Factors

The anatomical location of a tumor is closely related to the specific neurological and regional complications likely after surgery, as indicated in Table 62.3. This relates to surgical injury to the neighboring structures during resection such as the eloquent cerebellar cortex, nuclei, white matter tracts, and blood vessels. In terms of the neurological deficits caused by the tumor as opposed to that due to surgery, a slow-growing lesion due to a tumor is likely to have distinctive compensatory plastic

alterations in the normal surrounding brain compared to the rapid lesion induced by surgery. The compensatory plastic alterations in the surrounding brain may be a mechanism for the late presentation of large cerebellar tumors with minimal “cerebellar signs,” often only when the accompanying hydrocephalus decompensates.

Both the primary site of the tumor and the anatomical areas of extension also need to be considered for predicting the neurological and regional complications. The primary sites of the tumor can be categorized as the midline cerebellar vermis including floor of the fourth ventricle, cerebellar hemisphere, brainstem including diffuse and focal exophytic, and extrinsic including cerebellopontine angle tumors as well as other specific cranial nerve-related tumors. Extension may occur from the primary site: for example, from the cerebellar hemisphere to the midline or along one of the middle cerebellar peduncles, a midline tumor may cause splaying of bilateral cerebellar peduncles or invade the brainstem. These areas of involvement by extension are additional predictable risks for postoperative deficits. There is a predilection of

Table 62.3 Examples of associations between specific risk factors and complications, with potential interventions to mitigate or prevent these complications from occurring

Risk factors	Examples of risk complications	Potential mitigating interventions
<i>Baseline presenting features</i>		
Age	Infants have higher risk of hydrocephalus progression	Preoperative CSF diversion
Previous treatment (e.g., surgery, radiotherapy)	Infections, wound breakdown, hemorrhage	Achieve definitive surgery first time, intraoperative MRI
Hydrocephalus	CSF leak	Preoperative CSF diversion
Length of history	Invasion and extension of tumor, hydrocephalus	Earlier diagnosis
<i>Tumor location</i>		
Midline cerebellum and floor of the fourth ventricle	Posterior fossa syndrome/cerebellar mutism, hydrocephalus progression, truncal ataxia, vomiting	Surgical approaches including avoiding retraction
Cerebellar hemisphere	Appendicular ataxia, focal cognitive deficits	Surgical approach
Peduncle involvement	Increased risk of ataxia (unilateral) or posterior fossa syndrome (bilateral)	Preoperative and intraoperative monitoring
Cerebellopontine angle involvement	Hearing loss (unilateral), vertigo, facial palsy, facial sensory disturbance, bulbar palsy (dysphagia)	Intraoperative electrophysiological monitoring
Brainstem	Bulbar palsy (dysphagia), obstructive and central apneas, peripheral motor weakness	Intraoperative electrophysiological monitoring, limiting goal for extent of resection
<i>Tumor characteristics</i>		
Vascularity (e.g., choroid plexus tumors, cystic astrocytoma)	Hemorrhage	Preoperative embolization, chemotherapy, hemostasis
Size	Potential for retraction injury for large tumors	Retraction techniques, modified surgical approach
<i>Operative techniques</i>		
Intracranial access	CSF leak rate may be higher with craniectomy than craniotomy	Craniotomy, address hydrocephalus preoperatively, closure technique
Extent of resection/goal of resection	Gross total resection requirement (e.g., ependymoma) may predisposes to more neurological sequelae	Multidisciplinary presurgical treatment planning
Surgical approach	Retraction injury, cerebellar incision with nucleus and tract injury, skull base surgery with lower cranial nerve injury	Preoperative planning and intraoperative monitoring

specific tumor histologies for certain anatomical sites as detailed in earlier chapters, for example, ependymoma predilection for the lateral recess of the fourth ventricle and extension to the cerebellopontine angle and medulloblastoma predilection for the midline cerebellar vermis. Thus, there are associations between certain tumor histologies and specific postoperative complications.

For tumors of the midline cerebellar vermis and floor of the fourth ventricle or extension to

these areas from a primary hemispheric site, a common regional complication is progression of hydrocephalus, which is already present prior to surgery in the majority of children. The most characteristic neurological complication for a tumor in this location is posterior fossa syndrome/transient cerebellar mutism [7–9]. The extension of the tumor to involve the middle cerebral peduncles, brainstem invasion, and brainstem compression appear to be additional risk factors.

Posterior fossa syndrome (PFS) in its florid form remains an uncommon encountered sequela with approximately 25 % of patients detected in prospective series of varying cerebellar tumors [8, 10]. More frequent neurological complications for midline cerebellar tumors include worsening of gait ataxia and truncal instability, dysarthria including slow speech, dysphagia, prolonged vomiting independent of dysphagia, and gaze disturbances worsening diplopia [3, 4]. These neurological syndromes are likely to be related to injury to the deep cerebellar nuclei and proximal efferent cerebellar pathways in the peduncles to structures in the brainstem and thalami [11, 12]. The injury to the inferior vermis and dentate nuclei is related to worse neurocognitive outcomes [3]. Postoperative facial weakness and dysphagia may be more likely if there is brainstem invasion or adherence. These sequelae may be due to injury to the cranial nerve nuclei beneath the floor of the fourth ventricle (facial colliculus, sixth nerve, and hypoglossal nerves) during resection including the use of ultrasonic aspiration. However, this type of bulbar weakness can be expected to resolve, unlike cranial nerve lesions seen after resection of extrinsic tumors involving the cranial nerves themselves.

Modifications of surgical approaches have been suggested to avoid these neurological complications presumably caused by injury to the deep cerebellar nuclei and inferior vermis. Incision of the vermis, whether superior and inferior, and vermis resection for subvermian and transvermian approaches were previously thought to cause the posterior fossa syndrome (Pollack et al.). However, paravermian incisions and the telovelar approach (incision of the cerebellomedullary fissure) have not prevented these neurological complications including the posterior fossa syndrome occurring completely even if there has been an apparent reduction in frequency [13]. This may relate to the size of the tumor, with larger tumors of the fourth ventricle still requiring retraction causing concussive injury of sensitive structures such as the dentate nuclei and the cerebellar peduncles, which are already distorted by the tumor [14]. Additional attention to reducing retraction-related injury may reduce the neurological complications

above. Intraoperative neurophysiological monitoring and navigation techniques are likely to be useful to reduce the risk of neurological complications for tumors involving the floor of the fourth ventricle (see discussion below).

Cerebellar hemisphere tumors appear less likely to produce overt neurological and regional complications. Hydrocephalus progression is less common than for midline tumors unless the tumor is large enough to involve the brainstem. The most characteristic tumor histology at this site is astrocytoma. Pilocytic astrocytoma is usually cystic and readily resectable, predisposing to low risk of additional neurological complications although cystic tumors have higher risk of hemorrhage. Fibrillary astrocytomas may show extension into the ipsilateral cerebellar peduncle. These are higher risk for complications, due to injury to the cerebellar peduncle such as an increase in limb ataxia and tremor. As predictable given the lateralization of function in the cerebellar hemispheres, right cerebellar tumors are associated with language deficits and left cerebellar tumors with visuospatial deficits although these may well be present prior to surgery [2, 15].

Brainstem tumors of the midbrain, pons, and medulla are often associated with hydrocephalus and multiple cranial nerve deficits at presentation. The main consideration is whether it is feasible to perform resective surgery given the high risk of life-threatening complications due to the life-sustaining (autonomic) functions in neighboring structures. These include cardiorespiratory centers as well as bulbar nerve nuclei and descending motor pathways. Intraoperative cardiovascular instability often occurs during surgery to tumors that invade the brainstem and may limit the extent of resection. Focal enhancing and exophytic tumors are typically resectable, whereas diffuse intrinsic gliomas are not due to such concerns. Intraoperative neurophysiological monitoring is likely to have an increasingly important part to play in reducing neurological complications by identifying relevant nuclei and tracts [16]. Neuronavigation, intraoperative MRI, and ultrasound are additional techniques that are likely to further reduce these complications by improving targeting of the tumor and reducing injury to surrounding normal brain structures.

Tumors of the cerebellopontine angle (CPA) in children are typically ependymomas with extension from the lateral recesses of the fourth ventricle or exophytic brainstem tumors. The main issue for tumors in this site in children is adherence of the tumor to the brainstem and exiting lower cranial nerves and thus the potential for cranial nerve section (neurotmesis) of all the bulbar cranial nerves on one side. The need for complete resection is particularly important for ependymoma to prevent recurrence and mortality in this tumor which is so insensitive to other treatment modalities. This leads to significant problems with postoperative dysphagia and risk of aspiration necessitating tracheostomy and gastrostomy [17]. This predilection of ependymomas to involve the cerebellopontine angle and lateral recess of the fourth ventricle may explain the relatively high incidence of tracheostomy and gastrostomy performed (16 and 28 %, respectively) in Morris and colleagues' series of 96 children with infratentorial ependymoma. Other complications include injury to arterial vessels supplying the brainstem, facial weakness, and sensorineural hearing loss.

Extrinsic tumors of the posterior fossa are uncommon in children. These include vestibular schwannomas involving the facial (seventh) and the vestibulocochlear (eighth) nerves, as well as schwannomas of the ninth nerve around the jugular foramen and fifth nerve schwannomas near the trigeminal ganglion. The potential for additional cranial nerve-specific deficits after surgery is clear, and it is important to identify the degree of deficit prior to surgery. This is most reliably done for hearing and facial weakness, but other important symptoms and signs of facial sensation, lacrimation, taste, dizziness, and tinnitus should also be recorded and the possibility of worsening after surgery discussed [18]. Additional issues may arise from progression of regional problems present prior to surgery including brainstem compression and obstructive hydrocephalus. Specific neurological complications aside from sensorineural hearing loss and facial weakness include nervus intermedius lesion affecting taste, lacrimation dysfunction due to parasympathetic fiber injury, and facial numbness from fifth nerve lesions.

The surgical approach and access route to the brain will depend on factors such as tumor location and nearby critical structures, size of the tumor, and extent of resection required for effective treatment, but will also relate to individual surgeon preference. There may be important differences in complication rates for some approaches compared to others. Suboccipital craniotomy appears to have a lower incidence of postoperative CSF leak than suboccipital craniectomy [19]. Of 110 children with posterior fossa tumors operated on in Gnanalingham and colleagues' retrospective case series, the CSF leak and pseudomeningocele incidence was 24 % and 23 %, respectively, in those who had craniectomy, compared to 4 % and 9 % in those who had craniotomy. For deep-seated tumors in and around the ventral surface of the brainstem, for example, chordomas of the clivus, in the region of crucial vascular and neural structures, specialized skull base approaches tailored to the individual are required. This includes bone removal to create adequate exposure and less risk of direct and retraction injury to the critical blood vessels and cranial nerves, but with consequently increased risk of CSF leak compared to minimally invasive surgery.

62.3.1.2 Other Predisposing and Mitigating Factors

A number of other factors also impact on the risk of complications after surgery (Table 62.3). Some of these risk factors are present at baseline, that is, at diagnosis or prior to involvement of the neurosurgeon in the care of the child. Baseline risk factors include the age and sex of the child, child's general medical condition at presentation including presence of hydrocephalus, and length of history. Some of these baseline risks already present at diagnosis may be preventable although not necessarily directly by the neurosurgical team, for example, earlier community diagnosis of brain tumors may identify children before decompensation of hydrocephalus or distorted anatomy predisposes to additional surgical injury to eloquent structures.

The young age of the child may also be a risk factor for systemic and regional complications, for example, consequences of blood loss are

more problematic in infants. Younger age also appears to be a risk group for hydrocephalus progression after surgery [20]. For children presenting with hydrocephalus, there may be benefit in preventing unexpected postsurgical hydrocephalus progression, for example, in the midst of radiotherapy and chemotherapy that the child may proceed on to after surgery, by performing elective CSF diversion prior to resective surgery [5]. Endoscopic third ventriculostomy as the CSF diversion procedure is associated with lower risk of CSF infection than external ventricular drain and VP shunt.

Prior treatment including for tumor progression or recurrence may be a modifiable risk factor. Distortion of posterior fossa anatomy with scars from previous surgery, wound breakdown and infection risk, and tendency to hemorrhage after previous radiotherapy need to be considered. The solution is for the neurosurgeon to achieve the definitive extent of resection required first time for the most effective overall multimodality treatment of the tumor. This will help to avoid second look surgery with attendant risks as above. This is more likely to be achieved with a combination of multidisciplinary preoperative tumor diagnosis and treatment planning and appropriate intraoperative investigations and adjuncts to surgery. In terms of tumor diagnosis, the more informative the neuroimaging preoperatively (e.g., using relaxometry, contrast enhancement characteristics, and magnetic resonance spectroscopy of the lesion), the more likely that the appropriate surgical strategy can be chosen first time, avoiding the need to change strategy or need for second surgery when the final surgical pathology result dictates a different strategy from that conceived preoperatively. The extent of resection, and risk of neurological deficits associated with gross total resection close to eloquent areas, is determined by this surgical strategy which will also be facilitated by accurate intraoperative histology. Neuronavigation methods should allow minimization of injury during surgical approach to the tumor, although this effect may be more relevant in brainstem tumors rather than fourth ventricle and CPA tumors. Other intraoperative adjuncts to surgery that should aid

in reducing the need for second look surgery include intraoperative MRI (ioMRI) and ultrasound. Preliminary data from our institution has shown (personal communication, CM) that with the use of ioMRI in an initial series of 40 children for tumor resection surgery, further surgery during the same operative session was performed in 27 % of cases prior to waking the patient up. In addition, avoidable return to theater for second surgery within 6 months was analyzed between two equivalent cohorts prior to and since the routine use of ioMRI. A 14 % return for second surgery within 6 months of initial resective surgery was seen in the cohort prior to the use of ioMRI, compared to 0 % in the cohort since the routine use of ioMRI.

62.3.2 Specific Complications and Presenting Syndromes

In this section, we discuss specific complications of posterior fossa tumor surgery with a focus on the neurological and regional complications most relevant to the tumors encountered in childhood. From a practical point of view, the complications can be categorized by the time period following surgery at which they commonly present (Table 62.4). For the neurological complications, we have used the concept of presenting syndromes – clusters of signs and symptoms (e.g., facial weakness) or their functional consequences such as dysphagia and diplopia. This emphasizes the clinical presentation of the complication which is more reliably assessed than the presumed mechanism (e.g., cranial nerve lesion) which is more difficult to verify objectively. Clinical syndromes may result from multiple mechanisms (Table 62.2).

It is important to attempt to identify the underlying mechanism leading to the syndrome since this will impact on treatment or prognosis. For example, dysphagia may result from descending corticobulbar tract edema and contusion or from transection of bulbar cranial nerves – the latter can be expected to be longer lasting than the former. Where the mechanism underlying a syndrome is not currently known (e.g., posterior fossa syndrome), research into identifying the

Table 62.4 Time period after surgery during which specific complications are typically present

Time period after surgery	Complications presenting in time period
Perioperative	Hemodynamic instability, hemorrhage, prolonged coma/obtundation, hydrocephalus, pneumoencephalus
Early (<5 days)	Hydrocephalus, CSF leak, meningitis, most neurological syndromes including: posterior fossa syndrome, ataxia, visual disturbance, dysphagia/bulbar nerve palsy, neuro-respiratory problems, facial palsy, vomiting
Intermediate (<30 days)	CSF leak, meningitis, hydrocephalus progression
Late (>30 days)	Cognitive dysfunction, hydrocephalus progression
Very late	Superficial siderosis

Table 62.5 A checklist for establishing whether a child with an unexpected course in the early postoperative period has a treatable postsurgical complication

Checklist	Comments on diagnostic considerations
1 Review history: prior medical-behavioral problems, allergies, medications	Predisposition to psychogenic syndrome, anaphylaxis
2 Review perioperative nursing and surgical notes	Nonfunctioning CSF diversion, hemostasis, suturing
3 Airway, breathing, circulation, temperature	Hypoxemia, hypovolemia, blood loss, hypothermia, infection, pulmonary embolism
4 Evidence of raised ICP (dilated pupils, raised BP, bradycardia, decerebrate tonic posturing)	Hydrocephalus, herniation, intracranial hemorrhage, pneumoencephalus
5 Focal neurological signs	Cranial nerve section, parenchymal contusion and edema, raised ICP, vascular-ischemic injury
6 Review drug chart: drugs and infusions	Opiate and sedation overdose, analgesia underdose (pain), drug withdrawal
7 FBC, clotting, electrolytes, glucose, blood gas, ammonia	Hypoglycemia, anemia, coagulopathy
8 Infective and inflammatory markers, including CSF	Meningitis, systemic infection
9 CT head	Hydrocephalus, hemorrhage
10 Repeat review and consult other teams	No evident treatable cause

underlying mechanisms will encourage the development of methods to mitigate the risks in the future.

The initial nature of a complication – whether neurological, regional, or systemic – is often not clear, since the presentation may be with nonspecific symptoms and signs such as agitation, reduced interaction, and somnolence or vomiting. In many situations the underlying problem such as raised intracranial pressure, intracranial hemorrhage, or electrolyte disturbances requires urgent intervention to avoid more severe morbidity or even death. In Table 62.5, we provide a general clinical checklist to aid in identification of the underlying problem when faced with a child

presenting with a postoperative complication. A systematic approach such as indicated in Table 62.5 is important to exclude treatable underlying causes of a number of the clinical syndromes discussed below, for example, posterior fossa syndrome which is in essence a diagnosis of exclusion.

62.3.2.1 Neurological Syndromes Prolonged Coma and Altered Behavior

Prolonged unresponsive state and low conscious level after surgery may follow on from an obtunded state prior to surgery (often in association with acute hydrocephalus) or appear de novo after surgery. The child will typically be intubated and ventilated at this stage, and the problem may

only be noted when there is failure of planned extubation. There may be a lucid interval of a few days following surgery before the onset of the decreased conscious level. There is overlap with syndromes of altered behavior such as agitation, aggression, and withdrawal from social contact.

In this situation, following a differential diagnosis process as given, the clinical checklist of Table 62.5 is essential. If systemic causes such as hypoxia and hypoglycemia or regional causes such as hydrocephalus decompensation or meningitis have been excluded, the diagnosis is likely to be a variant of the posterior fossa syndrome [21].

Posterior Fossa Syndrome or Cerebellar Mutism

The posterior fossa syndrome (PFS) is a neurological complication that is characteristic of surgery for certain posterior fossa tumors in children. It is an acute neurobehavioral syndrome consisting of varying degrees of deficits in speech and language, affect, and volitional behavior in individual children. The most readily recognized deficit is the lack of speech output, hence the widely used alternative term “cerebellar mutism” for what is in essence the same condition [7, 22, 23]. The terms “transient cerebellar mutism” and “mutism with subsequent dysarthria” have also been applied to this condition by various authors, although these are diagnostic labels applied in retrospect. In most children, there are striking acute onset alterations of behavior with labile affect, reduced social interaction, and avolition (lack of motivated goal-directed voluntary behavior with preservation of automatic behaviors such as yawning). This altered behavioral state goes beyond the simple characterization of the syndrome as purely that of speech alone as the term “mutism” would imply. Indeed mutism is not seen in all patients who appear to have the same overall neurobehavioral syndrome. There are often other neurological deficits co-occurring with PFS that are not regarded as core components of the syndrome, such as ataxia, dysphagia, urinary retention, apraxia of eyelid opening, visual disturbance, and oromotor dyskinesia. These co-occurring deficits are likely to represent lesions of posterior fossa structures close to those

structures involved more directly in the pathophysiological mechanism of PFS.

The incidence of PFS, although infrequent in its most florid and severe form, appears to be more common than previously suggested. This is clear from more recent prospectively ascertained cohorts than from earlier small retrospective case series. In one prospective questionnaire-based survey of 450 children with medulloblastomas who were participants in one of two multicenter treatment trials, 24 % had the deficits characteristic of posterior fossa syndrome [8]. Of those with PFS, 42 % were judged to be severe based on the degree and persistence of the deficits. This is similar to the 29 % incidence from a prospective single-center cohort of 42 children with a wider range of cerebellar tumors assessed directly by a clinician as having cerebellar “mutism with subsequent dysarthria” postoperatively [7]. It is possible that there has been a true increase in incidence of PFS as a consequence of changing neurosurgical practice, for example, to achieve greater gross total resection rates of the underlying tumor with resultant increased surgical injury to neighboring structures [24].

A striking characteristic of PFS is the timing of onset. The onset is not typically from immediately following surgery, but rather follows a lucid period of between 1 and 2 days, with occasional children described to show onset as late as 5 days after resective surgery. This latent period may be masked by any background obtundation or other needs for intubation and ventilation that the child has because of their condition at presentation, for example, due to hydrocephalus. The latency to onset of the syndrome has led to various hypotheses regarding the underlying etiological mechanism (see below).

It is essential to exclude other more treatable disorders that may mimic PFS such as hydrocephalus progression and meningitis (Table 62.5). Similarly, any additional neurological deficits, such as descending motor tract injuries and cranial nerve palsies which may be primarily responsible for an accompanying dysphagia and limb weakness, need to be identified since this will impact on immediate management (e.g., ceasing oral intake of liquids) and prognosis [4].

The treatment of posterior fossa syndrome itself is currently supportive while awaiting the recovery of functions and rehabilitation for the persisting deficits. The more overt disturbances of behavior, physical dependency, and lack of speech improve over the course of days to months. The less visible deficits may persist much longer, for example, dysarthria which may be recognized as slow speech and more classical ataxic dysarthria [25]. The long-term cognitive problems appear to be consistent with the “cerebellar cognitive affective syndrome” [15, 26].

The pathophysiological mechanism of PFS is not established. Bilateral, multifocal injury to structures in the posterior fossa in the pons and proximal efferent cerebellar pathways (pECPs) appears to be necessary to produce the syndrome [12, 27, 28]. The pECP includes structures such as the dentate nuclei, the superior cerebellar peduncles, and the posterior mesencephalic tegmentum, injury to which may not be visualized on standard anatomical MRI but can be demonstrated with diffusion tensor imaging [27]. Diffusion tensor imaging in patients with PFS soon after surgery has demonstrated reduced fractional anisotropy, an indicator of abnormal white matter tract integrity, in the bilateral superior cerebellar peduncles and in remote cerebral cortical areas of the frontal and parietal lobes. Miller and colleagues reported high risk of developing PFS following bilateral pECP injury in their case-control study of PFS (OR=12, 95 % CI 1.12–129) [12]. The injury was detected using postoperative high-resolution MRI with standard sequences and diffusion-weighted imaging 3–4 weeks following surgery in a series of 11 patients with PFS and controls. Bilateral damage to the pECP was visualized in 6 of 11 patients, compared to only 1 of 11 controls without PFS. The pECP incorporates the dentatohalamocortical tracts, which are the polysynaptic route connecting output from the cerebellar vermis and hemispheres to the cerebral cortex particularly the prefrontal and temporal areas. Cerebellocerebral diaschisis is the remote dysfunction of cerebral cortical activity induced by interruption to the dentatohalamic tracts. This may explain the pattern of neurobehavioral problems seen in PFS that mimic primary lesions in

the frontal and temporal lobes (e.g., the abulia and akinetic mutism described in frontal lobe lesions). The impact on cerebral cortical activity has been demonstrated in studies at varying stages of PFS, and its recovery has also been demonstrated longitudinally using SPECT showing decreased cerebral perfusion either globally or in specific cerebral areas which could be correlated to specific behaviors demonstrated during the PFS [10].

The mechanism of injury to account for the delayed onset is not clear, nor indeed is the mechanism of recovery which can be protracted and incomplete. A direct intraoperative vascular-ischemic injury seems unlikely given the significant time lag to onset of symptoms of PFS after surgery. A pure surgical edema-related injury also seems unlikely given the protracted nature of PFS in the majority of children. Other proposed mechanisms which can cause delayed injury in other neurological conditions are delayed vasospasm, metabolic insult from abnormal neurotransmitter release, and microstructural axonal injury during surgery or as the result of the rapidly altered stresses and strains in the aftermath of removal of a slow-growing tumor.

A number of predictive risk factors for the occurrence of posterior fossa syndrome after surgery have been highlighted. The anatomical location of the tumor appears to be the most consistently reported risks from multiple cohorts. Midline as opposed to cerebellar hemisphere tumors, involvement of the cerebellar peduncles, invasion of the brainstem, and adherent to the floor of the fourth ventricle are at the highest risk [8, 9, 24]. This explains the majority of reported cases of PFS following medulloblastoma resection given the predilection of this tumor histology for these anatomical sites. Preoperative brainstem compression and a rostral position of the tumor in the fourth ventricle may also be predictive risk factors [27, 29]. Hydrocephalus does not appear to be a consistent risk factor for PFS particularly as it is common at presentation in posterior fossa tumors as a whole [10]. However, perioperative progression of hydrocephalus may be associated with PFS, or it should be considered as a treatable alternative cause to PFS for clinical presentation [25]. Other factors that have

not been consistently replicated across studies include age (younger children at increased risk) and tumor size, with one study finding medulloblastomas with diameter greater than 5 cm at increased risk [7].

The role of surgical factors as potentially modifiable risks for PFS also shows inconsistent findings across studies. Resection and length of incision of the vermis itself are not predictive of the occurrence of PFS [23, 30]. As discussed in the previous section of this chapter, the modified surgical approaches such as paravermian incisions and the telovelar approach have not eliminated the occurrence of PFS perhaps due to issues of retraction and injury to pECP and brainstem structures during tumor removal. The issue of individual neurosurgical skill has been analyzed, with no significant differences in risk when the tumor surgery is performed by a pediatric compared to a general neurosurgeon [8]. The extent of resection achieved has also been found inconsistently as a risk factor between studies, but analysis of the largest cohort did not demonstrate a significant relationship in medulloblastomas [24]. It is possible that partial resection indicates a tumor in a more inaccessible location, such as one with brainstem involvement which may thus predispose to PFS.

A multifaceted approach combining adequate preoperative planning, surgical resection goal, neuronavigation and intraoperative monitoring, reduced retraction, and ultrasonic aspirator injury is most likely to reduce the risk of occurrence of this serious neurological complication. There is an unexplored role for intraoperative MRI to predict PFS before its onset in an individual child and thus aids in the development of measures to mitigate its clinical course.

Ataxia-Limb Dysmetria-Gait Ataxia: The Cerebellar Syndrome

A degree of ataxia is common (58–82 %) at presentation of posterior fossa tumors, but the severity of impairment and functional impact on gait and activities of daily living is not typically recorded both pre and post surgeries in published series [2, 6]. This makes it difficult to identify the frequency of the cerebellar syndrome as a postsurgical neurological complication based on worsening

of symptoms and signs. However, it is clear from our clinical experience that ataxia can substantially worsen after surgery, for example, from being able to walk prior to surgery to being unable to sit up unaided and having head titubation requiring extended inpatient rehabilitation prior to any other tumor treatments. There will typically be associated visual disturbances (nystagmus and slow eye movements impacting on reading) and dysarthria (described below). Aside from surgical injury and anatomical causes, an increase in cerebellar signs may also be due to drug toxicity (e.g., phenytoin) which must be excluded.

The trajectory of ataxia is improvement over succeeding weeks, but with persistent deficits in postural equilibrium and upper limb control [11, 31]. Inferior cerebellar vermis lesions without deep cerebellar (fastigial, interposed, and dentate) nucleus involvement appear to cause transitory balance impairments, typically resolving within a year after surgery [32]. Splitting the vermis alone does not appear to be necessary or sufficient to cause persistent cerebellar syndrome. An animal model of surgical splitting of the posterior vermis recapitulates the features of a cerebellar syndrome which is however transient [33]. Injury to the deep cerebellar nuclei appears to lead to more persistent balance and upper limb control impairments [3]. These deep nuclei may be injured during surgery and retraction, for example, the fastigial nuclei are close to the midline above the superior part of the fourth ventricle.

Dysphagia, Dysarthria, Facial Nerve and Lower Cranial Nerve Palsies

As with other features of the cerebellar syndrome described above, dysphagia and dysarthria are often present at diagnosis but may worsen substantially following surgery. We consider these issues separately from the other aspects of the cerebellar syndrome due to the implications of dysphagia and underlying lower cranial nerve palsies for the medical stability of the patient in the immediate postoperative period and the common co-occurrence of these deficits with underlying lower cranial nerve palsies.

A recent retrospective study reported both pre- and postsurgical assessments of 27 children

with posterior fossa tumors for the presence or absence of dysarthria and dysphagia [4]. Worsening of dysphagia postoperatively was noted in nine children (33 %); only three of whom had dysphagia prior to surgery. This was accompanied by cranial nerve palsies in all except one child. There was a need for postoperative ventilation in four children and seven required a nasogastric or nasojejunal tube feeding for an extended period. Similarly, dysarthria was noted postoperatively in eight (30 %) children, with only one of these children having dysarthria prior to surgery. The postoperative dysarthria often followed a period of cerebellar mutism. Cranial nerve palsies were frequent. Both postoperative dysarthria and dysphagia were present in four children.

Dysphagia and bulbar cranial nerve palsies are essential to identify in the immediate postoperative period to avoid risk of aspiration and respiratory compromise. Careful assessment of children who have required a period of intubation and ventilation for dysphagia prior to reinitiating oral feeding is required. Importantly, the presence of dysphagia prior to surgery is a predictor for worsening dysphagia after surgery.

The mechanism for dysphagia and dysarthria may vary from child to child. Dysphagia may have an avolitional or apraxic component as seen in children with posterior fossa syndrome who are unable or unwilling to undertake the oral phase of feeding, but do not show problems with automatic functions such as clearance of saliva and yawning. Supranuclear mechanisms include injury to the descending corticobulbar tract in the brainstem. The cranial nerve nuclei in the floor of the fourth ventricle may also be injured during the removal of midline tumors or intrinsic focal brainstem tumors. Where the lesion is due to transient postoperative edema, the problems are likely to resolve. Transection of the cranial nerves themselves (neurotmesis) may occur during removal of extrinsic cranial nerve-specific tumors such as vestibular schwannoma or tumors involving the cerebellopontine angle and ventral brainstem, for example, ependymoma. Neurotmesis can be expected to have more persisting severe consequences. This may explain the frequent requirement

for gastrostomy (28 %) and tracheostomy (16 %) in a series of 96 children with ependymoma reported by Morris and colleagues, although it is not clear to what extent the problems were related to surgery rather than present at diagnosis [17].

Facial weakness is commonly present as a postoperative problem with dysphagia and dysarthria and resolution typically occurs according to the mechanism as discussed above. A less recognized problem in the pediatric literature is injury to the nervus intermedius, the sensory and parasympathetic component of the facial nerve, which has been reported to lead to an intrusive parasympathetic hypersensitivity syndrome (hypersalivation and lacrimation), parasympathetic underactivity, or reduced taste [34, 35].

The increased use of neuronavigation and intraoperative electrophysiological monitoring may reduce the incidence of dysphagia, dysarthria, and bulbar cranial nerve palsies in the future, although these are not able to currently identify the essential non-motor components, for example, the glossopharyngeal nerve for afferent component of the gag reflex [16].

Other Neurological Complications

Vomiting, often unaccompanied by any nausea or vertigo, following surgery remains an underascertained problem with very little literature on its characteristics. This is presumably because vomiting is taken to be a presenting sign of the tumor itself, given that hydrocephalus and features of raised intracranial pressure are so frequent at presentation. Postoperative vomiting may be taken also as a transient response to anesthesia. Furthermore, radiotherapy and chemotherapy that may follow surgery are also associated with vomiting (with nausea). However, in our clinical experience, there is a form of postoperative vomiting which does have different characteristics from that preceding surgery, for example, sensitivity to positional change, which occurs before other treatment modalities and can be very persistent despite anti-nausea and vomiting medications. Midline tumors of the vermis and fourth ventricle with peduncle involvement can cause a paroxysmal posturally evoked vomiting prior to surgery [36]. It is possible that surgical

injury may disrupt the outputs from the vermis to the vestibular nuclei that sense motion and thence to the area postrema, vomiting center [33]. Vascular injury to the posterior inferior cerebellar artery may induce similar problems.

Diplopia and vision disturbance may increase following surgery as a result of injury to cerebellar structures involved in eye movement control or due to a III, IV, or VI cranial nerve lesion. Very little is published on the mechanisms of vision disturbance, including findings pre and post surgery [6]. Traction injury can occur to the sixth nerve or direct injury to its nucleus in the floor of the fourth ventricle. Sixth nerve lesions tend to be more persistent than cerebellar eye movement problems. An animal model of posterior vermis surgical splitting demonstrated overshoot of saccades and decreased deceleration, low gain pursuit, gaze fixation interrupted by saccades, and a nystagmus that reduced spontaneously over a number of days. Whether these eye movement problems are found in children remains to be explored. A syndrome of transient cerebellar eye closure similar to apraxia of eyelid opening has been described in a child as part of a wider presentation with posterior fossa syndrome [37].

Hearing deficits subsequent to surgery are infrequently reported outside the context of vestibular schwannomas, which are uncommon in children. It is feasible that other tumors involving the cerebellopontine angle may lead to inadvertent sensorineural hearing loss during surgery, since the eighth nerve is sensitive to handling. However, hearing loss is not often assessed prior to surgery and may not be overt in the immediate postoperative period, and subsequent treatment with radiotherapy and chemotherapy which can both cause hearing loss will cloud the issue of causality. Nevertheless, surgery-induced hearing loss should be considered as a potential avoidable complication in certain tumors such as ependymomas, since hearing loss is the most common persisting severe neurosensory deficit [17]. Intraoperative electrophysiological monitoring and reduced handling of the eighth nerve are potential methods to reduce the risk of hearing loss.

Surgical injury to neurological structures essential for upper and lower respiratory function may lead to apnea and respiratory failure. This

may present with prolonged requirement for intubation and ventilation, with failure of extubation, unexpected respiratory collapse in the early postoperative period, or a more chronic presentation with nocturnal hypoventilation. Mechanical obstructive apnea may occur due to lesioning of lower cranial nerves including afferent component of protective reflexes or laryngospasm due to gastroesophageal reflux worsened by disruption of the vagus nerve. Such mechanisms may account for the relatively frequent requirement for tracheostomy (16 %) in the series of 96 children operated on for ependymoma [17]. Damage to respiratory centers in the brainstem could occur due to postoperative edema or hemorrhage. This may lead to obstructive apnea or central nocturnal hypoventilation [38, 39].

Seizures are rare as a presenting feature of posterior fossa tumors, and underlying treatable symptomatic causes should be considered in postoperative seizures. One series of children and adults following posterior fossa surgery recorded 5.9 % with a seizure, the majority within 3 h of surgery [40]. The underlying regional complications to be considered include venous air embolism, pneumoencephalus, hematoma, and worsening of hydrocephalus as well as general systemic complications (Table 62.4). Tonic decerebrate posturing due to coning, extrapyramidal reaction to medications, pain responses, and withdrawal from sedation may also be mistaken for a seizure.

Whether cognitive deficits can be regarded as a neurological complication of posterior fossa tumor, surgery is a controversial issue, particularly where data has come from children with malignant posterior fossa tumors who have been assessed in late-effect studies after intervening radiotherapy and chemotherapy [3]. Di Rocco and colleagues demonstrated using pre- and post-surgical neuropsychological assessment that many of the cognitive deficits present following posterior fossa tumor surgery (before other treatments such as radiotherapy) are detectable prior to surgery and often improve following surgery [2]. This is particularly the case for attention and visuospatial cognition. However, children who develop PFS after surgery do appear to have worse cognitive and affective function compared

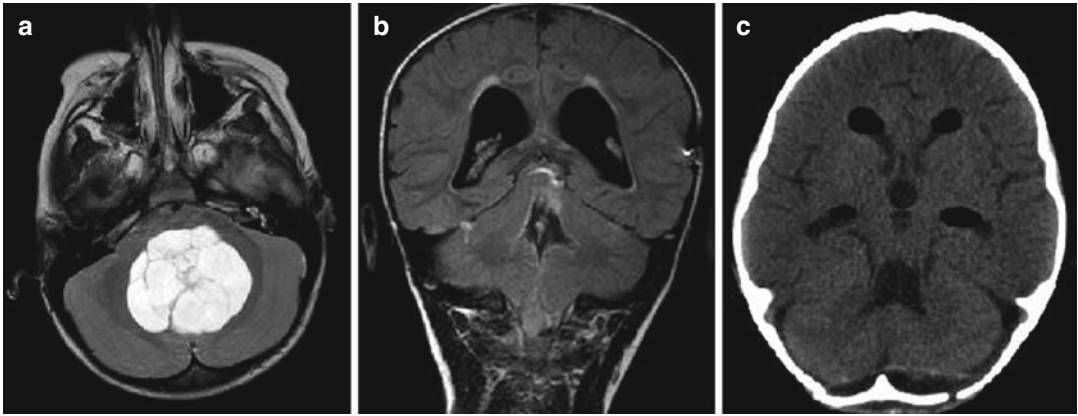


Fig. 62.3 A 6-year-old child presenting with a midline cerebellar pilocytic astrocytoma with symptoms of chronic raised intracranial pressure and minimal cerebellar syndrome. (a) Axial MRI T1 shows involvement of the floor of the fourth ventricle, distension of cerebellar peduncles, and compression of the brainstem. She is at risk of posterior fossa syndrome after surgery. CSF diversion with an EVD for hydrocephalus (not shown) was undertaken prior to resective surgery. (b) Immediate postoperative MRI coronal T2 FLAIR after gross total resection of tumor shows unilateral hyperintensity in the left proximal efferent cerebellar pathway. There is persisting evidence of hydrocephalus after EVD is removed. The child becomes

withdrawn, mute although socially aware. Non-mobile although only mild left cerebellar syndrome. The features are consistent with posterior fossa syndrome. (c) Axial CT scan on day 6 following surgery when new left sixth nerve palsy appeared. There is no new posterior fossa lesion but evidence of persisting hydrocephalus. A VP shunt was inserted leading to rapid but incomplete improvement of alertness and social interaction. Other features of posterior fossa syndrome, mild cerebellar syndrome, and sixth nerve palsy persisted for several weeks. This case demonstrates the difficulty of distinguishing posterior fossa syndrome from other independent treatable conditions such as persisting hydrocephalus

to other children with similar posterior fossa tumors. Regional and systemic complications, for example, meningitis, shunt infections in the perioperative period, the need for repeat surgery, and the presence of other perioperative neurological deficits, may also cause cognitive decline presumably due to surgery [41]. Splitting of the vermis with injury to the inferior vermis and bilateral dentate nucleus lesions were identified as potentially avoidable surgical factors that have been correlated with worse late cognitive outcomes in a series of 61 children treated for malignant posterior fossa tumor [3]. Thus, modifications to surgical techniques, avoiding posterior fossa syndrome and wider regional and systemic complications, are likely to play a part in improving overall cognitive outcomes.

62.3.2.2 Regional Complications Abnormalities of CSF Dynamics

Abnormalities of CSF dynamics include hydrocephalus, subdural hygromas, CSF leaks, and pseudomeningoceles which we consider together

since they frequently co-occur. Hydrocephalus is frequent at presentation prior to surgery, occurring in 71–90 % of children with posterior fossa tumors at diagnosis. Progression of hydrocephalus occurs in 10–62 % of cases following posterior fossa tumor surgery [5]. The accompanying signs and symptoms may be subtle, rather than overt evidence of decompensated raised intracranial pressure. Thus, there may be reduced level of responsiveness, slow rate of postoperative recovery, and features akin to posterior fossa syndrome (see case discussion in Fig. 62.3).

The majority of postoperative hydrocephalus progression occurs in the early postoperative period, but later progression after 30 days postoperatively may also occur.

Externally visible problems such as CSF leaks and pseudomeningoceles may also indicate the presence of underlying hydrocephalus which needs to be identified and managed. Specific risk factors for postoperative progression of hydrocephalus include midline fourth ventricle tumors and young age group. There has been much

discussion of the value of elective preoperative endoscopic third ventriculostomy in these children as a means of reducing the requirement for postoperative ventriculoperitoneal shunt placement, as discussed in an earlier chapter in this book.

CSF leak is a common yet avoidable phenomenon after posterior fossa surgery. CSF leak is a key issue since it predisposes to further complications including meningitis with all its own potential sequelae, leading to a cascade of further complications which will inevitably cause additional injury and prolong hospital length of stay. Attention to detail in surgical technique and evaluation of hydrocephalus and other risk factors can reduce this complication. The potential advantages of craniotomy over craniectomy in reducing CSF leak in posterior fossa tumor surgery have been discussed [19]. A variety of dural closure techniques have been described over the years with inevitable personal surgical preference and bias. A number of synthetic and other dural substitutes are in wide usage and availability aiming to minimize risk of CSF leakage and reduce potential adherence of the brain to the bone and tissues; none of which have been proven in their effectiveness.

CSF subdural hygromas and compartmentalized CSF collections including pseudomeningoceles also represent disordered CSF circulation requiring further intervention and prolonged hospitalization. They should be investigated and managed along the same lines as investigation for postoperative hydrocephalus and CSF leaks. Pseudomeningoceles often herald the delayed development of raised intracranial pressure. They may be managed conservatively with spontaneous resolution common in the absence of persistent raised ICP or hydrocephalus.

Intracranial Hemorrhage

Focal intracranial hemorrhage following surgery is an uncommon complication but potentially fatal. Vascular tumors, previous treatments such as radiotherapy, and tumors encasing large vessels are potential risk factors. Attention to tumor bed hemostasis and blood pressure control is likely to reduce the potential for hemorrhage. Intracranial hemorrhage may lead to consumption

of systemic clotting factors particularly in young infants, leading to more widespread life-threatening hemorrhage.

Diffuse Cerebellar Edema

With the routine use of perioperative high-dose steroids, diffuse postoperative cerebellar edema is an uncommon event following posterior fossa tumor surgery. The two cases reported by Ogiwara and colleagues were large cell medulloblastomas with leptomeningeal metastasis [42]. The onset was delayed beyond the first postoperative week so it is possible that surgery is not directly causative, but may rather be related to the leptomeningeal metastasis causing abnormal venous drainage. The cerebellar edema may cause upward transtentorial herniation which is life threatening or leads to persistent severe neurological deficit. Urgent posterior fossa decompression surgery may provide benefit.

Ischemic Stroke and Vasospasm

Ischemic infarcts including in the anterior cerebral circulation with evidence of underlying vasospasm have been reported in isolated cases following posterior fossa tumor surgery [21, 43]. The tendency to remote supratentorial vasospasm may be due to intraoperative factors including hemorrhage, blood replacement, and encasement of blood vessels by the tumor. A delayed onset of the infarct in the second week after surgery was a notable feature in these reported cases, which is consistent with the delayed onset typical of cerebral vasospasm in other situations such as following subarachnoid hemorrhage. Focal neurological deficits suggestive of middle cerebral artery vasospasm such as progressive hemiparesis and aphasia as well as globally reduced conscious level or “locked-in syndrome” suggestive of basilar vasospasm may occur. Diagnosis of early ischemia related to vasospasm may not be evident on routine CT scan or MRI scan, requiring diffusion-weighted sequences and magnetic resonance angiography (Fig. 62.4). The child presented in Fig. 62.4 was successfully treated by us with a combination of controlled hypervolemia, hypertension, and cerebral vasodilatation (intravenous nimodipine), reversing neurological

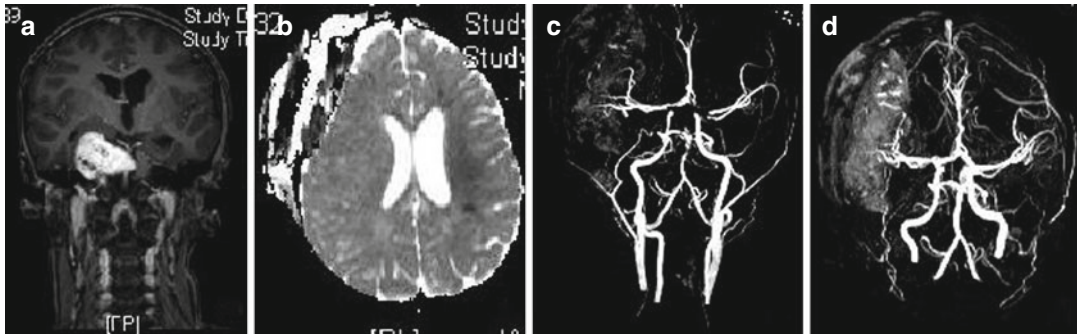


Fig. 62.4 A 13-year-old child presented with progressive right hemiparesis and aphasia which progressed to an early “locked-in” syndrome 9 days after resection of a large right trigeminal schwannoma requiring a skull base approach. **(a)** A preoperative MRI coronal T1 scan demonstrating extent of lesion in the vicinity of major verte-brobasilar arteries. **(b)** MRI axial diffusion-weighted imaging with ADC map demonstrates subtle areas of low diffusion (low signal) consistent with early ischemia in the left hemisphere. CT, MRI T1, T2, and FLAIR (not

shown) did not show any ischemia or infarction. **(c)** MR angiography of intracranial vessels demonstrates focal narrowing in the proximal internal carotid/proximal middle cerebral arteries and basilar artery consistent with vasospasm. **(d)** Repeat MR angiography after 3 days of treatment for vasospasm shows radiological improvement of vasospasm consistent with resolution of neurological deficits. Diffusion-weighted imaging and standard MRI sequences (not shown) were consistent with resolution of ischemia without established infarction

deficits accompanied with radiological improvement. Cerebral angiography is an alternative diagnostic method which in addition allows local intra-arterial vasodilator treatment.

Superficial Siderosis

This is a very late, rarely reported but possibly underrecognized complication that has been reported after cerebellar tumors surgically treated in childhood. The presentation has been in adult years, with a delay of two or three decades since surgery [44]. One of the patients in Anderson and colleagues’ series had been treated by surgery alone.

The clinical features include slow evolution of a bilateral sensorineural hearing loss, ataxia, optic neuropathy, upper motor neuron signs, and headache. Acute worsening may occur. The diagnosis is made on MRI sequences that are sensitive for iron deposition including T2* and gradient echo sequences which reveal hypointensities around the cerebellar folia. The CSF may show elevated inflammatory indices. The pathogenic mechanism is not clear. One possibility is chronic low-level bleeding into the subarachnoid CSF space with chronic toxicity due to hemoglobin breakdown products.

62.4 Conclusions and Future Prospects

We have discussed the common and lesser-known potential complications of posterior fossa surgery, along with proposed predictable risks based on patient, tumor, and surgical factors. We have identified methods and practices that if employed widely should reduce these risks. However, we have repeatedly noted the lack of a high-quality evidence base in each of these aspects of neurosurgical complications (i.e., incidence, risk factors, and solutions). This tempers the strength of the conclusions we can draw from analyzing the literature. Thus, we make the following suggestions for improving routine clinical practice for reducing surgical complications partly from the first principles and our own observations, while higher-quality evidence for effectiveness is gathered. Firstly, preoperative baseline risks in each child for the occurrence of surgical complications should be identified. Appropriate perioperative anesthetic and nursing care for the degree of risk must be available, as well as ready availability of pediatric-trained staff and facilities for the early differential diagnosis and management of evolving neurological

syndromes and systemic complications. A multidisciplinary neuro-oncology assessment prior to resective surgery is required including appropriate neuroradiology and oncology involvement to identify the goal and extent of resection. A CSF diversion procedure should be considered to reduce the many complications which can be exacerbated by hydrocephalus. Neuronavigation, intraoperative imaging, and electrophysiology should be employed where feasible. Methods for presurgical functional mapping of posterior fossa structures, particularly cerebellar function, and white matter tract tracing as available for supratentorial tumors should be developed. It is likely that no single intervention will make a difference to overall complication rates, rather a combination of the above practices together. This type of complex and incremental change in interventions does not lend itself well to classical patient-level randomized controlled trials, although provider-level cluster randomized trials should be possible.

It is imperative for internal departmental quality improvement that local rates of the specific neurological, regional, and systemic complications are routinely recorded, analyzed regularly, and fed back to the individual neurosurgeon and wider neuro-oncology team. With regard to this we suggest that all adverse events after surgery should be documented rather than just those that are overtly complications; that the salient neurological signs and symptoms are recorded pre and post surgery, along with an indication of severity such as level of disability; and that analysis of individual cases following serious adverse events should be performed using a structured process as proposed in our causality tool (Fig. 62.1).

Given the infrequent nature of some specific complications, such as posterior fossa syndrome, multicenter data collection on trends in these complication rates will be necessary. This raises the issue of inter-provider comparison of complication rates, much as with comparison of treatment effectiveness across centers. Inter-provider comparison does raise additional issues compared to the use of data collected locally for internal departmental quality improvement. The additional issues include identifying the most relevant, reliable, and feasible data to collect across centers. Preliminary work will need to

be performed gaining consensus across neurosurgeons at multiple centers on which complications to target as important, definitions of each complication, definitions of the denominator population at risk, baseline indicators of patient complexity (casemix variables), exclusion factors, and issues of data sharing. The feasibility of collecting the necessary data consistently over time must also be gauged. There is often a trade-off between the reliability of data and the feasibility of collecting such data. Routinely collected administrative data, for example, reimbursement claims data, may be less reliable and specific than prospective project-specific data collection at the bedside or from chart review, but it is often the most feasible system in terms of cost and long-term sustainability. Proxy indicators of complications in routinely collected data from administrative databases could include a number of the salient events and rescue treatments in our taxonomy of complications (Table 62.1). These include patient length of stay beyond an arbitrary threshold (e.g., the median length of stay for an uncomplicated postoperative course), return to theater within 30 days of surgery, admission to intensive care for more than 12 h of ventilation after surgery, salient procedures including tracheostomy and gastrostomy, and rate of school reentrance within a fixed time period.

In conclusion, the drive to understand and reduce surgical complications is a core component of improving the effectiveness of overall posterior fossa tumor treatment.

References

1. Dubey A, Sung W-S, Shaya M et al (2009) Complications of posterior cranial fossa surgery – an institutional experience of 500 patients. *Surg Neurol* 72:369–375
2. Di Rocco C, Chieffo D, Pettorini BL et al (2010) Preoperative and postoperative neurological, neuropsychological and behavioral impairment in children with posterior cranial fossa astrocytomas and medulloblastomas: the role of the tumor and the impact of the surgical treatment. *Childs Nerv Syst* 26: 1173–1188
3. Puget S, Boddaert N, Viguier D et al (2009) Injuries to inferior vermis and dentate nuclei predict poor neurological and neuropsychological outcome in children with malignant posterior fossa tumors. *Cancer* 115: 1338–1347

4. Mei C, Morgan AT (2011) Incidence of mutism, dysarthria and dysphagia associated with childhood posterior fossa tumour. *Childs Nerv Syst* 27: 1129–1136
5. Due-Tønnessen BJ, Helseth E (2007) Management of hydrocephalus in children with posterior fossa tumors: role of tumor surgery. *Pediatr Neurosurg* 43:92–96
6. Sønderkaer S, Schmiegelow M, Carstensen H et al (2003) Long-term neurological outcome of childhood brain tumors treated by surgery only. *J Clin Oncol* 21:1347–1351
7. Catsman-Berrevoets CE, Van Dongen HR, Mulder PG et al (1999) Tumour type and size are high risk factors for the syndrome of “cerebellar” mutism and subsequent dysarthria. *J Neurol Neurosurg Psychiatry* 67:755–757
8. Robertson PL, Muraszko KM, Holmes EJ et al (2006) Incidence and severity of postoperative cerebellar mutism syndrome in children with medulloblastoma: a prospective study by the Children’s Oncology Group. *J Neurosurg* 105:444–451
9. Ozgur BM, Berberian J, Aryan HE et al (2006) The pathophysiologic mechanism of cerebellar mutism. *Surg Neurol* 66:18–25
10. Catsman-Berrevoets CE, Aarsen FK (2009) The spectrum of neurobehavioural deficits in the Posterior Fossa Syndrome in children after cerebellar tumour surgery. *Cortex* 46:933–946
11. Schoch B, Konczak J, Dimitrova A et al (2006) Impact of surgery and adjuvant therapy on balance function in children and adolescents with cerebellar tumors. *Neuropediatrics* 37:350–358
12. Miller NG, Reddick WE, Kocak M et al (2010) Cerebellocerebral diaschisis is the likely mechanism of postsurgical posterior fossa syndrome in pediatric patients with midline cerebellar tumors. *AJNR Am J Neuroradiol* 31:288–294
13. Gudrunardottir T, Sehested A, Juhler M et al (2011) Cerebellar mutism: review of the literature. *Childs Nerv Syst* 27:355–363
14. Rajesh BJ, Rao BRM, Menon G et al (2007) Telovelar approach: technical issues for large fourth ventricle tumors. *Childs Nerv Syst* 23:555–558
15. Riva D, Giorgi C (2000) The cerebellum contributes to higher functions during development: evidence from a series of children surgically treated for posterior fossa tumours. *Brain* 123(Pt 5):1051–1061
16. Sala F, Manganotti P, Tramontano V et al (2007) Monitoring of motor pathways during brain stem surgery: what we have achieved and what we still miss? *Neurophysiol Clin* 37:399–406
17. Morris EB, Li C, Khan RB et al (2009) Evolution of neurological impairment in pediatric infratentorial ependymoma patients. *J Neurooncol* 94:391–398
18. Stripf T, Braun K, Gouveris H et al (2007) Influence of different approaches to the cerebellopontine angle on the function of the intermediate nerve. *J Neurosurg* 107:927–931
19. Gnanalingham KK, Lafuente J, Thompson D et al (2002) Surgical procedures for posterior fossa tumors in children: does craniotomy lead to fewer complications than craniectomy? *J Neurosurg* 97:821–826
20. Kumar V, Phipps K, Harkness W et al (1996) Ventriculo-peritoneal shunt requirement in children with posterior fossa tumours: an 11-year audit. *Br J Neurosurg* 10:467–470
21. Catsman-Berrevoets CE, Van Breemen M, Van Veelen ML et al (2005) Supratentorial arterial ischemic stroke following cerebellar tumor resection in two children. *Pediatr Neurosurg* 41:206–211
22. De Smet HJ, Baillieux H, Catsman-Berrevoets C et al (2007) Postoperative motor speech production in children with the syndrome of ‘cerebellar’ mutism and subsequent dysarthria: a critical review of the literature. *Eur J Paediatr Neurol* 11:193–207
23. Pollack IF, Polinko P, Albright AL et al (1995) Mutism and pseudobulbar symptoms after resection of posterior fossa tumors in children: incidence and pathophysiology. *Neurosurgery* 37:885–893
24. Korah MP, Esiasvili N, Mazewski CM et al (2010) Incidence, risks, and sequelae of posterior fossa syndrome in pediatric medulloblastoma. *Int J Radiat Oncol Biol Phys* 77:106–112
25. Huber JF, Bradley K, Spiegler BJ et al (2006) Long-term effects of transient cerebellar mutism after cerebellar astrocytoma or medulloblastoma tumor resection in childhood. *Childs Nerv Syst* 22:132–138
26. Wells EM, Walsh KS, Khademian ZP et al (2008) The cerebellar mutism syndrome and its relation to cerebellar cognitive function and the cerebellar cognitive affective disorder. *Dev Disabil Res Rev* 14: 221–228
27. Morris EB, Phillips NS, Laningham FH et al (2009) Proximal dentatohalamocortical tract involvement in posterior fossa syndrome. *Brain* 132:3087–3095
28. Kusano Y, Tanaka Y, Takasuna H et al (2006) Transient cerebellar mutism caused by bilateral damage to the dentate nuclei after the second posterior fossa surgery. Case report. *J Neurosurg* 104:329–331
29. Mcmillan HJ, Keene DL, Matzinger MA et al (2009) Brainstem compression: a predictor of postoperative cerebellar mutism. *Childs Nerv Syst* 25:677–681
30. Siffert J, Poussaint TY, Goumnerova LC et al (2000) Neurological dysfunction associated with postoperative cerebellar mutism. *J Neurooncol* 48:75–81
31. Konczak J, Schoch B, Dimitrova A et al (2005) Functional recovery of children and adolescents after cerebellar tumour resection. *Brain* 128:1428–1441
32. Schoch B, Hogan A, Gizewski ER et al (2010) Balance control in sitting and standing in children and young adults with benign cerebellar tumors. *Cerebellum* 9:324–335
33. Buzunov E, Ojemann JG, Robinson FR (2010) Rhesus macaque as an animal model for posterior fossa syndrome following tumor resection. *Pediatr Neurosurg* 46:120–126
34. Huy PT, Sauvaget E (2010) Unilateral rhinorrhea after translabyrinthine surgery due to parasympathetic hypersensitive syndrome: differentiation from cerebrospinal fluid leakage. *Otol Neurotol* 31:1160–1162

35. Irving RM, Viani L, Hardy DG et al (1995) Nervus intermedius function after vestibular schwannoma removal: clinical features and pathophysiological mechanisms. *Laryngoscope* 105:809–813
36. Drachman DA, Diamond ER, Hart CW (1977) Posturally-evoked vomiting; association with posterior fossa lesions. *Ann Otol Rhinol Laryngol* 86:97–101
37. Catsman-Berreoets CE, Van Dongen HR, Aarsen FK et al (2003) Transient cerebellar eye closure and mutism after cerebellar tumor surgery: long-term clinical follow-up of neurologic and behavioral disturbances in a 14-year-old girl. *Pediatr Neurosurg* 38:122–127
38. Matsuyama M, Nakazawa K, Katou M et al (2009) Central alveolar hypoventilation syndrome due to surgical resection for bulbar hemangioblastoma. *Intern Med* 48:925–930
39. Greenough G, Sateia M, Fadul CE (1999) Obstructive sleep apnea syndrome in a patient with medulloblastoma. *Neuro Oncol* 1:289–291
40. Suri A, Mahapatra AK, Bithal P (1998) Seizures following posterior fossa surgery. *Br J Neurosurg* 12: 41–44
41. Kao GD, Goldwein JW, Schultz DJ et al (1994) The impact of perioperative factors on subsequent intelligence quotient deficits in children treated for medulloblastoma/posterior fossa primitive neuroectodermal tumors. *Cancer* 74:965–971
42. Ogiwara H, Dipatri AJ Jr, Bowman RM et al (2011) Diffuse postoperative cerebellar swelling in medulloblastoma: report of two cases. *Childs Nerv Syst* 27:743–747
43. Lee TT, Ragheb J, Bruce JC et al (1998) Diffuse cerebral vasospasm with ischemia after resection of a cerebellopontine angle primitive neuroectodermal tumor in a child. *Pediatr Neurosurg* 29:300–303
44. Anderson NE, Sheffield S, Hope JK (1999) Superficial siderosis of the central nervous system: a late complication of cerebellar tumors. *Neurology* 52:163–169

Bahattin Tanrikulu, M. Memet Özek,
and Deniz Konya

63.1 Description

Vertebral column deformities after resection of posterior fossa tumors in children have been well documented [1–3]. These include mainly postlaminectomy kyphosis and cervical instability. Risk factors for postoperative vertebral column deformities include multiple levels of laminectomies, involvement of C2, cervical region, childhood, adjuvant radiotherapy, lateral extension of decompression, facetectomy, and number of levels resected [4–12].

63.2 Incidence and Prevalence

Bell et al. [8], Yeh et al. [13], and de Jonge et al. [14] reported a 44–88 % incidence of deformity. In these series, 33 %, 40 %, and 30 % of patients with deformity required surgical intervention with 45–79 months of follow-up. More patients might develop further deformity with longer follow-up.

B. Tanrikulu, M.D. • D. Konya, M.D.
Department of Neurosurgery, Marmara University,
School of Medicine, Istanbul, Turkey

M.M. Özek, M.D. (✉)
Division of Pediatric Neurosurgery,
Acibadem University, School of Medicine,
Istanbul, Turkey
e-mail: memetozek@gmail.com

63.3 Anatomy and Biomechanics

The adult vertebral column has four curvatures. The anteriorly concave thoracic and sacral curvatures are called kyphoses, whereas the posteriorly concave lumbar and cervical ones are called lordoses. The thoracic and sacral kyphoses are primary curvatures that develop during the fetal period because of flexed fetal position, whereas cervical and lumbar lordoses are secondary curvatures that develop during infancy and childhood (Fig. 63.1) [15].

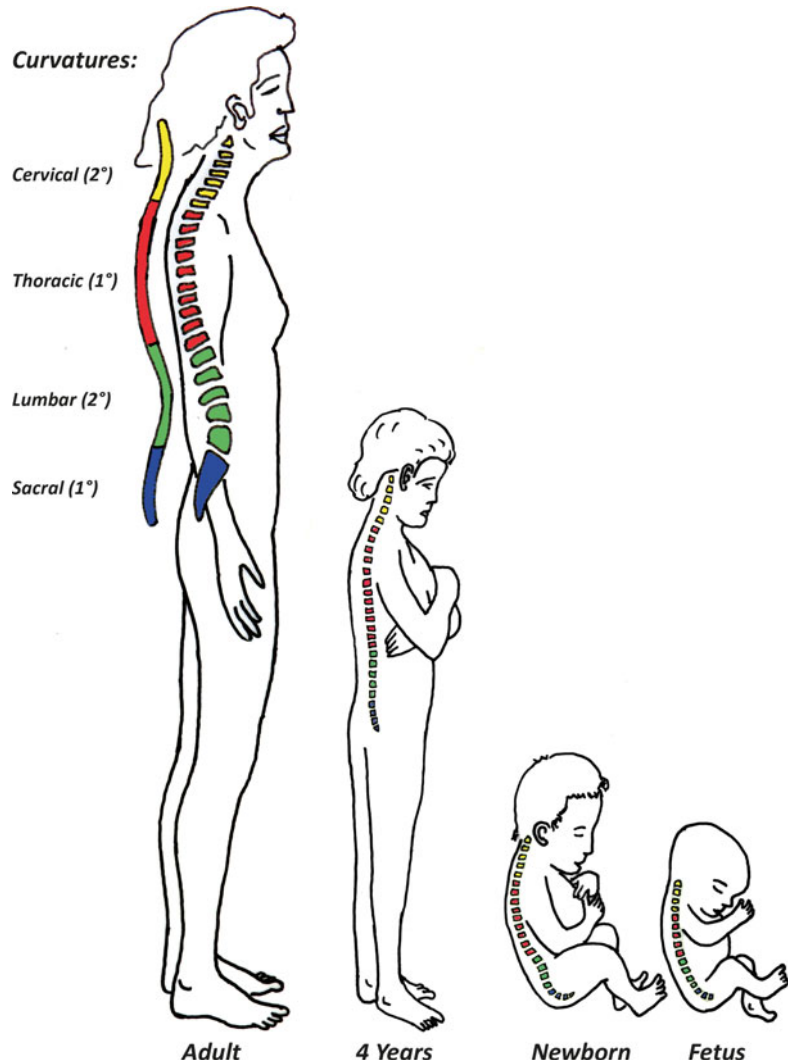
When we talk about postoperative kyphosis that develops after posterior fossa tumor operations in children, we generally mean change of curve from cervical lordosis to cervical kyphosis.

Cervical lordosis is defined as a piece of a circle from C2 to T1 by Harrison and colleagues [16]. However, adult data for the cervical lordosis may not actually apply to children from birth to early adolescence.

Bagnall et al. found that up to 9.5 weeks, 83 % of fetuses have a cervical lordosis. This means that by 9.5 weeks, most of the fetuses are starting to use their extensor cervical muscles to pull the cervical curve away from the fetal “C” shape. The lordosis increases during postnatal life when the baby raises his/her head and begins to sit up [17].

These spinal curvatures develop under the influence of multivectorial forces, and this delicate construction is kept in balance by the help of various bony and soft tissue structures (Fig. 63.2).

Fig. 63.1 The four curvatures of the adult vertebral column: “cervical, thoracic, lumbar, and sacral.” Thoracic and sacral ones exist during fetal life and are called primary (1°) curvatures. The cervical and lumbar ones develop during infancy and childhood and are named secondary (2°) curvatures



With the normal cervical spine lordosis, the weight-bearing axis lies posterior to the vertebral bodies and approximately two thirds of the load is carried by the posterior columns [18].

The loss of the posterior ligamentous and bony elements after cervical laminectomy may shift the weight-bearing axis forward. This results in loss of lordosis and a change towards a straight or kyphotic alignment. That subsequently moves the weight-bearing axis in front of the vertebral bodies. As this kyphotic deformity progresses, the anterior column tends to be compressed and the posterior columns are placed under tension (Fig. 63.3). The surgical trauma weakens the

posterior structures that stabilize the cervical vertebrae in their physiologic lordotic position. As a result, the kyphotic deformity progresses [19–21].

C2 and its muscular attachments are very important structures that protect physiologic cervical lordosis. Destruction of the second cervical vertebra leads to a highly unstable situation. The axis transfers the axial load of the two lateral masses of the atlas to three surfaces on the third cervical vertebra: the two articular facets and the vertebral body. Thus, pathological processes of this region are often treated less radically compared to other areas of the cervical spine [22].

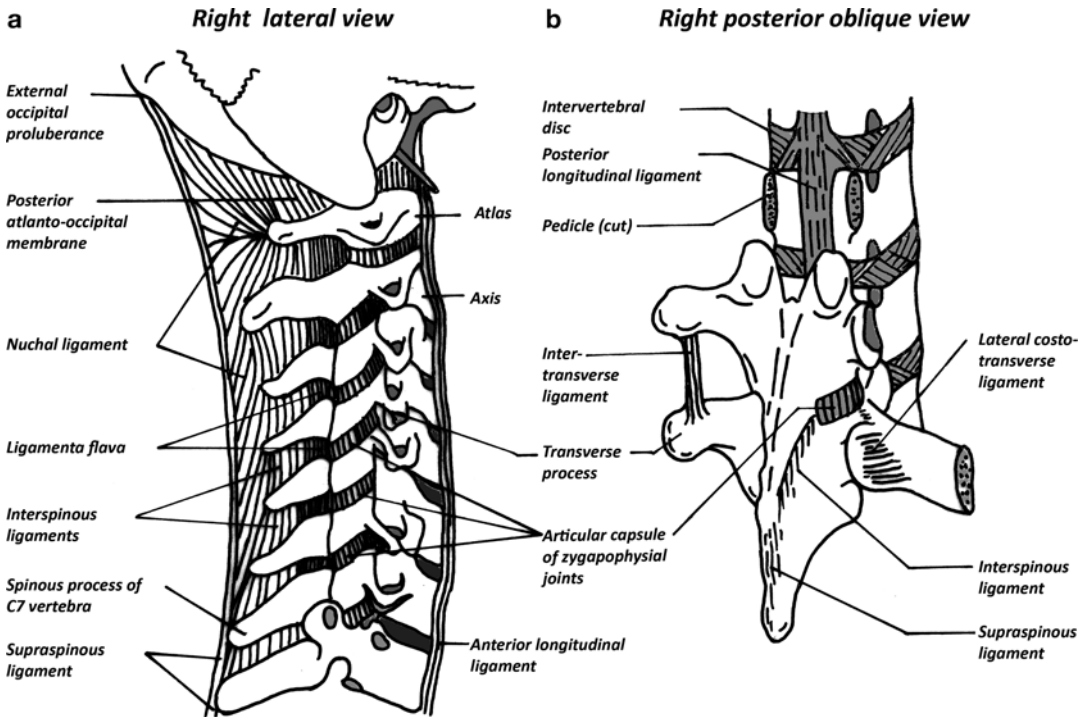


Fig. 63.2 (a) Right lateral view of the ligaments in the cervical region. (b) Posterolateral view of the ligaments in the cervicothoracic region

The extensor cervical back muscles especially the semispinalis cervicis group play a critical role in maintaining cervical lordosis. Consequently, the involvement of C2 and its muscular attachments in laminectomy operations may increase the risk of postlaminectomy kyphosis [23]. Because of the destruction of the posterior column and posterior stabilizing ligament complexes, increasing the number of lamina involved in laminectomy also increases the risk of postlaminectomy kyphosis [24].

63.4 Pathology and Etiology

Deformity develops secondary to a combination of load imbalance and instability [25]. Instability is defined as the “loss of the ability of the spine under physiologic loads to maintain its pattern of displacement so that there is no initial or additional neurological deficit, no major deformity, and no incapacitating pain” by White and Panjabi

[26]. Because of this, repetitive unbalanced physiological loads in combination with instability can lead to deformity [25]. The most common surgical procedure in the treatment of spinal and posterior fossa tumors has been laminectomy [27]. To limit postlaminectomy deformities, new techniques such as laminoplasty have been used. The prevalence of postlaminectomy deformities in the pediatric population is higher than in the adult population [27, 28].

There are significant differences between the pediatric and adult human spine. The pediatric spine is associated with greater viscoelasticity of its ligamentous structures. This allows the development of deformity when the supporting posterior structures are weakened. Posterior ligaments including the ligamentum flavum, interspinous and supraspinous ligaments, and the extensor spinal muscles normally counteract the flexion force of gravity on the cervical spine. After laminectomy, these stabilizing structures are damaged and make the spinal cord vulnerable to kyphosis [1].

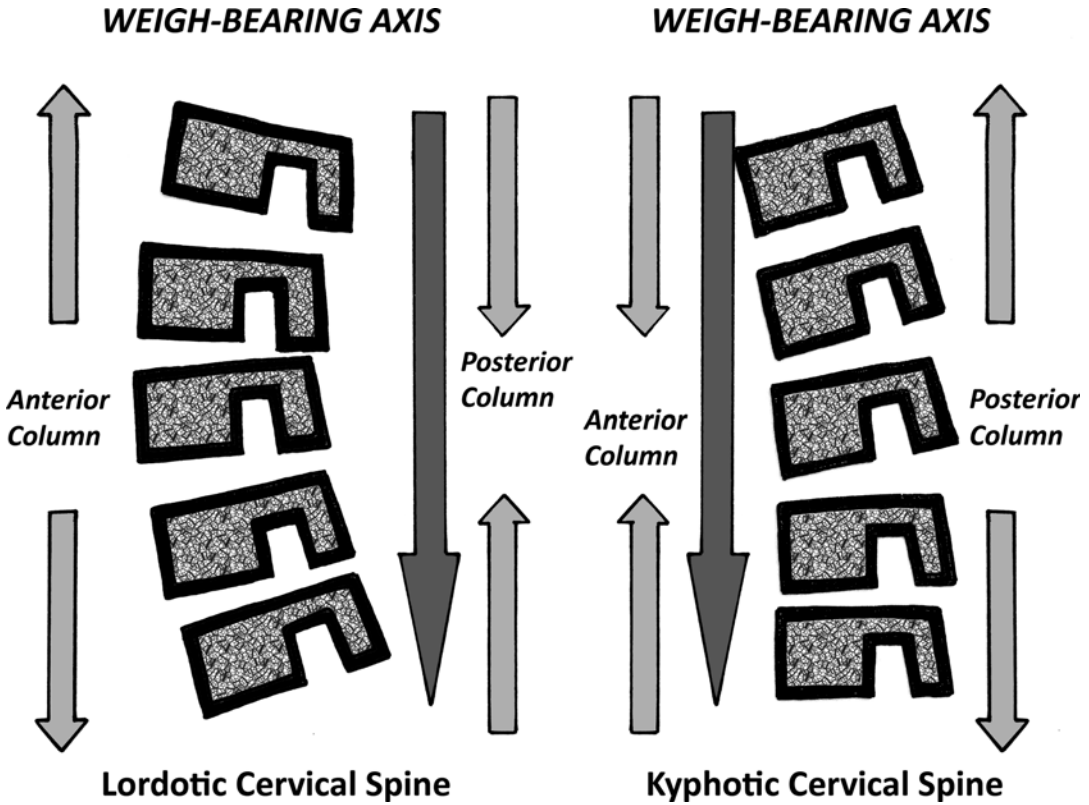


Fig. 63.3 Schematic drawings showing lordosis and kyphosis in the cervical spine. Kyphosis tends to be a self-progressive condition because the deformity causes the

weight-bearing axis in the cervical spine to move to a more ventral position in front of the vertebral bodies

Also in the pediatric patient, the cervical facets are in a more horizontal plane, the paraspinal muscles are not yet fully developed, ossification is ongoing, and the nucleus pulposus has a higher water content [1, 8, 10, 29]. These factors differ significantly from adults and these should be considered during surgery [25]. Therefore, the incidence of cervical postlaminectomy kyphosis is higher in pediatric patients than in adults [25].

The risk of spinal deformity in pediatric patients is thought to be due to C2 involvement, younger age, preoperative misalignment, irradiation, more elastic ligaments, more horizontal facets, ongoing ossification and remodeling process and weak paraspinal muscles [3, 8, 13, 29–31].

Bell and colleagues reviewed 89 patients with a mean age of 5.7 years who had an average of 4.7 levels removed between C2 and C7. After a

5-year follow-up, they found that 46 (52 %) of 89 patients developed cervical spinal deformity; however, they did not find a correlation between the number of levels removed and deformity [8].

Yasuoka and colleagues reviewed 248 patients younger than 25 years of age and concluded that patients younger than 15 years of age had a higher incidence of postlaminectomy deformity. Yasuoka and colleagues [32] found no link between deformity and gender or the number of laminae resected in their 58 patients [28].

Yeh and colleagues compared laminectomy and laminoplasty techniques with a 45-month follow-up. They found that increasing the number of laminae operated increases the risk of postlaminectomy kyphosis in the cervical region, whereas laminoplasty reduces the risk of postoperative kyphosis [13].

There are many case-control studies in literature concerning the involvement of the cervical vertebra above or below C2 in the laminectomy procedure. Most of them state that in suboccipital craniotomy, the involvement of cervical laminectomies below C2 increases kyphotic deformity in the cervical region.

This is because more fibrous bands and muscles are scarified in axial and subaxial laminectomies. In suboccipital craniotomy with C1 laminectomy, muscular and ligamentous attachments to the C2 spinous process should not be detached. Even partial involvement of the C2 lamina in the laminectomy procedure may leave enough structural integrity to compensate for laminectomy-related instability [25].

Cervical intradural tumors which involve multiple cervical levels and posterior fossa tumors which also involve cervical levels below C2 may require multilevel cervical laminectomy. Multilevel laminectomies also increase the risk of postlaminectomy kyphosis. Sciubba et al. reported that there is an increased risk of kyphosis in the pediatric population after patients had surgeries which require greater than three levels of laminectomies for the intradural tumor resection [24].

63.5 Treatment

There have been many attempts to limit the development or progression of deformity. Many authors suggest postoperative bracing [8, 27, 28, 31]. On the other hand, bracing may actually reduce the role of the paraspinal muscles and lead to atrophy.

Bracing is thought to play a limited role in the long-term management of preexisting deformity. It may prove useful for shorter periods, for early intervention, or perhaps to postpone surgical intervention until growth spurts pass [25].

To limit the chance of postlaminectomy vertebral deformities, the surgeon should first protect the C2 lamina, muscles, and ligaments that are attached on it. Also the surgeon should try not to damage facet joints. It is because most of the strong ligaments responsible for vertebral integrity have attachments to the C2 lamina, spinous process, and facet joints [33, 34].

There are different surgical procedures to limit postoperative vertebral deformity. Iatrogenic deformity mainly develops after dorsal tension band disruption. A variety of surgical procedures, especially laminoplasty techniques, have been tried to protect this structure [35].

There are not so many studies that show the actual benefit of laminoplasty over laminectomy in pediatric patients. Besides this, the most commonly accepted procedure in current practice is laminoplasty.

There are studies that propose instrumentation with fusion during initial surgery [14]; others advise close follow-up with x-rays every 6 months for the first year after surgery and then yearly controls with x-rays until bone maturity is achieved [28].

The time period between initial surgery and diagnosis of spinal deformity ranges from right after surgery to 74 months [14, 28, 36, 37]. Close follow-up and early diagnosis and intervention may prevent the progression of deformity. Not all patients with iatrogenic spinal deformity need to be surgically corrected so early because surgical correction may lead to many unnecessary and expensive procedures in these children.

Before making a decision about surgery, patients should be evaluated for cervical instability with flexion and extension x-rays using the criteria described by Panjabi et al. [21]. According to these criteria, the presence of more than 3.5 mm or 20 % sagittal plane displacement and more than 20° of sagittal plane rotation on flexion-extension x-rays and also the presence of 3.5 mm sagittal plane translation or more than 11° sagittal plane angulation on neutral x-rays are suggestive findings of instability. It should be noted that the Panjabi instability criteria were based on an adult spine research investigation, and there are no parallel studies to determine the criteria for instability in pediatric patients.

Patients with signs and symptoms of instability such as excessive pain, gross deformity and neurological symptoms should be treated surgically [25].

In surgery, anterior fixation, anterior and posterior fixation, and posterior fixation alone are options.

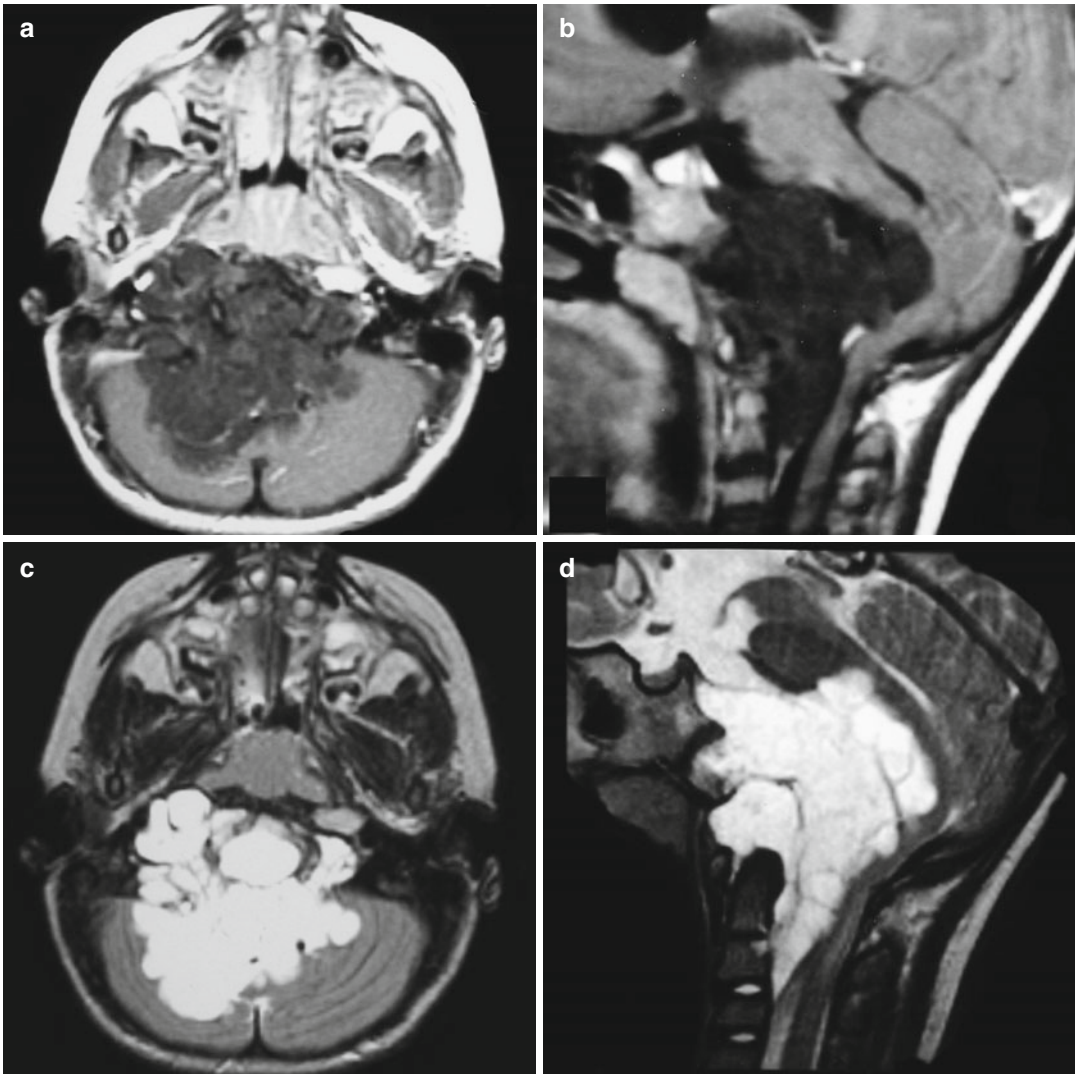


Fig. 63.4 (a) Axial T1-weighted cranial MRI of a 5-year-old boy presented with a 6-month history of progressive torticollis and hearing loss. (b) Sagittal T1-weighted cranial

MRI of the same patient with marked brain stem distortion. (c, d) Axial and sagittal T2-weighted cranial MRI. The lesion was radiologically diagnosed as clival chordoma

Posterior fixation is generally indicated in the setting of posterior column instability [38, 39]. One of the earliest posterior cervical fusion techniques was sublaminar wiring which was first described in the early 1890s for the management of deformity caused by Pott's disease [39]. Early strategies for craniovertebral junction or cervical spinal stabilization used simple onlay bone graft technique. Suboccipital and sublaminar wiring techniques were used for

stabilizing the onlay graft. However, to achieve optimal stability, more cervical vertebral levels should be involved in this technique which limits the patient's motion range [40, 41] (Figs. 63.4, 63.5, and 63.6).

Rod and wire techniques evolved later which provide more stability. The rod and wire technique involves bending a rod in U shape and fixing the rod and bone graft to the cervical spine and occiput (Figs. 63.7 and 63.8). The rod and

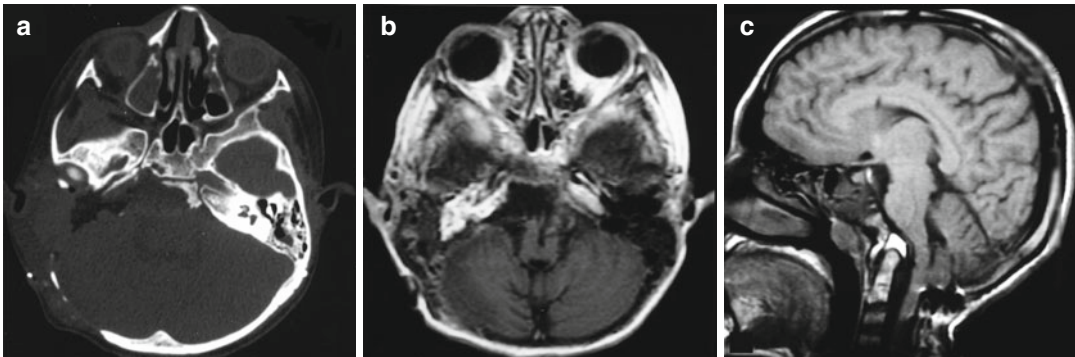


Fig. 63.5 (a) Axial postoperative head CT scan of the patient who was operated through the presigmoid route. Occipitocervical stabilization was performed with the suboccipital and sublaminar wiring technique.

(b) Postoperative axial T1-weighted MRI of the patient. (c) Postoperative sagittal T1-weighted MRI of the patient showing decompression of the brain stem with metallic artifacts by suboccipital and sublaminar wires

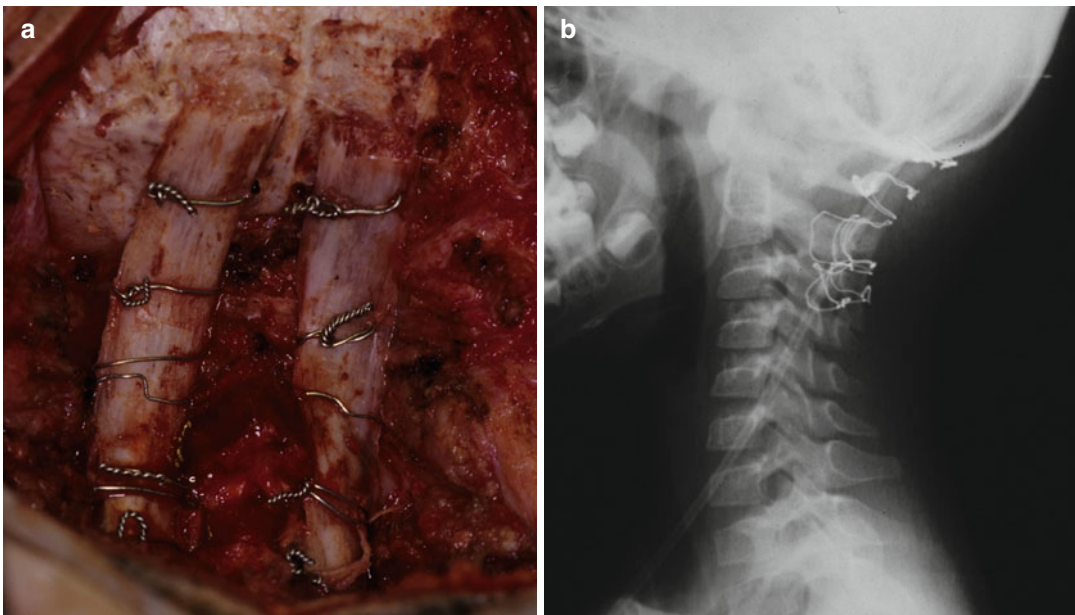


Fig. 63.6 (a) Intraoperative photograph of the patient. Ribs were used as an onlay bone graft which was held in place by suboccipital and sublaminar wires. (b) Lateral cervical x-ray showing craniocervical junction and its alignment

wire technique may be a suitable option in pediatric patients whose cervical spine anatomy may limit the use of screws [40, 41].

These former posterior cervical fusion techniques changed significantly through time to the

predominant use of lateral mass screw fixation techniques. These techniques are biomechanically stronger, more durable, and more rigid so they provide more stability to enhance bone fusion [39] (Figs. 63.9, 63.10, 63.11, and 63.12).

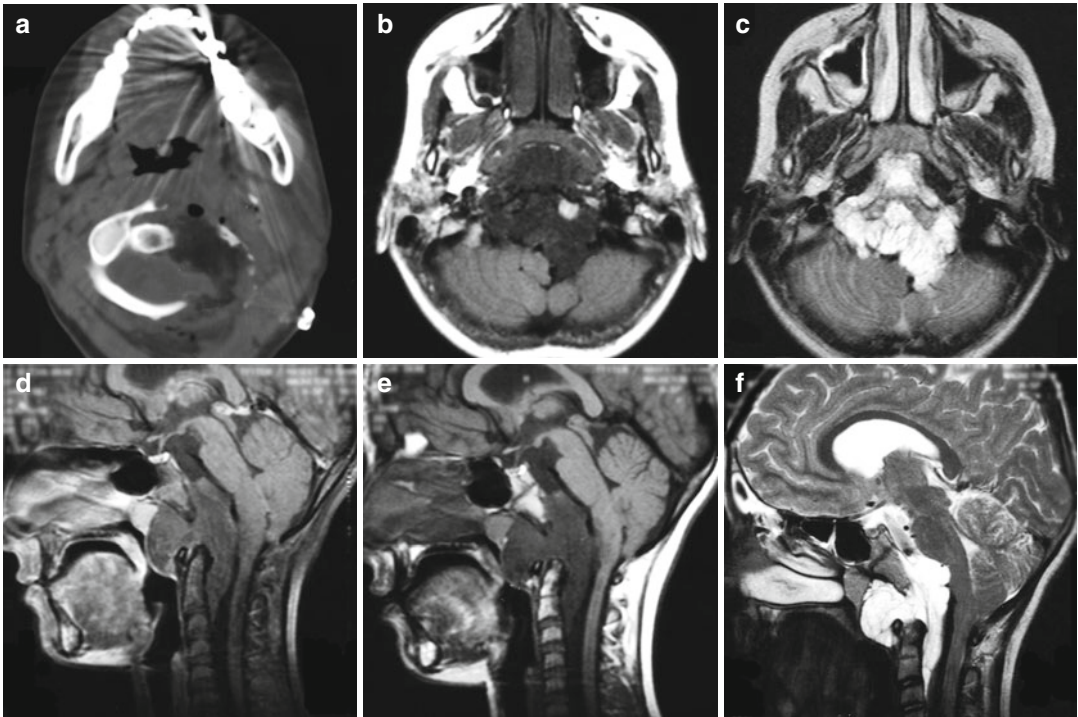


Fig. 63.7 (a) Axial head CT scan of a 12-year-old boy demonstrating a lesion-eroded C1. (b) Axial T1-weighted cranial MRI showing a hypointense mass lesion, which eroded the clivus, and the surrounding bony structures. (c) Axial T2-weighted cranial MRI showing a hyperintense lesion. (d) Contrast sagittal cranial MRI showing that the lesion is

minimally contrast enhancing. (e) T1-weighted non-contrasted sagittal plain MRI showing that the lesion compressed the brain stem and also it had grown retropharyngeally. (f) Sagittal T2-weighted image. The lesion was radiologically diagnosed as clival chordoma

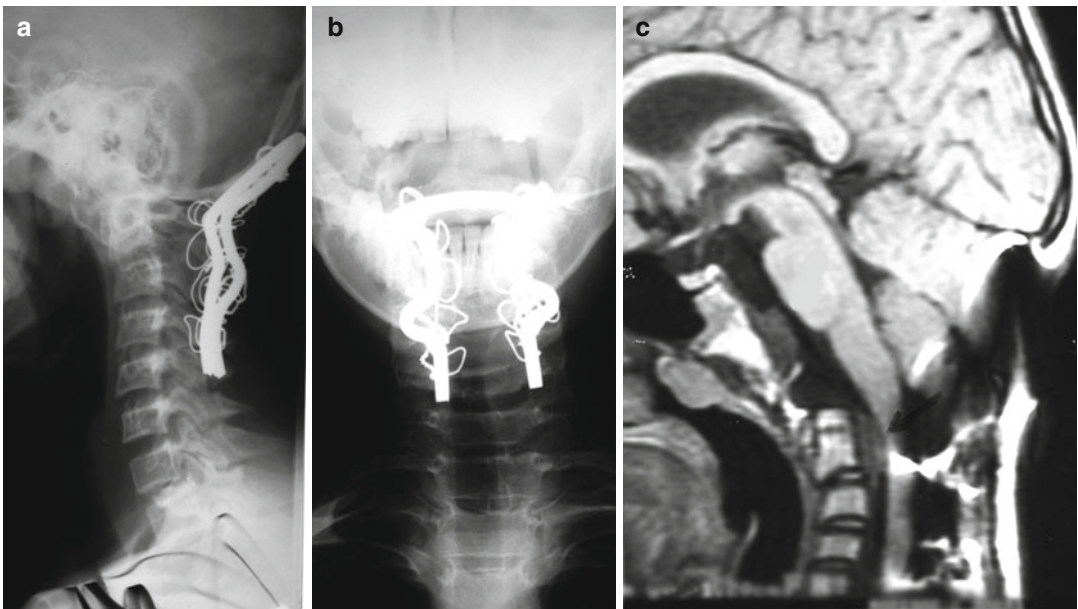


Fig. 63.8 (a, b) Postoperative lateral and anteroposterior cervical x-ray images of the same patient. Craniovertebral stabilization was performed with the rod and wire technique.

(c) Postoperative sagittal T1-weighted MRI of a patient with metallic artifacts due to rods and wires

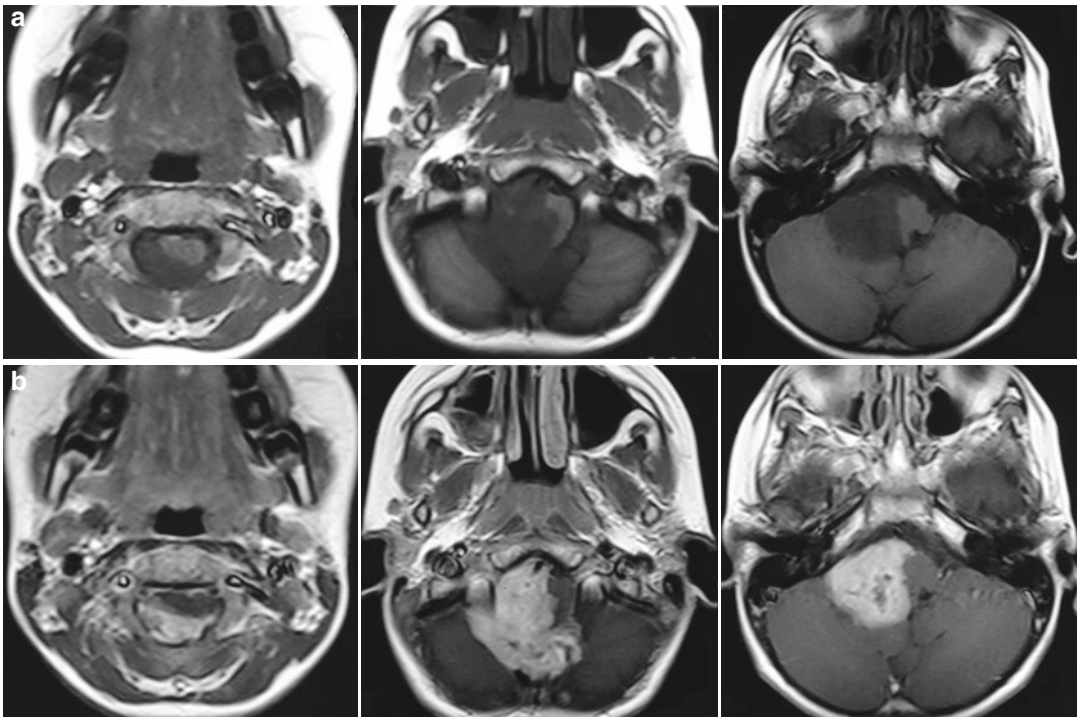


Fig. 63.9 (a) Axial T1-weighted cranial MRI of an 8-year-old boy presented with vomiting and progressive torticollis. A hypointense mass lesion in the fourth ventricle and right pontocerebellar angle was noted. (b) On axial contrasted cranial MRI scans, the lesion was contrast enhancing and radiologically diagnosed as medulloblastoma

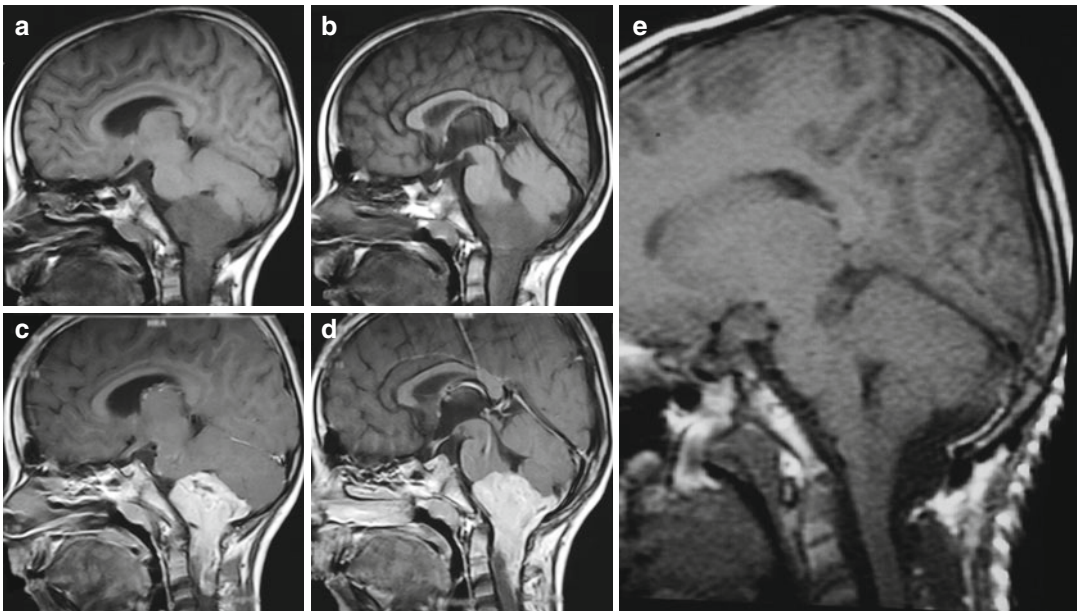


Fig. 63.10 (a, b) Sagittal T1-weighted cranial MRI images. (c, d) Axial T1-weighted cranial MRI with contrast. (e) Postoperative sagittal T1-weighted MRI of the patient

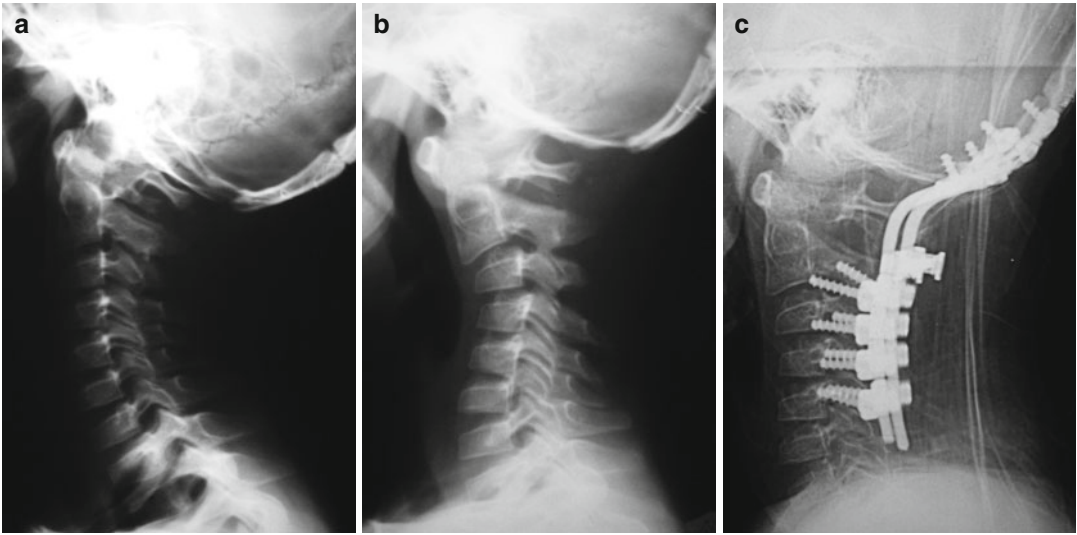


Fig. 63.11 (a) Early preoperative lateral cervical x-ray image of the patient. (b) The patient presented with new-onset torticollis and intractable neck pain. Lateral cervical x-ray was obtained showing C2-C3 dislocation. (c) Occipitocervical fusion was performed with occipitocervical rods and lateral mass screws

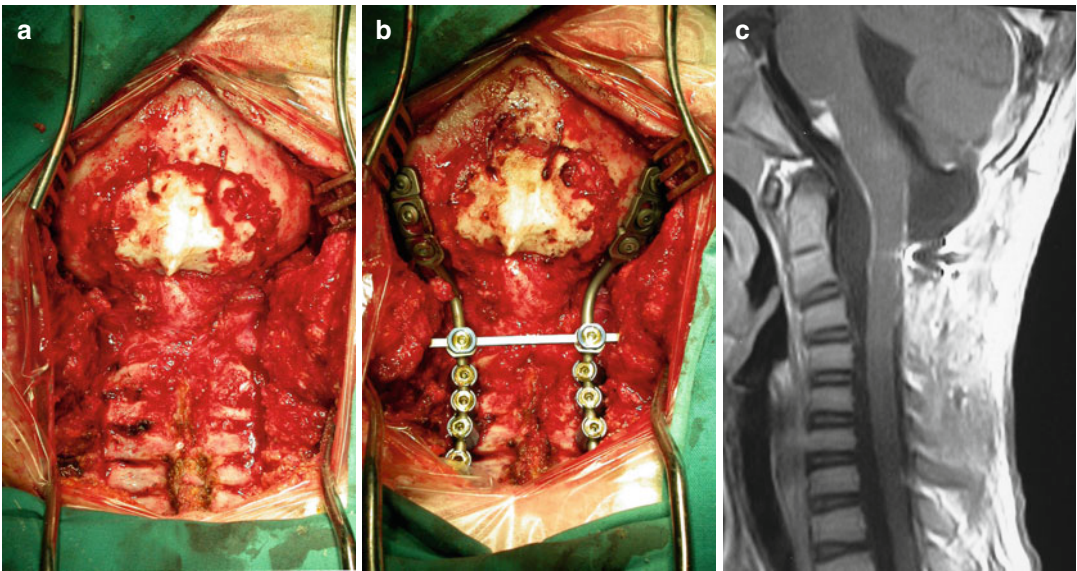


Fig. 63.12 (a) Perioperative photograph before occipitocervical instrumentation. (b) Perioperative photograph after occipitocervical instrumentation. (c) Postoperative sagittal T1-weighted MRI showing craniocervical junction and cervical vertebra alignment

References

- Steinbok P, Boyd M, Cochrane D (1989) Cervical spinal deformity following craniotomy and upper cervical laminectomy for posterior fossa tumors in children. *Childs Nerv Syst* 5(1):25–28
- Cochrane DD, Gustavsson B, Poskitt KP, Steinbok P, Kestle JR (1994) The surgical and natural morbidity of aggressive resection for posterior fossa tumors in childhood. *Pediatr Neurosurg* 20(1):19–29
- Gangemi M, Renier D, Daussange J, Hirsch JF, Rigault P (1982) Children's cervical spine instability after posterior fossa surgery. *Acta Neurol (Napoli)* 4(1):39–43
- Katsumi Y, Honma T, Nakamura T (1989) Analysis of cervical instability resulting from laminectomies for removal of spinal cord tumor. *Spine (Phila Pa 1976)* 14(11):1171–1176
- Raynor RB, Pugh J, Shapiro I (1985) Cervical facetectomy and its effect on spine strength. *J Neurosurg* 63(2):278–282
- Albert TJ, Vacarro A (1998) Postlaminectomy kyphosis. *Spine (Phila Pa 1976)* 23(24):2738–2745
- am Orde U, Glaesener JJ, Exner G, Gerner HJ (1993) Results of extensive cervical laminectomy. *Z Orthop Ihre Grenzgeb* 131(4):356–362
- Bell DF, Walker JL, O'Connor G, Tibshirani R (1994) Spinal deformity after multiple-level cervical laminectomy in children. *Spine* 19(4):406–411
- Butler JC, Whitecloud TS 3rd (1992) Postlaminectomy kyphosis. Causes and surgical management. *Orthop Clin North Am* 23(3):505–511
- McLaughlin MR, Wahlig JB, Pollack IF (1997) Incidence of postlaminectomy kyphosis after Chiari decompression. *Spine (Phila Pa 1976)* 22(6):613–617
- Inoue A, Ikata T, Katoh S (1996) Spinal deformity following surgery for spinal cord tumors and tumorous lesions: analysis based on an assessment of the spinal functional curve. *Spinal Cord* 34(9):536–542
- Guigui P, Benoist M, Deburge A (1998) Spinal deformity and instability after multilevel cervical laminectomy for spondylotic myelopathy. *Spine (Phila Pa 1976)* 23(4):440–447
- Yeh JS, Sgouros S, Walsh AR, Hockley AD (2001) Spinal sagittal malalignment following surgery for primary intramedullary tumours in children. *Pediatr Neurosurg* 35(6):318–324
- de Jonge T, Slullitel H, Dubousset J, Miladi L, Wicart P, Illes T (2005) Late-onset spinal deformities in children treated by laminectomy and radiation therapy for malignant tumours. *Eur Spine J* 14(8):765–771
- Kelly PJ (ed) (1999) *Clinically oriented anatomy*, 4th edn. Lippincott Williams & Wilkins, Philadelphia
- Harrison DD, Harrison DE, Janik TJ, Cailliet R, Ferrantelli JR, Haas JW, Holland B (2004) Modeling of the sagittal cervical spine as a method to discriminate hypolordosis: results of elliptical and circular modeling in 72 asymptomatic subjects, 52 acute neck pain subjects, and 70 chronic neck pain subjects. *Spine* 29(22):2485–2492
- Bagnall KM, Harris PF, Jones PR (1977) A radiographic study of the human fetal spine. 2. The sequence of development of ossification centres in the vertebral column. *J Anat* 124(Pt 3):791–802
- Pal GP, Sherk HH (1988) The vertical stability of the cervical spine. *Spine (Phila Pa 1976)* 13(5):447–449
- Goel VK, Clark CR, Harris KG, Schulte KR (1988) Kinematics of the cervical spine: effects of multiple total laminectomy and facet wiring. *J Orthop Res* 6(4):611–619
- Fassett DR, Clark R, Brockmeyer DL, Schmidt MH (2006) Cervical spine deformity associated with resection of spinal cord tumors. *Neurosurg Focus* 20(2):E2
- White AA 3rd, Panjabi MM, Thomas CL (1977) The clinical biomechanics of kyphotic deformities. *Clin Orthop Relat Res* 128:8–17
- Jeszszsky D, Fekete TF, Melcher R, Harms J (2007) C2 prosthesis: anterior upper cervical fixation device to reconstruct the second cervical vertebra. *Eur Spine J* 16(10):1695–1700
- Takeuchi K, Yokoyama T, Aburakawa S, Itabashi T, Toh S (2005) Anatomic study of the semispinalis cervicis for reattachment during laminoplasty. *Clin Orthop Relat Res* 436:126–131
- Sciubba DM, Chaichana KL, Woodworth GF, McGirt MJ, Gokaslan ZL, Jallo GI (2008) Factors associated with cervical instability requiring fusion after cervical laminectomy for intradural tumor resection. *J Neurosurg* 108(5):413–419
- Hwang SW, Riesenburger RI, Benzel EC (2007) Pediatric iatrogenic spinal deformity. *Neurosurg Clin N Am* 18(4):585–598
- White A, Panjabi M (1990) *Clinical biomechanics of spine*, 2nd edn. JB. Lippincott, Philadelphia
- Tachdjian MO, Matson DD (1965) Orthopaedic aspects of intraspinal tumors in infants and children. *J Bone Joint Surg Am* 47:223–248
- Yasuoka S, Peterson HA, MacCarty CS (1982) Incidence of spinal column deformity after multilevel laminectomy in children and adults. *J Neurosurg* 57(4):441–445
- Sim FH, Svien HJ, Bickel WH, Janes JM (1974) Swan-neck deformity following extensive cervical laminectomy. A review of twenty-one cases. *J Bone Joint Surg Am* 56(3):564–580
- Aronson DD, Kahn RH, Canady A, Bollinger RO, Towbin R (1991) Instability of the cervical spine after decompression in patients who have Arnold-Chiari malformation. *J Bone Joint Surg Am* 73(6):898–906
- Lunardi P, Licastro G, Missori P, Ferrante L, Fortuna A (1993) Management of intramedullary tumours in children. *Acta Neurochir (Wien)* 120(1–2):59–65
- Yasuoka S, Peterson HA, Laws ER Jr, MacCarty CS (1981) Pathogenesis and prophylaxis of postlaminectomy deformity of the spine after multiple level laminectomy: difference between children and adults. *Neurosurgery* 9(2):145–152
- Cusick JF, Yoganandan N, Pintar F, Myklebust J, Hussain H (1988) Biomechanics of cervical spine

- facetectomy and fixation techniques. *Spine (Phila Pa 1976)* 13(7):808–812
34. Zdeblick TA, Zou D, Warden KE, McCabe R, Kunz D, Vanderby R (1992) Cervical stability after foraminotomy. A biomechanical in vitro analysis. *J Bone Joint Surg Am* 74(1):22–27
 35. Shikata J, Yamamuro T, Shimizu K, Saito T (1990) Combined laminoplasty and posterolateral fusion for spinal canal surgery in children and adolescents. *Clin Orthop Relat Res* 259:92–99
 36. Cattell HS, Clark GL Jr (1967) Cervical kyphosis and instability following multiple laminectomies in children. *J Bone Joint Surg Am* 49(4):713–720
 37. Taddonio RF Jr, King AG (1982) Atlantoaxial rotatory fixation after decompressive laminectomy. A case report. *Spine (Phila Pa 1976)* 7(6):540–544
 38. Bransford RJ, Lee MJ, Reis A (2011) Posterior fixation of the upper cervical spine: contemporary techniques. *J Am Acad Orthop Surg* 19(2):63–71
 39. Molina C, Kretzer RM, Hu N, Umekoji H, Cunningham BW, Serhan H (2014) Comparative in vitro biomechanical analysis of a novel posterior cervical fixation technique versus conventional posterior-based constructs. *J Spinal Disord Tech* 27(1):40–47
 40. Schultz KD Jr, Petronio J, Haid RW et al (2000) Pediatric occipitocervical arthrodesis. A review of current options and early evaluation of rigid internal fixation techniques. *Pediatr Neurosurg* 33(4):169–181
 41. Oppenlander ME, Kalyvas J, Sonntag VK, Theodore N (2014) Technical advances in pediatric craniovertebral junction surgery. *Adv Tech Stand Neurosurg* 40:201–213

Endocrinologic Complications and Late Sequela of Childhood Posterior Fossa Tumors

64

Abdullah Bereket

64.1 Introduction

Primary malignant central nervous system (CNS) tumors are the second most common childhood malignancies, after hematologic malignancies, and are the most common pediatric solid organ tumor [1]. Although advances in surgical intervention, radiotherapy, and chemotherapy have improved the survival rates in children with CNS tumors, in general, and posterior fossa tumors, mortality and morbidity associated with these disorders persist.

Treatment of posterior fossa tumors consists of a combined modality approach that includes surgery, radiation therapy, and chemotherapy in most patients. Long-term survival is now achieved in majority of the patients, but each component of therapy can cause late complications that have a profound effect on the quality of life of survivors. Endocrine-reproductive disturbances are among the most common late effects in survivors of childhood cancers including posterior fossa tumors [2]. These often result in significant morbidity including poor growth, thyroid dysfunction, pubertal delay, gonadal toxicity/infertility, precocious puberty, adrenal insufficiency, and osteopenia. Understanding

how to improve the prevention, recognition, and treatment of endocrinopathies will improve the quality of life of these patients. Patients at risk for endocrine late effects are especially those who were treated with radiotherapy and/or high doses of alkylating agents, such as cyclophosphamide, ifosfamide, and busulfan [3]. However, in a study, 15/32 (47 %) of patients with posterior fossa tumors had evidence of endocrinopathy before RT, suggesting tumor-induced damage also plays some role in these complications [4].

Studies evaluating endocrine late consequences of posterior fossa tumors are mostly derived from children with medulloblastoma. After surgical excision, medulloblastomas are treated with external beam RT to the craniospinal axis, with an additional boost to the tumor site [5]. Contemporary radiation doses vary according to risk group. For average-risk disease, the whole brain and spine are typically treated with 23.4 Gy, with posterior fossa boost of 30.6 Gy to total dose of 54 Gy. For advanced-stage disease, 36 Gy is administered to the whole brain and spine, with a posterior fossa boost of 18 Gy to a total dose of 54 Gy. With low radiation doses (<30 Gy), GH deficiency usually occurs in isolation in about 30 % of patients, while with radiation doses of 30–50 Gy, the incidence of GH deficiency can reach 50–100 % and long-term gonadotropin, TSH, and ACTH deficiencies occur in 20–30, 3–9, and 3–6 % of patients, respectively. Precocious puberty can occur after radiation doses of <30 Gy in girls only and in

A. Bereket, M.D.
Division of Pediatric Endocrinology, Marmara
University Hospital, Istanbul, Turkey
e-mail: abdullahbereket@gmail.com

both sexes equally with a radiation dose of 30–50 Gy. Hyperprolactinemia, due to hypothalamic damage is mostly seen in young women after high-dose cranial irradiation and is usually subclinical [6].

Current protocols are investigating the use of reduced posterior fossa high-dose volume boost in order to spare normal brain from excess radiation exposure. Newer techniques, such as intensity-modulated RT and proton radiation therapy, are being evaluated to limit radiation to normal tissues [7]. Although higher doses of RT are associated with better tumor control [5], irradiation of the craniospinal axis in children is, in addition to neurologic complications, associated with poor skeletal growth, hypothyroidism, adrenal insufficiency, and hypogonadism, all of which may be minimized with lower doses of radiation and/or newer techniques. In a study comparing reduced dose (18 Gy) with conventional dose (23–39 Gy) of radiotherapy, adult heights of group 18 Gy were significantly better than those who received conventional dose (CD) and were not different from midparental heights, unlike group CD, whose adult heights were less than midparental heights. Of other endocrine sequelae, ten patients of the CD group were hypothyroid, three had adrenal insufficiency, three had hypogonadism, and two had early puberty. In contrast, within group 18 Gy, only one was hypothyroid and one had early puberty. Thus, endocrine morbidity was significantly reduced with 18 Gy CSRT in young children with medulloblastoma [8].

Because of the risks of serious complications, the initial management of pediatric patients with medulloblastoma has utilized adjuvant chemotherapy with decreased doses of RT in average-risk children or substituted chemotherapy for RT in the initial management of infants and young children. However, chemotherapy itself has unwanted long-term effects especially on the gonads. Depending on the cumulative doses, cyclophosphamide, ifosfamide, mechlorethamine, procarbazine, busulfan, melphalan, and cisplatin are associated with gonadotoxicity in both sexes [9].

64.2 Specific Endocrinologic Complications of Posterior Fossa Tumors

64.2.1 Poor Growth

Linear growth in childhood posterior fossa tumor survivors may be negatively influenced by both endocrine and non-endocrine factors. Non-endocrine factors include radiation-induced direct damage to the vertebral growth plates. Spinal irradiation damages both the epiphyseal plates and the bony matrix. Patients treated with spinal irradiation often manifest stunted spinal growth, which becomes most apparent during puberty [10]. In the year after the diagnosis of medulloblastoma, poor growth may result from ill health and anorexia, though an associated transient GH deficiency is known to occur during or immediately after cranial irradiation. It has been shown that the major factor in poor growth is retardation of spinal growth particularly during periods of accelerated growth [11]. Brauner et al. [12] showed in a prospective study of 16 children, aged 1.7–15 years at the time of treatment, who received cranial (31–42 Gy) and spinal radiation for medulloblastoma or ependymoma. Their growth was compared to that of 11 children given similar doses of cranial radiation only. At the 2-year follow-up, children treated by cranial and spinal radiation had a mean height of -1.46 ± 0.40 SD below the normal mean. In contrast, the children given only cranial radiation had a mean height of -0.15 ± 0.18 SD further supports that poor growth in these children are mainly due to spinal irradiation.

Another cause for the poor growth is GH deficiency. GH is the most sensitive hormone to radiation injury; thus, GH deficiency is the most common endocrinopathy seen in childhood cancer survivors following cranial irradiation. GH deficiency occurs in a dose- and time-related fashion with risk increasing as doses exceed 18 Gy of radiation and the time interval increases from treatment [13]. Shalet has shown that doses as low as >2.9 Gy cause GH deficiency [14]. In survivors of medulloblastoma, young age at treatment was a determinant of GH deficiency in adulthood [15].

In order for a timely recognition of growth retardation in children with posterior fossa tumors, regular monitoring of height and sitting height is essential. After reviewing the child's growth curves and treatment-related risk factors, GH stimulation testing is indicated in most cases based on documentation of poor growth. Failure of two GH stimulation tests, using two different pharmacologic agents known to increase GH secretion, is required for the diagnosis of GH deficiency. In patients who received irradiation, insulin-induced hypoglycemia may be the most sensitive and reliable pharmacologic test of GH status; however, it may cause serious hypoglycemia-related events and should only be done in experienced centers under close surveillance. IGF-1 and IGF-binding protein 3 (IGF-BP3), which are commonly used as surrogate markers of GH secretion in children assessed for short stature, are not reliable indicators of GH status following cranial irradiation or documented hypothalamo-pituitary injury due to tumoral expansion [16]. For children who prove to be GH deficient, a comprehensive consultation regarding the benefits and risks of GH therapy should be performed prior to the initiation of therapy. Although several studies have reported no evidence of increased risk of tumor recurrence associated with GH therapy [17], there are data showing a small risk of second neoplasms, particularly solid tumors, in childhood cancer survivors treated with GH [18].

Once the risks and benefits have been carefully discussed, GH therapy can be provided to patients with GH deficiency. In a report of 183 childhood cancer survivors treated with GH, higher final height was associated with a younger bone age at the time of initiation of GH and higher doses of GH, while a higher dose of spinal irradiation was negatively associated with final height [19].

64.2.2 Hypothyroidism

Thyroid hormone is important for normal development and metabolism in children and young adults. Survivors of posterior fossa tumors develop hypothyroidism in varying frequency and the etiology depending on the exposure and

the dose of radiation. Since both the neck and hypothalamo-pituitary area may have been exposed to radiation, they can develop primary hypothyroidism, central hypothyroidism, or a mixed form of hypothyroidism. The diagnosis of primary hypothyroidism is based on high serum TSH levels and low serum free T4 values, whereas in central and mixed hypothyroidism, low free T4 is accompanied by a normal or modestly elevated TSH. In a study investigating thyroid dysfunction in childhood posterior fossa tumors, hypothyroidism was found in 12/23 patients in the course of treatment, in two patients hormone deficits were diagnosed directly after irradiation, and in ten patients such condition was observed at the end of the whole therapy [20].

Primary hypothyroidism is seen more commonly than central hypothyroidism (38 % and 19 %) in medulloblastoma [21]. In that study, All seven children <5 years developed hypothyroidism, whereas the frequency of hypothyroidism was 60 % and 20 % in children of 5–10 years and >10 years respectively. Furthermore, hypothyroidism was documented in 83 % who had 23Gy+CT, 60 % who had 36Gy+CT, and 20 % who had 36Gy without CT. However, Ricardi et al. [22] have shown that the use of hyperfractionated craniospinal radiotherapy in the treatment of childhood posterior fossa primitive neuroectodermal tumors is associated with a lower risk of developing late thyroid dysfunction. Young age and the use of chemotherapy and conventional doses of radiotherapy are associated with a higher incidence of hypothyroidism. Levothyroxine is indicated for patients with TSH deficiency. Dose should be titrated to maintain normal free T4 levels. Serum TSH should be monitored to assess dosing adequacy and medication compliance.

64.2.3 Thyroid Neoplasms

Because of the exposure of the neck to radiation during craniospinal irradiation, children with posterior fossa tumors are at risk for both benign and malignant thyroid neoplasms [23]. The raised TSH values in association with the radiation damage to the

thyroid may be an important factor in carcinogenesis [24]. Thus, treatment with thyroxine to suppress elevated TSH may be appropriate in these patients. Treatment prior to 10 years of age and/or total doses of radiation between 20 and 29 Gy appear to confer the greatest risk for the development of thyroid cancer [23]. The association between radiation dose and thyroid cancer is curvilinear, with risk increasing at low to moderate doses and decreasing at doses >30 Gy due to cell-killing effect [25]. Among patients treated with radiation doses to the thyroid of ≤ 20 Gy, treatment with alkylating agents appears to increase thyroid cancer risk [26]. The risk of thyroid cancer persists throughout the adult life of at-risk survivors. There are case reports of thyroid carcinoma that developed 7–12 years after irradiation for medulloblastoma [27, 28]. The Children's Oncology Group (COG) currently recommends annual exam of the thyroid gland via careful palpation. Routine use of screening thyroid ultrasonography in childhood cancer survivors increases detection of small nodules of uncertain clinical significance and may result in unnecessary and excessive invasive procedures. This was illustrated in a study of pediatric Hodgkin lymphoma survivors who underwent routine screening thyroid ultrasonography. Although thyroid nodules were a common finding, only one case of malignant thyroid cancer was detected by ultrasound screening. Another six cases of thyroid cancer developed in the cohort, which were detected after clinical findings prompted further evaluation. All seven patients with thyroid cancer were alive at the time of data analysis [29]. Thus, in survivors of posterior fossa tumors, careful palpation and/or thyroid US annually is recommended. In patients who have suspicious nodules (based on ultrasonographic and clinical features), a fine needle aspiration is required to rule out malignancy. Continuous follow-up with US is needed in those with benign cytology.

64.2.4 Delayed/Arrested Puberty

Survivors of childhood posterior fossa tumors may have delayed or arrested puberty depending on their age due to hypogonadotropic hypogonadism or gonadal insufficiency. Those who have reached sexual maturity can also

develop treatment-related LH/FSH deficiency. Presentation in adult females includes secondary amenorrhea, and in males, loss of libido, erectile dysfunction, and reduced energy or stamina.

Delayed puberty is defined by lack of breast development in girls by 13 years of age and lack of testicular enlargement in boys by 14 years of age. Arrested puberty is nonprogression or lack of completion of puberty that has started. Those who are treated with doses of radiation >30–40 Gy to the hypothalamo-pituitary axis are at risk for deficits of LH and FSH called hypogonadotropic hypogonadism (low serum FSH and LH levels) [30]. In addition, survivors are at risk for primary gonadal dysfunction due to direct damage to the ovaries or testes (in which case serum FSH and LH are elevated and is called hypergonadotropic hypogonadism). Similar to those in hypothyroidism, some patients with gonadal failure may also have partial gonadotropin deficiency which prevents the elevation of gonadotropins and masks gonadal damage. Measurement of inhibin B and antimüllerian hormone (AMH) may be helpful in these circumstances. Cuny et al. [31] measured plasma inhibin B in 34 boys and 22 girls to evaluate the roles of hypothalamo-pituitary and spinal irradiations and chemotherapy in gonadal deficiency after treatment for medulloblastoma or posterior fossa ependymoma. Two boys had partial gonadotropin deficiency, combined with testicular deficiency in one boy. Six boys had increased levels of FSH, indicating tubular deficiency, combined with Leydig cell deficiency in five boys. The seven boys with inhibin B levels <100 ng/mL included the one with combined deficiencies and the six with testicular deficiency. Puberty did not progress in seven girls; three had gonadotropin deficiency, combined with ovarian deficiency in one, and four had increased FSH levels, indicating ovarian deficiency. Inhibin B and AMH levels were low in the girl with combined deficiencies, in the four girls with ovarian deficiency, and in four girls with normal clinical-biological ovarian function, including two who underwent ovarian transposition before irradiation. Thus, it appears that plasma concentrations of inhibin B and AMH are useful means of detecting primary gonad deficiency in patients with no increase in their plasma

gonadotropin levels because of radiation-induced gonadotropin deficiency.

The etiology of hypogonadotropic hypogonadism is clearly radiation exposure of brain. However, gonadal failure may result from radiation exposure to gonads and/or damage due to chemotherapy. Ovarian [32] and testicular [33] damage after abdominal irradiation in childhood is known for a long time. This is influenced not only by the total radiation dose but also by the fractionation and time sequence of treatment and the sex and age of the patient. Single doses of 6 Gy are probably 100 % effective in inducing permanent sterility in women of all ages [34]. Brown et al. [35] have shown that after spinal irradiation of 35 Gy, the scattered dose to the ovaries may be as high as 10 Gy, and by the use of skin dose meters, they calculated a cumulative dose of approximately 2.4 Gy to the testes. It has been shown that patients who had had CCNU but no spinal radiotherapy had evidence of primary gonadal damage [35].

64.2.4.1 Males

The human testis has two primary functions: sperm production and testosterone production. One or both of these functions may be damaged by cancer treatment. Germ cells and Sertoli cells form the seminiferous tubules where spermatogenesis occurs; Leydig cells are responsible for the production of testosterone.

Germ Cell Dysfunction

The following chemotherapeutic agents are associated with impaired spermatogenesis, which is dependent on the cumulative dose [9]: mechlorethamine, cyclophosphamide, ifosfamide, procarbazine, busulfan, melphalan (all alkylating agents), and cisplatin. Alkylating agents used in concert have additive gonadotoxic effects. Although earlier studies suggested that younger age at treatment was associated with a lower risk of germ cell loss, data are inconclusive. Sperm analysis is the only definitive test available to determine a survivor's ability to produce sperm. Although a variety of clinical (e.g., decreased testicular volume) and biochemical findings (e.g., raised plasma concentrations of

follicle-stimulating hormone [FSH] and reduced plasma concentrations of inhibin B) have been associated with impaired sperm production in population studies, none is suitable as a diagnostic for oligospermia due to poor sensitivity and/or specificity.

Leydig Cell Dysfunction

Leydig cells are susceptible to radiation-induced damage at higher doses than those associated with germ cell dysfunction; risk is directly related to testicular radiation dose and inversely related to age at treatment [36]. The majority of males who receive <20 Gy fractionated radiation to the testes will continue to produce normal amounts of testosterone [36]. However, most prepubertal males who receive radiation doses ≥ 24 Gy to the testis will develop Leydig cell failure. Chemotherapy alone rarely results in Leydig cell failure, although subclinical Leydig cell dysfunction has been reported following treatment with alkylating agents [9]. Ahmed et al. [37] showed that in a group of patients with medulloblastoma who received surgery and craniospinal radiation, only those who received chemotherapy had evidence of gonadal failure. They concluded that nitrosoureas were responsible for the gonadal damage in the children with procarbazine, also contributing to the damage in the three children who received this drug. The authors questioned the necessity of adjuvant chemotherapy in view of the limited proved value of adjuvant chemotherapy with nitrosoureas in the treatment of medulloblastoma and recognition of this serious complication of cytotoxic drug therapy. Leydig cell failure will result in failed entry if it occurs before pubertal onset or pubertal arrest if it occurs after the start of puberty. Affected males who have completed normal puberty may present with reduced libido, erectile dysfunction, decreased bone mineral density, and decreased muscle mass. Elevated serum levels of LH with low levels of testosterone are consistent with the diagnosis of Leydig cell failure. Males with Leydig cell failure should be referred to an endocrinologist for the initiation of testosterone replacement therapy.

64.2.4.2 Females

Ovarian dysfunction may result from treatment with gonadotoxic chemotherapy (especially

alkylating agents) or radiation impacting the ovaries [31, 32, 35, 38]. Due to the interdependence of the sex steroid-producing cells and oocytes within the ovarian follicle, ovarian failure results in impairment of both sex hormone production and fertility. Risk is directly correlated with cumulative dose and older age at exposure. Radiation doses to the ovary exceeding 10 Gy are associated with a very high risk of ovarian failure [39]. When ovarian transposition is performed prior to radiotherapy, however, many girls retain ovarian function [40]. Furthermore, Harden et al. [41] have shown that using MRI to localize the ovaries for positioning and a modified radiotherapy technique using a non-divergent beam edge inferiorly, it is possible to reduce the ovarian dose by 66 %. This technique was able to reduce the number of patients receiving <4 Gy to a single ovary from three to six. Irradiation at older age confers a greater risk. Women who have normal ovarian function at the end of treatment with potentially gonadotoxic therapy remain at risk for premature menopause later in life and should be counseled accordingly [42]. All patients treated with the gonadotoxic therapies should have periodic screening of LH and FSH measurements and Tanner staging to monitor pubertal progression. Elevated gonadotropin levels indicate ovarian dysfunction. Patients should be referred to an endocrinologist for the initiation of ovarian hormone replacement therapy.

64.2.5 Precocious Puberty

Central precocious puberty is defined as any sign of secondary sexual maturity before age 8 years in girls and age 9 years in boys which is caused by premature activation of the hypothalamo-pituitary-gonadal axis and subsequent early elevation of LH and FSH levels. In girls, this may lead to early menarche, defined by the onset of menstrual cycles prior to the age of 10 years. Advancement of bone age more than two standard deviations for chronological age is also a consistent finding in children with precocious puberty. In survivors of central nervous system (CNS) malignancies, or those treated with cranial

radiotherapy, puberty may progress at a rapid tempo with similar advancement of bone age and risk of short stature [43–45]. Childhood brain cancer survivors treated with cranial irradiation regardless of dosing (>18 Gy) are at risk for the development of central precocious puberty [43, 44]. Other risk factors include younger age at diagnosis, female sex, and increased body mass index [44]. Survivors of posterior fossa tumors who are noted to have a rapid tempo of pubertal development should be referred to an endocrinologist. Assessment of skeletal maturity via standard bone age and measurement of LH, FSH, and testosterone/estradiol levels should be done. A pelvic ultrasound, which assesses the size of the ovaries and uterus, also may be obtained in girls. Since central precocious puberty may cause rapid bone age advancement with resultant reduction in final height potential, it may be beneficial to temporally suppress the hypothalamo-pituitary-gonadal axis by employing long-acting formulations of gonadotropin-releasing hormone (GnRH) agonists. Such therapy may prevent further advancement in skeletal maturity, resulting in a modest improvement in final height.

64.2.6 Adrenocorticotrophic Hormone (ACTH) Deficiency

In healthy individuals, the hypothalamus releases corticotropin-releasing hormone and vasopressin, which stimulate the pituitary gland to secrete ACTH. ACTH prompts secretion of cortisol from the adrenal cortex. Cortisol is a regulatory hormone in gluconeogenesis, the body's response to stress, and has a major role in maintaining homeostasis. ACTH deficiency is infrequently encountered in posterior fossa tumor survivors related to high-dose irradiation >30 Gy to the hypothalamo-pituitary area [46, 47]. Transient ACTH deficiency may also result from prolonged use of pharmacologic doses of glucocorticoids. Patients with ACTH deficiency may present with fatigue, poor weight gain, and/or hypoglycemia. In times of stress or illness, unrecognized ACTH deficiency can be life-threatening. The patients should be screened annually for ACTH deficiency,

by obtaining a fasting morning cortisol level at 8 AM. At-risk patients with screening basal cortisol levels <10 mcg/dL (276 nmol/L), or those who are symptomatic, should be referred to an endocrinologist for dynamic testing of adrenal function. Tests for appropriate central regulation of adrenal function include the insulin tolerance test, glucagon stimulation test, metyrapone test, standard-dose cosyntropin test, and low-dose cosyntropin test. Patients with ACTH deficiency require glucocorticoid replacement therapy (e.g., hydrocortisone, prednisone, or prednisolone) at physiologic doses based on a daily production rate of hydrocortisone of 7 mg/m² per day. Under stress conditions, such as illness or surgery, glucocorticoid dosing should be increased to three times the normal replacement dose. If the patient is unable to tolerate oral therapy, an intramuscular injection of approximately 50 mg/m² of hydrocortisone sodium succinate (Solu-Cortef) should be administered. Every patient with ACTH deficiency should wear a medical identification bracelet, indicating the diagnosis of adrenal insufficiency, at all times.

64.2.7 Low Bone Mineral Density

Dual energy x-ray absorptiometry (DEXA) has traditionally been used to determine BMD, but results in children and adolescents must be interpreted according to age, height, and pubertal stage using normative Z scores rather than T scores. Children who have undergone irradiation for posterior fossa tumors have diminished total body and lumbar spine bone mineral density (BMD), as compared with those of the general population [48–50]. In most of these patients, BMD was lower than normal in both the lumbar column and in the femoral neck. However, bone mass loss was higher in the lumbar region than in the femoral neck, due to spinal radiation therapy and to the effect of hormonal deficiencies. Particularly hypogonadism, but also multiple hormonal deficiencies, is associated with lower BMD values. In a study, regional BMD has been measured using DEXA in adults following craniospinal irradiation for medulloblastoma between ages 4 and 19 years,

receiving doses of 35–40 Gy to the brain and spinal cord. Failure to achieve a normal BMD and mean reduction at the lumbar spine of 12.1 % and a mean reduction at the femoral neck of 14.3 % was observed [49]. No relationship was found between reduction in BMD at either site and age at irradiation, time elapsed since irradiation, or BMI at time of scanning. Biochemical and endocrine markers including corrected calcium, alkaline phosphatase, sex hormones, and IGF-1 were normal in all patients. The reduction in BMD outside the irradiated area suggests that indirect factors may be important in this effect. In another study done in survivors of posterior fossa tumors, the reduction in BMD was similar within all treatment groups (craniospinal irradiation and chemotherapy, only craniospinal irradiation, and only posterior fossa irradiation), which suggests that chemotherapy did not play a major role and that localized irradiation may have systemic effects [50]. This population often has balance and gait problems, so the risk of falling, coupled with osteopenia, may place them at considerably increased risk of fractures.

In addition to radiation and gonadotropin deficiency, growth hormone (GH) deficiency may contribute to low BMD in survivors of posterior fossa tumors. Sedentary lifestyle and suboptimal nutrition, which is often problematic in these groups of children, may also worsen BMD. Subjects at high risk for low BMD and those who experience fractures should undergo screening with bone density studies upon entry into a long-term follow-up program. Calcium and vitamin D supplementation and regular weight-bearing exercise should be encouraged in these children with borderline or low BMD. Sex hormone and GH replacement therapies should be implemented in those with hormone deficiencies to prevent pathological fractures, thus improving the quality of life.

References

1. Linabery AM, Ross JA (2008) Trends in childhood cancer incidence in the U.S. (1992–2004). *Cancer* 112(2):416
2. Hudson MM, Ness KK, Gurney JG, Mulrooney DA, Chemaitilly W, Krull KR, Green DM, Armstrong GT,

- Nottage KA, Jones KE, Sklar CA, Srivastava DK, Robison LL (2013) Clinical ascertainment of health outcomes among adults treated for childhood cancer. *JAMA* 309(22):2371–2381
3. Nandagopal R, Laverdière C, Mulrooney D, Hudson MM, Meacham L (2008) Endocrine late effects of childhood cancer therapy: a report from the Children's Oncology Group. *Horm Res* 69(2):65
 4. Merchant TE, Williams T, Smith JM, Rose SR, Danish RK, Burghen GA, Kun LE, Lustig RH (2002) Preirradiation endocrinopathies in pediatric brain tumor patients determined by dynamic tests of endocrine function. *Int J Radiat Oncol Biol Phys* 54(1):45–50
 5. Hughes EN, Shillito J, Sallan SE, Loeffler JS, Cassady JR, Tarbell NJ (1988) Medulloblastoma at the joint center for radiation therapy between 1968 and 1984. The influence of radiation dose on the patterns of failure and survival. *Cancer* 61(10):1992
 6. Darzy KH, Shalet SM (2009) Hypopituitarism following radiotherapy revisited. *Endocr Dev* 15:1–24
 7. St Clair WH, Adams JA, Bues M, Fullerton BC, La Shell S, Kooy HM, Loeffler JS, Tarbell NJ (2004) Advantage of protons compared to conventional X-ray or IMRT in the treatment of a pediatric patient with medulloblastoma. *Int J Radiat Oncol Biol Phys* 58(3):727
 8. Xu W, Janss A, Packer RJ, Phillips P, Goldwein J, Moshang T Jr (2004) Endocrine outcome in children with medulloblastoma treated with 18 Gy of craniospinal radiation therapy. *Neuro Oncol* 6(2):113–118
 9. Kenney LB, Cohen LE, Shnorhavorian M, Metzger ML, Lockart B, Hijjiya N, Duffey-Lind E, Constine L, Green D, Meacham L (2012) Male reproductive health after childhood, adolescent, and young adult cancers: a report from the Children's Oncology Group. *J Clin Oncol* 30(27):3408–3416
 10. Shalet SM, Gibson B, Swindell R, Pearson D (1987) Effect of spinal irradiation on growth. *Arch Dis Child* 62(5):461–464
 11. Broadbent VA, Barnes ND, Wheeler TK (1981) Medulloblastoma in childhood: long term results of treatment. *Cancer* 48:26–30
 12. Brauner R, Rappaport R, Prevot C, Czernichow P, Zucker JM, Bataini P, Lemerle J, Sarrazin D, Guyda HJ (1989) A prospective study of the development of growth hormone deficiency in children given cranial irradiation, and its relation to statural growth. *J Clin Endocrinol Metab* 68(2):346–351
 13. Darzy KH (2009) Radiation-induced hypopituitarism after cancer therapy: who, how and when to test. *Nat Clin Pract Endocrinol Metab* 5(2):88–99
 14. Shalet SM, Beardwell CG, Pearson D, Morris-Jones PH (1976) The effect of varying doses of cerebral irradiation on growth hormone production in childhood. *Clin Endocrinol (Oxf)* 5:287–290
 15. Heikens J, Michiels EM, Behrendt H, Ender E, Bakker PJ (1998) Fliers long-term neuro-endocrine sequelae after treatment for childhood medulloblastoma. *Eur J Cancer* 34(10):1592–1597
 16. Weinzimer SA, Homan SA, Ferry RJ, Moshang T (1999) Serum IGF-I and IGFBP-3 concentrations do not accurately predict growth hormone deficiency in children with brain tumours. *Clin Endocrinol (Oxf)* 51(3):339–345
 17. Packer RJ, Boyett JM, Janss AJ, Stavrou T, Kun L, Wisoff J, Russo C, Geyer R, Phillips P, Kieran M, Greenberg M, Goldman S, Hyder D, Heideman R, Jones-Wallace D, August GP, Smith SH, Moshang T (2001) Growth hormone replacement therapy in children with medulloblastoma: use and effect on tumor control. *J Clin Oncol* 19(2):480–487
 18. Ergun-Longmire B, Mertens AC, Mitby P, Qin J, Heller G, Shi W, Yasui Y, Robison LL, Sklar CA (2006) Growth hormone treatment and risk of second neoplasms in the childhood cancer survivor. *J Clin Endocrinol Metab* 91(9):3494
 19. Brownstein CM, Mertens AC, Mitby PA, Stovall M, Qin J, Heller G, Robison LL, Sklar CA (2004) Factors that affect final height and change in height standard deviation scores in survivors of childhood cancer treated with growth hormone: a report from the childhood cancer survivor study. *J Clin Endocrinol Metab* 89(9):4422–4427
 20. Sobol G, Musioł K, Kalina M, Kalina-Faska B, Miziamalarz A, Ficek K, Mandera M, Woś H, Malecka-Tendera E (2012) The evaluation of function and the ultrasonographic picture of thyroid in children treated for medulloblastoma. *Childs Nerv Syst* 28(3):399–404
 21. Paulino AC (2002) Hypothyroidism in children with medulloblastoma: a comparison of 3600 and 2340 cGy craniospinal radiotherapy. *Int J Radiat Oncol Biol Phys* 53(3):543–547
 22. Ricardi U, Corrias A, Einaudi S, Genitori L, Sandri A, di Montezemolo LC, Besençon L, Madon E, Urgesi A (2001) Thyroid dysfunction as a late effect in childhood medulloblastoma: a comparison of hyperfractionated versus conventionally fractionated craniospinal radiotherapy. *Int J Radiat Oncol Biol Phys* 50(5):1287–1294
 23. Bhatti P, Veiga LH, Ronckers CM, Sigurdson AJ, Stovall M, Smith SA, Weathers R, Leisenring W, Mertens AC, Hammond S, Friedman DL, Neglia JP, Meadows AT, Donaldson SS, Sklar CA, Robison LL, Inskip PD (2010) Risk of second primary thyroid cancer after radiotherapy for a childhood cancer in a large cohort study: an update from the childhood cancer survivor study. *Radiat Res* 174(6):741–752
 24. Conard RA, Rall JE, Sutow WW (1966) Thyroid nodules as a late sequela of radioactive fallout. *N Engl J Med* 274:1391–1399
 25. Sigurdson AJ, Ronckers CM, Mertens AC, Stovall M, Smith SA, Liu Y, Berkow RL, Hammond S, Neglia JP, Meadows AT, Sklar CA, Robison LL, Inskip PD (2005) Primary thyroid cancer after a first tumour in childhood (the Childhood Cancer Survivor Study): a nested case-control study. *Lancet* 365(9476):2014
 26. Veiga LH, Bhatti P, Ronckers CM, Sigurdson AJ, Stovall M, Smith SA, Weathers R, Leisenring W, Mertens AC, Hammond S, Neglia JP, Meadows AT,

- Donaldson SS, Sklar CA, Friedman DL, Robison LL, Inskip PD (2012) Chemotherapy and thyroid cancer risk: a report from the childhood cancer survivor study. *Cancer Epidemiol Biomarkers Prev* 21(1):92–101
27. Raventos A, Duszynski DO (1963) Thyroid cancer following irradiation for medulloblastoma. *AJR Am J Roentgenol* 89:175–181
 28. Andrew DS, Kerr IF (1965) Carcinoma of thyroid following irradiation for medulloblastoma. *Clin Radiol* 16:282–283
 29. Metzger ML, Howard SC, Hudson MM, Gow KW, Li CS, Krasin MJ, Merchant T, Kun L, Shelso J, Pui CH, Shochat SJ, McCarville MB (2006) Natural history of thyroid nodules in survivors of pediatric Hodgkin lymphoma. *Pediatr Blood Cancer* 46(3):314–319
 30. Sklar CA, Constine LS (1995) Chronic neuroendocrinological sequelae of radiation therapy. *Int J Radiat Oncol Biol Phys* 31:1113
 31. Cuny A, Trivin C, Brailly-Tabard S, Adan L, Zerah M, Sainte-Rose C, Alapetite C, Brugières L, Habrand JL, Doz F, Brauner R (2011) Inhibin B and anti-Müllerian hormone as markers of gonadal function after treatment for medulloblastoma or posterior fossa ependymoma during childhood. *J Pediatr* 158(6):1016–1022
 32. Shalet SM, Beardwell CG, Morris-Jones PH, Pearson D, Orrell DH (1976) Ovarian failure following abdominal irradiation in childhood. *Br J Cancer* 33:655–658
 33. Shalet SM, Beardwell CG, Jacobs HS, Pearson D (1978) Testicular function following irradiation of the human prepubertal testis. *Clin Endocrinol (Oxf)* 9:483–490
 34. Ash P (1980) The influence of radiation on fertility in man. *Br J Radiol* 53:271–278
 35. Brown HI, Lee TJ, Eden B, Bullimore JA, Savage CL (1983) Growth and endocrine function after treatment for medulloblastoma. *Arch Dis Child* 58:722–727
 36. Sklar C (1999) Reproductive physiology and treatment-related loss of sex hormone production. *Med Pediatr Oncol* 33(1):2
 37. Ahmed SR, Shalet SM, Campbell RH, Deakin DP (1983) Primary gonadal damage following treatment of brain tumors in childhood. *J Pediatr* 103(4):562–565
 38. Clayton PE, Shalet SM, Price DA, Jones PH (1989) Ovarian function following chemotherapy for childhood brain tumours. *Med Pediatr Oncol* 17(2):92–96
 39. Green DM, Whitton JA, Stovall M, Mertens AC, Donaldson SS, Ruymann FB, Pendergrass TW, Robison LL (2002) Pregnancy outcome of female survivors of childhood cancer: a report from the Childhood Cancer Survivor Study. *Am J Obstet Gynecol* 187(4):1070
 40. Barahmeh S, Al Masri M, Badran O, Masarweh M, El-Ghanem M, Jaradat I, Lataifeh I (2013) Ovarian transposition before pelvic irradiation: indications and functional outcome. *J Obstet Gynaecol Res* 39(11):1533–1537
 41. Harden SV, Twyman N, Lomas DJ, Williams D, Burnet NG, Williams MV (2003) A method for reducing ovarian doses in whole neuro-axis irradiation for medulloblastoma. *Radiother Oncol* 69(2):183–188
 42. Chemaitilly W, Mertens AC, Mitby P, Whitton J, Stovall M, Yasui Y, Robison LL, Sklar CA (2006) Acute ovarian failure in the childhood cancer survivor study. *J Clin Endocrinol Metab* 91(5):1723
 43. Armstrong GT, Chow EJ, Sklar CA (2009) Alterations in pubertal timing following therapy for childhood malignancies. *Endocr Dev* 15:25
 44. Oberfield SE, Soranno D, Nirenberg A, Heller G, Allen JC, David R, Levine LS, Sklar CA (1996) Age at onset of puberty following high-dose central nervous system radiation therapy. *Arch Pediatr Adolesc Med* 150(6):589–592
 45. Josan VA, Timms CD, Rickert C, Wallace D (2007) Cerebellar astrocytoma presenting with precocious puberty in a girl. Case report. *J Neurosurg* 107(1 Suppl):66–68
 46. Rose SR, Danish RK, Kearney NS, Schreiber RE, Lustig RH, Burghen GA, Hudson MM (2005) ACTH deficiency in childhood cancer survivors. *Pediatr Blood Cancer* 45(6):808
 47. Patterson BC, Truxillo L, Wasilewski-Masker K, Mertens AC, Meacham LR (2009) Adrenal function testing in pediatric cancer survivors. *Pediatr Blood Cancer* 53(7):1302
 48. Petraroli M, D'Alessio E, Ausili E, Barini A, Caradonna P, Riccardi R, Caldarelli M, Rossodivita A (2007) Bone mineral density in survivors of childhood brain tumours. *Childs Nerv Syst* 23(1):59–65
 49. Mithal NP, Almond MK, Evans K, Hoskin PJ (1993) Reduced bone mineral density in long-term survivors of medulloblastoma. *Br J Radiol* 66(789):814–816
 50. Krishnamoorthy P, Freeman C, Bernstein ML, Lawrence S, Rodd C (2004) Osteopenia in children who have undergone posterior fossa or craniospinal irradiation for brain tumors. *Arch Pediatr Adolesc Med* 158(5):491–496

Adam M. Scheinberg

65.1 Introduction

Rehabilitation is the combined and coordinated use of medical, social, educational and vocational measures for training or retraining an individual to their highest possible level of function. It utilises functional and social models rather than a predominantly disease-based model of care. Paediatric rehabilitation uses generic principles of functional intervention but incorporates the essentials of growth and development as part of expert child health knowledge to ensure that care is child-focused and family-centred. [1]

Children and adolescents with a wide range of health conditions including acquired brain injury, spinal cord injury, limb deficiency, and neuromuscular and movement disorders may benefit from a rehabilitation approach together with specific rehabilitation interventions. Although children with posterior fossa tumors are known to have both short- and long-term disability, there is little published literature describing rehabilitation outcomes for this specific patient group. Recommendations for treatment therefore are extrapolated from experience with the more diverse population of children with acquired brain injury.

A.M. Scheinberg, M.D.
Victorian Paediatric Rehabilitation Service,
Royal Children's Hospital, Murdoch Children's
Research Institute, Faculty of Medicine, Monash
University, 50 Flemington Rd, Parkville,
VIC 3052, Australia
e-mail: adam.scheinberg@rch.org.au

Brain tumors are the second most common malignancy and most common solid tumor of childhood. The posterior fossa is the most common site for brain tumors in children. Depending on the site, type of tumor, extent of surgical excision, and need for adjunctive treatments such as radiotherapy or chemotherapy, children present with a range of both early-onset and longer-term disability requiring input from the rehabilitation team. Although historically the cerebellum has been thought of as primarily a sensorimotor organ, research implicates wider functions including language, visual-spatial organization and memory, intellect, executive functions, and personality.

65.2 The Rehabilitation Approach

The rehabilitation team consists of many different health professionals working together in an interdisciplinary framework (Box 65.1). Because of the complexity of treating children with posterior fossa tumors, most of the team will be needed at one point or another. The success of what is typically a large team of health professionals working with a sick child and their distressed carers relies on competent clinicians, effective team collaboration, and excellent communication both between the health professionals and the family. Research has suggested factors such as collaborative leadership, shared philosophy of care (linked to family-centered goals) and ease of

interprofessional exchanges are vital [2]. Communication strategies for teams working with children with complex disabilities include regular care planning and family meetings, provision of written information to the family that documents goal plans and repetition of information given verbally. Tools to empower families to access and manage information about their child are freely available and have proven useful in rehabilitation settings [3].

Box 65.1

- Range of rehabilitation team health professionals who may be required for a child with posterior fossa tumor
- Pediatric rehabilitation specialist
- Occupational therapist
- Speech pathologist
- Physiotherapist
- Dietician
- Clinical nurse specialist
- Neuropsychologist
- Clinical psychologist
- Social worker
- Rehabilitation education specialist
- Working together with neurosurgeons, teachers, chaplains, oncologists, radiation-oncologists, palliative care team, and the child and family

Although the rehabilitation team may not become involved in the child’s care until after surgical removal of the tumor has occurred, anticipatory guidance is nonetheless vitally important to prepare families and the child for common complications such as weakness, dysphagia, ataxia, and possibly even mutism with associated dysarthria. Whenever possible, a meeting with one or more key members of the rehabilitation team prior to surgery can provide some reassurance to parents of the availability of services in the postoperative period and a familiar face for the child once they are managed on the hospital ward and ready to start a more formal rehabilitation program.

The International Classification of Functioning, Disability, and Health (ICF) has been proposed as the framework in which rehabilitation teams can assess and treat children [4, 5] (Fig. 65.1). The ICF system, developed by

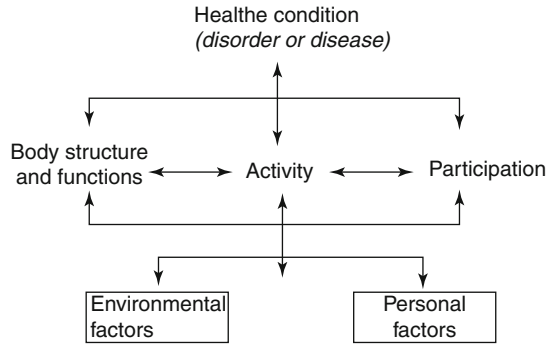


Fig. 65.1 The ICF model

the World Health Organization, focuses on the various aspects of health which are viewed in a framework that goes beyond considering just the individual’s health impairment to body structure and function, to also consider the impact of that impairment on a child’s daily activities and participation. The ICF describes “body functions and structures” as physiological functions of body systems or anatomical elements such as organs, limbs, and their components. “Activity” is the execution of specific tasks or actions by the individual, while “participation” is involvement in life situations. Contextual factors are external environmental factors (e.g., social attitudes or the child’s physical environment) and internal personal factors, such as gender, age, coping style, or other factors, that influence how disability is experienced by the individual. The ICF is intended to be a universal classification system and can also be used to code components of health. Within rehabilitation, the ICF is a useful tool to help ensure all aspects of health care are assessed and when necessary treated. To date, most research for children with posterior fossa tumors has focused within the body structure and function domain with little known about outcome in activity and participation domains.

65.2.1 Assessments

Assessments used by the rehabilitation team to help guide treatment and monitor progress will include those at the levels of body structure and function (e.g., videofluoroscopy for swallowing,

joint range of motion, Modified Tardieu Scale [6] for spasticity, ASIA Scale [7] for spinal injury, psychometric assessment), activity (e.g., Six-Minute Walk Test [8], Timed Up and Go [9], 2D or 3D gait analysis, WeeFIM™ (*Wee Functional Independence Measure*) [10], COPM (*Canadian Occupational Performance Measure*) [11], psychometric assessment) and participation (e.g., COPM [11], CAPE [12]).

Two measures we have found useful and relatively simple to apply in clinical practice are the WeeFIM™ [10] and COPM [11]. The WeeFIM™ can be used in children aged 6 months to 7 years, and older if they function below the functional level expected for a 7-year-old. It is useful for tracking disability status and a child's level of functional independence. The WeeFIM™ has 18 items covering the domains of self-care, mobility, and cognition. Each item is scored 1–7, with 1 being complete dependence through to 7 being complete independence. Comparison of an individual can be made with age-normed scores. The WeeFIM™ can be completed by any trained member of the team and in our setting is generally completed on admission to the inpatient rehabilitation program and again at the time of discharge. The COPM is a standardized outcome measure administered by semi-structured interview with the child or carers. The COPM measures changes in performance and satisfaction with tasks (or “occupations”) that are important to the child. Daily occupations, which are needed, wanted, and expected, are rated on a 10-point scale and those areas with the highest scores prioritized for rehabilitation intervention. The client then rates both their performance and satisfaction in each of the identified occupations on 10-point scales. Changes in scores between baseline assessment and reassessment can be calculated with change in score of two or more considered clinically significant (see Clinical Scenario below for an example of how these assessments may be used by the rehabilitation team).

Clinical Scenario

Sarah presented at 6 years of age with a 3-month history of progressive ataxia and dysarthria. She was an only child with both parents from

professional backgrounds. The family lived within driving distance of a tertiary pediatric hospital, the site at which she received medical services. Sarah was in her second year of school and there was no family history of cancer or neurological disease. Sarah's brain MRI scan showed a large heterogeneous lesion in the brainstem with an associated syrinx. She underwent a posterior fossa craniotomy. Tumor biopsy revealed pilocytic astrocytoma. She underwent chemotherapy, which was ceased prematurely due to poor tolerance. She subsequently progressed to radical resection of the remaining tumor.

Impairments following surgery included unilateral XIIth nerve palsy, asymmetric quadriparesis with spasticity in hip adductors and hamstrings, neurogenic bladder and bowel, and central hypoventilation requiring tracheostomy and ventilatory support. Over a 12-month period, her ventilation requirement reduced to overnight ventilator support only and she could tolerate a speaking valve on her tracheostomy.

She was initially referred to the rehabilitation team, following surgery, for an inpatient rehabilitation program. Table 65.1 shows her WeeFIM™ scores at the time of admission and again at the time of discharge from the hospital to her home. The WeeFIM™ norm score for a 6-year-old child in the self-care domain is 51, for mobility domain 34, and cognition domain 33. These are compared with Sarah's admission scores of 11, 7, and 21 in these respective domains. At the time of discharge, her WeeFIM™ score total had increased to 66.

Soon after referral to the rehabilitation program, Sarah's keyworker from the rehabilitation team completed her initial WeeFIM™ assessment and met with Sarah and her family to discuss the results and determine her treatment goals. These included independent floor mobility, bowel and bladder continence, and playing and talking with her peers for short periods without need for adult supervision. These goals were agreed to by her family and the team and formed the basis of her interdisciplinary inpatient rehabilitation program. The family used the KIT [3] to store information about Sarah and found this useful and empowering when meeting with the many different health professionals.

Table 65.1 Sarah's WeeFIM™ scores on admission and discharge

Domain	Item score		Domain score	
	Admission	Discharge	Admission	Discharge
Self-care				
Eating	1	3		
Grooming	1	2		
Bathing	1	2		
Dressing – upper body	2	3		
Dressing – lower body	1	3		
Toileting	1	2		
Bladder control	2	3		
Bowel control	2	3		
Domain total			11	21
Mobility				
Transfer chair/wheelchair	2	4		
Transfer toilet	1	4		
Transfer bath/shower	1	4		
Walk/wheelchair/crawl	2	5		
Stairs	1	1		
Domain total			7	18
Cognition				
Comprehension	5	5		
Expression	4	6		
Social interaction	4	5		
Problem solving	4	5		
Memory	4	6		
Domain total			21	27
Total			39	66

Table 65.2 illustrates how these goals may also be recorded and scored using the COPM. In our setting, the WeeFIM™ is used in the inpatient setting where the rehabilitation focus is more towards the ICF domains of body structure and function and activity. In the outpatient setting, we have found the COPM more useful as the child's goals and rehabilitation program move more towards activity and participation domains.

The rehabilitation team operationalized these goals with family and child education, a strengthening program to upper and lower limbs to improve transfers/floor mobility, and appropriate prescription of equipment such as a manual wheelchair. Botulinum toxin A was injected into hip adductors (adductor longus and gracilis) to reduce scissoring of legs when standing and stepping and improve cross leg sitting on floor. Advice was given on home and school modifications

including ramps, grab bars, and accessible toilets. A range of psychometric assessments were used to test cognition, behavior, and executive function. The psychologist informed both the team and family about her neuropsychological profile. Testing of executive function showed reduced ability to hold and manipulate information, and information processing speed was reduced. Information was then given in smaller chunks, both verbally and visually, repeated more often and with longer breaks to prevent cognitive fatigue. The school was informed and appropriate modifications made to Sarah's academic program. Funding was sought for a teacher's aide to assist Sarah with clean intermittent catheterization and daily bowel program. Involvement of a clinical psychologist to assist Sarah with return to school, self-perception, and mood was recommended but declined by the family.

Table 65.2 COPM scores at the start and end of outpatient rehabilitation program

Canadian occupational performance measure©				
	Initial assessment		Reassessment	
	Performance	Satisfaction	Performance	Satisfaction
1. Transfers floor to chair	3	2	6	5
2. Bowel/bladder continence	3	4	4	6
3. Playing/talking with peers	3	3	5	7
Change in performance = reassessment performance score 5 – initial performance score 3 = 2 ^a				
Change in satisfaction = reassessment satisfaction score 6 – initial satisfaction score 3 = 3 ^a				

^aTotal score = Total performance or satisfaction scores/number of problems

Once Sarah had completed her rehabilitation program, the COPM was completed and further review planned in 3 months time. The use of the COPM in the outpatient setting can assist in determining the timing, focus, location, and intensity of further outpatient rehabilitation interventions. A keyworker from the rehabilitation team made regular phone contact with the family to ensure Sarah was continuing to make progress and earlier reassessment was not required.

Throughout her childhood and adolescence, Sarah is likely to continue to require input from the rehabilitation team, particularly for independent mobility, bowel and bladder care, self-care, learning, and behavior. Regular resetting and measurement of her rehabilitation goals using the COPM or other goal setting tools will ensure that the rehabilitation team works with Sarah to improve her function in those areas deemed important to her. When Sarah is approaching adolescence, the rehabilitation focus may shift to focus more on vocational advice and planning, sexuality, peer relationships, and practical independence issues such as driving. Transition to adult health care services should be a planned, coordinated, and smooth process. Early discussion and anticipatory guidance for transition is essential.

social support of the child and family, as well as prevention of secondary impairments caused by either the tumor or subsequent treatment. The child may require splinting of upper or lower limb joints to prevent contracture. The occiput, sacrum, and heels are at risk of developing pressure areas if the child has prolonged immobilization. Regular skin monitoring, passive mobilization, and pressure-relieving gel or air mattress may be recommended. Nutrition needs close supervision by a dietician, particularly if the child has a prolonged period of enteral feeding. Prevention of aspiration secondary to dysphagia may require enteral feeding or modification to diet and posture. Speech pathology referral should be made for the assessment of swallowing function with videofluoroscopy or bedside assessment when this is not available. Bladder and bowel function may be affected. A renal ultrasound and baseline renal function should be checked in those children with neurogenic bladder. Generally constipation is easily managed with diet or laxatives. A neurogenic bowel and bladder may occur when tumor or the resection affects the descending long tracts and a more formalized bowel program and clean intermittent catheterization may be required. Early passive mobilization and a graded return to walking activity and self-care is a focus of the rehabilitation program in this early stage.

65.3 Acute Care: Inpatient Rehabilitation

Early rehabilitation care usually commences once the child is out of the intensive care and on the hospital ward after surgical resection of the tumor. The issues at this stage include ongoing education and

65.4 Later Care: Outpatient Rehabilitation

Later rehabilitation, typically towards the end of the hospital admission or once the child has been discharged home, includes therapy and/or

equipment to improve independent mobility and assistance with return to recreational and sporting activities. Depending on the child's level of disability, participation in community disability sports or provision of specialized sporting equipment may be appropriate. Schooling may be significantly disrupted during the child's initial period in the hospital and then by any residual disabilities, particularly cognitive and behavioral problems. Teachers and psychologists may need to adapt education programs and assist the child to talk with other students about their illness. Adolescence is a time of dramatic change and challenge for young persons. Adolescents who had their posterior tumor treated many years previously may develop concerns related to independence, sexuality, and peer relationships despite steady progress in these areas in childhood. Those adolescents who have cognitive impairment or problems in behavioral regulation are particularly at risk of poor social outcomes. Independence with self-care, transitions such as school to university or home to independent living, driving, using public transport, workplace safety, and managing finances are other issues which have a potential impact on quality of life for young adults with a history of posterior fossa tumor.

65.5 Rehabilitation Issues Specifically Related to Posterior Fossa Tumors

65.5.1 Ataxia

Ataxia describes a child's lack of coordination while performing voluntary movements and is caused by damage to the cerebellum or connecting neural pathways. Movements are clumsy, disjointed, or jerky. Tremor, hypotonia, weakness, dysarthria, and nystagmus may accompany ataxia. Ataxia is often a presenting symptom in children with posterior fossa tumors and may remain or worsen following surgery or adjunctive treatment. Clinical signs include past pointing with attempted finger nose pointing, wide based gait to compensate for instability and poor balance. Speech may be "scanning" or breathy.

Rehabilitation approaches for the child with ataxia are not well described, and as yet, there is no reliable ataxia-specific pediatric outcome measure used to assess an intervention. Most recommendations for the management of ataxia in children with posterior fossa tumors are extrapolated from the treatment of children with cerebral palsy or similar disorders. Ataxia is generally resistant to medical treatments; therefore, physical therapy is the mainstay of treatment. Physical therapy approaches may include proprioceptive training [13], balance exercises, and stabilization exercises. However, the wide variation in treatment approaches may be testament to their limited success, and compensatory strategies should accompany any treatment aimed directly at improving the ataxic movements. Methods for improving proprioception and balance in adults with ataxia due to cerebellar disease include vibration, suit therapy, proprioceptive neuromuscular facilitation, gait training, and balance board-ball exercises. In adults with severe ataxia, suspending weights from the extremities has been used with some success [14].

65.5.2 Dysphagia, Dysarthria, and Cerebellar Mutism

Dysphagia (impairment of swallowing) and dysarthria (a motor disorder of speech production) have both been frequently reported in children with posterior fossa tumors [15–17]. Cerebellar mutism, also well reported, is however less well defined and has been described as a postoperative clinical syndrome with diminished or absent speech, ataxia, hypotonia, and emotional lability, possibly due to damage to dentothalamocortical tracts [18]. Mei [15] has reported a retrospective chart audit of 27 children treated consecutively for posterior fossa tumor. Just over half the children had postsurgical mutism, dysarthria, or dysphagia. Children with any of these symptoms typically stayed in hospital twice as long as those without. There was a high association between mutism and subsequent dysarthria. Morgan [16] has also reported a small cohort of subjects with posterior fossa tumor who received preoperative

bedside evaluation of dysphagia. The evaluation was repeated 1–2 weeks following surgical resection of the tumor. No subjects had dysphagia preoperatively, but 73 % had dysphagia at 1–2 weeks post surgery with impairment of lip closure, chewing, and oral transit time. At 2 months post surgery, 75 % of subjects were managing a full oral diet. Other authors have reported larger cohorts but without preoperative assessment. Newman [17] reported significant swallowing difficulty in 24 children from a cohort of 127 children with posterior fossa tumors.

Speech pathology may be required preoperatively to provide anticipatory guidance on potential swallowing difficulties in the postoperative period. In the postoperative phase when dysphagia may present, the speech pathologist may recommend thickening of oral fluids, guidance on posture, and education of carers to assist the child with oral clearance. If dysphagia places the child at risk of aspiration, enteral feeding may be recommended. However, there is a paucity of evidence-based rehabilitation interventions for dysphagia, together with a lack of systematic referral of populations known to be at risk [19].

Similar to the treatment of dysphagia, there is little evidence to support specific treatment approaches to dysarthria in children with acquired brain injury. Morgan [20] grouped interventions for children with dysarthria firstly into those using perceptually based therapy and secondly those using instrumentally based biofeedback approaches. Perceptually based therapy uses repetition exercises without instrumentation such as lip and tongue exercises, breathing exercises, and voice drills. Instrumentally based biofeedback approaches include electropalatography, kinematics, and visual biofeedback acoustic treatment. The need for comprehensive child-focused rating scales, for dysarthria, is highlighted by this author [20].

Cerebellar mutism, also termed posterior fossa syndrome [21], was initially described by Hirsch [22]. Mutism typically develops 24–96 h after surgery to the tumor. The patient usually has normal vocalization ability, with expected ataxia, in the postoperative period prior to onset of the mutism [23]. Mutism may be accompanied by

supranuclear cranial nerve palsies, weakness, and a wide range of neurobehavioral abnormalities including emotional lability, apathy, and bizarre personality change. Recovery may take weeks to months but is generally positive in terms of mutism and affect. A recent longer-term study, however, suggests that children with cerebellar mutism syndrome perform significantly more poorly on psychometric tests of processing speed, attention, working memory, executive processes, and reading compared to children with similar disease and treatment but who do not develop mutism [18]. This suggests a particular need for close monitoring of psychometric and behavioral outcomes throughout childhood for this group of children.

Predicting which child will develop cerebellar mutism is difficult as the exact mechanism causing the syndrome is unclear. Postsurgical edema and ischemia, change in neurotransmitters, or interruption to cerebellar pathways such as the dentothalamocortical tract have all been implicated [18, 24]. Children with resection of large midline posterior fossa tumors appear to be at most risk, but all children, and their carers, who have surgery for posterior fossa tumor should be warned of this possible complication [21]. To date there are no specific evidence-based rehabilitation treatments for cerebellar mutism. Prevention of secondary complications, reassurance to the child and family, use of simple non-verbal communication devices, and a quiet non-stimulating environment are all helpful strategies while awaiting recovery. In the longer term, the use of compensatory strategies based on the results of neuropsychological testing has been raised as one possible treatment approach [18].

65.5.3 Weakness and Spasticity

Spasticity and weakness may develop, due to damage to the pyramidal long tracts, as a result of tumor or resection in the brainstem. A secondary mechanism of injury may be stretching of the periventricular white matter tracts by hydrocephalus, a frequent complication of posterior fossa tumors [25]. Spasticity is characterized by an increase in

the velocity-dependent excitability of muscle reflexes [26]. Spasticity causes involuntary muscle contraction and painful spasms and commonly coexists with weakness, poor coordination, and loss of dexterity. These impairments may lead to restricted, abnormal movement patterns.

Rehabilitation management of weakness and spasticity in children with acquired brain injury is well described in the literature. However, treatment approaches are not described specifically for children with posterior fossa tumor. In Australia, comprehensive rehabilitation programs delivered by interdisciplinary teams with input from neurosurgery and orthopedics have developed to manage both the cognitive and complex motor impairments caused by acquired brain injury in children [27]. Treatments for spasticity include casting and splinting, botulinum toxin A injections [28], oral medications such as baclofen [28], and in more severely involved children an implanted pump delivering baclofen into the intrathecal space [29]. Functional or passive care goals, including pain relief, should be discussed and when possible measured prior to treatment of spasticity. Reduction of spasticity alone is rarely the primary goal of treatment, but rather a way to facilitate functional goals that are relevant to the child or family [29, 30].

65.5.4 Cognition and Behavior

Long-term neuropsychological and behavioral sequelae in children with posterior fossa tumors have been summarized [31]. Impairments of cognition, working memory, attention, processing speed, visuospatial orientation, executive function, and affect are reported as long-term sequelae of posterior fossa tumor or associated treatment [18, 32]. The majority of reports are retrospective and include different tumor pathology and treatment approaches. Additional side effects of adjuvant therapy such as chemotherapy and radiotherapy complicate interpretation and generalization of results. Hydrocephalus and raised intracranial pressure have been noted to be risk factors for poorer cognitive outcome [33, 34]. Younger children are most at risk of poor

educational outcomes due to the long-term effect on their learning [31]. A progressive decline in intellectual quotient has been reported [35]. Baseline pre-intervention assessment is often difficult due to the child being acutely unwell and greater emphasis placed on practical and emotional preparation for surgery. Formal psychometric assessment is not possible in very young children. In some instances, a child may have been referred pre-morbidly to speech pathology or psychology for unrelated problems, for example, a learning disorder identified by the child's teacher. This information can prove useful when monitoring the child's progress after treatment of their tumor.

Few authors have described specific rehabilitation approaches to the cognitive and behavioral problems experienced by children with posterior fossa tumors. Van't Hooft [36] reported a pilot study of three children, treated for medulloblastoma, who received a condensed version of the SMART program (Swedish Memory and Attention ReTraining). SMART uses daily practice and games and specific attention and memory techniques. The program takes 30 min per day for 17 weeks (or 1 h per day for 10 weeks for the condensed version). The daily program is combined with relaxation and goal-focused tasks. Both auditory and visual skills are trained. Parents or carers are also given training to facilitate application of their child's new skills. Stress caused by providing the intensity of the program and the potential to draw attention to the child's deficits were noted as potential complications of the program. However, improvements in attention and memory and self-image and social interaction were also noted and warrant further investigation. Another author has described a single case study emphasizing the importance of long-term psychometric assessment and a close working relationship between the rehabilitation team, family, and education system [37]. Over a period of almost 10 years, psychometric evaluation of a child treated for cerebellar medulloblastoma at age 2 years demonstrated deficits in working and long-term memory, spatial orientation, visual agnosia, cognitive fatigue, attention, and executive function (problem solving,

behavioral regulation). Regular rehabilitation interventions (e.g., speech pathology for oral language used to compensate for visuo-constructive difficulty and facilitate writing abilities) were successful in facilitating the child's educational development. The authors noted the importance of communication between the rehabilitation team, family, and teachers and the need for regular rehabilitation team meetings to develop yearly therapy goal plans. The difficulty of balancing more intensive rehabilitation, which might highlight a child's deficits or marginalize them from peers within a mainstream school setting, against a less intensive approach which might be insufficient to remedy neurocognitive or physical problems is highlighted [37].

65.6 Rehabilitation and Palliative Care

Survival rates for children with posterior fossa tumors have improved dramatically over the past few decades [38]. Nonetheless, a significant number of children will have tumors which can only be partially resected, whose tumor is resistant to adjuvant therapy, or where there is tumor progression some years after initial treatment. For some children, early referral to the palliative care team may be more appropriate than to rehabilitation. For children with tumor recurrence, transition from the rehabilitation team to the palliative care team must be handled sensitively to avoid feelings of abandonment or hopelessness [39].

65.7 Summary

Children with posterior fossa tumors present with a wide and complex range of neurodeficits. Many will benefit from a rehabilitation approach to their care with specific rehabilitation interventions when indicated. Setting child and family relevant goals and measuring longer-term outcomes is an important role for rehabilitation teams providing services to this group of children. The lack of evidence for many of the

rehabilitation interventions provided to this patient group is both a challenge and opportunity for those working in the field.

Acknowledgments Thanks to Dr. Angela Morgan and Ms. Jane Galvin for proofreading and comments on the manuscript.

References

1. http://www.health.vic.gov.au/vprs/downloads/vprs_model_of_care.pdf. Accessed 15 Apr 2011
2. Sinclair LB, Lingard LA, Mohabeer RN (2009) What's so great about rehabilitation teams? An ethnographic study of interprofessional collaboration in a rehabilitation unit. *Arch Phys Med Rehabil* 90: 1196–1201
3. Stewart D, Law M, Burke Gaffney J et al (2006) Keeping it together: an information KIT for parents of children and youth with special needs. *Child: Care Health Dev* 32(4):493–500
4. Salghetti AM, Betto S, Russo E et al (2009) Projecting and programming rehabilitation based on ICF-CY format in a neuropsychiatric hospital unit. *Disabil Rehabil* 31(S1):S55–S60
5. <http://www.who.int/classifications/icf/en/>. Accessed 15 Apr 2011
6. Boyd R, Graham H (1999) Objective measurement of clinical findings in the use of botulinum toxin type A for the management of children with cerebral palsy. *Eur J Neurol* 6:S23–S35
7. <http://www.asia-spinalinjury.org/elearning/elearning.php>. Accessed October 2014
8. Geiger R, Strasak A, Tremi B et al (2007) Six-minute walk test in children and adolescents. *J Pediatr* 150(4): 395–399
9. Williams EN, Carroll SG, Reddihough DS et al (2005) *Dev Med Child Neurol* 47:518–524
10. Ottenbacher KJ, Taylor ET, Msall ME, Braun S, Lane SJ, Granger CV, Lyons N, Duffy LC (1996) The stability and equivalence reliability of the functional independence measure for children (WeeFIM)[®]. *Dev Med Child Neurol* 38(10):907–16. PubMed PMID: 8870612
11. Law M, Baptiste S, McColl MA et al (1998) Canadian occupational performance measure, 3rd edn. CAOT Publications ACE, Ottawa. www.caot.ca
12. King G, Law M, King S et al (2004) Children's Assessment of Participation and Enjoyment (CAPE) and Preferences for Activities of Children (PAC). Harcourt Assessment, San Antonio
13. Adler SS, Beckers D, Buck M (2000) PNF in practice. Springer, Heidelberg
14. Gibson-Horn C (2008) Balance-based torso-weighting in a patient with ataxia and multiple sclerosis: a case report. *J Neurol Phys Ther* 32(3):139–146
15. Mei C, Morgan AT (2011) Incidence of mutism, dysarthria and dysphagia associated with childhood

- posterior fossa tumour. *Childs Nerv Syst* 2011;27(7):1129–36
16. Morgan AT, Sell D, Ryan M et al (2008) Pre and post-surgical dysphagia outcome associated with posterior fossa tumour in children. *J Neuro-Oncol* 87:347–354
 17. Newman LA, Boop FA, Sanford RA et al (2006) Postoperative swallowing function after posterior fossa tumour resection in pediatric patients. *Childs Nerv Syst* 22:1296–1300
 18. Palmer SL, Hassall T, Evankovich K et al (2010) Neurocognitive outcome 12 months following cerebellar mutism syndrome in pediatric patients with medulloblastoma. *Neuro-Oncology* 12(12):1311–1317
 19. Morgan AT (2010) Dysphagia in childhood traumatic brain injury: a reflection on the evidence and its implications for practice. *Dev Neurorehabil* 13(3):192–203
 20. Morgan AT, Vogel AP (2008) Intervention for dysarthria associated with acquired brain injury in children and adolescents. *Cochrane Database Syst Rev* (3):CD006279. doi:10.1002/14651858.CD006279.pub2
 21. Vernon-Levett P, Geller M (1997) Posterior fossa tumors in children: a case study. *AACN Clin Issues* 8(2):214–226
 22. Hirsch JF, Renier D, Czernichow P et al (1979) Medulloblastoma in childhood: survival and functional results. *Acta Neurochir (Wien)* 48:1–15
 23. Pollock IF, Polinko P, Albright LA et al (1995) Mutism and pseudobulbar symptoms after resection of posterior fossa tumours in children: incidence and pathophysiology. *Neurosurgery* 37(5):885–893
 24. Morris EB, Phillips NS, Laningham FH et al (2009) Proximal dentatothalamic tract involvement in posterior fossa syndrome. *Brain* 132:3087–3095
 25. de Oliveira Santos R, Barros Jucá CE, Valera ET et al (2008) Hydrocephalus in posterior fossa tumors in children. Are there factors that determine a need for permanent cerebrospinal fluid diversion? *Childs Nerv Syst* 24(12):1397–1403
 26. Lance JW (1980) Symposium synopsis. In: Feldman RG, Young RR, Koella WP (eds) *Spasticity: disordered motor control*. Year Book Medical Publishers, Chicago, pp 485–494
 27. O'Flaherty S (2004) International perspectives on paediatric rehabilitation. *Pediatr Rehabil* 7(4):267–270
 28. Scheinberg A, Hall K, Lam LT et al (2006) Oral baclofen in children with cerebral palsy: a double-blind cross-over pilot study. *J Paediatr Child Health* 42:715–720
 29. Scheinberg A (2009) Clinical use of botulinum toxin. *Aust Prescr* 32(2):39–42
 30. Ward A, Hayden S, Dexter M et al (2009) Continuous intrathecal baclofen for children with spasticity and/or dystonia: goal attainment and complications associated with treatment. *J Paediatr Child Health* 45:720–726
 31. Stargatt R, Anderson V (2002) Neuropsychological outcomes of children treated for posterior fossa tumours: a review. *Brain Impair* 3(2):92–104
 32. Butler JM, Rapp SR, Shaw EG (2006) Managing the cognitive effects of brain tumour radiation therapy. *Curr Treat Options Oncol* 7:517–523
 33. Jacobs R, Northam E, Anderson V (2001) Cognitive outcome in children with myelomeningocele and perinatal hydrocephalus: a longitudinal perspective. *J Dev Phys Disabil* 13(3):389–404
 34. Ellenberg L, McComb JG, Siegel SE et al (1987) Factors affecting intellectual outcome in pediatric brain tumour patients. *Neurosurgery* 21:638–644
 35. Packer RJ, Sutton LN, Atkins TE et al (1989) A prospective study of cognitive function in children receiving whole brain radiotherapy and chemotherapy: 2-year results. *J Neurosurg* 70:707–713
 36. Van't Hooft I, Norberg AL (2010) SMART cognitive training combined with a parental coaching programme for three children treated for medulloblastoma. *NeuroRehabilitation* 26:105–113
 37. Callu D, Laroussinie F, Kieffer V et al (2008) Remediation of learning difficulties in children after treatment for a cerebellar medulloblastoma: a single-case study. *Dev Neurorehabil* 11(1):16–24
 38. Nejat F, El Khashab M, Rutka JT (2008) Initial management of childhood brain tumours: neurosurgical considerations. *J Child Neurol* 23:1136–1148
 39. Taggart D (2010) Late effects of treatment and palliative care. In: Gupta N, Banerjee A, Haas-Kogan D (eds) *Pediatric CNS tumors*, 2nd edn. Springer, Berlin, pp 336–353

Banu Çankaya and M. Kemal Kuşcu

66.1 Introduction

Pediatric cancer and related events pose a variety of challenges and stressors for children and their families. After the diagnosis of tumor, parents assume new roles in addition to their traditional parenting roles – to state the least, becoming advocates for their children and coordinators of their care [1]. Throughout the demanding and long treatment regime, families' lives revolve around disease-related stressors, such as management of the side effects of intervention, changes in the daily routines, and disruptions in previously existing social and family roles [2]. Much is known about the medical effects of brain tumors; however, despite the vital and irrefutable role of families in the care of their children with pediatric cancer, only few studies examined the effects of disease-related processes on children's and family members' psychological well-being. A review of 31 studies on survivors of childhood brain tumors shows that such medical event has impact on survivors' general psychological adjustment, social competence, internalizing and

externalizing behavioral problems, and quality of life [3].

Increasing knowledge about the effects of pediatric cancer, and posterior fossa tumor in particular, on families' psychological adjustment is important not only due to the central role families play in the care of their children but also due to the interplay between the course of cancer and the child's developmental process and parental and familial psychological functioning [2]. Research provides ample evidence for this interplay; parent, child, and sibling adaptation has been shown to have reciprocal influences [4–7]. In a prospective study at an oncology unit at the Women's and Children's Hospital in South Australia, it was shown that maternal distress at the time of cancer diagnosis significantly affected the psychological adjustment of their children 2 years after diagnosis [8]. The higher maternal anxiety, depression, insomnia, and somatic symptoms during diagnosis, the worse were the prospect for their children's emotional and behavioral problems.

This chapter reviews the current literature on psychological adjustment of families and children in pediatric oncology in general, and brain tumors in particular. It also aims to provide a framework for the practitioner in the field while working with families and children with neurosurgical procedures including the posterior fossa tumors. Compared to other types of tumor, brain tumors have a less positive prognosis, which is significantly associated with the intensity and

B. Çankaya, Ph.D.
Department of Psychology, Koç University,
Istanbul, Turkey

M.K. Kuşcu, M.D. (✉)
Department of Psychiatry, Marmara University,
School of Medicine, Istanbul, Turkey
e-mail: mkkusc@gmail.com

duration of psychological distress families might experience [9]. Furthermore, posterior fossa tumors is one of the most debilitating types with adverse acute and long-term effects on cognitive functioning and behavioral and affective regulation [10] – all of which potentially make the treatment and posttreatment adjustments more challenging for families. The implications of the literature for families of children with posterior fossa tumors must be interpreted with this consideration in mind.

66.2 Diagnosis: Impact of the Oncological Diagnosis of the Child in the Family

Cancer is often a feared, but not an expected diagnosis, and psychological stress is a natural response to obtaining this life-threatening diagnosis. For families of children with cancer, the stress response has been studied with respect to multiple emotional manifestations; the widely studied are depression, anxiety, feelings of uncertainty, and posttraumatic stress response [11]. These emotional symptoms are experienced by families to varying degrees depending on the interplay of multiple factors such as the phase of illness, context of diagnosis and treatment, and psychological vulnerabilities.

A significant factor involved in the long-term impact of pediatric cancer diagnosis on families is the process families experienced from the moment they felt something was “not right” with their children to the moment they find out about the final cancer diagnosis [12]. The diagnosis of pediatric cancer is not always made within initial visits to health professionals because initial symptoms of cancer are, most often than not, very vague and are at first misdiagnosed as common cold or flu. As the accurate diagnosis is usually belated for pediatric cancer and more so for brain tumors, right after the diagnosis, most parents’ confidence in their judgment about their children’s health decreases [13] and the delay in diagnosis adds to the difficulty of hearing about the cancer diagnosis [12].

At diagnosis, a distressing realization on the part of parents is that their children’s death is imminent without treatment including invasive procedures, and even with treatment, death may not be averted [14]. In one of the few studies on parents of children with a diagnosis of brain tumor, Freeman and colleagues [15] investigated problems parents experience during each phase of illness. The two most commonly experienced parental problems during the time of diagnosis were concerns about the cause of illness and the manner in which prognosis was communicated. Similarly, siblings of children with brain tumor also stressed the lack of communication about health information and prognosis as sources of important problems during diagnosis [16].

The lack of precise prognostic information and treatment regimes generates a feeling of uncertainty and fear of possible death [17], which persists for many families throughout the course of the illness. Uncertainty feelings are closely linked with thoughts of “what if’s,” leading to difficulties in making decisions, doubts about one’s capabilities in managing cancer, and feelings of insecurity [13]. Cancer symptoms and side effects of interventions, if not managed well, could trigger and intensify the uncertainty feelings regarding cancer trajectory [13], in turn leading to an increased risk for symptoms of posttraumatic stress [18]. In addition to these findings, the findings of a qualitative study are noteworthy; the experience of certainty in cancer diagnosis and treatment, rather than the uncertainty, may be perceived as more stressful [13]. The uncertainty of cancer trajectory may generate a sense of hope and hope could help families cope with difficult times throughout cancer treatment.

At the time of diagnosis, families face various challenges aside the uncertainty; they have to manage their own stress while managing their children’s care and treatment [19]. Coordinating their child’s care requires reorganization of family roles and daily routines. New restrictions to their daily living and extra work are distressing for families and could be hard to handle given the long-term cancer treatment regime [13]. Providing explanation of the diagnosis to their

children in an age-appropriate way and responding to their anxieties and fears are only few of the many difficult tasks of the diagnostic phase [14].

Most parents naturally experience a shock and psychological distress in response to the diagnosis of cancer; some may also experience impaired cognitive abilities such as having a difficult time processing, learning, and retaining information related to their child's illness and treatment. Research has not shown consistent evidence for this effect [20, 21]. Risk for psychiatric diagnosis is high for parents of children with cancer, but the majority does not experience psychiatric symptoms at a clinical level despite the challenges of cancer trajectory. Most reported symptoms are at preclinical levels and decrease over time [22]. Existing coping skills play a significant role in how parents overcome psychological distress. Parents with difficulties in emotion regulation and with preexisting risk conditions have the highest risk for psychiatric diagnosis following the cancer diagnosis.

Research findings indicate that it takes about a year to adjust to the diagnosis of childhood cancer [8, 23, 24]. During the adaptation period, most parents experience increased symptoms of depression and anxiety [25–29]. Anxiety symptoms have been shown to attenuate following the year of adaptation [2, 11]. In a prospective study, anxiety levels of parents of children diagnosed with cancer decreased to relatively normal levels 5 years after the diagnosis [11]. A small proportion of parents continue to experience higher levels of anxiety compared to parents of healthy children, which puts them under the risk for developing posttraumatic stress symptoms [30, 31]. Unlike anxiety symptoms, studies have shown inconsistent results for the course of depressive symptoms through the cancer trajectory [26, 32]. The initial depressive reaction of moderate to severe levels is more likely to persist over time.

A meta-analytic study on the effects of pediatric cancer on parents and families showed that mothers of children with cancer experienced higher distress compared to fathers of children with cancer and mothers of healthy children [2]. These findings have been accounted by the higher

frequency of contact of mothers with their children during their care [33, 34], but reporting biases of women compared to men could also explain these findings. This is not to say that fathers do not experience distress; findings suggest that they do, although not as high as mothers, but more than fathers of healthy children [2]. With respect to family functioning overall, mothers of children with cancer perceived higher levels of family conflict than mothers of children without cancer. Increased demands on logistic, financial, and emotional resources may account for higher conflict in families [2].

After the adaptation phase, most studies have shown no differences between families of healthy children and families of children with cancer. Similarly, in a prospective study with 212 mothers of children recently diagnosed with cancer [35], previously reported mild negative affect and depressive and posttraumatic symptoms decreased steadily 3 and 6 months after the diagnosis. Among posttraumatic symptoms, intrusion and hyperarousal, but not avoidance, decreased over time. It has to be noted, however, that for cancers of more severe type as brain tumors, and posterior fossa in particular, the resilience may be compromised and the risk may be higher.

In the aftermath following the adaptation phase to cancer diagnosis and course of treatment, posttraumatic stress symptoms are most common. For only 11–25 % of mothers and 10 % of fathers, these symptoms are as such to be diagnosed as a disorder (posttraumatic stress disorder (PTSD)) [36]. Avoidance of any cues related to cancer, intrusive thoughts, reexperiencing of stressful experiences related to their child's illness, and physiological arousal at cancer reminders are commonly experienced as posttraumatic stress (PTS) symptoms at subclinical levels by parents of children with cancer, approximately 37–44 % for mothers and approximately 33–36 % for fathers [36]. A study investigating the dyadic pattern of PTS symptoms in parents of children who survived cancer showed that most families have at least one parent who experiences moderate to severe levels of PTS symptoms [36, 37]. In Alderfer and colleagues' study, mothers most often experienced reexperiencing and emotional hyperarousal

symptoms, whereas fathers had difficulties with memory, concentration, and decision-making [36].

Social support is strongest during diagnosis and declines over time [38]. Considering the decline following diagnosis, it is important for providers to help families find and actively seek support from family, community, and hospital resources. Better adjustment of parents to childhood cancer is related to better social support [39, 40]; the risk for posttraumatic stress symptoms increased for parents who report lack of support [30, 41]. The positive association between social support and psychological distress experienced by parents was not consistently found for both fathers and mothers, some studies showed a stronger influence of social support on the psychological adjustment of mothers [41, 42], and others showed a stronger effect for fathers [38]. Overall, it is important to assess the availability of a support network for parents.

Studies on coping in children with cancer and their families are few in number [11]. There are two major approaches to categorizing coping strategies children employ, with overlaps in their definitions: emotion- and problem-focused coping [43, 44] and approach and avoidance strategies [45]. Problem-focused strategies involve efforts to affect the source of stress in the environment, such as planning, seeking instrumental support, problem solving, and logical analysis, whereas emotion-focused strategies involve efforts to cope with emotional response to the source of stress, such as optimism, humor, seeking emotional support, and relaxation. Approach strategy reflects efforts to handle the source of distress directly, and these strategies include seeking information, seeking guidance, problem solving, planning, and logical analysis. Avoidance strategy, on the other hand, reflects efforts put forth to divert away from the source of stress, such as wishful thinking, denial, behavioral and mental disengagement, self-blame, and emotional venting. Existing evidence suggests that different coping strategies are effective depending on various factors, including the stage of illness, controllability of the situation, and age of the ill child [46]. Emotion-focused strategies (e.g., seeking emotional and social support, acceptance, and

relaxation) were found useful in decreasing acute stress and overcoming the difficulties of the first few months following the diagnosis [46]; however, they are related to difficulties in psychological adjustment during active treatment and maintenance phases of illness [31]. The use of passive or palliative reactions leads to a short-term, but not long-term, relief and typically involves avoidance behavior and negative emotional expression, both of which were found to be associated with more depressive symptoms and anxiety in not only parents of children in active cancer treatment but also children that are cancer-free [47]. In active treatment and maintenance of treatment benefits, problem-focused and approach coping strategies are indicated [46, 47]. Age made a difference in the effectiveness of coping strategies; children of older ages used more cognitively oriented and emotion-focused coping strategies, while younger children used coping strategies directed more at changing the environment [48]. With increasing age, a wider range of coping strategies is used by children [49].

Routine psychiatric and psychological care and follow-ups for families of children with cancer have to be considered, especially for those with a recent diagnosis and for those with a prolonged course of treatment [9]. For instance, cognitive-behavioral treatment approaches, problem-solving skills training in particular [50], have been found to decrease distress in mothers of children recently diagnosed with cancer and have been recommended for mothers of children in treatment for cancer [51, 52].

For families with a prolonged course of illness and severe treatment regime, psychosocial services have to be intensified, and special care and referrals for routine and frequent follow-ups may be indicated [9].

Family members should be screened for pre-existing risk factors individually such as history of psychiatric problems, past trauma, and lower socioeconomic status [53]; those with preexisting vulnerabilities are more likely to have increased levels of symptoms and distress and are, in turn, in more need for support and psychological intervention [11].

Families also need to be screened for or asked about family functioning. Problems within the

family system are likely to make the cancer trajectory more challenging and distressing for family members. Less family cohesion and satisfaction were shown to be associated with heightened parental anxiety and posttraumatic stress symptoms in families of children with cancer [54]. Furthermore, family cohesion and the ability to express emotions and thoughts during the earlier phases of cancer diagnosis have been found inversely related to internalizing symptoms in children [9]. Treatments targeting family relationships and facilitating emotional expression and sharing could have protective long-term implications for parents and affected children. Research has shown support for family-based psychosocial interventions in decreasing distress related to childhood cancer [55].

Family management style (FMS) framework has been proposed as a road map in examining and understanding the strategies that are used by families in managing cancer diagnosis and treatment of children with cancer [56]. The major components of the FMS framework are the subjective definition of the child's cancer to the family, management behaviors related to the treatment of cancer and its integration into daily life, and perceived consequences. Subjective meaning of the child's cancer incorporates how families view their child with respect to his/her normalcy and capabilities; how families view illness with respect to its course, predictability, cause, and seriousness; and whether parents' views of illness and child are mutual. Management behaviors include avoidance, proactive, and reactive reactions to managing cancer and how it is integrated into the routines of daily living. Perceived consequences are related to the extent to which families focus on illness and family life in general and future expectations related to their child's illness.

In dealing with uncertainty, encouraging ongoing and open-ended communication within the families and between the health-care providers and families is vital. One has to consider that the posttraumatic aspect of cancer diagnosis might contribute to the sense of uncertainty as well. Families have also indicated that changing their future orientation to a focus on one day at a

time and assigning new meanings to cancer, like that cancer helped the family to feel closer to each other, were helpful strategies in managing uncertainty [57, 58].

Managing symptoms is one of the most important components of cancer care. Keeping symptoms under control, whenever possible, helps families cope with their feeling of uncertainty, feel empowered in protecting their children from distressing experiences, and have a sense of stability [58, 59]. Stability in this sense also could help families to live normalcy at certain spheres of their lives [13]. Being able to protect their children from distressing symptoms helps parents as well as siblings feel empowered during this process [60].

Studies have shown that families want to be informed about their child's health status to better cope with the illness and related uncertainty of future health [13, 58, 61]. Considering the potential protective quality of uncertainty at certain phases of illness [13], as a result of their qualitative study, suggested that much forethought be given to the type and time of information given to parents – parents' readiness and willingness to hear certain types of information may vary and could be critical in how they manage the information.

66.3 Surgery: Invasive Treatments Ensuing the Diagnosis of Cancer

Cancer treatment involves multiple repeated invasive procedures such as intravenous injections, venipunctures, and venous port access, chemotherapy, and surgical operations. Compared to other types of cancer diagnosis, most posterior fossa tumors call for hospitalization and surgical intervention. Many children and adolescents with cancer perceive the diagnostic and surgical procedures as the most stressful aspects of their illness [62]. Anticipatory stress prior to invasive procedures is inevitable for both children and their families. Children often manifest their anticipatory stress psychosomatically such as problems with sleeping, nausea, vomiting, and skin reactions [63].

Psychological and pharmacological interventions have been established to help children and their families manage symptoms of anxiety and fear related to distressing procedures and operations. Preoperational preparation programs date back to 1960s and mainly involved providing information related to surgery, building trust in the relationship between the medical staff and the child, and encouraging expression of emotions [64]. In the last two decades, the focus of research and practice has shifted from information-based programs to pharmacotherapy (e.g., sedative medications) and cognitive-behavioral coping skills training for children and their families [65–67].

Information-based preparation programs include narrative strategies, printed materials, puppet shows, tours, and films related to hospitalization and operational processes. These programs help families and children cope with anxiety that might stem from the unfamiliarity of hospital and operational procedures and help to increase their sense of control [68]. Certain factors such as age, previous experience with surgery, and duration of hospital stay prior to surgery were found to moderate the effect of information-based preparations in decreasing children's stress related to invasive surgical procedures [69]. Older children, compared to younger children, retained information better; younger children needed information-based preparation closer to the time of operation. Prior surgical experience sensitized children to hospital-relevant films and thus increased their arousal. Children who were hospitalized within a short period of time to surgery were more likely to respond to hospital- and surgery-relevant information with increased anxiety and were more likely to benefit from distracting films irrelevant to hospital or operation. Children who had been hospitalized for a longer period of time prior to the surgical operation benefitted from hospital-relevant informative films.

Cognitive-behavioral skills-oriented strategies include breathing exercises, relaxation, cognitive/attentional distraction using guided imagery, storytelling, and video game playing, filmed modeling via videos or a puppet show, behavioral rehearsal, contingency management (reinforcement/incentive schedules for increasing adherence

to treatment), and active coaching. Among these interventions, cognitive/attentional distraction and relaxation via storytelling have been found particularly effective in controlling nausea, pain, and anxiety [67, 70]. This strategy involves asking children to imagine a pleasant location or activity and telling stories or statements suggestive of a calm emotional state and wellness.

There is evidence in support of both the effectiveness of cognitive-behavioral interventions, and no differences were found in the effectiveness of cognitive-behavioral and pharmacological interventions [33, 65, 71]; however, little evidence supported the long-term benefits of either intervention [2, 65, 72].

Pharmacological interventions decrease the anticipatory and operational anxiety and helps with pain management, although with side effects of longer recovery period and greater medical risks. Cognitive-behavioral interventions involve few, if any, medical risks and do not involve a recovery period. Cognitive-behavioral strategies were found to increase coping skills and to reduce reported and observed preoperative anxiety, fear, and pain related to procedures like port access and venipunctures [65, 66]. Increased sense of mastery has been shown as a mechanism underlying the effectiveness of cognitive-behavioral strategies, and self-efficacy was shown to be a significant predictor of cognitive-behavioral intervention outcome [73]. This finding is in line with research indicating the effectiveness of emotion-focused strategies such as self-efficacy in reducing stress in uncontrollable situations prior to invasive procedures [46]. Despite these benefits, the cost-effectiveness in recruiting specialized personnel in teaching cognitive-behavioral skills have not yet been examined well, and its use has been limited in pediatric oncology [67].

Training parents to help their children deal with fear and procedural stress has been recommended as a strategy to increase the effectiveness as well as the feasibility of cognitive-behavioral interventions for children undergoing medical procedures [74]. In fact, research has shown that the effect of cognitive-behavioral interventions as preparatory programs prior to surgery is moderated by parental

anxiety [75] and certain parenting attitudes and parents' inconsistent use of prompts for distraction [76]. Parents who received training in both managing their own stress and coaching their children reported less distress, and their children experienced less fear compared to the families who were only shown puppetry film describing hospitalization and surgery procedures a week prior to hospitalization [77].

In sum, in addition to pharmacological interventions, increasing coping skills, mainly distraction and relaxation techniques, and information-based programs using films tailored to each individual patient could be recommended as the standard of care for children with cancer and their families prior to hospitalization and surgery [78]. It is strongly recommended that the active role of parents in the care of their children is encouraged in preparing for surgical procedures [68]. As parents take on more active roles, their sense of mastery is likely to stay intact or increase postoperatively. The ideal intervention appears to be teaching parents coping strategies with their own stress and training them to be coaches in helping their children cope with pain and anxiety. Parents have at least two major roles during hospitalization and surgical procedures [79]: One is that they exert themselves vigorously for the well-being of their children by staying nearby, being sensitive and responsive, facilitating knowledge, and offering consolation. Another major parental role is using the parental authority to actively assert the needs of their children. Medical health teams have to stay cognizant of and encourage these roles. Increasing the sense of mastery of both the parents and children preoperatively and postoperatively would potentially increase the resiliency of families in the long trajectory of cancer treatment.

66.4 Postoperative Phase: Coping with Impairment

Risk of cognitive impairment in brain tumor survivors is very high, with greatest risk indicated for the children of an age of 7 and younger [80]. Radiation and chemotherapy have been found to be associated with lower IQ and achievement

scores, and surgery can result in brain injury associated with deficits in attention, processing speed, executive functions, visual-perceptual skills, and memory [81, 82]. Cognitive problems in memory sequential processing, fine-motor coordination, and physical stamina have been indicated for older children who survive brain tumors. Affected children have to learn to deal with neurocognitive effects and physical deficits.

In their study on children's and siblings' concerns during different phases of brain tumor treatment [16], affected children were most concerned about changes in their physical abilities, appearance, and mood states after hospital discharge. Supportive family environment and spiritual support helped them most during this phase. Their siblings reported lack of help with schoolwork as the continuing problem, and supportive environment was reported to be helpful and important for them in overcoming various difficulties during this phase. Concerns during the adjuvant treatment phase was characterized most by information children received from their computers regarding their illness and the changes in their mood states for the affected child, and for siblings, the limitations on their activities and changes in appearance and moods of their affected sibling.

After the hospital discharge and during adjuvant treatments, parents reported lack of clarity regarding long-term sequelae of treatment as one of the most problematic concerns [15]. At the end of treatment, parents may also face a heightened uncertainty feeling about whether there will be future side effects, another malignancy, or relapse [83, 84].

The supportive interactions with hospital staff and providers decrease with respect to ongoing emotional, practical, and informational feedback, and this may leave parents with feelings of abandonment and parents may struggle to gain their confidence back in taking care of their children [84]. Families and children alike have to adjust to a newly defined daily routine and family environment outside the context of active treatments and interactions with medical or nurse providers. Also, ending efforts devoted to treatment may

lead parents to feel that they are not doing enough to prevent disease from relapsing and overprotectiveness, hypervigilance, confusion, and fear may result [85]. To the end of establishing a supportive environment, families have to seek support from multiple systems including physicians, psychologists, psychiatrists, and school personnel (e.g., administration, teachers, tutors).

Changes in personality and moods of their children affected the parental stress significantly during the hospital discharge phase, and what helped most were support from friends and family and treatments targeting pain relief [15]. In adjuvant treatment phase, lack of information regarding the cessation of treatment was related to increased stress. Also, inappropriateness in the way doctors communicated prognosis, difficulties with handling the child's changes in mood or personality, and affected children being younger increased parental stress.

66.5 Remission: Gaining the Social Competence

In remission, children with brain tumor were most concerned with the socialization process [16], and major adjustments occur regarding their integration to daily living at home, community, and friendship circles [84], going back to school, and keeping up with school work [86]. During this period, children may not be able to assume responsibilities and roles similar to those before treatment and as a result may need to readjust to daily living along with the process of redefining their roles within the family.

Missed time from school and related drawbacks could make this period more stressful for children. Studies to date have shown inconsistent findings about the effects of absenteeism from school after cancer treatment [86, 87]; however, some children are likely to experience difficulties in reuniting with their friends and establishing new friendships. Lack of support in the socialization process was reported as a major concern by at least a third of the children with brain tumors in the remission phase [16]. Psychological and neurocognitive affects of the disease and its treatment

make this transition even more difficult for affected children with brain tumors. In their reintegration to school, neurocognitive deficits and changes in appearance are sources of stress for affected children [84] and could make the transition to joining a peer group more difficult. Bruce and colleagues [86] found that during the time affected children returned to their social life at school, their friends showed reluctance to understand their illness, the treatment process, and its aftermath. The difficulties in communication with others and reestablishing friendships impaired their adjustment to school and social environment. Many children, in fact, did not want to disclose their conditions, which is likely to increase the lack of awareness about the tumor treatment and its effects, in turn leading to diminishing resources of support within peers [86].

The reintegration phase after treatment completion is a challenging period of reestablishing new routines and new roles for families, and during this period, parents cannot and should not be advised that they go back to their normal routine [84]. Normalcy has to be redefined by the family members. In doing so, families have to seek support from multiple resources including physicians, psychologists, psychiatrists, and school personnel (e.g., administration, teachers, tutors). In their qualitative study, Bruce et al. [86] recommended that families of childhood cancer survivors maintain an open and consistent communication within the family, ensure planning and preparation in advance, promote for their child's socialization in an ongoing communication between school and health-care providers, advocate for compensations for academic needs, and raise awareness and education of the school staff. Parents reported that being active in seeking support, being realistic and persistent, being attentive to other family members' well-being, ensuring active involvement of their children in the process, and keeping written reports were helpful in overcoming school challenges. Staying in collaboration with the school system and assuring support from staff were noted as key elements for parents in acquiring the help they need for their children. Children and youth were also recommended to seek assistance from

teachers and teaching resources such as copies of notes, teacher aides, and technological assistive devices. Facilitating an open communication between children and their teachers ensured better adjustment to school life.

The period after treatment completion continues to be a stressful time for families, not only due to reestablishing roles and routines within the family and school reintegration but also due to the prevailing feeling of uncertainty since the beginning of the diagnosis and treatment. The two most commonly reported problems of parents of children with brain tumor in remission were the lack of information related to possible long-term and delayed side effects of treatments and expectations for lifetime [15]. Lack of knowledge related to lifetime expectations and lack of expert doctors in the after care of their children were significantly associated with families' stress levels. The availability of expert knowledge related to their children's care and support from friends and family were the two most helpful resources for families in remission phase. As in other phases of illness, mothers experienced more stress than fathers in this phase of illness. In this period, siblings may struggle with feelings of resentment that may result from increased family responsibilities, taking time away from their friends, and attention increasingly and continuously devoted to the affected child [88]. Medical and mental health providers should work with families to help them attain coping skills to overcome their emotional challenges and deal with struggles related to restructuring and readjusting their family environment to the needs of the affected child's condition [84].

It is questionable whether traditional ways of measuring psychological adjustment capture the effects of a life-threatening and significantly debilitating medical condition on childhood cancer survivors and their families [89], and findings with respect to the psychological adjustment of childhood cancer survivors are inconclusive. For children who survive tumors affecting the central nervous system or those with changes in physical appearance, studies have indicated greater problems in peer relationships and social competence [87, 90]. Child survivors of brain tumor were also

found to have behavioral problems [91]. On the other hand, in another study on children and adolescent survivors of brain tumor and their families [92], affected children and adolescents reported feeling within the normal range with respect to their social and scholastic functioning, appearance, conduct, and self-worth, while their mothers rated them as having greater communication difficulties and problematic social interactions. Giving findings on the difficulties with social competence during the reintegration into school, several pilot studies have been conducted to examine the effects of social skills training on children with brain tumors [25, 93], providing preliminary support for these programs.

One of the most widely studied, concerning, and prevalent late effect of cancer diagnosis and treatment is the posttraumatic stress disorder at clinical and subclinical levels [97]. In many families, at least one parent is distressed with posttraumatic stress symptoms resulting from the cancer diagnosis of their child [36, 37]; psychosocial interventions for families of children in remission should be informed by trauma research. Targeting the posttraumatic stress symptoms, Kazak and colleagues [94] have developed a brief (4-session, 1-day) intervention program for childhood cancer survivors and their families, based on cognitive-behavioral and family systems approaches, called the Surviving Cancer Competently Intervention Program (SCCIP) and have proposed a pediatric psychosocial preventative health model (PPPHM) [95]. Evidence has been provided for the effectiveness of SCCIP in randomized clinical trials with caregivers of children newly diagnosed with cancer [96] and childhood cancer survivors and their fathers [97].

Some families expect the end of life and ultimately have to experience the death of their children resulting from cancer. When expecting the end of life, lack of information about the dying process and alternative treatments were the most commonly reported concerns of parents of children with brain tumor [15]. Helpful topics in this phase for families were the environment in which the child was to die and religious support. For siblings of dying children with brain tumor, pain treatment, their ability in soothing their affected

sibling, and harmony in the family were helpful [16]. Similar to their parents, siblings reported the lack of information about the dying process as a major problem, and most felt unprepared for the death of their affected sibling.

The deaths associated with childhood cancer can lead to great distress for a long period of time and posttraumatic stress symptoms for the remaining family members. Turmoil, grief, and disorganization of the family members are typical responses to losing a child, but there is not enough evidence showing whether and how these families seek help for their grief [53]. As a response to child death from cancer, it is likely that guilt feelings and sense of failure arise within all the systems concerning the child, including the health-care team [53]. It is recommended that a psychologist be part of the health-care team facilitating the process before and after the death of the child by being a role model and consultant to the health-care team and all the systems involved with the child and their families. Psychologists could clarify professional roles and boundaries of health-care teams while ensuring their emotional involvement with families. Current practice recommendations suggest that the possibility of death is not to be thwarted from the start of the treatment and treatments focus on the process of living with the possibility of death [53]. After a child's death, it is recommended that key health-care providers plan follow-up care that ideally would involve sending a card, attendance at funeral, follow-up phone calls, and invitation for a follow-up meeting with the whole team. Kazak and Noll provided recommendations for families with higher risk for developing psychological problems (such as those with higher family conflict or preexisting psychiatric condition) [53]. Suggestions included a three-session follow-up with focus on normalization of the grief process, remembering the child, and talking about the family's future in separate successive sessions. Support groups and continued psychotherapy are also implicated for families with higher risk for prolonged grief response and other psychological problems [53].

References

1. Kratz L, Uding N, Trahms CM et al (2009) Managing childhood chronic illness: parent perspectives and implications for parent-provide relationships. *Fam Syst Health* 27(4):303–313
2. Pai ALH, Greenley NG, Lewandowski A et al (2007) A meta-analytic review of the influence of pediatric cancer on parent and family functioning. *J Fam Psychol* 21(3):407–415
3. Fuemmeler BF, Elkin TD, Mullins LL (2002) Survivors of childhood brain tumors: behavioral, emotional, and social adjustment. *Clin Psychol Rev* 22(4):547–585
4. Dolgin MJ, Phipps S (1996) Reciprocal influences in family adjustment to childhood cancer. In: Baider L, Cooper C, Kaplan De-Nour A (eds) *Cancer and the family*. Wiley, Oxford, pp 73–92
5. Kazak AE, Alderfer M, Rourke MT et al (2004) Posttraumatic stress disorder (PTSD) and posttraumatic stress disorder symptoms (PTSS) in families of adolescent childhood cancer survivors. *J Pediatr Psychol* 29:211–219
6. Sahler OJ, Roghman KJ, Mulhern RK et al (1997) Sibling adaptation to Childhood Cancer Collaborative Study: the association of sibling adaptation with maternal well-being, physical health, and resource use. *J Dev Behav Pediatr* 18:233–243
7. Varni JW, Katz ER, Colegrove RJ et al (1996) Family functioning predictors of adjustment in newly diagnosed cancer: a prospective analysis. *J Child Psychol Psychiatry* 37:321–328
8. Sawyer Y, Antoniou G, Toogood I et al (2000) Childhood cancer: a 4-year prospective study of the psychological adjustment of children and parents. *J Pediatr Hematol Oncol* 22(3):214–220
9. Robinson KE, Gerhardt CA, Vannatta K et al (2007) Parent and family factors associated with child adjustment to pediatric cancer. *J Pediatr Psychol* 32(4):400–410
10. De Smet HJ, Baillieux H, Wackenier P et al (2009) Long-term cognitive deficits following posterior fossa tumor resection: a neuropsychological and functional neuroimaging follow-up study. *Neuropsychology* 23(6):694
11. Vrijmoet-Wiersma CM, van Klink JMM, Kolk AM et al (2008) Assessment of parental psychological stress in pediatric cancer: a review. *J Pediatr Psychol* 33(7):694–706
12. Dixon-Woods M, Findlay M, Young B et al (2001) Parents' accounts of obtaining a diagnosis of childhood cancer. *Lancet* 357(9257):670–674
13. Woodgate RL, Degner LF (2002) "Nothing is carved in stone!": uncertainty in children with cancer and their families. *Eur J Oncol Nurs* 6(4):191–202
14. Rabineau KM, Mabe A, Vega RA (2008) Parenting stress in pediatric oncology populations. *J Clin Hematol Oncol* 30(5):358–365

15. Freeman K, O'Dell C, Meola C (2004) Childhood brain tumors: parental concerns and stressors by phase of illness. *J Pediatr Oncol Nurs* 21:87-97
16. Freeman K, O'Dell C, Meola C (2003) Childhood brain tumors: children's and siblings' concerns regarding the diagnosis and phase of illness. *J Pediatr Oncol Nurs* 20:133-140
17. Stewart JL, Mishel MH (2000) Uncertainty in childhood illness: a synthesis of the parent and the child literature. *Sch Inq Nurs Pract* 14(4):299-319
18. Mishel MH (1999) Uncertainty in chronic illness. *Annu Rev Nurs Res* 17:269-294
19. Young B, Dizon-Woods M, Findlay M et al (2002) Parenting in a crisis: conceptualizing mothers of children with cancer. *Soc Sci Med* 55:1835-1847
20. Dermatis H, Lesko LM (1990) Psychological distress in parents consenting to child's bone marrow transplantation. *Bone Marrow Transplant* 6:411-417
21. Jedlicka-Kohler I, Gotz M, Eichler I (1996) Parents' recollection of the initial communication of the diagnosis of cystic fibrosis. *Pediatrics* 97:04-209
22. Greening L, Stoppelbein L (2007) Brief report: pediatric cancer, parental coping style, and risk for depressive, posttraumatic stress, and anxiety symptoms. *J Pediatr Psychol* 32(10):1272-1277
23. Fife B, Norton J, Groom G (1987) The family's adaptation to childhood leukemia. *Soc Sci Med* 24:159-168
24. Steele R, Long A, Reddy K et al (2004) Changes in maternal distress and child-rearing strategies across treatment for pediatric cancer. *J Pediatr Psychol* 28:447-452
25. Barrera MD, D'Agostino NM, Gibson J et al (2004) Predictors and mediators of psychological adjustment in mothers of children newly diagnosed with cancer. *Psychooncology* 13:630-641
26. Hoekstra-Weebers JEHM, Jaspers JPC, Kamps WA et al (1998) Gender differences in psychological adaptation and coping in parents of pediatric cancer. *Psychooncology* 7(1):26-36
27. Manne SL, Miller DL, Meyers P et al (1996) Depressive symptoms among parents of newly diagnosed children with cancer: a 6-month follow-up study. *Child Health Care* 25:191-209
28. Sloper P (2000) Predictors of distress in parents of children with cancer: a prospective study. *J Pediatr Psychol* 25:79-91
29. Yeh CH (2002) Gender differences of parental distress in children with cancer. *J Adv Nurs* 38(6):598-606
30. Best M, Streisand R, Catania L et al (2001) Parental distress during pediatric leukemia and posttraumatic stress symptoms (PTSS) after treatment ends. *J Pediatr Psychol* 26(5):299-307
31. Hoekstra-Weebers JEHM, Jaspers JPC, Kamps WA et al (1999) Risk factors for psychological maladjustment of parents of children with cancer. *J Am Acad Child Psychiatry* 38(12):1526-1535
32. Boman K, Lindahl A, Björk O (2003) Disease-related distress in parents of children with cancer at various stages after the time of diagnosis. *Acta Oncol* 42:137-146
33. Kazak AE, Biancamaria P, Boyer B et al (1996) A randomized controlled prospective outcome study of a psychological and pharmacological intervention protocol for procedural distress in leukemia. *J Pediatr Psychol* 21:615-631
34. Cook JA (1984) Influence of gender on the problems of parents of fatally ill children. *J Psychosoc Oncol* 2:71-91
35. Dolgin MJ, Phipps S, Fairclough DL et al (2007) Trajectories of adjustment in mothers of children with newly diagnosed cancer: a natural history investigation. *J Pediatr Oncol Nurs* 32(7):771-782
36. Alderfer MA, Cnaan A, Annunziato RA et al (2005) Patterns of posttraumatic stress symptoms in parents of childhood cancer survivors. *J Fam Psychol* 19(3):430-440
37. Kazak AE, Boeving C, Alderfer MA et al (2005) Posttraumatic stress symptoms during treatment in parents of children with cancer. *Jpn J Clin Oncol* 23(30):7405-7410
38. Wijnberg-Williams BJ, Kamps WA, Klip EC et al (2006) Psychological distress and the impact of social support on fathers and mothers of pediatric cancer patients: long-term prospective results. *J Pediatr Psychol* 31(8):785-792
39. Hoekstra-Weebers JE, Jaspers JP, Kamps WA et al (2001) Psychological adaptation and social support of parents of pediatric cancer patients: a prospective longitudinal study. *J Pediatr Psychol* 26:225-235
40. Smith MY, Redd WH, Peyser C et al (1999) Posttraumatic stress disorder in cancer: a review. *Psychooncology* 8:521-537
41. Manne S, Duhamel K, Redd WH (2000) Associations of psychological vulnerability factors to posttraumatic stress symptomatology in mothers of pediatric cancer survivors. *Psychooncology* 9:372-384
42. Barakat LP, Kazak AE, Meadows AT et al (1997) Families surviving childhood cancer: a comparison of posttraumatic stress symptoms with families of healthy children. *J Pediatr Psychol* 22:843-859
43. Folkman S, Lazarus RS (1980) An analysis of coping in a middle-aged community sample. *J Health Soc Behav* 21:219-239
44. Folkman S, Lazarus RS (1985) If it changes, it must be a process: study of emotion and coping during three stages of a college examination. *J Pers Soc Psychol* 48:150-170
45. Holahan CJ, Moos RH (1987) Personal and contextual determinants of coping strategies. *J Pers Soc Psychol* 52:946-955
46. Aldridge AA, Roesch SC (2007) Coping and adjustment in children with cancer: a meta-analytic study. *J Behav Med* 30(2):115-129

47. Lindahl-Norberg A, Lindblad F, Boman KK (2005) Parental traumatic stress during and after cancer treatment. *Acta Oncol* 44(4):382–388
48. Compas BE, Malcarne VL, Fondacaro KM (1988) Coping with stressful events in older children and adolescents. *J Consult Clin Psych* 56:405–411
49. Peterson L (1989) Coping by children undergoing stressful medical procedures: some conceptual, methodological, and therapeutic issues. *J Consult Clin Psych* 57:380–387
50. Nezu AM, Nezu CM, Friedman SH et al (1998) Helping cancer patients cope: a problem-solving approach. American Psychological Association, Washington, DC
51. Sahler OJ, Varni J, Fairclough D et al (2002) Problem-solving skills training for mothers of children with newly diagnosed cancer: a randomized trial. *J Dev Behav Pediatr* 23:77–86
52. Sahler OJZ, Fairclough DL, Phipps S et al (2005) Using problem solving skills training to reduce negative affectivity in mothers of children with newly diagnosed cancer: report of a multi-site randomized trial. *J Consult Clin Psych* 73:272–283
53. Kazak AE, Noll RB (2004) Child death from pediatric illness: conceptualizing intervention from a family/systems and public health perspective. *Prof Psychol Res Pract* 35(3):219–226
54. Kazak AE, Stuber ML, Barakat LP et al (1998) Predicting posttraumatic stress symptoms in mothers and fathers of survivors of childhood cancers. *J Am Acad Child Psychiatry* 37(8):823–831
55. Meyler E, Guerin S, Kiernan G et al (2010) Review of family-based psychosocial interventions for childhood cancer. *J Pediatr Psychol* 35(10):1116–1132
56. Dearrick JA, Thibodeaux AG, Mooney K et al (2006) Family management style framework: a new tool with potential to assess families who have children with brain tumor. *J Pediatr Oncol Nurs* 23(1):19–27
57. Clarke-Steffen L (1997) Reconstructing reality: family strategies for managing childhood cancer. *J Pediatr Oncol Nurs* 12(5):278–287
58. Cohen M (1995) The triggers of heightened parental uncertainty in chronic, life-threatening, childhood illness. *Qual Health Res* 5(1):63–77
59. Schmidt K, Eland J, Weiler K (1994) Pediatric cancer pain management: a survey of nurses' knowledge. *J Pediatr Oncol Nurs* 11(1):4–12
60. McGrath P (2001) Findings on the impact of treatment for childhood acute lymphoblastic leukemia on family relationships. *Child Fam Soc Work* 6: 229–237
61. Cohen M (1993) The unknown and the unknowable-managing sustained uncertainty. *West J Nurs Res* 15(1):77–96
62. Hedstrom M, Hadlung K, Skolin I et al (2003) Distressing events for children and adolescents with cancer: child, parent, and nurse perceptions. *J Pediatr Oncol Nurs* 20(3):120–132
63. Katz ER, Kellerman J, Siegel SE (1980) Distress behavior in children with cancer undergoing medical procedures: developmental considerations. *J Consult Clin Psych* 48:356–365
64. Vernon DTA, Foley JM, Sipowicz RR et al (1965) The psychological responses of children to hospitalization and illness. Charles C. Thomas, Springfield
65. Kuppenheimer WG, Brown RT (2002) Painful procedures in pediatric cancer: a comparison of interventions. *Clin Psychol Rev* 22:753–786
66. Powers SW (1999) Empirically supported treatments in pediatric psychology: procedure related pain. *J Pediatr Psychol* 24:131–145
67. Redd WH, Montgomery GH, DuHamel KN (2001) Behavioral intervention for cancer treatment side effects. *J Natl Cancer I* 93(11):810–823
68. O'Conner-Von S (2000) Preparing children for surgery: an integrative research review. *AORN J* 71(2): 334–343
69. Faust J, Melamed BG (1984) Influence of arousal, previous experience, and age on surgery preparation of same day of surgery and in-hospital pediatric patients. *J Consult Clin Psych* 52(3):359–365
70. Kirsh I, Montgomery G, Sapirstein G (1995) Hypnosis as an adjunct to cognitive-behavioral psychotherapy: a meta-analysis. *J Consult Clin Psych* 63:214–220
71. Jay SM, Elliot CH, Fitzgibbons I et al (1995) A comparative study of cognitive behavioral therapy versus general anesthesia for painful medical procedures in children. *Pain* 62:3–9
72. Kain ZN, Caramico LA, Mayes LC et al (1998) Preoperative preparation programs in children: a comparative examination. *Anesth Analg* 87:1249–1255
73. Reeb RN, Bush JP (1996) Preprocedural psychological preparation in pediatric oncology: a process-oriented intervention study. *Child Health Care* 25:265–279
74. Manne SL, Redd WH, Jacobsen PB et al (1990) Behavioral intervention to reduce child and parental distress during venipuncture. *J Consult Clin Psych* 58:565–572
75. Dahlquist LM, Gil KM, Armstrong FD et al (1986) Preparing children for medical examinations: the importance of previous medical examination. *J Health Psychol* 5(3):249–259
76. Pringle B, Hilley L, Gelfand K et al (2001) Decreasing child distress during needle sticks and maintaining treatment gains over time. *J Clin Psychol Med S* 8:119–130
77. Zastowny TR, Kirschenbaum DS, Meng AL (1986) Coping skills training for children effects on distress before, during, and after hospitalization for surgery. *Health Psychol* 5(3):231–247
78. O'Bryen KK, Peterson L, Saldana L (1997) Survey of pediatric hospitals' preparation programs: evidence of the impact of health psychology research. *Health Psychol* 16(2):147–154
79. Anderzén-Carlsson A, Kihlgren M, Svantesson M et al (2010) Parental handling of fear in children with cancer; caring in the best interests of the child. *J Pediatr Nurs* 25(5):317–326
80. Radcliffe J, Packer RJ, Atkins TE et al (1992) Three- and four-year cognitive outcome in children with

- noncortical brain tumors treated with whole-brain radiotherapy. *Ann Neurol* 32(4):551–554
81. Alvarez JA, Scully RE, Miller TL et al (2007) Long-term effects of treatments for childhood cancers. *Curr Opin Pediatr* 19(1):23–31
 82. Nathan PC, Patel SK, Dilley K et al (2007) Guidelines for identification of, advocacy for, and intervention in neurocognitive problems in survivors of childhood cancer: a report from the Children's Oncology Group. *Arch Pediatr Adolesc Med* 161(8):798–806
 83. Keene N, Hobbie W, Ruccione K (2000) Childhood cancer survivors: a practical guide to your future, Patient centered guides. O'Reilly & Associates, Sebastopol, CA.
 84. Labay LE, Mayans S, Harris MB (2004) Integrating the child into home and community following completion of cancer treatment. *J Pediatr Oncol Nurs* 21:165–169
 85. Haase J, Rostad M (1994) Experiences of completing cancer therapy: children's perspectives. *Oncol Nurs Forum* 21:1483–1492
 86. Bruce BS, Chapman A, MacDonald A et al (2008) School experiences of families of children with brain tumors. *J Pediatr Oncol Nurs* 25:331–339
 87. Reiter-Purtill J, Noll RB (2003) Peer relationships of children with chronic illness. In: Roberts MC (ed) *Handbook of pediatric psychology*. Guilford, New York, pp 176–197
 88. Spinetta JJ, Jankovic M, Eden T et al (1999) Guidelines for assistance to siblings of children with cancer: report of the SIOP working Committee on psychosocial issues in pediatric oncology. *Med Pediatr Oncol* 33(4):395–398
 89. Kazak AE (2005) Evidence-based interventions for survivors of childhood cancer and their families. *J Pediatr Psychol* 30(1):29–39
 90. Vance YH, Eiser C (2002) The school experience of the child with cancer. *Child Care Health Dev* 28(1):5–19
 91. Carlson-Green B, Morris RD, Krawiecki N (1995) Family and illness predictors of outcome in pediatric brain tumors. *J Pediatr Psychol* 20(6):769–784
 92. Radcliffe J, Bennett D, Kazak AE et al (1996) Adjustment in childhood brain tumor survival: child, mother, and teacher report. *J Pediatr Psychol* 21(4): 529–539
 93. Barakat L, Hetzke J, Foley B et al (2003) Evaluation of a social skills training group intervention with children treated for brain tumors: a pilot study. *J Pediatr Psychol* 28:299–307
 94. Kazak A, Simms S, Barakat L et al (1999) Surviving Cancer Competently Intervention Program (SCCIP): a cognitive-behavioral and family therapy intervention for adolescent survivors of childhood cancer and their families. *Fam Process* 38:175–191
 95. Kazak AE (2006) Pediatric psychosocial preventative health model (PPPHM): research, practice and collaboration in pediatric family systems medicine. *Fam Syst Health* 24(4):381–395
 96. Kazak AE, Simms S, Alderfer MA et al (2005) Feasibility and preliminary outcomes from a pilot study of a brief psychological intervention for families of children newly diagnosed with cancer. *J Pediatr Psychol* 30(8):644–655
 97. Kazak AE, Alderfer MA, Streisand R et al (2004) Treatment of posttraumatic stress symptoms in adolescent survivors of childhood cancer and their families: a randomized clinical trial. *J Fam Psychol* 18: 493–504

Index

A

- A9934, 152, 153
- A9961, 151, 162
- Abducens nerves, 95
- Abductor hallucis, 255
- Abductor pollicis brevis (APB), 255
- Abl* gene, 67
- Abnormal hemodynamics, 581
- Abscesses, 539, 788
- Absorption, 800
- Accessory nerves, 95, 246
- Acoustic neuroma, 41, 148, 763
- Acute side effects, 147
- ADC mapping, 517
- ADEM, 539
- Adjuvant
 - chemotherapy, 156, 371
 - radiation therapy, 668–669
 - therapy, 780, 800
- Adrenal insufficiency, 899
- Adrenocorticotrophic hormone (ACTH)
 - deficiency, 904–905
- Adult ependymomas, 383–384
- Adverse drug reactions, 866–869
- Adverse effects, 671, 863
- Agenesis, 786
- Aicardi syndrome, 131
- AIEOPSN9501, 357
- Air embolism, 183, 213, 458, 829
- Airway protection, 859
- Akt/mTOR pathway, 437, 679
- Ala cinerea, 116, 246
- Alanine (Ala), 301
- Alexander Monro II, 25
- Alisphenoid, 64
- Alkylating agents, 899, 903, 904
- Alpha-methyltyrosine scan, 746
- Altered behavior, 875–876
- Amifostine, 159
- Analgesia, 859
- Anaplastic astrocytomas (AA), 467, 472, 487, 495, 586
- Anaplastic ependymoma, 415
- Anaplastic medulloblastoma, 333
- Anaplastic pilocytic astrocytoma, 469
- Anaplastic tumors, 820
- Anaplastic variants, 297
- Anatomical features, brainstem, 511
- Anatomo-pathological study, 705
- Anatomy, posterior cranial fossa, 75–98
- Androgen receptor (AR), 697
- Anesthetic, 319–320
- Aneurysmal bone cyst, 220–222
- Angiocentric glioma, 419
- Angiogenesis, 389
- Angiomatosis, 126
- Angiopoietin, 615
- Anode, 244
- Antennapedia, 65
- Anterior tumour extension, 705
- Anterior cerebellar incisura, 86
- Anterior cerebellar notch, 102
- Anterior fixation, 891
- Anterior median fissure, 110
- Anteroinferior cerebellar artery (AICA), 88, 179
- Anterolateral approaches, 209–210, 216
- Anterolateral (preolivary) sulcus, 95
- Antiangiogenic, 492
 - agents, 425
 - drugs, 389
 - therapy, 615–617
- Anticipatory stress, 923
- Anticonvulsant, 856
- Anti-Ki67, 820
- Antimetabolites, 389–390
- Antimüllerian hormone (AMH), 902
- Anti-VEGF (vascular epithelial growth factor), 389
- Apex of the dens, 225
- Apnea, 851
- Apparent diffusion coefficient (ADC), 394, 433
- Apraxia, 239
- Aqueduct, 88, 326, 546, 844
- Aqueductal stenoses, 231
- Arachnoid cyst, 792
- Arachnoiditis, 790, 845
- Area acustica, 116
- Area postrema, 96, 115
- Armour, D., 4
- Armoured endotracheal tube, 843
- Articular facets, 888
- Aseptic meningitis, 412, 790, 794, 804, 844, 846

Aspiration pneumonia, 246, 412, 855
 Assisted technique, 803
 Associated hydrocephalus, 643
 Astrocytomas, 457, 585
 Asynergia, 119
 Ataxia, 119–120, 148, 799, 846, 865, 914
 Atlantal arch, 225
 Atlanto-occipital membrane, 77, 184, 190
 A-train, 258
 Aretic cephalocele, 792
 Atrophy, 891
 AT-RT. *See* Atypical teratoid-rhabdoid tumor (AT-RT)
 Atypical tumors, 816, 818, 820
 Atypical chordomas, 675
 Atypical choroid plexus papilloma (APP), 724, 745
 Atypical teratoid-rhabdoid tumor (AT-RT), 139, 147, 148, 151–152, 304, 539, 629, 633–641, 651, 667–671, 719
 Auditory pathways, 252
 Auditory tubercle, 115
 Aurora A, 662
 5-Aza-2'-deoxycytidin, 390

B

Baby SFOP Protocol, 357
 Bacterial meningitis, 790, 799
 BAERs. *See* Brainstem auditory-evoked responses (BAERs)
 Bailey, P., 50
 Balanced anesthesia, 828
 Ballance, C.A., 41
 Bartholow, R., 34
 Basilar artery, 190, 399
 Basilar sulcus, 95
 Basioccipital, 62–64
 BCNU, 611, 620
 Behavioral problems, 239, 927
 Behaviour, 916–917
 Behçet's disease, 539
 Bell, C., 32
 Benign tumors, 818
 Benzodiazepine, 850
 Bergmann cells, 67
 β -catenin, 342, 350, 439, 808
 Bevacizumab, 358, 389, 492, 616, 766
 Bilateral deafness, 765
 Biomarkers, 419–420, 423, 425
 Biopsy, 411, 574, 596, 643
 Biphasic pattern, 467
 Bipolar concentric probe, 242
 Bipolar stimulation, 242
 Biventral lobules, 93, 108
 Blackfan, K., 53
 B-nystagmus, 121
 Bochdalek's baskets, 726
 Bone absorption, 800
 Bone tumor, 693
 Bony matrix, 900
 Borchardt, M., 53

Brachyury, 676, 696
 Bracing, 891
 Bradycardia, 125, 458
 BRAF, 138
 duplication, 438
 mutations, 439, 490
 Bragg peak, 374
 Brain edema, 855
 Brain retraction, 217
 Brainstem, 79, 94–95, 240, 432, 557, 774, 827
 implants, 162
 tumors, 177, 511, 844
 Brainstem auditory evoked potentials (BAEPs), 252, 566, 764
 Brainstem auditory-evoked responses (BAERs), 242, 252
 Brainstem glioma (BSG), 148, 156–157, 164, 585, 595
 Brainstem mapping (BSM), 565, 579
 Brainstem/midbrain, 802, 803
 Brain tumor-polyposis syndrome, 268
 Branchial arch, 65
 Breathing exercises, 924
 Bright, R., 36
 Broca, P., 34
 Bromodeoxyuridine (BrdU), 475
 Bucy, P., 3
 Burdach, 252
 Busulfan, 614

C

Cadaveric dural grafts, 845
 Calamus scriptorius, 96, 246
 Calcification, 298, 399, 635, 775, 791, 798, 816
 Calvarial erosion, 816
 Canadian occupational performance measure (COPM), 911
 Canadian pediatric brain tumor consortium, 659
 Cancer genomics, 265
 Capillary telangiectasis, 791
 Capsule, 794, 798, 799, 803
 Carboplatin, 389, 433, 489, 610, 612, 616, 658, 659, 747
 Carmustine, 614
 Carmustine-impregnated polymers, 620
 CASP8, 277
 Caspase 3 activation, 663
 Cathode, 244
 Caudal vermis syndrome, 117
 Cavernomas, 539
 Cavernous malformations, 405
 Cavernous sinus, 213, 242
 Cavitron Ultrasonic Surgical Aspirator, 846
 CCG 921, 375
 CCNU, 355, 489
 CD 24, 696
 CD56, 418
 CD133, 385
 CDKN2A, 137, 677
 CDKN2B, 677

- CD4+ T lymphocytes, 388
 Central auditory pathway, 112
 Central Brain Tumor Registry of the United States (CBTRUS), 431
 Central hypothyroidism, 901
 Central lobule, 86
 Central precocious puberty, 904
 Central venous line, 644
 Central vesicles, 799
 Centromere protein F, 662
 Centro-pontine myelinolysis, 539
 Cephalic mesoderm, 62, 64–66
 Cephalosporin, 829
 Cerebellar abscess, 790
 Cerebellar astrocytomas, 49, 467
 Cerebellar ataxia, 829
 Cerebellar folia, 807, 809
 Cerebellar function, 856
 Cerebellar mutism, 329, 412, 463, 564, 649, 846, 856, 876–878, 914–915
 Cerebellar mutism syndrome (CMS), 161, 180, 846
 Cerebellar peduncles, 88, 513, 774, 779
 Cerebellar swelling, 320
 Cerebellar tumors, 844
 Cerebellar vermis, 177
 Cerebellomedullary angle, 856
 Cerebellomedullary cisterns, 801
 Cerebellomedullary fissure, 86, 88, 93, 94, 110, 178, 314
 Cerebellomesencephalic fissure, 88, 94, 108, 179
 Cerebellopontine angle (CPA), 43, 77, 193, 213, 241, 291, 334, 564, 763, 797, 799, 849, 856
 Cerebellopontine angle epidermoids, classification of, 798
 Cerebellopontine angle tumors, 148, 160, 327
 Cerebellopontine cistern, 764
 Cerebellopontine fissure, 88, 93–94, 108–110
 Cerebellum, 79
 Cerebral aqueduct, 95
 Cerebral edema, 855
 Cerebral peduncles, 112, 241, 244, 550
 Cerebral perfusion, 855, 860
 Cerebral perfusion pressure, 828
Cerebri Anatomie, 18
 Cerebrospinal fluid (CSF)
 drainage, 828
 flow, 846
 infection, 230, 845, 846
 leak/leakage, 412, 844, 845, 849, 865
 wound leak, 463
 Cervical flexures, 786
 Cervical instability, 887
 Cervical laminectomy, 888
 Cervical lordosis, 887, 888
 Cervical osteoplastic laminectomy, 582
 Cervical spine, 706
 Cervicomedullary brainstem, 240, 610
 Cervicomedullary gliomas, 519
 Cervicomedullary junction, 561
 Cervicomedullary lesions, 597
 Cervicomedullary tumors, 148, 164, 571, 595
 Cervicothoracic junction, 708
 Cervicothoracic region, 889
 C/guanylate cyclase C (NPR3), 342
 Chang's stage, 230
 Chemical meningitis, 791, 799, 804
 Chemosensitivity, 350
 Chemotherapy, 151–162, 305, 350, 364, 423, 432, 489, 821
 Chemotherapy following radiotherapy, 614–615
 Chiasm, 157
 CHI3L1, 387
 Child, age of, 609
 Childhood cancer survivors, 927
 Children's Cancer and Leukaemia Group (CCLG), 376
 Children's Cancer Study Group (CCSG), 351
 Children's Oncology Group (COG), 154, 157, 167, 354, 659
 Child's growth curves, 901
 Chipault, A., 43
 Chloroform, 31
 Cholesterol, 791, 798, 800
 Chondrocranium, 61, 63
 Chondroid chordomas, 675, 693
 Chondrosarcoma(s), 210, 222, 698
 Chordoid, 818
 Chordomas, 148, 220, 693
 anatomic localisation, 715–716
 chemotherapy, 712–713
 conventional radiotherapy, 711
 genetics of, 675–680
 management of, 710
 prognostic factors, 713
 proton therapy, 711–712
 radiotherapy, 711–712
 treatment of, 710–711
 treatment-related complications, 713
 tumor volume, 716
 Choroid plexus, 92, 94, 745
 Choroid plexus carcinoma (CPC), 304, 723, 745
 Choroid plexus papilloma (CPP), 140, 304, 418, 723, 745
 Choroid plexus tumor, 723–739
 Chromogranin A, 778
 Chromosomal abnormality, 816
 Chromosomal imbalances, 384, 387
 Chronic ulcers, 805
 Circular sinus, 461
 Cisplatin, 151–153, 158, 354, 372, 423, 611, 658, 747, 758
 Cisternal spaces, 798
 Cisterna magna, 88, 183, 399, 512, 788
 Cisterns, 801
 C1 laminectomy, 734
 Classic, variant, 333
 Clava, 114
 Clear cell, 818
 Clinical manifestations, 790–791
 Clinical target volume (CTV), 150, 156, 157, 163, 366, 498, 602

- Clival chordoma, 706, 892, 894
 Clival tumor extension, 705
 Clivus, 95, 209, 214, 693, 894
 chordomas, 683–691
 spine, 706
 Closure of the neural groove, 786
c-myc, 344
 C-MYC/N-MYC amplification, 358
 CNS embryonal tumors, 147, 152, 163
 Coagulation disorder, 843
 Cochlea/cochleae, 157, 252
 Cochlear nucleus, 252
 COG ACNS0121 trial, 156
 COG ACNS0831 trial, 156
 Cognition, 916–917
 Cognitive, 159–160
 decline, 370
 impairment, 925
 Cognitive/attentional distraction, 924
 Cognitive-behavioral skills-oriented strategies, 924
 Colliculi, 91
 Colliculus facialis, 115
 Collimator leaf, 369
 Combined approaches, 206–207
 Combined, suboccipital craniotomy, 180
 Communicating hydrocephalus, 799
 Comparative genomic hybridization (CGH), 479–481
 Compartments, 797, 802
 Complete surgical resection, 821
 Complications, 231, 329–330, 408, 412
 Compound muscle action potentials (CMAPs), 242
 Computed tomography (CT), 393, 449
 Concomitant chemotherapy, radiotherapy, 611–613
 Concorde, 183
 Concurrent chemotherapy, 610
 Conformal conventionally fractionated full dose irradiation, 425
 Conformal 3D non coplanar, 499
 Conformal radiation therapy, 152–155
 Conformal RT boost, 372
 Congenital aqueductal stenosis, 546
 Congenital dermal sinus, 786
 Connection, 785
 Contracture, 913
 Contrast enhancement, 637
 Convection-enhanced delivery (CED), 566, 621
 Conventional radiotherapy, 610
 Corkscrew-like electrodes, 254
 Corpora quadrigemina, 546
 Corpus pontobulbar, 111
 Correlate biological findings, 606
 Cortical dysplasia, 778
 Corticobulbar motor-evoked potential (CBT MEP), 242, 258–259
 Corticobulbar tract (CBT), 252, 566
 Corticocerebellar fibers, 104
 Corticospinal tract (CST), 116, 241, 244–245, 558, 565–566
 Corticotrophin-releasing hormone, 904
 Cortisol, 904
 Cosyntropin test, 905
 Cough, 828
 Coughing reflex, 246
 Cowden syndrome, 808
 CPA. *See* Cerebellopontine angle (CPA)
 CP angle lesions, 798
 CPC. *See* Choroid plexus carcinoma (CPC)
 CPP. *See* Choroid plexus papilloma (CPP)
 CPT-SIOP-2000, 738–739, 747
 Cranial motor nerve(s), 241, 243
 Cranial nerve palsies/palsy, 412, 791
 Cranial nerves, 75, 412, 463, 827
 Cranial nerve VI palsy, 239
 Craniocervical junction (CCJ), 209, 214, 215, 786
 Craniopharyngioma, 148
 Cranioplasty, 845
 Craniospinal axis, 899
 Cranio-spinal hinge, 61, 62
 Craniospinal irradiation (CSI), 151–165, 363, 425, 498, 669, 758
 Craniospinal metastases, 670
 Craniospinal radiation, 670
 Craniospinal radiotherapy (CSRT), 352
 Craniotomies/craniotomy, 189, 193, 321, 410
 Craniovertebral joints, 224
 Craniovertebral junction, 190, 892, 893, 896
 Craniovertebral stabilization, 894
 Creatine, 300
 Cribriform plate, 366
 Criteria, WHO, 820
 Crockard, H.A., 224
 Cromogranin, 340
 Crossbow incision, 50
 Cruveilhier, J., 34
 Crystals, 800
 CSF. *See* Cerebrospinal fluid (CSF)
 CSF-shunts, 829
 CSI. *See* Craniospinal irradiation (CSI)
 CST. *See* Corticospinal tract (CST)
 Culmen, 82, 86, 178
 Cumulative incidence (CI), 154
 Cuneate fasciculus, 95
 Cuneocerebellar pathway, 104
 Cuneocerebellar tract, 107
 Cushing, H.W., 35, 48
 CyberKnife, 166–167
 CYC. *See* Cyclophosphamide (CYC)
 CyclinD1, 662
 Cyclooxygenase 2(COX-2), 697
 Cyclophosphamide (CYC), 151–153, 354, 489, 610, 658, 747
 Cyst(s), 449, 785
 Cystic changes, 817
 Cystic tumor, 574, 817
 Cyst wall, 457, 798, 801
 Cytarabine, 614
 Cytokeratin AE1/AE3, 695
 Cytokeratins, 731
 Cytoreduction, 643

D

- Da Carpi, J.B., 6
 Dactinomycin, 758
 Dandy-Walker syndrome, 786
 Dandy, W.E., 31, 53, 192
 Dawbarn, R., 46
 3D conformal radiotherapy (3DCRT), 598
 3-Deazaneplanocin A, 390
 Decision-making, 573
 Declive, 82
 Decompress, 643
 Decompressive craniectomy, 41
 Decussation, 95
 “Dedifferentiated” chordoma, 694
 Defective closure, 785
 Dehydration, 860
 Delayed/arrested puberty, 902–903
 Deletion, 816
 De Martel, T., 45
 Dentate nucleus, 90, 408
 Dentate-rubro-thalamic tract, 104, 116
 Dentatohalamic tract, 104
 Dentatohalamocortical tract, 846
 Dentothalamocortical tract, 915
 Dermal sinus, 785, 786, 797, 800
 Dermal tract, 790
 Dermoid cysts, 785, 798
 Dermoid tumors, 797
 Desflurane, 859
 Desmoplasia, 777
 Desmoplastic infantile ganglioglioma, 537, 778
 Desmoplastic medulloblastoma (DMB), 272, 291, 337–339
 Desmoplastic/nodular histology, 350
 Desmoplastic/nodular variant, 333, 375
 Desquamation process, 788
 Detailed MRI workup, 577
 Dexamethasone, 852
 DFCI/IRS III, 657
 Diastematobulbia, 786
 Dibromodulcitol, 489
 Dickkopf-related protein 1 (DKK1), 342
 Differential diagnosis, 639–641
 Diffuse astrocytoma, 139, 471–472
 Diffuse brainstem gliomas, 557, 609
 Diffuse fibrillary astrocytomas, 490–491, 495
 Diffuse intrinsic pontine gliomas (DIPG), 519
 Diffuse intrinsic tumors, 595
 Diffuse tumors, 571
 Diffusion imaging, 516–517
 Diffusion tensor imaging (DTI), 433, 516
 Diffusion tensor imaging studies/tractography, 394
 Diffusion-weighted imaging (DWI), 394, 639, 800
 3 Dimensional conformal radiation (3DCRT), 368
 Diplopia, 125
 Direct (D) wave, 256
 Dishevelled, 133
 Distress, 928
 Distressing procedures, 924
DLL1, 385
 Dopamine, 829
 Dorsal column nuclei, 252
 Dorsal exophytic gliomas, 519
 Dorsally exophytic tumors, 571, 595
 Dorsal nucleus, 115
 Dorsal spinocerebellar fasciculus, 111
 Dorsal spinocerebellar fibers, 105
 Dorsal tubular structure, 704
 Dorsum sellae, 77
 Dosage, 604
 Downbeat nystagmus, 122
 Doxorubicin/cisplatin, 758
 Draining sinuses, 805
 Drop metastases, 305, 335, 411, 458
Drosophila melanogaster, 65
 Dryander, J., 6
 Duane’s retraction syndrome, 121
 Dura, 186
 attachment, 815
 mater, 66, 321
 Dural closure, 230
 Dural sinus, 794
 Dural substitutes, 845
 Dural tail, 817
 Dural thickening, 817
 Duroplasty, 187
 DUSP12, 387
 Du Verney, J.G., 27
 D-wave, 256
 Dysarthria, 791, 865, 878–879, 914–915
 Dysarthric features, 239
 Dysdiadochokinesia, 119
 Dysembryoplastic inclusion cysts, 539
 Dysembryoplastic neuro-epithelial tumor, 419, 778
 Dysmetria, 119, 120, 239
 Dysphagia, 148, 239, 863, 878–879, 914–915
 Dysphonia, 246
 Dysplastic cerebellar gangliocytoma, 305, 807
- E**
 Early puberty, 900
 Early surgery, 229
 Echordosis physaliphora, 675
 Ectoderm, 786
 Ectodermal elements, 786, 799
 Ectopic inclusion, 785
 EGFR. *See* Epidermal growth factor receptor (EGFR)
 Eight-drugs-in-one-day, 355
 Eight-in-one, 355
 Electrolytic balance, 859
 Electrooculographic monitoring, 242
 Eloquent area, 798
 EMA. *See* Epithelial membrane antigen (EMA)
 Embolization, 222, 817
 Embryo, 62–64, 67–69
 Embryogenesis, 786
 Embryology, 62, 72, 786
 Embryonal posterior fossa tumors, 151–152

- Embryonal tumor with abundant neuropil and true rosette (ETANTR), 719
- Emergency, 643
- Eminentia arcuata, 210
- Encephalocele, 791
- Encephalomalacia, 800
- Endochondral ossification, 63
- Endocrine, 159
- Endocrine-reproductive disturbances, 899
- Endocrinopathy/endocrinopathies, 899
- End of life, 927
- Endoscope-assisted microsurgical technique, 804
- Endoscopically assisted techniques, 803
- Endoscopic approaches, 226
- Endoscopic assistance, 803
- Endoscopic assisted removal, 804
- Endoscopic third ventriculostomy (ETV), 229, 316, 408, 547, 643, 845, 846
- Endoscopy-assisted microscopic resection, 408
- ENT surgeons, 710
- Eosinophilic granular bodies, 434, 467
- Ependyma, 242
- Ependymal rosettes, 415
- Ependymomas, 147, 148, 154–156, 177, 303, 383–390, 393, 407, 415, 452, 539, 900, 902
- EphAs, 69
- Ephrins A, 69
- Epidemiology, 785–786
- Epidermal cells, 785
- Epidermal growth factor receptor (EGFR), 137, 386, 440
inhibitor(s), 596, 619
signaling pathway, 135–136
- Epidermoid(s), 785, 799, 801, 803
lesions, 799
tumors, 797–805
- Epidural recordings, 256–257
- Epigenetic activity, 630
- Epigenome, 265
- Epilepsy, 124
- Epileptic seizure, 829
- Epiphyseal plates, 900
- Epipterygoid bone, 64
- Epithelial lining, 798
- Epithelial membrane antigen (EMA), 418, 696, 731, 820
- Epithelial rests, 785
- Epitheloid sarcoma, 222
- Epstein, 562
- ERBB1, 596
- Erectile dysfunction, 902, 903
- Erosion, 816
- Estienne, C., 14
- Estrogen receptor- β (ER- β), 697
- Ether, 31
- Etoposide, 358, 489, 610, 658, 747
- Eustachian tubes, 213
- EVD. *See* External ventricular drainage (EVD)
- EVD catheter, 856
- Ewings sarcoma, 222
- The Exo-occipital, 62–65
- Exophytic, 251, 511
- Exophytic brainstem tumors, 462, 564
- Exophytic component, 557
- Exophytic lesion, 798
- Exophytic tumors, 560, 609, 610
- Extensive nodularity medulloblastomas (MBEN), 357
- Extensive nodularity variants, 291
- Extensor cervical muscles, 887, 889
- Extensor digitorum communis, 255
- Extensor spinal muscles, 889
- External beam RT, 899
- External germinal layer, 334
- External granule layer (EGL), 70–72, 132
- External occipital protuberance, 75
- External ventricular drainage (EVD), 183, 229, 408, 645, 828, 829, 844–846, 856
- Extracellular matrix (ECM), 386
- Extracranial meningioma, 816
- Extradural exposure, 210
- Extraneural metastases, 307, 481
- Extraskeletal chordomas, 706
- Extrinsic oculomotor muscles, 242
- Extubation, 851, 859
- F**
- Facetectomy, 887
- Facet joints, 891
- Facial colliculus, 96, 108, 245
- Facial nerve
MEP, 768
nuclei, 242
transposition, 214
- Facial palsy, 797, 799
- Facial paresis, 240
- Falx cerebelli, 102, 178
- Family conflict, 928
- Family management style (FMS), 923
- Far-lateral approach, 177, 194–204
- Fasciculus cuneatus, 111
- Fasciculus gracilis, 111
- Fastigium, 88, 398, 726
- Fat cells, 789
- Fat droplets, 790
- Fatty content, 791
- FBXW7*, 385
- Fear, 924
- Feather, 368
- Fentanyl, 851
- Ferrier, D., 34
- Fetal inclusion, 785
- Fgf8* gene, 69, 70
- Fiber tracking, 517
- Fibrillary astrocytomas, 457, 511, 586
- Fibrillary histology, 437
- Fibrin glue, 849
- Fibroblastic type, 820
- Fibrous, 818
- Field in field, 368
- Finger/nose test, 120
- Fixation techniques, 893

- FLAIR MRI, 596
 FLAIR sequences, 516
 Flexner-Wintersteiner, 652
 Floccular part, 726
 Flocculi/flocculus, 86, 93
 Flocculonodular lobe, 92
 Floor of fourth ventricle, 240
 Floor, ventricle, 95–96, 856
 Fluid, 817
 Fluor-Desoxy-Glucose PET, 746
 Focal intrinsic medullary tumors, 519
 Focal intrinsic tumors, 564
 Focal tumors, 609
 Folium, 82
 Folium vermis, 103
 Follicle stimulating hormone (FSH), 902–904
 Follow-up studies, 541
 Foramen magnum, 77, 95, 178, 213
 Foramen of Magendie, 84, 179
 Foraminal tumors, 213
 Fourth ventricle, 4, 84, 86–88, 113–114, 177, 788, 844
 Fourth ventricle mapping technique, 251
 Fourth ventricular epidermoids, 804
 Foville's syndrome, 123
 Frazier, C., 48
 Frazier's point, 460
 Free-running electromyography (EMG), 242, 257–258
 French Society of Pediatric Oncology (SFOP), 352
 Fritsch, G.T., 34
 FSH. *See* Follicle stimulating hormone (FSH)
 Functional hearing preservation, 770
 Functional preservation, 576
 Funiculus separans, 96, 115
- G**
- Gag reflexes, 828
 Gait disturbances, 844
 Gait impairment, 240
 Galea, 845
 Galen of Pergamon, 4
 Gall, 252
 Gamma knife, 425, 433
 Gamma knife radiosurgery, 165–167, 805
 Gamma-secretase inhibitors (GSI), 389
 Gangliocytoma, 305, 591
 Ganglioglioma(s), 164, 419, 511, 537, 585, 591
 Ganglion cells, 777
 Gastrostomy, 240, 408
 Gastrulation, 62
 Gautier D'Agoty, J.F., 27
 Gefitinib, 619
 Gemistocytic component, 779
 Genetics, ependymomas, 383–390
 German Society for Paediatric Oncology and Haematology, 364, 660
 Germ cells, 903
 dysfunction, 903
 Germinomas, 244, 304
 GFAP. *See* Glial fibrillary acidic protein (GFAP)
- GH. *See* Growth hormone (GH)
 Gigli, L., 38
 Gigli saw, 38
 Glands, 789
 Glial fibrillary acidic protein (GFAP), 341, 418, 434, 587, 652, 731
 Glioblastoma (GBM), 418, 467, 472–475, 586
 Glioblastoma multiforme (GBM), 487, 495
 Glomus tumors, 213
 Glossopharyngeal nerves, 93, 191, 246
 Glossopharyngeal neuralgia, 55
 Glucagon stimulation test, 905
 Glutamate compounds, 817
 Glutamine compounds, 817
 Glutamine plus Glutamate (Glx), 301
 Glutathione, 817
 Glyosis, 788
 Gonadal insufficiency, 902
 Gonadal toxicity/infertility, 899
 Gonadotoxic therapy, 904
 Gonadotropin deficiency, 902
 Gonadotropin releasing hormone (GnRH), 904
 Gorlin syndrome, 71, 129, 267–268, 357
 Gracile fasciculus, 95
 Gracile tubercle, 115
 Grade 1 tumor, 816, 818
 Grade 2 tumor, 490, 816, 818
 Grade 3 tumor, 818, 820
 Gradient-echo imaging, 394
 Grading system, 818
 Grading, WHO, 815
 Gram positive cocci, 792
 Granular cells, 807
 Granulomatous meningitis, 790, 799
 Greater occipital nerve, 191
 Gross tumor volume (GTV), 149, 156, 157, 498, 602
 Group 3 tumor, 334, 350
 Group 4 tumor, 334, 350
 Growth hormone (GH), 900
 deficiency, 899, 900
 deficient, 901
 secretion, 901
 stimulation testing, 901
 therapy, 901
 Growth retardation, 670
 GTV. *See* Gross tumor volume (GTV)
 Guilt feelings, 928
 Guiot, G., 56
- H**
- Haematoma, 843, 844
 Haemorrhage, 843
 Hair follicles, 789
 Hair loss, 161
 Halsted, W.H., 48
 Hamartoma(s), 305, 548, 807
 Hannover classification, 764
 H2 antagonist, 844
 Hardware, PFT irradiation, 165, 166

- Harvard University, 53
 Headache, 123, 148
 Head Start II (HS II) regimens, 660
 Healthcare providers, 926
 Hearing, 503
 impairment, 239, 764
 loss, 158–159, 372, 492
 Heister, L., 21
 Helical IMRT, 670
 Helical tomotherapy, 365
 Hemangioblastoma, 50, 126, 305, 452, 539
 Hemianaesthesia, 799
 Hemifacial spasm, 124
 Hemihypertrophy, 807
 Hemiparesis, 799
 Hemispheres, 102
 Hemorrhage, 800
 Hereditary syndromes, 129–131
 Herniation, 298, 855
 HES1, 385, 389
 HEY1, 385, 389
 HFRT. *See* Hyperfractionated radiation therapy (HFRT)
 HGF/cMET signaling pathway, 136–137
 High cellularity, 639
 High conformality, 601
 High-dose chemotherapy, 610, 660–661
 Higher proliferation index (MIB-1), 822
 High grade II, 820
 High grade III, 820
 High grade astrocytoma, 457
 High grade gliomas, 491
 High-grade type, 821
 High risk MB
 chemotherapy, 354–357
 radiotherapy, 363
 High risk patients, radiotherapy, 375–376
 High serum TSH, 901
 Histological analysis, 388
 Histology/immunohistochemistry, 334, 433–441
 Histone deacetylase, 662
 Histone deacetylase inhibitors (HDACi), 389
 History, posterior fossa, 3–57
 HIT-SIOP PNET 4 trial, 354
 HIT-SKK'92, 357
 Hitzig, E., 34
 Hockey stick incision, 202
 Holmes, O.W., 4, 31
 Homer-Wright rosettes, 335, 652
 Horizontal conjugate gaze, 546
 Horizontal suboccipital fissure, 178
 Horizontal sulcus, 102
 Hormonal effects, 815
 Hormone replacement therapy, 159
 Horner's syndrome, 713
 Horsley, V.A.H., 34, 41
 Hot-cold spots, 368
Hox d4 gene, 65
hSNF5/INI1, 139, 657
 hTERT telomerase, 389
 Human telomerase reverse transcriptase (hTERT), 387
 Hunter, W., 8
 Hydrocephalus, 50, 123–124, 179, 229–235, 289,
 316–318, 334, 398, 407, 432, 459, 521, 560, 799,
 828, 829, 844–846, 849, 865
 Hydrocortisone solution, 792
 Hyperfractionated accelerated radiotherapy (HART), 356
 Hyperfractionated craniospinal radiotherapy, 901
 Hyperfractionated radiation therapy (HFRT), 354,
 373, 610
 Hypergonadotropic hypogonadism, 902
 Hypermethylation, 276
 Hyperosmolar agent, 856
 Hyperostosis, 816
 Hyperprolactinaemia, 900
 Hyperpyrexia, 790
 Hypersensitivity, 489
 Hyperthermia, 855
 Hypofractionated stereotactic radiotherapy (SCRT), 376
 Hypoglossal canal, 77
 Hypoglossal nerve, 95, 191
 Hypoglossal nuclei, 246
 Hypoglossal paralysis, 246
 Hypoglossal triangle, 96, 246
 Hypoglossus facial nerve anastomosis, 768
 Hypogonadism, 900, 903
 Hypogonadotropic, 903
 Hypogonadotropic hypogonadism, 902
 Hyponatremia, 828, 850, 860
 Hypothalamic infundibulum, 404–405
 Hypothalamic-pituitary axis, 902
 Hypothalamic-pituitary-gonadal axis, 904
 Hypothalamopituitary area, 901
 Hypothermia, 855
 Hypothyroidism, 900–902
 Hypotonia, 119–120, 846

I
 Ibuprofen, 828
 Idarubicin, 358
 IDH-1, 435
 Ifosfamide, 614, 658
 IGF-1, 901
 IGF-binding protein 3 (IGF-BP3), 901
 Imaging protocols, 518–519
 Imatinib, 619
 Immediate postoperative period, 843
 Immune-related genes, 388
 Immunohistochemical findings, 418
 Immunohistochemical stain, 820
 Immunostimulatory therapy, 617–618
 Impact, 920–923
 Impairment, 925–926
 IMRT. *See* Intensity modulated radiation therapy (IMRT)
 Inappropriate antidiuretic hormone secretion, 860
 Incidence, 431
 Inclusion lesions, 785
 Incomplete resection, 821
 Infants, 432
 Inferior cerebellar artery(ies), 411

- Inferior cerebellar peduncle, 88, 93, 104–107
 Inferior extension, 705
 Inferior foramen cecum, 95
 Inferior fovea, 96
 Inferior medullary velum, 86, 88, 313, 334
 Inferior oblique, 77
 Information-based preparation programs, 924
 Infracollicular incision, 547
 Infratemporal approach, 214
 Infratentorial supracerebellar approach, 180, 548, 552, 797, 803
 Inhibin B, 902, 903
 INII, 629, 652
 Inner acoustic canals, 404
 Inpatient rehabilitation, 913
 Instability, 889
 Insulin-induced hypoglycemia, 901
 Insulin tolerance test, 905
 Integrins, 386
 Intellectual impairment, 492
 Intellectual outcome, 371
 Intensity modulated proton therapy (IMPT), 374
 Intensity modulated radiation therapy (IMRT), 158, 499, 598–600, 670
 Intensive care unit, 855, 859
 Interferon-beta, 617
 Interhemispheric supratentorial approach, 803
 Interhemispheric transcallosal approach, 552
 Interleukin-12, 615
 Intermittent cranial nerve palsy, 790
 Internal acoustic meatus, 77
 Internal auditory canal (IAC), 768
 International Society of Paediatric Oncology (SIOP), 351, 364
 Internuclear ophthalmoplegia, 122, 240
 Interparietal, 62–66
 Interpeduncular fossa, 94, 112, 405, 554
 Interpeduncular sulcus, 91
 Interspinous ligaments, 889
 Interstimulus interval, 254
 Interstitial brachytherapy, 621
 Intervertebral foramina, 366
 Intracranial chordomas, 705–706
 Intracranial epidermoids, 797
 Intracranial haemorrhage, 882
 Intracranial hypertension, 124, 791
 Intracranial hypertensive syndrome (ICH), 705
 Intracranial pressure (ICP), 827–829, 845, 855
 monitoring, 232, 855, 856
 Intracystic, 800
 Intradural exposure, 210–211
 Intraocular meningiomas, 816
 Intraoperative-evoked potentials, 240
 Intraoperative magnetic resonance imaging (ioMR), 461, 578, 580
 Intraoperative neurophysiological methods, 578
 Intraoperative neurophysiologic monitoring (IONM), 239–259, 565, 648
 Intraoperative neurophysiology (ION), 240, 735–736
 Intraparenchymal epidermoids, 799
 Intratentorial approach, 803, 804
 Intrathecal chemotherapy, 668
 Intratumoral hemorrhage, 635
 Intravenous morphine, 828
 Intraventricular chemotherapy, 374, 745, 799
 Intraventricular CT, 357
 Intraventricular epidermoids, 798
 Intrinsic tumors, 609
 Involvement, brainstem and cranial nerves, 647
 (125)Iodine seeds, 377
 Irinotecan, 358, 389, 616
 Ischaemic stroke, 882–883
- J**
 JAK/STAT pathway, 679
 Jelly-like tumors, 703
 Jerk nystagmus, 122
 Johns Hopkins University, 48
 Jugular foramen (JF), 77, 178, 209, 213–214
 Jugular tubercle, 214
 Juvenile pilocytic astrocytomas (JPA), 147, 148, 495
 Juxtacondylar approach, 214
- K**
 Kawase approach, 210
 Keen, W.W., 38
 Keratin content, 800
 Ketorolac, 860
 Ki-67, 341, 419
 Kinesin family member 2C, 662
 Kinesin family number-27 (KIF27), 387
 Kinesin KIF11, 385
 KIT/PDGFR, 440
Klebsiella, 790
 Klippel-Feil syndrome, 786
 Knife radiosurgery, 805
 Kocher, T., 48
 Koch, R., 32
 Krause, F., 43, 189
 Kyphosis, 887, 890
- L**
 Lactate (Lac), 300
LacZ gene, 64
 Lamina, 891
 Laminectomy/laminectomies, 887, 889–891
 Laminin alpha 2 (LAMA2), 386
 Laminoplasty, 889–891
 Langerhans cell histiocytosis (LCH), 220, 539
 Large cell (LC), 297
 Large cell and anaplastic (LCA), 339–340
 Large cell variant, 333
 Lateral approaches, 211–213
 Lateral cerebrosplinal fasciculus, 111
 Lateral exophytic tumors, 571
 Lateral gaze disturbances, 245
 Lateral lemniscus, 107, 111, 112, 116

- Lateral longitudinal fasciculus, 550
 Lateral masses, 888, 893, 896
 Lateral mesencephalic sulcus, 244, 547
 Lateral position, 462
 Lateral recess/lateral recesses, 88, 93–94, 399
 Lateral rectus muscles, 242
 Lateral retrosigmoid approach, 564
 Lateral sinus, 82
 Lateral sulcus, 113
 Lay bone graft, 893
 Le Fort I maxillotomy, 219, 226
 Leonardo da Vinci, 6
 Leptomeningeal dissemination, 670
 Leptomeningeal spread, 305
 Lethargy, 123
 Leukoencephalopathy, 405
 Levothyroxine, 901
 Leydig cell deficiency, 902
 Leydig cell dysfunction, 903
 Leydig cells, 903
 LH, 902–904
 Lhermitte-Duclos disease (LDD), 305, 778, 807
 LH/FSH deficiency, 902
 Li-Fraumeni syndrome, 129, 266–267, 746
 Ligamentum flavum, 889
 Limb ataxia, 239, 856
 Limb paresis, 239
 Lindau, 50
 Linear growth, 900
 Lingula, 86, 103
 Lipid droplets, 791
 Lister, J., 32
 Lobus centralis, 103
 Lobus pyramidalis, 108
 Lobus uvula, 108
 Localized atypical choroid plexus papilloma, 750
 Localized choroid plexus carcinoma, 754
 Local radiotherapy, 660
 Locus ceruleus, 96
 LOH 17p, 589
 Lomustine/cisplatin, 151, 156, 354
 Longissimus capitis, 77
 Long term follow up, 504
 Long-term sequelae, 353
 Long-term side effects, 147
 Longus capitis, 77
 Longus colli, 77
 Lordosis/lordoses, 887, 890
 Loss of heterozygosity (LOH), 436
 Louis, A., 23
 Low bone mineral density, 905
 Low-dose cosyntropin test, 905
 Lower cranial nerve injury, 240
 Low grade focal, 595
 Low-grade gliomas, 431, 434, 609
 of tectum, 432
 Lumbar drain, 846
 Lumbar puncture, 412, 804, 845, 846
 Luschka, 88, 148, 154, 168, 179, 191, 303, 314, 399
 Lymphoma, 305, 539
- M**
 Macewen, W., 38
 Macrocephaly, 123–124
 Magendie, 88, 314, 399
 Magnetic resonance (MR), 449–451
 Magnetic resonance imaging (MRI), 393, 515, 596
 Magnetic resonance spectroscopy (MRS), 291, 298, 449, 817
 Malignant astrocytoma, 491, 561
 Malignant fibrillary astrocytomas, 609
 Malignant transformation, 469
 Malignant WHO grades, 818
 Mandibular glossotomy, 226
 Mandibular splitting, 219
 Mannitol, 860
 MAPK. *See* Mitogen-activated protein kinase (MAPK)
 Mapping techniques, 241–242
 Masseter, 243
 Maxillotomy, 223
 Mayfield, 184
 McBurney, C., 40
 Mdm2 overexpression, 678
 Meckel, J.F., 25
 Meckel's cave, 25, 213, 804
 Medial lemniscus, 112, 558
 Medial longitudinal fasciculus, 112, 246
 Medial longitudinal rafe, 252
 Median eminence, 96
 Median raphe, 110
 Median suboccipital approach, 177
 Medulla, 95, 179, 511
 Medulla oblongata, 110, 240
 Medullary pyramids, 95
 Medulla spinalis, 112
 Medulloblast, 334
 Medulloblastoma (MB), 49, 71–72, 124–125, 147, 148, 151–154, 177, 229, 287, 313, 333, 349, 363, 398, 452, 828, 845, 846, 895, 899–903
 extensive nodularity, 333
 low-risk, 163–164
 tumorigenesis, 265
 Medulloblastoma with extensive nodularity (MBEN), 339
 Medulloblastoma, 333, 337
 Megalencephaly, 807
 Megavoltage photons, 364
 Megavoltage RT, 363
 Melanotic medulloblastoma, 333, 337
 Membranous bone, 63
 Memorial Sloan-Kettering Cancer Center, 376
 Meninges, 61, 64, 66–67
 Meningiomas, 148, 162, 815–822
 Meningismus, 846
 Meningitis, 412, 788, 799
 Meningothelial tumor, 818
 MEPs. *See* Motor-evoked potentials (MEPs)
 Mesencephalic tumors, 545–555
 Mesencephalic gliomas, 545
 Mesencephalon, 88, 94

- Mesenchymal cells, 786
 Mesoderm, 62, 64–66
 Metabolic acidosis, 828
 Metastasis, 287, 305–307
 Metastatic atypical choroid plexus papilloma, 752
 Metastatic choroid plexus carcinoma, 756
 Metastatic mucinous adenocarcinoma, 699
 Metastatic spread, 401
 Metastatic tumor, risk, 709
 Metencephalon, 69, 70
 Methotrexate, 356, 611, 659, 758
 Metoclopramid, 852
 Metyrapone test, 905
 MGMT, 435
Mhox (Prx-1) gene, 65–66
 MIB-1, 435, 585, 820
 labeling index, 652, 696
 Michelangelo, 6
 microRNAs (miRNAs), 273, 435
 Microtubule-associated protein 2 (MAP2), 434
 Microvascular proliferation, 652
 Midazolam, 859
 Midbrain, 79, 112–113, 240, 511
 Middle cerebellar inferior fibers, 104
 Middle cerebellar peduncle, 88, 93, 95, 104, 179, 801
 Middle cerebellar superior fibers, 104
 Middle ear damage, 160–161
 Midline occipital sinus, 411
 Midline suboccipital craniotomy, 459, 564
 Midline suboccipital route, 802
 Midsagittal plane, 786
 Millard-Gubler syndrome, 123
 Mitigating factors, 873–874
 Mitogen-activated protein kinase (MAPK), 386, 778
 Mixed glio-neuronal phenotype, 776
 Mixed hypothyroidism, 901
 Möbius syndrome, 121
 Modern linear accelerator, 165, 166
 Modern radiation therapy, 149
 Modified accelerated fractionation radiotherapy (HART), 375
 Molecular analysis, 630
 Molecular biology, 129–140, 354, 675–680
 Molecular layer, 809
 Molecularly targeted therapies, 619–620
 Molecular subgroups, 272–273
 Monitoring techniques, 242
 Monoclonal antibody, 820
 Monopolar microneedle, 412
 Monopolar probe, 242
 Monosomy, 816
 Monticulus, 103
 Morand, S.F., 23
 Morbidities, 187
 Morgagni, G.B., 24, 25
 Morphine, 850
 Motor-evoked potentials (MEPs), 240, 242, 254–257, 565
 Motor neglect, 239
 Moyamoya disease, 490
 MRI-based neuronavigation, 648
 MR venography, 817
 MS-275, 662
 MST-312, 389
 mTOR pathway, 679
 MT3 proteins, 385
 Mucoid fluid, 788
 Multifocal, 816
 Mural nodule, 449
 Muscles, 889
 Musée Dupuytren, 34
 Mutism, 120, 844
MYC, 385, 389
MYCN, 137
 Mydriasis, 829
 Myelosuppression, 489
 Myelotoxicity, 364
 Myoinositol plus Glycine (mI), 301
- N**
 N-acetylaspartate (NAA), 300
 Naffziger, H.C., 48
 Nasal dermal sinus, 800
 National Cancer Institute's Surveillance Epidemiology End Results (SEER), 431
 Nausea, 123
 Necrosis, 161–162, 335
 NEFL70, 384
 Negative intracranial pressure, 828
 Neoadjuvant chemotherapy, 364, 733
 Nerve monitoring, 846
 NeuN, 778
 Neural crest, 63–66
 Neural ectoderm, 786
 Neural epidermal growth factor-like 2 (NELL2), 387
 Neuralgia, 799
 Neural stem cells (NSCs), 386
 Neural tube, 799
 Neural tube ectoderm, 798
 Neuraxis, 785
 Neuroanesthesia, 239, 458
 Neuroaxis, 797
 Neurocognition, 502–503
 Neurocognitive complications, 371
 Neurocognitive decline, 433
 Neurocognitive sequelae, 160
 Neuroendocrine, 503
 Neurofibromatosis (NF), 447, 468, 488, 816, 822
 NF1, 432, 489, 537, 585
 NF2, 763, 816, 820
 NF70, 778
 Neurofibromin, 436
 Neurofilament light polypeptide (NEFL70), 384, 388
 Neurological deficits, 863
 Neuronal differentiation, 336, 388
 Neuronal growth inhibitory factor, 385
 Neuronavigation, 192, 518, 846
 Neuronavigator, 394
 Neurophysiological monitoring, 564

- Neurothelium, 66
 Nevoid basal cell carcinoma, 289
 New drug delivery methods, 620–621
 Nitrosoureas, 903
 Nitrous oxide, 31
N-myc, 344
 Nodule, 86, 92, 104, 108
 Nonmetastatic medulloblastoma, 151–153
NOTCH1, 137
 Notch signaling pathways, 134–135, 385, 389
 Notch1 ubiquitination, 385
NOTCH4 VAV1, 137
 Notochord, 675, 693
 Nuclear-cytoplasmic ratio, 287
 Nucleolin, 387
 Nucleus ambiguous, 246
 Nystagmus, 125, 791, 799, 914
- O**
- Obalinski, A., 38
 Obex, 93, 114, 246, 398, 411
 Obstructive hydrocephalus, 794, 844
 Occipital artery, 190
 Occipital bone, 61–66, 75, 77
 Occipital bony defect, 791
 Occipital condyle, 203
 Occipital dermal sinus, 785
 Occipital musculature, 845
 Occipital protuberance, 849
 Occipital sinus, 178
 Occipital transtentorial approach, 257, 548, 551
 Occipitocervical junction, 190
 Occipitocervical rods, 896
 Occipitocervical stabilization, 893
 Occipitofrontalis, 190
 Oculomotor dysfunction, 240
 Oculomotor nerve, 94, 241
 Oculomotor nerve nuclei, 241, 243–244, 550
 Oculomotor nucleus, 121
 Oculomotor paresis, 550
 Oculomotor sulcus, 113
 Odansetron, 828
 Odontoid process, 95
Olig2, 418, 434
 Oligoastrocytoma, 537
 Oligodendroglioma, 537
 Oligospermia, 903
 Olivocerebellar pathway, 104, 105
 Ollier's disease, 447
 O6-methylguanine-DNA methyltransferase (MGMT), 618
 Oncogenesis pathways, 386–387
 Ondansetron, 844, 850, 860
 Onlay bone graft technique, 892
 Onternuclear ophthalmoplegia, 246
 Ontology analyses, 388
 Open door maxillotomy, 225–226
 Operative mortality, 53
 Operative technique
- complications, 329–330
 positioning, 320–321
 telovelar approach, 323–324
 transvermian approach, 325–327
 Opioid, 828
 Opisthotonos, 125
 Optic nerves, 157, 488
 Optic vesicles, 786, 799
 Orbicularis oculi, 243
 Orbitozygomatic approach, 554
 Organs at risk (OARs), 365
 Orthopaedic management, 711
 Oscilloscope, 242
 Osteopenia, 899
 Otic vesicles, 786, 799
 Ototoxic chemotherapy, 158, 159
 Ototoxicity, 372
 Outpatient rehabilitation, 913–914
 Ovarian deficiency, 902
 Ovarian dysfunction, 903
 Overprotectiveness, 926
 Oxaliplatin, 659
- P**
- Packer, R.J., 612
 Pain
 - management, 924
 - treatment, 927
 Palatal split, 225
 Palliative care, 917
 Palsy, 799
 Panjabi instability criteria, 891
 Panse, R., 46
 Papillary, 820
 Papilledema, 125, 232, 550
 Paracetamol, 828, 852
 Paragan gliomas, 213
 Paramedian unilateral suboccipital, 192
 Parapontine reticular formation, 245–246
 Paraspinal muscles, 890, 891
 Paré, A., 15
 Parental anxiety, 924
 Parinaud's syndrome, 122, 546
 Pasteur, L., 32
 Patchy enhancement, 775
 Pathology, dermoid tumors, 788–789
Pax gene, 786
 Peak, GSH, 817
 Pearly tumor, 798
 Pediatric ependymomas, 383–390
 Pediatric Hodgkin lymphoma, 902
 Pediatric neuro-intensive care unit (NICU), 849
 Pediatric Oncology baby protocol (POG1), 357
 Pediatric Oncology Group (POG), 157, 659
 Pediatric Oncology Group Trial 9031, 375
 Pendular nystagmus, 121
 Perfusion imaging, 517–518
 Perfusion-weighted imaging (PWI), 394
 Periaqueductal gray matter, 244

- Periaqueductal tumors, 519
 Pericranial graft, 845
 Pericranium patch, 849
 Perineural fibrosis, 804
 Periodic alternating nystagmus, 122
 Peri-operative mortality, 821
 Peritectal tumor, 522
 Peritoneal seeding, 230
 Peritumoral edema, 856
 Perivascular fibrosis, 804
 Perivascular pseudorosettes, 415
 Periventricular edema, 398
 Persistent hydrocephalus, 855
 Personalized medicine therapy, 389
 Peter Bent Brigham Hospital, 50
 Petroclival meningiomas, 210
 Petroclival space, 193
 Petrosal approaches, 212
 Petrosal fissure, 87
 Petrosal surface, 178
 Petrosectomy, 211
 Petrous apex, 213, 797
 Petrous bone, 77, 86, 209, 213
 PF boost, 363
 PHACE, 447
 Pharynx, 243
 Phosphocreatine, 300
 Photon linear accelerators, 364
 Physaliferous cells, 675
 Physaliphorous cells, 698
 Pial sutures, 582
 PICA. *See* Posteroinferior cerebellar artery (PICA)
 PI3K/AKT, 439
 Pilocytic astrocytomas (PA), 147, 177, 418, 447, 449,
 467, 487, 511, 591, 778
 Pilomyxoid astrocytomas (PMA), 434, 457, 469–471,
 477–478, 511, 537
 Pimple-like lesion, 791
 Pineal, 122
 Pineal regions tumors, 519
 p16INK4A, 662
 Pituitary-tumor transforming gene 1, 662
 Planning organ at risk volume (PRV), 603
 Planning target volume (PTV), 150, 156–158, 498, 602
 Plasma osmolality, 856
 Platelet-derived growth factor (PDGF), 386, 588
 Platelet-derived growth factor receptor (PDGFR)
 inhibitor, 619
 PDGFR α , 713
 PDGFR β , 713
 Platysma, 77
 Pleocytosis, 846
 Pleomorphic xanthoastrocytoma, 471, 491, 778
 Pleurospenoid, 64
 1p36 LOCUS, 678–679
 Pneumocephalus, 320, 799
 Pneumothorax, 829
 Podoplanin, 731
 POG 9233/34, 659
 Point of entry, in focal tumors of medulla, 579
 Polo-like kinase, 662
 Polyuria, 860
 Pons, 95, 112, 179, 240, 511, 550
 Pontine, 801
 glioma, 148
 tegmentum, 112
 tumors, 519, 558
 Pontocerebellar angle, 895
 Pontocerebellar fibers, 104
 Pontocerebellar tracts, 116
 Pontomedullary sulcus, 95
 Pontomesencephalic junction, 551
 Pontomesencephalic sulcus, 91, 94, 95
 Poor growth, 899–901
 Poor prognosis, 630
 Positioning, 320–321, 409, 458
 Positive cells, 820
 Postanesthesia care unit, 827–829
 Posterior tumor extension, 705
 Posterior cerebellar notch, 102
 Posterior clinoid process, 211
 Posterior cranial fossa, 75–98
 Posterior extension, 708
 Posterior fixation, 891
 Posterior fossa (PF), 3–57, 802
 brain tumor, 849
 dermoids, 785
 epidermoids, 797, 798
 epidermoid tumor anatomical classification, 798
 meningiomas, 816
 syndrome, 846, 876–878
 tumor, 147–170, 383, 827, 844, 855–856, 899–901
 Posterior inferior cerebellar artery (PICA), 179, 203, 726
 Posterior intermediate sulcus of the spinal cord, 95
 Posterior ligamentous, 888
 Posterior ligaments, 889
 Posterior medullary velum, 114
 Posterior perforated substance, 94, 112–113
 Posterior reversible encephalopathy syndrome
 (PRES), 405
 Posterior stabilization, 226–227
 Posteroinferior cerebellar artery (PICA), 88
 Posterolateral approach, 194–204, 213, 215
 Posterolateral (postolivary) sulcus, 95
 Postirradiation changes, 605
 Postirradiation chemotherapy, 151, 152, 154, 158
 Postlaminectomy deformities, 889
 Postlaminectomy kyphosis, 889
 Post-operative analgesia, 859
 Post-operative aseptic meningitis, 804
 Post-operative care, 465
 Postoperative complication, 582
 Postoperative hematoma, 855
 Postoperative infection, 856
 Postoperative monitoring, 859
 Postoperative MRI, 465, 856
 Posttraumatic stress disorder, 927
 Posttraumatic stress symptoms, 923
 Potassium channel Kv1.1, 342
 Pott, P., 21

- p16 protein, 590
 Prealbumin, 731
 Prebiventral fissure, 85
 Precentral cerebellar fissure, 90
 Precocious puberty, 899, 904
 Prednisone, 614
 Pre-irradiation chemotherapy, 610–611
 Premature menopause, 904
 Preoperative DTI, 576
 Preoperative embolization, 733
 Preoperative function, 583
 Prepontine cistern, 399
 Prepyramidal fissure, 85
 Preradiation chemotherapy, 610
 Presigmoid retrolabyrinthine, 211
 Presigmoid route, 893
 Prevalence, 431
 Primary curvatures, 887
 Primary germinal zone, 334
 Primary gonadal dysfunction, 902
 Primary hypothyroidism, 901
 Primary motor cortex, 254
 Primary vesicles, 799
 Primitive neuroectodermal tumors (PNETs), 333, 539, 561, 651, 719, 901
 PNET 3, 352
 PNET 3 trial, 364
 Procarbazine, 489, 903
 Procedural stress, 924
 Progesterone receptor (PR), 697
 Prognosis of pediatric CPTs, 738
 Prognostic biomarkers, 387
 Prognostic factor, 463
 Progression free interval, 597
 Progressive disease, 597
 Proliferation/proliferative index, 435, 820
 Prolonged coma, 875–876
 Prone position, 184, 409, 459
 Prophylactic antibiotics, 856
 Propofol, 828, 851
 Proton beam irradiation, 221
 Proton beam radiation therapy, 374
 Proton diffusion imaging, 515
 Proton metabolic imaging, 515
 Proton MR spectroscopy, 394, 517
 Proton radiation therapy, 900
 Proton therapy, 167–170, 499, 670, 703
 Pseudomatous, 818
 Pseudobulbar palsy, 230
 Pseudomeningocele, 185, 230, 412, 463, 794, 844–846
 pStat3, 679
 Psychiatric condition, 928
 Psychological care, 922
 Psychologist, 928
 Psychosocial coping, 919–928
 Psychosocial services, 922
 PTCH (Patched) gene, 267–268
 PTEN, 589, 679
 mutations, 436
 pathway, 807
 Pterional route, 802
 Pterional transsylvian route, 553
 Pterygoidal, 209
 Pubertal delay, 899
 Pupillary reflexes, 828
 Purkinje cells, 807
 Pylocytic astrocytomas, 303
 Pyramid, 178
- Q**
- Quadrangular lobules, 103
 Quadrigeminal cisterns, 204
 Quadrigeminal plate, 513, 548
 Quesnay, F., 22
- R**
- Radiation
 dose, 497
 necrosis, 405, 541
 volumes, 497–499
 Radiation-related treatment effects, 370
 Radiation therapy, 147–170, 309, 423, 433, 489, 668, 821
 techniques, 669–670
 Radiological classification, 408
 Radiologic complexity, 633
 Radionecrosis, 425
 Radiosensitive, 792
 Radiosensitization, 611
 Radiotherapy (RT), 363, 597
 cerebellar astrocytomas, 495–504
 Raised intracranial pressure, 546
 Ranitidine, 852
 Rapamycin, 679
 Rb gene, 677
 Re-arrangement, 816
 Receptor tyrosine kinase 1 (RTK1), 387
 Rectus capitis anterior, 77
 Rectus capitis lateralis, 77
 Rectus capitis posterior major, 77
 Rectus capitis posterior minor, 77
 Recurrent medulloblastoma, 376–377
 Recurrent tumors, 821
 Red nucleus/nuclei, 116, 550
 Reduced-dose CSRT, 354
 Reelin, 384
 Rehabilitation, 909–917
 Reintegration, 926
 Re-irradiation, 162, 164–165
 Relapse, 423
 Relapsed MB, 376
 Relaxation, 924
 Relaxation imaging, 515
 Religious support, 927
 RELN, 384
 Remifentanyl, 851, 859
 Removal, dermal sinus, 794
 Renal impairment, 492

- Repeated invasive procedures, 923
 Residual tumors, 465, 821
 Respiratory insufficiency, 582
 Restricted diffusion, 792
 Reticular formation, 112
 Retreatment, 504
 Retromastoid approach, 327, 459, 802
 Retrosigmoid approach, 177, 192–194, 213
 Retrosigmoid lateral-suboccipital approach, 768
 Rexinoid bexarotene, 662
 Rhabdoid cells, 651
 Rhabdoid predisposition syndrome, 657
 Rhabdoid tumor predisposition syndrome (rtps), 629
 Rhabdoid tumors, 820
 Rhombencephalitis, 539
 Rhombencephalo-cervical junction, 786
 Rhombencephalosynapsis, 71
 Rhombic lip, 70–71
 Rhomboid fossa, 111
 Rhomboid lip, 93
 Rhombomeres, 67–70
 Ridley, H., 18
 Rim, 817
 Ring enhancement, 596
 Risk factors for complications, 869–870
 Rod, 892, 894
 Rosenthal fibers, 418, 434, 467
 RT1 protocol, 154, 158
 Rubinstein-Taybi syndrome, 131
- S**
- Sacrococcygeal chordomas, 706, 707
 Sacrococcygeal region, 707
 Sacrum, 693
 Safe entry zone, 242
 Salt-wasting brain syndrome, 860
 Salvage chemotherapy, 376
 Salvage treatment, 670
 Sargent, P., 4
 Saucerotte, L.S., 23
 School, 926
 Schwannomas, 210, 820
 Sclerotome, 62
 Sebaceous, 789
 Sebum, 785
 Secondary amenorrhea, 902
 Secondary cerebral vesicles, 786, 799
 Secondary curvatures, 887
 Secondary malignancy/secondary malignancies, 309, 370, 489
 Secondary tumors, 162–163
 Second look surgery, 489, 659, 821
 Second malignancies, 503–504
 Secretions, 785
 Sedation, 859
 Seesaw nystagmus, 122
 Seizure, 124, 828, 856
 Semicircular canal, 210
 Semilunar lobule, 108
 Semi-sitting, 213
 Semispinalis capitis, 75
 Semmelweis, I.F., 31
 Sensorineural hearing, 489
 Septic meningitis, 790
 Sertoli cells, 903
 Sestamibi (MIBI-SPECT), 746
 Sevoflurane, 828, 851
 Shunt, 829
 Shunting or endoscopic third ventriculostomy (ETV), 844
 Shunting procedures, 229
 Shunt malfunction, 230
 Siderosis, 883
 Sigmoid sinus, 82, 191
 Simian virus 40 (SV40), 746
 Simple squamous epithelium, 789
 Simple stratified squamous epithelium, 798
 Simulation, 365
 Single-beam proton therapy, 162
 Single pulse technique, 256–257
 Single-stimulus-single-response, 256
 Singultus, 148
 Sinus, 800
 SIOP ependymoma trial, 424
 SIOP II, 352
 SIOP/UKCCSG PNET-3, 356
 Sitting position, 184, 320, 410, 460, 829, 850
 Sixth cranial nerve, 856
 SJMB96, 152
 Skin appendages, 798
 Skull base approaches, 209–218
 Slurred speech, 148
 SMARCB1 gene, 629, 657, 662
 Smoothened inhibitors, 358
 Social competence, 926–928
 Social support, 922
 Soemmering, S.T., 24
 Somatic, 161
 Somatosensory-evoked potentials (SEPs), 242, 252, 566
 Somites, 62, 64–66, 68, 69, 786
 Sonic hedgehog (SHH), 130, 267, 273, 334, 350, 440
 pathway, 71, 131–133
 Sorafenib, 663
 Space, infratentorial, 797
 Spasticity, 915–916
 Speech pathology, 915
 Sphenoidal fissure, 210
 Sphenooccipital synchondrosis, 220
 Spillage, 801, 804
 Spillage of content, 794
 Spinal accessory, 191
 Spinal cord, 158, 511
 monitoring, 240
 Spinal deformity, 412
 Spinal stabilization, 892
 Spinal thecal sac, 405
 Spinal trigeminal tract, 112
 Spinocerebellar, 104
 Spinothalamic tracts, 112

- Spinous process, 891
 Splenius capitis, 75
 Spongioblastoma, 469
 Spongioblastoma multiforme, 334
 Sporadic vestibular schwannomas, 766
 S-100 protein, 418, 434, 590, 696, 731
 Squamous cell carcinoma, 805
 SRGAP3-RAF1, 438–439
 Stabilization of the child, 644
 Staged surgeries, 408
 Standard-dose, 905
 Standard-risk MB, 363
Staphylococcus epidermidis, 790
 Starr, M.A., 40
 Stereotactic hypofractionated irradiation, 425
 Stereotactic interstitial brachytherapy, 377
 Stereotactic irradiation, 376
 Stereotactic radiosurgery, 433, 499, 600, 670
 Stereotactic radiotherapy (SRT), 601
 Stereotactic re-irradiation, 425
 Sternocleidomastoid, 75, 190
 Steroids, 407, 844, 856
 Stimulation parameters, 243
 Strabismus, 123
 Stratified squamous epithelium, 789
 Striae medullaris/medullares, 96, 111, 115, 116, 246
 Subarachnoid space, 790, 845, 846
 Subcapsular resection, 53
 Subdural type pressure transducer, 855
 Subependymal giant cell astrocytoma (SEGA), 437–438
 Suberoylanilide hydroxamic acid, 662
 Subfrontal transbasal approach, 214
 Subgaleal space, 849
 Sublaminar wires, 893
 Sublaminar wiring technique, 892
 Suboccipital approaches, 191, 192
 Suboccipital craniectomy, 77
 Suboccipital craniotomy, 178, 579, 645, 891
 Suboccipital exposure, 794
 Suboccipital fissure, 84
 Suboccipital supratentorial approach, 257
 Suboccipital surface, 83–86, 178
 Suboccipital technique, 892, 893
 Substantia nigra, 550
 Subtemporal approach, 189, 204–206, 209
 Subtemporal lateral approach, 257
 Subtemporal transtentorial approach, 552
 Subtotal resection, 815, 821, 855
 Sulcus limitans, 96
SULT4A1, 137
 Sunitinib, 663
 Superior and inferior colliculi, 545
 Superior cerebellar artery (SCA), 88, 179
 Superior cerebellar peduncle, 90, 103–104, 107, 179, 846
 Superior collicula, 244
 Superior foramen cecum, 94
 Superior fovea, 96
 Superior medullary velum, 88, 548
 Superior oblique, 77, 242
 Superior olivary complex, 252
 Superior petrosal sinus, 82, 210
 Superior rectus, 242
 Superior, tumor extension, 705
 Supine position, 365, 462
 Supracerebellar approach, 77, 803, 804
 Supracerebellar-infratentorial approach, 43
 Supracollicular incision, 547
 Supranuclear paralysis, 257
 Supra-occipital, 61–66
 Supraolivary fossette, 95
 Supraspinous ligaments, 889
 Supratentorial CSF tumor, 828
 Supratentorial ependymomas, 384, 386, 387
 Supratentorial space, 855
 Supratonsillar approach, 108
 Supratonsillar cleft, 86, 93
 Sural nerve graft, 768
 Surgery, 3–57, 821
 Surgical consent, 183
 Surgical optimization, 148
 Surveillance, 501–502
 Surveillance imaging, 401–406, 489
 Survival, 431
 Susceptibility weighed sequences, 516
 Susceptibility-weighted imaging (SWI), 394
 Sweat, 789
 Swelling, 791
 Sylvian aqueduct, 513
 syndrome, 122
 Sylvian fissure, 211
 Synaptophysin, 340, 652, 731, 778
 Syndrome of cerebellopontine angle, 52
- T**
- Taenia choroidea, 725
 Taeniae, 93
 Talacchi, 798
 Tamoxifen, 612
 Tancerdi, 804
 Targeted monoclonal antibody, 621
 Targeting epigenetic modifiers, 390
 Targeting mTOR pathway, 390
 Target volumes, 366, 601
 Taurine (Tau), 301
 Taxol, 358
 Tectal plate, 241, 243–244, 511
 Tectal plate tumors, 519
 Tectal tumors, 545
 Tectum, 94
 Tegmental midbrain tumors, 522
 Tegmental tumors, 550
 Tegmentum, 94, 244, 550
 Tela choroidea, 86, 93, 178, 313
 Telomerase, 677
 Telomerase inhibitors, 389
 Telomere, 436
 maintenance, 677
 Telovelar approach, 178, 180, 323–324, 407, 579
 Telovelar junction, 93, 313

- Telovelotonsillar cleft, 86, 93
Telovelotonsillar segment, 727
Temozolomide, 358, 389, 435, 491, 613, 758
Temporal fossa, 366
Tenascin C (TNC), 384–386, 388, 419
Tension, 799
Tension pneumocephalus, 410
Tentorial edge, 204
Tentorial fissure, 82, 107
Tentorial incisura, 77, 204
Tentorial surface, 178
Tentorium, 65, 77, 211, 244
Tentorium cerebelli, 178
Teratomas, dermoids, 786, 788
Testicular deficiency, 902
Testosterone, 903
Testosterone/estradiol levels, 904
TGF- β , 386
Thalamus, 550
Thallium-scan, 746
Therapeutic targets, 388
6-Thioguanine, 489
Thiotepa, 614, 659
Third ventriculostomy, 183, 459
Threshold, 252
Thrombocytopaenia, 489
Thrombospondin, 615
Thyroid
 carcinoma, 902
 dysfunction, 899
 gland, 902
 hormone, 901
 neoplasms, 901–902
 ultrasonography, 902
Thyroxine, 902
Tibialis anterior (TA), 255
T1 imaging, 516
T2 imaging, 516
Tinea capitis, 816
Tinnitus, 764
Tiothepa, 376
Titian, 6
TNFRSF14, 678
Tongue, 243
Tonsillar peduncle, 86
Tonsilloventral fissure, 85, 108
Tonsils, 108
Topoisomerase II alpha, 662
Topotecan, 358, 659
Torcula, 321, 794
Torcular, 185
Torkildsen shunt, 230
Torsional nystagmus, 122
Torticollis, 120, 125, 849, 895, 896
Total intravenous anesthesia (TIVA), 828
Total resection, 821
Toxicity, 502
TP53 gene, 140
 mutations, 266–267
Tracheal tube, 859
Tracheostomy, 240, 408
Tractography, 433
TRAIL pathway-related genes, 389
Tramadol, 860
Transcavernous approach, 211
Transcerebellomedullary fissure, 734
Transcochlear approach, 211, 213
Transcortical, craniotomy, 180
Transcranial electrical stimulation, 256–257
Transcriptional silencing, 390
Transcription factor EVI1, 388
Transcriptome, 265, 271–272
Transfacial approaches, 214
Transient GH deficiency, 900
Transient ischaemic attacks, 790
Transitional meningioma, 820
Transitional tumor, 818
Translabyrinthine approach, 46, 211, 212
Transoral approach, 215, 220
Transoral retractor system, 224
Transoral route, 219
Transpetrosal approach, 214
Transpharyngeal route, 219
Transthyretin, 731
Transvermian approach, 180, 325–327, 407
Transverse-sigmoid junction, 191
Transverse sinus, 178, 191
Trapezius, 75, 243
Trapezoid body, 112
Treatment-induced neurotoxicity, 310
Tremor, 120
Trephinations, 4
Trichostatin A, 389, 662
Trigeminal nerve, 94, 95
Trigeminal neuralgia, 55, 799
Trigeminthalamic tract, 108, 116
Trochlear nerve, 91, 242
Truncal, 844
Truncal ataxia, 119, 239, 856
TSC1 gene, 679
TSC2 gene, 679
TSC/mTORC1 pathway, 679
TSH deficiency, 901
T2 steady state sequences, 516
Tuberous sclerosis complex, 679
Tübingen algorithm, 766
Tumor, 803
 hemorrhage, 230
 resection, 646, 856
 spreading, 644
Tumorigenesis, 384–386
Tumor-infiltrating lymphocytes (TIL), 388
Tumor protein 53 (p53), 435, 587
 overexpression, 678
Tumor suppressor gene, 271
Turcot syndrome, 72, 129, 266, 447, 479
T4 values, 901
T2 weighted MRI, 157, 596
Tympanoplasty, 160
Tyrosine kinases, 679

U

UBOs, 537
 Ultrasonic aspirator, 647
 Ultrasounds, 647
 Under-expression, 786
 Unsteady gait, 791
 Up-beating vertical nystagmus, 122
 Upbeat nystagmus, 122
 Upward herniation, 230
 Uvula, 86, 92, 108, 178

V

Vagal triangle, 96, 115, 246
 Vagus nerves, 93, 115, 191, 246
 Valleculla, 86
 Valleculla cerebelli, 84
 Vascular endothelial growth factor, 615
 Vascular epithelial growth factor (VEGF), 440–441
 Vasculopathy, 503
 Vasopressin, 904
 Vasospasm, 882–883
 VEGF. *See* Vascular epithelial growth factor (VEGF)
 Vein of Labbé, 204
 Venipunctures, 924
 Venous air embolism, 410
 Venous hypertension, 458
 Venous sinuses, 788, 794
 Ventral spinocerebellar fasciculus, 111
 Ventral tegmentum, 112
 Ventricular dilation, 232
 Ventricular drainage, 829
 Ventricular system, 844
 Ventriculography, 53, 561
 Ventriculoperitoneal (VP) shunt, 183, 230, 305, 316, 408, 459, 547, 844–846
 Ventriculostomy, 855
 Vermian tumors, 846
 Vermis, 79, 102, 408
 Vermohemispheric fissure, 83, 108
 Vertebral artery, 77, 98, 190–191, 220, 412, 463
 Vertebral column chordomas, 706
 Vertebral column deformities, 887
 Vertical gaze deficiency, 550
 Vertigo, 764
 Vesalius, A., 6
 Vestibular schwannomas, 296, 763
 Vestibulocerebellar pathway, 104
 Vestibulocochlear nerve, 93
 Vicq d' Azyr, F., 26

Video game playing, 924
 VII palsy, 239
 Vimentin, 418, 434, 731
 Vincristine, 354, 433, 489, 610, 658, 747, 758
 Vincristine (VCR), 151–153, 156
 Virchow-Robbins spaces, 786
 Visual impairment, 239
 Vocal cords, 243
 Volume definition, 604
 Volumetric arc therapy, 601
 Volumetric modulated arc therapy (VMAT), 601
 Vomiting, 123, 148
 Von Hippel-Lindau disease, 126
 VP16, 747

W

Wagner, W., 38
 Warren, J.C., 31
 Wave I, 252
 Waves V, 252
 Weakness, 915–916
 WeeFIM, 911
 Wells, H., 31
 Wilkins, R.H., 44
 Willis, T., 18
 Windsor Castle, 8
 Wingless/WNT, 334
 Wire-reinforced endotracheal tube, 859
 Wire technique, 892, 894
 Wnt, 273, 350, 385, 439–440
 Wnt/ β -catenin, 133
Wnt1 gene, 64
 Wnt pathway, 268–269
 Wnt/protein kinase A pathways, 133
 Wnt signaling pathway, 133–134
 World Health Organization (WHO), 818, 820
 2007 classification, 415
 Grade II, 815
 Grade III, 815
 Wyeth, J., 37

Y

Y-knife, 766

Z

Zygomatic arch, 209